NUCLEAR SCIENCE ABSTRACTS

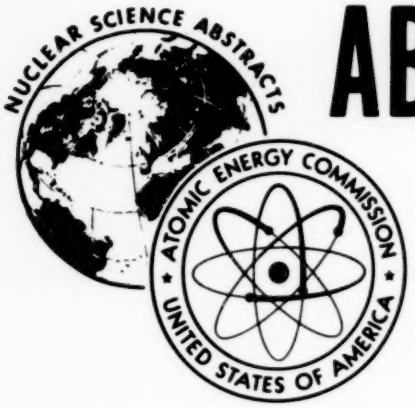

Volume 25 Number 12

Abstracts 26150-28911

June 30, 1971

UNITED STATES ATOMIC ENERGY COMMISSION
Division of Technical Information

REPORT COLLECTIONS IN THE UNITED STATES

The libraries listed below purchase and maintain microfiche collections of USAEC and foreign reports that are abstracted in *NSA*. Their collections also include *NSA* and its indexes, AEC's Technical Progress Reviews, AEC-sponsored translations, conference proceedings published by AEC, and various bibliographic tools. Most of these libraries have microfiche reader-printers or other photocopy facilities with which to reproduce enlarged copies from microfiche. Charges for reproduction services vary.

ALABAMA
Auburn, Auburn University
Tuskegee Institute, Tuskegee Institute

ALASKA
College, University of Alaska

ARIZONA
Tucson, University of Arizona

ARKANSAS
Fayetteville, University of Arkansas

CALIFORNIA
Davis, University of California
Los Angeles, University of California

COLORADO
Boulder, University of Colorado

DISTRICT OF COLUMBIA
Washington, Library of Congress (by deposit)

FLORIDA
Gainesville, University of Florida

GEORGIA
Atlanta, Georgia Institute of Technology

HAWAII
Honolulu, University of Hawaii

IDAHO
Pocatello, Idaho State University

ILLINOIS
Evanston, Northwestern University
Urbana, University of Illinois

INDIANA
Lafayette, Purdue University

IOWA
Ames, Iowa State University

KANSAS
Manhattan, Kansas State University

KENTUCKY
Lexington, University of Kentucky
Louisville, University of Louisville

LOUISIANA
Baton Rouge, Louisiana State University
New Orleans, Tulane University

MARYLAND
Baltimore, Johns Hopkins University
College Park, University of Maryland

MASSACHUSETTS
Cambridge, Massachusetts Institute of Technology
Worcester, Worcester Polytechnic Institute

MICHIGAN
Ann Arbor, University of Michigan

MISSISSIPPI
State College, Mississippi State University

MISSOURI
Kansas City, Linda Hall Library

NEVADA
Las Vegas, University of Nevada

NEW JERSEY
Princeton, Princeton University

NEW MEXICO
Albuquerque, University of New Mexico

NEW YORK
Albany, New York State Library
Albany, State University at Albany
Buffalo, State University of New York at Buffalo
Ithaca, Cornell University
New York, Columbia University
Rochester, University of Rochester
Syracuse, Syracuse University
Troy, Rensselaer Polytechnic Institute

NORTH CAROLINA
Raleigh, North Carolina State University

OHIO
Cincinnati, University of Cincinnati
Cleveland, Cleveland Public Library
Columbus, Ohio State University
Toledo, University of Toledo

OKLAHOMA
Norman, University of Oklahoma

PENNSYLVANIA
Philadelphia, University of Pennsylvania
Pittsburgh, Carnegie Library
University Park, Pennsylvania State University

PUERTO RICO
San Juan, University of Puerto Rico

SOUTH CAROLINA
Columbia, University of South Carolina

TENNESSEE
Knoxville, University of Tennessee
Nashville, Joint University Libraries
Oak Ridge, Oak Ridge Associated Universities

TEXAS
Austin, University of Texas
College Station, Texas A & M University
Houston, Rice University

UTAH
Salt Lake City, University of Utah

VIRGINIA
Blacksburg, Virginia Polytechnic Institute
Charlottesville, University of Virginia

WASHINGTON
Pullman, Washington State University
Seattle, University of Washington

WEST VIRGINIA
Morgantown, West Virginia University

WISCONSIN
Madison, University of Wisconsin

WYOMING
Laramie, University of Wyoming

The following governmental and international organizations offer for sale USAEC reports abstracted in *Nuclear Science Abstracts:*

National Technical Information Service, U. S. Department of Commerce
Springfield, Virginia 22151
International Atomic Energy Agency, Vienna, Austria
National Lending Library, Boston Spa, England

XU

NOTICE

A title page for Volume 25, Numbers 7–12, is included at the back of this issue for use in binding those issues.

CORRECTIONS

NSA Vol. 24, No. 23, Abst. 50188, line 6 should read: core is 9 in. in diameter and 10 in. high. A flux of 10^{11} n/sec

NSA Vol. 25, No. 5, Abst. 8754, last line of abstract should read: interaction with the physical environment. (auth) (Canada)

NSA Vol. 25, No. 6, Abst. 10583, line 8 should read: ALUMINUM ALLOYS—Al-Mn, crystal structure of quenched,

NSA Vol. 25, No. 6, Abst. 10583, line 28 should read: MANGANESE ALLOYS—Al-Mn, crystal structure of quenched,

NSA Vol. 25, No. 9, Abst. 19488, line 2 should read: LISIONS. II. ELASTIC ATOMIC COLLISIONS. Gryzinski, M.

XUM

Volume 25, Number 12, June 30, 1971

NUCLEAR SCIENCE ABSTRACTS

A semimonthly publication of the USAEC Division of Technical Information, Edward J. Brunenkant, Director, Published by the USAEC Division of Technical Information Extension, Robert L. Shannon, Extension Manager.

Nuclear Science Abstracts provides the only comprehensive abstracting and indexing coverage of international nuclear science literature. *Nuclear Science Abstracts* covers scientific and technical reports of the U. S. Atomic Energy Commission and its contractors, other U. S. Government agencies, other governments, universities, and industrial and research organizations. In addition, books, conference proceedings, individual conference papers, patents, and journal literature on a worldwide basis are abstracted and indexed. Each issue of *Nuclear Science Abstracts* includes four indexes: subject, personal author, corporate author, and report number.

The following organizations scan and abstract the nuclear science literature in their respective countries:

Atomic Energy of Canada Limited
Australian Atomic Energy Commission
Danish Atomic Energy Commission
Finnish Atomic Energy Commission
French Atomic Energy Commission
Japan Atomic Energy Bureau–Atomic Energy Research Institute
Institutt for Atomenergi (Norway)
Aktiebolaget Atomenergi (Sweden)
United Kingdom Atomic Energy Authority

Numerous organizations, societies, and publishers throughout the world provide *Nuclear Science Abstracts* with advance page-proof copy of their publications, e.g., in the United States the American Institute of Physics provides page-proof copy of its publications.

A list of the journals scanned regularly and the abbreviations used appears in Issue 1 (January 15) of each volume of *Nuclear Science Abstracts* and is supplemented in Issues 7, 13, and 19. Issue 1 of each volume also describes the scope and arrangement of the subject matter covered in *Nuclear Science Abstracts*. The subject matter covered is also described in TID-4552, *Subject Scope of Nuclear Science Abstracts*, available free from the USAEC Division of Technical Information Extension, P.O. Box 62, Oak Ridge, Tennessee 37830. An outline of the subject categories appears in the Contents of each issue.

AVAILABILITY OF PUBLICATIONS ABSTRACTED

Public availability of all U. S. Atomic Energy Commission reports is indicated in the report number indexes. The availability of other reports, when known, is also indicated. The availability of some unnumbered reports is given in the abstract.

Dissertations abstracted in *Dissertation Abstracts* and included in *Nuclear Science Abstracts* are available from University Microfilms, Inc., 315 N. First Street, Ann Arbor, Michigan 48103.

Information on the availability of the published literature and unpublished conference papers abstracted in *Nuclear Science Abstracts* can be obtained from the USAEC Division of Technical Information Extension, P.O. Box 62, Oak Ridge, Tennessee 37830.

HOW TO OBTAIN NUCLEAR SCIENCE ABSTRACTS

Nuclear Science Abstracts is available to the public on a subscription basis from the Superintendent of Documents, U. S. Government Printing Office, Washington, D. C. 20402.

For the 24 regular issues, the yearly rate is $42.00 for domestic subscribers and $52.50 for foreign subscribers. A single issue costs $1.75, domestic rates, or $2.19, foreign rates. Domestic rates apply to the United States, Canada, Mexico, and Central and South American countries except Argentina, Brazil, Guyana, French Guiana, Surinam, and British Honduras.

For a yearly subscription to the cumulative indexes, the rates are $38.00 for domestic subscribers and $47.50 for foreign subscribers.

The following cumulative indexes are available:

From Johnson Reprint Corporation, 111 Fifth Avenue, New York, N. Y. 10003:
Vols. 1–9, Subjects and Authors (1948–1950), $30.00.

From Superintendent of Documents, U. S. Government Printing Office, Washington, D. C. 20402:

Vols. 5–10, Subjects and Authors (1951–1956), $5.25.

Vols. 11–15, Subjects (1957–1961), $19.00.
Vols. 11–15, Personal Authors (1957–1961), $14.25.
Vols. 11–15, Corporate Authors (1957–1961), $2.50.

Vols. 16–20, Subjects (1962–1966), $36.00.
Vols. 16–20, Personal Authors (1962–1966), $22.50.
Vols. 16–20, Corporate Authors (1962–1966), $3.75.

Vol. 21, Subjects and Authors (1967), $16.00.
Vol. 22, Subjects and Authors (1968), $26.00.
Vol. 23, Subjects and Authors (1969), $25.75.
Vol. 24, Subjects and Authors (1970), $22.50.

Cumulative Report Number Index, Vols. 1-15 Revised, $4.00.
Cumulative Report Number Index, Vols. 16-20 Revised, $5.50.
Cumulative Report Number Index, Vols. 21-24, $4.25.

Nuclear Science Abstracts is available on an exchange basis to universities, research institutions, industrial firms, and publishers of scientific information. Government agencies may obtain *NSA* free of charge. Inquiries should be directed to the USAEC Division of Technical Information Extension, P. O. Box 62, Oak Ridge, Tennessee 37830.

XUM

INDEXES TO NSA

Comprehensive indexes appear in each issue and are cumulated quarterly and annually. Multivolume cumulations have been issued as indicated above.

All documents abstracted are indexed by subjects and personal authors. Report literature is indexed also by corporate author and report number. Each of these indexes in every issue is preceded by an introduction explaining in detail the organization of the index and the principles by which it is compiled. The reader is referred to these explanations for information not found in the brief summary below.

Personal Authors

Each author's name is indexed in the form appearing on the document abstracted:

ISHIHARA, T., Accumulation of fallout ^{137}Cs in newborn infants, 23:50538
ISHIHARA, Toyokuki, Shielding effect of paraffin, water, soil, concrete, Fe, and Pb for nigh-energy neutrons, 23:51748

Subjects

The subject index consisting of specific materials, objects, and processes is arranged alphabetically. Modifying phrases specific to these subjects in turn are arranged alphabetically under the subjects.

MELPHALAN
effects on proliferation of cultured antigen-stimulated spleen cells from mice, dose-response curve for, 23:50820
MEMBRANE FILTERS
design for removal of cell-free Streptococcus faecalus from bacteria cultures in fermentation tank, 23:49996 (UCRL-18667, pp 322-9)
MENDELEVIUM
separation from einsteinium and fermium by electrolysis, 23:49772 (UCRL-18667, pp 277-312)
separation from sodium acetate solutions by solvent extraction using sodium amalgam, 23:49772 (UCRL-18667, pp 277-312)
stability of divalent state of, 23:49772 (UCRL-18667, pp 277-312)

Corporate Authors

Technical report literature is indexed from the name of the organization or institution responsible for the issuance of the report.

51093 (LA-4164) FABRICATION OF BORON CARBIDE RINGS AND DISKS. Sheinberg, H.; Herrera, T.; Kostacopoulos, J. **(Los Alamos Scientific Lab., N. Mex.).** Apr. 25, 1969. Contract W-7405-eng-36. 11p. Dep. CFSTI.

is indexed as:

LOS ALAMOS SCIENTIFIC LAB., N. MEX.
Fabrication of boron carbide rings and disks, 23:51093 (LA-4164)

Report Numbers

Technical report literature is also indexed by report numbers. This index includes information on where individual reports may be obtained. While not reports, patents and conference papers are indexed here as a matter of convenience.

JPRS-	**(Non-AEC)**	
46949	23-51587	CFSTI
48330	23-52305	CFSTI
48331	23-52451	CFSTI
48481	23-50889	CFSTI
48743	23-51034	CFSTI
49025	23-51706	CFSTI (U. S. Sales Only)
JUL-	**(German)**	
571-RG	23-52269	Dep
578-PP	23-51624	Dep. CFSTI (U. S. Sales Only)
581-FN	23-51079	Dep. CFSTI (U. S. Sales Only)
584-RG	23-52313	Dep
586-FN	23-51035	Dep. CFSTI (U. S. Sales Only)
K-		
1777	23-50987	Dep. CFSTI
1778	23-50988	Dep. CFSTI
KFK-	**(German)**	
743	23-52461	Dep
743	23-52447	For translation see EURFNR-613
781/I	23-52462	Dep
824	23-52397	Dep. CFSTI (U. S. Sales Only)

TABLE OF CONTENTS

Volume 25, Number 12, June 30, 1971

Category	Page
CHEMISTRY	2581
Analytical Chemistry	2581
Chemical and Spectral Procedures	2581
Isotope Dilution Procedures	2583
Radiometric and Radiochemical Procedures	2584
Activation Procedures	2584
Inorganic, Organic, and Physical Chemistry	2586
Chemical Properties	2586
Isotope Effects and Exchange	2587
Physical Chemistry	2592
Radiation and Nuclear Chemistry	2594
Radiation Effects	2594
Radiation Processes	2595
Radiolysis	2595
Radioisotope Production	2599
Recoil Production and Reactions	2599
Radiochemistry	2599
Separation Processes	2599
EARTH SCIENCES	2603
Geology and Hydrology	2603
Meteorology	2603
Mineralogy and Exploration	2607
Oceanography	2607
Seismology	2608
ENGINEERING	2609
Nuclear Explosions	2609
Facilities and Equipment	2610
Heat Transfer and Fluid Flow	2611
Isotope Technology	2611
Materials Testing	2612
Radioactive Material Handling	2613
Vacuum Engineering	2614
INSTRUMENTATION	2615
Radiation Detection Instruments	2615
General Detectors and Monitors	2615
Nuclear Spectroscopic Instrumentation	2617
High Energy Physics Instrumentation	2619
Radiation Dosimeters	2620
Radiometric Instruments	2622
Miscellaneous Instruments and Components	2623
Radiation Effects on Instruments and Instrument Components	2624
LIFE SCIENCES	2626
Biochemistry, Physiology, and Molecular Biology	2626
Basic Processes	2626
Metabolism, Physiology, and Toxicology	2627
Radiation Effects	2632
Immunology	2637
Ecology	2640
Genetics and Cytogenetics	2640
Health Physics and Safety	2646
Radioactive Contamination and Decontamination	2646
Dosimetry and Monitoring	2647
Radiation Protection	2649
Safety Procedures	2650

Category	Page
LIFE SCIENCES (Cont'd.)	
Civil Defense	2651
Legal Aspects	2651
Medicine	2651
Protective Substances	2651
Radiation Sickness and Injuries	2654
Radiodiagnosis	2654
Radiotherapy	2659
Blast and Thermal Effects	2662
Radiation Effects on Animals	2662
Invertebrates	2663
Vertebrates	2665
Man	2679
Radiation Effects on Plants	2682
Radiation Effects on Microorganisms	2686
Radiosterilization and Radiopreservation	2688
METALS, CERAMICS, AND OTHER MATERIALS	2694
Metals and Alloys	2694
Corrosion and Erosion	2694
Preparation and Fabrication	2694
Properties Evaluations	2696
Structure and Phase Studies	2701
Radiation Effects	2704
Ceramics and Cermets	2704
Preparation and Fabrication	2704
Properties Evaluations	2705
Structure and Phase Studies	2706
Radiation Effects	2708
Plastics and Other Materials	2708
PHYSICS (GENERAL)	2709
Astrophysics and Cosmology	2709
Cosmic Ray Exposure Ages	2709
Stars	2709
Quasi-Stellar, Radio, and X-Ray Sources	2713
Solar Phenomena	2714
Galaxies	2718
Cosmology	2720
Planetary Phenomena	2721
Atomic and Molecular Physics	2722
Atomic, Electron, Ion, and Molecular Beams and Their Reactions	2722
Atomic and Molecular Properties	2722
Positronium, Muonium, and Mesic Atoms and Molecules	2723
Collision Phenomena	2723
Atomic Theory	2724
Cosmic Radiation	2724
Direct Energy Conversion	2726
Fluid Physics	2727
Geophysics (Upper Atmosphere)	2728
Low-Temperature Physics and Cryogenic Equipment	2741
Superfluidity	2741
Superconductivity	2743
Equipment and Devices	2745
Plasma and Thermonuclear Physics	2745
Confinement and Heating	2745
Diagnostics	2746

TABLE OF CONTENTS (continued)

Category	Page
PHYSICS (GENERAL) (Cont'd.)	
Kinetics (General)	2747
Kinetics (Experimental)	2747
Kinetics (Theoretical)	2748
Production	2749
Stability	2750
Thermonuclear Processes	2756
Wave Phenomena	2756
Shielding	2759
Solid-State Physics	2760
Radiation Effects	2760
Physical Properties	2763
Moessbauer Effects and NMR	2769
Theoretical Physics	2770
PHYSICS (HIGH-ENERGY)	2773
Particle Interactions and Properties (Experimental)	2773
Electromagnetic	2773
Weak	2773
Strong (Baryon-Induced)	2773
Strong (Meson-Induced)	2774
Particle Interactions and Properties (Theoretical)	2775
General	2775
Electromagnetic	2775
Weak	2777
Strong (General)	2778
Strong (Baryon No. = 0)	2779
Strong (Baryon No. = 1)	2780
Strong (Baryon No. ≥ 2)	2781
Particle Invariance Principles and Symmetries	2782
General	2782
Applications (Electromagnetic and Weak)	2782
Applications (Strong)	2782
Field Theories	2782
General	2782
Quantum Field Theory	2782
Gravitation and General Relativity	2784
Scattering Theory	2785
Particle Accelerators	2786
PHYSICS (NUCLEAR)	2791
Neutron Interactions with Matter	2791
Nuclear Properties and Reactions, A ≤ 5	2792
PHYSICS (NUCLEAR) (Cont'd.)	
Nuclear Properties and Reactions, 6 ≤ A ≤ 19	2793
Nuclear Properties and Reactions, 20 ≤ A ≤ 89	2796
Nuclear Properties and Reactions, A ≥ 90	2802
Nuclear Theory	2815
REACTOR TECHNOLOGY	2822
Commercial Power Reactors	2822
Operation and Economics	2824
Safety and Siting	2827
Steam and Power Conversion Systems	2829
Power Reactor Development	2829
Kinetics and Dynamics	2832
Control Systems	2833
Shielding	2834
Cooling Systems	2834
Fuels	2835
Auxiliary and Emergency Systems	2836
Operation and Economics	2837
Safety and Siting	2839
Power Conversion Systems	2841
Research and Test Reactors	2842
Rocket and Space Reactors	2845
Process Heat and Desalination Reactors	2846
Marine and Portable Power Reactors	2847
Production Reactors	2847
Reactor Theory	2847
Kinetics	2847
Dynamics	2849
Experimental Applications	2849
Reactor Components, Fuels, and Accessories	2849
GENERAL	2852
CORPORATE AUTHOR INDEX	INDEX-1
PERSONAL AUTHOR INDEX	INDEX-13
SUBJECT INDEX	INDEX-72
REPORT NUMBER INDEX	INDEX-174

STAFF OF NUCLEAR SCIENCE ABSTRACTS

John W. Norris
Managing Editor

Donald D. Davis
Assistant Managing Editor

David E. Bost
Production Manager

Sidney F. Lanier
Subject Heading Specialist

J. Paul Meredith
Descriptive Cataloging Specialist

Frederick E. Marsh, Jr.
Computer Index Coordinator

Clara L. Fox
Corporate Author Specialist

Helen W. White
Report Number Specialist

Section Editors

Everett J. Hoffman
Chemistry

Robert C. Kelly
Engineering; Earth Sciences; Metals, Ceramics, and Other Materials

Lee M. Thompson
General Physics

Charles E. Stuber
High Energy Physics; Instrumentation

Donald D. Davis
Life Sciences

Lawrence T. Whitehead
Nuclear Physics

James M. Jacobs
Reactor Technology

Evaluators

Thomas S. Chapman
Rose V. Jermain
John H. Mitchell
Mary H. Newman
Polly C. Summers

Abstractors

F. S. Armstrong*
Ellis R. Bedford
Mary M. Brown
Jane G. Buchanan
D. Lamar Cason
Gloria M. Caton
David C. Cunningham
James R. Dulaney
Helga B. Gerstner
Mary C. Grissom
Phyllis C. Hansen
Carolyn D. Houston
Elaine E. Huber
Rose V. Jermain
W. Hugh Kinser, Jr.
Lisbeth C. Lieberman
Betty L. McDowell
Patricia B. McEwen
Fay M. Martin
William D. Matheny
Dora H. Moneyhun
Jean F. Peckham
Henry D. Raleigh
Mona H. Raridon
Julia S. Redford
Jessie W. Rushing
Robert W. Rutkowski
Francis L. Sachs
Lila B. Smith
Anne G. Ward
Helen L. Ward
Milton O. Whitson
Juanita Wilson

*Atomic Energy of Canada, Ltd.

Charles R. Bruce
Publishing Coordinator

Communication concerning the editorial policy and content of *Nuclear Science Abstracts* should be addressed to the Managing Editor, *Nuclear Science Abstracts*, USAEC Division of Technical Information Extension, P. O. Box 62, Oak Ridge, Tennessee 37830.

Use of funds for printing this publication approved by the Director of the Bureau of the Budget, June 26, 1969.

XUM

Volume 25, Number 12 June 30, 1971

NUCLEAR SCIENCE ABSTRACTS

CHEMISTRY

Analytical Chemistry

Refer also to abstracts 27168 and 27169.

26150 ANALYSIS OF ZIRCONIUM COMPOUND. Mori, Yoshihiro (Shinshu Univ., Nagano, Japan). Shin Kinzoku; No. 52, 28-33(Mar 1970). (In Japanese).

Methods for separation of hafnium and zirconium and their subsequent analyses are reviewed. Ion exchange and solvent extraction are mentioned as separation methods. Chemical, neutron activation, and x-ray analysis methods are discussed. (TSS)

Chemical and Spectral Procedures

Refer also to abstracts 26331 and 26572.

26151 (CNEA-288) DETERMINATION OF THALLIUM IN MICROSAMPLES OF NATURAL VANADATES OF URANIUM BY ANODIC REDISSOLUTION. Botbol, Moises; Garcia, Enrique E.; Casabe, Jaime (Comision Nacional de Energia Atomica, Buenos Aires (Argentina)). 1970. 11p. (In Spanish). Dep. NTIS (U. S. Sales Only).

A method for determination of traces of thallium in microsamples of impure tyuyamunite $[Ca(UO_2)_2(VO_4)_2 \cdot nH_2O]$ is described. It requires no previous separations. The procedure is based on anodic stripping of the thallium after concentration in a hanging-drop mercury electrode by means of controlled-potential electrolysis. The procedure was applied to the determination of thallium in concentrations of the order of 0.02% on microsamples weighing between 2 and 4 mg. (auth)

26152 (JAERI-Memo-4267) SPECTROPHOTOMETRIC DETERMINATION OF TRACES OF URANIUM IN SODIUM. Toita, Yukio; Onishi, Hiroshi (Japan Atomic Energy Research Inst., Tokyo). Jan 1971. 10p. (In Japanese). Dep. NTIS (U. S. Sales Only).

A method is described for spectrophotometric determination of 1 to 6 μg of uranium in less than 3g of sodium. A weighed sample is converted into sodium carbonate with moist carbon dioxide. The sodium carbonate is neutralized and acidified with HCl. EDTA, ascorbic acid, and ammonium thiocyanate are added, and uranium is extracted with a mixture of tributyl phosphate and carbon tetrachloride. After washing of the organic phase, uranium is back-extracted with 1M hydrochloric acid. The back-extract is evaporated to dryness. The residue is dissolved in 9M HCl, and uranium is reduced to the quadrivalent state with zinc. Arsenazo III is added and the absorbance is measured at 665 nm. (auth) (Japan)

26153 (LA-4622) METHODS OF CHEMICAL ANALYSIS FOR FBR URANIUM-PLUTONIUM OXIDE FUEL AND SOURCE MATERIALS. Rein, James E.; Matlack, George M.; Waterbury, Glenn R.; Phelps, Robert T.; Metz, Charles F. (eds.) (Los Alamos Scientific Lab., N. Mex.). Feb 1971. Contract W-7405-eng-36. 155p. Dep. NTIS.

Twenty-four methods are given for the chemical specification analysis of FBR uranium-plutonium mixed oxide fuel and uranium dioxide insulator pellets, and for the source materials of ceramic grade uranium dioxide and plutonium dioxide used for their manufacture. The methods include dissolution procedures, uranium and plutonium assay, uranium and plutonium isotopic abundances, metal and nonmetal impurities, and other specifications relating to total gas, water, and the oxygen-to-metal ratio. (auth)

26154 (RFP-Trans-76) DETERMINATION OF TRACES OF IRON, NICKEL, AND CHROMIUM IN PLUTONIUM NITRATE SOLUTIONS WITHOUT PRIOR SEPARATION BY ATOMIC ABSORPTION SPECTROPHOTOMETRY. Ganivet, M.; Benhamou, A. Translated from Anal. Chim. Acta; 47: 81-90(1969). 14p. Dep. NTIS.

An abstract of this paper, prepared from the original language, appeared as NSA 25: 22.

26155 Vth INTERNATIONAL CONGRESS ON X-RAY OPTICS AND MICROANALYSIS, TUEBINGEN, GERMANY, SEPTEMBER 9th-14th, 1968. Moellenstedt, G.; Gaukler, K. H. (eds.). Berlin; Springer-Verlag (1969). 622p. $54.50. (In several languages). (CONF-680984).

The conference proceedings include ~100 papers divided into the following sections: (1) X-ray Optics; (2) Electron Probe Microanalysis, Physical Bases; (3) Electron Probe Microanalysis, Quantitative Analysis; (4) Instrumentation; (5) Microdiffraction; (6) Metallurgical and Mineralogical Applications; and (7) Biological Applications. Separate abstracts have been prepared for 5 of these papers. (B.L.M.)

For abstracts of individual papers see: 26156-26160.

26156 SHIELDED X-RAY MICROPROBE FOR THE ANALYSIS OF RADIOACTIVE SAMPLES. Macres, V. G.; Preston, O.; Yew, N. C.; Buchanan, R. (Materials Analysis Co., Palo Alto, Calif.). pp 248-9 of Vth International Congress on X-Ray Optics and Microanalysis, Tuebingen, Germany, September 9th-14th, 1968. /Moellenstedt, G. (ed.). Berlin; Springer-Verlag (1969).

From 5th International Congress on X-Ray Optics and Microanalysis, Tuebingen, Germany. See CONF-680984.

Special shielding of an electron microprobe for analysis of radioactive samples includes the main tungsten base shielding components, the column base and an intermediate chamber shielding ring; a tubular shield over the gun cable at the top of the column; and Kennertium plugs held in a shielding wall located at the rear of the spectrometer to block the cone or radiation escaping from the back of the spectrometer. During operation of the instrument, shielding equivalent to 4.3 in. of W in all directions from the specimen is provided. Results of peak to background measurements made on a stainless steel specimen in the presence of a 9-Ci ^{60}Co source with the shield microprobe and with an unshielded one are tabulated for comparison. (B.L.M.)

26157 ANALYSIS OF RADIOACTIVE MATERIALS BY MEANS OF AN ELECTRON MICROPROBE DEMONSTRATED ON UO_2-Mo AND UO_2-ZIRCALOY FUEL CERMETS. Giacchetti, G.; Raensch, J. (EURATOM, Karlsruhe, Ger.). pp 250-60 of Vth International Congress on X-Ray Optics and Microanalysis, Tuebingen, Germany, September 9th-14th, 1968. /Moellenstedt, G. (ed.). Berlin; Springer-Verlag (1969).

From 5th International Congress on X-Ray Optics and Microanalysis, Tuebingen, Germany. See CONF-680984.

Modifications of an industrial-type CAMECA microanalyzer for analysis of a specimen with a γ dose up to 100,000 mR/hr at 30 cm are described. The principal modification is a lead shielding of one of the spectrometer chambers to reduce or eliminate fluorescence of materials of the counting tube. The modified microprobe was used to analyze irradiated molybdenum- and Zircaloy-clad UO_2 fuel elements. (B.L.M.)

26158 MICROANALYSIS WITH A PROTON-PROBE. Poole, D. M.; Shaw, J. L. (Atomic Energy Research Establishment,

Harwell, Eng.). pp 319-24 of Vth International Congress on X-Ray Optics and Microanalysis, Tuebingen, Germany, September 9th–14th, 1968. /Moellenstedt, G. (ed.). Berlin; Springer-Verlag (1969).

From 5th International Congress on X-Ray Optics and Microanalysis, Tuebingen, Germany. See CONF-680984.

In addition to having a sensitivity somewhat better than that of the electron-probe, the proton-probe x-ray method forms a perfect partner for proton-excited nuclear γ emission analytical method. In this method a proton beam is used to generate γ's by nuclear reactions with the light elements such as oxygen and fluorine; identification and counting of the γ's enable the excited nuclei to be identified and their concentrations and spatial distributions to be studied. The γ-emission method is best suited to the analysis of light elements up to about atomic number 9 (fluorine), while the x-ray emission equipment described can be used for all elements of higher atomic number. Thus, addition to this apparatus of a suitable scintillation counter for γ-detection will enable high sensitivity analysis at or below 1 ppM to be carried out for all the elements at the same point on a sample without the necessity for transfer from one equipment to another. The method has a resolution of about 10 μm and a sensitivity presently about 10 ppM with excellent prospects for improvement to less than 1 ppM when certain modifications are carried out. (auth)

26159 INVESTIGATIONS ON SUPERCONDUCTING DIFFUSION LAYERS WITH AN ELECTRON BEAM MICROPROBE. Otto, G.; Wizgall, H. (Univ., Giessen, Ger.). pp 481-4 of Vth International Congress on X-Ray Optics and Microanalysis, Tuebingen, Germany, September 9th–14th, 1968. /Moellenstedt, G. (ed.). Berlin; Springer-Verlag (1969). (In German).

From 5th International Congress on X-Ray Optics and Microanalysis, Tuebingen, Germany. See CONF-680984.

Superconducting diffusion layers of the systems Nb–Sn, V–Si, and V–Ga containing intermetallic compounds of the A 15-structure were investigated with a JEOL electron probe microanalyzer of the type JXA-3A. The influence of different methods of diffusion as well as different conditions of preparation on the composition and thickness of the layers is shown. Diffusion wires of the system Nb–Sn prepared by vapor-phase diffusion consist of only one phase with a composition being richer in niobium than the stoichiometric phase Nb_3Sn. The composition of the A 15-phase on corresponding samples of the system V–Si is very close to V_3Si. Diffusion layers of the most thoroughly investigated system V–Ga include the two phases V_6Ga_5 and V_3Ga besides an outer layer V–Ga–Si built up at higher temperatures. In addition the phase V_2Ga_5 is found in layers prepared by the dipping process. There is one sample with a diffusion temperature of 1,000°C showing all phases of the phase diagram by Van Vucht, et al. (auth)

26160 ELECTRON PROBE MICROANALYSIS OF Ti(C,N) AND Zr(C,N) IN STEEL. Shiraiwa, T.; Fujino, N. (Sumitomo Metal Industries, Ltd., Amagasaki, Japan). pp 531-4 of Vth International Congress on X-Ray Optics and Microanalysis, Tuebingen, Germany, September 9th–14th, 1968. /Moellenstedt, G. (ed.). Berlin; Springer-Verlag (1969).

From 5th International Congress on X-Ray Optics and Microanalysis, Tuebingen, Germany. See CONF-680984.

The angular titanium precipitates (carbide or nitride) in steels, which have not been precisely identified hitherto, were analyzed by the electron probe microanalyzer, and it is found that their structures depend on the composition of matrix steel. In the solid solution type precipitate, the carbide concentration increases with the carbon content in the matrix, and it suggests the equilibrium at the precipitation. The appearance of the core structure precipitate means that the precipitation temperature is different for nitride and carbide, and nitride precipitates at an early stage in cooling and solidification of molten steel. But the reason why the core structure is observed in the Cr–Mo cast steel and the high chromium and nickel alloys cannot be interpreted, and it is necessary to investigate the effects of alloying elements on the precipitation. In the Cr–Mo cast steel, molybdenum is observed in titanium carbide. This precipitate is suggested to be a solid solution of Mo_2C in TiC. The color of titanium carbide is bluish white and nitride is orange yellow, and they are distinguished by optical microscopic observation. The similar modification of carbide and nitride is observed in zirconium precipitate in the low carbon steel. (auth)

26161 PHOTOMETRIC DETERMINATION OF RARE EARTHS OF THE YTTRIUM SUBGROUP WITH THE USE OF SALICYLFLUORONE AND 1,10-PHENANTHROLINE. Poluektov, N. S.; Sandu, M. A.; Lauer, R. S. (Inst. of General and Inorganic Chemistry, Odessa). Zh. Anal. Khim.; 26: 499-505(Mar 1971). (In Russian).

The interaction of the rare earth ions with salicylfluorone in the presence of 1,10-phenanthroline was studied spectrophotometrically. Complex compounds at a ratio of Me : Phen : Sfl = 1 : 1 : 2 are formed. Under these conditions two protons are displaced from two molecules of the colored ligand. Formation constants for La and Y compounds were calculated. A spectrophotometric method was developed for determining Er_2O_3 and Yb_2O_3 in a mixture with La_2O_3 at pH 4.4. (auth)

26162 DETERMINATION OF SAMARIUM MICROIMPURITY IN EUROPIUM OXIDE BY MEANS OF CRYSTAL PHOSPHOR LUMINESCENCE. Anikina, L. I.; Karyakin, A. V.; Le Viet Bin (Inst. of Geochemistry and Analytical Chemistry, Moscow). Zh. Anal. Khim.; 26: 511-13(Mar 1971). (In Russian).

Two modifications of the method for determining samarium in europium oxide by the luminescence spectra of crystal phosphors based on $CaWO_4$ and Eu_2O_3 (at a ratio of 100 : 2) with scanning of the spectrum were developed. By the first modification samarium is determined without any preliminary concentration with a sensitivity of 5×10^{-3}%. In the second modification samarium is separated beforehand by a chromatographic method on Teflon. The sensitivity of this variant is 2×10^{-5}%. (auth)

26163 EXTRACTION-PHOTOMETRIC DETERMINATION OF URANYL IONS BY MEANS OF 3-PYRIDINECARBOXYLIC ACID AND RHODAMINE B. Poluektov, N. S.; Bel'tyukova, S. V. (Inst. of General and Inorganic Chemistry, Odessa). Zh. Anal. Khim.; 26: 541-4(Mar 1971). (In Russian).

Uranyl ions form complex compounds with nicotinic acid (NA) and rhodamine B or crystal violet which can be extracted with benzene or with a mixture of benzene and acetone. Optimum conditions for the complex formation were studied. The ratio of the components UO_2^{2+} : NA : dye is 1 : 3 : 1. An extraction–photometric method for determining uranyl ions is suggested. (auth)

26164 RADIOACTIVE ANALYSIS TECHNIQUES. Martinelli, P. (CEA., Saclay, France). Tech. Mod.; 62: 424-27(Oct 1970). (In French).

Different methods of analysis using radioactivity are described: activation analysis, x-ray fluorescence, absorptiometry, diffusion of radiation, and the use of radioactive tracers. The use of sealed sources in analysis is emphasized. (France)

26165 SPECTROPHOTOMETRIC DETERMINATION OF PRASEODYMIUM, NEODYMIUM, SAMARIUM, AND EUROPIUM USING CHROMOTROPE 2 R AS A CHROMOGENIC REAGENT. Shah, Vasant L.; Sangal, S. P. (Univ. of Nagpur, India). Chim. Anal. (Paris); 53: 47-50(Jan 1971). (In French).

The optimum conditions for the spectrophotometric determination of praseodymium, neodymium, samarium, and europium using Chromotrope 2R as a chromogenic reagent, were studied. Other considerations studied include: the effect of pH on absorbance at 590 mμ, the determination of the range consistent with Beer's law, the molar extinction coefficient, and the sensitivity. The effects due to foreign ions were demonstrated. (France)

26166 APPLICATIONS OF ION-SELECTIVE ELECTRODES. Bazzelle, W. E. (E. I. du Pont de Nemours and Co., Inc., Wilmington, Del.). Anal. Chim. Acta; 54: 29-39(Mar 1971).

Various commercial electrodes were studied. The single crystal fluoride electrode is used for direct measurements as well as in titrations of fluoride with lanthanum(III) solution; 60% 2-propanol is the optimal medium for the titration of small amounts of fluoride. Small amounts of hydrogen peroxide do not interfere. The sulfike electrode is useful for the sequential titration of chloride, bromide, and iodide with silver nitrate solution, as well as in titrations of cyanide and thiocyanate; end-point breaks are greater than those obtained with a silver billet electrode. The divalent cation electrode is useful for EDTA titrations of calcium, barium, and sulfate. (auth)

26167 DETERMINATION BY X-RAY FLUORESCENCE OF BARIUM AND STRONTIUM IN BARIUM CARBONATE OF INDUSTRIAL GRADE. Hisano, Kingo; Oyama, Kiyoshi (Ishihara Sangyo Co., Ltd., Kusatsu, Japan). Jap. Anal.; 20: 228-30(Feb 1971). (In Japanese).

Barium and strontium were determined in barium carbonate of industrial grade by x-ray fluorescence following fusion of the sample with a flux containing sodium borate as a major component. The coefficients of variation for barium and strontium were reduced to 0.06 and 0.61%, respectively, by the use of titanium dioxide as the internal standard and the improvement of the borax fusion method. Results of this method agreed closely with those of the cation exchange separation method. (auth)

26168 STUDIES ON ANALYSIS OF RARE EARTHS. II. SPECTROGRAPHIC DETERMINATION OF RARE EARTHS AND

NON-RARE EARTH METALLIC ELEMENTS IN YTTRIUM OXIDE. Sato, Matsuki; Matsui, Hiroshi; Matsubara, Tadao (Shin-Etsu Chemical Industrial Co., Ltd., Takefu, Japan). Jap. Anal.; 20: 215-22(Feb 1971). (In Japanese).

A dc arc excitation method in a controlled atmosphere was applied successfully to the spectrographic determination of small amounts of 14 rare earths and 12 nonrare earth metallic elements in yttrium oxide. In order to establish the optimum conditions, studies were made on the effects of the argon to oxygen mixing ratio in the atmosphere, the selection of analytical line pairs, and the effect of the ignition temperature of yttrium oxalate. Base material was purified by cation exchange using EDTA as the eluant, then by homogeneous precipitation using diethyl oxalate. The intensities of the CN band spectra and the background were remarkably reduced by the use of argon–oxygen (4 : 1) mixed gas atmosphere. It was then possible to obtain analytical sensitivities several times stronger than in excitation in air. The lower limits for the determination of the impurities were: 0.01 to 0.1 ppM for Yb, Mg, Al, Si, Ca, Mn, Fe, Ni, and Cu; 0.1 to 1 ppM for Eu, Er, Tm, V, Cr, Sn, and Pb; 1 to 10 ppM for La, Pr, Nd, Gd, Tb, Dy, Ho, and Lu; and 20 ppM for Ce (as oxides, respectively). Coefficients of variation were 4.5 to 8.0% for rare earth impurities 5.5 to 15.9% for nonrare earth metallic impurities. (auth)

26169 DETERMINATION OF MICROAMOUNTS OF SILVER IN COPPER, ALUMINUM, AND THEIR ALLOYS BY SOLVENT EXTRACTION–ATOMIC ABSORPTION SPECTROPHOTOMETRY. Takahisa, Michio; Tsukahara, Iwao; Shibuya, Seiji (Central Research Lab., Tokyo). Jap. Anal.; 20: (Feb 1971). 188-93 (In Japanese).

An atomic absorption spectrophotometric method for the determination of microamounts of silver in copper, aluminum, and their alloys is presented. This method involves the extraction of silver diethyldithiocarbamate with benzene and the measurement of absorbance of the extract. The interferences from matrix elements such as copper, aluminum, uranium, nickel, and iron can be eliminated by addition of citric acid or EDTA. As little as 1 ppM of silver in copper, aluminum, and their alloys can be determined by this method. (J.G.B.)

26170 SPECTROCHEMICAL DETERMINATION OF ^{235}U. Fukushima, Hiroyuko; Nakajima, Tokunosuke (Japan Atomic Energy Research Inst., Tokai). Bunko Kenkyu: 19: No. 1, 38-42 (Feb 1970). (In Japanese).

The spectrochemical method for determination of ^{235}U utilizes a dc arc and Shimadzu 3.4 m plane grating spectrograph as an exciting light source and a spectrograph, respectively. The choice of AgCl–graphite as a buffer to evaporate uranium smoothly was made on the basis of the experimental results on intensity–time curve and on reproducibility. Intensity–time curves and reproducibility using various buffers were investigated. The 4244.124Å spectral line was used as an analytical line for ^{235}U. Reproducibility using various spectral lines as internal standard lines was investigated. Examples of analysis are presented. (Japan)

26171 ANALYSIS OF ZIRCALOY. Narita, Kiichi; Taniguchi, Masayuki; Mizuno, Tomomi; Harada, A.; Matsumura, Tetsuo (Kobe Steel, Ltd., Japan). Kobe Seiko Giho; 20: No. 2, 35-41 (Apr 1970). (In Japanese).

Methods for determining the ingredients of zircaloy, such as Cr, Fe, Ni, and Sn, by chemical methods are described. The method for determination of micro-ingredients such as Al, B, C, Cd, Cl, Co, Cu, Mn, Mo, Si, Ti, U, and W is also described. Methods for the determination of micro-ingredients such as Hf, B, Cd, and other elements by instrumental methods are described. Point-to-plate emission spectroscopic analysis, and fluorescent x-ray analysis were studied as methods for determining the alloy elements. Oxygen, hydrogen, and nitrogen in Zircaloy are determined by gas analysis, because they affect the properties of the alloy remarkably. (Japan)

26172 SPECTROPHOTOMETRIC DETERMINATION OF BERYLLIUM AND GALLIUM WITH CHROMAZUROL S AND CETYLTRIMETHYLAMMONIUM CHLORIDE. Shijo, Yoshio (Univ. of Utsunomiya, Japan); Takeuchi, Tsugio. Jap. Anal.; 20: 137-41(Feb 1971). (In Japanese).

Chromazurol S (CAS) reacts with beryllium and gallium to form water-soluble blue complexes in the presence of cetyltrimethylammonium chloride. The absorption maximum of the Be complex is at 612 mμ, and its absorbance is nearly constant at pH 5.3 to 5.6. The Ga complex has the same absorption maximum with constant absorbance at pH 4.4 to 4.8. As the result of the continuous variation method, the composition of the complexes is estimated to be 1 : 2 (Be : CAS) and 1 : 4 (Ga : CAS) in excess of reagents. Neither of these complexes obeys Beer's law, but the calibration lines at 619 mμ for Be and at 618 mμ for Ga are linear over the range of 6×10^{-7} to 6×10^{-6} M metals. The sensitivities are very high, the molar absorptivity being 9.1×10^4 for Be and 1.15×10^5 for Ga. Al, Th, U, Fe, Cu, V, Ti, Au, Zr, and Sn interfere with the determination. (auth)

26173 ELECTROMETRIC DETERMINATION IN CHROMATOGRAPHIC DEVELOPMENT. III. ELECTROMETRIC DETERMINATION OF ALKALINE EARTH METAL IONS DURING DEVELOPMENT OF ASCENDING PAPER CHROMATOGRAPHY AND THEIR SEPARATION FROM ALKALI METAL IONS. Chikui, Shumpei (Kobe Municipal Technical Coll., Japan). Jap. Anal.: 20: 167-73(Feb 1971). (In Japanese).

A quantitative analysis by detective current was applied for alkaline earth metal ions during their development in ascending paper chromatography. The applied dc tension is 3.0 V; and 5 to 100 μg of metallic salts is spotted on the filter paper. Optimum composition of the developer, relation between the concentration of ions, and maximum current or the product of current-time, effects of the precipitating agent, and effects of the chelating agent are given. Complete separation of alkaline earth metals from alkali metals, with the least spreading of R_f values, was achieved by the use of 80% ethanol as developer. The addition of potassium sulfate, potassium chromate, and EDTA-2Na gave good results in the mutual separation of alkaline earth metals. The measured deviation in electrometric values for 15 to 50 μg of each alkaline earth metal ion was less than 2.0 ± 0.5%. (auth)

26174 REACTIONS OF METAL IONS WITH CARBOXY DERIVATIVES OF PHENYLFLUORONE. Vrbsky, J.; Fogl, J. (Technische Hochschule, Prague). Collect. Czech. Chem. Commun.; 35: 2497-2501(Aug 1970). (In German).

Two previously undescribed derivatives of 2,6,7-trihydroxy-9-phenyl-3-isoxanthenone with a carboxyl group and a methyloxycarbonyl group were prepared. Under certain conditions they react with metallic salts to form orange to red colored complex salts. Their suitability for the photometric detection and determination of Cu(II), Bi(III), Ti(III), Sn(II), Sn(IV), Sb(III), As(V), Se(VI), Te(VI), W(VI), Mo(VI), V(V), V(IV), Ge(IV), Fe(II), Fe(III), In(III), La(III), Sc(III), Zr(IV), Th(IV), Ce(IV), U(VI), Nb(V), and Ta(V) was tested at pH 2.0 and 4.5. The results obtained are tabulated. (J.S.R.)

26175 RADIONUCLIDE X-RAY FLUORESCENCE ANALYSIS. II. DETECTION OF X-RAY FLUORESCENT RADIATION EXCITED BY NUCLEAR RADIATION. Varga, Stefan. Chem. Listy; 65: 28-44(Jan 1971). (In Czech).

The technique for the detection of x-ray fluorescent radiation excited by nuclear radiation, the analysis of disturbing effects, and methods for their elimination are discussed. (auth)

26176 FLAME-SPECTROPHOTOMETRIC DETERMINATION OF MICROQUANTITIES OF Li, Rb, Cs, AND Sr IN WATER. Prudnikov, E. D.; Shapkina, Yu. S.; Semov, M. P. (Leningrad State Univ. Inst. of Chemistry of Silicates, Moscow). Izv. Vyssh. Ucheb. Zaved., Khim. Khim. Tekhnol.; 14: 196-7(1971). (In Russian).

A direct determination of microquantities of Li, Rb, Cs, and Sr was achieved by using sensitive selective emission flame spectrophotometers. Experiments carried out with various waters found 1×10^{-5} mg/l Li, less than 5×10^{-5} mg/l of Rb and Cs, and 1×10^{-3} mg/l Sr in distilled water and 1×10^{-4} to 1×10^{-3} mg/l Li and 1×10^{-4} to 3×10^{-3} mg/l Rb in Karelian lake water and 0.1 × 0.6 mg/l Sr in soil water. In HF purified by distillation and ion exchange, 1×10^{-6}% Li, 1×10^{-5}% Rb, and less than 5×10^{-3}% Cs were determined. The accuracy of the analysis in waters containing 0.01 to 0.1 mg/l of Li, Rb, Cs, and Sr was equal to 3 to 5%; for microquantities the level of accuracy was lower. (R.V.J.)

Isotope Dilution Procedures

26177 (PG-Report-965) DETERMINATION OF ^{137}Cs AND ^{134}Cs IN SAMPLES FROM THE WINDSCALE EFFLUENT TREATMENT PLANT. Davies, A. G.; Wilson, J. J. (United Kingdom Atomic Energy Authority, Sellafield (England). Production Group). 1971. 13p. Dep. NTIS (U. S. Sales Only). UK 25p.

Several approaches to the determination of ^{137}Cs and ^{134}Cs in Windscale neutralised liquid effluent were assessed. An isotope dilution method involving the removal of ammonia by volatilisation, solvent extraction of the Cs with sodium tetraphenylboron–nitrobenzene, and γ spectrometry was selected and developed for routine application. A complete description of the analytical procedure is given. (auth) (UK)

Radiometric and Radiochemical Procedures

Refer also to abstracts 26317 and 26464.

26178 (BNWL-SA-3608) MEASUREMENT OF RADIATION EXPOSURE OF ASTRONAUTS BY RADIOCHEMICAL TECHNIQUES. Brodzinski, R. L. (Battelle-Northwest, Richland, Wash. Pacific Northwest Lab.). [1970]. Contract AT(45-1)-1830. 12p. (CONF-710304-5). Dep. NTIS.

From Symposium on natural and manmade radiation in space; Las Vegas, Nev. (1 Mar 1971).

The principal gamma-emitting radioisotopes produced in the body of astronauts by cosmic-ray bombardment, which have half-lives long enough to be useful for radiation dose evaluation, are ^{7}Be, ^{22}Na, and ^{24}Na. The sodium isotopes were measured in the preflight and postflight urine and feces, and those feces specimens collected during the manned Apollo missions, by analysis of the urine salts and the raw feces in large crystal multidimensional gamma spectrometers. The ^{7}Be was chemically separated, and its concentration measured in an all NaI(Tl), anticoincidence shielded, scintillation well crystal. The overall sensitivity of the experiment was reduced by almost all variables such as low concentrations of excreted cosmogenic radionuclides, high concentrations of injected radionuclides, low sample sizes, long delay periods before analysis, and uncertain excretion rates. The astronaut radiation dose in millirads, as determined by this technique, for the Apollo 7, 8, 9, 10, 11, 12, and 13 missions was 330, 160, <315, 870 ± 550, 31, 110, and <250, respectively. In view of these limitations this technique would be best applied to cases of unusually high exposures, such as that encountered from solar flares. (auth)

26179 (CNEA-285) THIN LAYER CHROMATOGRAPHY OF VARIOUS RADIOPHARMACEUTICALS. Alvarez, J.; de Salas, G. N. B.; Mitta, A. E. A. (Comision Nacional de Energia Atomica, Buenos Aires (Argentina)). 1970. 7p. (In Spanish). Dep. NTIS (U. S. Sales Only).

A rapid method for determination of radioactive impurities in several radiopharmaceuticals employing instant thin-layer chromatography is described. These methods are of value as a quick control at the plant and, also, before administering them to the patients. (auth)

26180 LIQUID SCINTILLATION COUNTING OF $^{14}CO_2$ IN A TOLUENE/TRITON X-100 SYSTEM. Murray, J. (Torry Research Station, Aberdeen, Scotland). Int. J. Appl. Radiat. Isotop.; 22: 209-12(Mar 1971).

The disadvantages of various trapping agents used to absorb the released $^{14}CO_2$ during manometric studies are given. An accurate and quick method for estimation of the evolved $^{14}CO_2$ from Warburg flasks, using the channels ratio technique is given. The method is based on use of a toluene/Triton X-100 scintillator solution. (UK)

26181 DETERMINATION OF RUTHENIUM IN FALLOUT SAMPLES. Hingorani, S. B.; Subba Rao, M. (Bhabha Atomic Research Centre, Bombay). Curr. Sci. (India); 40: 121-3(20 Mar 1971).

A rapid and quantitative chemical procedure was used to separate ruthenium from other fission products. Ruthenium-103 and Ru-106 were determined by counting of the beta activity. (J.G.B.)

26182 RADIOISOTOPE DERIVATIVE PROCEDURE FOR DETERMINATION OF EPINEPHRINE OR NOREPINEPHRINE. Blaedel, W. J.; Anderson, T. J. (Univ. of Wisconsin, Madison). Anal. Chem.; 43: 521-9(Apr 1971).

Epinephrine (E) and norepinephrine (NE) are quantitatively and stoichiometrically converted to labeled iodoaminochromes with high specific activity ^{125}I. Inactive iodoaminochrome of the sought-for catecholamine is added, and the activity purified and isolated by column chromatography. E is determinable in the range 0.01 to 1 μM range and NE in the range 0.1 to 1 μM. The relative precision is 1 to 2% at midrange. After an alumina adsorption step, the procedure is applicable to the determination of NE in urine. E cannot be determined in urine because of interference by dopamine. (auth)

26183 DETERMINATION OF SURFACE IMPURITY CONCENTRATION PROFILES BY NUCLEAR BACKSCATTERING. Ziegler, James F. (IBM Thomas J. Watson Research Center, Yorktown Heights, N. Y.); Baglin, John E. E. J. Appl. Phys.; 42: 2031-40(Apr 1971).

An analysis was made to extract the concentration profiles of impurities in the upper two microns of a substrate surface. The technique used is nuclear backscattering. Since the stopping power of materials is nonlinear with energy, detailed calculations are necessary to unfold the impurity distributions. The calculations were tested by analyzing arsenic impurities in silicon. Four MeV helium was used as the projectile. Because the reaction $^{28}Si(\alpha,\alpha)^{28}Si$ at 2 to 4 MeV occurs in a region of many energy levels in ^{32}S, a fitting technique was used to extract cross sections from an optical-model calculation of the reaction cross section. The experimental data were corrected by the technique of deconvolution for detector and electronic noise to obtain a final depth resolution of about 200 Å. The extracted impurity profile is shown to be as accurate as those obtained from neutron-activation profiling, differential Hall measurements, and differential resistivity measurements. (auth)

26184 AUTOMATED CALCULATION OF ^{14}C AND ^{35}S RADIOACTIVITY IN BIOLOGICAL SAMPLES BY EXTERNAL STANDARDIZATION AND A COMPUTER PROGRAM. Figdor, Sanford K. (Chas. Pfizer and Co., Inc., Groton, Conn.). Comput. Biomed. Res.; 3: 201-11(Jun 1970).

Recent technical advances in liquid scintillation spectrometers have resulted in the development of an automatic external standardization procedure to estimate quench and to simplify the process of converting observed radioactivity into corrected true radioactivity. In practice a radioactive sample is counted in the normal fashion and then briefly recounted in the presence of a fixed source of gamma radiation such as barium-133 or radium-226. The resultant Compton electrons are counted in two separate channels and the ratio of these counts plotted against quench (or efficiency) results in a general calibration curve suitable for converting observed counts for the nuclide under study into corrected true radioactivity. An example with carbon-14 is described in detail. This simplified counting method is ideally suited for direct automatic data processing with subsequent computer treatment of the data and a system is described by which this objective is achieved. (auth)

26185 ABOUT THE ABSOLUTE ACTIVITY MEASUREMENTS OF RADIOACTIVE NUCLIDES. Vuorinen, A. Otaniemi, Finland: Technical Univ. of Helsinki (1969). 87p.

Thesis.

Activation Procedures

26186 (BARC-529) NUCLEAR METHODS IN TRACE ANALYSIS: A REVIEW. Gangadharan, S. (Bhabha Atomic Research Centre, Bombay (India)). 1971. 57p. Dep. NTIS (U. S. Sales Only).

Nuclear methods of analysis, of which activation analysis forms a part, are briefly reviewed giving the basic principles of the methods and their potentialities and limitations. Several techniques, using different radiochemical methods of separation and varying degrees of instrumentation including computer-coupled automated systems, are briefly discussed. Sources of different projectiles, such as neutrons, charged particles and photons, and their uses are described. Depending on the nature of the problem encountered, the type of experiment varies from simple activation, followed by radiochemical separation prior to counting, to the measurement of prompt gammas/particles for nondestructive analysis and use of charged particles as microprobes. Typical examples are given for the techniques discussed in the section dealing with applications where the emphasis was placed on industrial and materials-science programs. Some of the topics discussed include routine on-line determination of oxygen in steel, analysis of ultra-pure materials such as semiconductor-grade silicon and surface analysis and depth profiles of impurities in very pure metal surfaces. Applications to other disciplines such as archaeology, agriculture, biology and medicine, forensic science and geochemistry are briefly mentioned. The review concludes with a summary and a comparative evaluation of nuclear analysis vis-a-vis other techniques. (131 references) (auth))

26187 (BNWL-1183-7) THE MEASUREMENT OF RADIATION EXPOSURE OF ASTRONAUTS BY RADIOCHEMICAL TECHNIQUES. Quarterly Research Report to the NASA Manned Spacecraft Center, October 5, 1970–January 3, 1971. Brodzinski, R. L. (Battelle-Northwest, Richland, Wash. Pacific Northwest Lab.). 15 Jan 1971. Contract AT(45-1)-1830. 39p. Dep. NTIS.

Gamma analyses of the neutron-activated fecal samples from the Apollo 12 and 13 missions were completed, and the data are being evaluated. Samples of the exposed Apollo 12 solar wind composition (SWC) foil and blank foils were obtained for analysis of the ^{210}Po (^{210}Pb,^{222}Rn) content. It is expected that the determination of the ^{210}Po content of these foils will yield the concentration of radon atoms incident on the foil while exposed to the lunar atmosphere, and this indirectly will permit an estimate of the average uranium concentration of the lunar surface. Proposals to measure the cosmic-ray intensity and energy spectra inside and

outside of late Apollo and Project Skylab spacecraft by exposing and subsequently analyzing pure metal foils, and to measure the elemental mass balance in Project Skylab astronauts by instrumental neutron activation analysis of the intake and excreta are summarized. (auth)

26188 (BNWL-SA-3803) ^{252}Cf NEUTRON ACTIVATION FOR TERRESTRIAL, SEA FLOOR, AND POSSIBLE PLANETARY SURFACE ANALYSIS. Perkins, R. W.; Haller, W. A.; Rieck, H. G. (Battelle-Northwest, Richland, Wash. Pacific Northwest Lab.). [1971]. 15p. (CONF-710402-2). Dep. NTIS.

From Meeting on neutron sources and applications; Augusta, Ga. (18 Apr 1971).

The high neutron emission rates presently available from ^{252}Cf sources have dramatically improved the potential applications of both laboratory and in situ neutron activation analyses of minerals. In recent laboratory studies of 200-lb ore samples, techniques were developed that permit the very rapid analysis of more than 16 elements at concentrations that are generally well below those of commercial interest. These developments were based on studies conducted with 260-μg and 1.8-mg ^{252}Cf sources for neutron activation and a 50-cc Ge(Li) diode for gamma spectrometric analysis. In feasibility studies carried out in several feet of water in an ocean tidal zone, it was demonstrated that elements such as Au, Ag, and Mn could be measured in concentrations as low as a few ounces per ton. The technology developed for either ground-based or shipboard laboratory mineral analysis, the technology and equipment being developed for in situ analysis of the floors of fresh and salt water basins, and the potential applications of this technology for planetary surface analysis are described. (auth)

26189 (KFK-1293) PNEUMATIC SYSTEM FOR ACTIVATION ANALYSIS WITH SHORT-LIVED RADIONUCLIDES. Ehret, R.; Domberg, H.; Lohner, H. (Kernforschungszentrum, Karlsruhe (West Germany). Laboratorium fuer Isotopentechnik). Oct 1970. 13p. (In German). Dep. NTIS (U. S. Sales Only).

A rabbit system is described for activation analyses covering short-lived radionuclides, with particular reference to application to oxygen analyses with 14-MeV neutrons. There is no piping material between the sample and the neutron target. The distance may be set to a minimum of 2.5 mm. Sample and standard are transported in a single piping system. After activation, sample and standard are automatically separated from each other. Samples may be used in any form. Compact samples do not call for additional cladding during transportation. For constructional reasons, an interruption of about 4 sec is provided between irradiation and measurement and, similar to the period of irradiation, recorded automatically. A minimum expenditure is required to build the system (about DM 10,000.-). (auth)

26190 (NYO-4150-9) DISTRIBUTION OF SOME CHEMICAL ELEMENTS BETWEEN DISSOLVED AND PARTICULATE PHASES IN THE OCEAN. Spencer, Derek W.; Brewer, Peter G.; Sachs, Peter L.; Smith, C. L. (Woods Hole Oceanographic Institution, Mass.). [1970]. Contract AT(30-1)-4150. 13p. Dep. NTIS.

Particulate matter from the Gulf of Maine was analyzed by instrumental neutron activation methods. The principal limitation in the technique is the variability in the chemical composition of Millipore filters. Amounts of Sc, Mn, Fe, Co, Hg, Zn, La, and Sb present were determined. (M.C.G.)

26191 RELATIVE MEASUREMENTS OF ACTIVITY WITH Ge(Li) DETECTORS. Debertin, K. (Physikalisch-Technische Bundesanstalt, Brunswick. Physikalisch-Technische Bundesanstalt, Berlin). Atomkernenergie; 17: 97-102(Mar 1971). (In German).

Ge(Li)-detectors are well suited for the relative measurement of decay rates of γ-emitting nuclides. The high energy resolution is especially effective, if the radiation sources to be compared contain other radionuclides in addition to the interesting one. The number of counts in the total absorption peak which is evaluated by a computer program is taken as a relative measure of the activity. In order to minimize the uncertainty caused by dead-times and pile-up effects at high counting rates the preamplifier is fed by pulser signals of constant frequency which suffer nearly the same fractional losses in the pulse height analysis system as the detector signals. The reliability of the method described is demonstrated by some examples. (auth)

26192 DETERMINATION OF IMPURITIES IN THORIUM AND ZIRCONIUM COMPOUNDS BY NEUTRON ACTIVATION ANALYSIS. Csath, G.; Oerdoegh, M.; Szabo, E. KFKI (Kozp. Fiz. Kut. Intez.) Kozlem.; 18: 139-52(1970). (In Hungarian).

A neutron activation analytical method for the determination of small concentrations of Cu, Ca, Mn, Co, Cr, and Zn contaminants in thorium and zirconium compounds used in telecommunication and reactor techniques is described. For thorium compounds paper chromatography is used for the preirradiation separation of the matrix element and methyl isobutyl ketone extraction and precipitation with cupferron for the isolation of the contaminants after irradiation. Precipitation with cupferron is used after irradiation of zirconium compounds. Individual impurities are determined by gamma spectrometry following chemical separation. (auth)

26193 THE DETERMINATION OF FLUORINE IN ROCK MATERIALS BY γ-ACTIVATION AND RADIOCHEMICAL SEPARATION. Hislop, J. S.; Pratchett, A. G.; Williams, D. R. (Atomic Energy Research Establishment, Harwell, Eng.). Analyst; 96: 117-22(Feb 1971).

A technique is described for the determination of fluorine in rock materials involving irradiation in a source of high energy γ-photons to induce the ^{19}F (γ,n) ^{18}F reaction. Fluorine-18 is then separated from the radioactive matrix by distillation and its activity measured either in the distillate or as precipitated calcium fluoride and compared with that of irradiated calcium fluoride standards. The technique was applied to the analysis of standard rock materials G1 (638 ppM), W1 (221 ppM), T1 (476 ppM) and to Apollo 11 lunar fines (76 ppM). Precautions are taken to eliminate interferences. The results obtained for the standard rocks are in good agreement with those of conventional methods but disagree with other activation results. The limit of detection of the method is 0.002 μg. (auth) (UK)

26194 STUDIES ON THE DISTRIBUTION OF CHEMICAL ELEMENTS IN GEOCHEMICAL SAMPLES BY AN ACTIVATION AUTORADIOGRAPHIC METHOD. Sakanoue, M.; Yoshioka, M.; Nakanishi, T.; Takagi, T. (Kanazawa Univ., Japan). Int. J. Appl. Radiat. Isotop.; 22: 177-83(Mar 1971).

By autoradiography combined with radioactivation overall distributions of several elements in geochemical samples were studied. For example, after irradiating, with thermal neutrons, a thin section of a granitic sample mounted on acrylite, the distributions of Al, Mn, Na and Fe were all revealed on photographic films to be in close contact with the sample surfaces, if three appropriate experimental factors (irradiation time, cooling time and exposure time) were chosen for each element. This method can be used widely in many fields. (auth) (UK)

26195 APPLICATION OF ACTIVATION ANALYSIS IN HOT SPRING CHEMISTRY AND SANITARY CHEMISTRY. Kawakami, Hiroyasu; Oda, Toshiyuki (Kyushu Univ., Beppu, Japan). Onken Kiyo; 21: No. 1, 47-56(Mar 1969). (In Japanese).

The pH of 400 ml of hot spring water was adjusted to 1.5 with sulfuric acid for determination of microgram amounts of mercury; the sample was shaken successively with three 5-ml portions of dithizone-chloroform solution and 5 ml of chloroform for ten min; the combined extracts were evaporated just to dryness under an infrared lamp; and the mercury dithizonate was redissolved in 2 ml of chloroform and absorbed on filter paper. Neutron irradiation was carried out with the TAIC-HTR reactor (2.1×10^{12} n/cm^2/sec) for 5 hrs. In a radioactivation method for determination of rare earth elements in hot spring water, rare earth elements were coprecipitated on Ca oxalate from 10 liters spring water, ignited, and then irradiated by KUR (4×10^{12} n/cm^2/sec). Samples were counted by 1024 PHA (3" $\times$ 3" NaI crystal and 0.4cc Ge(Li) detector). Hair samples were washed successively with neutral detergent, distilled water, acetone, and then distilled water and dried. Then 200-mg samples of hairs and standards were sealed individually with polyethylene envelopes and packed together in an irradiation capsule. Neutron irradiation was carried out with the TAIC-HTR reactor for 5 hrs. (auth) (Japan)

26196 PROMPT ACTIVATION ANALYSIS FOR LITHIUM UTILIZING AN Am-Be NEUTRON SOURCE. Ishii, Daido; Jinno, Kiyokatsu (Nagoya Univ., Japan). Radioisotopes (Tokyo); 19: No. 3, 165-8(Mar 1970). (In Japanese).

Samples containing lithium carbonate were irradiated with the neutrons from an Am-Be neutron source, and the spectrum of triton particles resulting from the reaction $^6Li(n,\alpha)^3H$ was measured. The triton peak area was plotted against the weight of lithium carbonate. It was demonstrated that this analytic method can be used as a selective analytical method for lithium. (Japan)

26197 URANIUM DETERMINATION IN CROP SOILS BY NEUTRON ACTIVATION. Corbean, Stela (Institutul de Cercetari Pentru Cereale si Plante Technice, Bucharest). Stiinta Solului; 8: No. 2, 57-69(1970). (In Rumanian).

A method is suggested for separating U from soils by ion exchange in 8M HNO_3 on Dowex 1 $\times$ 4, as well as a method for maintaining the 4^+ valence of ^{239}Np in 8M HNO_3. The sample is irradiated in a neutron flux of 10^{13}n/cm^2/sec for 30 hr. The ^{239}Np formed

from ^{238}U by the reaction (n,γ) is reduced with iron hydrazine in an 8M HNO_3 solution, and the reduced ^{239}Np is fixed on the resin. The ^{239}Np is eluted with 4N HCl. This method allows good separation of the ^{239}Np coming from the U and from other soil elements. (auth)

26198 PROMPT ACTIVATION ANALYSIS FOR BORON UTILIZING AN Am–Be NEUTRON SOURCE. Ishii, Daido; Jinno, Kiyokatsu (Nagoya Univ., Japan). Radioisotopes (Tokyo): 19: No. 4, 210-11(Apr 1970). (In Japanese).

Samples containing sodium borate were irradiated with the neutrons from an Am–Be neutron source, and the spectrum of α-particles resulting from the reaction $^{10}B(n,\alpha)^{7m}Li$ was measured. The 1.47-MeV α peak area was plotted against the weight of sodium borate. It was demonstrated that by this analytical method, nondestructive analysis can be made without the interference by other elements. (Japan)

26199 RETENTION OF RADIONUCLIDES ON METAL SULPHIDE PRECIPITATES. Gimesi, O. (Technical Univ., Budapest); Banyai, E.; Csajka, M.; Szabadhazy, A. Talanta; 17: 1183-9(Dec 1970).

The retention of various radionuclides on metal sulphide precipitates was studied. The sulphide precipitates quantitatively retained the common radionuclides. The condition for 100% retention in a thin layer is small particle size (a few μm) in the precipitate. This can be ensured by pulverization of the dried precipitate of metal sulphide. $^{203}Hg^{2+}$ is retained by mercury sulphide and $^{65}Zn^{2+}$ by zinc sulphide by isotopic exchange. The retention of foreign radioactive ions can be reduced or even eliminated by counter-carrier technique in cases where the retention is not due to chemical reaction, precipitate exchange. The isotopic exchange with mercury (II) sulphide and zinc sulphide enables mercury and zinc ions to be separated rapidly and determined in the presence of a number of interfering ions. (auth) (UK)

26200 INSTRUMENTAL ACTIVATION ANALYSIS OF Au, Br, Mn, Na, Ta, AND W USING A Ge/Li/ DETECTOR. Lambrev, V. G.; Akalaev, G. G.; Nekrasov, V. V. (Lab. of Activation Analysis, Moscow). Radiochem. Radioanal. Lett.; 6: 133-8 (3 Apr 1971).

The instrumental activation analysis of a fabric of unknown composition is described. After irradiation with reactor neutrons, the γ-radiation of the samples was measured using a Ge(Li) detector. In a series of measurements, six elements were recorded: Au, Br, Mn, Na, Ta, and W. For the purpose of quantitative determinations, the time parameters for each detected element were calculated on a computer and the activation was repeated using optimum conditions of analysis. (auth)

26201 LOSS OF MERCURY FROM CONTAINERS IN NEUTRON ACTIVATION ANALYSIS. Bate, L. C. (Oak Ridge National Lab., Tenn.). Radiochem. Radioanal. Lett.; 6: 139-44 (3 Apr 1971).

Experiments performed at ~50°C and a neutron flux of ~1×10^{12} ncm^{-2} sec^{-1} indicate that Hg radioactivity is lost from plastic containers when irradiations of 12 to 65 hr are made. Any irradiation longer than a few minutes should be made in quartz. (auth)

26202 DETERMINATION OF CARBON IN HIGH-PURITY SILICON BY γ PHOTON, DEUTERON, ^3He, AND α PARTICLE ACTIVATION. Engelmann, Ch.; Marschal, A. (CEN de Saclay, Gif-sur-Yvette, France). Radiochem. Radioanal. Lett.; 6: 189-94(3 Apr 1971). (In French).

Carbon was determined in high-purity silicon by activation with γ photons, deuterons, ^3He, and α particles, respectively. The results obtained by each of these methods are compared and it is shown that, while γ photons and deuterons give similar results, the other two activation processes lead to much higher values. This may be due to the presence of beryllium in the silicon, at concentrations of the order of 1 μg/g. (auth)

26203 DETERMINATION OF LEAD IN MILK POWDER. Dutilh, C. E.; Das, H. A. (Reactor Centrum Nederland, Petten). Radiochem. Radioanal. Lett.; 6: 195-201(3 Apr 1971).

Photon activation was applied to for the determination of lead in milk. The reaction involved is $^{204}Pb(\gamma,n)^{203}Pb$ ($T_{\frac{1}{2}}$ = 52 hr). This method is very convenient for the analysis of lead in biological samples. The absolute sensitivity is ~0.5 μg. (auth)

26204 DETERMINATION OF SODIUM IN ULTRABASIC ROCKS. Das, H. A.; de Koning, J.; Oosterom, M. G. (Reactor Centrum Nederland, Petten). Radiochem. Radioanal. Lett.; 6: 203-9(3 Apr 1971).

A method was developed for the selective determination of sodium in US Geological Survey standard rocks. A cadmium-cover technique was used with the neutron activation analysis of DTS-1 and PCC-1 standards. (J.C.B.)

Inorganic, Organic, and Physical Chemistry

Refer also to abstracts 27168, 27169, and 27291.

26205 FUNDAMENTAL NUCLEAR ENERGY RESEARCH, 1970. A Supplemental Report to the Annual Report to Congress for 1970 of the United States Atomic Energy Commission, January 1971. Washington, D. C.: Atomic Energy Commission (1971). 227p. GPO $2.75.

Topics covered include: basic physical research, reactor technology, environmental aspects and biological and medical research. (M.C.G.)

Chemical Properties

Refer also to abstracts 26345 and 26608.

26206 (ARH–1920) HYDROXYLAMINE NITRATE REDUCTION OF PLUTONIUM(IV): IRON CATALYSIS. Barney, G. S. (Atlantic Richfield Hanford Co., Richland, Wash.). Jan 1971. 15p. Dep. NTIS.

The effect of ferric ion on the kinetics of the reduction of plutonium (IV) with hydroxylamine nitrate was examined. It was found that iron catalyzes the reaction, especially in the latter stages of the reaction. The effect of iron concentration was compared with other factors that influence the rate and was found to be less significant than temperature, acidity, or hydroxylamine nitrate concentration. (auth)

26207 (BLG–448) EXPERIENCE ACQUIRED IN FLUID BFD PREPARATION OF UF_6 IN VIEW OF REACTOR FUEL PROCESSING. Schmets, J. J. (Centre d'Etude de l'Energie Nucleaire, Brussels (Belgium)). Oct 1970. 13p. Dep. NTIS (U. S. Sales Only).

Fluidization is considered as a method to produce UF_6 from spent nuclear fuels. Limitations are imposed to the application of this technique: physical and chemical properties of the irradiated fuel, the more or less extensive head-end step to obtain a suitable starting material, the exothermicity combined with the necessity to take into account temperature conditions for subsequent plutonium recovery, and nuclear criticality problems. The results obtained are reviewed in the frame of these boundary conditions. (auth)

26208 (BNWL-CC-2180) CATION-EXCHANGE CONVERSION OF HYDROXYLAMINE SULFATE TO HYDROXYLAMINE NITRATE. Wheelwright, E. J. (Battelle-Northwest, Richland, Wash. Pacific Northwest Lab.). 26 May 1969. Contract AT(45-1)-1830. 13p. Dep. NTIS.

A cation-exchange process is described that will permit the conversion of hydroxylamine sulfate to hydroxylamine nitrate for a chemical cost of approximately $0.02 per mole of hydroxylamine. Utilization of this process to supply hydroxylamine nitrate in plutonium reclamation (Z-plant) could save up to $200.00 per day. The three-step cation-exchange process requires only nitric acid and distilled water in addition to the exchange resin. (M.C.G.)

26209 (JINR–P12-5644) SIGN OF ASTATINE ION CHARGE IN $HClO_4$–$H_2Cr_2O_7$ SOLUTIONS. Tung, Do Kim; Dudova, I.; Khalkin, V. (Joint Inst. for Nuclear Research, Dubna (USSR). Lab. of Nuclear Problems). 1971. 8p. (In Russian). Dep. NTIS (U. S. Sales Only).

Oxidation of astatide and of astatine by dichromate in dilute aqueous solutions of perchloric acid leads to the production of positively charged ions of the fifth halogen. This is proved by the results of the experiments on astatine ion migration in an electrical field. (auth)

26210 (KFK–1312) EXPERIMENTAL CONTRIBUTION TO JOST MECHANISM IN SOLID-STATE REACTIONS. Kleykamp, H. (Kernforschungszentrum, Karlsruhe (West Germany). Institut fuer Material und Festkoerperforschung). Dec 1970. 17p. (In German). (CONF-690455–1). Dep. NTIS (U. S. Sales Only).

From Conference on transport processes in inorganic nonmetallic raw material and structure of these materials; Mainz, Germany (10 Apr 1969).

In solid-state reactions with two initial phases the double decomposition AX + BY = AY + BX takes on a particular form. After

reacting, following the Jost mechanism, the products form layers between the initial phases. The order of these layers depends on the mobility of the ions taking part in the reaction. Extreme cases are illustrated using microstructure pictures and microanalysis investigations as well as reaction kinetics observations. The reaction ZnS + CdO → ZnO + CdS is a process of simultaneous cation diffusion, the reaction UN + ZrO_2 → UO_2 + ZrN one of simultaneous anion diffusion. If the cations and anions are predominantly mobile in one component, then the Kirkendall effect will possibly occur to the products following the Jost mechanism. As examples, the reaction $PbCl_2$ + BaO → PbO + $BaCl_2$ and UAl_3 + Al → UAl_4 in the case of only one mobile component are discussed. (auth)

26211 (TRG-Report-2104) REACTION OF PTFE WITH LIQUID SODIUM, POTASSIUM AND NaK ALLOY. Allan, C. G.; Drummond, J. L. (United Kingdom Atomic Energy Authority, Dounreay (Scotland). Reactor Group). 18 Nov 1970. 5p. Dep. NTIS (U. S. Sales Only). UK 6p.

Small-scale tests were performed on the reaction between PTFE (poly(tetrafluoroethylene)) chips and sodium, 70:30 NaK, and potassium. Liquid metal temperatures were between 200 and 360°C and PTFE temperatures between 200 and 400°C. The PTFE charred and in some cases ignited, even in an inert atmosphere, but no explosions or violent reactions were encountered. (auth)

26212 PROTON MAGNETIC RESONANCE CATION SOLVATION STUDY OF URANYL PERCHLORATE, URANYL NITRATE, AND URANYL PERCHLORATE–HYDROCHLORIC ACID SOLUTIONS IN WATER–DIMETHYL SULFOXIDE–ACETONE MIXTURES. Fratiello, Anthony; Kubo, Vicki; Schuster, Ronald E. (California State Coll., Los Angeles). Inorg. Chem.; 10: 744-7(Apr 1971).

A competitive solvation and complex formation study was completed for solutions of $UO_2(ClO_4)_2$, $UO_2(NO_3)_2$, and $UO_2(ClO_4)_2$–HCl in water–dimethyl sulfoxide–acetone mixtures using a low-temperature proton magnetic resonance (PMR) technique. At temperatures in the −80 to −100° range, the ligand and proton exchange rates are slow enough to permit the direct observation of PMR signals for water and DMSO molecules in the UO_2^{2+} ion solvation shell. Signal areas gave a quantitative measure of the contribution of water and DMSO to the UO_2^{2+} ion solvation number. The difference between the sum of these contributions and the maximum value of 4 for this ion was used to estimate the amount of anion complexed. In all systems, DMSO is preferentially bound by the UO_2^{2+} at the expense of water. Solvation by DMSO is an energetically more favorable process than cation–anion complex formation. (auth)

26213 LIPID-METAL ION INTERACTION IN MONOMOLECULAR FILMS. Shah, Dinesh O. (Columbia Univ., Palisades, N. Y.). pp 155-89 of Effects of Metals on Cells, Subcellular Elements, and Macromolecules. /Maniloff, Jack (ed.). Springfield, Ill.; Charles C Thomas, Publisher (1970).

From 2, conference on toxicity; Rochester, N. Y. (12 Jun 1969). See CONF-690621.

The interaction of monovalent, divalent, and trivalent metal ions with fatty acid, alkyl phosphate, and phospholipid monolayers was investigated by measuring surface pressure, surface potential, and surface rheology. The position of metal ions in a two-dimensional lattice of monolayers was proposed from surface potential measurements. Unsaturation of hydrocarbon chains influences the intermolecular spacing,and, hence, interaction between metal ions and lecithin monolayers. The presence of an hydroxyl group in the three-position of sphingomyelin reduces the interaction of metal ions with phosphate groups in the monolayers. Interaction of divalent metal ions with cardiolipin or phosphatidylserine monolayers results in a reduction in average area per molecule. Interaction of potassium permanganate ($KMnO_4$), osmium tetroxide (OsO_4), and uranyl acetate with saturated and unsaturated lecithins, cholesterol, and cholestanol was studied. $KMnO_4$ and OsO_4 react with the double bonds in the fatty acid chains, whereas uranyl acetate reacts with the phosphate groups in lecithin monolayers. OsO_4 also reacts with the double bond in cholesterol, whereas $KMnO_4$ and uranyl acetate do not. Interactions in mixed monolayers of stearic acid–stearyl alcohol were studied at pH 2, 6, and 8.8 in the presence and absence of calcium ions in the subsolution. Existence of 1:2 and 1:3 molecular complexes of stearic acid:stearyl alcohol was deduced from surface pressure and potential measurements. Mixed monolayers of dicetyl phosphate, phosphatidic acid, dipalmitoyl and egg lecithins with cholesterol were investigated. The deviation from the additivity rule for average area and potential per molecule is explained on the basis of an "intermolecular cavity effect" and an ion-dipole interaction in mixed monolayers. (auth)

26214 FORMATION CONSTANTS OF SOME METAL COMPLEXES OF 5,7-DIIODO-8-HYDROXYQUINOLINE. Manku, G. C. S. (Hansraj Coll., Delhi). J. Inorg. Nucl. Chem.; 33: 385-6(Jan 1971).

The results of pH metric investigations are reported for determination of the formation constants (K) of some bivalent and tervalent metal ion complexes (including uranyl) of 5,7-diiodo-8-hydroxyquinoline in 3:1 v/v dioxan:water medium. The results indicate that in case of the bivalent ions, 1:2 metal:ligand complexes are formed, whereas in case of the lanthanon(III) ions, 1:3 complexes are produced under the experimental conditions. (auth) (UK)

Isotope Effects and Exchange

26215 (NYO-2150-59) PARAELECTRIC RESONANCE IN KCl:Li^+. MSC Report 1323. Herendeen, Robert Albert (Cornell Univ., Ithaca, N. Y. Materials Science Center). Jun 1970. 122p. Dep. NTIS.

Thesis.

Paraelectric resonance spectra of KCl: $^7Li^+$ and KCl: $^6Li^+$ are presented and analyzed for three different frequencies: 63, 24, and 9 GHz. Quantitative results for the case of static electric field (E_0) || [001] support the ⟨111⟩ off-center tunneling model of Gomez, Bowen, and Krumhansl. Values for the dipole moment (μ) and zero-field splitting, (δ): $\mu_7 = \mu_6 = 5.6 \pm 0.2$ Debye, $\delta_7 = 0.77 \pm 0.03$ cm^{-1}, $\delta_6 = 1.07 \pm 0.04$ cm^{-1}, were obtained. These agree with results from several other experimental techniques. Detailed analysis of lineshapes and intensities indicates the presence of large random internal strains and of random electric fields. The strains are on the order of those expected from dislocations, but a satisfactory explanation for the electric fields is still lacking. The 64 GHz spectrum for E_0 || [011] lends qualitative support to the model; this spectrum shows a negative resonance, or "hole," similar to a feature seen previously in ESR experiments on MgO: Ni^{2+} and MgO: Fe^{2+}. The model is shown to satisfy requirements for the occurrence of this negative resonance. (auth)

26216 METHOD OF ASSIGNING THE VIBRATION BANDS BY PROGRESSIVE ISOTOPE EXCHANGE. Padhye, M. R.; Karnik, R. R. (Univ. of Bombay). Curr. Sci. (India); 40: 129-31(20 Mar 1971).

A method based on different rates of hydrogenation was used for the assignment of vibration bands of benzohydroxamic acid. In completely deuterated benzohydroxamic acid, three bands were observed in the ND and OD stretching regions at 2450, 2250, and 2080 cm^{-1}. During rehydrogenation, these bands lost intensity and bands in the proton region gained intensity, the rate of gain or loss of intensity being a measure of the rate of rehydrogenation of the group responsible for the band. (J.G.B.)

26217 SECONDARY KINETIC ISOTOPE EFFECTS IN BIMOLECULAR NUCLEOPHILIC SUBSTITUTIONS. IV. THE TEMPERATURE DEPENDENCE OF THE DEUTERIUM EFFECT FOR THE REACTION OF N,N-DIMETHYL-d_6-ANILINE AND METHYL p-TOLUENESULFONATE. CORRELATION OF ISOTOPE EFFECTS ON ACTIVATION PARAMETERS. Leffek, K. T.; Matheson, A. F. (Dalhousie Univ., Halifax, N. S.). Can. J. Chem.; 49: 439-46(1 Feb 1971).

The temperature dependence of the isotope effect for the reaction of dimethylaniline and dimethyl-d_6-aniline with methyl p-toluenesulfonate in nitrobenzene solvent was measured, yielding the result, $(\Delta H_D^{\ddagger} - \Delta H_H^{\ddagger}) = -134 \pm 30$ cal mole^{-1}, $(\Delta S_D^{\ddagger} - \Delta S_H^{\ddagger}) = -0.15 \pm 0.09$ cal mol^{-1} degree^{-1}. This result was compared with 15 other temperature dependence studies by plotting $\Delta\Delta H^{\ddagger}$ per D atom vs. $T\Delta\Delta S^{\ddagger}$ per D atom. The points fall on two clearly separated straight lines. A similar correlation was found for a plot of $\Delta\Delta G^{\ddagger}$ per D atom vs $\Delta\Delta H^{\ddagger}$ per D atom. The significance of the correlation is discussed and a possible rationalization, in terms of mechanism and particularly the role of the solvent is given. (auth) (Canada)

26218 RAMAN SPECTRA OF THE CHLOROFLUOROSILANES IN THE GASEOUS, LIQUID, AND SOLID STATE; ANOMALOUS ^{35}Cl, ^{37}Cl ISOTOPE INTENSITY EFFECTS IN THE SPLITTING OF THE TOTALLY SYMMETRICAL SiCl STRETCHING MODE IN $SiCl_3F$ AND $SiCl_2F_2$. Hamada, K.; Ozin, G. A.; Robinson, E. A. (Univ. of Toronto). Can. J. Chem.; 49: 477-80(1 Feb 1971).

The Raman spectra of the chlorofluorosilanes are reported in their various phases together with vibrational assignments of the normal modes. The $^{35}Cl - ^{37}Cl$ isotope lines of the totally symmetrical SiCl stretching modes in $SiCl_3F$ and $SiCl_2F_2$ were partially resolved in the solid and liquid phases and their intensities were found to be approximately normal in the liquid

state but may show deviations in the solid state. Possible reasons for this behavior are discussed and the results are compared with similar effects observed for CCl_3F and $CHCl_3$. (auth) (Canada)

26219 SYNTHESIS AND ISOMERIZATION OF DEUTERATED CYCLOBUTENES. Honig, Milton Leslie. Brooklyn; Polytechnic Inst. of Brooklyn (1970). 129p. University Microfilms Order No. 70-26,062.

Thesis.

To elucidate details of the mechanism of thermally induced cyclobutene isomerization, the synthesis and isomerization of specifically deuterated cyclobutenes was undertaken. Kinetic isotope effects (α and β types) as well as stereochemical aspects were investigated. (Diss. Abstr. Int., B)

26220 MECHANISM OF THE BENZOIN CONDENSATION. Kuebrich, John P.; Schowen, Richard L.; Wang, Maw-song; Lupes, Mircea E. (Univ. of Kansas, Lawrence). J. Amer. Chem. Soc.; 93: 1214-20(10 Mar 1971).

The benzoin condensation in methanol at 44 to 66°C proceeds by addition of cyanide ion to benzaldehyde ($\Delta G^* \sim 12$ kcal/mol, $\Delta G^0_{298} = -0.74 \pm 0.04$ kcal/mol, $\Delta H^\circ = -9.9 \pm 0.2$ kcal/mol, $\Delta S^0 = -30.6 \pm 0.6$ eu), conversion of the adduct to a cyanocarbanion ($\Delta G^*_{298} = 21.31 \pm 0.02$ kcal/mol, $\Delta H^* = 10 \pm 0.5$ kcal/mol, $\Delta S^* = -38 \pm 3$ eu, relative to original reactants, $k_H/k_D = 4.3$ at 25° for C_6H_5CHO vs. C_6H_5CDO), and condensation of the carbanion with benzaldehyde ($\Delta G^*_{298} = 22.5 \pm 0.1$ kcal/mol, $\Delta H^* = 10 \pm 2$ kcal/mol, $\Delta S^* = -42 \pm 4$ eu, relative to original reactants). The scheme is essentially that of Lapworth, proposed over 65 years ago. (auth)

26221 BROMINE SCRAMBLING ACCOMPANYING BASE-CATALYZED ISOMERIZATION OF 1,2,4-TRIBROMOBENZENE. McLennan, D. J.; Bunnett, J. F. (Univ. of California, Santa Cruz. Univ. of Auckland, N. Z.). J. Amer. Chem. Soc.; 93: 1198-1201 (10 Mar 1971).

1,2,4-Tribromobenzene radiolabeled in the 1 position (1b) undergoes partial isomerization to 1,3,5-tribromobenzene (2b) during 15-min exposure to potassium anilide and aniline in liquid ammonia. Product 2b and recovered 1,2,4-tribromobenzene are equal in molar radioactivity to each other and to the 1b introduced. In the recovered 1,2,4-tribromobenzene, the radiolabel is equally distributed among the three bromine positions. For the bromine scrambling, a mechanism is proposed the key step of which is positive bromine transfer from 1,2,4,5-tetrabromobenzene to 2,4,5-tribromophenyl anion, forming products identical with the reactants except for possible differences in the location of the radiolabel. (auth)

26222 ISOMERIZATION AND DISPROPORTIONATION OF TRIHALOBENZENES CATALYZED BY POTASSIUM ANILIDE IN LIQUID AMMONIA. Bunnett, J. F.; Moyer, Charles E. Jr. (Brown Univ., Providence). J. Amer. Chem. Soc.; 93: 1183-90(10 Mar 1971).

On treatment with potassium anilide in liquid ammonia, 1,2,4-tribromobenzene (1) rearranges to 1,3,5-tribromobenzene and there is a small amount of disproportionation to di- and tetrabromobenzenes. Similarly, 1-iodo-2,4-dibromobenzene rearranges to its 1,3,5 isomer and also disproportionates. Potassium anilide in ammonia also causes isomerization and/or disproportionation of 1-bromo-2,4-dichlorobenzene, 1-iodo-2-bromo-4-chlorobenzene, and 1-iodo-2,4,6-tribromobenzene. A conceivable mechanism involving aryne intermediates is ruled out by several items of evidence. However, a mechanism involving a series of nucleophilic displacements by aryl anions on the halogen of an aryl halide, effecting the transfer of a positive halogen moiety so as to form a new aryl halide and a new aryl anion, accounts for most of the evidence. The ir spectra of deuterated 1 was different from that of normal 1. (auth)

26223 OXIDATION OF 2-METHOXYETHANOL TO METHOXYACETIC ACID BY NITRIC ACID SOLUTIONS. Strojny, E. J.; Iwamasa, R. T.; Frevel, L. K. (Dow Chemical Co., Midland, Mich.). J. Amer. Chem. Soc.; 93: 1171-8(10 Mar 1971).

The oxidation of 2-methoxyethanol by nitric acid in sulfuric acid solution was studied using 60-MHz nmr to follow the rate of disappearance of the alcohol. Nitric oxide evolution and N_2O_3 and HONO in solution were also monitored. An activation energy of 17.9 kcal/mol was obtained for the overall reaction in the temperature range 4 to 27°C. The rate of disappearance of 2-methoxyethanol follows first-order kinetics well in the range of 20 to 80% conversion. A plot of the logarithm of the rate constants vs. the acidity function H_0 gives a unit slope. A deuterium isotope effect of 3.9 was observed and indicates the rate-determining step involves cleavage of the 1-C–H bond. A mechanism is proposed that involves nitrosonium ion (NO^+) as the active oxidizing agent. A rapid equilibrium between 2-methoxyethanol and 2-methoxyethyl nitrite exists under the oxidation conditions. The oxidation of 2-methoxyethanol by nitrosonium fluoroborate was studied and provides additional support for the role assigned to nitrosonium ion. (auth)

26224 STEREOCHEMISTRY OF ALLYLIC REARRANGEMENTS. XVI. STEREOCHEMISTRY OF ION-PAIR RETURN IN THE trans-α,γ-METHYLPHENYLALLYL p-NITROBENZOATE SYSTEM. Goering, Harlan L.; Koermer, Gerald S.; Lindsay, Ernest C. (Univ. of Wisconsin, Madison). J. Amer. Chem. Soc.; 93: 1230-4(10 Mar 1971).

Ion-pair return from the ion-pair intermediate(s) common to trans-α-phenyl-γ-methylallyl and trans-α-methyl-γ-phenylallyl p-nitrobenzoates (I and II) gives the γ-phenylallylisomer(II). In aqueous acetone the α-phenylallyl isomer (I) undergoes simultaneous solvolysis and allylic isomerization to II, which is less reactive than I and accumulates. At higher temperatures the γ-phenylallyl isomer (II) solvolyzes without rearrangement. In this case the amount of return from the common intermediate(s) (III) can be determined by carboxyl oxygen equilibration. Ion-pair return results in partial loss of optical configuration. The amount lost starting with I was determined from the relative optical purities for the I → II isomerization and the amount lost starting with II (in this case racemization) was determined from the amount of racemization associated with return, ratio. Within experimental error the stereochemistry of return is the same starting with either I or II. In 90% acetone at 100°C return results in about 65% loss of optical configuration. (auth)

26225 STUDIES ON THE MECHANISM OF HYDROGEN TRANSFER IN THE COENZYME B_{12} DEPENDENT DIOLDEHYDRASE REACTION. II. Essenberg, Margaret K.; Frey, Perry A.; Abeles, Robert H. (Brandeis Univ., Waltham, Mass.). J. Amer. Chem. Soc.; 93: 1242-51(10 Mar 1971).

Rates of the following processes that occur during the conversion of DL-1,2-propanediol to propionaldehyde by dioldehydrase and coenzyme B_{12} were measured: tritium transfer from the C-1 position of the substrate to the C-5′ position of coenzyme B_{12}; tritium transfer from the C-5′ position of coenzyme B_{12} to the C-2 position of the product; and the overall tritium transfer from substrate to product. The kinetics of these transfer reactions were found to be consistent with a reaction sequence in which coenzyme B_{12} functions as an obligatory intermediate hydrogen carrier. When [5′ – ^{3}H] coenzyme B_{12} is used, tritium transfer to product occurs in one out of 250 turnovers. When deuterium is present on C-1 of the substrate, and the C-5′ positions of coenzyme B_{12} contain deuterium and tritium, tritium is transferred in one out of 14 turnovers. If a substrate contains deuterium on C-1, the probability of tritium transfer to the product derived from that molecule is enhanced 4 to 8 times over that with a substrate that does not contain deuterium. These results support a previous suggestion that an intermediate must exist containing three hydrogens, one contributed by the substrate and the two C-5′ hydrogens of coenzyme B_{12}, and that in any one turnover any of the three hydrogens can be transferred to the reaction product. When sufficient [^{3}H] coenzyme B_{12} is added to enzyme, the amount of tritium released to the reaction product is independent of the amount of [^{3}H] coenzyme B_{12} added, indicating that enzyme and coenzyme combine to form an undissociable complex. (auth)

26226 ELECTROPHILIC REACTIONS AT SINGLE BONDS. III. HYDROGEN–DEUTERIUM EXCHANGE AND PROTOLYSIS (DEUTEROLYSIS) OF ALKANES WITH SUPERACIDS. THE MECHANISM OF ACID-CATALYZED HYDROCARBON TRANSFORMATION REACTIONS INVOLVING THE σ ELECTRON PAIR DONOR ABILITY OF SINGLE BONDS (SHARED ELECTRON PAIRS) VIA THREE-CENTER BOND FORMATION. Olah, George A.; Halpern, Yuval; Shen, Jacob; Mo, Y. K. (Case Western Reserve Univ., Cleveland). J. Amer. Chem. Soc.; 93: 1251-6(10 Mar 1971).

It is shown that the protolytic attack takes place on the C–H or C–C bonds where the major part of the electron density in covalent single bonds resides and not on the hydrogen or carbon atoms themselves. Hydrogen–deuterium exchange in these reactions was observed with great preference for the bridgehead positions. (M.C.G.)

26227 INFLUENCE OF TRANSLATIONAL ENTROPY OF ACTIVATION ON REACTION RATES IN ISOTOPIC SOLVENTS. Tseng, Linda; Stewart, James A. (Univ. of North Dakota, Grand Forks). J. Amer. Chem. Soc.; 93: 1273-5(10 Mar 1971).

The influence of entropy on reaction rates in D_2O and H_2O was studied. It is shown that the solvent isotope effect on the translational entropy of activation due to differences in solvation between the reactant and the activated complex has a pronounced effect on the ratio k_{H_2O}/k_{D_2O}. The activation enthalpy is slightly

greater for the D_2O system. However, the entropy term is more negative. (M.C.G.)

26228 HYDROFORMYLATION OF 3-METHYL-1-HEXENE-3-d_1. EVIDENCE AGAINST DIRECT FORMYLATION OF A METHYL GROUP IN THE OXO REACTION. Casey, Charles P.; Cyr, Clifford R. (Univ. of Wisconsin, Madison). J. Amer. Chem. Soc.; 93: 1280-2(10 Mar 1971).

The hydroformylation of 3-methyl-1-hexene and its deuterated analog was studied and yields determined. NMR spectral studies were made of the products to determine the reaction mechanism. (M.C.G.)

26229 OXIDATIONS OF AQUEOUS CHROMIUM(II). II. CHROMIUM-CARBON BOND. Schmidt, Willfred; Swinehart, James H.; Taube, Henry (Stanford Univ., Calif. Univ. of California, Davis). J. Amer. Chem. Soc.; 93: 1117-23(10 Mar 1971).

An investigation of the formation and kinetic stability of complexes containing a chromium–carbon bond in an aqueous medium is described. Pentaaquochromium(III) ions carbon bonded to small acyclic anions such as are derived from isopropyl alcohol and diethyl ether are formed by the reduction of organic radicals with Cr(II). The organic radicals are produced by hydrogen abstraction with OH radicals. Aquation rates of the Cr(III) complexes when the organic ligands contain hydroxyl groups (alcohols) are described by the differential rate law $-d \ln [(H_2O)_5CrL^{2+}]/dt = k_1 + k_2[H^+]$. The rate laws for complexes having organic ligands that do not have a hydroxyl group (e.g., methyl or the radical derived from diethyl ether) do not show the term independent of hydrogen ion. A mechanism is proposed in which the activated complex contains a solvent molecule in a position so as to take advantage of hydrogen bonding with the organic ligand. (auth)

26230 DEUTERIUM ISOTOPE STUDY OF ELECTROGENERATIVE HYDROGENATION. MECHANISM OF HYDROGENATION OF ETHYLENE AT POSITIVE POTENTIALS. Langer, Stanley H.; Feiz, Iraj; Quinn, Colin P. (Univ. of Wisconsin, Madison). J. Amer. Chem. Soc.; 93: 1092-8(10 Mar 1971).

The electrogenerative hydrogenation of ethylene was studied in a flow system using deuterium in the anode compartment with $DClO_4$–D_2O electrolyte. On initiation of the reaction by allowing the system to generate a variable controlled current, deuterium scrambling took place in the product stream in both ethylene and product ethane. The nature and extent varied with the current and potential of the system. Results were analyzed in terms of a Kemball model using statistical and computer techniques. Facile exchange and reversible reaction are indicated between ethylene and its half-hydrogenated state; the rate-determining step is the addition of a second hydrogen atom. Mechanistic implications are discussed. The characteristic open-circuit potential at the ethylene electrode is probably associated with the formation of a half-hydrogenated state. Electrogenerative systems are shown to be useful for carrying out controlled isotope studies at electrodes under steady-state conditions. (auth)

26231 HYDROGEN- AND DEUTERIUM-EVOLUTION REACTIONS ON GOLD IN ACID SOLUTIONS. Kuhn, A. T.; Byrne, M. (Univ. of Salford, Eng.). Electrochim. Acta; 16: 391-9 (Mar 1971).

A study of the hydrogen-evolution reaction on gold electrodes is reported. Two mechanisms are shown to operate between 0.0 and 0.3 V(he). At low cds d log $i/d\eta$ = 2.3 RT/2F; it changes to 2 × 2.3 RT/F at higher cds. This indicates a transition from a Tafel to a Heyrovsky rate-determining step. H/D isotope effects are reported and discussed. Earlier work is reviewed. (auth) (UK)

26232 FAR-INFRARED AND ELECTRONIC SPECTRA OF SOME BIS-ETHYLENEDIAMINE AND RELATED COMPLEXES OF COPPER(II) AND THE RELEVANCE OF THESE DATA TO TETRAGONAL DISTORTION AND BOND STRENGTHS. Lever, A. B. P.; Mantovani, E. (York Univ., Toronto). Inorg. Chem.; 10: 817-26(Apr 1971).

The far-infrared spectra (500 to 200 cm^{-1}) of the complexes $Cu(N-N)_2X_2$ were assigned [(N–N) = ethylenediamine, 1,3-propylenediamine, and symmetric and asymmetric N,N-dimethyl- and N,N-diethylethylenediamines and X = Cl, Br, I, NCS, ClO_4, BF_4, and NO_3]. A straight-line correlation was observed between the square of the highest metal–nitrogen stretching vibration and the energy of the main electronic d–d band. The position of a complex on the line is a measure of its tetragonal distortion and of the in-plane bond strength. (auth)

26233 MATRIX ISOLATION STUDY OF BORAZINE AND BOROXINE. A VIBRATIONAL ANALYSIS. Kaldor, Andrew; Porter, Richard F. (Cornell Univ., Ithaca, N. Y.). Inorg. Chem.; 10: 775-85(Apr 1971).

A vibrational analysis of borazine based on the infrared spectra of matrix-isolated isotopic species $H_3B_3N_3H_3$, $H_3{}^{10}B_3N_3H_3$, and $D_3B_3N_3H_3$ and the gaseous Raman spectrum of $H_3B_3N_3H_3$ is presented. One of the E′ modes, ν_{16}, is reassigned to 1068 cm^{-1}. Two of the inactive A_2' modes, ν_8 and ν_{17}, are assigned to 1195 and 782 cm^{-1}, respectively. The literature assignment of the other modes is confirmed, although the position of the A_1' and E″ modes is slightly modified. Strong bands observed in the matrix spectrum of borazine in the regions 1440 and 2500 cm^{-1} but not resolved in the gas-phase spectra are satisfactorily interpreted as combination bands for a planar D_{3h} molecule without invoking matrix effects or postulating a species of lower symmetry. By using the information available for borazine it is possible, through a combination-band analysis, to assign all the fundamentals of boroxine. (auth)

26234 METAL ISOTOPE EFFECT ON METAL–LIGAND VIBRATIONS. VI. METAL COMPLEXES OF 8-HYDROXYQUINOLINE. Ohkaku, Noboru; Nakamoto, Kazuo (Marquette Univ., Milwaukee). Inorg. Chem.; 10: 798-805(Apr 1971).

Low-frequency infrared spectra (650 to 100 cm^{-1}) were obtained for isotopic pairs of some first-row transition metal oxinates (8-hydroxyquinolinates) of the types MQ_2 (M = $^{58,62}Ni$, $^{63,65}Cu$, and $^{64,68}Zn$), $MQ_2 \cdot 2H_2O$ (M = $^{54,57}Fe$, $^{58,62}Ni$, and $^{64,68}Zn$), $CuQ_2 \cdot 2H_2O$–$CuQ_2 \cdot 2D_2O$, and MQ_3 (M = $^{54,57}Fe$) where Q denotes an oxinate anion. Based on the observed isotopic shifts, the metal–oxygen and metal–nitrogen stretching bands were assigned in the regions of 332 to 210 and 300 to 190 cm^{-1}, respectively. Structures of several metal oxinates were elucidated from the number of isotope-sensitive bands and the general pattern of the spectra. The spectra of CoQ_2 and its dihydrated derivative were studied. The spectra of α and β forms of anhydrous CuQ_2 were compared and discussed. (auth)

26235 CRYSTAL AND MOLECULAR STRUCTURE AND VIBRATIONAL SPECTRUM OF THE VANADIUM(V) OXIDE TRINITRATE–ACETONITRILE COMPLEX, $VO(NO_3)_3.CH_3CN$. Einstein, F. W. B.; Enwall, E.; Morris, D. M.; Sutton, D. (Simon Fraser Univ., Burnaby, B. C.). Inorg. Chem.; 10: 678-86(Apr 1971).

The crystal and molecular structure and vibrational spectrum of the vanadium oxide trinitrate–acetonitrile complex $VO-(NO_3)_3 \cdot CH_3CN$ were determined. The compound crystallizes in the orthorhombic space group Pbca with eight monomeric molecules in a unit cell of dimensions a = 11.14 (3), b = 12.88 (3), c = 13.93 (4) Å. The calculated density is 1.95 (3) g cm^{-3} and the measured density 1.9 (1) g cm^{-3} Full-matrix least-squares refinement of 548 observed three-dimensional x-ray counter measured intensities led to a final conventional R index of 0.095. The configuration about the vanadium atom is that of a pentagonal bipyramid. The equatorial pentagon of five oxygen atoms is formed by the coordination of two bidentate nitrate groups and one unidentate nitrate group, with the vanadyl oxygen atom and the nitrogen of the acetonitrile group forming the apices. The vanadium atom is displaced 0.27 Å out of the plane toward the vanadyl oxygen atom. The V–O bond length to the unidentate nitrate group is 1.92 (2) Å; the lengths of the V–O bonds to the bidentate nitrate groups range from 2.02 (2) to 2.07 (2) Å. The V=O bond length is 1.55 (2) Å and acetonitrile is coordinated by a somewhat long V—N bond of 2.24 (3) Å. Infrared and Raman spectra for the complex were measured and assignments aided by recording Raman spectra on the complex prepared with isotopically substituted (^2H and ^{15}N) acetonitrile. Bands that arise from the bidentate and unidentate nitrate groups were distinguished. (auth)

26236 INFRARED SPECTROSCOPIC STUDY OF THE PHOTOLYTIC DECOMPOSITION OF METHYL AZIDOFORMATE. Wilde, R. E.; Srinivasan, T. K. K.; Lwowski, Walter (Texas Tech Univ., Lubbock, New Mexico State Univ., Las Cruces). J. Amer. Chem. Soc.; 93: 860-3(24 Feb 1971).

Methyl azidoformate has been photolyzed in rare-gas matrices near 4°K and in the solid state at 77°K. Methoxy isocyanate, formaldehyde, and isocyanic acid are proposed as possible photolysis products which are consistent with the infrared spectra. Mechanisms based on band-intensity changes upon prolonged photolysis are also proposed. New bands observed after photolysis of N_3COOCH_3 and N_3COOCD_3 in a neon matrix are tabulated. (auth)

26237 EFFECTS OF METALS ON PROTEIN STRUCTURE. Ulmer, David D. (Peter Brent Brigham Hospital, Boston). pp 11-37 of Effects of Metals on Cells, Subcellular Elements, and Macromolecules. /Maniloff, Jack (ed.). Springfield, Ill.; Charles C Thomas, Publisher (1970).

From 2. conference on toxicity; Rochester, N. Y. (12 Jun 1969). See CONF-690621.

The structural role of metal atoms in metalloproteins and relationships of structure to function are reviewed. A variety of experimental methods has become available for investigating

the effects of metals on protein structure. Measurement of the rate of hydrogen isotope exchange is discussed as a particularly interesting approach for probing the influence of metals on conformational motility as exemplified by studies of conalbumin, transferrin, metallothionein, and carboxypeptidase A. (J.G.B.)

26238 SELF-DIFFUSION OF LIQUID ^{6}Li AND ^{7}Li AS MEASURED BY NUCLEAR MAGNETIC RESONANCE. Krueger, G. J. (EURATOM, Ispra, Italy); Mueller-Warmuth, W.; Klemm, A. Z. Naturforsch.; 26a: 94-8(Jan 1971).

The self-diffusion coefficients of liquid ^{6}Li and ^{7}Li were measured using NMR spin echo techniques with pulsed gradients. In the experimental procedure, and in the sample preparation, particular attention was paid to a relative, rather than to an absolute measurement. At 190°C, the ratio of the self-diffusion coefficients was found to be $D_6(x_6 = 1)/D_7(x_7 = 1) = 1.09 \pm 0.06$, in agreement with the square root of the mass ratio $(m_7/m_6)^{1/2} = 1.08$. In an atomic mixture of 80% ^{6}Li and 20% ^{7}Li, $D_6(x_6 = 0.8)/D_7(x_6 = 0.8) = 1.03 \pm 0.08$ was obtained. (auth)

26239 SELF-DIFFUSION IN MOLTEN LITHIUM. ISOTOPIC MASS DEPENDENCE. Murday, J. S.; Cotts, R. M. (Cornell Univ., Ithaca, N. Y.). Z. Naturforsch.; 26a: 85-93(Jan 1971).

The liquid state self-diffusion coefficients of ^{6}Li and ^{7}Li in isotopically enriched ^{6}Li and ^{7}Li metal and in several isotopic alloys were measured by the nuclear magnetic resonance spin echo, pulsed magnetic gradient technique. At the melting point 180.5°C, the self diffusion coefficients were measured as $D_m^6 = (6.8 \pm 0.7) \times 10^{-5}$ cm^2/sec for ^{6}Li in 99% ^{6}Li, and $D_m^7 = (5.8 \pm 0.6) \cdot 10^{-5}$ cm^2/sec for ^{7}Li in 99.9% ^{7}Li. The ratio of measured values $(D_m^6/D_m^7) = 1.18 \pm 0.07$, which is greater than the square root of the mass ratio, $(m^7/m^6)^{1/2} = 1.08$. The isotopic ratio of self diffusion coefficients was observed to be less than the ratio of the mutual diffusion coefficients in almost pure ^{6}Li and almost pure ^{7}Li, $(D_{Mm}^6/D_{Mm}^7) = 1.35$, and the viscosity ratio, $(\eta^7/\eta^6) = 1.44$. The dependence of D upon isotopic alloy concentration appears to be relatively weak and linear in all but the very low concentrations. As a test of the experimental method, D was measured in liquid Na, H_2O, and D_2O. In liquid sodium at the melting point, $D = (3.7 \pm 0.3) \times 10^{-5}$ cm^2/sec. The Na measurement and the values of D in water are about 5% below other published data, but they are in agreement within experimental uncertainties. Results of this experiment contain systematic corrections amounting to 15 to 20% caused principally by the finite size of the droplets of the liquid metal samples. The corrections as well as the limitations of the technique in measurement of self diffusion coefficients in metals are discussed. (auth)

26240 DIFFERENTIAL DIFFUSION OF IMPURITIES IN ISOTOPIC LITHIUM MATRICES. Lodding, A.; Ott, A. (Chalmers Univ. of Tech., Goteborg). Z. Naturforsch.; 26a: 81-4 (Jan 1971).

The diffusion of ^{22}Na and ^{195}Au was investigated in solid, isotopically pure ^{6}Li and ^{7}Li metal. The Na tracer was found to diffuse by about 4% faster in ^{6}Li than in ^{7}Li. For Au the corresponding difference was 4% at the melting point, but as much as about 15% at $^2/_3$ T_m(°K). A formalism is given for the interpretation of diffusion experiments where the matrix isotope mass is varied. The present results for Na in Li can be plausibly explained in terms of the vacancy mechanism. For Au diffusion in Li, the interpretation appears incompatible with a simple vacancy mechanism, and the anomalous departure from the inverse root mass relationship can be connected with recently detected quantum effects in ^{6}Li–^{7}Li mutual diffusion. (auth)

26241 ISOTOPE EFFECTS IN CLOSE-PACKED METALS AND IN ALKALI HALIDES. Brown, R. C. (Univ. of Sheffield, Eng.); Worster, J.; March, N. H.; Perrin, R. C.; Bullough, R. Z. Naturforsch.; 26a: 77-80(Jan 1971).

A previously reported expression was obtained on the basis of Vineyard's rate theory, for the sharing of the kinetic energy of a diffusing isotope at the saddlepoint with other host atoms. The theory is expressed in terms of the (imaginary) frequency of the localized vibration in which the diffusing atom at the saddlepoint is coupled to its neighbors. Numerical results are presented for the case of a Cu isotope diffusing by the vacancy mechanism in a pure Cu lattice. The pair potential determined by Englert, Tompé and Bullough, which fits the phonon spectra and the stacking fault energy, was used in the calculation. The effects of coupling between the diffusing atom and its immediate neighbors are very small with this potential. The main coupling is found to be to the eight third-nearest neighbors. Treating the vibrations of these nine atoms, a sharing of kinetic energy is found, which is in quantitative agreement with the experimentally observed isotope effect, assuming a vacancy mechanism for self-diffusion. This situation for Cu is in marked contrast to Na, where it was shown in earlier work that the present theory could not explain the observed mass effect, assuming a vacancy mechanism for diffusion. The diffusion of Cs in the CsCl lattice is also discussed using the same theory. Following earlier work on NaCl, the localized normal mode considered is that in which the Cs isotope at the saddlepoint is at the center of a square with four Cl near-neighbor ions at the vertices. A formula for the sharing of kinetic energy is derived, and it is pointed out that, as for NaCl, the force constants, can be obtained from the classical approach of Mott and Littleton. An argument is proposed which suggests that, as with NaCl, the sharing of kinetic energy will be small. No experimental data appear as yet to be available for the CsCl structure. (auth)

26242 SEPARATIVE FLUODIFFUSION. Klemm, A. (Max-Planck-Institut fuer Chemie, Mainz). Z. Naturforsch.; 26a: 52-5(Jan 1971).

Earlier work on fluodiffusion is discussed. General phenomenological equations for fluodiffusion are given. It is shown that in a Poiseuille flow of a molecular mixture, separational fluodiffusion is expected to be much bigger in the direction of the flow than perpendicular to it. Experiments with liquid lithium are reported. They show a clear isotope effect, but it remains a question whether this effect is due to fluodiffusion or to an interaction of the lithium with the iron in which it was contained. (auth)

26243 MEASUREMENT OF LIFETIME AND g FACTORS BY LEVEL CROSSING AND OPTICAL DOUBLE RESONANCE IN THE OH AND OD FREE RADICALS. deZafra, Robert L.; Marshall, Alan; Metcalf, Harold (State Univ. of New York, Stony Brook). Phys. Rev., A; 3: 1557-67(May 1971).

Zero-field level crossing and optical double-resonance techniques were used to measure the lifetimes and g factors of several rotational substates in the $A^2\Sigma^+$ excited state of the OH and OD free radicals. Optical excitation was provided by a molecular lamp and individual emission transitions were observed through a monochromator in the beam of resonantly scattered light. The measured g factors are in agreement with results expected from pure case b coupling for this state. The measured lifetimes are 660 ± 22 and 598 ± 20 nsec for OH and OD, respectively; the mean value 629 ± 22 nsec is suggested. The optical double-resonance experiments allow a tentative lower limit to be placed on the excited-state hyperfine interaction. (auth)

26244 UV SPECTRUM OF THE $^{120}Sn^{35}Cl$ MOLECULE IN THE REGION BETWEEN 2800 AND 3450 A. Richter, W. (Technische Univ., Brunswick). Z. Phys. Chem. (Frankfurt); 71: 303-10(Oct 1970). (In German).

The uv spectrum of the SnCl molecule in the wavelength region between 2800 and 3450 Å was investigated using a sample enriched to 98.4% in ^{120}Sn. Values are given for the vibrational constants of the participating molecular levels. (M.C.G.)

26245 PRESSURE DEPENDENCE AND MECHANISMS OF NITROGEN ACTIVATION ON IRON. Schulz-Ekloff, G. (Max-Planck-Gesellschaft, Berlin). Ber. Bunsenges. Phys. Chem.; 75: 110-14(Feb 1971). (In German).

The pressure dependence of the nitrogen isotope exchange was determined at 350°C and 2 to 20 torr. The exchange rate is proportional to the square root of the nitrogen pressure. A mechanism of adsorption with rearrangement is proposed and discussed in connection with results found by investigations of the pressure dependence of nitrogen activation and of the surface complexes of the iron-nitrogen system. The mechanism is consistent with others that can be described by an Elovich-kinetic. (auth)

26246 STRUCTURE OF CHLORINATED POLY(VINYL CHLORIDE). I. DETERMINATION OF THE MECHANISM OF CHLORINATION FROM INFRARED AND NMR SPECTRA. Kolinsky, M. (Inst. of Macromolecular Chemistry, Prague); Doskocilova, D.; Scheider, B.; (and others). J. Polym. Sci., Part A-1; 9: 791-800(Mar 1971).

Infrared and NMR spectra of chlorinated poly(vinyl chloride) (CPVC) and of chlorinated α-deuterated poly(vinyl chloride) (α-d-CPVC) were measured. It was found that the CDCl unit of α-d-PVC does not undergo chlorination. By assuming an analogous mechanism of chlorination in normal PVC, the populations of all the three possible types of two-carbon sequences ($-CH_2-CHCl-$, $-CHCl-CHCl-$, $-CHCl-CCl_2-$) in CPVC could be determined. The mechanism of chlorination of PVC is discussed from the viewpoint of the previous findings on the conformational structure of this polymer. Differences in structure between suspension- and solution-chlorinated PVC were established. (auth)

26247 SUBSTITUENT EFFECT ON THE IR INTENSITIES OF CH STRETCHING VIBRATIONS OF BENZENE DERIVATIVES. Schmid, E. D.; Seydewitz, H. H. (Univ., Freiburg i. B.). Ber. Bunsenges. Phys. Chem.; 75: 141-9(Feb 1971). (In German).

A theoretical model for interpretation of the infrared intensities of aromatic CH-stretching vibrations is proposed. There are four essentials: the electric dipole moment that determines the infrared intensity is assumed as being mainly localized in the CH-bond-region; in benzene this bond-moment has the polarity C^+-H^-; it can be reversed by the influence of electron-withdrawing substituents; and the effects of the substituents on the CH-stretching-intensity are purely inductive and independent of the effects on the π-electron system. In the scope of this model the intensities of 20 m-substituted benzene derivatives can be predicted in satisfactory agreement with experimental data using empirical parameters from earlier work. The effects of deuterium on the spectra were determined for some of the compounds. (auth)

26248 INTERPRETATION OF THE VAPOR PRESSURE ISOTOPE EFFECT OF H_2S/D_2S. Gellai, B.; Jancso, G. (Central Research Inst. for Physics, Budapest). Ber. Bunsenges. Phys. Chem.; 75: 156-9(Feb 1971).

The reduced partition function ratios of H_2S-D_2S in the liquid and the solid phase were derived from available experimental data on the vapor pressure isotope effect. A model calculation led to the conclusion that molecular rotations in hydrogen sulfide are hindered in the solid. For the liquid phase there is a good agreement between the predictions of the model and the experimental data up to the region of high pressures. (auth)

26249 ION CYCLOTRON RESONANCE STUDIES OF IONIC REACTIONS IN ETHANE AND OF HYDROGEN EXCHANGE IN $D_2-C_2H_6$ AND $H_2-C_2D_6$ MIXTURES. Wexler, S.; Pobo, L. G. (Argonne National Lab., Ill.). J. Amer. Chem. Soc.; 93: 1327-35(24 Mar 1971).

Ionic reactions in pure gaseous ethane and in $D_2-C_2H_6$ and $H_2-C_2D_6$ mixtures were investigated with the technique of ion cyclotron resonance spectroscopy. The observations on ethane lead to the establishment of mechanisms for the formation of $C_2H_4^+$, $C_2H_3^+$, C_3, and C_4 ions and the protonated species $C_2H_7^+$ and $C_3H_3^+$. The results resolve conflicting conclusions about these ions derived from previous high-pressure mass spectrometric experiments. The mechanisms of exchange of hydrogen isotopes during the ionic reactions that take place in $D_2-C_2H_6$ and $H_2-C_2D_6$ mixtures were also determined. The modes observed serve as the basis for the sequences of reactions proposed to account for the nuclear-decay-induced and radioinduced Wilzbach labeling of ethane by tritium. (auth)

26250 PHOTOCHEMICAL TRANSFORMATIONS OF SMALL-RING CARBONYL COMPOUNDS. XXVIII. 1,5-HYDROGEN TRANSFER IN THE PHOTOCHEMISTRY OF AROYLAZIRIDINES. Padwa, Albert; Eisenhardt, William (State Univ. of New York, Buffalo). J. Amer. Chem. Soc.; 93: 1400-8(24 Mar 1971).

The photolysis in pentane of trans-N-tert-butyl-2-phenyl-3-benzoylaziridine was found to yield four products. The structures were assigned as 2,5-diphenyloxazole, (β-tert-butylamino)-trans-benzalacetophenone (A), N-tert-butylbenzalimine, and benzaldehyde. The course of the overall photoreaction was substantially altered for the cis-aziridine. Irradiation of cis-N-tert-butyl-2-phenyl-3-benzoylaziridine gave diphenyloxazole and N-tert-butylbenzalimine with no detectable quantities of A. Sensitization and emission studies indicate that the reaction is derived from the $n-\pi^*$ triplet state. The failure to quench implies that the reaction of the ketone is too rapid for diffusion of the excited state to quencher molecule. A mechanism involving transfer of an electron from nitrogen to the excited triplet state followed by a 1,5-proton transfer accounts for the formation of A. The 1,5-hydrogen transfer route does not seem to be important in the photolysis of the related α,β-epoxy ketone system. (auth)

26251 REACTIONS OF THE HYDROGEN ATOM IN SOLUTION. III. THE PHOTOLYSIS OF THIOLS. STUDIES OF TRITIUM-LABELED THIOLS. Pryor, William A.; Griffith, Michael G. (Louisiana State Univ., Baton Rouge). J. Amer. Chem. Soc.; 93: 1408-11(24 Mar 1971).

Propanethiol, tritiated at the S–H bond, was photolyzed in the presence of various organic hydrogen donors (QH). Tritium becomes incorporated both into the thiol side chain and into QH. A relation was derived between the rate of formation of labeled QH (i.e., d(QT)/dt) and the rate constant k_H for the reaction $H\cdot + QH \rightarrow H_2 + Q\cdot$ In order to avoid errors produced by changes in light flux from run to run, the rate of formation of QT was measured relative to the rate of formation of side-chain labeled thiol. This method gives correct values of k_H for alkanes where the Q–H bond being broken is much stronger than the RS–H bond. Compounds such as toluene which contain weak C–H bonds give spuriously high values of k_H. For these compounds the thiyl radical, and possibly also the carbon radical resulting from hydrogen abstraction from the side chain of the thiol, are able to convert QH to Q . The isotope effect k_T/k_H for the reaction of Q· with RSH or RST must be known before values of k_H can be calculated; this isotope effect can be evaluated directly in independent measurements and data are presented for several Q· radicals. (auth)

26252 REACTIONS OF THE HYDROGEN ATOM IN SOLUTION. IV. PHOTOLYSIS OF DEUTERATED THIOLS. Pryor, William A.; Stanley, James P. (Louisiana State Univ., Baton Rouge). J. Amer. Chem. Soc.; 93: 1412-18(24 Mar 1971).

A new method is reported for studying the reactions of hydrogen atoms in solution which is simpler and more direct than previous methods. The hydrogen atoms are produced by the photolysis of thiols, and they react with organic hydrogen donors: $QH + H\cdot \rightarrow Q\cdot + H_2(k_H)$. For convenience in analysis, RSD was used for studying the reactions of deuterium atoms. However, it is known that H and D atoms react with virtually the same constant, so that the data should be equivalent to data for the hydrogen atom. The technique used to obtain values of k_H involves measuring the HD to D_2 ratio produced as the QH to thiol solvent ratio is varied. The photolysis of thiols produces the thiyl radical as well as the hydrogen atom, but a series of control experiments has shown that the thiyl radical does not interfere with the analysis. Perhaps the most significant of these controls is that tert-butyl mercaptan and thiophenol, which have S–H bond dissociation energies differing by 13 kcal/mol, give results in excellent agreement. A comparison of our data with results obtained from the radiolysis of aqueous solutions shows excellent agreement for all compounds studied except ethanol and isopropyl alcohol. Good agreement with earlier data was obtained for saturated hydrocarbons obtained using tritiated thiols. (auth)

26253 ACYL TRANSFER REACTIONS FROM AND TO THE UREIDO FUNCTIONAL GROUP. IV. NEIGHBORING CARBOXYL GROUP GENERAL ACID CATALYSIS IN THE HYDROLYSIS OF AN O-ACYLISOUREA (2-AMINO-8-CARBOXY-4-OXO-3,1,4-BENZOXAZINE). Hegarty, A. F.; Pratt, R. F.; Giudici, T.; Bruice, T. C. (Univ. of California, Santa Barbara). J. Amer. Chem. Soc.; 93: 1428-34(24 Mar 1971).

2-Amino-4-oxo-3,1,4-benzoxazine (1) has previously been studied as a plausible model for the CO_2–biotin complex of biotin carboxylases. The effects of carboxyl substitution on the reactivity of this model system toward nucleophiles are examined. The compounds used were 2-amino-8-carboxy-4-oxo-3,1,4-benzoxazine and the 6- and 5-carboxyl isomers (2, 3, and 4 respectively). Kinetic analysis of the hydrolysis rates of these compounds indicates that although a 5-carboxyl group (adjacent to the reactive carboxyl site of the benzoxazine) does not promote hydrolysis, as judged by comparison with the 6-carboxy isomer where participation is impossible, an 8-carboxyl group (adjacent to the benzoxazine nitrogen atom, i.e. the leaving group) markedly does so. The reactivity in the latter case, thought to be that of a derivative of 2, is proposed to arise from intramolecular general acid catalysis. Catalytic efficiency is also seen in the morpholinolysis of 2. The kinetic solvent deuterium isotope effect on the hydrolysis of 2 was determined. (auth)

26254 ALIPHATIC SEMIDIONES. XV. 2,3-SEMIDIONES DERIVED FROM THE BICYCLO[n.1.0]ALKANES. Russell, Glen A.; McDonnell, John J.; Whittle, Philip R.; Givens, R. S.; Keske, R. G. (Iowa State Univ., Ames). J. Amer. Chem. Soc.; 93: 1452-66(24 Mar 1971).

The synthesis of bicyclo[2.1.0]pentane-, bicyclo[3.1.0]hexane-, bicyclo[4.1.0]heptane-, bicyclo[5.1.0]octane-, and bicyclo[6.1.0]-nonane-2,3-semidiones was investigated. Acyloin condensations of cis-1,2-cyclopropanedicarboxylic esters failed to yield bicyclopentane semidiones. Instead, the ring-opened cyclopentane-semidiones were formed. Acyloin condensation or oxidation of the 2- or 3-ketones in basic solution produced the bicyclo[3.1.0]-hexane-2,3-semidione. The hyperfine splittings observed in the ESR spectrum were assigned to the six hydrogen atoms by examination of a number of deuterium and alkyl derivatives. Extended Hückel self-consistent field calculations are reported which are in excellent agreement with the experimentally observed values. During this investigation it was determined that the α-methylene group in bicyclo[3.1.0]hexanesemidione underwent a highly stereoselective hydrogen–deuterium exchange in basic dimethyl sulfoxide solution wherein the exo hydrogen exchanged much more rapidly than the endo hydrogen. It was also observed that syn-6-alkylbicyclo[3.1.0]hexane-2,3-semidiones rearranged to the anti isomers with base catalysis. An electrocyclic mechanism is

suggested in which the bicyclo[3.1.0]hexane ring opens to a cyclohexadienyl intermediate which undergoes competing ring closure and aromatization. Overoxidation of the bicyclo[3.1.0]hexanesemidione leads to an o-semiquinone with molecular rearrangement in which C-6 of the bicyclic semidione is converted to C-3 in the semiquinone. A sigmatropic 1,4 migration followed by a cyclopropanol ring opening is suggested. A variety of tricyclic derivatives containing the bicyclo[3.1.0]hexanesemidione nucleus and showing interesting long-range ESR splittings were synthesized. Bicyclo[4.1.0]heptane-2,3-semidione appears to exist in two conformations depending upon the substitution pattern. The importance of long-range interactions is greatly reduced in the bicyclo[4.1.0]heptane system and inconsequential in the bicyclo-[5.1.0]octane- and bicyclo[6.1.0]nonane-2,3-semidiones. (auth)

26255 ALIPHATIC SEMIDIONES. XVI. SEMIDIONES DERIVED FROM THE BICYCLO[n.1.1]ALKANES. Russell, Glen A.; Whittle, Philip R.; Keske, Robert G. (Iowa State Univ., Ames). J. Amer. Chem. Soc.; 93: 1467-70(24 Mar 1970).

Bicyclo[2.1.1]hexane- and bicyclo[3.1.1]heptane-2,3-semidiones were examined by electron spin resonance spectroscopy in dimethyl sulfoxide solution. The long-range hyperfine splitting by the anti hydrogen atoms of the methano bridges decreases from 10 G in the hexane to 3.5 G in the heptane. Bicyclo[4.1.1]octane-3,4-semidione was prepared and studied between –80 and +60°. Ring inversion was fast at all temperatures. A ring-expansion reaction of bicyclo[2.1.1]hexane-2,3-diones to bicyclo[3.1.1]heptane-2,3-diones by reaction with the methylsulfinylcarbanion was detected. Deuterium exchange was used to study hydrogenation reactions. (auth)

26256 ALLYLIC AND HOMOALLYLIC OXIDATION OF CYCLOHEXENE AND CYCLOHEXENE-3,3,6,6-d_4 BY PALLADIUM(II) SALTS. EVIDENCE FOR COMPETING SYMMETRICAL AND OXYPALLADATION INTERMEDIATES. Wolfe, Saul; Campbell, P. G. C. (Queen's Univ., Kingston, Ont.). J. Amer. Chem. Soc.; 93: 1497-9(24 Mar 1971).

The mechanisms of allylic and homoallylic oxidations of cyclohexene and cyclohexene-3,3,6,6-d_4 by Pd(II) salts were studied. Deuterium isotope effects were used to study the oxidation. Results indicate that the two oxidation paths are the result of two competing processes, only one of which involves an oxypalladation adduct. (J.G.B.)

26257 ISORACEMIZATION OF N-CARBOBENZOXYAMINO ACID ESTER DERIVATIVES. Kovacs, J.; Cortegiano, H.; Cover, R. E.; Mayers, G. L. (St. John's Univ., New York). J. Amer. Chem. Soc.; 93: 1541-3(24 Mar 1971).

The racemization by α-hydrogen abstraction of N-carbobenzoxyamino acid active esters in a nonpolar solvent was found to proceed via isoracemization in the presence of triethylamine. Details of the mechanism were investigated by studying the base-catalyzed racemization and deuterium exchange of N-carbobenzoxy-S-benzyl-L-cysteine pentachlorophenyl ester in chloroform in the presence of triethylamine and monodeuteriomethanol. (J.G.B.)

26258 VIBRATIONAL SPECTRUM AND FORCE FIELD OF OSMIUM TETROXIDE. McDowell, Robin S.; Goldblatt, Maxwell (Los Alamos Scientific Lab., N. Mex.). Inorg. Chem.; 10: 625-30(Mar 1971).

Infrared spectra of the vapor and infrared and Raman spectra of CCl_4 solutions are reported for $Os^{16}O_4$ and $Os^{18}O_4$. Particular attention was given to measurement of the isotopic frequency shifts and the band contours, from which the Coriolis interaction constants are obtained. Anharmonicity corrections are estimated and the resulting harmonic frequencies are used to determine the general quadratic force constants of this molecule. The relative effectiveness of Coriolis constants and frequency shifts in determining the force field is compared. The valence stretching force constant, f_r = 8.32 mdyr/Å, supports the assumption of appreciable double-bond character for the Os–O bond. Standard-state thermodynamic functions for OsO_4 vapor are calculated for the temperature range 273 to 600°K. (auth)

26259 H_2O–D_2O SOLVENT ISOTOPE EFFECTS IN THE VOLUME AND EXPANSIVITY BEHAVIOUR OF SOME ORGANIC AND INORGANIC IONS. Conway, B. E.; Laliberte, L. H. (Univ. of Ottawa). Trans. Faraday Soc.; 66: 3032-47(Dec 1970).

Changes of structure of the water solvent caused by organic and inorganic ions were investigated by measurements of the H_2O–D_2O solvent isotope effect in the partial molar volumes $\bar{V}_2$ of alkali halides, tetraalkylammonium (TAA) and other ammonium type salts over a range of temperatures. The structure promoting hydrophobic ions have larger $\bar{V}_2$ in D_2O than in H_2O, while the more electrostricting simple inorganic ions have smaller volumes in D_2O than in H_2O. By means of an extrapolation procedure based on the additivity of $\bar{V}_2^0$ for homologous TAA salts, the individual ionic contributions to the solvent isotopic volume difference can be evaluated. On this basis, the results indicate that the anions are predominantly the species that are associated with the so-called structure breaking effects in the simple salt solutions while K^+ and the TAA cations exhibit an opposite kind of behavior. The solvent isotope effect in $\bar{V}_2$ for pyridine and H (as HOD) is also evaluated. Studies over a range of temperature enabled the partial molal expansibilities to be evaluated in H_2O and D_2O. (auth) (UK)

Physical Chemistry

Refer also to abstracts 26332 and 27283.

26260 (COO–1182-34) INFRARED SPECTRA OF UO AND UO_2 VAPOR CONDENSED IN RARE-GAS MATRICES. Leary, H. J. Jr.; Cater, E. D.; Friedrich, H. B.; Rooney, T. A. (Iowa Univ., Iowa City. Dept. of Chemistry). 10 Mar 1971. Contract AT-(11-1)-1187. 26p. Dep. NTIS.

The molecules UO and UO_2 were vaporized from tantalum and tungsten Knudsen cells containing variously a urania–uranium mixture, solid urania of natural isotopic composition, and solid urania, 60% enriched in ^{18}O, in the range 2300 to 2500°K. The molecules were trapped in argon and krypton matrices at 20°K and studied spectroscopically from 4000 to 100 cm^{-1}. Positively identified vibrational frequencies in argon matrices are 773 cm^{-1} for $U^{16}O$, 734 cm^{-1} for $U^{18}O$, and the frequencies 869, 853, and 825 cm^{-1} for one of the stretching modes of the UO_2 molecule of respective isotopic composition $U^{16}O_2$, $U^{16}O^{18}O$, and $U^{18}O_2$. The second stretching frequency and the bending frequency of UO_2 were not observed. (auth)

26261 (ORNL-tr-2439) NUCLEAR MAGNETIC RESONANCE STUDIES OF METAL HYDRIDES. Spalthoff, W. Translated for Oak Ridge National Lab., Tenn., from Z. Phys. Chem. (Frankfurt); 29: 258-76(1961). 19p. Dep. NTIS.

An abstract of this paper, prepared from the original language, appeared as NSA 16: 5741.

26262 IONIC RANGE OF ThO_2–15 WT. PERCENT Y_2O_3 AT HIGH OXYGEN ACTIVITIES. Salzano, F. J.; Auerbach, C.; Isaacs, H. S.; Minushkin, B. (Brookhaven National Lab., Upton, N. Y.). J. Electrochem. Soc.; 118: 416-18(Mar 1971).

The ionic transference numbers (t_i) of ThO_2–15 wt % Y_2O_3 was determined at oxygen activities corresponding to approximately 1 atm by (a) emf measurements utilizing air–O_2 and air–Pb/PbO cells and (b) four-point resistance measurements, both as a function of temperature. The expression $t_i = [1 + 8.3 \times 10^{-2} P^{1/4} \exp(3420/RT)]^{-1}$ was deduced from the emf measurements. The resistance data are in good agreement with these results, but the latter technique is not sensitive enough to discriminate easily between cases where $t_i < 1$ and where ionic and electronic contributions to the resistance are of comparable magnitude. (auth)

26263 ENTHALPY OF FORMATION OF URANIUM TETRACHLORIDE. Fitzgibbon, G. C.; Pavone, D.; Holley, C. E. Jr. (Los Alamos Scientific Lab., N. Mex.). J. Chem. Thermodyn.; 3: 151-62(Jan 1971).

The enthalpy of formation of uranium tetrachloride, $UCl_4(s)$, was determined from measurements of the enthalpies of solution of uranium metal and of $UCl_4(s)$ in 4M and 6M HCl containing added Na_2SiF_6 and combined with the enthalpy of formation of aqueous HCl of corresponding concentration. The necessity of making the measurements in the absence of dissolved oxygen is emphasized. The weighted mean of the two sets of measurements gives $\Delta H_f^0(UCl_4,s,298\ K) = -(243.4 \pm 0.7)$ kcal $mole^{-1}$. This result was compared with that obtained by a series of measurements including the enthalpies of solution of $UO_2(s)$ and $UCl_4(s)$ in sulfuric acid solutions. These latter measurements lead to a value for the enthalpy of formation of $UCl_4(s)$ of $-(244.0 \pm 1.0)$ kcal $mole^{-1}$. The weighted average of the two determinations gives $\Delta H_f^0(UCl_4,s,298\ K) = -(243.6 \pm 0.6)$ kcal $mole^{-1}$. (auth) (UK)

26264 THE MAGNETIC TRANSITION, HEAT CAPACITY, AND THERMODYNAMIC PROPERTIES OF URANIUM DIOXIDE FROM 5 TO 350°K. Huntzicker, James J.; Westrum, Edgar F. Jr. (Univ. of Michigan, Ann Arbor). J. Chem. Thermodyn.; 3: 61-76(Jan 1971).

The heat capacity of high-purity uranium dioxide was reexamined over the low-temperature range especially in the vicinity of the λ-type anomaly reported to occur at 28.7°K

as a consequence of magnetic ordering. The present study indicates a very sharp transition at 30.44°K with a maximum C_p of 391 cal mole^{-1} K^{-1}. The heat capacity at constant pressure C_p, the entropy S°, the enthalpy ($H° - H_0^0$), and Gibbs energy function ($G° - H°$)/T are tabulated and at 298.15°K have the following values: 15.20 cal mole^{-1} K^{-1}, 18.41 cal mole^{-1} K^{-1}, 2696 cal mole^{-1}, and −9.37 cal mole^{-1} K^{-1}. The heat capacity results are compared with those derived from the neutron scattering work and also with the theory of Allen. (auth) (UK)

26265 REDOX PROCESSES OF URANIUM(VI), (V), (IV), AND (III) IN ACETATE BUFFERS. Sipos, L. (Inst. Rudjer Boskovic, Zagreb); Galus, Z. Inorg. Nucl. Chem. Lett.; 7: 299-304(Mar 1971).

Polarographic investigations of the electrode behavior of uranium (VI), (V), (IV), and (III) in acetate buffers are discussed. Measurements were made at varying acetate concentrations and constant acidity, then at constant acetate concentration and varying acidities. When the acetate concentration is increased, the rate of uranium(V) disproportionation increases; increasing pH causes a decrease in disproportionation. Results indicate the presence of an adsorbed uranium(IV) on the electrode, a deterrent to the U(VI) to U(V) process. At least two and possibly three U(IV) species are present in the solutions studied. (J.G.B.)

26266 MECHANISTIC IMPLICATIONS OF THE ROLE OF PHENOL IN THE URANIUM(IV)–CHLORINE(III)–PHENOL REACTION. Grimley, Eugene B.; Buchacek, Robert; Gordon, Gilbert). (Univ. of Iowa, Iowa City). Inorg. Chem.; 10: 873-6 (Apr 1971).

Previous studies indicate the presence of a reactive chlorine intermediate in the reaction of uranium(IV) with chlorine(III) in acidic aqueous solutions and the scavenging of the intermediate by phenol additions to the system. Reaction rates were compared in order to determine which of the known chlorine species are able to react with phenol rapidly enough to account for the observed scavenger reaction. Results indicate the intermediate species to be chlorine and $[Cl_2O_2]$. At a pH of 1 or more, $[Cl_2O_2]$ appears to be the only intermediate. A mechanism for the reaction is proposed. (J.G.B.)

26267 CATALYSIS OF IONIC REACTIONS BY POLYELECTROLYTES. III. QUENCHING OF URANYL ION FLUORESCENCE BY IRON(II) IONS IN POLY(VINYLSULFONIC ACID) SOLUTION. Taha, Issam A.; Morawetz, Herbert (Polytechnic Inst. of Brooklyn). J. Amer. Chem. Soc.; 93: 829-33(24 Feb 1971).

Addition of poly(vinylsulfonate) (PVS) to uranyl solutions at pH 2 leads to a reduction of their fluorescence intensity probably due to self-quenching of the UO_2^{2+} concentrated in the vicinity of the polyanion. At pH 3, UO_2^{2+} binding to the polymer produces a greater reduction in fluorescence intensity and a change in the shape of the fluorescence spectrum similar to the change observed when the acidity of the medium is increased. Addition of ferrous ions to solutions containing uranyl and PVS leads first to rapid fluorescence quenching produced by concentration of ferrous and uranyl ions in the polymer domain. This is followed by a pronounced increase in fluorescence intensity as the Fe^{2+} ions displace uranyl ions from the polymer binding sites. Eventually, the fluorescence decreases again as a consequence of the quenching of free uranyl. This behavior proves that exchange of bound and free counterions is negligible over the lifetime of the excited uranyl ion. (auth)

26268 THORIUM FLUORIDE COMPLEXES. DETERMINATION OF THE STABILITY CONSTANTS USING THE FLUORIDE ION ACTIVITY ELECTRODE. Klotz, Paul; Mukherji, Anil; Feldberg, Stephen; Newman, Leonard (Brookhaven National Lab., Upton, N. Y.). Inorg. Chem.; 10: 740-3(Apr 1971).

Thorium(IV) in acidic media undergoes stepwise complexation with fluoride ion forming three soluble complexes, ThF_3^+, ThF_2^{2+}, ThF_3^+, and a precipitate, ThF_4. Using a titration technique and measuring the fluoride ion activity directly with a fluoride ion activity electrode, it was possible to evaluate the formation constants ${}^*\beta_n = [ThF_n^{4-n}][H^+]^n[Th^{4+}]^{-1}[HF]^{-n}$ for the complexes and the solubility product constant for the precipitate ${}^*K_{SO} = [Th^{4+}][HF]^4[H^+]^{-4}$ as log ${}^*\beta_1 = 4.52 \pm 0.05$, log ${}^*\beta_2 = 7.26 \pm 0.14$, log ${}^*\beta_3 = 8.9 \pm 0.3$, and log ${}^*K_{SO} = -15.17 \pm 0.15$. A calculation of the fraction of species present as a function of fluoride ion concentration using the value for ${}^*\beta_3$ indicates that the fraction of ThF_3^+ never exceeds 0.1 under the conditions investigated. Accordingly, the value for ${}^*\beta_3$ is at best approximate, and its elimination from the least-squares analysis of the data has almost no effect on the values of the other constants or on the standard deviations. Variation of the thorium ion concentration from 0.003 to 0.03M indicates that polynuclear species do not play an important role. Experiments carried out at acid concentrations of 0.1 and 1.0M show no evidence for acid-base equilibria of the thorium complexes. (auth)

26269 INFRARED ABSORPTION OF CRYSTALLINE THORIUM TETRAFORMATES. II. DETECTION OF POLYMORPHIC TRANSITIONS BY INFRARED SPECTROSCOPY: INTERPRETATION OF THE δ(OCO) VIBRATIONAL MODE SPLITTING IN THE CARBOXYLIC GROUP OF THORIUM TETRAFORMATES. Mentzen, Bernard F. (Institut National des Sciences Appliquees de Lyon, Villeurbanne, France). J. Solid State Chem.; 3: 20-5(Feb 1971).

Investigation of polymorphic transitions in the solid state by infrared spectroscopy is described. The reversibility of the $Th(HCOO)_4\alpha \rightleftharpoons Th(HCOO)_4\gamma$ allotropic transition was checked, and it was established that residual water molecules had a blocking effect on the $\gamma \rightarrow \alpha$ transition. The splitting of the δ(OCO) vibrational mode of the formate ion in the thorium tetraformates is discussed in terms of a vibrational analysis under the factor group. (auth)

26270 INFRARED ABSORPTION OF CRYSTALLINE THORIUM TETRAFORMATES. I. CHARACTERIZATION OF THORIUM TETRAFORMATES IN THE SOLID STATE BY INFRARED SPECTROSCOPY. Mentzen, Bernard F. (Institut National des Sciences Appliquees de Lyon, Villeurbanne, France). J. Solid State Chem.; 3: 12-19(Feb 1971).

The different thorium tetraformates were characterized by their infrared spectra, and the totality of the observed absorption bands assigned to vibrational modes in the powdered crystalline samples. Discussion of the experimental results led to the statement that in all the thorium tetraformates the coordination mode of the formate atoms is the same, the corresponding coordination polyhedron of the thorium atoms being a distorted Archimedean antiprism. It was also established that in the hydrated compounds the crystal water is essentially of the coordinated type, except for one of the three water molecules in the trihydrate, which seems to be distorted lattice water. The infrared spectra of the five polymorphic species of anhydrous thorium tetraformate exhibit residual water bands; these bands disappear completely at 153°C only. (auth)

26271 URANYL ION-ADENINE NUCLEOTIDES COMPLEXES. Feldman, Isaac; Rich, Kenneth E.; Agarwal, Raghunath P. (Univ. of Rochester, N. Y.). Contract W-7401-Eng-49. pp 117-29 of Effects of Metals on Cells, Subcellular Elements, and Macromolecules. /Maniloff, Jack (ed.). Springfield, Ill.; Charles C Thomas, Publisher (1970). (UR-49-1128).

From 2. conference on toxicity; Rochester, N. Y. (12 Jun 1969). See CONF-690621.

The structures and reactions of the complexes formed between uranyl ions and adenine nucleotides are of considerable interest because of their possible involvement in uranium inhibition of sugar transport into the cell and because of the use of uranyl compounds in tissue staining. Titrations indicated that in equimolar solution below pH 4.5 uranyl ion is chelated by each of the three adenine nucleotides, AMP, ADP, and ATP, in the same manner, the uranium being bonded by the adenine N_7 atoms, the ribose ring-oxygen atom, and an alpha-phosphate oxygen atom. Nuclear magnetic resonance spectra, proton and phosphorus, gave information about these systems in basic solution. Near pH 7.5 an equimolar mixture of uranyl nitrate and ADP(U−ADP) contains a dinuclear complex (i.e., 2 : 2) in which uranium is bound only to phosphate and in which the adenine rings are stacked to a greater degree than in a free ADP solution. This complex disproportionates to free ADP and a 2 : 1 complex as the pH is raised, the reaction being complete near pH 10. In the U−AMP system, an equimolar mixture at pH ~ 10.5 contains only a 2 : 2 sandwich-type complex with uranium bonded to the phosphate and to the ribose hydroxyl-oxygen atoms. This complex begins to disproportionate just below pH 10.5 to free AMP and 2 : 1 complexes (two forms). Above pH 8 the U−ATP system contains a 2 : 2 sandwich-type chelate, in which uranium is bonded to the β and γ phosphate groups and the ribose hydroxyl-oxygen atoms. Below pH 8 U−ATP hydrolyzes first to U−ADP, but above pH 9 it hydrolyzes first to U−AMP, pH 8 to 9 being the most stable region. (auth)

26272 THERMOCONDUCTOMETRIC INVESTIGATION OF PHOSPHATIDYLCHOLINE IN AQUEOUS TERTIARY BUTANOL SOLUTIONS IN THE ABSENCE AND PRESENCE OF METAL IONS. Hoogeveen, Joh. Th. (State Univ. of New York, Buffalo). pp 207-29 of Effects of Metals on Cells, Subcellular Elements, and Macromolecules. /Maniloff, Jack (ed.). Springfield, Ill.; Charles C Thomas, Publisher (1970).

From 2. conference on toxicity; Rochester, N. Y. (12 Jun 1969). See CONF-690621.

XUM

Under certain conditions, extracted and purified lecithin (phosphatidylcholine) forms membranes in vitro. Lecithin is dissolved in water containing tertiary butanol and NaCl at 60°C. When cooled at 0.3°C/min the isotropic lecithin solution turns into an opalescent system at a certain temperature. This phase transition coincides with an increase of the electrical resistance of the system. The increase of the resistance can be nullified by mechanical agitation proving that a three-dimensional structure exists in the opalescent phase. This structural behavior of lecithin appears to be thermoreversible. Over a pH-range of 5 till 9 the structural properties are not influenced. However, at higher pH values deterioration of lecithin occurs. The study of the action of different metal ions on the properties of lecithin resulted in the formulation of an affinity sequence: $UO_2^{++} > Fe^{+++} > Pb^{++} > Fe^{++} > Ca^{++} > Hg^{++}$. (auth)

26273 MASS SPECTROMETRIC DETERMINATION OF THE HEATS OF ATOMIZATION OF NdO_2, NdBO, AND $NdBO_2$ AND UPPER VALUES FOR THE DISSOCIATION ENERGIES OF NdAg AND Nd_2. Pupp, C.; Gingerich, K. A. (Texas A and M Univ., College Station). J. Chem. Phys.; 54: 3380-4(15 Apr 1971).

During evaporation of Nd and Ag from a boron nitride Knudsen cell the new molecules $NdO_{2(g)}$, $NdBO_{(g)}$, and $NdBO_{2(g)}$ were detected by mass spectrometric analysis. The enthalpies of the following reactions were determined by a third-law method: (1) $NdO_{2(g)} + Nd_{(g)} \rightarrow 2NdO_{(g)}$, $\Delta H_0^\circ = -10.5 \pm 1.2$ kcal mol^{-1}, (2) $NdBO_{(g)} \rightarrow Nd_{(g)} + BO_{(g)}$, $\Delta H_0^\circ = 77.4 \pm 1.9$ kcal mol^{-1}, (3) $Nd_{(g)} + NdBO_{2(g)} \rightarrow NdBO_{(g)} + NdO_{(g)}$, $\Delta H_0^\circ = 10.5 \pm 4.$ kcal mol^{-1}. From these reaction enthalpies, the heats of atomization of NdO_2, NdBO, and $NdBO_2$ were calculated: $NdO_{2(g)}$; $\Delta H_{0\,atom}^\circ = 323.5 \pm 12.5$ kcal mol^{-1}; $NdBO_{(g)}$: $\Delta H_{0atom}^\circ = 268.7 \pm 10$ kcal mol^{-1}; $NdBO_{2(g)}$: $\Delta H_{0atom}^\circ = 446.2 \pm 13$ kcal mol^{-1}. A discussion of the possible geometric arrangement of these molecules on the basis of thermochemical data is given. Upper limits for the bond energies of $Nd_{2(g)}$ and $NdAg_{(g)}$ are given as 39 and 50 kcal mol^{-1}, respectively. (auth)

26274 SPECTROPHOTOMETRIC STUDIES ON PLUTONIUM (IV) COMPLEXES IN AQUEOUS AND MIXED ORGANIC–NITRIC ACID SYSTEMS. Sherief, M. K.; Grass, F. (Univ., Vienna). Atomkernenergie; 17: 214-16(May 1971).

The absorption spectra of quadrivalent plutonium-239 in nitric acid, lithium nitrate, and mixed methyl alcohol aqueous systems were studied. The data indicate that the hexanitrato complex reaches its maximum (i.e., the Pu(IV) is changed completely to the hexanitrato complex) at 1.5N HNO_3 + 90% methyl alcohol. These results are attributed more to the effect of the medium on the complex formation than the concentration of the nitric acid. (auth)

Radiation and Nuclear Chemistry

Refer also to abstracts 26470, 26535, and 28379.

26275 (AEC-tr-7102/1) NUKLEONIKA. Translation of Nukleonika; 15: 1-144(1970). 132p. (TT-70-55010/1). Dep. NTIS.

26276 TRENDS IN THE UTILIZATION OF RADIATION AND RADIOISOTOPES. RADIATION CHEMISTRY. Oshima, Keiichi (Tokyo Univ.). Genshiryoku Kogyo; 16: No. 4, 107-9(Apr 1970). (In Japanese).

The present state and the prospect in the 1970's of the industrial use of radiation chemistry is reviewed. In the 1970's the following circumstances will be seen in the field of the industrial use of radiation chemistry: cost decreases of radioisotopes and accelerators will enable radiation chemical process to compete economically with conventional process; Nuclear reactors will be used widely, and as a result, the kinds of available radiation will be diversified; and, chemonuclear reactors will be used for radiation sources. The problems connected with these matters are discussed. In conclusion, it is stated that what should now be done in the radiation chemistry is to build the engineering systems of radiation chemistry as industrial process techniques. (Japan)

Radiation Effects

Refer also to abstracts 26638, 26657, 26658, and 27636.

26277 (ORO-3799-7) SPIN INTERACTIONS BETWEEN SLOW ELECTRONS AND AMINO ACID FILMS. Three Year Summary Report of Progress, June 1, 1968–February 28, 1971. Yeargers, Edward (Georgia Inst. of Tech., Atlanta. Engineering Experiment Station). 1 Mar 1971. Contract AT(40-1)-3799. 67p. Dep. NTIS.

The possibility of spin exchange between incident electrons and orbital electrons of evaporated films of aromatic amino acids is being investigated. The theoretical work was concerned with two problems: calculations of the energy levels, transition moments, and charge densities of the aromatic amino acids and the quantum mechanics of incident electron–orbital electron spin interactions. The experimental work, as proposed, was performed by irradiating amino acid films at 100°K and at pressures below 10^{-7}mm with electron beams of selected energies between 40 and 1000 eV. The light emitted as the result of such irradiation was analyzed according to wavelength and radiative lifetimes, these latter characteristics being indicative of the identity of the originating excited state. The results showed that electrons with these energies generated short-lived (singlet), long-lived (triplet), and other long-wavelength states (with lifetimes of about 50 msec.), the latter being characteristic of emission due to excitation by ionizing radiation. These long-wavelength states make it almost impossible to isolate triplet-singlet emission. These long-wavelength emitting transitions, however, are not generated by uv. (auth)

26278 KINETICS OF THE PYROLYSIS OF BERYLLIUM HYDRIDE. Schneider, G. R.; Nigh, W. G. (Rocketdyne, Canoga Park, Calif.). Combust. Flame; 15: 223-31(Dec 1970).

The kinetics of the pyrolytic decomposition of beryllium hydride, $BeH_2(s) \rightarrow Be(s) + H_2(g)$, was studied over the temperature range 205 to 250°C. When the fraction decomposed, α, is plotted versus time, the reaction exhibits a sigmoid-shaped curve typical of autocatalytic processes. The initial portion of the acceleratory phase ($0.1 < \alpha < 0.35$) has been correlated with a simple power law which is the result of using a model assuming random formation of beryllium nuclei and a linear growth rate of the nuclei. The data indicate that the exponent on t in the power law was 7 for 95.6% hydride and about 5 for 93.1% hydride. A contracting-volume model has been used to describe the final portion of the acceleratory phase and the deceleratory phase ($0.35 < \alpha < 0.80$ to 0.95). A first-order rate expression correlated the data for $\alpha > 0.80$. Values of the activation energy were found to be between 23 and 27 kcal/mole for the 95.6% hydride and between 23 and 30 kcal/mole for the 93.1% hydride for all of the models used. Any rate equation having the general form $f(\alpha) = (kt)^n$ will produce similar activation energies. The hydride pyrolysis rate was unaffected by beryllium metal addition, by extensive washing in n-hexane, ether, and benzene, or by exposure to mercury vapor. X-ray irradiation changed the pyrolysis rate in a way that was consistent with the production of more nucleation sites. Grinding the hydride also increased the decomposition rate but lowered the exponent on t in the power law from 7 to about 5. (auth)

26279 INTERACTION BETWEEN THYMIDYLIC ACID AND SULFHYDRYLAMINE RADIOPROTECTORS. Pullman, I. (Sloan-Kettering Inst. for Cancer Research, New York); Blumenthal, N. C.; Handler-Bernich, E. Radiat. Res.; 45: 476-86(Mar 1971).

The nature of the binding between certain sulfhydrylamine radioprotectors and diammonium deoxythymidylate (dTMP) was studied using ESR and x-ray diffraction techniques on solid systems prepared by freeze-drying and solution evaporation. ESR spectra taken after x-irradiation of an L-cysteine hydrochloride–dTMP system showed no spin transfer to the sulfur atom in contrast to the large amount of spin transfer exhibited by a cysteamine hydrochloride–dTMP system. X-ray diffraction powder patterns of the two unirradiated solid systems showed that no unreacted material was present. Over 99% of the reaction between cysteamine hydrochloride and dTMP proceeded via binding through an enolate form of the thymine ring. In the case of L-cysteine hydrochloride, approximately 40% of the reaction involved binding of the radioprotector to the phosphate group. Indirect arguments lead to the conclusion that very little of this reaction takes place through the enolate group. These observations are consistent with the hypothesis that for a significant amount of spin transfer to take place to the sulfur atom, the binding of the radioprotector must be predominantly through an enolate form of the nucleotide base. (auth)

26280 TRANSPORT OF FIXED GASES IN RADIATION-STABILIZED POLY(VINYL CHLORIDE). Nakagawa, Tsutomu; Hopfenberg, H. B.; Stannett, V. (North Carolina State Univ., Raleigh). J. Appl. Polym. Sci.; 15: 231-45(Jan 1971).

Poly(vinyl chloride) was reacted with sodium N-methyl dithiocarbamate to produce a modified PVC containing N-methyl dithiocarbamate varying degrees of substitution. The resulting adducts were markedly more stable when subjected to γ-radiation than the unmodified PVC. The transport parameters (permeability, solubility, and diffusivity) of fixed gases were determined in modified and unmodified films. Although the radiation stability was dramatically improved by this novel substitution, the barrier properties of the PVC were only slightly changed by the controlled substitution of N-methyl dithiocarbamate. (auth)

26281 RELATION BETWEEN THE POLYMER CONFORMATION AND THE ELASTIC MODULUS OF THE CRYSTALLINE REGION OF POLYMER. Sakurada, Ichiro; Kaji, Keisuke (Kyoto Univ.). J. Polym. Sci., Part C; No. 31, 57-76(1970).

The force required to stretch a polymer chain by 1% (f value) was calculated from experimental values of elastic moduli E_1 in the direction of molecular axis and the cross-sectional area of the molecule of 25 well known polymers (some γ-irradiated and others not irradiated). The f value is mainly dependent on the conformation of a molecule and almost independent of side groups. The f values of polymers of various types of conformation may be summarized as follows: T type, 4.5×10^{-5} dyne; TGT$\overline{G}$ type, 1.5×10^{-5} dyne; TG(3/1) type, 1×10^{-5} dyne; T′G′ (7/2) type, 0.58×10^{-5} dyne; T′G′(4/1) type, 0.36×10^{-5} dyne; TTGG type, 0.29×10^{-5} dyne; where T, G, and $\overline{G}$ mean trans, gauche and minus gauche, respectively, and the numbers in the paratheses denote helical structures. The reason for an anomalous apparent E_1 value of nylon 6 (α-form) previously reported was elucidated; it was confirmed that E_1 exhibits a value expected for a polymer with a nearly extended zigzag conformation. (auth)

Radiation Processes

26282 X-RAY INDUCED POLYMERIZATION OF GASEOUS VINYL CHLORIDE. EFFECT OF ADDITIVES. Grossoleil, J.; Herman, J. A. (Laval Univ., Quebec). Can. J. Chem.; 49: 363-70(1 Feb 1971).

X-radioinduced polymerization in the gas phase of pure vinyl chloride and of its mixtures with O_2, NO, SF_6, NH_3, CH_3NH_2, H_2O, HCl, and C_2H_2 were examined. About 75% of the polymerization proceeds via a radical mechanism. The experiments indicate that most of the additives are deactivating chain transfer agents. Gel permeation chromatography showed that the polymer is activated by x-ray absorption during the time it takes to fall to the bottom of the irradiation cell, and forms a branched polymer. (auth) (Canada)

26283 PRESENT STATUS OF INDUSTRIALIZATION OF RADIATION CURING AND ITS PROBLEMS. Arakawa, Tetsutaro (Mitsubishi Chemical Industries, Ltd., Kawasaki, Japan). Genshiryoku Kogyo: 16: No. 3, 40-3(Mar 1970). (In Japanese).

The characteristics of radiation curing are described. The coating materials that are suited to radiation curing are those such as unsaturated polyester–styrene systems. The comparison between radiation process and conventional heat process is presented. The present status of industrialization is also described. The following three factors are needed for industrialization of radiation curing: development of the coating materials for radiation curing; development of the low-energy electron accelerators for radiation curing; and users who joined the radiation curing technique with their products. The present status in Europe and America is described with attention to these three factors. Some problems of industrialization are also discussed. (Japan)

26284 VAPOUR-PHASE RADIATION-INITIATED THERMAL OXIDATION OF BENZENE BY MOLECULAR OXYGEN WITH FAST ELECTRON IRRADIATION. Timofeev, V. D.; Yur'ev, Z. N.; Klapishevskaya, Z. B.; Borisov, E. A. Petrol. Chem. (USSR) (Engl. Transl.); 10: No. 1, 5-11(1970).

Translated from Neftekhimiya; 10: No. 1, 5-11(1970).

During radiation-initiated thermal oxidation of benzene with molecular oxygen the dependence of phenol yield on temperature, benzene:oxygen ratio in the reacting mixture, contact time, concentration of cyclohexane additive was compared with phenol yields during thermal oxidation under the same conditions. Phenol yield in radiation-initiated thermal oxidation is always higher than the yield in thermal oxidation. Maximum phenol concentration achieved during the experiments was 4% wt. The radiation-initiated chemical yield of phenol with maximum concentration was 40 molecules per 100 eV radiation energy absorbed. Effective activation energy of phenol formation in thermal and radiation initiated thermal reaction was determined. (auth) (UK)

26285 VOLUME DEPENDENCE OF THE C_2 CORRECTION IN THE MOONEY–RIVLIN ELASTIC EQUATION OF STATE. Mark, J. E. (Univ. of Michigan, Ann Arbor). J. Polym. Sci., Part C; No. 31, 97-106(1970).

Stress-strain isotherms at 25°C are reported for a series of unswollen networks of cis-1,4-polybutadiene, which differ both in degree of crosslinking and in the volume at which the crosslinks were introduced. The former quantity was varied by variation of the amount of high-energy γ radiation used to bring about the crosslinking, the latter, by crosslinking the polymer in solution as well as in the bulk, undiluted state. The results are interpreted in terms of the equation $f^*/(\alpha - \alpha^{-2}) = 2C_1 + 2C_2\alpha^{-1}$ where f^* is the force per unit area of the undistorted, unswollen sample, α is the relative length of the sample, and C_1 and C_2 are empirical constants, the latter serving as a measure of the departure of the dependence of stress on strain from that indicated by the statistical theory of rubber elasticity. At equal values of the "modulus" $f^*/(\alpha - \alpha^{-2})$, the correction C_2 is found to be very small for networks prepared in solution and to increase markedly with increase in concentration of polymer in the system undergoing crosslinking. In addition, the networks prepared in solution exhibit considerably smaller nonequilibrium, relaxation effects than those crosslinked in the undiluted state. (auth)

26286 SURFACE COMPLEXES FORMED BY THERMAL AND RADIOLYTIC ADSORPTION OF GASES ON GRAPHITE. Feates, F. S.; Keep, C. W. (Atomic Energy Research Establishment, Harwell, Eng.). Trans. Faraday Soc.; 66: 3156-62 (Dec 1970).

The nature of the surface complexes formed when graphite is exposed to thermal or reactor-irradiated CO_2 or O_2, and their role in carbon gasification, were deduced by temperature programmed desorption to 1075°K. A series of complexes with discrete activation energies of desorption (21-274 kJ mol^{-1}) that desorb by first-order processes were observed. They are attributed to adsorption at carbon atoms on the graphite surface adjacent to edges and vacancies. The site responsible for radiolytic oxidation of graphite by CO_2 was tentatively identified from the variation in surface coverage and desorption energies in the presence of radiation or on addition of CO or CH_4 to the CO_2. (auth) (UK)

26287 APPLICATION OF NUCLEAR TECHNIQUES TO THE RECOVERY OF FADED PHOTOGRAPHS. Chatters, R. M.; Jacobs, Camille (Washington State Univ., Pullman). Isotop. Radiat. Technol.; 8: 309-14(1971).

Faded paper photographs, tintypes, and glass-plate negatives can be upgraded through neutron activation of the residual silver in the faded objects and subsequent exposure of photographic film or paper to the radiations from the long-half-life ^{110m}Ag so produced. The nuclear technique is presented as one method of faded-photograph recovery — not as the only or necessarily best method for so doing. (auth)

Radiolysis

Refer also to abstracts 26328, 26330, 26349, 26523, and 26623.

26288 (LB/G–2937) THE LET PARAMETER AND THE RADIOLYSIS OF Fe^{2+} SOLUTIONS BY LOW-ENERGY PROTONS. Pucheault, J.; Julien, R. Translated by R. G. P. Towndrow (Atomic Energy Research Establishment, Harwell (England)), from Radiochem. Radioanal. Lett.; 2: No. 1, 27-31(1969). 5p. Dep. NTIS (U. S. Sales Only).

An abstract of this paper, prepared from the original language, appeared as NSA 23: 47568.

26289 (NYO–2150-60) ELECTRON SPIN RESONANCE SPECTRUM OF FCN^- AND HCN^- IN KCl. MSC Report 1369. Othmer, Siegfried (Cornell Univ., Ithaca, N. Y. Materials Science Center). Jun 1970. 84p. Dep. NTIS.

Thesis.

The electron spin resonance spectra of FCN^- and HCN^- (produced by x irradiation of KCN-doped crystals) as substitutional impurities in KCl were studied at 9, 18, and 24 kMHz, and from 4 to 250°K. The FCN^- molecular ion was found to be bent to a bond angle of about 117°, the molecular plane coinciding with a (110) plane of the crystal. At 77°K a motionally averaged spectrum of (111) symmetry was observed, with rotation restricted by a barrier of about 30 cm^{-1}. Above 150°K the spectrum was isotropic, rotational freedom being governed by a barrier of about 400 cm^{-1}. The HCN^- spectrum, previously reported, was studied under higher resolution at K-band. At 30°K a spectrum of (111) symmetry was found. Treatment in terms of a motional averaging model indicates a higher trigonal barrier than was deduced for FCN^-. A preliminary report of the X-band spectrum of $ClCN^-$ at 77°K, a V_k-like spectrum of (110) symmetry, is given in an appendix. (auth)

26290 (NYO–3753-19) NATURE OF OXYGEN CONTAINING RADICALS IN RADIATION CHEMISTRY AND PHOTOCHEMISTRY OF AQUEOUS SOLUTIONS. Technical Progress Report, September 1, 1970–July 1, 1971. Czapski, Gideon (Hebrew Univ., Jerusalem (Israel). Dept. of Physical Chemistry). Contract AT(30-1)-3753. 34p. Dep. NTIS.

The reactions of Fe^{2+}, Cr^{2+}, V^{4+}, and Ti^{3+} with H_2O_2 in the

XUM

presence of 2-propanol were studied using the ESR flow technique. It was shown that all these "Fenton like" reagents form OH radicals that can react with the 2-propanol. From studies of the ESR intensities of the alcohol radical as a function of H_2O_2, Ti^{3+}, and that of added Ti^{4+}, Fe^{3+}, V^{5+}, and Cr^{3+} it was concluded that these ions react faster with CH_3COHCH_3 than with $CH_2-CHOH-CH_3$. The reaction of the alcohol radicals with H_2O_2 was also studied by radiolysis experiments. The unusual kinetics and properties of "Fenton like reagent" and OH and R radicals generated by these reagents previously reported are shown to be due to wrong kinetic assumptions. (auth)

26291 REPAIR AND DAMAGE BY MERCAPTANS IN ^{60}Co γ-RAY IRRADIATION OF ORGANIC COMPOUNDS IN AQUEOUS SOLUTION. Cohen, Saul G.; Lam, F. L. (Brandeis Univ., Waltham, Mass.). Radiat. Res.; 45: 462-75(Mar 1971).

Solutions of ~0.1 M 2-propanol and of ~0.1 M acetone in water were subjected to ^{60}Co γ radiolysis, dose rate 5×10^{22} eV/1/hr, over a range of pH in the presence and absence of a mercaptan, cysteine, or 2-mercaptoethanol. G values for formation of acetone from 2-propanol decrease with decreasing acidity, 2.6, 1.0, and 0.6 at pH 2.8, 5.7, and 9.7, respectively. Addition of mercaptan, 0.003 M, reduces G(acetone) to ~0.3. This is due largely to a repair mechanism, demonstrated by mercaptan-induced introduction of deuterium into 2-propanol during mercaptan protected radiolysis in D_2O: $(CH_3)_2\dot{C}OH + RSD \rightarrow (CH_3)_2CDOH + RS\cdot$. This reaction fully suppresses formation of pinacol, formed from propanol with G = 0.6 at pH 5.7 and 9.7 in absence of mercaptan. G values for formation of 2-propanol from acetone increase with decreasing acidity, from ~0 at pH 1.1 to ~0.7 at pH 6 and 9.2. Mercaptan, 0.003 M, greatly increases G(2-propanol) to 1.5 at pH 1.1, ~3 at pH 6 and 9.2. The same hydrogen transfer reaction repairs 2-propanol and damages acetone. 2,5-Hexanedione, formed with G ~ 1.3 from aqueous acetone in absence of mercaptan, is completely suppressed by mercaptan. The mechanisms of the reactions and significance to protection and damage by mercaptans in radiobiology are discussed. (auth)

26292 ESR STUDIES OF X-IRRADIATED SINGLE CRYSTALS OF N-BENZOYLALANINE. Lassman, G.; Damerau, W. (Deutsche Akademie der Wissenschaften, Berlin). Stud. Biophys.; 17: 195-6 (1969). (In German).

Single crystals of N-benzoylalanine deuterated in exchangeable positions and nondeuterated were investigated with ESR after x-irradiation at room temperature. Two different types of radicals are present, and their structure was confirmed by determination of principal values of the g- and hyperfine tensors. Type I dominates at room temperature and has the structure $CH_3-\dot{C}H-\overset{+}{N}H_2-CO-C_6H_5$. Type II is the radical $CH_3-\dot{C}(COO^{(-)})-\overset{+}{N}H_2-CO-C_6H_5$ stable even after annealing up to +140°C. (auth)

26293 MEASUREMENT OF THE MEAN GAMMA RAY ENERGY NECESSARY TO CREATE ION PAIRS IN DIELECTRIC LIQUIDS. Mathieu, Jacques; Blanc, Daniel; Patau, Jean-Paul (Univ., Toulouse). pp 57-89 of Phenomenes de Conduction dans les Liquides Isolants. Paris; Centre National de la Recherche Scientifique (1970). (In French).

From International Conference on Conduction Processes in Dielectric Liquids, Grenoble, France. See CONF-680983.

All the ions created by the passage of gamma radiation through a liquid cannot be collected. The theory of Jaffé was programmed; and by a method of successive approximations the parameters were adjusted to superimpose the theoretical characteristic curve and the experimental curve, which was established up to 200 kV cm^{-1}, within an accuracy of 1%. The purity of the liquid was such that a field of this intensity could be established without secondary effects, such as amplification in the liquid. The precision with which the saturation current was calculated did not exceed 10%, because the modification of the field by the space charge existing at the moment of irradiation was not considered. A special cell constructed entirely of plexiglass with metallized mylar electrodes was used. Since the exact intensity of a ^{60}Co source placed at the center of the radiation room was known the energy absorbed by the liquid could be accurately determined. There was only a small difference between the atomic numbers of the liquid and the chamber walls; consequently, the variation in the energy absorbed at the interface was small. Results are given for 21 compounds. These include isomers of octane and other branched alkanes. The measurement of the ionization occurring in alkane–CCl_4 mixtures demonstrates the role played by the ionization inhibitor in this last compound. The influence of the carbon chain structure on the mean ion-pair creation energy was studied. (auth) (France)

26294 STUDIES ON γ-RADIOLYSIS OF SULPHUR-CONTAINING AMINO ACIDS. II. VOLATILE PRODUCTS FROM S-n-PROPYL-L-CYSTEINE SULPHOXIDE AND S-ALLYL-L-CYSTEINE SULPHOXIDE IRRADIATED IN OXYGEN-FREE AQUEOUS SOLUTIONS. Nishimura, H.; (Hokkaido Univ., Sapporo); Mizutani, J.; Obata, Y.; Namiki, M. Tetrahedron; 27: 307-13(Jan 1971).

In connection with flavour deterioration accompanied by food irradiation, the volatile products from sulphoxide amino acids, S-n-propyl-L-cysteine sulphoxide (PCSO) and S-allyl-L-cysteine sulphoxide (ACSO) irradiated in oxygen-free aqueous solution were analysed. The major volatile products formed by γ radiolysis of PCSO were di-n-propyl sulphide and di-n-propyl disulphide, and those derived from ACSO were allyl alcohol, n-propyl allyl sulphide, and diallyl sulphide, which were isolated by GLC and identified by using mass spectrometry. From the experiments with N_2O or KBr addition during irradiation, i.e., from the scavenger effects, the formation processes of volatiles were partly elucidated. (auth) (UK)

26295 PULSE RADIOLYTIC INVESTIGATIONS OF HYDROXY-RADICAL REACTIVITIES IN MICELLAR SOLUTIONS. Patterson, L. K. (Carnegie-Mellon Univ., Pittsburgh); Bansal, Krishan M.; Fendler, J. H. J. Chem. Soc., D; No. 3, 152-3(10 Feb 1971).

Rate constants for reactions of OH· with charged and neutral surfactants are substantially smaller above the critical micelle concentrations than below them; rate constants for OH· addition to C_6H_6 are also smaller in micellar systems than in water. (auth) (UK)

26296 FREE RADICALS IN PYRIMIDINES: E.S.R. OF A γ-IRRADIATED SINGLE CRYSTAL OF 5-NITROURACIL. Benson, Brent (Southern Illinois Univ., Carbondale); Snipes, Wallace. Mol. Phys.; 20: 357-63(Feb 1971).

Free radicals were observed in γ-irradiated single crystals of 5-nitrouracil with the unpaired electron showing hyperfine interaction with one nitrogen atom. The principal values of hyperfine coupling are $A_x = 22.5$ G, $A_u = 25.2$ G, and $A_z = 40.0$ G, and the principal values of the spectroscopic splitting factor are $g_u = 2.0117$, $g_v = 2.0064$ and $g_w = 2.0027$. The relationship of the directions of the corresponding principal axes to the molecular orientations show that the unpaired electron must be located in an sp^2 orbital on either $N_{(1)}$ or $N_{(5)}$. Considerations of the mechanism of radical formation and comparison to radiation damage in other molecules make the $N_{(1)}$ location seem more probable. The π interaction of the nitro group on $C_{(5)}$ evidently prevents the formulation of free radicals with the unpaired electron on $C_{(5)}$. The carbon atom is the most common location of unpaired electron density in other pyrimidine free radicals. (auth) (UK)

26297 ION RECOMBINATION AND DELAYED EMISSION IN THE PULSE RADIOLYSIS OF LIQUID ISOPENTANE SOLUTIONS AT LOW TEMPERATURE. Baxendale, J. H.; Wardman, P. (Univ. of Manchester, Eng.). J. Chem. Soc., D; No. 4, 202-3 (24 Feb 1971).

Delayed emission (maximum at 380 nm) in the pulse radiolysis of biphenyl in liquid isopentane at –120°C persists up to microseconds and is correlated in time with the rate of decay of biphenyl ions. (auth) (UK)

26298 OPTICAL BLEACHING OF TRAPPED ELECTRONS IN γ-IRRADIATED ALKALINE ICE. LOCATION OF ENERGY LEVELS. Hamlet, Peter; Kevan, Larry (Wayne State Univ., Detroit). J. Amer. Chem. Soc.; 93: 1102-06(10 Mar 1971).

The optical bleaching of radiation-produced trapped electrons in glassy alkaline ice (10M NaOH) was studied by EPR. The optical bleaching rate shows no temperature dependence between 4 and 77°K; this indicates that the optical transition occurs directly to a continuum state and that no bound excited state exists for electrons trapped in this matrix. Between 90 and 140°K the optical bleaching rate decreases with temperature and is characterized by a negative activation energy of 0.05 eV. This indicates the existence of shallow traps. A similar temperature dependence is found for electrons produced by photoionization of ferrocyanide ion in alkaline ice. The shallow traps appear to provide a common path for combination of the optically detrapped electrons with their counterpart holes. Only 70% of the optically detrapped electrons ultimately react with the matrix hole, O^-, to cause loss of the O^- EPR signal, this per cent is independent of temperature and of radiation dose. The other electrons may react to form dielectrons and hole-electron charge pairs. (auth)

26299 TRANSFER OF RADIATION ENERGY FROM MACROMOLECULES TO SULFUR COMPOUNDS. A COMPARISON BETWEEN THE TRAPPING EFFICIENCY OF A THIOL AND ITS CORRESPONDING DISULFIDE. Sanner, Tore (Norwegian Radium Hospital, Oslo). Radiat. Res.; 44: 594-604(Dec 1970).

Electron spin resonance studies were carried out on irradiated

molecular mixtures containing a macromolecule (Sephadex, CM-Sephadex or DEAE-Sephadex) and a sulfur compound (reduced or oxidized penicillamine). The pH prior to freeze-drying was in all cases adjusted to predetermined values. The irradiation as well as the electron spin resonance measurements were carried out at 77°K. The transfer of radiation energy from uncharged Sephadex occurred more efficiently to oxidized penicillamine than to reduced penicillamine when the samples were freeze-dried from acid solutions, while the opposite was the case when the samples were freeze-dried from alkaline solutions. The pH prior to freeze-drying influenced greatly the temperature range where the major part of the transfer of unpaired spins occurred from the macromolecule to the disulfide. While no further energy transfer occurred to oxidized penicillamine when the samples were heated above room temperature, an extensive transfer of unpaired spins took place from the macromolecule to the thiol in the temperature range 293 to 333°K. This transfer seemed to involve mainly the dissociated form of the thiol. The results suggest that the pH prior to lyophilization influences the course of the secondary radical reactions occurring on heat treatment of the samples, while it has only a minor influence on the stability of the radicals present immediately after irradiation at 77°K. (auth)

26300 PRIMARY PROCESS IN THE DIRECT ACTION OF IONIZING RADIATION ON PROTEINS: ELECTRON PARAMAGNETIC RESONANCE OF A GLYCYLGLYCINE SINGLE CRYSTAL γ-IRRADIATED AT 77°K. Morishima, Hiroshi (Kyoto Univ.). Radiat. Res.; 44: 605-20(Dec 1970).

Single crystals of glycylglycine grown from aqueous and heavy water solutions were irradiated at 77°K with ^{60}Co γ rays in the dark, and the electron paramagnetic resonance of free radicals produced was studied under various conditions. The radical initially produced shows complicated hyperfine patterns depending on the direction of the applied magnetic field. Analysis of angular dependence of major hyperfine splitting gives the principal values, $A_x = 17$, $A_y = 27$, and $A_z = 9$ gauss, for the coupling tensors of two α-protons. Comparison of the observed hyperfine coupling constant with those of similar radicals and those from the spin density calculations suggests $NH_3^+-CH_2-CO-NH-\dot{C}H_2$ as the most probable structure. Upon warming, this is converted to a stable radical, $NH_3^+-CH_2-CO-NH-\dot{C}H-COO^-$, which is also obtained on visible light illumination at 77°K through the first order reaction with respect to the initial radical. (auth)

26301 ELECTRON SPIN RESONANCE IN GAMMA-IRRADIATED SINGLE CRYSTALS OF UNSATURATED ALIPHATIC HYDROCARBONS. Neilson, George Walter. Worcester, Mass.; Clark Univ. (1970). 167p. University Microfilms Order No. 71-15.

Thesis.

Several crystals of unsaturated organic molecules were subjected to gamma irradiation. The resulting radicals produced in these crystals were studied by electron spin resonance techniques. The principal investigation concerned two triply bonded molecules, acetylene dicarboxylic acid dihydrate ($HOOC-C\equiv C-COOH.2H_2O$), and acetylene dicarboxylic dipotassium salt dihydrate ($K^+OOC-C\equiv C-COO^-K^+.2H_2O$). The ESR spectrum of acetylene dicarboxylic acid showed two principal radicals in the crystal. One of the radicals, $HOOC-C(H)=\dot{C}-COOH$, was created when a proton from the waters of hydration added in to the triple bond. The hyperfine coupling between this proton and the unpaired electron was isotropic, 45.0 gauss. The principal g values were 2.0042, 2.0036, and 2.0024. The angle between the minimum principal g value and the intermolecular axis was 123°. The other radical, $HOOC-C(OH)=\dot{C}-COOH$, was created by the addition of a hydroxyl fragment at the triple bond. This hydroxyl molecule came from either the waters of hydration in the crystal or the carboxylate part of the molecule. The hyperfine coupling of the hydroxyl proton to the unpaired electron varied from 0 gauss to 3 gauss. The principal g values were 2.0042, 2.0037, and 2.0024. The angles between the principal g values and the molecular axes were the same for both radicals. The difference between the two radicals was in the magnitude of the hyperfine coupling. The unpaired electron resided in a σ bond in accordance with what was observed in the vinyl radical. The ESR spectrum of acetylene dicarboxylic dipotassium salt showed that there were at least three different radicals present in the crystal. The ESR spectra from two of these three were evident at room temperatures and the third dominated the spectra at 115°C. The first radical, $K^+OOC-C(OH)=\dot{C}-COO^-K^+$, gave rise to a singlet in the ESR spectra. The principal g values were 2.0043, 2.0037, and 2.0024, the same as in the acid. The other radical which was strong at room temperature, $K^+OOC-C(OH)=\dot{C}(H)$, gave rise to an anisotropic doublet. The principal values of the hyperfine tensor were −10g, −15.5g, and −24g. The isotropic hyperfine coupling was therefore −16.5g. The principal values of the g tensor were 2.0073, 2.0046, and 2.0030. At certain orientations of the crystal forbidden transitions appeared in the ESR spectrum. When a crystal was heated, the room temperature spectra diminished and a closely split doublet predominated. The splitting of this doublet varied between 0g and 4g. The principal g values were 2.0056, 2.0046, and 2.0036. In both the acid and its disalt it appeared that the waters of hydration contributed to the type of radical, which was observed. Whereas the radicals in the disalt were extremely stable, lasting well over two years, the radicals of the acid did not last much longer than eight hours. Besides producing radicals by gamma irradiation, powders of acetylene dicarboxylic acid and its salt were subjected to hydrogen atom bombardment. ESR spectra were observed, indicating that the hydrogen atoms had interacted with the unsaturated molecules. (Diss. Abstr. Int., B.)

26302 INACTIVATION AND REACTIVATION OF HEMOCYANIN BY RADIOLYTIC OH AND e^-_{aq}. Schubert, Jack; Ke, Charles H. (Univ. of Pittsburgh). J. Amer. Chem. Soc.; 93: 1282-4(10 Mar 1971).

In experiments with the oxygen-carrying copper protein, hemocyanin, it was found that in neutral, oxygen-free media, radiolytically produced OH eliminates the oxygen-carrying capacity by oxidizing the protein-bound copper to the cupric state, while the primary reducing species e^-_{aq} fully restores the oxygen-carrying capacity by reducing cupric copper to the cuprous state. The hemocyanin was irradiated in oxygenated media and then in oxygen-free media. (M.C.G.)

26303 RADIATION STUDIES OF ARYL GLYCOSIDES. PART I. THE EFFECTS OF γ-IRRADIATION ON ARYL GLUCOSIDES IN THE SOLID STATE. Moore, J. S.; Phillips, G. O. (Univ. of Salford, Eng.). Carbohyd. Res.; 16: 79-87(Jan 1971).

Gamma irradiation of crystalline aryl glucosides yields D-glucose and an equivalent amount of the corresponding phenol. The nature of the aglycon influences G(glycosidic scission) values, which vary from 1.2 for p-cresyl β-D-glucopyranoside to 0.3 for 2-naphthyl β-D-glucopyranoside. The greater radiation stability of aryl glycosides, compared with alkyl glycosides, is attributed to energy transfer, which varies in efficiency according to the nature of the aryl aglycon. Radical yields and the nature of the radical species produced on irradiation are dependent on the aglycon. G(glycosidic scission) values are lower at 77°K than at 298°K. The effects of γ irradiation on glycosides, 1-thioglycosides, and glycosylamines are compared. (auth)

26304 RADIATION STUDIES OF ARYL GLYCOSIDES. PART II. MECHANISM OF RADIOLYSIS OF PHENYL β-D-GLUCOPYRANOSIDE IN AQUEOUS SOLUTION. Phillips, G. O. (Univ. of Salford, Eng.); Filby, W. G.; Moore, J. S.; Davies, J. V. Carbohyd. Res.; 16: 89-103(Jan 1971).

The effects of ionizing radiation on aqueous solutions of phenyl β-D-glucopyranoside leads to glycosidic scission to yield equivalent amounts of D-glucose and phenol, and to hydroxylation of the aglycon. G(glycosidic scission) increases from 0.4 at mM to 1.0 at 10mM solute concentration. Pulse radiolysis studies indicate that the first intermediate is the hydroxycyclohexadienyl radical (1, λ_{max} 235 and 320 nm) derived from the glucoside; the molar extinction of 1 at 320 nm is 3,560. Two alternative reaction-paths for 1 were kinetically distinguished. One is a second-order process leading to hydroxylation of the aglycon and dimerization with $k_2 = 1.7\times10^9\ M^{-1}.sec^{-1}$. The alternative is a pH-dependent, first-order process ($k_1 \sim 10^3\ sec^{-1}$), leading to a carbonium ion which gives D-glucose and the phenoxyl radical (λ_{max} 400 nm) which yields phenol. The variation of G(phenoxyl) and G(glycosidic scission) with pH demonstrates that the unimolecular, heterolytic scission of the glucosyl-O bond in 1 is catalyzed by acid and alkali. Rate constants for the reaction of water radiolysis products with the glucoside were found to be $4\times10^9\ M^{-1}.sec^{-1}$ with OH radicals, $7\times10^7\ M^{-1}.sec^{-1}$ with e^-_{aq}, and $3.5\times10^7\ M^{-1}.sec^{-1}$ with H atoms. Spectra of the transients formed by reaction of e^-_{aq} and H atoms with the glucoside were determined. (auth)

26305 RADIATION STUDIES OF ARYL GLYCOSIDES. PART III. THE REACTIVITY OF ARYL GLUCOSIDES TOWARD HYDROXYL RADICALS AND HYDRATED ELECTRONS. Phillips, G. O. (Univ. of Salford, Eng.); Filby, W. G.; Moore, J. S.; Davies, J. V. Carbohyd. Res.; 16: 105-11(Jan 1971).

Rate constants for the reactions of hydrated electrons and OH radicals with the aryl aglycon of a series of substituted aryl glycosides were measured. The results are correlated by using the Hammett relationship $\log(k/k_s) = \rho\sigma$. For hydrated electrons, $\rho = +3.5$, and for OH radicals, $\nu = ca\ -0.3$, which show that electron-withdrawing groups greatly accelerate e^-_{aq} reactions but exert only a small retarding effect on OH radical reactions; electron-repelling groups exert an opposite effect. Glycosidic scission accompanies these reactions, and there is some similarity in the behavior of e^-_{aq} with alkaline hydrolysis ($\rho = +2.5$) and of OH radi-

XUM

cals with acidic hydrolysis ($\rho = -0.7$) of aryl glucosides. The results show that the sugar ring exerts an electron-attracting influence in relation to the aglycon. (auth)

26306 ELECTRON SPIN RESONANCE OF DEUTERATED DL-TARTARIC ACID SINGLE CRYSTALS IRRADIATED AT LOW TEMPERATURES. Cernansky, Barbara Ann. Tallahassee; Florida State Univ. (1970). 90p. University Microfilms Order No. 71-6980.

Thesis.

Electron spin resonance experiments were performed on single crystals of COODCHODCHODCOOD · D_2O, irradiated by 3-MeV or 50-kV x rays at 77 and 195°K, respectively, to a total dose of 2 to 4 Mrad. The data were taken at x-band with a standard reflection spectrometer employing high-frequency modulation, phase sensitive detection, and chart recording of the first derivative of the spectrum. At all temperatures from 77°K to 300°K there were more than one radical species present. At 77°K, the outstanding feature of the spectrum was a strong, nearly isotropic doublet. If the crystal was warmed to 188°K or alternatively was irradiated at 195°K, lines appeared which had a larger splitting than the initial doublet and which displayed considerable anisotropy. Upon continued warming these lines disappeared at 246°K, while the initial doublet persisted until 263°K. By 300°K, the spectrum had changed to a stable narrow doublet. The doublet at 77°K, with an isotropic coupling of 23.2 gauss, was attributed to a hyperfine interaction between an unpaired electron and a β-hydrogen arising from the radical anion [COODCHODCHODCOOD]$^-$, with the unpaired spin residing on the carboxyl carbon atom. As is usual in such radicals, the electron density distribution was approximately perpendicular to the plane of the carboxyl group in the undamaged molecule. The minimum g was close to the p orbital direction and, therefore, the unpaired electron was primarily in a $2p\pi$ orbital, but there was probably also a slight amount of s character present. At 195°K, the new lines were part of a quartet arising from a fairly large, nearly isotropic β-proton hyperconjugative coupling and an anisotropic α-proton coupling. The hyperfine tensor for the β-proton gave an isotropic coupling of 34.5 gauss. The magnitude of the hyperconjugative coupling is given by $a = B_0 + B_2\cos^2\theta$, θ being the angle between the C−H bond and the normal to the carbon plane. Assuming the usual tetragonal bonding for carbon gives an approximate value of 30° for θ. Taking $B_0 = 3.2$ gauss and $B_2 = 43.6$ gauss gave a calculated splitting of 35.9 gauss, in close agreement with the observed value. The principal values of the α-proton hyperfine tensor of −33.4, 23.0, and −10.7 gauss were very close to those obtained for α-proton couplings in other carboxylic acids. Putting the value of 22.3 gauss for the isotropic coupling into McConnell's relation, $a_H = Q\rho_\pi$, and giving Q its usual value of 22.5 gauss, a spin density, ρ_π, of 0.99 on the carbon atom was calculated. The spectrum at 195°K was due to the radical COODCHODĊHOD formed by breaking the C−C bond to a carboxyl group. It is likely that the unpaired electron is primarily in a $2p\pi$ orbital on the carbon atom with its axis of symmetry close to the normal to the carbon plane. As the irradiated crystal warmed to 300°K, the spectrum changed to a narrow doublet, unresolved at many orientations, with a maximum splitting of about five gauss. It was the same radical as was previously reported for room-temperature irradiated dl-tartaric acid: COODCHODĊODCOOD. The $2p\pi$ orbital of the unpaired electron was then normal to the -O-Ċ-C-O-group rather than to the carbon plane as in the previous radical. When deuterated dl-tartaric acid single crystals were irradiated at 77°K, ionic radical species were formed which decayed into other, neutral radicals as the crystals were warmed. At 77°K the radical anion [COODCHODCHODĊOOD]$^-$ was identified which persisted until 263°K, then decayed into CO_2^- and a nonparamagnetic species. The radical cation went through a more elaborate process, forming COODCHODĊHOD at 188°K. This persisted until 246°K at which point it began a process of hydrogen abstraction from an undamaged molecule to form the final stable free radical which was COODCHODĊODCOOD. (Diss. Abstr. Int., B)

26307 RADIOLYSIS OF OXYGENATED CYSTEINE SOLUTIONS AT NEUTRAL pH. THE ROLE OF RSS̄R AND O_2^-. Barton, J. P.; Packer, J. E. (Univ. of Manchester, Eng.). Int. J. Radiat. Phys. Chem.; 2: 159-66(Dec 1970).

It is shown that the species RSS̄R and RS· formed during the pulse radiolysis of aqueous solutions of cysteine react with oxygen with rate constants of $4.3 \pm 0.3 \times 10^9$ dm^3 mol^{-1} s^{-1} and about 8×10^9 dm^3 mol^{-1} s^{-1}, respectively. The reaction RSH + O_2^- $\xrightarrow{H^+}$ RS· + H_2O_2 is shown to proceed under γ radiolysis conditions at pH 7 with a rate constant greater than 5×10^4 dm^3 mol^{-1} s^{-1}. (auth) (UK)

26308 MULTIPLE PULSE RADIOLYSIS: SUCCESSIVE ACCUMULATION OF TWO HYDRATED ELECTRONS IN OXYGEN, NITROBENZENE, AND NITROMETHANE. Gruenbein, W.; Henglein, A.; Stevens, G.; Beck, G. (Hahn-Meitner-Institut fuer Kernforschung, Berlin). Ber. Bunsenges. Phys. Chem.; 75: 126-34(Feb 1971). (In German).

Aqueous solutions were irradiated with trains of high-energy electron pulses (pulse length: 2 to 10 μs; train length: ~100 μs). The changes in optical absorption and electrical conductivity were recorded. The radical anions O_2^-, $C_6H_5NO_2^-$, and $CH_3NO_2^-$, resulting from the reactions of the hydrated electron with dissolved O_2, $C_6H_5NO_2$, and CH_3NO_2, react with part of the electrons produced in the following pulses. A careful kinetic analysis using a computer was carried out for the three systems. It took notice of all possible reactions in each pulse including the side reaction of e_{aq}^- with the molecular hydrogen peroxide. It was found that the addition of the second electron is practically as fast as that of the first electron in all three cases. (auth)

26309 ION-MOLECULE REACTIONS IN THE CONDENSED-PHASE RADIOLYSIS OF HYDROCARBON MIXTURES. III. REACTIONS OF i-$C_4H_8^+$ AND TERT-$C_4H_9^+$ IONS ORIGINATING FROM NEOPENTANE. Collin, G. J.; Ausloos, P. (National Bureau of Standards, Washington, D. C.). J. Amer. Chem. Soc.; 93: 1336-40(24 Mar 1971).

The liquid-phase radiolysis of neopentane was investigated in the presence of various hydrocarbons and electron scavengers. It was found that the neopentane parent ion dissociates to yield tert-$C_4H_9^+$ and i-$C_4H_8^+$ ions. The yields of these ions which are intercepted in these experiments under optimum conditions are ~2.4 and ~0.9, respectively. The i-$C_4H_8^+$ ion reacts with various added alkanes by the H_2^- transfer mechanism: $C_4H_8^+ + RH_2 \rightarrow$ i-$C_4H_{10} + R^+$. The relative rates of reaction with different RH_2 additives were determined and show the same trends as those observed for these reactions in the gas phase. That is, the rate is seen to increase with an increase in the exothermicity of the reaction (as calculated from gas-phase thermodynamic data). The effect of the ΔH of reaction is, however, more pronounced in the liquid than in the gas phase. The tert-butyl ion reacts more slowly with alkane additives than does the isobutylene ion, but reacts effectively with a negative ion from CCl_4 to form tert-C_4H_9Cl. Neutralization of the tert-butyl ion leads to the formation of isobutylene and propylene. (auth)

26310 RADIATION CHEMISTRY OF LOW-TEMPERATURE AQUEOUS GLASSES. PART 4. DISTINGUISHABLE ELECTRON TRAPS IN NEUTRAL AND ALKALINE GLASSES. Buxton, G. V.; Dainton, F. S.; Lantz, T. E.; Sargent, F. P. (Univ. of Leeds, Eng.). Trans. Faraday Soc.; 66: 2962-73(Dec 1970).

Extensive studies of the photobleaching kinetics of e_T^- in aqueous alkaline glasses show (i) that electrons are trapped in potential wells of differing depths from which they can be selectively photobleached, and (ii) that trapping occurs within the Coulombic field of the positive charge produced concurrently with the electron. Examination of other aqueous glasses indicates that the trapped electron is located in a "water-walled" cavity. (auth) (UK)

26311 INFLUENCE OF LET ON THE RADICAL YIELDS IN FROZEN ALIPHATIC ALCOHOLS. Kroh, J.; Piekarska, A.; Slebocka, H.; Wypych, M. (Technical Univ., Lodz, Poland). Int. J. Radiat. Phys. Chem.; 2: 139-45(Dec 1970).

The effect of LET on the total radiation yields of radicals and trapped electrons in frozen ethanol, isopropanol, and n-propanol at −196°C was investigated by EPR. Solutions of alcohols containing 10 vol % of 1.0 mol dm^{-3} aqueous HNO_3 were irradiated with ^{210}Po α particles, ^{3}T β particles and ^{60}Co γ rays at the same dose rate 2.1×10^{16} eV dm^{-3} s^{-1} in the presence of air. The total radical yields, G(R·), for ethanol and isopropanol are: 8.6 and 6.6 for γ rays; 5.6 and 3.7 for β rays; and 0.63 and 0.48 for α rays, respectively. Deaerated solutions of alcohols containing 10 vol % H_2O were irradiated with ^{3}T β particles and ^{60}Co γ rays at the dose rate ca. 1.4×10^{17} eV dm^{-3} s^{-1}. The total radical yields, G(R·), for ethanol, n-propanol and isopropanol are: 5.1, 4.0, and 3.7 for β-irradiation and 7.1, 5.8, and 5.6 for γ-irradiation. The trapped electron yields, G(e_T^-), for ethanol, n-propanol, and isopropanol are: 1.3, 0.45, and 0.48 for β-irradiation and 2.2, 0.76, and 0.96 for γ-irradiation, respectively. Estimations indicate that the local heating effect, however important, may not be exclusively responsible for all the decrease in G value observed for high LET radiation. (auth) (UK)

26312 INTERMOLECULAR AND INTRAMOLECULAR FREE VALENCE TRANSFER IN GAMMA IRRADIATED CRYSTALLINE HEXADECANOIC AND CIS-9-OCTADECENOIC ACIDS. Faucitano, Antonio; Locatelli, Paolo; Faucitano Martinotti, Fausta; Perotti, Angelo. Atti Accad. Naz. Lincei, Rend., Cl. Sci. Fis., Mat. Natur.; 48: 523-9(May 1970).

ESR measurements were made on the mechanism of radical

transformation in a dilute solid solution of 10% elaidic acid in palmitic acid and in the urea occlusion compounds of palmitic and oleic acids γ-irradiated at −196°C. The measurements were made at room temperature for the solid solution and clathrates, and at −196°C for oleic acid. Results indicate that the free valence migration proceeds essentially through chains of intermolecular transfers, the intramolecular mechanism playing a negligible role. (J.G.B.)

26313 SPIN TRAPPING OF THE RADICALS FORMED BY γ-IRRADIATION OF SODIUM PHOSPHITE IN THE SOLID STATE. Adevik, Goeran; Lagercrantz, Carl (Univ. of Goteborg). Acta Chem. Scand.; 24: 2253-5(1970).

The solid samples, irradiated by γ-rays from a ^{60}Co source, were given about 3 M rad each and then dissolved in an aqueous solution of the nitroso scavenger, t-nitrosobutane. The ESR spectrum was consistent with the formation of $O_3P-N(O\cdot)-C(CH_3)_3^{2-}$ after the trapping of $\cdot PO_3^{2-}$ radicals. An identical spectrum was obtained when H_2O was replaced by D_2O as the solvent. (Denmark) (auth)

26314 REACTION OF NEON IONS WITH ETHYLENE. Gawlowski, J.; Niedzielski, J. (Warsaw Univ.). Radiochem. Radioanal. Lett.; 6: 161-7(3 Apr 1971).

The γ radiolysis of ethylene−neon mixtures was investigated over the range of neon pressures from 50 to 730 torr. G_{CH_4} and $G_{C_2H_2}$ have a maximum at p_{Ne} ~170 torr, G_H after an initial sharp increase level at higher neon pressures (above 170 torr), to reach an approximately constant value. It is suggested that the reaction yielding Ne_2^+ ions competes with the charge transfer from positive neon ions Ne^+ to ethylene. The rate constant for the reaction $Ne^+ + C_2H_4 = C_2H_2^+ + H_2 + Ne$ is ~10^{-12} cm^3 $molecule^{-1}$ sec^{-1}. (auth)

26315 GAS PHASE RADIOLYSIS OF HYDROGEN SULPHIDE. THE EFFECT OF ELECTRON AND PROTON SCAVENGERS ON $G(H_2)$. Forys, M.; Migdal, E. (Warsaw Univ.). Radiochem. Radioanal. Lett.; 6: 177-83(3 Apr 1971).

The effects of electron scavengers (CCl_4 and SF_6) and proton scavengers (NH_3 and i-C_4H_8) on $G(H_2)$ were studied in α-irradiated H_2S. Minor effects of both types of scavengers on $G(H_2)$ were observed. A possible explanation is based on the assumption that H_2S is an electron scavenger in the gas phase. (auth)

Radioisotope Production

Refer also to abstract 28772.

26316 RADIOISOTOPES, GENERAL CONCEPTS. Hours, R. (CEA., Saclay, France). Tech. Mod.; 62: 412-16(Oct 1970). (In French).

Fundamental information on radioelements is reviewed. The absorption and diffusion of α, β, γ particles and neutrons by matter are discussed. Production methods, detection, and measurement of radioisotopes are reviewed. (J.G.B.)

26317 EFFECT OF RADIONUCLIDE CONTAMINATION ON THE CALIBRATION OF ^{99}Mo. Lorenz, Erhard; Mauderli, Walter; Williams, Clyde M. (Univ. of Florida, Gainesville). J. Nucl. Med.; 12: 141-2(Mar 1971).

Methods for determining the amount of breakthrough of ^{99}Mo in ^{99m}Tc generators are discussed. A container of 4.8-mm lead and 1.3-mm stainless steel was used. It was found that ^{99}Mo used for calibration techniques should be as fresh as possible (less than 1 week) to minimize the effects of contaminants. (M.C.G.)

Recoil Production and Reactions

26318 PROPORTION OF ^{32}P PRODUCED BY $^{31}P(n,\gamma)$ AND $^{32}S(n,p)$ REACTIONS IN PHOSPHORUS−SULFUR COMPOUNDS. Ujimoto, Kikujiro; Asada, Hiroyuki; Takashima, Yoshimasa (Kyushu Univ., Fukuoka). Mem. Fac. Sci., Kyushu Univ., Ser. C; 7: No. 1, 67-74(Mar 1970).

Validity of reactor irradiation of phosphorus-sulfur compounds with and without cadmium shield was elucidated by investigation of ^{32}P recoil species produced by either the $^{31}P(n,\gamma)$ or the $^{32}S(n,p)$ reaction. The ratios of ^{32}P produced by both reactions in irradiated KH_2PO_4 and K_2SO_4 in the absence or the presence of a cadmium shield were obtained. On the basis of these ratios the proportions of the ^{32}P activity produced by the $^{32}S(n,p)$ and the $^{31}P(n,\gamma)$ reaction were calculated for several phosphorus-sulfur compounds. The results showed that more than 56% or 86% of the total activity arose from the $^{32}S(n,p)$ or the $^{31}P(n,\gamma)$ reaction in the presence or the absence of cadmium shield and that the reactor irradiation of phosphorus-sulfur compounds with and without cadmium shield is a convenient and relevant method for investigating ^{32}P recoil species produced by the $^{32}S(n,p)$ and $^{31}P(n,\gamma)$ reactions. The ^{34}S activity was <2% in the total activity. (auth) (Japan)

26319 METHOD OF OBTAINING AMERICIUM. Thompson, Stanley G. (to United States Atomic Energy Commission). U. S. Patent 3,554,867. 12 Jan 1971. Filed 23 Aug 1946.

A method is described for producing Am by subjecting natural U to a self-sustaining neutron chain reaction for a period of time sufficient to produce a transuranic fraction predominately Pu, which contains at least 0.01% ^{241}Pu, and aging the Pu for a further period of time such that the isotope decays to a detectable quantity of Am. The aged product is dissolved in an aqueous acidic solution, the Pu is oxidized to a valence state > 4+, and the Am, U, and fission products are removed by means of a water-insoluble rare earth carrier. The precipitate thus obtained is dissolved, fluorosilicate ions are introduced into the resulting solution, the solution is contacted with a water-insoluble rare earth carrier for the fission products, and the precipitate is separated. Sufficient HF is added to the supernatant liquid to render it about 3 to 6 M with respect to HF, the solution is contacted with a water-insoluble rare earth salt carrier for the Am, and the carrier precipitate is then separated. (B.L.M.)

26320 ^{83m}Kr GENERATOR. Moghissi, A. A.; Hupf, H. B. (Southwestern Radiological Health Lab., Las Vegas, Nevada). Int. J. Appl. Radiat. Isotop.; 22: 218-20(Mar 1971).

A convenient method of producing a ^{83m}Kr laboratory generator is by use of ^{83}Rb, which decays with an abundance of 77% to ^{83m}Kr. It is not necessary to use pure ^{83}Rb, which is difficult and expensive to produce and the half-life of 83 days is convenient for laboratory use. Details of the preparation of the ^{83}Rb and of the ^{83m}Kr generator are given. (UK)

Radiochemistry

Refer also to abstracts 26617, 26840, and 28379.

26321 REACTIONS OF HELIUM TRITIDE IONS WITH GASEOUS HYDROCARBONS. V. cis- AND trans-1,2-DIMETHYLCYCLOPROPANE. UNAMBIGUOUS EVIDENCE FOR GASEOUS PROTONATED CYCLOPROPANES. Cacace, Fulvio; Guarino, Angelo; Speranza, Maurizio (Univ., Rome). J. Amer. Chem. Soc.; 93: 1088-91(10 Mar 1971).

In order to gather direct chemical evidence for the occurrence of protonated cyclopropanes as intermediates in a gas-phase reaction, gaseous cis- and trans-1,2-dimethylcyclopropane were allowed to react with a gaseous Brønsted acid, the helium tritide ion formed from the β decay of molecular tritium. The cis and trans isomers gave the corresponding tritiated compounds retaining the configuration of the original molecules. The lack of any measurable cis-trans isomerization lends strong support to the view that the formation of the tritiated cycloalkanes, following the transfer of a triton from He^3H^+ to the substrate, proceeds via a cyclic intermediate, and does not involve the cleavage of the cyclopropane ring. These results corroborate the mechanistic interpretation of earlier experiments concerning the triton transfer from He^3H^+ to unsubstituted cycloalkanes, and provide unambiguous evidence for the intermediacy of protonated cyclopropanes in a gas-phase reaction. (auth)

26322 LABELING OF COPPER WIRE WITH ^{110m}Ag FOR SUBSEQUENT IDENTIFICATION. Bate, L. C.; Dyer, F. F. (Oak Ridge National Lab., Tenn.). Isotop. Radiat. Technol.; 8: 315-17(1971).

Labeling of copper electric cable with ^{110m}Ag was demonstrated as a suitable technique for use in subsequent identification of such cable in case of theft. The ^{110m}Ag, in solution, is applied inside the cable, i.e., on the surfaces of the wires that are twisted together to form the cable, with a hypodermic needle and allowed to dry. The label is not removed by several years of simulated weathering and can be detected by monitoring with a survey-type radiation meter. The technique can be carried out by a semiskilled person with a minimum of training. (auth)

Separation Processes

Refer also to abstract 26150, 26206, 26208, 26319, 26451, and 28633.

26323 (DOCKET-50201-67) WEST VALLEY REPROCESSING PLANT. Modification Schedule. (Nuclear Fuel Services, Inc., Rockville, Md.). 9 Apr 1971. 2p. Dep. NTIS.

XUM

26324 (DOCKET-50201-68) WEST VALLEY REPROCESSING PLANT. Final Safety Analysis Report, Revision 7. (Nuclear Fuel Services, Inc., Rockville, Md.). 14 Apr 1971. 15p. Dep. NTIS.

Revisions to the safety analysis report dealing with the effects of tornadoes, earthquakes, and various design parameters are presented. Codes and guide lines to govern the design and construction of buildings, structures, and equipment are listed. (M.C.G.)

26325 (DOCKET-50268-7) MIDWEST FUEL RECOVERY PLANT. Preliminary Safety Analysis Report, Amendment 10 (Includes Design and Analysis, Amendment 2 to Suppl. 1). (General Electric Co., San Jose, Calif. Nuclear Energy Div.). 22 Mar 1971. 26p. Dep. NTIS.

Supplementary information on earthquake and wind analyses of the plant is presented. A listing of previous correspondence and amendments is included. (M.C.G.)

26326 (KFK-911) AQUEOUS REPROCESSING OF THE FUEL ELEMENTS OF THE FAST BREEDER. THE COMBINED EXTRACTION AND SEPARATION OF MACROAMOUNTS OF PLUTONIUM AND URANIUM IN THE PUREX PROCESS. Ochsenfeld, W.; Schmieder, H.; Theiss, S. (Kernforschungszentrum, Karlsruhe (West Germany). Institut fuer Heisse Chemie). Oct 1970. 121p. (In German). (EUR-4167). Dep. NTIS (U. S. Sales Only).

For reprocessing irradiated fast breeder fuel elements by solvent extraction using 20% TBP-alkane, coextraction, co-backwash, and partitioning of uranium and plutonium were studied. In the coextraction and co-backwash countercurrent experiments, losses of plutonium and uranium to the aqueous raffinate (HAW) and to the organic extractant (HCW) remained below 0.1%. Partitioning of plutonium and uranium by reduction with uranium(IV) was studied intensively, and compared with reduction by ferrous sulfamate. Countercurrent experiments resulted in plutonium losses to the uranium stream (1BU) of less than 0.2%, while the decontamination of the plutonium product (1BP) from uranium yielded a decontamination factor of $\sim 10^3$. (auth)

26327 (ORNL-TM-3194) EQUIPMENT FOR THE DISSOLUTION OF CORE MATERIAL FROM SHEARED POWER REACTOR FUELS. Groenier, W. S. (Oak Ridge National Lab., Tenn.). Apr 1971. Contract W-7405-eng-26. 64p. Dep. NTIS.

A survey of all known existing equipment and concepts for the dissolution of sheared nuclear power reactor fuels was made. With respect to existing equipment, it was revealed that an effective device applicable to the dissolution of sheared LMFBR fuels does not exist. Dissolver concepts representing current approaches to the continuous dissolution of LMFBR fuels are described. Hopefully, these concepts have the necessary features to meet the requirements of residence time; mixing; fuel feeding, transport, and discharge; criticality; and off-gas collection. It appears that the development of an effective dissolver for LMFBR fuels will be feasible if the desirable features found in existing equipment and concepts are combined with the current approaches exemplified by the new concepts. (auth)

26328 (ORNL-tr-2410) SEMI-ANNUAL REPORT OF THE DEPARTMENT OF CHEMISTRY, JUNE-NOVEMBER 1969. (Commissariat a l'Energie Atomique, Fontenay-aux-Roses (France). Centre d'Etudes Nucleaires). Translated for Oak Ridge National Lab., Tenn., from Sections 2 and 7-11, pp 95-109; 245-436 of report CEA-N-1341. 189p. Dep. NTIS.

Six sections are included; an abstract was prepared for each. (J.G.B.)

For abstracts of individual sections see: 26329-26334.

26329 (ORNL-tr-2410, pp 1-13) TREATMENT OF MEDIUM- AND LOW-LEVEL EFFLUENTS. (Commissariat a l'Energie Atomique, Fontenay-aux-Roses (France). Centre d'Etudes Nucleaires). Translated from Section 2 of report CEA-N-1341.

An abstract of this paper, prepared from the original language, appeared as NSA 25: 6391. (J.G.B.)

26330 (ORNL-tr-2410, pp 14-78) STUDY OF AQUEOUS REPROCESSING METHODS: LABORATORY. (Commissariat a l'Energie Atomique, Fontenay-aux-Roses (France). Centre d'Etudes Nucleaires). Translated from Section 7 of report CEA-N-1341.

An abstract of this paper, prepared from the original language, appeared as NSA 25: 6393. (J.G.B.)

26331 (ORNL-tr-2410, pp 79-97) STUDY OF AQUEOUS PROCESSES: PILOT PLANT. (Commissariat a l'Energie Atomique, Fontenay-aux-Roses (France). Centre d'Etudes Nucleaires). Translated from Section 8 of report CEA-N-1341.

An abstract of this paper, prepared from the original language, appeared as NSA 25: 6394. (J.G.B.)

26332 (ORNL-tr-2410, pp 98-120) STUDY OF VOLATILITY REPROCESSING METHODS. (Commissariat a l'Energie Atomique, Fontenay-aux-Roses (France). Centre d'Etudes Nucleaires). Translated from Section 9 of report CEA-N-1341.

An abstract of this paper, prepared from the original language, appeared as NSA 25: 6395. (J.G.B.)

26333 (ORNL-tr-2410, pp 121-42) PREPARATION AND STUDY OF ACTINIDE ELEMENTS. (Commissariat a l'Energie Atomique, Fontenay-aux-Roses (France). Centre d'Etudes Nucleaires). Translated from Section 10 of report CEA-N-1341.

An abstract of this paper, prepared from the original language, appeared as NSA 25: 6396. (J.G.B.)

26334 (ORNL-tr-2410, pp 143-89) STUDY OF THE VITRIFICATION OF FISSION PRODUCT SOLUTIONS. (Commissariat a l'Energie Atomique, Fontenay-aux-Roses (France). Centre d'Etudes Nucleaires). Translated from Section 11 of report CEA-N-1341.

An abstract of this paper, prepared from the original language, appeared as NSA 25: 6397. (J.G.B.)

26335 (RO/EERL-71-1) DEVELOPMENT OF ION EXCHANGE PROCESSES FOR THE REMOVAL OF RADIONUCLIDES FROM MILK. Easterly D. G.; Brooks, I. B.; Hasuike, J. K. (Eastern Environmental Radiation Lab., Montgomery, Ala.); Weaver, Charles L. (Environmental Protection Agency, Rockville, Md. Radiation Office). Jan 1971. 33p. GPO $0.50.

Work was conducted on the removal of radionuclides from milk by ion exchange from the late fifties to June 1969. This progressed from laboratory-scale to a full-scale commercial process where the system was demonstrated to be feasible using fixed-bed ion exchange columns. For three full-scale combined anion-cation runs, an average of 99.3% of ^{131}I and 94.6% of ^{85}Si was removed. This process resulted in an increase in the total solids, ash, potassium, and citrate ions. The taste of the treated milk compared favorably with untreated milk, although some decrease in flavor score was noted. Good radionuclide removal was obtained using the pilot plant moving-bed system. These studies, although not extensive, showed 89, 99, and 99.5% removal for strontium, iodine, and cesium, respectively. Limited investigations of cesium removal showed this system to have much greater potential than the fixed-bed system. (auth)

26336 METHOD OF SEPARATING THE RARE EARTHS BY FRACTIONAL CO-DISTILLATION OF THEIR VOLATILE CHELATE DERIVATIVES. Harris, Charles W.; Sievers, Robert E.; Eisentraut, Kent J. (to Secretary of the Air Force). U. S. Patent 3,558,440. 26 Jan 1971. Filed 4 Jun 1968.

A method of separating by fractional distillation two or more nonvolatile compounds of rare earths comprises converting the compounds of the rare earths to their corresponding volatilizable chelate, distilling a mixture of the chelates and a co-distilling agent to obtain enriched fractions of the chelates in the co-distilling agent, collecting the enriched fractions, acidifying each of the fractions to form (a) a water-rare earth salt phase and (b) a co-distilling agent and ligand phase, and collecting the rare earth salt by stripping the rare earth salt of water. (Offic. Gaz.)

26337 SELECTIVE ION-EXCHANGE SEPARATION OF ALKALI METALS. Orlandini, Kent A.; Korkisch, Johann (to United States Atomic Energy Commission). U. S. Patent 3,554,709. 12 Jan 1971. Filed 17 Jun 1968.

A method of separating alkali metal values from other elements contained in an acid feed solution comprises evaporating the solution to near dryness and dissolving the resulting residue in a solvent solution consisting of 2-thenoyltrifluoroacetone in pyridine and passing the resulting organic feed solution over a cation-exchange resin bed so that the alkali metal values are retained on the resin and the other elements pass through the bed with the effluent. (auth)

26338 SEPARATION OF SCANDIUM FROM RARE EARTH ELEMENTS. Orlandini, Kent A.; Korkisch, Johann (to United States Atomic Energy Commission). U. S. Patent 3,554,693. 12 Jan 1971. Filed 7 Jan 1969.

A process for purifying scandium and for separating scandium values from the rare earths and other values comprises dissolving the values in an aqueous hydrochloric acid solution, which is then mixed with a water-miscible organic solvent containing an organic phosphorus compound selected from the group consisting of tri-octylphosphine oxide, bis(2-ethylhexyl) orthophosphate, and tri-n-butyl phosphate. The resulting mixture is passed over a cation exchange resin bed where the rare earths and other values are absorbed by the resin and the pure scandium values pass through the bed and are recovered from the effluent. (Offic. Gaz.)

XUM

26339 ABSORPTION BEHAVIOR OF RADIONUCLIDES, MAINLY RARE EARTH ELEMENTS, IN SEAWATER. Goda, Shiro (Kinki Univ., Osaka); Nishikawa, Yasuharu; Yashiki, Mikio; Shigematsu, Tsunenobu. Kinki Daigaku Genshiryoku Kenkyusho Nenpo; 7: 1-7(1968). (In Japanese).

Adsorption behavior of yttrium and rare earth elements in seawater on the wall of the vessel was studied as a function of pH and standing time. These elements in seawater may be presented in the colloidal state above pH = 5 and adsorbed on the vessel wall, filter paper, or suspended matter from the solution at pH = 5 to 8. Adsorption and desorption rates on various materials were observed to reach an equilibrium in about 5 to 7 days. In order to avoid the adsorption loss of those elements, the sample water should be kept in acidic medium (pH < 3). (auth) (Japan)

26340 SOLUBILITY OF TTA–URANYL CHELATE. Akiba, Kenichi; Suzuki, Nobuo; Kanno, Takuji (Tohoku Univ., Sendai). Kakuriken Kenkyu Hokoku; 2: No. 2, 150-2(Dec 1969). (In Japanese).

In the partition of U(VI)–TTA chelate between aqueous phase and organic phase, the anomaly of chelate partition was observed for a few solvents such as hexane. Since it was supposed that this anomaly resulted from the fact that the solubility of uranyl chelate is low in such system, the uranyl chelate labeled with ^{237}U was prepared, and its solubility in various inactive solvents was investigated. Uranyl chelate and solvent were shaked to be equilibrated, and by measuring the γ activity of supernatant liquid after centrifugal separation, the solubility was determined. The effect of shaking time was investigated. It took longer to equilibrate wet solvent than to equilibrate dry solvent. The solubility in hexane, cyclohexane, and heptane is very low. The relation between the solubility of U(VI)–TTA and the activity coefficient was investigated and is discussed. (Japan)

26341 COMPARATIVE STUDY ON ZIRCONIUM OXIDE FOR THE PREPARATION OF ^{113m}In GENERATOR. Sugii, Atsushi (Kumnamoto Univ., Japan); Oga[illegible], Naotake; Kawamura, Shoichi. Jap. Anal.; 20: 200-4(Feb 1971). (In Japanese).

In order to determine the separability of ^{113m}In from ^{113}Sn–^{113m}In, the adsorption behavior of these radionuclides for zirconium oxide were compared with those for hydrous zirconium oxide (HZO) under a variety of experimental conditions. From the batch distribution coefficients, the separability for these adsorbents was found to be nearly equal over the concentration range of hydrochloric acid as an external solution from 6.1×10^{-2} to 2.6×10^{-1}M. It was found from the column study that 70 to 85% of ^{113m}In free from ^{113}Sn was recovered either from the HZO column by passing through the hydrochloric acid solutions over the concentration range from 6.1×10^{-2} to 2.6×10^{-1}M or from zirconium oxide column from 3.7×10^{-2} to 4.2×10^{-1}M. The merit of zirconium oxide over HZO is that the former is inexpensive, affords wide concentration range of the eluate and keeps zirconium well from breaking through the column. X-ray diffraction patterns of zirconium oxide were considerably different from those of HZO. (auth)

26342 UTILISATION OF KINETICS IN SOLVENT EXTRACTION OF METALS. Canning, R. G. (Australian Mineral Development Labs., Frewville). AMDEL (Aust. Miner. Develop). Bull.: No. 10, 35-46(Oct 1970).

The utilization of kinetics in the solvent extraction of metals is discussed. Improved separations of components by use of very short contact times are indicated, and available types of short-contact-time equipment are briefly considered, with particular reference to shrouded turbines. Experimental results are quoted for the extraction of scandium and rare earths from a uranium-barren sulfate leach liquor containing trivalent iron (up to 5 g Fe_2O_3 per liter, using bis(2-ethylhexyl) phosphate in kerosene diluent as the extractant. Improved selectivities for scandium, yttrium, and lanthanides over trivalent iron are shown for extraction in a shrouded turbine system with approximately 2 seconds residence time, compared to extraction in a normal mixer vessel with 30 seconds residence time. Solvent losses by entrainment in the raffinate are reduced in the shrouded turbine system. (auth) (Australia)

26343 RARE-EARTH ELEMENTS SPOT-LIGHTED BY DEVELOPMENT OF THEIR SEPARATION TECHNIQUES. Hiyayama, Hiroshi (Shinetsu Chemical Industry Co. Ltd., Takefu, Japan). Kagaku Gijutsushi - MOL: 8: No. 2, 33-7(Jan 1970). (In Japanese).

Developments in the techniques of the separation and purification of rare earths are reviewed. The following topics are discussed: raw materials for rare earth elements (monazite, bastnasite, xenotime, etc.); production of the rare earth elements (ion exchange, solvent extraction, and reduction methods); and applications of the rare earth elements (in catalysts, fluorescent materials, ceramics, electronics, and in nuclear-related industries). (Japan)

26344 EXTRACTION METHODS IN THE ANALYTICAL CHEMISTRY OF MOLYBDENUM (A REVIEW). Busev, A. I.; Rodionova, T. V. (Moscow State Univ.). Zh. Anal. Khim.; 26: 578-89(Mar 1971). (In Russian).

Literature for the 1961 to 1969 period is reviewed. A bibliography of 137 references is included. (auth)

26345 APPARATUS FOR THE CONTINUOUS PRECIPITATION OF PLUTONIUM OXALATE. Auchapt, Pierre; Bouzou, Georges; Falcoz, Claude (to Commissariat a l'Energie Atomique). British Patent 1,224,248. 3 Mar 1971. Priority date 6 Sep 1967, France.

A continuous apparatus for the precipitation of plutonium oxalate to separate plutonium from aqueous solutions is made up of the following parts: a precipitator, a decanter, a first cylindro-conical transfer chamber, a first washing column, a second cylindro-conical transfer chamber, a second washing column, and a chamber for transfer of washed plutonium oxalate to a drying oven. The entire apparatus is constructed on a vertical axis, and no pumps are necessary for continuous operation. (B.L.M.)

26346 RECOVERY OF PLUTONIUM AND URANIUM FROM REACTOR FUEL ELEMENTS. Larsson, Alf; Hultgren, Ake (to Aktiebolaget Atomenergi). British Patent 1,219,146. 13 Jan 1971. Priority date 21 Apr 1967, Sweden.

A process for the recovery of Pu and U from a number of fuel elements irradiated to different levels comprises separately dissolving the elements that have been more irradiated and those that have been less irradiated to form separate aqueous acidic solutions; extracting the solution of the more irradiated elements with a solvent selective for Pu relative to U and fission products; recovering the Pu from the extract; combining the residual solution with the solution of the less irradiated elements; and extracting the combined solutions with a solvent selective for U and Pu relative to fission products. Finally, the extract is subjected to a process for separating the U and Pu. The Pu selective solvent may be a tertiary amine or a substituted quaternary ammonium compound, such as tridodecylamine or tridodecylmethylammonium nitrate; and the U and Pu selective solvent is TBP, dibutylcarbitol, diamyl butyl phosphate, or dibutyl phenyl phosphate. (B.L.M.)

26347 FISSION-PRODUCT XENON AND KRYPTON: AN OPPORTUNITY FOR LARGE-SCALE UTILIZATION. Rohrmann, C. A. (Battelle-Northwest, Richland, Wash.). Isotop. Radiat. Technol.; 8: 253-60(1971).

Xenon, as a fission product from nuclear-fuel processing, could be made potentially available in great quantities and at low costs compared to those of xenon from conventional liquid-air-processing sources. One year after discharge from a reactor, the fission-product xenon contains only insignificant amounts of activity from short-lived xenon radioisotopes. Residual activity will depend almost totally on the effectiveness of the krypton separation in removing the highly radioactive ^{85}Kr. Present technology appears capable of ensuring such removal. Comparisons of future fission-product and atmospheric xenon resources and costs are made. Physical properties of xenon and krypton are discussed. If the price becomes competitive, xenon may replace krypton in some applications, for example, as an inert gas in incandescent lamps. Another attractive major potential use of xenon is as an agent in surgery, where it has been found to be applicable in human anesthesia. (auth)

26348 MOLYBDENUM RECOVERY FROM ALKALINE SLAG. Akerman, Karol; Kozak, Danuta; Warulik, Wojciech. Przem. Chem.; 50: 28-30(Jan 1971). (In Polish).

Molybdenum recovery from slag formed during melting of lead contained in cupric dusts in Doerschel ovens is described. Alkaline slag contains 600 to 650 g of Mo per ton. Main recovery operations are: two-stage leaching of slag with water, precipitation of molybdenum in the form of trisulfide. Fractional precipitation for ensuring the purity of obtained product was proposed. The method of obtaining MoO_3 from slag is considered to be economically justified. (auth)

26349 EFFECT OF IONIZING RADIATION IN THE REPROCESSING OF IRRADIATED FUELS. Abellan, J. Ortega. Energ. Nucl. (Madrid); 15: 4-15(Jan-Feb 1971). (In Spanish).

A simplified idea is presented of the effect of ionizing radiation in the development or verification, on a laboratory scale, of a flow diagram for the reprocessing of irradiated fuels. In order to estimate the effect of ionizing radiation it is necessary to determine the radiant energy emitted by the fission products

XUM

and from these data to calculate the radiant energy that each component of the process absorbs. Since the degree of radiolysis that a substance undergoes is a function of the absorbed energy, it is possible to calculate the concentrations of the substances produced by radiolysis and to consider their effects by means of tests on a laboratory scale. (tr-auth)

26350 ADSORPTION OF URANIUM IN ARTIFICIAL SEA-WATER WITH TITANIC ACID. Ogata, Noboru (Japan Monopoly Corp., Tokyo); Inoue, Nobuko; Kakihana, Hidetake. Nippon Kaisui Gakkaishi; 24: No. 2, 68-72(Sep 1970). (In Japanese).

The adsorption of uranium in seawater using titanic acid as adsorbent was studied. The titanic acid was prepared by the neutralization method with alkali solution, by homogeneous precipitation with urea or ammonium acetate, and by hydrolysis using titanic sulfate as the starting material. The results of the study indicated that the amount of uranium adsorption in seawater was affected by conditions under which the titanic acid was prepared. The degree of uranium adsorption shows an increase if the homogeneity and acidity of the solution are maintained. When titanic acid was prepared by the neutralization method or by the homogeneous precipitation method with ammonium acetate, it became curdy and resulted in a greater amount of adsorbed uranium. Uranium adsorption increases as the temperature of seawater rises and the concentration of uranium contained in seawater increases. Uranium adsorption decreases due to an increase in salinity and co-existence of phosphate, fluoride, and copper, but this effect is so small that it can be neglected in seawater. Uranium adsorption in natural seawater was 20% less than that in artificial seawater. (auth) (Japan)

26351 APPLICATION OF THE RETAINING ION TECHNIQUE TO SEPARATION OF IONS BY ELECTROPHORETIC FOCUSING IONS. Pueschel, C. R.; Lima, F. W. (Instituto de Energia Atomica, Sao Paulo, Brazil). Radiochem. Radioanal. Lett.; 6: 145-50(3 Apr 1971).

Separation of lutetium and ytterbium by electrophoretic focusing ions can be achieved if copper ions are used in the cathodic solution containing the ligand. Copper ions are also added to the solution of rare earth ions which is to be spotted in the filter paper strip. The procedure is similar to the retaining ion technique developed for ion exchange separation of rare earth elements. (auth)

EARTH SCIENCES

Geology and Hydrology

Refer also to abstracts 26397, 26406, 26412, 26541, 26743, 26773, 27127, and 28710.

26352 (CONF-630513-1) ON THE METHOD AND TECHNIQUE OF GAMMA–GAMMA LOGGING OF UNDERGROUND BOREHOLES IN MERCURY AND IRON ORE DEPOSITS. Ochkur, A. P.; (and others). Translated by G. Hitoun (Australian Atomic Energy Commission Research Establishment, Lucas Heights), from pp 531-9 of Metodika, Tekhnika i Rezul'taty Geofizicheskoi Razvedki, Materialy Vsesoyuznoi Nauchno-Tekhnicheskoi Geofizicheskoi Konferentsii, 5th Novosibirsk, May 31–June 5, 1963. 17p. Dep. NTIS (U. S. Sales Only).

A short review is presented of developments in $\gamma-\gamma$ logging methods and equipment. The influence of boreholes on the value of the intensity of the scattered γ-radiation and on the sensitivity towards admixtures of heavy metals is considered for various constructions of borehole equipment. As a result of work with models of heaped Hg ores, it was established that the symmetrical probe length must not exceed 5 to 10 cm in dry boreholes. In deposits of heavy metals with irregular distribution of mineralization, it was necessary to use directional detection with an outboard installation in addition to a small probe. Comparisons of the results of $\gamma-\gamma$ sampling of boreholes with a chemical analysis of the core sample, sludge, and data obtained from exploitation of separate areas of ore bodies are tabulated. Gamma–gamma logging diagrams for iron ore deposits are shown. (Australia)

26353 (CONF-680112–, pp 37-52) NUCLEAR TECHNIQUES AND EQUIPMENT IN HYDROLOGY. Castagnet, Antonio C.; Gomez, Hector R. (Comision Nacional de Energia Atomica, Buenos Aires (Argentina)). (In Spanish).

A summary is presented of the studies made by the CNEA (Argentina) in the area of surface and subterranean hydrology using radioactive tracers. The different tracers used in surface and ground waters are reported, and the reasons for their selection are discussed. Radioactive tracers in fluvial or maritime sedimentology are considered, and the preliminary results give excellent qualitative or semiquantitative data. The instrumentation used in the measurements is described. (J.S.R.)

26354 (SC-R-70-4402) ENERGY PARTITIONING DURING HYPERVELOCITY IMPACT ON ROCKS. Hill, Leslie R. (Sandia Labs., Albuquerque, N. Mex.); Johnson, Wallace E. (Systems, Science and Software, La Jolla, Calif.). Dec 1970. 23p. (CONF-701119-1). Dep. NTIS.

From 12th Symposium on Rock Mechanics, Rolla, Mo.

As part of a continuing study of intense energy effects on the earth, such as explosive cratering for Plowshare, large scale hydrodynamic computer codes which numerically integrate the two-dimensional mass, momenta, and energy conservation equations were adapted for use on geological materials. Experimentally determined nonlinear dynamic equations of state and constitutive equations governing material strength are incorporated into a two-material Eulerian code, DORF. With the use of this code, impact studies were made of projectiles with arbitrary shapes in the r, z cylindrical plane normally incident on semi-infinite half-space targets. The impact of projectiles on rocks was studied empirically and experimentally; however, a theoretical approach is used here. Particular examples selected involve the impact of aluminum and iron projectiles on oil shale at velocities of 0.5 and 1.0 cm/μsec. These studies offer a quick and economic means to edit quantities unavailable in an experiment and to independently study the effect of varying parameters such as material shape, density, and strength, and impact velocity. Results reveal early time agreement with experimental high-speed photography as seen in the bowl-shaped crater and spray. Initial impact pressures at the projectile-target contact are in close accord with the one-dimensional Rankine–Hugoniot relations for the impact of dissimilar materials. These equations require local continuity of pressure and particle velocity across the interface and were found to hold locally, quite independent of projectile shape. Essentially all projectile energy is transferred quickly to the oil shale target (tens of microseconds). Over 75% of the original kinetic energy remains near the target surface. Energy losses in longer term processes, such as tensile spalling and comminution of ejecta, require additional analyses. (auth)

26355 (SRO-344-11) QUARTERLY REPORT, OCTOBER 1, 1970–DECEMBER 31, 1970. Duckworth, J. P. (Nuclear Fuel Services, Inc., West Valley, N. Y.). 21 Jan 1971. 7p. Dep. NTIS.

Environmental radiation monitoring activities at the West Valley (New York) Reprocessing Plant from Oct. 1970 to Jan. 1971 are reported. Results are given for measurements of the ^{131}I content in milk, the radioactivity of Cattaraugus Creek waters, and the ^{131}I and ^{85}Kr content in stack effluents. (L.C.L.)

26356 DETERMINATION OF SPECIFIC RELEASE OF RADON BY PROTECTIVE ENCLOSURES IN PREMISES. Shalak, N. I.; Krisyuk, E. M.; Tarasov, S. I. Gig. Sanit.; No. 2, 72-4(Feb 1970). (In Russian).

Two methods for determining the amount of radon emission from materials confined in buildings using the scintillation radonometer SR-2 are discussed. The static method has the advantage of simplicity, but it can only be used under conditions where the radon concentration increases linearly. The dynamic method does not have this restriction and has a higher sensitivity which is 5×10^{-16} Ci/m^2-sec. (tr-auth)

Meteorology

Refer also to abstracts 26205, 26355, 26404, 26559, 26683, and 26751.

26357 (CLOR-81/D) ORIGIN AND EVOLUTION OF THE RADIOACTIVE CLOUDS. Kownacka, Ludwika (Centralne Laboratorium Ochrony Radiologicznej, Warsaw (Poland)). 1970. 47p. (In Polish). Dep. NTIS (U. S. Sales Only).

The formation and evolution of radioactive clouds from nuclear explosion are described, and the problems of formation of radioactive particles, particle size distribution, and size and shape of the clouds are discussed. The dynamics of atmospheric processes associated with radioactive clouds are discussed. Detailed discussions of turbulent mixing and thermodynamic mechanisms which determine the increase and rise of the radioactive cloud in the atmosphere are presented. (auth)

26358 (CONF-700601) PRECIPITATION SCAVENGING (1970). Proceedings of a Symposium held at Richland, Washington, June 2–4, 1970. (Battelle-Northwest, Richland, Wash. Pacific Northwest Lab. Division of Biology and Medicine (AEC), Washington, D. C. Fallout Studies Branch). Dec 1970. 508p. Dep. NTIS.

Thirty-eight papers on precipitation scavenging were presented at the conference. A separate abstract was prepared for each of 33. Two appeared previously in NSA as 24: 41434 and 25: 4162. Three were not within the scope of NSA. (L.C.L.)

For abstracts of individual papers see: 26359–26391.

26359 (CONF-700601–, pp 6-10) PRIORITIES IN SCAVENGING RESEARCH. Engelmann, Rudolf J. (Division of Biology and Medicine (AEC), Washington, D. C. Fallout Studies Branch).

From Precipitation scavenging meeting; Richland, Wash. (2 Jun 1970).

In Precipitation scavenging (1970).

Many of the questions related to the problems in, information required for, and significance of scavenging research are briefly discussed. (L.C.L.)

26360 (CONF-700601–, pp 13-20) RADAR OBSERVATIONS OF CONVECTIVE STORM CIRCULATION AND ITS RELATION TO PRECIPITATION SCAVENGING. Lhermitte, Roger M. (Environmental Science Services Administration, Boulder, Colo. Wave Propagation Lab.).

From Precipitation scavenging meeting; Richland, Wash. (2 Jun 1970).

In Precipitation scavenging (1970).

The use of radar for probing convective storms is reviewed. Emphasis is placed on Doppler radar methods that probe precipitation-particle motion and thereby provide information on storm circulation. Also discussed is a vertically pointing Doppler radar, which enables the evaluation of precipitation particle size spectra from observations of vertical particle velocity distribution. Comments are included on the applicability of these methods to the study of scavenging by precipitation. (auth)

26361 (CONF-700601–, pp 21-35) SCAVENGING OF TRACER IN SEVERE STORMS. Dingle, A. Nelson (Michigan Univ., Ann Arbor. Dept. of Meteorology and Oceanography).

XUM

From Precipitation scavenging meeting; Richland, Wash. (2 Jun 1970).

In Precipitation scavenging (1970).

Design considerations for field experiments to study severe storms by tracer scavenging are presented. Criteria used in the selection of indium as an atmospheric tracer and in choosing the emission and placement techniques are discussed. Specific experiments using updraft inoculation and middle-level indraft air labeling are outlined, and idealized flight plans and deposition patterns for these are presented. Finally, the operational procedure used in our field experiments is given. (auth)

26362 (CONF-700601–, pp 37-48) INTERACTIONS OF CLOUD CONDENSATION NUCLEI AND ICE NUCLEI WITH CLOUD AND PRECIPITATION ELEMENTS: A REVIEW. Radke, L. F.; Scott, W. D.; Robertson, C. E. (Washington Univ., Seattle. Dept. of Atmospheric Sciences).

From Precipitation scavenging meeting; Richland, Wash. (2 Jun 1970).

In Precipitation scavenging (1970).

Ground and aircraft measurements showing the effects of rainfall, snowfall, and cloud formation and evaporation on the concentration of cloud condensation nuclei (CCN) and ice nuclei (natural and artificial) are reviewed. Cumulus clouds are shown to be sinks for CCN when they are growing and sources of CCN when they evaporate. The removal of sea-salt nuclei by precipitating stratiform over the ocean is detailed. Snowfall is shown to be relatively ineffective in scavenging artificial ice nuclei. The effect of the onset of rain during shower activity is discussed with reference to ice-nuclei concentration. (auth)

26363 (CONF-700601–, pp 49-68) ENTRY OF FREEZING NUCLEI INTO PRECIPITATION. Vali, Gabor (Wyoming Univ., Laramie. Natural Resources Research Inst.).

From Precipitation scavenging meeting; Richland, Wash. (2 Jun 1970).

In Precipitation scavenging (1970).

Variations of the concentrations of freezing nuclei in convective-type rain with variations of time and rate of rainfall were investigated. There appears to be a direct relation between rate of rainfall and nucleus content: almost 50% higher concentrations for each 10 mm/hr increase in rainfall rate. The nucleus content of hailstones is relatively uniform throughout the volumes of the stones. Rain and hail occurring simultaneously have very nearly identical concentrations of nuclei. It was concluded that freezing nuclei are transferred to cloud droplets by diffusion and take an active role in initiating precipitation. This concept is supported by the fact that appreciable fractions of the nuclei are only hundreths of microns in diameter. (auth)

26364 (CONF-700601–, pp 69-97) IN-CLOUD SCAVENGING ANALYSIS FROM COSMOGENIC RADIONUCLIDE MEASUREMENTS. Perkins, R. W.; Thomas, C. W.; Young, J. A.; Scott, B. C. (Battelle-Northwest, Richland, Wash. Pacific Northwest Lab.).

From Precipitation scavenging meeting; Richland, Wash. (2 Jun 1970).

In Precipitation scavenging (1970).

Measurements of the cosmogenic radionuclides ^{38}Cl (37.3 min), ^{39}Cl (55 min), and ^{24}Na (15 hr) in consecutive rainwater samples allowed a comparison of precipitation scavenging in two very dissimilar study areas. These cosmogenic radionuclides which are formed by spallation of atmospheric argon attach themselves to the natural aerosol and thus serve as tracers of precipitation scavenging processes. Rainwater from a large polyethylene-sheet collection area is passed continuously through Al_2O_3, cation, and anion beds where the radon daughter ^{214}Bi, ^{24}Na, and ^{214}Pb, and the radiochlorines, respectively, are collected. Direct counting of the ion-exchange beds on multidimensional gamma-ray spectrometers permits the ^{24}Na and radiochlorine measurements without significant interference from the radon daughters. At both the Quillayute, Wash. site, near the coast, and the Richland, Wash. site a few hundred kilometers inland, a very definite inverse relation between precipitation rate and cosmogenic radionuclide concentrations was observed. The cosmogenic radionuclide concentrations were several times lower for a given rainfall rate in the coastal rain than in the inland rain. This can be explained by the higher elevation for the inland rain formation where higher cosmogenic radionuclide production occurs and a greater evaporation during raindrop fall. The $^{39}Cl:{}^{38}Cl$ ratios were similar at the two locations, indicating similar time periods for the in-cloud development of raindrops. The $^{24}Na:{}^{38}Cl$ ratios were consistently higher at the inland site, which may reflect the addition of cosmogenic radionuclides from higher air masses. The cosmogenic radionuclides are discussed in terms of the various in-cloud precipitation formation processes which they help define. (auth)

26365 (CONF-700601–, pp 99-108) STABLE ELEMENTS OF THE ATMOSPHERE AS TRACERS OF PRECIPITATION SCAVENGING. Rancitelli, L. A.; Perkins, R. W.; Tanner, T. M.; Thomas, C. W. (Battelle-Northwest, Richland, Wash. Pacific Northwest Lab.).

From Precipitation scavenging meeting; Richland, Wash. (2 Jun 1970).

In Precipitation scavenging (1970).

Rainwater samples collected at Quillayute, Wash., were analyzed by a multielement technique of neutron activation analysis to estimate the origin and removal rates of atmospheric aerosols. The concentrations of 19 elements measured in each sample were compared with concentrations in seawater and the earth's crust to establish the origin of each element. The Na, Cl, and Br are primarily of marine origin; the Sc, Co, Mn, K, Cr, Rb, and Cs could come from continental dust. The Ag, Se, Sb, As, Zn, and possibly Cu appear to have origins independent of the marine aerosol or continental dust. Scavenging coefficients ranging from 0.5 to 3×10^{-4} sec^{-1} were estimated from the concentrations of Co, Fe, Sc, and Sb in rainwater and known trace-element profiles in the atmosphere. (auth)

26366 (CONF-700601–, pp 109-20) CONCENTRATION VARIATION OF SOME TRACE METALS IN PRECIPITATION FROM GREAT PLAINS THUNDERSTORMS. Steffe, Dirl H. (Chadron Atmospheric Research Inst., Nebr.).

From Precipitation scavenging meeting; Richland, Wash. (2 Jun 1970).

In Precipitation scavenging (1970).

In the summer of 1969, sequential rain and hail samples were collected from several thunderstorms in western South Dakota and Nebraska. Samples were collected in rapid time sequence at a fixed geographical point in the path of the most intense storm activity. The samples were later analyzed for concentrations of zinc and silver using an atomic absorption spectrophotometer with a sampling-boat attachment. Both silver and zinc concentrations generally decreased with time in the rain but sometimes varied sharply. The silver and zinc concentrations in hail were always as high as, or higher than, those of the accompanying rain. (auth)

26367 (CONF-700601–, pp 121-36) SCAVENGING BY SNOW AND ICE CRYSTALS. Sood, S. K.; Jackson, M. R. (IIT Research Inst., Chicago, Ill.).

From Precipitation scavenging meeting; Richland, Wash. (2 Jun 1970).

In Precipitation scavenging (1970).

The scavenging efficiency of naturally precipitating snow and ice crystals was determined for submicron polystyrene latex and sodium chloride aerosols. The effect of crystal habit, crystal dimensions, and particle size on scavenging efficiency was established. Experimental results show that scavenging efficiency is a function of both the crystal diameter and the particle diameter. (auth)

26368 (CONF-700601–, pp 137-47) SCAVENGING OF SOLUBLE DYE PARTICLES BY RAIN. Dana, M. Terry (Battelle-Northwest, Richland, Wash. Pacific Northwest Lab.).

From Precipitation scavenging meeting; Richland, Wash. (2 Jun 1970).

In Precipitation scavenging (1970).

A number of precipitation scavenging field experiments using uranin and rhodamine dye particles were conducted at an Olympic Peninsula (Wash.) field site. Most experiments employed air-jet atomization of a methanol solution of the tracer; variation of the solution concentration produced tracer plumes of selectable particle size. Mass median particle radii (unit density equivalent) for the experiments ranged from 0.4 to 7.5 μ. For particle radii of 3 μ and larger, experimental washout coefficients agreed well with those expected from the theory of inertial capture. Smaller particle experiments showed much higher washout than theory—as much as 10 times higher for particles of about 0.5-μ radius. There is some evidence that electrical effects contributed to the scavenging of the smaller particles. (auth)

26369 (CONF-700601–, pp 151-60) COLLECTION EFFICIENCIES OF RAINDROPS FOR SUBMICRON PARTICULATES. Adam, J. R.; Semonin, R. G. (Illinois State Water Survey, Urbana).

From Precipitation scavenging meeting; Richland, Wash. (2 Jun 1970).

In Precipitation scavenging (1970).

An experimental technique was developed to determine the scavenging efficiency of raindrops falling at terminal velocity for submicron biological aerosols. The experimental apparatus and methods used to produce the simulated raindrops and the

aerosol are discussed. Experimentally determined scavenging efficiencies of raindrops for 1-μ Bacillus subtilis spores are presented. The amount of material scavenged is very small, approximately 0.004% for a 2-mm-diameter drop. The scavenging efficiency increases exponentially with decreasing drop size to a value of 0.4% for a 0.4-mm drop. Also, electric charge on the drop dramatically increases the collection of the submicron particulates. (auth)

26370 (CONF-700601–, pp 161-7) COLLECTION EFFICIENCY OF WATER DROPLETS IN AgCl AEROSOL. Kerker, M.; Matijevic, E.; Hampl, V.; Cooke, D. (Clarkson Coll. of Tech., Potsdam, N. Y.).

From Precipitation scavenging meeting; Richland, Wash. (2 Jun 1970).

In Precipitation scavenging (1970).

A laboratory study of the collection efficiency of water droplets falling through an aerosol of AgCl particles with a narrow distribution of particle sizes is described. The aerosol was prepared thermally and is contained in a specially constructed chamber. The particle size distribution was obtained by light scattering; the mass concentration was determined by direct weighing after collection by thermal precipitation. A water droplet of known weight drops from a hypodermic syringe through a light beam; breaking the beam activates a circuit that automatically opens and shuts a pair of shutters at the entrance and the exit of the scavenging column and permits the droplet to fall through the aerosol. The amount of AgCl collected was determined both by neutron activation analysis and by a colorimetric microchemical analysis. Present results indicate a collection efficiency of less than 0.01% for an aerosol with radii in the range of 0.3 μ and with particle concentrations of about 10^6 liters^{-1}. (auth)

26371 (CONF-700601–, pp 169-86) COLLECTION EFFICIENCY IN WASHOUT BY RAIN. Berg, T. G. Owe (Berg (T. G. Owe), Inc., Garden Grove, Calif.).

From Precipitation scavenging meeting; Richland, Wash. (2 Jun 1970).

In Precipitation scavenging (1970).

Experimental data on collection efficiencies show some discrepancies among themselves and with respect to the theory. Thus collection on the back side of the scavenger has been reported as being in the range from nothing to 131 times that on the front side. The theory disregards collection on the back side. There are also discrepancies in the optimum scavenger size. These are explainable, but the collection on the back side poses a serious problem that needs study. (auth)

26372 (CONF-700601–, pp 187-204) SCAVENGING OF AEROSOL PARTICLES BY SPRAYS. McCormack, J. D.; Hilliard, R. K. (Battelle-Northwest, Richland, Wash. Pacific Northwest Lab.).

From Precipitation scavenging meeting; Richland, Wash. (2 Jun 1970).

In Precipitation scavenging (1970).

Eight experiments are described in which the washout of aerosol particles by aqueous sprays in a closed chamber was measured. The chamber volume was 750 m^3, and the average fall distance for drops was 11.6 m. Experimental conditions covered a range of those expected in a containment vessel following a loss-of-coolant accident in a pressurized water reactor, including room-temperature air. The washout of three types of aerosol particles was measured: water-soluble cesium and iodine particles and insoluble uranium oxide particles. The time-dependent mass concentrations of these aerosol materials were measured at many locations within the enclosed gas space. A model was developed which described the particle washout by relating the washout coefficient to the single-drop collection efficiency. The washout of all particle types was significantly higher than predicted by the model using particle sizes measured by cascade impactor sampling during the tests. Drop-collection efficiencies for capturing cesium and particulate iodine decreased with spraying time from about 0.04 to about 0.005. Efficiencies for uranium were about half the magnitude indicated for the soluble particles. (auth)

26373 (CONF-700601–, pp 213-16) PULSED-LASER HOLOGRAPHY FOR ANALYSIS OF PARTICLE SIZE AND DISTRIBUTION. Reich, F. R.; Hildebrand, B. P. (Battelle-Northwest, Richland, Wash. Pacific Northwest Lab.).

From Precipitation scavenging meeting; Richland, Wash. (2 Jun 1970).

In Precipitation scavenging (1970).

The principles of pulsed-laser holography and its application to particle studies are reviewed. Holography is an interferometric technique for recording a three-dimensional scene or volume on a two-dimensional medium such as film. The image retains the three-dimensionality of the scene along with depth of focus and parallax. This technique is useful for the study of particle distributions since the hologram can be made with a laser having pulse lengths in the microsecond to nanosecond range, in effect stopping any particle motion. Some experimental results demonstrating the technique are shown. (auth)

26374 (CONF-700601–, pp 247-59) EFFECT OF SOLUBILITIES OF GASES ON THEIR SCAVENGING BY RAINDROPS. Postma, A. K. (Battelle-Northwest, Richland, Wash. Pacific Northwest Lab.).

From Precipitation scavenging meeting; Richland, Wash. (2 Jun 1970).

In Precipitation scavenging (1970).

The degree to which gases are scavenged from the atmosphere by raindrops depends to a large extent on the solubility of the gas in the drop. Existing data on gas absorption by drops is reviewed to show the relative importance of solubility on scavenging in the atmosphere. Numerical examples of washout coefficients for a number of gases of interest show the influence of solubility and chemical reaction. Information needed to predict drop absorption rates for specific cases is reviewed. (auth)

26375 (CONF-700601–, pp 261-9) LABORATORY INVESTIGATIONS ON WASHOUT OF TRACE GASES. Beilke, S. (Frankfurt Univ. (West Germany). Institut fuer Meteorologie und Geophysik).

From Precipitation scavenging meeting; Richland, Wash. (2 Jun 1970).

In Precipitation scavenging (1970).

Laboratory investigations of the washout of SO_2, NO_2, and CO_2 are discussed. The order of magnitude of trace-gas washout coefficients was determined, and the reasons for different washout behavior of these three gases are explored. (auth)

26376 (CONF-700601–, pp 271-88) WASHOUT OF GASEOUS IODINE SPECIES. Coleman, L. F.; Postma, A. K. (Battelle-Northwest, Richland, Wash. Pacific Northwest Lab.).

From Precipitation scavenging meeting; Richland, Wash. (2 Jun 1970).

In Precipitation scavenging (1970).

Eight experiments for measuring the washout of airborne iodine species by aqueous sprays are described. The spray chamber volume was 750 m^3, and the average drop fall distance was 11.6 m. The spray drop size was 0.77 or 1.2 mm volume median diameter. Other parameters considered in this large-scale study were temperature, spray flow rate, and spray solution composition. Spray washout models are presented for elemental iodine and methyl iodide. Absorption rates measured for elemental iodine agree with a theoretical model based on mass transfer limited by gas-phase resistance. Methyl iodide washout was in agreement with a model based on absorption with simultaneous chemical reaction. (auth)

26377 (CONF-700601–, pp 289-92) EUROPEAN INTEREST IN ACIDIC PRECIPITATION: A REVIEW. Reiquam, H. (Battelle-Northwest, Richland, Wash. Pacific Northwest Lab.).

From Precipitation scavenging meeting; Richland, Wash. (2 Jun 1970).

In Precipitation scavenging (1970).

There is increasing concern, particularly in Scandinavia, over the long-range transport of air pollutants. Although hard data for verification are not available, there is circumstantial evidence that sulfur dioxide emitted in industrialized nations, such as Great Britain and West Germany, contributes to the acidity of precipitation far downwind. Some of that evidence is reviewed. Among the problems associated with this question are poor understanding of the reactions, reaction rates, and removal mechanisms, which determine the residence time of pollutants, and the lack of current data on air and precipitation chemistry worldwide. It might be anticipated that similar concern will develop in North America; an effective precipitation chemistry observation network would be an obvious first step toward providing factual response. (auth)

26378 (CONF-700601–, pp 293-303) WASHOUT OF SO_2 FROM THE PLUME OF A COAL-FIRED POWER PLANT. Hales, J. M.; Thorp, J. M.; Wolf, M. A. (Battelle-Northwest, Richland, Wash. Pacific Northwest Lab.).

From Precipitation scavenging meeting; Richland, Wash. (2 Jun 1970).

In Precipitation scavenging (1970).

Recent field measurements of washout by rain and snow of SO_2 in plumes from the 800-ft stacks at the world's largest mine-mouth electric power generating plant demonstrate some complexities arising from the interaction of meteorological and physicochemical factors. (auth)

XUM

26379 (CONF-700601–, pp 305-18) SCAVENGING OF SO_2 BY CONVECTIVE STORMS. Summers, Peter W. (Research Council of Alberta, Edmonton).

From Precipitation scavenging meeting; Richland, Wash. (2 Jun 1970).

In Precipitation scavenging (1970).

During the summer of 1968, a meteorological research aircraft made 15 hr of airborne SO_2 observations in central Alberta, Canada, with a continuous SO_2 analyzer. On several occasions the aircraft measurements enabled estimates to be made of the air, moisture, and SO_2 flux into the base of convective storms. Precipitation samples collected simultaneously by ground mobile units were analyzed for sulfate content by a conductometric titration method. Sulfur budgets for three storms indicate a high rainout efficiency, with ϵ in the range 0.19 to 0.65. (auth)

26380 (CONF-700601–, pp 319-24) MECHANISMS OF IODINE INJECTION FROM THE SEA SURFACE. Martens, Christopher S.; Harriss, Robert C. (Florida State Univ., Tallahassee. Dept. of Oceanography).

From Precipitation scavenging meeting; Richland, Wash. (2 Jun 1970).

In Precipitation scavenging (1970).

Experimental studies indicate that the total flux of iodine into the marine atmosphere is controlled by sea-surface temperature, ultraviolet light, and bubbling, with temperature being more important than ultraviolet light. The results of these experiments support the hypothesis of Duce, Woodcock, and Moyers that gaseous iodine is sorbed by aerosols in the atmosphere with relative enrichment being a function of aerosol surface area. (auth)

26381 (CONF-700601–, pp 325-51) MODEL FOR VARIATIONS WITH PARTICLE SIZE OF HALOGEN-ION RATIOS IN MARINE AEROSOLS. Robbins, John A. (Michigan Univ., Ann Arbor).

From Precipitation scavenging meeting; Richland, Wash. (2 Jun 1970).

In Precipitation scavenging (1970).

A mathematical model has been formulated to account for published chemical analyses of marine aerosol size fractions for iodine, bromine, and chlorine. The model assumes that iodine vapor is gained and bromine vapor is lost by particles at rates determined by gaseous diffusion around the particle. Both iodine and bromine may saturate a particle surface layer, although the detailed mechanism of saturation is not crucial to the model. By nonlinear least-squares fitting to observed data points, the model satisfactorily accounts for a decrease in the I/Cl ratio with increasing radius as r^2 for larger unsaturated particles and as r for smaller saturated particles, and the former shows an inverse dependence on wind speed. The model accounts for the observed minimum in Br/Cl ratio for intermediate size fractions and the inverse dependence of its depth on wind speed. The model requires that most of the aerosol mass sampled is derived from a fairly narrow band of particle ages in order to account for the observed composition variation with size fraction, and this assumption provides an explanation for dependence on wind speed. Among the specific questions raised in this mathematical study which may be tested experimentally are the band width of aerosol particle ages with wind speed and sampling location, the chemistry of iodine and bromine retention by particles, and the mechanism of bromine loss from particles. (auth)

26382 (CONF-700601–, pp 355-71) THEORY OF DIFFUSIVE AND IMPACTIVE SCAVENGING. Hidy, G. M. (North American Rockwell Corp., Thousand Oaks, Calif. Science Center).

From Precipitation scavenging meeting; Richland, Wash. (2 Jun 1970).

In Precipitation scavenging (1970).

Recent developments in a kinetic theory of hard-sphere aerosols are reviewed with particular emphasis on microphysical and microchemical processes involved in scavenging of gases and particles by rain clouds. Of particular interest are such topics as gas and particle diffusion to cloud and rain droplets, inertial deposition of particles on droplets, the role of rarified gas effects in such dynamical processes, the consequences of diffusiophoretic and thermal forces acting on aerosols near water droplets, removal of gases by homogeneous chemical reactions to form aerosols, chemical reactions inside and at the surface of droplets, and collision and coagulation of droplets and aerosols. It is suggested that elements of the idealized theory should provide a framework within which experiments may be interpreted or checked for consistency. Disagreement between theory and observation may point either to systematic experimental error or to poorly understood phenomena significant in the scavenging process. (auth)

26383 (CONF-700601–, pp 373-80) ATTACHMENT OF TRACE SUBSTANCES ON ATMOSPHERIC AEROSOLS. Brock, J. R. (Texas Univ., Austin).

From Precipitation scavenging meeting; Richland, Wash. (2 Jun 1970).

In Precipitation scavenging (1970).

Several factors which lead to characteristic distributions of trace substances in atmospheric aerosols are examined. The implications of these distributions in the study of atmospheric cleansing processes are discussed. (auth)

26384 (CONF-700601–, pp 381-3) RECENT CALCULATIONS OF COLLISION EFFICIENCIES. Hocking, L. M. (University Coll., London. Dept. of Mathematics).

From Precipitation scavenging meeting; Richland, Wash. (2 Jun 1970).

In Precipitation scavenging (1970).

Small particles collide when there is an approach mechanism to bring them together and an adhesion mechanism to prevent them from being separated. Two sets of calculations for collisions are discussed: one for liquid drops and one for solid particles. (auth)

26385 (CONF-700601–, pp 385-402) PROCESSES INFLUENCING EVOLUTION OF DROPLET OR AEROSOL SPECTRUM. Drake, R. L. (National Center for Atmospheric Research, Boulder, Colo.).

From Precipitation scavenging meeting; Richland, Wash. (2 Jun 1970).

In Precipitation scavenging (1970).

The state of the art of the scalar transport equation that arises in the study of an evolving size spectrum of aerosol particles or cloud water droplets is reviewed. The mathematical system investigated is an integrodifferential equation that contains terms accounting for coagulation or coalescence of particles, particle breakup, sedimentation of particles, particle scavenging, and droplet production due to condensation. This review includes the theoretical developments of Melzak, McLeod, and Morgenstern; the exact solutions of Golovin, Martynov, Bakanov, Scott, and Drake; the numerical models of Warshaw, Berry, Friedlander, Wang, Levin, and Sedunov; and other approximate methods of Enukashvili and Golovin. Also considered are results by the author concerning the upper and lower bounds of the power moments of the particle distribution and how these results affect the choice of the collection kernel in the integrodifferential equation. Finally, the author's ideas concerning the numerical solution of the coalescence equation by the method of perturbing the kernel and by similarity approximation are given. (auth)

26386 (CONF-700601–, pp 403-10) PARTICLE-FREE SPACE IN STEFAN FLOW. Vittori, Ottavio A.; Prodi, Vittorio (Comitato Nazionale per l'Energia Nucleare, Bologna (Italy)).

From Precipitation scavenging meeting; Richland, Wash. (2 Jun 1970).

In Precipitation scavenging (1970).

The dust-free space around evaporating surfaces was investigated in the laboratory. A vapor-diffusion field was established in plane-to-sphere and in plane-to-plane geometries. In the plane-to-plane field, the experimental parameters can be accurately controlled. In that configuration quantitative measurements were performed on the displacement velocity of the dark-space boundary. The actual velocity was found to be lower than the Stefan-flow velocity. This difference was interpreted in terms of Brownian diffusion of particles through the boundary. (auth)

26387 (CONF-700601–, pp 411-22) PHORETIC PROCESSES IN SCAVENGING. Slinn, W. G. N.; Hales, J. M. (Battelle-Northwest, Richland, Wash. Pacific Northwest Lab.).

From Precipitation scavenging meeting; Richland, Wash. (2 Jun 1970).

In Precipitation scavenging (1970).

A comparison is made of the roles played by thermophoresis, Brownian diffusion, and diffusiophoresis in the precipitation scavenging of aerosol particles. It is shown that for a certain range of particle sizes thermophoresis dominates if the latent heat associated with the phase transition of water is transferred through the air to or from the precipitation element by conduction. A graph of the resulting washout coefficient shows that thermophoresis enhances the below-cloud rain scavenging of aerosol particles with radii between 0.01 and 1.0 μ. The solution is presented for the appropriate convective-diffusion equation that describes thermophoretic effects in the in-cloud scavenging problem. (auth)

26388 (CONF-700601–, pp 433-46) SCAVENGING OF AEROSOLS BY RAIN: A NUMERICAL STUDY. Kortzeborn,

XUM

Robert N.; Abraham, Farid F. (IBM Scientific Center, Palo Alto, Calif.).

From Precipitation scavenging meeting; Richland, Wash. (2 Jun 1970).

In Precipitation scavenging (1970).

The washout process whereby small airborne particles are scavenged below the cloud level was studied. Previously published models of washout have assumed that the raindrop size distribution and the atmospheric conditions are identical at the ground and at cloud base and do not vary with time. The present model allows a spatially varying atmospheric profile and takes evaporation and coalescence of raindrops into account on a dynamic basis. These effects greatly alter washout at low elevations. The computational model is explained in detail. (auth)

26389 (CONF-700601–, pp 447-63) TROPOSPHERIC SCAVENGING OF ^{90}Sr AND ^{3}H. Krey, P. W.; Krajewski, B. (New York Operations Office (AEC), N. Y. Health and Safety Lab.).

From Precipitation scavenging meeting; Richland, Wash. (2 Jun 1970).

In Precipitation scavenging (1970).

Tropospheric inventories of tritium as HTO are calculated for the years 1963, 1964, and 1965 using data from the precipitation network of the International Atomic Energy Agency. From these inventories, from ^{90}Sr surface-air measurements, and from simple models of atmospheric transport, the half residence time of nuclear weapon particulate debris and the HTO tritium of recent stratospheric origin were computed. The previously reported half residence time of 30 days for ^{90}Sr was verified, and a surprisingly low overall half residence time of 10 days was found for HTO. This overall 10-day value is the result of tritium removal by precipitation and by vapor exchange with the oceans. The half residence time for HTO removed by precipitation is 28 days but only 16 days by vapor exchange. (auth)

26390 (CONF-700601–, pp 465-74) USE OF NATURAL RADIOACTIVITIES TO ESTIMATE LARGE-SCALE PRECIPITATION SCAVENGING. Machta, L.; List, R. J.; Smith, M. E. Jr.; Oeschger, H. (Environmental Science Service Administration, Silver Spring, Md. Air Resources Labs. Bern Univ. (Switzerland). Physikalisches Institut).

From Precipitation scavenging meeting; Richland, Wash. (2 Jun 1970).

In Precipitation scavenging (1970).

Beryllium-7 and argon-37 are naturally occurring cosmogenic radionuclides with similar half-lives. Relative productions as a function of altitude and latitude are identical. Beryllium-7 is subject to precipitation scavenging; argon-37, a noble gas, is not. A one-dimensional vertical diffusion model produces surface-air concentrations to fit the few surface-air ^{37}Ar measurements. Scavenging is added to the diffusion model to compare predictions with the observed ^{7}Be vertical profile. The diffusion–scavenging model can also be tested against the distribution of ^{210}Pb resulting from the decay of radon gas emitted from the earth's surface. The technique promises to provide useful information on large-scale precipitation scavenging. (auth)

26391 (CONF-700601–, pp 475-85) SCAVENGING PREDICTION USING RATIOS OF CONCENTRATIONS IN AIR AND PRECIPITATION. Engelmann, Rudolf J. (Division of Biology and Medicine (AEC), Washington, D. C. Fallout Studies Branch).

From Precipitation scavenging meeting; Richland, Wash. (2 Jun 1970).

In Precipitation scavenging (1970).

Data are presented which demonstrate that washout ratios (factors) are applicable to the prediction of scavenging by precipitation of widely varying particle sizes and even, perhaps, of gases. The explanation offered is compatible with observed variations of pollutant concentration in rain with rainfall rate and dew point, with the consistency of observed ratios, and with an elementary equation that is derived to explain the ratios. It is recommended that washout ratios be observed in the future, since such data may contribute to the understanding of precipitation processes and weather modification. (auth)

26392 (NIRS-RSD-27) RADIOACTIVITY SURVEY DATA IN JAPAN. Number 27, May 1970. (National Inst. of Radiological Sciences, Chiba (Japan)). 17p. Dep. NTIS (U. S. Sales Only).

The results of radioactivity monitoring in Japan from April 1969 to April 1970 are tabulated and include data on: ^{144}Ce, ^{137}Cs, and ^{90}Sr contents in airborne dusts and soils, and the ^{137}Cs and ^{90}Sr content in powdered milk, potable rainwater, source water, tea, and vegetables. (L.C.L.)

26393 (ORO-3944) STUDY OF TRITIATED HYDROGEN AND ITS COMPOUNDS IN THE ENVIRONMENT. Progress Report. Oestlund, H. Goete (Miami Univ., Fla. Rosenstiel School of Marine and Atmospheric Sciences). Mar 1971. Contract AT(40-1)-3944. 9p. Dep. NTIS.

Environmental monitoring activities from June 1970 to March 1971 for determining the ^{3}H and tritium water vapor content of ground level air, of the atmosphere to 31,000 ft, of rain, and of the environment near and within nuclear installations are described. Sampling equipment and methods used for tritium monitoring in the atmosphere near Miami, Florida and Fairbanks, Alaska are discussed and the results presented. (L.C.L.)

26394 ACTINIUM AEROSOLS DETERMINATION IN THE AIR IN THE PRESENCE OF OTHER RADIOACTIVE SUBSTANCES. Andreeva, O. S.; Kiselev, V. I.; Korzhov, L. N. Gig. Sanit.; No. 2, 69-71(Feb 1970). (In Russian).

Actinium-227 emits soft beta radiation and alpha radiation of insignificant intensity, not exceeding 1.5% of the total number of decays. Ac can be determined by the beta radiation of its short-lived daughter decay product, ^{223}Fr, which has a half-life of 21 min. A method for determining Ac aerosols is proposed based on the classical emission principle for determining Ac. (tr-auth)

Mineralogy and Exploration

Refer also to abstract 28764.

26395 (CONF-700903–15) DEMAND OF URANIUM ENRICHMENT SERVICES FOR SWEDEN'S NUCLEAR POWER PROGRAM, 1975–1985. Almgren, B. (Oskarshamnsverkets Kraftgrupp A.B., Stockholm (Sweden)); Edman, R. (Statens Vattenfallsverk, Stockholm (Sweden)). May 1970. 3p. Dep. NTIS (U. S. Sales Only).

From 4. Foratom Congress on industrial aspects of the nuclear fuel cycle in Europe; Stockholm, Sweden (21 Sep 1970).

The Swedish nuclear power program is briefly described. The separative work demand is estimated to be 600,000 kg in 1975, 1,300,000 kg in 1980, and 2,200,000 kg in 1985. It is stated that this demand for enrichment services is far too small for a diffusion plant of economic size in Sweden. A centrifuge plant could possibly be built in 1980's. (Sweden)

26396 (CONF-700903–16) URANIUM DEMAND AND SUPPLY. Gelin, R. (Aktiebolaget Atomenergi, Stockholm (Sweden)). Apr 1970. 14p. Dep. NTIS (U. S. Sales Only).

From 4. Foratom Congress on industrial aspects of the nuclear fuel cycle in Europe; Stockholm, Sweden (21 Sep 1970).

Uranium requirements are estimated under the assumption that only light water reactors are installed up to the middle of the 1980's. Uranium supply by bilateral agreements with countries which can deliver uranium and production from the Billingen deposits are considered. Uranium has been found in the Tåsjö area, but no economic method for uranium recovery has been developed. (Sweden)

Oceanography

Refer also to abstracts 26380 and 26381.

26397 (FRL-7) RADIOACTIVITY IN SURFACE AND COASTAL WATERS OF THE BRITISH ISLES, 1969. Mitchell, N. T. (Ministry of Agriculture, Fisheries and Food, Lowestoft (England). Fisheries Radiobiological Lab.). Mar 1971. 33p. Dep. NTIS (U. S. Sales Only).

Activities of the Fisheries Radiobiological Laboratory in monitoring the aquatic environment of the British Isles during 1969 are described and the result presented. Much of this effort was directed to fulfilling responsibilities for controlling radioactive waste discharges in England and Wales, but monitoring of waters off Ireland and Scotland is also included. The results show that adequate control of radioactive waste disposal has been achieved, and that radiation exposure of the public from these disposals is well within the dose limits prescribed by the International Commission on Radiological Protection. (L.C.L.)

26398 (RLO-2225-T-20-2) RADIOCARBON IN THE SEA. Fairhall, A. W.; Buddemeier, R. W.; Yang, I. C.; Young, A. W. (Washington Univ., Seattle). [1970]. 43p. Dep. NTIS.

Data are reported and analyzed on sampling and analysis of seawater for ^{14}C at several ocean locations throughout the world. Samples were also collected for total CO_2 analysis. The results are tabulated. (J.R.D.)

26399 (TID-25674) MARINE GEOCHEMISTRIES OF THE URANIUM ISOTOPES, ^{230}Th, AND ^{231}Pa. Turekian, K. K.; Chan,

L. H. (Yale Univ., New Haven, Conn. Dept. of Geology and Geochemistry). [1970]. 35p. Dep. NTIS.

The marine geochemistries of the uranium isotopes and their most long-lived daughters, ^{231}Pa and ^{230}Th, are discussed. Insights into the behavior of these nuclides, despite their apparently limited applicabilities, provide models for viewing the behavior of other trace elements in the oceans. (L.C.L.)

Seismology

Refer also to abstracts 26325 and 26402.

26400 (NVO–99-12) STRUCTURAL CONDITION STATUS REPORT. Nelson, William H. (Blume (John A.) and Associates Research Div., San Francisco, Calif.). May 1966. Contract AT(26-1)-99. 134p. Dep. NTIS.

Progress to date in structural condition survey efforts for Las Vegas and southern Nevada is summarized. Initial observations have been concentrated on Las Vegas structures, primarily the multi-story hotel and office buildings which are of greatest concern from a structural response damage vulnerability point of view. More recently efforts have been directed primarily toward observations of five typical residences in various parts of Las Vegas representing typical difficult foundation conditions. A second major area of effort is at the Nevada Test Site (NTS) and in the communities bordering the test site. Detailed surveys have been made at Mercury and at the Nuclear Rocket Development Station (NRDS), and reconnaissance surveys have been made of Indian Springs, Lathrop Wells, Beatty, Goldfield, Tonopah, Alamo, Moapa, Glendale, Overton, Henderson, and Boulder City. Structural condition surveys are principally concerned with the determination of the present state of the structure and the extent and kind of physical changes or deterioration which are occurring normally, i.e., in the intervals between and unaffected by ground motion from underground nuclear detonations. These changes are compared with those which are observed to occur as a result of ground motion from an underground nuclear detonation. Monitoring is done by visual observations and note-taking, photography, and by mechanical gages. These efforts are directed or oriented in the light of structural analyses of the existing building so that areas of high stress concentration or overloaded members are given priority for observation. Corollary efforts include determination and evaluation of foundation conditions for the effect of potential settlement or event-amplifying effects, and optical leveling to evaluate regional settlement processes. Regional settlement is well documented in Las Vegas and is attributed to ground water withdrawal by pumping. (auth)

26401 (NVO–1163-218) OBSERVED SEISMIC DATA, CALABASH EVENT. West, Lewis R.; Christie, Raymond K. (comps.) (Environmental Research Corp., Las Vegas, Nev.). Feb 1971. Contract AT(29-2)-1163. 66p. Dep. NTIS.

Results of the processing of the observed ground motions for the Calabash Event, an underground nuclear detonation on Yucca Flat, at the Nevada Test Site are presented. Pseudo-Relative Velocity Spectra at 5% damping were derived from the velocity seismograms. (auth)

ENGINEERING

Nuclear Explosions

Refer also to abstracts 26354, 26357, 26400, and 26401.

26402 (JAB–99–78) STRUCTURAL RESPONSE STUDIES FOR PROJECT RULISON. (Blume (John A.) and Associates Research Div., San Francisco, Calif.). Feb 1971. Contract AT-(26-1)-99. 183p. (PNE-R-46). Dep. NTIS.

Project RULISON, an experiment using an underground nuclear explosive to fracture and thereby increase production from a gas-bearing sandstone, was detonated in western Colorado on September 10, 1969. Comprehensive structural response investigations were required for the detailed prediction of response and damage to natural and man-made structures in the area, to eliminate hazards to the public and also to provide a quantitative assessment of probable damage repair cost. Detailed surveys and field evaluations needed to provide the basic information required for the response and damage predictions included inventorying the structural population out to 25 kilometers, observation and evaluation of earth structure stability and hazards (including earth and rock slopes, earth dams, and canals), a brief seismic history study, and engineering evaluations and recommendations as to specific hazards and appropriate corrective measures. Recommendations were provided for ground motion time-history instrumental recording. Mechanical gages for structure motion recording, crack movement measurement, and water wave observations were installed. Damage to structures occurred generally as predicted. A delay of the original shot date from May 1969 to September allowed slopes to dry out. As expected, there was an increase in stability, and little earth and rock slope movement occurred. Reservoir water levels were low, and some concern which had been expressed for the behavior of older earth dams was thereby eliminated. Initial analyses show correlation between response motion and damage occurrence, and further detailed analyses of the motion damage relationship are in progress. As of October 31, 1970, damage payments plus amounts offered in settlement of a few remaining claims totaled about $117,500. This compares well with the damage repair cost of $123,000 predicted for the 40-kiloton design yield. (auth)

26403 (NVO–1229–105(Pt.1)) EVALUATION OF THE PROJECT SHOAL SITE, FALLON, NEVADA, FOR DISPOSITION, INCLUDING IDENTIFICATION OF RESTRICTIONS. PART I. Gardner, M. C.; Nork, W. E. (Teledyne–Isotopes, Palo Alto, Calif.). Apr 1970. Contract AT(29-2)-1229. 42p. Dep. NTIS.

The site of the Project Shoal underground nuclear detonation was studied to develop criteria and recommendations for disposal of the site. Disposal of a nuclear event site should be considered from the standpoint of security, radiological safety, and structural safety in a logical sequence of criteria application. The chimney contains melt and debris whose analysis might reveal classified information. However, access to the chimney would require extensive drilling. Exclusion of drilling and mining from the site is recommended. Security considerations would not prevent release of the site to public domain. There are no radioactive materials at the site surface. Subsurface radioactive materials are confined to the rubble chimney and possibly some radiating fractures. Isolation of the radioactive area will continue into the foreseeable future. Further collapse of the present chimney roof to the ground surface is improbable, except in case of a major earthquake. Granitic rocks of the Sand Springs Range are in a local water recharge area. The potentiometric surface is above the rubble chimney. Water moves very slowly through fractures, and no radionuclides above Concentration Guide levels are forecast to enter the areas' alluvial formations. The site is recommended for release except for drilling and mining restrictions within a specified area. Inclusion of the site into the Fallon Naval Auxiliary Air Station is recommended. (auth)

26404 (PNE–527) FAR-OUT COLLECTION PROGRAM, Project SCHOONER. Tami, Thomas M. (Army Engineer Nuclear Cratering Group, Livermore, Calif.); Gibson, Thomas A. Jr.; Prindle, Austin L. (California Univ., Livermore. Lawrence Radiation Lab.). Jun 1970. 17p. Dep. NTIS.

The Far-Out Fallout Collection Program was an experimental program to collect and to analyze samples of long-range fallout from Plowshare nuclear cratering events. Samples of fallout from Schooner, a 31-kt cratering experiment, were collected at downwind distances ranging from 65 to 500 km from the detonation site. The field operations required to obtain the fallout samples and the radiochemistry techniques used to analyze the samples are described. Measured values of the gamma exposure rate resulting from fallout at downwind locations in eastern Nevada and western Utah are reported. The maximum recorded exposure rate 65 km from the detonation site was 130 mR/hr. Of the 80 fallout samples collected, 16 were radiochemically analyzed to determine the species and quantities of radionuclides present. The presence in each analyzed sample of up to 20 different radionuclides, including ^{90}Sr and ^{131}I, was determined. The radiochemistry results are expressed in terms of deposited radioactivity per unit area (pCi/m^2). (auth)

26405 (PNE–1002) GASBUGGY SEISMIC SOURCE AND SURFACE MOTION. Project Gasbuggy. Perret, William R. (Sandia Labs., N. Mex.). Dec 1969. 74p. (PNE-G-73). Dep. NTIS.

Four subsurface instrument stations were installed in a boring about 500 meters from the Gasbuggy shot hole to document the seismic source function for that event. Gasbuggy, a nuclear experiment designed to stimulate production of natural gas from the impervious Pictured Cliffs sandstone, was detonated at a depth of 1292 meters (4240 feet) at 1230:00.136 hours MST on December 10, 1967, about midway between Farmington and Dulce, New Mexico. The predicted nominal yield was equivalent to 26 kilotons of TNT, but final yield determination from postshot data was 29 ± 3 kiloton TNT-equivalence. Data from subsurface instrument stations indicated that they were probably close to, if not within, the region of elastic response of the rock near shot level and that reduced displacement potentials defined the seismic source. The mean peak potential was 7470 m^3 and the mean residual potential was 6470 m^3. Energy calculations indicate that about 1.75 percent of the explosive energy remained in the seismic source function at a radial range of 500 meters. Estimates based on reduced displacement indicate a yield equivalent to about 28 kilotons of TNT. Data from surface motion instruments distributed at six stations between surface zero and about twice shot depth show a normal spall pattern at all stations. (auth)

26406 (PNE–1009) GROUND WATER SAFETY EVALUATION. Project GASBUGGY. Sokol, Daniel (Teledyne-Isotopes, Palo Alto, Calif.). Sep 1970. Contract AT(29-2)-1229. 38p. (PNE-G-74). Dep. NTIS.

The most likely path for hydrologic transport of radionuclides from the Gasbuggy Site to possible water-use points is through the Ojo Alamo Sandstone. Groundwater in the Ojo Alamo Sandstone flows westward. The point at which groundwater in the Ojo Alamo Sandstone could mix with other water is along the San Juan River near the mouth of Los Pinos River, 38 kilometers northwest of the Gasbuggy Site. Based on available data, groundwater flowing from the Gasbuggy Site will take 5900 years to reach the confluence of the San Juan and Los Pinos Rivers. At the Gasbuggy Site, the total dissolved solids, sodium, and sulfate content of the groundwater occur in concentrations higher than acceptable for irrigation or domestic use. Tritium, ^{90}Sr, and ^{137}Cs will decay to concentrations below the appropriate concentration guides (CG) for the general public before reaching the San Juan River. Tritium will travel a maximum of 2100 m in no more than 309 yrs before decaying to a concentration of 1×10^{-3} $\mu Ci/ml$ (the CG for tritium). Because of their high K_d values, ^{90}Sr and ^{137}Cs will migrate no farther from the cavity than 320 m and 3.5 m, respectively, in 1,000 yrs. By this time, both nuclides will have decayed to well below the CG. (auth)

26407 (PNE–1112) PROJECT PRE-GONDOLA II SUMMARY REPORT. Day, W. C. (ed.) (Army Engineer Nuclear Cratering Group, Livermore, Calif.). Aug 1970. 116p. Dep. NTIS.

The design concept, objectives, technical programs and summarized results of Project Pre-Gondola II are presented. The site medium, the project layout, the explosive charge design, and the emplacement are described. The row-emplaced chemical charges were simultaneously detonated and produced a linear crater 490 ft long, from 142 to 214 ft wide, and from 34 to 57 ft deep. Surface motion spall velocities of 145 to 215 ft/sec were measured at and between surface ground zeros. A trench excavated through the crater lip indicates a maximum uplift of the original ground surface of about 8 ft. Some uplift extended as far as 250 ft from the centerline of the row. Subsurface displacements in the same region were determined and showed a good correlation with maximum ground stress measured during the detonation. Seismic amplitude attenuation was determined to be proportional to the frequency of the motion. A seismic amplitude yield scaling factor of $W^{0.8}$ was determined for the row detonation when compared to

the Pre-Gondola I detonations. Peak air overpressure was found to be inversely proportional to the distance from surface ground zero. The overpressures normal to the row orientation were about 50% greater than those at the same distances off the end of the row. The cloud had an average base surge radius of 1266 ft and a height of 800 ft. There was no visible main cloud. A laser radar cloud tracking system (lidar) operated from an aircraft, was successfully tested. The Pre-Gondola II detonation-generated shock wave was apparently not harmful to fish in the adjacent reservoir. (auth)

26408 (PNE-1117) PROJECT PRE-GONDOLA III, PHASE II SUMMARY REPORT CONNECTING ROW-CRATER EXPERIMENT. Lattery, J. E. (ed.) (Army Engineer Nuclear Cratering Group, Livermore, Calif.). Sep 1970. 68p. Dep. NTIS.

Project Pre-Gondola III Phase II was a row-crater experiment conducted on 30 October 1968 by the U. S. Army Engineer Nuclear Cratering Group at a site near Fort Peck, Montana. The primary experimental objective was to form a row-crater which would smoothly connect to the crater formed by a previous row-charge detonation, Pre-Gondola II. The row-charge consisted of seven 30-ton charges of nitromethane. These were emplaced in the clay-shale medium at depths averaging 53 ft with a typical horizontal spacing of 86 ft. Several technical programs by various governmental agencies and contractors measured the crater and significant side effects of the detonation. The detonation produced a crater having an apparent length of 610 ft, an average width of 191 ft, and an average depth of 48 ft. In combination with the preexisting crater, it formed a linear crater approximately 1100 ft in length. Technical programs were implemented to measure motions of surface ground zero, to compare preshot and postshot hydrologic, lithologic, and physical conditions of the site and cratered area, to measure long-range airblast, to determine the size and form of the dust cloud, to measure intermediate-range seismic motions, and to measure induced motions of the Fort Peck dam and associated structures. The final results and analyses are presented for all except the long-range airblast program. Final results for this last will be reported separately. (auth)

26409 (PNE-R-45) PROJECT RULISON POST-SHOT INVESTIGATIONS. Summary of Re-Entry Operations. Reynolds, Miles Jr. (Austral Oil Co., Inc., Houston, Tex.). Jan 1971. 28p. Dep. NTIS.

The Rulison Event, an underground nuclear explosion gas stimulation experiment, was detonated on Sept. 10, 1969. Drilling operations for reentry into the chimney commenced Apr. 28, 1970. The organization, drilling preparations, and drilling history of the reentry operations are summarized. (L.C.L.)

26410 (PNE-R-47) MOTION OF RIFLE GAP DAM RIFLE, COLORADO; PROJECT RULISON UNDERGROUND NUCLEAR DETONATION. Fowler, Jack (Army Engineer Waterways Experiment Station, Vicksburg, Miss.). Jan 1970. 32p. Dep. NTIS.

A summary of the maximum recorded Rulison Event-produced ground motions at Rifle Gap Dam is presented. Ground motions were measured by accelerometers (PAT), particle velocity transducers (PVT), and the strong-motion accelerographs. When compared to an earthquake, the level of motion observed on the dam during the Rulison Event was considered small; it was apparently well below any failure level. The motion of the base of the dam was about the same as that measured on the natural alluvium overburden materials downstream from the dam. The motion amplification factor between the base of the dam and the crest was considerably less than two. (auth)

26411 (SC-DC-71-3865) GROUND MOTION SUMMARY STATEMENT. Banister, John R. (Sandia Labs., Albuquerque, N. Mex.). [1970]. 8p. (CONF-710307-1). Dep. NTIS.

From Meeting of the seismological society of America; Riverside, Calif. (25 Mar 1971).

Information available from 1957 to 1970 on ground motion induced by underground nuclear explosions is briefly summarized. Close-in ground motion data measured and analyzed by Sandia and remote ground motion data from safety studies at the Nevada Operations Office of the AEC are discussed. (L.C.L.)

26412 (UCRL-50979) RESULTS OF POSTSHOT EXPLORATION OF THE GREELEY EVENT. Rawson, D. E.; Borg, I. Y. (California Univ., Livermore. Lawrence Radiation Lab.). 24 Nov 1970. 31p. Dep. NTIS.

Temperature and radiation logs made in a postshot drill hole (U20g PS-1D), which penetrates the Greeley chimney-cavity on Pahute Mesa, Nevada Test Site, indicate that the cavity radius is from 224 to 265 ft. The chimney height immediately after the event was about 1640 ft above the shot point. Propagation of the chimney to the surface occurred periodically following the event until a surface subsidence crater formed two to eight months later. Enlargement of the crater continued for several years in response to other Pahute Mesa events and natural earthquakes. As of April 26, 1968 (D + 1.35 years), the volume of the crater was 8.5% of that of the cavity, and the void space in the chimney was estimated to be 7.6% of the total chimney volume. The most distant fracturing, as evidenced by increased γ radiation in the postshot hole, occurs 2091 ft from the shot point. Extensive fracturing, permitting rapid inflow of displaced ground water, occurs 1100 ft and perhaps as far as 1700 ft from the shot point. The rate of inflow into the chimney area during the first year was about 2.4×10^2 gal/min. Two years after the shot, the water level was within 17 ft of the preshot level. (auth)

Facilities and Equipment

Refer also to abstracts 26345, 26559, 27062, 27665, 27883, 27884, and 27886.

26413 (N-71-10455) FREEZE, MELT VALVE AND DISPENSING SYSTEM FOR CESIUM. Morris, James F. (National Aeronautics and Space Administration, Cleveland, Ohio. Lewis Research Center). Nov 1970. 6p. (NASA-TM-X-2126; E-5884). NTIS.

Nuclear thermionic diodes for space electric power require cesium purity control, which vacuum packaging allows. However, dispensing small quantities of such a reactive element into prebaked evacuated capsules poses unique valving problems. One answer is the freeze, melt valve, an orifice that closes or opens as the cesium solidifies or liquifies locally. A single resistant metal contacts the corrosive liquid in a very simple, extremely compact, reliable flow regulator. These characteristics make it a good valve for reactive liquids in general. The design and operation of a freeze, melt valve used in vacuum encapsulating cesium for thermionic diodes is described. (auth) (STAR)

26414 (TID-4100(Suppl.62)) ENGINEERING MATERIALS LIST. Supplement 62. Smith, Richard J.; Sachs, Francis L.; Clark, Willie E. (eds.) (Division of Technical Information Extension (AEC), Oak Ridge, Tenn.). Mar 1971. 43p.

Twenty-two packages of engineering drawings and specifications are presented. Packages of drawings are included on linear pulse amplifiers, storage container and packaging, thermograph, melter pump, cavity-resonator microwave spectrometer, fission fragment analyzer, source holder, nonstable multivibrator, rotating step sector, Cm shipping cask, Cm process equipment, Crewe electron-energy-analyzing scanning microscope, display processing, digital oscilloscope plug-in units, Pu salt transport facility, large-scale mizer-settler facility, darkroom timer, Compton-suppressed Ge(Li) spectrometer, manipulator motion lock, and fluid-bed denitrator. A subject index is included. (L.C.L.)

26415 (TRG-Report-2121) THEORETICAL WAVING BEHAVIOUR OF MAGNOX FUEL ELEMENT FINS DUE TO COOLANT-GAS INDUCED CORROSION AND TO THERMAL CYCLING. Anderson, R. G. (United Kingdom Atomic Energy Authority, Springfields (England). Reactor Group). 23 Apr 1970. 49p. Dep. NTIS (U. S. Sales Only). UK 35p.

A comprehensive theory of struts which undergo spontaneous expansion and thermal cycling under conditions of axial restraint, stress relaxation and creep is developed. An approximate extension to finite plates is made. A preliminary check of the approximate plate theory against a numerical method shows good agreement. The theory is applied to explain many features of the in-pile and out-of-pile waving of Dungeness A fins. The effect of thermal cycling is found to have a rather higher relative weighting than that found in earlier work. Thermal cycling could be playing a substantial part in producing Category 10 deformations on Dungeness A fins though a much less important role in higher Category development. The strut theory and the plate approximation are new theoretical contributions to the behaviour of creeping structures and may have applications in other fields both inside and outside Fuel Element Analysis. (auth) (UK)

26416 THEORY AND PRACTICE OF LUBRICATION SYSTEMS. Nica, Alexandru. Bucharest; Publishing House of the Rumanian Academy (1969). 252p.

Translation of Sisteme de Lubrificatie by Alexandru Nica and P. A. J. Scott.

Information is presented on friction and wear, design of lubricating systems, construction of lubricating systems, effects of bearing characteristics on lubricant supply systems, lubricants and antifriction methods, and special lubrication systems such as magnetohydrodynamic and those used in radioactive environments. (J.R.D.)

26417 IRRADIATION APPARATUS IN COMBINATION WEB HANDLING MEANS. Martin, William J.; Ruppe, Charles R. (to Deering Milliken Research Corp.). U. S. Patent 3,564,238. 16 Feb 1971. Filed 8 May 1967.

A system for continuously irradiating chemically treated material employs an improved arrangement for permitting multiple passes of the treated material through the irradiation field while the distance between the layers of treated material passing through the field is maintained to improve the efficiency of the irradiation process. Ionizing irradiation apparatus is also included. (Official Gazette)

Heat Transfer and Fluid Flow

Refer also to abstracts 26435, 26441, 28660–28662, 28681, 28696, and 28819.

26418 (ANL–7734) EXPERIMENTAL STUDY OF A GAS JET PENETRATING A LIQUID COOLANT AND IMPINGING ON A HEATED SURFACE. Hoglund, B. M.; Anderson, R. P.; Bova, L. (Argonne National Lab., Ill.). Mar 1971. Contract W-31-109-eng-38. 42p. Dep. NTIS.

An experimental study of temperature transients induced in a heated wall as a result of a gas jet penetrating the coolant stream and impinging upon the wall is described. The experiment was performed in a water-cooled, electrically heated, rectangular flow channel, $0.050 \times 0.578 \times 18$ in. The test section was designed to allow a fixed volume of gas to be discharged through an orifice and impinge on the opposite wall. Thermocouples measured the resulting wall temperature transients. The test parameters were: coolant velocity of 10, 20, 30 fps; orifice diameter of 0.016, 0.025, 0.051 in.; plenum gas pressure of 500, 750, 1000 psia; and surface heat flux of 0.5×10^6, 1.0×10^6 Btu/hr-ft^2. Tests were run with and without bypass flow around the heated channel. Additional data were obtained from an unheated Lucite test section. Transient pressures and flow rates were measured, and high-speed motion pictures of the resulting gas jets and flow transients were obtained. It was concluded that an impinging gas jet is unlikely to produce failure in an adjacent fuel pin at the point of impingement. In every case, the surface at the point of impingement was cooled to a temperature less than the steady-state temperature. Only for cases where the channel was blown completely dry did the wall temperature exceed its initial steady-state value. (auth)

26419 (GEAP–10221–5) DEFICIENT COOLING FIFTH QUARTERLY PROGRESS REPORT, JULY 1–SEPTEMBER 30, 1970. (General Electric Co., San Jose, Calif. Atomic Power Equipment Dept.). Oct 1970. Contract AT(04-3)-189. 26p. Dep. NTIS.

A simplified transient analysis, for flow and/or pressure decay in a boiling system was coded for use with FORTRAN IV. The program was used to predict time of critical heat flow (CHF) in two actual runs. The results are very close, on the conservative side, to the actual data and other predictions obtained from a more complex code (SCAT) which calculates thermal conditions in a reactor core. Installation of the three-subchannel sampling system for the nine-rod test section was completed. Final inspection and hydro tests were completed to meet ASME code requirements. The TAPER code, for acquisition and reduction of transient data, has been expanded from seven- to fourteen-channel capability. Analysis of the transient flow as obtained by an orifice shows that the inertia term is practically negligible for cases of interest in this program. Thus, transient flow data can be reduced, with little error (about 1 to 2%), by use of standard steady state orifice techniques. (auth)

26420 (KFK–1300) THEORETICAL METHOD FOR CALCULATION OF TWO-PHASE FLOW WITH CHANGE OF PHASE IN A FLASH EVAPORATION. Gaballah, I. (Kernforschungszentrum, Karlsruhe (West Germany). Institut fuer Reaktorbauelemente). Nov 1970. 30p. (In German). Dep. NTIS (U. S. Sales Only).

A theory was developed for calculation of two-phase flow with change of phase. The basic equations were formulated and solved numerically. The results show that the steam temperature and the steam wetness at the inlet of the evaporator channel decrease very rapidly, but decrease only to a very small extent at low wetness of the steam and low degree of superheating. Also, the strong increase in the length required for evaporation with a low prescribed wetness and low prescribed degree of superheating at the end of the evaporator channel was shown. (auth)

26421 OPTIMUM CONTROL OF HEAT EXCHANGERS WITH INTERNAL HEAT GENERATION. Huang, H. S.; Yang, W. J. (Univ. of Michigan, Ann Arbor). Appl. Sci. Res. (The Hague); 23: No 1/2, 95-112(Oct 1970).

The optimum control of a heat exchanger having internal heat sources was investigated. Both the wall and coolant are treated as distributed-parameter systems. Under certain constraints inherent in the operating conditions and physical limitations of the heat exchanger, the control function of the system, i.e. the heat generation rate which minimizes the deviation of the temperature distribution from an assigned pattern at a given time, is found through the use of a linear programming method. The effects of physical parameters on the optimal control function and the temperature response and distribution are examined. Experimental results are presented which compare favorably with the theoretical analysis. Heat exchangers to which these results apply include the electrical heater, a chemical reactor in which a chemical reaction occurs within the solid walls and a heterogeneous nuclear reactor. (auth)

26422 FLOW OF A LIQUID METAL COOLANT PAST A HEAT GENERATING CYLINDER. Ishikawa, N.; Leipziger, S. (Inst. of Gas Tech., Chicago). Appl. Sci. Res. (The Hague); 23: No 1/2, 53-72(Oct. 1970).

The coupled problem whereby a solid heat generating cylinder is being cooled in steady state by a coolant in potential flow was investigated. An analytical method for determining the temperature distributions in the solid and the fluid is presented. Numerical studies for six Péclet numbers ($0.9 < Pe < 11.3$) and three thermal conductivity ratios ($0.31 < K < 3.1$) were carried out. The surface hot-spot temperature and center temperature are presented graphically as functions of the Péclet number with the thermal conductivity ratio as a parameter. The average Nusselt number is found to be proportional to the Péclet number to approximately the one-half power. For the special case of constant surface temperature (uncoupled problem), the variation of local Nusselt number with angle measured from the forward stagnation point is in excellent agreement with the result presented by other investigators. (auth)

Isotope Technology

Refer also to abstracts 26353, 26437, 26455, 26548, 27126, 28105, and 28106.

26423 (CEA-Bib-190) ISOTOPIC ELECTRICITY GENERATORS. Laveissiere, Francoise (Commissariat a l'Energie Atomique, Saclay (France). Centre d'Etudes Nucleaires). Jan 1971. 44p. (In French). Dep. NTIS (U. S. Sales Only).

Reports giving technical and economic information on the achievements of several countries (USA, France, UK, Euratom, USSR, and Canada) on isotopic electricity generators are presented. Each report contains information on the radioisotope used, activity of the source, output wattage, generator lifetime, manufacturer, type of conversion used, generator weight, and primary use. (auth)

26424 (CONF-700557–3) EXPECTED DEVELOPMENT OF METHODS FOR ENRICHING URANIUM IN EUROPE. Dreissigacker, H-L. Translated from Stroemungsmechanische Vorgaenge in Gaszentrifugen, DFVLR-Kolloquium, om 14. Mai 1970, Porz, Wahn, Germany. 6p. Dep. NTIS (U. S. Sales Only).

The present technical and economic states of the gaseous diffusion, gas centrifuge, and separation nozzle methods for U enrichment are described, and their potentials for development in Europe are re-assessed from the present-day point of view. The prospects of the three methods are qualitatively assessed and compared, particularly in view of the hoped-for European collaboration in the production of enriched uranium. (auth)

26425 (MLM–1796) HEAT SOURCE CAPSULE FABRICATION TECHNOLOGY PROGRAM: SEPTEMBER 1970–JANUARY 1971. Wendeln, D. E.; Wyder, W. C.; Tucker, P. A.; Newland, J. E. (Mound Lab., Miamisburg, Ohio). 5 Mar 1971. Contract AT-33-1-GEN-53. 104p. Dep. NTIS.

The Heat Source Capsule Technology Program was started in April of 1970, and in the period April 1 to September 1 a hydroform press was installed and the manufacturing engineering phases were completed. All special hydroform tooling, machining fixtures, and gages were designed, built, and inspected in this same period. With the delivery of the hydroform blanks basic hydroform parameter and tooling development phase was started. This phase has been completed on all six capsule parts of the Transit design. Further dimensional refinements are being made such as the development of compensated punches to reduce the internal spherical radii deviations (and wall thickness deviations) and to reduce the out-of-roundness of the body parts at the open end. The cutting tool and machining speeds and feeds development phase has been successfully completed, and the specially

designed cutting tools have been procured and are available for use. The machining fixtures and machining processes are being tried out and any discrepancies found are being corrected so that they reliably produce to "flight quality" tolerances. A detailed dimensional study of a group of five liner caps before and after annealing indicates that some minor dimensional changes have taken place. These changes are not considered to be significant. Metallographic analyses were performed on representative samples of all hydroform blank materials to assure the desired metallurgical quality. Subsequent detailed metallographic analysis was made of the structure of each formed component in both the as-formed and annealed conditions to determine grain size, micro-hardness, uniformity of micro-structure, and freedom from defects. In general, the structures of the hydroformed components were found to be superior to those of comparable components made by deep drawing in terms of control of a fine uniform grain size. (auth)

26426 (NUMEC-4189-4) RADIOISOTOPE POWERED CARDIAC PACEMAKER PROGRAM. Phase II. Quarterly Progress Report, November 1, 1970–January 31, 1971. (Nuclear Materials and Equipment Corp., Apollo, Pa. Energy Conversion Div.). Contract AT(30-1)-4189. 36p. Dep. NTIS.

Work performed from Nov. 1970 to Feb. 1971 on the development of a radioisotope-powered cardiac pacemaker is described. The subjects discussed include: program management; status of operational tests for reliability and quality assurance; preparations for leak testing of pilot production pacemakers; design, fabrication, and production status of pacemaker components; and data from electric shock, mechanical, vibration, and life testing of prototypes. (L.C.L.)

26427 (ORNL-IIC-30(Pt.4)) SELECTED ABSTRACTS OF WORLD LITERATURE ON PRODUCTION AND INDUSTRIAL USES OF RADIOISOTOPES (FROM NSA OCTOBER–DECEMBER 1970). Gerrard, Martha; Baker, P. S. (Oak Ridge National Lab., Tenn.). Apr 1971. Contract W-7405-eng-26. 37p. Dep. NTIS.

Approximately 320 abstracts of domestic and foreign publications on production and use of radioisotopes and radiation, selected from the October–December 1970 issues of Nuclear Science Abstracts, are presented. (auth)

26428 (SC-DR-710095) FOLLOW-ON TEST OF PROJECT FIRESCAN AS AN RTG HEAT SOURCE SEARCH AND DETECTION SYSTEM. Entrekin, J. L. (Sandia Labs., Albuquerque, N. Mex.). Feb 1971. 24p. Dep. NTIS.

The Firescan system was retested as an airborne detection system for use in the search, detection, and recovery of earth-impacted radioisotope heat sources. Test data and photographic results are presented. (auth)

26429 (SC-RR-71-21) WORLDWIDE CORRELATION OF SOIL AND POPULATION. Keller, L. L. Jr. (Sandia Labs., Albuquerque, N. Mex.). Jan 1971. 65p. Dep. NTIS.

The development of a data base containing the worldwide correlation of soil and population is discussed. A set of computer programs (SHAZ, POPDEN, and INVARA) designed for use with the data base is described. These programs are designed to aid in the investigation of the hazard to people from earth-impacted radioisotope capsules. (auth)

26430 EXPERIMENTAL MOCKUP SYSTEM (EMS) FOR SNAP-23A (2 Nov 1967) (Engineering Materials). (Westinghouse Electric Corp., Pittsburgh, Pa. Astronuclear Lab.). (CAPE-2063).
82 drawings.

The Experimental Mockup System (EMS) is a 60-W(e) terrestrial electrically-powered system, which simulates SNAP-23A. The EMS exhibits high reliability and provides a unit with size, weight, and power costs significantly less than previously built SNAP systems. The EMS is 24 in. OD and 27.4 in. high. In this system Ta is used as the barrier material between an Inconel heater assembly and a U–8Mo shield. The upper part of the heat source jacket is fabricated of Type 304 stainless steel with the remainder of the jacket formed of Inconel 718 which provides for strength and accommodates shield expansion. A mica sleeve is used between a stainless steel converter hot frame and a Cu heat source stud. An Al alloy radiator rejects 925 W(e) of heat to ambient air. Silicone grease promotes heat transfer between the stainless steel outer case and the radiator. Min-K 2000 provides system insulation. The electrical system consists of four preregulators and four power transformers. All circuitry is in encapsulated modules mounted on the radiator with BeO washers providing a thermally conductive path to the radiator for heat dissipation from the power transistors. For the Fueled Prototype Mockup System (FPMS) see CAPE-2064. (For details see TID-4100 Suppl. 63) (F.S.)

26431 FUELED PROTOTYPE MOCKUP SYSTEM (FPMS) SNAP 23A (17 Jun 1970) (Engineering Materials). (Westinghouse Electric Corp., Pittsburgh, Pa. Astronuclear Lab.). (CAPE-2064).
96 drawings.

A number of minor changes in the EMS (see CAPE-2063) are incorporated in the Fueled Prototype Mockup System (FPMS). The system is 30.9 in. high (3.5 in. higher than the EMS) and 24 in. in dia. Insulation thickness is increased 2 in. on top and 1.5 in. on the bottom with Min-K-2002 substituted for the Min-K-2000 used in the EMS. The outer radius of the axial-radiator fins has been lengthened ~2 in. The overall length of the fuel capsule has been increased to accommodate the fuel load, which also necessitates an increased shield length. The size of the hermetic seal on the convoluted base is increased to reduce heat loss. Inconel 625 is used in the base assembly, rain shield, converter cold frame, and the outer cover. The stud jacket and converter hot frame are fabricated of Type 304 stainless steel. (For details see TID-4100 Suppl. 63) (F.S.)

26432 ^{90}Sr HEAT SOURCES. Shor, Roberta; Lafferty, R. H. Jr.; Baker, P. S. Isotop. Radiat. Technol.; 8: 260-86(1971).

Current methods for the purification of fission product ^{90}Sr and the production of ^{90}Sr fuel forms are described. The SNAP-7A fuel is examined after 5½ years of operation. Excerpts were made from a full-length report on ^{90}Sr heat source production, source testing, and source properties. (auth)

26433 ORNL ISOTOPE KILOWATT PROGRAM. Fraas, A. P. (Oak Ridge National Lab., Tenn.). Isotop. Radiat. Technol.; 8: 341-5(1971).

Progress is reported on the Oak Ridge National Laboratory development of energy conversion systems which use radioisotope heat sources for the production of 1 to 10 kW(e) of electric power for terrestrial and undersea applications. An organic Rankine-cycle system using Dowtherm as the working fluid and a steam Rankine-cycle system are described. (L.C.L.)

26434 DEVELOPMENTS ABROAD ON RADIOISOTOPE-POWERED CARDIAC PACEMAKERS. Gerrard, Martha. Isotop. Radiat. Technol.; 8: 360-2(1971).

Cardiac pacemaker developments in Australia, France, Switzerland, and United Kingdom are briefly discussed. The design and operation of a ^{238}Pu-fueled pacemaker, implanted in a French woman on April 27, 1970, and a similar British pacemaker implanted in humans during July 1970 are described. Australian plans for developing a ^{147}Pm source pacemaker and Swiss plans for human implantations are mentioned. (L.C.L.)

26435 FLOW MEASUREMENTS WITH RADIOISOTOPES. Lafferty, Robert H. Jr. Isotop. Radiat. Technol.; 8: 287-309 (1971).

Methods of measuring flow with radioisotopes are reviewed. Various nonradioactive flowmeters are reviewed in an introductory section to put the methods using isotopes in the proper perspective. The advantages, disadvantages, and relative costs of various methods are compared. Radioisotopes may be used to measure flows of liquids or gases in a variety of ways: as tracers; to ionize a gas and then measure the flow rate of the ions; or with various mechanical flowmeters to indicate the movement of the flowing material. The precision and accuracy of flow measurements using radioisotope tracers are also discussed. (auth)

26436 I SIMPOSIO BRASILEIRO DE RADIOISOTOPOS, RIO DE JANEIRO, 23 A 17 DE JUNHO DE 1970. (First Brazilian Symposium on Radioisotopes, Rio de Janeiro, June 23–27, 1970). Rio de Janeiro; Comissao Nacional de Energia Nuclear (1970). 64p. (CONF-700641–(Absts.)).

Abstracts of the 65 papers presented at the First Brazilian Symposium on Radioisotopes are compiled. The topics discussed included the use of radioisotopes in chemistry and radiation protection, medicine, agronomy, biology, and in industry. (J.S.R.)

Materials Testing

Refer also to abstract 27242.

26437 (BNWL-SA-2865) NEUTRON RADIOGRAPHY WITH ^{252}Cf IN FORENSIC SCIENCE. Cason, John L. (Battelle-Northwest, Richland, Wash. Pacific Northwest Lab.). Oct 1969. Contract AT(45-1)-1830. 17p. Dep. NTIS.

Battelle–Northwest has established the use of ^{252}Cf for neutron

radiography and developed a portable neutron camera. This camera could be used for forensic science because it is portable, lightweight, efficient and easy to operate. A more compact camera could be developed for specific uses. Our experimental results demonstrate the usefulness of neutron radiography as a nuclear nondestructive method in forensic science. Tests include analyses of booby-trapped ammunition, bomb in a matchbook, powder residues in a gun barrel and narcotics hidden in a ball point pen. (auth)

26438 (DP-Report-432) QUALITY CONTROL, INSPECTION, AND TESTING OF THE SERIES I METALLURGICAL FUELS FOR THE FIRST CHARGE OF THE DRAGON REACTOR. Project DRAGON. Conde, J. F. G.; Holliday, J.; Good, P. D.; Keegan, J.; Edwards, M. I.; Frampton, P. D. (Atomic Energy Establishment, Winfrith (England)). Dec 1966. 81p. Dep. NTIS (U. S. Sales Only).

The results obtained in the pre-irradiation assessment of the fuel particles and cartridges for the four metallurgical fuel elements for the first charge of the Dragon Reactor are summarized to provide a source of reference for use in post-irradiation evaluation. (auth)

26439 (UJV-2545-R,T) NEUTRON RADIOGRAPHY AND ITS APPLICATION. Hrdlicka, Z. (Ceskoslovenska Akademie Ved, Rez. Ustav Jaderneho Vyzkumu). Jan 1971. 46p. (In Czech). Dep. NTIS (U. S. Sales Only).

Information from literature on the following topics was compiled for use in the development of neutron radiography in Czechoslovakia: concise development of the method and the main laboratories using it; special features of neutron radiography including the character of neutron interaction with matter, random distribution of neutron absorption cross-sections according to the atomic number, energy dependence of total and partial cross-sections, and insensitivity of current photographic materials to neutrons; accelerators, radioisotopes and nuclear reactors as neutron sources, their possibilities, availability and costs. Essential geometrical properties of the source and the methods of achieving them; photographic and nonphotographic neutron imaging detection methods, properties of converting materials for direct and transfer exposure methods, track-etch method, thermoluminescence method, and the possibilities of neutron radioscopy; availability and special features of fast, epithermal, thermal and cold neutron radiography; and review of application areas for neutron radiography. (auth)

26440 NONDESTRUCTIVE TESTING. McGonnagle, Warren J. (Chicago Wesley Memorial Hospital). pp 371-430 of Fracture. An Advanced Treatise. Vol. III. /Liebowitz, H. (ed.). New York; Academic Press Inc. (1971).

The use of physical phenomena to test materials, without damage to the material, has developed into nondestructive testing technology. In this technology, every form of energy and every property of materials has been utilized. The basic principles and applications of methods such as visual, liquid penetrant, thermal, penetrating radiation (x-ray and gamma-ray), ultrasonic, magnetic, electrical, and eddy current (electromagnetic) are discussed. (auth)

Radioactive Material Handling

Refer also to abstracts 26376, 26429, and 26550.

26441 (AECL-3802) THERMAL TEST CALCULATIONS FOR PACKAGES OF STEEL CONSTRUCTION. Taylor, W. R. (Atomic Energy of Canada Ltd., Chalk River (Ontario). Chalk River Nuclear Labs.). Jan 1971. 10p. (CONF-710210-1; SM-147/5). Dep. NTIS (U. S. Sales Only). AECL $0.50.

From Seminar on test requirements for packaging for the transport of radioactive materials; Vienna, Austria (8 Feb 1971).

Two Canadian packagings have been fabricated from steel for irradiated fuel shipments. A computer program has been developed to calculate package temperatures during and after Type B thermal tests. From these results, suitable packaging closures have been designed and the maximum fuel sheath temperatures have been estimated. One packaging is a solid casting with external cooling fins; the other has a wall cross-section which consists of seven 2 inch and two $\frac{3}{4}$ inch steel plates. A finite element calculation method is used. A digital computer calculates the transient temperatures for a three dimensional mathematical model. Equations which define heat transfer between the environment and the finite elements calculate element temperatures for each 0.005 hour time increment. Specific heat and thermal conductivity are defined as functions of temperatures. Different cooling modes may be defined and introduced in the calculations. The calculation method and the effects of different variables on the package temperatures are briefly described. (auth)

26442 (AECL-3803) DESIGN AND DEVELOPMENT OF PACKAGINGS FOR LOW ENRICHED FUEL BUNDLES. Taylor, W. R. (Atomic Energy of Canada Ltd., Chalk River (Ontario)). Jan 1971. 9p. (CONF-710210-2; SM-147/4). Dep. NTIS (U. S. Sales Only). AECL $0.50.

From Seminar on test requirements for packaging for the transport of radioactive materials; Vienna, Austria (8 Feb 1971).

A package has been designed to transport single unirradiated Candu-type fuel bundles between fuel manufacturers and reactor sites. The package consists of an extended 45 Imperial gallon drum, an 8 inch pipe and vermiculite insulation. A single fuel bundle is packed in a styrofoam mold and fitted into the 8 inch pipe. A shipment consists of forty packages, each with a 2.4 weight percent ^{235}U in U fuel bundle. A prototype packaging was loaded with a simulated fuel bundle and subjected to Type B destructive tests. A second packaging was subjected to Type A tests. The packaging did not rupture, the fuel bundle was not damaged, and package separation distances were maintained. An analysis showed that the packages would be nuclearly safe for normal and hypothetical accident conditions of transport. Future Canadian needs may require the transport of greater quantities of low enriched fuel bundles. Therefore, a second generation packaging is being designed. This packaging consists of a 45 Imperial gallon drum, rigid polyurethane foam insulation and a four fuel bundle compartment. The results of the test program and the proposed new packaging are described. (auth)

26443 (AED-C-13-7) BIBLIOGRAPHIES IN NUCLEAR SCIENCE AND TECHNOLOGY. SECTION 13. DECONTAMINATION. Philipp, Hermann; Wichmann, Erich (comps.) (Zentralstelle fuer Atomkernenergie-Dokumentation, Frankfurt am Main (West Germany)). Aug 1970. 46p. (In several languages). Dep. NTIS (U. S. Sales Only).

A bibliography on decontamination with emphasis on the most efficient and most current methods for removal of radionuclides is presented. Six separate sections deal with the following aspects: buildings, large areas, and installations; equipment, materials including clothing, food, and similar items; persons and animals; liquids; gases and aerosols; and miscellaneous items concerning decontamination equipment, installation, methods, and cost problems. (H.B.G.)

26444 (BNL-15601) DIFFICULTIES AND APPROACHES IN THE DEVELOPMENT OF INVENTORY CONTROL FOR NUCLEAR MATERIAL SAFEGUARDS. Suda, S. C. (Brookhaven National Lab., Upton, N. Y.). 20 Oct 1970. 14p. (CONF-701042-1). Dep. NTIS.

From 38. national meeting of the Operations Research Society of America; Detroit, Mich. (27 Oct 1970).

The objective of inventory control in nuclear material safeguards is to achieve a high degree of assurance that the amount and composition of special nuclear material declared on inventory by a facility does in fact correspond to the material in its possession. Methods for and the problems encountered in achieving this objective are discussed. (L.C.L.)

26445 (BRH/DMRE-71-1) SUMMARY OF FEDERAL REGULATIONS FOR PACKAGING AND TRANSPORTATION OF RADIOACTIVE MATERIALS. Conlon, Frank B.; Pettigrew, George L. (Bureau of Radiological Health, Rockville, Md. Div. of Medical Radiation Exposure). Feb 1971. 37p. GPO $0.50.

A summary of various governmental regulations in the US concerning the packaging and transportation of radioactive materials is presented, and is intended to serve as a guide to agencies or individuals interested in the requirements governing interstate shipment of radioactive materials. Information is included on: classification of radioactive materials; general and specific requirements for radioactive materials packages; quantity limitations for radioactive materials packages; labeling of radioactive materials packages; shipper's responsibilities; carrier's responsibilities; loading and storage of radioactive materials; and marking of vehicles containing radioactive materials. (L.C.L.)

26446 (DPSPU-71-124-1) SAFETY SUMMARY REPORT: LI D-1 PACKAGE (PACKAGING OF RADIOACTIVE AND FISSILE MATERIALS). Final Report. Rogers, R. F. (comp.) (Du Pont de Nemours (E. I.) and Co., Aiken, S. C. Savannah River Plant). Feb 1971. Contract AT(07-2)-1. 66p. Dep. NTIS.

Plutonium metal shipped in the LLD-1 package complies with AEC Manual Chapter 0529 (AECM 0529), "Safety Standards for the Packaging of Radioactive and Fissile Materials". The package withstands normal and hypothetical accident conditions with-

out release of plutonium and any array of packages remains subcritical. (auth)

26447 (HW-76299) RAIL ACCIDENT STATISTICS PERTINENT TO THE SHIPMENT OF RADIOACTIVE MATERIALS. Stewart, K. B. (General Electric Co., Richland, Wash. Hanford Atomic Products Operation). 21 Jan 1963. Contract AT(45-1)-1350. 72p. Dep. NTIS.

Statistical data on railroad accidents in the U. S. from 1958 to 1961 in which the damage costs exceeded $2000 are presented, and include information on accident date and location, kind of train, train speed, cause, and damage costs. This information was compiled for use in designing safe packaging for shipping radioactive materials and in determining routing and travel procedures which would minimize the probability of an accident involving these materials. (L.C.L.)

26448 (KFK-1263) TRANSPORT OF HIGH LEVEL VITRIFIED FISSION PRODUCTS. Bechthold, W. (Kernforschungszentrum, Karlsruhe (West Germany)). Sep 1970. 69p. (In German). Dep. NTIS (U. S. Sales Only).

The preconditions for the transportation from Karlsruhe to the abandoned ASSE salt mine (distance about 500 km) of welded cylindrical steel tubes containing heat-generating vitrified radioactive wastes from reprocessing plants were investigated. The investigations were based on the IAEA —"Regulations for the Safe Transport of Radioactive Materials." The necessary shielding of the shipping cask was determined as a function of various parameters and the requirements for removal of the fission product heat generated within the glass were calculated. The safety of the shipping cask in accidents during transport was investigated and anticipated transportation costs were calculated to determine the optimum transport requirements. (auth)

26449 (MLM-1790) METHOD AND DEVICE USED FOR THE SAFE HANDLING AND STORING OF FRAGILE X-RAY DIFFRACTION SPECIMENS. Eckstein, R. R.; Hudgens, C. R. (Mound Lab., Miamisburg, Ohio). 2 Apr 1971. Contract AT(33-1)-Gen-53. 9p. Dep. NTIS.

The design and use of equipment for the safe handling, transporting, and storing of fragile x-ray diffraction specimens which could contain radioactive and/or hygroscopic materials are described. (auth)

26450 (ORNL-TM-3298) ANALYSIS OF THE NEW BRUNSWICK LABORATORY SAMPLE CASK. Evans, J. H. (Oak Ridge National Lab., Tenn.). Mar 1971. Contract W-7405-eng-26. 58p. Dep. NTIS.

The New Brunswick Laboratory Sample Cask, which will be used to transport fuel element dissolver samples, was analytically evaluated to determine whether it complies with the applicable regulations governing packages in which radioactive materials are shipped. Computational procedures were used to determine the structural integrity and thermal behavior of the cask with respect to the general standards for packaging, structural standards, standards for normal conditions of transport, and the standards for the hypothetical accident conditions. The results of this evaluation show that the cask complies with all the applicable regulations. (auth)

26451 (SGAE-RT-33/1970) FUTURE MANAGEMENT OF RADIOACTIVE WASTES IN AUSTRIA. Schlosser, K.; Oszuszky, F. (Oesterreichische Studiengesellschaft fuer Atomenergie G.m.b.H., Seibersdorf. Institut fuer Reaktortechnik). Jul 1970. 16p. (CONF-700905-13). Dep. NTIS (U. S. Sales Only).

From Symposium on developments in the management of low and intermediate level radioactive wastes; Aix-en-Provence, France (7 Sep 1970).

The construction of a 600 MW(e) unit nuclear power station in Austria necessitates consideration of the management of future radioactive wastes originating from this source. The start of active operation of this plant, which will be probably situated on the Danube river, is envisaged in the middle of the seventies. In this respect the Austrian reactor operators will only be concerned with a small part of the activity to be treated so far as waste disposal is concerned. 99.9% of the fission products produced in nuclear reactors are handled in spent fuel reprocessing plants outside the country. In this connection the present and future national waste management policy in this country will have to be reviewed in particular with the forseen release of liquid wastes to the Danube, which is an international water system. Methods for ensuring safe radioactive waste disposal to such a river system without endangering its biological equilibrium and the cost of such waste management are discussed. The legal and economic aspects of waste management, the most suitable processes for waste treatment and storage, the cooperation required between waste producers and the national authorities and organizations responsible for a centralized service for waste collection, waste treatment, and ultimate storage are discussed. (auth)

26452 SHIPPING-CASK EVALUATION. Seagren, R. D. (Oak Ridge National Lab., Tenn.). Isotop. Radiat. Technol.; 8: 350-9 (1971). (CONF-700646-1).

From Radioisotope production technology development meeting; Oak Ridge, Tenn. (2 Jun 1970).

Radioisotope shipping-cask regulations and sources of information needed by the shipper are reviewed. (auth)

26453 SALT MINE REPOSITORY FOR RADIOACTIVE WASTES. Blomeke, J. O.; McClain, W. C. (Oak Ridge National Lab., Tenn.). Nucl. News; 14: No. 4, 35-8(Apr 1971).

Recognizing that a truly permanent solution is required to the problem of disposing of high-level liquid wastes, principally from the reprocessing of spent reactor fuels, the USAEC has promoted the development of processes for converting the liquid wastes to stable, solid forms and verification of the suitability of natural salt formations as a final repository for these materials. Background data on the use of salt formations for radioactive waste repositories, the factors which led to the tentative selection of a site near Lyons, Kansas for a demonstrational salt mine repository, and the work schedule which should result in a completed repository by January 1976 are presented. (L.C.L.)

26454 ARGUMENT FOR A RECOVERABLE HIGH-LEVEL WASTE CONTAINER. Meyer, Walter (Kansas State Univ., Manhattan). Nucl. News; 14: No. 4, 38-40(Apr 1971).

The chemical, geological, and hydrological factors which require that non-corrodible, recoverable shielded containers be developed to insure the long term safety of using salt mines for the disposal of high-level solidified radioactive wastes are discussed. (L.C.L.)

26455 MANUAL OF RADIOACTIVITY PROCEDURES. National Bureau of Standards Handbook 80. Washington, D. C.; National Bureau of Standards (1961). 166p. (NCRP-28). Available from Superintendent of Documents, GPO, Washington, D. C.

Radioactivity standardization procedures including the physics of some radiation detectors, principal methods for absolute standardization and relative standardization, and techniques of preparing standard solutions and samples for counting are discussed. The measurement of radioactivity for clinical and biological purposes is considered including instrumentation and preparation of reference standards, calibration and measurement prior to the use of the material, measurement of the radionuclide in the intact animal (human or otherwise), and measurement in aliquots or derived samples. Disposal limits for radioactive materials are summarized. An extensive list of references is included. (W.H.K.)

Vacuum Engineering

Refer also to abstracts 27440 and 28131.

INSTRUMENTATION

Radiation Detection Instruments

Refer also to abstracts 26578 and 28379.

General Detectors and Monitors

Refer also to abstracts 26191, 26455, 26529, 26535, and 27636.

26456 (ANU-P-516) MANUFACTURING PROCESS FOR SILICON SURFACE BARRIER RADIATION DETECTORS. England, J. B. A. (Australian National Univ., Canberra. Research School of Physical Sciences). Oct 1970. 43p. Dep. NTIS (U. S. Sales Only).

A detailed account is set out for the manufacture of silicon surface-barrier detectors on a small production line basis. Steps involved are (1) cleaning of silicon slices (categorized into new slices thicker than 0.5 mm, new slices thinner than 0.5 mm, and old slices for re-use); (2) preparing mounts by attaching gold electrical contacts; (3) etching (preparatory precautions, mixing of hydrofluoric/nitric acid etch, manual etching, quenching, dichromating and washing—detailed for both thick and thin slices); (4) mounting, and (5) evaporation of metal contacts. An alternative etching of slices using an ultrasonic generator is outlined, as is cold etching. Techniques for repairing counters are considered and comments on possible developments are made. (Australia)

26457 (CNEA-287) FABRICATION OF SEMICONDUCTOR DETECTORS OF Si(Li) FOR NUCLEAR REACTIONS. Erramuspe, H. J. (Comision Nacional de Energia Atomica, Buenos Aires (Argentina)). 1970. 31p. (In Spanish). Dep. NTIS (U. S. Sales Only).

A method is presented for the manufacture of Si(Li) semiconductor detectors using new techniques for control of depth of the total compensation zone and for automatic control for the drift process. Some characteristics of the detectors are given. (54 references) (tr-auth)

26458 DESIGN AND PERFORMANCE OF DOUBLE EMITTER TYPE SELF-POWERED NEUTRON DETECTORS. Seki-guchi, Akira; Koizumi, Yoshinobu (Tokyo Univ.). Tokyo Daigaku Kogakubu Fuzoku Sogo Shikenjo Nenpo; No. 29, 245-51(Sep 1970). (In Japanese).

Gamma-ray compensated beta self-powered detectors having two emitters were developed. The gamma-ray background of the output of neutron activated emitter was minimized by subtracting the current of the other emitter which is sensitive to gamma-rays only. The degree of compensation was investigated by the irradiation tests in the reactor core and using ^{60}Co gamma facility. The detectors were capable of functioning in the broader reactor power range by one decade or more than usual single emitter type. (auth) (Japan)

26459 PORTABLE ELECTRONIC UNIT ASSOCIATED WITH AN IONIZATION CHAMBER FILLED WITH A DIELECTRIC LIQUID. Bouet, J.; Prigent, R. (CEN, Fontenay-aux-Roses, France). Radioprotection; 4: 327-9(1969). (In French).

The design of a portable apparatus for measuring currents produced by ionization detectors is described. Photographs of the unit and a block diagram of the associated electronics are shown. Currents between 10^{-12} and 10^{-7} A can be determined. (J.F.P.)

26460 NEUTRON FLUX PLOTTING DEVICE. Porges, Karl G. (to United States Atomic Energy Commission). U. S. Patent 3,546,455. 8 Dec 1970. Filed 28 Jan 1969.

A spark chamber, placed in a flux of neutrons the spatial distribution of which is to be plotted, includes a pair of electrodes, one of which is formed of a resistive wire. A high-voltage supply is connected across the pair of electrodes to provide a potential difference therebetween. Disposed in the spark chamber are a fission foil for emitting fission fragments in response to receipt of neutrons, and a fission-fragment collimator placed between the fission foil and the pair of electrodes and comprising a shield with holes cut therethrough for only passing fission fragments from the fission foil having a predetermined trajectory. One end of the resistive-wire electrode is connected to a reference potential. The other end of the resistive-wire electrode is connected to the same reference potential via a pulse-coupling circuit including an output terminal. Pulses produced on the resistive-wire electrode in response to spark discharges initiated by fission fragments passing the collimator each have an amplitude proportional to the position of the spark along the resistive-wire electrode, and these pulses are coupled to a multichannel pulse-height analyzer via the output terminal and the pulse-coupling circuit. (auth)

26461 TRENDS OF DEVELOPMENT OF MODERN SEMICONDUCTOR IONIZING RADIATION DETECTORS. Bulatov, B. P. At. Energ. (USSR); 30: 285-95(Mar 1971). (In Russian).

An analysis of the up-to-date status in the field of semiconductor ionizing radiation detectors and some future trends of their development are presented. The analysis is done on the basis of numerous Soviet and foreign publications. Technical characteristics and practical use areas are considered. Factors determining resolution, efficiency, reliability and radiation resistance are analysed. A number of methods of continuous Compton distribution suppression as well as operation in strong magnetic and radiation fields are described. Technical characteristics of semiconductor materials which can be used in manufacturing semiconductor detectors are discussed. Presented are the results of recent studies in the field of development of new types of detectors which are stable and operable at room temperature including detectors for recording radiation with $E < 60$ keV, and as automatic spectrum treatment methods. (168 references) (auth)

26462 DEPENDENCE OF THE LIGHT OUTPUT OF LIQUID SCINTILLATION SYSTEMS ON SPECTRAL PROPERTIES OF COMPONENTS. Fodor-Csanyi, P.; Inzelt, Gy (Eoetvoes Lorand Univ., Budapest). Int. J. Appl. Radiat. Isotop.; 22: 159-64(Mar 1971).

On the basis of literary data it is concluded that the spectral characteristics (absorption and emission bands) of the components of liquid scintillation systems (solvents, scintillators, shifters, diluters, quenchers, additive materials etc.) definitely influence the light output of the systems. In the case of good scintillator + solvent pairs, the absorption bands of the solvent and scintillator overlap or are near to each other. The absorption bands of shifters are in the emission bands of the scintillators. The absorption bands of diluters are usually in a range of wave-length shorter than that of the absorption bands of the solvents. The absorption bands of additive materials increasing the light output overlap those of diluters, solvents and scintillators. The absorption bands of quenchers are usually in the absorption bands of solvents or scintillators. Therefore, a greater importance must be attached to radiation energy transfer. (auth) (UK)

26463 INTERFERENCE OF TISSUE SOLUBILIZERS WITH LIQUID SCINTILLATION COUNTING FLUORS. Dunn, Adrian (Univ. of North Carolina, Chapel Hill). Int. J. Appl. Radiat. Isotop.; 22: 212(Mar 1971).

It is stated that certain commercial tissue solvents interact with certain fluors used in liquid scintillation counting, and produce color-quenching so severe that their use in combination is not possible. Soluene 100 cannot be used with either butyl-PBD or Isopropyl-PBD scintillators, and the use of NCS Solubilizer with either of these two scintillators cannot be recommended. (UK)

26464 $4\pi\beta-\gamma$ COINCIDENCE ABSOLUTE MEASUREMENT OF NUCLIDES EMITTING SOFT CONVERSION ELECTRONS IN APPRECIABLE PROPORTIONS. Baba, H.; Umezawa, H.; Ishikawa, I.; Baba, S. (Japan Atomic Energy Research Inst., Tokai). Int. J. Appl. Radiat. Isotop.; 22: 141-8(Mar 1971).

A correction method was derived for the disintegration-rate measurement of nuclides emitting soft conversion electrons along the lines of the method developed in a previous paper (Baba et al. Int. J. Appl. Rad Isotop 21: 607(1970)). The resulting correction formulae were applied to the $4\pi\beta-\gamma$ coincidence absolute measurement of ^{161}Tb and of the $^{140}Ba-^{140}La$ mixed activity. The resulting disintegration rate was found to be a reasonable value with an uncertainty of, at most, 1% in either case. The proposed correction formulae were concluded to be particularly useful for the absolute determination of nuclides emitting conversion electrons of low energies, $\lesssim$30 keV. (auth) (UK)

26465 USE OF GAMMA CASCADE ISOTOPES IN THREE DIMENSIONAL FUNCTION MEASUREMENTS IN VIVO AND LAYER SCINTIGRAPHY. Schmitz-Feuerhake, Inge (Medizinische Hochschule, Hanover). Stud. Biophys.; 23: 37-41(1970). (In German).

It was demonstrated experimentally that 3-dimensional scintigrams are possible by applying γ-cascade isotopes. If isotopes

are used that, during decay, simultaneously emit two or more γ quanta, coincidence counting permits localization of the point of origin. The appropriate equipment is described. To obtain 3-dimensional measurements, several detectors must be hooked up for coincidence counting which, necessarily reduces counting rate. The principle is demonstrated with ^{75}Se by connecting a conventional scanner with two additional coincidence plastic scintillation detectors. By means of focusing slit collimators of sheet lead, layers of approximately 2-cm thickness could be presented most clearly. (H.B.G.)

26466 GAMMA COMPENSATED FISSION THERMOCOUPLE. Morrison, Roderick Gordon (to United States Atomic Energy Commission). U. S. Patent 3,564,246. 16 Feb 1971. Filed 5 Aug 1965.

A neutron flux measuring apparatus is described comprising the combination of a first and a second thermocouple connected in series in polarity opposition and each comprising an identical pair of dissimilar leads and a middle metallic spherical body having a diameter equal substantially to the mean free path of a thermal neutron in the uranium isotope, the neutron flux of which is being measured. One of the middle metallic bodies is of fissionable material and the other middle metallic body is of nonfissionable material but being equally gamma responsive. (auth)

26467 AMERICAN STANDARD: INTERRELATIONSHIP OF QUARTZ-FIBER ELECTROMETER TYPE DOSIMETERS AND COMPANION DOSIMETER CHARGERS. ANSI N 3.2 1965. New York; American Standards Association, Inc. (1965). 2p. Available from American National Standards Inst., New York.

A standard for specifying the interrelating mechanical and electrical properties so that quartz-fiber dosimeters may be used with any charger is presented. (W.H.K.)

26468 AMERICAN STANDARD: BASES FOR GM COUNTER TUBES. ANSI N 3.1 1965. New York; American Standards Association, Inc. (1965). 1p. Available from American National Standards Inst., New York.

Standard bases for GM counter tubes are designated as the 3-pin "Pee Wee" (JETEC-A3-1) and the 4-pin "Medium" base (JETEC-A4-9). Pin connections are dictated. (W.H.K.)

26469 DESIGN OF FREE-AIR IONIZATION CHAMBERS. Wyckoff, H. O.; Attix, F. H. National Bureau of Standards Handbook 64. Washington, D. C.; National Bureau of Standards (1957). 19p. Available from Superintendent of Documents, GPO, Washington, D. C.

General design characteristics are given for standard free-air type ionization chambers for x-rays from 50 to 500 kilovolts. Included are the plate-separation requirements, elimination of electric-field distortion, data on air-attenuation and scattering effects, current measurement techniques, and other relevant features. (auth)

26470 PHENOMENES DE CONDUCTION DANS LES LIQUIDES ISOLANTS. (Conduction Processes in Dielectric Liquids). International Conference Held in Grenoble, France, September 17–19, 1968. Paris; Centre National de la Recherche Scientifique (1970). 541p. (In French and English). (CONF-680983).

The following topics were treated: radiation induced conductivity in insulating liquids; breakdown and prebreakdown phenomena in insulating liquids; nature and mobility of charge carriers in insulating liquids; conduction mechanisms; applications of polar liquids; field measurement techniques. Separate abstracts were written for five of the thirty-four papers presented. (France)

For abstracts of individual papers, see: 26293, 26471, 26472, 26530, and 26531.

26471 IONIZATION CURRENTS INDUCED BY CORPUSCULAR RADIATIONS IN LIQUID DIELECTRICS. Chybicki, M. (Technical Univ., Danzig). pp 45-9 of Phenomenes de Conduction dans les Liquides Isolants. Paris; Centre National de la Recherche Scientifique (1970).

From International Conference on Conduction Processes in Dielectric Liquids, Grenoble, France. See CONF-680983.

The results of measurements of the intensity of ionization currents induced by α particles from ^{239}Pu and β particles from ^{204}Tl and ^{3}H in hexane and heptane as a function of the activities of these sources, the electric field, the polarity of the applied voltage, the distances between the electrodes of the ionization chamber and the temperature of the tested liquids were presented. The currents obtained were represented by the well known formula $I = I_0 + cE$, where E is the electric field strength and I_0 and c are both proportional to the radiation intensity. Only a small proportion of the ions produced by alpha particles in the liquid is collected by the electrodes. The value of the current I_0 includes only 0.2% of the total number of the ions produced, most of them being lost by recombination processes. These results are in agreement with a new model of charge collection in dielectric liquids. (France)

26472 APPLICABILITY OF THE THEORY OF INITIAL RECOMBINATION TO LIQUID FILLED IONIZATION CHAMBERS. Januszajtis, Andrzej (Technical Univ., Danzig). pp 51-6 of Phenomenes de Conduction dans les Liquides Isolants. Paris; Centre National de la Recherche Scientifique (1970).

From International Conference on Conduction Processes in Dielectric Liquids, Grenoble, France. See CONF-680983.

The theories proposed by Jaffé, Léa and Kramers to explain the experimental results obtained on the ionization current induced in liquids by ionizing radiations were compared with experiments. There is no correlation between the theory of Jaffé and experimental results. The two other theories are in agreement with experimental results as they contain adjustable parameters; but when these parameters are deduced in this way, their physical meaning is lost. The Adamczewski theory seems more promising. (France)

26473 PDP-8 SERIES STUDIES OF DYNAMIC RELOCATIONS OF RADIOACTIVE ISOTOPES. Kilthau, Gustave F. (Computer Corp. of America, Houston, Tex.). pp 69-73 of DECUS Proceedings. Maynard, Mass.; Digital Equipment Computer Users' Society (1970).

From Fall joint computer conference, Houston, Tex. (19 Nov 1970). See CONF-701101.

Computerization of the nuclear medical gamma imaging camera has entered into the commercial phase wherein turn-key systems, complete with standardized hardware and software, are now being supplied to the nuclear medical laboratory by Computer Corporation of America, Houston, Texas. The system design makes use of the PDP 8 series of digital computers. The combination of carefully selected hardware and software within these systems makes them productive in use with today's gamma cameras and flexible enough to provide for future uses and for future cameras. In nuclear medicine today there is an accelerating movement into the areas of study involving cellular physiology. Consequently, there is a need for tools with which to follow and to quantitate dynamic relocations of substances into and through various tissues and organs. The combination of the modern gamma camera and the CCA Scintillation Data System meets this set of needs. (auth)

26474 RECORDING AND USES OF α-PARTICLE TRACKS IN CELLULOSE NITRATE. Nicolae, M. Rev. Roum. Phys.; 15: 881-9(1970). (In French).

A systematic study on the possibility and conditions of using cellulose nitrate, obtained from commercial collodium, for α-track recording is presented. The optimal conditions of chemical etching, when the effectiveness of the α-particle recording reaches 100%, were established. The influence of the preliminary heating of the detector was also studied in detail. For purposes of quantitative determination the rate of energy loss and the range-energy curve in cellulose nitrate were established for α particles with energies between 3 and 10 MeV. When the efficiency of the α-particle track registration is 100%, the critical energy for α-particle recording in the cellulose nitrate of the type mentioned above was calculated as 4.1 MeV, which is in good agreement with other results for commercial sheets of cellulose nitrate. (auth)

26475 STANDARD METHOD FOR MEASURING THERMAL NEUTRON FLUX BY RADIOACTIVATION TECHNIQUES. ASTM E 262-70. Philadelphia; American Society for Testing and Materials (1970). 8p. Available from American Society for Testing and Materials, Philadelphia.

A general procedure for measuring an unknown thermal neutron flux by neutron activation techniques is defined. Three thermal-neutron activation procedures are detailed: cobalt method; standard foil technique using pure gold; and secondary standard foil techniques using pure indium, indium–aluminum alloy, and dysprosium–aluminum alloy. The techniques presented are limited to measurements at room temperature, but special problems in high-temperature environments are discussed. The useful neutron-flux ranges for each detector material are listed. (W.H.K.)

26476 STANDARD METHOD FOR MEASURING NEUTRON FLUX BY RADIOACTIVATION TECHNIQUES. ASTM E 261-70. Philadelphia; American Society for Testing and Materials (1970). 11p. Available from American Society for Testing and Materials, Philadelphia.

The basic theory, procedures, and calculations for neutron flux measurements by radioactivation techniques are presented. Reactor neutron spectra are divided into three energy ranges (thermal, resonance, and fast) which require different detectors and detec-

XUM

tion procedures that are discussed. Fission threshold detectors for fast neutrons are treated. Requirements for activation detector materials, irradiation procedures, and counting instruments and procedures are discussed. (W.H.K.)

26477 STANDARD METHOD FOR MEASURING FAST-NEUTRON FLUX BY RADIOACTIVATION OF IRON. ASTM E 263-70. Philadelphia; American Society for Testing and Materials (1970). 6p. Available from American Society for Testing and Materials, Philadelphia.

A standard method for measuring fast neutron fluxes using the threshold reaction $^{54}Fe(n,p)^{54}Mn$ is given. The reagents and materials are specified, and the irradiation, separation, and counting procedures are described. A NaI(Tl) scintillation gamma spectrometer is used. The necessary calculations are explained. (W.H.K.)

26478 OSO-G SATELLITE INSTRUMENTATION FOR MEASUREMENTS OF COSMIC X-RAYS IN THE ENERGY RANGE FROM 25 TO 190 keV. Brini, D.; Evangelisti, F.; Fuligni, F.; Vespignani, G. (Univ., Bologna). Nuovo Cim.; 2B: 193-207 (11 Apr 1971).

An experiment for the detection of solar and celestial X-rays in the energy range from about 20 keV to about 200 keV has been prepared for operation aboard the NASA satellite OSO-G. Details of design and assembly to meet flight specifications and scientific objectives are presented. The instrument is presently in orbital operation. (auth)

26479 STANDARD METHOD FOR MEASURING FAST-NEUTRON FLUX BY RADIOACTIVATION OF NICKEL. ASTM E 264-70. Philadelphia; American Society for Testing and Materials (1970). 5p. Available from American Society for Testing and Materials, Philadelphia.

A standard method for measuring fast neutron fluxes using the threshold reaction $^{58}Ni(n,p)^{58}Co$ is given. Material preparation and packaging and irradiation and counting procedures are described. A NaI(Tl) scintillation gamma spectrometer and a precision balance are used. Calculations are detailed. (W.H.K.)

26480 STANDARD METHOD FOR MEASURING FAST-NEUTRON FLUX BY RADIOACTIVATION OF SULFUR. ASTM E 265-70. Philadelphia; American Society for Testing and Materials (1970). 5p. Available from American Society for Testing and Materials, Philadelphia.

A standard method for measuring fast neutron fluxes using the threshold reaction $^{32}S(n,p)^{32}P$ is described. Sulfur can be used either the powder or pellet form. Aqueous separation techniques and pellet burning techniques are outlined. The counting technique is described, and the calculations are elaborated. (W.H.K.)

26481 STANDARD METHOD FOR MEASURING FAST-NEUTRON FLUX BY RADIOACTIVATION OF ALUMINUM. ASTM E 266-70. Philadelphia; American Society for Testing and Materials (1970). 5p. Available from American Society for Testing and Materials, Philadelphia.

A standard method for measuring fast neutron fluxes using the threshold reaction $^{27}Al(n,\alpha)^{24}Na$ is described. A thallium-activated sodium iodide scintillation gamma spectrometer and a precision balance are required in addition to high-purity aluminum foil or wire. The procedure and calculations are described. (W.H.K.)

26482 PULSE-TIME FLUCTUATION IN LARGE SCINTILLATION COUNTERS. Bagdasaryan, L. S.; Barsegyan, E. O.; Tashchyan, A. A. Izv. Akad. Nauk Arm. SSR, Ser. Fiz.; 5: 217-24(1970). (In Russian).

Time fluctuations in large fast scintillation counters are considered. Expressions for the trigger time of the Q-th photoelectron and its variance are obtained. An expression for the optimal size of a light guide is also presented. Time fluctuations for several types of counters are compared. (auth)

26483 SIGNIFICANCE OF SCATTERING IN CALIBRATING APPARATUS FOR THE MEASUREMENT OF FLUENCES AND NEUTRON DOSE EQUIVALENTS. Vialettes, H.; Cariou, J. M.; Duffar, M. (CEA, Saclay, France). Radioprotection; 5: 311-22(1970). (In French). (CONF-700505-24).

From 2nd Congress of the International Radiation Protection Association, Brighton, England.

The determination of correction factors for neutron scattering in calibrating fluxmeters and dosemeters was studied using (α,n) and other neutrons sources (Am–Li, E = 0.44 MeV, Am–F, E = 1.4 MeV, and Am–Be, E = 4.4 MeV) in experimental rooms with volumes ranging from 100 to 2000 m^3. It is shown that in some cases, the correcting factor can reach a 4 for fluence measurement and a factor of 2 for dose equivalent measurement. The percentage of scattering fluence may be considered constant with respect to neutron energy but varying as $V^{-\frac{1}{3}}$ (V = volume of the room). The dose equivalent does not vary significantly with the volume. The scattering percentage varies as $(d/R)^{2.17}$ (d = source detector distance, R = half the width of the room). The results were examined but it was not possible to find a simple relation between the fluence or the equivalent scattered dose or the percentage scattering and the source detector or source floor distances, or to find a relation between these two parameters. (auth) (France)

26484 SATELLITE-BORNE X-RAY SPECTROHELIOGRAPH. Herring, J. R. H. (University Coll., London); Glencross, W. M.; Parkinson, J. H.; Pounds, K. A. Proc. Roy. Soc. (London), Ser. A; 321: 493-502(9 Mar 1971).

A grazing incidence x-ray telescope for the study of the spatial and temporal variation of solar x radiation in the region 0.8 to 1.6 nm, with proportional counters and pulse height wavelength discrimination, is described in some detail. An accompanying slit system covering the 0.3 to 0.9 nm region provides a more rapid coverage of flares than the spacecraft raster period would otherwise allow. Results are given illustrating the types of data being received from this instrument, which has been operating correctly for 18 months. (auth) (UK)

26485 MAXIMUM ENERGY RESOLUTION FOR THIN dE/dx TYPE DETECTORS IN ENERGY RANGE E_α = 5 TO 9 MeV. Avdeichnikov, V. N.; Gridnev, G. F.; Lozhkin, O. V.; Perfilov, N. A. Izv. Akad. Nauk SSSR, Ser. Fiz.; 34: 210-17 (Jan 1970). (In Russian).

Energy-loss fluctuations in thin (10 to 40 μm) silicon dE/dx-type detectors were studied in order to obtain the basic characteristics of the energy-loss distribution functions for α particles with the energies from 5 to 9 MeV. The measurements were carried out using spectrometric α-particle sources of ^{148}Gd (E_α = 3.183 MeV), ^{226}Ra(E_α = 4.777, 5.486, 5.998, and 7.680 MeV), ^{241}Am(E_α = 5.482 MeV), and ^{228}Th(using only the line 8.786 MeV). (R.V.J.)

26486 SCINTILLATION CAMERA BASED ON DELAY-LINE TIME CONVERSION. Hiramoto, Toshiyuki; Tanaka, Eiichi; Nohara, Norimasa (National Inst. of Radiological Sciences, Chiba, Japan). J. Nucl. Med.; 12: 160-5(Apr 1971).

A scintillation camera based on delay-line time conversion for improved resolution for low-energy gamma emitters is described. Signals from the photomultipliers are fed to appropriate intermediate taps of a delay line so that the delay times are proportional to the coordinates of the photomultipliers on the crystal. The zero-crossing times of the mixed signals taken from both ends of the delay line can be made approximately proportional to the coordinates of scintillation events in the crystal. Then the difference of their zero-crossing times is detected and converted to a position signal. A block diagram is presented, and performance is discussed. (W.H.K.)

26487 PROPORTIONAL COUNTER FOR DETECTION OF EXOELECTRONS. Kriks, H.-J.; Schaare, W. PTB Mitt.: 81: 10-13(Feb 1971). (In German).

A proportional counter (methane-flow counter) is described, which was developed for the detection of thermally or optically stimulated exoelectrons. The characteristics of the counter were investigated in relation to several parameters. (auth)

26488 HIGHLY SENSITIVE METHOD FOR THE MEASUREMENT OF β-ACTIVE GASES IN THE PRESENCE OF NATURAL RADIOACTIVITY IN THE AIR. Ilari, O. (CNEN, Rome); Sciocchetti, G.; Wardaszko, T. Minerva Fisiconucl.; 14: 38-43(Jan-Mar 1970).

A method for the measurement of low concentrations of beta active gases in presence of natural radioactive gases in the atmosphere is described. The method of discrimination between artificial and natural gases is based on a simple correlation technique between the alpha and beta disintegrations of the Radon series members. A special scintillation chamber, of the dual phosphor type, has been used for the measurements; the chamber can also be employed as a desorption chamber in case of application of the gas enrichment procedure by active charcoal. The sensitivity of the method described for the ^{85}Kr fission gas was determined. (auth)

Nuclear Spectroscopic Instrumentation

Refer also to abstracts 26184, 26550, 26558, 28102, 28296, 28410, and 28766.

26489 (ANU-P-487(2)) COMPUTER REDUCTION OF COMPLEX SPECTRA. Ophel, T. R. (Australian National Univ., Can-

berra. Research School of Physical Sciences). [1970]. 81p. Dep. NTIS (U. S. Sales Only).

The problems of on-line and off-line computer analysis of complex spectra, with particular reference to particle and gamma ray spectra, are summarized. Details are given of an integrated set of on-line and off-line analysis programs for use with the IBM 1800, and of a universal program for the S360/50, INCRED, which incorporates all of the features of the 1800 programs and employs both linear and nonlinear fitting techniques. The programs are intended to perform all the basic reduction functions usually required and are structured so that modifications or additions to meet particular user requirements are readily made. The final section discusses line shape fitting of gamma ray spectra obtained with NaI and Ge(Li) detectors in the context of programs intended for use on the IBM 1800 and the S360/50. (auth)

26490 (ANU-P-514) SOME NOTES ON PARTICLE IDENTIFICATION USING THE ORTEC 423 IDENTIFIER. England, J. B. A. (Australian National Univ., Canberra. Research School of Physical Sciences). [1970]. 25p. Dep. NTIS (U. S. Sales Only).

A guide to preparation of a particle identification system using the ORTEC 423 is given. Typical block diagrams of circuits are given with recommended settings. A section is included on the selection, operation and performance of thin ΔE detectors. A selection of graphs that are generally required for particle identification experiments is included together with theoretical performance graphs for the 423 for the typical ranges of particle types and energies encountered in the ANU laboratory. (Australia)

26491 (INR-1213) SUBNANOSECOND TIMING IN NUCLEAR SPECTROSCOPY. Moszynski, M. (Institute of Nuclear Research, Warsaw (Poland)). 1970. 211p. (In Polish). Dep. NTIS (U. S. Sales Only).

Timing properties of nuclear-radiation detectors used in subnano-second-half-lives measurements are studied. A detailed study of timing properties of a scintillation counter that consisted of XP1021 photomultiplier and a Naton 136 or Ne111 scintillator with different dimensions are presented. The study gives an explanation of a time spread mechanism of the scintillation counter and, in particular, it removes a disagreement between experiments and the theory of timing. A time resolution of 132 ps for ^{60}Co has been obtained using Ne111 scintillators with 2.5 cm diameter and 1.0 cm height. Also, the timing properties of semiconductor detectors are described. In particular, the study of a time resolution obtainable with a surface barrier detector for α-particles shows that a plasma effect gives an essential contribution to the time spread of the detector. The best time resolution obtained with the 50 pF detector for 5.8 MeV α-particles in a coincidence measurement with conversion electrons with the 200 keV energy detected by the scintillation counter is equal to 180 ps. Further study of a pulse shape generated by α-particles in Si(Li) detectors brings a confirmation of the earlier postulated model of detector with a parabolic distribution of the electric field. As a result of the study of the pulse shape distribution from a large true coaxial germanium detector, a pulse shape selection method is developed and applied to nanosecond half-lives measurements. This method permits to obtain a fast and exponential slope of a prompt spectrum over more than four decades. By this method it has been possible to identify a very weak, delayed γ transition in ^{238}Pu. In the present state of the art in subnanosecond timing an identification of a delayed radiation appears to be a more serious problem than the determination of a half-life value. In order to solve this problem a system of two scintillation counters is applied. One counter with a plastic scintillator is used for a timing, the other one with a 3″ × 3″ NaI(Tl) scintillator for detection of Compton γ-quanta scattered from the plastic scintillator. The energy spectrum of summed pulses from both counters working in coincidence shows full energy peaks with the resolution ~10.5% for 662 keV γ-rays from ^{137}Cs. Properties of the summing counter for various energies are studied. The application of this counter for the identification of delayed radiation is illustrated for the ^{125}Sb source. (auth)

26492 (RCC-M-211) THE DERIVATION AND USE OF EXPERIMENTAL EFFICIENCY GRAPHS FOR GAMMA SPECTROMETRY IN THE PHYSICS DEPARTMENT AT THE RADIOCHEMICAL CENTRE. Tuck, A. G. (Radiochemical Centre, Amersham (England)). Aug 1967. 15p. Dep. NTIS (U. S. Sales Only).

The apparatus, procedure, and calculations for constructing an efficiency graph for a sodium iodide scintillation gamma spectrometer are described. Use of the efficiency graph and estimation of errors are discussed. (W.H.K.)

26493 BUNCHING OF NEUTRONS IN THE MeV REGION IN HIGH RESOLUTION NEUTRON SPECTROSCOPY. Peterlin, Tatjana M. (Institut Max von Laue-Paul Langevin, Grenoble, France). Atomkernenergie; 17: 93-6(Mar 1971).

A new method, based on the bunching of extremely slow neutrons directly on a detector, is proposed as means of attaining a reasonable intensity simultaneously with high resolution in both energy and momentum transfer; the error in energy transfer being on the order of 10^{-3} MeV and in momentum transfer about $6 \cdot 10^{-3}$ Å^{-1}. The spectrum of neutrons of the incident energy E_0 = 0,355 MeV which have been inelastically scattered at the target can be recorded at the same time for a wide range of energy transfers. (auth)

26494 USE OF MICROELECTRONICS IN LINEAR CIRCUITS FOR NUCLEAR SPECTROMETRY. Jollec, Claude; Raoult, Norbert; Ringeard, Claude (CEA, Saclay, France). Elec.-Electron. Mod.; 41: 17-20(Dec 1970-Jan 1971). (In French).

Microelectronics is particularly useful for the linear circuits employed in nuclear instrumentation for treating analog information. Each circuit forms the subassembly of an analog channel in nuclear spectrometry. A description is given of the way in which they are manufactured. A wide band amplifier, a linear gate circuit, and a stretcher circuit are described (principles of operation, mechanical, and electrical characteristics). (France)

26495 JOANIE: A MULTIANALYZER PROGRAM FOR PULSE HEIGHT ANALYSIS. Hully, Richard (Lowell Technological Inst., Mass.). pp 105-8 of DECUS Proceedings. Maynard, Mass.; Digital Equipment Computer Users' Society (1969).

From DECUS symposium, Wakefield, Mass. (12 May 1970). See CONF-690510.

JOANIE is a single parameter multianalyzer program designed for input and display of high speed nuclear data. The program is a revised version of DEC-9A-USAO-D program numbers 1 and 2 and operates under the environment of the PDP-9 Advanced Software System. Nearly all the basic commands from the DEC version have been incorporated with the addition of 14 new commands to significantly enlarge the flexibility of data manipulation. An extensive use of DECtape is employed for reopening and examining active files. The program also includes a complete Fail-Safe system, whereby data is saved on the active file in the event of an IOPS ERROR. (auth)

26496 USE OF A PDP-9 COMPUTER IN NUCLEAR SPECTROSCOPY MEASUREMENTS. Giannini, M.; Aquili, A. (CNEN, Rome). pp 109-14 of DECUS Proceedings. Maynard, Mass.; Digital Equipment Computer Users' Society (1969).

From DECUS symposium, Wakefield, Mass. (12 May 1970). See CONF-690510.

A PDP-9 (8-K words, 2 DECtapes, CRT display), interfaced to a double ADC converter, is used for single and two-parameter analysis of γ-ray spectra detected with large Ge(Li) detectors. The same system is also used for the off-line elaboration of the recorded data. (auth)

26497 SIMPLE PROGRAM FOR PULSE-HEIGHT ANALYSIS WITH TIME-SHARING FOR ROUTINES USING THE PERIPHERAL UNITS. Olsen, Birthe (Yale Univ., New Haven). pp 115-20 of DECUS Proceedings. Maynard, Mass.; Digital Equipment Computer Users' Society (1969).

From DECUS symposium, Wakefield, Mass. (12 May 1970). See CONF-690510.

A program for pulse-height analysis with single or extended precision has been developed for a PDP-8/I. The interrupt facility has been utilized to provide for simultaneous service of a number of different peripheral units. With this program it is possible to take in data for one spectrum at the same time as data is being displayed on the oscilloscope and data from a previous spectrum is being plotted on the Calcomp plotter and/or printed on the Teletype. The program is written in modular form and can easily be extended to serve an unlimited number of peripherals. (auth)

26498 DECUS PROCEEDINGS. PAPERS AND PRESENTATIONS OF DIGITAL EQUIPMENT COMPUTER USERS' SOCIETY, FALL SYMPOSIUM, HOUSTON, TEXAS, NOVEMBER 19-21, 1970. Maynard, Mass.: Digital Equipment Computer Users Society (1970). 335p. (CONF-701101).

Separate abstracts were prepared for 2 of the 53 papers presented. The remaining 51 papers were not within the scope of NSA. (W.H.K.)

For abstracts of individual papers see: 26473 and 26499.

26499 SPECTR: A PROGRAM FOR HANDLING AND ANALYZING MULTICHANNEL PULSE HEIGHT SPECTRA. Zurstadt,

D. H. (Univ. of Colorado, Boulder). pp 263-7 of DECUS Proceedings. Maynard, Mass.; Digital Equipment Computer Users' Society (1970).

From Fall joint computer conference, Houston, Tex. (19 Nov 1970). See CONF-701101.

Program SPECTR has been written to provide all of the operations required for handling large numbers of multichannel pulse height spectra and for accomplishing basic data reduction of the spectra. The final results of the data reduction are recorded on a master file along with the original spectra and important experiment setup parameters. Among the intermediate operations are included a wide variety of listing and plotting options, the extraction of peaks and peak areas, and the addition and subtraction of spectra from one another incorporating zero shifts and changes in gain. (auth)

26500 ADAPTATION OF A GAMMA-RAY SPECTRAL ANALYSIS PROGRAM FOR A PDP-9 COMPUTER. Donati, D. R.; Mathur, S. C. (Lowell Technological Inst., Mass.). pp 41-3 of DECUS Proceedings. Maynard, Mass.; Digital Equipment Computer Users' Society (1970).

From Digital Equipment Corporation Users Society spring symposium; Atlantic City, N. J. (4 May 1970). See CONF-700524.

A gamma-ray spectral analysis program GASPAN, developed by Barnes, has been adapted to run on a 16K PDP-9 computer. The program, in conjunction with the on-line data acquisition program JOANIE, is not in routine use for the analysis of gamma-ray spectra obtained by means of a high resolution GeLi spectrometer, in nuclear reactions produced by the LTI 5.5 MeV Van de Graaff accelerator. Due to the limited core memory available, extensive use of the Chaining technique has been made in adapting GASPAN to run on the PDP-9 computer. (auth)

26501 PRELIMINARY PROCESSING OF MULTIPLEXED TWO-PARAMETER GAMMA-SPECTROMETER DATA. Fager, J. E.; Kaye, J. H. (Battelle-Northwest, Richland, Wash.). pp 45-51 of DECUS Proceedings. Maynard, Mass.; Digital Equipment Computer Users' Society (1970).

From Digital Equipment Corporation Users Society spring symposium; Atlantic City, N. J. (4 May 1970). See CONF-700524.

A PDP-9 16k computer is used for preliminary processing of gamma spectrometer data. Data is accumulated off-line with a 4096-channel pulse-height analyzer multiplexed to store data from 4 detector systems simultaneously. Data is punched onto paper tape and read by a reel-type Digitronics reader interfaced to the PDP-9. A KSR-35 teletype has been mechanically modified to backspace under computer control allowing data to be point plotted with increased speed. Selected data can be punched onto cards by means of a standard 026 IBM Keypunch interfaced to the PDP-9. (auth)

26502 STABILIZATION OF THE MAGNETIC FIELD IN AN IRON $\pi\sqrt{2}\beta$ SPECTROMETER USING NUTATIONAL PROBES. Lyuti, I. N.; Gavrilyuk, V. I.; Kupryashkin, V. T.; (and others) (Inst. of Physics, Kiev). Izv. Akad. Nauk SSSR, Ser. Fiz.; 34: 828-34(Apr 1970). (In Russian).

A scheme of nonhomogeneous magnetic field formation with stabilization in two points was developed by attaching it to the frequency harmonics of the base generator. The instability of the magnetic field was $\pm 5 \times 10^{-6}$ during 5 hr and $\pm 1.1 \times 10^{-5}$ during 24 hr. The resolution of the $\pi\sqrt{2}\ \beta$-spectrometer pulse, using the developed system, reached 0.020% at the solid angle 0.009% of 4π and 0.025 to 0.035 at the solid angle 0.066% of 4π. (tr-auth)

26503 α SPECTROMETER FOR MEASURING THE DEGREE OF RADIOACTIVE EQUILIBRIUM BETWEEN ^{222}Rn AND ITS DAUGHTER PRODUCTS IN URANIUM MINES. Chapuis, A.; Lanegrasse, L.; Lopez, A. (Univ., Toulouse). Radioprotection; 5: 293-304(1970). (In French). (CONF-700505-22).

From 2nd Congress of the International Radiation Protection Association, Brighton, England.

The development of a portable α spectrometer for measuring the degree of radioactive equilibrium between Rn-222 and its daughter products in uranium mines is discussed. The detector is a 0.50 cm^2 silicon surface-barrier detector. The counting system consists of a detector, a preamplifier and amplifier, a scaler, and a power supply and is designed to fit into a 40 × 38 × 20 cm module. (auth) (France)

26504 TWO-DIMENSIONAL ANALYZER OF $\gamma\gamma$ COINCIDENCES WITH SEMICONDUCTOR DETECTORS OPERATING WITH AN ELECTRON COMPUTER MINSK-2 CAPABLE OF SELECTING DATA FROM THE DIGITAL WINDOWS DURING THE EXPERIMENT. Aleksandrov, V. S.; Duda, F.; Elizarov, O. I.; (and others). Izv. Akad. Nauk SSSR, Ser. Fiz.; 34: 69-77 (Jan 1970). (In Russian).

The block diagram is given for a $\gamma-\gamma$ coincidence system using semiconductor detectors and an electronic computer. Circuitry for the fast amplifier and time-to-amplitude converter is explained. Typical spectra are included for ^{153}Gd and ^{22}Na. (R.W.R.)

High Energy Physics Instrumentation

Refer also to abstracts 26554, 27959, and 28135.

26505 (JINR-P13-5636) MONOCHROMATIC METHOD FOR MEASUREMENT OF THE MEAN PROTON ENERGY IN 665 MeV BEAM USING THE VAVILOV-CHERENKOV RADIATION. Zrelov, V. P.; Musin, M. A.; Pavlovic, P.; Sulek, P.; Janik, R. (Joint Inst. for Nuclear Research, Dubna (USSR). Lab. of Nuclear Problems). 1971. 25p. (In Russian). Dep. NTIS (U. S. Sales Only).

The monochromatic method of measurement of the proton energy using the Vavilov–Cherenkov radiation and the interference filters with $\overline{\lambda}$ = 6000 Å and pass band $\Delta\lambda$ = 100 Å is described. The results of testing this method on the 665 MeV proton beam extracted from the synchrocyclotron of the Nuclear Problem Laboratory (JINR) are presented. The measurement accuracy of ±0.02% is achieved which exceeds the accuracy of the best previously known methods by 5 times. (auth)

26506 (JINR-P13-5637) APOCHROMATIC METHOD FOR MEASUREMENT OF THE MEAN PROTON ENERGY IN 657 MeV BEAM USING THE VAVILOV-CHERENKOV RADIATION. Zrelov, V. P.; Pavlovic, P.; Sulek, P. (Joint Inst. for Nuclear Research, Dubna (USSR). Lab. of Nuclear Problems). 1971. 28p. (In Russian). Dep. NTIS (U. S. Sales Only).

A new method of measurement of the mean proton energy over the Vavilov–Cherenkov radiation by using an apochromatic doublet of prisms to compensate the radiator dispersion is described. The results of testing this method on the 657 MeV proton beam extracted from the synchrocyclotron of the Nuclear Problem Laboratory (JINR) are presented. The accuracy of determining the mean energy is ±0.03% which exceeds the accuracy of the best previously known methods by 3 times. (auth)

26507 (NP-18764) UNIVERSAL MAGNETIC SPECTROMETER WITH 0,15 PERCENT RESOLVING POWER AT MAXIMUM PULSE OF 60 GeV/c. Ainutdinov, M. S.; Alikhanov, A. I.; Knyazev, V. M.; Lyubimov, V. A.; Pershin, I. I.; Shevchenko, V. G. (Gosudarstvennyi Komitet po Ispol'zovaniyu Atomnoi Energii SSSR, Moscow. Institut Teoreticheskoi i Eksperimental'noi Fiziki). 1970. 16p. (In Russian). Dep. NTIS (U. S. Sales Only).

A magnetic spectrometer is proposed to carry out the experiment at the Serpukhov proton accelerator. The spectrometer is composed of a streamer chamber 3.3 × 0.9 × 0.8 m^3 in volume placed in the magnetic field of H = 17 to 20 kG; a 6 meter magnet with the width of the magnetic path equal to 0.7 m (H = 17 kG); and a wire spark chamber. The momentum resolution of the spectrometer is 0.15% for P_{max} = 60 GeV/c. The aim is to study π^- + p interactions in the momentum interval 30 to 60 GeV/c and k^- + p and p + p interactions in the interval 20 to 40 GeV/c with the momentum transverse squared ≤1 GeV/c. (auth)

26508 (NP-18787) SEVERAL ASPECTS OF THE DESIGN AND THE CALCULATION OF ITEP 2-METER LIQUID-HYDROGEN BUBBLE CHAMBER. Stepanov, A. M. (Gosudarstvennyi Komitet po Ispol'zovaniyu Atomnoi Energii SSSR, Moscow. Institut Teoreticheskoi i Eksperimental'noi Fiziki). 1970. 22p. (In Russian). Dep. NTIS (U. S. Sales Only).

The design of the ITEP 2-metre liquid hydrogen bubble chamber is described. The designs and the calculations for the chamber body, expansion system, vacuum tank, and nitrogen shielding are discussed. (auth)

26509 (RHEL/R-212) A LASER ILLUMINATION SYSTEM FOR A HOUGH-POWELL DEVICE. Lawes, R. A.; Welford, W. T. (Rutherford High Energy Lab., Chilton (England)). Feb 1971. 38p. Dep. NTIS (U. S. Sales Only). UK 50p.

An HPD illumination system is described which uses an argon laser and requires a minimum of modification to the existing opto-mechanical structure. A diffraction limited measuring spot of 3μm diameter (at 50% intensity) is obtained at a power level of approximately 1μ watt. Photon noise effects are consequently reduced to negligible proportions for known applications of the machine. (auth)

26510 OUTPUT PROGRAM USED WITH ON-LINE DATA COLLECTION. Foss, M. H.; Bicker, R. H. (Carnegie-Mellon Univ., Pittsburgh). pp 133-6 of DECUS Proceedings. Maynard, Mass.; Digital Equipment Computer Users' Society (1969).

XUM

From DECUS symposium, Wakefield, Mass. (12 May 1970). See CONF-690510.

A PDP-7 is used to collect data as it is available from a wire spark chamber interface. The output program discussed operates with the interrupt on and thus does not interfere with data collection. Analysis of the spark chamber events uses the time not used for input or output of data. (auth)

26511 SLAC SPIRAL READER SYSTEM. Hu, Michael J. C. (Stanford Univ., Calif.). pp 137-42 of DECUS Proceedings. Maynard, Mass.; Digital Equipment Computer Users' Society (1969).

From DECUS symposium, Wakefield, Mass. (12 May 1970). See CONF-690510.

At the Stanford Linear Accelerator Center (SLAC) a modified spiral reader was built to measure bigger areas, and to handle different film formats. A PDP-9 computer was selected to control and to acquire data. Practically every I/O feature on the PDP-9 was used to minimize external electronic interface and to make the control program more efficient. The PDP-9 computer performs the following functions: It guides the operator through the measuring sequence and types out warning messages on the teletype if the operator makes an error. It passes the digitized data through the DMA channel to magnetic tape, and displays the data on the storage scope. It keeps track of the stage positions and the periscope position through the add-to-memory feature. It monitors the spiral reader for any electrical or mechanical malfunction. It checks operator's efficiency and performs bookkeeping on events measured and events rejected, etc. The entire spiral reader system at SLAC is in operation, and it is capable of producing over 70 events per hour. (auth)

26512 SCOLDS: SPARK CHAMBER ON-LINE DATA SYSTEM. Jones, Ray; Tilger, Clarence A. (Digital Equipment Corp., Maynard, Mass.). pp 143-5 of DECUS Proceedings. Maynard, Mass.; Digital Equipment Computer Users' Society (1969).

From DECUS symposium, Wakefield, Mass. (12 May 1970). See CONF-690510.

SCOLDS is a spark chamber on-line data system which accepts data from a spark chamber experiment, monitors it, and writes it on magnetic tape or DECtape. SCOLDS is constructed in modular form and functions within the framework of the keyboard monitor system. The keyboard monitor system is used for loading programs and the resident monitor is an integral part of SCOLDS. The main program resides in core and directs the use of these modules which have been loaded. SCOLDS responds to keyboard commands causing data taking to stop and start, histograms to be built from the data, and data to be written on magnetic tape or DECtape. (auth)

26513 FAST DETECTOR OF A RELATIVISTIC CHARGED PARTICLE PASSAGE. Khurshudyan, L. S. (Inst. of Physics, Erevan). Izv. Akad. Nauk Arm. SSR, Ser. Fiz.; 5: 225-7(1970). (In Russian).

A position-sensitive silicon detector preceded by a secondary emission foil and an accelerating grid is designed for the detection of relativistic charged particles with a resolution exceeding 1 mm. (W.H.K.)

26514 SPARK CHAMBERS IN HIGH-ENERGY PHYSICS. PART II. WIDE-GAP SPARK CHAMBERS. Dwurazny, Antoni; Knapik, Jerzy (Univ. of Lodz, Poland). Postepy Fiz.; 22: 3-23 (1971). (In Polish).

The article is the second part of a series of four, on the subject of spark chambers. After a short description of the time development of the spark discharge, a review of different types of wide-gap spark chambers is presented. Some practical applications are also given. (36 references) (auth)

26515 DETECTION OF X-RAY TRANSITION RADIATION BY MEANS OF A STREAMER CHAMBER. Avakyan, K. M.; Alikhanyan, A. I.; Garibyan, G. M.; Lorikyan, M. P.; Shikhlyarov, K. K. Izv. Akad. Nauk Arm. SSR, Ser. Fiz.; 5: 267-74 (1970). (In Russian).

A new method for x-ray transition radiation detection by a streamer chamber is suggested. The use of the chamber secures a separate observation of both the radiation and the particle. It is shown that the mean number of the transition quanta linearly increases in the electron energy 1.2 to 2.46 GeV. When the plastic foam was used instead of layered medium the efficiency of electron detection by transition radiation was 86%. (auth)

Radiation Dosimeters

Refer also to abstracts 26483, 26487, and 26756.

26516 (CLOR-82/D) X AND GAMMA THERMOLUMINESCENT DOSIMETER FOR ACCIDENTAL PERSONNEL DOSIMETRY PURPOSES. Koczynski, A.; Musialowicz, T.; Wolska-Witer, M.; Wysopolski, J. (Centralne Laboratorium Ochrony Radiologicznej, Warsaw (Poland)). 1970. 22p. (In Polish). Dep. NTIS (U. S. Sales Only).

The conditions of the usefulness of CaF_2: Mn prepared in the Central Laboratory for Radiological Protection were investigated for X and gamma accidental dose measurements in personnel dosimetry. Loose powder may be used in such dosimeter. The simple construction and properties of the dosimeter are given. (auth)

26517 (COO-1105-164) QUALITATIVE AND QUANTITATIVE FEATURES OF THE TERRESTRIAL SOLAR ULTRAVIOLET RADIATION ENVIRONMENT. McCullough, Edwin Charles (Wisconsin Univ., Madison). 1971. Contract AT(11-1)-1105. 129p. Dep. NTIS.

Thesis.

The various geometrical, astronomical and atmospheric factors which influence terrestrial solar uv are reviewed. A uv dosimeter whose spectral sensitivity approximates the erythemal (sunburn) response of human skin would provide a measure of the erythemal effectiveness of the uv radiation present at the time of measurement. Three photosensitive glasses were investigated as erythemally effective uv dosimeters. Thermoluminescent (TL) phosphors are small in size which makes them especially suited for in-vivo studies and personnel dosimetry. In addition, they require no electronics at the site of measurement and operate unattended. Investigations on the use of transferred TL in natural calcium fluoride (CaF_2: nat) as a uv dosimeter were carried out under both daylight and artificial illumination. The spectral sensitivity of transferred TL was found to be such that if the CaF_2: nat phosphor is used in a subtraction mode using a sharp cutoff filter, the dosimeter spectral sensitivity is similar to the erythema action spectrum of untanned human skin. Exposure times greater than 5 minutes in midday, mid-September sun produced a nonlinear response in the phosphor TL as a result of the bleaching of transfer TL peaks. This effect was shown to be eliminated through use of neutral density filters. Using CaF_2: nat phosphors, measurements of terrestrial solar uv have been carried out. These are compared to computed estimates based on atmospheric constituent data. Obtaining current values for the various atmospheric constituents (e.g. ozone) is discussed. The comparison of measured TL currents and minimal erythema times is discussed with regard to future improvement of CaF_2: nat as a thermoluminescent dosimeter of terrestrial solar uv. General features of the terrestrial solar uv radiation environment are also presented. (auth)

26518 (NP-18746) PERSONNEL MONITORING WITH RADIOPHOTOLUMINESCENT DOSIMETERS. Piesch, E. (Kernforschungszentrum, Karlsruhe (West Germany)). Nov 1970. 32p. Dep. NTIS (U. S. Sales Only).

A brief introduction is given on the dosimetric properties of silver-activated phosphate glass photoluminescent dosimeter systems. Based on the results of calibration test exposures and results of a five year routine dosimetry program, personnel monitoring with glass dosimeters is described. The technical requirements for the dose evaluation (identification of glass, washing of glass, predose, re-use of glass, measuring accuracy and reproducibility); the organization of a measurement service (working procedure, working period, cost); and the application in radiation monitoring (routine and accidental dosimetry, long-time dosimetry, activation dosimetry) are discussed. Also, some possibilities for further improvements are given. (auth)

26519 (NP-18747) NEW DEVELOPMENTS AND ASPECTS IN PHOSPHATE GLASS DOSIMETRY. Piesch, E. (Kernforschungszentrum, Karlsruhe (West Germany)). Nov 1970. 29p. Dep. NTIS (U. S. Sales Only).

In the past years a new method of differential fluorescence measurement was developed by which the glass is continuously scanned and a differential fluorescence intensity is measured and recorded directly as a function of the glass depth. By the new technique the radiation quality (10 to 600 keV) and the direction of the radiation incidence can be determined. Based on the results of extensive calibration exposures and phantom measurements new aspects of phosphate glass dosimetry are discussed, in particular the evaluation of radiation quality, the analysis of mixed radiation fields, the indication of the direction of the radiation incidence for frontal exposure and for exposure from behind, and the direct indication of the absorbed dose in the critical organs using an energy independent dosimeter with reduced influence of body orientation to radiation incidence. The advantages of the new dosimeter system are briefly discussed and compared to other dosimetric systems for personnel monitoring. (auth)

26520 (NYO-3409-9) ROLE OF TRAPPING PROCESSES IN SOLID STATE RADIATION DOSIMETRY. Progress Report, 1970–1971. (Pennsylvania State Univ., University Park. Materials Research Lab.). Feb 1971. Contract AT(30-1)-3409. 36p. Dep. NTIS.

Research on radiation dosimetry by polymer electret depolarization is described. Also, the characterization of non-luminescent near-insulating materials by the measurement of thermally stimulated currents and thermally stimulated depolarization is discussed. Radiation dose measurements based on carrier trap filling are considered. Equipment and results are discussed including the measurement of pyroelectric coefficients and the characterization of lunar materials. (W.H.K.)

26521 RESPONSE OF GLASS DOSIMETERS TO STRONG γ RADIATIONS. Gerard, F. (CEN, Fontenay-aux-Roses, France). Radioprotection; 4: 279-94(1969). (In French).

The coloration of glasses under γ radiation is a phenomenon used in dosimetry for a long time. The sphere of use is enlarged to the range between 10^4 and 5×10^5 rads, and an attempt is made to explain the decrease of the coloration with time. Some metaphosphate glasses with a cobalt oxide deposit were used; and their transmission measured after irradiation with γ radiation from ^{60}Co. The study of the absorption spectra, compared with those of nonirradiated glasses, shows the appearance of absorption bands. For dosimetry, measurement of the transmission of glasses at 3500 Å (350 nm) is advised for doses between 10^4 and 2×10^5 rads; and at 6000 Å (600 nm), for doses above 10^5 rads. The curves of the decrease of optical density as a function of time for various temperatures show two periods — one is rather short; the other, longer. Since first-order kinetics is applicable, one can construct a theoretical model. The existence of metastable traps is conjectured. With the help of this model a calibration curve is calculated, very near to the experimental curve, and the width of the energy level is determined exactly. (tr-auth)

26522 THERMOLUMINESCENT DOSIMETRY. van Wallendael, S. (MBLE, Brussels). Radioprotection; 4: 333-40(1969). (In French).

Thermoluminescent dosimetry is described covering the physics and use of natural calcium fluoride powder in a dosimeter, the response of calcium fluoride as a function of applied dose, the operation of miniature dosimeters, the luminescent emission as a function of heating time, and the use of these dosimeters to detect accidents. (J.F.P.)

26523 USE OF MANNITOL IN THE DOSIMETRY OF GAMMA RADIATION. Scherz, H.; Gruenewald, Th. (Bundesforschungsanstalt fuer Lebensmittelfrischhaltung, Karlsruhe, Ger.). Kerntechnik; 12: 501-3(Nov 1970). (In German and English).

Malonic dialdehyde is formed by gamma irradiation of 1% solutions of mannitol in 0.1 N NaOH saturated with N_2O. Its concentration is proportional to the absorbed dose. Malonic dialdehyde can be determined colorimetrically, down to low concentrations, by a highly sensitive reaction with 2-methylindole. The G-value for solutions saturated with N_2O is 4.99 ± 0.15. (auth)

26524 THERMOLUMINESCENT DOSIMETER BADGE. Korba, Alvin (to United States Atomic Energy Commission). U. S. Patent 3,562,480. 9 Feb 1971. Filed 25 Jul 1969.

A personnel dosimeter for detecting neutron radiation over a wide range of energies including two hemispheres of hydrogenous material with a ^{6}LiF phosphor and a ^{7}LiF phosphor imbedded in each hemisphere is described. One hemisphere has all of its surfaces covered with cadmium while the other hemisphere has only its curved surface covered with cadmium. Each ^{6}LiF, ^{7}LiF set of phosphors in each hemisphere measures different spectra of incident and body reflected neutrons. The difference in these measurements is correlatable to neutron dose over a wide range of neutron energies. (auth)

26525 PROPERTIES OF THERMOLUMINESCENCE DETECTORS DURING IRRADIATION WITH FAST ELECTRONS. Czaikowski, Peter-Michael (Univ. of Saarlandes, Saarbruecken, Ger.). Stud. Biophys.; 23: 101-8(1970). (In German).

LiF and CaF_2 dosimeters were studied. The commonly used evaluation, requiring more than three hours and leading to desensitization of the dosimeter, was replaced by a procedure that requires on the average six min per measurement. The most essential improvement consisted in the replacement of the silver heating plate by a tantalum foil that proved much more resistant to continuous changes of temperature. Experimental studies proved that the new type of lithium fluoride dosimeter is suitable for determining dose distributions during irradiation with fast electrons. (H.B.G.)

26526 EVALUATION OF THE CERIC–CEROUS SYSTEM AS AN IMPURITY-INSENSITIVE MEGARAD DOSIMETER. Matthews, R. W. (Australian Atomic Energy Commission Research Establishment, Lucas Heights). Int. J. Appl. Radiat. Isotop.; 22: 199-207(Mar 1971).

Results are given of a study of the rate of cerium (IV) reduction in ^{60}Co gamma irradiated cerium (IV) – cerium (III) – 0.4 molar sulphuric acid solutions prepared from water of various purities. At cerium (III) concentrations of 3.1 mmolar and above, the measured dose response was linear over a wide dose range. For any given cerium (III) concentration 3.1 mmolar or above there was no significant difference between the $G(Ce^{3+})$ obtained, whether solutions were prepared from water of the highest purity or mains water. Triple distillation of water and special cleaning of glassware are therefore unnecessary in ceric dosimetry if cerium (III) of this concentration is present in the solution and this facilitates routine application of the method. The cerium (III) yield from the solutions is as little affected by increased temperature as that from the traditional ceric dosimeter and photolytic stability is improved slightly. Buildup factors and LET effects need to be taken into account under degraded spectral conditions. (auth) (UK)

26527 NOTES ON PERSONNEL DOSIMETRY WITH ^{7}LiF TEFLON DISCS. Barbina, V.; Zecchin, R.; Di Chiara, F.; Englaro, G. C. (Ospedale Generale Regionale, Udine, Italy. Istituto di Radioterapia e Medicina Nucleare, Udine, Italy). Radiol. Med.; 56: 512-27(Jun 1970). (In Italian).

The authors discuss the suitability of thermoluminescent ^{7}LiF teflon discs for personnel dosimetry and investigate the results of over one year of trials and tests. When used with energy-compensating shields, the discs provide a wide-range personnel-monitoring device, offering a number of advantages over conventional film-badge dosimeters. Nevertheless, in the millirad dose range three major problems occur, resulting in poor measurement reproducibility; these are a nonnegligible dependence of readings on heating temperature, large background, and unsatisfactory variation of readings, getting worse with the reuse of the discs, due to sensitivity tolerances. The problems are closely examined by considering both theoretical causes and experimental data, and a method is developed to estimate simple corrections that reduce reading scattering within good limits. Finally, the minimum detectable dose is evaluated in terms of the reusability of the discs; a ten millirad dose is found as a minimum standard measurable quantity, for as many as 30 consecutive readings. (auth)

26528 APPLICATIONS OF THERMO AND PHOTOLUMINESCENT PHENOMENA IN HEALTH PHYSICS. Bernadou, J. M.; Blanquet, P.; Freour, P.; Beck, C. (Archives des Maladies Professionnelles de Medecine du Travail et de Securite Sociale, Paris. Institut National de la Sante et de la Recherche Medicale, Bordeaux). Arch. Mal. Prof. Med. Trav. Secur. Sociale; 31: 6 663-8(Dec 1970). (In French).

The applications of photoluminescent and thermoluminescent phenomena in dosimetry are discussed. The characteristics of dosemeters based on these processes are compared with those of the films and other dosemeters normally used. (France)

26529 RADIATION DOSIMETER WITH SEMICONDUCTOR DETECTORS. Alekseyunas, B. K.; Alishauskas, A. B.; Shirvaitis, A. I. (Vilnyus State Univ., USSR). Liet. Fiz. Rinkinys, Liet. TSR Mokslu Akad., Liet. TSR Aukst. Mokyklos; 10: 305-9(1970). (In Russian).

The radiation dosimeter consists of two small (diameter ~5 mm) Sb_2S_3 polycrystals and a dc amplifier. The dosimeter can be successfully applied to measure doses of X- and gamma rays in cavities of different materials and biological organisms. (auth)

26530 LIQUID FILLED IONIZATION CHAMBERS AS DOSIMETERS. Adamczewski, I. (Technical Univ., Danzig. Academy of Medicine, Danzig). pp 21-44 of Phenomenes de Conduction dans les Liquides Isolants. Paris; Centre National de la Recherche Scientifique (1970).

From International Conference on Conduction Processes in Dielectric Liquids, Grenoble, France. See CONF-680983.

Liquid-filled ionization chambers are discussed from a theoretical and a practical point of view. The experimental relations between the ionization current and the ionizing-particle flux are expressed in the form $I = I_0 + cE$. The coefficients of this formula depend on the nature and energy of the particles studied (photons, alpha, neutrons, ...). The ionization yields of a gas (air) and a liquid (hexane) were compared. The liquid gives much weaker ionization currents for the same quantity of energy absorbed. A gas–liquid ionization chamber was developed, whose response was independent of the energy of the ionizing radiation in the range 20

keV to 1,250 keV. Another ionization chamber filled with a mixture of hexane and CCl_4 was studied. The ionization current depends on the concentration of CCl_4; therefore, ionization chambers which correspond to adjustable effective atomic numbers could be developed for medical dosimetry. Thus, with this ionization chamber the atomic number corresponding to living tissues can be simulated. Detailed cross sections of different kinds of ionization chambers are shown. (auth) (France)

26531 IONIZATION CHAMBER FILLED WITH A MIXTURE OF N-HEXANE AND CARBON TETRACHLORIDE FOR PHANTOM MEASUREMENTS OF PHOTON RADIATIONS (X,γ). Terlecki, J. (Academy of Medicine, Danzig). pp 91-5 of Phenomenes de Conduction dans les Liquides Isolants. Paris; Centre National de la Recherche Scientifique (1970).

From International Conference on Conduction Processes in Dielectric Liquids, Grenoble, France. See CONF-680983.

A double-liquid-filled ionization chamber is described. This chamber incorporates a special liquid-chamber potential-compensating system (Jaffé law $I = I_0 + cU$), which renders the measurements insensitive to fluctuations in the applied potential U. The response is independent of the energy of the incident radiation over a large region; this region corresponds to the needs of radiotherapy. Radiation doses may be measured with this apparatus by using a water-filled phantom to simulate tissue. (auth) (France)

26532 PHOTOGRAPHIC DOSIMETRY AND X- AND GAMMA RAYS. Ehrlich, Margarete. National Bureau of Standards Handbook 57. Washington, D. C.; National Bureau of Standards (1954). 31p. Available from Superintendent of Documents, GPO, Washington, D. C.

Data and basic principles necessary for the photographic dosimetry of gamma and x rays are presented. Criteria for selection of photographic film, calibration, photographic processing, densitometry and interpretation, and storage of photographic emulsions are discussed. (W.H.K.)

26533 STOPPING POWERS FOR USE WITH CAVITY CHAMBERS. National Bureau of Standards Handbook 79. Washington, D. C.; National Bureau of Standards (1961). 90p. (NCRP–27). Available from Superintendent of Documents, GPO, Washington, D. C.

A critical review of the literature concerning the stopping power ratio that is used in the interpretation of cavity ionization measurements in radiation dosimetry is presented. The development of cavity theory is described, and the theory and experimental information on ranges and stopping powers of charged particles are discussed. Information from cavity chamber measurements is reviewed and compared with theory. Conclusions about the best currently available information on the stopping power ratios are given. (W.H.K.)

26534 MEASUREMENT OF ABSORBED DOSE OF NEUTRONS, AND OF MIXTURES OF NEUTRONS AND GAMMA RAYS. National Bureau of Standards Handbook 75. Washington, D. C.; National Bureau of Standards (1961). 92p. (NCRP–25). Available from Superintendent of Documents, GPO, Washington, D. C.

The concepts and units of radiation dosimetry, interaction of radiation with matter, and instruments and methods for dosimetry are discussed. Ionization devices, chemical methods, dosimetry by spectral measurements, fast neutron dosimetry with counting devices, intercomparison of fast neutron dosimeters, and measurement of first collision dose and absorbed dose are described. Dosimetry for radiobiological research, radiation protection, shielding and neutron physics studies, and radiation effects studies is discussed. (133 references.) (W.H.K.)

26535 STANDARD METHOD OF CALCULATION OF NEUTRON DOSE TO POLYMERIC MATERIALS AND APPLICATION OF THRESHOLD-FOIL MEASUREMENTS. ASTM D 2365-68. Philadelphia; American Society for Testing and Materials (1969). 18p. Available from American Society for Testing and Materials, Philadelphia.

Calculation of the neutron dose in polymeric materials based on the chemical composition of the material, the neutron spectrum, and the integrated flux exposure is described. Methods for neutron dose calculations for a known neutron spectrum, for an unknown neutron spectrum, and for thermal neutron capture reactions are presented. Also, procedures for measurement of integrated neutron fluxes with threshold foils are detailed. (W.H.K.)

26536 RELATIONSHIP BETWEEN ENCAPSULATION AND APPARENT FAST NEUTRON-INDUCED FADING IN TLD. Wallace, Robert H. (Purdue Univ., Lafayette, Ind.); Ziemer, Paul L.; Kastner, J.; Oltman, B. G. Health Phys.; 20: 221-4(Feb 1971).

Experimental evidence presented by Oltman et al (NSA 21: 36405) indicated that the combined thermoluminescent response of ^7LiF dosimeters exposed to gamma-only and fast neutron-only was greater than the response of a single thermoluminescent dosimeter exposed to both the gamma and fast neutrons. In order to resolve conflicting reports on the cause of this thermoluminescent γ response reduction or fading an experiment involving ^7LiF and $Li_2B_4O_7$: Mn was designed to reproduce the fading, describe the radiation parameters related to fading, and determine any sample treatment unrelated to irradiation which may affect the fading. The combined results for irradiated and unirradiated ^7LiF tend to show that the "fading" of fast neutron-irradiated ^7LiF originally reported is due in fact to the encapsulation process and associated with the heat-sealing of the polyethylene tubing. The original observation that the "fading" was a relatively constant amount regardless of irradiation treatment agrees with the finding of the present experiment. Furthermore, the findings that no fading occurred in glass-encapsulated ^7LiF or $Li_2B_4O_7$: Mn agrees completely with the experiment of Goldstein, Miller and Rago (NSA 24: 14325). The practical recommendation arising from the present work is that heat-sealed polyethylene for construction of ^7LiF dosimeters should be used with caution. (UK)

26537 POSSIBLE EXPLANATION IN APPARENT DISCREPANCIES OF RESULTS FROM COMMERCIAL SUPPLIERS OF FILM BADGES. Moss, Eugene C. (Medical Coll. of Virginia, Richmond). Health Phys.; 20: 225(Feb 1971).

It is commented that a very possible explanation of the inconsistencies noted by Crosby (24: 11850) in the results obtained from film badges could be that the filters are easily dislodged when badges fall. This tendency increases with the number of such drops and with the height from which they fall. (UK)

26538 PAIRED IONIZATION CHAMBERS FOR MEASUREMENT OF NEUTRONS AND GAMMA RAYS. Hiraoka, T.; Kawashima, K.; Inada, T.; Matsuzawa, H. (National Inst. of Radiological Sciences, Chiba, Japan). Strahlentherapie; 141: 64-8(Jan 1971).

Ionization chambers were made from polyethylene and filled with ethylene, from tissue equivalent plastic and filled with tissue equivalent gas, and from graphite and filled with carbon dioxide. On the basis of ^{60}Co gamma-ray calibration, the sensitivities of these chambers were quantitatively determined for fast neutrons and photons with energies between 0.01 and 10 MeV. Then, they were used as paired chambers to evaluate tissue dose for radiations produced by a Van de Graaff accelerator whereby deuterons were accelerated at 2.5 MeV and bombarded on thick Be targets. Estimated gamma-ray dose was roughly 20% of neutron dose. Fast neutron dose given by paired polyethylene and carbon chambers was 6% greater than that given by the Hurst counter, while that given by the tissue equivalent plastic and carbon chambers was 4% less than the latter. (auth)

26539 THERMOLUMINESCENT DOSIMETER OF LiF INCORPORATED IN SILICONE RUBBER. Bassi, P.; Busuoli, G.; Cavallini, A.; Rimondi, O. (CNEN, Bologna). Minerva Fisiconucl.; 13: 276-81(Oct-Dec 1969).

Discs of silicone rubber with LiF incorporated have been prepared. The use of discs is practical, whereas the use of loose powder is not. Discs have the same sensitivity and linearity as loose powder, with a higher energy dependence, and can be reused a certain number of times. (auth)

Radiometric Instruments

Refer also to abstract 26157.

26540 (ORO–3842-3) INSTRUMENT MANUAL FOR PROTOTYPE WET CONCRETE ANALYZER. Berry, P. F.; Hall, J. D. (Nuclear-Chicago Corp., Austin, Tex. Texas Nuclear Div.). 30 Sep 1970. Contract AT(40-1)-3842. 101p. Dep. NTIS.

The design, specifications, operation, calibration, maintenance and service procedures, and radiation safety aspects of radiometric instrument for the rapid, on-site determination of cement in wet concrete are presented. The instrument utilizes a low-energy americium-241 source and a high-energy cesium-137 source and a thallium-activated sodium iodide scintillation detector. (W.H.K.)

26541 MULTIPLE DETECTOR NEUTRON LOGGING APPARATUS. Schuster, Nick A. (to Schlumberger Ltd.). U. S. Patent 3,546,454. 8 Dec 1970. Filed 29 Nov 1967.

An illustrative embodiment of the invention discloses a borehole-effects compensation technique for a neutron logging tool. A third

neutron detector (or its physical equivalent) is joined to a two-neutron-detector formation-porosity logging tool. The third detector-equivalent is positioned within the tool at a distance relative to the neutron source and the other detectors that enables changes in the signal from the third detector caused by variations in the borehole environment to be generally distinguishable from changes in the signal from at least one of the other detectors. The signals from the third detector and one of the two other detectors are combined in order to compensate for the influence of the borehole environment. (auth)

26542 INSPECTION OF THE LAMINATES WITH THE BEAM OF ELECTRONS. Rudenko, V. N.; Karataev, V. D. (Tomsk Polytechnic Inst., USSR). Defektoskopiya; No. 1, 116-19(1971). (In Russian).

The use of accelerator (betatron) electron beams for regulating the thickness of light-element coatings on higher atomic number materials by means of backscattering electrons is discussed. The efficiency and limitations of the method are analyzed and compared with other radiation methods. Experimental data are presented on the reflection of electrons from Al coatings on lead, silicon, zinc, iron and titanium backing at electron energy from 2.4 to 6 MeV. (R.V.J.)

26543 IMPROVEMENTS IN MEANS FOR USING RADIATION FOR ASCERTAINING PROPERTIES OF WEBS. (to Valmet Oy). British Patent 1,228,694. 15 Apr 1971. Priority date 3 Apr 1968, Finland.

A radiometric instrument for measuring properties of a moving web, such as paper, is described. (W.H.K.)

26544 EFFECT OF CONCENTRATION GRADIENTS ON THE PERFORMANCE OF A NUCLEAR SEDIMENT CONCENTRATION GAGE. McHenry, J. R.; Coleman, N. L.; Willis, J. C.; (and others). (Dept. of Agriculture, Oxford, Miss.). Water Resour. Res.; 6: 538-48(Apr 1970).

A nuclear sediment concentration gage, using the attenuation of 22-keV X rays from cadmium-109 as a function of concentration, was evaluated in a series of laboratory tests conducted in a circulating water tunnel. Sediment concentration measurements were made with the X-ray beam directed up, down, and across the test flume section. Coarse sand, fine sand, and kaolin were used as sediments in concentrations of 100 to 30,000 ppm. The suspensions were passed through the water tunnel at velocities of 0.7 to 3 meters sec^{-1}. The response of the nuclear sediment concentration gage was not affected significantly by test position, type or size of particle, or velocity of sediment, but was a function of the total concentration of sediment in the test cross section. (auth)

Miscellaneous Instruments and Components

Refer also to abstracts 26156, 26360, 26373, 26428, 26495, 26497, 26498, 26755, 27189, 27252–27255, 27682, and 28135.

26545 (CEA-N-1430) HIGH-DYNAMIC RANGE RISE TIME TO AMPLITUDE CONVERTER. Prieur-Drevon, M.; Ros, J. (Commissariat a l'Energie Atomique, Grenoble (France). Centre d'Etudes Nucleaires). Feb 1971. 12p. (In French). Dep. NTIS (U. S. Sales Only).

A circuit providing output signals, the amplitude of which is proportional to the rise time of the input pulses defined between 20 and 70 percent of the maximum, is described. The dynamic range is 100:1 for the input pulse amplitude. The converted rise times range between 10 ns and 1.5 μs in 4 ranges. The circuit may also be used for detecting the time of arrival of pulses with variable amplitude and rise time. (auth) (France)

26546 (CEA-R-4166) CIRCUIT FOR DETECTING COINCIDENCES BETWEEN PULSES BY THE MEANS OF SEQUENTIAL GRAPHS. Chicheportiche, Armand (Commissariat a l'Energie Atomique, Saclay (France). Centre d'Etudes Nucleaires). Mar 1971. 55p. (In French). Dep. NTIS (U. S. Sales Only).

The practical problem of detection of coincidences between random pulses can only be conveniently solved by the means of binary analysis. The use of graphs with two coordinate axis associated with arrows corresponding to the commutations leads to an optimized representation of the system, the equations of which can thus be established and easily translated into logical schemes. The different sorts of hazards are systematically located and can be eliminated, when necessary, if a technological choice of the circuits has first been made. The definitions and the theorems of binary analysis, which are needed for understanding this study, are summarized in an appendix. (auth)

26547 (CERN-70-30(Vol.1), pp 307-19) FEASIBILITY OF DIRECT MASS DETERMINATIONS OF SHORT HALF-LIFE ISOTOPES. Johnson, W. H. Jr. (Minnesota Univ., Minneapolis. School of Physics).

In International conference on the properties of nuclei far from the region of beta-stability; Leysin, Switzerland (31 Aug 1970).

Mass measurements may be extended to isotopes far from stability by the technique of peak matching, in which the two members of a mass doublet alternately follow the same trajectory through a mass spectrometer. An ion beam is swept across the collector slit, and the output ion current is viewed on an oscilloscope. The accelerating voltage and deflection plate voltage are alternated on successive sweeps. The voltage difference required for superposition of successive sweeps can be used to determine the mass difference for the doublet. (R.W.R.)

26548 (MLM-1780) TECHNIQUE FOR DIRECT MEASUREMENT OF THERMAL POWER IN ASSAY CALORIMETERS. Otto, G. W.; Jordan, K. C. (Mound Lab., Miamisburg, Ohio). 9 Apr 1971. Contract AT-33-1-GEN-53. 12p. Dep. NTIS.

A new method for the direct measurement of the power input to a servo-controlled calorimeter is described. As applied to assay-type calorimeters the method reduced the analytical time in half and maintained or exceeded previous levels of accuracy in the determination of the thermal power of unknown samples. Additional benefits include applicability to all past and present calorimeters, and ready adaptability to automation by digital computer. (auth)

26549 (ORNL-tr-2462) [STUDY OF THE EXTRACTION AND THE SHAPING OF ION BEAMS IN PLASMA SOURCES]. Raiko, V. I. Translated by Martha Gerrard and J. J. Pinajian (Oak Ridge National Lab., Tenn.), from Kernenergie; 10: 85-9(1967). 16p. Dep. NTIS.

An abstract of this paper, prepared from the original language, appeared as NSA 21: 26285. (M.O.W.)

26550 (RT/ING-(71)1) EQUIPMENT FOR REMOTE CONTROL OF GAMMA SCANNING IN A HOT CELL. Cochi, C.; Babiloni, L. (Comitato Nazionale per l'Energia Nuclear, Rome (Italy)). 8 Jan 1971. 22p. (In Italina).an). Dep. NTIS (U. S. Sales Only).

An electronic equipment for the remote control of an in-cell gamma-scanning system is described. This equipment is designed to produce a longitudinal and rotating continuous or stepping movement, that allows the power distribution determination in cylindrical fuel rods of high or low gamma activity by scanning. A brief description of the gamma-scanning technique is also included (auth)

26551 ON-LINE ISOTOPE SEPARATOR DEVICE CONNECTED TO THE MELUSINE REACTOR (ARIEL PROJECT). Bocquet, J. P.; Brissot, R.; Crancon, J.; Ristori, C. (CEA, Grenoble, France). Bull. Inform. Sci.Tech. (Paris); No. 152, 71-8(Oct 1970). (In French).

An on line isotope separator was installed in order to study the short half-life isotopes (down to 1 s) produced in the fission of ^{235}U by thermal neutrons. The fission target is located near the core of the Melusine reactor. The fission fragments slow down in a thin silver foil and are pumped through the ion source of the separator. A fast moving belt located at the collector of the isotope separator allows measurements to be made on radioactive isotopes 1.5 s after collection. (France)

26552 USA STANDARD: SIGNAL CONNECTORS FOR NUCLEAR INSTRUMENTS. ANSI N 3,3 1968. New York; United States of America Standards Institute (1969). 7p. Available from American National Standards Inst., New York.

Standard coaxial connectors for signal cables for nuclear instruments are described. (W.H.K.)

26553 AMERICAN NATIONAL STANDARD: CRITICALITY ACCIDENT ALARM SYSTEM. ANSI N 16.2 1969. Hinsdale, Ill.; American Nuclear Society (1970). 4p. Available from American Nuclear Society, Hinsdale, Ill.

Guidelines for the establishment and maintenance of an alarm system to initiate personnel evacuation in the event of inadvertent criticality are presented. (W.H.K.)

26554 DECUS PROCEEDINGS. PAPERS AND PRESENTATIONS OF DIGITAL EQUIPMENT COMPUTER USERS' SOCIETY, SPRING SYMPOSIUM, WAKEFIELD, MASSACHUSETTS, MAY 12–13, 1969. Maynard, Mass.; Digital Equipment Computer Users Society (1969). 390p. (CONF-690510).

Separate abstracts were prepared for 11 of the 61 papers presented. The remaining 50 papers were not sufficiently within the scope of NSA. (W.H.K.)

For abstracts of individual papers see: 26495–26497, 26510–26512, 26555–26557, 28134, and 28135.

XUM

26555 TECHNIQUES FOR COMPILING LARGE FORTRAN PROGRAMS FOR A PDP-9 COMPUTER. Donati, Donald R.; Mathur, Suresh C. (Lowell Technological Inst., Mass.). pp 103-4 of DECUS Proceedings. Maynard, Mass.; Digital Equipment Computer Users' Society (1969).

From DECUS symposium, Wakefield, Mass. (12 May 1970). See CONF-690510.

The addition of a Chain Builder Program to the PDP-9 Advanced Software system has now provided the capability of compiling very large FORTRAN programs on the 16K memory configuration. Three nuclear structure programs, originally written for large computers with 32K or more core memory, have now been compiled for the PDP-9 computer at this laboratory. This work has demonstrated that small computers can now handle large scientific programming applications, which till recently required the availability of large and expensive computer configurations. (auth)

26556 DISC-BASED OPERATING SYSTEM FOR MASS SPECTROMETRY EXPERIMENTS. Frye, Roger E.; Slaughter, Barbara G.; Fraipont, Donald F. (Applied Data Research, Inc., Princeton, N. J.). pp 167-77 of DECUS Proceedings. Maynard, Mass.; Digital Equipment Computer Users' Society (1969).

From DECUS symposium, Wakefield, Mass. (12 May 1970). See CONF-690510.

An operating system for a 4K PDP-8 with 32K disc allows flexible control of mass spectrometry data collection and processing. Optional output devices include IBM compatible magnetic tape and a digital plotter. Spectral data are accepted through a low-cost interface from an on-line high or low resolution mass spectrometer, analog tape recorder, or high speed paper tape reader. Facilities provided by the system include: 1) Tuning of the interface and program parameters; 2) Calibration of reference compounds; 3) Data acquisition; 4) Scan file manipulation; 5) Digital plot; 6) Automatic identification of reference peaks; 7) Time to mass conversion; 8) Atomic composition report; 9) Quantitative spectrum; 10) Plotted spectrum; and 11) Permanent storage of scan data. (auth)

26557 COMPUTER CONTROLLED DYNAMIC CINERADIOGRAPHY. Fujimura, O.; Ishida, H.; Kiritani, S. (Tokyo Univ.). pp 279-83 of DECUS Proceedings. Maynard, Mass.; Digital Equipment Computer Users' Society (1969).

From DECUS symposium, Wakefield, Mass. (12 May 1970). See CONF-690510.

The high speed cineradiography can provide very effective means for the study of articulatory movements. The best possible way in principle for minimizing the dose problem is to use the x-ray exposure only when and where it is necessary for deriving immediately useful data. For this purpose, a new radiographic technique of "Computer Controlled Dynamic Cineradiography" has been proposed and preliminary experiments are now under way. Employing an on-line digital computer PDP-9 for controlling an x-ray microbeam produced by a special x-ray generator, the proposed system not only reduces the x-ray dose by a substantial factor but also provides a feasible and effective way for data processing in the study of articulatory movements. (auth)

26558 DECUS PROCEEDINGS. PAPERS AND PRESENTATIONS OF DIGITAL EQUIPMENT COMPUTER USERS' SOCIETY, SPRING SYMPOSIUM, ATLANTIC CITY, NEW JERSEY, MAY 4-5, 1970. Maynard, Mass.; Digital Equipment Computer Users' Society (1970). 361p. (CONF-700524).

Separate abstracts were prepared for 4 of the 47 papers presented. The remaining 43 papers were not sufficiently within the scope of NSA. (W.H.K.)

For abstracts of individual papers see: 26500, 26501, 28575, and 28713.

26559 SAMPLING OF RADIOACTIVE DEPOSITION THROUGH ION-EXCHANGE RESINS. De Bortoli, M. C.; Gaglione, P. (EURATOM, Ispra, Italy). Minerva Fisiconucl.; 13: 219-24 (Jul-Sep 1969). (CONF-680535-24).

From 14. national conference of the Italian Association for Health Physics and Protection from Radiation; Formia, Italy (29 May 1968).

A collector for radioactive fallout employing a column of ion-exchange resins has been developed and operated during two years. The comparison between the collection efficiency of the new collector and that of the evaporation collector (pot) shows that they are equivalent. The column collector is equipped with a filter, thus permitting the determination of the undissolved fraction of the radionuclides. This fraction has been found to depend on the amount of rain and the correlation equations are given for ^{90}Sr and ^{137}Cs. (auth)

Radiation Effects on Instruments and Instrument Components

Refer also to abstracts 27838 and 27852.

26560 (SC-DR-710045) TENTATIVE METHOD FOR EXPRESSING RADIATION HARDNESS. McKenzie, J. M. (Sandia Labs., Albuquerque, N. Mex.). Mar 1971. 42p. Dep. NTIS.

A technique is described for measuring neutron radiation hardness in terms of 14-MeV neutrons. A calibration procedure for the primary standard is given. This is based on a measured value, at 14.1 MeV, of the $^{19}F(n,2n)^{18}F$ cross section. An example describes the determination of the 14-MeV damage equivalence of an unknown neutron spectrum. A method to obtain the precision of the result is given. (auth)

26561 SOME EFFECTS OF THE NUCLEAR RADIATION ON SEMICONDUCTOR ELEMENTS. Opuchlik, M. Elektronika; 11: 475-9(1970). (In Polish).

The influence of nuclear radiation on semiconductors is examined taking into account the recombination and generation processes. As consequence of the changes in minority carriers lifetime caused by radiation, the current distribution in the p-n junction also varies. This fact imposes restrictions in selection of elements for devices operating in radiation environment. (auth)

26562 PERFORMANCE OF IMPACT AVALANCHE TRANSIT TIME DIODES UNDER THE INFLUENCE OF GAMMA AND NEUTRON RADIATION. Anderson, Wayne Arthur. Buffalo; State Univ. of New York (1970). 121p. University Microfilms Order No. 71-7143.

Thesis.

Several Impact Avalanche Transit Time (IMPATT) Microwave Diodes were studied while operating in the radiation beam from the Western New York Research Center's reactor. Computer solutions and experimental studies were used to evaluate radiation effects on IMPATT diodes. The experimental study involved the use of a Van de Graaff generator and nuclear reactor as sources of radiation. A microwave circuit was designed which placed the diode oscillator in the radiation region during diode oscillation. A mechanized, remote-controlled slide-screw turner was necessary due to the inaccessibility of the tuner during reactor studies. Both tuner and diode were located at the bottom of the reactor pool in a 30 foot pipe. The variable load permitted the accumulation of data to plot Rieke diagrams to further study radiation effects. The principal effects of radiation flux were an increased reverse bias current, cessation of oscillation for high flux densities, and a decreased rf power output. The principal effects of neutron fluence were an increased power output, increased oscillation frequency, increased negative resistance and reactance, and an increased reverse bias voltage. Rieke diagram constant power contours became smaller during and after irradiation. Frequency contours became shorter and shifted 60° counter-clockwise during irradiation. Radiation pulses caused the diodes to cease oscillating and then recover after about 15 minutes waiting time. Some diodes exhibited several simultaneous frequencies of oscillation all of which were equal to or higher than the pre-irradiation value. Passivated diodes were observed to be much more sensitive to gamma flux. These diodes ceased to oscillate at gamma fluxes lower than the point where non-passivated diodes still worked well. (Diss. Abstr. Int., B)

26563 NEUTRON DAMAGE IN EPITAXIAL GaAs LASER DIODES. Barnes, C. E. (Sandia Labs., Albuquerque, N. Mex.). J. Appl. Phys.; 42: 1941-9(Apr 1971).

The effects of neutron irradiation on the radiative, nonradiative, and threshold currents in epitaxial GaAs laser diodes have been studied at room temperature and 76°K. At 300°K for currents below the threshold, most of the current flows by recombination in the space-charge layer, but the radiative current is due to minority carriers thermally injected into the p-type region. Neutron irradiation does not significantly affect these current flow mechanisms. However, it does lead to a reduction in light intensity and an increase in total current through the introduction of nonradiative recombination centers which reduce the lifetime in both the space-charge and neutral regions. Neutron irradiation has less of an effect on the diode properties at 76°K. The radiative current, which is apparently due to tunneling, is rather insensitive to irradiation when the voltage is held constant. However, at constant current the light intensity decreases with neutron fluence although not as rapidly as in the constant current case at 300°K. Similar to the results at 300°K, the total current increases with irradiation; the additive current being due to space-charge recombination and nonradiative

tunneling. The laser threshold current increases with neutron irradiation by a multiplication factor which is approximately independent of temperature. The changes in J_T can be accounted for by assuming that the neutron-induced nonradiative recombination centers lead to a decrease in the internal stimulated quantum efficiency. Very little annealing of the light degradation was observed between 19 and 550°K. No neutron-induced time delay in laser turn on was detected. (auth)

26564 RADIATION AND MECHANICAL DAMAGE OF DIFFUSED LAYER OF SILICON SOLAR CELLS. Usami, Akira (Nagoya Inst. of Tech., Japan). Oyo Butsuri; 39: 1106-12(Dec 1970). (In Japanese).

It is found that the degradation rate of the open-circuit voltage is remarkably larger than that of the short-circuit current in silicon solar cells damaged by 40 keV protons. The reduction in the minority carrier lifetime of the diffused layer of a cell thus damaged is estimated by fitting the curve of the observed change in spectral response to the calculated one. Bombardment with a total flux of 1.71×10^{15} protons/cm^2 of 40 keV protons reduced the n-type diffused region lifetime by a factor of 5 in a particular case. The spectral response change by #2000 Al_2O_3 lapping on the surface of the silicon solar cell extends to a longer wave length region than that by #4000 Al_2O_3 lapping in which the degradation of the spectral response is observed mainly in the region of wavelength shorter than 600 mμ. This result is due to the decrease of the carrier lifetime in the diffused layer as shown by numerical analysis. (auth)

LIFE SCIENCES

Biochemistry, Physiology, and Molecular Biology

26565 ELECTRON MICROSCOPY, 1968. VOLUME II. Pre-Congress Abstracts of Papers Presented at the Fourth European Regional Conference Held in Rome, September 1–7, 1968. Bocciarelli, Daria Steve (ed.). Rome: Tipografia Poliglotta Vaticana (1968). 609p. (In several languages). (CONF-680942–(Vol.2)).

Pre-congress abstracts of papers on electron microscopy to be presented at the 4th European Regional Conference in Rome during 1968 are included in volume II. The abstracts are grouped into the following topical categories: biological techniques, biological scanning electron microscopy, cytochemistry, biomacromolecules, virus development and structure, tumors, nucleus, immunoelectromicroscopy, organelles, membrane structure, intercellular contact, permeability and transport, muscles, embryology, germical cells, endocrine glands, plant cell structure and differentiation, mineralized tissues, microorganisms, autoradiography, tissues, organs, systems, and sensorial organs. One abstract; "Demonstration of Radiation Induced Changes in the Fine Structure of Canine Retina" was within the scope of NSA. (E.R.B)

Basic Processes

Refer also to abstracts 26465, 26473, 26944, and 27134.

26566 (CEA-CONF–1711) STUDY OF THE CYCLIC VARIATION OF VOLUME OF THE HEART. COMPUTER TREATMENT OF MEASUREMENTS FURNISHED BY AN ISOTOPIC METHOD. Zwirn, P.; Viers, M.; Berbezier, J.; Sebaoun, E.; Lemaitre, J. (Commissariat a l'Energie Atomique, Cadarache (France). Centre d'Etudes Nucleaires). [1967]. 14p. (In French). (CONF-700833–1). Dep. NTIS (U. S. Sales Only).

From Symposium on dynamics studies with radioisotopes in clinical medicine and research; Rotterdam, Netherlands (31 Aug 1970).

The cyclic variation of the heart volume was studied in dogs injected with ^{131}I-labeled serum albumin. The method is based on the fact that a homogeneous radioactive liquid has an emission proportional to its volume and therefore the radioactivity recorded from the cardiac cavities filled with blood will be proportional to the volume of the cavities and will vary with the heart contraction. The method is reproducible and completely applicable to humans. It furnishes curves similar to those obtained by other techniques more complicated to perform and more traumatic to the patient. The different periodicity of successive cardiac cycles is normalized by Fourier series analysis by computer processing of the data. (J.S.R.)

26567 (STI/PUB–263) DYNAMIC STUDIES WITH RADIOISOTOPES IN MEDICINE. Proceedings Series. Proceedings of the Symposium Held in Rotterdam, 31 August–4 September 1970. (International Atomic Energy Agency, Vienna (Austria)). Feb 1971. 915p. (In English and French). (CONF-700833). IAEA $24.00.

The proceedings contain 70 papers dealing primarily with tracer techniques in function studies. The papers are grouped into the following topical sections; theoretical aspects, techniques and instruments, thyroid function studies, renal function studies, hepatic and splenic function studies, mineral metabolism studies, regional blood flow studies, cardiac function studies, and pulmonary function studies. (E.R.B.)

26568 SIMPLE METHOD FOR DETERMINING THE CONCENTRATION OF SERUM THYROXINE BY COMPETITIVE DISPLACEMENT ANALYSIS. Banos, Csaba; Tako, Jozsef; Gyoergyi, Sandor; Sztraka, Helen; Kapus, Istvan (Janos Hospital, Budapest. Semmelweis Univ. Medical School, Budapest). Nucl.-Med.; 9: 341-9(31 Dec 1970).

A simplified method for the determination of serum thyroxine is described. The mathematical formulation of the standard curve required for the competitive displacement analysis permits an evaluation of the serum thyroxine concentration with the use of two standard values instead of measuring the full curve. Thyroxine extracted from the unknown serum is added to the system containing thyroxine-binding globulin and ^{125}I-labeled thyroxine. The values calculated from the formula show a very close correlation with those obtained by comparison with the standard curve. (auth)

26569 USE OF AN ANALOGUE CIRCUIT FOR ON-LINE CORRECTION IN SIMULTANEOUS DOUBLE-TRACER STUDIES. Lange, D. (Univ., Heidelberg). Nucl.-Med.; 9: 385-96(31 Dec 1970). (In German).

In functional studies with two simultaneously administered radioisotopes, both functions may be followed by means of an on-line correction of the ratemeter output voltages with an analogue circuit, provided the gamma ray energies of the two radioisotopes differ sufficiently. The corrected curves are registered on a strip-chart recorder. The correction factors used for the partial subtraction of the signal voltage of the higher-energy isotope from that of the lower-energy isotope have to be determined by means of phantom measurements prior to the investigation. Taking ^{131}I as an example it is demonstrated that the correction factor increases with increasing tissue depth. However, an error in the localization of this isotope in the tissue-equivalent phantom of 4 cm results in an error of the correction factor of less than 10%. A simulated function study of the kidneys showed that the filtration rate (EDTA) alone could have been determined simultaneously with the primarily tubular excretion of ^{131}I-Hippuran. (auth)

26570 EARLY INTRACELLULAR EVENTS IN THE REPLICATION OF BACTERIOPHAGE T4 DEOXYRIBONUCLEIC ACID. V. FURTHER STUDIES ON THE T4 PROTEIN-DEOXYRIBONUCLEIC ACID COMPLEX. Miller, Robert C. Jr.; Kozinski, Andrzej W. (Univ. of Pennsylvania, Philadelphia). J. Virol.; 5: 490-501(Apr 1970).

Soon after infection parental deoxyribonucleic acid (DNA) enters a structure sedimenting fast to the bottom of a sucrose gradient. The addition of chloramphenicol (CM) prevents formation of this structure, whereas treatment with Pronase releases DNA which sediments thereafter with the speed characteristic of phenol-extracted replicative DNA. It is assumed therefore that the structure responsible for fast sedimentation of replicative DNA is a newly synthesized protein. Those fast sedimenting complexes contain preferentially the replicative form of parental DNA; this was proven by density labeling experiments. Progeny DNA labeled with ^{3}H-thymidine added after infection can also be detected preferentially in this fast-sedimenting moiety. The association of the DNA with the complexing protein is of a colinear or quasi colinear type. This was proven by introducing double strand scissions into DNA embedded in the replicative complex; double strand scissions do not liberate DNA from the fast sedimenting complex. Despite the apparent intimate relation between protein and DNA, DNA residing in complexes is fully sensitive to the action of nucleases. Shortly prior to the appearance of the fast-sedimenting complex, parental DNA displays still another characteristic: at about 3 min after infection, it sediments faster than reference, but sizeably slower than the complex which appears at roughly 4 to 5 min after infection. The transition between these two fast sedimenting types of moieties is not continuous. This fast-sedimenting intermediate, which appears at 3 min after infection, cannot be inhibited by the addition of CM either at the moment or prior to infection. Fast-sedimenting intermediate can be destroyed by sodium dodecyl sulfate, Pronase, or phenol extraction. The progeny DNA labeled with ^{3}H-thymidine between 3 and 3.5 min after infection can be recovered in fast sedimenting intermediate. The contribution of newly synthesized progeny DNA is so small that it cannot be detected as a shift of the parental density in a density labeling experiment. Small fragments of progeny DNA recovered in fast sedimenting intermediate are not covalently attached to parental molecules and represent both strands of T4 DNA. (auth)

26571 I. ESTIMATION OF MEAT COMPOSITION BY DIFFERENTIAL ABSORPTION OF GAMMA RAYS. II. EFFECTS OF PARENTAL SIZE ON CARCASS COMPOSITION AND PERFORMANCE OF LAMBS. Ringkob, Thomas Paul. Ithaca, N. Y.; Cornell Univ. (1970). 96p. University Microfilms Order No. 70-17,098.

Thesis.

A method for rapid estimation of fat content of fresh meat was examined which utilized γ attenuation to elucidate the composition of a two-phase system such as fat and lean. A two-phase system can be analyzed by using two energy sources which have different mass absorption coefficients for the two components being considered. The two isotopes, iodine-125 (27.4 keV) with a thin sheet of tin to filter out the higher energy photons and americium-241 (59.6 keV), were prepared as sealed point sources to produce monochromatic x-ray beams which were well-collimated. The emulsified meat sample was placed between the source and the detector. The sample was analyzed first with a 75 mCi ^{125}I source and then a 14 mCi ^{241}Am source. The ratio of the logarithms of

the attenuations of the ^{125}I to ^{241}Am was calculated. Reference standards of water and commercially rendered lard were used and the fraction of fat in the unknown sample was determined by interpolation. Correlations were –.9 or greater between estimated fat content by the γ ray attenuation technique and the ether extract content in the emulsified meat samples. However, the standard error of the estimate was too large for the individual meat samples to be of value to the meat industry. The influence of parental size on growth rate, carcass traits, and the chemical composition of the lamb carcass was also evaluated. Sixty lambs were produced by mating a small (54 kg.) and large (118 kg.) ram to a light (48 kg. average) and heavy (69 kg. average) group of ewes. Thirty lambs were randomly allotted to a light slaughter group (36 kg.) and a heavy slaughter group (48 kg.). Larger parents were associated with a faster rate of gain for the live animal, more carcass, more trimmed primals, and more grams of rack protein per day of age. (Diss. Abstr. Int., B)

26572 APPLICATION OF STABLE ISOTOPES IN MEDICAL AND BIOLOGICAL EXPERIMENTS. Bernat, Ivan; Cornides, Istvan. Honvedorvos; 22: 201-11(Jul-Sep 1970). (In Hungarian).

The determination of stable isotopes by mass spectrometry is described as well as chemical sample preparation. The method is used for measuring ^{15}N in heme. The results showed that in burn patients the average life span of erythrocytes was shortened to 111 days as compared to 120 days in normal persons. (H.B.G.)

26573 STUDIES ON THE MEDITERRANEAN FRUIT FLY IN TUNISIA. Feron, M. (Institut National de la Recherche Agronomique, Cantarel, France). pp 83-5 of Insect Ecology and the Sterile-Male Technique. Vienna; International Atomic Energy Agency (1969). (In French).

From Panel on Insect Ecology as Related to Control of Noxious Insects by the Sterile-Male Technique, Vienna, Austria. See STI/PUB-223; CONF-670853.

The work performed by Soria, Sigwalt and Yana of INRAT has provided some valuable basic knowledge of the ecology of Ceratitis capitata in Tunisia and of the efficacy of the different methods of study. A list of host-plants was established and this has contributed to crop protection; the eradication of certain dangerous plants reduced the rate of increase of the flies at certain times of the year. The release-recapture method with flies labelled with ^{32}P has permitted the authors to estimate the population level, which is quite low in winter (10 to 100 males per hectare). Various trapping methods (permanent traps, discontinuous and continuous trapping and release–recapture) have, in addition, contributed toward a better understanding of the variations in the population of this insect. (auth)

26574 ALPHA-PARTICLE AUTORADIOGRAPHY OF ALKALINE PHOSPHATASE INHIBITION BY CADMIUM. Landolt, R.; Gutwein, E. E. (Purdue Univ., Lafayette, Ind.). Int. J. Appl. Radiat. Isotop.; 22: 127-8(Feb 1971).

This paper is concerned with quantifying the inhibition of kidney alkaline phosphatase by cadmium using a modification of an existing alpha-particle autoradiographic technique in which ^{210}Pb was added to the metal salt used for staining the enzyme in tissue sections. (UK)

26575 EFFECTS OF PALMITIC ACID ON THE BINDING OF ^{131}I-INSULIN TO RAT LIVER MITOCHONDRIA. Katsumata, Kazuo (Nagoya Univ., Japan). Nagoya J. Med. Sci.; 32: 445-51(Mar 1970).

The effects of palmitic acid, inhibitors, uncouplers, and reduced and oxidized glutathione on the binding of ^{131}I-insulin and ^{131}I to isolated fresh or aged mitochondria were studied. The binding of ^{131}I-insulin to the fresh mitochondria was unexpectedly increased to a greater degree with the exogenous addition of palmitic acid, glutathione, acetaldehyde, and 2, 4-dinitrophenol to the medium. The fact indicated that the intactness of mitochondria was not prerequisite for the binding of ^{131}I-insulin to the isolated mitochondria. The binding of ^{131}I-insulin was compared to the fresh mitochondria and the aged mitochondria. ^{131}I-insulin bound to the aged mitochondria in a lesser degree. It is suggested that the binding of ^{131}I-insulin to the mitochondria might be related to the mitochondrial functional and conformational state. The binding of ^{131}I to the mitochondria was apparently different from that of ^{131}I-insulin. And the binding of ^{131}I was not altered by these uncouplers except in the case of acetaldehyde and ethyl alcohol. This implies that the process of binding of ^{131}I-insulin is different from that of ^{131}I. In the case of ^{131}I, it may have some connections with the ion transport mechanism. (auth) (Japan)

26576 ^{133}Xe CLEARANCE AND LIVER BLOOD FLOW. AN EXPERIMENTAL STUDY IN THE CAT. Darle, Nils (Goteborg Univ.). Acta Chir. Scand., Suppl.; 407: 1-64(1970).

The wash-out curve of intraportally administered ^{133}Xe, registered over the liver of the cat, was analysed. It was found that the wash-out curve consistently contained two components. The mean values of the half-times of the two components were 0.67 and 9.71 minutes, respectively. The components were thereafter named the fast and the slow component. The elimination curve over the liver after intraportal injection of ^{133}Xe was compared with the wash-out curve registered over the injection catheter as well as with the elimination curve registered over the lung. The results indicated that the fast component of the liver elimination curve reflects intrahepatic blood flow whereas the slow component reflects extrahepatic activity. The portal vein flow was registered with the aid of an optical drop-recorder and the recorded flow expressed in ml/min × 100 g liver tissue was compared with the flow values wash-out curve. In these experiments the recorded portal vein flow was less than 50% of the flow calculated from the simultaneously obtained wash-out curve from the liver. When the flow values from several experiments in the same animal were compared a linear relationship between the recorded flow and the calculated flow was, however, found. The blood flow calculated from the wash-out curve approximately corresponded to the total outflow of the liver, the mean value of the relationship of the flow values being 1.09. In the same animal changes in the total liver blood flow are reflected accurately in the values calculated from the wash-out curves. Because of inter-individual variations in total fat content of the liver and in the magnitude of the partition coefficient, flow values from different animals were, however, not comparable without corrections for possible variations of the partition coefficient. (auth) (Sweden)

26577 DETERMINATION OF CORTICAL BLOOD FLOW IN RABBIT FEMUR BY RADIOACTIVE MICROSPHERES. Lunde, P. K. M.; Michelsen, K. (Oslo Univ.). Acta Physiol. Scand.; 80: 39-44(Sep 1970).

The method for blood flow determination involving measurement of relative radioemission from radioactive microspheres retained in various tissues after intravascular injection was applied to minute tissue regions. ^{85}Sr-labeled plastic microspheres with a diameter of 15 ± 5 μ were injected in a retrograde manner into the aorta in 10 anesthetized adult rabbits. The tissues included were the m. quadriceps femoris tendon, the cortical bone, and the corresponding bone marrow from the left femur diaphysis. The unknown blood flows through these tissue regions were calculated by relating the measured radioactivity from tissue samples to a known blood flow and a known blood radioactivity in cannulated branches from the left posterior tibial artery. The blood flow values estimated by this technique were (g/min × g tissue): quadriceps femoris tendon –0.068 ± 0.044, bone marrow of femur diaphysis –0.250 ± 0.146, cortical bone of femur diaphysis –0.010 ± 0.007. (auth) (Sweden)

Metabolism, Physiology, and Toxicology

Refer also to abstracts 26740, 26839, 26943, 27012, and 27032.

26578 (CONF-680112–, pp 153-66) THE APPLICATION OF ATOMIC ENERGY TECHNIQUES TO INCREASE PRODUCTIVITY OF DOMESTIC LIVESTOCK. Lengemann, F. W. (New York State Veterinary Coll., Ithaca. Dept. of Physical Biology).

A review is presented of studies using radioisotopes for research on increasing productivity of farm animals. Studies were conducted on the comparative utilization of iodate and iodide as sources of iodine for dairy cattle using ^{131}I and ^{125}I as tracers. Radioisotopes of Ca were used in studies on Ca metabolism, and a table is presented to show the Ca maintenance requirements of cattle as a function of age. The use of unabsorbable radioactive markers in animal research is discussed; an example is the use of ^{91}Y as a marker in studies on Ca metabolism in chickens. The use of ^{14}C-polyethylene glycol for studies on secretion of mineral elements in milk is described. The use of neutron activation for determining levels of elements in tissues and secretions is discussed. A liquid scintillation type of whole-body counter for research on animal productivity is described; this instrument makes it possible to give extremely small doses of radioisotopes and to follow activity for longer periods of time than by other procedures. This technique was used for research on utilization of hemoglobin ^{59}Fe by sheep; effects of antihelminthic drugs on ^{59}Fe losses in lambs; excretion of fallout radioisotopes by cattle; and counting of ^{40}K to study body composition as a function of sex, age, diet, and hormonal treatments. Research on utilization of nonprotein nitrogen using ^{15}N is reviewed. Studies on the use of x-irradiated larvae as a vaccine against Dictyocaulus viviparous, a lung parasite of cattle, are described. (H.L.W.)

26579 DETERMINATION OF INTEGRATED PLASMA CONCENTRATIONS AND TRUE SECRETION RATES OF HUMAN

XUM

GROWTH HORMONE. Kowarski, A.; Thompson, R. G.; Migeon, C. J.; Blizzard, R. M. (Johns Hopkins Univ., Baltimore). J. Clin. Endocrinol. Metab.; 32: 356-60(Mar 1971).

A method is described that permits the measurement of the integrated concentration of growth hormone, or any substance whose concentration in blood fluctuates widely. This method employs a small portable constant withdrawal pump with heparin-coated plastic cannula and tubing that are inserted intravenously through a disposable needle. Similar metabolic clearance rates (MCR) of ^{131}I-HGH and nonradioactive HGH were found using a constant infusion technique. Changes in position, except for standing totally immovable, did not significantly alter the MCR, nor did it change the concentration of HGH. The true secretion rate of HGH was calculated in four normal female volunteers by multiplying their individual MCR of HGH by their integrated concentration of HGH. The secretion rates of HGH in these subjects ranged from 0.65 to 1.51 mg/24 hr. The secretion rate of HGH in an acromegalic patient was found to be 8.08 mg in 24 hr. (auth)

26580 DISCRETE FORMULATION AND ERROR MINIMIZATION IN APPLYING THE INTEGRO-DIFFERENTIAL EQUATION APPROACH TO MONO-COMPARTMENT DATA. Hart, Hiram E.; Sondheimer, James H. (City Coll., New York). Comput. Biol. Med.; 1: 59-74(Aug 1970).

A computer program, using the IBM 360 Scientific Subroutine Package, was used to calculate the distribution of a radioisotope tracer following intravenous injection in vascular systems as a function of time. The method allows each data point in a sequence of time intervals to be entered directly into the calculations. The method is more accurate than results obtained by careful long-term counting of the activity in successive blood samples. (C.H.)

26581 STUDY OF THE OBSERVED RATIOS BETWEEN ^{90}Sr/Ca AND ^{137}Cs/K IN THE DIET AND PASSAGE THROUGH HUMAN MILK. Calapaj, G. G.; Ongaro, D. (Univ., Padua). Nuovi Ann. Ig. Microbiol.; 18: 383-94(Sep-Oct 1967). (In Italian).

The average observed ratios (O.R.) ^{90}Sr/Ca and ^{37}Cs/K in the passage of these radioisotopes from diet to human milk were calculated. To this aim, groups of mothers that bore their children from 4 to 7 days earlier were kept on a controlled diet for four days. At the end of the fourth day, pooled samples of the milk of the donors of each group were prepared. ^{90}Sr, Ca, ^{137}Cs, and K were dosed in the pools and in the foodstuffs ingested by the mothers in the four days before milk drawing. Four experiments were performed for the ^{90}Sr/Ca and three for the ^{137}Cs/K. The O.R.s calculated from the intake of the fourth day alone did not differ significantly from those calculated on the basis of the daily average intake of the previous four days, so it was concluded that a metabolic equilibrium state was reached. The O.R. ^{90}Sr/Ca proved to be fairly constant and considerably less than unity; whereas the O.R. ^{137}Cs/K, besides being much greater than unity, showed an extremely large variability from one experiment to another. Since the ratios between the ingested and excreted potassium, shadow element of ^{137}Cs, remained fairly constant in the three experiments, a different metabolic behavior for ^{137}Cs in comparison with ^{90}Sr is suggested. The conclusion is drawn that the mother organism constitutes an efficient barrier against radiocontamination from ^{90}Sr of her feeding baby, whereas the same cannot be said for the radiocontamination from ^{137}Cs. (auth)

26582 INORGANIC PHOSPHORUS IN RED BLOOD CELLS OF MINERS IN URANIUM MINES. Nosek, J.; Bartonova, H. (Inst. of National Health in Uranium Industry, Pribram, Czech.). Cas. Lek. Cesk.; 108: 1263-4(10 Oct 1969). (In Czech).

In starving red blood cells in vitro, the concentration of inorganic phosphorus increased with time. Using the student t-test, no marked differences were found between miners and controls in the inorganic phosphorus level nor in its change during starvation of red blood cells. (auth) (NSA of Czech)

26583 EFFECT OF PRUSSIAN BLUE COMBINED WITH PILOCARPINE ON ^{137}Cs EXCRETION IN RATS. Havlicek, F.; Beran, M. (Military Research Inst. of Veterinary Medicine, Prague). Vet. Med. (Prague); 14: 465-70(Aug 1969). (In Czech).

Prussian Blue when present as a 1% admixture in the daily diet of rats decreased the retention of ^{137}Cs applied intraperitoneally and particularly led to a decreased ^{137}Cs accumulation in the liver, kidney, duodenum, and bones. A first portion of 15 and 62% was rapidly excreted by controls and by experimental animals, respectively. Further elimination continued with biological half-lives of 8 and 5.2 days, respectively. A repeated application of pilocarpine in doses of 4, 16, 40, and 160 mg per rat per day resulted neither in enhanced ^{137}Cs excretion nor in its redistribution. (NSA of Czech)

26584 LINKAGE OF RADIOCERIUM TO BLOOD SERUM PROTEINS STUDIED BY DIALYSIS TECHNIQUES. Slouka, V.; Bathova, M. (Military Medical Research and Postgraduate Inst., Hradec Kralove, Czech.). Sb. Ved. Pr. VLVDU Hradci Kralove; 41: 105-23(1969). (In Czech).

Cellophane "Visking" was used for dialysis procedures. In a 10^{-4}M $^{141}CeCl_3$ solution in TRIS-buffer (pH 7), the filtrability decreased because of hydrolysis linearly with time for 24 hrs; after that it remained unchanged. Results of a sedimentation experiment also proved that the hydrolytic process was completed in 24 hrs. Experiments involving various $CeCl_3$ carrier concentrations (from 10^{-11} to 10^{-3}M) showed a strong decrease in filtrability with decreasing concentration in the range 10^{-6} to 10^{-7}M; over the range of $10^{-11} - 10^{-8}$M the filtrability was about 10%. In the presence of rat plasma, human serum, 5% human γ-globulin, and 5% serum albumin, the results strongly depended on pH. The values corresponding to pH 3-3.5 were about one order higher than those observed at pH 6-7.5. At pH values of 5.0 to 6.0, where the strongest linkage to proteins is to be expected, the lowest filtrability was found. In the presence of serum ultrafiltrate the Ce filtrability was also reduced; the compounds binding Ce were not yet identified but they were found to absorb UV light at 254 nm. (NSA of Czech)

26585 PROBLEMS OF EXCRETION ANALYSIS AFTER REPEATED INTERNAL CONTAMINATION WITH STRONTIUM RADIOISOTOPES. Neruda, O.; Hradil, J. (Military Medical Research and Postgraduate Inst., Hradec Kralove, Czech.). Sb. Ved. Pr. VLVDU Hradci Kralove; 41: 43-65(1969). (In Czech).

Calculations of radiation doses due to repeated internal contamination from nuclear explosions during a nuclear war are discussed. Determination of ^{89,90}Sr in the organism is suggested as the best approach. Excretion analysis based on measuring ^{89,90}Sr in daily urine is the easiest way. Retention and excretion curves were plotted for human organism. The accuracy of the estimate depends on the knowledge of the time course of Sr intake; the intake has to be terminated several days prior to sampling urine. Otherwise, the activity of foodstuff has to be measured and appropriate corrections made. Excretion analysis can be combined with whole-body counting, however, the latter is very difficult because of the parameters of radionuclides of interest. The diagnosis of internal radiostrontium contamination is of interest for a prognosis of late consequences. A great statistical spread is expected as far as these consequences are concerned. (NSA of Czech)

26586 ESTIMATION OF ^{47}Ca IN FAECES. Bullamore, J. R. (General Infirmary, Leeds, Eng.). Int. J. Appl. Radiat. Isotop.; 21: 677-8(Nov 1970).

A method that combines the advantages of permanent homogenity in the faecal sample with an automatic counting procedure is described. Faeces were homogenised and an aliquot suspended in a gel in a container suitable for direct use in conventional automatic γ counting equipment. Patients were given 10 μCi of intravenous ^{47}Ca and a table of results obtained from duplicate samples is given. Self absorption in the faecal samples was found to be neglible. (UK)

26587 INITIAL UPTAKE, DISTRIBUTION, AND LOSS OF SOLUBLE ^{106}Ru IN MARINE AND FRESHWATER ORGANISMS IN LABORATORY CONDITIONS. van der Borght, O.; van Puymbroeck, S. (Belgian Nuclear Center, Mol). Health Phys.; 19: 801-11(Dec 1970).

The early uptake, distribution, and loss by some freshwater and marine organisms of ^{106}Ru in solution in the water and originating from nitrosyl nitrate complexes were studied during short periods (1 to 10 days) in laboratory conditions. Freshwater animals used were: Anodonta anatina (mussel), Lymnaea stagnalis, and Viviparus contectus (snails), and Alburnus lucidus (the bleak: a fish); marine organisms were: Fucus vesiculosus (an alga), Mytilus edulis (the mussel), Littorina littorea, and Purpura lapillus (two gastropods). The initial uptake and distribution of ^{106}Ru is similar when one compares the marine and the freshwater lamellibranch (Mytilus and Anodonta); but the fixation of Ru is much higher in the freshwater snail Viviparus than in the fish Alburnus. Surface adsorption is likely to play an important role in the radiocontamination of the organisms by soluble Ru. This is suggested by the high Ru content of thin structures in direct contact with water such as the byssus, the border of the shell and the operculum. The temperature dependence ($Q_{10} \simeq$ 1.8) of the initial uptake of Ru in the marine organisms suggests some metabolic interference, although it is striking that, both

in the alga and in the animals studied, this temperature dependence as well as the general kinetics of the uptake (sequence of two exponentials) are similar. (auth) (UK)

26588 HAEMOLYSIS OF RED BLOOD CELLS IN PROPYLENE GLYCOL SOLUTIONS IN MINERS FROM URANIUM MINES. Nosek, J.; Bartonova, H. (Inst. of National Health in Uranium Industry, Pribram, Czech.). Cas. Lek. Cesk.; 108: 1335-8 (31 Oct 1969). (In Czech).

Hemolysis was studied, in the presence of 40 to 50% propylene glycol, of red blood cells of miners from uranium mines and of a control group. The average time of osmotic hemolysis of native red blood cells was longer in miners than in controls. In in vitro experiments, a similar prolongation of the time of hemolysis was observed when the amount of 0.16 g of $UO_2(NO_3)_2 \cdot 6\,H_2O$ was added to 2 ml of the suspension. Lead salts were also able to prolongate the time of hemolysis, but only when present in relatively high concentrations that cannot be expected in vivo. This effect was potentiated when red cells preliminarily altered with uranyl salts were exposed to the effect of lead salts. Simultaneous action of these salts and of ionizing radiation may also be of importance in practice. (auth) (NSA of Czech)

26589 SIMPLE METHOD FOR THE STUDY OF THE UPTAKE OF RADIOACTIVE ^{32}P PHOSPHATE BY RED BLOOD CELLS. Hoeberichts, J. A.; Borst-Pauwels, G. W. F. H. (Univ., Nijmegen, Netherlands). Experientia; 26: 1407-8(15 Dec 1970).

A new method is reported for the study of the uptake of ^{32}P-labeled phosphate by erythrocytes. The new method avoids the elaborate washing procedure of the old method and consists essentially of one centrifugation and the determining of radioactivities of equal volumes of cell sediment and corresponding supernatant. The ratio of the activities is a measure of isotope uptake. (P.B.M.)

26590 ACCUMULATION OF CHROMIUM COMPLEXES IN SKELETAL TISSUE. Anghileri, Leopoldo J. (Univ. of Colorado, Denver. Veterans Administration Hospital, Denver). Nucl.-Med.; 9: 354-65(31 Dec 1970).

Studies of the in vivo distribution of ^{51}Cr-alloxantin complex in rats show a high uptake by bone. 24 hours after intravenous injection, approximately 20% of the complex remains in the body, and 50–65% is deposited in the skeleton. In vitro studies of its interaction with calcium carbonate and phosphate indicate a minimum of cation exchange, and therefore it is postulated that most of the interaction is due to a complex formation with the crystal lattice. (auth)

26591 SOME FACTORS INFLUENCING UPTAKE OF ^{75}Se-SELENOMETHIONINE BY THE PANCREATIC TISSUES OF THE RAT. Spaventi, S.; Rabadjija, L.; Cvrtila, D.; Filjak, K.; Sekso, M. (Institut fuer Radiologie und Nuklear-Medizin, Zagreb). Nucl.-Med.; 9: 366-74(31 Dec 1970).

Intravenous administration of pancreozymin and secretin under ether anaesthesia, in doses that increase pancreatic juice secretion in man, 90 min prior to the application of ^{75}Se-selenomethionine, does not increase the accumulation of this compound in the rat pancreas. Additional subcutaneous administration of insulin, or insulin and morphine, respectively, has no effect on the influence of pancreozymin and secretin on the ^{75}Se-selenomethionine accumulation in the pancreas. Lower ^{75}Se-selenomethionine accumulation in the pancreas of animals in all the experimental groups subjected to ether anaesthesia and surgical intervention prior to ^{75}Se-selenomethionine administration, as compared to that in intact animals, is perhaps attributable to the effect of stress. In the light of our findings indicating that insulin increases ^{75}Se-selenomethionine accumulation in the liver, its use in the pretreatment for isotope scanning of the pancreas does not seem justified, and may even be considered undesirable. (auth)

26592 ACTION OF GASEOUS TRITIUM ON MAMMALIAN DEOXYRIBONUCLEIC ACID. Blazicek, G. (Inst. of Biophysics, Brno). Stud. Biophys.; 23: 97-100(1970).

The tritium effect on DNA preparations of mammalian origin is reported. Using slightly modified procedures originally developed by WILZBACH, our attention was focused to the observation concerning certain variability that occurs in the rate of tritium incorporation into molecular structure of DNA originated from one mammalian source and follow the relationship to different values of molecular weight of the samples. (auth)

26593 CYCLING OF ^{65}Zn BY COLUMBIA RIVER PERIPHYTON IN A CLOSED LOTIC MICROCOSM. Cushing, Colbert E.; Rose, Fred L. (Battelle-Northwest, Richland, Wash.). Contract AT(45-1)-1830. Limnol. Oceanogr.; 15: 762-7(Sep 1970).

Studies of ^{65}Zn cycling by periphyton were performed in a closed, lotic microcosm under varying light regimes, community state, initial ambient concentrations, and stable divalent cation concentrations. Uptake of ^{65}Zn was considerable in continuous light, continuous darkness, a 12 hr photoperiod, or by killed communities, indicating a dominant adsorptive uptake mechanism. Uptake of ^{65}Zn was shown to be proportional to the initial ambient concentration of ^{65}Zn, which decreased during the course of an experiment. Increasing the concentration of stable zinc or magnesium proportionately decreased the uptake of ^{65}Zn, illustrating a competition for binding sites and supporting the adsorptive uptake theory. The similarity in function between the heterogeneous periphyton community and unialgal cultures or single species of plants is pointed out. (auth)

26594 EXPERIMENTAL STUDIES ABOUT INCORPORATION OF RADIOSTRONTIUM BY PIGS WITH SPECIAL REFERENCE TO THE EFFECT OF DIFFERENT CALCIUM CONCENTRATION IN FEED, AND TO THE PASSAGE THROUGH THE PLACENTA. II. DISTRIBUTION OF RADIOSTRONTIUM IN TISSUES OF SOWS AND THEIR FETUSES (LONG-TERM EXPERIMENTS WITH DOMESTIC PIGS). Werner, H. (Univ., Kiel). Strahlentherapie; 141: 86-92 (Jan 1971). (In German).

Twenty sows were studied. One group contained animals with an average age of eight months and an average weight of 200 pounds. The other group included 20-month-old animals weighing 400 pounds. During pregnancy, each animal received 0.1 μCi of ^{89}Sr. Strontium administration was started within a few days after impregnation. After a period of 105 days, and before birth of the litter, the animals were sacrificed and various tissues, including fetus and placenta, were analyzed for ^{89}Sr. Results of the experiments will be published in a subsequent issue. (H.B.G.)

26595 EFFECT OF TOTAL BODY GAMMA IRRADIATION ON THE PERCUTANEOUS ABSORPTION OF RADIOCESIUM. Stojanovic, Dragoslav; Milivojevic, Katarina (Boris Kidric Inst. of Nuclear Sciences, Belgrade). Strahlentherapie; 141: 93-5(Jan 1971).

The kinetics of ^{137}Cs absorption through the skin of rats contaminated one, three, and six days following irradiation with 600 rad of ^{60}Co gamma radiation were studied. Results showed that radiocesium absorption through the postirradiationally contaminated skin is much slower and less than that of contaminated controls. The absorption dynamics are a function of time elapsed between irradiation and contamination. The later the postirradiation contamination is carried out, the earlier a peak absorption is reached and radioactivity in the blood is at a lower level. The highest level of radioactivity, caused by radiocesium penetration, coincides with the most pronounced changes in the body after irradiation. (auth)

26596 ^{33}P AUTORADIOGRAPHY USED TO MEASURE PHOSPHATE UPTAKE BY INDIVIDUAL ALGAE. Fuhs, G. Wolfgang; Canelli, Edmondo (New York State Dept. of Health, Albany). Limnol. Oceanogr.; 15: 962-7(Nov 1970).

Diatoms from pure cultures and samples of lake phytoplankton were labeled with ^{33}P, and autoradiographs were prepared after concentration by centrifuge and membrane filter techniques. Conditions for labeling at a suitable intensity (1–3 dpm/1,000-μ^3 cell volume) were determined. The method is suitable for the detection of nonspecific binding of phosphorus by organic materials and of differential phosphorus uptake by members of a mixed population. It also was used to determine continuity of phosphorus uptake in a cultured diatom. (auth)

26597 CONCENTRATION OF RADIUM, THORIUM, AND URANIUM BY TROPICAL MARINE ALGAE. Edgington, David N. (Argonne National Lab., Ill.); Gordon, Solon A.; Thommes, Michael M.; Almodovar, Lutis R. Limnol. Oceanogr.; 15: 945-55(Nov 1970).

Twenty species of marine algae were collected between 1961 and 1968 from coastal waters of Puerto Rico and analyzed chemically for total organic material, protein nitrogen, and calcium, and radiochemically for the naturally occurring alpha particle emitters ^{226}Ra, ^{232}Th, and ^{238}U. Study of these data suggests that the concentration of radium, thorium, and uranium by tropical marine algae is controlled by two mechanisms: ion exchange or coprecipitation of the ion with the calcium carbonate matrix, and complex formation with either the protein nitrogen or some other component of the organic fraction. Radium and possibly thorium apparently is concentrated by both mechanisms, the dominant one depending on the phylum. For the Rhodophyta and the highly calcified Chlorophyta it is the former and for the Phaeophyta the latter. Uranium is concentrated by the first mechanism. (auth)

26598 DISTRIBUTION OF RADIOACTIVE ^{99}Mo IN TISSUE OF TEST ANIMALS. Bibr, B. (Isotopenlaboratorie, Prague); Lener, J. Vitalst. Zivilisationskr.; 15: 218-19(Dec 1970). (In German).

XUM

The preventive effects of molybdenum on the incidence of dental caries, the distribution and retention of radioactive ^{99}Mo in organs of rats of different age were examined. Subcutaneously the animals were given ^{99}Mo in the form of ammonium molybdate in a basic dose of 24 μCi per animal. The test animals were killed after varying intervals, and after weighing, the accumulated activity in the different organs was measured. Most of the accumulated radioactive ^{99}Mo was found in liver, kidneys, and spleen. There was a relatively low content in bones, teeth, myocardium and testes. The mechanism of Mo-incorporation in teeth and bones was discussed theoretically. (auth)

26599 TOXICITY OF INHALED PLUTONIUM. 2. Bair, W. J. (Battelle-Northwest, Richland, Wash.). Hoshasen Kagaku; 13: 217-21(Jan 1970). (In Japanese).

Plutonium oxide, prepared by sintering plutonium (^{239}Pu) oxalate at ca. 350 C, was inhaled by dogs and its toxicity was examined from the tissue distribution of $^{239}PuO_2$, dose and lethal rate relationship, and clinical changes, based on the data collected during about 10 years. Accumulation of $^{239}PuO_2$ in the lung is exponential and its half-life is 1000 days, while it remains in bronchial lymph nodes for one year. Its transition into the bones is slow and reaches 3 to 4% of lung deposition after 4 to 5 years. The average concentration of PuO_2 is higher in the lungs and mediastinal lymph nodes, and these organs would probably receive the maximum exposure to radiation. A dynamic simulation model of inhaled PuO_2, based on long-term data, showed that 15% and 60% of plutonium deposited in the deep part of the lung stays in the lung and in lymph nodes, respectively. Examination of the effect of the amount of PuO_2 inhaled on the life span showed that the animal died within one year when more than 0.1 μCi/g of plutonium was deposited (in the lung) while over 50% of the animals died within 6 to 7 years with smaller amounts. There were many cases of lung tumor in these animals and shortening of life was found to be due to the amount of PuO_2 inhaled. The first sign of pathological change is lymphocytopenia that accompanies destruction of the ability to produce heterophilic antigen. Other clinical changes are related to the beginning of respiratory ataxia. (Japan)

26600 PATTERN OF ESTERASES AND THEIR MICHAELIS CONSTANTS IN SPLEEN, LIVER, PLASMA, AND ERYTHROCYTES OF WHOLE-BODY IRRADIATED RATS. Valet, Guenter; Ruhenstroth-Bauer, Gerhard (Max-Planck-Institut fuer Biochemie, Munich). Strahlentherapie; 141: 114-18(Jan 1971). (In German).

The following items were examined between day 0 and 18 after x irradiation: Michaelis' constants of the esterases for pH 5.0 and 7.0 and the changes of the pattern of esterase activity in pH range 5.0 to 8.5 in particle-free spleen-, liver-, and erythrocyte extracts, as well as in the blood plasma of rats that were whole-body x-irradiated by 500 R (LR 38/30). By the activity determination with p-nitro-phenol-acetate several esterases or esterase groups in the extracts and in the plasma could be measured. (auth)

26601 DIFFERENCE IN THE DRIED THYROID BLOCK OF ^{131}I UPTAKE IN MALE AND FEMALE RATS. Kapitola, J.; Schreiberova, O. (Charles Univ., Prague). Physiol. Bohemoslov.; 19: 205-8(1970).

The effects of dried thyroid feeding on ^{131}I uptake by the thyroid of male and female rats were studied. In the first experiment the animals were allowed food ad libitum (food and dried thyroid consumption was somewhat higher in the males). The uptake of ^{131}I in the female controls was nonsignificantly higher than in the male controls (110%), but was significantly higher in blocked females than in blocked males (175%). In the second experiment feeding was modified so as to ensure that the intake of dried thyroid by the experimental males and females was the same (with generally lower food consumption). The uptake of ^{131}I in the female controls was higher than in the male controls (147%) and an even more pronounced difference was found between blocked females and males (166%). The results were not influenced by differences in the number of females in oestrus. The cause of this phenomenon, initially observed in mice, is still unknown. (auth)

26602 H-2-GLUCOSE AS TRACER IN TURNOVER STUDIES. Hetenyi, G. Jr.; Mak, D. (Univ. of Toronto). Can. J. Physiol. Pharmacol.; 48: 732-4(Oct 1970).

In rats, the reported difference between the slopes of the specific activities of plasma glucose following i.v. injection of either ^{3}H-2-glucose or ^{14}C-1-glucose was abolished by evisceration and nephrectomy. This proved that the difference observed in normal rats was due to the reincorporation of ^{14}C atoms into newly released glucose and not to a nonmetabolic tritium–proton exchange in plasma glucose. (auth) (Canada)

26603 THORIUM, ITS TOXICITY AND THE COUNTERMEASURE FOR SAFETY. Suzuki, Masashi; Mochizuki, Yoshio (National Inst. of Radiological Sciences, Chiba, Japan). Genshiryoku Kogyo; 16: No. 3, 32-9(Mar 1970). (In Japanese).

Thorium is going to be utilized as nuclear fuel together with uranium and plutonium which are utilized now. Thus, it is significant to study the toxicity and industrial hygiene of thorium. Its chemical toxicity seems to be low, but its radioactivity is dangerous. The chief danger in handling thorium originates from the external irradiation due to γ and β rays and from intake by inhalation. Inhaled thorium tends to remain in lungs for a long time and may cause lung cancer. Incepted thorium accumulates in liver, spleen, and bone marrow and may cause liver cancer and bone tumors. The carcinogenesis of ^{228}Th for bone is 14 times as high as that of ^{226}Ra for the same absorbed dose, and five times higher than that of ^{239}Pu. The permissible dose and the permissible concentration in air (3×10^{-11} μCi/c.c.) recommended by ICRP should be adopted as the safety standards for external irradiation and for thorium inhalation. For evaluating air contamination, it may be necessary to use personal samplers similar to the film badges now used for evaluating external irradiation. In order to determine the amount of thorium ingested, the thorium content in expiration, direct counting with a human counter, or urine analysis methods are available. (Japan)

26604 DISTRIBUTION OF INGESTED ZINC-65 IN THE TISSUES OF SOME MARINE CRUSTACEANS. Fowler, S. W. (Oregon State Univ., Corvallis); Small, L. F.; Dean, J. M. J. Fish. Res. Board Can.; 27: 1051-8(June 1970).

Autoradiographs of tissues of euphausiids and shrimps fed ^{65}Zn through a food chain showed the isotope located primarily in the interstitial spaces between muscle fibers, in the eye mainly between the rhabdoms and crystalline cones of adjacent ommatidia, within the exoskeleton, and on the interior surface of the exoskeleton. Comparisons of the autoradiographic evidence with concentrations of radiozinc and stable zinc in the various dissected tissues were in good agreement. The specific areas of ^{65}Zn localization were much the same as those seen in an earlier study of similar organisms that accumulated ^{65}Zn directly from sea water; thus, it appears that ^{65}Zn, and therefore zinc, is highly labile in marine crustaceans and will accumulate in certain specific locations regardless of the mode of uptake. The rates at which various tissues became saturated with ^{65}Zn were dependent upon mode of uptake, however. Because most of the ^{65}Zn was located intercellularly, and not intracellularly, most ingested zinc apparently accumulates in excess of the animals' needs and is not used metabolically. (auth) (Canada)

26605 ^{35}S UPTAKE OF GASTRIC WALL AND ITS EXCRETION INTO THE GASTRIC JUICE IN RATS WITH EXPERIMENTAL CLAMPING AND CLAMPING-CORTISONE ULCER. Hayashi, Tohru (Tokyo Medical Coll.). Nippon Shokakibyo Gakkai Zasshi; 67: No. 1, 27-46(Jan 1970). (In Japanese).

Experimental ulcers were induced by clamping and clamping-cortisone methods in rats and the effects of the ulcers on ^{35}S uptake by the gastric wall and of the ^{35}S secretion into the gastric juice were studied. The effects of different steroid hormones and nonsteroidal antiinflammatory drugs on the ^{35}S uptake of the gastric wall with ulcer were also studied. In two groups treated with cortisone acetate and prednisolone acetate, a clear dose-response curve was observed. However, in the groups treated with phosphate compounds, such a clear dose-response was not found. The group treated orally with prednisolone powder showed the same effect as the group treated intramuscularly. The ^{35}S uptake by the gastric wall was inhibited in both groups treated with acetylsalicylic acid and bucolom; but it was not inhibited in either group treated with indomethacin and phenylbutazone. (Japan)

26606 EFFLUX OF ^{22}Na AND ^{86}Rb FROM THE CRYSTALLINE LENS. Paterson, Christopher A. (Univ. of Colorado, Denver). Exp. Eye Res.; 10: 331-8(1970).

A lucite perfusion chamber was designed to study the efflux of labeled substances from the rabbit lens. ^{22}Na efflux was reduced by 10^{-5} M-ouabain and by lowered temperature, exhibiting a Q_{10} of 3.86. In the presence of ouabain, the Q_{10} was 1.2. ^{86}Rb (which behaves like potassium) efflux, on the other hand, was essentially unaffected by ouabain and lowering the temperature caused a slowing in efflux that corresponded to a Q_{10} of 1.2. Removal of the lens epithelium by manual decapsulation increased the efflux of ^{86}Rb, and rendered ^{22}Na efflux insensitive to ouabain. The Q_{10} of ^{22}Na efflux from the decapsulated lens was 1.3. These observations agree with the view that the lens is capable of actively extruding sodium and accumulating potassium and that the major site of transport is in the epithelium. It would also appear that the lens epithelium presents a considerable barrier to the passive flux of sodium and potassium. (auth)

26607 STUDY AND RESULTS OF MEDICAL EXAMINATIONS MADE AFTER THE INHALATION OF NATURAL URANIUM SOLUBLE COMPOUNDS. PART II. Chalabreysse, J. (CEA, Pierrelatte, France). Radioprotection; 5: 305-10(1970). (In French). (CONF-700505-23).

From 2nd Congress of the International Radiation Protection Association, Brighton, England.

In this present work that was completed in 1970, calculations made and results obtained in 1965 are reconsidered taking into account recommendations of the International Commission for Radiological Protection (I.C.R.P.) made in 1968 concerning the metabolism of natural uranium. It was possible to determine the initial body burden and the quantity remaining in the system at the day of the examination. These values were found to be less than those estimated in 1965. The limits are given for the quantities excreted into the urine during the first 24 hr after the inhalation of 2.5 mg of the so-called natural uranium compounds. After the initial purification process, 80% of the quantity retained by the lungs (0.625 mg) is eliminated. The threshold levels are defined beyond which the determination of the degree of contamination of an individual becomes obligatory; this value is 0.06 mg for natural uranium. (France)

26608 EFFECTS OF METALS ON CELLS, SUBCELLULAR ELEMENTS, AND MACROMOLECULES. Proceedings of the 2nd Conference on Toxicity, Rochester, N. Y., June 12-16, 1969. Maniloff, Jack; Coleman, James R.; Miller, Morton W. (eds.). Proceedings Publication of the Rochester Conferences on Toxicity. Springfield, Ill.; Charles C Thomas, Publisher (1970). 410p. (CONF-690621).

Separate abstracts were prepared on five chapters. One chapter, based on AEC Report UR-49-1248, was abstracted previously in NSA. Eleven additional chapters discuss various aspects of the molecular basis for the action of heavy metals on biological materials, structures, or processes. (C.H.)

For abstracts of individual chapters see: 26213, 26237, 26271, 26272, and 26609.

26609 RED BLOOD CELL: PENETRATION, DISTRIBUTION, AND TOXIC ACTIONS OF HEAVY METALS. Passow, Hermann (Univ. des Saarlandes, Homburg, Ger.). pp 291-344 of Effects of Metals on Cells, Subcellular Elements, and Macromolecules. /Maniloff, Jack (ed.). Springfield, Ill.; Charles C Thomas, Publisher (1970).

From 2. conference on toxicity; Rochester, N. Y. (12 Jun 1969). See CONF-690621.

Typical features of the penetration, distribution, and toxic effects of a number of heavy metals including Th and UO_2, on living cells are reviewed. Special emphasis is placed on a detailed description of selected metal actions on the red cell membrane: these include changes of electrophoretic mobility, agglutination, and the induction of permeability changes. The effects of lead and mercury on passive alkali ion permeability are discussed. They illustrate that, in spite of the ubiquity of binding sites for these metals, the observed toxic effects are quite specific: mercury induces an increase of the permeability to K and Na, but not to choline. Lead mainly augments K efflux but has comparatively little effect on Na movements. The detailed presentation of the available information is preceded by a short survey of the diversities and similarities of the interactions of the various metals with the red blood cell. (auth)

26610 RETENTION AND DISTRIBUTION OF ^{210}Pb IN THE ADULT BABOON. Cohen, Norman. New York; New York Univ. (1970). 228p. University Microfilms Order No. 71-68.

Thesis.

Measurements of the distribution and retention of ^{210}Pb in five adult female baboons and 19 rats were performed after single dose intravenous injection of $^{210}Pb(Cl_2)$. After two and up to 14 months post-injection, the removal rate of ^{210}Pb from the baboon skull can be represented by a single exponential function describing an effective half-life of 347 ± 33 days. The whole-body measurements over the same time period were best fit by the sum of two exponential components with effective half times of 9.0 ± 0.3 and 320 ± 30 days over the respective time periods of 0-40 and 41-420 days post-injection. Whole-body ^{210}Pb-moval rates, as determined from in vivo measurements of the rodent and the baboon were the same at the 0.025 significance level. Analysis of ^{210}Pb in excretion for three months post-injection, confirmed the significance of the fecal route as a mode of ^{210}Pb loss from the body almost equal to that of the urinary route for baboons. Liver, kidney, and spleen represent the major soft tissue uptake sites in both the baboon and the rat with the major concentrations occurring in the liver for the baboon and in the kidney for the rat. Location of the nuclide at one and two months post-injection was almost entirely in spongy bone trabeculae at endosteal surfaces. (Diss. Abstr.)

26611 DISTRIBUTION OF ^{65}Zn IN THE ENDOCHONDRAL GROWTH SITES OF THE MANDIBULAR CONDYLE AND THE PROXIMAL END OF THE TIBIA IN YOUNG RATS. AN AUTORADIOGRAPHIC AND GAMMA SCINTILLATION STUDY. Bergman, Bo (Umea Univ., Sweden). Odontol. Revy; 21: 261-74 (1970).

The distribution of ^{65}Zn in the endochrondral growth sites of the mandibular condyle and the proximal end of the tibia in young rats was studied autoradiographically. In addition, a quantitative study by means of scintillation measurements was performed in order to get a more thorough picture of the uptake of ^{65}Zn in various organs and tissues. It was found that the autoradiographic localization of ^{65}Zn was similar in the two growth regions. A high initial uptake was noted at the sites of mineralization at the erosion line. Seven days after injection, the uptake of ^{65}Zn at the erosion line was much weaker. The scintillation study showed that the concentration of ^{65}Zn in mandibular condyle was in the same (low) range as for kidney, spleen, and heart. The uptake in tibia epiphysis was significantly lower compared to mandibular condyle at all survival periods except 8 days, where no significant difference was observed between these two skeletal samples. In contrast to the mandibular condyle, the total ^{65}Zn concentration in the tibia epiphysis increased significantly from days 4 to 8 and was seen as a heavy accumulation of radiozinc in the developing epiphyseal spongiosa in the autoradiograms. (auth) (Sweden)

26612 ISODENSITOMETRIC EVALUATION OF ABSORBED DOSE RATES IN GROWING AND ADULT FELINE BONE RESULTING FROM CONTINUOUS EXPOSURE TO LOW LEVELS OF ^{90}Sr. Rosenstein, Laurence. Cincinnati; Univ. of Cincinnati (1970). 123p. University Microfilms Order No. 71-1134.

Thesis.

Attempts were made to measure absorbed dose rates (using quantitative radioautography) in particular bones from animals that had been continuously exposed to low levels of ^{90}Sr. The measurements were made in bones obtained from domestic cats of 50 (weanling) and 500 (adult) days of age in order to show the type of deposition found in young and adult animals. All experimental animals were obtained from mothers already having ^{90}Sr body burdens. Cats thus were exposed to ^{90}Sr in fetal life and during nursing. After 25 to 30 days of age, the radioisotope was mixed in the diet (0.5 μCi ^{90}Sr/100 grams of food) and continuously fed, ad libitum, to the experimental cats. Young cats receiving ^{90}Sr on a continuous basis showed heavy labeling and high absorbed dose rates (<3 Rads/day) in all bone regions. This type of deposition arose as a result of ^{90}Sr being transferred to and from bone by apposition-resorption. Augmentation-diminution as an effective ion transfer process was not very influential in this age group (with respect to absorbed dose rates). As the animal grew older, ^{90}Sr was added to and removed from bone predominantly through augmentation and diminution, respectively. This principally occurs in epiphyseal areas, between periosteal and endosteal bone in the shaft, and in much of the rib and vertebra. Higher depositions and correspondingly higher dose rates still were visible in areas of active growth. (Diss. Abstr. Int., B)

26613 MEASUREMENT AND ANALYSIS OF RADIOACTIVE FALLOUT OVER SOUTH AFRICA AND ITS BIOLOGICAL UPTAKE. Basson, J. K.; van As, D.; van der Westhuizen, M.; Vleggaar, Constance M. (Atomic Energy Board, Pelindaba). S. Afr. J. Sci.; 66: 214-24(Jul 1970).

Measurements of radioactive fallout over South Africa from nuclear weapon tests since 1963 are reported. Analyses of airborne activity and deposited fallout were made for a number of radionuclides. Special attention is given to the measurements resulting from the French nuclear detonations during 1966 to 67 in the South Pacific, with transit time and age analyses. The accumulation of 90-strontium and of 137-cesium in biological samples of significance to man, i.e., milk and human bone, were measured and the resulting doserate calculated. (auth)

26614 CALCIUM UPTAKE BY SUBTERRANEAN CLOVER BUR SHOWN BY USING ^{45}Ca. Ozanne, P. G. (CSIRO, Wembley, Australia); Werkhoven, C. H. E. At. Energy Aust.; 14: 16-18 ([1971]).

The movement of ^{45}Ca as $CaCl_2$ through the seeds of subterranean clover, was examined. Florets of the plant in flower were wrapped in wads of cotton wool and slipped into plastic vials. The cotton wool was moistened with a solution containing 240 ppm Ca labelled with 1 μCi/ml of ^{45}Ca. Plastic caps through which the peduncle passed were placed on the vials. After 2 months ^{45}Ca distribution was determined by sampling ashed sections of clover runners. Results showed that the bur developing

XUM

in contact with a Ca solution of a concentration within the range of those found in soils, absorbs sufficient Ca for healthy seed formation. (Australia)

26615 URANIUM IN VINE AND WINE. Davidescu, D.; Pavlovschi, Gh.; Davidescu, V.; Raducanu, E. Rev. Hort. Viticult.; 18: 93-100(1969). (In Rumanian).

In the soils of the Valea Călugăreasca and the Drăgăsani vineyards, mobile uranium ranges between 14 and 163 gamma per 100 g of soil. The distribution of uranium in various vine organs is not a simple process of suffusion. Higher accumulations are found in the stones. The variable uranium uptake into the different vine species affects this mineral content in wines. The maximum concentration was found in the Royal Feteasca (Maidenly) of the Valea Călugăreasca (300 gamma/1000 ml). (Rom. Sci. Abstr.)

26616 CHARACTERISTICS AND QUANTITATIVE PREDICTION OF THE CUMULATIVE STORAGE OF ^{90}Sr IN ARBOREAL PLANTS. Aleksakhin, R. M.; Naryshkin, M. A.; Bocharova, M. A. (Forestry Lab., Moscow). Dokl. Akad. Nauk. SSSR; 193: 1192-4(11 Aug 1970). (In Russian).

The laws governing the passage of artificial nuclides from the soil and their accumulation in perenial plants must be known in order to develop models to predict their accumulation in specific organs in humans and animals. Experiments were therefore carried out to determine the behavior of the most important fission product, ^{90}Sr by applying this radionuclide on the ground at the rate of 0.28 and 0.015 $\mu Ci/m^2$ in birch groves and pine forest. The ^{90}Sr was determined in wood specimens collected at various time periods. It was found that ^{90}Sr in birch keeps increasing continuously with time. This is due to the growth of the ^{90}Sr containing annual rains during the years after the application of the radionuclide; in addition the nuclide penetrates radially the trunk by diffusion from the external rings. The accumulation was found to be much slower in the pine trees because of the slower mineralization of the coniferous soil and the slower diffusion toward the core of the trunk. A formula was derived to predict the ^{90}Sr concentration in the trees as a function of time and the concentration in the soil. The predicted values agreed with experimental data. (TTT)

26617 INCORPORATION OF RADIOPHOSPHORUS INTO NUCLEIC ACIDS OF FROG EMBRYO. Trebichavsky, I.; Nedvidek, J. (Inst. of Microbiology, Prague. Charles Univ., Prague). Folia Biol. (Prague); 17: No. 1, 54-8(1971).

The nucleic acids of frog eggs and embryos were labeled with radiophosphorus, administered to the Rana temporaria L. female in the form of orthophosphate (200 μC) simultaneously with pituitary implantation. The metabolism of nucleic acids of developing embryos was studied by biochemical methods. The amount of RNA did not alter up to the gastrula stage, radioactivity in the RNA fraction changed quantitatively. In general, synthetic processes could be observed during, or after, gastrulation. The changes are discussed from the aspect of the presence and breakdown of stable mRNA and of new RNA and rRNA synthesis. Only a small amount of DNA was formed during the cleavage phase, when it was synthesized mainly from labeled precursors. Later on, after gastrulation, DNA synthesis increased. After the gastrula stage, the incorporation of radioactive phosphorus into the DNA fraction decreased. (auth)

26618 BETA RADIOACTIVITY IN SOME WINES FROM TRANSYLVANIA AND THE DOBRUJA. Luca, I.; Cotea, V.; Pasnicu, C.; Cotea, Victoria. Lucr. Stiint. Inst. Agron. Ion Ionescu De La Brad, Iasi; 315-22(1968). (In Rumanian).

The total beta radioactivity of wines in Transylvania was investigated. The radioactivity was due mostly to natural ^{40}K isotope. Other radionuclides such as ^{90}Sr, and ^{137}Cs, were also detected. (Rom. Sci. Abstr.)

Radiation Effects

Refer also to abstracts 26302, 26798, 26801, 26802, 26808, 27079, 27114, and 27123–27125.

26619 (COO-1793-6) PARTIAL PURIFICATION OF PHOTOREACTIVATING ENZYME FROM EUGLENA GRACILIS. Small, Gary D. (South Dakota Univ., Vermillion. Dept. of Biochemistry). [1970]. Contract AT(11-1)-1793. 11p. Dep. NTIS.

Photoreactivating enzyme was purified over 400 fold from green cells of Euglena gracilis. At this stage in the purification, the nuclease activity of the preparation is reduced to a very low level, permitting the accurate use of the transformation assay for photoreactivating enzyme activity. Properties of the purified enzyme are discussed. Graphs are presented to show chromatography of the enzyme on Sephadex G-100 and time course of repair of irradiated transforming DNA. (H.L.W.)

26620 EFFECTS OF γ-IRRADIATION ON THE ENZYME RELATING TO THE DEVELOPMENT OF CHARACTERISTIC ODOR OF ONIONS. Kawakishi, Shunro; Namiki, Kazuko; Nishimura, Hiroyuki; Namiki, Mitsuo (Nagoya Univ., Japan). J. Agr. Food Chem.; 19: 166-9(Jan-Feb 1971).

Effects of γ irradiation on the activity of cysteine sulfoxide lyase in onions and on the development of di-n-propyl disulfide in macerates of onions were investigated to elucidate the effects of irradiation on the quality of onions. The lyase activity was decreased apparently by irradiation with relatively lower doses utilized from sprout inhibition, 7 to 15 krad, but they were restored up to the level of the unirradiated control during storage for 3 mon at room temperature. The formation of the disulfide was also decreased by irradiation with the same doses, which corresponded to that observed in the lyase activity. These relations between the lyase activity and the amount of sulfide were not so conspicuous at higher doses, and some other factors such as radiolysis of the sulfoxide may be involved. (auth)

26621 EFFECT OF GAMMA RADIATION ON WHEAT STARCH AND ITS COMPONENTS. Ananthaswamy, H. N.; Vakil, U. K.; Sreenivasan, A. (Bhabha Atomic Research Centre, Bombay). J. Food Sci.; 35: 795-8(Nov-Dec 1970).

Studies on the susceptibility of irradiated wheat starch, amylose, and amylopectin to alpha and beta amylolysis reveal that they are more susceptible to enzyme actions, compared to their unirradiated controls; however, irradiated amylose seems to be comparatively more vulnerable. From irradiated starch, series of oligosaccharides of the maltose series are discernible, while glucose appears only above 200 Krad dose level. Quantitative analysis of the radiolytic breakdown products of starch reveal that at high dose levels (1 Mrad) maltose, maltotriose, and maltotetrose are the main products. Results on the separation of radiolytic breakdown products suggest they resemble those produced by alpha-amylolysis of starch. (auth)

26622 SUSCEPTIBILITY TO AMYLOLYSIS OF GAMMA-IRRADIATED WHEAT. Ananthaswamy, H. N.; Vakil, U. K.; Sreenivasan, A. (Bhabha Atomic Research Centre, Bombay). J. Food Sci.; 35: 792-4(Nov-Dec 1970).

Initial reducing sugars and diastatic activity, expressed as maltose value, are increased in irradiated wheat and are functions of dose levels in the range 20 to 200 Krad. Both alpha and beta-amylases retain their activities in irradiated wheat, but the sensitivities of starch to amylolysis are increased with radiation dose levels. Latent beta-amylase present in resting seeds is also radioresistant. Susceptibility of starch to radiation treatment is more pronounced with moist than dry grain. (auth)

26623 DEVELOPMENT OF CERTAIN PHYSICO-CHEMICAL PROPERTIES OF THE STARCH GRANULE AS A FUNCTION OF IRRADIATION CONDITIONS. Tollier, M. Th.; Guilbot, A. Staerke; 22: 296-304(1970). (In French).

Maize and potato starch of different water content were exposed to γ irradiation, and the development of certain properties of the starch granules was followed. These properties were judged by evaluating the picture in the optical microscope, solubility in alcohol at 80°GL and water at 20°C, as well as swelling and solubility in aqueous medium dependent on temperature. Examinations were carried out both independent of irradiation dose with constant water content and independent of water content with constant irradiation dose of 25 Mr. Results obtained make it possible to follow the degradation of starch macromolecules under the influence of irradiation, and at the same time show the protecting effect of water within the sample, especially with lower irradiation doses. The change in the swelling faculty and solubility of starch at different temperatures clearly shows the important role which the intermolecular associations play in this connection. (auth)

26624 SERUM AMINO ACIDS IN RATS IN THE COURSE OF ACUTE RADIATION INJURY. Rudnicki, Tadeusz; Wronski, Anastazy. Nukleonika; 15: 547-52(1970). (In Polish).

The lethal x ray dose causes alterations in the protein metabolism in rats resulting in changes in the free amino acid level in blood serum. The level of some of these acids, mostly of the endogeneous type, decreases shortly after irradiation, others, mostly exogeneous ones, show a distinct tendency to increase their level. There are some, however, which do not show any changes. (auth)

26625 PRODUCTION OF STRAND BREAKS IN MAMMALIAN DNA BY X-RAYS: AT DIFFERENT STAGES IN THE CELL CY-

CLE. Lett, J. T.; Sun, C. (Colorado State Univ., Fort Collins). Radiat. Res.; 44: 771-87(Dec 1970).

The formation of strand breaks induced by x rays in the DNA of Chinese hamster ovary cells was studied as a function of the position of the cells in the cycle by alkaline EDTA sucrose sedimentation. The efficiency of total strand breakage was found to be the same throughout the cell cycle and equal to 60 ± 10 eV per break. This figure was obtained from the best fit of a random distribution to the observed size distribution at high x ray doses; by computation from a direct evaluation of the number average molecular weight at low doses; and also at low x ray doses from the destruction of the monodisperse distributions associated with the structural chromosomal subunits. (auth)

26626 RELATION OF PROTEIN SYNTHESIS TO RADIATION-INDUCED DIVISION DELAY IN CHINESE HAMSTER CELLS. Bacchettil, Silvia; Sinclair, Warren K. (Argonne National Lab., Ill.). Radiat. Res.; 44: 788-806(Dec 1970).

The effects of x rays on the progression toward division and on the synthesis of proteins in Chinese hamster cells in G_2 phase were studied with the aim of clarifying the role played by protein synthesis in radioinduced division delay. The results were compared with those obtained in similar experiments with cycloheximide, an inhibitor of protein synthesis. The terminal point of action of x rays in arresting the progression of G_2 cells occurs at 90 to 60 min before division and is dose independent over the range 200 to 710 rads. However, the terminal point of action of cycloheximide is concentration dependent and occurs at 120 to 90 min before division for concentrations of 2 and 5 μg/ml, and at 90 to 60 min before division for 50 μg/ml. Therefore, only at the higher concentration is there coincidence with x rays in the time of the terminal points of action. The two agents, moreover, have opposite effects on the synthesis of proteins. Stimulation of uptake of ^{3}H-leucine in irradiated cells and an inhibition of this uptake in cells treated with cycloheximide were observed. These effects persist for at least one cell cycle after irradiation or removal of the drug. Additional data have suggested that cycloheximide could block cell progression by shutting off completely the protein synthetic process. When G_2 cells have been irradiated and then exposed to a pulse of cycloheximide, the radioinduced stimulation of protein synthesis was abolished and a nearly normal level of ^{3}H-leucine uptake was reestablished; however, division delay was further increased. Therefore, it appears that x rays do not cause division delay by inhibiting the synthesis of specific proteins or the synthetic process per se. It also appears that the extra synthesis of proteins is not responsible for the delay, since controlling it by addition of cycloheximide prevents cell division for even a longer time. The significance of the observed extra synthesis of proteins and a possible mechanism of action of x rays in inducing division delay are discussed. (auth)

26627 CELL SURVIVAL AND X-RAY-INDUCED DNA DEGRADATION IN MICROCOCCUS RADIODURANS. Driedger, A. A.; James, A. P.; Grayston, M. J. (Atomic Energy of Canada Ltd., Chalk River, Ont.). Radiat. Res.; 44: 835-45(Dec 1970).

Survival curves after x irradiation of Micrococcus radiodurans were done by micromanipulation in a manner so that each colony forming unit was visually accounted for. A measure of the survival of single cells was obtained by microdissection after the first postirradiation division and reinoculation of the progeny cells. More than 90% of the cells (distinguished from colony-forming units) formed colonies after 600 krads. Irradiated cells and their progeny gave rise to a significant number of microcolonies which were distinguished by very slow growth rates. About 90% of lethally irradiated cells underwent between 1 and 6 divisions after which death and lysis of all the progeny occurred. This suggests that radioinduced damage in some form persisted in the progeny of irradiated cells. Further evidence of persistent radioinduced damage was found in the decreased survival of the first generation progeny of irradiated cells. Complete survival follows radiation doses which are associated with the degradation of nearly 30% of the DNA to TCA-soluble fragments. From the assumptions that an intact genome is required for survival and that an undegraded complementary strand is required for repair replication at each site, it is concluded that x ray-induced DNA degradation involves only a single strand of DNA over each site over which it occurs. (auth)

26628 STAGE SENSITIVITY AND DOSE RESPONSE IN HUMAN LEUKOCYTES. Shepard, J. S. (Univ. of Massachusetts, Amherst); Ferrari, I. Radiat. Res.; 44: 855-66(Dec 1970).

In response to x irradiation, G_2 stage leukocytes are about 4 times more sensitive than G_0 stage cells, and S stage is intermediate when sensitivity is measured as percent abnormal cells. The yield of interchange type aberrations, however, is lowest for S cells. Chromosome terminal deletions increase as the dose, while dicentrics follow dose. (auth)

26629 IMPROVEMENT IN ALKALINE SUCROSE DENSITY GRADIENT SEDIMENTATION OF MAMMALIAN CELL DNA. Moroson, H.; Furlan, M. (Sloan-Kettering Inst. for Cancer Research, Rye, N. Y.). Radiat. Res.; 44: 713-26(Dec 1970).

The usual method of alkaline (0.1 – 0.5M NaOH) sucrose density gradient sedimentation of intact cells enables DNA molecular weight determinations with a minimum of shearing from bacterial protoplasts. This technique however was not successfully applied to intact mammalian cells because of higher molecular weight and contamination by protein, causing the DNA to sediment in a nonregular fashion. In addition, DNA aggregates may form which sediment to the bottom of the tube causing low recovery of the layered radioactive counts. This problem was overcome for Ehrlich ascites cells, by including 6M guanidinium chloride in the alkaline sucrose density gradient made 0.9M in sodium hydroxide. By this method, virtually complete recovery of the radioactivity layered upon the gradient is obtained in the recovered fractions, along with a reproducible DNA peak position. Neutral sucrose gradients of Ehrlich ascites cell DNA are also possible if 6M guanidinium chloride is included in the gradient. The effects of low doses of x rays on the molecular weight of single-stranded DNA in Ehrlich ascites cells obtained with and without 6M guanidinium chloride present in the alkaline sucrose gradient are presented. (auth)

26630 IRRADIATION OF PRIMARY HUMAN AMNION CELL CULTURES: EFFECTS ON DNA SYNTHESIS AND PROGRESSION THROUGH THE CELL CYCLE. Little, John B. (Harvard Univ., Boston). Radiat. Res.; 44: 674-99(Dec 1970).

The effects of radiation on progression through the life cycle were studied in very slowly proliferating, morphologically pure, cells derived directly from normal human tissue. Owing to a low mitotic activity balanced by some cell loss, these cells could be maintained for 2 mon in the same culture tubes without wide changes in net cell count. During the first 3 wk of growth the population consisted primarily of slowly proliferating cells in which S and G_2 were relatively short fixed phases of the life cycle, each lasting less than 24 hr. Because the estimated generation times averaged 14 to 20 days, most cells were in the presynthetic G_1 phase. The most prominent finding which differentiated the response of these cells from that of rapidly proliferating mammalian cells was the marked radiosensitivity of the initiation of DNA synthesis. There was a dose dependent decrease in the rate of flow of G_1 cells into S with 10 to 100 R, and progression was almost completely stopped for 3 to 10 days by 300 to 1000 R. On the other hand, the progression of cells already in S, which was slowed about 30% by 1000 R, as well as the flow of cells from S to G_2, and from G_2 into M were all affected similarly as in rapidly proliferating cells. The duration of the G_2 delay was proportionate to the long cell generation time but was minimal with exposures below 100 R. (auth)

26631 ELECTROPHORESIS AND IMMUNOELECTROPHORESIS PATTERNS FROM PROTEINS OF IRRADIATED MEAT, FISH, AND FOWL EGG. Bruaux, P.; Bugyaki, L.; Claeys, F.; Lafontaine, A.; van der Stichelen Rogier, M. (Institut d'Hygiene et d'Epidemiologie, Brussels). Atompraxis; 16: 390-4(Nov-Dec 1970). (In French).

The usefulness of starch gel electrophoresis and immuno electrophoresis in agar and in agarose as control methods for identification of irradiated meat, fish, and whole liquid fowl egg was evaluated. Significant modifications were observed in the starch gel electrophoretic patterns from the irradiated hen egg and in those realized with the sarcoplasmic extracts of irradiated beef. The protein modifications resulted from irradiation of stockfish are not discernible with these methods. (auth)

26632 THROMBOELASTROGRAPHIC RADIOBIOLOGICAL STUDIES OF THE BLOOD OF PATIENTS WITH GYNECOLOGIC CANCER FOLLOWING ADMINISTRATION OF IRRADIATED STREPTOKINASE-STREPTODORNASE. Stamm, H.; Szirmai, E.; Henderson, J. (Univ., Basel, Univ., Stuttgart). Acta Med. Iugoslav.; 23: 42-9(1969). (In German).

In cancer patients, the thromboelastogram was determined after addition to the blood of γ-irradiated or non-irradiated varidase. Behavioral differences of the two substances were compared, and it was concluded that irradiation changes some factors in the thromboelastogram. (H.B.G.)

26633 EFFECT OF X IRRADIATION ON YEAST RIBOSOMES IN VITRO. Ghosh, Nandini (Saha Inst. of Nuclear Physics, Calcutta). Int. J. Radiat. Biol.; 18: 567-75(1970).

With the gradual removal of Mg^{2+}, 80s ribosomes of Saccharomyces cerevisiae dissociate into 60s and 40s sub-units. Concurrently, the larger sub-unit 60s begins to unfold into a 50s form. X irradiation effects were observed both on intact 80s ribosomes and on dissociated sub-units. Irradiation of 80s ribosomes in a high Mg^{2+} buffer (0.005 M) showed no change in the sedimentation diagram. A gradual removal of Mg^{2+} from these ribosomes, however, resulted in the following processes at an enhanced rate with respect to the control: 80s → 60s + 40s; 60s → 50s; 50s + 40s → 25s + 6s. Irradiation of partially-dissociated ribosomes in a low Mg^{2+} buffer (0.00005 M) resulted in the direct dissociation of a part of 80s and direct unfolding of 60s into 50s and 50s into 40s. It was concluded that x rays affected the salt linkages which were responsible for formation of 80s ribosomes and maintaining structural compactness of sub-units. (auth) (UK)

26634 DNA REPAIR AND RADIATION SENSITIVITY IN HUMAN (XERODERMA PIGMENTOSUM) CELLS. Cleaver, J. E. (Univ. of California, San Francisco). Int. J. Radiat. Biol.; 18: 557-65(1970).

Human skin fibroblasts from neurological and other forms of the disease xeroderma pigmentosum performed repair replication after uv irradiation at 0 to 25% of normal levels. The reduced repair was correlated with reduced survival in terms of colony formation; normal and xeroderma pigmentosum fibroblasts had exponential survival curves with a D_0 of 29 ergs/mm^2 and 9 ergs/mm^2 respectively. The results demonstrate the importance of repair replication in the survival of irradiated mammalian cells and in the aetiology of xeroderma pigmentosum. Transformation by SV 40 virus did not appear to alter the level of repair replication in xeroderma pigmentosum. (auth) (UK)

26635 ON THE TWO MECHANISMS OF REPAIR OF ULTRAVIOLET-DAMAGED DNA IN VERTEBRATE CELLS. Regan, J. D. (Oak Ridge National Lab., Tenn.). Ann. Ist. Super. Sanita; 5: 355-9(1969).

Pyrimidine dimers can apparently be induced in the DNA of any type of vertebrate cell in culture by uv radiation, the mechanism of repair of the dimer is highly contingent upon the type of vertebrate cell involved and upon the post irradiation conditions. (auth)

26636 CHROMOSOME AND CHROMATID-TYPE ABERRATIONS INDUCED BY ^{60}Co IRRADIATION AND TRITIATED URIDINE IN HUMAN LEUKOCYTE CULTURES. Lindahl-Kiessling, K.; Santesson, B.; Boecoek, J.-A. (Uppsala Univ.). Chromosoma; 31: 280-4(1970).

Human short term leukocyte cultures were exposed to ^{60}Co and ^{3}H uridine irradiation. The cells were collected at the first mitotic event. In the cultures treated with ^{3}H uridine breaks of chromatid type were found, whereas the ^{60}Co irradiated cells had only breaks of chromosome type as long as the irradiation takes place before the onset of DNA synthesis. It is inferred that ^{3}H uridine causes damage to localized single stranded DNA loops separated during transcription in RNA synthesis and inaccessible to repairing. The results are interpreted as an indication that the chromosome (chromatid) continuity is dependent on one DNA double helix strand and that the subunits of the chromosome, as revealed by radiation, are in fact single-stranded DNA. (auth)

26637 OXYGEN EFFECT IN γ-IRRADIATED DNA. Luecke-Huhle, Christine; Braun, Arnim; Hagen, Ulrich (Kernforschungszentrum, Karlsruhe, Ger.). Z. Naturforsch.; 25b: 1263-7(Nov 1970).

Purified, dry DNA and dry nucleoprotein were irradiated with ^{60}Co γ rays under a nitrogen or oxygen atmosphere. The DNA was isolated from the irradiated nucleoprotein. In the DNA the following radiation induced changes were investigated: Double strand breaks, single strand breaks, and crosslinks between the DNA molecules. An oxygen effect (OER > 1) was found for all of these events except for crosslinks in irradiated DNA. In the nucleoprotein, the oxygen effect is more marked than in pure DNA. (auth)

26638 ELECTRON TRANSFER IN GAMMA-IRRADIATED COMPLEXES BETWEEN DNA NUCLEOTIDES AND PROFLAVINE. Gregoli, Silvano; Taverna, Carla; Bertinchamps, Albert (Univ. Libre, Brussels). Int. J. Radiat. Biol.; 18: 577-85(1970).

Stacking complexes between DNA or DNA nucleotides and proflavine were studied by ESR spectroscopy after γ irradiation. The final radiation damage was found to be completely localized on the dye even when the nucleotide, proflavine molar ratio greatly exceeded the equimolar ratio. The results are explained by the random formation of anionic radicals followed by a long range electron transfer via the stacking towards the constituents of greatest electron affinity. (auth) (UK)

26639 MACROMOLECULAR SYNTHESIS IN MICROCOCCUS RADIODURANS DURING POSTIRRADIATION INCUBATION. Kitayama, Shigeru; Matsuyama, Akira (Inst. of Physical and Chemical Research, Yamato, Saitama, Japan). Agr. Biol. Chem. (Tokyo); 34: 1095-1100(Jul 1970).

Macromolecular synthesis in M. radiodurans after irradiation with a wide range of doses was investigated in connection with the mechanism for cell killing in radioresistant bacteria. Incorporation of ^{14}C-amino acids into protein and ^{32}P into RNA was considerably inhibited by gamma irradiation at higher doses as well as synthesis of DNA. From the results obtained, it is possible to consider that inhibition of RNA and protein synthesis may have an important role in primary events leading to radiation lethality of this radioresistant bacterium. (Japan)

26640 RADIOSENSITIZING ACTION OF N-ETHYLMALEIMIDE. Tarasenko, A. G.; Nekrasova, I. V.; Graevskii, E. Ya. Dokl. Akad. Nauk SSSR; 193: 1406-8(21 Aug 1970). (In Russian).

N-ethylmaleimide (N-EM) is a very effective radiosensitizing agent. It was found earlier that N-EM is not present in the cells in its free state and the product of its radiolysis or interaction with radicals formed from water is not involved in the sensitizing action. The problem was further studied to determine whether the radiosensitizing effect involves a reduction of the thiol level in the cell. The compounds tested included 2-(2 aminoethyl)thio)-N-ethylsuccinimide, which is the reaction product of N-EM with mercaptoethylamine (N-EMMEA). Labeling with ^{35}S was used to determine the accumulation of N-EMMEA in the cell. The effect of E-EM and N-EMMEA on the radiosensitivity of the Ehrlich ascitic carcinoma cells was studied by incubation in a physiological solution with one of these agents in the absence of oxygen for 15 min at 37°C, subjecting them afterwards to 400R of x radiation. After irradiation the cells were administered to mice, extracting the ascitic cells and dyeing them with methylene blue. The results support the theory that radiosensitizing is related to the reduction of the level of endogenic thiols. Compounds which do not react directly with SH groups may reduce indirectly the level of thiols in the cells thus changing the metabolic processes. (TTT)

26641 EXAMINATIONS OF THE EFFECT OF IONIZING RADIATION ON DNA x RNA HYBRIDIZATION. Schroeder, Ellinor; Magdon, Erwin (Deutsche Akademie der Wissenchaften, Berlin). Strahlentherapie; 141: 96-9(Jan 1971). (In German).

With the hybridization technique of RNA and DNA, the effect of ionizing radiation is studied on the rapid synthesis of RNA in the liver of the rat. Because of the recovery of DNA, RNA is extracted two hours after irradiation, and after one hour incubation with carrier-free orthophosphate-^{32}P. A significant decrease of hybridization is observed after 10 kR, but no modification is found after 1.5 kR. (auth)

26642 MIGRATION AND SURVIVAL OF FIBROBLAST CULTURE IN CHICKEN FOLLOWING EXPOSURE TO X IRRADIATION. Olivo, Oliviero Mario; Valentini, Anna Fiorella (Univ., Bologna). Atti Accad. Naz. Lincei, Rend., Cl. Sci. Fis., Mat. Natur.; 48: 91-9(Jan 1970). (In Italian).

The action of Röntgen ionizing radiations from 1,000 R to 120,000 R on the migration and the survival of in vitro hanging drop cultivated chicken fibroblasts was investigated. Radial migration area was decreased with the growing of radiation doses. This action was immediate for 120,000 R but it showed an increasing latency for smaller doses. Culture survival lasted 6 to 9 days after doses ranging from 120,000 R to 20,000 R whereas at 10,000 R and 5,000 R it was of 20 to 25 days. 1,000 R reduced temporarily migration speed which went back to normality 15 days after irradiation. (auth)

26643 REPAIR OF X-RAY-INDUCED THYMINE DAMAGE IN MICROCOCCUS RADIODURANS. Hariharan, P. V.; Cerutti, P. A. (Princeton Univ., N. J.). Nature (London) New Biol.: 229: 247-9(24 Feb 1971).

Investigations were made to find out if bacterial cells could remove radiation damaged residues from their DNA. The DNA of Micrococcus radiodurans was labeled with thymidine-methyl (^{3}H) before irradiation with 150 krad of γ-rays at 0°C. The culture was incubated for different times at 37°C, at a concentration of 3×10^9 cells/ml, and samples withdrawn as a function of time, up to 140 min after irradiation. The culture medium and acid soluble extract of cell pellets in the samples were analyzed for radiolysis products of thymine, using an assay based on their selective reduction with sodium borolydride. The results indicate that damaged thymine was released from the DNA of a recovering culture in two phases: a rapid 30 min phase removing about 75% of the total product release, followed by a pause and a second phase, starting about 60 min after the beginning of the incubation

at 37°C, when the product was removed more slowly. A considerable amount of undamaged thymine was removed for each product, possibly indicating that extensive DNA degradation accompanied the removal of damaged residues. (UK)

26644 MECHANISM OF ACTION OF ULTRAVIOLET RADIATION ON PROTEINS. Vladimirov, Yu. A.; Roshchupkin, D. I.; Fesenko, E. E. (Inst. of Biological Physics, Pushchino, USSR). Biophysics (USSR) (Engl. Transl.): 15: 267-78(1970).

Translated from Biofizika; 15: 254-64(1970).

On exposure of proteins to inactivating doses of ultraviolet radiation, there is photolysis of only the aromatic amino acid residues and cystine. The latter amino acid is destroyed not only through inherent absorption but as a result of a photochemical reaction sensitized by aromatic amino acid residues. Hypotheses on the mechanism of this process are discussed and the literature reviewed. Inactivation of enzymes under the action of ultraviolet radiation is due to photolysis not of any but only of particular aromatic amino acid residues and cystine. Ultraviolet photolysis of the free amino acids and those forming part of proteins occurs through a stage of formation of free radicals. In the case of aromatic amino acids the formation of the radicals occurs as the result of photo-ionization also leading to the appearance of solvated electrons. The energetics of the process of photo-ionization and the structure of the free radicals of amino acids are discussed. (auth) (UK)

26645 DESOXYRIBONUCLEASES AND PHOSPHATASES OF THE RAT KIDNEY UNDER THE INFLUENCE OF WHOLE-BODY IRRADIATION AND 2,4,6-TRIETHYLENIMINO-S-TRIAZINE. Tempel, K.; Beurer, K. (Univ., Munich). Strahlentherapie; 141: 106-13(Jan 1971). (In German).

The increase of the activity of DNAse I must be considered as one of the most striking reactions of rat kidney following whole-body x-irradiation or injections of 2,4,6-triethyleneimino-s-triazine (TEM) (1170 to 2340 R or 1.2 to 2.4 mg/kg resp.). This increase appeared within twelve hours and attained its maximum after three days. When animals survived, enzyme activities of rats exposed to x rays normalized much faster as compared to TEM-treated animals. Three days after sublethal whole-body irradiation or three to seven days after injection of TEM (1.2 mg pro kg) DNA content was 30 to 80% higher than in controls. Activities of phosphatases and DNAse II increased slightly under the influence of irradiation or TEM in most instances. According to experiments concerning DNAse I reaction under the influence of whole-body irradiation, increase of enzyme-activity is to be reduced to enzyme induction, which may be mediated by glucocorticoids and/or increased substrate amount within the kidney. Mechanism of DNAse I reaction under the influence of TEM may be different from that after whole-body irradiation. (auth)

26646 CHEMICAL AND CONFORMATIONAL STUDIES OF GAMMA-IRRADIATED LYSOZYME. Herbert, Sarah Mary. Boulder, Colo.; Univ. of Colorado (1969). 115p. University Microfilms Order No. 70-16,490.

Thesis.

The phosphate soluble fraction of γ-irradiated lysozyme can be separated by column chromatography into a number of protein components. Detailed information on the nature of these fractions is essential in understanding chemical damage of irradiated enzymes. The chemical and physical properties of a major fraction, P3-I, eluting very close to native lysozyme were examined in depth. It was of interest to determine whether P3-I was undamaged lysozyme, one kind of damaged material, or a mixture of molecules which has been damaged in various ways. If this protein were damaged it was of interest to see how it differed from native lysozyme. In addition, the free radical distribution in the irradiated phosphate soluble fractions including P3-I was determined by labeling with tritiated hydrogen sulfide (HTS). The results suggest that P3-I is not a homogeneous material but consists of molecules which have been damaged in many ways, and in which no one molecule has suffered extensive damage. Both heat and pH perturbation spectra of the irradiated protein, when compared to native lysozyme, showed that part of the conformational damage to this irradiated molecule can be corrected by denaturation and renaturation. The heat denaturation curves confirmed this result. These data, together with the uv absorption spectra after denaturation by heat and alkaline pH, indicated that there were two levels of conformational damage to P3-I. There was conformational damage which was not reversible and presumed caused by chemical changes and there was that which was reversible and presumed not caused by chemical effects. Two mechanisms are proposed for the reversible conformational damage. One involves the formation of a hot spot during irradiation whereby very limited regions of the protein are subject to a rise in effective temperature sufficient to give atomic mobility within the solid molecule. The other mechanism involves the radiation formation of charged groups in hydrophobic centers of the protein which result in rearrangement of the hydrophobic groups to accommodate the charge. A mechanism for chemical damage from γ irradiation of proteins is proposed involving independent cumulative inactivation of amino acid residues. (Diss. Abstr. Int., B)

26647 FATTY ACIDS IN AN IRRADIATED CHICKEN PRODUCT. Cook, William Jackson Jr. Baton Rouge, La.; Louisiana State Univ. (1970). 75p. University Microfilms Order No. 70-18,522.

Thesis.

Lipid studies were conducted on samples of canned non-irradiated and irradiated chicken based pet food products. The fatty acids of these samples were isolated and identified using gas-liquid chromatography. Classes of lipids in the extracts of non-irradiated and irradiated samples were separated and tentatively characterized by thin-layer chromatography. Total extractable lipid was determined gravimetrically. Phospholipids, sterols, free fatty acids, triglycerides, and sterol esters were demonstrated on thin-layer plates in the samples of both non-irradiated and irradiated chicken products. The triglyceride class was observed to be the most abundant fraction of the total lipids in both types of samples. There were no differences detected between relative fatty acid composition of the total lipid extract or in the relative composition of the fatty acids of the triglyceride fractions of the non-irradiated and irradiated samples. (Diss. Abstr. Int., B)

26648 NUCLEIC ACID AND PROTEIN SYNTHESIS, AS MEASURED BY INCORPORATION OF TRACERS, DURING REGENERATION IN ULTRAVIOLET-TREATED BLEPHARISMA. Giese, A. C. (Stanford Univ., Calif.). Exp. Cell Res.; 64: 218-26(Jan 1971).

Regeneration of postperistomial pieces of Blepharisma intermedium was retarded by increasing doses of uv 265 nm; a dose of 3,200 ergs/mm^{-2} usually doubled the time for 50% regeneration while one greater than 5,600 ergs/mm^{-2} generally stopped regeneration. However, a dose of 4,000 ergs/mm^{-2} just detectably reduced incorporation of ^{14}C-uridine into RNA (RNAase-removable) in and near the macronucleus, doses of 4,400 ergs/mm^{-2} and more produced progressively greater effects, reduction of tracer incorporation being evident both in degree of labeling of individual cells and number of cells strongly labeled. Incorporation of ^{14}C-thymidine into DNA (DNAase-removable) in and around the macronucleus of those postperistomial pieces which showed any incorporation of Blepharisma was reduced by uv doses of 4,000 to 5,000 ergs/mm^{-2}, as was incorporation of ^{14}C-amino acids into proteins. Growth in bromodeoxyuridine did not sensitize fragments of Blepharisma to uv. Regeneration was retarded most by uv in cells irradiated immediately after cutting. However, incorporation of ^{14}C-uridine into postperistomial pieces continued throughout regeneration and was about equally sensitive to uv 4 after cutting as immediately afterwards. Regeneration was also retarded more if irradiated whole cells were cut soon after exposure than if cut later. However, incorporation of ^{14}C-uridine continued throughout regeneration and was about as sensitive to uv in those cut later as in those cut earlier. The macronuclear condensation cycle which accompanies regeneration was retarded by uv, the delay increasing with dose. (auth)

26649 PROTEIN SYNTHESIS IN THE LENS AND ITS DISTURBANCE. 2. ACCUMULATION OF ^{14}C-L-LEUCINE BY X-IRRADIATED AND NAPHTHALENE TREATED RABBIT LENSES. Koyama, Takeko (Okayama Univ., Japan). Nippon Ganka Gakkai Zasshi; 74: 747-52(Aug 1970). (In Japanese).

A series of experiments were conducted on the accumulation of amino acid ^{14}C-L-leucine in x-irradiated and naphthalene-treated rabbit lens cultured in the TC 199 medium, and the uptake of ^{14}C-L-leucine into these lenses was estimated. The results obtained were as follows: In the group of x-irradiated rabbit lenses, the incorporation of ^{14}C-L-leucine into lens protein and the uptake of ^{14}C-L-leucine into lens were increased in the early stage, and afterward, the latter decreased. In the group of x-irradiated rabbit lenses, opacity appeared only in the posterior subcapsular layer at the central region. In the group of naphthalene-treated rabbit lenses, the incorporation of ^{14}C-L-leucine into lens protein began to decrease soon after the beginning of naphthalene-treatment, but the total uptake of ^{14}C-L-leucine into the lens stayed normal for a long experimental period. In the group of naphthalene-treated rabbit lenses, the opacity spread to form a complete cataract within 3 months during the administration of naphthalene. It was suggested that the formation of 12-naphthoquinone-protein facilitated the denaturation of lens protein. The results of the present experiment suggest that the disturbance of protein synthesis is the most essential factor for cataract formation, but some other factors such as 1,2-

XUM

naphthoquinone seem to contribute to the denaturation of protein. (Japan)

26650 KINETICS OF CATALASE ACTIVITY IN SOLUTION AND IN A LIPOPROTEIN COMPLEX AND THE RELATIVE RESPONSE TO IONIZING RADIATION. Wright, Ann Elizabeth Foley. Houston, Tex.; Univ. of Texas (1970). 129p. University Microfilms Order No. 71-4544.

Thesis.

It is known that molecules change their available energy states and the reactivity of their functional groups when bound to other molecules. Evaluation of the magnitude of the change in enzymic activity with alteration of molecular structure would be helpful in the interpretation of the experimental results concerning: the fundamental role of enzymes whose dynamic function may involve partial existence in aqueous media and partial existence in association with phospholipids; variation in radiation response; variation in radiation protective effects; and relative biological effectiveness of radiation differing in LET values. The change induced in the reaction kinetics of catalase in decomposing hydrogen peroxide by complexing the protein with phospholipid micelles was significant. The amount of phospholipid bound by catalase was close to the amount bound by structural protein as shown by other studies. Radiation dose-response curves were determined for exposure to radiation at two different dose rates for catalase in solution, catalase–phospholipid complex, and catalase with 1 M glycerol added. Post-irradiation oxygen treatment was used to investigate the nature of the radiation damage. Addition of 1 M glycerol followed by irradiation resulted in an increase in activity of 40% over initial activity following a dose of 250K rads. Subsequent decrease in activity occurred at about the same rate as that of catalase alone or catalase in complex. After 250K rads at the high dose rate, catalase complexed with phospholipid had 56% remaining activity while catalase alone had only 45%. This difference was significant at the 95% confidence level. The model proposed to explain the experimental results was based on the theory of wave propagation in periodic arrays, with variation in the folding of the peptide chain and resultant difference in external shape of the molecule creating two different lattice structures. The difference in energy propagating characteristics of the two lattices gave rise to a difference in catalytic activity. Association with the phospholipid resulted in a molecular shape more favorable for optimum orientation of the molecules in the lattice. This orientation facilitated restitution of radiation damage to the molecule by increasing the rate of energy dispersal and of radical recombination. It is possible that the two species of catalase arise from the existence of catalase as a membrane bound component and as free catalase in the cytoplasm. To the degree that the viability of a cell or organism is dependent upon regulator properties deriving from supramolecular organization of enzymes, to that same degree will it be vulnerable to radiation damage. Thus, the more complex organisms would be more radiosensitive. Also, cells irradiated during mitosis, when radical formation would block the spontaneous chemical combinations resulting in the proper supramolecular organization, would suffer greater lethality than those in the stable membrane phases. (Diss. Abstr.)

26651 EFFECT OF PRE-IRRADIATION ON THE CONTENT OF GROWTH SUBSTANCES IN X_2-PLANTS OF BRASSICA OLERACEA VAR. ACEPHALA. Brugovitzky, Edith (Kernforschungsanlage, Juelich, Ger.). Physiol. Plant.; 24: 90-4(1971). (In German).

The auxin content of growth stimulated young plants (Brassica oleracea var. acephala) of the X_2-generation, originating from x-irradiated seeds (75 kR) was determined. Methanolic extracts were separated on thin-layer-chromatograms, which were analyzed by uv light and various chemical reactions. Quantitative determinations of growth substances were made using the Avena coleoptile-cylinder-test. The following results were obtained: X_2-plants had a higher content of IAA compared with unirradiated control samples; IAAm was detectable in only two out of 40 experiments; and two fluorescent substances were detected (a hydroxycinnamic acid derivative and a long chained unsaturated ketone or aldehyde, which is still unknown). (auth) (Sweden)

26652 EFFECTS OF UNILATERAL AND BILATERAL RENAL IRRADIATION ON PARAMETERS RELATED TO RENAL HYPERTENSION. Courtade, Elpiniki Tsinga. Rochester, N. Y.; Univ. of Rochester (1970). 232p. University Microfilms Order No. 71-8441.

Thesis.

In order to determine pathophysiologic mechanisms by which renal irradiation induces hypertension, male rats were studied at periodic scheduled sacrifice times after a single x-ray exposure of 2000 R to one or both temporarily exteriorized kidneys. Increased systolic blood pressure was noted after irradiation and was of greater severity in the bilaterally irradiated animals. In general, arteriolonephroschlerotic changes developed at a similar rate in the irradiated kidneys of the unilaterally and bilaterally irradiated animals until the final time interval when there was a greater degree of arteriolonephrosclerosis in the bilaterally irradiated animals. There was a reduction of the total renal mass in the irradiated kidneys, the degree of which depended on the amount of renal tissue exposed. The juxtaglomerular granulation index (JGI) was decreased in the irradiated kidneys. There was a rough inverse correlation between the average JGI of both kidneys and the blood pressure. Bilateral renal irradiation produced a diuretic effect of greater severity and duration than unilateral irradiation. An increased water intake and decreased concentration of sodium and potassium was associated with the increase in urine output. No changes occurred in the total excretion of sodium or potassium and in the serum concentration of sodium and potassium. The width of the zona glomerulosa remained relatively constant. These results are discussed in terms of possible mechanisms involved in the development of radioinduced hypertension. (Diss. Abstr.)

26653 LIGHT-MEDIATED REGULATION OF TMV-RNA PHOTOREACTIVATION. Murphy, Terence M.; Gordon, Milton P. (Univ. of Washington, Seattle). Photochem. Photobiol.; 13: 45-55(Jan 1971).

Nicotiana tabacum plants placed in the dark lost their ability to photoreactivate uv-irradiated 137 ergs/mm^2/min tobacco mosaic virus RNA over a course of approximately one week. When plants were returned to the light, they recovered their photoreactivation ability. The recovery occurred after a lag of at least 3 hr and was complete in 12 to 24 hr. Three hours or less of cool-white illumination (2400 ft-c) were necessary to induce recovery. Blue light was effective in inducing recovery, green light less effective, red and near-uv were ineffective. (auth) (UK)

26654 COMBINED HISTOCHEMICAL PROCEDURE TO DISTINGUISH BETWEEN MESENCHYMAL AND EPITHELIAL RETICULAR CELLS IN THE RAT THYMUS UNDER THE LIGHT MICROSCOPE. Bacsy, Ernoe; Oekroes, Istvan; Rappay, Gyoergy (Inst. of Experimental Medicine, Budapest). Acta Histochem.; 36: Suppl., 123-8(1970).

A combined procedure of staining for lipids and for acid phosphatase and non-specific esterase activity respectively, showed that whereas the thymus of rats previously exposed to the action of x rays contained lipids and intense acid phosphatase and non-specific esterase activity, the epithelial reticular cells exhibited primarily acid phosphatase activity and were poor in lipids and non-specific esterase. Staining for lipids and for acid phosphatase activity in one process enables ready distinction between mesenchymal and epithelial cells in sections for light microscopy. (auth)

26655 X-RAY-INDUCED SINGLE-STRAND BREAKS IN DNA OF E. COLI B/r: EFFECT OF IRRADIATION AND POSTIRRADIATION CONDITIONS. Lehnert, Shirley; Moroson, Harold (Sloan-Kettering Inst. for Cancer Research, Rye, N. Y.). Contract AT(30-1)-910. Radiat. Res.; 45: 299-310(Feb 1971).

Alkaline sucrose density gradient results indicate that aerobic x irradiation of log phase Escherichia coli B/r CSH is 4.5 times more effective than anoxic irradiation in producing single strand breaks in DNA. If 0.02 M EDTA, presumed to inhibit the rejoining enzyme, is present during irradiation, the yield of breaks is increased 6-fold in air and 10-fold in nitrogen, thus aerobic conditions are still more effective than anoxic in producing breaks. Holding bacteria at 0°C in buffer after aerobic or anoxic radiation resulted in 80 to 90% of the observed breaks being rejoined. Since rejoining takes place during irradiation, the yield of breaks is dose rate dependent. The oxygen effect on single strand breaks in log phase E. coli B/r may be related to radiation survival: however, survival is not improved by lowering the dose rate nor by postirradiation holding at 0°C conditions which result in the rejoining of breaks. Holding irradiated bacteria in buffer at 37°C results in only a small amount of rejoining, while considerable loss of label takes place due to DNA degradation. Holding at 37°C in growth medium, however, results in DNA degradation accompanied by a marked increase in molecular weight of TCA insoluble DNA. (auth)

26656 INFLUENCE OF GAMMA IRRADIATION ON SOME PHYSICAL AND CHEMICAL PROPERTIES OF GLUTEN PROTEINS. Lasztity, R.; Figuli, J. Elelmez. Ipar; 23: 321-5(1969).

The most significant physical properties (capacity of water absorption, stretching ability, spreadability, organoleptic properties) of dry gluten treated with ionizing rays do not undergo objectionable changes up to a dose of 0.18 Mrad. Over 1 Mrad. the important technological properties rapidly deteriorate and

are accompanied by disadvantageous chemical changes such as denaturation, disaggregation, change of the N-terminal groups, decrease of mean molecular weight. (Hung. Tech. Abstr.)

26657 EFFECT OF UV-IRRADIATION ON DNA IN DEPENDENCE OF THE DNA STRUCTURE. Wetzel, R.; Becker, M.; Zirwer, D. (Deutsche Akademie der Wissenschaften, Berlin). Stud. Biophys.; 13: 89-95(1969). (In German).

Investigations were performed on the influence of uv irradiation on the linear dichroism (LD) of oriented DNA films of different water content. From the results an effect of structure destabilization by uv irradiation is derived. This is possibly due to the breakage of H water bridges between the bases in consequence of their uv absorption. Water bridges which stabilize the DNA structure are probably an important factor for the uv sensibility of the DNA films at various water content. (auth)

26658 GEL FILTRATION STUDIES OF UV-IRRADIATED RIBONUCLEASE A. II. Mueller, H.-G. (Institut fuer Biophysik, Berlin). Stud. Biophys.; 13: 245-51(1969). (In German).

From photoderivates of ribonuclease irradiated with uv light the molecular weights were determined by means of gel filtration. The values obtained are between those of the monomer, dimer, or trimer form. In comparison with reduced ribonuclease the evidence is given that those are denaturation products. To a certain extent aggregates appear. (auth)

26659 INFLUENCE OF X-RAYS UPON THE MITOTIC ACTIVITY AND DNA SYNTHESIS IN ENDOMETRIAL GLANDULAR EPITHELIUM IN MICE. Jonek, J.; Klimkiewicz, Z.; Konecki, J. (Medical Academy, Zabrze-Rokitnica, Poland). Pol. Med. J.; 9: 1511-23(1970).

After irradiation of Porton strain mice with a whole body dose of 600 R an abrupt decrease of the mitotic index occurs in the dividing cells from the endometrial glands. This decrease persisted up to 12 hr after irradiation. The decrease of the mitotic index after irradiation could be due to an inhibition of transition of the examined cells from the premitotic into the mitotic phase proper. Under the influence of x rays an inhibition of DNA replication occurred in the mentioned cells which persisted for 36 hr after irradiation. (auth)

26660 IR SPECTROPHOTOMETRIC STUDY OF THE CHANGES INDUCED BY GAMMA IRRADIATION IN THE STRUCTURE OF PROTEINS AND NUCLEIC ACIDS. Furnica, Gh.; Ursu, V. Stud. Cercet. Biochim.; 12: 239-44(1969). (In Rumanian).

Studies of the protein spectra pointed out as characteristic the frequencies assigned to the N–H, C=O, and –CO–NH- bonds. In nucleic acids, frequencies that may characterize the C–N, C=N, P–O, and C–O bonds are evidenced. The irradiation of these polyelectrolytic biomacromolecules with doses of ^{60}Co γ rays in the range of 2×10^6R or 1.1×10^{20} eV/g, results in some intensity changes of their corresponding characteristic lines. The presence of a variable radiosensitivity to the action of γ irradiation of biopolyelectrolytes was detected. This sensitivity decreases in the following sequence: albumin, gammaglobulin, DNA, and RNA. (Rom. Sci. Abstr.)

26661 GEL FILTRATION STUDIES ON UV-IRRADIATED RIBONUCLEASE A. III. Mueller, H.-G. (Institut fuer Biophysik, Berlin). Stud. Biophys.; 17: 173-8(1969). (In German).

The irradiation of ribonuclease A by uv light enlarges the molecular Stokes radius of the enzyme. Simultaneously the quickness of diffusion of the photoderivatives will be decreased. Considerable modifications of the protein structure are the cause of this process. (auth)

Immunology

Refer also to abstracts 26918, 26919, 26985, 26986, 27001, and 27058.

26662 GRAFT-VERSUS-HOST REACTION MODIFIED BY IN VITRO PREINCUBATION OF MARROW WITH SUBCELLULAR ANTIGEN. Uphoff, Delta E.; Draper, Lawrence R. (National Cancer Inst., Bethesda, Md.). J. Nat. Cancer Inst.; 46: 139-41(Jan 1971).

The graft versus host reaction induced by inoculation of AKR marrow into lethally irradiated (AKR × CBA)F_1 and (CBA × AKR)F_1 hybrid recipients was prevented by the in vitro preincubation of AKR marrow with stromata of CBA erythrocytes for 35 min at 26°C. This subcellular antigen was as effective as, or more effective than, fresh preparations of intact erythrocytes. This validated the assumption that the critical factor in the incubation procedure was contact with tissue antigens rather than transfer to the recipient of viable stem cell contaminants in the erythrocyte preparation. (auth)

26663 ABROGATION OF PASSIVELY TRANSFERRED TUMOR IMMUNITY IN VIVO BY ANTIGENICALLY RELATED TUMOR CELLS. Wepsic, Harold T.; Bernstein, Irwin D.; Zbar, Berton; Borsos, Tibor; Rapp, Herbert J. (National Cancer Inst., Bethesda, Md.). J. Nat. Cancer Inst.; 46: 195-202(Jan 1971).

Systemic transfer of tumor immunity in syngeneic guinea pigs, accomplished by transfusion of peritoneal exudate cells, was abrogated after the intraperitoneal injection of live or x-irradiated tumor cells antigenically related to the immunity transferred. Passive transfer of immunity was not affected by the intraperitoneal injection of unrelated tumor cells. The relationships of time of inoculation and dose of tumor cells to abrogation of transferred immunity were studied. The transfer of tumor immunity was also abolished when antigenically related tumor cells were mixed with peritoneal exudate cells before inoculation. (auth)

26664 RADIATION EXPOSURE, AGING, AND IMMUNITY. 2. Kurusu, Akira (National Inst. of Radiological Sciences, Chiba, Japan). Hoshasen Kagaku; 13: 265-73(Apr 1970). (In Japanese).

From the effect of radiation exposure on immunity and from the observations on aging and immunity, a speculation is made that the mechanism of auto-immunity phenomenon might offer a way to solve the problem of radiation exposure and aging. Effect of radiation exposure on immune reaction may be seen from the abnormal increase of IgM antibody after whole-body x irradiation, 24 to 48 hours before antigen inoculation. There is a possibility of systemic effect even by local irradiation, by affecting immunity through lymphocytes and, as one of its mechanisms, the role of autoimmune phenomenon may play an important role. For this mechanism, there is a possibility of a change in the antigenicity of the cells or tissues in the irradiated locus, or its release into the blood, resulting in autoimmunity. Aging phenomenon begins already in the fetal period and progresses through the growing period over the whole life time. On the other hand, autoimmune phenomenon appears as a result of destruction of homeostatic control mechanism against immunological tolerance and produces marked increase of lysosomes and deposition of amyloids, and this condition is thought to facilitate formation of vascular damage and other adult diseases. (Japan)

26665 PARTICIPATION OF THREE CELL TYPES IN THE ANTI-SHEEP RED BLOOD CELL RESPONSE IN VITRO. SEPARATION OF ANTIGEN-REACTIVE CELLS FROM THE PRECURSORS OF ANTIBODY-FORMING CELLS. Tan, Teresita; Gordon, Julius (McGill Univ., Montreal). J. Exp. Med.; 133: 520-33(1 Mar 1971).

Recent studies have established that two cell types are involved in the synthesis of anti-sheep red blood cell (SRBC)[1] antibodies in vivo. One of these cells is thymus-derived and the other bone marrow-derived and thymus independent. It is the latter which gives rise to antibody forming cells (AFC). Both cell types were shown to be radiosensitive. In vitro, two cell types, a glass adherent and a nonadherent population, were separated and shown to be required for an anti-SRBC response; the former cell was found to be radioresistant. (auth)

26666 EFFECTS OF X-IRRADIATION AND ANTI-LYMPHOCYTE SERUM ON THE RESPONSES TO TUMOUR ALLOGRAFTS. Riches, A. C.; Thomas, D. Brynmor (Medical School, Birmingham, Eng.). Brit. J. Cancer; 24: 833-42(Dec 1970).

The growth of a CBA mammary adenocarcinoma was studied following transplantation to syngeneic and allogeneic recipients, with particular reference to the susceptibilities of the primary and secondary responses elicited by the tumor allografts, to impairment by whole-body x-irradiation and by treatment with rabbit-anti-mouse lymphocyte serum. In syngeneic recipients, the diameter of tumor implants increased linearly with time and there was no difference in the growth curves in females and males. Later tumor generations grew faster than earlier generations. In allogeneic recipients, there was a relationship between the tumor diameter on day 21 (T) and the dose of x-irradiation (D) administered before implantation: $T = 0.028\,D - 9.17$ for early tumor generations (SMT4) but this was obscured for later generations (SMT21). The primary response to tumor allografts was radiosensitive whereas the secondary response was radioresistant. This radioresistance of the secondary response persisted for at least 5 months after primary sensitization. Unlike whole-body x-irradiation, treatment with rabbit-anti-mouse lymphocyte serum suppressed both primary and secondary responses to tumor allografts. The possibility is considered that after exposure to

antigenic stimulation, an immunologically reactive cell population is formed which is radioresistant but sensitive to ALS, unlike the precursor cells from which this population is derived, which are radiosensitive and sensitive to ALS. (auth) (UK)

26667 PREPARATION OF HIGHLY RADIOACTIVE BOVINE ANTI-MOUSE LYMPHOCYTE ANTIBODY. Dresser, D. W. (National Inst. for Medical Research, London). Nature (London); 229: 630-2(26 Feb 1971).

It is shown that the ability of bovine anti-lymphocytic serum (ALS) antibody to prolong skin grafts can be increased by labeling the material with ^{125}I. Also the practicality of preparing purified bovine anti-mouse lymphocyte antibody using a column of insoluble immunoadsorbent, seems to be limited at the moment by the marked lability of ALS antibody in acid conditions. (UK)

26668 STUDIES OF IMMUNOLOGICAL MODIFICATIONS OF BLOOD COAGULATION INDUCED BY RADIOTHERAPY IN CANCER PATIENTS. di Lella, V.; D'Angelo, F.; Morucci, M.; Placanica, A. (Istituto di S. Spirito, Rome). Nunt. Radiol.; 34: 1403-15(Nov 1968). (In Italian).

A study was made of primary hemocoagulative factors during and after therapy in a number of patients with neoplasms of the uterus and the lungs. The prothrombin time, thromboelastograph, and platelet count were taken into consideration. Studies on antiplatelet antibodies were made simultaneously. The results obtained confirmed that radiotherapy in small doses stimulates the organism in the platelet-formation hypercoagulative direction, and higher doses stimulate in the platelet-deficiency hypocoagulative direction. The significance of the presence of antiplatelet antibodies and of their modification as a result of the irradiation is discussed. (tr-auth)

26669 IDENTIFICATION OF TWO-CELL POPULATIONS REQUIRED FOR IMMUNOCOMPETENCE. Brody, Thomas Bergman. Berkeley, Calif.; Univ. of California (1969). 79p. University Microfilms Order No. 70-17,517.

Thesis.

Two cell populations participating in the mouse immune response to sheep erythrocytes (SRBC) are identified. Cells of one population can attach SRBC by means of surface receptors. Cells with attached SRBC are called rosettes. Formed rosettes can be fractionated from other cells because of their high sedimentation velocity. Cells with surface receptors for SRBC are the cells in bone marrow which show synergism with thymus in response to SRBC in a cell transfer assay. Receptor-bearing cells may be fractionated from hematopoietic colony-forming units. Cells with receptors for antigen act as the direct cellular precursors of antibody producing cells. The degree of commitment of cells with receptors for SRBC antigens to respond to a restricted set of antigenic moieties is analyzed. Cells with receptors for SRBC antigens do not have receptors for erythrocytes of other species. However, the absolute restriction of SRBC-rosettes to respond only to SRBC antigens could not be demonstrated. The second cell population required for an immune response to SRBC acts in conjunction with receptor-bearing cells. This population is present in the peripheral lymphoid organs, e.g., spleen and Peyer's patches, and can be fractionated from the receptor-bearing cells of these organs. This auxiliary cell population is called the peripheral thymic population because its role in the immune response can be carried out by thymocytes. The differentiation of these two populations from cellular progenitors was studied in lethally irradiated mice. The receptor-bearing population differentiates from bone marrow progenitors much more rapidly than the peripheral thymic population. The differentiation from bone marrow progenitors of the cells with receptors for antigen is completely independent of thymus, while the differentiation of the peripheral thymic population is dependent upon thymus function. Peyer's patches may not be considered as solely primary lymphoid organs. Peyer's patches in adults have all the cell populations required for immunocompetence. In addition, Peyer's patches cannot be considered the initial source in the neonatal period of the cells with receptors for antigen, because these cells are present in the prenatal period in fetal liver. (Diss. Abstr. Int., B)

26670 COMPARISON OF COLONY-FORMING PERFORMANCE OF BONE MARROW CELLS IN SYNGENEIC AND ALLOGENEIC CELLULAR ENVIRONMENT WITHIN A SINGLE HOST. Lengerova, Alena; Matousek, V.; Viklicky, V.; Zeleny, V.; Boubelik, M. (Inst. of Experimental Biology and Genetics, Prague). Folia Biol. (Prague); 16: 385-90(1970).

The effects of allogeneic and syngeneic cellular environments on the capacity of bone marrow cells to form spleen colonies in irradiated hosts were compared. In order to eliminate one source of undesirable variation, the allogeneic and syngeneic conditions were created within a single host. F_1 hybrids of two H-2 congenic strains were splenectomized and both parent-strain spleens from neonatal donors were implanted under the capsule of one of their kidneys. Ten to 12 weeks later the animals were γ irradiated (850 R) and injected with 1.2×10^5 bone marrow cells of one parent-strain origin. The colony-forming performance was evaluated microscopically from series of histological sections of the syngeneic and allogeneic implants. Individual colonies were reconstructed and from their maximal cross section the volume of each colony was calculated assuming a spherical shape. Allogeneic inhibition of the colony-forming performance was reflected in both the number and mean volume of the colonies. The bearing of the microscopic and macroscopic techniques of scoring on the conclusion concerning the inhibitory effect of the allogeneic environment is discussed. (auth)

26671 SELECTIVE INHIBITION OF CELLS IN THE IMMUNE RESPONSE BY ACTINOMYCIN D. Kaufman, Stephen J. (Univ. of Colorado, Denver). J. Immunol.; 106: 781-5(Mar 1971).

A simple method is described for completely and selectively inhibiting one cell population that is required for in vitro and in vivo antibody responses to sheep erythrocyte antigens. This cell population, which is present in both 7-day immune spleen cells and in bone marrow-derived spleen cells, is completely inhibited by treatment with 0.01 μg/ml actinomycin D for 1 hr. These cells are also relatively resistant to radiation. A second cell type present in immune spleen cells is identified by resistance to this dose of actinomycin D, but is susceptible to a 10-fold higher concentration of the drug. (auth)

26672 REAPPEARANCE AND RELATIVE IMPORTANCE OF IMMUNOCOMPETENT CELLS IN THE THYMUS, SPLEEN, AND LYMPH NODES FOLLOWING LETHAL X-IRRADIATION AND BONE MARROW RECONSTITUTION IN MICE. Blomgren, Henric; Andersson, Birger (Karolinska Institutet, Stockholm). J. Immunol.; 106: 831-4(Mar 1971).

The development of the hemolysin response to sheep erythrocytes (SRBC) was studied in mice irradiated with 800 R and reconstituted within 2 hr with 10^7 isologous bone marrow cells (800 R:BM) as compared with untreated controls. The hemolysin response was absent in 800 R:BM mice when injected with SRBC on day 0 and was appreciably increased by adding thymic cells with the SRBC on day 0. Thereafter, it progressively reached higher peak titers during recovery of the animals from irradiation, as tested by the injection of SRBC along on days 10, 14, and 25 after irradiation, and reached somewhat higher peak titers by adding thymic cells with the SRBC on the same days after irradiation. The humoral antibody response against SRBC of mice which had previously been thymectomized, 800 R irradiated and bone marrow reconstituted was absent 14 days after treatment. Their hemolysin response could be restored by the injection of cells from thymus, spleen or lymph nodes from normal donors. After 800 R:BM of the cell donors this type of reactivity reappeared first in the thymus and thereafter in spleen and lymph nodes. It was concluded that immunocompetent cells of this type are generated within the thymus and are later seeded into other lymphoid organs. (auth)

26673 EVIDENCE FOR THYMIC DEPENDENCE OF PHA-REACTIVE CELLS IN SPLEEN AND LYMPH NODES AND INDEPENDENCE IN BONE MARROW. Blomgren, Henric; Svedmyr, Erik (Karolinska Institutet, Stockholm). J. Immunol.; 106: 835-41(Mar 1971).

The influence of the thymus on the in vitro phytohemagglutinin (PHA) response of spleen, lymph node and bone marrow cells was investigated in lethally irradiated, bone marrow-protected (800 R:BM) mice. Reactivity of the cells was measured by studying their incorporation of ^3H-thymidine in vitro. Nucleated cell content of the various sites during recovery was also obtained. In 800 R:BM mice, the PHA-response first appeared in cells of the bone marrow and later in those of the thymus, lymph nodes and spleen. It was markedly impaired in lymph node and spleen cells, but not in bone marrow cells during recovery (25 to 35 days after irradiation) when the mice were thymectomized 3 to 4 weeks prior to irradiation and protection by BM cells or fetal liver cells, as compared to similar cells during similar recovery in sham-thymectomized mice or in 800 R:BM mice given thymic cells with the bone marrow or fetal liver cells. Moreover, treatment of lymph node or bone marrow cells with an antiserum directed against an antigen specific for thymic lymphocytes or their descendants reduced the PHA-response of lymph node cells but not that of the bone marrow cells. These results suggest that the PHA-responses of lymph node and spleen cells are thymus-dependent while that of the bone marrow cells is thymus-independent. (auth)

26674 INVESTIGATION OF THE DETOXIFYING EFFECT OF ^{60}Co GAMMA RADIATION ON THE ANTIGENICITY OF NAJA NAJA VENOM IN RABBITS. Mittelstaedt, James Stanley. La-

fayette, Ind.; Purdue Univ. (1970). 102p. University Microfilms Order No. 71-2653.

Thesis.

The effects of γ radiation on detoxification of a neurotoxic snake venom, that of Naja naja, while allowing the radiation-altered venom to retain a significant portion of antigenic character, thus producing a neurotoxic venom toxoid was investigated. In order to standardize venom solutions, a procedure for Nesslerization of Naja naja venom was developed for determining the milligrams of nitrogen in each venom sample. Naja naja venom was found to contain 11.6% nitrogen. In addition to Nesslerization of the venom, a standard animal, that of the female Swiss strain mouse weighing 20 ± 1 gram, was chosen to be used in all LD_{50} tests. On the basis of the above LD_{50} test animal and standardization venom solutions, the LD_{50} for Naja naja venom was 0.53 micrograms of nitrogen per mouse (4.6 micrograms venom per mouse) and 0.026 milligrams nitrogen per kilogram body weight (0.230 milligrams venom per kilogram body weight). An approximate LD_{50} in male New Zealand White rabbits was found to be 0.013 milligrams nitrogen per kilogram body weight (0.113 milligrams venom per kilogram body weight) while the LD_{50} for the female rabbit was 0.011 milligrams nitrogen per kilogram body weight (0.098 milligrams venom per kilogram body weight). Three concentrations of Naja naja venom in aqueous solutions 0.1, 0.5, and 1.0 milligrams per milliliter, were exposed to various amounts of ^{60}Co γ radiation from 6,000 to 230,000 R. The change in LD_{50} value of the irradiated venom was determined. The increase was an exponential function, varying directly with the total R exposure with the concentration of the venom and inversely in aqueous solution during irradiation. The results indicate that the inactivation of the toxin molecule was a single hit reaction. Venom at a concentration of 1.0 milligrams per milliliter was selected for further study, after exposure to 10,000, 50,000 and 150,000 R, to determine the effect of radiation exposure on antigenicity. From the results of neutralization tests, it appeared that venom exposed to 10,000 and 50,000 R retained a large degree of antigenicity while the venom exposed to 150,000 R had little antigenicity. These results were confirmed by immunodiffusion analysis. (Diss. Abstr. Int., B)

26675 NEW PHENOMENON OF USEFULNESS IN THE RADIOIMMUNOASSAY OF PLASMA ADRENOCORTICOTROPIC HORMONE. Matsukura, Shigeru; West, Charles D.; Ichikawa, Yoichi; (and others) (Univ. of Utah, Salt Lake City). J. Lab. Clin. Med.; 77: 490-500(Mar 1971).

A new technique for radioimmunoassay of adrenocorticotropic hormone (ACTH) using ^{125}I was developed based on the discovery of an increase in the proportional binding of ACTH to antibody when small increments of ACTH are added to relatively high concentrations of antisera. A progressive increase in the bound/free (B/F) ratios occurs instead of the conventional decrease. This paradoxical binding was used to develop an accurate and convenient method for measuring ACTH levels in unextracted plasma. Antisera that are unsuitable for conventional radioimmunoassay can be used. The method has proven to be highly reliable and is now used routinely. (auth)

26676 AUTOANTIBODIES TO INTRINSIC FACTOR: THEIR DETERMINATION AND CLINICAL USEFULNESS. Rothenberg, Sheldon P.; Kajani Kantha, K. R.; Ficarra, Anthony (New York Medical Coll.). J. Lab. Clin. Med.; 77: 476-84(Mar 1971).

A new radioimmunoassay procedure has been developed for the simultaneous detection of blocking and binding anti-intrinsic factor antibodies in human serum and gastric juice with the use of a much lower ^{57}Co-labeled B_{12} concentration than heretofore employed. This has resulted in a sensitive assay, because at a 99% confidence level, the serum from 74% of pernicious anemia (PA) patients had blocking antibody and 48% binding antibody. No serum antibody was detected in patients with folate-deficient megaloblastic anemia. The gastric juice of 4 of 7 PA patients had blocking antibody, but none contained binding antibody. The same basic methodology has also been adapted as a simple immunoassay for intrinsic factor concentration in gastric juice. A deficiency of gastric intrinsic factor can be helpful in the diagnosis of PA where the test for serum anti-intrinsic factor antibodies is negative. The application of these procedures to facilitate the etiologic diagnosis of megaloblastic anemias and to screen for latent PA in patients with certain other medical illnesses has been reviewed. (auth)

26677 ELECTRON MICROSCOPIC CHANGES FOLLOWING CANINE CARDIAC ALLOGRAFTS: THE EFFECTS OF IRRADIATION. Weymouth, Richard J.; Seibel, Hugo R.; Craig, Shirley S.; Graham, Walter H.; Lower, Richard R. (Medical Coll. of Virginia, Richmond). Amer. J. Anat.; 129: 169-76[(1970)].

Orthotopic cardiac allotransplantation was performed on ten adult mongrel dogs. At the time of acute rejection (decline in QRS voltage to at least one-half of the post-operative level) a cardiac biopsy was removed from the left ventricle of each dog and followed by 300 R of local x irradiation on five consecutive days. After a full course of x irradiation (1500 R) to each dog, a second biopsy was removed from the left ventricle. In this way, each dog acted as its own control in order to determine the effects of x irradiation on cardiac transplants and the rejection phenomenon. The electron microscopic findings at the time of acute rejection involved primarily the myocytes and their cellular organelles in that the A, I, and Z bands were less distinct and there was significant enlargement and cytological distortion of the mitochondria, endoplasmic reticulum, and T tubules. Endothelial hyperplasia of the smaller blood vessels was also more apparent in the pre-irradiation biopsies. Following irradiation the ultrastructural changes appeared to be reversed in six of the ten dogs; mitochondria and other organelles of the myocytes were more normal and the banding of the fibers was more distinct. Vascular alterations were less and the tissue approached normal cytological architecture. Pre- and post-irradiated cardiac tissues were not different in two animals and in two other animals the post-irradiated tissues appeared more abnormal than those showing acute rejection. Local irradiation as a method of immunosuppression in cardiac transplants is discussed. (auth)

26678 CONTRIBUTION TO THE STUDY OF RECOVERY PROCESSES IN THE HAEMOPOIETIC TISSUE AFTER IRRADIATION: EFFECT OF INTRAPERITONEAL INJECTION OF MILK UPON HAEMOPOIETIC STEM CELLS, BLOOD PICTURE, AND SURVIVAL OF IRRADIATED MICE. Juraskova, Vera (Inst. of Biophysics, Brno). Folia Biol. (Prague); 19: No. 1, 41-9(1971).

In C57BL mice exposed to $LD_{50/30}$ to $LD_{100/30}$ of x rays, the effect of an intraperitoneal injection of milk was analyzed on the survival and hemopoietic recovery in the spleen, using the method of endogenous spleen colony formation. The maximum effect was observed after 1 to 1.5 ml of milk injected 2 to 1 day prior to the exposure: the increase in the survival rate could be quantitatively expressed as a dose reduction factor of approximately 1.24. An intraperitoneal injection of 1 ml of milk 24 hr before the exposure to 400 R or 600 R favorably affected the spleen weight and the WBC and RBC counts in peripheral blood. In unirradiated animals, the milk injection caused only transient changes. The effect of milk injection upon the survival of hemopoietic bone marrow and spleen stem cells after 300 R was evaluated with the method of exogenous spleen colony formation. An increased number of bone marrow and spleen stem cells was found in the pretreated mice compared to the controls at all the time intervals tested, i.e., between 10 min. and 8 days following the exposure. The degree and the nature of the differences found is discussed in relation to the known effect of radiation on stem cells and blood forming tissue. (auth)

26679 EFFECT OF RADIATION DOSE, DOSE RATE, AND QUALITY ON THE IMMUNE RESPONSE. Gottlieb, Charles Frederick. Knoxville, Tenn.; Univ. of Tennessee (1970). 88p. University Microfilms Order No. 71-348.

Thesis.

The effects of fission spectrum neutrons and 250 Kvp x rays on formation of humoral antibody were studied, both in terms of total dose and dose rate of exposure. The results were compared with earlier ^{60}Co studies. Mice (C3BF1) were injected with sheep red blood cells two hours after irradiation, and the immune response was measured over a 35 day period. With neutron irradiation, antibody formation was found to be dependent upon the total dose, but independent of the exposure rate (range of 2.5 to 82 rads/min). In contrast, the immune response after x or γ irradiation was found to be dependent on both the dose and dose rate. Maximum dose rate differences occurred with 500 rads of x rays, the 7.6 rads/min group yielding a tenfold higher response than the 67 rads/min group. The maximum depression with either neutron or x irradiation occurred when antigen was given 12 hr after exposure, compared to 24 hr after exposure for ^{60}Co. For x rays, a dose rate difference was clearly apparent only when antigen was given from 24 hr before to 12 hr after irradiation, compared to ^{60}Co, which exhibited dose rate differences from 3 days before to more than 15 days after irradiation. The dose rate dependence in terms of radiation quality was found to be ^{60}Co > X rays > neutrons. The exposure rate effect was demonstrated to be present at the cellular level by culturing irradiated spleen cells in lethally-irradiated syngenetic recipients. Using two assays of the immune response (intact animals and cultured spleen cells), plus animal mortality data, RBE's were calculated for neutrons and ^{60}Co to be about 3.3 (range of 2.4 to 4.8) and 0.9 (range of 0.7 to 1.0) respectively. (Diss. Abstr. Int., B)

26680 RADIOSENSITIVITY OF THE INDUCTIVE AND PRODUCTIVE PHASES OF ANTIBODY. Nikolaev, A. I.; Rozgon, M. I.; Safaeva, I. B. Zh. Mikrobiol., Epidemiol. Immunobiol.; No. 7, 117-22(Jul 1969). (In Russian).

The effect of x irradiation on hemagglutinin titer, the number of live nuclear cells, and the absolute and a relative number of antibody forming cells in the spleen of albino mice was studied. The mice were subjected to x irradiation in a dose of 400, 500, and 700 at various periods of inductive and productive phases of antibody formation. It was revealed that in comparison with others, the antibody forming cells of mouse spleen were more resistant to irradiation. Administration of the antigen soon after the irradiation caused a radioprotective effect in the nuclear cells of the spleen of animals irradiated with the x ray doses below the sublethal. This effect was brought to the minimum in irradiation of the animals with high doses. Irradiation of the animals at various periods of the antibody formation productive phase caused a reduction in the number of nuclear and antibody forming cells in the spleen, thus serving as a cause of reduction of the antibody titer. Irradiation of animals at various periods before the immunization increased the duration of the inductive phase of antibody formation on account of depression of processes of proliferation of antibody forming cells. (auth)

Ecology

Refer also to abstracts 26745, 26751, 27076, 27137, and 27150–27157.

26681 (BNWL–1528) FOOD AND FEEDING OF JUVENILE CHINOOK SALMON IN THE CENTRAL COLUMBIA RIVER IN RELATION TO THERMAL DISCHARGES AND OTHER ENVIRONMENTAL FEATURES. Becker, C. D. (Battelle-Northwest, Richland, Wash. Pacific Northwest Lab.). 1 Jan 1971. Contract AT(45-1)-1830. 68p. Dep. NTIS.

The relationship of thermal discharges from Hanford reactors to food and feeding of juvenile chinook salmon (Oncorhynchus tshawytscha) in the central Columbia River, Washington was studied in 1968 and 1969. The primary objectives were to evaluate the food composition and feeding activities of the fish and determine if heated effluents influenced their welfare. Environmental conditions, i.e. seasonal changes in river temperatures and flow volumes, in relation to thermal requirements of young chinook are detailed. Data on food organisms utilized by the fish are presented for 1968 and 1969, whereas analyses for possible thermal effects are based on the more extensive 1969 data. Young chinook at Hanford consumed primarily various stages of aquatic insects, of which adult and larvae Tendipedidae (Diptera) were of dominant importance. Other major food organisms were the order Collembola and the families Notonectidae (Hemiptera) and Hydropsychidae (Trichoptera). Small fry fed almost exclusively on tendipedids. The food composition was essentially similar in 1968 and 1969. Over 95 percent of food organisms utilized originated in the river ecosystem. Analyses to detect thermal effects were made on parameters dealing with food, feeding and growth compiled from fish collected at three sites above (coldwater stations) and three sites below (warmwater stations) the effluent discharges. The following comparisons were made: food organisms utilized, feeding activity, mean insects per feeding fish, seasonal increases in fish length, fish length-weight relationships, coefficients of condition, and dry weight of stomach contents. All data were characterized by considerable variation between and within individual stations. No consistent differences attributable to thermal increments were evident. The lack of detectable effects is apparently due to the fact that the main discharge plumes occur in midriver and the effluents are well mixed before reaching inshore feeding areas. The transient nature of fish at each sampling site, influenced by changes in regulated river discharge, and the availability of food organisms in the river drift were ecological factors affecting critical thermal evaluation in situ. (auth)

26682 (NYO–2579-20) RADIOECOLOGY OF SMALL VERTEBRATE SPECIES UNDER NATURAL ENVIRONMENTS. Progress Report, December 1, 1969–November 30, 1970. (Pittsburgh Univ., Pa.). Contract AT(30-1)-2579. 47p. Dep. NTIS.

Experiments were conducted on population mechanics and energetics of the eastern chipmunk (Tamias striatus) and of the northern pocket gopher (Thomomys talpoides) and the effects of exposure to γ radiation on populations of both species. In order to assess the effects of radiation on chipmunk populations, the following studies were carried out: evaluation of food produced on plots and annual consumption by chipmunks; determination of total annual activity; correlation of activity with oxygen metabolism; and determination of standard metabolism under varying conditions of the annual cycle. Studies were continued on irradiation of individuals and populations of pocket gophers under natural conditions. A drawer type irradiator with a 110 curie ^{137}Cs source was used, and live trapping was carried out on isolated plots in the Beartooth Mountains in Wyoming. Analyses were made of vegetation species and stomach contents in terms of calorific equivalents. Survivorship curves were constructed for male and female chipmunks based on results of seven years of experiments on irradiation of free ranging individuals. An appendix is included on biology of the eastern chipmunk with descriptions of sites and population plots. (H.L.W.)

26683 MARINE ECOLOGY AND ATOMIC ENERGY. CHIEFLY ON MARINE ECOLOGICAL STUDIES BY ISOTOPE TECHNIQUE. Saiki, Masamichi (National Inst. of Radiological Sciences, Chiba, Japan). Radioisotopes (Tokyo); 19: 328-36(Jul 1970). (In Japanese).

A review is given on the relation of marine ecology and atomic energy. Atomic energy is closely connected with marine ecology in relation to the disposal of radioactive waste into sea and the safety management of marine radioactivity. On the other hand, marine ecology has made remarkable progress by the use of isotopes. Several marine ecological studies by isotope techniques are presented. The close connection between marine ecology and atomic energy has established marine radioecology as a new field of ecology. Marine radioecology gives the basic knowledge necessary for the radiation protection of mankind. Recent studies in this new field are presented. (Japan)

26684 ^{210}Po IN SOILS AND PLANTS. Hanson, Wayne Richard. Fort Collins, Colo.; Colorado State Univ. (1970). 221p. University Microfilms Order No. 71-5336. Thesis.

Polonium-210 used as a radionuclide fuel for SNAP electrical generators may present a long term hazard if accidental release of the isotope were to contaminate agricultural soils. Absorption of $^{210}PoO_2$ in soils studied by bulk determination of distribution coefficients (K_d) indicated retention in the top soil samples was with silt content. Greater than 98% of the $^{210}PoO_2$ was retained by the first 2 cm of soil with K_d's greater than 100. Top soil samples with K_d's less than 100 indicated $^{210}PoO_2$ would be retained by the lower soil horizons. Hazards to water supplies by movement of ^{210}Po through soil would be minimal. Chemical species of ^{210}Po in soil solution examined by electrophoresis and dialysis experiments indicated both positive and negative species existed. Dialysis experiments indicated approximately 34% of the ^{210}Po in soil solution passed through a semi-permeable membrane. Plant uptake of $^{210}PoO_2$ added to three different soils was measured and expressed as a transfer coefficient, U, where $U = {}^{210}Po/g$ dry plant tissue$/{}^{210}Po/g$ dry soil. Transfer coefficients of 11 different fruit, grain, leafy, and root crops ranged from 10^{-2} to 10^{-6}. The transfer coefficients remained constant for the majority of plant tissues examined, although the distribution coefficients differed for the three soils used. Calculations using the transfer coefficients for estimating dietary intake of ^{210}Po from vegetables indicated a potential long-term ingestion hazard to the population. Protein hydrolyzates of wheat and spinach were separated by paper chromatography to investigate organic forms of polonium in plants. One possible organic form of polonium was observed. Measurements of naturally occurring ^{210}Po in the soil samples indicated a range of 0.22 to 3.47 pCi/g in top soils. Polonium-210 measured in the vegetation used for controls in the greenhouse experiments indicated the primary source of the isotope was the fallout of airborne ^{210}Po and its radioactive precursors. (Diss. Abstr.)

Genetics and Cytogenetics

Refer also to abstracts 26771, 26911, 26931, 26982, 27042, 27072, 27073, 27080, 27087–27090, 27097, 27116, 27128, and 27164.

26685 (CONF-680112–, pp 85-93) A COMPARATIVE STUDY OF THE MUTATION FREQUENCY AND GENETIC BEHAVIOR OF MUTANTS INDUCED BY ACUTE AND CHRONIC GAMMA IRRADIATION IN COMMON BEANS (PHASEOLUS VULGARIS L.). Moh, C. C.; Alan, J. J. (Inter-American Inst. of Agricultural Sciences, San Jose (Costa Rica)).

Seeds of Phaseolus vulgaris were given acute doses of 4, 8, and 12 kR from a ^{137}Cs source. For chronic irradiation plants were grown concentrically around a ^{137}Cs source; plants grown at a dose level of 25, 50, and 75 R per day received an approximate accumulated dose of 2, 4, and 6 kR, respectively. Tabu-

lated results show that the mutation frequency induced by chronic radiation was as high as that induced by acute radiation. Mutations were classified as chlorophyll and morphological. Acute irradiation of seeds resulted in 40% chlorophyll and 60% morphological mutations, while chronic plant irradiation resulted in 77% chlorophyll and 23% morphological mutations. Studies on the genetic behavior of induced mutations showed that of the mutants induced by acute radiation, 74% segregated according to Mendelian ratios; of the mutants induced by chronic radiation, less than 50% segregated according to Mendelian ratios. (H.L.W.)

26686 (CONF-680112–, pp 95-111) USES OF IONIZING RADIATIONS IN THE GENETICS OF VEGETABLE PLANTS. Favret Ewald A. (Instituto Nacional de Tecnologia Agropecuaria, Castelar (Argentina). Instituto de Fitotecnia). (In Spanish).

Some examples of the artificial mutation of cereals using radiations and ethyl sulfonates in order to improve the yield of the cereals are given and discussed. The techniques and mutations obtained are described. Examples of barley mutations resistant to various plant diseases are reported. The high protein content of some of the mutated cereals is discussed. (J.S.R.)

26687 CAROTENOIDS SYNTHESIZED BY UV-INDUCED MUTANTS OF A NON-ACID-FAST STRAIN OF MYCOBACTERIUM PHLEI. Kolmanova, A.; Hochmannova, J.; Malek, I. (Inst. of Microbiology, Prague). Folia Microbiol. (Prague); 15: 426-30(1970).

The composition of the cell pigment of three mutants (PN_1, PN_2, PN_3) of a non acid fast strain of Mycobacterium phlei (PN) induced with uv radiation was investigated. It was found that the mutants contain carotenes typical for the original parent strain, but that the quantity of the colorless precursor, phytoene, is substantially lower, and, on the contrary, the amount of lycopene is increased (especially in mutants PN_2 and PN_3). In addition, all mutants synthesized xanthins in considerable quantities: the PN_1 mutant above all with the β-carotene carbon skeleton, whereas for the PN_2 and PN_3 mutants xanthins with the lycopene structure were typical. The hit of the genome of the original strain caused by the mutagen is thus manifested even in the synthesis of secondary metabolites. (auth)

26688 SEGREGATION PATTERN IN THE M_3 GENERATION OF RICE (ORYZA SATIVA L.) ORIGINATING AFTER SINGLE, PRE- AND POST-IRRADIATION TREATMENT WITH DIETHYL SULPHATE. Bose, S.; Ghose, M. (Calcutta Univ.). Sci. Cult. (Calcutta); 36: 404-5(Jul 1970).

Studies were made on the segregation pattern in the M_3 generation of Oryza sativa. Diethyl sulfate treatment given before and after x irradiation resulted in mutants with segregation patterns for awning, lemma, palea, and rice color. (P.B.M.)

26689 INDUCED MUTABILITY OF THE FUNGUS WHICH IS THE VECTOR OF VERTICILLIUM COTTON WILT. Novotel'nova, N. S.; Pystina, K. A. (Botanical Inst., Leningrad). Mikol. Fitopatol.; 2: No. 4, 290-301(1968). (In Russian).

The fungus Verticillium dahliae was given a γ ray dose of 200,000 to 300,000 R from ^{60}Co. Conidiae from infected cotton plants were irradiated. Strain 141 was black and microsclerotial, while strain 65 was colorless and did not form microsclerotia. Old, 30 to 50 day cultures were used. After irradiation the cultures were grown in darkness, and observations were made on the cultural and morphological appearances of the strains. Irradiation suppressed the growth of conidia from a length of 300 microns in unirradiated conidia to about 5 to 10 microns length in irradiated conidia. After irradiation the colonies differed in size, color, and degree of sporulation. No mutants were observed on irradiating pigment free strain 65. The irradiation of black strain 141 produced a series of mutants with new properties which were transmitted over many generations. The mutants were also irradiated, and were shown to produce reversions. The properties of six mutants are described in detail. The morphology of the mycelia and the sporulation of the initial strains and mutants are described. The mutants differed in size and form of the conidia. Both strains caused wilt in cotton plants. The study showed the importance of employing induced mutability in investigating polymorphic strains of fungi. (TTT)

26690 GENETIC EFFECT ON RADIATION SENSITIVITY CONSISTENT WITH A SINGLE GENE LOCUS HYPOTHESIS. Spalding, J. F.; Popp, Diana M.; Popp, R. A. (Los Alamos Scientific Lab., N. Mex.). Radiat. Res.; 44: 670-3(Dec 1970).

Two sublines of strain RFM mice with different radiation sensitivity characteristics were used to investigate the genetic involvement of a radioresistance factor. Resistant and nonresistant sublines, their F_1 cross and the F_1 backcross to each parent subline were exposed to low level continuous γ rays, and radioresistance characteristics were determined by mean survival time. The F_1 backcross was H-2 tested, and mice were tested for radioresistance according to genotype $H\text{-}2^{ff}$ or $H\text{-}2^{fk}$. The data are consistent with the hypothesis that this radioresistance factor is controlled at a single gene locus with resistance dominant to sensitivity. However, the H-2 gene did not prove to be directly responsible for the difference in radiation resistance between the two lines. (auth)

26691 INDUCTION OF CELLULAR DNA SYNTHESIS BY SUPERCOILED SV40 DNA IN X-IRRADIATED MOUSE 3T3 CELLS. Rozenblatt, Shmuel; Winocour, Ernest (Weizmann Inst. of Science, Rehovot, Israel). Virology; 43: 300-3(Jan 1971).

The initiation of cellular DNA synthesis by polyoma virus and simian virus SV40 was documented. Evidence suggesting that this property of the virus is a function of the viral genome was obtained from experiments which showed that the property was sensitive to inactivation by nitrous acid, uv, and γ irradiation and that empty virus particles did not stimulate the activities of enzymes involved in the synthesis of cell DNA. Evidence that supercoiled SV40 DNA alone induced cellular DNA synthesis in x-irradiated mouse 3T3 cells is presented. (P.B.M.)

26692 LACK OF POLARITY OF DNA INJECTION BY ESCHERICHIA COLI PHAGE λ. Sharp, John D.; Donta, Sam; Freifelder, David (Brandeis Univ., Waltham, Mass.). Contract AT(30-1)-3797. Virology; 43: 176-84(Jan 1971).

The DNA fragments injected by x-irradiated phase λ were isolated from bacteria and analyzed for buoyant density by isopycnic centrifugation in Cs_2SO_4 density gradients containing Hg^{2+}. The density distribution showed that the amount of material contributed by each of the ends is not significantly different from that obtained for DNA isolated directly from unirradiated phages. Since x-irradiated phage injects only a single fragment from the end normally injected first up to the first doublestrand break it can be concluded that the phage population is divided equally between those phages that inject the right end first and those that inject the left end first. Complementation studies with x-irradiated phage showed activity of genes from both the right and left arms of the genetic map, but with different efficiencies. The pattern of these efficiencies suggests that the right arm contains the principal promoter for genes R, A, and the rest of the left arm. This pattern also suggests the existence of additional weak promoters between genes A and B, and between H and K. (auth)

26693 INTERRUPTION OF DNA INJECTION BY X-IRRADIATION OF PHAGE λ. Sharp, John D.; Freifelder, David (Brandeis Univ., Waltham, Mass.). Virology; 43: 166-75(Jan 1971).

When λ phage is irradiated, it loses the capacity to inject all of its DNA into Escherichia coli. Autoradiographic measurement of the amount of DNA injected by x-irradiated phages leads to the conclusion that only a single DNA fragment is injected, a piece extending from the end normally injected first to the first double strand break. This partial injection accounts for about half of the lethal effects of x irradiation in phage λ. Loss of adsorptive capacity and gross destruction of the phage head are shown to contribute only very slightly to the inactivation process. (auth)

26694 CORRELATION OF LINKAGE GROUPS WITH CHROMOSOMES IN THE MOSQUITO, AEDES AEGYPTI. McDonald, P. T.; Rai, K. S. (Univ. of Notre Dame, Ind.). Contract AT(11-1)-38. Genetics; 66: 475-85(Nov 1970). (COO-38-740).

Two radioinduced reciprocal translocations were used to determine the correlation between the three pairs of chromosomes and three linkage groups of the yellow fever mosquito, Aedes aegypti. Linkage group one, containing the sex locus, is the smallest chromosome and is designated chromosome 1. The two autosomes, carrying genes corresponding to linkage groups two and three are designated chromosome 2 and chromosome 3, respectively, with chromosome 2 being the longer autosome. The available data indicate that recombination may not be uniform throughout the lengths of the chromosomes in this species. (auth)

26695 INTRAGENIC RECOMBINATION OF ASCOSPORE COLOR MUTANTS IN ASCOBOLUS AND ITS RELATIONSHIP TO THE SEGREGATION OF OUTSIDE MARKERS. Stadler, David R.;Towe, Agnes M.; Rossignol, Jean-Luc (Univ. of Washington, Seattle). Genetics; 66: 429-46(Nov 1970).

Twenty-six w17 alleles causing colorless ascospores were isolated in Ascobolus immersus. Tetrads were analyzed for recombination at this locus in two situations: frequencies of gene conversion (3 : 1 or 1 : 3 segregation) were determined in crosses of the various mutants to $w17^+$, and the frequencies of wild type recombinants were measured in pairwise crosses between the mutants. Linked markers were isolated on both sides of the w17 locus, fpr (fluorophenylalanine resistance) is 3 map units to the right of w17, and colt (colonial at 37°C) is 10 units to the left. No chiasma interference was shown in 562 asci from 3 point crosses, although the two regions are in the same chromosome

arm. Preliminary mapping information on the mutant sites at w17 is compatible with an order based on increasing rates of gene conversion. Attempts were made to order the sites on the basis of both recombination frequencies and marker combinations accompanying intragenic recombination. However, the interpretation of recombination frequencies was limited by the finding that our stocks were segregating for genetic elements which have pronounced effects on these frequencies. Similar patterns of segregation of outside markers were found in gene conversion asci from mutant × wild type crosses and in recombination asci from mutant × mutant crosses; this indicates that both situations involve the same basic intragenic event. (auth)

26696 POST-NATAL DEVELOPMENT OF PHENOTYPE. Proceedings of a Symposium Held in Liblice, Czechoslovakia, September 18–22, 1967. Kazda, Stanislav; Denenberg, Victor H. (eds.). London; Butterworth and Company Limited (1970). 420p. 160s. (CONF-670997).

A separate abstract was prepared for one of the 32 papers presented. Other papers discuss the influence of post-natal conditions on the neurological, psychological, social, humoral, metabolic, structural, and sexual development of phenotype in organisms. (E.R.B.)

For an abstract of an individual paper see: 26930.

26697 INDUCED MUTATIONS IN PLANTS. Sigurbjoernsson, Bjoern. Sci. Amer.; 224: No. 1, 86-95(Jan 1971).

Experiments were performed on various economic plants to induce beneficial mutations. The principal mechanism for inducing mutations is γ and x irradiation of seeds, although mutations are also induced by treating seeds with mutagenic chemicals, EMS. Mutations affect the chemistry of the hereditary material, the DNA and RNA. Mutations affect the structure of chromosomes, causing aberrations, inversions, and translocations. (P.B.M.)

26698 INDUCED MUTABILITY OF PHYTOPATHOGENIC FUNGI. Levitin, M. M. (All-Union Inst. of Plant Protection, Leningrad). Mikol. Fitopatol.; 2: No. 1, 18-24(1968). (In Russian).

This review briefly systematizes the main studies on obtaining and using induced mutants of phytopathogenic microorganisms. The lethal and mutagenic effects of uv and ionizing radiation on various spores and fungi are presented. Morphological and physiological changes in mutants are described. Mutants are used mainly to study the particular genetics of phytopathogenic microorganisms. By this means it is possible to map genes, determine the ploidy and number of chromosomes in fungi, and to supply markers in various kinds of genetic experiments. Induced mutants can be used to study the pathogenicity of disease vectors. Mutants sometimes produce new virulent strains of fungi. Auxotrophic mutants requiring nicotinic acid, biotin, riboflavine, and various biological amines are frequently avirulent. The work on the relation between dietary factors and virulence is reviewed. These studies can be used to develop new species of agricultural plants which are resistant to fungi diseases. (TTT)

26699 INDUCTION OF AUXOTROPHIC MUTATION IN STREPTOMYCES ERYTHREUS IA 64-575. Ostrowska-Krysiak, Barbara; Kadzikiewicz, Teodora (Inst. of Antibiotics, Warsaw). Acta Microbiol. Pol., Ser. B; 2: 159-63(1970).

Uv light causes 90, 99, and 99.9% inactivation and variability of spores of Streptomyces erythreus IA 64–575. It was found that in populations treated with mutagenic agents the frequency of mutations to auxotrophy was several times higher than in the control. Similar doses of mutagenic agents applied for induction of reversal mutation in his⁻ mutant of S. erythreus IA 64–575 confirmed the effectiveness of uv light action in induction of the strain variability. The auxotrophic mutants selected during the studies were characterized by enzymatic blocks in synthesis of methionine, valine, isoleucine, tryptophan, histidine, and adenine. (auth)

26700 A SERIES OF HYBRID CELLS CONTAINING DIFFERENT RATIOS OF PARENTAL CHROMOSOMES FORMED BY TWO STEPS OF ARTIFICIAL FUSION. Murayama-Okabayashi, Fumiko; Okada, Yoshio; Tachibana, Takehiko (Osaka Univ. National Cancer Center Research Inst., Tokyo). Proc. Nat. Acad. Sci. U. S. A.; 68: 38-42(Jan 1971).

Double hybridization of Ehrlich ascites tumor cells (ETC) and L cells was performed. In the first step, a hybrid (LE) and ETC and L_{AG} (a mutant of L cells, resistant to 10 μg/ml of 8-azaguanine) and a hybrid (LL) of L_{AG} and L_{BrdU} (a mutant of L cells, resistant to 100 μg/ml of 5-bromodeoxyuridine) were prepared by the use of artificial fusion by uv-irradiated HVJ (Sendai virus). In the second step the LE hybrid and ETC, or the LL hybrid and ETC, were fused again by UV–HVJ. The hybrids (LEE and LLE) were segregated during culture. Thus, the series of hybrids L, LLE, LE, LEE, and ETC was obtained. The morphological feature and karyological characters of these hybrids and the distribution of antigens corresponding to each parent on their cell surfaces supported the above identification of the series of hybrids obtained by double hybridization. All three hybrids acquired new characters, such as the ability to form large colonies in soft agar and large tumors on the chorioallantoic membrane of chicken eggs, unlike either parent. The tumor forming capacity of the series was ETC > LEE > LE > LLE; L cells formed no tumor in mouse abdomen under the test conditions. (auth)

26701 STUDIES IN THE M_3 GENERATION OF SOME M_2 MUTANTS IN RICE (ORYZA SATIVA L.) ORIGINATING FROM DIETHYL SULPHATE TREATMENT AND FROM COMBINED TREATMENT OF DIETHYL SULPHATE AND X-RAYS. Bose, S.; Ghose, M. (Calcutta Univ.). Sci. Cult. (Calcutta); 36: 343-5 (Jun 1970).

Oryza sativa was x-irradiated and diethyl sulfate-treated to produce mutants of economic and commercial value. (P.B.M.)

26702 PARTIAL PISTILLOIDY IN RICE FOLLOWING IRRADIATION. Sapre, A. B. (Inst. of Science, Nagpur, India). Sci. Cult. (Calcutta); 36: 333(Jun 1970).

Sterile hybrids Oryza latifolia and O. minuta were γ-irradiated with the intention of producing viable mutants. On embryological investigation it was found that the sterile hybrids were lacking anthers. In early development the anthers were transformed into stigma like filaments. (P.B.M.)

26703 GENETICS AND SELECTION OF BEAUVERIA BASSIANA (BALS.) VUILL., AN ENTOMOPATHOGENIC FUNGUS. I. LETHAL AND MUTAGENIC EFFECTS OF ULTRAVIOLET AND X-RAYS. Levitin, M. M.; Kirsanova, R. V.; Yurchenko, L. V. (All-Union Research Inst. of Plant Protection, Leningrad. Inst. of Genetics and Selection on Industrial Microorganisms, Moscow. Ioffe Inst. of Physics and Tech., Leningrad). Genetika; 7: No. 1, 104-11(Jan 1971). (In Russian).

Studies were done to show the lethal and mutagenic effects of ultraviolet (uv) and x rays on the entomopathogenic fungus Beauveria bassiana. For all the strains the dose survival curve was of a sigmoid type for the uv rays and of an exponental type for x rays. LD_{90} for the uv was 4944 and 8404 to 8528 erg/mm² in the strains K_2 and K-87 respectively. For the x rays LD_{90} was 14 to 15.7 kr. Radioinduced mutants were isolated. They differed from the wild type in their morphological and cultural characters. The dependence of the frequency of mutants on the doses of uv and x rays was established. Auxotrophic mutants requiring methionine, arginine or ornithine, methionine, or cysteine or cystine, histidine, leucine, or norleucine, valine or norvaline, choline, thiamine, biotin, nicotinic acid, adenine, and uracyl were induced by uv radiation. The dependence of the frequency of auxotrophic mutants on the uv doses was established. The frequency of reversion of the adenine requiring mutant to the prototrophic state was studied. (auth)

26704 COMPARATIVE STUDY OF THE ABILITY OF CHROMOSOMES IN CELLS OF TWO SUBLINES OF THE EHRLICH ASCITES TUMOR TO RECOVERY AFTER X IRRADIATION. Voitovitskii, V. K. (Kazakh Inst. of Oncology and Radiology, Alma-Ata, USSR). Genetika; 7: No. 1, 92-7(Jan 1971). (In Russian).

After verificational x irradiation, the chromosomal aberrations in cells of two sublines of the hyperdiploid Ehrlich ascites tumor: parental subline (control) and x ray resistant subline (experiment) were studied during three days. In the control the largest number of the aberrations were discovered in 48 hr (23.3%). In 24 and 72 hr the number of the aberrations amounted to 3.3% and 8%, respectively. In the experiment the largest number of the aberrations were discovered in 24 hr (14.4%). In 48 and 72 hr the number of the aberrations amounted to 2 to 3%. Average number of the aberrations per cell was in the control –7.5 and in the experiment –4.5. In the experiment, chromatid exchanges, monocentric rings, dicentric and tricentric chromosomes predominated. In the control, on the contrary, chromatid and isochromatid lesions, acentric segment (pairs) predominated. The author explained x ray resistance of the experimental subline of Ehrlich ascites as a very high ability of chromosomes of cells in this tumor to recovery. (auth)

26705 CHANGES OF GENETIC LOADS IN EXPERIMENTAL POPULATIONS OF DROSOPHILA MELANOGASTER WITH RADIATION HISTORIES. Tobari, Izuo; Murata, Motoi (National Inst. of Radiological Sciences, Chiba, Japan). Jap. J. Genet.; 45: 387-97(Oct 1970).

The random load, A, and the inbreeding load, B in four experimental populations, which were derived from a successively irradiated population of Drosophila melanogaster with a dose of 5,000 R of x rays, were examined. The experimental populations A, B, C, and D were subjected to the accumulative radiation exposures of 10,000, 25,000, 50,000, and 75,000 R, respectively. With the cessation of the irradiation, both the A and B values decreased exponentially in successive generation. Furthermore, the random load appeared to reach the original level more rapidly than the inbreeding load. That is, the random load appeared to arrive close to the original level within 11 to 16 generations after the cessation of the irradiation, while it took longer time for the inbreeding load to drop to the original level. Especially, the amount of the inbreeding load in Population D was still significantly greater than in the control population. The analysis of the data indicated that most of the radioinduced mutant genes, which had dominant or semidominant effect reducing the Darwinian fitness, were relatively rapidly eliminated from the populations in the early generations after the cessation of the irradiation, and after that the slightly detrimental mutants were left in the populations. (auth)

26706 NEW SOYBEAN VARIETIES RAIDEN AND RAIKO INDUCED BY GAMMA-RAY IRRADIATION. Tohoku Nogyo Shikenjo Kenkyu Hokoku; No. 40, 65-105(Mar 1970). (In Japanese).

In order to cultivate early ripening varieties of Japanese soybeans, the air-dried seeds of the nematode-tolerant line Tohoku No. 6 (Nema-Shirazu) were irradiated with 10 krad of ^{60}Co γ radiation in 1960 and two mutant lines, Raiden and Raiko, were obtained. The maturing times of these two lines are 25 and 15 days earlier than that of the original variety. Other characteristics are as follows: tolerance to nematode cysts; resistance to A and B strains of mosaic virus and stunt virus, susceptibility to C and D virus strains, resistance to scab, and high productivity. The protein content of the seeds of the mutant lines is higher. (Japan)

26707 CO-TRANSDUCTION WITH serB OF A PLEIOTROPIC MUTATION AFFECTING COLICIN E2 REFRACTIVITY, ULTRAVIOLET SENSITIVITY, RECOMBINATION PROFICIENCY, AND SURFACE PROPERTIES OF ESCHERICHIA COLI K12. Threlfall, E. J.; Holland, I. B. (Univ. of Leicester, Eng.). J. Gen. Microbiol.; 62: 383-98(Aug 1970).

A cetB locus, determining E2 refractivity at low temperature, was mapped at minute 89 on the Escherichia coli K 12 chromosome and was 94% linked to the hsp loci. A second locus, cetA, which controlled expression of cetB in some way, was found to be 70% co-transducible with and to the right of thr. Both cetB and cetC, another locus which determined E2 refractivity, were 21% co-transducible with serB and the cetC locus therefore also probably lies close to hsp. Mutations of the cetC locus appeared to be pleiotropic and the additional characteristics of these mutants, uv sensitivity, detergent sensitivity, recombination deficiency, filament formation, and abortive λ growth were all fully co-transducible with E2-refractivity. In addition, uv resistant revertants of CetC mutants simultaneously reverted to all wild type characteristics including E2 sensitivity. The nature of the recombination deficiency of some CetC mutants was examined and both episomal and chromosomal gene transfer to the mutants found to be normal. PI transduction frequencies with CetC mutants were, however, also normal and it is suggested that the mutants may be deficient in some recombination step unique to Hfr $\times$ F^- crosses. (auth) (UK)

26708 PROPERTIES OF BACTERIOPHAGE T4 MUTANTS DEFECTIVE IN GENE 30 (DEOXYRIBONUCLEIC ACID LIGASE) AND THE rII GENE. Karam, J. D.; Barker, B. (Sloan-Kettering for Cancer Research, New York). J. Virol.; 7: 260-6(Feb 1971).

In Escherichia coli K-12 strains infected with phage T4 which is defective in gene 30 [deoxyribonucleic acid (DNA) ligase] and in the rII gene (product unknown), near normal levels of DNA and viable phage were produced. Growth of such T4 ligase-rII double mutants was less efficient in E. coli B strains which show the "rapidlysis" phenotype of rII mutations. In pulse-chase experiments coupled with temperature shifts and with inhibition of DNA synthesis, it was observed that DNA synthesized by gene 30-defective phage is more susceptible to breakdown in vivo when the phage is carrying a wild-type rII gene. Breakdown was delayed or inhibited by continued DNA synthesis. Mutations of the rII gene decreased but did not completely abolish the breakdown. T4 ligase-rII double mutants had normal sensitivity to ultraviolet irradiation. (auth)

26709 ANOTHER TWO GENES CONTROLLING MITOTIC INTRAGENIC RECOMBINATION AND RECOVERY FROM UV DAMAGE IN ASPERGILLUS NIDULANS. I. UV SENSITIVITY, COMPLEMENTATION, AND LOCATION OF SIX MUTANTS. Fortuin, J. J. H. (Rijksuniversiteit, Utrecht). Mutat. Res.; 11: 149-62(Feb 1971).

Six uv sensitive mutants of Aspergillus nidulans are described. The strains can be divided into four complementation groups on the basis of tests of the uv sensitivity of heterokaryons. The four groups were designated uvsB, C, D, and E, respectively. A uvsB and a uvsC mutant have been described previously. UvsB and uvsC are located on chromosomes IV and VIII, respectively. The loci uvsD and uvsE are situated on chromosome V; uvsD is linked with nicA, uvsE with riboD. All uvs mutations studied are recessive in diploids and heterokaryons. Dormant conidia of uvsC and uvsE mutants are as sensitive to inactivation by uv irradiation as are wild type conidia. The uv sensitivities of uvsC and uvsE conidia increase with increasing periods of incubation at 37° before irradiation. Dormant conidia of uvsB and D mutants are uv sensitive. The uv sensitivity of these mutants is also enhanced by preincubation. In the dose range studied, uvsB and D mutants are more uv sensitive than are uvsC and E mutants. The uvsB and D mutants may be defective in excision repair, and the uvsC and E mutants may be defective in recombination repair. (auth)

26710 INDUCED MUTATIONS IN TRITICUM DURUM. Desai, Puloma A. (Indian Agricultural Research Inst., Delhi). Indian J. Genet. Plant Breed.; 29: No. 1, 115-22(1969).

Dry dormant seeds of three varieties of Triticum durum (N. P. 410, N. P. 411, and N. P. 412) were treated with fast neutrons, gamma rays, and ethyl methanesulfonate. Chimeral changes were observed in ear characters in the M_2 generation. Chlorophyll mutations were observed in the M_2 generation. The spectrum was rather wide indicating thereby the occurrence of a large number of non-reduplicated loci in the genomic constitution with reference to chlorophyll development. The frequency of viable mutations was generally low. The highest value recorded was 1.82% (on the basis of number of mutations per 100 M_2 plants). The mutation spectrum was found to be very restricted and this suggests that there are only a few loci at which phenotypic buffering does not exist. This finding supports the conclusion arrived at from studies in nullitetra plants, that in T. durum the chromosomes of the A and B genomes have considerable homeologous relationships. For obtaining a larger number of mutations in a species like T. durum with a partly disomic and partly polysomic genetic architecture, it will be essential to continue the screening for mutations to later generations. (auth)

26711 CYTOGENETICAL IDENTIFICATION OF X-RAY-INDUCED TRANSLOCATIONS IN MALE MICE. Bath, Daniel White Jr. University, Miss.; Univ. of Mississippi (1970). 99p. University Microfilms Order No. 70-16,391.
Thesis.

Cytogenetical analyses were made of translocations induced in x-irradiated mice. Genetical analyses showed that four lines involve two marked linkage groups. Three lines involve linkage groups I and VIII and one involves groups VIII and XIV. Five additional lines showed linkage between one marked group and partial sterility. Coincidence values indicated negative interference across the point of breakage between the markers employed in all the doubly marked translocations. Enhancement of crossing-over was inversely proportional to the length of the involved segment. Cytological demonstration of translocations was made in 26 of 29 partially sterile lines examined. From pachytene analysis of genetically identified translocations, linkage groups I and XIV were localized to chromosomes A and P, respectively. These and other data placed linkage group VII in chromosome F. Cytological analysis of double translocation heterozygotes has supported genetical data T(8:14)5Ba/T(1:8)80Ba and T(8:14)5Ba/T(1:8)157Ba have one rearranged chromosome in common. Approximate positions of pink-eye, brown, and satin in linkage groups I, VIII, and XIV are postulated, and centromere locations relative to points of breakage and markers employed were established. Translocation homozygotes were obtained for one line, T(1:8)157Ba, and were viable and fully fertile. Data on the relative fertility of the semisterile lines as derived from breeding tests and autopsies of pregnant females are also given. (Diss. Abstr. Int., B)

26712 ULTRA-VIOLET INDUCED MUTATIONS TO GROWTH FACTOR REQUIREMENT AND PENICILLIN RESISTANCE IN A BLUE-GREEN ALGA. Srivastava, B. S. (Banaras Hindu Univ., India). Arch. Mikrobiol.; 66: 234-8(1969).

After exposures to uv, two mutant strains of Phormidium mucicola, which are stable and inheritable, were isolated. Strain 5/5 mL-1 is a photoheterotrophic mutant requiring addition of an organic growth factor to the basal medium that appears fulfilled by either casein hydrolysate, glucose, acetate, or vitamin mixture and fails to grow heterotrophically. The mr/p strain shows resistance up to 10.24 μg/ml of penicillin whereas the parent does not survive beyond a penicillin dose of 0.1 μg/ml. (auth)

26713 CHANGES IN THE FREQUENCY OF CROSSING-OVER IN X-IRRADIATED DROSOPHILA MELANOGASTER FEMALES. Puro, Jaakko (Univ. of Turku, Finland). Ann. Zool. Fenn.; 7: 341-8(1970).

The effects of different doses of x irradiation on crossing-over were studied simultaneously in distal segments of structurally normal autosomes and of autosomes having unequal parts of the left arms mutually exchanged. In this genetic system, the type of effect produced (increase or decrease of recombination) was found to depend on whether or not spontaneous crossing-over was affected by proximity to the centromere. The results lend support to the hypothesis that, in general, any external agent expected to reduce crossing-over is likely to exert its strongest action in the regions that are least influenced by the centromere effect, i.e., in the distal segments of the chromosome. On the other hand, in regions influenced by the centromere effect, x-radioinduced recombination generally more than counterbalances the decrease, the result being a net increase in the crossover frequency. (auth)

26714 COMPARISON OF MUTATION INDUCTION IN DIPLOID AND TETRAPLOID RICE. Sree Rangasamy, S. R.; Sree Ramulu, K. (Agricultural Coll. and Research Inst., Coimbatore, India). Theor. Appl. Genet.; 40: 312-15(1970).

A comparative assessment of the frequency and spectrum of chlorophyll mutations in the M(2) and M(3) of three diploids and one tetraploid of rice after x irradiation was made. A linear relationship of the frequency of mutations with the dose of mutagen, as well as a saturation effect was also evident. Among the three diploids, the maximum frequency of mutations was observed in T. N. 1, followed by G. E. B. 24 and A. S. D. 8. The diploid of G. E. B. 24 showed a higher frequency of mutations than the tetraploid when measured on the M(1) plant basis only. The diploids showed a higher rate of mutations in the M(2) than in the M(3). There was no relationship between the frequency of different types of chlorophyll mutations and the dose of x rays. Albina occurred in greater proportion than the other types of mutations in the diploids as well as in the tetraploid. The diploid showed a wider spectrum in the M(2) whereas the tetraploid recorded the maximum types of mutations in the M(3). Striking differences in the spectrum and the relative frequency of each type were observed among the three diploids and also between the diploid G. E. B. 24 and its tetraploid. (auth)

26715 MUTAGENESIS IN SORGHUM. Goud, J. V.; Nayar, K. M. D.; Rao, M. G. (Univ. of Agricultural Sciences, Bangalore, India). Indian J. Genet. Plant Breed.; 30: 81-90(Mar 1970).

Although mutation studies are very common in major cereals like wheat, barley, rice, and oats, such studies in the major millets like Fowar (Sorghum vulgare), Bajra (Pennisetum typhoides), Ragi (Eleusine coracana) and Navane (Setaria italica) are scanty. It is a well established fact that induced mutagenesis is a very potent tool to create variability in the population. Sorghum being an important crop, probably third in importance of all India acreage and production, deserves attention by the mutation breeders. It is with this interest in view that systematic mutation studies were started in this crop by subjecting the seeds of two varieties of sorghum to gamma irradiation. (auth)

26716 INCREASED MUTATION FREQUENCY AND WIDER MUTATION SPECTRUM IN BARLEY INDUCED BY COMBINING GAMMA-RAYS WITH ETHYL METHANE SULPHONATE. Sharma, R. P. (Indian Agricultural Research Inst., Delhi). Indian J. Genet. Plant Breed.; 30: 180-6(Mar 1970).

The generation of genetic variability by induced mutagenesis provides a base for strengthening plant improvement programs. Various classes of chemical and physical mutagens differ in their efficiency in inducing mutations and in the spectrum of mutations induced. Experiments were carried out using Hordeum vulgare. Combinations of different mutagens, if their mutation induction process is independent and capable of interaction should increase the mutation frequency and alter the mutation spectrum. The results of an experiment designed to assess the mutagenic effects of gamma rays and ethyl methane sulfonate (EMS) used in combination are reported. (auth)

26717 COMBINED EFFECT OF PHYSICAL AND CHEMICAL MUTAGENS ON MUTATION FREQUENCY IN ASPERGILLUS NIDULANS. Sharma, R. P. (Indian Agricultural Research Inst., Delhi). Indian J. Genet. Plant Breed.; 30: 199-211(Mar 1970).

Different mutagens may produce a given phenotypic change through different pathways of action. Studies on combined treatments with different mutagens showed that the efficiency of one mutagen can be modified by combining it with another mutagen. It was suggested that mutagens in combined treatments, besides initiating changes in DNA, may also affect the fixation or recovery of potential mutations. The combined effects of gamma rays and ethyl methane sulfonate are studied, when given in sequence, on mutation frequency in Aspergillus nidulans. (auth)

26718 FERTILE DWARF AND THREE OTHER MUTANTS OF CICER. Athwal, D. S.; Bhalla, S. K.; Sandhu, S. S.; Brar, H. S. (Punjab Agricultural Univ., Ludhiana, India). Indian J. Genet. Plant Breed.; 30: 261-6(Mar 1970).

With the ultimate aim of establishing a genetic map, studies were initiated to develop a collection of mutants with contrasting characters in chickpea, Cicer arietinum. Many spontaneous mutations were recorded in this crop plant by various workers. Although isolated studies on the genetics of mutant characters were undertaken, no organized attempt was made to maintain these mutants at one center and to identify the number of loci involved and their linkage relationships. Sixteen x ray induced and spontaneous mutations were reported in Cicer. Eight of these mutants that were viable and possessed normal or moderate seed fertility were maintained and used in genetic studies. Eight independent loci, one for each mutant, were identified. In crosses of these mutants with available genetic stocks for contrasting flower and seed colors, several cases of linkage were observed. (P.B.M.)

26719 CYTOGENETICS OF TWO RADIATION-INDUCED, SEX-LINKED TRANSLOCATIONS IN THE YELLOW-FEVER MOSQUITO, AEDES AEGYPTI. Rai, K. S.; McDonald, P. T.; Asman, Sr. M. (Univ. of Notre Dame, Ind.). Contract AT(11-1)-38. Genetics; 66: 635-51(Dec 1970). (COO-38-746).

The cytogenetics of two x radioinduced, sex-linked reciprocal translocations in Aedes aegypti and the potential of translocations for possible genetic control purposes are described. Data on the mating competitiveness, fecundity, and longevity of males heterozygous for one of these translocations are also included. (P.B.M.)

26720 SCREENING PROCEDURE FOR DETECTION OF PUTATIVE DELETIONS IN PROXIMAL HETEROCHROMATIN OF DROSOPHILA. Baldwin, Madeleine C.; Suzuki, David T. (Univ. of British Columbia, Vancouver). Contract AT(45-1)-1924. Mutat. Res.; 11: 203-13(Feb 1971).

The probable redundant nature of proximal heterochromatin in Drosophila may prevent the detection of loci in this region by point mutations. Formation of attached autosomes and their detachment require asymmetrical exchanges which can generate proximal deletions detectable by their lethality when homozygous. Of 162 detached γ-induced compound-3 chromosomes, 66 were found to be lethal when homozygous. Of these, 51 were located between ri and pp around the centromere and fell into 3 different patterns of complementation. (auth)

26721 MECHANISM OF RING CHROMOSOME FORMATION AND SOMATIC CROSSING-OVER. Dubinin, N. P.; Nemtseva, L. S. (Inst. of General Genetics, Moscow). Mutat. Res.; 11: 187-202(Feb 1971).

Studies of chromosomal structural changes in metaphase of the first root tip mitoses of Crepis capillaris, after irradiation by fast neutrons, gamma, and x radiation of dry seeds, have led to the discovery of a new type of chromosome variability, i.e., a phenomenon in which ring chromosomes vest or encircle other chromosomes or single chromatids. It is suggested that the encircling arises from a rigid loop made by a chromosome strand after being cut at the contact point into 3 fragments. During the reunion of the fragments the middle one may close forming a ring encircling a chromosome made up of the 2 terminal fragments. After replication, 2 sister chromatid rings encircled 2 sister chromatids. Subject to mitotic crossing over between sister encircling rings a single ring is formed encircling 2 sister chromatids twice in an 8-shaped pattern. Six other configurations of the phenomenon of vesting have been observed which can be accounted for by the assumption that inner chromatids slipped out of encircling rings at the point of crossing over through breaches produced at the point of exchange. (auth)

26722 DIFFERENTIAL MUTATION OF THE β-GALACTOSIDASE GENE OF ESCHERICHIA COLI. Brock, R. D. (Commonwealth Scientific and Industrial Research Organization, Canberra, Australia). Mutat. Res.; 11: 181-6(Feb 1971).

A range of mutagenic agents was tested using the β-galactosidase locus of Escherichia coli where the gene can be held in the active (induced) or inactive (noninduced) state while replication is inhibited. Treatment with alkylating agents diethyl sulfate (DES), ethyl methanesulfonate (EMS), and N-methyl-N'-nitro-N-nitrosoguanidine (MNG) induced a higher frequency of mutation when applied to the active gene than when applied to the inactive gene. Gamma rays and base analogues 5-bromodeoxyuridine (BUdR) and 2-aminopurine (AP) had the same mutagenic efficiency for both active and inactive genes. These results support the view that alkylating agents act directly upon the nucleotide bases which become

available to the mutagen when the DNA double helix is opened for the synthesis of messenger RNA. (auth)

26723 CHROMOSOMAL ABERRATIONS AND MORTALITY OF X-IRRADIATED MAMMALIAN CELLS: EMPHASIS ON REPAIR. Dewey, W. C.; Miller, H. H.; Leeper, D. B. (Colorado State Univ., Fort Collins). Proc. Nat. Acad. Sci. U. S. A.; 68: 667-71(Mar 1971).

Chromosomal aberrations induced by x rays in synchronized Chinese hamster cells correlated well with mortality as the radiosensitivity was made to vary by a factor of 4 by treating the cells with colcemid or 5-bromodeoxyuridine and by irradiating the cells in different parts of the cell cycle. 37% survival was observed when the cells sustained about one aberration per cell. Furthermore, the positive correlation was observed during repair of damage. Repair was measured by the reduction in damage observed either as the incubation period between two doses was increased (repair of sublethal lesions), or as the cells were held at 20°C after a single dose of radiation (repair of potentially lethal lesions). Repair of both sublethal and potentially lethal lesions occurred with a halftime of about 12 min and was inhibited at 0°C. These correlations strongly support the hypothesis that x ray-induced cell death results from damage in chromatin structures. (auth)

26724 CHROMOSOMAL REJOINING IN THE ABSENCE OF UNSCHEDULED DNA SYNTHESIS. Shaeffer, James; Vincent, Russell A. Jr.; Merz, Timothy (Johns Hopkins Univ., Baltimore). Mutat. Res.; 11: 256-7(Feb 1971).

Investigations were carried out to show that chromosome repair and unscheduled DNA synthesis involve different processes. Stock cultures of rat kangaroo kidney cells were x-irradiated with 200 R at an exposure rate of 150-R/min. At various times after irradiation metaphase cells were harvested and aberrations were scored on air-dried slides of the fixed cells. In cultures fixed 16 hr after irradiation, the aberrations involving rejoining are primarily of the chromatid type. In the cultures fixed 24 hr after irradiation, there is an increased appearance of dicentrics, or G_1 chromosome aberrations. These data show that chromosome rejoining processes are operative in this cell line and that the chromosome rejoining process is not identical to that of unscheduled DNA synthesis. (P.B.M.)

26725 VISUALIZATION BY SCANNING ELECTRON MICROSCOPY OF ACHROMATIC LESIONS (GAPS) INDUCED BY X-RAYS IN CHROMOSOMES OF VICIA FABA. Scheid, W.; Traut, H. (Univ., Muenster, Ger.). Mutat. Res.; 11: 253-5(Feb 1971).

The scanning electron microscope Stereoscan was used to visualize achromatic lesions or gaps induced by x rays in chromosomes of the broad bean Vicia faba. In order to induce gaps, 10-day-old seedlings were irradiated with 100 R applied in 1 min. Gaps were observed at metaphase but induced mostly in late interphase. For the scanning electron microscopical analysis only gaps completely traversing the diameter of the chromatid were selected. (P.B.M.)

26726 DOMINANT LETHAL MUTATIONS IN THE DESCENDANTS OF IRRADIATED MALE MICE. I. INVESTIGATION OF THE DOSE-EFFECT RELATION AND THE DIFFERENCES BETWEEN WHOLE- AND PARTIAL-BODY IRRADIATION IN MEIOTIC AND POSTMEIOTIC GERM CELL STAGES. Schroeder, Johannes Horst; Hug, Otto (Gesellschaft fuer Strahlenforschung, Neuherberg, Ger.). Mutat. Res.; 11: 215-45(Feb 1971). (In German).

Hybrid male mice were x-irradiated with doses ranging from 50 to 1100 R and mated with nonirradiated females to determine the number of dominant lethal mutations in the progeny. The mutagenic effectiveness of whole-body irradiation was compared with that of isolated gonad irradiation. The examination of the contents of uteri of females mated to sham-treated males served as controls. The losses found in females that were mated to irradiated males in the 3rd to 5th wk after irradiation follow a sigmoid curve up to a maximum between 600 and 710 R. After irradiation with 1100 R the incidence of dominant lethal mutations was found to be reduced again. The fractionation of 1100 R into two equal doses separated by a 24-hr interval shows a higher effectiveness than single acute irradiation with the same dose. (P.B.M.)

26727 INDUCTION OF CHROMOSOMAL ABERRATIONS IN PIG KIDNEY CELLS BY FAR-RED LIGHT. Gordon, S. A.; Stroud, A. N.; Chen, C. H. (Argonne National Lab., Ill.). Radiat. Res.; 45: 274-87(Feb 1971).

Exposure of pig kidney cells in monolayer culture to far red light (FRL), near 750 nm in wavelength, raises the frequency of chromatid aberrations. Dose response curves for this effect of FRL reach a maximum at incident energies of ca. 50 $mJ \cdot cm^{-2}$ and then decline. Lowering the temperature of the cells during exposure increases the aberration yield. When cells were exposed to FRL at various times after subculture, they showed peaks in the aberration yield when the intervals were about 16 and about 22 hrs. These maxima correspond to the early S and G_2 stages of the cell cycle of the synchronized fraction of the population, as determined by pulse labeling with tritiated thymidine. The induction of chromosome damage by FRL is interpreted as a consequence of a decrease in repair of a high spontaneous aberration frequency or an impairment of chromosome synthesis. (auth)

26728 ROLE OF VARIETY IN EXPERIMENTAL MUTAGENESIS OF COTTON. Konoplya, S. P.; Fursov, V. N. Izv. Akad. Nauk Turkm. SSR, Ser. Biol. Nauk; No. 6, 50-5(1969). (In Russian).

In the second year mutation nurseries of the Iolotan' cotton breeding station six varieties of cotton were investigated from 1965 to 1966. The γ ray and thermal neutron effects on the investigated cotton seeds revealed morphological genetic changes. Among the varieties investigated, qualitative and spectrum differences of the obtained mutations were discovered. According to the mutability, the varieties under investigation were divided into three groups namely: little mutability, occurring in small amounts, as the result of mutagen influence and insufficient spectrum; moderate mutability, the result of each mutagen influence; and highly mutable varieties when a broad spectrum and great amount of mutations are observed. (auth)

26729 MUTAGENESIS INDUCED BY UV-IRRADIATION IN STRAINS OF B. SUBTILIS VARYING IN THEIR SENSITIVITY TO UV-IRRADIATION. Likhoded, L. Ya.; Kuryushkina, A. A. (Inst. Epidemiology and Microbiology, Moscow). Zh. Mikrobiol., Epidemiol. Immunobiol.; No. 12, 5-7(Dec 1969). (In Russian).

The incidence of spontaneous and uv mutations in streptomycin locus of different strains of Bacillus subtillis was subjected to study. Mutation incidence proved to be increased in strains which had lost the ability to excise pyrimidine dimers. In recombination deficient strains with reduced transformability, the incidence of mutations, spontaneous, and induced by low uv doses, showed a slight increase. However, the maximum mutation frequency in recombination deficient strains was less than in bacteria of a wild strain. It was suggested that mutagenesis is related to some processes required for recombinations. (auth)

26730 EFFECTS OF ^{131}I AND X RADIATION ON THE CHROMOSOMES OF PERIPHERAL BLOOD LEUKOCYTES. Satcher, David. Cleveland; Case Western Reserve Univ. (1970). 167p. University Microfilms Order No. 71-1745.

Thesis.

The specific aims of the research were to identify the approximate dose level at which significant and demonstrable chromosome damage begins, and to effectively relate radiation dosage to chromosome damage. Chromosomes of peripheral blood leukocytes were examined from a relatively large number of patients exposed to a wide range of x irradiation and ^{131}I from low diagnostic levels, to high level x ray therapy. From this study of the chromosomes of patients exposed to diagnostic x irradiation (mainly barium enemas and UGI series) within the range of 12 to 48 rads surface doses or 3 to 12 rads/liter blood, a significant increase in the frequency of chromosome aberrations was found after exposure for the overall group; and no significant change in chromatid aberrations or aneuploid frequency was noted. After dividing the patients in this range (3–12 rads/liter) into three groups and analyzing the results statistically, it was concluded that significant damage begins between 8 to 9 rads/liter or 32 to 36 rads surface dosage. The chromosomes from 10 patients treated with low level ^{131}I (6–19.7 mc) were evaluated. For the patients as a group, an increase in the frequency of chromosome aberrations was found which reached a peak at 24 hrs and fell to almost control level by one week post-treatment. No relationship was found between dose of ^{131}I ingested and the increase in frequency in chromosome aberrations in time. (TSS)

26731 LONG-CHAIN MUTANTS OF STREPTOCOCCUS FAECALIS INDUCED BY ULTRAVIOLET IRRADIATION. Lominski, I.; Shaikh, M. Rafi (Univ. of Glasgow). J. Med. Microbiol.; 1: 219-20(Nov 1968).

Among the streptococci, which are characterized as a genus by chain formation, the species Streptococcus faecalis is exceptional in forming short aggregates of 4 to 6 cells or no chains at all. The organism can be made to grow as a chain forming phenotypic variant in the presence of a number of chemically unrelated compounds of which Suramin is the most useful. A strain was also found which, although biochemically and serologically identical with S. faecalis, grew spontaneously in long chains. Both types of chain are readily broken down by filtrates of ordinary cultures and by lysozyme; lysozyme in turn was found to be powerfully inhibited by Suramin. It was assumed

as a working hypothesis that separation of bacterial cells is an enzymic process; the enforced formation of chains by chemicals would be due to their inhibitory effect on the cell separating enzyme, and strains that spontaneously formed long chains would represent enzyme defective mutants. It seemed possible therefore that ultraviolet irradiation might produce chaining mutants from nonchaining strains. (P.B.M.)

26732 STUDY OF IRRADIATION EFFECTS ON MITOSIS IN LUCERNE IN R_0, R_1, AND R_2. Craciun, T.; Nasta, A. Lucr. Stiint. Inst. Agron. N. Balescu, Bucuresti, Ser. C; 10: 59-64(1967). (In Rumanian).

Gamma radiations (in doses of 500, 10,000 and 15,000 R) disturbed the mitotic mechanism of lucerne cells. After irradiation, some lucerne seeds perish, others germinated, but generated unviable plantlets, and others showed chromosomal abnormalities. (Rom. Sci. Abstr.)

26733 MODIFICATION OF THE CHEMICAL AND RADIATIVE MUTAGENESIS AND METABOLISM. Dubinina, L. G.; Dubinin, N. P. (Inst. of General Genetics, Moscow). Dokl. Akad. Nauk SSSR: 193: 1167-70(11 Aug 1970). (In Russian).

In view of the strong effects of radiation on chromosomes during the period after the synthesis of DNA, the mutagenesis was studied after treatment of Crepis capillaris seeds with ethyleneimine (EI) and by irradiation. A definite time sequence in the overall yield of the variations was found regardless of the special stage of the cell growth cycle. Experiments on the mutagenicity of seeds kept artificially at the presynthesis (G_1 phase) stage, and with seeds going through the normal cycle, yielded the same picture of the modification of the mutagenic process. This makes it desirable to reexamine the widely held viewpoint that the mutagenic sensitivity of chromosomes varies with the cell growth cycle. The results showed that the sensitivity is highest during the S phase, but soaked seeds yielded similar results during the G_1 phase. Radiation was found to cause chromosome changes primarily during the S phase while EI affects them mostly during the G_1 stage. The action of alkylizing compounds may be affected by changes in the intracellular conditions and by external factors. (TTT)

26734 DISTRIBUTION OF X-RAY-INDUCED ACHROMATIC LESIONS (GAPS) WITHIN AND BETWEEN THE ARMS OF THE M-CHROMOSOME OF VICIA FABA. Scheid, W.; Traut, H. (Univ., Muenster, Ger.). Stud. Biophys.; 17: 125-30(1969).

The distribution of x ray-induced gaps within and between the arms of the M-chromosome of Vicia faba has been investigated. Significantly more gaps are observed in the middle than in the end regions of each arm. The distribution of gaps between the three arms deviates significantly from that expected on the basis of their relative lengths. (auth)

26735 STUDIES ON MUTATION BREEDING OF TOMATO. I. MORPHOLOGICAL VARIANCES APPEARED IN R_1 GENERATION OF γ-IRRADIATED TOMATO SEEDS. Choi, J. K.; Won, J. L.; Kim, M. Z. (Radiation Research Inst., Seoul). J. Nucl. Sci. (Seoul); 10: No. 2, Part 2, 73-8(1970). (In Korean).

In order to induce useful mutants with male sterility and others in tomatoes, seeds were treated with γ rays of 30 to 50 kR doses. The following responses were observed in R_1 generation: germination rate was not affected with treatments although germination was delayed; seedling height, root length, and number of roots in seedling stage were significantly decreased with increasing doses and roots were more sensitive than shoot; days to flowering increased pollen fertility, and plant height were decreased as doses increased; and fruit weight, size, and number of seeds per fruit were reduced with increasing doses. (auth)

26736 RADIATION BIOPHYSICAL INVESTIGATIONS OF ARABIDOPSIS THALIANA. III. INDUCTION OF MUTATIONS BY X-RAY, PROTONS, AND ALPHA-PARTICLES. Ivanov, V. I. (Institut fuer Medizinische Radiologie, Obninsk, USSR); Sanina, A. V.; Timofeeff-Ressovsky, H. A.; (and others). Stud. Biophys.; 13: 111-17(1969). (In German).

Air dry seeds of Arabidopsis thaliana were irradiated with 0.1 MeV x rays, 6.3 MeV protons, and 25.1 MeV alpha particles at doses ranging from 1 to 20 krad, in order to study the frequencies of chlorophyll and embryonic lethals in M(1) pods. No difference in the mutagenic effectiveness of the applied radiations were observed. (auth)

26737 INVESTIGATIONS ON POTATO PLANTS (SOLANUM TUBEROSUM) OBTAINED FROM IRRADIATED TUBERS. Chita, O.; Paunel, F.; Georgescu, L. Bul. Stiint. Univ. Craiova; 10: 125-34(1969). (In Rumanian).

The effects of γ rays ^{60}Co in the range of 1000 R and 10,000 R on potato plants of the Carpatin variety are studied. Irradiation delivered previous to planting resulted in morphological changes of the leaves, stalks, and tubers proportional to the dose. Low γ ray doses (1000 to 6000 R) had a stimulating effect. (Rom. Sci. Abstr.)

Health Physics and Safety

26738 NATIONAL HEALTH AND MEDICAL RESEARCH COUNCIL. A REVIEW OF PUBLICATIONS RELATING TO MATTERS OF RADIATION HEALTH. Australas. Radiol.; 14: 451-3(Nov 1970).

Short resumes of publications of the N.H. and M.R.C. are given. The publications appear in the form of codes of practice and deal with control and safe handling of sealed radioactive sources used in radiation therapy (other than teletherapy), the use of ionizing radiations in secondary schools, nursing staff exposed to ionizing radiations from radioactive substances, safe handling of corpses containing radioactive substances, minimizing radiological hazards to patients (an interim statement), revised radiation protection standards for individuals exposed to ionizing radiations, radiation hygiene in dentistry, control and safe handling of sealed radioactive sources used in industrial radiography, and notes on medical procedure for radiation accidents and radioactive contamination. All publications are oriented to the Australian situation, and are published in Canberra by the N.H. and M.R.C. (Australia)

Radioactive Contamination and Decontamination

Refer also to abstracts 26335, 26406, 26429, 26443, 26607, 26684, and 27036.

26739 (MLM-1795) ENVIRONMENTAL MONITORING REPORT: JULY-DECEMBER 1970 AND 1970 SUMMARY. (Mound Lab., Miamisburg, Ohio). 15 Apr 1971. Contract AT-33-1-GEN-53. 51p. Dep. NTIS.

The average concentrations of polonium-210, plutonium-238, and tritium detected in the environment surrounding Mound Laboratory, Miamisburg, Ohio, are presented for the second half of 1970 and for the entire year. (The data for the first half of 1970 were presented in Mound Laboratory document MLM-1784.) The average concentrations of these radioisotopes in the Great Miami River and at the air sampling stations were well within the stringent standards adopted by the Atomic Energy Commission. The highest average concentration of these radioisotopes at any of the water sampling stations during the second half of 1970 was less than during the first half of 1970 by as much as 36%. The highest average concentration of polonium-210 at the air sampling stations during the second half of 1970 was 14% more than during the first half of 1970 (0.08% of RCG vs. 0.07% of RCG), however, the highest average concentration of the other two radioisotopes was less by as much as 57%. (auth)

26740 (NP-18728) LEVELS OF ^{137}Cs IN MAN IN U.A.R. DURING YEAR 1970. El-Assaly, F. M.; Alloush, A. A. (Atomic Energy Establishment, Cairo (Egypt). Radiation Protection Dept.). Jul 1970 4p. Dep. NTIS (U. S. Sales Only).

Results are reported from whole-body measurements of the content of ^{137}Cs in 30 adult human subjects residing in Egypt during 1970. Results are compared with measurements made in 1967 and 1968. (C.H.)

26741 HUMAN RADIATION EXPOSURES FROM NUCLEAR POWER REACTORS. Sagan, Leonard A. (Palo Alto Medical Clinic, Calif.). Arch. Environ. Health; 22: 487-92(Apr 1971).

The possible hazards to human populations from nuclear power plant effluents are reviewed. It is pointed out that available data on radioactive effluents from nuclear power plants provides evidence of a wide margin of safety from normal operations. Levels of radioactivity have consistently been below permissible limits. Growth of the industry is unlikely to increase the hazard and current research on breeder reactors and better methods of waste management is likely to result in the reduction of radioactive contamination even below currently predicted levels. (C.H.)

26742 CONTROL OF RADIOACTIVE POLLUTION IN A NORTH SEA OYSTER FISHERY. Preston, Alan (Fisheries Radiobiological Lab., Lowestoft, Eng.). Helgolaender Wiss. Meeresunters.; 17: 269-79(1968).

The radiological situation in the Blackwater estuary is reviewed. Some data are produced to contrast the behavior of particulate and soluble nuclides in this estuarine environment and it is demonstrated that ^{65}Zn, ^{60}Co, and ^{55}Fe probably reach the oysters on fine silt particles. The conclusion of the pre-operational assess-

ment is confirmed, that oysters are the critical material and ^{65}Zn is the critical radionuclide. At present, oysters are the only material in which measurable concentrations of activity exist throughout the estuary. The maximum dose-rates experienced by exceptional oyster consumers are less than 0.2% of the I.C.R.P. permissible dose limits for members of the public. A system is developed to relate oyster contamination, and consequently discharge rate of radioactivity, to any distance from the power station outfall. (auth)

26743 CHEMICAL AND HYGIENIC STUDIES ON NATURAL RADIOACTIVE SPA. 2. NATURAL RADIOACTIVE NUCLIDES IN HOT SPRING WATER AT MISASA SPA AREA. Kametani, Katsuaki; Kido, Yasumasa; Hasegawa, Akira; Ikebuchi, Hideharu; Urakubo, Goro (National Inst. of Hygienic Sciences, Tokyo). Eisei Kagaku; 16: 9-14(Feb 1970). (In Japanese).

Samples of hot spring water at Misasa spa area were collected several times from June 1963 to December 1965, and concentrations of the natural level of radioactivity from ^{226}Ra, natural U, ^{222}Rn, Ca ion, Cl ion, SO_4 ion were determined. The sampling places were distributed to cover all areas of the spa in order to know the mean value of radioactivity level. Among those 15 sampling places, springs containing rather higher concentration of radioactive nuclides were crowded at the center part of Misasa area, corresponding to the north side of Santoku river. Besides, the concentration of ^{226}Ra in spring water was far higher than the radioactive equilibrium value calculated from the content of natural U. The habitants in this area have a custom to drink the spring water usually, so hygienic problem was discussed comparing the maximum permissible concentration recommended by ICRP and NBS in the USA. The mean value of natural U was 2 μg/liter, and that of ^{226}Ra was 5.4 pCi/litter. Comparing with $1/_{30}$ of the maximum permissible concentration in water recommended by ICRP, the concentration of natural U was much lower, but the value of ^{226}Ra was near to $1/_{30}$ of recommended concentration. The mean value of the concentration of ^{222}Rn in spring water was 1.5×10^{-2} μCi/liter and much higher than $1/_{30}$ of the maximum permissible concentration recommended by NBS. (auth) (Japan)

26744 DEPOSITION OF URANIUM IN THE BONES OF ANIMALS. Otgonsuren, O.; Perelygin, V. P.; Chultem, D. At. Energ. (USSR); 29: 301-2(Oct 1970). (In Russian).

Although the concentration of uranium in the bones of animals is the same as in other organs, earlier studies revealed that the bones of fossil remains of mammal and fish bones contained increased amounts of uranium and sodium. Sensitive, dielectric-type charged-particle detectors were used to determine again the deposition of uranium in the bones of dinosaurus and giant turtle shells found in the southern Gobi region of Mongolia. The ground specimens were exposed to a thermal neutron flux of about 10^{14} n/cm^2 in the IBR reactor. The glass and plastic detectors used were etched with HF and KOH, respectively, to develop the tracks of fission fragments. The results indicated that the fossilized bones contained 10^{-3} to 10^{-4} g/g of uranium while the bones of laboratory mice contained only 10^{-6} g/g. The increase of the uranium content has been attributed to geochemical factors such as the selective accumulation of uranium by the bones from the aqueous solutions by substituting calcium atoms for the UO_2 ions during extended geological periods. This conclusion agrees with the finding of T. Muto et al. The great sensitivity of dielectric detectors makes it possible to extend these studies to the level of very low uranium concentrations of the order of 10^{-9} to 10^{-10} g/g of U. (TTT)

26745 RADIOACTIVITY OF THE SESTON AND WATERS OF THE BLACK SEA AND THE ALGA (CYSTOSERIA BARBATA) FROM THE RUMANIAN CONTINENTAL SHELF DURING 1964–1967. Georgescu, Iulia I. (Polytechnic Inst., Bucharest); Skolka, H. Rev. Roum. Phys.; 15: 945-58(1970). (In French).

Following the combined analysis of the α, β, and γ activities of samples obtained during 1964 to 1967 from the Rumanian continental shelf, namely: seston, ferromanganous concretions, continental fallout, seawater, and selected algae (Cystoseria barbata), it was concluded that the least contamination by fission products was found at the mouth of the Danube in the Black Sea, while in the region of Portita there was a tendency to concentrate the artificial and natural radionuclides of the U–Ra series. During 1964 to 1967, a rapid decrease was noted in the artificial radioactivity of the marine environment, notwithstanding the very slight contamination in 1967 due, in part, to the fresh debris from the Chinese atmospheric nuclear tests of June 17 and December 24, 1967. For example, ^{131}I accumulated in Cystoseria in September 1967 and it was revealed in the spring of 1968 in the shrimp Upogebia pusila. (tr-auth)

26746 RADIOLOGICAL POPULATION EXPOSURE IN THE ENVIRONMENT OF NUCLEAR POWER PLANTS. Boettger, P.; Schatz, A. BBC-Nachr.; 52: 250-3(1970). (In German).

Radioactive beams can produce acute sickness (at very high doses) and somatic and genetic injuries in man. No damage is to be expected at very low doses for large population groups. The natural radiation background has to be considered. A nuclear power reactor represents a hazardous source because of its fission products. The activity release into the environment can be kept low during normal operation and during disturbances so that no hazard to the population exists. This was demonstrated for an AGR type reactor. (INIS)

26747 ESTIMATE OF THE RISK OF INTERNAL CONTAMINATION IN MAN BY RADIOACTIVE WATER POLLUTION. Bittel, R.; Lacourly, G. (CEN, Fontenay-aux-Roses, France). Radioprotection; 5: 281-91(1970). (In French). (CONF-700505–41).

From 2nd Congress of the International Radiation Protection Association, Brighton, England.

The journal listing appearing here refers to a paper that was previously abstracted and published in NSA as a part of the original conference proceedings. It appeared in NSA Vol. 24 as abstract 48526. (E.R.B.)

26748 ESTIMATION OF THE DOSE TO SKIN FROM RADIOACTIVE PARTICULATE CONTAMINATION OF CLOTHING. Stevens, D. C.; Stephenson, J.; Bruce, G. S. (United Kingdom Atomic Energy Authority, Harwell, Eng.). Ann. Occup. Hyg.; 14: 1-9(Mar 1971).

The dose to the skin from particles containing radioactive strontium, caesium and cobalt embedded in clothing, was investigated. Each particle on clothing covering the trunk of the body irradiated an area of 1 to 2 cm^2. The particle activity which would give a dose rate of 1 rad/hr over 1 cm^2 skin was found to be 1 to 2 μCi for the three nuclides studied (^{60}Co, ^{137}Cs and $^{90}Sr/^{90}Y$). The results are also expressed in terms of the counting rates observed on counters used for routine surveys. The contamination by strontium titanate of protective clothing worn during decontamination of shielded cells, was statistically analysed. The median particulate activity was 0.06 μCi ($^{90}Sr + ^{90}Y$). Laundering the clothing removed 60% of particulate activity, and 50% by number, and many of the particles not washed off retained their position on the clothing. It was calculated that 95% of personnel engaged in decontamination would receive in a 13-week period less than 15 rad/cm^2 skin from the most active particles on their clothing. It is suggested that the present limit for clothing contamination by beta emitters is not entirely satisfactory for high activity particles. (auth) (UK)

Dosimetry and Monitoring

Refer also to abstracts 26178, 26355, 26356, 26392, 26488, 26503, 26534, 26535, 26790, 26849, 26858, 26865, 26870, 26882, 26894, 26931, and 27027.

26749 (NP–18732) TECHNICAL REPORT ON ANNUAL OCCUPATIONAL RADIATION EXPOSURE DOSE LEVELS FOR U.A.R. ATOMIC ENERGY WORKERS DURING THE PERIOD 1962–1969. Sayed, A. M. (Atomic Energy Establishment, Cairo (Egypt). Radiation Protection Dept.). 2 Jul 1970. 4p. Dep. NTIS (U. S. Sales Only).

Data are presented on the annual radiation dose received by atomic energy personnel in Egypt during 1962 through 1969. The number of personnel increased from 800 to 2,000 during this period. Annual doses were classified as less than 0.05, 1.5, and 5.0 rem or over 5.0 rem (7 persons during the period). (C.H.)

26750 (ORNL-tr–2455) RADIATION DOSES AT THE ALTITUDE OF SUPERSONIC TRANSPORT FLIGHTS. Allkofer, O. C.; Simon, M. Translated by R. Gregg Mansfield (Oak Ridge National Lab., Tenn.), from Atompraxis; 16: 186-95(1970). 16p. Dep. NTIS.

Supersonic transport flights (SST) will take place at an altitude of 19 to 25 km, which may result in exposure of the personnel to radiation doses in excess of the permissible dose of 5 rem/yr. Estimates were made of the radiation dose rates due to cosmic radiation, heavy primary particles, and solar radiation at this altitude. The special problem of very strong solar flares that occur only rarely is discussed. It was concluded that the yearly flight time for the crew of a supersonic aircraft might possibly be limited by the radiation dose and dose rate encountered during some flights. (C.H.)

26751 (UCRL–50163(Pt.7)) PREDICTION OF THE DOSAGE TO MAN FROM THE FALLOUT OF NUCLEAR DEVICES. VII. ESTIMATION OF THE MAXIMUM DOSE RATE FROM THE CONTINUOUS RELEASE OF RADIONUCLIDES TO THE BIOSPHERE.

Pratt, Michael W. (California Univ., Livermore. Lawrence Radiation Lab.). 2 Nov 1970. 77p. Dep. NTIS.

A method is described for estimating the maximum internal dose rate to man that could result from the continuous release, at a constant rate, of any given radionuclide to the biosphere. Calculations pertaining to the equilibrium dose rate to bone and whole body are presented to illustrate the method. The results of the analysis are shown to provide a new departure for the establishment of maximum permissible concentration (MPC) values in air and water that take into account the concentration factor associated with the entry of a radionuclide into food chains. They are also shown to be useful as a guide in establishing the maximum rate of radionuclides to the environment that could occur without exceeding allowable dosage limits. (auth)

26752 ABSORBED FRACTIONS FOR SMALL VOLUMES CONTAINING PHOTON-EMITTING RADIOACTIVITY. Ellett, W. H. (Oregon State Univ., Corvallis); Humes, R. M. J. Nucl. Med., Suppl.; 12: No. 5, 25-32(Mar 1971).

The absorbed fraction is the ratio of the energy absorbed in a given target volume to the energy emitted by a radioactive source. The use of absorbed fractions to calculate the dose from radionuclides within the body has been described in previous MIRD publications. Values of absorbed fractions for photon emitters in relatively small, unit-density absorbing volumes (1 to 500 g) containing either a central point or a uniformly distributed photon source, obtained by computer calculation, have been published. Data are presented that supplement the tables of absorbed fractions published in MIRD Pamphlet 3 for absorbing volumes of 300 g and larger. The data differ in one important respect from absorbed fractions published earlier. In the results given it is assumed that the volume containing the activity is imbedded within a large scattering medium of the same composition. Backscattered radiation from these surroundings is included in the absorbed fractions tabulated. The composition of the unit-density absorbing medium used as an analog for soft tissue is listed. The mean free path, and the total attenuation and energy-transfer coefficients of the material are listed for the source energies considered, and comparison of absorbed fractions in this material and in other tissue analogs is given. (C.H.)

26753 DISTRIBUTION OF ABSORBED DOSE AROUND POINT SOURCES OF ELECTRONS AND BETA PARTICLES IN WATER AND OTHER MEDIA. Berger, Martin J. (National Bureau of Standards, Washington, D. C.). J. Nucl. Med., Suppl.; 12: No. 5, 5-23(Mar 1971).

Data are presented on the distribution of absorbed dose around point-isotropic sources of electrons and beta particles, i.e., around sources that emit particles uniformly in all directions and have dimensions that are negligibly small compared with the ranges of the emitted particles. Absorbed-dose distributions as functions of distance from the source are tabulated for monoenergetic electron sources at nine energies between 4 MeV and 25 keV, and for 75 beta-emitting radionuclide sources. The tabulations were prepared for water and are given in such a form that they can readily be adapted to other media of low average atomic number and arbitrary density. For soft tissue with unit density practically no adjustment of the water data is required. The tabulated results pertain only to a medium with constant density and homogeneous composition and to source-medium configurations in which the leakage of particles across the boundaries of the medium is unimportant. These restrictive assumptions have been made for the following reasons: they provide a reasonably close approximation to the conditions often encountered in medical internal dosimetry; they are, in the present state of the art, the only basis on which a substantial body of data can readily be assembled; and they make it possible to calculate absorbed-dose distributions for extended line, surface, or volume sources by doing simple integrals over point-source distributions. The data can thus be used as input for the solution of a variety of electron and beta-particle dosimetry problems. (C.H.)

26754 EXTRACORPOREAL IRRADIATION OF BLOOD BY BETA-EMITTING ISOTOPES: PRINCIPLES OF DOSE CALCULATIONS. Slatkin, D. N.; Robertson, J. S. (Brookhaven National Lab., Upton, N. Y.). Radiat. Res.; 44: 846-54(Dec 1970).

A method for the calculation of the radiation dose rate to extracorporeal blood flowing through a cylindrical beta irradiator is developed. Turbulent and laminar blood flow are treated separately. Sample calculations of the absolute and normalized dose rate profiles in several idealized strontium-90 irradiators are presented. (auth)

26755 FIRST EXPERIENCES IN THE USE OF A COMPUTER SYSTEM IN CLINICAL RADIATION PHYSICS. Leetz, H.-K. (Univ. of Saarlandes, Saarbruecken, Ger.). Stud. Biophys.; 23: 89-95(1970). (In German).

Described is the installation of a computer system for on- and off-line handling of problems associated with dose measurement and dose calculation encountered in clinical radiation physics. For clinical use, a special detector was developed that converts, during scanning of the patient, cartesian into polar coordinates, stores them in the memory, and releases them as punch tape. The installation has been in operation for 40,000 hours. (H.B.G.)

26756 CONTRIBUTION TO THE FILM DOSIMETRY OF HIGH-ENERGY RAYS. III. CONCERNING A FILM DOSIMETRIC STANDARDIZATION PROCEDURE, APPROPRIATE ESPECIALLY FOR APPLICATION IN RADIOTHERAPY, RENDERING POSSIBLE THE EMPIRIC CONSIDERATION OF THE INFLUENCE OF RADIO-ENERGY SPECTRUM, INDEPENDENT OF DEVELOPMENT AND SHAPE OF THE BLACKENING CURVE. Rassow, Juergen (Ruhr Univ., Essen). Strahlentherapie; 141: 47-55(Jan 1971). (In German).

It is possible, by simultaneous development of standard-irradiated reference film badges, to decisively diminish with each measuring film the influence of errors caused by emulsion and developing fluctuations. A standardization is quoted on this base rendering possible a simple empiric consideration of the influences of the radioenergetic spectrum on the correlation dose: film density value. The energy factor F_E, valid for the dose maximum of a vertical field, mainly depends on the quality of incident radiation. The phantom depth factor F_p takes into consideration the spectrum alterations depending on the size of field, the direction of incident radiation, as well as other parameters. (auth)

26757 CONTRIBUTION TO IRRADIATION PLANNING IN ELECTRON THERAPY OF BRONCHIAL CARCINOMA. Heuss, Kurt (Allgemeine Ortskrankenkasse, Cologne). Strahlentherapie; 141: 25-31(Jan 1971). (In German).

Isodoses in four sections of thoracic phantoms with different compositions are shown for three different betatron irradiation techniques (fixed electron fields, electron moving-beam techniques, and opposing bremsstrahlung fields, at 43 MeV). The tumor dose is calculated depending on mean density and on the thickness measured in g/cm^2 of the irradiated body section. For individual treatment planning measurement of radiation transmittancy of the lungs is necessary. Two different methods are discussed. (auth)

26758 SIMULATION OF MOVING BEAM THERAPY AND GRID SIZE IN ELECTRONIC CALCULATION OF SINGLE FIELDS AND STANDARD PLANS OF TELECOBALT THERAPY. Rosenow, Ulf; Bode, Dietrich (Univ., Goettingen, Ger.). Strahlentherapie; 141: 56-63(Jan 1971). (In German).

By simulation measures, the effects of gradual changes in the calculation points on consecutive interpolation and on the distribution of isodose lines in simple fields and standard irradiation plans were examined. A diminution of the point distances below 1 cm did not effect a further improvement of accuracy. Furthermore, mobile irradiations were simulated via different angle regions under a number of vertical fields. It became evident that an equally good accuracy in different pendulum angles is attained by a fixed number of field positions for each pendulum angle and should not fall below 20°. (auth)

26759 GONADAL DOSE IN MALE RADIOTHERAPY PATIENTS. Green, James D.; Bushong, Stewart C. (Baylor Coll., Houston, Tex.). Radiology; 98: 661-3(Mar 1971).

Lithium fluoride thermoluminescent dosimeters were used to measure the gonadal dose in male patients undergoing radiotherapy on a 2-MV Van de Graaff accelerator. The patients were selected from two treatment groups, and the gonadal dose was measured and expressed as a function of the tumor dose. The gonadal dose was 0.0112 and 0.045% of the tumor dose for radiation therapy to the head and thorax, respectively. Phantom measurements showed that most of the radiation reaching the gonads was transmitted axially through the body, and therefore it is not possible to reduce this dose measurably with simple shielding. (auth)

26760 ESTIMATION OF DOSE TO GONADS FROM GAMMA EMITTERS PRESENT IN THE BODY. Snyder, W. S.; Ford, M. R.; Warner, G. G. (Oak Ridge National Lab., Tenn.). Radioprotection; 5: 271-80(1970). (CONF-700505-20).

From 2nd Congress of the International Radiation Protection Association, Brighton, England.

A Monte Carlo type computer code was developed for estimating the specific absorbed fraction of photon energy PHI (X – Y), i.e., fraction of energy absorbed in Y, per gram, of that released in X, where X is an organ of the body containing a source of photons distributed uniformly therein and Y is a target organ. The code involves a mathematical anthropomorphic phantom whose organs approximate those of their prototypes in size, shape, composition, and density. (auth) (France)

26761 PROBLEM OF AUTOMATIC DOSE PLANNING. Benedetti, G. R.; Dobry, H. (Siemens AG, Erlangen, Ger.). Stud. Biophys.; 23: 225-31(1970). (In German).

The use of a computer for the evaluation of measured dose radiation distributions for therapy is discussed. The data are used in conjunction with the dose planning program. Comparison between calculated and measured distribution levels for high-energy x radiation and gamma radiation indicates the accuracy attained. The effects of wedge filters and body inhomogenities on dose distribution are considered. The program may also be used for other types of radiation, such as electrons. (C.H.)

26762 MEETING ON THE PROBLEMS CONCERNING THE PROTECTION OF PERSONNEL HANDLING SHORT-LIVED RADIOELEMENTS IN HOSPITALS, SACLAY, FRANCE, MAY 12, 1970. J. Biol. Med. Nucl.; Special No., 1-22(1970). (In French). (CONF-700552).

Seven papers are included; separate abstracts were prepared for each. (France)

For abstracts of individual papers see: 26763–26768 and 26776.

26763 PROBLEMS RAISED IN HOSPITAL SERVICES BY THE USE OF SHORT-LIVED RADIOELEMENTS. Bru, A. (Hopital de la Grave, Toulouse). J. Biol. Med. Nucl.; Special No., 11(1970). (In French).

From Meeting on the problems concerning the protection of personnel handling short-lived radioelements in hospitals; Saclay, France (12 May 1970). See CONF-700552.

Many problems arise in hospitals concerning the protection of personnel handling radioelements. Hospital staff are subjected to many risks and it is essential to take the necessary precautions so that the dose received by assistants or nurses is kept to a minimum. (auth) (France)

26764 NOTES ON SAFETY NORMS. Dousset, M. (CEA, Fontenay-aux-Roses, France). J. Biol. Med. Nucl.; Special No., 12(1970). (In French).

From Meeting on the problems concerning the protection of personnel handling short-lived radioelements in hospitals; Saclay, France (12 May 1970). See CONF-700552.

The safety norms set limits to the irradiation of different tissues, using a quantity known as dose equivalent which is expressed in Rems. In the use of short-lived radioelements the whole body irradiation limits are: 3 Rems per quarter; 5 (N-18) Rems for an accumulated dose, N being the age of the worker. These limits are 1.3 Rem per quarter for women of child bearing age, and 1.5 Rem per year for pregnant women. The irradiation limit for the hands and fingers is 15 Rems per quarter. (auth) (France)

26765 DOSIMETRY AND SHIELDING DURING THE USE OF ^{99m}Tc AND ITS COMPOUNDS. Robillard, J.; Bloquel, J. (Centre Regional de Lutte contre le Cancer, Caen, France). J. Biol. Med. Nucl.; Special No., 13(1970). (In French).

From Meeting on the problems concerning the protection of personnel handling short-lived radioelements in hospitals, Saclay, France (12 May 1970). See CONF-700552.

Several compounds of ^{99m}Tc are used. The irradiation dose received by personnel during the different manipulations is measured with the Intertechnique radiationmeter and with luminescent dosimeters. All the measurements show that the doses absorbed by staff using ^{99m}Tc are negligible at the level of the face and abdomen if correct shielding is used. Only the hands receive a dose which is nevertheless acceptable, and can be reduced further by sheathing the syringe with lead. (auth) (France)

26766 IRRADIATION RISKS TO PERSONNEL IN CHARGE OF PATIENTS UNDERGOING EXAMINATIONS WITH ^{99m}Tc. Parmentier, C.; Chavaudra, J.; Burlot, A. (Institut Gustave Roussy, Villejuif, France). J. Biol. Med. Nucl.; Special No., 16(1970). (In French).

From Meeting on the problems concerning the protection of personnel handling short-lived radioelements in hospitals, Saclay, France (12 May 1970). See CONF-700552.

In order to establish the risks of ^{99m}Tc irradiation, the dose rate distribution was studied during scintigraphy at several points in the examination room; the doses received by the technician moving around the room during the scintigraphy were then read at the level of the gonads and chest. The figures found were almost twenty times lower than those of the norms in force. (auth) (France)

26767 DOSIMETRY DURING THE HANDLING OF ^{113m}In GENERATORS AND ITS COMPOUNDS. Valeyre, J. (Centre Regional de Lutte contre le Cancer, Reims). J. Biol. Med. Nucl.; Special No., 17(1970). (In French).

From Meeting on the problems concerning the protection of personnel handling short-lived radioelements in hospitals, Saclay, France (12 May 1970). See CONF-700552.

The use of ^{113m}In and its generators has raised serious shielding problems because of the danger of irradiation to the hands and especially the fingers. The preparation that most often keeps the operator near the source exposes the hands to 4 mRems for 20 mCi. Perfusion techniques, lead-shielded syringes, and containers are very useful in lowering the dose absorbed. The hands of an operator carrying out two elutions of 20 mCi a day are exposed to less than 10 mRems, i.e., below the accepted dose for the whole body and certainly for the hands. The doses measured at the finger tips with pen dosimeters were 4 mRems for the index and 3 for the thumb. (auth) (France)

26768 COMMENTS ON THE IRRADIATION OF THE HANDS DURING PREPARATION OF ^{99m}Tc AND ^{113m}In LABELED COMPOUNDS WITH C.E.A. KITS. Henry, R. (CEA, Saclay, France). J. Biol. Med. Nucl.; Special No., 19(1970). (In French).

From Meeting on the problems concerning the protection of personnel handling short-lived radioelements in hospitals, Saclay, France (12 May 1970). See CONF-700552.

The preparation of compounds labeled with ^{99m}Tc and ^{113m}In carries no risk of whole-body irradiation because of the attenuation of dose rate with distance. Exposure is restricted to a local irradiation of the hands during the preparation. Measurements were carried out using thermoluminescent films placed at the finger tips. The doses measured range from 275 to 380 mRems for ^{99m}Tc and from 330 to 860 mRems for ^{113m}In. These figures can be considerably reduced by shielding the syringes with lead. (France)

26769 REVIEW OF THE PHYSICAL DATA USED IN RADIUM AND RADON DOSIMETRY. Sofer, D. H. (Commonwealth X-Ray and Radium Lab., Parkville, Australia). Australas. Radiol.; 14: 443-50(Nov 1970).

Values of physical data on which the dosimetry of radium and radon sources is based are recommended in an attempt to achieve uniformity in Australia. Radon activity is measured assuming a value of 0.98 Ci/g for the specific activity of radium (N.S.C.). Specific γ constant of radium is defined as the exposure rate in air at 1 cm from a point source of 1 mg of radium filtered by 0.5 mm of platinum and is given as 8.25 $Rcm^2\ mg^{-1}\ hr^{-1}$. For a point source of 1 mCi Rn the value obtained was 8.49 $R\ cm^2\ mCi^{-1}\ hr^{-1}$. Tabulations were made of γ output F(d), for Pt filtration from 0.3 to 10.0 mm and for ratio of exposure in water to exposure in air from Ra sources for distances from 2 to 14 cm. Integrated exposure is proportional to $H(t) = 1/\lambda\ [1 - \exp(-\lambda t)]$. For radium $H_{Ra}(t) = t$; for radon $H_{Rn}(t) = 132.4\ [1 - \exp(-0.007551\ t)]$. Exposure at a point near a filtered point X_p, for radium is taken as $8.25\ m \cdot F(d) \cdot G(r)t$ and for radon as $X_p = 8.49\ A \cdot F(d) \cdot G(r) \cdot H(t)$ for activity A, and dependence on distance from source $G(r) = (1/r^2)$. Tables are set out of milligram hours required to deliver 1000 R at selected points near filtered line sources with wall thicknesses 0.5 and 1.0 mm Pt and lengths 2.5 and 8 cm. (Australia)

26770 ESTIMATE OF THE DOSE OF IONOGENIC RADIATIONS ABSORBED BY AIRPORT PERSONNEL CARRYING OUT THE GROUND OPERATIONS CONNECTED WITH THE TRANSPORT OF PACKAGES CONTAINING RADIOACTIVE MATERIALS. Perini, A. (Ispettorato Medico Centrale del Lavoro, Rome); Susanna, A. Securitas; 54: 821-40(1969). (In Italian). (RT/PROT-(70)6).

A study was made of the conditions in which the various operations connected with the air transport of packages containing radioactive materials were carried out. The operations studied included embarkation and disembarkation, handling, and storage, as well as acceptance and delivery of the packages, and particular attention was paid to the problems of protecting the personnel against radiation. The study was carried out at the Forlanini Airport at Milan-Linate. It was found that the critical group of workers is the one concerned with handling the arriving packages in the store. At the actual level of traffic involving packages with radioactive contents it was found that the dose absorbed was of the order of 350 mRem/annum. The study also arrived at an estimate of the radiation dose absorbed by the whole of the airport staff affected by the traffic between April 1967 and April 1968 and determined the frequency of such transports from both a quantitative and a qualitative point of view. (auth)

26771 CURRENT POSSIBILITIES OF BIOLOGIC DOSIMETRY. Tuscany, R. Cas. Lek. Cesk.; 109: 1036-8(23 Sep 1970). (In Czech).

An attempt was made to critically evaluate the utilization of radioinduced chromosome aberrations in biological dosimetry. The results of current studies are reported. (tr-auth)

Radiation Protection

Refer also to abstract 27013.

26772 TESTING OF DENTAL ROENTGEN APPARATUSES TO THEIR RADIATION SAFETY BY MEANS OF THE ROPAK METHOD. Babor, R.; Sonnabend, E. (Gesellschaft fuer Strahlenforschung mbH: Munich. Deutsche Gesellschaft fuer Zahn-, Mund- und Kieferheilkunde, Munich). Deutsch. Zahnaertztl. Z.; 25: 577-85(1970). (In German).

The control of x-ray apparatuses for dentists with respect to radiation protection according to the Ropak-method is a research project of the Federal Ministry of Health in collaboration with the working group of radiology and the Federation of German Dentists with the aim to check the x-ray apparatuses of about 30,000 dentists in the Federal Republic and West Berlin. A special x-ray film that is sent to the dentists, exposed by them and then evaluated by the control center, shows in particular the following defects: too high doses, unfavorable radiation quality, too large fields, deficient screening and unfavorable dark chamber technique. After evaluation of the exposed films and detection of defects suggestions for improvement are made. (auth)

26773 RADIOACTIVE AEROSOLS CHARACTERISTICS IN FRENCH URANIUM MINES. Pradel, J. (CEA, Fontenay-aux-Roses, France); Chapuis, A.; Lopez, A.; Cabrol, Ch. Radioprotection; 5: 263-70(1970). (In French). (CONF-700505-19).

From 2nd Congress of the International Radiation Protection Association, Brighton, England.

Important parameters concerning the protection of French uranium miners were considered. These parameters include the concentration of ultrafine radioactive ions, the concentration of condensation nuclei and the particle size spectrum, and polarity and nature of the radioactive aerosols. The concentration of ultrafine radioactive ions varies between 8 and 20%. The particle size spectra for radioactive nuclei of either polarity were similar and ranged from 0.02 to 0.10 μ. (auth) (France)

26774 HISTORY OF RADIATION PROTECTION. Morgan, Karl Z. (Oak Ridge National Lab., Tenn.). Mater. Eval.; 29: 19A-20; 22A; 24A-6; 32A(Mar 1971).

The history of man's awareness of the benefits and risks from ionizing radiation is reviewed. Data are given on the natural background radiation dose received by the average person in the United States, the early estimations of tolerance dose, and types of radiation damage from total exposure to x or γ radiation. A comparison was made of the consequences of x ray diagnostic exposure presently received by the U. S. population with the consequences of hypothetical exposure of 0.85 mrem/yr to the population from nuclear industries. The basic assumptions made by national and international organizations which make recommendations for radiation protection are given. The role of the health physicist in the field of radiation research and protection is outlined. (E.E.H.)

26775 RADIATION PROTECTION AROUND THE MEDICAL CYCLOTRON AT HAMMERSMITH HOSPITAL. Jones, T.; Bewley, D. K.; Vonberg, D. D. (Hammersmith Hospital, London). Radiology; 98: 665-71(Mar 1971).

The health physics problems experienced with use of a cyclotron for medical purposes are discussed. Particular reference is given to the hazards associated with the production of short-lived radioisotopes for use in diagnostic procedures, the use of fast neutrons for radiotherapy, and cyclotron maintenance. The information presented is of interest in the design and operation of a proposed medical cyclotron laboratory. (C.H.)

26776 PRESENTATION OF SHIELDING MATERIALS. Douis, M. (CEA, Saclay, France). J. Biol. Med. Nucl.; Special No., 20(1970). (In French).

From Meeting on the problems concerning the protection of personnel handling short-lived radioelements in hospitals; Saclay, France (12 May 1970). See CONF-700552.

The C.E.A. Radioelement Department has designed several devices for the protection of operators handling ^{99m}Tc and ^{113m}In. The first is the Elumatic, which performs semiautomatic elutions from ^{99m}Tc and ^{113m}In generators. The second is the Steripompe for the automatic transport of radioactive solutions from one flask to another. The third includes several models of syringe guards. (auth) (France)

26777 PODIATRIC X-RAY PROTECTION FOR DIAGNOSTIC APPLICATIONS. A REPORT PREPARED BY THE AD HOC COMMITTEE ON PODIATRIC X-RAY PROTECTION, AMERICAN PODIATRY ASSOCIATION. J. Amer. Podiat. Ass.; 60: 432-47(Nov 1970).

Recommendations pertaining to equipment design, use, and operating conditions for podiatric x rays and for radiation protection surveys and personnel monitoring are presented by a committee of the American Podiatry Association. It provides basic standards that may be used in the preparation of regulatory protection codes, but is not specifically written for literal adoption as legal regulations. (E.E.H.)

26778 RADIATION MODEL OF MAN FOR ANALYSIS OF FUTURE SPACE MISSIONS. Kase, Paul G.; Ryan, Lois M. (Martin-Marietta Corp., Denver). Advan. Astronaut. Sci.; 27: 513-48(1970).

From 16. annual meeting on space station and manned planetary exploration; Anaheim, Calif. (8 Jun 1970). See CONF-700643.

A detailed, computerized, radiation-shielding model of the human body is described and examples relating it to the planning of radiation protection during future space missions are reported. The model has two configurations (standing and seated), and more than 2200 individual geometric shapes are used to depict the external conformation, skeleton, and principal organs. The exterior dimensions are those of the 50th-percentile Air Force man, and the skeleton and organs were scaled to conform from life-size models. Protection of the crew usually requires additional weight, and it is desirable to know the margins of safety in order to minimize weight penalties. Some parts of the body are insensitive to radiation when compared to other parts, and in marginal situations it is necessary to compare the radiation doses at several points to identify the limiting dose. The extensive detail of this model fulfills this need. (C.H.)

26779 EFFICACY OF ADDITIONAL SHIELDING IN TELE-COBALT THERAPY. Hofner, W.; Kaercher, K. H.; Riedl, P. (Univ., Vienna). Wein. Klin. Wochenschr.; 83: 148-9(5 Mar 1971). (In German).

For three standard methods of ^{60}Co therapy, additional shielding is advisable. The protection of eyes is necessary to prevent cataract formation. Shielding of the larynx by lead block, 3.5 × 6.6 × 5.4 cm, prevents dryness, hoarseness, and swallowing difficulty in patients with cancer of the mesopharynx or metastatic nodes in the lymphatic glands of the neck. In addition, protection of the kidneys is necessary during irradiation of para-aortal lymph nodes. (H.B.G.)

Safety Procedures

26780 NUCLEAR SAFETY IN AMERICAN RADIOCHEMICAL PROCESSING PLANTS. Unger, W. E.; Browder, F. N.; Mann, S. Nucl. Safety; 12: 234-46(May-Jun 1971).

With the projected rapid growth of nuclear electric-power generation and the accompanying growth in reprocessing of spent nuclear fuel, the whole area of nuclear and radiochemical safety becomes increasingly important. There is an indicated worldwide need for information on accepted practices, recommended methods, and regulations for safe operation in radiochemical processing plants. Experience and developments in the United States are described to illustrate safety considerations in all stages from site selection and licensing through design, construction, operation, and maintenance of processing plants. (auth)

26781 RESTRICTED RELEASE OF PLUTONIUM: PART 1. OBSERVATIONAL DATA. Hunt, D. C. Nucl. Safety; 12: 85-9 (1971).

A study was made of the possible hazard outside an enclosure due to incidental release of plutonium from the enclosure following the uncontrolled release of plutonium within the enclosure. The existing data on such restricted plutonium releases are reviewed. Observations based on both accident experience and experiments designed to study the restricted release were considered. The conclusion, based on the observational data, is that restricted release is unlikely to lead to dangerous free release of a plutonium aerosol. A remarkable example of this was the fire at the Rocky Flats Plant on May 11, 1969. Only a minute amount of the plutonium involved in the fire escaped from the building in which the fire occurred, and no plutonium was detected beyond the plant boundaries. (auth)

26782 RESTRICTED RELEASE OF PLUTONIUM. PART 2. THEORY. Hunt, D. C. Nucl. Safety; 12: 203-16(May-Jun 1971).

A study was made of the possible hazard outside an enclosure due to uncontrolled release of plutonium within the enclosure. A model of restricted release was developed. The model predicts free-release source strengths as a function of the variables assumed to describe the release. An illustration of the use of the theoretical methods is given by applying them to the Rocky Flats critical-mass-facility test cell. These particular calculations show that the actual release would be significantly less than the allowable ^{239}Pu MPC value for insoluble material in controlled

areas if nominal values are assumed for all release parameters. A parametric study indicated that the calculated results are most sensitive to the rate of release of plutonium within the enclosure and to the assumed thermal equilibrium conditions within the enclosure. (auth)

26783 OCULAR OCCUPATIONAL ACCIDENTS CAUSED BY IONIZING RADIATION. Dollfus, M.-A. pp 155-67 of Problems of Industrial Medicine in Ophthalmology. Vol. 1-2. /Merte, H.-J. (ed.). Basel; S. Karger AG (1969). (In French).

From 1. symposium of the International Study Group for Ergophthalmology; Munich, Germany (14 Aug 1966) - 2. symposium of the International Study Group for Ergophthalmology; Amsterdam, Netherlands (18 Jun 1968). See CONF-660843-(Vol.1); CONF-680675-(Vol.2).

Reviewed are hazards encountered in nuclear industry and uranium mines and during the use of radioisotopes and radiation generators. Cataracts caused by cyclotrons, radioisotopes, and x- or gamma-ray generators, and eye damage in the watchmaking industry are assessed. Technical and medical preventive measures, with indications of the maximum permissible dose to the lens and radiation-induced lesions recognized in France as being of occupational origin are discussed with respect to relevant French regulations. (auth)

26784 SPACE STATIONS. Based on Space Station, Safety, and International Sessions of AAS 16th Annual Meeting, June 8-10, 1970, Anaheim, California. Larmore, L.; Gervais, R. L. (eds.). Advances in the Astronautical Sciences. Volume 27. Tarzana, Calif.; American Astronautical Society (1970). 602p. (CONF-700643).

Twenty-two papers discuss various aspects of space station safety. A separate abstract was prepared on one paper. (C.H.)

For an abstract of an individual paper see: 26778.

Civil Defense

26785 (ORNL-tr-2306) CIVIL DEFENSE. Akimov, N. I. (ed.). Translated by S. J. Rimshaw and edited by Joanne Gailar and Cresson H. Kearny (Oak Ridge National Lab., Tenn.), from Grazhdanskaya Oborona. Moscow; Kolos (1969). 337p. Dep. NTIS.

Chapter headings include: Civil Defense in a Nuclear War; Organization of Civil Defense; Personal Protective Equipment; Shelters for Protecting the Population; Reception and Relocation of Dispersed Personnel and Evacuated People; Instruments for Radiation, Chemical, and Bacteriological Survey and Dosimetric Control; Assessing the Effects of Weapons of Mass Destruction on People, Animals, Foodstuffs, Plants, Fodder, and Sources of Water; Protection of Same; Rendering First Aid and Mutual Aid in Time of Disaster; Responses of the Rural Population to Threat of Attack and to Various Civil Defense Signals; Civil Defense Plan for a Rural District; Executing the Civil Defense Plan on a Collective or State Farm; How Formations of a Rural County, Collective Farm, or State Farm Perform Rescue Work in a Stricken City; Mechanical Equipment Used for Decontamination, Plant Protection, and Veterinary Treatment of Animals; and Training the Rural Population in Civil Defense. (E.R.B.)

26786 EFFECTS OF FALLOUT IN AGRICULTURE. Hall, R. A. (Dept. of Agriculture, New South Wales). Civil Def. Bull.; 12: No. 3, 28-32(Jul 1970).

A brief account is given of some procedures to be taken for food conservation following a nuclear attack. Acceptable fallout dosages to cattle and other farm animals, with resultant distribution within livestock of long half life fission products, ^{89}Sr, ^{90}Sr, ^{137}Cs, ^{131}I, are considered. Factors influencing surface contamination of plants are considered, but more of a problem is the long term uptake of fission products from the soil. Storage prerequisites of grain and water and control of animal products are discussed. (Australia)

Legal Aspects

Refer also to abstract 26455.

26787 BUSHWHACKING, LICENSURE, AND SENATOR BARTLETT. Donnelly, Warren H. (Library of Congress, Washington, D. C.). Radiol. Technol.; 42: 248-58(Jan 1971).

The status in January 1971 of Federal legislation concerning standards for licensing x-ray technicians who operate diagnostic dental or medical equipment is reviewed. (C.H.)

Medicine

Refer also to abstracts 26205, 26777, and 28379.

26788 IONIZING RADIATION EXPOSURE FROM DIAGNOSTIC PROCEDURES. Kunz, E. (Inst. of Radiation Hygiene, Prague). Cas. Lek. Cesk.; 108: 1089-92(5 Sep 1969). (In Czech).

Contemporary estimates are discussed of the hazard of late somatic and genetic damages after exposure to small doses of ionizing radiation during diagnostic application of x rays. After an exposure to 1 rad, the probabilities of lesions in bone marrow, thyroid gland (adults), thyroid gland (infants), testes, and other tissues are as follows: 1.5×10^{-6} to 3×10^{-5}, 3×10^{-5} to 4×10^{-5}, 10^{-4}, 2×10^{-3} to 4×10^{-3}, and 3×10^{-5} to 6×10^{-5}, respectively. Data are presented on the frequency of x ray examinations in Czechoslovakia, taking into account various kinds of diagnostic procedure. The average genetically important dose and the mean dose in the bone marrow per person per year amount to 33 and 185 mrad, respectively. This cannot be considered acceptable since this exposure is very often unnecessary for achieving the informations desired. The exposure can be reduced not only by means of ingenious technical instruments (electronic amplifiers, magnetic records, etc) but also by using simple, easy, and well known methods (limitation of the area irradiated. shortening of the time of examination, proper development of the film, proper filtration, etc). (NSA of Czech.) (auth)

26789 PROCEEDINGS OF THE SIXTY-SECOND ANNUAL MEETING OF THE AMERICAN ASSOCIATION FOR CANCER RESEARCH, APRIL 8-10, 1971, CHICAGO, ILLINOIS. Weinhouse, Sidney (ed.). Proc. Amer. Ass. Cancer Res.; 12: 1-123(Mar 1970). (CONF-710405-(Absts.)).

Abstracts of 413 papers presented at the meeting are presented, including one paper on tritium carcinogenesis in mice and one paper on the effects of radiotherapy on peripheral blood lymphocytes in patients with breast carcinoma. (C.H.)

26790 GRUNDBEGRIFFE FUER DIE ANWENDUNG DER RADIOAKTIVITAET IN DER MEDIZIN. (Basic Concepts for the Use of Radioactivity in Medicine). Rach, Klaus. Stuttgart; S. Hirzel Verlag (1966). 52p.

Discussed are general properties of radioactive substances as well as calculation of dose, absorbed dose, and biologically effective dose. Equipment for detection of ionizing radiation is described especially with respect to γ spectrometry. Diagnostic application of radioisotopes is considered from the standpoint of functional disturbances, localization of tumors, and presentation of specific organs. Therapeutic use of radioisotopes is treated for open sources and also for sealed sources. Radiation burden to the patient and radiation hazards to medical personnel are discussed and practical procedures for radiation protection are outlined. (H.B.G.)

26791 CARCINOGENESIS: A BROAD CRITIQUE. A Collection of Papers Presented at the Twentieth Annual Symposium on Fundamental Cancer Research, Houston, Texas, 1966. Baltimore; Williams and Wilkins Company (1967). 786p. $16.00. (CONF-660314).

Separate abstracts were prepared for two papers. One abstract appeared previously in NSA (20: 20442). An additional 34 papers were presented on various aspects of carcinogenesis. (H.L.W.)

For an abstract of an individual paper see: 27111

Protective Substances

Refer also to abstracts 26640, 26650, 26895, 27014, 27068, and 27122.

26792 EFFECT OF THE TIME INTERVAL BETWEEN THE RADIOPROTECTIVE COMPOUND ADMINISTRATION AND THE BEGINNING OF IRRADIATION ON THE PROTECTIVE ACTION, EVALUATED ACCORDING TO THE WEIGHT LOSS OF THE SUBMAXILLARY GLAND. Vodicka, I.; Petyrek, P. (Military Medical Research and Postgraduate Inst., Hradec Kralove, Czech.). Sb. Ved. Pr. VLVDU Hradci Kralove; 43: 31-44(1969). (In Czech).

The effects of the time interval between an intraperitoneal application of cystamine, tetramethylcystamine, or AET and the beginning of whole-body γ irradiation at doses of 300 to 1000 R on the weight loss of the submaxillary gland in female rats were studied. With cystamine the maximum protective action was observed after 10 min. After 20 min the protective action disappeared. The dose reduction factor ranged between 1.25 and 2. For AET the maximum protective action was observed 35 min after application, whereas for tetramethylcystamine two maxima were manifested: at 30 and 85 min. (NSA of Czech.)

26793 ACUTE TOXIC AND RADIOPROTECTIVE EFFECTS OF CYSTAMINE COMBINED WITH EITHER AET OR SEROTONINE. Dostal, M. (Military Medical Research and Postgraduate Inst., Hradec Kralove, Czech.). Sb. Ved. Pr. VLVDU Hradci Kralove; 43: 93-185(1969). (In Czech).

Toxic and radioprotective actions of cystamine, cystamine + AET, and cystamine + serotonine mixtures in mice were compared. The animals were irradiated with ^{60}Co γ rays. LD_5, LD_{50}, and LD_{95} values were determined after application of individual radioprotective compounds. For these compounds, mean protective doses (ED_5, ED_{50}, ED_{95}) were determined. For both AET and cystamine ED_{95} corresponded to LD_5. Toxicity of cystamine was 1.26 times higher than that of AET, however, AET was not safer than cystamine since no significant difference was found between their ED_{95} and LD_5 values. Cystamine + AET mixtures (from 3 : 1 to 2 : 3) showed a toxicity significantly lower than cystamine and similar to that of AET. Their protective effect was slightly higher than that of cystamine and lower than that of AET. Neither the toxic nor the protective action of AET was affected by mixing it with cystamine. The cystamine + serotonine mixture (10 : 1) exhibited an insignificantly increased toxicity when compared with that of cystamine alone. Serotonine was capable of a protective effect greater by a factor of 7.34 than the effect of cystamine. The above mentioned mixture (10 : 1) had an effect 1.8 times greater than cystamine alone. (NSA of Czech.) (auth)

26794 CHANGES OF HEART FREQUENCY AND BLOOD PRESSURE IN RABBITS AFTER APPLICATION OF CYSTAMINE, AMINOETHYLISOTHIOURONIUM BROMIDE HYDROBROMIDE (AET), AND OF THEIR MIXTURE IN RADIOPROTECTIVE DOSES. Kuna, P.; Vokrouhlicky, L. (Military Medical Research and Postgraduate Inst., Hradec Kralove, Czech.). Sb. Ved. Pr. VLVDU Hradci Kralove; 43: 67-92(1969). (In Czech).

The influence of cystamine and AET on the heart frequency and blood pressure in rabbits was studied. Protective doses were preliminarily determined by applying these compounds and subsequently exposing the animals to 1000 r of ^{60}Co γ rays. In intact, unanesthetized rabbits infusion of cystamine and AET resulted in an immediate decrease in heart frequency. The most remarkable changes occurred in the second minute after starting the application. Neither decreasing the application rate nor changing pH (adjusting the NaOH normality from 2.5 to 7.5) resulted in any suppression of the effect. The mean arterial pressure was significantly depressed at 30 sec after starting the cystamine application. A recovery was observed in the next 30 sec. A deep hypotensia appearing immediately after an intravenous AET application (150 mg/kg of body weight) remained significant up to the 20th min. Combined application of cystamine + AET (1 : 1 or 1 : 3) resulted in similar effects. (NSA of Czech.)

26795 COMPARISON OF THE ACTION OF CERTAIN RADIOPROTECTIVE COMPOUNDS ON THE WEIGHT LOSS OF SUBMAXILLARY GLANDS WITH THEIR EFFECT ON RAT LETHALITY. Vodicka, I.; Petyrek, P. (Military Medical Research and Postgraduate Inst., Hradec Kralove, Czech). Sb. Ved. Pr. VLVDU Hradci Kralove; 43: 45-65(1969). (In Czech).

The radioprotective effectiveness of cystamine, tetramethylcystamine, AET, cysteine, 5-hydroxytryptamine, and noradrenaline was compared based on the following two parameters indicating the radiation injury: weight loss of the submaxillary gland on the 4th day after irradiation, and lethality over 30 days following the irradiation. Rats were exposed to 500, 700, 900, and 1000 R of ^{60}Co γ rays. Dose reduction factors (DRF) were calculated with respect to both parameters. For the individual compounds the DRF values were as follows: cystamine 1.29, 1.33; tetramethylcystamine 1.34, 1.29; AET 1.18, 1.08; cysteine 1.38, 1.32; noradrenaline 1.11, 1.12. (NSA of Czech.) (auth)

26796 BIOLOGICAL FACTORS AFFECTING THE RADIOPROTECTIVE EFFICIENCY OF S-2-[3-AMINOPROPYLAMINO] ETHYLPHOSPHOROTHIOIC ACID (WR-2721). $LD_{50(30)}$ DOSES. Yuhas, John M. (Oak Ridge National Lab., Tenn.). Radiat. Res.; 44: 621-8(Dec 1970).

The ability of graded single doses of WR-2721 to raise the x ray $LD_{50(30)}$ of adult females of four inbred mouse strains (A/J, BALB/cJ, C57BL/6J, and DBA/2J) was studied. Protective responses expressed as a dose reduction factor or DRF ($LD_{50(30)}$ treated/$LD_{50(30)}$ untreated) show significant strain differences. These differences are not correlated with differences in body weight (which are used to calculate the drug dose per animal) or with differences in inherent resistance (i.e., strains with low untreated $LD_{50(30)}$ values do not show higher or lower DRF values than strains with high untreated $LD_{50(30)}$ values). However, the differences do correlate with differences in tolerance to the toxic side effects of the drug. Both radiosensitive (A/J) and radioresistant (DBA/2J) strains that are sensitive to the toxic side effects of the drug show a rapid increase in the DRF as a function of drug dose, whereas the radiosensitive (BALB/cJ) and radioresistant (C57BL/6J) strains that are resistant to the toxic side effects of the drug show a less rapid increase. It was shown that the plasma acid phosphatase activity and the toxicity of this drug are inversely correlated in these strains. Since removal of the phosphate in the plasma would reduce cellular permeability of the drug, the association of high acid phosphatase activity, low toxicity, and relatively low protection is not unexpected. (auth)

26797 GRADUAL DEVELOPMENT OF RADIOPROTECTION IN HeLa S_3 CELLS DURING TREATMENT WITH β-MERCAPTOETHYLGUANIDINE. Sato, Fumiko; Shikita, Mikio; Terasima, Toyozo; Akaboshi, Sanya (National Inst. of Radiological Sciences, Chiba, Japan). Radiat. Res.; 44: 660-9(Dec 1970).

β-Mercaptoethylguanidine Br · HBr (MEG) was less effective than cysteamine (MEA) in protecting HeLa S_3 cells against x irradiation. Protection by MEG developed gradually with time of incubation, whereas the action of MEA was very rapid. Low temperature reduced the development of protection in the cases of MEA and MEG, but to a larger extent in the latter case. Washing of the MEA-treated cells resulted in a rapid decay of the protective potency. On the other hand, MEG-treated cells remained similarly protected for 15 min after removal of MEG from the culture medium. N,N′-Dimethyl derivative of MEG was less protective than MEG. Prolonged incubation did not improve the activity of the dimethyl MEG. Experiment with the use of ^{14}C-labeled MEG showed that the time course of development of protection closely resembled the time course of radioactivity incorporation into the cells. After the cells were incubated with ^{14}C-MEG, distribution of radioactivity among subcellular particles was examined. Approximately one third of the radioactivity was found in the nuclear fraction. A large portion of this nuclear radioactivity was not extractable with acid. (auth)

26798 EFFECTS OF NOVOCAIN ON THE ISOLATED PERFUSED HEART OF RATS AFTER X-IRRADIATION. Martinkova, J.; Grossmann, V.; Goutier, R. (Charles Univ., Hradec Kralove, Czech. CEEN, Mol, Belgium). Strahlentherapie; 141: 119-25 (Jan 1971).

An increase in the depressive action of novacain on the pulse rate was observed in an isolated rat heart after an x-ray whole-body irradiation with a dose of 600 or 1000 R. In both cases, the changes became manifest as early as 24 hours after irradiation. On application of a lower dose of radiation, the changes in the reactivity of the irradiated heart were normalized towards the sixth day. At the same time, a decreased activity of pseudocholinesterase as an enzyme playing an important role in novocain biotransformation was confirmed both in the myocardium and in the blood serum of irradiated rats. (auth)

26799 STUDIES OF PROTECTIVE EFFECT OF INOSINE AGAINST RADIATION INJURY. Ueda, Hiroshi (Kobe Univ., Japan). Nippon Igaku Hoshasen Gakkai Zasshi; 29: 1465-73 (Apr 1970). (In Japanese).

The mechanism of the protective action of inosine against γ radioinduced injuries of stem cells, especially with reference to the site of the action, was investigated from the standpoint of cell kinetics. When injury of the function of bone marrow induced by irradiation was analyzed in cell groups in vivo, the inhibition of the thrombocyte content and the increase of 5-hydroxytryptamine content was observed in peripheral blood. It is suggested that when the interval of irradiation is selected properly, the action of inosine is increased. Inosine was used clinically for the protection against the side effects of fractionated γ irradiation used for therapy of lung cancer. A remarkable effect was obtained, based on observations of bone marrow function. (Japan)

26800 TEMPORAL COURSE OF GAS METABOLISM AND RADIOPROTECTIVE EFFECT AFTER APPLICATION OF AET, SEROTONINE, NATRIUM-FLUORO-ACETATE, AND HISTAMINE IN MICE. Misustova, J.; Novak, L.; Hosek, B. (Tschechoslowakische Akademie der Wissenschaften, Brno). Strahlentherapie; 141: 126-31(Jan 1971). (In German).

The time behavior of respiratory exchange, body temperature, and radioprotection after application of protective doses of AET, histamine, serotonin, and sodium fluoroacetate was studied in male mice of H-strain. It was found that a time correlation exists between the inhibition of oxygen consumption and the rise of protection in all studied substances. The decrease of body temperature as a consequence of the inhibition of respiratory exchange is one hour delayed. From a comparison of the duration of protection and the duration of the decrease of oxygen consumption mainly for histamine and FAc, it follows that the rise of protection begins contemporary with the fast decrease of the respiratory exchange. It is supposed that this sudden change should have the greater

XUN

significance for the degree of protection than the value of decrease alone. (auth)

26801 FURTHER STUDIES ON PROTECTION OF DNA AGAINST IONIZING RADIATION. Kollmann, George; Castel, Norman; Shapiro, Bernard (Albert Einstein Medical Center, Philadelphia). Int. J. Radiat. Biol.; 18: 587-94(1970).

The protection of irradiated DNA against structural damage (measured by changes in molecular weight) and against functional damage (measured by DNA primer activity, RNA chain-length, and the effect of irradiated DNA on unirradiated DNA primer activity in enzymatic RNA synthesis) was studied. Bis(2-guanidoethyl) disulfide (GED) gave good protection against both structural and functional damage. Pentamethylene diguanidine (PMDG), which has no radical scavenging group, was not protective and cystamine, which shows less binding than GED to DNA, gave weak protection against functional damage. The mechanism of protection postulated is localized radical scavenging. (auth) (UK)

26802 INFLUENCE OF SUBSTANCES WHICH CHANGE THE RATE OF DEPOLYMERIZATION OF A COLLAGEN GEL ON ITS RADIOSENSITIVITY. Van Caneghem, P.; Lapierre, Ch. M. (Univ., Liege). Compt. Rend. Soc. Biol.; 164: 910-13(1 Dec 1970). (In French).

Glutaraldehyde and pyridoxal, which greatly delay the redissolution of gelified collagen, have only a pseudoprotective effect, unlike substances carrying thiol groups that are true protectors of collagen in solution against the polymerizing action of x rays. In the same way, borohydride and hydrazine, which greatly accelerate clarification, are pseudosensitizers. Penicillamine seems to have a combined effect. These results can be explained by assuming that the latter reagents act on bonds other than those induced by x rays and protected by thiols. (France)

26803 EFFECT OF METHYLENE BLUE ON LACTIC DEHYDROGENASE LEVEL AND LACTIC DEHYDROGENASE ISOENZYMES OF RATS EXPOSED TO GAMMA IRRADIATION. Sang, Y. N.; Seung, H. C. (Kyung Hee Univ., Seoul). Annot. Zool. Jap.; 43: No. 2, 79-87(Jun 1970).

Albino rats were given single 360 rad doses of whole-body gamma radiation 28 to 32 minutes following an intraperitoneal injection of physiological saline or methylene blue (38 mg/kg). Lactic dehydrogenase (LDH) activity in serum and LDH isoenzymes in serum, liver, heart, and testis were determined at various time intervals after exposure. Methylene blue delayed the LDH rise at 15 and 64 hours after exposure. The increase in serum LDH level after exposure is a reflection of an immediate increase in the H-type, band one of LDH isoenzymes. The protective action of methylene blue against the pathological effects of gamma irradiation in rats is discussed. (auth) (Japan)

26804 POSSIBLE EXISTENCE OF ANTIRADIOPROTECTIVE EFFECT OF CATECHOLAMINES. Kulinskii, V. I. (Inst. of Postgraduate Medical Training, Kharkov). Byull. Eksp. Biol. Med.; 71: No. 1, 31-4(Jan 1971). (In Russian).

During the irradiation of mice with a dose of 806 Rad, isadrine (N-isopropylnoradrenaline, 2.3 mg/kg) significantly reduced the antiradiation effect of high doses of noradrenaline (1.84 mg/kg) and mesatone (phenylephrine, 8.2 mg/kg). This effect was completely eliminated by anapriline (propranolol, 8.7 mg/kg). Anapriline potentiated the radioprotective effect of noradrenaline (0.92 mg/kg—from 28 to 87%) and adrenaline (1 mg/kg), but not mesatone. A hypothesis is presented to the effect that catecholamines are endowed with an antiprotective action realized via beta$_1$-receptors. Blocking of this action revealed the potential prophylactic activity. A combination of dibenamine, anapriline and noradrenaline produces a high protective effect (73%) with a low toxicity (the dose of noradrenaline employed was 320 times lower than LD_{50}). (auth)

26805 MECHANISM OF ACTION OF RADIATION PROTECTIVE AGENTS: IN VIVO DISTRIBUTION AND METABOLISM OF CYSTEAMINE-S-PHOSPHATE (MEAP). Shapiro, Bernard; Kollmann, George; Martin, David (Albert Einstein Medical Center, Philadelphia). Radiat. Res.; 44: 421-33(Nov 1970).

The distribution and chemical nature of the protective agent in various tissues of 8 to 10 wk old C57 BL/6J male mice, given a protective dose of ^{32}P- and ^{35}S-labeled cysteamine-S-phosphate (MEAP) of high specific activity were studied. Results were obtained at 10, 20, and 30 min after an intraperitoneal injection of 400 mg/kg MEAP. Distribution was measured by concentration of the labels in the various tissues. Metabolism was studied by chromatography of tissue homogenates. The tissues contained mainly cysteamine-cystamine, some protein-bound cysteamine, and some MEAP at 20 min, the time of maximum protection. At 30 min when little MEAP was present in the tissues, the animals were still protected. Taurine and sulfate were the main excretory products and only 7.4% ^{35}S was excreted by 30 min. The results indicate that protection is due to the dephosphorylation of MEAP and generation of cysteamine-cystamine in the tissues. The advantages of MEAP are: the temporary masking of the sulfhydryl group, thus reducing loss and toxicity due to binding of the agent before it reaches the tissues, and the generation of the protective form at the critical site. Such compounds with different SH-masking groups, which can be metabolized off in certain tissues, offer interesting possibilities for differential protection in tumor bearing animals. (auth)

26806 ANTI-INFLAMMATORY EFFECT OF BENZYDAMINE. Harrison, R. G.; O'Donnell, P. J. (General Hospital, Northampton, Eng. Bayer Products Co., Surbiton, Eng.). Toxicol. Appl. Pharmacol.; 17: 355-60(Sep 1970).

A study of 1-benzyl-3-dimethylaminopropoxy-1H-indazole hydrochloride (Benzydamine), claimed to possess analgesic and anti-inflammatory properties, was carried out in albino rabbits to determine anti-inflammatory action on x radioinduced skin inflammation. Benzydamine, given either intravenously or orally, in doses considerably in excess of the therapeutic range, exerted only a moderate suppressive action on the inflammatory response to ionizing radiation in terms of a reduction in increased vascular permeability of rabbit skin. Benzydamine would appear to have a weaker anti-inflammatory effect than well documented drugs such as aspirin and phenylbutazone. The results with laboratory animals did not correlate with the good effects that have been claimed in clinical studies. No changes in hepatic functions or hematopoiesis were noted in a 7-week period of chronic administration of Benzydamine. (auth)

26807 RADIOPROTECTIVE EFFECT OF AET AND SEROTONIN IN GROWING RATS, IRRADIATED FRACTIONALLY WITH SMALL DOSES OF ROENTGEN RAYS. Nikolov, Iv.; Baev, I. Rentgenol. Radiol.; 8: No. 1, 90-6(1969). (In Bulgarian).

The radioprotective properties of AET (aminoethylisothiouronium bromide) and serotonin, in fractional daily irradiation of young rats with 27.5 Rad, in the course of 10 days, were studied. The animals were divided into 6 groups. The first group was treated with AET and irradiated with a total corporal dose of 275 Rad. The second group was treated with serotonin and irradiated in the same way. The third group was subjected to irradiation, only. Two groups were treated with AET and serotonin, without being irradiated. The last group was not treated with radioprotectors and was not irradiated. The weight of the growing animals between the 2nd and 5th m was used as an indicator of the radioprotective effect. The results showed that AET exhibited a protective effect in fractional sublethal irradiation, while serotonin did not. (Abst. Bulg. Sci. Med. Lit.)

26808 PHOTOSENSITIZING EFFECT OF TRISORALEN ON DNA SYNTHESIS IN HUMAN CELLS GROWN IN VITRO. Trosko, J. E.; Isoum, M. (Michigan State Univ., East Lansing). Int. J. Radiat. Biol.; 19: 87-92(1971).

Experiments were made to find the effects of 2537 Å and 3600 Å radiation on the incorporation of ^3H-thymidine into the DNA of control and trisoralen-treated human amnion cells (AV_3). Cells received an incident dose of 400 ergs/mm^2 of 2537 Å and 48×10^5 ergs/cm^2 of 3600 Å radiation. Although DNA synthesis was reduced in cells irradiated with 2537 Å light, trisoralen did not sensitize this inhibition. DNA synthesis in trisoralen-treated cells (2×10^{-5}M) was drastically inhibited by 3600 Å light at 8.2×10^4 ergs/mm^2 DNA synthesis in cells treated only with trisoralen was not altered. The incorporation of ^3H-thymidine into DNA of 3600 Å irradiated (2.4×10^5 ergs/cm^2) AV_3 cells was measured at the following concentrations of trisoralen: 0, 2×10^{-8}M, 2×10^{-7}M, 2×10^{-6}M, 2×10^{-5}M. The effect of various doses of 3600 Å radiation on trisoralen-treated cells (2×10^{-5}M) was measured four hours after irradiation. DNA synthesis was reduced to 5% of the unirradiated control by 2×10^4 ergs/mm^2. Trisoralen photoproducts did not appear to interfere with the uv induction of pyrimidine dimers, or with the excision step of the repair of uv induced pyrimidine dimers, but male dimers appeared to be excised in the cells with the trisoralen photoproducts in their DNA. (UK)

26809 INDUCED CELL PROLIFERATION AND THE INITIATION OF SKIN TUMOUR FORMATION IN MICE BY ULTRAVIOLET LIGHT. Pound, A. W. (Univ. of Queensland, Brisbane). Pathology; 2: 269-75(1970).

A single short exposure of the skin of mice to ultraviolet light did not produce any tumors, but a significant number of tumors developed when the exposure was followed by repeated applications of croton oil. Ultraviolet radiation therefore behaves as an initiating agent, resembling the action of some other carcinogens for the skin of mice. Treatment of the skin of the mice with acetic acid, xylene or croton oil 20 hours before irradiation

increased the number of tumors. It is considered that cells induced to proliferate are more susceptible to the carcinogenic effect of ultraviolet radiation than their normal counterparts. (Australia)

Radiation Sickness and Injuries

Refer also to abstracts 27024 and 27048.

26810 LOCAL THERAPY OF BLADDER RADIATION INJURIES. Bauer, K. M. Med. Welt.; No. 17, 790-2(25 Apr 1970). (In German).

Discussed are etiology, symptomatology, and diagnosis of various stages of radioinduced bladder inflammation. From a differential diagnostic standpoint, typical cystoscopic findings are discussed. For local therapy, the bladder was instilled alternately with two solutions. The first one contained hydrocortisone, Vitamin A, and sterile olive oil; the second contained the blood extract actihemyl. As demonstrated by endovesical photographs, excellent results were obtained in 32 patients. (H.B.G.)

26811 RADIATION ENTEROCOLITIS: A REPORT OF SEVEN CASES. SOME ASPECTS OF PATHOLOGY AND MANAGEMENT. Alp, M. H.; Seymour, A. E.; Grant, A. Kerr (Queen Elizabeth Hospital, Woodville, Australia). Aust. N. Z. J. Surg.; 40: 144-51 (Nov 1970).

A report of seven patients with radiation damage to the intestinal tract is presented. As a group, they exhibit the full spectrum of complications. The pathological and histological changes are described. Appropriate medical and surgical management is discussed. (auth) (Australia)

26812 STUDIES ON RADIORESTORATIVE CHEMICALS AND THEIR CLINICAL APPLICATION. Fukuda, Masasi; Abe, Mitsuyuki (Kyoto Univ.). Nippon Igaku Hoshasen Gakkai Zasshi; 30: No. 2, 178-83(May 1970).

From the clinical point of view, substances which are effective even if they are given after irradiation are more important than the radioprotective substances which are effective only when administered shortly before exposure. Research studies on radiorestorative substances showed that uridine monophosphate, vitamin B_6, and taurine have radiorestorative effects in the sense of an increase in the survival rate of irradiated mice when they are given after irradiation. The efficacy of these chemicals and the mechanisms of their action is discussed. Clinical application of these substances to radiation-induced leukopenia also are reported. (auth) (Japan)

26813 UROLOGIC MANAGEMENT OF INJURIES TO THE BLADDER AFTER GYNECOLOGIC RADIOTHERAPY. Lenz, P.; Meridies, R.; Schmitz, W. (Urologische Univ., Duesseldorf). Z. Urol. Nephrol.; 63: 411-6(Jun 1970). (In German).

During the decade from 1958 to 1968, 365 women were treated for bladder injury caused by radiotherapy of gynecological tumors. Both pathogenesis and clinical picture are described for early and late radiation damage to the bladder. As primary treatment, continuous perfusion of the bladder was performed with acetic acid solution of increasing concentrations. Of the 365 women, 163 were treated as hospital patients while the remaining were handled as out patients. In 72%, treatment caused objective improvement and subjective freedom from complaints. Surgical intervention became necessary in 43 patients. (H.B.G.)

26814 OPERATIVE UROLOGIC MANAGEMENT OF URETERAL INJURIES AFTER OBSTETRIC-GYNECOLOGIC INTERVENTION AND RADIATION. Lenz, P.; Meridies, R.; Schmitz, W. (Urologische Univ., Duesseldorf). Z. Urol. Nephrol.; 63: 423-9(Jun 1970). (In German).

During the past decade, 157 patients were surgically treated for ureter lesions originating from obstetrical and radiation procedures. In approximately two thirds of the patients, uretrocystoneostomies were performed. For plastic operations in the lower third of the ureter, the extraperitoneal approach was used exclusively. The anastomosis was established by forming an oblique submucosal channel. Implantations were successful in approximately 80% of the cases. Failures resulted from insufficiency of the anastomosis, recurrent carcinoma, or severe intractable infection. (tr-auth)

Radiodiagnosis

Refer also to abstracts 26455, 26486, 26557, 26676, 27036, and 27050.

26815 (BRH/DMRE-71-2) X-RAY FLUOROSCOPIC SCREENS: HISTORY, CRYSTAL KINETICS, PRELIMINARY REPORT ON "AGING". Properzio, William S.; Trout, E. Dale (Bureau of Radiological Health, Rockville, Md.). Feb 1971. 49p. GPO $0.60.

A brief history is presented of the development and use of fluoroscopic screens for diagnostic radiography. It is pointed out that the incorporation of new types of phosphors in x-ray fluoroscopic screens has resulted in a reduction of the radiation dose to the patient by a factor of eight to ten. Results are included from a long-range study of factors that reduce the light output of fluoroscopic screens. (C.H.)

26816 RADIOGRAPHIC AND SCINTIGRAPHIC METHODS FOR THE STUDY OF HYDATIDS OF THE KIDNEYS. Sacco, M.; Fanelli, A. (Univ., Rome). Nunt. Radiol.; 34: Suppl. I, 57-66(1968). (In Italian).

The results from the combination of various methods of radiological examination of a case of left kidney hydatidosis were reported. The renal scintigraphic examination, little used up to the present even for the relative infrequency of the illness, supported the clinical diagnosis. The diagnosis was confirmed by surgery. (tr-auth)

26817 X-RAY BEAM PROFILES AND ORAL RADIOGRAPHY. Weissman, Donald D.; Feinstein, Richard B. (Univ. of California, Los Angeles). Oral Surg., Oral Med., Oral Pathol.; 31: 546-55(Apr 1971).

Methods for reduction of the dose of x radiation received by tissues of the mouth during dental radiography are described. The use of rectangular field instrumentation, high-speed films, open-end cones for the control of scattered radiation, and an x ray beam of not more than three inch diameter at the cone are recommended. (C.H.)

26818 USE OF ^{99m}Tc FOR CEREBRAL SCINTIGRAPHY. Cavallo, V.; Leccisotti, A.; Perria, C.; Davini, V. (Univ., Sassari, Italy). Nunt. Radiol.; 34: Suppl. I, 3-20(1968). (In Italian).

The results of the scintigraphic examination with ^{99m}Tc of 130 patients in which there were 34 cases of infected cerebral lesions were reported. Twenty-nine of these had definite areas of pathological accumulation of the radioisotope. In 5 of these the scintigraphic results were negative, and the diagnosis was made on the basis of neuroradiological examinations. Of the 29 patients with pathological accumulations of the radioisotope, the radioisotopic results and the neuroradiological examinations agree; in the other 4 patients the neuroradiological examination was normal. On the basis of literature data and the present examinations it was concluded that the cerebral scintigraphy with ^{99m}Tc is a simple and efficient diagnostic method, complementary to, but not substituting for the traditional neuroradiological examination. It can give useful data for surgical and radiation therapy for neoplasms. It is elective for the detection of infected vascular lesions and metastases. (tr-auth)

26819 DUAL RADIOISOTOPIC METHOD FOR DIAGNOSIS OF PULMONARY EMBOLISM. Isotop. Radiat. Technol.; 8: 346-7 (1971).

A simple and sensitive method to aid in the diagnosis of pulmonary embolism by distinguishing it from other causes of perfusion abnormality is described that consists of the simultaneous scanning of pulmonary arterial blood flow with ^{131}I or ^{113m}In and ventilation rate with ^{133}Xe. The dual procedure is more accurate than the determination of blood flow alone. Results of tests on 20 subjects, ten of whom had documented pulmonary embolism in which the embolic lung was underperfused and well ventilated, five patients with other pulmonary diseases that caused abnormalities of ventilation equaled or exceeded those of perfusion, and five controls are reported. The method is simple to perform and gives a low radiation exposure to the patient so that it may be repeated to follow the course of disease or the efficacy of treatment. The total time for perfusion scanning is 45 min and for ventilation scanning, 30 min or less. (C.H.)

26820 PATTERNS FOR DIFFERENTIATION OF POSTERIOR FOSSA NEOPLASMS AS DETECTED BY BRAIN SCANS. DeLand, Frank H.; James, A. Everette Jr.; Wagner, Henry N. Jr. (Johns Hopkins Medical Institutions, Baltimore). Nucl.-Med.; 9: 303-16(31 Dec 1970).

The histological characteristics of neoplasms that occur in the posterior cranial fossa can often be predicted by a knowledge of the patient's age and the specific anatomical location of the tumor. Dividing the posterior fossa into midline, cerebella fossa and cerebellopontine angle provides a scheme to characterize abnormal accumulations or radioactivity according to their anatomical locations. Midline lesions arise from bases activity on the lateral view and are in the midline on the posterior view.

Lesions of the cerebellar fossa may be adjacent to but do not appear to arise from the basal structures and are not in the midline. Cerebellopontine angle tumors are adjacent to and appear to arise from the normal radioactivity at the skull base but lie lateral to the midline. The expected distribution of histological types of neoplasms in each area according to age is discussed. (auth)

26821 SCINTIGRAPHIC LOCALISATION OF THE KIDNEYS FOR PERCUTANEOUS RENAL BIOPSY. Zimacek, J.; Mydlik, M.; Pokorna, I.; Melnicak, P.; Mrinak, J. (Safarik-Univ., Kosice, Czech.). Nucl.-Med.: 9: 317-26(31 Dec 1970). (In German).

Reported is the scintigraphic localization of the kidneys, prior to percutaneous renal biopsy, using ^{197}Hg Neohydrine (Chlormerodrine). This method was performed successfully in 37 patients and was found to be very accurate. The method has no inconvenience for the patient and, in addition, it has the advantage that it can be performed without immediate connection with renal biopsy. Effectiveness and usefulness of the scintigraphic visualization in renal insufficiency are discussed and the advantages as well as disadvantages of this method are compared with other diagnostic approaches, commonly used for kidney localization in percutaneous renal biopsy. (auth)

26822 DIAGNOSTIC VALUE OF THE QUOTIENTS OF PRECORDIAL OVER PREPULMONARY COUNTING RATE FROM Na^{131}I IN NORMAL PERSONS AND PATIENTS WITH CARDIAC DISEASE. Bluemchen, G.; Lenz, F.; Hoffmann, G. (Univ., Freiburg i. B.). Nucl.-Med.: 9: 326-40(31 Dec 1970). (In German).

Nine patients with myocardial infarction, 9 healthy students, 7 patients with coronary insufficiency, and 17 patients with peripheral arterial disease but without cardiac disease received 20 μCi of Na ^{131}I intravenously. Its accumulation was determined precordially and over the right half of the chest for several days. In comparison with the normal subjects, the precordial counting rate in the patients with myocardial infarction was not increased. The quotient of precordial over prepulmonary counting rate, tested statistically up to 35 hours after injection, is useless in the differential diagnosis of myocardial infarction. Small differences in methodology might be responsible for the difference between these negative results and the positive findings reported by Dreyfuss and coworkers. (auth)

26823 THYROID TUMOUR SCANNING WITH $^{197}HgCl_2$. PRELIMINARY NOTE. Artagaveytia, Daniel; Degrossi, Osvaldo J.; Pecorini, Victorio (Hospital Escuela Jose de San Martin, Buenos Aires). Nucl.-Med.: 9: 350-3(31 Dec 1970).

Thirteen patients with cold thyroid nodules were scanned after administration of $^{197}HgCl_2$. All nodules were examined histologically. Of the 8 nodules that had concentrated the radionuclide, 7 proved to be carcinomatous and one to be a fetal adenoma. The remaining 5 nodules with a negative scan were all colloid adenomata. These findings suggested that $^{197}HgCl_2$ may be a valuable scanning agent for the detection of malignant tumors. (auth)

26824 INTERPRETATION OF BRAIN SCANS BY COMPUTER ANALYSIS. Popham, Mary G. (National Hospital for Nervous Diseases, London); Bull, J. W. D.; Emery, E. W. Brit. J. Radiol.: 43: 835-47(Dec 1970).

A method for the analysis of radionuclide (^{197}Hg chlormerodrin) brain scans is described. Lateral scans were compared area for area with a mean pattern derived from the scans of clinically normal patients. In making the comparison, allowance was made for the errors arising both from the finite number of counts recorded in each area and from the patient to patient variation, and the latter was shown to be acceptably small. Antero-posterior and postero-anterior scans were also analyzed by making a direct comparison of the counts occurring in symmetrically placed 2 × 2 cm areas on opposite sides of the head. Using criteria that give 5% false positive scans, the analysis yielded no false negatives in visually abnormal scans; detected nine abnormalities in 35 scans that were judged normal by a group of observers, but related to abnormal subjects, and made 23 correct assessments in 30 scans that the observers found equivocal. (auth) (UK)

26825 MEASURING THE EFFECTIVE RENAL PLASMA FLOW BY MEANS OF WHOLE-BODY CLEARANCE OF ^{131}I-HIPPURIC ACID. Pixberg, H. U.; Just, G. (Medizinische Hochschule, Hanover). Deut. Med. Wochenschr.: 96: 156-61 (11 Jan 1971). (In German).

Whole-body clearance was obtained by a new catheterless method using ^{131}I. It measures the temporal decrease of the cleared substance not only in the vascular space but also in the body as a whole after intravenous injection. From the differential ratio and plasma concentration 20 and 25 minutes after injection the clearance can be calculated by Fick's principle. If, instead by whole-body counters, the measurement is made using relatively small catheters, different levels of the catheter must be taken into account. Furthermore, the time interval of 20 and 25 minutes until blood samples are taken must be strictly observed, because the clearance formula is valid only in this range. Combined with radioisotope nephrography quantitative results can be obtained for effective renal plasma flow and other renal functions. Since the method is simple and without danger, whole-body clearance is highly suitable for nephrological diagnosis. (auth)

26826 UNILATERAL DETERMINATION OF EFFECTIVE RENAL PLASMA FLOW BY RADIOISOTOPES. May, P.; Oberhausen, E.; Kirsch, W. (Univ., Homburg, Ger.). Deut. Med. Wochenschr.; 96: 152-5(22 Jan 1971). (In German).

A new method of measuring effective renal plasma flow in each kidney separately is described. It uses external gamma radiation after injection of ^{131}I-hippuran. Comparison of this method with the classical PAH clearance in 17 patients demonstrated good agreement. Separate unilateral measurement of renal plasma flow by radioisotopes, used together with urographic methods, provides important clues for choosing conservative and surgical treatment in case of unilateral renal disease. (auth)

26827 POSSIBLE CARCINOGENIC EFFECTS OF RADIATIONS ON THE UTERUS. Bird, C. C.; Willis, R. A. (Dept. of Pathology, Aberdeen, Scotland. Dept. of Pathology, London). Brit. J. Cancer; 24: 759-68(Dec 1970).

The carcinogenic effects of radium and x-rays on the rat uterus were investigated. Malignant endometrial tumors, usually adenocarcinomas, were produced in a small proportion of treated rats. One rat treated with x-rays developed an adeno-sarcoma (possibly carcino-sarcoma) of the endometrium. Benign mixed polypoidal endometrial tumors occurred also in radium and x-ray treated rats and in non-radiated controls; radiation increased the incidence of these tumors and may have induced malignant transformation in some. The incidence of lymphosarcomas and mammary tumors in the strain of rat used appeared to be influenced by radiation treatment. Review of the literature of human cases of mixed uterine tumors showed that in women over 40 years, more than one-fifth of the reported cases had a history of previous pelvic radiation; with other kinds of uterine malignancy a history of prior radiation treatment was considerably less. (auth) (UK)

26828 CORRELATION BETWEEN BRAIN TUMOR DETECTABILITY ON BRAIN SCAN AND PROTEIN LEVELS OF THE SPINAL FLUID. Pinsky, Steven M.; Hoffer, Paul B.; Flom, Richard; Quinn III, James L.; Gottschalk, Alexander (Univ. of Chicago, Argonne Cancer Research Hospital, Chicago, Chicago Wesley Memorial Hospital). Radiology; 98: 672-3(Mar 1971).

Fifty-eight patients with brain tumors had spinal fluid protein determinations and pertechnetate brain scans before surgery. Twenty-five patients had elevated spinal fluid protein levels; of these, 22 (88%) had positive scans, 33 had normal protein levels, and 17 (52%) had positive brain scans. There is a positive correlation between brain tumor detectability on brain scans and spinal fluid protein levels. (auth)

26829 NUKLEARMEDIZIN FUNKTIONSDIAGNOSTIK. (Diagnosis of Organ Function in Nuclear Medicine). Emrich, Dieter. Stuttgart; Georg Thieme Verlag (1971). 379p. DM 110,-. Intercontinental Medical Book Corporation, New York.

The general section discusses instrumentation, preparation of radiopharmaceuticals, kinetics of radionuclides, dosimetry in biological radiation effects studies, and electronic evaluation of data. The special section considers hematology, radioimmunological procedures for hormone assay, iodine metabolism, steroid metabolism, pancreatic function, cardiology, lung examinations, gastroenterology, water and electrolyte balance, and renal function. In a final section, techniques and applications of whole-body counting are discussed. (H.B.G.)

26830 CHANGES IN LIVER AND SPLEEN SCANS OF PATIENTS DURING TREATMENT WITH TWO HYPOLIPIDEMIC DRUGS. Dujovne, Carlos A.; Strauss, Harry W. (Johns Hopkins Univ., Baltimore). Radiology; 98: 682-4(Mar 1971).

Liver and spleen scans using ^{99m}Tc-labeled sulfur colloid were performed in 5 patients with hyperlipoproteinemia at the time of clofibrate, nafenopin, or placebo treatment. No clinical or laboratory hepatic abnormalities were detected except in one patient. A shift in colloid distribution was found during treatment with active drugs in 3 patients. This was not present when these patients were treated with a placebo. (auth)

26831 RADIATION DOSE WITH THE ORTHOMETRIC VIEW IN X-RAY PELVIMETRY. De Villiers, P. D. (Verwoerd Hospital, Pretoria). S. Afr. Med. J.; 44: 820-2(11 Jul 1970).

XUM

The use of the Thoms's view in x ray pelvimetry should be considered a medical crime. On the other hand, the risk to the pregnant mother of withholding an x ray examination where indicated, is probably 20 times as great as the radiation hazard. The orthometric inlet view reduced radiation by 95% compared with Thoms's view. (auth)

26832 SCINTIGRAPHY OF CARCINOMA USING $^{197}HgCl_2$. Canossi, G. C.; de Maria, D.; Romagnoli, R. (Univ., Modena, Italy). Nunt. Radiol.; 34: 1347-75(Nov 1968). (In Italian).

The results obtained with mercury bichloride, $^{197}HgCl_2$, in scintigraphic scanning of 147 malignant and benign neoplasms are reported. The $^{197}HgCl_2$ was intravenously injected at an average dose of 1 mCi and the scintigraphy was done after 24 to 40 and 48 to 60 hrs. The mercury accumulated progressively in tissues which had alterations of the cellular membrane and a higher content of mitochondrial sulfhydryl groups. In benign tumors the radioactivity declined linearly to the background and in malignant tumors it gives a positive image of the tumor after 48 hrs. In 37 benign neoplasms of various types and locations, there was a positive scintigraph) after 48 hrs in only one case of fibrocystic mastopathy. In 110 malignant neoplasms, the scintigraph was positive up to the 60th hr and beyond with the exception of one small mammary scirrhus and three renal sites where the behavior of the $^{197}HgCl_2$ was similar to that of chloromerodrin, giving negative images. The scintigraphy with $^{197}HgCl_2$ appeared suitable for routine use in a radioisotopic diagnostic center. It can resolve with sufficient accuracy clinical-radiological questions on the benign or malignant nature of neoformations, especially when they are located in the facial, cervical, and thorax regions. (tr-auth)

26833 DETECTION OF POSTOPERATIVE BRONCHOPLEURAL FISTULAS BY RADIONUCLIDE FOG INHALATION. Greyson, N. D.; Rosenthall, L. (Montreal General Hospital). Can. Med. Ass. J.; 103: 1366-8(19 Dec 1970).

Postoperative bronchopleural fistulas may be demonstrated quickly and safely by inhalation of nebulized ^{99m}Tc-albumin, or other similar radiopharmaceuticals. Posterior scintiphotographs of the distribution of the inhaled radioactive material were obtained with the γ scintillation camera while the patient was in the upright and lateral decubitus positions. The observation of radioactive material in the pleural cavity indicated an abnormal communication. The radiation-absorbed doses for lung and total body were well within acceptable limits when a ^{99m}Tc tag was used. About 15 min were required to complete this relatively safe diagnostic test. (auth) (Canada)

26834 INVESTIGATION OF THE USE OF A DIGITAL COMPUTER FOR PROCESSING RADIOISOTOPE SCAN DATA. McClain, William James. Knoxville, Tenn.; Univ. of Tennessee (1969). 221p. University Microfilms Order No. 70-17,835. Thesis.

Radioisotope scanning, or the in vivo mapping of the distribution of a radioisotope-labeled drug in a human body, is a very useful diagnostic procedure in the field of nuclear medicine. Activity maps, displayed as two-dimensional plots with varying intensities, provide a means by which clinicians can detect abnormal or malfunctioning tissue in vital organs. Two major factors that limit the detectability of tumors in a scan display are the response of the imaging system and the statistical variations in the detected counts. The former results from the low-frequency response of the detector; the latter from the statistical nature of photons emitted when radioisotope concentrations are necessarily low to minimize damage to healthy tissue. The effectiveness of a digital computer in overcoming these limitations was studied. The investigation included the development of the hardware and software required for on-line computer operation. The theoretical background and results of the use of six algorithms are included. Common data obtained from a scan of the standard IAEA phantom having a fifty percent tumor-to-background contrast were used. The data were displayed on a laboratory cathode-ray oscilloscope to provide a comparison of the detectability of tumors in the processed data. The results proved that the information content of radioisotope scans can be enhanced by digital-computer processing. Proper implementation of the computer in this application, however, requires an on-line operation, immediate display, and specialized resources. The specialized computer resources are necessary to permit selection of algorithms that perform tasks as needed. (Diss. Abstr. Int., B)

26835 IONIC ^{135m}Ba: A NEW AGENT FOR BONE SCANNING. Hosain, Fazle; Syed, Ibrahim B.; Wagner, Henry N. Jr.; Poggenburg, J. K. (Johns Hopkins Medical Institutions, Baltimore. Oak Ridge National Lab., Tenn.). Radiology; 98: 684-6(Mar 1971).

^{135m}Ba was produced by an n,γ reaction using enriched ^{134}Ba. It has a half-life of 28.7 hr and emits 268 keV photons. This agent, in the ionic form, was evaluated as a bone seeking element. Scans between one and two days after injection were suitable for the localization of bone lesions. ^{135m}Ba is an improvement over ^{85}Sr in scanning. (auth)

26836 TRAUMATIC INTRAPERICARDIAL HERNIATION OF THE TRANSVERSE COLON MASQUERADING AS A PERICARDIAL EFFUSION ON THE SCAN. Alexander, D. C.; Torrance, D. J. (Univ. of California, Los Angeles, Harbor General Hospital, Torrance, Calif.). Radiology; 98: 627-8(Mar 1971).

A case of traumatic rupture of the diaphragm with herniation of the transverse colon and omentum into the pericardial sac is presented with scan findings. Subsequent (postoperative) development of pericardial effusion made possible a comparison of scans in intrapericardial hernia and pericardial effusion. In this instance, they are identical. (auth)

26837 COMBINED INFERIOR VENA CAVOGRAPHY, ILIAC VENOGRAPHY, AND LUNG IMAGING WITH ^{99m}Tc ALBUMIN MACROAGGREGATES. Rosenthall, Leonard (Montreal General Hospital). Radiology; 98: 623-6(Mar 1971).

A technique is described for visualizing the iliac veins, inferior vena cava, and lungs to locate thrombi and pulmonary thromboembolism. Bilateral simultaneous injection of the pedal veins with ^{99m}Tc macroaggregates of human serum albumin and rapid sequence pictures of the abdomen with a gamma ray scintillation camera are followed by lung scintiphotography using the same injected material. The method was successful in uncovering occult thrombi and pulmonary thromboembolism and is recommended as a screening and monitoring procedure for patients who may have these difficulties. (auth)

26838 SCINTISCANNING WITH A ^{99m}Tc PERTECHNATE PERFUSION. Scopinaro, G.; Sanguineti, M. (Galliera Hospitals, Genoa). Minerva Radiol.; 15: 179-86(Jul-Aug 1970). (In Italian).

Blood pool or organ vascularization scintiscanning requires the use of a tracer that will remain in the vascular compartment for a sufficiently long time and with constant activity. The scintillation counter is the most suitable instrument for this type of exploration owing to the very short time required. It is also suitable for the use of ^{99m}Tc pertechnetate. A method characterized by the slow perfusion of this substance and the use of conventional linear scintiscans giving information similar to that provided by the scintillation chamber is described. (auth)

26839 DURATION OF RADIOACTIVITY IN THE MILK OF A NURSING MOTHER FOLLOWING ^{99m}Tc ADMINISTRATION. Vagenakis, Apostolos G.; Abreau, Cynthia M.; Braverman, Lewis E. (St. Elizabeth's Hospital, Boston. Tufts Univ., Boston). J. Nucl. Med.; 12: 188(Apr 1971).

A 24-year-old married white female developed seizures during an otherwise uneventful pregnancy. Five weeks after delivery of a normal baby, a brain scan was carried out following the intravenous administration of 10 mCi of ^{99m}Tc-sodium pertechnetate. Since she was nursing at the time of the brain scan, milk was extracted from the breasts by a breast pump for four days following the administration of the sodium pertechnetate and the amount of radioactivity was immediately determined. There was a significant amount of radioactivity in the milk 22 hr after the administration of the radioactive pertechnetate. Because of the short half-life of ^{99m}Tc very little radioactivity was found in the sample obtained 46 hr after the brain scan. No radioactivity was detectable at 70 and 94 hr. (C.H.)

26840 EVALUATION OF ^{99m}Tc-DTPA PREPARED BY THREE DIFFERENT METHODS. Atkins, H. L.; Cardinale, K. G.; Eckelman, W. C.; (and others) (Brookhaven National Lab., Upton, N. Y.). Radiology; 98: 674-7(Mar 1971).

Comparison of the biological behavior of three DTPA compounds incorporating technetium-99m showed that only two of these compounds are true chelates. The third compound, produced with a kit, is similar in behavior to that of the renal scanning agent ^{99m}Tc–Fe-ascorbic acid. (auth)

26841 STUDY OF REGIONAL LUNG FUNCTION TESTS USING THE ^{131}I AND ^{133}Xe DOUBLE ISOTOPE TRACER METHOD. Ogino, Noriyuki (Tokyo Medical Coll.). Nippon Kyobu Geka Gakkai Zasshi; 18: 202-20(Mar 1970). (In Japanese).

A mixed-solution of ^{131}I and ^{133}Xe was injected into the cubital vein of patients following breath holding. One scintillation counter was used to count the radioactivity of ^{131}I, and another counter was synchronized for counting radioactivity from ^{133}Xe. In general, ^{131}I circulated in the pulmonary capillaries without escape from circulating blood and ^{133}Xe was diffused to the alveoli through the capillary walls. It was concluded that circulatory and respiratory function, including alveolar diffusion, could be measured by means of the double tracer method using ^{133}Xe and ^{131}I. The value of the

method as a means of measuring regional lung function preoperatively, to decide the limits for lung resection, and for the measurement of lung function following surgery is discussed. (Japan)

26842 SCINTIGRAPHY OF LUNG CANCER USING ^{203}Hg PRETREATED WITH GLUTATHIONE. Hara, Toshihiko; Hirata, Masanobu; Iio, Masaaki; Baba, Harukata (National Sanatorium of Nakano, Tokyo). Nippon Kyobu Rinsho; 29: 525-31(Jul 1970). (In Japanese).

The scintillation scanning of the lungs using radioactive mercuric chloride has been proved to be useful as a screening method for the detection of lung carcinoma. One of the difficulties for wide application of this method is the poor resolution of the scintigraphs caused by the high level of radioactivity in the blood. Mercuric chloride, when mixed with the equivalent amount of glutathione just before the intravenous injection, prevents binding of mercuric chloride with blood cells, and induces rapid and preferential uptake by malignant tissue. For the routine examination one millicurie of $^{203}HgCl_2$ is quite enough, and by this method the accuracy of scintigrams of lung cancer has been improved. Autoradiography, using lung sections resected from patients to whom ^{203}Hg-mercuric chloride and glutathione was administered a day before the operation, revealed that the radioactivity was localized solely in malignant lesions of the lung. (auth) (Japan)

26843 UNIQUE CASE OF AMEBIC ABSCESS OF THE LIVER. Cohen, Marvin B. (Veterans Administration Hospital, Sepulverda, Calif. Temple Hospital, Los Angeles). J. Nucl. Med.; 12: 192-5(Apr 1971).

Numerous reports have emphasized the exceptional value of hepatic photoscanning in helping to establish a diagnosis of an amebic abscess of the liver. Photoscanning has also been shown to be of rather unique value in following the response to therapy of this disease. A unique case of proven multiple amebic abscesses of the liver is reported in which two definite localized abnormalities persisted on the ^{198}Au colloid scan for more than 2 to 5 years after the beginning of the drug treatment. (C.H.)

26844 DEMONSTRATION OF COLLATERAL PATHWAYS AFTER SUPERIOR VENA CAVAL OBSTRUCTION WITH THE SCINTILLATION CAMERA. Krishnamurthy, G. T.; Winston, M. A.; Weiss, E. R.; Blahd, W. H. (Veterans Administration Center, Los Angeles. Univ. of California, Los Angeles). J. Nucl. Med.; 12: 189-91(Apr 1971).

Obstruction of the superior vena cava leads to the development of collateral channels that transport the venous blood from the upper part of the body to the inferior vena cava and thus aid in the return of blood to the heart. These collateral channels are numerous and are located along the anterior and posterior aspects of the chest and abdomen. A case is reported that illustrates the usefulness of radioisotope venography performed with the scintillation camera using ^{99m}Tc-sodium pertechnetate in the demonstration of collateral venous channel formation following superior vena caval obstruction. It would appear that the smaller venous pathways can also be observed with the scintillation camera. (C.H.)

26845 RADIOLABELED CHOLESTEROL AS AN ADRENAL SCANNING AGENT. Blair, Richard J.; Beierwaltes, William H.; Lieberman, Lionel M.; (and others) (Univ. of Michigan, Ann Arbor). J. Nucl. Med.; 12: 176-82(Apr 1971).

Iodocholesterol, labeled with ^{125}I, and cholesterol, labeled with ^{14}C, were evaluated in dogs for possible use as adrenal scanning agents. Results showed that the dog adrenal cortex showed satisfactory uptake of ^{125}I-iodocholesterol when a dose of 300 μCi was given with or without ACTH stimulation. Data on the ratios of adrenal cortex-liver radioactivity following the administration of both tracers are included. (C.H.)

26846 UNUSUAL RADIOLOGICAL FEATURES IN 4 CASES OF BONE METASTASIS. Bottero, G. (Univ., Turin). Minerva Radiol.; 15: 194-8(Jul-Aug 1970). (In Italian).

Four cases of bone metastasis with unusual radiological pictures are presented. Clear-cell renal tumour was the primary neoplasm in two cases. The findings are discussed and emphasis is laid on the difficulties that sometimes attend the radiological diagnosis of bone metastases of unknown origin. (auth)

26847 IMPORTANCE OF BONE MARROW SCINTISCANS IN THE DETECTION OF SKELETAL METASTASES. Sannazzari, G. L.; Agati, G.; Bottero, G. (Univ., Turin). Minerva Radiol.; 15: 187-93(Jul-Aug 1970). (In Italian).

Marrow scintiscans with colloidal ^{198}Au are of importance in the search for skeletal metastases. Areas of low, or even nil, activity at a very early stage give a substantial indication of the extent of marrow involvement. Search may be made in bone segments with active hemopoietic marrow, particularly the spinal column, cranium, sternum, pelvis, and the proximal epiphyses of the femur and humerus. The method compares favorably with conventional radiography as far as early diagnosis is concerned. It may also be used in conjunction with ^{89}Sn scanning, since both offer useful information for use in diagnosis and therapy. (auth)

26848 CRITICAL EVALUATION OF ^{99m}Tc–Fe–ASCORBIC ACID COMPLEX AS A RENAL SCANNING AGENT. Winston, M. A.; Halpern, S. E.; Weiss, E. R.; Endow, J. S.; Blahd, W. H. (Veterans Administration Center, Los Angeles. Univ. of Southern California, Los Angeles). J. Nucl. Med.; 12: 171-5(Apr 1971).

Iron-ascorbic acid complex, labeled with ^{99m}Tc, was evaluated for use for kidney scanning. Results showed that it is an adequate but not outstanding scanning agent. (C.H.)

26849 CONTRIBUTION OF LOW-ENERGY GAMMA EMITTERS TO THE SCINTIGRAM. Saegusa, Kenji; Kakehi, Hirotake (Chiba Univ. School of Medicine, Japan). Radioisotopes (Tokyo); 20: 134-41(Mar 1971). (In Japanese).

Low-energy γ emitters with short physical half lives are useful as scanning agents, because a larger amount of radioactivity can be applied to a patient without raising radiation dose to a possible hazard, and the shielding effectiveness for γ rays increases. A good quality scintigram, with little background cannot always be obtained in organ scintigraphy. The reason is that low energy γ rays produce a larger amount of scattered rays than those of the medium energies over 200 keV. For measurements of scattered rays, eight nuclides with energies ranging from 30 to 412 keV were used with thyroid- and liver-phantoms. The fraction of scattered rays in a photopeak was determined by the ratio of the area of the scattered region to that of the photopeak that was found in the window of ±10%. The fraction of scattered rays was higher in ^{197}Hg and lower in ^{203}Hg. In ^{131}I, however, the fraction was a little higher than ^{203}Hg, because of the γ ray penetration of the collimator septa. The best energy for γ rays used in scanning was 250 keV from the viewpoint of the shielding effectiveness and the incidence of scattered rays. (auth)

26850 BRAIN SCANNING: CEREBRAL SCINTIGRAPHY. Rasmussen, P.; Buhl, J.; Busch, H.; Haase, J.; Harmsen, Aa. (Rigshospitalet, Copenhagen). Nord. Med.; 84: 1134-9(Sep 1970).

Brain scanning on 981 patients, admitted to neurosurgical and neurological departments, is reported. The scanning proved positive in 77% of 501 patients with confirmed intracranial lesions. The accuracy was greatest (more than 90%) in malignant gliomas and meningiomas, least (53%) in benign gliomas. There was a high accuracy (81%) in lesions of a supratentorial site and a low accuracy (42%) in patients having lesions in the posterior fossa. Comparison of the results obtained by EEG and by scanning revealed good conformity in 47%, questionable conformity in another 21%, and in 3% both studies were negative. In 59% there was agreement between arteriography and scanning, total accuracy, 88%. A good agreement between peg and scanning was found in 39%, total accuracy, 84%. In one-quarter of the cases, scanning could be designated as the best method in detecting the extent and localization of the lesion. Scanning is well-suited for diagnosing meningiomas, malignant gliomas and for assessing the multiplicity of metastases. Consecutive scanning may be used to check the course of the lesions in patients with infarcts and localized encephalitis. Scanning does not show a greater accuracy than the other diagnostic methods, but it affords a valuable supplement and increases the diagnostic accuracy. (auth) (Sweden)

26851 LYMPH NODE SCANNING WITH COLLOIDAL RADIOACTIVE GOLD. Herting, Sv. E.; Buechler Frederiksen, P.; Jagt, T.; Jeppesen, P. (Radium Center, Odense, Denmark). Acta Radiol., Diagn.; 10: 359-68(Sep 1970).

Isotope lymphography with colloidal radioactive gold was carried out over a period of one year in 77 patients suffering from malignant disease. Contrast lymphography was performed in connection with the scanning in 47 of the patients, and the results were used as a standard for comparison. In the remaining 30 patients, the surgical and clinical findings were used as a basis for the evaluation. The good agreement obtained suggested that lymph node scanning is sufficiently safe and accurate as a screening test and for control examinations. (auth) (Sweden)

26852 SCINTILLATION CAMERA AND RECTILINEAR SCANNER FOR DETECTION OF SPACE-OCCUPYING INTRACRANIAL LESIONS. Pedersen, Mogens; Haase, Jens (Odense Hospital, Denmark). Acta Radiol., Diagn.; 10: 534-44(Nov 1970).

Two hundred and thirteen patients were investigated with a γ camera and a rectilinear scanning system with ^{99m}Tc for tumors

XUM

and other intracranial conditions. No essential differences between the two methods as regards diagnostic accuracy were apparent although the γ camera appeared to possess considerable practical advantages. (auth) (Sweden)

26853 COMPARISON OF SCHILLING TEST AND PLASMA LEVEL OF CYANOCOBALAMIN ^{57}Co. Coiner, Diane (Veterans Administration Hospital, Portland, Oreg.); Walsh, John R. J. Amer. Med. Ass.; 215: 1642-5(8 Mar 1971).

Because of several undesirable features of the widely used Schilling test, results of this test and plasma levels of cyanocobalamin ^{57}Co were compared in 111 patients. The plasma test resulted in good separation of values between normal subjects and patients with vitamin B_{12} absorption defects. One patient with malabsorption had an unexplained falsely normal plasma concentration. On the other hand, over 5% of normal and over 50% of uremic patients had false-positive results of the Schilling test and normal plasma levels. The plasma test is more helpful than the Schilling test for patients with renal insufficiency and mental disturbances. It is a helpful adjuvant to the Schilling test to avoid mistakes in interpretation and repetitive tests. However, because of the consequences of missing a diagnosis of vitamin B_{12} deficiency, the plasma test cannot be recommended exclusively as a substitute for the urine test at this time. (auth)

26854 CARDIAC CATHETERIZATION. III. ANGIOCARDIOGRAPHY. Brandt, P. W. T.; O'Brien, K. P.; Glancy, D. L. (Green Lane Hospital, Auckland, New Zealand. National Heart Inst., Bethesda, Md.). Australas. Radiol.; 14: 398-408(Nov 1970).

Angiocardographic techniques, complications and hazards, recording and applications are reviewed. Attention is given to injection siting and technique, and contrast media. Electrical and radiation hazards from x ray apparatus during diagnostic procedures were also considered. Serial film and ciné angiocardiography are described. Uses in assessing valvular incompetence and associated cardiac diseases are indicated. (28 references). (Australia)

26855 REPORT OF THE TWENTIETH BAKER TRAVELLING FELLOW. Andrews, J. T. (Royal Melbourne Hospital, Victoria). Australas. Radiol.; 14: 363-72(Nov 1970).

Brief descriptions of research and facilities available in nuclear medicine departments in various centers are given, as a result of visits made on a world trip. Isotope scanning procedures discussed include thyroidal investigations with ^{131}I, ^{132}I, and ^{99}Tc, bone scanning with ^{85}Sr and ^{99}Tc, cerebral scanning with ^{133}Xe, ^{197}Hg, ^{99}Tc, and ^{169}Yb, renal scanning with ^{131}I, and pericardial scanning with ^{32}P. Developments in Malaysia, UK, Sweden, USA, Canada, Japan, and Italy are briefly covered. Gamma camera developments were also investigated. (37 references). (Australia)

26856 STATISTICAL ANALYSIS OF RADIOISOTOPE SCAN DATA. Boxerman, Stuart B. St. Louis; Washington Univ. (1970). 180p. University Microfilms Order No. 70-26,894.

Thesis.

The feasibility of developing an algorithm to detect a space-occupying lesion in a rectilinear scan was investigated. A ring-to-core test was introduced that provided a model for identifying abnormal regions in an organ. Statistically, this test involves the comparison of two Poisson-distributed observations having parameters in a given ratio. The problem of detecting a lesion at an unknown location in the organ was considered. The use of a series of overlapping dependent tests was found to result in the detection of more lesions than a series of non-overlapping independent tests. The relative performance of alternative testing schemes was compared analytically. Simulation techniques were found to be necessary to obtain actual detection probabilities associated with dependent testing configurations. In all of the testing schemes investigated, maintaining the false alarm rate at a suitable level was imperative. Finally, a simulation study was performed for a typical set of parameters, and the detection probability was obtained. (Diss. Abstr. Int., B)

26857 FURTHER OBSERVATIONS ON THE USE OF THE SERUM THYROXINE ESTIMATION IN THE IN-VITRO ASSESSMENT OF THYROID FUNCTION. Murray, I. P. C.; Joasoo, A.; Parkin, J. (Prince of Wales Hospital, Randwick, New South Wales). Med. J. Aust.; 1: No. 2, 78-7(9 Jan 1971).

A review of the results of serum total thyroxine estimation in 705 patients demonstrated that a high degree of diagnostic accuracy was achieved provided that no alteration in thyroxine-binding globulin was present. In this situation, the free thyroxine factor, derived from the serum thyroxine estimation and the triiodothyronine-resin uptake, was a useful method to obtain a correct assessment of thyroid function. Misleading results may be obtained in euthyroid patients who are seriously ill as the result of non-thyroid disorders. In these sick euthyroid patients, a simple technique that reflects the free thyroxine concentration has been found to be of value. A further comparison of Tetrasorb and Res-O-Mat T. kits demonstrated that modifications to the latter have resulted in increased reproducibility and diagnostic accuracy. The use of the serum thyroxine estimation as an index of the thyroid response to the thyroid stimulation and suppression tests was evaluated. (auth) (Australia)

26858 EFFECTS OF TECHNICAL IMPROVEMENTS ON PATIENT DOSES IN X-RAY DIAGNOSIS. Schott, O. (Siemens AG, Erlangen, Ger.). Radiologe; 10: 353-7(Sep 1970). (In German).

Every technical improvement in x-ray diagnosis must be examined with respect to a favorable compromise between diagnostic information to be obtained and radiation burden to the patient. Various improvements of conventional technqiues that reduce radiation are outlined. For image intensifiers and TV screens, the analysis shows that sometimes a decreased radiation burden can be obtained; however, with some of these improvements, the gain in diagnostic accuracy must be paid for by a high patient dose. (tr-auth)

26859 UPTAKE- AND METABOLIC STUDIES OF THE LABELLED COMPOUNDS IN MALIGNANT TUMORS. Lee, Jang Kyu; Koh, Chang Soon; Chang, Ko Chang; Chang, M. D. (Radiological Research Inst., Seoul). J. Nucl. Sci. (Seoul); 10: No. 2, Part 2, 99-100(1970). (In Korean).

The labeled compounds which have high avidity to all kinds of malignant tumors, namely, the multipurpose scan agents are indispensable, but are not fully developed. It has recently been found that the positive scans of the malignant tumors show bigger than the actual size, hence, the early detection of the tumors is easier by this method. Studies were done using ^{75}Se-selenite, ^{95}Nb-oxalate in animals, and ^{131}I-iodouracil, ^{131}I-fibrinogen, and ^{131}I-antifibrinogen in man for tumor localization. (P.B.M.)

26860 RADIOISOTOPIC SCINTIGRAPHY IN DIAGNOSIS OF LIVER ABSCESS. Toth, Z. (Center of Radiobiology and Radiologic Protection, Warsaw). Pol. Med. J.; 9: 1352-6(1970).

On the grounds of experiences gained with radioisotopic scintigraphy, used as the examination method on 22 patients with clinical diagnosis of liver abscess, values of this diagnostic procedure for detection and localization of liver abscesses were pointed out. (auth)

26861 VALUE OF RADIOISOTOPE SCINTIGRAPHY IN THE DIAGNOSIS OF LIVER CIRRHOSIS. Toth, Z. (Center of Radiobiology and Radiologic Protection, Warsaw). Pol. Med. J.; 9: 1346-51(1970).

The value of radioisotope scintigraphy in the diagnosis of liver cirrhosis was assessed in examination of 131 patients. The investigations were done with ^{131}I-rose bengal visualizing the liver parenchyma and ^{198}Au colloidal gold for demonstration of the system of reticulo endothelial cells in the liver. They served for simultaneous evaluation of the usefulness of both tracers for the diagnosis of liver cirrhosis. The effectiveness of radioisotope scintigraphy in the detection of changes in the liver parenchyma is considerable in cases of liver cirrhosis. A combined investigation with the use of both these tracers (^{131}I RB and ^{198}Au) increases considerably the value of scintigraphy in the detection and evaluaton of the grade of changes in liver cirrhosis. (auth)

26862 CLINICAL STUDY ON THE VALUE OF A SCORING SYSTEM OF THE SCANNING IMAGES IN LIVER CIRRHOSIS. Chang, Ko Chang; Lee, Jang Kyu (Radiological Research Inst., Seoul). J. Nucl. Sci. (Seoul); 10: No. 2, Part 2, 5-23(1970). (In Korean).

Although the radioisotope liver scan has primarily been of use in the detection of the intra hepatic space occupying lesions, there has been an increasing awareness of its use in evaluation of liver functions. The degree of hepatomegaly, changes in shape and mottling radiodensity on each lobe and splenic visualization in the liver scans done with colloidal radiogold were numerically expressed as scores under the arbitrary standard in 210 patients with liver cirrhosis, 50 patients with liver abscess, and 100 patients with carcinoma of the liver. The clinical value of this scoring system was studied with special regards to the correlation between the radiogold hepatic uptake half time and conventional liver function tests. (auth)

XUM

Radiotherapy

Refer also to abstracts 26757, 26758, 26761, 26799, 26973, 27037, 27038, 27040, 27044, 27049, 27052, 27055–27057, 27059, and 28132.

26863 TREATMENT OF CARCINOMA PENIS BY RADIUM MOULD. Narain, Prem (Inst. of Radiology and Cancer Research, Kanpur, India). Punjab Med. J.; 20: 195-202(Dec 1970).

Results are reviewed for 24 cases of small superficial carcinomas of the penis treated with contact γ therapy using ^{226}Ra molds that delivered a skin dose of 5,500 to 6,000 R during the total exposure time of 90 to 100 hr over a 10 day period. Good response was obtained in all but three cases. Methods used for making the molds and for calculating the local radiation dose are described. (C.H.)

26864 ADVANCED TREATMENT SCHEMES WITH HIGH-ENERGY RADIATION CONSIDERING THE OXYGEN EFFECTS ON ANOXIC TUMOR CELLS. Wideroee, R. Kerntechnik; 12: 504-7(Nov 1970).

A discussion of radiation treatment schemes for deep-seated tumors with various types of radiation based upon radiobiological findings is given. The first condition to be fulfilled is that the repopulation of damaged normal tissue in the tumor bed must be repaired to a high degree in the intervals between irradiations. A second condition for successful treatment is that tumor cells, and especially the anoxic ones, must be reduced to a very small degree, about 10^{-9}. In this case, the recently investigated reoxygenation and conversion processes taking place during fractionated radiation treatment are of outstanding importance. A clinically successful high-intensity treatment scheme, that employs high-energy electrons with the first dose of 900 rad followed by weekly doses of 500 rad until a sufficient total dose is reached administered while breathing hyperbasic oxygen, that demonstrates the importance and basic soundness of the calculated results is described and explained. (C.H.)

26865 RADIATION TREATMENT PLANNING FOR A 42 MeV BETATRON: EXPERIENCE WITH AN ALDERSON-RANDO PHANTOM. Heuss, Kurt (Allgemeine Ortskrankenkasse, Cologne). Stud. Biophys.; 23: 19-26(1970) (In German).

For planning radiation treatment with electrons, tissue-equivalent phantoms are very useful. The distribution of bones and other inhomogeneities within the phantom must be checked. Only small deviations in dose distribution result when many small ionization chambers were used simultaneously within one section of the phantom. Comparison of the dose distribution within an Alderson phantom and within a homogeneous polystyrene phantom gives the limits for the influence of inhomogeneities upon the tumor dose. Often, measurements of radiation transmission of the body of the patient are needed. (auth)

26866 CYLINDRICAL ADENOMA OF THE PAROTID GLAND. Marcorelli, E. (Univ., Rome). Nunt. Radiol.; 34: Suppl. I, 79-88(1968). (In Italian).

The case of cylindrical adenoma of the parotid gland is reported. The principal histological aspects of such tumors are briefly summarized with particular regard to the problem of their histogenesis. The particular difficulty of the anatomoclinical evaluation of the malignancy is the absence of local infiltration or of metastatic dissemination. The concept of malignant potentiality of the neoplasm from the initial stage was confirmed, agreeing with the definition of cancer in pleomorphic adenoma for such types of tumors. The problem of prognosis is reviewed in the light of a wide statistical range of cases of metastasized cylindromata existing in the literature. The necessity of pre- and post-operative radiotherapy, associated with radical surgery, is emphasized. (tr-auth)

26867 CONTRIBUTION TO THE ELECTRON DEEP THERAPY BY MEANS OF PENDULUM IRRADIATION. V. APPLICATION OF THE TELECENTRICAL SMALL ANGLE PENDULUM TECHNIQUE FOR RADIOTHERAPY OF TUMOURS IN THE ABDOMINAL REGION. Rassow, Juergen; Sack, Horst (Ruhr Univ., Essen). Strahlentherapie; 141: 5-12(Jan 1971). (In German).

Advantageous application possibilities for telecentrical small-angle pendulum therapy by means of fast electrons are demonstrated by four examples (tumor of urinary bladder, gynecological recurrent tumor of the pelvic wall, renal tumor). An advantage of the described technique is the steep dose drop in depth as well as on both sides, which leads to a greatest possible protection of the unaffected adjacent organs. (auth)

26868 RADIOTHERAPY OF VOCAL-CORD LEUKOPLAKIA. Hommerich, K. W.; Ernst, H.; Schubert, B. (Freie Univ., Berlin). Strahlentherapie; 141: 18-24(Jan 1971). (In German).

In drawing up a plan of treatment for epithelial hyperplasia of the vocal cords, not only should the diagnosis be taken into consideration, but the case must be selected with regard to its aptitude for radiotherapy, according to its complete histological condition. Thus only those cases of leukoplakia are to be selected for radiotherapy in which the hyperplasia is caused by a reaction of the epithelium on a small-cellular submucous inflammation. It may be stated that the regression of the epithelial hyperplasia is the consequence of a subepithelial sedation. Under the hypothesis that the radiation dose alone effects the destruction of the cellular inflammatory substrates, success can also be achieved by a dose of 2300 rad; therefore Leukoplakia with atypias should be treated by a total dose of 5000 rad. (auth)

26869 HIGH DOSE-RATE INTRACAVITARY RADIATION THERAPY UNDER HYPERBARIC OXYGENATION. Wakabayashi, Masaru (Hokkaido Univ., Sapporo). Gan No Rinsho; 16: 377-80(Apr 1970). (In Japanese).

Radiotherapy of the uterine cervical carcinoma was carried out with some improvement in the time-dose distribution during intracavitary irradiation. The dose was calculated by the Manchester system and a high-dose short irradiation of a total of 15 Ci from a ^{60}Co γ source was given. In the short-time irradiation, the oxygen effect was utilized to increase radiation sensitivity of the carcinoma to achieve complete cure of cancer and, at the same time, to reduce the therapeutic dose required. The patient was placed in a high-pressure chamber of 3 atm, with respiration of pure oxygen, and 500 R γ was administered for 1 to 2 minutes to point A. The same 500 R dose was repeated under the same condition one week later to bring the total intracavitary radiation dose to 1000 R. External irradiation using a Telecobalt γ therapy unit was also given by the split field method after intracavitary irradiation, and 4500 to 5000 R was delivered to the pelvic cavity during 4 to 5 weeks. This therapy was carried out on 20 cases, comprising four cases of stage II and 16 cases of stage III carcinoma. Histologically, these consisted of 18 cases of squamous cell carcinoma and two cases of adenocarcinoma. One case died of other diseases during the treatment and two cases had recurrence one to eight months after therapy. These recurrence cases were in stage III. Intracavitary radiation therapy under hyperbaric oxygenation seemed to be satisfactory as a temporary treatment. (Japan)

26870 DOSE MEASUREMENT OF ^{90}Sr-APPLICATOR, CLINICAL RESULTS IN THE TREATMENT OF PTERYGIUM AND ITS RELATION TO BETA-RAY CATARACT. Yamada, Eiichi (Tokyo Metropolitan Police Hospital). Ganka; 12: 33-41(Jan 1970). (In Japanese).

The β dose of ^{90}Sr applicator used for prevention of recurrence after pterygium operation was measured physically. Recurrence rate of pterygium was examined in 144 cases of operated patients given this irradiation during the 10 years from 1957 to 1966, together with occurrence of β-ray induced cataract in these people as a side effect. Proximal irradiation of the operated site was made with β-rays from the ^{90}Sr applicator immediately after surgery for 3 to 4 days. Since β-rays are likely to be absorbed or dispersed under various conditions, it is necessary to know the characteristic of an applicator in order to carry out safe and sufficient radiotherapy. Surface dose of the ^{90}Sr applicator was 730 rads and the dose at the depth of 3 mm was 18.5% of the surface dose. Recurrence of pterygium occurred in 9 out of 153 eyes or 5.88%, indicating the effectiveness of irradiation. Cataract was seen in 17 of 39 eyes or 43.6% of the total followed for over three years. There were three cases of cataract seen in this group of patients. From these results, it is assumed that the effective dose for prevention of pterygium recurrence would be 3000 to 4000 rep (roentgen equivalent physical dose) and the permissible dose to the lens of 300 to 500 rep. (Japan)

26871 CANCER OF THE UTERINE CERVIX. Gazzera, Giuseppe (Ospedale Maria Vittoria, Turin). G. Batteriol., Virol., Immunol. Ann. Osp. Maria Vittoria Torino; 62: 627-82 (Sep-Oct 1969). (In Italian).

The various surgical, radiological, and medical methods for the treatment of cancer of the uterine cervix were examined and critically compared with respect to their efficiency in the treatment of different stages of cancer. Recommendations are made for the most desirable therapy for different types and stages of cancer. (J.S.R.)

26872 ^{60}Co TELETHERAPY OF PITUITARY ADENOMAS. Carlson, David H.; Marsh, Spinks H. (Hartford Hospital). Radiology; 98: 655-9(Mar 1971).

XUM

^{60}Co radiotherapy was administered in 42 of 51 patients with pituitary adenoma, with or without surgery. An 88% improvement rate in visual fields was noted overall, 80% with irradiation alone. An overall control rate of 90% was obtained, 85% by irradiation alone. There were no serious complications. The use of super-voltage treatment as the initial step in the control of pituitary adenomas is recommended. (auth)

26873 SYNOVIOTHESIS (SYNOVIOTHERAPY BY RADIO-ISOTOPES) STUDIES OF MORE THAN 400 CASES AND FUTURE PROSPECTS. Roucayrol, J.-C.; Delbarre, F.; Cayla, J.; Menkes, C.; Aignan, M.; Ingrand, J. (Hopital Cochin, Paris). J. Biol. Med. Nucl.; 4: No. 18, 18-23(1969). (In French).

The results of 417 synoviortheses on 225 patients made with intra-articular injections of ^{198}Au, ^{90}Y, and ^{32}P are reported. The majority of the patients had arthritis at all stages, principally rheumatoid polyarthritis. The techniques used are summarized and the studies made to reduce the risks connected with this therapy and to adapt it to each particular case are described. Approximately 80% showed good results with at least half showing lasting results. The therapy is not traumatic as it is limited to one injection in some cases. (J.S.R.)

26874 MEDICAL TREATMENT FOR THE AMELIORATION OF MALIGNANT PULMONARY NEOPLASMS USING IRRADIATION WITH THE 42 MeV BETATRON. Garbagna, P.; Nicolato, A. (Univ., Pavia, Italy). Nunt. Radiol.; 34: 1395-1401(Nov 1968). (In Italian).

A study was made of 230 cases of pulmonary neoplasms cured with the 42-MeV betatron. The use of the betatron in clinical controls and in medical cures that tend to eliminate or alleviate the secondary effects of the presence of the tumor and those caused by the radiation itself is reported. (tr-auth)

26875 KOEBNER PHENOMENON-LIKE MANIFESTATION OF A RETOTHEL SARCOMA OF THE SKIN FOLLOWING X-RAY TREATMENT. Weber, G.; Stock, E. (Staedtische Krankenanstalte, Nuernberg, Ger.). Arch. Klin. Exp. Dermatol.; 239: 191-9(1970). (In German).

X-ray treatment of a retothel sarcoma of the skin brought about complete involution of the tumors in an otherwise typical course of the disease. After an interval of three months retothel sarcoma infiltrations corresponding in size exactly to that of the x-ray tube reappeared within the x-ray treated area of the back. They were homogeneously localized in the unchanged, i.e., formerly healthy skin as well as in the area of the previously x-ray treated and thereafter completely involuted tumors. Thus the assumption is justified that the x-ray treatment of the normal skin leads to a locus minoris resistentiae in which—equivalently to a Koebner phenomenon—a fresh tumor eruption established itself. (auth)

26876 SUPERHIGH VOLTAGE IRRADIATION OF BLADDER TUMOR. Katsume, Michito; Fujieda, Junichiro; Ohmuro, Hiroshi; Sato, Shosaku; Irie, Goro (National Hospital, Sapporo). Hinyokika Kiyo; 16: 371-83(Aug 1970). (In Japanese).

Tumors of the bladder were treated by external irradiation with the 6 MeV linear accelerator. Results of the treatment, secondary effects, and late effects were investigated. Most cases tolerated the radiation and were able to receive a sufficient therapeutic dose. Observation of 52 cases one to twelve months later showed that the tumor had disappeared in 23 cases. Shrinkage of the tumor occurred 3 to 4 months after irradiation in the low grade group and 5 months after irradiation in the high grade group. Results were comparable to those of total cystectomy. The following principles were established for treatment of tumors of the bladder: single and low grade tumors should be treated by open or transurethral surgery; in aged or poor risk cases, in which surgery is not recommended, external irradiation should be tried first; multiple or high grade tumors should be treated by irradiation first followed by six months observation. (Japan)

26877 RESULTS OF X-RAY IRRADIATION OF THE THYMUS GLAND IN MYASTHENIA GRAVIS. Raczkiewicz, J. Neurol., Neurochir. Psychiat. Pol.; 4: 357-9(May-Jun 1970). (In Polish).

Radiotherapy of the thymus gland was applied in nine myasthenic patients treated in the Dept. of Neurology, General Hospital Nr 1 in Bydgoszcz. The inhibitory effect of radiotherapy on the progress of myasthenia was observed in 55% of the cases. The benefit from radiotherapy of the thymus gland was also observed when combined with the carotid sinus block and denervation. (auth)

26878 NEW TELECENTRIC SMALL ANGLE PENDULUM TECHNIQUE, SPECIFIC FOR PRIMARILY UNSCATTERED ELECTRONS. Rassow, Juergen (Ruhr Univ., Essen). Stud. Biophys.; 23: 211-18(1970). (In German).

A telecentric small angle pendulum technique is described for use in electron beam therapy. The technique gives a larger dose at depth in a very small field compared with conventional techniques. (C.H.)

26879 GENERAL ASPECTS OF FAST NEUTRON THERAPY. Bewley, D. K. (Hammersmith Hospital, London). Stud. Biophys.; 23: 177-86(1970).

The effectiveness of fast neutron beams for cancer therapy was evaluated using the beam from a cyclotron. The physical properties of the neutron beam were compared with a ^{60}Co γ beam. The 30 MeV fast neutron beam was comparable to γ in tissue penetration, but not in the degree of skin-sparing afforded. It is pointed out that the use of fast neutrons for therapy requires cumbersome and expensive apparatus and that shielding from stray radiations is a particular problem. The smaller risk of bone necrosis and fracture resulting from the reduced absorbed dose in bone may represent a specific advantage in the use of fast neutrons. (C.H.)

26880 STUDY ON THE CONSERVATIVE TREATMENT OF RETINOBLASTOMA. Kiribuchi, Mitsunori (National Cancer Center, Tokyo). Nippon Ganka Gakkai Zasshi; 74: 1058-66 (Sep 1970). (In Japanese).

Results are reported for 21 cases of retinoblastomas treated with radiotherapy. The methods employed in the treatment included external irradiation using mega-voltage x rays, radon-222 seeds inserted in the sclera for contact radiation, electron beam emitted from a betatron, and intra-carotid infusion and retrograde infusion of anti-cancer drugs to ophthalmic artery. The majority of patients from group one to group three attained useful vision following therapy by external exposure to 3500 to 4000 R x radiation. Although direct irradiation of the tumor by the electron beam emitted from the treatment tube of a betatron in contact with the sclera was useful, further studies on the single dose and the irradiation technique are needed. The only effective treatment for the far-advanced cases from groups 3 to 6 were retrograde infusion of anti-cancer drugs into the ophthalmic artery, but it was impossible to obtain useful vision except for one case of group 6 who recovered his sight owing to the disappearance of retinal detachment after treatment. For such progressed cases, bone marrow transfusion from parent to patient is being tried as one method of promoting the tendency of spontaneous regression which this tumor retains. (auth) (Japan).

26881 THYROID CRISIS FOLLOWING ^{131}I THERAPY FOR HYPERTHYROIDISM. Hara, M. (Niigata Univ., Japan); Sato, T.; Izumi, M.; Imai, T. Naika; 25: 952-4(May 1970). (In Japanese).

Two cases of thyroid crisis are reported which occurred after ^{131}I therapy for hyperthyroidism. Thyroid crisis is difficult to discriminate from severe thyroid toxicosis, infections, or shock. The crisis occurred within two weeks after radioiodine therapy and this period agrees with the time period for increase in blood thyroid hormone. The main cause may be a sudden out-surge of hormone due to destruction of thyroid by radioiodine, but there is the possibility of increase in free-type thyroid hormone without increase in PBI. Since there have been reports on many cases of crisis with combined symptoms, it is possible that some individuals have lowered tolerance to thyroid hormone due to some combined disease and the body could not cope with the thyroid hormone increase caused by radioiodine therapy. There is no difference from other crises in clinical symptoms and treatment. For prevention of such crisis, it is necessary to measure ^{131}I uptake directly before starting the treatment in order to prevent the thyroid taking up more ^{131}I than would be expected, and adjusting the dose accordingly. In severe cases, anti-thyroid agent should be given to improve the general condition. (Japan).

26882 TREATMENT DOSES OF ^{131}I-LABELED CHLOROQUINE ANALOG IN NORMAL AND MALIGNANT MELANOMA DOGS. Lieberman, Lionel M.; Boyd, Charles M.; Varma, Vijay M.; Bergstrom, Terry J.; Beierwaltes, William H. (Univ. of Michigan, Ann Arbor). Contract AT(11-1)-2031. J. Nucl. Med.; 12: 153-9(Apr 1971).

Whole-body absorbed doses from both β and γ radiation were estimated for dogs following the intravenous injection of iodine-131-incorporated chloroquine analog. The β dose absorbed by malignant melanomas following injection of iodine-131-incorporated chloroquine analog was also measured. Results showed that tumoricidal doses of β radiation in melanoma tumors were reached without delivering prohibitive radiation doses to the eye or whole-body. (C.H.)

26883 GAS TARGET SOURCE FOR NEUTRON RADIATION THERAPY. Kelsey, C. A. (Univ. of Wisconsin, Madison); Boone, M. L. M.; Hevezi, J. M.; Wiley, A. L. Jr.; Spalek, G. C. Radiology; 98: 686-8(Mar 1971).

The design criteria for a 10^{13} neutron/sec. source suitable for radiation therapy are discussed. The possibility of employing a differentially pumped gas target containing gaseous tritium is considered. It is concluded that a differentially pumped gas target is technically feasible and can provide the source strength required for neutron cancer therapy. (auth)

26884 REVERSAL OF LIVER SCAN IMAGE AFTER RIGHT-SIDED RENAL RADIOTHERAPY. Samuels, Larry D.; Grosfeld, Jay L.; Kartha, Mukund (Ohio State Univ., Columbus. Children's Hospital, Columbus, Ohio). J. Amer. Med. Ass.; 215: 1816-18 (15 Mar 1971).

Fourteen children who received postoperative radiation therapy for Wilms' tumor were given serial liver scans. There was progressive alteration of the shape of the liver following radiation therapy to the right renal fossa, producing a reversal of the usual liver image. After left renal fossa irradiation there was little alteration in liver configuration. In light of this evidence, greater attention must be paid to shielding the liver from undesired irradiation. (auth)

26885 TRIPLE COMBINATION THERAPY OF MALIGNANT TUMORS OF THE HEAD AND NECK. ON THE CARCINOMA IN PARANASAL SINUSES. Sato, Yasuo (Tokyo univ.). Jibi To Rinsho; 15: 312-23(Jun 1970). (In Japanese).

Combined therapy using surgery, radiotherapy, and regional chemotherapy for the treatment of malignant neoplasms of the nose and paranasal sinuses was evaluated. 5-Fluorouracil (5-FU) alone or together with 5-bromodeoxyuridine (BUDR) were used as radiation-sensitizing agents. In order to eradicate the tumor a radiation dose of as much as 10,000 Rads was administered. However, when 5-FU and BUDR were infused simultaneously during telecobalt γ therapy and the necrotic tumor mass in the antrum sucked out every day, the eradication of the tumor mass was achieved within the total tumor dose of 4,000 Rads. In treating tumors which had extended to the ethmoid sinuses, this combined therapy was rather insufficient in the rate of tumor disappearance. In order to compensate the insufficient drug concentration in these regions, the cleaning of the ethmoid sinuses was done from the antrum, and in some cases mixed gas of 5% CO_2 and 95% O_2 was inhaled during radiotherapy to increase radiation effects. Even if the tumor still existed after the combined therapy, the partial resection of the maxilla or intracavitary γ irradiation using ^{137}Cs tubes was enough to eradicate the residue of the tumor. This method of treatment showed a definite improvement in saving the extent of surgery. No total resection of the maxilla has been required in the last four years. Consequently, a great number of patients were enabled to return to their former work soon after the completion of the therapy. (auth) (Japan)

26886 CANCER OF THE UTERINE CERVIX; JANEWAY LECTURE, 1970. Fletcher, Gilbert H. (Univ. of Texas, Houston). Amer. J. Roentgenol., Radium Ther. Nucl. Med.; 111: 225-42(Feb 1971).

An assessment is made of radiation response, dosimetry, and combined irradiation and surgery for the treatment of cancer of the uterine cervix. The complexity of dosimetry for intercavitary radium therapy is emphasized and the irradiation of lymphatics is discussed. (F.M.M.)

26887 POST-IRRADIATIONAL RECURRENT EPIDERMOID CARCINOMA OF THE UTERINE CERVIX. Kurohara, Samuel S.; Vongtama, Vitune Y.; Webster, John H.; George III, Frederick W. (Univ. of Southern California, Los Angeles. Roswell Park Memorial Inst., Buffalo). Amer. J. Roentgenol., Radium Ther. Nucl. Med.; 111: 249-59(Feb 1971).

During 1920 to 1954 there were 1,165 patients judged to have had recurrent cancers within a 10 year period following radiologic treatment of 4,308 cases of squamous cell carcinoma of the uterine cervix. Forty-seven per cent of recurrences was detected by ¾ year, 60% by 1 year, 73% by 2, and 100% by 9 years of follow-up for recurrences after radiotherapy. Thirty-seven per cent were pure cervical recurrences, 10.3% pure vaginal, 2.4% pure cervical and vaginal, 24.7% parametrial with or without central disease, 10.8% distant with or without pelvic disease. In 14.3% of cases the exact sites of recurrences were not determined. Retreatment was administered by individualized methods of roentgen irradiation and/or radium application. Only 11 cases were subjected to radical surgery. The overall 5 year survival was 15%. However, the results varied from 0 to 88% when the sites of recurrences, initial stages, previous radiation factors, and retreatment modalities were considered. Details of symptoms and signs in order of their appearances, time of recurrence and results of retreatment are presented in relationship to site of recurrence, initial clinical stage and initial radiation treatment factors. (auth)

26888 MALIGNANT MELANOMA, ITS TREATMENT BY THE ENDOLYMPHATIC ADMINISTRATION OF RADIOACTIVE ISOTOPES. Ariel, Irving M. (Pack Medical Foundation, New York). Amer. J. Roentgenol., Radium Ther. Nucl. Med.; 111: 310-22(Feb 1971).

The treatment of malignant melanoma by a combination of surgery and endolymphatic isotopic therapy is based on experimental evidence that the dose of irradiation delivered by this route will destroy microscopic-sized deposits of cancer. In lymph nodes bearing cancer, there is marked destruction of melanoma in the lymph nodes after the endolymphatic administration of 40 mCi of ^{131}I ethiodol. This was accomplished with no demonstrable interference to lymph flow due to marked differences in sensitivity to irradiation of the lymph nodes and the lymphatic vessels. The lymph nodes are radiosensitive, and the lymphatic vessels are radioresistant. Endolymphatically administered ^{131}I ethiodol delivers a sufficient irradiation (50,000 to 100,000 Rads β) to the lymph nodes in humans to destroy microscopic-sized deposits of melanoma cells lodged within the lymph nodes. The primary melanoma is treated by orthodox surgical techniques. Several patients with satellitoses have markedly benefited from endolymphatic isotope therapy. Two patients with distant metastases so treated showed no improvement and endolymphatic isotopes are not indicated for such patients. (F.M.M.)

26889 GLIOBLASTOMA MULTIFORME. AN ANALYSIS OF THE RESULTS OF POSTOPERATIVE RADIOTHERAPY ALONE VERSUS RADIOTHERAPY AND CONCOMITANT 5-FLUOROURACIL. Edland, Robert W.; Javid, Manucher; Ansfield, Fred J. (Univ. of Wisconsin, Madison). Amer. J. Roentgenol., Radium Ther. Nucl. Med.; 111: 337-42(Feb 1971).

Between January 1962 and December 1966, 32 patients with a histologically confirmed diagnosis of astrocytoma Grade 3 or 4 (glioblastoma multiforme) were entered into a cooperative, prospectively randomized study to compare the effects of postoperative, high dose, supervoltage radiotherapy alone (17 cases) versus a similar course of postoperative radiotherapy and concomitant systemic 5-fluorouracil chemotherapy (15 cases). The average survival from diagnosis (incomplete removal) was 11.7 months in the radiotherapy only group and 11.5 months in the combined therapy group. Two patients are still alive, 1 at 37 months treated by irradiation alone and 1 at 26 months who received combined therapy. It was concluded that combined therapy with 5-fluorouracil offers no advantage, from the standpoint of duration or caliber of survival, over high dose postoperative radiotherapy alone in the management of patients with glioblastoma multiforme. (auth)

26890 RADIOTHERAPY OF PRIMARY LYMPHOMA OF THE ORBIT. Foster, Stanley C.; Wilson, Charles S.; Tretter, Patricia K. (Columbia-Presbyterian Medical Center, New York). Amer. J. Roentgenol., Radium Ther. Nucl. Med.; 111: 343-9(Feb 1971).

Thirty-three patients with primary lymphoma of the orbit were treated. Thirty had radiotherapy, and three had surgery alone as initial treatment. Local recurrence occurred in five, and in each case was successfully retreated. The recurrences were anterior in low dosage areas. Nine developed generalized disease, usually within 1 year after treatment. Two of these patients died of lymphoma. It appeared that the patients with reticulum cell or mixed cell type lesions were more prone to generalized disease. The results indicated that local control can be obtained, and that in a significant percentage of patients the disease does not generalize. In four of the nine patients that developed neck lymph generalized disease, the eye symptoms were controlled. Complications of treatment were few utilizing orthovoltage technique that facilitates adequate shielding of the lens and cornea. (auth)

26891 RESULTS IN TREATMENT OF PURE SEMINOMA OF THE TESTIS. Castro, Joseph R.; Gonzalez, Mario (Univ. of Texas, Houston). Amer. J. Roentgenol., Radium Ther. Nucl. Med.; 111: 355-9(Feb 1971).

Irradiation of the iliac and paraaortic lymphatics to the dose of 2,500 Rads appeared sufficient for Stage I seminoma. Elective irradiation of the mediastinum and left supraclavicular area was not indicated. For patients with Stage II disease irradiation the iliac and paraaortic lymphatics followed by the mediastinum and left supraclavicular area is suggested. Aggressive treatment of Stage III_A patients will result in control of the disease in most patients. There was no indication for irradiating the opposite testicle, since the incidence of bilateral testicular seminoma or metastasis to the other testicle was quite low. (auth)

26892 VARIABLE BLOCK-SURFACE-DISTANCE (BSD) FOR ADJUSTMENT OF SHADOW SIZE IN MANTLE THERAPY. Maruyama, Yosh; Khan, Faiz M. (Univ. of Minnesota, Minneapolis).

XUM

Amer. J. Roentgenol., Radium Ther. Nucl. Med.; 111: 382-7(Feb 1971).

The problem of blocking an irradiation field during radiotherapy was considered based upon geometric principles. Precise adjustments of field shadowing can be made according to the method described. Considerable adjustment of shielded areas can be obtained by a block table that can be varied in its vertical position. A practical method is described. (auth)

26893 ANALYSIS OF THE TREATMENT OF STAGE I AND STAGE II CARCINOMAS OF THE UTERINE CERVIX. Easley, James D.; Fletcher, Gilbert H. (Univ. of Texas, Houston). Amer. J. Roentgenol., Radium Ther. Nucl. Med.; 111: 243-8 (Feb 1971).

The irradiation treatment of patients with cancer of the uterine cervix, Stage I or Stage II, cannot be standardized. Considerable radicalism has to be used to control massive cancers. The incidence of severe complications, which could be diminished is not prohibitive being approximately 2%, but more patients would die from uncontrolled cancer. (auth)

26894 DOSAGE TOLERANCE OF PELVIC STRUCTURES WITH ^{60}Co ROTATION RADIATION THERAPY. Koeck, George P.; Hillsinger, William R. (United Hospitals of Newark, N. J.). Amer. J. Roentgenol., Radium Ther. Nucl. Med.; 111: 260-8(Feb 1971).

A study was made on 263 patients that had been treated by cobalt-60 rotation therapy to determine the tissue tolerance of pelvic structures. It was found that a tissue dose of 7000 Rads to the rectum and 6500 to 7000 Rads to the bladder produced a high incidence of morbidity. In ovarian carcinoma, a tissue dose of 4500 to 5000 Rads to the entire pelvis was well tolerated. Minimal bladder complications were found with a dose of 6600 Rads but there were no rectal complications with a dose of 3000 Rads. (F.M.M.)

26895 REVIEW OF EXPERIENCE WITH IRRADIATION OF BRAIN METASTASIS. Nisce, Lourdes Z.; Hilaris, Basil S.; Chu, Florence C. H. (Memorial Hospital for Cancer and Allied Diseases, New York). Amer. J. Roentgenol., Radium Ther. Nucl. Med.; 111: 329-33(Feb 1971).

A series of 560 patients with intracranial metastases, treated by irradiation, is reviewed and the results are reported. In this series palliation was obtained in 54% of the total number of patients, and 80% of the 376 patients that completed the planned course of irradiation, and were available for evaluation. The mean duration of remission was 5 months and the median duration 3 months. The use of supervoltage irradiation and adjuvant corticosteroids reduced radiation reactions and permitted easier administration of irradiation, but there was no influence on the overall response rate or duration of response when compared to 250 kVp irradiation without adjuvant corticosteroids. The results were comparable with those reported previously. Since most patients have multiple metastatic foci in brain, total brain irradiation to a dose of 3,500 Rads in 3 to 4 weeks is advocated. (auth)

26896 SUPERVOLTAGE RADIATION RESPONSE IN EPIDERMOID CARCINOMA OF THE ESOPHAGUS. Sharma, U.; Gopinath, N.; Haldar, P. K. (All India Inst. of Medical Sciences, New Delhi) Indian J. Cancer; 7: 288-95(Dec 1970).

The results of 43 cases of epidermoid carcinoma of esophagus treated with ^{60}Co radiation have been assessed. Statistically, long time survivals are very few, but the palliation offered by supervoltage therapy is great. A dosage level of 5000 to 5500 R in 4 to 4.5 wk for radical and 3000 to 3500 R in 2 to 3 wk for palliative treatment have been advocated. (auth)

Blast and Thermal Effects

26897 BALNEOTHERAPY OF RADIATION INJURY. 28. ANNUAL REPORT OF RESEARCH INSTITUTE OF BEPPU HOT SPRING UTILIZATION BY ATOMIC BOMB SUFFERERS. 11. Hatta, Osamu (Genshi Bakudan Hibakusha Beppu Onsen Riyo Kenkyusho, Oita, Japan); Arima, Masashi. Oita-ken Onsen Chosa Kenkyu-kai Hokoku; No. 21, 62-4(Mar 1970). (In Japanese).

The effectiveness of balneotherapy for the treatment of residents of Japan exposed to atomic bombs at Hiroshima and Nagasaki was investigated. Results of the hot spring cure between April 1969 and March 1970 were studied. The number of utilizers for this fiscal year was 2011, 321 more than those for the last fiscal year. There were more utilizers in May, October, and November and less in July, August, and December, and women utilizers were more than men. The utilizers who stayed for more than a week were 851 (42.31%), and among them 17 persons were selected by their own hope for being helped by balneal effect. Of these 17, eight persons were not exposed directly to atomic bomb explosion, but entered into the city within several days after the explosion. Before the hot spring cure, there were seven cases of abnormal maximum blood pressure, one case each of oligocythemia, oligochromemia, and leukocytosis, and two cases of leukopenia. After spa treatment, two cases of abnormal maximum blood pressure, one case each of oligocythemia and leukocytosis recovered to normal, and one case of oligochromemia and two cases of leukopenia were improved nearly to normal. (Japan)

26898 SMALLEST FORMS OF PAPILLARY CARCINOMA OF THE THYROID. A STUDY OF 141 MICROCARCINOMAS LESS THAN 0.1 CM IN GREATEST DIMENSION. Sampson, Richard J.; Key, Charles R.; Buncher, C. Ralph; Iijima, Soichi (Hiroshima Univ.). Arch. Pathol.; 91: 334-9(Apr 1971).

Thyroid papillary carcinomas were categorized according to histologic evidence for tumor growth or invasiveness. Noninvasive circumscribed microcarcinomas were associated with a significant preponderance of male patients ($P < 0.01$), whereas no significant difference between sex distribution was noted in the group with "invasive" microcarcinomas. There was no significant difference in tumor prevalence relative to radiation dose at the time of the atomic bombs for the invasive microcarcinomas, and suggestive relationship ($P = 0.10$) was noted for the group with circumscribed microcarcinomas. The circumscribed microcarcinomas are interpreted as tumors that have been given no stimulus to grow because of a relative lack of endogenous promoting factor. Thus, they could be of any age, and the possible induction of some of these neoplasms at the time of the bombs suggests that some may have been present for an extended period. (auth)

Radiation Effects on Animals

Refer also to abstracts 26704 and 26808.

26899 ARTIFICIAL HEART PROGRAM CONFERENCE, Proceedings, Washington, D. C., June 9–13, 1969. Hegyeli, Ruth Johnsson (ed.). Bethesda, Md.; Department of Health, Education, and Welfare (1969). 1139p. GPO $10.00. (CONF-690655).

A separate abstract was prepared for one paper. The other 91 papers (chapters) are grouped into the following topical sections: development of materials for use in circulatory assist devices; analysis of the effects of materials on blood and tissues; blood flow through pumps and valves; cardiac control parameters; oxygenator development; circulatory assist devices; physiological effects of circulatory assist devices in animals; instrumentation applicable to artificial heart development and use; percutaneous leads; biological fuel cells; effects of additional endogenous heat; and implantable energy system. (E.R.B.)

For an abstract of an individual paper see: 26931.

26900 EFFECT OF IONIZING IRRADIATION ON BLOOD COAGULATION FACTOR ACTIVITY. Stamm, H.; Szirmai, E. (Univ., Basel. Abteilung fuer Strahlenhaematologie, Stuttgart. Inst. of Nuclear Engineers, London). Acta Med. Iugoslav.; 24: 185-91(1970). (In German).

Immediately after addition to human blood of Factor VIII (AHG-Behring) or Factors II, V, VII, and IX (Acc 76-Behring), its clotting barely changes. After 24 hours incubation in recalcified citrate blood, however, clotting occurs twice as fast after addition of the factors than without them. Irradiation of the Factors with 2000 R of ^{60}Co gamma does not affect their activity. Above a certain concentration, thrombin addition to blood leads to immediate clotting with unphysiological fibrin formation. Irradiation with 2000 R of ^{60}Co gamma fails to influence this action. (tr-auth)

26901 QUALITATIVE LEUCOCYTE CHANGES DUE TO TOTAL X-RAY IRRADIATION. Oyvin, I. A.; Koroleva, L. V. (Inst. of Medical Radiology, Obninsk, USSR). Stud. Biophys.; 23: 143-7 (1970). (In German).

The effects of homologous leucocyte preparations (lysosomes, granulocytic substance, destroyed leucocytes) on the skin vessel permeability were studied in experiments on Wistar rats and rabbits. The ability of leucocyte preparations to cause hemorrhages was also investigated. It was proved that i.c. administration of leucocyte preparation caused skin blood vessel permeability derangement and hemorrhages in skin and underlying tissues. Leucocyte preparations made of animals on the fourth day after x ray irradiation (600 R for rats and 800 R for rabbits) preserve the ability of causing hemorrhaging but lose the ability of affecting blood vessel permeability. The results may be valuable for the interpretation of the pathogenesis of a weakened development of early phases of inflammation in irradiated animals. (auth)

XUM

26902 RETROGRADE INJURY OF THE RETINA BY IONIZING RADIATION. Kanbai, G. G. Azerb. Med. Zh.; 46: No. 11, 9-13(1969). (In Russian).

Retrograde injury of the eye as a result of lethal and sublethal radiation is illustrated. The destruction of external and internal layers is discussed. (J.S.R.)

26903 RESPONSE OF EQUINE SMALL LYMPHOCYTES WITH AND WITHOUT PHYTOHEMAGGLUTININ TO X-IRRADIATION IN VITRO. Brannon, Richard Bland. Fort Collins, Colo.; Colorado State Univ. (1970). 172p. University Microfilms Order No. 71-5330.

Thesis.

Small lymphocytes were isolated from the peripheral blood of horses and incubated at 37°C in Eagle's medium supplemented with 20% fetal calf serum. The addition of phytohemagglutinin to the cultures resulted in increased RNA and protein synthesis, the enlargement of the small lymphocyte into a lymphoblast-like cell, the initiation of DNA synthesis, and cell division. The lymphoblast-like cell (D_{37} = 200 rads) was more resistant to x-irradiation then the very sensitive small lymphocyte (D_{37} = 20 rads). Survival was measured 24 hours after irradiation by means of phase-contrast microscopy. The criteria used to judge viability under the microscope were supported by autoradiographs which measured ^{3}H uridine and ^{3}H leucine incorporation. A dose of 100 rads, which kills all small lymphocytes and few of the lymphoblast-like cells, was used to investigate which of the changes occurring during the transformation of the small lymphocyte was responsible for the increased resistance to x-irradiation. It was determined that DNA synthesis was not necessarily involved in cell survival. A positive correlation was found, however, between the rate of RNA and protein synthesis which the cell had attained at the time of irradiation and the survival of the cell. The incorporation of bromodeoxyuridine into the lymphoblast-like cell did not affect the 24-hour survival of the cell. (Diss. Abstr.)

26904 IMPORTANCE OF DIRECT AND INDIRECT INFLUENCE OF IONIZING IRRADIATION IN RADIATION LEUCOSOGENESIS. Aleksandrov, S. N.; Galkovskaya, K. F.; Gubareva, A. V. (Central Research Roentgeno-Radiological Inst., Leningrad). Vop. Onkol.; 16: No. 11, 80-5(1970). (In Russian).

In irradiated mice, in which the bone marrow was autotransplanted immediately after irradiation, the frequency of development of myeloid leukosis is decreased along with the increase of a radiation dose, i.e., with the increasing role of non-irradiated (transplanted) stem cells and their generations in repopulation of hemopoietic organs. This supports the fact that a direct effect of ionizing radiation is of major importance in pathogenesis of radiation myeloleukosis. Contrary to that, the incidence of reticulosis and lymphoid leukosis in irradiated animals, subjected or not subjected to transfusion of autologous myelocariocytes, was found to be identical. Ionizing radiation seems to play an important role in development of the mentioned neoplasms. It was found that autotransplantation of bone marrow in non-irradiated mice produced a 5 to 6 fold increase in frequency of myeloleukosis development, as compared to the biological control. (auth)

26905 FORMATION OF FIBROBLAST COLONIES IN MONOLAYER SPLENIC CULTURES OF IRRADIATED AND INTACT MICE. Fridenshtein, A. Ya.; Kuzmenko, G. N. (Inst. of Epidemiology and Microbiology, Moscow). Byull. Eksp. Biol. Med.; 71: No. 1, 74-8(Jan 1971). (In Russian).

Colonies of fibroblasts that are apparently clones, grow in monostratal cultures of mice spleen. The number of colonies reflect the concentration of cell precursors for fibroblasts in the initial cellular suspensions and depend linearly upon the number of explanted cells. It comprises about 20 colonies per spleen. After irradiation in a dose of 150 R in the regenerating spleen the number of colony-forming cells on the 5th to 30th days increases by 6 times on the average. On the 12th day after irradiation with a dose of 600 R the number of these cells in the spleen sharply declines, whereas after irradiation with a dose of 825 R they disappear. (auth)

26906 CHANGES IN BIOLOGICAL EFFECTIVENESS OF A FAST NEUTRON BEAM WITH DEPTH IN TISSUE-EQUIVALENT MATERIAL. Evans, Richard G.; Pinkerton, Arthur; Djordjevic, Bozidar; Mamacos, James; Laughlin, John S. (Sloan-Kettering Cancer Inst., New York). Contract AT(30-1)-910. Radiat. Res.; 45: 235-43(Feb 1971).

A neutron beam of modal energy 6 MeV obtained by bombarding a beryllium target with ^{3}He ions accelerated by the Institute cyclotron was employed to study the biological effectiveness of fast neutrons with depth in tissue equivalent material. The end point used was the reproductive integrity of cultured HeLa cells as judged by colony forming ability after irradiation. Survival curves obtained after irradiating attached cells at different depths with fast neutrons show a complete lack of shoulder. Split dose experiments supported this observation in that there is little recovery of radioresistance in the period immediately after the first neutron exposure. The relative biological effectiveness (RBE) of the neutron beam compared to ^{60}Co radiation decreases monotonically from about 3.4 at 2.4 cm depth to about 2.3 at 16 cm depth in the phantom. (auth)

26907 RATE OF THE INITIAL FORMATION OF MICROCOLONIES IN THE GAMMA IRRADIATION OF SOTS CELLS IN VARIOUS PHASES OF THE MITOTIC CYCLE. Gubin, V. A.; Komolov, I. S. (Inst. of Biophysics, Moscow). Radiobiologiya; 10: 527-31(1970). (In Russian).

The effects of γ radiation on a synchronous culture lead to a substantial decrease in the rate of initial proliferation of the cells. The maximum changes arise in the case of irradiation during the period of mitosis and in the phase of DNA synthesis; the least arise at the beginning of the G_1 phase. The role of the phases of the cycle is associated with the change in the specific significance of the individual processes (delay of the beginning of division, increase in the time of mitosis, mitotic death) that are responsible for the slowness of proliferation. (auth)

26908 RADIOMIMETIC EFFECT OF ACTINOMYCIN C ON TUMORS OF GLIAL ORIGIN CULTURED IN VITRO. Kaluza, Jozef; Stefanicka-Wiechowa, Alina (Lab. of Neurosurgical Pathology, Krakow). Arch. Immunol. Ther. Exp.; 18: 220-4 (1970).

The radiomimetic effect of actinomycin C in concentration 5×10^{-14} and 5×10^{-15} followed by a single dose of x irradiation of 8000 R on tumors of glial origin cultured in vitro was studied. Tumors of the astrocytoma group responded with degeneration and decay of cells in the growth zone in 70% if a concentration of 5×10^{-14} was used or in 50% if concentration of 5×10^{-15} was applied to the medium. (auth)

Invertebrates

Refer also to abstracts 26619, 26648, 26694, 26705, 26713, 26719, 26720, 27151, 27152, 27154, and 27155.

26909 EFFECT OF IRRADIATION ON THE INFECTIVE STAGE LARVAE OF THE NEMATODE, OESOPHAGOSTOMUM COLUMBIANUM AND THEIR USE AS A VACCINE. Dhar, D. N.; Singh, Kunwar Suresh (Indian Veterinary Research Inst., Izatnagar, Egypt). J. Helminthol.; 44: No. 1, 11-26(1970).

The effect of x irradiation on the survival, behavior and immunogenicity of the infective (3rd stage) larvae of Oesophagostomum columbianum was studied. The findings reported were: irradiation with up to 160,000 R does not significantly alter the survival of the larvae when stored at 4°C and at room temperature (26 to 32°C) for a period of 42 days, irradiation at 15,000 R to 40,000 R results in progressively fewer adults developing but more nodules being formed in the intestinal wall. Irradiation at 80,000 R results in the larvae failing to develop and establish in the host, irradiation at 15,000 R to 40,000 R progressively changed the male : female ratio from 1 : 3 to 1 : 22.6, irradiated larvae develop and mature comparatively late and the eggs appear later in the feces of the host; many of these are infertile, a single dose of infective larvae irradiated at 40,000 R stimulated acquired immunity in the host and hence increased nodule formation. Accordingly immunization by irradiated infective larvae is not a practical measure, and a scheme for the control of oesophagostomiasis through the use of irradiated larvae and herd management was suggested. (auth)

26910 VISUAL EFFECTS OF IONIZING RADIATION IN THE NOCTUID MOTH, HELIOTHIS ZEA. Schafer, Kenneth Lisle Jr. Tallahassee; Florida State Univ. (1970). 94p. University Microfilms Order No. 71-7097.

Thesis.

A collection of experiments combining behavioral, electrophysiological, and photochemical techniques were designed to probe the problem of visual receptor excitation induced by low levels of x-ray, gamma, and beta radiation. Interactions between light and ionizing radiation as well as similarities between the two modes of stimulation were investigated in an attempt to provide information concerning the mechanism of transduction for ionizing stimuli in the visual system. Behavioral studies utilized motor responses to low intensity visual stimuli which can be elicited in the dark adapted moth by pulses of light and various types of ionizing radiation. In these experiments frequency of flight functions were obtained for both gamma (^{60}Co) and 90 kv

XUM

x-ray stimuli which provided an excellent means for comparing threshold energies of gamma and x-radiation necessary for eliciting motor activity. A second group of studies consisted of a systematic investigation of steady state reduction in the photically evoked electroretinogram produced by background lights gamma, and x-irradiation. It was found that the effects of gamma and light backgrounds could be matched with respect to changes in both the amplitude and waveform of the electroretinogram elicited with light flashes. X-radiation was compared with gamma radiation in this experiment also, and it was found that equal reduction of the photically evoked electroretinogram was obtained when exposure rates of the two background stimuli were equal. The effectiveness of light and beta radiation as visual stimuli during the dark adaptation process was studied after light adaptation of the eye. In the final group of experiments, photochemical techniques were employed to study the bleaching of visual purple with gamma radiation. Rhodopsin extracted from cattle retinas was irradiated with gamma at an exposure rate low enough to prevent thermal denaturation of the rhodopsin. Substantial reductions in 11-cis concentration were observed in the irradiated samples, but no evidence was obtained to indicate a normal 11-cis to all trans isomerization of the visual purple. (Diss. Abstr.)

26911 ACTION OF ACTINOMYCIN D ON MITOTIC ACTIVITY AND ON X-RAY-INDUCED PROPHASE REVERSION IN NEUROBLASTS OF CHORTOPHAGA VIRIDIFASCIATA (DE GEER). Stephens, Ralph Edmund. Knoxville, Tenn.; Univ. of Tennessee (1970). 71p. University Microfilms Order No. 71-7680.

Thesis.

Embryos of the grasshopper Chortophaga viridifasciata (DeGeer) equivalent to 14 days development at 26°C were utilized to determine the dependency of the recovery process from x-ray-induced prophase reversion on RNA synthesis. Neuroblasts were studied in hanging drop cultures at 28°C and in autoradiographed and stained squash preparations. Actinomycin D (AMD), an antibiotic, was utilized to inhibit DNA dependent RNA synthesis in this investigation. In hanging drop cultures lacking yolk, AMD at concentrations of 4 μg/ml and 10 μg/ml has no effect on the midmitotic time intervals, but decreases the mitotic rate to less than 25% of the control rate. In cultures containing yolk, 4 μg AMD/ml has no effect on the mitotic rate, but 10 μg AMD/ml depresses the rate by almost 75%. RNA synthesis was determined from autoradiographs of ^{3}H-uridine incorporation. The incorporation observed was RNase sensitive. The average autoradiographic grain count, representing RNA synthesis, for cells in all stages, increased after the first half hour at a constant rate of almost 9 grains per hour. Cells treated with 10 μg AMD/ml also demonstrated a constant level of RNA synthesis, but at a rate approximating 70% of the control rate. Embryos in the egg case were exposed to 64 R x-irradiation. Neuroblasts which were irradiated in middle prophase were observed to revert to early prophase and recover, progressing to prometaphase in an average time of 281 minutes after x-raying. When embryos were treated with 10 μg AMD/ml in addition to x-irradiation the average time necessary for the cells to reach prometaphase was increased to at least 480 minutes and most cells which were observed for more than 24 hours (data not used in average) did not recover. In cells which did not recover abnormal nucleoli were always observed. It was concluded from this investigation that: yolk is necessary to maintain a high mitotic rate in handling drop cultures; RNA synthesis is necessary for recovery from x-ray-induced prophase reversion; and the normal function of nucleoli is inhibited by AMD in telophase of nonirradiated cells and in prophase of cells exposed to 64 R x-irradiation. (Diss. Abstr.)

26912 REACTIONS OF THE SEA ANEMONE, ANTHOPLEURA XANTHOGRAMMICA, TO ELECTROMAGNETIC RADIATIONS IN THE VISIBLE, ULTRAVIOLET, AND X-RAY RANGES. Clark, Ervil Delwyn. Corvallis, Oreg.; Oregon State Univ. (1971). 100p. University Microfilms Order No. 71-6775.

Thesis.

The behavioral repertoire of the sea anemone, Anthopleura xanthogrammica, was investigated to test for the occurrence of any immediate response to various regions of the electromagnetic spectrum. Monochromatic radiations in the visible and ultraviolet spectral regions were produced by a 150-watt xenon lamp or a 200 watt mercury vapor lamp coupled to a Bausch and Lomb high intensity diffraction grating monochromator. X-rays were produced by a Maxitron 300 kVp x-ray machine. Small-area (1.75 × 2.5 cm) exposures were given to: the tentacles and oral disc, the column, the peristome, and the pedal disc. The effective dose of each wavelength, sufficient to evoke a specific criterion of response, was determined for each reaction. The relative efficiency for effective wavelengths was calculated after correction for relative quantum efficiency. Action spectra, based on the relative efficiency data, showed different stimulative efficiency ranges and maxima in five distinct behavioral responses as follows: tentacle flexion, from 340 nm to 600 nm with peaks at 360 nm and 500 nm, tentacle retraction, from 248 nm to 400 nm with a peak at 280 nm, oral disc flexion, from 350 nm to 600 nm with a peak at 360 nm, column cavitation, from 345 nm to 450 nm with a peak at 350 nm, and peristome depression, from 350 nm to 400 nm with a peak at 360 nm. The occurrence of these prompt reactions to x-ray, ultraviolet, and visible radiations indicates that a highly organized receptor system is not essential for radiation effects to be manifested in behavior. (Diss. Abstr.)

26913 PHYSICAL, CHEMICAL, AND BIOLOGICAL CONTROL OF THE ALFALFA WEEVIL (HYPERA POSTICA: CURCULIONIDAE). Burgess, Edward Eugene. Knoxville, Tenn.; Univ. of Tennessee (1969). 138p. University Microfilms Order No. 70-17,802.

Thesis.

Studies on the alfalfa weevil (Hypera postica Gyllenhal) consisted of a threefold investigation; namely, physical control by means of γ irradiation of the larval and pupal stages; chemical control by means of various experimental insecticides; and biological control by means of a parasitic nematode DD136 and parasitic hymenopterous insects. The study also contained a description of the systematic position and nomenclature of the alfalfa weevil. Third instar larvae were irradiated at 2000 R, 4000 R, 6000 R, 8000 R, and 10,000 R, and complete mortality followed in larval and pupal stages. From irradiated fourth instar larvae, 100 percent mortality occurred at 4000 R and higher rates in the pupal stage. Below 4000 R (2000 R down to 500 R), mortality decreased with an occurrence of abnormalities in the adult stage. Irradiated pupae of 1700 R to 10,000 R demonstrated significant differences, but were less sensitive to radiation than the larval stage. A decline in mortality and abnormalities was noted with an increase in age of the pupal stage. The experimental data obtained from various insecticide applications indicated that of all the insecticides tested, Furadan gave the best overall performance with one application. It was found in laboratory tests that a nematode parasite DD136 gave very significant larval and adult mortality rates. Hymenopterous parasites were released periodically from 1962 to 1968 in order to aid in control of the alfalfa weevil, however, the areas sampled in this study gave negative results. (Diss. Abstr.)

26914 RADIATION DAMAGE AND REPAIR AFTER WHOLE-BODY OR PARTIAL-BODY IRRADIATIONS OF TENEBRIO MOLITOR LARVAE. Jayaraman, Swaminathan. Urbana, Ill.; Univ. of Illinois (1970). 111p. University Microfilms Order No. 71-5134.

Thesis.

The time course of mortality, the dose response, the incidence of delayed pupation and developmental abnormalities, and the post-eclosion life span of adults were scored after x-irradiation of Tenebrio molitor larvae. The influence of larval age at the time of irradiation, of their parents' age at the time of egg-laying, of dose-fractionation, and of partial-body irradiations on the above criteria were investigated. There was always a lag between the time of irradiation and the onset of mortality, and the irradiated larvae had two patterns of survival depending upon the size of the dose delivered. The LD_{50} for survival to pupation was found to be around 3.1 KR. Dose-fractionation studies (using two and multiple fractions) indicated not only a significant increase in survival to pupation and eclosion but also the existence of fast and slow components of recovery. The fast component of recovery was found to be temperature dependent and cold treatment during inter-fraction intervals alone was found to be effective. Irradiation of either the middle third alone or of the posterior third alone resulted in a significant increase in survival to pupation and eclosion as compared to that of either whole body or anterior third alone or anterior and posterior thirds alone. It seems therefore that the critical targets leading to pupation delay and lethality are probably located in the anterior third of T. molitor larvae, possibly the neuro-endocrine system. The incidence of developmental abnormalities was affected by the magnitude of dose, by dose-fractionation and by the age of the larvae at the time of exposure. There was no significant reduction in life span of grossly normal-appearing adults obtained from irradiated larvae and the apparent differences in life span of male and female adults were found not to be significant. No significant influence of larval or of parental ages on the radiosensitivity of these larvae was found for most criteria scored with the exception of the aforementioned incidence of developmental abnormalities. (Diss. Abstr.)

26915 EFFECTS OF CHRONIC IRRADIATION AND TEMPERATURE ON POPULATIONS OF THE AQUATIC SNAIL, PHYSA HETEROSTROPHA. Cooley, James Louis. Knoxville, Tenn.; Univ. of Tennessee (1970). 96p. University Microfilms Order No. 71-7619. Thesis.

Three separate, but related, studies were conducted to determine the effects of chronic irradiation and temperature on laboratory and natural populations of the aquatic snail Physa heterostropha. In the laboratory, at 25 C, dose rates of chronic gamma irradiation of 1, 2, 5, 10, and 25 rads/hr caused a significant decrease in the fecundity of snails. A dose rate of 25 rads/hr would cause extinction of a population in one generation; 10 rads/hr, in one or two generations. Dose rates of 1, 2, and 5 rads/hr would not lead to an immediate extinction; the reduction in fecundity increased with increasing dose rate. The percentage of eggs hatching was decreased by all dose rates except 1 rad/hr. Dose ratios of 10 and 25 rads/hr significantly increased growth. The life span of adult snails was shortened significantly by all dose rates except 1 rad/hr. Laboratory populations were exposed to dose rates of 1, 2, and 5 rads/hr at 15°C. Only a dose rate of 5 rads/hr significantly decreased fecundity. Hatching of eggs was significantly decreased by dose rates of 2 and 5 rads/hr. The effects of chronic irradiation on snail populations were determined to be greater at the higher temperature of 25°C. A temperature of 25°C, as compared with 15°C, caused a significant increase in the fecundity of laboratory populations. Temperature elevation did not have an effect on the hatching of eggs. The elevated temperature was judged to be nondetrimental to snail populations for the conditions of this laboratory study. A natural population of Physa living in an area where it is exposed to chronic environmental radiation of 0.65 rad/day was studied. An acute gamma radiation study indicated that this population has not developed resistance to radiation. A $LD_{50(30)}$ dose of 47,900 rads was determined. When compared to a control population, the frequency of capsule production in the population exposed to chronic environmental radiation was reduced. A corresponding reduction in egg production was not found due to an increased number of eggs per capsule. It was suggested that the compensation for the reduced capsule production by increased number of eggs per capsule was brought about by natural selection. Results from the three studies imply that radioactive and thermal pollution from nuclear power reactors probably will not have an adverse effect on Physa heterostropha populations. (Diss. Abstr.)

26916 EFFECTS OF GAMMA RADIATION ON THE LARVAL MIDGUT OF THE INDIAN-MEAL MOTH, PLODIA INTERPUNCTELLA (LEPIDOPTERA: PHYCITIDAE). Ashraf, Mohammad; Brower, John H.; Tilton, Elvin W. (Dept. of Agriculture, Savannah). Radiat. Res.; 45: 349-54(Feb 1971).

The normal midgut of Plodia interpunctella consisted of an epithelial layer, a thin basement membrane, an inner circular muscle coat, and outer bundles of longitudinal muscles. The major cytological damage associated with radiation exposure was displayed by the midgut epithelium. Damage ranged from moderate cell disruption 4 days after treatment with 5 krads to almost complete histolysis following 50 krads. The regenerative cells that renew the epithelial lining of the midgut were particularly sensitive to radiation damage resulting in an inability to replace the midgut epithelium. (auth)

26917 EFFECTS OF FAST NEUTRONS AND ^{60}Co γ-RAYS ON ARTEMIA. Iwasaki, Tamiko; Maruyama, Takashi; Kumamoto, Yoshikazu; Kato, Yoshio (National Inst. of Radiological Sciences, Chiba, Japan). Radiat. Res., 45: 288-98(Feb 1971).

The effects of a single exposure to 2 MeV fast neutrons were compared with the effects of exposure to ^{60}Co γ ray irradiation on dry eggs of Artemia salina. Comparison of the survival data showed that neutrons were 2.1, 2.8, and 4.8 times as effective as γ irradiation in producing mortality of nauplii at 1, 2, and 3 days after hatching. Irradiation with fast neutrons produces severe chromosomal abnormalities and leads to a depression in mitotic activity. On the basis of the cytological observations, the relative biological effectiveness of fast neutrons was about 2 with reference to γ rays. (auth)

26918 IMMUNITY TO DICTYOCAULUS VIVIPARUS IN CALVES. III. VACCINATION WITH LARVAE ATTENUATED BY TRIETHYLENE MELAMINE (TEM) OR X-IRRADIATION AND PROTECTION AGAINST FIELD CHALLENGE. Cornwell, R. L.; Jones, R. M. (Pfizer Group, Sandwich, Eng.). Res. Vet. Sci.; 11: 569-74(Nov 1970).

Calves vaccinated with Dictyocaulus viviparus larvae attenuated either with triethylene melamine (TEM) or by x irradiation were exposed together with unvaccinated calves to a heavily infected pasture. Severe clinical disease occurred in the unvaccinated calves resulting in three fatalities out of eight calves. Vaccinated calves withstood the challenge showing moderate clinical signs with lower respiratory rates, minimal fecal larval excretion, and increased body weight gains compared with unvaccinated controls. Both types of vaccine produced similar responses. (auth)

26919 IMMUNITY TO DICTYOCAULUS VIVIPARUS IN CALVES. II. VACCINATION WITH NORMAL LARVAE OR LARVAE ATTENUATED BY TRIETHYLENE MELAMINE (TEM) OR X-IRRADIATION AND EXPOSURE TO EXPERIMENTAL CHALLENGE. Cornwell, R. L.; Jones, R. M. (Pfizer Group, Sandwich, Eng.). Res. Vet. Sci.; 11: 560-8(Nov 1970).

Calves vaccinated with 2 doses of 1,000 Dictyocaulus viviparus larvae attenuated with triethylene melamine (TEM), together with calves similarly dosed, but with normal larvae, and untreated controls, were challenged with 10,000 normal larvae. The TEM vaccine was fully attenuated and non-pathogenic, and protected calves against the challenge that produced severe symptoms in, and killed, two of the four controls. Mild clinical signs occurred in the vaccinates after challenge with increased respiratory rate and low grade fecal larval output (6% of controls) but weight gain was maintained. The calves receiving normal larvae showed moderate clinical signs with high respiratory rate, weight loss, and fecal larval excretion. The challenge did not exacerbate the symptoms and appeared to have no effect on the course of the initial infection that was eliminated with a return to normal weight gain. The initial weight loss was, however, not regained. In another experiment calves vaccinated at intervals of 2 to 4 weeks with 2 doses of 1,000 D. viviparus larvae attenuated with TEM were compared with calves vaccinated with x-irradiated or normal larvae with a 4-week interval between doses and, together with untreated controls, exposed to a challenge of 7,500 larvae. The groups vaccinated with TEM-attenuated larvae showed no untoward clinical effects during vaccination but a slight reduction in weight gain was apparent and a few fecal samples were positive for larvae. The irradiated larval vaccine was not associated with reduced weight gain and only one fecal sample was positive for larvae. Following challenge, mild clinical symptoms were present in all the vaccinates with low levels of fecal larval output and moderately elevated respiratory rates. Weight gain continued steadily in contrast to controls that suffered severely from the challenge with one fatality, substantial weight loss and high respiratory rate and fecal larval excretion. One death occurred in the TEM vaccinated group receiving vaccine at a 2-week interval. The group receiving normal larvae suffered moderately from the initial infections but did not appear to be affected in any way by the challenge infection. (auth)

Vertebrates

Refer also to abstracts 26588, 26612, 26625, 26626, 26652, 26654, 26659, 26666, 26669–26673, 26677–26680, 26682, 26690, 26711, 26723, 26724, 26726, 26727, 26792–26796, 26803, 26809, 26812, and 26827.

26920 (AD-711041) SIMULATION AND MEASUREMENT OF SOLAR-FLARE PROTON EXPOSURES. Final Report, November 1968–August 1969. Burton, Ben S.; Parker, C. Varren Jr.; Boles, Larry A.; Alexander, Edward F.; Nelson, John B. (Nuclear-Chicago Corp., Austin, Tex. Texas Nuclear Div.). Jun 1970. Contract F41609-69-C-0012. 20p. (SAM-TR-70-38). NTIS.

Analytical and experimental technics were developed for simulating solar-flare proton exposures. These technics were used to expose a series of animals (Macaca mulatta) to specified depth-dose distributions. The exposures were made with the nominal 300-MeV proton beam of the NASA Space Radiation Effects Laboratory synchrocyclotron. Details of the simulation and physical dosimetry measurements are presented. (auth) (USGRDR)

26921 (LF-tr-49) RADIATION (^{90}Sr) INDUCED PULMONARY CARCINOMA IN RATS. Altmann, H. W.; Hunstein, W.; Stutz, E. Translated by A. A. Horvath (Lovelace Foundation for Medical Education and Research, Albuquerque, N. Mex.), from Naturwissenschaften; 46: 85-6(1959). 4p. Dep. NTIS.

Radioinduced carcinomas were observed in the lungs of rats within five months following implantation of ^{90}Sr-filled capsules (6 × 2 mm dimension) that emitted a β dose at the surface ranging between 27 and 62 μCi. The containers remained in the body of the animals and were removed only at autopsy. All of the 134 rats used in the study developed carcinomas within eight months following ^{90}Sr implantation. (C.H.)

26922 (ORO-3260-3-A) LONG-TERM EFFECTS OF RADIATION: MAMMALIAN BEHAVIOR. Final Report, February 1968–July 31, 1970. Furchtgott, Ernest (Tennessee Univ., Knoxville, Dept. of Psychology). Contract AT(40-1)-3260. 16p. Dep. NTIS.

The purpose of this project was to investigate behavioral aging changes in mice irradiated as young adults and which have passed the acute radiation syndrome. Mice of the RF/Up strain were exposed to 800 rad in 4 fractionated doses of x rays between the age of 74 and 116 days. Beginning after irradiation and continuing to the age of 16 mon some animals were tested longitudinally and some cross sectionally in an open field, for general activity in a small box with an ultrasonic device and for swimming speed.

XUM

None of the measures showed any radioinduced aging changes though the irradiated animals did have a shortened life span and reduced body weight. It was concluded that the most sensitive behavioral index of aging, decreased activity, was not affected by radiation. (auth)

26923 RHEOLOGY OF FRESH, AGED, AND GAMMA-IRRADIATED EGG WHITE. Tung, M. A.; Richards, J. F.; Morrison, B. C.; Watson, E. L. (Univ. of British Columbia, Vancouver). J. Food Sci.; 35: 872-4(Nov-Dec 1970).

Rheology of unmixed egg white at 2°C was studied with a narrow-gapped rotational viscometer over a 20 fold range of shear rates. For a constant shear rate, egg white consistency decreases with time and approaches an equilibrium value in a few minutes. Flow behavior is pseudoplastic at 2°C between shear rates of 8.1 to 147 sec^{-1} and the shear stress-shear rate relation is accurately described by the power law and Casson models. The effects of gamma irradiation dose on Haugh unit score and equilibrium shear stress were discussed. (auth)

26924 DOSE REDUCTION FACTOR FOR RADIATION LETHALITY IN MICE AS A FUNCTION OF THE DOSE OF MERCAPTOETHYLAMINE. Hasegawa, A. T.; Landahl, H. D. (Univ. of Chicago). Radiat. Res.; 44: 738-47(Dec 1970).

Dose reduction factors (DRF) were determined for various doses of mercaptoethylamine (MEA) administered either intravenously or intraperitoneally to mice before whole body x irradiation. MEA doses ranging from 125 to 600 mg/kg were administered intravenously while MEA doses as high as 750 and 900 mg/kg were administered intraperitoneally. The toxicity of MEA was greater in mice kept at 30°C than in those kept at 22°C. The detoxification rate for MEA was about 90 mg/kg/hour. Pentobarbital administration, either in a single or in multiple injections, after irradiation and control of environmental temperature was used to counteract the toxicity following high doses of MEA. The acute mortality rate after large doses of MEA was high. The DRF values were approximately proportional to the MEA dose up to 600 mg/kg. The highest DRF (2.81) was obtained with an intravenous MEA dose of 600 mg/kg. (auth)

26925 TRITIUM: SOME EFFECTS OF CONTINUOUS EXPOSURE IN UTERO ON MAMMALIAN DEVELOPMENT. Cahill, Daniel F.; Yuile, Charles L. (Univ. of Rochester, N. Y.). Radiat. Res.; 44: 727-37(Dec 1970).

Pregnant rats were maintained at constant body activities of tritiated water ranging through 1 to 100 μCi/ml of body water throughout pregnancy. These activities provided whole body doses to the embryo and fetus of approximately 0.3 to 30.0 rads/day. The activity level of progeny was normal with respect to external and internal morphology. Statistically significant findings at various HTO levels included: micrencephally, sterility, stunting, litter size reduction, and increased resorption. Decreases in the absolute and relative weights of a number of term fetus organs were closely proportional to dose. Histologically all organs were normal except the gonads. Tritium incorporation into fetal organs was directly proportional to, and 20 to 30% of, the average maternal body water HTO activity prevailing during gestation. Postnatal observations showed that by 180 days stunting was no longer evident in irradiated females but persisted in males irradiated at 50 to 100 μCi/ml. Within 270 days 5 tumors had arisen in irradiated animals compared to 1 in a control animal. Continuous exposure to an HTO activity of 1 μCi/ml during pregnancy was found to be consistent with the production of offspring in which the only deviations from the controls noted were an increased length and a slight increase in weight of the liver and heart evident only in neonates. (auth)

26926 RADIOPROTECTIVE EFFECT OF RETICULOENDOTHELIAL SYSTEM BLOCKADE IN MICE. Mori, K. J.; Nakamura, S. (Osaka Prefectural Inst. of Public Health). Experientia; 26: 1386-7(15 Dec 1970).

The reticulendothelial system (RES) acts as a primary host defense mechanism against effects of self substances and intruded foreign materials. The RES is radioresistant. It was reported that after exposure of mice to x radiation cell debris occurred in the blood stream and was sequestered by RES. The blockage of RES by overloading with particulate material (carbon particles) provides the animals with a greater degree of tolerance to radiation by interfering with the phagocytosis of injured blood cells. (P.B.M.)

26927 SITE OF THE TARGET REGION FOR RADIATION-INDUCED MITOTIC DELAY IN CULTURED MAMMALIAN CELLS. Munro, T. R. (Strangeways Research Lab., Cambridge, Eng.). Radiat. Res.; 44: 748-57(Dec 1970).

Irradiation of the cytoplasm of Chinese hamster fibroblasts with large doses of α particles from a polonium-tipped microneedle did not delay their proliferation. 1000 R of x rays and small numbers of α particles penetrating a few microns into the nucleus produced 8 to 9 hr and 16 hr mitotic delay, respectively. Hence the targets for mitotic delay are either nuclear or in the immediately perinuclear cytoplasm. (auth)

26928 MINIATURE PIG PERFORMANCE AFTER FRACTIONATED SUPRALETHAL DOSES OF IONIZING RADIATION. Chaput, Raymond L.; Kovacic, Roger T. (Armed Forces Radiobiology Research Inst., Bethesda, Md.). Radiat. Res.; 44: 807-20(Dec 1970).

Miniature pigs, trained to traverse, on cue, a two chambered shuttlebox, received fractionated and unfractionated doses of pulsed mixed gamma-neutron radiation. Performance was significantly better when 6,800 to 13,000 rad doses were delivered in two equal fractions, 5 hr apart, than when given in a single pulse; the early transitory incapacitation period was shorter and the pigs recovered more rapidly to an acceptable performance level. Performance was also significantly better after an 8800 rad fractionated dose given as two 4400 rad fractions from ½ to 51 hr apart than after an 8600 rad unfractionated dose. Furthermore, the pigs generally had less severe clinical symptoms (convulsions and coma) after the second half than after the first half of the fractionated doses. When the first dose was reduced to 3400 or to 1700 rads, however, early transient incapacitation did occur after the subsequent 4800 to 5000 rad dose and was more frequently accompanied by convulsions when the initial dose was only 1700 rads. Mean survival times of pigs receiving the fractionated doses were significantly longer than that of pigs receiving equivalent unfractionated doses. (auth)

26929 DOSE-RELATED LOCAL AND SYSTEMIC EFFECTS OF INHALED ^{236}Pu AND ^{239}Pu DIOXIDE IN DOGS. Yuile, C. L.; Gibb, F. R.; Morrow, P. E. (Univ. of Rochester, N. Y.). Radiat. Res.; 44: 821-34(Dec 1970).

Pulmonary and lymph node lesions and leukopenia which developed in dogs after ^{239}Pu and ^{236}Pu dioxide inhalation were related to various radiation dose parameters, over a wide range of postexposure time intervals (16 to 468 days). The degree of radiation pathology in lungs was found to increase with increasing accumulated alpha doses above 1500 to 2000 rads and up to about 15,000 rads. In general no damage to tracheobronchial lymph nodes was evident unless radiation changes were also present in the lungs. The degree and extent of the lymph node changes did not correlate well with estimates of total lymph node dose, but there was a relatively good relationship with dose rate (rads per day) to the lymph nodes adjacent to trachea and main bronchi. Radiation changes in both types of tissue, and due to both plutonium isotopes, were unrelated to length of postexposure period except for increasing fibrosis with time. In contrast, the leukopenia which developed was related to mean, post exposure, fixed tissue burdens but not to rad dose except in experiments of similar duration. The findings indicate that the lung lesions reflect total accumulated pulmonary doses while lymph nodes are more sensitive to dose rate. It is suggested that the leukopenia developed as a result of irradiation of circulating cells by localized deposits of plutonium in lymph nodes and probably lungs, rather than to depression of hematopoiesis and or lymphopoiesis. (auth)

26930 LATE EFFECTS OF IRRADIATION IN INFANCY ON THE MOUSE OVARY. Peters, Hannah (Finsen Lab., Copenhagen). pp 193-202 of Post-Natal Development of Phenotype. /Kazda, Stanislav (ed.). London: Butterworth and Co. Ltd. (1970).

From Conference on the Post-Natal Development of Phenotype, Prague, Czechoslovakia. See CONF-670997.

The late effects of radiation in infancy on the ovary are discussed in relation to the following. The morphological development of the ovary. An immediate post-irradiation reduction in the number of oocytes led to premature depletion of oocytes and follicles in the ovary. An accumulation of corpora lutea was later followed by their confluence and the formation of luteomas. Foci of cell proliferation in the luteomas led to mixed tumor formation that infiltrate the surrounding tissues. The reproductive performance of the irradiated animals showed a reduced total reproductive capacity and a shortened fertility span. A hormonal imbalance developed in the radiated animals as an expression of a disturbed pituitary–ovarian interrelation that is initiated by the radiation induced prematurely aged ovary. (auth)

26931 EFFECTS OF INTRACORPOREAL HEAT AND RADIATION ON DOGS. Norman, J. (Sears Surgical Research Labs., Boston); Pegg, C.; Sandberg, G.; Lee, R.; Huffman, F. pp 901-11 of Artificial Heart Program Conference. /Hegyeli, Ruth Johnsson (ed.). Bethesda, Md.: Dept. of Health, Education, and Welfare (1969).

From Artificial Heart Program Conference, Washington, D. C. See CONF-690655.

The body must be capable of dissipating the reject heat from the power source that drives the blood pump(s) of an implantable circulatory support system. If the energy source is a radioisotope, the body must also tolerate nuclear radiation exposure. In these studies, the effects of additional heat and nuclear radiation imposed on dogs by implanting a blood-cooled heat exchanger in the thoracic cavity using ^{238}Pu capsules as well as RES (radiation equivalent sources) capsules that simulate the ^{238}Pu neutron and γ radiation environment were characterized. Within the observation periods (16 watt ^{238}Pu, 18 mos.; 24 watt ^{238}Pu, 10 mos.; RES, 10, 10, and 8 mos.), all radioisotope dogs were in apparent good condition except for chromosomal changes in their lymphocytes cultured in vitro after phytohemmaglutinin stimulation, similar to those found in patients after radiation therapy. Serial hematologic, endocrine, hepatic, and renal function tests were within normal limits. These continuing studies indicate that the temperature regulation mechanisms of mongrel dogs adjust to dissipate additional endogenous heat loads up to 0.8 watt/kg (corresponding to a heat flux of 1 watt/cm^2 and a maximum blood temperature rise of 4°C within the exchanger) and that the anticipated reject heat and dose-rate levels from an implantable circulatory support system may be permissible. (auth)

26932 COMBINED SURGICAL AND RADIATION INJURY. IV. EFFECT OF ANTIMICROBIALS ON THE WOUND HEALING PATTERN OF THE X-IRRADIATED RAT. Donati, Robert M. (St. Louis Univ. Veterans Administration Hospital, St. Louis). Arch. Surg. (Chicago); 102: 132-5(Feb 1971).

The effect of treatment with tetracycline, streptomycin, or chloramphenicol on mortality and wound healing patterns of irradiated and nonirradiated rats was assessed. The administration of tetracycline and streptomycin diminished the mortality in combined radiation and surgical injury; chloramphenicol, streptomycin, or tetracycline did not change the normal wound healing pattern in nonirradiated animals, nor did the administration of these antimicrobials restore the wound healing pattern in the irradiated animal to normal. These data suggest that infection may not play a primary role in the delay in wound contraction attendant to radiation injury. (auth)

26933 DEVELOPMENT OF CALCIFICATIONS AFTER WHOLE-BODY X IRRADIATION OF DHT (DIHYDROTACHYSTEROL)-SENSITIZED RATS. I. THE IONIZING IRRADIATION AND CALCIPHYLACTIC SYNDROME. Petyrek, P.; Mraz, J. Medical Research and Postgraduate Inst., Hradec Kralove, Czech.). Sb. Ved. Pr. VLVDU Hradci Kralove; 43: 3-15(1969). (In Czech).

Fifty white rats (males and females) were divided into five groups receiving the following treatments respectively: group one—exposed to whole-body x radiation at a dose of 500 R—a control group; group two—received dihydrotachysterol (DHT) at 1 mg/100 g per os—also a control group; groups three, four, and five were all exposed to whole-body x radiation at a dose of 500 R and were given DHT at 1 mg/100 g per os 24 hr before, at the time of, and 24 hr following irradiation, respectively. Five days following irradiation, four rats from each group were treated with Oxymykoin Spofa (tetracycline) at 5 ml/100 g and 24 hr later they were killed. The accumulation of the tetracycline in calcified tissues was studied as was its uv fluorescence. The 30-day survival of the remaining six rats in each group was studied. On the 29th day following irradiation, the surviving rats were given tetracycline (5 ml/100 g) and on the 30th day they were sacrificed for uv fluorescence studies. Mortality among the control groups was lower than among the experimental groups (17% and 50 to 83%, respectively). In groups three and four, the accumulation and fluorescence of Ca and tetracycline in certain tissues were higher than in the other groups. In group five, the mortality and accumulation of Ca and tetracycline were smaller than in groups three and four. The rats of all of the groups that were killed on the 30th day following irradiation had no calcifications in the tissues. Tetracycline fluorescence was observed only in the skeleton. (tr-auth)

26934 EFFECT OF BLEEDING AFTER IRRADIATION ON SURVIVAL OF THREE STRAINS OF LETHALLY-IRRADIATED MICE WITH DIFFERENT RADIOSENSITIVITY. Sugahara, T.; Tanaka, T. (Kyoto Univ.). Int. J. Radiat. Biol.; 18: 395-7 (1970).

A table is given of 30 day survival rates for 3 strains of mice, bled of 5% of their body weight after whole-body x irradiation. In all cases the survival rate was higher in bled than in non-bled mice. In dd/YF mice at 700 R and 900 R the results were statistically significant. In the C57BL/6 mice the results were significant only at 700 R and in NC (the most radiosensitive strain) there was no significance. (UK)

26935 BIOCHEMICAL CHANGES IN SERUM OF INTACT AND IRRADIATED DOGS AFTER INTRAVENOUS AET ADMINISTRATION. Arient, M.; Kourilek, K.; Pospisil, J.; Dienstbier, Z.; Kyral, V. (Charles Univ., Prague. Central Military Hospital, Prague). Cas. Lek. Cesk.; 108: 1470-8(28 Nov 1969). (In Czech).

The effects of intravenous administration of AET (in the dose of 100 mg/kg body weight) on certain biochemical parameters in intact dogs and in those exposed to 600 R of x rays were studied. The following parameters were investigated: non-protein nitrogen, total proteins, thymol, bilirubin, cholesterol, Na^+, K^+, Cl^-, Ca^{2+}, inorganic phosphorus, glutamic–pyruvic acid transaminase, glutamic–oxalacetic acid transaminase, and lactic acid dehydrogenase (total and individual isoenzymes). Significant metabolic lesions were found to result from AET administration. Liver, heart, and kidney were particularly damaged. In the activities of the following enzymes the most marked changes were observed: glutamic–oxalacetic acid transaminase, glutamic–pyruvic acid transaminase, and lactic acid dehydrogenase. (NSA of Czech.)

26936 RESTORATION OF RADIATION DAMAGE IN RAT THYMOCYTES BY ADENINE. Yamada, Takeshi; Ohyama, Harumi (National Inst. of Radiological Sciences, Chiba, Japan). Int. J. Radiat. Biol.; 18: 433-8(1970).

Adenine (5 or 10 mmoles) added exogenously to rat thymocytes after x irradiation with 8 kR, restored the ATP content of irradiated cells to normal level and reduced radiation cell death. 1 mmole of adenine was ineffective. When added to cells at later time after irradiation, adenine became less effective. Adenine also increased oxygen uptake by irradiated thymocytes and decreased degradation of adenine nucleotides to hypoxanthine. (auth) (UK)

26937 ACUTE RADIATION INJURY IN NEONATALLY THYMECTOMIZED GERM-FREE MICE. HEMATOPOIETIC AND MORPHOLOGIC CONSEQUENCES. Doughty, William E.; Anderson, Robert E.; Howarth, John L.; Tokuda, Sei (Univ. of New Mexico, Albuquerque). Arch. Pathol.; 91: 119-26(Feb 1971).

The role of the thymus in the acute (150-day) recovery of germ free mice from a single exposure to 700 rad of ^{60}Co γ radiation was reported. The results demonstrate that the acute hematological response to such exposure is but slightly modified by neonatal thymectomy but that there is a significant difference (9.3% vs 18.3%) in 30-day survival favoring the nonoperated over the thymectomized mice. (auth)

26938 RBE OF NEGATIVE PIONS IN 2-DAY-OLD ASCITES TUMORS. Feola, J. M.; Raju, M. R.; Richman, C.; Lawrence, J. H. (Univ. of California, Berkeley). Radiat. Res.; 44: 637-48(Dec 1970).

The relative biological effectiveness (RBE) of a 90-MeV negative pion beam at the peak of the depth dose distribution compared with ^{60}Co rays for a 5-day-old tumor was found to be 5.4 ± 1.8. In the investigation, the RBE of negative pions was measured for a 2-day-old lymphoma. Partial pressure of oxygen (pO_2) was measured in vivo with a microelectrode. The 5-day-old tumors were found to be hypoxic; the 2-day-old tumors showed a pO_2 of about 7.0 mm Hg. The dose rate of pions at the peak position was increased in this experiment to about 25 to 30 rads/hr by focusing the beam. The resulting beam was small, and only one mouse at a time could be irradiated. Mice were exposed to doses ranging between 60 and 150 rads. (P.B.M.)

26939 COLONY-FORMING UNITS IN RAT PARABIONTS. Sodicoff, Marvin (Temple Univ., Philadelphia). Radiat. Res.; 44: 758-70(Dec 1970).

Plasma of rats made leukopenic by irradiation can, upon injection into a normal rat, elicit a peripheral leukocytosis which is due, at least in part, to the release of large numbers of neutrophils from the bone marrow. Utilizing the radiation protective technique of postirradiation parabiosis, it was investigated whether the unirradiated partner of an irradiated parabiont would manifest any changes in the stem cell compartment of its bone marrow, i.e., colony forming units (CFU) as a result of its union to an irradiated partner. The pattern of hematopoietic recovery in the irradiated parabiont as measured by total femoral cellularity and CFU content was also investigated. Results indicated that in the unirradiated partner of an irradiated (leukopenic) parabiont the CFU increase to 3.5 times their original number; only part of this increase is attributed to the phenomenon of parabiosis itself. After an early fall in bone marrow cellularity and CFU concentration, the irradiated parabiont begins to recover both cellularity and CFU content, the latter, however, shows fluctuations which are discussed. A general scheme is proposed for the mechanism of postirradiation protection against the hematopoietic form of radiation death. (auth)

XUM

26940 RELATIVE SENSITIVITY OF VARIOUS AREAS OF THE RETINA TO LASER RADIATION. Lappin, P. W.; Coogan, Philip S. (Air Force School of Aerospace Medicine, Brooks Air Force Base, Tex.). Arch Ophthalmol. (Chicago); 84: 350-4(Sep 1970).

Threshold damage doses for helium nion (HeNe) laser radiation were determined in 20 Rhesus monkey eyes at seven selected sites, ranging from 50° nasal to 30° temporal to the macula. The mean damage threshold at the macula was found to be lowest of all examined sites, while the area between the optic disc and the macula was highest. Planimetry measurements of the retinal structures on an excised eye showed the comparative thickness of the nerve fiber layer to be most consistent with the relative sensitivity at the various sites. This layer was found to be thickest at the areas least sensitive to laser irradiation, suggesting that the optic nerve fibers act as an attenuating medium. The high sensitivity of the macula is attributed chiefly to the high density of pigment granules in the macular pigment epithelial cells. (auth)

26941 ACUTE EFFECTS OF X-RADIATION ON SPINAL CORD MOTONEURONS. A FUNCTIONAL AND ULTRASTRUCTURAL STUDY IN THE CAT. Carregal, Enrique J. A.; Cravioto, Humberto (Univ. of Southern California, Los Angeles). Contract AT(11-1)-113. Bull. Los Angeles Neurol. Soc.; 35: 89-103(Jul 1970).

Studies were done to investigate the immediate, acute effects of x irradiation on a particular nervous system function, both from a functional and an ultrastructural point of view. The spinal monosynpatic reflex in the cat was chosen as the test function. The acute effects of x rays on the electrophysiological properties of the motoneurons of the spinal cord were reported, but have not dealt specifically with the properties underlying the integrative function of the monosynaptic reflexes (post activation depression, facilitation and post tetanic potentiation). The ventral horn of the spinal cord was studied with the electron microscope and its ultrastructure is well known. (P.B.M.)

26942 MYELO-RESTORATIVE CAPACITIES AND IMMUNOCOMPETENCE OF BONE MARROW CELLS OF THE MOUSE CULTIVATED IN VITRO. Halpern, B.; Liacopoulos-Briot, M.; Crepin, Y.; Lambert, F.; Martial-Lasfargues, C. (College de France, Paris. INSERM, Paris. CNRS, Paris). Ann. Inst. Pasteur, Paris; 119: 87-99(Jul 1970). (In French).

Mouse isogenic and allogenic bone marrow cells were cultured in vitro in the presence and absence of phytohemagglutinin (PHA) for 48 hr. They were studied as to their capacity to restore the myeloid function and to induce graft versus host reaction in 100% lethally irradiated animals. Cultured cells, whether isogenic or allogenic were found able, when given in adequate amounts, to restore completely the hematopoietic functions and to insure definite survival of lethally irradiated animals. The addition of PHA did not significantly modify the results. Allogenic cells, whether fresh or cultured in the presence or absence of PHA, regularly caused a secondary syndrome of similar severity resulting in a mortality close to 100%. The colonization of the recipient by the transplanted cells was proved by a state of chimerism, evidenced by chromosome markers (CBA T6T6) and by the definite acceptance of donor skin grafts. (auth)

26943 LATE CONSEQUENCES OF WHOLE-BODY IRRADIATION. Moravek, F. (Military medical Research and Postgraduate Inst., Hradec Kralove, Czech.). Sb. Ved. Pr. VLVDU Hradci Kralove; 43: 187-204(1969). (In Czech).

A review with 73 references dealing with chromosome aberrations, bone marrow injuries, infection complications, reparation processes, cataract, tumors, and leukemia is presented. (NSA of Czech)

26944 ELIMINATION OF ^{131}I-LABELLED HETEROLOGOUS ANTIGEN FROM THE BLOOD OF CHICKENS AFTER TOTAL BODY X-IRRADIATION. Krejci, J.; Prochazka, Z.; Hampl, J. (Veterinary Research Inst., Brno. University School of Veterinary Medicine, Brno). Folia Microbiol. (Prague); 15: 485-91 (1970).

A study was made on the effect of ionizing radiation upon the rate of elimination of ^{131}I-labelled human serum albumin (HSA ^{131}I) from the blood and upon antibody formation in chickens irradiated with 1,2 00R (i.e. with LD_{50}) and injected with antigen 30 min, 6 days or 14 days after irradiation. The elimination curve from unirradiated control birds followed the typical three phase pattern. The effect of irradiation was most marked with chickens injected with antigen 6 days after irradiation, resulting in an extension of the second phase with practically no third phase at all. Exposure to irradiation 30 min prior to antigen administration resulted in an extension of the second phase by 2 days as compared to the controls, with the onset of the third phase occurring on day 7. Irradiation 14 days prior to antigen administration resulted in an extension of the second phase by 1 day as compared to the controls, with the onset of the third phase occurring on day 6. Elimination of HSA ^{131}I in the second phase was more rapid than that of ^{131}I-labeled chicken serum albumin (CSA ^{131}I) no matter whether the chickens were irradiated or not. This suggests that the capacity of specific antigen uptake is not affected by irradiation. Antigen elimination curves from control irradiated groups given CSA ^{131}I followed the same pattern as that found in control unirradiated birds injected with homologous antigen. (auth)

26945 STUDIES OF THE RELATIVE BIOLOGICAL EFFECTIVENESS OF FAST NEUTRONS (15 MeV NEUTRONS) ON THE INFLUENCE OF CATARACT DEVELOPMENT IN DIFFERENT DOSE RANGES. Ruether, W.; Graul, E. H. (Phillips Univ., Marburg, Ger.). Atompraxis; 16: 406-9(Nov-Dec 1970). (In German).

In experimental studies on rabbits' eyes the relative biological effectiveness of fast neutrons (15 MeV neutrons) on the cataract development was determined. In the first experiment 100 rad 15 MeV neutrons respectively 500 rad ^{60}Co γ radiation and in the second experiment 750 rad 15 MeV neutrons respectively 500 rad ^{60}Co γ radiation were applied. After several months rabbits showed incipient opacities of the lens. That means a relative biological effectiveness of 5 respectively 2 was determined; i.e. under these circumstances fast neutrons have a different value of effectiveness. The incipient opacities of the lens irradiated with 15 MeV neutrons formed mature cataracts more rapidly than after ^{60}Co γ irradiation. (auth)

26946 VULNERABILITY OF DEVELOPING BRAIN: I. SOME LASTING EFFECTS OF X-IRRADIATION. Dobbing, John; Hopewell, J. W.; Lynch, Anthony; Sands, Jean (Univ. of Manchester, Eng. St. Mary's Hospital Medical School, London). Exp. Neurol.; 28: 442-9(1970).

The heads of 7 day old rats were exposed to x irradiation (600 R) and the animals allowed to survive to 7.5 mon of age when their brains were examined. There was a large, selective, residual deficit of cerebellar weight amounting to 61% of controls. The deficit in number of cells was somewhat less than the deficit in weight, leading to a substantial increase in its cellularity. These changes were accompanied by residual deficits in cholesterol concentration, especially in the brain stem. The results provide yet another example of the differential susceptibility of the cerebellum when its growth is interfered with at a time when it is normally growing rapidly. Permanent deficits were induced at a late stage of development corresponding approximately to the perinatal period of human brain growth. (auth)

26947 PROLIFERATIVE AND PHAGOCYTIC CAPACITY OF THE RETICULOENDOTHELIAL SYSTEM OF SUBLETHALLY IRRADIATED MICE. Fred, Richard K.; Dobson, Ernest L.; Kelly, Lola S.; Shore, Moris L. (Bureau of Radiological Health, Rockville, Md. Univ. of California, Berkeley). RES, J. Reticuloendothel. Soc.; 7: 453-70(Apr 1970).

The response of the reticuloendothelial system (RES) to glucan treatment was studied in sublethally irradiated specific pathogen free (SPF) mice. Glucan is believed to induce proliferation of the RES with a concomitant increase in the RE phagocytic activity. Whole body ^{60}Co γ irradiation initially inhibited the increase in RE phagocytic activity ordinarily produced by glucan. Almost normal response, however, was seen when the glucan was given 3 to 7 days postirradiation. The effect of sublethal irradiation directly on RES phagocytic function was investigated. A marked spontaneous increase was observed in the RE phagocytic activity postirradiation in conventional mice. This spontaneous increase was inhibited by treatment with nonabsorbable antibiotics. Further, SPF mice did not ordinarily display as marked a spontaneous increase in RE phagocytic function postirradiation as conventional mice. (auth)

26948 DIFFERENCE OF ACTION BETWEEN HEPATIC EXTRACTS AND SMALL DOSES OF ROENTGEN RAYS ON THE MITOTIC ACTIVITY OF THE PARTIALLY HEPATECTOMIZED LIVER. Zelioli-Lanzini, Francesco (Ospedale Civile, Asola, Italy). Osp. Ital. Chir.; 20: 523-7(Jun 1969). (In Italian).

Different action of hepatic extracts and of low x-ray doses (80 r) on the regeneration of liver in partially hepatectomized rats was studied. Beneficial action both opotherapic and with treatment of the liver was observed. It is emphasized that the first one carries on its activity in the partly resected gland; the second one operates after a little rest of the liver. (auth)

26949 IMPORTANCE OF THE CONDITIONED REFLEX METHOD IN NEURORADIOLOGY. Semagin, V. N. (Inst. of

Higher Nervous Activity and Neurophysiology, Moscow). Zh. Vyssh. Nerv. Deyateln. im. I. P. Pavlova; 18: 11-8(Jan-Feb 1968). (In Russian).

In experiments with a six-member stereotype, motor food conditioned reflexes were elaborated in 26 young male rats antenatally irradiated with a 1 R dose, and in 25 non-irradiated male rats of the Wistar line. Statistical processing characterizing the artificial, natural, and intersignal reflexes showed that irradiation of an embryo on the 18th day of its development with a 1 R dose exerts an impairing action on its brain. It affects the brain functions of the adult animal as manifested in weakened processes of excitation and inhibition, as well as in diminished stability of the conditioned reflex stereotype. The conditioned reflex method is a highly sensitive objective method of detecting radiation lesions in the central nervous system. (auth)

26950 BALNEOTHERAPY OF RADIATION INJURY. 27. EXPERIMENTAL STUDY ON THE PROTECTIVE EFFECT OF HOT SPRING BATH AGAINST NEUTRON AND GAMMA-RAY INJURY. 3. Arima, Masashi; Tsuji, Hideo (Kyushu Univ., Beppu, Oita, Japan). Oita-ken Onsen Chosa Kenkyu-kai Hokoku; No. 21, 58-61(Mar 1970). (In Japanese).

Single whole-body irradiation was given to male ddN-strain mice with the combination of neutrons of 200 rad dose and ^{137}Cs-gamma-ray of 300 R dose. Thereafter, irradiated mice were subjected to hot spring balneotherapy and the recovery of their bone marrow was studied by bone marrow culture. No significant difference was observed between control and bathed groups. (Japan)

26951 DOSE-RATE EFFECTS IN THE PRENATALLY IRRADIATED RAT. Strange, John Ruble. Knoxville, Tenn.; Univ. of Tennessee (1970). 96p. University Microfilms Order No. 71-7681.

Thesis.

The objectives of this study were to determine if a dose-rate effect exists in rats born to females exposed to ^{60}Co gamma radiation on the 11th and 18th days of gestation. Previous work had shown these periods to have high frequencies of eye damage and abnormal testes development. A dose-response curve established for young irradiated on the 11th day revealed minimal eye response to 50 R and near maximal response for total doses of 150 R and 200 R. A dose of 100 R gave responses which involved only eye damage and did not alter the viability of the young. A comprehensive study using a total dose of 100 R and dose rates of 1, 2, 3.3, 5, 10, 25, and 47 R/min was completed. Results revealed a rapid increase in eye damage up to 3.3 R/min with gradual, but not significant, further increases at 5 and 10 R/min. Dose rates of 25 and 47 R/min showed significantly fewer defects than the 10 R/min group. Animals which were irradiated on the 18th day of gestation with 50 R total dose at rates of 1, 3, 10, 25, and 47 R/min showed body weight depression through 210 days of age. Testes evaluations were made at 28, 49, 70, 91, and 210 days of age. At 28, 49, 70, and 91 days a dose-rate response was present as determined by evaluating the most advanced cell type in 500 seminiferous tubule cross-sections in 16 animals from each group. A rapid increase in damage was associated with increasing dose rate up to 10 R/min. Dose rates of 25 and 47 R/min were found to be significantly less damaging than the 10 R/min group. By 210 days of age all groups had recovered and showed no differences from the controls. Total recovery time was a function of initial damage rather than recovery rates since all irradiated groups recovered in a parallel fashion. Breeding studies undertaken with a group of males irradiated on the 18th day of gestation resulted in no depression of litter size or of the number of young born dead. A kinetic model to explain this dose-rate phenomenon is presented which states that at low dose rates the damage incurred is a function of total dose per unit time minus a portion of that dose rendered ineffective by the cell's repair mechanisms. However, at some point the intensity ceases to play the major role as the shorter total exposure time reduces the chances of hitting a cell in a sensitive period. (Diss. Abstr.)

26952 RADIATION SENSITIVITY OF NEW ZEALAND BLACK MICE AND THE DEVELOPMENT OF AUTOIMMUNE DISEASE AND NEOPLASIA. Morton, Jane I.; Siegel, Benjamin V. (Univ. of Oregon, Portland). Proc. Nat. Acad. Sci. U. S. A.; 68: 124-6(Jan 1971).

Young New Zealand Black (NZB) mice manifested extremely high resistance to the lethal effects of acute exposures to ionizing radiation, with a dose necessary to kill 50% of the animals within 30 days, $LD_{50(30)}$, of 964 R at 30 days of age and of 856 R for 90 day old mice. In contrast, Coombs' positive 9 mon old NZB mice (with low primary immune response) were highly susceptible ($LD_{50(30)}$ = 543 R), possibly because of anemia-stimulated erythropoiesis leading to a depletion of stem cells. The radiation resistance of young NZB mice, combined with previous observations of their immunologic hyper-responsiveness, support the concept that NZB mice possess an unusually large pool of hematopoietic stem cells, an abnormality which may predispose them to the development of autoimmune disease and neoplasia. (auth)

26953 COMPARATIVE STUDIES ON REJOINING OF DNA-STRAND BREAKS INDUCED BY X-IRRADIATION IN MAMMALIAN CELL LINES IN VITRO. Horikawa, M.; Nikaido, O.; Tanaka, T.; Nagata, H.; Sugahara, T. (Kyoto Univ.). Exp. Cell Res.; 63: 325-32(Dec 1970).

Single strand breaks of the DNA in cultured mouse L cells, porcine kidney stable (PS) cells, and Ehrlich ascites tumor cells were induced to almost the same degree in alkaline sucrose gradient, as a linear function of dose. However, it was shown by the alkaline sucrose gradient method and autoradiographic observations of unscheduled DNA synthesis in x-irradiated cells that these three cell lines can repair to almost the same degree the single strand breaks in DNA induced by x irradiation. These results agree well with the fact that there are no striking differences in sensitivity to x irradiation among these three cell lines obtained by the colony forming method. Hamster lung (HL) cells, an x ray resistent cell line obtained by screening from various mammalian cell lines in vitro, seem to have a higher activity of repair enzyme that joins together most of the single strand breaks of DNA induced by x irradiation. Significant rejoining activity of damaged double strand DNA from these cell lines in the neutral sucrose gradient was not demonstrated. These findings suggest that double strand breaks of DNA induced by x irradiation are the lesions principally responsible for the lethal effect of ionizing radiation in mammalian cells in vitro. (auth)

26954 COMPARISON OF THE EFFECTIVENESS OF A SINGLE AND FRACTIONATED IRRADIATION OF SPERMATOZOIDS ON PRENATAL DEATH IN RABBITS. Nuzhdin, N. I.; Nizhnik, G. V. (Inst. of Biological Physics, Pushchino, USSR). Dokl. Akad. Nauk SSSR; 194: 1211-13(11 Oct 1970). (In Russian).

Sperm were collected and mixed. Spermatozoids were irradiated in vitro with single, ^{60}Co γ doses of 600 and 300 R and with a fractionated dose of 300 R twice with a 60 min time interval between the 300 R doses. Female rabbits were inseminated artificially and subjected to autopsy to determine the embryonic losses. It was found that the number of implantation sites with respect to yellow fertilization bodies was 30% for a single irradiation dose of 600 R and 49% for two 300 R doses. Embryo losses with respect to yellow bodies were 71% for the single 600 R dose and 55% for two 300 R doses. A single 300 R dose gave 69% implantation sites, and only a 31% loss of yellow bodies. The postimplantation losses were small in all experiments. The survival of implanted embryos was high. Most of the embryos died before implantation. It is concluded that fractionating the dose decreases the harmful effect of radiation. (TTT)

26955 INFLUENCE ON LIVER OF RADIATION AS DEMONSTRATED BY SCINTILLATION SCANNING. Nagase, Katsuya (Juntendo Univ., Tokyo); Saito, Toshimi. Nippon Igaku Hoshasen Gakkai Zasshi; 30: No. 2, 167-76(May 1970). (In Japanese).

During radiotherapy the liver is sometimes irradiated, depending on the direction of the radiation beam. The liver will show changes in the direction of the liver blood flow, the liver tissues, and the liver scintigram. The effects of 4500 R γ radiation from cobalt 60 units were followed in dogs by observing the liver scintigram every week, and then comparison with the first scintigram before radiation. Observations made one week following γ irradiation showed no distinction between the use of ^{198}Au colloid and ^{131}I Rose Bengal for making the liver scintigram. No difference was found in radiographs at that time. Observations two weeks following irradiation of the liver scintigrams made with ^{131}I Rose Bengal showed the shadow of the irradiated part was worse than the other parts, indicating radiation injury. Scintigrams made using ^{198}Au colloid showed that there was a particular and complete reaction in the irradiated region. Observation made three weeks following irradiation showed slight improvement over the two weeks stage. (Japan)

26956 PROLIFERATIVE ACTIVITY OF THE STEM CELLS IN THE BONE-MARROW OF MICE AFTER SINGLE AND MULTIPLE IRRADIATIONS (TOTAL-OR PARTIAL-BODY EXPOSURE). Croizat, H.; Frindel, E.; Tubiana, M. (Institut Gustave-Roussy, Villejuif, France). Int. J. Radiat. Biol.; 18: 347-58(1970).

After a whole-body irradiation of 150 rads, an increase in the proportion of S cells observed during the first day suggested that the bone marrow is stimulated by an unknown but probably compensatory mechanism. In the first hours after a partial-body irradiation with the same dose, the proliferative activity of the protected bone-marrow increased, and at 24 hrs all the stem cells seemed to be engaged in a mitotic cycle. In the irradiated areas, the same phenomenon occurred, but later. During a course

XUM

of subtotal daily irradiation, the number of stem cells in the shielded area decreased and leveled off around 10% of its initial value. The number of stem cells in the irradiated zone plateaued at a lower value. The progressive depletion of the protected bone marrow observed during the beginning of the course of radiotherapy and the plateau observed later seemed to be due to a migration of hematopoietic cells between the protected and the irradiated regions. (auth) (UK)

26957 DIFFERENCE IN SURVIVAL OF JEJUNAL CRYPT CELLS AFTER RADIATION DELIVERED AT DIFFERENT DOSE RATES. Hornsey, Shirley (Hammersmith Hospital, London). Brit. J. Radiol.; 43: 802-6(Nov 1970).

A comparison of the effects of dose-rate on the acute intestinal syndrome measured by animal survival five days after whole-body irradiation and on cell survival of the epithelial cells of the jejunum measured by clone production after local irradiation showed a close correlation between the two tests of radiation damage. The greater sensitivity of animals measured by death within five days of irradiation to higher dose-rates was observed at the cellular level also. Irradiation of adjacent segments of jejunum suggests that the dependence of sensitivity on dose-rate is inherent in the cells rather than due to radioinduced change in the environment of the cells. (auth) (UK)

26958 RESPONSE OF STEM CELLS OF INTESTINAL MUCOSA TO IRRADIATION WITH 14 MeV NEUTRONS. Withers, H. R. (Univ. of Texas, Austin); Brennan, J. T.; Elkind, M. M. Brit. J. Radiol.; 43: 796-801(Nov 1970).

The responses of stem cells of the intestinal mucosa in mice to 200-kVp x rays and 14-MeV neutrons, as measured by an in situ cell survival assay system, were compared. The slopes of the dose-survival curves were not markedly different, but the shoulder of the neutron curve was narrower. Consistent with this, neutron-irradiated cells repaired less sublethal injury. Nevertheless, the repair between 14-MeV neutron exposures was appreciable and greater than that found by others using cyclotron neutrons of mean energy 8 MeV. (auth) (UK)

26959 TISSUE CONTENT OF NORADRENALINE AND 5-HYDROXYTRYPTAMINE IN THE RAT AFTER IONIZING RADIATION. Johnsson, J.-E.; Owman, Ch.; Sjoeberg, N.-O. (King Gustavus V Jubilee Clinic, Malmoe, Sweden. General Hospital, Malmoe, Sweden. Univ. of Lund, Sweden). Int. J. Radiat. Biol.; 18: 311-16(1970).

In attempts to elucidate functional differences between various types of adrenergic nerves, rats were given 850 R whole-body x irradiation, previously found by others to produce a marked reduction in tissue catecholamine levels. This treatment, however, did not overtly affect the noradrenaline concentration in the heart, vas deferens, or in the brain as demonstrated in fluorometric determinations and by fluorescence microscopy 24 or 48 hrs after treatment. Also 5-hydroxytryptamine in the brain remained unchanged. If anything, there was a tendency to a slight increase in cardiac noradrenaline after 48 hrs and in the brain 5-hydroxytryptamine 24 hrs after the treatment. (auth) (UK)

26960 HISTOLOGICAL EXAMINATION OF PARODONTIUM AFTER IRRADIATION OF THE RAT TRUNK AT A DOSE OF 600 R. Klimek, H.; Krzywicki, J. (Clinic of Conserving Stomatology, Warsaw). Cesk. Stomatol.; 69: 198-202(Jul 1969). (In Czech).

Results of a detailed histological examination of changes in the parodontium of rats at various time intervals after an exposure to 600 R are reported. The intensity of pathological changes of the dental apparatus produced by irradiation was found to increase from the 5th to the 25th day after exposure. Possible reasons for the different degree of damage in individual teeth of an animal are discussed. (NSA of Czech.)

26961 EFFECT OF IONIZING RADIATION ON THE HEART. Bruscagli, C.; Fazzini, P. F.; Marchi, F.; Mincione, G. (Univ., Rome. Univ., Florence). Arch. De Vecchi Anat. Patol. Med. Clin.; 54: 315-28(Dec 1968). (In Italian).

In order to define the alterations in the heart caused by ionizing radiation, an experimental study was made on rabbits exposed to a complex radiation of 4200 R (tissue dose) given over the course of a month on alternate days. The animals were sacrificed 15 and 30 days following irradiation. The heart showed clear decisive effects. This was found by subacute fibrin pericarditis and regressive necrotic phenomena of the miocardiac fiber with occasional tendency to fibrosis. The regressive phenomena affected the right ventricle in all the experimental animals and the sub-endocardiac and intramural muscular layers of the left ventricle. No alterations were observed in the coronary arterial branches, extra and intramural, and in the cardiac valves. (tr-auth)

26962 EXPERIMENTAL STUDIES OF THE EFFECT OF ^{95}Zr–^{95}Nb ON MICE. 4. EFFECTS OF THE INTERNAL IRRADIATION OF SUBCUTANEOUSLY INJECTED ^{95}Zr–^{95}Nb ON THE REPRODUCTIVE FUNCTION OF MALE MICE. Morishige, Toshiko (Kyushu Univ., Fukuoka). Igaku Kenkyu; 40: 68-76 (Feb 1970). (In Japanese).

Previous reports have shown $^{95}Zr-^{95}Nb$ administered to mice is distributed in the organs of reproduction as well as the others, and the biological half life of it in these organs, especially in the testis, is relatively long. On the basis of these results, the effect of the internal irradiation of $^{95}Zr-^{95}Nb$ on the reproductive function of adult male mice was examined experimentally. Seven adult mice subcutaneously received 8 μCi $^{95}Zr-^{95}Nb$ and oxalate per one gram of body weight. Each male mouse was mated for a week with two females on the 1st, 4, 9, 14, 20, or 30th week of the injection. The results were as follows: The copulation rate of the male mice decreased following the injection and recovered after the 30th week. The pregnancy rate of the female mice mated with these male mice also decreased from the 4th to 20th week when the females were absolutely sterile, and thereafter gradually recovered. The incidence of dead embryos increased rapidly from 4th week, reached 100% on the 14th week, and began to decrease from the 30th week. Blackened spots caused by $^{95}Zr-^{95}Nb$ were found microautoradiographically in the interstitial stroma with a peak of its density between the 9th and 14th week. The histopathological findings revealed a diminishing of spermatogonia in the seminiferous epithelium on the 4th week and disappearance of spermatozoa from the seminiferous tubules from the 9th to 14th week and recovery of spermatogenesis after the 30th week. (Japan)

26963 ROLE OF RADIOSENSITIVE TISSUES IN THE MECHANISM OF POST-RADIATION GLUCONEOGENESIS. Kendysh, I. N.; Moroz, B. B. (Inst. of Biophysics, Moscow). Dokl. Akad. Nauk SSSR; 195: 1242-4(11 Dec 1970). (In Russian).

The radioinduced increase of glucose and glycogen in liver of rats from indogeneous substrata during irradiation was studied with young male rats weighing 150 μC treated interperitoneally with 150 μC-1-C^{14} 18 hr. before exposure to γ radiation of 750 r with 450 r/min dose. Results showed that the content of glucose in the blood increased after 6 hr., reached the maximum in 24 hr. and normalized on the 6th day. The increase of glycogen in the liver increased after 24 hr reaching the peak after 48 hr and normalized on the 6th day following the exposure. The observed post radiative changes in the hydrocarbon exchange in the liver were due to the increased glucogenesis at the expense of reutilization of metabolites separated from destroyed radiosensitive tissues. (R.V.J.)

26964 CHRONIC MYELOGENOUS LEUKEMIA IN HODGKIN'S DISEASE: IMMUNOFLUORESCENCE OF CELLS. Swaim, William R. (Veterans Administration Hospital, Minneapolis. Univ. of Minnesota, Minneapolis); Windschitl, Harold E.; Doscherholmen, Alfred; Bankole, Rufus O.; Bates, Henry A. Cancer; 27: 569-73 (Mar 1971).

A patient with Hodgkin's disease is described who developed chronic myelogenous leukemia 8½ years after the start of radiation therapy. This therapy was fractional and was administered to most of the patient's skeleton. The radiation was an important factor in the development of leukemia. The presence of positive reactions to the antileukemic fluorescent antibodies may be consistent with the hypothesis that viruses are concerned with human leukemia. (auth)

26965 GENETIC EFFECTS OF CUMULATIVE MATERNAL IRRADIATION ON GROWTH AND AGE AT SEXUAL MATURITY IN RATS. Davison, J.; Havenstein, G. B.; Chapman, A. B. (Univ. of Wisconsin, Madison). Contract AT(11-1)-697. Genetics; 66: 695-708(Dec 1970).

Studies were done on the genetic effects of cumulative maternal x irradiation on growth and age at sexual maturity in rats. (auth)

26966 OXYGEN EFFECT ON THE PRODUCTION OF RADIATION-INDUCED MYELITIS IN RATS. Asbell, Sucha Order; Kramer, Simon (Thomas Jefferson Univ. Hospital, Philadelphia). Radiology; 98: 678-81(Mar 1971).

The lower cervical and upper thoracic cords of 117 rats were exposed to single doses of 2,500 to 4,500 R x radiation in air or 100% O_2 at 1 and 3 ATA. Myelitis developed in all animals within 3½ to 9¾ mon. A 14% oxygen enhancement effect was seen at 2,500 R; this decreased until 3,500 R, after which no significant difference could be detected. (auth)

26967 DEVELOPMENT OF A TRANSIENT FATTY LIVER AFTER RELEASE FROM A TEN-DAY STAY IN HYPOXIA CORRESPONDING TO AN ALTITUDE OF 6000 m. Tribukait, B.;

Lindberg, K. (Karolinska Institutet, Stockholm). Beitr. Pathol. Anat. Allg. Pathol.; 140: 419-29(1970). (In German).

Immediately after a ten-day stay in hypoxia corresponding to an altitude of 6000 m, the fat content in the liver of mice was increased by about 40%. The distribution of the fat corresponded to a centrilobulare fatty liver. Subsequently the fat content increased up to double the normal with a maximum value three to four days after the termination of the hypoxia and normalized after about eight days. Here the distribution of the fat was diffuse. Possible mechanisms of this post-hypoxic fat accumulation are discussed. Furthermore the results are discussed in respect to the decreased radiation sensitivity of mice following a stay in hypoxia. (auth)

26968 AUDIOGENIC SEIZURE SUSCEPTIBILITY OF RATS X-IRRADIATED IN UTERO DURING FIRST ONE-THIRD OF PREGNANCY. Geller, Lester M. (Columbia Univ., New York). Exp. Neurol.; 29: 268-80(Nov 1970).

Groups of Sherman rats exposed in utero to a maternal dose of 250 R of x radiation, during the first one-third of pregnancy, were tested for susceptibility to sound-induced seizures at a median age of 175, 230, or 258 days. There was no significant difference between any irradiated group and control animals of comparable age in either number of running attacks or seizures. A need for caution in generalizing from these findings to other samples of rats, tested at equivalent ages, was noted. The suggestion by others of decreased susceptibility in 4-month-old offspring of Sprague-Dawley rats exposed to lower doses of x radiation, on gestational day 5 or 10, was found to be inadequately supported by their data. Well-known differences in audiogenic seizure susceptibility in relation to age in normal animals, underscore the importance of the age-at-testing variable in evaluating susceptibility in the prenatally x-irradiated rat, as well as the need for longitudinal studies in making that determination. Beyond its special consideration in seizure studies, the variable of test age appears to be of fundamental importance in elaborating the functional consequences of prenatal x irradiation. A reduction of the already limited number of behavioral changes said to occur in rats surviving x irradiation during the preorganogenetic period is reported. In view of the absence of light microscopic evidence of damage to their brains, a search for functional alterations in such animals would seem to be particularly challenging. (auth)

26969 STUDIES ON THE INFLUENCE OF RADIATION ON SYNCHRONIZED L CELLS DURING DEPRESSION OF MACROMOLECULAR SYNTHESIS. Baker, Max Leslie. Fayetteville, Ark.; Univ. of Arkansas (1970). 117p. University Microfilms Order No. 70-17,214.

Thesis.

Recent evidence indicates that cultured mammalian cells in a state of complete energy deprivation not only can repair radiation injury, but the repair may actually be enhanced by the energy deprived state. Some have also suggested that at least part of the post-irradiation effects seen in paired dose studies may be due to some synchronizing effect of the radiation. For this reason, a series of studies were undertaken to determine the effects of these forms of energy deprivation on post-irradiation survival of cells in different phases of the life cycle. Earle's strain L-929 cell line (derived originally from normal mouse subcutaneous tissue) was used in all the experiments. In the single cell survival experiments, the methods outlined by Puck and Marcus were used. The double thymidine technique was used to synchronize the cells. Suspensions of the cells were assayed for DNA, RNA, protein, and ATP content under the various treatments. The results with asynchronous cells showed that a state of depressed macromolecular synthesis alone is not necessarily indicative of an increased post-irradiation survival state. Rather, other factors such as inhibition or malfunction of electron transport, or inhibition of specific enzymes such as the nucleases must be considered. (Diss. Abstr. Int., B)

26970 SERUM PROTEIN AND HEMOGLOBIN ALTERATIONS IN THE GAMMA-IRRADIATED SPANISH GOAT. Travis, James Carlus. College Station, Tex.; Texas A and M Univ. (1970). 110p. University Microfilms Order No. 70-16,768.

Thesis.

The serological and immunological manifestations of radiation injury in continuously and acutely irradiated Spanish goats were studied in order to determine mechanisms of γ-radiation damage. Four groups of male Spanish goats were irradiated continuously for approximately four years at doses of 0, 2, 7, and 15 R/day, and one group was irradiated acutely with a dose of 1200 R. Blood samples were collected periodically from all groups during the course of the experiment and from several animals just prior to radiation death. Cellulose acetate electrophoresis of serum proteins and glycoproteins revealed a decreased albumin and an increased β^2-globulin in all irradiated goats that gave overt signs of sickness. Immunoelectrophoresis on agar-gel demonstrated three proteins in the β^2 electrophoretic fraction. One arc, designated β^2-M, was greatly augmented in all terminal samples, and was, therefore, the source of the increased β^2-globulin electrophoretic fraction. Sephadex G-200 column chromatography and electrophoresis provided data which demonstrated that the β^2-M globulin was a macroglobulin. This protein appeared possibly to have hemoglobin-binding properties when hemoglobin was observed in the macroglobulin peak with column chromatography of terminal sera. Fifty-two percent of all continuously irradiated goats exhibited a hemoglobin electrophoretically different from the normal adult types. This hemoglobin was absent in all control animals. Because of observations that irradiated goats near death exhibited reduced total hemoglobin, it is suggested that radiation destroyed erythrocyte stem cells, thus yielding lower erythrocyte counts and lowered hemoglobin values, and that increased hemoglobin-binding capacities and synthesis of hemoglobin C were resulting compensatory mechanisms. It is speculated that the macroglobulinemia of terminal sera was the product of a homogenous population of lymphocytoid cells similar to Waldenstorm's macroglobulinemia in humans, and that this condition was radioinduced. (Diss. Abstr. Int., B)

26971 PEAK VERSUS AVERAGE POWER IN MICROWAVE INDUCTION OF LENTICULAR CATARACTS. Fisher, Leslie John. Medford, Mass.; Tufts Univ. (1969). 90p. University Microfilms Order No. 70-18,002.

Thesis.

The eyes of rabbits were exposed to pulsed and CW microwave radiation at several combinations of peak and average powers to determine the relative importance of peak and average microwave powers in the induction of cataracts. Experiments were performed using peak power as the independent variable. Other exposures were made along constant dose curves. Average power was found to be the significant factor in cataract formation but the higher the average power used, the lower was the dose required for opacity induction. Hourly observations were reported of the development of microwave induced cataracts from equatorial lines at three hours post-irradiation, to equatorial striations at five hours post-irradiation, to posterior cortical opacities and vesicle strings at seventy-two hours post-irradiation. (Diss. Abstr. Int., B)

26972 SIGNIFICANCE OF RADIATION-INDUCED MODIFICATIONS IN THE COMPARATIVE TERATOLOGY OF THE NERVOUS SYSTEM. Ostertag, B. (Univ., Tuebingen, Ger.). Deut. Z. Nervenheilk.; 197: 239-54(1970). (In German).

The changes in the nervous system in mouse embryos and in infant mice, brought about by single doses of x radiation were studied. The strictly hemilateral exposure to radiation of the pregnant animal allowed for accurate comparisons between irradiated and untreated animals of the same litter. As to the teratogenic variation, the age of individual embryos appeared to be more crucial than the duration of the pregnancy. Both a phase specificity in the maturation of organs and, in particular, cortical disorders may be recognized in the already present anlage of the pallium. Here deviations, defects, and transient overshooting developments of structures become manifest. The radioinduced spinal cord lesions correspond to dysrhophia found in man at young age. The surviving infant animals (irradiated on the 11th day after conception) were generally retarded compared to their litter mates, displaying multiple malformations and functional lesions of the nervous system in addition to conjugated deformities. (auth)

26973 EXPERIMENTS FOR TESTING THE EFFECT OF THERAPEUTICAL ROENTGEN IRRADIATION ON ANIMAL SKIN FROM GREAT DISTANCE. Fettich, Janez (Dermatology, Medical Faculty, Ljubljana, Yugoslavia). Med. Pregl. (Novi Sad); 22: 441-6(1969). (In Slovene).

Following therapeutical distance x radiation with soft unfiltered rays to the skin of guinea pigs, the effects on hematopoiesis and epithelium of the testicles were investigated. Changes in the epithelium of the testicles were noted during the 12th week. It was possible to detect changes in hematopoiesis only after comparison of red blood cell curves between irradiated and unirradiated animals for 40 weeks. It was concluded that the usual doses of therapeutic radiation do not produce damage that can be found on a hemogram, but definite damage is done to the testicles, which must be protected during radiotherapy. The testicles and the hematopoietic system of guinea pigs react similarly to that of humans and the results can be used in therapeutical practice. (auth)

26974 REGENERATION OF PROLIFERATIVE ACTIVITY IN THE PROGENY OF MURINE LYMPHOMA CELLS L5178Y IR-

XUM

RADIATED WITH X-RAYS. Beer, J. Z.; Ziemba-Zak, B.; Rosiek, O.; (and others) (Inst. of Nuclear Research, Warsaw). Bull. Acad. Pol. Sci., Ser. Sci. Biol.; 18: 581-4(1970).

Cultured mouse leukemic lymphoblasts L 51784 were irradiated with 200 kV x rays at a dose rate of 5.74 rad/sec. The growth kinetics of the sublines obtained by cloning were studied. For sublines derived from single cells, a reduced growth rate was observed following irradiation of the cultures with 200 and 300 rads. The repair mechanism of mammalian cells is discussed. (F.M.M.)

26975 EFFECTS OF ALTERED PROPULSION ON RAT SMALL INTESTINAL FLORA. Summers, Robert W.; Kent, Thomas H. (Univ. of Iowa, Iowa City). Gastroenterology; 59: 740-4(Nov 1970).

Intestinal peristalsis has been stated to be an important factor regulating small bowel bacterial flora. The midintestinal flora were studied in rats under conditions of altered propulsion. The results failed to confirm the striking changes in flora and histological appearance produced by a ganglion-blocking agent previously reported. Agents that moderately retarded propulsion (mecamylamine, chlorisondamine, and morphine) produced only a slight increase in some organisms, in comparison to the gross overgrowth associated with the extreme stagnation from ileal obstruction. Treatments that mildly accelerated propulsion (tolazoline, neostigmine, and fasting) reduced the population of only a few organisms. An overgrowth of bacteria in two situations where propulsion was actually accelerated was found, indomethacin-induced ulceration and whole body x irradiation. Marked morphological mucosal changes were present in both of these situations. It appeared that extreme forms of stagnation were necessary to produce significant bacterial overgrowth in the small intestine of rats, and striking bacterial overgrowth can occur in the absence of retarded small intestinal propulsion, especially if there is mucosal damage. (auth)

26976 LATE INJURIES INDUCED BY RADIATION. II. STUDIES ON MICE. Muramatsu, Susumu; Sato, Fumiaki (National Inst. of Radiological Sciences, Chiba, Japan). Seibutsu Kagaku; 21: 189-98(Aug 1970). (In Japanese).

The similarity of the chronic effects of radiation on animals to the characteristics of natural aging is pointed out. The high incidence of leukemia and malignant tumors, especially ovarian tumors, is discussed. It was found that the tumorigenic effect of neutron beams was greater than that of γ and x radiation, and tumors occurred after a short incubation period even with low doses. Inhibition of growth, cataracts, and decrease in weight of organs were also observed. Investigations were also conducted on genetic effects and radiation protection. (Japan)

26977 DEVELOPMENT OF CALCIFICATIONS AFTER WHOLE-BODY IRRADIATION IN RATS SENSITIZED WITH DHT. II. EFFECTS OF VARIOUS γ-RAY DOSES. Petyrek, P.; Mraz, J.; Vodicka, I. (Military Medical Research and Postgraduate Inst., Hradec Kralove, Czech). Sb. Ved. Pr. VLVDU Hradci Kralove; 43: 17-29(1969). (In Czech).

The effects of whole-body ^{60}Co γ irradiation at doses of 500, 600, 700, and 800 R were studied on the development of calcifications in rats sensitized with DHT (dihydrotachysterol) in a dose of 0.5 mg per 100 g of body weight. DHT was applied 24 hrs after the irradiation. Calcifications in the duodenum and cecum occurred only after exposure to doses of 500 and 600 R. In the myocard only irregular occurrence of calcifications was observed. Exposure to doses of 700 and 800 R resulted in a decrease in the development of typical calcification. Results of quantitative Ca determination by the manganometric method agreed with those obtained by measuring the fluorescence intensity of the Ca-tetracycline complex. (NSA of Czech)

26978 DEVELOPMENT OF CALCIFICATIONS AFTER WHOLE-BODY IRRADIATION IN RATS SENSITIZED WITH DHT. I. IONIZING RADIATION AND THE CALCIPHYLAXIS SYNDROME. Petyrek, P.; Mraz, J. (Military Medical Research and Postgraduate Inst., Hradec Kralove, Czech). Sb. Ved. Pr. VLVDU Hradci Kralove; 43: 3-15(1969). (In Czech).

The development of calcifications was studied in rats sensitized with dihydrotachysterol (DHT) after a 500 R whole-body dose of x radiation. In rats sensitized with DHT and irradiated, a higher mortality was observed than that caused by either irradiation or DHT application alone. An increased formation of calcifications was found in certain tissues (particularly in the large and small intestine) when sensitized animals were irradiated. When performed either 24 hrs or just prior to irradiation, the sensitizing process was more effective than when performed 24 hrs after irradiation. (NSA of Czech)

26979 ACUTE-PHASE REACTANTS AND LYSOSOMAL ENZYMES IN THE BLOOD OF RATS WITH EXPERIMENTAL INFLAMMATION OR RADIATION INJURY. Koj, A. (Jagiellonian Univ., Krakow). Folia Biol. (Krakow); 18: 275-86(1970).

Changes in the blood plasma concentration of fibrinogen, haptoglobin, ceruloplasmin, and seromucoid, and the activity of three lysosomal hydrolases, acid phosphatase, arylsulphatase, and β-glucuronidase were determined in the blood plasma and liver of rats injected with turpentine, x-irradiated, or both. Local inflammation produced an increase in the plasma level of all four acute-phase reactants with a maximum observed between 24 and 48 hrs after injury. Exposure of rats to 800 R of hard x rays resulted in a much smaller rise in the concentration of these proteins. Changes in the activity of the lysosomal enzymes differed in the groups of rats. (E.E.H.)

26980 RADIATION INJURY AND RECOVERY IN HEMATOPOIETIC ORGANS AND LIVER OF MICE. Kasahara, Atsushi (Kyushu Univ., Fukuoka). Fukuoka Igaku Zasshi; 61: No. 3, 168-84(Mar 1970). (In Japanese).

Whole body irradiation of 300 R was delivered to ddN male mice with 200 kVP x-rays. Peripheral blood, bone marrow, liver, spleen and inguinal lymph nodes of irradiated mice were examined from the first day to 30 days after irradiation. Following total body irradiation of mice, damage was seen mainly in the bone marrow, peripheral leucocytes, nucleated cells in differential count, and the spleen. The damage of bone marrow was noted earlier but recovery started also earlier than in the other organs. The spleen showed a marked sensitivity with evidence of earlier damage than the other visceral organs. Recovery of the splenic damage was seen about 10 days earlier than that of peripheral blood. There was no particular change in liver and inguinal lymph nodes. (Japan)

26981 RADIATION-INDUCED RESIDUAL INJURY IN THE HEMATOPOIETIC SYSTEM OF THE MOUSE. MacVittie, Thomas Joseph. Buffalo; State Univ. of New York (1970). 186p. University Microfilms Order No. 71-7187.

Thesis.

C57Bl/6J female mice were exposed to zero, 200, 300, and 400R whole-body x-irradiation. At various intervals from 1 to 46 weeks post exposure, an equal number of exposed and control (sham exposed) mice were each either bled a total 66 per cent of their calculated blood volume (cbv) or injected with a total 40 μg of bacterial endotoxin (Salmonella abortus equi), i.e., 33 per cent cbv or 20 μg of endotoxin at each of two periods separated by 24 hours. At 66 hours after the initiation of the stimulation, the total skeletal marrow content of erythroid and myeloid cells was determined by means of an ^{59}Fe labeling technique as previously described by Gong et al., (Radiat. Res., 37: 467-77(1969)). Control and x-irradiated animals that were not bled or injected with endotoxin were studied along with the above groups of bled control and irradiated and endotoxin injected control and irradiated mice. The following is a summary of findings: The magnitude of the erythroid or myeloid cellular increase at 66 hours post stimulation (previously determined to be the optimal time for maximum hematopoietic effect in nonirradiated animals) was always lower in the x-irradiated animals than in the control, at any given time interval, from 1 to 46 weeks post exposure. The exponential loss of RI with time was found to be similar in both the erythropoietic and myelopoietic systems, suggesting that the site of residual damage was located at the pluripotential or common stem cell level. The amount of RI found in either the erythroid or myeloid systems, at any given time after six weeks post exposure, is directly related to the dose of x-irradiation given, while the rate of RI loss was found independent of the exposure dose. Based on the several observations above, it was deduced that RI is an indication of the presence of damaged cells within a compartment that is normal in size, rather than a reflection of a stem cell pool that has a smaller than normal number of cells. In the study of the spleen, it was found that bleeding induced a significant amount of splenic hematopoietic activity in both control and x-irradiated animals. In the bled x-irradiated animals, however, such activity was found depressed throughout most of the study period. However, by the 40th week, it had returned to within normal values. (Diss. Abstr.)

26982 RELATIONSHIP BETWEEN X-RAY INDUCED TERATOGENY AND CHROMOSOME ABERRATIONS IN GOLDEN HAMSTER EMBRYOS. Jones, William Elvin. Corvallis, Oreg.; Oregon State Univ. (1971). 72p. University Microfilms Order No. 71-6781.

Thesis.

The relationship between x-ray induced chromosome aberrations and x-ray induced embryonic abnormalities was studied. Golden hamsters were irradiated during four stages of gestation: the blastocyst stage, 4.5 days post-copulation; the primitive streak stage, 6.5 days post-copulation; the organogenesis stage, 9.5 days post-

copulation; and the period of fetal growth, 11.5 days post-copulation. The incidence of induced embryonic abnormalities as a consequence of irradiation in these various stages was 26 percent, 100 percent, 88 percent, and 0 percent respectively. Irradiation during the primitive streak stage produced the greatest variety of teratisms. The number of induced chromosome aberrations was found to remain constant, regardless of the stage in which irradiation occurred. Thirty-six percent of the cells contained some sort of chromosome aberration six hours post-irradiation, however, the number of aberrations was only seventeen percent three days post-irradiation. It was concluded that irradiation causes chromosome aberrations, which in turn, may be responsible for cellular death. Cellular death causes the development of embryonic abnormalities if it occurs at a particularly critical stage of development. Therefore the chromosome aberrations are indirectly responsible for the embryonic abnormalities but there is no correlation between the numbers of chromosome aberrations and the numbers and types of embryonic abnormalities. (Diss. Abstr.)

26983 INHIBITION OF RIBOSOMAL RNA SYNTHESIS IN X-IRRADIATED HeLa CELLS. Bases, R.; Mendez, F.; Nicolino, R. (Albert Einstein Coll. of Medicine, New York). Radiat. Res.; 44: 456-77(Nov 1970).

The effects of ionizing radiation on ribosomal RNA synthesis were studied in suspension cultures of HeLa-S-3 cells. After irradiation cells were incubated with ^{3}H uridine and their labeled RNA was prepared from whole cells or from their isolated polyribosomes and ribosomes. In the first hour following 1000 rads ribosomal RNA synthesis was depressed 30 to 50%. This was accompanied by a reduction in the amount of newly synthesized ribosomal subunits entering the cell cytoplasm and being recruited into polyribosomes. The rate of ribosomal RNA synthesis returned toward normal levels by 24 hours after irradiation. Labeled messenger RNA was isolated from polyribosomes of cells incubated for 15 minutes with ^{3}H uridine immediately after 1000 rads. No inhibition of messenger RNA synthesis could be detected in these cells or in irradiated cells whose ribosomal RNA synthesis was completely and selectively inhibited by lucanthone. (auth)

26984 PROTEOLYTIC ACTIVITY IN ISOLATED PERFUSED LIVER OF NORMAL AND X-IRRADIATED RATS. Kocmierska-Grodzka, D.; Gerber, G. B. (Nuclear Energy Study Center, Mol, Belgium). Radiat. Res.; 44: 338-44(Nov 1970).

Uptake and catabolism of ^{131}I-labeled denatured albumin was studied in perfused liver isolated from fed, starved, and starved x-irradiated (24 hours after 800 R) rats. Uptake of albumin and proteolytic activity was greater in starved rats than in fed rats. X irradiation depressed the uptake of albumin by the liver but did not affect or even increase proteolytic activity. (auth)

26985 RESTORATION OF THE HYBRID EFFECT SUPPRESSED BY WHOLE-BODY IRRADIATION. Oth, Daniel; Oswald, Patrick; Burg, Constant (Institut National de la Sante et de la Recherche Medicale, Nancy). Jap. J. Exp. Med.; 39: 649-52(Dec 1969). (In Japanese).

Tumor TP-8 is a methylcholanthrene-induced sarcoma specific for the inbred Swiss/B strain mice, and accepted in a significantly lower percentage in (Swiss/B × C3H/He) F_1 hybrid mice than in the indigenous strain. Hybrid mice exposed to 500 R or 550 R whole-body irradiation became fully susceptible to parental tumors grafted one day later. The effect of this immunodepression was comparatively stronger in F_1 hybrids than in syngeneic mice treated in the same manner. In these hybrids, intraperitoneal or intravenous injection of normal hybrid bone marrow cells, mixtures of hybrid bone marrow and splenic cells, or splenic cells, were effective in restoring the antitumoral resistance. It was concluded that the hybrid effect can be controlled by immunodepression and immunorestoration, and this suggests that a higher immune reaction to these antigens could be developed in the F_1 hybrids through the action of an allele of the parent to which the tumor is foreign. (Japan).

26986 ROLE OF CIRCULATING LEUKOCYTES IN THE PRODUCTION OF VIRUS-INHIBITING FACTOR OR INTERFERON. Nagano, Yasuiti; Maehara, Nobutoshi; Nakamura, Wataru (Kitasato Inst., Tokyo). Jap. J. Microbiol.; 14: 209-13(May 1970).

The relationship between the number of circulating leukocytes and amount of virus-inhibiting factor (IF) (or interferon) appearing in blood stream in response to injection of Escherichia coli endotoxin or Newcastle disease virus (NDV) was studied in mice after whole-body x irradiation. Two days after irradiation with 500 R, the leukocyte count fell to 7% of the normal value. Production of IF however, was not depressed when induced with endotoxin two days after irradiation, while NDV induced a slightly lower titer of IF than that found in non-irradiated mice. When induced 5 days after irradiation, though leukocyte count remained at 8 to 9% of the normal value, IF titers attained were only $\frac{1}{3}$ and $\frac{1}{4}$ of the control value with endotoxin and NDV, respectively. In mice given 1000 R before two days, leukocyte number was less than 1% of the normal value, while IF titers reached $\frac{1}{2.7}$ and $\frac{1}{3}$ of that in the control mice with endotoxin and NDV, respectively. The lack of parallel between the leukocyte count and amount of IF produced suggest that circulating leukocytes do not produce IF (auth) (Japan)

26987 ACUTE CHANGES OF THE CNS CAUSED BY THE EFFECT OF IONIZING RAYS: STUDY OF EDEMA. Cervos-Navarro, J. (Univ., Bonn). Acta Neurol. (Naples); 24: 307-11(Mar-Apr 1969). (In Italian).

Microscopic examination of the x-irradiated monkey brain (Macaca mulatta) showed conspicuous distention of the extracellular space. Forty-eight hours after irradiation the distention became maximal and caused loss of histological connections between cellular elements. On the 3rd day the extracellular space began to diminish again and on the 6th day no differences between irradiated brains and controls were observed. (auth)

26988 FETAL AND OVARIAN EFFECTS OF GAMMA IRRADIATION IN FEMALE COTTON RATS (SIGMODON HISPIDUS). Turnipseed, Marvin Roy. Athens, Ga.; Univ. of Georgia (1970). 59p. University Microfilms Order No. 71-3792.
Thesis.

Laboratory born and reared cotton rats (Sigmodon hispidus) were used to study the effects of γ radiation on the ovaries, fetuses, and general reproductive ability. The ovary or fetus was exteriorized during the irradiation. The oocyte $LD_{50(10)}$ for monoparous females is 842 R. The LD_{50} for 5-day embryos is 387 R. The LD_{50} for 12-day fetuses is bracketed by 650 and 700 R. The 20-day fetal $LD_{50(30)}$ is 1609 R. Probit regression equations were determined for the total number of oocytes and for two classes of oocytes and for the 5- and 20-day fetuses. The body posterior to the kidneys was irradiated in 0 to 1-, 15-, 30-, and 60-day old cotton rats with an adult $LD_{50(30)}$ dose and their reproductive ability determined, after they matured, for four months. All reproductive ability was destroyed by irradiation in the 0 to 1-day group while the reproductive capacity in the 15-, 30-, and 60-day groups was equal with each other and with that of their respective controls. Cotton rats have a generally high radioresistance and their ovaries have viable ova after exposure to dose levels above the adult $LD_{50(30)}$. (Diss. Abstr. Int., B)

26989 EFFECTS OF ULTRAVIOLET LIGHT ON MOUSE L CELLS. Domon, Masaharu. Toronto; Univ. of Toronto (1969). Available from National Library of Canada at Ottawa.
Thesis.

The effects of uv irradiation on mammalian cells in vitro at cellular level were investigated. By use of mouse L cells in suspension culture, the following three questions were studied under low exposure of uv by which 20% or more of the cells survive: the effects of uv irradiation on the progression of the cell through the cell cycle, the effects of uv irradiation on the proliferative capacity of the cells, and whether the damage produced by uv in the cell was altered during post-irradiation incubation. The first question was studied by use of an autoradiographic technique using radioactive thymidine to label the cells. The experimental results indicated that cell populations irradiated in G_1 or G_2 phase show no delay in their movement to S phase or mitosis respectively, but cell populations irradiated in S phase have a delay in their progression to G_2 phase. In addition, the delay in reaching mitosis for cell populations irradiated in late G_1 phase was entirely accountable for by an S phase delay. Thus, uv irradiation of the cell mainly produced a specific delay in the progression of the cell through the S phase. The second question was investigated using synchronized cell populations. The measurements showed that cell populations irradiated in late G_1 or early S phase have a larger fraction of cells that failed to reach mitosis than cells irradiated in late S phase. The fraction of cells that failed to reach the first mitosis after irradiation was approximately equal to the fraction of cells that lost their colony forming ability. This indicated that the effects of uv irradiation on cell colony forming ability are expressed before the first cell division after irradiation. The third question was studied by use of the toxic effect of caffeine on the ability of uv irradiated cells to progress about the cell cycle and to form colonies. It was observed that cells irradiated in S phase and incubated immediately in the presence of caffeine rapidly lost their capacity to form colonies, but when irradiated cells were allowed to progress right through S phase in the absence of caffeine, they became resistant to its action. This indicated that an alteration of the damaged site in the cell has occurred during the passage of the cell through S phase. From these conclusions, a general picture about the cellular effects of low uv exposures on mammalian cells can be derived. That is, cells in the DNA synthesis phase were the most suscepti-

ble to uv irradiation, expressed the presence of uv damage in the cell, and altered the nature of uv damage. (auth)

26990 DAUNOMYCIN AND ANTITUMOR IMMUNOLOGIC DEFENSE: ITS INFLUENCE ON THE GROWTH OF EHRLICH ASCITES CANCER. Nicolin, A.; Beretta, G. (Univ., Milan). Arch. Ital. Patol. Clin. Tumori; 12: 69-78(Jan-Jun 1969). (In Italian).

The effects of pretreatment with a single dose of daunomycin on the development of Ehrlich ascites tumors in mice were investigated using various doses and time intervals between daunomycin treatment and tumor implantation. Daunomycin did not show an immunosuppressive activity when compared with 5-fluorouracil in parallel experiments. Daunomycin, on the other hand, seemed to increase the animal resistance and survival. In animals pretreated with daunomycin and x irradiation, the immunosuppressive action was potentiated, and only the x-irradiated animals survived. The possibility that daunomycin, through an activation of the lymphatic system, induced sensitization to the lytic effect of x irradiation is hypothesized. (auth)

26991 DECREMENTS IN THE VISUAL ACUITY OF RHESUS MONKEYS (MACACA MULATTA) AS A DELAYED EFFECT OF OCCIPITAL CORTEX IRRADIATION. Graham, Ernest S. (Aeromedical Research Lab., Holloman AFB, N. Mex.); Farrer, Donald N.; Carsten, Arland L.; Roizin, Leon. Radiat. Res.; 45: 373-83(Feb 1971).

The visual acuity of four rhesus monkeys was measured before and after exposure of the occipital lobes to 3500 rads of 250 kVp x radiation. Two additional animals served as nonirradiated control animals. Acuity was measured with a four-choice discrimination problem involving Landolt rings. The initial statistical difference between the acuity of the experimental and control groups occurred 119 days after exposure. The initial observation of blindness (10.0 minutes of arc or greater) in the four experimental animals occurred between 149 and 195 days after exposure. Control animals showed no significant change in acuity through 203 days of postexposure acuity testing. EEG testing 210 days after exposure failed to demonstrate any photo evoked response in the four experimental animals. Neuropathology was completed on the four experimental animals; the results, including histochemical observations, are reported. (auth)

26992 SURVIVAL TIME AND DOSE-RESPONSE FOLLOWING SUPRALETHAL IRRADIATION OF DOGS. Block, P. C.; Taylor, J. F.; Ainsworth, E. J. (Naval Radiological Defense Lab., San Francisco). Radiat. Res.; 45: 384-98(Feb 1971).

Incapacitation and times of death were studied in beagles following supralethal doses of either ^{60}Co γ or pulsed reactor radiations. The dose range investigated was 3,800 to 20,000 rads. Direct comparison of the effects of reactor radiations and ^{60}Co γ radiations at two doses, ~11,500 and 14,000 to 15,000 rads, indicated incapacitation and survival time were not influenced by either dose rate or type of radiation. Radiation dose responses could be grouped in two broad categories, at doses of 3800 and 7600 rads the survival times of 8 dogs ranged from 67 to 98 hr with the first signs of incapacitation observed between 48 and 72 hr, at doses of 14,000 and 20,000 rads only 1 of 16 dogs survived more than 29 hr, and all dogs were incapacitated within 100 min. There was no evidence for recovery from radioinduced incapacitation after the signs were first observed. (auth)

26993 RESPONSE OF MAXIMAL AND SUBMAXIMAL ACTION POTENTIALS FROM FROG SCIATIC NERVE TO 200-kV X-RAYS. Gaffey, C. T. (Univ. of California, Berkeley). Radiat. Res.; 45: 311-25(Feb 1971).

Maximal action potentials (MAP) from isolated, frog sciatic nerve were recorded before and during x irradiation. MAP amplitudes were not changed by 10 kR of 200 kV x rays in 19 trials; in 16 other experiments the MAP amplitudes were not altered by 100 kR of x irradiation. Sixteen nerves were irradiated until complete suppression of the MAP was evidenced, which required 300 kR (average) of x rays. Rapid attenuation of the MAP amplitude was initiated with 160 to 200 kR of x rays. Twelve nerves exhibited a 4 to 10% increase of the MAP amplitude prior to rapid attenuation; four other nerves revealed only decreases in the MAP amplitude with x rays in excess of 160 kR. In these experiments the maximal threshold stimulus (MTS) to evoke a MAP remained unchanged below 100 kR of x rays; during attenuation of the MAP amplitude the MTS increased. The duration of the MAP increased in all nerves exposed to 20 kR of x rays even though the MAP amplitude remained unaffected. In some cases 10 kR of x rays provoked changes in the duration of the MAP. Submaximal action potentials (SMAP) generated by 57 nerves were recorded before and during exposure to x irradiation. The SMAP amplitude remained unchanged in 31 nerves (54.4%), increased in 20 nerves (35.1%), and decreased in 6 nerves when exposed to 10 kR of x rays. These findings failed to support the claim that 10 kR of x rays only heightened SMAP amplitudes. Nerves that always produced stable SMAPs during the control period were insensitive to irradiation. Nerves which exhibited a temporal increase or decrease in the SMAP amplitude during the preirradiation interval tended to be provoked into a similar SMAP amplitude change with 200 kV x rays. (auth)

26994 EARLY AND LATE EFFECTS OF TRITIATED THYMIDINE UPON THE REPLICATION OF SPLENIC LYMPHOCYTES. Post, Joseph; Hoffman, Joseph (New York Univ., N. Y. Goldwater Memorial Hospital, Welfare Island, New York). Contract AT(30-1)-2778. Radiat. Res.; 45: 335-48(Feb 1971).

Studies were made of the early and late effects of ^{3}H-TdR labeling of DNA upon the replication of spleen lymphocytes in 3 week old Wistar strain rats. The administration of 1 μCi/g body weight was associated with an asymmetrical mitotic labeling curve in which the first cycle was fairly well defined but the subsequent two cycles were less so. After 0.4 μCi/g, two cycles were observed of similar duration to those after 1 μ Ci. Following 2 and 10 μCi/g the pattern was disrupted. The effects were greater with the higher labeling dose and were related to the level of radiation and not to that of thymidine pool dilution. Five wk after 2 and 10 μCi/g, when autoradiographic evidence of retained radioactive labeling was absent, the cycle patterns were still altered. Four mon after 10 μCi/g the pattern was restored to that of age controls. The differences between the responses of spleen lymphocytes, on the one hand, and of previously studied coexistent hepatocytes and ileal cells, on the other, are reviewed. (auth)

26995 PRODUCTION OF CIRCULATING RAT INTERFERON IN MICE–RAT RADIOCHIMERAS. De Maeyer-Guignard, J.; De Maeyer, E.; Jullien, P. (Institut du Radium, Paris). pp 397-404 of L'Interferon. Paris; Institut National de la Sante et de la Recherche Medicale (1970). (In French).

From Conference on interferon; Lyon, France (6 Jan 1969). See CONF-690127.

C_3H/He mice were exposed to a total-body x irradiation of 1000 R, and were subsequently given 10^7 xenogeneic Wistar rat marrow cells. In these rat-to-mouse chimeras, the serum interferon producing capacity after injection of Newcastle disease virus (NDV) was examined four weeks after grafting. Normal levels of circulating interferon were produced. The interferon, however, had the species specificity of rat interferon, being 20 times more active in rat embryo fibroblasts than in mouse embryo fibroblasts. Moreover, it behaved like rat interferon when filtered by Sephadex G-100 dextran gel, displaying one activity peak in the 90,000 molecular weight range and two incompletely separated peaks of respectively 32,000 and 24,000, in the 30,000 molecular weight region. The fact that interferon is of the donor type in rat-to-mouse chimeras infers that the circulating interferon induced by NDV is made in bone-marrow derived cells. (France)

26996 INFLUENCE OF THE THYMUS IN THE REGENERATIVE PROCESS OF CERVICAL LYMPH NODES IN IRRADIATED MICE. Catalini, Nicola; Gibertini, Giancarlo; Filoni, Sergio (Univ., Rome). Atti Accad. Naz. Lincei, Rend., Cl. Sci. Fis., Mat. Natur.; 48: 543-9(May 1970). (In Italian).

The role played by the thymus in the regenerative process of cervical lymph nodes was investigated in whole-body irradiated mice and in thymus-shielded mice. In the lymph nodes of the shielded animals a lower percentage of pycnotic lymphocytes and a significantly higher mitotic index, detectable at an earlier stage, were found. It was concluded that a continuous migration of thymocytes towards x-ray damaged lymph nodes occurs in this group of animals. (auth)

26997 REGIONAL SHIFTS IN THE VERTERBRAL COLUMN OF INBRED MICE TREATED WITH X-RAYS OR FCdR. Ohmori, Kazuo (Johann Wolfgang Goethe Univ., Frankfurt am Main). Wilhelm Roux' Arch. Entwicklungsmech. Organismen; 166: 124-35(1970). (In German).

In three inbred-strains of mice (C57BL/6, C57BL/10, and C57BL/Ks) 5-fluoro-2'-deoxycytidine (FCdR) and x rays were applied at several stages of pregnancy. The shiftings of the regions of the vertebral column in the offspring were examined. There were several critical periods concerning differentiation of the cervical ribs. Critical periods for differentiation of lumbar ribs were at day VIII and day IX of pregnancy. X rays and FCdR, applied at day IX, inhibited the formation of cervical ribs. The appearance of the 13th ribs was inhibited by x rays at day X + 20 hr of pregnancy. The appearance of the 13th ribs was inhibited by FCdR at day IX; lumbar ribs have their critical period at the same time. First ribs were never absent in the control and ex-

perimental series. At day IX + 20 h x rays were induced at a third time to cervical ribs. This showed the importance of a broadly timed experiment. The border between the lumbar and the sacral region was very sensitive to exogeneous influences; in the controls asymmetrical vertebrae fixed at the pelvic girdle were rather frequent. (auth)

26998 PRIMARY REACTION OF THE HYPOPHYSEAL-ADRENAL SYSTEM TO THE EFFECT OF IONIZING RADIATION. Rogozkin, V. D.;Romashko, O. O. Byull. Eksp. Biol. Med.; 71: No. 1, 14-16(Jan 1971). (In Russian).

The primary reaction of the hypophyseal-adrenocortical system of rats in response to the effect of ionizing radiation was studied. An increase of the hormone-forming and secretory functions of the adrenals in irradiation with a dose of 650 R was recorded 5 minutes thereafter. Within 20 minutes, the levels of corticosterone of the plasma and adrenals did not differ from those in control animals. (auth)

26999 INFLUENCE OF IRRADIATION ON THE URINARY EXCRETION OF DEOXYCYTIDINE AND BETA-AMINOISOBUTYRIC ACID IN MONKEYS. Fedorova, T. A.; Tarakanova, M. P.; Mazurik, V. K.; Rubachev, P. G. Byull. Eksp. Biol. Med.; 71: No. 1, 34-7(Jan 1971). (In Russian).

In 15 M. rhesus monkeys weighing 2–2.5 kg urinary excretion of desoxycytidine (DC) and beta-aminoisobutyric acid (BAIBA) in health and after total gamma-irradiation in a dose of 620 R from the first to the 27th day was studied. In healthy monkeys, the diurnal urinary excretion of DC fluctuated within the limits of 5.11–58.12 μg, averaging 29.84 ± 1.48 μg, whereas BAIBA varies from 105 to 751 μg, averaging 379 ± 29 μg. In irradiated monkeys, the diurnal urinary excretion of DC increased on the 1st to 3rd, 6th to 8th and 8th to 24th day after irradiation (by 3.6–2 times, by 1.8 and 2–3.4 times respectively) and BAIBA on the 1st to 2nd, 5th to 6th and 7th day (by 2.7–2 and 2 times respectively) with a subsequent reduction of the urinary content of BAIBA from the 9th to 21st day to subnormal values, and normalization towards the 24th to 27th day. The possible mechanisms causing changes in the urinary excretion of DC and BAIBA in irradiated monkeys are discussed. (auth)

27000 EFFECT OF X-IRRADIATION ON THE WOUND RESPONSE OF THE RAT LENS EPITHELIUM. Lindgren, Alice Marilyn Lindell. Iowa City, Iowa; Univ. of Iowa (1970). 166p. University Microfilms Order No. 71-5784.

Thesis.

Albino male rats, 3 to 4 months of age, were utilized for all experiments. After the animals were anesthetized, the pupil was dilated with Mydriacyl and the anterior surface of the lens was wounded with a 28-22 gauge hypodermic needle which was inserted through the anterior chamber perpendicularly to the corneal surface. Before or after wounding, the eyes only were irradiated with 1000 rads of x-rays (HVL = 0.99 mm Cu, 250 Kvp, 30 ma, 170-180 rads/min). Cells were counted in areas of the epithelium, 100 × 100 u, as delineated by a microscope eyepiece reticule at 500 ×. The percentage of labeled mitotic figures, the average percentages of labeled or mitotic cells and standard errors of the means, the average number of cells per 0.01 mm^2 and the standard error of the mean, and the duration of S and G_2 were determined. An IBM 360 computer was used for many of the calculations. A Dupont 310 curve analyzer was utilized to interpret some of the plotted data. Wounding generated a stimulus that traveled outward from the wound at a rate of at least 300 u/hr. In response, the intermitotic cells began DNA synthesis at about 14 hours after wounding; this phase of the response reached a maximum at 18 hours and gradually diminished. Mitosis began at 24 hours, reached a maximum at 30 hours and gradually subsided. To determine the effect of x-irradiation on the intermitotic cells and to evaluate their recovery with time, the lens was irradiated with 1000 rads of x-rays at various times before and after wounding. X-irradiation two hours before the S phase did not block DNA synthesis but did delay mitosis. X-irradiation 1 hour before wounding suppressed and delayed both DNA synthesis and mitosis. As the time interval between irradiation and wounding was increased, DNA synthesis and mitosis appeared earlier in time and the number of cells responding increased, indicating that recovery had occurred in the intermitotic cells. (Diss. Abstr.)

27001 RADIATION, INFECTION, AND MACROPHAGE FUNCTION. IV. EFFECT OF RADIATION ON THE PROLIFERATIVE ABILITIES OF MONONUCLEAR PHAGOCYTES IN TUBERCULOUS LESIONS OF RABBITS. Chandrasekhar, Saroj; Shima, Kiyoshi; Dannenberg, Arthur M. Jr.; (and others) (Johns Hopkins Univ., Baltimore. Biological Science Lab., Frederick, Md.). Infec. Immunity; 3: 254-9(Feb 1971).

Rabbits were irradiated with 400 to 600 rads 2 to 3 days before they were infected with BCG or with virulent tubercle bacilli. Biopsies were periodically removed from the resulting lesions and incubated for 1 hr with ^{3}H-thymidine in vitro under hyperbaric oxygen. Twelve to 16 days after radiation there was a reduction in the percentage of mononuclear cells (macrophages and some lymphocytes) that had incorporated ^{3}H-thymidine in the lesions. At this time, the lesions of the irradiated group were smaller than those of controls. These results can be explained by the reduction in the number of new mononuclear cells that entered the lesions of the irradiated group and support the tenet that local mononuclear cell division occurs mainly in cells that have recently emigrated from the blood stream. An alternate, but less likely, explanation of these results would be that radiation caused the bone marrow to release a higher percentage of defective mononuclear cells that were unable to divide, i.e., incorporate ^{3}H-thymidine, in the lesions. The reduction produced by radiation in both local cell infiltration and local cell division would decrease the number of macrophages available to control the tuberculous infection in the host. (auth)

27002 X-RAY-INDUCED UNSCHEDULED DNA SYNTHESIS IN MAMMALIAN CELLS: RELATION TO CELL SURVIVAL AND CHROMOSOME REJOINING, VARIATION WITH CELL CYCLE STAGE, AND EFFECT OF METABOLIC INHIBITORS. Shaeffer, James Dennis. Baltimore; Johns Hopkins Univ. (1970). 94p. University Microfilms Order No. 70-26,735.

Thesis.

Studies were made on the extent of unscheduled DNA synthesis in several mammalian cell lines and the biological meaningfulness of the process in terms of cell survival. The relative extent of x ray induced unscheduled DNA synthesis was measured in six mammalian cell lines: HeLa, mouse L-929, human embryonic kidney, rat kangaroo kidney, human laryngeal tumor, and human peripheral lymphocyte. Relative radiosensitivities (D_0) and recovery ratios were measured in the HeLa, mouse L-929, and rat kangaroo kidney lines. There was no apparent correlation between relative unscheduled DNA synthesis and radiosensitivity or between relative unscheduled DNA synthesis and recovery ratio in these cell lines. These observations are in agreement with the conclusion that cell survival following x irradiation does not depend on unscheduled DNA synthesis. Puromycin, a protein synthesis inhibitor, inhibited unscheduled DNA synthesis although it has been found not to inhibit cell recovery. Likewise, dinitrophenol, an uncoupler of oxidative phosphorylation, inhibited unscheduled DNA synthesis, whereas it has previously been found to enhance cell recovery. Cell lines containing more chromosomes showed greater amounts of unscheduled DNA synthesis. One cell line, the rat kangaroo kidney line, showed no apparent unscheduled DNA synthesis following either x ray or uv irradiation. The rat kangaroo kidney line did show chromosome rejoining following x irradiation. This finding supports the conclusion that unscheduled DNA synthesis and chromosome rejoining represent different repair processes. The extent of unscheduled DNA synthesis appeared to be independent of cell cycle stage. (Diss. Abstr. Int., B)

27003 ANIMAL EXPERIMENTAL STUDIES ON THE PATHOGENESIS OF RADIOGENIC BONE INJURIES IN THE MANDIBLES OF ADULT RABBITS. II. HISTOMETRIC DATA. Grimm, G. (Martin-Luther-Univ., Halle-Wittenberg, Ger.). Deut. Zahn-, Mund- Kieferheilk.; 54: 352-62(Jun 1970). (In German).

Results of histometric investigations of the lower jaws of adult rabbits by radiation, under conventional conditions of treatment are reported, which illustrate the course of radiogenic bone damage in dependence on time and the radiation. The statistical analytical counting of the various degeneration stages of the bone cells permits the quantitative determination of the osteocyte diminution in dependence on mathematical functions, that can be statistically secured. (auth)

27004 COMPARATIVE EFFECTS OF X RAYS AND VISIBLE LIGHT ON THE RECONSTITUTION OF THE EARLY POTENTIALS (ERP) OF THE ISOLATED FROG EYE PREVIOUSLY ABOLISHED WITH SEVERE LIGHT EXPOSITION. Debenedetti, A.; Grossi, V.; Lucaroni, A. (Univ., Perugia, Italy). Boll. Soc. Ital. Biol. Sper.; 45: 1371-3(15 Nov 1969). (In Italian).

Previous studies have shown that the early potentials of the in vitro frog eye annihilated by severe light exposure can be reconstituted by a light source after readaptation to dark. A study was made to determine if analogous results could be obtained with the use of x rays as the reconstituting light source. The results showed that a period of readaptation to the dark for 10 min was sufficient for almost complete reconstitution of the early potentials (ERPO in the eye of controls after their annihilation by strong illumination). The administration of x rays of 75,000 R/min for the same period of time apparently did not interfere with the reconstitution of the potentials. The illumination of the eye with visible light (200 lux for 10 min) significantly reduced the reconstitution. (J.S.R.)

XUM

27005 EFFECT OF HOMOTRANSPLANTATION OF BONE MARROW ON THE HEALING OF LIVER WOUNDS IN SEVERE COMBINED RADIATION TRAUMA. Ogii, P. E.; Chumak, A. S. Vestn. Khir.; 103: 37-41(Aug 1969). (In Russian).

Rabbits were irradiated with a dose of 1096 rad and subjected to additional mechanical injury to the liver. Delayed healing of the hepatic wound was demonstrated in comparison with the control series. Transplants of bone marrow, made within 24 hrs to 6 days after the combined radiation injury, contributed to amelioration of the radiation injury, increased the percentage of survivors, and accelerated the healing processes of the liver. Clinical, hematological, and histological evidence indicated that the best results were obtained with animals given bone marrow transplants during the first three days following injury. (auth)

27006 EFFECTS OF PRIOR WHOLE-BODY GAMMA IRRADIATION ON PROTEIN BIOSYNTHESIS IN VITRO BY SUBCELLULAR COMPONENTS FROM RAT LIVER. Davidson, David Edward Jr. Washington, D. C.; Georgetown Univ. (1970). 192p. University Microfilms Order No. 70-26,656.
Thesis.

A decrease in the synthesis of protein in vitro by subcellular components from the livers of irradiated rats was observed. Possible mechanisms responsible for this defect were investigated. Female Sprague–Dawley rats weighing 100–150 grams were exposed to an LD 50/30 dose of uniform whole-body cobalt-60 γ radiation (820 R). Incubation mixtures containing microsomal fractions from irradiated rats were less active in incorporating ^{14}C-leucine than control mixtures. The ratio of RNA to protein in the irradiated microsomal fractions was decreased, but not to an extent which would entirely account for the reduced incorporation. This reduction in RNA to protein may reflect the release of ribosomes from the endoplasmic reticulum in vivo. Liver ribosomal fractions from irradiated rats, incubated with the purified enzyme fraction and sRNA, were less active in incorporating ^{14}C-leucine than control ribosomes. Decreased incorporation by irradiated ribosomal fractions was observed at all intervals from day 3 to day 27. The mechanism of a slight decrease in enzyme fraction activity between days 12 and 27 is not known. Monosomes and disomes obtained from sucrose density gradients were found to be free of functional messenger RNA. These messenger-free ribosomes incorporated ^{14}C-phenylalanine into protein in vitro when polyuridylic acid messenger was supplied exogenously. No difference in incorporation between irradiated and control samples was noted, suggesting indirectly that in unfractionated ribosomal fractions the decreased synthetic activity must have been due to a difference in the endogenous mRNA. The sucrose density gradient profiles of irradiated ribosomal fractions showed no evidence of changes in size distribution of polysomal aggregates. A slight increase in the area under the monosome peak was attributed to an increase in ferritin in irradiated samples. Evidence that the proteins synthesized by irradiated ribosomal fractions in vitro are qualitatively different was obtained in dual label experiments in which incorporation of lysine by irradiated ribosomal fractions was less inhibited than the incorporation of leucine, alanine, or phenylalanine. (Diss. Abstr. Int., B)

27007 EFFECTS OF IONIZING RADIATIONS ON ALBUMIN BIOSYNTHESIS AND CELL PERMEABILITY. Shihabi, Zakariya Kamel. Vermillion, S. D.; Univ. of South Dakota (1970). 88p. University Microfilms Order No. 71-1153.
Thesis.

Irradiation was used as a model system to study the regulation of albumin synthesis in the rat. Both the subcellular system and in vivo pulse labeling studies were performed. Irradiation decreased the incorporation of ^{14}C-leucine into microsomal albumin in the cell free system and in the starved rat. The previous effect was associated in both cases mainly with the microsomes and to a lesser extent in the cell sap. Irradiation caused a 37% decrease in the uptake of ^{14}C-orotic acid into the polysomal RNA, while starvation did not affect this step. Starvation affected the capacity of the ribosomes to incorporate phenylalanine in the presence of poly U, while irradiation did not. Irradiation caused an increased incorporation of ^{14}C-algal hydrolysate into microsomal albumin and the circulating serum albumin in in vivo studies. It was concluded that irradiation affects albumin synthesis at the level of RNA synthesis (transcription), while starvation acts at the level of the ribosomes (translational). Irradiation, furthermore, caused a significant change in the cell permeability of many tissues in the body. (TSS) (Diss. Abstr. Int., B)

27008 MORPHOLOGIC AND FUNCTIONAL CHANGES IN TESTICULAR INTERSTITIAL TISSUE OF THE RAT AFTER CRYPTORCHIDISM OR X IRRADIATION. Niewenhuis, Robert J. Cincinnati; Univ. of Cincinnati (1970). 116p. University Microfilms Order No. 71-1529.
Thesis.

Both cryptorchidism and x irradiation are known to cause structural changes in the interstitial cells of the testes as well as alterations in androgen production. Studies were made on these alterations in great detail and to gain additional knowledge about the mechanism by which both of the above conditions affect androgen production in the interstitial cells. Adult male rats were divided into six groups: (1 and 2) those surgically rendered either unilaterally or bilaterally cryptorchid; (3 and 4) those exposed to either unilateral or bilateral testicular x irradiation; (5) a group of bilaterally cryptorchid rats which had one testis returned to the scrotum after 20 days; and (6) a group of unilaterally cryptorchid animals which were treated with 100 I.U. of human chorionic gonadotrophin for 21 days. Functional changes were determined by the the histochemical demonstration of 3_B hydroxysteroid dehydrogenase activity and morphologic changes were determined by electromicroscopy. Cryptorchidism caused a distinct decrease in 3_B hydroxysteroid dehydrogenase activity in rat testicular interstitial cells, thus indicating a decrease in androgen production in these cells. Local irradiation (1000R) to both testes produced a four-fold decrease in the testosterone blood level after 35 days, as measured by gas-liquid chromatography. This corresponded to a significant decrease in ventral prostate weights. Cryptorchidism caused an increase in the amount of smooth endoplasmic reticulum arranged in vesicles within interstitial cells and a corresponding decrease in tubular or lamellar arrangement. Histochemical results and morphologic changes indicated that cryptorchidism and x irradiation produce their effect upon interstitial cells by different mechanisms. Both cryptorchidism and x irradiation appeared to cause a change in the basic type of fibrillar connective tissue. This change involved a decrease in the number of microfibrils with a corresponding increase in the amount of unit collagen fibrils. Shrinkage of the seminiferous tubules resulting in a dispersion of microfibrils throughout the increased extracellular space may play a role in the decreased density of the connective tissue in the experimental testes. Convolutions of the boundary tissue with a distinct increase in numbers of unit collagen fibrils in the inner noncellular layer was seen in the testes subjected to both experimental conditions. (Diss. Abstr. Int., B)

27009 DELAYED EFFECTS OF CANINE OVARIAN IRRADIATION. Lee, Arthur Clair. Fort Collins, Colo.; Colorado State Univ. (1970). 158p. University Microfilms Order No. 71-2446.
Thesis.

The ovaries of 65 sexually mature female beagles were irradiated with single doses of 250 kVp x rays given as local exposures to the individually isolated organs. The exposures ranged from 600 to 6,000 R. Postirradiation observation for the occurrence of estrus and subsequent breeding of all animals with clinical and/or cytological evidence of estrus were carried out for a maximum of seven such periods. The conception rate for females in the 900 R group was 50%. Immediate postirradiation sterility was present during the first three heat periods for the 1,300 R dogs but two of them produced litters at their fourth estrus and the remaining observation time did not allow determination of the permanence of the resumed function. All of the females that received 1,700 R or greater were sterile. Estrus occurred in all exposure groups through 3,000 R and in five individual dogs at higher levels. A dose dependent reduction in ovarian weights and volumes and in uterine weights was found. The uterine weights appeared to be more sensitive and were at a minimum beginning at approximately 1,700 R. Histologically the oocytes, primordial follicles, and growing follicles were subject to qualitative changes and reduction in numbers. At 1,700 R there was less than 11% of the number of primordial follicles found in control ovaries and growing follicles were present to the extent of 20% of control numbers. In both cases there was further reduction at higher exposure levels. (Diss. Abstr. Int., B)

27010 RESPONSE OF STREPTOZOTOCIN DIABETIC RATS TO IONIZING RADIATION. Thorson, Theodore Melvin. Evanston, Ill.; Northwestern Univ. (1970). 257p. University Microfilms Order No. 71-1987.
Thesis.

Research was conducted to determine whether rats made diabetic with streptozotocin were more sensitive to the effects of x ray exposure than non-diabetic rats. The radiation LD_{50} after 30 days was determined both for the streptozotocin diabetic and non-diabetic animals. The results showed the diabetic animals to be more radiation sensitive. Glucose tolerance tests were performed on diabetic and non-diabetic rats following x ray exposure. Irradiation at exposure levels of 300, 450, and 600 R was found to have a detrimental effect on the outcome of the GTT up to 15 days post exposure. Circulating plasma glucose, insulin, and electrolyte levels were

measured, after exposure to 600 R, to 48 hrs post irradiation. The results of these determinations were presented and discussed. The effect of irradiation on the ability of insulin to retard potassium efflux from irradiated muscle was investigated. This study indicated no impairment of insulin action but did show an increased rate of potassium loss following exposure up to 18 hrs. (Diss. Abstr. Int., B)

27011 SYNERGISM BETWEEN RADIATION AND ESTROGEN IN THE PRODUCTION OF MAMMARY CANCER IN THE RAT. Segaloff, Albert; Maxfield, William S. (Alton Ochsner Medical Foundation, New Orleans. Ochsner Clinic, New Orleans). Cancer Res.; 31: 166-8(Feb 1971).

A × C rats, in which continuous administration of diethylstilbestrol produces a high incidence of mammary carcinoma as opposed to their essentially zero spontaneous incidence, were given radiation of one mammary chain while they were under the systemic influence of diethylstilbestrol. The animals irradiated without the diethylstilbestrol, with the same dose and at the same time, developed fewer mammary carcinomas after a much longer latent period (minimum, 75 weeks), but those animals irradiated while under the influence of the estrogen had many more mammary carcinomas (the first at 18 weeks) than those given the diethylstilbestrol alone. This is interpreted as substantial synergism between the two modalities in mammary carcinogenesis. (auth)

27012 ERYTHROPOIESIS IN MICE WITH GRAFT-VERSUS-HOST REACTION: ^{59}Fe DISTRIBUTION IN NORMAL AND X-IRRADIATED MICE AND MICE WITH GRAFT-VERSUS-HOST REACTION. Smitananda, Nitaya; McRae, J.; Nelson, D. S. (Univ. of Sydney). Pathology; 3: 31-8(Jan 1971).

The kinetics and distribution of ^{59}Fe were studied in normal and sublethally x-irradiated (C57B1/6J × A/J) F_1 mice and in mice with graft-versus-host reaction produced by intravenous injection of C57B1/6J lymph node cells after sublethal x irradiation. In normal mice, erythropoiesis occurred in spleen as well as in bone marrow. In mice with graft-versus-host reaction, red cell ^{59}Fe incorporation was decreased and plasma clearance was slower than in both normal and x-irradiated control mice. There was grossly decreased erythropoiesis in bone marrow and spleen and increased storage and excretion of iron. In contrast, a pattern of accelerated erythropoiesis was seen in x-irradiated control mice, in which red cell ^{59}Fe uptake was increased, plasma clearance was faster and liver uptake was lower than in normal mice. In the x-irradiated control mice the increased erythropoiesis appeared to occur mainly in the spleen. (auth) (Australia)

27013 EFFECTS OF IONIZING RADIATION ON THE EYE. Krokowski, E. (Stadtkrankenhauses, Kassel, Ger.). pp 139-54 of Problems of Industrial Medicine in Ophthalmology. Vol. 1-2. /Merte, H.-J. (ed.). Basel; S. Karger AG (1969). (In German).

From 1. symposium of the International Study Group for Ergophthalmology; Munich, Germany (14 Aug 1966) - 2. symposium of the International Study Group for Ergophthalmology; Amsterdam, Netherlands (18 Jun 1968). See CONF-660843-(Vol.1); CONF-680675-(Vol.2).

The most radiosensitive part of the eye is the lens. Because of simple anatomical structure and low biological variability, the lens permits an exact analysis of radiation effects. Animal experiments permit assessment of lens damage with respect to dose and type of radiation. Relation between age of the animal and the latent period between exposure and appearance of lens disturbances are established. Practical applications are discussed in regard to radiation exposure in industry, medicine, and nuclear accidents. Also discussed are possibilities of eye protection as well as recommendations for tolerance doses. (auth)

27014 EYE CHANGES CAUSED BY FAST NEUTRONS (15 MeV) AND THE PROTECTIVE ACTION OF CHEMICALS. Jacobi, K. W. (Univ., Cologne); Ruether, W. pp 275-83 of Problems of Industrial Medicine in Ophthalmology. Vol. 1-2. /Merte, H.-J. (ed.). Basel; S. Karger AG (1969). (In German).

From 1. symposium of the International Study Group for Ergophthalmology; Munich, Germany (14 Aug 1966) - 2. symposium of the International Study Group for Ergophthalmology; Amsterdam, Netherlands (18 Jun 1968). See CONF-660843-(Vol.1); CONF-680675-(Vol.2).

Groups of twenty rabbits each were irradiated with 15-MeV neutrons and ^{60}Co γ radiation, respectively. Doses administered to the eye were 750 rad of neutrons and 1500 rad of ^{60}Co γ radiation. Within 3 to 10 months, cataracts developed in all animals. Neutrons were twice as effective as ^{60}Co γ. Neutron-induced cataracts progressed more rapidly than those caused by gamma radiation. The radioprotective action of serotonin, adenosino-monophosphate, and cysteamine was studied. These chemicals caused cataracts to appear later and reduced their severity. (H.B.G.)

27015 CHANGE IN THE FUNCTIONAL STATE OF ERYTHROPOIESIS DURING PROLONGED FRACTIONATED IRRADIATION. Muksinova, K. N.; Voronin, V. S.; Luzanov, V. M.; Murzina, L. D. (Inst. of Biophysics, Moscow). Radiobiologiya; 10: 541-7(1970). (In Russian).

Rats of the Wistar line were γ irradiated from a ^{137}Cs source at a dose of 50 R per day for a period of 2.5 months, and the morphology and functional state of erythropoiesis were studied. The rate of liberation of erythrocytes, volume of blood, incorporation of radioiron into the bone marrow and spleen cells, as well as the reaction to erythropoietin, were determined using ^{59}Fe and ^{32}P. In the irradiated animals, erythrocytic equilibrium is reached over a prolonged period, which is explained by conservation of the area of concentration and functional state of erythropoiesis. The cause of the disturbance of equilibrium is damage to the circulating erythrocytes, substantially exceeding their production. (auth)

27016 INFLUENCE OF DIETARY CALCIUM AND FLUORINE ON THE RADIORESISTANCE OF BACILLUS-CARRYING ANIMALS. Knizhnikov, V. A.; Grozovskaya, V. A. (Inst. of Biophysics, Moscow). Radiobiologiya; 10: 617-19(1970). (In Russian).

Investigations were conducted on 150 rats from a stock with 18% paratyphus bacillus carriers. The animals, divided into two groups, received diets with different contents of calcium and fluorine. Two months after placement on the diet, the animals were subjected to fractionated γ irradiation on an ÉGO-2 apparatus with a total dose of 800 R for a week. The experimental animals, which received supplementary amounts of calcium and fluorine, began to die later than the controls. Bacillus carrying lowered the resistance of the animals to irradiation. (auth)

27017 INFLUENCE OF RADIOPROTECTORS ON THE CONTENT OF CATECHOLAMINES IN MOUSE TISSUES. Kulinskii, V. I.; Miller, L. P. (Second Clinical Hospital, Kharkov). Radiobiologiya; 10: 596-9(1970). (In Russian).

Mexamine and cystamine produce substantial changes in the content of catecholamines in a number of tissues of mice. During the first 10 min, both protectors lead to an identical rapid decrease in the noradrenalin content in the spleen. In the small intestines, cystamine gave the same effect; when mexamine was administered, signs of mobilization of noradrenalin were observed only in the first 5 min. The dynamics of the changes studied are in good agreement with the time peculiarities of the protection of radiovulnerable tissues by protectors. (auth)

27018 HISTOLOGY AND HISTOCHEMISTRY OF THE EMBRYONIC CHICK MANDIBLE FOLLOWING X RADIATION. Bailey, Barbara Ann. Norman, Okla.; Univ. of Oklahoma (1970). 143p. University Microfilms Order No. 71-1476.

Thesis.

The anomalous mandibular development of the chick embryo resulting from x irradiation was studied grossly, histologically, and histochemically. The most sensitive period for the mandibular development of chick embryos, due to x irradiation was determined to be 5 days of incubation or stage 27. Reduction in mandibular length and curvature of the lower jaw cartilage were common anomalous phenomena. A common response following x irradiation was the production of a blister or hematoma beneath the mandible. These blisters could not be positively correlated with anomalous mandibular development. The normal sites of cell death were studied in 3 through 9 day (stage 18–35) embryos. A possible correlation between nerve growth and cell death of the surrounding tissue was suggested. Cell deaths around the distal ends of Meckel's cartilage through the 7th day may aid distal cartilage elongation. (TSS)

27019 RESPIRATION AND OXIDATIVE PHOSPHORYLATION OF BONE MARROW TISSUE OF IRRADIATED RABBITS AFTER HOMOTRANSPLANTATION OF BONE MARROW ELEMENTS. Malovichko, I. I.; Shamray, A. E. (Kiev Medical Inst.). Vrach. Delo; No. 3, 132-5(1970). (In Russian).

Three groups of rabbits were used to study radiation effects on oxidative phosphorylation and respiration: controls, rabbits irradiated with 1200 to 1250 R, and rabbits irradiated and treated with bone marrow transplants. In rabbits irradiated with 1200 to 1250 R phosphorylation was reduced to 83% of normal on the 3rd day, and to 69% of normal on the 7th day after irradiation. All animals died 8 to 12 days after irradiation. The rabbits treated with bone marrow transplants were studied 7, 13, 20, and 30 days, and 2 and 5 months after irradiation, showed continual progressive increase in oxidative phosphorylation, from 64.8% to 90% of normal. It was concluded that the stimulating effect of transplanted bone marrow

is connected with the introduction into the organism of nucleoprotein complexes, with the nuclei of donor cells, and with the hematological condition of the animal. (JPRS)

27020 SPECTROPHOTOMETRIC CHARACTERIZATION OF DNA AFTER IRRADIATION IN VIVO. VI. SOME PHYSIOCHEMICAL PROPERTIES OF NEWLY SYNTHETIZED DNA IN THE REGENERATION OF IRRADIATED RAT LIVER. Furnica, M.; Georgescu, P.; Botez, G. Stud. Cercet. Biochim.; 12: 333-40(1969). (In Rumanian).

After partial hepatectomy (60% excised liver) rats were exposed to 900 R for 15 hrs. The newly synthetized DNA from the regenerated liver of irradiated rats was extracted after 10 days. No physico chemical modifications were noted. Some changes similar to those recorded in the liver DNA of non-hepatectomized irradiated rats were observed, a poor heat DNAase-induced hyperchromic effect, Tm = 90°, and a higher transition range ($\Delta^2/_3$). These modifications are presumably due to the unusual recovery of DNA strands in the rats exposed to lethal doses. (Rom. Sci. Abstr.)

27021 LEUKEMOGENIC EFFECT OF X RAYS IN BALB MICE: EFFECT OF SPLENECTOMY. Saal, Fortuna; Pasqualini, Christiane Dosne; Rabasa, S. L. (Academia Nacional de Medicina, Buenos Aires). Medicina (Buenos Aires); 30: 365-71(Jul-Aug 1970). (In Spanish).

The leukemogenic effect of x rays was studied in adult BALB mice of both sexes and compared to that of ^{32}P. Different doses of whole body irradiation were applied to groups of 40 mice at the age of 2 months: 1 × 400, 2 × 200, 2 × 400, 3 × 150, and 4 × 170 rad, with a weekly interval between each fractionated dose. Splenectomy was performed 1 month before the irradiation. It can be concluded that irradiation is responsible for the appearance of thymomas in the BALB strain in which leukemias, either spontaneous or induced by diverse agents, never involve the thymus; moreover, splenectomy increases the incidence of thymomas without increasing the total incidence of leukemia in x-irradiated animals. (P.B.M.)

27022 CHANGES IN THE CONCENTRATION OF FREE AMINO ACIDS IN THE LIVER OF IRRADIATED AND PARTIALLY HEPATECTOMIZED RATS. Izvoranu, M. Stud. Cercet. Biol., Ser. Zool.; 21: 251-7(1969). (In Rumanian).

The concentration changes of some free amino acids in the liver of rats after irradiation with 1000 R and partial hepatectomy were discussed. The differentiated amino acid balance in the experimental groups shows a close relation between dose and the mode of x ray delivery which influences the liver regeneration after hepatectomy. (Rom. Sci. Abstr.)

27023 EFFECT OF γ-RAY MICRODOSES ON SOME METABOLIC INDEXES DURING WHITE RAT ADAPTATION TO HYPOTHERMIA. Pora, E. A.; Manciulea, S. Stud. Cercet. Biol., Ser. Zool.; 21: 327-32(1969). (In Rumanian).

Very low radiation doses of 656 μ ^{65}Co daily, increase the mortality rate of white rats under hypothermia (temperature of 20°). This effect is presumably due to an enhanced enzymatic activity that produces a series of biochemical lesions in the cellular organites. A higher transaminase activity was recorded, with the consequent tissular proteolysis in irradiated animals, leading to their death. (Rom. Sci. Abstr.)

27024 EXPRESS METHODS OF INITIAL SELECTION AND STUDY OF CHEMICAL MEANS OF PROTECTION FROM RADIATION INJURY. Kudryashov, Yu. B. Vestn. Mosk. Univ., Biol. Pochvoved.; No. 2, 51-70(Mar-Apr 1970). (In Russian).

The rather extensive literature on the subject of chemical means of protection from radiation injuries is reviewed, and a series of original experiments on the subject are presented, testing a number of chemicals for their probable prophylactic properties and mode of action. It was found that the degree of decrease in the level of the redox potential in animal tissues after introduction of a chemical agent is correlated with the degree of radio protective action. Decrease in cellular level of lipid oxidation products prior to irradiation increases the resistance of the cell to ionizing radiation. Mercamine is the most effective and rapidly acting prophylactic agent; followed by those chemicals which liberate in the body mercamine. (JPRS)

27025 EFFECT OF 1200 R OF X RADIATION ON THE GROWTH OF BONE AND DENTINE IN THE MANDIBLE. Adkins, K. F. (Univ. of Queensland, Brisbane). Ala. J. Med. Sci.; 5: 409-14(Oct 1968).

The effects produced by 1200 R of x radiation on growing bone and dentine in the mandible were studied in albino rats. Foreshortening of the irradiated mandibles was apparent within 7 days. There was some indication that the most severe effects resulted when the radiation was administered in a single dose but statistical analysis failed to show any significant differences between the three dose/time patterns used. There were no statistically significant dimensional differences between the femurs which were protected during irradiation. Reduction in the amount of dentine apposition was apparent 28 days following 2 × 600 R of x radiation. No other quantitative aberrations were noted in dentine. (auth)

27026 X-RADIATION AND THE MANDIBULAR CONDYLE. Adkins, K. F. (Univ. of Queensland, Brisbane). Ala. J. Med. Sci.; 5: 415-20(Oct 1968).

The effects produced in the condyles of rats by 1200 R of x radiation were studied histologically. The marrow spaces were rapidly depleted of hemopoietic tissues and considerable fibrosis subsequently developed. Differentiation of mesenchymal cells into osteoblasts was temporarily impeded and as a result ossification close to the cartilage was reduced. Isolated functional chondrocytes were identified in the bony regions well away from the cartilage bone interface. No similar features were seen in control animals. The femurs that were protected during irradiation were also studied histologically but no aberrations were noted. (auth)

27027 INFLUENCE OF IRRADIATION DOSE ON THE LATENCY TIME OF CATARACTS IN RABBITS. DETERMINATION OF THE RELATIVE BIOLOGICAL EFFICIENCY OF 14 MeV NEUTRONS. Haye, C.; Legeay, G.; Bazin, J. P.; Quechon, H. (Institut du Radium, Paris). Ann. Ocul. (Paris); 203: 749-67 (1970). (In French).

The relative biological efficiency of the cataract-producing effect of monoenergetic 14 MeV neutrons was studied in rabbits. The criteria for opacification of the crystalline lens correspond to well-defined stages which allow the responses to be studied as a function of both the doses absorbed and the latency time. The graphs show the existence of an induction threshold or latency time. In the intervals, where the latency time is dependent on dose, it is possible to determine a relative biological efficiency with respect to gamma rays, which depends on the stage of the cataract. (France)

27028 FUNCTIONAL AND MORPHOLOGICAL CHANGES IN OVARIES OF MICE FOLLOWING PROLONGED LOW-DOSE γ IRRADIATION. Gelashvili, K. D. (Tbilisi State Univ., USSR). Soobshch. Akad. Nauk Gruz. SSR; 61: 481-4(Feb 1971). (In Russian).

A morphometrical investigation was made of some cells of the mouse ovary, such as granulose and theca cells of growing and mature follicules, as well as of yellow body cells. The animals were exposed to γ ray irradiation of ^{60}Co for 15 months, receiving 0.036 R daily. Some regular displacements were observed in the sphere of karyo and cytoplasma and nuclear plasmatic relations, with manifestations of structural changes in the ovaries, the latter being the basis of functional changes revealed in experiments. (auth)

27029 INDIVIDUAL DIFFERENCES IN THE RADIATION TOLERANCE OF RATS AND THEIR RELATIONSHIP TO THE DIFFERENCES IN THE PRE-IRRADIATION STRESS RESPONSE. Pospisil, M.; Zakopalova, I. (Inst. of Biophysics, Brno). Stud. Biophys.; 17: 197-204(1969).

The mean values of Na/K ratio of urine, collected from rats placed separately in metabolic cages for a 5-day period of interrupted fasting, indicate a relationship to the mortality of animals x-irradiated 3 days later with an exposure of 700 R. Individual average values of Na/K ratio are considered as an indicator of various stress reactivity of the animals with the participation of the hormones of adrenal cortex. Extreme variants of the preirradiation stress reactivity, the low and high average values of Na/K ratio, were found to predict the unfavorable prognosis of the post-irradiation syndrome. (auth)

27030 CHANGES OF PLASMA KININASE ACTIVITY IN IRRADIATED ANIMALS. Gaponiuk, P. Ya.; Umarchodgaev, E. M. (Medical Radiology Inst., Obninsk, USSR). Stud. Biophys.; 13: 225-30(1969).

Studies were done to determine the changes of plasma kininase activity in acute x ray disease in male rats. In all animals acute irradiation disease developed. Maximum mortality (40%) with all signs of gastro-intestinal disturbance was observed in 3 days after irradiation. The changes of blood plasma kininase activity post irradiation are summarized. The results show that within 3 hr following irradiation the blood plasma kininase activity increased. On the 13th day following irradiation the blood plasma kininase activity markedly increased and exceeded the control level in normal animals 1.9 times. (P.B.M.)

27031 RIBONUCLEIC ACID SYNTHESIS IN ENDOMETRIAL EPITHELIUM IN MICE AFTER WHOLE-BODY X-RAY IRRADIA-

TION. Konecki, J.; Klimkiewicz, Z. (Medical Academy, Zabrze-Rokitnica, Poland). Pol. Med. J.; 9: 1524-31(1970).

The autoradiographic technique was applied (tritium-labeled uridine) in investigations of RNA synthesis in the endometrial epithelium in mice, irradiated previously with a whole body dose of 600 R. It was demonstrated that a decrease of labeled uridine incorporation into RNA occurs in the irradiated mice, the lowest values being detected in samples collected 30 min after irradiation. About 36 hr after irradiation, uridine incorporation into the endometrial epithelium RNA showed a rising tendency. (auth)

27032 EFFECT OF DIETARY SELENIUM ON THE SURVIVAL OF RATS EXPOSED TO CHRONIC WHOLE BODY IRRADIATION. Hurt, H. D.; Cary, E. E.; Allaway, W. H.; Visek, W. J. (Cornell Univ., Ithaca, N. Y.). J. Nutr.; 101: 363-6(Mar 1971).

Rats fed a basal low selenium, vitamin E adequate diet or the basal diet supplemented with 0.5 ppM of selenium as selenomethionine for 6 wk were exposed to ^{60}Co γ irradiation at a dose rate of 9.4 R/hr for 20 hr daily. The preirradiation body weight, blood selenium, and liver selenium concentrations averaged 130 g, 0.070 and 0.072 ppM, respectively, for the selenium-depleted rats. Respective values for the supplemented rats were 150 g, 0.585 and 0.940 ppM. No differences in preirradiation hematocrit, erythrocyte concentrations, or leukocyte concentrations were observed between the two groups. These indices showed characteristic declines after irradiation with no differences between treatments. The length of survival after irradiation was not related to the selenium content of the tissues. (auth)

27033 REGENERATION OF CELL POPULATIONS OF INTESTINAL EPITHELIUM AFTER IRRADIATION. Kononenko, A. M.; Volke, J.; Farafonow, G. W. (Zentral Wissenschaftliches Roentgen-Radiologisches Forschungsinstitut, Leningrad). Stud. Biophys.; 17: 157-64(1969). (In German).

The transient behavior and the regeneration process of the cell population of intestinal epithelium of white mice is investigated after x irradiation with 400 rad. The period of investigation extends for 30 days after the irradiation. It was possible to point out, that the regeneration process is not terminated after the first restoration of normal values (3 days after irradiation). The transient behavior demonstrates the existence of two different oscillation systems. A slow variable component remembers the transient behavior of regulation systems, another faster component points out the character of day–night rhythm. (auth)

27034 DECREASE IN PETHIDINE DEMETHYLATING ACTIVITY OF ISOLATED RAT LIVER MICROSOMES FOLLOWING WHOLE-BODY X-IRRADIATION. Kvasnickova, E.; Lejsek, K.; Hais, I. M. (Charles Univ., Hradec Kralove, Czech.). Experientia; 27: 130-1(15 Feb 1971).

Studies were done on the effects of whole-body x irradiation on the enzymatic pethidine demethylating system of isolated rat liver microsomes. The activity of the enzymatic system was measured in isolated microsomes by the estimation of formaldehyde released from pethidine after 1-hr incubation. (P.B.M.)

27035 PROTEASE ACTIVITY CHANGES IN RABBIT LUNG MACROPHAGES, SPLEEN CELLS, AND POLYMORPHONUCLEAR LEUCOCYTES AFTER WHOLE-BODY X-IRRADIATION. Kotulova, Daniela; Stefanovic, J. (Comenius Univ., Bratislava). Folia Biol. (Prague); 17: No. 1, 26-32(1971).

Changes correlated to the time after irradiation and to the type of cells examined were found in intracellular protease activity in rabbits irradiated with a whole-body x ray exposure dose of 500 R. Enzymatic activity in the polymorphonuclear leucocytes rose within only 4 hr after irradiation and still persisted at a significantly high level on the third day. The activity increase in the lung macrophages appeared later, between the sixth and tenth day after irradiation. Changes in the protease activity of spleen cell extracts were biphasic in character. Initially, a significant increase was recorded on the first day after irradiation, with maximum values on the second day. Subsequently, protease activity fell, reaching the minimum value on the sixth day, but afterwards it rose again up to the tenth day. (auth)

Man

Refer also to abstracts 26603, 26628, 26668, 26730, 26783, 26797, 26799, 26811, 26835, 26836–26838, 26875, 26881, 26893, 26894, and 26898.

27036 (CONF-691057) BIOLOGICAL EFFECTS OF RADIATIONS. International Seminar, Sao Paulo, October 6–17, 1969. Eston de Eston, Tede; Rapp de Eston, Veronica (eds.) (Sao Paulo Univ. (Brazil). Centro de Medicina Nuclear). 1970. 389p. (In several languages).

Papers were presented on the following research projects: effects of radiation on cellular components; effects of radiation on the cell; effects of radiation on the gonads; effects of ionizing radiation on embryonic development of man and animals; the radiation syndromes; the bone marrow syndrome; effects of ionizing radiation on the digestive tract; cell renewal systems; the action of radiation on nervous tissues; action of hormones and biogenic amines on systemic reactions following irradiation; effects of radiation on life span of animals and man; radioinduced cancer and leukemia; effects of long-term ionizing radiation on conjunctival, renal, and pulmonary tissue; long-term toxicity of radioactive substances; chemical protection against radiation; treatment of acute radiation syndrome in man; bone marrow grafts in experimental radiopathology; natural radioactivity; radiodiagnosis using ionizing radiation and radioactive substances; radioactive contamination; recommendations of the International Commission on Radiation Protection; general methods of research in radiobiology; and biological effects of radiation and their consequences for development of peaceful uses of nuclear energy. (H.L.W.)

27037 AQUEOUS HUMOR DYNAMICS FOLLOWING PITUITARY IRRADIATION IN DIABETIC PATIENTS WITH RETINOPATHY. Caygill, Wayne M. (Univ. of California, San Francisco). Amer. J. Ophthalmol.; 71: 826-7(Apr 1971).

Hypopituitarism, induced in diabetic patients with retinopathy by alpha particle pituitary irradiation with 8000 to 12,500 rads did not appear significantly to alter intraocular pressure or scleral rigidity up to three years afterward. However, the facility of aqueous outflow and flow concurrently decreased so that the intraocular pressure after pituitary irradiation remained unchanged. It is not clear whether this decrease was related to the change in pituitary function or merely a consequence of passing time in the diabetic population. (auth)

27038 INCIDENCE OF MULTIPLE PRIMARY CANCERS. IV. CANCERS OF THE FEMALE BREAST AND GENITAL ORGANS. Schottenfeld, David; Berg, John (Memorial Hospital for Cancer and Allied Diseases, New York. National Cancer Inst., Bethesda, Md.). J. Nat. Cancer Inst.; 46: 161-70(Jan 1971).

The incidence of multiple primary cancers of other organs or tissues was studied in patients with carcinomas of the breast, ovary, endometrium, and cervix uteri, vagina, or vulva. The index patients were treated during 1949 to 62 and their observed frequency of new primary cancers was compared with the age and site specific incidence rates reported by the population based central registry. The incidence of metachronous primary carcinomas in the opposite breast was 6.1/year/1,000 patients, or 4.5 times expectation, in the patients with carcinoma of the breast, the incidence of multiple primary carcinomas of the ovary was 0.6/year/1,000 patients, or twice the normal risk, but one-tenth the risk for incurring a primary carcinoma in the opposite breast. The risk for incurring a metachronous primary carcinoma of the breast by a patient with a previous ovarian carcinoma was 3 to 4 times the normal risk. In patients with endometrial carcinoma, the risk of a subsequent breast carcinoma was 1.25 to 2.0 times the normal risk. The demonstration of a positive association of multiple primary carcinomas of the breast, ovary, and endometrium suggests demographic characteristics and etiologic factors common to these diseases. At least 3 of the 5 observed multiple, primary, soft tissue sarcomas developed as sequelae of previous breast cancers —1 arising in irradiated tissue and 2 in a lymphedematous upper extremity. (auth)

27039 STUDY OF HUMAN RADIATION SENSING AND DARK ADAPTOMETRY USING X-RAYS. Hellerstein, Lewis J.; Ballinger, Edwin R. (School of Aerospace Medicine, Brooks AFB, Tex.). Radiat. Res.; 44: 629-36(Dec 1970).

Thirty one patient volunteers underwent dark adaptometry studies before and after a true or sham series of skull x rays. There was no significant change in the cone plateau or rod cone break which could be attributed to the radiation. Although it did not reach our criterion for statistical significance, there was a suggestion that the rod plateau was decreased following radiation. Incorporated into the study was a radiation sensing test using the Townes' view of the skull series. There was no evidence that the subjects could detect the radiation under the usual clinical conditions. A second study confirmed that humans can easily detect the presence of radiation from a standard set of skull x rays while dark adapted. (auth)

27040 IRRADIATION AND RADIOCONTAMINATION DURING PREGNANCY. Sternberg, Joseph (Univ. of Montreal). Amer. J. Obstet. Gynecol.; 108: 490-513(Oct 1970).

The injuries provoked by ionizing radiation during the early stages of life were extensively studied. The chief purpose is to familiarize the practicing obstetrician with the incidences and the consequences of a voluntary or inadvertent application of a radiation procedure to a pregnant woman. The widespread use of nuclear energy for industrial purposes will lead to situations in which pregnant women will be exposed to accidental environmental radiocontamination. (P.B.M.)

27041 PITUITARY RADIOTHERAPY. Levene, Martin B. Radiol. Clin. N. Amer.; 5: 333-48(Aug 1967).

Reviews are given on the effects of x radiotherapy of the pituitary gland in man. The most serious effect associated with radiotherapy of the pituitary gland is radionecrosis of the brain. The necrosis may remain clinically latent and only be discovered at autopsy. Cases of brain necrosis following 4500 R in 4 wk are reported. (P.B.M.)

27042 DEVELOPMENT OF QUANTITATIVE BASES FOR RADIATION PROTECTION. Pochin, E. E. (University Coll., London). pp 119-25 of Environmental Aspects of Nuclear Power Stations. Vienna; International Atomic Energy Agency (1971).

From Symposium on environmental aspects of nuclear power stations; New York (10 Aug 1970). See STI/PUB-261; CONF-700810.

No valid assessment can be made of the adequacy of radiation protection measures without some assessment of the risk, or of the maximum likely risk, that is entailed in any given radiation exposure. For the low doses with which radiation protection measures are concerned, and for doses delivered at low dose rates, this requirement necessarily presents considerable difficulties, since no quantitative information exists as to the frequency of harmful effects produced in man by exposure to small doses of ionizing radiation delivered at low dose rates. Some numerical data have been obtained on the frequency of certain types of harm, particularly in the induction of malignancies in various body tissues or organs, by relatively high doses in the region of hundreds of rads. Inferences need then to be made from the incidences observed at high doses delivered at high dose rates to the incidences (or, at least, to the maximum likely incidences) to be expected at low doses delivered at low dose rates, although the latter may overestimate considerably the true risk in these circumstances. In the same way an estimate is required of the possible genetic effects of a particular exposure of a given number of people, both for mutations or chromosomal aberrations likely to be expressed in different ways in the immediate progeny of the subjects exposed, and for the frequency of such effects occurring in later generations within the population as a whole. To evaluate the likely hazard from any environmental contamination, therefore, it is necessary to assess the scale, composition, and probability of releases from potential sources, the size and age distribution of populations that may be exposed, the levels of whole-body or particular tissue exposure that might occur under various meteorological conditions, the extent to which these exposures might be curtailed by remedial action and the totality of biological hazard that might result from the doses received. (auth)

27043 CHILDHOOD CANCER IN RELATION TO PRENATAL EXPOSURE TO ATOMIC-BOMB RADIATION. Jablon, Seymour; Kato, Hiroo (Japanese National Inst. of Health, Hiroshima, Atomic Bomb Casualty Commission, Hiroshima). Lancet; 2: 1000-3(14 Nov 1970).

The juvenile cancer experience of 1292 children exposed prenatally in 1945 to the atomic bombs in Hiroshima and Nagasaki was studied. There was no significant excess of mortality from leukemia or other cancers. This experience is not consistent with the specific model for carcinogenesis as a result of prenatal x ray, advanced by another group, which postulates a linear dose response curve and an estimate for cancer deaths in the first 10 yrs of life of 572 per million person-rad. Only by drastically revising this value for the linear coefficient can the Japanese data be made consistent with this model. (auth) (UK)

27044 RADIATION-INDUCED FIBROSARCOMA. Gane, N. F. C.; Lindup, Rhona; Strickland, P.; Bennett, M. H. (Mount Vernon Hospital, Northwood, Eng.). Brit. J. Cancer; 24: 705-11 (Dec 1970).

Six cases of fibrosarcoma arising in previously irradiated tissues are reported out of a total of 220 cases of fibrosarcoma treated at Mount Vernon Hospital during 23 years. This rare occurrence may follow at any interval from 3 to 38 years after irradiation, usually after high dosage. Four of six cases are known to have died of the disease. The literature regarding radiation-induced fibrosarcoma is reviewed and it is suggested that excision or amputation may be curative, if undertaken early enough. (auth) (UK)

27045 HISTOLOGIC TYPES OF LUNG CANCER AMONG URANIUM MINERS. Saccomanno, Geno (Veterans Administration Hospitals, Grand Junction, Colo.); Archer, Victor E.; Auerbach, Oscar; (and others). Cancer; 27: 515-23(Mar 1971).

A panel of pathologists classified 121 cases of lung cancer from American uranium miners by cell type, and 138 cases of cancer in nonminers. Undifferentiated carcinomas showed a higher incidence with increasing radiation exposure and age and cigarette matched controls. At high radiation exposures the WHO 2B cell type accounted for more than half the total. An average of 15.9 yr elapsed from the beginning of mining to development of cancer. It was longest among the highly exposed men and was shortest among men with small cell, undifferentiated carcinoma who had less than 700 Work Level Months exposure. In all age and cigarette groups, radiation exposure increased the small cell, undifferentiated, but decreased the epidermoid tumors. Age showed an increase in epidermoid carcinoma. Undifferentiated small cell types were slightly increased among the lowest exposure groups. These increases and an excess of these cell types among South African gold miners seem to establish a trend. (auth)

27046 THORIUM-SERIES IN CIGARETTES AND IN LUNGS OF SMOKERS. Joyet, G. (Univ. of Zurich). Experientia; 27: 85-9(15 Jan 1971).

The potential hazards of the uptake of the thorium series in lungs of cigarette smokers was investigated. It was found to be dependent on the radiation dose delivered to the tissues. The average values of the thorium-232 content for 120 cigarettes is given. (P.B.M.)

27047 RADIATION EFFECTS ON THE EYE. Geeraets, Walter J. (Virginia Commonwealth Univ., Richmond). Ind. Med. Surg.; 39: 441-50(Oct 1970).

The effects of five types of radiation namely ionizing, uv, near ir, far ir, and microwaves on the eye are discussed. The radiation in these regions poses potential dangers to the human eye, against which protection and control are of high importance. Dangers of overexposure are discussed, with suggested permissible exposure levels. (auth)

27048 RADIOTHERAPY HEART DISORDERS. Giard, P. J. Sci. Med. Lille; 88: 449-59(1970). (In French).

The heart no longer appears as an organ insensitive to radiotherapy. Two kinds of lesion are observed: direct radionecrosis lesions and indirect lesions of the myocardium connected with vascular lesions. These lesions rapidly become associated with local conjunctive reactions. The resulting clinical manifestations are often delayed and may call for surgery. Earlier disorders may arise, warranting a corticoid treatment. (France)

27049 APPEARANCE OF SKIN HAEMANGIOMA 15 YEARS AFTER RADIATION LESION. Donati, E. (Ospedale Civile Maggiore, Verona, Italy. Univ., Bologna). Minerva Radiol.; 15: 207-12(Jul-Aug 1970). (In Italian).

A close interdependence between the onset of a hemangioma and prior radiation treatment was noted following exposure of an area of the skin to repeated high-dose irradiation. After a long latency period (15 years), a skin hemangioma was observed in a site seriously altered by chronic irreversible radiodermatitis. The case is of interest for its presentation as an example of a benign process caused by radiation employed (intercavitary Ra-226 γ and external x) for the treatment of a malignant tumor of an internal organ (in this case, uterine cancer, clinically cured at the time of observation). (auth)

27050 THORIUM INDUCED CARCINOMA OF THE MAXILLARY SINUS. Schmitz, Gerald L.; Peters, Richard; Lehman, Roger H. (Veterans Administration Center, Wood, Wis. Marquette Schools of Medicine and Dentistry, Milwaukee). Laryngoscope; 80: 1722-32(Nov 1970).

A case of carcinoma of the maxillary sinus following thorium-instillation is presented. The physical properties of thorium are discussed. A review of the literature revealed several similar cases, each with long latent periods. Because of the long latent period and the extensive use of thorium in the past, the finding of foreign bodies of metallic density in the sinuses should suggest the the removal of the foreign material and proper therapy if an underlying neoplasm is present. (auth)

27051 PROBLEMS OF INDUSTRIAL MEDICINE IN OPHTHALMOLOGY. VOLUME 1-2. 1st Symposium of the International Study Group for Ergophthalmology, Munich, 1966 - 2nd Symposium of the International Study Group for Ergophthalmology, Amsterdam, 1968. Merte, H.-J. (ed.). Basel; S. Karger AG (1969). 395p. $17.75. (In several languages). (CONF-660843-(Vol.1); CONF-680675-(Vol.2)).

Twenty-one papers are included; separate abstracts were prepared for three. The remaining presentations deal with work-connected ophthalmological problems and their prevention. (H.B.G.)

For abstracts of individual papers see: 26783, 27013, and 27014.

27052 URETERAL STRICTURES AFTER RADIATION THERAPY FOR CARCINOMA OF THE UTERINE CERVIX. Slater, James M.; Fletcher, Gilbert H. (Univ. of Texas, Houston). Amer. J. Roentgenol., Radium Ther. Nucl. Med.; 111: 269-72(Feb 1971).

The status of the ureters in uterine cancer patients treated by irradiation only was evaluated. Ureteral obstruction caused by fibrosis without complicating factors is a rare occurrence. Approximately 10% of the ureteral obstructions resulting from disease are relieved by radiotherapy. (F.M.M.)

27053 NEURO-MUSCULAR TESTS OF AGING IN HIROSHIMA SUBJECTS. Hollingsworth, Dorothy R.; Hollingsworth, J. William; Bogitch, Seymour; Keehn, Robert J. (Atomic Bomb Casualty Commission, Hiroshima). J. Gerontol.; 24: 276-83 (Jul 1969).

Three tests of neuro-muscular function were administered to atomic bomb survivors (Ss) attending the clinic of the Atomic Bomb Casualty Commission in Hiroshima, Japan. All three readings, strength of hand grip, reaction time in a light-extinction test, and the voltage required to detect vibration, clearly varied with the age of the Ss. No changes definitely related to radiation were detected. Only for hand grip strength was there evidence that the relationship between age and test score varied significantly between exposure groups, but no significant association between grip strength and rad-dose was found in Ss within 2,000 meters of hypocenter. The differences between exposure groups were more likely to have resulted from socioeconomic variation by geographical area than from variation in the level of radiation. (auth)

27054 PROLONGED EXPOSURE TO IONIZING RADIATION IN A BOY WITH APLASTIC ANAEMIA OF FANCONI TYPE. Guminski, Tadeusz; Struminska, Jadwiga (Inst. of Pediatrics, Krakow). Przegl. Lek.; No. 9, 724-5(30 Sep 1970). (In Polish).

A case study of a six-year old boy with aplastic anemia of the Fanconi type is presented. The additional factor influencing the course of the disease was prolonged exposure to pigment containing radium. (auth)

27055 ECCRINE POROMA: TWO UNUSUAL VARIANTS. Penneys, Neal S.; Ackerman, A. Bernard; Indgin, Sidney N.; Mandy, Stephen H. (Univ. of Miami, Fla.). Brit. J. Dermatol.; 82: 613-5(Jun 1970).

Two eccrine poromas are reported. One was a recurrent lesion on the nose containing many mitotic figures. The other occurred in an area of chronic radiation dermatitis. (auth)

27056 REACTION OF NERVOUS TISSUE TO APPLICATION OF IONIZING RADIATION. Jedlicka, Pavel (Charles Univ., Prague). Acta Univ. Carolinae, Med.; 15: 433-7(1969).

Experiences with an early and late reaction of nervous tissue to ionizing radiation as a consequence of radiotherapy of nervous tissue are described. An early reaction appeared in the course of radiotherapy, most frequently at the start of the treatment or after an increase of the daily dose, particularly in patients with a marked nervous tissue edema existing prior to the start of irradiation. Its most frequent manifestation was a rise of the intracranial pressure and less often accentuation of the topical neurological finding. The course of the reaction was indicative of the development of a nervous tissue edema. In the treatment of an early reaction, application of corticoids proved to be most useful. A late reaction of the nervous tissue to radiation was observed only in a single patient. This observation was interesting because of the histological finding of a destruction of the white matter in the site of application of radiation. This destruction exhibited signs of an entirely fresh progression of the process, even though more than one year had elapsed since the operation and radiotherapy. Destruction of the nervous tissue took place without a clear participation of the vascular system. Personal experiences were compared with those reported in literature. Evaluation of the nervous tissue tolerance for radiation as a biological factor was attempted. (auth)

27057 CYTOGENETIC AND CLINICAL SEQUELLAE OF INTRAUTERINE RADIATION EXPOSURE IN A GIRL 4 YEARS AND 6 MONTHS AFTER EXPOSURE. Kucerova, M. (Czechoslavak Academy of Sciences, Prague). Cesk. Pediat.; 25: 185-8 (Apr 1970). (In Czech).

The child, exposed in utero in the 5th to 6th month of pregnancy to the therapeutic doses of x rays for Ca coli uteri in her mother, has been under clinical and cytogenetical observation for four consecutive years. The girl showed signs of psychomotoric retardation, microcephalia, and epilepsy with the exception of the latter all in accordance with other reports. High incidence of chromosomal aberrations was found in peripheral lymphocytes, showing no decrease but rather increasing tendency in the past four years. (auth)

27058 IMMUNOHEMATOLOGICAL STUDIES OF MARSHALL ISLANDERS SIXTEEN YEARS AFTER FALLOUT RADIATION EXPOSURE. Conard, Robert A.; Demoise, Charles F.; Scott, William A.; Makar, Michael (Brookhaven National Lab., Upton, N. Y.). J. Gerontol.; 26: 28-36(1971).

Age related and/or radioinduced age effects on immunohematological criteria were tested in a Marshallese population of about 150 people, 50 of whom had been exposed to fallout radiation in 1954. In the unexposed group the following age-correlated changes were noted: a decreasing percentage transformation of peripheral blood lymphocytes by phytohemagglutinin stimulation indicating decreasing immunological competence of lymphocytes; significant increase in gamma globulin reflected also in increases in IgG, IgA immunoglobulins and also increase of K light chains. These latter findings are believed to be associated with age-accumulated effects of repeated exposures to infectious agents and perhaps to increased autoimmune reactions. In the irradiated population there were certain significant differences in the findings compared with the unexposed population that may indicate radiation effects. A relative depression of platelet and neutrophil levels of the peripheral blood was noted. Some slight degree of depression of peripheral blood elements has, however, been noted since exposure. Also noted were reduced gamma globulin levels (also IgG, IgA, and L light chains by immunodiffusion analysis), more pronounced in older age groups which may indicate a radioinduced aging effect. Evidence, however, for relative loss of immunological capacity in the exposed population has not been evident based on the incidence or severity of diseases compared with the unexposed population. (auth)

27059 DEVELOPMENT OF A FIBROSARCOMA IN A ROENTGENODERMA FOLLOWING CHOAUL'S X-IRRADIATION OF A HEMANGIOMA IN EARLY INFANCY. Undeutsch, Walter (Univ., Tuebingen, Ger.). Aerztl. Forsch.; 24: 290-3(10 Oct 1970). (In German).

A case of a fibrosarcoma is described that developed on the base of a Roentgenoderma following x irradiation (according to Chaoul) of a hemangioma in early infancy. With regard to the literature and own experience a cautious and critical treatment of a hemangioma is recommended. (auth)

27060 MEDICAL STUDY OF KOREAN ATOMIC BOMB SURVIVORS. Lee, Jang Kyu; Chang, Ko Chang; Kim, Jin Yong; Yun, Taik Koo; Moon Suc Kyong (Radiological Research Inst., Seoul). J. Nucl. Sci. (Seoul); 10: No. 2, Part 2, 41-6(1970). (In Korean).

A medical survey was carried out on the Korean atomic bomb survivors, who have returned home from Hiroshima and Nagaski after the World War II. According to the Korean Association of Atomic Bomb Survivors, there are 3,008 registered survivors and their offsprings living in Korea. Studies were made on 90 original survivors and their offsprings. It consisted of 65 males and 25 females. The comprehensive checks were carried out with prepared medical charts and various tests were also done on blood, feces, urine, liver function, and chest x rays. In some selected cases, special x-ray check-ups and brain scanning were done. The results of the survey are as follows: chief complaints; headache 35 cases (39%), weakness of extremities 15 cases (17)%, indigestion 10 cases (11%), and general malaise 8 cases (9%), clinical findings; gastrointestinal disturbance 22 cases (24%), enlarged liver 19 cases (21%), hypertension 11 cases (12%), and burn scar 11 cases (12%), pathological findings; hepatopathy 6 cases, albuminuria 5 cases, glucosuria 5 cases, and anemia 3 cases, and physical diagnosis; burn scar 11 cases (3 kelloid cases), hypertension 11 cases, tuberculosis 10 cases, chronic gastritis 8 cases, and neurosis 8 cases. Among these, the symptoms and findings which could be attributed to the atomic bomb effects would be 3 cases with anomaly of extremities and muscular atrophy, 2 cases with psychosis and 2 cases with muscular dystrophy. (auth)

27061 CHANGES OF THE SALIVARY GLAND FUNCTION AFTER ^{60}Co IRRADIATION IN PATIENTS WITH TUMOR OF THE HEAD AND NECK. Kang, Shin Koo (Radiological Research Inst., Seoul). J. Nucl. Sci. (Seoul); 10: No. 2, Part 2, 35-9(1970). (In Korean).

Sialography reflects the concentration, and excretory functions of the salivary glands simultaneously. Studies were made on the effects of ^{60}Co irradiation on these functions in the patient with tumors of the head and neck evaluated by means of sialography using ^{131}I. (auth)

Radiation Effects on Plants

Refer also to abstracts 26616, 26621, 26622, 26651, 26686, 26688, 26689, 26695, 26697, 26698, 26701–26703, 26706, 26709, 26710, 26712, 26714–26718, 26721, 26725, 26728, 26732, and 26733–26737.

27062 (IAEA-R-459) STANDARD NEUTRON IRRADIATION FACILITY EXPERIENCE IN THAILAND. Hayodom, V.; Khambanonda, P.; Saimongkol, U. (International Atomic Energy Agency, Vienna (Austria)). 6p. NTIS (U. S. Sales Only).

Work done under the IAEA research contract within the framework of the IAEA coordinated research program on neutron seed irradiation is described. Four experiments were carried out on barley seed (Himalaya CI 000620), using the standard neutron irradiation facility (SNIF). Based on two calibrations, dosimetry errors might be expected to be as large as 10%. Seedling growth from irradiated seeds was tested in Austria and Thailand. D 50 values of seeds grown in Austria were lower; larger variations in seedling height were found in seeds grown in Thailand. Measurements of dose rate and dose ratio (neutron/gamma), and variations in k-factors for indium and sulphur with distance were measured. A preliminary study made use of rhodium foils in the SNIF, indicating a marked improvement over indium and sulphur. (INIS)

27063 MITOTIC DELAY IN TWO BIOCHEMICALLY DIFFERENT G1 CELL POPULATIONS IN CULTURED ROOTS OF PEA (PISUM SATIVUM). Van't Hof, Jack; Kovacs, C. J. (Brookhaven National Lab., Upton, N. Y.). Radiat. Res.: 44: 700-12(Dec 1970).

The mitotic delay of two biochemically different G1 cell populations of cultured 48 hr stationary phase (S.P.) and synchronized pea root meristems was measured after exposure to 300 R of γ rays. The indices of delay were the transition from G1 to S and the time required for the population to divide (G1 → S → G2 → M). The criteria for biochemical differences were the time required to enter the S period and the sensitivity of DNA synthesis initiation to actinomycin D, puromycin, and cycloheximide. The population of S.P. meristems was delayed in G1 for approximately 5 hr but subsequently traversed S and G2 at a control rate; puromycin treatment prevented all cells from advancing to S for at least 12 hr and none divided for 24 hr. Actinomycin D treatment failed to stop about 10% of the G1 cells from moving to S, and a few of these eventually divided. Synchronized cells at the G1/S boundary progressed to S unimpaired but were delayed somewhere in either S or G2 and they appeared in mitosis 6 to 7 hr later than the controls. When irradiated and treated with an inhibitor, these cells were not prevented from advancing to S. It was concluded that defective protein synthesis was the cause of delay in all irradiated G1 cells and that the time and cycle period where it occurred varied and was dependent on whether the requisite proteins for functional completion of a given period were already formed at the moment of exposure. (auth)

27064 EFFECT OF GIBBERELLINE ON GROWTH, CONTENT OF CHLOROPHYLL, AND RESPIRATION IN GERMS SUBJECTED TO X-RAY IRRADIATION. Grebinskii, S. O.; Dudok, E. P. (Lvov State Univ.). Fiziol. Biokhim. Kul't. Rast.; 1: No. 1, 44-7(1969). (In Russian).

The treatment of x-irradiated corn, pea, and wheat seedlings with gibberellin eleminates the effects of the radiation on chlorophyll content, growth, and respiration. (auth)

27065 EFFECT OF RADIATION ON THE SPORE GERMINATION OF THE CELLULAR SLIME MOLD DICTYOSTELIUM DISCOIDEUM. Hashimoto, Y.; Yanagisawa, K. (Isotope Research Inst., Tokyo). Radiat. Res.; 44: 649-59(Dec 1970).

Spores of the cellular slime mold Dictyostelium discoidenum produce and secrete a substance called an autoinhibitor which inhibits their germination, and when the concentration of this substance increases, spore germination is repressed. However, it was found that when the spores are irradiated with certain doses of γ ray, the speed and percentage of germination increase even in the presence of such an inhibiting substance. This is not the result of the damage done to the autoinhibitor. The possible reasons for this promotion of germination by γ irradiation are discussed. (auth)

27066 NATURE OF GROWTH STIMULATION OF VICIA FABA ROOTS DURING IRRADIATION AT LOW DOSE-RATES. Woodham, C. H.; Bedford, J. S. (Vanderbilt Hospital, Nashville). Int. J. Radiat. Biol.; 18: 501-5(1970).

Primary roots of Vicia faba were irradiated at dose rates of 1.3 and 7 rads per hour in the presence and absence of 2×10^{-5} gammes per litre of the synthetic auxin, alpha naphthalene acetic acid. The temporary stimulation of root growth observed during irradiation at 1.3 rads per hour was completely eliminated when the synthetic auxin was present. The results tend to support the contention that the temporary stimulation is a consequence of a disturbance in the auxin economy in the root. (auth) (UK)

27067 PHYSIOLOGY OF DISKS OF IRRADIATED TOMATO FRUIT. I. INFLUENCE OF CUTTING AND INFILTRATION ON RESPIRATION, ETHYLENE PRODUCTION, AND RIPENING. Lee, T. H.; McGlasson, W. B.; Edwards, R. A. (Univ. of New South Wales, Kensington, Australia). Radiat. Bot.; 10: 521-9 (Nov 1970).

Fruits were picked at the 65 and 83% stages of development and subjected to a γ radiation dose of 200 krad. At various times after irradiation, disks of pericarp tissue were cut aseptically and this stimulated initial respiration and ethylene production. Respiration declined rapidly during the first 2 hrs except in disks of non-irradiated, 65% stage fruit which showed an induced respiration that began at 1 hr and reached a peak at 2 to 3 hr. Within 3 days after cutting, respiration in all disks stabilized at rates similar to those of corresponding whole fruit. Ethylene production in all disks continued to rise after cutting. Maximum rates, up to 100 times higher than in whole fruit, were reached at 5 hr and at 10 hr in disks of non-irradiated and irradiated fruit respectively. Ethylene production by disks of both non-irradiated and irradiated fruit subsequently declined and stabilized at similar rates. These rates were respectively 20 to 50 times and 5 to 7 times those of matched samples of whole fruit. Vacuum infiltration of disks of non-irradiated fruit with water generally resulted in small and brief increases in respiration and ethylene production additional to those stimulated by cutting alone, but infiltration did not affect the rates in disks of irradiated fruit. Ripening in disks was similar to that in whole fruit. Disks passed through a respiratory climacteric of similar magnitude and duration and which was accompanied by increased ethylene production, appearance of lycopene and development of a normal ripe fruit aroma. (auth) (UK)

27068 CHANGES IN RADIOSENSITIVITY OF STREPTOMYCES CACAOI SPORES DURING GERMINATION. Nagatsu, Chizuko; Matsuyama, Akira (Inst. of Physical and Chemical Research, Yamato, Saitama, Japan). Agr. Biol. Chem. (Tokyo); 34: 860-9(Jun 1970).

Changes in sensitivity to gamma and ultraviolet radiations of germinating spores of Streptomyces cacaoi var. asoensis were investigated. The results obtained are as follows: The period highly sensitive to gamma irradiation was found at about 100 to 110 min of incubation in a germination medium, which was different in the timing from that sensitive to heat. The patterns of changes in sensitivity to gamma and ultraviolet radiations during germination were not identical. The presence of chloramphenicol in the germination medium remarkably abolished changes in radiosensitivity of spores during the germination treatment. Mitomycin C also inhibited the development of radiation resistance during the late phase of germination. Radioprotective effects of freezing and ethanol as a radical scavenger lead us to the view that indirect-type actions of radiation on spores may operate to increase radiosensitivity during the early phase of germination. The scheme for phase transitions in sensitivities to gamma and ultraviolet radiations during germination was presented in relation to the macromolecular synthesis and heat resistance. Different patterns of the time course were observed on sensitivities to gamma and ultraviolet radiations and heat. (Japan)

27069 EFFECTS OF IONIZING RADIATION ON DRIED SPORES OF OSMUNDA REGALIS. II. MODIFICATION OF SURVIVAL AND ITS CORRELATION WITH FREE RADICAL CHANGES. Dodd, N. J. F.; Ebert, M. (Christie Hospital and Holt Radium Inst., Manchester, Eng.). Int. J. Radiat. Biol.; 18: 463-73(1970).

Spores were irradiated and cultured to measure their survival. Radiation damage could be modified by treating with NO, O_2, and water during and after irradiation. The radiation damage in anoxically irradiated spores, stored in N_2, remained open to full enhancement by O_2 for several hours, but the rate of this process decreased with time. Enhancement of damage by O_2 could be prevented by treatment with NO or water. The opposing effects of NO and O_2 were used to titrate the rate of development of the radiobiological oxygen effect. The behavior of radioinduced species could be described by a kinetic model. The modification of radiation damage by O_2 involved the formation and the decay of a peroxy radical intermediate. A correlation of survival data with ESR data is given in terms of the models. (auth) (UK)

27070 EFFECTS OF MODIFYING FACTORS ON THE RESPONSE OF RICE SEEDS TO γ-RAYS AND FISSION NEUTRONS. Constantin, M. J.; Conger, B. V.; Osborne, T. S. (Univ. of

Tennessee, Oak Ridge). Contract AT(40-1)-GEN-242. Radiat. Bot.; 10: 539-49(Nov 1970).

Experiments were conducted with Oryza sativa L. cv. "Bluebonnet" to determine the effects of modifying factors on seed response to γ rays and fission neutrons. Dose rate did not affect the seed response to γ rays when storage oxygen effects were minimized. Seed sensitivity to γ rays increased as water content was either decreased from 12 to 13% to approximately 3% or increased to approximately 20%. D_{50} for seeds with 2.7% water irradiated in vacuo was 4.77 or 59.09 krad when seeds were soaked under oxic or anoxic conditions, respectively; OER was 12.4. Although a major role of seed water content is to mediate the extent of the oxygen effect, results suggest also that the increase in water content from 2.7 to 13% afforded a degree of protection which is oxygen independent. Storage effects were observed during as well as after irradiation in seeds with less than 13% water when the oxygen effect was not eliminated. In contrast, increasing the water content from 3.8 to 16.3% had little or no effect on seed sensitivity to fission neutrons; however, seeds containing 20% water exhibited relatively higher sensitivity. The increase in damage at 20.3% water content was probably caused by the increase in dose from the hydrogen and an increase in metabolic and physiologic activity. D_{50} for seeds at 2.7% water irradiated with fission neutrons in vacuo was 1.9 or 2.7 krad when soaked under oxic or anoxic conditions, respectively; OER was 1.44. There was no conclusive evidence of a storage effect following neutron irradiation of Bluebonnet rice seed. The RBE for fission neutrons based on seedling growth reduction was 2.5 or 21.9 for seeds with 2.7% water soaked under oxic or anoxic conditions, respectively. (auth) (UK)

27071 EFFECT OF TEMPERATURE ON SURVIVAL OF γ-IRRADIATED SEEDS OF ARABIDOPSIS THALIANA. Daly, K. R. (Brookhaven National Lab., Upton, N. Y.). Experientia; 27: 81-3 (15 Jan 1971).

The question of how the gamma irradiation of dry seeds and post treatment growing temperatures may interact to influence the response of plants of Arabidopsis thaliana was investigated. Evidence is presented for temperature sensitivity of radiation injury in seeds which is unrelated to induced free radicals. (P.B.M.)

27072 PATHOGENICITY RESULTING FROM MUTATION AT THE b LOCUS OF USTILAGO MAYDIS. Day, P. R.; Anagnostakis, S. L.; Puhalla, J. E. (Connecticut Agricultural Experiment Station, New Haven). Proc. Nat. Acad. Sci. U. S. A.; 68: 533-5(Mar 1971).

The genetic basis of the ability of the fungus, Ustilago maydis, to induce neoplastic galls in the corn plant Zea mays is discussed. Pathogenic mutants of U. maydis were produced by uv irradiation of cultures of nonpathogenic diploids homozygous at the b locus. The mutants formed smaller neoplasms, produced fewer teliospores, and showed higher frequencies of meiotic failure and lower rates of basidiospore survival than did the wild type fungus. (auth)

27073 RELATIVE SUSCEPTIBILITIES OF CAFFEINE-SENSITIVE AND CAFFEINE-RESISTANT STRAINS OF CANDIDA ALBICANS TO INACTIVATION AND MUTATION BY ULTRA - VIOLET RADIATION. Sarachek, A.; Bish, J. T.; Ireland, Rosalee (Wichita State Univ., Kan.). Contract AT(11-1)-1772. Arch. Mikrobiol.; 74: 244-57(1970).

Stable variants having increased resistance to growth inhibition by caffeine were obtained from four different absolute, amino acid auxotrophs of Candida albicans. Differences in growth rates and expression of auxotrophy between the resistant [Caf(R)] variants and their sensitive [Caf(S)] progenitors suggest that caffeine resistance arises through suppressor mutations that affect the fidelity of messenger RNA translation. Both Caf(S) and Caf(R) strains of C. albicans are more susceptible to inactivation by uv radiation when grown at 37°C rather than 25°C following exposure. Post-irradiation growth on caffeine potentiates uv inactivation of all Caf(S) strains at both temperatures. Depending on its origin, a Caf(R) strain may show greater, lesser or the same intrinsic susceptibility to uv inactivation as its Caf(S) parent at 25°C or at 37°C and may or may not be refractory to post-irradiation contact with caffeine. Caf(R) variants independently isolated from a given auxotroph are alike in inactivational responses whereas those obtained from different auxotrophs are dissimilar. This implies that different suppressor mutations are unique in the way they affect expression of potentially lethal uv damage and that only one kind of suppressor is obtained by selection for caffeine resistance in a particular auxotroph. The histidine-requiring Caf(R) strain WB-2CR is much more resistant to uv inactivation than its Caf(S) parent WB-2. Moreover, post-irradiation survival of WB-2CR is unaffected by caffeine. However, WB-2CR and WB-2 are equally susceptible to uv-induced reversion to prototrophy. In both strains, caffeine does not enhance uv-induced reversion at 25°C or 37°C and exhibits an antimutagenic activity at high uv dosage at 37°C. The findings reinforce previously reported indications that, in C. albicans, caffeine-sensitive excision-repair of uv damaged DNA does not occur and caffeine potentiates uv cellular inactivation by disturbing post-irradiation synthesis of protein essential for recovery from non-genetic damage. (auth)

27074 CHANGES IN CARBOHYDRATES AND ORGANIC ACIDS IN LEAVES AND ROOTS OF COTTON AND MAIZE PLANTS IN DEPENDENCE ON THE DOSE OF PRESOWING GAMMA IRRADIATION OF SEEDS. Marfina, K. G.; Ibragimov, A. P. (Inst. of Experimental Plant Biology, Tashkent). Fiziol. Rast.; 15: 1064-7(1968). (In Russian).

The effects of γ rays on organic acids in the leaves and roots of corn and cotton plants following seed exposure were studied. Interrelationships between carbohydrates and organic acids and between carbohydrates and fats were observed. Presowing γ irradiation exerted an effect on the quantitative composition of organic acids and, with doses of 10,000 R, on the qualitative composition. The amount of citric acid decreased with the γ dose whereas acid X increased. It was assumed that seed irradiation affects the synthesis of acid X. (auth)

27075 EFFECT OF CHRONIC LOW LEVEL GAMMA RADIATION OF POLYTRICHUM COMMUNE HEDW. Grossman, Herbert Harry. University Park, Pa.; Pennsylvania State Univ. (1970). 149p. University Microfilms Order No. 71-6309.
Thesis.

Spores, gametophores and sporocytes of Polytrichum commune were subjected to 1,000, 1,600, 2,200 and 2,800 roentgens of chronic gamma radiation. Some of the gametophores were desiccated following irradiation. Spores, detached leaves and stem segments with leaves from irradiated and control material were placed on Knops' agar medium and maintained in a growth chamber for 15 weeks after which the plants were transferred to soil. The gametophores and spores exhibited some radioresistance, but a marked radiosensitivity was observed in the sporocytes. There was a mild and somewhat delayed inhibitory effect on the growth of the young shoots from spores and cuttings of the gametophores. The effect was more noticeable after the shoots had been growing in soil for six months. The radiation generally had a stimulatory effect on protonemal growth, and 1,000 R had a stimulatory effect on leaf proliferation as well as on size of shoots and protonemal cells from desiccated and non-desiccated gametophore cuttings. The stimulatory and inhibitory responses may have been brought about by changes in the hormone balance in the plants, initiated by the action of the radiation. The similarity in size and anatomy of the irradiated and control shoots from spores and gametophore cuttings to that of specimens collected in the field indicated that the light, temperature and humidity in the growth chamber as well as the nature of the substrate had some influence on the growth of the irradiated and control plants. Some of the spores from irradiated sporocytes produced protonemata with cells of atypical size and shape. These filaments died within five weeks. The protonemata from the remaining spores produced shoots with stunted growth. No visible chromosome damage was noted in the irradiated sporocytes and the irregular protonemal filaments and stunted shoots may have been due to either the production of free radicals in the cytoplasm or base deletion or wrong pairing in the DNA molecules of the chromosomes. Conditions in the growth chamber and the nature of the substrate probably had some influence on spore germination. Further research is needed in order to discover the precise combination of factors, in addition to radiation, involved in the growth of the irradiated and control plants. Before this can be achieved the biochemistry of mosses must be thoroughly explored. (Diss. Abstr.)

27076 ECOLOGICAL ASPECTS OF RESPONSES OF LIRIODENDRON TULIPIFERA L. AND ACER SACCHARINUM L. TO FAST NEUTRON RADIATION AND REDUCED LIGHT. Harris III, William Franklin. Knoxville, Tenn.; Univ. of Tennessee (1970). 218p. University Microfilms Order No. 71-7642.
Thesis.

Seedlings of yellow poplar and silver maple were irradiated as dormancy was breaking with doses of fast neutron radiation ranging to 500 rads. Plants were grown in 100, 50, and 25% of full sunlight for the duration of the two-year study. Plants were watered daily and fertilized in the spring of each year. Morphological variables that were measured included: leaf emergence, terminal and lateral bud mortality, developed of leaf aberrations, leaf histology, terminal and lateral shoot growth in length and leaf area development. Results of examination of morphological responses indicated that production of aberrant foliage represented a poor criterion for assessment of damage to a landscape following exposure to ionizing

XUM

radiation since there was neither a dose-effect relationship nor an interspecific interphase chromosome volume relationship. Terminal and lateral bud mortality were the only responses independent of reduced light. This result supported a previously stated hypothesis and suggests a corollary of the hypothesis to include the independence of bud responses to variation in environmental light. However, if bud mortality criteria are used to assess radiation damage, baseline data on natural terminal bud death are necessary. For example, natural terminal bud death varied by a factor of three between the two species used in the present study. Other responses of morphological variables were confounded with effects along a gradient of reduced light. They were confounded in the sense that either the direction or magnitude of the response was altered. Changes in the magnitude of a response indicated a degree of synergism between stresses of reduced light and exposure to ionizing radiation. Changes in the direction of response implied a degree of independence between the two types of stress. For example terminal growth of yellow poplar was independent of light only at doses in excess of 300 rads. At lower doses, reduced light stimulated terminal growth. Leaf area development showed consistent depressions following irradiation in the 0 to 115-day period post-irradiation between 1968 and 1969 experimental units. However, recovery later in the season varied widely between years and would be expected on the landscape as a consequence of both intrinsic and extrinsic factors. The results of examination of morphological responses indicate that the use of morphological variables alone to assess damage to higher plants following irradiation is not warranted. Bud mortality criteria represent the best variables to measure since they are independent of light intensity effects. Leaf area development, although variable, is also recommended because it determines the photosynthetic potential of the plants. This study quantified some of the physiological responses of irradiated plants. Physiological responses that were examined included: net photosynthesis, biomass production, carbohydrate accumulation and water relations. Physiological responses that were observed were not independent of structural modifications, but did reflect species differences in radiosensitivity. The net photosynthetic capacity of seedlings, for example, was a function of total leaf area development. Photosynthetic capacity, however, was modified by: annual variation in leaf area recovery, reduced rates of net photosynthesis per unit area early in the season and earlier senescence of irradiated seedling foliage. Reductions in seasonal net photosynthetic potential were to levels one-third those of control yellow poplar seedlings and one-half those of control silver maple seedlings. (Diss. Abstr.)

27077 RADIATION INDUCED MORPHOLOGICAL ABNORMALITIES IN RICE (ORYZA SATIVA L.). Basu, A. K.; Basu, Rabindra Krishna (Bose Inst., Calcutta). Trans. Bose Res. Inst. (Calcutta); 31: 151-5(Dec 1968).

Morphological abnormalities of various kinds were observed in the M(1) generation of three varieties of rice grown after treatment of seeds with x rays, ^{32}P, ^{35}S and of plants with ^{60}Co. The abnormalities included lethal dwarf, sterile dwarf, twisted leaf chimera, chlorophyll mosaic, rolled leaf, tiller branching vegetatively, bifurcated panicle, and spikelet with awn. These were visibly not associated with chromosomal abnormalities excepting in sterile dwarf that manifested chromosomal aberrations during meiosis. Most of the morphological abnormalities occurred as chimeras and progeny tests of these plants indicated no immediate genetic background of the abnormalities. The induction of morphological abnormalities was thought to be due to physiological disturbances following irradiations. A case of polyembryony was recorded in the M(2) generation. Both members of the twin seedling were diploid. The origin of multiple seedlings was believed to be due to altered embryonic development. (auth)

27078 EFFECT OF X-RAYS, ^{32}P AND ^{35}S ON GERMINATION AND SURVIVAL IN RICE (ORYZA SATIVA L.). Basu, A. K.; Basu, Rabindra Krishna (Bose Inst., Calcutta). Trans. Bose Res. Inst. (Calcutta); 31: 157-64(Dec 1968).

The effects of x rays, ^{32}P, and ^{35}S on seed germination and survival of plants till maturity in three varieties of winter rice were studied. Germination and survival decreased with increase in x-ray dosage. Dehusked seeds were found to be more radiosensitive than husked ones. Treatments with ^{32}P and ^{35}S often showed increased germination and survival over those of the respective controls and were considered as a stimulative effect. With equal dosages applied, ^{32}P usually produced more lethality than ^{35}S. The three varieties of rice manifested differences in radiosensitivity among themselves. The differential killing effect of the mutagens was thought to be due to differences in ion density and in seed size and thickness of seed coat. (auth)

27079 EFFECT OF GAMMA RADIATION ON THE SYNTHESIS OF SCOPOLETIN AND SCOPOLIN IN GRAPEFRUIT PEEL IN RELATION TO RADIATION DAMAGE. Riov, J.; Goren, R.; Monselise, S. P.; Kahan, R. S. (Hebrew Univ., Rehovot, Israel. Soreq Nuclear Research Centre, Yavne, Israel). Radiat. Res.; 45: 326-34(Feb 1971).

Two unknown compounds, featuring blue fluorescence under uv light on thin layer chromatography plates, were found to accumulate in the peel of gamma-irradiated grapefruit. The two compounds were isolated and identified as scopoletin (6-methoxy-7-hydroxy-coumarin) and scopolin (7-glucoside of scopoletin). Both the content of the two compounds and radiation damage (peel pitting) were positively correlated with radiation doses up to 300 krads. Irradiation with 300 krads also increased the incorporation of phenylalanine-^{14}C into the scopoletin molecule. Rate of incorporation and content of free and hydrolyzed scopoletin increased with time following the irradiation. Phenolic compounds which accumulate in the peel after irradiation contribute to the formation of radiation damage in citrus fruits. (auth)

27080 PHOTOREVERSAL OF ULTRAVIOLET-INDUCED DIVISION DELAY IN SACCHAROMYCES CEREVISIAE. Goodin, L. J.; Johnson, R. G.; Morrison, H. Gail (Trent Univ., Peterborough, Ont.). Radiat. Res.; 45: 440-8(Feb 1971).

Diploid yeast cells of Saccharomyces cerevisiae strain X841 were used in a study of uv-induced division delay and its reduction by photoreactivation through post irradiation exposure to visible light. It was found that the uv-induced delay in initial budding of the cells and the increase in first generation time were essentially eliminated after a sufficiently long photoreactivation period. Also, if the difference between first generation times of irradiated and control cells was taken as a measure of the uv damage causing delay, then residual damage after photoreactivation was found to decrease exponentially with increasing time of photoreactivation at constant dose rate. No lengthening of the second generation time was found, even for cells which were not photoreactivated. (auth)

27081 EFFECT OF X RAYS ON THE NUCLEUS AND ON THE NUCLEAR DNA OF THE APICAL MERISTEM OF DILL STEM. Chkhubianishvili, E. I. Soobshch. Akad. Nauk Gruz. SSR; 61: 669-71(Mar 1971). (In Russian).

A study of the effects of x rays on the nucleus size and the amount of DNA of meristematic zone of the stem revealed that the swelling of the nucleus was caused by the radiation. An increase of the dose of radiation facilitated this process. The DNA content decreased with an increase of the dose. The dose of 5,000 R decreases the amount of DNA by 35 to 52% and the dose of 10,000 R by 50 to 72%. (auth)

27082 EFFECT OF IONIZING RADIATION ON THE GROWTH OF WHEAT. Gamkrelidze, L. M. Soobshch. Akad. Nauk Gruz. SSR; 61: 665-7(Mar 1971). (In Georgian).

The effects of ionizing radiation on the seeds and germs of durum and soft wheat were studied. Dry and wet seeds, as well as six day radicles, were irradiated. The irradiation was carried out by the PYM-17 x ray machine at doses of 1000 to 8000 R. Corn sproutings of irradiated dry seeds do not differ from the control ones. Irradiation of wet seeds caused growth braking, excluding those irradiated with 1000 R. Irradiation of six day radicles has shown that the plant treated with 1000 R grows more intensively during the first days after irradiation, but the other doses depress the plant growth. Investigations have revealed that the durum wheat is more resistant than the soft one. (auth)

27083 EFFECTS OF RADIATION ON SAFFLOWER. Chatterji, A. K.; Prasad, N. (Indian Inst. of Tech., Kharagpur, India). Sci. Cult. (Calcutta); 36: 513-14(Sep 1970).

The cytological and morphological changes in the x(1) generation of the cultivated safflower, Carthamus tinctorius, as a result of x irradiation are reported. The dry seeds were irradiated at 10 to 40 kR at the rate of 6 kR/min. (P.B.M.)

27084 EFFECTS OF γ RADIATION ON PENICILLIUM EXPANSUM L. I. SOME FACTORS INFLUENCING THE SENSITIVITY OF THE FUNGUS. Chou, T. W.; Singh, B.; Salunkhe, D. K.; Campbell, W. F. (Utah State Univ., Logan). Radiat. Bot.; 10: 511-16(Nov 1970).

The effects of media, age of spores, delayed plating, heat treatment, and chemical sensitizers on the lethality of gamma radiation to Penicillium expansum L. were determined. Higher survival was obtained when irradiated conidia were plated on the Czapek's agar medium. Six month old conidia were more radiosensitive than 1 to 2 week old conidia. Recovery from radiation injuries was observed when irradiated spores were held in suspension for several days at 23°C; however, no recovery was evident at 1°C. Heat treatment (58°C for 4 min) before or after irradiation increased the radiation effect. Difolatan, iodoacetic acid, and sec-butylamine were effective radiation sensitizers. (auth)

27085 EFFECTS OF GAMMA RADIATION IN CONCURRENCE WITH CERTAIN ENVIRONMENTAL CONDITIONS ON LETHAL AND PHYSIO-CHEMICAL RESPONSES OF PENICILLIUM EXPANSUM L. Chou, Tsong-wen. Logan, Utah; Utah State Univ. (1970). 101p. University Microfilms Order No. 70-26,965.

Thesis.

In vitro investigations were conducted to study the lethal effect of γ radiation on the fruit spoilage fungus Penicillium expansum under certain environmental conditions, and to study some physio chemical changes in the fungus induced by the radiation which may be related to the death of the fungus or its ability to invade fruits. The radiosensitivity of P. expansum conidia was influenced by such factors as nutritional condition of the post irradiation media, age of the spores, delayed plating, heat treatment, and chemical sensitizers. Higher survival was obtained when irradiated conidia were plated on Czapek solution agar (sugar salts medium) than on potato dextrose agar; yeast extract added in Czapek's medium hastened colony growth but reduced survival. The 6 month old conidia were more radiosensitive than the 1 wk old conidia. (TSS)

27086 EFFECT OF X-RAYS ON PLANT GROWTH, FLOWERING, AND FRUITING IN IMPATIENS BALSAMINA L. Bose, S.; Mukherjee, D. (Calcutta Univ.). Indian J. Sci. Ind.; 1: 172-7 (1967).

Dry seeds of Impatiens balsamina var. Scarlet treated with x ray doses from 10 kR to 110 kR showed sharp decline in percentage of germination from 30 kR onwards. In the x ray treated series, bifurcation and fasciation of stem and dwarf plants were observed. (Indian Sci. Abstr.)

27087 RELATIONSHIP BETWEEN RESPONSE TO RADIATIONS AND NATURE OF POLYPLOIDY IN SOME CROP PLANTS. Krishnaswami, R. (IARI, Coimbatore, India). Caryologia; 21: 303-10(1968).

Use of response to radiations as a tool in assessing the nature of polyploidy is the aim of this study. Four crop sp. viz., barley Hordeum vulgare (diploid and avtotetraploid), bread wheat (Triticum aestivium) tobacco (Nicotiana rustica), and Upland cotton (Gossypium hirsutum) were chosen. Dry seeds were irradiated with x rays, γ rays and fast neutrons. Observations on sterility and incidence of morphological changes in the M_1 and frequency of chlorophyll and viable mutations in M_2 suggest that the extent of genetic diploidization may increase in the following order. Autotetraploid H. vulgare → T. aestivum → N. rustica → G. hirsutum. The above study would hence suggest that an assessment of radiation response to a polyploid plant would be worth while for the purpose of supplementing the available knowledge on the nature of polyploidy in it. (Indian Sci. Abstr.)

27088 STUDIES IN TRICHODERMA GLAUCUM WITH SPECIAL REFERENCE TO THE EFFECTS OF THERMAL NEUTRONS, GAMMA, AND ULTRAVIOLET RADIATION. Khatri, A. A. Bombay; Univ. of Bombay (1967).

Thesis.

Studies were undertaken on the mutagenic effects of thermal neutrons, γ, and uv radiations on the soil fungus, Trichoderma glaucum. Radiosensitivity of the conidispores of the fungus to the above mentioned radiations was discussed. Morphological and biochemical mutants were isolated as well as the antifungal antibiotic, gliotoxin. All the mutants synthesized lesser amounts of gliotoxin than the wild strain. (Indian Sci. Abstr.)

27089 EFFECT OF GAMMA-RAYS ON SOME PEA SPECIES. Scumpu, N.; Ionescu, M. Lucr. Stiint. Inst. Agron. Ion Ionescu De La Brad, Iasi; 267-76(1968). (In Rumanian).

A study was undertaken on the effect of γ rays on cell division, pollen germination, and viability. Pea seeds of the I.C.A. 53 and Uladovschi 303 variety were used in the experiments. The ratio of chromosomal aberrations was higher in the former variety both in mitosis and meiosis, whereas pollen viability and germination was increased in the Uladovschi 303 type. The I.C.A. 53 variety proved to be more radiosensitive. (Rom. Sci. Abstr.)

27090 INCIDENCE-RATE AND TYPES OF CHLOROPHYLL MUTANTS IN FLAX INDUCED BY GAMMA RAYS AND SOME ALKYLATING AGENTS. Bianu, M.; Marki, A. Stud. Cercet. Biol., Ser. Bot.; 22: No. 1, 75-85(1970). (In Rumanian).

A comparative study was undertaken on the mutagenic effect of some alkylating agents (Endoxan, ethylmethanesulfonate, nitrosomethylurea, and triethylenemelamine) and of gamma rays. Ethylmethanesulfonate and nitrosomethylurea induced maximum chlorophyll mutants in Linum usitatissimum. The frequency and spectrum of alkylator-induced chlorophyll mutants differs from that of gamma rays. The former results in a frequency fall of albina mutants, and a greater incidence of xantha and viridis mutants after a gamma ray treatment. The frequency of gamma ray-exposed albina and viridis mutants increased proportional to dose. The number of recessives is higher, an atypical segregation being recorded. Out of 1045 chlorophyll mutants only 5 proved semi dominant. (Rom. Sci. Abstr.)

27091 EFFECT OF X RAYS ON CELL SIZE IN LEAVES OF VEGETABLES. Chkhubianishvili, E. I. (Inst. of Botany, Tbilisi, USSR). Soobshch. Akad. Nauk Gruz. SSR; 61: 417-20(Feb 1971). (In Russian).

A study of the effects of x rays on the cell size of the leaves of spinach, lettuce, and dill has revealed that radiation favors the growth of cells. The threshold dose for the growth processes of the cells of spinach leaves is 5000 R, whereas the cells of lettuce and dill attain maximum size with the dose of 8000 R. (auth)

27092 INFLUENCE OF A STORAGE PERIOD BETWEEN DRYING AND IRRADIATION ON THE ACTION OF X-RAYS IN RESTING BARLEY SEEDS. 2. CHANGES IN RADIOSENSITIVITY UNDER DIFFERENT CONDITIONS OF STORAGE. Peisker, M. (Deutsche Akademie der Wissenschaften zu Berlin, Gatersleben, Ger.). Stud. Biophys.; 13: 127-34(1969). (In German).

The increase of radiosensitivity in resting barley seeds after drying over P_2O_5 is based in part on a reversible sensibilization of the seeds to x rays by the process of water extraction. Therefore the radiation injury diminishes after cessation of the drying treatment even then, if the water content of the seeds does not increase. However, the disappearance of the sensibilization is accelerated by water uptake. Water uptake brings about another relation between water content and radiosensitivity than changes of water content in the inverse direction. The diminution of radiosensitivity is greater after storage at 27°C than at 5°C, whereas at −20°C there are no changes in the action of x rays. (auth)

27093 RADIATION INDUCED CHROMOSOMAL ABERRATIONS AND GROWTH INHIBITION IN SOME AGRICULTURAL PLANT SPECIES. Grothe, K.-T. (Arndt Univ., Greifswald, Ger.). Stud. Biophys.; 13: 119-26(1969). (In German).

The frequency of disturbed anaphases and telophases in the first mitosis of the radicle and the radioinduced growth inhibition of the radicle of flax, hemp, radish, and rye were analyzed after x irradiation of the air dried seeds. It was found that the radioinduced rate of disturbed anaphases or telophases in rye and hemp was the same after irradiation, with the mean effective dose of growth inhibition ED 50. The more radioresistant (in regard to the growth inhibition) radish and flax were able to tolerate a higher rate of mitotic disturbed cells after irradiation with the ED 50 than the radiosensitive rye and hemp. (auth)

27094 STUDY OF THE BIOCHEMICAL ACTIVITY OF ANASTOMOSE STRAINS OF ASPERGILLUS NIGER UNDER THE EFFECTS OF X-RAYS. Pashev, Il.; Kibarska, T.; Parchev, N. Izv. Mikrobiol. Inst., Bulg. Akad. Nauk.; 20: 15-20(1969). (In Bulgarian).

A study was made of the effect resulting from the influence of x rays on anastomose cultures obtained through anastomosis between two single cells from various Aspergillus niger strains. The numerous mutants thus produced were investigated morphologically, physiologically, and biochemically as well as with regard to their capacity of synthetizing an acid. The anastomose strains have an increased sensitivity towards roentgen influences. Irradiation with 7000 R results in mutants with a 10 to 20% increased productivity. (auth)

27095 ROLE OF HIGH ENERGY COMPOUNDS IN THE PROCESSES OF POSTIRRADIATION RECOVERY OF YEAST. Krasnopevceva, N. G.; Smirnov, M. N. (Inst. of Medical Radiology, Obninsk, USSR). Stud. Biophys.; 17: 191-4(1969).

Saccharomyces ellipsoideus cells which are x-irradiated recover during incubation in sterile tap water or in buffer solutions. Experiments were done to determine the role of ATP synthesis in this recovery process. (P.B.M.)

27096 RECOVERY OF YEAST AFTER IRRADIATION AND PROTEIN SYNTHESIS. Krasnopevceva, N. G.; Smirnov, M. N. (Inst. of Medical Radiology, Obninsk, USSR). Stud. Biophys.; 17: 187-9(1969).

The role of protein synthesis in the processes of recovery after x irradiation of Saccharomyces ellipsoideus is investigated. Based on indirect data no correlation between protein synthesis and the restoration of irradiated cells has been found. Results are given on the use of cycloheximide, an antibiotic inhibiting protein synthesis in yeast, to study the relation between postirradiation recovery and protein synthesis in irradiated yeast cells. (auth)

27097 STUDIES ON THE AMYLASE AND PROTEASE ACTIVITIES OF ASPERGILLI BY UV-IRRADIATION METHOD. Lee,

XUM

Bae Ham; Chung, Sung Koo (Kon-Kuk Univ., Seoul). J. Nucl. Sci. (Seoul); 10: No. 2, Part 2, 1-4(1970). (In Korean).

Experiments were performed using uv irradiation in order to obtain Aspergillus mutants with increased amylase activities. The results obtained are as follows; by uv irradiation on Aspergillus oryzae 12, A. niger 55, and A. usamii 56, mutants were produced. Three promising strains, A. oryzae 12-321, A. oryzae 12-830, and A. niger 55-1273, were selected from them for industrial brewing, progeny test proved that the enzyme activities of the selected mutants were quite stable and homogenous. A. oryzae 12-830 was found to be an excellent strain for α-amylase activity, A. niger 55-1273 an excellent strain for β-amylase activity, and A. oryzae 12-321 a powerful strain for both α and β-amylase activities, and changes in proteinase activity were inconclusive. (auth)

Radiation Effects on Microorganisms

Refer also to abstracts 26627, 26639, 26643, 26655, 26687, 26691–26693, 26699, 26708, 26722, 26729, 26731, 26975, 27143, and 27164.

27098 CHARACTERISTICS OF TRANSDUCING GROUP A STREPTOCOCCAL BACTERIOPHAGES A5 AND A25. Malke, H. (Deutsche Akademie der Wissenschaften, Jena, Ger.). Arch. Gesam. Virusforsch.; 29: 44-9(1970).

The virulent, transducing, DNA containing group A streptococcal bacteriophages A5 and A25 are 58 mμ in head size and have a flexible, noncontactile tail with a length of 180 mμ. The morphologic outline of the head is hexagonal. Treatment of the bacteriophages with potentially lethal uv radiation produced damages which were repairable by the Hcr^+ streptococcal host strain K56, the host cell reactivable sector being 0.9. These properties together with a demonstrable serological cross reaction show a close relationship between the two phage strains. (auth)

27099 OPTIMIZING THERMAL AND RADIATION EFFECTS FOR BACTERIAL INACTIVATION. Reynolds, M. C.; Garst, D. M. (Sandia Labs., Albuquerque, N. Mex.). Space Life Sci.; 2: 394-9(Dec 1970).

The temperatures required for dry-heat spacecraft sterilization were known to degrade heat sensitive components. Thermoradiation, the simultaneous application of dry heat and γ radiation, can provide the same degree of microbial inactivation as dry heat alone while substantially reducing component degradation. This is made possible by the synergistic effects produced when relatively low levels of these agents (e.g., 90 to 350 krads and 60° to 105°C) are applied simultaneously, thus permitting the use of lower temperatures and a reduced duration of heat exposure. The effects of temperature, radiation dose rate, and relative humidity on microbial inactivation during thermoradiation exposure were established. (auth)

27100 BIOLOGIC ACTIVITY OF DAUNOMYCIN (NSC-82151) IN MICROBIAL SYSTEMS. Pittillo, Robert F.; Hunt, Dale E. (Southern Research Inst., Birmingham, Ala.). Cancer Chemother. Rep.; 52: 707-13(Dec 1968).

Daunomycin, an antibiotic reported effective in the chemotherapy of various malignant diseases, was evaluated in a variety of bacterial systems in an attempt to gain new information or develop techniques to supplement successful clinical application of this drug. Daunomycin is a radiation sensitizer for Streptococcus faecalis. A strain of S. faecalis resistant to 6-mercaptopurine (6-MP; NSC-755) is uniquely sensitive to daunomycin inhibition. Various strains of S. faecalis could be adapted to growth in the presence of daunomycin, but permanent resistance to daunomycin was not conferred. Such adaptation did result in significant permanent cross resistant to 6-MP and 1-β-D-arabinofuranosylcytosine (NSC-63878; cytosine arabinoside). Several purines, notably xanthine, reversed or prevented daunomycin inhibition of S. faecalis, but a variety of other naturally occurring metabolites sensitized the cells to daunomycin action—a phenomenon that may be related to daunomycin toxicity for mammals. A microbiologic assay procedure for daunomycin was developed. (auth)

27101 KINETIC ANALYSIS OF SPORE INACTIVATION IN A COMPOSITE HEAT AND GAMMA RADIATION ENVIRONMENT. Dugan, V. L. (Sandia Labs., Albuquerque, N. Mex.). Space Life Sci.; 2: 498-505(Mar 1971).

Presented is the analysis of a combined environment of dry heat and gamma radiation when applied for the purpose of spacecraft sterilization. The nature of the synergistic inactivation effect of dry heat and radiation on bacterial spores is explained using a semiempirical mathematical model, and the dependence of the inactivation rate upon a temperature dependent, nonlinear function of radiation dose rate is presented. An analysis of the temperature required for a defined population reduction with a defined upper limit on radiation dose and time is described. Also discussed is the dependency of the dose required for a defined population reduction on the radiation dose rate at any selected temperature. (auth)

27102 EFFECT OF UV IRRADIATION, MERTHIOLATE, AND THYMOL ON INTERFERENTIAL PROPERTIES OF TICK-BORNE ENCEPHALITIS VIRUS (TE). Dabek-Szreniawska, Malgorzata (Maria Curie-Sklodowska Univ., Lublin). Acta Microbiol. Pol., Ser. A; 2: 139-42(1970).

Tick-borne Encephalitis (TE) virus, strain K_S, adapted to cultures of Detroit 6 cells and to mice irradiated with uv rays or affected by thymol, shows an increased interferential activity in homologous tissue cultures. UV rays are more active stimulators of the interferential activity than thymol. (auth)

27103 GENETIC ANALYSIS BY TRANSDUCTION OF RHIZOBIUM MELILOTI MUTANTS WITH CHANGED SYMBIOTIC ACTIVITY. Kowalski, Mieczyslaw (Maria Curie-Sklodowska Univ., Lublin). Acta Microbiol. Pol., Ser. A; 2: 115-22(1970).

Rhizobium meliloti strain L5-30 effective and prototrophic was mutagenized by uv irradiation. 135 clones were selected and tested for auxotrophy and effectiveness. More than 40% of clones lost effectiveness. Among them one lysine dependent mutant was found. Both transduction of lysine dependent mutant to prototrophy and its spontaneous reversion did not restore effectiveness. Attempts were made to transfer effectiveness marker to 11 ineffective mutants by transduction. Direct selection of effective transductants on plants did not provide significant results. (auth)

27104 TRANSDUCING PHAGES OF RHIZOBIUM MELILOTI. Kowalski, Mieczyslaw (Maria Curie-Sklodowska Univ., Lublin). Acta Microbiol. Pol., Ser. A; 2: 109-14(1970).

From among 21 temperate phages of Rhizobium meliloti 12 were able to transfer streptomycin resistance. Lysates obtained by multiplication of bacteria and by uv induction transduced streptomycin resistance marker with the frequency from about 10^{-5} to 10^{-7} depending on phage lysate preparation. (auth)

27105 KORNBERG POLYMERASE AND THE REPAIR OF IRRADIATED T4 BACTERIOPHAGE. Smith, Sheila Maynard; Symonds, N.; White, Patricia (Univ. of Sussex, Brighton, Eng.). J. Mol. Biol.; 54: 391-3(14 Dec 1970).

Three types of experiments are reported which show an increased sensitivity to uv irradiation of wild type phage T4 when the host Escherichia coli carries a mutation affecting the production of the bacterial Kornberg polymerase. (auth)

27106 STUDIES ON THE EFFECT OF CONSTANT MAGNETIC FIELD ON TOBACCO MOSAIC VIRUS SYNTHESIS IN TOBACCO LEAVES. Maj, Zbigniew; Dutczak, Krzysztof (Dept. of Plant Physiology, Krakow). Acta Microbiol. Pol., Ser. A; 2: 143-8 (1970).

Investigations were carried out on the effect of constant magnetic field (1200 Oesterds) on TMV synthesis in isolated leaf discs of tobacco (cv. White Burley). The effects of the 48 and 72 hr exposure were examined biologically by inoculation of Nicotiana glutinosa half leaves with homogenates of the appropriate discs. Homogenates obtained from discs after 48 hours exposure to the magnetic field contained 38% less infective viruses in comparison with those exposed for 72 hr as well as with the control, untreated discs. Experiments on the influence of a similar magnetic field on purified TMV preparation in vitro gave no effects. (auth)

27107 SENSITIVITY TO INACTIVATION BY ULTRAVIOLET LIGHT OF CERTAIN FUNCTIONS OF POLYOMA VIRUS: CELL SURFACE ANTIGEN. Meyer, G.; Birg, Francoise (Cancer Inst. of Marseilles). J. Gen. Virol.; 9: 127-31(Nov 1970).

Ultraviolet irradiation of polyoma virus inactivated different functions of the virus genome. This inactivation was related to the radiation dose. It was found that the uv radiation target size of the nuclear T antigen is one-half that of the ability to form plaques, and that the radiation target size of the homograft rejection antigen is one-sixth that of the latter. UV irradiation was applied in a similar manner in order to study the cell surface antigen. Quantitative analysis showed that the radiation target size for this antigen is one-half that of the ability to form plaques (infectivity). The difference in responses of the cell surface antigen and in the homograft rejection antigen observed after irradiation of the virus can be due either to differences in sensitivities of the techniques used or to a difference in antigenicity. Experiments with defective polyoma strains favored a difference in antigenicity. (auth) (UK)

27108 INACTIVATION BY ULTRAVIOLET RADIATION AT DIFFERENT WAVELENGTHS OF THE RNA ISOLATED FROM POTATO VIRUS X. Govier, D. A.; Kleczkowski, A. (Rothamsted Experimental Station, Harpenden, Eng.). Photochem. Photobiol.; 12: 345-53(Nov 1970).

The action spectra and quantum yields for photoreactivable, non-photoreactivable, and total damage caused by uv in the RNA isolated from potato virus X differed from those for similar types of damage in the whole virus. The differences result from the virus protein partly protecting the RNA from damage, and the degree of protection depended on the wavelength of uv and on the salt concentration of the irradiated solution (borate buffer). The action spectra for the different types of damage in the RNA all resembled the absorption spectrum of the RNA, but did not exactly parallel it. The photoreactivable sectors of the RNA and of the whole virus were greater at 290 nm than at 230 nm but, whereas that of the virus increased rectilinearly, that of the RNA had a pronounced minimum at about 250 nm. At wavelengths longer than 240 nm, the photoreactivable sector of the virus exceeded that of the RNA, because, at these wavelengths, the virus protein protected the RNA more against non-photoreactivable damage than against photoreactivable damage. (auth) (UK)

27109 REPAIR OF ALKYLATION-INDUCED DAMAGE IN ESCHERICHIA COLI AND ITS BACTERIOPHAGE λ. Ronen, A.; Atidia, J. (Hebrew Univ., Jerusalem). Mutat. Res.; 11: 175-9 (Feb 1971).

Repair of the primary alkylation-induced damage in Escherichia coli K12 and bacteriophage λ is affected by mutations in genes known to be also involved in the repair of uv-induced damage. The repair of phage damaged by alkylation does not affect the delayed (secondary) damage. Rec⁻ cells are less able than wild type to reactivate phage λ damaged by alkylation. (auth)

27110 TRANSDUCTION IN GROUP A STREPTOCOCCI BY ULTRAVIOLET IRRADIATED BACTERIOPHAGES. Colon, A. E.; Cole; R. M.; Leonard, C. G. (Nat. Inst. of Allergy and Infectious Diseases, Bethesda, Md.). Can. J. Microbiol.; 16: 201-2(Mar 1970).

Thirteen strains of five group A streptococcal serotypes were efficiently transduced to streptomycin resistance by uv-irradiated virulent bacteriophages. (auth) (Canada)

27111 IRRADIATION OF ONCOGENIC VIRUSES: DISSOCIATION OF VIRAL FUNCTIONS. Latarjet, R.; Cramer, R.; Golde, A.; Montagnier, L. (Institut du Radium, Orsay, France). pp 677-95 of Carcinogenesis: a Broad Critique. Baltimore; Williams and Wilkins Co. (1967).

From 20. annual symposium on fundamental cancer research; Houston, Tex. (7 Mar 1966).

Studies on the dissociation of infectivity and oncogenicity in the polyoma and simian virus 40 were conducted using ultraviolet, gamma, and x radiation. It was found that oncogenicity was five times as radiation-resistant as infectivity in the polyoma virus. Gamma irradiation of Rous sarcoma virus made it possible to obtain defective virions that were still oncogenic but no longer infectious. It was thought that the radiation injured a part of the viral genome necessary for production but not indispensable for oncogenicity. Studies on the formation of hyperproducing virions by irradiation are described. It was observed that among pocks (microtumors) produced by virions that survived doses of 320, 630, and 950 kr some showed a hyperproduction of virus. Investigations on isologous interference were conducted using Rous sarcoma virus and Gross virus. It was shown that ultraviolet irradiation of Rous sarcoma virions inhibited viral production as much as 95% in mixed infections with nonirradiated virus. A discussion is presented of possible mechanisms of these phenomena. (H.L.W.)

27112 ABSENCE OF REPAIR REPLICATION FOLLOWING ULTRAVIOLET IRRADIATION OF AN EXCISION-DEFICIENT MUTANT OF ESCHERICHIA COLI. Cooper, P. K.; Hanawalt, P. C. (Stanford Univ., Calif.). Photochem. Photobiol.; 13: 83-5(Jan 1971).

Cultures of Escherichia coli strain AB2497 F⁻ thy⁻ uvr⁺ and its excision deficient derivative AB2500 F⁻ thy⁻ uvrA6 were prelabeled with ^{32}P, irradiated with a 15-W uv lamp and subsequently the thymine supplements were replaced with tritium labelled 5-bromouracil. Assay was carried out by liquid scintillation spectrometry. The ratio of ^{3}H to ^{32}P in the normal density peak fractions of the re-banded parental density DNA was used as an indication of the amount of repair replication. In the uvr⁺ strain, irradiation with 93 ergs/mm² almost doubled the amount of non-conservative replication over the control value, 279 ergs/mm² producing a further increase. In the uvrA6 strain, the level of non-conservative replication decreased after ultraviolet radiation. (UK)

27113 RADIOBIOLOGICAL STUDY OF THE FORMATION OF INTERFERON IN THE KIDNEY CELLS OF MONKEYS INFECTED WITH N.D.V. Coppey, J.; Markovits, P. (Institut du Radium, Paris). pp 407-9 of L'Interferon. Paris; Institut National de la Sante et de la Recherche Medicale (1970). (In French).

From Conference on interferon; Lyon, France (6 Jan 1969). See CONF-690127.

The radiosensitivity of the virus replication and interferon formation mechanisms in Newcastle disease virus infected monkey kidney cells was investigated. The cells were irradiated before or at different moments after infection. It was found that the radioresistance of the virus replication increases during the eclipse phase; this increase requires the synthesis of proteins apparently coded by the viral genome. Four phases were seen in the radiosensitivity of the interferon formation. From the analysis of these phases the synthesis kinetics of a messenger RNA implicated in interferon formation can be inferred. (France)

27114 STORAGE TEMPERATURE EFFECTS ON THE PROTEOLYTIC ACTIVITY OF RADIATION-SURVIVING BACTERIA IN OYSTERS. Liuzzo, Joseph A.; Farag, Mohammed K.; Novak, Arthur F. (Louisiana State Univ., Baton Rouge). Contract AT(40-1)-2951. J. Food Sci.; 36: 287-8(Mar 1971).

The activity of 2 radiation surviving and strongly proteolytic strains of Pseudomonas and Achromobacter were compared to the activity of 2 lesser active strains of Neisseria and Bacillus in fresh oysters during iced (32°F) and refrigerated (40°F) storage for 15 days. Gamma radiation doses used for the oysters were 100 and 800 kRad. The activity of the former bacteria was higher than that of the latter 2 at both temperatures and radiation doses. Neither the nonirradiated nor the irradiated uninoculated oysters displayed significant increases in proteolytic activity when they were ice-stored for 15 days, but storage at 40°F for the same period resulted in significant activity increases in the nonirradiated. This emphasizes irradiation and storage temperature as related factors. A slight decrease in pH at 15 days in both nonirradiated and 100 kRad-irradiated oysters corresponded to the increase in bacterial numbers. (auth)

27115 RADIATION DESTRUCTION OF VIBRIO PARAHAEMOLYTICUS. Matches, Jack R.; Liston, J. (Univ. of Washington, Seattle). Contract AT(45-1)-1549/1730. J. Food Sci.; 36: 339-40(Mar 1971).

The effects of gamma irradiation on 27 strains of Vibrio parahaemolyticus isolated from sediment, seawater, and shellfish are reported. Numbers of viable cells surviving irradiation were determined at 22°C by the drop plate method with trypticase soy agar medium made up with seawater. Samples were irradiated in the ^{60}Co Mark II food irradiator at a dose rate of 300 kRad/hr and a temperature of 24°C. Irradiation was especially lethal at low doses for Vibrio parahaemolyticus and therefore can be controlled easily in seafoods by exposure to pasteurizing doses of irradiation. (P.B.M.)

27116 GENETIC CONTROL OF RADIORESISTANCE OF THE CELL AND SOME GENERAL PROBLEMS OF GENETICS. Zakharov, I. A. (Physical-Technical Inst., Leningrad). Tsitol. Genet.; 4: 123-39(Mar-Apr 1970). (In Russian).

A review of genetics and a discussion of the photosensitivity and radioresistance of various microorganisms and their mutants are presented. (JPRS)

27117 IN-VITRO STUDIES OF RAT VIRUSES. II. EFFECTS OF HEAT, X-IRRADIATION, AND CARCINOGENIC DRUGS. Lum, G. S. (Univ. of Cincinnati). Oncology; 24: 416-30(1970).

Continuous incubation of rat embryo cells at 42°C suppressed both the appearance and the yield of RV and L-S strain of rat virus. The effect of this temperature is probably on attachment and the very early phase of viral development. When heat is applied during the later phase viral titers are enhanced. The addition of D_2O nullifies the effect of heat with titers surpassing those at 37°C for the first 5 days. Exposure of primary cultures to 800 rad of x irradiation before inoculation with rat viruses decreased the viral titer while less exposure had no effect. The virus cycles and titers of persistently-infected cells were unaffected by x irradiation. (P.B.M.)

27118 INFLUENCE OF THE DOSE RATE AND CONDITIONS OF α-IRRADIATION ON RADIOSENSITIVITY OF E. COLI B/R, B, AND B_{s-1}. Myasnik, M. N.; Petin, V. G.; Morozov, I. I. (Inst. of Medical Radiology, Obninsk, USSR). Stud. Biophys.; 17: 79-84 (1969).

The effects of dose rate and preirradiation conditions on the α-radiosensitivity of Escherichia coli B/r, B, and B s-1 are discussed. Survival curves of E. coli B/r, B, and B s-1 exposed to

a high dose rate of α particles and grown on fish bone agar (FBA) and wort agar (WA) before irradiation are given. (P.B.M.)

27119 GROWTH PATTERNS OF UV-IRRADIATED E. COLI B IN SALINE. Myasnik, M. N. (Inst. of Medical Radiology, Obninsk, USSR); Safiyasov, Zh. S.; Akhmedova, D. U.; Simonyan, N. V.; Korogodin, V. I. Stud. Biophys.; 17: 63-70(1969).

It has been shown that Escherichia coli B can grow in saline [1]. In contrast to the situation with ordinary nutrient media, bacterial growth in saline is demonstrable only with low cell concentration in the suspension and is characterized by relatively low cell yields in the final growth phase. The growth rate and cell number during the stationary phase (M-concentration) are a function of incubation temperature. In view of the fact that bacterial growth in saline is dependent on the initial cell concentration in the suspension, the growth patterns in suspensions of various densities when the viable cell counts in them were reduced by exposure to various doses of uv were ascertained. This question is of fundamental significance for radiation microbiology, because the holding of uv-irradiated cells in so called starvation media is widely employed to study post irradiation recovery. (auth)

27120 BIOPHYSICAL STUDIES WITH LUMINOUS BACTERIA. V. PROTECTION AGAINST X-RAYS BY NUCLEIC ACID COMPOUNDS. Koessler, Franz (Zentralinstitut fuer Arbeitsmedizin, Berlin). Stud. Biophys.; 13: 185-90(1969). (In German).

Data about the protection effect of exogenous nucleic acid substances against radiation damage of luminous bacteria is presented. In the experiments performed with x rays there is also a protection effect by RNA or adenosine. Beside an increase of bioluminescent and respiration reactions the rate of survivals is enhanced too. (auth)

27121 INDUCTION OF MUTATION IN STREPTOCOCCUS DIACETILACTIS BY NITROSOGUANIDINE AND ULTRAVIOLET IRRADIATION. Kuila, R. K.; Ranganathan, B.; Dutta, S. M.; Laxminarayana, H. (National Dairy Research Inst., Karnal, India). J. Dairy Sci.; 54: 331-4(Mar 1971).

A culture of Streptococcus diacetilactis was exposed to the mutagenic action of N-methyl-N'-nitro-N-nitrosoguanidine and uv irradiation, singly and in combination. There was considerable variation in total acidity and production of flavor compounds for cultures, irrespective of the mutagenic treatment, indicating possible genetic changes in exposed cells. An average of 0.3% titratable acidity was obtained for mutants in contrast to 0.45% for the untreated culture. Eight mutants obtained after combined treatment produced higher amounts of diacetyl. One of the mutants M(1) did not coagulate milk up to 48 hr compared to the performance of other isolates and the parent culture. The capacity to produce acid was partially impaired in this mutant strain. There were no significant differences between it and the parent culture in production of volatile acidity, diacetyl, acetoin, and proteolytic activity. However, mutant strain M(1) produced nearly double the amount of acetaldehyde. (auth)

27122 BIOPHYSICAL STUDIES WITH LUMINOUS BACTERIA. IV. REDUCTION OF THE UV-EFFECT BY NUCLEIC ACID SUBSTANCES. Koessler, Franz (Zentralinstitut fuer Arbeitsmedizin, Berlin). Stud. Biophys.; 13: 177-84(1969). (In German).

DNA, RNA, and nucleosides as adenosine, guanosine, and inosine decrease the effect of uv light on bioluminescence and respiration of Vibrio luminosus if the substances are present in the suspension of bacteria during the irradiation. There is also a shortening of the lag phase of growth which is prolonged by uv. The effect may not be only a physical protection but also a physiological one. It is supposed that adenosine or another compound takes part in these metabolism processes which are related to recovery. (auth)

27123 EFFECT OF 5-FLUOROURACIL POSTTREATMENT ON SENSITIVITY TO ULTRAVIOLET RADIATION AND COURSE OF MESSENGER RNA SYNTHESIS IN ESCHERICHIA COLI CELLS. Brozmanova, J.; Sedliakova, M.; Stefunkova, E.; Slezarikova, V. (Inst. of Biology, Bratislava). Folia Microbiol. (Prague); 16: 114-25(1971).

The effect of 5-fluorouracil (5-FU) posttreatment and uracil starvation on sensitivity to uv radiation and on the course of messenger RNA synthesis was studied in the strains Escherichia coli 15 $T^-U^-his^-$, Escherichia coli BU^-, and Escherichia coli Br. 5-FU posttreatment in liquid medium increased the number of surviving cells, while posttreatment in uracil medium either did not affect resistance or lowered it. A correlation was sought between increased resistance and messenger RNA synthesis (or stabilization). Messenger RNA synthesis was studied by means of pulse labeling with radioactive precursor and the amount of m RNA was determined by measuring total RNA proteosynthetic activity. It was found that the amount of RNA with messenger activity increased in cells treated with 5-FU, but that it decreased during cultivation in uracil medium. It is assumed that the 5-FU induced increase in resistance is based on the preferential promotion of repair processes under conditions of a reduced turnover and the consequent stabilization of the m RNA molecules. The possible mechanism of this promotion is discussed. (auth)

27124 REPAIR OF IRRADIATED TRANSFORMING DEOXYRIBONUCLEIC ACID IN WILD TYPE AND A RADIATION-SENSITIVE MUTANT OF MICROCOCCUS RADIODURANS. Moseley, B. E. B.; Mattingly, Alice (Univ. of Edinburgh). J. Bacteriol.; 105: 976-83(Mar 1971).

The survival of biological activity in irradiated transforming deoxyribonucleic acid (DNA) has been assayed in the wild type and a radiosensitive mutant of Micrococcus radiodurans. The frequency of transformation with unirradiated DNA was lower in the mutant to about the same extent as the mutant's increased sensitivity to radiation. However, in both the wild type and the mutant, the irradiated DNA that was incorporated into the bacterial genome was repaired to the same extent as determined by the loss of transforming activity with increasing radiation dose. This applied to DNA irradiated either with ionizing or uv radiation. The rate of inactivation of biological activity after uv radiation was the same in any of the DNA preparations tested. For ionizing radiation, the rate of inactivation varied up to 40 fold, depending on the DNA preparation used, but for any one preparation was the same whether assayed in the wild type or the radiosensitive mutant. When recipient bacteria were irradiated with ionizing or uv radiation immediately before transformation, the frequency of transformation with unirradiated DNA fell, rapidly and exponentially in the case of the sensitive mutant but in a more complicated fashion in the wild type. The repair of DNA irradiated with ionizing radiation was approximately the same whether assayed in unirradiated or irradiated hosts. Thus, irradiation of the host reduced the integration of DNA but not its repair. (auth)

27125 EFFECT OF NALIDIXIC ACID ON SEMICONSERVATIVE REPLICATION AND REPAIR SYNTHESIS AFTER ULTRAVIOLET IRRADIATION IN ESCHERICHIA COLI. Eberle, Helen; Masker, Warren (Univ. of Rochester, N. Y.). J. Bacteriol.; 105: 908-12(Mar 1971).

Both semiconservative deoxyribonucleic acid replication and extensive repair synthesis, in Escherichia coli after uv irradiation, appear to be blocked by nalidixic acid. These findings suggest that the agent(s) responsible for both of these modes of replication, or some necessary common process or structure, is affected by this drug. (auth)

27126 APPLICATION OF LARGE GAMMA RADIATION SOURCE TO THE TREATMENT OF PARASITES IN HUMAN EXCRETA. Ha, Chung Woo; Lee, Hyun Duk (Atomic Energy Research Inst., Seoul). J. Nucl. Sci. (Seoul); 10: No. 2, Part 1, 11-21(1970). (In Korean).

Investigations were made on the possibility of using gamma radiation for the treatment of parasites in human excreta. Various cost break downs were made up for sources, essential supporting facilities, and equipment for a ^{60}Co facility. Following are the provisional concluding remarks: Total source activity must be greater than 1,134,933.3 Ci to treat excreta when the processing rate is 3.6 Kl per hour, and the cost for the plant was estimated as much as $0.908 million. (auth)

Radiosterilization and Radiopreservation

Refer also to abstract 26647.

27127 (CONF-680112) PROCEEDINGS OF THE CONFERENCE ON NUCLEAR ENERGY AND AGRICULTURAL PRODUCTIVITY, SANTIAGO, CHILE, JANUARY 9–12, 1968. (Comision Interamericana de Energia Nuclear). 245p. (In English and Spanish).

Twenty-two papers on nuclear energy and agricultural productivity are included. A separate abstract was prepared for each of 11; one paper was previously abstracted in NSA as 22:23131. Ten are not within the scope of NSA. (L.C.L.)

For abstracts of individual papers see: 26353, 26578, 26685, 26686, and 27128–27134.

27128 (CONF-680112–, pp 1-7) A REPORT ON THE PROGRAMME OF THE JOINT FAO/IAEA DIVISION OF ATOMIC ENERGY IN FOOD AND AGRICULTURE. Fried, Maurice (Joint FAO/IAEA Div. of Atomic Energy in Agriculture, Vienna (Austria)).

The applications of radiation and radioisotopes to activities of the joint FAO/IAEA program are described for the following areas: soils, irrigation, and crop production; insect eradication and pest control; pesticide residues and food protection; plant breeding and genetics; animal production and health; and food preservation. (H.L.W.)

27129 (CONF-680112–, pp 123-8) REVIEW OF METHOD OF STERILE INSECT RELEASE TO CONTROL AND ERADICATE INSECT POPULATIONS. Taylor, E. A. (Agricultural Research Service, Beltsville, Md.).

Comparative studies on the control of insect populations showed that the method of release of sterile male insects in each succeeding generation had a progressively greater effect on the reproductive potential of the native population than the use of insecticides. The feasibility of using the method of release of sterile males is based on the following basic requirements: an efficient method of mass rearing; techniques of sterilization that have no serious adverse effects on the mating capability, competitiveness, or vigor of the species; a practical and efficient means of disseminating the sterile insects into the environment; and assurance that introduction of the number of insects required to suppress the natural population will not create undue hazards or loss to crops, livestock, or man. A discussion is given of the advantages of integrating the techniques of sterile insect release with programs involving the use of parasites, predators, pathogens, or cultural measures. Studies are described on the control of codling moths, Carpocapsa pomonella, using the technique of sterile male release at Yakima, Washington. Problems of practical application, such as the most efficient methods of rearing and handling, are discussed. (H.L.W.)

27130 (CONF-680112–, pp 129-42) FRUIT PESTS IN BOLIVIA. de Fernandez, M. Luisa H. (Ministerio de Agricultura, La Paz (Bolivia)). (In Spanish).

The genera Ceratitis and Anastrepha cause the greatest damage to fruit crops in Bolivia. A review of the literature on the life cycle and habits of this insect is given. Its geographic dispersion in the country is defined. The methods used to control it are discussed at length. A joint plan for the irradiation of the pupae was adopted among the countries of Bolivia, Peru, and Chile. The results of this sterilization effort are not yet available. (J.S.R.)

27131 (CONF-680112–, pp 143-50) COOPERATIVE PROGRAM ON THE INVESTIGATION OF THE MED FLY IN CENTRAL AMERICA. Samperio, Jorge Gutierrez (Organismo Internacional Regional de Sanidad Agropecuaria, San Salvador (El Salvador). Departamento de Sanidad Vegetal). (In Spanish).

The release of radiation-sterilized med flies for the eradication of this pest was investigated in two test areas, one in Panama and the other in Nicaragua. The results were promising. The techniques used for the artificial reproduction of the flies and their irradiation are described. (J.S.R.)

27132 (CONF-680112–, pp 221-39) RADIATION PRESERVATION OF FOODS. Whitehair, L. A. (National Institutes of Health, Bethesda, Md.).

A discussion of principles involved in food irradiation includes destruction or inhibition of the growth of microorganisms, inactivation of autolytic enzymes, penetration of ionizing radiations into food, and types of ionizing radiations, such as γ, x rays, and high speed electrons. A summary of major potential applications of food irradiation includes sterilization, pasteurization, disinfection, disinfestation, sprout inhibition, inhibition of ripening, and product improvement. A review of major wholesomeness considerations is concerned with effects on nutritive value; possible induction of carcinogenic substances by irradiation; induction of other toxic substances by irradiation; destruction of microorganisms by irradiation; and induction of radioactive substances from the radiation source. A table is included to show irradiated foods and packaging materials approved by the Food and Drug Administration. (H.L.W.)

27133 (CONF-680112–, pp 241-3) USES OF IRRADIATION IN THE AGRICULTURAL PRODUCTION IN ARGENTINA. Castagnet, Antonio C. (Comision Nacional de Energia Atomica, Buenos Aires (Argentina). Gerencia de Energia). (In Spanish).

A resume is given of the studies made on the uses of irradiation in the agricultural production in Argentina. These include physicochemical analysis of irradiated wheat, inhibition of the sprouting of potatoes, economic study of the preservation of potatoes by irradiation, irradiation of bovine blood albumine and meat preservation, and design and construction of a semi-industrial irradiation installation. (J.S.R.)

27134 (CONF-680112–, pp 245-6) USES OF RADIOISOTOPES IN AGRICULTURE IN ECUADOR. Estrada A., Raul (Escuela Politecnia Nacional, Quito (Ecuador). Instituto de Ciencias Nucleares). (In Spanish).

A resume is given of the study of the agricultural uses of radioisotopes made in Ecuador. These are experiments on the biosynthesis of radioactive pyrethrin and rotenone and inhibition of the maturation of oranges by means of radiation. Positive results were obtained in the latter study. (J.S.R.)

27135 (IAEA-R-362-F) RELATIONSHIP BETWEEN RADIATION DAMAGES TO CITRUS FRUITS AND CHANGES IN ENZYMES AND OTHER CONSTITUENTS OF THE PEEL. PART OF A COORDINATED PROGRAMME ON ASPECTS OF TISSUE PHYSIOLOGY IN FOOD PRESERVATION BY IRRADIATION. Monselise, S. P.; Riov, J. (International Atomic Energy Agency, Vienna (Austria)). May 1970. vp. NTIS (U. S. Sales Only).

Radiation damage to citrus fruit is particularly evident in peel which shows pitting within days of exposure. A seasonal investigation of irradiation effects was made on developing Shamouti orange fruits. Generally, the radioinduced depression in ascorbic acid and reducing sugars tended to become less marked with increasing fruit age. Radioinduced changes in enzymatic activities (peroxidase, catalase) in flavedo and albedo differed markedly. Experiments on Valencia oranges and grapefruit showed no clear-cut dose rate effects (except a clear decrease with increasing dose in ascorbic acid in flavedo tissue of grapefruit, plus increases in peroxidase and catalase activity). Irradiation with 0.5 and 1.5 MeV electrons caused more pitting in orange peel than γ rays. Chemical effects were similar. Damage was more extensive at the stem end. Prevention of excessive water loss (wax treatment) may considerably reduce radiation damage. Radioinduced accumulation of phenolics in cells was observed in irradiated peel. Irradiation greatly increased both respiration rate and ethylene output. Ethylene produced under irradiation stress induced a very marked increase in PAL (phenylalanine ammonia-lyase) activity. Protein synthesis (inhibited by cycloheximide) was necessary at both levels of ethylene evolution and PAL induction. Irradiation with 400 krad almost completely inhibited total protein synthesis; 100 krad caused a 50% reduction. Irradiation also caused a marked increase in scopoletin (6-methoxy-7-hydroxycoumarin) and its 7-glucoside scopolin. Sugar degradation and respiration rates resulting from irradiation were studied in young and mature oranges. (auth)

27136 (NP-tr-1932) EFFECT OF IONIZING RADIATION ON THE KEEPING QUALITY OF SLICED PORK. Kiss, Istvan; Kalman, Bala; Farkas, Jozsef. Translated from Husipar; 19: No. 3, 101-4(May–Jun 1970). 11p.

Experiments were carried out to determine the effects of γ processing on the organoleptic properties and storage life of sliced pork. The meat was wrapped in plastic foil before irradiation (0.65 Mrad) and stored at refrigerator temperature (0 to 4°C). Results showed no adverse effects on organoleptic properties and an increase of two to three fold (up to 16 days) in the storage life of the processed meat. (C.H.)

27137 (STI/PUB-223) INSECT ECOLOGY AND THE STERILE-MALE TECHNIQUE. Panel Proceedings Series. Proceedings of a Panel on Insect Ecology as Related to Control of Noxious Insects by the Sterile-Male Technique Held in Vienna, 7–11 August 1967. (International Atomic Energy Agency, Vienna (Austria)). Oct 1969. 108p. (In French and English). (CONF-670853). IAEA $4.00.

Separate abstracts were prepared for nine papers presented at the conference. An additional three papers on ecology of insect pests are included, but were not abstracted for NSA. (H.L.W.)

For abstracts of individual papers see: 26573 and 27150–27157.

27138 (TID-25543) MARINE PRODUCTS DEVELOPMENT IRRADIATOR PROGRAM: IRRADIATED FRESH SHRIMP SHIPPING STUDIES. Annual Report, October 1, 1967–September 30, 1968. Kaylor, John D.; Murphy, Edward J.; Green, John H.; Hill, Wilma S. (National Marine Fisheries Service, Gloucester, Mass. Gloucester Fisheries Products Technology Lab.). Oct 1970. Contract AT(49-11)-3005. 103p. Dep. NTIS.

If fresh, raw, headless shrimp are packaged and γ irradiated at a minimum absorbed dose of 100 to 200 kilorads, a one to two log cycle reduction of bacterial numbers will usually result and a commercially desirable extension of shelf life of at least a week is obtained. The present system in which interstate carriers use ice alone or ice in addition to mechanical refrigeration results in internal shrimp temperatures below 40°F. Modern interstate shipping practices, therefore, would not be a limiting factor in the distribution of irradiated shrimp. (auth)

27139 EFFECT OF γ-IRRADIATION ON BEEF MYOGLOBIN. Clarke, Reginald; Richards, James F. (Univ. of British Columbia, Vancouver). J. Agr. Food Chem.; 19: 170-4(Jan-Feb 1971).

Absorption spectra of γ-irradiated (1.0 Mrad) samples of metmyoglobin, myoglobin, or a mixture of oxy and metmyoglobin in an oxygen or nitrogen atmosphere suggested that the iron was in the Fe^{3+} form but the normal metmyoglobin structure was destroyed. The Soret absorbance of hemin and, to a lesser extent, myoglobin underwent a progressive decrease as irradiation dose increased from 0 to 6 Mrad. Treatment of myoglobin with H_2S and γ radiation singly and in combination provided spectral evidence that sulfmyoglobin per se cannot account for the absorption spectrum of irradiated myoglobin. The fluorescent spectra of irradiated hemin and irradiated myoglobin which were not similar to that of protoporphyrin were suggested to be due to the presence of a chole heme protein formed by rupture of the hemin nucleus. (auth)

27140 EFFECT OF GAMMA IRRADIATION ON POST-HARVEST PHYSIOLOGY OF FRUITS. Thomas, Paul; Sreenivasan, A. (Bhabha Atomic Research Centre, Trombay, India). J. Sci. Ind. Res.; 29: 414-23(Sep 1970).

Technical problems involved in the use of ionizing radiations for extending the shelf life of fruits by controlling ripening and senescence were reviewed. Emphasis was laid on the effects of γ irradiation on respiration and ethylene production, enzymes and hormones, tissue texture, changes in chemical constituents like carbohydrates, organic acids, vitamins and pigments, and related physiological and biochemical properties. (auth)

27141 L'IRRADIATION DES POMMES DE TERRE, SYMPOSIUM, BRUXELLES, 1 ET 2 OCTOBRE 1969. (Symposium on the Irradiation of Potatoes, Brussels, October 1–2, 1969). Cahier d'Information du Bureau EURISOTOP 45. Brussels, Bureau EURISOTOP (1970). 173p. (In several languages). (CONF-691056).

Ten papers are included that discuss various aspects of the γ processing of potatoes to prevent sprouting and increase storage life. The economic and commercial aspects of marketing radiation-processed potatoes are also considered. (C.H.)

27142 PRESENT SITUATION OF THE DEVELOPMENT OF FOOD IRRADIATION IN U.S.A. AND OTHER FOREIGN COUNTRIES. Furusawa, Yoichi (Ministry of Health and Welfare, Tokyo). Shokuhin Eisei Kenkyu; 20: 906-16(Sep 1970). (In Japanese).

Food irradiation developments in U.S.A., Denmark, and Holland are reviewed. At Hawaii Irradiated Food Laboratory in the U.S.A. papaya and mango are irradiated by 25 krad to exterminate noxious insects, and their preservation period is prolonged. The radiation source is ^{60}Co with the capacity of 200,000 Ci, and processing capacity is two tons per hour. At the Univ. of California, according to the plan of AEC to develop irradiated food, irradiation is applied to citrus fruits, grapes, mushrooms, and strawberries to prolong their preservation period. Effective results were observed for strawberries and mushrooms. Gamma doses of 20 to 50 krad for the extermination of vermin in wheat and wheat flour, and 5 to 15 krad for the prevention of germination of potatoes have been investigated by AEC at four laboratories. A study, mainly on canned food, has been made in the army laboratory. In Denmark, this problem is now under study by the Atomic Energy Commision and by a meat laboratory. In Holland, the study of irradiation on potatoes has been performed at Food Irradiation Laboratory and Agricultural Radiation Laboratory. (Japan)

27143 IRRADIATION OF FOOD. Lancet; 2: 1024(1970).

The main hazards expected from the irradiation of food are mutagenicity and carcinogenicity. Some experiments showed that irradiated food and food components have mutagenic and cytotoxic effects, but there is no positive evidence of carcinogenicity though tests were few. Sterilization of food which may contain an aerobic bacteria requires doses of the order of 5 megarads, which change the food flavor though smaller doses of about 100,000 rads increase the shelf life. The acceptance of irradiation of stored wheat and wheat products with doses of up to 75,000 rads (against insect infestation) and of potatoes and onions with doses up to 15,000 rads (to prevent sprouting) is acceptable. The data on the onions are unsatisfactory, as a high intake of onions was toxic to the test animals. (UK)

27144 EFFECT OF GAMMA IRRADIATION ON THE REHYDRATION CAPACITY OF FREEZE-DRIED MEAT. Brendl, J.; Klein, S. (Technologische Hochschule, Prague). Nahrung; 14: 579-85(1970). (In German).

The rehydration capacity of freeze-dried meat that had been irradiated before or after drying was studied. It was found that the rehydration capacity is harmed in samples irradiated prior to drying. The greater the gamma dose applied to the raw meat prior to drying, the greater is the decrease of the amount of bound water in the rehydrated meat homogenate. In meat irradiated after freeze-drying, temporary improvement of the rehydration capacity cannot be excluded. Prolonged storage of such a meat produces a noticeable reduction of its rehydration capacity. The higher the gamma dose applied immediately after drying and the longer the storage in a sealed polyethylene film at room temperature, the less is the amount of bound water in the rehydrated meat. (auth)

27145 HISTOLOGICAL IDENTIFICATION OF IRRADIATED POTATOES. Penner, H. (Bundesforschungsanstalt fuer Lebensmittelfrischhaltung, Karlsruhe, Ger.). Z. Lebensm.-Untersuch. Forsch.; 144: 99-101(1970). (In German).

The prospect of commercial irradiation of potatoes makes it necessary to develop methods that enable government agencies to identify irradiated potatoes. It is possible to use the well known inhibition of wound periderm formation by irradiation for such an identification. (auth)

27146 RADIATION PRESERVATION OF FISH. I. GWYNIAD. Ehlermann, D.; Muenzner, R. (Bundesforschungsanstalt fuer Lebensmittelfrischaltung, Karlsruhe, Ger.). Z. Lebensm.-Untersuch. Forsch.; 141: 196-200(1969). (In German).

Freshly caught, whole gwyniads (Coregonus Wartmanni Bloch) from Lake Constance were packed in plastic films impermeable to oxygen and water vapor, irradiated with 10 MeV electrons and stored under wet ice. Samples were examined for organoleptical, chemical and microbiological quality during six weeks. Shelflife of unirradiated controls was nine days, a dose of 100 krad prolonged sheflilife to 23 days. Samples irradiated with 200 or 400 krad spoiled even later, but these higher doses caused changes in flavor. (auth)

27147 RADIATION PRESERVATION OF FISH. III. CARP. Ehlermann, D.; Muenzner, R. (Bundesforschungsanstalt fuer Lebensmittelfrischhaltung, Karlsruhe, Ger.). Z. Lebensm.-Untersuch. Forsch.; 142: 12-17(1970). (In German).

Freshly slaughtered whole carp (Cyprinus carpio L.) were gutted, immediately packed in plastic film impermeable to oxygen and water vapor, irradiated with 10 MeV electrons, and stored under wet ice. Samples were examined for sensorical, chemical, and microbiological quality during 5 weeks. Shelf-life of unirradiated controls was 15 days, a dose of 0.5 Mrad prolonged shelf-life, to about 35 days. Lower doses caused correspondingly shorter shelflife, higher doses up to 1.5 Mrad only reduced bacterial counts further, but additional shelflife was not achieved; the optimal dose therefore was 0.5 Mrad. No negative effect of irradiation on flavor of carp was observed; some members of the taste panel consistently rated irradiated samples higher than the nonirradiated. In comparison with other freshwater species investigated by us, the chances for practical application of the irradiation process to carp seem particularly favorable. (auth)

27148 RADIATION PRESERVATION OF FISH. II. TROUT. Ehlermann, D.; Muenzner, R. (Bundesforschungsanstalt fuer Lebensmittelfrischhaltung, Karlsruhe, Ger.). Z. Lebensm.-Untersuch. Forsch.; 142: 7-12(1970). (In German).

Whole rainbow trout (Trutta iridea W. Gibb.) were gutted, immediately packed in plastic films impermeable to oxygen and water vapour, irradiated with 10 MeV electrons, and stored under wet ice. Samples were examined for organoleptical, chemical and microbiological quality during five weeks. Shelflife of unirradiated controls was 15 days, a dose of 50 krad prolonged shelflife to 21 days. Doses of 100 and 200 krad caused a certain loss of the typical fine flavour of trout, without substantial further improvement of shelflife. A dose of 400 krad prevented spoilage for over 5 weeks but affected flavor markedly. In comparison with other fish species, trout is particularly sensitive to irradiation. The chances for practical application of the radiation process therefore appear less favorable in this case. (auth)

27149 STUDY OF IRRADIATED-PASTEURIZED FISHERY PRODUCTS. Ronsivalli, L. J.; King, F. J.; Ampola, V. G.; Holston, J. A. (Bureau of Commercial Fisheries, Gloucester, Mass.). Isotop. Radiat. Technol.; 8: 321-40(1971).

The results are given of a study of the maximum shelf life of γ irradiated and nonirradiated commercial-grade cod fillets, prime-quality haddock fillets, and prime-quality pink and brown shrimp. The increase in shelf life provided by irradiation is inversely proportional to the storage temperature. Gas chromatography was used to study the effects of radiation or storage, or both, on the chemical composition of cod and haddock fillets and to assess the similarity in chemical composition between irradiated and non-irradiated fish of both species. (auth)

XUM

27150 POPULATION STUDIES OF THE CHERRY FRUIT FLY, RHAGOLETIS CERASI L. Leski, R. (Research Inst. of Pomology, Skierniewice, Poland). pp 1-7 of Insect Ecology and the Sterile-Male Technique. Vienna; International Atomic Energy Agency (1969).

From Panel on Insect Ecology as Related to Control of Noxious Insects by the Sterile-Male Technique, Vienna, Austria. See STI/PUB-223; CONF-670853.

A summary of recent investigations into the ecology of the cherry fruit fly, Rhagoletis cerasi L., is given. These studies indicate that, from an ecological viewpoint, the cherry fruit fly may be a good candidate for control or eradication by the sterile-male technique. (auth)

27151 RADIATION-INDUCED STERILITY IN THE CONTROL OF THE OLIVE FRUIT FLY DACUS OLEAE (GMEL). Manikas, G. (Ministry of Agriculture, Athens); Baldwin, W. F. pp 21-3 of Insect Ecology and the Sterile-Male Technique. Vienna; International Atomic Energy Agency (1969).

From Panel on Insect Ecology as Related to Control of Noxious Insects by the Sterile-Male Technique, Vienna, Austria. See STI/PUB-223; CONF-670853.

In the application of the sterile-male method of control, some prior information on the required ratios of sterile flies/normal flies is of primary importance. Initial experiments in large cages built over mature olive-bearing trees in the orchard at the College of Agriculture, Athens, have been completed, and the results have shown that the number of damaged fruit is drastically reduced with ratios of 4:1, 6:1 and 8:1 irradiated/normal laboratory flies. At the last ratio only 4% of the fruit showed any damage other than oviposition scars, and we have concluded that this ratio might give good control in field application, especially when populations are low during the early spring. (auth)

27152 POPULATION DYNAMICS OF THE SCREW-WORM FLY, COCHLIOMYIA HOMINIVORAX (COQUEREL), WITH RESPECT TO CONTROL BY THE STERILE-MALE TECHNIQUE. Hightower, B. G. (Agricultural Research Service, Mission, Tex.). pp 25-31 of Insect Ecology and the Sterile-Male Technique. Vienna; International Atomic Energy Agency (1969).

From Panel on Insect Ecology as Related to Control of Noxious Insects by the Sterile-Male Technique, Vienna, Austria. See STI/PUB-223; CONF-670853.

The current program to control screw-worms with the sterile-male technique involves an area in northern Mexico 1500 miles long and 300 miles wide together with parts of the States of Texas, Arizona, New Mexico, and California. Since it is beyond the capability of the program to release sterile flies simultaneously in the entire control zone, priorities for treatment are based on estimates of regional and seasonal variations in screw-worm populations. The research support for this program includes efforts to determine the time-space relationship of these changes in populations. Ancillary studies include the behavioral characteristics of both native and released flies, especially in regard to mating habits and dispersal. Trapping records made after mass releases of laboratory-reared, marked flies are used to obtain information on the local distribution and movements of sterile flies. Released flies tend to congregate along watercourses in hot, dry weather, but these concentrations are transitory. Some of the released flies disperse rapidly for distances up to 180 miles, but the inefficiency of present trapping methods requires artificially large concentrations of released flies and poses concomitant difficulties in interpreting data on recoveries. Bait animals are used to collect egg masses as a means of determining ratios of sterile to fertile egg masses after releases of sterile flies. These data are used in evaluating various fly release techniques. Methods of integrating research findings with information on the incidence of screw-worm cases are also discussed. (auth)

27153 DEMOGRAPHIC MODELS OF POPULATION RESPONSE TO STERILE-RELEASE PROCEDURES FOR PEST CONTROL. Geier, P. W. (Commonwealth Scientific and Industrial Research Organization, Canberra, Australia). pp 33-41 of Insect Ecology and the Sterile-Male Technique. Vienna; International Atomic Energy Agency (1969).

From Panel on Insect Ecology as Related to Control of Noxious Insects by the Sterile-Male Technique, Vienna, Austria. See STI/PUB-223; CONF-670853.

Existing models to describe demographic effects of sterilized contingents released in field populations were found to be unrealistic and potentially misleading. In particular, they failed to consider the functioning of density-related processes and stabilizing mechanisms in the life systems of target populations. Attempts were made to account for the operation of such agencies in theoretical instances, which suggested a number of inferences immediately relevant to the feasibility and optimalization of sterile-release procedures. Tentative conclusions are drawn regarding strategy planning in pest control. (auth)

27154 THE ABILITY OF STERILIZED IRRADIATED MALES OF DACUS CUCURBITAE COQ. AND DACUS ZONATUS (SAUNDERS) TO COMPETE WITH NORMAL MALES. Qureshi, Z. A. (Atomic Energy Agricultural Research Centre, Tandojam, Pakistan). pp 43-6 of Insect Ecology and the Sterile-Male Technique. Vienna; International Atomic Energy Agency (1969).

From Panel on Insect Ecology as Related to Control of Noxious Insects by the Sterile-Male Technique, Vienna, Austria. See STI/PUB-223; CONF-670853.

A preliminary study was conducted to evaluate the competitive ability of normal versus gamma-irradiated males of Dacus cucurbitae Coq. and Dacus zonatus (Saunders). Five- to six-day-old pupae of both species were irradiated with 9 kR from a ^{60}Co source of 250 Ci. Both sexes of the emerging flies were completely sterilized and there was no apparent serious effect on either vigour or behavior. When sterile males, normal males and females were caged in the laboratory at the ratio 5:1:1, no reproduction occurred. Field cage studies with D. cucurbitae indicated, however, that ratios greater than 9:1:1 would be necessary for complete cessation of reproduction. (auth)

27155 METHODS OF ESTIMATING THE SIZE OF POPULATIONS OF CODLING MOTHS, CARPOCAPSA POMONELLA (L.), FOR STERILE-MOTH RELEASE PROGRAMS. Butt, B. A. (U. S. Dept. of Agriculture, Yakima, Wash.); Steiner, L. F. pp 57-61 of Insect Ecology and the Sterile-Male Technique. Vienna; International Atomic Energy Agency (1969).

From Panel on Insect Ecology as Related to Control of Noxious Insects by the Sterile-Male Technique, Vienna, Austria. See STI/PUB-223; CONF-670853.

The United States Department of Agriculture at Yakima, Washington, and the Canadian Department of Agriculture at Summerland, British Columbia, are currently releasing gamma-irradiated codling moths, Carpocapsa pomonella (L.), in semi-isolated orchards. The following methods have been used to estimate size of the native populations of codling moths as a basis for determining the release rate of sterile males necessary for effective control: The rate of emergence of native moths is estimated on the basis of prevailing temperatures, numbers of moths captured in traps, and rate of emergence of diapausing larvae in screen cages. The total population entering diapause is estimated by examining all cull fruit at harvest for the number of exit holes and of nearly mature live larvae. The ratio of sterile:native males captured in traps is used to estimate the fluctuating abundance of native moths. The number of natives captured in relation to the number of moths released gives a useful estimate of the size of the native spring-brood population. (auth)

27156 METHODS OF ESTIMATING THE SIZE OF POPULATIONS OF STERILE PEST TEPHRITIDAE IN RELEASE PROGRAMS. Steiner, L. F. (U. S. Dept. of Agriculture, Honolulu, Hawaii). pp 63-72 of Insect Ecology and the Sterile-Male Technique. Vienna; International Atomic Energy Agency (1969).

From Panel on Insect Ecology as Related to Control of Noxious Insects by the Sterile-Male Technique, Vienna, Austria. See STI/PUB-223; CONF-670853.

The ecology of such tephritids as the Mediterranean fruit fly, Ceratitis capitata (Wiedemann), the oriental fruit fly, Dacus dorsalis Hendel, and the melon fly, D. cucurbitae Coquillett, prevents accurate estimates of the size of total populations. Among the most important of these biotic factors are the sensitivity of the three species to environmental changes that affect longevity, the ability of the insects to move long distances and to multiply rapidly, and the ease with which they find new host sites as needed. Expected sizes of populations can be estimated from previous trap records and from release-recovery data if the sterile-insect release program is to involve temporary suppression in semi-isolated localities where small but concentrated areas of high-value crops exist. The same methods may be used when the program is intended to eradicate an incipient outbreak if the infested zone is surrounded by a fly-free area. In addition, in such isolated regions the marked sterile:wild ratio of flies obtained in male lure traps will indicate the rate of release required and the progress in eradication. However, for large eradication programs involving a long established infestation, a survey of at least a year should be made to estimate requirements. The preferred method for such an estimate is use of male lure traps containing trimedlure, methyl eugenol, or cue-lure. (These synthetic lures are far more uniformly efficient in attracting male flies than the most attractive liquid baits.) The catches per trap per day of non-competitive males in representative sample areas can then

XUM

be multiplied by a factor that approximates the minimum number of traps required per square mile to attract all male flies before they become sexually mature. (The factor represents a hypothetical situation in which there is no competition between traps and no part of the square mile is unexposed to an effective concentration of lure.) This factor is first multiplied by 2 to correct for females released but not caught in the non-competitive traps; then the sum is multiplied by the catch per trap day and by the square miles of an area surveyed. The resulting figure is the daily natality for the total area. Another factor, based on release-recovery data, that compensates for the high rate of loss occurring in fruit fly release programs is used to estimate the required release rate. With this method, the data obtained during the year or more of pretreatment surveys can be used to estimate the number of sterile flies needed and the best time for starting releases. Also, the trap catches made during the few weeks immediately before the start of the program permit reasonably accurate estimates of the ratio of sterile to wild flies that can be anticipated from a given release rate. Subsequently, the ratio of marked sterile and wild flies captured can be used to make any adjustments needed. (auth)

27157 MEDITERRANEAN FRUIT FLY RESEARCH IN HAWAII FOR THE STERILE FLY RELEASE PROGRAM. Steiner, L. F. (U. S. Dept. of Agriculture, Honolulu, Hawaii). pp 73-82 of Insect Ecology and the Sterile-Male Technique. Vienna; International Atomic Energy Agency (1969).

From Panel on Insect Ecology as Related to Control of Noxious Insects by the Sterile-Male Technique, Vienna, Austria. See STI/PUB-223; CONF-670853.

Research on the use of sterile fly releases to control the Mediterranean fruit fly, Ceratitis capitata (Wiedemann), in Hawaii involves the development of a strain with easily recognizable genetic markers; breeding into laboratory strains increased longevity and increased capability of mating, foraging and dispersal; investigation into the effects of various methods of release on fly longevity, vigor, and survival; improvements in larval rearing medium to produce more vigorous flies at a lower cost than the current $20 per million flies; development of more efficient traps; improvement in methods of population detection, surveillance, and size estimation; evaluation of new ultra-low volume bait-spray formulations for possible use in suppressing heavy concentrations of native flies before or during programs; investigation of the potential value of methods of annihilating males and improving them to supplement the sterile release method; and continued detailed research on behavior and ecology relating to rhythms, confinement during emergence, sexual behavior, and adult movement. (auth)

27158 SHIPBOARD IRRADIATION OF SHRIMP. Champion, Robert Morrell. Baton Rouge, La.; Louisiana State Univ. (1970). 78p. University Microfilms Order No. 70-18,521.

Thesis.

An investigation was designed and conducted for the purpose of evaluating the feasibility of low-dose γ radiation processing of shrimp at sea using the first portable on-shipboard irradiator developed for this purpose. The irradiation unit was installed aboard the U. S. Bureau of Commercial Fisheries research vessel Oregon, and shrimping cruises were conducted in Atlantic and Gulf of Mexico shrimping grounds. Irradiation, handling, storage, and transportation procedures were developed which were compatible with the nature of the product. After irradiation and ice-storage aboard ship, the shrimp were transported to the Louisiana State University Department of Food Science and Technology Laboratories for chemical, physical, microbiological, and organoleptic testing. Results demonstrated the on-shipboard irradiated shrimp to be superior to shrimp irradiated after ice-storage of four days, and to the non-irradiated, ice-stored control. The on-shipboard irradiator was later removed from the Oregon, and relocated at a dockside site in Grand Isle, Louisiana. Shrimp were purchased through commercial channels from shrimpers who could ascertain that the product was not more than five hours out of the water. These shrimp were packaged, irradiated immediately and returned to the Department of Food Science and Technology for subsequent testing. A field test involving 1500 servicemen as judges was conducted at Fort Lee, Virginia with dockside irradiated and nonirradiated shrimp. Results indicated that dockside irradiated shrimp, while lower in overall quality than on-shipboard irradiated shrimp, as measured by laboratory and sensory methods, are superior in these attributes, and remain palatable longer under iced-storage than shrimp receiving no radiation treatment. (Diss. Abstr. Int., B)

27159 ORGANOLEPTIC CHEMICAL AND MICROBIOLOGICAL ASPECTS OF IRRADIATED PORTUGUESE SAUSAGES. Simoes, J. Henriques (Estacao de Estudos de Tecnologia Animal, Oeiras, Portugal); d'Abreu, F. M. Marques; Martins, A. A. R. Lopes; Ferreira, C. A. Goncalves. Zentralbl. Veterinarmed., Beih.; No. 11, 227-38(1970).

Samples of a typical Portuguese smoked sausage, canned in different atmospheres, were x irradiated with doses from 0.64 to 2 Mrads, and then stored in different conditions. Although the total bacterial content was highly reduced, no shelf life increase was noted and no significant organoleptic and chemical changes were observed. (auth)

27160 EFFECT OF GAMMA IRRADIATION ON THE PECTIC SUBSTANCES OF STRAWBERRIES AT DIFFERENT MATURITY STAGES. Belli-Donini, M. L.; Taggi, R. (CNEN, Rome). Ind. Conserve; 45: No. 1, 23-8(Jan-Mar 1970). (In Italian). (RT/BIO-(70)33).

Red Gauntlet strawberries were picked at different maturity stages and irradiated at 200 krad with a ^{60}Co source. After irradiation the strawberries were held at a temperature of 0 to 3°C and a relative humidity of 90 to 95%. The effects of irradiation on pectic substances and pectin-methylesterase activity, as well as the changes in oxygen uptake, were studied. According to the stage of ripeness at which the strawberries were irradiated different responses to the irradiation were found with regard to pectin metabolism and oxygen uptake. (auth)

27161 RADIATION STERILIZATION OF AN OPHTHALMIC OINTMENT CONTAINING HYDROCORTISONE AND CHLORAMPHENICOL. IV. BACTERIOLOGICAL ASPECTS. Bartha, Tibor; Hangay, Gyoergy; Haraszti, Maria. Acta Pharm. Hung.; 40: 226-32(1970). (In Hungarian).

The dose for radiation sterilization of an ophthalmic ointment containing hydrocortisone acetate and chloramphenicol was measured. A culture of Streptococcus faecalis $A_3$1 as well as a spore culture of B. pumilus E 601 were used as artificial agents for infection. A method was developed for treating irradiated samples of ointment to determine surviving germ counts after irradiation with different doses. In addition, the natural bacterium flora of the ointment was determined both from a qualitative and quantitative point of view. The increase of resistance in the medium of the ointment indicated by earlier experiments was determined also in a quantitative manner; it was found that the resistance was approximately doubled; the value of D_{10} increased from 0.21 to 0.33. On the basis of these results and taking actual germ counts into consideration, the effective sterilizing dose was found to be as large as 2.5 Mrad for this preparate. (auth)

27162 COLOR STABILITY OF FRESH BEEF AS AFFECTED BY IONIZING RADIATION DOSE RATE AND ADDED INORGANIC PHOSPHATE. Ballantyne, William Wallace. East Lansing, Mich.; Michigan State Univ. (1970). 102p. University Microfilms Order No. 71-2025.

Thesis.

A method that employs a pasteurizing dose of ionizing radiation was developed for the centralized cutting of consumer-sized fresh beef cuts to provide a 21-day distribution and shelf life. A critical factor in this process is the development of a bright red color in meat at the time of retail sale. The color of fresh meat is primarily dependent upon the chemical form of the heme-containing protein pigment, myoglobin. Reflectance spectrophotometric methods were used to study pigment form conversions resulting from electron and γ irradiation. The pigment form was a factor of the atmospheric conditions at the time of irradiation. When oxygen was available during the irradiation period, oxidation was dose-rate dependent. Except at the highest electron dose rates studied, the effect did not seem to alter the ability of the vacuum-held beef slices to oxygenate after 21 days of storage. A 10% solution of sodium tripolyphosphate was used before packaging and irradiation as a dip treatment to reduce exudation or "drip" from fresh beef slices. Treated slices had less oxidized pigment after 21 days of vacuum storage than control slices. (Diss. Abstr. Int., B)

27163 PROCESS FOR INACTIVATING ENZYMES IN MEAT TO BE STABILIZED BY RADIATION. Shults, Gary W.; Wierbicki, Eugene (to Secretary of the Army). U. S. Patent 3,554,773. 12 Jan 1971. Filed 29 Feb 1968.

A process is described for the radiation stabilization of fresh beef wherein the beef is first blanched to inactivate proteolytic enzymes and then stabilized with high energy ^{60}Co γ radiation. The improvement consists of increasing the salt content of beef to a level from between 0.5 to 1.5% by weight by pumping and/or marinating with a concentrated salt solution prior to blanching whereby the beef enzymes are rendered susceptible to inactivation at lower temperatures or the same temperature for shorter times than was heretofore possible. (Official Gazette)

27164 EFFECTS OF RADIATION PASTEURIZATION ON SALMONELLA. II. INFLUENCE OF REPEATED RADIATION-

GROWTH CYCLES ON VIRULENCE AND RESISTANCE TO RADIATION AND ANTIBIOTICS. Previte, J. J.; Chang, Y.; Scrutchfield, W.; El-Bisi, H. M. (Army Natick Labs., Mass.). Can. J. Microbiol.; 17: 105-10(Jan 1971).

Populations derived from Salmonella typhimurium surviving 1, 5, or 10 exposures to 0.5 Mrad did not show any increase in resistance to antibiotic discs containing 5 μg of tetracycline, 5 μg of chloromycetin, or 50 units of polymyxin. The frequency of resistance to 3 μg of tetracycline, 10 units of ampicillin, 120 μg of chloromycetin, or 30 μg of streptomycin per milliliter of agar did not increase among progeny derived from either of two strains of S. typhimurium surviving 5 to 10 exposures to 0.5 Mrad. So, too, the virulence and radiation resistance of three strains of S. typhimurium exposed to radiation-growth cycling remained essentially unchanged or decreased. A mixture which originally contained 10 different serotypes of Salmonella was cycled at 0.23 Mrad. After 10 exposures the frequency of resistance of the progeny to ampicillin, chloromycetin, and streptomycin increased 87-, 55- and 13-fold respectively. The LD_{50} was essentially the same, but the radiation resistance (D value) increased from 0.053 Mrad in controls to 0.074 Mrad. The evidence presented seems to indicate that mutants are attained more readily from Salmonella cultures recycled at 0.25 Mrad or less than from those recycled at 0.5 Mrad. The pathogenicity of either one was usually essentially unchanged or reduced. (auth) (Canada)

27165 EFFECT OF GAMMA IRRADIATION ON THE POST-HARVEST PHYSIOLOGY OF FIVE BANANA VARIETIES GROWN IN INDIA. Thomas, Paul; Dharkar, S. D.; Sreenivasan, A. (Bhabha Atomic Research Centre, Trombay, India). J. Food Sci.; 36: 243-7(Mar 1971).

Gamma irradiation of 20 to 40 kRad inhibits the ripening changes in preclimacteric bananas without affecting the fruit quality. Both fruit maturity at harvest and postirradiation storage temperature markedly influence the response to irradiation. The optimum dose and the maximum tolerable dose varied among the five varieties screened. Ability of the banana fruit to withstand higher doses of γ irradiation depends on the physiological status of the fruit at time of irradiation. Irrespective of varietal differences, irradiation of preclimacteric bananas to doses above 50 kRad resulted in severe skin discoloration and fruit splitting. Irradiation under anoxia did not markedly reduce the radiation injury, suggesting that factors other than ozone formed during irradiation in air may contribute the radiation damage. Fruits on the climacteric could tolerate up to 200 kRad but no effect on ripening rate was observed. Ethylene or 2,4-D could reverse γ-induced inhibition of ripening in bananas. Irradiation seems to decrease the sensitivity of banana fruit to the ripening action of exogenously added ethylene. (auth)

27166 ADVANCES IN PRESERVATION OF FOOD BY IRRADIATION. Randeria, B. V. (General Food Corp., Bombay). Food Ind. J.; 1: 12-15(1967).

The irradiation food process was reviewed. Potential applications of ionizing radiations in the food industry, various devices and advantages were discussed. Irradiation of fish was discussed in detail. Scope for irradiation methods was pointed out. (Indian Sci. Abstr.) (auth)

27167 PRESENT STATUS OF NATIONAL RESEARCH PROJECT ON FOOD IRRADIATION; SPROUT INHIBITION OF POTATOES. Sato, Tomotaro (Japan Atomic Energy Research Inst., Takasaki). Nippon Genshiryoku Gakkaishi; 13: 135-8 (Mar 1971). (In Japanese).

Results are given on the effects of radiation on sprout inhibition in potatoes. Data indicate that potato sprouts can be inhibited for 8 mo when irradiated within 3 mo of harvest with doses between 7 to 15 Krad. Further investigations conclude no potential health hazards to man following ingestion of the irradiated potatoes. (P.B.M.)

XUM

METALS, CERAMICS, AND OTHER MATERIALS

Metals and Alloys

Refer also to abstract 28632.

27168 PLUTONIUM-DOKUMENTATION. Referate-Zeitschrift mit Anhang Transplutonium-Elemente. Februar 1971. Band 5, Heft 2. 196 Referate (Register-Nr.426-788), 50 Referate (Register-Nr.58T-107T). (Plutonium-Documentation. Abstract Journal with Appendix on Transplutonium Elements. February 1971. Vol. 5, No. 2. 196 Abstracts (Register No. 426-788), 50 Abstracts (Register No. 58T-107T)). Karlsruhe, Ger.; Gesellschaft fuer Kernforschung m.b.H (1971). 122p. (In German and English).

27169 PLUTONIUM-DOKUMENTATION. Referate-Zeitschrift mit Anhang Transplutonium-Elemente. Januar 1971. Band 5, Heft 1. 225 Referate (Register-Nr.1-425), 57 Referate (Register-Nr.1T-57T). (Plutonium-Documentation. Abstract Journal with Appendix on Transplutonium Elements. January 1971. Vol. 5, No. 1. 225 Abstracts (Register No. 1-425, 57 Abstracts (Register No. 1T-57T)). Karlsruhe, Ger.; Gesellschaft fuer Kernforschung m.b.H (1971). 133p. (In German and English).

27170 FRACTURE. AN ADVANCED TREATISE. VOLUME III. ENGINEERING FUNDAMENTALS AND ENVIRONMENTAL EFFECTS. Liebowitz, H. (ed.). New York: Academic Press Inc. (1971). 771p. $35.00.

The information is presented in twelve chapters. A separate abstract was prepared for each of five chapters. Those chapters for which no abstracts were prepared are concerned with crack growth, plasticity, notch analysis, fracture, creep, and stress-corrosion. (J.R.D.)

For abstracts of individual chapters see: 26440, 27175, 27242, 27243, and 27270.

Corrosion and Erosion

27171 CORROSION AND PASSIVATION OF THIN MOLYBDENUM FILMS. Lee, L. H.; Doo, V. Y. (IBM Components Div., Hopewell Junction, N. Y.). J. Electrochem. Soc.; 118: 443-6(Mar 1971).

Corrosion behavior of thin molybdenum films was investigated in the environments of air, fluorochemical liquid coolant ($C_5F_{11}NO$), and deionized (DI) water in the 70 to 100°C temperature range. A striking similarity both in kinetics and mechanism was observed for the corrosion of molybdenum film in dry air and dry coolant ($C_5F_{11}NO$), as well as moist air and wet coolant ($C_5F_{11}NO/H_2O$). Molybdenum remained inert in dry environments and corroded in the wet media. In addition, molybdenum formed a nonprotective, porous corrosion film and dissolved in DI water at 85°C. The simultaneous presence of water and oxygen in these environments was the controlling factor on the corrosion of molybdenum films. An effective passivation of thin molybdenum films can be provided by either a single layer of silicon dioxide or a composite layer of silicon nitride over silicon dioxide on the metal film. (auth)

27172 IMPROVEMENTS RELATING TO ANODISING BERYLLIUM. Cotton, Joseph Bernard; Giles, Robert Duncan. (to Imperial Metal Industries (Kynoch) Ltd.). British Patent 1,222,653. 17 Feb 1971. Filed 22 Mar 1967.

In accordance with the invention a method of protecting beryllium articles from corrosion comprises anodising in an aqueous bath containing at least 10/l of a sodium salt which is a borate or phosphate (preferably di-sodium tetraborate (borax) or sodium metaborate, or monosodium phosphate). The invention also covers beryllium articles provided with an anodic corrosion-protective layer in an aqueous bath containing at least 10/l of a sodium salt which is a borate or a phosphate. (UK)

27173 STRESS CORROSION CRACKING OF ZIRCONIUM IN METHANOL/HYDROCHLORIC ACID SOLUTIONS. De, P. K.; Elyaperumal, E.; Balachandra, J. Trans. Soc. Advan. Electrochem. Sci. Technol.; 5: 15-20(Jan-Mar 1970).

Zr containing Hf < 200, C 760, H 16, O 1550, Si 70, Fe 85, and other impurities 10 ppM was tested for its resistance to stress corrosion cracking in CH_3OH/HCl mixtures. Samples cold worked to 50% showed excellent resistance to stress corrosion cracking. In annealed specimens intensity of corrosion was max in 0.4% HCl. Loss of ductility was associated with H embrittlement during exposure. A diffusion controlled mechanism of crack formation, whose rate increased with temperature, is suggested. General corrosion was negligible in all cases. (Metals Abstr.)

27174 REACTIONS OF V–Zr–Cr– AND V–Ti–Cr ALLOYS IN LIQUID SODIUM HAVING LOW OXYGEN ACTIVITIES. Borgstedt, Hans Ulrich (Kernforschungszentrum, Karlsruhe, Ger.). Corros. Sci.; 11: 89-105(Feb 1971). (In German).

V–Zr–Cr and V–Ti–Cr alloys, which are used as fuel cladding materials in nuclear reactors, have been studied to evaluate their compatibility to flowing liquid Na at 500 to 600°C. The corrosion phenomena and kinetics are strongly influenced by the O_2 content of the liquid Na; with less than 1 ppM O_2 the weight gain of the alloys is governed by a parabolic rate law, and oxide layers cannot be observed. At higher O_2 activities (1 to 10 ppM) oxide layers are formed on the alloys, and the specimens suffer linear weight-losses. At low O_2 concentrations the O_2 dissolved in the alloys is related to the O_2 concentration in the Na. At 600°C the saturated O_2 content of the alloys was 4000 to 5000 ppM. At higher O_2 concentrations in the Na than necessary to saturate the alloys oxide layers are formed that are removed by the flowing liquid metal. The rate constants of the parabolic reactions at 500 to 600°C lead to values of the activation energy of 10 to 18 kcal/mole. The pick-up of C of this group of alloys is less important than the O_2 exchange, and the reactions are influenced by the alloy composition, especially by the content of Ti. The alloys of this group should be useful for fuel claddings in reactor cooling circuits, which do not suffer the pick-up of C and O_2 below a limit level during the operation. (auth) (UK)

27175 ENVIRONMENTAL CRACKING IN HIGH-STRENGTH MATERIALS. Johnson, H. H. (Cornell Univ., Ithaca, N. Y.). pp 679-720 of Fracture. An Advanced Treatise. Vol. III. /Liebowitz, H. (ed.). New York; Academic Press Inc. (1971).

The major evidence bearing on environment and crack growth in high-strength structural materials is reviewed and discussed. The effect of environment on subcritical crack growth and fracture is considered for stresses, both cyclic and static, less than the net section yield strength. The applicability of fracture mechanics concepts to environmental cracking is considered, and it is shown that the stress-intensity factor may be viewed as the driving force for environmental flaw growth under both cyclic and static load. In terms of threshold values for crack growth, this allows a correlation of test results from different specimen geometries and also a correlation between test results and service failures. The significance of time-to-failure tests is considered briefly. Environmental cracking under static load is considered. Steel and titanium alloys in various environments of water, water vapor, hydrogen, and oxygen are discussed. For steels, crack growth in water and saturated water vapor is a thermally activated process with an activation energy that agrees well with the measured value for diffusion of hydrogen in a high-strength steel. The role of oxygen in inhibiting environmental cracking in vapor environments is discussed. The combined effects of cyclic stress and aggressive environment are considered. Many of the behavior patterns in static loading are observed to carry over to cyclic loading. One exception is that the protective role of oxygen in vapor environments is no longer observed. A lack of data for stress-intensity ranges less than the threshold is noted. Engineering applications are emphasized. Relationships among flaw size, threshold stress intensities in different environments, and proof and operating stresses are presented graphically and their interpretation is discussed. For 4340 steel, the role of yield strength level is summarized in a diagram that indicates that environmental cracking is the major problem at yield strengths in excess of 180 ksi, whereas fatigue crack growth is the major problem at lower strength levels. (auth)

Preparation and Fabrication

Refer also to abstracts 26425 and 27886.

27176 (INIS-mf-9) DEVELOPMENTS IN OXIDATION AND CORROSION RESISTANT MATERIALS. Elayathu, N. S. D.; Balachandra, J. (Department of Atomic Energy, Bombay (India). Chemistry and Metallurgy Committee). 1970. 23p. (CONF-700218-4). NTIS (U. S. Sales Only).

From Symposium on materials science research; Bangalore, India (24 Feb 1970).

Some aspects of the development of oxidation and corrosion-resistant materials and protective coatings to meet the needs

of various fields are reviewed. The behavior of the materials can be almost tailored to suit the demands by suitable modification of their composition, working and heat treatment, surface finish and coating, singly or in combination. The choice of zirconium alloys for structural and cladding purposes in nuclear reactors is discussed. The future trends in some of the materials are indicated. (INIS)

27177 (JUL-681-RX) HIGH-TEMPERATURE BRAZING OF THERMOELEMENTS AND PIPE DUCTS ON REACTOR PLUGS FOR REACTOR EXPERIMENTS. Lehrheuer, W.; Lison, R. (Kernforschungsanlage, Juelich (West Germany). Zentralinstitut fuer Reaktorexperimente). Jul 1970. 49p. (In German). Dep. NTIS (U. S. Sales Only).

Brazing studies were made with two solders and three construction materials in all possible combinations. No tests of the mechanical properties nor the effects of a heat treatment on the solder joints were carried out. The only heat treatment was the cooling time caused by the slowness of the oven. The BNi-5 solder is suitable for soldering on the austenitic high-alloy steel 1.4541. Joining of high-alloy steel with Nb or Ta is to be only conditionally recommended. They contain no fissures but after introduction to increased temperatures fissures are expected because of an interdiffusion of Nb and solder or high-alloy steel elements. Joining of Nb-Nb, Ta-Ta, and Nb-Ta with BNi-5 solder is not useful because of the fissures occurring. The BNi-7 solder is more difficult to handle than BNi-5. For the joining of high-alloy steel to high-alloy steel, the temperature pattern in the oven available was not the best for a solder-material diffusion. The brittle phases could be only unsatisfactorily decomposed and in the separation, long fissures occur in the solder. This solder can not be recommended for joining of Ta-Nb, Ta-Ta, and Nb-Nb. (tr-auth)

27178 (N-71-10353) DETERMINATION OF WELDABILITY AND ELEVATED TEMPERATURE STABILITY OF REFRACTORY METAL ALLOYS. V. WELDABILITY OF TUNGSTEN BASE ALLOYS. Lessmann, G. G.; Gold, R. E. (Westinghouse Electric Corp., Pittsburgh, Pa. Astronuclear Lab.). Sep 1970. Contract NAS3-2540. 110p. (NASA-CR-1611; WANL-PR(P)-17). NTIS.

The weldability of unalloyed tungsten and two tungsten alloys was evaluated. The alloys were evaluated as arc cast material and for the ternary alloy also as a powder metallurgy product. The most important aspect of welding unalloyed tungsten was that it was very sensitive to thermal shock. High preheat temperatures (to 1400°F) alleviated this problem. The W-25 Re alloy had improved thermal shock resistance but was shown to be basically hot tear sensitive in gas tungsten arc welding. Preheat temperatures of 1400°F were again beneficial. The powder metallurgy W-25 Re-30 Mo alloy displayed excellent weldability whereas the arc cast material displayed extensive hot tearing and poor weldability. The anomalous hot tearing behavior of the arc cast W-25 Re-30 Mo alloy was ascribed to a very high sensitivity to oxygen contamination. The effects of post weld annealing, joint preparation, and aging for 1000 hours at temperatures to 3000°F were evaluated. The high temperature tensile strength of base metal, gas tungsten arc welds and electron beam welds in W-25 Re-30 Mo was determined. (auth) (STAR)

27179 (N-71-10454) THERMAL CYCLING ON A 3-in.-DIAMETER NIOBIUM-1 PERCENT ZIRCONIUM TO 316 STAINLESS STEEL TRANSITION JOINT. Cameron, Harry M. (National Aeronautics and Space Administration, Cleveland, Ohio. Lewis Research Center). Nov 1970. 11p. (NASA-TM-X-2118; E-5798). NTIS.

The effect of thermal cycling on the integrity of a Nb-1Zr to stainless steel 3-inch diameter tubular coextruded joint was investigated. The joint was cycled 78 times between 300 and 1550°F and 500 times between 1450 and 1600°F. Extensive post-test examination revealed no metallurgical changes or deterioration of the bond between the two metals. Some diametral contraction was measured in the transition area. (auth) (STAR)

27180 (NLCO-1080) THORIUM METAL PRODUCTION. Briggs, G. G.; Cavendish, J. H. (National Lead Co. of Ohio, Cincinnati). Jan 1971. Contract AT(30-1)-1156. 57p. (CONF-710305-1). Dep. NTIS.

From 100. annual AIME centennial meeting; New York, N. Y. (1 Mar 1971).

Modifications to the Ames ThF_4 reduction process for the production of thorium metal were developed to make the operation safer and capable of providing higher quality metal. The improvements developed included: a precipitation process for production of dense crystalline ThF_4 amenable to rapid filtration and efficient washing; use of nonhygroscopic ZnF_2 instead of $ZnCl_2$ as a source of zinc in the reduction charge. This greatly reduced the potential for hydrogen generation by reaction between moisture and the calcium metal in the charge, thereby reducing the explosion hazard (especially in the charge blending operation); and use of ZnF_2 in the reduction process also made it feasible to use CaF_2 slag from the reaction as liner material for the reduction vessels. This development significantly improved the purity of the metal produced. The process developed has been in routine production for several months. (auth)

27181 (ORNL-TM-3193) MANUAL FOR ASTM A-533 GRADE B, CLASS 1 STEEL (HSST PLATE 03) PROVIDED TO THE INTERNATIONAL ATOMIC ENERGY AGENCY. Childress, C. E. (Oak Ridge National Lab., Tenn.). Mar 1971. Contract W-7405-eng-26. 58p. Dep. NTIS.

The fabrication history of the first two steel plates (HSST plates 01 and 02) for evaluation was presented in USAEC report ORNL-4313. Two additional 12-in.-thick A-533 grade B steel plates were purchased for evaluation. The data relative to these plates are described in USAEC report ORNL-4313-2. This report is devoted primarily to the third plate (plate 03). On completion of fabrication, heat treatment, and testing at the mill, plate 03 was cut into smaller subdivisions called plate sections. Appropriately sized plate sections, depending on the types of tests to be performed, were assigned to research facilities, universities, testing agencies. Practically all of the material assigned to date was from the plate periphery. Most of the remaining plate material is designated as International Atomic Energy Agency (IAEA) material. The fabrication history of plate 03, along with most of the technical data derived from tests involving peripheral material, is presented. (auth)

27182 (R-69-CAP-8) ATTACHMENT OF THERMOCOUPLES TO ZIRCALOY TUBES BY INDUCTION BRAZING. Flemons, R. S. (Canadian General Electric Co., Ltd., Peterborough (Ontario). Atomic Power Dept.). 30 May 1969. 74p.

Special techniques were developed to attach low profile thermocouples to Zircaloy fuel sheaths using Zr-5% Be brazing alloy. The braze was heated in high vacuum using an induction heater with an SCR controller. The brazing temperature was controlled using an infrared pyrometer coupled to the SCR controller. (auth)

27183 PRODUCTION OF TUNGSTEN POWDER FROM MECHANICALLY ACTIVATED TUNGSTIC ACID. Schrader, Richard; Westphal, Hartmut. Neue Huette; 15: 581-5(Oct 1970). (In German).

Following mechanical activation, WO_3 can be reduced by hydrogen to tungsten powder with large surface and low oxygen content. To stabilize the fine grain powder, obtained at 700°C, the pyrophoric tungsten had to be treated in a hydrogen-benzole environment. The same environment also reduced the oxygen content of non-pyrophoric tungsten powder and, thereby, favorably affected the subsequent transformation into tungsten carbide. The experimental method consisted of the following steps: production of fine grain tungsten powder with low O_2 content through mechanical activation for 10 to 30 min; 120 min. reduction of WO_3 by hydrogen at 700°C; coverage of the material with a hydrogen-benzole stream for about 10 min.; and cooling under hydrogen atmosphere. (H.B.G.)

27184 CAST PERMANENT MAGNETS OF COBALT, COPPER, AND CERIUM: PROCESS AND PERFORMANCE CHARACTERISTICS. Cullen, Thomas J. (Sel-Rex Corp., Nutley, N. J.). J. Appl. Phys.; 42: 1535-6(15 Mar 1971).

From 16th Annual Conference on Magnetism and Magnetic Materials, Miami Beach, Fla. See CONF-701104.

A process for casting magnets of the cobalt, copper, rare-earth type weighing as much as several pounds was developed. The characteristics of the alloys are highly reproducible between castings. The uniformity of performance within a casting is excellent. The residual induction of a typical cerium alloy casting is 5600 G. The coercive force is 4800 Oe. The variation of induction with temperature in the region of a load line of 2 is 0.08%/°C from room temperature to 100°C. (auth)

27185 WELDABILITY OF CERTAIN Mo ALLOYS. Gurevich, S. M. (Inst. of Welding, Kiev); Nerodenko, M. M.; Alekseenko, G. N.; Biryukova, T. A.; Shchukin, A. A. Avtomat. Svarka; No. 3, 27-9(Mar 1971). (In Russian).

The weldability of Mo-base alloys with additions of carbon and either Fe, Co, Ni, or Ir is discussed. It was found that the weldability was best when alloyed with Ni or Ir. (R.V.J.)

27186 EXPLOSIVE WELDING OF TUBULAR COMPONENTS Doherty, A. E. ASTME Tech. Paper No. AD69-818. Dearborn, Mich.: American Society of Tool and Manufacturing Engineers (1969). 13p.

Explosive welding parameters which must be controlled for a

XUM

given weld are type of explosive, placement, material standoff, and product configuration. The production of a reliable Al/stainless steel tubular transition joint from 6061 and 5083 Al and 304 stainless steel using a high-rate angular welding technique is described. The joints are tested under service conditions. Tests included shop welding practices, thermal shock, pulsating loads, shear and bend tests and rotating-beam fatigue tests. Metallurgical examinations of the weld are also made. The production of nuclear-reactor boiler tubing comprised of an outer jacket of 316 stainless steel and an inner liner of commercially pure Ta by explosive welding techniques is described. Titanium/stainless steel transition joints for spacecraft fuel systems produced by explosive welding are also discussed. (Metals Abstr.)

27187 HIGH CONDUCTIVITY COPPERS. Vaidyanath, L. R.; Bhandary, V. S. East. Metals Rev.; 23: No. 11, 115-17(10 Apr 1970).

Manufacture of high conductivity Cu metals is considered in relation to technique and possible sources of poor castings. Details of the manufacture and preferred composition of master alloys for the preparation of pure Cu and Cu–Cr, Cu–Cd, Cu–Be, Cu–Te, and Cu–Ag alloys are given. The applications of each alloy are indicated. (Metals Abstr.)

27188 COOPERATION OF REINFORCED-CONCRETE CONSTRUCTION AND STEEL CONSTRUCTION. Geiger, G. (Eidgenoessische Technische Hochschule, Kleindoettingen, Switzerland); Ruh, F. Neue Tech., B; 11: 128-32(1969). (In German).

The four forms in which reinforced-concrete construction and steel construction can be used together are tabulated. The effect of the joint use under each of these conditions on the building process is investigated. (J.S.R.)

27189 USE OF FIELD ION MICROSCOPY IN STUDIES OF THE VAPOUR DEPOSITION OF METALS. Bassett, D. W. (Imperial Coll. of Science and Tech., London). Surface Sci.; 23: 240-58(Oct 1970).

Techniques are outlined which exploit the atomic resolution of the field ion microscope for detailed studies of the nucleation step in metal vapor deposition. Formation of adatom clusters from single adatoms, and the structure, stability, mobility, and growth of such clusters are shown to be amenable to detailed study. (auth)

27190 ZIRCONIUM-BASE ALLOYS. Osadchuk, R. (to Atomic Energy of Canada Ltd.). Canadian Patent 859,053. 22 Dec 1970.

The alloy contains about 0.5 to 5 wt % Nb, about 0.005 to 1 wt % Be and optionally Sn, Cu, Fe, Cr, Mo, V, W, Ta, Ni, Y, Sb and Te (up to 10 wt %) with balance Zr. The alloys are particularly suited for use as structural materials in nuclear reactors. (F.S.A.)

27191 Zr Hf NEWSLETTER, NOVEMBER 1970. Akron, N. Y.; AMAX Specialty Metals Division (1970). 17p.

Developmental and other information is presented on Hf, Zr metal, Zr-base alloys, use of Zr as an additive to other alloys, production of Hf and Zr, production of zirconates, and production of zirconium borides, carbides, nitrides, silicides, beryllides, and germanides. 251 references are included. (J.R.D.)

27192 ELECTROLYTIC PROCESS FOR ULTRA-FINE BERYLLIUM [POWDER]. Hanson, G. T.; Griffiths, V. G. TMS Paper Selection No. A70-34. New York; Metallurgical Society of AIME (1970). 17p. $3.00.

The design, construction and operating parameters of a molten salt electrolytic cell are discussed. A novel feature of the cell was a liquid Hg cathode, which allowed formation of a quasi-amalgam from which Be metal powder of an extremely fine grain size was produced. Hot pressing of these amalgams resulted in Be compacts that showed retention of the fine grain sizes, in general considered to be finer than commercial practice. (Metals Abstr.)

27193 [RECENT RESEARCH ON] METALS JOINING. Mortland, J. E.; Evans, R. M. DMIC Rev.; 3p(20 May 1970).

Recent research on the joining of Ti alloys and steels includes work on: bonding Ti–6Al–6V–2Sn to itself in vacuum using titanium hydride as a reactive bonding agent; a diffusion welding method for fabricating hollow compressor blades from Ti–6Al–4V alloy; the effects of weld defects and of repair welds on static and fatigue properties of Ti–6Al–4V weldments; a new heat treatable β alloy, Ti–11.5 Mo–6Zr–4.5 Sn, for fastener applications; welding of HY 130 steel by the gas-W-arc, hot-wire gas-W-arc, pulsed-power gas-metal-arc, narrow-gap gas-metal-arc and submerged-arc processes; a heat treatable HY-130 filler metal consisting of 0.1% C, 0.67% Mn, 2.38% Ni, 0.45% Cr and 0.95% Mo, and a double austenitizing and tempering treatment for improving the toughness of HY 130 steel weldments. (Metals Abstr.)

27194 [RECENT RESEARCH ON] METALWORKING. Olofson, C. T.; Byrer, T. G.; Boulger, F. W. DMIC Rev.; 4p(19 Apr 1970).

Recent research on metalworking includes the following topics: roll forming of structural and airfoil shapes from Ti–8Al–1Mo–1V alloy and a superalloy; ball swaging of welded Ti–6Al–4V alloy tubing; shear spinning of ingot-sheet Be to form cones; development of a new β Ti alloy composed of Ti–11.5Mo–6.0Zr–4.5Sn that provides a combination of cold workability with high strength; an extrusion and cold drawing program for forming long, complex structural shapes from a newly developed β III Ti alloy (Ti–11.5Mo–6.0Zr–4.5Sn) and a study of the effect of surface alterations such as the presence of untempered martensite, over-tempered martensite, austenite reversion, cracks, tears and residual stresses on the fatigue strength and stress corrosion of high-strength steels such as A4340 and D6ac. (Metals Abstr.)

27195 URANIUM ALLOYS. Blanchard, Pierre; Lehmann, Jeanne; Virot, Andre (to Commissariat a l'Energie Atomique). British Patent 1,228,390. 15 Apr 1971. Priority date 23 Aug 1967, France.

A uranium alloy suitable for use in preparing fuel elements used in CO_2-cooled reactors is described. The alloy is fine-grained and is composed of 0.8 to 1.5 wt % Mo, 0.08 to 0.15 wt % Al, 0.02 to 0.08 wt % of an element selected from the group comprising Sn, Cr, and Fe. The remainder is U. (J.R.D.)

27196 MATERIAL FORMING AND WELDING NUCLEAR PRESSURE VESSELS. Bunn, W. B.; Randolph, D. D. (Combustion Engineering, Inc., New York). Nucl. Eng. Int., 16: 53-7(Jan-Feb 1971).

Fabrication techniques used by U. S. manufacturers of steel pressure vessels for light water systems are reviewed. Descriptions are given of forming and thermal treatments for forgings and plate. The technology of welding vessels, cladding, and external attachments is discussed. Corrosion aspects are briefly considered. (UK)

27197 ELECTRON BEAM WELDING. PRINCIPLES AND PRACTICE. Meleka, A. H. (ed.). London; McGrail-Hill (1971). 341p. Pound 7.

The subject is dealt with under the following headings: history of electron-beam welding, generation and control, thermal effects, equipment, metallurgical considerations, component design, applications, and production engineering. (UK)

Properties Evaluations

Refer also to abstracts 26159, 26160, 26238–26242, 27910, 27911, and 28680.

27198 (BMI-X-10276) EFFECTS OF HYDRIDE PRECIPITATION ON THE TENSILE PROPERTIES OF IRRADIATED ZIRCALOY-2. Final Report. Kangilaski, Mihkel; Perrin, James S.; Wullaert, Richard A. (Battelle Memorial Inst., Columbus, Ohio). Mar 1970. Contract NObs-94029. 25p. Dep. NTIS.

For Bettis [Atomic Power Lab., Pittsburgh, Pa.].

Metallographic examination of a tapered tensile specimen, whose gage section had been subjected to tensile stresses ranging from 5,000 to 30,000 psi during cooling from 680°F, indicated that a stress of at least 30,000 psi was necessary to orient hydride platelets perpendicular to the stress axis in irradiated Zircaloy-2. The effect of 170 ppM of hydrogen on the tensile properties of Zircaloy-2 specimens irradiated to a fast fluence of 5×10^{21} nvt (>1 MeV) was also determined. The unoriented zirconium hydride platelets caused a minor reduction in strength of the unnotched Zircaloy-2 specimens at room temperature and reduced the values of reduction in area at 500 F. The orientation of zirconium hydride platelets perpendicular to the tensile axis did not significantly influence the tensile strength of unnotched samples, but decreased the reduction in area of irradiated Zircaloy-2 at both room temperature and 500°F. The notch strength ratio (NSR) of irradiated Zircaloy-2 was not significantly influenced by additions of hydrogen and stress orientation of the zirconium hydride platelets. (auth)

27199 (CEA-CONF-1671) STUDY OF INTERNAL FRICTION PEAKS IN MOLYBDENUM AFTER IRRADIATION WITH NEUTRONS AT 27°K. Pichon, R.; Bichon, P.; Moser, P. (Commissariat a l'Energie Atomique, Grenoble (France). Centre d'Etudes Nucleaires). [1970]. 16p. (In French). (CONF-700624–3). Dep. NTIS (U. S. Sales Only).

From Conference on Anelastic Effects due to Defects and Phase Transformations in Solids, Lausanne, Switzerland.

The internal friction peaks in Mo after irradiation with neutrons at 27°K were studied. The results obtained show the importance of relaxation phenomena associated with the reorientation and with the

migration of interstitials to the stage I recovery of the resistivity. In the vicinity of stage III no peak can be associated with the migration of a second type interstitial. The model proposed then is a model with the interstitial migrating freely to the stage I_E recovery of the resistivity. Although any stage of electric resistivity does not present the characteristics desired, that is a second-order reaction, this objection can be removed by supposing that the major part of the free interstitials created will fall back into their mother hole; the rest will be trapped by the impurities present in non-negligible concentration in the metal used. (tr-auth)

27200 (CONF-691114-7) DEVELOPMENT OF NUCLEAR REACTOR BEARINGS FOR 1500°F SPACE OPERATION. Horton, P. H.; Kurzeka, W. J. (Atomics International, Canoga Park, Calif.). [nd]. Contract AT(04-3)-701. 7p. ASME, New York $1.50.

From 90. annual meeting on American Society of Mechanical Engineers; Los Angeles, Calif. (16 Nov 1969).

Several material combinations were evaluated for use in compact nuclear reactor control bearings of the spherical self-aligning type operating at 1500°F in high vacuum for 50,000 hrs. An approach to accelerate long-term effects by friction, dwell, and wear tests and materials contact interaction tests at 100 F above the design temperature is explained. Results of this research indicated that carbon-graphite (P5) against flame-plated Al_2O_3 is a satisfactory bearing material couple for this use. Bonded TiC may also be satisfactory but exhibits higher friction. (L.C.L.)

27201 (EUR-4549) SOME EXPERIMENTAL RESULTS ON THE SORPTION OF CAESIUM BY TUNGSTEN AND GRAPHITE. De Beni, G. F.; Gautsch, O.; Wahl, H. (European Atomic Energy Community, Ispra (Italy). Joint Nuclear Research Center). 24 Jul 1970. 22p. Dep. NTIS (U. S. Sales Only). EUR FF 4.45.

A submicron W powder, a nuclear graphite, and a pyrolytic graphite sample were loaded with Cs at sample temperatures between 600 and 800°C and Cs vapor pressure from about 0.01 to 30 mm Hg to see whether such systems could be used as Cs reservoirs in thermionic converters. The amounts of Cs sorbed by the samples at a given temperature as a function of time were measured by a radioactive tracer method using ^{134}Cs. From these sorption curves the saturation loadings and the corresponding equilibrium pressures of the Cs vapor were determined. The Cs saturation loadings on the W powder ranged at different temperature and pressure conditions, from 1.0 to 1.4 mgCs/gW. The sorbed Cs was strongly fixed to the powder and to obtain at a given constant temperature a release of 0.1 mgCs/gW pressure decreases of more than 20% were required. For a loading of 1.2 mg/g vapor pressures of 1 to 10 mm Hg were obtained in the temperature range of 600 to 800°C. The low loadings and their small changes may result in difficulties for a practical use in a converter. The graphite samples attained saturation loadings of up to 1500 mg/g and the loading isotherms showed transition stages corresponding to compounds between $C_{24}Cs$ and $C_{10}Cs$ roughly. In the temperature range of 700 to 800°C these compounds had vapor pressures between 1 and 10 mm Hg. For a pressure decrease of 20% Cs amounts of 10 to 200 mg/g were released. The pressure, temperature and loading characteristics of the Cs-graphite systems are more suitable for a practical use in a converter than those of the tested W powder. (auth)

27202 (EUR-4562) HOW TO USE THE CODE, COMET. Lecloux, M. (European Atomic Energy Community, Ispra (Italy). Joint Nuclear Research Center). 1971. 74p. (In French). Dep. NTIS (U. S. Sales Only). EUR FF 11,-.

In report EUR 4049 i by M. Fantozzi the mathematical formulation of the calculation of mechanical and thermal stresses in the cladding of a fuel element was given. This document explains the structure of the calculation code deriving from it and gives the necessary information for the correct use of the code. (auth)

27203 (INIS-mf-2) HIGH TEMPERATURE SUPER ALLOYS WITH PARTICULAR REFERENCE TO TITANIUM AND ITS ALLOYS. Bhattacharjee, S. K. (Department of Atomic Energy, Bombay (India). Chemistry and Metallurgy Committee). 1970. 18p. (CONF-700218-1). NTIS (U. S. Sales Only).

From Symposium on materials science research; Bangalore, India (24 Feb 1970).

The mechanical properties and application of titanium and its binary and ternary alloys are discussed. Some characteristic mechanical properties such as yield strength, total elongation percentage in the temperature range of 400 to 800°C of selected cobalt, nickel, niobium, iron, titanium and zirconium base high-temperature super-alloys are discussed. Mention is also made of some of the metal-ceramic alloys for the purpose of comparison. While the mechanical and metallurgical properties of these alloys can be further improved along with finding of newer alloys, their application also will continue to increase in an expanding field. Zr-Ru-alloys and their room temperature tensile and total strain properties are mentioned. As the data show, Zr-Ru-alloy had a unique combination of oxidation resistance coupled with good creep properties and excellent elongation. (INIS)

27204 (INIS-mf-3) MATERIALS FOR REACTOR TECHNOLOGY. Rao, N. K.; Balaramamoorthy, K. (Department of Atomic Energy, Bombay (India). Chemistry and Metallurgy Committee). 1970. 15p. (CONF-700218-11). NTIS (U. S. Sales Only).

From Symposium on materials science research; Bangalore, India (24 Feb 1970).

The problems involved in the selection of appropriate materials for reactor use such as nuclear fuels, cladding, pressure tubes and pressure vessels are reviewed. High quality materials such as ferritic or austenitic steels for pressure vessels, zirconium alloys and stainless steels for fuel, cladding, and reactor core components were dealt with emphasis on the special properties required, namely, corrosion resistance, yield strength, and aging. A special mention is made of Rajastan Atomic Power Project, India, as to the reactor materials selected for RAPP reactor. (INIS)

27205 (INIS-mf-19) CONTRIBUTION OF POWDER METALLURGY TECHNIQUES TO MATERIALS SCIENCE. Reshamwala, A. S.; Tendolkar, G. S. (Department of Atomic Energy, Bombay (India). Chemistry and Metallurgy Committee). 1970. 25p. (CONF-700218-14). NTIS (U. S. Sales Only).

From Symposium on materials science research: Bangalore, India (24 Feb 1970).

The techniques of powder metallurgy consist not only in consolidating metal and metal-nonmetal aggregate but also in fabricating individual particles. As such the present paper is divided into three sections viz.: materials in powder form; methods of consolidation; and applications. The section on materials in powder form emphasizes the fact that powder particles needed for a particular purpose are not just ground materials but are precision particles of controlled composition, purity, shape, and size distribution, conforming to strict metallurgical specifications to suit the application for which they are intended. The advantages of the use of pyrolytic carbon coated UO_2 particles as fuel elements, to reach higher burn-up in nuclear reactors are mentioned. In the second section, a short resume of the various techniques of consolidation of metal and nonmetal aggregates is presented with special reference to their advantages, limitations and capabilities. The section on applications describes mainly two areas viz., the applications where powder metallurgy techniques offer superior properties than those offered by the conventional ones and the applications where the powder method is the only alternative. These are illustrated by considering the fabrication of beryllium and development of dispersion strengthened products such as SAP (sintered aluminum powder), TD-Nickel (thoria dispersed nickel) and dispersion strengthened lead. Information on electrical contacts, ferrites, ESD (elongated single domain) magnets is provided to emphasize that these types of materials can only be fabricated by powder metallurgical techniques. (INIS)

27206 (KFK-Ext.Ber.-8/70-1) SELFWELDING OF REACTOR STRUCTURAL MATERIALS IN SODIUM ENVIRONMENT AT HIGH TEMPERATURES. Benndorf, K. (Kernforschungszentrum Karlsruhe (West Germany). Inst. fuer Reaktorentwicklung). Apr 1970. 21p. (In German). NTIS (U. S. Sales Only).

With the purpose of investigating the self-welding tendency of structural materials in the light of the sodium-cooled fast breeder reactor to be built, static load tests in sodium were carried out on these materials. Besides austenitic materials also a stabilized ferritic steel and a nickel-base alloy as well as several hard facing and hard metal alloys were used in the tests. The test temperatures were 580 and 700°C, the compressive load ranged up to 5 kp/mm^2, and the tests lasted for 168 hrs. The results showed a more or less pronounced tendency of all the materials to weld together. Solely the nickel-base alloy, which up to now was only investigated in one experiment, did not weld together — with one exception. (auth) (INIS)

27207 (N-70-42045) LONG-TIME CREEP BEHAVIOR OF TANTALUM-10 TUNGSTEN IN HIGH VACUUM. Titran, Robert H.; Klopp, William D. (National Aeronautics and Space Administration, Cleveland, Ohio. Lewis Research Center). Oct 1970. 22p. (NASA-TN-D-6044). NTIS.

The high vacuum creep behavior of tantalum-10 tungsten in the 2000 to 2600°F range was studied for times up to 10,000 hours. The creep strength was found to be related to grain size, the secondary creep rate increasing with decreasing grain size. The exponential

XUM

factor n relating creep rate to applied stress was found to increase with increasing grain diameter. Analysis of the creep curves showed that after an initial period of decreasing creep rate, the creep rate gradually increased with time. Creep strain during the nonlinear second-stage creep was proportional to time to the 1.5 power. (STAR) (auth)

27208 (N-71-10352) DETERMINATION OF WELDABILITY AND ELEVATED TEMPERATURE STABILITY OF REFRACTORY METAL ALLOYS. II. LONG-TIME TEMPERATURE STABILITY OF REFRACTORY METAL ALLOYS. Lessmann, G. G.; Gold, R. E. (Westinghouse Electric Corp., Pittsburgh, Pa. Astronuclear Lab.). Sep 1970. Contract NAS3-2540. 171p. (NASA-CR-1608; WANL-PR(P)-14). NTIS.

The thermal stability of refractory metal alloys which showed promise for application in high temperature space power systems was determined. Electron beam and gas tungsten arc welds were evaluated as well as base metal. Only the very fabricable niobium and tantalum base alloys were evaluated. The alloys included T-111, T-222, Ta-10W, FS-85, D-43, B-66, C-129Y, Cb-752, and SCb-291. These represent all of the commercial alloys prominent at the inception of the aging studies. The fabricable alloys were screened for high temperature stability over long exposure times. Bfd testing for ductility changes as reflected in the bend transition temperature was emphasized as a screening technique. Tensile testing, hardness-determinations, and extensive optical and electron metallography were also employed. Fracture modes of the alloys were also studied. Some aging effects were noted in all of the alloys studied. None of these effects would be detrimental in normal application of these materials. These effects ranged from simple grain growth in the case of Ta-10W and SCb-291 to classic overaging response in the D-43 alloy. (STAR) (auth)

27209 (N-71-11662) ALLOY SOFTENING IN GROUP VIA METALS ALLOYED WITH RHENIUM. Stephens, Joseph R.; Witzke, Walter R. (National Aeronautics and Space Administration, Cleveland, Ohio. Lewis Research Center). Nov 1970. 27p. (NASA-TN-O-7000; E-5680). NTIS.

An investigation was conducted to determine the effect of temperature and composition on alloy softening in group VIA metals Cr, Mo, and W alloyed with Re. Results showed that alloy softening was similar in all three alloy systems occurring at homologous temperatures less than 0.16 and at Re concentrations less than 16 atom percent. Rhenium content required to produce a hardness minimum diminished rapidly in all three systems with increasing test temperature. The similarities in hardness behavior in these three alloy systems suggest a common softening mechanism which may arise from lowering the Peierls stress. (STAR) (auth)

27210 (SC-DR-710124) REACTION OF MULBERRY WITH VARIOUS GASES. Sallach, R. A. (Sandia Labs., Albuquerque, N. Mex.). Feb 1971. 20p. Dep. NTIS.

The reaction of Mulberry (U-7.5 wt % Nb-2.5 wt % Zr) with the gases CO_2, H_2O, N_2, and O_2 was surveyed. With CO_2 a linear reaction was found at 600°C. With the other gases, parabolic reactions were generally found; deviations were attributed to spalling of reaction product. Catastrophic reactions with H_2O and O_2 were observed at 600°C. The reactivity of the gases can be ordered as $O_2 \sim H_2O > N_2 \geq CO_2$. (auth)

27211 (UCRL-20301) MECHANICAL PROPERTIES OF LAVES PHASES. Sasaki, Go (California Univ., Berkeley. Lawrence Radiation Lab.). Dec 1970. Contract W-7405-eng-48. 69p. Dep. NTIS.
Thesis.

Primary interest in Laves phases in iron binary systems with transition elements lies in their effects as dispersed precipitates. The characteristics of Laves phases themselves should be made clear before discussing precipitation hardening. Mechanical properties of Laves phases, $NbFe_2$, $TaFe_2$, $TiFe_2$, $ZrFe_2$, and $HfFe_2$ were studied by use of a micro Vickers hardness tester. The highest strength (over Hv. 1000) was obtained in $NbFe_2$ and $TaFe_2$, while the strength of $TiFe_2$ and $ZrFe_2$ was comparatively low (Hv. 859). The observation of the deformation around the hardness indentation showed that $TaFe_2$, $ZrFe_2$, and $HfFe_2$ seemed to deform partially with plastic form. $NbFe_2$ and $TaFe_2$, which had almost the same strength but deformed differently were chosen for the study of their effects on the mechanical properties of the iron base binary alloys. Both higher strength and better ductility were obtained in the Fe-1.9 at. % Ta alloy than in Fe-1.78 at. % Nb alloy. A remarkable denuded zone at the retained δ grain boundaries was observed in the Fe-1.78 at. % Nb alloy. (auth)

27212 CHANGE OF SIGN OF THE HALL COEFFICIENT IN LIQUID ALLOYS. Busch, G.; Guentherodt, H.-J.; Kuenzi, H. U. (Eidgenoessische Technische Hochschule, Zurich). Phys. Lett.; 34A: 309-10(5 Apr 1971).

The Hall coefficients were measured of several liquid alloys of normal metals with transition metals which show a positive Hall coefficient in the liquid state: Cu-Ce and Fe-Ge. It was found that the Hall coefficients are also positive for the transition metal rich alloys, decrease with increasing concentration of the normal metals, pass through zero, and finally approach the negative Hall coefficients of the liquid normal metals. (auth)

27213 MATERIALS FOR THE NUCLEAR REACTOR TECHNOLOGY. Dressler, G. (Metallgesellschaft AG., Frankfurt am Main); Westphal, H. Metallgesellschaft; No. 13, 41-9(1970). (In German).

The canning materials used for the fuel containing tubes of the reactor fuel elements are discussed. A description is given of the material properties and the production of the fuel cans. In thermal reactors mainly zirconium alloys were used while in fast breeder reactors chromium, nickel, vanadium, and molybdenum alloys were applied. (INIS)

27214 AUSTENITIC STAINLESS STEELS FOR USE IN NUCLEAR REACTORS. Allio, Robert J.; Thomas, Kenneth C.; Ferrari, Harry M. (to Westinghouse Electric Corp.). U. S. Patent 3,563,728. 16 Feb 1971. Filed 12 Mar 1968.

An austenitic stainless steel for use in a water-cooled nuclear reactor is described wherein the steel is in contact with coolant at elevated temperature and pressure. The alloy is characterized by a low neutron capture cross-section, is highly resistant to stress corrosion in the presence of chlorides and has a relatively high strength. It consists essentially of by weight, from 17 to 22% nickel, from 14 to 19% chromium, from 0.007 to 0.015% carbon, a maximum of 0.015% nitrogen, the total of carbon and nitrogen not exceeding 0.025%, a maximum of 1.5% manganese, and 0.02% cobalt (manganese and cobalt are elements which when exposed to a neutron flux are transformed at least in part to radioactive isotopes of high activity) a maximum of 0.5% silicon, other impurities not exceeding 0.5%, and the balance iron. A nuclear fuel element cladding employing this steel is also described. (Official Gazette)

27215 INTERNAL FRICTION STUDIES IN SOME TITANIUM AND ZIRCONIUM BASED ALLOYS. Doherty, J. E.; Gibbons, D. F. (Case Western Reserve Univ., Cleveland). Acta Met.; 19: 275-82(Apr 1971).

The internal friction spectra of some titanium and zirconium alloys were measured from 4 to 300°K. These spectra showed a peak in the vicinity of 180°K (at 120 kHz). This peak was found to be associated with the beta phase and not with $\beta-\omega$ interface as was previously suggested by Nelson et al. These data are discussed in terms of the special electronic properties of the titanium group elements. An analysis of the omega structure suggested that, on alloying with other transition metals, the titanium group elements could exist in two different electronic configurations. The existence of these two electronic species in the bcc beta phase resulted in stabilized or bound vacancies which accounted for the anomalous diffusion behavior in the titanium group elements. These vacancies and their stabilizing complex constituted defects in the bcc lattice and these defects were responsible for the internal friction peak observed in the vicinity of 180°K in bcc titanium group element alloys. (auth)

27216 ELASTIC PRECURSOR DECAY IN TANTALUM. Gillis, Peter P. (Univ. of Kentucky, Lexington); Hoge, Kenneth G.; Wasley, Richard J. J. Appl. Phys.; 42: 2145-6(Apr 1971).

Uniaxial stress tests were conducted at higher rates in order to reconcile the Hugoniot elastic limit (HEL) with theory. Specimens were subjected to symmetrical projectile impact, and the stress-time pulse was measured at the rear face. Projectile velocity and tilt were also measured. The decay of the HEL wavefront stress with distance was determined and found to be lower than the predicted values. This discrepancy can be reconciled if the dislocation density increases prior to the HEL from the initial value of 10^6 cm^{-2} to 10^8 cm^{-2} Calculations confirm this hypothesis, and it is concluded that finite risetimes of stress wavefronts produce increases in dislocation densities. (D.L.C.)

27217 MEASUREMENT OF MEAN PARTICLE SIZE OF TUNGSTEN AND TUNGSTEN CARBIDE POWDERS BY FISHER SUB-SIEVE SIZER NOT DEPENDENT ON POROSITY. Aoyama, Tadaaki (New Japan Metal Co. Ltd., Osaka). Funtai Oyobi Funmatsuyakin; 17: No. 4, 161-7(Nov 1970). (In Japanese).

An equation for the specific surface area of powder, not dependent on the porosity for F-SSS, was derived from the Kozeny-Carman formula: $S_x = [K\sqrt{\rho_p(x-\epsilon)}]\sqrt{(h_1 - h_2/h_2)}\sqrt{(\epsilon^3/L)}$. Using the equation, measurements of mean particle size of tungsten and tungsten carbide powders were determined at different packing methods, sample weights and porosities. The equation applied to tungsten powder, but not satisfactorily to tungsten carbide powder since the latter possibly had an unstable packing structure.

The particle size was affected only slightly by the packing method, as examined by analysis of variance. The obtained correction factor x was about 0.95 for tungsten and about 1.0 for tungsten carbide powder. (auth) (Japan)

27218 DETERMINATION OF PORE DISTRIBUTIONS IN TUNGSTEN AND TUNGSTEN CARBIDE POWDERS BY MERCURY-POROSIMETER. Suzuki, Kunio (New Japan Metal Co. Ltd., Osaka). Funtai Oyobi Funmatsuyakin; 17: No. 4, 155-60(Nov 1970). (In Japanese).

Distributions of pore sizes greater than 100 Å in tungsten and tungsten carbide powders were determined by a Hg-porosimeter, (with the Hg-pressure up to about 1000 kg/cm^2). Pore sizes were corrected, assuming that the total surface area of pores calculated from the pore distribution curves was consistent with that by BET method. Relations between mean particle size obtained by permeability method (Fisher Sub-Sieve Sizer) and mean pore size determined by a Hg-porosimeter were recognized. Ratio of mean particle size to mean pore size was about 1.0 for tungsten and about 0.5 for tungsten carbide powders. The discrepancy would be probably due to differences in pore shape between the powders. Pore distribution curves of each sample were characteristic of its shape. In almost all samples, one maxima peak was present, but in an exceptional case, in one of the tungsten powders, two peaks were observed. (auth) (Japan)

27219 MATERIALS AND FUELS FOR NUCLEAR REACTORS. Bar-Or, A. Mada; 14: No. 2, 104-10(1970). (In Hebrew).

Nuclear reactors are made mainly of metals. These metals are subjected to extreme working conditions, e.g., high temperature, corrosive fluids, and radiation. The appropriate selection and improvement of metals for adaptation to the working conditions are described. (INIS)

27220 EFFECT OF SMALL ADDITIONS OF VANADIUM AND NICKEL ON SOME PROPERTIES OF CAST TITANIUM. Kashchuk, V. A.; Cherkashin, A. I. Sb. Nauch. Tr., Tomsk. Inzh.-Stroit. Inst.; 16: 3-9(1969). (In Russian).

A study was made of the effect of small additions (0.09 to 0.95%) of V (99.8 to 99.9% purity) or Ni (Ni ≥ 99.99% purity Co ≤ 0.005%) on the microstructure, resistivity, and microhardness of cast iodide Ti. The Ti alloys were prepared in graphite crucibles using high frequency equipment, the V and Ni being added as alloys. The C content in all cases was 0.3 to 0.4%. Ni was twice as effective as V in grain refining and gave a maximum effect at 0.95% concentration. The resistivity and microhardness increased with increase in V content up to 0.95%. (Referativnyi Zh.)

27221 INFLUENCE OF STRUCTURE AND TESTING CONDITIONS ON THE MECHANICAL PROPERTIES OF LOW-ALLOYED MOLYBDENUM. Danyushchenkov, I. A.; Ivashchenko, R. K.; Mil'man, Yu. V.; Trefilov, V. I.; Yakushina, A. I. Probl. Prochnosti; No. 12, 58-63(Dec 1970). (In Russian).

A correlation is established between the mechanical characteristics produced in testing of Type TSM-2A sheet molybdenum with various structural states in tension and flexure. It is demonstrated that the ratio of these characteristics decreases slightly as the deformation rate is increased. The plasticity characteristics are independent of the deformation rate if the test temperature is much higher than the temperature of transition to the brittle state, and decrease rapidly as the deformation rate increases if the test temperature is near the temperature of transition to the brittle state. (JPRS)

27222 TWO APPLICATIONS OF THE MICROHARDNESS TEST. Veado, Juarez Tavora. Metalurgia (Sao Paulo); 26: 393-7(May 1970). (In Portugese).

Microhardness testing was used to study radiation damage in KCl as a result of neutron bombardment and solid-state diffusion of Zn into SAP (sintered Al powder). In the diffusion experiments, standard curves of Zn concentration vs microhardness in the diffusion zone were plotted from a study of one of the specimens. These curves were then used to determine Zn concentration in other specimens solely on the basis of microhardness values. Special attention was given to developing a method of preparing specimen surfaces for the hardness tests. In the other application, the variation in microhardness of KCl with the integrated flux of neutrons was determined. In this case, the KCl served as a simplified model of a ceramic fuel material. (Metals Abstr.)

27223 EFFECT OF PERIOD V TRANSITION METALS ON THE STRUCTURE AND PROPERTIES OF TITANIUM. Cherkashin, A. I.; Kashchuk, V. A. Sb. Nauch. Tr., Tomsk. Inzh.-Stroit. Inst.; 16: 144-8(1969). (In Russian).

A study was made of the effect of small additions (0.05 to 1.5%) of Mo, Nb, and Y on the microstructure, resistivity, and microhardness of Ti. The alloys were prepared as described previously. Mo and Nb have practically no effect on grain size. Y at concentrations >0.3% markedly refines the structure with a max effect at 1.2%. The effect of the elements in the concentration range 0.4 to 1.4% on the resistivity and microhardness is opposite to their effect on grain size. The action of these elements on the properties of Ti is considered, taking into account their dimensional and structural factors and their electronic structure. (Referativnyi Zh.)

27224 OXYGEN ADSORPTION, RECONSTRUCTION, AND THIN OXIDE FILM FORMATION ON CLEAN METAL SURFACES: Ni, Fe, W, AND Mo. Horgan, A. M.; King, D. A. (Univ. of East Anglia, Norwich, Eng.). Surface Sci.; 23: 259-82(Nov-Dec 1970).

A kinetic investigation is reported of the interaction of molecular oxygen with nickel, iron, tungsten, and molybdenum films deposited in ultrahigh vacua, covering the pressure range from 10^{-9} to 10^{-3} torr, and temperatures between 77 and 373°K. On each of the metals and under all conditions examined the sticking probability s for oxygen on the clean surface was found to be very close to unity (>0.99). The sticking probability-coverage profile for nickel shows a minimum at one quarter of a monolayer, which is more pronounced at higher temperatures, and is associated with a phase change of the adsorbate: up to this coverage oxygen is non-dissociatively bound on the surface. Adsorption on the high-coverage phase proceeds with a higher value of s, whence the minimum in the s-profile. At a monolayer coverage s drops to $<10^{-4}$ before a slow process sets in, involving a further substantial uptake of oxygen: the rate of this process is independent of temperature in the range 195 to 290°K, and proportional to the pressure. On iron, only a monolayer uptake is obtained at temperatures <190°K, but at room temperature the equivalent of 3 monolayers are sorbed when s has fallen to 10^{-4}. Five distinguishable and reproducible stages are noted in the s-profile, the discontinuities being associated with phase changes in the surface layer. The final stage of the process has an activation energy of 20 ± 5 kcal/mole, and the rate is proportional to the pressure ($P < 10^{-4}$ torr). Four stages are noted in the adsorption of oxygen on tungsten and molybdenum films; the final stage on tungsten has an activation energy of 5 kcal/mole, and the rate is again proportional to the pressure ($P < 10^{-3}$ torr). About 2 monolayers are taken up at room temperature before s falls to 10^{-7}. Desorption spectra are obtained to characterize low adsorption heat states on these films. In all cases the populations in these γ states are low by comparison with, for example, those found for nitrogen on tungsten or titanium. (auth)

27225 SURFACE AND BULK CARBURIZATION OF TUNGSTEN SINGLE CRYSTALS. Ollis, D. F.; Boudart, M. (Stanford Univ., Calif.). Surface Sci.; 23: 320-46(Nov-Dec 1970).

The initial phases of high-temperature (T > 2000°K) carburization of oriented tungsten single crystals by hydrocarbons at low pressures ($10^{-8} - 10^{-2}$ torr) were examined with LEED, x-ray diffraction, and optical microscopy. Results utilizing a variety of single crystal orientations (and a polycrystalline foil sample) confirm the main result of a preliminary report: all surfaces are initially quite reactive toward the decomposition of the hydrocarbons used (methane, cyclopropane), but only the two most densely packed faces, W(110) and W(100), form stable surface structures which are extremely resistant to further bulk corrosion. The stable carburized surface structures on the (100) and (110) surfaces are interpreted as coincidence lattices with the densely packed basal plane of α-ditungsten carbide parallel to the original W(hkl) surface. X-ray diffraction measurements from bulk W_2C formed on these surfaces at the highest pressures ($10^{-3} - 10^{-2}$ torr) indicate that in the bulk W_2C, the predominant orientation is a relatively "open" plane, $W_2C(10.1)$, exactly parallel to the original W(hkl). Optical microscopy reveals that eventually a roughly constant density of 5 to 10 × 10^5 crystallites/cm^2 of the bulk corrosion product, W_2C, forms on all surfaces (including a polycrystalline foil) except the two stable surfaces, W(100) and W(110). The difference in reactivity of the carburized surface structures on the W(100) and W(110) versus all other samples is attributed to a very incomplete thermal accommodation of the incoming hydrocarbon molecules by the former structures. (auth)

27226 ADSORPTION OF HYDROGEN ON W (100). Adams, D. L.; Germer, L. H. (Cornell Univ., Ithaca, N. Y.). Surface Sci.; 23: 419-22(Nov-Dec 1970).

A combined LEED/flash desorption study of H absorption on W(100) is described. Results of the investigation indicate that the β_2 desorption peak observed is associated with the C(2 × 2) LEED pattern, which is evidence that this binding state consists of H atoms in a C (2 × 2) array. Results are also the basis for a hypothesis that the surface structures responsible for the β_1 peak have not been correctly identified. (J.R.D.)

XUM

27227 COLUMBIUM [NIOBIUM] ALLOY DEVELOPMENT WITH BORON, HAFNIUM, AND TUNGSTEN. Babitzke, H. R.; Oden, L. L.; Kelly, H. J. Report of Investigation No. 7388. Washington, D. C.; Department of Interior, Bureau of Mines (1970). 30p.

As part of a continuing project to develop refractory metal alloys for high-temperature structural applications, solid solution and precipitation strengthening techniques were applied to improve the properties of Nb alloys. The purpose was to investigate the effects of Hf, W, and B on the formability, strength, and oxidation resistance of Nb. The experiment was of factorial design with two replications which called for 72 ingots of 36 basic compositions, weighing 150 g each. Hafnium, W, and B were evaluated at 3, 3, and 4 levels, respectively. Values of alloy content are all in atomic percent. The highest strength observed was 29000 lb/in^2 at 1200°C for alloys Nb–15Hf, Nb–7.5Hf–5W–2B, and Nb–15Hf–5W–2B. At 1200°C, the ternary alloy Nb–15Hf–5W, which showed good properties in previous investigations, was the most resistant to oxidation. For B additions, the alloys oxidized more readily with increasing amounts of this element. The fabricability of the alloys high in B became increasingly difficult, resulting in an inadequate number of alloys required for a complete statistical analysis for all the tests. As a result of the decrease in ductility, an insufficient quantity of tensile samples was available for a proper analysis for the high-temperature strength data. (Metals Abstr.)

27228 RECOVERY OF LOW-TEMPERATURE FAST NEUTRON IRRADIATED TUNGSTEN. Takamura, Saburo; Hanada, Reimon; Okuda, Shigeo; Kimura, Hiroshi (Japan Atomic Energy Research Inst., Tokai. Tohoku Univ., Sendai). J. Phys. Soc. Jap.; 30: 1091-5(Apr 1971).

The recovery of W after fast neutron irradiation at about 10°K with various treatments was investigated by electrical resistivity measurements and the recovery structure determined from 15 to 420°K. The stage I below 90°K of W consists of at least five substages after fast neutron irradiation. Radiation doping enhances the amount of recovery in stages I and II. In W, the effect of doping does not vanish when doped specimen is annealed at 400°C, where stage III is completed. This is in contrast with Mo where the enhancement vanishes when doped specimen is annealed above stage III. (auth)

27229 TITANIUM–ZIRCONIUM–GERMANIUM BRAZING ALLOY. Canonico, Domenic A.; Cole, Nancy C.; Houck, Clarence W. (to United States Atomic Energy Commission). U. S. Patent 3,565,591. 23 Feb 1971. Filed 28 Mar 1969.

A new and improved ternary alloy was developed having particular utility in brazing parts made of graphite or a refractory metal selected from the group consisting of titanium, zirconium, hafnium, vanadium, niobium, chromium, tantalum, tungsten, and molybdenum, and alloys containing this metal as a predominant alloying ingredient. The brazing alloy consists essentially of, by weight, 55 to 75 percent titanium, 15 to 35 percent zirconium, and 10 to 20 percent germanium. (auth)

27230 EFFECT OF SMALL ADDITIONS OF VANADIUM, CHROMIUM, AND MANGANESE ON THE [STRUCTURE AND] PROPERTIES OF CAST ZIRCONIUM. Filippov, V. F.; Kashchuk, V. A. Sb. Nauch. Tr., Tomsk. Inzh.-Stroit. Inst.; 16: 126-31 (1969). (In Russian).

A study was made of the resistivity, microhardness, and the degree of grain refinement of Zr alloys containing 0.05 to 16% Mn, Cr, or V. Curves for grain refinement vs concentration of the added element show that those for Mn and Cr have a max at ~0.6%. The order of increased modifying action and of increasing effect on resistivity and microhardness is V, Cr, Mn. The results are discussed in terms of the electronic mechanism of alloy component interaction. (Referativnyi Zh.)

27231 EFFECT OF PRECIPITATES ON FATIGUE STRENGTH. Ogirima, Masahiko; Hirayama, Toshinari (Hitachi Ltd., Kokubunji, Japan). J. Jap. Inst. Metals; 35: 135-40(Feb 1971). (In Japanese).

Many high-strength alloys, such as Cu-Be alloy, Al-Cu-Mg-Zn alloy (duralumin), 17-7 PH stainless steel, and maraging steel are strengthened by dispersing fine precipitates into a matrix. However, the increase of fatigue strength by precipitation hardening is usually smaller than the values expected from other mechanical properties. For example, carbon steel has a value $\sigma_w/\sigma_B = 0.4 \sim 0.5$ (σ_w: fatigue limit, σ_B: tensile strength), but as for duralumin, $\sigma_w/\sigma_B = 0.2 \sim 0.3$. These properties particular to fatigue strength of precipitation-hardening alloys are assumed to be mainly due to the generation of lattice vacancies or interstitials during fatigue process. So, the effect of excess vacancies on the aging process during fatigue is very interesting. The effects of point defeats generated by fatigue during the aging process and the influence of fine precipitates on fatigue strength were investigated for Cu-Be alloy, Fe-Ni-Ti alloy, and Fe–Cr–Mo alloy which have relatively high recrystallization temperatures. The fatigue strength of these alloys was found to increase by precipitating fine particles in the matrix. The precipitating process was accelerated by the generation of lattice vacancies and interstitials during fatigue. When precipation-hardening alloys were aged isothermally, the increase rate of fatigue strength was larger than that of other mechanical properties. However, the absolute value for the increase of fatigue strength was small as compared with other mechanical properties. The influence of the size and distribution of fine precipitate on fatigue strength was investigated using a transmission electron microscope. (auth)

27232 AGING CHARACTERISTICS OF Cu–30 PERCENT Ni–Be–Ti ALLOYS. Amano, Yoshitugu; Miki, Masamichi (Himeji Inst. of Tech., Japan). J. Jap. Inst. Metals; 35: 113-19 (Feb 1971). (In Japanese).

For the purpose of obtaining high-strength copper alloys with high corrosion resistance, aging characteristics and tensile properties of Cu-30% Ni containing 0.47 wt % Be and 0.5 to 1.8 wt % Ti were investigated by means of hardness test, x-ray diffraction, optical and electron microscopy (reprica method) and tensile testing. These alloys showed a maximum hardness value at 500 to 600°C when aged at 300 to 800°C for 1 hr after water quenching from 1050°C, and the maximum hardness increased with the addition of titanium. It was concluded that age hardening (occurred by heating at 600°C after water quenching from 1050°C) was due to the precipitation process of NiBe (β) and $Ni_3Ti(\eta)$, and that the precipitation process of NiBe contributed to the hardening at an earlier stage of aging and the precipitation process of Ni_3Ti at a later stage of aging. The added titanium suppressed the grain boundary reaction which developed by the precipitation of NiBe and restrained the over-aging of these alloys, but Ni_3Ti precipitates grew from the grain boundary in the high titanium alloys aged for a long time. The alloy containing both beryllium and titanium showed a Kb value higher than that of the alloy containing beryllium. (auth)

27233 EFFECT OF Zr ON THE STABILITY OF A Ti–15 Mo BASE BETA ALLOY. Otani, Shitoshi; Nishigaki, Minoru (Kobe Steel, Ltd., Japan). J. Jap. Inst. Metals; 35: 97-102(Feb 1971). (In Japanese).

The effect of Zr additions (0 to 40 wt %) on the stability of a metastable beta titanium alloy, Ti-15 wt % Mo, was investigated. The measurement of the mechanical properties in various annealing conditions revealed that the stability of Ti-15 Mo-Zr alloy changed abruptly at about 5% Zr. When the alloys containing less than 5% Zr were slow-cooled from the beta region, hardening and embrittlement due to the decomposition of beta was remarkable, and when quenched, a low yield/tensile strength ratio was shown because of martensitic strain transformation. On the other hand, the mechanical properties of the alloys containing more than 5% Zr did not depend on the rate of cooling from the beta region, and the alloys were stable mechanically and thermally. The TTT diagram obtained by an automatic transformation apparatus and the changes in the mechanical properties during aging showed that Zr in a metastable beta alloy, Ti-15 Mo, suppressed and retarded the omega precipitation. The beta stabilizing power of Zr which was calculated from the slope of $\beta/\alpha + \beta$ solvus in the Ti-Zr equilibrium diagram was weak, but the above-mentioned beta stabilizing effect of Zr in the Ti-15 Mo alloy was as strong as that of Mo. (auth)

27234 SURFACE POTENTIAL OF HYDROGEN ON TUNGSTEN (100), (110), AND (112) SINGLE CRYSTAL SURFACES. Hopkins, B. J.; Usami, S. (Univ. of Southampton, Eng.). Surface Sci.; 23: 423-6(Nov-Dec 1970).

A discussion is presented on discrepancies in results of experiments conducted to determine the surface potential change due to hydrogen adsorption on (100) W crystal surfaces. Further experimental results showed that the discrepancy occurred because different techniques were used; in the earlier experiment, H exposure was not continued to saturation. Data on work functions at crystal planes are included to illustrate the discussions. (J.R.D.)

27235 LEED STUDIES OF ARGON CRYSTALS ON NIOBIUM (100) SURFACE. Dickey, J. M.; Farrell, H. H.; Strongin, M. (Brookhaven National Lab., Upton, N. Y.). Surface Sci.; 23: 448-52(Nov-Dec 1970).

Results of LEED studies of Ar crystals grown on the (100) surface of Nb are presented which show that the Ar crystal grows in register with the Nb substrate. (J.R.D.)

27236 [RECENT RESEARCH ON] MECHANICAL PROPERTIES OF METALS. Campbell, J. E. DMIC Rev.; 6p(8 May 1970).

Experimental results are given for the fracture toughness and fatigue properties of four 7000-series Al alloys (7075-T6510, 7178-T6510, 7075-T73510 and X7080-T7E42), and three armor steels. Dynamic tensile testing of high-purity Al(99.99%), com-

mercial-purity Al(99.4%), and alpha-brass and high-frequency fatigue testing of 316 stainless steel and Ti–6Al–2Mo–4Zr–2Sn alloy are reported. Hot hardness test results on irradiated and unirradiated specimens of high-temperature alloys include Mo, Mo alloys, W, W alloys, Nb and Nb–1Zr alloy, Ta and Ta–10W alloy, V, V alloys, Co, Co alloys, Incoloy 800, Re, stainless steels, and A302-B steel. Mechanical properties of carburized and nitrided stainless steels are listed. (Metals Abstr.)

27237 ADSORPTION OF URANIUM ON TUNGSTEN SINGLE CRYSTAL PLANES. Collins, R. A.; Blott, B. H. (Univ. of Southampton, Eng.). J. Phys., D (London); 4: 102-13(Jan 1971).

Uranium adsorption on the (110), (112), (100), (111), (113) and (116) planes of tungsten field emitter substrates was studied. Measurements of work function against coverage at 295, 950, and 1120°K were found to be in good agreement with previous contact potential difference and photoelectric measurements. A Topping point dipole depolarization model was used to determine dipole moments and effective adsorbate polarizabilities. This model is found to be only partially adequate in describing the adsorption process, deviation from the theory being most evident for the (100) plane. (auth) (UK)

27238 CHANGE IN SOLUBILITY OF CERIUM, PRASEODYMIUM, AND NEODYMIUM IN CHROMIUM AS A FUNCTION OF TEMPERATURE. Kobzenko, G. F.; Kholodov, A. G.; Ivanchenko, V. G.; Martinchuk, E. L.; Kashevs'ka, O. M. (Inst. of Metal Physics, Kiev). Dopov. Akad. Nauk Ukr. RSR, Ser. A; No. 11, 1045-8(1970). (In Ukrainian).

Metallographic, x-ray crystal, and durometric analyses were used to determine the solubility of cerium, praseodymium, and neodymium in chromium. Solubility curves were plotted in a temperature range of 1000 to 1800°C. The effect of rare earth content on microhardness (plasticity) of chromium-base solid solutions was studied. (auth)

27239 PROCESS OF REACTION DIFFUSION OF SILICON INTO NIOBIUM. Sirota, N. N.; Sokolov, S. N. (Inst. of Solid State Physics and Semiconductors, Minsk). Dokl. Akad. Nauk BSSR; 15: 14-17(Jan 1971). (In Russian).

The process of reaction diffusion of Si into Nb at isothermal annealing temperatures from 800 to 1100°C was studied. Diffusion coefficients, preexponential factors, activation energy for reaction diffusion of Si into Nb in the given range of temperatures were calculated. (R.V.J.)

27240 AXIAL RATIOS OF HEXAGONAL METALS. Cousins, C. S. G. (Univ. of Exeter, Eng.). J. Phys., C (London); 3: L197-9(Dec 1970).

Calculations of the equilibrium axial ratios of beryllium, magnesium, zinc, and cadmium based on the optimized model potential are compared. The condition for a large axial ratio is examined. A recent empirically determined change in the normalized energy-wavenumber characteristic in the structure region for zinc and cadmium helps to satisfy this condition and consequently improves the axial ratio prediction. (auth) (UK)

27241 ADSORPTION OF ZIRCONIUM ON TUNGSTEN SINGLE CRYSTAL PLANES. Collins, R. A.; Blott, B. H. (Univ. of Southampton, Eng.). J. Phys., D (London); 4: 114-17(Jan 1971).

The adsorption of zirconium on the (110), (112), (100), (111) and (310) planes of tungsten field emitter substrates was studied. Work function against coverage measurements were made and the dipole moment and effective adsorbate polarizability determined for (100) adsorption. Comparison is made with contact potential difference measurements. As for uranium adsorption, the modified Topping point dipole depolarization model is found to be inadequate in describing adsorption on the (100) plane. (auth) (UK)

27242 FATIGUE OF HIGH-STRENGTH MATERIALS. Ronay, Maria (Columbia Univ., New York). pp 431-82 of Fracture. An Advanced Treatise. Vol. III. /Liebowitz, H. (ed.). New York; Academic Press Inc. (1971).

Fatigue is understood in terms of accumulating irreversible microplastic deformations that become critical only at concentrations of strain. The effect of cyclic straining on the bulk properties of high-strength materials involving strain softening are discussed. Fatigue-crack initiation in high-strength materials is compared to initiation in soft metals and metal composites. Mechanisms of crack propagation in high-strength materials are discussed, together with a unique and very favorable crack-propagation mechanism in shear that has been found in a high-strength steel. On the basis of an energy approach to fatigue-crack propagation, it is shown that crack-propagation laws for any metal will be bounded by a $da/dN = \text{const}\ K^6 - S_e$ law delimiting the case of perfect elasticity and a $da_s/dN = \text{const}\ K^2$ law (for crack propagation by shear) delimiting the case of maximum ductility. The laws for most metals are located between these extremes, and any power of K between 2 and 6 can govern the macroscopic fatigue-crack propagation, depending on the ratio and nature of the micro-events and, thus, on material and strain range. (auth)

27243 ADSORPTION-INDUCED BRITTLE FRACTURE IN LIQUID-METAL ENVIRONMENTS. Westwood, A. R. C. (Martin Marietta Corp., Baltimore); Preece, C. M.; Kamdar, M. H. pp 589-644 of Fracture. An Advanced Treatise. Vol. III. /Liebowitz, H. (ed.). New York; Academic Press Inc. (1971).

Solid metals can be caused to behave in a brittle manner by exposure to a variety of physical or chemical environments. Perhaps the most dramatic examples of such effects, however, result from exposure to surface-active liquid metals. Specimens prestressed above some critical value fail virtually instantly on being wetted by an appropriate liquid metal, and "brittle" crack propagation rates of order 100 cm/sec have been recorded in otherwise ductile metals under such environmental conditions. Such effects are presently considered to result from adsorption-induced reductions in the cohesive strength of atomic bonds at regions of stress concentration in the solid metal; e.g., at the tips of cracks or in the vicinity of piled-up groups of dislocations. The results of a number of recent investigations on this type of liquid-metal embrittlement are described and the prerequisites and possible mechanisms for its occurrence are discussed. Also discussed are the effects of such variables as chemical composition of the solid- and liquid-metal phases, temperature, prestrain, and rate of loading, on severity of embrittlement. The possible correlations between severity of embrittlement and electronegativity, the use of "inert carrier" liquid metals, possible means of inhibiting liquid-metal embrittlement, and criteria for brittle failure are examined. (auth)

Structure and Phase Studies

27244 (BNWL–1545) X-RAY COMPARISON OF BETA PLUTONIUM GRAIN SIZE. Allen, R. P.; Arrowsmith, H. W.; Nelson, R. D. (Battelle-Northwest, Richland, Wash. Pacific Northwest Lab.). Jan 1971. Contract AT(45-1)-1830. 14p. Dep. NTIS.

The relative grain size of alpha plutonium, beta plutonium formed from the alpha phase (β_α), beta plutonium formed from the gamma phase (β_γ), and gamma plutonium was determined using an elevated-temperature x-ray metallographic technique. Fine-grained alpha that was transformed $\alpha \rightarrow \beta \rightarrow \gamma \rightarrow \beta \rightarrow \alpha$ at 3°C/min gave fine-grained β_α, coarse-grained gamma, and coarse-grained β_γ. The alpha formed from the coarse-grained β_γ and the subsequent β_α were both coarsened by the gamma phase heat treatment. Conversely, $\alpha \rightleftharpoons \beta$ transformation cycling refined the grain size of the alpha and the β_α. A specimen of coarse-grained alpha (300 to 500 μ average grain diameter) was slowly transformed $\alpha \rightarrow \beta$ at 5°C/hr to maximize the β_α grain size and then rapidly transformed $\beta \rightarrow \gamma \rightarrow \beta$ at 20°C/min to minimize the β_γ grain size. The resultant β_α was again much finer grained than the β_γ, confirming the existence of a characteristic difference in the average grain size of β_α and β_γ. (auth)

27245 (INIS-mf-15) TRANSMISSION ELECTRON MICROSCOPIC STUDIES OF COLD-ROLLED ZIRCONIUM. Mukhopadhyay, P.; Banerjee, S.; Krishnan, R. (Department of Atomic Energy, Bombay (India). Chemistry and Metallurgy Committee). 1970. 14p. (CONF-700218–7). NTIS (U. S. Sales Only).

From Symposium on materials science research; Bangalore, India (24 Feb 1970).

A study of the room-temperature deformed structure by cold rolling of crystal bar zirconium is reported. It was observed that apart from the expected increase in the dislocation density, the nature of the dislocation configuration changed with increasing degrees of cold work. Slip trace and selected area diffraction analyses showed that though slip occurred pre-ponderantly on prismatic planes of the type $(10\bar{1}0)$, pyramidal glide was also operative. The samples rolled at low degree of reductions per pass appeared to deform only by slip, whereas both slip and twinning were seen to be the deformation modes when the reduction per pass was greater. The presence of hydride precipitates with the associated dislocations and the interaction of dislocations with these precipitates were observed. Movements of dislocations induced by electron beam heating within the microscope and the interaction of the trails left by them were also studied. (auth) (INIS)

27246 (JUL–675–FF) INVESTIGATION OF THE DISLOCATION STRUCTURE OF A Ni SINGLE CRYSTAL WITH MAGNETIC SMALL-ANGLE SCATTERING OF NEUTRONS. Durcansky, Georg (Kernforschungsaniage, Juelich (West Germany). Institut fuer Festkoerperforschung). Jul 1970. 76p. (In German). Dep. NTIS (U. S. Sales Only).

XUM

The dislocation structure of a Ni single crystal deformed under tension at room temperature up to the middle of the hardening region II was studied by means of the magnetic small-angle scattering of neutrons. The method of neutron photography was used for the study of the scattering intensity as a function of the direction of the scattering vector because it allows a total scattering diagram to be taken simultaneously. The evaluation of the photoplates was done on a completely automatic installation. Perpendicular to the primary slip plane, a strong scattering intensity was observed. It was caused by coherent scattering of dislocated groups. A relatively large scattering fraction can be attributed to primary individual dislocations which scatter at 60° deformation. The dislocations found of the critical and conjugated slip plane scatter so that they have a line direction between 60 and 90°. Indications on reaction products between dislocations of the primary and the critical slip planes were found. Scattering by secondary or reaction products was also observed. The scattering intensity as a function of the contribution of the scattering vector and of the imposed magnetic field follows the regularity predicted by theory. (tr-auth)

27247 PHASE EQUILIBRIA IN THE SYSTEM VANADIUM–TANTALUM–HAFNIUM. Guzei, L. S.; Sokolovskaya, E. M.; Sokolova, I. G.; Ronami, G. N.; Kuznetsova, S. M. Vestn. Mosk. Univ., Ser. II, Khim.; 11: 696-9(Nov-Dec 1970). (In Russian).

The phase diagram of system V–Ta–Hf was investigated by different methods of physicochemical analysis. The ternary Laves phase was shown to be formed in the solid state. The binary Laves phases TaV_2 and HfV_2 were found to form the succession of solid solutions. (auth)

27248 CALORIMETRIC INVESTIGATION OF LONG-RANGE ORDERING IN THE CADMIUM–MERCURY SYSTEM. Misra, S.; Rao, G. S.; Singh, H. P. (Banaras Hindu Univ., India). Acta Met.; 19: 331-6(Apr 1971).

The energies of long-range ordering at 81°K of ω-phase Cd–Hg alloys of compositions $CdHg_2$, Cd_2Hg, and of intermediate compositions were measured in a liquid alloy solution calorimeter. The values showed a continuous variation with composition with a minimum for the equiatomic alloy. The results were analysed in terms of near-neighbor interactions and strain energy of solid solutions. The interpretation is in satisfactory agreement with a preferential mode of atomic substitution in the off-stoichiometric ordered alloys. A continuity of the ordered phase field extending from $CdHg_2$ to Cd_2Hg is inferred in accord with published superconductivity results. (auth)

27249 TRI-AXIAL PERIODIC MODULATED STRUCTURE IN METALLIC ALLOYS. Tyapkin, Yu. D. (Central Scientific Research Inst. for Ferrous Metallurgy, Moscow); Jibuti, M. V. Acta Met.; 19: 365-71(Apr 1971).

The calculation of the diffuse scattering of x-rays (the intensity of the satellite reflections about the Bragg reflections from supersaturated solid solution) was carried out for the description of the structure of some metallic alloys in the initial stages of the decomposition of the supersaturated solid solution with the help of the model of a tri-axial modulated periodic structure (the modulation of the interplanar spacing and the scattering power in three ⟨100⟩ directions simultaneously). The comparison of the results of quantitative measurements of the satellite intensity in various directions away from the Bragg maxima (in the directions ⟨100⟩ and ⟨110⟩) for the initial stage of aging of the Fe–Be alloys with 16.5 and 19.5 at. % Be after annealing at 400° with the results of calculation proved the correctness of the proposed model. The study of the satellite intensity in various directions depending on different parameters of the model (on the period of modulation L and the degree of modulation Δa/a) permits an explanation based on the proposed model, the observations in the previously studied alloys with the modulated periodic structure (in such alloys as CuNiFe, CuNiCo, ticonal others), in contrast to the Fe–Be alloys, of satellites only in the directions ⟨100⟩. (auth)

27250 SUPERDISLOCATIONS IN Ni_3V. Moreen, Harry A.; Polonis, D. H.; Taggart, R. (Univ. of Washington, Seattle). J. Appl. Phys.; 42: 2151-2(Apr 1971).

A Ni–18 at. % V alloy was strained 2% under tension after a series of quenching, rolling, and annealing treatments. Transmission electron microscopy showed that Ni_3V had precipitated in a "tweed" morphology with the particles parallel to the ⟨110⟩ directions, and superdislocations of pairs and sets of four were observed. The existence of superdislocations of a/2 ⟨110⟩ pairs and sets of four is consistent with the DO_{22} structure of Ni_3V. The apparent stacking fault energy from the spacing of the a/2 ⟨110⟩ dislocations is 8 erg/cm^2. (D.L.C.)

27251 THERMAL CYCLING TEST FOR PLATES CONTAINING DISPERSIONS. Cintra, Sebastiao Hermano Leite; Gentile, Erberto Francisco; de Souza Santos, Tharcisio Damy. Metalurgia (Sao Paulo); 26: 417-20(May 1970). (In Portuguese).

Apparatus and test methods for the study of structural transformations in the core of fuel plates are described. The test is an accelerated simulation of the conditions to which a plate would be subjected in the reactor. After a 4 hr start-up period, the apparatus operates continuously for 5 days, with a cycle time of 11 min, 32 sec. Some results on a core containing a dispersion of Al in 65% U_3O_8 that had been subjected to 431 cycles are included. (Metals Abstr.)

27252 MEASUREMENTS OF ATOMIC ORDER WITH THE FIELD-ION MICROSCOPE. Son, U. T.; Hren, J. J. (Univ. of Florida, Gainesville). Surface Sci.; 23: 177-97(Oct 1970).

Field-ion studies of several near stoichiometric alloys exhibiting long-range order were made with the intent of extracting quantitative data on atomic ordering parameters. The alloys studied include PtCo, Ni_4Mo, FePt, and $FePt_3$. Methods of calculating the long-range order parameter directly from a field-ion micrograph (direct counting and optical transformation) have been developed and detailed techniques are described. Optical transforms of computer simulated masks indicate that order parameters can be deduced within 4% accuracy. Similar measurements from experimental images are considerably less accurate, but there is promise that this may be greatly improved in the near future. The direct counting method is employed to determine the long-range order parameter of the alloy FePt as a function of temperature. These values are compared with those calculated by the theories of Bragg and Williams and Cowley and with experimental x-ray data. All values were in good agreement with one another in the low-temperature range; however, they diverged considerably as the temperature approached T_c. The primary reason for this divergence is due to an observed region in which two phases (ordered and disordered) coexist in equilibrium. The experimental evidence supports an ordering mechanism based upon nucleation and growth near the critical temperature, accompanied by a homogeneous transformation within each domain. (auth)

27253 OBSERVATIONS OF GRAIN BOUNDARIES WITH THE FIELD ION MICROSCOPE. Bayuzick, R. J.; Goodrich, R. S. (Vanderbilt Univ., Nashville). Surface Sci.; 23: 225-39(Oct 1970).

Several interesting grain boundaries have been observed in tungsten. The typical boundary has a very complex topography which is quite different from that predicted by the various grain boundary models. Using both trace analysis on single micrographs and analysis of the movement of boundary traces during field evaporation, it was found that the boundaries are curved surfaces. Several types of observations show that individual planar segments do not persist over more than a few atom diameters. (auth)

27254 METALLURGICAL APPLICATIONS OF THE FIELD-ION MICROSCOPE. Ralph, B. (Cambridge Univ., Eng.). Surface Sci.; 23: 130-43(Oct 1970).

A brief review of recent metallurgical studies with the field-ion microscope is presented. While the information is primarily concerned with two-phase alloy investigations, recent studies of radiation damage, dislocations, and grain boundaries are mentioned. In the area of two-phase studies it is shown that crystallographic data, size distributions, particle shape, and homogeneity can all be derived from field-ion micrographs in a quantitative fashion. These data complement those which may be obtained by other techniques. (auth)

27255 FIELD-ION STUDIES OF MICROSTRUCTURES AND TRANSFORMATIONS IN LONG-RANGE-ORDERED ALLOYS. Lefevre, B. G. (Georgia Inst. of Tech., Atlanta). Contract AT(40-1)-3908. Surface Sci.; 23: 144-59(Oct 1970).

The FIM has been shown in recent years to be a useful tool in the study of microstructures of ordered alloys. Although most of the studies have been of a qualitative nature they have shown that it is possible to obtain detailed information about rotational and translational domain boundaries, order–disorder interfaces, and local variations in the degree of order. This type of information can be particularly useful in the study of order–disorder transformations. (auth)

27256 ELECTRON DIFFRACTION AT CRYSTAL SURFACES. IV. COMPUTATION OF LEED INTENSITIES FOR MUFFIN-TIN MODELS WITH APPLICATION TO TUNGSTEN (001). Jennings, P. J.; McRae, E. G. (Bell Telephone Labs., Inc., Murray Hill, N. J.). Surface Sci.; 23: 363-88(Nov-Dec 1970).

Low energy electron diffraction intensities have been computed for "muffin-tin" models representing atomically-clean crystal surfaces and surfaces formed by the adsorption of foreign atoms. Computational results are reported for specific model potentials corresponding to tungsten crystal with a (001) surface and hydrogen adsorbed on tungsten (001) to form various surface structures of centered (2 × 2) periodicity. No attempt has been made to optimize the model potentials or to allow for inelastic scattering processes. The computational method is a combination of the generalized Dar-

XUM

win method (Part I in the series) with Kambe's method for simple monolayers. The scattering ability of tungsten and hydrogen atom layers and the appropriate band-structure section for tungsten are determined at intermediate stages in the intensity computation. Results are reported for the energy range (0 to 54 eV). The main features of the computed intensity curve for tungsten appeared to be related more directly to scattering resonances of a single layer of atoms than to the Bragg conditions referring to the free-electron description. The presence of a surface potential barrier has a substantial effect on intensity curves. The computational results are compared with the observed intensity versus energy curve for tungsten (001) in the energy range 0 to 20 eV. The computation accurately locates two peaks observed at 8 and 17 eV, but the model cannot account for a third peak observed at 4 eV. An interpretation as a displaced resonance of the surface monolayer is suggested. The computations for hydrogen on tungsten indicate that integral-order beam intensities are only slightly affected by a hydrogen layer. The computed intensities for fractional-order beams are comparable with the intensities for neighboring integral-order beams, and are extremely structure-sensitive. The chief mechanism for the appearance of fractional-order beams is inter-layer multiple scattering. (auth)

27257 ISOTHERMAL TRANSFORMATION OF Ti–Mo BINARY ALLOY. Otani, Shitoshi; Nishigaki, Minoru (Kobe Steel, Ltd., Japan). J. Jap. Inst. Metals; 35: 92-7(Feb 1971). (In Japanese).

The aim of the present work was to obtain more detailed information on the phase transformation of metastable beta-type titanium alloys, Ti-(12 ~ 20)Mo. Preliminary investigations revealed that an automatic transformation apparatus Formastor-F was applicable to titanium alloys. The phase changes of these alloys during isothermal transformation were mainly detected by the changes in dimension, hardness, and microstructure using this apparatus, and then TTT diagrams were obtained. The start point of the contraction coincided with the point where quenched omega transformed to aged omega in the TTT diagram, and the starting point of expansion or the contraction end point also coincided with the point where softening due to the omega→alpha transformation occurred. The contraction and hardening of these three alloys were maximum at 400 to 450°C. In the Ti-15 Mo specimens isothermally transformed at 650 and 700°C, the alpha phase precipitated along the grain boundary, while the alpha phase precipitated in the grain at 500 to 600°C. This indicated that the beta→alpha reaction was not so easy as the beta→omega→alpha reaction and occurred only at grain boundary at high temperature. (auth)

27258 STUDY OF THE ZIRCONIUM–NICKEL–ALUMINUM SYSTEM. Burnashova, V. V.; Markiv, V. Ya. Visn. L'viv. Derzh. Univ., Ser. Khim.; No. 11, 34-7(1969). (In Ukrainian).

X-ray and microstructural analyses were used to study the Zr–Ni–Al system in the region bounded by Zr, $ZrAl_2$, ZrNiAl, $ZrNi_2Al$, Ni_2Al, and Ni. Determinations of the phase equilibria at 800°C established the existence of the ternary compounds Zr_6NiAl_2 and Zr_5Ni_4Al, and refined the composition of the compound $ZrNi_2Al_4$. The following data were obtained from studying single crystals of the compounds Zr_6NiAl_2 and $ZrNi_2Al_4$: Zr_6NiAl_2 had an hexagonal lattice with a = 7.92, c = 3.34Å, c/a = 0.42, space group D_6^4–$P6_322$, N = 9; $ZrNi_2Al_4$ had a tetragonal lattice with a = 4.01, c = 14.41 A, c/a = 3.59, space group D_{4h}^4–P4/mnc or C_{4V}^4–P4nc, N = 14. (Metals Abstr.)

27259 RECRYSTALLIZATION OF V–20 PERCENT Ti ALLOY. Ogawa, Yutaka; Nagasaki, Ryukichi (Japan Atomic Energy Research Inst., Tokai). J. Jap. Inst. Metals; 35: 162-9(Feb 1971). (In Japanese).

The recrystallization of vanadium and its alloy containing 20% titanium was studied by hardness measurement, tensile testing, x-ray diffraction, and optical and electron microscopy. The materials were cold rolled to 20 and 50% in reduction and subsequently annealed in vacuum for 1 hr in the temperature range from 500 to 1100°C. The strength of the V–20% Ti alloy decreased at temperatures between 500 and 700°C upon heating after the cold rolling, while in the pure vanadium the decrease occurred less sharply in the temperature range from 500 to 1100°C. Microscopic observation and x-ray diffraction analysis revealed that the recrystallization was complete at 900°C in both materials. The recrystallization nuclei were formed through well-defined subgrain growth in the V–20% Ti alloy, whereas in the pure vanadium the nuclei were formed by a process of strain-induced boundary migration. In both materials, there was no definite correspondence between the decrease in strength and the recrystallization process observed by optical and electron microscopy. The dislocations in the pure vanadium remained locally after heating above 900°C, while in the V–20% Ti alloy dislocations disappeared almost completely after heating above 900°C and precipitates were observed. (auth)

27260 DEVELOPMENTS IN THE STRUCTURAL CHEMISTRY OF ALLOY PHASES. Symposium Held at Cleveland, Ohio, October, 1967. Giessen, B. C. (ed.). Metallurgical Society of AIME Proceedings. New York; Plenum Publishing Corporation (1969). 298p. $12.50. (CONF-671092).

Eight papers were presented at the conference. A separate abstract was prepared for each of five papers. Papers for which no abstracts were prepared are concerned with crystal chemistry and structure of giant cells. (J.R.D.)

For abstracts of individual papers see: 27261–27264 and 27304.

27261 ALLOY PHASE STABILITY CRITERIA. Engel, Niels N. (Georgia Inst. of Tech., Atlanta). pp 25-40 of Developments in the Structural Chemistry of Alloy Phases. /Giessen, B. C. (ed.). New York; Plenum Publishing Corp. (1969).

From Conference on Developments in the Structural Chemistry of Alloy Phases, Cleveland, Ohio. See CONF-671092.

Mixing of atoms with the same type of electron distribution generally does not lead to electronic changes which cause compound formation. This has been shown for systems of copper and the nearest transition metal neighbors, titanium and the nearest transitional metal neighbors, and aluminum and thirteenth and fourteenth column elements. Mixing of atoms with different electron distributions often cause electronic changes in either of the atoms whereby new and more stable bonding patterns may develop, as found in copper-early transition metal systems, titanium-normal metal systems, titanium-late transition metal or aluminum-transition metal systems. Compound diagrams are presented in which each type of compound corresponds to a horizontal line which can often be traced through several compound diagrams. Such an arrangement of compounds with the same structure and bonding pattern generally exhibits a stability maximum. For the case of transition metal-second period element compounds, a bonding pattern is presented which explains the main features of these very hard, high melting phases. (auth)

27262 STRUCTURAL PROPERTIES OF SOME σ-PHASE RELATED PHASES. Shoemaker, Clara B.; Shoemaker, David P. (Massachusetts Inst. of Tech., Cambridge). pp 107-39 of Developments in the Structural Chemistry of Alloy Phases. /Giessen, B. C. (ed.). New York; Plenum Publishing Corp. (1969).

From Conference on Developments in the Structural Chemistry of Alloy Phases, Cleveland, Ohio. See CONF-671092.

A survey is given of tetrahedrally close-packed structures which are dense packings of atoms of slightly different sizes with only tetrahedral interstices. The coordination numbers present are 12, 14, 15, and 16. The radii of the atoms depend on the chemical composition of the phase and increase with the coordination number. In the higher coordinations (14, 15, 16) the atoms are definitely nonspherical, each having in effect two different radii. (auth)

27263 ALLOY CHEMISTRY OF THORIUM, URANIUM, AND PLUTONIUM COMPOUNDS. Dwight, A. E. (Argonne National Lab., Ill.). pp 181-226 of Developments in the Structural Chemistry of Alloy Phases. /Giessen, B. C. (ed.). New York; Plenum Publishing Corp. (1969).

From Conference on Developments in the Structural Chemistry of Alloy Phases, Cleveland, Ohio. See CONF-671092.

Discussions are presented concerned with intermetallic compounds between the A elements thorium, uranium, and plutonium and X elements from the chromium group through the Si group. Thorium, U, and Pu differ from the transition elements in the crystal structure of their compounds, in that Th, U, and Pu form compounds with definite stoichiometric ratios and never form sigma phases or other compounds which are characterized by variable composition. Furthermore, the thoride elements tend to form compounds with an average atomic volume greater than that predicted from the atomic volumes of the elements, while transition elements generally form compounds which show a contraction in the average atomic volume. Thoride-rich compounds crystallize in uncommon crystal structures, but thoride-poor compounds have structures which are commonly found in transition element compounds. Crystal structure data are presented for: U_2RhNi, NaTl-type, a_0 = 6.419 Å and five isostructural compounds; ThRhAl, Fe_2P-type, a_0 = 7.183 Å, c_0 = 4.120 Å and 28 isostructural compounds; and UCo_3, $PuNi_3$-type, a_0 = 4.849 Å, c_0 = 24.317 Å. Thoride-rich compounds with nickel exhibit larger average atomic volumes than those with cobalt. The relation of this anomalous behavior to similar observations on titanium compounds is discussed. (auth)

27264 CONSTITUTION OF NON-EQUILIBRIUM ALLOYS AFTER RAPID QUENCHING FROM THE MELT. Giessen, B. C. (Northeastern Univ., Boston. Massachusetts Inst. of Tech., Cambridge). pp 227-81 of Developments in the Structural Chemistry of Alloy Phases. /Giessen, B. C. (ed.). New York; Plenum Publishing Corp. (1969).

XUM

From Conference on Developments in the Structural Chemistry of Alloy Phases, Cleveland, Ohio. See CONF-671092.

A description of current experimental techniques for the quenching of molten alloys at very high cooling rates is presented and a comprehensive review of the effects of rapid quenching (especially by the splat cooling technique) on the alloy constitution is given. 153 binary and 28 ternary systems are treated; references available to December 1968 are included. (auth)

Radiation Effects

Refer also to abstracts 26205, 27837, 28682, 28691, and 28765.

27265 (INIS-mf-5) IRRADIATION EFFECTS ON REACTOR STRUCTURAL MATERIALS. Sivaramakrishan, K. S.; Sharma, B. D.; Rodriguez, P. (Department of Atomic Energy, Bombay (India). Chemistry and Metallurgy Committee). 1970. 16p. (CONF-700218-16). NTIS (U. S. Sales Only).

From Symposium on materials science research; Bangalore, India (24 Feb 1970).

Irradiation induced hardening in reactor structural materials is reviewed from both engineering as well as fundamental points of views. Dose damage characteristics, irradiation effects on impact properties, and recovery behavior of radiation damage in zirconium-base alloys and steel both austenitic and ferritic are included. The current concepts of radiation hardening mechanism are discussed briefly. (INIS)

27266 (RD/B/N-1812) EFFECTS OF HIGH FLUX NEUTRON IRRADIATION ON THE MICROSTRUCTURE OF METALS. Fisher, S. B.; Williams, K. R. (Central Electricity Generating Board, Berkeley (England). Berkeley Nuclear Labs.). Dec 1970. 24p. (FRDC/FEWP/P-(70)559). Dep. NTIS (U. S. Sales Only).

The fast reactor development sequence DFR-PFR-Civil Fast Reactor involves an increase in fast neutron flux. The consequences of such an increase on the microstructure of cladding material are discussed as far as is possible with available data from in-reactor and high-voltage electron microscope studies. (auth) (UK)

27267 (UJV-2371.R,T.) A RADIATION EXPERIMENT ON A MODEL OF A FINNED TUBULAR FUEL ELEMENT. I. DESIGN AND PREPARING OF THE EXPERIMENT. Derian, L.; Masek, V.; Kadlec, J. (Ceskoslovenska Akademie Ved, Rez. Ustav Jaderneho Vyzkumu). Apr 1970. 47p. (In Czech). NTIS(U. S. Sales Only).

The design is described of a tubular test element of uranium metal enriched to 6.5% with ^{235}U, coated on both sides with longitudinally finned magnesium alloy tubes of the Magnox type. The element was hermetically sealed by welded end faces made of the same alloy. A description is given of a radiation experiment designed to verify the dimensional stability and the technological preparedness of the production of fuel elements which are to be operated under radiation and thermal cycling. During the experiment, the temperature changes in the test element, radiation growth, and long-term coating tightness were measured. The experiment will be performed in the medium-pressure gas loop of the VVRS reactor at the Institute of Nuclear Research. (INIS)

27268 (WHAN-FR-38) EFFECTS OF NEUTRON IRRADIATION, AT THERMAL REACTOR TEMPERATURES, ON THE PROPAGATION VELOCITY OF ULTRASONIC WAVES IN A533-B STEEL. Hunter, D. O. (Hanford Engineering Development Lab., Richland, Wash.). Dec 1970. Contract AT(45-1)-2170. 23p. Dep. NTIS.

Ultrasonic measurements at 4 MHz and 10 MHz were made on some A533-B tensile and fracture specimens both before and after irradiation from 1 to 9×10^{19} nvt (E > 1 MeV), and at irradiation temperatures of 503 to 550°F. Velocity changes were less than ±0.15%; attenuation changes were small and caused in part by degraded surface smoothness. Due to the fact that ultrasonic changes are very small, do not predictably relate to neutron fluence, and do not correlate with mechanical changes, the method does not appear feasible for assessment of irradiation damage in steel irradiated at thermal reactor temperatures. These findings contrast to those of earlier work which showed readily measurable elasticity changes in steels irradiated at temperatures below 300 to 350°F, and apparent large elasticity changes in stainless steels irradiated to high fluences at 700 to 1400°F. (auth)

27269 DEFECT ANNEALING IN NEUTRON IRRADIATED NIOBIUM. Martkoplishvili, G. S.; Naskidashvili, I. A.; Maisuradze, N. A. (Inst. of Physics, Tbilisi, USSR). Soobshch. Akad. Nauk Gruz. SSR; 61: 569-72(Mar 1971). (In Russian).

The recovery spectrum of Nb irradiated at 120 to 500°K with fast neutrons was investigated by measuring the electrical resistance. Two peaks were found in the recovery spectrum of the electrical resistance at 190°K and 440°K. It was found that the impurity atoms of oxygen greatly affect the process of recovery within the limits of the third stage of annealing. (auth)

27270 FRACTURE MECHANISMS AND RADIATION EFFECTS. Bement, A. L. Jr. (Battelle-Northwest, Richland, Wash.); Hoagland, R. G.; Smidt, F. A. Jr. Contract AT(45-1)-1830. pp 535-87 of Fracture. An Advanced Treatise. Vol. III. /Liebowitz, H. (ed.). New York; Academic Press Inc. (1971).

A description is presented of current fracture theory and how it relates to the irradiation hardening and embrittlement of metals. Selected experimental evidence is presented to illustrate correlations, applications of theory, and areas requiring further work. Most of the discussion centers on iron and steel, although the concepts reviewed are generally applicable to a broad range of materials. Preparatory to examining effects, several aspects of the nature of neutron radiation-induced defects are discussed both in terms of defects resulting from momentum exchanges (collision reactions) and from nuclear transmutation reactions. According to current understanding of radiation damage, it is shown that defects can harden the material both directly, by interaction with dislocations, and indirectly, through alteration of the kinetics of metallurgical reactions such as precipitation. Since a material derives its resistance to crack initiation and propagation primarily from its ability to deform plastically, several effects of radiation damage on dislocation motion are examined. The specific nature of the influence of radiation-induced defects on the motion of dislocations is revealed in studies of the thermally activated flow behavior of several irradiated metals and, in particular, iron. Other information is included on the changes in the yield point in polycrystalline metals due to neutron irradiation, providing an interpretation of irradiation-damage effects in accord with the Hall-Petch analysis in its original and in a more recent and modified form. The implications of results from studies of the flow-stress dependence on neutron fluence are discussed in terms of the conditions defining the initiation and propagation of cracks in irradiated polycrystalline and monocrystalline materials. In the initiation or formation of cracks by the double-pileup model, one particular role of radiation damage is shown to be related to the size of dislocation arrays which can be supported by the shear stress. On the other hand, a crack, once formed, will require less energy for propagation if the extent of dislocation multiplication and motion is restricted by the presence of defect clusters. The radiation-damage dependence of the pertinent material parameters defining the conditions for crack initiation and propagation are examined in some detail. Consideration is also given to loss of strain hardenability and changes in strain-rate sensitivity resulting from neutron irradiation. Investigations of the complex nature of the interaction between impurities and radiation-induced defects are reviewed. The susceptibility to radiation embrittlement is shown to be related to the presence of impurities and is probably the result of the formation of certain defect-impurity atom complexes. Data from several sources are presented illustrating the importance of fabrication variables, with respect to microstructure and phase distribution, to the susceptibility to radiation embrittlement. (auth)

Ceramics and Cermets

Refer also to abstracts 27168, 27169, and 28632.

27271 POLYBLENDS AND COMPOSITES. Conference Held at Brooklyn, New York, June 6-7, 1969. Bruins, Paul F. (ed.). Appl. Polym. Symp.; No. 15, 1-292(1970). (CONF-690651).

Sixteen papers were presented at the conference. A separate abstract was prepared for each of three papers. Papers for which no abstracts were prepared are concerned with aircraft composite materials, and polyblends. (J.R.D.)

For abstracts of individual papers see: 27277, 27278, and 27307.

Preparation and Fabrication

27272 (CONF-700903-18) FUEL MANUFACTURING IN SWEDEN. Widell, Bjoern (ASEA-ATOM, Vasteras (Sweden)). May 1970. 6p. Dep. NTIS (U. S. Sales Only).

From 4. Foratom Congress on industrial aspects of the nuclear fuel cycle in Europe; Stockholm, Sweden (21 Sep 1970).

Fuel element fabrication in Sweden is described. Safety considerations, material supplies, and manufacturing costs are discussed, and operating experiences are given. (Sweden)

XUM

27273 PROCESS FOR PREPARATION OF CERAMICS OF FISSIONABLE MATERIALS. Francois, Bernard; Gremeret, Roger (to Commissariat a l'Energie Atomique). U. S. Patent 3,564,081. 16 Feb 1971. Priority date 9 Mar 1967, France.

Starting from a powder, especially a powder of uranium oxide, a first compression at a pressure P is carried out to obtain granules of the desired size. Then, after crushing these granules and sifting, a second compression at a pressure p lower than P is carried out. Finally, sintering is carried out, for example between 1300 and 1700°C. This leads to ceramics having an open porosity, and the porosity appears to be higher as the difference P−p is greater. (Official Gazette)

27274 METHOD FOR PRODUCING STOICHIOMETRIC URANIUM DIOXIDE COMPOSITIONS. Fairbanks, Norman P.; McGurty, James A. (to United States Atomic Energy Commission). U. S. Patent 3,573,036. 30 Mar 1971. Filed 15 Nov 1966.

A method is described for fabricating a nuclear fuel element comprised of a body of uranium dioxide in a matrix selected from refractory metals or refractory metal alloys, sintering said body in a non-oxidizing atmosphere to a desired density at a temperature above 1700°C, thereby producing hypostoichiometric urania, and contacting the resulting cermet with wet hydrogen at a temperature in the range 1000 to 1500°C until substantial stoichiometry has been attained. (Official Gazette)

27275 COATED NUCLEAR FUEL PARTICLES AND METHOD OF OPERATING A NUCLEAR REACTOR USING SUCH PARTICLES. (to Gulf General Atomic Inc.). British Patent 1,227,505. 7 Apr 1971. Priority date 20 Sep 1968, United States.

A method for the preparation of pyrolytic carbon-coated nuclear fuel particles having excellent structural stability at high temperatures and under fast neutron irradiation is described. Fuel particles of UC_2, UO_2, PUO_2, or ThO_2 may be coated by this method. (J.R.D.)

27276 PREPARATION OF NUCLEAR FUEL ELEMENTS. (to Canadian General Electric Co., Ltd.). British Patent 1,228,317. 15 Apr 1971. Priority date 17 Jun 1968, Canada.

A method of preparing enriched nuclear fuel elements is described which includes impregnating the fuel member, drying the fuel, and converting the enrichment material to metallic oxide. The element contains uranium dioxide with controlled quantities of plutonium dioxide. (J.R.D.)

27277 NEW COMPOSITES: MORPHOLOGY AND PROPERTIES. Mark, Herman F. (Polytechnic Inst. of Brooklyn). Appl. Polym. Symp.; No. 15, 3-8(1970).

From Polyblends and Composites Conference, Brooklyn, N. Y. See CONF-690651.

Information contained in a general introduction to a series of lectures on specific aspects of composite technology is presented. An analysis of relations between the microgeometry or morphology of composite systems and their properties is included. (J.R.D.)

27278 IMPORTANCE OF FABRICATION TECHNOLOGY IN TRANSLATION OF FIBER AND MATRIX PROPERTIES TO ADVANCED COMPOSITES. Friedlander, H. N.; Calfee, John D. (Chemstrand Research Center, Inc., Durham, N. C.). Appl. Polym. Symp.; No. 15, 9-50(1970).

From Polyblends and Composites Conference, Brooklyn, N. Y. See CONF-690651.

A review of composite fabrication technology is presented. Information is included on definitions, matrix types, fiber fabrication, mechanics of fiber orientation and load distribution, tensile properties, use of long and short fibers, and examples of applications. (J.R.D.)

Properties Evaluations

Refer also to abstracts 27191, 27217, 27218, 27239, 27293, 27307, 27906, 27910, 28686, and 28689.

27279 (INIS-mf-11) KINETICS OF THE HIGH-TEMPERATURE OXIDATION OF DISPERSION-STRENGTHENED NICKEL–NIOBIA ALLOYS. Rao, T. H.; Vasu, K. I. (Department of Atomic Energy, Bombay (India). Chemistry and Metallurgy Committee). 1970. 46p. (CONF-700218-13). NTIS (U. S. Sales Only).

From Symposium on materials science research; Bangalore, India (24 Feb 1970).

The oxidation resistance of nickel decreased considerably with the presence of a dispersed phase of Nb_2O_5 up to 5 vol %. In pure sintered nickel, oxidation in the range 700 to 950°C was found to be a two-stage process; an initial logarithmic oxidation with an activation energy of 19 ± 2 kcal/mole, which was followed by a parabolic oxidation with an activation energy of 47 ± 2 kcal/mole. In composite nickel-niobia alloys, on the other hand, a three-stage oxidation process was observed: an initial logarithmic oxidation, an intermediate linear growth and a final, general parabolic process. In the initial activated adsorption step, the adsorbed oxygen atoms on the metal generated fewer adsorption sites than were invalidated, resulting in a logarithmic oxidation with an activation energy of 11 to 19 kcal/mole. With subsequent growth of the thin oxide film, an equilibrium situation will be reached where the site generation and invalidation are equal. If more sites are generated than are invalidated, adsorption becomes very rapid, and another mechanism such as the diffusion of the cation through the oxide film controls further oxidation. Above 750°C, the oxidation product was a $NiO-Nb_2O_5$ solid solution which was non-adherent, glassy and transparent. The presence of the higher valent Nb^{5+} ion in the NiO lattice modified its defect structure in such a way as to enhance the oxidation rate of nickel. (INIS)

27280 (INIS-mf-12) DEVELOPMENT OF HIGH TEMPERATURE CERAMIC MATERIALS. Kulkarni, A. K.; Moorthy, V. K. (Department of Atomic Energy, Bombay (India). Chemistry and Metallurgy Committee). 1970. 11p. (CONF-700218-5). NTIS (U. S. Sales Only).

From Symposium on materials science research; Bangalore, India (24 Feb 1970).

The influence of composition and manufacturing conditions on the properties of the commonly used refractories is discussed on the basis of the respective phase diagrams. The factors to be considered for development of super refractories are reviewed and the difference in properties of super refractories and conventional refractories explained on the basis of the extent of glass formation. A brief mention of refractory materials UO_2, ThO_2, and ZrO_2 for special applications is included. (INIS)

27281 (INIS-mf-13) RESEARCHES ON CERAMIC MATERIALS IN INDIA. Sen, S.; Kumar, S. (Department of Atomic Energy, Bombay (India). Chemistry and Metallurgy Committee). 1970. 23p. (CONF-700218-15). NTIS (U. S. Sales Only).

From Symposium on materials science research; Bangalore, India (24 Feb 1970).

A review on the researches carried out in India during the present decade on ceramic raw materials and products is presented. The review covers: mica; ceramic and refractory raw materials and finished products; phase transformation and phase equilibrium studies; high temperature processes in oxide ceramics; ferroelectric and ferro-magnetic ceramics; and other ceramic products and processes. In the discussion on oxide ceramics, properties of beryllia, thoria, urania, and 99.9% pure oxides of niobium and tantalum were enumerated. (INIS)

27282 (INIS-mf-14) THE INFLUENCE OF MICROSTRUCTURE ON THE PROPERTIES OF CERAMIC PRODUCTS. Rao, S. V. K.; Moorthy, V. K. (Department of Atomic Energy, Bombay (India). Chemistry and Metallurgy Committee). 1970. 10p. (CONF-700218-12). NTIS (U. S. Sales Only).

From Symposium on materials science research; Bangalore, India (24 Feb 1970).

Commercial ceramic products are essentially constituted of polycrystalline minerals, glassy or crystalline bonding phases, and voids. It is realized that the properties of the products depend on the inter-relationships between these three constituents. The thermal conductivity depended on the macrostructural (texture) features like the distribution and extent of the voids in the product. Strength behavior at room temperature and at elevated temperatures depended mainly on the nature and distribution of the bonding, generally in a glassy phase. Macrostructural features such as orientation of the grains, grain size, and distribution, influenced magnetic and electrical properties. Though the exact relations between structural features and the physical properties were not yet precisely established, microstructural studies were of considerable help in the development of ceramic materials with the desired properties. This is particularly illustrated in the case of UO_2 pellets used as nuclear fuel. (INIS)

27283 (N-71-10590) THERMODYNAMIC PROPERTIES OF TERNARY REFRACTORY CARBIDES. III. ZIRCONIUM–HAFNIUM–CARBON. Technical Report, July 1, 1967–June 30, 1969. Hoch, Michael; Yamauchi, S. (Cincinnati Univ., Ohio). Dec 1969. Contract F33615-67-C-1565. 30p. (NASA-CR-111120; AFML-TR-69-209(Pt.3)). NTIS.

The thermodynamic properties of ternary zirconium hafnium carbide having the sodium chloride-type structure were studied, using the time-of-flight mass spectrometer. The ratios of the activities of the components were measured as a function of composition at 2440°K. From the variation of the ratio of activities

XUM

with composition, the pairwise interaction energies were obtained. The metal-metal interaction energy = 1.9 + or − 0.3 kcal/mole was similar to that in the body-centered cubic zirconium-hafnium metallic system. The difference between the zirconium-carbon and hafnium-carbon interaction energy was a function of composition. (STAR) (auth)

27284 REDUCTION OF POWDERED U_3O_8 BY LIQUID ALUMINUM. de Souza Santos, Tharcisio D. Metalurgia (Sao Paulo); 26: 283-9(Apr 1970). (In Portuguese).

Experiments are described on U_3O_8 in the form of loose powder, with liquid Al or liquid Al−U alloys as the reducers. Under the best of the operating conditions tested, charges of U_3O_8 powders were reduced by liquid Al protected by a cryolite cover or cryolite with 10% LiF. Recovery of U in such case was as high as 92%, and the U content in the resulting Al−U alloy was ~45%. The purpose of the work was to define the conditions of reduction of powdered U_3O_8 and study the influence of the principal variables on the separation and recovery of the products of fission and recovery of residual U from research reactor fuel plates. (Metals Abstr.)

27285 CALCULATION OF STRESS IN FAST REACTOR FUEL ELEMENTS. Matthews, J. R. (Atomic Energy Research Establishment, Harwell, Eng.). Atomwirt., Atomtech.; 16: 27-8(Jan 1971).

Four computer programs were developed to investigate the mechanical interaction of a cylindrical swelling fuel and its clad. The first model, NERFIX, considered the equilibrium interaction when the clad was rigid, the second, NERFS, was also for the equilibrium case but allowed creep deformation of the clad. The other two models calculated the transient behavior; CYLND, describing both fuel and clad, while, CAND, considered only the clad. The models were applied to a hypothetical case of an oxide type fuel, clad with 316 stainless steel and of reference dimensions. The fuel was assumed theoretically dense but with an axial hole reducing the smear density to 80%. (auth)

27286 IONIC DOMAIN FOR Y_2O_3-DOPED ThO_2 AT LOW OXYGEN ACTIVITIES. Hardaway III, John B.; Patterson, John W.; Wilder, D. R.; Schieltz, Jon D. (Iowa State Univ., Ames). J. Amer. Ceram. Soc.; 54: 94-8(Feb 1971).

The emf method was used to determine the lower limit of oxyge activity for essentially pure anionic conduction in $Th_{0.85}Y_{0.15}O_{1.925}$ from 775 to 1000°C. The results showed that the oxygen transference number was ≥0.99 when $\log P_{O_2} \geq -6.5\ (10^4/T°K) + 29$. (auth)

27287 DEFORMATION OF UO_2 AT HIGH TEMPERATURE. Canon, R. F.; Roberts, J. T. A.; Beals, R. J. (Argonne National Lab., Ill.). J. Amer. Ceram. Soc.; 54: 105-12(Feb 1971).

The effects of temperature, strain rate, and grain size on the mechanical properties of UO_2 were investigated using the four-point bending techniques. Strain rates were varied by two orders of magnitude, and test temperatures up to 1800°C were used. Data are presented on the ultimate tensile stress, yield stress, and plastic strain-to-fracture. Below the brittle-to-ductile transition temperature, T_c, the material fractured in a brittle manner, with no macroscopic plastic deformation. Between T_c and a second transition at a higher temperature, T_i, a small amount of plastic deformation was measured before fracture. Beyond T_i the strength of UO_2 decreased continuously, and extensive plasticity was observed. This high-temperature plasticity was characterized by a thermally activated rate-controlling process; this behavior was consistent with observations of creep behavior under high stresses. The following phenomenological equations for the strain rate fit the data for the material with 8-μm grain size above T_i:

$$\dot{\epsilon} = \frac{2}{T}\,\sigma_p^{4.23} \exp - \left(\frac{82{,}000}{RT}\right)/h$$

and

$$\dot{\epsilon} = \frac{2}{T}\,\sigma_{ssf}^{4.23} \exp - \left(\frac{87{,}000}{RT}\right)/h,$$

where σ_p and σ_{ssf} are the proportional limit and steady-state flow stress, respectively, and temperature T is in °K. (auth)

27288 SURFACE RELAXATION KINETICS OF URANIUM DIOXIDE. Maiya, P. S. (Argonne National Lab., Ill.). Acta Met.; 19: 255-62(Apr 1971).

Surface relaxation techniques were used to investigate surface and vapor-phase diffusion in stoichiometric uranium dioxide. A series of sinusoidal profiles, with wavelengths in the range 8 to 40 μ, were produced on the (100), (110), and (111) surfaces of UO_2. The relaxation to flatness of these profiles, due to capillary forces, was measured at temperatures from 1660 to 2035°C in a helium atmosphere. From the wavelength dependence of the decay constant, it was established that the relaxation kinetics were controlled predominantly by the diffusion of UO_2 vapor in helium. The vapor-phase diffusion coefficients were determined from the relaxation times associated with surface smoothing, and were compared with the predictions of kinetic theory. The agreement was within a factor of 2 to 4, and was within the limits of uncertainty of various kinetic parameters. The anisotropy of the measured relaxation rates and the relative importance of surface, volume and vapor-phase diffusion in UO_2 are discussed. (auth)

27289 THERMAL CONDUCTIVITY OF SINTERED CARBIDES AT ELEVATED TEMPERATURE. Michel, W. Tech. Mitt. Krupp, Forschungsber.; 27: No. 3-4, 79-82(Dec 1969). (In German).

The thermal conductivity of sintered WC−Co and WC−TiC−TaC−Co specimens was measured at 200 to 700°C to determine the effect of temperature on thermal properties. The composition of the alloys investigated is given in detail, and the measuring device is described. In all cases an increase of thermal conductivity with temperature was found. (Metals Abstr.)

27290 EMISSIVITY OF DIBORIDES OF TRANSITION METALS FROM GROUPS IV–VI. Samsonov, G. V.; Kunits'kii, Yu. A. (Inst. of Problems in Material Studies, Kiev). Dopov. Akad. Nauk Ukr. RSR, Ser. A; No. 11, 1048-50(1970). (In Ukrainian).

The work function of diborides was established to be less than that of pure metals and it decreases with increase of metals in the third transition group. Qualitative estimations are presented of the nature of transition metal diborides heat emission. Me−B and B−B bonds are of decisive importance in the diborides properties. (auth)

27291 REACTION OF OXIDES OF RARE EARTH ELEMENTS WITH BORON DURING SHOCK COMPRESSION. Adadurov, G. A.; Breusov, O. N.; Dremin, A. N.; Drobyshev, V. N. Zh. Neorg. Khim.; 15: 2887-9(Nov 1970). (In Russian).

The effects of shock waves on the oxides of lanthanum, neodymium, gadolinium, yttrium, ytterbium, and their mixtures with amorphous boron were studied. It was found that the phase transformations of the oxides and the formation of the corresponding hexaborides were controlled by high temperatures and reacted with crystalline imperfections which occurred upon the passage of the shock front. The shock waves prevent high residual temperatures and, therefore, do not promote chemical reactions because residual crystalline imperfections increase the mobility of atoms in the lattices of the compounds. (tr-auth)

Structure and Phase Studies

27292 (GEMP-714) DETERMINATION OF SOLIDUS–LIQUIDUS TEMPERATURES IN THE UO_{2+x} SYSTEM ($-0.50 < x < 0.20$). Latta, R. E.; Fryxell, R. E. (General Electric Co., Cincinnati, Ohio. Nuclear Systems Programs). Oct 1969. Contract AT(40-1)-2847. 38p. Dep. NTIS.

Solidus and liquidus temperatures for urania were determined to ±15°C over the composition range $UO_{1.50}$ to $UO_{2.23}$. The congruent composition was $UO_{2.00}$ (2865°C) and the monotectic composition was $UO_{1.46}$ (2425°C). The data were obtained by a highly refined thermal arrest technique, using samples totally enclosed in tungsten or rhenium. The absolute accuracy of the temperature measurements was verified by melting Ta, Mo, and Al_2O_3 (sapphire) as standard materials. The small bias caused by thermal gradients which existed in the sample during dynamic heating and cooling conditions was evaluated and was included in the ±15°C estimate of overall reliability. For oxygen excess compositions, there was general agreement in the data for W contained and Re contained samples in spite of the extremely different types of interaction between sample and container in the two systems. Rhenium dissolved in molten UO_{2+x} and separated out as the element on cooling with no net change in the urania. On the other hand, tungsten which dissolved in the melt separated out during cooling as a mixture of dendritic W and U_xWO_3 which had a perovskite structure. The remaining urania exhibited a lattice parameter corresponding to the stoichiometric composition. (auth)

27293 (RT/ING-(70)21) NUCLEAR FUEL CHARACTERIZATION. Allegro, A.; Ferrante, E.; Francia, M.; Modugno, G.; Stampa, L. (Comitato Nazionale per l'Energia Nucleare, Casaccia (Italy). Centro di Studi Nucleari). 1970. 15p. (CONF-700556-1). Dep. NTIS (U. S. Sales Only).

From Italian-Polish meeting; Warsaw, Poland (26 May 1970).

A careful investigation of the parameters influencing solid state densification phenomena is essential for obtaining ceramic fuel material, with pre-established form and dimensions, from

ceramic grade powders. The problem was studied by developing investigation methods and characterizing starting powders, where surfaces and porosities provide the forces which cause sintering phenomena; products deriving from the various operations of the fabrication processes; and finished materials. Moreover, a careful study of the microstructural variations of nuclear fuel, undergoing conditions simulating those typical of in-pile fuel operation is very important for an evaluation of the behavior of fuel under irradiation. Simulation studies and experiments carried out with different heating systems are described. (auth)

27294 STUDY OF THE REACTIVITY OF U_3O_8/Al DISPERSIONS. Gentile, Erberto Francisco; Cintra, Sebastiao Hermano Leite; Tracanella, Roberto Barata. Metalurgia (Sao Paulo); 26: 305-9(Apr 1970). (In Portuguese).

Fuel plates rolled to a total thickness of 2.45 mm, containing 65% dispersions of U_3O_8 in Al and clad with Al alloys were studied to identify the phases other than U_3O_8 and Al that were observed in the cores of the plates. The phases were tentatively identified as UO_2 and/or UAl_4. Their formation was attributed to the rupture of the Al_2O_3 barrier by a process of deformation during rolling, as well as a shear process caused by differential contraction and expansion between the ceramic and metallic phases during thermal alternation. The U_3O_8 powder used in the plates was in the -325-mesh range, with specific surface of 0.96 m^2/g and low density (7.3 g/cm^3). These properties, which are much below international specifications, probably influenced the outcome of the tests. (Metals Abstr.)

27295 HIGH-TEMPERATURE PHASE EQUILIBRIA IN THE $PbTiO_3$–$PbZrO_3$ SYSTEM. Moon, Ronald L.; Fulrath, Richard M. (Univ. of California, Berkeley). J. Amer. Ceram. Soc.; 54: 124-5(Feb 1971).

Phase equilibria in the $PbO-TiO_2-ZrO_2$ system above 900°C were studied by analyzing the heating curves of homogeneous powders. A three-phase region (liquid + ZrO_2 + PZT) was found to exist at high temperatures. The results agreed with those obtained by quenching methods. The quenching diagram was modified with lower solidus and liquidus temperatures and a peritectic temperature of 1360 rather than 1340°C. (G.M.C.)

27296 COMPOSITION AND MICROSTRUCTURE OF STABILIZED HAFNIUM DIOXIDE. Buckley, John D. (Langley Research Center, Hampton, Va.); Wilder, David R. Amer. Ceram. Soc. Bull.; 50: 254-5(Mar 1971).

X-ray diffraction and electron microprobe x-ray techniques were used to identify phases in and composition of hafnia bodies stabilized with CaO, Y_2O_3 and MgO. (auth)

27297 X-RAY- AND NEUTRON-DIFFRACTION STUDY OF ORDERING IN SOME ALLOYS OF THE TITANIUM–ZIRCONIUM–OXYGEN SYSTEM. Fykin, L. E.; Vavilova, V. V.; Kornilov, I. I.; Ozerov, R. P.; Solov'ev, S. P. (Inst. of Physical Chemistry, Moscow. Inst. of Metallurgy, Moscow). Dokl. Akad. Nauk SSSR; 194: 1374-7(21 Oct 1970). (In Russian).

Neutron and x-ray studies were made of a specimen of the ternary Ti–Zr–O system and of a series of specimens in homogeneous $Ti_{2-y}Zr_{1+y}O_x$ phases. The influence of oxygen and divergence from the stoichiometric state on the structure of the alloys was determined, and neutronograms for a $Ti_{0.62}Zr_{0.38}$–O specimen are given, as well as tabulated data on atomic ordering and diffraction maxima in the metals of the system. (R.V.J.)

27298 TWO-PHASE REGION IN TiC–Mo–30 PERCENT Ni ALLOYS. Suzuki, Hisashi; Hayashi, Kozi; Terada, Osamu (Tokyo Univ.). J. Jap. Inst. Metals; 35: 146-50(Feb 1971). (In Japanese).

The phenomena relating to the two-phase region in TiC–Mo–30% Ni alloys was studied in order to obtain basic information on the properties of TiC–Mo–Ni alloy systems. TiC–(0 ~ 30)% Mo–30% Ni alloys were vacuum-sintered at 1300 to 1450°C. The average cooling rate from sintering temperatures to 700°C was about 24°C/min. The width and location of two-phase region in each alloy seemed not to be affected by the sintering temperatures. The two-phase region of the straight alloy was in the range of 18.1 to 19.3% C (calculated in terms of the carbon content in carbide). The two-phase region in the straight alloy was extended with increasing addition of Mo. For example, the phase region of the 30% Mo alloy existed in the range of 12.7 to 14.5% C. The added Mo appeared to dissolve in titanium carbide in the form of Mo_2C. Compositions of the binder and carbide phases of each alloy showed a definite variation in the two-phase region with carbon content, as was confirmed in various WC–Co base alloys. The dissolved amount of Ti in the binder phase of the straight alloy was found to change sharply in the two-phase region from a minimum of about 3% (in the highest carbon alloy) to a maximum of about 10% (in the lowest carbon alloy). Even in the alloys containing Mo, the dissolved amount of Ti was nearly the same as in the straight alloy, but in this case Mo also dissolved in the range from about 0 to 6% depending on the Mo and the carbon contents. The dissolved amount of Ni in titanium carbide was about 0.4% in the straight alloy. The amount of Mo dissolved in the ϵ phase was about 5% in the alloys containing Mo. The corrosion and oxidation resistance of the alloys were confirmed to vary as can be expected from the change in composition of the binder phase. (auth)

27299 X-RAY STUDY OF THE CHROMIUM–MANGANESE–BORON SYSTEM. Talagus, V. S.; Kuz'ma, Yu. B. Visn. L'viv. Derzh. Univ., Ser. Khim.; No. 11, 21-4(1969). (In Ukrainian).

The Cr–Mn–B system was studied by x-ray and microstructural analyses, and an isothermal section constructed at 800°C. Continuous series of solid solutions were shown to exist for CrB_2-MnB_2, $Cr_3B_4-Mn_3B_4$, and Cr_2B-Mn_4B. The solubility of Mn in CrB was 10 at. % with lattice constants a = 2.971, b = 7.839, and c = 2.931 Å; that of Mn in Cr_5B_3 was ~5 at. % with a = 5.461 and c = 10.088 Å. The solubility of Cr in MnB was 20 at. %. (11 references) (Metals Abstr.)

27300 PHASE EQUILIBRIA IN THE TITANIUM–VANADIUM–BORON AND TITANIUM–MANGANESE–BORON SYSTEMS. Kuz'ma, Yu. B.; Paitash, T. P.; Baidala, S. I. Visn. L'viv. Derzh. Univ., Ser. Khim.; No. 11, 18-20(1969). (In Ukrainian).

X-ray and microstructural analyses were used to study the Ti–V–B and Ti–Mn–B systems. Isothermal sections were obtained at 1400 and 800°C. The compound TiB dissolved V up to 25 at. % and the compound VB dissolved Ti up to 15 at. %, with the lattice constants of the limiting composition being a = 3.11, b = 8.19, and c = 3.000 Å. V_3B_2 dissolved Ti up to 15 at. % with a = 5.75 and c = 3.04 Å. No solid solutions based on binary compounds were found in the Ti–Mn–B system. (Metals Abstr.)

27301 CRYSTAL STRUCTURE OF THE BORON–THORIUM SYSTEM. A NEW BORIDE WITH TYPE YB_{66} STRUCTURE. Naslain, Roger (CNRS, Talence, France); Etourneau, Jean; Kasper, John S. J. Solid State Chem.; 3: 101-11(Feb 1971). (In French).

A δ phase single crystal was obtained in the boron–thorium system by slow cooling of a liquid corresponding to an atomic ratio B/Th = 70. The structure was established from two sets of 650 independent reflexions. Absorption correction was made necessary by the thorium atoms. From least-squares refinement, Fourier syntheses and electron density maps it appears that the δ phase is isotypic with the yttrium boride YB_{66}. The crystal is cubic with a = 23.53 Å; the space group is Fm3c, O_h^5. There are 1584 boron atoms and 24 thorium atoms in the unit cell; 1248 boron atoms are contained in 13 icosahedron units corresponding to the formula $B_{12}(B_{12})_{12}$. B–B bonds within icosahedra range from 1.749 to 1.911 Å. The shortest inter-icosahedral bond is 1.598 Å, the longest 1.837 Å. The remaining boron atoms are statistically distributed in channels resulting from packing of the $B_{12}(B_{12})_{12}$ units and form nonicosahedral cages as in YB_{66}. The thorium atoms are inserted in the channels; the thorium–boron bonds range from 2.71 – 2.84 Å. (auth)

27302 INVESTIGATIONS INTO THE Eu–Eu_2O_3, THE Eu–Pt–Eu_2O_3, THE Sm–Sm_2O_3, AND THE Yb–Yb_2O_3 SYSTEMS. Bedford, R. G.; Catalano, E. (Univ. of California, Livermore). J. Solid State Chem.; 3: 112-24(Feb 1971).

The binary system Eu–Eu_2O_3 has been examined in detail over the composition range EuO to Eu_2O_3 at 1500°C. Only three oxide phases were found: EuO, Eu_3O_4, and Eu_2O_3. Both EuO and Eu_3O_4 exhibit very narrow composition limits, while the monoclinic sesquioxide is stable over the composition range $EuO_{1.45}$ to $EuO_{1.50}$ at 1500°C. The melting points found for the three phases were 1900°C for EuO, 2000°C for Eu_3O_4, and 2300°C for Eu_2O_3. Europium was quantitatively extracted from EuO by reaction with platinum in sealed capsules at 1500°C, which resulted in the formation of an intermetallic phase plus a higher oxide of europium. The most europium-rich intermetallic phase found in these studies, $EuPt_{2+x}$, has the fcc $MgCu_2$ structure and is stable over the composition range $EuPt_{2.0}$ to $EuPt_{2.8}$ at 1500°C. Besides $EuPt_2$, two phases were encountered in the Eu–Pt alloys which contained more than 75 at. % Pt. These are tentatively designated as Eu_2Pt_7 and $EuPt_3$. No crystalline phases other than the sesquioxides were found in the Sm–Sm_2O_3 or the Yb–Yb_2O_3 systems. (auth)

27303 INVESTIGATION OF REACTIONS IN SOLID PHASES IN THE SYSTEMS Y_2O_3–Al_2O_3 AND Y_2O_3–Ga_2O_3 WITH THE LUMINESCENCE SPECTRA OF EUROPIUM. Trofimov, A. K.; Savinova, I. R. Zh. Neorg. Khim.; 15: 2994-7(Nov 1970). (In Russian).

The luminescence spectra of europium was assumed as the basis of qualitative and semiquantitative estimate of chemical reactions

XUM

in the solid phases between the oxides of yttrium and aluminum or gallium. Samples were prepared by ammonia precipitation of the mixture of hydroxides activated by europium and dried and roasted for 2 hours at 800 to 1300°C. By comparing the luminescence spectra of europium with the oxides and their compounds, a curve was obtained that illustrated the region of existence of each compound. Relations of composition and calcination temperatures were also established. (tr-auth)

27304 METAL-RICH METAL-METALLOID PHASES. Stadelmaier, H. H. (North Carolina State Univ., Raleigh). pp 141-80 of Developments in the Structural Chemistry of Alloy Phases. /Giessen, B. C. (ed.). New York; Plenum Publishing Corp. (1969).

From Conference on Developments in the Structural Chemistry of Alloy Phases, Cleveland, Ohio. See CONF-671092.

A review is presented of borides, carbides, nitrides, and oxides of transition elements, often in combination with non-transitional elements. In the metal rich compounds the metalloid atom is isolated and surrounded by six or eight transition metal atoms in close contact with each other. The metalloid atom is therefore interstitial, sometimes in the strict sense that the phase fields include metalloid-free ("unfilled") compositions. Five structure types are singled out because they occur extensively. There may be some initial objection to having borides, carbides, nitrides, and oxides lumped together in one class. It is indeed rare, but not impossible, to find an individual structure type that spans the entire range from borides to oxides. On the other hand, there is so much overlap between types that a common classification does seem justified. (auth)

Radiation Effects

Refer also to abstracts 27839, 28633, 28687, 28688, 28691, and 28765.

27305 (N-70-35897) GAMMA RADIATION CHARACTERISTICS OF PLUTONIUM DIOXIDE FUEL. Gingo, P. J.; Dore, M. A. (Jet Propulsion Lab., Pasadena, Calif.). 15 Jun 1970. Contract NAS7-100. 37p. (NASA-CR-110136; JPL-TR-32-1481). NTIS.

An extensive investigation was performed to characterize the net gamma ray source intensity and spectrum for PuO_2 fuel. All major sources were considered, including the gamma radiation from the various plutonium isotopes and their decay, and the decay of fission products, as well as gammas due to spontaneous fission and (α,n) reactions with ^{18}O and other light elements. Particular attention was paid to ^{236}Pu and its daughter products. These sources are tabulated for 20 energy groups ranging from 1 keV to 7 MeV. For each of the age-dependent composite source spectra determined, gamma ray fluxes are calculated for three different thicknesses of fuel in a typical PuO_2-fueled capsule. The gamma fluxes are determined at the capsule surface, as well as at several exterior points. (auth) (STAR)

Plastics and Other Materials

Refer also to abstracts 26281, 27188, 27222, and 27271.

27306 POSITRON ANNIHILATION IN IRRADIATED TEFLON. Hsu, F. H.; Hadley, J. H. Jr. (Georgia State Univ., Atlanta). Phys. Lett.; 34A: 317-18(5 Apr 1971).

Positron annihilation measurements in Teflon irradiated in air and vacuum show that the intermediate lifetime (τ_3) component is not due to a pick-off process. The primary effect to radiation is a reduction in the intensity of the τ_3 component. (auth)

27307 ADVANCED FILAMENTRY COMPOSITES FOR PRIMARY AIRCRAFT STRUCTURES. Dastin, S. (Grumman Aircraft Engineering Corp., Bethpage, N. Y.). Appl. Polym. Symp.; No. 15, 81-92(1970).

From Polyblends and Composites Conference, Brooklyn, N. Y. See CONF-690651.

Advanced filamentary composites considered for primary aerospace structural applications, particularly boron-epoxy, are discussed and several typical examples are given. Mechanical property data, preliminary design allowables, and resultant weight savings are presented along with the generalized manufacturing and quality control techniques presently employed. (auth)

XUM

PHYSICS (GENERAL)

Astrophysics and Cosmology

Cosmic Ray Exposure Ages

27308 NOBLE GAS ABUNDANCES IN LUNAR MATERIAL: COSMIC-RAY SPALLATION PRODUCTS AND RADIATION AGES FROM THE SEA OF TRANQUILITY AND THE OCEAN OF STORMS. Bogard, D. D. (Manned Spacecraft Center, Houston, Tex.); Funkhouser, J. G.; Schaeffer, O. A.; Zaehringer, J. J. Geophys. Res.; 76: 2757-79(10 Apr 1971).

The major noble gas component in lunar rocks can be ascribed to spallation reactions of galactic cosmic rays. Other noble gas components arise from radiogenic decay of K, U, and Th, gases implanted on exterior rock surfaces by the solar wind, adsorbed atmospheric gases, and possibly from solar-flare interactions. No evidence was found in lunar rocks of either primordial noble gases or the decay products of extinct radionuclides. The isotopic compositions of the spallation-produced isotopes of neon and of ^{36}Ar and ^{38}Ar are shown to be similar to those found in stone meteorites. Small variations in the spallation ^{21}Ne/^{22}Ne ratios may exist. Spallation ^{4}He, and therefore the spallation ^{4}He/^{3}He ratio, could not be determined because of the large radiogenic component. Spallation xenon spectra were determined in a large number of rocks from both Apollo 11 and 12. In general, the spectra are similar to spallation xenon in stone meteorites, except that large and variable excesses of ^{131}Xe exist. The measured spallation ^{131}Xe/^{128}Xe in surface or near-surface samples of forty crystalline rocks ranged from 2.2 to 5.1. These large ^{131}Xe excesses are attributed to a lower energy spectrum in these rocks, either because of high shielding or solar-flare protons. Spallation krypton spectra were determined in a smaller number of crystalline rocks, and for masses 78 through 83 the spectra are similar to krypton in stone meteorites. Spallation krypton 84 occurs in lower relative yield than in meteorites, and there is a difference in the spallation ^{84}Kr/^{83}Kr ratio between Apollo 11 rocks and Apollo 12 rocks. These variations in spallation ^{84}Kr are attributed to differences in the chemistry of Apollo 11 and Apollo 12 rocks, and specifically the high and variable Y and Zr concentrations. The concentrations of the major spallation-produced noble gas isotopes ^{3}He, ^{21}Ne, ^{38}Ar, and ^{126}Xe in the lunar rocks can be expressed primarily as a function of the exposure times of the rocks and of the concentrations of the principal target elements. Plots of ^{21}Ne/Mg + Si versus ^{3}He, ^{38}Ar/Ca versus ^{3}He, and ^{126}Xe/Ba versus ^{3}He yield essentially linear relationships within analytical errors, and there is no consistent evidence of major random diffusion losses. Assuming 2π geometry for cosmic-ray bombardment of the lunar surface, and typical ^{3}He production rates for stone meteorites, spallation production rates were calculated for the noble gases in lunar crystalline rocks per unit weight of the principal target elements as: (units of 10^{-8} cc STP/g target/10^{6} years) ^{21}Ne/Mg + Si = 0.56, ^{38}Ar/Ca = 1.7, and ^{126}Xe/Ba = 0.13. These values are not unlike those obtained for stone meteorites. Utilizing the derived noble gas production rates as a function of chemistry, cosmic-ray exposure ages of rocks from both the Sea of Tranquility and Ocean of Storms based on ^{3}He, ^{21}Ne, ^{38}Ar, and ^{126}Xe were calculated. Where data exist, these were compared with ages based on ^{3}H–^{3}He, ^{22}Na–^{22}Ne, ^{39}Ar–^{38}Ar, and ^{81}Kr–Kr. Except for a few rocks that may exhibit gas losses, the various exposure ages generally agree within experimental uncertainties. The range of exposure ages is 30 to 500 m.y. for the Sea of Tranquility and 30 to 300 m.y. for the Ocean of Storms; the predominant characteristic of the ages is their wide scatter. Proximity of rocks on the lunar surface is apparently not sufficient criterion for assuming their common origin from a single cratering event. The fact that no lunar rock analyzed, except a glass splatter, exhibited an exposure age less than 30 m.y. implies that burial in the regolith may constitute a part of the history of lunar rocks, and that erosion and break-up rates of rocks on the lunar surface is less efficient than for stone meteorites in space. (auth)

Stars

Refer also to abstract 28308.

27309 (ANU-P-471) EXPERIMENTAL INVESTIGATION OF ^{16}O + ^{12}C NUCLEAR BURNING AT STELLAR ENERGIES. Patterson, J. R. (Adelaide Univ., (Australia). Dept. of Physics); Nagorcka, B. N.; Symons, G. D.; Zuk, W. M. (Australian National Univ., Canberra. Dept. of Nuclear Physics). [1970]. 19p. Dep. NTIS (U. S. Sales Only).

The ^{12}C(^{16}O,α)^{24}Mg and ^{12}C(^{16}O,p)^{27}Al reactions were studied for center-of-mass energies from 4.54 to 8.53 MeV to provide experimental data on their cross sections in the region of astrophysical interest. Excitation functions and angular distributions were measured and used to estimate the total and partial reaction cross sections for energies down to 3 MeV, at which ^{16}O + ^{12}C nuclear burning is expected to be important in stars. The cross sections for these reactions show a pronounced resonance structure similar to that found in the ^{12}C + ^{12}C system. These "quasi-molecular" resonances are grouped just below the Coulomb barrier energy and do not appear to extend below 6 MeV in the ^{12}C + ^{16}O system. (auth) (Australia)

27310 (CERN–70-30(Vol.2), pp 735-57) DYNAMICS OF THE RAPID NEUTRON CAPTURE PROCESS. Cameron, A. G. W.; Delano, M. D.; Truran, J. W. (Yeshiva Univ., New York, Belfer Graduate School of Science, National Aeronautics and Space Administration, New York, Goddard Inst. for Space Studies).

In International conference on the properties of nuclei far from the region of beta-stability; Leysin, Switzerland (31 Aug 1970).

Previous studies of the rapid neutron-capture mechanism of nucleosynthesis ("r" process) were carried out with the assumption of constant temperature and density during the reactions. The "dynamics" of such a process thus consists essentially of the beta decay of neutron-rich isotopes in local statistical equilibrium for a given Z. An attempt to improve the treatment of this process is made by employing a nuclear-reaction network containing 6000 nuclei whose neutron capture cross sections, neutron binding energies, beta decay rates, and delayed neutron branching ratios are calculated from nuclear systematics based upon a mass formula. Beta-decay rates much larger than in the work of Seeger, Fowler, and Clayton are found. It was demonstrated that charged-particle reactions in an expanding neutron-rich supernova envelope are likely to form ^{79}Ni seed nuclei. The rapid neutron capture from this seed nucleus for various expanding supernova envelope adiabats is studied. Neutron captures do not proceed rapidly until the temperature falls to about 1.5×10^{9} °K. Virtually all of the neutrons have been captured by the time the temperature falls to 6×10^{8} °K. Delayed-neutron effects tend to produce a small odd–even abundance effect in the final material, consistent with observed abundances. The influence of cooling and expansion of the material on the final abundances is demonstrated to be substantial for this choice of temperature and density conditions. (auth)

27311 (CERN–70-30(Vol.2), pp 759-68) NUCLEI IN NEUTRON MATTER. Boerner, G. (Max-Planck-Institut fuer Physik und Astrophysik, Munich (West Germany)).

In International conference on the properties of nuclei far from the region of beta-stability; Leysin, Switzerland (31 Aug 1970).

The amounts of nuclei present in a neutron star are calculated using the standard methods of nuclear-matter theory and the Reid soft-core potential under various assumptions. (R.W.R.)

27312 THE DISTRIBUTION OF GAS AND DUST IN THE ORION NEBULA. Muench, G.; Persson, S. E. (California Inst. of Tech., Pasadena). Astrophys. J.; 165: 241-58(15 Apr 1971).

Photoelectric measurements of Balmer-line intensities at 4000 points on the Huyghenian region of the Orion Nebula, with an angular resolution of 3 arc sec, were analyzed to show the following: (1) The differential reddening that affects nebular radiation can be accounted for only if dust particles are mixed with the ionized gas and the wavelength dependence of the dust-absorption coefficient is the same as that determined for the Trapezium stars. (2) The intensity and reddening gradients, on the average, have the same sign. This fact indicates that dust is well mixed with the gas and that, statistically, fluctuations in gas density are positively correlated with variations in dust density. The behavior of the intensities of the He I lines at 10830, 7065, and 5876 Å, measured at 150 points covered by Balmer-line observations, can be understood only if dust, absorbing resonantly trapped λ10830 photons, is mixed with the gas. (auth)

27313 OPTICAL STUDIES OF CASSIOPEIA A. II. UBV PHOTOMETRY OF FIELD STARS. van den Bergh, Sidney (Univ. of Toronto). Astrophys. J.; 165: 259-63(15 Apr 1971).

UBV photometry is reported for seventy-eight stars located within 300″ of the center of expansion of Cas A. These observations show that there are no OB stars with $A_v < 6$ mag within 4 pc of the supernova. The origin of the H II region surrounding Cas A is briefly discussed. (auth)

27314 EXTENDED MODEL ATMOSPHERES FOR THE CENTRAL STARS OF PLANETARY NEBULAE. Cassinelli, Joseph P. (Univ. of Washington, Seattle). Astrophys. J.; 165: 265-84(15 Apr 1971).

Procedures for the construction of spherical stellar model atmospheres are developed and applied to the calculation of three gray and three nongray model atmospheres for the central stars of planetary nebulae. The models are calculated under the classical assumptions of hydrostatic, radiative, and local thermodynamic equilibrium. Radiative transfer for spherical geometry and the $1/r^2$ dependence of gravity are taken into account. The transfer equation is solved by using the discrete-S_N method of Carlson and Lathrop and a difference form of the diffusion-approximation equation. The atmospheres are brought to radiative equilibrium by using modifications to spherical geometry of the flux-correction procedure of Unsöld for the gray case, and of the temperature-correction procedure of Lucy for the nongray case. Models which have luminosity constant with r to within 1.5% are calculated. All of the models have the same geometrical extension, and in each case the geometrical depth from $\langle\tau\rangle = 0.001$ to $\langle\tau\rangle = 1.0$ is approximately equal to the radius of curvature of the atmosphere at $\tau = 1.0$. The three nongray models have temperatures, at $\langle\tau\rangle = \frac{2}{3}$, of 3.7×10^{4}°, 4.9×10^{4}°, and 9.5×10^{4}°K. The emergent continuous flux of the models shows emission edges at the Balmer and Lyman limits and strong absorption edges in the far-ultraviolet. These features are explained as being due to the rapid increase of the temperature with optical depth and by geometrical enhancement of the Schuster mechanism. The flux distribution in the visual and infrared matches rather well the continuum of the Wolf–Rayet stars observed by Kuhi. (auth)

27315 MASS LOSS FROM M STARS. Gehrz, R. D.; Woolf, N. J. (Univ. of Minnesota, Minneapolis). Astrophys. J.; 165: 285-94(15 Apr 1971).

Infrared observations of M giants and supergiants show that circumstellar dust shells are frequently present. The observations permit the radii and densities of the dust shells to be determined. It is shown that radiation pressure drives the particles through the gas at a velocity that varies with the density. The momentum coupling drives the gas out of the star. Velocities of gas ejection are estimated and compared with optical and radio measures. Rates of mass ejection are calculated for a number of stars. These rates are compared with the rates required to maintain the interstellar medium at its present density. (auth)

27316 EVOLUTIONARY MODELS OF STARS OF 15 AND 30 $M_\odot$. Simpson, Erik E. (Univ. of California, Berkeley). Astrophys. J.; 165: 295-316(15 Apr 1971).

Evolutionary models are computed for stars of 15 and 30 $M_\odot$ with a composition given by the mass abundances X = 0.75, Y = 0.23, Z = 0.02. Parallel calculations are carried out with and without allowance for semiconvection or full convection in shells of intermediate mass. In the case of semiconvection, the stability criterion that has been adopted is $dT/dP = (dT/dP)_{ad}$. After the main-sequence phases the models with intermediate mixing develop fully convective shells that greatly alter the behavior of the models during core helium burning. The models with the convective shells spend much of their helium-burning lifetimes as blue supergiants, whereas the models without convective shells rapidly become red supergiants. From an examination of the observations of h and χ Persei it is concluded that the convective-shell models are more likely to be physically correct. (auth)

27317 NARROW- AND BROAD-BAND PHOTOMETRY OF RED STARS. VI. LUMINOSITIES AND TEMPERATURES FOR OLD DISK-POPULATION RED STARS OF HIGH LUMINOSITY. Eggen, O. J. (Australian National Univ., Canberra). Astrophys. J.; 165: 317-34(15 Apr 1971).

(UBVRI) observations of red giants in old disk-population groups and clusters are discussed. The form of the red-giant sequence changes radically for masses near that of the brighter Hyades stars ($\sim 2.5 M_\odot$) with the giant sequences of less massive stars of the old disk population crossing that of the Hyades at R – I near +0.4 mag (log T_e near 3.65) and rejoining it near +1.2 mag (log T_e near 3.50). Also, the giant sequences for both the old and young (Hyades) disk populations show a discontinuity that is not predicted by the interior models. The boundary of the instability region for red variables is near R – I = +0.8 mag (log T_e near 3.55). The quasi-periodic, small-amplitude variables of the young (Hyades) disk population have characteristic periods that are about one-half that of old disk variables of the same temperature. The old disk-population variables are also distinguished by a marked, large-amplitude, secondary oscillation with a period about an order of magnitude longer than the characteristic period. The reddest, and longest-period variables in both populations are nearly indistinguishable by their light curves alone. Observations of two old disk-population, early-type carbon stars, both possible members of the Wolf 630 Group, show them to be indistinguishable in the (M_{bol}, R – I) plane from normal stars of the same temperature. Similar results are obtained for a late-type (R8) carbon star of the young disk population that forms a wide pair with a normal K-type giant. (auth)

27318 A PHOTOMETRIC STUDY OF FOUR CLASSICAL CEPHEIDS. Schmidt, E. G. (Australian National Univ., Canberra). Astrophys. J.; 165: 335-63(15 Apr 1971).

Model atmospheres were used to calculate continuum energy distributions and broad-band colors for comparison with spectral scans and broad-band photometry of the Cepheids U Sgr, η Aql, S Nor, and Y Oph. The effect of line blocking on the B – V, V – R, and R – I colors was determined from the measured colors and scans, and the color excesses were found. The scale and variations of the temperatures of these stars are discussed in the light of available data. The variation of blanketing as a function of turbulent velocity, temperature, and gravity is discussed; and it is found that the blanketing variations are consistent with the variations of the atmospheric parameters. The radii of these Cepheids were determined from the monochromatic light curves and model atmospheres. It was found that, due to blanketing effects, the radii derived by the usual Wesselink method may be too large by up to 30% for some Cepheids. (auth)

27319 PHOTOELECTRIC PHOTOMETRY OF THE DWARF CEPHEID HD 199757. Chambliss, Carlson R. (Georgetown Coll. Observatory, Washington, D. C.). Astrophys. J.; 165: 365-8(15 Apr 1971).

The dwarf Cepheid HD 199757 was observed on three nights with U, B, V photometry at the Cerro Tololo Inter-American Observatory. The period was found to be 0.0671835d, making it one of the shortest known among the dwarf Cepheids. No significant variations in the light curve from cycle to cycle were found. The colors of HD 199757 are normal for its spectral type. (auth)

27320 BINARY STARS AMONG CATACLYSMIC VARIABLES. XII. PHOTOELECTRIC OBSERVATIONS FROM THE SOUTHERN HEMISPHERE. Mumford, George S. (Tufts Univ., Medford, Mass.). Astrophys. J.; 165: 369-80(15 Apr 1971).

Results of photoelectric observations of various cataclysmic variables are presented. The U Geminorum star Z Cha was found to be an eclipsing binary of short period; periodic brightness variations of Nova RR Pic were confirmed; BV Cen may show periodic features identifiable with an eclipse; no changes from previously established periods of EX Hya and WZ Sge were found. (auth)

27321 PAIR CORRELATIONS IN STELLAR SYSTEMS. Miller, R. H. (Univ. of Chicago). Astrophys. J.; 165: 391-7 (15 Apr 1971).

The structure of the pair correlation in stellar dynamical systems was investigated through numerical experiments on small (32-body) systems. A very strong negative pair correlation prevents two particles from approaching each other too closely in the μ-space. There is weak attraction in the projection to configuration space. The dominant dependence appears to be on the pair energy. Possible forms for the pair correlation function are suggested. The result implies that all s-particle correlation functions are important up to and including the n-particle correlation in an n-body system. (auth)

27322 SPECTROPHOTOMETRY OF NOVA SERPENTIS 1970. Wagner, Raymond L.; Tull, Robert G.; Byrd, Gene G.; Loren, Robert B. (Univ. of Texas, Austin). Astrophys. J.; 165: 431-7 (15 Apr 1971).

Spectrophotometric observations of Nova Serpentis 1970 near maximum light are reported. The observations were used to derive the absolute energy distribution of the nova. (auth)

27323 EFFECTS OF DUST AND LYMAN-ALPHA RADIATION ON THE DYNAMICAL EVOLUTION OF PLANETARY NEBULAE. Kovach, William Stephen. Columbus, Ohio; Ohio State Univ. (1970). 110p. University Microfilms Order No. 71-7495.

Thesis.

The dynamics of spherically expanding envelopes illuminated by a very hot central star such as observed in some planetary nebula is investigated. It is assumed that the expanding envelope consists of an H II region surrounded by an optically thick H I region containing a mixture of hydrogen and dust grains. It is further assumed that Lyman-alpha photons are unable to diffuse into the H I region while they are in the core of the line but are able to cross the H II region unattenuated. The resulting reflec-

tions from the expanding ionization front, analogous to a moving mirror, Doppler shifts the Lyman-alpha photon from the core into the red wing of the line. Since the optical thickness in the wing is much less than the core, the Lyman-alpha photon will be able to diffuse into the H I region after a number of reflections. The dust imbedded in the gas, however, is able to absorb almost all the Lyman-alpha photons before they reach the outer boundary of the H I region. The resulting reradiation of the Lyman-alpha energy into the infrared region is evaluated for different dust densities as a function of time. Only graphite dust particles are considered. To determine if the dust is able to survive in the H II region, once the ionization front has passed, the sputtering, due to collisions with protons, and evaporation rate of the grains are calculated. The dynamical equations are integrated by evaluating the forces due to the Lyman-alpha pressure, Lyman continuum pressure, and the gas pressure of the H II region. The resulting models were compared to the infrared observations and the expansion velocity of the planetary nebula NGC 7027. It was found that for nebula containing .1 $M_\odot$ or less, Lyman-alpha could accelerate them to a velocity of 20 km/sec in 1500 years. The calculated infrared flux distributions can match quite well the observations of NGC 7027. (Diss. Abstr. Int., B)

27324 SOME RELATIVISTIC INTEGRAL THEOREMS. Forrester, David A. (Cambridge Univ., Eng.). Mon. Notic. Roy. Astron. Soc.; 151: 149-56(1971).

The general relativistic form of a well-known classical integral theorem is obtained. Upper and lower bounds are then found for the gravitational potential energy, and some expressions are given for the average pressure of a relativistic star. Some limits on a pressure integral are given. (auth) (UK)

27325 A NOTE ON NEUTRAL STABILITY AGAINST CONVECTION IN GENERAL RELATIVITY. Forrester, David A. (Cambridge Univ., Eng.). Mon. Notic. Roy. Astron. Soc.; 151: 157-9(1971).

The conditions obtained by Islam (Mon. Notic. Roy. Astron. Soc., 150: 237(1970)) for the nonexistence of neutral modes of convection in general relativity have been relaxed slightly. For the condition $p \leq \beta\rho$ where p is the pressure and ρ is the density of mass-energy including internal energy, $\beta = 0.15$ for $l = 2$ and $\beta = 1.83$ for $l = 3$ (l is the spherical harmonic index of the mode). (auth) (UK)

27326 ANGULAR MOMENTUM PROBLEM IN STAR FORMATION. Prentice, A. J. R.; ter Haar, D. (Oxford Univ.). Mon. Notic. Roy. Astron. Soc.; 151: 177-84(1971).

The difficulties of theories of star formation are discussed, especially the problems of shedding of angular momentum and of magnetic flux. It is shown that in the Reddish-Wickramasinghe grain-cloud theory the collapse of the grain-cloud will for the first 10^7 year or so proceed "spoke-like," which means that the grains will, during their collapse, lose angular momentum to the neutral gas component in such a way that they essentially retain their original angular velocity. In this way the grain-cloud may lose at least 99% of its original angular momentum. (auth) (UK)

27327 BETA CEPHEI STARS: A LINEAR NONADIABATIC ANALYSIS OF RADIAL OSCILLATIONS. Davey, William Robert. Boulder, Colo.; Univ. of Colorado (1970). 92p. University Microfilms Order No. 71-5883.

Thesis.

In an attempt to provide a theoretical interpretation of this class of variable stars, the pulsational stability toward infinitesimal radial oscillations of stellar evolutionary models near the observed region of the H-R diagram occupied by β Cephei stars was investigated. A linearized, fully nonadiabatic stability analysis incorporating the extra thermal-imbalance terms caused by the lack of thermal equilibrium in the static models was used as a test for pulsational stability. The immediate post-main-sequence evolutionary phases were examined first. Evolutionary sequences for stars of 10 and 15 $M_\odot$ were constructed from the homogeneous main sequence through hydrogen exhaustion in the core. All of the models were found to be stable against small-amplitude radial oscillations in the fundamental mode and in several of the lowest few overtones. Next, the immediate pre-main-sequence gravitational contraction phases were investigated. Several 15 $M_\odot$ models that passed through the β Cephei region during their gravitational contraction to the main sequence were examined for stability. These pre-main-sequence models also proved to be completely stable. Because all of the models in these "normal" phases of evolution were found to be stable, yet another evolutionary track for a 2.5 $M_\odot$ star was constructed, which was the product of significant mass loss from a heavier star during the red-giant stage of evolution. This highly evolved star was greatly overluminous for its mass and did pass through the β Cephei region. Unfortunately, these lower-mass models were also found to be stable. The main conclusion of this study is that no destabilizing mechanism has been found within a single stellar model calculated that can excite radial pulsations. It also appears that the additional effects of thermal imbalance terms probably can be safely neglected in future stability studies of stellar models evolving into the β Cephei region. (Diss. Abstr. Int., B)

27328 STELLAR WINDS AND RELATED FLOWS. Holzer, Thomas Edward. San Diego, Calif.; Univ. of California (1970). 326p. University Microfilms Order No. 71-4230.

Thesis.

A review is presented in which certain aspects of steady, radial flows of significance in astrophysics and space physics are discussed. Most emphasis is placed on the relatively formal and well-established features of the general theory of such flows, the purpose being to show that the results are of wide applicability and may be used in discussing not only stellar winds, but also galactic winds, comet winds, the polar wind (and related processes in planetary ionospheres), and of course the classical accretion problem. Certain specific flow problems are considered in some detail. The interaction of the solar wind with interstellar hydrogen and helium is dealt with, and it is shown that this interaction provides a suitable mechanism for producing He^+ ions in the solar wind. A detailed discussion is given of plasma transport in the upper atmosphere of the Earth, with special emphasis on the polar wind, the most complex of the physical phenomena considered here. Kinetic and hydrodynamic models of an expanding ion exosphere are compared. It is found that the flow characteristics of a constituent flowing supersonically throughout the exosphere are well described by ordinary hydrodynamic equations with isotropic pressure, while temperature anisotropies can be described with modified CGL-type equations. A brief description of the basic equations that can be used to describe the neutral atmosphere of a comet is given. Synthetic energy per charge spectra of solar wind ions is calculated and compared with observational data. Among other things evidence is found for the presence of ^{56}Fe ions in the solar wind. A diffusion coefficient appropriate to accidentally resonant charge exchange is calculated for thermal nonequilibrium conditions. This result is used in the calculations. (Diss. Abstr. Int., B)

27329 STELLAR DIAMETERS FROM OCCULTATIONS. Berg, Richard Allen. Charlottesville, Va.; Univ. of Virginia (1970). 90p. University Microfilms Order No. 70-26,603.

Thesis.

In search of angular structure in stellar sources, the Virginia dual-channel photometer was used at McCormick Observatory's Fan Mountain Station (32-inch reflector) and Kitt Peak National Observatory (#2 36-inch reflector) to record occultations of stars by the Moon. The results of observations of seven occultations are summarized. Upper limit values quoted represent mean errors of observation. In terms of gross angular structure, occultations of stars provide excellent opportunities for discovery of very close binaries, especially those with low-inclination orbits where spectroscopic methods fail. Angular diameter determinations are sensitive to signal/noise, bandwidth smoothing, aperture smoothing, and time-constant smoothing. Using the instrumental system described, the practical limit to resolution is on the order of 0.001 and is set principally by bandwidth smoothing. (TSS) (Diss. Abstr. Int., B)

27330 LIGHT VARIATIONS OF CLOSE BINARIES CONFORMING TO THE ROCHE MODEL. Cochran, Gordon Vance. Charlottesville, Va.; Univ. of Virginia (1970). 109p. University Microfilms Order No. 71-6702.

Thesis.

Close binary models, based on the Roche stellar model, were computed and monochromatic light curves deduced. These computations were carried out by direct numerical methods employing a grid of 3280 points over the surface of each star, except in the case of the reflection effect calculations which used a coarser grid. To determine the reflection effect, it was assumed that all radiation from all visible areas of the companion falling on an element of area add to the intrinsic net flux there and act to produce a higher effective temperature. The monochromatic energy distribution is, then, obtained by Planck's law after the reflection corrections for both components have been computed by an iterative method. Comparison with observed light curves of MR Cygni and EG Cephei indicate the inadequacy of the ellipsoidal model for close systems. Difficulties encountered in matching the observations with curves computed from the present model are interpreted as being due, mainly, to the simplified treatment of the reflection effect. Future refinements of the present model should make possible the determination of the physical parameters of close, but not contact, eclipsing binary systems and could also make possible the analysis of shallow eclipse curves and noneclipse curves. (Diss. Abstr. Int., B)

XUM

27331 EVOLUTION OF CLOSE BINARIES. V. STATIONARY MODELS REPRESENTING THE END OF THE PHASE OF RAPID MASS LOSS IN CASE A. Horn, J.; Kriz, S.; Plavec, M. (Astronomical Inst., Ondrejov, Czech.). Bull. Astron. Inst. Czech.; 21: 45-54(1970).

Mass exchange in close binary systems, where the mass-losing component has not-yet-exhausted hydrogen in its convective core, consists of a rapid and a slow phase. The outcome of the rapid phase can be computed by means of a sequence of stationary models. Such calculations were made for five values of the initial masses of the mass-losing component (9, 7, 6, 5, and 4 $M_\odot$, respectively), for four different evolutionary stages, and for equidistant values of the initial mass ratio. The models are tabulated. (auth)

27332 WHITE-DWARF ENVELOPE STRUCTURE AND ITS EFFECT ON THE THERMAL COOLING RATE. Lacis, Andrew Andrejs. Iowa City, Iowa; Univ. of Iowa (1970). 244p. University Microfilms Order No. 71-5778.

Thesis.

White dwarf envelope models were computed for a pure helium composition as well as for a composition containing a 0.1% metal abundance. The envelope equation was developed in terms of a temperature–degeneracy formulation which was found to be both numerically convenient and useful in analyzing the relationship between the different physical quantities of the envelope. Asymptotic relations were derived for the temperature distribution in the nondegenerate surface layers and the highly degenerate interior. The effect of different opacities on the interior core temperature was analyzed. A limiting value for the internal core temperature was established in the limit $\eta \to \infty$. By taking full account of degeneracy effects and including also the Coulomb correction to the equation of state, it was found that the internal temperature may be represented in the form $T_c = T_0(L/M)^{0.4}$. This differs from the previous results both in the constant factor T_0 and also in the exponential dependence on the L/M ratio. (TSS) (Diss. Abstr. Int., B)

27333 SPECTRUM AND A QUANTITATIVE ANALYSIS OF THE Ap STAR ALPHA DRACONIS. Zverko, J. (Astronomical Observatory, Skalnate Pleso, Czech.). Bull. Astron. Inst. Czech.; 21: 56-61(1970).

Three spectrograms, obtained by the 193-cm telescope's coudé spectrograph at Observatoire du Haute Provence, were used for measuring the equivalent line widths in the spectrum of the peculiar star α Draconis. A comparison of the observed contours of H_γ with the theoretical ones computed by Mihalas (1965) gave the best agreement for the values $\theta_{eff} = 0.6$, log g = 2 and $\theta_{eff} = 0.5$, log g = 3. The excitation temperature increases with increasing ionization potential of the ionized elements. The abundance anomalies are as follows: Si is in excess by a factor of 5, Cr is in excess by a factor of 3, Sr is perhaps in slight excess. (auth)

27334 EVOLUTION OF CLOSE BINARIES. VI. CASE B OF MASS EXCHANGE IN SYSTEMS 4 + 3.2$M_\odot$ AND 4 + 1.6$M_\odot$. Harmanec, P. (Astronomical Inst., Ondrejov, Czech.). Bull. Astron. Inst. Czech.; 21: 113-31(1970).

Two examples of case B of mass exchange were computed to estimate the effect of basic initial parameters of systems on the course and the results of mass exchange. In the case of 4 + 3.2$M_\odot$ the changes in inner structure of the mass-losing star are discussed in detail. It seems that the resulting mass of the original primary might be independent of the initial mass ratio, that the resulting orbital period might be independent of initial mass of the primary and that the resulting surface hydrogen content might be independent of both of those parameters. Validity of those results should be checked for different evolutionary stages of the primary. (auth)

27335 THERMODYNAMICS UNDER CONDITIONS OF HOT MATTER NEUTRONIZATION AND THE HYDRODYNAMIC STABILITY OF STARS AT LATE STAGES OF EVOLUTION. Imshennik, V. S.; Chechetkin, V. M. (Inst. of Applied Mathematics, Moscow). Sov. Astron. AJ (Engl. Transl.); 14: 747-57(Mar-Apr 1971).

Under the assumption that neutrinos and antineutrinos can escape freely from the central region of a star, the thermodynamics of matter is studied in the following wide range of variation of the density and temperature: 10^8 g/cm$^3 \lesssim \rho \lesssim 10^{12}$ g/cm^3, 5×10^9 °K $\lesssim T \lesssim 20 \times 10^9$ °K. In this region, an important role is played by hot matter neutronization. The thermodynamics considered is a variant of the thermodynamics of a physical system with a variable number of particles. The analysis is based on the assumption of statistical equilibrium of nuclear reactions and kinetic equilibrium of β processes. This assumption is justified by comparing the characteristic times of nuclear processes and β processes. On the basis of the thermodynamical data and the characteristic times of the important processes, certain conclusions are drawn concerning the development of hydrodynamic instability of stars. Since β processes take place very slowly, neutronization cannot lead to a rapid development of fast hydrodynamic compression. A direct numerical calculation with allowance for the neutronization kinetics can establish the onset of such a compression. (auth)

27336 VELOCITY DISTRIBUTION OF STARS OF EQUAL MASS IN CLUSTERS. Kaliberda, V. S. (Leningrad State Univ.). Sov. Astron. AJ (Engl. Transl.); 14: 773-7(Mar-Apr 1971).

Translated from Astron. Zh.; 47: 960-6(Sep-Oct 1970).

The velocity distribution of stars in nonrotating stellar systems is found for systems consisting of stars of equal mass. The number of stellar encounters is taken into account. The energy removed by dissipating stars and the rate of dissipation are found. It is found that mass dispersion accelerates the evolution of the stellar systems. (auth)

27337 OBSERVATIONS OF COMET-SHAPED NEBULAE AND GLOBULES. Dibai, E. A. (Shternberg State Astronomical Inst., USSR). Sov. Astron. AJ (Engl. Transl.); 14: 785-93(Mar-Apr 1971).

Translated from Astron. Zh.; 47: 977-88(Sep-Oct 1970).

Observations of cometary nebulae and globules carried out with a 125-cm reflector over the period 1963–1968 are reported. Most of the negatives were obtained with a reducing camera (f/2), and with a red glass filter transmitting the Hα line. Some of the bright nebulae were studied photoelectrically and spectrographically. The cometary nebulae are characterized by both ionized and neutral gases. The density and mass of the ionized gas can be determined from the absolute intensity of the Hα line through the use of photoelectric standards. Additional gas-dynamic considerations are necessary for the neutral gas. In the case of globules having emission rims and embedded in an H II region, the rim is presumably a stationary ionization front. Then the pressures in the ionized gas (the rim) and in the neutral gas (the globule) are equal. The density and temperature in the border are determined from observations, while the temperature in the globule is found from Kaplan's calculations (300 to 1000°). One thus has a density jump of ρ (H I) = (20 to 50)ρ (H II) at the ionization front. Furthermore, the globules are often at the ends of long dark channels. The density and mass of the channels may be estimated under the assumption that the material is in the gravitional field of all the diffused nebula. For channel dimensions small in comparison with the radius of the H II region, the density distribution has a barometric behavior. Relations are given for evaluating the density and mass of the cometary nebulae and globules. The masses of the cometary nebulae lie in the range 0.1 to 100 $M_\odot$ (for large globules), while their typical sizes range from a fraction of a parsec to several parsecs. A morphological classification of the cometary nebulae is given that coincides with that given by Badalyan. The first class contains stars having a low nebula reflectivity at the focus of the emission rim (at the center of the globule). The second class contains classical "comets" with stars at their vertices. The third class includes arcs or "commas," and the fourth includes biconical structures. It is concluded that these types of cometary nebulae are due to certain kinds of macroscopic motion in diffuse nebulae. (auth)

27338 INVESTIGATION OF PLANETARY NEBULAE IN THE NEAR ULTRAVIOLET REGION OF THE SPECTRUM. Kostyakova, E. B. (Shternberg State Astronomical Inst., USSR). Sov. Astron. AJ (Engl. Transl.); 14: 794-7(Mar-Apr 1971).

Translated from Astron. Zh.; 47: 989-93(Sep-Oct 1970).

Study of the continuous spectra of planetary nebulae in the ultraviolet yields information that is valuable in establishing the processes behind their luminosity. Inferences as to physical conditions in a nebula and its electron temperature can be drawn from the energy distribution in the Balmer continuum. Simultaneous measurements of the continuous spectrum in the region of the Balmer continuum and the Balmer discontinuity D make is possible to determine the physical parameters n_e and T_e of the nebulae independently of all other methods. (auth)

27339 PHOTOMETRIC ASPECTS OF TYPE I SUPERNOVAE. Pskovskii, Yu. P. (Shternberg Astronomical Inst., USSR). Sov. Astron. AJ (Engl. Transl.); 14: 798-805(Mar-Apr 1971).

Translated from Astron. Zh.; 47: 994-1003(Sep-Oct 1970).

Methods of estimating the time of occurrence and the maximum brightness of Type I supernovae from the average light curve, the point of slope change, and the variation in the form of the spectrum are discussed and their accuracy is estimated. Data on the maxima of 27 Type I supernovae are presented. The color–phase relations and the form of the ascending branch of the light curve are reviewed and refined. The light curve of the galactic Kepler's supernova is analyzed. (auth)

27340 NORMAL COLOR INDICES OF CEPHEIDS. III. Nikolov, N. S.; Ivanov, G. R. Sov. Astron. AJ (Engl. Transl.); 14: 806-12(Mar-Apr 1971).

XUM

Translated from Astron. Zh.; 47: 1004-11(Sep-Oct 1970).

A calibration of the $(U-B)_0$ spectrum relation for Cepheids was derived, by means of which the normal $(U-B)_0$ color of a given Cepheid was found directly from a determination of its spectral class, without resorting to the reddening curves in the two-color diagram. By using the spectral classes of Cepheids given in the system of Γ photometry, normal $(U-B)_0$ colors were determined for approximately 130 Cepheids at maximum and minimum. The dependence of U − B excess on the phase of the brightness variation (being a consequence of the dependence of E_{U-B} on the spectrum) was also derived, and by means of it one can find E_{U-B} for any phase of brightness variation if one knows $E_{U-B\varphi}$ and $E_{B-V\varphi}$ for some phase φ and has a curve of the B − V variation for the star in question. This dependence was taken into account when calibrating the spectrum−$(U-B)_0$ relation. (auth)

27341 INFLUENCE OF, AND ALLOWANCE FOR, THE BACKGROUND IN PHOTOGRAPHIC PHOTOMETRY. Sincheskul, V. N.; Sincheskul, B. F. (Poltava Gravimetric Observatory, Kiev). Sov. Astron. AJ (Engl. Transl.); 14: 855-60(Mar-Apr 1971).

Translated from Astron. Zh.; 47: 1066-72(Sep-Oct 1970).

An account is given of the results of research conducted on the influence of background of various densities on the photographic images of stars. It is shown that, with an increase in the density of the background, the diameter of stellar images decreases, the decrease being unequal for stars of different magnitudes. A method is proposed for taking into account the influence of the background when determining photographic magnitudes. It consists of two stages: first, at the time of the measurements, allowance is made for the background that enters the measuring aperture of the instrument together with the image of a star; and then during reduction, allowance is made for the decrease in stellar image size. A comparison of photographic magnitudes obtained by this method with photoelectric magnitudes shows good agreement, considering the great range of background density fluctuation (from 0.65 to 2.15). (auth)

27342 X-RAY SOURCES IN BINARY SYSTEMS. Guseinov, O. Kh. (Shemakha Astrophysical Observatory, Baku). Sov. Astron. AJ (Engl. Transl.); 14: 912-13(Mar-Apr 1971).

Translated from Astron. Zh.; 47: 1143-5(Sep-Oct 1970).

A neutron star that belongs to a binary system along with a star that is losing mass may be a variable x-ray source. The factors responsible for variability of such an x-ray source and some observable effects that may be produced in the atmosphere of the visible component are discussed. Special attention is drawn to the identification of x-ray sources with binary stars and the possibility of distinguishing neutron and collapsed stars from white dwarfs. Estimates are obtained for the power of the x-ray emission and for an upper bound on the number of observable x-ray sources which may be neutron stars in binary systems. (auth)

27343 SPECTRAL TYPE OF THE BRIGHTEST COMPONENT OF THE TRIPLE SYSTEM 44 i BOOTIS. van't Veer, F. (Institut d'Astrophysique, Paris). Astron. Astrophys.; 11: 197-9 (Mar 1971).

The spectral type of the slowly revolving brightest component of the triple system 44 i Boo was studied using spectra taken at the Dominion Astrophysical Observatory Victoria in 1922. At that time the separation between the brightest component and the two others (which form an eclipsing contact binary) was sufficiently large, so that separate spectra could be taken. This study confirms the hypothesis suggested by a photometric study in eight colors of the eclipsing system in a previous paper (Kurpinska and van't Veer, 1970) according to which the spectral type of the third and brightest component is earlier (F5V) than previously supposed (GφV). One can conclude that the conspicuous reddening of 44 i Boo during the maxima is not an intrinsic phenomenon of the eclipsing system but merely due to the presence of the third component. (auth)

27344 MAGNETIC FIELD DECAY OF NEUTRON STARS. Chanmugam, G.; Gabriel, M. (Univ., Liege). Astron. Astrophys.; 11: 268-9(Mar 1971).

The time scales for the magnetic field decay of neutron stars are determined, taking into account their nonuniform conductivity. It is found that these time scales are at least 10^3 times the value used by Gunn and Ostriker in their models describing various pulsar properties. (auth)

27345 CURVE OF GROWTH ANALYSIS OF δ CEP. van Paradijs, J. A. (Univ., Amsterdam). Astron. Astrophys.; 11: 229-310(Mar 1971).

Nine spectrograms of δ Cep, taken with the 200″ Palomar telescope at a dispersion of 4.5 Å/mm, were analyzed by (monolayer) curve of growth methods. Values of θ_{exc} were derived from Fe I and Cr II. The microturbulent velocity is shown to vary regularly during the pulsation cycle. Abundance determinations of 25 elements relative to Fe showed that the chemical composition of the atmosphere of δ Cep does not differ significantly from that of the Sun. From the asymmetry of the line λ4508 of Fe II the existence of a velocity gradient in the atmosphere is inferred. A similar conclusion is drawn from the study of 25 moderately strong lines. This agrees well with Jacobsen's earlier observations of differential radial velocities. These last two data, together with the phase dependence of the density variation, are interpreted as evidence for a running wave in the atmosphere of δ Cep. (auth)

27346 CORRECTIONS TO PREVIOUSLY PUBLISHED PHOTOGRAPHIC OBSERVATIONS OF SIRIUS B. van Albada, G. B. (Univ., Amsterdam). Astron. Astrophys.; 11: 317-19(Mar 1971).

Previously published photographic observations of Sirius B, which had been obtained with a rudimentary objective grating consisting of only five wires, were corrected for the effect of an image shift predicted by Hertzsprung. Since the contraction of the photographic emulsion had already been eliminated, the observations should now be essentially free from systematic errors. The results confirm previously observed deviations from the presently accepted orbit. (auth)

Quasi-Stellar, Radio, and X-Ray Sources

Refer also to abstract 27342.

27347 GRAVITATIONAL RED-SHIFT. Ross, D. K. (Iowa State Univ., Ames). Nuovo Cim.; 2B: 55-62(11 Mar 1971).

The usual expression for the gravitational redshift z is calculated exactly in both the standard and isotropic forms of the Schwarzschild metric. The differing results are found to be meaningless and metric-dependent until they are put in terms of quantities directly observable from earth. The importance of expressing physical quantities in terms of observables is stressed. (auth)

27348 SEARCH FOR OPTICAL CIRCULAR POLARISATION IN THE CRAB NEBULA. Landstreet, J. D. (Univ. of Western Ontario, Can.); Angel, J. R. P. Nature (London); 230: 103(12 Mar 1971).

It has been suggested that the magnetic field associated with the Crab Nebula that causes relativistic particles to emit synchrotron radiation may be an oscillating 30 Hz electromagnetic field from the pulsar, rather than a static field. If this is so, the nebula should show a circular polarization of the order of a few percent in visible light, and of opposite sense in the NW and SE regions of the nebula, assuming that the spin axis of the pulsar is in the direction of linear polarization. An attempt to detect the predicted circular polarization is described, using a polarimeter on the 82-inch telescope at McDonald Observatory, in Nov. 1970. The technique adopted eliminated effects due to the strong linear polarization of the nebula. No significant polarization was detected. (UK)

27349 OBSERVATIONS OF RADIO RECOMBINATION LINES OF HYDROGEN, HELIUM, AND CARBON. Churchwell, Edward Bruce. Bloomington, Ind.; Indiana Univ. (1970). 210p. University Microfilms Order No. 71-6831.

Thesis.

Basic formulae that describe the emission of radio-recombination lines are reviewed. Using these formulae an analysis of observed hydrogen, helium, and carbon radio recombination lines is carried out. An analysis of the H109α, H137β, H157γ, and H172δ line widths at λ6 cm for Orion A and M17 gives evidence for Stark broadening; however, the magnitude of this broadening appears to be less than that predicted by the most recent theoretical computations in Griem (1967). Using a non-LTE analysis of the hydrogen line intensities, it it is shown that the α and higher-order lines all predict the same electron temperature in a given H II region and departures from LTE decrease with increasing transition order in H II regions with a high emission measure. Interpretation of the electron temperature, electron density, and emission measure derived from a non-LTE analysis of hydrogen lines leads to a model in which the line emission is primarily produced in high-density condensations embedded in an extended low-density plasma. From the helium and hydrogen radio-recombination line intensities the relative abundance of ionized helium in 22 galactic H II regions is inferred. Twelve sources are found to have an average number ratio $[N(He^+)/N(H^+)] = 0.089 \pm 0.009$; four have a ratio $[N(He^+)/N(H^+)] = 0.058 \pm 0.007$; and six show no helium line at all. The assumptions on which these determinations are based are discussed, as well as possible astrophysical interpretations of the three groups of sources. Carbon line emission was observed in seven galactic H II

regions, the line parameters for which are reported. The nature of the line formation process for the carbon radio-recombination lines is considered. From the observations and theoretical considerations a model is proposed in which the carbon lines originate in cool, dense condensations where hydrogen is neutral or only partially ionized either embedded in or located at the edge of H II regions. If such a model is correct, carbon radio-recombination line emission may be a valuable probe for protostars in or near galactic H II regions. (Diss. Abstr. Int., B)

27350 RADIO OBSERVATIONS OF THE PULSE PROFILES AND DISPERSION MEASURES OF TWELVE PULSARS. Craft, Harold Dumont Jr. Ithaca, N. Y.; Cornell Univ. (1970). 354p. University Microfilms Order No. 71-4972.

Thesis.

For the newly discovered pulsating radio stars, pulsars, much information concerning the nature of the source can be deduced from careful measurements of the shapes and timing of the pulses from each of these sources. At radio frequencies such measurements are complicated by the interstellar plasma, which introduces a frequency-dependent time delay to each pulse. This thesis discusses some of the techniques for and results of measurements of pulse profiles and dispersion measures of the first twelve pulsars known to be within view of the Arecibo Observatory. All measurements were made at that observatory utilizing frequencies between 430 and 40.12 MHz. Time resolution of the pulses ranged from tens to tenths of a millisecond. (TSS) (Diss. Abstr. Int., B)

27351 ANGULAR STRUCTURE OF THE QUASAR 3C 147. Donaldson, W.; Smith, H. Mon. Notic. Roy. Astron. Soc.; 151: 253-8(1971).

Continuous, twenty-four hour, observations of the quasi-stellar radio source 3C 147 were made at 1422 and 2694 MHz with the Jordrell Bank-Malvern long-baseline interferometer. The visibility function obtained at 2694 MHz shows that the source has a complex structure at this frequency. 80% of the flux is emitted by 3C 147B, consisting of two small components ($0.07 \times 0.04''$) separated by 0.14″ in position angle 55°. The remaining 20% of the flux is emitted by a larger component, 3C 147A, separated from 3C 147B by 0.55″. Comparison with other very long-baseline observations suggests that the angular separation of the components of 3C 147B is strongly dependent on frequency. (auth) (UK)

27352 EXPANDING NEUTRAL HYDROGEN IN VIRGO. Fejes, I. (Kapteyn Astronomical Lab., Groningen, Netherlands). Astron. Astrophys.; 11: 163-70(Mar 1971).

A concentration of neutral hydrogen with positive velocities lower than 40 km s^{-1} is found in the galactic region $280° \leq l \leq 340°$, $+32.5° \leq b \leq +57.5°$. In the same region there are also weak negative velocity components. The region is partly surrounded by ridges of continuum radiation. These characteristics may be interpreted as due to a large-scale expansion in the H I medium. (auth)

27353 STATISTICALLY COMPLETE SAMPLE OF RADIO-SOURCES AT 1400 MHz. Witzel, A.; Veron, P.; Veron, M. P. (Observatoire, Meudon, France). Astron. Astrophys.; 11: 171-87(Mar 1971).

1400-MHz flux densities are given for 315 extragalactic radio sources with fluxes ≥ 2.0 f.u. in the declination range $-5° < \delta < +70°$ exclusive of a strip of 5° on both sides of the galactic equator, in order to provide a sample of radio sources well suited for a statistical analysis. The fluxes were determined on the basis of the data given in several recent 21-cm catalogues after adjusting the scales to the scale of Kellermann et al. (1969). The completeness of this sample is estimated to be about 94%. The distribution of the spectral index $\alpha(178, 1400)$ is described for 305 of these sources that show a sharp peak around $\alpha = 0.75$ and a broad wing on the flat spectra side, including 66 sources having $\alpha < 0.4$. Flux density measurements at 11- and 6-cm wavelengths are reported. Together with previously published measurements all the sources of the sample were measured at these two wavelengths (with the exception of 1600 + 33). The same observations were used to determine the right ascension of the sources (Nancay measurements) or the right ascension and the declination (Green Bank measurements). The radio positions are given. (auth)

Solar Phenomena

Refer also to abstracts 26484, 26517, 27443, 27470, 27471, 27531, 27532, 27543, 27553, and 27555–27574.

27354 HIGH ENERGY FLARE RADIATION. De Jager, C. (Astronomical Inst., Utrecht). Astrophys. Space Sci. Libr.; 19: 25-33(1970).

From 3rd Intercorrelated Satellite Observations Related to Solar Events, Noordwijk, Netherlands. See CONF-690971.

Flare-associated photon and particle fluxes are characterized by short rise times and longer-lasting decays. High-energy x-ray photon emission decays faster than low-energy x radiation, which together with the observed shapes of the energy spectra, suggests that the emission is due to a high-energy flare-associated plasma, whose projected position is, certainly in the first phase, closely associated with the first-appearing bright elements of the optical flare. It is suggested that this plasma emits both the non-thermal (hard) x burst as well as the quasi-thermal softer x bursts, but the nonthermal component is mainly confined to the first phase of the flare. During the further thermalization of the plasma the average particle energy decreases, while the high-energy plasma cloud seems to expand and to exchange energy with the ambient gas, so that the number of involved particles increases. The phase of energetic-particle acceleration may be explained with Alfvén and Carlqvist's circuit-interruption model. (auth)

27355 PARTICLE EVENT FORECASTING. Svestka, Zdenek (Astronomical Inst., Ondrejov, Czech.). Astrophys. Space Sci. Libr.; 19: 90-101(1970).

From 3rd Intercorrelated Satellite Observations Related to Solar Events, Noordwijk, Netherlands. See CONF-690971.

The solar-particle events are classified according to the classification scheme proposed by Smart and Shea. Main characteristics of proton-active regions are then summarized: magnetically complex type of the region, increase of the magnetic-field gradient, δ-configuration and A-configuration of the sunspot group, intensification and hardening of the microwave and x-ray spectrum, increased activity in the x-ray and microwave spectral regions, permanent emission of ~1 MeV proton flux, and loop–prominence-system occurrence. Characteristic properties of proton flares in the Hα light, x-ray, and radio spectrum also are mentioned, as well as the influence of the flare position on the solar disk on the particle flux recorded in the Earth's surroundings. Basic principles of the long-term forecasts are explained. Active longitudes, complexes of activity, permanent proton flux, and traveling impulses of solar activity are mentioned. (auth)

27356 PROPOSED SOLAR PROTON EVENT CLASSIFICATION SYSTEM. Smart, D. F.; Shea, M. A. (Air Force Cambridge Research Labs., Bedford, Mass.). Astrophys. Space Sci. Libr.; 19: 102-7(1970).

From 3rd Intercorrelated Satellite Observations Related to Solar Events, Noordwijk, Netherlands. See CONF-690971.

A preliminary proton event classification system based upon the proton flux in the immediate vicinity of the Earth was presented at the Inter-Union Commission on Solar–Terrestrial Physics Plenary meeting, Jan. 1969. The system is based on the logarithm (base 10) of the solar proton flux in unit of cm^{-2} sec^{-1} $sterad^{-1}$. A reference level of 10 MeV is recommended. Each solar proton event would be classified by a three-digit number: the first digit would represent neutron monitor response; the second, riometer response; and the third describe the proton intensity with E > 10 MeV. The three-digit number is confined to the response of Earth-based sensors and satellites in an Earth–Moon system orbit. The basic criteria is represented by the third digit, the satellite-measured proton intensity. Negative index numbers were incorporated to allow for the classification of small events. Tables are given listing riometer and neutron monitor locations meeting the necessary criteria for meeting the classification system. (J.C.W.)

27357 X-RAY OBSERVATIONS BETWEEN 1 AND 55 A OF THE FEBRUARY 25th FLARE. Brinkman, A. C. (Space Research Lab., Utrecht); De Graaff, W.; Shaw, M. L. Astrophys. Space Sci. Libr.; 19: 413-18(1970).

From 3rd Intercorrelated Satellite Observations Related to Solar Events, Noordwijk, Netherlands. See CONF-690971.

Data from satellite observations of the February 25, 1969 solar flare at soft x-ray frequencies are presented. Temporal variations of the intensity at four different wavelength bands are shown and compared. The variation of the spectrum during the flare is considered. (auth)

27358 RELATIVISTIC GRAVITY IN THE SOLAR SYSTEM. I. EFFECT OF AN ANISOTROPIC GRAVITATIONAL MASS ON THE EARTH-MOON DISTANCE. Will, Clifford M. (California Inst. of Tech., Pasadena). Astrophys. J.; 165: 409-12(15 Apr 1971).

Some relativistic theories of gravity (not including general relativity) predict that the passive gravitational masses of the Sun and planets should be anisotropic tensors. This paper calculates the perturbation in the Earth–Moon distance due to the

predicted anisotropy in the Earth's passive mass. It is found to be at the 10^{-2} cm level, hence unmeasurable with today's lunar laser ranging technology. Also shown to be undetectable are planetary orbits due to the predicted anisotropy of the Sun's passive mass. (auth)

27359 PHOTOELECTRON SHEATH NEAR A PLANAR PROBE IN INTERPLANETARY SPACE. Grard, R. J. L.; Tunaley, J. K. E. (European Space Research and Tech. Center, Noordwijk, Netherlands). J. Geophys. Res.; 76: 2498-2505(1 Apr 1971).

Estimating the extent of the photoelectron sheath and associated electric field around a spacecraft in interplanetary space is important for the interpretation of probe measurements. In addition, the theory is relevant to predicting the sheath parameters around bodies such as the Moon. In the present study, a general treatment of the photoelectron sheath in a vacuum is undertaken, typical sheath profiles are given, and the effects of a tenuous ambient plasma are also discussed. Finally, an attempt is made to ascribe orders of magnitude to the physical parameters of the photoelectron sheath. (auth)

27360 SURFACE POTENTIAL OF A PHOTOEMITTING PLATE. Fu, Jerry H. M. (Univ. of Maryland, College Park). J. Geophys. Res.; 76: 2506-9(1 Apr 1971).

In earlier work [Guernsey and Fu, 1970] the potential distribution in the neighborhood of a photoemitting plate immersed in plasma was studied. The result indicates that two steady-state potential distributions can exist, namely one in which the potential decreases from its plate value to zero monotonically and one in which it decreases from its plate value to a negative minimum and then increases to zero (overshoot type). In the present work, a Maxwellian distribution is assumed for the emitting photoelectrons instead of a Fermi-shape distribution. Furthermore, the difference of the surface potential for these two types of distributions is investigated in more detail. The result shows that this difference can exist only if $1 < T_e/T_v < n_v/n_e$, where T_e, T_v, n_e, n_v, are the temperatures and number densities of plasma electrons and photoelectrons. (auth)

27361 SOLAR SOURCES AND THE COSMIC-RAY TRANSPORT EQUATION. Gleeson, L. J. (Monash Univ., Clayton, Australia). J. Geophys. Res.; 76: 2510-11(1 Apr 1971).

The solution governing the transport equation of the modulation of galactic cosmic rays in the interplanetary region utilizes the numerical method introduced by Fisk, (J. Geophys. Res., 76: 221(1971)). The method uses a transformation $u(r,T) = r^{\gamma}U(r,T)$, $(0 < \gamma < 1)$, to have an inner boundary condition $u \to 0$ as $r \to 0$; this transformation also ensures that there are no inadvertent sources at the origin $r = 0$, providing that k remains finite and that $rV/k \to 0$ as $r \to 0$. The method is restricted to problems in which the cosmic rays are of galactic origin and cannot be used to include sources at the origin (solar sources). It is shown that sources at the origin can be treated by Fisk's method if a new transformation of the independent variable U(r,T) is used. The method has also been used to investigate the interplanetary cosmic-ray flux associated with steady-state solar sources. (J.C.W.)

27362 RECURRENCE OF 10.7-cm SOLAR FLUX AND OF SUNSPOT ACTIVITY OVER THE 11-YEAR SOLAR CYCLE. Das Gupta, M. K.; Sarkar, S. K. (Univ. of Calcutta). Indian J. Pure Appl. Phys.; 8: 734-5(Nov 1970).

The true nature of the so-called 27-day periodicity in both the variable component of 10.7-cm solar flux and the sunspot activity was examined over the 11-year solar cycle by the superposed epoch method. It was observed that the two phenomena are closely associated in all the phases of the 11-year solar cycle. The average periodicities of both are found to be identical, being 27.5, 26, and 25 days in the increasing, peak, and declining phases, respectively, of the 11-year solar cycle. The 27-day cycle shows a marked asymmetry since the average-time duration for the change of the solar flux from minimum to peak is a few days shorter than that for the change from the peak to the following minimum. (auth)

27363 PFP OBSERVATIONS. I. RESULTS OF SPECIAL OBSERVATIONS FOR THE PROTON FLARE PROJECT, 1969. Hakura, Yukio (Radio Research Lab., Tokyo). Denpa Kenkyusho Kiho; 16: No. 83, 69-70(Mar 1970). (In Japanese).

The Proton Flare Project (PFP) was adopted as one of the research programs during the IASY (1969–1971). The researches in this field are historically surveyed and the significance of the PFP project is discussed. High-energy (10-GeV) solar protons were first observed by Forbush in 1942. During the IGY (1957–8), the anomalous absorption of radio waves due to the solar proton (polar-cap absorption) was found. Forecasting of the proton flare and the accompanying geomagnetic storm was attempted by IUWDS during the IGY. The systematic study of the relation of the proton flare and geomagnetic storm was carried out by IAU in 1966. The proton flare on July 7, 1966 was successfully forecast. PFP research teams selected the PFP interval once in a year during IASY, from May 1 to July 31 in 1969, for the special observation. The period June 5 to June 18, 1969, when two active regions appeared on the solar surface, was called the PFP retrospective interval and extensive research was carried out, including the proton flare on June 8. (Japan)

27364 CENTIMETER AND DECIMETER SOLAR BURSTS IN RELATION TO THE PHASE OF THE S COMPONENT OF SOLAR RADIO EMISSION. Das Gupta, M. K.; Sarkar, S. K. (Univ. of Calcutta). Indian J. Pure Appl. Phys.; 8: 736-8(Nov 1970)

Occurrences of different types of solar radio bursts at frequencies 606, 1415, 2695, 4995, and 8800 MHz for the period November 1966 to April 1969 were examined in relation to the phase of the slowly varying component (S component) of solar radio emission. It was found that bursts of all types at these frequencies occur more frequently in the rising than in the declining phase of the S component. The true nature of the periodic variation of the S component was further examined by the well-known Chree method. It was concluded that the predominance of bursts in the rising phase may be related to the greater rate of change of the S component in this phase. (auth)

27365 [Fe I] LINES: THEIR TRANSITION PROBABILITIES AND OCCURRENCE IN SUNSPOTS. Grevesse, N.; Nussbaumer, H.; Swings, J. P. (Univ., Liege). Mon. Notic. Roy. Astron. Soc.; 151: 239-52(1971).

Magnetic dipole and electric quadrupole transition probabilities were calculated for all the transitions in the configurations $3d^74s$ and $3d^64s^2$ of Fe I. Configuration interaction was included. A search with the Kitt Peak solar telescope was made in sunspots for the lines corresponding to the strongest predicted transitions. Lines of the multiplets a^5D-a^3P, a^5D-b^3F, and a^5D-a^5P were tentatively identified. Their equivalent widths confirm the high solar iron abundance: $\log N_{Fe} = 7.5$. The possible presence of [Fe I] lines in the absorption spectrum of Arcturus is also discussed. (auth) (UK)

27366 STUDIES OF GRANULAR VELOCITIES. II. STATISTICAL ANALYSIS OF TWO HIGH-RESOLUTION SPECTROGRAMS. Mehltretter, J. P. (Fraunhofer Institut, Freiburg i. B.). Solar Phys.; 16: 253-71(Feb 1971).

Continuum brightness and Doppler velocity fluctuations in the lines λ6301.5 and λ6302.5 Å of FeI, measured in two selected spectrograms, were analyzed by standard statistical (power- and coherence-spectrum) methods. It is shown qualitatively that the oscillatory component of the velocity fluctuations (at spatial wavelengths >4″) decreases, while the supposedly "granular" component (at spatial wavelengths <4″) as well as the coherence between brightness and velocity fluctuations increases with optical depth. The spatial resolution of the spectrograms is estimated by comparing the observed power spectrum of brightness fluctuations with spectra found in the literature, assuming the combined instrumental and seeing spread function to be Gaussian. The resolution thus determined is $\sigma = 1.24'' \pm 0.07''$. If the measured values are corrected accordingly, a true brightness rms of 10 to 14% is obtained, depending upon the shape of the power spectrum chosen for comparison, and a velocity rms at continuum optical depth of 1.3 km/sec. It is shown, however, that using the same correction function for the velocity power spectrum as for the brightness possibly gives rise to misestimating the velocity rms. (auth)

27367 DETERMINATION OF SOLAR DOPPLER WIDTHS BY GOLDBERG'S METHOD. Dunn, A. R. (Rensselaer Polytechnic Inst., Troy, N. Y. Kitt Peak National Observatory, Tucson, Ariz.); Olson, E. C. Solar Phys.; 16: 272-85(Feb 1971).

The so-called "Goldberg" or "profile intercomparison" method of determining Doppler widths from spectral line profiles was used to analyze a group of high-quality solar profiles observed with the McMath solar telescope at the Kitt Peak National Observatory. The observations consisted of profiles of eight lines of calcium and chromium, made at either four or five positions on the solar disk. A depth dependence of solar microturbulence could not be derived by applying the Goldberg method to a single pair of lines at a single disk position. When the depth dependence was determined from line pairs at different disk positions, a depth-dependent turbulence model was obtained. The final model was anisotropic with radial and tangential components increasing with depth in the atmosphere. (auth)

27368 ANALYTIC SOLUTIONS TO THE UNNO TRANSFER EQUATION FOR THE STOKES PARAMETERS IN A MILNE–EDDINGTON ATMOSPHERE. Hagyard, M. J. (Marshall Space Flight Center, Ala.). Solar Phys.; 16: 286-7(Feb 1971).

XUM

The mathematical expressions derived by Moe(1968) for the solutions to the transfer equations for the Stokes parameters as derived by Unno(1956) are adapted to the more-restricted problem of a Milne–Eddington atmosphere. This is felt to be of interest in connection with sunspots. (W.D.M.)

27369 EMPIRICAL SOLAR CONTINUUM MODELS. Remo, J. L. (Franklin Inst., Swarthmore, Pa.). Solar Phys.; 16: 288-92(Feb 1971).

A model of the solar photosphere is derived on the basis of observed absolute intensities and limb darkening of the continuous spectrum between 5,000 and 19,450 Å. (auth)

27370 INTERPRETATION OF THE SOLAR CONTINUUM FROM 1680 to 600 A. MODEL OF THE TRANSITION REGION PHOTOSPHERE–CHROMOSPHERE AND OF THE CHROMOSPHERE. Cuny, Yvette (Smithsonian Astrophysical Observatory, Cambridge, Mass. Harvard Coll. Observatory, Cambridge, Mass. High Altitude Observatory, Boulder, Colo.) Solar Phys.; 16: 293-313(Feb 1971).

An interpretation is given of the observations of the continuous solar radiation in the spectral range 600 to 1700 Å. The model allows for deviations from LTE of H, C, Si, and S, and is in hydrostatic equilibrium. The predicted intensity from 1680 to 1520 Å has virtually no dependence on the electron temperature variation in the optical depth range 10^{-3} to 4×10^{-6}, at 5000 Å; the brightness temperature is compatible with a low electronic temperature minimum near the optical depth 10^{-4}. The model of the low chromosphere is characterized by a steep temperature gradient. The model satisfies observations at millimeter wavelengths. (auth)

27371 CALCULATIONS OF TWO-DIMENSIONAL MODELS OF THE LOWER SOLAR CHROMOSPHERE. Cannon, C. J. (Univ. of Sydney). Solar Phys.; 16: 314-27(Feb 1971).

Several two-dimensional models of the lower solar chromosphere were computed using relative RMS line center intensity variations and mean limb-darkening curves observed in Mg b and NaD. These calculations indicated that the small-scale fluctuations observed at line center in these lines may result from density and electron temperature fluctuations in the lower chromosphere, while the large-scale fluctuations may result from either fluctuations in the deeper-lying continuum or horizontal and vertical differential velocity fields. (auth)

27372 CENTER TO LIMB VARIATION OF THE SEPARATION OF THE Mg II, H_2, AND K_2 EMISSION PEAKS. Greve, A. (C. Zeiss, Oberkochen, Ger.). Solar Phys.; 16: 328-35(Feb 1971).

From observations of the center to limb variation of the emission peaks of the Mg II, H, and K lines the optical thickness of the emitting layer for a simplified geometrical model was calculated to be ≈300. The source function was approximated by a second-order polynomial. The turbulent velocities of the emitting layer were found to be ≈6.8 km/sec, in agreement with other observations. (auth)

27373 λ 4097.3 NIII EMISSION IN THE CHROMOSPHERIC SPECTRUM. Lambert, D. L. (Univ. of Texas, Austin). Solar Phys.; 236-9(Feb 1971).

The recent tentative identification of a chromospheric emission line at λ = 4097.342 Å with the N III transition $3s^2S_{\frac{1}{2}}-3p^2P^0_{\frac{3}{2}}$ is discussed. It is shown that the observed intensity is inconsistent with the observed flux in the xuv resonance lines and considerably greater than the predicted intensity from the chromosphere–corona transition zone. Microphotometry of a plate shows that the "line" is a short interval of continuum between absorption lines. (auth)

27374 MOLECULAR SPECTRUM OF SUNSPOTS. Webber, John C. Solar Phys.; 16: 340-61(Feb 1971).

The sunspot spectrum shows many molecular lines, of which some have been identified. These lines are formed farther out in the sunspot atmosphere than the atomic lines or the continuum, and are thus useful for probing the outer layers. Photographic spectrograms were obtained for three different sunspots under carefully selected seeing conditions, showing molecular absorption lines due to MgH, CaH, and TiO. Analysis led to estimates of the effective rotational temperatures of each; in the case of CaH, no definite conclusions could be drawn. Predicted rotational temperatures and observational f-values were calculated on the basis of model umbral atmospheres due to several authors. A new model was derived from the molecular lines measured here, and shown to differ widely from previous models. The usefulness of photographic spectra for this purpose is seriously questioned, and suggestions are made for new observations. (auth)

27375 UNUSUAL ROTATION OF A SUNSPOT SEPTEMBER 30 TO OCTOBER 8, 1969. Miller, Richard A. (Manila Observatory). Solar Phys.; 16: 371-8(Feb 1971).

The rotation of a leader sunspot in plage region No. 10344, first 130° counterclockwise, then 142° clockwise in only eight days, was investigated. Proper motion of translation of the components of this spot was found more important for flare activity than was rotational motion. (auth)

27376 NEW EMPIRICAL MODEL OF A SUNSPOT UMBRA. Yun, Sik Hong (Franklin Inst., Swarthmore, Pa.). Solar Phys.; 16: 379-83(Feb 1971).

A model for the T, τ relation in the umbra of a sunspot was derived from the observed infrared continuous limb darkening of the spots' umbrae. (auth)

27377 MAGNETIC FIELDS AND MOTIONS IN SUNSPOTS AT DIFFERENT ATMOSPHERIC LEVELS. Abdussamatov, H. I. (Pulkovo Observatory, USSR). Solar Phys.; 16: 384-97(Feb 1971).

The distribution of the magnetic field and radial velocities in the sunspot group were investigated simultaneously at two atmospheric levels (Hα and 6302.499 Å) of the Sun inside the area of 35″ × 80″ photographically (Abdussamatov, 1970) using the method of escalation. The outward motion of matter in the spot umbra was detected. Distributions of the magnetic field at both levels are well correlated. The magnetic field motions are observed in the sunspot. The vertical gradient H decreases slightly in the direction of increasing H. The minimum of brightness I in sunspots corresponds to the maximum of H. (auth)

27378 MAGNETOSTATIC SUNSPOT MODEL WITH TWISTED FIELD. Yun, Sik Hong (Franklin Inst., Swarthmore, Pa.). Solar Phys.; 16: 398-403(Feb 1971).

It is shown that the internal structure of sunspots is affected only to a small degree by the presence of the azimuthal component of the sunspot magnetic field. The magnetostatic theory of sunspots developed by Schlüter and Temesvary (1958) is extended to include such an effect. In the present study, the radial dependence of the azimuthal component of the field is adopted from the observation of Stepanov (1965). A typical sunspot of an effective temperature of 4000 K is considered and its detailed structure is presented. (auth)

27379 ECLIPSE MEASUREMENTS NEAR 1.2 cm WAVELENGTH ON SEPTEMBER 11, 1969. El-Raey, Mohamed (Univ. of California, Berkeley). Solar Phys.; 16: 404-12(Feb 1971).

Measurements performed at wavelength 1.18 cm during the September 11, 1969, partial solar eclipse are described. No significant limb brightening was detected. However, a high coronal contribution to the emission at this wavelength was observed. Separation between the emission from the center of a unipolar spot of diameter ≈ ½ to 1 arc min and its plage region of diameter ≈3 to 4 arc min was possible. (auth)

27380 PROBLEM OF THE FLARE-LIKE EMISSION IN SODIUM LINES. Gurtovenko, E. A. (Main Astronomical Observatory, Kiev). Solar Phys.; 16: 413-16(Feb 1971).

Unusual and intense emission in the D_1, D_2 lines was registered photoelectrically in an undisturbed region near the center of the solar disk on July 28, 1966. Various aspects of the possibility that the emission might originate in either artificial or natural comets by processes of resonance scattering or fluorescence were analyzed. It is shown that the observed emission can only be located on the solar surface. Some aspects of the problem are discussed briefly. (auth)

27381 IMPULSIVENESS OF MICROWAVE BURSTS AND ITS ASSOCIATION WITH SUNSPOT TYPES. Matsuura, O. T.; Nave, M. F. F. (Univ. Mackenzie, Sao Paulo, Brazil). Solar Phys.; 16: 417-22(Feb 1971).

A statistical analysis on 220 impulsive microwave bursts showed a marked preference to occur in sunspots of type D, E, and F (after Zürich classification). Assuming a shock mechanism for accelerating electrons, this tendency seems to be related to the size of the magnetic loops. (auth)

27382 EXPLOSIVE PHASE OF SOLAR FLARES. Harvey, Karen L. (Lockheed Solar Observatory, Saugus, Calif.). Solar Phys.; 16: 423-30(Feb 1971).

The explosive phase of a flare can be defined by a simple photometric measurement of Hα film records of the flare development. Using the quantitative definition, improved correlations are found between the start of the explosive phase and the start of 10.7-cm radio bursts and Sudden Frequency Deviations compared to earlier correlations of the same data using visual estimates of the start of the explosive phase. Explosive development may be confined to only part of a flare. (auth)

27383 SOLAR SOFT X RAYS AND SOLAR ACTIVITY. II. SOFT X RAY EMISSION DURING SOLAR FLARES. Thomas,

XUM

Roger J. (Univ. of Michigan, Ann Arbor. Goddard Space Flight Center, Greenbelt, Md.); Teske, Richard G. Solar Phys.; 16: 431-53(Feb 1971).

Flare-associated soft x-ray bursts (8 to 12 Å) were examined for 283 events observed by OSO-III. These bursts are shown to be predominantly thermal in nature. Their time profiles are roughly similar to those of the associated Hα flares, although the x-ray burst begins about two minutes earlier, on the average. The strength of the soft x-ray burst is directly related to the area and brilliance of the flare, the age and "flare-richness" of the associated plage, and the general level of solar activity at the time of the burst. The peak enhancements in the soft x-ray and Hα emission rates during flares are of the same order of magnitude, as are the total flare energies radiated at these wavelengths. It is estimated that soft x radiation accounts for up to 10% of a flare's total electromagnetic emission. (auth)

27384 LOCATION AND SIZE OF A SOLAR HARD X RAY BURST ON SEPTEMBER 27, 1969. Takakura, T.; Ohki, K.; Shibuya, N.; (and others) (Tokyo Univ.). Solar Phys.; 16: 454-64(Feb 1971).

The location and size of a solar impulsive hard x-ray burst were determined in one dimension to a considerable precision with a balloon-borne x-ray modulation collimator. The center of the x-ray source was on the line passing through the center of a big Hα flare region of 3 arc min. The size of the x-ray source was remarkably smaller and may have been one arc min or less. (auth)

27385 ORIGIN OF FLARE PRODUCED HARD X RAYS. Milkey, R. W. (Los Alamos Scientific Lab., N. Mex.). Solar Phys.; 16: 465-8(Feb 1971).

The question of whether or not the x-ray bursts associated with solar flares are produced by thermal processes or require a nonthermal electron energy distribution is of great importance to the development of flare theories. Some authors (Takakura, 1969; Kane, 1969; Hudson et al., 1969) have used a nonthermal electron distribution, usually a power law distribution, to explain the shape of the hard (E > 10 keV) x-ray spectrum. The purpose of this note is to point out that in some cases thermal emission from a volume in which a strong temperature gradient is present may mimic the behavior of a nonthermal spectrum. Therefore it may not be necessary to invoke the presence of these high-energy, nonthermal, electrons in order to explain flare x-ray emission. (W.D.M.)

27386 COMMENT ON SOLAR FLARE IRON LINE EMISSION AT 1.9 A. Phillips, K. J. H.; Culhane, J. L. (Mullard Space Science Lab., London). Solar Phys.; 16: 469-71(Feb 1971).

The controversy which has developed over the past three years on the identification of a line feature at 1.9 Å, prominent in solar flare spectra, is discussed. It is concluded that an anomalous concentration of Fe XXV ions at the measured temperatures is not now required. Other sources of error apart, the assumption of ionization equilibrium does not apparently lead to discordant results. (W.D.M.)

27387 EFFECT OF ALFVEN WAVES ON MHD FAST SHOCKS. Scholer, M.; Belcher, J. W. (California Inst. of Tech., Pasadena). Solar Phys.; 16: 472-83(Feb 1971).

The Rankine–Hugoniot equations for hydromagnetic shocks are extended to include the energy and momentum flux due to Alfvén waves incident on the shock. The shock relations are solved numerically for a wide variety of parameters typical of interplanetary conditions. The presence of the waves can cause appreciable changes in the structure of fast shocks of low Mach number. (auth)

27388 SOLAR PROTON EVENT CLASSIFICATION SYSTEM. Smart, D. F.; Shea, M. A. (Air Force Cambridge Research Labs., Bedford, Mass.). Solar Phys.; 16: 484-7(Feb 1971).

The system described is the result of a preliminary proton event classification system proposed during the Inter-Union Commission on Solar–Terrestrial Physics Plenary Meeting held in London in Jan. 1969. The system is based on the solar proton flux in the vicinity of the Earth measured in units of cm^{-2} sec^{-1} $ster^{-1}$ at the time of maximum intensity, and is intended to convey the response of three types of sensors to a solar-particle event. (W.D.M.)

27389 COMMENTS ON SOLAR ACTIVITY, 27-DAY VARIATIONS, AND LONG-TERM MODULATION OF COSMIC-RAY INTENSITY BY V. K. BALASUBRAHMANYAN AND D. VENKATESAN. Lockwood, J. A. (Univ. of New Hampshire, Durham). Solar Phys.; 16: 488-9(Feb 1971).

In order to clarify the relationship between Forbush decreases and the 11-year variation, direct spacecraft measurements should be made of either the radial cosmic-ray density gradient as a function of time during the solar modulation cycle, or the interplanetary field fluctuations at several AU. Until such results are available, the question of whether the 11-year variation arises from a series of large and sudden drops, from which only partial recovery occurs or gradually remains unresolved. (W.D.M.)

27390 MOLECULES IN SUNSPOTS. Woehl, H. (Univ., Goettingen, Ger.). Solar Phys.; 16: 362-72(Feb 1971).

Spectra of umbrae of several sunspots in the wavelength region 4000 to 8000 Å scanned photoelectrically at the Göttingen Locarno Observatory were used in order to search for absorption lines of molecules. Several thousands of lines of known molecules were reidentified. Newly identified molecules are CoH, NiH, and H_2O. The Zeemann effect on molecular lines of MgH and CaH in spectra of umbrae was detected. (auth)

27391 OBSERVATIONS OF CHROMOSPHERIC FLARES AT ONDREJOV OBSERVATORY DURING THE YEARS 1964–1968. Hrebik, F.; Kvicala, J.; Krivsky, L.; Olmr, J. (Astronomical Inst., Ondrejov, Czech.). Bull. Astron. Inst. Czech.; 21: 170-92(1970).

This paper is a continuation of ten preceding reports, which contained data on chromospheric flares observed at Ondřejov from 1948 up to the end of the year 1963, and covers the period of the years 1964–1968. The data on 447 flares, associated 9400-, 808-, 536-, and 260-MHz events, and 27-kHz SEA observed and recorded during the years 1964–1968 are summarized. The corresponding curves of the H_α line-width changes are plotted. (auth)

27392 REFLECTION, REFRACTION, AND COUPLING OF MHD WAVES AT A DENSITY STEP. Stein, Robert F. (Harvard Coll. Observatory, Cambridge, Mass.). Astrophys. J., Suppl. Ser.; 22: No. 192, 419-43(Apr 1971).

The transmission and reflection coefficients for MHD waves incident on a density step are calculated. All three modes (fast, slow, and Alfvén) are coupled together except when the magnetic field is in the plane of incidence or the plane of the interface. Results for arbitrary orientations of the interface normal, the magnetic field, and the incident wave vector are shown in a series of graphs. Strong coupling between modes occurs for incident wave vectors nearly parallel to the magnetic field. The fast and Alfvén modes are coupled for $P_{mag} > P_{gas}$, the slow and Alfvén modes are coupled for $P_{mag} < P_{gas}$, and all three modes are coupled for $P_{mag} \approx P_{gas}$. The slow and Alfvén modes are decoupled for $P_{mag} > P_{gas}$. (auth)

27393 PROPAGATION OF MAGNETO-ACOUSTIC WAVES ALONG THE GRAVITATIONAL FIELD IN AN ISOTHERMAL ATMOSPHERE. Bel, N. (Institut d'Astrophysique, Paris); Mein, P. Astron. Astrophys.; 11: 234-40(Mar 1971).

The local dispersion equation obtained by McLellan and Winterberg (1968) for magneto-acoustic waves propagating in an isothermal atmosphere was studied. Wave propagation vectors along the gravitational field, for an arbitrary direction of the magnetic field, were considered. The propagation of the waves is shown to depend on two parameters, namely the ratios of the Alfvén velocity and of the Alfvén velocity for the vertical component of the magnetic field to the speed of sound. For typical values of these two parameters, representative curves were obtained for the phase and the amplitude of the waves as functions of the frequency. Two modes were found, which are the counterparts of the usual fast and slow magneto-acoustic waves. A comparison with the case of an isothermal and compressible atmosphere without a magnetic field shows that the new mode is the slow one. It was found that the magnetic field decreases the hydrodynamic cut-off frequency and that, for large values of the magnetic field, the fast and the slow modes can intersect. The theoretical curves thus obtained make possible a direct comparison with observational data concerning the solar atmosphere. (auth)

27394 RELATIONSHIP BETWEEN VELOCITY FIELDS AND MAGNETIC FIELDS IN THE SOLAR ATMOSPHERE. Gopasyuk, S. I.; Tsap, T. T. (Crimean Astrophysical Observatory, Moscow). Sov. Astron. AJ (Engl. Transl.); 14: 813-17(Mar-Apr 1971).

Translated from Astron. Zh.; 47: 1012-18(Sep-Oct 1970).

The relationship between the velocity fields and the magnetic fields in the active and quiet regions of the solar atmosphere was studied. The radial velocities and magnetic fields were measured on a double magnetograph in the lines Fe I λ 5250 Å, Ca I λ 6103 Å, and Hα. The maxima of the magnetic "hills" in both the active and quiet regions are on a line of zero radial velocity or in the immediate vicinity of such a line. Near the zero lines, where there are magnetic hills, the velocity direction indicates both compression and expansion of the gas near the zero line. In about 43% of the cases, gas is flowing away from the zero lines. (auth)

27395 HYDROGEN IONIZATION AND THE EXCITATION OF QUIESCENT PROMINENCES. Kiryukhina, A. I. (Shternberg State Astronomical Inst., USSR). Sov. Astron. AJ (Engl. Transl.); 14: 818-24(Mar-Apr 1971).

Translated from Astron. Zh.; 47: 1019-29(Sep-Oct 1970).

It was found from measurements of the continuous spectra of prominences that the n(H II)/n(H I) value characterizing the degree of ionization of hydrogen varies greatly from prominence to prominence. A direct dependence was found between the ratio of He_ζ and H_δ equivalent line widths and hydrogen ionization and the mean density of neutral hydrogen atoms along the line of sight. Corresponding graphic dependences were constructed, as well as the graphic dependence of the H_δ equivalent line width on the total number of neutron hydrogen atoms along the line of sight. The constructed curves were used for 40 prominences with known T_{kin} and v_t values for determining the values: n(H II)/n(H I), n(H I), n_e, $\alpha = h_{eff}/H$, and H, the thicknesses of prominences along the line of sight. It is shown that ionization in prominences is not dependent on the T_{kin}, n_e, and H values but is a result of the fine structure of prominences. "Metallic" and "ordinary" prominences differ primarily in the degree of hydrogen ionization. (auth)

27396 THERMAL MODEL OF SOLAR CORONA ACTIVE REGIONS. Beigman, I. L.; Vainshtein, L. A. (Lebedev Inst. of Physics, Moscow). Sov. Astron. AJ (Engl. Transl.); 14: 825-30 (Mar-Apr 1971).

Translated from Astron. Zh.; 47: 1030-7(Sep-Oct 1970).

X-ray fluxes in the resonance lines ($\lambda < 25$ Å) of the most abundant ions in the solar corona were computed. The computed fluxes were used in an analysis of experimental data published by various authors (1963–1967) within the framework of thermal models of active coronal regions. The two groups of available data can be described either by a model with a definite temperature and an emission measure of about 0.1 Baumbach (case a) or by a model of a region with a high emission measure and smooth temperature variation (case b). (auth)

27397 INNER CORONA POLARIZATION DURING THE SOLAR ECLIPSE OF SEPTEMBER 22, 1968. Nikol'skii, G. M.; Sazanov, A. A. (Inst. of Terrestrial Magnetism, Ionosphere, and Radio-Wave Propagation, Moscow). Sov. Astron. AJ (Engl. Transl.); 14: 831-4(Mar-Apr 1971).

Translated from Astron. Zh.; 47: 1038-43(Sep-Oct 1970).

Polarimetric photographs of the inner corona with the polaroid in different positions (spectral region 5000 to 7000 Å) were obtained during the total solar eclipse of September 22, 1968 (Yurgamysh, Southern Urals) with a Maksutov telescope (1 m/10). Isophotes for three photographs were constructed as a result of photometric processing. The isophotes were used in constructing isolines of the degree of polarization for altitudes $\leq 0.25\ R_\odot$. The degree of polarization was exceptionally high, 30 to 60% (accuracy ±10%); this indicates a considerable degree of inhomogeneity in the distribution of matter in the inner corona. (auth)

27398 OBSERVATIONS OF SOLAR RADIO BURSTS WITH HIGH SPECTRAL RESOLUTION. Markeev, A. K.; Chernov, G. P. (Inst. of Terrestrial Magnetism, Ionosphere, and Radio-Wave Propagation, Moscow). Sov. Astron. AJ (Engl. Transl.); 14: 835-9(Mar-Apr 1971).

Translated from Astron. Zh.; 47: 1044-6(Sep-Oct 1970).

Preliminary results are given of observations with a spectrograph with high resolution in the range of 190 to 220 MHz. Besides the usual Type-I bursts, short bursts were observed whose parameters suggested those called "spikes." Also, fast-drifting bursts with the following parameters are described: duration at fixed frequency ~0.1 sec, instantaneous frequency bandwidth $\Delta f \sim 1$ to 1.5 MHz, bandwidth of occupied frequencies 6 to 30 MHz, $df/dt \sim$ 20 to 40 MHz/sec, and degree of polarization close to 100%. In "chains" of Type-I bursts, a drifting cutoff of burst intensity on the high-frequency side is observed. (auth)

27399 STATIC SOLAR HII ZONE. Krasnobaev, K. V. (Inst. of Cosmic Research, Moscow). Sov. Astron. AJ (Engl. Transl.); 14: 840-4(Mar-Apr 1971).

Translated from Astron. Zh.; 47: 1047-52(Sep-Oct 1970).

A static solar H II zone is considered. A system of equations for ionization balance and energy, transfer of ultraviolet radiation, and gravitational equilibrium is numerically solved. The results of the computations show that the extent of the Strömgren zone is quite great—of the order of 10^3 au—and the temperature of the interstellar gas surrounding the Sun is about 10^4 °K. These results are compared with other data on the solar H II zone. (auth)

27400 EFFECT OF MACROTURBULENCE ON FRAUNHOFER LINE PROFILES. Gurtovenko, E. A.; Ratnikova, V. A. (Main Astronomical Observatory, Moscow). Sov. Astron. AJ (Engl. Transl.); 14: 845-8(Mar-Apr 1971).

Translated from Astron. Zh.; 47: 1053-7(Sep-Oct 1970).

Macroturbulence in the solar photosphere and its relationship to the form of Fraunhofer line profiles are briefly discussed. The effect of macroturbulence on the central intensities of different absorption-line profiles is evaluated. (auth)

27401 THOMSON SCATTERING AS A COOLING MECHANISM FOR THE SOLAR CORONA. Illarionov, A. F.; Syunyaev, R. A. (Inst. of Applied Mathematics, Moscow). Sov. Astron. AJ (Engl. Transl.); 14: 910-11(Mar-Apr 1971).

Translated from Astron. Zh.; 47: 1141-3(Sep-Oct 1970).

Compton scattering of photospheric radiation by coronal electrons will lead to cooling of the electrons and an insignificant departure of the spectrum of the scattered light from the emission spectrum of the disk. This cooling mechanism will contribute a few percent of the total energy losses of the corona; it will predominate over the radiative cooling mechanism at distances greater than $2.5\ R_\odot$. (auth)

Galaxies

27402 INTERSTELLAR $^{12}C^{16}O$, $^{13}C^{16}O$, AND $^{12}C^{18}O$. Penzias, A. A. (Bell Telephone Labs., Inc., Holmdel, N. J.); Jefferts, K. B.; Wilson, R. W. Astrophys. J.; 165: 229-40(15 Apr 1971).

J = 1 to J = 0 line radiation due to interstellar $^{12}C^{16}O$, $^{13}C^{16}O$, and $^{12}C^{18}O$ was measured in the directions of a number of well-known objects. Strip maps in declination and right ascension across W51, Sgr A, and Sgr B2 are presented. The peak opacities observed were typically near 70, corresponding to column densities close to 10^{19} molecules cm^{-2}. (auth)

27403 GALACTIC WINDS. Johnson, H. E.; Axford, W. I. (Univ. of California, San Diego). Astrophys. J.; 165: 381-90 (15 Apr 1971).

The steady, radial flow of a perfect gas in a spherically symmetric galaxy is analyzed, taking into account the emission of gas from the stars comprising the galaxy and allowing for the presence of a central gravitating source or sink of gas. The equations of motion are reduced to a concise form which involves a single ordinary differential equation for the Mach number in terms of the radial distance. A variety of solutions with outward and inward flow is found, including cases in which the flow is partly inward and partly outward. (auth)

27404 NEUTRAL-PION DECAY AND THE GAMMA RADIATION FROM OUR GALAXY. Cavallo, G.; Gould, R. J. (Univ. of California, San Diego, La Jolla). Nuovo Cim.; 2B: 77-92 (11 Mar 1971).

From the demodulated cosmic-ray spectrum, the production spectrum of γ rays from π^0 decay is computed, the π^0 mesons being produced (singly, multiply, and from isobar decay) in collisions of cosmic-ray protons and alpha particles with hydrogen and helium nuclei of the interstellar gas. The computed spectrum is characteristically broad and flat for photon energies in the neighborhood (factor of 2) of $\frac{1}{2}m_\pi c^2 = 67.5$ MeV. Applied to the interpretation of the Clark–Garmire–Kraushaar experiment, the calculated γ-ray flux from the general galactic disk is in agreement with the observations. However, to explain the observed peak flux from the galactic center a core source with therein at least several times the local interstellar emissivity is required. (auth)

27405 ABSENCE OF RADIO EMISSION FROM MAFFEI I. Oort, J. H. Nature (London); 230: 103-5(12 Mar 1971).

It has been suggested that the infrared object discovered by Maffei during a search for T Tauri variables is the nucleus of an exceptionally close giant elliptical galaxy, the main body of which is obscured by absorption in our Galaxy. Although the observations point strongly in this direction, the suggestion is a considerable extrapolation from the actual observations and additional information on the properties of the object is desirable. In the work described, the field surrounding Maffei I was examined over a period of 12 hours with the synthesis radio telescope at Westerbork to look for continuous radiation at 1415 MHz; the result was negative. The survey presented indicates that no giant elliptical galaxy is known to have a radio luminosity smaller than 5×10^{38} but the available data are insufficient to exclude the possibility of the existence of giant ellipticals with radio luminosities of the order of 10^{34}. It can only be stated that Maffei I is at least four orders of magnitude fainter in radio luminosity than the faintest observed giant ellipticals. Further work is going on. (UK)

27406 COMPUTER SIMULATIONS OF PROCESSES IN GALACTIC DYNAMICS. Quirk, William Joseph. New York; Columbia Univ. (1970). 108p. University Microfilms Order No. 71-6242.

Thesis.

Computer n-body calculations were carried out to simulate galactic evolution. Three types of systems were simulated: pure gas, pure star, and pure gas evolving into mixed star and gas. To simulate a property of real galaxies, namely, that two body gravitational interactions are unimportant, n in these calculations was made large, roughly 100,000. The bodies were of two types: either "stars"—point particles with only gravitational interactions—or "gas clouds"—particles that have inelastic collisions with each other as well as gravitational interactions. The "gas cloud" component of the n-body system resembles a gas in two ways: it is dissipative and its particles have a finite mean free path. The effects of magnetic fields, cosmic rays, supernovae, ionization of hydrogen regions by young stars and many other phenomena were ignored. (TSS) (Diss. Abstr. Int., B)

27407 GAMMA RAYS AND THE DISTRIBUTION OF COSMIC RAYS IN THE GALAXY. Ulmer, Melville Paul. Madison, Wis.; Univ. of Wisconsin (1970). 168p. University Microfilms Order No. 70-22,077.

Thesis.

An interpretation is provided of the OSO III gamma-ray results of Clark, Garmire, and Kraushaar, 1968. Reevaluation of the estimate of the OSO III gamma-ray detector's efficiency shows that the flux from the galactic anticenter ($|l^{II}| > 130°$, $|b^{II}| < 15°$) is explained by assuming the gamma-ray flux originates from the decay of collisionally-produced π^0 mesons. Assuming this mechanism is responsible for all of the observed gamma-ray flux from the galactic plane, cosmic-ray distributions are derived that would produce the observed galactic longitude dependence of the gamma-ray data. The general features of the most reasonable models suggest a cosmic-ray density that increases by more than a factor of 10 from the Earth to within 4 kpc of the galactic center. Nonthermal radio noise predictions are made, using the cosmic-ray distributions that were used to make gamma-ray predictions. The nonthermal radio noise data agree with the observations if the galactic magnetic field strength is assumed to be constant or decreases slightly from near the Earth to the galactic center. (Diss. Abstr. Int., B)

27408 POLARIZATION OF μ CEPHEI AND GRAPHITE CORE–ICE MANTLE GRAINS. Svatos, J. (Charles Univ., Prague). Bull. Astron. Inst. Czech.; 21: 54-5(1970).

It is shown that the theoretical curve for graphite core–ice mantle grains having parameters $R_0 = 0.05\mu$ and $R = 0.13\mu$ gives a good fit with the observational points according to Coyne and Gehrels (1966). (auth)

27409 STELLAR CONTENT OF THE NUCLEI OF NEARBY GALAXIES. I. M31, M32, AND M81. Spinrad, Hyron; Taylor, Benjamin J. (Univ. of California, Berkeley). Astrophys. J., Suppl. Ser.; 22: No. 193, 445-84(Apr 1971).

Photoelectric scanner observations with spectral resolutions of 16 and 32 Å were obtained for the nuclei of the nearby galaxies M31, M32, and M81. The objective was to synthesize model galaxies from individual local stars observed with the same equipment. In the models many groups of stars representing different segments of the H–R diagram were blended together to match the galaxy observations suitably—the scanner I(λ) measures made from λ3300 to λ10700 and infrared colors to 3.4 μ. Both lines and continua were included. The spectral features measured (molecular bands of TiO, CN, CH, CaH, and MgH; plus atomic lines of Na I, Ca I and Ca II, Mg I and the Balmer lines of hydrogen) were chosen so as to maximize the likelihood of achieving almost-unique models to represent the stellar content of the nuclei of galaxies. Given a few astrophysical constraints (mainly a continuous luminosity function), good-fitting models which are relatively unique can be obtained for M31. The solutions for M32 and M81 are somewhat less satisfactory. Alternative solutions are presented, mainly to illustrate some of the difficulties with previous models. Main conclusions for the center of M31 are as follows: a) There is a strongly dwarf-enriched lower main-sequence, leading to a stellar M/L = 44 for the best models. Dwarfs contribute ~30% of the V light in these models and somewhat more in the near-infrared. b) The main-sequence turnoff point is at a slightly hotter temperature than the Sun, an observation implying a rather old stellar population. However, some star formation continued until 4 billion years ago. c) The stars in the nucleus are very strong-lined, with an average metal abundance much higher than the Sun's and probably somewhat in excess of that found in old super-metal-rich open clusters like M67. No weak-lined stars are allowed in the M31 model; i.e. Population II plays no role. The best M32 models are quite different. They require a mildly metal-poor globular-cluster-like population as a base. The solution for the M81 nucleus is complicated by the presence of many emission lines. They could be associated with the small radio source there. The best models for M81 have more gM's than the M31 model; this is required to match the stronger M81 infrared continuum flux. (auth)

27410 STABILITY PROBLEM OF OSCILLATIONS ALONG THE AXIS OF SYMMETRY IN A GALAXY. II. THE FIRST ORDER PERTURBATIONS IN A GENERAL RESONANCE CASE. Andrle, P. (Astronomical Inst., Prague). Bull. Astron. Inst. Czech.; 21: 132-9(1970).

The properties of galactic orbits of a test particle (a star) being in close proximity to the axis of symmetry are considered. In an unperturbed case the considered movement is supposed to be created by two oscillations perpendicular to each other. It was shown previously that the oscillations are stable in the most general case without any commensurabilities. Here, the ratio of the frequencies of both oscillations is equal to r/s, where r and s are natural numbers. The studied oscillations are sometimes unstable. Supposing the perturbing term $a_{ij}\varpi^i z^j$ (which is to be added to a spheroid potential expressing in cylindrical co-ordinates ϖ, ϑ, z) one can conclude that studied oscillations can be unstable if $r \leq i$, $s \leq j$. Two special examples are solved. (auth)

27411 STRUCTURE OF THE GALAXY AND THE VISIBLE PICTURE OF THE MILKY WAY. Pavlovskaya, E. D.; Sharov, A. S. (Shternberg State Astronomical Inst., USSR). Sov. Astron. AJ (Engl. Transl.); 14: 849-54(Mar-Apr 1971).

Translated from Astron. Zh.; 47: 1058-65(Sep-Oct 1970).

The visible brightness of the Milky Way in relation to galactic longitude is considered for a number of galactic structure models. It is shown that, for various suppositions concerning stellar and absorbing matter distributions, the brightness maxima may be both in the directions of the spiral arms and in the spaces between them. Real inhomogeneties in star and dust distributions further complicate the visible picture of the Milky Way. All of this makes the surface photometry of the Milky Way an unreliable means of uncovering the spiral structure of the Galaxy. Within the limits of the model used, the high brightness of the northern Milky Way in comparison to the southern connot be explained. It may be connected with the difference in average light absorption in these two parts of the Milky Way. (auth)

27412 NUMERICAL EXPERIMENTS WITH A ONE-DIMENSIONAL GRAVITATIONAL SYSTEM BY A EULER-TYPE METHOD. Janin, Guy (Observatory, Geneva). Astron. Astrophys.; 11: 188-96(Mar 1971).

Evolutions of one-dimensional gravitational water-bag models are computed with a Euler-type method. More accurate than the Lagrange-type one, this method shows in a very suggestive manner the separation of the system into a stable core of uniform phase density and a halo formed by thin filaments. If the systems have a space extension greater than the Jeans length, the fragmentation into subsystems due to the Jeans instability appears only if the initial distribution of points is irregular. (auth)

27413 EVIDENCE FOR A SOURCE OF AN EXTRATERRESTRIAL HYDROGEN LYMAN-ALPHA EMISSION: THE INTERSTELLAR WIND. Bertaux, J. L.; Blamont, J. E. (CNRS, Verrieres, France). Astron. Astrophys.; 11: 200-17(Mar 1971).

A series of three special maneuvers commanded to the OGO-5 satellite in September 1969, December 1969, and April 1970 allowed to map the intensity of the 1216-Å Lyman-α emission coming from outside the geocorona, as measured by a photometer with a 80-Å bandwidth and a 0.66° circular field of view. The spatial distribution of this emission, presented in celestial and galactic coordinates, shows no small-scale features, but a maximum of 530 Rayleighs near the ecliptic plane and a minimum of 200 Rayleighs in the opposite direction; these results are in good agreement with those of Thomas and Krassa (1971). The results present no galactic symmetry, but one cannot rule out the existence of an isotropic galactic emission of less than 200 Rayleighs. The 50° apparent displacement of the maximum region between the September 1969 and April 1970 observations is interpreted as the parallax effect of the Earth's motion on its orbit, an evidence that the emission in this direction originates from a distance of ≃3 AU from the Sun. Another evidence is the time variation of the intensity measured in the direction of the North ecliptic pole. The results give strong support to the theory that, in its motion towards the apex, the Sun crosses neutral atomic hydrogen of interstellar origin, giving rise to an apparent interstellar wind; however, the direction of the maximum intensity is found 45° away from the apex direction, and near the ecliptic plane, a fact which might not be fortuitous. (auth)

27414 OGO 5 MEASUREMENTS OF THE LYMAN ALPHA SKY BACKGROUND. Thomas, G. E.; Krassa, R. F. (Univ. of Colorado, Boulder). Astron. Astrophys.; 11: 218-33(Mar 1971).

A series of satellite measurements of the Lyman alpha sky background radiation at radial distances from the Earth of more than 80,000 km is described. A two-channel ultraviolet photometer on OGO 5, responding to the spectral regions 1050 to 1800 Å and 1225 to 1800 Å, measured the spatial variations of the 1216 Å background during three spin-up manoeuvres in September 1969, December

1969, and April 1970. Observations of a large number of hot stars were useful in determining the viewing direction as a function of time. It is shown that a weighted difference of the signals from the two channels represents the Lyman-α 1216 Å background, free from the contribution of unresolved stars. The results are presented in the form of iso-intensity contour maps in ecliptic, celestial, and galactic coordinate systems. The most significant result is the discovery of a prominent maximum in intensity (570 Rayleighs) and a less pronounced minimum (240 Rayleighs) both located near the ecliptic and separated by about 180°. Comparison of the results from the September and April observations indicates the existence of time variations in the spatial structure of up to 70 Rayleighs. The present results are in excellent agreement with those of Bertaux and Blamont (1971) and with less-extensive measurements by previous investigators. An upper limit of about 250 Rayleighs is found for the contribution of galactic sources, which would be expected to be very nearly isotropic. The most likely origin of the observed emission is scattering of solar Lyman-alpha from interstellar hydrogen that is swept into the vicinity of the Earth from the direction of the apparent apex of motion of the solar system. The observed displacements of the maximum and minimum along the ecliptic over a 6-month period are explained by a parallax effect due to the Earth's motion in its orbit. This explanation requires that the effective scattering region be located well within the solar system. (auth)

27415 CORRELATION BETWEEN GAS AND DUST? Wesselius, P. R.; Sancisi, R. (Kapteyn Astronomical Lab., Groningen, Netherlands). Astron. Astrophys.; 11: 246-56(Mar 1971).

The distributions of dust, as derived from the galaxy counts by Shane and Wirtanen (1967), and of neutral hydrogen, as taken from the 21-cm survey by Tolbert (1971), are compared. Both gas and dust are concentrated to the galactic plane, but they do not depend on galactic latitude in the same way. Therefore the material was analyzed in strips of constant latitude with a width of 10° and 2.5°. Using Kendall's rank correlation test and choosing a significance level of 0.01 a "general" correlation was not found between gas and dust. In most of the strips at latitudes below 40° a significant positive correlation was found. Gould's Belt and four other r were investigated separately. Neutral hydrogen and dust are correlated in the two parts of Gould's Belt, i.e., Scorpius–Ophiuchus in the direction of the galactic center at positive latitudes and Orion–Taurus–Perseus in the anticenter direction below the plane. A positive correlation is found also in the region at intermediate positive latitudes, between longitudes 60° and 280°. In Gould's Belt and in the latter region the ratio of neutral hydrogen to dust density ranges between 40 and 140. (auth)

27416 SURVEY OF HIGH-VELOCITY AND INTERMEDIATE-VELOCITY H I CLOUDS WITH 12.5' ANGULAR RESOLUTION. Rickard, J. J. (Univ. of Maryland, College Park. Carnegie Inst. of Washington, D. C. California Inst. of Tech., Pasadena). Astron. Astrophys.: 11: 270-8(Mar 1971).

A survey of the sky from RA = 8h 45m to 11h 45m from Dec = 50° to 85° was made with the 300-ft radio telescope at the NRAO at Green Bank, West Virginia. Some 3000 low-noise 21-cm line profiles were obtained. No new small high-velocity clouds were discovered; but parts of HVC A and HVC CII lie within the survey limits. Several intermediate-velocity clouds were examined. The differences among the various clouds are discussed. These clouds appear to be hot H I clouds of various spin temperatures at large distances from the galactic plane. Some theoretical problems related to their existence at large z distances are investigated. (auth)

27417 NEUTRINO LIMITS ON ANTIMATTER SOURCES OF ENERGY IN SEYFERT GALAXIES. Steigman, G.; Strittmatter, P. A. (Inst. of Theoretical Astronomy, Cambridge, Eng.). Astron. Astrophys.; 11: 279-85(Mar 1971).

Muon-neutrinos (and antineutrinos) produced in matter–antimatter annihilation can serve to test the hypothesis that strong infrared sources derive their energy from annihilation. By comparing the number of μ-neutrinos produced in a typical annihilation with the energy in the electron–positron and gamma-ray components, the minimum flux of μ-neutrinos may be predicted once the infrared flux is known. The spectrum of neutrinos produced in annihilation was computed. Assuming the product of the space density and ir luminosity of Seyfert galaxies varies with redshift (Z) as $L(Z)\,n(Z) = L_0\,n_0(1+Z)^{m+3}$, the flux of μ-neutrinos contributed by all Seyfert galaxies out to a given redshift was computed for m = 0.3 and 6.5. Further, assuming the 3°K and 0.3 mm background radiation fields to be caused by a burst of "Seyfert type" objects at appropriate redshifts, the μ-neutrino flux was computed. When these results are compared with present limits on the flux of μ-neutrinos at the Earth, it emerges that annihilation probably does not supply the energy the ir sources require. (auth)

27418 ABUNDANCES AND REDDENING OF THE NUCLEI OF SEYFERT GALAXIES. Andrillat, Yvette; Souffrin, Suzy (Faculte des Sciences, Montpellier, France. Institut d'Astrophysique, Paris). Astron. Astrophys.; 11: 286-98(Mar 1971). (In French).

Two new problems arise after emission line reddening is found in the spectrum of Seyfert galaxies nuclei: (1) The physical conditions of the emissive gas in the Seyfert nuclei have to be reconsidered, as they were determined from the ratio of emission-line intensities. Indeed, the selective absorption has to be taken into account in the determination of line intensities. (2) It is important to find out if the continuum is reddened or not, as the continuous emission might be much larger than usually assumed. In particular, if a similar reddening has to be applied to the continuum as for the lines, it follows that the continuum is absorbed by a factor 10 or 100 according to the reddening law. The physical conditions of the galaxies studied by Wampler were redetermined and some values of the abundance ratios A(O)/A(N)/A(Ne) were deduced with very few hypotheses. When the line intensities and the physical conditions of the Seyfert nuclei are well known, it was found that the abundances are similar to those of planetary nebulae. In no significant case, the abundances differ drastically from those of planetary nebulae. A stellar population for two nuclei was found and an attempt was made to try to fit the equivalent widths of the Seyfert nuclei absorption lines with calculated equivalent widths for different stellar populations and for different contributions of the nonstellar continuum. It was found that: (a) the dominant spectral type of the stars in these Seyfert nuclei are K and M. The Seyfert nuclei was usually classified as A or F0 as their absorption lines, even intrinsically intense, disappear in a nonstellar continuum, very intense in the uv range. (b) The continuum is not appreciably reddened. The second part of the study was made using the hypothesis of normal abundances in the stars of the nuclei, as the abundances found in the emissive gas seem to be normal. (auth)

27419 ANALYSIS OF THE LOW FREQUENCY RADIO CONTINUUM IN THE GALAXY. Stephens, S. A. (Kamerlingh Onnes Laboratorium, Leiden). Astron. Astrophys.; 11: 311-16 (Mar 1971).

A detailed analysis of the galactic radio continuum above 0.4 MHz towards the halo directions was carried out using knowledge of the energy spectrum of cosmic-ray electrons in the Galaxy. It was found that, if the intercloud medium is in a thermally stable phase at about 9000°K, one can make a reliable estimate of the electron density in the cool clouds, which are mainly responsible for the absorption of the low-frequency continuum radiation. Analysis of the radio spectrum favors the model of the interstellar medium proposed by Field, Goldsmith, and Habing with a lower electron density of 0.02 cm^{-3} for the clouds at z = 0, with a filling factor of about 0.02. It was also found that in the absence of clouds, one can set a lower limit of 4000°K to the temperature of the intercloud medium, which seems to discredit the model proposed by Hjellming, Gordon, and Gordon. (auth)

27420 ORIENTATION IN PHYSICAL PAIRS OF GALAXIES. Gorbachev, B. I. (Novocherkassk Polytechnical Inst., USSR). Sov. Astron. AJ (Engl. Transl.); 14: 781-4(Mar-Apr 1971).
Translated from Astron. Zh.; 47: 972-6(Sep-Oct 1970).

All the close interacting galactic pairs in the MCG catalog, which furnishes estimates of the inclinations of the components' equatorial planes, were used to find the distribution of pairs with respect to the difference Δi between the inclinations of the components and the difference $\Delta\theta$ between the positional angles of the major galactic axes. A preferential orientation of the galaxies in pairs was found. (auth)

Cosmology

Refer also to abstracts 28087, 28441, and 28444.

27421 (ITF-70-105-E) ON A MODEL OF THE EXPANDING UNIVERSE. Wataghin, G. V. (Akademiya Nauk Ukrainskoi SSR, Kiev. Institut Teoreticheskoi Fiziki). 1970. 11p. Dep. NTIS (U. S. Sales Only).

The evolution of the expanding Universe is interpreted as a uniform 4-dimensional dilatation of space–time and the corresponding contraction of momentum–energy parameters. A simple interpretation of the Hubble effect is obtained. (auth)

27422 IMPLICATIONS OF THE INVERSE-SQUARE-LAW MODEL. Saari, Donald G. (Northwestern Univ., Evanston, Ill.). Astrophys. J.; 165: 399-407(15 Apr 1971).

Newtonian gravitational systems are considered and the behavior of the n-body problem as time approaches infinity is discussed.

This gives the Newtonian version of the spatial distribution of clusters. Also, the value of Hubble's constant for Newtonian systems is derived. The virial theorem is studied from two viewpoints. The first is to show the dynamical consequences of the assumption $2T - U = 0$, and the second is to consider the probability that a system will eventually approach this state. All of the results assume only the inverse-square law as the force law. Hence the conclusions could be interpreted as a test of the validity of the inverse-square law and/or which phenomenon can be explained by simply the dynamics of the problem. (auth)

27423 THE POSSIBILITY OF DETECTABLE FLUXES OF COSMIC γ RAYS WITH ENERGY ABOVE 10^{19} eV. Wdowczyk, J. (Inst. of Nuclear Research, Lodz, Poland); Tkaczyk, W.; Adcock, C.; Wolfendale, A. W. J. Phys., A(London); 4: L37-9(Mar 1971).

Under the assumption that cosmic rays are of extragalactic origin above 10^{18} eV it is shown that the presence of the 2.7°K blackbody radiation may lead to a detectable flux of very energetic γ rays. (auth) (UK)

27424 TIME-REVERSAL SYMMETRY VIOLATION AND THE OSCILLATING UNIVERSE. Aharony, Amnon; Ne'eman, Yuval (Tel-Aviv Univ., Israel). Int. J. Theor. Phys.; 3: 437-41(Dec 1970).

The expressions for the fractional number of K^0's and $\bar{K}^0$'s in a neutral kaon beam are discussed with reference to time-reversal asymmetry. The suggested relation between the sign of Reϵ (ϵ is the Lee–Wu T-violation parameter) and the cosmological arrow of time if CPT is broken is further clarified. (auth) (UK)

27425 HOMOLOGICAL FOUNDATION FOR SCALE PROBLEMS IN PHYSICS. Atkin, R. H. (Univ. of Essex, Eng.); Bastin, Ted. Int. J. Theor. Phys.; 3: 449-66(Dec 1970).

First steps towards a discrete theory of observation are developed by using algebraic topological concepts and are shown to account for finite limits of resolution. The cohomology ring on a basic simplicial complex is claimed as the natural language of physical theory. This is illustrated by specific examples and a complete set of generators for such a ring will be called the Eddingtonian of a system. The concept of tensorial covariance is logically replaced by that of an isomorphism between base homologies induced by a bijective simplicial map. This is applied to velocity space to produce an abstract form of the Lorentz–Einstein relativity theory and also to discuss an experimental diffraction arrangement devised by Bohm and Aharonov. The latter is shown to be homologically equivalent to the problem of the redshift, and consequently throws light on the question of galactic recession. (auth) (UK)

27426 ANTIMATTER IN THE UNIVERSE. OMNES: R. (Paris Univ., Orsay, France). Nature (London); 230: 26-8 (5 Mar 1971).

Models of nucleosynthesis are discussed which might give clues to the possible existence of aggregations of antimatter in the Universe. (auth) (UK)

27427 GROWTH OF PERTURBATIONS IN AN EXPANDING UNIVERSE OF FREE PARTICLES. Bisnovatyi-Kogan, G. S.; Zel'dovich, Ya. B. (Inst. of Applied Mathematics, Moscow). Sov. Astron. AJ (Engl. Transl.); 14: 758-62(Mar-Apr 1971).

Translated from Astron. Zh.; 47: 942-7(Sep-Oct 1970).

A study is made of the growth of perturbations in a collision-free medium on the background of the exact solution for an expanding universe with the critical density. The Newtonian theory of gravitation is used. The solution of the linearized transport equation is obtained by the method of "integration along trajectories." The results obtained for long waves coincide with the hydrodynamic treatment. For short waves, aperiodic damping is obtained, in contrast to the hydrodynamic result. It is shown that the presence of streams on the distribution function exerts a stabilizing influence on the growth of perturbations; the gravitational interaction does not lead to two-stream instability. (auth)

27428 MIXMASTER UNIVERSES AND THE COSMOLOGICAL PROBLEM. Doroshkevich, A. G.; Novikov, I. D. (Inst. of Applied Mathematics, Moscow). Sov. Astron. AJ (Engl. Transl.); 14: 763-9(Mar-Apr 1971).

Translated from Astron. Zh.; 47: 948-56(Sep-Oct 1970).

A solution describing a model of a mixmaster universe is analyzed quantitatively. The propagation of light in such a model is studied. It has been shown that the solution consists of periods (cycles) of monotonic expansion of the Universe in one direction and oscillations in the two other directions. In the next cycle, the monotonic expansion occurs along one of the other directions, etc. It is shown that during an expansion lasting n cycles there is a catastrophically large change of scale (with the exception of degenerate cases). The scale changes by not less than $(u_{0,1})^2(u_{0,2})^2 \ldots (u_{0,n})^2$ orders, where $u_{0,i}$ is the number of oscillations in the i-th cycle. For a scale change from the quantum-gravitational 10^{-33} cm to the present day 10^{28} cm, not more than three cycles with two or three oscillations in each cycle are possible. If the number of oscillations is greater than 10, there could not be more than one cycle. At best, light does not have sufficient time to go around the Universe in all directions more than two or three times. This is evidently insufficient to equalize temperature inhomogeneities. (auth)

27429 IONIZATION AND HEATING OF INTERGALACTIC GAS. Prilutskii, O. F.; Rozental, I. L. (Inst. of Cosmic Research, Moscow). Sov. Astron. AJ (Engl. Transl.); 14: 770-2 (Mar-Apr 1971).

Translated from Astron. Zh.; 47: 957-9(Sep-Oct 1970).

The ionization and heating of intergalactic gas by ultraviolet radiation is considered. The source of the ultraviolet radiation is assumed to be cosmic electrons interacting with the relict radiation by the inverse Compton effect process. Under this assumption it turns out that the degree of ionization in the intergalactic gas can be high. The heating of intergalactic gas due to ultraviolet radiation turns out to be negligible. (auth)

27430 CORRELATION OF FLUCTUATIONS IN GRAVITATING MEDIA. Genkin, I. L. (Astrophysical Inst., Alma-Ata, USSR). Sov. Astron. AJ (Engl. Transl.); 14: 778-80(Mar-Apr 1971).

Translated from Astron. Zh.; 47: 967-71(Sep-Oct 1970).

The reasons were examined for the differences between the results obtained by various authors in their determinations of the sizes of the correlation region for certain stellar-dynamic characteristics. A correlation function for density fluctuations was obtained. To some degree it reflects the hierarchical structure of the stellar world. (auth)

Planetary Phenomena

27431 IONOSPHERE OF MARS BELOW 80 km ALTITUDE. I. QUIESCENT CONDITIONS. Whitten, R. C.; Poppoff, I. G.; Sims, J. S. (Ames Research Centre, Moffett Field, Calif.). Planet. Space Sci.; 19: 243-50(Feb 1971).

A model of the positive and negative ion chemistry of the Martian ionosphere below 80 km is developed. It is shown that the principal positive ion species are expected to be O_2^+, CO_2^+, and H_3O^+ and its hydrates; the principal negative ions species are CO_3^-, CO_4^- and perhaps CO^-. The model shows that the ionosphere of Mars above 25 km is quite insensitive to the concentrations of atomic oxygen and ozone, and to the values of those rate coefficients that have not yet been measured. Below 25 km, sufficient knowledge does not yet exist to construct a unique ionospheric model. It is concluded that Mars should have a very definite D region and a permanent low-lying electron layer that becomes quite distinct at night. (auth) (UK)

27432 EXTREME-ULTRAVIOLET DAYGLOW OF JUPITER. Carlson, R. W.; Judge, D. L. (Univ. of Southern California, Los Angeles). Planet. Space Sci.; 19: 327-43(Mar 1971).

Processes involving both resonant scattering and fluorescence of the incident solar flux in the wavelength region 300 Å – 1300 Å were considered for the upper atmosphere of Jupiter, and calculations were performed for the intensities of the spectral features that would be observed from outside the atmosphere. (auth) (UK)

27433 MARINER 6 AND 7 ULTRAVIOLET SPECTROMETER EXPERIMENT: UPPER ATMOSPHERE DATA. Barth, C. A.; Hord, C. W.; Pearce, J. B.; (and others) (Univ. of Colorado, Boulder). J. Geophys. Res.; 76: 2213-27(1 Apr 1971).

Mariner 6 and 7 observations of the Mars upper atmosphere show the ultraviolet emission spectrum to consist of the CO_2^+ A–X and B–X bands, the CO a–X and A–X bands, the CO^+ B–X bands, the C I 1561- and 1657-A lines, the O I 1304-, 1356-, and 2972-A lines, and the H I 1261-A line. Laboratory measurements and theoretical calculations show that the CO_2^+ band systems are produced by the combination of photoionization excitation of CO_2 and fluorescent scattering of CO_2^+. An analysis of the vibrational populations of the CO Cameron bands shows that they may be produced from photon or electron dissociative excitation of CO_2. The vibrational distribution of the CO fourth positive bands is the same in the Mars spectrum as in a laboratory CO_2 dissociative excitation spectrum, except from the bands that are self-absorbed by CO in the Mars atmosphere. Since the C I 1561- and 1657-A lines and the O I 1356- and 2972-A lines may be produced in the laboratory by CO_2 dissociative excitation processes, these are the most likely sources in the Mars atmosphere. The

altitude distribution of all the emissions is the same, except for the H I 1261-A and O I 1304-A lines and part of the CO_2^+ A–X bands. The scale heights indicate a cold, predominantly CO_2 atmosphere. The O I 1304-A line emission extends to much higher altitudes than the CO_2 emissions showing that atomic oxygen is present. Its profile suggests that it is excited by more than one mechanism. Fluorescent scattering of the CO_2^+ A–X and B–X bands indicates the presence of CO_2^+, but CO_2^+ is not necessarily an abundant ion. Lyman-α radiation with a single scale height extending several radii from the planet establishes the presence of atomic hydrogen in the Mars exosphere. (auth)

27434 HIGH-RESOLUTION RADIO OBSERVATIONS OF THE PLANET VENUS AT A WAVELENGTH OF 6 CM. Hall, R. W.; Branson, N. J. B. A. (Cavendish Lab., Cambridge, Eng.). Mon Notic. Roy. Astron. Soc.; 151: 185-96(1971).

The Cambridge One-Mile radio telescope was used at a wavelength of 6 cm to obtain maps of the planet Venus with a resolution of 6" × 21" arc. A number of possible models for the atmosphere of Venus are considered, and it appears that the surface pressure is 110 ± 15 atmospheres and the surface temperature 790 ± 20°K. Approximately 0.4% water vapor is present in the lower atmosphere. Some features are found on the disc of the planet, and temperature variations of up to 50°K may occur over the surface of Venus. (auth) (UK)

27435 IO, AN ALFVEN-WAVE GENERATOR. Schmahl, Edward Joseph. Boulder, Colo.; Univ. of Colorado (1970). 142p. University Microfilms Order No. 71-5927.

Thesis.

Io, the nearest of Jupiter's four large satellites, controls the emission probability of about half of Jupiter's decametric radiation. Io can excite hydromagnetic waves and/or particle streams in various ways. One of the most efficient of these mechanisms is the dipole radiation of Alfven waves. Induction effects cause Io to have a sizeable dipole moment. Its magnitude and direction depend on Io's core conductivity and the amplitude of variation of Jupiter's magnetic field as seen by Io. A reasonable estimate of this moment is 10^{22} gauss cm^3. A low-frequency solution of Maxwell's equations coupled to the linearized Vlasov equation indicates that shear Alfven waves will be radiated with a power on the order of 8×10^9 watts. It is suggested that these waves, which are largely unattenuated, are the means of interaction between Io and the ionosphere of Jupiter. (Diss. Abstr. Int., B)

Atomic and Molecular Physics

Atomic, Electron, Ion, and Molecular Beams and Their Reactions

Refer also to abstract 26549.

27436 (WASH–1159) CONFERENCE ON HEAVY ION SOURCES HELD AT U. S. ATOMIC ENERGY COMMISSION, WASHINGTON, D. C., FRIDAY, MARCH 13, 1970. (Division of Research (AEC), Washington, D. C.). 260p. (CONF-700337). Dep. NTIS.

Separate abstracts were prepared for seventeen of the articles. Three brief summary-type articles, including the overall conference summary, were not abstracted. Five of the articles included have already appeared in NSA: see NSA 23: 10461 and 24: 15157, –21810, -28228, and -37178. (M.O.W.)

For abstracts of individual papers see: 27437–27439, 27678, 27688, 27694–27697, 27723, and 28124–28130.

27437 (WASH–1159, pp 113-19) DEEP INELASTIC COLLISIONS AND AUGER PROCESSES. Snell, A. H. (Oak Ridge National Lab., Tenn.).

From Conference on heavy ion sources; Washington, D. C. (13 Mar 1970).

In Conference on heavy ion sources.

The history of production of highly charged ions, the mechanisms involved (principally Auger processes), and possibilities for improved production methods are reviewed briefly. (A.G.W.)

27438 (WASH–1159, pp 141-6) POSSIBLE SINGLE IMPACT SOURCE FOR MULTIPLY CHARGED IONS. Zucker, A. (Oak Ridge National Lab., Tenn.).

From Conference on heavy ion sources; Washington, D. C. (13 Mar 1970).

In Conference on heavy ion sources.

The use of the ELMO mirror machine for producing ions of hydrogen and helium is described. Diagrams showing the doubly ionized helium and the singly ionized molecular hydrogen emission peaks are given. (M.O.W.)

27439 (WASH–1159, pp 147-55) PRODUCTION OF MULTIPLY STRIPPED IONS IN MAGNETICALLY CONFINED HIGH-ENERGY ELECTRON CLOUDS. Trivelpiece, A. W. (Maryland Univ., College Park).

From Conference on heavy ion sources; Washington, D. C. (13 Mar 1970).

In Conference on heavy ion sources.

The University of Maryland Electron Ring Injection and Containment (ERIC) device is discussed as an example of a possible source of multiply stripped heavy ions for particle accelerators. (auth)

27440 SURFACE AND VACUUM PHYSICS INDEX. VOLUME 6, NO. 2, 1971. Bibliography, Author Index, Subject Index in Alphabetical Order, Cumulative Subject Index in Logical Order. Frankfurt am Main; Zentralstelle fuer Atomkernenergie-Dokumentation (1971). 65p.

This listing includes 285 references on various aspects of surface and vacuum physics. (A.G.W.)

Atomic and Molecular Properties

Refer also to abstracts 27895 and 28400.

27441 (ANL–7784) HYPERFINE INTERACTIONS: TABLES OF ISOTROPIC AND ANISOTROPIC PARAMETERS FOR THE ATOMS HYDROGEN TO BISMUTH. McMillan, J. A.; Halpern, T. (Argonne National Lab., Ill.). Mar 1971. Contract W-31-109-eng-38. 14p. Dep. NTIS.

The hyperfine-interaction paramagnetic Hamiltonian is discussed. Tables of expectation values for the atoms hydrogen to bismuth are given for the contact term and for the principal values of the dipole–dipole interaction, reduced to g = 2. An empirical relation is given that permits one to evaluate the change in $\langle r^{-3} \rangle$ with charge in transition metal ions. (auth)

27442 OPTICAL PROPERTIES OF Cr–Mn AND Cr–V ALLOYS. Crandell, M. E. (Muskingum Coll., New Concord, Ohio); Schroeder, K. J. Appl. Phys.; 42 1710-12(15 Mar 1971).

From 16th Annual Conference on Magnetism and Magnetic Materials, Miami Beach, Fla. See CONF-701104.

The optical reflectance of chromium alloys with up to 10 at. % manganese or 50 at. % vanadium was measured at room temperature for photon energies from 0.475 to 2.24 eV. The Cr–Mn alloy system shows a very slight shift of the chromium absorption edge to higher photon energies, whereas the addition of vanadium shifts the absorption edge to lower photon energies. For the alloy with 10 at. % V, the edge disappears to values below the measured photon energy range. The direction of the shift of the absorption edge can be explained qualitatively in a rigid band model with transitions from the t_{2g} band to the Fermi level. This model was previously proposed to explain optical reflection data of chromium–iron alloys. (auth)

27443 CROSS-SECTIONS AND REACTION RATES FOR ELECTRON-IMPACT IONIZATION OF LITHIUMLIKE AND SODIUMLIKE POSITIVE IONS. Mathur, K. C.; Tripathi, A. N.; Joshi, S. K. (Univ. of Roorkee, India). Astrophys. J.; 165: 425-9(15 Apr 1971).

An extension of the classical binary-encounter model is used to calculate the cross sections for ionization of lithium- and sodium-like ions by electron impact. The ionization rate coefficient is also calculated for these ions under the assumption of a Maxwellian distribution for the velocity of the incident electrons. (auth)

27444 EXCHANGE INTERACTION OF MULTI-ELECTRON ATOMS. Duman, E. L.; Smirnov, B. M. Opt. Spectrosc. (USSR) (Engl. Transl.); 29: 229-33(Sep 1970).

Translated from Opt. Spektrosk.; 29: 425-34(Sep 1970).

The energy of exchange interaction of atoms with similar ionization potentials was calculated for large interatomic distances. The result obtained is used to construct the intermolecular interaction potential of inert gas atoms. This potential is used to calculate the basic characteristics of inert gas crystals (sublimation energy, distance between nearest atoms, Debye temperature) and also the coefficients of self-diffusion of inert gas atoms and the elastic-scattering cross sections of these atoms. (auth)

27445 RELATIVE VALUES OF OSCILLATOR STRENGTHS OF SPECTRAL LINES. Komarovskii, V. A.; Penkin, N. P.; Nikiforova, G. P. Opt. Spectrosc. (USSR) (Engl. Transl); 29: 116-18(Aug 1970).

Translated from Opt. Spektrosk.; 29: 220-5(Aug 1970).

The relative values of the oscillator strengths of 275 lines in the absorption spectrum of Sm I are measured by the hook method

of D. S. Rozhdestvenskii. The lines are located in the 7800- to 3200-Å region and originate in transitions from the ground state $4f^6 6s^2\,{}^7F$ of the atom to its excited states. A comparison of the theoretical intensities of several spectral lines in the $^7F - {}^7G$ multiplet of Sm I with experiment showed that there is no L–S coupling in the samarium atom. (auth)

Positronium, Muonium, and Mesic Atoms and Molecules

Refer also to abstracts 27306 and 27865.

27446 TWO-FREQUENCY PRECESSION OF MUONIUM IN MAGNETIC FIELD. Gurevich, I. I.; Ivanter, I. G.; Meleshko, E. A.; (and others). Zh. Eksp. Teor. Fiz.; 60: 471-84(Feb 1971). (In Russian).

A new phenomenon, two-frequency precession of the μ^+-meson of muonium in a transverse magnetic field, is predicted and studied experimentally. Two-frequency precession is employed for determining the magnitude of hyperfine splitting of free muonium atoms in ice, germanium, and quartz. Cessation of μ^+-meson precession in a strong magnetic field is studied theoretically. The effect of incoherent interactions between muonium and the medium on precession of the μ^+-meson spin in muonium atoms is considered. (auth)

27447 POSSIBILITY OF A SINGLE POSITRON BOUND STATE IN AN ELECTRON LIQUID. Baldo, M.; Pucci, R. (Univ., Catania, Italy. Istituto Nazionale di Fisica Nucleare, Catania, Italy). Lett. Nuovo Cim.; 1: 87-95(16 Jan 1971).

Two approximation schemes are used to show that at metallic densities the main contribution to the positron self-energy comes from the positron–plasmon interaction and that, in turn, this interaction gives rise to a plasmon–positron bound state. It is also seen that at low densities the dynamical effects become negligible and an electron–positron bound state seems to appear (quasi-positronium formation). The transition region between the two situations seems to be near a density parameter of $r_s \simeq 8$. (A.G.W.)

Collision Phenomena

Refer also to abstracts 27616, 28126, and 28127.

27448 (IAE-2001) EXPERIMENTAL LIMITATIONS OF THE METHOD OF MERGING BEAMS FOR STUDYING ION-ATOM COLLISIONS. Belyaev, V. A. (Institut Atomnoi Energii, Moscow (USSR)). 1970. 23p. (In Russian). Dep. NTIS (U. S. Sales Only).

Data from experimental studies of ion–atom collisions show the efficiency and feasibility of further development of the method of merging beams. The details of the method and results achieved are discussed. (R.V.J.)

27449 (INR-P-1217) CLASSICAL THEORY OF ATOMIC COLLISIONS. II. ELASTIC ATOMIC COLLISIONS. Gryzinski, Michal (Institute of Nuclear Research, Warsaw (Poland)). 1970. 132p. Dep. NTIS (U. S. Sales Only).

This is an English version of report number INR-P-1225, which was written in Polish. An abstract of INR-P-1225 previously appeared as NSA 25: 19488. (A.G.W.)

27450 DIFFERENTIAL CROSS SECTIONS FOR EXCITATION OF RESOLVED VIBRATIONAL STATES IN $H^+ + H_2(v = 0)$ NON-REACTIVE COLLISIONS. Udseth, H.; Giese, Clayton F.; Gentry, W. Ronald (Univ. of Minnesota, Minneapolis). J. Chem. Phys.; 54: 3642-3(15 Apr 1971).

Differential cross sections for the processes $H^+ + H_2(v = 0) \rightarrow H^+ + H_2(v = 0, 1, 2)$ were measured at an initial center-of-mass kinetic energy of 10 eV. In a plot of the data, peaks due to scattering into the ground and first two excited vibrational states of H_2 are clearly resolved, and the $v = 3$ peak is perceptible. The relative probability of vibrational excitation increases with increasing scattering angle. Q values are calculated for the H_2 final states $v = 1, 2, 3$. (A.G.W.)

27451 ANGULAR DISTRIBUTION OF THE SCATTERING OF Ar BY N_2 AND Ne. Anlauf, K. G.; Bickes, R. W. Jr.; Bernstein, R. B. (Univ. of Wisconsin, Madison). J. Chem. Phys.; 54: 3647-8(15 Apr 1971).

Improved measurements of differential scattering of Ar by N_2 were carried out. The observed cross section follows classical behavior, $I(\theta) \propto \theta^{-\frac{1}{2}}$, at low angles, but the fully averaged calculated $I(\theta)$ still retains undulatory deviations about this angular dependence. Computations carried out with a variety of L–J (n,6) potentials failed to successfully reproduce the data in the rainbow region. Previous results on Ar scattering by Ne are summarized. (A.G.W.)

27452 ENERGETICS OF HeH^+ FORMED IN H_2^+–He COLLISIONS. Leventhal, J. J. (Univ. of Missouri, St. Louis). J. Chem. Phys.; 54: 3279-82(15 Apr 1971).

Kinetic-energy distributions of forward-scattered HeH^+ ions resulting from H_2^+ – He collisions were experimentally determined for H_2^+ laboratory kinetic energies in the range 1.7 to 12.5 eV. These distributions have two main peaks over most of this primary-ion energy range. The lower-energy peak, which appears to correspond to completely inelastic collisions, is believed to result from enhanced collection efficiency; this conclusion is supported by energetic considerations. The behavior of the higher-energy peak, which corresponds to ions formed in the forward direction (center of mass), is consistent with theoretical calculations for the HeH^+ species. (auth)

27453 PAULI EXCITATION OF ATOMS IN COLLISION. Laubert, Roman. New York; New York Univ. (1970). 93p. University Microfilms Order No. 71-2311.

Thesis.

Cross sections were determined for K-shell ionization of Al by energetic ions of N, O, Ne, and Ar and for K-shell ionization of Ne in collisions with C, Ne, and Al. The measurements were made in the energy range of 100 to 350 keV. Data on collisions of Ne with Al were extended to 3.2 MeV. The ionization cross sections were determined by measuring the number of characteristic x rays emitted when an energetic ion is incident on the target. The cross sections obtained were some 10^3 to 10^5 times larger than Coulomb excitation cross sections. The cross sections can be attributed to the exchange forces set up during collision by the Pauli exclusion principle in the overlapping electron clouds of the interpenetrating atoms. This forces the electrons into transient quasi-molecular configurations leaving the atoms in excited states after separation. This mechanism, referred to as the Pauli excitation of atoms in collision, accounts qualitatively for the gross features of the observed phenomena. (TSS) (Diss. Abstr. Int. B)

27454 CROSS SECTION FOR EXCITATION OF THE Cs II RESONANCE LINES IN THE $Cs^+ + He$ PROCESS NEAR THE THRESHOLD. Devdariani, A. Z.; Bobashev, S. V. (Leningrad State Univ.). Zh. Eksp. Teor. Fiz.; 60: 485-8(Feb 1971). (In Russian).

The cross section for excitation of the Cs II resonance line emitted in the $Cs^+ + He$ reaction in the vicinity of the threshold region is calculated theoretically. The calculations are carried out in accordance with the assumption that the turning and pseudointersection points approach each other; in this case a quantum mechanical study of motion of the atoms is necessary. Despite the kinetic energy of the atoms exceeding 100 eV, it is found that a previously developed theory for slow atomic collisions involving energies below 10 eV can be applied. The results of the calculations are in good agreement with the experimental data. (auth)

27455 CHARGE EXCHANGE BETWEEN NEGATIVE AND POSITIVE IONS. Radtsig, A. A.; Smirnov, B. M. (Inst. of High Temperatures, Moscow). Zh. Eksp. Teor. Fiz.; 60: 521-6(Feb 1971). (In Russian).

Charge exchange between a positive and negative ion is considered in the limit of small electron binding energy in the negative ion. In this case a transition of the valency electron to a large number of atomic excited states is possible, and hence the process may be regarded as penetration of the electron through the potential barrier in the ion field. The charge-exchange cross section is found for linear collision trajectories. The results are compared with the experimental data. (auth)

27456 CHARGE EXCHANGE BETWEEN A NEGATIVE ION AND HIGH-ENERGY PROTON. Kunike, M. (Leningrad State Univ.). Zh. Eksp. Teor. Fiz.; 60: 53-61(Jan 1971). (In Russian).

Charge exchange between a negative ion and a proton is considered for proton energies $E \gtrsim 10$ keV. For a negative hydrogen ion the initial and final electron states are described by symmetrized electron functions. The bound states for arbitrary negative ions are described by two-parameter one-electron functions. The cross sections for electron capture by protons in states characterized by a principal quantum number n are calculated. Four-dimensional symmetry of the hydrogen-atom wave function is used in summing over the orbital and magnetic quantum numbers. (auth)

27457 IONIZATION CONSTANT OF THE PENNING PROCESS. Smirnov, B. M. (Inst. of High Temperature, Moscow). Zh. Eksp. Teor. Fiz.; 60: 66-8(Jan 1971). (In Russian).

XUM

The Penning effect (ionization of atoms in collisions with metastable atoms) is investigated for the most common case when the ionization probability per collision is small. A general expression for the ionization constant is derived, from which it follows that in the limit of low temperatures the constant is inversely proportional to the square root of the temperature and at extremely high temperatures is independent of the temperature. The ionization-electron spectrum is independent of temperature at extremely low and high temperatures. The relative number of molecular ions produced in the Penning process decreases with increasing temperature and is independent of temperature at extremely low temperatures. Some of the results obtained are confirmed experimentally. (auth)

27458 SECONDARY RAINBOWS AND INTERFERENCE IN ELASTIC SCATTERING OF H^+ BY Ar. Weise, H. P.; Mittmann, H. U.; Ding, A.; Henglein, A. (Hahn-Meitner-Institut fuer Kernforschung, Berlin). Z. Naturforsch.; 25a: 1154-5(Jul 1970). (In German).

The secondary rainbows and interferences in the elastic scattering of H^+ ions by Ar were investigated in the laboratory system at incident-ion energies of 10 and 25 eV. The intensity of the scattered H^+ ions was determined as a function of the scattering angle. The measurement of the dependence of the angle at which the maxima of the primary and secondary rainbows and the minimum between adjacent rainbows appear showed that the angle increases as the energy decreases. The $Ar-H^+$ distance at the potential minimum r_m was calculated, and the mean value was greater than the equilibrium distance in the isoelectric HCl molecule. (J.S.R.)

27459 SPECTRUM OF THE INELASTIC COLLISION INTEGRAL IN MOLECULAR MIXTURES. Podlubnyi, L. I. (Moscow Energy Inst.). Zh. Eksp. Teor. Fiz.; 60: 356-71(Jan 1971). (In Russian).

The linearized collision integral for a multitemperature molecular mixture is expressed in terms of the correlation functions describing the intrinsic degrees of freedom of the colliding particles. The effect of inelastic collisions on the shape of the Boltzmann operator spectrum is discussed in the impulse approximation for the particular case of collisions between structureless particles and diatomic molecules. The dependence of the spectrum on the relation between particle mass and form of the collision pseudopotential is studied. Transition from the Boltzmann integral operator to a finite-order differential operator is considered for the case of a large mass difference between the colliding particles. A Fokker–Planck type of equation for eigenvalues of the Boltzmann operator (s-spectrum) is solved for electrons in a weakly ionized plasma of homonuclear molecules by the WKB method with allowance for rotational transitions. (auth)

27460 CONFIGURATION-INTERACTION STUDY OF X-RAY AND FAST-ELECTRON SCATTERING FACTORS FOR LIGHT ATOMIC SYSTEMS. Tanaka, Kiyoshi; Sasaki, Fukashi (Hokkaido Univ., Sapporo). Int. J. Quant. Chem.; 5: 157-75(Mar 1971).

A study of x-ray and fast-electron scattering by light atoms and ions was carried out in the first Born approximation. Coherent and incoherent scattering factors calculated with configuration-interaction wave functions are compared with those obtained with Hartree–Fock wave functions. These configuration-interaction wave functions involve only L-shell correlation. It is shown that the changes in the coherent scattering factors due to configuration interaction are not negligible and that the electron correlation effects on the incoherent scattering factors are important. Tables of coherent and incoherent scattering factors for light atomic systems are given. (auth)

27461 COMPTON SCATTERING OF GAMMA RAYS BY ELECTRONS BOUND IN HEAVY ATOMS. Schumacher, M. (Univ., Goettingen, Ger.). Z. Phys.; 242: 444-57(1971).

The energy spectra of 661.6-keV gamma rays scattered incoherently by lead were measured for the scattering angles 62°, 85°, and 135° using a germanium detector. The differential cross sections $d\sigma/d\Omega dE_{\gamma'}$ obtained from the experiment were compared with form-factor calculations using relativistic s-electron wave functions for the initial state and relativistic Coulomb wave functions for the unbound state. A good agreement has been obtained for large energies $E_{\gamma'}$ of the scattered quanta. (auth)

27462 ROLE OF ELECTRONIC RESONANCE STATES IN HEAVY PARTICLE ATOMIC COLLISIONS. Mizuno, Junya. San Diego, Calif.; Univ. of California (1970). 172p. University Microfilms Order No. 71-7979.

Thesis.

The collision between a negative ion and an atom via the electronic resonance states is investigated. The effect of the electronic resonance states that strongly couple with the electron-detachment channel is accounted for by a set of complex potentials. The theories and methods for the electronic resonance states are discussed. The coupled equations for nuclear motion are derived. The semi-classical methods for complex potentials are discussed. Finally, the general theories are applied to the specific example of the $H^- - H$ collision. Numerical results are given and compared with the available experimental data. (Diss. Abstr. Int., B)

27463 EXCITATION FUNCTIONS OF He I SPECTRAL LINES EMITTED DUE TO COLLISIONS OF He^+ IONS AND H_2 MOLECULES. Polyakova, G. N.; Erko, V. F.; Zats, A. V. Opt. Spectrosc. (USSR) (Engl. Transl.); 29: 219-20(Aug 1970). Translated from Opt. Spektrosk.; 29: 412-14(Aug 1970).

The charge-transfer process $He^+ + H_2 \rightarrow He^* + H_2^+$ was studied at He^+ energies of 100 eV to 30 keV. The excitation functions of nine spectral lines of He, emitted in transitions from the S, P^0, and D upper levels of the He atom, were measured. The $\sigma(v)$ curves (σ is the effective excitation cross section of the spectral line and v is the relative velocity of the colliding particles) for the nine lines are compared, and tentative explanations for the differences are suggested. (A.G.W.)

Atomic Theory

Refer also to abstract 27943.

27464 USE OF INFORMATION THEORY IN LOCALIZING ELECTRONS IN ATOMS AND MOLECULES. Aslangul, Claude (CNRS, Paris). Compt. Rend., Ser. B; 272: 1-4(4 Jan 1971). (In French).

A transformation of the information contained in the vector representation of a quantum system is proposed. Application to the Schrödinger description leads to a natural expression in the cell model theory. A criterion for the probability distribution based on entropy considerations is defined; this permits classification by partitioning of atoms and molecules into cells. (auth) (France)

27465 USE OF COULOMB GREEN FUNCTIONS IN ATOMIC CALCULATIONS. I. Safronova, U. I. Opt. Spectrosc. (USSR) (Engl. Transl.); 29: 234-6(Sep 1970).

Translated from Opt. Spektrosk.; 29: 435-9(Sep 1970).

One- and two-particle Coulomb Green functions in the coordinate and momentum representations are discussed. (auth)

27466 ANALYSIS OF REDUCED DENSITY MATRICES IN THE COORDINATE REPRESENTATION. I. DEFINITIONS AND BASIC FORMULAS. Sperber, Gunnar (Univ. of Florida, Gainesville). Int. J. Quant. Chem.; 5: 177-87(Mar 1971).

The probability interpretation of density matrices is reviewed, and certain quantities are suggested for study by means of diagrams. The case of a "spin-symmetric ensemble" is further discussed. (auth)

27467 ANALYSIS OF REDUCED DENSITY MATRICES IN THE COORDINATE REPRESENTATION. II. THE STRUCTURE OF CLOSED-SHELL ATOMS IN THE RESTRICTED HARTREE–FOCK APPROXIMATION. Sperber, Gunnar (Univ. of Florida, Gainesville). Int. J. Quant. Chem.; 5: 189-214(Mar 1971).

The electron density and the Fermi hole of the ground states of the atoms He, Be, Ne, Mg, Ar, Ca, Zn, and Kr are studied in the restricted Hartree–Fock approximation. The use of single Slater-type orbitals for the free atoms is also discussed. (auth)

Cosmic Radiation

Refer also to abstracts 27361, 27389, 27404, 27513, 27952, 27954, and 28050.

27468 NEW ASPECT OF AIR SHOWER OBSERVATION. Tanahashi, Goro (Tokyo Univ.). Kagaku (Tokyo); 40: 294-300(Jun 1970). (In Japanese).

Air-shower research and observation become very difficult when the primary energy exceeds 10^{17} eV since a very large number of detectors are arranged over a large area to compensate for the low frequency of the event. Atmospheric scintillation due to air showers was examined quantitatively, and the possibility of air-shower observation by means of scintillation light was discussed. Preliminary observation was made by the Cornell group to detect the atmospheric scintillation due to air showers. At the Institute for Nuclear Study, Tokyo Univ., preliminary observations have been made since 1968. CRT record

of the light pulse was shown, and the incident energy was estimated to be $10^{19 \pm 0.5}$ eV. During 100 hours of observations, fifteen records of air-shower scintillation were obtained within 3 km from the observatory. The frequency was one order of magnitude smaller than expected. (Japan)

27469 PROPAGATION OF SOLAR AND GALATIC COSMIC RAYS OF LOW ENERGIES IN INTERPLANETARY MEDIUM. Vernov, S. N.; Chudakov, A. E.; Vakulov, P. V.; (and others) (Moscow State Univ.). Astrophys. Space Sci. Libr.; 19: 53-89(1970).

From 3rd Intercorrelated Satellite Observations Related to Solar Events, Noordwijk, Netherlands. See CONF-690971.

Results of measurements of low-energy cosmic rays from Zond-3, Venus-2, Venus-3, and Venus-4 space probes for the period from 1965 to 1967 are summarized, as well as preliminary results from Venus-5 and Venus-6 space probes. It was found on the basis of solar cosmic-ray bursts and Forbush decreases of galactic cosmic rays that the solar cosmic rays propagate rapidly from ejection region near the Sun along the beam of magnetic lines of force emerging from the active region on the Sun and slowly when they are retarded in the region of the field knee created by the shock wave from the burst and move together with the knee at the velocity of the wave. The observed retardation of shock waves from the bursts results in disappearance of Forbush decreases and accumulation of solar cosmic rays at distances of ~2 AU from the Sun. On the basis of the observations of variations in galactic cosmic rays, the variation parameters (amplitude, steepness of the fall) are determined by the dynamics, latitude, and development phase of active regions. (auth)

27470 SOLAR COSMIC-RAY INCREASE ON 25 FEBRUARY–5 MARCH, 1969 ACCORDING TO MEASUREMENTS FROM VENUS-5 AND VENUS-6 SPACE PROBES. Vernov, S. N.; Kontor, N. N.; Lyubimov, G. P.; Pereslegina, N. V.; Chuchkov, E. A. (Moscow State Univ.). Astrophys. Space Sci. Libr.; 19: 460-70(1970).

From 3rd Intercorrelated Satellite Observations Related to Solar Events, Noordwijk, Netherlands. See CONF-690971.

During the period from Feb 25 to March 5, 1969 the Venus-5 and Venus-6 space probes detected an increase in solar cosmic-ray protons with $E_p > 1$ MeV and electrons with $E_e > 0.05$ MeV. The increase had a complex form and was due to a series of solar flares occurring in a single active region. The main flares occurred on Feb. 24 and 27, 1969. A scheme for the development of a disturbance in the interplanetary medium caused by the above-mentioned flares is considered on the basis of the analysis of the form of increase for various proton energies, anisotropy of protons with $E_p = 1$ to 4 MeV, and the increase in electrons with $E_e > 0.05$ MeV together with solar and geophysical events. (auth)

27471 OBSERVATIONS RECORDED BY THE LEEDS UNIVERSITY COSMIC-RAY DETECTOR ON BOARD THE ESRO II SPACECRAFT DURING THE SOLAR FLARE OF FEBRUARY 25th, 1969. Jakeways, R.; Marsden, P. L.; Calder, I. R. (Univ. of Leeds, Eng.). Astrophys. Space Sci. Libr.; 19: 486-91(1970).

From 3rd Intercorrelated Satellite Observations Related to Solar Events, Noordwijk, Netherlands. See CONF-690971.

Results showing the fluxes of electrons and low-energy protons observed during the solar flare of Feb. 25, 1969 are presented. Design and operational performance of the Leeds detector, S 29, are given. The maximum mean counting rate observed corresponded to a flux of solar protons of 1.4 ± 0.2 particles cm^{-2} sterad^{-1} sec^{-1}, but since the first observation from the spacecraft was made about an hour after the maximum enhancement in neutron-monitor rates observed on the ground, it is quite likely that the actual maximum flux was higher than this. The solar proton rate was observed to decay exponentially with a time constant of 225 ± 20 min and there is no evidence of any further substantial fluctuations in the low-energy proton counting rate during the next few days. Data show the existence of fluctuations in rate observed during the polar-cap pass at maximum. Spatial variations of a similar nature were noted, and differences were noted between north and south polar data. Two models suggested to describe the entry of fast particle of solar origin into the magnetosphere are discussed: the connected-line model and the ring-current model. Results here agree with the ring-current model since it can explain the enhancements in intensity observed near the auroral zones. (J.C.W.)

27472 27-DAY OSCILLATION IN THE COSMIC-RAY INTENSITY AND SHORTER PERIODICITIES. Lovera, G.; Oldano, C. (Politecnico, Turin). Nuovo Cim.; 2B: 28-37(11 Mar 1971).

Average diurnal data of cosmic-ray intensity, recorded in the time intervals between July 1955 and December 1958 (maximum solar activity, IGY) and between November 1963 and April 1965 (minimum solar activity, IQSY) at Huancayo with one neutron monitor and one ionization chamber, and at Resolute Bay with one neutron monitor and one cubic telescope of G–M counters, were analyzed with respect to the recurrent variations of the 27-day period and of shorter periods (approximately 12 days and 6 days). Results of the analysis are herein reported and discussed. It emerges that: the amplitude values obtained at the same time with different counters are of the same order of magnitude; in the period of maximum solar activity these values are much higher and more correlated (solar modulation effect) than in the period of minimum solar activity (local atmospheric effects). (auth)

27473 LOW-ENERGY COSMIC RAYS NEAR EARTH. Gleeson, L. J. (Monash Univ., Clayton, Australia); Krimigis, S. M.; Axford, W. I. J. Geophys. Res.; 76: 2228-35(1 Apr 1971).

Observations of protons with kinetic energy >0.31 MeV in interplanetary space during quiet times made from the spacecraft Explorer 33 show that there is an anisotropy of ~15%, the maximum flux being directed approximately radially outward from the Sun. This observation, and the corresponding radial gradient results reported by S. M. Krimigis, are shown to be in very good agreement with those expected from a model in which the observed protons are convected outward at the solar-wind speed. It is concluded that these particles have come from an interior region and that the most probable source is the Sun, but the possibility that they are of galactic origin, although remote, cannot be positively excluded. (auth)

27474 POWER SPECTRUM OF SCINTILLATIONS OF A TWO-COMPONENT RADIO SOURCE. Chivers, H. J. A. (Univ. of California, San Diego, La Jolla). J. Geophys. Res.; 76: 2526-30(1 Apr 1971).

It has been shown that the power spectrum of the scintillations from a two-component extraterrestrial radio source should show a cosine distribution that is the result of overlapping of the diffraction patterns from the two components, with some frequency components in the two spectra being in phase while others are out of phase. The effects of source size and shape on the observed spectra of ionospheric scintillations are shown on some spectra obtained by using the Cygnus-A radio source. The cosine modulation is seen in the slope change at 0.17 Hz. It is explained that in some observations when the cosine modulation is not seen, the scintillation spectrum merges with the noise background at about 0.3 Hz. (J.C.W.)

27475 ELECTRIC CHARGE OF INTERACTING COSMIC-RAY PARTICLES AT SEA LEVEL. Ashton, F.; King, J. (Durham Univ., Eng.). J. Phys., A (London); 4: L31-4(Mar 1971).

The magnitude of the electric charge of sea-level cosmic-ray particles producing energy transfers greater than or approximately equal to 25 GeV in a 22.9 cm thick steel target was measured. The charge distribution shows a peak at the electron charge and an apparent high-charge tail. Spurious effects contributing to the high-charge tail are knock-on electrons and nuclear interactions in the proportional counter walls, which are used to measure the charge. The limit obtained on the flux of 4e/3, 5e/3, and 7e/3 quarks is less than 8.2×10^{-10} cm^{-2} s^{-1} sr^{-1}. (auth) (UK)

27476 MUON BUNDLES IN EXTENSIVE AIR SHOWERS. Wdowczyk, J. (Inst. of Nuclear Research, Lodz, Poland); Wolfendale, A. W. J. Phys.; A (London); 4: L34-7(Mar 1971).

It is suggested that coherent production of pions in pion–air nucleus interactions is responsible for the bundles of muons observed in extensive air showers. (auth) (UK)

27477 THEORETICAL ANALYSIS OF EXTENSIVE AIR SHOWERS. V. GENERAL ANALYSIS OF MUONS ABOVE 1000 GeV. Adcock, C.; Coats, R. B.; Wolfendale, A. W.; Wdowczyk, J. (Univ. of Durham, Eng.). J. Phys., A (London); 4: 276-90(Mar 1971).

Previous calculations (Adcock et al., J. Phys., A, 2: 574-83 (1969)) were extended to yield predictions of the frequencies of multiple muons in the comprehensive experiment of Cannon and Stenerson, (J. Phys., A, 4: 266-75(1971)). It is shown how comparison with experiment can give information about the magnitude of the mean transverse momentum $\langle p_t \rangle$ of the parent pions, the form of the multiplicity law, and the magnitude of the primary cosmic-ray intensity, all in the region of 2×10^3 GeV primary energy. Comparison is also made with the previous experiments and the areas of agreement and disagreement are explored. Combining all the experimental data, the average transverse momentum is somewhat less than that given by Adcock et al. (J. Phys., A, 3: 697-707(1970)) from an analysis of the Utah data alone and is 0.5 ± 0.06 GeV/c (for the p_t distribution given by Elbert et al. in 1968) at primary energies in the region of 2×10^3 GeV. (auth) (UK)

Direct Energy Conversion

27478 FUNDAMENTALS OF THE SINGLE-STAGE TWO-PHASE CONDENSATION PROCESS BASED ON THE CARNOT CYCLE FOR LIQUID-METAL MHD CONVERTERS. Radebold, Reinhart. Wiss. Ber. AEG-Telefunken; 43: 229-34(1970). (In German).

The liquid-metal MHD processes on the basis of the Rankine process exhibit various drawbacks: due to the simple, single-stage injection condensation, increasing mixing losses are obtained with increasing thermodynamic efficiency. If multistage additive mixing of the liquid phase (two-phase transformation) is employed instead, this coupling may be eliminated and the losses reduced, but then the problem of the noticeable thermal capacity of the working medium is encountered. Consequently the liquid added to the various stages must be preheated by heat exchange in the relaxation jet. However, the low-equilibrium sound velocity of the two-phase flow of high humidity causes constant changes between subsonic and supersonic velocities in the various stages and, secondly, the material flow enters the heat source at the condensation temperature of the working medium and must be heated additionally. The process based on the Carnot cycle is characterised by a relatively small change: by the heat exchange in the relaxation jet not only the material flow injected into the jet is heated but also the working medium entering the heat source. Hence the heat source works at an almost constant, above all enhanced, temperature. Moreover, so much heat is extracted from the relaxing two-phase flow in the jet that the terminal velocity of the medium is very low, i.e., firstly, the losses in mixing are sufficiently low, and secondly, a single injection stage is adequate for full condensation. The thermodynamic fundamentals are indicated. Under these conditions only a slight temperature difference may be allowed for the internal heat exchange, and there the principal difficulty is encountered of the single-stage process based on the Carnot cycle. But it is found from the estimates (flow losses in the jet are disregarded) that the condensation on the jet surface is adequate to convey the necessary heating flows with technically justifiable jet dimensions. With a jet length L = 50 cm, which is twice as long as the usual type, and its ratio to the diameter L/D = 15, ~100 W/cm^2 may be transferred at a 15°C temperature difference, i.e., thermal quantities such as are customary in high-speed reactors. (auth)

27479 OPTIMIZATION OF THE SINGLE-STAGE TWO-PHASE CONDENSATION PROCESS BASED ON THE CARNOT CYCLE FOR LIQUID-METAL MHD CONVERTERS. Freund, Juergen (Technische Univ., Berlin). Wiss. Ber. AEG-Telefunken; 43: 235-40(1970). (In German)

The single-stage process based on the Carnot cycle is optimized with respect to the various significant process parameters. The starting point is the fact that the relaxing two-phase flow continues to lose its ability to do work with increasing preheating temperature T_v but, on the other hand, the thermodynamic efficiency grows with rising T_v. An optimum is shown. The position of the optimum temperature changes due to the losses in the jet, which are considered here, and due to the losses occurring on the additive mixing of cold liquid for condensation. It is easiest to appraise the appropriate influences by considering the internal efficiency, which is thoroughly investigated. It is found that isentropic flow efficiency and preheating temperature are significant parameters, and they thus occur in the diagrams. The results of the calculation are shown. Three types of optimum condition may be differentiated: (1) By the choice of preheating temperature at given temperatures for jet entry, condensation and undercooling, maximum internal efficiencies may be adjusted. (2) By the choice of jet entry and undercooling temperatures (at a given temperature difference between the two) at a given condensation temperature or by selecting the condensation temperature at given jet entry and undercooling temperatures, the adiabatic temperature decrease being kept constant in the jet in both cases, maximum internal efficiencies may be adjusted. (3) By the choice of preheating temperature a given temperature for jet entry, condensation and undercooling, minimum jet outlet diameters may be adjusted, which are important for mass optimization. (auth)

27480 DIRECT CONVERSION OF NUCLEAR RADIATION ENERGY. Miley, George H. Monograph Series on Nuclear Science and Technology. Hinsdale, Ill.; American Nuclear Society (1970). 528p. $34.90. (TID-25672).

Methods for converting nuclear radiation directly without resorting to a heat cycle are presented. The concepts discussed primarily involve direct collection of charged particles released by radioisotopes and by nuclear and thermonuclear reactors. Areas considered include basic energy conversion, charged-particle transport theory, secondary-electron emission, and leakage currents and associated problems. Applications to both nuclear instrumentation and power sources are discussed. (M.H.R.)

27481 STUDY OF A CYLINDRICAL LINEAR MHD MACHINE IN THE OPEN-CYCLE REGIME. Andreev, A. M.; Ostapenko, V. P. Magn. Gidrodin., Akad. Nauk Lat. SSR; No. 1, 110-15(Jan-Mar 1970). (In Russian).

Expressions are presented for the distribution of magnetic field in the gap and the yoke of the magnetic circuit of a linear-induction MHD machine in the ideal open-cycle regime. It is found that in the machine gap, besides straight traveling and pulsating magnetic fields, there also exists a reverse traveling field. In the yoke of the magnetic circuit, besides the indicated fields, an additional pulsating field appears. Experimental investigations were conducted on a model of a linear cylindrical MHD machine. The magnetic fields in the gap and the core and the inductive resistances of the coil were studied. Good agreement of the experimental and calculated data was obtained. (tr-auth)

27482 EXCITATION IN THE GAP OF A LINEAR INDUCTION MACHINE OPERATING WITH VARIABLE-VELOCITY WAVE FIELD. Rashchenkin, A. P. Magn. Gidrodin., Akad. Nauk Lat. SSR; No. 1, 116-20(Jan-Mar 1970). (In Russian).

Design requirements are established for the gap of a linear induction machine with a traveling-wave field, generally with variable amplitude and phase velocity, with induction by a symmetrical system of t-phase currents. Conditions are also derived under which potentials in the phases of the windings will be symmetrical. In the formulation of the problem it was supposed that, in the gap of the machine was a specified field of the form of a traveling wave with variable velocity along the channel and with variable amplitude. According to this field the position of currents in the region, and their magnitude and phase were determined. Then restrictions were applied that the amplitudes of these currents be equal, and the phase shift of the adjacent currents would differ by a constant angle. With the given conditions the field may be induced by the symmetrical t-phase current system. (tr-auth)

27483 STRUCTURE OF THE GENERAL SOLUTION OF BOUNDARY-VALUE PROBLEMS DESCRIBING LONGITUDINAL END EFFECTS IN MHD CHANNELS AT ARBITRARY R_m NUMBERS. Kozyrenko, V. E. Magn. Gidrodin., Akad. Nauk Lat. SSR; No. 1, 129-30(Jan-Mar 1970). (In Russian).

In previous work the solution of specific edge problems indicated that the analytical investigation of longitudinal end effects in conduction-type MHD channels at not very small magnetic Reynolds numbers R_m may be achieved efficiently using the method of successive approximations and with the absence of anisotropy of conductivity — the Keldysh–Sedov theorem. The respective analysis was completed, determining the induced magnetic field distribution in MHD channels in zero and first approximations. The analysis of the edge problems, which determine the distribution of the induced magnetic field in MHD channels in subsequent approximations, shows that the process of their solution and also the solutions themselves turn out to be extremely simple. (M.H.R.)

27484 PARAMETERS OF AN ASYNCHRONOUS LIQUID-METAL MHD GENERATOR. Kim, K. I. Magn. Gidrodin., Akad. Nauk Lat. SSR; No. 1, 98-109(Jan-Mar 1970). (In Russian).

An asynchronous MHD generator (AMHDG), as well as the usual asynchronous machine, may be characterized by a certain set of parameters. However, with primary concern being maintenance of physical size, known from the theory of electrical machines, these parameters must be refined in accordance with the distinctive characteristics of the AMHDG. Formulas are presented for the AMHDG parameters, obtained by considering the limitations of its dimensions and the velocity profile of liquid metals in a transverse section of the channel. It seems that, in contrast to the usual asynchronous machine design, substitutions in the AMHDG may not be fully equivalent. This discrepancy is eliminated by refinement in equalizing the power balance. (tr-auth)

27485 MOTION OF A PLASMA CLUSTER IN A CHANNEL WITH VARIABLE INDUCTANCE. Sinkevich, O. A.; Krylova, L. M. Magn. Gidrodin., Akad. Nauk Lat. SSR; No. 1, 28-34 (Jan-Mar 1970). (In Russian).

The effect on the motion of a plasma cluster of the inductance of the external circuit of the working channel and the intrinsic variation of its inductances was studied. The analytical relation of the cluster velocity with time was obtained. Formulas for the calculation of energy characteristics of the MHD generator in different regimes are given. The effect of the inductance in the circuit of the generator on its characteristics (electric current, power), calculated according to the obtained formulas, is shown. (tr-auth)

Fluid Physics

Refer also to abstract 27806.

27486 NEUTRAL STABILITY OF AN INCOMPRESSIBLE MAGNETOHYDRODYNAMIC HALF-JET AT LOW REYNOLDS NUMBER. Deshpande, Narayan V. (Univ. of Rochester, N. Y.). Phys. Fluids; 14: 779-81(Apr 1971).

The effect of an applied magnetic field on the instability of a laminar, free boundary layer formed between two parallel streams of semi-infinite extent was studied. It is shown that the stabilizing effect of the magnetic field does not give rise to any minimum critical Reynolds number. The fluid is assumed to have infinite electrical conductivity. (auth)

27487 ENERGY FLUX IN INCOMPRESSIBLE MAGNETOHYDRODYNAMIC PLANE WAVES. Skiles, Durward D.; Kunkel, Wulf B. (Univ. of California, Berkeley). Phys. Fluids; 14: 1029-31(May 1971).

The energy flux in plane magnetohydrodynamic waves in general includes a mechanical contribution pv in addition to the usual Poynting vector S, even when the fluid is incompressible. Thus, S need not be coplanar with the group and phase velocities of such waves. (auth)

27488 VARIATIONAL PRINCIPLE AND CANONICAL VARIABLES IN MAGNETOHYDRODYNAMICS. Zakharov, V. E.; Kuznetsov, E. A. Dokl. Akad. Nauk SSSR; 194: 1288-9(21 Oct 1970). (In Russian).

A variational principle was formulated by B. I. Davydov (Dokl. Akad. Nauk, 69: No. 2, 165(1949)) for the hydrodynamics of an ideal fluid, and it was shown that (λ,μ) and (ρ,ϕ) were pairs, where $v = (\lambda/\rho)\nabla\mu + \nabla\phi$. In this note, a similar problem is resolved for the magnetohydrodynamics of an ideal fluid. (R.V.J.)

27489 STUDY OF SUPERSONIC MHD-CHANNEL FLOWS WITH COMPRESSION SHOCK. Kostenko, P. P.; Frolov, S. D. Magn. Gidrodin., Akad. Nauk Lat. SSR; No. 1, 23-7(Jan-Mar 1970). (In Russian).

The possible causes of the formation of shock waves and the characteristic tendencies of their development in the variable working regimes of a supersonic MHD channel are noted. Equations are developed for the description of one-dimensional flow of an equilibrium-dissociated gas in a supersonic channel MHD generator from calculations of dissociation, friction, and heat transfer effects in a normal shock. The position and intensity of the shock are found by the sample method and amount to finding a channel cross section, such that the presence of a shock guaranteed the combined observation of conditions at entry and exit and the condition for coupling parameters in normal compression shock. Recommendations are given according to a sampling of the approximation formula for the analytical presentation of tabular data concerning the dependence of enthalpy, entropy, and the gas constant of dissociated gas on pressure and temperature. Certain results of calculations are cited as an example. (tr-auth)

27490 EFFICIENCY OF A THREE-DIMENSIONAL MHD-CHANNEL. Ignatenko, M. M. Magn. Gidrodin., Akad. Nauk Lat. SSR; No. 1, 39-44(Jan-Mar 1970). (In Russian).

The electric field in an MHD channel of rectangular cross section with end electrodes is calculated, when a homogeneous external magnetic field is concentrated in the electrode zone or extended for a certain distance beyond the electrodes. The effects on channel efficiency of heterogeneity of velocity along the cross section of the channel and extension of the magnetic field beyond the electrodes are studied. (tr-auth)

27491 RAYLEIGH'S PROBLEM IN MAGNETOHYDRODYNAMICS WITH SUCTION. Pandey, Girish Chandra (Defence Science Lab., Delhi). Def. Sci. J. (New Delhi); 20: 71-5(Jan 1970).

Extension of Rayleigh's problem to magnetohydrodynamics with suction when the plate is nonmagnetic and nonconducting is considered. The suction velocity is assumed to be varying as the minus one-half power of time. Series solutions for velocity and skin friction are obtained under the assumption that the hydromagnetic parameter K is small. It is seen that the skin friction increases with increasing magnetic field. (auth) (IAA)

27492 DISTRIBUTION OF ELECTRIC FIELD IN CONDUCTING CYLINDER WITH ELECTRODES OF FINITE SIZE. Chekin, B. V.; Shchelukhin, E. M. Magn. Gidrodin., Akad. Nauk Lat. SSR; No. 1, 45-8(Jan-Mar 1970). (In Russian).

The electric field distribution in cylindrical and annular channels of finite length with electric current introduced through finite electrodes located on the lateral surface of the channel is described. It is assumed that the electric conductivity of the fluid is isotropic, and the velocity is zero. The expressions obtained can be used to calculate the potential in the channels of different MHD devices. (tr-auth)

27493 OPTIMUM MAGNETOHYDRODYNAMIC FLOWS. Pleshanov, A. S. Magn. Gidrodin., Akad. Nauk Lat. SSR; No. 1, 49-55(Jan-Mar 1970). (In Russian).

It is shown that in a quasi-one-dimensional approach, at small magnetic Reynolds numbers, the problem of optimization of a linear conduction MHD generator according to either thermodynamic or gasdynamic functions has the same solution. However, the regions of variation of the required functions, where the necessary extremum condition of the function is fullfilled—the Legendre condition—are different for different functions. The analytical solution of the optimization problem according to Joule dissipation or energy of a channel of constant cross section is obtained. It is shown in a general case that the optimum inclusion of a shock wave in a generated regime, as a rule, is impossible. The analytical solution of the problem of optimization according to power is obtained, allowing for constant heat flux in the channel walls. The effect of friction on certain obtained results is analyzed. (tr-auth)

27494 MOTION OF ALTERNATE LAYERS OF CONDUCTING LIQUID AND NONCONDUCTING GAS IN A TRANSVERSE MAGNETIC FIELD. Zimin, E. P.; Eismont, O. A. Magn. Gidrodin., Akad. Nauk Lat. SSR; No. 1, 56-62(Jan-Mar 1970). (In Russian).

The quasi-one-dimensional steady flow stream, formed by alternate layers of inviscid, non-heat-conducting, ideal, nonconducting gas and viscous electric-conducting liquid in transverse magnetic and electric fields, is considered. Approximate solutions for three special cases are obtained by the perturbation method: flows with small Mach number, with small values of the relative mass of liquid layers, and with a large number of successive layers. It is shown that, in the first two cases, the behavior of the stream is qualitatively analogous to the flow of a conducting homogeneous gas. In the latter, however, it is characteristic that the suppression of the stream occurs at a value of the Mach number, generally speaking, different from unity. (tr-auth)

27495 LAMINAR MAGNETOGASDYNAMIC BOUNDARY LAYER AT NONCONDUCTING SURFACE WITH ARBITRARY DISTRIBUTION OF PARAMETERS IN THE FLOW CORE. Benenson, E. B. Magn. Gidrodin., Akad. Nauk Lat. SSR; No. 1, 83-8(Jan-Mar 1970). (In Russian).

A non-self-similar solution, correct for a wide range fluctuation of parameters, is obtained. The effect of temperature on thermal capacity and gas constants is taken into account. The Chapman–Rubezina formula is used for the viscosity. The effect of flow parameters in the flow core on the boundary-layer characteristics is shown. (tr-auth)

27496 UNSTEADY MAGNETOHYDRODYNAMIC FLOW OF A VISCOPLASTIC MEDIUM OVER AN INFINITE PLATE. Vishnyakov, V. I.; Makarov, A. M. Magn. Gidrodin., Akad. Nauk Lat. SSR; No. 1, 69-76(Jan-Mar 1970). (In Russian).

The unsteady motion of Shvedova–Bingham plastics, possessing electric conductivity, was examined in half-space over an infinite plate, with a constant magnetic field applied perpendicularly. The characteristic anomaly of the indicated motion is the presence of two-zone viscous flow, separated by a zone of quasi-solid motion. The classes of flows are separated, for which solutions of the corresponding problems may be obtained in the form of power series. Asymptotic solutions of problems for small values of time, describing certain classes of flows, are given. It is shown that the presence of the magnetic field leads to the increase of the dimensions of the quasi-solid center. (tr-auth)

27497 PROPAGATION OF SHEAR WAVES IN CONDUCTING VISCOUS-PLASTIC MEDIUM. Kosachevskii, L. Ya. Magn. Gidrodin., Akad. Nauk Lat. SSR; No. 1, 77-80(Jan-Mar 1970). (In Russian).

A one-dimensional problem is considered concerning the propagation, in a conducting viscoplastic medium, of shear waves induced by a pulsed boundary perturbation in a constant homogeneous magnetic field. Using the operational method, the velocity and stress distributions are found, and an equation for the determination of the nonstationary boundary of the viscoplastic and rigid zones is also obtained. This equation is solved numerically for a specific value of the external magnetic field. (tr-auth)

27498 FLUID FLOW WITH TEMPERATURE-DEPENDENT TRANSPORT COEFFICIENTS IN PLANE CHANNELS. Filippov, S. S. Magn. Gidrodin., Akad. Nauk Lat. SSR; No. 1, 81-5(Jan-Mar 1970). (In Russian).

The effect of the dependence of the coefficients of viscosity and electric conductivity on temperature in the laminar flow of an incompressible liquid between parallel nonconducting walls

XUM

in crossed electric and magnetic fields (the latter applied perpendicularly to the walls) is studied. There is a pressure gradient along the stream. The nonisothermal analogs of Hartmann, Poiseuille, and Couette flows are described by a nonseparable system of nonlinear equations for velocity and temperature as special cases, as a function of a sampling of values of the problem parameters and the boundary conditions for the velocity. However, in contrast to the case of constant transport coefficients, the character of the flow substantially depends on the boundary conditions at the temperature; the asymmetric temperature distribution causes the asymmetry of the velocity profile. Cases of both decreases and increases of transport coefficients with temperature increase were examined in accordance with the different character of this relation in liquid metals, electrolytes, and ionized gases. The results of numerical solutions are illustrated graphically. (tr-auth)

27499 CONCENTRATION DISTRIBUTION OF BINARY MIXTURES IN FILMS MOVING ALONG THE WALLS OF ROUND PIPES IN THE PRESENCE OF AN EXTERNAL NONUNIFORM MAGNETIC FIELD. Voronina, S. M.; Atroshchenko, L. S. Magn. Gidrodin., Akad. Nauk Lat. SSR; No. 1, 86-92(Jan-Mar 1970). (In Russian).

An analytic distribution formula for components of a binary mixture in a fluid film was obtained in the form of a highly convergent infinite series. The magnetic part was separated, and the extent of the effect of the magnetic field on the redistribution of components and the length of the initial part is determined. In the absence of a magnetic field the known distribution formula is obtained. It is shown that the magnetic field significantly intensifies the process of redistribution of components and reduces the length of the initial part; it is possible to improve the design parameters of the film dividers by means of an external nonhomogeneous magnetic field. (tr-auth)

27500 MHD-ROTATION OF CONDUCTING FLUID IN A CYLINDRICAL VESSEL. Dremov, V. V.; Kapusta, A. B. Magn. Gidrodin., Akad. Nauk Lat. SSR; No. 1, 93-7(Jan-Mar 1970). (In Russian).

The problem of three-dimensional motion of conducting liquid confined along the length of a cylindrical vessel of circular cross section under the influence of a rotating magnetic field formed by one pair of poles was examined for small magnetic and hydromagnetic Reynolds numbers. The system of equations for the azimuthal component of the velocity and the vorticity was solved by the method of least parameters. Expressions were found for the azimuthal velocity and vorticity of the zero approximation. According to the results of the calculations, diagrams were constructed for the distribution of azimuthal velocity along the radius and length of the vessel for different geometric parameters of the system. (tr-auth)

27501 APPARATUS FOR STUDY OF MOTION OF CONDUCTING EMULSIONS IN ELECTRIC AND MAGNETIC FIELDS. Zaletaev, S. P.; Ivanov, U. I. Magn. Gidrodin., Akad. Nauk Lat. SSR; No. 1, 135-7(Jan-Mar 1970). (In Russian).

Apparatus for the study of the motion of two-phase electric-conducting emulsions in an electromagnetic field is described. The relation of the electric conductivity of the emulsion to the ratio flow rate of mercury and an electrolyte is cited. The optimum frequency region for the measurement of electroconductivity by the contact method is given. Certain characteristics of the flow of electroconducting emulsions are given. (tr-auth)

27502 MEASUREMENTS OF THE VELOCITY PROFILE IN CROSSED ELECTRIC AND MAGNETIC FIELDS. Bocheninskii, V. P.; Tananaev, A. V. Magn. Gidrodin., Akad. Nauk Lat. SSR; No. 1, 137-9(Jan-Mar 1970). (In Russian).

The methodology of measurement of mean velocities in the presence of electric and magnetic fields is considered. New experimental results are presented that confirm the conclusions concerning the independence of the velocity distribution from the electric field. (tr-auth)

Geophysics (Upper Atmosphere)

Refer also to abstracts 27356, 27470, 27471, 27473, and 27682.

27503 LUNAR AND SOLAR DAILY VARIATION OF THE GEOMAGNETIC FIELD AT WATHEROO, WESTERN AUSTRALIA. Green, Pauline; Malin, S. R. C. (Inst. of Geological Sciences, Herstmonceux, Eng.). J. Atmos. Terrest. Phys.; 33: 305-18(Mar 1971).

Mean hourly values of magnetic declination, horizontal intensity, and vertical intensity observed at Watheroo (1919–1958) were analyzed to determine their solar and luni-solar diurnal components. Results, showing the variations of the first four harmonic components with season, degree of magnetic activity, and annual sunspot number, are tabulated and discussed. (auth) (UK)

27504 RELATIONSHIP BETWEEN H RANGES AT EQUATORIAL AND MIDDLE LATITUDES. Kane, R. P. (Physical Research Lab., Ahmedabad, India). J. Atmos. Terrest. Phys. 33: 319-27(Mar 1971).

The quiet-day H ranges at the equatorial station Trivandrum and the midlatitude station Alibag for 1964 show low correlations (<+0.50) in all seasons. It is found that on many days D_{st}-type effects are observed at all stations. Also, the ranges depend largely upon the position of S_q focus in the northern hemisphere. If corrections for these are applied, correlations improve considerably (~+0.80) for about 90% days. There are, however, a few days of abnormally high and/or low H ranges that remain unexplained. These could be due to meridional and vertical ionospheric currents or due to nonionospheric (magnetospheric?) contributions. (auth) (UK)

27505 COUPLING PROCESSES IN THE D AND E REGIONS AT LOW AND MEDIUM FREQUENCIES. III. THE COUPLING ECHO AND THE TRANSITION THROUGH CRITICAL COUPLING. Altman, C.; Postan, A. (Technion-Israel Inst. of Tech., Haifa). J. Atmos. Terrest. Phys.; 33: 329-41(Mar 1971).

Night-time electron-density distributions are used to study coupling echo reflections from the X = 1 level at various frequencies. Overall reflection-matrix elements R_{11}, R_{12} (= R_{21}) and R_{22} are calculated as functions of the variable upper height of ionospheric slabs based on the bottom of the ionosphere. At each frequency calculations are performed for various values of θ, the angle between the geomagnetic field and the vertical. Two types of coupling echoes are found. The true coupling echoes depend directly on the interface matrix elements, r_{12} and r_{21}, of the elementary thin layers into which the ionosphere has been divided, near the X = 1 level. They appear in the angular range $0 < \theta \lesssim 2\theta_c$, where θ_c is the angle of critical coupling, and approach a maximum near the upper limit $\theta \approx 2\theta_c$. They are generally characterized by the three reflection-matrix elements, R_{11}, R_{12} and R_{22}, being roughly equal in absolute value at the X = 1 level. For much higher angular values, $\theta \gtrsim 4\theta_c$, the coupling echo coefficient R_{12} (= R_{21}) at the X = 1 level is given as the geometric mean of the direct extraordinary and ordinary reflection coefficients, R_{11} and R_{22}, respectively, R_{22} having increased markedly and R_{11} showing a corresponding marked decrease. This type of coupling echo is due to a Z-coupling CTR process. The response to a vertically incident wave linearly polarized in the magnetic meridian and reflected from the X = 1 level is determined numerically, and results agreeing with the observations of Kelso et al. (1951) are obtained, although the propagation mechanism is more complicated than is generally assumed. (auth) (UK)

27506 PROPAGATION OF ELF AND VLF RADIO WAVES BENEATH AN INHOMOGENEOUS ANISOTROPIC IONOSPHERE. Barr, R. (King's Coll., London). J. Atmos. Terrest. Phys.; 33: 343-53(Mar 1971).

The attenuation and phase velocity of elf and vlf radio waves propagating under a realistic anisotropic ionosphere were calculated. The anisotropy produced by the Earth's magnetic field was found to have its greatest effect on propagation at frequencies in the range 1 to 4 kHz where differences in attenuation of greater than 45 dB/1000 km were observed between west-to-east and east-to-west propagation in the least-attenuated mode. The computed values of attenuation constant were found to be in very good agreement with the existing experimental data except for the heavily attenuated region. The computed values of phase velocity, however, do not show such a good agreement with experimental data. It is concluded that if future experimental observations of attenuation constant and phase velocity are to be of any practical value for determining ionosphere profiles, the azimuth of the propagation paths for which these constants are determined must also be recorded. (auth) (UK)

27507 LONGITUDINAL VARIATION OF THE MIDLATITUDE IONOSPHERE PRODUCED BY NEUTRAL-AIR WINDS. I. NEUTRAL-AIR WINDS AND IONOSPHERIC DRIFTS IN THE NORTHERN AND SOUTHERN HEMISPHERES. Challinor, R. A.; Eccles, D. (Radio and Space Research Station, Slough, Eng.). J. Atmos. Terrest. Phys.; 33: 363-9(Mar 1971).

At middle latitudes horizontal neutral-air winds produce important vertical ionospheric drifts that vary appreciably with longitude at any particular local time. These variations are caused mainly by changes in the direction of the Earth's mag-

netic field; longitudinal variations of the neutral-air winds themselves are of secondary importance. The longitudinal variation of the vertical upward drift velocity has two maxima in the northern hemisphere; in the southern hemisphere, however, a single maximum occurs at approximately 0600 UT. (auth) (UK)

27508 LONGITUDINAL VARIATION OF THE MIDLATITUDE IONOSPHERE PRODUCED BY NEUTRAL-AIR WINDS. II. COMPARISONS OF THE CALCULATED VARIATIONS OF ELECTRON CONCENTRATION WITH DATA OBTAINED FROM THE ARIEL I AND ARIEL III SATELLITES. Eccles, D.; King, J. W.; Rothwell, P. (Radio and Space Research Station, Slough, Eng.). J. Atmos. Terrest. Phys.; 33: 371-7(Mar 1971).

The equation of motion of the neutral atmosphere and the ionospheric continuity equation were solved simultaneously to calculate longitudinal variations of electron concentration for particular local times and heights above the F-layer peak at middle latitudes in both the northern and southern hemispheres. There is good agreement between the major features of the calculated variations and those observed by means of the Ariel I and Ariel III satellites. The theory not only satisfactorily explains the 0700 UT effect observed at middle latitudes in the southern hemisphere, but also predicts the existence of the two electron concentration maxima observed in the northern hemisphere. The differences between the behavior in the two hemispheres are attributable to the fact that the morphology of the Earth's magnetic field is different in the two hemispheres. In the southern hemisphere the direction of the field varies with longitude in such a way that the longitudinal variation of electron concentration at any fixed local time exhibits a single maximum; at different local times the maximum occurs at different longitudes but always at approximately 0700 UT. In the northern hemisphere the field is such that two electron concentration maxima are produced; these are separated by approximately 180° of longitude and, in contrast to the behavior observed in the southern hemisphere, there appears to be no simple Universal Time effect. (auth) (UK)

27509 STORM-TIME VARIATION OF F2-LAYER ELECTRON CONCENTRATION. Jones, K. L. (Radio and Space Research Station, Slough, Eng.). J. Atmos. Terrest. Phys.; 33: 379-89(Mar 1971).

Storm-time variations of electron content measured at Auckland, New Zealand and of F2-layer critical frequency measured at Australasian stations were examined. Increases of electron content are found to be associated with a class of S events, which are defined in terms of magnetic D_{st} variations. The results of previously published storm-time variations were reconsidered. It is suggested that the variety of forms of F2-layer storm variations is due to the coexistence of two opposing effects on electron concentrations. (auth) (UK)

27510 ORIGIN OF STORM INCREASES OF MIDLATITUDE F-LAYER ELECTRON CONCENTRATION. Jones, K. L.; Rishbeth, H. (Radio and Space Research Station, Slough, Eng.). J. Atmos. Terrest. Phys.; 33: 391-401(Mar 1971).

A theory is presented to explain the increases in midlatitude F-layer electron concentration which are sometimes observed during magnetic storms. It is supposed that heating in the auroral zone changes the horizontal winds at midlatitudes, thus causing changes in the F layer. With the aid of a simple numerical method developed to estimate the increases of N_mF2 during storms, it is shown that this mechanism can explain some local-time and longitude variations of the occurrence and magnitude of such increases. (auth) (UK)

27511 SOME FEATURES OF DISTURBANCES IN THE IONOSPHERE F REGION DURING THE RED AURORA OF THE TYPE A. Evlashina, L. M.; Evlashin, L. S. (Polar Geophysical Inst., Murmansk, USSR). J. Atmos. Terrest. Phys.; 33: 403-11(Mar 1971).

It is shown that red aurora of type A (λ6300 to 6364-Å) in the auroral zone are accompanied by a sporadic layer F2s. It is shown also that in the polar-cap area (St. Heiss), in the years of the maximum cycle of solar activity (IGY), the probability of occurrence of both red aurora of the type A and of sporadic layer F2s on magneto-quiet days has a maximum near local noon. It is concluded that the nature of these two events is the same in the auroral region. It is suggested that events are most probably caused by low-energy electrons. This conclusion is confirmed by recent direct measurements in a satellite with a nearly polar orbit. (auth) (UK)

27512 SEASONAL VARIATIONS OF ELECTRON DENSITIES BELOW 100 km AT MIDLATITUDES. IV. PRELIMINARY MODEL CALCULATIONS. Manson, A. H.; Merry, M. W. J. (Univ. of Saskatchewan, Saskatoon). J. Atmos. Terrest. Phys.; 33: 413-28(Mar 1971).

Calculations of electron-production rates due to photoionization, $q_s(\chi,h)$, and particle precipitation, $q_p(h)$, were performed for the mid-latitude ionosphere from 70 to 140 km during periods of quiet solar activity. A simple model in which E and D regions are defined by Lyman β, euv (30 to 120 Å), Lyman α and x rays (2 to 10 Å) was used. Seasonally varying atmospheric models were used: these include constant, annual and semiannual models. A seasonally constant profile of nitric oxide was used. Results of calculations are shown for solar-zenith angles, $\chi = 37°$, 60°, and 72°, typical of noon values for summer, equinox and winter seasons. (auth) (UK)

27513 VARIATIONS OF THE COSMIC-RAY LAYER IN THE LOWER IONOSPHERE. Velinov, P. (Geophysical Inst., Sofia). J. Atmos. Terrest. Phys.; 33: 429-36(Mar 1971).

The variations of the cosmic-ray layer situated in the lower part of the D region and formed by the galactic cosmic rays are considered. The variations of the electron-production rate are studied more in detail. They, in conformity with the derived equation, are divided into three groups: meteorological, geomagnetic, and variations of an extraterrestrial origin. Examples are given for the experimental recording of some more important variations and for their quantitative explanation. (auth) (UK)

27514 ROLE OF RECOMBINATION IN THE PRE-DAWN ENHANCEMENT OF λ6300 A [O I] AIRGLOW. Schaeffer, R. C. (Univ. of Adelaide). J. Atmos. Terrest. Phys.; 33: 437-49 (Mar 1971).

The pre-dawn enhancement of λ6300 Å [O I] airglow was investigated at Adelaide (L lat. 45.3°S) and its morphology found to be associated with sunrise at the magnetic conjugate point. The use of a time-latitude isophote diagram in presenting observational data and in identifying pre-dawn enhancements is described. The study of variations of local ionospheric parameters reveals the major role of recombination of local F-region electrons in the phenomenon. It is suggested that the associated vertical movement of the F-region ionization is influenced by photoelectrons from the sunlit atmosphere in the conjugate region. (auth) (UK)

27515 GEOGRAPHIC DISTRIBUTION OF THE IONOSPHERIC EVENING ANOMALY AND ITS RELATION TO THE GLOBAL PATTERN OF NEUTRAL WINDS. Papagiannis, Michael S.; Mullaney, Henry (BOSTON Univ.). J. Atmos. Terrest. Phys.; 33: 451-9(Mar 1971).

By plotting world contour maps of the index $I(t) = 10\{f_0F2(1200) - f_0F2(t)\}/f_0F2(1200)$ that describes the magnitude of the evening anomaly (the higher than expected evening values of the critical ionospheric frequency in the summer hemisphere), patterns were obtained that show that the anomaly is more pronounced in regions of westerly declination in the northern hemisphere and easterly declination in the southern hemisphere, as well as in regions where there is a poleward divergence of the magnitude meridians. By studying neutral-wind patterns computed by other authors, the conclusion was reached that the neutral winds, by dragging the ionospheric plasma which is essentially constrained to move along the lines of force of the Earth's magnetic field, play a very important role in determining the geographic variations in the intensity of the evening anomaly. (auth) (UK)

27516 OBSERVED REDISTRIBUTION OF E-REGION IONIZATION BY NEUTRAL WINDS. Constantinidies, E.; Bedinger, J. F. (GCA Tech. Div., Bedford, Mass.). J. Atmos. Terrest. Phys.; 33: 461-72(Mar 1971).

Sequential measurements of electron-density profiles are compared with the ionization-drift velocities derived from simultaneously obtained neutral-wind velocities. The measurements resulted from a series of five rocket flights launched at Wallops Island during a 6-hr period in the morning of February 22, 1968. The electron-density profiles were measured with a Langmuir probe during rocket ascent and the wind profiles were determined from vapor trails released during descent. The computed ion-drift velocities describe accurately the upper portion of the electron-density profiles characterized by a slowly descending layer of enhanced electron density. The small and slowly varying drift velocities in the lower E region cannot be so simply related to the complex structure observed in the electron density. The data from the upper portion of the electron-density profiles are used to calculate the value of the recombination coefficient. This value compares well with laboratory measurements. (auth) (UK)

27517 DEPENDENCE OF HORIZONTAL DRIFT AND ANISOTROPY OF IRREGULARITIES ON THE RELATIVE SPACING OF THE AERIALS. Sastri, J. Hanumath; Rao, B. Ramachandra (Andhra Univ., Waltair, India). J. Atmos. Terrest. Phys.; 33: 507-10(Mar 1971).

The results of preliminary study of the statistical properties

XUM

of the ground diffraction patterns using an array of five aerials are presented. It is found that the estimated magnitudes of true drift speed and structure size depend on the relative separation of the aerials used for evaluating them. (auth) (UK)

27518 NOTE ON THE EXTRATERRESTRIAL RING CURRENT UNDER VERY QUIET MAGNETIC CONDITIONS. Yacob, A.; Bhargava, B. N. (Colaba Observatory, Bombay). J. Atmos. Terrest. Phys.; 33: 515-18(Mar 1971).

The presence of a ring current under extremely quiet magnetic conditions is established from an examination of the mean daily horizontal intensity of the Earth's magnetic field over a 37-yr period. With an increase in the index Ap of magnetic activity the horizontal intensity is shown to decrease linearly. Departures from the linear relationship, however, occur when Ap assumes values of about 45 and 90. It is suggested that these departures may be due to increased pressure on the magnetospheric boundary associated with the M-region and flare plasma respectively. (auth) (UK)

27519 IN SITU OBSERVATIONS OF HIGH-LATITUDE F-REGION IRREGULARITIES. Frihagen, J.; Jacobsen, T. (Norwegian Defence Research Establishment, Kjeller). J. Atmos. Terrest. Phys.; 33: 519-22(Mar 1971).

A rocket-borne impedance probe measured electron density in the F region from L ~ 6.5 to L ~ 11. Patches of strong irregularities were observed throughout much of the flight, the first one in the region north of an auroral arc. Between patches weaker irregularities of a few percent change in electron density were present. Very strong electron-density gradients were observed. (auth) (UK)

27520 INVESTIGATION OF THE DAYTIME LOWER IONOSPHERE OVER THE EQUATOR USING LANGMUIR PROBE AND PLASMA NOISE PROBE. Prakash, Satya; Subbaraya, B. H.; Gupta, S. P. (Physical Research Lab., Ahmedabad, India). J. Atmos. Terrest. Phys.; 33: 129-35(Feb 1971).

A Langmuir probe and plasma noise-probe payload launched from Thumba on 29 August, 1968 at 1415 hr IST explored the equatorial D region at ~60 km. The electron-density profiles obtained from the Langmuir-probe currents do not show any pronounced layering in the D region. They exhibit a steep rise below 70 km and above about 85 km while in the intermediate region the slope is relatively small. These profiles are compared with two other electron-density profiles available in literature for the equatorial lower ionosphere. Most of the observed differences are found to be explicable in terms of the difference in solar activity prevalent when these profiles were obtained. A comparison was also made with two electron-density profiles obtained at similar conditions of solar activity and for similar solar-zenith angles, but over the middle latitudes. No marked differences between the equatorial and middle latitude profiles could be observed. The plasma-noise probe measured the electron-density irregularities in the scale-size range 1 to 15 m present in the medium. Irregularities were found to be present almost throughout the height region 65 to 105 km, with amplitudes ranging from a few tenths to a few percent. The results are compared with other available results on the electron-density irregularities obtained using different techniques. (auth) (UK)

27521 SOLUTION OF THE COUPLED IONOSPHERIC CONTINUITY EQUATIONS AND THE EQUATIONS OF MOTION FOR THE IONS, ELECTRONS, AND NEUTRAL PARTICLES. Ruester, R. (Max-Planck-Institute fuer Aeronomie, Lindau, Ger.). J. Atmos. Terrest. Phys.; 33: 137-47(Feb 1971).

The time-dependent continuity equations for four different ion species and the equations of motion for the ions, electrons, and neutral particles are discussed and a method of solving them numerically is described. The calculations include the effects of neutral-air winds, electric fields, viscosity, Coriolis force, geomagnetic declination, a time-dependent incoming flux, and different electron, ion, and neutral particle temperatures. The various assumptions which have to be made in order to solve the equations, and some limitations of the present work, are also discussed. (auth) (UK)

27522 LOWER IONOSPHERE. Thomas L. (Scientific Research Council Radio and Space Research Station, Slough, Eng.). J. Atmos. Terrest. Phys.; 33: 157-95(Feb 1971).

Current ideas about the D region at middle latitudes are reviewed. The main features of the height distribution of electron concentration and its diurnal variation are presented, but no attempt is made to describe the morphology of the region. The height distributions of minor neutral constituents are examined, and their role in the ionization processes and in the positive-ion and negative-ion chemistry is discussed. Attention is concentrated on solar-minimum conditions but the changes expected with increasing solar activity are also indicated. Finally, D-region phenomena observed during winter and following certain magnetic storms are described and possible explanations are presented. (auth) (UK)

27523 AURORAL OVAL PLANETARY ENERGETICS. Feldshtein, Ya. I. (Inst. of Terrestrial Magnetism, Ionosphere, and Radio-Wave Propagation, Moscow); Starkov, G. V. J. Atmos. Terrest. Phys.; 33: 197-203(Feb 1971).

The energy associated with a polar substorm is deduced from photographs of the aurora. (auth) (UK)

27524 SPORADIC-E AND ATMOSPHERIC PRESSURE WAVES. Shrestha, K. L. (Univ. of Queensland, Brisbane). J. Atmos. Terrest. Phys.; 33: 205-11(Feb 1971).

It is shown that the phenomena of sporadic-E ionization, cold fronts, and microbarometric activity are related. The method of superimposed epoch applied to sporadic-E parameters indicated that on the frontal days sporadic E tends to occur more frequently and with higher critical frequency than for the 10 preceding and 10 following days. No such effects were observed in the case of the blanketing frequency of sporadic E, f_bE_s. The data used are for Brisbane and cover a period of almost two years. Generation of atmospheric waves in the frontal region appears to cause the enhancement of microbarometric oscillations. A part of this wave energy leaking to ionospheric heights is suggested as the possible cause of the enhancement of sporadic E. It is not clear whether the wind shear provided by the waves themselves, or the turbulence they generated, was responsible for the sporadic-E enhancement. No effect of geomagnetic activity on the frequency of occurrence and the critical frequency of sporadic E, for the chosen period, is discernible. (auth) (UK)

27525 STABLE AURORAL RED ARCS OBSERVED FROM ADELAIDE DURING 1967-69. Schaeffer, R. C.; Jacka, F. (Univ. of Adelaide). J. Atmos. Terrest. Phys.; 33: 237-50 (Feb 1971).

Observations of Stable Auroral Red arcs from Adelaide (L lat. 45.3°S) on four occasions in the period September, 1967 to October, 1969 are reported. A noted feature was the low intensity of λ6300-Å emission from the arcs, with values ranging from 300 R down to 50 R. On two occasions, small components of λ5577-Å emission were detected in the region of the arc and an explanation is offered in terms of the dissociative recombination of O_2^+. Occurrences of oblique ionogram echoes at Christchurch, New Zealand, during optical observation of arcs at Adelaide are also reported. Some evidence for local time control of arc alignment and latitudinal movement is presented. Methods of height determination are discussed. (auth) (UK)

27526 ELECTRON DENSITY DISTRIBUTIONS IN THE LOWER IONOSPHERIC REGIONS FROM MULTI-FREQUENCY A_1 ABSORPTION DATA. Ganguly, S. (Bose Inst., Calcutta). J. Atmos. Terrest. Phys.; 33: 221-7(Feb 1971).

Attempts were made to derive the height distribution of electron density in the D and the E region of the ionosphere, from the multifrequency A_1-absorption data. Available cross-modulation profiles for moderately low latitudes were used to fix the lower bound of ionization distribution. The method of deriving the profiles is essentially a process of trial and error, where the observed experimental values are matched with those derived from the proposed models. (auth) (UK)

27527 IONIZATION OF THE E REGION BY PRECIPITATING ELECTRONS. Ivanov-Kholodni, G. S.; Kazatchevskaya, T. V. (Inst. of Applied Geophysics, Moscow). J. Atmos. Terrest. Phys.; 33: 285-7(Feb 1971).

The results of rocket measurements at middle latitudes at high solar-zenith angle $Z_\odot$ are compared with existing hypothesis of corpuscular ionization in the E region. (auth) (UK)

27528 RELATIVE EFFECTS OF ELECTRIC FIELDS AND ATMOSPHERIC COMPOSITION CHANGES ON THE ELECTRON CONCENTRATION IN THE MIDLATITUDE F LAYER. Ruester, R. (Scientific Research Council Radio and Space Research Station, Slough, Eng.). J. Atmos. Terrest. Phys.; 33: 275-80 (Feb 1971).

The coupled ionospheric continuity equations and the equation of motion for the neutral atmosphere were solved in order to investigate the relative importance of the effects of (a) electric fields, (b) neutral air winds and (c) atmospheric composition changes on the behavior of the midlatitude F layer. Calculations using the diurnal variation of the electric field given by Matsushita (1969) indicate that the field increases the electron concentration near the peak of the F layer by about 7% by day and reduces it by 28% at night. The effects of the neutral air winds produced by thermospheric pressure gradients are considerably

greater; further, if various slightly different, but nonetheless reasonable, atmospheric models are used in the calculations, the calculated values of electron concentration vary over a range of up to 92%. It appears that, in order to make accurate calculations of the electron concentration in the midlatitude F layer, it is more important to use reliable information about the composition of the neutral atmosphere than to take into account the effects of the electric fields calculated from dynamo theory. (auth) (UK)

27529 EFFECTS OF ELECTRIC FIELDS AND ION DRAG IN THE MIDDLE-LATITUDE F REGION. Bramley, E. N.; Ruester, R. (Scientific Research Council Radio and Space Research Station, Slough, Eng.). J. Atmos. Terrest. Phys.; 33: 269-74(Feb 1971).

Calculations of the diurnal variations in the critical frequency and height of the peak electron density were made for the middle-latitude F2 layer in order to investigate the effects of an east-west electric field. These calculations involve simultaneous solutions of the continuity equation for the ions and the equations of motion of the ions and the neutral atmosphere. Results given show the behavior both with and without the electric field calculated by Matsushita (1969) using dynamo theory. These results are compared with those of previous calculations in which the effect of ion drag on the atmospheric motion was ignored. It is found that ion drag is more effective by day than by night in reducing the changes caused by the electric field. (auth) (UK)

27530 CHARACTERISTICS OF TRAVELLING IONOSPHERIC PERTURBATIONS OVER WALTAIR USING PHASE PATH TECHNIQUE. Reddi, C. Raghava; Rao, B. Ramachandra (Andhra Univ., Waltair, India). J. Atmos. Terrest. Phys.; 33: 251-66(Feb 1971).

The phase-path technique is a very sensitive experimental method for detecting travelling ionospheric perturbations in the F2 region and is capable of giving much information on the various characteristics of the perturbations. The travelling-wave perturbations over Waltair, scaled from phase-path records of O and X components in the F2-region echoes on 5.6 MHz, were found to have periods in the range 3 to 39 min. Smaller periods were of more frequent occurrence than larger periods and the most frequently observed period was about 9 min. An average wave perturbation in the F2 region could be represented by the equation $A = 46.49\ K \sin 2\pi t/K$ where A is in meters, K the period of the disturbances in the general range 3 to 39 min and t is the time in minutes. The phase speed of the perturbations was in the range 2.5 to 14 km/min. Perturbations with shorter periods were found to travel faster than larger periods. It was shown that the above variation of the speed of the perturbations with period leads to the conclusion that the group speed of the perturbations is twice their phase speed. (auth) (UK)

27531 INTERCORRELATED SATELLITE OBSERVATIONS RELATED TO SOLAR EVENTS. Proceedings of the Third ESLAB/ESRIN Symposium Held in Noordwijk, Netherlands, September 16-19, 1969. Manno, V.; Page, D. E. (eds.). Astrophysics and Space Science Library. Volume 19. New York; Springer-Verlag New York Inc. (1970). 644p. $38.20. (CONF-690971).

Abstracts were prepared for the 51 papers presented at the conference on solar flare-associated interplanetary and terrestrial phenomena. (J.C.W.)

For abstracts of individual papers see: 27354-27357, 27469-27471, and 27532-27575.

27532 SURVEY OF INTERPLANETARY AND TERRESTRIAL PHENOMENA ASSOCIATED WITH SOLAR FLARES. Axford, W. I. (Univ. of California, San Diego, La Jolla). Astrophys. Space Sci. Libr.; 19: 7-22(1970).

From 3rd Intercorrelated Satellite Observations Related to Solar Events, Noordwijk, Netherlands. See CONF-690971.

Various interplanetary and terrestrial phenomena associated with solar flares are reviewed. An analogy of a solar flare and magnetospheric substorm is made. Sources of disturbances in the solar wind following a flare are analyzed. Other solar flare-associated phenomena discussed include solar x-ray bursts, energetic solar particles, galactic cosmic rays, ionospheric effects, and geomagnetic storms. (J.C.W.)

27533 SATELLITE OBSERVATIONS OF SOLAR COSMIC RAYS. McDonald, Frank B. (Goddard Space Flight Center, Greenbelt, Md.). Astrophys. Space Sci. Libr.; 19: 34-52(1970).

From 3rd Intercorrelated Satellite Observations Related to Solar Events, Noordwijk, Netherlands. See CONF-690971.

Solar-particle phenomena are grouped into four categories and satellite observations are discussed. Flare-associated events display a close association with solar flares, x-ray and microwave radio emission, and a diffusive particle propagation for both electrons and nucleons. Recurrent events sometimes appear on the next rotation after a flare-associated event, contain electrons and protons displaying essentially the same time history, and apparently originate in the same active region as that producing the original flare. Energetic particles associated with an active center display no velocity dispersion and appear to be co-rotating with the active center. Energetic storm particle events are large increases of low-energy electrons and protons that appear immediately behind strong interplanetary shock waves on certain occasions. (J.C.W.)

27534 SOLAR-WIND DISTURBANCES ASSOCIATED WITH SOLAR ACTIVITY. Hundhausen, A. J. (Los Alamos Scientific Lab., N. Mex.). Astrophys. Space Sci. Libr.; 19: 111-29(1970).

From 3rd Intercorrelated Satellite Observations Related to Solar Events, Noordwijk, Netherlands. See CONF-690971.

Geomagnetic activity has been attributed to particle emission from active solar regions. The occurrence of geomagnetic storms subsequent to large solar flares has been explained by the arrival at Earth of material ejected by the flare. Recurrent geomagnetic activity has been interpreted as the effect of persistent streams emitted from long-lived active regions on the rotating Sun. These phenomena observed by satellites are reviewed. (J.C.W.)

27535 VARIATIONS OF SOLAR-WIND FLUXES OBSERVED ON BOARD VENERA-5 AND VENERA-6 FROM JANUARY 21 TO MARCH 21, 1969 AND PULSATIONS OF THE EARTH'S ELECTROMAGNETIC FIELD CAUSED BY THESE VARIATIONS. Gringauz, K. I.; Troitskaya, V. A.; Solomatina, E. K; Shchepetnov, R. V. (Inst. of the Physics of the Earth, Moscow). Astrophys. Space Sci. Libr.; 19: 130-9(1970).

From 3rd Intercorrelated Satellite Observations Related to Solar Events, Noordwijk, Netherlands. See CONF-690971.

Preliminary comparison was made of data obtained from solar-wind fluxes on board Venera-5 and Venera-6 from January 21 to March 21, 1969 and from recording of pulsations and short-period disturbances of the Earth's electromagnetic field at the Soviet Observatory "Borok" ($\Phi = 53°$, $A = 123°$). The considerable increases of solar-wind fluxes as a rule were accompanied by considerable disturbances of the Earth's electromagnetic field so that there is no doubt about their causality. (auth)

27536 MAGNETIC-FIELD VARIATION IN INTERPLANETARY SPACE. Wilcox, John M. (Univ. of California, Berkeley). Astrophys. Space Sci. Libr.; 19: 140-51(1970).

From 3rd Intercorrelated Satellite Observations Related to Solar Events, Noordwijk, Netherlands. See CONF-690971.

Magnetic-field variations and structures in interplanetary space are described and related to the Sun. Discrete flare-related effects in the interplanetary medium occur within a large-scale interplanetary sector pattern related to a solar sector pattern that is ordered over a large extent in heliographic latitude and longitude. A random-walk transport of photospheric field lines slightly modifies the overall ordered pattern, but sector boundaries appear to resist the random-walk process. There is a delay of approximately one solar rotation between appearance of an active region and its possible effect on the interplanetary sector pattern. A flare occurrence is most probable near a solar sector boundary. (auth)

27537 PLASMA MEASUREMENTS ACROSS THE BOW SHOCK AND IN THE MAGNETOSHEATH. Hundhausen, A. J. (Los Alamos Scientific Lab., N. Mex.). Astrophys. Space Sci. Libr.; 19: 155-69(1970).

From 3rd Intercorrelated Satellite Observations Related to Solar Events, Noordwijk, Netherlands. See CONF-690971.

The changes in plasma properties that occur at the bow shock are studied from instrument data on satellites and space probes. It is the post-shock or magnetosheath plasma that is in contact with the magnetopause and that transmits interplanetary disturbances to the magnetosphere. Changes in bow shock and magnetopause position that occur in response to solar-wind variations, and that in turn induce changes in the geomagnetic field are discussed. (J.C.W.)

27538 INTERACTION OF SOLAR ENERGETIC PARTICLES WITH THE EARTH'S BOW SHOCK AND MAGNETOPAUSE. Singer, Sidney (Los Alamos Scientific Lab., N. Mex.). Astrophys. Space Sci. Libr.; 19: 170-80(1970).

From 3rd Intercorrelated Satellite Observations Related to Solar Events, Noordwijk, Netherlands. See CONF-690971.

The temporal and directional properties and the energy spectrum of energetic protons in the interplanetary medium, the magnetosheath, and the magnetotail are intercompared to determine the interactions of energetic particles with the bow shock and the magnetopause. Vela observations of May, 1967 and Feb., 1969 solar-particle events are summarized. Detectable interactions

XUM

with the Earth's bow shock are usually observed only at proton energies below a few MeV. The bow shock does not act as a barrier that slows the penetration of energetic particles. The interaction most commonly observed is an enhancement of the lower-energy fluxes in the magnetosheath, which sometimes is as large as a factor of 2. Certain changes in the directional characteristics of the protons show no consistent trends. The magnetopause tends to act as a multiple-scattering or diffusing barrier for energetic particles. (J.C.W.)

27539 MAGNETIC AND ELECTRIC FIELD CHANGES ACROSS THE SHOCK AND IN THE MAGNETOSHEATH. Scarf, F. L. (TRW Systems, Redondo Beach, Calif.); Coleman, P. J.; Fredricks, R. W.; Kennel, C. R.; Russell, C. T. Astrophys. Space Sci. Libr.; 19: 181-9(1970).

From 3rd Intercorrelated Satellite Observations Related to Solar Events, Noordwijk, Netherlands. See CONF-690971.

The structure of the Earth's bow shock is studied from Pioneer 8 and OGO-5 data from March 14 to April 5, 1968. Correlated solar events show that the two-stream current instability can be triggered by strong magnetic-field compressions that are not directly associated with the bow shock. Field configurations that yield intense vlf electrostatic turbulence include those near null regions (probably associated with reconnection) and those associated with large-amplitude oblique magnetosonic waves. (J.C.W.)

27540 SOLAR PARTICLE OBSERVATIONS OVER THE POLAR CAPS. Paulikas, G. A.; Blake, J. B.; Vampola, A. L. (Aerospace Corp., El Segundo, Calif.). Astrophys. Space Sci. Libr.; 19: 193-204(1970).

From 3rd Intercorrelated Satellite Observations Related to Solar Events, Noordwijk, Netherlands. See CONF-690971.

The report summarizes the recent measurements of spatial (latitude) distributions and angular distributions of solar particles obtained aboard the USAF–OAR satellites 1966-70A (OV3-3), 1967-72D (OVI-12), and 1968-59A (OVI-15). Solar potons and alpha particles with energies less than 10 MeV/nucleon and solar electrons with energies down to 40 keV were observed over the polar caps. The connection between the limits of trapping and the access and cutoff latitudes for solar particles is compared. It is concluded that some scattering of low-energy solar protons, but not electrons, is required in order to account for the experimental observations of solar particles over the polar caps. Direct entry of particles through the flanks of the magnetosphere appears to play a role in supplying particles to the polar caps. (J.C.W.)

27541 ACCESS OF SOLAR PARTICLES TO SYNCHRONOUS ALTITUDE. Lanzerotti, L. J. (Bell Telephone Labs., Murray Hill, N. J.). Astrophys. Space Sci. Libr.; 19: 205-28(1970).

From 3rd Intercorrelated Satellite Observations Related to Solar Events, Noordwijk, Netherlands. See CONF-690971.

When a source of solar-originated particles is present in interplanetary space, comparable fluxes of these particles with similar spectral characteristics are usually observed inside the magnetosphere at synchronous altitudes. The temporal and spectral changes in the access of these solar protons and α particles to synchronous altitude are discussed and reviewed. Possible consequences of the presence of substantial fluxes of low-energy solar protons deep inside the magnetosphere are also discussed. (auth)

27542 ENTRY OF LOW-ENERGY SOLAR PROTONS INTO THE MAGNETOSPHERE. Bostrom, Carl O. (Johns Hopkins Univ., Silver Spring, Md.). Astrophys. Space Sci. Libr.; 19: 229-38(1970).

From 3rd Intercorrelated Satellite Observations Related to Solar Events, Noordwijk, Netherlands. See CONF-690971.

Some aspects of the temporal and spatial variations of low-energy solar protons are examined by comparing data from the polar-orbiting satellite 1963 38C with measurements in interplanetary space by Explorers 33 and 34. Selected periods during the events of September 1966 and May 1967 are used to show a variety of features in the polar-region latitude profiles. The proton intensity in the low-latitude rim of the polar region appears to track the interplanetary flux of solar protons more readily than does the polar intensity. The rim straddles the energetic electron trapping boundary, and the rim intensity is frequently greater than the polar plateau flux. The intersatellite comparisons and latitude profiles are discussed in terms of model requirements. (auth)

27543 TRAPPED PARTICLE POPULATION CHANGES ASSOCIATED WITH SOLAR EVENTS. Roederer, Juan G. (Univ. of Denver). Astrophys. Space Sci. Libr.; 19: 239-50(1970).

From 3rd Intercorrelated Satellite Observations Related to Solar Events, Noordwijk, Netherlands. See CONF-690971.

The sequence of time variations occurring during a magnetospheric storm is followed, and the important changes occurring in the energetic-particle population of the magnetosphere during this time are given. Adiabatic changes and nonadiabatic effects are discussed. Morphology of the trapped-particle variations during the storm is given. Trapped-particle population changes associated with the solar events are caused by the effects of solar-wind discontinuities on the magnetosphere. (J.C.W.)

27544 GEOMAGNETIC STORMS AT ATS 1. Coleman, Paul J. Jr. (Univ. of California, Los Angeles). Astrophys. Space Sci. Libr.; 19: 251-79(1970).

From 3rd Intercorrelated Satellite Observations Related to Solar Events, Noordwijk, Netherlands. See CONF-690971.

It is concluded that the effects of a sudden commencement usually include an increase in the tail current along with the increase in the compression of the geomagnetic cavity. Nine of the 18 storms occurring in the first half of 1967 are discussed and include the initial phase, main-phase decrease, main-phase minimum, and the recovery phase. A summary of the storm-associated pulsations is given at the synchronous equatorial orbit of the ATS 1. (J.C.W.)

27545 MAGNETOSPHERIC ELECTRIC FIELDS. Voelk, H.; Haerendel, G. (Max-Planck-Institut fuer Physik und Astrophysik, Garching, Ger.). Astrophys. Space Sci. Libr.; 19: 280-96(1970).

From 3rd Intercorrelated Satellite Observations Related to Solar Events, Noordwijk, Netherlands. See CONF-690971.

Observational results concerning the high-latitude magnetosphere are discussed. The mapping of ionospheric electric fields into the magnetosphere is discussed. Electrostatic-probe measurements with sounding rockets have been made and field phenomena connected with auroral displays have been observed. Satellite flights show the onset of an intense irregularity structure poleward from the auroral zones, and low-energy ion-flux anisotropies have been detected using retarding potential analyzers. Balloon experiments with electrostatic probes in the auroral zone recorded electric-field distributions for a day. Barium ion-cloud experiments in the auroral ionosphere and an ion-cloud experiment in the distant magnetosphere are described. (J.C.W.)

27546 EXPERIMENTAL OBSERVATIONS IN THE MAGNETOTAIL DURING AN INTERPLANETARY DISTURBANCE. Hones, Edward W. Jr. (Los Alamos Scientific Lab., N. Mex.). Astrophys. Space Sci. Libr.; 19: 299-308(1970).

From 3rd Intercorrelated Satellite Observations Related to Solar Events, Noordwijk, Netherlands. See CONF-690971.

Observations were made simultaneously by two Vela satellites — one in the solar wind and one in the plasma sheet of the magnetotail — before and during the first seven hours of a weak sc storm that started May 1, 1967. A sudden compression in the plasma in the plasma sheet was observed a few minutes after the sc at the Earth. A sudden moderate helium enrichment of the solar wind, occurring $3\frac{1}{2}$ hours after the sc, was followed within minutes by the sharp onset of negative bays in the midnight sector of the auroral zone and by sudden diminution of plasma intensity in the plasma sheet. A discontinuity in the solar wind may affect the Earth many minutes (8 to 15) before its effects are felt at ~18 R_E in the center of the magnetotail. (J.C.W.)

27547 TEARING INSTABILITIES IN THE MAGNETOSPHERE. Schindler, K. (European Space Research Inst., Frascati, Italy). Astrophys. Space Sci. Libr.; 19: 307-15(1970).

From 3rd Intercorrelated Satellite Observations Related to Solar Events, Noordwijk, Netherlands. See CONF-690971.

Studies concerning plasma instabilities in the magnetosphere that involve topological changes of the magnetic-field configuration are described. There is evidence that magnetic-field loops are formed in the magnetospheric tail, but an attempt is made to show that similar processes may occur in other parts of the magnetosphere. The neutral sheet is treated as one region in a series of others, where tearing instabilities play a role. (J.C.W.)

27548 CURRENT PROBLEMS IN POLAR-CAP ABSORPTION. Reid, George C. (Univ. of Colorado, Boulder. ESSA Research Labs., Boulder, Colo.). Astrophys. Space Sci. Libr.; 19: 319-34(1970).

From 3rd Intercorrelated Satellite Observations Related to Solar Events, Noordwijk, Netherlands. See CONF-690971.

PCA represents the ionospheric response to the large fluxes of solar protons and heavier nuclei that are generated by certain flares. These particles create abnormally large amounts of ionization in the lower part of the ionosphere, giving rise to radio-propagation effects that can be readily detected by a wide variety of techniques. PCA phenomena were observed after the great cosmic-ray flare of Feb. 23, 1956 and the proton flares that followed the event. Important features of PCA that have been studied in the following twelve years are outlined. The ground-base observations provide knowledge on the manner in which solar protons enter the

magnetosphere and on the processes responsible for the loss of electrons in the lower ionosphere. Simultaneous observations by satellite confirm the data. (J.C.W.)

27549 INTERDISCIPLINARY INVESTIGATIONS OF THE AURORAL PHENOMENA. Zhulin, I. A. (Inst. of Terrestrial Magnetism, Ionosphere, and Radiowave Propagation, Moscow). Astrophys. Space Sci. Libr.; 19: 335-40(1970).

From 3rd Intercorrelated Satellite Observations Related to Solar Events, Noordwijk, Netherlands. See CONF-690971.

Problems and difficulties of the interdisciplinary analysis of auroral phenomena are discussed using investigations in magnetically conjugate points. In March–April, 1968, a series of balloon launchings was performed in the northern (Arkhangelsk region) and southern (Kerguelen Island) conjugate subauroral zones ($L \approx 3.85$). During this experiment a better conjugacy was achieved than during all the other known flights of balloons (approximately 50 km). On the basis of calculations made by Roederer, the influence upon conjugacy of the daily migration of conjugate points due to the change of spatial position of the geomagnetic-field axis was estimated. On April 1, 1968, three events of auroral-electron precipitation were recorded. In the energy spectrum of these electrons the presence of soft and hard components was revealed (characteristic energies 6 and 30 keV). In one of the events the presence of the maximum in the exponential spectrum near 90 keV (nearly monoenergetic flux of electrons) was revealed. Possibilities for the intercorrelated analysis of obtained data in comparison with satellite data (especially from ESRO-1) are discussed. (auth)

27550 ASPECTS OF AURORAL MORPHOLOGY. Davis, T. Neil (Univ. of Alaska, College). Astrophys. Space Sci. Libr.; 19: 341-50(1970).

From 3rd Intercorrelated Satellite Observations Related to Solar Events, Noordwijk, Netherlands. See CONF-690971.

The temporal relationship of the auroral substorm to increases in the total particle kinetic energy within the trapping region and, also, the characteristics of auroras near the equatorward boundary of the typical display indicate a close physical connection between acceleration processes causing auroras and growth of the ring current. Conjugate studies of auroras during disturbed epochs indicate sizable distortions in the geomagnetic field at the higher latitudes; these distortions may be caused by meridional asymmetry in the ring current as well as by magnetopause and neutral sheet currents. (auth)

27551 ACCELERATION AND PRECIPITATION OF VAN ALLEN ELECTRONS DURING MAGNETOSPHERIC SUBSTORMS. Parks, George K. (Univ., Toulouse). Astrophys. Space Sci. Libr.; 19: 351-63(1970).

From 3rd Intercorrelated Satellite Observations Related to Solar Events, Noordwijk, Netherlands. See CONF-690971.

Data from the ATS-1 auroral particle correlation experiment shows that magnetospheric and auroral processes are intimately related and that Van Allen electrons of $E > 50$ keV are accelerated during magnetospheric substorms. In particular, it is shown that (1) intense auroral precipitation does not occur randomly, but only during periods when the outer zone electron fluxes increase, (2) electron pitch-angle distribution in the equatorial plane during substorms is peaked toward 90°, (3) the pitch-angle distribution changes in time and depends on the flux, and (4) lifetimes of freshly energized Van Allen electrons are considerably shorter than their drift periods. It will be shown that the observations can be explained consistently in terms of energy and pitch-angle diffusion processes accompanying whistler-cyclotron resonance interaction. (auth)

27552 INTRODUCTION TO THE ESRO SPACECRAFT ESRO-II/IRIS, ESRO-I/AURORAE AND HEOS-I. Page, D. E. (ESLAB, Noordwijk, Netherlands). Astrophys. Space Sci. Libr.; 19: 367-81(1970).

From 3rd Intercorrelated Satellite Observations Related to Solar Events, Noordwijk, Netherlands. See CONF-690971.

ESRO-II was launched in May 1968, ESRO-I in early October 1968, and HEOS-I in early December 1968. The three satellites observed the solar event of Feb. 25, 1969. The main features of the satellites and the experiments are described. (J.C.W.)

27553 GROUND OBSERVATIONS OF THE SOLAR EVENT OF FEBRUARY 25, 1969. Lenhart, K. G. (ESOC, Darmstadt, Ger.). Astrophys. Space Sci. Libr.; 19: 382-404(1970).

From 3rd Intercorrelated Satellite Observations Related to Solar Events, Noordwijk, Netherlands. See CONF-690971.

In order to give a broad basis for correlation of satellite data with ground-based measurements for the solar event of February 25, 1969, ground-based observations centered on this period were collected. The data presented include solar measurements (magnetic fields, radio emission, sunspots) and effects caused on the Earth (ionospheric effects, magnetic measurements, and neutron-monitor data). (auth)

27554 SUBSTORM INFLUENCES ON vhf CONTINUOUS WAVE AURORAL BACKSCATTER. Czechowsky, P.; Lange-Hesse, G. (Max-Planck-Institut fuer Aeronomie, Lindau, Ger). Astrophys. Space Sci. Libr.; 19: 405-12(1970).

From 3rd Intercorrelated Satellite Observations Related to Solar Events, Noordwijk, Netherlands. See CONF-690971.

On Feb. 26, 1969 an ssc was observed as a consequence of the events recorded on Feb. 25, 1969; the storm reached its peak on Feb. 27. During this time vhf auroral backscatter echoes were recorded with the network in Northern Germany and Scandinavia. These observations are compared with simultaneous geomagnetic records that include location, direction, and intensity variation of the polar electrojet (PEJ). The ion-acoustic wave theory of Farley is used as a basis in the discussion. An analysis of the single event demonstrates a close correlation between the PEJ and the backscattering of vhf radio waves. The geomagnetic deviations coincide in nearly all details with the amplitude variations of the backscattered signals. (J.C.W.)

27555 SOLAR PARTICLE EVENT OF FEBRUARY 25, 1969. HEOS-1 INTERPLANETARY MAGNETIC FIELD MEASUREMENTS. Hedgecock, P. C. (Imperial Coll. of Science and Tech., London). Astrophys. Space Sci. Libr.; 19: 419-26(1970).

From 3rd Intercorrelated Satellite Observations Related to Solar Events, Noordwijk, Netherlands. See CONF-690971.

HEOS-1 measurements of the interplanetary magnetic field during the particle event of February 25, 1969 are reported. The measurements provide virtually continuous coverage from 0130 Z on February 25 until 0700 Z on February 27, when HEOS-1 re-entered the magnetosphere. Preliminary values for the power spectra of the field fluctuations are quoted. (auth)

27556 INTERPLANETARY MAGNETIC FIELD MEASURED BY PIONEER 8 DURING THE FEBRUARY 25, 1969 EVENT. Mariani, F. (Univ., Rome); Bavassano, B.; Ness, N. F. Astrophys. Space Sci. Libr.; 19: 427-35(1970).

From 3rd Intercorrelated Satellite Observations Related to Solar Events, Noordwijk, Netherlands. See CONF-690971.

Observations aboard Pioneer 8 during the Feb. 25, 1969 event are discussed in relation to measurements obtained by other near-Earth satellites at that time. Several long-lasting strong flares were observed on the Sun, one cosmic-ray proton event and three sc geomagnetic storms were observed on Earth, and si disturbances were detected. A very active region, McMath No. 9946, was present in the northern hemisphere of the Sun. Two worldwide geomagnetic storms were observed on Feb. 26 and 27. Presence of shocks in the interplanetary medium can be expected to be associated with them. An illustration is presented of the time sequence of the events on the Sun, on Pioneer 8, and on the Earth beginning with the effect of the flare of 2300 Feb. 24, 1969. (J.C.W.)

27557 OBSERVATION OF SOLAR-WIND DISCONTINUITIES FROM FEBRUARY 24 TO FEBRUARY 28, 1969. Bonetti, A. (Univ., Florence); Moreno, G.; Candidi, M.; (and others). Astrophys. Space Sci. Libr.; 19: 436-47(1970).

From 3rd Intercorrelated Satellite Observations Related to Solar Events, Noordwijk, Netherlands. See CONF-690971.

Interplanetary-plasma data at 1 AU obtained with experiment S-73 on board of HEOS-A during the last week of February 1969 were analyzed. A well-defined shock wave, traveling with a velocity of 600 to 700 km/sec, was observed and is most likely related to a large solar flare. A second shock wave occurring a few days later is also recognizable. A preliminary analysis of data within the magnetosheath is presented; the possible interaction between a solar wind discontinuity and the magnetosheath is reported. (auth)

27558 OBSERVATIONS OF THE SPECTRA AND TIME HISTORY OF PROTONS IN INTERPLANETARY SPACE, FEBRUARY 25–28, 1969. Barouch, E.; Engelmann, J.; Gros, M.; Koch, L.; Masse, P. (CEN, Saclay, France). Astrophys. Space Sci. Libr.; 19: 448-59(1970).

From 3rd Intercorrelated Satellite Observations Related to Solar Events, Noordwijk, Netherlands. See CONF-690971.

Visual and radio observations are reported from instruments aboard HEOS A1 and IRIS satellites during the flare sequence Feb. 24–28, 1969. Two Centaure Rockets were launched on Feb. 25. Time sequence of the particle flux close to Earth is presented. The energy spectra are analyzed, and it is shown that it is important to observe solar-flare phenomena with a battery of detectors, permitting a broad spectral range to be examined simultaneously. It is concluded that the passage of solar cosmic particles into the magnetosphere over the polar cap was unhindered down to 2 MeV in this event. Although falling on a smooth curve, the inten-

XUM

sity spectrum does not follow a simple power or exponential law. Fluctuations in intensity from 24 to 200 MeV were observed during the decrease of the event. The overall behavior of the particle flux can be explained by the detailed study of the different shock waves in the interplanetary medium. (J.C.W.)

27559 LOW-ENERGY PROTON MEASUREMENTS IN INTERPLANETARY SPACE ON BOARD THE HEOS-1 SATELLITE. Balogh, A.; Hynds, R. J. (Imperial Coll. of Science and Tech., London). Astrophys. Space Sci. Libr.; 19: 471-7(1970).

From 3rd Intercorrelated Satellite Observations Related to Solar Events, Noordwijk, Netherlands. See CONF-690971.

Directional measurements of low-energy (1 to 13 MeV) protons in interplanetary space obtained during the February 25, 1969 solar-proton event are presented. The time history of the anisotropies is presented and discussed in connection with magnetic-field measurements taken on the same spacecraft. (auth)

27560 SOLAR PARTICLE EVENT OF FEBRUARY 25, 1969. DIRECTIONAL MEASUREMENTS OF SOLAR PROTONS WITH ENERGIES GREATER THAN 360 MeV ON HEOS-1. Engel, A. R. (Imperial Coll. of Science and Tech., London). Astrophys. Space Sci. Libr.; 19: 478-85(1970).

From 3rd Intercorrelated Satellite Observations Related to Solar Events, Noordwijk, Netherlands. See CONF-690971.

Measurements made on the HEOS-1 spacecraft during the particle event of February 25, 1969 are reported. Directional measurements were made on protons >360 MeV and omnidirectional measurements on protons >30 MeV. Results indicate that diffusion of the particles has occurred in interplanetary space. Initially the particle flux is highly anisotropic. There is an evident discrepancy between the direction of maximum particle flow and the magnetic-field direction measured on the same spacecraft. A strong bi-directional anisotropy is noted, indicating some back-scattering process beyond the Earth. (auth)

27561 ESRO I SATELLITE OBSERVATIONS OF 1 to 30 MeV PROTONS DURING THE 25th FEBRUARY 1969 SOLAR EVENT. Thomas, G. R.; Dalziel, R.; Donaldson, W. (Science Research Council, Ditton Park, Eng.). Astrophys. Space Sci. Libr.; 19: 492-8(1970).

From 3rd Intercorrelated Satellite Observations Related to Solar Events, Noordwijk, Netherlands. See CONF-690971.

Observations of solar protons over the northern polar cap during the February 25, 1969 solar event are described. The time history of the proton distributions is described, and an asymmetry is found between the morning and evening sides. It is suggested that in the early stages of the event the protons had access to the polar cap both by diffusion into the geomagnetic tail and by direct entry through the dayside neutral point on the high-latitude magnetopause. (auth)

27562 ROCKET MEASUREMENTS OF PROTONS AND α-PARTICLES DURING THE FEBRUARY 25, 1969 SOLAR EVENT. Wiberenz, G.; Witte, M. (Univ., Kiel). Astrophys. Space Sci. Libr.; 19: 499-507(1970).

From 3rd Intercorrelated Satellite Observations Related to Solar Events, Noordwijk, Netherlands. See CONF-690971.

Two Centaure rockets were launched during an ESRO PCA campaign 7.3 and 14.6 hours after the February 25, 1969 solar event. Energy spectra of protons between 30 and 120 MeV and of α-particles between 24 and 75 MeV/nucleon are presented and compared with other particle measurements on board the same rockets. Proton-to-α ratios for the energy/nucleon range 24 to 75 MeV/N are 88 ± 15 and 190 ± 50 for the two flights. Implications of the time-varying proton-to-α ratio are discussed in terms of a diffusion model of propagation. (auth)

27563 ROCKET OBSERVATIONS OF PROTONS AND α-PARTICLES AT ANDOEYA AFTER THE SOLAR FLARES OF 24th–25th FEBRUARY 1969. Van Beek, H. F.; Stevens, G. A. (Space Research Lab., Utrecht). Astrophys. Space Sci. Libr.; 19: 508-14 (1970).

From 3rd Intercorrelated Satellite Observations Related to Solar Events, Noordwijk, Netherlands. See CONF-690971.

During the polar-cap absorption event occurring after the flares of 24th and 25th February 1969, three rockets were launched successfully at Andenes (Norway). Riometer and magnetometer recordings show that the PCA event is a fairly weak one. The energy spectra of protons and α-particles in the range from 2.3 to 70 MeV obtained during these flights are given. The α/proton ratio found is 0.013 in the range 4 to 20 MeV/nucleon at both flights. The mean free path of the protons is estimated to be 0.06 AU. (auth)

27564 ELECTRON DENSITY OBSERVATIONS DURING THE PCA EVENT OF 25 FEBRUARY 1969. Jespersen, M. (Danish Space Research Inst., Lyngby); Troeim, J.; Landmark, B. Astrophys. Space Sci. Libr.; 19: 515-19(1970).

From 3rd Intercorrelated Satellite Observations Related to Solar Events, Noordwijk, Netherlands. See CONF-690971.

Results from rocket observations of electron density during the PCA event of February 25, 1969 are discussed. Results were obtained in two Sidewinder–Arcas rockets. The electron densities are related to results from high-energy-particle measurements. The effective loss rates derived are interpreted in terms of a two-ion model of recombination. It is shown that the interpretation is consistent with similar results obtained during quiet and auroral absorption conditions. (auth)

27565 ROCKET-BORNE D-REGION PROBE MEASUREMENTS. Murdin, J.; Bowling, T. S. (Mullard Space Science Lab., Dorking, Eng.). Astrophys. Space Sci. Libr.; 19: 520-3 (1970).

From 3rd Intercorrelated Satellite Observations Related to Solar Events, Noordwijk, Netherlands. See CONF-690971.

After the onset of the Feb. 25, 1969 solar-proton event, two Arcas rockets were launched to measure the positive-ion density at 60 to 70 km. The experiment utilized a cylindrical electrostatic probe consisting of a 10-cm-long, rhodium-plated steel wire of 0.05-cm diameter biased at −2.7 volt with respect to the rocket body. Probe current and positive-ion density profiles are given as a function of altitude. (J.C.W.)

27566 ELECTRON DENSITY MEASUREMENTS IN THE THERMAL PLASMA OF THE MAGNETOSPHERE USING A LANGMUIR PROBE. Freeman, R.; Norman, K.; Willmore, A. P. (University Coll., London). Astrophys. Space Sci. Libr.; 19: 524-34(1970).

From 3rd Intercorrelated Satellite Observations Related to Solar Events, Noordwijk, Netherlands. See CONF-690971.

Ambient electron density and temperature in the magnetosphere was measured aboard OGO-V using a Langmuir probe during the Feb. 25, 1969 solar-proton event. The results are compared with previous data taken preceding the solar event. The experimental observations of the plasmapause-boundary position and its relation to the K_p index are consistent with previous results. The sudden commencement of Feb. 26, 1969, appeared to cause no major disturbances in the thermal plasma in the magnetosphere, and no significant changes in the positions of the bow shock and magnetopause were observed on the two satellite passes investigated. The position of the plasmapause boundary was consistent with the level of magnetic activity. (J.C.W.)

27567 IONOSPHERIC MEASUREMENTS BY THE ESRO-I SATELLITE DURING THE FEBRUARY 25th, 1969 SOLAR PROTON EVENT. Raitt, W. J. (University Coll., London). Astrophys. Space Sci. Libr.; 19: 535-48(1970).

From 3rd Intercorrelated Satellite Observations Related to Solar Events, Noordwijk, Netherlands. See CONF-690971.

Measurements on local electron density and temperature variations for complete near-Earth satellite orbits are presented for periods before and after the solar proton event of February 25, 1969. No large-scale effects on the ionospheric structure were detected from this relatively small sample of data. (auth)

27568 ESRO I SATELLITE OBSERVATIONS OF 45 TO 450 keV ELECTRONS DURING THE PERIOD FEBRUARY 24–MARCH 3, 1969. Thomas, G. R.; Smith, P. A.; Dalziel, R. (Science Research Council, Ditton Park, Eng.). Astrophys. Space Sci. Libr.; 19: 549-56(1970).

From 3rd Intercorrelated Satellite Observations Related to Solar Events, Noordwijk, Netherlands. See CONF-690971.

Results are presented for trapped and precipitated electrons observed at northern high latitudes during morning- and evening-side passes of the ESRO I satellite in the period February 24 to March 3, 1969. Variations of the integral intensities >50 keV and of the latitudes at which the peak intensities occur are examined in relation to magnetic activity and local time. The energy spectra of the trapped and precipitated electrons are compared, and variations of the spectra are related to local time and latitude. (auth)

27569 ESRO I MEASUREMENTS OF LOW-ENERGY AURORAL PARTICLES FROM FEBRUARY 23 TO MARCH 2, 1969. Riedler, W. (Kiruna Geophysical Observatory, Sweden). Astrophys. Space Sci. Libr.; 19: 557-66(1970).

From 3rd Intercorrelated Satellite Observations Related to Solar Events, Noordwijk, Netherlands. See CONF-690971.

Results of satellite electron and proton measurements in the energy range 1 to 13 keV are reported. Three different electron spectra can be distinguished: a hard type, a high-intensity soft type, and a low-intensity soft type. These appear in distinct regions: two hard zones, one probably coinciding with the auroral oval, one with the auroral zone, a high-intensity soft belt and a low-intensity soft polar-cap region. Proton precipitation was highest in the dusk and noon sectors. Anisotropies and changes

of zone boundaries during the observed period February 23 to March 2, 1969 are reported. (auth)

27570 OBSERVATION OF THE FEBRUARY 26, 1969 INTERPLANETARY SHOCK WAVE. Hundhausen, A. J.; Bame, S. J.; Montgomery, M. D. (Los Alamos Scientific Lab., N. Mex.). Astrophys. Space Sci. Libr.; 19: 567-70(1970).

From 3rd Intercorrelated Satellite Observations Related to Solar Events, Noordwijk, Netherlands. See CONF-690971.

Data are given from 0004 to 0240 UT on Feb. 26, 1969 when the Vela 4B spacecraft was near the Earth's bow shock at 19.2 R_E. An interplanetary shock wave, which caused the sudden commencement reported at ground stations shortly before 0200 UT, was observed at 0152 UT. An observational description of the shock is given and its possible correlation with the Feb. 25 event is made. In an attempt to associate the shock wave with the flare event, difficulties arise, but possibilities presented include: the shock normal may have been tilted away from the radial direction, so that the shock propagation speed has not been correctly derived; the shock may have been decelerated near the Earth by a thin region of dense interplanetary plasma; and the disturbance may have been produced by a small flare, such as the 1B flare observed at 0440 UT on Feb. 23. (J.C.W.)

27571 ASSOCIATION OF ENERGETIC STORM PARTICLES WITH INTERPLANETARY SHOCK WAVES. Singer, Sidney (Los Alamos Scientific Lab., N. Mex.). Astrophys. Space Sci. Libr.; 19: 571-82(1970).

From 3rd Intercorrelated Satellite Observations Related to Solar Events, Noordwijk, Netherlands. See CONF-690971.

Energetic storm particle (ESP) events associated with the Feb. 25, 1969, May 1967, and Jan. 9, 1968 solar energetic particle events are reported. The nature of the ESP event, the relationship of the ESP event to the interplanetary shock, and the penetration of energetic storm particles into the magnetotail are discussed. It is concluded that ESP events are associated with shock waves and are not seen when other kinds of solar-wind discontinuities are detected. ESP events are associated with protons of energy less than several MeV; the intensity and energy spectrum of protons >20 MeV are not usually affected by the event. The ESP event is characterized by a slow increase in flux intensity beginning several hours before shock arrival and, frequently, by an abrupt, stepped decay. The degree of enhancement of the particle flux is variable, and perhaps depends on the strength of the shock. Comparisons of time history of ESP events seen by Vela satellites inside and outside the magnetopause show that ESP's do not have free and immediate access to the magnetotail. (J.C.W.)

27572 GM OBSERVATIONS OF AURORAL PARTICLES AND GROUND OBSERVATIONS DURING THE FEBRUARY 25th SOLAR EVENT. Stauning, Peter (Ionosphere Lab., Lyngby, Denmark); Skovli, Gunnar; Bahnsen, Axel. Astrophys. Space Sci. Libr.; 19: 583-91(1970).

From 3rd Intercorrelated Satellite Observations Related to Solar Events, Noordwijk, Netherlands. See CONF-690971.

An array of Geiger counters aboard ESRO-I is devoted to studying fast variations and fine structure in the intensities and in the angular spectra of energetic (>40 keV) auroral electrons. Results presented were obtained during the Feb. 25, 1969 solar event. The counting rates for all detectors are very low when the satellite is close to the magnetic pole. At such low fluxes and well inside the polar cap the high-energy solar protons could make a significant contribution to the fluxes observed during the solar-flare event. During auroral zone passes, the relative contribution from high-energy solar protons or radiation-belt protons is very small compared to the contribution from the electrons and might be neglected for most purposes. These data from S71D are compared with the S71C data on energetic proton fluxes. (J.C.W.)

27573 OBSERVATION OF LOW-ENERGY SOLAR PROTONS DURING THE FEBRUARY 25, 1969 EVENT. Soeraas, F.; Aarsnes, K.; Lindalen, H. R. (Univ. of Bergen, Norway). Astrophys. Space Sci. Libr.; 19: 592-8(1970).

From 3rd Intercorrelated Satellite Observations Related to Solar Events, Noordwijk, Netherlands. See CONF-690971.

Protons in the energy range 100 keV to 6 MeV were observed over the northern polar cap for a period of five days following the solar flare of Feb. 25, 1969. The S71C experiment was flown aboard the ESRO-I satellite launched into a near-polar orbit. The instrumentation will measure protons belonging to the radiation belt and transient phenomena such as solar and auroral protons. There exists an enormous variation both in intensities and spectral hardness of the protons observed. (J.C.W.)

27574 HIGH-ENERGY SOLAR ELECTRONS. Bland, C. J. (Univ., Milan); Degli Antoni, G.; Dilworth, C.; (and others). Astrophys. Space Sci. Libr.; 19: 599-609(1970).

From 3rd Intercorrelated Satellite Observations Related to Solar Events, Noordwijk, Netherlands. See CONF-690971.

Observations of high-energy solar-electron flux enhancements are reported for Dec. 1969 to June, 1969. The four main events recorded during the S-79 experiment (aboard HEOS-A1) include enhancements on Feb. 25, Feb. 27, Mar. 30, and Apr. 12, 1969. The flares of Feb. 25 and Mar. 30 are compared, after which the flares of Feb. 27 and Apr. 12 are compared. Common characteristics for the latter two include their small size, no correlation with large radio bursts, no correlation with neutron monitor enhancements, and their occurrence following the larger events. It is postulated that there exists a semi-transparent barrier at some 10 to 20 AU from the Sun that would reflect back part of the electrons produced during the large flares. Another hypothesis considered is that the electrons detected are due to invisible solar activity, perhaps from the same active areas on the Sun as the large flares preceding them. Results on Venus 6 differ from those on the HEOS experiment. (J.C.W.)

27575 OGO-5 MEASUREMENTS OF ELECTRONS ABOVE 500 MeV. Swanenburg, B. N. (Kamerlingh Onnes Lab., Leiden). Astrophys. Space Sci. Libr.; 19: 610-13(1970).

From 3rd Intercorrelated Satellite Observations Related to Solar Events, Noordwijk, Netherlands. See CONF-690971.

A cosmic-ray electron detector is flown on board the OGO-5 satellite. The long-term variation of the electron intensity above 500 MeV is clearly observed. Short-term decreases related to solar events show a similar energy dependence. (auth)

27576 PRECIPITATION PATTERN FOR AURORAL keV ELECTRONS AND PROTONS. Riedler, W.; Borg, H. (Kiruna Geophysical Observatory, Sweden). Phys. Norv.; 4: No. 2, 69-72(1970).

Precipitation patterns for keV electrons and protons are presented, as they were observed by ESRO 1A (Aurorae) over the northern polar cap during autumn 1968. Two hard electron zones, one coinciding with the auroral oval, the other one with the auroral zone, and several soft electron zones can be distinguished. Both isotropic and anisotropic proton precipitation could be observed. (auth) (Norway)

27577 ON THE PITCH-ANGLE DEPENDENCE OF AURORAL ELECTRON FLUXES IN THE keV RANGE. Holmgren, L.-A.; Christophersen, P.; Riedler, W. (Kiruna Geophysical Observatory, Sweden). Phys. Norv.; 4: No. 2, 85-91(1970).

Some results of ESRO 1 A(Aurorae) measurements of low-energy electrons (1 to 6 keV) obtained during October-December 1968 are presented. Two points of the pitch-angle distribution are monitored, namely 10 and 80° with respect to the magnetic-field line. Thirty-four northward Tromsø passes covering the eccentric dipole-time range 23-01 are analyzed. The pitch-angle distributions are found to depend on magnetic activity. Both 1-keV and 6-keV electrons reach isotropy within a factor of 2 when $Kp \leq 7$. For $Kp \leq 6$ a pronounced difference is observed in the pitch-angle distribution of 1-keV electrons as compared to 6 keV. The 1-keV electrons can remain isotropic throughout the whole precipitation zone, or in some cases show anisotropies peaking along the field line (10°) in the high-intensity soft zone. On the other hand the 6-keV electrons show isotropy in the hard zone and peaks normal to the field line (80°) at the soft equatorward edge of the hard zone and in the high-intensity soft zone. A persistent feature of all anisotropies is found to be an associated softening of the spectra, mostly in both 10 and 80°. No evidence for the dependence of degree of isotropy on flux magnitude is found. One case of extreme anisotropy along the field line (10°) is reported for 1-keV electrons. (auth) (Norway)

27578 RELATION OF LOW-ENERGY PARTICLE PRECIPITATION TO THE LUMINOUS AURORA OBSERVED FROM ESRO-1A. Deehr, C. S.; Gustafsson, G. A.; Omholt, A.; (and others). Phys. Norv.; 4: No. 2, 101-7(1970).

A comparison of electron and proton spectra in the 1- to 13-keV range was made with photometric observations of the luminous aurora in the midnight meridian from the satellite ESRO-1A. The electron flux was characterized by isotropic pitch-angle distribution, softer spectral profile on the edges than in the center of the main precipitation region, and occasional relatively hard spikes. The protons exhibited an anisotropic pitch-angle distribution near the edges of the main precipitation region. The photometer data showed N_2^+ (4278 A) to be more than 50 times brighter than H_β in the electron precipitation region, although this region contained the main flux of isotropic pitch-angle proton precipitation also. The N_2^+ (4278 A)/H_β ratio dropped to 5 on the edge of the auroral

zone, where the satellite observed only high pitch-angle protons. (auth) (Norway)

27579 PROTON PRECIPITATION IN THE NOON-MIDNIGHT MERIDIAN AND ITS RELATION TO GEOMAGNETIC ACTIVITY. Aarsnes, K.; Amundsen, R.; Lindalen, H. R.; Soeraas, F. Phys. Norv.; 4: No. 2, 73-83(1970).

Proton precipitation at high latitudes in the noon-midnight meridian plane was studied. Proton data from an experiment onboard the satellite ESRO 1A covering periods with quiet as well as disturbed geomagnetic conditions were used. The precipitation region was found at higher invariant latitudes on the dayside than on the nightside. With increasing geomagnetic disturbances the precipitation region expanded and moved equatorwards. Generally the intensity increased. In the time period covered, low energy solar protons were recorded over the polar region. An example of proton precipitation connected with a geomagnetic substorm is described. (auth) (Norway)

27580 OBSERVATIONS OF ELECTRONS IN THE AURORAE (ESRO-1A) SATELLITE. Skovli, G. Phys. Norv.; 4: No. 2, 109-12(1970).

The S-71D scientific experiment onboard the polar-orbiting satellite Aurorae is briefly described. An example showing a real-time quick-look display is given. During a two-month period the scatter in the day-to-day observations of the maximum fluxes is shown, and from the same period, the dependence of the maximum fluxes versus the magnetic disturbance. (auth) (Norway)

27581 AURORAL LUMINOSITY PATTERNS OVER NORTHERN SCANDINAVIA DURING A NUMBER OF ESRO-1A (AURORAE) PASSAGES. Gustafsson, G. (Kiruna Geophysical Observatory, Sweden). Phys. Norv.; 4: No. 2, 113-19(1970).

Maps of auroral forms based on all-sky camera recordings were drawn for 4 passages of the satellite ESRO 1A. The location of the auroral structures is related to particle measurements of protons and electrons in the 1 to 13-keV range. It was found that the flux of 6-keV precipitated electrons is very closely related to the auroral emission. Precipitated 1.3-keV electrons and, particularly during high magnetic activity, also 2.9-keV electrons are anticorrelated with the aurora. (auth) (Norway)

27582 PRELIMINARY RESULTS OF ESRO-1A (AURORAE) OBSERVATIONS OF VARIATIONS IN THE LOW-ENERGY ELECTRON SPECTRUM AND THEIR RELATION TO MAGNETIC ACTIVITY. Liszka, L.; Borge, H.; Riedler, W. (Kiruna Geophysical Observatory, Sweden). Phys. Norv.; 4: No. 2, 121-5 (1970).

Some aspects of observations of low-energy electrons (1 to 6 keV) measured on the ESRO-1A satellite during October-December 1968 are presented. The steepness of the electron-energy spectrum between 1 and 6 keV has been studied. A distinct softening of the energy spectrum observed in the evening sector at the southern boundary of the auroral zone, the soft edge, has been found. The steepness of the spectrum is negatively correlated with the geomagnetic K_p index. In a few cases effects of the particle flux and the steepness of the spectrum of low-energy electrons on the true electron-density profiles of the F layer were studied. A significant influence of the particles was found only for the steepness of the electron spectrum above a certain level. (auth) (Norway)

27583 ON THE MORPHOLOGY AND DYNAMICS OF AURORAL-ZONE ELECTRON PRECIPITATION FROM BALLOON MEASUREMENTS OF BREMSSTRAHLUNG. Trefall, H.; Pytte, T.; Broenstad, K.; (and others). Phys. Norv.; 4: No. 2, 161-9(1970).

A review is given of the local-time dependence of auroral-zone x-ray events, with examples taken from one whole day of simultaneous recordings with three balloons. In addition to showing features already well known, the recordings presented here also confirm the existence of some less-well-known types of electron-precipitation events, like westward-moving pulsation trains in the morning, and large-scale coherent pulsation events around geomagnetic noon. Furthermore, several cases of impulsive x-ray events were recorded in association with the onset of magnetic substorms or with impulsive disturbances in the geomagnetic field. It is suggested that electron acceleration normally occurs along the auroral oval eastwards from the midnight sector, and that the precipitation events observed during the day are caused by pitch-angle scattering into the atmosphere of drifting electrons. (auth) (Norway)

27584 SIMULTANEOUS VARIATIONS IN PARTICLE FLUXES AND MAGNETIC FIELD CONFIGURATION AFTER THE MAJOR PARTICLE INJECTION OF JANUARY 28, 1967. Lindgren, S. (Univ. of Uppsala). Phys. Norv.; 4: No. 2, 127-32(1970).

For three weeks following the January 28, 1967 particle event, the flux of solar particles was high enough to allow a study of how the propagation can be affected by the configuration of the magnetic field. A few illustrations are given of different kinds of such effects, using particle and magnetic-field data from experiments on IMP-3. It is also suggested that the field can be strongly disturbed by high densities of solar particles (protons above 500 keV). (auth) (Norway)

27585 IONOSPHERIC PLASMA DRIFTS DERIVED FROM WAKE MEASUREMENTS. Knott, K. (ESTEC, Noordwijk, Netherlands); Brommundt, G.; Schumann, G. Planet. Space Sci.; 19: 345-55(Mar 1971).

A technique was developed whereby the direction of the plasma wake produced by a sounding rocket is obtained by measuring the electrostatic field at the surface of the vehicle. From the orientation of the wake the direction of ionospheric plasma drift is derived. Two experiments were carried out at high latitude, one during evening twilight under slightly disturbed conditions. A strong plasma drift towards the west was detected. At a second flight in morning twilight a small drift towards the east was prevailing. As a by-product from a comparison of both flights, which took place under different plasma conditions, an upper limit of 0.1 for the plasma rarefaction in the wake can be given. (auth) (UK)

27586 POLARIZATION FIELDS PRODUCED BY WINDS IN THE EQUATORIAL F REGION. Rishbeth, H. (SRC Radio and Space Research Station, Slough, Eng.). Planet. Space Sci.; 19: 357-69(Mar 1971).

Neutral-air winds blowing across the magnetic field cause a slow transverse drift of the positive ions, perpendicular to both the winds and the magnetic field. This drift sets up an electric polarization field which can only be neutralized by currents flowing along magnetic-field lines and through the E layer. But at night the E-layer conductivity may be too small to close this circuit, so that polarization fields build up in the F layer, causing the plasma to drift with the wind. This polarization effect may influence the behavior of the nighttime equatorial F layer and contribute to superrotation of the atmosphere. (auth) (UK)

27587 IONOSPHERE DURING A SOLAR ECLIPSE. Torr, Marsha R.; Torr, D. G. (National Inst. for Telecommunications Research, Johannesburg). J. Atmos. Terrest. Phys.; 33: 527-37(Apr 1971).

Two different partial solar eclipses are examined, each for two different stations. A comprehensive version of the steady-state ionospheric continuity equation is solved for theoretical comparison. It is shown that it is not possible to reproduce the ionospheric eclipse effects satisfactorily using solar euv radiation as the only source of ionization. The resultant drop in N_mF2 is so much larger than is observed that another source, unaffected by the eclipse, must be acting throughout the eclipse. This is found to apply to both mid- and high-latitude stations. The inclusion of a corpuscular source of ionization yields theoretical results in better agreement with the observed than when it is not included. The second source is the major one in the F2 region and contributes negligibly to the production rate below 165 km. (auth) (UK)

27588 MAPS OF THE VERTICAL F LAYER DRIFTS CAUSED BY HORIZONTAL WINDS AT MID LATITUDES. Rishbeth, H.; Kelley, D. M. (SRC Radio and Space Research Station, Slough, Eng.). J. Atmos. Terrest. Phys.; 33: 539-45(Apr 1971).

The F layer of the ionosphere shows appreciable variations with geographic longitude, at a given latitude and local time, that appear to be largely due to winds. Maps of the longitude variations of vertical drift computed from an approximate theory are presented. (auth) (UK)

27589 EFFECTS OF THE AURORAL ELECTROJET ON THE SCATTERING AND ADSORPTION OF FAST ELECTRONS IN THE UPPER ATMOSPHERE. Wedde, T. (Norwegian Defence Research Establishment, Kjeller). J. Atmos. Terrest. Phys.; 33: 547-55(Apr 1971).

A single-scattering Monte Carlo technique is used in studying the effects horizontal electric currents in the ionosphere exert on the scattering and absorption of precipitated electrons of energies > 1 keV. The computer programme developed for this task allows arbitrary energy and angular distributions to be employed. It is found that in the vicinity of the current, appreciable distortion in the local electron density occurs. The electrojet also causes anomalies in the electron albedo, and increases as well as decreases may occur. (auth) (UK)

27590 AURORAL ELECTRON CHARACTERISTICS DEDUCED FROM GROUND-BASED OBSERVATIONS. O'Brien, Brian J. (Univ. of Sydney). J. Atmos. Terrest. Phys.; 33: 679-84(Apr 1971).

It is shown that the variability and complexity of auroral-electron spectra and pitch-angle distributions are so extreme that their deduction only from simple ground-based experiments in present use must be generally avoided. (auth) (UK)

27591 NATURE AND AVERAGE MAGNITUDE OF THE SOURCES OF TRANSIENT EXCITATION OF SCHUMANN RESONANCES. Jones, D. Llanwyn; Kemp, D. T. (King's Coll., London). J. Atmos. Terrest. Phys.: 33: 557-66(Apr 1971).

The amplitude-frequency spectra of 100 elf transient electromagnetic disturbances propagated within the Earth–ionosphere cavity and received in Cornwall, England, were determined in absolute units. Using a simplified analysis, based on computed spectra, the current moment of the average source discharge was estimated. The current moment of the derived source decays exponentially with time, with a time constant of 28 msec. The total charge moment change during the discharge is inferred to be 4×10^6 C.m. Waveforms of the signals generated by the source model were computed and are compared with observed waveforms. (auth) (UK)

27592 NEW TECHNIQUE FOR THE ANALYSIS OF TRANSIENT ELF ELECTROMAGNETIC DISTURBANCES WITHIN THE EARTH–IONOSPHERE CAVITY. Kemp, D. T.; Jones, D. Llanwyn (King's Coll., London). J. Atmos. Terrest. Phys.: 33: 567-72 (Apr 1971).

A numerical study of the wave impedance of elf signals that have propagated in the Earth-ionosphere cavity is described. It is found that the wave impedance and its variation with frequency uniquely determines the source–observer separation and the attenuation constant of the Earth–ionosphere waveguide. The technique is readily applicable to experimental data. (auth) (UK)

27593 AURORAL-ZONE X-RAY EVENTS AND THEIR RELATION TO POLAR MAGNETIC SUBSTORMS. Sletten, A.; Stadsnes, J.; Trefall, H. (Univ. of Bergen). J. Atmos. Terrest. Phys.: 33: 589-604(Apr 1971).

The general relationship between auroral-zone x-ray events produced by precipitating electrons, and magnetic-bay activity, was studied. Every x-ray event, irrespective of the local time at which it was observed, could be associated with a negative disturbance in the geomagnetic H-component in the midnight sector of the auroral zone. And in most cases, a polar magnetic substorm of global character could be identified. X-ray events observed in the local midnight sector are prompt with respect to the associated magnetic disturbance, but it was found that those which occur later tend to be delayed, and those observed after 0600 hr LMT are always delayed. The average delay increases with increasing separation of the region of electron precipitation from the instantaneous midnight sector, that is interpreted as an effect of drift of electrons in the magnetosphere from an acceleration region on the nightside of the Earth. Reasons are given for assuming that the acceleration region is usually rather narrow in latitude, and may extend from about magnetic midnight to dawn. (auth) (UK)

27594 MORPHOLOGY OF AURORAL-ZONE X-RAY EVENTS. I. DYNAMICS OF MIDNIGHT EVENTS. Bjordal, J. (Univ. of Bergen); Trefall, H.; Ullaland, S.; (and others). J. Atmos. Terrest. Phys.: 33: 605-26(Apr 1971).

Simultaneous multiple balloon measurements were performed of x ray bremstrahlung from electrons ≥30 keV precipitated into the auroral zone during polar magnetic substorms. Observations in the midnight sector showed that the precipitation region is normally narrow in the north-south direction, but has probably a large extension in the east-west direction. It has been found that impulsive electron-precipitation events frequently occur in the midnight sector near the onset of a negative bay. Indications of rapid poleward motion were found for such events. During the growing phase of the negative bay, the precipitation region may move equatorward as often as poleward between $L \simeq 5$ and $L \simeq 7$. Towards the end of the substorm the electron precipitation usually moves poleward to $L \simeq 7$ or beyond. When magnetograms indicate the existence of an apparently well-defined electrojet, the precipitation region also seems to be well delimited, and its motions well correlated with simultaneous motions of the auroral electrojet. Following the initial impulsive precipitation, the energy spectrum of the precipitated electrons shows a gradual softening at least throughout the expanding phase of the substorm, irrespective of the direction of motion of the precipitation region. There seems to be a close agreement between the development of an x-ray substorm in the midnight sector and Akasofu's picture of the dynamics of the auroral substorm. (auth) (UK)

27595 ABSORPTION OF HF RADIO WAVES REFLECTED AT OBLIQUE INCIDENCE FROM THE IONOSPHERE IN WINTER. Evans, R. E.; Jones, T. B. (Univ. of Leicester, Eng.). J. Atmos. Terrest. Phys.: 33: 627-33(Apr 1971).

During the winter period large changes can occur in the electron density of the lower ionosphere within the height range 80 to 95 km. The propagation characteristics of obliquely incident hf (2 to 3 MHz) radio waves are particularly sensitive to these electron-density changes since reflection occurs at this level. Experimental observations of the noon absorption for the 2.61-MHz transmission from Norddeich to Lindau, W. Germany, during the winter 1961–62, confirm that considerable day-to-day variations exist, with upper and lower limits of 77 and 23 dB respectively for this period. The absorption loss and reflection height for this circuit have been calculated, by means of a ray-tracing method, for a number of winter electron density-height distributions recently discussed by Thomas (1968) and Beynon and Rangaswamy (1969). The calculated absorption losses for these profiles lie within the range of the experimental observations; however, the day-to-day variability indicates that a unique model should probably be developed for each winter day. (auth) (UK)

27596 INTERPRETATION OF IONOSPHERIC RADIO DRIFT MEASUREMENTS. III. VALIDATION OF CORRELATION ANALYSIS BY COMPUTER SIMULATION. Pitteway, M. L. V.; Wright, J. W.; Fedor, L. S. (Environmental Research Labs., Boulder, Colo.). J. Atmos. Terrest. Phys.: 33: 635-60(Apr 1971).

A computer is used to simulate fading records that might have been observed in a spaced-antenna drift experiment. The model for computer analysis permits scattering centers to be located at random positions, then moved stepwise across the sky to simulate a drift; random changes are also studied. The output format matches that of actual experimental equipment, and the simulated records are used to validate standard correlation analysis programs. Correlation analysis correctly detects the mean direction and speed of the diffraction pattern produced in this way, and estimates a random velocity fluctuation magnitude directly related to the random changes in the model. The statistically rigorous formulation of correlation analysis by Fedor (1967) is shown to estimate reasonable error limits for the wanted parameters. (auth) (UK)

27597 AIRBORNE IONOSPHERIC AND OPTICAL MEASUREMENTS OF NOONTIME AURORA. Whalen, James A.; Buchau, Jurgen; Wagner, Rosemarie A. (Air Force Cambridge Research Labs., Bedford, Mass.). J. Atmos. Terrest. Phys.: 33: 661-78 (Apr 1971).

The results are reported of a series of three local noon flights by the AFCRL Flying Ionospheric Laboratory through the latitude of the auroral oval. The flights, performed in December 1968 over the Arctic Ocean, maintained local magnetic noon while scanning back and forth in latitude for durations of 5 to 10 hr each for a total of 16 latitude scans and 20 hr all in darkness and at nearly constant K_p(2- to 3-). Coordinated in these airborne measurements were an ionospheric sounder, all-sky cameras, and photometers. Parameters analyzed are f_0E, $h'E$, $h'E_s$, f_{min}; the presence of discrete aurora overhead; the intensities of N_2^+ 4278 Å, O I 5577 Å and O I 6300 Å measured by a photometric technique that discriminates between discrete and nondiscrete aurora. (auth) (UK)

27598 F-LAYER DYNAMO. Rishbeth, H. (Radio and Space Research Station, Slough, Eng.). Planet. Space Sci.: 19: 263-7(Feb 1971).

It is stated that horizontal winds in the thermosphere, driven by the daily pressure variations due to solar heating, set in motion the charged particles of the ionospheric F region, the principal motion being a drift of ions and electrons along magnetic field lines. In addition there is a much slower sideways drift of the positive ions, resulting from a combination of the gyration around field lines and the collisional force imposed by the neutral-air wind. An account is given of the current system set up by this ion drift in the mid-latitude F layer, and it is noted that at night a substantial proportion of the total ionospheric current may flow in the F layer. Since this current arises from the action of winds blowing across the magnetic field it may be appropriate to call it the F-layer dynamo current, and it bears some resemblance to the better known E-layer dynamo current, set up by tidal winds in the lower ionosphere. The F-layer current system produced a ground-level magnetic field of about 1 gamma. The ion drift also tends to set up polarisation fields in the F layer, which are effectively short-circuited by the E layer by day, but only partially at night. (UK)

27599 PHASE AND AMPLITUDE STUDY OF AURORAL PULSATIONS. Parkinson, T. D. (Univ. of Pittsburgh). Planet. Space Sci.: 19: 251-62(Feb 1971).

To supplement a rocket investigation of the auroral green line,

XUM

data from some auroral pulsations were analyzed by direct integration of the time-dependent continuity equations for each of the sources now thought to contribute. It is shown that indirect processes are not incompatible with studies of auroral pulsations, and that a non-negligible contribution to the green-line intensity comes from dissociative recombination. Calculations using the theoretical $O(^1S)$ lifetime show that the remaining green line must come from a direct or very fast process; however, if the $O(^1S)$ lifetime can be reduced, significant portions of the green line can come from the transfer of energy from $N_2(A^3\Sigma_u^+)$ to atomic oxygen. (auth) (UK)

27600 AURORAL INTENSITY RATIO OF O I (6300 A) AND O I (5577 A). Parkinson, T. D. (Kitt Peak National Observatory, Tucson, Ariz.); Ziff, E. C. Planet. Space Sci.; 19: 267-70 (Feb 1971).

Reference is made to Murcray (Planet. and Space Sci., 17: 1429(1969)), who studied the 6300-Å O red-line and the 5577-Å O green-line emissions in a quiet auroral arc using rocket-borne photometers. From the obtained intensity ratio Murcray claimed that the ratio of excitation of the red line to that of the green line was 10 at 120 to 330 km. That such large amounts of red emission at 120 km, and an altitude-independent excitation ratio, could have been observed is thought to be surprising in view of the very large quenching of the red at lower altitudes. It is suggested that Murcray's analysis contained two errors, one minor and one major, and that the excitation ratios should have been 2500 at 120 km, 670 at 160 km, and 90 at 220 km. It is considered that Murcray's values are just upper limits. Some data are also discussed that allow the limits on the excitation ratio to be set considerably lower. The observation of red-line emission below 150 km is contrary to the findings of the present authors, who observed no source of red-line emission below 160 km. Murcray's data were obtained with sidewise-viewing photometers, which could not make the altitude differentiation claimed, whereas the present authors employed forward-viewing instruments. (UK)

27601 PARTICLE INFLUX AND THE MIDLATITUDE NIGHTTIME E REGION AT SOLAR MINIMUM. Manson, A. H. (Univ. of Saskatchevan, Saskatoon). Planet. Space Sci.; 19: 270-2(Feb 1971).

Reference is made to the comprehensive study of the origin of the nighttime ionosphere (80 to 200 km) by Ogawa and Tohmatsu (Rep. Ionosph. Space Res., Japan, 20: 395(1966)), and some of the data given are considered to be in error. It was considered to be of interest to consider quantitatively the role of precipitated electrons in the nighttime E region, and three aspects of the problem are discussed: (a) the morphology of the midlatitude nighttime E region as revealed by radiowave and rocket data; (b) estimates of the precipitated flux of electrons as revealed by satellite and photometer data; and (c) calculation of ionisation rates. It was evident from the calculations that the flux of electrons in the range 10^2 to 10^3 cm^{-3} is a significant source of ionisation in the nighttime E region, especially at 80 to 140 km. It was also found that the correlation between geomagnetic activity and particle precipitation is not good at mid-latitudes, and hence correlations between geomagnetic activity and the peak of the E region near 100 km is not to be expected. (UK)

27602 CAUSE OF A TYPE OF MAGNETIC VARIATION ON QUIET DAYS. Mizzi, C.; Schlapp, D. M. (Univ. of Exeter, Eng.). Planet. Space Sci.; 19: 273-4(Feb 1971).

Reference is made to Mayaud (Atlas of K indices, IAGA Bull., Paris, No. 21: 90(1967)), who considered ways in which determination might be made as to whether or not a particular magnetic variation belongs to the regular daily variation (S_R). The present communication gives some evidence based on Mayaud's criterion that "a variation that appears synchronous in Universal Time can be identified as not belonging to S_R." Possible causes for magnetic variations on abnormally quiet days are discussed. (UK)

27603 INFLUENCE OF FIELD-ALIGNED CURRENTS ON AURORAL-ELECTRON TEMPERATURES. Rees, M. H. (Univ. of Colorado, Boulder); Jones, R. A.; Walker, J. C. G. Planet. Space Sci.; 19: 313-25(Mar 1971).

A precipitating flux of auroral electrons produces a flow of reverse current to maintain electrical neutrality in the ionosphere. The transport effects associated with such a current act as heat sinks for the electron gas, resulting in auroral-electron temperatures that are lower at high altitude than they would be in the absence of the current. In a typical aurora the difference approches 1000°K above 700 km. There are electric fields associated with the parallel currents, but their magnitude is only a few microvolts per meter. (auth) (UK)

27604 OBSERVATIONS OF MAGNETIC-FIELD-ALIGNED ANISOTROPY FOR 1- AND 6-keV POSITIVE IONS IN THE UPPER IONOSPHERE. Hultqvist, Bengt; Borg, Hans; Riedler, Willi; Christophersen, Peter (Kiruna Geophysical Observatory, Sweden). Planet. Space Sci.; 19: 279-95(Mar 1971).

Measurement of the fluxes at about 10° and 80° pitch angle of 1- and 6-keV positive ions on board the near Earth polar orbit satellites ESRO 1A (Aurorae) and ESRO 1B (Boreas) are reported. 202 transits through the auroral particle precipitation zone were investigated. About 80% of these occurred in the eccentric dipole time evening and midnight sectors. The remaining ones were obtained in the morning–noon sector. The depleted-loss-cone type of anisotropy was found to occur at the equatorward edge of the particle zone in all cases from the nightside studied. In going polewards this region was generally followed by a latitude range with isotropy. Further polewards the positive ion flux inside the loss cone was often much higher than outside it. This field-aligned anisotropy was always found to be associated with energetic electron fluxes. It sometimes appeared over large regions and was in one case present for 6 hr. These observations may be interpreted in terms of an electric double layer near or in the ionosphere. (auth) (UK)

27605 WAVE-PACKET PROPAGATION IN AN AMPLIFYING MEDIUM AND ITS APPLICATION TO THE DISPERSION CHARACTERISTICS AND TO THE GENERATION MECHANISMS OF Pc 1 EVENTS. Gendrin, R. (Groupe de Recherches Ionospheriques, Saint-Maur, France); Lacourly, S.; Roux, A.; (and others). Planet. Space Sci.; 19: 165-94(Feb 1971).

The formulae that give the propagation characteristics of a wave packet in a dispersive and amplifying medium are established. Application is made to the propagation of Pc1 elements through a magnetosphere constituted of a cold plasma and a high-energy proton population. It is shown that the spectral shape, in a frequency–time coordinate system, of the Pc1 elements is related to two terms: $\nu = d^2\omega/dk^2$, which represents the variation of the group velocity with frequency and which depends only on the cold plasma characteristics, and $\mu = -d^2\gamma/dk^2$, in which γ is the amplification coefficient depending on the frequency and which is related to the high-energy particle distribution function. When $\nu \gg \mu$, only the usual dispersion effects occur, but a new method is found for determining the line of force on which the micropulsations are generated, without making any assumption about the cold plasma density distribution inside the magnetosphere. It is also possible to deduce some characteristics about the high-energy proton distribution. Theoretical computations are presented that give the frequency variation of the amplification coefficient as a function of the e-folding energy and the anisotropy factor of these high-energy protons. Applications are made to ~30 pearl events that are analysed in detail according to this theory. When $\mu \gtrsim \nu$, other effects do appear. After a preliminary phase, the pearl elements can become parallel for a while, or even re-erect before lying again; the duration of each element gives an indication about the number of interacting particles. The conditions for the validity of the quasi-linear theory, and some other nonlinear effects related with the interpretation of Pc1 micropulsations are also discussed. (auth) (UK)

27606 DP 2 AND POLAR SUBSTORM. Nishida, Atsuhiro (Tokyo Univ.). Planet. Space Sci.; 19: 205-21(Feb 1971).

The morphological distinction between DP 2 fluctuations and polar substorms (DP 1) is explained, and the relation between these two modes of the disturbance is examined. It is found that although DP 1 and 2 tend to occur together, they are not coherent, indicating that they are driven by different electric-field systems. The distinction between DP 2 fluctuations and sudden impulses is also discussed. (auth) (UK)

27607 COMMENTS ON A PROPOSED MAGNETOSPHERIC MODEL. Frank, L. A. (Univ. of Iowa, Iowa City). J. Geophys. Res.; 76: 2512-15(1 Apr 1971).

The principal features of a new proposed model of the magnetosphere are given. The energy source for magnetospheric and auroral phenomena, length of the magnetotail, the relationship of the polar cusp and the auroral oval and electrojet, and polar and magnetospheric substorms are discussed. These examples provide a working guide to the various applications of this proposed magnetospheric model. (J.C.W.)

27608 OXYGEN ION–ION NEUTRALIZATION REACTION AS RELATED TO TROPICAL ULTRAVIOLET NIGHTGLOW. Olson, Ronald E.; Peterson, James R.; Moseley, John (Stanford Research Inst., Menlo Park, Calif.). J. Geophys. Res.; 76: 2516-19(1 Apr 1971).

Multistate Landau–Zener calculations were performed to help understand the tropical ultraviolet night glow at thermal and near-thermal energies. Olson et al. previously described the method, but the more recently developed semi-empirical method for esti-

mating the necessary coupling matrix elements is used. The crossing parameters and product destination for the reaction $0^+ + 0^- \rightarrow 0^* + 0 + \Delta E$ are tabulated. The calculations were made at several energies and the relative contributions to the total cross section from the various product states are shown. It has been suggested that the intensity ratios for 1304- and 1356-A emissions observed in the nighttime uv tropical airglow may give a possible means of distinguishing between excitation mechanisms. From the calculations it can be determined that the predicted ratio of 1304- to 1356-A emissions from the ion–ion reaction is about 0.9. (J.C.W.)

27609 ATOMIC OXYGEN AND CARBON DIOXIDE IN THE LOWER THERMOSPHERE. Offermann, D.; von Zahn, U. (Univ., Bonn). J. Geophys. Res.; 76: 2520-2(1 Apr 1971).

A helium-cooled ion source was developed to determine atomic oxygen intensity in the lower thermosphere and to delineate the measurement of the oxygen from CO_2, which was believed to have been produced by atomic oxygen at the ion source walls. The new design allows for minor influence of the walls on the measured density. On Oct. 13, 1970, the instrument was flown on a Skylark rocket above Sardinia at 118 to 288 km. At an altitude of 120 km the ratio of the measured ion currents of atomic and molecular oxygen was 2.75 and by assuming that there was no mass discrimination in the ion source, the ratio of the measured densities is found to be $n(0)/n(0_2) = 3.5$. In 1967 von Zahn had discussed that the ratio might be as high as 4 at 120 km. Only trace amounts of CO_2 were detected. The presence of CO_2 in the lower thermosphere has an important bearing on the ion formation in the D region. (J.C.W.)

27610 DIVERGENCE OF ION VELOCITY IN THE E REGION DUE TO VERTICAL WINDS. Whitehead, J. D. (Air Force Cambridge Research Labs., Bedford, Mass.); Hooke, W. H. J. Geophys. Res.; 76: 2523-5(1 Apr 1971).

The magnetoshear theory of sporadic E shows that a shear in the neutral winds at E-region heights produces a vertical ion motion that varies with height, and that the convergence of this motion produces the increases in ion density known as sporadic-E layers. While the ion motion is often so convergent that the ion density increases several times above the ambient, hydrodynamic constraints apparently prevent the neutral air density from changing by anything like this amount. The effect of these constraints is visible in the relatively simple theory that describes motions of the internal atmospheric gravity-wave type. Neutral atmospheric motions are nearly nondivergent for waves of small vertical wavelength and long period, which appear to be of fundamental importance to upper atmospheric dynamics. It is shown that with these constraints, the contributing circumstances are sometimes cancelled by other contributions to the ion convergence, particularly those resulting from horizontal variations in the horizontal neutral winds. (J.C.W.)

27611 GEOMAGNETIC FIELD INCLINATION DETERMINED BY CALIBRATING THE FARADAY ROTATION OF AN INCOHERENTLY SCATTERED SIGNAL. Cohen, Robert (Environmental Research Labs., Boulder, Colo.). J. Geophys. Res.; 76: 2487-97(1 Apr 1971).

The differential ionospheric Faraday rotation per unit height of an incoherent-scatter signal is proportional to BN cos θ, where B is the geomagnetic field intensity, N is the electron density, and θ is the angle between B and the wave vector. When θ is near 90°, cos θ is a very sensitive function of θ, so that geomagnetic field models do not provide a sufficiently accurate estimate of θ for the ionospheric F region. Consequently, for the spatial region above the Jicamarca Radar Observatory of the Instituto Geofisico del Peru, Lima (11.95°S, 76.87°W; surface dip ~2°), an experimental determination of B cos θ was made by comparing maximum Faraday rotation rates with simultaneous ionosonde measurements of N_{max}, the maximum electron density of the ionosphere. This procedure provided a precise and convenient absolute calibration of the Faraday-rotation records. Furthermore, the average value of B cos θ, in conjunction with model values of B, was used to find θ and thence the geomagnetic dip angle. This value of dip angle was more accurate then values derived from available geomagnetic-field models. (auth)

27612 LABORATORY MODEL FOR RADIO-STAR SCINTILLATION AND OTHER DIFFRACTION PHENOMENA. Morgan, M. Granger (Univ. of California, San Diego, La Jolla). J. Geophys. Res.; 76: 2469-86(1 Apr 1971).

The diffraction of a radio-star signal by a thin, weak, random phase-changing screen such as the Earth's ionosphere or the solar wind was modeled in the laboratory by using 40-kHz airborne ultrasonic sound and a diffracting screen of warm turbulent air. A phase-coherent system and temperature probes mounted in the diffracting region have provided information not available in typical radio-star observations. The experiment was designed with the idea of exploring more complicated screen geometries, particularly thick or strong diffracting screens or both. Considerable difficulties encountered in producing a satisfactory model even for the thin weak screen precluded the study of more complex geometries. Agreement with theory was obtained for the thin weak screen, and an on-line laboratory computer allowed a full application of a number of signal processing techniques, particularly for the determination of the screen-drift velocity. It is concluded that further progress by modeling cannot be accomplished without unreasonably large investments of time and money. (auth)

27613 COMPARISON OF KINETIC AND HYDRODYNAMIC MODELS OF AN EXPANDING ION EXOSPHERE. Holzer, Thomas E.; Fedder, Joel A.; Banks, Peter M. (Univ. of California, San Diego, La Jolla). J. Geophys. Res.; 76: 2453-68(1 Apr 1971).

The results of calculations based on kinetic and hydrodynamic models of a collisionless-ion exosphere are compared, and it is found that the density and velocity of an ionic constituent flowing supersonically throughout the exosphere can be adequately described by ordinary hydrodynamic equations with isotropic pressure. This suggests that the basic flow characteristics of the polar wind can be determined by hydrodynamic equations throughout the polar ionosphere. A set of CGL-type hydrodynamic equations (for anisotropic pressure) that include the effects of energy and momentum transfer processes (e.g., collisions) are derived, and it is shown that such equations are applicable to problems of polar-wind and solar-wind temperature anisotropies, as well as to related flow problems. (auth)

27614 DIURNAL VARIATION OF NITRIC OXIDE IN THE UPPER ATMOSPHERE. Strobel, Darrell F. (Kitt Peak National Observatory, Tucson, Ariz.). J. Geophys. Res.; 76: 2441-52(1 Apr 1971).

A detailed theoretical model with measured values of solar flux, absorption cross sections, and chemical-rate constants for input data is used to study the diurnal variation of [NO] in the upper atmosphere. Two models for sources of $N(^2D)$ are considered: in model 1 all NO^+ recombinations result in $N(^2D)$ production and in model 2 photoelectron dissociation of N_2 and ion–atom interchange of N_2^+ and O are the sources. Results are compared with the recent rocket measurements reported by L. G. Meira, Jr. (1970), and very good agreement is obtained for both models. For the D region, where Lyman α is the source of ionization, a decrease in electron density for model 1 and an increase for model 2 is predicted for increasing solar activity. D-region electron-density measurements may be helpful in selecting the appropriate model. Below 150 km the distribution of [NO] is nearly time-independent. Above 150 km the diurnal variation of [NO] is small and never exceeds a factor of 4 in the model. The sensitivity of the solutions of the eddy-diffusion coefficient K is studied, and below the turbopause the NO density increases as K decreases. (auth)

27615 ROCKET TWILIGHT OBSERVATIONS OF H I 1216-A HORIZON BRIGHTENING NEAR 150 KILOMETERS. Buckley, J. L. (Johns Hopkins Univ., Baltimore); Moos, H. W. J. Geophys. Res.; 76: 2437-40(1 Apr 1971).

Two rocket observations of Ly α with a solar-zenith angle of 120° indicated that the ratio of the brightness near the solar horizon to that near the zenith and antisolar points was 1.6 ± 0.2 and 1.8 ± 0.2, respectively. The first was predawn and the second post-sunset. In the second observation, the brightness close to the antisolar direction varied less than 15% between 135 and 105 km. These phenomena are consistent with geocoronal models of multiple scattering of solar Ly-α radiation. (auth)

27616 EXCITATION OF NITROGEN BY FAST PROTONS AND ELECTRONS. Sheridan, W. F. (Air Force Cambridge Research Labs., Bedford, Mass); Oldenberg, O.; Carleton, N. P. J. Geophys. Res.; 76: 2429-36(1 Apr 1971).

Cross sections are measured for excitation of the (0,0) first negative band by protons in the range 5000 to 25,000 eV and by electrons in the range 45 to 25,000 eV. Upper limits are given for the very weak proton excitation of the first and second positive systems. To find the cross sections for the primary collisions and to avoid secondary effects, measurements are extrapolated to zero pressure. Not all intensities emitted are proportional to the pressure. The processes responsible for these deviations, excitation by neutral atoms and collisional deactivation, are investigated. (auth)

27617 ULTRAVIOLET EMISSIONS FROM ATOMIC NITROGEN IN THE AURORA. Prasad, S. S.; Green, A. E. S. (Univ.

of Florida, Gainesville). J. Geophys. Res.; 76: 2419-28(1 Apr 1971).

Excitation of the far-ultraviolet emissions (λλ 1134, 1200, 1493, and 1743 A) from atomic nitrogen in auroras is considered. For the nonresonance radiations (λλ 1493 and 1743 A) the excitation mechanism is the electron-impact dissociation of N_2 resulting in a highly excited N atom. This is also the predominant mechanism for the resonance radiations. In this case, however (especially for λ 1200 A), auroral observations indicate some imprisonment effects as well. As such, the altitude profiles of λ 1200- and 1134-A emission intensities can provide useful information about the atomic nitrogen density in the auroral ionosphere. Further measurements are therefore very desirable. (auth)

27618 EVIDENCE FOR A SOLAR-WIND ORIGIN OF AURORAL IONS FROM LOW-ENERGY ION MEASUREMENTS. Whalen, B. A.; Miller, J. R.; McDiarmid, I. B. (National Research Council, Ottawa). J. Geophys. Res.; 76: 2406-18(1 Apr 1971).

A rocket-borne ion spectrometer capable of separating and detecting H^+, He^+, and He^{++} with energies between 2 and 24 keV was flown into an early-evening proton aurora from Fort Churchill, Canada. The measurements made with a Black Brant 4 at altitudes to 775 km enabled the positive-ion composition of the primary auroral precipitation to be determined above the masking effects of atmospheric interactions. The proton differential energy spectrum was found to peak at 8 keV with an intensity of 1.5×10^5 $(cm^2 \text{ sec ster keV})^{-1}$, that is orders of magnitude less than some previously obtained values between 2 and 10 keV. No statistically significant flux of He^+ was observed. The He^{++} intensity at 15 keV was measured to be $7 \pm 3.5 \times 10^3$ $(cm^2 \text{ sec sterad keV})^{-1}$ and an upper limit of 5×10^3 was set at 7.5 keV. The He^{++}/H^+ ratios determined from these data were combined with the two previously reported measurements at higher energies to obtain an auroral He^{++} differential energy spectrum. The H^+ and He^{++} energy spectra were used to calculate an integrated He^{++}/H^+ flux ratio of approximately 4%. Some comments on characteristics of auroral-particle acceleration mechanisms are presented. The observation of auroral He^{++} and H^+ ions of approximately the same ratio as in the solar wind, and the apparent lack of He^+ ions, is interpreted as strong evidence for a direct solar-wind origin of the particles. (auth)

27619 LOW-LATITUDE DS COMPONENT OF GEOMAGNETIC STORM FIELD. Kawasaki, K.; Akasofu, S. I. (Univ. of Alaska, College). J. Geophys. Res.; 76: 2396-2405(1 Apr 1971).

Relationships between the low-latitude DS component and the intensity of the auroral electrojet are examined for several intense geomagnetic storms. It is shown that the magnitude of the DS component fluctuates considerably during the course of a storm and that magnetospheric substorms are responsible for the fluctuations. In particular, during the main phase many substorms are associated with a temporary decrease of DS during its early phase and with a subsequent increase during a later phase. Therefore there temporarily occurs a strong anticorrelation between DS and the electrojet intensity. The origin of the DS component is discussed in the light of recent particle observations by the synchronous satellite ATS 5. (auth)

27620 EVIDENCE FOR MAGNETIC FIELD ALIGNED CURRENTS DURING THE SUBSTORMS OF MARCH 18, 1969. Haerendel, G. (Max Planck-Institut fuer Physik und Astrophysik, Garching, Ger.); Hedgecock, P. C.; Akasofu, S. I. J. Geophys. Res.; 76: 2382-95(1 Apr 1971).

The magnetic perturbation field on the ground is analyzed for the first three substorms on March 18, 1969, in terms of a three-dimensional magnetospheric–ionospheric current system. The electric field at field lines originating in the morning side of the polar cap is within certain limits inferred from the motions of a barium plasma cloud released during the second substorm at a distance of 12.4 R_E. The field, pointing nearly northward, would not be able to drive ionospheric currents that could generate the magnetic perturbations observed at a nearby observatory. Transverse magnetic perturbations of 9.5 γ maximum amplitude, in phase with the surface data, were measured on Heos 1 during the second and third substorms. These data taken together suggest the existence of magnetic-field aligned currents flowing from the near tail along the horns of the plasma sheet into the morning side of the auroral oval. The total strength of the currents was on the order of 5×10^5 A. Irregular pulsations of the transverse perturbation field at the satellite with a mean period of 13 min were observed between the second and third substorms. They were in phase with similar fluctuations on the ground. (auth)

27621 FAST TIME-RESOLVED SPECTRAL ANALYSIS OF VLF BANDED EMISSIONS. Coroniti, F. V.; Fredricks, R. W.; Kennel, C. F.; Scarf, F. L. (TRW Systems Group, Redondo Beach, Calif.). J. Geophys. Res.; 76: 2366-81(1 Apr 1971).

Several classes of vlf-banded emissions acquired by the short-antenna Ogo 5 electric-field detector are investigated by using high time-resolution spectral techniques. The fastest temporal resolution of statistically independent spectra is 50 msec; individual spectra are taken every 12.5 msec. Vlf banded rising chorus spectra possessed single and/or multiple frequency-modulated bursts; discrete single modes with unchanging center frequencies are often observed to be part of the banded chorus spectrum. Inverted or falling banded chorus spectra also contained frequency-modulated bursts and single modes, but with greater structural complexity than rising chorus. The spectrum of a banded "hisslike" emission was dominated by multiple discrete single modes with constant center frequencies. A narrow-band emission with frequencies slightly above one-half the local electron cyclotron frequency consisted of single modes and groups of unresolved modes that were not frequency-modulated. Finally an emission at $\frac{3}{2}$ the local electron cyclotron frequency exhibited an almost uniform spectral density across its 200-Hz bandwidth. Since this preliminary study contains only a limited quantity of data, the reported spectral structures probably neither exhaust nor are necessarily typical of all classes of banded vlf emissions. (auth)

27622 OGO 5 MEASUREMENTS OF THE PLASMASPHERE DURING OBSERVATIONS OF STABLE AURORAL RED ARCS. Chappell, C. R.; Harris, K. K.; Sharp, G. W. (Lockheed Palo Alto Research Lab., Calif.). J. Geophys. Res.; 76: 2357-65 (1 Apr 1971).

Ambient H^+ ion concentration was measured in the plasmasphere during two intense magnetic storms that were accompanied by occurrences of stable auroral red (SAR) arcs. The H^+ ion-density profiles were measured by the ion mass spectrometer on Ogo 5 during the periods October 29 to November 7, and October 10 to 17, 1968. Correlations of the H^+ ion densities in the plasmasphere were made with the D_{st} and Kp magnetic indices and with ground observations of the 6300-A SAR arcs. This study shows that the SAR arcs are observed in the rapid recovery phase of the storm in the 10 to 20 hours following injection of ring-current particles, and that the plasmasphere is drastically reduced in size during the storm, with the SAR arc located in L value near the position of the plasmapause. The arc is found to occur in the ionosphere at the base of flux tubes that have ambient H^+ ion densities of 100 to 1000 ions/cm^3 near the magnetic-equatorial plane. (auth)

27623 MULTIPLY COUPLED OSCILLATIONS OF FIELD LINES IN THE MAGNETOSPHERE: MODULATION OF TRAPPED PARTICLES AND IONOSPHERIC CURRENTS. Cladis, John B. (Lockheed Palo Alto Research Lab., Calif.). J. Geophys. Res.; 76: 2345-56(1 Apr 1971).

A new field-line resonance is proposed to explain some coherent modulations of trapped proton and electron fluxes with correlated magnetic-field variations that have been observed in the outer magnetosphere. The resonance is excited by the ∇B drift of energetic trapped particles that have an inhomogeneous distribution in the direction of the drift motion. The field lines oscillate as standing waves in the meridional plane and form a wave pattern in the azimuthal direction that moves with a phase velocity equal to the mean azimuthal drift velocity of the particles. Particles that drift near the phase velocity become bunched in the potential wells of the wave; other trapped particles undergo radial motions, tending to follow the motions of the field lines. Analytical solutions based on a simplified model of the magnetosphere are used to interpret experimental observations. The characteristics of the wave field that appear at the surface of the Earth are discussed, and an experiment involving ground measurements of the field is suggested as a means of obtaining spatial information of particle-injection processes. (auth)

27624 SOLAR-CYCLE MODULATION OF THE RADIATION-BELT PROTON FLUX. Dragt, Alex J. (Univ. of Maryland, College Park). J. Geophys. Res.; 76: 2313-44(1 Apr 1971).

The solar-cycle time variations to be expected in the trapped radiation-belt proton flux are predicted on the assumption of a neutron decay source. Suitable models for the Earth's atmosphere and magnetic field should allow for the prediction of the time variations expected for protons of any energy and pitch angle at any point in space. Attention is paid to a derivation from the Boltzmann equation of the simplified proton transport equation commonly used in discussing energetic protons at low L values. (auth)

27625 DIFFERENTIAL ENERGY SPECTRUM OF GEOMAGNETICALLY TRAPPED PROTONS WITH INJUN 5 SATELLITE.

Pizzella, G.; Randall, B. A. (Univ. of Iowa, Iowa City). J. Geophys. Res.; 76: 2306-12(1 Apr 1971).

The proton energy spectrum in the radiation belt was measured with the Injun 5 satellite for the period August 29 through November 15, 1968 in the energy range 0.3 to 74 MeV. The most salient features of the differential energy spectrum are: (a) in the inner belt there is a minimum at about 2 MeV, and (b) in the outer belt the E_0 parameter at constant invariant radial distance is proportional to $L^{-1.74 \pm 0.12}$. (auth)

27626 RADIAL DIFFUSION OBSERVATIONS IN THE EARTH'S OTHER RADIATION BELT. Parsignault, D. R. (American Science and Engineering, Cambridge, Mass.). J. Geophys. Res.; 76: 2298-2305(1 Apr 1971).

The intensities and differential energy spectra of electrons between 1 and 3.6 MeV were obtained with an instrument flown on polar-orbiting AF Satellite OV1 9 during May and June 1967, which almost coincided with the time of maximum solar activity. A severe depletion was observed of the outer-belt electrons with $E_e > 0.94$ MeV coincident with the onset of the magnetic storm of May 25, and the subsequent growth of the peak flux at $L \simeq 3.0$ (pre-storm $L \simeq 3.8$). Over the region $2.5 \lesssim L \lesssim 5$, and on May 23, 24, and June 16, the e-folding energies (E_0) versus L distributions were found to be characteristic of the bimodal diffusion process. After the May 25 storm, the E_0 distributions were independent of L, and a spectral hardening was observed from $\langle E_0 \rangle = 482 \pm 67$ keV (May 27) to the prestorm value of $\langle E_0 \rangle = 567 \pm 57$ keV (June 14). On June 5, a secondary electron maximum appeared at L = 3.40, which then diffused outward across field lines, with a velocity $\propto L^{10.6 \pm 2.0}$. (auth)

27627 POSSIBLE MECHANISMS FOR FORMATION OF THE RING-CURRENT BELT. Swift, Daniel W. (Univ. of Alaska, College). J. Geophys. Res.; 76: 2276-97(1 Apr 1971).

A numerical model for the magnetosphere is used to investigate possible mechanisms for the injection of low-energy protons into the magnetosphere. The proton-distribution function is assumed to consist of two monoenergetic components. The effects of day–night asymmetries in the geomagnetic field, the Earth's rotation, and a finitely conducting ionosphere are included in the model. The model was used to determine if one group of particles could result in the injection of another group of particles. The calculations indicated that coupling between particles of different energies would be ineffective in injecting particles. Another numerical experiment sought to determine the effect of the internal polarization fields of the injected particles on particle injection by an externally imposed convection electric field. It was found that the external field tended to be canceled out by the internally generated field. The calculations indicate that an external convection field is unlikely to result in the injection of significant particles deep within the magnetosphere unless the effective ionospheric conductivity is very high, as might exist in an ionosphere bombarded by auroral ionization. Another experiment was used to investigate the effect of the Earth's rotation and the asymmetric geomagnetic field in causing injection. It was found that significant injection of 80-eV/γ particles occurred on a time scale of a day without any assist from external electric fields. It is pointed out that much faster and deeper injection may occur if a self-consistent model of the geomagnetic field were used in the calculations. A mechanism of this type would also require the existence of a highly conductive ionosphere. A final numerical experiment suggests that certain features of the auroral substorm could result from rapid changes in the effective ionospheric conductivity. (auth)

27628 HEAT CONDUCTION AND NONSTEADY PHENOMENA IN THE SOLAR WIND. Hundhausen, A. J.; Montgomery, Michael D. (Los Alamos Scientific Lab., N. Mex.). J. Geophys. Res.; 76: 2236-44(1 Apr 1971).

The role of heat conduction in the solar wind is assessed by a dimensional analysis of the electron energy equation. The relaxation time for transient perturbations of electron temperature is shown to be $\sim 4 \times 10^4$ sec for reasonable solar-wind parameters. For phenomena requiring longer times to propagate or develop (e.g., disturbances propagating near the solar-wind speed) the electron energy equation can be approximated as time-independent. Two such specific classes of solar-wind variations, namely overtaking streams and shock waves, are considered as sources of electron-temperature perturbations. In both cases heat conduction is found to be so efficient as to smooth out the electron temperature, thus causing any increase to be much smaller than would be observed for protons. The few available pertinent observations of electron temperature are consistent with this analysis. A few effects of electron heat conduction on small-scale phenomena (e.g., the modification of the Rankine–Hugoniot relations applicable to interplanetary shocks) are briefly discussed. (auth)

27629 TWO-DIMENSIONAL SIMULATION OF FLARE-ASSOCIATED DISTURBANCES IN THE SOLAR WIND. De Young, D. S. (National Radio Astronomy Observatory, Green Bank, W. Va.); Hundhausen, A. J. J. Geophys. Res.; 76: 2245-53(1 Apr 1971).

The propagation of flare-associated disturbances through the interplanetary medium is examined by using numerical solutions of time-dependent two-dimensional hydrodynamic flow in spherical coordinates. The study is limited to blast-wave phenomena, and the dependence on initial disturbance energy and angular extent is examined. For constant energy disturbances initially occupying cones of half angle up to ~15° at 0.1 AU, the angular dependence of the transmit time to 1 AU and of the shock shape at 1 AU is very small. For disturbance energies at 0.1 AU of a few times 10^{30} ergs, transit times to 1 AU are ~65 hours. The calculated disturbance shapes at 1 AU and the transit times are found to be in good agreement with the observational data. (auth)

27630 TWO BASIC MODES OF INTERACTION BETWEEN THE SOLAR WIND AND THE MAGNETOSPHERE. Nishida, Atsuhiro; Maezawa, Kiyoshi (Tokyo Univ.). J. Geophys. Res.; 76: 2254-64(1 Apr 1971).

From Explorer 33 and 35 interplanetary-plasma and magnetic-field data, it is confirmed that there are at least two basic modes in the interaction mechanism between the solar wind and the magnetosphere. The first is the change in the magnetospheric dimension that results from changes in the solar-wind dynamic pressure exerted at the magnetopause, and the second is the fluctuation in the magnetospheric DP 2 electric field that is related to fluctuations in the north–south component of the interplanetary magnetic field. Whereas the first can be interpreted essentially by the classical Chapman–Ferraro theory, the second suggests that the interplanetary electric field penetrates deep into the magnetosphere. (auth)

27631 RELATIONSHIP OF THE PLASMA SHEET, RING CURRENT, TRAPPING BOUNDARY, AND PLASMAPAUSE NEAR THE MAGNETIC EQUATOR AND LOCAL MIDNIGHT. Frank, L. A. (Univ. of Iowa, Iowa City). J. Geophys. Res.; 76: 2265-75(1 Apr 1971).

The complex structure of the near-Earth termination of the plasma sheet in the pre- and post-midnight sectors of the magnetosphere near the magnetic equator was observed with a sensitive electrostatic analyzer array flown on Ogo 3 during June and July 1966. The trapping boundary for energetic electrons $E \gtrsim 40$ keV was found to be within the extraterrestrial proton ring current and near its outer edge. The region characterized by an exponential decrease of electron energy densities (or average electron energy) with decreasing radial distance, i.e., the earthward edge of the plasma sheet, is located in the post-midnight sector such that its inner boundary is coincident with the plasmapause position. This inner boundary of the earthward edge of the plasma sheet is at 1 to 3 R_E beyond the plasmapause position in the pre-midnight sector. An electron trough characterized by relatively low, constant electron energy densities lies between the plasmapause and the inner boundary of the earthward edge of the plasma sheet in the pre-midnight sector. The plasmapause is within the region of the proton ring current. The near-earth termination of proton ring current is usually at ~0.5 to 1 R_E inside the plasmapause position. The trapping boundary for energetic electrons is usually coincident with or beyond the outer boundary of the earthward edge of the plasma sheet. The earthward edge of the plasma sheet and the electron trough are within the proton ring current. During the main phases of two moderate geomagnetic storms on June 25 and July 9, the interrelationships of these various boundaries and regions remained similar to those observed during periods of relative magnetic quiescence as the entire distribution moved earthward. For two measurements available during a polar magnetic substorm and a main-phase magnetic storm July 9 in the pre-midnight sector, the electron trough disappears and the structure appears to be similar to that for the post-midnight sector. (auth)

Low-Temperature Physics and Cryogenic Equipment

Refer also to abstract 27912.

Superfluidity

27632 (RLO–1388-599) ω^{-1} SUM RULES AND LONG RANGE CORRELATIONS IN BINARY SOLUTIONS. Campbell, C. E. (Washington Univ., Seattle. Dept. of Physics). Dec 1970. 18p. Dep. NTIS.

The $1/\omega$ sum rules are derived for two component uniform

many-body systems. The density fluctuations are quantized for the case when both components satisfy Bose statistics. Information about the long-wave-length behavior of the liquid structure functions is deduced from both the sum rules and the zero-point density fluctuations. (auth)

27633 (RLO-1388-603) GROUND STATE OF ^{4}He MONOLAYERS ADSORBED ON INERT SUBSTRATE. Campbell, C. E.; Schick, M. (Washington Univ., Seattle. Dept. of Physics). [1971]. 25p. Dep. NTIS.

The properties of a system of ^{4}He atoms at absolute zero interacting via a Lennard-Jones potential and constrained to motion in two dimensions by an otherwise inert substrate are investigated. Results of a semiclassical calculation indicate that the ground state is that of a self-bound liquid. It further indicates that a close-packed solid configuration is not self-bound. A quantum-mechanical variational calculation is performed to obtain an upper bound on the energy of the system. A result of -0.61°K per particle is obtained at a density of 0.035 Å^{-2}. The relationship between this calculation and recent experiments on ^{4}He monolayers is briefly discussed. (auth)

27634 (RLO-1388-604) EFFECTS OF LATERAL SUBSTRATE FIELDS ON HELIUM MONOLAYERS. Campbell, C. E.; Dash, J. G.; Schick, M. (Washington Univ., Seattle. Dept. of Physics). [1971]. 10p. Dep. NTIS.

Heat capacities of He monolayers on graphite show qualitative differences between ^{3}He and ^{4}He, contrary to the usual theories of 2D quantum fluids. The differences are attributed to weak lateral fields due to substrate inhomogeneities and, using a 2D ideal gas model, qualitative agreement is found between theoretical and observed heat capacities. (auth)

27635 (RLO-1388-605) SUBSTRATE MEDIATED INTERACTION BETWEEN ADSORBED ATOMS. Schick, M.; Campbell, C. E. (Washington Univ., Seattle. Dept. of Physics). [1971]. 27p. Dep. NTIS.

An effective interaction between atoms adsorbed on a substrate is calculated. The interaction arises from the exchange of phonons in the substrate and makes a density-dependent contribution to the ground-state energy per particle of the adsorbed system. Results are applied to submonolayer helium film adsorbed on argon-plated copper studied by Stewart and Dash. It is shown that, for this system, the interaction is attractive and contributes to the ground-state energy per particle an amount of the order of -1°K, a significant fraction of the observed binding energy. The role of the effective interaction in bringing about the enhancement of the binding energy and the formation of dense clusters observed by Stewart and Dash is discussed. (auth)

27636 EFFECT OF PRESSURE ON THE LUMINESCENCE OF HELIUM II. Lee, William David. Charlottesville, Va.; Univ. of Virginia (1970). 101p. University Microfilms Order No. 70-26,606.

Thesis.

Alpha-particle-induced luminescence of liquid helium-II at temperatures between 1.5 and 0.3°K and at pressures from the vapor pressure to 16 atm was investigated. It was found that the pulse height intensity decreases with temperature to about 0.6°K, being approximately constant below that point, while the total scintillation intensity remains approximately constant to about 1.2°K, below which point it decreases sharply to a temperature of about 0.5°K, rising again below this temperature. Thus, it was shown that the pulse-height decrease is at least partly due to delayed photon emission. At constant temperature, both the pulse-height and total intensities exhibit a minimum as a function of pressure at about 1 atm. It is shown that the temperature dependence of the pulse height can be fitted quite well by an expression depending exponentially on the normal fluid density. This is interpreted in terms of a radiative destruction frequency for metastable states in the liquid. A similar model applied to the decrease in total intensity is interpreted as indicating nonradiative destruction at the walls of the sample chamber. It is also shown that the increase in total intensity at lowest temperatures is consistent with a T^{-3} law, which suggests increased production or survival of excited states at lowest temperatures and higher pressures through the correlation with the inverse of the phonon number density. Although these correlations have been demonstrated, it is concluded that insufficient evidence is presently available to ascribe the effects to any microscopic physical mechanism. The pressure dependence of the pulse height was fitted with an empirical relation, but no physical interpretation was found to motivate the expression. (Diss. Abstr. Int., B)

27637 THEORY OF SUPERFLUID FERMI SYSTEMS. Prabhu, Rashmiraj Balkrishna. Columbus, Ohio; Ohio State Univ. (1970). 85p. University Microfilms Order No. 71-7540.

Thesis.

The ladder-approximation formalism is studied for the superfluid Fermi systems. The fermions are assumed to be spinless and interacting via an arbitrary nonretarded two-body potential. It is first shown how to set up the self-consistent equations in the ladder approximation for the superfluid system using the Nambu formalism. The equations are then studied, neglecting the particle–hole interaction. The integral equation for the vertex part is solved using a separable potential. A study is then made of the diagonal parts of the self-energy and vertex matrices. It is shown how to approximate these by the corresponding normal state functions and the errors involved in doing so. A separate treatment is given for the off-diagonal parts. It is shown that by properly renormalizing the interaction the equations can be cast in a form such that the integration region is around the Fermi surface. These equations lay the foundation of the theory of the superfluid Fermi liquid. Finally, a perturbation theoretical study is made of the imaginary part of the diagonal element of the self-energy matrix. Its behavior near the Fermi surface is established. It is shown that the behavior is markedly different from the one in the normal state. The implications of this in the single-particle tunneling phenomena are pointed out. It is shown that normal-to-superconductor-tunneling experiments should reveal this behavior if the data is extended beyond the range already investigated. (Diss. Abstr. Int., B)

27638 INTERACTION OF ELECTRONS WITH VORTICITY IN HEAT-FLUSHED He II. Spangler, Glenn Edward. Charlottesville, Va.; Univ. of Virginia (1970). 114p. University Microfilms Order No. 70-26,612.

Thesis.

A technique was developed that allows the use of incandescent 5-μ tungsten filaments as electron sources in superfluid helium. The technique is possible because of the formation of a stable bubble about the filament when the power input fed to the filament exceeds a certain critical level. This bubble then effectively insulates the filament from the bath, allowing filament temperatures in excess of 2000°K to be obtained. The placement of these filaments in a cylindrical diode arrangement allowed characteristic curves to be obtained and currents as high as 5.0×10^{-7} amps to be collected through 1 cm of liquid with 2500 volts. Incorporation of the tungsten filaments in a triode of plane geometry resulted in the discovery of an anomalous current. This current develops for a minimum critical accelerating filament-grid field of about 600 volts/cm and thereafter is capable of traversing macroscopic distances of liquid in a zero electric field. Evidence is presented that this anomalous current is composed of 9-keV charged vortex rings that derive their energy from the action of the Hall and Vinen drag force exerted on them by the heat-flushed normal fluid velocity field. Comments are made on the possible relationship that may exist between this anomalous current and the "persistent" current of Brushi, Maraviglia, and Mazzoldi. (Phys. Rev., 143; 84 (1966)) (Diss. Abstr. Int., B)

27639 NORMAL COMPONENT DENSITY OF ^{3}He–^{4}He SOLUTIONS AT TEMPERATURES DOWN TO 0.4°K. Sobolev, V. I.; Esel'son, B. N. (Physical-Technical Inst. of Low Temperatures, Kharkov). Zh. Eksp. Teor. Fiz.; 60: 240-50(Jan 1971). (In Russian).

The normal component density was measured by the oscillating disk stack technique in ^{3}He–^{4}He solutions containing up to 0.54 ^{3}He by weight at temperatures from the λ point down to 0.4°K. The Bose and Fermi branch parameters of the elementary excitation spectrum in the solutions are estimated on basis of the data thus obtained. (auth)

27640 DISPERSION OF FIRST SOUND IN SUPERFLUID ^{3}He–^{4}He SOLUTIONS DUE TO DAMPING OF THE NORMAL COMPONENT. Dyumin, N. E.; Rudavskii, E. Ya. (Physical-Technical Inst. of Low Temperatures, Kharkov). Zh. Eksp. Teor. Fiz.; 60: 830-7(Feb 1971). (In Russian).

Propagation of sound in narrow channels filled with superfluid ^{3}He–^{4}He solutions is studied at frequencies between 35 and 110 kc. Dispersion of sound velocity due to partial damping of the normal component is observed; the dispersion depends on the degree of damping and concentration of ^{3}He. The dependences of sound velocity and absorption on temperature, oscillation frequency, and concentration of ^{3}He which are derived are found to be in satisfactory agreement with the theoretical predictions. (auth)

27641 GROUP THEORY OF SUPERFLUIDITY. Solomon, A. I. (Dublin Inst. for Advanced Studies). J. Math. Phys. (N. Y.); 12: 390-4(Mar 1971).

The method of using a dynamical group to generate the energy spectrum of a given Hamiltonian is applied to the case of a super-

fluid Bose system. Here the relevant group is found to be SU(1,1) [or $\Pi_k \otimes SU(1,1)_k$ for a multilevel system]. The energy eigenvalues and eigenfunctions are obtained by means of the group. (auth)

27642 TOPICS IN SUPERFLUIDS. Vinen, W. F. (Univ. of Oregon, Eugene). pp 99-193 of Statistical Physics, Phase Transitions, and Superfluidity. Vol. 2. /Chretien, M. (ed.). New York; Gordon and Breach, Science Publishers, Inc. (1968).

The following subjects are covered: superfluid flow in helium II, experiments on quantization of circulation in superfluid helium, critical velocities in liquid helium, superfluid flow in superconductors, experiments on quantization flux lines in cylinders of superconductors, Josephson tunneling, quantum interferometers, and flux line motion. (M.H.R.)

Superconductivity

Refer also to abstracts 27910 and 27936.

27643 (ITF-70-90-E) ON THE MODEL HAMILTONIAN OF THE THEORY OF SUPERCONDUCTIVITY. Petrina, D. Ya.; Yatsishin, V. P. (Akademiya Nauk Ukrainskoi SSR, Kiev. Institut Teoreticheskoi Fiziki). 1970. 21p. (CONF-700648-3). Dep. NTIS (U. S. Sales Only).

From third conference on statistical physics and physical kinetics; L'vov, USSR (Jun 1970).

The model Hamiltonian of the theory of superconductivity in an infinite volume is investigated for the excited states. It is proved that the model Hamiltonian coincides with the approximation one. The meaning of the approximation Hamiltonian in an infinite volume is specified on the excited states. The correlation functions at zero temperature and infinite volume are defined. (auth)

27644 (KHFTI-70-8) DIMENSIONAL EFFECT IN MAGNETIZATION OF STRONG SUPERCONDUCTORS. Lazarev, B. G.; Ovcharenko, O. N. (Akademiya Nauk Ukrainskoi SSR, Kharkov. Fiziko-Tekhnicheskii Institut). 1970. 11p. (In Russian). Dep. NTIS (U. S. Sales Only).

Behavior of magnetized Nb-Zr-Ti, Nb-Ti, and Nb-Zr alloys as a function of the structure of the alloys was studied. In the cast state, or in a single phase, the magnetization depended only slightly on the magnetic field strength, but was strongly influenced by the dimension (diameter) of the specimen. The same effect held for a homogeneous superconductor and deformed alloys. In two-phase alloys, deformed and heat treated, the magnetization curve varied strongly with reduced diameter of the cylindrically shaped specimens. (tr-auth)

27645 FLUX FLOW IN SUPERCONDUCTING THIN FILMS . Byrd, James Donald Jr. Charlottesville, Va.; Univ. of Virginia (1970). 123p. University Microfilms Order No. 71-6655.

Thesis.

Measurements on superconducting thin film systems are presented in this dissertation. The samples consist of two narrow films superposed with a wide film in the form of a dc transformer. A search was made for any anomalous behavior suggestive of a collective oscillation of the flux lattice. Although no evidence for collective modes was observed, anomalous phase shifts between the voltages on the different films are observed. These phase shifts are observed with a dc current in the wide or primary film, while a smaller ac current of low frequency (20 Hz to 10 KHz) is applied to one of the narrow or secondary films. At a frequency of 6 KHz, a phase shift as large as 60° is observed between this driving secondary voltage and the primary voltage. No phase shift is observed between the primary voltage and the other secondary voltage. These measurements are discussed in the framework of flux flow. Included also is a general discussion of the mixed state and flux flow with particular emphasis on thin-film applications. Several qualitative models are presented for interpreting the results. (Diss. Abstr. Int., B)

27646 INVESTIGATION OF THE SUPERCONDUCTING STATE OF NIOBIUM-TITANIUM SOLID SOLUTIONS. Sukharevskii, B. Ya.; Shchetkin, I. S.; Fal'ko, I. I. (Physical-Technical Inst. of Low Temperatures, Kharkov). Zh. Eksp. Teor. Fiz.; 60: 277-82(Jan 1971). (In Russian).

The superconducting transition in niobium-titanium solid solutions is investigated by the specific heat technique. The dependence of the superconductivity parameters (superconducting transition temperature, energy gaps and pre-exponential factors) on titanium concentration in the solid solutions is found. A good correlation is observed between the energy gap ratio, transition temperature, and pre-exponential factors. (auth)

27647 MACROSCOPIC ELECTRODYNAMICS AND THERMAL EFFECTS IN THE SUPERCONDUCTOR INTERMEDIATE STATE. Andreev, A. F.; Dzhikaev, Yu. K. (Inst. of Physical Problems, Moscow). Zh. Eksp. Teor. Fiz.; 60: 298-311(Jan 1971). (In Russian).

A complete set of equations is found that describes related electromagnetic and thermal effects in the intermediate state of Type-I superconductors. The kinetic coefficients (specific resistance, thermal conductivity, and thermoelectricity tensors) are calculated for all types of structures, viz. for a lamellar structure and for filamentary structures with normal and superconducting filaments. Formulas for the Ettinghausen effect are derived that agree satisfactorily with the available experimental data. The velocity of the structure in stationary conditions due to the action of a current and temperature gradient is calculated. (auth)

27648 DEPENDENCE OF THE ELECTRON DISLOCATION STOPPING POWER IN A SUPERCONDUCTOR ON TEMPERATURE AND VELOCITY. Kaganov, M. I.; Natsik, V. D. (Inst. of Physical Problems, Moscow. Physical-Technical Inst. of Low Temperatures, Kharkov). Zh. Eksp. Teor. Fiz.; 60: 326-9(Jan 1971). (In Russian).

The temperature-velocity dependence of the electron dislocation stopping power due to scattering of normal electrons by dislocations and also to production of electron-hole pairs is investigated. The plot of stopping force as a function of velocity V has a break at $V = 2\Delta(T)/\hbar q_m$ where $\Delta(T)$ is the energy gap of the superconductor at a temperature T and $q_m \approx a^{-1}$ (a is the size of the dislocation nucleus). The temperature dependence of the stopping power is analyzed, and it is shown that it cannot be reduced to the temperature dependence of the energy gap $\Delta(T)$ and the number of normal electrons N(T). (auth)

27649 EFFECT OF LOW FREQUENCY FLUCTUATIONS ON SUPERCONDUCTING TUNNELLING. Galkin, A. A.; Borodai, B. I.; Zil'berman, L. A.; Ivanchenko, Yu. M.; Svistunov, V. M. (Donetsk Physical-Technical Inst., USSR). Zh. Eksp. Teor. Fiz.; 60: 651-8(Feb 1971). (In Russian).

The effect of low-frequency fluctuations on the volt-ampere characteristics and magnetic dependences of the critical Josephson junction current is investigated. It is shown that low-frequency noise in the circuit leads to the appearance of a resistive state and a nonoscillating dependence of the tunnel superconducting current on magnetic field strength. The experimental results are compared with the theory developed for this case. (auth)

27650 MOTION OF VORTEXES IN SUPERCONDUCTORS OF THE SECOND KIND. Krasnov, Yu. K.; Shukhman, V. A. (Inst. of Physics, Tbilisi, USSR). Zh. Eksp. Teor. Fiz.; 60: 659-64 (Feb 1971). (In Russian).

Motion of Abrikosov vortex lines in Type-II superconductors is considered phenomenologically for $\varkappa \gg 1$ and T = 0°K in the presence of a transport current which in the general case depends on time. An effective Ohm law is introduced for the transport current and the effective resistance in the mixed state is determined by means of the law. A phenomenological generalization of the results is proposed in which elastic properties of the vortex line are taken into account. The problem of the vibrational spectrum of the vortex line is solved. The existence of helicoidal oscillations is demonstrated. An expression for the relaxation time of such oscillations is obtained. The effective resistance for a varying current arising in the mixed state as a result of excitation of vibrational degrees of freedom of the vortex lines is calculated. The resistance exhibits a resonance behavior which depends on frequency of the external harmonic current. (auth)

27651 PLASMA OSCILLATIONS AND METASTABLE STATES IN JOSEPHSON TUNNEL JUNCTIONS. Gorbonosov, A. E.; Kulik, I. O. (Physical-Technical Inst. of Low Temperatures, Kharkov). Zh. Eksp. Teor. Fiz.; 60: 688-94(Feb 1971). (In Russian).

The electrodynamics of weak superconductivity in finite-width tunnel junctions is investigated. When account is taken of the boundary conditions at the junction borders, phenomena of the "magnetic overheating" type arise in both the Meissner and mixed states. A diagram of state is set up for a finite-width tunnel junction in an arbitrary magnetic field. In contrast to the situation encountered in ordinary superconductors, the absolute stability boundary of the metastable superconducting state coincides with the upper boundary of existence of the Meissner solutions. Josephson plasma oscillations in semi-infinite junction are studied in the Meissner and mixed states. (auth)

XUM

27652 UHF METHODS FOR INVESTIGATION OF THE DYNAMIC CHARACTERISTICS OF THIN SUPERCONDUCTING FILMS. Peskovatskii, S. A.; Eru, I. I.; Kashchei, V. A. (Inst. of Radio Physics and Electronics, Novosibirsk, USSR). Zh. Eksp. Teor. Fiz.; 60: 775-81(Feb 1971). (In Russian).

Several methods for investigating experimentally the uhf dynamic characteristics of thin superconducting films are proposed. With their aid, it is found that, in thin lead films, the recovery rate of destructed superconductivity is 1×10^9 to 2×10^{10} sec^{-1}. (auth)

27653 DAMPING OF MAGNETIC SURFACE LEVELS IN SUPERCONDUCTORS. Blank, A. Ya.; Fal'kovskii, L. A. (Inst. of Theoretical Physics, Moscow). Zh. Eksp. Teor. Fiz.; 60: 797-805(Feb 1971). (In Russian).

Damping of magnetic surface levels in a superconductor due to scattering of excitations by the surface roughnesses is calculated. In the semiclassical spectrum range, damping increases with growth of the glancing angle. (auth)

27654 SUPERCONDUCTIVITY OF ZIRCONIUM–TRANSITION METAL COMPOUNDS HAVING THE $CuAl_2$-TYPE STRUCTURE. McCarthy, Shaun Leaf. San Diego, Calif.; Univ. of California (1970). 137p. University Microfilms Order No. 71-4231.

Thesis.

As-cast Zr_2Rh (T_c = 11.3°K) has the highest superconducting transition temperature (T_c) of any noncubic structure stable at room temperature, as well as the highest T_c in the $CuAl_2$ structure class. The lattice of this compound is, however, unstable when cold-worked by grinding. There is a sharp drop in the T_c accompanied with an expansion of the unit cell. No symmetry change was observed, but this cannot be discounted. The T_c of the new form of Zr_2Rh is ~5°K. No instability is observed in the isomorphic, isoelectronic compounds Zr_2Co and Zr_2Ir which have the lower transition temperatures 5.0 and 7.3°K, respectively. The properties of T_c of the $CuAl_2$-type compounds of Zr_2Co, Zr_2Ni, Zr_2Rh, Zr_2Fe, and Zr_2Ir are discussed with respect to alloying and heat treatment. Dilute pseudo-binary alloys of transition metal elements with Zr_2Rh produced lower transition temperatures suggesting that the valence electron concentration of 5.67 electrons/atom gives a maximum in T_c for this structure. Results for Zr_2Co and Zr_2Ir show that their transition temperatures are raised when the electron concentration is increased by alloying. A peak is seen near 5.7 electrons/atom. No such behavior occurs for Zr_2Rh when higher valence state elements replace Zr or Rh in the lattice. A peak in the room temperature magnetic susceptibility in the Zr_2Co-Zr_2Ni system occurs near the same electron concentration as the peak in T_c. Similar susceptibility behavior occurs in the Zr_2Rh-Zr_2Ni system, however, with no peak in T_c. The anomalous behavior of Zr_2Rh may be due to the observed lattice instability. Results of susceptibility measurements on Zr_2Ir and its isomorphic alloys indicate correlation between T_c and susceptibility. An anticorrelation occurs for Zr_2Co suggesting the presence of Coulomb interactions. A sharp symmetric drop was also observed in T_c for Zr_2Co near the stoichiometric composition. No anomalous behavior occurs in the susceptibility over this composition range. A systematic behavior of the T_c for isoelectronic pseudobinary systems was observed and related to previously reported results on other systems. These systematics allow one to increase the T_c of alloys or compounds for systems involving 3-d or 5-d late transition elements and 3-d or 4-d elements in the Ni group. Verification was observed in the cases of Mo_3Os (T_c = 11.68°K), Mo_3Ir (T_c = 8.4°K), and Ti_3Ir (T_c = 4.8°K) by isoelectronic alloying with Ru and Rh, respectively. The T_c ordering in isoelectronic alloys correlates with susceptibility suggesting that differences between the impurity atoms and those in the host result in a change in the density of states. An appendix contains T_c results on the compound Zr_3Co (Zr_3CoO_x?) reported here as being superconducting at 3.9°K. A variation of the transition temperature with Zr source suggests that the Zr_3CoO_x phase may be stabilized even at a few hundred ppm oxygen. Bcc-stabilized Zr–Co alloys (1 to 15 at. %) formed by very rapid quenching from the melt were found to be not superconducting above 1.2°K. It is concluded that the reported superconductivity for arc-quenched alloys is due to the intermediate compound Zr_3Co. The crystallographic structure parameter was measured by the powder method for Sn_2Co, Th_2Al, and Zr_2Rh, all $CuAl_2$-type compounds. $x(Sn_2Co) = 0.1620 \pm 0.0007$, $x(Th_2Al) = 0.1636$ and $x(Zr_2Rh) = 0.168 \pm 0.001$. The value for Zr_2Rh is equal to the single crystal result of Zr_2Co. New superconductors found in the course of this study were Zr_2Ir (T_c = 7.3°K, $CuAl_2$-type), Zr_2Ga (T_c = 0.4°K, $CuAl_2$-type), Zr_3Ir (T_c = 2.13°K, β-U type), Hf_2Ir (T_c = 0.91°K, Ti_2Ni-type). (Diss. Abstr. Int., B)

27655 SUPERCONDUCTIVITY AT HIGH PRESSURE. Brandt, N. B.; Ginzburg, N. I. Sci. Amer.; 224: No. 4, 83-8; 90; 92-4(Apr 1971).

The history and current state of experiments designed to measure the effects of compression on the superconducting properties of certain metals are reviewed. The possibility of the creation of new, higher-temperature superconductors is mentioned. (M.H.R.)

27656 HIGH-TEMPERATURE SUPERCONDUCTIVITY? Matthias, Bernd T. Comments Solid State Phys.; 3: 93-6(Oct-Nov 1970).

A brief review of the lack of reality in experimental and theoretical predictions concerning superconductors with high transition temperatures is presented. It is pointed out that most high-transition-temperature superconductors are metastable at best. These instabilities increase as the transition temperature increases until the crystal will not form in the first place. (M.H.R.)

27657 INTERMEDIATE STATE IN TYPE-II SUPERCONDUCTORS. Seeger, A. Comments Solid State Phys.; 3: 97-104(Oct-Nov 1970).

The possibility of a state analogous to the intermediate state existing in Type-II superconductors is discussed. Results reported are in conflict with the Ginzburg–Landau theory. It is concluded that the existence of an attractive long-range interaction between flux lines was established not only by the observations on the intermediate state, but also by measurements of the true magnetization of Type-II superconductors. (M.H.R.)

27658 TEMPERATURE DEPENDENCE OF CRITICAL CURRENT IN Nb_3Sn RIBBON. Matsunaga, Sakuro (Japan Atomic Energy Research Inst., Tokai); Ueda, Kazuo. Jap. J. Appl. Phys.; 10: 480-4(Apr 1971).

The temperature dependence of critical current in vapor-deposited Nb_3Sn ribbon was measured in the temperature region above 4.2°K in magnetic fields below 55 kOe. The results are analyzed by Coffey's model. For the magnetic field of 30 kOe, the experimental values in the temperature region from 4.2 to 12°K agree with those calculated by the model, but in the region above 12°K the experimental values become smaller than the calculated values. The temperature at which the experimental values deviate from the calculated values decreases with increasing magnetic field. This temperature is about 8°K in the magnetic field of 55 kOe. (auth)

27659 PREPARATION OF JOSEPHSON JUNCTIONS BY PLASMA OXIDATION OF Nb. Graeffe, R.; Wiik, T. (State Inst. for Technical Research, Otaniemi, Finland). J. Appl. Phys.; 42: 2146-7(Apr 1971).

Josephson $Nb/Nb_xO_y/Pb$ junctions may be prepared by oxidation of Nb films during a O_2 glow discharge, with the maximum Josephson current being determined by the glow discharge time. A 1300-Å-thick Nb pattern is deposited through a mask on a heated glass substrate in vacuum. The substrate is cooled, O_2 is introduced to a pressure of 10 mtorr, and the glow discharge is started and then stopped when the desired maximum Josephson current is reached (50 to 100 mA after 15 sec, 0.2 mA after 40 sec). The system is pumped down and the substrate degassed. Finally, a 2000-Å-thick Pb pattern and then an Au contact pattern are deposited. The stability of the junctions is good. (D.L.C.)

27660 EVIDENCE FOR ELECTRON–ELECTRON SCATTERING IN THE ELECTRICAL RESISTIVITY OF In. Bressan, O. J.; Ridner, A. E.; Luengo, C. A.; Alascio, B. (Univ. Nacional, Cuyo, Argentina). Solid State Commun.; 8: 2129-33(15 Dec 1970).

Experimental measurements of the electrical magnetoresistivity of high-purity indium at low temperatures were performed and indicate that: a generalized Kohler's rule can be used to describe all experiments; a reliable method is therefore obtained for extrapolating the zero magnetic field resistivity to temperatures below the superconducting transition temperature; and clear-cut and reliable data show that no T^2 dependence of the resistance is found; therefore no evidence of electron–electron interaction appears, contrary to information previously reported in the literature. (auth) (UK)

27661 MECHANISM OF SUPERCONDUCTIVITY. Makiej, Boleslaw (Inst. of Low Temperatures and Structural Research, Wroclaw). Postepy Fiz.; 22: 39-48(1971). (In Polish).

A brief review of the basic experimental facts and an account of the theory of Type-I and Type-II superconductivity were given. (auth)

27662 INVESTIGATION OF KONDO ALLOYS AND COMPOUND BY THE SUPERCONDUCTIVE PROXIMITY EFFECT.

Hauser, J. J.; Hamann, D. R.; Kammlott, G. W. (Bell Telephone Labs., Murray Hill, N. J.). Phys. Rev., B; 3: 2211-23 (1 Apr 1971).

The proximity effect between a superconductor and a normal metal is sensitive to the presence, amount, and state of order of the impurity spin in the normal metal. The present experiments were performed with $Cu_{0.99}Fe_{0.01}$, $Cu_{1-x}Mn_x$ (x = 0.0025, 0.05), $Cu_{0.9975}Co_{0.0025}$ Kondo alloys, and with the Kondo compound $CeAl_2$. The alloys were sputtered first at temperatures ranging from about −100 to 530°C, followed by Pb sputtering at 77°K. Electron diffraction showed that the Cu alloy films prepared at −100°C were quasi-amorphous and did not have the structure of bulk Cu. In such a state, regardless of the Kondo temperature of the bulk alloys, the magnetic impurities in the dilute alloys behave as random free spins; the spin depairing in the superconductive proximity effect is almost independent of the type of host metal (Cu or Mo) or the type of impurity (Fe, Mn, Co) and is proportional to the amount of impurity present. The $Cu_{0.95}Mn_{0.05}$ alloy, when deposited at −100°C, becomes ferromagnetic at 5.5°K and the magnetic transition is clearly exhibited by the proximity effect. Alloys prepared at and above room temperature have the bulk Cu structure. In the temperature range of the measurements (1 to 7.2°K) which is well below the Kondo temperature of $Cu_{0.99}Fe_{0.01}$ (≈13°K as determined by resistivity), the $Cu_{0.99}Fe_{0.01}$ alloy films with the bulk Cu structure behave as an almost spinless system. The Cu−Mn alloys with the bulk Cu structure are antiferromagnetic at low temperature and give rise to a spin-depairing factor about 10 times smaller than the one corresponding to free random spins. The same qualitative result was obtained with Cr films, where the free-spin state can be achieved by sputtering at 77°K. The proximity-effect experiments were also performed with the Kondo compound $CeAl_2$; above 3.5°K, $CeAl_2$ behaves as a spinless system, which implies that $CeAl_2$ has a Kondo temperature above 7.2°K. The antiferromagnetic transition at 3.5°K is clearly shown by the proximity effect. (auth)

Equipment and Devices

27663 (ORNL-tr-2436) PROTECTION OF LARGE SUPERCONDUCTING COILS. Bronca, G.; Krikorian, J.; Neel, J.; Vassal, G.; Burnier, P.; Moreau, J. Translated by R. Gregg Mansfield (Oak Ridge National Lab., Tenn.), from Nucl. Instrum. Methods; 79: 309-14(1970). 12p. Dep. NTIS.

When a quenching occurs in a large coil, the dissipation of the energy will increase the temperature of the superconductor and the pressure in the cryostat. The study of these phenomena showed that, using the usual protection device, pressure and temperature can be held at a low value and make the coil safe even if the protection is switched on one second after detection of the quenching. Experimental results obtained on a 10-MJ coil confirm the theory. (auth)

27664 (RHEL/R-208) THE EVOLUTION OF THE PUMPING GROUPS USED ON THE RUTHERFORD LABORATORY ^{3}He REFRIGERATOR. Cragg, D. A. (Rutherford High Energy Lab., Chilton (England)). Dec 1970. 11p. Dep. NTIS (U. S. Sales Only). UK 17p.

Modifications have been made to the pumping groups used on the Rutherford Laboratory Helium-3 Refrigerator. These modifications and the reasons for them are reported here, together with the resulting improvement in performance. (auth) (UK)

27665 PROPAGATION OF AN ELECTROMAGNETIC WAVE IN A SUPERCONDUCTING COAXIAL CYLINDRICAL GUIDE. Zepp, Gerard (Clermont-Ferrand Univ., France). Compt. Rend., Ser. B; 272: 95-7(11 Jan 1971). (In French).

The propagation of an electromagnetic wave in a coaxial cylindrical guide made of superconducting material (or possibly of two different superconducting materials) is studied. The analytical expressions for the attenuation coefficient and the phase shift are determined. (France)

27666 HYPERFINE ENHANCED NUCLEAR MAGNETIC COOLING IN VAN VLECK PARAMAGNETIC INTERMETALLIC COMPOUNDS. Andres, K.; Bucher, E. (Bell Telephone Labs., Murray Hill, N. J.). J. Appl. Phys.; 42: 1522-7(15 Mar 1971). From 16th Annual Conference on Magnetism and Magnetic Materials, Miami Beach, Fla. See CONF-701104.

In strongly Van Vleck paramagnetic rare-earth alloys or compounds, large hyperfine fields can be induced at the rare-earth nucleus with moderate external fields. These fields are useful to generate low temperatures by the method of nuclear adiabatic demagnetization. Experiments in the Van Vleck paramagnets $PrPt_5$ and $PrTl_3$ are described in which end temperatures of 3.5 and 1.5 mK are obtained starting from about 60 mK and 20 kOe. The possibility of nuclear ferromagnetism in $PrTl_3$ is discussed and compared with observations. (auth)

Plasma and Thermonuclear Physics

27667 PLASMA PHYSICS INDEX. VOLUME 6, NO. 2, 1971. Bibliography, Author Index, Subject Index. Frankfurt am Main; Zentralstelle fuer Atomkernenergie-Dokumentation (1971). 122p.

This listing includes 421 articles on various aspects of plasma physics. (M.O.W.)

27668 TECHNOLOGY INDEX FOR PLASMAPHYSICS RESEARCH AND FUSION REACTORS. VOLUME 5, NO. 2, 1971. Bibliography, Author Index, Subject Index, Appendix. Frankfurt am Main; Zentralstelle fuer Atomkernenergie-Dokumentation (1971). 57p.

This listing includes 286 articles on various aspects of plasma physics. (M.O.W.)

Confinement and Heating

27669 (IAE-1972) DURATION OF CHARGED PARTICLES CONTAINMENT IN A TRAP WITH MAGNETIC MIRROR. Sivukhin, D. V. (Institut Atomnoi Energii, Moscow (USSR)). 1970. 47p. (In Russian). Dep. NTIS (U. S. Sales Only).

A simplified problem on the duration of charged-particle containment in a trap with magnetic mirrors is reduced to the solution of the kinetic equation in the center of the trap. The magnetic and electric fields are determined from the kinetic equation and their influence is taken into account by the boundary conditions for the distribution function. The kinetic Landau equation is used for resolving (in zero and first approximation) the problem of Coulomb scattering of the light particles by heavy particles in traps with magnetic mirrors. Formulas are obtained for the mean time of light particle containment. With additional physical factors, a formula was obtained for the mean time of containment of ions of real plasma in the trap. The latter almost coincides with Budker's formula. (R.V.J.)

27670 PLASMA HEATING BY STRONG SHOCK WAVES. Gross, R. A. (Columbia Univ., New York); Miller, B. Methods Exp. Phys.; 9: 169-212(1970).

The design and construction details of electromagnetic devices for producing hot plasmas by means of very high-speed shock waves are described. Results achieved by shock heating are summarized. (M.O.W.)

27671 TRAPPING AND CONTAINMENT OF A CESIUM PLASMA IN A MAGNETIC MIRROR. Kesner, Jay (Columbia Univ., New York). Phys. Fluids; 14: 868-77(Apr 1971).

Time-dependent plasma behavior was observed by injecting plasma pulses, created by means of a rotating shutter, into a Q machine. Reflection of short collisionless plasma pulses from a single magnetic mirror was observed, and a comparison of the experimental results with a computer simulation was used to obtain information about the ion velocity distribution function and about the dynamics of plasma−mirror interaction. Buildup and decay of plasma in a magnetic mirror well was studied by injecting dense, collisional plasma pulses into the Q machine at the mirror throat. The density of plasma at the midplane of the mirror was seen to increase significantly due to trapping and the containment times observed were about 10 msec (approximately 10 transit times). The plasma decay rate was slower than would be expected for a collisionless mirror. A model, based on Coulomb scattering for the trapping and decay processes, gives predictions in good agreement with the experimental results. (auth)

27672 HEATING OF COUNTERSTREAMING ION BEAMS IN AN EXTERNAL MAGNETIC FIELD. Papadopoulos, K.; Davidson, R. C.; Dawson, J. M.; (and others) (Naval Research Lab., Washington, D. C.). Phys. Fluids; 14: 849-57(Apr 1971).

Ion heating by a strong ion−ion two-stream instability perpendicular to a magnetic field in the presence of a relatively cold electron background ($T_e \ll m_i V_d^2$) is considered. The magnetic field strength is such that the ion trajectories are straight, whereas the electrons are bound to the field lines ($kr_{Le} \ll 1 \ll kr_{Li}$). Theory is presented for both quasi-linear and nonlinear stages of the evolution of the system for the case that the instability is electrostatic [$(B^2/8\pi)(1+\beta) > nm_i V_d^2/8$] and is compared with a series of computer simulation experiments. It is found that the quasi-linear theory gives a fairly accurate description of spatially averaged plasma properties until the ion beams have been sufficiently modulated

for ions to be trapped by the waves. In the subsequent nonlinear stage, stabilization occurs when the ion-trapping period is equal to the reciprocal growth rate associated with the instability. The directed ion beam energy is mainly converted into random ion energy. The possible role of this instability in high Mach number shocks is discussed. (auth)

27673 PARTICLE DIFFUSION IN TURBULENT ELECTRIC FIELDS. Flynn, Robert W. (Massachusetts Inst. of Tech., Cambridge). Phys. Fluids; 14: 956-9(May 1971).

The statistics of charged-particle dynamics in turbulent plasmas were studied in a numerical experiment which models a turbulent plasma as a system of uncorrelated plasma waves. The ensemble averaged distribution function roughly "diffuses" in velocity space in both weak and strong field regimes. The experimental data are consistent with Dupree's prediction of a diffusion coefficient having a broadened wave–particle resonance and scaling quadratically in the electric field strength for weak fields, and proportional to $E^{\frac{4}{3}}$ for stronger fields. (auth)

27674 CONSERVATIVE TRAPPING OF CHARGED PARTICLES IN A STATIC MAGNETIC FIELD. Hogan, W. A.; Lamborn, B. N. A. (Florida Atlantic Univ., Boca Raton). Phys. Fluids; 14: 1006-10(May 1971).

Trajectories of charged particles injected tangentially into the midplane of a physically reasonable static mirror field were analyzed by computer. Conditions necessary for the nonadiabatic transfer of particle energy from the plane perpendicular to the field to the direction parallel to the field are discussed. It is shown that this energy transfer can be qualitatively predicted from the Mathieu equation. Two exchange mechanisms are observed; when the requirements for parametric resonance are satisfied energy is transferred into the longitudinal degree of freedom, and when the particle exhibits the characteristic looping behavior energy may be transferred between the transverse and longitudinal degrees of freedom. The coupled nonlinear equations of motion for single particles are numerically integrated using the fourth-order Runge–Kutta method. Based on the results of the various computer experiments, an effective trapping time is obtained. (auth)

27675 ANOMALOUS HEATING OF PLASMA ELECTRONS DRIVEN BY A LARGE TRANSVERSE FIELD AT $\sim\omega_{pe}$. Kruer, W. L.; Dawson, J. M. (Princeton Univ., N. J.). Phys. Fluids; 14: 1003-5(May 1971).

Numerical experiments on a plasma driven by a large-amplitude transverse field oscillating at nearly twice the electron plasma frequency are presented. The large wave drives the electrostatic plasma waves unstable. When these unstable waves grow to large amplitude, they efficiently transfer energy to the plasma particles. A simple theory to explain the results is presented. (auth)

27676 DYNAMIC CONTROL OF CUSP LOSS. Sato, T.; Miyake, S.; Watari, T. (and others) (Nagoya Univ., Japan). pp 310-14 of Feedback and Dynamic Control of Plasmas. /Chu, T. K. (ed.). New York; American Institute of Physics (1970).

From Symposium on feedback and dynamic control of plasmas; Princeton, N. J. (18 Jun 1970).

Experimental results and computer simulation studies on the dynamic control of cusp loss are presented. The steady-state plasma is fed into a cusped magnetic field along the spindle axis. The plasma density at the center is 10^{11} cm^{-3}, and $T_e \simeq T_i \simeq 10$ eV. The rf electric field whose frequency is near the ion cyclotron frequency is applied perpendicularly to the line cusp and to both point cusps. When the rf field is applied the ion density at the center increases by a factor of two and its mean energy reaches up to 50 eV. From the increase of ion density, the increase of decay time by about a factor of ten is estimated. The number density of high-energy ions above 100 eV confined in the cusp increases by a factor of over fifty. The computer simulation of the rf effect on the line loss suppression indicates a good agreement with the experimental results. (auth)

27677 HOT ELECTRON CONFINEMENT IN A CUSPED MAGNETIC FIELD BY ECRH WRAPPING. Aihara, S.; Fujiwara, M.; Hosokawa, M.; Ikegami, H. (Nagoya Univ., Japan). pp 315-19 of Feedback and Dynamic Control of Plasmas. /Chu, T. K. (ed.). New York; American Institute of Physics (1970).

From Symposium on feedback and dynamic control of plasmas; Princeton, N. J. (18 Jun 1970).

The confinement of a hot electron plasma in a cusped magnetic field is studied. The hot electron plasma whose temperature is about 30 keV is produced in the electron cyclotron resonance region within the cusped magnetic field by a 20-msec pulse of 6.4 GHz having a power up to 5 kW. During the afterglow plasma, a weak 6.4-GHz microwave power is supplemented. Up to 150 W of supplemented power, the decay time increases linearly up to about 30 msec, about three times that without the supplement. With further increase of the power, the decay time decreases. The increase in the plasma containment time is explained to be due to the force $\langle F \rangle = -[(e^2/4m)\nabla E^2/\omega^2 - \Omega_e^2]$. (auth)

Diagnostics

Refer also to abstracts 27769, 27795, and 27809.

27678 (WASH–1159, pp 172-83) DETECTION OF HIGHLY STRIPPED HEAVY IONS IN A LOW-PRESSURE LINEAR PINCH DEVICE. Lie, T. N. (Catholic Univ. of America, Washington, D. C.).

From Conference on heavy ion sources; Washington, D. C. (13 Mar 1970).

In Conference on heavy ion sources.

Highly stripped heavy ions were observed in the discharge using spectroscopic analysis. The kinetics of the discharge is also described in order to give the time history of the high-temperature plasma formation. Finally, the possible application of the present device as an ion source is briefly discussed. (M.O.W.)

27679 MICROWAVE SCATTERING FROM PLASMAS. Marshall, T. C. (Columbia Univ., New York). Methods Exp. Phys.; 9: 37-59(1970).

Elementary scattering theory for electromagnetic waves on plasma fluctuations is reviewed. Some experimental tests of the theory are mentioned along with boundary effects. Fluctuation problems are outlined. Experimental apparatus for transmitting and detecting microwaves is briefly described. (M.O.W.)

27680 PLASMA DIAGNOSTICS BY LIGHT SCATTERING. DeSilva, A. W. (Univ. of Maryland, College Park); Goldenbaum, G. C. Methods Exp. Phys.; 9: 61-113(1970).

The following sections are presented: (1) theory of light scattering, (2) major design parameters of a scattering experiment, (3) optical systems, and (4) interpretation of data. (M.O.W.)

27681 CYLINDRICAL PROBE IN A FLOWING PLASMA. Swift-Hook, D. T.; Andrews, J. G. (Central Electricity Generating Board, Southampton, Eng.). J. Phys. A (London); 4: L21-4(Mar 1971).

The theory developed by Andrews and Swift-Hook (J. Phys. A., 4: 142-57(1971)) for a spherical probe in a flowing plasma can be applied to a cylindrical probe. As with a sphere, a stagnation point forms downstream and there is a small change in floating potential and in ion saturation current. These changes are smaller than for a sphere and opposite in sign; it might just be possible to obtain some indication of the flow velocity from them. Apart from this, existing low pressure, subsonic probe theories are substantially correct numerically. (auth) (UK)

27682 RELATION BETWEEN INTEGRAL ELECTRON FLUX AND CURRENT IN RETARDING-POTENTIAL PLASMA PROBES. Matthews, D. L. (Univ. of Maryland, College Park). J. Atmos. Terrest. Phys.; 33: 511-14(Mar 1971).

A relationship for retarding probes is derived, expressing the integral electron flux in the plasma in terms of the probe current and its first derivative with respect to the retarding potential. Certain applications of this result to probes on spacecraft are discussed. (auth) (UK)

27683 RESONANCE CONES IN THE FIELD PATTERN OF A RADIO FREQUENCY PROBE IN A WARM ANISOTROPIC PLASMA. Fisher, R. K.; Gould, . W. (California Inst. of Tech., Pasadena). Phys. Fluids; 14: 857-67(Apr 1971).

An experimental and theoretical investigation of the angular distribution of the electric field of a short radio-frequency probe in a plasma in a magnetic field is described. The field is observed to become very large along a resonance cone whose axis is parallel to the static magnetic field and whose opening angle is observed to vary with incident probe frequency, cyclotron frequency, and plasma frequency in agreement with simple cold plasma dielectric theory. The relationship of these cones to the limiting phase- and group-velocity cones that appear in the theory of plane wave propagation is discussed. The addition of electron thermal velocities (warm plasma effects) is examined in the limit of a large static magnetic field. A fine structure appears inside the cones and is shown to result from an interference between a fast electromagnetic wave and a slow plasma wave. This interference structure is observed experimentally and measurements of the angular interference spacing are shown to agree with the warm plasma theory. The use of measurements of the resonance cones and structure as a diagnostic tool to determine the plasma density and electron temperature in a plasma in a magnetic field is discussed. (auth)

27684 LOCAL DENSITY MEASUREMENTS BY NONLINEAR MIXING OF ELECTROMAGNETIC WAVES. Cano, R.; Fidone, I.; Zanfagna, B. (CEN, Fontenay-aux-Roses, France). Phys. Fluids; 14: 811-17(Apr 1971).

A diagnostic scheme for local measurements of the electron density in low-β plasmas using the nonlinear mixing of electromagnetic waves is presented. The basic assumption is made that the three interacting waves satisfy the synchronism relations. A number of nonlinear processes are examined for different magnetic configurations. Experimental results obtained with a steady-state plasma ($10^{10} < ne < 10^{12}$ cm^{-3}) are reported to illustrate the method. (auth)

27685 MEASUREMENTS IN A NONEQUILIBRIUM PLASMA BOUNDARY LAYER. Brown, R. T.; Mitchner, M. (Stanford Univ., Calif.). Phys. Fluids; 14: 933-40(May 1971).

Measurements and related analyses of the electron temperature and electron number density in an atmospheric pressure laminar thermal boundary layer adjacent to a cooled wall are described. The analyses proceed from consideration of the coupled electron continuity and electron energy equations with boundary conditions appropriate to NaK-seeded argon. It is shown that the theoretical results can be interpreted in terms of three characteristic lengths: δ, the thermal boundary layer thickness, l_E, the characteristic length for electron energy exchange, and l_I, the characteristic length for ionization. Electron temperature profiles were measured experimentally in the boundary layer described above using a spectroscopic technique, and electron number density profiles were measured using a small traversing probe developed by the authors. The experimental results, obtained for various values of the lengths l_E and l_I, were found to be in good agreement with the theory. (auth)

27686 ENERGY ANALYSIS OF CESIUM IONS IN A Q MACHINE. Motley, R. W.; Kawabe, T. (Princeton Univ., N. J.). Phys. Fluids; 14: 1019-23(May 1971).

Energy analysis of cesium ions in the collision-dominated plasma of a double-ended Q machine is reported. The ion temperature, found to be between 3000 and 6000°K, is always greater than the temperature of the hot ionizing plates. Also, the measured temperature is almost 50% greater than can be accounted for solely by thermal and electrostatic energy associated with the acceleration of ions in the plasma sheath. (auth)

Kinetics (General)

27687 (NP-18758) BREMSSTRAHLUNG OF RELATIVISTIC PLASMA. Tsytovich, V. N. (Akademiya Nauk SSSR, Moscow. Institut Fiziki). 1971. 36p. (In Russian). Dep. NTIS (U. S. Sales Only).

A general theory of bremsstrahlung is constructed, considering the processes of spontaneous and induced emission and the influence of emission processes on the distribution of plasma particles (quasi-linear effects). (tr-auth)

27688 (WASH-1159, pp 193-5) PERPENDICULAR INJECTION OF RELATIVISTIC ELECTRON BEAMS INTO MAGNETIC MIRRORS. Fleischmann, Hans H. (Cornell Univ., Ithaca, N. Y. Lab. of Plasma Studies).

From Conference on heavy ion sources; Washington, D. C. (13 Mar 1970).

In Conference on heavy ion sources.

An experiment similar to the Astron device for trapping a relativistic electron beam in a magnetic mirror trap is briefly described. (M.O.W.)

27689 METHODS OF EXPERIMENTAL PHYSICS. VOLUME 9. PLASMA PHYSICS. PART A. Griem, Hans R.; Lovberg, Ralph H. (eds.). New York; Academic Press Inc. (1970). 485p. $22.50.

Separate abstracts were prepared for the 10 included chapters. (M.O.W.)

For abstracts of individual chapters see: 27670, 27679, 27680, 27690, 27705, 27727-27730, and 27800.

27690 COLLISIONLESS SHOCK WAVES IN LABORATORY PLASMAS. Hintz, E. (Kernforschungsanlage, Juelich, Ger.). Methods Exp. Phys.; 9: 213-74(1970).

The discussion considers the case of collisionless shock waves for $\beta \ll 1$, $\theta = 90°$, where θ is the angle between the direction of propagation and the magnetic field. Some theoretical models for the formation and structure of shock waves are described along with experimental methods for producing collisionless shocks. (M.O.W.)

27691 AXIALLY SYMMETRIC HYDROMAGNETIC EQUILIBRIA WITH SPHERICAL PLASMA-VACUUM INTERFACES. Yeh, Tyan; Morikawa, G. K. (New York Univ., N. Y.). Phys. Fluids; 14: 781-5(Apr 1971).

Solutions representing axially symmetric hydromagnetic equilibria with spherical plasma-vacuum interfaces are extended from a low-pressure paramagnetic regime to a high-pressure diamagnetic regime. (auth)

27692 THE CONTRIBUTION OF ELECTRONIC EXCITATION TO THE TOTAL SPECIFIC HEATS OF HIGH-TEMPERATURE GASES: A MISINTERPRETED ABSENCE. Capitelli, M.; Ficocelli, E. (Univ., Bari, Italy). J. Plasma Phys.; 5: 115-121 (Jan 1971).

It is shown that the reported absence of a contribution of electronic excitation to the total specific heats of helium and nitrogen (10,000 to 35,000°K, 10^{-1} to 10 atm) should be attributed to the presence of compensation effects among the various terms into which the total specific heat can be separated and that these terms are influenced by the electronic contribution. (auth) (UK)

27693 MEASUREMENTS OF WAVE-PARTICLE INTERACTION IN A SINGLE-ENDED Q MACHINE. Andersen, S. A.; Christoffersen, G. B.; Jensen, V. O.; Michelsen, P.; Nielsen, P. (Danish Atomic Energy Commission Research Establishment, Risoe). Phys. Fluids; 14: 990-8(May 1971).

A Green-function technique is used to solve the linearized Vlasov equation for the perturbed ion velocity distribution function, f(x,v, t), in a case where a short-density pulse is released into a plasma. Some characteristic features in the calculated curves are caused by wave-particle interaction. Experimentally, short-density pulses are generated in the plasma in a single-ended Q machine by application of electrical square pulses to a grid immersed in the plasma column. The perturbed ion velocity distribution function in the density pulse is measured by means of an electrostatic energy analyzer. The features showing the wave-particle interaction appear in the experimental results. (auth)

Kinetics (Experimental)

27694 (WASH-1159, pp 184-9) ACCELERATION AND STRIPPING OF IONS BY INTENSE RELATIVISTIC ELECTRON BEAMS. Rostoker, Norman (Cornell Univ., Ithaca, N. Y. Lab. of Plasma Studies).

From Conference on heavy ion sources; Washington, D. C. (13 Mar 1970).

In Conference on heavy ion sources.

Two experiments are briefly described: (1) the injection of a relativistic electron beam into a torus, and (2) injection of the beam through a cusp field. Bremsstrahlung measurements are briefly described for the toroidal experiments. The existence of highly stripped ions is discussed. (M.O.W.)

27695 (WASH-1159, pp 196-203) ION PRODUCTION WITH INTENSE ELECTRON BEAMS. Yonas, G. (Physics International Co., San Leandro, Calif.).

From Conference on heavy ion sources; Washington, D. C. (13 Mar 1970).

In Conference on heavy ion sources.

The injection of an electron beam into a neutral gas is briefly discussed. The transport of ions along with the beam is described. (M.O.W.)

27696 (WASH-1159, pp 204-18) ION ACCELERATION WITH HIGH ν/γ ELECTRON BEAMS. Rander, J.; Ecker, B.; Yonas, G. (Physics International Co., San Leandro, Calif.).

From Conference on heavy ion sources; Washington, D. C. (13 Mar 1970).

In Conference on heavy ion sources.

The experiments consisted of injecting a pulsed electron beam into a gas-filled drift chamber. Ions formed and accelerated in the chamber were analyzed downstream. Some results are described. (M.O.W.)

27697 (WASH-1159, pp 219-26) ION MOMENTUM ANALYSIS OF COLLECTIVELY ACCELERATED ION SPECIES. Graybill, S. E.; Uglum, J. R. (Ion Physics Corp., Burlington, Mass.).

From Conference on heavy ion sources; Washington, D. C. (13 Mar 1970).

In Conference on heavy ion sources.

The velocity of ion species collectively accelerated by a high-current electron beam was recorded by measuring their time-of-flight. The experimental apparatus for momentum analysis of these beams is described. The ions measured were H, D, He, N, and Ar. (M.O.W.)

XUM

27698 CONTROLLED AVALANCHE CAUSED BY ELECTRON CYCLOTRON ACCELERATION. Watt, F.; Hand, T. W.; Schneider, E. E. (Univ. of Newcastle-upon-Tyne, Eng.). J. Phys.; A (London); 4: L25-7(Mar 1971).

Results are given of an investigation into an electron avalanche produced by microwaves at the electron cyclotron resonance frequency in the presence of crossed electric and magnetic fields. (auth) (UK)

27699 SCATTERING OF ELECTRONS BY ELECTROSTATIC FLUCTUATIONS IN A MAGNETIZED PLASMA. Walsh, J. E.; Bancroft, D.; Hawkins, C.; Layman, R. W. (Dartmouth Coll., Hanover, N. H.). Phys. Fluids; 14: 878-84(Apr 1971).

The scattering of beam electrons in a beam-formed, magnetized plasma was measured experimentally. Evidence for an effective inverse mean free path that depends upon the intensity and width of the beam excited fluctuations is presented. The model used to interpret the experiment is based upon an elementary application of the Fokker–Planck equation and the theory of Brownian motion. It includes the effects of velocity space diffusion. Mean free paths between 10 and 10^3 cm are found to be in agreement with the predictions of the model. The ordinary collisional attenuation of the beam under the same operating conditions is several orders of magnitude smaller. (auth)

27700 ELECTRON-BEAM RELAXATION IN A PLASMA. Levitskii, S. M.; Shashurin, I. P. (Kiev State Univ.). Nucl. Fusion; 11: 111-17(Mar 1971).

The interrelationship between the oscillation amplitude and the form of the energy distribution function of beam electrons is studied under conditions where the electron beam predominantly excites longitudinal plasma oscillations. It is shown that the intensity of the oscillations stops growing when the distribution function assumes the form of a plateau extending to thermal velocities of the plasma electrons. Experimental measurements of the beam relaxation distance as a function of the parameters of the plasma–beam instability are in qualitative agreement with theory. Initial modulation of an electron beam by means of a monochromatic signal of sufficiently high amplitude, leading to a considerable narrowing of the oscillation spectrum, reduces the relaxation distances and the number of anomalously fast electrons in the beam. (auth)

27701 ROTATION OF A GLOW DISCHARGE IN A HOMOPOLAR DEVICE. Diamond, S. A.; Turcotte, D. L. (Cornell Univ., Ithaca, N. Y.). Phys. Fluids; 14: 928-32(May 1971).

The rotation of a glow discharge in the homopolar geometry was studied experimentally. In helium the motion of the discharge is independent of the current level and is attributed to ion drift with the neutrals stationary. In argon at low currents the rotational speed is proportional to the current and the discharge acts like a magnetohydrodynamic pump. At higher pressure in argon the discharge contracts and the rotational speed increases by nearly an order of magnitude. (auth)

27702 SUPRESSION OF LONGITUDINAL ELECTRON OSCILLATION BY BEAM MODULATION. Nakamura, Yoshihara; Kojima, Shoji (Tokyo Univ. of Education). pp 264-5 of Feedback and Dynamic Control of Plasmas. /Chu, T. K. (ed.). New York; American Institute of Physics (1970).

From Symposium on feedback and dynamic control of plasmas; Princeton, N. J. (18 Jun 1970).

The suppression of beam-excited longitudinal electron oscillations by beam-density modulation in an axially and transversely finite beam–plasma system was studied. The modulation frequency is in the vicinity of the frequency of the oscillation, neighboring modes, or higher harmonics. (auth)

27703 NONLINEAR PERTURBATIONS AND ELECTRON SCATTERING IN A BEAM PLASMA. Walsh, J. E.; Bancroft, D.; Layman, R. W.; Lewis, P. B. (Dartmouth Coll., Hanover, N. H.). pp 266-73 of Feedback and Dynamic Control of Plasmas. /Chu, T. K. (ed.). New York; American Institute of Physics (1970).

From Symposium on feedback and dynamic control of plasmas; Princeton, N. J. (18 Jun 1970).

The scattering of electrons by fluctuations, out of an electron beam in a beam–plasma, is measured experimentally. Evidence for a nonlinear effective inverse mean free path that depends upon the intensity and width of the fluctuations is presented. One finds that some control over the scattering process can be obtained when external oscillators of the natural oscillations are used to perturb the natural fluctuation spectrum. It is possible to both enhance and decrease velocity space diffusion in this way. (auth)

Kinetics (Theoretical)

Refer also to abstracts 27737, 27739, and 27811.

27704 (NP-18759) PLASMA BREMSSTRAHLUNG FROM RELATIVISTIC PARTICLES IN A TURBULENT PLASMA. Tsytovich, V. N. (Akademiya Nauk SSSR, Moscow. Institut Fiziki). 1971. 33p. (In Russian). Dep. NTIS (U. S. Sales Only).

Two mechanisms of relativistic-particle emission in turbulent plasma are discussed: (1) induced and spontaneous emission during Compton scattering on nonresonant turbulent plasma oscillations, previously described by the author, and (2) the process of a new bremsstrahlung effect during scattering on resonant turbulent oscillations. The spectral composition and angular distribution of the radiation and the particle energy losses due to the plasma bremsstrahlung are analyzed. The influence of multipole scattering (the Landau–Pomeranchuk effect) on the emission processes was studied. The intensity of the plasma bremsstrahlung shows a slight dependence on the particle mass and is, in particular, higher for the ions. The effect of turbulent expansion of the Cherenkov resonance was interpreted as resulting from the multiple scattering of particles on the resonances of plasma pulsations. (tr-auth)

27705 ATOMIC PROCESSES. Elton, R. C. (Naval Research Lab., Washington, D. C.). Methods Exp. Phys.; 9: 115-68(1970).

The following are discussed: (1) effects of atomic processes observable in plasmas, (2) how such observations can be utilized for analysis in terms of specific plasma parameters, and (3) what information concerning fundamental atomic processes can be obtained from a plasma that has been well diagnosed by other means. The important equilibrium models that have evolved are reviewed, and formulation of the rate equations required for certain models is discussed. The various atomic processes occurring in and influencing a plasma are defined, and convenient formulas are given for estimating the relevant process reaction rate. (M.O.W.)

27706 APPROXIMATION OF THE GENERAL FORMULAE FOR GYRO AND SYNCHROTRON RADIATION IN A VACUUM AND ISOTROPIC PLASMA. Wild, J. P.; Hill, E. R. (CSIRO, Epping, N. S. W.). Aust. J. Phys.; 24: 43-52(1971).

Approximate expressions are derived for the Bessel function $J_n(nx)$ and its derivative with respect to nx, valid when $0 \leq x \leq 1$ and for $1 \leq n \leq \infty$. The expressions, which are accurate to within a few per cent, are used to derive general formulas for the power spectrum and polarization of gyro and synchrotron radiation emanating from a vacuum and a "weak" (isotropic) plasma. (auth)

27707 PENETRATION TO SECOND ORDER OF AN ELECTROSTATIC FIELD INTO A WARM PLASMA. Zawadzki, E. M.; Lewak, G. J. (Univ. of California, San Diego, La Jolla). J. Plasma Phys.; 5: 73-87(Jan 1971).

Using a reformulation of ordinary perturbation theory to first and second order, explicit solutions for the penetration of electrostatic waves into a semi-infinite Vlasov plasma are presented. Two types of electron velocity distribution are used, the uniform step ("water-bag" model) and the Maxwellian. The existence of propagating modes below the plasma frequency, behavior of the second harmonic field and the formation of a narrow sheet of electrons near the bounding wall are displayed. Replacement of boundary fields with equivalent charge and current sources is discussed. (auth) (UK)

27708 NOTE ON THE EXISTENCE OF STATIONARY SHOCK WAVES IN COLLISIONLESS PLASMAS. Pfirsch, D. (Institut fuer Plasma-Physik, Garching., Ger.); Schindler, K. J. Plasma Phys.; 5: 123-30(Jan 1971).

Wave propagation perpendicular to a magnetic field is discussed. Variables depend on x only. The medium is collision-free, described by the Vlasov theory. It is shown that there exist two, and only two, unique constants of the motion that are independent of y, z and t, and that at least one of them depends on x. Thus a necessary condition for the existence of stationary shocks is fulfilled. Examples show that the existence proof also suggests a practical tool for solving problems. The oblique case which is also briefly discussed turns out to be qualitatively different in that, owing to the presence of reflected particles, a uniform upstream state cannot be prescribed a priori. (auth) (UK)

27709 PLASMA EXPANSION INTO A VACUUM. Widner, M.; Alexeff, I.; Jones, W. D. (Oak Ridge National Lab., Tenn). Phys. Fluids; 14: 795-6(Apr 1971).

The expansion of a semi-infinite, uniform plasma into a vacuum is studied by computer simulation. The solution resembles an analytic similarity solution except for a discontinuous front that precedes the plasma at a velocity of about

XU

$3(kT/M_i)^{\frac{1}{2}}$. Thus, previous speculation that the initial burst of ions would be accelerated to velocities comparable to that of the thermal velocity of the plasma electrons on the basis of a fluid model alone is found to be not valid. (auth)

27710 NONLINEAR BEHAVIOR OF THE ONE-DIMENSIONAL WEAK BEAM–PLASMA SYSTEM. Joyce, Glenn; Knorr, Georg; Burn, Thomas (Univ. of Iowa, Iowa City). Phys. Fluids; 14: 797-801(Apr 1971).

The effect of a weak beam of electrons on a Maxwellian plasma is studied by numerically integrating the Vlasov equation in one dimension. The solution is carried past the point of maximum electrostatic energy. After reaching its maximum value, the electrostatic energy fluctuates about its maximum. Some modes that are linearly stable grow due to mode coupling with the unstable modes. The relative amount of energy in the fastest-growing mode is shown to depend on the periodicity length of the system. (auth)

27711 EFFECT OF THE VIBRATIONAL EXCITATION OF N_2 MOLECULES ON THE FREQUENCY OF e–N_2 ELASTIC COLLISIONS IN A NITROGEN PLASMA. Cottereau, Marie-Joseph; Valentin, Pierre (Rouen Univ., Mont-Saint-Aignan, France). Compt. Rend., Ser. B; 272: 40-3(4 Jan 1971). (In French).

An attempt is made to estimate the effect of collisions of the type $N_{2\nu} + e \rightarrow N_{2\nu}^- \rightarrow N_{2\nu'} + e$ on the electron collision frequency in a nitrogen plasma at about 6000°K. (auth) (France)

27712 COMMENT ON NEGATIVE DIFFUSION COEFFICIENTS IN QUASI-LINEAR THEORY. Montgomery, David (Univ. of Iowa, Iowa City); Bodner, Stephen. J. Plasma Phys.; 5: 131-3(Jan 1971).

A recent paper on quasi-linear theory by Klozenberg and Bernstein is commented upon. It is argued that improper treatment of the perturbed electron distribution for damped waves has led to a diffusion-type equation with a negative diffusion coefficient. (auth) (UK)

27713 REPLY TO THE COMMENT ON NEGATIVE DIFFUSION IN COEFFICIENTS IN QUASI-LINEAR THEORY BY DAVID MONTGOMERY AND STEPHEN BODNER. Bernstein, Ira B. (Yale Univ., New Haven); Klozenberg, J. P. J. Plasma Phys.; 5: 135(Jan 1971).

The criticisms of Montgomery and Bodner (preceding paper) seem to stem from a misunderstanding of the claims in the paper of the authors (1970) in part perhaps semantic. The derivation criticized was intended to apply only to those particle velocities v corresponding to the range in phase velocities β_k/k for which there is an appreciable wave excitation. (auth) (UK)

27714 EFFECT OF TEMPERATURE NONUNIFORMITY ON THE POSITIVE COLUMN OF A GAS DISCHARGE. Lindgren, R. G.; Gavalas, G. R. (California Inst. of Tech., Pasadena). Phys. Fluids; 14: 923-7(May 1971).

The effect of temperature nonuniformity on the voltage–current characteristic of the positive column of a gas discharge is studied theoretically. The coupled electron diffusion and neutral temperature equations are solved by perturbation and numerically. It is found that at currents corresponding to the abnormal glow and higher, the voltage drop of the positive column decreases with increasing current, but this result is quite sensitive to the experimental data. Numerical results are obtained for an H_2 discharge. (auth)

27715 RELATIVISTIC ACCELERATION OF CHARGED PARTICLES BY AN ELECTROMAGNETIC PULSE. Noerdlinger, Peter D. (New Mexico Inst. of Mining and Tech., Socorro). Phys. Fluids; 14: 999-1002(May 1971).

The kinetic energy imparted to a charged particle by an electromagnetic pulse is $\frac{1}{2}q^2\Phi^2/mc^2$, where Φ is the "magnetic flux" in the pulse. The particle can acquire any velocity $<c$ in the propagation direction, but not more than $2^{-\frac{1}{2}}c$ in the transverse direction. An ionized medium is able to perturb the wave significantly whenever $\omega^2 < \omega_p^2$, no matter how powerful the wave. (auth)

27716 COMMENT ON REVISED QUASI-LINEAR EQUATIONS DEALING WITH WAVE-NUMBER SPECTRA. Abraham-Shrauner, Barbara (Washington Univ., St. Louis). J. Plasma Phys.; 5: 137-9(Jan 1971).

It is pointed out that the revised quasi-linear equations found recently by Klozenberg and Bernstein (1970) for continuous wave-number spectra, which are a simplified version of those derived earlier for discrete wave spectra, can be derived easily from the conventional quasi-linear equations by analytic continuation. (auth) (UK)

27717 QUASI-LINEAR THEORY IN THE NONRESONANT REGION. Bodner, Stephen E. (Univ. of California, Livermore). J. Plasma Phys.; 5: 141-4(Jan 1971).

By solving for the changes $\langle\Delta v\rangle$ and $\langle\Delta v\Delta v\rangle$ for a particle, it is shown that there is no diffusion equation for nonresonant particles when the electric field wave is damping. By indirect means it is then shown for this case that the appropriate quasi-linear solution for $f_1(k,v,t)$ is proportional to $\partial f_0(v,0)/\partial v$ rather than $\partial f_0(v,t)/\partial v$. (auth) (UK)

27718 RESONANCES OF A PLANE PLASMA CONDENSER IN CROSSED ELECTRIC AND MAGNETIC FIELDS. Nikolov, N. A. (Sofia Univ.). J. Plasma Phys.; 5: 145-50(Jan 1971).

Resonance frequencies of a plane plasma condenser in crossed electric and magnetic fields were determined using the two-component magnetic hydrodynamical equations. The perturbed plasma parameters (ion and electron densities and velocities and the electric field in the plasma), due to an external ac electric field, were found. The calculated resonance is not exact since dissipative processes were neglected. (auth) (UK)

27719 TRANSVERSE PARTICLE DIFFUSION IN STOCHASTIC FIELDS. Indykul, V. P. (Inst. of Physics and Tech., Kharkov). Ukr. Fiz. Zh. (Russ. Ed.); 16: 38-42(Jan 1971). (In Russian).

The space diffusion of plasma perpendicularly to a magnetic field in stochastic fields was examined. Propagation of circularly polarized and longitudinal waves in plasma was also investigated. The diffusion coefficients for arbitrary frequencies and arbitrary Larmor radii were obtained, taking into account collisions and thermal motion of the particles and finite correlation time of the field Fourier components. (auth)

27720 SOME ASPECTS OF PLASMA MOTION ACROSS AN INHOMOGENEOUS MAGNETIC FIELD. Voloshko, A. Yu.; Silenok-Bel'skii, G. A.; Solodovchenko, S. I. (Inst. of Physics and Tech., Kharkov). Ukr. Fiz. Zh. (Russ. Ed.); 16: 43-8(Jan 1971). (In Russian).

The influence of charged-particle velocity distribution upon the plasma stream motion across an inhomogeneous, magnetic field is studied. The influence of other plasma charges is estimated in the resulting electric field. The active energy exchange among plasma particles is shown to take place in a typical case. This process is accompanied by strong kinetic energy oscillations of particles which may be responsible for observed plasma stream instabilities, as well as particle scattering. The plasma stream thickness is also shown to increase infinitely in some cases. (auth)

27721 DISTRIBUTION OF A PULSED CURRENT IN A CYLINDRICAL CONDUCTOR OF VARIABLE CONDUCTIVITY. Demirkhanov, R. A.; Kirov, A. G.; Burdiashvili, M. Sh. (Physical-Technical Inst., Sukhumi, USSR). Nucl. Fusion; 11: 107-9(Mar 1971).

Numerical calculations of the current density distribution over the cross section of a cylindrical conductor were made when (a) the conductivity of the cylinder depends on time as $t^{\frac{1}{2}}$ for sinusoidal current and, (b) the time dependences of the current shapes and the conductivity are taken from experiments. An analytical solution is given of the nonstationary equation for the skin effect for constant conductivity of the cylinder when the function describing the time dependence of the current can be expanded in a Fourier series. (auth)

27722 VELOCITY DISTRIBUTION OF RAPID IONS WITH SUPERTHERMAL VELOCITY IN A NONISOTHERMAL PLASMA. Dnestrovskii, Yu. N. (Moscow State Univ.); Kostomarov, D. P. Nucl. Fusion; 11: 141-6(Mar 1971).

The ion velocity distribution in a nonisothermal plasma with $T_e \neq T_i$ is considered. The difference between this distribution and the Maxwellian distribution is studied. It is shown that under certain conditions the number of rapid ions with superthermal velocity may be much larger than in the Maxwellian distribution with the same temperature. (auth)

Production

27723 (WASH–1159, pp 162-7) HIGHLY STRIPPED IONS IN LASER SOURCES. Harrison, H. F. A. (United Kingdom Atomic Energy Authority, Abingdon (England). Culham Lab.).

From Conference on heavy ion sources; Washington, D. C. (13 Mar 1970).

In Conference on heavy ion sources.

The use of a 500-MW, Q-spoiled laser for producing a highly ionized plasma is discussed. Diagrams showing temperature and velocity measurements of an iron plasma are given. (M.O.W.)

27724 HOT DENSE PLASMAS FORMED BY LASER FOCUSING ON A TARGET. Consoli, T. (CEN, Grenoble, France). High Temp. - High Pressures; 2: 259-90(1970). (In French).

Generation of plasmas by focusing a laser beam on a gas or a solid target, either supported or levitated, is reviewed. The experimental setups and diagnostic methods are described and ionization theories are briefly reviewed, including the case when a magnetic field is present. The plasmas produced experimentally by this process are described, with particular emphasis on the work done in the USA and in France. (auth) (UK)

27725 FUSION CHAIN REACTIONS. III. THE PRODUCTION OF MeV PLASMAS. McNally, J. Rand Jr. (Oak Ridge National Lab., Tenn.). Nucl. Fusion; 11: 191-3(Mar 1971).

The production of proton or deuteron plasmas having $\beta \sim 1$ and $n\tau \gg 10^{14} s/cm^3$ is discussed. The plasma is produced by H_2^+ injection and trapping in magnetic mirrors. Curves showing trapping and loss rates are given. (M.O.W.)

Stability

Refer also to abstract 27672.

27726 (LA-4598) FEEDBACK SYSTEMS ON LINEAR θ PINCHES WITH HELICAL FIELDS. Thomassen, K. I. (Los Alamos Scientific Lab., N. Mex.). Aug 1970. Contract W-7405-eng-36. 14p. Dep. NTIS.

Stabilization of a θ-pinch plasma column by $l = 0$ and $l = 1$ coils to produce helical fields is discussed. The nature of the forces produced by helical fields is outlined and a nonlinear "bang-bang" feedback system is proposed for controlling plasma position. (auth)

27727 HIGH-FREQUENCY INSTABILITIES. Perkins, W. A. (Univ. of California, Berkeley). Methods Ex. Phys.; 9: 275-304(1970).

Driving mechanisms for hf instabilities in plasmas are discussed. The general types of particle distributions that tend to be unstable are illustrated. Linear theory is briefly discussed, and the dispersion-relation approach to predict instabilities is described. The theory for parallel and perpendicular wave vectors is presented. (M.O.W.)

27728 LOW-FREQUENCY INSTABILITIES. Yoshikawa, S. (Princeton Univ., N. J.). Methods Exp. Phys.; 9: 305-43(1970).

An attempt is made to classify the low-frequency instabilities in a collisionless plasma. Rough classifications include flute-like modes, drift instabilities (including ballooning mode), and the trapped-particle mode. Methods used in classifying these instabilities are described. (M.O.W.)

27729 COLLISIONAL DRIFT INSTABILITIES. Hendel, H. W.; Chu, T. K. (Princeton Univ., N. J.). Methods Exp. Phys.; 9: 345-94(1970).

Drift waves in a one-dimensional plasma slab are described theoretically. Drift-wave identification in a Q-machine plasma is described. The following topics are also discussed: (1) mode stabilization, (2) critical fluctuations, (3) amplitudes in stable and unstable regimes, and (4) enhanced radial plasma transport caused by collisional drift waves. (M.O.W.)

27730 INSTABILITIES OF HIGH-BETA PLASMAS. Bodin, H. A. B. (Culham Lab., Abingdon, Eng.). Methods Exp. Phys.; 9: 395-449(1970).

Systems for producing high-β plasmas are described. A theory is given for ideal and non-ideal MHD instabilities. Diagnostic techniques for high-β plasmas are described. (M.O.W.)

27731 INSTABILITIES IN PERPENDICULAR COLLISIONLESS SHOCK WAVES. Gary, S. P. (Coll. of William and Mary, Williamsburg, Va.); Biskamp, D. J. Phys., A (London); 4: L27-31(Mar 1971).

A comparison of the ion acoustic instability with the $E \times B$ electron drift instability leads to predictions concerning observations of enhanced fluctuations in perpendicular collisionless shock waves. (auth) (UK)

27732 STABILITY OF THE SCREW PINCH WITH HALL CURRENT. Malik, S. K. (Univ. of Wisconsin, Madison). J. Plasma Phys.; 5: 65-71(Jan 1971).

The stability of the screw pinch is investigated taking into account the presence of Hall current in Ohm's law. The dispersion relation is obtained as the exact solution of the characteristic value equations governing the general perturbations. It is found that the Hall current has no effect on the hydromagnetic stability of the screw pinch. (auth) (UK)

27733 STABILITY OF A TRAPPED-PARTICLE EQUILIBRIUM. Goldman, Martin V. (Univ. of California, Los Angeles. Univ. of California, Livermore); Berk, Herbert L. Phys. Fluids; 14: 801-4(Apr 1971).

A simple periodic Bernstein-Greene-Kruskal equilibrium is constructed in which trapped electrons make a small contribution to the reactive part of the one-wave dispersion relation. This contribution is found to have an important effect on stability of the wave against decay into sidebands. Enhanced growth rates and frequency shifts are calculated. (auth)

27734 CONVECTION CELL PRODUCED BY LOW-FREQUENCY FLUTE INSTABILITIES. Ohkawa, Tihiro (Gulf General Atomic Inc., San Diego, Calif.). Phys. Fluids; 14: 818-21(Apr 1971).

The structure of convection cells in a closed line system is studied. It was found that the isothermal plasma confined in a magnetic well will not dynamically reach the steady-state convecting state. The presence of a small amount of cold plasma will lead to the formation of a convection cell. (auth)

27735 PLASMA CONVECTION PRODUCED BY ION-DRIVEN DRIFT INSTABILITY. Ohkawa, Tihiro (Gulf General Atomic, Inc., San Diego, Calif.). Phys. Fluids; 14: 822-5(Apr 1971).

The low-frequency drift instability is discussed as a possible cause for plasma convection. The presence of cold plasma near the wall makes the ion-driven drift mode unstable. The resultant transport may have a rate given by the Bohm formula estimated at the temperature of the cold component. (auth)

27736 EXPLOSIVE INSTABILITIES IN SIMULATED PLASMAS. Byers, J. A.; Rensink, M. E.; Smith, J. L.; Walters, G. M. (Univ. of California, Livermore). Phys. Fluids; 14: 826-9(Apr 1971).

Nonlinear instabilities arising from the interaction of two positive energy waves and one negative energy wave were observed on a one-dimensional superparticle computer model for perpendicularly propagating, linearly stable cyclotron waves. For the case in which all three-wave amplitudes are initially equal, the theoretical predictions and experimental results on the growth of these instabilities are in good qualitative and quantitative agreement. Saturation is observed when the electrostatic energy grows to about 1% of the kinetic energy in the system, sufficient to cause significantly large changes in the equilibrium orbits. The "forward scattering" theory of Fukai, Krishan, and Harris is used to explain the qualitative behavior of the wave amplitudes and phases just prior to saturation. (auth)

27737 NUMERICAL SIMULATION OF THE WEIBEL INSTABILITY IN ONE AND TWO DIMENSIONS. Morse, R. L.; Nielson, C. W. (Los Alamos Scientific Lab., N. Mex.). Phys. Fluids; 14: 830-40(Apr 1971).

Particle-in-cell simulation methods for doing full electromagnetic simulations of collisionless plasma phenomena are described and applied to the Weibel instability in one and two dimensions. Magnetic particle trapping and subsequent mode coalescing are seen. Magnetic field energy is seen to reach 10% of the total particle energy. The different electromagnetic simulation methods are compared. (auth)

27738 EFFECT OF HELICAL INSTABILITY ON THE RADIAL DENSITY AND POTENTIAL DISTRIBUTION. Imazu, S.; (Nigata Univ., Nagaoka, Japan); Maruyama, T.; Sato, H.; Nakano, Y. Phys. Fluids; 14: 841-8(Apr 1971).

Helical instability of a positive column in a longitudinal magnetic field is investigated, assuming that the perturbed densities have finite amplitudes and that the densities of electrons and ions are perturbed independently. A relationship between the perturbed densities of charged particles and the corresponding electric field is determined by solving Poisson's equation. Furthermore, the equations describing the behavior of steady-state densities are readily solved by transforming them into the integral equation of Volterra's type. With this treatment, simplified equations of the radial distribution of the steady-state density and potential are found as functions of the amplitude of the superimposed helix for the helical mode ($m = 1$) and the phase shift between the perturbed densities of electrons and ions. The results are compared with experimental data and found to be in fair agreement with experimental values of the radial density and potential distribution. The measurements also show the onset of modes 2, 3, and a low-frequency oscillation as a function of magnetic field intensity. (auth)

27739 MODIFICATION OF THE QUASI-LINEAR EQUATIONS. Abraham-Shrauner, Barbara (Washington Univ., St. Louis). Phys. Fluids; 14: 889-91(Apr 1971).

Modified quasi-linear equations are derived for the marginally and weakly stable states of an initially unstable plasma. Comparison with computer simulations indicate the equations may explain two-dimensional but not one-dimensional plasma stabilization. (auth)

27740 WEAK-TURBULENCE ANALYSIS OF THE TWO-STREAM INSTABILITY. Smith, D. F.; Fung, P. C. W. (Stanford Univ., Calif.). J. Plasma Phys.; 5: 1-30(Jan 1971).

The effects of nonlinear interaction of plasma waves in the weak-turbulence approximation on a stream–plasma system subject to the two-stream instability are studied. The momentum distribution of the stream is assumed to be a Gaussian function and the background plasma is assumed to be a Maxwellian with a temperature T. The nonlinear wave–particle interaction of induced scattering on the polarization clouds of ions may lead to stabilization if the stream plasma waves in the resonant cone are scattered into the nonresonant region, and vice versa, leading to a well-defined average energy density in plasma waves much less than the energy density of the stream. Nonlinear scattering also causes transformation of plasma waves into electromagnetic radiation near the fundamental of the electron plasma frequency of the background plasma, and combination of two plasma waves leads to electromagnetic radiation near the second harmonic of this frequency. Expressions are given for the latter process for emission and absorption for arbitrary values of the ratio of the wave number of plasma waves to the wave number of the electromagnetic wave. The major features of the whole phenomenon are illustrated with the help of a numerical example, with conditions typical for the solar corona in which case an ion stream would be stabilized, but an electron or neutral stream (with the chosen density) would not. (auth) (UK)

27741 STABILIZATION OF DRIFT WAVES BY A NONUNIFORM HIGH-FREQUENCY FIELD. Gutkin, T. I.; Boleslavskaya, G. I. (Physical-Technical Inst., Sukhumi, USSR). Nucl. Fusion; 11: 167-74(Mar 1971).

The interaction of a high-frequency electromagnetic field with a magnetized inhomogeneous plasma is considered. From kinetic and Maxwellian equations a system of equations is obtained that describes the linear oscillations of an inhomogeneous plasma. The dispersion relation is given for the potential oscillations. The results are obtained for the limiting case of long waves $k_\perp \rho_A \to 0$. Three types of drift instability are considered: (a) electronic drift instability; (b) slow ion-acoustic waves, and (c) drift-temperature instability. It is shown that, by applying an hf field having a certain frequency and intensity, it is possible to enlarge the region of stability against drift oscillations in an inhomogeneous magnetized plasma. When an hf field is applied, the stability region for a fast ion-acoustic wave grows considerably in the direction of negative values of η_e. Stabilization occurs as a result of the increased oscillation frequency that accompanies the application of the hf field, and this in turn intensifies Landau damping by the electrons. The stabilizing effect on the hf field pressure is associated with a Doppler shift resulting from plasma particle drift with velocity $g/\omega_{H\alpha}$ (g is the effective acceleration due to gravity with allowance for the potential forces in a nonperturbed state). The sign of the growth rate of the slow ion-acoustic wave does not change when the hf field is applied, but its value decreases considerably. The hf magnetic field stabilizes the drift-temperature instability for negative values of η_i. (auth)

27742 FEEDBACK STABILIZATION IN PLASMAS. Thomassen, K. I. (Massachusetts Inst. of Tech., Cambridge). Nucl. Fusion; 11: 175-86(Mar 1971).

By using feedback control techniques a variety of plasma instabilities were suppressed. In all cases these instabilities have long wavelengths, low azimuthal wave numbers, and simple radial dependence. This minimizes control problems associated with the spatial variation of the mode. Drift waves, gravitational flutes, ion sound waves, Kelvin–Helmholtz "edge oscillations," and other instabilities were feedback-stabilized using a variety of control systems. This review attempts to illuminate the problems of feedback control in plasmas by a study of the work in this field. (auth)

27743 STABILITY OF MICROWAVE-HEATED PLASMAS. Guest, G. E.; Sigmar, D. J. (Oak Ridge National Lab., Tenn.). Nucl. Fusion; 11: 151-9(Mar 1971).

Magnetically confined plasmas, created and heated by electromagnetic fields near the electron gyrofrequency, can support several modes of instability driven by inherent temperature anisotropy or possible loss-cone effects. If $T_\parallel \ll T_\perp$, both electrostatic and electromagnetic waves can grow in time; while if $T_\parallel \to T_\perp$, electrostatic waves at the hybrid frequency can be driven unstable by the loss-cone effect. Here the relevant known criteria are reviewed, and several new criteria to describe the stabilization of the temperature-anisotropy modes as $T_\parallel \to T_\perp$ are developed. The results of a detailed analysis of the electrostatic loss-cone mode, for which temporal growth rates greater than anticipated electron bounce frequencies are obtained only for electron densities near microwave cutoff, are also reported. (auth)

27744 INSTABILITIES OF A HIGH-PRESSURE PLASMA CONTAINED BY A DENSE BLANKET OF NEUTRAL GAS. Mikhailovskii, A. B.; Friedman, A. M.; Tsypin, V. S. (Inst. of Atomic Energy, Moscow). Nucl. Fusion; 11: 123-6(Mar 1971).

Instabilities are examined in an inhomogeneous plasma whose pressure, p, is balanced by the pressure of a dense blanket of neutral gas and is large compared with the pressure of the magnetic field, $B^2/8\pi$, $\beta \equiv 8\pi p/B^2 \gg 1$. It was shown earlier that with $\partial \ln B/\partial \ln n \geq 0$ (n being the plasma density) instabilities may arise in such plasma with a growth rate of the order of the gradient frequency, $\gamma \simeq \omega_n$, and a longitudinal wave number $k_z \omega_n/v_{T_i}$, v_{T_i} being the thermal velocity of the ions. Where $\partial \ln B/\partial \ln n < 0$ such dangerous instabilities do not arise; hence this represents the most favorable conditions of containment. However, it is shown that even in these conditions the plasma is not free of instabilities. It is established that with $\partial \ln B/\partial \ln n < 0$ perturbations with a large k_z value can arise, e.g. $k_z \gtrsim \omega_n/v_{T_i}$. However, the growth k rate of such perturbations is small by comparison with the frequency $\gamma \approx (k_\perp \rho_i)^2 \sqrt{\beta}\omega_{ni}$ (where $k_\perp$ is the transverse wave number and ρ_i the Larmor ion radius). (auth)

27745 STABILIZING EFFECT OF A HIGH-FREQUENCY MAGNETIC FIELD ON THE TRAPPED-PARTICLE INSTABILITY. Ross, D. W.; Pogutse, O. P. (International Centre for Theoretical Physics, Trieste, Italy). Nucl. Fusion; 11: 127-31(Mar 1971).

The stabilizing effect which an oscillating magnetic field of frequency Ω perpendicular to the main toroidal field has on the collisionless trapped-particle instability is studied for frequencies in the range $\omega_{be} < \Omega < \Omega_i$, where ω_{be} is the electron bounce frequency and Ω_i is the ion cyclotron frequency. It is found that the fastest-growing modes are stabilized when $\epsilon^{\frac{1}{2}} k_\perp \bar{v}_e B_l/\Omega B_0 > 1$, where $k_\perp$ is the wave number perpendicular to the main field $\vec{B}_0$, $\bar{v}_e$ is the electron thermal velocity, B_l is the amplitude of the oscillating field, and $\epsilon^{-1} = R_0/r$, the aspect ratio. The extension of the calculation to other modes is discussed, and an additional example is given. (auth)

27746 EFFECTS OF COLD PLASMA ON THE NEGATIVE MASS INSTABILITY OF A RELATIVISTIC ELECTRON LAYER. Lau, Y. Y.; Briggs, R. J. (Massachusetts Inst. of Tech., Cambridge). Phys. Fluids; 14: 967-76(May 1971).

The stability of a cylindrical layer of gyrating relativistic electrons (E layer), both in vacuum and in a cold plasma, is examined. The beam model assumes concentric particle orbits and allows for a finite thickness of the E layer. It is shown that the background plasma can stabilize the lower azimuthal modes (modes with their frequency less than the cold cyclotron frequency, or azimuthal wavenumber l less than the relativistic mass factor γ). The mechanism of stabilization can be interpreted in terms of an inductive impedance at the beam edge due to the cold plasma. The interaction of the beam with the plasma at the upper hybrid frequency is discussed briefly. (auth)

27747 UNIVERSAL DRIFT INSTABILITY IN A COLLISIONAL PLASMA. Bhadra, Dilip K. (Gulf General Atomic Co., San Diego, Calif.). Phys. Fluids; 14: 977-86(May 1971).

The effect of electron–ion collisions on the "universal" drift instability in an inhomogeneous plasma, using a Fokker–Planck collision operator, is considered and compared with the results obtained using the Bhatnagar, Gross, and Krook model. It is found that for small collision frequency, the BGK model gives a destabilizing effect while the Fokker–Planck model indicates a stabilizing effect. For larger values of collision frequency, growth rates for collisional drift waves increase in both models but the growth rate obtained from the Fokker–Planck model is not nearly as high as would be expected from the results derived from the Krook model calculations. For very large collision frequency, growth rates tend to vanish in both models. (auth)

27748 HYDROMAGNETIC STABILITY OF THE BENNETT PINCH. Harris, Edward G.; Kaneko, Shobu (Univ. of Tennessee, Knoxville. Oak Ridge National Lab., Tenn.). Phys. Fluids; 14: 987-9(May 1971).

The hydromagnetic energy principle is applied to the derivation of a sufficient condition for the hydromagnetic stability of the linear Bennett pinch. The instabilities can be divided into unlocalized modes in which the most dangerous ones are the kink mode and localized modes. A sufficient condition for stability of the kink mode is $\beta_z < (9/25)\ (r_0/R)^2$ for $(r_0/R)^2 < 3.75$ where β_z is the toroidal β and r_0 and $2\pi R$ are the mean radius and the length of the pinch, respectively. The linear Bennett pinch is unstable for localized Suydam modes. But these unstable modes can be stabilized if

the pinch is bent into a torus. The above stability condition against the kink instability may be considered as a sufficient condition for stability of a toroidal Bennett pinch. (auth)

27749 DYNAMIC STABILIZATION OF THE SCREW PINCH. Berge, G.; Freidberg, J. P. (Los Alamos Scientific Lab., N. Mex.). Phys. Fluids; 14: 1035-6(May 1971).

A method is presented for dynamically stabilizing the m = 1 mode in a screw pinch. (auth)

27750 BOUNDARY CONDITIONS FOR CONVECTIVE WAVE INSTABILITIES IN MIRROR MACHINES. Berk, Herbert L. (Univ. of California, Livermore). Phys. Fluids; 14: 1036-8 (May 1971).

Wave behavior at the ends of a mirror machine is sensitive to the shape of the electron distribution and the containment forces. However, it is shown by dimensional considerations that wave damping without reflection can be achieved experimentally. (auth)

27751 TEARING-MODE INSTABILITY. Gibson, R. D. (Teesside Polytechnic, Middlesbrough, Eng.); Kent, A. Quart. J. Mech. Appl. Math.; 24: 63-80(Feb 1971).

The instability that arises in a layer of fluid of finite conductivity in the presence of a sheared magnetic field is considered. Using the method of matched asymptotics the limit of small resistivity is treated and stability criteria are derived. A uniformly valid asymptotic treatment of the logarithmic singularity (a feature of singular perturbation problems of the type treated herein) is presented. (auth) (UK)

27752 FEEDBACK AND DYNAMIC CONTROL OF PLASMAS. AIP Conference Proceedings Held at Princeton, N. J., June 1970. Number 1. Chu, T. K.; Hendel, H. W. (eds.). New York; American Institute of Physics (1970). 374p. (CONF-700616-(Vol.1)).

Separate abstracts were prepared for 43 of the included articles. (M.O.W.)

For abstracts of individual papers see: 27676, 27677, 27702, 27703, and 27753-27791.

27753 FEEDBACK STABILIZATION OF A VLASOV PLASMA. Cotsaftis, M. (Centre d'Etudes Nucleaires, Fontenay-aux-Roses, France). pp 1-5 of Feedback and Dynamic Control of Plasmas. /Chu, T. K. (ed.). New York; American Institute of Physics (1970).

From Symposium on feedback and dynamic control of plasmas; Princeton, N. J. (18 Jun 1970).

The complete Maxwell-Vlasov equations, together with feedback, are analyzed in the quasi-homogeneous case, using the Nyquist criterion. A class of feedback loops, satisfying sufficient conditions for stability but depending on the wave number k, is found. If the instability satisfies certain properties, a subclass of feedback loops, independent of the wave number, can be constructed. The classical amplification-delay feedback, generally used in experiments, does not belong to the subclass; and therefore designing an adapted feedback loop is of importance. Applications of the general theory to the low-frequency electrostatic microinstability and the double-beam instability are given. (auth)

27754 GEOMETRICAL LIMITATIONS IN PLASMA FEEDBACK SYSTEMS. Crowley, Joseph M. (Univ. of Illinois, Urbana). pp 12-16 of Feedback and Dynamic Control of Plasmas. /Chu, T. K. (ed.). New York; American Institute of Physics (1970).

From Symposium on feedback and dynamic control of plasmas; Princeton, N. J. (18 Jun 1970).

Based on the dispersion relation of the individual mode, a stability criterion accounting for the geometrical effects that inherently limit detection and enforcing processes of feedback systems while neglecting the nonlinear mode coupling effects, is formulated. If the criterion predicts instability, the plasma should be considered unstable. If the criterion predicts stability below a certain value of feedback gain, however, the plasma may in fact be unstable under those conditions; but a reduction in gain will always lead to stability. The agreement between stable operating regions predicted by this criterion and by earlier exact analysis shows acceptable agreement for design purposes. (auth)

27755 GENERALIZED BOUNDARY CONDITIONS OF PLASMA FEEDBACK SYSTEMS. Lindman, E. L. (Univ. of Texas, Austin). pp 17-22 of Feedback and Dynamic Control of Plasmas. /Chu, T. K. (ed.). New York; American Institute of Physics (1970).

From Symposium on feedback and dynamic control of plasmas; Princeton, N. J. (18 Jun 1970).

General boundary conditions of plasma-feedback systems that use electrodes simultaneously as both sensor and suppressor at plasma boundaries are discussed. Difference equations describing the electrical properties of the boundary are derived and converted to differential equations that lead to a boundary dispersion relation describing the boundary modes and their interaction with the plasma. Application to Kelvin-Helmholtz instability is given. (auth)

27756 PLASMA STABILIZATION BY FEEDBACK. Taylor, J. B.; Lashmore-Davies, C. N. (United Kingdom Atomic Energy Authority, Abingdon, Eng.). pp 23-6 of Feedback and Dynamic Control of Plasmas. /Chu, T. K. (ed.). New York; American Institute of Physics (1970).

From Symposium on feedback and dynamic control of plasmas; Princeton, N. J. (18 Jun 1970).

A simple model is discussed that illustrates the general features of plasma stabilization by an external feedback system. This indicates that different phase relations in the feedback loop are needed to stabilize differing classes of electrostatic instability. (auth)

27757 STABILIZATION OF A LOW-DENSITY PLASMA IN A SIMPLE MAGNETIC MIRROR BY FEEDBACK CONTROL. Lashmore-Davies, C. N. (United Kingdom Atomic Energy Authority, Abingdon, Eng.). pp 27-32 of Feedback and Dynamic Control of Plasmas. /Chu, T. K. (ed.). New York; American Institute of Physics (1970).

From Symposium on feedback and dynamic control of plasmas; Princeton, N. J. (18 Jun 1970).

Stabilization of an electrostatic flute-type instability occurring in a simple magnetic mirror by feedback techniques is discussed. In the first part of the paper a diffuse plasma is considered. The effect of varying the locations of the sensing and suppressing systems is found to alter the stability threshold significantly. In the second part a sharp-boundary plasma is considered, and phase shift and frequency response are included in the feedback terms. (auth)

27758 PLASMA CONTROL WITH INFRARED LASERS. Chen, F. F. (Univ. of California, Los Angeles). pp 33-7 of Feedback and Dynamic Control of Plasmas. /Chu, T. K. (ed.). New York; American Institute of Physics (1970).

From Symposium on feedback and dynamic control of plasmas; Princeton, N. J. (18 Jun 1970).

An extraordinary electromagnetic wave of large amplitude will produce a quasi-linear dc drift of electrons relative to ions that can be modulated for feedback stabilization of low-frequency waves. The effect occurs at the upper hybrid resonance. A promising way to penetrate the cutoff in a fusion plasma is to use the nonlinear interaction of two CO_2 laser beams to produce a difference frequency near ω_h. The cold plasma analysis was extended for this process, and it was found that the intensities required are not unreasonable even when thermal effects are taken into account. (auth)

27759 FEEDBACK STABILIZATION OF HYDROMAGNETIC CONTINUA: REVIEW AND PROSPECTS. Melcher, J. R. (Massachusetts Inst. of Tech., Cambridge). pp 38-53 of Feedback and Dynamic Control of Plasmas. /Chu, T. K. (ed.). New York; American Institute of Physics (1970).

From Symposium on feedback and dynamic control of plasmas; Princeton, N. J. (18 Jun 1970).

Three types of analytical models for determining adequate feedback spatial and temporal resolution are distinguished for representing dynamics with finite sampling: piecewise continuous, ("spliced") discrete coupled modes, and coupled wavetrains. The stabilization of the $z-\theta$ pinch is used for comparing the various representations, particularly as they represent a quasi-one-dimensional model for the m = 1 modes, and specific stability regimes are given. The advantages of the modal and wavetrain approaches in describing three-dimensional effects are illustrated, with the wavetrain approach shown as particularly convenient for systems having many potentially unstable wavelengths within the system boundaries, hence necessitating many sampling stations. A discussion of difficulties in stabilizing interchange modes is given, and nonlinear forms of "bang-bang" feedback obviating these difficulties suggested. (auth)

27760 NONLINEAR STABILIZATION OF A CONTINUUM. Millner, A. R.; Parker, R. R. (Massachusetts Inst. of Tech., Cambridge). pp 54-9 of Feedback and Dynamic Control of Plasmas. /Chu, T. K. (ed.). New York; American Institute of Physics (1970).

From Symposium on feedback and dynamic control of plasmas; Princeton, N. J. (18 Jun 1970).

Nonlinear, or "bang-bang," feedback, in which a constant corrective force of arbitrary strength is applied to the plasma for as long a time as the local average of the surface displacement is

XU

positive, is discussed for the stabilization of MHD modes. It is shown that, in addition to obvious bandwidth and impedance-level problems, linear feedback cannot stabilize modes for which the perturbation amplitude is constant along the lines of the external magnetic field. Plasma stability with "bang–bang" feedback scheme is studied using an energy principle (Liapunov function). Although attention is focused on modes whose amplitude is constant along B_0, the proposed scheme can be applied to stabilize all other modes as well. (auth)

27761 VIDEOTYPE SAMPLING IN THE FEEDBACK STABILIZATION OF ELECTROMECHANICAL EQUILIBRIA. Dressler, John L. (Massachusetts Inst. of Tech., Cambridge). pp 60–7 of Feedback and Dynamic Control of Plasmas. /Chu, T. K. (ed.). New York; American Institute of Physics (1970).

From Symposium on feedback and dynamic control of plasmas; Princeton, N. J. (18 Jun 1970).

The feedback control of hydromagnetically contained plasmas with dimensions large compared to potentially unstable wavelengths requires a large number of spatially distributed feedback sensors and drivers. The multiplicity of signals to be amplified and processed suggests the use of computers or other discrete-time devices that handle signals on a "time-sharing" basis. Typically, scanning techniques are envisioned to sense and drive, thus introducing to an analytical representation discreteness in both time and space. A general method, based on the Fourier superposition of wavetrains, is developed to describe infinite continuum systems with discrete spatial and temporal feedback. Dynamics are represented by a generalization of the dispersion equation, with Z transforms used to provide closed-form expressions if the discreteness is in space or in time only. The Bers–Briggs criterion is generalized to differentiate between absolute instabilities and amplifying waves with the discrete feedback. A quasi-one-dimensional model for the m = 1 mode of the $z-\theta$ pinch is studied to delineate effects of spatial and temporal sampling rates on stability regimes. (auth)

27762 FEEDBACK CONTROL OF KRUSKAL–SHAFRANOV MODES. Clarke, J. F.; Dory, R. A. (Oak Ridge National Lab., Tenn.). pp 68–73 of Feedback and Dynamic Control of Plasmas. /Chu, T. K. (ed.). New York; American Institute of Physics (1970).

From Symposium on feedback and4ynamic control of plasmas; Princeton, N. J. (18 Jun 1970).

Kruskal–Shafranov modes on a cylindrical plasma are examined with respect to possible active feedback stabilization. Active stabilization of these modes, which would make tokamak reactors more realizable, is found to be possible in principle but to present great practical difficulties. The application of the technique to a reactor-type plasma is considered. (auth)

27763 FEEDBACK CONTROL PROBLEMS IN TOKAMAKS. Furth, H. P.; Rutherford, P. H. (Princeton Univ., N. J.). pp 74–9 of Feedback and Dynamic Control of Plasmas. /Chu, T. K. (ed.). New York; American Institute of Physics (1970).

From Symposium on feedback and dynamic control of plasmas; Princeton, N. J. (18 Jun 1970).

In the basic tokamak experiment, the copper shell is a highly satisfactory feedback control device. For certain extensions of the tokamak operation—for example, to compression heating—it is, however, convenient to remove the copper shell. External feedback control of the equilibrium position is then a natural substitute. A more complex problem is the feedback stabilization of MHD modes. The interchange instabilities, against which linear magnetic feedback is ineffective, are fortunately stabilized by the minimum-average-B property of the toroidal tokamak. Feedback stabilization of a type of thermal instability that results in major-radius shifts is discussed. (auth)

27764 FEEDBACK STABILIZATION OF A HIGH-β, SHARP-BOUNDARIED PLASMA COLUMN WITH HELICAL FIELDS. Ribe, F. L. (Los Alamos Scientific Lab., N. Mex.); Rosenbluth, M. N. pp 80–3 of Feedback and Dynamic Control of Plasmas. /Chu, T. K. (ed.). New York; American Institute of Physics (1970).

From Symposium on feedback and dynamic control of plasmas; Princeton, N. J. (18 Jun 1970).

A sharp-boundaried high-β Stellarator of l-fold helical symmetry is MHD unstable, particularly to the m = 1, long-wavelength mode. For this mode the instability is driven by $l \pm 1$ fields introduced by the unstable displacement. Compensating fields (or, equivalently, plasma distortions) to counteract the instability can be introduced externally and controlled by a feedback arrangement. The self-adjointness property of the MHD energy-principle operator is used to derive the relationship between the external fields and the unstable displacement. (auth)

27765 NONLINEAR COLLISIONLESS INTERACTION BETWEEN ELECTRON AND ION MODES AND FEEDBACK STABILIZATION IN FUSION PLASMAS. Wong, A. Y.; Baker, D. R.; Booth, N. (Univ. of California, Los Angeles). pp 84–93 of Feedback and Dynamic Control of Plasmas. /Chu, T. K. (ed.). New York; American Institute of Physics (1970).

From Symposium on feedback and dynamic control of plasmas; Princeton, N. J. (18 Jun 1970).

An efficient method of interaction with ion modes in fusion and space plasmas through the excitation of resonant electron modes is proposed. The feasibility was demonstrated in laboratory experiments over a wide density range (10^8 to 10^{10}/cm^3) and a wide ion frequency range (1 kHz to 500 kHz). The collisionless nature of the nonlinear interaction between electron and ion modes is emphasized, leading to the feasibility of feedback stabilization in hot collisionless fusion plasmas. Measurements of nonlinear coupling coefficients are presented that support the theoretical mode–mode coupling model. (auth)

27766 REMOTE FEEDBACK STABILIZATION OF DRIFT INSTABILITY BY MICROWAVES. Chu, T. K.; Hendel, H. W.; Perkins, F. W.; Simonen, T. C. (Princeton Univ., N. J.). pp 94–102 of Feedback and Dynamic Control of Plasmas. /Chu, T. K. (ed.). New York; American Institute of Physics (1970).

From Symposium on feedback and dynamic control of plasmas; Princeton, N. J. (18 Jun 1970).

A modulated microwave source is used in remote feedback stabilization of the collisional drift instability in a Q-machine cesium plasma at $n \simeq 5 \times 10^{10}$ cm^{-3}. The microwave heats electrons by resonance absorption at interior plasma locations selected by adjusting the microwave frequency to the local upper-hybrid frequency $[f_{ce}^2 + f_{pe}^2]^{\frac{1}{2}} \simeq 11$ GHz. Penetration of the evanescent exterior plasma region is achieved by introducing a weak magnetic field gradient ($\nabla B/B \approx 0.03$ cm$^{-1} \ll \nabla n/n \approx 1$ cm^{-1}) with an iron block placed outside the plasma column. The modulation phase (<180°) and microwave amplitude (≈0.1 mW) necessary for stabilization agree qualitatively with a linear theory including a modulated heat source. Upon stabilization, improved plasma confinement is measured. (auth)

27767 EXPERIMENTS AND INTERPRETATION OF RESULTS CN THE FEEDBACK STABILIZATION OF VARIOUS PLASMA INSTABILITIES. Keen, B. E. (United Kingdom Atomic Energy Authority, Abingdon, Eng.). pp 103–13 of Feedback and Dynamic Control of Plasmas. /Chu, T. K. (ed.). New York; American Institute of Physics (1970).

From Symposium on feedback and dynamic control of plasmas; Princeton, N. J. (18 Jun 1970).

Experimental results are reported on the feedback stabilization of a "drift-type" instability and on the remote sensing and feedback stabilization by amplitude modulation with electron–cyclotron resonance heating of ion-sound instability. For the "drift-type" instability, results are interpreted in terms of an equation of Van der Pol type; for the ion-sound instability, in terms of a theory predicting the variation of instability amplitude and frequency due to the feedback modulation of electron temperature. Comparison between the theory and experiment shows good agreement. (auth)

27768 FEEDBACK SUPPRESSION OF COLLISIONLESS, MULTI-MODE DRIFT-CENTRIFUGAL WAVES IN A MIRROR-CONFINED PLASMA. Lindgren, N. E.; Birdsall, C. K. (Univ. of California, Berkeley). pp 114–18 of Feedback and Dynamic Control of Plasmas. /Chu, T. K. (ed.). New York; American Institute of Physics (1970).

From Symposium on feedback and dynamic control of plasmas; Princeton, N. J. (18 Jun 1970).

Simultaneous suppression of several modes of the drift-centrifugal wave in a collisionless plasma was achieved by using as many independent feedback systems, each one tuned to a different mode. This is an improvement over broadband systems in which suppression of one mode has generally led to enhancement of other modes. (auth)

27769 FEEDBACK APPLICATIONS TO BASIC PLASMA INSTABILITY EXPERIMENTS. Simonen, Thomas C. (Princeton Univ., N. J.). pp 119–28 of Feedback and Dynamic Control of Plasmas. /Chu, T. K. (ed.). New York; American Institute of Physics (1970).

From Symposium on feedback and dynamic control of plasmas; Princeton, N. J. (18 Jun 1970).

Feedback was applied, as a diagnostic technique, to measure properties of low-frequency instabilities. Feedback-stabilized plasmas provide equilibria in which the temporal growth of instabilities to nonlinear saturation levels and the effect of instability on confinement can be measured by switching feedback

XUM

off. Enhancement of instability amplitudes by positive feedback above the decay-instability threshold value, can be employed to destabilize parametrically excited decay modes. Experiments with theories illustrating such feedback applications to the collisional drift instability are described. (auth)

27770 CHARACTERISTICS OF A MODIFIED FEEDBACK CONTROL METHOD APPLIED TO EDGE OSCILLATIONS IN A Q MACHINE. Mueller, G. L. J.; Corbin, J. C.; Palmer, R. S. (Aerospace Research Labs., Wright Patterson AFB, Ohio). pp 129-37 of Feedback and Dynamic Control of Plasmas. /Chu, T. K. (ed.). New York; American Institute of Physics (1970).

From Symposium on feedback and dynamic control of plasmas; Princeton, N. J. (18 Jun 1970).

Experimental results on the feedback control of an "edge-type" oscillation in a Q machine, using a fixed-amplitude drive signal phase- and frequency-locked to the plasma oscillation, are reported. Results are compared with stationary solutions of a theoretical model described by a second-order linear differential equation. In connection with this theory, growth rates and ac coupling between suppressor probe and plasma are measured and compared with calculated values. The method provides a means of measuring radial plasma losses caused by this instability. (auth)

27771 PASSIVE FEEDBACK STABILIZATION. Carlyle, David C. (Univ. of Texas, Austin). pp 138-41 of Feedback and Dynamic Control of Plasmas. /Chu, T. K. (ed.). New York; American Institute of Physics (1970).

From Symposium on feedback and dynamic control of plasmas; Princeton, N. J. (18 Jun 1970).

A single-ended Q-machine was modified to provide for the study of generalized boundary conditions. The sections of the segmented boundary can be interconnected through passive components to provide passive feedback. The ion density fluctuation amplitude of the Kelvin–Helmholtz instability, for densities of ~10^8 to 10^9 cm^{-3} and magnetic fields of ~1 to 2 kG, decreased by 20 to 40% when feedback is applied. The dc peak density is increased by ~10 to 30% upon stabilization. The effect shows a definite dependence on the capacitance and resistance in the passive circuitry. (auth)

27772 FEEDBACK STABILIZATION OF THE TRANSVERSE KELVIN–HELMHOLTZ INSTABILITY: EXPERIMENT AND THEORY. Chu, T. K.; Hendel, H. W.; Jassby, D. L.; Simonen, T. C. (Princeton Univ., N. J.). pp 142-8 of Feedback and Dynamic Control of Plasmas. /Chu, T. K. (ed.). New York; American Institute of Physics (1970).

From Symposium on feedback and dynamic control of plasmas; Princeton, N. J. (18 Jun 1970).

By modulating the electron current flow to an electrostatic probe immersed in the plasma, the Kelvin–Helmholtz instability driven primarily by transverse velocity shear at the edge of a Q-machine plasma column is feedback stabilized. The measured feedback gain and phase delay and the oscillation frequency shift are in reasonable agreement with predictions from linear-theory quadratic-form representations constructed from the appropriate radial wave equation. Upon stabilization. the plasma density in the plasma interior increases. (auth)

27773 FEEDBACK EXPERIMENTS ON MULTIMODE IONIZATION WAVES. Garscadden, A.; Bletzinger, P. (Aerospace Research Labs., Wright Patterson AFB, Ohio). pp 149-59 of Feedback and Dynamic Control of Plasmas. /Chu, T. K. (ed.). New York; American Institute of Physics (1970).

From Symposium on feedback and dynamic control of plasmas; Princeton, N. J. (18 Jun 1970).

The influence of feedback and external driving signals on growth and saturation of ionization waves in a finite-length positive column discharge was investigated. Inserting a frequency-swept driving signal, the ionization wave response exhibits eigenmodes that are equally spaced on the wavenumber axis. In the absence of any external perturbation, only one mode is spontaneously excited. By external feedback the dominant ionization wave can be caused to mode jump. With external electrodes, the mode changes occurred from the cathode and propagated with a finite velocity (approximately that of the group velocity of the waves). Measurements of the spatial gain and its saturation for different discharge currents (or gain) are compared with the Landau saturation formula to give gain and saturation coefficients. (auth)/

27774 OBSERVATION OF PLASMA DISPLACEMENT DUE TO DIPOLE CURRENT NEAR A HIGH-BETA PLASMA COLUMN. Newton, A. A.; Junker, J.; Bodin, H. A. B. (United Kingdom Atomic Energy Authority, Abingdon, Eng.). pp 166-9 of Feedback and Dynamic Control of Plasmas. /Chu, T. K. (ed.). New York; American Institute of Physics (1970).

From Symposium on feedback and dynamic control of plasmas; Princeton, N. J. (18 Jun 1970).

Plasma displacement due to dipole current near a high-beta plasma column is observed and interpreted. Its application to high-beta plasma feedback experiments is discussed. (auth)

27775 FEEDBACK EXPERIMENTS IN A HOT ELECTRON PLASMA. Haste, Glenn (Oak Ridge National Lab., Tenn.). pp 177-87 of Feedback and Dynamic Control of Plasmas. /Chu, T. K. (ed.). New York; American Institute of Physics (1970).

From Symposium on feedback and dynamic control of plasmas; Princeton, N. J. (18 Jun 1970).

A plasma formed by electron cyclotron heating operates in one of two modes: a high-density mode above a transition pressure (~5×10^{-6}) and a low-density mode below. Below the transition pressure the plasma is unstable to flutes due to the electron drift. It was found that instability signals that are fed back to an electrode at the radial edge of the plasma alter the instability markedly. The frequency spectrum is reduced from a broad spectrum to a single frequency associated with self-induced oscillations. The fluctuations in electron density associated with the flute signals are eliminated. The mean density remains about at the same level when feedback is applied. (auth)

27776 FEEDBACK STABILIZATION OF THE RAREFIED PLASMA CYCLOTRON INSTABILITY. Chuyanov, V. A.; Liktenshtein, V. Kh.; Panov, D. A.; Zhil'tsov, V. A. (Kurchatov Inst. of Atomic Energy, Moscow). pp 188-98 of Feedback and Dynamic Control of Plasmas. /Chu, T. K. (ed.). New York; American Institute of Physics (1970).

From Symposium on feedback and dynamic control of plasmas; Princeton, N. J. (18 Jun 1970).

A surface of finite conductivity placed parallel to the plasma boundary can absorb enough energy to suppress the long-wavelength, unstable, low-increment oscillations. Feedback systems with regulated amplification and phase shift work like such a surface. Using such regulated feedback control as artificial damping, experiments were carried out in the OGRA-2 mirror machine. The results demonstrated the possibility of suppressing unstable cyclotron oscillations of different mode structure and showed that the broadening of the confined ion spectra is connected with the symmetrical mode of oscillation and the axial expansion of the plasma is connected with the antisymmetrical mode. (auth)

27777 DYNAMIC STABILIZATION OF PLASMA INSTABILITIES. Lashinsky, Herbert (Univ. of Maryland, College Park); Dewan, Edmond M. pp 199-205 of Feedback and Dynamic Control of Plasmas. /Chu, T. K. (ed.). New York; American Institute of Physics (1970).

From Symposium on feedback and dynamic control of plasmas; Princeton, N. J. (18 Jun 1970).

Methods for dynamic stabilization of plasma instabilities can be divided into two classes: (1) closed-loop and (2) open-loop. In the former case the correction forces are derived from the instability; in the latter case they are essentially independent. The two approaches are discussed, and analog-computer results that demonstrate open-loop dynamic stabilization of the van der Pol oscillator are described. Possible applications to the suppression of plasma instabilities are discussed. (auth)

27778 DYNAMIC STABILIZATION OF A CONFINED PLASMA. Samain, A. (Centre d'Etudes Nucleaires, Fontenay-aux-Roses, France). pp 206-9 of Feedback and Dynamic Control of Plasmas. /Chu, T. K. (ed.). New York; American Institute of Physics (1970).

From Symposium on feedback and dynamic control of plasmas; Princeton, N. J. (18 Jun 1970).

The stabilization of a magnetically confined plasma by the presence of an hf potential is discussed. The amplitude of the hf potential may be reduced if it is modulated with a short period along the direction of the density gradient. (auth)

27779 DYNAMIC STABILIZATION OF DRIFT WAVES IN A COLLISIONLESS PLASMA BY AC ELECTRIC FIELDS. Dobrowolny, M. (CNEN, Frascati, Italy). pp 210-13 of Feedback and Dynamic Control of Plasmas. /Chu, T. K. (ed.). New York; American Institute of Physics (1970).

From Symposium on feedback and dynamic control of plasmas; Princeton, N. J. (18 Jun 1970).

The influence of an ac electric field parallel to the confining magnetic field on low-frequency instabilities in an inhomogenous collisionless low-β plasma was considered. Stabilization effects were found for a majority of unstable drift waves. Corresponding stability criteria in terms of the electric field amplitude and conditions on the modulation frequency are given. (auth)

27780 DYNAMIC STABILIZATION OF THE DRIFT DISSIPATIVE INSTABILITY BY AN INHOMOGENEOUS RF FIELD. Lepechinsky, D.; Rolland, P.; Teichmann, J. (Centre d'Etudes Nucleaires, Saclay, France). pp 214-20 of Feedback and Dynamic Control of Plasmas. /Chu, T. K. (ed.). New York; American Institute of Physics (1970).

From Symposium on feedback and dynamic control of plasmas; Princeton, N. J. (18 Jun 1970).

The effect of an rf electric field of frequency Ω oriented parallel to a static magnetic field, and having a gradient in the radial direction of the plasma column, on the drift dissipative instability is studied using two-fluid equations. When Ω is greater than the collision frequency of the electrons, the presence of a gradient of the rf field reduces the minimum value of this field required for complete stabilization by more than an order of magnitude when compared with the value for the case of zero rf gradient. (auth)

27781 INFLUENCE OF HIGH-FREQUENCY FIELD ON PLASMA INSTABILITIES. Ivanov, A. A.; Murav'ev, V. F. (Kurchatov Inst. of Atomic Energy, Moscow). pp 221-5 of Feedback and Dynamic Control of Plasmas. /Chu, T. K. (ed.). New York; American Institute of Physics (1970).

From Symposium on feedback and dynamic control of plasmas; Princeton, N. J. (18 June 1970).

The results of theoretical investigations of high-frequency stabilization of plasma instabilities are reported. The ordinary wave and helicon-type wave are shown to suppress electrostatic instabilities with frequencies small compared to the frequency of the stabilizing wave. The comparison of two modes of stabilization showed that for "loss-cone" instability helicon stabilization is more preferable. An explanation of the stabilization mechanism is given. (auth)

27782 ELECTRON–ION COLLISION EFFECTS ON PARAMETRIC INSTABILITY. Stern, R. A. (Bell Telephone Labs., Whippany, N. J.). pp 226-30 of Feedback and Dynamic Control of Plasmas. /Chu, T. K. (ed.). New York; American Institute of Physics (1970).

From Symposium on feedback and dynamic control of plasmas; Princeton, N. J. (18 Jun 1970).

The choice of high-frequency fields in dynamic stabilization schemes is often limited, because the stabilizing field may serve as a pump for driving parametric instabilities in the plasma. The dependence of the parametric instability growth rate on electron–ion collisions in a plasma is investigated. Sharp enhancement of the complex plasma conductivity near $\omega \approx \omega_p$, in the presence of ion correlations, is shown to have dramatic effects on this growth rate. (auth)

27783 DYNAMIC STABILIZATION OF HIGH-β PLASMAS. Troyon, F. (Centre de Recherches en Physique des Plasmas, Lausanne, Switzerland). pp 231-8 of Feedback and Dynamic Control of Plasmas. /Chu, T. K. (ed.). New York; American Institute of Physics (1970).

From Symposium on feedback and dynamic control of plasmas; Princeton, N. J. (18 Jun 1970).

A discussion of various types of dynamic stabilization schemes for high-β plasmas with sharp boundary is presented. The influence of the plasma model on stability is illustrated by exact numerical calculations that indicate the problems of parametric excitation of resonances. As a particular case, the results of Wolf's fluid experiments are reproduced. (auth)

27784 DYNAMIC STABILIZATION OF MHD INSTABILITIES. Wobig, H.; Tasso, H. (Institut fuer Plasmaphysik GmbH, Garching, Ger.). pp 239-44 of Feedback and Dynamic Control of Plasmas. /Chu, T. K. (ed.). New York; American Institute of Physics (1970).

From Symposium on feedback and dynamic control of plasmas; Princeton, N. J. (18 Jun 1970).

The stability of the periodic solutions of the time-dependent MHD equations in the Eulerian form is investigated. The Floquet theory for systems with periodic coefficients is generalized to this problem. An expansion procedure with respect to the amplitude ϵ of the oscillating solution about a static equilibrium is applied to calculate the stability conditions. (auth)

27785 DYNAMIC STABILIZATION OF THE m = 1 INSTABILITY IN A BUMPY THETA PINCH. Berge, G. (Univ. of Bergen). pp 245-9 of Feedback and Dynamic Control of Plasmas. /Chu, T. K. (ed.). New York; American Institute of Physics (1970).

From Symposium on feedback and dynamic control of plasmas; Princeton, N. J. (18 Jun 1970).

The possibility of dynamic stabilization of slightly bumpy axisymmetric systems was investigated using a general theory that can be regarded as a generalization of the well-known energy principle. The equilibrium is taken to be one in which there is a sharp boundary, with a surface current but no current in the main body of the plasma. An oscillatory external magnetic field then sets up oscillatory motion in the plasma column. The problem is made solvable by assuming the sharp boundary to have a prescribed motion. This motion will, in general, cause induced currents to flow in the plasma. A sufficient condition for dynamic stabilization of this system is obtained. (auth)

27786 PRELIMINARY RESULTS ON THE DYNAMIC STABILIZATION OF THE DRIFT-DISSIPATIVE INSTABILITY. Alcock, M. W.; Keen, B. E. (United Kingdom Atomic Energy Authority, Abingdon, Eng.). pp 250-4 of Feedback and Dynamic Control of Plasmas. /Chu, T. K. (ed.). New York; American Institute of Physics (1970).

From Symposium on feedback and dynamic control of plasmas; Princeton, N. J. (18 Jun 1970).

Preliminary results are presented showing that the "drift-dissipative" instability in helium and hydrogen afterglow plasmas is dynamically stabilized by an oscillating magnetic field B_θ of frequency ω. Oscillations at the fundamental frequency ($\omega_\theta \sim$ 4 kHz) are suppressed with $B_\theta/B_z \sim 1\%$; some signal at $2\,\omega_\theta$ remains. Larger-amplitude drives were required to suppress this second harmonic. Experiments were also performed to determine how the critical field for stabilization B_θ^{crit} varies as a function of the oscillating frequency ω (in the range 8 kHz to 100 kHz), both for suppression of the fundamental instability frequency ω_θ, and for its second harmonic at $2\,\omega_\theta$. (auth)

27787 SUPPRESSION OF DRIFT INSTABILITY BY RF ELECTRIC FIELD. Nishida, Y.; Tanibayashi, M.; Ishii, K. (Nagoya Univ., Japan). pp 255-9 of Feedback and Dynamic Control of Plasmas. /Chu, T. K. (ed.). New York; American Institute of Physics (1970).

From Symposium on feedback and dynamic control of plasmas; Princeton, N. J. (18 Jun 1970).

Suppression of the drift instability is achieved by applying a homogeneous rf electric field in a dc discharge diffused plasma. The instability amplitude is reduced by more than 25 db. The suppressing rf frequency depends on neutral pressure but is nearly independent of plasma density. These phenomena are discussed by means of a model of high-frequency plasma conductivity. (auth)

27788 DYNAMIC STABILIZATION OF A TWO-STREAM INSTABILITY. Decker, J. F.; Levine, A. M. (Bell Telephone Labs., Whippany, N. J.). pp 260-3 of Feedback and Dynamic Control of Plasmas. /Chu, T. K. (ed.). New York; American Institute of Physics (1970).

From Symposium on feedback and dynamic control of plasmas; Princeton, N. J. (18 Jun 1970).

In a certain pressure range, the Whippany ECR collisionless plasma was observed to be unstable to a two-stream ion instability. The frequency spectra of the instability was related to the double humped ion distribution function measured with an energy analyzer. By modulating the power source of the plasma, a time-dependent variation of plasma parameters was introduced. This was used to stabilize the microinstability. As the frequency of the modulation was varied relative to that of the instability, regions of stabilization and destabilization were observed. (auth)

27789 DYNAMIC STABILIZATION OF THE Z PINCH. Phillips, J. A.; Forman, P. R.; Haberstich, A.; Karr H. (Los Alamos Scientific Lab., N. Mex.). pp 274-85 of Feedback and Dynamic Control of Plasmas. /Chu, T. K. (ed.). New York; American Institute of Physics (1970).

From Symposium on feedback and dynamic control of plasmas; Princeton, N. J. (18 Jun 1970).

Results of dynamic stabilization of the m = 1 kink instability of a low-current z pinch (≤40 kA) by (1) high-frequency linear-quadrupole magnetic fields and (2) high-frequency oscillating B_z magnetic fields are described. In method (1) the m = 1 instability of wavelengths of the order of the interelectrode spacing (~56 cm) are stabilized but the short-wavelength instabilities of 5 to 12 cm are dominant and are not suppressed. The observed instabilities have a reduced growth rate with stabilization in agreement with MHD theory. The stabilizing field is also seen to (a) distort the cross section of the plasma column into an ellipse whose major axis increases with time and (b) to increase the total number of electrons in the discharge above the initial gas filling due to release of gas from the walls. MHD theory predicts growth times larger than the duration of the experiment for dynamic stabilization of an oscillating B_z magnetic field, method (2). Experimentally significant (~kA) j_θ discharge currents are driven parallel to the B_θ fields of the z pinch near the walls by the stabilization fields. These j_θ currents shield out most

XUM

of the time varying fields from the central region and prevent a test of the simple theory. Longitudinal limiters parallel the axis help to suppress these j_θ currents and stable times are increased by ~75%. These experiments on dynamic stabilization of the z pinch have been marginally effective in slowing down the growth rate of the m = 1 instability. Complete stability theoretically requires higher frequencies and currents than those used in the experiment, but these would be technically difficult. However, the data also show that, as the dynamic field strengths and frequencies are raised, there may be undesirable dangerous side effects: (1) the growth of driven oscillations and (2) the shielding out of the hf fields by induced currents in the residual plasma outside the pinched plasma column, which may prevent dynamic stabilization from being effective. (auth)

27790 DYNAMIC STABILIZATION EXPERIMENT ON A LINEAR SCREW PINCH. Becker, G.; Gruber, O.; Herold, H. (Institut fuer Plasmaphysik, Garching, Ger.). pp 286-92 of Feedback and Dynamic Control of Plasmas. /Chu, T. K. (ed.). New York; American Institute of Physics (1970).

From Symposium on feedback and dynamic control of plasmas; Princeton, N. J. (18 Jun 1970).

In a linear screw pinch (T_i = 50 to 350 eV; β = .5 to .7) helical m = 1 instabilities with growth rates ω_i of about .3 to 3×10^6 sec^{-1} were observed. A modulation of the quasi-stationary B_{z0} field component with amplitude ratios $\xi = B_z/B_{z0}$ up to .2 and with frequencies ω_s of 7 and 10×10^6 sec^{-1} was applied for dynamic stabilization. A reduction of the growth of the m = 1 mode could be achieved, provided that $\xi\omega_s$ was higher than a critical value for a given ω_i. Dynamic shear of the field lines in the plasma boundary and inertial effects appeared during the enforced radial oscillation of the plasma surface. An upper limit for $\xi\omega_s$ beyond which breakdown close to the wall occurred was observed. (auth)

27791 DYNAMIC STABILIZATION OF HYDRODYNAMIC INTERCHANGE INSTABILITIES: A MODEL FOR PLASMA PHYSICS. Wolf, G. H. (Institut fuer Plasmaphysik, Garching, Ger.). pp 293-304 of Feedback and Dynamic Control of Plasmas. /Chu, T. K. (ed.). New York; American Institute of Physics (1970).

From Symposium on feedback and dynamic control of plasmas; Princeton, N. J. (18 Jun 1970).

Dynamic stabilization and parametric resonances of superposed fluids with sharp and diffuse interfaces are described. An analogous method is used to derive the stabilizing potential for the short-wavelength flutes for the standing-wave scheme of a high-β plasma column. (auth)

Thermonuclear Processes

27792 (IAE-1986) NUCLEAR DATA FOR THERMONUCLEAR REACTORS. Chernilin, Yu. F.; Yan'kov, G. B. (Institut Atomnoi Energii, Moscow (USSR)). 1970. 36p. (In Russian). Dep. NTIS (U. S. Sales Only).

The design of a thermonuclear reactor is described and the pertinent nuclear data are analyzed. A brief review is made of published data (through 1969) on ^{6}Li, ^{7}Li, and Nb as effective materials for nuclear reactor operation. An attempt is made to show that the data on nuclear interactions in the power region, determined by thermonuclear neutrons, are insufficient and that further neutronic calculations for blanket assemblies of fusion power reactors are imperative. (R.V.J.)

27793 TORSATRON WITHOUT TOROIDAL FIELD COILS AS A SOLUTION OF THE DIVERTOR PROBLEM. Gourdon, C.; Marty, D.; Maschke, E. K.; Touche, J. (CEN, Fontenay-aux-Roses, France). Nucl. Fusion; 11: 161-6(Mar 1971).

The torsatron without toroidal field coils is a configuration of the stellarator type obtained with a particularly simple set of conductors (l helical windings and a vertical field). Here the case l = 3 is studied by numerical calculation. It is found that good magnetic surfaces exist. High values of rotational transform ($\iota/2\pi \simeq 3$) and shear ($\Theta \simeq 0.5$) can be obtained simultaneously with a relatively low mirror ratio along the field lines ($B_{max}/B_{min.} \simeq 1.2$). The absence of separate toroidal field coils allows the design of an efficient divertor. (auth)

27794 OPERATING CHARACTERISTICS OF DISC-FOCUS DENSE PLASMA. Puttarudraiah, Sathyavathiamma Magadi. Columbus, Ohio; Ohio State Univ. (1970). 141p. University Microfilms Order No. 71-7542.

Thesis.

Three disc focus plasma discharge devices consisting of plasma chambers of different diameters were constructed and studied. The principle of pinch effect is used for confinement of the plasma. The experiment aimed at determining the dimensions of the discharge chamber, for which the performance of the chamber would be optimum. Operating characteristics of each of the three discharge devices were studied at different initial pressures and condenser bank voltages. For each gas filling pressure, the total current, I, through the plasma volume and the time rate of variation of the current, dI/dt, were measured using a Rogowski coil. The voltage between the electrodes was monitored by a high voltage probe. The plasma was photographed by an Image Converter Camera in "streak" and "frame" modes. Time integrated pinhole and stereoscopic pictures of the plasma focus were taken. (TSS) (Diss. Abstr. Int., B)

27795 PROPOSED METHOD OF MEASURING THE POLOIDAL MAGNETIC FIELD IN DIFFUSE TOROIDAL PINCHES. Murakami, M.; Clarke, J. F. (Oak Ridge National Lab., Tenn.). Nucl. Fusion; 11: 147-9(Mar 1971).

A method of using the Thomson scattering of a CO_2 laser beam is proposed to measure the poloidal magnetic field produced by the plasma current in diffuse toroidal pinches of the Tokamak type. The method is based on resolving the relative shape of the cyclotron lines, whose broadening is introduced by "misalignment" due to the poloidal field with respect to the large toroidal magnetic field on which the scattering system is aligned. A small improvement in currently available transversely excited atmospheric CO_2 lasers is necessary to perform the measurement. (auth)

27796 FUSION CHAIN REACTIONS. I. McNally, J. Rand Jr. (Oak Ridge National Lab., Tenn.). Nucl. Fusion; 11: 187-9(Mar 1971).

A qualitative discussion is presented on the concept of charged-particle fusion chain reactions in which protons (deuterons, tritons, ^{3}He, or energetic alphas) may catalyze the nuclear burning of ^{6}Li or other nuclear fuels, quite analogous to chemical chain reactions except for the energy scale of the events. (M.O.W.)

27797 FUSION CHAIN REACTIONS. II. McNally, J. Rand Jr. (Oak Ridge National Lab., Tenn.). Nucl. Fusion; 11: 189-91(Mar 1971).

The effect of the lithium-6–deuteron reaction on a fusion chain process is discussed. (M.O.W.)

27798 REVERSED FIELD EQUILIBRIA IN AXIALLY SYMMETRIC ELECTRON CURRENT LAYERS. Fisher, Shalom (New York Univ., N. Y.). Phys. Fluids; 14: 962-6(May 1971).

Self-consistent, nonrelativistic E-layer equilibria in two dimensions are calculated by numerical methods. A rigid-rotor model for the electron distribution, together with a neutralizing ion background, leads to a nonlinear equation for the magnetic flux function ψ. Solutions to this equation are displayed, and the existence of bifurcations or nonuniqueness is demonstrated. (auth)

27799 NEUTRON PRODUCTION IN A PLASMA FOCUS DISCHARGE WITH AND WITHOUT AXIAL MAGNETIC FIELD. Bernstein, M. J.; Hai, F. (Aerospace Corp., El Segundo, Calif.). Phys. Fluids; 14: 1010-18(May 1971).

The D–D neutron emission from a 27-kJ plasma focus discharge was investigated with and without the effects of an applied axial magnetic field. With no applied field, the ratio of axial to radial neutron fluxes varied from 1.5 down to 1.2 for gas fillings of 4 to 10 torr; the ratio of fluxes was greater for a round anode tip than for a flat end. An axial field of 1200 G (trapped flux of 57,000 Maxwells) reduced the average neutron yield from 10^{10} to 10^9, reduced the average energy of the axially emitted neutrons from 2.9 to 2.8 MeV, and caused the effective neutron source to shift away from the anode surface; the width of the neutron energy spectra remained about 500 keV. With an applied field, the ratio of axial to radial neutron fluxes increased from 1.2 early in the pulse to 1.5 at peak intensity. Streak photography with and without axial field revealed that neutron production began when the plasma column first pinched and that peak neutron emission occurred when the plasma luminosity faded; the axial field delayed the onset of peak emission by up to 80 nsec. The observations do not agree with a thermonuclear model of neutron production, but the results are consistent with a model of deuteron acceleration in crossed fields. (auth)

Wave Phenomena

27800 PLASMA WAVES AND ECHOES. Gentle, K. W. (Univ. of Texas, Austin). Methods Exp. Phys.: 9: 1-36(1970).

A brief theoretical description is given of electron plasma waves and ion acoustic waves. Experimental techniques for observing these waves are described. A brief discussion of the theory of plasma wave echoes and their detection is given. (M.O.W.)

27801 PROPAGATION OF AN ELECTROMAGNETIC PULSE THROUGH INHOMOGENEOUS PLASMA. Singh, K. P.; Shukla,

XUM

P. K.; Singh, R. N. (Inst. of Tech., Varanasi, India). Int. J. Electron.; 30: 249-54(Mar 1971).

The propagation of electromagnetic waves through inhomogeneous plasma is considered. The results obtained by earlier workers were suitably modified. The effect of electron collision frequency is discussed. (auth) (UK)

27802 OSCILLATION DUE TO COLLISION-INDUCED INSTABILITY IN MERCURY PLASMA. Idehara, T.; Ishida, Y. (Fukui Univ., Japan). Phys. Lett.; 34A: 336-7(5 Apr 1971).

An oscillation ascribed to a collision-induced instability is observed near the electron cyclotron frequency and its second harmonic in mercury plasma. (auth)

27803 PROPAGATION OF ELECTROMAGNETIC WAVES IN PLASMAS. Ginzburg, V. L. International Series of Monographs in Electromagnetic Waves, Volume 7. Oxford; Pergamon Press, 1970. 615p. Pound 8.

Translated by J. B. Sykes and R. J. Tayler.

The subject is dealt with under the following headings: the fundamental theory of electromagnetic wave propagation in plasmas, wave propagation in a homogeneous isotropic plasma, wave propagation in a homogeneous magnetoactive plasma, wave propagation in an inhomogeneous isotropic plasma, wave propagation in an inhomogeneous magnetoactive plasma, reflection of radio waves from ionospheric layers, radio-wave propagation in cosmic conditions, and nonlinear phenomena in a plasma in a variable electromagnetic field. (UK)

27804 ELECTROMAGNETIC WAVE PROPAGATION THROUGH A BOUNDED TIME-SPACE PERIODIC COLD PLASMA. Askne, J. (Chalmers Univ. of Tech., Goteborg). Int. J. Electron.; 30: 201-18(Mar 1971).

A plane wave is incident upon a bounded, cold plasma with a density varying periodically in time and space due to a high-power wave. The modulation of the medium will produce a spectrum of reflected and transmitted components in different directions and with different frequencies. Inside the medium parametric effects will occur. The analysis takes into account all the time and space harmonics inside the medium and the reflection and transmission coefficients outside the medium. Four different types of wave interaction are obtained. Particularly, the case of traveling-wave amplification is extensively studied by means of approximate analysis as well as computer analysis. It is found that when the width of the medium exceeds a critical value, a gain saturation is obtained and degenerate oscillations may occur. If the pump wave propagates obliquely, the maximum angular separation will be between the amplified components. (auth) (UK)

27805 SPACE-CHARGE WAVES IN SOLIDS. Jonscher, A. K.; Rodger, K. S. (London Univ.). J. Phys., C (London); 4: 194-200(1971).

The conventional Boltzmann–Vlasov equations are solved for the case of a hot plasma with collisions such as may correspond to the conduction electrons in a semiconductor. A collision term is used which contains two relaxation times corresponding approximately to the usual momentum and energy relaxation times. This collision term is so constructed that it does not give rise to a spurious generation of particles by collisions, a defect found in some of the earlier treatments of this topic. A general dispersion relation is obtained for space charge waves propagating in such a plasma and this represents an extension of the previous results obtained by Landau and by Pines and Schrieffer. In the limit of a cold plasma this dispersion relation reduces to results familiar from cold plasma theory. (auth) (UK)

27806 SIMILARITIES BETWEEN ION WAVES IN PLASMAS AND GRAVITY WAVES IN INCOMPRESSIBLE FLUIDS. Lam, S. H.; Sanmartin, Juan R. (Princeton Univ., N. J.). Phys. Fluids; 14: 786-91(Apr 1971).

Some similarities between ion waves in plasmas and gravity waves in incompressible fluids are investigated. It is shown that for zero ion temperature the ion-wave dispersion relation is similar to that of gravity waves in a stratified liquid between rigid, horizontal walls; for large wavelength the ion waves behave as the surface gravity waves of shallow-water theory. The general character of the pattern of ion waves arising in steady plasma flows is analyzed for arbitrary ion temperature, wavelength, and acoustic Mach number (which is based on the ion-acoustic speed), and is compared to the pattern of surface gravity waves in steady water flows when surface tension is taken into account. (auth)

27807 EXTERNAL CONTROL OF ION WAVES IN A PLASMA BY HIGH-FQUENCY FIELDS. Kaw, P. K.; Dawson, J. M. (Princeton Univ., N. J.). Phys. Fluids; 14: 792-4(Apr 1971).

It is shown that a high-frequency field, with a frequency close to the electron plasma frequency and a strength less than that required to excite parametric instabilities, can be used to externally control, in a very significant way, the frequency and damping of ion waves in a plasma. (auth)

27808 ELECTROSTATIC ELECTRON OSCILLATIONS IN CYLINDRICAL, NON-NEUTRAL PLASMAS. Linson, Lewis M. (Avco Everett Research Lab., Everett, Mass.). Phys. Fluids; 14: 805-11(Apr 1971).

The character and stability of electrostatic electron waves that propagate both parallel to B (wave-number β) and perpendicular to B (azimuthal mode number l) in non-neutral plasmas in cylindrical geometry are studied. The background ions are taken to be infinitely massive and so provide a partial neutralization of the unperturbed electron space charge; this neutralization ranges from the completely un-neutralized electron plasma case to the more familiar case of a completely neutral plasma. It is found that the axisymmetric mode ($l = 0$) is stable for arbitrary radial density variation when the charge density is not too high. For $l \geq 1$ and electron and ion densities constant out to $r = a$ and zero beyond, the system is stable for all frequencies independent of the degree of neutralization and the location of a conducting outer wall. The dispersion relation is analogous to that for a neutral plasma permitting separate low- and high-frequency propagation bands. For low frequencies and low, nonincreasing electron, ion, and net charge densities, it is found that the presence of a resonant layer (zero frequency as seen by the electrons) within the electron cloud is necessary but not sufficient for instability. In general, finite axial wavenumber increases the tendency towards stability. (auth)

27809 MEASUREMENTS OF DRIFT-WAVE POTENTIAL OSCILLATIONS IN THE PRESENCE OF TEMPERATURE OSCILLATIONS. Motley, R. W.; Ellis, R. F. (Princeton Univ., N. J.). Phys. Fluids; 14: 886-9(Apr 1971).

Floating-potential oscillations on a Langmuir probe are found to lead density oscillations in drift wave instabilities of a thermally ionized cesium plasma. This contradiction of the isothermal theory is attributed to oscillations of the electron temperature. (auth)

27810 TIME-ASYMPTOTIC PERTURBATION THEORY IN WEAK PLASMA TURBULENCE. I. MACROSCOPIC DESCRIPTION. Elsaesser, Klaus (Max-Planck-Institut fuer Physik und Astrophysik, Munich). J. Plasma Phys.; 5: 31-7(Jan 1971).

The time-asymptotic method of nonlinear mechanics is used to solve the hierarchy equations of low-amplitude wave correlations. Starting with a formal description of individual dispersive and undamped waves, the usual kinetic equation for the energy spectrum and the three-wave correlation in the lowest order (three-wave processes) are derived. It is shown that the equations are automatically closed ("quasi-Gaussian") even in the case where the correlations have the same order of magnitude as the corresponding moments. (auth) (UK)

27811 TIME-ASYMPOTOTIC PERTURBATION THEORY IN WEAK PLASMA TURBULENCE. II. VLASOV DESCRIPTION. Elsaesser, Klaus (Max-Planck-Institut fuer Physik und Astrophysik, Munich). J. Plasma Phys.; 5: 39-49(Jan 1971).

In electrostatic turbulence under appropriate conditions it is shown that one can have an equation for ϕ_k (time variation of electrostatic potential amplitude) which is essentially instantaneous in time. The coefficients in this equation are uniquely determined by the Poisson equation of the corresponding order. By applying time-asymptotic methods of Bogolyubov and Mitropolski to the corresponding hierarchy equations, a kinetic equation for the spectrum $\langle|\varphi_k|^2\rangle$ is obtained. The resonant-mode coupling terms agree with the usual ones. But the nonlinear Landau damping terms are complemented by additional terms which are, at least formally, nonzero. For simplicity, the calculations were only done for the weakly unstable (and weakly damped) modes. (auth) (UK)

27812 INTERACTION OF ELECTROSTATIC WAVES IN COLLISIONLESS PLASMAS. Lewak, G. J. (Univ. of California, San Diego, La Jolla). J. Plasma Phys.; 5: 51-63(Jan 1971).

The interaction of three electrostatic waves in a collisionless plasma is treated to fourth order neglecting the wave–particle interaction (damping). Using the principles of energy conservation, and invariance under time reversal, conditions on the coupling constants are derived, enabling the solution to be expressed as a function of only two coupling constants. Phase plane diagrams of the solutions are sketched showing that the only singular points are stable equilibria. It is suggested how the theory may be applied to the explanation of the "floating-spike" resonance observable when one-half the hybrid frequency is the difference between the plasma and gyrofrequencies. (auth) (UK)

XUM

27813 MEASUREMENT OF MICROWAVE REFLEXION FROM A LONGITUDINALLY MAGNETIZED PLASMA-FILLED COAXIAL WAVEGUIDE. Oldfield, M. L. G.; Franklin, R. N. (Oxford Univ.). J. Plasma Phys.; 5: 89-105(Jan 1971).

The voltage reflèction coefficient from a vacuum–plasma boundary in a coaxial transmission line with an axial magnetic field B_0 applied was measured. The results agree well with a previously published theory for conditions where the microwave-, plasma-, electron collision-, and electron cyclotron frequencies are of the same order. (auth) (UK)

27814 PARAMETRIC EXCITATION IN AN INHOMOGENEOUS PLASMA. Chen, C. S. (Univ. of California, San Diego, La Jolla). J. Plasma Phys.; 5: 107-113(Jan 1971).

An infinite, inhomogeneous electron plasma driven by a spatially uniform oscillating electric field is investigated. The multi-time perturbation method is used to analyze possible parametric excitations of transverse waves and to evaluate their growth rates. It is shown that there exist subharmonic excitations of: (1) a pair of transverse waves in an unmagnetized plasma and (2) a pair of one right and one left circularly polarized wave in a magnetoplasma. Additionally, parametric excitation of two right or two left circularly polarized waves with different frequencies can exist in a magnetoplasma. The subharmonic excitations are impossible whenever the density gradient and the applied electric field are perpendicular. However, parametric excitation is possible with all configurations. (auth) (UK)

27815 EFFECT OF DISSIPATION ON NONLINEAR COUPLING PHENOMENA. Stenflo, Lennart (Uppsala Univ.). Phys. Scr.; 2: 50-2(1970).

The coupling coefficients, which account for the nonlinear interaction between three longitudinal plasma waves, are calculated. The results depend significantly on effects due to energy-dependent collision frequencies and carrier masses. (auth) (Sweden)

27816 INVESTIGATION OF LOW-FREQUENCY PLASMA OSCILLATIONS BY MEANS OF AMPLITUDE MODULATION OF MICROWAVE RADIATION. Bakai, A. S.; Ermakov, A. I.; Nazarov, N. I. (Inst. of Physics and Tech., Kharkov). Ukr. Fiz. Zh. (Russ. Ed.); 16: 12-18(Jan 1971). (In Russian).

It is shown that in a plasma–beam system the plasma density fluctuations caused by low-frequency waves produce not only transformation of the Langmuir waves to transverse ones, which are emitted, but also an amplitude modulation of these waves. Investigation of the amplitude modulation of uhf emission from plasma at frequency close to the electron plasma one makes it possible to determine the spectrum of low-frequency plasma oscillations (their frequency being much lower than that of electron plasma). Besides, the amplitude of low-frequency oscillations may be estimated from the depth of amplitude modulation of uhf emission. (auth)

27817 DERIVATION OF A CONNECTION FORMULA USING A PARTIAL WRONSKIAN. Baldwin, D. E.; Parlange, J.-Y. (Yale Univ., New Haven). Phys. Fluids; 14: 1031-3(May 1971).

A partial Wronskian is employed to derive the previously known Stokes parameters of the fourth-order equation coupling plasma oscillations to Bohm–Gross waves. (auth)

27818 CONDITIONS FOR THE EXISTENCE OF SHOCK-LIKE SOLUTIONS OF KORTEWEG–DE VRIES EQUATION WITH DISSIPATION. Pfirsch, D.; Sudan, R. N. (International Centre for Theoretical Physics, Trieste, Italy). Phys. Fluids; 14: 1033-5(May 1971).

Necessary conditions on dissipative-operators for the existence of shock-like solutions of the Korteweg–de Vries equation, which limit the damping tolerable at long wavelengths, are derived. (auth)

27819 EXPERIMENTAL INVESTIGATION OF TEMPORAL LANDAU DAMPING AND WAVE ECHOES IN COLLISIONLESS PLASMA. Rohde, Robert Sterbenz. Chicago; Illinois Inst. of Tech. (1970). 114p. University Microfilms Order No. 71-6040.

Thesis.

Temporal Landau damping of ion plasma waves and temporal plasma echoes were investigated experimentally by using standing waves. The experimental conditions were such that the waves could be either self-excited or externally excited and their oscillation frequency and amplitude could be controlled. The responses are coherently detected by sampling techniques. The experimental results on Landau damping agree well with the theory of B. Fried and R. Gould. That is, in a collisionless plasma, waves may decay in time exponentially by resonant absorption. On the other hand, it is found by the method of superposition that if two plasma waves are launched separately in time and decay by the Landau damping process, a third wave called the echo will spontaneously appear at a definite time later. These results, although obtained by an indirect method, agree within experimental error with the theory of Gould and O'Neil. As a by-product of this investigation, plasma beats were also observed. This phenomena may be attributed to the presence of two types of ion waves corresponding to two different masses. (Diss. Abstr. Int., B)

27820 THERMONUCLEAR COMBUSTION WAVE. Alikhanov, S. G.; Konkashbaev, I. K. (Nuclear Physics Inst., Novosibirsk, USSR). Nucl. Fusion; 11: 119-22(Mar 1971).

The existence of a steady-state thermonuclear combustion wave in dense plasma is demonstrated. The parameters of the wave are determined by numerical integration of the plasma balance equations. The possibility of constructing a flow reactor incorporating a self-sustaining thermonuclear reaction is examined. (auth)

27821 PROPAGATION OF ELECTROMAGNETIC WAVES IN A PLASMA WITH A SHEARED MAGNETIC FIELD. Fidone, I.; Granata, G. (CEN, Fontenay-aux-Roses, France). Nucl. Fusion; 11: 133-9(Mar 1971).

The propagation of an extraordinary wave in a toroidal plasma is investigated taking into account small shear. It is shown that an ordinary component can be generated at the upper hybrid frequency. The amplitude of the ordinary wave is proportional to the spatial derivative of $\theta = B_\theta/B_0$, where B_0 is the main magnetic field and B_θ the poloidal component. The result is of a form suggesting a diagnostic scheme for measuring the local value of $d\theta/dr$. A numerical application is given for the case of a T-3 Tokamak. (auth)

27822 LONGITUDINAL OSCILLATIONS OF A LORENTZIAN ELECTRON GAS. Lee, W. W.; Hirsch, R. H.; Denavit, J. (Northwestern Univ., Evanston, Ill.). Phys. Fluids; 14: 941-51 (May 1971).

The combined nonlinear and collisional effects on the Landau damping of longitudinal electron oscillations are studied using the Lorentz gas model to represent electron–neutral and electron–ion interactions. Three types of interactions are considered: hard-sphere collisions, inverse fifth-power interactions, and inverse square interactions. A perturbation analysis of the nonlinear kinetic equation is carried out following Montgomery's expansion technique. For hard-sphere collisions, the collisional damping and the nonlinear change in Landau damping are determined analytically. For inverse fifth-power interactions and inverse square interactions, the same results are obtained numerically by expanding the distribution function in Legendre polynomials to sufficiently high order to adequately represent its variations in the resonance region. (auth)

27823 EXPERIMENTAL OBSERVATION OF THE DEFORMATION OF THE ELECTRON DISTRIBUTION FUNCTION DUE TO A DAMPED ELECTROSTATIC WAVE. Guillemot, M.; Olivain, J.; Perceval, F.; Scharer, J. (CEA–CEN, Fontenay-aux-Roses, France). Phys. Fluids; 14: 952-5(May 1971).

The change in the electron distribution function due to a damped electron plasma wave is observed by means of an electron energy analyzer. The results show that the number of particles with velocities greater than that of the wave phase velocity is increased and that the number of particles with velocities less than the wave decreases. The distance between the antenna and analyzer is varied to show the increase in the deformation of the velocity distribution due to wave–particle interaction through space. For sufficiently high wave power and large separation a plateau is formed in the vicinity of the wave phase velocity. (auth)

27824 NONLINEAR LANDAU DAMPING AND BEAT WAVE TRAPPING. Ott, Edward; Dum, Christain Thomas (Cornell Univ., Ithaca, N. Y.). Phys. Fluids; 14: 959-61(May 1971).

The nonlinear interaction of two coherent waves with particles of velocity near $(\omega_1 - \omega_2)/(k_1 - k_2)$ is investigated. For times short compared with the trapping time in the beat wave, one recovers the usual nonlinear Landau damping result, previously derived for the incoherent (turbulent) case. For two coherent waves, however, trapping severely limits the validity of this result. (auth)

27825 COUPLING OF WAVES IN NONUNIFORM PLASMA. Chakraborty, B. (Jadavpur Univ., Calcutta). J. Math. Phys. (N. Y.); 12: 529-33(Mar 1971).

The mutual coupling of transverse and longitudinal high-frequency waves of both electron and ion fluid motions of perturbation in slowly varying nonmagnetized equilibrium plasma is studied. Also, the particular problem of coupling of ion acoustic and electromagnetic waves is considered in detail. The power of electro-

XUM

magnetic radiation generated by an ion acoustic wave and also, in reverse, from the latter to the former is evaluated. (auth)

Shielding

Refer also to abstracts 26533, 26535, 28677, and 28784.

27826 (DEMO–70/11) MEASUREMENT OF THE COEFFICIENT OF GAMMA ABSORPTION OF MATERIALS USED FOR NUCLEAR CONSTRUCTIONS. Mavroyannakis, E.; Antoniades, J. (Democritus Nuclear Research Center, Athens (Greece)). Jul 1970. 15p. (In French). Dep. NTIS (U. S. Sales Only).

An experimental device for the measurement of the γ absorption cross section was described. The radiation sources used and the measurement techniques are discussed. The values of absorption coefficients measured for Cd, Al, 18/8 stainless steel, Fe, UO_2, Si, Sb, Pb, Ni, Plexiglas, paraffin, paraffin Bl, bitumen, teflon, gum, marble, and porcelain are tabulated and compared with theoretical values when possible. (J.S.R.)

27827 (DESY–70/59) FLUORESCENCE EXCITATION OF ULTRA-SOFT X-RAY EMISSION SPECTRA USING SYNCHROTRON RADIATION. Feser, K.; Mueller, J.; Wiech, G.; Faessler, A. (Deutsches Elektronen-Synchrotron, Hamburg (West Germany)). Nov 1970. 11p. Dep. NTIS (U. S. Sales Only).

Attempts were made to use the synchrotron radiation of the 7.5-GeV electron synchrotron DESY for the fluorescence excitation of ultra-soft x-ray emission spectra. The very intense background produced by the scattered radiation of short wavelengths could be reduced so that it was possible to observe the K-emission bands of carbon (45 Å), boron (67 Å), and beryllium (114 Å). The results are compared with data obtained by electron excitation. (auth)

27828 (DP–1246) ^{252}Cf SHIELDING GUIDE. Stoddard, D. H.; Hootman, H. E. (Du Pont de Nemours (E. I.) and Co., Aiken, S. C. Savannah River Lab.). Mar 1971. Contract AT(07-2)-1. 82p. Dep. NTIS.

Neutron and gamma-ray dose rates were calculated for ^{252}Cf source interaction with most common shielding materials. Information has been compiled to assist ^{252}Cf evaluators and prospective users in determining: radiations involved with the use of ^{252}Cf; personnel dose guides and shipping dose rate levels for ^{252}Cf; comparative thicknesses of different shield materials required for a specific ^{252}Cf dose reduction; and approximate flux levels for neutron activation and background radiation levels in applications. (auth)

27829 EXPERIMENTS AND CALCULATIONS FOR GAMMA RAYS STREAMING THROUGH PENETRATION IN SHIELDING STRUCTURE. Yamaki, Hideo (Hitachi Ltd., Ibaraki, Japan); Kitazume, Mitsuyuki; Fukushima, Yutaka; Uchida, Shunsuke. Hitachi Hyoron; 52: 373-7(Apr 1970). (In Japanese).

Streaming from pipes, penetrating holes, and other gaps in primary shielding of a reactor is studied. A new computing code for streaming (by the ray analysis method) gave good results. These results coincide with experimental results within a factor of 2. Experiments were performed by changing the parameters (duct diameter, duct length, off-set position, off-set width). The radioactive source was the HTR (Hitachi Training Reactor) and the shielding material was light water. The results were concerned with the quantitative influence of parameters on the maximum streaming dose rate. (1) Effect of off-set width. Of course, the larger the width, the smaller the streaming rate. By this experiment, the change in the rate is the steepest about the position of d/r = 2.0 (duct width). (2) Effect of off-set position. Ordinarily, the larger the value (l_1/l), the larger the maximum streaming dose rate, but by this experiment, at the position where l_1/l was 0.625 the maximum streaming rate became a minimum. Other results are also presented. (Japan)

27830 L-SHELL PHOTOELECTRIC CROSS-SECTIONS FOR LOW ENERGY GAMMA-RAYS IN LEAD. Singh, Mohanjit; Sood, B. S. (Punjab Univ., Patiala, India). Curr. Sci. (India); 40: 129(20 Mar 1971).

L-shell photoelectric cross sections for γ rays of 84, 145, and 279 keV in Pb were calculated from measurements of the intensity of fluorescent L x rays following the photoelectric interaction. Comparison of the results with various theoretical predictions shows that screening effects for the L shell are significant and cannot be neglected. (A.G.W.)

27831 GENERALIZATION OF γ-ALBEDO CALCULATIONS ON THE BASIS OF SIMILARITY THEORY. Ochkur, A. P.; Pshenichnyi, G. A.; Marenkov, O. S. This paper was summarized in At. Energ. (USSR); 28: 494-5(Jun 1970) as paper No. 399/5479. (In Russian).

Similarity theory was used to generalize certain Monte Carlo albedo calculations for low-energy γ rays (below 300 keV) for an isotropic point source at the surface of semi-infinite reflector. On the basis of similarity and dimensionality theory, the dependence of the integral reflected γ-flux N on the medium density and the total bulk attenuation coefficient for the primary γ radiation is written. (TSS)

27832 BREMSSTRAHLUNG SPECTRUM OF ENERGETIC β PARTICLES TRAVERSING SINGLE CRYSTALS IN LATTICE-DIRECTED TRAJECTORIES. Nip, Hans C. H.; Kelly, J. C. (Univ. of New South Wales, Sydney). Phys. Rev., B.; 3: 2884-7 (1 May 1971).

For lattice-directed trajectories, the Fourier spectrum of the interaction between an energetic ($\gtrsim 10^5$ eV) β particle and the lattice atoms is different from the Fourier spectrum of the interaction with randomly distributed target atoms by significant terms of frequencies near sv/2a. Here s is an integer, v is the velocity of the β particle parallel to the low-index crystallographic direction, and 2a is the interatomic spacing in this low-index direction in the reference frame of the β particle. It is suggested that these frequencies will dominate the bremsstrahlung spectrum of an energetic β particle traversing a single crystal in a lattice-directed trajectory. This effect is considered in terms of the quantal time-dependent perturbation theory. Its magnitude is estimated using the classical theory of radiation. (auth)

27833 ANALYSIS OF ENERGY-LOSS DATA FOR 0.2 TO 0.5-MeV/amu p, α, AND N IN Se. Nakata, Hiroshi. Phys. Rev., B; 3: 2847-51(1 May 1971).

The analysis of experimental energy-loss data for 0.2- to 0.5-MeV/amu p, α, and N ions in Se was made to obtain certain quantities. Data on standard media are also shown for comparison. The results indicate that the effective-charge parameter for N is quite different from unity. The variation of the relative mean excitation energy measured by α particles is not linear in terms of Z_2. The parameter ξ for N is slightly larger than the theoretical value (Z_1^3). The electronic stopping cross section for N, which lies between two theoretical values, is not exactly proportional to the projectile velocity, suggesting that nitrogen as a projectile shows a peculiar behavior particularly unlike other ions. (auth)

27834 NEW SEMI-RANDOM SAMPLING TECHNIQUES FOR MONTE CARLO CALCULATIONS. Woolson, William Andrew. University Park, Pa.; Pennsylvania State Univ. (1970). 87p. University Microfilms Order No. 71-6374.

Thesis.

The multi-dimensional distribution of the sample numbers employed in Monte Carlo programs is of critical importance for producing reliable and efficient calculations. Two new semi-random sampling techniques called Embedded Systematic Sampling (ESS) and Generalized Systematic Sampling (GSS) were designed to provide Monte Carlo sample numbers which have a good multi-dimensional distribution. Basically, ESS improves the previous semirandom sampling technique of Systematic Sampling (SS) and GSS extends the properties of Systematic Sampling to sample spaces of large dimensions. It was theoretically shown that to the same order of magnitude as the variances, the variance of these new sampling methods was less than the variance resulting from random sampling and systematic sampling. These calculations imply that regardless of the specific properties of the Monte Carlo problem, the use of the new sampling methods would result in less variance than the use of conventional random sampling methods. A Monte Carlo program, which simulated a one dimensional continuous random walk, provided experimental comparisons of the new semirandom sampling methods with random sampling and previous methods of semi- and nonrandom sampling. The results of these experiments indicated that ESS offered a significant variance reduction over random sampling but only marginal improvement over SS. In more complex calculations involving large sampling spaces, GSS appeared to be the best sampling technique tested; it had less variance than random sampling and another semirandom sampling method and had less error than the nonrandom sampling method. The practical criterion for comparing the efficiencies of various Monte Carlo sampling methods, however, is not the variance for a given number of histories but the variance for a given computation time. Judging the new sampling techniques by this criterion, it was found that employing Generalized Systematic Sampling in Monte Carlo programs would result in more efficient calculations if the variance reduction resulting from the simple Monte Carlo experiments was indicative of the variance reduction that would result in more complex Monte Carlo programs. (Diss. Abstr. Int., B)

27835 ENERGY DISSIPATION NEAR AN INTERFACE: A MORE REALISTIC APPROACH TO ELECTRON RANGE AND STOPPING POWER. Charlton, D. E. (Sir George Williams Univ., Montreal). Radiat. Res.; 44: 575-93(Dec 1970).

Spencer's (Nat. Bur. Stand. Monogr., No. 1 (1959)) treatment of the energy dissipated near point isotropic electron sources is incorporated into the convenient formalism introduced by Charlton and Cormack (Radiat. Res., 17: 34-49(1962)) in their treatment of the interface problem. This approach leads to functions that are dependent both upon the initial electron energy and the medium in which the energy is being dissipated—factors not introduced into prior treatments. Dose distributions based on the functions derived in this paper are compared to distributions calculated from data presented by other authors. These comparisons suggest that dose distributions predicted by some of the simpler models of electron passage through matter are remarkably good and that one of the frequently-referred-to models must be rejected as a basis for dosage calculation. Functions are presented in tabular and graphical form for plane and spherical interfaces for electrons with high and low initial energies traveling through various media. (auth)

27836 CALCULATION OF X-RAY PRODUCTION IN ALLOY TARGETS BY NEW APPROACH USING MONTE CARLO METHOD. Shimizu, Ryuichi; Ikuta, Takashi; Nishigori, Nobuko; Murata, Kenji (Osaka Univ.). Jap. J. Appl. Phys.; 9: 1429-30(Nov 1970).

The Monte Carlo method is used to calculate the x-ray production in a two-component alloy resulting from electron scattering. The procedure is based on Bethe's formula for the energy loss and Lewis's multiple scattering treatment for the angular distribution. The approach is applied to a copper–aluminum alloy, and depth distributions for both scattered electrons and characteristic x rays are given for the alloy and its components. (R.W.R.)

Solid-State Physics

Refer also to abstracts 26470, 27303, and 27440.

Radiation Effects

Refer also to abstracts 26472, 26561, and 27832.

27837 (AERE-R-6506) SELF-IRRADIATION DAMAGE IN α-PLUTONIUM. Hall, R. O. A.; Mortimer, M. J. (Atomic Energy Research Establishment, Harwell (England)). Aug 1970. 13p. Dep. NTIS (U. S. Sales Only).

The change in the resistivity of high purity α-plutonium, due to self-irradiation damage with time of holding in liquid helium, was measured. A small term, additional to the two terms previously reported, was found. A detailed analysis showed that a good fit was obtained using: $(\rho - \rho_0) = 1.920(1 - \exp(-0.65 \times 10^{-3}t)) - 0.400(1 - \exp(-0.192 \times 10^{-2}t)) - 0.230(1 - \exp(-0.172 \times 10^{-3}t))\mu\Omega m$. This analysis was also applied to earlier results on lower-purity α-plutonium and to a Pu–1% Np alloy. (auth)

27838 (ANL-Trans-874) EFFICIENCY OF X-RAY LUMINESCENCE AND THERMOLUMINESCENCE OF LITHIUM FLUORIDE CRYSTALS. Grube, M.; Schwarz, K. Translated for Argonne National Lab., Ill. from Latv. PSR Zinat. Akad. Vestis, Fiz. Teh. Zinat. Ser.; No. 4, 37-43(1970). 11p. Dep. NTIS.

The effect of activation by magnesium and calcium on thermoluminescence and x-ray luminescence of LiF crystals was investigated. Activation by magnesium strongly influences thermoluminescence yield, but it has little effect on x-ray luminescence efficiency. With an Mg concentration of 0.3 wt %, the maximum observed thermoluminescence yield is 10^{10} quanta/g·rad. Calcium impurities act mainly to increase the thermoluminescence in the crystal with mixed activators—LiF : Mg (0.3 wt %), Ca (0.01 wt %, as used for dosimetry). (auth)

27839 (CEA-N-1171) WIGNER ENERGY IN IRRADIATED OXIDES BeO, MgO, Al_2O_3, AND SiO_2. Roux, Andre (Commissariat a l'Energie Atomique, Saclay (France). Centre d'Etudes Nucleaires). Dec 1969. 95p. (In French). Dep. NTIS (U. S. Sales Only).

Thesis. Submitted to Univ. of Lyon, Faculte des Sciences, Lyon, France.

Stored energy in BeO, MgO, Al_2O_3 (sintered) and SiO_2 (vitrous) is weak and appears at a very large range of temperatures. The measurement of this energy was performed with an immersion calorimetric apparatus up to high temperature (1200°C). The results indicate relations between stored energy and dimensional changes (density or lattice parameters). Interpretation of the results shows that in the four oxides, most of the Wigner energy may be attributed to Frenkel defects. In MgO a theoretical computation of defect energies indicates a preponderance of the positive-ion Frenkel pairs. (auth)

27840 (IPP-7/3) INFLUENCE OF LATTICE DEFECTS ON BACKSCATTERING OF PROTONS AND HELIUM IONS FROM NIOBIUM SINGLE CRYSTALS. Schulze, H. (Institut fuer Plasmaphysik, G.m.b.H., Garching (West Germany)). Dec 1970. 38p. (In German). Dep. NTIS (U. S. Sales Only).

The backscattering of 100-keV protons and helium ions from a niobium single crystal was measured by the single- and double-alignment techniques as a function of both temperature and bombardment dose. In the investigated range from −80 to 800°C, the measured intensities of H^+ backscattered from an annealed single crystal agree well with Lindhard's theory of the temperature dependence of backscattering. From the backscattering intensities measured by the single- and double-alignment techniques it is possible to determine the lattice-defect concentration in the surface and in the first hundred atomic layers. For a niobium single crystal annealed to 1300°C, this concentration is $N_{GF}/N_0 \approx 10^{-4}$ and is almost temperature-independent in the given range. With a bombardment dose of 2×10^{18} protons/cm^2 or 3×10^{17} He^+ ions/cm^2 injected in a ⟨111⟩ direction, so many defects were produced in an ~20-Å-thick surface layer at 20°C that this layer may be regarded as amorphous. In the 100-Å-thick layer below, the radiation damage remained comparatively small at $\sim 10^{-3}$. If bombardment is made at 800°C, no increase of the lattice defects is observed since the radiation damage can apparently anneal again. (auth)

27841 (NYO-3463-23) EFFECT OF ELECTRIC FIELD AND TEMPERATURE ON THE RADIATIVE LIFETIME OF THE F CENTER. Report 1329. Stiles, Lynn F. Jr. (Cornell Univ., Ithaca, N. Y. Materials Science Center). Jun 1970. 135p. Dep. NTIS.

Thesis.

The radiative lifetime of the excited F center at 4.2°K and the changes in the radiative lifetime induced by an applied electric field and by increasing temperature were measured in KCl, KF, and NaF with sufficient precision to test recent models for the relaxed excited states. The results are in semi-quantitative agreement with the predictions of the mixed-state model recently proposed by Bogan and Fitchen. The quantities measured were the luminescent decay time τ (using a pulse sampling technique), the relative luminsecent yield η (using conventional techniques), and the emission line shape function. Lifetimes at 4.2°K were 717 ± 15 nsec for KCl, 380 ± 20 nsec for KF, and 117 ± 5 nsec for NaF. Changes in lifetime were measured for [100]-applied dc fields of 0 to 140 kV/cm at 4.2°K. These results add convincing support for the mixed-state model. Its ability to explain other recent experiments on the excited F center is discussed, as well as some of its limitations, which suggest that a vibronic model will be required for a more accurate analysis. (auth)

27842 (RD/B/N-1850) BUBBLE MOBILITY ON DISLOCATIONS AND RANDOM DIFFUSION STUDIES. Beere, W. B. (Central Electricity Generating Board, Berkeley (England). Berkeley Nuclear Labs.). Dec 1970. 20p. Dep. NTIS (U. S. Sales Only).

Krypton and helium bubbles were precipitated on dislocations in copper foils and the root mean square migration distances measured during isothermal annealing. Helium bubbles either remained fixed, coalesced, or migrated to the foil surface. Krypton bubbles showed a maximum in the root mean square migration distance for bubbles of 7 nm radius. The effects of bubble pinning and coalescence upon migration distances were calculated and, together with the effect of correlation of surface atomic jumps, were compared with experimental observations. It was shown that previous expressions for the mobility do not adequately describe the experimental root mean square random migration distances. (auth) (UK)

27843 SHALLOW TRAPS IN p-TYPE GERMANIUM CONVERTED FROM n-TYPE BY ELECTRON IRRADIATION. Saito, Haruo; Fukuoka, Noboru; Tatsumi, Yukichi (Osaka Univ.). Jap. J. Appl. Phys.; 10: 389(Mar 1971).

P-type Ge containing Sb were irradiated by 1.5-MeV electrons at 77°K and then given isochronal anneals. The electric conductivity was measured after recooling to 77°K in the dark and under illumination; from the difference between the two, traps are present. Three annealing stages were observed: 80 to 150°K, 160 to 220°K, and above 230°K. These traps and annealing stages are also observed for As-, Ga-, In-, and Al-doped Ge, and the trapping level is concluded to lie 0.23 eV below the conduction band. The traps are stable at 77°K and are annealed out at ~250°K. The shallow trap density depends only on irradiation dose, and the trap is probably a vacancy–interstitial pair. (D.L.C.)

27844 ION-IMPLANTATION DOPING OF ZINC SULPHIDE THIN FILMS. Brown, M. R.; Cox, A. F. J.; Shand, W. A.; Williams, J. M. (Signals Research and Development Establishment, Christchurch, New Zealand). Solid State Commun.; 9: 37-40 (1 Jan 1971).

The ion-implantation doping of zinc sulphide thin films with terbium, erbium, and manganese is reported, and it is shown that the resultant cathode-excited emission is characteristic of the implanted ion. (auth) (UK)

27845 INFRARED STUDY OF DEFECTS PRODUCED IN n-TYPE SILICON BY ELECTRON IRRADIATION AT LOW TEMPERATURES. Bean, A. R.; Newman, R. C. (Univ. of Reading, Eng.). Solid State Commun.; 9: 271-4(15 Feb 1971).

The infrared local mode absorption produced by irradiation of n-type silicon by 2-MeV electrons at temperatures in the range 100 to 140°K was investigated. A new band at 884 cm^{-1} was observed and interpreted as due to a vacancy–oxygen complex (A-centre) with a trapped electron. (auth) (UK)

27846 OPTICAL STUDY OF AN IONIC CRYSTAL BY MEANS OF PULSED ELECTRON IRRADIATION. 4. Ueda, Masayasu; Hirai, Masamitsu; Kondo, Yasuhiro; Yoshinari, Takehisa (Tohoku Univ., Sendai). Kakuriken Kenkyu Hokoku; 2: No. 2, 119-22(Dec 1969). (In Japanese).

During irradiation of a KCl single crystal with the pulsed electron beam of 15-ns pulse width, an absorption band appearing in the uv region was assigned to an H center, and it was found that it vanished with the same time constant as that of F center. This appears to confirm that the F center and H center vanish to make a pair. The absorption band with a peak at 660 nm was also observed, and was due to the trapping of electrons in the triplet state of a V_k center. This species has a lifetime of 0.3 ms in the vicinity of liquid-helium temperature. From the variation of the lifetime with temperature, the decay energy of the triplet state was estimated to be 0.018 eV. (Japan)

27847 SHALLOW DONOR STATE PRODUCED BY PROTON BOMBARDMENT OF SILICON. Zohta, Yashuhito; Ohmura, Yamichi; Kanazawa, Mamoru (Tokyo Shibaura Electric Co., Ltd., Kawasaki, Japan). Jap. J. Appl. Phys.; 10: 532-3(Apr 1971).

Proton bombardment of both n- and p-type Si at 200 to 400 kV and room temperature was found to produce a shallow donor state. Junctions were formed, and the carrier concentration was determined by the Copeland and capacitance methods. The results show that new carriers lie at a depth of from 2 to 4 μ and that the depth increases with proton energy. (D.L.C.)

27848 DEFECT STUDIES IN NEUTRON AND GAMMA-IRRADIATED SILICON. MaGee, Tommy Joe. New Orleans; Tulane Univ. (1970). 350p. University Microfilms Order No. 71-8069.

Thesis.

The defect structure induced in silicon after neutron and gamma irradiation was investigated utilizing electron microscopy, electron paramagnetic resonance, Hall effect–resistivity measurements, and space-charge-limited current observations. The defect structure in the neutron-irradiated samples tended to reflect a significant amount of complexity compared to that observed in the gamma-irradiated samples. Whereas gamma irradiation produces only isolated point defects or simple coupled point defect assemblages, neutron irradiation produces both point defects and large disordered regions composed of interstitials or vacancies. N-type silicon samples were irradiated at a temperature 250°C with fast neutrons to a total exposure of 2×10^{19} nvt. EPR studies at 9.4 GHz indicated the presence of silicon N centers which disappeared at anneal temperatures in excess of 610°C. Transmission electron microscopy revealed the presence of clusters in the unannealed samples of approximately 40 Å in diameter. Upon annealing, the cluster density decreased, but the average size increased, with an average of 56 Å recorded after an anneal of 700°. The resistivity decreased as the anneal temperature was increased. Trapping centers were observed and identified in space-charge-limited current experiments at 0.4 eV below the conduction band. These centers were not observed at anneal temperatures in excess of 200°C. This loss of trapping centers and the reduction in resistivity and EPR intensity, coupled with the increase in cluster size at higher anneal temperatures, was interpreted as evidence for direct interaction between point defect centers and clusters, thereby explaining the observed growth of disordered regions with annealing. Deformed and undeformed n-type silicon samples were irradiated at room temperature to a level of 7×10^7 R. Both silicon A centers and deep levels were introduced in the gamma-irradiated samples. The introduction rate of defect centers was lowered slightly in the deformed irradiated samples. Reverse annealing of A centers was recorded for all samples independent of dopant impurity. Annealing of deep levels differed in the deformed irradiated samples in that a distinct reverse-annealing stage was detected that could be attributed to trapping of defects by dislocation lines. Slight variations in the deep-level anneal curves could be noted in relation to differences in the induced dislocation structure, as observed in electron-microscopy examinations and Hall-effect measurements. (Diss. Abstr. Int., B)

27849 EFFECT OF STRESS ON THE LUMINESCENCE SPECTRUM OF IRRADIATED SILICON. Jones, Colin Elliott. Urbana, Ill.; Univ. of Illinois (1970). 198p. University Microfilms Order No. 71-5141.

Thesis.

Silicon crystals irradiated with neutrons, high-energy electrons, or gamma rays at room temperature show two strong luminescence bands in the near-infrared. Both bands have a sharp zero-phonon line followed by a series of broad phonon-assisted peaks. The higher-energy band associated with a zero-phonon line at 0.97 eV is independent of any impurities, while the lower-energy band with a zero-phonon line at 0.79 eV is seen only in silicon containing oxygen. Data on the temperature and stress dependence of the luminescence bands were taken in order to obtain information on the type of defects and the optical transitions involved. The narrow line widths observed for the zero-phonon lines show that the transitions do not involve a free carrier. The zero-phonon broadening and the major phonon-assisted structure can be related to interactions with the momentum conserving transverse acoustical phonons. The energies and form of the bands do not fit the usual mechanisms involving an exciton bound to a neutral or ionized donor or acceptor. An exciton bound to a neutral defect that has a trapping level nearly as deep as the binding energy determined from the luminescence is a possible mechanism. The zero-phonon line at 0.79 eV is a doublet showing thermal population effects that relate it to two levels in the initial state. The lack of any association with impurities, the annealing, and the stress data for the bands associated with the 0.97-eV zero-phonon line all support an identification of these bands with the divacancy. The oxygen dependence and the thermal stability of the bands associated with the 0.79-eV zero-phonon line lead to a tentative identification of these bands with the K center or G-15 center seen in EPR. A model for this defect, tentatively suggested by the EPR investigators, consists of two nearest-neighbor substitutional oxygen atoms in a [221] crystal orientation. The stress data are not completely explained by this model, and a [100] defect model would also fit the stress splitting. (Diss. Abstr. Int., B)

27850 LOW-TEMPERATURE ANNEALING OF ELECTRON IRRADIATED GERMANIUM. Hyatt, William Dennis. Urbana, Ill.; Univ. of Illinois (1970). 95p. University Microfilms Order No. 71-5132.

Thesis.

N-type germanium (4×10^{14} Sb/cm^3) was irradiated with 1.1-MeV electrons at 5°K. The defects produced were studied by measuring the voltage-dependent capacitance of a metal–germanium junction formed at the surface of a germanium sample. These measurements were made at 10°K and directly gave the fixed charge density near the surface of the sample. The production and recovery of defects seen near the surface is the same as seen in bulk experiments. A 0.5-MeV electron beam was used to cause radiation annealing of the defects at 5°K. The fraction recovered during radiation annealing is directly proportional to $\sqrt{t}$. A model based on diffusion-limited recovery theory is used to explain these results. This model is also used to discuss the results of previous experiments. The temperature dependence of the observed recovery at 5°K gave a defect migration energy of 0.0044 ± 0.0008 eV. (Diss. Abstr. Int., B)

27851 CHANNELING IN FLUORITE CRYSTALS. Bacharach, Stephen Laurence Irwin. Ithaca, N. Y.; Cornell Univ. (1970). 123p. University Microfilms Order No. 71-1049.

Thesis.

A study of channeling phenomena in fluorite crystals was performed, utilizing a 3-MeV linear accelerator. Rutherford backscattered protons were used to investigate the effects on channeling of temperature, ion bombardment, and diatomic composition. A new method of analyzing temperature dependence, by calculation of an energy-independent dechanneling cross section, is presented and applied to the present work. Lattice averaging was used to compare the experimentally observed angular width of channeling to theory. For a diatomic crystal, the usual lattice averaging techniques are shown to give poor results when applied to two sublattices with greatly differing Z. A new method for computing the average row potential is developed and experimentally tested. This method agreed well with the experimental results and may explain the anomalously low angular widths obtained for UO_2 by other authors. Finally, an unexpected blocking phenomenon was discovered following proton bombardment. The blocking was extremely temperature-sensitive. Further in-

XUM

vestigation suggested that the blocking may be due to the release of implanted hydrogen (protons), thus indicating that channeling may be useful as a probe in gas release studies. (Diss. Abstr. Int., B)

27852 GAMMA IRRADIATION OF LITHIUM-DRIFTED SILICON. Kool, W. H.; Goedbloed, J. J.; Ammerlaan, C. A. J. (Univ., Amsterdam). J. Appl. Phys.; 42: 2024-30(Apr 1971).

Boron-doped silicon, compensated by the lithium ion drift method, was irradiated at room temperature with ^{60}Co gamma rays. Resistivity and Hall-effect measurements show the samples to be p-type immediately after irradiation. Kept near room temperature, the p-type conductivity of the samples spontaneously increases because lithium donors are lost by precipitation on irradiation-produced defects. Also other defects are introduced that have an electron energy level at $E_v + (0.25 \pm 0.03)$ eV in float zone and at $E_v + (0.30 \pm 0.03)$ eV in oxygen-rich silicon. The latter level is ascribed to the association of oxygen with an interstitial silicon atom. (auth)

27853 PARAMAGNETIC DEFECTS IN TiO_2 PRODUCED BY RADIATION. Purcell, T.; Weeks, R. A. (Oak Ridge National Lab., Tenn.). J. Chem. Phys.; 54: 2800-10(1 Apr 1971).

Single crystals of TiO_2, space group D_{4h}^{14}, reactor irradiated at 140°K and measured at 78°K, without warmup, exhibit intense electron spin resonance spectra. The most intense component of these spectra has an orientation dependence expected of a substitutional site. Two other less intense components of the spectra could be associated with interstitial sites or perturbed substitutional sites. The concentration of each of these was ~0.1, the concentration of the intense component. These three spectral components and a blue-black color were no longer observed after warming to 300°K. An additional radiation with ^{137}Cs gamma rays at 77°K gave a new intense resonance having an orientation dependence expected for an interstitial site. Weak satellite lines observed for one orientation were attributed to hyperfine interaction with ^{47}Ti and ^{49}Ti. Good agreement between the observed orientation dependence and that calculated from a spin Hamiltonian for which $S = \frac{1}{2}$ and for which D_{4h}^{14} point symmetry is used was found for each species. On the basis of concentration, g values, and hyperfine interactions, the two most intense spectral components are attributed to singly charged oxygen vacancies and interstitial Ti^{3+} ions. (auth)

27854 ISOTHERMAL ANNEALING OF BORON IMPLANTED SILICON. Seidel, T. E.; MacRae, A. U. (Bell Telephone Labs., Murray Hill, N. J.). Radiat. Eff.; 7: 1-6(Jan 1971).

Isothermal annealing studies of boron-implanted silicon were made at temperatures above 600°C for boron doses in the range of 10^{14} to 10^{15} ions/cm^2. A 5-eV activation energy is obtained in the temperature range 600 to 900°C. This value is the same as that associated with the generation and subsequent migration of vacancies in silicon. This indicates that the mechanism responsible for the increase in electrical activity of the implanted boron is due to the thermal generation of vacancies and the diffusion of these vacancies or vacancy complexes to interstitial boron atoms, which then become substitutional. The characteristic annealing times are dose-dependent. No simple integral-order kinetic process will explain all the data. Good agreement between the data and a calculation is obtained if it is assumed that the characteristic annealing times are position-dependent. Detailed data are presented that provide the time and temperature necessary to obtain complete electrical activity of boron-implanted silicon over several orders of magnitude of incident dose. (auth)

27855 LOW ENERGY BORON IMPLANTATION PROFILES IN SILICON FROM JUNCTION DEPTH MEASUREMENTS. Sebillotte, P.; Badanoiu, M.; Ndocko, V. B.; Siffert, P. (Centre de Recherches Nucleaires, Strasbourg). Radiat. Eff.; 7: 7-15(Jan 1971).

Boron-implanted nuclear-particle detectors prepared with high-resistivity material (up to 50,000 Ω cm) are needed. The properties of these p–n junctions depend to a certain amount on the impurity distribution existing several orders of magnitude below the top of the distribution. Therefore, only the junction location method can be employed to study the distribution of implanted boron. In this method a series of n-type silicon samples, differing each from the other by an increase in resistivity, are implanted with boron. The depth of the p–n junction corresponds to the point of the profile where the concentration N_A is equal to that of the substrate N_D (this latter being well known from the resistivity of the starting material). If the location of the junction can be measured, the profile can then be constructed point by point. The junction location is visualized generally by copper staining. This procedure has been used for boron implantations at energies higher than 50 keV. There is a problem due to the small penetration of the boron ion, and, for high-resistivity materials, it is difficult to know the true limits of the zones stained with copper. In our problem, when heavy particle detectors are desired, it is necessary to implant at lower energies than those indicated previously (<20 keV). A new technique derived from the junction depth method was developed which is useful even at very low implant energy (≈10 keV). It consists in measuring the energy loss by 100-keV protons when crossing the entrance window of the p–n junctions used as detectors. The method is described and the possible errors are analyzed and evaluated. The distribution of 15-keV boron ions implanted under several experimental conditions is studied. Emphasis is given to the defects resulting from the silicon bombardment. (auth)

27856 LATTICE LOCATION AND DOPANT BEHAVIOR OF GROUP II AND VI ELEMENTS IMPLANTED IN SILICON. Gyulai, J.; Meyer, O.; Pashley, R. D.; Mayer, J. W. (California Inst. of Tech., Pasadena). Radiat. Eff.; 7: 17-24(Jan 1971).

Outdiffusion, lattice location, and electrical behavior of Zn, Cd, Hg and Se, Te implanted into silicon at 50 keV were investigated by backscattering and channeling of 1-MeV He^+ ions and by Hall effect and sheet resistivity measurements. All the species exhibited outdiffusion with thermal processing. A significant fraction of Zn, Cd, and Hg, when implanted into a substrate at 350°C, occupied regular interstitial lattice sites, while 50 to 60% of the Se and Te atoms were on substitutional lattice sites. Selenium implanted at room temperature and Hg implanted into a substrate of 350°C exhibited depth-dependent lattice location. The implanted layers showed n-type behavior: the maximum value of number of carriers/cm^2 was less than the number of implanted ions/cm^2 in all cases. The highest electrical activity was observed for Se corresponding to 25% of the substitutional component. (auth)

27857 USE OF CHANNELING-EFFECT TECHNIQUES TO LOCATE INTERSTITIAL FOREIGN ATOMS IN SILICON. Andersen, J. U.; Andreasen, O.; Davies, J. A.; Uggerhoej, E. (Univ. of Aarhus, Denmark). Radiat. Eff.; 7: 25-34(Jan 1971).

When the channeling-effect technique is used to determine the lattice location of an impurity that is not completely substitutional, quantitative interpretation of the results requires knowledge of the interaction yield between a channeled beam and an interstitial atom. This problem was investigated for Yb implanted into silicon. Along the ⟨110⟩ direction, a peak of almost a factor of two is observed in backscattering yield from the Yb atoms, using a 1-MeV He beam. The height and angular width of the peak is satisfactorily interpreted in terms of flux-peaking of the channeled beam in the central region of the ⟨110⟩ channels. The existence of such a large flux-peaking effect seriously complicates quantitative determination of the location of nonsubstitutional impurities. However, it is still possible to establish rather accurately the lattice position of the impurity, provided the measured minimum yields and angular widths of the ⟨111⟩ and ⟨100⟩ dips are taken into account. (auth)

27858 ANALYSIS OF ION IMPLANTED DIAMOND. Davidson, L. A.; Chou, S.; Gibbons, J. F.; Johnson, W. S. (Stanford Univ., Calif.). Radiat. Eff.; 7: 35-44(Jan 1971).

Ion implantation allows controlled introduction of impurities into diamond. A basic problem is to determine if the implanted layers are dominated by substitutional doping or radiation damage effects. Optical and electrical measurements on the implanted diamonds revealed (1) a degradation of the band gap and sample coloration, (2) no optical absorption levels that would be characteristic of hydrogenic ionization levels, (3) resistivity activation energies of 0.2 to 0.3 eV independent of the ion specie, and (4) no measurable Hall effect. Phosphorous-implanted layers in diamond were analyzed by means of the proton channeling technique. It was shown that (1) the diamond retained the implanted phosphorous atoms during a vacuum anneal at 950°C which restored crystalline order, (2) the implanted phosphorous atoms did not assume either substitutional or tetrahedral interstitial sites, (3) the measured projected range for 70-keV phosphorous in diamond of 450 ± 115 Å was consistent with theoretical range calculations, and (4) a stable monolayer of oxygen atoms (5.5×10^{15}/cm^2) exists on the {111} surface of implanted and annealed diamond. The results of the crystal analysis show that these electrical and optical properties are dominated by radiation damage and not substitutional doping mechanisms. (auth)

27859 LOW TEMPERATURE CHANNELING MEASUREMENTS OF ION IMPLANTATION LATTICE DISORDER IN SINGLE CRYSTAL SILICON. Picraux, S. T.; Weisenberger, W. H.; Vook, F. L. (Sandia Labs., Albuquerque, N. Mex.). Radiat. Eff.; 7: 101-7(Jan 1971).

Lattice disorder for 200-keV Sb implantations into silicon was studied by channeling-effect analysis using 400-keV proton backscattering. Implantation and analysis were performed at low tem-

peratures in the same system without warmup. In the temperature region between 85°K and room temperature, the disorder production per incident ion at low doses is implantation-temperature-dependent. Approximately 18,000 silicon scattering centers per incident 200-keV Sb ion are observed for 90°K implantations, and this value is nearly a factor of three greater than at room temperature. Isochronal anneal curves of low-fluence, low-temperature implantations show significant annealing below room temperature. The observed disorder production per incident ion decreases with increasing implantation temperature at temperatures 50 to 100°K lower than annealing occurs following 85 or 90°K implants. Strong similarities of the implantation temperature dependence and anneal behavior of the disorder exist for Sb and B implantations into silicon and suggest that much of the lattice disorder produced by ion implantation can be understood in terms of the basic properties of the silicon target material. (auth)

27860 PREFERENTIAL ETCHING OF ION-BOMBARDED GaAs. Arnold, G. W.; Whan, R. E. (Sandia Labs., Albuquerque, N. Mex.). Radiat. Eff.; 7: 109-14(Jan 1971).

Ion bombardment of GaAs above fluences of the order of 2×10^{13} 400-keV Xe-ions/cm^2 produces a highly strained surface that is elevated several hundred Angstroms above the adjacent masked surface. The irradiated area etches rapidly to yield circular etch pits ~0.3 μ in depth and 0.2 μ in diameter. At lower fluences, observations show much less expansion, slower crystalline etching, and some evidence of triangular etch pits and slip planes. These results are attributed to expansion in the implanted layer that results in high surface strain and the generation of dislocations to accommodate the mismatch of lattice parameters. (auth)

27861 SPATIAL DISTRIBUTION OF DEFECTS IN ION BOMBARDED SILICON AND GERMANIUM. Boegh, E.; Hoegild, P.; Stensgaard, I. (Univ. of Aarhus, Denmark). Radiat. Eff.; 7: 115-21(Jan 1971).

The damage produced in Si and Ge by 10 to 400-keV heavy-ion bombardment was measured by using the channeling technique. By optimizing the experimental conditions, the depth distribution of the damage can be measured with a depth resolution of ~10% in the range of 50 to 10000 Å. A short description is given of the method and the apparatus used in these measurements. The results of the measurements may be summarized as follows: (i) The measured depth distributions demonstrate the necessity of taking the energy transported by recoils away from their point of origin into account. (ii) The average damage depth and the depth straggling agree with recent theoretical calculations of the distribution of energy deposited by ions in solids. (iii) The damage production exhibits a dose rate dependence indicative of room-temperature annealing. This is supported by the observation of the annealing effect of a 0.5-MeV He bombardment. (iv) Channeling of a heavy ion has a marked influence on the damage produced by the ion. The depth and the width of a damage distribution created by a channeled implantation are larger than those of a distribution from a nonchanneled implantation, whereas the damage production in the former case is smaller than in the latter. (auth)

27862 ANNEALING OF DAMAGE IN ION IMPLANTED GALLIUM ARSENIDE. Harris, J. S.; Eisen, F. H. (North American Rockwell Corp., Thousand Oaks, Calif.). Radiat. Eff.; 7: 123-8 (Jan 1971).

Photoluminescence measurements at 77°K and Rutherford scattering of 450-keV protons were used to study radiation damage and annealing in ion-implanted GaAs. The characteristic band edge luminescence (8225 Å) in GaAs is completely quenched by ion implantation. Photoluminescence measurements on samples isochronally annealed show a single annealing stage at 600°C. A luminescence peak at 9140 Å is introduced into the spectra of all implanted and annealed samples. This peak is attributed to an acceptor level created by As vacancies. The intensity of the peak is greatly reduced by protecting the surface of implanted layers with SiO_2 during annealing. Rutherford-scattering measurements on isochronally annealed samples reveal two annealing stages. A 300°C annealing stage is observed on samples that have an initial aligned yield less than random, while a 650°C stage is observed on samples that have an initial aligned yield equal to random. (auth)

27863 ANNEALING OF DAMAGE PRODUCED BY BORON ION IMPLANTATION OF SILICON SINGLE CRYSTALS. Chadderton, L. T.; Eisen, F. H. (North American Rockwell Corp., Thousand Oaks, Calif.). Radiat. Eff.; 7: 129-38(Jan 1971).

Using the techniques of Rutherford scattering, electron microscopy, and infrared absorption, the damage produced by implantation of 100- to 400-keV boron (^{11}B) ions in silicon single crystals, held at room and liquid nitrogen temperatures, was examined and the annealing behavior investigated. The rapid annealing of disorder in the range between room temperature and 325°C, as observed by the Rutherford scattering of channeled analyzing particle beams, correlates with a shrinkage of the 1.8-μ divacancy infrared absorption band and with a coarsening of some of the defects observed in the electron microscope. Amorphous zones observed in samples implanted with 10^{15} boron ions/cm^2 at liquid nitrogen temperature do not anneal until temperatures in the vicinity of 450°C are attained. The consequences of aggregation of point defects, first as small crystallographic clusters, for temperatures in the vicinity of 300°C, and then as large circular dislocation loops following isochronal anneals up to 1000°C, were observed for specimens implanted at liquid nitrogen temperature. Details of this and of substantial differences observed in room temperature-implanted samples are discussed. (auth)

27864 FLUX AND FLUENCE DEPENDENCE OF DISORDER PRODUCED DURING IMPLANTATION OF ^{11}B IN SILICON. Eisen, F. H.; Welch, B. (North American Rockwell Corp., Thousand Oaks, Calif.). Radiat. Eff.; 7: 143-8(Jan 1971).

The flux and fluence dependence of disorder produced in silicon during the implantation of ^{11}B was investigated at room temperature, −50°C, and −120°C. Implantations were carried out with 200-keV ^{11}B ions using current densities in the range from 0.06 to 15 μA/cm^2, and the disorder monitored by measuring the energy spectra of backscattered protons that were incident on the sample at 450 keV parallel to a ⟨110⟩ axis. Significant differences in the dependence of the disorder on ^{11}B flux and fluence were observed between the implantations performed at room temperature and those carried out at the two lower temperatures. (auth)

Physical Properties

Refer also to abstracts 27184, 27212, 27215, 27220, 27223, 27230, 27662, and 27666.

27865 (CEA-R-4138) INVESTIGATION OF ELECTRONIC LATTICE STRUCTURE BY POSITRON ANNIHILATION IN SOME INSULATORS. Coussot, Gerard (Commissariat a l'Energie Atomique, Saclay (France). Centre d'Etudes Nucleaires). Feb 1971. 142p. (In French). Dep. NTIS (U. S. Sales Only).

Thesis. Submitted to Univ. of Paris, Faculte des Sciences, Orsay, France.

The angular distribution of gamma quanta resulting from positron annihilation in single insulator crystals was measured with long-slit-geometry apparatus for intense positron sources (^{64}Cu ≃ 1 Ci). Two new phenomena were observed in the angular correlation curves. In the fcc MgO, UO_2, and CaF_2 crystals, modulations appeared at angles corresponding to the limit of the first Brillouin zone in relation to the crystallographic direction studied. In SiO_2, MgF_2, MnF_2 crystals, a narrow peak at 0 mrad and a fine structure superimposed on the broad distribution, were resolved. The fine structure correlated with the narrow component is characterized by modulations appearing at angles corresponding to the projection of reciprocal lattice vectors along the crystallographic direction investigated. The narrow peak at $p \simeq 0$ suggests the formation of a bound state (positron−electron). If this bound state is described by a Bloch wave, the modulations observed correspond to the Fourier components that contribute to every reciprocal lattice vector $\vec{p} = \vec{G}$ ("umklapp" process). This model predicts that the "umklapp" process in polycrystals must produce a change in slope that can be experimentally observed. A systematic research of optimal observation conditions shows that the intensity of the narrow component is closely correlated with the purity and the perfection of the crystal where p−Ps is presumably formed, as suggested by magnetic experiments. (France)

27866 (NYO-3504-56) DEFECTS IN METAL CRYSTALS. Annual Progress Report. Balluffi, R. W.; Seidman, D. N. (Cornell Univ., Ithaca, N. Y.). Feb 1971. Contract AT(30-1)-3504. 21p. Dep. NTIS.

Attention was focused on point defects (vacancies, interstitials, and solute atoms), line defects (dislocations), and planar defects (dislocation arrays, grain boundaries, and surfaces). Progress was made in the following areas: (a) annealing kinetics of vacancy defects in quenched gold at elevated temperatures; (b) electron microscope study of low- and high-angle grain boundaries in gold; (c) field-ion microscope (FIM) and electrical-resistivity study of vacancy defects in platinum; (d) FIM and electrical-resistivity study of vacancy defects in tungsten; (e) in-situ FIM studies of defects in tungsten irradiated with tungsten ions; (f) in-situ FIM studies of defects in platinum irradiated with platinum ions; (g) field-ion microscopy of gold; and (h) heating of FIM specimens. (auth)

XUM

27867 (UCRL-51006) ELECTRICAL RESISTANCE OF YTTERBIUM AS A FUNCTION OF TEMPERATURE AND PRESSURE. Lilley, E. M.; Stephens, D. R. (California Univ., Livermore. Lawrence Radiation Lab.). 4 Feb 1971. 13p. Dep. NTIS.

The piezoresistance of ytterbium from three sources was measured at pressures up to 40 kbar and at temperatures between 21 and 90°C under hydrostatic and quasi-hydrostatic conditions. From the data, from calculations of Hugoniot state temperatures, and from the geometrical effect of plane strain on resistance, the piezoresistance of ytterbium along the Hugoniot was calculated. The computed results agree with the experimental Hugoniot data of Brown for the same samples to within 10%. Although resistance hysteresis upon unloading from the Hugoniot is observed in shock studies, no measurable hysteresis was seen at constant temperatures below the fcc-to-bcc transition. Only minor resistance hysteresis is predicted on the basis of the temperature differences between the Hugoniot and the release states. The fcc-to-bcc transition in ytterbium, which occurs between 37 and 39 kbar at room temperature, is predicted to occur between 34 and 35 kbar along the Hugoniot as the transformation pressure decreases with increasing temperature. (auth)

27868 ESTIMATION OF CORRELATION EFFECTS IN TRANSITION METALS AND ALLOYS FROM PRESSURE AND RELATED EXPERIMENTS. Wohlfarth, E. P. (Imperial Coll.of Science and Tech., London); Bartel, L. C. Phys. Lett.; 34A: 303-4 (5 Apr 1971).

The ratio I/I_b, where I and I_b, respectively, are the effective and bare interactions between the itinerant electrons, was estimated on the basis of high-pressure and related experiments to be generally greater than $\frac{1}{2}$ for Ni_3Ga, Ni-Rh, Invar, and $ZrZn_2$, indicating weak correlation effects for these materials. (auth)

27869 PROCEEDINGS OF THE SIXTEENTH ANNUAL CONFERENCE ON MAGNETISM AND MAGNETIC MATERIALS, 17-20 NOVEMBER 1970, HELD AT MIAMI BEACH, FLORIDA. J. Appl. Phys.; 42: 1243-1816(15 Mar 1971). (CONF-701104).

Two hundred eight papers and 41 abstracts are included which are grouped into 44 sessions. Some of the topics covered are: bubble domains, critical phenomena, rare earths, transition metals, magnetism in biology and medicine, films, resonance, spin diffusion and anisotropic scaling, photoemission and photoconductivity, magneto-optics, astrophysical magnetism and continental drift, semiconductors and pnictides, hard and soft magnetic materials, relaxation, exchange-enhanced metals, orthoferrites, solid O_2 and H_2, ultrasonic attenuation and sublattice magnetization, anisotropy and magnetostriction, EPR hyperfine effects, spin waves, optical properties, Moessbauer spectroscopy, crystal fields and metal-insulator transitions, thermomagnetic recording, and chalcogenides. Separate abstracts were prepared for 35 of the papers. (D.L.C.)

For abstracts of individual papers see: 27184, 27442, 27666, 27870-27898, and 27920-27922.

27870 MAGNETIC AND ELECTRICAL CHARACTERISTICS OF $REPd_3$ INTERMETALLIC COMPOUNDS. Hutchens, R. D.; Rao, V. U. S.; Greedan, J. E.; Wallace, W. E.; Craig, R. S. (Univ. of Pittsburgh). J. Appl. Phys.; 42: 1293-4(15 Mar 1971).

From 16th Annual Conference on Magnetism and Magnetic Materials, Miami Beach, Fla. See CONF-701104.

Magnetic characteristics of 12 $REPd_3$ (RE = a rare earth) compounds were studied between 4 and 300°K. Electrical resistivity measurements were made on the Ce, Gd, and Ho compounds. All compounds are paramagnetic at room temperature; all except $CdPd_3$, $SmPd_3$, and $EuPd_3$ exhibit Curie-Weiss behavior with paramagnetic moments in close agreement with that expected for the free tripositive ion. The susceptibility behavior of $CePd_3$ is ascribed to the Kondo phenomenon (spin compensation) while that of $SmPd_3$ and $EuPd_3$ to the narrowness of the multiplet spacings. This interpretation for $CePd_3$ is supported by its resistivity-temperature behavior. Evidence for magnetic ordering is found only for $GdPd_3$, which seems to order ferromagnetically below 7°K. (auth)

27871 ELECTRICAL RESISTIVITY AND MAGNETIZATION OF Gd-Th AND Gd-Mg ALLOYS. Mellon, D. W.; Legvold, S. (Ames Lab., Iowa). J. Appl. Phys.; 42: 1295-7(15 Mar 1971).

From 16th Annual Conference on Magnetism and Magnetic Materials, Miami Beach, Fla. See CONF-701104.

Electrical resistivity and magnetization measurements were made over the 4.2 to 300°K temperature range on single-crystal $Gd_{1-x}Th_x$ and on polycrystalline $Gd_{1-x}Mg_x$ samples with $0 < x < 0.15$. This work was done because quadrivalent Th increases the number of conduction electrons and hence raises E_F, whereas divalent Mg decreases the number of conduction electrons and so lowers E_F. Fermi surface changes might then be expected. The most interesting result was obtained with $Gd_{0.88}Mg_{0.12}$, which showed an increase in resistivity with decreasing temperature below 260°K. The magnetic measurements indicated that all samples ordered ferromagnetically. (auth)

27872 MAGNETIC PROPERTIES OF THE SYSTEM Au_4R (R = Er, Tm, AND Yb). Sill, L. R.; Mass, W. J.; Fedro, A. J.; Shaffer, J. C.; Kimball, C. W. (Northern Illinois Univ., DeKalb). J. Appl. Phys.; 42: 1297-8(15 Mar 1971).

From 16th Annual Conference on Magnetism and Magnetic Materials, Miami Beach, Fla. See CONF-701104.

Magnetic measurements were made from 6.1 to 300°K on chemically ordered RAu_4(R = Er, Tm, Yb) with the bct $MoNi_4$ structure. No magnetic ordering was found for any of the compounds in this temperature range. The temperature dependence of the reciprocal susceptibility for each specimen satisfied an equation which included both Curie-Weiss and temperature-independent terms. The paramagnetic Curie temperature for each specimen had a negative value and the magnetic moments of the rare earths were those appropriate to the trivalent ion. An RKKY calculation indicates that $ErAu_4$ and $TmAu_4$ should magnetically order at ~5° and below 2°K, respectively. (auth)

27873 DOMAIN WALLS IN FERROMAGNETIC Dy AND Tb. Egami, T.; Graham, C. D. Jr. (Univ. of Pennsylvania, Philadelphia). J. Appl. Phys.; 42: 1299-1300(15 Mar 1971).

From 16th Annual Conference on Magnetism and Magnetic Materials, Miami Beach, Fla. See CONF-701104.

The spin structure and energy of ferromagnetic domain walls in Dy and Tb are calculated, using an iterative method that takes into account exchange interactions, magnetocrystalline anisotropy, and magnetoelastic anisotropy. The domain walls are found to be very thin (less than 20 atom layers) and to have relatively high energy (~10 erg/cm^2), as compared to the ferromagnetic transition metals. An intrinsic coercive force for wall motion is predicted for these very thin walls; it is analogous to the Peierls-Nabarro force on a dislocation, and is estimated to be of the order of 1 kOe for Dy and 30 Oe for Tb at absolute zero. (auth)

27874 MAGNETIC PROPERTIES OF EUROPIUM: PRESSURE AND IMPURITY EFFECTS. Menyuk, N.; Dwight, K.; Kafalas, J. A. (Massachusetts Inst. of Tech., Lexington). J. Appl. Phys.; 42: 1301-2(15 Mar 1971).

From 16th Annual Conference on Magnetism and Magnetic Materials, Miami Beach, Fla. See CONF-701104.

Magnetic properties of europium in the vicinity of the transition temperature T_t were studied as functions of hydrostatic pressure. A marked drop in the moment, consistent with a first-order transition, is observed at atmospheric pressure, but the sharpness of this transition decreases at higher pressures. The variation of T_t with pressure is nonlinear above 4 kbar, with $\Delta T_t/\Delta P = 0.45° \pm 0.03°K/kbar$ in the limit $P \to 0$. This value corresponds, via the Clausius-Clapeyron relation, to twice the volume change previously estimated on the basis of direct thermal-expansion measurements. In addition, it is found that $d\theta/dP < 0$, where θ is the paramagnetic Curie temperature. Below T_t, the magnetic susceptibility of europium is known to rise anomalously. Although the sample was nominally "high-purity" europium, the presence of a ferromagnetic component is observed at 4.2°K. In addition, the temperature variation of the susceptibility is shown to be consistent with a presence of a small amount of some ferromagnetic europium salt with $T_c \sim 16.5°K$ in the bulk of the sample. (auth)

27875 FERROMAGNETISM OF $ZrZn_2$. Knapp, G. S.; Fradin, F. Y.; Culbert, H. V. (Argonne National Lab., Ill.). J. Appl. Phys.; 42: 1341-6(15 Mar 1971).

From 16th Annual Conference on Magnetism and Magnetic Materials, Miami Beach, Fla. See CONF-701104.

The magnetic properties of $ZrZn_2$ and related alloys and compounds are discussed. In particular, the pseudo-$ZrZn_2$ alloy system $ZrCu_{2-x}Al_x$ was studied, where $0.76 \leq x \leq 1.5$. The results of specific heat, magnetic susceptibility, and NMR measurements are presented to show that the Fermi level of $ZrCu_{1.1}Al_{0.9}$ lies at the top of a sharp narrow d-band peak that is about 0.1 eV in half-width and has a maximum value of 2.7 states (eV-Zr atom spin)$^{-1}$. It also is shown that $ZrZn_2$ has a sharp narrow peak in the d-band density of states at the Fermi level. This peak has a half-width of about 0.05 eV and has a maximum value of 5.4 states (eV-Zr atom spin)$^{-1}$. The ferromagnetism of $ZrZn_2$ is understandable in terms of this feature of the band structure. The occurrence of a high narrow peak at the Fermi level is the most favorable condition for the existence of itinerant ferromagnetism. (auth)

27876 PHOTOEMISSION STUDIES OF f STATES AND VALENCE BANDS IN SEVERAL RARE-EARTH AND URANIUM COM-

XUM

POUNDS. Eastman, D. E. (IBM Thomas J. Watson Research Center, Yorktown Heights, N. Y.); Kuznietz, Moshe. J. Appl. Phys.; 42: 1396-1402(15 Mar 1971).

From 16th Annual Conference on Magnetism and Magnetic Materials, Miami Beach, Fla. See CONF-701104.

Photoemission spectroscopy measurements of f states and valence band energies are reported for EuS, GdS, and US using photon energies for 5 to 41 eV. The energy dependence of photoemission spectra permits the "l" character of various levels to be identified. Characteristic energy-dependent emission strengths of "p", "d", and "f" states are observed. In a typical case, the emission strength of the $4f^7$ level in EuS increases about 100-fold relative to the ~2.9-eV-wide valence "p" band (which lies just below the $4f^7$ level) as $\hbar\omega$ increases from 10 to 41 eV. Metallic GdS shows a "d"-like conduction band at the Fermi level E_F, a 4.5-eV-wide "p"-band centered at ~5 eV below E_F, and a $4f^7$ level at 9 eV below E_F. Uranium monosulphide shows a narrow "f-d" conduction band at E_F and a 4.7-eV-wide "p"-band centered at 4.7 eV below E_F. (auth)

27877 THERMOPOWER OF DILUTE ALLOYS OF CERIUM IN LANTHANUM. Grobman, Warren D. (IBM Thomas J. Watson Research Center, Yorktown Heights, N. Y.). J. Appl. Phys.; 42: 1456-7(15 Mar 1971).

From 16th Annual Conference on Magnetism and Magnetic Materials, Miami Beach, Fla. See CONF-701104.

A large negative peak in the thermoelectric power S of the La-Ce Kondo system was measured at low temperature. This result is qualitatively different than that of Sugawara. Measurements were made in the range $4.2°K \leq T \leq 350°K$ for four compositions: 0.03-, 0.5-, 2-, and 5-at. % Ce. The size of the peak was in the range −1.5 to −2. $\mu V/K$ and occurred at ~20°K. The shape of the curves, and the temperature at which the peak occurred, were nearly independent of composition for $T < 150°K$, while the curves were somewhat sample dependent at higher temperatures. While significant amounts of metallic impurities were present, they probably do not contribute a peak in the thermopower. However, on the basis of these measurements one cannot rule out the possibility that the peak is intrinsic to La. (auth)

27878 MAGNETIC PROPERTIES OF DILUTE ALLOYS OF SCANDIUM. Isaacs, L. L.; Lam, D. J.; Fradin, F. Y. (Argonne National Lab., Ill.). J. Appl. Phys.; 42: 1458-9(15 Mar 1971).

From 16th Annual Conference on Magnetism and Magnetic Materials, Miami Beach, Fla. See CONF-701104.

Previous experiments have shown that small quantities of cerium will induce a spin-compensated state in the d^1 elements yttrium and lanthanum. The magnetic susceptibility of scandium alloys with 0.02 to 2-at. % cerium was measured over the temperature range of 4 to 300°K. No evidence for a spin-compensated state is found. Addition of gadolinium was shown to polarize the scandium matrix. To study the influence of a heavy rare earth with nonzero orbital angular momentum on the polarization of the scandium matrix, a series of dilute dysprosium alloys were studied. The effect of dysprosium is found to be similar to that of gadolinium. Also, the influence of the nonmagnetic alloying elements titanium and thorium on scandium was investigated in order to separate the various factors affecting the magnetic properties of dilute scandium alloys. (auth)

27879 EVIDENCE OF THE INTRINSIC METALLIC CHARACTER OF SOME RARE-EARTH PNICTIDES. Gambino, R. J.; Eastman, D. E.; McGuire, T. R.; Moruzzi, V. L.; Grobman, W. D. (IBM Thomas J. Watson Research Center, Yorktown Heights, N. Y.). J. Appl. Phys.; 42: 1468-9(15 Mar 1971).

From 16th Annual Conference on Magnetism and Magnetic Materials, Miami Beach, Fla. See CONF-701104.

From measurements of the low-temperature specific heat of bulk crystals of YSb and GdSb and photoemission spectra from a single crystal of GdSb, it is concluded that these compounds are intrinsic metals. The electronic contribution to the specific heat of YSb was found to be 0.9 mJ/mole deg^2 which may be compared with 0.65 for Ag, a good metal. Photoemission spectra for GdSb show structure at the Fermi level E_F which is consistent with an s-like band at E_F which overlaps a "valence band" with a peak at 2.2 eV below E_F. This band picture offers an alternative explanation for the absorption spectra which have been interpreted as evidence for a large bandgap in the rare-earth pnictides. (auth)

27880 EFFECT OF SUBSTITUTIONAL ANIONS ON THE MAGNETIC PROPERTIES OF THE MONONITRIDES OF URANIUM AND GADOLINIUM. Kuznietz, Moshe (Argonne National Lab., Ill.). J. Appl. Phys.; 42: 1470-2(15 Mar 1971).

From 16th Annual Conference on Magnetism and Magnetic Materials, Miami Beach, Fla. See CONF-701101.

The mononitrides of uranium and gadolinium have the NaCl-type structure and are good electrical conductors. UN is antiferromagnetic of type I ($T_N \sim 50°K$); GdN is ferromagnetic ($T_C \sim 70°K$). In UN, limited oxygen substitution raises T_N, while carbon substitution lowers T_N, and $UN_{0.9}C_{0.1}$ does not order. Oxygen substitution in GdN lowers the paramagnetic Curie temperature θ, and $GdN_{0.95}O_{0.05}$ and $GdN_{0.90}O_{0.10}$ do not order or, at most, have short-range antiferromagnetic order; carbon substitution in GdN raises T_C or θ. The different orderings in UN and GdN and the variations in T_N or T_C due to anion substitution are accounted for by a simple model, originally proposed for UX compounds, in terms of variations in the number Z of conduction electrons per cation. Assuming U^{4+} and Gd^{3+} cations and N^{3-} anions, and RKKY-type interactions between the localized f electrons, the observed ordering in UN is most stable for $Z \sim 1$ and in GdN for $Z \sim 0.1$. Substituting O^{-2} anions for nitrogen increases Z in both UN and GdN; carbon substitution decreases Z. The variations of magnetic ordering and θ with Z are discussed for anion-substituted GdN and UN as well as other monopnictides of Gd and U. (auth)

27881 CRYSTAL-FIELD SPLITTING AND SPIN WAVES IN ANTIFERROMAGNETIC CeSb. Busch, G.; Stutius, W.; Vogt, O. (Eidgenoessisches Technische Hochschule, Zurich). J. Appl. Phys.; 42: 1493-4(15 Mar 1971).

From 16th Annual Conference on Magnetism and Magnetic Materials, Miami Beach, Fla. See CONF-701104.

The specific heat of crystalline samples of $Ce_xY_{1-x}Sb$ (x = 1, 0.2, 0.1, and 0) and LaSb was measured for temperatures between 1.5 and 70°K. The Néel temperature of CeSb is found to be 16.0 (±0.2)°K. The magnetic specific heat between 1.5 and 3.8°K is proportional to T^2. This temperature dependence is correlated with spin waves in the anisotropic magnetic structure of CeSb. The crystal-field splitting of the $^2F_5$ ground state of the Ce^{3+} ion in CeSb is 24 ± 2°K. (auth)

27882 CRITICAL FIELDS DETERMINING MAGNETIC COERCIVITY IN MICROPARTICLES OF $SmCo_5$ AND $LaCo_5$. Zijlstra, H. (Philips Research Labs., Eindhoven, Netherlands). J. Appl. Phys.; 42: 1510-15(15 Mar 1971).

From 16th Annual Conference on Magnetism and Magnetic Materials, Miami Beach, Fla. See CONF-701104.

Magnetic hysteresis curves measured by a specially designed magnetometer on a single particle taken from a ground $SmCo_5$ powder show that the coercivity is determined by pinning of domain walls. Heat treatment at 100°C in air reduces the pinning force. Magnetizing the particle in a strong field increases the pinning force. A wall-pinning model is proposed to explain this effect. The coercivity of a particle taken from the powder after electrolytic etching seems to be determined by nucleation of domain walls. Heat treatment at 100°C in air does not significantly influence the field at which nucleation occurs. The coercivity of an $LaCo_5$ particle is determined by pinning. The pinning force is reduced by hydrogen absorption. (auth)

27883 CAST PERMANENT MAGNETS OF THE Co_5RE TYPE WITH MIXTURES OF CERIUM AND SAMARIUM. Nesbitt, E. A.; Chin, G. Y.; Gallagher, P. K.; Sherwood, R. C.; Wernick, J. H. (Bell Telephone Labs., Inc., Murray Hill, N. J.). J. Appl. Phys.; 42: 1530-2(15 Mar 1971).

From 16th Annual Conference on Magnetism and Magnetic Materials, Miami Beach, Fla. See CONF-701104.

Previous studies of the effect of composition on the magnetic properties of arc-cast alloys in the vicinity of $Co_{3.5}CuFe_{0.5}Ce$ yielded maximum energy products from 4 to 10×10^6 G Oe, residual inductions from 4000 to 6400 G, and intrinsic coercive forces from 5000 to 12,000 Oe. The partial substitution of samarium for cerium in alloys in this vicinity results in an improvement in permanent magnet properties, with maximum energy products from 4.6 to 12.3×10^6 G Oe, residual inductions 4300 to 7150 G, and intrinsic coercive forces from 4000 to 13,400 Oe. Freezing points of these alloys were determined using differential thermal analysis. The dependence of magnetic saturation on temperature was determined for several of these alloys from room temperature to 1.5°K. The saturation increases gradually with decreasing temperature without anomaly. The temperature coefficient of saturation magnetization between 25 and −100°C was found to be 0.1%/°C for the alloy $Co_{3.5}CuFe_{0.5}Ce$, 0.06%/°C for the alloy $Co_{3.5}Cu_{1.35}Fe_{0.4}Sm$. Intermediate values were obtained for mixtures of Ce and Sm. The temperature coefficient of saturation magnetization was reduced to practically zero by the partial substitution of Gd for Ce. (auth)

27884 INITIAL OBSERVATIONS: COBALT-MISCHMETAL-SAMARIUM PERMANENT MAGNET ALLOYS. Benz, M. G.; Martin, D. L. (General Electric Research and Development Center, Schenectady, N. Y.). J. Appl. Phys.; 42: 1534-5(15 Mar 1971).

From 16th Annual Conference on Magnetism and Magnetic Materials, Miami Beach, Fla. See CONF-701104.

Several authors have reported successful fabrication of high-energy-product (20 MG Oe) Co_5R-type cobalt–samarium permanent magnets. In earlier papers preparation of such magnets by a liquid-phase sintering process sequence that includes powder preparation, magnetic alignment, pressing, sintering, and magnetizing was described by the present authors. They also described preparation of ternary compositions, primarily Co–Sm–Pr, by this process. In an effort to utilize more abundant rare-earth metals, the cobalt–mischmetal–samarium system was studied. Initial results indicate that a substantial fraction of the samarium may be replaced with mischmetal while retaining high magnetic properties (BH_{max} = 20 MG Oe). (auth)

27885 MAGNETIZATION DISCONTINUITIES IN COBALT–RARE-EARTH PARTICLES. Becker, J. J. (General Electric Research and Development Center, Schenectady, N. Y.). J. Appl. Phys.; 42: 1537-8(15 Mar 1971).

From 16th Annual Conference on Magnetism and Magnetic Materials, Miami Beach, Fla. See CONF-701104.

Hysteresis loops of single particles of Co_5Sm have previously shown that magnetization discontinuities (jumps) occur at fields H_n that are quite discrete and whose values depend on the previous magnetizing field H_m. Some effects of chemical polishing and air aging on the values of H_n and their H_m dependence in Co_5Sm particles are described. Jumps have now been observed in Co_5Y. A particle of Co_5Y showed a rectangular hysteresis loop with H_n = 3800 Oe for H_m of only 4100 Oe, the loop remaining unchanged for H_m up to 30 kOe, and a maximum energy product of 27.6×10^6 G Oe. (auth)

27886 EVALUATION OF THE UTILITY OF A $(Pr,Nd)Co_5$ ALLOY FOR PERMANENT MAGNETS. Tsui, J. B. Y.; Strnat, K. J.; Harmer, R. S. (Univ. of Dayton, Ohio). J. Appl. Phys.; 42: 1539-40(15 Mar 1971).

From 16th Annual Conference on Magnetism and Magnetic Materials, Miami Beach, Fla. See CONF-701104.

Neodymium substitution for Pr in $PrCo_5$ increases Curie point and saturation and lowers the coercive force of powders. Attritor-milled powders of $Pr_{0.87}Nd_{0.13}Co_5$ have up to ${}_MH_c$ = 4100 Oe. They can be improved only insignificantly by treating the particles with citric or dilute nitric acid. Magnets having $(BH)_{max}$ = 4.5 and 5.5 MG Oe were pressed from such powders. A magnet of 13 MG Oe was produced by liquid-phase sintering. (auth)

27887 MAGNETIC PROPERTIES OF CeBi, NdBi, TbBi, and DyBi. Nereson, N.; Arnold, G. (Los Alamos Scientific Lab., N. Mex.). J. Appl. Phys.; 42: 1625-7(15 Mar 1971).

From 16th Annual Conference on Magnetism and Magnetic Materials, Miami Beach, Fla. See CONF-701104.

The magnetic properties of four REBi compounds, where RE is Ce, Nd, Tb, and Dy, were investigated by neutron diffraction on powder samples; all of these compounds are antiferromagnetic below Néel temperatures T_N of 26, 25, 18, and 13°K, respectively. The magnetic structure of both CeBi and NdBi consists of (001) ferromagnetic planes coupled antiferromagnetically with the spin direction along the [001] axis. TbBi has a magnetic structure which consists of (111) ferromagnetic planes coupled antiferromagnetically with a [111] spin direction. The magnetic structure of DyBi could be either type A or B of MnO; the spin direction could not be determined from the present powder sample. CeBi and NiBi possess antiferromagnetic ordering of the first kind whereas TbBi and DyBi have the second kind. The development of antiferromagnetic ordering below T_N follows a Brillouin function for CeBi and NdBi but TbBi and DyBi show considerable deviation. The saturation ordered moments for CeBi and NdBi are 6% less than the calculated values whereas for TbBi and NdBi the moments are 12% less than the expected values. (auth)

27888 SPIN-WAVE DISPERSION RELATION IN RARE-EARTH METALS. Nicklow, R. M. (Oak Ridge National Lab., Tenn.). J. Appl. Phys.; 42: 1672-9(15 Mar 1971).

From 16th Annual Conference on Magnetism and Magnetic Materials, Miami Beach, Fla. See CONF-701104.

Recent measurements of the spin-wave dispersion relations for Gd, Dy, and Ho metal by triple-axis neutron spectrometry are reviewed. Measurements along the c axis were carried out for each metal at several temperatures, and for Gd additional measurements along the a and b axes were made at 78°K. Information about the Fourier-transformed exchange interaction $J(q)$ was obtained from data analyses, which are based on a simple Hamiltonian containing only exchange interactions for Gd and a Hamiltonian containing exchange interactions plus appropriate anisotropy interactions (the usual frozen lattice model) for Dy and Ho. For both Dy and Ho a satisfactory analysis of the data requires the use of anisotropy interaction parameters which are not in good agreement with the results of macroscopic measurements. The neutron data suggest the existence of other anisotropy interactions, perhaps magnetoelastic, in addition to those usually considered in the frozen lattice Hamiltonian. The dispersion relation for Dy in the ferromagnetic phase has a pronounced minimum, and hence $J(q)$ has a maximum, for q in the vicinity of the wave vector that is appropriate for the spiral structure just above T_c. (auth)

27889 UNIAXIAL STRESS EXPERIMENTS AND MAGNETO-ELASTIC INTERACTIONS IN RARE EARTHS. Bartholin, H.; Beille, J.; Bloch, D.; Boutron, P.; Feron, J. L. (CNRS, Grenoble, France). J. Appl. Phys.; 42: 1679-88(15 Mar 1971).

From 16th Annual Conference on Magnetism and Magnetic Materials, Miami Beach, Fla. See CONF-701104.

The effect of uniaxial stress on the magnetic transition temperatures of gadolinium, terbium, and dysprosium was determined. The problem of stress homogeneity received particular attention. From the variation with stress of the Curie (Gd) or Néel (Tb, Dy) temperatures, spontaneous magnetostriction in Gd, Tb, and Dy is quantitatively interpreted. (auth)

27890 MICTOMAGNETISM IN Pd–Cr and V–Mn ALLOYS. Chakravorty, S.; Panigrahy, P.; Beck, Paul A. (Univ. of Illinois, Urbana). J. Appl. Phys.; 42: 1689-9(15 Mar 1971).

From 16th Annual Conference on Magnetism and Magnetic Materials, Miami Beach, Fla. See CONF-701104.

Face-centered cubic Pd–Cr alloys with 25 to 35% Cr, quenched from 1200°C, have an average paramagnetic moment $\bar{\mu}_{Cr}$ of 0.5 – 1.2 μ_B. Below T_f = 36 to 76°K the moments are largely frozen, without long-range magnetic order, but ferromagnetic clusters of up to about 24 μ_B account for the thermomagnetic or isothermal remanence. These giant moments can be aligned in successive small thermally activated steps by cooling in a magnetic field. Once aligned, the giant moments can be turned collectively by much smaller fields. The bcc V–Mn alloys with 50 to 76% Mn have similar magnetic properties, but with supergiant moments of more than 1000 μ_B, as quenched from 1200°C. For the Pd alloys with more than 25% Cr the minimum fields and temperatures necessary to align the moments are decreased considerably by annealing at 400°C, when the ferromagnetic clusters acquire dipole moments of up to 3600 μ_B, as measured in the superparamagnetic state, above T_f. The total moment of all supergiant clusters in the annealed 33% Cr alloy is equal to the thermomagnetic remanence of this alloy at 4.2°K. In the quenched as well as in the annealed condition, the alloys with 29% and 33% Cr show the largest thermomagnetic remanence, presumably because the tendency for atomic ordering is largest at these compositions. (auth)

27891 PARAMAGNETISM OF HIGH-CONCENTRATION MANGANESE IN bcc VANADIUM. von Meerwall, E. Univ. of Illinois, Urbana), Schreiber, D. S. J. Appl. Phys.; 42: 1695-6(15 Mar 1971).

From 16th Annual Conference on Magnetism and Magnetic Materials, Miami Beach, Fla. See CONF-701104.

The nuclear magnetic resonance and magnetic susceptibility in bcc V–Mn was studied from 0% to 70% Mn. Above 45% Mn, a rather sharp rise is found in a heretofore only weakly concentration-dependent paramagnetism, as well as decreases in both ^{51}V and ^{55}Mn Knight shifts. This increase in paramagnetism in V–Mn, as well as in V–Fe, is identified with the onset of occupation of the higher-lying 3d subband and occurs earlier near the solute atoms of higher nuclear charge. A simple model incorporating this solvent–solute difference in the band structure forms the basis for a partitioning of the susceptibility and the Knight shift. An emerging temperature dependence in χ becomes Curie–Weiss-like at the highest Mn concentrations. (auth)

27892 DEPENDENCE OF THE s–f EXCHANGE COUPLING PARAMETER ON RARE-EARTH ATOMIC NUMBER. Levy, Peter, M. (New York Univ., N. Y.). J. Appl. Phys.; 42: 1702-3(15 Mar 1971).

From 16th Annual Conference on Magnetism and Magnetic Materials, Miami Beach, Fla. See CONF-701104.

The s–f exchange coupling parameter Γ_{sf} was independently determined for the rare-earth dialuminides from a variety of phenomena. All the results show a similar variation of the parameter across the rare-earth series. The origins of this variation are discussed. (auth)

27893 NEUTRON CRYSTAL-FIELD SPECTROSCOPY IN RARE-EARTH METALLIC COMPOUNDS. Turberfield, K. C. (Brookhaven National Lab., Upton, N. Y.); Passell, L.; Birgeneau, R. J.; Bucher, E. J. Appl. Phys.; 42: 1746-54(15 Mar 1971).

From 16th Annual Conference on Magnetism and Magnetic Materials, Miami Beach, Fla. See CONF-701104.

XUM

The technique of inelastic neutron scattering was applied to the problem of crystal fields in rare-earth metallic compounds. It is shown that in compounds where the Stark energies are somewhat greater than exchange energies, the complete energy-level diagram can be readily obtained from the inelastic neutron spectra and hence the corresponding crystal-field parameters may be deduced. This is illustrated by a series of measurements performed on the praseodymium monopnictides, PrBi, PrSb, PrAs, PrP, and monochalcogenides PrTe, PrSe, PrS. It is found that the spectra can be reproduced in detail using ordinary crystal-field theory together with a simple approximation to the instrumental resolution function. In addition, all of the crystal-field levels in all seven compounds studied can be quantitatively accounted for using a nearest-neighbor point-charge model with an effective charge of –2. This is in spite of marked variations in covalency, carrier concentration and, indeed, in the widths of the crystal-field transitions themselves over the series. (auth)

27894 PREPARATION AND STRUCTURE OF Fe-DOPED EuO FILMS. Ahn, K. Y.; Tu, K. N.; Reuter, W. (IBM Thomas J. Watson Research Center, Yorktown Heights, N. Y.). J. Appl. Phys.; 42: 1769-70(15 Mar 1971).

From 16th Annual Conference on Magnetism and Magnetic Materials, Miami Beach, Fla. See CONF-701104.

A large increase in ferromagnetic Curie temperature from 69.5°K to ~190°K was observed in EuO films doped with Fe. These films retain most of the large magneto-optic rotation of EuO (at 4.2°K) desired for beam addressable memories. However, the increase in T_c permits the operation of these devices at the more convenient liquid-nitrogen temperature. Films were prepared by simultaneous evaporation of Eu, Eu_2O_3, and Fe at pressure of 2×10^{-5} torr. The amount of T_c increase is strongly dependent upon composition. For example, films with the highest T_c require $Fe/Fe + Eu \sim 0.07$ and excess Eu with a typical weight ratio of $Eu/Eu_2O_3 \sim 1.3$ as compared to ~0.9 for pure EuO. The analysis by Seeman–Bohlin x-ray diffractometer shows the same NaCl structure as that of pure EuO with a slightly larger lattice parameter (5.1564 Å). The doping also causes a reduction of grain size (from 200 to 120 Å) and a tendency toward preferred orientation. Results of electron microprobe spectroscopy and Moessbauer measurements show that the iron is predominantly present in the metallic state and the europium in the Eu^{2+} state. The dependence of physical properties on fabrication parameters is critically examined. (auth)

27895 DEPENDENCE OF THE E_1 REFLECTIVITY STRUCTURE IN EuO ON TEMPERATURE AND DOPING. Grant, Paul M. (IBM Research Lab., San Jose, Calif). J. Appl. Phys.; 42: 1771-2(15 Mar 1971).

From 16th Annual Conference on Magnetism and Magnetic Materials, Miami Beach, Fla. See CONF-701104.

The temperature dependence of the E_1 reflectivity peak ($4f^7 \rightarrow 4f^6 5d$ transition) in both intrinsic and Gd-doped single-crystal EuO over the range 20 to 300°K was measured. It is observed that this structure occurs consistently at lower energies in Gd-doped EuO vis-a-vis intrinsic for all temperatures covered. X-ray data indicate a smaller lattice constant for the doped material, thus substantiating the direction of the shift on the basis of an overlap model. A strong Burstein–Moss effect would have shifted the peak oppositely to that observed. The onset of the "red shift" associated with magnetic ordering in the bulk occurs at a higher temperature for the doped material consistent with its higher T_c, but the shift is not as closely correlated with this temperature as it is for intrinsic EuO. These results suggest a localized model for the E_1 excitation. (auth)

27896 MAGNETIC SUSCEPTIBILITY OF Eu_2O_3. Kern, S.; Kostelecky, R. (Colorado State Univ., Fort Collins). J. Appl. Phys.; 42: 1773-4(15 Mar 1971).

From 16th Annual Conference on Magnetism and Magnetic Materials, Miami Beach, Fla. See CONF-701104.

Huang and Van Vleck have recently attributed the "excess" in susceptibility of Eu_2O_3 over that calculated from the spectroscopic data of Eu^{3+} diluted in Y_2O_3 to orbitally dependent exchange processes. Measurements of $(Eu_xY_{1-x})_2O_3$ by Grill and Schieber done above 95°K, on the other hand, have indicated that the susceptibility increases, rather than decreasing to the dilute calculated value, as x decreases. The susceptibility of Eu^{3+} in Y_2O_3 was carefully remeasured down to helium temperatures and it was found that the susceptibility and crystal-field splitting remains relatively constant over the entire range of concentration. Calculations showed that the effects of spin–orbit and crystal field mixing of states do not explain the magnitude of the discrepancy, nor would the presence of the monoclinic phase of the sesquioxide, which also exhibits a similar "excess" of susceptibility over the spectroscopically determined value. (auth)

27897 MAGNETIC AND MAGNETO-OPTICAL PROPERTIES OF Fe-DOPED EuO FILMS. McGuire, T. R.; Petrich, G. F.; Olson, B. L.; Moruzzi, V. L.; Ahn, K. Y. (IBM Thomas J. Watson Research Center, Yorktown Heights, N. Y.). J. Appl. Phys.; 42: 1775-7(15 Mar 1971).

From 16th Annual Conference on Magnetism and Magnetic Materials, Miami Beach, Fla. See CONF-701104.

EuO films with ~8 wt % Fe have saturation magnetic moments of about 180 emu/g at 4.2°K and Curie temperatures (T_c) as high as 200°K (for pure EuO, $\sigma = 232$ emu/g, $T_c = 69.5$°K). The temperature dependence of the magnetization does not scale relative to pure EuO but deviates from the normal magnetization curve in that it exhibits a long tail extending from about 100°K up to T_c. Optical absorption data at 6°K in the range 0.3 to 2.5 μ indicate a characteristic peak at $\lambda = 0.6$ μ (due to the 4f-5d transition) with $\alpha = 2.2 \times 10^5$/cm, about 50% higher than pure EuO. The wavelength dependence of the normal Faraday rotation at 4.2°K is similar in shape to pure EuO; both peak at 0.7 μ but the peak rotation of the Fe-doped film (6×10^5 deg/cm) is about 30% lower than pure EuO. Moessbauer measurements of ^{151}Eu show mainly Eu^+ with an isomer shift of –12.25 mm/sec as in bulk EuO. At 4.2°K the ^{151}Eu hyperfine field is 280 ± 5.6 kOe (pure EuO ≈ 300 kOe). The isomer shift of the doublet observed on the ^{57}Fe resonance at 300°K is characteristic for metallic iron. It is concluded that only a small fraction of the Fe is effectively doping the EuO films. (auth)

27898 ANNEALING STUDY OF EuO FILMS DOPED WITH IRON AND EUROPIUM. Suits, J. C.; Lee, Kenneth; Winters, H. F.; Phipps, P. B. P.; Kyser, D. F. (IBM Research Lab., San Jose, Calif.). J. Appl. Phys.; 42: 1777-8(15 Mar 1971).

From 16th Annual Conference on Magnetism and Magnetic Materials, Miami Beach, Fla. See CONF-701104.

Fe-doped and Eu-doped EuO films when annealed in vacuum exhibit large changes in the magnetic, electrical, optical, and magneto-optical properties. Annealing for 5 min at 500°C causes the Curie temperature to drop from 150° to 70°K. This effect is related to the insolubility of iron and excess europium in EuO. The annealing temperature for the iron is somewhat higher (500°C) than the annealing temperature for the excess europium (300°C). (auth)

27899 OPTICAL PROPERTIES OF TUNGSTEN SINGLE CRYSTALS. Nomerovannaya, L. V.; Kirillova, M. M.; Noskov, M. M. (Inst. of Physics of Metals, Sverdlovsk, USSR). Zh. Eksp. Teor. Fiz.; 60: 748-58(Feb 1971). (In Russian).

The frequency dispersion of the dielectric permeability $\epsilon(\omega)$ of tungsten single crystal samples was measured in the (110) and (100) planes and in the spectral range between 20 and 0.265 μ (0.062 – 4.9 eV). The plasma frequency of conductivity electrons is determined. Features of interband transitions are studied. Low-energy conductivity spikes at energies of 0.33 and 0.40 eV are observed that are related to spin–orbit splitting of the bands near the Fermi level. The results are discussed on the basis of recent concepts regarding the structure of energy bands in tungsten. (auth)

27900 DOPPLERONS IN CADMIUM. Fisher, L. M.; Lavrova, V. V.; Yudin, V. A.; Konstantinov, O. V.; Skobov, V. G. (All-Union Electrotechnical Inst., Moscow. Ioffe Inst. of Physics and Tech., Leningrad). Zh. Eksp. Teor. Fiz.; 60: 759-74(Feb 1971). (In Russian).

Oscillations of the surface resistance of single-crystal cadmium plates in a magnetic field normal to the surface and parallel to the hexagonal axis were observed experimentally and studied theoretically. At a frequency of 1 MHz the oscillations exist in a range between 7.5 and 13.5 kOe. With growth of frequency, the boundary fields increase proportionally to the cube root of the frequency. The oscillation period increases with the field, varying by 30 to 50%. Near the upper boundary the period attains its extreme value, which depends only on the plate thickness. The oscillations are related to excitation of an electromagnetic wave ("dopplerons") due to doppler-shifted cyclotron resonance of the lens electrons. A theoretical analysis shows that, near the upper boundary, the doppler oscillations change into oscillations of the Gantmakher–Kaner type. The curvature of the lens at the reference point could be determined by measuring the oscillation period, $k_F = 1.49 \pm 0.08$ A^{-1}. The experimental boundaries of the region of existence of dopplerons and the variation of the period satisfactorily agree with theoretical predictions of the free-electron model. (auth)

27901 MAGNETIZATION AND ELECTRICAL CONDUCTIVITY STUDIES OF SOME TRANSITION METAL OXIDE GLASSES. Catchings III, Robert M. Detroit; Wayne State Univ. (1970). 143p. University Microfilms Order No. 71-390.

Thesis.

Bulk magnetization versus temperature studies, nuclear magnetic resonance studies, and dc electrical conductivity studies were performed on the glass systems: iron–sodium borate (Fe_2O_3–Na_2O–B_2O_3), cobalt–aluminum silicate (CoO–Al_2O_3–SiO_2), and iron–lithium–sodium borate (Fe_2O_3–Li_2O–Na_2O–B_2O_3). The investigation was concerned with the study of magnetic ordering and electrical conduction in amorphous materials, namely glasses. Glass samples containing large concentrations of some transition metal ions were prepared. Magnetic transitions, characteristic of an antiferromagnetic type of ordering, were observed in some of the glasses of the three systems studied. Also, some glass samples of the iron–sodium borate system were found to be semiconductors. The possibility that the magnetic ordering arises from microcrystals in the glass samples is examined in detail. In some instances it appears that the ordering may be caused by fine crystalline particles in the samples, and in other instances the magnetic ordering may be due to the amorphous material. (Diss. Abstr. Int., B)

27902 NONVERTICAL INTERBAND TRANSITIONS IN GRAPHITE BY INELASTIC ELECTRON SCATTERING. Zeppenfeld, K. (Univ., Hamburg). Z. Phys.: 243: 229-43(1971). (In German).

Characteristic energy-loss measurements are carried out on natural graphite single crystals. The frequency- and wave-vector-dependent dielectric constant $\epsilon(\omega,q)$ for $q \perp c$-axis is determined by Kramers–Kronig Analysis. The results are interpreted in terms of nonvertical interband transitions $E(k) \rightarrow E(k+q)$ between the π-bands within the two-dimensional approximation. (auth)

27903 MAGNETIC STRUCTURE OF α-Tb_2C_3. Atoji, Masao (Argonne National Lab., Ill.). J. Chem. Phys.; 54: 3504-9(15 Apr 1971).

Neutron-powder-diffraction measurements have shown that, in the body-centered cubic α-Tb_2C_3 below 33 ± 4°K, two out of four body-diagonally linked Tb arrays become antiferromagnetic linear chains but the two remaining Tb arrays exhibit no ordered moment. The nearest Tb atoms between the different ordered spin arrays are related ferromagnetically. Six alternative ways of choosing two body-diagonal antiferromagnetic arrays are mutually equivalent due to the crystal symmetry but not to the multiplet degeneracy in powder diffractometry. The moments are most likely directed along the face diagonal that lies in the plane formed by two body diagonals parallel to the ordered spin arrays. The next probable moment direction lies longitudinally along any one of the two ordered arrays. The saturation moment per magnetically ordered Tb in these collinear spin structures is very insensitive to the selection of the moment direction and approximates closely the free Tb^{3+} value of 9 μ_B. An equivalent multiaxial antiferro-structure is obtained by combining two collinear magnetic structures with the mutually orthogonal face-diagonal moments. In this alternative biaxial structure, all Tb atoms possess the same saturation-ordered moment of $9/\sqrt{2}\ \mu_B$. A sizeable magnetic diffuse scattering having the modulation of an apparently ferromagnetic short-range order was observed in the magnetically long-range-ordered region. (auth)

27904 MAGNETIC STRUCTURE OF α-Ho_2C_3. Atoji, Masao; Tsunoda, Y. (Argonne National Lab., Ill.). J. Chem. Phys.; 54: 3510-3(15 Apr 1971).

The antiferromagnetic structure of α-Ho_2C_3 as revealed by neutron powder diffraction is stabilized below 19 ± 1°K and is markedly different from the ordered spin structure of the isostructural α-Tb_2C_3 (the cubic body-centered Pu_2C_3 type). Two out of four body diagonally linked arrays of Ho atoms become the ferromagnetically ordered chains and the remaining two arrays show one-dimensional antiferromagnetic alignment. Among three nearest Ho–Ho neighbors bridging between the different body-diagonal arrays are two antiferromagnetic pairs and one ferromagnetic pair. The moment direction is most likely parallel to one of the ferromagnetic linear arrays. The maximum spontaneous moment is $7.3 \pm 0.2\ \mu_B$ which is considerably smaller than the free Ho^{3+} value of 10 μ_B. The temperature dependency of the spontaneous magnetization is approximated by the Brillouin function with $S = 1 \pm \frac{1}{2}$ but departs significantly from the free ion function with $J(g-1) = 2$. The magnetically ordered phase exhibits a sizeable magnetic diffuse scattering having the characteristics of a ferromagnetic short-range order and this persists down to near 0°K. (auth)

27905 DAMPING OF DISLOCATIONS IN NIOBIUM BY PHONON VISCOSITY. Mason, Warren P.; MacDonald, Douglas E. (George Washington Univ., Washington, D. C.). J. Appl. Phys.; 42: 1836-42(Apr 1971).

Attenuation measurements were made of the body-centered crystal niobium for three waves along the ⟨110⟩ direction. The room-temperature measurements are consistent with dislocations lying in the (110) planes with glide directions along the ⟨100⟩ axes. The fast shear has the largest attenuation, which was measured over a temperature range from 30 to 300°K with frequencies from 10 to 150 MHz. The attenuation can be divided into a square-law attenuation and a dislocation component. The dislocation component can be used to evaluate a drag coefficient that is nearly constant down to 78°K. It rises at low temperatures indicating an electron drag effect. The constant region is consistent with a phonon viscosity damping with a crystal having a peak in the thermal conductivity. The electron drag confirms a theoretical calculation giving a drag inversely proportional to the electrical resistivity. (auth)

27906 PROPERTIES OF VANADIUM DIOXIDE THERMAL FILAMENTS. Kitchen, W. J. Jr.; Proto, G. R. (Univ. of Maryland, College Park). J. Appl. Phys.; 42: 2140-2(Apr 1971).

The thin-film structure was analyzed, and equations were derived for the current and voltage as functions of filament parameters. Measurements of the dc I–V characteristic for switching between two top-surface electrodes and of the filament width and voltage drop vs current were made on evaporated VO_2 films. The results show that, for the switched film, the voltage is nearly independent of current, and the filament width varies linearly with current, as expected from the thermal transport model. (D.L.C.)

27907 ELECTRONIC STRUCTURE OF CUBIC REFRACTORY CARBIDES. Ramqvist, Lars (Axel Johnson Inst. for Industrial Research, Nynaeshamn, Sweden). J. Appl. Phys.; 42: 2113-20 (Apr 1971).

Recent electron (ESCA) and x-ray emission and absorption spectra for the cubic refractory carbides of Group IVb (TiC, ZrC, HfC) and Group Vb (VC, NbC, TaC) are summarized. Based on an interpretation of the experimental data by using self-consistent-field calculations on free atoms and ions and supported by an approximately self-consistent augmented-plane-wave calculation on TiC, a model of the electronic structure is presented. The metal atoms are positive and the carbon atoms negative in the refractory carbide. The electrostatic (Madelung) energy of a cubic carbide is less than one-third of the total binding energy and equals the heat of formation of the carbide. (auth)

27908 EXTRAORDINARY HALL EFFECT IN PARAMAGNETIC GADOLINIUM. Wald, Francine J.; Juretschke, H. J. (Polytechnic Inst. of Brooklyn). Phys. Rev., B; 3: 2412-18(15 Apr 1971).

The extraordinary Hall coefficient R_s of gadolinium was measured in the temperature range 300 to 360°K by analysis of the dc voltages accompanying electron spin resonance in thin oriented gadolinium films. These results extend the single-crystal data of R_s for M parallel to c, known up to 275°K, into the paramagnetic range and give a temperature-independent value $R_s = -1.4 \times 10^{-9}$ V cm/AG at high temperatures. Combined with conventional Hall-effect measurements, the data also yield the strongly temperature-dependent ordinary Hall constant for the same orientation in this temperature range. (auth)

27909 CHEMICAL TRANSPORT OF SILICON AND GERMANIUM DURING ANNEAL TREATMENT. Sigurd, D.; Johansson, N. G. E. (Research Inst. for Physics, Stockholm). Radiat. Eff.; 7: 139-41(Jan 1971).

A Si disk was annealed on top of a Ge disk in dry Ar for 30 min at 550 to 925°C, and ^4He ion elastic scattering analyses showed that a monolayer of Ge formed on the Si. No difference was found for direct contact or spacings of 0.2 or 0.4 mm. Similar results were observed for graphite in contact with Sb-implanted Si at 1000°C. The effect of wet Ar was also investigated. (D.L.C.)

27910 LOW-TEMPERATURE SPECIFIC HEAT 1.5 TO 20 K, MAGNETIC SUSCEPTIBILITY 80 TO 300 K AND SEARCH FOR SUPERCONDUCTIVITY ABOVE 0.05 K OF VANADIUM CARBIDE; LOW TEMPERATURE SPECIFIC HEAT OF COPPER 1.5 TO 20 K. Bloom, Danning Wilford. Boulder, Colo.; Univ. of Colorado (1970). 212p. University Microfilms Order No. 71-5869.

Thesis.

The specific heat and magnetic susceptibility of four vanadium-carbide single-crystal samples, having carbon atom/vanadium atom ratios varying from 0.76 to 0.87, were measured. In addition, a search for superconductivity in these samples was made down to 50 mK. The specific heat results give good qualitative agreement with theoretical predictions by R. G. Lye of the location of a peak in the electronic density of states. However, the amplitude of the observed peak is considerably less than that predicted. The magnetic susceptibility χ of each of the samples was measured in the range 77 to 300°K using a vibrating-sample magnetometer. The results agree with previous susceptibility measurements on various VC_x samples. However, the results do not agree with the spe-

cific heat results in that they do not reflect the bump in the density of states versus energy curve. Also, they have a positive $d\chi/dT$ (except for $VC_{0.87}$, for which $d\chi/dT < 0$), contrary to that which might be expected from the specific heat results. It is concluded that the orbital paramagnetism, rather than the spin paramagnetism of the conduction electrons, dominates the compositional dependence of the magnetic susceptibility and is responsible for the apparent discrepancy in the temperature dependence. The superconducting transition temperature was sought, using a mutual inductance method. The samples did not go superconducting above 50 mK. Using recent accomplishments in the theory of superconductivity, this allows one to estimate that the electron–phonon interaction parameter is less than 0.3. Measurement and comparison of the specific heat (1.5 to 20°K) were carried out on two very pure copper samples having very different residual resistivity ratios (2000, 30,000). It is found that the electronic specific heat of the sample with the greatest residual resistivity ratio is about 1% lower than that of the less electronically pure sample. However, their Debye characteristic temperatures are the same within experimental error. (Diss. Abstr. Int., B)

27911 THERMIONIC PROPERTIES OF REFRACTORY INTERMETALLIC COMPOUNDS IN THE BINARY SYSTEMS CHROMIUM–RHENIUM, MOLYBDENUM–RHENIUM, AND TUNGSTEN–RHENIUM. Miller, C. Samuel. Denver; Univ. of Denver (1970). 139p. University Microfilms Order No. 71-6037.

Thesis.

The Group VIA–Re binary systems are characterized by the presence of several intermediate phases. The σ phase is present in all of the systems, but the α-Mn phases occur in only the Mo–Re and W–Re systems. The occurrence of these intermediate phases appears to be governed largely by electronic factors and is predictable on the basis of electron/atom ratio. The thermionic work functions of the intermediate-phase materials were experimentally determined. A correlation between the work function and the screening of the outermost electrons in the Group VIA metals was found. As might be expected for purely metallic substances, the work functions were relatively high, in the range 4.5 to 5.0 eV, and in each case were bracketed by the work functions of the pure constituents. A discontinuous change in the average work function with composition is proposed, based on a thermodynamical treatment of the electron vapor. (Diss. Abstr. Int., B)

27912 STATISTICAL PHYSICS, PHASE TRANSITIONS, AND SUPERFLUIDITY. VOLUME 2. Chretien, M.; Gross, E. P.; Deser, S. (eds.). Brandeis University Summer Institute in Theoretical Physics, 1966. New York; Gordon and Breach, Science Publishers, Inc. (1968). 487p. $25.00.

Four topics are included; separate abstracts were prepared for three. The fourth topic is "Thermal Fluctuations and the Scattering of Light." (M.H.R.)

For abstracts of inavvidual chapters see: 27642, 27913, and 27947.

27913 LECTURES ON THE ISING MODEL OF PHASE TRANSITIONS. Montroll, Elliott W. (Univ. of Rochester, N. Y.). pp 195-267 of Statistical Physics, Phase Transitions, and Superfluidity. Vol. 2. /Chretien, M. (ed.). New York; Gordon and Breach, Science Publishers, Inc. (1968).

The following topics are covered: recent experiments on critical phenomena, the Ising model, the matrix approach to lattice statistics, combinatorial approach to the Ising model, dimer statistics and the evaluation of two dimensional Ising partition function, correlation and spontaneous magnetization on 2D lattices, and an analysis of 3D series expansions. (M.H.R.)

Moessbauer Effects and NMR

27914 (CERN–70-30(Vol.1), pp 361-81) ON-LINE MEASUREMENTS OF SPIN AND MOMENTS OF NUCLEAR GROUND STATES. Otten, E. W. (European Organization for Nuclear Research, Geneva (Switzerland). Heidelberg Univ. (West Germany). Physikalisches Institut (I)).

In International conference on the properties of nuclei far from the region of beta-stability; Leysin, Switzerland (31 Aug 1970).

Methods for the determination of spins and moments of nuclear ground states for short-lived isotopes are discussed. The methods include on-line nuclear magnetic resonance, on-line atomic beam resonance, and on-line optical pumping. (36 references) (R.W.R.)

27915 (NP–18702) LECTURES ON HYPERFINE INTERACTIONS, A FIELD BETWEEN NUCLEAR PHYSICS AND SOLID STATE PHYSICS, LEUVEN, 1969. Bodenstedt, E. (Bonn Univ. (West Germany)). 363p. Dep. NTIS (U. S. Sales Only).

Twenty-three lectures are presented, giving a definition of hyperfine interactions and discussing the uses of hyperfine interactions in research fields. Some of these uses are: Moessbauer effect, perturbed angular correlation, NMR, magnetic hyperfine fields, Coulomb recoil implantation, rotational states, electric quadrupole moments and interactions, electric monopoles, and relaxation. The final lecture lists the kind of problems that can be investigated with hyperfine interactions. Two appendices discuss (1) the weight of photons and its detection by Moessbauer effect, and (2) the symmetry properties of nature and the violation of parity in weak interactions. (TSS)

27916 QUADRUPOLAR EFFECTS IN THE ^{51}V NMR OF V-BASED TRANSITION-METAL ALLOYS. von Meerwall, E.; Rowland, T. J. (Univ. of Illinois, Urbana). Solid State Commun.; 9: 305-7(15 Feb 1971).

The ^{51}V NMR absorption line shape and peak-to-peak intensity loss in V-based transition metal alloys were studied. Simulations of the line, assuming it to be composed of first-order quadrupolar powder patterns, were fitted to the experimental spectra, yielding uniformly small quadrupole interactions, whose size appears to be correlated with the severity of the lattice distortion due to alloying. (auth) (UK)

27917 NEW METHOD FOR DIFFERENTIAL PERTURBED ANGULAR CORRELATION MEASUREMENTS. Raghavan, R. S.; Raghavan, P. (Technische Univ., Munich). Nucl. Instrum. Methods; 92: 435-7(1971).

A new method suitable for differential angular correlations perturbed by large hyperfine interactions is described. Using this technique, the CdFe hyperfine field at 293°K was measured to be 368 ± 4 kG. (auth)

27918 EFFECTS OF COAXIAL MAGNETIC AND ELECTRIC FIELDS ON TIME-INTEGRAL PAC WITH SPECIAL REFERENCE TO RARE-EARTH ISOTOPES. Karlsson, E.; Bajaj, M. M.; Bostroem, L. (Univ. of Uppsala). Phys. Scr.; 2: 60-4 (1970).

Effects of coaxial magnetic and electric fields on time-integral PAC are studied theoretically. Formulas are developed for the angular shift in the correlation pattern and for the P factor usually measured in a four-detector setup. The formulas are applied to all the trivalent rare-earth ions, for which values of electric and magnetic hyperfine interaction frequencies are calculated at zero temperature. The effect on the angular shift for different values of the lifetime of the excited states is calculated for use in the interpretation of g-factor measurements at low temperatures. As an example of the temperature dependence of the hyperfine fields and angular shifts, one case was calculated for the temperature region 0 to 150°K. (auth) (Sweden)

27919 CALCULATION OF DIFFERENTIAL ANGULAR CORRELATION FACTORS FOR NON-COAXIAL ELECTRIC AND MAGNETIC FIELDS. Bostroem, L.; Karlsson, E.; Zetterlund, S. (Univ. of Uppsala). Phys. Scr.; 2: 65-9(1970).

The influence of noncoaxial magnetic and electric fields on radioactive nuclei embedded as impurities in ferromagnetic materials is considered. The attenuation factor $G_{22}(t)$, as defined in perturbed angular correlation theory, is calculated for different angles β_0 between the directions of the magnetic field and the electric field gradient and for different ratios of the magnetic and electric frequencies. The method was tested for Cd in ferromagnetic gadolinium. (auth) (Sweden)

27920 ^{139}La NMR STUDIES IN $LaIn_3$. Welsh, L. B. (Northwestern Univ., Evanston, Ill.); Gambino, R. J.; Toxen, A. M. J. Appl. Phys.; 42: 1545-6(15 Mar 1971).

From 16th Annual Conference on Magnetism and Magnetic Materials, Miami Beach, Fla. See CONF-701104.

Normal-state nuclear magnetic resonance studies of the superconductor $LaIn_3$ were made in order to investigate the origin of the large temperature-dependent normal-state susceptibility χ attributed to exchange enhancement of the La d-electron spin susceptibility. The ^{139}La Knight shifts, linewidth, and nuclear-spin relaxation times (T_1 and T_2) were measured with cw and pulsed techniques from 1.6 to 300°K. The Knight shifts (+0.402% ± 0.002% at 1.6°K and +0.371% ± 0.002% at 300°K) vary linearly with χ. The relaxation times vary from T_1T = 1.1 ± 0.05 sec °K at 4.2°K to T_1T = 1.6 ± 0.1 sec °K at 300°K. The small magnitude and temperature dependence of the La T_1 and Knight shift as well as the value of the Korringa product K^2T_1T/S of 1.28 at 4.2°K appears in the independent band approximation to be inconsistent with the expected large La d-band hyperfine contribution. This suggests a breakdown of the independent band approximation in $LaIn_3$ due to interference effects between the various hyperfine interactions. (auth)

27921 MAGNETIC PROPERTIES OF DILUTE Pd(Gd) ALLOYS. Guertin, R. P. (Tufts Univ., Medford, Mass.); Foner, S.; McNiff, E. J. Jr.; Praddaude, H. C. J. Appl. Phys.; 42: 1550-1(15 Mar 1971).

From 16th Annual Conference on Magnetism and Magnetic Materials, Miami Beach, Fla. See CONF-701104.

Magnetic moment measurements on $Pd_{1-x}Gd_x$ alloys for $0.002 \leq x \leq 0.05$, $1.5 \leq T \leq 4.2°K$, and $0 \leq B_0 \leq 150$ kG are reported. The saturation moment per Gd atom is independent of Gd concentration and is equal to that of Gd^{3+} within experimental error. An empirical formula is given that fits the magnetic isotherms to better than 1% over the entire field range. (auth)

27922 INVESTIGATION OF THE MAGNETIC BEHAVIOR OF SOME CONDUCTING Am SYSTEMS. Dunlap, B. D.; Lam, D. J.; Kalvius, G. M.; Shenoy, G. K. (Argonne National Lab., Ill.). J. Appl. Phys.; 42: 1719-20(15 Mar 1971).

From 16th Annual Conference on Magnetism and Magnetic Materials, Miami Beach, Fla. See CONF-701104.

A number of Am compounds were investigated by bulk magnetic and nuclear gamma resonance (NGR) measurements. For the latter type of investigations, the compounds were used as a source for the 59.6-keV resonance in ^{237}Np. AmSb, Am_3Se_4, and Am_3Te_4 show no magnetic ordering down to 4.2°K, and the NGR isomer shifts show that the Am ions are present in the trivalent state. The susceptibility of AmSb is temperature-independent. Similarly, no ordered magnetism is seen in Am_2C_3, although Np_2C_3 has a ferromagnetic transition at 109°K. These results show the tendency of conducting Am compounds to form a trivalent, nonmagnetic state. The results are discussed in terms of a crystal-field calculation which includes J mixing caused by the large crystal-field interaction present in actinide compounds. (auth)

27923 QUADRUPOLE EFFECTS IN NMR SPECTRA ON SHORT-LIVED β-RADIOACTIVE NUCLEI, ^{12}B AND ^{12}N. Minamisono, Tadanori; Matuda, Kozi; Mizobuchi, Akira; Sugimoto, Kenzo (Osaka Univ.). J. Phys. Soc. Jap.; 30: 311-22(Feb 1971).

Quadrupole effects in NMR on $^{12}B(T_{\frac{1}{2}} = 20$ ms) and $^{12}N(T_{\frac{1}{2}} = 11$ ms) were investigated by using the polarized nuclei produced and implanted through nuclear reactions and the resultant asymmetric β decay. The implantation media were polycrystalline bcc metals (Nb, Mo, Ta, and W), TiB_2, and ZrB_2. To increase the observable effects in NMR, a frequency-modulated r-f field was employed. The spectra in bcc metals show the characteristics of quadrupole interaction for nuclear spin $I = 1\hbar$, and the determined coupling constants depend largely on the periodic groups of the related elements. The spectra in the bcc metals, together with those in the fcc metals (Al, Cu, Pt, and Au), indicate that the major implanted sites are interstitial. From the results on TiB_2 and ZrB_2 and the known values on ^{11}B, the ratio of quadrupole moments is determined as $|Q(^{12}B)/Q(^{11}B)| = 0.42 \pm 0.04$, and the moment of ^{12}B is deduced to be $|Q(^{12}B)| = 0.017_1 \pm 0.001_6$ b. (auth)

27924 MOESSBAUER EFFECT STUDY OF HYPERFINE INTERACTIONS IN ^{145}Nd. Kaindl, G. (Univ. of California, Berkeley). Z. Phys.; 240: 100-22(1970).

The magnetic hyperfine splitting of the 72.5-keV γ rays of ^{145}Nd was investigated in intermetallic compounds of Nd and in the paramagnetic salts $Nd_xY_{1-x}Cl_3 \cdot 6H_2O$ (with $x = 0.02$ and $x = 0.05$) at 4.2°K. With the magnetic hyperfine tensor A of $Nd_{0.01}Y_{0.99}Cl_3 \cdot 6H_2O$ known from EPR spectroscopy, the analysis of the unresolved magnetic hyperfine spectra yields $I_e = \frac{5}{2}$ for the spin of the 72.5-keV state, in contradiction to a previous result. The multipolarity of the 72.5-keV γ transition was found to be essentially M1 with $\delta^2 = 0.010 \pm 0.014$, and the magnetic moment of the 72.5-keV state was determined as $\mu(\frac{5}{2}) = -0.319 \pm 0.004$ nm. For various divalent and trivalent Nd compounds, as well as for metallic Nd, the isomer shift of the 72.5-keV γ line was measured. A value for the change of the mean square nuclear charge radius during the 72.5-keV γ transition of $\Delta\langle r^2\rangle = +(1.9 \pm 0.9) \cdot 10^{-3}$ fm² was deduced, using electron density differences from free-ion Hartree-Fock calculations. (auth)

Theoretical Physics

Refer also to abstracts 28063 and 28078.

27925 (CNRS-CPT-70-P-325) CONSTRAINTS IMPOSED UPON A STATE OF A SYSTEM THAT SATISFIES THE K.M.S. BOUNDARY CONDITION. Sirugue, M.; Winnink, M. (Centre National de la Recherche Scientifique, Marseilles (France). Centre de Physique Theorique). 1970. 14p. Dep. CFSTI (U. S. Sales Only).

Using the uniqueness of the Kubo-Martin-Schwinger automorphism the set of automorphisms that commutes with it was investigated. The results were applied to gauge invariant quasi-free states of a fermion system. (auth)

27926 (CNRS-CPT-70-P-352) A CLASS OF ANALYTIC PERTURBATIONS FOR SCHRODINGER HAMILTONIANS. I. THE ONE-BODY PROBLEM. Aguilar, J.; Combes, J. M. (Centre National de la Recherche Scientifique, Marseilles (France). Centre de Physique Theorique). 1970. 18p. Dep. NTIS (U. S. Sales Only).

A class of symmetric relatively compact perturbations satisfying analyticity conditions with respect to the dilatation group in R^n is considered. Absence of a continuous singular part for the Hamiltonians is proved, together with the existence of an absolutely continuous part having an $[0, \infty]$ spectrum. The point spectrum consists of a finite multiplicity of isolated energy bound states standing in a bounded domain. Bound-state wave functions are analytic with respect to the dilatation group. Some properties of resonance poles are investigated. (France)

27927 (FEI-203) SPINNING TOP PROBLEM IN QUANTUM MECHANICS. Gal, E. V. (Gosudarstvennyi Komitet po Ispol'zovaniyu Atomnoi Energii SSSR, Moscow. Fiziko-Energeticheskii Institut). 1970. 7p. (In Russian). Dep. NTIS (U. S. Sales Only).

The author reviews the problem of constructing wave functions of an asymmetrical spinning top (gyroscope) in quantum mechanics. It is demonstrated that the functions can be derived from spherical-conical wave functions with the aid of the appropriate operators for the increasing (decreasing) of the projection of the gyroscope's moment onto an external axis. It is also shown that the operators of projections of the gyroscope's moment constitute generators for the motions of a point in the third sphere. (tr-auth) (JPRS)

27928 (INR-P-1203) ON THE INTERACTION OF HARMONIC OSCILLATORS WITH RADIATION FIELD. Rzazewski, K.; Zakowicz, W. (Institute of Nuclear Research, Warsaw (Poland)). 1970. 18p. Dep. NTIS (U. S. Sales Only).

The radiation of charged harmonic oscillators is investigated. Detailed classification of the states of oscillators from the point of view of their radiation is given. The superradiant behavior of certain states is derived. Exact solution to the problem of interaction with one mode in the lossless cavity is discussed. (auth)

27929 (ITF-70-62-E) SOME PECULARITIES OF COGNITION OF MICROWORLD. Lomsadze, Yu. M.; Kaliberda, S. G. (Akademiya Nauk Ukrainskoi SSR, Kiev. Institut Teoreticheskoi Fiziki). 1970. 22p. Dep. NTIS (U. S. Sales Only).

A preliminary attempt is made to comprehend critically, anew, the Copenhagen explication of quantum mechanics and to appreciate the contribution of the Soviet physicists to it. The "gnoseological" conception is also suggested, having the purpose of reflecting the specific role of the quantum measurement in the natural-science cognition of nature. (auth)

27930 (ITF-70-101-E) ON A CONSEQUENCE OF THE GRIBOV-FROISSART FORMULA. Yatsun, V. A. (Akademiya Nauk Ukrainskoi SSR, Kiev. Institut Teoreticheskoi Fiziki). 1970. 20p. Dep. NTIS (U. S. Sales Only).

Some restrictions on the partial-wave amplitudes which follow from the Grobov-Froissart formula are obtained. These restrictions are in the lower and upper estimates of the determinants composed of the partial amplitudes. (auth)

27931 (JINR-E2-5575) GLOBAL AND LOCAL STRUCTURE OF RELATIVISTIC QUANTUM SYSTEMS. Khoruzhii, S. S.; Sushko, V. N. (Joint Inst. for Nuclear Research, Dubna (USSR). Lab. of Theoretical Physics). 1971. 78p. Dep. NTIS (U. S. Sales Only).

On the basis of general algebraic description of quantum system with superselection rules, developed earlier by the authors, the detailed investigation is made of the global, local and asymptotic structure of such systems. Essential part of the investigation consists in the study of equivalence properties of coherent superselection sectors. It is demonstrated that the field character of a quantum system is associated with a definite asymptotic behavior in space-like directions. (auth)

27932 PARTICLE METHOD FOR THE NUMERICAL SOLUTION OF THE TIME-DEPENDENT SCHROEDINGER EQUATION. Weiner, J. H.; Askar, A. (Brown Univ., Providence). J. Chem. Phys.; 54: 3534-41(15 Apr 1971).

A method for the solution of the time-dependent Schrödinger equation in two dimensions is presented, which is based on the hydrodynamic analogy to quantum mechanics. The continuum introduced in that analogy is approximated by a finite number

of particles, whose trajectories are computed. The procedure is applied here to the dynamics of a Gaussian wave packet on a two-dimensional quadratic potential surface containing a saddle point. Comparison with the known analytical solution indicates that the method is capable of accurate results with substantially less computer time required than in methods previously employed. This particular check problem was chosen because of its close relationship to the wave-packet dynamics of chemical reaction rates. (auth)

27933 NUMERICAL CALCULATION OF THE S-STATE ENERGY EIGENVALUES FOR A LOCAL POTENTIAL. Kermode, M. W. (Liverpool Univ.). J. Phys., A (London); 4: L3-5(Jan 1971).

A numerical method for calculating the S-state energy eigenvalues for a local potential is given. The method makes use of a first-order differential equation that is easily derived from the Schroedinger equation. (auth) (UK)

27934 EXACTLY SOLVABLE QUANTUM-MECHANICAL N-BODY PROBLEM. Magyari, E.; Meder, L. F. (Univ. of Craiova, Romania). Rev. Roum. Phys.; 15: 1039-48(1970).

An unequal mass N-particle system interacting pairwise by harmonic forces of arbitrary intensities is treated in the framework of quantum mechanics. An exact analytical solution of the Schroedinger eigenvalue problem is given in terms of normal mode frequencies. Some simply solvable particular cases of practical interest in nuclear physics are picked out. The degeneracy of energy levels is systematically studied. (auth)

27935 SOLUTION OF THE MATHIEU EQUATION IN THE WKB APPROXIMATION. Richardson, M. J. (State Univ. of New York, Stony Brook). Amer. J. Phys.; 39: 560-5(May 1971).

The Schroedinger equation for a particle in a one-dimensional sinusoidal potential is the Mathieu equation. The usual solution of this equation is in terms of a stability analysis and is given by power series expansions. The Mathieu equation is discussed as a Schroedinger equation, and stability is interpreted in terms of allowed and forbidden energy bands. It is shown how simple physical arguments and use of the WKB approximation lead easily to the stability diagram given but not derived in most texts. (auth)

27936 DENSITY OPERATOR AND MULTITIME CORRELATION FUNCTIONS FOR OPEN SYSTEMS. Haake, Fritz (Harvard Univ., Cambridge, Mass.). Phys. Rev., A; 3: 1723-34(May 1971).

The dynamics of an open system $\mathscr{S}$ are described in terms of a nonunitary time evolution operator. The latter is defined to solve the generalized master equation for the density operator of $\mathscr{S}$ as obtained using Zwanzig's projector technique. Multitime correlation functions of observables of $\mathscr{S}$ are expressed in terms of this time evolution operator. The results generalize well-known fluctuation dissipation (or regression) theorems valid for Markovian motions of open systems. Moreover, they can be used to combine density-operator and Green's-function methods in dealing with open systems. As an example, the retarded electron–electron interaction in superconductors is treated. (auth)

27937 DERIVATION OF THE PRYCE–FOLDY–WOUTHUYSEN TRANSFORMATION. Cohen, H. A. (La Trobe Univ., Victoria, Australia). Amer. J. Phys.; 39: 409-12(Apr 1971).

A simple and instructive derivation of the Pryce–Foldy–Wouthuysen transformation is given in terms of rotations in two dimensions. (auth)

27938 DEVELOPMENT OF THE WKB APPROXIMATION BY USE OF TRANSFORMATIONS. Engelke, Ray (Univ. of New Mexico, Albuquerque). Amer. J. Phys.; 39: 428-30(Apr 1971).

The WKB wave functions for one-dimensional nonrelativistic problems are derived by a simple transformation method. By applying the Liouville substitution to Schroedinger's equation, and then neglecting certain "small" terms in the transformed equation, one arrives at the WKB solutions. The terms neglected in obtaining the WKB solutions are explicit. No asymptotic expansions are used in the derivation. Use of a known criterion from the theory of differential equations gives assurance that the WKB solutions are asymptotic to exact solutions of Schroedinger's equation in certain cases. (auth)

27939 MODULATED DECAY IN A TWO-LEVEL QUANTUM SYSTEM. Bali, L. M.; Higgins, R. B. (London Univ.). Phys. Lett.; 34A: 191-2(22 Feb 1971).

The radiative decay in a two-level system with the excited state coupled by an external perturbation is investigated. The results obtained differ from those of Keller and Robiscoe [Phys. Rev., 188: 82(1969)] who claim to have discovered a new type of modulation factor. (auth)

27940 QUANTUM MECHANICS FOR HAMILTONIANS DEFINED AS QUADRATIC FORMS. Simon, Barry Martin. Princeton N. J.; Princeton Univ. (1970). University Microfilms Order No. 70-23,639.

Thesis.

Quantum mechanics is considered for Hamiltonians with potentials in the classes, $R \cap L^1$, R, $R + (L^\infty)_\epsilon$, $R + L^\infty$, where R is the set of potentials V with

$$\int \frac{|V(x)|\,|V(y)|}{|x-y|^2}\, d^3x \times d^3y < \infty$$

These generalize the classes based on L^2 potentials and allow singularities almost as bad as r^{-2} (instead of only as bad as $r^{-\frac{1}{2}}$ in the L^2 case). While $H_0 + V$ may not be defined on a large set as an operator sum, as a sum of quadratic forms it defines a form with an associated self-adjoint Hamiltonian. The following aspects of these Hamiltonians are considered in the two body case: (1) discreteness of the negative spectrum, (2) domains of essential self-adjointness, (3) time-dependent Hamiltonians, (4) Feynman path integrals, (5) integral equations for bound states, (6) bounds on the number of bound states, (7) absence of positive energy bound states, (8) existence of wave operators, (9) completeness of wave operators, (10) eigenfunction expansions, (11) asymptotic completeness for a non-empty subclass, (12) time-independent scattering theory, (13) forward dispersion relations, and (14) analyticity in the Lehmann ellipse. In the n-body case, it is demonstrated that Hunziker's theorem on the position of the continuum carries over to potentials with $V \epsilon R + (L^\infty)_\epsilon$. (Diss. Abstr. Int., B)

27941 SELF-INTERACTION CORRECTIONS IN A NON-RELATIVISTIC STOCHASTIC THEORY OF QUANTUM MECHANICS. de la Pena-Auerbach, L.; Cetto, Ana M. (Univ. Nacional, Mexico City). Phys. Rev., D; 3: 795-800(15 Feb 1971).

The radiation damping terms of classical electrodynamics are introduced into a set of stochastic equations of nonrelativistic quantum mechanics to study their effects on the energy levels of a stationary system to first order in perturbation theory. In the potential case there appear correction terms to Schroedinger's equation, one of which is calculated by solving a subsidiary equation. In particular, we obtain for the Lamb shift an expression of essentially stochastic origin, whose structure is in complete agreement with known results. According to this calculation, which has the advantage of being devoid of divergence problems, the nonrelativistic spinless contribution to the Lamb shift of the 2s level amounts to 60% of the total effect. (auth)

27942 DETERMINISTIC QUANTUM INTERFERENCE EXPERIMENTS. Aharonov, Yakir (Yeshiva Univ., New York); Pendleton, Hugh; Petersen, Aage. Int. J. Theor. Phys.; 3: 443-8(Dec 1970).

It is explained why quantum interference may pertain to a single degree of freedom, and it is demonstrated how it can be exhibited by deterministic experiments involving a single particle. (auth) (UK)

27943 MOLECULAR QUANTUM ELECTRODYNAMICS. Woolley, R. G. (Oxford Univ.). Proc. Roy. Soc. (London), Ser. A; 321: 557-72(9 Mar 1971).

A comparison is made of the conventional quantum mechanical hamiltonian for the interaction of molecular systems with the electromagnetic field and the alternative multipole formulation given recently (Atkins & Woolley 1970). The conventional hamiltonian is first derived by using Dirac's generalized hamiltonian theory in which the Coulomb gauge condition is introduced as a supplementary condition. The interpretation of the unitary transformation that connects the two Hamiltonians is analyzed further in terms of the arbitrariness of the phase of the wave functions of charged particles in the presence of the electromagnetic field, and finally examine the problem of exhibiting explicitly the binding energies of the molecular systems. (auth) (UK)

27944 LEAST-SQUARES ANALYSIS OF THE UNCERTAINTY PRINCIPLE. Forkosch, John. Amer. J. Phys.; 39: 425-8 (Apr 1971).

The statistical best-fit line corresponding to an error term that is taken as the uncertainty product between two conjugate parameters is found. The average error per observation attributable to this line is then assumed to be greater than a certain minimum value. This restriction results in the finding that successive measurements cannot be obtained arbitrarily close together. (auth)

27945 JORDAN ALGEBRAS AND QUANTIZABLE DYNAMICAL SYSTEMS. Hurt, N. E. (Univ. of Massachusetts, Amherst). Lett. Nuovo Cim.; 1: 473-4(13 Mar 1971).

It is shown that the class of quantizable dynamical systems given by geodesic flow of spheres and real, complex, and quarternionic projective spaces are classified by the set of pure states of simple formal real Jordan algebras. (L.B.S.)

27946 PHASE EQUATION FOR ELECTRON MOTION IN A TRAVELING-WAVE FIELD WITH SYNCHRONOUS ENERGY AS AN INDEPENDENT VARIABLE. Zhileiko, G. I.; Movsisyan, L. M. (Moscow Power Engineering Inst.). Izv. Akad. Nauk Arm. SSR, Ser. Fiz.; 5: 205-9(1970). (In Russian).

A solution for the phase equation with synchronous energy as an independent variable is investigated for the deflection of phase from equilibrium value in a traveling-wave field, taking into account the space-charge fields. The necessary traveling-wave fields and the laws for the change of the equilibrium phase are found for the given solution of the phase equation. (auth)

27947 FLUCTUATION AND COHERENCE PHENOMENA IN CLASSICAL AND QUANTUM PHYSICS. Lax, Melvin (Bell Telephone Labs., Inc., Murray Hill, N. J.). pp 269-478 of Statistical Physics, Phase Transitions, and Superfluidity. Vol. 2. /Chretien, M. (ed.). New York; Gordon and Breach, Science Publishers, Inc. (1968).

The following topics are covered: a summary of methods of attack; the mean behavior of masers and lasers; spectral measurement and correlations; Markov processes; Langevin processes; the rotating-wave Van der Pol oscillator; further properties of the Fokker–Planck process; coherent state representation; density operator equations; a dynamic quantum–classical correspondence; quantum theory of damping; the damped harmonic oscillator; atomic equations of motion; coupled systems; independent reservoirs; the stochastic model of a maser; a broad atomic line case; and photodetection fluctuations. (M.H.R.)

27948 EXACT ANALYTIC SOLUTIONS OF TRANSPORT EQUATIONS. Birkhoff, Garrett (Harvard Univ., Cambridge, Mass.); Abu-Shumays, Ibrahim K. J. Math. Anal. Appl.; 32: 468-81(Dec 1970).

A number of new exact analytic solutions of monoenergetic transport equations in free p-dimensional x space R^p are constructed. These solutions are intended to provide improved approximations of actual neutron distributions in finite domains. It is first shown that any time-independent solution of the Helmholtz equation in p-dimensional space having suitably bounded order of growth is a scalar flux of the integral transport equation. Next, exponentially time-dependent solutions of neutron transport equations are constructed from time-independent ones. Finally, two more extensive new families of solutions of the equations for (time-dependent) neutron transport are constructed; these solutions, exponentially time-decaying solutions and polynomial solutions, apparently can not be derived from time-independent solutions. (R.W.R.)

27949 PHENOMENOLOGICAL FOUNDATION OF QUANTUM LOGIC. Fay, G. (Chelsea Coll. of Science and Tech., London). Acta Phys. Acad. Sci. Hung.; 29: 27-33(1970).

On general physical grounds and from symmetry considerations, some important lattice theoretical properties of quantum logic are derived. (auth)

XUM

PHYSICS (HIGH ENERGY)

Particle Interactions and Properties (Experimental)

Refer also to abstracts 27976 and 27977.

Electromagnetic

27950 (DESY–71/9) ELECTROPRODUCTION OF SINGLE π^+ MESONS ON HYDROGEN. Driver, C.; Heinloth, K.; Hoehne, K.; Hofmann, G.; Karow, P.; Schmidt, D.; Specht, G.; Rathje, J. (Deutsches Elektronen-Synchrotron, Hamburg (West Germany)). Feb 1971. 49p. Dep. NTIS (U. S. Sales Only).

The electroproduction of single π^+-mesons on hydrogen, $e + p \rightarrow e' + \pi^+ + n$, was investigated by measuring coincidences between the scattered electron and the produced π^+-meson. The differential cross sections as functions of s_0, q^2, t and ϕ_{eq} were determined. (auth)

27951 (NP–18725) QUASIELASTIC ELECTRON–DEUTERON SCATTERING FOR FOUR MOMENTUM TRANSFERS IN THE RANGE $0.2(GeV/c)^2 < q^2 < 0.85(GeV/c)^2$. Klein, H. (Kernforschungszentrum, Karlsruhe (West Germany). Institut fuer Experimentelle Kernphysik). Sep 1970. 77p. (In German). Dep. NTIS (U. S. Sales Only).

In an electron–deuteron scattering experiment at DESY, the reaction $e + d \rightarrow e + p + n$ was investigated with a coincidence device for momentum transfers in the range $0.2(GeV/c)^2 < q^2 < 0.85(GeV)^2$. The direction and momentum of the scattered electrons were measured with a spark chamber spectrometer. The recoil protons were detected with a counter hodoscope and their scattering angles were registered. The accumulated measurement data were stored and processed on-line with a process computer. Within the measurement error of 6%, the measured electron effective cross sections $d^3\sigma/d\Omega_3 dE_3$ agree well with the values which were calculated according to a theoretical work of Durand III. The measured proton angular distributions are in good agreement with the theoretical calculations of McGee. The measurement results ratify the validity of the scaling law for the magnetic neutron factor, whereas there is no indication for the effect of final state interactions or meson exchange currents. The square of the electric neutron form factor was determined in which the usual nucleon form factors were assumed as known. (tr-auth)

27952 NEW STUDIES OF CHERENKOV RADIATION IN EXTENSIVE AIR SHOWERS. Grindlay, J. E. (Smithsonian Astrophysical Observatory, Cambridge, Mass. Harvard Coll. Observatory, Cambridge, Mass.). Nuovo Cim.; 2B: 119-38(11 Mar 1971).

New experimental studies of the angular, spectral and temporal properties of Čerenkov light produced in cosmic-ray extensive air showers (EAS) are reported. These data appear to be best explained by a two-component model for the origin of the Čerenkov light with production occurring not only (predominantly) at the electron maximum but also at greater atmospheric depths from unscattered, nearly "on-axis" particles, such as expected in the EAS core. Monte Carlo calculations to be published of EAS cores support this hypothesis. An individual EAS may thus be detected at its maximum of electromagnetic development and at its core simultaneously. New experiments employing these techniques are discussed and the important implications for the possible identification of the primary particle initiating the EAS detected are considered. Experiments are now in progress using the methods reported to search for cosmic γ-ray sources as well as to study the primary cosmic-ray mass spectrum at energies $E_0 \gtrsim 10^{12}$ eV. (auth)

27953 TOTAL PHOTOPRODUCTION CROSS SECTION OF HADRONS ON NUCLEI. Heynen, V.; Meyer, H.; Naroska, B.; Notz, D. (Deutsches Elektronen-Synchrotron, Hamburg). Phys. Lett.; 34B: 651-4(12 Apr 1971).

The total cross section for photoproduction of hadrons $\sigma(\gamma A)$ was measured on 7 nuclei (Be, C, Al, Ti, Cu, Ag and Au) at 5.4 GeV photon energy. In addition the energy dependence of $\sigma(\gamma A)$ was measured for Be, C and Ti between 1.5 and 5.7 GeV. A small shadow effect is observed which is in reasonable agreement with the prediction of the vector dominance model. (auth)

Weak

27954 MULTIPLE MUONS DEEP UNDERGROUND. Cannon, T. M.; Stenerson, R. O. (Univ. of Utah, Salt Lake City). J. Phys., A (London); 4: 266-75(Mar 1971).

A sample of 176,723 single cosmic ray muon events, 2802 two-muon events, and 225 three-muon events were collected and analyzed to obtain muon rates adjusted for an equivalent detector having a constant normal area of 20 m^2. The measurements span the range of zenith angles between 40 and 70° and slant depths of standard rock between 2×10^5 g cm^{-2} and 6.5×10^5 g cm^{-2}, corresponding to minimum muon energies at ground level of between 750 and 8000 GeV. (auth) (UK)

27955 SCATTERING OF HIGH ENERGY MUONS ON ELECTRONS. Wixon, Norman J. Buffalo; State Univ. of New York (1970). 114p. University Microfilms Order No. 71-6130. Thesis.

The elastic interaction of negative and positive mu mesons with atomic electrons in nuclear emulsion was studied in this experiment. The incident mu mesons were produced at the Brookhaven A.G.S. with peak momenta of 5.0 GeV/c μ^-, 10.1 GeV/c μ^+, and 14.5 GeV/c μ^-. The events were found by an "along the track" scanning technique. The secondary electrons thus found were measured for their ejection angle and secondary energy. Secondary electrons with energies from 7.7 MeV to approximately 3,500 MeV were studied and compared to the Bhabha cross section. Previous research workers have been in disagreement as to the behavior of the muon–electron cross section, several have reported an anomalously large cross section for energy transfers > 100 MeV in comparison to the Bhabha prediction. One research group has reported this anomaly to lie with the positive and not with the negative mu mesons. However, most of the previous experiments were conducted with cosmic ray muons which introduce several difficulties: (i) the pion background is uncertain; (ii) the incoming muon momentum is not known; (iii) the use of thick targets necessitates serious corrections for multiple scattering and radiation loss. The use of the well defined accelerator beam of mu mesons gives us control over (i) and (ii). For the conditions the pion contamination was approximately 1 in 10^7 with well defined muon beam energy spectra. The choice of nuclear emulsion as a target material allowed a high degree of spatial resolution resulting in an accurate determination of the event vertex and secondary electron ejection angle with no serious corrections for multiple scattering. This precision has allowed one to determine the secondary electron energy to an average precision of 15% over the entire spectrum. The results show that there is no deviation from the Bhabha cross section for the scattering of negative mu mesons up to transferred energies in the region of 3 GeV. The results also show no deviation from the Bhabha cross section for the scattering of positive mu mesons up to transferred energies in the region of 1.5 GeV. The results of previous research workers who have reported an anomalously large cross section in the region of the spectrum studied are discussed. (Diss. Abstr. Int., B)

Strong (Baryon-Induced)

Refer also to abstracts 28046 and 28166.

27956 NEUTRON–PROTON SCATTERING AT 152 MeV. Palmieri, J. N. (Oberlin Coll., Ohio. Harvard Univ., Cambridge, Mass.); Wolfe, Janet P. Phys. Rev., C; 3: 144-8(Jan 1971).

The differential cross section for neutron-proton scattering was measured at 152 ± 1 MeV. Protons were detected in the angular range of 5 to 50° relative to the incident beam direction, corresponding to neutron scattering angles of 169 to 78° in the c.m. system. The angular distribution is consistent with earlier data at the smaller proton angles, but significant discrepancies are apparent at angles greater than 25°. (auth)

27957 PROTON–PROTON ELASTIC SCATTERING FROM 9.6 TO 13.6 MeV. Jarmie, Nelson; Jett, J. H.; Detch, J. L. Jr.; Hutson, R. L. (Los Alamos Scientific Lab., N. Mex.). Phys. Rev., C; 3: 10-19(Jan 1971).

Accurate differential-cross-section data for proton–proton elastic scattering are presented at 9.690, 9.918, and 13.600 MeV. These data agree with current energy-dependent phase-shift analyses and resolve discrepancies between previous sets of data and between those data and the phenomenological analysis. (auth)

27958 SCATTERING OF HIGH ENERGY PROTONS FROM NUCLEI. Palevsky, H. (Brookhaven National Lab., Upton, N. Y.). Acta Phys. Pol.; B2: 79-93(Jan-Mar 1971).

Experimental studies of the interaction of 1 GeV protons with nuclei that were performed at the Brookhaven Cosmotron are described. The method of measurements is briefly described, and

some of the results pertinent to the study of nucleon correlations in the nucleus are given. (L.B.S.)

27959 MEASUREMENT OF THE DIFFRACTION SCATTERING OF PIONS AND PROTONS FROM COMPLEX NUCLEI USING MULTIWIRE PROPORTIONAL COUNTERS. Segler, Samuel Louis. Urbana, Ill.; Univ. of Illinois (1970). 94p. University Microfilms Order No. 71-5230.

Thesis.

The development and testing of multiwire proportional counters is considered. The use of a proportional counter system in an experiment to study the diffraction scattering of protons and positive pions from various complex nuclei is discussed. A good precision experiment is made considerably simpler due to the high resolution characteristic of the multiwire proportional counters. The differential and total cross sections for 1 GeV/c positive pion and proton scattering from complex nuclei were measured at the Argonne ZGS. The targets used were carbon, aluminum, copper, and lead. A combination of scintillation, Cherenkov, and multiwire proportional counters was used to obtain the data. The total cross sections were calculated from the observed transmissions and are in good agreement with existing data. The differential cross sections were obtained from the proportional counter hodoscope and are the first measurements at high energy for pions. Two optical models are described and compared with the results. Radius parameters are obtained for each nucleus from the slope of the differential cross section and fit to an equation of the form $R = r_0 A^{\frac{1}{3}} + C$ where A is the atomic number. The parameter r_0 is found to be 1.12 ± .02 fm and c is .61 ± .08 fm. (Diss. Abstr. Int., B)

Strong (Meson-Induced)

27960 (DESY-71/8) ANALYSIS OF THE REACTION $\pi^+p \rightarrow \rho^0\Delta^{++}$ AT 11.7 GeV/c INCIDENT MOMENTUM. PART I. AN EXPERIMENTAL INVESTIGATION. Maddock, R. O.; Pinter, G. F.; Evans, D.; (and others) (Deutsches Elektronen-Synchrotron, Hamburg (West Germany)). Feb 1971. 35p. Dep. NTIS (U. S. Sales Only).

The difficulty in determining the total and the differential cross sections of the double resonance process $\pi^+p \rightarrow \rho^0\Delta^{++}$ is discussed and a method of determining these is given which involves only few theoretical assumptions. The total cross section is (.32 ± .04) mb. The joint decay angular distribution is analysed in terms of statistical tensor and density matrix elements. The data are consistent with pion exchange. (auth)

27961 (PURC-4159-16) AN EXPERIMENTAL STUDY OF OMEGA NEUTRAL DECAYS. Technical Report No. 5. Dakin, James T. (Princeton Univ., N. J. Dept. of Physics). Feb 1971. Contract AT(30-1)-4159. 129p. Dep. NTIS.

The neutral decay modes of the ω meson (784 MeV) were studied in an experiment at the Princeton-Pennsylvania Accelerator. A sample of 532 ω neutral decays from the reaction $\pi^-p \rightarrow \omega n$ were identified from the times-of-flight and angles of the neutrons. The momentum of a single γ from each decay was measured in a wide-aperture pair spectrometer. The γ momentum was transformed to the ω c.m. system. The resulting γ (c.m.) spectrum was compared with spectra for various ω decay modes generated by a Monte Carlo program. The principal ω neutral decay, $\omega \rightarrow \pi^0\gamma$, was observed with a branching ratio $(\omega \rightarrow \pi^0\gamma)/(\omega \rightarrow \text{neutrals}) = (65 \pm 7)\%$. The upper limit for the decay $\omega \rightarrow \eta\gamma$ was $(\omega \rightarrow \eta\gamma)/(\omega \rightarrow \text{neutrals}) < 25\%$ (90% confidence limit). A multi-body decay, probably $\omega \rightarrow \pi^0\pi^0\gamma$, was observed with a branching ratio $(\omega \rightarrow \pi^0\pi^0\gamma)/(\omega \rightarrow \text{neutrals}) = (35 \pm 7)\%$. (auth)

27962 REACTION $\pi^-p \rightarrow \pi^+\Delta^-$ AT CMS ENERGIES 1640 TO 1760 MeV. Brody, A. D. (Stanford Univ., Calif.); Cashmore, R. J.; Kernan, A.; (and others). Phys. Lett.; 34B: 665-70(12 Apr 1971).

A partial wave analysis of the quasi-two body reaction $\pi^-p \rightarrow \Delta^-\pi^+$ has led to two solutions. In both solutions, A and B, the total πN decay of the $N^*(D_{15})$ is accounted for by the Δπ channel whereas only in solution B does the Δπ channel correspond to the total πN decay of the $N^*(F_{15})$. The relative sign of the couplings of the resonances to Δπ is also different between solutions, being negative in solution A and positive in solution B. The results are used to predict the decay rates of other members of the octets. (auth)

27963 MEASUREMENT OF THE POLARIZATION PARAMETER IN K^+p ELASTIC SCATTERING AT 1.60, 1.80, 2.11, and 2.31 GeV/c. Barnett, B. A. (Univ. of Maryland, College Park); Laasanen, A. T.; Steinberg, P. H.; (and others). Phys. Lett.; 34B: 655-8(12 Apr 1971).

The polarization parameter for K^+p elastic scattering was measured at 1.60, 1.80, 2.11 and 3.31 GeV/c incident momenta over the entire angular range with an emphasis on the backward region. The results in the extreme backward region appear to be small and consistent with zero. (auth)

27964 OBSERVATION OF THE FOUR-PION DECAY MODE OF THE D(1285) MESON IN pi^-p REACTIONS AT 16 GeV/c. Boesebeck, K. (Technische Hochschule, Aachen); Honecker, R.; Lauscher, P.; (and others). Phys. Lett.; 34B: 659-62(12 Apr 1971).

A narrow peak is observed at 1283 ± 6 MeV in the $(\pi^+\pi^+\pi^-\pi^-)$ mass distribution in the reactions $\pi^\pm p \rightarrow \pi^\pm p(4\pi)^0$ at 16 GeV/c. This is interpreted as evidence for a four-pion decay mode of the D-meson. It is shown that this enhancement is mainly ρππ. The cross section for $\pi^\pm p \rightarrow \pi^\pm pD^0$, with $D^0 \rightarrow \pi^+\pi^+\pi^-\pi^-$ is 16 ± 5 μb and 6.0 ± 1.5 μb for incident π^+ and π^-, respectively. An upper limit of 1.8 is established for the ratio of $(\eta\pi^+\pi^-)$ to $(\pi^+\pi^+\pi^-\pi^-)$ decay modes of the D-meson. (auth)

27965 $\pi^\pm p$ BACKWARD ELASTIC SCATTERING FROM 2.18 TO 5.25 GEV/C. Sidwell, Ronald Arden. Bloomington, Ind.; Indiana Univ. (1970). 100p. University Microfilms Order No. 71-6907.

Thesis.

Differential cross sections are presented for pion−proton elastic scattering in the angular range $-0.6 \gtrsim \cos\theta_{c.m.} \gtrsim -0.98$ at 15 incident π^+ momenta from 2.18 to 5.25 GeV/c and five incident π^- momenta from 2.38 to 3.00 GeV/c. The π^+p angular distributions rise steeply near 180° at all momenta. For laboratory momenta ≳2.75 GeV/c they show a minimum at $u \simeq -0.17$ $(GeV/c)^2$ and a broad maximum near $u \simeq -0.5$ $(GeV/c)^2$, where u is the square of the four momentum transfer between the incoming pion and outgoing proton. The structure of the π^-p angular distributions undergoes a marked change in the momentum range studied. A pronounced dip in the cross section at 180° which is observed at momenta ≲2.50 GeV/c evolves into a steeply rising peak at 2.80 and 3.00 GeV/c. A minimum in the differential cross sections appears in the 3.00 GeV/c data at $\theta_{c.m.} \simeq 155°$. A shallow minimum is indicated for all momenta near $\theta_{c.m.} \simeq 135°$. Qualitatively good agreement with the experimental results is obtained with a direct channel resonance model. The π^+p data are compared with a Regge model which considers the exchange of the A_δ and N_α Regge trajectories. The qualitative success of both the direct channel resonance model and the Regge model lends support to the concept of duality. (Diss. Abstr. Int., B)

27966 ANTI-LAMBDA PRODUCTION IN 10 GeV/c K^+ PROTON INTERACTIONS. Barnham, K. W. J. (Univ. of Birmingham, Eng.); Colley, D. C.; Jobes, M.; (and others). Nucl. Phys.; B28: 291-307 (1971).

Data are presented on $\bar{\Lambda}$ production in 10 GeV/c K^+p interactions. A low-mass enhancement is found in the $\bar{\Lambda}$ N system in quasi-three-body final states but the nature of this enhancement is not clear. The generalized Veneziano model is applied to the final state $\bar{\Lambda}$ pp and a reggeised multi-peripheral model to the three- and four-body final states. In each case agreement with the data is only qualitative. (auth)

27967 COHERENT K^-d INTERACTIONS AT 12.6 GeV/c. Denegri, D.; Antich, P.; Callahan, A.; (and others) (Johns Hopkins Univ., Baltimore). Nucl. Phys.; B28: 13-33(1971).

Coherent interactions in a 2.5 event/μb K^-d exposure are reported. The predominant channel studied is $K^-d \rightarrow K^-\pi^+\pi^-d$ (415 events). Strong Q- and L-production is found in the (Kππ) system. The production mechanism determines $I = \frac{1}{2}$ for both enhancements and a spin-parity in the series $0^-, 1^+, 2^-, \ldots$. A spin-parity analysis shows the Q to be a 1^+ object, while the L is 1^+ or 2^-, although a higher spin cannot be excluded. The cross sections for Q and L production and other final states are presented. (auth)

27968 STUDY OF THE $K^0\pi^+p$ FINAL STATE PRODUCED IN K^+p INTERACTIONS AT 10 GeV/c. Barnham, K. W. J. (Univ. of Birmingham, Eng.); Colley, D. C.; Jobes, M.; (and others). Nucl. Phys.; B28: 171-83(1971).

The results are presented of a study of 1173 uniquely identified events of the $K^0\pi^+p$ final state produced in 10 GeV/c K^+p interactions. This final state is dominated by the quasi-two-body processes $K^+p \rightarrow K^0N^{*2+}(1238)$, $K^+p \rightarrow K^{*+}(890)p$ and $K^+p \rightarrow K^{*+}(1420)p$. The background is very low and there is little overlapping of resonance bands. Cross sections, t-distributions and decay angular distributions are presented for the contributing reaction channels. Dips are observed near t = 0 in the differential cross sections for all three processes. The decay angular distributions for the $N^{*2+}(1238)$ and the $K^{*+}(890)$ agree with those expected for production via vector meson exchange, though there is an asymmetry in the $K^{*+}(890)$ distribution suggesting interference between the dominant p-wave and a background wave of opposite parity.

Analysis of the $K^{*+}(1420)$ distributions favors 2^+ or 3^- for the spin parity of that resonance. The generalized Veneziano model was applied to the final state being studied, and though it agrees qualitatively with the results in most respects, its predictions for the $K^{*+}(1420)$ decay distributions are found to be in gross disagreement with the data. (auth)

Particle Interactions and Properties (Theoretical)

General

Refer also to abstract 28493.

27969 (PURC-4159-19) PHENOMENA IN MULTIPARTICLE PRODUCTION PROCESSES. Abarbanel, Henry D. I. (Princeton Univ., N. J. Joseph Henry Labs.). Mar 1971. Contract AT-(30-1)-4159. 19p. (CONF-710413-1). Dep. NTIS.

From American Physical Society meeting; Washington, D. C. (26 Apr 1971).

A review is given of multiparticle production experiments and the kinds of results that have emerged within the last two years. The limiting behavior of the cross sections are discussed. Inclusive production that bears directly on the question of the nature of diffractive dissociation or equivalently on the structure of the Pomeranchuk singularity in J-plane physics is treated. (L.B.S.)

27970 BASIS CONCEPTS OF A STRUCTURE THEORY OF ELEMENTARY PARTICLES. PART II. RELATIVISTIC THEORY OF THE EXTENDED ELECTRON. Bagge, Erich (Institut fuer Reine und Angewandte Kernphysik, Kiel). Atomkernenergie; 17: 75-87(Mar 1971). (In German).

In this structure theory of elementary particles the droplet theory will be extented to the relativistic case on the basis of Diracs equation of the electron. Also here the extended electron can have different values of inner excitation energy. Already in the state of lowest angular momentum there is a continuum of possible excitation energies which is brought to a direct connection with the β-continuum of radioactive decay of nuclei. A detailed investigation shows that for an extended electron there has to be distinguished between the eigen-angular momentum $n\hbar$ ($n = 1, 2, 3, \ldots$) and the spin $\hbar/2$ of the particle. The eigen-angular momentum can be received by integration over all contributions of differential angular momenta varying from point to point for different distances from the axis of rotation. The spin on the other side is a property of state, which has the same value at all points in space and which is essential for the behavior of the particle in external fields. The two results we received: that there exists a continuum of possible inner excitation energies for the electron and that the eigen-angular momenta of this particle have full number values show that there is no real need for the postulation of a neutrino in β-decay. Therefore it is supposed that all experiments to prove the existence of this particle with the help of reactors, accelerators or in the cosmic radiation should be reinterpreted in a new way. (auth)

27971 PERTURBATION TREATMENT OF THE BETHE-SALPETER EQUATION FOR TIGHTLY BOUND FERMION-ANTIFERMION SYSTEMS. Keam, R. F. (Univ. of Auckland, N. Z.). J. Math. Phys. (N. Y.); 12: 515-28(Mar 1971).

A perturbation theory is developed for the ladder approximation Bethe-Salpeter equation that describes bound spin-½ fermion-antifermion systems of small total mass. A new exact analytical solution for a zero-mass system is presented and the perturbation theory is applied to it. Some time-reversal properties of the equation are also examined. (auth)

27972 NONRELATIVISTIC CURRENT ALGEBRAS AS UNITARY REPRESENTATIONS OF GROUPS. Goldin, Gerald A. (Univ. of Pennsylvania, Philadelphia). J. Math. Phys. (N. Y.); 12: 462-87(Mar 1971).

It is possible that a complete physical theory can be written entirely in terms of operators such as current densities, rather than in terms of field operators. The current densities in these models correspond in general to distributions of unbounded operators. Such a theory is reviewed for the case of nonrelativistic quantum mechanics. It is found that one can exponentiate the current algebra to obtain a group, which may then be represented by unitary (hence bounded) operators in Hilbert space. This procedure is analogous to exponentiating the canonical commutation relations and obtaining the Weyl group. For nonrelativistic quantum mechanics without spin, the group is the semidirect product JAK Schwartz space $J(R^3)$ with a group K of certain C_∞ diffeomorphisms from R^3 onto itself. For $f\epsilon J$ and $\varphi\epsilon K$, the composition mapping $(f, \varphi) \rightarrow f^{\varphi}$ defines the semidirect product law. The Gel'fand-Vilenkin formalism for "nuclear Lie groups" is suitable for the representation theory of such a group. Almost all of the physical information is contained in a cylindrical measure μ on J', the dual of the nuclear space J. The Fourier transform of μ can be interpreted as an expectation functional with respect to the state of lowest energy. The nonrelativistic Fock representation (including the theory of n particles in a box) is examined in this formalism. Conditions on μ are systematically developed which suffice to recover all of the infinitesimal generators on a common, dense, invariant domain in the Hilbert space. For the Weyl group slightly weaker conditions than for the semidirect product case would suffice. Gaussian measures in J', as well as the measures defining n-particle representation of JAK, satisfy these conditions. (auth)

27973 RELATIVISTIC HARMONIC OSCILLATORS WITH INTRINSIC SPIN STRUCTURE. Cook, P. A. (Univ. of Kent, Canterbury, Eng.). Lett. Nuovo Cim.; 1: 419-26(6 Mar 1971).

A simple model is presented that involves a system of two Dirac spinor particles with nonlocal interactions so constructed as to produce a harmonic-oscillator structure in these states. A simple analog in a two-dimensional space-time is also discussed. The spectrum of the four-dimensional model is obtained and the results are discussed. (L.B.S.)

27974 LIMITING PARTIAL CROSS-SECTIONS. Benecke, J. (Max-Planck-Institut fuer Physik und Astrophysik, Munich). Nuovo Cim.; 2A: 615-31(1 Apr 1971).

One-particle distributions, as defined in the hypothesis of limiting fragmentation, are discussed. It is shown that a dip in the distribution of target fragments for small values of the laboratory momentum is consistent with a divergent multiplicity of these target fragments. Further, a relationship between the energy dependence of inelastic-channel cross sections and of topological cross sections is established. The distributions of individual transverse momenta in inelastic ep and pp collisions are compared. (auth)

27975 FIRST-ORDER WAVE EQUATION FOR INTEGRAL SPIN. Shamaly, A.; Capri, A. Z. (Univ. of Alberta, Edmonton). Nuovo Cim.; 2B: 236-53(11 Apr 1971).

A general method of finding first-order wave equations without subsidiary conditions for integer spin and finite mass is described. Spins 0, 1, 2 and 3 are examples used to illustrate this method. (auth)

27976 HIGH ENERGY PHYSICS INDEX. VOLUME 9, NO. 5, 1971. Frankfurt am Main; Zentralstelle fuer Atomkernenergie-Dokumentation (1971). 78p.

27977 HIGH ENERGY PHYSICS INDEX. VOLUME 9, NO. 7, 1971. Frankfurt am Main; Zentralstelle fuer Atomkernenergie-Dokumentation (1971). 73p.

27978 COHERENT AND INCOHERENT REACTIONS AND DIFFRACTION. Margolis, B. (McGill Univ., Montreal). Acta Phys. Pol.; B2: 57-77(Jan-Mar 1971).

Lectures are presented on the many uses of heavy atomic nuclei in high-energy particle physics. Some topics treated include: elastic and inelastic scattering of high-energy hadrons on heavy nuclei; Glauber theory and eikonal approximation; production in the infinite energy limit; coherent and incoherent production at finite energy; diffractive processes on protons; and K-regeneration and elastic K-scattering. (L.B.S.)

27979 STABILITY OF ZERO-MASS PARTICLES. Levy-Leblond, J.-M. (Laboratoire de Physique Theorique, Paris). Lett. Nuovo Cim.; 1: 467-8(13 Mar 1971).

A general argument is given to the effect that a particle with zero mass is necessarily stable. It is shown that dynamic effects are unable to provoke instability. (L.B.S.)

Electromagnetic

Refer also to abstracts 27404, 28004, and 28070.

27980 (DESY-71/7) ELASTIC ELECTRON-DEUTERON SCATTERING AND THE ELECTRIC NEUTRON FORM FACTOR AT FOUR MOMENTUM TRANSFERS: 5 $FERMI^{-2} < q^2 < 14$ $FERMI^{-2}$. Galster, S.; Klein, H.; Moritz, J.; Schmidt, K. H.; Wegener, D.; Bleckwenn, J. (Deutsches Elektronen-Synchrotron, Hamburg (West Germany)). Feb 1971. 38p. Dep. NTIS (U. S. Sales Only).

The cross section for elastic electron-deuteron scattering was measured for ten four-momentum transfers squared in the range $5\ f^{-2} < q^2 < 14\ f^{-2}$. From the measured cross sections the

sum $A(q^2)$ of charge and quadrupole form factors was determined. The experimental values are compared with theoretical predictions including relativistic corrections. Different deuteron wave functions and different parametrizations for the electric neutron form factor G_{EN} were used. The best fit to the experimental data was found with the wave function of Feshbach-Lomon and the parametrization $G_{EN}(q^2) = -(\mu_N\tau/1 + 5.6\tau)G_{EP}(q^2)$, $\tau = (q^2/4M^2)$. (auth)

27981 (DESY-71/11) ELECTROPRODUCTION OF ω-MESONS AS A TEST OF THE $\rho\omega\pi$-VERTEX. Fraas, H. (Deutsches Elektronen-Synchrotron, Hamburg (West Germany)). Mar 1971. 24p. Dep. NTIS (U. S. Sales Only).

A simple model for electroproduction of ω-mesons is presented. The non-diffractive part is described by elementary OPE without corrections, combined with vector-meson dominance. For the diffractive production-amplitudes helicity conservation in the direct channel is assumed. The differential cross section and the spin-density matrix of the ω-mesons are discussed particularly emphasizing the dependence on the mass of the virtual photon and the possibility to test the mass-dependence of the $\rho\omega\pi$-coupling constant. (auth)

27982 (DESY-71/12) COMPARISON OF PION ELECTROPRODUCTION DATA WITH VECTOR MESON DOMINANCE PREDICTIONS. Fraas, H.; Schildknecht, D. (Deutsches Elektronen-Synchrotron, Hamburg (West Germany)). Mar 1971. 18p. Dep. NTIS (U. S. Sales Only)

Single pion electroproduction results are compared with predictions obtained within the vector meson dominance model. The large longitudinal contribution observed in pion electroproduction is successfully predicted from data on pion photoproduction and on production of vector mesons by pions from nucleons. (auth)

27983 ELECTRIC POLARIZABILITY OF THE NUCLEON AND THE HARMONIC-OSCILLATOR SYMMETRIC QUARK MODEL. Ragusa, S. (Univ. Federal de Sao Carlos, Sao Paulo, Brazil). Lett. Nuovo Cim.; 1: 416-18(6 Mar 1971).

The electric polarizability of the nucleon is studied in the symmetric quark model, taking harmonic-oscillator wave functions for the spatial part. The electric polarizability of the neutron and of the proton was found to be 5.5×10^{-43} cm^3. (L.B.S.)

27984 CLASSICAL CHARGED TACHYONS AND THEIR ELECTROMAGNETIC INTERACTION WITH ORDINARY RELATIVISTIC CHARGED PARTICLES: A SIMPLE FORMULATION. Leiter, D. (Univ. of Windsor, Ont.). Lett. Nuovo Cim.; 1: 395-8(6 Mar 1971).

The structure of a Lagrangian theory of charged tachyons and charged tardyons interacting via a classical Maxwell field is outlined. The properties of the associated equations of motion are discussed. (L.B.S.)

27985 PAIR ANNIHILATION AT A POTENTIAL BARRIER IN TIME. Walter, J. F.; Marx, E. (Drexel Univ., Philadelphia). Nuovo Cim.; 2B: 1-8(11 Mar 1971).

The probability of pair annihilation is determined for charged scalar particles in an external electromagnetic field that is switched on for a finite interval, within the context of relativistic quantum mechanics of a single particle. The results of numerical calculations are presented in several graphs. It is found that this probability is extremely small for fields of the magnitude usually found in the laboratory. A general expression is also obtained for the spreading of the wave packet that represents a free relativistic scalar particle. (auth)

27986 ENERGY AND MOMENTUM OF A CLASSICAL ELECTRON IN SPECIAL RELATIVITY. Benumof, Reuben (Staten Island Community Coll., N. Y.). Amer. J. Phys.; 39: 392-8(Apr 1971).

An equation for the energy of a "classical" electron is derived from Maxwell's equations. The reason for carefully specifying the time at which certain integrations are performed is established The momentum of the electron is treated in a similar manner. The results are in complete agreement with the special theory of relativity. (auth)

27987 COULOMB SCATTERING OF HIGH ENERGY PARTICLES BY A CYLINDRICAL BLOCK. Durand, Alain (Ecole Militaire Interarmes, Coetquidan, France). Compt. Rend., Ser. B; 272: 386-9(8 Feb 1971). (In French).

The distribution of particles scattered by a cylindrical block is determined. Energy losses and the boundaries of the scattering medium are taken into account. (France)

27988 CHARGE INVARIANCE AND ELECTRON MASS FROM THE ULTIMATE SPEED EXPERIMENT. Steinberg, M. S. (Smith Coll., Northampton, Mass.). Amer. J. Phys.; 39: 582-3(May 1971).

It is pointed out how the data exhibited in the PSSC film titled The Ultimate Speed may be exploited to arrive at two additional useful conclusions, namely, the Lorentz invariance of electric charge and the numerical value of the rest mass of the electron. (L.B.S.)

27989 PHOTOPRODUCTION OF η MESONS ON NUCLEONS AT HIGH ENERGIES. Kobylinskii, N. A. (Inst. of Theoretical Physics, Kiev). Ukr. Fiz. Zh. (Russ. Ed.); 16: 61-6(Jan 1971). (In Russian).

Processes of photoproduction of η-mesons on nucleons at high energies are considered in terms of a model taking into account ρ- and ω-poles and ρP- and ωP-cuts. Pole residua and cut discontinuities for the amplitude of η-meson production are connected with those for π^0-meson production by SU(6)-symmetry and vector dominance model. The model allows available experimental data to be described and a number of predictions to be made. (auth)

27990 MESON PHOTOPRODUCTION ON NEUTRONS AT HIGH ENERGIES. Rekalo, M. P. (Inst. of Physics and Tech., Kharkov). Ukr. Fiz. Zh. (Russ. Ed.); 16: 29-37(Jan 1971). (In Russian).

Different reactions of hadron photoproduction on neutrons are considered which permit information to be obtained on electromagnetic hadron interaction in addition to that dealing with hadron photoproduction on protons. It is shown that investigation of the reaction $\gamma + n \rightarrow p + \pi^-$ allows isotopic structure of the radiative decay amplitudes of the nucleon resonances with isotopic spin $1/2$ to be elucidated and the isotopic spin change rule for electromagnetic hadron interaction to be tested. The investigation of the reaction $\gamma + n \rightarrow \Delta^0 + \pi^0$ would permit removing the uncertainty in theoretical models for the reactions $\gamma + N \rightarrow \Delta + \pi$. It is shown that the reactions $\gamma + n \rightarrow \Delta^0 + \omega$ and $\gamma + n \rightarrow p + \rho^-$ are very sensitive to the one-pion amplitude and therefore make it possible to determine the constants of $(\omega\pi\gamma)$- and $(\rho\pi\gamma)$-interaction. The investigation of the neutral vector meson photoproduction on neutrons and deuterons allows the predictions of the quark model and the Regge-pole model to be checked. The cross sections of the reactions $\gamma + N^* \rightarrow N + V^0$ are predicted. (auth)

27991 PROTON FORM FACTORS. Bilen'kaya, S. I.; Kazarinov, Yu. M.; Lapidus, L. I. (Joint Inst. for Nuclear Research, Dubna, USSR). Zh. Eksp. Teor. Fiz.; 60: 460-7(Feb 1971). (In Russian).

All experimental data available as of May 1970 and pertaining to the differential cross sections for scattering of electrons by protons in the transferred momentum range $0.3 \leq q^2 \leq 225$ F^{-2} are treated with the purpose of determining the form factors and radius of the proton. Various types of dependence of the form factors on q^2 are considered. As a result of treatment of the data, parameter values are obtained which yield the best fit for the experimental data in various ranges of q^2. It is shown that it is not possible to obtain a statistically satisfactory description of all the data in the range $0.3 \leq q^2 \leq 225$ F^{-2} for the forms of parametrization of form factors considered. The data of the various groups can be made consistent with each other only if renormalization which takes into account all possible systematic errors is carried out and a satisfactory description can be obtained only for $q^2 < 30$ F^{-2}. (auth)

27992 $\eta \rightarrow 3\pi$ DECAY PUZZLE. Mohapatra, R. N. (State Univ. of New York, Stony Brook). Nuovo Cim.; 2A: 707-32 (1 Apr 1971).

The various problems associated with understanding the $\eta \rightarrow 3\pi$ decay are reviewed. Pole models and the conventional current-current model for the electromagnetic Hamiltonian are discussed in detail, and it is shown that they fail to explain the decay rate, although the slope in the Dalitz plot comes out in agreement with experiment in almost all models. A scalar density model for the electromagnetic Hamiltonian is studied and it is shown that the ensuing σ-terms induce a certain degree of freedom; the effect of the σ-terms on the decay rate is exhibited. A reason behind the universality of the slope in the Dalitz plot is given. (auth)

27993 LOW-ENERGY THEOREMS FOR COMPTON SCATTERING ON TARGETS OF ARBITRARY SPIN. Lin, K. Y. (CERN, Geneva). Nuovo Cim.; 2A: 695-706(1 Apr 1971).

New low-energy theorems for Compton scattering on targets of arbitrary spin are derived. The second-order (in photon energy ω) low-energy theorems derived in the previous paper for spin-1 targets are shown to be valid for targets of any spin, provided we interpret the spin operator S for spin 1 in these theorems as the spin operator for any spin. Third-order low-energy theorems are derived. It is shown that the amplitudes are determined to the third order in ω by the electric charge, the dipole magnetic moment, the quadrupole electric moment, the octupole magnetic moment, and ten structure-dependent

XU

constants. The method can be used to derive higher-order low-energy theorems. (auth)

27994 EVIDENCE FOR ELECTRON-POSITRON PAIR ELECTROPRODUCTION. Balakin, V. E.; Bukin, A. D.; Pakhtusova, E. V.; Sidorov, V. A.; Khabakhpashev, A. G. (Inst. of Nuclear Physics, Novosibirsk, USSR). Phys. Lett.; 34B: 663-4(12 Apr 1971).

The process of pair electroproduction was observed in the electron-positron interaction at the energy 2×510 MeV. The work was done with the colliding beam machine VEPP-2 in Novosibirsk. The cross section of this process and the azimuth angular distribution for large out-of-flight angles of the produced particles were measured. (auth)

27995 DOES W_1 SCALE. Chen, F. C. (United Coll., Hong-Kong). Phys. Lett.; 34B: 625-7(12 Apr 1971).

It is shown that the proton inelastic structure function W_1 exhibits small but definite and systematic deviation from scale-invariant behavior in the region where it has been experimentally determined. The reason why this is compatible with the scaling of νW_2 in the same region is also discussed. (auth)

27996 POLARIZATION EFFECTS DURING THE PHOTOPRODUCTION OF ELECTRON–POSITRON PAIRS CONSIDERING ELECTROMAGNETIC MULTIPOLE NUCLEAR MOMENTS. Kerimov, B. K.; El Gavkhari, A. Izv. Akad. Nauk SSSR, Ser. Fiz.; 34: 204-9(Jan 1970). (In Russian).

Cross sections, differential in angle and energy, were obtained in Born approximation for the process of electron–positron (or muon) pair formation by γ quanta. Simultaneously, calculations considered electric quadrupole Q, magnetic dipole μI, and octupole Ω moments of target nuclei and the longitudinal polarization of spins (helicity) participating in particle production. A general formula describing the influence of electromagnetic multipole moments of the point nucleus on the degree of longitudinal polarization of positrons (electrons) is also obtained. It is shown that efficient transmission of helicity in magnetic photopair production reaches a maximum magnitude in the upper spectrum boundary. The higher-energy positron of the pair escaping in reverse ($\theta_+ \to 180°$) had the helicity of the incoming high-energy γ quantum. (R.V.J.)

27997 PAIR PRODUCTION IN COLLISIONS OF HIGH-ENERGY CHARGED PARTICLES. Baier, V. N.; Fadin, V. S. (Inst. of Nuclear Physics, Novosibirsk, USSR). Lett. Nuovo Cim.; 1: 481-5(13 Mar 1971).

Cross sections of the electroproduction processes at high energies are obtained in the double-logarithmic approximation. (L.B.S.)

27998 COMMENTS ON THE LETTER LIMITS ON THE ELECTROMAGNETIC PRODUCTION OF HEAVY LEPTONS. Mann, A. K. (Univ. of Pennsylvania, Philadelphia). Lett. Nuovo Cim.; 1: 486-8(13 Mar 1971).

Two observations are noted: (1) The lifetime of a heavy lepton L decaying as $L^\pm \to l + \nu_e + \nu_L$ increases rapidly as M_L decreases, which combines with the effect of time dilation to reduce severely the number of μe pairs arising from the pair production of leptons with $M_L \leq 500$ MeV. (2) If the heavy lepton L and its neutrino ν_L are assumed to couple to hadrons in a manner similar to that with which the lighter charged leptons e and μ are coupled to hadrons, then the predominant decay mode of L (for $M_L \leq 1$ GeV) will be $L^\pm \to \pi^\pm + \nu_L$. (L.B.S.)

27999 PHENOMENOLOGICAL INVESTIGATION OF INELASTIC ELECTRON–PROTON SCATTERING. Nachtmann, O. (Laboratoire de Physique Theorique et Hautes Energies, Orsay, France) Nucl. Phys.; B28: 282-90(1971).

Contour lines for the structure function νW_2 are drawn. Scaling behavior is clearly exhibited for $\omega \gtrsim 8$. For larger ω a diffractive mechanism seems to dominate. Combining data from inelastic ep scattering with those from photoproduction and complex nuclei the region of validity of the vector-dominance model is studied. A qualitative change seems to take place at $Q^2 \approx 0$. (auth)

28000 DERIVATIVE AMPLITUDES IN PHOTOPRODUCTION. Mueller, H. J. W. (Univ., Munich). Nucl. Phys.; B28: 125-40(1971).

Partial-wave decompositions of amplitudes for reactions of nonspinless particles generally involve derivatives of Legendre functions. In an approach suggested by Fubini and Rebbi the invariants are constructed in such a way that their amplitudes possess simple scalar-like partial-wave decompositions and are therefore particularly suitable for Reggeization and applications of current algebra. Here the usefulness of the derivative approach is explored by application to a non-trivial example-pion photoproduction. The results are of interest both as an application of the method and as a compact treatment of photoproduction amplitudes. (auth)

28001 PARTONS AND DUALITY IN DEEP INELASTIC LEPTON SCATTERING. Landshoff, P. V.; Polkinghorne, J. C. (Cambridge Univ., Eng.). Nucl. Phys.; B28: 240-52(1971).

The parton approach, with the partons identified as quarks, is combined with a dual model to describe deep inelastic lepton scattering. The partons are introduced through a non-perturbative field-theory formalism, which is shown to reproduce many of the results of more phenomenological approaches. Duality is imposed by assuming that exotic states correspond to a purely diffractive contribution, and by constructing a Veneziano-like model for the non-diffractive contribution. It is found that the difference between the cross sections on proton and neutron is just less than one third of the experimental cross section for electroproduction on the proton. The proton cross section is well explained by assuming that the diffractive contribution is small. (auth)

28002 PARTON THEORY BASED ON THE DUAL RESONANCE MODEL. Nielsen, H. B. (NORDITA, Copenhagen); Susskind, L.; Kraemmer, A. B. Nucl. Phys.; B28: 34-50(1971).

The consequences of replacing the continuous string model of hadrons by an infinite but discrete chain of partons are considered. It is shown that such a replacement leads to a sensible theory of form factors and deep inelastic electroproduction cross sections. Experimental data concerning these quantities are used to estimate the departure from the continuum limit. It is found that a hadron is probably a fairly loosely knit structure. (auth)

Weak

Refer also to abstract 28059.

28003 (PURC–4159-22) PHENOMENOLOGY OF WEAK INTERACTIONS. Treiman, S. B. (Princeton Univ., N. J. Joseph Henry Labs.). Apr 1971. Contract AT(30-1)-4159. 23p. (CONF-710309-1). Dep. NTIS.

From Conference on the phenomenology of particle physics; Pasadena, Calif. (25 Mar 1971).

A review is given of some recent developments in weak interaction physics. Some topics discussed are CP violation, second class currents, and inelastic neutrino reactions. (L.B.S.)

28004 CHIRAL SYMMETRY AND NONLEPTONIC-RADIATIVE HYPERON DECAY. Holstein, B. R. (Princeton Univ., N. J.). Nuovo Cim.; 2A: 561-78(1 Apr 1971).

Nonleptonic-radiative hyperon decay—$\alpha \to \beta\gamma$—is studied from the point of view of current algebra and simple chiral Lagrangians. Equivalence between the approaches is shown and attempts to fit current experimental data are discussed. Predicted values in such models are found to be in apparent disagreement with present experiments. (auth)

28005 LEPTON–HADRON PROCESSES AT HIGH ENERGY. Bjorken, J. D. (Stanford Linear Accelerator Center, Calif.). Acta Phys. Pol.; B2: 5-34(Jan-Mar 1971).

The kinematical description and state of data for lepton-induced hadron interactions are briefly reviewed. The nature of the current commutators and light cone behavior are discussed. Two classes of dynamic models for interpreting the deep-inelastic data are discussed—the parton model and diffraction-like models. Quantum electrodynamics at infinite moment is studied to gain some insight into the nature of the models for semileptonic processes. (L.B.S.)

28006 INELASTIC NEUTRINO–NUCLEON SCATTERING AT HIGH ENERGY AND SUGAWARA MODEL, STRESS TENSOR, AND SPECTRAL SUM RULES. Palmer, David Ray. Boulder, Colo.; Univ. of Colorado (1970). 110p. University Microfilms Order No. 71-5920.

Thesis.

Inelastic neutrino-nucleon scattering is considered within the context of Harari's duality model. It is argued that the Regge residue function associated with the vector-axial interference term should be rapidly damped at large $|q^2|$. A causal representation is used to show a rapidly damped residue function is consistent with scale invariance and Regge asymptotic behavior. The scaling function $F_3(\omega)$ is then shown to approach a nonzero constant as $\omega = |q^2|/\nu \to 0$ in contrast to previously suggested behavior. Using PCAC, the asymptotic limit of the scaling function $F_3(\omega)$ as $\omega \to 0$ is calculated to be 0.25. This value is lower than the experimental values in the lowest accessible ω-region indicating that the diffractive region has not been reached. A prescription is presented for modifying the stress tensor of the Sugawara model in order that

it become consistent with general postulates of field theory. The prescription involves redefining the stress tensor as the limit of a spatially nonlocal operator. Within the context of the modified theory, sum rules are derived by considering the vacuum expectation value of equal-time stress tensor commutators. It is shown that a convergent Weinberg's second sum rule in the framework of the Sugawara model leads to a null theory. The existence of a nontrivial Sugawara model leads to a specific behavior of the cross section for positron-electron annihilation into hadrons at high energies. (Diss. Abstr. Int., B)

Strong (General)

Refer also to abstract 28100.

28007 (CERN-71-8) SPIN FORMALISMS. Lectures given in the Academic Training Programme of CERN 1969-1970. Chung, Suh Urk (European Organization for Nuclear Research, Geneva (Switzerland)). 25 Mar 1971. 81p. Dep. NTIS (U. S. Sales Only).

A comprehensive view of the various spin formalisms used in the study of the elementary particles is presented. Particular emphasis is given to the description of resonances decaying into two, three, or more particles and to the methods of determining the spin and parity of resonances with sequential decay modes. (L.B.S.)

28008 (UCRL-73073) HADRON SPECTROSCOPY. Mac Gregor, Malcolm H. (California Univ., Livermore. Lawrence Radiation Lab.). 19 Feb 1971. 85p. (CONF-710106-6). Dep. NTIS.

From Conference on fundamental interactions at high energy; Coral Gables, Fla. (20 Jan 1971).

The available hadron data are arranged in such a way as to reveal any systematic experimental regularities. The discussion covers a comparison of hadronic and nuclear rotational bands, baryon and hyperon rotational bands, dibaryon states, meson and kaon rotational bands, $N\bar{N}$ resonances, basic mass quanta, the mass matrix, excitation towers, and A_2 splitting. Geometries of spinning and spinless mass quanta, experimental evidence for a spin-1 ABC response, the (M, η^1, δ^-) and (H, π_N, ϕ) resonance groups as single I = 1 particles, Kemmer branching ratios and lifetime systematics are included. Also discussed are baryon number, predictions and clarifications, and dynamical tests of symmetries. A compilation of experimental hadron data is included. (J.F.P.)

28009 NATURE OF HADRON ROTATIONAL LEVELS. Mac Gregor, M. H. (Univ. of California, Livermore). Lett. Nuovo Cim.; 1: 427-36(6 Mar 1971).

It is demonstrated that a nuclear physics approach might be used in classifying baryon and hyperon resonances. A classification of rotational levels is attempted based on an L(L + 1) interval rule for the energies. (L.B.S.)

28010 EVIDENCE FOR LINEAR MESON SYSTEMATICS WITH BARYON NUMBER N = 2. MacGregor, M. H. (Univ. of California, Livermore). Lett. Nuovo Cim.; 1: 437-41(6 Mar 1971).

Interval relationships are displayed by a plot of narrow meson and kaon resonances and narrow or S-state baryon and hyperon resonances (baryon number N = 1). It is pointed out that a recent experimental result extends this interval relationship to the Ap system (N = 2). It is pointed out that the N = 2 resonance can be used as a confirmation of the existence of an N = 1 resonance for which the experimental data are somewhat inconclusive. (L.B.S.)

28011 IMPACT PICTURE AND THE EIKONAL APPROXIMATION. Cheng, H.; Wu, T. T. (Deutsches Elektronen-Synchrotron, Hamburg). Phys. Lett.; 34B: 647-50(12 Apr 1971).

A detailed study of the ϕ^3-theory shows that the impact picture is correct, while the eikonal approximation is not valid. A relatively simple experimental test, at the CERN Intersecting Storage Ring, of the impact picture is discussed. (auth)

28012 SELF-CONSISTENT RISING CROSS-SECTIONS. Finkelstein, J.; Zachariasen, F. (CERN, Geneva). Phys. Lett.; 34B: 631-4(12 Apr 1971).

It is shown that the multiperipheral model, when corrected for absorption, can accommodate increasing total cross sections. In this case, a particle appears as a totally absorbing disk, with a radius which increases with energy; this property is independent both of the properties of the production amplitudes when not all the subenergies are large, and also of the details of the absorption. If one does use the absorbed multiperipheral matrix element over all of phase space, then the resulting bootstrap has a self-consistent solution given by $T(s,t) = 4\pi$ is $R_0 \log s(-t)^{-\frac{1}{2}} J_1 (R_0 \log s(-t)^{\frac{1}{2}})$. (auth)

28013 ANALYTICITY STRUCTURE OF SIMPLE SINGLE-PARTICLE EXCHANGE MODELS FOR HIGH-ENERGY INTERACTIONS. Rivers, R. J. (Imperial Coll. of Science and Tech., London). Phys. Lett.; 34B: 635-7(12 Apr 1971).

It is shown that the requirement that a simple single-particle exchange model gives a four-point tree diagram with Regge behavior precludes its use as a Born term in a perturbatively unitary field theory. (auth)

28014 VENEZIANO n-POINT FUNCTION: SYMMETRIC REPRESENTATIONS AND THEIR IMPLICATIONS. Koba, Z. (Niels Bohr Inst., Copenhagen). Acta Phys. Pol.; B2: 111-27 (Jan-Mar 1971).

One aspect of the recent developments in the study of the Veneziano model, i.e., symmetric representations of the n-point function and their implications is studied. An elementary introduction to the conventional way of construction of the Veneziano n-point function is given. (auth)

28015 NON PERTURBATIVE PARTON MODEL OF CURRENT INTERACTIONS. Landshoff, P. V.; Polkinghorne, J. C.; Short, R. D. (Cambridge Univ., Eng.). Nucl. Phys.; B28: 225-39(1971).

A formulation of the parton picture of current interactions is given without recourse to perturbation theory. In deep inelastic electron scattering the structure functions W_1 and νW_2 scale but the corresponding functions $\overline{W}_1$ and $\nu\overline{W}_2$ for electron-positron annihilation processes at high energy are likely to be divergent. Form factors for particles other than the partons themselves go to zero at infinite momentum transfer. The relation between the rate of decrease of the nucleon form factors and the behavior of νW_2 near $\omega = 1$ is shown to depend upon further specific properties of parton-nucleon dynamics and so to be model dependent. Some similarities between the parton picture and a recently proposed Veneziano-like amplitude are discussed. A difference is that the parton picture permits the incorporation of the pomeron. (auth)

28016 SCALING AND DUALITY IN STRONG INTERACTIONS. Rittenberg, V.; Rubinstein, H. R. (Weizmann Inst. of Science, Rehovot, Israel). Nucl. Phys.; B28: 184-8(1971).

It is shown that the dual resonance models scale by themselves even in the absence of electromagnetism. Though the result is derived in a crude model the scaling condition seems general and predicts scaling for the normal trajectories and not for the pomeron. (auth)

28017 EXPERIMENTAL CONSEQUENCES OF THE CONJECTURE THAT THE QUARK MODEL ADDITIVITY FRAME IS THE JACKSON FRAME. Bialas, A. (Jagellonian Univ., Krakow. Inst. of Nuclear Physics, Krakow); Kotanski, A.; Zalewski, K. Nucl. Phys.; B28: 1-12(1971).

It is proposed to fix the additivity frame of the quark model by identifying it with the Jackson frame of reference. The consequences of this choice are discussed for (i) resonance production by polarized particles, (ii) production of higher-spin resonances, (iii) production of the A_1 and Q bumps. (auth)

28018 s-WAVE INTERFERENCE IN THE f^0 RESONANCE REGION. Beaupre, J. V. (Technische Hochschule, Aachen); Deutschmann, M.; Graessler, H.; (and others). Nucl. Phys.; B28: 77-84(1971).

The anomalous shape of the decay angular distribution of the f^0 resonance can be explained by an interference of the resonating d-wave with an isospin zero s-wave, whose phase stays near 90° in the f^0 region. (auth)

28019 SEPARABLE INTERACTIONS AND HIGH ENERGY SCATTERING. Bawin, M. (Indiana Univ., Bloomington). Nucl. Phys.; B28: 109-17(1971).

A model for the elastic scattering of two particles in the presence of inelastic processes is proposed, in which a complex nonlocal potential simulating the presence of inelastic channels is taken to be separable. In particular, the form of a complex separable interaction leading to linear Regge trajectories, Regge behavior and a finite cross section at infinite energy is given. The model can also be used as a guide as to what properties a separable potential fitting some low and intermediate energy data should have. Possible application can be made in the three-body problem. (auth)

28020 POMERANCHUK SINGULARITY IN THE VENEZIANO MODEL AND UNITARITY. Blagojevic, M.; Lalovic, D. (Boris Kidric Inst. of Nuclear Science, Belgrade). Nucl. Phys.; B28: 118-24(1971).

A recent suggestion, that in the unitarized Veneziano amplitude the Pomeranchuk contribution may come out as a non-resonant background, is analyzed quantitatively. It is shown that the ap-

proximate form of the proposed unitarization can not reproduce the Pomeranchuk contribution. (auth)

28021 DUAL SYMMETRIC THEORY AND THE HARMONIC OSCILLATOR MODEL OF HADRONS. Gallardo, Juan Carlos. New York; Yeshiva Univ. (1970). 102p. University Microfilms Order No. 71-5683.

Thesis.

A general dual vertex with one of the legs on the leading trajectory was constructed. The basic assumption is to consider the spin-J external particle interacting with the local momentum density of the quarks in the framework of the dual harmonic oscillator model of hadrons. This vertex enables one to construct the tree graphs with spinning external particles (on the leading trajectory) preserving the intrinsic simplicity and manifestly factorization of the harmonic oscillator formalism. The properties of a dual local electromagnetic current (scalar photons) are investigated. The form factors behave as negative integer-powers of q^2 where the exponent depends on the spin of the hadron. The amplitudes with a single current show fixed poles at negative integers but in complete agreement with several speculations, the leading fixed pole is canceled out; this is, presumably, due to the composite nature of the hadrons. Although a difficulty is encountered in the calculation of two current amplitudes, the model has interesting properties which agree at least qualitatively with the present experimental evidence. (Diss. Abstr. Int., B)

Strong (Baryon No. = 0)

28022 (DESY-71/10) RELATIVISTIC SCALAR QUARK MODEL WITH STRONG BINDING. Boehm, M.; Joos, H.; Krammer, M. (Deutsches Elektronen-Synchrotron, Hamburg (West Germany)). Mar 1971. 37p. Dep. NTIS (U. S. Sales Only).

The dynamics of strong binding of heavy scalar particles (quarks) are discussed with the help of the Bethe–Salpeter equation with a smooth ladder type kernel. For this purpose the Bethe–Salpeter amplitudes are expanded into 0(4) spherical functions and the remaining "hyperradial" equation is solved by a variational method. These calculations are considered as a model of mesons as bound states of heavy quarks. The low lying mesons form linear trajectories with a slope of 1 GeV^{-2}. The modification of the vector meson dominance form factor by the bound state wavefunctions is calculated and found to be in good agreement with experiment. (auth)

28023 (NP-18763) κ-MESON DECAY IN THE VECTOR THEORY WITH THE NONCONSERVED CURRENT. Achasov, N. N. (Akademiya Nauk SSSR, Novosibirsk. Institut Matematiki). 1967. 8p. Dep. NTIS (U. S. Sales Only).

The constants for the coupling of $\varkappa$ meson with pseudoscalar mesons and baryons are obtained in the vector theory by taking phenomenologically into account $\varkappa\kappa^*$ transitions in the virtual lines and assuming for the vector current with $\Delta S = 1$ the relation $\partial_n S_n = -Zm_\varkappa^2 m\varkappa'(x)$ to be very close to them in its physical meaning. For example, $\Gamma_\varkappa = 22$ MeV was obtained for $\varkappa \to \kappa\pi$. (auth)

28024 (NP-18766) SUM RULES FOR $\pi\pi$-SCATTERING. Baranov, A. I.; Wall, A. N.; Serebryakov, V. V. (Akademiya Nauk SSSR, Novosibirsk. Institut Matematiki). 1967. 11p. Dep. NTIS (U. S. Sales Only).

A number of sum rules for pion–pion partial amplitudes was obtained making use of the low energy interpretation of the dispersion relation for the fixed momentum transfer, from which there follows a real relationship between the scattering lengths and parameters of the known resonances and high energy contributions as well as indication on the possible existence of a new I = 0 and J = 1 = 4 bipion resonance with a mass of about 2 GeV. (auth)

28025 (NP-18768) THE AMPLITUDE OF FORWARD SCATTERING OF THE PROCESS $\pi^+\pi^0 \to \pi^+\pi^0$. Belinicher, V. I. (Akademiya Nauk SSSR, Novosibirsk. Institut Matematiki). 1967. 10p. Dep. NTIS (U. S. Sales Only).

It is noted that the account of ρ meson contribution in the amplitude of the process $\pi^+\pi^0 \to \pi^+\pi^0$ described by N. G. Antonion was not sufficiently correct. It is shown that less rigorous restrictions on the scattering length and the cross section follow from the assumptions made. (auth)

28026 (NP-18774) POSSIBLE QUASINUCLEAR NATURE OF HEAVY MESONIC RESONANCES. Dalkarov, O. D.; Mandelzweig, V. B.; Shapiro, I. S. (Gosudarstvennyi Komitet po Ispol'zovaniyu Atomnoi Energii SSSR, Moscow. Institut Teoreticheskoi i Eksperimental'noi Fiziki). 1970. 12p. Dep. NTIS (U. S. Sales Only).

It is shown that nucleon–antinucleon potential interaction gives rise to a number of nuclear-like nonrelativistic bound states appearing as heavy mesonic resonances (with masses close to the double nucleon mass). (auth)

28027 (RLO-1388-602) CURRENT ALGEBRA AND ANALYTICITY: BOOTSTRAPPING THE RHO AND SIGMA WITH THE PION DECAY CONSTANT SETTING THE SCALE. Brown, Lowell S. (Washington Univ., Seattle. Dept. of Physics); Goble, Robert L. (Minnesota Univ., Minneapolis. Dept. of Physics). Jan 1971. 11p. Dep. NTIS.

Simple one-parameter forms for the S and P waves of pion scattering that obey current algebra constraints and allow for a resonance are constructed. The parameters are completely determined by solving self-consistently three-subtracted forward dispersion relations in a region up to 1 GeV. Resonances for the ρ and σ are produced with the mass scale set by the pion decay constant, but the dispersion relations require the "exotic" T = 2, S-wave be nonresonant. (auth)

28028 (SU-1206-242) s-CHANNEL HELICITY CONSERVATION CONSTRAINTS ON t-CHANNEL EXCHANGES. Blackmon, Maurice L.; King, Marcia J.; Wali, Kameshwar C. (Syracuse Univ., N. Y. Dept. of Physics). Jan 1970. 34p. (NYO-3399-242). Dep. NTIS.

Equations relating t-channel Regge residue functions are derived assuming s-channel helicity is conserved. When these equations are extrapolated to the positive t region, they become constraints on coupling constants for the exchanged particles. One can show that if one insists on helicity conservation in reactions $\pi\pi \to \pi S$ ($\pi N \to \pi N^*$), then the exchanged particles have a unique coupling and that they have angular momentum J such that $J \geq S$ ($J \geq S + \frac{1}{2}$) where S is the angular momentum of the meson resonance S (baryon resonance N^*). Detailed examples are given. (auth)

28029 APPLICATION OF THE DISPERSIVE SUM RULE METHOD TO MESON SYSTEMS. McKisic, James Michael. Columbus, Ohio; Ohio State Univ. (1970). 99p. University Microfilms Order No. 71-7516.

Thesis.

The dispersive sum rule method of Fubini and Furlan is applied to a study of pion–kaon, kaon–kaon and kaon–antikaon elastic scattering processes and to a study of SU(3) × SU(3) symmetry breaking. In the case of pion–kaon scattering, sum rules derived for the s-wave $I = \frac{1}{2}$ and $I = \frac{3}{2}$ scattering amplitudes under the assumptions of current algebra, PCAC, PCVC, single particle pole dominance and the assumption that the SU(3) × SU(3) symmetry breaking part of the strong-interaction Hamiltonian transforms according to the $(3,3^*) + (3^*,3)$ representation of the group. The off-shell corrections are evaluated, and the isospin-antisymmetric combination of scattering lengths is found to be consistent with previous calculations based on current algebra, phenomenological Lagrangian models and recent multiple term Veneziano models, but smaller than those predicted from the leading term Veneziano model. In addition, a kappa meson mass and width is predicted, consistent with a recent experimental indication. Similar methods are applied to the case of K–K and K–$\bar{K}$ elastic scattering with the principal exceptions that off-shell corrections are estimated by a smoothness assumption, and there is no investigation of symmetry breaking. In an attempt to reconcile the Veneziano model with current algebra, qualitative indications are found for the existence of a rich resonance spectrum near the KK threshold. (Diss. Abstr. Int., B)

28030 NONRELATIVISTIC COMPOSITE PARTICLE MODEL FOR MESONS. Namiki, Mikio; Fujimura, Kimio; Ohba, Ichiro; Yap, S. P. (Waseda Univ., Tokyo). Waseda Daigaku Rikogaku Kenkyusho Hokoku; No. 47, 83-91(May 1970).

On the basis of nonrelativistic composite particle model the Schrödinger equation is employed to describe the internal dynamics of the composite particles such as mesons. Some characteristic properties of the bound states are analyzed by numerical calculation by making use of a square well potential and a Woods–Saxon potential. It is found that the mass levels of meson states can be reproduced if appropriate values of potential parameters are adopted. The results thus obtained for the Woods–Saxon potential are more consistent with the experimental data than those obtained for the square well potential. Calculation of the internal kinetic energy seems to show that its values can be consistent with the nonrelativistic treatment. The electromagnetic form factor of the pion and spin-orbit force for P-wave ground state are also calculated. The best fitted expectation value of the spin-orbit potential is found to be equal to 28.5 MeV, which seems somewhat too small in comparison with the mass splitting between the $1^{+\prime}$-nonet ($^1P_1$) and 1^+-nonet ($^3P_1$), since according to Iizuka's theory this should be about 100 MeV. (auth)

28031 KAON MASS MEASUREMENT FROM KAONIC ATOM X-RAY ENERGIES: THE 4f-3G KAONIC TRANSITION IN CHLORINE. Kunselman, R. (Univ. of Wyoming, Laramie). Phys. Lett.; 34B: 485-7(29 Mar 1971).

From measurements of kaonic atom x-ray energies the negative kaon mass is measured to be 493.87 ± 0.19 MeV. The effects of the strong interaction between the kaon and nucleus cause the X rays from the 4f-3d transition in chlorine (Z = 17) to be shifted by −0.94 ± 0.40 keV. This shift was used to estimate the strong interaction shifts needed for the mass measurement. (auth)

28032 P-WAVE ππ SCATTERING AMPLITUDE WITH CDD POLES. Antoniou, N. G.; Baier, R. (CERN, Geneva). Lett. Nuovo Cim.; 1: 443-7(13 Mar 1971).

It is shown that a unitarized model for the P-wave ππ scattering amplitude can be constructed having a left-hand cut discontinuity given by the Lovelace-Veneziano representation. N/D equations are used, and it is assumed that all particles in this channel are described predominantly by inelastic CDD poles. By requiring consistency with the Lovelace-Veneziano representation near the ρ-meson a condition is obtained which leads to a value for the intercept of the ρ-f trajectory, in good agreement with the phenomenological one. A reasonable picture of the pion form factor in the timelike and in the spacelike regions is obtained on the basis of this model. (L.B.S.)

28033 NECESSITY OF EXOTIC MESONS, PARITY DOUBLETS, OR REGGE CUTS. Finkelstein, J. (CERN, Geneva). Nucl. Phys.; B28: 73-6(1971).

It is shown that the assumptions of duality and of Regge-pole behavior imply the necessity of exotic contributions to meson–meson scattering amplitudes, unless there is parity doubling for leading meson trajectories at t = 0. (auth)

28034 MULTI-PARTICLE EIKONAL MODEL WITH HIGH ENERGY S-CHANNEL HELICITY CONSERVATION. Gunion, J. F. (Stanford Univ., Calif.); Roberts, R. G. Nucl. Phys.; B28: 205-9(1971).

Using a modified version of the Baker–Blankenbecler formalism unitary corrections are applied to the generalized Veneziano model and an eikonal model is obtained for all types of reactions. The "Pomeranchuk" contribution in the model conserves s-channel helicity. (auth)

Strong (Baryon No. = 1)

Refer also to abstract 27962.

28035 ARGAND-DIAGRAM ANALYSIS OF THE POMERON COUPLING TO THE KN AND $\bar{K}N$ SYSTEM. Hogan, W.; (Northeastern Univ., Boston); Srivastava, Y.; Restignoli, M.; Violini, G. Lett. Nuovo Cim.; 1: 409-15(6 Mar 1971).

The conjecture that Argand diagrams for S-channel helicity amplitudes should show resonance circles is tested for the case of the $\bar{K}N$ and KN system. The possible existence of the Z* resonance is also examined. An analysis of the data based on CERN phase shifts was found to be inconclusive. (L.B.S.)

28036 IMAGINARY PARTS OF REGGE TRAJECTORIES, DUALITY CONCEPT, AND MESON–NUCLEON SCATTERING. Minami, S. (Osaka City Univ.). Lett. Nuovo Cim.; 1: 404-8 (6 Mar 1971).

It was previously pointed out that the imaginary parts of nonstrange and strange baryon trajectories can be expressed by $\xi(s) \equiv \mathrm{Im}\alpha(s) = 0.14(s-1)$ and $\xi(s) = 0.13(s-2.2)$, respectively. The following problems are studied: (1) How to examine experimentally whether $\xi(s)$ is not equal to zero at $s \leq 0$; (2) the effects of $\mathrm{Im}(\alpha)$ on the differential cross section of backward pion–nucleon scattering; (3) the properties of $\xi(s)$ for meson trajectories; and (4) the duality concept for the case where $\xi(s)$ is not equal to zero at $s \leq 0$. (L.B.S.)

28037 SU(3) × SU(3) CHIRAL LAGRANGIAN MODEL FOR $\bar{K}N$ INTERACTIONS. Hogan, Mary Elizabeth Mogge. Tallahassee, Fla.; Florida State Univ. (1970). 138p. University Microfilms Order No. 71-7032.

Thesis.

A chiral Lagrangian model of meson–baryon scattering is used to develop a theory of KN, πΣ, and πΛ interactions. The meson and baryon fields are assumed to transform as nonlinear realizations of SU(3) × SU(3). In addition to pseudoscalar meson and $J^P = 1/2^+$ baryon fields, vector meson, $J^P = 1/2^-$ baryon, $J^P = 3/2^+$ baryon and $J^P = 3/2^-$ baryon fields are introduced to describe one-particle exchange contributions. The chiral symmetry is broken by Lagrangians bilinear in either the baryon or pseudoscalar fields. An extensive formalism is developed in order to obtain physical predictions from the model. The partial wave amplitudes obtained from the chiral Lagrangian model are unitarized by a K-matrix formalism. Total cross sections are calculated for the processes $\bar{K}N \to \bar{K}N$, $\bar{K}N \to \pi\Sigma$, $\bar{K}N \to \pi\Lambda$, $\pi\Sigma \to \pi\Sigma$, $\pi\Lambda \to \pi\Sigma$, and $\pi\Lambda \to \pi\Lambda$. $\bar{K}N$, $\pi\Lambda$, and π scattering lengths are also calculated. Not all of the predictions agree with experiment. Methods of improving the model are suggested. (Diss. Abstr. Int., B)

28038 STUDY OF THE REACTIONS $\pi^-p \to K^+\Sigma^-$ AND $\pi^+p \to K^+Y^{*+}$ FROM 2.75 TO 14.0 GeV/c. Bashian, Allen. Stony Brook, N. Y.; State Univ. of New York (1970). 66p. University Microfilms Order No. 71-8093.

Thesis.

The reactions $\pi^-p \to K^+\Sigma^-$ and $\pi^-p \to K^+Y^*_{1385}$, which are single meson exchange forbidden, were studied in an experiment at the Brookhaven AGS. With π mesons incident on a liquid hydrogen target, a wire spark chamber-bending magnet spectrometer was used to measure the momentum of the forward K^+. Missing mass analysis of all events showed no evidence for either reaction in the peripheral region of 0–5° lab product angle. For $K^+\Sigma^-$ production, an upper limit for the forward cross section is obtained under two assumptions: a flat distribution in momentum transfer and a distribution identical to that of the companion allowed reaction $\pi^+p \to K^+\Sigma^-$. For either case, the cross section for $K^+\Sigma^-$ is found to be $\lesssim .01\ \sigma(K^+\Sigma^+)$ from 2.75 to 4.5 GeV/c and $\lesssim .005\ \sigma(K^+\Sigma^+)$ at 6. and 10. GeV/c. The upper limit for the cross section is found to be ∼.5 ± .5 μ bn from 2.75 to 4.5 GeV/c, ∼.2 ± .2 μ bn at 6 GeV/c, and ∼0.0 ± .1 at 10 GeV/c. For the reaction $\pi^-p \to K^+Y^-_{1385}$, an upper limit for the forward cross section is calculated based on the assumption of a flat t-distribution. The values found are ∼1. ± 1. μ bn between 3. and 4. GeV/c; at 4.5 and 6. GeV/c, the cross section for forward production is consistent with 0. The companion allowed reaction $\pi^+p \to K^+Y^{*+}$ was also studied from 3.5 to 14.0 GeV/c. Differential cross sections for the process are presented and are found to exhibit a forward dip in the region $|t| \leq .16$. (auth)

28039 GRAPHICAL ILLUSTRATION OF ISOSPIN ANALYSIS IN SINGLE-PION PRODUCTION. Bjoerneboe, J.; Koba, Z. (Univ. of Copenhagen); Toernquist, N. Phys. Lett.; 34B: 638-40(12 Apr 1971).

Predictions of charge independence for processes with three isospin channels are obtained from a pyramid constructed using measured integrated and spin-averaged cross sections. The exchange isospin amplitudes in processes XN → XπN, where X = N, K, $\bar{K}$, π are studied in detail. (auth)

28040 PURE STATES, POLARIZED TARGETS, AND BARYON SPIN DETERMINATION. Donohue, J. T. (Univ., Nice). Phys. Lett.; 34B: 628-30(12 Apr 1971).

A relation is found between the spin J of a fermion resonance, the sum of the squares of the statistical tensors t_L^M for even L, and the degree of target polarization for the reaction M + B(P) → M + B* on a polarized target. In principle an unambiguous spin determination can be made by observing the parity-conserving decays of B* for two different values of the target polarization |P|. (auth)

28041 ANALYSIS OF MESON–BARYON SCATTERING PROCESSES RELATED BY SU(3) IN A UNITARIZED VENEZIANO MODEL. Gunion, J. F. (Stanford Univ., Calif.); Roberts, R. G. Nucl. Phys.; B28: 210-24(1971).

A previously developed eikonal-like model is extended to analyze meson–baryon scattering. Unitarity is partly described by introducing all the coupled two-particle channels which are related to each other by the requirements of SU(3), duality, factorization and absence of exotics. The pomeron is interpreted as the manifestation of multiparticle unitarity rather than as a t-channel Regge exchange. With a small number of parameters good agreement with data was obtained on twelve processes. One parameter, the F/D ratio for t-channel spin-flip coupling, is shown to play a crucial role in understanding the differing behaviors of various cross sections and polarizations. (auth)

28042 REACTION $K^-P \to \Lambda K^+K^-$ AND THE GENERALIZED VENEZIANO MODEL. Schreiner, P. A. (Univ. of California, Los Angeles); Stork, D. H.; Ross, R. T.; Clark, A. G.; Lyons, L. Nucl. Phys.; B28: 85-96(1971).

New data for the reaction $K^-p \to \Lambda K^+K^-$ at 3.3 GeV/c were used to investigate the five-particle generalized Veneziano model. The amplitude is constrained by symmetry properties of the crossed channels and by non-exchange degeneracy of the N^*_α trajectory. The Harari–Rosner dual quark model determines the trajectories which couple to the K^+K^- system. Reasonable choices for the other

trajectories lead to good agreement with these data as well as data at higher and lower beam momentum. The pomeron exchange contribution to the reaction is shown to be small; however, both pseudoscalar and vector kinematic factors are required for detailed agreement with the angular distributions. The model fails to account for the crossing-symmetric reaction $K^+p \to \Lambda K^+K^+$. (auth)

28043 K^+p REGGEIZED PHASE SHIFT ANALYSIS. Lovelace, C.; Wagner, F. (CERN, Geneva). Nucl. Phys.; B28: 141-70(1971).

KN and $\bar{K}N$ absorptive Regge fits at high energies, and phase-shift analysis of K^+p at 26 energies below 2 GeV/c were completed. They used the same Veneziano formula for the high partial waves. The shortest path solution turned out to be that closest to the Regge extrapolation in low waves also. A consistent picture of K^+p is obtained from 0 to 16 GeV/c. Agreement with the KN^* channel is also better than before. Though an exotic resonance is not completely excluded, K^+p scattering can be accurately described without one. The KAN coupling constant is $g_A^2 = 10.5 \pm 1.5$. (auth)

28044 REDEMPTION OF THE DUAL DESCRIPTION OF PRODUCTION PROCESSES BY UNITARITY. THE RELEVANCE OF THE EIKONAL MODEL. Gunion, John F.; Roberts, R. G. (Univ. of California, San Diego, La Jolla). Nucl. Phys.; B28: 189-204(1971).

Using the Baker–Blankenbecler formalism unitarity corrections are applied to the Veneziano model and its generalization to many-point functions. As a result an eikonal-like pole-cut model is obtained for elastic scattering and for production processes. The dip at $t = -0.9$ GeV^2 in K^-p scattering is particularly well described. The processes $K^-p \to \pi^-Y^{*+}$ and $\pi^+p \to K^+Y^{*+}$ are considered in detail and it is found that inclusion of unitarity corrections allows the assumptions of factorization, exchange degeneracy and duality to be retained in contrast to the previous applications of the generalized Veneziano model to these reactions and leads to an improvement in the agreement with data. (auth)

Strong (Baryon No. ≥ 2)

Refer also to abstracts 28073 and 28482.

28045 (DESY-71/6) IMPACT PICTURE AND THE EIKONAL APPROXIMATION. Cheng, Hung; Wu, Tai Tsun (Deutsches Elektronen-Synchrotron, Hamburg (West Germany)). Feb 1971. Contract AT(30-1)-4101. 11p. Dep. NTIS.

A detailed study of the ϕ^3-theory shows that the impact picture is correct, while the eikonal approximation is not valid. A relatively simple experimental test, at the CERN Intersecting Storage Ring, of the impact picture is discussed. (auth)

28046 ANALYSIS OF THE KANTOR AMPLITUDES AND RECENT LOW-ENERGY PROTON–PROTON SCATTERING EXPERIMENTS. Furuichi, S. (Rikkyo Univ., Tokyo); Suemitsu, H.; Yonezawa, M.; Watari, W. Nucl. Phys.; A165: 211-24 (1971).

The behavior of the $^3P_0$ phase shift for proton–proton scattering in the energy range 25 to 50 MeV is discussed. It is shown that theoretical analysis of the Kantor amplitudes predicts a larger $^3P_0$ phase shift than the experimental value currently accepted. The existing experimental data are examined by means of a phase-shift analysis to see how the individual spin-correlation data affect the $^3P_0$ phase shift. (auth)

28047 CALCULATION OF THE THREE-BODY MODEL VERTEX PART $^3H \to n + d$. Orlov, Yu. V. Vestn. Mosk. Univ., Ser. III. Fiz. Astron.; 11: 487-94(Sep-Oct 1970). (In Russian).

The vertex part of virtual decay (or synthesis) of $^3H \rightleftharpoons n + d$ in the three-body models was calculated. The wave functions of ground state of ^3H nuclei were found by two methods, the K harmonics method and by resolving the Faddeev equations in separate approximations. Analytical expressions were obtained for various vertex functions. Considerations for the many-body system resulted in much slower and smoother descending vertex with increased transmitted pulse Q; however, in the separable approximation this effect was exaggerated. The vertex function depends on which of the two particles (n or d) is on the mass surface. The vertex diminished faster with the growth of Q and slower, according to the absolute magnitudes, when deuteron was virtual and neutron real. Data obtained were in agreement with the results of the prior analysis of (d, ^3H) and (^3H, d) reactions for light nuclei in peripheral model. (R.V.J.)

28048 DISTORTED WAVE EFFECTS IN PION INTERACTIONS WITH NUCLEI. Jones, William Benjamin. Charlottesville, Va.; Univ. of Virginia (1970). 143p. University Microfilms Order No. 70-26,587.

Thesis.

Theoretical studies of the related problems of pion absorption and pion propagation within nuclear matter were made. Because of energy and momentum conservation considerations, pure (as opposed to radiative) pion absorption on a single nucleon does not occur. Since, as a result, pion absorption takes place only upon nucleons bound in a nucleus, any attempt at explaining this process presupposes some understanding of pion propagation within the range of strong forces. The latter may be studied by means of either pion-nucleus scattering or pi-mesic atoms. Since pion wave functions generated in a successful phenomenological treatment of pion-nucleus scattering are not necessarily valid inside the nucleus, one must seek other means of testing them and/or provide logical support for the optical model used to generate them. Thus, a theoretical treatment of pion absorption employing such wave functions may be regarded as a test thereof, as well as of the absorption theory. To place the pion wave functions upon a firmer foundation and thus to sharpen the test of the absorption theory, a study of the Kroll modification of the Kisslinger optical model of pion-nucleus scattering has been undertaken. Called the Lorentz–Lorenz effect in analogy to the electromagnetic parallel, this modification results if zero-range anti-correlations among scattering centers are introduced into the multiple scattering derivation of the pion-nucleus optical model. Except for the real part of the central potential, which is unaffected, the Kroll modification of the Kisslinger model brings the phenomenologically determined parameters of this optical model into much better agreement with those given by multiple scattering theory and, in the 50 MeV range, eliminates the disturbing negative or pure imaginary values of the effective mass otherwise occurring. The differential cross section for proton emission following positive pion absorption by ^{12}C was calculated in the formalism of first order perturbation theory using distorted waves for the absorbed and emitted particles and using wave functions generated by a Woods–Saxon well for the neutron-hole state of the residual nucleus, to which the reaction provides access. This reaction is especially suited for testing the oft-employed perturbation theory approach to pion absorption phenomena because of its straight-forward nature both experimentally and theoretically. Only one particle, a proton, need be detected in the final state. Compared to absorption processes more often studied involving the emission of two nucleons or radiation, this reaction is relatively free of complicating nucleon pair correlation, final state interaction, electromagnetic and collective effects. The proton cross sections calculated are less sharply peaked in the forward direction and much more stable than those previously obtained using plane waves for the unbound particles and harmonic oscillator wave functions for the bound neutron. The most dramatic feature of the more realistic theory is an enhancement of three orders of magnitude produced by the distortion of the pion wave function. The proton distortion, primarily due to the absorptive part of the central potential, is responsible for a fivefold reduction in the proton cross section. It is, therefore, about two hundred times larger than the plane-wave result and some thirty times larger than presently available experimental findings. Pion wave functions generated by both the Kisslinger and Kroll–Kisslinger models produce about the same result. Cross sections calculated with the latter are perhaps fifteen per cent smaller and more sharply peaked in the forward direction. Unless it can be shown that neglected considerations play a larger role than one would tend to expect, the perturbation theory approach to pion absorption would appear to be of dubious value. (Diss. Abstr. Int., B)

28049 REGENERATION OF K^0 MESONS ON A DEUTERON AT HIGH ENERGIES. Babaev, Z. R.; Margvelashvili, P. I. (Tbilisi State Univ., USSR). JETP Lett. (USSR) (Engl. Transl.); 12: 337-9(20 Nov 1970).

Translated from Zh. Eksp. Teor. Fiz., Pis'ma Red.; 12: 483-6 (20 Nov 1970).

The differential cross section and phase of the amplitude of the coherent regeneration process $K_2d \to K_1d$ were calculated from postulated dispersion relations for forward scattering of K mesons by deuterons and using isotopic invariance of strong interaction. The calculations were made either under the assumption that the Pomeranchuk theorem is violated or in the Regge-pole model. (L.B.S.)

28050 EXPERIMENTAL INFORMATION ABOUT MULTIPLE MESON PRODUCTION AT SUPER-HIGH ENERGIES. Gierula, J.; Wolter, W. (Inst. of Nuclear Physics, Krakow). Acta Phys. Pol.; B2: 95-110(Jan-Mar 1971).

Some advantages of the use of log tan θ variable in the analysis of the experimental data on the multiple particle production at very high energies are given. A selection of a few well established observations concerning this phenomenon in collisions at TeV energies is presented. (auth)

28051 HYPERNUCLEI AND HYPERNUCLEAR SPECTROSCOPY. Pniewski, J. (Univ., Warsaw). Acta Phys. Pol.; B2: 129-42(Jan-Mar 1971).

A short account is given of the problems investigated or already solved in hypernuclear studies and the perspectives for the future are mentioned, especially in the case of the hypernuclear spectroscopy. Some of the results presented at the Hypernuclear Conference in Argonne (Proceedings of International Conference on Hypernuclear Physics, Argonne 1969) are summarized. (auth)

28052 RECENT HIGH-ENERGY p-p SCATTERING EXPERIMENTS AND THE OPTICAL-MODEL PREDICTIONS. Saifuddin (Univ. of Islamabad, Rawalpindi, Pakistan). Lett. Nuovo Cim.; 1: 475-6(13 Mar 1971).

Recent experimental results on pp scattering above 10 GeV are compared with previous optical model predictions (Nuovo Cimento 55 A, 690 (1968)) and are found to be in good agreement. The importance of the optical-model calculations and predictions for future high-energy hadron-hadron scattering experiments is emphasized. (L.B.S.)

Particle Invariance Principles and Symmetries

General

Refer also to abstract 27424.

28053 STRUCTURE OF THE COMBINATORIAL GENERALIZATION OF HYPERGEOMETRIC FUNCTIONS FOR SU(n) STATES. Wu, Alfred C. T. (Univ. of Michigan, Ann Arbor). J. Math. Phys. (N. Y.); 12: 437-440(Mar 1971).

The combinatorics of the boson operator formalism in the construction of the SU(n) states provide a natural scheme for the appearance of certain generalized hypergeometric functions. It is shown that, while special cases exist where the functions thus generated belong to the class of generalized hypergeometric functions defined by Gel'fand et al. as being the Radon transforms of products of linear forms, the general cases apparently do not. This is already so at the SU(4) level. (auth)

28054 UNITARY IRREDUCIBLE REPRESENTATIONS OF SU(2,2). III. REDUCTION WITH RESPECT TO AN ISO-POINCARE SUBGROUP. Yao, Tsu (Univ. of Pittsburgh). J. Math. Phys. (N. Y.); 12: 315-42(Mar 1971).

The unitary irreducible representations of SU(2,2), the covering group of the conformal group, are reduced with respect to an iso-Poincaré subgroup E(3,1). Explicit representations of the 15 generators of SU(2,2) in terms of differential operators in the function space of $|\eta, \xi, \epsilon; s, t, m\rangle$, $|\omega, \xi, \epsilon; r, t, m\rangle$, and $|\xi, \epsilon; t, m\rangle$, the basis vectors for "timelike," "spacelike," and "lightlike" UIR's for E(3,1), respectively, are given. The matrix elements between a basis vector in the maximal compact subgroup SU(2) × SU(2) × U(1) and a basis vector in E(3,1) are calculated for all 14 different classes of UIR's of SU(2,2). It is found that two classes are reducible with respect to "lightlike" representations, two classes are reducible with respect to "timelike" representations, eight classes are reducible with respect to "spacelike" representations, and two classes contain both "timelike" and "spacelike" representations of E(3,1). (auth)

28055 PROPOSED EXTENSION OF THE REGGE POLE MODEL TO INCLUDE THE ISOTOPIC SPIN SYMMETRY. Cobb, Donald Dean. Iowa City, Iowa; Univ. of Iowa (1970). 88p. University Microfilms Order No. 71-5726.

Thesis.

A group theoretical model of high-energy hadron scattering is proposed which incorporates the isotopic spin symmetry into the Regge pole model. The semisimple Lie group SU(2,2) is assumed to be an appropriate "little group" for scattering at large s and fixed, negative t. As a first step in the construction of this model, an explicit form is given for the representations of the principal, nondegenerate series of SU(2,2). The content of unitary, irreducible representations of the subgroup SU(1,1) × SU(2) in a representation of the principal, nondegenerate series is then found. SU(1,1) is the appropriate Poincaré little group for scattering at fixed, negative t and SU(2) is interpreted as the isotopic spin group. (Diss. Abstr. Int., B)

28056 FADDEEV'S EQUATIONS IN THE SU(3) REPRESENTATION OF A THREE-PARTICLE STATE. Hochberg, S. (Imperial Coll. of Science and Tech., London); Lee, S. P. Y.; Sibbel, R. Nucl. Phys.; B28: 308-16(1971).

Following a recent first formulation of Faddeev's equations in the SU(3) representation of a three-particle state, a numerical computation was performed for the bound state of three identical particles with and without spins. The results are in agreement with values obtained by authors using a different approach. (auth)

28057 SCALING AND DILATION INVARIANCE. Kugler, M. (Weizmann Inst. of Science, Rehovot, Israel); Nussinov, S. Nucl. Phys.; B28: 97-108(1971).

The solution of a large class of Bethe–Salpeter equations for dilation invariant field theories are investigated, and the asymptotic behavior of the solutions as ν and q^2 become infinite is examined. In the Bjorken limit ($\omega q^2 = 2m\nu \to \infty$) dilation-invariant field theories do not scale. Scaling can be recovered only by breaking dilation invariance, when an ultra-violet cut-off is introduced. (auth)

Applications (Electromagnetic and Weak)

28058 INFINITE MULTIPLETS WITH SU(3). Kyriakopoulos, E. (Democritos Nuclear Research Center, Athens). Nucl. Phys.; B28: 61-72(1971).

An infinite multiplet model was constructed for mesons containing SU(3). The model is based on the mapping of the group $SU(3)/Z_3$ into SO(8), and on the fact that the n-dimensional spherical harmonics can be accommodated into a single irreducible representation of the group SO(n,2). In this relativistic SU(6) type scheme only SU(3) representations of triality zero appear. An infinite component wave equation is given. The form factors of pseudoscalar mesons are calculated. (auth)

Applications (Strong)

Refer also to abstracts 28016 and 28029.

28059 SYMMETRY BREAKING AND THE CABIBBO ANGLE. Bane, John Campbell. Boulder, Colo.; Univ. of Colorado (1970). 116p. University Microfilms Order No. 71-5866.

Thesis.

The semi-strong symmetry breaking interaction and the strangeness-changing weak interactions are explained as being self-consistent responses to the existence of strong, electromagnetic, and strangeness conserving weak interactions. Electromagnetic and strangeness conserving weak interactions (drivings) are used to define preferred directions in a symmetric, strong interaction framework. The resulting system of nonlinear equations has solutions with the phenomenological form of the semi-strong interactions and with a nonzero Cabibbo angle. Two different cases are considered; the strong interactions are assumed to be SU(3) symmetric and SU(3) × SU(3) symmetric. Assuming the strong interactions to be SU(3) symmetric, a solution of the phenomenological form $H = \bar{H} - (U_8 + dU_3)$ results, where d = O(EM). $\bar{H}$ is the SU(3) symmetric piece of the Hamiltonian. This solution has a semi-strong component in the hypercharge (U_8) direction and an electromagnetic "tadpole" component in the U_3 direction. It is shown that the 27-plet pieces of the weak and electromagnetic drivings must be included in order to have a nonzero Cabibbo angle. Assuming the strong interactions to be SU(3) × SU(3) symmetric, a solution of the phenomenological form $H = \bar{H} - (U_8 + CU_8 + dU_3)$ results, where $C \approx -1.25$ and d = O(EM). $\bar{H}$ is the SU(3) × SU(3) symmetric piece of the Hamiltonian. U_i are the members of a $(3,\bar{3}) + (\bar{3},3)$ representation of SU(3) × SU(3). The solution has these interesting features: It has a semi-strong component in the direction of the hypercharge. It satisfies the PCAC (partially conserved axial current) hypothesis. It has a nonzero, discrete Cabibbo angle. It is shown that the 27-plet piece of the weak driving must be included in order to get a nonzero Cabibbo angle. (Diss. Abstr. Int., B)

Field Theories

General

Refer also to abstract 27959.

Quantum Field Theory

Refer also to abstracts 28011 and 28057.

28060 (IC-69/121) INFORMAL MEETING ON RENORMALIZATION THEORY, 25–29 AUGUST 1969. Summaries. (Inter-

national Centre for Theoretical Physics, Trieste (Italy)). Sep 1969. 96p. (CONF-690820-(Summ.)).

Summaries of papers on renormalization in quantum field theory are presented. (J.F.P.)

28061 TOPOLOGY FOR MINKOWSKI SPACE. Nanda, S. (Regional Engineering Coll., Orissa, India). J. Math. Phys. (N. Y.); 12: 394-401(Mar 1971).

One of Zeeman's conjectures that the group of homeomorphisms of the finest topology on Minkowski space that induces the 3-dimensional Euclidean topology on spacelike hyperplanes is the one generated by the inhomogeneous Lorentz group and dilatations is proven. (auth)

28062 DYNAMICAL APPROACH TO THE CLOCK PARADOX. Quale, Andreas (Univ. of Oslo). Amer. J. Phys.; 39: 434-41 (Apr 1971).

The problem of establishing a dynamical connection between the proper time rate of a standard clock and its physical environment is considered, and the relevance of this for the famous "clock paradox" controversy is discussed. In particular, the possibility of "explaining" this phenomenon as due to a physical interaction between the gravitational field and the clock, governing the rate of the latter, is investigated. It is found that one may always introduce formally an "effect" by the field on the clock rate, and thus "resolve the paradox," as has been done in the literature; however, this "effect" is physically trivial, arising from a conventional choice of coordinates, and can always be "normalized away," irrespective of the field environment of the clock. It is argued that a nontrivial "dynamical resolution" of the clock paradox must yield a way of predicting the effect of the field on the proper time rate of a clock from local field observations, without observing this rate directly on the clock. It is shown that this requires a number of restrictions to be imposed on the gravitational field environment of the clock and that the field equations of standard relativity theory are not sufficiently restrictive in this respect. Hence, the clock paradox cannot, in principle, be explained as a genuine dynamical phenomenon within this theory. (auth)

28063 PADE APPROXIMANT IN THEORETICAL PHYSICS. Baker, George A. Jr.; Gammel, John L. (eds.). Mathematics in Science and Engineering. Volume 71. New York; Academic Press Inc. (1970). 391p. $17.50.

The topics covered are the Pade approximant method and some related generalizations, application of Pade approximants to dispersion force and optical polarizability computations, bounds for averages using moment constraints, turbulent diffusion, linear integral equations, series of derivatives of σ-functions, Hilbert space, and the connection of the Pade approximants with stationary variational principles and the convergence of certain Pade approximants. Also approximate N/D solutions, solution of the N/D equations, Pade approximants as a computational tool for solving the Schroedinger and Bethe–Salpeter equations, solution of the Bethe–Salpeter equation, application to meson-baryon scattering, and the nucleon–nucleon system are discussed. (J.F.P.)

28064 VIRTUAL PROCESSES AND VIRTUAL PARTICLES: REAL OR FICTITIOUS. Bunge, Mario (McGill Univ., Montreal). Int. J. Theor. Phys.; 3: 507-8(Dec 1970).

The notions of a virtual process and a virtual quantum, central in current field theories, are usually justified by means of the so-called fourth indeterminacy relation between energy and time. But since the latter formula is meaningless in quantum theory, virtual processes and virtual quanta turn out to be fictitious. A number of consequences follow. (auth) (UK)

28065 DOUBTS ABOUT MACH'S PRINCIPLE. McCrea, W. H. (Univ. of Sussex, Brighton, Eng.). Nature (London); 230: 95-7(12 Mar 1971).

It is suggested that Mach's principle, in any simple form, is largely illusory, but attempts at deeper and more sophisticated formulations are difficult. An argument is presented that the principle gives a simple physical reason for the apparent connection between local inertial properties and remote matter in the universe. Laboratory experiments with Foucault pendulums, gyroscopes or other entirely local means enable establishment of a unique local reference frame that is considered nonrotating. The question arises, however, as to what respect it is nonrotating. A standard of nonrotation is obviously not provided by, say, the earth, the sun or the galaxy, since one can speak meaningfully of the nonzero rotation of these systems; there remains only the background of the remotest objects in the universe. The arguments presented are in terms of special relativity, but are equally valid in general relativity, with certain elaborations, and in the latter case comparisons can be made with the case of gravitation. The discussion includes the significance of the cosmological constant. (UK)

28066 HILBERT SPACES OF FUNCTIONAL POWER SERIES. Rzewuski, J. (Univ., Wroclaw). Bull. Acad. Pol. Sci., Ser. Sci., Math., Astron. Phys.; 18: 677-85(Dec 1970).

A generalization of results of estimates for the convergence domain and asymptotic behavior of functional power series from previous work is given. This work was done for the purpose of establishing rigorous foundations for the method of generating functionals in quantum field theory. The topics covered are Hilbert spaces of functional power series, operators, and connection with Fock spaces. (J.F.P.)

28067 DESCRIPTION OF N–θ SECTOR IN LEE MODEL USING THE FIELD OPERATOR WITH CONTINUOUS SPECTRUM OF ASYMPTOTIC ENERGIES. Lukierski, J.; Oziewicz, M. (Univ., Wroclaw). Bull. Acad. Pol. Sci., Ser. Sci., Math., Astron. Phys.; 18: 695-700(Dec 1970).

It is shown how to introduce the Lagrangian formalism with a field operator having a continuous asymptotic energy spectrum describing the N–θ sector. The field-theoretic description of the N–θ sector and the solution and renormalization procedure are discussed. (J.F.P)

28068 LORENTZ-COVARIANT LAGRANGIANS AND CAUSALITY. Aichelburg, P. C.; Ecker, G.; Sexl, R. U. (Univ., Vienna). Nuovo Cim.; 2B: 63-76(11 Mar 1971).

A class of Lorentz-covariant Lagrangians is described which seem to violate causality in the sense that the propagation velocity of wave fronts and particles can be larger than the velocity of light. As a simple model of a Lagrangian of this type a point particle coupled to a massless rank-two tensor is considered. While it seems kinematically possible to accelerate a particle through the Minkowski light-cone, it turns out that dynamical reasons prevent this. The reaction force due to the radiation emitted by the particle diverges when the particle approaches the Minkowski light-cone. This simple model seems to indicate that Lorentz covariance is indeed sufficient to guarantee causality and no restrictions concerning the type of couplings which may be contained in the Lagrangian are necessary. (auth)

28069 ANNIHILATOR OF ENERGY–MOMENTUM SPECTRA IN QUANTUM FIELD THEORY. Chen, Etang (East Carolina Univ., Greenville, N. C.). Nuovo Cim.; 2B: 161-6(11 Apr 1971).

It is shown that in a quantum field theory the annihilator of energy-momentum spectra has empty interior. (auth)

28070 NONLINEAR EFFECTS IN QUANTUM ELECTRODYNAMICS. Costantini, V. (Univ., Rome); De Tollis, B.; Pistoni, G. Nuovo Cim.; 2A: 733-87(1 Apr 1971).

The fourth-rank vacuum polarization tensor, which is related to the lowest-order nonlinear interaction between four electromagnetic fields in quantum electrodynamics, is exactly calculated in terms of rational, logarithm and dilogarithm functions when two of the four electromagnetic fields describe photons off the mass shell. This task has been accomplished by a not exceedingly laborious effort with the aid of double dispersion relations which proved to be a very convenient tool for the treatment of these problems (in particular, photon–photon scattering). From the explicit expression of the polarization tensor the exact amplitudes for photon–photon scattering, photon splitting and photon coalescence into photons on nuclei were easily obtained. Moreover the real and imaginary parts of Delbrück scattering are given in the form of threefold integrals over the momentum transferred to the nucleus by one of the two virtual photons. This can be compared with the fivefold and sixfold integrals for the imaginary and real part, respectively, available in the existing literature on Delbrück scattering. Finally an explicit expression is given for the differential cross section of Delbrück scattering in the limit of low energies. (auth)

28071 QUANTIZATION OF AN ESSENTIALLY NONLINEAR FIELD. Blohincev, D. I. (Joint Inst. for Nuclear Research, Dubna, USSR). Nuovo Cim.; 2A: 632-40(1 Apr 1971).

An essentially nonlinear field implies here a field obeying a certain equation with characteristics depending on the field itself or its derivatives. The simplest example of quantization of an essentially nonlinear system with one degree of freedom is first considered. Then a method of quantization of the essentially nonlinear field of the type of the Born-Infeld field is described. (auth)

28072 MECHANISM FOR THE ORIGIN OF REGGE ASYMPTOTIC BEHAVIOR IN QUANTUM FIELD THEORY. Brandt, R. A.; Orzalesi, C. A. (New York Univ., N. Y.). Phys. Lett.; 34B: 641-6(12 Apr 1971).

XUM

A mechanism is proposed for obtaining Regge asymptotic behavior from operator product expansion near the light cone. With canonical singularities, a consequence is the quantization condition $\alpha_R(t = m_R^2 - m_\lambda^2) = \frac{1}{2}N_{AB}^R$ = half-integer for any particles A and B which can couple to the Reggeon R. This is found to be in excellent agreement with experiment. (auth)

28073 SCATTERING OF COMPOSITE PARTICLES AT VERY HIGH ENERGY WITH APPLICATIONS TO QUANTUM ELECTRODYNAMICAL PROCESSES. Czyz, W. (Inst. of Nuclear Physics. Krakow). Acta Phys. Pol.; B2: 35-56(Jan-Mar 1971).

It is shown that a straightforward generalization of the multiple diffractive scattering model used in high energy nuclear collisions leads to the correct expressions for the high energy limits of the cross sections of various quantum electrodynamical processes. (auth)

28074 VACUUM POLARIZATION TENSOR AND EQUAL-TIME COMMUTATORS IN QUANTUM ELECTRODYNAMICS. Leo, R. A.; Minguzzi, A.; Soliani, G. (Univ., Lecce, Italy). Lett. Nuovo Cim.; 1: 477-80(13 Mar 1971).

Some consequences coming from the assumption that the vacuum expectation value of the equal-time commutator (seagull term) exists and is a local operator are discussed. The following points are proved: the Bjorken limit of the vacuum polarization tensor is dictated by the sea-gull term; the relation between the sea-gull and the Schwinger term is the relation predicted by the canonical formalism plus minimal electromagnetic interaction; and the photon wave-function renormalization constant Z_3 is a finite quantity obeying the condition $0 < Z_3 < 1$. (L.B.S.)

28075 EFFECT OF DIRECT CURRENT ON THE FUNCTION OF THE BRAIN CORTEX SYMMETRIC AREAS IN IRRADIATED ANIMALS. Medyanik, I. A. (Kiev State Univ.). Fiziol. Zh., Akad. Nauk Ukr. RSR; 17: 26-32(Jan-Feb 1971). (In Ukrainian).

The effect was studied of direct current on work of the brain cortex symmetric areas in irradiated animals (after a single x irradiation of the dog head by a dose of 400 R). It is established that anodization (3 mA, 3 min) of the brain cortex in the irradiated animals during a month removes the phase disturbances in the conditioned reflex activity of the symmetric areas in the cortex of both hemispheres, its asymmetry arising under the effect of brain irradiation as well as parabiotic phase states and accelerates the recovery of the initial level of the functional manifestations in these areas, i.e. decreases the degree and depth of the disturbances in the activity of the nervous system appearing under the effect of penetrating radiation. Cathodization of the brain cortex has an opposite effect. The parabiotic inhibition that arose in the symmetric areas of the brain cortex of the irradiated animals is preserved and deepened by the effect of the cathode and is removed by the direct current anode, i.e. it is of catelectronegative nature. (auth)

28076 AXIOMATIC APPROACH TO QUANTUM FIELD THEORY AND MANY BODY PROBLEM. VOLUME I A. V Winter School of Theoretical Physics in Karpacz, February 17-March 2, 1968. Acta Univ. Wratislaviensis; No. 98, 1-217(1968).

Separate abstracts were prepared for the eight lectures included. (J.F.P.)

For abstracts of individual lectures see: 28077-28084.

28077 STRUCTURE ANALYSIS OF QUANTUM FIELD THEORY. Haag, R. (Univ., Hamburg). Acta Univ. Wratislaviensis; No. 98, 9-17(1968).

This review of the structure analysis of quantum field theory covers the choice of mathematical objects and their physical interpretation, and relations between the mathematical objects which are necessary and desirable to ensure agreement of the interpretation with the gross qualitative features of experience with the phenomena. Also discussed are the compatibility and interdependence of various structural mathematical assumptions, consequences of such assumptions for the phenomena, and the construction of models. (J.F.P.)

28078 REPORT ON ERGODIC STATES. Haag, R. (Univ., Hamburg). Acta Univ. Wratislaviensis; No. 98, 18-22(1968).

In this discussion of ergodic states a C^* algebra and a group whose elements act as an automorphism on the algebra are considered. Applications are mentioned for equilibrium states of statistical mechanics and relativistic field theory. (J.F.P.)

28079 PROBLEM OF MOMENTS AND REPRESENTATIONS WIGHTMAN TYPE FUNCTIONALS BY CONTINUAL INTEGRALS. Berezanskii, Yu., M. (Inst. of Mathematics, Kiev). Acta Univ. Wratislaviensis; No. 98, 23-51(1968).

Generalizations of the power problem of moments and applications of these generalizations to an investigation of Wightman functionals are discussed. Fewer axioms of field theory are taken into account, and all fields which satisfy these axioms or all Wightman-type functionals, namely the axioms of positiveness and local commutativity are described. (J.F.P.)

28080 STRUCTURE OF THE ALGEBRA ASSOCIATED TO FREE FIELDS. Dell'Antonio, G. F. (Univ., Naples). Acta Univ. Wratislaviensis; No. 98, 52-97(1968).

Results are outlined which give a complete algebraic characterization of the only and trivial systems known to satisfy the relevant set of axioms. A brief general survey of the algebraic approach to the theory of relativistic fields and of infinite thermodynamic systems is given. The structure of the free Fermi gas at finite density and of the relativistic free scalar field is analyzed. (J.F.P.)

28081 LIE FIELDS. Efremov, A. V. (Joint Inst. for Nuclear Research, Dubna, USSR). Acta Univ. Wratislaviensis; No. 98, 98-109(1968).

The model of vector Lie fields in axiomatic field theory is discussed. It is found that this model is trivial though less trivial than generalized free fields in the sense that the vertex function out of the mass shell is not zero. (J.F.P.)

28082 INTEGRAL REPRESENTATIONS OF VACUUM EXPECTATION VALUES WITH ACCOUNT FOR LOCAL COMMUTATIVITY. Gachok, V. P. (Inst. of Theoretical Physics, Kiev). Acta Univ. Wratislaviensis; No. 98, 110-22(1968).

The derivation of relations following from the axiom of positive definiteness is considered. The result is that any Wightman functional can be put in correspondence with a process with distribution $\Theta_{n;\lambda}$. (J.F.P.)

28083 HAAG'S THEOREM. Garczynski, W. (Univ. of Wroclaw). Acta Univ. Wratislaviensis; No. 98, 123-84(1968).

The discussion of the Haag theorem includes a review of criteria related to the Haag theorem for the free character of a field, proof of the Haag theorem, and generalized Haag theorem in scattering theory. (J.F.P.)

28084 PRACTICAL USE OF ALGEBRAIC CONCEPTS IN QUANTUM FIELD THEORY. Guenin, M. (Univ., Geneva). Acta Univ. Wratislaviensis; No. 98, 185-217(1968).

Concepts developed by various axiomatic and especially algebraic approaches are used to make rigorous the Lagrangian approach. The Haag theorem and the description of the time evolution of a system, quadratic interaction, the vacuum, the scalar field model, and renormalization are treated. (J.F.P.)

Gravitation and General Relativity

Refer also to abstracts 27347 and 27358.

28085 EINSTEIN TENSOR AND ITS GENERALIZATIONS. Lovelock, David (Univ. of Waterloo, Ont.). J. Math. Phys. (N. Y.); 12: 498-501(Mar 1971).

The Einstein tensor G^{ij} is symmetric, divergence free, and a concomitant of the metric tensor g_{ab} together with its first two derivatives. All tensors of valency two with these properties are displayed explicitly. The number of independent tensors of this type depends crucially on the dimension of the space, and, in the 4-dimensional case, the only tensors with these properties are the metric and the Einstein tensors. (auth)

28086 GRAVITATIONAL RADIATION DAMPING OF SLOWLY MOVING SYSTEMS CALCULATED USING MATCHED ASYMPTOTIC EXPANSIONS. Burke, William L. (California Inst. of Tech., Pasadena). J. Math. Phys. (N. Y.); 12: 401-18(Mar 1971).

The slow-motion approximation for radiating systems is treated as a problem in singular perturbations. By using the method of matched asymptotic expansions, one can construct approximations valid both in the near zone and the wave zone. The outgoing-wave boundary condition applied to the wave-zone expansion leads, by matching, to a unique and easily calculable radiation resistance in the near zone. The method is developed and illustrated with model problems from mechanics and electromagnetism; these should form a useful and accessible introduction to the method of matched asymptotic expansions. The method is then applied to the general relativistic problem of gravitational radiation from gravitationally bound systems, where a significant part of the radiation can be attributed to nonlinear terms in the expansion of the metric. This analysis shows that the formulas derived from the standard linear approximation remain valid for gravitationally

XUM

bound systems. In particular, it shows that according to general relativity bodies in free-fall motion do indeed radiate. These results do not depend upon any definition of gravitational field energy. (auth)

28087 COSMOLOGICAL MODELS IN AN EXTENSION OF YILMAZ' THEORY OF GRAVITATION. Tupper, B. O. J. (Univ. of New Brunswick, N. J.). Nuovo Cim.; 2B: 148-56(11 Mar 1971).

The field equations of Yilmaz' new approach to general relativity are extended to the case when matter is present and are used to find cosmological models. It is shown that the theory includes both steady-state and Robertson-Walker type models which are not the same as those found in the usual relativistic cosmology. (auth)

28088 GRAVITATIONAL SHOCK WAVES FROM TACHYONS. Schulman, L. S. (Indiana Univ., Bloomington). Nuovo Cim.; 2B: 38-44(11 Mar 1971).

The gravitational field predicted by general relativity for a tachyon is in many ways similar to the shock wave produced by an object moving faster than the signal velocity in a medium. It is an intense wave and for a dense macroscopic tachyon it is capable of exciting Weber's gravitational radiation detection apparatus across astronomical distances. (auth)

28089 GENERAL-RELATIVISTIC AND NEWTONIAN GRAVITATIONAL ENERGY TRANSFER. Cooperstock, F. I.; Booth, D. J. (Univ. of Victoria, B. C.). Nuovo Cim.; 2B: 139-47 (11 Mar 1971).

Bondi's Newtonian inductive energy transfer by gravitation is rederived and new forms are presented to exhibit the lack of uniqueness of the Newtonian gravitational Poynting vector. Einstein's power transfer theory is employed in a straightforward manner to deduce the energy transfer for weak fields in general relativity. The relativistic and classical expressions, developed in terms of the multipole moments of the matter distributions participating in the interaction, coincide in the limit as $c \to \infty$. (auth)

Scattering Theory

Refer also to abstracts 27930, 28056, and 28083.

28090 SCATTERING OF WAVES IN MANY DIMENSIONS. Adawi, I. (Univ. of Missouri, Rolla). J. Math. Phys. (N. Y.); 12: 358-9(Mar 1971).

Scattering by a spherical potential is discussed in all dimensions by one formulation using the partial-wave expansion method. The optical theorem relating the total scattering cross section σ to the forward scattering amplitude f(0) is derived. (auth)

28091 HARMONIC ANALYSIS OF THE SCATTERING AMPLITUDE AND THE POINCARE MODEL OF LOBACEVSKIJ GEOMETRY. Viano, G. A. (Istituto di Scienze Fisiche, Genoa. Istituto Nazionale di Fisica Nucleare, Genoa). Lett. Nuovo Cim.; 1: 399-403(6 Mar 1971).

The geometry underlying the t-channel expansion of the scattering amplitude, i.e. the hyperbolic geometry, is considered. The Poincaré model of the Lobacevskij geometry is constructed. The connection that exists between the Joos expansion and the Poincaré model of the hyperbolic geometry is examined through Helgason's approach to the non-Euclidean Fourier analysis. (L.B.S.)

28092 STUDY OF MACDOWELL SYMMETRY, CONSPIRACY, AND FERMION REGGE TRAJECTORIES. Lang, Joseph Edward. Urbana, Ill.; Univ. of Illinois (1970). 113p. University Microfilms Order No. 71-5160.

Thesis.

Nondynamical constraints on the scattering amplitude are derived and applied to the Regge pole model. In particular, the effects of MacDowell symmetry and the conspiracy constraints are derived for fermion Regge trajectory and residue functions. It is shown that two solutions of the constants — analogous to the "conspiratorial" and "evasive" solutions for boson Regge poles — exist. The conspiratorial ($M = \frac{1}{2}$) solution of the constraints implies that the first derivative of the fermion Regge trajectory with respect to the energy vanishes. Experimental tests for the existence of $M = \frac{1}{2}$ trajectories are suggested. (Diss. Abstr. Int., B)

28093 PROMOTION PHENOMENON FOR THREE PARTICLE EXCHANGE. Blau, Irwin (Massachusetts Inst. of Tech., Cambridge). Stud. Appl. Math.; 49: 389-99(Dec 1970).

In the two particle exchange, it has been shown that the asymptotic form of the scattering amplitude at high energies behaves differently for $t = 4\mu^2$ and $t \neq 4\mu^2$. The three particle exchange is considered for $t = 9\mu^2$ and $t \neq 9\mu^2$. For t near but not equal to $9\mu^2$ in the three particle exchange, the asymptotic behavior of the scattering amplitude is also discussed. (auth)

28094 ANALYTIC PROPERTIES AND BOUND-STATE DEGENERACY IN NONLOCAL POTENTIALS. Gutkowski, D.; Scalia, A. (Univ., Catania, Italy. Istituto Nazionale di Fisica Nucleare, Catania, Italy). Nuovo Cim.; 2A: 641-61(1 Apr 1971).

It is proved that for a class of nonlocal potentials the zeros of the Jost function $D_l(-k)$, lying in the complex upper half k-plane, may lie only on the imaginary axis. A necessary and sufficient condition is given in order for these zeros to have multiplicity m. It is proved that the order of that multiplicity is equal to the degeneracy of the corresponding bound state. An upper bound is given for the number of zeros of $D_l(-k)$ in the complex k-plane; a necessary and sufficient condition for the existence of Ma poles for the function $S_l(k)$ is given; a sufficient condition is given for the existence of extinct bound states. At last a relation is obtained between the number of poles (with their multiplicity) both in the upper and lower complex half k-planes. (auth)

28095 SPECTRUM OF AN OPERATOR INTRODUCED BY FESHBACH IN THE FORMULATION OF THE OPTICAL POTENTIAL. Bertero, M. (Univ., Genoa. Istituto Nazionale di Fisica Nucleare, Genoa. CNR, Genoa). Nuovo Cim.; 2A: 605-14 (1 Apr 1971).

The spectrum of an operator introduced by Feshbach in the theory of the optical potential is analysed in the case of a 3-particle system. A conjecture made by Feshbach on the structure of the spectrum is proved. (auth)

28096 MATHEMATICAL APPROACH TO THE DERIVATION OF THE THEORETICAL OPTICAL POTENTIAL. Bertero, M.; Passatore, G. (Univ., Genoa. Istituto Nazionale di Fisica Nucleare, Genoa. CNR, Genoa). Nuovo Cim.; 2A: 579-604 (1 Apr 1971).

A rigorous analysis of the foundations and of the properties of the theoretical optical potential is attempted. It is shown that, under suitable conditions on the two-body potentials, the optical potential exists both in a time-dependent and in a time-independent theory and is a bounded operator. This property does not require the boundedness of the two-body potentials. The analytic and asymptotic properties of the optical potential in the energy plane are obtained. The connection between the time-independent and time-dependent formulation is discussed in a rigorous way. (auth)

28097 CONSTRAINTS ON THE PARTIAL AMPLITUDES OF AN ANNIHILATION CHANNEL. Malkov, E. I. (Ioffe Inst. of Physics and Tech., Leningrad). Phys. Lett.; 34B: 618-20(12 Apr 1971).

A set of inequalities, each involving finite number of the partial waves of an annihilation channel, is derived. It is equivalent to positivity of the absorptive parts of the amplitude in the crossed channels, which correspond to elastic scattering. (auth)

28098 DISCUSSION ON THE ASYMPTOTIC LOWER BOUND OF CROSSING-EVEN AMPLITUDES AND DISPERSION RELATIONS FOR THEIR INVERSES. Gensini, P. (Univ., Lecce, Italy). Lett. Nuovo Cim.; 1: 464-6(13 Mar 1971).

A brief discussion is presented of the lower bounds of crossing-even amplitudes with a positive definite imaginary part of the right-hand cut, starting from the bounds obtained by Jin and Martin and using the known properties of their zeros and poles. The possibility of writing dispersion relations for the inverses of the amplitudes is shown. (L.B.S.)

28099 KINEMATIC SINGULARITIES IN MULTI-PARTICLE PROCESSES DERIVED FROM BASIC PROPERTIES OF SPINOR AMPLITUDES. Johannesson, Nils (Univ. of Lund, Sweden). Nucl. Phys.; B28: 51-60(1971).

Scattering amplitudes for multi-particle processes have, in general, like helicity or Bali–Chew–Pignotti amplitudes, kinematic singularities when considered as functions of the invariant variables. These singularities are derived from the fundamental covariance and analyticity properties of spinor amplitudes. The ambiguity in expressing scattering amplitudes via spinor amplitudes is used to regularize the spinor amplitudes on each special singularity surface through regularization of the four-momentum components. The kinematic singularities are thus isolated in the coefficients describing the transformation from the spinor amplitudes to the scattering amplitudes under study. The singularities can then be exhibited in a straightforward manner. (auth)

28100 ASYMPTOTIC PROPERTIES OF SCATTERING AMPLITUDES AND THEIR EXPERIMENTAL CONSEQUENCES.

XUM

Eden, R. J.; Kaiser, G. D. (Cambridge Univ., Eng.). Nucl. Phys.; B28: 253-82(1971).

Bounds are obtained on the asymptotic behavior of scattering amplitudes that violate the Pomeranchuk theorem and correspond to asymptotically-constant total cross sections. It is proved that the differential cross sections have forward peaks whose height grows like $B \ln^2(s)$ and whose width shrinks like $B' \{\ln(s)\}^{-2}$. It is proved that the amplitudes have zeros in the region $|t| \sim B'' \{\ln(s)\}^{-2}$, and bounds are obtained on the constants B, B' and B''. A range of possible experimental consequences is studied and it is found that interference between Coulomb interactions and strong interactions plays a major role in determining whether the new theoretical results can be observed in practice. A narrow strong peak in the Coulomb region cannot be excluded and may invalidate some experimental procedures for obtaining the phases of forward amplitudes and total cross sections. (auth)

28101 CALCULATIONS OF THREE-BODY SCATTERING AMPLITUDES. Pieper, Steven Charles. Urbana, Ill.; Univ. of Illinois (1970). 135p. University Microfilms Order No. 71-5202. Thesis.

Two techniques for the calculation of three-body scattering amplitudes are developed and studied. The first is a variational principle based on the Faddeev equations. In form it resembles a Schwinger principle. The wave functions that are varied are products of the two-body potentials and the normal three-body wave function. This results in a very simple asymptotic behavior, even for energies above the breakup threshold. Numeric results are presented for s-wave calculations using separable potentials for elastic, rearrangement and breakup scattering. The convergence is rapid and the technique seems very successful. Accuracies on the order of several parts per million are easily achieved. The specific forms of the equations for problems involving two or three identical bosons are also presented and the breakup calculations for these cases are presented as Dalitz plots. The second technique is based on the analytic structure in the total energy of the three-body T-matrix. The T-matrix is computed for energies less than the physically allowed energies and the results of these calculations are then numerically analytically continued to the physical region. Because the wave function has very simple asymptotic behavior beneath threshold, these calculations are easy to do. Calculations have again been done for separable potentials so the results can be compared with the results from the first technique. It is concluded that this is a reliable technique for scattering beneath the breakup threshold and that useful results are achieved for positive total energies, if there is not too much breakup scattering. The technique is then applied to a local s-wave calculation using Yukawa potentials. A Kohn type variational principle is used to find the beneath threshold T-matrices. The final results show good convergence and, with the above mentioned limitation, this appears to be a good technique for local calculations. (Diss. Abstr. Int., B)

Particle Accelerators

Refer also to abstracts 26507, 26775, 26883, 27436, 27439, 27836, 28161, and 28315.

28102 (ANU-P-502) NOTES ON NUCLEAR SPECTROSCOPY INSTRUMENTATION. Ophel, T. R. (Australian National Univ., Canberra. Research School of Physical Sciences). [1970]. 39p. Dep. NTIS (U. S. Sales Only).

A summary is given of equipment that has been developed in the ANU laboratories for spectroscopy measurements. Illustrations and descriptions are provided for 50 cm dia scattering chambers, general purpose gamma ray and neutron scattering chambers, D-shaped chambers, target holders and ladders, preparation and use of unstable target materials, cold traps and counter coolers, target modulation techniques, sodium iodide detector mounts and shielding, accelerator calibration, a detector test chamber, and collimators. A list is given of available radioactive sources and a discussion on background in semiconductor detectors and contaminants in gamma ray spectra is appended. (Australia)

28103 (ANU-P-519) BEAM OPTICS CALCULATIONS FOR CYCLOTRON-TANDEM INJECTION SYSTEM. Treacy, P. B. (Australian National Univ., Canberra. Research School of Physical Sciences). [1971]. 14p. Dep. NTIS (U. S. Sales Only).

A summary of calculations made on beam trajectories with focusing elements to be placed between the present EN tandem accelerator and a future negative-ion cyclotron at ANU is given. Calculations are dependent on cyclotron beam phase space characteristics as measured at Livermore. There is thought to be some uncertainty in these. A simplified Gaussian optics analysis is given and the lens layout is described. The proposed injection system is considered suitable provided an aperture of about 0.5 in. is inserted in the 20° magnet. (Australia)

28104 (BNL-16000) BNL SUMMER STUDY ON AGS UTILIZATION, 1970. Toohig, T. E. (ed.) (Brookhaven National Lab., Upton, N. Y.). 1970. 385p. Dep. NTIS.

Thirty-nine papers are presented on the status and plans for the AGS conversion project. Topics include beams and beam layouts, high-resolution spectrometers, computers and instrumentation, experiments for the converted AGS, and an outlook to the future. (W.H.K.)

28105 (CERN-70-30(Vol.1), pp 109-41) EXPERIMENTAL TECHNIQUES USING ISOL SYSTEMS (REVIEW OF OPERATING SYSTEMS). Talbert, W. L. Jr. (European Organization for Nuclear Research, Geneva (Switzerland)).

In International conference on the properties of nuclei far from the region of beta-stability; Leysin, Switzerland (31 Aug 1970).

A summary of ISOL systems that are in operation is presented. Emphasis is placed on the techniques employed in various systems, such as target and transport line configurations, ion-source and -separator types, and ion-beam handling of separated beams to detector stations. The performance of existing systems is outlined in a general way for the purpose of suggesting the types of studies that are currently possible. (50 references) (auth)

28106 (CERN-70-30(Vol.1), pp 153-62) RECOIL ATOM MASS ANALYSER (RAMA). Nitschke, J. M. (Centre National de la Recherche Scientifique, Orsay (France). Centre de Spectrometrie Nucleaire et de Spectrometrie de Masse).

In International conference on the properties of nuclei far from the region of beta-stability; Leysin, Switzerland (31 Aug 1970).

The recoil-atom mass analyzer in operation at Orsay is described. After an explanation of the physical layout of the system, the transit time and transmission of this on-line isotope separator system are discussed. (R.W.R.)

28107 (CERN-70-30(Vol.2), pp 1003-5) EXPERIMENTAL TECHNIQUES FOR NUCLEAR STRUCTURE STUDIES IN THE TIN-REGION AT OSIRIS. Borg, S.; De Geer, L.-E.; Holm, G. B.; Rydberg, B. (Stockholm Univ. (Sweden). Research Inst. for Physics).

In International conference on the properties of nuclei far from the region of beta-stability; Leysin, Switzerland (31 Aug 1970).

The OSIRIS target-ion source produces a number of neighboring elements with efficiencies of the same order of magnitude. Although A is well known, Z is not. Techniques for coping with this difficulty are explained. (R.W.R.)

28108 (ITEF-761) REGULATOR FOR HIGH VOLTAGE CAPACITOR BANK. Kozodaev, A. M.; Lazarev, N. V. (Gosudarstvennyi Komitet po Ispol'zovaniyu Atomnoi Energii SSSR, Moscow. Institut Teoreticheskoi i Eksperimental'noi Fiziki). 1970. 11p. (In Russian). Dep. NTIS (U. S. Sales Only).

The high voltage capacitor bank of 2.8 μF is charged through the unregulated rectifier, connected to the secondary winding of the step-up transformer. Regulation of the capacitor bank voltage of 10 to 40 kV with an accuracy of ±0.1% at any periodic or unperiodic discharges, at separated time intervals greater than 0.7 sec, is accomplished with an SCR 3-phase bridge connected between the primary winding and the supply line. (auth)

28109 (JINR-P9-5610) DEUTERON ACCELERATION IN THE LA9-INJECTOR OF THE JINR SYNCHROCYCLOTRON. Beznogikh, Yu. D.; Zinov'ev, L. P. (Joint Inst. for Nuclear Research, Dubna (USSR). Lab. of High Energy). 1971. 18p. (In Russian). Dep. NTIS (U. S. Sales Only).

A brief physical substantiation of the deuteron acceleration in the second drift multiplicity in the proton linear accelerator with the grid focusing is given. Decrease of the accelerating interval length by a factor of two by means of special caps on the drift tubes and application of the combined 2-gap buncher allows one to get the accelerated deuteron beam intensity of the same order as for the proton beam. (auth)

28110 (JINR-P9-5622) COMPUTATIONAL STUDY OF THE NON-LINEAR REGIME OF THE RADIATION INSTABILITY DEVELOPMENT OF THE RELATIVISTIC ELECTRON RINGS. Bonch-Osmolovskii, A. G.; Makhankov, V. G.; Tsytovich, V. N.; Shchinov, B. G. (Joint Inst. for Nuclear Research, Dubna (USSR). Lab. of Computing Techniques and Automation). 1971. 33p. (In Russian). Dep. NTIS (U. S. Sales Only).

The instability evolution of a relativistic thin electron ring is numerically investigated. The results of the exact non-linear equation, considering interactions of 10 harmonics of the coherent radiation, are obtained. Both the radiation effects and the

negative mass effects for a ring in the free space are considered. (auth)

28111 (KFK–1218) A 12 cm BORE SUPERCONDUCTING DC QUADRUPOLE LENS. Fessler, N. (Kernforschungszentrum, Karlsruhe (West Germany). Institut fuer Experimentelle Kernphysik); Bogner, G.; Kuckuck, H.; Kullmann, D. (Siemens A. G., Erlangen (West Germany)). May 1970. 11p. (CONF-700503–9). Dep. NTIS (U. S. Sales Only).

From 3. international conference on magnet technology; Hamburg, Germany (19 May 1970).

An optimization with respect to a high solid angle acceptance in a parallel focus-target-doublet leads to the following parameters of the first quadrupole: straight length = 1m, warm bore = 12 cm, field at the circumference of the aperture = 30 kG. The winding concept is that of Beth, Sampson, Krueger and Snyder (BNL). The poles are wound with suitable, selected Nb_3Sn tape. Improved winding techniques have been developed to get a mechanical solid structure. First experiments with one test pole and first measurements on the complete quadrupole are described. (auth)

28112 (KHFTI–70-17) STRUCTURE OF ELECTRON CLUSTERS IN AN INJECTOR WITH A STEP-LIKE VARYING WAVE PHASE VELOCITY. Vishnyakov, V. A.; Grishaev, I. A.; Grizhko, V. M.; Kolosov, V. I.; Krasnikov, V. D.; Melnicheko, V. V.; Fursov, G. L. (Akademiya Nauk Ukrainskoi SSR, Kharkov. Fiziko-Tekhnicheskii Institut). 1970. 11p. (In Russian). Dep. NTIS (U. S. Sales Only).

Theoretical and experimental data are given on the structure of clusters formed by injection with a step-wise variable wave-phase rate. The possibility of improving the efficiency parameters of the 2 GeV electron accelerator by using an injector with step-wise varying wave-phase-rate is discussed. (tr-auth)

28113 (LYCEN–7054) DEVELOPMENT OF A TEST BENCH FOR MULTICHARGED ION SOURCES. APPLICATION TO THE STUDY OF AXIAL REFLEX SOURCES. Bajard, Marcel (Lyon Univ. (France). Institut de Physique Nucleaire). Jul 1970. 46p. (In French). Dep. NTIS (U. S. Sales Only).

Thesis.

A test bench for multicharged ion sources was designed and constructed. Likely modifications such as the adaptation of an emittance measuring system, or the use of a Wien filter for separating the isotope beams, were foreseen. Tests on axial extraction reflex sources led to the realization of a construction favoring the production of multicharged ions, and to the definition of the optimum source parameters. An extraction geometry giving a beam of good characteristics was developed after a series of tests. The sources were tested with nitrogen, neon and argon. The study was limited to ions with four charges, which corresponded to $\xi = Z/A > 0.1$. This value of ξ is very much better than the minimum value envisaged in linear ion accelerator projects ($\xi_{min} > 0.06$). The various possible improvements to the system are: the use of a pulsed arc in such a way as to produce an enhanced yield of multicharged ions and a prolonging of the source life, the use of a better designed escape field permitting higher extraction potentials, and the use of an efficient focussing system to improve detection. (auth)

28114 (NP–18634) RADIATION EFFECTS ON DYNAMICS OF RELATIVISTIC ELECTRON RINGS. Kolemenskii, A. A. (Akademiya Nauk SSSR, Moscow. Institut Fiziki). 1970. 28p. (In Russian). Dep. NTIS (U. S. Sales Only).

Consideration is given to the general problem of how radiation emission effects can be used to improve the characteristics of electron rings and to increase the acceleration efficiency. In addition to an induced (betatron) electric field, systems with a high-frequency field are also considered. Thus the results can be applied to the motion of electrons in other systems where the orbital radius and other parameters vary substantially (ring phasotrons, certain types of accumulators, etc.). The equation of motion of an electron in the presence of synchrotron radiation is given for a relativistic case. Expressions are given for the nonequilibrium motion of the radiation-emitting electron. Radiation compression of a ring takes place relatively slowly (on the order of milliseconds or longer), if strong magnetic fields are not involved. The radiation emission effects can be used to form electron rings having optimal parameters. (TTT)

28115 (PURC–4159-17) AUTOMATIC TARGET CYCLING SYSTEM FOR TOTAL CROSS SECTION MEASUREMENTS. Devlin, T. J. (Rutgers-The State Univ., New Brunswick, N. J. Dept. of Physics); McFadden, J. T. (Princeton-Pennsylvania Accelerator, Princeton, N. J.); Mischke, R. E. (Princeton Univ., N. J. Joseph Henry Labs.). [1970]. 14p. Dep. NTIS.

The construction and operation of an automatic target cycling system is described. It is designed to move three targets cyclicly into a particle beam for preset intervals which are proportional to the beam flux. The system has been successfully used in a measurement of n-p and n-d total cross sections. (auth)

28116 (UCRL–20165) PRINTED-CIRCUIT STEERING COILS. Avery, Robert T.; Lambertson, Glen R.; Pike, Chester D. (California Univ., Berkeley. Lawrence Radiation Lab.). Feb 1971. Contract W-7405-eng-48. 2p. (CONF-710308–2). Dep. NTIS.

From National particle accelerator conference; Chicago, Ill. (1 Mar 1971).

Beam steering coils utilizing "turns" etched on printed-circuit boards have been constructed and tested. This approach offers an economical method for achieving high-quality, compact steering coils. The circuit-boards are rolled into a cylinder and inserted inside a short steel tube. Boards for vertical and horizontal steering are located in separate layers. For our application, three coil sizes were constructed with inside diameters of 25 cm, 20.6 cm, and 17.3 cm respectively. Active length is 0.6 of the inside diameter in all cases. The coils produce an integrated deflection field in either the vertical or horizontal direction of ~316 Gauss-cm when excited with 5 A at ~30 V. The conductor pattern on the circuit-board was designed to produce a nearly uniform angular deflection for all rays transmitted, in spite of the short length/diameter ratio. The magnetic field integrated over a length of 152 cm was measured at several radii and azimuths. Values at 0.4 and 0.8 of bore radius were within ~0.5% and ~1.5% respectively of the central value. Suggestions for further refinement of deflection uniformity are presented. (auth)

28117 (UCRL–20166) NON-INTERCEPTING MONITOR OF BEAM CURRENT AND POSITION. Avery, Robert T.; Faltens, Andris; Hartwig, Edward C. (California Univ., Berkeley. Lawrence Radiation Lab.). Feb 1971. Contract W-7405-eng-48. 3p. (CONF-710308–3). Dep. NTIS.

From National particle accelerator conference; Chicago, Ill. (1 Mar 1971).

A compact monitor has been developed which measures beam current and beam position without intercepting or appreciably affecting the particle beam being measured. It is a broad band device which prevents the development of beam disturbing resonant modes. Although developed specifically for use on a short-pulse electron induction accelerator, it might be applied to other accelerator beams of pulsed or rf-bunched nature. The monitor consists of a resistive band inserted in the beam pipe wall with connections for reading the voltage across the band at each vertical and horizontal axis intercept. For pulsed or rf beams, return current equal in magnitude to the beam current flows on the beam pipe inside wall and through the resistive band. If the beam is centered, equal voltage appears on all four monitor connections. If the beam is off-center, the return currents are unsymmetrical and unequal voltages appear at the monitor connections. Beam current is proportional to the sum of all monitor voltages, while beam position is approximately proportional to the difference in voltage at opposing monitors. Tests and operating experience confirm its operation. (auth)

28118 (UCRL–20177) MECHANICAL FEATURES OF ELECTRON-RING COMPRESSORS. Avery, R. T.; Chupp, W. W.; Hernandez, H. P.; Meneghetti, J. R.; Salsig, W. W. (California Univ., Berkeley. Lawrence Radiation Lab.). Feb 1971. Contract W-7405-eng-48. 3p. (CONF-710308–4). Dep. NTIS.

From National particle accelerator conference; Chicago, Ill. (1 Mar 1971).

The technology of electron-ring compressors draws more heavily on controlled thermonuclear research than on conventional accelerators. This is dictated by the rapidly rising, intense magnetic fields (>50 kG in <1 ms), the required ultrahigh vacuum ($\approx 10^{-9}$ torr), and the need for extensive diagnostics and instrumentation during the development phase. Interesting mechanical features of the Berkeley Compressor 3, Compressor 4, and Compressor 5 electron-ring research apparatus are described, including ceramic chamber design, ceramic-metal and ceramic-ceramic joining techniques, cryo-pumping, vacuum bake-out practices, and novel diagnostic probes suitable for ultrahigh vacuum service. (auth)

28119 (UCRL–20194) BEVATRON EXTERNAL PROTON BEAM FACILITIES. Elioff, T.; Lou, K. H.; Sah, R. C. (California Univ., Berkeley. Lawrence Radiation Lab.). Feb 1971. Contract W-7405-eng-48. 4p. (CONF-710308–6). Dep. NTIS.

From National particle accelerator conference; Chicago, Ill. (1 Mar 1971).

A septum magnet beam-splitting system has been successfully operated at the Bevatron. This system has made possible a more flexible placement of secondary particle beams and the simultaneous sharing of the external proton beam between two end stations.

XUM

A second beam-splitting system is under construction, and simultaneous beam sharing among three end stations will soon be possible. Other developments which will greatly increase the total flux of the external proton beam are also discussed. (auth)

28120 (UCRL-20406) AN EXTERNAL HEAVY ION SOURCE FOR THE BERKELEY 88-INCH CYCLOTRON. Clark, D. J.; Steyaert, J.; Carneiro, A.; Elo, D.; Frazier, P.; Morris, D.; Renkas, M. (California Univ., Berkeley. Lawrence Radiation Lab.). Mar 1971. Contract W-7405-eng-48. 10p. (CONF-710308-5). Dep. NTIS.

From National particle accelerator conference; Chicago, Ill. (1 Mar 1971).

A heavy ion source of the PIG type has been installed on the axial injection line at the 88-Inch Cyclotron. It is now in the testing phase. Arc powers up to 4 kW have been run, and hydrogen and nitrogen beams have been injected and accelerated in the cyclotron. (auth)

28121 (UCRL-20620) VACUUM CRYOPUMPING A HEAVY ION SOURCE IN A HIGH VOLTAGE TERMINAL. Wolgast, Richard C. (California Univ., Berkeley. Lawrence Radiation Lab.). Feb 1971. Contract W-7405-eng-48. 5p. (CONF-710308-12). Dep. NTIS.

From National particle accelerator conference; Chicago, Ill. (1 Mar 1971).

Two coldfingers differentially cryopump the heavy ion source of the SuperHilac 3-MV injector. One coldfinger near the source freezes most of the source gas load and provides adequate clean vacuum for source operation. The second coldfinger near the beam entrance into the high voltage column produces high vacuum to reduce ion beam loss through charge exchange and accidental electrical discharges. The 20°K temperature is produced by a small refrigerator in the terminal, and is transmitted to the coldfingers by hydrogen-charged heat pipes. The effective system pumping speed for air at the source measures 180 l/s. While running beams of argon ions, pressures are 8×10^{-5} at the source and 5×10^{-6} mm Hg at the column entrance. The integral of pressure with distance along the terminal beam path is 1.8×10^{-3} mm Hg-cm. (auth)

28122 (UCRL-20633) SOME CONSIDERATIONS IN PLANNING FOR SUPERHILAC TIMESHARE OPERATION WITH BOTH HEAVY AND LIGHT ION BEAMS. Selph, Frank B. (California Univ., Berkeley. Lawrence Radiation Lab.). Mar 1971. Contract W-7405-eng-48. 9p. (CONF-710308-10). Dep. NTIS.

From National particle accelerator conference; Chicago, Ill. (1 Mar 1971).

One of the important problems to be solved for any accelerator, with the exception of those intended for a single purpose such as injection, is providing adequately for multiple use of the machine. Of particular importance is the possibility of timeshare operation, in which two or more experimental setups can be supplied with beam at the same time. The SuperHilac will accelerate ions of all mass numbers, with final energy continuously variable from 2.6 to 8.5 MeV/nucleon. Normally, to change particle and energy in the Hilac requires a careful retuning of many machine parameters and (optimistically) an hour of machine time. For the SuperHilac it is proposed to provide particles of different charge-to-mass ratio on alternate pulses, so that, for example, half of the pulses would be light ions, delivered to one experimental area, and the other half heavy ions, delivered to another experimental area. Consequently a number of new problems need to be solved. These occur at injection, with accelerating and focusing the beams in the linac, in the stripper area, and at the exit from the machine. (auth)

28123 (UCRL-73075) LRL (LIVERMORE) 100-MeV LINEAR ELECTRON ACCELERATOR AND FACILITY. Fultz, S. C.; Whitten, C. L.; Gallagher, W. J. (California Univ., Livermore. Lawrence Radiation Lab.). 2 Mar 1971. 8p. (CONF-710308-1). Dep. NTIS.

From National particle accelerator conference; Chicago, Ill. (1 Mar 1971).

The 100 MeV electron accelerator and facility at Livermore have been designed for undertaking investigations in neutron physics and nuclear photoreactions. This has required versatility in the performance of the accelerator and in the layout of the beam transport system. The accelerator is a 5-section S-band device with beam pulse capability of 5ns, 10A at 1800 pps to 3μs 650 ma at 300 pps. A tungsten converter after the third section produces a positron beam capable of acceleration to 80 MeV. The accelerator can operate in the transient or steady state modes. The magnets used to steer the high current pulses are achromatic and can pass a momentum spread of ±15%. Other beam lines are achromatic and can pass a momentum spread of ±5%. (auth)

28124 (WASH-1159, pp 1-10) STATUS AND OUTLOOK FOR ARC-DISCHARGE SOURCES. Main, Robert (California Univ., Berkeley. Lawrence Radiation Lab.).

From Conference on heavy ion sources; Washington, D. C. (13 Mar 1970).

In Conference on heavy ion sources.

The operation and characteristics of arc discharge heavy-ion sources are discussed. Geometry, electron temperature, extraction process, pulsed operation, charge state, lifetime, and materials are considered. (W.H.K.)

28125 (WASH-1159, pp 13-33) ION SOURCES FOR MULTIPLY CHARGED HEAVY IONS. Bennett, J. R. J. (Rutherford High Energy Lab., Chilton (England)).

From Conference on heavy ion sources; Washington, D. C. (13 Mar 1970).

In Conference on heavy ion sources.

A review is given of existing sources of multiply charged heavy ions. Particular emphasis is on cyclotron applications. Most sources are of the P.I.G. type and the performance of the various models is compared. New methods have recently been suggested for producing high charge states of very heavy particles. Some are based on plasmas used in thermonuclear research. A very brief account is given of a few of these devices. Finally, acceleration and stripping of ions is mentioned for completeness, as it can be a very effective way of producing highly charged ions. (33 references). (auth)

28126 (WASH-1159, pp 34-41) RECENT WORK ON STRIPPING AND PICKUP OF ELECTRONS BY FAST HEAVY IONS. Grodzins, Lee (Massachusetts Inst. of Tech., Cambridge).

From Conference on heavy ion sources; Washington, D. C. (13 Mar 1970).

In Conference on heavy ion sources.

Charge stripping data for heavy-ion accelerators are reviewed. Single collision cross section measurements for the pickup or loss of electrons by heavy ions are discussed. (W.H.K.)

28127 (WASH-1159, pp 45-57) EQUILIBRIUM CHARGE-STATE DISTRIBUTIONS OF HEAVY IONS (1 TO 14 MeV). E-Report No. 430. Ryding, G.; Wittkower, A. (High Voltage Engineering Corp., Burlington, Mass.).

From Conference on heavy ion sources; Washington, D. C. (13 Mar 1970).

In Conference on heavy ion sources.

Equilibrium charge state distributions have been determined for iodine, bromine, chlorine, and aluminum ions traversing various targets with energies between 1 and 14 MeV. The mean charge $\bar{i}$ and the distribution width σ in an oxygen target are described by the semi-empirical relationships: $\bar{i} = 1.76\ E^{\frac{1}{3}}$ and $\sigma = 0.27\ Z_P^{\frac{1}{3}}$ (velocities greater than $3.5\ 10^8$ cm/sec) where E is the projectile energy in MeV and Z_P is the nuclear charge of the projectile. (auth)

28128 (WASH-1159, pp 88-112) THE "HIPAC" AS A SOURCE OF HIGHLY STRIPPED HEAVY IONS. Daugherty, J. D.; Eninger, J. E.; Janes, G. S.; Levy, R. H. (Avco-Everett Research Lab., Everett, Mass.).

From Conference on heavy ion sources; Washington, D. C. (13 Mar 1970).

In Conference on heavy ion sources.

The HIPAC Ion Source is a novel device intended to produce very highly stripped heavy ions; the achievement of this objective would permit the acceleration of heavy ions in relatively modest cyclotrons, linacs, etc. The problem of stripping heavy ions by successive electron impacts is discussed in general terms. The HIPAC Ion Source is then described using for illustrative purposes a nominal set of characteristic parameters. A torus 20 cm in major radius is estimated to yield 10^{13} ions/sec of Kr^{20+} or 10^{11} ions/sec of U^{60+}. The current status of experimental work on the concept is briefly reviewed. (auth)

28129 (WASH-1159, pp 168-71) SPARK SOURCE. Zwally, H. Jay (Maryland Univ., College Park. Inst. for Fluid Dynamics and Applied Mathematics).

From Conference on heavy ion sources; Washington, D. C. (13 Mar 1970).

In Conference on heavy ion sources.

A spark source of multiply-charged heavy ions is described. The design and operating parameters are discussed, and m/z identifications of the time-of-flight spectrum are made. (W.H.K.)

28130 (WASH-1159, pp 227-51) INTENSITY AND PHASE-SPACE LIMITATIONS OF VARIOUS HEAVY-ION ACCELERATION METHODS. Reiser, M.; Viola, V. (Maryland Univ., College Park).

XUM

From Conference on heavy ion sources; Washington, D. C. (13 Mar 1970).

In Conference on heavy ion sources.

A heavy ion accelerator suitable for production of new transuranic elements should be capable of providing beams of any given element with energies in excess of 6 MeV per nucleon. Intensities should be of the order of 10^{11} particles per second or more. Proposed heavy ion linacs and cyclotrons which use conventional ion sources with preacceleration and stripping can readily achieve the desired energies. However, by conservative estimates the intensities provided by these acceleration methods should be low by one to two orders of magnitude, the cyclotron yielding the larger number of particles. New types of ion sources, such as plasma-containment devices, laser-produced plasmas etc., are potentially capable of producing short pulses of high-charge state ions ($Z > 20$) which could be accelerated directly without stripping. However, even if 10^{11} particles could be produced per pulse, it is estimated that, depending on pulse length, the space charge limit of the accelerator could reduce the intensity by several orders of magnitude. The electron ring accelerator should be a promising alternative to the other schemes. Calculations show that ion energies in the range of 1000 to 2000 MeV should be feasible by the simple expansion method. For ion masses $M > 80$ the energy is practically independent of the mass. No high charge states are required, and intensities of 10^{11} ions per second or more can be expected. (auth)

28131 PARTICLE ACCELERATOR VACUUM CHAMBERS IN ALUMINUM OXIDE CERAMICS. Droscha, H. Kerntechnik; 12: 477-9(Nov 1970). (In German and English).

The use of vacuum-chamber segments of aluminium oxide ceramic, with internal sintered-in metal strips and external metal ring connections, makes is possible to improve considerably the performance of circular accelerators. (auth)

28132 MEDICAL 6 MeV LINEAR ACCELERATOR MADE IN JAPAN. Kitabatake, Takashi (Nagoya Univ., Japan); Sano, Hogara; Machiyama, Yoshihiko; Kitagawa, Toshio; Ueda, Toshio. Nagoya J. Med. Sci.; 32: 359-77(Mar 1970).

A 6 MeV medical linear accelerator manufactured by the Mitsubishi Heavy Industries, Ltd., has been installed in the Aichi Cancer Center Hospital. This is the first unit of this type made in Japan. This paper gives a brief description of the unit, reports the results of a series of tests for radiation and mechanical accuracy, and summarizes the one year history of calibration and stability. One of the most striking characteristic is a mechanism that deflects the electron beam at 180 degrees and uses a two step deflection magnet system. The maximum x-ray output was 465 R/min at one meter from the target with the actual maximum energy of 5.75 MeV. The unit has been used for clinical radiotherapy for the past year, and treatment was only interrupted one day because of mechanical trouble. (auth) (Japan)

28133 DYNAMIC ACCELERATED PROTON BEAM CHARACTERISTICS IN IHEP 70-GeV ACCELERATOR. Gridasov, V. I.; Zelenov, B. A.; Zelin, V. A.; Myznikov, K. P. At. Energ. (USSR); 30: 266-70(Mar 1971). (In Russian).

The methods of measuring phase characteristics of the beam in the process of acceleration are presented. Results of the measurements processed on a computer, taking into account the real characteristics of the RF circuit, are presented. Phase oscillation amplitudes and an energy spread in the beam are determined. A dependence of the beam dimensions on its energy is given. It is shown that the amplitude of betatron oscillations damps adiabatically with the increasing magnetic field up to $H = 9000$ e only. After this there appear nonlinear effects connected with a saturation of the iron of the accelerator magnets. The functions of particle distribution in amplitudes of vertical and radial betatron oscillations are determined, taking into account the contribution of the radial-phase oscillations. (auth)

28134 CONTROL AND MONITORING OF THE SLAC ACCELERATOR UTILIZING A PDP-9 SYSTEM. Struven, Warren C. (Stanford Univ., Calif.). pp 121-7 of DECUS Proceedings. Maynard, Mass.; Digital Equipment Computer Users' Society (1969).

From DECUS symposium, Wakefield, Mass. (12 May 1970). See CONF-690510.

A PDP9 system is being installed to supplement the manual controls and visual readout of the SLAC accelerator and to provide data logging from some 3000 points. Initially, malfunctioning klystrons will be sensed and suitable spares will be switched to multiple beams. Switching will be slow at first (up to 0.7 seconds) but a future parallel system will switch klystrons within one interpulse period (2.7 ms). Summarized data will be readout weekly or bi-weekly from the disk. Later, magnetic tape will be used to transfer data from the disk to an IBM 360-91 for extensive off-line data reduction. Beam steering, focusing and spectrum control will be implemented. (auth)

28135 ON-LINE HIGH ENERGY PHYSICS ANALYSIS WITH A PDP-9. Shrager, P.; Snape, G.; Teitelbaum, L. (Univ. of Pennsylvania, Philadelphia). pp 129-32 of DECUS Proceedings. Maynard, Mass.; Digital Equipment Computer Users' Society (1969).

From DECUS symposium, Wakefield, Mass. (12 May 1970). See CONF-690510.

A software system written for the PDP-9 and used on-line to a high energy physics experiment is described. The system is designed to perform the following functions: logging of data from spark chambers onto a magnetic tape, monitoring the experimental apparatus, and performing on-line analysis. The amount and type of analysis to be performed is decided at time of system initialization, but can be changed during execution at the will of the experimenter. The system relies heavily on an X–Y display unit for monitoring the hardware and keeping the physicist abreast of the progress of the experiment. (auth)

28136 MICROTRON TYPE ELECTRON ACCELERATOR. Komar, A. P.; Fominenko, V. P.; Chizhov, V. P. (to Ioffe Physical Tech. Inst.). Russian Patent 244,519. 10 Oct 1969. Filed 26 Mar 1968. (In Russian).

Descriptions are given of a linear accelerator with rotating two-section magnetic system with magnetic bypasses differently distributed in relation to the direction to the electrons and supplied with the entrance and exit sheers for magnetic focusing. The linear accelerator is erected between two C-shaped pivot-magnets with a steady homogeneous magnetic field (two-sector magnet). On each electron orbit in the gaps between the magnet are placed quadrupole focusing lens systems in order to augment the inherent unstableness of radial and vertical particle motion in the two-sector magnet. (R.V.J.)

28137 SPUTTER-TYPE PENNING DISCHARGE FOR METALLIC IONS. Gavin, Basil F. (to United States Atomic Energy Commission). U. S. Patent 3,566,185. 23 Feb 1971. Filed 12 Mar 1969.

An ion source in which ions of normally solid materials are easily produced is described. A plasma is generated in a gas adjacent the solid material from which ions are to be produced. The solid is negatively charged and the gas plasma ions bombard the solid, sputtering off ions of the solid. This is accomplished through the use of a Penning discharge with a cold cathode-type source and a centrally positioned and negatively charged dynode upon which the solid material is mounted, the dynode being electrically connected to the cathode and provided with an exit slit through which the metallic ions are extracted from a plasma potential. (auth)

28138 LIQUID HYDROGEN TARGET UTILIZING A SMALL MECHANICAL REFRIGERATOR. Doi, Yoshikuni; Fujii, Tadao; Kitami, Toyokichi; Okuno, Hideki; Takamatsu, Kunio (Tokyo Univ.). Jap. J. Appl. Phys.; 10: 468-71(Apr 1971).

A liquid hydrogen target system utilizing a small mechanical refrigerator (6 W at 20°K) has been developed for high energy physics experiments at the electron synchrotron of Institute for Nuclear Study. The hydrogen gas is liquefied at the cold head of the refrigerator and is maintained as a liquid either in a reservoir or in a target container. A development of the pneumatic-type cold valve has enabled a rapid transfer of hazardous liquid hydrogen between a condenser and a thin target container. The liquid hydrogen target of 500 ml can be made ready for the experiment within 7 h and maintained automatically in a steady state for about 1,000 h without any manual operation. (auth)

28139 AZIMUTHAL ASYMMETRY OF THE MAGNETIC FIELD STRENGTH OF THE EREVAN SYNCHROTRON ELECTROMAGNET. Esin, S. K.; Sadoyan, K. A.; Tumanyan, A. R. (Inst of Physics, Erevan). Izv. Akad. Nauk Arm. SSR, Ser. Fiz.; 5: 197-204(1970). (In Russian).

Basic causes leading to azimuthal asymmetry of the magnetic field strength at the level of injection fields of the ring accelerator electromagnet are determined and certain methods of reducing its quantity are described. (auth)

28140 MAXIMUM CURRENT OF THE CIRCULAR ACCELERATOR OR STORAGE RING. Baryshev, A. I. (Inst. of Physics, Erevan). Izv. Akad. Nauk Arm. SSR, Ser. Fiz.; 5: 244-9 (1970). (In Russian).

Synchrotron oscillation stability is investigated, taking into account the voltage induced in the cavities by electrons themselves. It is shown that the maximum accelerating current in conditions of negative detuning of the cavity depends on the

transmitter power and energy gain; at the same time it is independent of the synchrotron oscillation damping rate. When the cavity detuning is positive, the maximum current depends significantly on damping rate. (auth)

28141 HIGH RESULUTION DETECTION UNIT FOR CHARGED PARTICLES. Gales, S.; Bartol, F.; Schapira, J. P. (Univ. Paris, Orsay, France). Rev. Phys. Appl.; 5: 835-9(Dec 1970). (In French).

A scattering chamber for charged particle studies incorporating five Peltier cooled surface barrier detectors, capable of assuming any angle and position on a rotating plate, was developed. The charge preamplifiers are directly connected to the detectors and are incorporated in the vacuum system of the chamber; a rotating plate at the bottom of the chamber facilitates the electrical connections. After 10 hours of pumping a vacuum of 10^{-6} mm of Hg was achieved. A resolution of 16 keV was obtained for the $^{31}P + p$ elastic scattering reaction at 3200 MeV. (auth) (France)

28142 ELECTRON OPTICS OF SAGITTAIRE. Aucouturier, J.; Huber, H.; Jaouen, J. (Thomson-CSF, Orsay, France). Rev. Tech. Thomson-CSF; 2: 655-80(Dec 1970). (In French).

In order to fulfill therapeutic requirements, an apparatus was developed consisting of an electron linear accelerator and an additional rotary head presenting an appropriate target for the production of photons. The electron beam focusing system was designed from theoretical considerations and its performance checked using the hodoscope method. The results obtained are in good agreement with those predicted, both with respect to the dimensions of the beam on the target and the uniformity of the dose over the field covered. (auth) (France)

28143 INFLUENCE OF RESONANT PHENOMENA ON THE INCOHERENT SPACE CHARGE ACCELERATED IN A BETATRON. Scarlat, F. (Inst. of Nuclear Physics, Bucharest). Stud. Cercet. Fiz.; 22: 821-6(1970). (In Rumanian).

It is well known that the resonance phenomena taking place in particle accelerators due to the variation of motion equation parameters or to the harmonic components of some external forces lead to the limitation of the accelerated particle numbers. The limit number of the electrons in the beam for the most important resonances is determined at two betatrons of 8 and 25 MeV. The results show that at 50-keV injection energy this number lies between 10^{10} and 10^{11} electrons per pulse for both betatrons. (auth)

XUM

PHYSICS (NUCLEAR)

Neutron Interactions with Matter

Refer also to abstracts 26883, 27893, 27948, 28656, 28798, 28814, and 28815.

28144 (CNEN-RT/FIMA-69-5) COLLIMATION CORRECTIONS IN SMALL ANGLE SCATTERING OF NEUTRONS. Antonini, M. (Comitato Nazionale per l'Energia Nucleare, Rome (Italy)). 1970. 28p. NTIS (U. S. Sales Only).

A numerical technique is developed for correcting experimental data of small-angle diffuse scattering of neutrons for the effect of instrumental resolution in the static approximation. The unfolding method does not require any particular a priori theoretical prediction on the form of the differential cross section while the resolution is assumed to be product of two independent Gaussian functions representing the effect of the finite angular divergence of the incident and scattered beams in the scattering plane (horizontal collimation) and in the normal plane (vertical collimation). The validity of the procedure is tested under various typical experimental conditions, and the results are discussed also in connection with random errors affecting the input data. (INIS)

28145 (EIR-188) INTEGRAL EQUATION OF TRANSPORT IN ONE-DIMENSIONAL CYLINDRICAL GEOMETRY: POLYNOMIAL APPROXIMATION AND LINEAR ANISOTROPIC DIFFUSION. I. THEORY. Ligou, J. (Eidgenoessisches Institut fuer Reaktorforschung, Wuerenlingen (Switzerland)). Dec 1970. 54p. (In French). Dep. NTIS (U. S. Sales Only).

It is shown how, in the framework of a one-dimensional cylindrical geometry, it is possible to suppress for the most part the first insufficiency (hypothesis of uniform emission) and how to incorporate the linear anisotropy of the diffusion (P1 matrices) without supplementary complexity. After a review of the general equations, the essential ideas concerning the choice of the polynomial retained and the generalization of the resulting collision probabilities are presented. The quantities which generalize the collision probabilities and which constitute the greater part of the calculations are evaluated. (tr-auth)

28146 (EUR-4601) JN-METD1: A FORTRAN-IV PROGRAMME FOR SOLVING NEUTRON TRANSPORT PROBLEMS WITH ISOTROPIC SCATTERING IN BARE SPHERES AND HOMOGENEOUS SLABS BY THE j_N METHOD. Asaoka, T. (European Atomic Energy Community, Ispra (Italy). Joint Nuclear Research Center). 16 Sep 1970. 90p. Dep. NTIS (U. S. Sales Only). EUR F,Fr. 13.80.

The mathematical solution of neutron transport problems in a bare sphere and infinite homogeneous slab according to the new analytical j_N method, spherically symmetric scattering in the laboratory system being assumed is summarized. Also described in detail is a Fortran-IV computer program JN-METD1 for accurately solving both the stationary and time-dependent problems. (auth)

28147 (JUL-683-MA) PROGRAM FOR SOLUTION OF THE STATIONARY NEUTRON TRANSPORT EQUATION WITH SPHERICAL SYMMETRY. Hnake, W.; Horlitz, E. (Kernforschungsanlage, Juelich (West Germany). Zentralinstitut fuer Angewandte Mathematik). Jul 1970. 24p. (In German). Dep. NTIS (U. S. Sales Only).

The method previously described for the treatment of the stationary neutron transport equation in spherical symmetry with the boundary condition that nothing flows into the reactor from the outside was programmed. In the method an equation system is to be solved whose coefficients are three-dimensional integrals. The program is in two independent parts with a preliminary program which is described individually. An example is given of the use of the program. The program itself is given. (J.S.R.)

28148 (ORNL-TM-3266) EDITOR: A PROCESSING CODE FOR ENDF/B FORMAT DATA. Thompson, C. L.; Stockton, J. R.; Petrie, L. M.; Wright, R. Q.; Penny, S. K. (Oak Ridge National Lab., Tenn.). 16 Feb 1971. Contract W-7405-eng-26. 33p. (ENDF-142). Dep. NTIS.

EDITOR is a FORTRAN IV computer code designed to print, in readable form, the contents of ENDF/B format nuclear cross-section data tapes. In addition, EDITOR allows copying, altering mode, merging, punching and otherwise manipulating the data which appears on one or more ENDF tapes. (auth)

28149 (ORNL-tr-2419) ANISN SYSTEM: DESCRIPTION AND SERVICE INSTRUCTIONS FOR THE ANISN DISCRETE ORDINATE PROGRAM AND SUBROUTINES. Devillers, Christian (Commissariat a l'Energie Atomique, Fontenay-aux-Roses (France). Centre d'Etudes Nucleaires). Translation of report CEA-N-1358. 90p. Dep. NTIS.

An abstract of this paper, prepared from the original language, appeared as NSA 25: 14863.

28150 (RCN-134) EXTENSION OF THE DERIVATION OF THE DIFFUSION LENGTH FOR NEUTRONS IN A MEDIUM WITH SMALL ABSORPTION. Woldringh, H. H. (Reactor Centrum Nederland, Petten). Jan 1971. 6p. Dep. NTIS (U. S. Sales Only).

The explicit expression for the first-order correction of the diffusion length for neutrons in a medium with small absorption is derived. This constitutes an extension to the work of Davison, who gives an implicit equation for this correction. (auth)

28151 (TUBIK-21) REVIEW OF METHODS FOR HANDLING OF STATIONARY NEUTRON TRANSPORT PROBLEM. Lindauer, Erwin (Technische Universitaet, Berlin (West Germany). Institut fuer Kerntechnik). Oct 1970. 268p. (In German). Dep. NTIS (U. S. Sales Only).

An instruction program and workbook for the review of the methods for the treatment of neutron transport problems are presented. The topics considered are the Boltzmann equation, simplification of the transport equation, P_1, diffusion, and group diffusion approximations, one-, two-, and multigroup diffusion calculations, source iteration and Fermi approximation, synthetic method of source iteration as eigenvalue problem, methods with discretization of the angle, and moderator nucleus. (J.S.R.)

28152 NORMAL MODE EXPANSION IN NEUTRON THERMALIZATION THEORY WITH A SIMPLE SCATTERING KERNEL. Yamagishi, Tomejiro (Osaka Univ.). J. Nucl. Sci. Technol. (Tokyo); 8: 153-61(Mar 1971).

Elementary solutions to the energy-dependent Boltzmann equation with a one-term degenerate scattering kernel are derived in plane geometry, and the weight function W(z) is obtained which makes these solutions mutually orthogonal over the half-range interval of the continuum. The weight function greatly facilitates determination of the expansion coefficients in general solutions and is applied to the problems in infinite half space. The diffusion length (discrete space eigenvalue) ν_0 is exactly expressed by using the half-range characteristic function X(z). In a 1/v-absorbing medium, as the absorption concentration q increases from zero to a critical value q^*, the diffusion length decreases from infinity to the end of the continuum $1/\Sigma_{min}$. For $q \geq q^*$, ν_0 vanishes and the neutron density can be represented by the transient term alone, whose exact expression is obtained. (auth)

28153 NEUTRON COLLIMATOR. Desandre-Navarre, Christian; Lacruche, Gilbert (to Commissariat a l'Energie Atomique). British Patent 1,227,929. 15 Apr 1971. Priority date 1 Jul 1969, France.

The neutron collimator comprises an assembly of contacting parallel hollow needles which are of substantially equal length and at least the inside surface of which is formed of neutron-absorbing material. The assembly is fitted into one or more bearing rings and the whole assembly is driven by a motor and rotated about a center axis parallel to the needles. (W.H.K.)

28154 GREEN'S FUNCTION OF TIME-ENERGY DEPENDENT NEUTRON TRANSPORT EQUATION. Minn, Hokee; Pac, Pong Youl (Seoul National Univ.). J. Korean Nucl. Soc.; 2: 263-8(Dec 1970).

The spectrum of the continuous transfer operator arising in a time-energy-dependent neutron transport equation is analyzed. Four theorems concerning the spectrum are proved. A convolution theorem of the generalized Mellin energy transform is given. The completeness theorem necessary for a final solution is proved. A unique time decay constant $1 - c$ is found, which is dominant asymptotically. (auth)

28155 GENERAL ENERGY-DEPENDENT TRANSPORT EQUATION WITH FISSION. Lee, Un Chul; Pac, Pong Youl (Seoul National Univ.). J. Korean Nucl. Soc.; 2: 255-62(Dec 1970).

The general anisotropic transport equation with fission is studied. These calculations utilize the fact that the operator can be split into scattering and fission operators when the completeness of general anisotropy is proved. Applying these operators to the equation makes it easy to extract the slowing-down transient of zero-measure and completely solves the transport equation. In addition, the number of the eigenvalues of the second anisotropy is classified with Cs unknown, B_1 and B_2 known constants. (auth)

XUM

28156 PULSED ENERGY DEPENDENT NEUTRON TRANSPORT. Minn, Hokee (Seoul National Univ.). J. Korean Nucl. Soc.; 2: 249-54(Dec 1970).

The time–energy transient characteristics of the pulsed neutron transport problem with an inelastic kernel in the fast domain are found exactly with a continuous energy transfer operator. A discrete time eigenvalue is found which is asymptotically dominant. The complete solution consists of three parts: a time–energy separable mode that is asymptotically dominant and a nonseparable mode which is made up by two parts—a pure energy slowing-down transient and a mixture of time and energy transient which is negligible asymptotically. (auth)

28157 AGE OF FISSION NEUTRONS TO INDIUM RESONANCE IN WATER AND POLYETHYLENE. Kanda, Keiji; Hayashi, Masatoshi; Nakagawa, Haruo; Shibata, Toshikazu (Kyoto Univ.). Annu. Rep. Res. Reactor Inst., Kyoto Univ.; 3: 93-106(1970).

The age of fission neutrons to indium resonance energy was measured in two materials, water and polyethylene, by using a fission plate 27 cm in diameter combined with the KUR heavy-water thermal column. In the experiment the infinite-plane-detector method was employed, where the age is half of the second moment of the slowing-down flux distribution at the 1.46-eV resonance of indium. The calculation of the age was done with Greuling–Goertzel and Selengut–Goertzel approximations. In both materials the former approximation was in good agreement with the experimental values, while the latter gave considerably larger values. (auth)

28158 INFLUENCE OF DIFFERENT CRYSTAL MODELS ON THERMAL NEUTRON SCATTERING IN BERYLLIUM OXIDE AND GRAPHITE. Schroeder, Guenter (Kernforschungsanlage, Juelich, Ger.). Atomkernenergie; 17: 103-12(Mar 1971). (In German).

For the moderator materials beryllium oxide and graphite the effect of phonon spectra, derived from different crystal models, on thermal-neutron scattering calculations is tested by the computer code COLLI. Several phonon spectra of beryllium oxide (models of Sinclair, Borgonovi, and linear chain) reproduce adequately the observed values of specific heat and the scattering law. The differences in calculations of the energy-transfer cross sections (scattering kernel) can be ignored, particularly for higher neutron energies and moderator temperatures. It is not necessary to regard different oscillation amplitudes of beryllium and oxygen atoms, so that much of the computer time can be saved. For both graphite phonon spectra (Young and Koppel, Carvalho) calculated and measured values of the scattering law coincide quite well. Through nuclear calculations for a HTGR low-enriched spherical fuel element it is pointed out that the effect of different scattering properties on the neutron spectrum, the averaged cross sections, the fission neutrons produced per absorption, and the moderator temperature coefficient can be ignored if scattering kernels are calculated up to sufficiently high neutron energies by exact scattering models instead of the free-gas model. (auth)

28159 ROLE OF ENERGY DEPENDENCE IN PROBLEMS OF TRANSPORT THEORY. Ershov, Yu. I.; Shikhov, S. B. This paper was summarized in At. Energ. (USSR); 28: 422(May 1970) as paper No. 387/5499. (In Russian).

The integral equation of neutron transport with an isotropic scattering indicatrix in a homogeneous medium is considered; the use of integral transforms yields results not only for plane geometry, but also for an arbitrary nonconcave volume. (R.W.R.)

28160 PRINCIPLE OF BOUNDARY SOURCES IN NEUTRON TRANSPORT THEORY. Rumyantsev, G. Ya. This paper was summarized in At. Energ. (USSR); 26: 447-8(May 1969) as paper No. 288/5010. (In Russian).

An infinite medium with an anisotropic source distributed over a certain closed surface is considered, and several theorems applying to the neutron distribution in such a medium are given. These theorems are then used to solve Boltzmann's equation in bounded media, in particular, flat plates. A rule for substituting boundary sources for the medium boundaries is formulated. The principle of boundary sources reduces the problem of the neutron distribution in a plate to a system of singular integral equations that directly relates the angular distribution of the neutrons entering the plate to the distribution of emerging neutrons. These equations can be used independently of Boltzmann's equation in albedo methods of transport theory. (R.W.R.)

28161 PULSED NEUTRON RESEARCH. III. Yamamuro, Nobuhiro; Arai, Eiichi; Aizawa, Otohiko; Maekawa, Hiroshi; Uchiyama, Yuichi (Tokyo Inst. of Tech.). Bull. Tokyo Inst. Technol. (Engl. Ed.): No. 90, 139-49(Mar 1969).

Some features of the recent pulsed-neutron research in this laboratory were described. To obtain a high-intensity pulsed beam current having a short width, a very-high-frequency oscillator for the ion source has been built and the improvements of the pulsing system and the beam transport system have been performed. These were described first. By means of this apparatus the pulsed experiments for lead block and natural uranium assembly were carried out, and a result is shown. Because the accelerator was improved in beam intensity, the experiments on neutron spectra in pure water and poisoned water were examined. It was found that the spectrum measurement by time-of-flight technique can be made within a reasonable time. The preliminary result is shown. (Japan)

Nuclear Properties and Reactions, A≤ 5

Refer also to abstracts 26547, 28073, 28291, 28344, 28351, 28401, 28510, and 28753.

28162 (IAE–2000) WAVE FUNCTION AND BOUND ENERGY OF NUCLEI ^{3}H(^{3}He) TAKING INTO ACCOUNT THE TENSOR INTERACTION OF NUCLEONS. Dzyuba, B. M.; Pustovalov, V. V.; Rybachenko, V. F.; Sadovoi, A. A.; Efros, V. D. (Gosudarstvennyi Komitet po Ispol'zovaniyu Atomnoi Energii SSSR, Moscow. Institut Atomnoi Energii). 1970. 20p. (In Russian). Dep. NTIS (U. S. Sales Only).

The K-harmonics method is used to calculate the binding energy and the wave functions of ^{3}H and ^{3}He. A system of ten equations is obtained, which takes into account all harmonics of the K = 0, 2, 4 values and all the L = 0, 1, 2 values. The solution of five equations (K = 0, 2, 4; L = 0; K = 2, L = 2) gives the ^{3}H binding energy for different forms and parameters of the potentials, which is too small as compared with that calculated without tensorial forces. Approximate consideration of two more equations for the components of the function with K = 4, L = 2 increases appreciably the absolute value of the ^{3}H bound energy. The admixture of the mixed symmetry function is considerably reduced, which seems to create the problem of agreement of calculated values of the charge form factors ^{3}H and ^{3}He with experimental data. (auth)

28163 (ITF–70–100–P) ENERGY LEVELS OF THREE-PARTICLE SYSTEM. Ovcharenko, V. I.; Simenog, I. V.; Filippov, G. F. (Akademiya Nauk Ukrainskoi SSR, Kiev. Institut Teoreticheskoi Fiziki). 1970. 72p. (In Russian). (CONF-700117–1). Dep. NTIS (U. S. Sales Only).

From 2d. conference on nuclei; Leningrad, USSR (Jan 1970).

Bound states of the three-particle system are studied by the method of reciprocal interaction parameter expansion. The dependence of energy levels, mean-square radii, and other physical quantities of the system on the interaction parameter is investigated. A complete set of zero-approximation Hamiltonian eigenfunctions is proposed. The basic functions of a number of low states are given explicitly. With these functions the matrix elements of $\Sigma_{i<j} r_{ij}^{2\lambda}$ are calculated, and expressions for energies and mean-square radii of the bound states of the three-particle system are found as a sum of the first several terms of the series in reciprocal of the interaction parameter. In conclusion, the dependence of energy levels and mean-square radii on the interaction parameter (g) is discussed in detail. (auth)

28164 (LA–4576) ACCURATE CROSS-SECTION MEASUREMENTS OF THE REACTIONS T(p,p)T, T(p,d)D, T(p,^{3}He)N, AND T(p,p')T AT 13,600 MeV. Detch, J. Lewis Jr. (Argonne National Lab., Ill.). Dec 1970. Contract W-7405-eng-36. 123p. Dep. NTIS.

Differential cross sections were measured with absolute accuracies of about 1.0% and relative accuracies of about 0.7% using a thin-walled tritium gas target and silicon surface barrier detector telescope in conjunction with an on-line computer for mass identification and data handling. The angular scattering distributions for T(p,p)T, T(p,d)D, and T(p,^{3}He)N, and the proton asymmetries of $T(\vec{p},\hat{p})T$ were measured at a proton laboratory energy of 13.600 MeV. In addition, differential cross sections for T(p,p)T were measured at energies of 16.230 and 19.480 MeV to provide supporting data for existing mass-4 studies at these energies. Related data is compared and preliminary attempts to analyze the data with an energy independent phase shift analysis program are discussed. Several sets of single channel phase shift solutions are given for maximum angular momentum L-values of three. These solutions are not unique. Simultaneous two and three channel analyses were inconclusive. Polarization asymmetry measurements using the Los Alamos Lamb Shift polarized ion source show a maximum analyzing power of about +0.70 at 13.600 MeV for $T(\vec{p},\hat{p})T$. These values are related to existing analyzing power measurements of $^3He(\vec{p},\hat{p})^3He$ and $T(\vec{p},\hat{p})T$ near this energy. The errors and data analysis are discussed in detail. The compensation ef-

fects of multiple scattering in the gas target foils are treated by explicit calculation and experimental verification. (auth)

28165 ANGULAR DISTRIBUTION OF PHOTONEUTRONS FROM DEUTERIUM. Evwaraye, Andrew Oteku. Saskatoon; Univ. of Saskatchewan (1969). 106p. University Microfilms Order No. 71-3205.

Thesis.

A photon beam of Eγmax = 125 MeV, produced by an electron linear accelerator, was used to irradiate a deuteron target. The deuteron target was viewed simultaneously by five neutron detectors located respectively at 30, 60, 90, 112 and 142° to the incident photon beam. The measured angular distributions were compared with the theoretical calculations using Hamada–Johnston and Boundary Condition Model potentials. The results of this experiment were also compared with previous measurements where they overlap. Good agreement was found between the present measurements and theoretical predictions in the energy region of Eγ ≤ 40 MeV. The shape of the angular distributions in this energy region is approximately $\sin^2\Theta$ as expected. There is no strict agreement between the present measurements and the theoretical predictions at Eγ ≤ 55 MeV. Though the non-phenomenological potential, the Boundary Condition model potential, appears to give better predictions of the angular distributions than the Hamada-Johnston potential. The apparent disagreement between the present work and previous experiments at backward angles is interpreted to be due to the large uncertainties in the background subtraction in the forward proton angles, as all previous workers detected in the outgoing protons in the reaction D (γ,p) n. The large isotropic contribution observed is interpreted to be due to tensor forces both in the ground and final states as well as spin-orbit forces in the final state. (Diss. Abstr. Int., B)

28166 SOME EVIDENCE FOR THE CONVERGENCE OF THE INFINITE SERIES OF NONRELATIVISTIC GRAPH CONTRIBUTIONS FOR THE (n–d) ELASTIC SCATTERING AMPLITUDE. Komarov, V. V. (Moscow State Univ.); Serebryakov, S. G.; Popova, A. M. Phys. Lett.; 34B: 275-6(1 Mar 1971).

The absolute value of the total (n + d) cross-section at an incident neutron energy of from 20 to 60 MeV was calculated, using the optical theorem. The zero-angle elastic scattering amplitude was taken in successive approximations with respect to the number of non-relativistic graphs from the infinite series representing this amplitude. The convergence parameter (α/k_0) was determined where $(-\alpha^2/m)$ is the deuteron binding energy and $(k_0^2/2m)$ is the initial neutron energy. It has been shown that the S-wave two-nucleon approximation gives the absolute value of the total (n + d) cross section with approximately 10% precision. (auth)

28167 CLUSTER-MODEL EVALUATION OF NEUTRON CROSS SECTIONS FOR LIGHT-WEIGHT NUCLEI. Iotti, Robert Charles. Manhattan, Kan.; Kansas State Univ. (1970). 138p. University Microfilms Order No. 71-4437.

Thesis.

The four-nucleon reaction is formulated using the resonating group (cluster) model for the neutron-helium-3 and proton-triton groupings. Two coupled integro-differential equations describing the possible reactions are derived for each value of the total spin and angular momentum of the system. Analytical forms for the nonlocal and direct interactions are obtained by employing an equivalent central potential with a Gaussian shape, and wavefunctions for the ground states of the helium-3 and triton clusters also of Gaussian shape. The exchange dependence of the potential is chosen to be of the Serber type. Other authors have shown this type to yield satisfactory agreement with experimental values for the range of energies considered. The coupled integro-differential equations are solved numerically and the total and differential cross sections for the ^{3}He(n,n)^{3}He and ^{3}He(n,p)T reactions are reported for incident neutron energies of 1, 3.6, and 6 MeV. The ^{3}He(n,n)^{3}He cross sections, both total and differential, are in fairly good agreement with the experimental values except at 1 MeV, where the calculated cross section is too low at all angles. The shape of the angular distribution curve, however, matches quite well with the experimental one; in particular the minima of the distribution are predicted correctly. At the higher energies, the larger values of the calculated cross section at large angles could be attributed to the presence of another open channel, ^{3}He(n,d)D, which is of course not accounted for in the present theoretical treatment. The elastic scattering cross sections do not significantly differ from those calculated by other authors, who considered the elastic-scattering channel as the only open exit channel. The calculated total cross section for the ^{3}He(n,p)T channel is consistently too low. The angular distribution curves exhibit the qualitative features found in the experimental ones, i.e., the minima shift toward larger angles as the energy increases, and their position is well predicted. The small values predicted for the Serber interaction at the larger angles are expected, since this interaction yields too large a value at those angles for the elastic scattering cross section. (Diss. Abstr. Int., B)

28168 LEVELS IN ^{5}He EXCITED IN THE ELASTIC d–^{3}H SCATTERING. Kilian, K.; Treiber, H.; Strausz, R.; Fick, D. (Univ., Erlangen, Ger.). Phys. Lett.; 34B: 283-5(1 Mar 1971).

Using vector polarized deuterons, excitation functions of elastic scattering on tritons were obtained for the differential cross section and the analyzing power. A resonance with unnatural parity was found at $E_d \approx 5$ MeV. The structure of this resonance and theoretical calculations for mass-five nuclei are discussed. (auth)

28169 NEUTRON TOTAL CROSS SECTIONS, 2.5 TO 15 MeV. II. EFFECTS OF NUCLEAR DEFORMATION. Glasgow, Dale W. (Battelle-Northwest, Richland, Wash. Aerospace Research Labs., Wright-Patterson AFB, Ohio); Foster, D. Graham Jr. Contract AT(45-1)-1830. Phys. Rev., C; 3: 604-20(Feb 1971).

A spherical nonlocal optical-model analysis was performed on a homogeneous set of moderate-precision neutron total cross sections for 78 elements and 14 separated isotopes. The presence of fluctuations in the cross sections prevents the effective application of the optical model for nuclei with A < 45 unless the data are averaged over many experimental resolution widths. The dependence of the magnitude of the fluctuations on the ground-state spin of the target nucleus was observed. The analysis of the data for 46 spherical or soft nuclei within the regions 46 ≤ A ≤ 150 and 188 ≤ A ≤ 206, 2 transitional nuclei within the region ≥ 185 ≤ A ≤ 187, and 19 hard-deformed nuclei within the regions 152 ≤ A ≤ 184 and 228 ≤ A ≤ 239 clearly indicates the effects of nuclear deformation. The spherical nonlocal optical potential of Perey and Buck describes (within 3%) the interaction of fast neutrons (3.0 ≤ E_n ≤ 15.0 MeV) with 46 spherical or soft nuclei. The analysis yields considerably less accurate (17%) results for the 19 hard-deformed nuclei. The surface thickness is approximately the same for all spherical nuclei (with the possible exception of light nuclei below A = 46), to the extent that the nonlocal optical potential has the same form as the nuclear-matter distribution. The systematic nature of the deviations of the data from the theoretical predictions leads to a conjecture which spans the mass range 45 ≤ A ≤ 239. (auth)

28170 NEUTRON TOTAL CROSS SECTIONS, 2.5 TO 15 MeV. I. EXPERIMENTAL. Foster, D. Graham Jr.; Glasgow, Dale W. (Battelle-Northwest, Richland, Wash.). Contract AT(45-1)-1830. Phys. Rev., C; 3: 576-603(Feb 1971).

Measurements of the total cross section, for neutrons between 2.5 and 15 MeV, of 78 natural elements and 14 artificial or isotopically enriched samples spanning the range from hydrogen to plutonium are presented. The measurements were made by transmission in good geometry (inscattering <0.3%), using time-of-flight analysis of the continuous spectrum of neutrons from a pulsed Li(d,n) source. Data were taken with moderate energy resolution (2 to 4%) and moderate precision (1 to 3% at each point) at a density of three or four points per resolution interval, in order to avoid leaving gaps. Systematic errors do not exceed 2%, except in particular cases. The method leads naturally to small samples, so that it was possible to include all of the stable elements except the noble gases. The resulting homogeneous set of data supplies a reference surface for the intercomparison of results from other laboratories. Detailed comparisons are made with virtually all previous measurements in this energy range, and the systematic properties of the major ones are summarized. The completeness of the set helps to reveal a number of systematic properties of the interaction of fast neutrons with nuclei over the entire range of masses. (auth)

Nuclear Properties and Reactions, 6 ≤ A ≤ 19

Refer also to abstracts 26547, 27309, 27914, 27923, 27953, 27970, 28073, 28169, 28170, 28274, 28275, 28289–28291, 28293, 28344, 28400, 28401, 28440, 28441, 28452, 28496, and 28509.

28171 (CERN–70-30(Vol.1), pp 601-2) NUCLEAR MOLECULES FORMED IN THE ELASTIC ^{16}O + ^{16}O SCATTERING. Greiner, W.; Helling, G.; Pruess, K.; Scheid, W. (Frankfurt Univ. (West Germany). Institut fuer Theoretische Physik).

In International conference on the properties of nuclei far from the region of beta-stability; Leysin, Switzerland (31 Aug 1970).

In ^{16}O elastic scattering by ^{16}O one observes intermediate structure with a width of about 0.5 MeV. A theory is proposed

XUM

to describe this intermediate structure by inelastic excitations of low-energy states in the individual nuclei. The molecular-type potential used has virtual states for angular momenta exceeding l = 10 that produce the wide gross structure of the elastic cross section. (R.W.R.)

28172 CALCULATION OF NUCLEON WIDTHS OF THE LOWEST T = 3/2 STATES OF ^{13}N AND ^{13}C. Arima, A.; Yoshida, S. (Rutgers-The State Univ., New Brunswick, N. J.). pp 73-9 of Nuclear Isospin. /Anderson, John D. (ed.). New York; Academic Press, Inc. (1969).

From 2. conference on nuclear isospin; Pacific Grove, Calif. (13 Mar 1969). See CONF-690310.

28173 ANGULAR MOMENTUM TRANSFER IN ^{18}O(^{3}He,t) ^{18}F. Duhm, H. H.; Detraz, C.; Finlay, R. (Max-Planck-Institut fuer Kernphysik, Heidelberg). pp 263-7 of Nuclear Isospin. /Anderson, John D. (ed.). New York; Academic Press, Inc. (1969).

From 2. conference on nuclear isospin; Pacific Grove, Calif. (13 Mar 1969). See CONF-690310.

28174 FURTHER INDICATIONS FOR T-DEPENDENCE OF ANGULAR DISTRIBUTIONS. Mairle, G.; Becker-Bender, G.; Kaschl, G. Th.; and others (Max-Planck-Institut fuer Kernphysik, Heidelberg. Kernforschungsanlage, Juelich, Ger.). pp 291-6 of Nuclear Isospin. /Anderson, John D. (ed.). New York; Academic Press, Inc. (1969).

From 2. conference on nuclear isospin; Pacific Grove, Calif. (13 Mar 1969). See CONF-690310.

28175 MEASUREMENT OF THE MASS OF ^{9}Li. Nettles, P. H.; Hensley, D. C.; Tombrello, T. A. (California Inst. of Tech., Pasadena). pp 819-24 of Nuclear Isospin. /Anderson, John D. (ed.). New York; Academic Press, Inc. (1969).

From 2. conference on nuclear isospin; Pacific Grove, Calif. (13 Mar 1969). See CONF-690310.

28176 AN EXPERIMENTAL TEST OF THE BARSHAY–TEMMER THEOREM VIA THE REACTIONS ^{10}B(α,^{7}Li$_{g.s.}$)^{7}Be$_{g.s.}$ AND ^{10}B(α,^{7}Be$_{g.s.}$)^{7}Li$_{g.s.}$. Richter, A.; Fortune, H. T.; Ziedman, B. (Argonne National Lab., Ill.). pp 825-30 of Nuclear Isospin. /Anderson, John D. (ed.). New York; Academic Press, Inc. (1969).

From 2. conference on nuclear isospin; Pacific Grove, Calif. (13 Mar 1969). See CONF-690310.

28177 ISOSPIN IMPURITIES OF SOME ^{18}F STATES OBSERVED VIA ^{14}N(α,α)^{14}N* (2.311 MeV). Tollefsrud, P. B. (Univ. of Wisconsin, Madison). pp 837-42 of Nuclear Isospin. /Anderson, John D. (ed.). New York; Academic Press, Inc. (1969).

From 2. conference on nuclear isospin; Pacific Grove, Calif. (13 Mar 1969). See CONF-690310.

28178 CHARGED PARTICLE EMISSION FOLLOWING PION CAPTURE IN NUCLEI. Castleberry, P. J.; Coulson, L.; Minehart, R. C.; Ziock, K. O. H. (Univ. of Virginia, Charlottesville). Phys. Lett.; 34B: 57-8(18 Jan 1971).

The charged particles emitted following pion capture in thin (0.05 g/cm^2) targets of Li, Be, ^{10}B, C, O, Mg, S, Ca, Co and Pb were identified and their energy spectra were measured as well as the integrated branching ratios above threshold energies of 6, 8 and 9 MeV for the proton, deuteron and triton mode, respectively. (auth)

28179 ROLE OF CONFIGURATION STATES IN ISOSPIN FORBIDDEN PROTON DECAYS OF T = 3/2 STATES. Auerbach, N.; Lev, A. (Tel Aviv Univ., Israel). Phys. Lett.; 34B: 13-16(18 Jan 1971).

A calculation of several contributions to the partial width of the isospin-forbidden proton decays of T = 3/2 states was made for a number of nuclei. It was found that the dominant term in the partial width amplitude arises from the Coulomb mixing of the T = 3/2 states with their configuration states. The consequences of a possible charge-dependence and charge asymmetry of the nuclear force are discussed and their contribution to the partial width is estimated. (auth)

28180 CALCULATION OF QUADRUPOLE MOMENTS, DEFORMATIONS: AND SHAPE OF LIGHT NUCLEI WITHIN K-HARMONIC METHOD. Grin, Yu. T.; Kochetov, A. B. Yadern. Fiz.; 12: 1154-62(Dec 1970). (In Russian).

The mean square radii, form, quadrupole moments and deformations of ^{8}Be, ^{12}C, and ^{16}O nuclei in the ground state are calculated in the K-harmonic method, in the lowest K approximation. (auth)

28181 ESTIMATE OF THE BINDING ENERGY OF ^{16}O WITH MATRIX ELEMENTS OF EFFECTIVE INTERACTION. Grypeos, M. E. (Democritus Nuclear Research Center, Athens. International Centre for Theoretical Physics, Trieste, Italy). Phys. Lett.; 34B: 481-4(29 Mar 1971).

An estimate of the binding energy of ^{16}O nucleus is given using matrix elements of effective interaction determined by means of a variational method with a "healing condition". A "minimum condition" is also derived for these matrix elements. (auth)

28182 PRODUCTION CROSS SECTIONS OF LITHIUM AND BERYLLIUM ISOTOPES IN ^{12}C BY HIGH-ENERGY PROTONS AND ALPHA PARTICLES. Fontes, P.; Perron, C.; Lestringuez, J.; Yiou, F.; Bernas, R. (CNRS, Orsay, France). Nucl. Phys.; A165: 405-14(1971).

The formation cross sections of ^{6}Li, ^{7}Li and ^{7}Be, ^{9}Be, ^{10}Be by high-energy protons and α particles in a ^{12}C target have been determined by a high sensitivity mass-spectrometric technique. A method for extracting lithium and beryllium from the irradiated graphite without interference by natural contamination has been developed. Cross sections have been measured for 150 and 600 MeV protons as well as 100 to 140 MeV α-particles. The ^{9}Be and ^{10}Be cross sections from ^{12}C are significantly higher than the corresponding ones on ^{16}O measured previously. The implications of the high values of α-induced cross sections on the study of cosmic-ray propagation are briefly discussed. (auth)

28183 RELATIVISTIC CORRECTIONS TO THE ASYMMETRY OF HIGH-ENERGY NEUTRONS EMITTED IN POLARIZED MUON CAPTURE BY NUCLEI. Piketty, C. A. (Faculte des Sciences, Orsay, France); Procureur, J. Nucl. Phys., B26: 390-412 (1971).

The effects of relativistic corrections on neutron asymmetry in polarized μ-capture by light nuclei (^{12}C–^{28}Si–^{32}S–^{40}Ca) were studied. By describing the nucleus by the Fermi-gas model, for which the relativistic problem can be treated exactly, it is shown that relativistic corrections up to the (inverse nucleon mass)$^{-2}$ (and only) contribute appreciably. Next, using the harmonic-oscillator shell model for the nucleus, it is shown that the M^{-2} corrections do increase significantly the asymmetry that gets positive, increasing with energy and in qualitative agreement with recent experiments. The asymmetry turns out to be rather insensitive to both spin–orbit coupling and final-state interaction. On the contrary, the neutron spectrum depends strongly on the final-state interaction; when included (even in a very crude way), the calculated spectrum fits closely the experiments. (auth)

28184 ANOMALIES OF ENERGY DISTRIBUTION OF α-PARTICLES IN p + ^{11}B → 3α REACTION. Komarov, V. V.; Popova, A. M.; Romanovskii, E. A.; Kalacheva, Z. F.; Sal'man, Kh. Izv. Akad. Nauk SSSR, Ser. Fiz.; 34: 84-8(Jan 1970). (In Russian).

Data obtained on the energy distribution of α particles in the reaction ^{11}B(p,3α) revealed resonances related to the interactions between two α particles in the 0^+ and 2^+ states of the ^{8}Be nucleus. The width of these resonances proved to be much smaller than the width of resonances observed during the scattering of two free α particles. The theory of multi-particle reactions is used for determining the reasons for the observed narrowing of the resonances. Comparisons of theoretical and experimental data showed that the narrowing phenomenon was the result of the third-particle influence on the scattering of the two other particles. (R.V.J.)

28185 VERTEX FUNCTION FOR THE ^{6}Li → α + d PROCESS. Abdel Rida, Al Khor; Blokhintsev, L. D. (Moscow State Univ.). Izv. Akad. Nauk SSSR, Ser. Fiz.; 34: 190-3(Jan 1970). (In Russian).

A three-body model (α particle, neutron, and proton) was used for determining the vertex function describing the virtual decay of ^{6}Li → α + d. (R.V.J.)

28186 APPLICATION OF MATHEMATICAL STATISTICS METHOD FOR CALCULATING CROSS SECTIONS OF ^{16}O(γ,n)^{15}O REACTIONS. Ivanchenko, V. G.; Ratner, B. S. (Lebedev Inst. of Physics, Moscow). Izv. Akad. Nauk SSSR, Ser. Fiz.; 34: 175-8(Jan 1970). (In Russian).

Calculations of cross sections for the photonuclear reaction ^{16}O(γ,n)^{15}O were carried out using the method suggested by V. G. Ivanchenko, and the results were compared with the results of the existing method using the yield curve. Measurements were made on a synchrotron with the maximum γ-quantum energy of 30 MeV and a detection system consisting of a 35 × 30 NaI(Tl) crystal, pulse amplifier, and 100-channel analyzer. The yield curve was measured from the threshold to 22.15 MeV at 0.1 MeV intervals. (R.V.J.)

28187 MASS AND HALF-LIFE OF ^{9}C. Mosher, J. M.; Kavanagh, R. W.; Tombrello, T. A. (California Inst. of Tech., Pasadena). Phys. Rev., C; 3: 438-41(Feb 1971).

The mass of ^{9}C was measured by counting delayed protons near the ^{7}Be(^{3}He,n)^{9}C threshold. The data are consistent with an s-wave threshold at $E^*_{^3He}$ = 8980 ± 5 keV, giving a ^{9}C mass excess of 28,907 ± 4 keV, and confirming the reported deviation of the A = 9,

XUM

lowest T = 3/2 quartet from the quadratic mass formula. The half-life of ^{9}C, measured with a multiscaler, is 126.5 ± 2 msec. (auth)

28188 LARGE ISOSPIN MIXING IN ^{16}O STATES NEAR 18 MeV. Bernstein, E. M.; Shamu, R. E.; Kuo, L. Y.; (and others) (Western Michigan Univ., Kalamazoo). Phys. Rev., C; 3: 427-9 (Feb 1971).

Differential cross sections were measured for the mirror reactions $^{12}C(\alpha,n_0)^{15}O$ and $^{12}C(\alpha,p_0)^{15}N$ for incident energies between 13 and 16 MeV. A striking feature of the data is the existence of a pair of states in ^{16}O; one (17.63 MeV) appears to emit protons and not neutrons, the other (18.10 MeV) appears to emit neutrons and not protons. The total lab widths of these levels are ~180 keV for the 17.63-MeV level and ~250 keV for the 18.10-MeV level. The (α,p) angular distribution near the center of the 17.63-MeV state is similar to the (α,n) angular distribution near the center of the 18.10-MeV state. The results indicate large isospin mixing in the 18.10-MeV state. Evidence that the two states comprise an isospin-mixed doublet formed by strong mixing of a T = 0 and T = 1 state is presented. (auth)

28189 EFFECTIVE OPERATORS IN NUCLEI. Siegel, Stanley Gordon. New Brunswick, N. J.; Rutgers–The State Univ. (1970). 270p. University Microfilms Order No. 71-3103.

Thesis.

The concept of effective charge is used to study the electric multipole moments and transition rates in nuclei in the oxygen and calcium regions of the periodic table. Particular attention is given to quadrupole moments and single-particle electric quadrupole transitions in ^{15}O, ^{15}N, ^{17}O, ^{17}F, ^{39}Ca, ^{39}K, ^{41}Ca, and ^{41}Sc. The effective-charge formalism is developed by means of perturbation theory. A full second-order calculation is performed for ^{17}O and ^{17}F, and a slow convergence (or possible non-convergence) of the perturbation series is indicated. Within the framework of perturbation theory, two other approximation schemes are treated. Each of these schemes—termed the Tamm–Dancoff (TDA) and random-phase approximations (RPA)—consists of a subset of (bubble) diagrams from the full perturbation series. These bubble diagrams can be summed conveniently to all orders in the two-body potential. Electric quadrupole effective charges are calculated in the TDA and RPA with several different "semi-realistic" and "realistic" two-nucleon interactions. The effect of replacing harmonic oscillator by Woods–Saxon radial wave functions in the one-body radial integral $\langle j|r^l|j\rangle$ (l = positive integer) is studied, and the relevance of this effect to the effective charge is discussed. Finally, the effective-charge formalism is generalized to treat the problem of TDA and RPA renormalized two-body matrix elements. Applications to the nuclei ^{18}O, ^{18}F, and ^{18}Ne are given. (Diss. Abstr. Int., B)

28190 ISOSPIN PURITY AT HIGH EXCITATION ENERGIES AS EVIDENCED BY CROSS CORRELATIONS OF MIRROR-CHANNEL FLUCTUATIONS. Detraz, C.; Moss, C. E.; Zafiratos, C. D.; Zaidins, C. S. (Univ. of Colorado, Boulder). Phys. Rev. Lett.; 26: 448-50(22 Feb 1971).

The Ericson fluctuations of the mirror decays $^{15}O + {}^{7}Li$ and $^{15}N + {}^{7}Be$ of a ^{22}Na compound state near 53-MeV excitation energy are found to be correlated; this correlation provides evidence that isospin is a good quantum number at this high excitation energy. (auth)

28191 SHORT NOTE ON EVEN-PARITY STATES OF ^{16}O. Nagai, Hiroyuki (Kyushu Inst. of Tech., Fukuoka); Itaya, Mitsuo. Bull. Kyushu Inst. Technol., Math., Natur. Sci.; No. 17, 47-54 (Mar 1970).

In the double-closed-shell nuclei such as ^{16}O and ^{40}Ca, all nuclear states except the ground state arise from core excitation. The most striking facts in both nuclei are that even-parity excited states, particularly the first excited 0^+ state, are very low, and that the monopole transition from this state to the ground state is very large. In this short note, the authors attempt to explain these properties of the even-parity excited states of ^{16}O. The unperturbed (zero-th order) excitation energy of the even-parity states was estimated to be about 30 to 50 MeV, while experimental value was 6.06 MeV. They attributed the large reduction of the excitation energy not to configuration interaction or the off-diagonal elements of energy matrix, but to unperturbed configuration energy or diagonal matrix elements. They adopted the harmonic-oscillator shell model and calculated the excitation energy of the first excited 0^+ state by employing standard shell-model technique. The calculated value is 11.23 MeV. The calculated monopole matrix element between the ground and excited states is 2.6×10^{-26} cm^2, which is in fair agreement with experimental value. (Japan)

28192 NEW EXPERIMENTAL DATA FOR NEUTRON POLARIZATION FROM $^{11}B(\alpha,n_0)^{14}N$ REACTION, AT LOW ENERGIES. Molea, M.; Pencea, C.; Salagean, O.; Ciocanel, A. (Inst. of Atomic Physics, Bucharest). Rev. Roum. Phys.; 15: 1053-4(1970).

The angular distribution of the neutron polarization from the reaction $^{11}B(\alpha,n)^{14}N$ at 3.4 and 3.8 MeV was measured from 0 to 110°. The data for incident energies between resonances do not change their shape and maximum locations (about 40 and 100°), while the distributions taken at the resonance energies are shifted about 10°. It is concluded that the mechanism of the $^{11}B(\alpha,n)^{14}N$ reaction at low energies is based on multi-level interference in the compound nucleus ^{15}N. (R.W.R.)

28193 ELECTRODISINTEGRATION OF CARBON. Wong, Cho Fai. Saskatoon; Univ. of Saskatchewan (1970). 142p. University Microfilms Order No. 71-3219.

Thesis.

Energy spectra and angular distributions of protons from ^{12}C and ^{13}C produced by electron beams of energies E_0 = 45.9 and 43 MeV, respectively, were measured by using a magnetic spectrometer and solid-state detectors. The (e,pe') cross sections were converted to the corresponding (γ,p) cross sections by using the E1 virtual photon spectrum. Both the energy spectrum and angular distribution of protons from ^{13}C indicate that the center of the giant resonance is at 22.5 MeV excitation and is predominantly of the $p_{\frac{1}{2}}^{-1}d_{\frac{5}{2}}$ configuration. The angular distribution of ^{12}C was found to be forward peaked at large energies. The measurement on ^{13}C shows a broadening of the giant resonance peak, which is centered at around 24 MeV excitation energy and assigned predominantly T = 3/2. Compared with real-photon measurements, these measurements show a larger cross section in the low-energy region ($E_p \leq 5$ MeV), which cannot be explained by the non-ground-state transitions alone. The center of the giant resonance in ^{13}C is higher than that of ^{12}C by approximately 1.5 MeV, the difference of the thresholds of (γ,p) from the two carbon isotopes. If the energy scales are shifted by this amount, the energy spectra of ^{12}C and ^{13}C resemble each other except for possible J splitting and T splitting; in particular, the four finer peaks in the 24-MeV region of ^{13}C may correspond to the J splitting of the levels at 22.5 and 25.5 MeV in ^{12}C by the coupling of a $p_{\frac{1}{2}}$ neutron to the core. The angular distribution of ^{13}C indicates that protons are primarily due to d-wave emission with slight evidence of a larger magnitude in the directions forward of 90° at higher energies. Thus, the angular distributions of both ^{12}C and ^{13}C indicate a predominant d-wave emission. The result of the present measurements suggests that, for the most part, the valence neutron acts as a spectator during the photoexcitation of the giant resonance in carbon. (Diss. Abstr. Int., B)

28194 HIGH-ENERGY PHOTOPROTONS FROM BERYLLIUM. Costa, S. (Univ., Turin); Ferrero, L.; Pasqualini, L.; Sanzone, M. Lett. Nuovo Cim.; 1: 448-52(13 Mar 1971).

Some preliminary results are reported on the proton emission from ^{9}Be induced by quasi-monochromatic photons. Proton spectra were measured at several bremsstrahlung end-points of 50 to 90 MeV. Yield curves were obtained for proton emission at fixed energy, which revealed a resonant behavior in the unfolded cross sections. The proton cross sections were also measured. The data were fitted with the quasi-deuteron model. The ratio between the single-particle cross sections for the emission of 1p and 1s shell protons was calculated and found to be in good agreement with experiment. (L.B.S.)

28195 ISOSPIN PURITY AND DELAYED-PROTON DECAY: ^{17}Ne AND ^{33}Ar. Hardy, J. C.; Esterl, John E.; Sextro, R. G.; Cerny, Joseph (Univ. of California, Berkeley). Phys. Rev., C; 3: 700-18(Feb 1971).

β-delayed proton and γ-ray measurements were used to study the decay of ^{17}Ne and ^{33}Ar. Their half-lives were measured as 109.0 ± 1.0 and 173.0 ± 2.0 msec, respectively, and absolute ft values were determined for their β-decay branches. Precise level energies were measured in ^{17}F and ^{33}Cl, and an earlier discrepancy concerning energies in ^{17}F was resolved. The log ft value for the superallowed decay branch of ^{17}Ne was measured to be 3.29, which indicates an isospin purity of ≥95% for the lowest T = 3/2 state in ^{17}F. In addition, the antianalog configuration is located in ^{17}F and is shown to be the most probable source of the small isospin mixing present in the analog state in that nucleus. The log ft value measured for the superallowed decay branch from ^{33}Ar was 3.34 ± 0.05, a value which suggests an impurity of ~10% in the lowest T = 3/2 state in ^{33}Cl. There is circumstantial evidence that this mixing occurs with four T = 1/2 states which lie within 350 keV of the analog state. (auth)

28196 ELASTIC SCATTERING OF ^{16}O BY ^{48}Ti, ^{40}Ca, ^{27}Al, ^{12}C, ^{7}Li, AND ^{6}Li. Orloff, J.; Daehnick, W. W. (Univ. of Pittsburgh). Phys. Rev., C; 3: 430-8(Feb 1971).

A number of isotopically enriched light targets were bombarded with ^{16}O ions of 36- to 48-MeV energy (lab), and ten elastic angular distributions were measured. All cross sections show strongly destructive interference of nuclear and Coulomb scattering at angles above 30 to 60° cm, and fall orders of magnitude below the

XUM

Coulomb cross section. The data were fitted reasonably well with conventional optical-model calculations, and $\langle\chi^2\rangle$ values between 0.5 and 5.2 could be obtained for all targets. Typically, four-parameter fits were adequate. For the heavier targets the parameter sets are not unique, but were found to have continuous well-depth-geometry ambiguities, which were investigaged in some detail. A procedure to produce in situ clean targets of highly reactive elements is described. (auth)

28197 COMMENT ON THE RESOLUTION OF PHASE-EQUIVALENT DISCRETE AMBIGUITIES IN THE OPTICAL-MODEL ANALYSIS OF $^{16}O + ^{16}O$. Eck, John S. (Kansas State Univ., Manhattan). Phys. Rev., C; 3: 949-52(Feb 1971).

A method, described earlier, which has been shown to help resolve the question of phase-equivalent discrete ambiguities in the optical-model-potential description of heavy-ion scattering is applied to the case of $^{16}O + ^{16}O$ elastic scattering. (auth)

28198 LOW-ENERGY NEUTRON–OXYGEN SCATTERING DERIVED FROM TWO-BODY FORCES. MacKellar, Alan D. (Univ. of Kentucky, Lexington); Reading, J. F.; Kerman, A. K. Contract AT(30-1)-2098. Phys. Rev., C; 3: 460-5(Feb 1971).

Low-energy n-^{16}O elastic scattering phase shifts are calculated from potential matrix elements using nuclear-reaction theory. As in bound-state calculations, it is found to be essential to include second-order contributions. When this is done the theoretical calculations which contain essentially no adjustable parameters reproduce the experimental phase shifts reasonably well, the disagreement between theory and experiment being generally no larger than the spread in the theoretical results produced by different two-body forces. A nonlocality of the optical potential arises naturally out of the calculation. It is possible to see the effect of this by comparing the internal wave function to that obtained using a Woods–Saxon well with parameters adjusted to give the same phase shift, i.e., one can investigate the Perey effect. The scattering wave function is found to be about 30 to 50% smaller in the potential region than the corresponding wave function calculated from the Woods–Saxon well. (auth)

28199 OPTICAL-POTENTIAL SCATTERING OF NUCLEONS BY CARBON AT MEDIUM ENERGIES. Chalmers, Joseph S. (Univ. of Louisville, Ky.). Phys. Rev., C; 3: 968-72(Feb 1971).

The elastic scattering of nucleons by carbon, at incident energies of 142, 210, and 330 MeV, is calculated from an optical potential retaining all terms to second order in the N–N amplitudes. The amplitudes are calculated using recent N–N phase-parameter sets obtained by the Yale, Livermore, and Michigan State Groups. Nuclear correlation functions of both the Fermi and Brueckner–Gammel types are used to represent nuclear structure. Comparison with experiment is made in order to distinguish among different N–N phase-parameter sets, and among different types of nuclear correlation functions. (auth)

28200 INTERNAL BREMSSTRAHLUNG ACCOMPANYING THE ORBITAL-ELECTRON CAPTURE IN ^{7}Be. Lancman, H.; Lebowitz, Jacob (Brooklyn Coll.). Phys. Rev., C; 3: 465-8(Feb 1971).

The spectrum of the internal bremsstrahlung accompanying the electron-capture decay of ^{7}Be was measured in coincidence with the 477-keV γ rays. From the extrapolated end-point energy of the spectrum, the transition energy to the first excited state of ^{7}Li was determined to be 395 ± 25 keV. The intensity of the internal bremsstrahlung in the energy range from 120 to 360 keV was determined to be $(5.45 \pm 1.1) \times 10^{-5}$ per ordinary nonradiative 1s capture (based on a theoretically predicted L/K ratio of 12.4×10^{-2}) as compared with the value of 7.86×10^{-5} predicted by the theory of Martin and Glauber. (auth)

28201 DYNAMICAL CORRELATION IN ^{6}Li AND INELASTIC ELECTRON SCATTERING. Lodhi, M. A. K. (Texas Tech Univ., Lubbock). Phys. Rev., C; 3: 503-8(Feb 1971).

A simple nucleon-nucleon correlation function was invoked in the independent-particle shell-model (IPSM) wave functions of ^{6}Li. This was assumed due to a substantial residual two-body interaction in addition to the IPSM Hamiltonian of ^{6}Li. Using the variational principle, the excitation energy of the first excited state of ^{6}Li was obtained in good agreement with the experimental value. The nuclear form factor for the inelastic electron scattering and the reduced transition probability were calculated and compared with experimental data and other calculated results. (auth)

28202 INVESTIGATION OF STATES IN ^{17}O VIA NEUTRON-POLARIZATION MEASUREMENTS IN THE $^{13}C(\alpha,n)^{16}O$ REACTION. Baker, W. L.; Busch, C. E.; Keane, J. A.; Donoghue, T. R. (Ohio State Univ., Columbus). Phys. Rev., C; 3: 494-502(Feb 1971).

Neutron-polarization angular distributions were measured at six α-particle energies between 3.36 and 4.80 MeV for the $^{13}C(\alpha,n_0)^{16}O$ reaction in order to investigate the level structure of ^{17}O between 8.7 and 10.2 MeV. These measurements were analyzed together with the previous cross-section data of Walton, Clement, and Boreli and Kerr, Morris, and Risser using an S-matrix search code to yield a number of J^π assignments to ^{17}O levels in this energy interval. Although most assignments agreed with previous results, the assignment for the 9.95-MeV state must be changed to $^5/_2^+$. The existence of broad states near 8.7 and 9.6 MeV were confirmed and assigned J^π values of $^1/_2^-$ and $^3/_2^-$, respectively. (auth)

28203 LIFETIME OF THE 981-keV STATE IN ^{8}Li. Throop, M. J. (Univ. of Iowa, Iowa City); Youngblood, D. H.; Morrison, G. C. Phys. Rev., C; 3: 536-43(Feb 1971).

The lifetime of the 981-keV state in ^{8}Li produced in the $D(^{7}Li,p)^{8}Li^*$ reaction was measured by the two-backing variant of the Doppler-shift attenuation method. The resulting mean life was $\tau_m = 10.1 \pm 4.5$ fsec. This result is in agreement with the shell-model prediction of Cohen and Kurath, and also with that of Barker. The large error limits preclude a detailed test of either prediction. (auth)

28204 SURVEY OF (p,t) REACTIONS IN THE 1p SHELL. Kahana, S. (Brookhaven National Lab., Upton, N. Y.); Kurath, D. Phys. Rev., C; 3: 543-51(Feb 1971).

A comprehensive survey of 21 (p,t) reactions for a wide range of 1p-shell nuclei is made using zero-range distorted-wave Born-approximation codes and previously calculated two-particle fractional parentage coefficients. Average optical parameters are used for the proton and triton potentials in an attempt to relate magnitudes of transitions in different nuclei. A reasonable fit is obtained to the experimental data, but there remain discrepancies in strong transitions for target nuclei with $A \geq 14$. An effect of (2s-1d) admixture which acts differently in L = 0 and L = 2 transfer is proposed as a likely explanation of this difficulty. (auth)

28205 STUDY OF ^{12}C STATES USING THE $^{11}B(^{3}He,d)^{12}C$ REACTION. Reynolds, G. M.; Rundquist, D. E.; Poichar, R. M. (Univ. of Michigan, Ann Arbor). Phys. Rev., C; 3: 442-7(Feb 1971).

States in ^{12}C were studied using the $^{11}B(^{3}He,d)^{12}C$ reaction at a ^{3}He energy of 44.0 MeV. Energy spectra were obtained to 26-MeV excitation in ^{12}C. The results indicate the presence of a positive-parity state at 11.16 ± 0.05 MeV having a width of 550 ± 100 keV. It is suggested to be the 2^+ member of an α-cluster band based on the 0^+ state at 7.65 MeV. There is no evidence of a state at 14.7 MeV. The 4^-, $(p_{\frac{3}{2}})^{-1}(d_{\frac{5}{2}})$ T = 0 and T = 1 states are located at 18.27 and 19.56 MeV, respectively. In the region of the giant dipole resonance in ^{12}C, there is a peak at 22.4 MeV. (auth)

Nuclear Properties and Reactions, $20 \leq A \leq 89$

Refer also to abstracts 26547, 27836, 27914, 27953, 28169, 28170, 28178, 28179, 28183, 28189, 28195, 28196, 28289–28291, 28293, 28294, 28340, 28344, 28400, 28401, 28413, 28421, 28440, 28441, 28505, and 28509.

28206 (ANU-P-508) NOTE ON THE CROSS SECTION OF THE $^{25}Mg(\tau,\gamma)^{28}Si$ REACTION. Davidson, W. F.; Black, J. L.; Najam, M. R. (Australian National Univ., Canberra, Research School of Physical Sciences); Spicer, B. M. (Melbourne Univ., Parkville (Australia). School of Physics). [1970]. 8p. Dep. NTIS (U. S. Sales Only).

The differential cross section for the $^{25}Mg(^{3}He,\gamma)^{28}Si$ reaction was measured at $E_{^{3}He}$ 4.44, 6.08, 6.15, and 8.26 MeV, using a large NaI crystal spectrometer. The smallness of the observed cross section suggests that 3p–3h states play an insignificant role in explaining the intermediate structure observed above the ^{28}Si giant resonance in a recent study of the $^{28}Si(\gamma,n)^{27}Si$ reaction. (auth) (Australia)

28207 (ANU-P-517) A STUDY OF RESONANCES IN THE $^{29}Si(p,\gamma)^{30}P$ REACTION. Din, G. U.; Davis, J. R. (Australian National Univ., Canberra. Dept. of Nuclear Physics). [1970]. 18p. Dep. NTIS (U. S. Sales Only).

Gamma-ray decay schemes of 14 resonances in the $^{29}Si(p,\gamma)^{30}P$ reaction in the range E_p = 900–2200 keV were obtained with high resolution Ge(Li) detectors. Consistent resonance decay schemes were derived, along with decay schemes of bound levels. Decay to bound levels at 3.84, 4.74, 4.94, 5.21, 5.51, and 5.70 MeV was observed in this reaction for the first time. New results were obtained for the decay of some of the bound levels. The reported level at 4.458 MeV was confirmed. The decay schemes of the E_p = 1110, 1664, 1850, 1975, and 2070 keV resonances indicate they are predominantly T = 0 levels, whereas the 2105 and 2115 keV reso-

nances are probably the split analogue of a T = 1 level in ^{30}Si. (auth)

28208 (ANU-P-521) SEARCH FOR HIGH-SPIN STATES IN ^{27}Al. Carter, K. W.; Kean, D. C.; Piluso, C. J.; Spear, R. H. (Australian National Univ., Canberra. Research School of Physical Sciences). [1971]. 24p. Dep. NTIS (U. S. Sales Only).

A search has been made for high-spin states in ^{27}Al in the range of excitation energies E_x from 4.8 to 8.0 MeV using the reactions $^{12}C(^{16}O,p)^{27}Al$ and $^{24}Mg(\alpha,p)^{27}Al$. Gamma-ray branching ratios and proton-gamma angular correlations have been measured for prospective high-spin states. Although no unambiguous spin and parity assignments were obtained, it is argued that states at E_x = 5499, 6716, 6952, 7226, and 7441 keV probably have spins and parities $11/2^+$, $9/2^+$, $11/2^+$, $9/2^+$ or $11/2^+$, and $13/2^+$, respectively. An attempt is made to interpret the results in terms of the strong-coupling rotational model. (auth) (Australia)

28209 (CERN-70-30(Vol.1), pp 383-5) MEASUREMENT OF THE SPIN AND NUCLEAR MAGNETIC MOMENT OF THE 408 msec ^{20}Na. Bonn, J.; Otten, E. W.; von Platen, Ch. (Heidelberg Univ. (West Germany). Physikalisches Institut (I)); Linder, W.; Mueller, H.; Schweickert, H. (Kernforschungszentrum, Karlsruhe (West Germany). Zyklotron-Laboratorium).

In International conference on the properties of nuclei far from the region of beta-stability; Leysin, Switzerland (31 Aug 1970).

^{20}Na from the reaction $^{20}Ne(d,2n)^{20}Na$ at 30 MeV was polarized by the method of spin exchange with ^{87}Rb. The asymmetry of the β decay was time dependent with a maximum value of 2.5%. Numerical evaluation of the $\Delta F = 0$ resonances yielded $\mu_I(^{20}Na)$ = 0.368(3) nm. (R.W.R.)

28210 (CERN-70-30(Vol.1), pp 447-55) BETA-NEUTRINO CORRELATIONS AND RECOIL NUCLEAR ALIGNMENT EFFECTS IN LIGHT DELAYED PARTICLE EMITTERS. Macfarlane, Ronald D. (Niels Bohr Institutet, Copenhagen (Denmark). Texas Agricultural and Mechanical Univ., College Station); Nickels, Robert J. (Niels Bohr Institutet, Copenhagen (Denmark)); Oakey, Neil S. (Texas Agricultural and Mechanical Univ., College Station).

In International conference on the properties of nuclei far from the region of beta-stability; Leysin, Switzerland (31 Aug 1970).

The beta-delayed alpha decay of ^{20}Na is discussed. Realistic $\beta^+-\nu$ directional correlation coefficients and the nuclear longitudinal polarization and alignment of the β-recoils can be obtained from the shape of the peaks in the singles α spectrum. (R.W.R.)

28211 (CERN-70-30(Vol.1), pp 517-18) REASSESSMENT OF SOME NEUTRON YIELDS FROM THE LONGER-LIVED DELAYED NEUTRON EMITTERS. del Marmol, P.; Fettweis, P.; Perricos, D. C. (Centre d'Etude de l'Energie Nucleaire, Mol (Belgium)).

In International conference on the properties of nuclei far from the region of beta-stability; Leysin, Switzerland (31 Aug 1970).

The delayed-neutron (dn) activity of ^{137}I, measured with respect to that of the 56-sec dn activity of ^{235}U, yielded a dn ratio $^{137}I/^{87}Br = 4.85 \pm 0.20$. Also measured after chemical separation, the ratio $^{88}Br/^{87}Br$ was 1.7 ± 0.2. Delayed-neutron yields per 10^4 fissions were found to be 5.8 ± 0.4 for ^{87}Br, 28.1 ± 2.3 for ^{137}I second dn group, and 9.9 ± 1.4 for ^{88}Br second dn group. The neutron emission probability was measured to be 2.1 ± 0.3 for ^{87}Br and 8.6 ± 1.2 for ^{137}I. Half-lives for these isotopes were 55.6 ± 0.3 sec (^{87}Br) and 24.7 ± 0.2 sec (^{137}I). All results are compared with those of other investigators. (R.W.R.)

28212 (CERN-70-30(Vol.1), pp 519-20) DELAYED NEUTRON EMISSION FROM SELENIUM ISOTOPES: IDENTIFICATION OF ^{89}Se. Tomlinson, L.; Hurdus, M. H. (Atomic Energy Research Establishment, Harwell (England)).

In International conference on the properties of nuclei far from the region of beta-stability; Leysin, Switzerland (31 Aug 1970).

The isotopes ^{87}Se, ^{88}Se, and ^{89}Se were produced by the thermal-neutron fission of ^{235}U and then separated within 1 sec of their formation using high-speed radiochemistry. ^{89}Se is a new isotope, identified for the first time. Half-lives and neutron branching ratios for these isotopes are given and compared with published values. (R.W.R.)

28213 (CERN-70-30(Vol.2), pp 911-15) ON- AND OFF-BEAM GAMMA SPECTROSCOPY ON NEUTRON DEFICIENT ISOTOPES OF Ge, Se, Br, AND Kr. Nolte, E.; Kutschera, W.; Shida, Y.; Morinaga, H. (Technische Universitaet, Munich (West Germany)).

In International conference on the properties of nuclei far from the region of beta-stability; Leysin, Switzerland (31 Aug 1970).

Neutron-deficient isotopes in the Kr region were produced by bombarding targets of enriched nickel isotopes with 42- to 57-MeV ^{16}O and 36-MeV ^{12}C beams. Gamma spectra were measured at 0 and 90° with two Ge(Li) detectors. Excitation functions for gamma yields are shown for the reactions $^{60}Ni(^{16}O,pn)^{74}Br$, $^{60}Ni(^{16}O,2p)^{74}Se$, and $^{60}Ni(^{16}O,2n)^{74}Kr$. Level schemes are proposed for ^{74,76,78}Kr, ^{72,74}Se, and ^{68}Ge. The new isotope ^{72}Br decays with a half-life of ~1.7 min to the 2_1^+ and 2_2^+ states in ^{72}Se. (R.W.R.)

28214 (CERN-70-30(Vol.2), pp 1105-13) PRODUCTION AND DECAY PROPERTIES OF SOME SHORTLIVED COBALT NUCLEI. Jongsma, H. W.; de Lange, J. C.; Boddendijk, J. C.; Kamermans, T.; Verheul, H. (Vrije Universiteit, Amsterdam (Netherlands). Natuurkundig Laboratorium).

In International conference on the properties of nuclei far from the region of beta-stability; Leysin, Switzerland (31 Aug 1970).

Several new gamma transitions were observed in the decay of the following isotopes: ^{62}Co (13.5 min), ^{62}Co (1.4 min), ^{62}Cu (9.73 min), and ^{63}Co (26.7 sec). (auth)

28215 (CERN-70-30(Vol. 2), pp 1137) DECAY OF ^{90}Nb, ^{89m,89}Nb, ^{85m,85}Y AND ^{85m}Sr. Arlt, R.; Kracik, B.; Musiol, G.; Tran Thanh Minh (Joint Inst. for Nuclear Research, Dubna (USSR)).

In International conference on the properties of nuclei far from the region of beta-stability; Leysin, Switzerland (31 Aug 1970).

Spin-parity assignments are given for the energy levels of ^{85}Sr, ^{89}Zr, and ^{90}Zr obtained from beta decay of the corresponding mother nuclei produced by proton bombardment. (R.W.R.)

28216 (COO-1746-54) BETA-GAMMA CIRCULAR POLARIZATION CORRELATION AND NUCLEAR MATRIX ELEMENTS OF ^{76}As. Smith, H. A.; Simms, P. C. (Purdue Univ., Lafayette, Ind. Dept. of Physics). [1971]. 27p. Dep. NTIS.

The $\beta-\gamma$ circular polarization correlation P_γ for the 2.41-MeV β transition of ^{76}As was measured as an average value over the energy interval E_β = 1.4 to 2.0 MeV at an average angle $\theta_{\beta\gamma}$ = 158 degrees. Previous experimental data, this new value for P_γ, and theoretical arguments are used to set limits on the nuclear matrix elements and to investigate the diagonality of the Coulomb hamiltonian. The analysis shows that matrix elements which change the angular momentum by 0, 1, and 2 units all contribute with approximately equal strength to the transition. The matrix element analysis indicates that the A_3 term in P_γ is negligible compared to the A_1 term. When A_3 is set equal to zero, the experimental data gives the following value for P_γ: P_γ(1.4 MeV < E_β < 2.0 MeV, $\theta_{\beta\gamma}$ = 180°) = 0.105 ± 0.02. (auth)

28217 (LUNP-7013) PROTON HOLE STATES EXCITED BY MONOENERGETIC GAMMA-QUANTA. Wene, Clas-Otto (Lund Inst. of Tech. (Sweden). Dept. of Nuclear Physics). Oct 1970. 24p. Dep. NTIS (U. S. Sales Only).

Elements that can be procured in thin foils were irradiated with monoenergetic gamma quanta from the reaction $^7Li(p,\gamma)^8Be$. The energies of the photoprotons from the foil were measured with silicon surface barrier detectors. The conditions under which these protons give information about proton hole states are discussed. Results from runs on a foil of natural copper are given. (auth) (Sweden)

28218 (NP-18674) STATISTICAL MODEL CALCULATIONS OF ^{56}Fe NEUTRON CROSS SECTION. Bloom, S. D.; Green, J. M.; Hubbard, H. W.; Moszkowski, S. A. (RAND Corp., Santa Monica, Calif.). Sep 1970. 30p. (R-591).

Certain neutron cross sections for ^{56}Fe are calculated and results are compared with available experimental data. The unknown excited states of the daughter nucleus at states higher than the highest experimental results were characterized by means of Kanestrom's theory, which describes the number density of the high-lying states as a function of excitation energy and nuclear spin. The Kanestrom statistical model was grafted onto the NEARREX computer program (see RM-5899). The revised code generates excited states for both (n,p) and (nn') reactions and accounts for the competition between these reactions. The single particle level spacing, the spin parameter, and the pairing energy parameter were chosen to fit 4 independent sets of data: the experimental values for the distribution of excited states of ^{56}Fe and ^{54}Mn, and also the total low energy (nn') and (n,p) cross sections on ^{56}Fe. Subsequent calculations, based on these parameters, were self-consistent over a wide range of high neutron energies and agreed with the experimental data. (35 references.) (auth)

28219 (NRCN-254) THE MEASUREMENT OF ENERGY LEVELS' WIDTH IN THE 6-9 MeV REGION. Has, M. (Israel Atomic Energy Commission, Beersheba. Nuclear Research Center-Negev). May 1970. 46p. (In Hebrew). NTIS (U. S. Sales Only).

Energy-level widths in the region 6 to 9 MeV were measured in various nuclei using resonance scattering of nickel capture gamma rays. It was done by measuring the $\langle\sigma_{\gamma\gamma}\rangle$ cross section, the self-absorbing effect, and the temperature effect. The results are as follows: 0.21 ± 0.04 eV for ^{66}Zn, 0.09 ± 0.02 eV for ^{80}Se, 0.1 ± 0.05 eV for ^{86}Sr, 0.12 ± 0.03 eV for ^{120}Sn, 0.24 ± 0.06 eV for ^{130}Te, and 6.5 ± 0.5 eV for ^{150}Sm. Axel's theory was used in analyzing the results. (TSS)

28220 (UJV-2553-F) THE ELECTROEXCITATION OF ^{32}S IN THE REGION OF THE DIPOLE RESONANCE. Bely, Yu. I.; Kabachnik, N. M.; Neudatchin, V. G.; Yudin, N. P.; Majling, L.; Rizek, J. (Ceskoslovenska Akademie Ved, Rez. Ustav Jaderneho Vyzkumu). [1970]. 22p. Dep. NTIS (U. S. Sales Only).

The C1 + E1 and M2 form factors for inelastic scattering of high-energy electrons by ^{32}S in the region of the giant dipole resonance were calculated. The wave functions of excited states were obtained in terms of a microscopic "particle-hole" approach of the shell model taking into account the configurational splitting and coupling of the particle-hole excitations to one- and two-phonon states. This corresponds to the diagonalization of the 64 × 64 matrix for the 1^- states and of the 85 × 85 matrix for the 2^- states. A good fit with the experimental data of Afanasyev and coworkers for the ^{32}S excitation curve at different momentum transfers $q \leq 1$ fm^{-1} was obtained though the agreement of the γ-quanta absorption cross sections and the (γ,n) reaction with the experiment is not satisfactory. It is emphasized that the cross sections (γ,γ), (γ,p_0) and (p,γ_0), the photonucleon spectra and the transverse electron scattering form factors are particularly sensitive to the configurational composition of wave functions in different regions of the ^{32}S excitation curve. The available experimental data confirm the presence of the configurational splitting of the giant resonance, however, a more comprehensive investigation of this interesting phenomenon is desirable. (auth)

28221 DECAYS OF ^{70a}Cu, ^{70b}Cu, AND ^{67}Ni. Taff, L. M.; Koene, B. K. S.; Van Klinken, J. (Rijksuniversiteit, Groningen, Netherlands). Nucl. Phys.; A164: 565-75(1971).

Three activities observed after 14 MeV neutron irradiation of ^{70}Zn have been assigned to two isomers of ^{70}Cu(^{70a}Cu, $T_{\frac{1}{2}}$ = 5 ± 1 s, and ^{70b}Cu, $T_{\frac{1}{2}}$ = 42 ± 3 s) and to ^{67}Ni($T_{\frac{1}{2}}$ = 18 ± 4 s). Ge(Li) single γ-ray spectra, NaI–Ge(Li)$\gamma\gamma$ coincidences, plastic scintillation single β-ray spectra and plastic-Ge(Li) $\beta\gamma$ coincidences were measured. Levels in ^{70}Zn are proposed at 884.8 (2^+), 1786.5 (4^+) and 3038.2 (>3, $^-$) keV on the basis of coincidence spectra. Evidence suggests spins and parities of (1^+) and (5^-) for ^{70a}Cu and ^{70b}Cu, respectively. A probable level in ^{67}Cu is suggested at 1072.2 keV from the decay of ^{67}Ni. Many additional γ-rays were observed but were too weak for coincidence studies and could not be placed in the decay schemes. Some results of reaction studies are discussed. (auth)

28222 ANALOG RESONANCES FORMED IN ISOSPIN FORBIDDEN REACTIONS AND SPLITTING OF THE E1 GIANT RESONANCE. Hanna, Stanley S. (Stanford Univ., Calif.). pp 3-27 of Nuclear Isospin. /Anderson, John D. (ed.). New York; Academic Press, Inc. (1969).

From second conference on nuclear isospin; Pacific Grove, Calif. (13 Mar 1969). See CONF-690310.

28223 PROPERTIES OF ANALOG RESONANCES FORMED IN DIRECT REACTIONS DECAYING VIA ISOSPIN-FORBIDDEN MODES. McGrath, Robert L. (State Univ. of New York, Stony Brook). pp 29-50 of Nuclear Isospin. /Anderson, John D. (ed.). New York; Academic Press, Inc. (1969).

From second conference on nuclear isospin; Pacific Grove, Calif. (13 Mar 1969). See CONF-690310.

28224 GAMMA-RAY TRANSITIONS IN LIGHT NUCLEI. Endt, P. M. (Rijksuniversiteit, Utrecht). pp 51-63 of Nuclear Isospin. /Anderson, John D. (ed.). New York; Academic Press, Inc. (1969).

From second conference on nuclear isospin; Pacific Grove, Calif. (13 Mar 1969). See CONF-690310.

28225 SOME M1 TRANSITIONS WITH $\Delta = 1$ IN ^{24}Mg, ^{27}Al AND ^{28}Si. Lawergren, B.; Nessin, N.; Taylor, I. J. (Columbia Univ., New York). pp 113-16 of Nuclear Isospin. /Anderson, John D. (ed.). New York; Academic Press, Inc. (1969).

From second conference on nuclear isospin; Pacific Grove, Calif. (13 Mar 1969). See CONF-690310.

28226 ^{51}Ti GROUND-STATE ANALOGUE. Maripuu, S. (Utrecht Univ.). pp 119-22 of Nuclear Isospin. /Anderson, John D. (ed.). New York; Academic Press, Inc. (1969).

From second conference on nuclear isospin; Pacific Grove, Calif. (13 Mar 1969). See CONF-690310.

28227 ISOBARIC ANALOG STATES IN (γ,p) REACTIONS ON N = 50 NUCLEI. Shoda, K.; Sugawara, M.; Saito, T.; Miyase, H. (Tohoku Univ., Sendai). pp 125-30 of Nuclear Isospin. /Anderson, John D. (ed.). New York; Academic Press, Inc. (1969).

From second conference on nuclear isospin; Pacific Grove, Calif. (13 Mar 1969). See CONF-690310.

28228 EVIDENCE FOR SPLITTING OF A BOUND ISOBARIC ANALOG STATE IN ^{58}Co. Becchetti, F. D. Jr. (Univ. of Minnesota, Minneapolis); Dehnhard, D.; Dzubay, T. G. Contract AT(11-1)-1265. pp 171-7 of Nuclear Isospin. /Anderson, John D. (ed.). New York; Academic Press, Inc. (1969).

From second conference on nuclear isospin; Pacific Grove, Calif. (13 Mar 1969). See CONF-690310.

28229 L = O TRANSITIONS TO O^+ STATES OF N = 29 NUCLEI. Belote, T. A.; Dorenbusch, W. E.; Rapaport, J. (Massachusetts Inst. of Tech., Cambridge). Contract AT(30-1)-2098. pp 253-6 of Nuclear Isospin. /Anderson, John D. (ed.). New York; Academic Press, Inc. (1969).

From second conference on nuclear isospin; Pacific Grove, Calif. (13 Mar 1969). See CONF-690310.

28230 PROPOSAL OF $d3/2^{-1}p3/2$ ANALOGUE STATES IN ^{40}Ca. Bommer, J.; Fuchs, H.; Grabisch, K.; Roeschert, G. (Hahn-Meitner-Institut fuer Kernforschung, Berlin). pp 257-62 of Nuclear Isospin. /Anderson, John D. (ed.). New York; Academic Press, Inc. (1969).

From second conference on nuclear isospin; Pacific Grove, Calif. (13 Mar 1969). See CONF-690310.

28231 NUCLEAR STRUCTURE STUDIES OF ^{51}V BY ^{50}Ti (^{3}He,d) REACTION. Maheshwari, P. N. (Bhabha Atomic Research Centre, Bombay). pp 281-9 of Nuclear Isospin. /Anderson, John D. (ed.). New York; Academic Press, Inc. (1969).

From second conference on nuclear isospin; Pacific Grove, Calif. (13 Mar 1969). See CONF-690310.

28232 A SEARCH FOR ISOSPIN MIXING USING THE (^{3}He,t) REACTION. Roos, P. G. (Univ. of Maryland, College Park); Goodman, C. D. pp 297-301 of Nuclear Isospin. /Anderson, John D. (ed.). New York; Academic Press, Inc. (1969).

From second conference on nuclear isospin; Pacific Grove, Calif. (13 Mar 1969). See CONF-690310.

28233 ^{24}Mg$(\alpha,d)^{28}$Al–A TEST OF THE $\Delta T = O$ SELECTION RULE. Zafiratos, C. D. (Univ. of Colorado, Boulder). pp 303-5 of Nuclear Isospin. /Anderson, John D. (ed.). New York; Academic Press, Inc. (1969).

From second conference on nuclear isospin; Pacific Grove, Calif. (13 Mar 1969). See CONF-690310.

28234 PARTICLE-CORE STRUCTURE IN THE SPECTRA OF THE STRONTIUM NUCLEI. Cosman, E. R.; Kalish, R.; Kossler, J.; and others (Massachusetts Inst. of Tech., Cambridge). pp 309-13 of Nuclear Isospin. /Anderson, John D. (ed.). New York; Academic Press, Inc. (1969).

From second conference on nuclear isospin; Pacific Grove, Calif. (13 Mar 1969). See CONF-690310.

28235 ANALOG SPIN MIXING IN ^{49}Sc. Payne, G. L.; Perez, J. D. (Univ. of Maryland, College Park). pp 353-9 of Nuclear Isospin. /Anderson, John D. (ed.). New York; Academic Press, Inc. (1969).

From second conference on nuclear isospin; Pacific Grove, Calif. (13 Mar 1969). See CONF-690310.

28236 ANALYSIS OF ELASTIC AND INELASTIC ANALOGUE-STATE RESONANCES USING COUPLED OPTICAL EQUATIONS. Spencer, J. E.; Cosman, E. R.; Kerman, A. K.; Enge, H. A. (Massachusetts Inst. of Tech., Cambridge). pp 421-5 of Nuclear Isospin. /Anderson, John D. (ed.). New York; Academic Press, Inc. (1969).

From second conference on nuclear isospin; Pacific Grove, Calif. (13 Mar 1969). See CONF-690310.

28237 FINE STRUCTURE OF THE ISOBARIC ANALOGS OF THE GROUND AND SECOND EXCITED STATES OF ^{63}Ni. Browne, J. C. (Duke Univ., Durham, N. C.); Lindstrom, D. P.; Moses, J. D. pp 573-8 of Nuclear Isospin. /Anderson, John D. (ed.). New York; Academic Press, Inc. (1969).

From second conference on nuclear isospin; Pacific Grove, Calif (13 Mar 1969). See CONF-690310.

28238 POLARIZATION MEASUREMENTS FOR ^{88}Sr(p,p)^{88}Sr NEAR ISOBARIC ANALOG RESONANCES. Ellis, J. L.; Haeberli, W. (Univ. of Wisconsin, Madison). pp 585-9 of Nuclear Isospin. /Anderson, John D. (ed.). New York; Academic Press, Inc. (1969).

From second conference on nuclear isospin; Pacific Grove, Calif. (13 Mar 1969). See CONF-690310.

28239 STUDY OF ISOBARIC ANALOGUE RESONANCES IN ELASTIC SCATTERING OF POLARIZED PROTONS FROM ^{88}Sr, ^{90}Zr, ^{92}Zr, ^{94}Zr, ^{92}Mo, ^{142}Ce, ^{144}Nd, ^{146}Nd. Clausnitzer, G.; Fleischmann, R.; Graw, G.; Wienhard, K. (Univ., Erlangen, Ger.). pp 629-33 of Nuclear Isospin. /Anderson, John D. (ed.). New York; Academic Press, Inc. (1969).

From second conference on nuclear isospin; Pacific Grove, Calif. (13 Mar 1969). See CONF-690310.

28240 RESONANCE STRUCTURE IN THE ^{88}Sr(p,p') OCTUPOLE TRANSITION. Cosman, E. R. (Massachusetts Inst. of Tech., Cambridge); Kalish R.; Armstrong D. D.; Britt, H. C. Contract AEC(30-1)-2098. pp 635-7 of Nuclear Isospin. /Anderson, John D. (ed.). New York; Academic Press, Inc. (1969).

From second conference on nuclear isospin; Pacific Grove, Calif. (13 Mar 1969). See CONF-690310.

28241 SPIN ASSIGNMENT FOR TWO ISOBARIC ANALOG RESONANCES IN ^{76}Se FROM THE NEUTRON DECAY. Finckh, E.; Jahnke, U.; Schreiber, B.; Weidinger, A. (Hahn-Meitner-Institut, Berlin). pp 655-9 of Nuclear Isospin. /Anderson, John D. (ed.). New York; Academic Press, Inc. (1969).

From second conference on nuclear isospin; Pacific Grove, Calif. (13 Mar 1969). See CONF-690310.

28242 ISOBARIC ANALOG RESONANCES IN PROTON SCATTERING FROM ^{86}Kr. Hollas, C. L.; Hiddleston, H. R.; Mistry, V. D.; Riley, P. J. (Univ. of Texas, Austin). pp 667-71 of Nuclear Isospin. /Anderson, John D. (ed.). New York; Academic Press, Inc. (1969).

From second conference on nuclear isospin; Pacific Grove, Calif. (13 Mar 1969). See CONF-690310.

28243 COULOMB DISPLACEMENT ENERGIES FOR EXCITED STATES IN NUCLEI AROUND ^{28}Si. Martin, S.; Santo, R. (Max-Planck-Institut fuer Kernphysik, Heidelberg). pp 813-17 of Nuclear Isospin. /Anderson, John D. (ed.). New York; Academic Press, Inc. (1969).

From second conference on nuclear isospin; Pacific Grove, Calif. (13 Mar 1969). See CONF-690310.

28244 INELASTIC SCATTERING OF VERY LOW ENERGY PIONS FROM NUCLEI. Mackintosh, R. S. (Australian National Univ., Canberra). Phys. Lett.; 34B: 465-8(29 Mar 1971).

Inelastic scattering of 10-MeV pions leading to the 2^+ state of ^{24}Mg is studied theoretically. The possibility of obtaining information concerning the nuclear structure and the pionic optical potential subject to the experimental possibilities is demonstrated. (auth)

28245 CONFIGURATION MIXING AND EFFECTIVE CHARGES. De Kock, P. R.; Glaudemans, P. W. M. (State Univ., Utrecht). Phys. Lett.; 34B: 280-2(1 Mar 1971).

The E2 transition rates between low-lying states in ^{33}S were investigated within various shell model spaces. In addition the groundstate quadrupole moments of sd-shell nuclei were calculated with pure configurations. The magnitude of the effective charge, which compensates for truncations in the shell model space, was studied as a function of shell model space for ^{33}S and of mass number for the quadrupole moments. (auth)

28246 DECAY STUDY OF ^{76}Br. Ladenbauer-Bellis, I. M.; Bakhru, H.; Bakhru, R. (Yale Univ., New Haven). Can. J. Phys.; 49: 54-60(1 Jan 1971).

The decay of bromine-76 was studied using high resolution Ge(Li) detectors in singles and coincidence mode. Bromine-76 was produced via various reactions, i.e., ^{75}As(α,3n),^{76}Br and ^{65}Cu(^{14}N,3n), ^{76}Kr(14.8 h decay to ^{76}Br). The results of these experiments verified the previously reported levels of ^{76}Se, studied by (d,d') reaction. In addition to the previously described transitions, the following levels in ^{76}Se were observed: 1689.5, 1942, 2890, 2949, 3600, 3910, 4030, 4140, 4570 keV. Accurate energies for the various γ rays were obtained using several Ge(Li) detectors in conjunction with a PDP-8/I computer. The mass difference between ^{76}Br/^{76}Se was measured to be 4680 ± 100 keV. A comparison of the level schemes of the even-even, neutron deficient Se isotope is given. (auth) (Canada)

28247 THE CONTACT DENSITY OF CONDUCTION ELECTRONS IN IRON AND THE ISOMER SHIFT OF ^{57}Fe. Pleiter, F.; Kolk, B. (Univ., Groningen, Netherlands). Phys. Lett.; 34B: 296-8(1 Mar 1971).

The contact density of conduction electrons is derived from measured conversion electron spectra of ^{57}Fe in different metallic hosts. For iron, the result is $\rho_C(0) = (8.9 \pm 0.9)\ a_0^{-3}$ is the Bohr radius). Combination of the isomer shift determined from Mössbauer spectra and the relative conversion of conduction electrons yields the change in the mean charge radius $\Delta R/R = -(0.45 \pm 0.15) \times 10^{-3}$ (auth)

28248 PARAMETERS OF OPTICAL NUCLEAR MODEL ACCORDING TO ELASTIC SCATTERING OF POLARIZED NEUTRONS WITH ENERGY 3.2 MeV. Kashuba, I. E.; Korzh, I. A. (Inst. of Physics, Kiev). Ukr. Fiz. Zh.; 15: 1036-40(Jun 1970). (In Russian).

Experimental data on elastic scattering of 3.2-MeV polarized neutrons by Ti, Cr, Fe, Cu, Zn, and Zr were analyzed using the optical model. Parameters were obtained which gave satisfactory agreement with the data. (TSS)

28249 COUPLING OF QUASIPARTICLES AND ANHARMONIC VIBRATIONS: A = 33 AND 34. Castel, B. (Queen's Univ., Kingston, Ont.); Stewart, K. W. C.; Harvey, M. Nucl. Phys.; A162: 273-88(1971).

A version of the intermediate coupling vibrational model, in which quasiparticle and anharmonic core effects are considered, is described. A detailed application of the model to A = 33 and 34 nuclei is presented. Comparison is made with the classical version of the model and shows that substantial improvement on it can be obtained. The calculated low-lying structure of ^{33}S, ^{33}Cl and ^{34}S compares well with the known properties of these nuclei. (auth)

28250 EXCITED STATES OF ^{52}Cr AND GROUND STATE SPIN OF ^{52}V IN THE DECAY OF ^{52}V. Okano, Kotoyuki; Uehara, Shinichi; Kawase, Yoichi (Kyoto Univ.). Annu. Rep. Res. Reactor Inst., Kyoto Univ.; 3: 166-8(1970).

Gamma singles and coincidence spectra from the decay of ^{52}V were measured using Ge(Li) and NaI(Tl) detectors. The decay scheme determined from the spectra was compared with previous data. The data was used in conjunction with results of decay studies on ^{52}Mn to establish the ^{52}V ground state spin-parity as 3^+. (J.W.R.)

28251 STUDY OF THE ^{40}Ar(d,p)^{41}Ar REACTION AT DEUTERON ENERGY BELOW THE COULOMB BARRIER. Corleo, G.; Cunsolo, A.; Foti, A.; Di Toro, M.; Pappalardo, G. (Univ., Catania, Italy. Istituto Nazionale di Fisica Nucleare, Catania, Italy). Lett. Nuovo Cim.; 1: 169-73(23 Jan 1971).

Surface barrier silicon detectors were used to detect the protons from the ^{40}Ar (d,p) reaction at $E_d = 1.960$ MeV. Angular distributions were measured at 15 to 170° in steps of approximately 10°. The absolute values of the cross section were determined by comparison with the Rutherford cross section for deuteron elastic scattering. A DWBA analysis of the data was performed and spectroscopic factors for the ^{41}Ar levels were extracted. (J.W.R.)

28252 ATOMIC BEAM INVESTIGATION OF THE HYPERFINE STRUCTURE OF ^{51}Cr. Aedelroth, K. E.; Rosen, A. (Chalmers Tekniska Hoegskola, Goteborg). Ark. Fys.; 40: 457-63 (1970).

The atomic-beam magnetic resonance method was used to measure the ground state hyperfine structure of ^{51}Cr(28 d). The dipole coupling constant and the quadrupole coupling constant are found to be /a/ = 69.701 (2) MHz and /b/ <0.050 MHz. From the measured hfs and the known values of a and μ_I for ^{53}Cr the nuclear magnetic moment for ^{51}Cr is calculated to be $\mu_I = (-)$ 0.934 (5) n.m. including a diamagnetic correction. (auth) (Sweden)

28253 ^{41}Sc–^{41}Ca COULOMB ENERGY DIFFERENCE. Negele, J. W. (Univ. of Copenhagen). Nucl. Phys.; A165: 305-26(1971).

Various contributions to the difference between the ground-state energies of the mirror nuclei ^{41}Sc and ^{41}Ca are evaluated, with particular emphasis on the effect of the Coulomb induced neutron-proton density difference in the core. The resulting theoretical energy difference is 0.58 MeV less than the observed difference. It is argued that it is unreasonable to attempt to resolve this discrepancy by changing the radius of the valence wave function and that the most plausible explanation is the small charge asymmetry of the nuclear force. (auth)

28254 ENERGY LEVELS IN ^{70}Ga. Sawa, Zdzislaw P. (Forskningsinstitutet foer Atomfysik, Stockholm). Phys. Scr.; 2: 233-7(1970).

Locations of levels in ^{70}Ga were experimentally obtained in a ^{69}Ga(d,p)^{70}Ga reaction at $E_d = 7.1$ MeV in which the final energy resolution achieved was 35 to 40 keV. Deexcitation of levels reached by the ^{70}Zn(p,nγ)^{70}Ga process at $E_p = 3.55$ MeV and at two reduced energies was also studied with Ge(Li) detectors. In an appendix information about levels in ^{72}Ga is presented. (Sweden)

28255 INVESTIGATION OF THE EXCITED STATES OF ^{40}Ca BY THE (p,p') REACTION AT 185 MeV. Kaelline, J.; Tibell, G.; Johansson, A. (Uppsala Univ.). Phys. Scr.; 2: 195-203(1970).

In an experiment on inelastic scattering of 185-MeV protons

from ^{40}Ca differential cross sections have been determined for scattering from individual excited states of the target nucleus. The measurements have been extended over the angular range 4° to 40° (lab. system), and the results are presented in the form of angular distributions of the most prominent peaks in the energy spectra. The identification with known states of ^{40}Ca is made by the determination of the excitation energy, and, in the cases where the energy resolution (approximately 250 keV, FWHM) is not sufficient, by the shape of the angular distributions. The results are compared with previously published measurements on other nuclei at the same incoming proton energy as well as with inelastic scattering data at lower energies. In particular, it is shown that the results on the two closed-shell nuclei ^{16}O and ^{40}Ca are very similar and that these nuclei behave differently from other 1p- and 2s−1d-shell nuclei studied. (auth) (Sweden)

28256 POLARIZATION IN THE EXCITATION OF THE 3^- LEVEL AT 3.74 MeV IN ^{40}Ca BY 185 MeV PROTONS. Ingemarsson, A.; Kaellne, J. (Uppsala Univ.). Phys. Scr.; 2: 191-4(1970).

The polarization of 185-MeV protons inelastically scattered from the 3^- level at 3.74 MeV in ^{40}Ca has been measured in the angular region 10° to 42.5° (lab. system). The total energy resolution was 0.28 and 0.50 MeV (FWHM) for the two different targets used. The angular distribution obtained is in qualitative agreement with calculations performed in the distorted-wave impulse approximation. (auth) (Sweden)

28257 NUCLEAR STRUCTURE STUDY OF ^{23}Ne AND ^{21}Ne BY MEANS OF THERMAL NEUTRON CAPTURE IN NATURAL NEON. Selin, E. (Chalmers Tekniska Hoegskola, Goteborg). Phys. Scr.; 2: 169-79(1970).

The energies and intensities of thermal-neutron capture γ-rays from natural neon have been measured with a Ge(Li) detector in pair- and anti-coincidence spectrometer arrangements. Internal target of neon gas has been used. The reaction Q-value and excitation energies have been determined. Cross sections for thermal neutron capture in ^{20}Ne and ^{22}Ne have been deduced. The level schemes of ^{21}Ne and ^{23}Ne are discussed on the basis of the Nilsson model. Calculations with and without inclusion of Coriolis interaction have been made for ^{23}Ne. These are compared with corresponding calculations on ^{25}Al and ^{23}Na. (auth) (Sweden)

28258 STUDY OF THE REACTION ^{73}Ge(n,γ)^{74}Ge. Hasselgren, A. (Chalmers Tekniska Hoegskola, Goteborg). Phys. Scr.; 2: 23-30(1970).

The energies and intensities of thermal-neutron capture gamma rays from ^{74}Ge were measured with a Ge(Li) detector. An internal target of enriched ^{73}Ge was used. The reaction Q-value and excitation energies were determined. The decay scheme of ^{74}Ge is discussed in view of the vibrational model. (auth) (Sweden)

28259 ENERGY LEVELS OF ^{24}Mg FROM THE ^{23}Na(p,α_0)^{20}Ne REACTION. Luukko, A.; Antila, A.; Bister, M.; Piiparinen, M. (Helsinki Univ.). Phys. Scr.; 2: 159-62(1970).

The ^{23}Na(p,α_0)^{20}Ne reaction was investigated in the energy region E_p = 590 to 1810 keV; 16 resonances were observed. The angular distributions of α particles were measured in 14 cases. Analysis of the distributions allowed the following assignments for the resonance states: 592 keV 3^-; 744 keV 2^+; 919 keV 0^+, 1^-, 2^+; 1091 keV 1^-, 2^+; 1136 keV 1^-, 2^+; 1163 keV 0^+, 1^-, 2^+; 1010 keV 3^-; 1284 keV 1^-; 1417 keV 2^+; 1458 keV $3^-(1^-)$; 1500 keV 2^+; 1556 keV (2^+); and 1650 keV (1^-). The population probabilities of different magnetic substates and the formation parameters of the resonances are given. (auth) (Sweden)

28260 PHOTONEUTRON REACTIONS ON COPPER. Ishkhanov, B. S.; Kapitonov, I. M.; Lazutin, E. V.; Piskarev, I. M.; Shevchenko, V. G. Vestn. Mosk. Univ., Ser. III. Fiz. Astron.; 11: 606-13(Nov-Dec 1970). (In Russian).

The structure of photoneutron differential cross section in copper was studied. The energy dependence of cross sections of photoneutron reactions on copper at excitation from the threshold to 30 MeV was determined. Theoretical and experimental data were compared. (R.V.J.)

28261 ELASTIC AND INELASTIC SCATTERING AND MODEL OF EXCITED CORE STATE IN A = 23 to 35 REGION. Antropov, A. E.; Zarubin, P. P.; Kudryashov, V. I.; (and others). (Leningrad State Univ.). Izv. Akad. Nauk SSSR, Ser. Fiz.; 34: 153-60(Jan 1970). (In Russian).

Data obtained on quantum characteristics and differential and integrated cross sections of particle scattering by ^{23}Na, ^{24}Mg, ^{25}Mg, ^{26}Mg, ^{33}S, ^{34}S, and ^{35}Cl nuclei are analyzed. (R.V.J.)

28262 ELASTIC PROTON SCATTERING ON MEDIUM-A NUCLEI. Prokopenko, V. S.; Tokarevskii, V. V.; Shcherbin, V. N. Izv. Akad. Nauk SSSR, Ser. Fiz.; 34: 126-35(Jan 1970). (In Russian).

Differential cross sections of elastic scattering of 6.9-MeV protons by ^{45}Sc, $^{46-50}$Ti, ^{50,52}Cr, ^{56,58}Fe, ^{59}Co, ^{58,60,61,62,64}Ni, ^{63,65}Cu, ^{51}V, and ^{64,66,67,70}Zn nuclei were measured. Data obtained on differential cross sections were analyzed using the nuclear optical model. (R.V.J.)

28263 DIFFERENTIAL CROSS SECTION AND POLARIZATION DURING ELASTIC SCATTERING OF PROTONS ON IRON AND COBALT. Prokopenko, V. S.; Klimenko, A. S.; Pucherov, N. N.; Chirko, V. I. (Inst. of Physics, Kiev). Izv. Akad. Nauk SSSR, Ser. Fiz.; 34: 122-5(Jan 1970). (In Russian).

Differential cross sections and polarizations of protons elastically scattered by ^{56}Fe and ^{59}Co were measured using a semiconductor spectrometer with resolution of not less than 70 keV and analyzed by the comparison method. The results of the measurements and calculations of the differential cross section, carried out using the optical model of elastic scattering, are presented as ratios to Rutherford $\sigma(\theta)/\sigma_R(\theta)$. The order of error for the $\sigma(\theta)\sigma_R(\theta)$ did not exceed 10%. (R.V.J.)

28264 ELASTIC AND INELASTIC PROTON SCATTERING ON ^{24}Mg, ^{25}Mg, AND ^{26}Mg. Antropov, A. E.; Zarubin, P. P.; Orlov, B. N.; Plavko, A. V.; Sorokin, A. I. (Leningrad State Univ.). Izv. Akad. Nauk SSSR, Ser. Fiz.; 34: 106-15(Jan 1970). (In Russian).

Angular distributions of elastic and inelastic scattering of protons by ^{24}Mg, ^{25}Mg, and ^{26}Mg were measured at three energies of the incoming protons (close to 6 MeV). Published data on elastic and inelastic proton scattering by magnesium isotopes at proton energies from 4.8 to 18 MeV are displayed. The mechanism of elastic and inelastic scattering and the lower levels of these nuclei are discussed. (R.V.J.)

28265 SCATTERING OF 14.2 MeV NEUTRONS ON MAGNESIUM. Myachkova, S. A.; Nefedov, V. V. (Lebedev Inst. of Physics, Moscow). Izv. Akad. Nauk SSSR, Ser. Fiz.; 34: 179-81(Jan 1970). (In Russian).

Differential cross sections for elastic and inelastic scattering of 14.2-MeV neutrons by ^{24}Mg were measured; the cross section for excitation of the 1.4-MeV level is given from 30 to 140°. Energy spectra of the scattered neutrons revealed neutron groups corresponding to levels at 4.2, 5.3, and 6.1 MeV in ^{24}Mg. Cross sections at 60° were obtained for these levels. A single-crystal spectrometer with γ-ray pulse-shape discrimination was used for these measurements. (R.V.J.)

28266 EFFECTS OF NUCLEAR SHELLS AND ANGULAR MOMENTUM IN EVAPORATIVE DEEXCITATION. Gilat, Jacob; Grover, J. Robb (Brookhaven National Lab., Upton, N. Y.). Phys. Rev., C; 3: 734-45(Feb 1971).

A detailed statistical-model analysis was carried out of recently reported proton and α spectra for the complex nuclear reactions ^{63}Cu + ^{12}C (55 MeV, lab) and ^{64}Zn + ^{11}B (43 MeV, lab). In both systems the compound nucleus ^{75}Br* is formed with the same excitation energy of 50 MeV, but the distribution of angular momentum is expected to be significantly different. Observed differences in the experimental spectra were accordingly interpreted in terms of assumed differing angular momentum distributions. In the calculations it was found possible to achieve agreement with the data within experimental error for plausible but widely differing sets of important but unknown systemic properties, viz., the distribution of angular momentum in the ^{75}Br*, and the level densities to high excitation of the several nuclei involved. However, it was always found necessary to include the effect of the proximity of the closed proton shell at Z = 28. The behavior of the calculated α emission for individual nuclei shows important differences of detail between reasonable sets of input data, although for all such sets the production ratio [(total protons)/(total α particles)] decreases with increasing angular momentum of the compound nucleus. It is significant that one of the data sets giving satisfactory agreement with experiment included level densities calculated numerically up to the high energies involved using a realistic shell model. These calculations have already been shown to give values in agreement with reliable experimental level densities, which are, however, only available for lower energies. Since additional data on the same system are needed to reduce the ambiguities, specific suggestions for further experiments are offered, and examples of how such experiments can be useful are worked out. (auth)

28267 STUDY OF THE LOW-LYING EXCITED STATES OF ^{29}Al. III. MEAN LIFETIMES AND INTERPRETATION. Jones, A. D. W.; Becker, J. A.; McDonald, R. E. (Lockheed Palo Alto Research Lab., Calif.). Phys. Rev., C; 3: 724-33(Feb 1971).

Lifetimes or, alternatively, limits for lifetimes of low-lying levels in ^{29}Al were obtained employing the Doppler-shift-attenuation method. The levels were excited by the ^{27}Al(t,p)^{29}Al reaction and measurements were made of the γ-ray spectrum in coinci-

dence with reaction protons. Measured mean lifetimes, or limits, [E_x (τ_m), in MeV(psec)] for the first six levels of ^{29}Al are: 1.402 (3.3), 1.762(<0.05), 2.228(<0.08), 2.875(<0.15), 3.071(<0.05), and 3.191(0.21 ± 0.10). A partial level scheme of ^{29}Al for excitation energy $E_x \leq 4.5$ MeV based on previously reported information is presented. Properties of these levels are interpreted according to the Nilsson model on the basis of (1) a direct-reaction investigation and (2) γ-ray angular-correlation investigations as previously reported. The properties of ^{29}Al are shown to be consistent with a prolate deformation characterized by $\eta \approx +3$. (auth)

28268 NUCLEAR-STATE WIDTHS OF MEDIUM-WEIGHT NUCLEI IN THE CONTINUUM. Fessenden, P.; Gibbs, W. R.; Leachman, R. B. (Los Alamos Scientific Lab., N. Mex.). Phys. Rev., C; 3: 807-23(Feb 1971).

The technique of fluctuation averaging was utilized with (p,α) reactions to measure subkilovolt average widths Γ of excited states for six medium-weight nuclei. The following compound-nucleus widths were determined: 386 ± 80, 465 ± 111, and 390 ± 100 eV at excitations of 15.24, 17.02, and 17.00 MeV, respectively, for the ^{76}Se compound nucleus; 114 ± 40, 150 ± 66, 206 ± 34, and 190 ± 65 eV at excitations of 17.36, 18.80, 18.90, and 20.85 MeV, respectively, for ^{90}Zr; 111 ± 46 and 312 ± 85 eV at excitations of 15.50 and 17.72 MeV, respectively, for ^{104}Pd; 36 ± 30 and 101 ± 30 eV at excitations of 15.06 and 16.27 MeV, respectively, for ^{108}Cd; 128 ± 64 eV at an excitation of 15.98 MeV for ^{110}Cd; and 58 eV at an excitation of 19.29 MeV for ^{116}Sn. In all these measurements, excitation functions were measured over a span of several hundred keV in steps of 5- to 15-keV proton energy. The accurately known instrumental resolutions required by the method were primarily determined from the target thicknesses, which were about 10 keV. The required dominance of compound-nucleus reactions was obtained by the use of sufficiently low incident energies and by observations at backward angles. Excitation functions over a span of several MeV and angular distributions were measured in order to select regions of negligible direct reactions. Comparison of these measurements with widths calculated from the statistical model of the nucleus suggests the need for reduced level densities. The measured widths show no evidence for shell effects. (auth)

28269 STUDIES OF (d,p) REACTIONS OF CERTAIN Ti AND Cr ISOTOPES. Alekseev, V. V.; Polyanskii, V. N.; Terenetskii, K. O.; Tokarevskii, V. V.; Shcherbin, V. N. (Inst. of Physics, Kiev. Kiev State Univ.). Izv. Akad. Nauk SSSR, Ser. Fiz.; 34: 194-200(Jan 1970). (In Russian).

Differential cross sections for deuteron stripping reactions at 13.6 MeV in ^{48,49}Ti and ^{50,52}Cr nuclei into ground and first excited states were measured over a large range of angles. The results obtained were correlated with results obtained by the distorted-wave method. (R.V.J.)

28270 HIGH-RESOLUTION INVESTIGATION OF THE ^{30}Si (p,γ)^{31}P AND ^{30}Si(τ,d)^{31}P REACTIONS. Wolff, Andre Charles. Utrecht; Utrecht State Univ. (1970). 59p.

Thesis.

The γ-ray spectra of 46 resonances in the ^{30}Si(p,γ)^{31}P reaction are given, along with the angular distribution measurements of primary and secondary γ-ray transitions at seven resonances. The excitation energies of 36 bound states up to 7.3 MeV and the reaction Q value were determined. The branching ratios of these states and of the resonances are given. Mean lifetimes or upper limits of lifetimes are reported for 20 levels. There are two levels at about 5.0 MeV excitation, with energies differing by less than 1 keV. The strengths of six resonances in the ^{30}Si(p,γ)^{31}P reaction were measured, and spectroscopic factors of 24 bound states were extracted from the ^{30}Si(τ,d)^{31}P reaction at a τ (=^{3}He) energy of 12 MeV. The measurements led to a unique spin and/or parity assignments for 17 levels, whereas the spin was limited to two values for seven states. (R.W.R.)

28271 IN-BEAM INTERNAL CONVERSION SPECTROSCOPY. Robert, Kearny Quinn Jr. New Orleans; Tulane Univ. (1970). 161p. University Microfilms Order No. 71-8082.

Thesis.

An in-beam internal conversion spectrometer was used to collect electron and gamma-ray spectra simultaneously from targets that were placed at the source position of the spectrometer and bombarded with positive ions from a 3 MV Van de Graaff accelerator. Internal conversion coefficients were derived by use of the NPG method with the 662-keV transition in ^{137}Ba as a standard. Reported here are the results for twenty transitions in ten medium- and low-medium-mass nuclei (^{19}F, ^{27}Al, ^{54}Cr, ^{54}Mn, ^{55}Mn, ^{55}Fe, ^{59}Ni, ^{65}Zn, ^{71}Ge, and ^{75}Se) populated by proton-induced nuclear reactions. Transition energies, branching ratios, absolute and relative cross sections, gamma-ray angular distributions, as well as the absolute internal conversion coefficients, were obtained and are compared to theoretical predictions and to the results of other experiments. A realistic effective-charge model is proposed and shown to be essentially equivalent to the renormalization model. Consistent sets of K-shell screening parameters and screening factors for the lighter elements are obtained. A table of point-nucleus unscreened dipole and quadrupole internal conversion coefficients for 23 energies (50 keV to 10,000 keV) for 10 atomic numbers (Z = 3 to 8, 10, 20, 25, 30) is presented. (Diss. Abstr. Int., B)

28272 DECAY OF ^{66}Ge. Dzhelepov, B. S.; Mozzhukhin, A. V.; Popova, T. I.; Prikhodtseva, V. P. Izv. Akad. Nauk SSSR, Ser. Fiz.; 34: 29-41(Jan 1970). (In Russian).

The gamma-ray spectrum of ^{66}Ge was measured using Ge(Li) spectrometers with sensitive areas of 5, 9, and 12 cm^2. Twenty-six lines out of the 44 lines recorded belonged to ^{66}Ge. The measured time intervals in relation to the intensities of the 381-keV (^{66}Ge) and 1039-keV (^{66}Ga) gamma transitions and the known intensities of the 1039-keV gamma ray (in decay %) were used for determining the intensities of ^{66}Ge γ rays (in decay %). The decay scheme of ^{66}Ge was constructed and the log-ft values were calculated; the quantum characteristics of the ^{66}Ge levels are discussed. (R.V.J.)

28273 MEASUREMENTS OF AVERAGE CROSS SECTIONS FOR SOME THRESHOLD REACTIONS FOR NEUTRONS WITH FISSION-TYPE REACTOR SPECTRUM. Kimura, Itsuro; Kobayashi, Katsuhei; Shibata, Toshikazu (Kyoto Univ.). J. Nucl. Sci. Technol. (Tokyo); 8: 59-69(Feb 1971).

The fast-neutron spectrum in the core of the Kyoto University Reactor (KUR) was measured by using seven threshold reactions, a ^{6}Li sandwich counter, and nuclear emulsion plates; and the results were compared with theoretical calculations by the S_n method. It was found that the shape of the fast-neutron spectrum was approximately the same as that of fission neutrons. Making use of these neutrons with fission-type spectrum, measurements were made of the average cross sections for twelve threshold reactions [^{46}Ti(n,p)^{46}Sc, ^{47}Ti(n,p)^{47}Sc, ^{48}Ti(n,p)^{48}Sc, ^{28}Si(n,p)^{28}Al, ^{29}Si(n,p)^{29}Al, ^{30}Si(n,α)^{27}Mg, ^{51}V(n,α)^{48}Sc, ^{64}Zn(n,p)^{64}Cu, ^{92}Mo(n,p)^{92m}Nb, ^{93}Nb(n,2n)^{92m}Nb, ^{204}Pb(n,n')^{204m}Pb, and ^{204}Pb(n,2n)^{203}Pb]. For the purpose of comparison, the average cross sections for six among these reactions were measured also with neutrons from a fission plate. The results agreed within experimental error with those obtained for neutrons in the KUR core. A Ge(Li) counter was mainly used for the measurement of γ-rays emitted from induced activities. (auth)

28274 ELASTIC SCATTERING OF CARBON AND NITROGEN IONS. Kohno, Isao; Nakajima, Shyunji; Tonuma, Tadao; Odera, Masatoshi (Inst. of Physical and Chemical Research, Yamato, Japan). J. Phys. Soc. Jap.; 30: 910-18(Apr 1971).

Elastic scattering of ^{14}N and ^{12}C particles by ^{12}C, ^{27}Al, ^{28}Si, and ^{58}Ni at ^{14}N energies of 65 to 88 MeV and ^{12}C energies of 49.3 to 83.5 MeV was studied. Angular distributions were measured at laboratory angles extending from 7 to 35 degrees at 1- or 1.5-degree intervals; the results changed with the value of the Coulomb parameter (η) regardless of the target and projectile combination. These various angular distributions were analyzed by the optical model with a Woods–Saxon potential; they were fitted very well with a real potential depth of 50 to 70 MeV and geometrical parameters similar to those found in ^{3}Fe and α elastic scattering. (auth)

28275 GAMMA RAYS FROM THERMAL NEUTRON CAPTURE IN NITROGEN AND NATURAL NEON. Bellmann, D. (Institut fuer Reine und Angewandte Kernphysik, Kiel). Atomkernenergie; 17: 145-8(Mar 1971).

The gamma radiation following thermal-neutron capture by nitrogen and neon was measured by a Ge(Li) detector. Precise determinations of the gamma energies and intensities are given for ^{15}N, ^{21}Ne, ^{22}Ne, and ^{23}Ne. The thermal-neutron capture cross sections for ^{20}Ne, ^{21}Ne, and ^{22}Ne are estimated. (R.W.R.)

28276 ENERGIES OF SOME ^{25}Al LEVELS FROM THE ^{24}Mg (p,γ)^{25}Al REACTION AND THE COULOMB-ENERGY DIFFERENCES OF ANALOG ROTATIONAL BANDS. Everling, F.; Morgan, G. L.; Miller, D. W.; Seagondollar, L. W.; Tillman, P. W. Jr. (North Carolina State Univ., Raleigh. Triangle Universities Nuclear Lab., Durham, N. C.). Can. J. Phys.; 49: 402-6(15 Feb 1971).

Gamma rays from the ^{24}Mg(p,γ)^{25}Al reaction at the 1201- and 1485-keV resonances were measured with a 20 cm^3 Ge(Li) detector. Excitation energies obtained for known levels in ^{25}Al are (in keV) 1612.5 ± 0.5, 1789.6 ± 1.3, 3424.3 ± 0.6, and 3696.3 ± 1.1. By using the known 1201.4 ± 1.0 keV resonance energy, a more precise Q value of 2271.4 ± 1.2 keV is obtained, 16 keV lower than the previous value, which had a 6-keV uncertainty. A brief discussion of the Coulomb-energy differences of ^{25}Al and ^{25}Mg analog rotational bands in relation to the ^{24}Mg ground-state band is given,

XUM

and the situation is compared with that at mass number A = 21. (auth) (Canada)

28277 THE $^{86}Sr(\tau,\alpha)^{85}Sr$ REACTION AT E_τ = 17.5 MeV. Bucurescu, D. (Inst. of Atomic Physics, Bucharest); Ivascu, M.; Titirici, M.; Spilling, P. Rev. Roum. Phys.; 15: 1049-51(1970).

Angular distributions for the reaction $^{86}Sr(\tau,\alpha)^{85}Sr$ were measured from 6 to 80° at a $\tau(\equiv^3He$ energy of 17.5 MeV. DWBA analysis yielded l-transfer values and spin–parity assignments for the level scheme constructed. (R.W.R.)

28278 GAMMA-RAY SPECTROSCOPY OF ^{76}As. Iizawa, Katsuyuki; Kitamura, Isao; Kawade, Kiyoshi; (and others) (Nagoya Univ., Japan). J. Phys. Soc. Jap.; 30: 901-9(Apr 1971).

The decay of ^{76}As was investigated by using a Ge(Li) detector and Ge(Li)–NaI(Tl) coincidence methods. Sixteen new gamma rays were observed, and eleven of them were assigned in a proposed decay scheme. Four new levels were found at 2026.4, 2348, 2365.1, and 2514 keV. Spins and parities of the levels at 2026.4, 2655.7, and 2669.8 keV were estimated from log-ft values of beta transitions that fed these levels. The existence of 563.4- and 772.1-keV gamma rays emitted from the 0^+ and 4^+ levels, which are considered to be levels of two-phonon triplet states and have been observed by Coulomb excitation and inelastic scattering, was confirmed. The character of the 1691.5- and 1788.1-keV levels as three-phonon states is discussed. (auth)

28279 TOTAL CROSS SECTIONS FOR KILOVOLT NEUTRONS OF EVEN–ODD NUCLEI IN HE REGION OF THE 3s STRENGTH-FUNCTION RESONANCES. Cho, Mann (Atomic Energy Research Inst., Seoul); Bak, Hae-ill; Frohner, F. H.; Muller, K.-N. J. Korean Nucl. Soc.; 2: 241-8(Dec 1970).

Neutron total cross sections of separated isotopes were measured with a time-of-flight spectrometer. The neutron energy ranged from 10 to 250 keV, and the energy resolution was between 0.2 and 0.5 nsec/m. The measured cross sections were shape-analyzed in terms of an R-matrix multilevel formula; thus, neutron widths and spins for up to 50 resonances per isotope could be determined. Average neutron widths, level densities, and strength functions were derived. The spin dependence of strength functions and the distribution of widths and spacings were investigated. (auth)

28280 PROJECTED HARTREE–FOCK AND CORE-PARTICLE COUPLING FOR A = 29 AND 30. Castel, B.; Stewart, K. W. C. (Queen's Univ., Kingston, Ont.). Phys. Rev., C; 3: 964-8(Feb 1971).

A projected Hartree–Fock calculation of the properties of ^{28}Si is used as the basis for a core-quasiparticle coupling treatment of ^{29}Si, ^{29}P, and ^{30}Si. Very good agreement with the known properties of these nuclei is achieved in this calculation with a variation of essentially one parameter, the coupling strength. (auth)

28281 MEAN LIVES AND ANGULAR CORRELATIONS IN ^{57}Co WITH THE $^{54}Fe(\alpha,p\gamma)^{57}Co$ REACTION. Burton, K. S.; McIntyre, L. C. Jr. (Univ. of Arizona, Tucson). Phys. Rev., C; 3: 621-9(Feb 1971).

The reaction $^{54}Fe(\alpha,p\gamma)^{57}Co$ with incident α-particle energies of 9 and 10 MeV was used to investigate the properties of ^{57}Co levels below 3 MeV in excitation. Using the Doppler-shift-attenuation method, mean lives were obtained for 11 excited levels. These results are as follows: τ(1.22 MeV) = 0.084 ± 0.018, τ(1.68 MeV) = 0.26, τ(1.76 MeV) = 0.36 ± 0.07, τ(1.89 MeV) = 0.12 ± 0.03, τ(1.92 MeV) = 0.03 ± 0.02, τ(2.31 MeV) = 0.32 ± 0.09, τ(2.48 MeV) = 0.036, τ(2.60 MeV) = 0.11 ± 0.03, τ(2.73 MeV) = 0.11 ± 0.03, τ(2.80 MeV) = 0.04 ± 0.02, and τ(2.87 MeV) = 0.05 ± 0.02, all in psec. In addition multipole mixing ratios were obtained for several transitions. Arguments are given for a spin assignment of J = 7/2 to the 2.31-MeV level. (auth)

28282 NEUTRON ACTIVATION CROSS SECTIONS FOR As, Br, Rb, AND Sr ISOTOPES AT 14.4 MeV. Rao, P. Venugopala (Emory Univ., Atlanta); Wood, R. E.; Palms, J. M.; Fink, R. W. Phys. Rev., C; 3: 629-35(Feb 1971).

Activation cross sections at an incident neutron energy of 14.4 ± 0.3 MeV are measured for the (n,2n), (n,p), and (n,α) reactions on isotopes of As, Br, Rb, and Sr, by using the mixed-powder method and γ detection by Ge(Li) spectrometer. The use of a stoichiometric chemical compound as an alternative to the mixed-powder technique, where one of the constiuents serves as the neutron flux monitor, is investigated and is recommended, whenever applicable, over all other methods for measurement of relative activation cross sections. (auth)

28283 COULOMB EXCITATION OF THE FIRST 2^+ STATE OF ^{24}Mg. Vitoux, D.; Haight, R. C.; Saladin, J. X. (Univ. of Pittsburgh). Phys. Rev., C; 3: 718-24(Feb 1971).

Coulomb excitation of the first excited state of ^{24}Mg was investigated by means of coincidence experiment using a position-sensitive detector. Interpreting the data according to the semi-classical theory and correcting for quantal effects, a reduced transition probability of $B(E2; 0^+ \rightarrow 2^+) = 0.042 \pm 0.002\ e^2\ b^2$ and a static quadrupole moment of $Q_{2+} = -0.305 \pm 0.064$ e b were obtained. (auth)

28284 STUDY OF THE LEVEL STRUCTURE OF ^{50}Ti AND ^{51}Ti USING THE $^{49}Ti(n,\gamma)$ AND $^{50}Ti(n,\gamma)$ REACTIONS. Tenenbaum, J. (Nuclear Research Center, Negev, Israel); Moreh, R.; Wand, Y.; Ben-David, G. Phys. Rev., C; 3: 663-71(Feb 1971).

The capture γ-ray spectrum resulting from thermal-neutron capture in ^{49}Ti and ^{50}Ti was measured using a 30- and a 10-cm^3 Ge(Li) detector, and angular-correlation measurements were carried out using NaI(Tl) detectors. Some 16 γ lines corresponding to transitions between levels of ^{50}Ti, and 9 γ lines corresponding to transitions between levels of ^{51}Ti were observed. The neutron separation energies of ^{50}Ti and ^{51}Ti were determined to be 10.938 ± 0.008 and 6.377 ± 0.007 MeV, respectively. The following assignments of spins for some levels (in MeV) of ^{50}Ti and the first excited level of ^{51}Ti were made: 1.555 (2^+), 2.675 (4^+), 4.151 [2^+, 3^+, 4^+, (5^+)], 4.178 (2^+, 3^+, 4^+), 4.887 [2^+, 3^+, 4^+, (5^+)] 5.195 (2^+, 3^+, 4^+), 5.382 [2^+, 3^+, 4^+, (5^+)], 5.948 [3^+, 4^+, (5^+)] for ^{50}Ti and 1.164 ($1/2^-$) for ^{51}Ti. There are some indications that only the 3^- capture-state spin contributes to the population of the low-lying levels in ^{50}Ti. The results of a comparison between the measured strengths of exciting the ^{50}Ti levels in the (n,γ) and (d,p) reactions are discussed. (auth)

28285 NUCLEAR LEVEL DENSITIES AND REACTION MECHANISMS FROM CONTINUUM NEUTRON SPECTRA. Grimes, S. M.; Anderson, J. D.; McClure, J. W.; Pohl, B. A.; Wong, C. (Univ. of California, Livermore). Phys. Rev., C; 3: 645-63(Feb 1971).

The neutron spectra produced by the $^{51}V(p,n)^{51}Cr$, $^{59}Co(p,n)^{59}Ni$, $^{48}Ti(\alpha,n)^{51}Cr$, and $^{56}Fe(\alpha,n)^{59}Ni$ reactions were measured at five angles between 15 and 135° for proton energies between 7.8 and 14.7 MeV, and for α energies between 11.5 and 22.7 MeV. Spectra at low energies were used to obtain the spin-weighted level density of the residual nuclei ^{51}Cr and ^{59}Ni. Comparison of these spectral shapes with those obtained at higher energies made possible a separation of the higher-energy spectra into compound and non-compound contributions. The deduced compound-nuclear cross sections to given groups of levels were related to the integrals of the level densities of the residual nuclei; the variation of these cross sections with energy was used to extend the level-density measurements beyond the neutron binding energy. A constant-temperature level-density form is found to be appropriate for ^{51}Cr and ^{59}Ni up to residual excitation energies of 14 MeV. Values of the moment of inertia of the residual nuclei were extracted from the magnitude of the asymmetry of the compound-nuclear angular distributions. The characteristics of the noncompound portion were compared with those expected from direct- and pre-equilibrium-reaction mechanisms. It is concluded that no convincing evidence for a pre-equilibrium component is observed in the (α,n) spectra; the (p,n) data show behavior consistent with contributions from both pre-equilibrium- and direct-reaction mechanisms. A value of approximately 160 keV was obtained for the widths of the participating doorway states from a model-dependent calculation based on the magnitude of the pre-equilibrium (p,n) cross section. (auth)

Nuclear Properties and Reactions, A ≥ 90

Refer also to abstracts 26547, 26551, 27168, 27169, 27914, 27953, 28169, 28170, 28178, 28211, 28215, 28219, 28227, 28239, 28268, 28273, 28440–28442, 28445, 28500, 28501, 28503, 28504, 28508, and 28509.

28286 (ANU-P–511) SPECTROSCOPIC FACTORS FROM $^{124}Sn(d,p)^{125}Sn$ ABOVE AND BELOW THE COULOMB BARRIER. Powell, D. L.; Dallimore, P. J.; Davidson, W. F. (Australian National Univ., Canberra. Research School of Physical Sciences). [1971]. 20p. Dep. NTIS (U. S. Sales Only).

Angular distributions for the reaction $^{124}Sn(d,p)^{125}Sn$ leading to the unresolved ground and 0.026 MeV levels and to the 0.210, 0.936, 1.257, 1.362, and 1.540 MeV levels of ^{125}Sn have been measured with deuteron energies of 5.1 and 12.0 MeV. Spectroscopic factors and transferred orbital angular momentum values have been extracted using the DWBA theory. The dependence of the spectroscopic factor on the approximations of the theory has been compared at energies above and below the Coulomb barrier. (auth) (Australia)

28287 (ANU-P-518) 9/2⁻[514] STATE IN ^{185}Re. Evans, M.; Ellis, A. E.; Leigh, J. R.; Newton, J. O. (Manchester Univ. (England). Dept. of Physics). [1971]. 6p. Dep. NTIS (U. S. Sales Only).

For Australian National Univ., Canberra. Research School of Physical Sciences.

Gamma rays following the ^{186}W(d,3n)^{185}Re reaction have been observed. Evidence is given for rotational bands based on the 5/2⁺[402] and 9/2⁻[514] states. The half-life of the 9/2⁻ state has been measured and found to be 33 ± 3 ns. (auth) (Australia)

28288 (CEA-R-4121) EFFECT OF THE CHARGE ON ^{252}Cf FISSION FRAGMENTS ON THE NEUTRON EMISSION PROCESS. Nifenecker, Herve (Commissariat a l'Energie Atomique, Saclay (France). Centre d'Etudes Nucleaires). Jan 1971. 166p. (In French). Dep. NTIS (U. S. Sales Only).

Thesis. Submitted to Univ. of Paris, Orsay.

Simultaneous measurements of the x-ray emission, neutron emission, and kinetic energies of ^{252}Cf fission fragments were made. The charge, the total kinetic energy, and the neutron emission by the individual fragments were determined. For light fragments of charge between 40 and 46 and the complementary heavy fragments, the first and second moments of the kinetic energy and neutron number distributions were obtained. It was thus possible to deduce the proportions of excitation energy shared between the two fragments and to determine which part of the excitation contributed to the deformation energy of the fragments. The intrinsic excitation energy of the fragments, at scission, was found to be approximately 13 MeV; the pairing energy term associated with the parity of the proton number appeared mostly in the form of intrinsic excitation energy. The increase in excitation energy necessary for a fragment to emit an additional neutron was determined and indicated that, when the deformation energy of the fragments is high, conditions favor gamma-ray emission rather than neutron emission. (auth) (France)

28289 (CERN-70-30(Vol.1), pp 1-19) THEORETICAL CONSIDERATIONS ON NUCLEI FAR FROM STABILITY. Sorensen, R. A. (Carnegie-Mellon Univ., Pittsburgh, Pa.).

In International conference on the properties of nuclei far from the region of beta-stability; Leysin, Switzerland (31 Aug 1970).

The question as to just which nuclei are stable is still an open one. Mass formulas are examined as a means of predicting stability. Pairing correlations in N = Z nuclei are discussed. The regions of the nuclide chart where deformation occurs are considered, as well as the effects of shell closure on the double-humped fission barrier. Finally, the energetics for decay of nuclei far from the stability line are reviewed. (R.W.R.)

28290 (CERN-70-30(Vol.1), pp 21-45) SPECIAL EXPERIMENTAL TECHNIQUES USED IN THE STUDY OF NUCLEI FAR FROM STABILITY. Klapisch, R. (Centre National de la Recherche Scientifique, Orsay (France). Centre de Spectrometrie Nucleaire et de Spectrometrie de Masse).

In International conference on the properties of nuclei far from the region of beta-stability; Leysin, Switzerland (31 Aug 1970).

Techniques for studying nuclei far from stability are reviewed, with emphasis on light nuclei. Particle identification by dE/dx-E telescope or magnetic analyzer is discussed; either can be used alone, or they can be combined. High-energy reactions can be relatively efficient for the production of light, neutron-rich nuclei as compared with heavy-ion reactions; the difference may be four orders of magnitude in cross section. On-line mass spectrometers can be used to determine half-lives in the millisecond range. Other techniques briefly described include the focusing parabola mass spectrograph, the gas-filled mass separator, and the helium-jet technique. (R.W.R.)

28291 (CERN-70-30(Vol.1), pp 165-216) CURRENT SEMI-EMPIRICAL MASS EQUATIONS AND IMPROVED SHELL MODEL NUCLEAR MASSES. Comay, E.; Liran, S.; Wagman, J.; Zeldes, N. (Hebrew Univ., Jerusalem (Israel). Dept. of Theoretical Physics).

In International conference on the properties of nuclei far from the region of beta-stability; Leysin, Switzerland (31 Aug 1970).

Mass equations are broadly classified into those emerging from the picture of the nucleus as a liquid drop and those based on the opposite notion of independent particle motion. The Bethe-Weizsaecker equation is used to calculate the average nuclear energy in the droplet model, and various corrections to this result are computed. The shell-model mass equation is given and discussed. Finally, the Garvey-Kelson mass relations are explained. (52 references) (R.W.R.)

28292 (CERN-70-30(Vol.1), pp 263-73) DETERMINATION OF ATOMIC MASSES FOR FAR UNSTABLE NUCLEI BY EXTRAPOLATION. Wapstra, A. H. (Instituut voor Kernphysisch Onderzoek, Amsterdam (Netherlands)).

In International conference on the properties of nuclei far from the region of beta-stability; Leysin, Switzerland (31 Aug 1970).

Procedures used to obtain estimates of the atomic masses of nuclides that cannot be calculated from known experimental data are described. (R.W.R.)

28293 (CERN-70-30(Vol.1), pp 275-306) CONSTRUCTION OF MASS FORMULAS DESIGNED TO BE VALID FOR NEUTRON-RICH NUCLEI. Truran, J. W.; Cameron, A. G. W. (Yeshiva Univ., New York. Belfer Graduate School of Science. National Aeronautics and Space Administration, New York. Goddard Inst. for Space Studies); Hilf, E. (Wuerzburg Univ. (West Germany). Physikalisches Institut. Yeshiva Univ., New York. Belfer Graduate School of Science).

In International conference on the properties of nuclei far from the region of beta-stability; Leysin, Switzerland (31 Aug 1970).

A semi-empirical atomic mass formula aimed at providing improved estimates of the masses of neutron-rich nuclei is constructed. In addition to the four standard terms whose coefficients are determined by a least-squares fit to masses—the volume, volume symmetry, surface, and Coulomb energy terms—a number of additional terms are also included. Criteria for the selection of appropriate coefficients for these terms included the assumption that the shell corrections to the reference mass formula should be separable in Z and N and well behaved. This criterion allowed the assignment of reasonable coefficients both to a Wigner-type term, which predominantly affects the masses of light nuclei, and to a surface symmetry term. A higher-order volume symmetry term is included as prescribed by Myers and Swiatecki, and a curvature term of negative sign is included in order to give a reasonable fit to the Stanford determinations of nuclear Coulomb energies. Still higher-order volume and surface symmetry terms are included with reasonable but arbitrary assignments of coefficients in order to prevent nuclei with very small charges from having positive neutron binding energies out to indefinitely large neutron numbers. It is found that the liquid droplet model formula of Myers and Swiatecki can not be used in the form suggested by those authors; their determination of the nuclear symmetry effect in the nuclear interior suffers from the premature dropping of terms, and hence the resulting truncated mass formula cannot be fitted to masses in a satisfactory self-consistent fashion. (auth)

28294 (CERN-70-30(Vol.1), pp 321-9) MASS-DIFFERENCES IN THE NEUTRON-RICH Sr REGION. Macias-Marques, M. I.; Foucher, R.; Cailliau, M.; Belhassen, J. (Paris Univ., Orsay (France). Institut de Physique Nucleaire).

In International conference on the properties of nuclei far from the region of beta-stability; Leysin, Switzerland (31 Aug 1970).

The β rays emitted by neutron-rich Rb isotopes and their daughter nuclei were detected with a particle telescope. The Q values Q_{β^-} of the β decay are given for ^{93}Rb through ^{96}Rb and ^{93}Sr through ^{95}Sr. It is concluded that the n-n pairing energy in the $g_{\frac{9}{2}}$ subshell is at least 2.9 MeV in the Sr nuclei, while for the $d_{\frac{5}{2}}$ subshell it is about 1.7 MeV in the Sr and Zr nuclei. It is found that n-n pairing changes weakly with Z, but it changes strongly with N and in the same sense as the angular momentum. (R.W.R.)

28295 (CERN-70-30(Vol.1), pp 331-40) EXPERIMENTAL Q-VALUES FAR FROM STABILITY. Lindahl, A.; Nielsen, O. B.; Rasmussen, I. L. (Niels Bohr Institutet, Copenhagen (Denmark)).

In International conference on the properties of nuclei far from the region of beta-stability; Leysin, Switzerland (31 Aug 1970)

A measurement of the β^+ decay of ^{194}Au to ^{194}Pt is reported. The experimental arrangement and the β^+-γ coincidence spectrum are given. The value for Q_β is 5.0 ± 0.2 MeV. (R.W.R.)

28296 (CERN-70-30(Vol.1), pp 341-51) Q-VALUES OF SOME NUCLIDES ON THE NEUTRON-RICH SIDE OF STABILITY. Rudstam, G.; Lund, E.; Westgaard, L.; Grapengiesser, B. (Forskningsradens Laboratorium, Studsvik (Sweden)).

In International conference on the properties of nuclei far from the region of beta-stability; Leysin, Switzerland (31 Aug 1970).

The development of a "Q-meter" spectrometer for measuring total nuclear decay energies is described. A silicon detector for β particles is placed between two NaI detectors which should have a high efficiency in summing the pulses of gamma rays cascading from a given excited level to the ground state of the daughter nucleus. Results for the Q values for β decay of ^{90}Rb, ^{132}I, ^{133}Sb, ^{133}Te, ^{135}I, ^{139}Cs, and ^{141}Ba are given. (R.W.R.)

28297 (CERN-70-30(Vol.1), pp 353-60) BETA DECAY ENERGIES OF SOME NEUTRON DEFICIENT NUCLIDES. Beck, E. (Max-Planck-Institut fuer Kernphysik, Heidelberg (West Ger-

XUM

many). European Organization for Nuclear Research, Geneva (Switzerland)).

In International conference on the properties of nuclei far from the region of beta-stability; Leysin, Switzerland (31 Aug 1970).

Beta spectra of short-lived neutron-deficient isotopes of cadmium, iodine, iridium, platinum, silver, and xenon were measured; the Q values for these β decays are given. (R.W.R.)

28298 (CERN-70-30(Vol.1), pp 387-94) ATOMIC-BEAM MEASUREMENTS IN THE RARE-EARTH REGION. Lindgren, I.; Nyqvist, H.; Rosen, A.; Aedelroth, K. E. (Chalmers Tekniska Hogskola, Goteborg (Sweden)); Ekstroem, C.; Olsmats, M.; Wannberg, B. (Uppsala Univ. (Sweden). Inst. of Physics).

In International conference on the properties of nuclei far from the region of beta-stability; Leysin, Switzerland (31 Aug 1970).

The heavier rare earths, Tb, Dy, Ho, Er, Tm, and Lu, were investigated by means of atomic-beam methods. Spin measurements and proposed Nilsson-model nuclear level assignments are given and discussed. Preliminary results for the magnetic dipole and electric quadrupole moments of ^{157}Dy and ^{161}Er are also given. (R.W.R.)

28299 (CERN-70-30(Vol.1), pp 435-46) STRAIGHTFORWARD ELUCIDATION OF COMPLEX SHELL-MODEL STATES BY THE β DECAY OF NUCLEI FAR FROM STABILITY. McHarris, Wm. C.; Eppley, R. E.; Warner, R. A.; Todd, R. R.; Kelly, W. H. (Michigan State Univ., East Lansing).

In International conference on the properties of nuclei far from the region of beta-stability; Leysin, Switzerland (31 Aug 1970).

Several nuclei moderately far from stability but close to the major closed shell at N = 82 are discussed; these nuclei exhibit complex but straightforward decay patterns, which can be explained with simple shell-model arguments. The configurations of these (odd-mass) nuclei, involving one or more high-spin states, are such that their $\beta^+\epsilon$ decay is forced to populate unique and well-defined three-quasi-particle states in the daughter nuclei. Thus, information can be obtained about the structures of states lying near 2 MeV that often is not available for states much closer to the ground state. The systems considered are ^{139}Nd–^{139}Pr, ^{141}Sm–^{141}Pm, and ^{145}Gd–^{145}Eu. (R.W.R.)

28300 (CERN-70-30(Vol.1), pp 457-86) PROTON EMITTER STUDIES IN THE REGION OF Z > 50. Karnaukhov, V. A.; Bogdanov, D. D.; Petrov, L. A. (Joint Inst. for Nuclear Research, Dubna (USSR)).

In International conference on the properties of nuclei far from the region of beta-stability; Leysin, Switzerland (31 Aug 1970).

The possibilities of obtaining nuclear information by means of delayed proton emitters are considered. Results on the search for proton decay from the nuclear ground state are then presented. The advantages of nuclei in the region of Z > 50, compared to lighter ones, really exist and make heavy nuclei, in some respects, more predominant. (auth)

28301 (CERN-70-30(Vol.1), pp 487-96) DELAYED-PROTON EMISSION FROM NEUTRON-DEFICIENT ISOTOPES OF XENON AND MERCURY. Hornshoej, P.; Wilsky, K.; Hansen, P. G.; Johson, B.; Kugler, E.; Alpsten, M.; Andersson, G.; Appelqvist, A.; Bengtsson, B. (European Organization for Nuclear Research, Geneva (Switzerland)).

In International conference on the properties of nuclei far from the region of beta-stability; Leysin, Switzerland (31 Aug 1970).

The delayed-proton-emitting isotopes ^{115}Xe, ^{117}Xe, ^{179}Hg, ^{181}Hg, and ^{183}Hg were investigated; half-lives and other characteristics of these isotopes are reported. The delayed-proton spectra from ^{181}Hg and ^{115}Xe are given, and a calculation in the spirit of the statistical model is carried out for the latter. Spin and parity $(5/2 \text{ or } 7/2)^+$ are assigned to ^{115,117}Xe; and $3/2^-$, to ^{181}Hg. The ground state of ^{183}Hg probably has even parity. (R.W.R.)

28302 (CERN-70-30(Vol.1), pp 523-31) ALPHA DECAY OF NEUTRON DEFICIENT ISOTOPES OF MERCURY AND RADON AND THEIR DAUGHTERS. Hornshoej, P.; Wilsky, K. (Aarhus Univ. (Denkmark). Fysisk Institut); Alpsten, M.; Hansen, P. G. (European Organization for Nuclear Research, Geneva (Switzerland)); Lindahl, A.; Nielsen, O. B. (Niels Bohr Institutet, Copenhagen (Denmark)).

In International conference on the properties of nuclei far from the region of beta-stability; Leysin, Switzerland (31 Aug 1970).

Neutron-deficient isotopes of Hg (with its Au and Pt daughters) and Rn (with Po and At daughters) were produced, and a survey of the knowledge of the systematic trends in α decay obtained with these isotopes is presented. Data include α spectra, Q values, partial half-lives, and reduced α widths for Hg, Pt, Rn, and Po. (R.W.R.)

28303 (CERN-70-30(Vol.1), pp 533-44) SEARCH FOR NEW α-EMITTERS WITH N = 86 AND N = 87. Toth, K. S.; Hahn, R. L. (Oak Ridge National Lab., Tenn.).

In International conference on the properties of nuclei far from the region of beta-stability; Leysin, Switzerland (31 Aug 1970).

Several new radioactive species in the 82-neutron region were produced by bombarding various rare-earth targets with 100-MeV ^{3}He and 100-MeV ^{14}N ions. New information on the half-lives and α-decay energies (where applicable) is provided for the following nuclides: ^{157}Yb, ^{156}Yb, ^{156}Tm (low-spin isomer), ^{151}Er, ^{154}Ho (high-spin isomer), ^{153}Ho (high-spin isomer), and ^{150}Ho. Yield curves for ^{150}Dy, ^{151}Dy, ^{151}Ho, ^{151m}Ho, ^{152}Ho, ^{152}Er, and ^{153}Er are given as a function of bombarding energy for ^{3}He ions on ^{156}Dy. The α-decay energy systematics in this region are discussed. (R.W.R.)

28304 (CERN-70-30(Vol.1), pp 545-6) PRODUCTION AND DECAY PROPERTIES OF THORIUM AND PROTACTINIUM ISOTOPES OF MASS 221-225 FORMED IN HEAVY ION REACTIONS. Valli, K.; Hyde, E. K.; Borggreen, J. (California Univ., Berkeley. Lawrence Radiation Lab.).

In International conference on the properties of nuclei far from the region of beta-stability; Leysin, Switzerland (31 Aug 1970).

Alpha decay chains initiated by $^{222-225}$Pa and $^{221-225}$Th were produced by bombardments of Tl, Pb, and Bi targets with beams of C, F, N, Ne, and O. Energy values, intensities, half-lives, and genetic relations of the individual peaks are determined. (R.W.R.)

28305 (CERN-70-30(Vol.1), pp 567-74) SEARCH FOR NEW ISLANDS OF FISSION ISOMERISM. Bjoernholm, Sven; Borggreen, Joern; Hyde, Earl K. (Niels Bohr Institutet, Copenhagen (Denmark)).

In International conference on the properties of nuclei far from the region of beta-stability; Leysin, Switzerland (31 Aug 1970).

Gold-197 was bombarded with beams of ^{11}B, ^{12}C, ^{14}N, and ^{16}O between the Coulomb barrier and 10.3 MeV/amu. In no case was delayed fission observed; the cross-section limits for decay in the time range 2 ns to 1 hr were about 40 nb. (R.W.R.)

28306 (CERN-70-30(Vol.1), pp 575-87) SEARCH FOR SPONTANEOUSLY FISSIONING ISOMERS PRODUCED WITH 600 MeV PROTONS. Boos, A. H.; Brandt, R.; Molzahn, D.; Montgomery, D. (Marburg Univ. (West Germany). Institut fuer Kernchemie).

In International conference on the properties of nuclei far from the region of beta-stability; Leysin, Switzerland (31 Aug 1970).

Experiments were performed to produce spontaneously fissioning isomers in the interaction of 600-MeV protons with elements like uranium, thorium, and bismuth. No such isomers could be detected having an assumed half-life of 10 sec $\leq T_{\frac{1}{2}} \leq$ 20 d; the upper limit for the production cross section is between $10^{-32} \geq \sigma \geq 10^{-34}$ cm^2. Furthermore, no spontaneously fissioning isomers could be observed for sec half-lives ($\sigma \leq 10^{-30}$cm^2). (10 references) (auth)

28307 (CERN-70-30(Vol.1), pp 589-99) ON-LINE INVESTIGATION OF INDEPENDENT CESIUM YIELDS IN ^{235}U FISSION: IDENTIFICATION OF ^{145}Cs. Forman, L.; Balestrini, S. J.; Wolfsberg, K. (Los Alamos Scientific Lab., N. Mex.); Jeter, T. R. (Ballistic Research Labs., Aberdeen Proving Ground, Md.).

In International conference on the properties of nuclei far from the region of beta-stability; Leysin, Switzerland (31 Aug 1970).

The independent fission yields of ^{138}Cs, ^{139}Cs, ^{141}Cs, ^{142}Cs, ^{143}Cs, and ^{145}Cs were measured utilizing the Bernas-type on-line surface ionization technique with a fast-burst reactor neutron source. The nuclides were mass-separated by a magnetic lens and collected along a focal surface. After separation, the focal surface was examined for activity associated with each mass number. The data, normalized to radiochemical values, at masses 138, 139, and 141 give the following independent yields: ^{138}Cs, 0.322 ± 0.077; ^{139}Cs, 1.27 ± 0.19; ^{141}Cs, 2.58 ± 0.41; ^{142}Cs, 1.46 ± 0.39; ^{143}Cs, 0.98 ± 0.17; ^{145}Cs, $0.100^{+0.055}_{-0.042}$. (auth)

28308 (CERN-70-30(Vol.2)) INTERNATIONAL CONFERENCE ON THE PROPERTIES OF NUCLEI FAR FROM THE REGION OF BETA-STABILITY, LEYSIN, SWITZERLAND, AUGUST 31–SEPTEMBER 4, 1970. (European Organization for Nuclear Research, Geneva (Switzerland)). 23 Nov 1970. 510p. (CONF-700815-(Vol.2)).

Separate abstracts were prepared for 44 of the 46 papers in this volume; the remaining 2 were previously abstracted in NSA. For abstracts of the latter papers, see CONF-700815 in a cumulative report number index. (R.W.R.)

For abstracts of individual papers see: 27310, 27311, 28107, 28213–28215, 28309–28343, and 28446–28448.

28309 (CERN-70-30(Vol.2), pp 605-44) THEORETICAL PREDICTIONS FOR SUPERHEAVY NUCLEI. Nix, J. R. (Los Alamos Scientific Lab., N. Mex.).

In International conference on the properties of nuclei far from the region of beta-stability; Leysin, Switzerland (31 Aug 1970).

XUM

An island of nuclei in the vicinity of 114 protons and 184 neutrons is expected to be relatively stable with respect to spontaneous fission, α decay, and β decay, although the precise shape and extent of the island is unknown. Nuclei with approximately 124 protons are also possibly fairly stable with respect to spontaneous fission, but they would decay rapidly by α and β emission. The way to produce superheavy nuclei is by heavy-ion reactions. Of the alternatives available, direct transfer reactions and compound-nucleus formation, possibly in overshoot reactions to the region of $^{308}124$, offer the most hope. The chemical properties of the superheavy elements through element 120 should be similar to those of the preceding group of elements in the periodic table. The fission of a superheavy nucleus should release somewhat more kinetic energy and substantially more neutrons than the fission of a conventional nucleus. (129 references) (auth)

28310 (CERN-70-30(Vol.2), pp 646-53) EXTRAPOLATIONS TO THE Z = 164 REGION. Bengtsson, Ragnar (Lund Inst. of Tech. (Sweden). Dept. of Mathematical Physics).

In International conference on the properties of nuclei far from the region of beta-stability; Leysin, Switzerland (31 Aug 1970).

A gap at Z = 164 is conspicuous for the set of nuclear parameters used for A ≈ 300, and it may persist to the A = 400 to 500 region, when it becomes relevant. A calculation using the Strutinsky shell-correction method results in a prolate barrier which is considerably thinner than the oblate one. The resulting fission half-lives are smaller than those of earlier calculations. The longest half-life in this region apparently belongs to $^{468}164$; it is of the order of ten milliseconds. (R.W.R.)

28311 (CERN-70-30(Vol.2), pp 654-75) SHELL MODEL PARAMETERS OF THE Z = 114 REGION. Gustafsson, Christer (Lund Inst. of Tech. (Sweden). Dept. of Mathematical Physics).

In International conference on the properties of nuclei far from the region of beta-stability; Leysin, Switzerland (31 Aug 1970).

The shell structure and the corresponding shell-correction energy are not qualitatively changed with a modest change of the potential of such a kind that the observed actinide and rare-earth single-particle level order is reproduced. Still, the extrapolation with A appears a relatively difficult problem. The great sensitivity of the predicted fission half-lives in the A ≈ 300 region to the values of the extrapolated values of spin–orbit splitting and l_t^2 correction is exemplified by the "favorable" and "unfavorable" cases treated in this calculation. It should be emphasized that the "unfavorable" one of the extrapolated cases is in a way unduly "unfavorable" as other neutron and even proton (Z = 124) gaps then require considerations. It should be noted that in this "unfavorable" case the fission half lives are decisive relative to the α half-lives. In this case, consequently, the most long-lived elements center around Z = 114 (and N = 182) rather than Z = 110. (auth)

28312 (CERN-70-30(Vol.2), pp 676-88) TWO-CENTRE POTENTIAL AND THE $(\Delta V \times p \text{ vector})^2$ TERM. Johansson, Thomas (Lund Inst. of Tech. (Sweden). Dept. of Mathematical Physics).

In International conference on the properties of nuclei far from the region of beta-stability; Leysin, Switzerland (31 Aug 1970).

Two changes of the modified oscillator model, which might be important for strongly deformed nuclei, give shapes appropriate for fission and also give realistic level schemes at equilibrium. However, it appears desirable in the future also to include ΔV_s into the generalized l term, and to obtain a better understanding of the $\langle l^2 \rangle_N$ term or a generalization thereof. (auth)

28313 (CERN-70-30(Vol.2), pp 689-99) EFFECTS OF THE P_3 AND P_5 DISTORTIONS ON THE FISSION BARRIERS OF THE SUPERHEAVY ELEMENTS. Moeller, Peter (Lund Inst. of Tech. (Sweden). Dept. of Mathematical Physics).

In International conference on the properties of nuclei far from the region of beta-stability; Leysin, Switzerland (31 Aug 1970).

The effect of asymmetric distortions on the fission barriers for ^{236}U and the superheavy nuclei are investigated. Distortions including the ground state of the nuclei are included. Fission barriers and potential-energy surfaces are given for ^{236}U and $^{294}110$. (R.W.R.)

28314 (CERN-70-30(Vol.2), pp 700-8) ODD-PARTICLE EFFECT ON THE FISSION BARRIER. Ohlen, Gunnar (Lund Inst. of Tech. (Sweden). Dept. of Mathematical Physics).

In International conference on the properties of nuclei far from the region of beta-stability; Leysin, Switzerland (31 Aug 1970).

The extra particle in odd-A nuclei strongly affects the spontaneous-fission half-life. The even–even energy surface is calculated by using the single-particle potential and the Strutinsky shell-correction method. The odd-A energy surface is then obtained by adding the quasi-particle energy to the even–even energy surface calculated with an even–even BCS solution that has an average number of particles that is odd. Fission barriers for Pu and element 112 are given, as well as lower limits on the half-lives of some superheavy elements. (R.W.R.)

28315 (CERN-70-30(Vol.2), pp 723-33) SEARCH FOR SUPERHEAVY ELEMENTS ON THE ACCELERATOR ALICE. Lefort, Marc; Riou, Michel (Paris Univ., Orsay (France). Institut de Physique Nucleaire).

In International conference on the properties of nuclei far from the region of beta-stability; Leysin, Switzerland (31 Aug 1970).

Methods for producing superheavy elements using 400-MeV Kr beams are reviewed. Means of identifying the nuclides produced by various spectrometers and solid-state detectors are discussed. (R.W.R.)

28316 (CERN-70-30(Vol.2), pp 779-812) NEW ASPECTS OF INTERMEDIATE NUCLEI. Kumar, Krishna (Oak Ridge National Lab., Tenn.).

In International conference on the properties of nuclei far from the region of beta-stability; Leysin, Switzerland (31 Aug 1970).

Nuclei in two transition regions are discussed: spherical to deformed shapes (e.g., ^{150}Sm–^{152}Sm) and prolate to oblate shapes (e.g., $^{190}_{78}$–^{192}Pt). The various theoretical techniques used to study these nuclei are reviewed, with emphasis on the results from the pairing-plus-quadrupole model. The calculations are compared with experimental results for a number of different parameters. (R.W.R.)

28317 (CERN-70-30(Vol.2), pp 829-45) SOME NEW ASPECTS OF DEFORMED NUCLEI. Elbek, Bent (Niels Bohr Institute, Copenhagen (Denmark)).

In International conference on the properties of nuclei far from the region of beta-stability; Leysin, Switzerland (31 Aug 1970).

The types of nuclear reactions used to study deformed nuclei are briefly reviewed. It is found that Coriolis coupling is important for understanding a large number of phenomena observed in deformed nuclei. The coupling of single-particle levels associated with the crossing of Nilsson levels with the same spin and parity but belonging to different oscillator shells is also discussed. The properties of β vibrations are touched upon, and the ground-state bands of even–even nuclei are treated. (R.W.R.)

28318 (CERN-70-30(Vol.2), pp 847-82) EXTRAPOLATIONS TO THE Z = 40–60 REGION OF ELEMENTS. Ragnarsson, Ingemar (Lund Inst. of Tech. (Sweden). Dept. of Mathematical Physics).

In International conference on the properties of nuclei far from the region of beta-stability; Leysin, Switzerland (31 Aug 1970).

In order to test the method of shell-parameter extrapolations used in the superheavy region, the same prescription is used to treat the regions below the rare earth region. The Strutinsky shell-correction method is used with two different sets of values for κ and μ. The results of the theory, including masses and quadrupole moments, are compared with experiment. It appears that some of the discrepancy may result from the employment of the liquid-drop parameters in the Strutinsky shell-correction method. (R.W.R.)

28319 (CERN-70-30(Vol.2), pp 905-10) LIFETIME MEASUREMENTS ON NEUTRON DEFICIENT EVEN-EVEN ISOTOPES OF Xe AND Ba. Sann, H. J.; Dehnhardt, W.; Kistner, O. C.; Kump, P.; Kutschera, W.; Povh, B. (Max-Planck-Institut fuer Kernphysik, Heidelberg (West Germany). Heidelberg Univ. (West Germany). Physikalisches Institut (I)).

In International conference on the properties of nuclei far from the region of beta-stability; Leysin, Switzerland (31 Aug 1970).

The lifetimes of the first 2^+ states of ^{120}Xe, ^{122}Xe, ^{128}Ba, and ^{130}Ba were measured by the recoil Doppler-shift technique using the (^{16}O,4n) reaction on isotopes of Pd and Cd. Typical spectra are shown for the ^{110}Pd(^{16}O,4n)^{122}Xe reaction at 75 MeV. Deformation parameters and transition probabilities for the four isotopes are reported. (R.W.R.)

28320 (CERN-70-30(Vol.2), pp 917-30) PROMPT GAMMA TRANSITIONS IN PRIMARY FRAGMENTS FROM NEUTRON-INDUCED FISSION. Horsch, F. (Kernforschungszentrum, Karlsruhe (West Germany). Institut fuer Angewandte Reaktorphysik).

In International conference on the properties of nuclei far from the region of beta-stability; Leysin, Switzerland (31 Aug 1970).

Prompt gamma transitions in moving fission fragments of specific masses were investigated in thermal-neutron fission of ^{235}U. The masses of coincident fission fragments were deduced from their correlated kinetic energies as determined by two Si surface-barrier detectors. Gamma spectra were measured by means of a Ge(Li) detector surrounded by an $8'' \phi \times 9''$ NaI(Tl) crystal in Compton-suppression mode. The high velocity of the fission fragments was used to restrict with geo-

metric means the effective time resolution to about 10^{-9} sec after fission. The sign of the observed Doppler shift allowed the assignment of gamma-ray lines to single members of fragment pairs. The properties of individual neutron-rich nuclei far off the stability line were studied. The gross energy tendency of 54 identified gamma-ray lines as a function of mass is in agreement with the assumption that the de-excitation is predominantly collective. In the magic regions A = 88 to 92 and A = 130 to 134 only gamma rays were observed whose energies fit well into the systematics of low-lying vibrational transitions in neighboring nuclei. In the framework of such systematics it seems highly probable that the $2^+ \rightarrow 0^+$ transitions in the neutron-rich even–even nuclei ^{134}Te and ^{132}Te were identified. The specific assignment of 6 other lines in these magic regions as $2^+ \rightarrow 0^+$ transitions in the possible candidates ^{88,90,92}Kr, ^{94,96}Sr, and ^{130}Sn is discussed. (auth)

28321 (CERN–70-30(Vol,2), pp 931-8) STUDY OF SOME NEUTRON-DEFICIENT NUCLIDES WITH HIGH RESOLUTION X-RAY DETECTOR AND MASS SEPARATION. Chu, Y. Y. (Brookhaven National Lab., Upton, N. Y.).

In International conference on the properties of nuclei far from the region of beta-stability; Leysin, Switzerland (31 Aug 1970).

Several neutron-deficient nuclides of hafnium and heavy rare earths were produced by (^{3}He,xn) reactions at 30 to 60 MeV. Ge(Li) detectors with thin windows were used to resolve K x rays of the various nuclides produced. Isotopic separation was employed for nuclides whose half-lives were greater than about ten minutes. Half-lives and decay schemes are presented for ^{169}Hf and ^{168}Lu; for the latter, relative intensities of observed gamma rays are given for different means of production. Half-lives for ^{162}Yb and ^{162}Tm are also reported. (R.W.R.)

28322 (CERN–70-30(Vol,2), pp 939-47) DECAY OF SOME NUCLEI FAR FROM THE STABILITY LINE STUDIED WITH STANDARD SPECTROSCOPIC TECHNIQUES. de Boer, F. W. N.; Cardoso, M. H.; Goudsmit, P. F. A.; Koldewijn, P.; Konijn, J.; Meijer, B. J. (Instituut voor Kernphysisch Onderzoek, Amsterdam (Netherlands)).

In International conference on the properties of nuclei far from the region of beta-stability; Leysin, Switzerland (31 Aug 1970).

The (^{3}He,xn) and (p,xn) reactions were used to produce and study a number of isotopes in the rare-earth region. Half-lives, mode of production, and gamma rays measured are reported for ^{158}Tm, ^{159}Tm, ^{160}Tm, ^{164m}Tm, ^{158}Yb, ^{160}Yb, ^{163}Yb, ^{170}Ta, ^{171}Ta, ^{171m}Ta, ^{172}W, and ^{176}Os. Gamma spectra observed in the decay of ^{164m}Tm, ^{170}Ta, ^{171}Ta, ^{171m}Ta, ^{172}W are shown. A proposed decay scheme for ^{164m}Tm is given. (R.W.R.)

28323 (CERN–70-30(Vol,2), pp 949-55) ROTATIONAL BANDS IN $^{171\ 173\ 175}$Hf FROM (PARTICLE, xn) REACTIONS. Rezanka, I.; Hultberg, S.; Ryde, H. (Stockholm Univ. (Sweden). Research Inst. for Physics); Rasmussen, J. O.; Bernthal, F. M.; Alonso, J. (Yale Univ., New Haven, Conn. Heavy Ion Accelerator Lab.).

In International conference on the properties of nuclei far from the region of beta-stability; Leysin, Switzerland (31 Aug 1970).

The structure of ^{171,173,175}Hf was studied by means of the gamma spectroscopy of (particle, xn) reactions. The level structure of the $\frac{1}{2}^-$[521], $\frac{5}{2}^-$[512], and $\frac{7}{2}^+$[633] rotational bands is identified up to high spins. Rotational parameters for the odd-parity bands are given. With a simple model and basic nuclear constants the even-parity bands are reproduced to no worse than 8 keV for all levels observed; only the 3 attenuation factors for the Coriolis matrix elements were varied in obtaining the fit. (R.W.R.)

28324 (CERN–70-30(Vol,2), pp 957-65) POSSIBLE NUCLEAR CO-EXISTENCE IN ODD-MASS Ir NUCLEI. Baecklin, A.; Hedin, G. (Forskningradens Laboratorium, Studsvik (Sweden)); Malmskog, S. G.; Berg, V. (Forsvarets Forskningsanstalt, Stockholm (Sweden). Stockholm Univ. (Sweden)).

In International conference on the properties of nuclei far from the region of beta-stability; Leysin, Switzerland (31 Aug 1970).

The decays of ^{189}Pt → ^{189}Ir, ^{191}Pt → ^{191}Ir, ^{191}Os → ^{191}Ir, and ^{193}Os → ^{193}Ir were studied using solid state detectors, magnetic spectrometers, and prompt and delayed coincidences. New levels with the following spin–parity assignments and half-lives were found: ^{193}Ir: 299.45 ± 0.09 keV, $I^\pi = \frac{7}{2}^-$, $T_{\frac{1}{2}} = 0.19 \pm 0.03$ ns; 598.26 ± 0.15 keV, $I^\pi = \frac{3}{2}^-$; 740.46 ± 0.15 keV, $I^\pi = \frac{5}{2}^-$ ^{191}Ir: 391.14 ± 0.05 keV, $I^\pi = \frac{7}{2}^-$, $T_{\frac{1}{2}} = 0.24 \pm 0.02$ ns; 659.06 ± 0.08 keV, $I^\pi = \frac{3}{2}^-$, $T_{\frac{1}{2}} < 0.12$ ns. ^{189}Ir: 615.70 ± 0.08 keV, $I^\pi = \frac{7}{2}^-$, $T_{\frac{1}{2}} = 0.18 \pm 0.02$ ns; 1184.54 ± 0.11 keV, $I^\pi = \frac{5}{2}^-$, $T_{\frac{1}{2}} < 0.08$ ns. In all three Ir nuclei the values of B(E2; $\frac{7}{2}^- \rightarrow \frac{11}{2}^-$) are close to the values of B(E2; $2^+ \rightarrow 0^+$) in neighboring, essentially spherical, even nuclei. Energies and transition probabilities indicate that the $\frac{7}{2}^-$ states are analogous to the $\frac{7}{2}^-$ states found in the odd mass Au nuclei; i.e., they are associated with an essentially spherical shape of the nucleus. This is in contrast to the low-lying positive parity states, which in all three nuclei can be arranged into rotational bands, which may be assigned as the Nilsson states $\frac{3}{2}^+$[402] and $\frac{1}{2}^+$[400]. From the B(E2) values of the intra-band transitions, deformations $\delta = 0.25$ for ^{189}Ir and $\delta = 0.12$ in ^{191}Ir and ^{193}Ir are obtained. (auth)

28325 CERN–70-30(Vol.2), pp 967-84) IDENTIFICATION OF μs ISOMERS AMONG PRIMARY FISSION FRAGMENTS. Grueter, J. W.; Sistemich, K.; Armbruster, P.; Eidens, J.; Lawin, H. (Kernforschungsanlage, Juelich (West Germany). Institut fuer Neutronenphysik).

In International conference on the properties of nuclei far from the region of beta-stability; Leysin, Switzerland (31 Aug 1970).

The isomeric x rays and γ rays emitted by fission products from the thermal-neutron fission of ^{235}U in the time window between 1 μs and 80 μs after the fission event were investigated. Isomeric transitions were detected at the fission product masses A = 88, 93, 96 to 100, and 132 to 136 with about 90% of the γ lines being emitted in the regions A = 96 to 100 and A = 132 to 136. An identification of the isomeric nuclides was achieved in most cases. In the mass region 96 to 100 all identified or possible isomers have 58 or 59 neutrons. The identified isomers in the region A = 132 to 136 are ^{134}Te and ^{136}Xe with N = 82. The isomerism is discussed. (34 references) (auth)

28326 (CERN–70-30(Vol,2), pp 985-1000) SOME STUDIES ON NEUTRON-RICH NUCLEI. Herrmann, G.; Kaffrell, N.; Trautmann, N.; Denig, R.; Herzog, W.; Huebscher, D.; Kratz, K. L. (Mainz Univ. (West Germany). Institut fuer Anorganische Chemie und Kernchemie).

In International conference on the properties of nuclei far from the region of beta-stability; Leysin, Switzerland (31 Aug 1970).

The half-lives of the neutron-rich isotopes ^{90}Br, ^{91}Br, ^{92}Br, ^{139}I, ^{140}I, and ^{141}I were measured by direct and indirect γ-ray spectroscopic methods to be between 0.25 and 2.3 sec. Gamma spectra are given for short-lived Tc fission products; 5.9-sec ^{192}Re, ^{192m}Os; 3.0-min ^{164}Tb; and 2.3-min ^{238}Pa. These results were used to produce level schemes for ^{106}Ru, ^{192}Os, ^{164}Dy, and ^{238}U. (R.W.R.)

28327 (CERN–70-30(Vol,2), pp 1001-3) ^{132}Sn-REGION STUDIED BY MEANS OF THE OSIRIS FACILITY. Holm, G. B. (Forsvarets Forskiningsanstalt, Stockholm (Sweden)).

In International conference on the properties of nuclei far from the region of beta-stability; Leysin, Switzerland (31 Aug 1970).

Reasons for the investigation of the ^{132}Sn region are presented. Half-lives and Q_β values in for nuclides in the region are given. (R.W.R.)

28328 (CERN–70-30(Vol,2), pp 1006-7) PROTON STATES IN THE TIN-REGION. Holm, G. B.; Borg, S.; Rydberg, B. (Forsvarets Forskiningsanstalt, Stockholm (Sweden). Stockholm Univ. (Sweden). Research Inst. for Physics).

In International conference on the properties of nuclei far from the region of beta-stability; Leysin, Switzerland (31 Aug 1970).

Beta–gamma coincidence measurements were made on the decay of ^{133}Sn. At higher beta energies only a 963-keV gamma ray remains; it is interpreted as de-exciting the $d_{\frac{5}{2}}$ state to the $g_{\frac{7}{2}}$ ground state. The half-life of the decay is 1.7 sec. Gamma rays of 267, 604, and 871 keV were observed in the decay of ^{135}Te. The intensity results favor assigning the 267-keV transition as M1 and the 871 as E2. It appears that the three-quasi-particle $\frac{5}{2}$ state occurs at an excitation of about 0.8 MeV; since this is close to the one-quasi-particle state, the two states mix strongly and repel each other. (R.W.R.)

28329 (CERN–70-30(Vol,2), pp 1008-10) NEUTRON HOLE STATES IN THE TIN-REGION. Holm, G. B.; Andersson, G. I.; Borg, S.; De Geer, L.-E. (Forsvarets Forskningsanstalt, Stockholm (Sweden). Stockholm Univ. (Sweden). Research Inst. for Physics).

In International conference on the properties of nuclei far from the region of beta-stability; Leysin, Switzerland (31 Aug 1970).

A 0.3-sec activity is assigned to the beta decay of ^{131}In. The 2431-keV gamma ray probably represents a transition from the $g_{\frac{9}{2}}$ ground state of ^{131}In to the $g_{\frac{7}{2}}$ state in ^{131}Sn. The origin of a 330-keV gamma is discussed. No isomeric states were detected belonging to ^{131}Sn. The decays of ^{129}In and ^{127}In were also studied. (R.W.R.)

28330 (CERN–70-30(Vol.2), pp 1010-11) LEVELS IN DOUBLY-EVEN TELLURIUM ISOTOPES. Kerek, A.; Bergstroem, I.; Borg, S.; Carle, P.; Holm, G.; Rydberg, B. (Stockholm Univ. (Sweden). Research Inst. for Physics. Forsvarets

Forskningsanstalt, Stockholm (Sweden)).
In International conference on the properties of nuclei far from the region of beta-stability; Leysin, Switzerland (31 Aug 1970).

The level systematics of doubly-even Te was studied by means of (α, 2nγ) reactions for the isotopes $^{114-126}$Te, while the levels of $^{128-132}$Te were populated in doubly-odd Sb decay. The 2^+ and 4^+ levels show a vibrational pattern for $114 \leq A \leq 128$, while in the heavier isotopes the shell effect is noticeable. The energy of the 6^+ state is nearly constant (1800 keV) for $118 \leq A \leq 132$. (R.W.R.)

28331 (CERN-70-30(Vol.2), pp 1012-14) EVIDENCE FOR A HIGH-SPIN THREE QUASIPARTICLE STATE IN ^{133}I PRODUCED IN FISSION. Bergstroem, I.; Borg, S.; Holm, G. B.; Rydberg, B. (Stockholm Univ. (Sweden). Research Inst. for Physics. Forsvarets Forskningsanstalt, Stockholm (Sweden)).
In International conference on the properties of nuclei far from the region of beta-stability; Leysin, Switzerland (31 Aug 1970).

A 9-sec component with A = 133 was found among the products of nuclear fission. All available evidence indicates the existence of a high-spin ($\sim 15/2$), negative-parity state in ^{133}I. The reasoning leading to this conclusion is explained. (R.W.R.)

28332 (CERN-70-30(Vol.2), pp 1015-21) DECAY OF ^{110}Sb, ^{111}Sb, ^{112}Sb, ^{113}Sb, AND ^{114}Sb. Sunier, J. W.; Singh, M.; DeVries, R. M.; Thompson, G. E. (California Univ., Los Angeles).
In International conference on the properties of nuclei far from the region of beta-stability; Leysin, Switzerland (31 Aug 1970).

Two previously unknown isotopes, ^{110}Sb and ^{111}Sb, were produced by (p,3n) and (p,2n) reactions on ^{112}Sn. The gamma spectra following their beta decay were studied, as well as those of ^{112}Sb, ^{113}Sb, and ^{114}Sb, produced by (p,xn) reactions on ^{112}Sn and/or ^{114}Sn. Half-lives, partial decay schemes, and typical gamma spectra are given. The systematics of the energy levels of the product tin nuclei is discussed. (R.W.R.)

28333 (CERN-70-30(Vol.2), pp 1023-9) LOW-LYING STATES IN ODD-MASS POLONIUM ISOTOPES. Astner, G.; Jonson, B.; Alpsten, M.; Appelqvist, Aa. (European Organization for Nuclear Research, Geneva (Switzerland)).
In International conference on the properties of nuclei far from the region of beta-stability; Leysin, Switzerland (31 Aug 1970).

Alpha-gamma coincidence measurements were carried out to obtain excitation energies for levels in ^{201,203,205}Po from alpha decay of radon. Levels in ^{203,205,207,209}Po were studied by electron-capture decay in astatine by using Ge(Li) and Si(Li) detectors and a double-focusing beta spectrometer; $\gamma-\gamma$ coincidence measurements were also made. Level diagrams with spin-parity assignments and multipolarities are given and compared with those in the corresponding lead isotones. (R.W.R.)

28334 (CERN-70-30(Vol.2), pp 1031-43) PROPERTIES OF THE LOW-LYING LEVELS IN THE EVEN Pt AND Os NUCLEI. Erdal, B. R.; Finger, M.; Foucher, R.; (and others) (European Organization for Nuclear Research, Geneva (Switzerland)).
In International conference on the properties of nuclei far from the region of beta-stability; Leysin, Switzerland (31 Aug 1970).

Low-lying levels in the even neutron-deficient Os and Pt nuclei ($182 \leq A \leq 192$) were investigated. Lifetimes and B(E2)'s were measured. The results and possible theoretical interpretations are discussed. Three principal conclusions are drawn: low-lying levels in Pt nuclei seem to be organized in bands, and the β band-head is strongly mixed with the ground band; the energy of the levels of the proposed β and γ bands present minima for masses A = 186 to 190; a marked variation of the energy and of the relative position of the levels takes place between masses 186 to 190. (27 references) (R.W.R.)

28335 (CERN-70-30(Vol.2), pp 1045-55) ISOMERISM IN ODD AND ODD-ODD NUCLEI WITH MASS NUMBER $185 \leq A \leq 191$. Erdal, B. R.; Finger, M.; Foucher, R.; (and others) (European Organization for Nuclear Research, Geneva (Switzerland)).
In International conference on the properties of nuclei far from the region of beta-stability; Leysin, Switzerland (31 Aug 1970).
Results from the study of isomeric states in a number of odd-A and odd-odd nuclei in the Pt region are presented. In some cases these results are correlated with decay-scheme investigations. Because of the experimental method used, only isomers with half-lives longer than a few seconds or in the nsec to μsec range could be detected. The assignment of the Nilsson-model characteristics is attempted for some of the observed excited states. (41 references) (R.W.R.)

28336 (CERN-70-30(Vol.2), pp 1057-68) NUCLEAR SPECTROSCOPY OF IODINE ISOTOPES WITH $A \geq 134$. Achterberg, E. O.; de Aisenberg, E. Y.; Iglesias, F. C.; (and others) (Comision Nacional de Energia Atomica, Buenos Aires (Argentina)).
In International conference on the properties of nuclei far from the region of beta-stability; Leysin, Switzerland (31 Aug 1970).
The heavy fragments from ^{235}U fission were searched for heavy I isotopes. Semiconductor detectors were used to record singles and coincidence spectra of electrons and gamma rays. Gamma energies and intensities, conversion coefficients, and multipolarities are given for the decay of ^{134}I. Similar results are given for the decay of ^{139}Xe, as well as for several other sources in the A = 133 to 137 mass region. The half-life of ^{134m}I was found to be 3.50 ± 0.12 min. (R.W.R.)

28337 (CERN-70-30(Vol.2), pp 1069-74) ENERGY LEVELS IN $^{114\ 116\ 118\ 120\ 122}$Cd POPULATED IN THE DECAY OF Ag ISOTOPES. Baecklin, A.; Fogelberg, B.; Hedin, G. (Forskningradens Laboratorium, Studsvik (Sweden)).
In International conference on the properties of nuclei far from the region of beta-stability; Leysin, Switzerland (31 Aug 1970).

The decays of Ag isotopes to even Cd isotopes with $114 \leq A \leq 122$ were investigated. The following levels are populated (energies in keV): ^{114}Ag → ^{114}Cd($T_{1/2} < 10$s): 558(2^+), 1134(0^+). ^{116}Ag → ^{116}Cd($T_{1/2}$ = 3 min): 513.5(2^+), 1154.0(0^+), 1212.8(2^+), 1922. ^{116}Ag → ^{116}Cd($T_{1/2}$ = 10s): 513.5(2^+), 1219(4^+), 2026. ^{118}Ag → ^{118}Cd($T_{1/2}$ = 4.5s): 487.1(2^+), 1165, 1269(2^+). ^{120}Ag → ^{120}Cd($T_{1/2}$ = 1.3s): 505.5(2^+), 1203, 1324(2^+). ^{122}Ag → ^{122}Cd (short): 569(2^+) (tentative). (auth)

28338 (CERN-70-30(Vol.2), pp 1075-9) DECAY STUDIES OF NEUTRON DEFICIENT Ga AND Zn ISOTOPES. Dulfer, G. H.; Beertema, H. E.; Wigmans, M. E. J.; Verheul, H. (Vrije Universiteit, Amsterdam (Netherlands). Natuurkundig Laboratorium).
In International conference on the properties of nuclei far from the region of beta-stability; Leysin, Switzerland (31 Aug 1970).
Spectroscopy was performed on neutron deficient Ga and Zn isotopes. The decay of 31-sec ^{63}Ga was investigated with Ge(Li) detectors. A decay scheme is presented. Preliminary results are given from the study of the decay of 15-min ^{65}Ga. (auth)

28339 (CERN-70-30(Vol.2), pp 1081-91) NUCLEAR SPECTROSCOPY OF SOME LIGHT Tl ISOTOPES. Fenyes, T.; Mahunka, I.; Mahunka, M.; Mate, Z.; Piotrowski, A.; Tron, L.; Tyrroff, H.; Vandlik, J.; Zaitseva, N. G. (Joint Inst. for Nuclear Research, Dubna (USSR)).
In International conference on the properties of nuclei far from the region of beta-stability; Leysin, Switzerland (31 Aug 1970).
Neutron-deficient Tl isotopes were produced by irradiating PbF_2 powder with 660-MeV protons. The ^{191}Tl isotope was identified, and its half-life was measured. The gamma spectra of ^{190}Tl, ^{191}Tl, and ^{193}Tl and the conversion-electron spectrum of ^{193}Tl were also measured. Internal conversion coefficients for ^{193}Tl are reported. The separation of Tl from the target material is explained in some detail. (R.W.R.)

28340 (CERN-70-30(Vol.2), pp 1093-1103) NEUTRON-RICH NUCLIDES OBTAINED USING THE OSIRIS FACILITY. Grappengigsser, B.; Lund, E.; Rudstam, G. (Forskningradens Laboratorium, Studsvik (Sweden)).
In International conference on the properties of nuclei far from the region of beta-stability; Leysin, Switzerland (31 Aug 1970).
Fission fragments recoiling out of a ^{235}U target were caught by a graphite cloth in the ion source. The temperature of the ion source was kept high enough to release eighteen of the elements produced by fission so fast that it was possible to detect their short-lived isotopes after electromagnetic mass separation. No chemical separation except the element-dependent separator efficiency was used. Several methods for the determination of the half-life of the radioactive nuclides were employed. The decays were counted by means of the following systems: a 4π β counter made of plastic scintillating material; a neutron detector consisting of BF_3 tubes; an anthracene crystal with beta pulses sorted according to energy; and Ge(Li) and Si(Li) detectors for following the decay of gamma rays, x rays, and conversion electrons. The results are collected in a table containing half-life determinations of 75 nuclides or isomers, 32 of them new or with half-lives significantly different from published data. (auth)

28341 (CERN-70-30(Vol.2), pp 1115-18) LIFETIMES OF EXCITED NUCLEAR LEVELS. Malmskog, S. G.; Berg, V.; Hoeglund, A. (Aktiebolaget Atomenergi, Studsvik (Sweden). Stockholm Univ. (Sweden). Inst. of Physics).
In International conference on the properties of nuclei far from the region of beta-stability; Leysin, Switzerland (31 Aug 1970).
Probabilities for E2 transitions in several Au isotopes are reported. Half-lives are given for the 79.5-keV level in ^{134}I and the 190.3-keV level in ^{141}La. (R.W.R.)

XUM

28342 (CERN-70-30(Vol.2), pp 1119-21) SHORT-LIVED ISOMERS OF ^{136}I AND ^{138}Cs DECAYING VIA METASTABLE STATES OF ^{136}Xe AND ^{138}Ba. Monnand, E.; Blachot, J.; Carraz, L. C.; Moussa, A. (Commissariat a l'Energie Atomique, Grenoble (France). Centre d'Etudes Nucleaires).

In International conference on the properties of nuclei far from the region of beta-stability; Leysin, Switzerland (31 Aug 1970).

In the study of fission products, isomers were discovered in ^{136}I (48 sec) and ^{138}Cs (3.1 min). These states populate (among others) a 2.8-μsec, 1892.3-keV state in ^{136}Xe and a 0.8-μsec, 2091-keV state in ^{138}Ba, respectively. Decay schemes of isomeric ^{136}I and ^{138}Cs are given. (R.W.R.)

28343 (CERN-70-30(Vol.2), pp 1125-7) RECENT STUDIES OF SHORT-LIVED GASEOUS FISSION PRODUCTS AND THEIR DAUGHTERS. Talbert, W. L. Jr. (Ames Lab., Iowa).

In International conference on the properties of nuclei far from the region of beta-stability; Leysin, Switzerland (31 Aug 1970).

Gamma-ray decay studies are outlined for short-lived gaseous fission products and their daughters for decay chains with A = 90, 91, 92, 140, 141, and 142. (R.W.R.)

28344 (JAERI-1200) COMPARISON OF THERMAL NEUTRON CROSS SECTIONS. Tsuchihashi, Keiichiro (Japan Atomic Energy Research Inst., Tokyo). May 1970. 13p. (In Japanese). Dep. NTIS (U. S. Sales Only).

The thermal-neutron cross sections (except for the scattering cross sections) contained in the JNDC set (1966), UK files (1967), and ENDF/B files (1967) are converted into ENDF/A format. A processing program was developed in order to use these cross sections for multigroup calculations. The 30 group cross sections and Westcott parameters, which are obtained by the processing program, are compared. It is found that a few cross sections in the JNDC set are seriously different from those in UK files and ENDF/B files. As for most cross sections, however, the differences are sufficiently minor that any cross sections can be used for reactor calculations. (auth)

28345 (JINR-E3-5483) (n,α) REACTION: A NEW CHANNEL FOR STUDYING THE NATURE OF NEUTRON RESONANCES. Popov, Yu. P. (Joint Inst. for Nuclear Research, Dubna (USSR). Lab. of Neutron Physics). 1970. 22p. Dep. NTIS (U. S. Sales Only).

The measurements of the (n,α) reaction cross sections and α-particle spectra in individual resonances performed in the Laboratory of Neutron Physics (JINR) showed the efficiency of further development of this branch of neutron spectroscopy. The results of the first studies of the (n,α) reaction on resonance neutrons, the problems to be solved by experimentalists and the perspectives of acquisition of new data on the nature of neutron resonances and parameters of the optical model are considered. (auth)

28346 (JINR-E4-5567) NONROTATIONAL STATES OF ODD-N DEFORMED NUCLEI IN THE REGION $153 \leq A \leq 171$. Malov, L. A.; Solov'ev, V. G.; Fedotov, S. I. (Joint Inst. for Nuclear Research, Dubna (USSR). Lab. of Theoretical Physics). 1971. 17p. Dep. NTIS (U. S. Sales Only).

The ground and excited states of odd-N nuclei in the region $153 \leq A \leq 171$ were calculated in the framework of the superfluid nuclear model. The calculations were performed with the Saxon-Woods single-particle energies and wave functions. A satisfactory agreement of the experimental and theoretical data was obtained. (auth)

28347 (JINR-P3-5553) ALPHA DECAY OF THE RESONANCE STATES OF ^{148}Sm. Wilhelm, I.; Popov, Yu. P.; Przytula, M.; Rumi, R. F.; Stempin'ski, M. (Joint Inst. for Nuclear Research, Dubna (USSR). Lab. of Neutron Physics). 1970. 16p. (In Russian). Dep. NTIS (U. S. Sales Only).

The spectra of eleven resonance states in the reaction ^{147}Sm (n,α) ^{144}Nd are analyzed. The spin identification of resonances is made. The questions of partial α-widths distribution and of the probability of emission of α-particles with different orbital moments are considered. The effects of the highly excited-state structure on the α-decay are discussed. (auth)

28348 (JINR-P6-5617) NEW ISOTOPES OF IRIDIUM. Nadzhakov, E.; Bochev, B.; Venkova, Ts.; Shcheglovski, Z.; Kutsarova, T.; Kalpakchieva, R. (Joint Inst. for Nuclear Research, Dubna (USSR). Lab. of Nuclear Reactions). 1971. 23p. (In Russian). Dep. NTIS (U. S. Sales Only).

In compound-nucleus reactions resulting in neutron evaporation, far neutron-deficient iridium isotopes were produced by bombarding Ho with ^{22}Ne and ^{20}Ne heavy ions. The isotopes were identified according to the genetic relations with the daughter isotopes of Os and Re. New isotopes of ^{181}Ir (10 ± 2 min), ^{180}Ir (6.5 ± 1.5 min), and ^{179}Ir (4 ± 1 min) are reported. (auth)

28349 (KAPL-P-3930) NEUTRON CROSS SECTIONS AND STRENGTH FUNCTIONS OF ^{147}Sm AND ^{150}Sm. Eiland, H. M.; Weinstein, S.; Seemann, K. W. (Knolls Atomic Power Lab., Schenectady, N. Y.). [1971]. Contract W-31-109-eng-52. 7p. (CONF-710301-2). Dep. NTIS.

From third conference on neutron cross sections and technology; Knoxville, Tenn. (15 Mar 1971).

The total cross sections of ^{147}Sm and ^{150}Sm were determined by transmission measurements upon samples of high isotopic purity. Measurements were made at the RPI Linear Accelerator with a lithium-glass scintillation detector at 25 meters. Energy resolution varied from 2 to 10 nsec/m. Resonance parameters were extracted for ^{147}Sm resonances up to 1200 eV and for ^{150}Sm resonances up to 1500 eV. The results are given. (auth)

28350 (KFK-tr-350) INVESTIGATION OF THE α DECAY OF ISOTOPES OF ELEMENT 105. Druin, V. A.; Demin, A. G.; Kharitonov, Yu. P.; Akap'ev, G. N.; Rud', V. I.; Sun-Tszin-Yan, G. Ya.; Chelnokov, L. P.; Gavrilov, K. A. (Joint Inst. for Nuclear Research, Dubna (USSR)). Translated by Rosemarie Corssen (Kernforschungszentrum, Karlsruhe, Ger.), from report JINR-P7-5161. 11p. (In German). Dep. NTIS (U. S. Sales Only).

The α decay of element 105, produced by the irradiation of ^{243}Am with ^{22}Ne ions at 120 MeV, was investigated. A long-lived (half-life of 35 sec) and a short-lived (half-life of 1.4 sec) activity were observed. The long-lived activity was attributed to element 103, but the short-lived activity with an α decay energy of 9.10 MeV was attributed to element 105. The effective cross section for the nuclear reaction leading to its synthesis was evaluated as $\approx 2 \times 10^{-33}$ cm^2. The isotope of element 105 emitting the 9.1 MeV activity could not be ascertained. (J.S.R.)

28351 (KFK-tr-352) EMISSIONS OF ^{6}He THROUGH NUCLEAR FISSION BY HEAVY IONS. Pulativ, D. D.; Polikanov, S. M. (Joint Inst. for Nuclear Research, Dubna (USSR)). Translated by Rosemarie Corssen (Kernforschungszentrum, Karlsruhe, Ger.), from report JINR-P7-5192. 12p. (In German). Dep. NTIS (U. S. Sales Only).

The emissions of ^{6}He during the fission of ^{238}U and ^{197}Au by ^{12}C and ^{16}O at energies of 82 and 137 MeV, respectively, were investigated. In order to estimate the effect connected with the β decay of ^{6}He, measurements were taken in three motion cycles of the collector in front of the detectors. The existence of a short-lived activity was proved, and the yield and half-life of this activity were determined. The data obtained was discussed with respect to the mechanism for the emission of ^{6}He. (J.S.R.)

28352 (N-71-10060) MEASURED ELECTRON CONVERSION RATIOS FOR THE 1064-keV γ RAY OF ^{207}Bi. Beck, Sherwin M. (National Aeronautics and Space Administration, Langley Station, Va. Langley Research Center). Nov 1970. 40p. (NASA-TN-D-6057; L-6015). NTIS.

The electron conversion ratios for the 1064-keV gamma ray of ^{207}Bi were determined from the conversion-electron spectra obtained by using lithium-drifted silicon detectors. The spectrometer system had an energy resolution between 4 and 5 keV at 1 MeV, which was sufficient to separate the L- and M-shell conversion-electron lines. Sixty-one measurements were made with four Si(Li) detectors. The average values obtained for the conversion ratios of K-, L-, and M-shell electrons were K/L = 3.90, K/M = 11.23, K/L + M = 2.90, and L/M = 2.89. (auth)

28353 (NP-18695) LIFETIMES OF EXCITED STATES IN HEAVY NUCLEI. Ton, Hendrik (Vrije Universiteit, Amsterdam (Netherlands)). 1970. 99p. Dep. NTIS (U. S. Sales Only).

Thesis.

The research includes gamma-ray transition probabilities in deformed nuclei, experimental methods and apparatus for the measurement of short lifetimes, and lifetimes of 2+ and 4+ rotational states in heavy even-even nuclei. Also discussed are lifetimes of rotational states in thorium-229 and uranium-235 and lifetimes of high-spin states in platinum-194, platinum-196, mercury-198, and mercury-200. (J.F.P.)

28354 (NP-18723) FISSION PRODUCT YIELD IN THE FISSION OF ^{235}U, ^{238}U, ^{239}Pu, AND ^{241}Pu WITH NEUTRONS OF DIFFERENT ENERGIES. Hofmann, P. (Kernforschungszentrum, Karlsruhe (West Germany). Institut fuer Material- und Festkoerperforschung). 12 Nov 1970. 155p. (In German). Dep. NTIS (U. S. Sales Only).

The compatibility of nuclear fuels with cladding materials of the breeder reactor constitutes a decisive problem with respect to their lives. Since the nuclear fuel is modified chemically by the formation of fission products, compatibility investigations on pure nuclear fuels are no longer sufficient for high burnups. Hence, compatibility investigations must be carried out with simulated fission products added to the nuclear fuel. This requires

that the composition and yield of the fission products of a nuclear fuel be known as a function of the neutron energy and the time. Consequently, the stable and long-lived fission products of the isobaric fission product decay series were determined which are formed during fission of ^{235}U, ^{239}Pu, and ^{241}Pu by thermal neutrons (0.025 eV) and ^{235}U, ^{238}U, and ^{239}Pu by fast neutrons (1 MeV, 14 MeV, fission spectrum). In determining the fission product yields negative β-decays and splitting of isobaric decay chains by emission of delayed neutrons were taken into account. (n,γ)-reactions of the fission products which are the transition of one isobaric decay series to another were considered only in the fission of ^{235}U, ^{238}U, and ^{239}Pu by fast neutrons (fission spectrum). These fission product yields were compared with those obtained in the absence of (n,γ)-reactions. The comparison reveals that during the fission of ^{239}Pu the fission yields of the lanthanides, zirconium, yttrium, and molybdenum are higher when neutron capture reactions of fission products are taken into account. (auth)

28355 (TID-25659) EXPERIMENTAL AND THEORETICAL INVESTIGATION OF NUCLEAR FISSION INDUCED BY LOW-ENERGY NUCLEAR PARTICLES. Progress Report. Bacharach, S. L.; Deutsch, R. W. (Catholic Univ. of America, Washington, D. C. Dept. of Nuclear Science and Engineering). 29 Jan 1971. Contract AT(40-1)-3951. 35p. Dep. NTIS.

Measurements were made of the delayed fission of ^{237}Pu produced by 9.0 to 14.0 MeV deuterons bombardment of ^{237}Np. Two isomers with half lives of 112 ± 10 and 1090 ± 310 nanoseconds were identified. This is the first time that these two isomers have been measured simultaneously. The relative yields of these isomers show that the 112 ns isomer increases relative to the 1090 ns isomer as the deuteron energy decreases, which indicates a possible inconsistency in the Strutinsky double humped potential. A method for predicting the prompt neutron yields from thermal neutron fission was developed, based upon available measured characteristics of ^{233}U, ^{235}U and ^{239}Pu thermal neutron fission. This method can be applied to determine prompt neutron yields from unmeasured thermal neutron fissionable elements that are present in long burning nuclear reactors. (auth)

28356 (UCRL-50400(Vol.3)) AN INDEX TO THE EXPERIMENTAL DATA OF NEUTRON-INDUCED REACTIONS. Howerton, R. J.; Perkins, S. T.; Altamirano, C. P.; Hill, K. L. (California Univ., Livermore. Lawrence Radiation Lab.). [nd]. 812p. Dep. NTIS.

An index to the data of neutron-induced reactions contained in the Experimental Cross Section Information Library (ECSIL), as of October 1, 1970, is presented. Three permutations of the reaction index, a key to current conventions, and a summary table are presented. (auth)

28357 (UJV-2540-F) QUASIPARTICLE DESCRIPTION FOR INDIUM. Alzetta, R.; Gmitro, M.; Gambhir, Y. K. (Ceskoslovenska Akademie Ved, Rez. Ustav Jaderneho Vyzkumu). [1970]. 31p. Dep. NTIS (U. S. Sales Only).

The quasiparticle model was applied to the description of the nuclear properties of the low-lying states of In isotopes. The $\mathcal{H}$ is diagonalized in the space obtained by coupling zero- and two-quasineutron configurations with the proton-hole states in N = Z = 50 core, using a renormalized Tabakin interaction. The inclusion of two-hole one-particle proton configurations, consistent with the experimental findings in the $^{114}Cd(^3He,d)^{115}In$ reaction, in a weak coupling approximation in which the quasineutron excitation modes are first generated independently, and then coupled to the proton hole excitations to obtain the configuration space for the diagonalization work, is also studied quantitatively. The energy spectrum of the ^{115}In nucleus is calculated and discussed. (auth)

28358 FORWARD ELASTIC SCATTERING OF 9 MeV GAMMA RAYS. Moreh, R. (Nuclear Research Centre, Beer-Sheva, Israel); Salzmann, D.; Ben-David, G. Phys. Lett.; 34B: 494-6 (29 Mar 1971).

The elastic scattering cross section of 9-MeV photons from lead and uranium targets was measured at forward angles between 7° and 20° with a Ge(Li) detector. The contribution of Delbruck scattering was found to be dominant, while that of Rayleigh scattering is probably negligible. (auth)

28359 ISOBARIC ANALOGUE RESONANT (p,γ) REACTIONS ON ^{92}Mo. Ejiri, H.; Ferguson, S. M.; Halpern, I.; Heffner, R. (Univ. of Washington, Seattle). pp 65-71 of Nuclear Isospin. /Anderson, John D. (ed.). New York; Academic Press, Inc. (1969).

From second conference on nuclear isospin; Pacific Grove, Calif. (13 Mar 1969). See CONF-690310.

28360 E1 TRANSITIONS FROM ANALOG STATES IN ^{90}Zr. Hughes, T. A. (IBM Scientific Center, Houston, Tex.); Fallieros, S. pp 109-12 of Nuclear Isospin. /Anderson, John D. (ed.). New York; Academic Press, Inc. (1969).

From second conference on nuclear isospin; Pacific Grove, Calif. (13 Mar 1969). See CONF-690310.

28361 ISOBARIC ANALOG STATES IN (γ,p) REACTIONS ON Sn ISOTOPES. Shoda, K.; Sugawara, M.; Saito, T.; Miyase, H. (Tohoku Univ., Sendai). pp 131-6 of Nuclear Isospin. /Anderson, John D. (ed.). New York; Academic Press, Inc. (1969).

From second conference on nuclear isospin; Pacific Grove, Calif. (13 Mar 1969). See CONF-690310.

28362 ISOBARIC ANALOG STATES IN (γ,p) REACTIONS ON N = 82 NUCLEI. Shoda, K.; Sugawara, M.; Saito, T.; Miyase, H. (Tohoku Univ., Sendai). pp. 137-42 of Nuclear Isospin. /Anderson, John D. (ed.). New York; Academic Press, Inc. (1969).

From second conference on nuclear isospin; Pacific Grove, Calif. (13 Mar 1969). See CONF-690310.

28363 SPREADING OF THE ANTIANALOGUE STATES IN ^{91}Nb. Vourvopoulos, G. (Florida A and M Univ., Tallahassee. Florida State Univ., Tallahassee); Shoup, R.; Fox, J. D.; Ball, J. B. pp 205-14 of Nuclear Isospin. /Anderson, John D. (ed.). New York; Academic Press, Inc. (1969).

From second conference on nuclear isospin; Pacific Grove, Calif. (13 Mar 1969). See CONF-690310.

28364 R-MATRIX ANALYSIS OF PROTON INELASTIC SCATTERING THROUGH ISOBARIC ANALOG RESONANCES. Thompson, W. J. (Florida State Univ., Tallahassee). pp 427-31 of Nuclear Isospin. /Anderson, John D. (ed.). New York; Academic Press, Inc. (1969).

From second conference on nuclear isospin; Pacific Grove, Calif. (13 Mar 1969). See CONF-690310.

28365 SPECTATOR PARTICLES AND RESONANCES. Moore, Fred C.; Endriss, M.; Grosse, E.; Heusler, A.; von Brentano, P. (Max-Planck-Institut fuer Kernphysik, Heidelberg). pp 579-83 of Nuclear Isospin. /Anderson, John D. (ed.). New York; Academic Press, Inc. (1969).

From second conference on nuclear isospin; Pacific Grove, Calif. (13 Mar 1969). See CONF-690310.

28366 A COMPARISON OF ANALOGUE RESONANCE STUDIES AND COULOMBSTRIPPING IN ^{208}Pb. Dost, M.; Harney, H. L. (Max-Planck-Institut fuer Kernphysik, Heidelberg). pp 639-42 of Nuclear Isospin. /Anderson, John D. (ed.). New York; Academic Press, Inc. (1969).

From second conference on nuclear isospin; Pacific Grove, Calif. (13 Mar 1969). See CONF-690310.

28367 INELASTIC PROTON DECAY OF THE g_9 ANALOGUE RESONANCE IN ^{209}Bi. Dyer, P.; Zaidi, S. A. A. (Univ. of Texas, Austin). pp 643-50 of Nuclear Isospin. /Anderson, John D. (ed.). New York; Academic Press, Inc. (1969).

From second conference on nuclear isospin; Pacific Grove, Calif. (13 Mar 1969). See CONF-690310.

28368 POLARIZATION MEASUREMENTS FOR $^{92}Zr(p,p)^{92}Zr$ NEAR ISOBARIC ANALOG RESONANCES. Ellis, J. L.; Haeberli, W. (Univ. of Wisconsin, Madison). pp 651-4 of Nuclear Isospin. /Anderson, John D. (ed.). New York; Academic Press, Inc. (1969).

From second conference on nuclear isospin; Pacific Grove, Calif. (13 Mar 1969). See CONF-690310.

28369 NEUTRON PARTICLE-HOLE STATES IN ^{130}Te. Hiddleston, H. R.; Mistry, V. D.; Hollas, C. L.; Riley, P. J. (Univ. of Texas, Austin). pp 661-6 of Nuclear Isospin. /Anderson, John D. (ed.). New York; Academic Press, Inc. (1969).

From second conference on nuclear isospin; Pacific Grove, Calif. (13 Mar 1969). See CONF-690310.

28370 ISOBARIC ANALOG RESONANCES IN PROTON ELASTIC SCATTERING FROM ^{110}Cd, ^{112}Cd, ^{114}Cd. Mistry, V. D.; Hollas, C. L.; Hiddleston, H. R.; Riley, P. J. (Univ. of Texas, Austin). pp 673-8 of Nuclear Isospin. /Anderson, John D. (ed.). New York; Academic Press, Inc. (1969).

From second conference on nuclear isospin; Pacific Grove, Calif. (13 Mar 1969). See CONF-690310.

28371 SINGLE-PARTICLE ANALOG STATE ANOMALIES IN THE SCATTERING OF PROTONS FROM ^{197}Au, ^{196}Pt, AND ^{184}W. Schiffer, J. P.; Kienle, P.; Morrison, G. C. (Argonne National Lab., Ill.). pp 679-84 of Nuclear Isospin. /Anderson, John D. (ed.). New York; Academic Press, Inc. (1969).

From second conference on nuclear isospin; Pacific Grove, Calif. (13 Mar 1969). See CONF-690310.

28372 COMPARISON OF SPECTROSCOPIC FACTORS FROM (p,p_0) AND (d,p) REACTIONS ON BARIUM ISOTOPES.

XUM

Williams, N.; von Ehrenstein, D.; Nolen, J. A. Jr.; Morrison, G. C. (Argonne National Lab., Ill.). pp 695-700 of Nuclear Isospin. /Anderson, John D. (ed.). New York; Academic Press, Inc. (1969).

From second conference on nuclear isospin; Pacific Grove, Calif. (13 Mar 1969). See CONF-690310.

28373 DECAY SCHEMES FOR THE ISOMERS OF ^{148}Pm AND THE CROSS SECTIONS FOR THEIR PRODUCTION BY NEUTRON CAPTURE IN ^{147}Pm. Mowatt, R. S.; Walker, W. H. (Atomic Energy of Canada Ltd., Chalk River, Ont.). Can. J. Phys.; 49: 108-17(1 Jan 1971). (AECL-3749).

The γ-ray spectra arising from the decay of 41-day ^{148}Pm^{m} and 5-day ^{148}Pm^{g} produced by the irradiation of 2.6-year ^{147}Pm in a thermal reactor neutron flux were measured with a Ge(Li) detector. The absolute probabilities for γ-ray emission were determined from an analysis of the spectra and used to construct an improved decay scheme for the two isomers and to obtain their production cross sections. The ^{147}Pm thermal neutron cross sections obtained after making a small correction for epithermal capture are 84 ± 10 b and 72.4 ± 3.0 b for the production of the ^{148}Pm^{g} and ^{148}Pm^{m} activities respectively, in good agreement with the results of Fenner and Large, but significantly smaller than other recent measurements. (auth) (Canada)

28374 STRIPPING AND PICKUP REACTIONS BETWEEN MASSES 90 AND 120. Diehl, Richard Curtis. Pittsburgh; Univ. of Pittsburgh (1970). 149p. University Microfilms Order No. 71-4460.

Thesis.

The (d,p) reactions leading to $g_{\frac{9}{2}}$ and $h_{\frac{11}{2}}$ states behave anomalously in the isotopes of Ru, Pd, Cd, and In but not in the Sn isotopes. The ratios of the spectroscopic factors for l = 4 transitions to various $^{7}/_{2}^{+}$ states in the Pd isotopes vary markedly with bombarding energy. This represents a breakdown in basic one-nucleon-transfer theory. This breakdown was found not to extend to l = 0 and l = 2 transitions. The (d,t) reactions on ^{96}Mo, and ^{100}Mo were studied with 17-MeV incident deuterons. The experimental angular distributions of the triton groups were compared with DWBA calculations to determine the l values and the spectroscopic factors. The I^{π} and excitation energy of the levels are compared with previous work. The most striking result was the breakdown of the quasiparticle picture for the l = 0 transfers to states of ^{99}Mo. Seventeen MeV deuteron induced (d,t) reactions on ^{110}Pd, ^{108}Pd, and ^{104}Ru were investigated to complement previous (d,p) studies. Further anomalous behavior was found for the $g_{\frac{9}{2}}$ and $h_{\frac{11}{2}}$ states. Many new states were found and some previous $l - \pi$ assignments were changed. (Diss. Abstr. Int., B)

28375 NUCLEAR DATA SHEETS FOR A = 208. Lewis, M. B. (Oak Ridge National Lab., Tenn.). Nucl. Data, Sect. B; 5: 243-85(Mar 1971).

Level schemes, spin and parity assignments, and decay properties are presented for all nuclei with mass number A = 208. Experimental data and adopted values are given along with conclusions as to the spin and parity assignments. The presentation of the nuclear properties is given in the light of the data and current theoretical ideas. Where reasonably well established, shell-model configurations have been noted for many levels in ^{208}Pb and ^{208}Bi. Compilers have attempted to point out inconsistencies in the data and resolve the discrepancies when possible. No reaction data exist for ^{208}Tl although this nucleus could be studied by ^{210}Pb(d,a) since ^{210}Pb targets have been fabricated. Although the levels in ^{208}Pb have been studied in many ways, the neutron stripping and proton pickup data are not entirely satisfactory owing to either too low a bombarding energy or experimental resolution. There are no lifetime measurements for excited states in ^{208}Bi except for an isomeric level. All tabulated C^2S and C^2S' direct-reaction strengths are derived from distorted-wave Born approximation reaction theory unless otherwise noted. The reader is referred to the individual papers for details of these calculations as well as those regarding the analysis of decay of isobaric analog resonances. (auth)

28376 NUCLEAR DATA SHEETS FOR A = 209. Martin, M. J. (Oak Ridge National Lab., Tenn.). Nucl. Data, Sect. B; 5: 287-317(Mar 1971).

Detailed level schemes and the experimental reaction and decay data on which they are based are presented for all the nuclei with mass number A = 209. The experimental data are evaluated, inconsistencies and discrepancies are noted, adopted values for level and gamma energies, gamma intensities and other nuclear properties are given. Conclusions regarding spin assignments as well as some configuration assignments are presented. (auth)

28377 NUCLEAR DATA SHEETS FOR A = 211. Pancholi, S. C. (Oak Ridge National Lab., Tenn. Univ. of Delhi); Martin, M. J. Nucl. Data, Sect. B; 5: 319-38(Mar 1971).

A review of information available on level schemes and decay characteristics for all nuclei with mass number A = 211 is presented. Experimental data and their evaluation, adopted values, comparisons with theory, and arguments for spin and parity assignments are given. Inconsistencies and discrepancies in the level schemes are discussed (in particular the level schemes of ^{211}At and ^{211}Po). (auth)

28378 NUCLEAR DATA SHEETS FOR A = 207. Schmorak, M. R.; Auble, R. L. (Oak Ridge National Lab., Tenn.). Nucl. Data, Sect. B; 5: 207-42(Mar 1971).

The available experimental data pertaining to the nuclear structure of nuclei with A = 207 are compiled; the results from various decay and reaction measurements are compared and evaluated. Inconsistencies and discrepancies in the level schemes are discussed. Level properties, gamma-ray properties, and comments are presented following the data on the relevant nucleus. (auth)

28379 APPLICATIONS OF NUCLEAR PHYSICS. Fremlin, J. H. New York; Hart Publishing Company, Inc. (1970). 373p. $15.00.

The topics covered include elementary nuclear theory, radioactivity, radiation detectors, radiation measurement techniques, radioisotope production, radiochemistry, radioisotopic dating, radiobiology, miscellaneous applications, and safety precautions. Detailed appendices and a bibliography are included. (J.W.R.)

28380 IN-BEAM NUCLEAR MAGNETIC RESONANCE OF THE 159 μs LEVEL IN ^{115}Sn. Braeuer, N.; Focke, B.; Lehmann, B.; Matthias, E.; Riegel, D. (Freie Univ., Berlin). Phys. Lett.; 34B: 54-6(18 Jan 1971).

The γ-ray distribution of the $^{11}/_{2}^{-}$, 159 μs state in ^{115}Sn was disturbed by nuclear magnetic resonance yielding a magnetic moment $|\mu|$ = 1.361 ± 0.004 nm. The relaxation time for the excited ^{115}Sn nuclei in liquid indium metal is τ_R = 0.75 ± 0.18 ms. (auth)

28381 MAGNETIC MOMENTS OF THREE EXCITED STATES IN ^{149}Pm. Seo, Takeshi (Kyoto Univ.); Hayashi, Takeo; Aoki, Atsushi. Annu. Rep. Res. Reactor Inst., Kyoto Univ.; 3: 173-9(1970).

The decay of ^{149}Nd was studied using Ge(Li) and NaI(Tl) γ-ray detectors. The decay scheme of previous studies was reconfirmed. The g-factors for levels at 114, 189, and 270 keV in ^{149}Pm were measured by observing the perturbed angular correlations of the γ rays. Lifetimes for the levels were determined from β and conversion electron measurements. (J.W.R.)

28382 TWO-PHONON STATES IN ^{104}Pd. Okano, Kotoyuki; Kawase, Yoichi; Uehara, Shinichi (Kyoto Univ.). Annu. Rep. Res. Reactor Inst., Kyoto Univ.; 3: 162-5(1970).

Gamma singles and coincidence spectra from the decays of 43-sec ^{104}Rh and 4.41-min ^{104m}Rh were measured using Ge(Li) and NaI(Tl) detectors. A new level at 1333.6 keV in ^{104}Pd was observed. It is suggested that this is the O^+ member of the two phonon triplet. (J.W.R.)

28383 FISSION YIELDS AND BRANCHING RATIOS OF ^{85}Kr IN THERMAL NEUTRON FISSION OF ^{233}U, ^{235}U, ^{239}Pu, AND ^{241}Pu. Lisman, F. L.; Abernathey, R. M.; Foster, R. E. Jr.; Maeck, W. J. (Idaho Nuclear Corp., Idaho Falls). Contract AT(10-1)-1230. J. Inorg. Nucl. Chem.; 33: 643-9(Mar 1971).

The thermal fission yields and effective branching ratios of 10.76 yr ^{85}Kr were determined by mass spectrometric and gas chromatographic techniques for ^{233}U, ^{235}U, ^{239}Pu, and ^{241}Pu. The determined thermal fission yields of ^{85}Kr for ^{233}U, ^{235}U, ^{239}Pu, and ^{241}Pu are 0.512 ± 0.012, 0.2880 ± 0.0035, 0.1300 ± 0.0031, and 0.0864 ± 0.0028 per cent respectively. The measured corresponding effective branching ratios are 0.2296 ± 0.0028, 0.2176 ± 0.0024, 0.2260 ± 0.0018, and 0.2235 ± 0.0033. There appears to be a difference between the branching ratio obtained for ^{233}U and ^{235}U. (auth) (UK)

28384 YIELDS OF RUTHENIUM ISOTOPES FROM THE SPONTANEOUS FISSION OF ^{238}U. Swindle, D. L.; Wright, R. J.; Kuroda, P. K. (Univ. of Arkansas, Fayetteville). J. Inorg. Nucl. Chem.; 33: 876-9(Mar 1971).

Attempts were made to measure yields at mass numbers 103 and 106 (a region hitherto little studied) using a depleted U sample of isotopic composition 99.989% ^{238}U and 0.011% ^{235}U. The fission product activity had been allowed to build up for 2 years, leading to a saturation activity of ^{104}Ru and 75% saturation for ^{106}Ru. Details are given of the method for separation of Ru from the U solution. The decay of the Ru samples was followed using a low back-

ground β-counting system, and an Al absorber was employed to shield the low energy β's associated with ^{103}Ru from the ^{106}Ru activity. Two sets of determinations were made. Saturation activities for ^{103}Ru and ^{106}Ru per gram of U were calculated to be $1.5 \pm 0.5 \times 10^{-4}$ and $0.20 \pm 0.05 \times 10^{-4}$ dps, respectively, values corresponding to fission yields of 2.35 and 0.325 ± 0.08%. It is shown how these results fit into the ^{238}U spontaneous fission mass distribution; the results seem reasonable when compared with data obtained by other investigators. (UK)

28385 DISTRIBUTION OF LOW-MASS FISSION YIELDS IN THE 14.8-MeV NEUTRON INDUCED FISSION OF ^{238}U AND ^{232}Th. Swindle, D. L.; Wright, R. J.; Ward, T. E.; Kuroda, P. K. (Univ. of Arkansas, Fayetteville). J. Inorg. Nucl. Chem.; 33: 651-6 (Mar 1971).

The fission yields of ^{238}U and ^{232}Th in the mass region A = 73–81 were radiochemically determined for 5 mass chains. The absolute activities for these nuclides were determined by gross beta counting and the cumulative fission yields were measured relative to ^{99}Mo. These data were utilized to define the slope of the left wing in the light peak of the mass yield curves for ^{238}U and ^{232}Th. A comparison of these fission yields was made with corresponding mirror points, assuming 3.5 and 4.5 secondary neutrons emitted per fission of ^{238}U and ^{232}Th respectively. (auth) (UK)

28386 NEW ISOTOPES ^{176}Os AND ^{177}Os. DECAY SCHEME FOR $^{177\ 176\ 179\ 180}$Re AND $^{176\ 179\ 180}$Os. DECAY SCHEME FOR ^{179}Re. Arl't, R.; Gromov, K. Ya.; Zaitseva, N. G.; (and others) (Joint Inst. for Nuclear Research, Dubna, USSR). Izv. Akad. Nauk SSSR, Ser. Fiz.; 34: 702-12(Apr 1970). (In Russian).

Os isotopes were prepared by irradiation of metallic gold and mercury oxide by 660-MeV proton beams followed by chemical separation of fractions. Re isotopes were obtained as Os daughter isobars. The half-lives of light isotopes were found: ^{176}Os(3.0 min), ^{177}Os(3.5 min), ^{178}Os(6.0 min), ^{179}Os(7.3 min), ^{180}Os(22.0 min), and ^{181}Os(110 and 2.7 min). ^{176}Os and ^{177}Os isotopes were identified on the basis of the genetic bond with the daughter isobars W and Ta. The ^{179}Re decay scheme was constructed using the data obtained on ^{179}Re γ emission and published data on conversion electrons. (tr-auth)

28387 NEW ISOTOPES ^{133}Pr, ^{134}Nd, AND ^{135}Nd. DECAY SCHEMES FOR ^{134}Pr AND ^{135}Pr. Abdurazakov, A. A.; Arl't, R.; Babadzhanov, R.; (and others) (Joint Inst. for Nuclear Research, Dubna, USSR. Tashkent State Univ.). Izv. Akad. Nauk SSSR, Ser. Fiz.; 34: 796-803(Apr 1970). (In Russian).

A gamma spectrometer with a Ge(Li) detector was used for studying γ-ray spectra of short-lived neutron deficient praseodymium and neodymium isotopes. New isotopes ^{133}Pr($T_{½}$ = 7 ± 3 min), ^{134}Nd($T_{½}$ = 8.0 ± 1.5 min), and ^{135}Nd($T_{½}$ = 5.5 ± 0.5 min) were identified. New data were obtained for the decay schemes of ^{134}Pr(17 ± 2 min) and ^{135}Pr($T_{½}$ 27 ± 3 min). (tr-auth)

28388 HALF-LIVES OF THE NEW ISOTOPES ^{99}Rb, ^{98}Sr, AND $^{145\ 146}$Cs. Tracy, B. L.; Chaumont, J.; Klapisch, R.; (and others) (CNRS, Orsay, France). Phys. Lett.; 34B: 277-9(1 Mar 1971).

On-line mass spectrometer techniques for the separation of Rb and Cs were used to detect products from the 50-MeV proton induced fission of ^{238}U. The new isotopes ^{99}Rb, ^{98}Sr and $^{145-146}$Cs were observed and their half-lives measured. Also the half-life of ^{98}Rb was measured for the first time. Additional half-lives were obtained for $^{96-97}$Rb and ^{97}Y, and upper limits were set for ^{97}Sr and ^{98}Y. (auth)

28389 STUDIES OF RADIOACTIVE DECAY OF NEUTRON DEFICIENT ISOTOPES OF Pt, Ir, AND Os. Bakiev, S. A.; Kordyukevich, V. O.; Kryukova, L. N.; Murav'eva, V. V.; Sorokin, A. A. (Moscow State Univ.). Izv. Akad. Nauk SSSR, Ser. Fiz.; 34: 59-61(Jan 1970). (In Russian).

A spectrometer with a Ge(Li) detector was used for studying γ-radiation of ^{189}Pt, ^{188}Pt, ^{189}Ir, and ^{185}Os. Intensities and energies of γ lines were measured. (R.V.J.)

28390 SPECTRA OF PROTONS IN THE ^{238}U(t,pf) REACTION. Almazov, A. V.; Andreev, M. F.; Zavgorodnii, V. A.; (and others). Izv. Akad. Nauk SSSR, Ser. Fiz.; 34: 136-7(Jan 1970). (In Russian).

The spectra of coincidence protons in the fission reaction ^{238}U(t,pf) were measured at triton energies of 12.54 MeV. The neutron fission threshold of ^{239}U obtained from the measured spectra was equal to +0.065 ± 0.07 MeV. Similarily, the threshold of ^{234}U measured according to the reaction ^{233}U(t,pf) was equal to +0.65 ± 0.15 MeV. (R.V.J.)

28391 PHOTONEUTRON CROSS SECTIONS OF ^{203}Tl AND ^{205}Tl. Antropov, G. P.; Mitrofanov, I. E.; Prokof'ev, A. I.; Russkikh, V. S. Izv. Akad. Nauk SSSR, Ser. Fiz.; 34: 116-21 (Jan 1970). (In Russian).

Cross sections of (γ,n) reactions with ^{203}Tl and ^{205}Tl were measured using thallium oxide targets enriched with 87% ^{203}Tl and 96.5% ^{205}Tl irradiated in a betatron by 30-MeV electrons. Tabulated integral measurements of the cross sections were correlated with the data on $\sigma_{\gamma n}(E_\gamma)$ for ^{208}Pb and ^{209}Be. The spallation energy of the giant resonance observed in the curves of $\sigma_{\gamma n}$ for ^{203}Tl and ^{205}Tl permitted calculation of the internal quadrupole moments of the nuclei studied. (R.V.J.)

28392 POSITRON DECAY IN ^{194}Au AND ^{188}Ir. Ageev, V. A.; Mitrokhovich, N. F.; Feoktistov, A. I. (Kiev State Univ.). Izv. Akad. Nauk SSSR, Ser. Fiz.; 34: 201-3(Jan 1970). (In Russian).

Studies of the ^{194}Au β^+ spectrum by a 4π coincidence scintillation β^+ spectrometer revealed a component at 930 ± 30 keV (0.14 ± 0.07%, log ft = $8.0^{+0.3}_{-0.2}$). In the ^{188}Ir β^+ spectrum there were found components at 1650 ± 30 keV (log ft = 7.9) and 1030 ± 50 keV (log ft = 8.6). (R.V.J.)

28393 ISOTOPIC EFFECTS IN PHOTONUCLEAR REACTIONS. Osokina, R. M.; Yadrovskii, E. L. Izv. Akad. Nauk SSSR, Ser. Fiz.; 34: 182-9(Jan 1970). (In Russian).

Giant-dipole-resonance states with $I^\pi = 1^-$ and $T_< = T_0$ in ^{114}Sn, ^{120}Sn, and ^{124}Sn nuclei and isobaric-analog states with $I^\pi = 1^-$, $T_> = T_0 + 1$ in ^{114,118,120,122}, and ^{124}Sn nuclei were studied within the framework of shell models for interacting quasi-particles. Data obtained were used for analyzing the experimental results on photospallation of ten isotopes. The Fermi-boundary-expansion influence on the nuclear photoeffect is discussed. (R.V.J.)

28394 HIGH-SPIN ROTATIONAL STATES IN ^{168}Yb, ^{169}Yb, AND ^{170}Yb. Selin, E. (Chalmers Tekniska Hoegskola, Goteborg); Hjort, S. A.; Ryde, H. Phys. Scr.; 2: 181-9(1970).

Levels within three rotational bands in the odd-A nuclide ^{169}Yb have been excited in the ^{167}Er(α,2n)^{169}Yb reaction. The positive-parity ground-state band is strongly perturbed. The observed energy levels and relative transition rates within this band are compared with the results of a Coriolis coupling calculation. Good agreement is obtained if the theoretical Coriolis coupling strength is reduced for the orbitals close to the Fermi surface. With $g_s = g_{s\text{free}}$ and non-adiabatic wavefunctions the experimental E2/M1 mixing ratios are reproduced for the $½^+$ [633] ground-state band. The magnetic moment for the ground-state has been calculated and is compared with the measured one for the isotone ^{167}Er. This comparison indicates that the mechanism which reduces the Coriolis matrix elements may also be effective in preventing interband M1 transitions with $|\Delta K| = 1$. The results of a Coriolis coupling calculation for N = 5 bands are also discussed. The rotational levels in the doubly-even nuclides ^{168}Yb and ^{170}Yb are observed up to the 10^+ member. (auth) (Sweden)

28395 ENERGY SURFACES DURING FISSION OF ^{226}Ra, ^{238}U, AND ^{246}Cf. Gamalya, I. A.; Cherdantsev, P. A. (Tomsk Polytechnic Inst., USSR). Izv. Vyssh. Ucheb. Zaved., Fiz.; No. 10, 143-6(1970). (In Russian).

Energy surfaces of Ra, U, and Cf nuclei were studied in the parameter space of the asymmetry parameter κ, parameter of ellipsoidal fragments α, and distance from the light fragments ζ. The calculated surfaces of ^{226}Ra(α,ζ), ^{246}Cf(α,ζ), ^{226}Ra(κ,ζ), ^{238}U(κ,ζ), and ^{246}Cf(κ,ζ) are given in graphical form. (R.V.J.)

28396 NUCLEAR MAGNETIC MOMENT AND HYPERFINE STRUCTURE ANOMALY OF ^{103}Ag AND NUCLEAR SPIN OF 13 m ^{102}Ag. Wannberg, B.; Joensson, J. O.; Sanner, L. (Uppsala Univ.). Phys. Scr.; 2: 238-42(1970).

The hfs of ^{103}Ag ($T_{½}$ = 66 min) has been investigated with the atomic-beam magnetic-resonance (ABMR) method. $\Delta\nu$ and μ_I have been determined independently, and the results are $\Delta\nu$ = 39,700 (500) MHz and μ_I = + 4.45 (5) n.m. The hfs anomaly Δ^{103}_{107} has been determined to be +3.4 (1.7)%. Theoretical calculations give Δ^{103}_{107} = 3.9%. For I = 5, there is a component with a half-life of 13 min which may be ^{102}Ag or ^{102}Ag + ^{100}Ag. Furthermore, signals with a half-life of 9(2) minutes have been obtained for I = 9/2. This activity is ascribed to ^{101}Ag. (auth) (Sweden)

28397 MULTIPOLE CHARACTER OF SOME GAMMA TRANSITIONS IN ^{152}Sm. Helppi, H.; Hattula, J. (Jyvaskyla Univ., Finland). Phys. Scr.; 2: 155-8(1970).

The multipole character of some transitions connecting the quadrupole and octupole vibrational bands to the ground-state rotational band in ^{152}Sm was determined by measuring directional correlations using a Ge(Li)–NaI(Tl) spectrometer. A total of 14 correlations were measured. From these measurements it can be concluded that the $2^+_\beta - 2^+$, 689 keV, $2^+_\gamma - 2^+$, 964 keV and $3^+_\gamma - 2^+$, 1,112 keV transitions are essentially pure

XUM

E2, and $3^- - 2_\gamma^+$, 1,457 keV, $3^- - 4^+$, 1,213 keV and $2^- - 2^+$, 1,408 keV transitions contain less than 2% M2. (auth) (Sweden)

28398 ENERGY LEVELS OF ^{176}Yb FROM THE DECAY OF ^{176}Tm AND ^{176m}Yb. Tuurnala, T.; Pursiheimo, V.; Liukkonen, E. (Helsinki Univ.). Phys. Scr.; 2: 163-8(1970).

The decay of ^{176}Tm was studied by means of Ge(Li) detectors and some gamma–gamma as well as gamma–beta coincidence arrangements. For the half-life of ^{176}Tm a value of 1.9 ± 0.1 min was measured. A total of 31 gamma rays were assigned to the decay of ^{176}Tm. According to the proposed level scheme these depopulate 19 levels in ^{176}Yb, of which those at 977, 1360, 1599, 1673, 2142, 2372, 2411, 2954 and 3188 keV are new. Spin and parity assignments are suggested for some of these levels and for the ground state of ^{176}Tm. In addition, four gamma transitions possibly belonging to an isomer in ^{176}Tm were found with energies 116.3, 122.3, 193.6 and 199.0 keV and with half-life 1.4 ± 0.1 min. Also the decay of ^{176m}Yb was reinvestigated, the results obtained being consistent with the previous data. (auth) (Sweden)

28399 LIMITING CROSS SECTIONS FOR FISSION ISOMERS WITH NANOSECOND LIFETIMES PRODUCED IN HEAVY-ION REACTIONS. Ruddy, Frank H.; Namboodiri, M. N.; Alexander, John M. (State Univ. of New York, Stony Brook). Phys. Rev., C; 3: 972-4(Feb 1971).

Targets of Pr, Ce, Nd, Ir, Au, and Pb were bombarded with heavy ions in order to produce fission isomers with nanosecond lifetimes. In all cases, limits for detection were set which were much lower than the cross sections previously reported for these systems. It is concluded that fission isomerism was not observed in the previously reported experiments. (auth)

28400 CATALOGUE OF γ-RAYS EMITTED BY RADIONUCLIDES. Wakat, M. A. (E. I. du Pont de Nemours and Co., Aiken, S. C.). Contract AT(07-2)-1. Nucl. Data. Sect. A; 8: 445-666(Jan 1971).

A catalog is presented of the γ rays emitted by radionuclides, arranged in order of increasing γ-ray energy. Each items consists of γ-ray energy, abundance, half-life, production mode, and the energies and abundances of two of the more abundant γ rays associated with it. One section covers nuclides with a half-life less than one day. A second section covers those nuclides with a half-life greater than one day; this section also includes all naturally occurring nuclides and the K_α, K_β, L_α, L_β, and L_γ x rays of the elements. The catalog is designed for use in connection with the high-resolution analytical γ-ray spectroscopy made possible by semiconductor detectors. (auth)

28401 TABULATION OF GAMMA–GAMMA DIRECTIONAL-CORRELATION COEFFICIENTS. Taylor, H. W. (Univ. of Toronto); Singh, B.; Prato, F. S.; McPherson, R. Nucl. Data, Sect. A; 9: 1-83(Feb 1971).

The coefficients in the gamma–gamma directional-correlation function $W(\theta) = 1 + A_2(\delta)P_2(\cos\theta) + A_4(\delta)P_4(\cos\theta)$ where δ is the mixing ratio for γ_1 or γ_2 are tabulated for 445 selected spin sequences of the form $I_1 \xrightarrow{L_1 L_1'} I_2 \xrightarrow{L_2} I_3$ or $I_1 \xrightarrow{L_1} I_2 \xrightarrow{L_2 L_2'} I_3$. In most cases L_1 and L_2 are either 1 or 2, L_1' and L_2' are $L_1 + 1$ and $L_2 + 1$, respectively. A small number of coefficients for first–third correlations is included. Integral spin values are limited to the range $0 \rightarrow 8$; half-integral spins, to the range $\frac{1}{2} \rightarrow 11/2$. (auth)

28402 PARITY ASSIGNMENTS OF SOME ^{98}Mo RESONANCES. Migneco, E.; Theobald, J. P.; de Jonge, S. (EURATOM, Geel, Belg.). Lett. Nuovo Cim.; 4: 1220-2(19 Dec 1970).

Yields for the neutron capture resonances at 429, 612, and 818 eV in ^{98}Mo were measured at 35 and 145°. Comparison with theoretical curves suggests p-wave character for these resonances. (R.W.R.)

28403 OPTIMUM PARAMETERS OF THE ^{238}U NEUTRON OPTICAL POTENTIAL. Anikin, G. V.; Dovbenko, A. G.; Kazakova, L. Ya.; (and others). This paper was summarized in At. Energ. (USSR); 28: 420-1(May 1970) as paper No. 385/5440. (In Russian).

An optical-model search code is described which includes real, imaginary (surface and volume), and real spin–orbit terms in the potential. Different weights are allowed for the total cross sections and the angular distributions of elastically scattered neutrons. Energy-dependent optical-potential parameters are given for ^{238}U over the range 0.075 to 15 MeV. Total cross sections agree with experiment within 3%; and angular distributions, 10 to 15%. (R.W.R.)

28404 TOTAL NEUTRON CROSS SECTIONS OF GROSS FISSION PRODUCTS. Jung, H. H.; Priesmeyer, H. G. (Univ., Kiel). Atomkernenergie; 17: 144(Mar 1971).

Uranium, enriched to 90%, was irradiated to a burnup of about 40%. The transmission of this sample was then measured by a fast-chopper time-of-flight spectrometer at a resolution of 0.16 μsec/m. The total neutron cross section of the gross fission products at 4.6 to 23 eV is given. (R.W.R.)

28405 DECAY OF ^{134}Cs. Sud, S. P.; Trehan, P. N. (Panjab Univ., Chandigarh, India). J. Phys. Soc. Jap.; 30: 919-22(Apr 1971).

The decay of ^{134}Cs was investigated by using single-crystal, γ–γ-coincidence, sum–peak-coincidence and γ–γ angular-correlation techniques. There is no evidence for the 1580-keV level proposed by Nagpal. The directional correlation measurements of the 1038–605-keV cascade favor a 3^+ spin assignment for the 1643-keV level of ^{134}Ba. (auth)

28406 DECAY OF 14-min ^{112}In. Itagaki, Shinjiro; Takeda, Yasushi; Sugiyama, Kazusuke (Tohoku Univ., Sendai). J. Phys. Soc. Jap.; 30: 923-6(Apr 1971).

The gamma rays following the decay of 14-min ^{112}In were studied with a 24-cm^3 Ge(Li) detector. The energies and relative intensities of the gamma rays are 606.4 ± 0.5 keV (23.4%), 618.2 ± 0.4 keV (100.0%), 1252.6 ± 0.9 keV (5.6%), 1278.0 ± 1.4 keV (0.2%), 1306.3 ± 1.7 keV (0.1%), and 1488.9 ± 1.3 keV (1.2%). The excited levels of ^{112}Cd at 618 keV, 1225 keV, 1306 keV, 1489 keV, 1871 keV, and 2503 keV are considered to be 2^+, 0^+, 2^+, 2^+, 0^+, and 2^+, respectively. The population of the 1225-keV 0^+ state by beta feeding is also discussed. (auth)

28407 ENERGY RELEASED BY BETA RADIATION FOLLOWING FISSION. I. ^{235}U DATA. MacMahon, T. D.; Wellum, R.; Wilson, H. W. (Scottish Research Reactor Centre, Glasgow). J. Nucl. Energy; 24: 493-501(Dec 1970).

A series of experiments to measure the rate of energy release by beta radiation following ^{235}U fission were carried out at the Scottish Research Reactor Centre, East Kilbride, by using the UTR-100 reactor. A novel feature of the technique is the use of a magnetic field to discriminate between beta and gamma radiation. (auth) (UK)

28408 CALCULATION OF KINETIC ENERGY AND MOST-PROBABLE CHARGE IN FISSION. Okamoto, Hironobu; Nakahara, Hiromichi; Nishi, Tomota (Kyoto Univ.). J. Phys. Soc. Jap.; 30: 927-31(Apr 1971).

Kinetic energies and most-probable charges in fission were calculated for ^{235}U + n, ^{252}Cf, and ^{226}Ra + p by applying the statistical model of Fong. The mass formula of Myers and Swiatecki was employed to evaluate fragment deformation energies. The most-probable scission configuration for a given mass division was obtained by maximizing the effective intrinsic excitation energy of the complementary fragments, which was given as a function of their charges and deformation parameters. The general trends of the kinetic energy distribution and the charge distribution in fission could be reproduced fairly well. (auth)

28409 MEASUREMENT OF AVERAGE CROSS SECTION FOR THE ^{232}Th(n,f) REACTION FOR THE FISSION-TYPE REACTOR SPECTRUM. Kobayashi, Kathuhei; Kimura, Itsuro (Kyoto Univ.). Annu. Rep. Res. Reactor Inst., Kyoto Univ.; 3: 84-92(1970).

The average cross section for the ^{232}Th (n,f) reaction was measured for a quasi-fission neutron spectrum. A Ge(Li) counter was used for the measurements of the gamma rays from the irradiated thorium sample without chemical processing. The relative fission yields for five nuclides, ^{140}Ba, ^{135}Xe, ^{132}Cs, ^{95}Zr, and ^{91}Sr, were obtained; and the values, normalized to the value of ^{140}Ba preferred by Bresesti et al., agreed with the earlier data. From these results, the average cross section for the ^{232}Th (n,f) reaction is found to be 67 ± .6 mb. (auth)

28410 DECAY OF EXCITED NUCLEAR STATES STUDIED BY ELECTRON DIRECTIONAL CORRELATION METHODS. Samuelsson, Erik Lennart Mauritz. Uppsala; Univ. of Uppsala (1969). 131p. Almqvist and Wiksell, Stockholm, Sweden. Thesis.

A four-detector electron directional correlation (EDC) spectrometer consisting of three independent magnetic lenses and NaI(Tl) γ-detectors was constructed. The focussing properties of the electron spectrometer with envelope ring focus baffle are treated in detail and investigated experimentally by photographic ray tracing and by studying line profiles for different focussing parameters. The origin and intensity of background signals observed in a magnetic lens spectrometer were investigated and methods how to minimize such signals are discussed. From correlation measurements with the EDC-spectrometer conversion coefficients and particle parameters in ^{207}Pb were obtained. Consistent results for the multipolarity of some transitions in the complex decay of ^{172}Lu could be determined. The multipolarity mixture of $2^+ - 2^+$ transitions in the even–even nuclei ^{184}W and

^{190}Os was studied. Measured coincidence information from several radioactive sources can be used to estimate upper limits for double internal conversion as shown by an investigation of the decay of $^{114}In_m$. The measured results for the two-quanta probability are about one order of magnitude lower than theoretical estimates available at present. (Diss. Abstr. Int., B)

28411 (p,t) REACTION ON EVEN–EVEN DEFORMED NUCLEI. Sugiyama, Yasuharu (Japan Atomic Energy Research Inst., Tokai); Kokame, Jun; Suehiro, Teruo; (and others). J. Phys. Soc. Jap.; 30: 602-10(Mar 1971).

The (p,t) reactions on ^{158}Gd, ^{164}Dy, ^{172}Yb, ^{176}Hf, and ^{184}W were studied with 51.7-MeV protons. Triton spectra were measured with a broad-range magnetic spectrometer with a 200-proportional-counter array. The cross sections for the states of the ground-state rotational band, which were found to depend on mass number, are analyzed by the distorted-wave Born-approximation. In particular, the Y_4 deformation parameter β_4 for each nucleus is obtained from the cross section for the 4^+ state of the ground-state rotational band. The cross sections for the first excited 0^+ states are found to have a mass-number dependence, and this dependence is compared with the prediction based on the pairing vibrational mode. (auth)

28412 DEVIATION FROM THE ξ APPROXIMATION IN THE BETA TRANSITION OF ^{122}Sb. Yamada, Shigeru; Hayashi, Takeo (Kyoto Univ.). Annu. Rep. Res. Reactor Inst., Kyoto Univ.; 3: 1-8(1970).

Beta–gamma angular correlations of the first-forbidden beta transitions of ^{122}Sb were measured. The ξ approximation was found to be valid in the β_1 transition to the first excited state of ^{122}Te. In the case of the β_2 transition to the second excited state, however, the result of the measurement indicates that the β_2 transition does not follow the ξ approximation. The result of the analysis for the case of the β_2 transition for exact electron radial wave functions that include finite-nuclear-size corrections shows that there exists cancellation among the nuclear matrix elements, and, therefore, that deviation from the ξ approximation was observed. The nuclear matrix elements determined by the present calculation are given. (auth)

28413 THRESHOLD PHOTONEUTRON CROSS SECTIONS FOR $^{206\ 207\ 208}$Pb, $^{56\ 57}$Fe, $^{52\ 53}$Cr, $^{24\ 25\ 26}$Mg, AND ^{19}F. Baglan, R. J.; Bowman, C. D.; Berman, B. L. (Univ. of California, Livermore). Phys. Rev., C; 3: 672-99(Feb 1971).

The threshold photoneutron cross sections for ^{206,207,208}Pb, ^{56,57}Fe, ^{52,53}Cr, ^{24,25,26}Mg, and ^{19}F were measured to about 1 MeV above the (γ,n) threshold. Cross sections are presented and analyzed for the parameters of over 200 resonances. The results bear on several phenomena of interest in nuclear physics; these include E1 strength functions, analog states, doorway states, the M1 giant resonance, and nonresonant neutron capture. (auth)

28414 EXCITED STATES OF ^{138}Ce. Julian, Glenn M. (Miami Univ., Oxford, Ohio); Fessler, Theodore E. Phys. Rev., C; 3: 751-5(Feb 1971).

Sources of 2.02-h ^{138m}Pr and 1.44-min ^{138}Pr were made by the (p,n) reaction on enriched ^{138}Ce, and sources of 5.7-h ^{138}Nd were produced by the (α,2n) reaction on enriched ^{136}Ce. Eighteen γ rays plus annihilation radiation were attributed to the decay of ^{138m}Pr, and twelve γ rays plus annihilation radiation were attributed to the decay of ^{138}Pr. The level scheme of ^{138}Ce is discussed. Evidence is given for the existence of a (2^+) level of ^{138}Ce at 1510.9 keV, near the previously reported 0^+ and 4^+ levels at, respectively, 1477.0 and 1826.4 keV. (auth)

28415 ENERGY LEVELS IN ^{235}Np. Gorman, D. J.; Asaro, F. (Univ. of California, Berkeley). Phys. Rev., C; 3: 746-51(Feb 1971).

The energy levels in ^{235}Np were studied through the α decay of ^{239}Am and the electron-capture decay of ^{235}Pu. A level was observed at 34.1 keV and assigned to the ground-state rotational band with Nilsson quantum numbers $5/2^+$ [642]. Levels at 49.0, 91.6, and 146.8 keV were assigned to the $5/2^-$ [523] rotational band. The lifetime of the 49.0-keV state was measured as 6.9 nsec, and the half-life of the ^{235}Pu was redetermined to be 24.3 min. (auth)

28416 GAMMA RAYS IN COINCIDENCE WITH K X RAYS OF Cs AND Ba FISSION PRODUCTS OF ^{252}Cf. Eddy, N. W. (Sir George Williams Univ., Montreal); Roy, R. R. Phys. Rev., C; 3: 877-82(Feb 1971).

A method of identifying the atomic number of γ-ray spectra of ^{252}Cf fission products by means of K x-ray and γ-ray coincidence techniques was applied to Cs (Z = 55) and Ba (Z = 56) fission products. The separation of the K α x-ray peak centroids for this pair is only 1.2 keV, while the full width at half maximum of these peaks [using a Si(Li) detector] is 1.6 keV. It is shown that by using computer analysis, assignment of γ lines to either Cs or Ba may still be achieved with a high degree of reliability. 22 γ transitions have been analyzed in the energy range 125–300 keV. 12 of these have been tentatively assigned to Cs, and 10 to Ba. (auth)

28417 SHELL-MODEL STRUCTURE OF ^{209}Bi. Alford, W. P.; Schiffer, J. P.; Schwartz, J. J. (Univ. of Rochester, N. Y.). Phys. Rev., C; 3: 860-76(Feb 1971).

The level structure of ^{209}Bi was investigated using both stripping and pickup reactions. The ^{207}Pb(^{3}He,d) and ^{207}Pb(α,t) reactions permit the identification of a series of doublets arising from the coupling of a proton in the $h_{9/2}$, $f_{7/2}$, $i_{13/2}$, $f_{5/2}$, and $p_{3/2}$ single-particle states with a neutron hole in the $p_{1/2}$ shell. The ^{209}Bi(d,t) and ^{209}Bi(^{3}He,α) reactions populate the multiplets arising from coupling of a neutron hole in the $p_{1/2}$, $f_{5/2}$, $p_{3/2}$, $i_{13/2}$, $f_{7/2}$, and $h_{9/2}$ states with a proton in the $h_{9/2}$ shell. A detailed analysis shows that the total strength in each multiplet is close to that for the corresponding single-particle or single-hole transition on ^{208}Pb. In addition to the strong transitions leading to states of these multiplets, some relatively weak transitions are observed which provide a measure of the mixing of different configurations. The structure and purity of the particle-hole multiplets below about 3-MeV excitation are in good agreement with shell-model calculations. (auth)

28418 α DECAY FROM HIGH-SPIN ISOMERS IN ^{153}Ho AND ^{154}Ho. Toth, K. S.; Hahn, R. L. (Oak Ridge National Lab., Tenn.). Phys. Rev., C; 3: 854-9(Feb 1971).

α-emitting high-spin isomeric states in ^{153}Ho and ^{154}Ho were found by bombarding targets of ^{142}Nd and ^{144}Nd with nitrogen ions accelerated in the Oak Ridge isochronous cyclotron. In the experiments, recoil nuclei ejected from the thin targets were stopped in helium gas, swept through an orifice, and deposited on the surface of a wheel. After bombardment, the wheel was turned by remote control to place the collected activity in front of an α-particle Si(Au) spectrometer for assay. The previously unreported high-spin isomer in ^{153}Ho was found to have a half-life of 2.0 ± 0.1 min and an α-decay energy of 3.91 ± 0.01 MeV. The β decay of the 3.25-min ^{154}Ho high-spin isomer had been investigated earlier by Ward and Neiman. In the present study it was found that the isomer also emits α particles with an energy of 3.72 ± 0.01 MeV. The nuclidic assignments of these two new α emitters were based primarily on (1) a comparison of yield curves for their production with yield curves for the production of the known pairs of α-emitting isomers in ^{151}Ho and ^{152}Ho, and (2) cross bombardments which demonstrated that the α groups could not be due to decay from previously unknown isomers in dysprosium and terbium nuclei in the investigated mass region. (auth)

28419 MASS-SPECTROMETRIC SEARCH FOR NEON AND ARGON ISOTOPES IN TERNARY FISSION OF ^{235}U. Kugler, G.; Clarke, W. B. (McMaster Univ., Hamilton, Ont.). Phys. Rev., C; 3: 849-53(Feb 1971).

A search was carried out for neon and argon isotopes produced in ternary fission of ^{235}U, using high-sensitivity mass spectrometry. The following upper limits—expressed in atoms per binary fission—were obtained: ^{20}Ne < 5.8×10^{-8}, ^{21}Ne < 3.4×10^{-10}, ^{22}Ne < 5.9×10^{-9}, ^{36}Ar < 2.4×10^{-9}, ^{37}Ar < 2.2×10^{-9}, ^{38}Ar < 2.0×10^{-9}, ^{39}Ar < 7.8×10^{-10}, ^{40}Ar < 6.9×10^{-7}, ^{42}Ar < 2.2×10^{-9}. Except in the case of ^{40}Ar, these limits are lower by 1 to 4 orders of magnitude than indicated from results of triple-coincidence experiments carried out by previous workers. Assuming unique formation of ^{40}Ar, the upper limit for this nuclide is a factor of 5 lower than the triple-coincidence frequency. (auth)

28420 MOESSBAUER EFFECT IN THE 121.2-keV TRANSITION IN ^{147}Sm. Parker, F. T.; Hardy, K. A.; Walker, J. C. (Johns Hopkins Univ., Baltimore). Phys. Rev., C; 3: 841-9(Feb 1971).

The Moessbauer effect was observed in the decay of the $5/2^-$ 121.2-keV state of ^{147}Sm. Sources were ^{147}Pm in a mixed Pm–Sm oxide matrix and ^{147}Eu in Sm_2O_3. Both types of sources gave single Lorentzian lines when used with an Sm_2O_3 absorber. The ^{147}Eu source was used with a samarium iron garnet absorber to obtain the excited-state nuclear moments. The magnetic dipole moment is found to be $-0.445 \pm 0.25\mu_N$. Using an atomic-beam measurement of the ground-state quadrupole splitting, an estimate of -0.31 ± 0.12 b is obtained for the excited-state quadrupole moment. Three light rare-earth odd-neutron nuclei have now been studied by the Moessbauer effect: ^{145}Nd, ^{147}Sm, and ^{149}Sm. The g factors for the low-lying levels of these nuclei cluster about −0.22. The present theoretical models are not particularly successful in accounting for the magnetic moments. (auth)

28421 NONRANDOM DISTRIBUTIONS OF NEUTRON RESONANCE LEVELS. Ideno, Kazumi; Ohkubo, Makio (Japan Atomic Energy Research Inst., Tokai). J. Phys. Soc. Jap.; 30: 620-31(Mar 1971).

Analysis of correlations between spacings of arbitrary pairs of neutron resonance levels for intermediate and heavy nuclei is described. It is found that pairs of levels separated at particular spacings appear very frequently and the observed levels are also preferentially distributed at periodical positions with particular periods. These correlations are found in the observed resonances of ^{75}As, ^{121}Sb, ^{123}Sb, ^{146}Nd, ^{166}Er, ^{174}Yb, ^{177}Hf, ^{234}U, ^{240}Pu, etc. It is shown that these regular level distributions are rarely expected for statistically distributed levels. (auth)

28422 DEEXCITATION OF THE 662-keV STATE IN ^{137}Ba BY THE INTERNAL COMPTON EFFECT. Ljubicic, A.; Hrastnik, B.; Ilakovac, K.; Jurcevic, M.; Basar, I. (Inst. Ruder Boskovic, Zagreb). Phys. Rev., C; 3: 824-31(Feb 1971).

A double-decay process in which the transition energy is distributed between one photon and one K conversion electron was investigated in the decay of the 662-keV state in ^{137}Ba. For the energy interval of emitted photons from 50 to 150 keV, the result of $T_{K\gamma}/T_K = (2.2 \pm 0.2) \times 10^{-3}$ was obtained. The measured energy and angular distributions are compared with the Spruch–Goertzel theory in which the process is treated as the internal Compton effect. Some deviations from the theory are observed in both distributions. The contribution of nuclear intermediate states is negligible in the range of energies which was investigated. (auth)

28423 COULOMB EXCITATION OF LEVELS IN ^{105}Pd. Bolotin, H. H.; McClure, D. A. (Argonne National Lab., Ill.). Phys. Rev., C; 3: 797-806(Feb 1971).

The low-lying excited states of ^{105}Pd were investigated by means of Coulomb excitation using 4.4 to 8.0-MeV α-particle projectiles. The γ-ray spectrum resulting from the deexcitation of these levels was recorded at each bombarding energy with the aid of a large-volume high-resolution Ge(Li) detector. Thirteen transitions were observed that result from direct E2 excitation of 10 excited states up to an excitation energy of 782 keV. The B(E2↑) values from the ground state to each of these 10 levels was determined. Several E2 transitions were found to be strongly enhanced over estimates of single-particle speed, a pattern suggestive of collective behavior. The measured B(E2) values, together with some inferred M1 transition speeds, are compared with predictions of a weak-coupling core-excitation model. (auth)

28424 NUCLEAR LEVELS IN ^{177}Lu AND ^{175}Lu. Minor, Michael M. (Florida State Univ., Tallahassee); Sheline, Raymond K.; Jurney, E. T. Phys. Rev., C; 3: 766-84(Feb 1971).

One- and three-quasiparticle states were investigated in ^{175}Lu and ^{177}Lu using (d,p), (d,t), and thermal (n,γ) reactions on isotope-separated targets of ^{176}Lu. The (d,p) and (d,t) studies utilized 12-MeV deuterons and a broad-range magnetic spectrograph; the (n,γ) studies used Ge(Li) and Si(Li) spectrometers. The ground-state one-quasiparticle band $^{7}/_{2}^{+}$[404] through the $^{17}/_{2}^{+}$ member and four tentative three-quasiparticle bands are observed in ^{175}Lu. Members of the following one-quasiparticle bands are observed in ^{177}Lu: $^{7}/_{2}^{+}$[404] ground state, $^{9}/_{2}^{-}$[514], $^{5}/_{2}^{+}$[402], and $^{1}/_{2}^{+}$[411]; in addition the following three-quasiparticle bands are observed in ^{177}Lu: $^{23}/_{2}^{-}$[p404↓ + n514↓ + n624↑], $^{11}/_{2}^{+}$[p514↑ + n624↑ + n514↓], $^{13}/_{2}^{+}$ and $^{15}/_{2}^{+}$[p404↓ + n514↓ ± n510↑], K + 2 γ vibration built on the $^{1}/_{2}^{+}$[404] ground state, tentatively $^{17}/_{2}^{+}$[p404↓ + n514↓ + n512↓], and tentatively $^{13}/_{2}^{+}$ and $^{15}/_{2}^{+}$[p404↓ + n514↓ ± n521↓]. The neutron separation energy of ^{177}Lu was measured as 7072.7 ± 2.0 keV, and the Q value for the reaction ^{176}Lu(d,t)^{175}Lu as −25 ± 15 keV. Identification of differential cross-section patterns to various members of three-quasiparticle rotational bands in both the (d,p) and (d,t) reactions indicates that this spectroscopic tool is also valuable for three-quasiparticle states. A sum rule is suggested and experimentally evaluated for the total differential cross sections in the (d,p) reaction to rotational members of the two different bands resulting from parallel and antiparallel coupling of the last neutron. (auth)

28425 LEVELS IN ^{184}Pt, ^{186}Pt, AND ^{188}Pt. Huebel, H.; Naumann, R. A.; Spejewski, E. H. (Princeton Univ., N. J.). Phys. Rev., C; 3: 756-65(Feb 1971).

The nuclear decay chains beginning with the neutron-deficient isotopes ^{184}Hg, ^{186}Hg, and ^{188}Hg were studied using isotopically separated sources from the Princeton on-line isotope-separator facility. Ge(Li) and Si(Li) singles spectra and Ge(Li)–Ge(Li) coincidence spectra were obtained and used in constructing level schemes for the corresponding platinum daughters. Systematics of experimental energy levels and ratios B(E2, 2′ → 2)/B(E2, 2′ → 0) for all known even platinum isotopes are given. (auth)

28426 FRAGMENT PRODUCTION IN THE INTERACTION OF 5.5-GeV PROTONS WITH URANIUM. Poskanzer, A. M.; Butler, Gilbert W.; Hyde, Earl K. (Univ. of California, Berkeley). Phys. Rev., C; 3: 882-904(Feb 1971).

The energy spectra of nuclear fragments produced by the interaction of 5.5-GeV protons with uranium were determined at several laboratory angles by means of dE/dx-E measurements with semiconductor-detector telescopes. Individual isotopes of the elements from hydrogen to carbon were resolved, and from nitrogen to argon the study was continued for the elements without isotopic separation. The evaporation-like energy spectra were integrated to obtain angular distributions and total cross sections for the isotopes of helium through carbon. Total cross sections for many rare isotopes were also estimated. The yield surface constructed from these cross sections has a ridge-like shape positioned one neutron in excess of the line of β stability. The yields fall off more steeply on the neutron-deficient side and exhibit odd-even effects reflecting those of the mass surface. The energy spectra of the neutron-deficient isotopes differ from the others in that the high-energy parts of the spectra are more pronounced and flatter, and the angular distributions are more forward peaked. Some of the energy spectra were fitted with calculated curves based on the isotropic evaporation of fragments from a system moving along the beam axis. The apparent Coulomb barriers obtained from this analysis were about one half the nominal Coulomb barriers, and the apparent nuclear temperatures fell in the 10- to 13-MeV range. For the highest-energy fragments observed at 90° the apparent temperatures rose to 20 MeV. From the forward-backward shifts in energy it was deduced that the average velocity of the moving system is about 0.006c and that there is a positive correlation between this velocity and the velocity of the fragments in the moving system. However, all of the data are more peaked forward in intensity than can be explained by this simple two-step model. Radiochemical cross sections are also presented for the production of ^{7}Be from uranium, silver, and aluminum, and for ^{22}Na from aluminum. (auth)

28427 ISOBARIC ANALOG RESONANCES IN PROTON ELASTIC AND INELASTIC SCATTERING FROM ^{130}Te. Hiddleston, H. R.; Hollas, C. L.; Mistry, V. D.; Riley, P. J. (Univ. of Texas, Austin). Phys. Rev., C; 3: 905-20(Feb 1971).

Proton elastic scattering data are analyzed in the framework of a single-particle theory to obtain energies, partial widths, total widths, and spectroscopic factors for 14 isobaric analog resonances in ^{131}I. Excitation functions and fits are presented and the results are compared with those of similar analyses as well as with those of (d,p) investigations. A total of 42 excited states in ^{130}Te were identified from the inelastic spectra at the various resonances. Groups of states at the d_{5}, f_{5}, and p_{5} resonances were analyzed as neutron particle-neutron hole states, and fits to the angular-distribution data for these states are presented. The analysis provides proton partial widths, spectroscopic factors, and assignment of possible spins and parities for these states. The ^{130}Te inelastic results are compared with those of other nuclei in the N = 82 mass region. (auth)

28428 LEVEL STRUCTURE OF ^{109}Cd FROM THE DECAY OF ^{109}In. Bakhru, H. (Yale Univ., New Haven. State Univ. of New York, Albany); Ladenbauer-Bellis, I. M.; Rezanka, I. Phys. Rev., C; 3: 937-44(Feb 1971).

The excited levels of ^{109}Cd were investigated from the decay of ^{109}In with high-resolution Ge(Li) and Si(Li) detectors as well as with standard scintillation counters. ^{109}In was produced by the (α,n) reaction on enriched ^{106}Cd. This reaction produced ^{109}Sn, which decays with a short half-life to ^{109}In. Levels of the following energies (in keV) were established in ^{109}Cd: 59.5, 203.3, 347.4, 426.2, 623.8, 673.7, 721.5, 822.5, 997.5, 1352.2, 1475.6, 1539.8, 1622.5, and 1772.6. The use of two Ge(Li) detectors in connection with the PDP-8/I and a program for two-dimensional analysis with a 4096-dual analog-to-digital converter revealed the presence of several previously unreported transitions in ^{109}In. Based on the $\gamma-\gamma$ and $\beta-\gamma$ coincidence results, a consistent level scheme for ^{109}Cd is given. The spin and parity assignments of levels of ^{109}Cd are discussed. (auth)

28429 ANOMALIES IN THE DISTORTED-WAVE BORN-APPROXIMATION ANALYSIS OF ^{140}Ce(d,p)^{141}Ce. Brown, R. A.; Mlekodaj, R. L. (Florida State Univ., Tallahassee). Contract AT(40-1)-2434. Phys. Rev., C; 3: 954-8(Feb 1971).

The present results are compared with those of ^{140}Ce(n,γ)^{141}Ce and ^{140}Ce(p,p)^{140}Ce analog experiments. The (n,γ) and (d,p) results do not yield consistent spin assignments for six states between 1809- and 2523-keV excitation in ^{141}Ce. The use of conventional distorted-wave Born-approximation theory in the analysis of the (d,p) data is questioned. The available (p,p) analog data does not support either the (n,γ) or (d,p) spin assignments. (auth)

28430 BETA–GAMMA BAND MIXING IN ^{152}Sm. Hamilton, J. H.; Coffman, F. E.; Ramayya, A. V.; Baker, K. (Vanderbilt Univ., Nashville). Phys. Rev., C; 3: 960-3(Feb 1971).

High-resolution singles and 4096 × 2048 Ge(Li)–Ge(Li) coincidence-spectrum measurements were made to clarify the properties of the β and γ vibrational bands in ^{152}Sm. A $2_\gamma \rightarrow 2_\beta$ transition is placed from coincidence experiments and $B(E2; 2_\gamma \rightarrow 2_\beta)/B(E2; 2_\gamma \rightarrow 2_g) = 1.3 \pm 0.4$. The $B(E2; 3_\gamma \rightarrow 2_\beta)/B(E2; 3_\gamma \rightarrow 2_g) < 0.6$. Of the six transitions out of the 2_γ and 2_β levels, the intensities of four were revised from coincidence measurements and new branching ratios obtained. The $2_\gamma \rightarrow 4_g$ transition intensity is shown to be too low to allow a one-parameter fit to the γ-band branching ratios. (auth)

28431 STUDIES OF ^{99}Pd γ RADIATION. Anton'eva, N. M.; Grigor'ev, E. P.; Katykhin, G. S.; Nikitin, M. K.; Protasova, L. F. (Leningrad State Univ.). Izv. Akad. Nauk SSSR, Ser. Fiz.; 34: 54-8(Jan 1970). (In Russian).

The γ-ray spectrum for ^{99}Pd($T_{\frac{1}{2}}$ = 22 min) was measured by a Ge(di) detector. Data obtained on the energy and intensity of γ transitions and the available published data were used for constructing the ^{99}Pd decay scheme. Comparisons are made with the properties of ^{99}Rh and ^{101}Rh. (R.V.J.)

28432 EXCITATION OF ^{169}Tm LEVELS WITH 633 AND 718 keV ENERGIES DURING ^{169}Yb DECAY. Aleksandrov, V. S.; Balalaev, V. A.; Dzhelepov, B. S.; Ter-Nersesyants, V. E. (All-Union Scientific-Research Inst. of Metrology, Leningrad). Izv. Akad. Nauk SSSR, Ser. Fiz.; 34: 42-53(Jan 1970). (In Russian).

Spectra of internal-conversion electrons and ^{169}Yb γ rays at energies exceeding 300 keV revealed transitions corresponding to the 633-keV ($I^\pi K = \frac{5}{2} + \frac{3}{2}$) and 718-keV ($I^\pi K = \frac{1}{2} + \frac{3}{2}$) levels in ^{169}Tm, which were observed previously in reactions. Data obtained verified the level energies and the $K^\pi = \frac{3}{2}^+$ band characteristics, the multiplicity of transitions was determined. In the spectra of ^{169}Yb there appeared transitions with the energies of 336.2, 370.86, 379.0, and 387 keV. The distribution of transitions in the ^{169}Tm decay scheme is discussed. (R.V.J.)

28433 STUDIES OF ^{169}Yb LEVELS IN ^{169}Lu DECAY. Bonch-Osmolovskaya, N. A.; Grigor'ev, E. P.; Liptak, Ya.; Urbanets, Ya. (Joint Inst. for Nuclear Research, Dubna, USSR. Leningrad State Univ.). Izv. Akad. Nauk SSSR, Ser. Fiz.; 34: 12-28(Jan 1970). (In Russian).

The gamma-ray spectrum of ^{169}Lu was measured using a Ge(Li) detector. Analysis of these results and data obtained from nuclear reactions and conversion-electron spectra of ^{169}Lu were used for construction of the ^{169}Lu decay scheme. (R.V.J.)

28434 MEASUREMENT OF QUADRUPOLE-DIPOLE MIXING AMPLITUDES OF GAMMA TRANSITIONS BETWEEN COLLECTIVE STATES OF EVEN–EVEN NUCLEI USING THE ANGULAR CORRELATION METHOD. Krane, Kenneth Saul. Lafayette, Ind.; Purdue Univ. (1970). 158p. University Microfilms Order No. 71-2640.

Thesis.

Gamma–gamma directional-correlation measurements were performed in order to test the predictions of various nuclear models regarding the multipole mixing ratios of gamma transitions from collective levels in even–even nuclei. The multi-pole mixing ratios were determined in terms of explicitly defined reduced electromagnetic matrix elements, and were determined for collective vibrational, rotational, and transitional even–even nuclei. Results of the measurement, given in terms of the nucleus under investigation and the energy (in keV) of the mixed-multipole gamma transition, were as follows: ^{110}Cd — $\delta(447) = -0.45 \pm 0.20$, $\delta(620) = -0.80 \pm 0.50$, $\delta(678) = -0.25 \pm 0.20$, $\delta(687) = -1.1^{+0.4}_{0.3}$, $\delta(707) = -1.0 \pm 0.3$, $\delta(818) = -1.20 \pm 0.15$, $\delta(1384) = -0.37 \pm 0.03$, and $\delta(1505) = -0.55 \pm 0.10$; ^{124}Te — $\delta(722) = -3.7 \pm 0.3$; ^{160}Dy — $\delta(215) = -0.18 \pm 0.10$, $\delta(299) = 0.005 \pm 0.010$, $\delta(392) = 0.01 \pm 0.06$, $\delta(879) = -13.5 \pm 3.0$, $\delta(962) = -18.0 \pm 5.0$, $\delta(1176) = 0.02 \pm 0.02$, and $\delta(1272) = -0.03 \pm 0.03$; ^{186}Os — $\delta(630) = -10^{+9}_{0}$ and $\delta(773) = -12^{+4}_{3}$; ^{188}Os — $\delta(478) = -12.3 \pm 2.8$ and $\delta(635) = -6.9 \pm 3.2$; ^{190}Os — $\delta(371) = -8.5 \pm 1.0$ and $\delta(569) = -9.0 \pm 1.5$; ^{194}Pt — $\delta(294) = 14.3 \pm 2.1$; and ^{196}Pt — $\delta(333) = -6.5 \pm 0.3$. The results obtained for the ^{110}Cd gamma transitions indicated considerable deviations from the vibrational model. The results for ^{160}Dy are consistent with the rotational model, if there is band mixing in the negative parity states. The results for the mixing ratios in the osmium–platinum region are in excellent agreement with the predictions of the Kumar–Baranger pairing-plus-quadrupole model. (Diss. Abstr. Int., B) (TSS)

28435 DECAY OF ^{110m}Ag TO ^{110}Cd. Kracikova, T. I. (Charles Univ., Prague). Czech. J. Phys.; 20: 1138-48(1970).

The gamma-ray spectrum of the decay of ^{110m}Ag was measured with Ge(Li) detectors. A total of 32 gamma rays associated with the decay of ^{110m}Ag were observed; and their intensities, determined. A number of gamma-ray transitions were not observed previously. The K-electron internal conversion coefficients were found from the relative gamma intensities used in conjunction with published K-conversion electron intensities. It is proposed that the level scheme of ^{110}Cd has new levels at 1410.4, 1443.2, and 2237.7 keV in addition to the previously known levels. The spins and parities of the new levels are discussed. (auth)

28436 DECAY OF ^{169}Lu. Balalaev, V. A.; Dzhelepov, B. S.; Medvedev, A. I.; (and others) (All-Union Scientific-Research Inst. of Metrology, Leningrad). Izv. Akad. Nauk SSSR, Ser. Fiz.; 34: 2-11(Jan 1970). (In Russian).

Conversion-electron spectra of ^{169}Lu were measured at 460 to 1500 keV, revealing several previously unknown transitions. Energies of several transitions in other regions were corrected. Data are given on the known transitions taking place during ^{169}Lu decay. These data, combined with published data on the levels of ^{169}Yb, enabled the ^{169}Lu decay scheme to be verified. (R.V.J.)

28437 GAMMA SPECTRA FROM CAPTURE OF RESONANCE NEUTRONS BY Rh, Ta, AND Au NUCLEI. Burgov, N. A.; Danilyan, G. V.; Efimov, I. A.; Kazachkovskii, O. D.; Pavlov, V. S. Izv. Akad. Nauk SSSR, Ser. Fiz.; 34: 89-96(Jan 1970). (In Russian).

Results are given for measurements of spectra from γ-ray capture of resonance neutrons by Rh, Ta, and Au. The measurements were carried out by means of a magnetic Compton γ spectrometer with a resolving power of ~1%. All three spectra revealed transitions not observed during the capture of thermal neutrons (thus revealing some previously unknown levels). The relative partial widths of observed transitions and the spins and parities of the populated levels in ^{104}Rh, ^{182}Ta, and ^{198}Au were calculated. (R.V.J.)

28438 DECAY OF ^{97}Zr. Miminoshvili, Z. N.; Murav'eva, V. V.; Sorokin, A. A. (Moscow State Univ.). Izv. Akad. Nauk SSSR, Ser. Fiz.; 34: 62-8(Jan 1970). (In Russian).

A double-coincidence spectrometer with a NaI(Tl) crystal and semiconductor Ge(Li) and Si(Li) detectors was used for measuring the γ spectrum and γ–γ and γ–e coincidence spectra for ^{97}Zr ($T_{\frac{1}{2}}$ = 17 hr) decay. The decay scheme for ^{97}Zr was constructed. (R.V.J.)

Nuclear Theory

Refer also to abstracts 26205, 27915, 27958, 27978, 28095, 28096, 28245, 28258, 28308–28310, 28312, 28314, and 28318.

28439 (AECL-3801) EVALIN: A CDC 6600 FORTRAN IV CODE TO PERFORM AN EXTENDED VARIATIONAL APPROXIMATION FOR LIGHT AND INTERMEDIATE NUCLEI. Cusson, R. Y.; Lee, H. C. (Atomic Energy of Canada Ltd., Chalk River (Ontario)). Jan 1971. 116p. Dep. NTIS (U. S. Sales Only). AECL $2.50.

A computer code is described that performs an extended Hartree–Fock variational calculation for the intrinsic state of lighter nuclei having up to 82 protons and 82 neutrons. An exact treatment of the kinetic energy of the center-of-mass and the Coulomb two-body interaction is developed. The self-consistent orbitals can mix all the basis states including the time-reversed pairs but are restricted to having good parity; this results in an improved variational approximation, which can be applied to odd nuclei. The neutron and proton wavefunctions are treated separately so as to exhibit the isospin violation due to the Coulomb force. The matrix elements of the nuclear interaction must be supplied as initial data. The initial trial wavefunction is taken to be that of the Nilsson model. Most calculated quantities are found to be within 10% of their experimental values, for nuclei with $4 \leq A \leq 40$. (auth)

28440 (CERN-70-30(Vol.1)) INTERNATIONAL CONFERENCE ON THE PROPERTIES OF NUCLEI FAR FROM THE REGION OF BETA-STABILITY, LEYSIN, SWITZERLAND, AUGUST 31–SEPTEMBER 4, 1970. (European Organization for Nuclear Research, Geneva (Switzerland)). 1970. 602p. (CONF-700815–(Vol.1)).

Separate abstracts were prepared for 33 of the 37 papers in this volume; the remaining 4 were previously abstracted in NSA. For abstracts of the latter papers, see CONF–700815 in a cumulative report number index. (R.W.R.)

28441 (CERN-70-30(Vol.1), pp 217-62) MASS LAW WITH MODEL-BASED SHAPE-DEPENDENT SHELL TERMS. Seeger, P. A. (Los Alamos Scientific Lab., N. Mex.).

In International conference on the properties of nuclei far from the region of beta-stability; Leysin, Switzerland (31 Aug 1970).

Shell terms based on the Nilsson model with Strutinsky normalization and BCS pair correlations are included in the least-squares determination of liquid-drop parameters in order to obtain more reliable values for extrapolation. Equilibrium shapes are described by quadrupole and hexadecapole (P_2 and P_4) moments. Fit-

XUM

ting is done both to the mass table and to the experimental reaction and mass-doublet data, for various combinations of liquid-drop and shell-correction terms. The r process is calculated using this and one other new mass law. An appendix includes calculated binding energies, equilibrium shapes and skin–parity assignments for Z = 20 to 120 nuclei. (auth)

28442 (CERN–70-30(Vol.1), pp 397-419) GROSS THEORY OF BETA-DECAY AND THE NUCLEI FAR FROM THE REGION OF BETA-STABILITY. Yamada, Masami (Waseda Univ., Tokyo (Japan). Science and Engineering Research Lab.); Takahashi, Kohji; Koyama, Shin-Ichiro (Waseda Univ., Tokyo (Japan). Dept. of Applied Physics).

In International conference on the properties of nuclei far from the region of beta-stability; Leysin, Switzerland (31 Aug 1970).

The importance of the Gamow–Teller matrix element for these decays and the Fujita–Ikeda Theory are briefly discussed. Beta decay is next described at a statistical theory whose object is the gross properties of the decay and not the individual transitions. This theory is treated in the context of the Fermi-gas model. Strength functions are shown for isotopes of Ir, Pt, Au, Hg, Bi, Po, At, and Rn. Strength functions are also given for some delayed-nucleon precursors. In addition, the half-lives of many of the nuclides are calculated. (R.W.R.)

28443 (CERN–70-30(Vol.1), pp 421-33) COMPOUND-NUCLEUS ASPECTS OF BETA DECAYS WITH HIGH Q VALUES. Damkjaer, A.; Duke, C. L.; Hornshoej, P.; Wilsky, Hansen, P. G.; Jonson, B.; Nielsen, O. B.; Rudstam, G. (European Organization for Nuclear Research, Geneva (Switzerland)).

In International conference on the properties of nuclei far from the region of beta-stability; Leysin, Switzerland (31 Aug 1970).

Beta strength functions for nuclei with N > Z are surveyed. The technique of using a total-absorption gamma spectrometer to find the energy of the level fed in beta decay is described. The calculation of average strength functions is discussed. The energy distribution of the beta strength appears to be very wide. The origin of the strength and the influence of pairing seem to be understood qualitatively. Applications for the determination of Q values and for prediction of the beta half-lives of very exotic nuclear species are mentioned. (R.W.R.)

28444 (CERN–70-30(Vol.1), pp 497-516) PROPERTIES OF NUCLEI FAR OFF THE β-STABILITY VALLEY. Berlovich, E. E. (Akademiya Nauk SSSR, Leningrad. Fiziko-Tekhnicheskii Institut).

In International conference on the properties of nuclei far from the region of beta-stability; Leysin, Switzerland (31 Aug 1970).

Some effects characteristic of nuclei far off the β-stability line are reviewed; features of the structure of these nuclei, two-neutron decay at the boundary of the neutron stability region, delayed decays with the emission of ^{3}He and ^{3}H, delayed fission, double β decay, contributions of higher orders to β transitions of the $0^+ \rightarrow 0^+$ type, and nucleon synthesis of superheavy elements in supernova explosions are considered. (44 references) (auth)

28445 (CERN–70-30(Vol.1), pp 553-66) RESONANT FISSION WITH DAMPING. Bondorf, J. P. (Niels Bohr Instiutet, Copenhagen (Denmark)).

In International conference on the properties of nuclei far from the region of beta-stability; Leysin, Switzerland (31 Aug 1970).

Some effects of the doubly humped fission barrier in the decay of the compound nucleus by fission are discussed. The fission penetrability is calculated in an "optical model of fission" in which the real potential characteristic of each saddle-point channel is assumed to be doubly humped. The coupling of the vibrational states in the intermediate well to more complicated states is described by an imaginary potential. Thus, the damping of the fission-channel states is made in the same way as in the conventional optical model for particle scattering. The problem of subsequent distribution of the dissipated flux is discussed. The theory is illustrated by the ^{239}Pu(d,pf) reaction. (15 references) (auth)

28446 (CERN–70-30(Vol.2), pp 813-27) SOME INTERESTING ASPECTS OF THE VMI MODEL. Scharff-Goldhaber, Gertrude (Brookhaven National Lab., Upton, N. Y.).

In International conference on the properties of nuclei far from the region of beta-stability; Leysin, Switzerland (31 Aug 1970).

The variable-moment-of-inertia model is explained. This model is able to describe ground-state bands of all even–even nuclei of at least moderate mass that do not contain a filled nucleon shell from a simple semiclassical point of view. (R.W.R.)

28447 (CERN–70-30(Vol.2), pp 1129-32) CO-EXISTENCE OF DIFFERENT STRUCTURES IN VARIOUS DOMAINS OF THE PERIODIC TABLE. Schuette, D.; Gerling, W.; Bleuler, D. (Bonn Univ. (West Germany)).

In International conference on the properties of nuclei far from the region of beta-stability; Leysin, Switzerland (31 Aug 1970).

Some parts of the periodic table are characterized by nuclei with a "pure" structure, such as the spherical or alpha-particle type. Between these domains, however, there are many nuclides which correspond to no ideal case; it seems reasonable to suppose that they may be described in a first approximation by a linear superposition of the "pure" wave functions. Work on a mathematical model for an N-fermion problem that might exhibit such behavior is outlined. (R.W.R.)

28448 (CERN–70-30(Vol.2), pp 1133-5) ONE BOSON EXCHANGE POTENTIAL AND NUCLEAR MATTER PROPERTIES. Erkelenz, K.; Holinde, K.; Bleuler, K. (Bonn Univ. (West Germany). Institut fuer Theoretische Kernphysik).

In International conference on the properties of nuclei far from the region of beta-stability; Leysin, Switzerland (31 Aug 1970).

A one-boson exchange potential (OBEP) is used to describe the nucleon–nucleon interaction and to calculate the binding energy and saturation density of nuclear matter. It is concluded that the ratio of repulsion (core region) to attraction (intermediate range) in the S-wave states of the OBEP must be improved. (R.W.R.)

28449 (ISS–70/17) STATUS OF SOME RELEVANT PROBLEMS IN NUCLEAR PHYSICS. Amaldi, U. Jr. (Istituto Superiore di Sanita, Rome (Italy). Laboratori di Fisica). 30 Jun 1970. 29p. Dep. NTIS (U. S. Sales Only).

The fundamental problem of nuclear physics is the calculation of the structure of nuclei from the knowledge of the nucleon–nucleon interaction. The sources of the experimental facts are reviewed and compared with the results of theory in the first part of the present contribution. In the second part the basis of the Brueckner nuclear theory is briefly outlined, and the results of recent theoretical calculations are presented. By comparing theoretical predictions and experimental data the conclusion is reached that, while the saturation properties of nuclear matter and the surface properties of nuclei are reasonably well understood, the deep single-particle states and the high-momentum components of the nuclear wave function deserve more study, both from the theoretical and the experimental points of view. (auth)

28450 (N–70-42846) EXPANDED FORTRAN 4 PROGRAM FOR ELASTIC SCATTERING ANALYSES. Smith, Margaret M.; Giamati, Charles C. (National Aeronautics and Space Administration, Cleveland, Ohio. Lewis Research Center). Sep 1970. 110p. (NASA-TN-D–6000; E–5607). NTIS.

The SCATLE program is a FORTRAN 4 nuclear-optical-model program that is a revision and extension of program SCAT4. Program SCATLE is described as a user's guide. The SCATLE program calculates elastic scattering cross sections, polarizations, phase shifts, and triple scattering values. An automatic search varies the nuclear parameters to improve agreement between calculated and experimental cross sections and polarizations. Several nuclear potential forms are available. (auth) (STAR)

28451 (N–71-10999) COULOMB CORRECTIONS TO THE BETHE–HEITLER CROSS SECTIONS FOR ELECTRON–NUCLEUS BREMSSTRAHLUNG. Morgan, S. H. Jr. (National Aeronautics and Space Administration, Huntsville, Ala. George C. Marshall Space Flight Center). Oct 1970. 104p. (NASA-TN-D–6038; M–436). NTIS.

The bremsstrahlung differential cross section is obtained using both the Born approximation and a partial-wave expansion. The cross sections are evaluated for energies in the 0.2 and 2.0 MeV range and compared with the experimental results for different scattering media. A comparison is made between the two theoretical approaches to obtain a correction to the Born approximation. The corrected Born approximation gives relatively good results in the 0.1 to 2.0 MeV range but is not applicable to higher energies. (auth) (STAR)

28452 (NP–18717) EFFECTIVE NUCLEAR INTERACTIONS AND LEVEL PROPERTIES FOR THE LIGHTER NUCLEI IN THE 1p-SHELL. Kumar, Naresh (Australian National Univ., Canberra). Mar 1970. 221p. Dep. NTIS (U. S. Sales Only).

Thesis.

Shell model calculations using the effective interaction approach of Talmi are reported for nuclei of mass numbers 6 to 9. Difficulty experienced in the simultaneous fitting of excitation energies of levels in these nuclei is discussed, and the possible connection of this difficulty with the deformations of ^{8}Be and ^{9}Be is indicated. After the inclusion of these deformations in a phenomenological way, the obtained effective interaction is shown to give either equally good or better agreement with the experimental data than the ones achieved by previous authors, and the resulting two-body matrix elements

of the effective interaction are found to resemble the ones obtained by starting from the free two-nucleon interactions. An analysis of the $^{7}Li(p,\alpha)^{4}He$ reaction data obtained with the use of both polarized and unpolarized beams of protons and using the multi-level R-matrix theory is reported. This analysis gives information about the α-emitting states of ^{8}Be lying in the region of ^{20}MeV excitation energies. Predictions of the above mentioned shell model calculations were found useful in this analysis, and evidence was found for two new levels in ^{8}Be. (auth)

28453 (NYO-4032-37) MODEL SPACE CALCULATION OF THE QUASI-PARTICLE INTERACTION FOR NUCLEAR MATTER. Poggioli, R. S.; Jackson, A. D. (State Univ. of New York, Stony Brook. Dept. of Physics). [1969]. 23p. Dep. NTIS.

Landau's theory of Fermi liquids is outlined, and a microscopic approach to the calculation of the quasi-particle interaction $f(k_1,k_2)$ for nuclear matter is detailed. A model space is introduced in order to take especial care of the contribution of low-lying states to $f(k_1,k_2)$. The model space is constructed to include only those states in which all particles have momentum less than $2k_f$. The effect of the high momentum states is absorbed into the definition of the effective interaction to be used within the model space. An examination of Brueckner-Bethe theory leads to the choice of a truncated G-matrix as a good approximation for this model interaction. A simple perturbative approach is attempted within the model space. The quasi-particle interaction is calculated to second order (in the model interaction). Good values are obtained for the effective mass and symmetry energy, but the calculated compression modulus is too small. It is hoped that third order corrections will improve the results, but no definitive statement about the convergence of this approach is possible at this stage. (auth)

28454 (RT/FI-(70)38) TENSORIAL FORMULATION AND GEOMETRIC INTERPRETATION OF A MULTI LEVEL MULTI CHANNEL FORMULA FOR NUCLEAR RESONANCES. Motta, M. (Comitato Nazionale per l'Energia Nucleare, Rome (Italy)). 26 Aug 1970. 33p. (In Italian). Dep. NTIS (U. S. Sales Only).

A tensoral formulation of a simplified multi-level multi-channel formula for nuclear resonances is presented. The formulation is obtained by the representation of the cross section for a given reaction as an Hermitian form in a space referred to curvilinear axes which are directly related to the Breit-Wigner single level curves. Using conformal mapping a geometrical interpretation is given in which the cross section is obtained by reflection of points on the complex plane with respect to circles, one for each level. As an example, the two-level formula is deduced by the general formula. (auth)

28455 NUCLEAR ISOSPIN. Proceedings of the Conference, Asilomar-Pacific Grove, California, March 13-15, 1969. Anderson, John D.; Bloom, Stewart D.; Cerny, Joseph; True, William W. (eds.). New York; Academic Press, Inc. (1969). 866p. $22.00. (CONF-690310).

Sixty-seven of the 73 papers included are listed by title only. The remaining 6 papers have previously appeared in NSA. (J.W.R.)

For abstracts of individual papers see: 28172-28177, 28222-28243, 28359-28372, and 28456-28480.

28456 IS THE EFFECTIVE CHARGE CORRECTION LARGER FOR A NEUTRON THAN FOR A PROTON. Siegel, Stan; Zamick, Larry (Rutgers - The State Univ., New Brunswick, N. J.). pp 143-6 of Nuclear Isospin. /Anderson, John D. (ed.). New York; Academic Press, Inc. (1969).

From second conference on nuclear isospin; Pacific Grove, Calif. (13 Mar 1969). See CONF-690310.

28457 CHARGED-EXCHANGE REACTIONS. Madsen, V. A. (Oregon State Univ., Corvallis). pp 149-69 of Nuclear Isospin. /Anderson, John D. (ed.). New York; Academic Press, Inc. (1969).

From second conference on nuclear isospin; Pacific Grove, Calif. (13 Mar 1969). See CONF-690310.

28458 EXCITATION OF ANALOGUE STATES BY STRIPPING AND PICK-UP REACTIONS. Barnes, C. A. (California Inst. of Tech., Pasadena). pp 179-203 of Nuclear Isospin. /Anderson, John D. (ed.). New York; Academic Press, Inc. (1969).

From second conference on nuclear isospin; Pacific Grove, Calif. (13 Mar 1969). See CONF-690310.

28459 ENERGY DEPENDENCE OF DIRECT ISOSPIN-VIOLATING (d,α) REACTIONS. Noble, J. V. (Univ. of Pennsylvania, Philadelphia). pp 233-8 of Nuclear Isospin. /Anderson, John D. (ed.). New York; Academic Press, Inc. (1969).

From second conference on nuclear isospin; Pacific Grove, Calif. (13 Mar 1969). See CONF-690310.

28460 ALLOWED NEUTRON DECAY OF HIGHLY EXCITED ($T_o + \frac{1}{2}$) COMPOUND NUCLEUS STATES. Anderson, J. D.; Kerman, A. K. (Univ. of California, Livermore). pp 247-51 of Nuclear Isospin. /Anderson, John D. (ed.). New York; Academic Press, Inc. (1969).

From second conference on nuclear isospin; Pacific Grove, Calif. (13 Mar 1969). See CONF-690310.

28461 SEARCH FOR AN IMAGINARY ISOVECTOR INTERACTION IN THE OPTICAL MODEL POTENTIAL IN ^{3}He INDUCED REACTIONS. Hansen, Luisa F.; Stelts, Marion L. (Univ. of California, Livermore). pp 269-74 of Nuclear Isospin. /Anderson, John D. (ed.). New York; Academic Press, Inc. (1969).

From second conference on nuclear isospin; Pacific Grove, Calif. (13 Mar 1969). See CONF-690310.

28462 ISOSPIN COUPLING IN DEUTERON STRIPPING REACTIONS. Hooper, M. B. (Nuclear Physics Lab.; Oxford). pp 275-80 of Nuclear Isospin. /Anderson, John D. (ed.). New York; Academic Press, Inc. (1969).

From second conference on nuclear isospin; Pacific Grove, Calif. (13 Mar 1969). See CONF-690310.

28463 FINE STRUCTURE OF ANALOG RESONANCES. Mahaux, C. (Univ. of Liege). pp 337-52 of Nuclear Isospin. /Anderson, John D. (ed.). New York; Academic Press, Inc. (1969).

From second conference on nuclear isospin; Pacific Grove, Calif. (13 Mar 1969). See CONF-690310.

28464 DETERMINATION OF SPECTROSCOPIC FACTORS. Weidenmueller, Hans A. (Yale Univ., New Haven). Contract AT(30-1)-3223. pp 361-84 of Nuclear Isospin. /Anderson, John D. (ed.). New York; Academic Press, Inc. (1969).

From second conference on nuclear isospin; Pacific Grove, Calif. (13 Mar 1969). See CONF-690310.

28465 GENERAL REMARKS. Robson, D. (Florida State Univ., Tallahassee). pp 385-99 of Nuclear Isospin. /Anderson, John D. (ed.). New York; Academic Press, Inc. (1969).

From second conference on nuclear isospin; Pacific Grove, Calif. (13 Mar 1969). See CONF-690310.

28466 MICROSCOPIC CALCULATION FOR THE ESCAPE WIDTH OF ANALOG STATES. Auerbach, Naftali; Huefner, Joerg; Kerman, A. K.; Shakin, C. M. (Massachusetts Inst. of Tech., Cambridge). pp 403-8 of Nuclear Isospin. /Anderson, John D. (ed.). New York; Academic Press, Inc. (1969).

From second conference on nuclear isospin; Pacific Grove, Calif. (13 Mar 1969). See CONF-690310.

28467 THE ROLE OF THE ANTI-ANALOG STATE IN THE DECAY OF THE ANALOG STATE. Auerbach, Naftali; Huefner, Joerg; Kerman, A. K.; Shakin, C. M. (Massachusetts Inst. of Tech., Cambridge). pp 409-14 of Nuclear Isospin. /Anderson, John D. (ed.). New York; Academic Press, Inc. (1969).

From second conference on nuclear isospin; Pacific Grove, Calif. (13 Mar 1969). See CONF-690310.

28468 ANALOG FINE STRUCTURE AND ASYMMETRY. Moldauer, P. A. (Argonne National Lab., Ill.). pp 415-19 of Nuclear Isospin. /Anderson, John D. (ed.). New York; Academic Press, Inc. (1969).

From second conference on nuclear isospin; Pacific Grove, Calif. (13 Mar 1969). See CONF-690310.

28469 PROTON-INDUCED ANALOG RESONANCES. Morrison, G. C. (Argonne National Lab., Ill.). pp 435-80 of Nuclear Isospin. /Anderson, John D. (ed.). New York; Academic Press, Inc. (1969).

From second conference on nuclear isospin; Pacific Grove, Calif. (13 Mar 1969). See CONF-690310.

28470 RESULTS AND INTERPRETATION OF ANALOG RESONANCE EXPERIMENTS. Stein, Nelson (Yale Univ., New Haven). Contract AT(30-1)-3223. pp 481-534 of Nuclear Isospin. /Anderson, John D. (ed.). New York; Academic Press, Inc. (1969).

From second conference on nuclear isospin; Pacific Grove, Calif. (13 Mar 1969). See CONF-690310.

28471 PROTON EMISSION FROM ISOBARIC ANALOG RESONANCES FORMED IN DIRECT REACTIONS AND ISOBARIC ANALOG RESONANCES EFFECTS IN (d,p) AND (p,d) CROSS SECTIONS. Richard, Patrick (Univ. of Texas, Austin). pp 535-67 of Nuclear Isospin. /Anderson, John D. (ed.). New York; Academic Press, Inc. (1969).

XUM

From second conference on nuclear isospin; Pacific Grove, Calif. (13 Mar 1969). See CONF-690310.

28472 INTEREST OF ANALOG STATE STUDIES IN DEFORMED NUCLEI. Cassagnou, Y.; Foissel, P.; Levi, C.; Mitting, W.; Papineau, L. (Centre d'Etudes Nucleaires, Saclay, France). pp 625-7 of Nuclear Isospin. /Anderson, John D. (ed.). New York; Academic Press, Inc. (1969).

From second conference on nuclear isospin; Pacific Grove, Calif. (13 Mar 1969). See CONF-690310.

28473 A MODIFIED SCHIFFER PROCEDURE FOR SPECTROSCOPIC FACTORS FROM ANALOGUE RESONANCES. Seitz, H. (Max-Planck Institut fuer Kernphysik, Heidelberg). pp 685-8 of Nuclear Isospin. /Anderson, John D. (ed.). New York; Academic Press, Inc. (1969).

From second conference on nuclear isospin; Pacific Grove, Calif. (13 Mar 1969). See CONF-690310.

28474 ISOBARIC ANALOG STATES FOR NEUTRON SPECTROSCOPIC FACTORS. Thompson, W. J. (Florida State Univ., Tallahassee); Ellis, J. L. pp 689-94 of Nuclear Isospin. /Anderson, John D. (ed.). New York; Academic Press, Inc. (1969).

From second conference on nuclear isospin; Pacific Grove, Calif. (13 Mar 1969). See CONF-690310.

28475 COULOMB ENERGIES. Schiffer, J. P. (Argonne National Lab., Ill. Univ. of Chicago). pp 733-55 of Nuclear Isospin. /Anderson, John D. (ed.). New York; Academic Press, Inc. (1969).

From second conference on nuclear isospin; Pacific Grove, Calif. (13 Mar 1969). See CONF-690310.

28476 ISOSPIN IMPURITY IN BOUND STATES. Mekjian, A. Z. (Rutgers - The State Univ., New Brunswick, N. J.). pp 763-79 of Nuclear Isospin. /Anderson, John D. (ed.). New York; Academic Press, Inc. (1969).

From second conference on nuclear isospin; Pacific Grove, Calif. (13 Mar 1969). See CONF-690310.

28477 ISOBARIC SPIN IN NUCLEAR FISSION. Kelson, I. (Tel-Aviv Univ., Israel). pp 781-7 of Nuclear Isospin. /Anderson, John D. (ed.). New York; Academic Press, Inc. (1969).

From second conference on nuclear isospin; Pacific Grove, Calif. (13 Mar 1969). See CONF-690310.

28478 SOME SYSTEMATICS OF COULOMB DISPLACEMENT ENERGIES. Atkinson, Jay; Bloom, S. D. (Univ. of California, Livermore). pp 799-806 of Nuclear Isospin. /Anderson, John D. (ed.). New York; Academic Press, Inc. (1969).

From second conference on nuclear isospin; Pacific Grove, Calif. (13 Mar 1969). See CONF-690310.

28479 SHELL-MODEL DESCRIPTION OF COULOMB DISPLACEMENT ENERGIES IN THE LIGHT NUCLEI. Jaenecke, Joachim (Univ. of Michigan, Ann Arbor). pp 807-12 of Nuclear Isospin. /Anderson, John D. (ed.). New York; Academic Press, Inc. (1969).

From second conference on nuclear isospin; Pacific Grove, Calif. (13 Mar 1969). See CONF-690310.

28480 HIGHER ORDER INTERFERENCE EFFECTS IN HINDERED ALLOWED β-DECAY AND THE MATRIX ELEMENT RATIO $C_v[1]C_{A_1}[\sigma]$. Sastry, K. S. R. (Univ. of Massachusetts, Amherst). pp 831-6 of Nuclear Isospin. /Anderson, John D. (ed.). New York; Academic Press, Inc. (1969).

From second conference on nuclear isospin; Pacific Grove, Calif. (13 Mar 1969). See CONF-690310.

28481 SHAPE-FLUCTUATION MODEL OF GROUND-STATE BANDS IN EVEN-EVEN NUCLEI. Satpathy, M. (Berhampur Univ., India); Satpathy, L. Phys. Lett.; 34B: 377-80(15 Mar 1971).

A shape-fluctuation (SF) model for the energy levels of the ground-state bands in even-even nuclei is proposed invoking the idea of the J-dependence of the intrinsic wave function. In addition to permitting an excellent fit of the energy levels, the model yields in each state the contribution to the energy due to shape fluctuation, which provides a measure of the variation of the intrinsic shape in the ground-state band. (auth)

28482 EFFECTIVE FOUR-BODY INTERACTION IN LIGHT NUCLEI. Camiz, P. (Univ., Rome. Istituto Nazionale di Fisica Nucleare, Rome); D'Andrea, A.; Olivieri, E.; Scalia, M. Nuovo Cim.; 2A: 393-400(21 Mar 1971).

The binding nuclear energies in the shells $1p_{\frac{3}{2}}$, $1d_{\frac{5}{2}}$, $1d_{\frac{3}{2}}$, and $1f_{\frac{7}{2}}$ were calculated with a mass formula including generalized pairing interaction and an effective four-body interaction acting between nucleons coupled to J = 0 and T = 0. The introduction of the four-body force considerably improves previous results: the correlation between the new parameter and the others is discussed in a qualitative way. (auth)

28483 DIFFRACTION RADIATION BY A LINE CHARGE MOVING PAST A COMB: A MODEL OF RADIATION LOSSES IN AN ELECTRON RING ACCELERATOR. Hazeltine, R. D. (Inst. for Advanced Study, Princeton, N. J.); Rosenbluth, M. N.; Sessler, A. M. J. Math. Phys. (N. Y.); 12: 502-14(Mar 1971).

A calculation is given of the radiated-energy loss from a charged rod which moves at constant speed past an infinite set of parallel semi-infinite conducting plates of infinitesimal thickness, with the rod taken parallel to and at a fixed distance from the plate edges. The problem is analyzed using the Wiener-Hopf technique, and the resulting formulas are evaluated analytically in the limits of high rod speed and low rod speed, and compared with numerical evaluation over the full range of speeds. (auth)

28484 EFFECT OF SPIN-SPIN AND SPIN-ORBIT FORCES ON THE DECOUPLING PARAMETERS. Chernyshev, A. S. (Voronizh State Univ., USSR). Yadern. Fiz.; 12: 1194-1202(Dec 1970). (In Russian).

The effect of spin-spin forces on the orbital component of the decoupling parameter a is considered using the method of the finite Fermi-system theory. It is shown that the value of the correction is of the same order as the one-particle matrix element. The effect of the residual spin-orbit quasi-particle interaction on the a value is also considered. The contribution from this term in the amplitude is of systematic nature and amounts to 30 to 40% of the effect from spin-spin forces. (auth)

28485 NUCLEAR REARRANGEMENT PROCESSES IN AN EXACT N-BODY THEORY. Vanzani, V. (Univ., Padua. Laboratori Nazionali di Legnaro, Legnaro, Italy. Istituto Nazionale di Fisica Nucleare, Padua). Nuovo Cim.; 2A: 525-43(21 Mar 1971).

Nuclear rearrangement processes are investigated within the framework of the Yakubovskii approach to the N-body problem. Transition operator components having prescribed connectedness properties are proposed in order to extract from exact equations the relevant reaction mechanisms. Specific applications to single-particle and two-particle transfer reactions are treated. (auth)

28486 THREE-BODY MODEL FOR ^{6}Li INDUCED REACTIONS. Osman, A. (Cairo Univ.). Phys. Lett.; 34B: 478-80 (29 Mar 1971).

The ^{6}Li-induced reactions are presented on a soluble three-body model. Taking for the ^{6}Li nucleus a deuteron + alpha cluster structure, the angular distributions for its stripping and elastic scattering on a target nucleus X are calculated. Good agreement with the experimental measurements is obtained. (auth)

28487 ANGULAR CORRELATION OF NUCLEONS GENERATED DURING THE REACTIONS OF DECAYING DEUTERONS IN THE FIELD OF NUCLEI. Gaivoronskaya, T. V.; Komarov, V. V. Ukr. Fiz. Zh.; 15: 949-58(Jun 1970). (In Russian).

Nucleon angular correlations in the deuteron decay of compound nuclei were analyzed theoretically. The analysis, based on the general multiparticle scattering theory, permits a set of correlation maxima in the angular distributions of the nucleons to be obtained. This set is found to be in good agreement with the experimental data. A new effect in nucleon scattering by excited nuclei was predicted by the theory. (auth)

28488 MICROSCOPIC ANALYSIS OF THE (γ,p) AND (γ,n) REACTIONS AT MEDIUM PHOTON ENERGIES. Weise, Wolfram; Huber, Max G. (Univ., Erlangen, Ger.). Nucl. Phys.; A162: 330-48(1971).

The photonuclear reactions (γ,p) and (γ,n) have been analyzed for photon energies 40 MeV < E_γ < 140 MeV on the basis of a shell-model picture modified by short-range nucleon-nucleon correlations. The cross sections turn out to depend sensitively on the details of the correlation factor, i.e. on the exchange of high momenta between otherwise independently moving nucleons. As in the case of the (γ,pn) reaction, the results of the calculations for ^{16}O indicate that precise measurements of the (γ,p) and (γ,n) cross sections do contain information on the properties of the nuclear wave functions at small internucleonic distances. (auth)

28489 TENSOR POLARIZABILITY IN THE GIANT DIPOLE RESONANCE REGION AND COLLECTIVE BEHAVIOUR. Arenhoevel, H. (Max-Planck-Institut fuer Chemie, Mainz); Gneuss, G.; Rezwani, V. Phys. Lett.; 34B: 249-51(1 Mar 1971).

The extended dynamic collective model of the giant dipole resonance has been used to calculate elastic and inelastic γ-scattering by even-even nuclei. For the examples given it turns out that the scalar polarizability leads only to elastic γ-scattering, i.e., inelastic γ-scattering to 0^+-states is neg-

XUM

ligible. However, the tensor polarizability leading to the inelastic γ-scattering into 2^+-states is of appreciable size and gives valuable additional information on the collective character of the nucleus. (auth)

28490 STATES OF INTERMEDIATE CHARGE SYMMETRY AS LOW-LYING, 0^+ COLLECTIVE EXCITATIONS OF MEDIUM WEIGHT NUCLEI. Chen, Hsi-tseng; Richardson, R. W. (New York Univ.). Phys. Lett.; 34B: 271-4(1 Mar 1971).

A method for calculating the states of the charge-independent pairing Hamiltonian that have intermediate charge symmetry is presented. The states are shown to be collective 0^+ excitations with energies that fall well within the gap in the single-particle spectrum. (auth)

28491 ELECTRON EXCITATION–GAMMA DECAY REACTION IN HEAVY NUCLEI AND INVESTIGATION OF p–p CORRELATIONS IN NUCLEI VIA HIGH ENERGY ELECTRON SCATTERING. Whitehill, Don Earl. Austin, Tex.; Univ. of Texas (1970). 117p. University Microfilms Order No. 71-213.

Thesis.

Two separate theoretical investigations are presented. Both involve the use of high-energy electron scattering to study nuclear structure. Results are presented in both cases for the coincidence detection of the final electron and other final particles. Coincidence experiments would facilitate the investigation of specific aspects of nuclear structure which are inaccessible when only the final electrons are detected. The reaction $e + A \rightarrow e' + A' \rightarrow A'' + \gamma$ is suggested as a means for investigating low-lying excited states of heavy nuclei. The formalism for the $e - \gamma$ coincidence cross section and the γ-detection differential cross section is given. By detecting the decay photon, the problems caused by the inability to attain sufficient energy resolution for the electrons are circumvented. The effect of the static Coulomb field of the nucleus, which is important for heavy nuclei, is taken into account in the electron wave functions. Results are given for several different nuclei. Both the coincidence cross section and the γ-detection differential cross section appear to offer a feasible method for investigating excited states in heavy nuclei. In fact, the differential cross section for the decay photons might be detectable in many cases with present day accelerators. More information about the excited states can be obtained from the $e - \gamma$ coincidence cross section than from the differential cross section for the decay photons. The possibility of using the reaction A(e,e' pp)B to investigate proton-proton correlations in nuclei is discussed. The proposed method requires coincidence detection of the final electron and two final protons. The formalism for the cross section is given to the lowest order in the electromagnetic coupling constant and neglecting final state interactions. Wave functions for the harmonic oscillator potential are used with the correlation function $f(r) = 1 - e^{-\beta^2 r^2}$. Antisymmetrization of the wave functions is not taken into account. It is found that the portion of the cross section which is sensitive to the correlation has a very small magnitude. (Diss. Abstr. Int., B)

28492 EXTENSION OF A SCHEMATIC THEORY OF NUCLEAR REACTIONS TO INCLUDE ISOSPIN AND ISOBARIC ANALOGUE RESONANCES. Mello, P. A.; Moshinsky, M. (Univ. Nacional de Mexico, Mexico City). Rev. Mex. Fis.; 19: 339-66 (1970).

In a previous paper one of the authors discussed a schematic theory of nuclear reactions in which both the colliding particles and the compound system are described as point particles, the main advantage being that the time-dependent analysis of the problem is considerably simplified. In the present paper the schematic theory is extended to include the isotopic spin formalism in the specific example of a two-channel problem involving isobaric analog resonances. (auth)

28493 RADIATIVE CORRECTIONS TO BETA DECAY SPECTRA AND THE NEUTRINO REST MASS. Jarlskog, Cecilia (Lund Univ., Sweden). Ark. Fys.; 40: 509-12(1970).

The effect of radiative corrections on the beta decay spectra is examined with emphasis on the beta decay of tritium and the question of the rest mass of the electron neutrino. It is found that the experimental conclusions on the rest mass of the electron neutrino are not altered by radiative corrections and that these corrections are appreciable in the low-energy region of spectra from decays with large energy release. (auth) (Sweden)

28494 NEW VALUES FOR K/β BRANCHING COEFFICIENTS. Zyryanova, L. N.; Suslov, Yu. P. Izv. Akad. Nauk SSSR, Ser. Fiz.; 34: 101-5(Jan 1970). (In Russian).

Tabulated data are given of the relative probability of K-electron capture and β^+ decay. New values for K/β^+ were obtained for self-consistent atomic potentials, which took the finite nuclear dimensions into account according to the model of a uniformly charged sphere. The difference between the new and old data comprised from 2 to 10%. (R.V.J.)

28495 RELATIVISTIC EVALUATION OF ELECTRON CAPTURE EXCHANGE EFFECT. Suslov, Yu. P. (Leningrad State Univ.). Izv. Akad. Nauk SSSR, Ser. Fiz.; 34: 97-100(Jan 1970). (In Russian).

Relativistic calculations were made for correction factors describing exchange and overlap effects during electron capture in the Bahcall theory. A self-consistent Hartree–Fock–Slater potential and the final dimensions of the nucleus according to the simulated uniformly charged sphere were used in the calculations. Within the region of small atomic numbers the data obtained are close to the results obtained by Bahcall, while for the $Z > 38$ the calculations have no precedent. The correction factors (with the exchange and overlapping in the K-, L_I-, and M_I-capture taken into account) are tabulated for $14 \leq Z \leq 98$ and may be used in the experimental data for electron capture. (R.V.J.)

28496 POLARIZATION IN TWO-NUCLEON STRIPPING REACTIONS AT LOW ENERGIES. Vysotskii, G. L.; Chegoryan, M. A. (Inst. of Physics and Tech., Kiev). Izv. Akad. Nauk SSSR, Ser. Fiz.; 34: 147-52(Jan 1970). (In Russian).

Polarization effects appearing in two-nucleon stripping reactions, (^{3}He,p), (T,p), (α,d), etc., are considered in the energy range in which resonance excitation of the complex nuclei is possible in addition to the direct mechanisms. Numerical calculations are given for the $^{13}C(^3He,p)^{14}N$ reaction at low energy, in which the deuteron is captured into the s shell of the target nucleus. (R.V.J.)

28497 RESONANCE NARROWING EFFECT IN TWO-PARTICLE INTERACTIONS PRODUCING THREE PARTICLES. Komarov, V. V. (Moscow State Univ.). Izv. Akad. Nauk SSSR, Ser. Fiz.; 34: 78-83(Jan 1970). (In Russian).

In nuclear reactions producing three particles but with the energy distribution of only one of the particles measured, resonances from interactions between the two other particles have been found when their relative energy was equal to the energy of the bound or quasi-bound state. A method based on the general theory of multiparticle scattering for describing resonances and energy distributions of products from a reaction emitting three particles is discussed. It is assumed that the reaction results from a direct interaction or through a compound nucleus. (R.V.J.)

28498 PERIPHERAL MODEL FOR NUCLEAR REACTIONS AND COMPARISONS OF THE MODEL WITH OTHER EXPERIMENTS AND THEORIES. Dolinskii, E. I. Izv. Akad. Nauk SSSR, Ser. Fiz.; 34: 165-74(Jan 1970). (In Russian).

Calculations of direct nuclear reactions according to the peripheral model were correlated with experimental data on differential cross sections for the (d,p), (d,t), and (^{3}He,α) reactions with eight nuclei in a large range of incident particle energies. It is shown that the peripheral model describes the differential cross sections as well as the distorted-wave model; in addition, it has its advantages because, in contrast to the distorted-wave model, the peripheral model is based on a relatively small number of nonsimulated general physical postulates and contains a smaller number of unknown adjusted fitted parameters. (R.V.J.)

28499 MAGNETIC DIPOLE AND ELECTRIC QUADRUPOLE MOMENTS OF ODD-MASS NUCLEI. Korolev, A. M. (Inst. of Physics, Kiev). Izv. Akad. Nauk SSSR, Ser. Fiz.; 34: 161-4 (Jan 1970). (In Russian).

Magnetic dipole and electric quadrupole moments of the ground and excited states of odd-mass spherical nuclei were studied using a generalized Bohr model and taking into account the excitations in the core of an arbitrary large number of phonons. Considerations for collective effects in magnetic moments of the ground states of odd-mass nuclei resulted in some deviations from the Schmidt line bringing their magnitudes closer to the experimental values. (R.V.J.)

28500 ABNORMALITIES IN ELASTIC NEUTRON SCATTERING AT SMALL ANGLES. Gorlov, G. V.; Lebedeva, N. S.; Morozov, V. M. Izv. Akad. Nauk SSSR, Ser. Fiz.; 34: 138-46(Jan 1970). (In Russian).

Anomalous neutron scattering at small angles by heavy nuclei has been observed in some previous experiments. However, other experiments with these nuclei in the identical energy range did not observe any abnormalities. An analysis of the existing theory and interpretation of the available data established a lack of proof for the existence of anomalous scattering. (R.V.J.)

28501 THEORY OF EXCITED STATES OF DEFORMED EVEN–EVEN NUCLEI. Karaev, R.; Sharipov, Sh. (Tashkent State Univ.). Dokl. Akad. Nauk Uzb. SSR; No. 5, 23-4(1970). (In Russian).

The theory of collective excitations of the quadrupole type, which takes into account the deformation of the nucleus during

XUM

excitation, explains a number of regularities observed in the excitation spectrum of even–even and odd atomic nuclei such as: energy of the excited level, arrangement of spins, probability of electromagnetic transitions between excited levels, and average values of quadrupole electric moments in each excited state. The type of excited states of deformed, even–even atomic nuclei depends substantially on two dimensionless parameters which characterize the longitudinal and radial deformation of the nuclear surface. Level energies and spins are calculated for ^{152}Sm, and are compared with experimental values. At high deformations there is a noticeable effect on level energies and arrangement of spins. (TTT)

28502 ISOMER RATIO FOR (b,xn,yp,γ) REACTIONS. Liggett, G.; Sperber, D. (Rensselaer Polytechnic Inst., Troy, N. Y.). Phys. Rev., C; 3: 447-54(Feb 1971).

A method for the calculation of isomer ratios in reactions in which the compound nucleus decays by the emission of a few particles followed by γ emission is presented. It is shown that the calculated value of the isomer ratio is sensitive to the spin cutoff parameter, the amount of quadrupole admixture in the γ-ray cascade, and the presence of discrete levels. In most cases good agreement between experimentally measured and calculated values of isomer ratios is obtained. (auth)

28503 CALCULATION OF THE FACTORS OF RESONANCE SELF-SHIELDING IN FISSILE MATERIALS. Knapp, J. (Univ., Stuttgart). Atomkernenergie; 17: 19-24(Feb 1971). (In German).

A method for an exact calculation of the factors of resonance self-shielding f in fissile materials is described. The cross sections are computed with the multilevel formalism of Adler. Some examples show that the f factors are dependent on the moderator and the cross sections of uranium. For ^{235}U the f factors between 1 eV and 46.5 eV are calculated for various temperatures and various proportions of absorber to moderator and are compared with the values of the ABN data set. (auth)

28504 MECHANISM OF FISSION OF HEAVY NUCLEI. Facchini, U.; Saetta-Menichella, E. (CISE, Milan, Univ., Milan). Energ. Nucl. (Milan); 18: 124-8(Feb 1971).

A unified picture of the mechanism of fission of heavy nuclei is given to clarify the various aspects of the proposed model for scission. The existence of a barrier sharper than the Coulombian one is found. The barrier parameters are not very different for the various pairs of fragments, but the small variations in the parameters produce significant variations in the final properties of the fragments. Numerical results are given for the case of 15.5-MeV neutrons on ^{235}U. (R.W.R.)

28505 FOUR-BODY CORRELATIONS IN LIGHT NUCLEI. THE GROUND-STATE CORRELATIONS AND THE EXCITED LEVEL STRUCTURE. Fukushima, Yoshihiro; Kamimura, Masayasu; Takada, Kenjiro (Kyushu Univ., Fukuoka). Mem. Fac. Sci., Kyushu Univ., Ser. B: 4: No. 2, 39-45(Dec 1969).

By using the theory of the four-body correlations in light nuclei proposed by Marumori and Suzuki, the effect of the ground-state correlations on the level structure in the nucleus of the closed core plus four particles is investigated. A very simplified two-level model is used for this aim. It is found that the ground-state correlations have little influence on the relative level structure. A brief discussion on the relation between this model and the surface-delta-interaction model is also included. (auth) (Japan)

28506 SUM RULES FOR THE MOSHINSKY BRACKETS. Aguilera-Navarro, V. C.; Brody, T. A.; Flores, J. (Univ. Nacional de Mexico, Mexico City). Rev. Mex. Fis.; 19: 303-9(1970).

Sum rules and symmetry relations for the generalized Moshinsky transformation coefficients are derived. A number of relations valid only for the ordinary Moshinsky brackets are also derived. (auth)

28507 ISOBARIC ANALOGUE STATES. Bayman, B. F. (Univ. of Minnesota, Minneapolis). Rend. Scu. Int. Fis. Enrico Fermi; 40: 380-427([1970]). (COO-1764-64).

The formalism for the description of isobaric analog states is reviewed. Tests of isobaric spin purity and the energy splitting of the isobaric multiplet are described, and Coulomb-energy differences between isobaric analog states in medium-weight nuclei are considered. The external mixing approximation is presented. Information that may be obtained from scattering resonances is discussed. (R.W.R.)

28508 NUCLEAR CHARGE DISTRIBUTION IN FISSION FRAGMENTS. Iyer, M. R.; Ganguly, A. K. (Bhabha Atomic Research Centre, Bombay). Phys. Rev., C; 3: 785-97(Feb 1971).

A model is proposed for the fissioning nucleus which in the early stages of the fission process undergoes charge polarization into two parts, each with a number of neutrons corresponding to the ground-state β-stable nuclides for the two charges. The rest of the neutrons are then randomly distributed between the two impending fragments, as in an order-disorder process. The model is checked in detail for the thermal-neutron fission of ^{235}U. The yield distributions of fission fragments having the same charge Z along isotopic lines (isotopic distributions) are found to be single peaked but not exactly Gaussian. The $\bar{\nu}$(Z) distribution is found to closely resemble the experimental $\bar{\nu}$(A) distribution. The distribution of total isotopic yield versus Z, calculated from the isotopic distributions given by the model and experimental fragment-mass yield distribution, shows odd-even Z effects in the form of well-defined fine structure except in the high-slope region. The isotopic distributions, taken in conjunction with total isotopic yield versus Z distribution, give the usual approximately Gaussian distribution along isobaric lines (charge distribution) and provides a rationale for the variation in spread of the distributions. The variation of the mean charge Z_p of the isobaric distributions is studied by plotting the parameter $Z_p - Z_{UCD}$ (Z_{UCD} being the charge for a mass given by unchanged charge density), as a function of the mass A. This function obtained in the present work shows very good agreement with that calculated from published Z_p values for products. The fine structure observed in this function is found to correspond to the fine structure in the fragment-mass yield distribution. Distributions of total isotopic yield versus Z for the thermal-neutron fission of ^{233}U and ^{239}Pu and the spontaneous fission of ^{252}Cf are also presented. In these distributions, the higher-Z peak is found to be clustered around 54 (±2). The mass of 141 (±5), where the peaks in the fragment-mass yield curves are obtained, also has these Z's as the most probable charges. In all these distributions, odd-even Z effects are pronounced. The function $Z_p - Z_{UCD}$ for the four cases studied shows vertical shift as well as horizontal shift of the peaks in the distributions with increasing charge and mass of the fissioning nucleus. (auth)

28509 RENORMALIZATION CONSTANTS IN THE RANDOM-PHASE APPROACH. Weigel, M. (Univ. of California, Berkeley); Garside, L.; Haug, P. K. Phys. Rev., C; 3: 563-75(Feb 1971).

The renormalized random-phase-approximation equations are solved for a density-dependent particle-hole force emerging from the nucleon–nucleon interaction. Migdal's renormalization constants are determined for ^{16}O and ^{40}Ca assuming Woods–Saxon states for the quasiparticle and quasihole propagation, and compared with the renormalization constants for a harmonic-oscillator propagation. In both cases the assumption of good isospin is made. Furthermore, the renormalization constants in the ^{16}O, ^{40}Ca, ^{48}Ca, and ^{208}Pb problem were redetermined in order to test the assumption of a mass-number-independent renormalization constant. For this purpose the standard harmonic-oscillator states for the quasi-single-particle (-hole) propagation (no good isospin) was used. (auth)

28510 SEPARABLE-EXPANSION METHOD FOR THE THREE-NUCLEON SYSTEM. Fuda, Michael G. (State Univ. of New York, Buffalo). Phys. Rev., C; 3: 485-93(Feb 1971).

A previously developed separable expansion for the two-particle T matrix is applied to calculating the properties of the three-nucleon system, using spin-dependent static central potentials. The force model is identical to one that was previously employed by Brayshaw and Buck. Results are presented for the triton binding energy, the doublet and quartet scattering lengths, and for the doublet and quartet s-wave phase shifts below and above the three-body breakup threshold. It is found that two or three terms of the expansion in each two-particle spin state give staisfactory convergence in the doublet state of the three-nucleon system. Only one term is needed for the quartet state. The over-all agreement with experiment is good, but some possibly significant discrepancies are found between the theoretical and experimental quartet phase shifts above the breakup threshold. Also, it is shown that a two-particle T matrix or an approximation to one which satisfies the off-shell unitarity relation and has the correct behavior at the bound-state poles leads to three-particle scattering amplitudes which satisfy the three-particle off-shell unitarity relations. The proof does not depend on the existence of a two-particle energy-independent Hermitian potential. (auth)

28511 MAXIMUM-OVERLAP ORBITALS, AN ENERGY VARIATIONAL PRINCIPLE, AND PERTURBATION THEORY. Kobe, Donald H. (North Texas State Univ., Denton). Phys. Rev., C; 3: 417-26(Feb 1971).

The maximum-overlap orbitals first proposed by Brenig, in which the overlap between the true wave function and a Slater determinant is maximized, is shown to be equivalent to Loewdin's exact self-consistent-field theory. By defining an energy functional and varying it, some points in Loewdin's theory are clarified. The ground-state energy is expanded in perturbation theory, and it is pointed out that some diagrams could become

XUM

divergent. In order to eliminate these diagrams, Bogoliubov's principle of compensation of dangerous diagrams (PCDD) is extended to finite fermion systems. In these systems, the PCDD states that the sum of all the diagrams leading from the vacuum to a single particle-hole state must be set equal to zero. This condition is the Brillouin–Brueckner condition, which is also obtained from the other methods. The form of the PCDD obtained here is different from another form that leads to Loewdin's natural orbitals, and the difference is discussed. (auth)

28512 INFLUENCE OF BREAKUP CHANNELS ON THE ANALYSIS OF DEUTERON STRIPPING REACTIONS. Harvey, J. D.; Johnson, R. C. (Univ. of Surrey, Eng.). Phys. Rev., C; 3: 636-45(Feb 1971).

It is shown by explicit calculations that the adiabatic treatment of certain deuteron breakup channels predicts differential cross sections for (d,p) and (p,d) reactions, involving 20-MeV deuterons and a wide range of targets, similar to results obtained with the distorted-wave method but with large suppression of the contributions from low partial waves. An improved fit to angular distributions is obtained in many cases. (auth)

28513 SEMIEMPIRICAL GENERALIZED ONE-BOSON-EXCHANGE POTENTIALS. Stagat, R. W.; Riewe, F.; Green, A. E. S. (Univ. of Florida, Gainesville). Phys. Rev., C; 3: 552-62(Feb 1971).

Four generalized one-boson-exchange-potential (GOBEP) models are examined. The first is a highly realistic model which includes only well-established mesons and which takes account of the resonance width of the isoscalar scalar ϵ meson. Two others are adaptions of this model, each containing a phenomenological term to help improve the fits to high-energy phase shifts. The final model does not assume charge independence of the nuclear force. Meson–nucleon form factors derived from a generalized field theory are used throughout, and a new fitting procedure is introduced which makes allowances for the uncertainties in the theoretical model. The models are compared and evaluated in terms of both the F test for a fit to the phase shifts and the second-derivative matrix method for a fit to observable data. The basic intention is to provide realistic GOBEP models suitable for nuclear-structure and nuclear-matter calculations. (auth)

28514 NEUTRON–PROTON INTERACTION IN ODD–ODD DEFORMED NUCLEI. Jones, Heber D.; Onishi, Naoki; Hess, Tom; Sheline, Raymond K. (Florida State Univ., Tallahassee). Contract AT(40-1)-2434. Phys. Rev., C; 3: 529-35(Feb 1971).

Calculations of the energy splittings between the parallel and antiparallel coupling states of odd neutron and odd proton in deformed nuclei were made for both zero-range and finite-range nuclear forces. The energy splittings for both types of forces agree with the corresponding experimental energies. Calculations have also been made for the odd-even shift in K = 0 bands. Finite-range interactions improve the agreement between experiment and theory for the odd-even shift, but the results are still unsatisfactory. It is shown that a tensor force is important in reproducing the experimental odd-even shift, especially in the case where $\Sigma_n + \Sigma_p = 1$. (auth)

28515 RELATION BETWEEN NUCLEAR BINDING AND EXCITATION ENERGIES. Dutta, A. K. (Calcutta Univ.). Phys. Rev., C; 3: 480-5(Feb 1971).

In the isobaric parabola equation for ground-state energies expressed as $-E(A,Z) = -E^0(A) + \beta(Z-Z^0)^2$, the magnitude of β decreases with increasing A, and has superposed irregular deviations at particular values of A. Very similar deviations from smoothly decreasing curves are also observed when the excitation energies for nuclei with odd and even mass number are drawn separately against nucleon number for different states of excitation. It is, therefore, believed that the variation of excitation energies from smooth curves is caused by the corresponding variation of the second term in the above equation. Therefore, an attempt was made to formulate relations which would determine the average expected ground-state energies and excitation energies for odd- and even-mass nuclei in the form of isobaric parabolas. It was possible to obtain these expressions in terms of the hypothetical energy per nucleon $\mathscr{E}^0_n(A)$ in nuclei composed of α particles combined in an ideal state. The deviations are obtained by comparing the experimentally determined values with those obtained from the formulated relations, and are correlated to determine the energies of nuclei in different excited states. The ideal energy per nucleon in a nucleus of actual nuclear size with A nucleons is determined by the hypothesis that even–even nuclei in the ideal condition, without the associated repulsive energy caused by Coulomb forces, would be composed of α particles only. The binding energy in such a symmetric nucleus of prescribed size is considered as the ideal energy of the nucleus. It is obtained by taking the experimental binding energy with the Coulomb and asymmetry energies. It increases systematically with A. The nucleonic composition and nuclear energy in actual nuclei are obtained by replacing some of the protons of the ideal composition by neutrons in order to minimize Coulomb-repulsive effects, and by subtracting the energy decrease due to asymmetry and the repulsive energy caused by Coulomb forces from the energy in the ideal condition. The replaced number of protons or the subtracted amounts of energy are determined by nucleonic forces in the ideal nucleus and hence by the ideal nucleonic energy $\mathscr{E}^0_n(A)$. The possibility of representing the ideal energy of nuclei with different nucleon numbers by such smooth relations suggests that the α particles forming ideal nuclei are statistically distributed in different energy shells corresponding to different nucleon numbers. The occupation and disengagement probabilities of states and the energy associated with these states give us a statistical background for the relations determining nuclear charge and energies for ground and excited states. (auth)

28516 ISOSPIN IMPURITIES IN THE NUCLEAR GROUND STATES. Mohan, Radhe (Duke Univ., Durham, N. C. Rutgers–The State Univ., New Brunswick, N. J.); Danos, M.; Biedenharn, L. C. Phys. Rev., C; 3: 468-79(Feb 1971).

Isospin impurities in the ground states of some even–even nuclei are calculated in the shell model including the effective residual interactions and in the three-fluid model. It is shown that the residual interactions reduce the calculated impurities by an order of magnitude. The impurities given by the three-fluid model are even smaller. Comparison of the present results is made with those of the two-fluid model. (auth)

28517 TRANSITION QUADRUPOLE MOMENTS AND THE VARIABLE-MOMENT-OF-INERTIA MODEL FOR EVEN–EVEN NUCLEI. Varshni, Y. P.; Bose, S. (Univ. of Ottawa). Phys. Rev., C; 3: 958-60(Feb 1971).

An expression is proposed for the transition quadrupole moment in terms of the mass number and the moments of inertia of the initial and final states as obtained from the variable-moment-of-inertia model. The expression is shown to give reasonable results for $0^+ \rightarrow 2^+$, $2^+ \rightarrow 4^+$, and $4^+ \rightarrow 6^+$ transitions. For $6^+ \rightarrow 8^+$ transitions the calculated values appear to be a little higher than the experimental ones. (auth)

28518 COMMENTS ON INTERMEDIATE-COUPLING AND ADDITIONAL EXCITATION MODES. Beres, William P.; Dorenbusch, William E. (Wayne State Univ., Detroit). Phys. Rev., C; 3: 952-4(Feb 1971).

An extension of the intermediate-coupling model of Thankappan and True that would include incoherent 2p-1h modes of excitation is suggested. (auth)

28519 LINEARIZED VERSION OF THE HARTREE–FOCK METHOD. Mann, A. (Hebrew Univ., Jerusalem. Indiana Univ., Bloomington); Gross, R. Phys. Rev., C; 3: 945-8(Feb 1971).

An approximate version of the Hartree–Fock method is proposed. This approximate version involves the solution of a set of linear equations. An application to a solvable model with a nontrivial Hartree–Fock solution yields good results. (auth)

28520 OFF-SHELL EFFECTS IN NUCLEAR MATTER. Haftel, Michael I. (Naval Research Lab., Washington, D. C.); Tabakin, Frank. Phys. Rev., C; 3: 921-36(Feb 1971).

The binding energy of nuclear matter is examined for exactly phase-shift-equivalent potentials. These potentials are generated by applying a short-range unitary transformation to the Reid soft-core potential. All potentials have a one-pion-exchange tail. For the potentials studied, variations of up to 9.5 MeV in the binding energy and 0.33 F^{-1} in the saturation density occur. The variations in binding energy are linearly correlated with the wound integral κ for those potentials that give nearly the same deuteron electric form factor. An increase in κ leads to less binding in nuclear matter. The sensitivity of the binding energy is somewhat greater to the $^3S_1 + {}^3D_1$ contribution to κ than to the $^1S_0$ contribution to κ. A theoretical explanation, based on the modified Moszkowski–Scott separation approximation, is given to account for the sensitivity of the binding energy to the $^1S_0$ and $^3S_1 + {}^3D_1$ contributions to κ. The relation of κ and the binding energy of nuclear matter to the off-shell elements of the T matrix are discussed. Far-off-shell elements ($q \gtrsim 6$ F^{-1}) play a significant role in nuclear matter. (auth)

REACTOR TECHNOLOGY

Commercial Power Reactors

Refer also to abstracts 26741 and 28637.

28521 (AECL–3670, pp 39–44) RELIABILITY FROM THE SUPPLIER'S VIEWPOINT. Frederick, L. G. (General Electric Co., San Jose, Calif. Atomic Power Equipment Dept.).

In Proceedings of the AECL symposium on reliability.

The application and influence of reliability methodology in nuclear reactor and steam supply system design are discussed. Reliability techniques used in the nuclear power industry are examined. 13 references. (H.D.R.)

28522 (CONF-700550) NOR-POWER '70. International Power System Fair and Symposium, Oslo, May 19–24, 1970. Session: Nuclear Energy, May 20, 1970. ([Institutt for Atomenergi, Kjeller (Norway)]). 82p.

Included are 4 papers on nuclear power plant development in Norway, the United Kingdom, Sweden, and Germany. A separate abstract was prepared for each paper. (H.D.R.)

For abstracts of individual papers see: 28523–28526.

28523 (CONF-700550–, Paper 1) NUCLEAR POWER IN NORWAY. Ager-Hanssen, Henrik (Institutt for Atomenergi, Kjeller (Norway)). 13p.

In Nor-Power '70. Session: nuclear energy, May 20, 1970.

In considering the planning, licensing, construction and operation of nuclear power stations in Norway, the choices between light water, gas-cooled, heavy water and fast breeder reactors, siting and containment questions and the economic factors are discussed. The licensing situation and the Norwegian engineering and production potential are briefly surveyed. The activities of the Institutt for Atomenergi are described. (Norway)

28524 (CONF-700550–, Paper 2) NUCLEAR POWER INDUSTRY OF THE UNITED KINGDOM. Ghalib, S. A. (Nuclear Power Group Ltd., Knutsford (England)). 13p.

In Nor-Power '70. Session: nuclear energy, May 20, 1970.

The structure of the nuclear power industry in Great Britain is explained and the design, construction and fuel services defined. The current nuclear power program in Britain is surveyed. (Norway)

28525 (CONF-700550–, Paper 3) SWEDISH NUCLEAR MANUFACTURING INDUSTRIES: TODAY AND TOMORROW. Halle, Lars (Asea-Atom, Vasteras (Sweden)). 20p.

In Nor-Power '70. Session: nuclear energy, May 20, 1970.

Following descriptions of the Swedish nuclear power program and the Swedish nuclear manufacturing industry, the ASEA-ATOM BWR is described. The future development of nuclear power in Sweden is discussed. (Norway)

28526 (CONF-700550–, Paper 4) TECHNOLOGY AND ECONOMICS OF NUCLEAR POWER PLANTS CONSTRUCTED BY KRAFTWERK UNION IN GERMANY AND ABROAD. Frewer, Hans (Kraftwerk Union A. G., Erlangen (West Germany)). 41p.

In Nor-Power '70. Session: nuclear energy, May 20, 1970.

The technical-commercial structure of the Kraftwerk Union is briefly described, following which its experience in power reactor construction is stated. A number of technical factors in the development of the concern's BWR and PWR types are described and the technical and economic factors leading to the choice of a D_2O reactor for Atucha are stated. The concern's work on fast reactors is briefly stated and the place of nuclear power in the total power program, nuclear power for process steam and desalination, and nuclear ship propulsion are discussed. (Norway)

28527 (DUN-SA–166) NUCLEAR ENERGY AND ELECTRICAL GENERATION. Peacock, D. W. (Douglas United Nuclear, Inc., Richland, Wash.). 10 Mar 1971. Contract AT(45-1)-1857. 12p. Dep. NTIS.

Some of the fundamental aspects of nuclear power as they are related to the environmental impact of electric power generation are discussed. The three aspects examined are the need for more electric power, radioactivity releases from reactors, and thermal pollution. (H.D.R.)

28528 (RD/B/N–1784) CORRELATION OF MEASURED AND CALCULATED STRAINS IN THE TOP-HALF OF THE OLDBURY PRESTRESSED CONCRETE PRESSURE VESSEL R1 FOR THE PERIOD 1965 TO 1970. Carmichael, G. D. T.; Hornby, I. W.; Irving, J. (Central Electricity Generating Board, Berkeley (England). Berkeley Nuclear Labs.). Jan 1971. 55p. Dep. NTIS (U. S. Sales Only).

Strain gauges installed in the Oldbury, Reactor 1, pressure vessel have been monitored since startup in 1967. Readings obtained indicate the strain behavior of the vessel under prestress and pressure loads at the operating temperature cross falls. Changes in stress and strain due to creep under prestress and operational loading were calculated using an iterative time-step technique allied with a finite element method of elastic analysis. The theoretical results obtained are compared with the strains measured. It is concluded that the greater part of the creep strain in the vessel occurred prior to start-up of the reactor and that strains under operating conditions are dominated by thermo-elastic effects. Under all conditions of loading the predicted stresses in the vessel are well within the limits set in the design specification. (auth) (UK)

28529 (STI/PUB–267) SMALL AND MEDIUM POWER REACTORS, 1970. Proceedings Series. Proceedings of a Symposium Held in Oslo, 12–16 October 1970. (International Atomic Energy Agency, Vienna (Austria)). Feb 1971. 544p. (In several languages). (CONF-701046). IAEA $14.00.

Information on small and medium power reactors is presented under the following headings: status of light water reactors for small and medium power applications; status of heavy water and gas-cooled reactors for small and medium power applications; improved designs and advanced concepts; multi-purpose small and medium power reactor systems, and special applications; cost experience and projects for small and medium power reactors; fuel cycle evaluation; and outlook for nuclear power in developing countries. Separate abstracts are included for each of the 31 papers presented. (D.C.C.)

For abstracts of individual papers see: 28538–28541, 28576–28583, 28637–28642, 28663, 28715–28724, 28792, and 28793.

28530 ENVIRONMENTAL COST OF ELECTRIC POWER. Abrahamson, Dean E. Scientists' Inst. for Public Information Workbook. New York; Scientists' Institute for Public Information (1970). 36p. $3.50.

The environmental aspects of electric power production in the U. S. are examined. Fundamental questions of power costs versus benefits discussed include: are there ways to generate power that are less costly in environmental terms than ways now in use; can power plants be made more efficient; can wastes from power production be controlled; what legal measures can be taken to protect the environment; how can we evaluate present and experimental power sources; how can power plants be sited to produce the least environmental damage; and why do we need more power. (48 references) (H.D.R.)

28531 STROITEL'STVO YADERNYKH USTANOVOK. IZDANIE TRET'E, DOPOLNENNOE I PERERABOTANNOE. (Construction of Nuclear Installations. Third Revised and Supplemented Edition). Komarovskii, A. N. Moscow; Atomizdat (1969). 504p.

An analysis is made of published data and various recomendations are given pertaining to the design and construction of nuclear installations. General problems concerning nuclear reactors, biological protection and physical and technological properties of shielding materials are covered. The design and construction of reactor shielding, water shielding and reactor vessels construction using prestressed reinforced concrete are discussed. The site selection, ventilation, turbines, and architectural design of the power plant building on the surface and underground are described. General data on assembly and erection of monolythic concrete and reinforced concrete structures, reactor vessels and shielding shells, steel shielding, hermetically closed reactor buildings and general construction problems are discussed. (R.V.J.)

28532 INVESTIGATION OF Pu ISOTOPES BUILD-UP IN NOVO-VORONEZH APS FUEL. Gabeskiriya, V. Ya.; Belokopytov, V. S.; Miller, O. A.; (and others). At. Energy. (USSR); 30: 247-50(Mar 1971). (In Russian).

The decrease of ^{235}U quantity and the building-up of Pu isotopes in dependence of the fuel burn-up fraction in the Novo-Voronezh APS reactor have been measured. It is shown that at 23 kg/t U burn-up fraction of fuel the Pu fission contribution to the total burn-up attains 50%, the content of the heavy isotopes ^{240}Pu, ^{241}Pu and ^{242}Pu in the accumulated Pu being 40%. (auth)

XUM

28533 FUTURE WORLD ELECTRICITY NEEDS. pp 45-56 of Environmental Aspects of Nuclear Power Stations. Vienna; International Atomic Energy Agency (1971).

From Symposium on environmental aspects of nuclear power stations; New York (10 Aug 1970). See STI/PB-261; CONF-700810.

An analysis of the consumption of electrical energy in the recent past is given. This is correlated with the relevant macroeconomic variables such as income, population, industrialization and urbanization. Projections over the medium- and long-term periods are taken into account with other factors such as the economic and technological possibilities of substitution between electrical and nonelectrical sources of energy. Using alternative hypotheses concerning the growth factors, separate projections of future electricity demands are made at the global and regional levels. (4 references.) (auth)

28534 ST. LAURENT DES EAUX POWER REACTOR PROTOTYPE OF VANDELLOS. Crespi Gonzalez, Maria Alicia. Energ. Nuc. (Madrid); 14: 153-70(Mar-Apr 1970). (In Spanish).

The treaty which placed the St. Laurent power plant within the French nuclear program and its antecedents and lines of evolution are reported. A historical resume is made of the individual steps of its construction, with emphasis on the principal elements. (tr-auth)

28535 ELECTRONIC INSTRUMENTATION AND CONTROL OF THE JOSE CABRERA POWER REACTOR. del Val Cob, J. L. Energ. Nucl. (Madrid); 14: 121-30(Mar-Apr 1970). (In Spanish).

A general description is given of the power station. The pulse channels, intermediate channels, power channels for the measurement of the neutron flux are described. The electronic and operational logics are discussed. The instrumentation in the core and the functions of the control system of the reactor are described. (tr-auth)

28536 REVIEW OF ENGINEERING STANDARDS DEVELOPMENT FOR NUCLEAR POWER SYSTEMS. Joslin, W. Murray; Moore, James S.; Russ, John C. Nucl. Safety; 12: 217-26(May-Jun 1971).

The efforts being made by the American National Standards Institute, Inc., the American Nuclear Society, and the Institute of Electrical and Electronics Engineers in promoting engineering standards-development programs for nuclear power systems are discussed. Some examples are given of the difficulties and the satisfactions, and some suggestions are made for solving the problems. The reviewers present a general conclusion that the time elapse from inception to adoption needs to be shortened and that more participation and closer coordination are needed among groups having overlapping interests. (auth)

28537 TENTATIVE REGULATORY SUPPLEMENTARY CRITERIA FOR ASME CODE-CONSTRUCTED NUCLEAR PRESSURE VESSELS. Washington, D. C.; Atomic Energy Commission (1967). 49p. Available from United States Atomic Energy Commission, Washington, D. C.

Proposed general design criteria for nuclear power plant construction requires that nuclear pressure vessels be designed, fabricated, and inspected to quality standards which supplement those specified by existing engineering codes. Regulatory criteria developed to supplement ASME Nuclear Vessel Code specifications as to safety objectives and long-term reliability are presented. (H.D.R.)

28538 ATOMIC POWER PLANT WITH A WATER-COOLED, GRAPHITE-MODERATED REACTOR FOR COMBINED POWER AND HEAT GENERATION. Abramov, V. M. (Central Reactor Inst., Leningrad); Bogdanov, N. V.; Bondarenko, A. V.; (and others). pp 363-71 of Small and Medium Power Reactors, 1970. Vienna; International Atomic Energy Agency (1971). (In Russian).

From Small and medium power reactors symposium; Oslo, Norway (12 Oct 1970). See STI/PUB-267; CONF-701046.

A power plant is described having a reactor-turbine system with a capacity of 12×10^3 kW(e) and heat-generating capacity of 25 Gcal/h. The reactor has a thermal capacity of 62×10^3 kW and a steam capacity of 96 t/h. The thermal system is of the single-circuit type with a 65-ata saturated-steam cycle and with intermediate moisture separation between the turbine cylinders at 3-2.5 ata. The reactor is a U-graphite facility with fuel channels containing six tubular fuel elements each. The circulation system consists of six separate and closed circuits associated with a single drum-separator. A U-9% Mo dispersed in a Mg matrix is used as fuel. The fuel-element cladding is of stainless steel. The fuel loading is 7.6 t of U, 3% enriched in ^{235}U. The duration of the run involving partial reloading of fuel channels is 1000 days (1000×24 h). The efficiency of the fuel elements chosen has been confirmed by the operation of similar elements in the reactors of the First and Beloyarsk nuclear power plants and by special tests conducted on experimental elements in the reactor of the First plant. The Bilibin nuclear thermal power station, which has four such facilities, is now under construction in Chukotka, USSR. (auth)

28539 FIRST NUCLEAR POWER PLANT IN KOREA. Kim, S. C. (Korea Electric Co., Seoul). pp 415-30 of Small and Medium Power Reactors, 1970. Vienna; International Atomic Energy Agency (1971).

From Small and medium power reactors symposium; Oslo, Norway (12 Oct 1970). See STI/PUB-267; CONF-701046.

The installation of nuclear power in Korea is studied. The addition of a nuclear plant will require enriched uranium which will be an entirely new fuel in Korea. The results of the investigation indicate that the installation of a 600-MW(e) nuclear plant is not only feasible but is necessary to generate economical power in Korea. (auth)

28540 PROBLEMS OF INTRODUCING SMALL AND MEDIUM POWER REACTORS TO DEVELOPING COUNTRIES WITH PARTICULAR REFERENCE TO THE CREATION OF A SPECIAL NUCLEAR FUND. Matin, A. (Pakistan Atomic Energy Commission, Karachi). pp 493-503 of Small and Medium Power Reactors, 1970. Vienna; International Atomic Energy Agency (1971).

From Small and medium power reactors symposium; Oslo, Norway (12 Oct 1970). See STI/PUB-267; CONF-701046.

Various problems relating to introduction of small and medium power reactors (SMPRs) in developing countries are discussed. These problems normally deal with the establishment of technical and economic feasibility, selection of suitable size and type of reactor, selection of vendor and the arrangement of financing on favorable terms. (5 references.) (auth)

28541 POTENTIAL DEMAND FOR NUCLEAR POWER IN DEVELOPING COUNTRIES. Roberts, J. T. (International Atomic Energy Agency, Vienna). pp 505-16 of Small and Medium Power Reactors, 1970. Vienna; International Atomic Energy Agency (1971).

From Small and medium power reactors symposium; Oslo, Norway (12 Oct 1970). See STI/PUB-267; CONF-701046.

The total installed electrical generating capacity in developing countries (defined as those for which UNDP technical assistance has been approved for 1970) is projected to increase from 157 GW(e) in 1970 to 246 GW(e) in 1975, 379 GW(e) in 1980, and 555 GW(e) in 1985. These figures correspond to 14.7% of total world electrical capacity (excluding mainland China) in 1970, slowly increasing to 17.2% in 1985, for countries which have about two-thirds of the world population. The total nuclear electrical capacity in developing countries is predicted to increase from 1.2 GW(e) in 1970 to 5.8 in 1975, 35 in 1980, and 86 GW(e) in 1985. These figures correspond to 6% of world nuclear totals in 1970, increasing to 12% by 1985. The predicted market for nuclear power plant orders from developing countries during the next ten years is thus about 80 GW(e), i.e. the difference between the 1975 and 1985 totals since a backlog of about five years falls between placing an order and putting it into operation. Considerable uncertainty exists in this estimate of demand, probably greater than 30%, because of uncertainties in the assumptions. Of particular importance is the assumption of the availability of the required approximately $13,000 million of foreign exchange financing on terms which the developing countries can afford. Of the 80 GW(e) total about 30 should be ordered during the next five years if the 1985 prediction is to be met. On a geographical basis, the 80 GW(e) total is made up approximately as follows: Latin America 18, Asia 19, Israel and UAR 2, Comecon Europe 19, and other European countries and Turkey 23 GW(e). (auth)

28542 TSURUGA: TRIUMPH OF TEAMWORK. Ferguson D. F.; Kilsby, E. R. Power Eng.; 75: No. 4, 40-2(Apr 1971).

The Tsuruga Nuclear Power Station began commercial operation 47 months and 23 days from the contract date, a record for completion of a large nuclear power station. Some of the design, construction, and government licensing requirements problems, and their solutions, are described. (H.D.R.)

28543 STRATEGY AND TACTICS IN NUCLEAR FUEL MANAGEMENT. Fornaciari, P. (ENEL-CPN, Rome). Energ. Nucl. (Milan); 18: 149-53(Mar 1971).

Some nuclear fuel management problems are described. It

is pointed out that most of those considered concern utilities more than reactor designers or nuclear fuel suppliers: a real interest in this field arose only in recent years with the increasing number of nuclear power plants in operation. Typical problems are those concerning the determination of the best fuel cycle length (or best batch size), of the best period for refueling and of the way to avoid shutdowns in peak load periods, the investigation of the advantage for operation beyond the fuel cycle's end (stretch-out or derating), the enrichment optimization. Solutions to these problems are presented. (3 references) (auth)

28544 NUCLEAR POWER. Moore, R. V. (ed.). London; Cambridge University Press (1971). 200p. £3.40

The development of nuclear power is discussed under the following headings: development and brief history; economics and the effect of introducing nuclear stations into a generating system; fission process and the fissile materials involved; reactor physics and core design; reactor instrumentation; Oldbury nuclear power station; Dungenness "B" nuclear power station; high-temperature gas-cooled reactors and Dragon; the Yankee p.w.r. station at Haddam Neck, Connecticut; the Jersey Central b.w.r. station at Oyster Creek; the s.g.h.w. reactor at Winfrith; the Canadian natural uranium heavy-water reactor (CANDU); the fast-breeder reactor at Dounreay; safety and siting; and future developments. (UK)

28545 AIR HANDLING PLANT OF THE OBRIGHEIM NUCLEAR POWER STATION. Kruger, M.; Seggewies, H. Heiz-Luft-Haustech.; 21: 191-5(Jun 1970). (In German).

The air conditioning and ventilation installations at the 300 MW Obrigheim nuclear power station are described. The main purpose of the installation is controlled exhaust of air from the reactor building, reactor auxiliary plant building, and the store for radioactive waste. (UKAEA Info. Bull.)

Operation and Economics

Refer also to abstract 28638.

28546 (AECL-3670) PROCEEDINGS OF THE AECL SYMPOSIUM ON RELIABILITY, CHALK RIVER NUCLEAR LABORATORIES, CHALK RIVER, ONTARIO, OCTOBER 14 AND 15, 1970. Blackstein, F. P. (ed.) (Atomic Energy of Canada Ltd., Chalk River (Ontario)). Dec 1970. 127p. (CONF-701041). AECL $2.50.

Included are 10 papers on various aspects of nuclear power plant equipment and systems reliability. Separate abstracts were prepared for each of 9 papers. (H.D.R.)

For abstracts of individual papers see: 28521 and 28547–28554.

28547 (AECL-3670, pp 13-20) NUCLEAR GENERATING UNIT PERFORMANCE: AN OPERATOR VIEWPOINT. Kelly, R. J. (Hydro-Electric Power Commission of Ontario, Toronto).
In Proceedings of the AECL symposium on reliability.

A technique for the evaluation of the performance of a mature nuclear station is described. Complete performance standards for the generating unit are specified, based on criteria in the areas of production reliability, cost and safety. Unit imperfections are then shared among the various systems, and finally among the individual components. (Canada)

28548 (AECL-3670, pp 23-37) SURVEY OF EXPERIENCE WITH EQUIPMENT AVAILABILITY. Ringlee, R. J. (Power Technologies, Inc., Schenectady, N. Y.).
In Proceedings of the AECL symposium on reliability.

The use of reliability concepts, models, and measures of performance in planning electric power generation reserve is discussed. The need for international standardization of outage definitions and information collection procedures is examined. 29 references. (H.D.R.)

28549 (AECL-3670, pp 45-55) RELIABILITY FACTORS AFFECTING POWER PLANT MECHANICAL EQUIPMENT. Lewis, P.; Schwarz, H.; Waldron, W. (Mechanical Technology Inc., Latham, N. Y.).
In Proceedings of the AECL symposium on reliability.

Mechanical equipment for power stations require assurance that on-stream time will be maximized and that unscheduled outages be virtually eliminated. The degree to which this can be achieved is contingent upon the actions of the three participating parties: namely, the architect engineers, the manufacturers, and the users. In broad terms these actions are: (1) system design philosophy and capability; (2) manufacturing quality control standards and performance execution and documentation; and (3) operation and maintenance procedures and continuous education of all the user employees. (auth) (Canada)

28550 (AECL-3670, pp 59-63) QUALITY ASSURANCE IN RELATION TO NUCLEAR POWER PLANTS. Philip, W. S. (Atomic Energy of Canada Ltd., Sheridan Park (Ontario)).
In Proceedings of the AECL symposium on reliability.

Quality assurance is a requirement of reliability and is a shared responsibility between those who design and manufacture equipment and those who install and maintain it. Standards and regulations to assure quality in the nuclear field have been established by various organizations, and assurance of quality is a criterion in formulating contract requirements, selecting bidders, and evaluating tenders. Interaction between owners and suppliers to assure quality in design, planning, and procurement and manufacture is discussed. (Canada)

28551 (AECL-3670, pp 65-70) MAINTENANCE FROM THE STATION OPERATOR'S POINT OF VIEW. Ryder, J. (Hydro-Electric Power Commission of Ontario, Toronto).
In Proceedings of the AECL symposium on reliability.

The conditions which a station operator is likely to encounter doing maintenance in a nuclear unit at maturity are examined, based on experience at Douglas Point to date. A main concern is access to equipment, both at power and shutdown, so that adequate maintenance can be done for reliable operation. Reliability with minimum maintenance is especially important for equipment in radiation areas. (Canada)

28552 (AECL-3670, pp 73-81) SPECIAL ASPECTS OF RELIABILITY AND MAINTAINABILITY IN NUCLEAR STATIONS. Wolfe, W. A. (Atomic Energy of Canada Ltd., Chalk River (Ontario). Chalk River Nuclear Labs.).
In Proceedings of the AECL symposium on reliability.

Calculations on the pumps for the heat transport system of a power reactor are used to show that reliability is a function of the reliability and maintainability of the individual components. The following questions are asked: how often will a pump fail? what is the resulting reliability? what is the effect of standby pumps? how much repair time is needed? does radiation impede repair? In order to accomplish high intrinsic capability with minimum repair times, equipment must be designed and installed for easy and quick maintenance, components must be improved until their failure is due to limitations of materials and applications, and designers, suppliers, operators and maintainers must be properly educated in these areas. (Canada)

28553 (AECL-3670, pp 83-8) INFORMATION RETRIEVAL AND RELIABILITY ANALYSIS. Blackstein, F. P. (Atomic Energy of Canada Ltd., Chalk River (Ontario). Chalk River Nuclear Labs.).
In Proceedings of the AECL symposium on reliability.

The need for the development and application of analytical reliability evaluation methods for nuclear plant systems is discussed. Methods for acquisition and retrieval of reliability data and mathematical analysis of nuclear systems based on the data bank are examined. 10 references. (H.D.R.)

28554 (AECL-3670, pp 89-96) DESIGN AND DEVELOPMENT FOR RELIABILITY. Melvin, J. G. (Atomic Energy of Canada Ltd., Chalk River (Ontario). Chalk River Nuclear Labs.).
In Proceedings of the AECL symposium on reliability.

The capability of a nuclear generating station depends on the reliability and maintainability of the individual components. Four quantities must be known or assumed as basic data for system capability analysis: component failure rate, component population, repair time, and local radiation field. These quantities must be considered in all phases of the project: concept, system design, equipment design and selection, and maintenance planning. Reliability data are needed as a basis for decisions in many areas of design. Existing nuclear stations are the principal source of this information and substantial efforts to obtain it are justified. (Canada)

28555 (DOCKET-1155-112) LA CROSSE BOILING WATER REACTOR. Unplanned Reactor Shutdown While Performing a Technical Specification Test on Power/Flow Safety System Channel No. 1. (Dairyland Power Cooperative, La Crosse, Wis.). 15 Apr 1971. 2p. (DPC-71-8). Dep. NTIS.

28556 (DOCKET-50003-67) INDIAN POINT STATION, UNIT NO. 1. Abnormal Occurrence Report: Time-Delay Switch on High Pressure Boron Addition System Pump No. 12 Inopera-

tive on Routine Test. (Consolidated Edison Co. of New York, Inc., New York). 13 Apr 1971. 2p. Dep. NTIS.

28557 (DOCKET-50010-84) DRESDEN NUCLEAR POWER STATION, UNIT 1. Abnormal Occurrence Report: Failure of a Primary Drum Low Level Scram Relay. (Commonwealth Edison Co., Chicago, Ill.). 7 Apr 1971. 2p. Dep. NTIS.

28558 (DOCKET-50016-108) ENRICO FERMI ATOMIC POWER PLANT, UNIT 1. [Operations] Report, November 1970. (Power Reactor Development Co., Detroit, Mich.). 6 Apr 1971. 14p. (PRDC-EF-87). Dep. NTIS.

28559 (DOCKET-50016-109) ENRICO FERMI ATOMIC POWER PLANT, UNIT 1. [Operations] Report, December 1970. (Power Reactor Development Co., Detroit, Mich.). 9 Apr 1971. 12p. (PRDC-EF-88). Dep. NTIS.

28560 (DOCKET-50133-53) HUMBOLDT BAY POWER PLANT, UNIT NO. 3. Abnormal Occurrence Report: Blown Fuse in Automatic Circuitry for the Off-Gas Isolation Valve. (Pacific Gas and Electric Co., San Francisco, Calif.). 7 Apr 1971. 2p. Dep. NTIS.

28561 (DOCKET-50155-78) BIG ROCK POINT NUCLEAR PLANT. Seventh Semiannual Report of Operations, May 1-October 31, 1967. (Consumers Power Co., Jackson, Mich.). 13 Dec 1967. 11p. Dep. NTIS.

28562 (DOCKET-50171-83) PEACH BOTTOM ATOMIC POWER STATION, UNIT 1. Monthly Operations Report No. 60, February 1971. (Philadelphia Electric Co., Pa.). 20 Apr 1971. 9p. Dep. NTIS.

28563 (DOCKET-50206-111) SAN ONOFRE NUCLEAR GENERATING STATION, UNIT 1. Operation Report, March 1971. (Southern California Edison Co., Los Angeles). Mar 1971. Contract AT(30-1)-3270. 6p. (NYO-3270-47). Dep. NTIS.

28564 (DOCKET-50237-145) DRESDEN NUCLEAR POWER STATION, UNIT 2. Condition Relating to Operation in Which 2/3 "A" Standby Gas Treatment System Malfunctioned. (Commonwealth Edison Co., Ill.). 2 Mar 1971. 2p. Dep. NTIS.

28565 (DOCKET-50237-151) DRESDEN NUCLEAR POWER STATION, UNIT 2. Loss of Electric Power to the Low Pressure Coolant Injection System. (Commonwealth Edison Co., Chicago, Ill.). 8 Mar 1971. 2p. Dep. NTIS.

28566 (DOCKET-50237-155) DRESDEN NUCLEAR POWER STATION, UNIT 2. Wiring Error Discovered on April 4, 1971. (Commonwealth Edison Co., Chicago, Ill.). 21 Apr 1971. 4p. Dep. NTIS.

A wiring error on the backup power supply to the reactor injection valves of the low pressure coolant injection system which caused a phase reversal is described. (D.C.C.)

28567 (DOCKET-50261-55) H. B. ROBINSON UNIT NO. 2. Part-Length Bank Maneuvering. (Carolina Power and Light Co., Raleigh, N. C.). 31 Mar 1971. 8p. Dep. NTIS.

28568 (DOCKET-50261-56) H. B. ROBINSON UNIT NO. 2. Difficulties with Lube Oil System of Emergency Diesel Generators. (Carolina Power and Light Co., Raleigh, N. C.). 7 Apr 1971. 2p. Dep. NTIS.

28569 (DOCKET-50261-57) H. B. ROBINSON UNIT NO. 2. Bearing Failure Due to Loss of Flow of Lubricating Oil. (Carolina Power and Light Co., Raleigh, N. C.). 7 Apr 1971. 5p. Dep. NTIS.

28570 (DOCKET-50261-58) H. B. ROBINSON UNIT NO. 2. Tests on Safety Injection System. (Carolina Power and Light Co., Raleigh, N. C.). 13 Apr 1971. 2p. Dep. NTIS.

28571 (DOCKET-50266-46) POINT BEACH NUCLEAR PLANT, UNIT 1. Abnormal Occurrence Report: Unscheduled Release of Radioactivity. (Wisconsin Electric Power Co., Milwaukee). 7 Apr 1971. 3p. Dep. NTIS.

28572 BLOCK IN-PLANT RADIATION BY DESIGN. Wascher, Robert E.; Howard, James O. Elec. Light Power (Boston); 49: No. 4, 35-7(Mar 1971).

The various means by which radiation environments are produced in nuclear power reactors are examined. The importance of radiation considerations in a plant's design stages to ensure successful operation and maintenance procedures is discussed. (H.D.R.)

28573 ECONOMIC-FINANCIAL EXPERIENCE IN ARGENTINA WITH POWER REACTOR CONSTRUCTION. Csik, Jose Bela Energ. Nucl. (Madrid); 14: 131-6(Mar-Apr 1970). (In Spanish).

The studies and design planning of the Atucha reactor power plant, previous to the acceptance and evaluation of energy demands, are described. The details of the acceptance of the reactor are given. The total cost is given and discussed. (tr-auth)

28574 NUCLEAR DISTRICT HEATING: A STUDY FOR THE TOWN OF LUND. Josefsson, L.; Thunell, J. (South Swedish Power Co., Malmoe). pp 687-92 of Environmental Aspects of Nuclear Power Stations. Vienna; International Atomic Energy Agency (1971).

From Symposium on environmental aspects of nuclear power stations; New York (10 Aug 1970). See STI/PUB-261; CONF-700810.

In an attempt to reduce urban atmospheric pollution, a design study has been made on piping heat from the future No. 2 unit of the Barsebeck nuclear power plant 15 km to Lund. Technical data are given, and the economic factors are discussed. (auth)

28575 COMPUTERIZED INFORMATION RETRIEVAL FOR NUCLEAR REACTOR SYSTEMS. Blackstein, F. P. (Atomic Energy of Canada Ltd., Chalk River, Ont.). pp 33-6 of DECUS Proceedings. Maynard, Mass.; Digital Equipment Computer Users' Society (1970).

From Digital Equipment Corporation Users Society spring symposium; Atlantic City, N. J. (4 May 1970). See CONF-700524.

In studying reliability of nuclear reactor systems it is imperative to maintain accurate histories of components as related to time of failure, operations performed and subsequent observations. The initiation and utilization of a computerized information retrieval system recently commissioned at the Chalk River Nuclear Laboratories are described. Presently, the system is used to datalog specific information from the Douglas Point Nuclear Generating Station but the broader implications are being studied with a view to further expansion. (auth)

28576 CONSTRUCTION AND INITIAL OPERATION OF THE TSURUGA POWER STATION. Asada, C. (Japan Atomic Power Co., Tokyo). pp 45-62 of Small and Medium Power Reactors, 1970. Vienna; International Atomic Energy Agency (1971).

From Small and medium power reactors symposium; Oslo, Norway (12 Oct 1970). See STI/PUB-267; CONF-701046.

The construction of the Tsuruga Power Station was started on April 22, 1966, and fuel loading took place on schedule at the end of September 1969. After five and a half months of subsequent startup tests, the station began commercial operation in mid-March 1970 since when, on the whole, the station was operated smoothly. The station is a boiling-water reactor, similar to those of Oyster Creek and Nine Mile Point stations, with an initial operating power of 331 MW(e). However, because of the improved core performance, the plant equipment has been designed for a 10% power stretch. The station is characterized by its flask-type dry-well as well as by a single-cycle design employing a flow control system. Various stages of construction, the startup tests, and the operating conditions including load factors during initial operation and major operational problems and their countermeasures are described. (auth)

28577 UNITED STATES UTILITY EXPERIENCE WITH INTERMEDIATE LIGHT-WATER REACTORS. Coe, R. J.; Vandenburgh, D. E. (Yankee Atomic Electric Co., Westboro, Mass.). pp 63-91 of Small and Medium Power Reactors, 1970. Vienna; International Atomic Energy Agency (1971).

From Small and medium power reactors symposium; Oslo, Norway (12 Oct 1970). See STI/PUB-267; CONF-701046.

Accumulated operating experiences with seven United States light-water-reactor plants ranging in size from 75 to 615 MW(e) are reviewed. The seven plants are equally divided between pressurized-water and boiling-water types: Dresden, Big Rock Point and Humboldt Bay being BWRs and the others PWRs. The oldest plant of all is Dresden which has been in service ten years, and the newest, Haddam Neck Plant, in service for two years. Except for the Yankee plant, not much is available in the way of economics and operating costs. All these plants were privately financed, and, therefore, in computing power costs, fairly high fixed-charge rates must be used; on the other hand, fuel costs are relatively low, so that over-all power costs are acceptable as long as high-capacity factors can be maintained. The deficiencies which caused troubles and down-times have been identified and corrected, so that capacity factors and reliability are improving. (auth)

XUM

28578 TECHNICAL AND ECONOMIC EXPERIENCE GAINED IN OPERATING THE JOSE CABRERA NUCLEAR POWER STATION AT ZORITA, SPAIN. Bertolotti, G. (Union Electrica, SA, Madrid). pp 93-108 of Small and Medium Power Reactors, 1970. Vienna; International Atomic Energy Agency (1971). (In Spanish).

From Small and medium power reactors symposium; Oslo, Norway (12 Oct 1970). See STI/PUB-267; CONF-701046.

The José Cabrera Nuclear Power Station (160 MW(e) gross) has been in commercial operation for over one year. The power station has certain special features which may be of interest to those who are proposing to build intermediate-power plants in the near future: it is the only commercial power station with the single-circuit PWR; it is very compact (for example, there are no separate new and spent fuel storage buildings and no separate reactor auxiliary building, the facilities in question being housed within the reactor containment building); the only duplication of equipment is that necessary for reasons of safety, emphasis being placed in the design of maximum simplicity of the systems and equipment and on quality rather than quantity. For the first time in a commercial power station with a PWR, Zircaloy has been used as the fuel-element cladding material. In addition, four very advanced fuel types have been loaded into the core for testing under a research and development program being conducted jointly by the Spanish Nuclear Energy Board and the reactor constructors. This program is part of a general effort being made to find ways of reducing the costs of electricity generation. The operating cost structure of the José Cabrera Nuclear Power Station is described. The way in which costs are affected by the technical decisions taken at the design stage and the operating criteria currently applied is analyzed. The influence of preventive maintenance on generating costs and on availability is studied. (auth)

28579 OPERATIONAL EXPERIENCE WITH THE VK-50 REACTOR FACILITY. Khakimov, A. A. (State Committee for the Use of Atomic Energy, Moscow); Solov'ev, Yu. A.; Zabelin, A. I.; (and others). pp 117-29 of Small and Medium Power Reactors, 1970. Vienna; International Atomic Energy Agency (1971). (In Russian).

From Small and medium power reactors symposium; Oslo, Norway (12 Oct 1970). See STI/PUB-267; CONF-701046.

The principal operational results obtained over a period of four years in the experimental VK-50 facility, which has a pressure-vessel-type boiling-water reactor, are presented. Particular attention is paid to problems connected with the operation of the basic equipment, water-operating conditions and radiation conditions. The results of re-designing the techological layout are given. Operational experience has shown that the reactor is highly stable and simple to control; the flow-sheet can be considerably simplified and the reactor power and run can be increased further. Recommendations on designing low-power nuclear plants with pressure-vessel-type boiling-water reactors are given. (3 references.) (auth)

28580 ROLE OF HEAVY-WATER REACTORS IN THE INDIAN NUCLEAR POWER PROGRAM. Meckoni, V. N. (Bhabha Atomic Research Centre, Trombay, India). pp 173-83 of Small and Medium Power Reactors, 1970. Vienna; International Atomic Energy Agency (1971).

From Small and medium power reactors symposium; Oslo, Norway (12 Oct 1970). See STI/PUB-267; CONF-701046.

The nuclear power program in India, in the first phase, is based on heavy-water reactors. Prospects for capital cost reductions are quite favorable, which make the heavy-water reactor attractive especially in the medium power range of 200 to 600 MW(e). Some of the areas where cost reductions are possible are reviewed with respect to the Madras Atomic Power Station. The potential of heavy-water reactors to initiate a permissible fuel cycle to meet the nuclear future power demand in India is also reviewed. (auth)

28581 TECHNOLOGICAL STATUS OF THE STEAM-GENERATING HEAVY-WATER REACTOR (SGHWR). Moore, J. (United Kingdom Atomic Energy Authority, Risley, Eng.). pp 185-209 of Small and Medium Power Reactors, 1970. Vienna; International Atomic Energy Agency (1971).

From Small and medium power reactors symposium; Oslo, Norway (12 Oct 1970). See STI/PUB-267; CONF-701046.

The 100-MW Steam-Generating Heavy-Water Reactor has now been in operation at Winfrith for 2½ years. During commissioning and operation data on fuel performance, reactor physics, reactor kinetics and heat transfer have been obtained to check calculation methods and performance predictions based on data obtained from the supporting research and development program. The reactor has proved to be flexible in operation and no major problems have arisen to affect basic design of the core and coolant systems or of the type of engineering components used in them. Two specific technical aspects warranting comment are experience in control of water chemistry, and access to the reactor core. Faulty ion-exchange beds caused deposition on fuel leading to fuel failure during the first year's operation. Data on failure mechanisms have been obtained and the Powdex ion-exchange plant now gives excellent control of water chemistry. Six experimental zirconium–niobium pressure tubes which had not been correctly heat treated were successfully changed using conventional engineering techniques. After cleaning the primary circuit, access to the pipework enabled cutting and welding operations to be made without having to use remotely operated equipment. Reactor physics properties are now fully understood and no further work is required to develop theory or to make experiments on zero energy and subcritical assemblies. Detailed heat-transfer studies with a 9-MW test facility in which full-size elements with the correct coolant conditions are simulated are almost completed. Further work in the general area of performance assessment consists of continued examination of fuel-cycle variations affecting form factor and also detailed examination of factors affecting the choice of dryout margin, both of which could lead to further economies in design. Operating experience and results obtained from the R. & D. program have confirmed choice of the same channel and fuel geometry for commercial design as has been used in the Winfrith reactor, making that reactor a good demonstration to confirm commercial design. The main function of the reactor is its continued use to statistically test fuel. (17 references.) (auth)

28582 POTENTIAL CONTRIBUTION OF NUCLEAR POWER TO THE ON-SITE GENERATION OF ELECTRIC AND STEAM POWER IN JAPANESE INDUSTRIES. Yabe, G.; Okazaki, M. (Asahi Chemical Industry Co. Ltd., Tokyo). pp 319-29 of Small and Medium Power Reactors, 1970. Vienna; International Atomic Energy Agency (1971).

From Small and medium power reactors symposium; Oslo, Norway (12 Oct 1970). See STI/PUB-267; CONF-701046.

An enormous energy demand is estimated to be necessary to support the continuous development of the Japanese economy. By 1985, the total installed capacity of the electric power generators will reach 277,000 MW (including 47,000 MW on site) and more than a third of which, or 102,000 MW (including 22,000 MW on site), will be nuclear power. The potential market of the small and medium nuclear reactors is promising. Nuclear power is of great advantage for preventing air pollution and solving the eternal problems concerning transportation and fuel-oil storage. A survey was made of the market for nuclear power reactors with thermal outputs of 3,000, 1,000, 500, or 250 MW(t) applied to large industrial plants or complexes. More than two hundred on-site nuclear reactors with a thermal output from 250 to 3,000 MW(t) may be installed by 1985. The technology for designing and constructing small reactors with generating costs that are competitive with fossil-fuel power plants has not yet developed. Medium or small reactors should be standardized so that construction costs could be reduced. Japan is an industrialized country that has developed its own nuclear industry which is able to supply complete nuclear power reactors. Now interest is directed towards the future world development of technology and engineering connected with small and medium power reactors. (auth)

28583 PROSPECTS OF INTERMEDIATE-SIZE POWER REACTORS. Khan, M. A. (International Atomic Energy Agency, Vienna). pp 395-414 of Small and Medium Power Reactors, 1970. Vienna; International Atomic Energy Agency (1971).

From Small and medium power reactors symposium; Oslo, Norway (12 Oct 1970). See STI/PUB-267; CONF-701046.

The current technical and economic status of nuclear power reactors in the intermediate size range (100–500 MW), their availability, the potential of reducing their costs, and the specific measures which could be taken to improve their competitive position and widen their application are discussed. So far, 138 plants below 500 MW(e) (out of a total of about 230) have been built or are under construction and have accumulated 300 reactor years of satisfactory operating experience. From the technological standpoint plants in this size range could be built with greater confidence than very large plants incorporating design extrapolation and innovations. (auth)

28584 DEVELOPMENT OF ATOMIC ENERGY: VIEWED FROM ENERGY DEMANDS. Sakon, Tomosaburo (Ministry of International Trade and Industry, Tokyo). Genshiryoku Kogyo; 16: No. 4, 13-17(Apr 1970). (In Japanese).

The development of atomic energy, viewed from the standpoint of energy demands, is described in the following: energy demand-and-supply situation in Japan; dealing with the characteristics of coal, oil, hydraulic power, and atomic energy; position of nuclear (electric) power generation in Japan, including its economy, inclusion in the grid, etc.; state of nuclear power generation in Eu-

XUM

ropean countries and the United States; and revision of the energy demands in Japan, dealing with the relation with a marked advance in GNP. (Japan)

28585 EXPERIENCES AT THE KWL (NUCLEAR POWER PLANT LINGEN) WITH THE STEAM PRODUCING SYSTEM UP TO THE FIRST FUEL ELEMENT REPLACEMENT. Deublein, O. (Kernkraftwerk Lingen GmbH, Ger.). Atomwirt., Atomtech.; 16: 177-80(Apr 1971). (In German).

At the KWL, performance until the first fuel element replacement reached an operational readiness of 91% and a utilization of 83% is described. After exhaustion of its excess reactivity, the reactor could be operated and regulated for an additional 12.5 months. During the time of operation, increasing radioactivity within the primary circuit caused some difficulties as to monitoring and repairing of certain parts. Following reloading, the first core showed several damaged fuel rods. Altogether, operation thus far revealed no undesirable effects upon the environment, and the radioactivity contained in effluent water and gas was far below permissible levels. (tr-auth)

28586 FOUR YEARS OF OPERATIONAL EXPERIENCE WITH MZFR. Armbruster, H. (Kernkraftwerk-Betriebsgesellschaft mbH, Leopoldshafen, Ger.). Atomwirt., Atomtech.; 16: 181-4 (Apr 1971). (In German).

The heavy water pressure reactor MZFR (57 MW(e) power) became operational in 1966 for the purpose of obtaining data about electricity production, testing of advanced fuel elements, and the availability of experimental radiation loops. During the first years of operation, numerous shutdown periods were caused by inexperience with the new reactor system. Between fall of 1969 and spring of 1971, the MZFR reached an operational safety that promises a high degree of efficiency for this type of modern reactor. Exchange of fuel elements under nominal load proceeded smoothly. At a pressure of 90 at, the daily loss of D_2O was less than 2.5 kg. (H.B.G.)

Safety and Siting

28587 (DOCKET-50016-107) ENRICO FERMI ATOMIC POWER PLANT, UNIT 1. Change No. 24 to Technical Specifications of Provisional Operating License No. DPR-9. (Division of Reactor Licensing (AEC), Washington, D. C.). 14 Apr 1971. 3p. Dep. NTIS.

Revised technical specifications are presented concerning secondary containment requirements for emergency liquid sodium system. (D.C.C.)

28588 (DOCKET-50133-54) HUMBOLDT BAY POWER PLANT, UNIT NO. 3. Facility License No. DPR-7, Amendment 2. (Division of Reactor Licensing (AEC), Washington, D. C.). 16 Apr 1971. 4p. Dep. NTIS.

Authorization for revised methods of regulating personnel access to high radiation areas is presented. (D.C.C.)

28589 (DOCKET-50133-55) HUMBOLDT BAY POWER PLANT, UNIT NO. 3. License No. DPR-7; Technical Specifications Proposed Change No. 34. (Pacific Gas and Electric Co., San Francisco, Calif.). 15 Apr 1971. 4p. Dep. NTIS.

Revised technical specification definitions are presented for average and maximum fuel burnup. (D.C.C.)

28590 (DOCKET-50146-71) SAXTON REACTOR. License No. DPR-4; Technical Specifications Change Request No. 42. (Saxton Nuclear Experimental Corp., Pa.). 15 Apr 1971. 4p. Dep. NTIS.

Revised technical specifications are presented concerning release limits for radioactive effluents and leak rate testing schedule for the containment structure. (D.C.C.)

28591 (DOCKET-50171-82) PEACH BOTTOM ATOMIC POWER STATION, UNIT 1. Change No. 13 to Technical Specifications of Provisional Operating License No. DPR-12. (Division of Reactor Licensing (AEC), Washington, D. C.). 8 Apr 1971. 28p. Dep. NTIS.

Revised technical specifications are presented concerning personnel and administrative controls. (D.C.C.)

28592 (DOCKET-50213-102) CONNECTICUT YANKEE ATOMIC POWER PLANT. License No. DPR-14. Technical Specifications Proposed Change No. 17, Suppl. 1. (Connecticut Yankee Atomic Power Co., Hartford). 12 Apr 1971. 10p. Dep. NTIS.

Revised technical specifications are presented concerning in-service inspection requirements, gaseous and liquid radioactive effluents, and calibration requirements of pressurizer level instrumentation. (D.C.C.)

28593 (DOCKET-50213-103) CONNECTICUT YANKEE ATOMIC POWER PLANT. License No. DPR-14. Technical Specifications Proposed Change No. 18, Suppl. 1. (Connecticut Yankee Atomic Power Co., Hartford). 8 Apr 1971. 10p. Dep. NTIS.

Revised technical specifications are presented concerning design parameters and operations aspects of Core 3 with zircaloy clad assemblies and neptunium target rods. (D.C.C.)

28594 (DOCKET-50213-104) CONNECTICUT YANKEE ATOMIC POWER PLANT. License No. DPR-14. Technical Specifications Proposed Change No. 19, Suppl. 1. (Connecticut Yankee Atomic Power Co., Hartford). 8 Apr 1971. 7p. Dep. NTIS.

Revised technical specifications are presented for core limits and low pressure trip setpoint. (D.C.C.)

28595 (DOCKET-50220-62) NINE MILE POINT NUCLEAR STATION. Provisional Operating License No. DPR-17, Amendment 2 (Authorization for Power Increase to 1850 Megawatts (Thermal)). (Division of Reactor Licensing (AEC), Washington, D. C.). 14 Apr 1971. 58p. Dep. NTIS.

Revised technical specifications for 1850 MW(t) operation are presented. Operational safety limits and environmental monitoring requirements are included. (D.C.C.)

28596 (DOCKET-50237-146) DRESDEN NUCLEAR POWER STATION, UNIT 2. Facility License DPR-19; Technical Specifications Proposed Change No. 9 to Appendix A. (Commonwealth Edison Co., Chicago, Ill.). 5 Mar 1971. 177p. Dep. NTIS.

Revised technical specifications are presented for Dresden Power Reactor Unit 2. (D.C.C.)

28597 (DOCKET-50237-148) DRESDEN NUCLEAR POWER STATION, UNIT 2. Change No. 9 to Technical Specifications and Bases (Appendix A to Provisional Operating License No. DPR-19). (Division of Reactor Licensing (AEC), Washington, D. C.). 15 Mar 1971. 180p. Dep. NTIS.

Revised technical specifications are presented for Dresden Power Reactor Unit 2. (D.C.C.)

28598 (DOCKET-50237-152) DRESDEN NUCLEAR POWER STATION, UNIT 2. Special Reports on Nine Topics to February 16, 1971 AEC Request. (Commonwealth Edison Co., Chicago, Ill.). 22 Mar 1971. 36p. Dep. NTIS.

Additional information concerning Dresden Power Reactor Unit 2 is presented under the following headings: vibration criteria for jet pump supports; minimization or elimination of venting; investigation of failures of radioactive liquid waste system; installation of radioactive offgas system; evaluation of failed fuel; reactor asymmetrical neutron flux distribution; corrective actions to assure main steam line isolation valve operability; corrective actions related to malfunctions on LPCI and isolation condenser valves; and seismic test program for instrument and electrical system. (D.C.C.)

28599 (DOCKET-50237-153) DRESDEN NUCLEAR POWER STATION, UNITS 2 AND 3. Proposed Modification No. 71-2 to Final Safety Analysis Report. (Commonwealth Edison Co., Chicago, Ill.). 6 Apr 1971. 4p. (DOCKET-50249-63). Dep. NTIS.

Revised information is presented concerning additional pressure sensors for the turbine electrohydraulic control system oil piping. (D.C.C.)

28600 (DOCKET-50237-154) DRESDEN NUCLEAR POWER STATION, UNIT 2. Facility License DPR-19; Proposed Change No. 10 to Appendix A. (Commonwealth Edison Co., Chicago, Ill.). 14 Apr 1971. 3p. Dep. NTIS.

Revised technical specifications are presented concerning in-service inspection requirements for pressure vessel and cooling system piping. (D.C.C.)

28601 (DOCKET-50244-69) ROBERT EMMETT GINNA NUCLEAR POWER PLANT, UNIT NO. 1. Change No. 5 to Technical Specifications of Provisional Operating License No. DPR-18. (Division of Reactor Licensing (AEC), Washington, D. C.). 15 Apr 1971. 5p. Dep. NTIS.

Revised technical specification is presented concerning an end-of-life reactivity shutdown margin of 1.9%. (D.C.C.)

XUM

28602 (DOCKET-50245-21) MILLSTONE NUCLEAR POWER STATION, UNIT 1. Order Extending Provisional Construction Permit Completion Date. (Division of Reactor Licensing (AEC), Washington, D. C.). 24 Nov 1969. 3p. Dep. NTIS.

28603 (DOCKET-50245-65) MILLSTONE NUCLEAR POWER STATION, UNIT 1. Application for Amendment to Provisional Construction Permit No. CPPR-20. (Connecticut Light and Power Co., Hartford. Hartford Electric Light Co., Conn. Western Massachusetts Electric Co., Greenfield. Millstone Point Co., Wethersfield, Conn.). 3 Nov 1969. 5p. Dep. NTIS.

A request for an extension of the completion date stated in the provisional construction permit is presented. The requested change would provide for a January 1, 1971, completion date instead of the existing January 1, 1970 date. (D.C.C.)

28604 (DOCKET-50245-66) MILLSTONE NUCLEAR POWER STATION, UNIT 1. Additional Information on Scram Trip Circuitry. (Millstone Point Co., Hartford, Conn.). 29 Dec 1969. 2p. Dep. NTIS.

28605 (DOCKET-50249-64) DRESDEN NUCLEAR POWER STATION, UNIT 3. Facility Operating License No. DPR-25; Proposed Change No. 2 to Appendix A. (Commonwealth Edison Co., Chicago, Ill.). 14 Apr 1971. 3p. Dep. NTIS.

Revised technical specifications are presented concerning in-service inspection requirements for pressure vessel and cooling system piping. (D.C.C.)

28606 (DOCKET-50250-43) TURKEY POINT PLANT, UNITS NO. 3 AND NO. 4. Environmental Report, Suppl. 1. (Florida Power and Light Co.). 7 Apr 1971. 7p. (DOCKET-50251-39). Dep. NTIS.

Additional information is presented concerning electrical power requirements and capacities for Florida during 1971 and 1972. (D.C.C.)

28607 (DOCKET-50255-37) PALISADES PLANT. Correction to Provisional Operating License No. DPR-20. (Division of Reactor Licensing (AEC), Washington, D. C.). 15 Apr 1971. 3p. Dep. NTIS.

A correction in the possession limit for ^{137}Cs is presented. (D.C.C.)

28608 (DOCKET-50267-28) FORT ST. VRAIN NUCLEAR GENERATING STATION, UNIT 1. Preliminary Safety Analysis Report, Amendment 19. (Public Service Co. of Colorado, Denver). 6 Apr 1971. 286p. Dep. NTIS.

Revised design parameters of the Fort St. Vrain Power Reactor Unit 1 are presented. Included also are additional data on the reactor requested by the Division of Reactor Licensing. Radiation monitoring data for the site during January to December 1970 are presented. (D.C.C.)

28609 (DOCKET-50271-49) VERMONT YANKEE NUCLEAR POWER STATION. Preliminary Safety Analysis Report, Amendment 24. (Vermont Yankee Nuclear Power Corp., Rutland). 16 Apr 1971. 158p. Dep. NTIS.

Financial data on the owners of Vermont Yankee Power Reactor are presented. The 1970 Annual Reports of the Central Vermont Public Service Corporation, Green Mountain Power Corporation, New England Power Corporation, Connecticut Light and Power Company, Central Maine Power Company, Public Service Company of New Hampshire, Hartford Electric Light Company, Cambridge Electric Light Company, Eastern Utilities Associates, and Western Massachusetts Electric Company are included. (D.C.C.)

28610 (DOCKET-50280-38) SURRY POWER STATION, UNITS 1 AND 2. Summary of Data Collected by the Onsite Meteorological Measurements Program at the Hog Island Site Instrument Installation, November 2, 1967-July 17, 1969. (Virginia Electric and Power Co., Richmond). 23 Apr 1971. 54p. (DOCKET-50281-38). Dep. NTIS.

28611 (DOCKET-50289-34) THREE MILE ISLAND NUCLEAR STATION, UNIT 1. Preliminary Safety Analysis Report, Amendment 19 (Includes Final Safety Analysis Report Modifications, Appendix 5A). (Metropolitan Edison Co., Reading, Pa. Jersey Central Power and Light Co., Morristown, N. J. Pennsylvania Electric Co., Johnstown). 15 Apr 1971. 83p. Dep. NTIS.

The results are presented of the aircraft impact study, which includes the analysis of the reactor building shell for various locations of loadings and plate analysis for loadings on wall and roof slab designs for structures other than the reactor building shell. Additional studies are described which determine if the aircraft impact loading will produce a loss of prestress force in the reactor building shell and, if the loss of prestress does occur, what effect this loss would have on the structure. The possibility of the spalling of the anchors of the lines due to an aircraft impact on the reactor building shell is analyzed. 26 references. (D.C.C.)

28612 (DOCKET-50293-46) PILGRIM NUCLEAR POWER STATION. Suggestions of Advisory Committee on Reactor Safeguards. (Division of Reactor Licensing (AEC), Washington, D. C.). 15 Apr 1971. 4p. Dep. NTIS.

28613 (DOCKET-50293-47) PILGRIM NUCLEAR POWER STATION. Notice of AEC Consideration of Issuance of Facility Operating License. (Division of Reactor Licensing (AEC), Washington, D. C.). 19 Apr 1971. 4p. Dep. NTIS.

28614 (DOCKET-50293-48) PILGRIM NUCLEAR POWER STATION. Withdrawal of Requests of January 12, 1971 and February 12, 1971. (Boston Edison Co., Mass.). 16 Apr 1971. 2p. Dep. NTIS.

A withdrawal of a request for counsel on weld reinforcements for piping systems is presented. (D.C.C.)

28615 (DOCKET-50309-33) MAINE YANKEE ATOMIC POWER STATION. Preliminary Safety Analysis Report, Amendment 22. (Maine Yankee Atomic Power Co., Westboro, Mass.). 21 Apr 1971. 163p. Dep. NTIS.

Additional data requested by the Division of Reactor Licensing on the Maine Yankee Power Reactor are presented. (D.C.C.)

28616 (DOCKET-50338-28) NORTH ANNA POWER STATION, UNIT 1. Construction Permit Nos. CPPR-77 and CPPR-78, Amendment No. 1. (Division of Reactor Licensing (AEC), Washington, D. C.). 14 Apr 1971. 5p. (DOCKET-50339-27). Dep. NTIS.

Additional provisions are submitted to the construction permit for protection of the environment. (D.C.C.)

28617 (DOCKET-50338-29) NORTH ANNA POWER STATION, UNITS 1 AND 2. Preliminary Safety Analysis Report, Amendment 14. Modifications to the Containment Spray System. (Virginia Electric and Power Co., Richmond). 23 Apr 1971. 6p. (DOCKET-50339-28). Dep. NTIS.

28618 (DOCKET-50348-19) JOSEPH M. FARLEY NUCLEAR PLANT, UNITS 1 AND 2. Preliminary Safety Analysis Report, Amendment 14. (Alabama Power Co., Birmingham). 9 Apr 1971. 293p. (DOCKET-50364-13). Dep. NTIS.

Revised design parameters of the Joseph M. Farley Power Reactor Units 1 and 2 are presented. Included also are additional data on the reactor requested by the Division of Reactor Licensing. (D.C.C.)

28619 (DOCKET-50367-12) BAILLY GENERATING STATION, NUCLEAR I. Preliminary Safety Analysis Report, Amendment 5. (Northern Indiana Public Service Co., Hammond). 19 Apr 1971. 300p. Dep. NTIS.

Revised design parameters of the Bailly Power Reactor Unit 1 are presented. Included also are additional data on the reactor requested by the Division of Reactor Licensing. (D.C.C.)

28620 (DOCKET-50368-8) ARKANSAS NUCLEAR ONE, UNIT 2. Preliminary Safety Analysis Report, Suppl. 3. (Arkansas Power and Light Co., Little Rock). 31 Mar 1971. 258p. Dep. NTIS.

Revised design parameters of the Arkansas Nuclear One Power Reactor Unit 2 are presented. Included also are additional data on the reactor requested by the Division of Reactor Licensing. (D.C.C.)

28621 (STI/PUB-261) ENVIRONMENTAL ASPECTS OF NUCLEAR POWER STATIONS. Proceedings Series. Proceedings of a Symposium Held in New York, 10-14 August 1970. (International Atomic Energy Agency, Vienna (Austria)). Jan 1971. 982p. (In several languages). (CONF-700810). IAEA $25.00.

Topics discussed include: standards for the control of effluents; nuclear power as an energy source; effluent control and monitoring; considerations affecting steam power station site selection; and benefit-risk assessments. Separate abstracts are presented for 7 of the 59 papers included. Fifty-one papers have been previously abstracted and listed in NSA. A paper discussing the gaseous and solid effluents from fossil-fueled power plants is also included. (D.C.C.)

For abstracts of individual papers see: 27042, 28533, 28574, and 28623-28626.

XUM

28622 NUCLEAR POWER AND THERMAL POLLUTION: ZION, ILLINOIS. Gustafson, Philip F. (Argonne National Lab., Ill.). Bull. At. Sci.; 26: No. 3, 17-23(Mar 1970).

The technical problems of power production and pollution are examined, with particular reference to the effects of the Zion Nuclear Power Plant on Lake Michigan. The basic cooling problems of power plants are described and the possible effects of thermal discharges into Lake Michigan are discussed. It is concluded that under anticipated levels of nuclear power generation on Lake Michigan, there is no cause for concern from either a thermal or radiation standpoint. (H.D.R.)

28623 METHODS OF EFFLUENT CONTROL IN NUCLEAR PLANTS. Krishnamoorthy, P. N. (Bhabha Atomic Research Centre, Bombay). pp 317-24 of Environmental Aspects of Nuclear Power Stations. Vienna; International Atomic Energy Agency (1971).

From Symposium on environmental aspects of nuclear power stations; New York (10 Aug 1970). See STI/PUB-261; CONF-700810.

Current methods of effluent control developed to meet standards set in respect of nuclear facilities are discussed. Problems related to the control of thermal pollution from some of these facilities are also considered. Methods of treatment of solid, liquid, and gaseous radioactive effluents prior to disposal or dispersal to the environment are discussed. (auth)

28624 MANAGEMENT OF EFFLUENTS FROM JAPC'S NUCLEAR POWER STATIONS. Yoshioka, T.; Itakura, T.; Hashimoto, T. (Japan Atomic Power Co., Tokyo). pp 439-51 of Environmental Aspects of Nuclear Power Stations. Vienna; International Atomic Energy Agency (1971).

From Symposium on environmental aspects of nuclear power stations; New York (10 Aug 1970). See STI/PUB-261; CONF-700810.

There are two commercial nuclear power stations in operation in Japan, both owned by the Japan Atomic Power Company. One is a magnox type 160 MW(e), in Tokai, and the other is a BWR type, 330 MW(e), in Tsuruga. The latter was completed in March 1970. There are also seven under construction, all of which are light-water type reactors. The effluent management procedures conducted at Tsuruga Station (light-water reactor) are described. The program includes: gas effluent management; liquid effluent management; and environmental monitoring. (auth)

28625 RADIOLOGICAL SURVEILLANCE STUDIES AT A BOILING WATER NUCLEAR POWER REACTOR. Kahn, B.; Blanchard, R. L.; Krieger, H. L.; (and others) (Dept. of Health, Education, and Welfare, Cincinnati). pp 535-48 of Environmental Aspects of Nuclear Power Stations. Vienna; International Atomic Energy Agency (1971).

From Symposium on environmental aspects of nuclear power stations; New York (10 Aug 1970). See STI/PUB-261; CONF-700810.

Radionuclides in water, gases, and airborne particles were measured at the Dresden Nuclear Power Station and in its environs in order to provide the technical basis for surveillance programs at nuclear power stations. Concentrations of radionuclides in the primary coolant and the off-gas were determined on several occasions; at the same time, radioxenon concentrations and external radiation exposures were measured near the plume within 1 to 2 km of the stack, and the radionuclide content of effluent water was measured near the point of discharge. Samples of food, feed and water from the immediate environment were also analyzed for specific radionuclides. Results of radionuclide analyses and radiation exposure calculations are presented, and analytical techniques for measuring radionuclides at low concentrations and in complex mixtures are indicated. (8 references.) (auth)

28626 ENVIRONMENTAL ASPECTS OF KARACHI NUCLEAR POWER PLANT. Nasim, M. (Pakistan Atomic Energy Commission, Karachi). pp 781-9 of Environmental Aspects of Nuclear Power Stations. Vienna; International Atomic Energy Agency (1971).

From Symposium on environmental aspects of nuclear power stations; New York (10 Aug 1970). See STI/PUB-261; CONF-700810.

The Karachi Nuclear Power Plant is located on the Arabian Sea Coast, 11 miles west of the City of Karachi. Prominent factors in the licensing process for the plant are the design characteristics of the plant in relation to its release to the environment of radioactive waste and the nature and characteristics of the specific environment in which the plant is located. Basic to the above factors is the review of the plant's radioactive waste discharge system, the specific radionuclide and anticipated normal discharges and public health implication of the presence of these radionuclides. In order to ensure that environmental dose limits for routine exposures are not exceeded, a program for the environmental survey of the site has been initiated. Environmental surveillance data would also be used as a basis for estimating population exposure. The program is basically directed at the identification of possible routes (called exposure pathways) of contamination to the population. These include air and water pathways and fish and agriculture food crops. (7 references.) (auth)

28627 RADIATION IN PERSPECTIVE: SOME COMPARISONS OF THE ENVIRONMENTAL RISKS FROM NUCLEAR- AND FOSSIL-FUELED POWER PLANTS. Hull, Andrew P. (Brookhaven National Lab., Upton, N. Y.). Nucl. Safety; 12: 185-96(May-Jun 1971).

Fossil- and nuclear-fueled steam plants seem the practical means for meeting immediate power needs. The use of nuclear-fueled plants is being restricted in several instances because reactor-related hazards have been exaggerated. Ninety power reactors, in the United States and abroad, have generated 2.5×10^{11} kWh over 650 reactor years without serious incidents. Comparison of routine discharges of hazardous agents from different types of steam power plants shows that nuclear-fueled plants produce the lowest concentrations of such agents relative to protection standards. Radioactive releases associated with the Brookhaven Graphite Research Reactor are comparable to the upper amounts anticipated from 1000-MW(e) reactors, and the measured Brookhaven external radiation levels, deposition, and aquatic concentrations suggest that the radiation level in the vicinity of large power reactors should be insignificant. The calculated risk ($\sim 10^{-7}$/year) of fatal injury from the anticipated maximum exposures of a few millirems per year above natural background is small compared with that of other accepted hazards of everyday living. 31 references. (auth)

28628 SEISMIC AND GEOLOGIC SITING CRITERIA FOR NUCLEAR POWER PLANTS. TENTATIVE REGULATORY CRITERIA. Washington, D. C.; Atomic Energy Commission (1969). 29p. Available from United States Atomic Energy Commission, Washington, D. C.

The principal seismic and geologic criteria which guide the USAEC in evaluating proposed sites for nuclear power plants and the seismic design suitability of the plants are presented. (H.D.R.)

28629 HURRICANE PROTECTION DESIGN. McLemore, R. H. Power Eng.; 75: No. 4, 49-51(Apr 1971).

The Crystal River Power Reactor, Unit 3 is located about one and one-half miles from the Gulf of Mexico. Design considerations applied to ensure protection of the plant from major hurricanes are discussed. The hazards from flooding, the impact of waves, and critical erosion of land are evaluated. (H.D.R.)

28630 FEASIBILITY OF THE SEA-BOTTOM ATOMIC POWER STATIONS. Kurabe, M. (Kawasaki Heavy Industries, Ltd., Kobe, Japan). FAPIG (Tokyo); No. 57, 4-17(May 1970). (In Japanese).

It is expected that the acquisition of nuclear-power generation sites near the area of power consumption will be increasingly difficult. Then, the site in the ocean, at the sea-bottom, comes into the spotlight. In this respect, Japan is most favored, surrounded by seas. The condition of sea-bottoms is relatively agreeable; the finding of sites near the consumers area is no problem. The technical feasibility and economic aspect of sea-bottom nuclear power stations is described including: the advantages; the types of reactor plant; the arrangement of a power station; PWR ice containment plant; turbine and generator; operation; output cables; and containment vessel. (Japan)

Steam and Power Conversion Systems

28631 DESIGN DETAILS OF THE BOILER FOR A 330 MW HTGR POWER STATION. Schutzendubel, W. G. Energie; 22: 113-20(Apr 1970). (In German).

The design of the boiler for a 330 MW(e) gas cooled high temperature reactor in Fort St Vrain nuclear power station is presented in which helium is cooled from 775 to 345°C and superheated steam is generated at 171 ata and 540°C and reheated steam at 40.8 ata and 539°C. The steam circuits, radiation shields, tube temperatures and operation are described. (UKAEA Info. Bull.)

Power Reactor Development

Refer also to abstracts 26205 and 28790.

28632 (EURFNR-824) FAST BREEDER PROJECT. First Quarterly Report, 1970. (Kernforschungszentrum, Karlsruhe

XUM

(West Germany)). Translation of report KFK-1270/1. 164p. Dep. NTIS.

Work performed under United States–Euratom Fast Reactor Exchange Program.

REACTOR FUEL ELEMENTS—development of fast breeder, fabrication and irradiation testing programs for
—cladding materials for fast breeder, development of, (E/T)
REACTOR FUELS—development of fast breeder, fabrication and irradiation testing programs for
REACTORS, BREEDER—development during January to March 1970
REACTORS, FAST—development during January to March 1970
—physics parameters of, (E/T)
—safety studies on, (E/T)
—core monitoring in, instrumentation and signal processing for, (E/T)
—cooling systems for, corrosion product and fission product activity levels in, (E)
—core for, thermodynamic and hydrodynamic design of, (E/T)
REACTORS, RESEARCH—design parameters of FR-3
SODIUM—corrosive effects of liquid, on fast breeder reactor materials, (E/T) (H.D.R.)

28633 (GA-10399) HTGR BASE PROGRAM QUARTERLY PROGRESS REPORT FOR THE PERIOD ENDING NOVEMBER 30, 1970. (Gulf General Atomic Co., San Diego, Calif.). 31 Dec 1970. Contract AT(04-3)-167. 99p. Dep. NTIS.

CESIUM—vaporization from graphite, (E)
GRAPHITE—radiation effects on dimensional stability of boronated and hafnated, neutron, (E)
HIGH TEMPERATURE LATTICE TEST REACTOR—physics parameters of HTGR lattices in, (E/T)
NEUTRONS—effects on dimensional stability of boronated and hafnated graphite, (E)
REACTOR FUEL ELEMENTS—reprocessing cycle development for gas cooled, (E)
—fabrication of coated particle type gas cooled, for recycle testing
REACTOR FUELS—radiation effects testing of coated particle
—reprocessing of coated particle, fluid bed oxidation procedures in, (E)
REACTORS, GAS COOLED—development of 1000 MW(e) HTGR concept during September through November 1970
—fission product release and transport in high temperature, (E/T)
—fuel elements for high temperature, fabrication and irradiation testing of recycle, (E/T)
—fuel elements for high temperature, plant designs and costs for reprocessing
REACTORS, POWER—development of 1000 MW(e) HTGR concept during September through November 1970 (H.D.R.)

28634 (NP-18782) CONCEPTUAL STUDIES OF A 1000-MWe NUCLEAR POWER STATION WITH A STEAM-COOLED, FAST BREEDER REACTOR. Mueller, R. A. (Kernforschungszentrum, Karlsruhe (West Germany). Institut fuer Reaktorentwicklung). Dec 1970. 70p. (In French). Dep. NTIS (U. S. Sales Only).

Referring to the Reference Design of a 1000 MW(e) Steam Cooled Fast Breeder Reactor D 1 the factors determining the design and layout of a large steam cooled fast breeder reactor are given. The methods are discussed in detail, which allow reliable afterheat removal and reactor flooding to perform refueling. As a development of the mentioned Reference Study a reactor design is indicated allowing easy inspection of the pressure vessel and simple dismantling of all internals. The safety features of the plant are also improved by modification to the refueling pool and the main steam lines. As a result the water content of this pool can be used for rapid flooding of the reactor cavity in case of a serious accident. 8 references. (auth)

28635 GASEOUS-FUELED NUCLEAR REACTORS FOR ELECTRICAL POWER PRODUCTION. Gritton, Eugene C.; Pinkel, Benjamin (to United States Atomic Energy Commission). U. S. Patent 3,558,935. 26 Jan 1971. Filed 13 Nov 1968.

Nuclear reactors are described in which fissile fuel material in gaseous form is utilized as an energy source for the production of electrical power. The active core region of such reactors comprises gaseous fuel disposed within a cavity or cavities and surrounded by a material having both reflector and moderator properties. A high temperature liner is provided to contain the gaseous fuel while permitting it to attain temperatures where heat transfer by thermal radiation predominates within the cavity or cavities. The heat reaching the cavity wall or walls is converted to electrical energy by several methods including the use of thermionic converters immediately adjacent the wall or walls or located remotely therefrom, or by using a circulating thermodynamic working fluid in combination with the thermionic converters and passing it through a conventional turboelectric generator loop. (auth)

28636 MOLTEN SALT REACTOR EXPERIMENT (MSRE): CHEMICAL ASPECTS. Grimes, W. R.; Bamberger, C. E. (Oak Ridge National Lab., Tenn.). Energ. Nucl. (Madrid); 14: 137-52(Mar-Apr 1970). (In Spanish).

A brief history and general description is given of the MSRE. The purely chemical aspects of the reactor, fuel, coolant, construction materials, and compatibility of materials are then considered. Phase diagrams of the fluorides, chemical and oxide equilibria, and general chemical behavior of such materials are discussed. A series of predictions on the future of the MSRE concept is presented. (35 references.) (tr-auth)

28637 ASPECTS OF BOILING-WATER MEDIUM-POWER REACTORS. Haga, I.; Kraemer, W. (ASEA-ATOM AB, Vaesteras, Sweden). pp 19-31 of Small and Medium Power Reactors, 1970. Vienna; International Atomic Energy Agency (1971).

From Small and medium power reactors symposium; Oslo, Norway (12 Oct 1970). See STI/PUB-267; CONF-701046.

A brief description of the design of the Oskarshamn I plant is given. Special emphasis is put on features characterizing the boiling-water reactor design. Trends in reactor development in the period since Oskarshamn I was ordered are indicated. An analysis of the capital cost variation with plant size is included. The analysis is based on recent nuclear power plant cost figures for unit sizes above the medium- and small-power range. However, estimates are made of the variations in capital costs into the lower power range. (9 references.) (auth)

28638 WESTINGHOUSE EXPERIENCE WITH MEDIUM-SIZE REACTORS AND SOME FACTORS TO BE CONSIDERED IN SELECTING A NUCLEAR PLANT. McGrath, R. G. (Westinghouse Electric Corp., Pittsburgh). pp 109-16 of Small and Medium Power Reactors, 1970. Vienna; International Atomic Energy Agency (1971).

From Small and medium power reactors symposium; Oslo, Norway (12 Oct 1970). See STI/PUB-267; CONF-701046.

The experience, technical features, and relationship to larger units of medium-size plants are reviewed. The experience has already included the operation of several generations of plants, all of which have contributed to the success of the pressurized-water reactor as a reliable source of energy for the electric power industry. The operating experiences of the Ginna station, which entered commercial operation in March 1970, and the Beznau station which began full-scale operation in December 1969 are reviewed. The technical features of medium-size plants are very similar to those of larger units and reflect the systematic, evolutionary development of the PWR. In concept the units are not size dependent. Although there are a few differences, basically the medium-size plants differ from larger units only in the capacity of components. This affords maximum opportunity for all units to benefit from prior and contemporary experience with other units. Some of the factors that should be considered by those interested in purchasing nuclear plants are discussed. The advantages and the relative economics associated with the purchase of a nuclear steam supply system which does not exactly match the preferred rating are analyzed. (auth)

28639 CONCEPTUAL DESIGN OF A MEDIUM-OUTPUT INTEGRATED PWR PRODUCED FROM COMPONENTS SERIES INTENDED FOR LARGER UNITS. Margen, P. H. (Aktiebolaget Atomenergi, Studsvik, Sweden). pp 251-71 of Small and Medium Power Reactors, 1970. Vienna; International Atomic Energy Agency (1971).

From Small and medium power reactors symposium; Oslo, Norway (12 Oct 1970). See STI/PUB-267; CONF-701046.

To obtain an economic plant in the medium-size range despite the initially limited market for this type of plant, one should aim at a radical simplification in basic design; and utilization as far as possible of components produced in series for larger units. Design modifications are described. (9 references.) (auth)

28640 OPTIMIZATION OF PARAMETERS FOR SMALL NUCLEAR POWER SOURCES CONTAINING WATER-COOLED, WATER-MODERATED REACTORS. Andreev, P. A. (Central Reactor Inst., Leningrad); Marinich, A. M.; Sergeev, Yu. A. pp 273-91 of Small and Medium Power Reactors, 1970. Vienna; International Atomic Energy Agency (1971). (In Russian).

From Small and medium power reactors symposium; Oslo, Norway (12 Oct 1970). See STI/PUB-267; CONF-701046.

XUM

One method of reducing the cost of power generated by nuclear power sources is the integrated optimization of the physical, thermal-hydraulic, thermodynamic and design parameters. Design optimization was carried out with reference to three types of nuclear power sources incorporating water-cooled, water-moderated reactors: thermal power stations using condensation turbines, with provision for intermediate bleeding of steam for heating purposes; thermal power stations with backpressure turbines; and single-purpose facility for centralized heat supply. Facilities containing reactors with thermal capacity from 10 to 200 MW were considered. For purposes of calculation, an algorithm (an integrated mathematical model of nuclear power sources with water-cooled, water-moderated reactors) and a computer program were worked out. These were used to make a study of facilities having integral and multi-block layout of the reactor and steam-generator systems and making use of natural and forced circulation of the coolant in the first and second circuits of the nuclear steam-generation system. The variants with the optimum combination of the parameters were subjected to comparative analysis and a selection was made on the basis of the minimum calculated cost of power and heat generation. (6 references.) (auth)

28641 CONCEPT FOR A SMALL NUCLEAR STEAM-GENERATING SYSTEM WITH AN INTEGRATED CONSTRUCTION. Fischer, R. (INTERATOM, Bensberg, Ger.); Bohmann, W. pp 293-303 of Small and Medium Power Reactors, 1970. Vienna; International Atomic Energy Agency (1971).

From Small and medium power reactors symposium; Oslo, Norway (12 Oct 1970). See STI/PUB-267; CONF-701046.

The integrated self-pressurized water reactor is particularly suited for small power stations. It is a logical land-based application of a further development of the FDR-reactor, which has been operating on the N. S. "Otto Hahn" since 1968 with very good results. A description of the integrated power reactor is given with special regard to its well proved components which are applied to pressurized and boiling reactors. Special features of this reactor type are the good control and safety characteristics. (8 references.) (auth)

28642 STEAM-GENERATING HEAVY-WATER REACTOR AS ENERGY SOURCE FOR POWER AND WATER PRODUCTION WHEN COUPLED TO MULTI-STAGE-FLASH OR VAPOUR RECOMPRESSION DISTILLATION PLANT. Chambers, S.; Wood, F. C. (Atomic Energy Establishment, Winfrith, Eng.). pp 345-62 of Small and Medium Power Reactors, 1970. Vienna; International Atomic Energy Agency (1971).

From Small and medium power reactors symposium; Oslo, Norway (12 Oct 1970). See STI/PUB-267; CONF-701046.

Optimization studies of the SGHWR with backpressure turbines exhausting to MSF units are reported in the range of reactor sizes up to 1500 MW(t) and electrical outputs up to 200 MW(net) and 300 MW(gross). The effect of the choice of power credit is shown to be highly important while the effect of choice of exhaust pressure or maximum brine temperature in the range of 190 to 250°F is relatively unimportant, in respect of water-production cost. Characteristics of the system of coupling are discussed and measures to increase flexibility in operation are considered. The hold-up of brine in large multi-stage distillation plants necessitates a slow response to changing conditions and suggests that in a load-following or peaking role the vapor recompression distiller could be suitable. Some characteristics of vapor recompression coupled to SGHWR are discussed and it is concluded that integral dual-purpose power and water systems involving the use of SGHWR are technically and economically attractive over a broad field of operational requirement. (9 references.) (auth)

28643 OCEAN NUCLEAR-POWER PLANT; TECHNICAL FEASIBILITY AND ECONOMY. Sakuta, Masaaki (Fuyo Ocean Development and Engineering Co. Ltd., Tokyo). Genshiryoku Kogyo; 16: No. 6, 10-18(Jun 1970). (In Japanese).

Ocean nuclear power plants, feasibility and economics, are described in the following: marine structures and nuclear power plants, dealing with the types of installation in sea water, and the necessity for compactness of a nuclear power plant; technical aspects of ocean nuclear power plants, dealing with the artificial-island procedure, plant operation, etc.; cost of ocean nuclear power plants, well competitive with the conventional type; and problems in ocean nuclear power plants. (Japan)

28644 NUCLEAR TECHNOLOGY INDUSTRY IN THE FEDERAL REPUBLIC OF GERMANY. Neue Tech., B; 11: 179-84(1969). (In German).

The development of a nuclear technological industry in the Federal Republic of Germany is briefly reviewed. The dominant role played by the government in the early years is emphasized and the entry of the private sector into this field is described. The present nuclear industry of the country is described. (J.S.R.)

28645 HEAVY-WATER-COOLED AND-MODERATED BOILING-WATER REACTOR. Ruf, R.; Stueger, R. Canadian Patent 867,000. 23 Mar 1971. Priority date 26, Jan 1967, Germany.

This reactor type has separate cooling and moderating flow paths and includes a steam separator for separating the gaseous and liquid phases of cooling water issuing from it. The gaseous phase is supplied to a steam generator. The liquid phase is mixed with moderator water issuing from the reactor and a first portion of the mixture is supplied as cooling water. The second portion of the mixture is supplied to the reactor as moderator water after passage through a moderator cooler. Circulation of this second portion is effected by a reaction jet conveyor driven by the cooling water emerging from the steam generator. (F.S.A.)

28646 GAS TURBINE PLANTS. (to Sulzer Brothers Ltd.). British Patent 1,227,606. 7 Apr 1971. Priority date 27 Jul 1967, Switzerland.

REACTORS, GAS COOLED — design with closed cycle carbon dioxide gas turbines and two compression and expansion stages

REACTORS, POWER — design with closed cycle carbon dioxide gas turbines and two compression and expansion stages (H.D.R.)

28647 GAS TURBINE AND NUCLEAR REACTOR PLANTS. Strub, Rene (to Sulzer Brothers Ltd.). British Patent 1,227,580. 7 Apr 1971. Priority date 27 Jul 1967, Switzerland.

REACTORS, GAS COOLED — design with closed cycle carbon dioxide gas turbine and means for maintaining constant pressure at reactor inlet

REACTORS, POWER — design with closed cycle carbon dioxide gas turbine and means for maintaining constant pressure at reactor inlet (H.D.R.)

28648 NUCLEAR REACTOR AND GAS TURBINE PLANTS. (to Sulzer Brothers Ltd.). British Patent 1,228.617. 15 Apr 1971. Priority date 27 Jul 1967, Switzerland.

REACTORS, GAS COOLED — design with closed cycle carbon dioxide gas turbine and means for turbine speed control

REACTORS, POWER — design with closed cycle carbon dioxide gas turbine and means for turbine speed control (H.D.R.)

28649 IMPROVEMENTS IN OR RELATING TO NUCLEAR REACTORS. Boothroyd, Milton Woodall (to United Kingdom Atomic Energy Authority). British Patent 1,226,106. 24 Mar 1971. Filed 21 Jun 1967.

Reference is made to reactors employing cluster type fuel elements. In such reactors the coolant flow path is usually through longitudinal spaces between the cluster rods. There may be many such clusters and it is generally desirable that temperature differences of coolant emerging from paths in the same core should be minimized as far as possible. One way of equalizing the temperature distribution in the outlet coolant is to divide the core cross section into a number of channels and restrict the flow rate in the lower rated flow paths so that the cooling effect in these flow paths is less and the outlet temperature higher; but this arrangement, which uses an orifice plate, gives only coarse control. In the system described differential restriction of the flow along the various flow paths is effected by inserting in each flow path an elongated member, fixedly mounted, the central portion of which obstructs a predetermined amount of flow area, while the portion surrounding the central portion does not materially obstruct the flow. A finned rod may be employed that provides a solid central portion that obstructs a predetermined amount of the flow area while the fins obstruct the flow by a lesser amount. The system is particularly applicable to fast reactor cores employing breeder fuel in cluster form around the core. (UK)

28650 KINETIC INTENSE NEUTRON GENERATOR REACTOR. King, L. D. Percival (to United States Atomic Energy Commission). U. S. Patent 3,573,167. 30 Mar 1971. Filed 6 Jun 1968.

A nuclear reactor capable of producing on a continuous basis an intense neutron flux is described. The reactor comprises a small core region, a large containment vessel, pumping means to continuously and rapidly move a liquid nuclear fuel through the core and inject it into the said vessel in such a manner that the geometry of the fuel in the core under static conditions is supercritical. (auth)

28651 IMPORTANCE AND TECHNIQUE OF FAST BREEDER REACTORS. Eisner, J. H. Energ. Tech.; 22: 122-6(Apr 1970). (In German).

After discussing the economic necessity for a type of nuclear reactor able to utilize the ample supplies of ^{238}U for energy generation the fast breeder reactor, the breeding process, neutron economy and its technical and physical characteristics are de-

XUM

scribed. Circuit arrangements and design details of fuel elements are presented. (UKAEA Info. Bull.)

28652 IMPROVEMENTS IN OR RELATING TO METHODS AND APPARATUS FOR INSERTING RODS INTO A FRAME. Tindale, John Basil; Burgess, James Henry (to United Kingdom Atomic Energy Authority). British Patent 1,225,782. 24 Mar 1971. Filed 6 Sep 1967.

A method is described for inserting close fitting rods into a frame that has grids for locating the rods to form a parallel array in the frame. It is particularly applicable to the insertion of nuclear reactor fuel pins into grid-containing wrappers for assembling a reactor core, as in fast reactor construction, an operation which presents some difficulties and may easily damage the pins, owing to their thin stainless steel walls and their length, which may also result in errors of location. The method involves the use of loose fitting pilot rods that engage the ends of the first rods, together with a thrust head and propelled rollers. Transducers may be used to provide an output signal corresponding to the applied thrusts, together with means controlled by these signals to interrupt the propulsion if the thrust exceeds a predetermined value. Loading means for the rods are described. (UK)

28653 GAS TURBINE PLANTS. (to Sulzer Brothers Ltd.). British Patent 1,228,616. 15 Apr 1971. Priority date 27 Jul 1967, Switzerland.

REACTORS, GAS COOLED — design with closed cycle carbon dioxide gas turbines and automatic control of throttle and gas flow

REACTORS, POWER — design with closed cycle carbon dioxide gas turbines and automatic control of throttle and gas flow (H.D.R.)

Kinetics and Dynamics

Refer also to abstracts 28760, 28799, and 28804.

28654 (CEA-N-1344(2)) COREGRAF 2: ADJUSTMENT AND COMPARISON WITH EXPERIMENT. Charbonneau, Serge; Hoffmann, Alain; Laponche, Bernard; Luffin, Jean; Morier, Francis (Commissariat a l'Energie Atomique, Saclay (France). Centre d'Etudes Nucleaires). Mar 1971. 155p. (In French). Dep. NTIS (U. S. Sales Only).

The COREGRAF code for calculation of graphite moderated lattices was compared to experiment and, as a result, a number of adjustments were made. For fresh lattices, calculations were compared to experiments made in Marius and Cesar: buckling measurements by flux maps and progressive replacement, fine measurements of the disadvantage factor, the fast fission factor, spectral indices, leakage determination based on the values of diffusion coefficient and graphite constants, measurement of the temperature coefficient by integral and differential methods. These comparisons led to an adjustment of the ^{238}U resonance integral and of the variation of the ^{235}U fission cross-section as a function of energy. Measurements made on power steps at the starting-up of power reactors were used to adjust xenon absorption. For irradiated lattices, calculations were compared to chemical and isotopic analyses of fuel irradiated in power reactors and to the reactivity measurements on the Latina reactor. Another adjustment of the ^{238}U resonance integral was made, which is specific to the calculation of the number of nuclei of an irradiated fuel. Cross sections of the plutonium isotopes (^{239}Pu, ^{240}Pu, and ^{241}Pu) were also adjusted. The adjusted code has been applied to the calculation of the neutron balance of graphite gas cooled reactors and a number of specifications for use have been defined. 78 references. (auth) (France)

28655 (EURFNR-830) OPTIMIZATION OF SODIUM-COOLED FAST BREEDERS BY NONLINEAR PROGRAMMING METHODS. Heusener, G. (Kernforschungszentrum, Karlsruhe (West Germany). Institut fuer Reaktorentwicklung). Translation of report KFK-1238. 104p. Dep. NTIS.

Work performed under United States–Euratom Fast Reactor Exchange Program.

Methods of nonlinear programming are used to optimize fast breeder reactors. Two different procedures, a systematic one (method of steepest descent) and a statistical one (evolution strategy) are described. Their advantages and disadvantages are discussed. As example for the application of these methods, a core optimization for sodium cooled 1000 MW(e) breeder reactors with oxide and carbide fuel is considered. In order to reduce the needed computer time, approximations in nuclear computations are necessary. A procedure is described that allows a fast and sufficiently accurate estimation of the nuclear results. The optimization is performed with regard to two different criteria. The resulting design characteristics are discussed. Using importance quantities, which are obtained as part of the solution, the influence of the design limits upon the optimization criterion is predicted quantitatively. By recalculating some special cases the reliability of the predictions is demonstrated. 49 references. (auth)

28656 (EURFNR-842) MEASUREMENT OF NEUTRON SPECTRA WITHIN THE 1 eV TO 10 keV ENERGY RANGE BY MEANS OF THE SANDWICH TECHNIQUE. Mueller, M. (Kernforschungszentrum, Karlsruhe (West Germany). Institut fuer Angewandte Reaktorphysik). Translation of report KFK-1233. 112p. Dep. NTIS.

Work performed under United States–Euratom Fast Reactor Exchange Program.

Twenty-one different resonance absorbers were investigated theoretically and experimentally in order to check their suitability as sandwich detectors for the determination of neutron spectra in fast reactors below the energy of 10 keV. The obtainable accuracy of the measured results of all detectors was found to be influenced strongly by the hardness of the neutron spectrum. By means of the absolute cross sections of gold and manganese the results could be given absolutely. The accuracy of the measurements was 10–20% for spectra similar to those in a fast steam-cooled breeder reactor and 20–40% for spectra similar to those in a fast sodium-cooled breeder reactor. 32 references. (auth)

28657 (HEDL-TME-71-36) GROUP CONSTANTS FOR FAST REACTOR CALCULATIONS. Kidman, R. B.; Schenter, R. E. (Hanford Engineering Development Lab., Richland, Wash.). Mar 1971. Contract AT(45-1)-2170. 299p. (ENDF-143). Dep. NTIS.

A current 29-group fast reactor cross section library consisting of 34 different isotopes is presented. The multigroup constants were generated by ETOX (a code which calculates group constants for nuclear reactor calculations) using the Evaluated Nuclear Data File, ENDF/B Version II, for the fundamental nuclear data input. The library is also used to make some representative calculations on several critical assemblies. 9 references. (auth)

28658 INFLUENCE OF COATED-PARTICLE STRUCTURE IN THERMAL-NEUTRON-SPECTRUM ENERGY RANGE. Hansen, U.; Teuchert, E. (Kernforschungsanlage, Juelich, Ger.). Nucl. Sci. Eng.; 44: 12-17(Apr 1971).

The heterogeneity due to lumping the fuel in coated particles affects the thermal-neutron spectrum. A calculational model is discussed which, apart from some simplifying assumptions about the statistical distribution, allows a rigorous computation of effective cross sections for all nuclides of the heterogeneous medium. It is based on an exact computation of the neutron-penetration probability through coating and kernel. The model is incorporated in a THERMOS code providing a double heterogeneous cell calculation that can be repeated automatically at different time steps in the depletion code system MAFIA-V.S.O.P. A discussion of the effects of the coated-particle structure is given by a comparison of calculations for heterogeneous and homogeneous fuel zones in pebble bed reactor elements. This is performed for enriched UO_2 fuel and for a ThO_2-PuO_2 mixture in the grains. Depending on the energy-dependent total sigmas in the kernels, the changes of the cross sections range from 0.1 up to 45%. The influence on the spectrum-averaged sigmas of the nuclides in the fresh UO_2 fuel is lower than 1%. For the emerging ^{240}Pu it increases up to 3.3% during irradiation. For the ThO_2-PuO_2 fuel, the averaged sigmas of the isotopes vary from 0.5 to 5.7% depending on the state of irradiation. Correspondingly, there is an influence on the plutonium isotopic composition, on breeding ratios, and on the tilt of k_{eff} during burnup which is discussed in detail. (11 references) (auth)

28659 EXPERIMENT ON INVESTIGATION OF NEUTRON PHYSICS OF STEAM-COOLED FAST REACTORS AT SNEAK. Engelmann, Peter (Kernforschungszentrum, Karlsruhe, Ger.). Acta Phys. Austr.; 29: 54-85(1969). (In German).

A review is given of the experimental studies on SNEAK for the neutron physics characteristics of steam-cooled fast reactors. A brief description is given of SNEAK and the experimental devices. The two types of integral experiments carried out on SNEAK are basic studies on neutron physics and critical experiments for planned power reactors. A review is given of the measurement programs and results. Detailed descriptions are given of the Doppler measurements for the testing of the $\alpha = \langle\sigma_\gamma/\sigma_f\rangle$ ratio of ^{239}Pu and the method of progressive substitution for the determination of the critical mass of pure Pu systems for measurements on zone assemblies. (20 references) (J.S.R.)

28660 CRITICAL HEAT FLUX UNDER CONDITIONS PREVAILING IN A BOILING-WATER REACTOR. Haiduc, C.; Vinitchi, V. Stud. Cercet. Energ. Electroteh.; 20: 542-53(1970). (In Rumanian).

The critical heat flux q_{cr}, the flux for which nucleate boiling is replaced by the quasistable film boiling, represents the limit of the heat load of the fuel elements, and thus of the power to be generated in the reactor. In view of the importance of this problem for the clarification of the boiling phenomenon in boiling water reactors and for bulk boiling, the heat transfer problems related to the critical flux were studied under natural convection, using test loops with smooth, cylindrical, electrically heated fuel element models. The tests involved determination of the angle of inclination and the phenomenon of hysteresis during boiling. A new critical equation which may be used to calculate q_{cr} on smooth, vertical, cylindrical fuel elements, was obtained for a broad pressure range of $1 < p < 225$ atm, and fuel element diameters of $d_e > 5$ mm, containing a new similarity criterion of $(\mu/\mu'')^{0.5}$. This expression is characteristic for the influence of the ratio of the viscosity of the liquid with respect to the viscosity of the steam on q_{cr}. The data calculated by the newly derived critical boiling equations compares better with experimental values than those obtained by means of most of the other equations reported in the literature. (14 references) (TTT)

28661 MULTIREGION HEAT TRANSFER ANALYSIS FOR DISPLACED CENTRAL, CORNER, AND SIDE ELEMENTS OF UNBAFFLED LMFBR FUEL ROD BUNDLES. Johannsen, K.; Ullrich, R.; Wolf, L. (Technische Univ., Berlin). Nucl. Eng. Des.; 15: 29-32(Mar 1971).

Some results of a single-rod multiregion analysis for fully developed slug-flow heat transfer to displaced central, corner and side elements of LMFBR fuel rod bundles are presented. The analysis was performed under the assumption that the heat generation within the fuel may be taken constant and thermal resistances at the interfaces may be neglected. (8 references) (auth)

28662 TRANSIENT HEAT CONDUCTION MODEL FOR REACTOR FUEL ELEMENTS. Lewis, E. E. (Northwestern Univ., Evanston, Ill.). Nucl. Eng. Des.; 15: 33-40(Mar 1971).

A two region, lumped-parameter model is developed for the treatment of thermal transients in reactor fuel elements. The fuel-region heat conduction is treated by a fundamental mode approximation to the time-dependent Green's function. The model also accounts for the thermal resistance of the fuel-cladding gap and the cladding-coolant interface, and for the non-negligible heat capacity of both the fuel and cladding regions. The thermal resistance of the cladding is neglected. The resulting differential equations are similar to those that are obtained from the lumped-parameter model of Tong. The results from the fundamental mode model and the Tong model are compared to exact analytical results that are obtained for a number of highly idealized problems. The fundamental mode model is then used to treat a series of highly idealized loss-of-coolant transients. The fundamental mode model has been incorporated into the FLASH-2 code to treat more realistic accident transients. (13 references) (auth)

28663 REACTOR PHYSICS DESIGN TECHNIQUE FOR BURNABLE POISON AND ENRICHMENT-ZONED CORES. Pyne, H.; Feil, J.; Poiter, R.; Barnett, M. (United Kingdom Atomic Energy Authority, Winfrith, Eng.). pp 227-49 of Small and Medium Power Reactors, 1970. Vienna; International Atomic Energy Agency (1971).

From Small and medium power reactors symposium; Oslo, Norway (12 Oct 1970). See STI/PUB-267; CONF-701046.

Economic designs of small pressurized-water reactors tend to be based on complete core replacement fuel management schemes and to make full use of burnable poison techniques. As a result it is a design objective to minimize both the power peaking factors and the core $k_{(effective)}$ (i.e. defined with control rods out of the core) over the core life. The appropriate techniques for doing this are the selection of appropriate, variable fuel enrichment zones, the detailed design of the burnable poison loading and self-shielding and the choice of an optimum control-rod programming scheme. This leaves the designer with a larger number of variables to optimize and it is suggested that a useful first step is to minimize the peaking factors and the core $k_{(effective)}$ for the case with no control-rod insertion. The optimum control program is then defined as one which presents the minimum disturbance to the uncontrolled flux. The problem of choosing fuel enrichments and burnable poison loadings to achieve these design objectives for the uncontrolled core are described for a core with two radial enrichment zones. The effectiveness of these techniques is shown by applying them to the design of the Burnable Poison Water Reactor (BPWR) developed for civil marine application. (2 references.) (auth)

28664 ECONOMICAL AND TECHNICAL PROPERTIES OF THE SODIUM-COOLED HIGH-POWER BREEDER REACTOR WITH CARBIDE FUEL. Affeldt, Burkhard; Kilian, Peter; Reinke, Peter. Wiss. Ber. AEG-Telefunken; 43: 200-9(1970). (In German).

The economic aspects of Na cooling in combination with UC–PuC fuel in order to define a system having the highest possible breeding gain in a high-power breeder reactor are considered. As a reference concept in accordance with economic criteria, a reactor core 0.8 m high and 2 m in diameter, comprising rods 8 mm in diameter, resulted from the parameter studies. The rods are operated with the highest possible linear rod power (1080 W/cm) and high burn-up (10^5 MWd/t on an average). At these fuel rod and reactor dimensions the so-called inventory costs pass through a flat minimum. Moreover, the parameter studies yielded a connection between fissile material and breeding rate in the sense that a low breeding rate is associated with an economically favorable high fissile material load. Further parameter calculations were directed towards the influence of burn-up, breeder jacket dimensions and linear rod power. In order to examine the stability and safety behavior reactor-kinetic calculations were performed. As expected the reactor design proved to be stable, i.e., the reactor power tends to return to the original state in the presence of small defects. Rapid changes of coolant circulation or reactivity were examined by means of a kinetic computer program. Such extreme operational changes cause coolant simmering and fuel melting, which stand in contrast to high-speed reactors with oxydic fuel. The simulation of the safety system in the dynamic model showed that the reactor core may be disconnected without damage in the event of all conceivable faults (in contrast to the hypothetical faults considered previously). In conclusion the behavior of the sodium combination layer between the carbide fuel and jacket material was examined. 7 references. (auth)

28665 ANALYTICAL MODEL FOR DESCRIBING THE FREQUENCY RESPONSE AND STABILITY BEHAVIOR OF LIGHT-WATER MODERATOR PRESSURIZED POWER REACTORS. Hoeld, A.; Stahl, D. (Technische Univ., Munich). Atomkernenergie; 17: 167-74(May 1971). (In German).

A linear one-dimensional reactor-dynamic model is presented which describes in an analytical way the frequency response and stability behavior of a pressurized (light) water reactor (or loop) with respect to perturbations in reactivity (or heating power), subcooling or mass flow (both at the entrance to the primary reactor or the secondary steam transformer circuit) and steam load or system pressure (on the secondary side of the steam transformer). 2 references. (auth)

28666 EQUIVALENCE RELATION FOR RESONANCE ABSORPTION BASED ON NUMERICALLY CALCULATED COLLISION PROBABILITIES. PART 1. Schriewer, J. (Gutehoffnungshuette Sterkrade AG, Oberhausen, Ger.). Atomkernenergie; 17: 185-8(May 1971).

The heterogeneous resonance integral (N.R. or I.M. approximations) is reduced to the homogeneous case by applying a so-called escape cross-section, formally dependent on the first-flight collision probability in the fuel lumps. In order to avoid the use of rotational approximations a method is given to calculate collision probabilities for homogeneous fuel or fuel grains contained in a lattice of cylindrical or annular zones. An example indicates how simple analytical expressions for collision probability and escape cross-section are obtainable from but a few numerical evaluations. 4 references. (auth)

Control Systems

Refer also to abstract 28721.

28667 (HEDL-SA-170) EUROPEAN LIQUID METAL COOLED BREEDER REACTOR INSTRUMENTATION: A TRIP SUMMARY. Swanson, Carl D. (Hanford Engineering Development Lab., Richland, Wash.). Mar 1971. Contract AT(45-1)-1270. 22p. (CONF-710412-1). Dep. NTIS.

From Instrument Society of America meeting; Richland, Wash. (13 Apr 1971).

Impressions of a tour of European reactor installations and support facilities made in October 1969 are presented. Visits were made to fast breeder reactor installations at Cadarache in France, Karlsruhe in Germany, and at four sites in the United Kingdom. The basic emphasis of the visits was to discuss sodium-cooled fast reactor instrumentation and control technology development at the various installations. (H.D.R.)

28668 (WCAP-7406) PART LENGTH ROD CONTROL SYSTEM. Blanchard, A. E. (Westinghouse Electric Corp.,

XUM

Pittsburgh, Pa. Nuclear Energy Systems Div.). Mar 1971. 23p. Dep. NTIS.

A functional description of the control system used for operating the part length rod drive mechanisms in present Westinghouse pressurized water reactors is presented. The system has been designed to satisfy the requirements for two, three, and four loop plants. Detailed descriptions of the major subassemblies which comprise the system, the operational features of these sub-assemblies and the overall operational capabilities of the entire system are presented. (auth)

28669 (WCAP-7571) ROD POSITION MONITORING. Blanchard, A. E. (Westinghouse Electric Corp., Pittsburgh, Pa. Nuclear Energy Systems Div.). Mar 1971. 17p. Dep. NTIS.

Rod Position Monitoring in Westinghouse Pressurized Water Reactors is performed by two independent indication systems. The demand position indication is generated within the part length and full length rod control systems and furnishes an indication of the position that a group of rods should assume in response to command signals generated within each control system. The actual position indication is generated within the analog rod position indication system and furnishes individual indication of the actual position each rod has assumed in response to the control system command signals. Both actual and demand position information is displayed on the control board and both are monitored by the plant computer as part of the rod deviation monitoring program. A detailed functional description of the analog rod position indication system is presented and a general description of the demand position indication system is also included. (auth)

28670 CONNECTIONS FOR NUCLEAR REACTOR CONTROL ROD DRIVES. (to Siemens Aktiengesellschaft). British Patent 1,225,460. 17 Mar 1971. Priority date 21 Dec 1968, Germany.

REACTOR CONTROL ELEMENTS—drives coupling system for liquid metal cooled reactor
REACTORS, LIQUID METAL-COOLED—control rod drive coupling system for (D.C.C.)

28671 NUCLEAR REACTORS. (to Siemens Aktiengesellschaft). British Patent 1,226,514. 31 Mar 1971. Priority dated 17 Jan 1969, Germany.

REACTOR CONTROL ELEMENTS—drives for liquid sodium cooled, description of coupling system for
REACTORS, LIQUID METAL-COOLED—control rod drives for, description of coupling system for (D.C.C.)

28672 NUCLEAR REACTOR POWER MONITOR SYSTEM. Parkos, Gerald R.; Minor, Gregory C.; Collett, Wells I. (to General Electric Co.). U. S. Patent 3,565,760. 23 Feb 1971. Filed 23 Oct 1967.

A system is described for monitoring the power level of a nuclear reactor and for automatically protecting against excessive local and bulk power levels and for automatically blocking control rod withdrawal to prevent fuel damage. A plurality of nuclear detectors are located within the reactor core, the number and location being selected to provide signals representative of the power level throughout the core. The system utilizes core symmetry and detector signal averaging to provide fault tolerance and to reduce equipment requirements. (auth)

28673 NEUTRON-ABSORBING MEMBER. (to Commissariat a l'Energie Atomique). British Patent 1,225,947. 24 Mar 1971. Priority date 7 Mar 1969, France.

REACTOR CONTROL ELEMENTS—design of helium vented rod type, for liquid sodium cooled reactors
REACTORS, LIQUID METAL-COOLED—control elements for, description of helium vented rod type (D.C.C.)

28674 REACTOR INSTRUMENTATION. Haebler, D. V. Combustion; 42: No. 2, 23-5(Aug 1970).

The safe operation of nuclear power plants is basically a function of the reactor safety system. This system includes the analog measuring devices, an inter-connecting logic and the shutdown system e.g. the control rods of the reactor. The logic between limit functions on one hand and the relay which initiates the counteraction on the other hand is the safety system. The larger the reactor the greater is the number of signals to be accommodated and the safety system logic grows accordingly. The trends of this development are discussed. (12 references.) (auth)

28675 SPECIAL FEATURES OF MEASUREMENTS AND CONTROL FOR NUCLEAR POWER STATIONS COMPARED WITH CONVENTIONAL PLANTS. Weidmann, J.; Ettemeyer, R. Mitt. Ver. Grosskesselbetr.; 50: 94-9(Apr 1970). (In German).

The measurements necessary in nuclear power stations differ from those in conventional plants and the requirements on the measuring instruments are presented. Controls of BWR, PWR and gas cooled reactor plants are described and compared with conventional plant. Criteria of reactor safety are set out. (UKAEA Info. Bull.)

28676 HYDRAULIC CONTROL ROD DRIVE SYSTEM. Germer, John H. (to United States Atomic Energy Commission). U. S. Patent 3,573,166. 30 Mar 1971. Filed 24 Jul 1968.

A system for controlling a nuclear reactor utilizing pressurized coolant for raising control rods out of the reactor core is described. The system positions individual control rods or groups thereof in either an all-in or an all-out position, and incorporates means for assuring fail-safe operation and for position indication of the rods. The simplicity of the system makes it feasible to provide a sufficient number of weak control rods to permit all-in or all-out operation without excessive increments of reactivity. The individual control rods in large thermal reactors, for example, may be operated in groups widely dispersed throughout the core, sufficiently spaced that the rods have little or no interaction; while a fast reactor is much more closely-coupled. While this system is particularly applicable to sodium-cooled fast reactors, it can be adapted to other types of reactors. (auth)

Shielding

28677 (ORNL-tr-2451) STATUS REPORT ON THE STUDY OF THE UPPER NEUTRON SHIELDS OF PHENIX ON 15 APRIL 1969. Brandicourt, G.; (and others) (Commissariat a l'Energie Atomique, Fontenay-aux-Roses (France). Centre d'Etudes Nucleaires). Translated for Oak Ridge National Lab., Tenn.), from report CEA-N-1349. 23p. Dep. NTIS.

Calculations on the upper shielding of the Phenix Fast Reactor are presented for four options and are compared to the design study reference option. The four options are: (1) ordinary graphite; (2) dense graphite; (3) stainless steel; and (4) a mixture of graphite and iron. The shielding options are compared as to: neutron attenuation; radiation damage; cost; activation of materials located over the shield; and consequences of a fuel element cladding failure. 8 references. (H.D.R.)

28678 INSTRUMENT LINES PENETRATING PRIMARY REACTOR CONTAINMENT. AEC Safety Guide 11 1971. Washington, D. C.; Atomic Energy Commission (1971). 3p. Available from United States Atomic Energy Commission, Washington, D. C.

General Design Criteria 55 and 56 require that each line that penetrates primary reactor containment and is part of the reactor coolant pressure boundary or that is connected directly to the containment atmosphere have one automatic valve inside and one automatic valve outside containment "unless it can be demonstrated that the design is acceptable on some other defined basis." A suitable basis which may be used to implement General Design Criteria 55 and 56 for demonstrating the acceptability of a particular group of these lines, namely, instrument lines is presented. (auth)

Cooling Systems

28679 (EUR-4553) STAZ-2: PROGRAMME FOR THE THERMOHYDRAULIC ANALYSIS OF A CHANNEL OF A WATER-MODERATED AND COOLED NUCLEAR REACTOR CORE OPERATING IN THE STATIONARY STATE. Besi, A.; Magri, V.; Previti, G.; Antognetti, G. F. (FIAT, Turin (Italy). Sezione Energia Nucleare, ANSALDO S.p.A., Genoa (Italy)). Mar 1971. 72p. (In Italian). Dep. NTIS (U. S. Sales Only). EUR Lit. 1,250.

The STAZ-2 code, programmed for the IBM 704 computer, is intended for the thermohydraulic analysis of a channel of a water-moderated and cooled nuclear reactor operating in the stationary state. The code takes into consideration cores with a single passage and closed channels with fuel elements of the type of a bundle of sheathed rods or of the slab type, and calculates the distribution of the coolant and fuel, the distribution of the density and the voids, the load losses and the DNB ratio (the ratio of the critical thermal flux and the actual thermal flux). 13 references. (auth)

28680 (GEAP-10207-23) REACTOR PRIMARY COOLANT SYSTEM RUPTURE STUDY. Quarterly Report No. 23, October-December 1970. (General Electric Co., Sunnyvale, Calif. Breeder Reactor Development Operation). Jan 1971. Contract AT(04-3)-189. 58p. Dep. NTIS.

PIPES—failure in reactor cooling systems, probability analysis of
—crack initiation and growth in reactor cooling system, effects of low-cycle fatigue on, (E)
REACTORS, BOILING—cooling systems for, testing of low-cycle fatigue life of carbon and stainless steel piping in, (E)
REACTORS, WATER-COOLED—cooling systems for, failure mechanisms in piping of, (E/T)
STEEL—crack initiation and growth in carbon and Type 304 stainless, effects of low-cycle fatigue on, (E) (D.C.C.)

28681 (GEAP-10221-6) DEFICIENT COOLING. Sixth Quarterly Progress Report, October 1–December 31, 1970. (General Electric Co., San Jose, Calif. Atomic Power Equipment Dept.). Dec 1970. Contract AT(04-3)-189. 18p. Dep. NTIS.

Nine-rod subchannel sampling with typical grid spacers, 4 inches upstream of the sampling section, was accomplished for the first time with the simultaneous sampling of three unique subchannels in the 3 × 3 array. Data were taken with 80 to 100°F water at 100 and 1000 psig, several exit qualities, and mass velocities of 0.5, 1.0, 1.5, and 2×10^6 lb/h-ft^2. The single phase runs showed a good mass balance between the total measured flow and that calculated from subchannel measurements. It was concluded that the center subchannel measurements were reliable. The corner and side subchannel measurements are under some question due to a possibility of leakage past the sampling tube gaskets. The general effect of the grid spacer, when data is compared to that in a clean channel with button spacers instead of grids, is to decrease flow in the center channels and increase it in the side and (apparently) the corner channels. The two-phase data showed a mass defect of over 10% which was attributed to loss of sampling seals discovered at disassembly. This data will be rerun with redesigned sampling tubes which should avoid leakage. (auth)

28682 (JAERI-1202) EVALUATION OF INTEGRITY FOR FAST NEUTRON IRRADIATION EMBRITTLEMENT OF JPDR PRESSURE VESSEL. Fujimura, Tadato; Namatame, Hiroshi; Kodaira, Tsuneo; Suzuki, Komei (Japan Atomic Energy Research Inst., Tokai. Tokai Research Establishment). May 1970. 17p. (In Japanese and English). Dep. NTIS (U. S. Sales Only).

JPDR has operated for a total of 14,096 hrs (18,501 MWD) at the equivalent full power of 45 MW(t) from 1963 to 1969. JAERI is now proceeding with the project to double-up the thermal power of JPDR (JPDR-II) program. In order to confirm the integrity of its pressure vessel concerning the neutron irradiation embrittlement, the surveillance test has been performed three times up to the present. The results of surveillance tests are presented. 16 references. (auth)

28683 THERMAL SHOCK TO REACTOR PRESSURE VESSELS. AEC Safety Guide 2 1970. Washington, D. C.; Atomic Energy Commission (1970). 2p. Available from United States Atomic Energy Commission, Washington, D. C.

Proposed General Design Criterion 35 specifies design and operating conditions necessary to assure that the reactor coolant pressure boundary will behave in a nonbrittle manner. To provide protection against loss of coolant accidents, present designs provide for the injection of large quantities of cold emergency coolant into the reactor coolant system. The effect on the reactor pressure vessel of this cold water injection is of concern because the reactor vessel is subjected to greater irradiation than other components of the reactor coolant pressure boundary and, thus, has a greater potential for becoming brittle. A suitable program which may be used to implement General Design Criterion 35 to assure that the reactor pressure vessel will behave in a nonbrittle manner under loss of coolant accident conditions is described. (auth)

28684 PRESTRESSED CONCRETE PRESSURE VESSELS FOR NUCLEAR REACTORS. de la Camara, Santiago Norena. Energ. Nucl. (Madrid); 14: 391-402(Sep-Oct 1970). (In Spanish).

The development of prestressed concrete pressure vessels for nuclear reactors is explained with emphasis on the reasons for their use in graphite-gas reactors. The characteristics of some pressure vessels constructed or under construction are tabulated, and the distinct types and forms of the vessels are compared. The future possibilities of prestressed concrete pressure vessels and their possible use in reactors other than the graphite-gas type are discussed. The problems caused by prestressed concrete pressure vessels are presented in a general review. The studies being made in the development of this type of pressure vessel and in the reduction of its present costs are also presented. (tr-auth)

Fuels

Refer also to abstracts 26418 and 26438.

28685 (BAW-1355) 1000-MWe LMFBR ACCIDENT ANALYSIS AND SAFETY SYSTEM DESIGN STUDY. TOPICAL REPORT. EFFECTS OF IRRADIATION-INDUCED METAL SWELLING ON THE REFERENCE DESIGN. Goulding, B. J. (Babcock and Wilcox Co., Lynchburg, Va. Nuclear Power Generation Dept.). Nov 1970. Contract 31-109-38-2339. 233p. Dep. NTIS.

For Argonne National Lab., Ill.

The work performed to ascertain the effects of irradiation-induced metal growth on core components subjected to operating characteristics as defined by 1000-MW(e) LMFBR reference design is reviewed. Four metal growth correlations were reviewed and compared. Several possible solutions were evaluated in separate studies, and the results from these studies formed the basis for defining a modified design. This modified design, which utilizes a core clamp device, resulted in a reduction of peak volumetric growth from 35 to 18%. The economic penalty associated with this reduction is less than 0.4 mill/kWh. (32 references) (auth)

28686 (BMI-1898) PROGRESS ON DEVELOPMENT OF FUELS AND TECHNOLOGY FOR ADVANCED REACTORS DURING OCTOBER–DECEMBER 1970. Progress Report. Keller, Donald L. (Battelle Memorial Inst., Columbus, Ohio). Jan 1971. Contract W-7405-eng-92. 110p. Dep. NTIS.

Activities in the development of uranium–plutonium nitride fuels for LMFBR applications, studies of high temperature fuels for advanced fast reactors, and studies of creep of reactor fuel materials are summarized. A separate abstract was prepared for each of the three sections included. (H.D.R.)

For abstracts of individual sections see: 28687–28689.

28687 (BMI-1898, Sect.A) URANIUM–PLUTONIUM NITRIDE FUELS FOR LMFBR APPLICATIONS. (Battelle Memorial Inst., Columbus, Ohio). 38p.

In Progress on development of fuels and technology for advanced reactors during October–December 1970.

EXPERIMENTAL BREEDER REACTOR-II—fuel pins for, fabrication and irradiation testing of plutonium nitride–uranium nitride
LIQUID METAL FAST BREEDER REACTOR—fuels for, development of plutonium nitride–uranium nitride, (E)
NITROGEN—diffusion in plutonium nitride–uranium nitride fuels, self, (E)
PLUTONIUM NITRIDES—PuN–UN, self-diffusion of nitrogen in, (E)
—PuN–UN, irradiation testing of fuels of
RADIATION TARGET CANS—fabrication of fuel irradiation capsule for EBR-2
REACTOR FUEL ELEMENTS—development of sodium-bonded stainless steel clad plutonium nitride–uranium nitride, (E)
—performance of stainless steel clad plutonium nitride–uranium nitride, during transient irradiation, (T)
REACTOR SAFETY EXPERIMENTS—fuel element irradiation in TREAT, analysis of stainless steel clad plutonium nitride–uranium nitride, (T)
URANIUM NITRIDES—PuN–UN, self-diffusion of nitrogen in, (E)
—PuN–UN, irradiation testing of fuels of (H.D.R.)

28688 (BMI-1898, Sect.B) TECHNOLOGY OF NUCLEAR FUELS FOR ADVANCED FAST REACTORS. (Battelle Memorial Inst., Columbus, Ohio). 52p.

In Progress on development of fuels and technology for advanced reactors during October–December 1970.

LIQUID METAL FAST BREEDER REACTOR—fuels for, high temperature irradiation performance of, (E/T)
PLUTONIUM NITRIDES—PuN–UN, radiation effects on high temperature swelling, fission gas release, and microstructure of, (E/T)
PLUTONIUM OXIDES PuO_2—PuO_2–UO_2, radiation effects on high temperature swelling, fission gas release, and microstructure of, (E/T)
REACTOR FUELS—radiation effects on performance of fast, at high temperature, (E/T)
—fission gas diffusion and bubble growth in, (E/T)
URANIUM CARBIDES—radiation effects on high temperature swelling, fission gas release, and microstructure of, (E/T)
URANIUM NITRIDES—PuN–UN, radiation effects on high temperature swelling, fission gas release, and microstructure of, (E/T)
—radiation effects on high temperature swelling, fission gas release, and microstructure of, (E/T)
URANIUM OXIDES UO_2—PuO_2–UO_2, radiation effects on high temperature swelling, fission gas release, and microstructure of, (E/T)

—radiation effects on high temperature swelling, fission gas release, and microstructure of, (E/T)
—fission gas diffusion and bubble growth in, (E/T)
—stoichiometry control of, (E) (H.D.R.)

28689 (BMI–1898, Sect.C) CREEP OF REACTOR FUEL MATERIALS. (Battelle Memorial Inst., Columbus, Ohio). 14p.

In Progress on development of fuels and technology for advanced reactors during October–December 1970.

LIQUID METAL FAST BREEDER REACTOR—fuels for, creep testing of ceramic
PLUTONIUM OXIDES PuO_2—PuO_2–UO_2, creep of, effects of microstructure, stress, temperature, and fissicn process on, (E)
REACTOR FUELS—creep testing of fast ceramic
URANIUM OXIDES UO_2—PuO_2–UO_2, creep of, effects of microstructure, stress, temperature, and fission process on, (E)
—creep of, effects of microstructure, stress, temperature, and fission process on, (E) (H.D.R.)

28690 (EURFNR–836) STOICHIOMETRY SHIFT IN AN OXIDE FUEL ELEMENT AT HIGH BURNUP. Holleck, H.; Kleykamp, H. (Kernforschungszentrum, Karlsruhe (West Germany). Institut fuer Material- und Festkoerperforschung). Translation of report KFK–1181. 66p. Dep. NTIS.

Work Performed under United States–Euratom Fast Reactor Exchange Program.

The contributing factors leading to a change in stoichiometry of an oxide-fuel during burnup are discussed. The arising fission products alter the average final stoichiometry, while gas equilibria above the oxide determines the stoichiometry at a particular point. The thermodynamics of the mixed oxide and of the fission product oxides were studied. Experimental results concerning irradiated samples are discussed and related to equilibrium states in fuels with high burnup. 62 references. (auth)

28691 (GEAP–10028–37) SODIUM-COOLED REACTORS FAST CERAMIC REACTOR DEVELOPMENT PROGRAM. Quarterly Report No. 37, November 1970–January 1971. (General Electric Co., Sunnyvale, Calif. Breeder Reactor Development Operation). Mar 1971. Contract AT(04-3)-189. 109p. Dep. NTIS.

FAST CERAMIC REACTOR—fuel elements for, development during November 1970 to January 1971
—core for, design and kinetic analyses of
—safety of, transient overpower and coolant loss effects on
LIQUID METAL FAST BREEDER REACTOR—fuel elements for, development of stainless steel clad plutonium oxide (PuO_2)–uranium oxide (UO_2)
NEUTRONS, FAST—effects on mechanical properties and swelling of stainless steel fuel element cladding, (E)
PLUTONIUM OXIDES PuO_2—PuO_2–UO_2, radiation effects testing of fuels of
—PuO_2–UO_2, properties of fuels of, mechanical, physical, and thermal, (E)
REACTOR FUEL ELEMENTS—performance of defected mixed uranium oxide (UO_2)–plutonium oxide (PuO_2), in flowing sodium, (E)
—cladding for mixed uranium oxide (UO_2)–plutonium oxide (PuO_2) fast, development and testing of stainless steel
—radiation effects testing of mixed uranium oxide (UO_2)–plutonium oxide (PuO_2) fast
STAINLESS STEEL—radiation effects on swelling and mechanical properties of Type 304, Type 316, and Type 347, fast neutron, (E)
URANIUM OXIDES UO_2—PuO_2–UO_2, radiation effects testing of fuels of (H.D.R.)

28692 (JAERI-memo-4248) ANALYSIS OF INSTRUMENTATION DATA FROM IFA-150 IRRADIATED IN HBWR. Ichikawa, Michio; Morishima, Atsuyoshi; Taketani, Kiyoaki (Japan Atomic Energy Research Inst., Tokyo). Dec 1970. 26p. (In Japanese). Dep. NTIS (U. S. Sales Only).

Irradiation of IFA-150 (Instrumented Fuel Assembly) was started in May 1968 in HBWR and ended in March 1970 with burnup of 11,400 MWD/T. IFA–150 was irradiated with IFA–149, which is of the same design and contains the same fuel as that in IFA–150. The data obtained from these assemblies are quite similar. IFA–150 was aimed to prove the integrity of the fuel rods for JPDR-II project. The fuel rods with diameter of 12.23 mm were arranged in 3 × 3 square lattice. Fuel rods were provided with 2 fission gas transducers, 3 oxide center thermocouples and 8 fuel rod elongation monitors. The data from the instrumentation are analyzed. The maximum linear heat rating of the fuel rods was calculated to be 420 W/cm. 15 references. (Japan)

28693 LOCKING MECHANISM FOR NUCLEAR FUEL ELEMENTS. (to SNAM Progetti SpA). British Patent 1,226,919. 31 Mar 1971. Priority date 24 Sep 1968, Italy.

REACTOR FUEL ELEMENTS—grid locking device for liquid metal cooled rod type
REACTORS, LIQUID METAL-COOLED—fuel elements for, grid locking device for rod type (D.C.C.)

28694 IMPROVEMENTS IN OR RELATING TO NUCLEAR REACTORS. (to Gulf General Atomic Inc.). British Patent 1,226,021. 24 Mar 1971. Priority date 9 Jun 1967, United States.

REACTOR FUEL ELEMENTS—design of gas cooled vented bundle arranged pin type
REACTORS, GAS-COOLED—fuel element assemblies for, description of vented bundle arranged pin type (D.C.C.)

28695 FUEL ASSEMBLIES FOR NUCLEAR REACTORS. Ekwall, Per (to Allmanna Svenska Elektriska Aktiebolaget). British Patent 1,226,826. 31 Mar 1971. Priority date 2 Aug 1967, Sweden.

REACTORS, FAST—fuel element assemblies for steam cooled, description of bundle arranged spaced rod type
REACTORS, SUPERHEATING—fuel elements assemblies for steam cooled fast, description of bundle arranged spaced rod type
REACTOR FUEL ELEMENTS—design of steam cooled bundle arranged spaced rod type (D.C.C.)

28696 SURFACE ROUGHENED FUEL RODS IN LARGE, FAST GAS-COOLED REACTORS. Christensen, E. R. (Technical Univ., Langby, Denmark). J. Nucl. Energy; 24: 573-6 (Dec 1970).

A model for heat transfer calculations of surface roughened fu rods in gas-cooled reactors is set up. Various degrees of roughness of fuel rods are introduced by means of a concept of fictitious maximum fuel rod surface temperature. (auth) (UK)

Auxiliary and Emergency Systems

28697 (CENPD–11) REACTOR PROTECTION SYSTEM DIVERSITY. Copperşmith, W. Carlton; Kling, Charles L.; Shesler, Albert T.; Tashjian, Benjamin M. (Combustion Engineering, Inc., Windsor, Conn. Nuclear Power Dept.). Feb 1971. 168p

The Combustion Engineering Reactor Protection System and other protective functions which are not part of the Reactor Protection System are described, and an evaluation of the Reactor Protective System is presented for the following incidents: Control Element Assembly Withdrawal; Control Element Assembly Drop; Loss of Reactor Coolant Flow; Excess Load; Loss of Load; and Loss of Feedwater. (auth)

28698 (NP–18778) CLADDING MONITORING IN SODIUM-COOLED REACTORS BY DETECTION OF DELAYED NEUTRONS. Jacobi, S.; Schmitz, G. (Kernforschungszentrum, Karlsruhe (West Germany). Labor fuer Elektronik und Messtechnik). Feb 1971. 21p. (In German). Dep. NTIS (U. S. Sales Only).

The detection of fuel pin failures in sodium cooled reactors by monitoring of delayed neutrons is examined. Experimental measurements in the KNK reactor which have led to the design of an improved system for the SNR are described. Calculations are presented to show that the smallest detectable free fuel pin surface is between 0.2 and 2 cm^2. Diagrams indicate the effects of transit time from core to monitor on the neutron activity concentration. 14 references. (auth)

28699 MONITORING OF POWER DISTRIBUTION IN NUCLEAR REACTOR CORES. Emely'anov, I. Ya.; Konstantinov, L. V.; Postnikov, V. V. At. Energ. (USSR); 30: 275–85(Mar 1971). (In Russian).

Modern techniques and sensitive elements applied for power distribution monitoring are considered. Methods of mathematical treatment of discretely located sensitive element signals for restoring continuous power distribution are discussed. Trends in the development of in-core monitoring systems are discussed. (70 references) (auth)

28700 INSULATION AND COOLING SYSTEM FOR A NUCLEAR REACTOR CONDENSER COMPARTMENT. (to Westinghouse Electric Corp.). British Patent 1,226,930. 31 Mar 1971. Priority date 23 Apr 1969, United States.

REACTOR CONTAINMENT SYSTEMS—design of ice condenser, for pressurized water reactor

REACTORS, PRESSURIZED-WATER—containment system for, refrigeration system and thermal insulation for ice condenser
THERMAL INSULATION—design of pressurized water reactor ice condenser containment system (D.C.C.)

28701 NET POSITIVE SUCTION HEAD FOR EMERGENCY CORE COOLING AND CONTAINMENT HEAT REMOVAL SYSTEM PUMPS. AEC Safety Guide 1 1970. Washington, D. C.; Atomic Energy Commission (1970). 1p. Available from United States Atomic Energy Commission, Washington, D. C.

Proposed General Design Criterion 41 requires that the emergency cooling and containment heat removal systems be capable of accomplishing their required safety functions assuming partial loss of installed capacity. In current designs the ability to accomplish these safety functions reliably depends in part on the proper performance of system pumps which, in turn, depends on the conditions under which the pumps must operate. One of these conditions is suction pressure. A suitable relationship between increases in containment pressure caused by postulated loss of coolant accidents and the net positive suction head (NPSH) of emergency core cooling and containment heat removal system pumps which may be used to implement General Design Criterion 41 is described. (auth)

28702 CONTROL OF COMBUSTIBLE GAS CONCENTRATIONS IN CONTAINMENT FOLLOWING A LOSS OF COOLANT ACCIDENT. AEC Safety Guide 7 1971. Washington, D. C.; Atomic Energy Commission (1971). 3p. Available from United States Atomic Energy Commission, Washington, D. C.

General Design Criterion 41 requires that systems to control hydrogen, oxygen, and other substances which may be released into the reactor containment be provided as necessary to control their concentrations following postulated accidents to assure that containment integrity is maintained. An acceptable method of implementing this criterion is described. (auth)

28703 FUEL FAILURE MONITOR FOR PRESSURIZED WATER REACTORS. Power Eng.: 75: No. 4, 72(Apr 1971).

A continuous, direct-reading system for monitoring failures in fuel element claddings is described. The system consists of a scintillation detector which monitors a continuous sample of the coolant for fission products and two ratemeter/analyzers to make the measurement and trigger the alarms. (H.D.R.)

28704 INDEPENDENCE BETWEEN REDUNDANT STANDBY (ONSITE) POWER SOURCES AND BETWEEN THEIR DISTRIBUTION SYSTEMS. AEC Safety Guide 6 1971. Washington, D. C.; Atomic Energy Commission (1971). 2p. Available from United States Atomic Energy Commission, Washington, D. C.

General Design Criterion 17 requires that onsite electrical power systems have sufficient independence to perform their safety functions assuming a single failure. An acceptable degree of independence between redundant standby (onsite) power sources and between their distribution systems is described. (auth)

28705 SELECTION OF DIESEL GENERATOR SET CAPACITY FOR STANDBY POWER SUPPLIES. AEC Safety Guide 9 1971. Washington, D. C.; Atomic Energy Commission (1971). 3p. Available from United States Atomic Energy Commission, Washington, D. C.

General Design Criterion 17 requires that the onsite (standby) power supply for a nuclear power plant be of sufficient capacity and capability to assure that specified acceptable fuel design limits and design conditions of the reactor coolant pressure boundary are not exceeded as a result of anticipated operational occurrences, and the core is cooled and containment integrity and other vital functions are maintained in the event of postulated accidents. Diesel generator sets have been widely used as the power source for the standby power supplies. An acceptable basis for the selection of diesel generator sets of sufficient capacity and margin to implement General Design Criterion 17 is presented. (auth)

Operation and Economics

Refer also to abstracts 26396 and 26558.

28706 (DOCKET-50231-74) SOUTHWEST EXPERIMENTAL FAST OXIDE REACTOR. Quarterly Plant Operations Report No. 7, November 1, 1970–January 31, 1971. (General Electric Co., Sunnyvale, Calif. Breeder Reactor Development Operation). 8 Apr 1971. 29p. Dep. NTIS.

28707 (DOCKET-50231-75) SOUTHWEST EXPERIMENTAL FAST OXIDE REACTOR. Natural Circulation Testing of the Reactor Coolant System. (General Electric Co., Sunnyvale, Calif. Breeder Reactor Development Operation). 6 Apr 1971. 32p. Dep. NTIS.

28708 (DOCKET-50231-77) SOUTHWEST EXPERIMENTAL FAST OXIDE REACTOR. Summary of Results From Testing of the Fast Reactivity Excursion Device. (General Electric Co., Sunnyvale, Calif. Breeder Reactor Development Operation). 12 Apr 1971. 28p. Dep. NTIS.

28709 (DOCKET-50231-78) SOUTHWEST EXPERIMENTAL FAST OXIDE REACTOR. Malfunction of Reactor Vessel Overflow Line Valve and Safety System Relay. (General Electric Co., Sunnyvale, Calif. Breeder Reactor Development Operation). 16 Apr 1971. 5p. Dep. NTIS.

28710 (HEDL-TME-71-26) ENVIRONMENTAL ENGINEERING PROGRAMS. Quarterly Technical Progress Report, October–December 1970. Hofmann, P. L. (comp.) (Hanford Engineering Development Lab., Richland, Wash.). Jan 1971. Contract AT-(45-1)-2170. 23p. Dep. NTIS.

Technical progress in programs for studying the environmental effects of waste heat from nuclear power plants is reported. The development of the COL HEAT and TOPLYR systems for simulating the environmental effects of thermal generation, the regional modeling of surface water temperatures resulting from planned nuclear power plants, and methods for evaluating nuclear power plant heat dissipation methods are included. (L.C.L.)

28711 (ORNL-TM-3253) MSRE PROCEDURES FOR THE PERIOD BETWEEN EXAMINATION AND ULTIMATE DISPOSAL (PHASE III OF DECOMMISSIONING PROGRAM). Guymon, R. H. (Oak Ridge National Lab., Tenn.). 10 Feb 1971. 41p. Dep. NTIS.

The condition of the MSRE and procedures to be followed after the post-operation examinations and before the ultimate disposal of the fissile and radioactive material in the reactor are described. The fuel salt will be kept frozen in the sealed drain tanks, within secondary containment whose only opening is through filters to a stack. Surveillance will consist of remote monitoring and daily visits by X-10 plant personnel. Personnel access will be controlled by the security fence around the reactor building. The MSRE Procedures specify remedial actions for abnormal conditions. Also specified are procedures and responsibilities for maintenance, modifications, and removal of surplus equipment. 9 references. (auth)

28712 REPORT OF THERMAL NEUTRON REACTOR STUDY GROUP. Yuhara, Hiroshi; Hiyama, Tetsuo (Japan Atomic Power Co., Tokyo). FAPIG (Tokyo): No. 55, 155-7; 171(Dec 1969). (In Japanese).

A brief review of the result of studies concerning thermal power reactors by the "Thermal Neutron Reactor Study Group" is presented. AGR, CANDU-PHW, SGHWR, CANDU-BLW, HTGR and MSR were investigated from the technical and economical points of view. The result of studies on AGR and CANDU-PHW are described. Technical advantages are seen in the design of AGR. The cost of construction and power generation, and the actual proof as a practical reactor, however, are still uncertain. CANDU-PHW is a heavy water moderated and cooled reactor having good neutron economics by the use of natural uranium. The required amount of natural uranium is not much, and the enrichment of uranium is not necessary. The cost of construction is expensive, and the cost of fuel is cheap. The report also indicated that it is necessary to study the Pu cycle. (Japan)

28713 COMPUTER SIMULATION OF NUCLEAR REACTOR SYSTEM'S CAPABILITY. Blackstein, F. P.; Wolfe, W. A. (Atomic Energy of Canada Ltd., Chalk River, Ont.). pp 37-9 of DECUS Proceedings. Maynard, Mass.; Digital Equipment Computer Users' Society (1970).

From Digital Equipment Corporation Users Society spring symposium; Atlantic City, N. J. (4 May 1970). See CONF-700524.

The effects of improving component reliability and maintainability on the overall plant capability are discussed. The simulation and programming techniques for a rapid and accurate prediction of nuclear reactor capability are described. A Monte Carlo analysis on the PDP-9 deals with numerous subsystems each containing many components. With minor modifications, the analysis may be applied to the PDP-8 computer series. (auth)

28714 POWER REACTOR STRATEGIES AND THEIR EFFECT ON FUEL CYCLE REQUIREMENTS. Boxer, L. W. (European Nuclear Energy Agency, Paris). Nucl. News; 14: No. 3, 39-43 (Mar 1971).

The influence of fuel demand and available economic fuel re-

sources on the future growth of nuclear power is examined. The results of an European Nuclear Energy Agency study on uranium and thorium resources and production capacity depending on various reactor strategies employed in Western Europe and a given rate of growth of nuclear installed capacity over the next 40 years are presented and discussed. (H.D.R.)

28715 MEDIUM-POWER BOILING-WATER REACTORS FOR DEVELOPING COUNTRIES. Seyfferth, L. (Allgemeine Elektricitaets-Gesellschaft, Frankfurt am Main). pp 3-17 of Small and Medium Power Reactors, 1970. Vienna; International Atomic Energy Agency (1971).

From Small and medium power reactors symposium; Oslo, Norway (12 Oct 1970). See STI/PUB-267; CONF-701046.

The BWR reactor's suitability for developing countries is studied. A description of the experience in construction and the operation of nuclear power plants in various sizes and power ranges should be interesting for developing and less industrialized countries. The design parameters of the most recent medium-size power reactor are presented. The cost structure of the boiling-water reactor nuclear steam supply system and what can influence it are analyzed. The local supply of components from such countries for the reactor system is discussed. (auth)

28716 STANDARDIZED LINE OF PRESSURE-VESSEL TYPE BOILING-WATER REACTORS. Sokolov, I. N.; Bulkin, Yu. M.; Tokarev, Yu. I.; Barskii, M. L. (Inst. of Atomic Energy, Moscow). pp 33-44 of Small and Medium Power Reactors, 1970. Vienna; International Atomic Energy Agency (1971). (In Russian).

From Small and medium power reactors symposium; Oslo, Norway (12 Oct 1970). See STI/PUB-267; CONF-701046.

The advantage of using low- and medium-power reactors in the USSR stems from the fact that there are extensive areas (chiefly local mining areas) in the north and northeast, where organic fuel is very costly. A standardized line of pressure-vessel-type boiling-water-cooled, water-moderated reactors with unit capacities of 12, 25, 50, and 100 MW(e) has been developed to supply electrical power and heat to these regions. The choice of the type of reactor for use in remote regions is determined by the following considerations: the pressure-vessel type design makes it possible to carry out the basic construction work for the reactor in the factory; the single-circuit system used in the facility reduces its cost; the natural circulation of the coolant inside the pressure vessel provides a reliable system of heat removal under all operating conditions; and low-enrichment uranium dioxide in zirconium cladding makes for an economical fuel cycle. The operational reliability of reactors of this type has been confirmed by five years' experience with the VK-50 facility at Melekess. Data are given on power generation and specific investment costs of power plants of the series in question, as a function of the remoteness of the area of construction and local conditions, such as base or peak load, generation of only one type of power, and nature of water supply. The influence of the number of units (reactor-turbine) in a single power plant on its economics and on the possibility of operation under autonomous conditions is analyzed. Efforts are being made to increase the power intensity in the core by improving heat exchange and reducing the volume coefficient of non-uniform energy release. (8 references.) (auth)

28717 BELGONUCLEAIRE AND SIEMENS PWRs FOR SMALL AND MEDIUM POWER REACTORS. Storrer, J. (BelgoNucleaire SA, Brussels); Gallois, G.; Kafka, P. pp 131-60 of Small and Medium Power Reactors, 1970. Vienna; International Atomic Energy Agency (1971).

From Small and medium power reactors symposium; Oslo, Norway (12 Oct 1970). See STI/PUB-267; CONF-701046.

The successive stages of growth the electricity consumption of a country goes through are described. A market study which was performed in 1966-1968 for small power reactors (20 to 120 MW(e)) is reviewed. The advantages and improvements of the PWR are outlined. The expected costs over the 50- to 500-MW(e) range are finally indicated, together with the generation costs per kilowatt-hour. (8 references.) (auth)

28718 CANADIAN APPROACH TO DESIGNING AND BUILDING FOREIGN NUCLEAR POWER STATIONS. Johnston, R. C. (Canadian General Electric Co. Ltd., Peterborough, Ont.). pp 163-72 of Small and Medium Power Reactors, 1970. Vienna; International Atomic Energy Agency (1971).

From Small and medium power reactors symposium; Oslo, Norway (12 Oct 1970). See STI/PUB-267; CONF-701046.

On May 30, 1970 the construction of Canada's first foreign nuclear power station was completed. The favorable progress against a tight schedule and under difficult conditions was the result of a few key decisions on organization and handling of the project. These decisions are discussed and are related to actual progress and performance. (auth)

28719 USING THE HIGH-TEMPERATURE REACTOR FOR POWER GENERATION BELOW 500 MW(e). Lockett, G. E. (OECD High Temperature Reactor Project, Winfrith, Eng.). pp 211-23 of Small and Medium Power Reactors, 1970. Vienna; International Atomic Energy Agency (1971).

From Small and medium power reactors symposium; Oslo, Norway (12 Oct 1970). See STI/PUB-267; CONF-701046.

The high-temperature helium-cooled reactor has developed through a number of phases to the point where exploitation of the system for large-scale power generation is beginning. Earlier work was concentrated on systems using highly enriched fissile material but the study of systems using uranium of low enrichment has made the system more attractive commercially in Europe at the present time. Previous Dragon Project power reactor studies have led towards the development of low-enriched homogeneous design but they have been based on large units, not less than 500 MW(e). Smaller systems are described, and some preliminary predictions on station costs are presented. Some of the general aspects of the high-temperature reactor concept are also briefly described. To illustrate the design possibilities an outline arrangement of a reactor for a 250-MW(e) power plant is included and a general description of its main features are given. The engineering solutions used follow directly from the larger systems and there is no difficulty in producing a good sound design. Cost predictions are, however, based at this stage on a simple evaluated extrapolation from the 1968/1969 costing of a 630-MW(e) plant. (auth)

28720 UNITED KINGDOM REACTORS AVAILABLE FOR COMMERCIAL OPERATIONS IN THE OUTPUT RANGE UP TO 500 MW. Bainbridge, G. R.; Parry, A.; Marques de Souza, J. A. (United Kingdom Atomic Energy Authority, Risley, Eng.). pp 375-94 of Small and Medium Power Reactors, 1970. Vienna; International Atomic Energy Agency (1971).

From Small and medium power reactors symposium; Oslo, Norway (12 Oct 1970). See STI/PUB-267; CONF-701046.

The available reactor types are described which are considered to be competitive in the range 0 to 500 MW. The economics of burnable poison pressurized-water reactors and steam-generating heavy-water-moderated reactors as developed for this size range in the United Kingdom are dealt with in detail, the BPWRs at the lower end of the scale and SGHWRs in the larger sizes. The cost of any nuclear power station is dependent upon many factors such as the customer's specification, site conditions, type of contract, single or multiple units, in addition to the type of reactor. The distinction is drawn between an indicative price and one associated with a known set of such factors and including a detailed cost assessment, which can lead to a quite different result. Reference is made to the fuelling arrangements for reactors, and the effects of these and the operation methods on the electricity generating costs. A comparison is introduced between the generating costs of nuclear and oil-fired stations, and it can be seen that in the very small sizes nuclear stations are likely to be competitive only in remote areas or for special applications. (auth)

28721 SOME TECHNICAL ASPECTS AND THE ECONOMY OF THE AEG-BWR FUEL CYCLE. Mattern, J. (AEG-Telefunken, Frankfurt am Main). pp 433-40 of Small and Medium Power Reactors, 1970. Vienna; International Atomic Energy Agency (1971).

From Small and medium power reactors symposium; Oslo, Norway (12 Oct 1970). See STI/PUB-267; CONF-701046.

Three aspects concerning incorporation of a 300- to 500-MW(e) boiling-water reactor in a fairly small grid are analyzed. The first question is how to start the reactor from cold conditions even in an extreme case, where no or little energy is available. Because of the excellent natural recirculation capabilities of the BWR this can be done in a reasonable time with the aid of power supplied by emergency diesel power. The diesel capacity required does not exceed that for emergency cooling purposes. The second point is the behavior of the boiling-water reactor in view of the load-following requirements of a small grid. It is demonstrated that large power ramps and power steps can be accommodated. Even in the case of a load rejection and turbine trip the reactor can be held on line. The third point is how the fuel cycle can be designed for the requirement of small grids, where it is difficult to forecast projected power supplies. The described procedure, which is based on the decrease of void content in the reactor core at the end of the burnup cycle, offers additional possibilities of cost savings. (auth)

28722 FUEL-CYCLE EVALUATION CRITERIA FOR AN INTERMEDIATE-POWER REACTOR. Lartigue, J.; Ortega, R. F. (Comision Nacional de Energia Nuclear, Mexico City). pp 441-58 of Small and Medium Power Reactors, 1970. Vienna; International Atomic Energy Agency (1971). (In Spanish).

From Small and medium power reactors symposium; Oslo, Norway (12 Oct 1970). See STI/PUB-267; CONF-701046.

Results and criteria applied by a group studying fuel sale offers submitted to the Federal Electricity Commission and the National Nuclear Energy Commission in connection with the construction of Mexico's first power reactor are described. The reactor is an intermediate-power reactor which is to go into commercial operation within the Mexican electricity generating system in 1975. Seven tenders relating to four reactor types (PWR, BWR, HWR, AGR) in the range 540–660 MW(e) were studied; in some cases, alternatives were offered in respect of rated power, fuel regime and other features of an economic nature. In carrying out its evaluation, the group considered a number of factors which are important from the point of view of defining the fuel cycle and determining its associated costs as completely as possible. These factors included: the feasibility of using uranium mined in Mexico; the possibility of local fuel fabrication; the prospects for using the plutonium. The economic effect of various kinds of short- and long-term cost escalation at different stages in the fuel cycle is analyzed. It is felt that the evaluation criterion described will be of use in future evaluations of intermediate-power reactors to be built in Mexico. (12 references.) (auth)

28723 FACTORS DETERMINING THE INTRODUCTION OF NUCLEAR POWER STATIONS IN DEVELOPING COUNTRIES: THE CASE OF CHILE. Alvarado, S. (Comision Chilena de Energia Nuclear, Santiago de Chile); Friedmann, E.; Covarrubias, A. pp 459-76 of Small and Medium Power Reactors, 1970. Vienna; International Atomic Energy Agency (1971). (In Spanish).

From Small and medium power reactors symposium; Oslo, Norway (12 Oct 1970). See STI/PUB-267; CONF-701046.

Background material on the energy situation and electricity generation in Chile is presented. The factors which may favor or hinder the introduction of nuclear power stations in developing countries are discussed. The case of Chile is taken as an example. Various general conclusions are drawn and an explanation is given for the fact that Chile is considering short-term nuclear solutions although, by conventional standards, such solutions do not appear to constitute the most economic approach. Certain measures of an international or regional nature which might facilitate the integration of nuclear power stations in the electric power systems of developing countries are described. (14 references.) (auth)

28724 PROBLEMS ENCOUNTERED IN THE INITIATION OF A NUCLEAR POWER PROGRAM IN TURKEY. Aybers, N. (Technical Univ., Istanbul). pp 477-91 of Small and Medium Power Reactors, 1970. Vienna; International Atomic Energy Agency (1971).

From Small and medium power reactors symposium; Oslo, Norway (12 Oct 1970). See STI/PUB-267; CONF-701046.

There are many concealed difficulties in beginning a nuclear power program in a developing country. The installation of such a power station makes little sense if it does not fit into a long-range nuclear power program within the framework of the general policy of the utilization of energy resources. All cost considerations favor larger reactors, but there are difficulties in integrating a large nuclear power station into the relatively small interconnected system of a developing country. However, medium-size reactors might prove economic in high fuel cost areas. Therefore, the particular circumstances in each individual country must be evaluated. Much preparatory work is required before making a start with a nuclear power supply, and a number of special problems may arise. The problems faced by a developing country about to install its first nuclear power station are discussed. Factors involved in the decision to have recourse to nuclear power are examined, and topics such as optimal size selection, policy for nuclear fuel cycle and the choice of a reactor type are reviewed. The results of these analyses as applied specifically to Turkey are presented. To put the problem in the correct frame a survey of nuclear energy perspectives in Turkey is made, showing a market for medium-size nuclear power plants during the next 20 years. (8 references.) (auth)

28725 PERSONNEL SELECTION AND TRAINING. AEC Safety Guide 8 1971. Washington, D. C.; Atomic Energy Commission (1971). 1p. Available from United States Atomic Energy Commission, Washington, D. C.

Subdivision 50.34 (b) (6) (i) of 10 CFR Part 50 requires that nuclear power plant operating license applications include information concerning organizational structure, personnel qualifications, and related matters. An acceptable method of implementing this portion of the Commission's regulations with regard to personnel qualifications is described. (auth)

Safety and Siting

28726 (AI-AEC-12986) LMFBR SAFETY PROGRAMS QUARTERLY TECHNICAL PROGRESS REPORT, OCTOBER-DECEMBER 1970. (Atomics International, Canoga Park, Calif.). 22 Feb 1971. Contract AT(04-3)-701. 41p. Dep. NTIS.

LIQUID METAL FAST BREEDER REACTOR—safety programs during October to December 1970
—coolant combustion accidents in, release and transport of aerosols and energy from sodium, (E/T)
—kinetics of, effects of sodium coolant boiling on, (E/T)
REACTOR FUEL ELEMENTS—explosion in liquid sodium of uranium oxide (UO_2), mechanical energy conversion efficiency and particle size distribution from, (E)
REACTOR SAFETY—coolant combustion accidents in liquid metal cooled reactors, release and transport of aerosols and energy from sodium
SODIUM—combustion in liquid metal cooled reactor accidents, release and transport of aerosols and energy from, (E/T)
—boiling in liquid metal cooled reactors, initiation and thermal hydraulics aspects of, (E/T) (H.D.R.)

28727 (ANL-7607) SAS1A: COMPUTER CODE FOR THE ANALYSIS OF FAST-REACTOR POWER AND FLOW TRANSIENTS. Carter, J. C.; Fischer, G. J.; Heames, T. J.; MacFarlane, D. R.; McNeal, N. A.; Sha, W. T.; Sanathanan, C. K.; Youngdahl, C. K. (Argonne National Lab., Ill.). Oct 1970. Contract W-31-109-eng-38. 294p. Dep. NTIS.

The SAS1A computer code is a comprehensive code designed for analyzing both flow and power transients for the large LMFBR cores. The models, numerical methods, and programming details used in its development as well as the input–output, including a sample problem, are described. Since SAS1A is intended to be a complete accident package, the analysis can be carried from a normal operating state of the reactor up to and through thresholds for irreversible fuel and/or cladding damage, finally terminating in core disassembly (if prior calculated events so dictate). SAS1A is the first in a planned series of SAS codes which are currently under development. The code is available in CDC-3600 and IBM-360 (75) versions from the Argonne Code Center. 18 references. (auth)

28728 (ANL-7701) VENUS: TWO-DIMENSIONAL COUPLED NEUTRONICS-HYDRODYNAMICS COMPUTER PROGRAM FOR FAST-REACTOR POWER EXCURSIONS. Sha, W. T.; Hughes, T. H. (Argonne National Lab., Ill.). Oct 1970. Contract W-31-109-eng-38. 114p. Dep. NTIS.

A new computational model for fast-reactor disassembly analyses is presented. The model utilizes the space-independent neutronics, two-dimensional (RZ) Lagrangian hydrodynamics, and an energy-density-dependent equation of state. The reactivity feedbacks due to Doppler broadening and material motion are explicitly taken into account. This model can analyze both high- and low-density systems in contrast with the modified Bethe–Tait methods, which are valid only for the low-density systems. A unique feature of this model is its pointwise description of core material contents so that an appropriate equation of state corresponding to sodium-in and sodium-out conditions can be assigned. Another is its rigorous treatment of implosion effects at any arbitrary boundary surface, such as a void region surrounded by a nonvoid region or at the interface of two regions of a zoned core. The total energy release during a nuclear excursion calculated from this model is much lower (except for a completely voided core) than the values obtained from the modified Bethe–Tait methods. 43 references. (auth)

28729 (BAW-1342) 1000-MWe LMFBR ACCIDENT ANALYSIS AND SAFETY SYSTEM DESIGN STUDY. TOPICAL REPORT. ACCIDENT ANALYSIS METHODS. Scott, J. H.; Stevenson, M. G.; Moore, R. W. (Babcock and Wilcox Co., Lynchburg, Va. Power Generation Div.). Nov 1970. Contract 31-109-38-2339. 117p. Dep. NTIS.

For Argonne National Lab., Ill.

The methods and models that will be used in the Accident Analysis and Safety System Design Study (AASSDS) are described. In most cases the rationale for methods selection is given; in other cases, only a single model seemed adequate for a particular application, and this is stated. Insofar as possible, the way that selected methods will be applied to the analysis is indicated. In addition, significant problem areas in fast reactor safety are discussed along with their importance to accident analyses. In some cases, prospective solutions are discussed. The appendix provides detailed descriptions of the computer programs that will be used in the accident analyses but are not widely known in the nuclear industry. 43 references. (auth)

XUM

28730 (BAW–1349) 1000-MWe LMFBR ACCIDENT ANALYSIS AND SAFETY SYSTEM DESIGN STUDY. TOPICAL REPORT. CANDIDATE SECONDARY CONTAINMENT SUPPORT SYSTEMS. Honig, H.; Burris, J. R.; DuBois, Q. B. (Babcock and Wilcox Co., Lynchburg, Va. Power Generation Div.). Nov 1970. Contract 31-109-38-2339. 127p. Dep. NTIS.

For Argonne National Lab., Ill.

The work performed to complete Activity 244 (Review and Identify Candidate Secondary Containment Support Systems) of the 1000-MW(e) LMFBR Accident Analysis and Safety System Design Study is described. Resultant temperature and pressure effects of spray fires and pool fires were investigated to determine features and systems that might be required to protect the public. A literature survey on reactor containments was conducted to determine the minimum practical leak rate to be expected from the containment building. Environmental calculations were then made using this leak rate as a means of determining the maximum allowable concentration of fission products, sodium-24, and plutonium in the containment building. Suggested features and systems are presented as possible candidates. 24 references. (auth)

28731 (BAW–1350) 1000-MWe LMFBR ACCIDENT ANALYSIS AND SAFETY SYSTEM DESIGN STUDY. ACCIDENT-INITIATING CONDITIONS. PART 1. FLOW ABNORMALITIES. Topical Report. Scott, J. H.; Moore, R. W. (Babcock and Wilcox Co., Lynchburg, Va. Nuclear Power Generation Dept.). Nov 1970. Contracts 31-109-38-2339; 847-0501. 103p. Dep. NTIS.

For Argonne National Lab., Ill.

Two broad categories of initiating conditions with the reactor at power were investigated: flow abnormalities arising in the primary loop and abnormalities arising in the secondary loop. The TART computer program with point kinetics and multiregion thermal model was used to study these transient conditions. In addition, the analog computer model was used to investigate certain phenomena relating to abnormalities of the secondary loop. The following abnormalities of the primary loop were investigated: (1) Complete loss of six primary pumps; (2) Complete loss of two primary pumps; and (3) Double-ended break in a 28-inch primary pipe. Instantaneous loss of the heat sink was the only event investigated under secondary loop abnormalities. Appropriate sensitivity studies were performed for each of the two broad categories investigated. The results of these calculations indicate that no fuel melting or cladding failure occurs for any transient so long as the protective system functions normally. As to flow abnormalities in the primary loop, three levels of protection may be by passed before failure thresholds are approached. If one postulates such partial failure of the protection system and a rapid flow decay, then high cladding temperatures occur in the hot pin. These temperatures are probably sufficient to cause some cladding failure. On the basis of these studies it is concluded that no irreversible damage results from identifiable flow abnormalities unless partial failure of the protection system is postulated. At least three levels of protection must fail (three simultaneous faults) before even limited cladding failure can occur. Thus, the probability that flow abnormalities at full power will lead to gross core damage is extremely small. (auth)

28732 (BAW–1351) 1000-MWe LMFBR ACCIDENT ANALYSIS AND SAFETY SYSTEM DESIGN STUDY. CANDIDATE EMERGENCY DECAY HEAT REMOVAL SYSTEMS. Topical Report. Honig, A. L.; Mercado, A. L. (Babcock and Wilcox Co., Lynchburg, Va. Nuclear Power Generation Dept.). Nov 1970. Contracts 31-109-38-2339; 847-0501. 85p. Dep. NTIS.

For Argonne National Lab., Ill.

Candidate systems for emergency decay heat removal were identified and developed to the extent required for an initial screening of questionable systems. These systems were based on anticipated requirements which were arbitrarily imposed pending results from other activities which will establish the functional requirements for the emergency decay heat removal system. The possibility of containing molten fuel was examined along with various ways of cooling it. This investigation covered: (a) meltdown pan features and requirements to determine the possibility of containing molten fuel from a hypothetical seven-fuel assembly meltdown inside the core vessel, (b) a sodium-cooled pan located outside the primary tank to accommodate the entire molten core as a last-ditch cooling system, and (c) characteristics governing the potential for natural circulation of primary sodium under a range of thermal duties. Based on a simplified melt-through model, the results of a transient thermal analysis indicate that for a hypothetical seven-fuel assembly meltdown, melt-through can be reasonably precluded as long as the pony motors are operable and provide 5% of the total flow rate In the event of a total core meltdown, the transient-temperature analysis indicates that natural convection cooling is a very effective means in preventing melt-through. 19 references. (auth)

28733 (BAW–1352) 1000-MWe LMFBR ACCIDENT ANALYSIS AND SAFETY SYSTEM DESIGN STUDY. CANDIDATE PRIMARY CONTAINMENT SAFETY FEATURES. Topical Report. Dossett, J. S.; Masseth, F. X. (Babcock and Wilcox Co., Lynchburg, Va. Nuclear Power Generation Dept.). Nov 1970. Contracts 31-109-38-2339; 847-0501. 90p. Dep. NTIS.

For Argonne National Lab., Ill.

The work performed to complete Activity 243 (Identify and Review Candidate Primary Containment Safety Features) of the 1000-MW(e) LMFBR Accident Analysis and Safety System Design Study is described. A literature survey was conducted to determine the potential accident conditions in the primary containment and to find potential candidate solutions to the problems. Underwater TNT-equivalent explosions were assumed, and the resultant loading conditions were calculated. Suggested features are presented as possible methods of solution. 12 references. (auth)

28734 (BAW–1354) 1000-MWe LMFBR ACCIDENT ANALYSIS AND SAFETY SYSTEM DESIGN STUDY. CANDIDATE PROTECTIVE FEATURES. Topical Report. Wilson, R. C. (Babcock and Wilcox Co., Lynchburg, Va. Nuclear Power Generation Dept.). Nov 1970. Contracts 31-109-38-2339; 847-0501. 68p. Dep. NTIS.

For Argonne National Lab., Ill.

The work performed to complete Activity 241 (Review and Identify Candidate Protective Features) of the 1000-MW(e) LMFBR Accident Analysis and Safety System Design Study is described. A literature survey was conducted to determine the approach to protection taken in other LMFBR designs, and to identify protective features (especially instruments) that may be available. An updated estimate of possible protective requirements was prepared to help guide the effort. An initial assessment resulted in identification of several possible candidate features. The major unresolved problem area is in determining and providing the protection needed for local accidents that may initiate within a fuel assembly. 59 references. (auth)

28735 (BAW–1360) 1000-MWe LMFBR ACCIDENT ANALYSIS AND SAFETY SYSTEM DESIGN STUDY. ACCIDENT INITIATING CONDITIONS. PART 2. REACTIVITY INSERTIONS. Scott, J. H. (Babcock and Wilcox Co., Lynchburg, Va. Nuclear Power Generation Dept.). Oct 1970. Contract 31-109-38-2339. 37p. Dep. NTIS.

For Argonne National Lab., Ill.

The consequences of reactivity insertions arising from definable malfunctions or events have been investigated. The specific events that were identified, without regard to credibility, are as follows: single rod withdrawn at 30 in./s; continuous withdrawal of four regulating rods at shim speed; gas bubble(s) entrained in the coolant; loading accidents; moderator entrainment; sudden fuel movement; and drop in inlet temperature. All of these accidents were investigated to some extent; the last four were eventually dropped when the investigations indicated that the events required to produce dangerous conditions were extremely improbable. In addition to the mechanistic study outlined above, a series of calculations was performed to determine the dynamic response of the reactor to arbitrary ramp reactivity insertions. This permitted the defining of parameters related to the protection system design, and the determining of intrinsic stability of the reactor. The results of these investigations are summarized. (10 references) (auth)

28736 (DOCKET-50231–76) SOUTHWEST EXPERIMENTAL FAST OXIDE REACTOR. Change No. 3 to Technical Specifications of Provisional Operating License No. DR-15. (Division of Reactor Licensing (AEC), Washington, D. C.). 12 Apr 1971. 7p. Dep. NTIS.

Revised technical specifications are presented for release limits for radioactive effluents and qualifications of personnel. (D.C.C.)

28737 (IN–1445) THETA1-B: A COMPUTER CODE FOR NUCLEAR REACTOR CORE THERMAL ANALYSIS. Hocevar, C. J.; Wineinger, T. W. (Idaho Nuclear Corp., Idaho Falls). Feb 1971. Contract AT(10-1)-1230. 112p. Dep. NTIS.

A digital computer code, THETA1-B, was developed to study the thermal response characteristics of a nuclear fuel rod subjected to a postulated loss-of-coolant accident environment. The energy equations for both the fuel rod and the adjacent fluid channel are solved. A heat transfer model is employed to link the solutions of the two energy equations. This model has been developed on the basis of heat transfer correlations available in the open literature. The code has the capability of modeling electrically heated test

XUN

elements. This feature allows the postulated heat transfer model to be evaluated in terms of experimental heat transfer data obtained during decompression tests. (33 references) (auth)

28738 (NP-18781) DANGER CONTAINED IN A STEAM-COOLED FAST BREEDER REACTOR AND THE DOSE VALUE RELEASED TO THE ENVIRONMENT IN A SEVERE ACCIDENT. Mueller, R. A. (Kernforschungszentrum, Karlsruhe (West Germany). Institut fuer Reaktorentwicklung). Dec 1970. 57p. (In German). Dep. NTIS (U. S. Sales Only).

The requirements to be met by the containment system of the 1000 MW(e) steam cooled fast breeder reactor D 1 are analyzed using the method proposed by Blässer and Wirtz. For this purpose the "quantity of danger" of the predominant fission products and the nuclear fuel contained in the reactor core is calculated. By use of "outflow factors" the "effective danger outflow" is obtained for the maximum credible accident. Taking into account a "meteorological propagation factor" this yields directly the dose values. It is shown that a double containment is required for the respective plant to achieve sufficiently low dose values. 12 references. (auth)

28739 (RT/ING-(70)25) CONTAINMENT DESIGN CRITERIA FOR SODIUM COOLED FAST REACTORS. Bruzzi, L.; Cicognani, G.; Tavoni, R.; Travaglini, N. (Comitato Nazionale per l'Energia Nucleare, Rome (Italy)). 12 Nov 1970. 28p. (In Italian). Dep. NTIS (U. S. Sales Only).

The differences between the containment philosphy for sodium cooled fast reactors and for other types of reactors in connection with the selected "Design Basis Accident" are discussed. The general containment design criteria for fast reactors are analyzed; in particular the design criteria adopted for the reference fast power reactor PCC are identified and defined. (auth)

28740 RELIABILITY ANALYSIS FOR THE EVALUATION OF REACTOR SYSTEMS. Maurer, Hans A. Tech. Ueberwach.; 10: 412-14(Dec 1969). (In German).

The reliability analysis is a useful means for comparing systems in order to find out possible constructive defects in the design of a circuit and to point out measures of improvement. Due to the errors in empirically determined data no quantitative data can be obtained yet. When using calculating formulas care must be taken to make sure that the simplifications made are also practicable for the case in question. It is considered necessary to collect a large number of representative data. Since no quantitative information concerning the safety of a system or a total analysis is possible yet with the means available a reliability analysis cannot yet be used as a basis for an authorization procedure. (auth)

28741 USE OF ACTUATORS AS LOGIC ELEMENTS IN RELATION TO FAIL-SAFE DESIGN. Epler, E. P.; Ditto, S. J. Nucl. Safety; 12: 226-33(May-Jun 1971).

Some of the principles governing current designs of electrical or electronic voting logic systems can be applied to the design of control and protection systems where the voting logic is at the level of the large electromechanical devices that act directly to control a process. This application is of particular benefit in systems for which there may be a significant penalty for failure in the so-called safe mode as well as in the unsafe mode. Such systems have frequently made use of "failure-to-danger" techniques, which in some areas might lead to a compromise of safety objectives. The use of actuators as logic elements allows the design of simpler systems, with more complete testability, and can provide an ultimate gain in safety. (auth)

28742 ASSUMPTIONS USED FOR EVALUATING THE POTENTIAL RADIOLOGICAL CONSEQUENCES OF A LOSS OF COOLANT ACCIDENT FOR PRESSURIZED WATER REACTORS. AEC Safety Guide 4 1970. Washington, D. C.; Atomic Energy Commission (1970). 6p. Available from United States Atomic Energy Commission, Washington, D. C.

Section 50.34 of 10 CFR Part 50 requires that each applicant for a construction permit or operating license provide an analysis and evaluation of the design and performance of structures, systems, and components of the facility with the objective of assessing the risk to public health and safety resulting from operation of the facility. The design basis loss of coolant accident (LOCA) is one of the postulated accidents used to evaluate the adequacy of these structures, systems, and components with respect to the public health and safety. Acceptable assumptions are presented that may be used in evaluating the radiological consequences of this accident for a pressurized water reactor. In some cases, unusual site characteristics, plant design features, or other factors may require different assumptions which will be considered on an individual case basis. (auth)

28743 ASSUMPTIONS USED FOR EVALUATING THE POTENTIAL RADIOLOGICAL CONSEQUENCES OF A LOSS OF COOLANT ACCIDENT FOR BOILING WATER REACTORS. AEC Safety Guide 3 1970. Washington, D. C.; Atomic Energy Commission (1970). 13p. Available from United States Atomic Energy Commission, Washington, D. C.

Section 50.34 of 10 CFR Part 50 requires that each applicant for a construction permit or operating license provide an analysis and evaluation of the design and performance of structures, systems, and components of the facility with the objective of assessing the risk to public health and safety resulting from operation of the facility. The design basis loss of coolant accident (LOCA) is one of the postulated accidents used to evaluate the adequacy of these structures, systems, and components with respect to the public health and safety. Acceptable assumptions are presented that may be used in evaluating the radiological consequences of this accident for a boiling water reactor. In some cases unusual site characteristics, plant design features, or other factors may require different assumptions which will be considered on an individual case basis. (auth)

28744 ASSUMPTIONS USED FOR EVALUATING THE POTENTIAL RADIOLOGICAL CONSEQUENCES OF A STEAM LINE BREAK ACCIDENT FOR BOILING WATER REACTORS. AEC Safety Guide 5 1971. Washington, D. C.; Atomic Energy Commission (1971). 4p. Available from United States Atomic Energy Commission, Washington, D. C.

Section 50.34 of 10 CFR Part 50 requires that each applicant for a construction permit or operating license provide an analysis and evaluation of the design and performance of structures, systems, and components of the facility with the objective of assessing the risk to public health and safety resulting from operation of the facility. The steam line break accident is one of the postulated accidents used to evaluate the adequacy of these structures, systems, and components with respect to the public health and safety. Acceptable assumptions that may be used in evaluating the radiological consequences of this accident for a boiling water reactor are presented. (auth)

Power Conversion Systems

28745 IMPROVEMENTS TO ENERGY PRODUCTION PLANTS (to Societe Babcock-Atlantique). French Patent 1,593,817. 1 Jun 1970. Filed 29 Nov 1968. (In French).

A motive power production process is described, of use in particular to adapt a condensation steam cycle unit, supplying a variable-demand network, to a constant-output heat source such as a nuclear reactor. During slack hours or periods of low demand on the network, steam is removed from the condensation cycle and the heat stored in the form of useful heat by transfer to a liquid. This is used in peak hours as a heat source to supply an absorption cycle energy production unit which includes the degassing of an aqueous ammonia solution, the superheating and expansion of the gas with energy production and its reabsorption by the depleted solution in the degasser. The corresponding motive power device is also described. It contains a liquid reservoir, means of storing heat in this liquid by heat exchange with steam extracted from the condensation cycle, and an independent energy production unit using the reservoir as a heat source and including an aqueous ammonia solution degasser, a gas turbine, and an absorber adapted to receive the depleted solution leaving the degasser and enrich it by absorption of the gas escaping from the turbine. (auth) (France)

28746 IMPROVEMENTS IN VAPOR GENERATORS. (to Combustion Engineering Inc.). British Patent 1,224,856. 10 Mar 1971. Priority date 4 Jun 1968, United States.

BOILERS—design of molten salt and liquid metal cooled reactor
REACTORS, LIQUID METAL-COOLED—boilers for
REACTORS, MOLTEN-SALT—boilers for (D.C.C.)

28747 METHOD OF AND APPARATUS FOR THE PRODUCTION OF POWER. Mailliet, Ennemond (to Commissariat a l'Energie Atomique). British Patent 1,227,386. 7 Apr 1971. Priority date 30 Jun 1967, France.

REACTORS, GAS COOLED—power production system for, with means for heat storage during off-peak operation
REACTORS, POWER—power production system for gas cooled, with means for heat storage during off-peak operation (H.D.R.)

28748 CALCULATION AND DESIGN OF BOILERS IN NUCLEAR POWER STATIONS. Upmalis, A. Waerme; 76: No. 1/2, 1-8(1970). (In German).

A review is presented of the literature dealing with the calcula-

XUM

tion of boilers for use in nuclear power stations, especially the heat transfer and stresses. The arrangement of the boiler tubes, horizontal or vertical, is discussed and typical designs of both types of boiler presented. Of special interest are the boilers for the nuclear ship "Otto Hahn" in which cross-counterflow is used for the once-through boiler and the boiler for the helium-neon cooled reactor at Julich power station which was helically wound tubes. (UKAEA Info. Bull.)

28749 IMPROVEMENTS IN HEAT EXCHANGERS. Peters, Martin Charles; Perrin, Alfred James (to Babcock and Wilcox Ltd.). British Patent 1,225,967. 24 Mar 1971. Filed 22 Mar 1967.

Reference is made to heat exchangers of the tubular type as used in liquid metal cooled nuclear reactors. The heat exchanger described is designed to overcome some of the problems which arise with such exchangers, notably localized and fluctuating overheating and unstable fluid flow in the tubes, which could lead to tube failure due to thermal stresses. The construction includes sleeves or collars which define stagnant liquid metal flow spaces either around individual tube regions or groups of individual tube regions which are liable to the foregoing problems. This arrangement restricts the rate of heat transfer to a rate less than that giving rise to these problems, while allowing full heat transfer over the remainder of the tubes. The sleeves or collars may be supported from a grid plate. (UK)

28750 COMPARISON OF VARIOUS STEAM CIRCUITS AND OPTIMIZATION OF STEAM TEMPERATURE FOR SODIUM-COOLED FAST BREEDERS. Fischer, R.; Geruschkat, K.; Ratzel, W. (INTERATOM, Bensberg, Ger.). Atomwirt., Atomtech.; 16: 191-3(Apr 1971). (In German).

To optimize the design of sodium-cooled fast breeder reactors, steam circuits and optimal temperature gradients were studied for a 300 MW(e) and a 1000 MW(e) installation. Investigation proceeded in four steps: changes in efficiency and cost were analyzed for intermediate heat exchanger, steam producer, and steam power plant; the economy of the reactor was computed under various conditions for constant electricity production; the consumption of the reactor itself was calculated; and cost of the fuel cycle was calculated and included in the overall computation. Results were compiled in four tables. With respect to future large scale power plants, a steam circuit was selected that possessed thermal drying and a steam temperature of 500°C. (H.B.G.)

28751 STEAM GENERATING ASSEMBLY FOR USE IN THE INTERIOR OF A PRESSURE VESSEL OF A PRESSURIZED WATER NUCLEAR REACTOR. Kumpf, H. Canadian Patent 866,999. 23 Mar 1971. Priority date 14 Jun 1967, Germany.

The assembly consists of primary fluid channels extending vertically through and above the reactor core. Lateral outlets are provided. Heat exchanger modules suspended from the top of the pressure vessel above the core and between the channels comprise an upper and lower collection chamber and straight secondary fluid conveying elements. The heat transfer surfaces are directly exposed to the interior of the pressure vessel for engagement by a flow of heated primary fluid in a horizontal direction from the lateral outlets of the primary fluid channels. (F.S.A.)

Research and Test Reactors

Refer also to abstract 28659.

28752 (ANL–7759) ZPR-3 ASSEMBLIES 48, 48A, AND 48B: THE STUDY OF A DILUTE PLUTONIUM-FUELED ASSEMBLY AND ITS VARIANTS. Broomfield, A. M.; Hess, A. L.; Amundson, P. I.; Baird, Q. L.; Bennett, E. F.; Davey, W. G.; Gasidlo, J. M.; Keeney, W. P.; Long, J. K.; McVean, R. L. (Argonne National Lab., Ill.). Dec 1970. Contract W-31-109-eng-38. 158p. Dep. NTIS.

ZPR-3 Assembly 48 and its variants were relatively simple and small Pu-fueled fast critical systems. All the cores were composed with plates of Pu diluted with plates of depleted U, Na, and graphite, in addition to the necessary steel drawers and matrix tubes. In Assembly 48, the atomic ratio of U to Pu in the core was approximately 4:1, with the ^{240}Pu isotopic fraction of 6%, and the blanket was 12 in. of depleted U. Assembly 48A had the same core composition, except that part of the radial blanket was replaced by an Inconel reflector. Worths of simulated B_4C control rods were measured in the Inconel reflector. In Assembly 48B, the core contained a small central zone where the ^{240}Pu isotopic content in the Pu was raised to an average of approximately 17%. The program of Assembly 48 experiments described includes the measurements of critical masses, central fission ratios, central reactivity coefficients, heterogeneity effects, Na-voiding worth, neutron spectrum, ^{238}U and Pu Doppler effect, material-worth and reaction-rate traverses, and foil activations. In Assembly 48A, attention was confined to the worths of B_4C rods and their influence on reaction rates and material worths. In Assembly 48B, a limited selection of the Assembly 48 measurements was repeated, including the worths of Na-voiding and the Doppler effect in ^{238}U. 36 references. (auth)

28753 (BLG–450) IMPROVEMENTS IN THE USE OF THE $^6Li(n,\alpha)t$ REACTION FOR IN-CORE NEUTRON SPECTRUM MEASUREMENTS. De Leeuw-Gierts, G.; De Leeuw, S. (Centre d'Etudes de l'Energie Nucleaire, Brussels (Belgium)). Dec 1970. 15p. Dep. NTIS (U. S. Sales Only).

An improved method to exploit fully the physical characteristics of the $^6Li(n,\alpha)t$ reaction for neutron spectrometry is described. It is shown how, by analyzing simultaneously the energies of the two emitted particles by means of a two-parameter analyzer, one can eliminate and measure the background, generated by gamma radiation or competitive reactions, while measuring the $E_\alpha + E_t$ or E_t spectrum. Solutions to the drawbacks of E_t spectrometry, i.e., screening of the responses to low neutron energies by the high neutron energy tail (phenomenon common to all indirect techniques) and partial superposition of the E_α distribution to the triton one, are stated and illustrated. Finally an improvement related to the use of the $E_\alpha = E_t$ parameter for in-core measurements is reported. 8 references. (auth)

28754 (CEA-N–1405) MEASUREMENT OF THE TRANSFER FUNCTION OF A REACTOR BY REACTIVITY MODULATION. Carre, Jean-Claude; Costa Oliveira, Jaime M. (Commissariat a l'Energie Atomique, Fontenay-aux-Roses (France). Centre d'Etudes Nucleaires). Feb 1971. 82p. (In French). Dep. NTIS (U. S. Sales Only).

In order to experimentally investigate transfer functions a reactivity modulator covering a large frequency range (0.01 to 100 Hz) and digital recording equipment for measuring the variations in the number of neutrons collected by a detector were developed. Measurements of transfer functions in the critical state were made for three thermal reactor configurations: MINERVE with part of the lattice center modulated with heavy water, ERMINE (MINERVE reactor with a portion of fast lattice at its center), and ULYSSE with various detector positions. Subcritical measurements were made on MINERVE. The measurements made indicate the importance of space effects in reactor dynamics at high frequencies. The neutron generation time for ERMINE was found to be 106 ± 5 μs; this value is in agreement with values obtained using the α Rossi method, and the method of correlating signals from two detectors. 17 references. (auth) (France)

28755 (CEA-N–1406) MEASUREMENT OF THE KINETIC PARAMETERS OF THE MINERVE REACTOR FROM ANALYSIS OF THE NEUTRON FLUCTUATIONS. Carre, Jean-Claude; Costa Oliveira, Jaime M.; Roullier, Francoise (Commissariat a l'Energie Atomique, Fontenay-aux-Roses (France). Centre d'Etudes Nucleaires). Feb 1971. 56p. (In French). Dep. NTIS (U. S. Sales Only).

The kinetic parameters of a reactor can be determined by analyzing the degree of correlation in the information obtained from one or two detectors of adequate efficiency. The parameters which can be measured include the transfer function at the measurement point, the neutron generation time, and the reactor power. The method was applied to the ERMINE reactor, which is a thermal reactor, coupled at its center to part of a fast lattice. Intercorrelation measurements yielded a generation time of 107 ± 6μs. This value is compared with values obtained with the same lattice using the α Rossi method and the modulation method. Autocorrelation measurements with a single chamber gave a value of 33 ± 4 W for the operating power, which is in agreement with the previously estimated value. 26 references. (auth) (France)

28756 (EURFNR–803) STRUCTURE AND WORKING OF THE ON-LINE SYSTEM FOR SNEAK DATA PROCESSING AND CONTROL OF EXPERIMENTS. van Velze, P.; Walze, H. (Kernforschungszentrum, Karlsruhe (West Germany). Institut fuer Angewandte Reaktorphysik). Translation of report KFK–1188. 62p. Dep. NTIS.

Work performed under United States–Euratom Fast Reactor Exchange Program.

On-line computer application in the field of nuclear reactor experiments is discussed. A technical description of the installation for computerized data acquisition and experiment control at the fast zero power reactor SNEAK is given. The main part of the system consists of a third generation type 24 bit-computer in DTL technique. Its core memory has a capacity of 16 K words. A line printer, a digital plotter, and 2 magnetic tapes

comprise its periphery. For the acquisition of measured data a very flexible buffer/counter-system has been built. For program controlled data transfer the acquisition system is connected to 5 parallel input channels. In addition a direct memory access channel is available. With control- and sense lines the computer can influence and check an experimental procedure. Typical applications are the calibration of the reactor control rods, material worth measurements, axial and radial fission rate traverses, neutron spectroscopy and automatic tests of experimental equipments. The on-line system has been found to be more reliable than the method based upon data acquisition with punched paper tapes and off-line reduction of experimental data. Previously, for example, it took up to 4 days to obtain a control rod calibration curve. Now it is plotted immediately after the calibration procedure. For certain experiments the manual control of the system has been greatly simplified. (auth)

28757 (GEAP-10010-27) SOUTHWEST EXPERIMENTAL FAST OXIDE REACTOR DEVELOPMENT PROGRAM. Twenty-Seventh Quarterly Report, November 1970–January 1971. Pflasterer, G. R.; Becker, R. A. (comps.) (General Electric Co., Sunnyvale, Calif. Breeder Reactor Development Operation). Feb 1971. Contract AT(04-3)-540. 62p. Dep. NTIS.

REACTOR FUEL ELEMENTS—fabrication of plutonium oxide (PuO_2)—uranium oxide (UO_2) pellet type
—inspection of plutonium oxide (PuO_2)–uranium oxide (UO_2) pellet type
SOUTHWEST EXPERIMENTAL FAST OXIDE REACTOR—fuel elements for, fabrication and inspection of plutonium oxide (PuO_2)–uranium oxide (UO_2) pellet type
—startup testing of plutonium oxide (PuO_2)–uranium oxide (UO_2) fueled
—physics measurements for plutonium oxide (PuO_2)–uranium oxide (UO_2) fueled, (E/T)
—maintenance during November 1970 to January 1971
—operations during November 1970 to January 1971 (D.C.C.)

28758 (JAERI-1204) PRIMARY COOLING WATER DECOMPOSITION IN REACTORS. Tone, Hirohito; Yamamoto, Katsumune; Okagawa, Seigo; Yokouchi, Ichiro; Atomura, Masakatu (Japan Atomic Energy Research Inst., Oarai. Oarai Research Establishment). May 1970. 11p. (In Japanese and English). Dep. NTIS (U. S. Sales Only).

The decomposition rate of water (or heavy water) as a moderator-coolant in JRR-2 (heavy water moderated reactor) and JMTR was observed at the high power operations. The specific heavy water decomposition rate in JRR-2 was 5 ± 0.7 (gr(D_2O)/MW · hr) at reactor power of 10 MW. During 10 MW operation of JRR-2, the heavy water conditions such as pH, ionic impurities and temperature, were maintained in the following mentioned values: pH of 6.5 ± 0.5, conductivity less than 1 μmho/cm, D_2O_2 concentration of 2 ± 0.5 ppM, O_2 concentration of 0.55 ± 0.15 ppM and the temperature between 47°C and 55°C. The primary cooling water decomposition in JMTR was examined between reactor power of 1.2 MW and 50 MW. When the cooling water temperature was 50°C, the specific decomposition rate was 10.6 ± 1 (gr (H_2O)/MW · hr) at 10MW, 4.5 ± 0.5 (gr (H_2O)/MW · hr) at 50MW. During these reactor operation of JMTR, the cooling water conditions were maintained as the following: pH of water between 5.5 and 6, conductivity less than 2μmho/cm, H_2O_2 concentration 16 ± 1 ppM and O_2 concentration 14.8 ± 0.5 ppM. The decomposition rate in JMTR much higher than that in JRR-2 accounts for increased dissolved oxygen concentration in the cooling water of JMTR. An increase in cooling water temperature favors the back reaction. As a result, the higher temperature favors lower net decomposition. 11 references. (auth)

28759 (JAERI-Memo-4272) PULSED NEUTRON EXPERIMENT ON FCA I-5. Hiraoka, Toru; Nakano, Masafumi; Konishi, Toshio (Japan Atomic Energy Research Inst., Tokyo). Jan 1971. 22p. Dep. NTIS (U. S. Sales Only).

Pulsed neutron experiments were carried out on a bare spherical core and a series of cylindrical cores composed of only 20% enriched U metal to measure the limited range of negative reactivity where the fundamental decay is observed. The linear relation between the prompt neutron decay constant, α, and the reactivity measured by multiplication method was observed to hold down to −12% Δk/k. The results of the calculations of α_c and k_{eff} agree well with the experimental data. The difference in α_c with the core geometry could not be observed. Distortions of the prompt neutron decay were observed at large negative reactivities. They may be due to insufficient multiplication of neutrons. (auth) (Japan)

28760 (JPRS-52907) IBR: FAST PULSED REACTOR. Shabalin, E. Translated from Nauka Zhizn; No. 10, 2-8(1970). 12p. NTIS.

Fast neutron reactors, which will provide the basis of atomic power in the coming years, are widely known. Much less well known is the IBR [fast pulsed reactor]. The operating principle of the IBR is discussed together with its application in experimental physics. (auth)

28761 (NASA-CR-72409) CAVITY REACTOR ENGINEERING MOCKUP CRITICAL EXPERIMENT. Pincock, G. D.; Kunze, J. F.; Wood, R. E. (General Electric Co., Idaho Falls, Idaho. Nuclear Systems Programs); Hyland, R. E. (National Aeronautics and Space Administration, Cleveland, Ohio. Lewis Research Center). 22 May 1968. Contracts AT(40-1)-2847; C-67747-A. 23p. (GESP-31; CONF-680601-59). Dep. NTIS.

From 14. annual meeting of the American Nuclear Society, Toronto, Ontario (9 Jun 1968).

Cavity reactor critical experiments performed with various configurations fueled with solid uranium sheets or gaseous UF_6 are described. Some of the critical mass and related data obtained in the experiments are presented. (H.D.R.)

28762 (ORNL-TM-3369) OAK RIDGE RESEARCH REACTOR QUARTERLY REPORT, OCTOBER–DECEMBER 1970. Hurt III, S. S.; Tabor, W. H. (Oak Ridge National Lab., Tenn.). 22 Mar 1971. Contract W-7405-eng-26. 36p. Dep. NTIS.

The ORR operated 92.2% of the time during October, November, and December of 1970 at an average power level of 29.9 MW/operating hour. There was a slight increase (~10% as compared with the average for 1969) in the radioactivity of the reactor water caused by a small leak of fission gases from a fuel element. The exact method of escape was not discovered, however, the leak caused no significant problems and the leaky element was isolated. Twenty-one fuel elements were declared spent during the quarter, with an average burnup of 51.3%. Fuel elements spent during the year totaled 104, as compared with only 87 for 1969; however, the average for three years (1968, 1969, 1970) is 93.6 per year which compares quite favorably with the number anticipated (99 per year) when the fuel content per new element was increased to 240 g. The reactor was scheduled down on nine occasions and encountered four unscheduled shutdowns, one of which resulted in an unscheduled refueling. Consequently, unscheduled downtime was high (4.2% of the total) as compared with recent experience but was still rather insignificant. Modifications and maintenance requirements during the quarter are described. (auth)

28763 (RISO-205) EXPERIMENTAL INVESTIGATIONS OF THE RELEASE OF RADIOACTIVITY UNDER ACCIDENTAL CONDITIONS IN A REACTOR CONTAINMENT BUILDING. Zak, W. M.; Walmod-Larsen, O. (Danish Atomic Energy Commission, Risoe. Research Establishment). Apr 1970. 117p. Dep. NTIS (U. S. Sales Only).

Experimental measurements of the dynamic as well as the static spread pattern of large amounts of airborne radioactivity suddenly released in the DR3-reactor shell at Risö were made by means of releases of ^{41}Ar. A method of data treatment was worked out by which the data from the different measurement points and releases could be standardized and therefore directly compared. An evaluation of the preferred ventilation conditions and evacuation routes in the case of a sudden release of activity was made. Only one or two minutes elapse before significant increases in the activity concentrations are observed in and around the crane well. The control room, the elevator stairs and the personnel air lock are not affected until after several minutes. Recommendations on the present system are given. 3 references. (auth)

28764 MARINE MANGANESE NODULES STUDIED USING NUCLEAR REACTOR. Wiggins, Peter F. (Naval Academy, Annapolis, Md.); Duffy, Dick; El Kady, Ahmed. Nav. Eng. J.; 83: 31-4(Feb 1971).

As ore deposits of important elements become depleted on land masses, man will look to the ocean floor for metals of economic interest. Manganese nodules, which can be pumped from the ocean floor, contain valuable elements. The prompt photon emission which follow neutron capture can be used for location and analysis of these elements. A 10 kW pool-type research reactor thermal column supplied the neutrons for this application of nuclear spectroscopy. (9 references) (auth)

28765 LOOP FOR THE RADIATION STUDY OF THE ELECTRICAL CONDUCTIVITY OF MATERIALS IN THE VVR REACTOR. Kharlamov, A. G.; Zakharova, N. P.; Batalov, A. A.; Zaikin, Yu. I.; Kolyadin, V. I. At. Energ. (USSR); 29: 289-91 (Oct 1970). (In Russian).

The "RIM" radiation research loop of the VVR reactor has been modified to measure the electrical conductivity of materials. The loop channel, placed near the core, was exposed to a fast and thermal neutron flux with E > 0.5 MeV of 4×10^{12} and 1×10^{13}

n/cm^2 sec, respectively, at a nominal reactor power level of 2 MW. The loop was provided with an evacuation and a gas supply system to carry out measurements under various conditions, including also water cooling and electrical heating. The conductivity was measured by the conventional potentiometric method. Several tests may be carried out simultaneously in the channel made of seamless pipe. The experiments were installed during the shutdown periods of the reactor. The experiments carried out included irradiation of graphite and beryllium specimens for a period of 100 hours at the 2 MW power level by integral fast and thermal neutron fluxes of 1.5×10^{19} and 4×10^{19} n/cm^2, while the temperature of the specimens was kept within the range from 120 to 170°C. It was found that the electrical conductivity of beryllium hardly changed while that of the graphite along the C axis was reduced 1.5 fold. (TTT)

28766 ABSOLUTE DETERMINATION AND AXIAL RADIAL DISTRIBUTION OF BURN-UP FOR REACTOR LATTICE CELLS. Schaechter, L.; Popa, P.; Hacman, D. (Inst. of Atomic Physics, Bucharest). Rev. Roum. Phys.; 15: 777-81(1970).

The axial and radial burnup distributions of fuel elements irradiated in the UUR-S Bucharest reactor are measured. A γ-scanning device was used for the measurements. (10 references) (D.C.C.)

28767 COLD NEUTRON SOURCE IN JUELICH. Doose, C.; Preussner, A.; Stelzer, F.; Stiller, H.; Tholen, A. (Kernforschungsanlage, Juelich, Ger.). Cryogenics; 11: 107-13(Apr 1971).

Using liquid H_2, condensed by cooled He gas, reactor neutrons can be moderated to subthermal energies. For energies between 5 and 0.3 MeV the neutron flux is increased by factors of between 5 and 26. The H_2 condensation is carried out in a thermosiphon system inside the beam part of the reactor. The in-pile installation and the principles of operational and safety controls are described. (auth) (UK)

28768 OPTIMIZED DYNAMIC CONTROL OF THE IRRADIATION LOOP OF THE PEGASE REACTOR. Guintrand, Claude (CEA, Cadarache, France). Automatisme; 16: 15-22(Jan 1971). (In French).

The optimized dynamic control of the testing equipment of the PEGASE reactor is analyzed. The facilities, and the experimental data obtained, are discussed. It is shown how a self adapting configuration can be used and a simple mathematical model developed for optimizing the control. In this way the costs can be minimized. The introduction of a special reference input signal substantially improves the performance of the optimized circuit, providing much smoother running and a consequent reduction in the stresses occurring in the equipment; the reliability of the equipment is thus improved. A series of simulations demonstrated the improvements brought about by the method. (auth) (France)

28769 PILE PHYSICS EXPERIMENT BY MEANS OF TOF NEUTRON DIFFRACTION. Kimura, Motoharu; Watanabe, Noboru; Oyamada, Masayuki; Yamada, Yukio; Takahashi, Fuminobu (Tohoku Univ., Sendai). Kakuriken Kenkyu Hokoku; 2: No. 2, 100-5(Dec 1969).

Measurement of the time-dependent thermalization spectrum of small BeO system was performed using TOF neutron diffraction method for different buckling. The measured result was compared with a model by numerical calculation. It was found that the measured result is in fairly good agreement with the approximation using the first term only in the Placzek expansion for the thermalization kernel. For better agreement with the measurement, the Debye temperature of BeO should be about 1050°K, rather than 1200°K as reported previously, or than 950°K as estimated recently from the die-away experiment. (auth) (Japan)

28770 MEASUREMENT AND INTERPRETATION OF THE AVERAGE NEUTRON TEMPERATURE DURING A POWER SURGE OF THE TRIGA MARK II REACTOR. Fleck, C. M.; Miesterl, J. (Oesterreichische Hochschule, Vienna). Acta Phys. Austr.; 29: 152-9(1969). (In German).

The neutron temperature during a power surge at the TRIGA Mark II reactor was measured by means of an activation probe. The pattern of the core temperature was calculated by the Fuchs–Nordheim model and the specific heat of the core was determined with a temperature-dependent insert. For the pattern of the neutron temperature during the surge a simple linear dependence with the core temperature was assumed. Mean values over the surge were given for this proportionality constant and for the neutron temperature. These values can be represented as linear functions of the released energy or of the maximum reactor power. (5 references) (tr-auth)

28771 ELECTRICAL FACILITIES OF THE BRAUNSCHWEIG RESEARCH AND MEASURING REACTOR (FMRB). Runge, E.-G. PTB Mitt.; 80: 355-65(Oct 1970). (In German).

The core-configuration of the Research and Measuring Reactor of the Physikalisch-Technische Bundesanstalt (FMRB) consisting of two loosely coupled fission zones or reactor cores requires two identical groups of neutron measuring channels. In each group there are one logarithmic pulse-channel and one linear dc-channel with switchable measuring ranges. The logarithmic dc-channels and the linear dc-channels with one fixed measuring range acting on the safety circuits during normal reactor operation are installed threefold, their functions being controlled by comparison of their output signals. Schematic diagrams are given to show the coolant loops and the heavy-water system and the corresponding control points. Reactor protection is performed by "two-out-of-three"-coincidence circuits. A speaker system, an industrial television device, and stationary health physics instruments are part of the signal equipment. According to special requirements for the operation of the reactor and of experiments the electrical supply network is manyfold as to availability and voltages offered. (31 references.) (auth)

28772 ACCOUNT OF THE RADIOISOTOPES PRODUCTION PROGRAMME AT THE NUCLEAR RESEARCH CENTER DEMOCRITOS, ATHENS, GREECE. Constantinides, M. G. (Democritus Nuclear Research Center, Athens). pp 47-56 of Research Reactor Utilization. Vol. 1. Vienna; International Atomic Energy Agency (1970). (CONF-700204-11).

From IAEA meeting on research reactor utilization; Rome, Italy (2 Feb 1970).

The radioisotope production program of the Nuclear Research Center "Democritos" is described. A brief account of the development of these activities from 1962 to the present is presented. For the future, plans are being made to build a radiopharmaceutical laboratory to include the production of the most used labelled compounds of iodine-131, mercury-197 and mercury-203, selenium-75, and radiopharmaceuticals of technetium-99m. A large radioisotopes dispensing center is to be put into operation, through which will pass all Greek demands for radioisotopes, including the 100,000 mCi per year now being imported. A method for production of technetium-99m is also described. (INIS)

28773 NEW REPOSITIONING DRIVES FOR THE SOURCE-RANGE DETECTORS FOR THE STARTUP CHANNELS OF THE REACTOR FMRB. Runge, E.-G. (Physikalisch-Technische Bundesanstalt, Brunswick). Kerntech. Atomprax.; 13: 135-40 (Mar 1971). (In English and German).

The source range neutron flux detectors used for monitoring the startup of a reactor must be retracted from their initial measuring positions as the startup proceeds into the power range. Various repositioning drive facilities suitable for reactors of the swimming pool type are described. The description of a new facility designed specifically for the FMBR with a deflected roller chain is presented. The position signalling is divided into two ranges of unequal reading accuracy. 13 references. (auth)

28774 EXPERIENCE AND RESEARCH WITH THE GREEK REACTOR. Chrysochoides, N. G.; Mitsonias, C.; Perricos, D. C. (Democritus Nuclear Research Center, Athens). pp 27-45 of Research Reactor Utilization. Vol. 1. Vienna; International Atomic Energy Agency (1970). (CONF-700204-6).

From IAEA meeting on research reactor utilization; Rome, Italy (2 Feb 1970).

A few modifications in the electronic, electrical and mechanical systems of the GRR-1 reactor installed at the Nuclear Research Center "Democritus" are described. Three out of the six beam tubes are presently being used for experiments; beam tube No. 3 is used as a neutron source for a double-axis single-crystal spectrometer. A system for the fast measurement of irradiated thin samples has been installed in beam tube No. 4 and a neutron chopper is installed in beam tube No. 5. Some of the facilities in the reflector—four pneumatic transfer systems—and in the thermal column are also given. Two programs on delayed neutron research are at present in progress, namely the delayed neutron energy spectrum measurements and the determination of delayed neutrons group relative yields in fissionable nuclides of light masses that have not been studied before. (auth) (INIS)

28775 EXPERIMENTS AT THE MUNICH RESEARCH REACTOR FRM. von Egidy, T.; Boening, K.; Heidemann, A.; Koester, L.; Rabenstein, D. (Technische Hochschule, Munich). pp 225-49 of Research Reactor Utilization. Vol. 1. Vienna; International Atomic Energy Agency (1970). (CONF-700204-12).

From IAEA meeting on research reactor utilization; Rome, Italy (2 Feb 1970).

The measurement of conversion electrons after slow neutron capture has been accomplished by the use of magnetic spectrometers and a semi-conductor spectrometer. The use of neutron conducting tubes for neutron capture gamma ray measurements is discussed, and a neutron crystal spectrometer with extremely high energy resolution is described. Low-temperature irradiation of solids with fast neutrons has been applied. To determine neutron scattering amplitudes a neutron gravity refractometer was used. (INIS)

28776 SHORT COMMUNICATION ON THE UTILIZATION OF THE TR-1 RESEARCH REACTOR OF THE CEKMECE NUCLEAR RESEARCH CENTER. Ozemre, A. Y. pp 117-22 of Research Reactor Utilization. Vol. 1. Vienna; International Atomic Energy Agency (1970). (In French). (CONF-700204-4).

From IAEA meeting on research reactor utilization; Rome, Italy (2 Feb 1970).

The main areas of utilization of the research reactor TR-1 are described. In the field of radioisotope production, from 1963 to 1969 2018 shipments of radioactive isotopes with a total activity of 248.75 Ci were produced. The radioisotope production is based mainly on the following isotopes: ^{198}Au, ^{99}Mo, ^{99m}Tc, ^{31}Si, ^{82}Br, ^{24}Na, ^{42}K, ^{203}Hg, ^{192}Ir, ^{32}P and ^{122}Sb. Another use of the research reactor is in the field of radioactivation analysis, as well as the use of the reactor as a source of gamma rays for investigations of the polymerization of certain chemical substances, for example methacrylonitrile. Among the physical investigations the determination of the ratio of the number of neutrons with energies over 0.4 eV to neutrons with higher energies in the neutron capture of ^{238}U was studied. Some other physical investigations have been realized using an MAN diffractometer. A certain part of the neutron spectrometry measurements have been made by means of a spectrometer constructed in the Nuclear Research Center. Other physical experiments conducted on the research reactor are described. (INIS)

28777 REVIEW OF RESEARCH ACTIVITIES USING THE UA-RR-1. Hamouda, I.; El-Garhy, M.; El-Shanshoury, I. (Atomic Energy Establishment, Inshas, Egypt). pp 149-66 of Research Reactor Utilization. Vol. 1. Vienna; International Atomic Energy Agency (1970). (CONF-700204-13).

From IAEA meeting on research reactor utilization; Rome, Italy (2 Feb 1970).

The purpose of installing the UA-RR-1 reactor in the United Arab Republic is to conduct research in the fields of physics, chemistry and biology, to produce radioisotopes and to provide training in reactor engineering. The research activities carried out in the fields of physics and materials, and the program of isotope production are described. The physics research is directed towards: neutron spectrum measurements, neutron flux measurements, neutron data, neutron capture gamma ray investigations, neutron thermalization experiments, shielding experiments, neutron diffraction and inelastic scattering studies, and reactor theory and calculations. The materials research deals with: radiation damage and corrosion investigations. The radiochemistry research work and production of radioisotopes covers about thirty varieties of preparations of more than twenty kinds of isotopes, chemically processed or unprocessed. (INIS)

28778 REPORT ON RESEARCH PROGRAMMES AT THE REACTOR TRIGA MARK II AT THE INSTITUTE JOZEF STEFAN, LJUBLJANA. Dimic, V.; Najzer, M. (Nuclear Inst. Jozef Stefan, Ljubljana, Yugoslavia). pp 167-76 of Research Reactor Utilization. Vol. 1. Vienna; International Atomic Energy Agency (1970). (CONF-700204-10).

From IAEA meeting on research reactor utilization; Rome, Italy (2 Feb 1970).

A program of basic research is being conducted at the reactor TRIGA Mark II (250kW). The principal physics experiments accomplished during the first three years of reactor operation include the investigation of ferroelectrics and liquid crystals by the time of flight spectrometer using a semimonochromatic neutron beam obtained by a beryllium filter. For this purpose the cold neutron source has been installed into the tangential beam hole. Very recently, the double axis neutron spectrometer was constructed. The single crystal scintillation spectrometer, ^{6}Li semiconductor sandwich detector and set of threshold detectors are used for the fast neutron spectrometry where quite an extensive program is carried on. A CDC 1700 on-line computer is used as a data acquisition equipment. The work on this machine is in progress. (auth) (INIS)

28779 NEUTRON INELASTIC SCATTERING AND NEUTRON DIFFRACTION AT THE VINCA HEAVY WATER REACTOR. Brajovic, V.; Jovic, Dj.; Konstantinovic, J.; Zivanovic, M. (Boris Kidric Inst. of Nuclear Science, Belgrade). pp 185-206 of Research Reactor Utilization. Vol. 1. Vienna; International Atomic Energy Agency (1970). (CONF-700204-5).

From IAEA meeting on research reactor utilization; Rome, Italy (2 Feb 1970).

Currently, for the purpose of studying phenomena in solid state physics, five horizontal reactor channels are used. By means of a neutron spectrometer neutron inelastic scattering measurements are being conducted using the diffraction method. With this spectrometer the dynamics of spin systems (dispersion law, exchange integral, life of magnon, crystal anisotropy, etc.) have been studied. With the aid of a neutron time-of-flight spectrometer a series of experiments was performed with the purpose of investigating localized and virtual magnon levels in the systems Ni(V), Ni(Cr), etc. A neutron crystal spectrometer has been adopted for the Be-detector method. At the end of this year, the spectrometer for magnetic critical neutron scattering will be put into operation. By using the natural crystal of magnetite as monochromator and the Fermi chopper, a resolution of about 3% was obtained. A neutron diffractometer with monocrystal (Cu(111)) as a monochromator and BF_3 detector is used successfully. Theoretical work has been done on current problems of ferroelectric, dielectric and magnetic properties of solids. (INIS)

28780 STATUS REPORT TO THE STUDY GROUP MEETING ON THE UTILIZATION OF RESEARCH REACTORS IN ISRAEL. Ben-David, G.; Shaked, H. (Israel Atomic Energy Commission, Tel Aviv). pp 89-116 of Research Reactor Utilization. Vol. 1. Vienna; International Atomic Energy Agency (1970). (CONF-700204-7).

From IAEA meeting on research reactor utilization; Rome, Italy (2 Feb 1970).

Some examples of recent work using research reactors in Israel are presented. (INIS)

28781 EXPERIMENTAL PHYSICS RESEARCH AT THE DEMOCRITOS REACTOR. Kostikas, A. (Democritus Nuclear Research Center, Athens). pp 57-72 of Research Reactor Utilization. Vol. 1. Vienna; International Atomic Energy Agency (1970). (CONF-700204-3).

From IAEA meeting on research reactor utilization; Rome, Italy (2 Feb 1970).

The experimental physics projects that have been completed or are currently pursued at the 1 MW swiming pool reactor operating at the N.R.C. Democritos are described. It covers the 6 year period since the previous meeting in Athens of the study group on research reactor utilization. (auth) (INIS)

28782 MAJOR SHUTDOWN OF HIFAR IN 1970. Wood, A. C. (Australian Atomic Energy Commission Research Establishment, Lucas Heights). At. Energy Aust.; 14: No. 1, 8-15([1971]).

Work undertaken on the primary cooling circuit, the secondary cooling circuit and the shield cooling circuit during an extended shut down of HIFAR is described. Two of the main stainless steel heat exchangers which had developed tube leaks from stress corrosion and had been temporarily repaired with epoxy resin were replaced. Neoprene diaphragms in the main check valves were replaced if they showed signs of cracking. Measures taken to limit personnel contamination during maintenance are described. Several lengths of pipework were removed to facilitate internal examination of remaining pipework. A cast stainless steel elbow was replaced and used for destructive examination. It showed no modification of existing structure. Examination of the aluminum reactor vessel using television showed no anomalies. The condition of the vessel and of the primary circuit pipework was regarded as satisfactory. Interior surfaces of all the pipework in the secondary circuits were cleaned with water jets. Some gate valves required replacement due to wear at the junction between the gate and drive spindle. Improved methods of water treatment were expected to benefit the secondary circuits. Repairs to copper cooling coils of the thermal shield were effected following development of cutting techniques on a mockup of a concrete biological shield with steel reinforcement. Leaks at other locations have since developed but it is anticipated that further repairs can be carried out if necessary. (Australia)

Rocket and Space Reactors

28783 (AI-AEC-Memo-12717) REFERENCE ZIRCONIUM HYDRIDE REACTOR THERMOELECTRIC SYSTEM. (Atomics International, Canoga Park, Calif.). 15 Jun 1969. 176p. Dep. NTIS.

The results of an engineering study of nuclear reactor—thermoelectric power systems suitable for space missions are presented. The reference system design is a ZrH reactor similar to SNAP-8 coupled to four parallel power-conversion sections incorporating

PbTe tubular thermoelectric modules. A nominal power level of 25 kW(e) and a minimum lifetime of 20,000 hours are specified. Aspects of the engineering effort reported include: parametric performance data over a suitable power range above and below 25 kW(e) to illustrate the trade-offs available between power, weight, area, temperature, etc.; preliminary design and performance requirements for key system components; and conceptual designs of systems adapted for specific space missions. 11 references. (H.D.R.)

28784 (ORNL-TM-3365) APPLICATION OF DOT-MORSE COUPLING TO THE ANALYSIS OF THREE-DIMENSIONAL SNAP SHIELDING PROBLEMS. Straker, E. A.; Childs, R. L.; Emmett, M. B. (Oak Ridge National Lab., Tenn.). 1 Apr 1971. Contract W-7405-eng-26. 25p. (CONF-710304-6). Dep. NTIS.

From Symposium on natural and manmade radiation in space; Las Vegas, Nev. (1 Mar 1971).

Many radiation transport problems can best be solved by using both discrete ordinates and Monte Carlo techniques with a coupling between the two techniques occurring at a geometry interface. A general discussion of two possible coupling schemes is given. The calculation of the reactor radiation scattered from a docked service and command module is used as an example of coupling discrete ordinates (DOT) and Monte Carlo (MORSE) calculations. (auth)

28785 NUCLEAR ROCKET ENGINE DEVELOPMENT PROGRAM. JOINT HEARINGS BEFORE THE COMMITTEE ON AERONAUTICAL AND SPACE SCIENCES, UNITED STATES SENATE, AND THE JOINT COMMITTEE ON ATOMIC ENERGY, CONGRESS OF THE UNITED STATES, NINETY-SECOND CONGRESS, FIRST SESSION, FEBRUARY 23 AND 24, 1971. Washington, D. C., Joint Committee on Atomic Energy, 1971. 139p. GPO.

The application of nuclear energy to space systems through the nuclear rocket engine development program is discussed. Specific emphasis of the discussions is to explore the decision, and the consequences, to stop the development of the NERVA engine. (H.D.R.)

28786 SPACE SHUTTLES AND INTERPLANETARY MISSIONS. Based on Shuttle, Precursor Missions, and Planetary and Lunar Space Station Sessions of AAS 16th Annual Meeting, June 8–10, 1970, Anaheim, California. Larmore, L.; Gervais, R. L. (eds.). Advances in the Astronautical Sciences. Volume 28. Tarzana, Calif.; American Astronautical Society (1970). 484p. (CONF-700643).

Included are 17 papers on planning and engineering requirements for the establishment of space stations and for manned planetary missions. A separate abstract was prepared for each of three papers treating the uses of nuclear propulsion in manned missions. (H.D.R.)

For abstracts of individual papers see: 28787–28789

28787 PERSPECTIVE AND SYSTEMS ENGINEERING OF MANNED PLANETARY FLIGHT. Ehricke, Krafft A. (North American Rockwell Corp., Downey, Calif.). Advan. Astronaut. Sci.; 28: 337-92(1970).

From 16. annual meeting on space station and manned planetary exploration; Anaheim, Calif. (8 Jun 1970). See CONF-700643.

The objectives of the manned planetary flight program are discussed in relation to flight requirements beyond the capabilities of unmanned missions and the cost of implementing such a program. Exploration missions to Mercury through Jupiter are examined as to planning, vehicle, and propulsion system requirements. Missions in which the NERVA nuclear propulsion system could be utilized are briefly described. (H.D.R.)

28788 EARTH DEPARTURE TECHNIQUE FOR USE IN MANNED INTERPLANETARY MISSIONS USING THE NERVA ENGINE. McAdoo, Stewart F. Jr.; Funk, Jack (Manned Spacecraft Center, Houston, Tex.). Advan. Astronaut. Sci.; 23: 437-55(1970).

From 16. annual meeting on space station and manned planetary exploration; Anaheim, Calif. (8 Jun 1970). See CONF-700643.

The use of nuclear propulsion would increase greatly the available payload for spacecraft and experiments and reduce the required number of launches for specific manned interplanetary missions. However, if a direct injection onto interplanetary trajectory is used, the initial thrust-to-weight ratio must be approximately 0.15 to 0.2. To achieve such thrust-to-weight ratios, a new, large engine must be developed, or several of the NERVA engines would have to be used simultaneously. An alternate approach to these systems developments is the development of a mission plan that does not require them. A multiorbit injection technique is described that eliminates the need for these systems developments. The development of a steering equation for use in analyzing vehicle performance with multiorbit injection is presented. A survey is made to determine the optimum initial thrust-to-weight ratio using multiorbit injection for missions having departure-velocity requirements similar to those required for manned Mars missions. Operational aspects of the technique are discussed. (auth)

28789 MANNED PLANETARY MISSIONS WITH REUSABLE NUCLEAR SHUTTLES. Riedesel, R. G.; Cowls, R. S. (McDonnell Douglas Astronautics Co., Huntington Beach, Calif.). Advan. Astronaut. Sci.; 28: 457-73(1970).

From 16. annual meeting on space station and manned planetary exploration; Anaheim, Calif. (8 Jun 1970). See CONF-700643.

The application of reusable nuclear shuttles to manned planetary missions in the late 1980's and early 1990's is examined. A comparison of expendable and reusable shuttle operating modes is made, considering total propellant requirements, number of nuclear shuttles required, nuclear shuttle propellant capacity, costs, and complexity of operations. The 1988 Mars landing mission with an inbound Venus swingby is used as the baseline for the comparison. Elliptical and circular orbit assembly modes are also compared for the reusable nuclear shuttle. (auth)

Process Heat and Desalination Reactors

Refer also to abstracts 28538 and 28642.

28790 (ORNL-4668) NUCLEAR DESALINATION PROGRAM ANNUAL PROGRESS REPORT ON ACTIVITIES SPONSORED BY THE ATOMIC ENERGY COMMISSION FOR PERIOD ENDING OCTOBER 31, 1970. Anderson, T. D.; Gill, A. B. (comps.) (Oak Ridge National Lab., Tenn.). Apr 1971. Contract W-7405-eng-26. 32p. Dep. NTIS.

The program activities on the application of nuclear energy to desalting and other processes which benefit from low-cost heat and electricity are summarized. Studies aimed at developing useful data and techniques that will allow independent evaluations of nuclear plant designs and applications included: (1) nuclear desalting plant coupling; (2) dual-purpose plant control; (3) nuclear desalting applications; and (4) agro-industrial complexes. Activities of the Nuclear Desalination Information Center are summarized. (H.D.R.)

28791 POSSIBILITY OF NUCLEAR ENERGY FOR METALLURGICAL AND CHEMICAL PROCESSES. Wenzel, Werner (Technische Hochschule, Aachen). Tech. Ueberwach.; 10: 407-11(Dec 1969). (In German).

By means of nuclear power stations integrated into metallurgical plants it will be possible to reduce the cost of iron and steel production. The heat required for the reduction of iron ore can be directly drawn from a high-temperature pile and led via heat exchangers to the reduction process during the first step towards the production of iron sponge. The useful heat still remaining in the reactor coolant will be used for the generation of electrical energy for the metallurgical plant. (auth)

28792 SMALL LOW-TEMPERATURE ORGANIC-COOLED AND MODERATED REACTORS (ROVI) TO BE COUPLED TO A DESALINATION PLANT. Di Menza, R. (Comitato Nazionale per l'Energia Nucleare, Rome). pp 305-16 of Small and Medium Power Reactors, 1970. Vienna; International Atomic Energy Agency (1971).

From Small and medium power reactors symposium; Oslo, Norway (12 Oct 1970). See STI/PUB-267; CONF-701046.

Small nuclear reactors of simplified design and therefore requiring a low capital investment to be used mainly to operate a desalination plant and to produce, if required, small quantities of electrical energy are described. A study on organic-cooled and moderated reactors (ROVI), designed to operate at low temperature for the above purposes, is discussed. This particular type of reactor was chosen because it involved many cost-saving simplifications. Technical and economical evaluations indicate that the range of convenient and economic applicability of the ROVI reactors was restricted to plant sizes varying approximately from 100 to 400 MW(t). The preliminary design of a plant including a desalination section driven by a prototype 220-MW(t) reactor and

capable of producing the electricity needed for its self-sufficiency has been completed and is described. (3 references.) (auth)

28793 WELL REACTOR. Jamne, E. (Institutt for Atomenergi, Kjeller, Norway). pp 331-44 of Small and Medium Power Reactors, 1970. Vienna; International Atomic Energy Agency (1971).

From Small and medium power reactors symposium; Oslo, Norway (12 Oct 1970). See STI/PUB-267; CONF-701046.

A design study on a small, steam-producing reactor—the "well reactor"—is presented. This is a boiling-water reactor which is placed in a water-filled well, and where the reactor vessel is open at the bottom so that the primary steam pressure corresponds to the static head of water above the vessel. From a safety point of view the reactor has a number of advantages, and it should be simple to operate. It can be used for delivery of process steam for desalination or for general industrial purposes. The results of a preliminary economical study of a 70-MW unit for a desalination plant are given. An economic comparison with oil-fired units is presented. (auth)

28794 USES OF HIGH TEMPERATURE REACTORS FOR THE GENERATION OF PROCESS HEAT. Bode, K. H. (Brown Boveri/Krupp Reaktorbau GmbH, Cologne). Kerntech. Atomprax.; 13: 109-17(Mar 1971). (In English and German).

Dual purpose plants generating both electric power and process heat are described. Such plants can be used for generating process or heating steam and for the desalination of seawater. In addition, the further development of high temperature reactor types with high cooling gas outlet temperatures will make possible the economic realization of processes for the conversion and upgrading of fossil raw materials such as natural gas, coal and oil. 22 references. (auth)

Marine and Portable Power Reactors

28795 UNDERWATER ARCTIC OIL TRANSPORT. Golay, Marcel J. (Perkins-Elmer Corp., Norwalk, Conn.). Nav. Eng. J.; 83: 75-85(Feb 1971).

The essential technical characteristics of very large unfoldable oil-carrying submarine barges, and their economic advantages, are discussed. (auth)

28796 ITEMS OF TESTS AND EXPERIMENTS FOR THE NUCLEAR SHIP MUTSU. Yamagata, Masao (Japan Nuclear Ship Development Agency, Tokyo). Genshiryokusen; No. 82, 2040-55(Aug 1970). (In Japanese).

The survey and research ad hoc committee deliberated on the experimental navigation of Mutsu for nine months, and submitted a report. The technical committee approved the report. First, three working groups of the survey and research ad hoc committee collected 320 experimental items concerning confirmation of the performance, check-up of the design coefficients, confirmation of the secular change and the data to decide the presence of expendable installations for the nuclear ship Mutsu. 183 items of them were adopted after prudent deliberation, and were summarized in "the collective table for the testing and experimental items for the nuclear ship Mutsu." These items were classified into three groups, and the method for disposing of each group was decided. As for those items which need new experimental materials and men for being carried out, "the investigation sheets $\frac{1}{3}$-$\frac{3}{3}$ for the tests and experiments for the nuclear ship Mutsu" were summarized. In the collective table, classification, item number, item, purpose, detail, the period of execution and the aim of the study are shown for each item. These items, their detail, experimental apparatuses, and others must be re-examined every time according to the change of situation. The conclusions in outline will be obtained during the life time of first core, and it will take about one year after the completion of the experimental navigation to analyze and summarize the results. (Japan)

Production Reactors

28797 MAINTENANCE OF ON-LINE COMPUTERS USED WITH NUCLEAR PRODUCTION REACTORS. New, I. B. Jr. (E. I. du Pont de Nemours and Co., Aiken, S. C.). Contract AT(07-2)-1. ISA (Instrum. Soc. Amer.) Trans.; 9: 355-62(1970).

At the Savannah River Production Reactors, four on-line computer systems were installed to monitor 3500 process variables in each area and to simplify operation by machine calculations based on these process variables. The computers compare critical variables with calculated limits at frequent intervals and automatically change reactor power based on these comparisons. The extensive maintenance program, including personnel selection and training, is described. (H.D.R.)

Reactor Theory

28798 (NYU-4090-1) SUMMARY REPORT ON INVESTIGATIONS OF TRANSFER MATRIX METHOD. Aronson, Raphael (New York Univ., N. Y.). 25 Feb 1971. Contract AT(30-1)-4090. 16p. Dep. NTIS.

Mathematical and numerical aspects involved in the solution of the transport equation by the Transfer Matrix method are examined. Included in the various tasks summarized are: convergence of discrete eigenvalues; radiation transfer; and complex eigenvalues. 10 references. (H.D.R.)

Kinetics

Refer also to abstracts 28654, 28666, 28679, 28754, 28755, 28769, and 28770.

28799 (CEA-N-1385) REACTIVITY MEASUREMENTS USING THE CONTINUOUS RUN TECHNIQUE. Eckert, Hans G.; Jacquemart, Rene (Commissariat a l'Energie Atomique, Cadarache (France). Centre d'Etudes Nucleaires). Feb 1971. 39p. (In French). Dep. NTIS (U. S. Sales Only).

The reactivity of a reactor can be determined by the continuous run technique, a signal being continuously measured which is proportional to the power. The method is particularly suitable for the calibration of absorbers in reactor physics, such as control elements or safety rods. The theoretical aspects of the method and the knowledge acquired from tests made on the mock-up of the high flux Franco-German reactor are presented. The results are compared with those obtained using other methods, such as divergences and pulsed neutron techniques. 6 references. (auth) (France)

28800 (COO-2109-3) STABILITY DOMAINS IN NONLINEAR POINT REACTOR DYNAMICS. Kendall, James Michael (Arizona Univ., Tucson. Dept. of Nuclear Engineering). Jan 1971. Contract AT(04-3)-670. 47p. Dep. NTIS.

Thesis.

The nonlinear point reactor kinetics model with linear reactivity feedback is studied to determine stable regions of the state space. Geometric and Liapunov techniques are used to determine system stability and effects of system parameters on the stable region. In studying the one temperature region model with effective lifetime kinetics and a power coefficient, a transformation is obtained which simplifies analysis of the system. Using this transformation an exact solution is found for parameter values such that the system is a nonlinear center. In addition, a Liapunov function is developed which proves asymptotic stability for an infinite sector of the phase space. The stable region shown by this method is compared to those shown by previous techniques for a given set of parameters. In applying the method to the two temperature region model with effective lifetime kinetics, a set of trajectories asymptotically approaching lines of constant reactivity is shown to exist. An infinite region bounded by three intersecting planes with the property that all trajectories crossing the planes move toward the interior of the region is determined. The parameter condition required for existence of this region is shown to be identical to the condition for the existence of stable limit cycles previously stated. Numerical examples studied indicate the region described above is one of bounded trajectories, i.e., all trajectories with finite initial conditions within the region remain bounded. Possible applications of the method to higher order systems is discussed. Preliminary studies indicate a set of trajectories asymptotic to lines of constant reactivity exists for these models, and that this set may be of assistance in an attempt to define regions of stability. 7 references. (auth)

28801 (DP-MS-70-78) JOSHUA LATTICE PHYSICS SUBSYSTEM. Honeck, H. C.; Pryor, R. J.; Henderson, C. E.; Hightower, W. H. (Du Pont de Nemours (E. I.) and Co., Aiken, S. C. Savannah River Lab.). 18 Mar 1971. 8p. (CONF-710302-1). Dep. NTIS.

From Meeting on new development in reactor mathematics and applications; Idaho Falls, Idaho (29 Mar 1971).

The Lattice Physics Subsystem of the JOSHUA system accepts a description of an infinite lattice and computes spectra, reaction rates, and few-group cross sections. A brief description of the

subsystem is presented and some of the features and results are discussed. (H.D.R.)

28802 (EUR-4554) TIGER: PROGRAMME FOR THE CALCULATION OF THE THERMAL CROSS SECTIONS IN A LIGHT-WATER NUCLEAR REACTOR. Criscuolo, L.; Paterlini, V. (FIAT, Turin (Italy). Sezione Energia Nucleare. ANSALDO S.p.A., Genoa (Italy)). Mar 1971. 88p. (In Italian). Dep. NTIS (U. S. Sales Only). EUR Lit. 1,560.

The Tiger programme calculates the thermal spectrum in a fuel cell with particular reference to the zones to which the latter is subdivided (fuel, cladding and moderator). The heterogeneity of the cell is taken into consideration by defining in each of the 310 thermal microgroups of a scheme similar to the SOFOCATE, average thermal cross sections weighted on the local cell fluxes, calculated by means of the Amouyal and Benoist model. With such a homogenisation, depending on the energy, it is possible to use a thermalisation model based on a homogeneous medium. The model used in the Tiger is SOFOCATE. As required, it is possible to obtain from the Tiger thermal constants averaged over one of the following spectra: Maxwellian; Wigner and Wilkins (light moderator); and Wilkins (heavy moderator) with a cut-off higher than the energy interval, variable up to 2 eV. 5 references. (auth)

28803 (EUR-4555) WIGNER: PROGRAMME FOR THE CALCULATION OF THE MEAN THERMAL CROSS SECTIONS IN THE REACTOR CORE AND FOR THE PUNCHING OF LOAD DATA FOR CALCULATING THE EPITHERMAL CROSS SECTIONS. Claps, M.; Console, M.; Moncassoli, A. M.; Paterlini, V. (FIAT, Turin (Italy). Sezione Energia Nucleare. ANSALDO S.p.A., Genoa (Italy)). Mar 1971. 128p. (In Italian). Dep. NTIS (U. S. Sales Only). EUR Lit. 2,180.

The object of the Wigner programme is to improve the methods of nuclear planning of the reactor core. It combines the most up-to-date methods of calculation in a single programme so as to indicate with two consecutive machine runs the average thermal and epithermal cross sections in the core. The Wigner programme embodies the Tempest programme for the calculation of the thermal spectrum and punches the cards for the FORMEGA programme for the evaluation of the epithermal and rapid spectrum, enabling the operator to make a successive calculation with the FORMEGA programme. Use is also made of the most up-to-date techniques for the calculation of the heat damage factors and the epithermal self-screening factors (Amouyal-Benoist method with Maxwellian and Wigner-Wilkins cross sections; calculation of the resonance transparency factor by a semi-empirical formula showing good agreement with the Monte Carlo method). The thermal calculation is recycled in order to assess the damage factors with Wigner-Wilkins cross sections. One characteristic of the Wigner programme is the extreme simplicity of the data required for the calculation. Only the geometrical data, temperatures and densities are needed. The results of the calculation consist of thermal cross sections and punch cards for the epithermal calculation. The programme is written in FORTRAN-IV by means of a 32K-IBM-7040. (auth)

28804 (EURFNR-835) INFLUENCE OF REAL DEAD-TIME SIMULATION ON THE DYNAMIC BEHAVIOR OF THE COMPUTER MODEL OF THE AUTOMATICALLY CONTROLLED Na-2 REACTOR. Koepp, C. (Kernforschungszentrmum, Karlsruhe (West Germany). Institut fuer Reaktorentwicklung). Translation of report KFK-1179. 65p. Dep. NTIS.

Work Performed under United States-Euratom Fast Reactor Exchange Program.

The results of the Na-2 reactor control studies which were carried out with the digital dynamic simulator DAS2 on the IBM 360/65 computer are presented. A certain number of studies were done on the IBM 360/91 computer; for these it was necessary to make some changes in the control cards. The aim was to discover whether the generally applied simulation of the dead-time relations in the model by first-order time delays yields a better automatic control behavior than does simulation by real dead-time members. 5 references. (auth)

28805 (EURFNR-898) CALCULATION OF FLUX DISTRIBUTIONS IN REACTOR SUB-REGIONS WITH GENERALIZED MULTIPLE COLLISION PROBABILITIES. Mayer, L. (Kernforschungszentrum, Karlsruhe (West Germany). Institut fuer Neutronenphysik und Reaktortechnik). Nov 1970. 22p. (KFK-1334). Dep. NTIS (U. S. Sales Only).

Work Performed under United States-Euratom Fast Reactor Exchange Program.

The theory of multiple collision probabilities for one-dimensional problems has been extended for handling thick zones and strongly anisotropic fluxes. This entails the treatment of space dependent scattering sources and anisotropic fluxes at the boundaries of subzones. For plane geometry anisotropic scattering sources have been included. A multigroup collision probability code STOWA based on the extended theory has been written. It may be used in connection with diffusion calculations or independently and may perform cell calculations or determine flux distributions in special layers of a reactor, e.g. in the blanket or the shielding. Results are given and compared to other transport codes and measurements. Different approximations to angular scattering on hydrogen are evaluated with the code. 15 references. (auth)

28806 (RD/B/N-1837) AXIAL BUCKLING MEASUREMENTS IN B.N.L. MARK II STACKS: RESULTS AND INTERPRETATION. Waterson, R. H. (Central Electricity Generating Board, Berkeley (England). Berkeley Nuclear Labs.). Jan 1971. 49p. (RPC/RPNK/P-(70)80). Dep. NTIS (U. S. Sales Only).

Measurements of axial buckling on a number of lattices were made in order that the correct axial leakage could be accounted for in XY diffusion code calculations. The experiments and their analysis are described, and a comparison is made with theoretical values. A theoretical overestimate of 6-10% of the axial buckling is reported. Attempts to discover the cause of this discrepancy are described. A theoretical underestimate of migration area asymmetry of about 10% is the most likely cause. (auth) (UK)

28807 (ZJE-101) DIFFERENCE METHOD OF SOLUTION OF TWO-DIMENSIONAL MULTIGROUP TIME-INDEPENDENT DIFFUSION EQUATIONS. Krysl, V. (SKODA Concern, Pilsen (Czechoslovakia). Nuclear Power Plant Div.). 1971. 20p. Dep. NTIS (U. S. Sales Only).

A numerical solution of a two-dimensional system of time independent multigroup diffusion equations is presented. On principle it is very simple to expand this method for a three-dimensional problem, but in such a case from the point of view of economical solution it is more advantageous to use the synthesis technique. The system of partial differential equations is being replaced by a system of difference linear algebraical equations. The DIFFIT-code procedure in ELLIOTT-AUTOCODE for NE 803 B and NE 503 was worked out. This procedure serves mainly for calculations of the reactor core. Further the REDIFFIT-code variant for radiation shielding calculations by using the removal-diffusion method was worked out. The number of mesh-points for the computers named above is 1000, the number of chosen groups is 30. The slowing-down of neutrons from the given group into all lower groups was taken into consideration. By a suitable choice of the boundary conditions it is possible to use these procedures for one-dimensional problems (plane and cylinder). (auth)

28808 PROBLEM OF NUMERICAL CALCULATIONS FOR REACTORS. Nathschlaeger, P.; Putz, F.; Wagner, J. (Oesterreichische Studiengesellschaft fuer Atomenergie GmbH, Vienna). Acta Phys. Austr.; 29: 251-6(1969). (In German).

The difficulties found in the numerical calculation of reactors are discussed and the development of synthesis methods to avoid these difficulties is reviewed. (9 references) (J.S.R.)

28809 QUESTION CONCERNING THE DECREASE OF CRITICAL MASS OF A REACTOR BY MEANS OF ZONES WITH CONSTANT DENSITY OF THERMAL NEUTRONS. Zima, T. E.; Kostritsa, A. A. Izv. Akad. Nauk Kaz. SSR, Ser. Fiz.-Mat.; No. 6, 73-7(Nov-Dec 1969). (In Russian).

28810 INVESTIGATION OF THE ASYMPTOTIC STABILITY IN THE LARGE OF THE LINEAR MODEL OF THE CIRCULATING FUEL REACTOR. Adamski, J. (Technical Univ., Warsaw). Bull. Akad. Pol. Sci., Ser. Sci. Tech.; 18: 1005-11(1970).

The asymptotic stability in the large of the circulating fuel reactor was analyzed. This type of a reactor is described by means of space independent differential-difference linear equations. Bellman's theorem was applied to solve the problem. Two numerical examples are solved to illustrate the theory. (auth)

28811 STUDY OF THE EFFECTS OF ^{135}Xe ON A THERMAL REACTOR USING A DIRECT NUMERICAL SOLUTION. Bingham, Billy Elias. Charlotsville, Va.; Univ. of Virginia (1970). 131p. University Microfilms Order No. 70-26,565.

Thesis.

A numerical solution technique was developed to study both the fundamental and the higher-order modes of the stability of a thermal reactor as affected by xenon-135 feedback; the technique was applied to typical one-dimensional problems. For the higher-order stability modes, a set of iodine-135, xenon-135, neutron distribution, and heat balance equations were solved at each mesh point. The fundamental mode was suppressed by maintaining a constant outlet temperature of the coolant flowing through the reactor. The computer program XEIOD, written in ALGOL, had a run time of about 15 minutes on the Burroughs B5500 for a typical transient study. Typical solution times for

current production codes are on the order of several hours. The XEIOD program was used for a parametric survey with these resulting conclusions: (1) By increasing the flux level in a reactor with no power level-control, the reactor passed through a region where the power level was unstable. (2) Zoning the core to flatten the flux shape reduced the size boundary of the stable reactor core. (3) The physical location of the control rod within the core had a noticeable effect on the size boundary of the stable reactor core. (4) The size boundary depended on the type of reactor fuel in the core and was primarily a function of the delayed xenon-135 production. (Diss. Abstr. Int., B)

28812 COMPARISONS OF TRANSPORT AND DIFFUSION THEORY CALCULATIONS OF PERFORMANCE CHARACTERISTICS FOR LARGE FAST REACTORS. Rohan, Paul Edward. Urbana, Ill.; Univ. of Illinois (1970). 172p. University Microfilms Order No. 71-5217.

Thesis.

A detailed comparison of transport and diffusion theory calculations of performance characteristics for large fast reactor assemblies is made. Included in the performance characteristics are the breeding ratio, sodium void coefficients and Doppler coefficients. In addition, k-effective, and the scalar and directed fluxes from diffusion and transport theory are also compared. Six assemblies in all are studied. These include 400, 770 and 4400 liter slabs and cylinders. The assemblies are UC or PuC–UC fueled and sodium cooled. Variations arising from nuclear data are eliminated from the performance characteristics calculations by using the same cross section sets for all computations. The calculations are performed using transport and diffusion theory perturbation codes with DTF-IV or MACH-1 generated fluxes. (Diss. Abstr. Int., B)

28813 APPLICATIONS OF OPTIMAL CONTROL THEORY TO SPACE–TIME REACTOR KINETICS. Specker, Steven Robert. Ames, Iowa; Iowa State Univ. (1970). 96p. University Microfilms Order No. 71-7332.

Thesis.

The development and application of a technique for determining optimal control programs for a space-dependent nuclear reactor is presented. Various numerical optimization methods for solving trajectory optimization problems are discussed. The natural Mode Approximation method is used to reduce the space and time dependent multi-group diffusion equations to a system of coupled, nonlinear, ordinary differential equations involving the time coefficients of the modal expansion and the control variable. State variable techniques are used to formulate a specific problem in terms of a trajectory optimization problem. The method of conjugate gradients in conjunction with a penalty function approximation is adapted to obtain an algorithm for the iterative solution of the optimization problems. The theory is applied to a bare slab reactor model described by the two-energy group, one delayed group diffusion equations. Optimal control schemes are presented for fixed transition time, minimum control energy power level changes. Comparisons are made with point kinetics and finite difference methods. (Diss. Abstr. Int., B)

28814 CALCULATION OF TEMPERATURE EFFECTS ON REACTOR NEUTRON SPECTRA. Stefan, Horia (Inst. of Nuclear Physics, Bucharest). Stud. Cercet. Fiz.; 22: 767-94(1970). (In Rumanian).

The rethermalization cross section method is treated and covers the variational method, the temperature-dependent diffusion equation, the Cadilhac and Purica methods, and a thermodynamic approximation. (J.F.P.)

Dynamics

Refer also to abstract 28665.

Experimental Applications

28815 (BNWL-tr-66) NEUTRON TRANSPORT BY A MOVING MEDIUM. Vasiliev, G. Y.; Kaminker, D. M.; Konoplev, K. A.; Kostritza, A. A. Translated for Battelle-Northwest, Richland, Wash., from At. Energ. (USSR); 28: 356-7(1970). 6p. Dep. NTIS.

The effects of a moving column of water on transport of neutrons in a beam perpendicular to the water filled tube were investigated. Experimental values of the diffusion coefficients obtained are found to compare favorably with calculations and with previously measured values. The results indicate that the neutron diffusion coefficient in water is independent of the turbulence. (H.D.R.)

28816 (RD/B/N-1518) MANGANESE REACTION RATE MEASUREMENTS IN B.N.L. REACTORS. Beynon, A. J.; Waterson, R. H. (Central Electricity Generating Board, Berkeley (England). Berkeley Nuclear Labs.). Jul 1970. 43p. (RPC/RPNK/P-(71)7). Dep. NTIS (U. S. Sales Only).

Manganese reaction rates were measured in a range of axially uniformly fuelled reactors designed to test theoretical techniques available for CAGR performance problems. Parameters considered were relative channel powers in the core, cross channel gradients, cross pin gradients, fuel axial and radial fine structure and moderator cell fine structure. The arrays of fuel used included vacancies and differing fuel weights and enrichments. (auth) (UK)

28817 METHOD BASED ON REACTIVITY MEASUREMENTS FOR DETERMINING THE PORTION OF FISSION ATTRIBUTABLE TO EPITHERMAL NEUTRONS. Demin, V. E.; Smirnov, O. N. At. Energ. (USSR); 29: 372-4(Nov 1970). (In Russian).

A method was developed to determine what portion of the fission may be due to epithermal neutrons. The determination was based on measurements of reactivity changes in the system. These changes are produced by substituting elements containing fissionable materials by identical, cadmium-clad ones or by unclad and cadmium-clad elements containing either fissionable, absorbing, or scattering materials. The high precision of the experimental results indicated that the method is well suited for the study of heterogeneous reactors. The experiment described involved flat, $100 \times 100 \times 0.5$ mm elements, consisting of a heterogeneous mixture of polyfluoroethylene resin and U_3O_8 with 90% enriched ^{235}U, clad with the same resin. Elements containing various amounts of boron were used as absorber. The fuel element was replaced by the absorbing element, then by the cadmium-clad fuel element and then by the cadmium-clad absorbing element, measuring the respective reactivity changes. (TTT)

28818 EXPERIMENTAL INVESTIGATION OF NEUTRON PULSES THROUGH AN INTERFACE AND MODERATOR LATTICE. Harper, Boyd Elbert Jr. Los Angeles; Univ. of California (1970). 258p. University Microfilms Order No. 71-3820.

Thesis.

Thermal neutron flux time and space dependence was investigated experimentally using a neutron pulse, for diffusion of neutrons through: (1) an assembly of graphite moderator, (2) an interface of two dissimilar moderators, styrofoam and graphite, and (3) a lattice formed by alternate layers of styrofoam and graphite. The thermal neutron source was produced by moderating 14 MeV neutron pulses in graphite to thermal energies. Flux space dependence was observed by taking measurements with a boron trifluoride chamber at several locations in each assembly. Flux time dependence was observed by recording the neutron density with time at each detector location, using a multichannel analyzer. Data analysis consisted of: (1) smoothing the neutron pulse time histories at each location by least squares methods, (2) taking the numerical Laplace transform of the discrete, smoothed counts per channel versus time data to convert it from the time to frequency domain, and (3) calculating neutron diffusion parameters and spatial distributions from the experimental data using diffusion theory. (Diss. Abstr. Int., B)

Reactor Components, Fuels, and Accessories

Refer also to abstracts 26157, 26458, 26460, 26550, 27195, 27202, 27219, 27275, 27276, and 27829.

28819 (EUR-4552) EXPERIMENTAL DETERMINATION OF THE TURBULENT DIFFUSIVITY COEFFICIENT IN A BUNDLE OF RODS WITH AND WITHOUT SPACER GRIDS. Debernardi, M.; Valtancoli, A. (FIAT, Turin (Italy). Sezione Energia Nucleare. ANSALADO S.p.A., Genoa (Italy)). Mar 1971. 26p. (In Italian). Dep. NTIS (U. S. Sales Only). EUR Lit. 500,-.

The turbulent diffusivity coefficient of the coolant is a factor to be considered in the thermohydraulic planning of the core in determining the engineering factor of a hot channel, or directly as an input datum of thermohydraulic codes. This coefficient is determined experimentally by means of the tracer method, by injecting water of a temperature exceeding that of the water circulating in the section being tested. The geometry within which the water flows was formed by a bundle of rods arranged in the form of a square lattice; the pitch/diameter ratio was 1.31. The determinations were made both without spacer grids and with spacer grids of the ferrule type. The determinations were successively made with an inclined grid device adapted to increase the transfer of mass through the channels of the bundle. The pitch/diameter ratio

XUM

of the present experiment is the highest of those of similar experiments of which these results have been recorded. A comparison of the results with those of other experiments shows that the coefficient of turbulent diffusivity increases with an increasing pitch/diameter ratio. The sequence of the tests shows the influence on the turbulent mixing of spacer grids with a special geometrical arrangement. 3 references. (auth)

28820 (EUR-4556) ANALYTICAL METHOD FOR REPRESENTING CYLINDRICAL B_4C ABSORBERS IN TWO-DIMENSIONAL DIFFUSION CALCULATIONS. Rama, P. G.; Claps, M. (FIAT, Turin (Italy), Sezione Energia Nucleare, ANSALDO S.p.A., Genoa (Italy)). Mar 1971. 38p. (In Italian). Dep. NTIS (U. S. Sales Only). EUR Lit. 750,-.

Since the 1/V curve of the epithermal collision cross-sections of boron does not pose the difficulties inherent in the treatment of resonances, an analytical method has been developed for calculating the efficiency of B_4C cluster rods, its validity being checked by examining critical experiments performed in the presence of B_4C absorbers. Comparison of the calculated and measured values shows that the computation method described here is valid to an error of 4 to 5% for estimating the efficiency of B_4C clusters. 13 references. (auth)

28821 FISSION-GAS RELEASE FROM NUCLEAR FUELS WITH IN-PILE GAS-LOOP. Inoue, Kiyoshi; Taniguchi, Kaoru; Doi, Akira; Osawa, Yasuo (Hitachi Ltd., Kawasaki, Japan). Hitachi Hyoron; 51: 197-202(Mar 1969). (In Japanese).

Nuclear-fuel irradiation experiments were begun using the gas-loop installed in the Hitachi Training Reactor. Fission-gas release from UO_2 during irradiation was studied. The UO_2 specimen was externally heated by electric heating in order to simulate the condition under which it is burned in power reactors. The gas-loop was improved step by step so that the experiment can be carried out under high temperature irradiation. The in-core assemblies in which UO_2 is mounted were also improved. It was found that the annealing of lattice defects in UO_2 played an important role in fission-gas release at irradiation temperatures below 1200°C. New information was obtained on fission-gas release from fissioning UO_2 at temperatures conductive to grain growth (around 2000°C). (Japan)

28822 FAST RESPONSE CONTROL OF REACTOR POWER ON THE BASIS OF γ RADIATION INTENSITY. Emel'yanov, I. Ya.; Konstantinov, L. V.; Postnikov, V. V.; Potapkin, V. I.; Serebrennikov, Yu. M. At. Energ. (USSR); 29: 298-9(Oct 1970). (In Russian).

The delayed γ radiation complicates the control of reactor power based on in-core γ detectors. In order to clarify this problem the time correlation between the γ radiation intensity and the number of fission events in the core or in some of its specific regions was investigated. The value of the coefficients encountered in the formulas concerning the prompt and delayed γ radiation was found to depend on the reactor type involved. The effect of the burnout may be conveniently calculated by known equations. A main goal of using γ detectors lies in the determination of the fission rate or its distribution within the core. The use of derived formulas for such a purpose was experimentally tested on the IRT reactor. The calculated amplitude-frequency characteristics and the time dependence determined from the energy emitted by the γ quanta after the fission event were plotted, comparing also the readings of neutron and γ chambers. The neutron chamber readings were found to differ from the calculated fission rate by less than 4%. The error in the calculation of the fission rate under transient conditions may be reduced by using a higher number of exponents. The method may also be used to eliminate the inertia of the direct charge instruments. (TTT)

28823 A CYLINDRICAL REINFORCED CONCRETE PRESSURE VESSEL FOR NUCLEAR REACTORS. Vaessen, Franz (to Hochtief AG Fuer Hoch-Und Tiefbauten, Vorm. Gebr. Helfmann). British Patent 1,224,278. 10 Mar 1971. Priority date 9 Aug 1969, Germany.

PRESSURE VESSELS—design of prestressed reinforced concrete cylinder shaped

REACTORS—pressure vessels for, description of prestressed reinforced concrete cylinder shaped (D.C.C.)

28824 NUCLEAR REACTOR FUEL ELEMENT ASSEMBLIES. (to Atomic Energy of Canada Ltd.). British Patent 1,225,470. 17 Mar 1971. Priority date 27 Mar 1969, United States.

REACTOR FUEL ELEMENTS—design of spaced 19 rod bundle assemblies of (D.C.C.)

28825 FUEL ELEMENT REPLACEMENT APPARATUS FOR USE IN CONJUNCTION WITH A VERTICAL-CHANNEL NUCLEAR REACTOR. Buzzi, Umberto; Dufresne, Jacques; Farfaletti-Casali, Flaviano (to EURATOM). British Patent 1,226,308. 24 Mar 1971. Priority date 5 Feb 1969, Italy.

REACTOR LOADING MACHINES—design of low profile horizontal, for vertical core reactors (D.C.C.)

28826 IMPROVEMENTS IN OR RELATING TO NUCLEAR FUEL ELEMENTS AND THE MANUFACTURE THEREOF. (to Gulf General Atomic Inc.). British Patent 1,226,207. 24 Mar 1971. Priority date 25 Jun 1967, United States.

REACTOR FUEL ELEMENTS—design of packed bed pyrolytic carbon coated particles in resin filler

—fabrication of packed bed pyrolytic carbon coated particles in resin filler (D.C.C.)

28827 NUCLEAR REACTOR FUEL ELEMENT ASSEMBLY. (to Atomic Energy of Canada Ltd.). British Patent 1,226.929. 31 Mar 1971. Priority date 15 Apr 1969, United States.

REACTOR FUEL ELEMENTS—design of spaced 19 rod assemblies (D.C.C.)

28828 IMPROVEMENTS IN AND RELATING TO GRAPHITE MODERATED NUCLEAR REACTORS. Quick, Martin Vinicombe; Roberts, Geoffrey Alfred; Yellowlees, John Mackinlay (to Nuclear Power Group Ltd.). British Patent 1,226,264. 24 Mar 1971. Filed 30 May 1969.

It has been proposed that the graphite blocks should be replaceable during the operating life of a graphite moderated nuclear reactor. In such cases the fuel is located within the blocks and is removable with them. The use of keying systems, especially between blocks of adjacent columns, can lead to difficulties, including the high forces needed to withdraw the blocks. In the system described at least some of the uppermost blocks have laterally displaceable members adapted to engage the sides of displaceable members of corresponding uppermost blocks of adjacent columns, to maintain within predetermined limits a fixed column spacing. These members are retractable to allow removal of the uppermost and other blocks of a column. The displaceable members may be displaced by an actuating member adapted to be moved in the direction of the longitudinal axis of the blocks, and preferably acting through rollers to reduce the force required. This actuating member may take the form of a wedge actuated by lowering or raising a weight by means of a grab. If the column of blocks houses a control rod, a guide tube can be used as the actuating member. The individual blocks of a column may be spigotted together. (UK)

28829 IMPROVEMENTS IN OR RELATING TO FILTERS. Marshall, Dennis Albert George. British Patent 1,225,751. 24 Mar 1971. Filed 30 Dec 1966.

Reference is made to filters such as are used for removing particulate material from nuclear reactor gas streams or gas streams from other installations. The aim of the filter described is guaranteed removal of at least 99.9% of the particulate matter. It comprises two or more plies of honeycomb material slightly offset relative to each other and containing granules of activated carbon. The peripheral edges of the plies are covered by layers of foamed plastic sealed into a moulded plastic surrounding frame. A great advantage of this construction is that it prevents "tracking" or leakage of particles between the peripheral portions of the filtering medium and the surrounding frame. The plies of honeycomb material may be formed of resin-impregnated paper, and a metal grille may be interposed between the plies or between each pair of adjacent plies where more than two are provided, these grilles being coated with a thermoplastic material that bonds the grilles to the plies and holds the plies together. Methods of manufacturing such filters are described. (UK)

28830 NUCLEAR REACTOR STANDPIPES. Prince, Norman (to United Kingdom Atomic Energy Authority). British Patent 1,225,360. 17 Mar 1971. Filed 26 Jan 1968.

During reloading of a fuel element channel, through a standpipe, there is a tendency for the coolant flow through the channel to increase to a value called the "empty channel flow," which can be ten or more times the flow with a fuel stringer in position. Insertion of a stringer against this flow is difficult and the stringer receives a severe buffeting that can damage it. This buffeting can be avoided by arranging the reactor so that the coolant flow is in the direction of stringer insertion, but with top refuelling this would effectively increase the weight of the stringer. In the arrangement described the reactor has an internal coolant plenum, a standpipe extending from outside the reactor core structure to the plenum, and a charge tube extending from a fuel element channel to the plenum. The standpipe and charge tube are in spaced end-to-end alignment and interconnected by a tubular valve closure member to afford a passage extending from the channel to outside the core structure. Means are provided, operable from outside, for rotating the valve closure member within the standpipe. The charge tube

XUM

and valve closure member have co-operating wall apertures forming a port for coolant flow between the charge tube and the plenum, this port being variable in size by rotation of the valve closure member. (UK)

28831 GAS COOLED NUCLEAR REACTORS. Shaw, Michael Kevin; Long, Everett (to English Electric Co. Ltd.). British Patent 1,225,487. 17 Mar 1971. Filed 23 May 1967.

Reference is made to reactor gas circulating systems having a circulator unit removably housed in an aperture in the concrete pressure vessel wall. In the system described a removable primary pressure containment means is provided that closes off the aperture externally, together with a secondary pressure containment means that will limit the escape of coolant when the primary containment means is removed. Full constructional details are given. Objects of this system are to provide means for secondary containment without the need to rely on axial movement of the circulator shaft and impeller, and to eliminate the special equipment necessary to accommodate such axial movement; also to provide secondary containment that is accessible without removing the circulator unit, and having no moving parts; also to provide secondary containment even when the circulator unit is operating, so that no action is necessary to establish such containment in the event of failure of the primary containment. (UK)

28832 SOUND ABSORBING DEVICES. Harrington, Peter Bryan; Barclay, Arthur (to Nuclear Design and Construction Ltd.). British Patent 1,225,771. 24 Mar 1971. Filed 28 Mar 1967.

A sound absorbing device is described for fitting to the wall of a gas duct, such as a gas circulator intake duct of a gas-cooled nuclear reactor. The device includes a perforated plate, with a layer of metal wire mesh adjacent to the surface of the plate nearer to the wall, together with an arrangement adjacent to the mesh for defining a number of resonant chambers each communicating via the mesh with a number of plate perforations. The arrangement may include baffles extending between the mesh and the wall. Alternatively the arrangement may include one or more open boxes, each box being located with its opening adjacent to the mesh. (UK)

28833 COMPRESSOR FOR A HIGH PRESSURE HELIUM CIRCUIT FOR COOLING HIGH TEMPERATURE FUEL ELEMENTS DURING IRRADIATION EXPERIMENTS. Melzer, E.; Meyer, J. (Deutsche Forschungs- und Versuchsanstalt fuer Luft- und Raumfahrt E. V., Goettingen, Ger.). Kerntech. Atomprax.; 13: 118-21 (Mar 1971). (In English and German).

A compact compressor is described in which a high pressure rise is obtained for a low mass flow rate at a high intake pressure. The rotor is in the shape of a truncated cone, with straight borings from the inner to the outer diameter serving as stream tubes. The rotor is driven by a frequency controlled, high speed, three-phase induction motor located inside the compressor casing. 4 references (auth)

28834 IMPROVEMENTS RELATING TO NUCLEAR REACTORS. (to Combustion Engineering, Inc.). British Patent 1,228,610. 15 Apr 1971. Priority date 5 Dec 1967, United States.

REACTOR FUEL ELEMENTS — end retaining member for, with means for control of longitudinal thermal expansion (H.D.R.)

28835 NOISE EFFECT OF VIBRATING CONTROL ELEMENTS. Barrett, Paul R. (Univ. of New South Wales, Sydney). Atomkernenergie; 17: 175-84(May 1971).

The effect of control element vibrations on the reactivity of a reactor and as a general source of neutron flux noise is examined for the cases of a large regular array of control elements, arrays of control elements arranged in groups, each group containing a regular array, and a finite reactor containing a small number of control elements. Finally the case of control elements so widely separated that there is negligible neutron interaction between them is discussed; in this latter situation there is no significant reactivity effect but there are strong local effects on the neutron flux with stochastic noise effects owing to the random components of the control element vibrations. 5 references. (auth)

28836 IMPROVEMENTS IN AND RELATING TO WATER-COOLED NUCLEAR REACTORS. Wadmark, Lars Olof Tor (to Aktiebolaget Atomenergi). British Patent 1,165,689. 1 Oct 1969. Priority date 3 Dec 1965, Sweden.

REACTOR LOADING MACHINE — guide tubes for, description of reactor bottom penetrating

REACTORS, WATER COOLED — refueling tube for, description of bottom penetrating (H.D.R.)

28837 IMPROVEMENTS IN OR RELATING TO NUCLEAR REACTOR FUEL ELEMENTS. D'Eye, Royston Walter Mastin; Shennan, John Vincent; Cutts, Burton (to United Kingdon Atomic Energy Authority). British Patent 1,225,970. 24 Mar 1971. Filed 20 Dec 1967.

Reference is made to sheathed cluster type fuel elements. The fuel element described is characterized by a sheath of SiC containing oxide fuel, with means interposed between sheath and fuel for absorbing fission fragments and preventing chemical reaction. For this purpose a layer of pyrolytic carbon may be deposited on the sheath interior, or alternatively a layer of Al_2O_3 or BeO may be employed, or a sprayed coating of Si. The oxide fuel may be in the form of a stack of solid or hollow pellets, or full sheath length solid, or a hollow rod. The fuel may also be in the form of a mass of vibrocompacted particles. Suitable gaps may be initially provided in the coatings to accommodate gaseous fission products and/or thermal expansion of the fuel, or where the interposed material is low density pyrolytic carbon and is crushable. (UK)

XUM

GENERAL

28838 (ANL–7764) NOTES ON ELECTRON PARAMAGNETIC RESONANCE SPECTROSCOPY. McMillan, Juan A. (Argonne National Lab., Ill.). Dec 1970. Contract W-31-109-eng-38. 112p. Dep. NTIS.

28839 (ANL/ES–4) PHOTOGRAPHIC METHOD FOR DETERMINING VELOCITY DISTRIBUTIONS WITHIN THERMAL PLUMES. Asbury, J. G.; Grench, R. E.; Nelson, D. M.; Prepejchal, W.; Romberg, G. P.; Siebold, P. (Argonne National Lab., Ill.). Feb 1971. Contract W-31-109-eng-38. 20p. Dep. NTIS.

28840 (ANL/ES-CC–8) CHICAGO AIR POLLUTION SYSTEMS ANALYSIS PROGRAM. LONG-RANGE PLANNING IN AIR RESOURCE MANAGEMENT. Cohen, A. S.; Croke, E. J.; Hurter, A.; Norco, J. E.; Roberts, J. J. (Argonne National Lab., Ill.). Jan 1971. Contract W-31-109-eng-38. 137p. Dep. NTIS.

28841 (BMI–171-133) FRESHWATER VERTEBRATE AND INVERTEBRATE ECOLOGY OF AMCHITKA ISLAND. Amchitka Bioenvironmental Program. Annual Progress Report, July 1, 1969–June 30, 1970. Neuhold, John M.; Helm, William T. (Utah State Univ., Logan). 1 Apr 1971. Contract AT(26-1)-171. 15p. Dep. NTIS.
For Battelle Memorial Inst., Columbus, Ohio.

28842 (CALT–822-26) MOESSBAUER STUDY OF BiF_3 TYPE ORDERING IN METASTABLE FeGa ALLOYS. Newkirk, L. R.; Tsuei, C. C. (California Inst. of Tech., Pasadena. W. M. Keck Lab. of Engineering Materials). Apr 1971. Contract AT(04-3)-822. 13p. Dep. NTIS.

28843 (CALT–822-27) HYPERFINE MAGNETIC INTERACTIONS IN Fe–Ga SOLID SOLUTIONS. Newkirk, L. R.; Tsuei, C. C. (California Inst. of Tech., Pasadena. W. M. Keck Lab. of Engineering Materials). Apr 1971. Contract AT(04-3)-822. 22p. Dep. NTIS.

28844 (CALT–822-28) TWO CURRENTS CONDUCTION IN KONDO ALLOYS. Hasegawa, Ryusuke (California Inst. of Tech., Pasadena. W. M. Keck Lab. of Engineering Materials). Apr 1971. Contract AT(04-3)-822. 7p. Dep. NTIS.

28845 (COO–256-102) ELECTROCHEMICAL RESEARCH IN AMINE SOLVENTS. Final Report. Schaap, Ward B.; Schmidt, Frederic C. (Indiana Univ. Foundation, Bloomington). Mar 1971. Contract AT(11-1)-256. 12p. Dep. NTIS.

28846 (COO–1469-178) ORBIT: ONLINE REDUCED BANDWIDTH INFORMATION TRANSMISSION. Report No. 430. Oberbeck, Peter Ernst Rudolf (Illinois Univ., Urbana. Dept. of Computer Science). Feb 1971. Contract AT(11-1)-1469. 87p. Dep. NTIS.
Thesis.

28847 (COO–1599-32) ROLE OF CARBON IN HARD-WATER LAKES. Wetzel, Robert G. (Michigan State Univ., Hickory Corners. W. K. Kellogg Biological Station). [1971]. Contract AT(11-1)-1599. 35p. Dep. NTIS.

28848 (COO–1631-27) CARBOHYDRATE AND NUCLEIC ACID METABOLISM IN THE DEVELOPING AMPHIBIAN. Annual Progress Report, February 1, 1970–January 31, 1971. (Wisconsin Univ., Madison. Dept. of Physiological Chemistry). 1 Feb 1971. Contract AT(11-1)-1631. 12p. Dep. NTIS.

28849 (COO–1683-32) MERODIPLOIDY AND EXPRESSION OF EPISOMAL GENES IN PSEUDOMONAS PUTIDA. Chakrabarty, A. M.; Queener, S. F.; Gunsalus, I. C. (Illinois Univ., Urbana. Dept. of Biochemistry). [1971]. 10p. Dep. NTIS.

28850 (COO–1701-16) RETINAL CONE RECEPTOR AS AN IDEAL LIGHT COLLECTOR. Winston, Roland (Chicago Univ., Ill.); Enoch, Jay M. (Washington Univ., St Louis, Mo.). [1971]. 8p. Dep. NTIS.

28851 (COO–2118-5) ILLIAC III REFERENCE MANUAL. VOLUME I: THE COMPUTER SYSTEM. Report No. 433. Atkins, D. E.; Borovec, R. T.; Goyal, L. N.; Katoh, L. M.; Lansford, R. M.; Schwebel, J. C.; Tareski, V. G. (Illinois Univ., Urbana. Dept. of Computer Science). 17 Feb 1971. Contracts AT(11-1)-1018; AT(11-1)-2118. 106p. Dep. NTIS.

28852 (CU–4203-1) COMPREHENSIVE STUDY OF THE SEISMOTECTONICS OF THE ALEUTIAN ARC. Annual Progress Report. (Columbia Univ., Palisades, N. Y. Lamont-Doherty Geological Observatory). Feb 1971. Contract AT(30-1)-4203. 10p. Dep. NTIS.

28853 (DESY–SR–71/1) OPTICAL ABSORPTION OF GASEOUS METHANE, ETHANE, PROPANE, AND BUTANE, AND REFLECTION OF SOLID METHANE AND ETHANE IN THE VACUUM ULTRAVIOLET. Koch, E. E.; Skibowski, M. (Deutsches Elektronen-Synchrotron, Hamburg (West Germany)). Feb 1971. 11p. Dep. NTIS (U. S. Sales Only).

28854 (EGG–1183-1465) WIDE LATITUDE PROCESSING OF TRI-X-ORTHO OSCILLOGRAPHIC FILM. Tech. Report No. L-974. Shaffer, R. M.; Dutton, D. M. (EG and G, Inc., Las Vegas, Nev.). 15 Jan 1970. 47p. Dep. NTIS.

28855 (GAT–T–1649) PRECISE COMPUTERIZED IN-LINE COMPRESSIBLE FLOW METERING. Mustard, G. L. (Goodyear Atomic Corp., Piketon, Ohio). 11 Feb 1971. Contract AT(33-2)-1. 18p. (CONF-710507–1). Dep. NTIS.
From Symposium on flow: its measurement and control in science and industry; Pittsburgh, Pa. (9 May 1971).

28856 (HEDL–TME–71-39) TOPLYR: A TWO-DIMENSIONAL THERMAL ENERGY TRANSPORT CODE. Sonnichsen, J. C. Jr.; Kolesar, D. C. (Hanford Engineering Development Lab., Richland, Wash.). Jan 1971. Contract AT(45-1)-2170. 41p. Dep. NTIS.

28857 (INR–1269) MAGNETIC STRUCTURE OF A MANGANESE-SUBSTITUTED ZINC FERRITE BY NEUTRON DIFFRACTION. Fayek, Mohamed Khorshid (Institute of Nuclear Research, Warsaw (Poland)). 1971. 74p. Dep. NTIS (U. S. Sales Only).

28858 (LA-tr–71-25) POLYVINYL CHLORIDE IMPRESSIONS FOR INDIRECT CARBON REPLICAS IN ELECTRONIC MICROSCOPY. Faberge, Alexander C. Translated from J. Microscop.; 6: 157-68(1967). 11p. Dep. NTIS.

28859 (LA-tr–71-27) VELOCITIES OF PARTICLES OF A REFRACTORY MATERIAL INJECTED INTO AN ARC PLASMA JET. Lemoine, A.; Le Goff, P. Translated for Los Alamos Scientific Lab., N. Mex., from Chim. Ind., Genie Chim.; 102: 1304-11(1969). 16p. Dep. NTIS.

28860 (LA-tr–71-28) PROBLEMS CONNECTED WITH THE GRAPHICAL INTERACTION OPERATOR-COMPUTER. De Lotto, I. (Centro Informazioni Studi Esperienze, Milan (Italy)). Translated from S. I. F. Congress Conference, Bologna, Italy, Oct 1967. 21p. (CONF–671093–1). Dep. NTIS.

28861 (MIT–905-162) PROGRESS REPORT [ON INSTRUMENTAL CHEMISTRY AND HOT ATOM CHEMISTRY], FOR THE YEAR ENDING DECEMBER 31, 1970. (Massachusetts Inst. of Tech., Cambridge). Contract AT(30-1)-905. 31p. Dep. NTIS.

28862 (NAL–55) NAL 1970 ARCHAEOLOGICAL SURVEY: THE PREHISTORIC OCCUPATIONS OF THE NATIONAL ACCELERATOR LABORATORY SITE. Early, Ann M. (National Accelerator Lab., Batavia, Ill.). Nov 1970. 9p. Dep. NTIS.

28863 (NYO–2391-111) STUDIES OF RESONANT PHONON SCATTERING IN KCl:Li USING HEAT PULSES AND MICROWAVE PHONON GENERATION. MSC Report 1311. Channin, Donald Jones (Cornell Univ., Ithaca, N. Y. Materials Science Center). Jun 1970. 106p. Dep. NTIS.
Thesis.

28864 (NYO–3973-8) COINCIDENCE-MOESSBAUER STUDIES OF SOLID STATE PHENOMENA. Progress Report, June 1, 1970–May 31, 1971. Hoy, Gilbert R. (Boston Univ., Mass.). Feb 1971. Contract AT(30-1)-3973. 16p. Dep. NTIS.

28865 (NYO–3976-4) TECHNICAL PROGRESS REPORT, JUNE 1, 1970–MAY 31, 1971. Mazur, A. (New York Blood Center, N. Y.). Contract AT(30-1)-3976. 4p. Dep. NTIS.

28866 (NYO–3976-5) PREPARATION AND PROPERTIES OF SIX RAT RED CELL HEMOGLOBINS. Stein, S.; Cherian, M. G.; Mazur, A. (New York Blood Center, N. Y. City Coll., New York. Dept. of Chemistry). [1970]. 22p. Dep. NTIS.

28867 (NYO–3993-1) AUTOMATED PRIMARY PRODUCTIVITY MEASUREMENTS IN WATER BODIES. PHASE I. FEASIBILITY AND PRELIMINARY DESIGN STUDIES. Levin, Gilbert V.; Simons, Daniel J.; Plakas, Chris (Biospherics,

Inc., Rockville, Md.). 10 Feb 1969. Contract AT(30-1)-3993. 144p. Dep. NTIS.

28868 (NYO-4075-10) PROGRESS REPORT, MAY 1, 1970-APRIL 30, 1971. Artman, Joseph O. (Carnegie-Mellon Univ., Pittsburgh, Pa.). 1 Mar 1971. Contract AT(30-1)-4075. 6p. Dep. NTIS.

28869 (NYO-4078-3) HYDROSTATIC EXTRUSION OF HARD CORE CLAD ROD. Zoerner, William (Lehigh Univ., Bethlehem, Pa.). 1971. 37p. Dep. NTIS.
Thesis.

28870 (NYO-4097-2) FATIGUE-ENHANCEMENT OF DIFFUSION. Progress Report, June 1, 1970-May 31, 1971. Herman, Herbert (State Univ. of New York, Stony Brook). Contract AT(30-1)-4097. 12p. Dep. NTIS.

28871 (ORNL-tr-1991) DYNAMIC TESTS ON TANGENTIAL PIPE FITTINGS. PART 1. TEST RESULTS. Stockman, Godfried; Sijs, Arnold. Translated for Oak Ridge National Lab., Tenn., from report CRIF-MT-28. 27p. Dep. NTIS.

28872 (ORNL-tr-2133) DIAGRAMS FOR THE DETERMINATION OF THE RISK OF FAILURE OF STRUCTURES. Manuzio, Caterina. Translated for Oak Ridge National Lab., Tenn., from Ann. Inst. Tech. Batiment Trav. Publics; 22: 249-57(1969). 15p. Dep. NTIS.

28873 (ORNL-tr-2445) STUDIES ON THE INFLUENCE OF DIFFERENT TRAUMAS ON PREGNANCY IN THE LABORATORY MOUSE. Bloch, Suzanne; Rippmann, Ernst T. Translated for Oak Ridge National Lab., Tenn., from Z. Psychosom. Med.; 14: 33-45(1968). 20p. Dep. NTIS.

28874 (ORNL-tr-2447) APPLICATION OF PHARMACOLOGY TO ANIMAL GROUP PSYCHOLOGY. Kita, Tomitaro; Hata, Taeko; Murakami, Tetsuo. Translated for Oak Ridge National Lab., Tenn., from Nippon Yakurigaku Zasshi; 65: 363-7(1969). 9p. Dep. NTIS.

28875 (ORNL-tr-2457) THEORY OF INTERMOLECULAR NUCLEAR MAGNETIC RELAXATION OF ADSORBED MOLECULES. PART I. Beckert, D. Translated by R. Gregg Mansfield (Oak Ridge National Lab., Tenn.), from Ann. Phys. (Leipzig); (5/6), 20: 220-9(1967). 12p. Dep. NTIS.

28876 (ORNL-tr-2458) THEORY OF INTERMOLECULAR NUCLEAR MAGNETIC RELAXATION OF ADSORBED MOLECULES. PART II. Beckert, D. Translated by R. Gregg Mansfield (Oak Ridge National Lab., Tenn.), from Ann Phys. (Leipzig); (1/2), 23: 98-103(1969). 7p. Dep. NTIS.

28877 (ORO-2572-27) FINAL TECHNICAL REPORT [ON COMPUTER PROJECT], JUNE 1, 1959-MARCH 31, 1970. Orvedahl, Walter (Rice Univ., Houston, Tex.). 19 Jun 1970. Contract AT(40-1)-2572. 43p. Dep. NTIS.

28878 (ORO-3328-13) DEFORMATION SUBSTRUCTURE IN POLYCRYSTALLINE ALUMINA. Becher, Paul F. (North Carolina State Univ., Raleigh). 30 Jun 1970. Contract AT(40-1)-3328. 13p. Dep. NTIS.

28879 (RLO-1750-41) CHEMICAL BUDGET OF THE COLUMBIA RIVER. Park, P. Kilho; Osterberg, Charles L.; Forster, William O. (Oregon State Univ., Corvallis. Dept. of Oceanography). [1970]. 27p. Dep. NTIS.

28880 (RLO-1750-59) TWO NEW GREGARINE PARASITES FROM THE SPATANGOID-URCHIN BRISASTER LATIFRONS. Brownell, Charles; McCauley, James E. (Oregon State Univ., Corvallis. Dept. of Oceanography). [1970]. 14p. Dep. NTIS.

28881 (SC-DC-713920) CLIMATOLOGY OF ATMOSPHERIC DIFFUSION PREDICTION VARIABLES. Church, Hugh W.; Luna, Robert E. (Sandia Labs., Albuquerque, N. Mex.). [1971]. 18p. Dep. NTIS.

28882 (SC-DR-68-796) CIRCUIT FOR MEASURING FREQUENCY DEPENDENT COMPLEX ADMITTANCE AND IMPEDANCE. Snelling, J. B. (Sandia Labs., Albuquerque, N. Mex.). Nov 1968. 12p. Dep. NTIS.

28883 (SC-DR-70-510) USER'S MANUAL FOR THE TWO-DIMENSIONAL AXISYMMETRIC TRANSIENT HEAT CONDUCTION MATERIAL ABLATION COMPUTER PROGRAM (ASTHMA) Moyer, C. B.; Blackwell, B. F.; Kaestner, P. C. (Sandia Labs., Albuquerque, N. Mex.). Dec 1970. 215p. Dep. NTIS.

28884 (SC-DR-70-680) COMPUTERIZED ULTRASONIC DATA ACQUISITION SYSTEM. Bennett, L. C.; Shurtleff, W. W. (Sandia Labs., Albuquerque, N. Mex.). Oct 1970. 29p. Dep. NTIS.

28885 (SC-DR-70-856) A SYSTEM THAT ENABLES A PDP-9 COMPUTER TO UTILIZE A CDC-160A COMPUTER AS A PERIPHERAL CONTROLLER. Borgman, C. R. (Sandia Lab., Albuquerque, N. Mex.). Mar 1971. 95p. Dep. NTIS.

28886 (SC-DR-710033) GENERALIZED INTEGRATED CIRCUIT. Skogmo, David G. (Sandia Labs., Albuquerque, N. Mex.) Mar 1971. 26p. Dep. NTIS.

28887 (SC-DR-710086) EVALUATION OF THE IMPEDANCE PROBE METHOD OF SHOCK SPEED MEASUREMENT. Mulac, A. J.; Guzman, J. A. (Sandia Labs., Albuquerque, N. Mex.). Apr 1971. 15p. Dep. NTIS.

28888 (SC-DR-710192) ADVANCED FILAMENT-WOUND CARBON COMPOSITE. Guess, T. R.; Butler, B. L.; Theis, J. D. (Sandia Labs., Albuquerque, N. Mex.). Mar 1971. 41p. Dep. NTIS.

28889 (SC-RR-70-356) DETERMINATION OF THE ACTIVATION ENERGY FOR THE PRECIPITATION OF Al_6Mn IN Al-3.4 W/O Mn ALLOY. Karnowsky, Maurice M. (Sandia Labs., Albuquerque, N. Mex.). Mar 1971. 44p. Dep. NTIS.

28890 (SC-RR-70-852) COMPACTNESS BY BOUNDED L_p-VARIATION. Hicks, D. L.; Epstein, B. (Sandia Labs., Albuquerque, N. Mex.). Feb 1971. 16p. Dep. NTIS.

28891 (SC-RR-710122) CHARACTERIZATION OF THE IONIC SPECIES INCIDENT ON THE CATHODE IN A GLOW DISCHARGE. Houston, J. E.; Uhl, J. E. (Sandia Labs., Albuquerque, N. Mex.). Mar 1971. 36p. Dep. NTIS.

28892 (TID-5001(10th Rev.)) SUBJECT HEADINGS USED BY THE USAEC DIVISION OF TECHNICAL INFORMATION. Lanier, Sidney F. (ed.) (Division of Technical Information Extension (AEC), Oak Ridge, Tenn.). Feb 1971. 272p. Dep. NTIS.

28893 (TID-25679) OAK RIDGE NATIONAL LABORATORY VERTICAL TUBE EVAPORATOR PILOT PLANT ANNUAL REPORT FOR FISCAL YEAR 1969. Research and Development Progress Report No. 600. (Stearns-Roger Corp., Denver, Colo.). Aug 1970. Contract 14-01-0001-2535. 71p. GPO $1.00.
For Oak Ridge National Lab., Tenn.

28894 (TID-25682) STRUCTURAL STUDIES OF METAL COORDINATION COMPOUNDS. Terminal Report, 1959-1969. Quagliano, James V. (Florida State Univ., Tallahassee). Contract AT(40-1)-2503. 20p. Dep. NTIS.

28895 (TID-25683) MOLECULAR DYNAMICAL STUDIES OF THE PHASE TRANSFORMATION OF IRON UNDER PRESSURE. Tsai, D. H.; MacDonald, R. A. (National Bureau of Standards, Washington, D. C.). 11 Mar 1971. Contract AT-(49-16)-3003. 36p. Dep. NTIS.

28896 (UCID-15754) ENGINEERING VIEW OF THE LRL OCTOPUS COMPUTER NETWORK. Pehrson, David L. (California Univ., Livermore. Lawrence Radiation Lab.). 17 Nov 1970. 32p. Dep. NTIS.

28897 (UCLA-34-P-172-1) PARTICLE SIZE DISTRIBUTION EFFECTS IN PRECIPITATION HARDENING. Second Annual Progress Report, April 1, 1970-January 31, 1971. Ardell, A. J. (California Univ., Los Angeles. School of Engineering and Applied Science). Feb 1971. Contract AT(04-3)-34. 31p. Dep. NTIS.

28898 (UCRL-20613) STUDIES ON THE MOST PRIMITIVE PRECURSOR CELLS OF THE HEMOPOIETIC SYSTEM. Lin, David H. Y. (California Univ., Berkeley. Lawrence Radiation Lab.). Feb 1971. Contract W-7405-eng-48. 49p. Dep. NTIS.
Thesis.

28899 (UCRL-20624) INTERMEDIATES IN THE BIOSYNTHETIC CONVERSION OF THEBAINE TO CODEINE IN PAPAVER SOMNIFERUM. Parker, Harriet Inez (California Univ, Berkeley. Lawrence Radiation Lab.). Mar 1971. Contract W-7405-eng-48. 105p. Dep. NTIS.
Thesis.

28900 (UCRL-72748) TRIAXIAL BIDIRECTIONAL INTEGRATING 4-LEVEL ACCELERATION AMPLITUDE RECORDER LEA69-3100. Morrison, Jasper J. (California Univ., Livermore. Lawrence Radiation Lab.). Mar 1971. 8p. (CONF-710409-1). Dep. NTIS.
From 17. annual meeting and equipment exposition; Los Angeles, Calif. (26 Apr 1971).

XUM

28901 (UCRL-73063) AIR POLLUTION: OUR ECOLOGICAL ALARM AND BLESSING IN DISGUISE. Elisaesser, Hugh W. (California Univ., Livermore. Lawrence Radiation Lab.). Feb 1971. 6p. (CONF-710410-1). Dep. NTIS.
From 6. space congress conference; Cocoa Beach, Fla. (1 Apr 1971).

28902 (UCRL-73080) NUMERICAL IMAGE RESTORATION. Ekstrom, M. P.; Rater, O. L. (California Univ., Livermore. Lawrence Radiation Lab.). 10 Mar 1971. 5p. (CONF-710506-1). Dep. NTIS.
From IEEE region 6th conference; Sacramento, Calif. (11 May 1971).

28903 (UCRL-73103) ANALOG-TO-DIGITAL CONVERTER TO DIGITIZE VOLTAGE TRANSIENTS. Eckard, Royce D. (California Univ., Livermore. Lawrence Radiation Lab.). 15 Apr 1968. 53p. (CONF-710212-1). Dep. NTIS.
From Analog-to-digital symposium; Albuquerque, N. Mex. (2 Feb 1971).

28904 (UR-49-1429) MODIFICATION OF ANION AND CATION PERMEABILITY OF THE HUMAN RED CELL MEMBRANE BY AMINO AND SULFHYDRYL REACTIVE REAGENTS. Knauf, Philip Andrew (Rochester Univ., N. Y. Dept. of Radiation Biology and Biophysics). 1970. 132p. Dep. NTIS.
Thesis.

28905 (UR-49-1440) ON THE ENERGETICS OF ACTIVE TRANSCELLULAR CALCIUM TRANSPORT BY THE CHORIO-ALLANTOIC MEMBRANE OF THE EMBRYONIC CHICK. Garrison II, James Carlton (Rochester Univ., N. Y.). 1971. 104p. Dep. NTIS.
Thesis.

28906 (UR-49-1444) ON THE POSSIBLE ROLE OF CRYSTALS IN THE ORIGINS OF LIFE: ADSORPTION, CATALYSIS, AND PYROPHOSPHATE FORMATION BY HYDROXYAPATITE. Burton, Frederick Glenn (Rochester Univ., N. Y. Dept. of Radiation Biology and Biophysics). 1971. 106p. Dep. NTIS.
Thesis.

28907 (Y-1725) PREPARATION OF CONTROL TAPE FOR AN R-θ INSPECTION MACHINE. Wilson, C. W.; Hensley, W. R. (Union Carbide Corp., Oak Ridge, Tenn. Y-12 Plant). 9 Apr 1971. Contract W-7405-eng-26. 56p. Dep. NTIS.

28908 (Y-1755) CORRECTION OF INSPECTION DATA FOR PART MISALIGNMENT UTILIZING A SMALL COMPUTER. Bookhart, T. W.; Easterday, R. J.; Walter, W. Q. (Union Carbide Corp., Oak Ridge, Tenn. Y-12 Plant). 16 Apr 1971. Contract W-7405-eng-26. 40p. Dep. NTIS.

28909 (Y-1782) CUBIC INTERPOLATION FOR NUMERICALLY CONTROLLED MACHINES. Miskell, R. V. (Union Carbide Corp., Oak Ridge, Tenn. Y-12 Plant). 31 Mar 1971. Contract W-7405-eng-26. 54p. Dep. NTIS.

28910 (Y-1783) CAPACITANCE GAGE FOR DIMENSIONAL MEASUREMENT. Henry, J. J. (Union Carbide Corp., Oak Ridge, Tenn. Y-12 Plant). 20 Apr 1971. Contract W-7405-eng-26. 26p. Dep. NTIS.

28911 (Y-1787) EDDY CURRENT MEASUREMENTS WITH A COIL ENCIRCLING A TWO-CONDUCTOR ROD. Mundt, F. D (Union Carbide Corp., Oak Ridge, Tenn. Y-12 Plant). 8 Apr 1971. Contract W-7405-eng-26. 87p. Dep. NTIS.

CORPORATE AUTHOR INDEX

In the Corporate Author Index, technical report literature is indexed by the organization or institution responsible for issuing the report. Entries are given for all report literature and for published literature for which a corporate author approach is especially desirable, e.g., symposium and conference proceedings.

Each entry under a corporate author gives the publication title and the *NSA* volume and abstract numbers. Report numbers, where applicable, are given in parentheses at the end of the entry.

A

AARHUS UNIV. (DENMARK). FYSISK INSTITUT.
Alpha decay of neutron deficient isotopes of mercury and radon and their daughters, 25:28302 (CERN-70-30(Vol.1), pp 523-31)
ADELAIDE UNIV. (AUSTRALIA). DEPT. OF PHYSICS.
Experimental investigation of $^{16}O + ^{12}C$ nuclear burning at stellar energies, 25:27309 (ANU-P-471)
AGRICULTURAL RESEARCH SERVICE, BELTSVILLE, MD.
Sterile insect release to control and eradicate insect populations, 25:27129 (CONF-680112-, pp 123-8)
AKADEMIYA NAUK SSSR, LENINGRAD. FIZIKO-TEKHNICHESKII INSTITUT.
Properties of nuclei far off the β-stability valley, 25:28444 (CERN-70-30(Vol.1), pp 497-516)
AKADEMIYA NAUK SSSR, MOSCOW. INSTITUT FIZIKI.
Bremsstrahlung of relativistic plasma, 25:27687 (NP-18758)
Plasma bremsstrahlung from relativistic particles in a turbulent plasma, 25:27704 (NP-18759)
Radiation effects on dynamics of relativistic electron rings, 25:28114 (NP-18634)
AKADEMIYA NAUK SSSR, NOVOSIBIRSK. INSTITUT MATEMATIKI.
Amplitude of forward scattering of the process $\pi^+\pi^0 \to \pi^+\pi^0$, 25:28025 (NP-18768)
kappa-meson decay in the vector theory with the nonconserved current, 25:28023 (NP-18763)
Sum rules for $\pi\pi$-scattering, 25:28024 (NP-18766)
AKADEMIYA NAUK UKRAINSKOI SSR, KHARKOV. FIZIKO-TEKHNICHESKII INSTITUT.
Dimensional effect in magnetization of strong superconductors, 25:27644 (KHFTI-70-8)
Structure of electron clusters in an injector with a step-like varying wave phase velocity, 25:28112 (KHFTI-70-17)
AKADEMIYA NAUK UKRAINSKOI SSR, KIEV. INSTITUT TEORETICHESKOI FIZIKI.
Consequence of Gribov--Froissart formula, 25:27930 (ITF-70-101-E)
Energy levels of three-particle system, 25:28163 (ITF-70-100-P)
Model Hamiltonian of theory of superconductivity, 25:27643 (ITF-70-90-E)
Model of expanding universe, 25:27421 (ITF-70-105-E)
Some peculiarities of cognition of microworld, 25:27929 (ITF-70-62-E)
AKTIEBOLAGET ATOMENERGI, STOCKHOLM (SWEDEN).
Uranium demand and supply, 25:26396 (CONF-700903-16)
AKTIEBOLAGET ATOMENERGI, STUDSVIK (SWEDEN).
Isomerism in odd and odd--odd nuclei with mass number 185 less than or equal to A less than or equal to 191, 25:28335 (CERN-70-30(Vol.2), pp 1045-55)
Lifetimes of excited nuclear levels, 25:28341 (CERN-70-30(Vol.2), pp 1115-18)
Low-lying states in odd-mass polonium isotopes, 25:28333 (CERN-70-30(Vol.2), pp 1023-9)
Properties of low-lying levels in even Pt and Os nuclei, 25:28334 (CERN-70-30(Vol.2), pp 1031-43)
ALABAMA POWER CO., BIRMINGHAM.
Joseph M. Farley Nuclear Plant, Units 1 and 2. Preliminary safety analysis report, Amendment 14, 25:28618 (DOCKET-50348-19)
AMES LAB., IOWA.
Recent studies of short-lived gaseous fission products and their daughters, 25:28343 (CERN-70-30(Vol.2), pp 1125-7)
ANSALDO S.p.A., GENOA (ITALY).
Analytical method for representing cylindrical B_4C absorbers in two-dimensional diffusion calculations, 25:28820 (EUR-4556)
Experimental determination of the turbulent diffusivity coefficient in a bundle of rods with and without space grids, 25:28819 (EUR-4552)
STAZ-2: program for thermohydraulic analysis of channel of water-moderated and cooled nuclear reactor core operating in stationary state, 25:28679 (EUR-4553)
TIGER: program for the calculation of thermal cross sections in light-water nuclear reactor, 25:28802 (EUR-4554)
WIGNER: program for calculation of mean thermal cross sections in reactor core and for punching of load data for calculating the epithermal cross sections, 25:28803 (EUR-4555)
ARGONNE NATIONAL LAB., ILL.
1000-MWe LMFBR accident analysis and safety system design study. Candidate primary containment safety features. Topical report, 25:28733 (BAW-1352)
1000-MWe LMFBR accident analysis and safety system design study. Candidate emergency decay heat removal systems. Topical report, 25:28732 (BAW-1351)
1000-MWe LMFBR accident analysis and safety system design study. Accident-initiating conditions. Part 1. Flow abnormalities. Topical report, 25:28731 (BAW-1350)
1000-MWe LMFBR accident analysis and safety system design study. Candidate protective features. Topical report, 25:28734 (BAW-1354)
1000-MWe LMFBR accident analysis and safety system design study, 25:28729 (BAW-1342)
1000-MWe LMFBR accident analysis and safety system design study. Topical report. candidate secondary containment support systems, 25:28730 (BAW-1349)
Accurate cross-section measurements of reactions T(p,p)T, T(p,d)D, T(p,^{3}He)N, and T(p,p')T at 13.600 MeV, 25:28164 (LA-4576)
Chicago air pollution systems analysis program, 25:28840 (ANL-ES-CC-8)
Electron paramagnetic resonance spectroscopy, 25:28838 (ANL-7764)
Experimental study of a gas jet penetrating a liquid coolant and impinging on a heated surface, 25:26418 (ANL-7734)
Hyperfine interactions: tables of isotropic and anisotropic parameters for the atoms hydrogen to bismuth, 25:27441 (ANL-7784)
Photographic method for determining velocity distributions within thermal plumes, 25:28839 (ANL/ES-4)
SASIA: a computer code for the analysis of fast-reactor power and flow transients, 25:28727 (ANL-7607)
VENUS: a two-dimensional coupled neutronics-hydrodynamics computer program for fast-reactor power excursions, 25:28728 (ANL-7701)
ZPR-3 assemblies 48: 48A, and 48B: the study of a dilute plutonium-fueled assembly and its variants, 25:28752 (ANL-7759)
ARIZONA UNIV., TUCSON. DEPT. OF NUCLEAR ENGINEERING.
Stability domains in nonlinear point reactor dynamics, 25:28800 (COO-2109-3)
ARKANSAS POWER AND LIGHT CO., LITTLE ROCK.
Arkansas Nuclear One, Unit 2. Preliminary safety analysis report, Suppl. 3, 25:28620 (DOCKET-50368-8)
ARMY ENGINEER NUCLEAR CRATERING GROUP, LIVERMORE, CALIF.
Far-out collection program. Project Schooner, 25:26404 (PNE-527)
Project pre-Gondola II summary report, 25:26407 (PNE-1112)
Project pre-Gondola III, phase II summary report, 25:26408 (PNE-1117)
ARMY ENGINEER WATERWAYS EXPERIMENT STATION, VICKSBURG, MISS.
Motion of Rifle Gap Dam Rifle, Colorado; Project Rulison underground nuclear detonation, 25:26410 (PNE-R-47)
ASEA-ATOM, VASTERAS (SWEDEN).
Fuel manufacturing in Sweden, 25:27272 (CONF-700903-18)
Swedish nuclear manufacturing industries: today and tomorrow, 25:28525 (CONF-700550-, Paper 3)

XUM

ATLANTIC RICHFIELD HANFORD CO., RICHLAND, WASH.
Hydroxylamine nitrate reduction of plutonium(IV): iron catalysis, 25:26206 (ARH-1920)
ATOMIC ENERGY COMMISSION, WASHINGTON, D. C.
Fundamental nuclear energy research, 1970, 25:26205
ATOMIC ENERGY ESTABLISHMENT, CAIRO (EGYPT). RADIATION PROTECTION DEPT.
Annual occupational radiation exposure dose levels, 25:26749 (NP-18732)
Levels of ^{137}Cs in man in U.A.R. during year 1970, 25:26740 (NP-18728)
ATOMIC ENERGY ESTABLISHMENT, WINFRITH (ENGLAND).
Quality control, inspection, and testing of Series I metallurgical fuels for first charge of Dragon reactor, 25:26438 (DP-Report-432)
ATOMIC ENERGY OF CANADA LTD., CHALK RIVER (ONTARIO).
Conference on reliability, Chalk River, Ontario, 10/70, 25:28546 (AECL-3670)
Design and development of packagings for low enriched fuel bundles, 25:26442 (AECL-3803)
EVALIN: CDC FORTRAN IV code to perform an extended variational approximation for light and intermediate nuclei, 25:28439 (AECL-3801)
ATOMIC ENERGY OF CANADA LTD., CHALK RIVER (ONTARIO). CHALK RIVER NUCLEAR LABS.
Design and development for reliability, 25:28554 (AECL-3670, pp 89-96)
Information retrieval and reliability analysis, 25:28553 (AECL-3670, pp 83-8)
Special aspects of reliability and maintainability in nuclear stations, 25:28552 (AECL-3670, pp 73-81)
Thermal test calculations for packages of steel construction, 25:26441 (AECL-3802)
ATOMIC ENERGY OF CANADA LTD., SHERIDAN PARK (ONTARIO).
Quality assurance in relation to nuclear power plants, 25:28550 (AECL-3670, pp 59-63)
ATOMIC ENERGY RESEARCH ESTABLISHMENT, HARWELL (ENGLAND).
Delayed neutron emission from selenium isotopes, 25:28212 (CERN-70-30(Vol.1), pp 519-20)
Self-irradiation damage in α-plutonium, 25:27837 (AERE-R-6506)
ATOMICS INTERNATIONAL, CANOGA PARK, CALIF.
Development of nuclear reactor bearings for 1500°F space operation, 25:27200 (CONF-691114-7)
Prog. rpt. on LMFBR safety programs, 10--12/70, 25:28726 (AI-AEC-12986)
Reference zirconium hydride reactor thermoelectric system, 25:28783 (AI-AEC-Memo-12717)
AUSTRAL OIL CO., INC., HOUSTON, TEX.
Project Rulison post-shot investigations, 25:26409 (PNE-R-45)
AUSTRALIAN NATIONAL UNIV., CANBERRA.
Effective nuclear interactions and level properties for the lighter nuclei in the 1p-shell, 25:28452 (NP-18717)
AUSTRALIAN NATIONAL UNIV., CANBERRA. DEPT. OF NUCLEAR PHYSICS.
Experimental investigation of $^{16}O + ^{12}C$ nuclear burning at stellar energies, 25:27309 (ANU-P-471)
Resonances in $^{29}Si(p,\gamma)^{30}P$ reaction, 25:28207 (ANU-P-517)
AUSTRALIAN NATIONAL UNIV., CANBERRA. RESEARCH SCHOOL OF PHYSICAL SCIENCES.
9/2-[514] state in ^{185}Re, 25:28287 (ANU-P-518)
Beam optics calculations for cyclotron-tandem injection system, 25:28103 (ANU-P-519)
Computer reduction of complex spectra, 25:26489 (ANU-P-487(2))
Cross section of $^{25}Mg(tau,\gamma)^{28}Si$ reaction, 25:28206 (ANU-P-508)
Manufacturing process for silicon surface barrier radiation detectors, 25:26456 (ANU-P-516)
Nuclear spectroscopy instrumentation, 25:28102 (ANU-P-502)
Particle identification using ORTEC 423 identifier, 25:26490 (ANU-P-514)
Search for high-spin states in ^{27}Al, 25:28208 (ANU-P-521)
Spectroscopic factors from $^{124}Sn(d,p)^{125}Sn$ above and below the Coulomb barrier, 25:28286 (ANU-P-511)
AVCO-EVERETT RESEARCH LAB., EVERETT, MASS.
HIPAC as a source of highly stripped heavy ions, 25:28128 (WASH-1159, pp 88-112)

B

BABCOCK AND WILCOX CO., LYNCHBURG, VA. NUCLEAR POWER GENERATION DEPT.
1000-MWe LMFBR accident analysis and safety system design study. Candidate emergency decay heat removal systems. Topical report, 25:28732 (BAW-1351)
1000-MWe LMFBR accident analysis and safety system design study. Accident-initiating conditions. Part 1. Flow abnormalities. Topical report, 25:28731 (BAW-1350)
1000-MWe LMFBR accident analysis and safety system design study. Candidate protective features. Topical report, 25:28734 (BAW-1354)
1000-MWe LMFBR accident analysis and safety system design study. Candidate primary containment safety features. Topical report, 25:28733 (BAW-1352)
1000-MWe LMFBR accident analysis and safety system design study. Topical report. Effects of irradiation-induced metal swelling on the reference design, 25:28685 (BAW-1355)
1000-MWe LMFBR accident analysis and safety system design study. Accident initiating conditions. Part 2. reactivity insertions, 25:28735 (BAW-1360)
BABCOCK AND WILCOX CO., LYNCHBURG, VA. POWER GENERATION DIV.
1000-MWe LMFBR accident analysis and safety system design study. Topical report. candidate secondary containment support systems, 25:28730 (BAW-1349)
1000-MWe LMFBR accident analysis and safety system design study, 25:28729 (BAW-1342)
BALLISTIC RESEARCH LABS., ABERDEEN PROVING GROUND, MD.
Independent cesium yields in ^{236}U fission: identification of ^{145}Cs, 25:28307 (CERN-70-30(Vol.1), pp 589-99)
BATTELLE MEMORIAL INST., COLUMBUS, OHIO.
Creep of reactor fuel materials, 25:28689 (BMI-1898, Sect.C)
Effects of hydride precipitation of the tensile properties of irradiated Zircaloy-2. Final report, 25:27196 (BMI-X-10276)
Prog. rpt. on Amchitka bioenvironmental program, annual, 7/69--6/70, 25:28841 (BMI-171-133)
Prog. rpt. on development of fuels and technology for advanced reactors, 10--12/70, 25:28686 (BMI-1898)
Technology of nuclear fuels for advanced fast reactors, 25:28688 (BMI-1898, Sect.B)
Uranium--plutonium nitride fuels for LMFBR applications, 25:28687 (BMI-1898, Sect.A)
BATTELLE-NORTHWEST, RICHLAND, WASH. PACIFIC NORTHWEST LAB.
Californium-252 neutron activation for terrestrial, sea floor, and possible planetary surface analysis, 25:26188 (BNWL-SA-3803)
Cation-exchange conversion of hydroxylamine sulfate to hydroxylamine nitrate, 25:26208 (BNWL-CC-2180)
Conference on precipitation scavenging, 1970, Richland, Wash, 25:26358 (CONF-700601)
Effect of solubilities of gases on their scavenging by raindrops, 25:26374 (CONF-700601-, pp 247-59)
European interest in acidic precipitation, 25:26377 (CONF-700601-, pp 289-92)
Food and feeding of juvenile chinook salmon in Central Columbia River in relation to thermal discharges and other environmental features, 25:26681 (BNWL-1528)
In-cloud scavenging analysis from cosmogenic radionuclide measurements, 25:26364 (CONF-700601-, pp 69-97)
Measurement of radiation exposure of astronauts by radiochemical techniques, 25:26178 (BNWL-SA-3608)
Neutron radiography with ^{252}Cf in forensic science, 25:26437 (BNWL-SA-2865)
Phoretic processes in scavenging, 25:26387 (CONF-700601-, pp 411-22)
Prog. rpt. on measurement of radiation exposure of astronauts, 10/5/70--1/3/71, 25:26187 (BNWL-1183-7)
Pulsed-laser holography for analysis of particle size and distribution, 25:26373 (CONF-700601-, pp 213-16)
Scavenging of aerosol particles by sprays, 25:26372 (CONF-700601-, pp 187-204)
Scavenging of soluble dye particles by rain, 25:26368 (CONF-700601-, pp 137-47)
Stable elements of the atmosphere as tracers of precipitation scavenging, 25:26365 (CONF-700601-, pp 99-108)
Washout of gaseous iodine species, 25:26376 (CONF-700601-, pp 271-88)
Washout of SO_2 from plume of a coal-fired power plant, 25:26378 (CONF-700601-, pp 293-303)
X-ray comparison of beta plutonium grain size, 25:27244 (BNWL-1545)
BERG (T. G. OWE), INC., GARDEN GROVE, CALIF.
Collection efficiency in washout by rain, 25:26371 (CONF-700601-, pp 169-86)
BERN UNIV. (SWITZERLAND). PHYSIKALISCHES INSTITUT.
Use of natural radioactivities to estimate large-scale precipitation scavenging, 25:26390 (CONF-700601-, pp 465-74)
BETTIS ATOMIC POWER LAB., PITTSBURGH, PA.
Effects of hydride precipitation of the tensile properties of irradiated Zircaloy-2. Final report, 25:27198 (BMI-X-10276)
BHABHA ATOMIC RESEARCH CENTRE, BOMBAY (INDIA).
Nuclear methods in trace analysis: a review, 25:26186 (BARC-529)
BIOSPHERICS, INC., ROCKVILLE, MD.
Automated primary productivity measurements in water bodies, 25:28867 (NYO-3993-1)
BLUME (JOHN A.) AND ASSOCIATES RESEARCH DIV., SAN FRANCISCO, CALIF.
Structural condition status report, 25:26400 (NVO-99-12)
Structural response studies for Project Rulison, 25:26402 (JAB-99-78)
BONN UNIV. (WEST GERMANY).
Co-existence of different structures in various domains of the periodic table, 25:28447 (CERN-70-30(Vol.2), pp 1129-32)
Lectures on hyperfine interactions, a field between nuclear physics and solid state physics, Leuven, 1969, 25:27915 (NP-18702)

XUM

BONN UNIV. (WEST GERMANY). INSTITUT FUER THEORETISCHE KERNPHYSIK.
One boson exchange potential and nuclear matter properties, 25:28448 (CERN-70-30(Vol.2), pp 1133-5)
BOSTON EDISON CO., MASS.
Pilgrim Nuclear Power Station. Withdrawal of requests of January 12, 1971 and February 12, 1971, 25:28614 (DOCKET-50293-48)
BOSTON UNIV., MASS.
Prog. rpt. on coincidence-Moessbauer studies of solid state phenomena, 6/70--5/71, 25:28864 (NYO-3973-8)
BROOKHAVEN NATIONAL LAB., UPTON, N. Y.
BNL summer study on AGS utilization, 1970, 25:28104 (BNL-16000)
Difficulties and approaches in the development of inventory control for nuclear material safeguards, 25:26444 (BNL-15601)
Some interesting aspects of the VMI model, 25:28446 (CERN-70-30(Vol.2), pp 813-27)
Study of some neutron-deficient nuclides with high resolution x-ray detector and mass separation, 25:28321 (CERN-70-30(Vol.2), pp 931-8)
BUREAU OF RADIOLOGICAL HEALTH, ROCKVILLE, MD.
X-ray fluoroscopic screens: history, crystal kinetics, preliminary report on aging, 25:26815 (BRH/DMRE-71-2)
BUREAU OF RADIOLOGICAL HEALTH, ROCKVILLE, MD. DIV. OF MEDICAL RADIATION EXPOSURE.
Summary of federal regulations for packaging and transportation of radioactive materials, 25:26445 (BRH/DMRE-71-1)

C

CALIFORNIA INST. OF TECH., PASADENA. W. M. KECK LAB. OF ENGINEERING MATERIALS.
Hyperfine magnetic interactions in Fe--Ga solid solutions, 25:28843 (CALT-822-27)
Moessbauer study of BiF_3 type ordering in metastable FeGa alloys, 25:28842 (CALT-822-26)
Two currents conduction in Kondo alloys, 25:28844 (CALT-822-28)
CALIFORNIA UNIV., BERKELEY. LAWRENCE RADIATION LAB.
Bevatron external proton beam facilities, 25:28119 (UCRL-20194)
External heavy ion source for Berkeley 88-inch cyclotron, 25:28120 (UCRL-20406)
Intermediates in the biosynthetic conversion of thebaine to codeine in Papaver somniferum, 25:28899 (UCRL-20624)
Mechanical features of electron-ring compressors, 25:28118 (UCRL-20177)
Mechanical properties of laves phases, 25:27211 (UCRL-20301)
Most primitive precursor cells of hemopoietic system, 25:28898 (UCRL-20613)
Non-intercepting monitor of beam current and position, 25:28117 (UCRL-20166)
Planning for superhilac timeshare operation with both heavy and light ion beams, 25:28122 (UCRL-20633)
Printed-circuit steering coils, 25:28116 (UCRL-20165)
Production and decay properties of thorium and protactinium isotopes of mass 221-225 formed in heavy ion reactions, 25:28304 (CERN-70-30(Vol.1), pp 545-6)
Status and outlook for arc-discharge sources, 25:28124 (WASH-1159, pp 1-10)
Vacuum cryopumping a heavy ion source in a high voltage terminal, 25:28121 (UCRL-20620)
CALIFORNIA UNIV., LIVERMORE. LAWRENCE RADIATION LAB.
Air pollution: our ecological alarm and blessing in disguise, 25:28901 (UCRL-73063)
Analog-to-digital converter to digitize voltage transients, 25:28903 (UCRL-73103)
Electrical resistance of ytterbium as a function of temperature and pressure, 25:27867 (UCRL-51006)
Engineering view of the LRL OCTOPUS computer network, 25:28896 (UCID-15754)
Far-out collection program. Project Schooner, 25:26404 (PNE-527)
Hadron spectroscopy, 25:28008 (UCRL-73073)
Index to experimental data of neutron-induced reactions, 25:28356 (UCRL-50400(Vol.3))
LRL (Livermore) 100-MeV linear electron accelerator and facility, 25:28123 (UCRL-73075)
Numerical image restoration, 25:28902 (UCRL-73080)
Prediction of the dosage to man from the fallout of nuclear devices. VII. Estimation of the maximum dose rate from the continuous release of radionuclides to the biosphere, 25:26751 (UCRL-50163(Pt.7))
Results of postshot exploration of the Greeley Event, 25:26412 (UCRL-50979)
Triaxial bidirectional integrating 4-level acceleration amplitude recorder, 25:28900 (UCRL-72748)
CALIFORNIA UNIV., LOS ANGELES.
Decay of ^{110}Sb, ^{111}Sb, ^{112}Sb, ^{113}Sb, and ^{114}Sb, 25:28332 (CERN-70-30(Vol.2), pp 1015-21)
CALIFORNIA UNIV., LOS ANGELES. SCHOOL OF ENGINEERING AND APPLIED SCIENCE.
Prog. rpt. on particle size distribution effects in precipitation hardening, annual, 4/70--1/71, 25:28897 (UCLA-34-P-172-1)

CANADIAN GENERAL ELECTRIC CO., LTD., PETERBOROUGH (ONTARIO). ATOMIC POWER DEPT.
Attachment of thermocouples to zircaloy tubes by induction brazing, 25:27182 (R-69-CAP-8)
CARNEGIE-MELLON UNIV., PITTSBURGH, PA.
Prog. rpt., annual, 5/70--4/71, 25:28868 (NYO-4075-10)
Theoretical considerations on nuclei far from stability, 25:28289 (CERN-70-30(Vol.1), pp 1-19)
CAROLINA POWER AND LIGHT CO., RALEIGH, N.C.
H. B. Robinson Unit No. 2. Bearing failure due to loss of flow of lubricating oil, 25:28569 (DOCKET-50261-57)
H. B. Robinson Unit No. 2. Difficulties with lube oil system of emergency diesel generators, 25:28568 (DOCKET-50261-56)
H. B. Robinson Unit No. 2. Part-length bank maneuvering, 25:28567 (DOCKET-50261-55)
H. B. Robinson Unit No. 2. Tests on safety injection system, 25:28570 (DOCKET-50261-58)
CATHOLIC UNIV. OF AMERICA, WASHINGTON, D. C.
Detection of highly stripped heavy ions in a low-pressure linear pinch device, 25:27678 (WASH-1159, pp 172-83)
CATHOLIC UNIV. OF AMERICA, WASHINGTON, D. C. DEPT. OF NUCLEAR SCIENCE AND ENGINEERING.
Experimental and theoretical investigation of nuclear fission induced by low-energy nuclear particles. Progress report, 25:28355 (TID-25659)
CENTRAL ELECTRICITY GENERATING BOARD, BERKELEY (ENGLAND). BERKELEY NUCLEAR LABS.
Axial buckling measurements in BNL Mark II stacks, 25:28806 (RD/B/N-1837)
Bubble mobility on dislocations and random diffusion studies, 25:27842 (RD/B/N-1850)
Correlation of measured and calculated strains in top-half of Oldbury prestressed concrete pressure vessel R1, 1965--1970, 25:28528 (RD/B/N-1784)
Effects of high flux neutron irradiation on the microstructure of metals, 25:27266 (RD/B/N-1812)
Manganese reaction rate measurements in [Berkeley Nuclear Lab.] reactors, 25:28816 (RD/B/N-1518)
CENTRALNE LABORATORIUM OCHRONY RADIOLOGICZNEJ, WARSAW (POLAND).
Origin and evolution of the radioactive clouds, 25:26357 (CLOR-81/D)
X and gamma thermoluminescent dosimeter for accidental personnel dosimetry purposes, 25:26516 (CLOR-82/D)
CENTRE D'ETUDE DE L'ENERGIE NUCLEAIRE, BRUSSELS (BELGIUM).
Experience acquired in fluid bed preparation of UF_4 in view of reactor fuel processing, 25:26207 (BLG-448)
Improvements in use of $^6Li(n,\alpha)t$ reaction for in-core neutron spectrum measurements, 25:28753 (BLG-450)
CENTRE D'ETUDE DE L'ENERGIE NUCLEAIRE, MOL (BELGIUM).
Reassessment of some neutron yields from the longer-lived delayed neutron emitters, 25:28211 (CERN-70-30(Vol.1), pp 517-18)
CENTRE NATIONAL DE LA RECHERCHE SCIENTIFIQUE, MARSEILLES (FRANCE). CENTRE DE PHYSIQUE THEORIQUE.
Class of analytic perturbations for Schrodinger Hamiltonians. I, 25:27926 (CNRS-CPT-70-P-352)
Constraints imposed upon a state of a system that satisfies the K.M.S. boundary condition, 25:27925 (CNRS-CPT-70-P-325)
CENTRE NATIONAL DE LA RECHERCHE SCIENTIFIQUE, ORSAY (FRANCE). CENTRE DE SPECTROMETRIE NUCLEAIRE ET DE SPECTROMETRIE DE MASSE.
Recoil atom mass analyser (RAMA), 25:28106 (CERN-70-30(Vol.1), pp 153-62)
Special experimental techniques used in the study of nuclei far from stability, 25:28290 (CERN-70-30(Vol.1), pp 21-45)
CENTRE NATIONAL DE LA RECHERCHE SCIENTIFIQUE, PARIS (FRANCE).
Conference on conduction processes in dielectric liquids, Grenoble, France, 9/68, 25:26470
CENTRO INFORMAZIONI STUDI ESPERIENZE, MILAN (ITALY).
Problems connected with the graphical interaction operator-computer, 25:28860 (LA-tr-71-28)
CESKOSLOVENSKA AKADEMIE VED, REZ. USTAV JADERNEHO VYZKUMU.
Electroexcitation of ^{32}S in region of dipole resonance, 25:28220 (UJV-2553-F)
Neutron radiography and its application, 25:26439 (UJV-2545-R,T)
Quasiparticle description for indium, 25:28357 (UJV-2540-F)
Radiation experiment on a model of a finned tubular fuel element. I, 25:27267 (UJV-2371.R,T.)
CHADRON ATMOSPHERIC RESEARCH INST., NEBR.
Concentration variation of some trace metals in precipitation from great plains thunderstorms, 25:26366 (CONF-700601--, pp 109-20)
CHALMERS TEKNISKA HOGSKOLA, GOTEBORG (SWEDEN).
Atomic-beam measurements in the rare-earth region, 25:28298 (CERN-70-30(Vol.1), pp 387-94)
CHICAGO UNIV., ILL.
Retinal cone receptor as an ideal light collector, 25:28850 (COO-1701-16)
CINCINNATI UNIV., OHIO.
Thermodynamic properties of ternary refractory carbides. III, 25:27283 (N-71-10590)
CITY COLL., NEW YORK. DEPT. OF CHEMISTRY.
Preparation and properties of six rat red cell

XUM

hemoglobins, 25:28866 (NYO-3976-5)
CLARKSON COLL. OF TECH., POTSDAM, N. Y.
Collection efficiency of water droplets in AgCl aerosol, 25:26370 (CONF-700601-, pp 161-7)
COLUMBIA UNIV., PALISADES, N. Y. LAMONT-DOHERTY GEOLOGICAL OBSERVATORY.
Prog. rpt. on seismotectonics of Aleutian arc, annual, 2/71, 25:28852 (CU-4203-1)
COMBUSTION ENGINEERING, INC., WINDSOR, CONN. NUCLEAR POWER DEPT.
Reactor protection system diversity, 25:28697 (CENPD-11)
COMISION INTERAMERICANA DE ENERGIA NUCLEAR.
Conference on nuclear energy and agricultural productivity, Santiago, Chile, 1/68, 25:27127 (CONF-680112)
COMISION NACIONAL DE ENERGIA ATOMICA, BUENOS AIRES (ARGENTINA).
Determination of thallium in microsamples of natural vanadates of uranium by anodic redissolution, 25:26151 (CNEA-288)
Fabrication of semiconductor detectors of Si(Li) for nuclear reactions, 25:26457 (CNEA-287)
Nuclear spectroscopy of iodine isotopes with a greater than or equal to 134, 25:28336 (CERN-70-30(Vol.2), pp 1057-68)
Nuclear techniques and equipment in hydrology, 25:26353 (CONF-680112-, pp 37-52)
Thin layer chromatography of various radiopharmaceuticals, 25:26179 (CNEA-285)
COMISION NACIONAL DE ENERGIA ATOMICA, BUENOS AIRES (ARGENTINA). GERENCIA DE ENERGIA.
Uses of irradiation in agricultural production in Argentina, 25:27133 (CONF-680112-, pp 241-3)
COMISSAO NACIONAL DE ENERGIA NUCLEAR DE BRASIL, RIO DE JANEIRO.
Conference on radioisotopes, Rio de Janeiro, 6/70, 25:26436
COMITATO NAZIONALE PER L'ENERGIA NUCLEARE, BOLOGNA (ITALY).
Particle-free space in Stefan flow, 25:26386 (CONF-700601-, pp 403-10)
COMITATO NAZIONALE PER L'ENERGIA NUCLEARE, CASACCIA (ITALY). CENTRO DI STUDI NUCLEARI.
Nuclear fuel characterization, 25:27293 (RT/ING-(70)21)
COMITATO NAZIONALE PER L'ENERGIA NUCLEARE, ROME (ITALY).
Collimation corrections in small angle scattering of neutrons, 25:28144 (RT/FIMA-69-5)
Containment design criteria for sodium cooled fast reactors, 25:28739 (RT/ING-(70)25)
Equipment for remote control of gamma scanning in a hot cell, 25:26550 (RT/ING-(71)1)
Tensorial formulation and geometric interpretation of a multi level multi channel formula for nuclear resonances, 25:28454 (RT/FI-(70)38)
COMMISSARIAT A L'ENERGIE ATOMIQUE, CADARACHE (FRANCE). CENTRE D'ETUDES NUCLEAIRES.
Cyclic variation of volume of the heart, 25:26566 (CEA-CONF-1711)
Reactivity measurements using the continuous run technique, 25:28799 (CEA-N-1385)
COMMISSARIAT A L'ENERGIE ATOMIQUE, FONTENAY-AUX-ROSES (FRANCE). CENTRE D'ETUDES NUCLEAIRES.
ANISN system: description and service instructions for ANISN discrete ordinate program and subroutines, 25:28149 (ORNL-tr-2419)
Measurement of the kinetic parameters of the MINERVE reactor from analysis of the neutron fluctuations, 25:28755 (CEA-N-1406)
Measurement of the transfer function of a reactor by reactivity modulation, 25:28754 (CEA-N-1405)
Preparation and study of actinide elements, 25:26333 (ORNL-tr-2410, pp 121-42)
Semi-annual report of the Dept. of Chemistry, 6--11/69, 25:26328 (ORNL-tr-2410)
Status report on the study of the upper neutron shields of PHENIX on 4/15/69, 25:28677 (ORNL-tr-2451)
Study of aqueous processes: pilot plant, 25:26331 (ORNL-tr-2410, pp 79-97)
Study of aqueous reprocessing methods: laboratory, 25:26330 (ORNL-tr-2410, pp 14-78)
Study of the vitrification of fission product solutions, 25:26334 (ORNL-tr-2410, pp 143-89)
Study of volatility reprocessing methods, 25:26332 (ORNL-tr-2410, pp 98-120)
Treatment of medium- and low-level effluents, 25:26329 (ORNL-tr-2410, pp 1-13)
COMMISSARIAT A L'ENERGIE ATOMIQUE, GRENOBLE (FRANCE). CENTRE D'ETUDES NUCLEAIRES.
High-dynamic range rise time to amplitude converter, 25:26545 (CEA-N-1430)
Short-lived isomers of ^{126}I and ^{128}Cs decaying via metastable states of ^{126}Xe and ^{128}Ba, 25:28342 (CERN-70-30(Vol.2), pp 1119-21)
Study of internal friction peaks in molybdenum after irradiation with neutrons at 270°K, 25:27199 (CEA-CONF-1671)
COMMISSARIAT A L'ENERGIE ATOMIQUE, SACLAY (FRANCE). CENTRE D'ETUDES NUCLEAIRES.
Circuit for detecting coincidences between pulses by the means of sequential graphs, 25:26546 (CEA-R-4166)
COREGRAF 2: adjustment and comparison with experiment, 25:28654 (CEA-N-1344(2))
Effect of charge on ^{252}Cf fission fragments on neutron emission process, 25:28288 (CEA-R-4121)
Electronic lattice structure by positron annihilation in insulators, 25:27865 (CEA-R-4138)
Isotopic electricity generators, 25:26423 (CEA-Bib-190)
Wigner energy in irradiated oxides BeO, MgO, Al_2O_3, and SiO_2, 25:27839 (CEA-N-1171)
COMMONWEALTH EDISON CO., CHICAGO, ILL.
Dresden Nuclear Power Station, Unit 1. Abnormal occurrence report: failure of a primary drum low level scram relay, 25:28557 (DOCKET-50010-84)
Dresden Nuclear Power Station, Unit 2. Condition relating to operation in which 2/3 "A" Standby Gas Treatment System malfunctioned, 25:28564 (DOCKET-50237-145)
Dresden Nuclear Power Station, Unit 2. Facility License DPR-19; technical specifications Proposed Change No. 9 to Appendix A, 25:28596 (DOCKET-50237-146)
Dresden Nuclear Power Station, Unit 2. Facility License DPR-10; Proposed Change No. 10 to Appendix A, 25:28600 (DOCKET-50237-154)
Dresden Nuclear Power Station, Unit 2. Loss of electric power to the Low Pressure Coolant Injection System, 25:28565 (DOCKET-50237-151)
Dresden Nuclear Power Station, Unit 2. Special reports on nine topics to February 16, 1971 AEC request, 25:28598 (DOCKET-50237-152)
Dresden Nuclear Power Station, Unit 2. Wiring error discovered on April 4, 1971, 25:28566 (DOCKET-50237-155)
Dresden Nuclear Power Station, Unit 3. Facility Operating License No. DPR-25; Proposed Change No. 2 to Appendix A, 25:28605 (DOCKET-50249-64)
Dresden Nuclear Power Station, Units 2 and 3. Proposed modification No. 71-2 to final safety analysis report, 25:28599 (DOCKET-50237-153)
CONNECTICUT LIGHT AND POWER CO., HARTFORD.
Millstone Nuclear Power Station, Unit 1. Application for amendment to provisional construction permit No. CPPR-20, 25:28603 (DOCKET-50245-65)
CONNECTICUT YANKEE ATOMIC POWER CO., HARTFORD.
Connecticut Yankee Atomic Power Plant. License No. DPR-14. Technical specifications Proposed Change No. 18, Suppl. 1, 25:28593 (DOCKET-50213-103)
Connecticut Yankee Atomic Power Plant. License No. DPR-14. Technical specifications Proposed Change No. 19, Suppl. 1, 25:28594 (DOCKET-50213-104)
Connecticut Yankee Atomic Power Plant. License No. DPR-14. Technical specifications Proposed Change No. 17, Suppl. 1, 25:28592 (DOCKET-50213-102)
CONSOLIDATED EDISON CO. OF NEW YORK, INC., NEW YORK.
Indian Point Station, Unit No. 1. Abnormal occurrence report, time-delay switch on high pressure boron addition system pump No. 12 inoperative on routine test, 25:28556 (DOCKET-50003-67)
CONSUMERS POWER CO., JACKSON, MICH.
Big Rock Point Nuclear Plant. Seventh semiannual report of operations, May 1--October 31, 1967, 25:28561 (DOCKET-50155-78)
CORNELL UNIV., ITHACA, N. Y.
Prog. rpt. on defects in metal crystals, annual, 2/71, 25:27866 (NYO-3504-56)
CORNELL UNIV., ITHACA, N.Y. LAB. OF PLASMA STUDIES.
Acceleration and stripping of ions by intense relativistic electron beams, 25:27694 (WASH-1159, pp 184-9)
Perpendicular injection of relativistic electron beams into magnetic mirrors, 25:27688 (WASH-1159, pp 193-5)
CORNELL UNIV., ITHACA, N. Y. MATERIALS SCIENCE CENTER.
Effect of electric field and temperature on radiative lifetime of F center, 25:27841 (NYO-3463-23)
Electron spin resonance spectrum of FCN^- and HCN- in KCl, 25:26289 (NYO-2150-60)
Paraelectric resonance in KCl:Li^+, 25:26215 (NYO-2150-59)
Resonant phonon scattering in KCl:Li, 25:28863 (NYO-2391-111)

D

DAIRYLAND POWER COOPERATIVE, LA CROSSE, WIS.
La Crosse Boiling Water Reactor. Unplanned reactor shutdown while performing a technical specification test on power/flow safety system channel No. 1, 25:28555 (DOCKET-1155-112)
DANISH ATOMIC ENERGY COMMISSION, RISOE. RESEARCH ESTABLISHMENT.
Experimental investigations of the release of radioactivity under accidental conditions in a reactor containment building, 25:28763 (RISO-205)
DEMOCRITUS NUCLEAR RESEARCH CENTER, ATHENS (GREECE).
Measurement of the coefficient of gamma absorption of materials used for nuclear constructions, 25:27826 (DEMO-70/11)
DEPARTMENT OF ATOMIC ENERGY, BOMBAY (INDIA). CHEMISTRY AND METALLURGY COMMITTEE.
Contribution of powder metallurgy techniques to materials science, 25:27205 (INIS-mf-19)
Development of high temperature ceramic materials, 25:27280 (INIS-mf-12)
Developments in oxidation and corrosion resistant

materials, 25:27176 (INIS-mf-9)
High temperature super alloys with particular reference to titanium and its alloys, 25:27203 (INIS-mf-2)
Influence of microstructure on properties of ceramic products, 25:27282 (INIS-mf-14)
Irradiation effects on reactor structural materials, 25:27265 (INIS-mf-5)
Kinetics of the high-temperature oxidation of dispersion-strengthened nickel--niobia alloys, 25:27279 (INIS-mf-11)
Materials for reactor technology, 25:27204 (INIS-mf-3)
Researches on ceramic materials in India, 25:27281 (INIS-mf-13)
Transmission electron microscopic studies of cold-rolled zirconium, 25:27245 (INIS-mf-15)
DEUTSCHES ELEKTRONEN-SYNCHROTRON, HAMBURG (WEST GERMANY).
Analysis of the reaction $\pi^+ p \to rho^0 \Delta^{++}$ at 11.7 GeV/c incident momentum, 25:27960 (DESY-71/8)
Comparison of pion electroproduction data with vector meson dominance predictions, 25:27982 (DESY-71/12)
Elastic electron--deuteron scattering and electric neutron form factor at four momentum transfers: 5 Fermi^{-2} < q^2 < 14 Fermi^{-2}, 25:27980 (DESY-71/7)
Electroproduction of ω-meson as a test of the rhoww-vertex, 25:27981 (DESY-71/11)
Electroproduction of single π^+ mesons on hydrogen, 25:27950 (DESY-71/9)
Fluorescence excitation of ultra-soft x-ray emission spectra using synchrotron radiation, 25:27827 (DESY-70/59)
Impact picture and the eikonal approximation, 25:28045 (DESY-71/6)
Optical absorption of gaseous methane, ethane, propane, and butane, and reflection of solid methane and ethane in the vacuum ultraviolet, 25:28853 (DESY-SR-71/1)
Relativistic scalar quark model with strong binding, 25:28022 (DESY-71/10)
DIVISION OF BIOLOGY AND MEDICINE (AEC), WASHINGTON, D. C. FALLOUT STUDIES BRANCH.
Conference on precipitation scavenging, 1970, Richland, Wash, 25:26358 (CONF-700601)
Priorities in scavenging research, 25:26359 (CONF-700601-, pp 6-10)
Scavenging prediction using ratios of concentrations in air and precipitation, 25:26391 (CONF-700601-, pp 475-85)
DIVISION OF REACTOR LICENSING (AEC), WASHINGTON, D. C.
Dresden Nuclear Power Station, Unit 2. Change No. 9 to technical specifications and bases (Appendix A to Provisional Operating License No. DPR-19), 25:28597 (DOCKET-50237-148)
Enrico Fermi Atomic Power Plant, Unit 1. Change No. 24 to technical specifications of Provisional Operating License No. DPR-9, 25:28587 (DOCKET-50016-107)
Humboldt Bay Power Plant, Unit No. 3. Facility License No. DPR-7, Amendment 2, 25:28588 (DOCKET-50133-54)
Millstone Nuclear Power Station, Unit 1. Order extending provisional construction permit completion date, 25:28602 (DOCKET-50245-21)
Nine Mile Point Nuclear Station. Provisional Operating License No. DPR-17, Amendment 2 (authorization for power increase to 1850 megawatts (thermal)), 25:28595 (DOCKET-50220-62)
North Anna Power Station, Unit 1. Construction Permit Nos. CPPR-77 and CPPR-78, Amendment No. 1, 25:28616 (DOCKET-50338-28)
Palisades Plant. Correction to Provisional Operating License No. DPR-20, 25:28607 (DOCKET-50255-37)
Peach Bottom Atomic Power Station, Unit 1. Change No. 13 to technical specifications of Provisional Operating License No. DPR-12, 25:28591 (DOCKET-50171-82)
Pilgrim Nuclear Power Station. Notice of AEC consideration of issuance of facility operating license, 25:28613 (DOCKET-50293-47)
Pilgrim Nuclear Power Station. Suggestions of Advisory Committee on Reactor Safeguards, 25:28612 (DOCKET-50293-46)
Robert Emmett Ginna Nuclear Power Plant, Unit No. 1. Change No. 5 to technical specifications of Provisional Operating License No. DPR-18, 25:28601 (DOCKET-50244-69)
Southwest Experimental Fast Oxide Reactor. Change No. 3 to technical specifications of Provisional Operating License No. DR-15, 25:28736 (DOCKET-50231-76)
DIVISION OF RESEARCH (AEC), WASHINGTON, D. C.
Conference on heavy ion sources, Washington, D. C., 3/70, 25:27436 (WASH-1159)
DIVISION OF TECHNICAL INFORMATION EXTENSION (AEC), OAK RIDGE, TENN.
Engineering materials list, 25:26414 (TID-4100(Suppl.62))
Subject headings used by the USAEC Division of Technical Information, 25:28892 (TID-5001(10th Rev.))
DOUGLAS UNITED NUCLEAR, INC., RICHLAND, WASH.
Nuclear energy and electrical generation, 25:28527 (DUN-SA-166)
DU PONT DE NEMOURS (E.I.) AND CO., AIKEN, S. C. SAVANNAH RIVER LAB.
Californium-252 shielding guide, 25:27828 (DP-1246)
Joshua lattice physics subsystem, 25:28801 (DP-MS-70-78)
DU PONT DE NEMOURS (E.I.) AND CO., AIKEN, S. C. SAVANNAH RIVER PLANT.
Safety summary report: LLD-1 package, 25:26446 (DPSPU-71-124-1)

E

EASTERN ENVIRONMENTAL RADIATION LAB., MONTGOMERY, ALA.
Development of ion exchange processes for the removal of radionuclides from milk, 25:26335 (RO/EERL-71-1)
EG AND G, INC., LAS VEGAS, NEV.
Wide latitude processing of Tri-X-Ortho oscillographic film, 25:28854 (EGG-1183-1465)
EIDGENOESSISCHES INSTITUT FUER REAKTORFORSCHUNG, WUERENLINGEN (SWITZERLAND).
Integral equation of transport in one-dimensional cylindrical geometry. I, 25:28145 (EIR-188)
ENVIRONMENTAL PROTECTION AGENCY, ROCKVILLE, MD. RADIATION OFFICE.
Development of ion exchange processes for the removal of radionuclides from milk, 25:26335 (RO/EERL-71-1)
ENVIRONMENTAL RESEARCH CORP., LAS VEGAS, NEV.
Observed seismic data, Calabash event, 25:26401 (NVO-1163-218)
ENVIRONMENTAL SCIENCE SERVICES ADMINISTRATION, BOULDER, COLO. WAVE PROPAGATION LAB.
Radar observations of convective storm circulation and its relation to precipitation scavenging, 25:26360 (CONF-700601-, pp 13-20)
ENVIRONMENTAL SCIENCE SERVICES ADMINISTRATION, SILVER SPRING, MD. AIR RESOURCES LABS.
Use of natural radioactivities to estimate large-scale precipitation scavenging, 25:26390 (CONF-700601-, pp 465-74)
ESCUELA POLITECNICA NACIONAL, QUITO (ECUADOR). INSTITUTO DE CIENCIAS NUCLEARES.
Uses of radioisotopes in agriculture in Ecuador, 25:27134 (CONF-680112-, pp 245-6)
EUROPEAN ATOMIC ENERGY COMMUNITY.
Analytical method for representing cylindrical B_4C absorbers in two-dimensional diffusion calculations, 25:28820 (EUR-4556)
Experimental determination of the turbulent diffusivity coefficient in a bundle of rods with and without spacer grids, 25:28819 (EUR-4552)
STAZ-2: program for thermohydraulic analysis of channel of water-moderated and cooled nuclear reactor core operating in stationary state, 25:28679 (EUR-4553)
TIGER: program for the calculation of thermal cross sections in light-water nuclear reactor, 25:28802 (EUR-4554)
WIGNER: program for calculation of mean thermal cross sections in reactor core and for punching of load data for calculating the epithermal cross sections, 25:28803 (EUR-4555)
EUROPEAN ATOMIC ENERGY COMMUNITY, ISPRA (ITALY). JOINT NUCLEAR RESEARCH CENTER.
How to use the code, COMET, 25:27202 (EUR-4562)
JN-METD1: FORTRAN-IV programme for solving neutron transport problems with isotropic scattering in bare spheres and homogeneous slabs by the j/sub N/ method, 25:28146 (EUR-4601)
Some experimental results on the sorption of caesium by tungsten and graphite, 25:27201 (EUR-4549)
EUROPEAN ORGANIZATION FOR NUCLEAR RESEARCH, GENEVA (SWITZERLAND).
Alpha decay of neutron deficient isotopes of mercury and radon and their daughters, 25:28302 (CERN-70-30(Vol.1), pp 523-31)
Beta decay energies of some neutron deficient nuclides, 25:28297 (CERN-70-30(Vol.1), pp 353-60)
Compound-nucleus aspects of beta decays with high Q values, 25:28443 (CERN-70-30(Vol.1), pp 421-33)
Conference on properties of nuclei far from region of beta-stability, Leysin, Switzerland, 8--9/70, 25:28440 (CERN-70-30(Vol.1))
Conference on properties of nuclei far from region of beta-stability, Leysin, Switzerland, 8--9/70, 25:28308 (CERN-70-30(Vol.2))
Delayed-proton emission from neutron-deficient isotopes of xenon and mercury, 25:28301 (CERN-70-30(Vol.1), pp 487-96)
Experimental techniques using ISOL systems (review of operating systems), 25:28105 (CERN-70-30(Vol.1), pp 109-41)
On-line measurements of spin and moments of nuclear ground states, 25:27914 (CERN-70-30(Vol.1), pp 361-81)
Spin formalisms, 25:28007 (CERN-71-8)

F

FIAT, TURIN (ITALY). SEZIONE ENERGIA NUCLEARE.
Analytical method for representing cylindrical B_4C absorbers in two-dimensional diffusion calculations, 25:28820 (EUR-4556)
Experimental determination of the turbulent diffusivity coefficient in a bundle of rods with and without spacer grids, 25:28819 (EUR-4552)
STAZ-2: program for thermohydraulic analysis of channel of water-moderated and cooled nuclear reactor core operating in stationary state, 25:28679 (EUR-4553)

XUM

TIGER: program for the calculation of thermal cross sections in light-water nuclear reactor, 25:28802 (EUR-4554)
WIGNER: program for calculation of mean thermal cross sections in reactor core and for punching of load data for calculating the epithermal cross sections, 25:28803 (EUR-4555)
FLORIDA POWER AND LIGHT CO.
Turkey Point Plant, Units No. 3 and No. 4. Environmental report, Suppl. 1, 25:28606 (DOCKET-50250-43)
FLORIDA STATE UNIV., TALLAHASSEE.
Prog. rpt. on structual studies of metal coordination compounds, 1959--69, 25:28894 (TID-25682)
FLORIDA STATE UNIV., TALLAHASSEE. DEPT. OF OCEANOGRAPHY.
Mechanisms of iodine injection from the sea surface, 25:26380 (CONF-700601-, pp 319-24)
FORSKNINGSRADENS LABORATORIUM, STUDSVIK (SWEDEN).
Energy levels in ^{114} ^{116} ^{118} ^{120} ^{122}Cd populated in decay of Ag isotopes, 25:28337 (CERN-70-30(Vol.2), pp 1069-74)
Neutron-rich nuclides obtained using OSIRIS facility, 25:28340 (CERN-70-30(Vol.2), pp 1093-1103)
Possible nuclear co-existence in odd-mass Ir nuclei, 25:28324 (CERN-70-30(Vol.2), pp 957-65)
Q-values of some nuclides on the neutron-rich side of stability, 25:28296 (CERN-70-30(Vol.1), pp 341-51)
FORSVARETS FORSKNINGSANSTALT, STOCKHOLM (SWEDEN).
Evidence for high-spin three quasiparticle state in ^{133}I produced in fission, 25:28331 (CERN-70-30(Vol.2), pp 1012-14)
Levels in doubly-even tellurium isotopes, 25:28330 (CERN-70-30(Vol.2), pp 1010-11)
Neutron hole states in the tin-region, 25:28329 (CERN-70-30(Vol.2), pp 1008-10)
Possible nuclear co-existence in odd-mass Ir nuclei, 25:28324 (CERN-70-30(Vol.2), pp 957-65)
Proton states in the tin-region, 25:28328 (CERN-70-30(Vol.2), pp 1006-7)
Tin-132-region studied by means of OSIRIS facility, 25:28327 (CERN-70-30(Vol.2), pp 1001-3)
FRANKFURT UNIV. (WEST GERMANY). INSTITUT FUER METEOROLOGIE UND GEOPHYSIK.
Laboratory investigations on washout of trace gases, 25:26375 (CONF-700601-, pp 261-9)
FRANKFURT UNIV. (WEST GERMANY). INSTITUT FUER THEORETISCHE PHYSIK.
Nuclear molecules formed in elastic ^{16}O + ^{16}O scattering, 25:28171 (CERN-70-30(Vol.1), pp 601-2)

G

GENERAL ELECTRIC CO., CINCINNATI, OHIO. NUCLEAR SYSTEMS PROGRAMS.
Determination of solidus-liquidus temperatures in the UO/sub 2+x/ system (-0.50 < x < 0.20), 25:27292 (GEMP-714)
GENERAL ELECTRIC CO., IDAHO FALLS, IDAHO. NUCLEAR SYSTEMS PROGRAMS.
Cavity reactor engineering mockup critical experiment, 25:28761 (NASA-CR-72409)
GENERAL ELECTRIC CO., RICHLAND, WASH. HANFORD ATOMIC PRODUCTS OPERATION.
Rail accident statistics pertinent to the shipment of radioactive materials, 25:26447 (HW-76299)
GENERAL ELECTRIC CO., SAN JOSE, CALIF. ATOMIC POWER EQUIPMENT DEPT.
Deficient cooling. Sixth quarterly progress report, October 1--December 31, 1970, 25:28681 (GEAP-10221-6)
Prog. rpt. on deficient cooling, 7--9/70, 25:26419 (GEAP-10221-5)
Reliability from the supplier's viewpoint, 25:28521 (AECL-3670, pp 39-44)
GENERAL ELECTRIC CO., SAN JOSE, CALIF. NUCLEAR ENERGY DIV.
Midwest Fuel Recovery Plant. Preliminary safety analysis report, Amendment 10 (includes design and analysis, Amendment 2 to Suppl. 1), 25:26325 (DOCKET-50268-7)
GENERAL ELECTRIC CO., SUNNYVALE, CALIF. BREEDER REACTOR DEVELOPMENT OPERATION.
Prog. rpt. on SEFOR, 11/70--1/71, 25:28757 (GEAP-10010-27)
Prog. rpt. on sodium-cooled reactors fast ceramic reactor development, 11/70--1/71, 25:28691 (GEAP-10028-37)
Reactor primary coolant system rupture study. Quarterly Report No. 23, October--December 1970, 25:28680 (GEAP-10207-23)
Southwest Experimental Fast Oxide Reactor. Malfunction of reactor vessel overflow line valve and safety system relay, 25:28709 (DOCKET-50231-78)
Southwest Experimental Fast Oxide Reactor. Natural circulation testing of the reactor coolant system, 25:28707 (DOCKET-50231-75)
Southwest Experimental Fast Oxide Reactor. Quarterly plant operations report No. 7, November 1, 1970--January 31, 1971, 25:28706 (DOCKET-50231-74)
Southwest Experimental Fast Oxide Reactor. Summary of results from testing of the fast reactivity excursion device, 25:28708 (DOCKET-50231-77)
GEORGIA INST. OF TECH., ATLANTA. ENGINEERING EXPERIMENT STATION.
Prog. rpt. on spin interactions between slow electrons and amino acid films, 6/68--2/71, 25:26277 (ORO-3799-7)
GESELLSCHAFT FUER KERNFORSCHUNG m.b.H., KARLSRUHE (WEST GERMANY).
Plutonium-documentation. Vol. 5, No. 1, 1971, 25:27169
Plutonium-documentation. Vol. 5, No. 2, 1971, 25:27168
GOODYEAR ATOMIC CORP., PIKETON, OHIO.
Precise computerized in-line compressible flow metering, 25:28855 (GAT-T-1649)
GOSUDARSTVENNYI KOMITET PO ISPOL'ZOVANIYU ATOMNOI ENERGII SSSR, MOSCOW. INSTITUT ATOMNOI ENERGII.
Wave function and bound energy of nuclei ^{3}H(^{3}He) taking into account tensor interaction of nucleons, 25:28162 (IAE-2000)
GOSUDARSTVENNYI KOMITET PO ISPOL'ZOVANIYU ATOMNOI ENERGII SSSR, MOSCOW. INSTITUT TEORETICHESKOI I EKSPERIMENTAL'NOI FIZIKI.
Design and calculation of ITEP 2-meter liquid-hydrogen bubble chamber, 25:26508 (NP-18787)
Possible quasinuclear nature of heavy mesonic resonances, 25:28026 (NP-18774)
Regulator for high voltage capacitor bank, 25:28108 (ITEF-761)
Universal magnetic spectrometer with 0.15 percent resolving power at maximum pulse of 60 GeV/c, 25:26507 (NP-18764)
GOSUDARSTVENNYI KOMITET PO ISPOL'ZOVANIYU ATOMNOI ENERGII SSSR, OBNINSK. FIZIKO-ENERGETICHESKII INSTITUT.
Spinning top problem in quantum mechanics, 25:27927 (FEI-203)
GULF GENERAL ATOMIC CO., SAN DIEGO, CALIF.
Prog. rpt. on HTGR base programs, 11/30/70, 25:28633 (GA-10399)

H

HANFORD ENGINEERING DEVELOPMENT LAB., RICHLAND, WASH.
Effects on neutron irradiation, at thermal reactor temperatures, on the propagation velocity of ultrasonic waves in A533-B steel, 25:27268 (WHAN-FR-38)
European liquid metal cooled breeder reactor instrumentation: a trip summary, 25:28667 (HEDL-SA-170)
Group constants for fast reactor calculations, 25:28657 (HEDL-TME-71-36)
Prog. rpt. on environmental engineering, 10--12/70, 25:28710 (HEDL-TME-71-26)
TOPLYR: two-dimensional thermal energy transport code, 25:28856 (HEDL-TME-71-39)
HARTFORD ELECTRIC LIGHT CO., CONN.
Millstone Nuclear Power Station, Unit 1. Application for amendment to provisional construction permit No. CPPR-20, 25:28603 (DOCKET-50245-65)
HEBREW UNIV., JERUSALEM (ISRAEL). DEPT. OF PHYSICAL CHEMISTRY.
Prog. rpt. on nature of oxygen containing radicals in radiation chemistry and photochemistry of aqueous solutions, 9/70--7/71, 25:26290 (NYO-3753-19)
HEBREW UNIV., JERUSALEM (ISRAEL). DEPT. OF THEORETICAL PHYSICS.
Current semiempirical mass equations and improved shell model nuclear masses, 25:28291 (CERN-70-30(Vol.1), pp 165-216)
HEIDELBERG UNIV. (WEST GERMANY). PHYSIKALISCHES INSTITUT (I).
Lifetime measurements on neutron deficient even--even isotopes of Xe and Ba, 25:28319 (CERN-70-30(Vol.2), pp 905-10)
Measurement of the spin and nuclear magnetic moment of ^{26}Na, 25:28209 (CERN-70-30(Vol.1), pp 383-5)
On-line measurements of spin and moments of nuclear ground states, 25:27914 (CERN-70-30(Vol.1), pp 361-81)
HIGH VOLTAGE ENGINEERING CORP., BURLINGTON, MASS.
Equilibrium charge-state distribution of heavy ions (1 to 14 MeV), 25:28127 (WASH-1159, pp 45-57)
HYDRO-ELECTRIC POWER COMMISSION OF ONTARIO, TORONTO.
Maintenance from the station operator's point of view, 25:28551 (AECL-3670, pp 65-70)
Nuclear generating unit performance: an operator viewpoint, 25:28547 (AECL-3670, pp 13-20)

I

IBM SCIENTIFIC CENTER, PALO ALTO, CALIF.
Scavenging of aerosols by rain, 25:26388 (CONF-700601-, pp 433-46)
IDAHO NUCLEAR CORP., IDAHO FALLS.
THETA1-B: a computer code for nuclear reactor core thermal analysis, 25:28737 (IN-1445)
IIT RESEARCH INST., CHICAGO, ILL.
Scavenging by snow and ice crystals, 25:26367 (CONF-700601-, pp 121-36)
ILLINOIS STATE WATER SURVEY, URBANA.
Collection efficiencies of raindrops for submicron particulates, 25:26369 (CONF-700601-, pp 151-60)
ILLINOIS UNIV., URBANA. DEPT. OF BIOCHEMISTRY.
Merodiploidy and expression of episomal genes in Pseudomonas putida, 25:28849 (COO-1683-32)

XUM

ILLINOIS UNIV., URBANA. DEPT. OF COMPUTER SCIENCE.
Illiac III Reference Manual. Vol. I, 25:28851 (COO-2118-5)
ORBIT: Online Reduced Bandwidth Information Transmission, 25:28846 (COO-1469-178)
INDIANA UNIV. FOUNDATION, BLOOMINGTON.
Prog. rpt. on electrochemical research in amine solvents, final, 3/71, 25:28845 (COO-256-102)
INSTITUT ATOMNOI ENERGII, MOSCOW (USSR).
Duration of charged particles containment in a trap with magnetic mirror, 25:27669 (IAE-1972)
Experimental limitations of the method of merging beams for studying ion-atom collisions, 25:27448 (IAE-2001)
Nuclear data for thermonuclear reactors, 25:27792 (IAE-1986)
INSTITUT FUER PLASMAPHYSIK, G.M.B.H. GARCHING (WEST GERMANY).
Influence of lattice defects on backscattering of protons and helium ions from niobium single crystals, 25:27840 (IPP-7/3)
INSTITUTE OF NUCLEAR RESEARCH, WARSAW (POLAND).
Classical theory of atomic collisions. II, 25:27449 (INR-P-1217)
Interaction of harmonic oscillators with radiation field, 25:27928 (INR-P-1203)
Magnetic structure of a manganese-substituted zinc ferrite by neutron diffraction, 25:28857 (INR-1269)
Subnanosecond timing in nuclear spectroscopy, 25:26491 (INR-1213)
INSTITUTO NACIONAL DE TECNOLOGIA AGROPECUARIA, CASTELAR (ARGENTINA). INSTITUTO DE FITOTECNIA.
Uses of ionizing radiations in the genetics of vegetable plants, 25:26686 (CONF-680112-, pp 95-111)
INSTITUTT FOR ATOMENERGI, KJELLER (NORWAY).
Conference on international power system, Oslo, 5/70, 25:28522 (CONF-700550)
Nuclear power in Norway, 25:28523 (CONF-700550-, Paper 1)
INSTITUUT VOOR KERNPHYSISCH ONDERZOEK, AMSTERDAM (NETHERLANDS).
Decay of some nuclei far from the stability line studied with standard spectroscopic techniques, 25:28322 (CERN-70-30(Vol.2), pp 939-47)
Determination of atomic masses for far unstable nuclei by extrapolation, 25:28292 (CERN-70-30(Vol.1), pp 263-73)
INTER-AMERICAN INST. OF AGRICULTURAL SCIENCES, SAN JOSE (COSTA RICA).
Frequency and behavior of mutants induced by gamma irradiation in beans, 25:26685 (CONF-680112-, pp 85-93)
INTERNATIONAL ATOMIC ENERGY AGENCY, VIENNA (AUSTRIA).
Conference on dynamic studies with radioisotopes in medicine, Rotterdam, 8--9/70, 25:26567 (STI/PUB-263)
Conference on environmental aspects of nuclear power stations, New York, 8/70, 25:28621 (STI/PUB-261)
Conference on insect ecology and the sterile-male technique, Vienna, 8/67, 25:27137 (STI/PUB-223)
Conference on small and medium power reactors, 1970, Oslo, 10/70, 25:28529 (STI/PUB-267)
Relationship between radiation damages to citrus fruits and changes in enzymes and other constituents of the peel, 25:27135 (IAEA-R-362-F)
Standard neutron irradiation facility experience in Thailand, 25:27062 (IAEA-R-459)
INTERNATIONAL CENTRE FOR THEORETICAL PHYSICS, TRIESTE (ITALY).
Conference on renormalization theory, 8/69, 25:28060 (IC-69/121)
ION PHYSICS CORP., BURLINGTON, MASS.
Ion momentum analysis of collectively accelerated ion species, 25:27697 (WASH-1159, pp 219-26)
IOWA UNIV., IOWA CITY. DEPT. OF CHEMISTRY.
Infrared spectra of UO and UO_2 vapor condensed in rare-gas matrices, 25:26260 (COO-1182-34)
ISRAEL ATOMIC ENERGY COMMISSION, BEERSHEBA. NUCLEAR RESEARCH CENTER-NEGEV.
The measurement of energy levels' width in the 6-9 MeV region, 25:28219 (NRCN-254)
ISTITUTO SUPERIORE DI SANITA, ROME (ITALY). LABORATORI DI FISICA.
Status of some relevant problems in nuclear physics, 25:28449 (ISS-70/17)

J

JAPAN ATOMIC ENERGY RESEARCH INST., OARAI. OARAI RESEARCH ESTABLISHMENT.
Primary cooling water decomposition in reactors, 25:28758 (JAERI-1204)
JAPAN ATOMIC ENERGY RESEARCH INST., TOKAI. TOKAI RESEARCH ESTABLISHMENT.
Evaluation of integrity for fast neutron irradiation embrittlement of JPDR pressure vessel, 25:28682 (JAERI-1202)
JAPAN ATOMIC ENERGY RESEARCH INST., TOKYO.
Analysis of instrumentation data from IFA-150 irradiated in HBWR, 25:28692 (JAERI-Memo-4248)
Comparison of thermal neutron cross sections, 25:28344 (JAERI-1200)
Pulsed neutron experiment on FCA I-5, 25:28759 (JAERI-Memo-4272)
Spectrophotometric determination of traces of uranium in sodium, 25:26152 (JAERI-Memo-4267)
JERSEY CENTRAL POWER AND LIGHT CO., MORRISTOWN, N. J.
Three Mile Island Nuclear Station, Unit 1. Preliminary safety analysis report, Amendment 19 (includes final safety analysis report modifications, Appendix 5A), 25:28611 (DOCKET-50289-34)
JET PROPULSION LAB., PASADENA, CALIF.
Gamma radiation characteristics of plutonium dioxide fuel, 25:27305 (N-70-35897)
JOINT COMMITTEE ON ATOMIC ENERGY (U. S. CONGRESS).
Nuclear rocket engine development program, 25:28785
JOINT FAO/IAEA DIV. OF ATOMIC ENERGY IN AGRICULTURE, VIENNA (AUSTRIA).
Program of FAO/IAEA in food and agriculture, 25:27128 (CONF-680112-, pp 1-7)
JOINT INST. FOR NUCLEAR RESEARCH, DUBNA (USSR).
Decay of ^{89}Nb, /sup 89m,89/Nb, /sup 85m,85/Y and /sup 85m/Sr, 25:28215 (CERN-70-30(Vol.2), pp 1137)
Emissions of ^{8}He through nuclear fission by heavy ions, 25:28351 (KFK-tr-352)
Investigation of α decay of isotopes of element 105, 25:28350 (KFK-tr-350)
Nuclear spectroscopy of some light Tl isotopes, 25:28339 (CERN-70-30(Vol.2), pp 1081-91)
Proton emitter studies in region of Z > 50, 25:28300 (CERN-70-30(Vol.1), pp 457-86)
JOINT INST. FOR NUCLEAR RESEARCH, DUBNA (USSR). LAB. OF COMPUTING TECHNIQUES AND AUTOMATION.
Non-linear regime of radiation instability development of relativistic electron rings, 25:28110 (JINR-P9-5622)
JOINT INST. FOR NUCLEAR RESEARCH, DUBNA (USSR). LAB. OF HIGH ENERGY.
Deuteron acceleration in LA9-injector of JINR synchrocyclotron, 25:28109 (JINR-P9-5610)
JOINT INST. FOR NUCLEAR RESEARCH, DUBNA (USSR). LAB. OF NEUTRON PHYSICS.
Alpha decay of resonance states of ^{149}Sm, 25:28347 (JINR-P3-5553)
Reaction (n,α): new channel for studying nature of neutron resonances, 25:28345 (JINR-E3-5483)
JOINT INST. FOR NUCLEAR RESEARCH, DUBNA (USSR). LAB. OF NUCLEAR PROBLEMS.
Apochromatic method for measurement of mean proton energy in 657 MeV beam, 25:26506 (JINR-P13-5637)
Monochromatic method for measurement of mean proton energy in 665 MeV beam, 25:26505 (JINR-P13-5636)
Sign of astatine ion charge in $HClO_4$--$H_2Cr_2O_7$ solutions, 25:26209 (JINR-P12-5644)
JOINT INST. FOR NUCLEAR RESEARCH, DUBNA (USSR). LAB. OF NUCLEAR REACTIONS.
New isotopes of iridium, 25:28348 (JINR-P6-5617)
JOINT INST. FOR NUCLEAR RESEARCH, DUBNA (USSR). LAB. OF THEORETICAL PHYSICS.
Global and local structure of relativistic quantum systems, 25:27931 (JINR-E2-5575)
Nonrotational states of odd-N deformed nuclei in region 153 less than or equal to A less than or equal to 171, 25:28346 (JINR-E4-5567)

K

KERNFORSCHUNGSANLAGE, JUELICH (WEST GERMANY). INSTITUT FUER FESTKOERPERFORSCHUNG.
Dislocation structure of a Ni single crystal with magnetic small-angle scattering of neutrons, 25:27246 (JUL-675-FF)
KERNFORSCHUNGSANLAGE, JUELICH (WEST GERMANY). INSTITUT FUER NEUTRONENPHYSIK.
Identification of μ s isomers among primary fission fragments, 25:28325 (CERN-70-30(Vol.2), pp 967-84)
KERNFORSCHUNGSANLAGE, JUELICH (WEST GERMANY). ZENTRALINSTITUT FUER ANGEWANDTE MATHEMATIK.
Program for solution of the stationary neutron transport equation with spherical symmetry, 25:28147 (JUL-683-MA)
KERNFORSCHUNGSANLAGE, JUELICH (WEST GERMANY). ZENTRALINSTITUT FUER REAKTOREXPERIMENTE.
High-temperature brazing of thermoelements and pipe ducts on reactor plugs for reactor experiments, 25:27177 (JUL-681-RX)
KERNFORSCHUNGSZENTRUM, KARLSRUHE (WEST GERMANY).
Fast Breeder Project, 25:28632 (EURFNR-824)
New developments and aspects in phosphate glass dosimetry, 25:26519 (NP-18747)
Personnel monitoring with radiophotoluminescent dosimeters, 25:26518 (NP-18746)
Transport of high level vitrified fission products, 25:26448 (KFK-1263)
KERNFORSCHUNGSZENTRUM, KARLSRUHE (WEST GERMANY). INSTITUT FUER ANGEWANDTE KERNPHYSIK.
Prompt gamma transitions in primary fragments from neutron-induced fission, 25:28320 (CERN-70-30(Vol.2), pp 917-30)
KERNFORSCHUNGSZENTRUM, KARLSRUHE (WEST GERMANY). INSTITUT FUER ANGEWANDTE REAKTORPHYSIK.
Measurement of neutron spectra within the 1 eV to 10 keV energy range by means of the sandwich technique, 25:28656 (EURFNR-842)
Structure and working of the on-line system for SNEAK

XUM

data processing and control of experiments, 25:28756 (EURFNR-803)

KERNFORSCHUNGSZENTRUM, KARLSRUHE (WEST GERMANY). INSTITUT FUER EXPERIMENTELLE KERNPHYSIK.
Quasielastic electron--deuteron scattering for four pulse transfers in range 0.2 $(GeV/c)^2 < q^2 < 0.85(GeV/c)^2$, 25:27951 (NP-18725)
Superconducting dc quadrupole lens, 25:28111 (KFK-1218)

KERNFORSCHUNGSZENTRUM, KARLSRUHE (WEST GERMANY). INSTITUT FUER HEISSE CHEMIE.
Aqueous reprocessing of fuel elements of fast breeder, 25:26326 (KFK-911)

KERNFORSCHUNGSZENTRUM, KARLSRUHE (WEST GERMANY). INSTITUT FUER MATERIAL UND FESTKOERPERFORSCHUNG.
Experimental contribution to Jost mechanisms in solid-state reactions, 25:26210 (KFK-1312)
Fission product yield in the fission of ^{235}U, ^{238}U, ^{239}Pu, and ^{241}Pu with neutrons of different energies, 25:28354 (NP-18723)
Stoichiometry shift in an oxide fuel element at high burnup, 25:28690 (EURFNR-836)

KERNFORSCHUNGSZENTRUM, KARLSRUHE (WEST GERMANY). INSTITUT FUER NEUTRONENPHYSIK UND REAKTORTECHNIK.
Calculation of flux distributions in reactor sub-regions with generalized multiple collision probabilities, 25:28805 (EURFNR-898)

KERNFORSCHUNGSZENTRUM, KARLSRUHE (WEST GERMANY). INSTITUT FUER REAKTORBAUELEMENTE.
Theoretical method for calculation of two-phase flow with change of phase in a flash evaporation, 25:26420 (KFK-1300)

KERNFORSCHUNGSZENTRUM, KARLSRUHE (WEST GERMANY). INSTITUT FUER REAKTORENTWICKLUNG.
Conceptual studies of a 1000-MWe nuclear power station with a steam-cooled, fast breeder reactor, 25:28634 (NP-18782)
Danger contained in a steam-cooled fast breeder reactor and the dose value released to the environment in a severe accident, 25:28738 (NP-18781)
Influence of real dead-time simulation on dynamic behavior of computer model of automatically controlled Na-2 reactor, 25:28804 (EURFNR-835)
Optimization of sodium-cooled fast breeders by nonlinear programming methods, 25:28655 (EURFNR-830)
Selfwelding of reactor structural materials in sodium environment at high temperatures, 25:27206 (KFK-Ext.Ber.-8/70-1)

KERNFORSCHUNGSZENTRUM, KARLSRUHE (WEST GERMANY). LABOR FUER ELEKTRONIK UND MESSTECHNIK.
Cladding monitoring in sodium-cooled reactors by detection of delayed neutrons, 25:28698 (NP-18778)

KERNFORSCHUNGSZENTRUM, KARLSRUHE (WEST GERMANY). LABORATORIUM FUER ISOTOPENTECHNIK.
Pneumatic system for activation analysis with short-lived radionuclides, 25:26189 (KFK-1293)

KERNFORSCHUNGSZENTRUM, KARLSRUHE (WEST GERMANY). ZYKLOTRON-LABORATORIUM.
Measurement of the spin and nuclear magnetic moment of ^{20}Na, 25:28209 (CERN-70-30(Vol.1), pp 383-5)

KNOLLS ATOMIC POWER LAB., SCHENECTADY, N. Y.
Neutron cross sections and strength functions of ^{147}Sm and ^{150}Sm, 25:28349 (KAPL-P-3930)

KRAFTWERK UNION A.G., ERLANGEN (WEST GERMANY).
Technology and economics of the nuclear power plants constructed by Kraftwerk Union, 25:28526 (CONF-700550-, Paper 4)

L

LEHIGH UNIV., BETHLEHEM, PA.
Hydrostatic extrusion of hard core clad rod, 25:28869 (NYO-4078-3)

LOS ALAMOS SCIENTIFIC LAB., N. MEX.
Feedback systems on linear THETA pinches with helical fields, 25:27726 (LA-4598)
Independent cesium yields in ^{238}U fission: identification of ^{145}Cs, 25:28307 (CERN-70-30(Vol.1), pp 589-99)
Mass law with model-based shape-dependent shell terms, 25:28441 (CERN-70-30(Vol.1), pp 217-62)
Methods of chemical analysis for FBR uranium--plutonium oxide fuel and source materials, 25:26153 (LA-4622)
Theoretical predictions for superheavy nuclei, 25:28309 (CERN-70-30(Vol.2), pp 605-44)

LUND INST. OF TECH. (SWEDEN). DEPT. OF MATHEMATICAL PHYSICS.
Effects of P_3 and P_5 distortions on fission barriers of superheavy elements, 25:28313 (CERN-70-30(Vol.2), pp 689-99)
Extrapolations to Z = 164 region, 25:28310 (CERN-70-30(Vol.2), pp 646-53)
Extrapolations to Z = 40 - 60 region of elements, 25:28318 (CERN-70-30(Vol.2), pp 847-82)
Odd-particle effect on the fission barrier, 25:28314 (CERN-70-30(Vol.2), pp 700-8)
Shell model parameters of Z = 114 region, 25:28311 (CERN-70-30(Vol.2), pp 654-75)
Two-centre potential and the (del V x p vector)^2 term, 25:28312 (CERN-70-30(Vol.2), pp 676-88)

LUND INST. OF TECH. (SWEDEN). DEPT. OF NUCLEAR PHYSICS.
Proton hole states excited by monoenergetic gamma-quanta, 25:28217 (LUNP-7013)

LYON UNIV. (FRANCE). FACULTE DES SCIENCES.
Wigner energy in irradiated oxides BeO, MgO, Al_2O_3, and SiO_2, 25:27839 (CEA-N-1171)

LYON UNIV. (FRANCE). INSTITUT DE PHYSIQUE NUCLEAIRE.
Development of a test bench for multicharged ion sources, 25:28113 (LYCEN-7054)

M

MAINE YANKEE ATOMIC POWER CO., WESTBORO, MASS.
Maine Yankee Atomic Power Station. Preliminary safety analysis report, Amendment 22, 25:28615 (DOCKET-50309-33)

MAINZ UNIV. (WEST GERMANY). INSTITUT FUER ANORGANISCHE CHEMIE UND KERNCHEMIE.
Some studies on neutron-rich nuclei, 25:28326 (CERN-70-30(Vol.2), pp 985-1000)

MANCHESTER UNIV. (ENGLAND). DEPT. OF PHYSICS.
9/2-[514] state in ^{185}Re, 25:28287 (ANU-P-518)

MARBURG UNIV. (WEST GERMANY). INSTITUT FUER KERNCHEMIE.
Search for spontaneously fissioning isomers produced with 600 MeV protons, 25:28306 (CERN-70-30(Vol.1), pp 575-87)

MARYLAND UNIV., COLLEGE PARK.
Intensity and phase-space limitations of various heavy-ion acceleration methods, 25:28130 (WASH-1159, pp 227-51)
Production of multiply stripped ions in magnetically confined high-energy electron clouds, 25:27439 (WASH-1159, pp 147-55)

MARYLAND UNIV., COLLEGE PARK. INST. FOR FLUID DYNAMICS AND APPLIED MATHEMATICS.
Spark source, 25:28129 (WASH-1159, pp 168-71)

MASSACHUSETTS INST. OF TECH., CAMBRIDGE.
Prog. rpt. on instrumental chemistry and hot atom chemistry, annual, 12/31/70, 25:28861 (MIT-905-162)
Recent work on stripping and pickup of electrons by fast heavy ions, 25:28126 (WASH-1159, pp 34-41)

MAX-PLANCK-INSTITUT FUER KERNPHYSIK, HEIDELBERG (WEST GERMANY).
Beta decay energies of some neutron deficient nuclides, 25:28297 (CERN-70-30(Vol.1), pp 353-60)
Lifetime measurements on neutron deficient even--even isotopes of Xe and Ba, 25:28319 (CERN-70-30(Vol.2), pp 905-10)

MAX-PLANCK-INSTITUT FUER PHYSIK UND ASTROPHYSIK, MUNICH (WEST GERMANY).
Nuclei in neutron matter, 25:27311 (CERN-70-30(Vol.2), pp 759-68)

MECHANICAL TECHNOLOGY INC., LATHAM, N. Y.
Reliability factors affecting power plant mechanical equipment, 25:28549 (AECL-3670, pp 45-55)

MELBOURNE UNIV., PARKVILLE (AUSTRALIA). SCHOOL OF PHYSICS.
Cross section of $^{28}Mg(tau,\gamma)^{28}Si$ reaction, 25:28206 (ANU-P-508)

METROPOLITAN EDISON CO., READING, PA.
Three Mile Island Nuclear Station, Unit 1. Preliminary safety analysis report, Amendment 19 (includes final safety analysis report modifications, Appendix 5A), 25:28611 (DOCKET-50289-34)

MIAMI UNIV., FLA. ROSENSTIEL SCHOOL OF MARINE AND ATMOSPHERIC SCIENCES.
Prog. rpt. on tritiated hydrogen and its compounds in the environment, 3/71, 25:26393 (ORO-3944)

MICHIGAN STATE UNIV., EAST LANSING.
Straightforward elucidation of complex shell-model states by β decay of nuclei far from stability, 25:28299 (CERN-70-30(Vol.1), pp 435-46)

MICHIGAN STATE UNIV., HICKORY CORNERS. W. K. KELLOGG BIOLOGICAL STATION.
Role of carbon in hard-water lakes, 25:28847 (COO-1599-32)

MICHIGAN UNIV., ANN ARBOR.
Model for variations with particle size of halogen-ion ratios in marine aerosols, 25:26381 (CONF-700601-, pp 325-51)

MICHIGAN UNIV., ANN ARBOR. DEPT. OF METEOROLOGY AND OCEANOGRAPHY.
Scavenging of tracer in severe storms, 25:26361 (CONF-700601-, pp 21-35)

MILLSTONE POINT CO., HARTFORD, CONN.
Millstone Nuclear Power Station, Unit 1. Additional information on scram trip circuitry, 25:28604 (DOCKET-50245-66)

MILLSTONE POINT CO., WETHERSFIELD, CONN.
Millstone Nuclear Power Station, Unit 1. Application for amendment to provisional construction permit No. CPPR-20, 25:28603 (DOCKET-50245-65)

MINISTERIO DE AGRICULTURA, LA PAZ (BOLIVIA).
Fruit pests in Bolivia, 25:27130 (CONF-680112-, pp 129-42)

MINISTRY OF AGRICULTURE, FISHERIES AND FOOD, LOWESTOFT (ENGLAND). FISHERIES RADIOBIOLOGICAL LAB.
Radioactivity in surface and coastal waters of the British Isles, 1969, 25:26397 (FRL-7)

MINNESOTA UNIV., MINNEAPOLIS. SCHOOL OF PHYSICS.
Feasibility of direct mass determinations of short half-life isotopes, 25:26547 (CERN-70-30(Vol.1), pp 307-19)

XUM

MOUND LAB., MIAMISBURG, OHIO.
Environmental monitoring report: July--December 1970 and 1970 summary, 25:26739 (MLM-1795)
Heat source capsule fabrication technology program: September 1970--January 1971, 25:26425 (MLM-1796)
Method and device used for the safe handling and storing of fragile x-ray diffraction specimens, 25:26449 (MLM-1790)
Technique for direct measurement of thermal power in assay calorimeters, 25:26548 (MLM-1780)

N

NATIONAL ACCELERATOR LAB., BATAVIA, ILL.
NAL 1970 archaeological survey, 25:28862 (NAL-55)
NATIONAL AERONAUTICS AND SPACE ADMINISTRATION, CLEVELAND, OHIO. LEWIS RESEARCH CENTER.
Alloy softening in group VIA metals alloyed with Re, 25:27209 (N-71-11662)
Cavity reactor engineering mockup critical experiment, 25:28761 (NASA-CR-72409)
Expanded FORTRAN 4 program for elastic scattering analyses, 25:28450 (N-70-42846)
Freeze, melt valve and dispensing system for Cs, 25:26413 (N-71-10455)
Long-time creep behavior of tantalum--10 tungsten in high vacuum, 25:27207 (N-70-42045)
Thermal cycling on a 3-in.-diameter Nb--1 percent Zr to 316 stainless steel transition joint, 25:27179 (N-71-10454)
NATIONAL AERONAUTICS AND SPACE ADMINISTRATION, HUNTSVILLE, ALA. GEORGE C. MARSHALL SPACE FLIGHT CENTER.
Coulomb corrections to Bethe--Heitler cross sections for electron--nucleus bremsstrahlung, 25:28451 (N-71-10999)
NATIONAL AERONAUTICS AND SPACE ADMINISTRATION, LANGLEY STATION, VA. LANGLEY RESEARCH CENTER.
Measured electron conversion ratios for 1064-keV γ ray of ^{207}Bi, 25:28352 (N-71-10060)
NATIONAL AERONAUTICS AND SPACE ADMINISTRATION, NEW YORK. GODDARD INST. FOR SPACE STUDIES.
Construction of mass formulas designed to be valid for neutron-rich nuclei, 25:28293 (CERN-70-30(Vol.1), pp 275-306)
Dynamics of the rapid neutron capture process, 25:27310 (CERN-70-30(Vol.2), pp 735-57)
NATIONAL BUREAU OF STANDARDS, WASHINGTON, D. C.
Molecular dynamical studies of the phase transformation of iron under pressure, 25:28895 (TID-25683)
NATIONAL CENTER FOR ATMOSPHERIC RESEARCH, BOULDER, COLO.
Processes influencing evolution of droplet or aerosol spectrum, 25:26385 (CONF-700601-, pp 385-402)
NATIONAL INST. OF RADIOLOGICAL SCIENCES, CHIBA (JAPAN).
Radioactivity survey data in Japan, 5/70, 25:26392 (NIRS-RSD-27)
NATIONAL INSTITUTES OF HEALTH, BETHESDA, MD.
Radiation preservation of foods, 25:27132 (CONF-680112-, pp 221-39)
NATIONAL LEAD CO. OF OHIO, CINCINNATI.
Thorium metal production, 25:27180 (NLCO-1080)
NATIONAL MARINE FISHERIES SERVICE, GLOUCESTER, MASS. GLOUCESTER FISHERIES PRODUCTS TECHNOLOGY LAB.
Prog. rpt. on marine products development irradiator program: irradiated fresh shrimp shipping studies, annual, 10/67--9/68, 25:27138 (TID-25543)
NEW YORK BLOOD CENTER, N.Y.
Preparation and properties of six rat red cell hemoglobins, 25:28866 (NYO-3976-5)
Prog. rpt., 6/70--5/71, 25:28865 (NYO-3976-4)
NEW YORK OPERATIONS OFFICE (AEC), N. Y. HEALTH AND SAFETY LAB.
Tropospheric scavenging of ^{90}Sr and ^{3}H, 25:26389 (CONF-700601-, pp 447-63)
NEW YORK STATE VETERINARY COLL., ITHACA. DEPT. OF PHYSICAL BIOLOGY.
Atomic energy techniques to increase productivity of domestic livestock, 25:26578 (CONF-680112-, pp 153-66)
NEW YORK UNIV., N. Y.
Summary report on investigations of transfer matrix method, 25:28798 (NYU-4090-1)
NIELS BOHR INSTITUTET, COPENHAGEN (DENMARK).
Alpha decay of neutron deficient isotopes of mercury and radon and their daughters, 25:28302 (CERN-70-30(Vol.1), pp 523-31)
Beta-neutrino correlations and recoil nuclear alignment effects in light delayed particle emitters, 25:28210 (CERN-70-30(Vol.1), pp 447-55)
Experimental Q-values far from stability, 25:28295 (CERN-70-30(Vol.1), pp 331-40)
Resonant fission with damping, 25:28445 (CERN-70-30(Vol.1), pp 553-66)
Search for new islands of fission isomerism, 25:28305 (CERN-70-30(Vol.1), pp 567-74)
Some new aspects of deformed nuclei, 25:28317 (CERN-70-30(Vol.2), pp 829-45)
NORTH AMERICAN ROCKWELL CORP., THOUSAND OAKS, CALIF. SCIENCE CENTER.
Theory of diffusive and impactive scavenging, 25:26382 (CONF-700601-, pp 355-71)
NORTH CAROLINA STATE UNIV., RALEIGH.
Deformation substructure in polycrystalline alumina, 25:28878 (ORO-3328-13)
NORTHERN INDIANA PUBLIC SERVICE CO., HAMMOND.
Bailly Generating Station, Nuclear I. Preliminary safety analysis report, Amendment 5, 25:28619 (DOCKET-50367-12)
NUCLEAR-CHICAGO CORP., AUSTIN, TEX. TEXAS NUCLEAR DIV.
Instrument manual for prototype wet concrete analyzer, 25:26540 (ORO-3842-3)
Prog. rpt. on simulation and measurement of solar-flare proton exposures, final, 11/68--8/69, 25:26920 (AD-711041)
NUCLEAR FUEL SERVICES, INC., ROCKVILLE, MD.
West Valley Reprocessing Plant. Final safety analysis report, Revision 7, 25:26324 (DOCKET-50201-68)
West Valley Reprocessing Plant. Modification schedule, 25:26323 (DOCKET-50201-67)
NUCLEAR FUEL SERVICES, INC., WEST VALLEY, N.Y.
Prog. rpt., 10--12/70, 25:26355 (SRO-344-11)
NUCLEAR MATERIALS AND EQUIPMENT CORP., APOLLO, PA. ENERGY CONVERSION DIV.
Prog. rpt. on radioisotope powered Cardiac Pacemaker Program, 11/70--11/71, 25:26426 (NUMEC-4189-4)
NUCLEAR POWER GROUP LTD., KNUTSFORD (ENGLAND).
Nuclear power industry of the United Kingdom, 25:28524 (CONF-700550-, Paper 2)

O

OAK RIDGE NATIONAL LAB., TENN.
Analysis of the New Brunswick Laboratory Sample Cask, 25:26450 (ORNL-TM-3298)
Application of DOT--MORSE coupling to the analysis of three-dimensional SNAP shielding problems, 25:28784 (ORNL-TM-3365)
Deep inelastic collisions and Auger processes, 25:27437 (WASH-1159, pp 113-19)
EDITOR: processing code for ENDF/B format data, 25:28148 (ORNL-TM-3266)
Equipment for the dissolution of core material from sheared power reactor fuels, 25:26327 (ORNL-TM-3194)
Manual for ASTM A-533 grade B, class 1 steel (HSST plate 03) provided to the International Atomic Energy Agency, 25:27181 (ORNL-TM-3193)
MSRE procedures for period between examination and ultimate disposal, 25:28711 (ORNL-TM-3253)
New aspects of intermediate nuclei, 25:28316 (CERN-70-30(Vol.2), pp 779-812)
Nuclear desalination program annual progress report on activities sponsored by the Atomic Energy Commission for period ending October 31, 1970, 25:28790 (ORNL-4668)
Possible single impact source for multiply charged ions, 25:27438 (WASH-1159, pp 141-6)
Prog. rpt. on research reactor, 10--12/70, 25:28762 (ORNL-TM-3369)
Prog. rpt. on Vertical Tube Evaporator Pilot Plant, annual, 1969, 25:28893 (TID-25679)
Search for new α-emitters with N = 86 and N = 87, 25:28303 (CERN-70-30(Vol.1), pp 533-44)
Selected abstracts of world literature on production and industrial uses of radioisotopes, 25:26427 (ORNL-IIC-30(Pt.4))
OESTERREICHISCHE STUDIENGESELLSCHAFT FUER ATOMENERGIE G.M.B.H., SEIBERSDORF. INSTITUT FUER REAKTORTECHNIK.
Future management of radioactive wastes in Austria, 25:26451 (SGAE-RT-33/1970)
OREGON STATE UNIV., CORVALLIS. DEPT. OF OCEANOGRAPHY.
Chemical budget of Columbia River, 25:28879 (RLO-1750-41)
Two new gregarine parasites from the spatangoid-urchin Brissaster latifrons, 25:28880 (RLO-1750-59)
ORGANISMO INTERNACIONAL REGIONAL DE SANIDAD AGROPECUARIA, SAN SALVADOR (EL SALVADOR). DEPARTAMENTO DE SANIDAD VEGETAL.
Cooperative program on the investigation of the Med Fly in Central America, 25:27131 (CONF-680112-, pp 143-50)
OSKARSHAMNSVERKETS KRAFTGRUPP A.B., STOCKHOLM (SWEDEN).
Demand of uranium enrichment services for Sweden's nuclear power program, 1975--1985, 25:26395 (CONF-700903-15)

P

PACIFIC GAS AND ELECTRIC CO., SAN FRANCISCO, CALIF.
Humboldt Bay Power Plant, Unit No. 3. Abnormal occurrence report: blown fuse in automatic circuitry for the off-gas isolation valve, 25:28560 (DOCKET-50133-53)
Humboldt Bay Power Plant, Unit No. 3. License No. DPR-7; technical specifications Proposed Change No. 34, 25:28589 (DOCKET-50133-55)
PARIS UNIV., ORSAY (FRANCE).
Effect of charge on ^{252}Cf fission fragments on neutron emission process, 25:28288 (CEA-R-4121)
PARIS UNIV., ORSAY (FRANCE). FACULTE DES SCIENCES.
Electronic lattice structure by positron annihilation in insulators, 25:27865 (CEA-R-4138)

XUM

PARIS UNIV., ORSAY (FRANCE). INSTITUT DE PHYSIQUE NUCLEAIRE.
Mass-differences in neutron-rich Sr Region, 25:28294 (CERN-70-30(Vol.1), pp 321-9)
Search for superheavy elements on accelerator ALICE, 25:28315 (CERN-70-30(Vol.2), pp 723-33)
PENNSYLVANIA ELECTRIC CO., JOHNSTOWN.
Three Mile Island Nuclear Station, Unit 1. Preliminary safety analysis report, Amendment 19 (includes final safety analysis report modifications, Appendix 5A), 25:28611 (DOCKET-50289-34)
PENNSYLVANIA STATE UNIV., UNIVERSITY PARK. MATERIALS RESEARCH LAB.
Prog. rpt. on role of trapping processes in solid state radiation dosimetry, annual, 1970--1971, 25:26520 (NYO-3409-9)
PHILADELPHIA ELECTRIC CO., PA.
Peach Bottom Atomic Power Station, Unit 1. Monthly operations report No. 60, February 1971, 25:28562 (DOCKET-50171-83)
PHYSICS INTERNATIONAL CO., SAN LEANDRO, CALIF.
Ion acceleration with high v/γ electron beams, 25:27696 (WASH-1159, pp 204-18)
Ion production with intense electron beams, 25:27695 (WASH-1159, pp 196-203)
PITTSBURGH UNIV., PA.
Prog. rpt. on radioecology of small vertebrate species under natural environments, 12/69--11/70, 25:26682 (NYO-2579-20)
POWER REACTOR DEVELOPMENT CO., DETROIT, MICH.
Enrico Fermi Atomic Power Plant, Unit 1. Operations report, November 1970, 25:28558 (DOCKET-50016-108)
Enrico Fermi Atomic Power Plant, Unit 1. Operations report, December 1970, 25:28559 (DOCKET-50016-109)
POWER TECHNOLOGIES, INC., SCHENECTADY, N.Y.
Survey of experience with equipment availability, 25:28548 (AECL-3670, pp 23-37)
PRINCETON-PENNSYLVANIA ACCELERATOR, PRINCETON, N. J.
Automatic target cycling system for total cross section measurements, 25:28115 (PURC-4159-17)
PRINCETON UNIV., N.J. DEPT. OF PHYSICS.
Experimental study of omega neutral decays, 25:27961 (PURC-4159-16)
PRINCETON UNIV., N.J. JOSEPH HENRY LABS.
Automatic target cycling system for total cross section measurements, 25:28115 (PURC-4159-17)
Phenomena in multiparticle production processes, 25:27969 (PURC-4159-19)
Phenomenology of weak interactions, 25:28003 (PURC-4159-22)
Public Health Service. National Institutes of Health, Bethesda, Md.
Artificial heart program conference, Washington, D. C., 6/69, 25:26899
PUBLIC SERVICE CO. OF COLORADO, DENVER.
Fort St. Vrain Nuclear Generating Station, Unit 1. Preliminary safety analysis report, Amendment 19, 25:28608 (DOCKET-50267-28)
PURDUE UNIV., LAFAYETTE, IND. DEPT. OF PHYSICS.
Beta--gamma circular polarization correlation and nuclear matrix elements of ^{76}As, 25:28216 (COO-1746-54)

R

RADIOCHEMICAL CENTRE, AMERSHAM (ENGLAND).
Derivation and use of experimental efficiency graphs for γ spectrometry in the Physics Department at the Radiochemical Centre, 25:26492 (RCC-M-211)
RAND CORP., SANTA MONICA, CALIF.
Statistical model calculations of ^{56}Fe neutron cross section, 25:28218 (NP-18674)
REACTOR CENTRUM NEDERLAND, PETTEN.
Extension of the derivation of the diffusion length for neutrons in a medium with small absorption, 25:28150 (RCN-134)
RESEARCH COUNCIL OF ALBERTA, EDMONTON.
Scavenging of SO_2 by convective storms, 25:26379 (CONF-700601-, pp 305-18)
RICE UNIV., HOUSTON, TEX.
Prog. rpt. on computer project, final, 6/59--3/70, 25:28877 (ORO-2572-27)
ROCHESTER UNIV., N. Y.
Energetics of active transcellular calcium transport by chorioallantoic membrane of the embryonic chick, 25:28905 (UR-49-1440)
ROCHESTER UNIV., N. Y. DEPT. OF RADIATION BIOLOGY AND BIOPHYSICS.
Modification of anion and cation permeability of the human red cell membrane by amino and sulfhydryl reactive reagents, 25:28904 (UR-49-1429)
Possible role of crystals in origins of life, 25:28906 (UR-49-1444)
RUTGERS--THE STATE UNIV., NEW BRUNSWICK, N. J. DEPT. OF PHYSICS.
Automatic target cycling system for total cross section measurements, 25:28115 (PURC-4159-17)
RUTHERFORD HIGH ENERGY LAB., CHILTON (ENGLAND).
Evolution of pumping groups used on Rutherford Laboratory ^{3}He Refrigerator, 25:27664 (RHEL/R-208)
Ion sources for multiply charged heavy ions, 25:28125 (WASH-1159, pp 13-33)
Laser illumination system for Hough--Powell device, 25:26509 (RHEL/R-212)

S

SANDIA LABS., ALBUQUERQUE, N. MEX.
Advanced filament-wound carbon composite, 25:28888 (SC-DR-710192)
Characterization of the ionic species incident on the cathode in a glow discharge, 25:28891 (SC-RR-710122)
Circuit for measuring frequency dependent complex admittance and impedance, 25:28882 (SC-DR-68-796)
Climatology of atmospheric diffusion prediction variables, 25:28881 (SC-DC-713920)
Compactness by bounded L/sub p/-variation, 25:28890 (SC-RR-70-852)
Computerized ultrasonic data acquisition system, 25:28884 (SC-DR-70-680)
Determination of the activation energy for precipitation of Al_6Mn in Al--3.4 w/o Mn alloy, 25:28889 (SC-RR-70-356)
Energy partitioning during hypervelocity impact on rocks, 25:26354 (SC-R-70-4402)
Evaluation of the impedance probe method of shock speed measurement, 25:28887 (SC-DR-710086)
Follow-on test on project firescan as an RTG heat source search and detection system, 25:26428 (SC-DR-710095)
Gasbuggy seismic source and surface motion, 25:26405 (PNE-1002)
Generalized integrated circuit, 25:28886 (SC-DR-710033)
Ground motion summary statement, 25:26411 (SC-DC-713865)
Reaction of Mulberry with various gases, 25:27210 (SC-DR-710124)
System that enables PDP-9 computer to utilize CDC-160A computer as a peripheral controller, 25:28885 (SC-DR-70-856)
Tentative method for expressing radiation hardness, 25:26560 (SC-DR-710045)
User's manual for two-dimensional axisymmetric transient heat conduction material ablation computer program, 25:28883 (SC-DR-70-510)
Worldwide correlation of soil and population, 25:26429 (SC-R-7121)
SAO PAULO UNIV. (BRAZIL). CENTRO DE MEDICINA NUCLEAR.
Conference on biological effects of radiations, Sao Paulo, 10/69, 25:27036 (CONF-691057)
SAXTON NUCLEAR EXPERIMENTAL CORP., PA.
Saxton Reactor. License No. DPR-4; technical specifications Change Request No. 42, 25:28590 (DOCKET-50146-71)
SIEMENS A.G., ERLANGEN (WEST GERMANY).
Superconducting dc quadrupole lens, 25:28111 (KFK-1218)
SKODA CONCERN, PILSEN (CZECHOSLOVAKIA). NUCLEAR POWER PLANTS DIV.
Difference method of solution of two-dimensional multigroup time-independent diffusion equations, 25:28807 (ZJE-101)
SOUTH DAKOTA UNIV., VERMILLION. DEPT. OF BIOCHEMISTRY.
Partial purification of photoreactivating enzyme from Euglena gracilis, 25:26619 (COO-1793-6)
SOUTHERN CALIFORNIA EDISON CO., LOS ANGELES.
San Onofre Nuclear Generating Station, Unit 1. Operation report, March 1971, 25:28563 (DOCKET-50206-111)
STATE UNIV. OF NEW YORK, STONY BROOK.
Prog. rpt. on fatigue-enhancement of diffusion, annual, 6/70--5/71, 25:28870 (NYO-4097-2)
STATE UNIV. OF NEW YORK, STONY BROOK. DEPT. OF PHYSICS.
Model space calculation of the quasi-particle interaction for nuclear matter, 25:28453 (NYO-4032-37)
STATENS VATTENFALLSVERK, STOCKHOLM (SWEDEN).
Demand of uranium enrichment services for Sweden's nuclear power program, 1975--1985, 25:26395 (CONF-700903-15)
STOCKHOLM UNIV. (SWEDEN).
Possible nuclear co-existence in odd-mass Ir nuclei, 25:28324 (CERN-70-30(Vol.2), pp 957-65)
STOCKHOLM UNIV. (SWEDEN). INST. OF PHYSICS.
Lifetimes of excited nuclear levels, 25:28341 (CERN-70-30(Vol.2), pp 1115-18)
STOCKHOLM UNIV. (SWEDEN). RESEARCH INST. FOR PHYSICS.
Evidence for high-spin three quasiparticle state in ^{133}I produced in fission, 25:28331 (CERN-70-30(Vol.2), pp 1012-14)
Experimental techniques for nuclear structure studies in the Tin-region at OSIRIS, 25:28107 (CERN-70-30(Vol.2), pp 1003-5)
Levels in doubly-even tellurium isotopes, 25:28330 (CERN-70-30(Vol.2), pp 1010-11)
Neutron hole states in the tin-region, 25:28329 (CERN-70-30(Vol.2), pp 1008-10)
Proton states in the tin-region, 25:28328 (CERN-70-30(Vol.2), pp 1006-7)
Rotational bands in ^{171} ^{173} ^{175}Hf from (particle, xn) reactions, 25:28323 (CERN-70-30(Vol.2), pp 949-55)
SYRACUSE UNIV., N. Y. DEPT. OF PHYSICS.
s-channel helicity conservation constraints on t-channel exchanges, 25:28028 (SU-1206-242)
SYSTEMS, SCIENCE AND SOFTWARE, LA JOLLA, CALIF.
Energy partitioning during hypervelocity impact on rocks,

T

TECHNISCHE UNIVERSITAET, BERLIN (WEST GERMANY). INSTITUT FUER KERNTECHNIK.
Review of methods for handling of stationary neutron transport problem, 25:28151 (TUBIK-21)

TECHNISCHE UNIVERSITAET, MUNICH (WEST GERMANY).
On- and off-beam gamma spectroscopy on neutron deficient isotopes of Ge, Se, Br, and Kr, 25:28213 (CERN-70-30(Vol.2), pp 911-15)

TELEDYNE--ISOTOPES, PALO ALTO, CALIF.
Evaluation of Project Shoal site, 25:26403 (NVO-1229-105(Pt.1))
Ground water safety evaluation. Project Gasbuggy, 25:26406 (PNE-1009)

TENNESSEE UNIV., KNOXVILLE. DEPT. OF PSYCHOLOGY.
Prog. rpt. on long-term effects of radiation, final, 2/68--7/70, 25:26922 (ORO-3260-3-A)

TEXAS AGRICULTURAL AND MECHANICAL UNIV., COLLEGE STATION.
Beta-neutrino correlations and recoil nuclear alignment effects in light delayed particle emitters, 25:28210 (CERN-70-30(Vol.1), pp 447-55)

TEXAS AGRICULTURAL AND MECHANICAL UNIV., COLLEGE STATION. CYCLOTRON INST.
Beta-neutrino correlations and recoil nuclear alignment effects in light delayed particle emitters, 25:28210 (CERN-70-30(Vol.1), pp 447-55)

TEXAS UNIV., AUSTIN.
Attachment of trace substances on atmospheric aerosols, 25:26383 (CONF-700601-, pp 373-80)

U

UNION CARBIDE CORP., OAK RIDGE, TENN. Y-12 PLANT.
Capacitance gage for dimensional measurement, 25:28910 (Y-1783)
Correction of inspection data for part misalignment utilizing a small computer, 25:28908 (Y-1755)
Cubic interpolation for numerically controlled machines, 25:28909 (Y-1782)
Eddy current measurements with a coil encircling a two-conductor rod, 25:28911 (Y-1787)
Preparation of control tape for an R-THETA inspection machine, 25:28907 (Y-1725)

UNITED KINGDOM ATOMIC ENERGY AUTHORITY, ABINGDON (ENGLAND). CULHAM LAB.
Highly stripped ions in laser sources, 25:27723 (WASH-1159, pp 162-7)

UNITED KINGDOM ATOMIC ENERGY AUTHORITY, DOUNREAY (SCOTLAND). REACTOR GROUP.
Reaction of PTFE with liquid sodium, potassium, and NaK alloy, 25:26211 (TRG-Report-2104)

UNITED KINGDOM ATOMIC ENERGY AUTHORITY, SELLAFIELD (ENGLAND). PRODUCTION GROUP.
Determination of ^{137}Cs and ^{134}Cs in samples from the Windscale effluent treatment plant, 25:26177 (PG-Report-965)

UNITED KINGDOM ATOMIC ENERGY AUTHORITY, SPRINGFIELDS (ENGLAND). REACTOR GROUP.
Theoretical waving behavior of Magnox fuel element fins due to coolant-gas induced corrosion and to thermal cycling, 25:26415 (TRG-Report-2121)

UNITED STATES-EURATOM FAST REACTOR EXCHANGE PROGRAM.
Calculation of flux distributions in reactor sub-regions with generalized multiple collision probabilities, 25:28805 (EURFNR-898)
Fast Breeder Project, 25:28632 (EURFNR-824)
Influence of real dead-time simulation on dynamic behavior of computer model of automatically controlled Na-2 reactor, 25:28804 (EURFNR-835)
Measurement of neutron spectra within the 1 eV to 10 keV energy range by means of the sandwich technique, 25:28656 (EURFNR-842)
Optimization of sodium-cooled fast breeders by nonlinear programming methods, 25:28655 (EURFNR-830)
Stoichiometry shift in an oxide fuel element at high burnup, 25:28690 (EURFNR-836)
Structure and working of the on-line system for SNEAK data processing and control of experiments, 25:28756 (EURFNR-803)

UNIVERSITY COLL., LONDON. DEPT. OF MATHEMATICS.
Recent calculations of collision efficiencies, 25:26384 (CONF-700601-, pp 381-3)

UPPSALA UNIV. (SWEDEN). INST. OF PHYSICS.
Atomic-beam measurements in the rare-earth region, 25:28298 (CERN-70-30(Vol.1), pp 387-94)

UTAH STATE UNIV., LOGAN.
Prog. rpt. on Amchitka bioenvironmental program, annual, 7/69--6/70, 25:28841 (BMI-171-133)

V

VERMONT YANKEE NUCLEAR POWER CORP., RUTLAND.
Vermont Yankee Nuclear Power Station. Preliminary safety analysis report, Amendment 24, 25:28609 (DOCKET-50271-49)

VIRGINIA ELECTRIC AND POWER CO., RICHMOND.
North Anna Power Station, Units 1 and 2. Preliminary safety analysis report, Amendment 14. Modifications to the containment spray system, 25:28617 (DOCKET-50338-29)
Surry Power Station, Units 1 and 2. Summary of data collected by the onsite meteorological measurements program at the Hog Island site instrument installation, November 2, 1967--July 17, 1969, 25:28610 (DOCKET-50280-38)

VRIJE UNIVERSITEIT, AMSTERDAM (NETHERLANDS).
Lifetimes of excited states in heavy nuclei, 25:28353 (NP-18695)

VRIJE UNIVERSITEIT, AMSTERDAM (NETHERLANDS). NATUURKUNDIG LABORATORIUM.
Decay studies of neutron deficient Ga and Zn isotopes, 25:28338 (CERN-70-30(Vol.2), pp 1075-9)
Production and decay properties of some shortlived cobalt nuclei, 25:28214 (CERN-70-30(Vol.2), pp 1105-13)

W

WASEDA UNIV., TOKYO (JAPAN). DEPT. OF APPLIED PHYSICS.
Gross theory of beta-decay and the nuclei far from the region of beta-stability, 25:28442 (CERN-70-30(Vol.1), pp 397-419)

WASEDA UNIV., TOKYO (JAPAN). SCIENCE AND ENGINEERING RESEARCH LAB.
Gross theory of beta-decay and the nuclei far from the region of beta-stability, 25:28442 (CERN-70-30(Vol.1), pp 397-419)

WASHINGTON UNIV., ST. LOUIS, MO.
Retinal cone receptor as an ideal light collector, 25:28850 (COO-1701-16)

WASHINGTON UNIV., SEATTLE.
Radiocarbon in the sea, 25:26398 (RLO-2225-T-20-2)

WASHINGTON UNIV., SEATTLE. DEPT. OF ATMOSPHERIC SCIENCES.
Interactions of cloud condensation nuclei and ice nuclei with cloud and precipitation elements, 25:26362 (CONF-700601-, pp 37-48)

WASHINGTON UNIV., SEATTLE. DEPT. OF PHYSICS.
Current algebra and analyticity, 25:28027 (RLO-1388-602)
Effects of lateral substrate fields on helium monolayers, 25:27634 (RLO-1388-604)
Ground state of ^3He monolayers adsorbed on inert substrate, 25:27633 (RLO-1388-603)
ω^{-1} sum rules and long range correlation in binary solutions, 25:27632 (RLO-1388-599)
Substrate mediated interaction between adsorbed atoms, 25:27635 (RLO-1388-605)

WESTERN MASSACHUSETTS ELECTRIC CO., GREENFIELD.
Millstone Nuclear Power Station, Unit 1. Application for amendment to provisional construction permit No. CPPR-20, 25:28603 (DOCKET-50245-65)

WESTINGHOUSE ELECTRIC CORP., PITTSBURGH, PA. ASTRONUCLEAR LAB.
Weldability and elevated temperature stability of refractory metal alloys. V, 25:27178 (N-71-10353)
Weldability and elevated temperature stability of refractory metal alloys. II, 25:27208 (N-71-10352)

WESTINGHOUSE ELECTRIC CORP., PITTSBURGH, PA. NUCLEAR ENERGY SYSTEMS DIV.
Part length rod control system, 25:28668 (WCAP-7406)
Rod position monitoring, 25:28669 (WCAP-7571)

WISCONSIN ELECTRIC POWER CO., MILWAUKEE.
Point Beach Nuclear Plant, Unit 1. Abnormal occurrence report: unscheduled release of radioactivity, 25:28571 (DOCKET-50266-46)

WISCONSIN UNIV., MADISON.
Qualitative and quantitative features of the terrestrial solar ultraviolet radiation environment, 25:26517 (COO-1105-164)

WISCONSIN UNIV., MADISON. DEPT. OF PHYSIOLOGICAL CHEMISTRY.
Prog. rpt. on carbohydrate and nucleic acid metabolism in developing amphibian, annual, 2/70--1/71, 25:28848 (COO-1631-27)

WOODS HOLE OCEANOGRAPHIC INSTITUTION, MASS.
Distribution of some chemical elements between dissolved and particulate phases in the ocean, 25:26190 (NYO-4150-9)

WUERZBURG UNIV. (WEST GERMANY). PHYSIKALISCHES INSTITUT.
Construction of mass formulas designed to be valid for neutron-rich nuclei, 25:28293 (CERN-70-30(Vol.1), pp 275-306)

WYOMING UNIV., LARAMIE. NATURAL RESOURCES RESEARCH INST.
Entry of freezing nuclei into precipitation, 25:26363 (CONF-700601-, pp 49-68)

Y

YALE UNIV., NEW HAVEN, CONN. DEPT. OF GEOLOGY AND GEOCHEMISTRY.
Marine geochemistries of the uranium isotopes, ^{230}Th, and ^{231}Pa, 25:26399 (TID-25674)

YALE UNIV., NEW HAVEN, CONN. HEAVY ION ACCELERATOR LAB.
Rotational bands in ^{171} ^{173} ^{175}Hf from (particle, xn) reactions, 25:28323 (CERN-70-30(Vol.2), pp 949-55)

XUM

YESHIVA UNIV., NEW YORK. BELFER GRADUATE SCHOOL OF SCIENCE.
Construction pf mass formulas designed to be valid for neutron-rich nuclei, 25:28293 (CERN-70-30(Vol.1), pp 275-306)
Dynamics of the rapid neutron capture process, 25:27310 (CERN-70-30(Vol.2), pp 735-57)

Z

ZENTRALSTELLE FUER ATOMKERNENERGIE-DOKUMENTATION, FRANKFURT AM MAIN (WEST GERMANY).
Bibliographies in nuclear science and technology, Sect. 13, No. 7, 1970, 25:26443 (AED-C-13-7)
High energy physics index, Vol. 9, No. 5, 1971, 25:27976
High energy physics index, Vol. 9, No. 7, 1971, 25:27977
Plasma physics index, Vol. 6, No. 2, 1971, 25:27667
Surface and vacuum physics index, Vol. 6, No. 2, 1971, 25:27440
Technology index for plasmaphysics research and fusion reactors, Vol. 5, No. 2, 1971, 25:27668

PERSONAL AUTHOR INDEX

Authors' names are indexed in the form appearing in the abstracted publication. Each entry under an author's name gives the publication title and the *NSA* volume and abstract numbers. Report numbers, where applicable, are given in parentheses at the end of the entry.

Because of problems involved in the mechanical preparation of this index, all accent marks are omitted. The following changes in spelling have been introduced to reduce some of the confusion which might result from omitting the accents:

Germanic	ä	appears as ae
Germanic	ö	oe
Germanic	ü	ue
Scandinavian	ϕ	oe

A

AARSNES, K., Low-energy solar protons during the Feb. 25, 1969 event, 25:27573
Proton precipitation in noon--midnight meridian, 25:27579
ABARBANEL, Henry D. I., Phenomena in multiparticle production processes, 25:27969 (PURC-4159-19)
ABDEL RIDA, Al Khor, Vertex function for ^{6}Li + α + d process, 25:28185
ABDURAZAKOV, A. A., New isotopes ^{133}Pr, ^{134}Nd, and ^{135}Nd, 25:28387
ABDUSSAMATOV, H. I., Magnetic fields and motions in sunspots at different atmospheric levels, 25:27377
ABE, Mitsuyuki, Radiorestorative chemicals and their clinical application, 25:26812
ABELES, Robert H., Studies on the mechanism of hydrogen transfer in the coenzyme B_{12} dependent dioldohydrase reaction. II, 25:26225
ABELLAN, J. Ortega, Effect of ionizing radiation in the reprocessing of irradiated fuels, 25:26349
ABERNATHEY, R. M., Fission yields and branching ratios of ^{85}Kr in thermal neutron fission of ^{233}U, ^{235}U, ^{239}Pu, and ^{241}Pu, 25:28383
ABRAHAM, Farid F., Scavenging of aerosols by rain, 25:26388 (CONF-700601-, pp 433-46)
ABRAHAM-SHRAUNER, Barbara, Modification of the quasi-linear equations, 25:27739
Revised quasi-linear equations dealing with wave-number spectra, 25:27716
ABRAHAMSON, Dean E., Environmental cost of electric power, 25:28530
ABRAMOV, V. M., Atomic power plant with water-cooled, graphite-moderated reactor for combined power and heat generation, 25:28538
ABREAU, Cynthia M., Duration of radioactivity in the milk of a nursing mother following /sup 99m/ Tc administration, 25:26839
ABU-SHUMAYS, Ibrahim K., Exact analytic solutions of transport equations, 25:27948
ACHASOV, N. N., kappa-meson decay in the vector theory with the nonconserved current, 25:28023 (NP-18763)
ACHTERBERG, E. O., Nuclear spectroscopy of iodine isotopes with a greater than or equal to 134, 25:28336 (CERN-70-30(Vol.2), pp 1057-68)
ACKERMAN, A. Bernard, Eccrine poroma, 25:27055
ADADUROV, G. A., Reaction of oxides of rare earth elements with boron during shock compression, 25:27291
ADAM, J. R., Collection efficiencies of raindrops for submicron particulates, 25:26369 (CONF-700601-, pp 151-60)
ADAMCZEWSKI, I., Liquid filled ionization chambers as dosimeters, 25:26530
ADAMS, D. L., Adsorption of hydrogen on W (100), 25:27226
ADAMSKI, J., Investigation of the asymptotic stability in the large of the linear model of the circulating fuel reactor, 25:28810
ADAWI, I., Scattering of waves in many dimensions, 25:28090
ADCOCK, C., Possibility of detectable fluxes of cosmic γ rays with energy above 10^{19} eV, 25:27423
Theoretical analysis of extensive air showers. V, 25:27477
ADEVIK, Goeran, Spin trapping of radicals formed by γ-irradiation of sodium phosphite in solid state, 25:26313
ADKINS, K. F., Effect of 1200 R of x radiation on growth of bone and dentine in mandibular condyle, 25:27026
X-radiation and the mandibular condyle, 25:27025
AEDELROTH, K. E., Atomic-beam measurements in the rare-earth region, 25:28298 (CERN-70-30(Vol.1), pp 387-94)
Hyperfine structure of ^{51}Cr, 25:28252
AFFELDT, Burkhard, Economical and technical properties of the sodium-cooled high-power breeder reactor with carbide fuel, 25:28664
AGARWAL, Raghunath P., Uranyl ion-adenine nucleotides complexes, 25:26271
AGATI, G., Importance of bone marrow scintiscans in the detection of skeletal metastases, 25:26847
AGEEV, V. A., Positron decay in ^{190}Au and ^{188}Ir, 25:28392
AGER-HANSSEN, Henrik, Nuclear power in Norway, 25:28523 (CONF-700550-, Paper 1)
AGUILAR, J., Class of analytic perturbations for Schrodinger Hamiltonians. I, 25:27926 (CNRS-CPT-70-P-352)
AGUILERA-NAVARRO, V. C., Sum rules for Moshinsky brackets, 25:28506
AHARONOV, Yakir, Deterministic quantum interference experiments, 25:27942
AHARONY, Amnon, Time-reversal symmetry violation and the oscillating universe, 25:27424
AHN, K. Y., Magnetic and magneto-optical properties of Fe-doped EuO films, 25:27897
Preparation and structure of Fe-doped EuO films, 25:27894
AICHELBURG, P. C., Lorentz-covariant Lagrangians and causality, 25:28068
AIGNAN, M., Synoviothesis (synoviotherapy by radioisotopes) studies of more than 400 cases and future prospects, 25:26873
AIHARA, S., Hot electron confinement in a cusped magnetic field by ECRH wrapping, 25:27677
AINSWORTH, E. J., Survival time and dose-response following supralethal irradiation of dogs, 25:26992
AINUTDINOV, M. S., Universal magnetic spectrometer with 0.15 percent resolving power at maximum pulse of 60 GeV/c, 25:26507 (NP-18764)
AIZAWA, Otohiko, Pulsed neutron research. III, 25:28161
AKABOSHI, Sanya, Gradual development of radioprotection in HeLa S_3 cells during treatment with β-mercaptoethylguanidine, 25:26797
AKALAEV, G. G., Instrumental activation analysis of Au, Br, Mn, Na, Ta, and W, 25:26200
AKAP'EV, G. N., Investigation of α decay of isotopes of element 105, 25:28350 (KFK-tr-350)
AKASOFU, S. I., Evidence for magnetic field aligned currents during the substorms of Mar. 18, 1969, 25:27620
Low-latitude DS component of geomagnetic storm field, 25:27619
AKERMAN, Karol, Molybdenum recovery from alkaline slag, 25:26348
AKHMEDOVA, D. U., Growth patterns of uv-irradiated E. coli B in saline, 25:27119
AKIBA, Kenichi, Solubility of TTA--uranyl chelate, 25:26340
AKIMOV, N. I., Civil defense, 25:26785 (ORNL-tr-2306)
ALAN, J. J., Frequency and behavior of mutants induced by gamma irradiation in beans, 25:26685 (CONF-680112-, pp 85-93)
ALASCIO, B., Electron--electron scattering in electrical resistivity of In, 25:27660
ALCOCK, M. W., Preliminary results on the dynamic stabilization of the drift-dissipative instability, 25:27786
ALEKSAKHIN, R. M., Characteristics and quantitative prediction of cumulative storage of ^{90}Sr in arboreal plants, 25:26616
ALEKSANDROV, S. N., Influence of ionizing irradiation in radiation leucosogenesis, 25:26904
ALEKSANDROV, V. S., Analyzer of γγ coincidences with semiconductor detectors, 25:26504
Excitation of ^{169}Tm levels, 25:28432

ALEKSEENKO, G. N., Weldability of certain Mo alloys, 25:27185
ALEKSEEV, V. V., Reactions (d,p) of Ti and Cr isotopes, 25:26269
ALEKSEYUNAS, B. K., Radiation dosimeter with semiconductor detectors, 25:26529
ALEXANDER, D. C., Traumatic intrapericardial herniation of the transverse colon masquerading as a pericardial effusion on the scan, 25:26836
ALEXANDER, Eduard F., Prog. rpt. on simulation and measurement of solar-flare proton exposures, final, 11/68--8/69, 25:26920 (AD-711041)
ALEXANDER, John M., Limiting cross sections for fission isomers with nanosecond lifetimes produced in heavy-ion reactions, 25:28399
ALEXEFF, I., Plasma expansion into a vacuum, 25:27709
ALFORD, W. P., Shell-model structure of ^{209}Bi, 25:28417
ALIKHANOV, A. I., Universal magnetic spectrometer with 0.15 percent resolving power at maximum pulse of 60 GeV/c, 25:26507 (NP-18764)
ALIKHANOV, S. G., Thermonuclear combustion wave, 25:27820
ALIKHANYAN, A. I., Detection of x-ray transition radiation by means of a streamer chamber, 25:26515
ALISHAUSKAS, A. B., Radiation dosimeter with semiconductor detectors, 25:26529
ALLAN, C. G., Reaction of PTFE with liquid sodium, potassium, and NaK alloy, 25:26211 (TRG-Report-2104)
ALLAWAY, W. H., Effect of dietary selenium on the survival of rats exposed to chronic whole body irradiation, 25:27032
ALLEGRO, A., Nuclear fuel characterization, 25:27293 (RT/ING-(70)21)
ALLEN, R. P., X-ray comparison of beta plutonium grain size, 25:27244 (BNWL-1545)
ALLIO, Robert J., Austenitic stainless steels for use in nuclear reactors, 25:27214
ALLKOFER, O. C., Radiation doses at the altitude of supersonic transport flights, 25:26750 (ORNL-tr-2455)
ALLOUSH, A. A., Levels of ^{137}Cs in man in U.A.R. during year 1970, 25:26740 (NP-18728)
ALMAZOV, A. V., Spectra of protons in ^{238}U(t,pf) reaction, 25:28390
ALMGREN, B., Demand of uranium enrichment services for Sweden's nuclear power program, 1975--1985, 25:26395 (CONF-700903-15)
ALMODOVAR, Lutis R., Concentration of radium, thorium, and uranium by tropical marine algae, 25:26597
ALONSO, J., Rotational bands in ^{171} ^{173} ^{175}Hf from (particle, xn) reactions, 25:28323 (CERN-70-30(Vol.2), pp 949-55)
ALP, M. H., Radiation enterocolitis, 25:26811
ALPSTEN, M., Alpha decay of neutron deficient isotopes of mercury and radon and their daughters, 25:28302 (CERN-70-30(Vol.1), pp 523-31)
  Delayed-proton emission from neutron-deficient isotopes of xenon and mercury, 25:28301 (CERN-70-30(Vol.1), pp 487-96)
  Low-lying states in odd-mass polonium isotopes, 25:28333 (CERN-70-30(Vol.2), pp 1023-9)
ALTAMIRANO, C. P., Index to experimental data of neutron-induced reactions, 25:28356 (UCRL-50400(Vol.3))
ALTMAN, C., Coupling processes in D and E regions at low and medium frequencies. III, 25:27505
ALTMANN, H. W., Radiation (^{90}Sr) induced pulmonary carcinoma in rats, 25:26921 (LF-tr-49)
ALVARADO, S., Factors determining introduction of nuclear power stations in developing countries, 25:28723
ALVAREZ, J., Thin layer chromatography of various radiopharmaceuticals, 25:26179 (CNEA-285)
ALZETTA, R., Quasiparticle description for indium, 25:28357 (UJV-2540-F)
AMALDI, U. Jr., Status of some relevant problems in nuclear physics, 25:28449 (ISS-70/17)
AMANO, Yoshitugu, Aging characteristics of Cu--30 percent Ni--Be--Ti alloys, 25:27232
AMMERLAAN, C. A. J., Gamma irradiation of lithium-drifted silicon, 25:27852
AMPOLA, V. G., Study of irradiated-pasteurized fishery products, 25:27149
AMUNDSEN, R., Proton precipitation in noon--midnight meridian, 25:27579
AMUNDSON, P. I., ZPR-3 assemblies 48: 48A, and 48B: the study of a dilute plutonium-fueled assembly and its variants, 25:28752 (ANL-7759)
ANAGNOSTAKIS, S. L., Pathogenicity resulting from mutation at the b locus of Ustilago maydis, 25:27072
ANANTHASWAMY, H. N., Effect of gamma radiation on wheat starch and its components, 25:26621
  Susceptibility to amylolysis of gamma-irradiated wheat, 25:26622
ANDERSEN, J. U., Use of channeling-effect techniques to locate interstitial foreign atoms in silicon, 25:27857
ANDERSEN, S. A., Wave--particle interaction in single-ended Q machine, 25:27693
ANDERSON, J. D., Allowed neutron decay of highly excited ($T_0^{+1}/_2$) compound nucleus states, 25:28460
  Nuclear level densities and reaction mechanisms from continuum neutron spectra, 25:28285
ANDERSON, John D., Nuclear isospin. Proceedings of the conference, Asilomar--Pacific Grove, California, March 13--15, 1969, 25:28455
ANDERSON, R. G., Theoretical waving behavior of Magnox fuel element fins due to coolant-gas induced corrosion and to thermal cycling, 25:26415 (TRG-Report-2121)
ANDERSON, R. P., Experimental study of a gas jet penetrating a liquid coolant and impinging on a heated surface, 25:26418 (ANL-7734)
ANDERSON, Robert E., Acute radiation injury in neonatally thymectomized germ-free mice. Hematopoietic and morphologic consequences, 25:26937
ANDERSON, T. D., Nuclear desalination program annual progress report on activities sponsored by the Atomic Energy Commission for period ending October 31, 1970, 25:28790 (ORNL-4668)
ANDERSON, T. J., Radioisotope derivative procedure for determination of epinephrine or norepinephrine, 25:26182
ANDERSON, Wayne Arthur, Performance of impact avalanche transit time diodes under the influence of gamma and neutron radiation, 25:26562
ANDERSSON, Birger, Reappearance and relative importance of immunocompetent cells in the thymus, spleen, and lymph nodes following lethal x-irradiation and bone marrow reconstitution in mice, 25:26672
ANDERSSON, G., Delayed-proton emission from neutron-deficient isotopes of xenon and mercury, 25:28301 (CERN-70-30(Vol.1), pp 487-96)
ANDERSSON, G. I., Neutron hole states in the tin-region, 25:28329 (CERN-70-30(Vol.2), pp 1008-10)
ANDREASEN, O., Use of channeling-effect techniques to locate interstitial foreign atoms in silicon, 25:27857
ANDREEV, A. F., Macroscopic electrodynamics and thermal effects in the superconductor intermediate state, 25:27647
ANDREEV, A. M., Cylindrical linear MHD machine in open-cycle regime, 25:27481
ANDREEV, M. F., Spectra of protons in ^{238}U(t,pf) reaction, 25:28390
ANDREEV, P. A., Optimization of parameters for small nuclear power sources containing water-cooled, water-moderated reactors, 25:28640
ANDREEVA, O. S., Actinium aerosols determination in the air in the presence of other radioactive substances, 25:26394
ANDRES, K., Hyperfine enhanced nuclear magnetic cooling in Van Vleck paramagnetic intermetallic compounds, 25:27666
ANDREWS, J. G., Cylindrical probe in a flowing plasma, 25:27681
ANDREWS, J. T., Report of twentieth Baker travelling fellow, 25:26855
ANDRILLAT, Yvette, Abundances and reddening of nuclei of Seyfert galaxies, 25:27418
ANDRLE, P., Stability problem of oscillations along axis of symmetry in galaxy. II, 25:27410
ANGEL, J. R. P., Search for optical circular polarization in the Crab Nebula, 25:27348
ANGHILERI, Leopoldo J., Accumulation of chromium complexes in skeletal tissue, 25:26590
ANIKIN, G. V., Optimum parameters of ^{238}U neutron optical potential, 25:28403
ANIKINA, L. I., Determination of Sm microimpurity in Eu oxide, 25:26162
ANLAUF, K. G., Angular distribution of the scattering of Ar by N_2 and Ne, 25:27451
ANSFIELD, Fred J., Glioblastoma multiforme. An analysis of the results of postoperative radiotherapy alone versus radiotherapy and concomitant 5-fluorouracil, 25:26889
ANTICH, P., Coherent K-d interactions at 12.6 GeV/c, 25:27967
ANTOGNETTI, G. F., STAZ-2: program for thermohydraulic analysis of channel of water-moderated and cooled nuclear reactor core operating in stationary state, 25:28679 (EUR-4553)
ANTON'EVA, N. M., Palladium-99 γ radiation, 25:28431
ANTONIADES, J., Measurement of the coefficient of gamma absorption of materials used for nuclear constructions, 25:27826 (DEMO-70/11)
ANTONINI, M., Collimation corrections in small angle scattering of neutrons, 25:28144 (RT/FIMA-69-5)
ANTONIOU, N. G., P-wave πN scattering amplitude with CDD poles, 25:28032
ANTROPOV, A. E., Elastic and inelastic scattering in A = 23 to 35 region, 25:28261
  Proton scattering on ^{24}Mg, ^{25}Mg, and ^{26}Mg, 25:28264
ANTROPOV, G. P., Photoneutron cross sections of ^{203}Tl and ^{205}Tl, 25:28391
ANTTILA, A., Energy levels of ^{24}Mg, 25:28259
AOKI, Atsushi, Magnetic moments of three excited states in ^{149}Pm, 25:28381
AOYAMA, Tadaaki, Measurement of mean particle size of W and W carbide powders, 25:27217
APPELQVIST, A., Delayed-proton emission from neutron-deficient isotopes of xenon and mercury, 25:28301 (CERN-70-30(Vol.1), pp 487-96)
APPELQVIST, Aa., Low-lying states in odd-mass polonium isotopes, 25:28333 (CERN-70-30(Vol.2), pp 1023-9)
AQUILI, A., Use of a PDP-9 computer in nuclear spectroscopy measurements, 25:26496
ARAI, Eiichi, Pulsed neutron research. III, 25:28161
ARAKAWA, Tetsutaro, Present status of industrialization of radiation curing and its problems, 25:26283

ARCHER, Victor E., Histologic types of lung cancer among uranium miners, 25:27045
ARDELL, A. J., Prog. rpt. on particle size distribution effects in precipitation hardening, annual, 4/70--1/71, 25:28897 (UCLA-34-P-172-1)
ARENHOEVEL, H., Tensor polarizability in the giant dipole resonance region and collective behaviour, 25:28489
ARIEL, Irving M., Malignant melanoma, its treatment by the endolymphatic administration of radioactive isotopes, 25:26888
ARIENT, M., Biochemical changes in serum of intact and irradiated dogs after intravenous AET administration, 25:26935
ARIMA, A., Calculation of nucleon widths of the lowest T = 3/2 states of ^{13}N and ^{13}C, 25:28172
ARIMA, Masashi, Balneotherapy of radiation injury. XXVII, 25:26950
Balneotherapy of radiation injury. XXVIII, 25:26897
ARLT, R., Decay of ^{90}Nb, /sup 89m,89/Nb, /sup 85m,85/Y and /sup 85m/Sr, 25:28215 (CERN-70-30(Vol.2), pp 1137)
New isotopes ^{133}Pr, ^{134}Nd, and ^{135}Nd, 25:28387
New isotopes ^{176}Os and ^{177}Os, 25:28386
ARNBRUSTER, H., Four years of operational experience with MZFR, 25:28586
ARNBRUSTER, P., Identification of μ s isomers among primary fission fragments, 25:28325 (CERN-70-30(Vol.2), pp 967-84)
ARMSTRONG D. D., Resonance structure in the $^{88}Sr(p,p')$ octupole transition, 25:28240
ARNOLD, G., Magnetic properties of CeBi, NdBi, TbBi, and DyBi, 25:27887
ARNOLD, G. W., Preferential etching of ion-bombarded GaAs, 25:27860
ARONSON, Raphael, Summary report on investigations of transfer matrix method, 25:28798 (NYU-4090-1)
ARROWSMITH, H. W., X-ray comparison of beta plutonium grain size, 25:27244 (BNWL-1545)
ARTAGAVEYTIA, Daniel, Thyroid tumour scanning with $^{197}HgCl_2$, 25:26823
ARTMAN, Joseph O., Prog. rpt., annual, 5/70--4/71, 25:28868 (NYO-4075-10)
ASADA, C., Construction and initial operation of Tsuruga Power Station, 25:28576
ASADA, Hiroyuki, Proportion of ^{32}P produced by $^{31}P(n,\gamma)$ and $^{32}S(n,p)$ reactions in phosphorus--sulfur compounds, 25:26318
ASAOKA, T., JN-METD1: FORTRAN-IV programme for solving neutron transport problems with isotropic scattering in bare spheres and homogeneous slabs by the j/sub N/ method, 25:28146 (EUR-4601)
ASARO, F., Energy levels in ^{239}Np, 25:28415
ASBELL, Sucha Order, Oxygen effect on the production of radiation-induced myelitis in rats, 25:26966
ASBURY, J. G., Photographic method for determining velocity distributions within thermal plumes, 25:28839 (ANL/ES-4)
ASHRAF, Mohammad, Effects of gamma radiation on the larval midgut of the Indian-meal moth, Plodia interpunctella (Lepidoptera: Phycitidae), 25:26916
ASHTON, F., Electric charge of interacting cosmic-ray particles at sea level, 25:27475
ASKAR, A., Particle method for the numerical solution of the time-dependent Schroedinger equation, 25:27932
ASKNE, J., Electromagnetic wave propagation through a bounded time--space periodic cold plasma, 25:27804
ASLANGUL, Claude, Use of information theory in localizing electrons in atoms and molecules, 25:27464
ASMAN, Sr. M., Cytogenetics of two radiation-induced, sex-linked translocations in the yellow-fever mosquito, Aedes aegypti, 25:26719
ASTNER, G., Low-lying states in odd-mass polonium isotopes, 25:28333 (CERN-70-30(Vol.2), pp 1023-9)
ATHWAL, D. S., Fertile dwarf and three other mutants in Cicer, 25:26718
ATIDIA, J., Repair of alkylation-induced damage in E. coli and its bacteriophage lambda, 25:27109
ATKIN, R. H., Homological foundation for scale problems in physics, 25:27425
ATKINS, D. E., Illiac III Reference Manual. Vol. I, 25:28851 (COO-2118-5)
ATKINS, H. L., Evaluation of /sup 99m/Tc-DTPA prepared by three different methods, 25:26840
ATKINSON, Jay, Some systematics of coulomb displacement energies, 25:28478
ATOJI, Masao, Magnetic structure of α-Ho_2C_3, 25:27904
Magnetic structure of α-Tb_2C_3, 25:27903
ATOMURA, Masakatu, Primary cooling water decomposition in reactors, 25:28758 (JAERI-1204)
ATROSHCHENKO, L. S., Concentration distribution of binary mixtures in films moving along the walls of round pipes in the presence of an external nonuniform magnetic field, 25:27499
ATTIX, F. H., Design of free-air ionization chambers, 25:26469
AUBLE, R. L., Nuclear data sheets for A = 207, 25:28378
AUCHAPT, Pierre, Precipitation of Pu C_2O_4, 25:26345
AUCOUTURIER, J., Electron optics of sagittaire, 25:28142
AUERBACH, C., Ionic range of ThO_2--15 wt. percent Y_2O_3 at high oxygen activities, 25:26262
AUERBACH, N., Role of configuration states in isospin forbidden proton decays of T = 3/2 states, 25:28179
AUERBACH, Naftali, Microscopic calculation for the escape width of analog states, 25:28466
The role of the anti-analog state in the decay of the analog state, 25:28467
AUERBACH, Oscar, Histologic types of lung cancer among uranium miners, 25:27045
AUSLOOS, P., Ion-molecule reactions in the condensed-phase radiolysis of hydrocarbon mixtures. III. Reactions of i-$C_4H_8^+$ and tert-$C_4H_9^+$ ions originating from neopentane, 25:26309
AVAKYAN, K. M., Detection of x-ray transition radiation by means of a streamer chamber, 25:26515
AVDEICHNIKOV, V. M., Energy resolution for dE/dx detectors, 25:26485
AVERY, R. T., Mechanical features of electron-ring compressors, 25:28118 (UCRL-20177)
AVERY, Robert T., Non-intercepting monitor of beam current and position, 25:28117 (UCRL-20166)
Printed-circuit steering coils, 25:28116 (UCRL-20165)
AXFORD, W. I., Galactic winds, 25:27403
Low-energy cosmic rays near Earth, 25:27473
Survey of interplanetary and terrestrial phenomena associated with solar flares, 25:27532
AYBERS, N., Problems encountered in initiation of nuclear power program in Turkey, 25:28724

B

BABA, H., 4πβ--γ coincidence absolute measurement of nuclides emitting soft conversion electrons in appreciable proportions, 25:26464
BABA, Harukata, Scintigraphy of lung cancer using ^{203}Hg, 25:26842
BABA, S., 4πβ--γ coincidence absolute measurement of nuclides emitting soft conversion electrons in appreciable proportions, 25:26464
BABADZHANOV, R., New isotopes ^{133}Pr, ^{134}Nd, and ^{135}Nd, 25:28387
BABAEV, Z. R., Regeneration of K^0 mesons on deuteron at high energies, 25:28049
BABILONI, L., Equipment for remote control of gamma scanning in a hot cell, 25:26550 (RT/ING-(71)1)
BABITZKE, H. R., Niobium alloy development with B, Hf, and W, 25:27227
BABOR, R., Testing of dental Roentgen apparatuses to their radiation safety, 25:26772
BACCHETTIL, Silvia, Relation of protein synthesis to radiation-induced division delay in Chinese hamster cells, 25:26626
BACHARACH, S. L., Experimental and theoretical investigation of nuclear fission induced by low-energy nuclear particles. Progress report, 25:28355 (TID-25659)
BACHARACH, Stephen Laurence Irwin, Channeling in fluorite crystals, 25:27851
BACSY, Ernoe, Combined histochemical procedure to distinguish between mesenchymal and epithelial reticular cells in the rat thymus under the light microscope, 25:26654
BADANOIU, M., Low energy boron implantation profiles in silicon from junction depth measurements, 25:27855
BAECKLIN, A., Energy levels in ^{114} ^{116} ^{118} ^{120} ^{122}Cd populated in decay of Ag isotopes, 25:28337 (CERN-70-30(Vol.2), pp 1069-74)
Possible nuclear co-existence in odd-mass Ir nuclei, 25:28324 (CERN-70-30(Vol.2), pp 957-65)
BAEV, I., Radioprotective effect of AET and serotonin in growing rats, irradiated fractionally with small doses of roentgen rays, 25:26807
BAGDASARYAN, L. S., Pulse-time fluctuation in large scintillation counters, 25:26482
BAGGE, Erich, Basis concepts of structure theory of elementary particles. II, 25:27970
BAGLAN, R. J., Threshold photoneutron cross sections for ^{206} ^{207} ^{208}Pb, ^{54} ^{57}Fe, ^{52} ^{53}Cr, ^{24} ^{25} ^{26}Mg, and ^{19}F, 25:28413
BAGLIN, John E. E., Determination of surface impurity concentration profiles by nuclear backscattering, 25:26183
BAHNSEN, Axel, Auroral particles and ground observations during the Feb. 25th solar event, 25:27572
BAIDALA, S. I., Phase equilibria in the titanium--vanadium--boron and titanium--manganese--boron systems, 25:27300
BAIER, R., P-wave πN scattering amplitude with CDD poles, 25:28032
BAIER, V. N., Pair production in collisions of high-energy charged particles, 25:27997
BAILEY, Barbara Ann, Histology and histochemistry of the embryonic chick mandible following x radiation, 25:27018
BAINBRIDGE, G. R., United Kingdom reactors available for commercial operations, 25:28720
BAIR, W. J., Toxicity of inhaled plutonium. II, 25:26599
BAIRD, Q. L., ZPR-3 assemblies 48: 48A, and 48B: the study of a dilute plutonium-fueled assembly and its variants, 25:28752 (ANL-7759)
BAJAJ, M. M., Effects of coaxial magnetic and electric fields on time-integral PAC with special reference to rare-earth isotopes, 25:27918
BAJARD, Marcel, Development of a test bench for

multicharged ion sources, 25:28113 (LYCEN-7054)
BAK, Hae-Ill, Total cross sections for kilovolt neutrons of even--odd nuclei in he region of the 3s strength-function resonances, 25:28279
BAKAI, A. S., Investigation of low-frequency plasma oscillations by means of amplitude modulation of microwave radiation, 25:27816
BAKER, D. R., Interaction between electron and ion modes and feedback stabilization, 25:27765
BAKER, George A. Jr., Pade approximant in theoretical physics, 25:28063
BAKER, K., Beta--gamma band mixing in ^{152}Sm, 25:28430
BAKER, Max Leslie, Influence of radiation on synchronized L cells, 25:26969
BAKER, P. S., ^{90}Sr heat sources, 25:26432
Selected abstracts of world literature on production and industrial uses of radioisotopes, 25:26427 (ORNL-IIC-30(Pt.4))
BAKER, W. L., States in ^{17}O via neutron-polarization measurements in ^{13}C(α,n)^{16}O reaction, 25:28202
BAKHRU, H., Decay of ^{76}Br, 25:28246
Level structure of ^{109}Cd from decay of ^{109}In, 25:28428
BAKHRU, R., Decay of ^{76}Br, 25:28246
BAKIEV, S. A., Decay of neutron defficient isotopes of Pt, Ir, and Os, 25:28389
BALACHANDRA, J., Developments in oxidation and corrosion resistant materials, 25:27176 (INIS-mf-9)
Stress corrosion cracking of Zr in methanol/hydrochloric acid solutions, 25:27173
BALAKIN, V. E., Evidence for electron-positron pair electroproduction, 25:27994
BALALAEV, V. A., Decay of ^{169}Lu, 25:28436
Excitation of ^{169}Tm levels, 25:28432
BALARAMAMOORTHY, K., Materials for reactor technology, 25:27204 (INIS-mf-3)
BALDO, M., Possibility of a single positron bound state in an electron liquid, 25:27447
BALDWIN, D. E., Derivation of connection formula using partial Wronskian, 25:27817
BALDWIN, Madeleine C., Detection of putative deletions in proximal heterochromatin of Drosophila, 25:26720
BALDWIN, W. F., Radiation-induced sterility in the control of the olive fruit fly, 25:27151
BALESTRINI, S. J., Independent cesium yields in ^{236}U fission: identification of ^{145}Cs, 25:28307 (CERN-70-30(Vol.1), pp 589-99)
BALI, L. M., Modulated decay in a two-level quantum system, 25:27939
BALL, J. B., Spreading of the antianalogue states in ^{91}Nb, 25:28363
BALLANTYNE, William Wallace, Color stability of fresh beef as affected by ionizing radiation dose rate and added inorganic phosphate, 25:27162
BALLINGER, Edwin R., Study of human radiation sensing and dark adaptometry using x-rays, 25:27039
BALLUFFI, R. W., Prog. rpt. on defects in metal crystals, annual, 2/71, 25:27866 (NYO-3504-56)
BALOGH, A., Low-energy proton measurements in interplanetary space, 25:27559
BAMBERGER, C. E., Molten Salt Reactor Experiment (MSRE): chemical aspects, 25:28636
BAME, S. J., Observation of the Feb. 26, 1969 interplanetary shock wave, 25:27570
BANCROFT, D., Nonlinear perturbations and electron scattering in a beam plasma, 25:27703
Scattering of electrons by electrostatic fluctuations in a magnetized plasma, 25:27699
BANE, John Campbell, Symmetry breaking and the Cabibbo angle, 25:28059
BANERJEE, S., Transmission electron microscopic studies of cold-rolled zirconium, 25:27245 (INIS-mf-15)
BANISTER, John R., Ground motion summary statement, 25:26411 (SC-DC-713865)
BANKOLE, Rufus O., Chronic myelogenous leukemia in Hodgkin's disease: immunofluorescence of cells, 25:26964
BANKS, Peter M., Comparison of kinetic and hydrodynamic models of an expanding ion exosphere, 25:27613
BANOS, Csaba, Simple method for determining the concentration of serum thyroxine by competitive displacement analysis, 25:26568
BANSAL, Krishan M., Pulse radiolytic investigations of hydroxy-radical reactivities in micellar solutions, 25:26295
BANYAI, E., Retention of radionuclides on metal sulphide precipitates, 25:26199
BARANOV, A. I., Sum rules for ππ-scattering, 25:28024 (NP-18766)
BARBINA, V., Personnel dosimetry with ^{7}LiF Teflon discs, 25:26527
BARCLAY, Arthur, Sound absorbing devices, 25:28832
BARKER, B., Properties of bacteriophage T4 mutants defective in gene 30 (deoxyribonucleic acid ligase) and the rII gene, 25:26708
BARNES, C. A., Excitation of analogue states by stripping and pick-up reactions, 25:28458
BARNES, C. E., Neutron damage in epitaxial GaAs laser diodes, 25:26563
BARNETT, B. A., Polarization parameter K$^+$p elastic scattering GeV/c, 25:27963
BARNETT, M., Reactor physics design technique for burnable poison and enrichment-zoned cores, 25:28663
BARNEY, G. S., Hydroxylamine nitrate reduction of plutonium(IV): iron catalysis, 25:26206 (ARH-1920)
BARNHAM, K. W. J., Anti-lambda production in 10 GeV/c K$^+$ proton interactions, 25:27966
K^{0}s$^+$p final state produced in K$^+$p interactions at 10 GeV/c, 25:27968
BAR-OR, A., Materials and fuels for nuclear reactors, 25:27219
BAROUCH, E., Spectra and time history of protons in interplanetary space, Feb. 25--28, 1969, 25:27558
BARR, R., Propagation of elf and vlf radio waves beneath an inhomogeneous anisotropic ionosphere, 25:27506
BARRETT, Paul R., Noise effect of vibrating control elements, 25:28835
BARSEGYAN, E. O., Pulse-time fluctuation in large scintillation counters, 25:26482
BARSKII, M. L., Standardized line of pressure-vessel type boiling-water reactors, 25:28716
BARTEL, L. C., Correlation effects in transition metals and alloys, 25:27868
BARTH, C. A., Mariner 6 and 7 ultraviolet spectrometer experiment: upper atmosphere data, 25:27433
BARTHA, Tibor, Radiation sterilization of an ophthalmic ointment containing hydrocortisone and chloramphenicol. IV, 25:27161
BARTHOLIN, H., Uniaxial stress experiments and magnetoelastic interactions in rare earths, 25:27889
BARTOL, F., High resolution detection unit for charged particles, 25:28141
BARTON, J. P., Radiolysis of oxygenated cysteine solutions at neutral pH, 25:26307
BARTONOVA, H., Haemolysis of red blood cells in propylene glycol solutions in miners from uranium mines, 25:26588
Inorganic phosphorus in red blood cells of miners in uranium mines, 25:26582
BARYSHEV, A. I., Maximum current of the circular accelerator or storage ring, 25:28140
BASAR, I., Deexcitation of the 662-keV state in ^{137}Ba by the internal Compton effect, 25:28422
BASES, R., Inhibition of ribosomal RNA synthesis in x-irradiated HeLa cells, 25:26983
BASHIAN, Allen, Reactions π$^-$p → K$^+$Σ$^-$ and π$^-$p → K$^+$Y^{0*-} from 2.75 to 14.0 GeV/c, 25:28038
BASSETT, D. W., Use of field ion microscopy in studies of the vapour deposition of metals, 25:27189
BASSI, P., Thermoluminescent dosimeter of LiF incorporated in silicone rubber, 25:26539
BASSON, J. K., Measurement and analysis of radioactive fallout over South Africa, 25:26613
BASTIN, Ted, Homological foundation for scale problems in physics, 25:27425
BASU, A. K., Effect of x-rays, ^{32}P and ^{35}S on germination and survival in rice, 25:27078
Radiation induced morphological abnormalities in rice (Oryza sativa L.), 25:27077
BASU, Rabindra Krishna, Effect of x-rays, ^{32}P and ^{35}S on germination and survival in rice, 25:27078
Radiation induced morphological abnormalities in rice (Oryza sativa L.), 25:27077
BATALOV, A. A., Loop for radiation study of electrical conductivity of materials in the VVR reactor, 25:28765
BATE, L. C., Labeling of copper wire with /sup 110m/Ag for subsequent identification, 25:26322
Loss of mercury from containers in neutron activation analysis, 25:26201
BATES, Henry A., Chronic myelogenous leukemia in Hodgkin's disease: immunofluorescence of cells, 25:26964
BATH, Daniel White Jr., Cytogenetical identification of x-ray-induced translocations in male mice, 25:26711
BATHOVA, M., Linkage of radiocerium to blood serum proteins studied by dialysis techniques, 25:26584
BAUER, K. M., Local therapy of bladder radiation injuries, 25:26810
BAVASSANO, B., Interplanetary magnetic field measured by Pioneer 8 during the Feb. 25, 1969 event, 25:27556
BAWIN, M., Separable interactions and high energy scattering, 25:28019
BAXENDALE, J. H., Ion recombination and delayed emission in the pulse radiolysis of liquid isopentane solutions at low temperature, 25:26297
BAYMAN, B. F., Isobaric analogue states, 25:28507
BAYUZICK, R. J., Observations of grain boundaries with the field ion microscope, 25:27253
BAZIN, J. P., Influence of irradiation dose on latency time of cataracts in rabbits, 25:27027
BAZZELLE, W. E., Applications of ion-selective electrodes, 25:26166
BEALS, R. J., Deformation of UO_2 at high temperatures, 25:27287
BEAN, A. R., Defects produced in n-type silicon by electron irradiation, 25:27845
BEAUPRE, J. V., S-wave interference in the f^0 resonance region, 25:28018
BECCHETTI, F. D. Jr., Evidence for splitting of a bound isobaric analog state in ^{58}Co, 25:28228
BECHER, Paul F., Deformation substructure in polycrystalline alumina, 25:28878 (ORO-3328-13)
BECHTHOLD, W., Transport of high level vitrified fission products, 25:26448 (KFK-1263)
BECK, C., Applications of thermo and photoluminescent

phenomena in health physics, 25:26528
BECK, E., Beta decay energies of some neutron deficient nuclides, 25:28297 (CERN-70-30(Vol.1), pp 353-60)
BECK, G., Multiple pulse radiolysis: successive accumulation of two hydrated electrons in oxygen, nitrobenzene, and nitromethane, 25:26308
BECK, Paul A., Micromagnetism in Pd--Cr and V--Mn alloys, 25:27890
BECK, Sherwin M., Measured electron conversion ratios for 1064-keV γ ray of ^{207}Bi, 25:28352 (N-71-10060)
BECKER, C. D., Food and feeding of juvenile chinook salmon in Central Columbia River in relation to thermal discharges and other environmental features, 25:26681 (BNWL-1528)
BECKER, G., Dynamic stabilization experiment on a linear screw pinch, 25:27790
BECKER, J. A., Low-lying excited states of ^{29}Al. III, 25:28267
BECKER, J. J., Magnetization discontinuities in cobalt--rare-earth particles, 25:27885
BECKER, M., Effect of uv-irradiation on DNA in dependence of DNA structure, 25:26657
BECKER, R. A., Prog. rpt. on SEFOR, 11/70--1/71, 25:28757 (GEAP-10010-27)
BECKER-BENDER, G., Further indications for t-dependence of angular distributions, 25:28174
BECKERT, D., Theory of intermolecular nuclear magnetic relaxation of adsorbed molecules. I, 25:28875 (ORNL-tr-2457)
Theory of intermolecular nuclear magnetic relaxation of adsorbed molecules. II, 25:28876 (ORNL-tr-2458)
BEDFORD, J. S., Growth of Vicia faba roots during irradiation, 25:27066
BEDFORD, R. G., Investigations into the Eu--Eu_2O_3, the Eu--Pt-Eu_2O_3, the Sm--Sm_2O_3, and the Yb--Yb_2O_3 systems, 25:27302
BEDINGER, J. F., Observed redistribution of E-region ionization by neutral winds, 25:27516
BEER, J. Z., Regeneration of proliferative activity in progeny of murine lymphoma cells L5178Y irradiated with x-rays, 25:26974
BEERE, W. B., Bubble mobility on dislocations and random diffusion studies, 25:27842 (RD/B/N-1850)
BEERTEMA, H. E., Decay studies of neutron deficient Ga and Zn isotopes, 25:28338 (CERN-70-30(Vol.2), pp 1075-9)
BEIERWALTES, William H., Radiolabeled cholesterol as an adrenal scanning agent, 25:26845
Treatment doses of ^{131}I-labeled chloroquine analog in normal and malignant melanoma dogs, 25:26882
BEIGMAN, I. L., Thermal model of solar corona active regions, 25:27396
BEILKE, S., Laboratory investigations on washout of trace gases, 25:26375 (CONF-700601-, pp 261-9)
BEILLE, J., Uniaxial stress experiments and magnetoelastic interactions in rare earths, 25:27889
BEL, N., Propagation of magneto-acoustic waves along the gravitational field in an isothermal atmosphere, 25:27393
BELCHER, J. W., Effect of Alfven waves on MHD fast shocks, 25:27387
BELHASSEN, J., Mass-differences in neutron-rich Sr Region, 25:28294 (CERN-70-30(Vol.1), pp 321-9)
BELINICHER, V. I., Amplitude of forward scattering of the process $\pi^+\pi^0 \to \pi^+\pi^0$, 25:28025 (NP-18768)
BELLI-DONINI, M. L., Effect of gamma irradiation on the pectic substances of strawberries at different maturity stages, 25:27160
BELLMANN, D., Gamma rays from thermal neutron capture in nitrogen and natural neon, 25:28275
BELOKOPYTOV, V. S., Investigation of Pu isotopes build-up in Novo-Voronezh APS fuel, 25:28532
BELOTE, T. A., L = 0 transitions to 0^+ states of N = 29 nuclei, 25:28229
BEL'TYUKOVA, S. V., Extraction-photometric determination of uranyl ions, 25:26163
BELY, Yu. I., Electroexcitation of ^{32}S in region of dipole resonance, 25:28220 (UJV-2553-F)
BELYAEV, V. A., Experimental limitations of the method of merging beams for studying ion-atom collisions, 25:27448 (IAE-2001)
BEMENT, A. L. Jr., Fracture mechanisms and radiation effects, 25:27270
BEN-DAVID, G., Forward elastic scattering of 9 MeV gamma rays, 25:28358
Level structure of ^{50}Ti and ^{51}Ti using ^{49}Ti(n,γ) and ^{50}Ti(n,γ) reactions, 25:28284
Utilization of research reactors in Israel, 25:26780
BENECKE, J., Limiting partial cross-sections, 25:27974
BENEDETTI, G. R., Problem of automatic dose planning, 25:26761
BENENSON, E. B., Laminar magnetogasdynamic boundary layer at nonconducting surface, 25:27495
BENGTSSON, B., Delayed-proton emission from neutron-deficient isotopes of xenon and mercury, 25:28301 (CERN-70-30(Vol.1), pp 487-96)
BENGTSSON, Ragnar, Extrapolations to Z = 164 region, 25:28310 (CERN-70-30(Vol.2), pp 646-53)
BENHAMOU, A., Determination of traces of iron, nickel, and chromium in plutonium nitrate solutions, 25:26154 (RFP-Trans-76)
BENNDORF, K., Selfwelding of reactor structural materials in sodium environment at high temperatures, 25:27206 (KFK-Ext.Ber.-8/70-1)
BENNETT, E. F., ZPR-3 assemblies 48: 48A, and 48B: the study of a dilute plutonium-fueled assembly and its variants, 25:28752 (ANL-7759)
BENNETT, J. R. J., Ion sources for multiply charged heavy ions, 25:28125 (WASH-1159, pp 13-33)
BENNETT, L. C., Computerized ultrasonic data acquisition system, 25:28884 (SC-DR-70-680)
BENNETT, M. H., Radioinduced fibrosarcoma, 25:27044
BENSON, Brent, Free radicals in pyrimidines: ESR of a γ-irradiated single crystal of 5-nitrouracil, 25:26296
BENUMOF, Reuben, Energy and momentum of a classical electron in special relativity, 25:27986
BENZ, M. G., Cast permanent magnets of Co, Cu, and Ce: process and performance characteristics, 25:27884
BERAN, M., Effect of Prussian Blue combined with pilocarpine on ^{137}Cs excretion in rats, 25:26583
BERBEZIER, J., Cyclic variation of volume of the heart, 25:26566 (CEA-CONF-1711)
BERES, William P., Intermediate-coupling and additional excitation modes, 25:28518
BERETTA, G., Daunomycin influence on Ehrlich ascites cancer, 25:26990
BEREZANSKII, Yu. M., Problem of moments and representations Wightman type functionals by continual integrals, 25:28079
BERG, John, Incidence of multiple primary cancers. IV. Cancers of the female breast and genital organs, 25:27038
BERG, Richard Allen, Stellar diameters from occultations, 25:27329
BERG, T. G. Owe, Collection efficiency in washout by rain, 25:26371 (CONF-700601-, pp 169-86)
BERG, V., Lifetimes of excited nuclear levels, 25:28341 (CERN-70-30(Vol.2), pp 1115-18)
Possible nuclear co-existence in odd-mass Ir nuclei, 25:28324 (CERN-70-30(Vol.2), pp 957-65)
BERGE, G., Dynamic stabilization of the m = 1 instability in a bumpy theta pinch, 25:27785
Dynamic stabilization of the screw pinch, 25:27749
BERGER, Martin J., Distribution of absorbed dose around point sources of electrons and beta particles in water and other media, 25:26753
BERGMAN, Bo, Distribution of ^{65}Zn in tibia in rats, 25:26611
BERGSTROEM, I., Evidence for high-spin three quasiparticle state in ^{133}I produced in fission, 25:28331 (CERN-70-30(Vol.2), pp 1012-14)
Levels in doubly-even tellurium isotopes, 25:28330 (CERN-70-30(Vol.2), pp 1010-11)
BERGSTROM, Terry J., Treatment doses of ^{131}I-labeled chloroquine analog in normal and malignant melanoma dogs, 25:26882
BERK, Herbert L., Convective wave instabilities in mirror machines, 25:27750
Stability of a trapped-particle equilibrium, 25:27733
BERLOVICH, E. E., Properties of nuclei far off the β-stability valley, 25:28444 (CERN-70-30(Vol.1), pp 497-516)
BERMAN, B. L., Threshold photoneutron cross sections for ^{206} ^{207} ^{208}Pb, ^{56} ^{57}Fe, ^{52} ^{53}Cr, ^{24} ^{25} ^{26}Mg, and ^{19}F, 25:28413
BERNADOU, J. M., Applications of thermo and photoluminescent phenomena in health physics, 25:26528
BERNAS, R., Production cross sections of Li and Be isotopes in ^{12}C by high-energy protons and alpha particles, 25:28182
BERNAT, Ivan, Application of stable isotopes in medical and biological experiments, 25:26572
BERNSTEIN, E. M., Large isospin mixing in ^{16}O states near 18 MeV, 25:28188
BERNSTEIN, Ira B., Reply to comment on negative diffusion in coefficients in quasi-linear theory, 25:27713
BERNSTEIN, Irwin D., Abrogation of passively transferred tumor immunity in vivo by antigenically related tumor cells, 25:26663
BERNSTEIN, M. J., Neutron production in plasma focus discharge, 25:27799
BERNSTEIN, R. B., Angular distribution of the scattering of Ar by N_2 and Ne, 25:27451
BERNTHAL, F. M., Rotational bands in ^{171} ^{173} ^{175}Hf from (particle, xn) reactions, 25:28323 (CERN-70-30(Vol.2), pp 949-55)
BERRY, P. F., Instrument manual for prototype wet concrete analyzer, 25:26540 (ORO-3842-3)
BERTAUX, J. L., Evidence for source of extraterrestrial H Lyman-alpha emission, 25:27413
BERTERO, M., Mathematical approach to the derivation of the theoretical optical potential, 25:28096
Spectrum of an operator introduced by Feshbach in formulation of optical potential, 25:28095
BERTINCHAMPS, Albert, Electron transfer in γ-irradiated nucleotides and proflavine, 25:26638
BERTOLOTTI, G., Experience gained in operating Jose Cabrera Nuclear Power Station, 25:28578
BESI, A., STAZ-2: program for thermohydraulic analysis of channel of water-moderated and cooled nuclear reactor core operating in stationary state, 25:28679 (EUR-4553)
BEURER, K., Rat kidney under whole-body irradiation and 2,4,6-triethylenimino-s-triazine, 25:26645

BEWLEY, D. K., General aspects of fast neutron therapy, 25:26879
Radiation protection around the medical cyclotron at Hammersmith Hospital, 25:26775
BEYNON, A. J., Manganese reaction rate measurements in [Berkeley Nuclear Lab.] reactors, 25:28816 (RD/B/N-1518)
BEZNOGIKH, Yu. D., Deuteron acceleration in LA9-injector of JINR synchrocyclotron, 25:26109 (JINR-P9-5610)
BHADRA, Dilip K., Universal drift instability in a collisional plasma, 25:27747
BHALLA, S. K., Fertile dwarf and three other mutants in Cicer, 25:26718
BHANDARY, V. S., High conductivity coppers, 25:27187
BHARGAVA, B. N., Extraterrestrial ring current under very quiet magnetic conditions, 25:27518
BHATTACHARJEE, S. K., High temperature super alloys with particular reference to titanium and its alloys, 25:27203 (INIS-mf-2)
BIALAS, A., Quark model additivity frame, 25:28017
BIANU, M., Incidence-rate and types of chlorophyll mutants in flax induced by gamma rays and some alkylating agents, 25:27090
BIBR, B., Distribution of radioactive ^{99}Mo in tissue of test animals, 25:26598
BICHON, P., Study of internal friction peaks in molybdenum after irradiation with neutrons at 27°K, 25:27199 (CEA-CONF-1671)
BICKER, R. H., Output program used with on-line data collection, 25:26510
BICKES, R. W. Jr., Angular distribution of the scattering of Ar by N_2 and Ne, 25:27451
BIEDENHARN, L. C., Isospin impurities in the nuclear ground states, 25:28516
BILEN'KAYA, S. I., Proton form factors, 25:27991
BINGHAM, Billy Elias, Study of the effects of ^{135}Xe on a thermal reactor using a direct numerical solution, 25:28811
BIRD, C. C., Carcinogenic effects of radiations on the uterus, 25:26827
BIRDSALL, C. K., Feedback suppression of drift-centrifugal waves in mirror-confined plasma, 25:27768
BIRG, Francoise, Inactivation by uv light of Polyoma virus: cell surface antigen, 25:27107
BIRGENEAU, R. J., Neutron crystal-field spectroscopy in rare-earth metallic compounds, 25:27893
BIRKHOFF, Garrett, Exact analytic solutions of transport equations, 25:27948
BIRYUKOVA, T. A., Weldability of certain Mo alloys, 25:27185
BISH, J. T., Relative susceptibilities of caffeine-sensitive and caffeine-resistant strains of Candida albicans to inactivation and mutation by ultraviolet radiation, 25:27073
BISKAMP, D., Instabilities in perpendicular collisionless shock waves, 25:27731
BISNOVATYI-KOGAN, G. S., Growth of perturbations in an expanding universe of free particles, 25:27427
BISTER, M., Energy levels of ^{24}Mg, 25:28259
BITTEL, R., Estimate of the risk of internal contamination in man by radioactive water pollution, 25:26747
BJOERNEBOE, J., Graphical illustration of isospin analysis in single-pion production, 25:28039
BJOERNHOLM, Sven, Search for new islands of fission isomerism, 25:28305 (CERN-70-30(Vol.1), pp 567-74)
BJORDAL, J., Morphology of auroral-zone x-ray events. I, 25:27594
BJORKEN, J. D., Lepton--hadron processes at high energy, 25:28005
BLACHOT, J., Short-lived isomers of ^{136}I and ^{138}Cs decaying via metastable states of ^{136}Xe and ^{138}Ba, 25:28342 (CERN-70-30(Vol.2), pp 1119-21)
BLACK, J. L., Cross section of ^{28}Mg(tau,γ)^{28}Si reaction, 25:28206 (ANU-P-508)
BLACKMON, Maurice L., s-channel helicity conservation constraints on t-channel exchanges, 25:28028 (SU-1206-242)
BLACKSTEIN, F. P., Computer simulation of nuclear reactor system's capability, 25:28713
Computerized information retrieval for nuclear reactor systems, 25:28575
Conference on reliability, Chalk River, Ontario, 10/70, 25:28546 (AECL-3670)
Information retrieval and reliability analysis, 25:28553 (AECL-3670, pp 83-8)
BLACKWELL, B. F., User's manual for two-dimensional axisymmetric transient heat conduction material ablation computer program, 25:28883 (SC-DR-70-510)
BLAEDEL, W. J., Radioisotope derivative procedure for determination of epinephrine or norepinephrine, 25:26182
BLAGOJEVIC, M., Pomeranchuk singularity in the Veneziano model and unitarity, 25:28020
BLAHD, W. H., Critical evaluation of /sup 99m/Tc--Fe--ascorbic acid complex as a renal scanning agent, 25:26848
Demonstration of collateral pathways after superior vena caval obstruction with the scintillation camera, 25:26844
BLAIR, Richard J., Radiolabeled cholesterol as an adrenal scanning agent, 25:26845
BLAKE, J. B., Solar particle observations over the polar caps, 25:27540
BLAMONT, J. E., Evidence for source of extraterrestrial H Lyman-alpha emission, 25:27413
BLANC, Daniel, Mean gamma ray energy necessary to create ion pairs in dielectric liquids, 25:26293
BLANCHARD, A. E., Part length rod control system, 25:28668 (WCAP-7406)
Rod position monitoring, 25:28669 (WCAP-7571)
BLANCHARD, Pierre, Uranium alloys, 25:27195
BLANCHARD, R. L., Radiological surveillance studies at a boiling water nuclear power reactor, 25:28625
BLAND, C. J., High-energy solar electrons, 25:27574
BLANK, A. Ya., Damping of magnetic surface levels in superconductors, 25:27653
BLANQUET, P., Applications of thermo and photoluminescent phenomena in health physics, 25:26528
BLAU, Irwin, Promotion phenomenon for three particle exchange, 25:28093
BLAZICEK, G., Action of gaseous tritium on mammalian deoxyribonucleic acid, 25:26592
BLECKWENN, J., Elastic electron--deuteron scattering and electric neutron form factor at four momentum transfers: 5 Fermi^{-2} < q^2 < 14 Fermi^{-2}, 25:27980 (DESY-71/7)
BLETZINGER, P., Feedback experiments on multimode ionization waves, 25:27773
BLEULER, D., Co-existence of different structures in various domains of the periodic table, 25:28447 (CERN-70-30(Vol.2), pp 1129-32)
BLEULER, K., One boson exchange potential and nuclear matter properties, 25:28448 (CERN-70-30(Vol.2), pp 1133-5)
BLIZZARD, R. M., Determination of integrated plasma concentrations and true secretion rates of human growth hormone, 25:26579
BLOCH, D., Uniaxial stress experiments and magnetoelastic interactions in rare earths, 25:27889
BLOCH, Suzanne, Influence of different traumas on pregnancy in laboratory mouse, 25:28873 (ORNL-tr-2445)
BLOCK, P. C., Survival time and dose-response following supralethal irradiation of dogs, 25:26992
BLOHINCEV, D. I., Quantization of an essentially nonlinear field, 25:28071
BLOKHINTSEV, L. D., Vertex function for ^{6}Li + α + d process, 25:28185
BLOMEKE, J. O., Salt mine repository for radioactive wastes, 25:26453
BLOMGREN, Henric, Evidence for thymic dependence of PHA-reactive cells in spleen and lymph nodes and independence in bone marrow, 25:26673
Reappearance and relative importance of immunocompetent cells in the thymus, spleen, and lymph nodes following lethal x-irradiation and bone marrow reconstitution in mice, 25:26672
BLOOM, Danning Wilford, Specific heat, magnetic susceptibility, and superconductivity of vanadium carbide and specific heat of copper, 25:27910
BLOOM, S. D., Some systematics of coulomb displacement energies, 25:28478
Statistical model calculations of ^{56}Fe neutron cross section, 25:28218 (NP-18674)
BLOOM, Stewart D., Nuclear isospin. Proceedings of the conference, Asilomar--Pacific Grove, California, March 13--15, 1969, 25:28455
BLOQUEL, J., Use of /sup 99m/Tc and its compounds, 25:26765
BLOTT, B. H., Adsorption of uranium on tungsten single crystal planes, 25:27237
Adsorption of zirconium on tungsten single crystal planes, 25:27241
BLUEMCHEN, G., Diagnostic value of the quotients of precordial over prepulmonary counting rate from Na^{131}I, 25:26822
BLUMENTHAL, N. C., Interaction between thymidylic acid and sulfhydrylamine radioprotectors, 25:26279
BOBASHEV, S. V., Cross section for excitation of the Cs II resonance lines in the Cs^+ + He process near the threshold, 25:27454
BOCCIARELLI, Daria Steve, Conference on electron microscopy, Rome, 9/68. II, 25:26565
BOCHAROVA, M. A., Characteristics and quantitative prediction of cumulative storage of ^{90}Sr in arboreal plants, 25:26616
BOCHENINSKII, V. P., Measurements of the velocity profile in crossed electric and magnetic fields, 25:27502
BOCHEV, B., New isotopes of iridium, 25:28348 (JINR-P6-5617)
BOCQUET, J. P., On-line isotope separator device connected to Melusine reactor, 25:26551
BODDENDIJK, J. C., Production and decay properties of some shortlived cobalt nuclei, 25:28214 (CERN-70-30(Vol.2), pp 1105-13)
BODE, Dietrich, Simulation of moving beam therapy and grid size in electronic calculation of single fields and standard plans of telecobalt therapy, 25:26758
BODE, K. H., Uses of high temperature reactors for the generation of process heat, 25:28794
BODENSTEDT, E., Lectures on hyperfine interactions, a field between nuclear physics and solid state physics, Leuven, 1969, 25:27915 (NP-18702)
BODIN, H. A. B., Instabilities of high-beta plasmas,

25:27730
Plasma displacement due to dipole current near high-beta plasma, 25:27774
BODNER, Stephen, Negative diffusion coefficients in quasi-linear theory, 25:27712
BODNER, Stephen E., Quasi-linear theory in the nonresonant region, 25:27717
BOEGH, E., Spatial distribution of defects in ion bombarded silicon and germanium, 25:27861
BOEHM, M., Relativistic scalar quark model with strong binding, 25:28022 (DESY-71/10)
BOENING, K., Experiments at the Munich research reactor FRM, 25:28775
BOEOEK, J.-A., Chromosome and chromatid-type aberrations induced by ^{60}Co irradiation and tritiated uridine in human leukocyte cultures, 25:26636
BOERNER, G., Nuclei in neutron matter, 25:27311 (CERN-70-30(Vol.2), pp 759-68)
BOESEBECK, K., Four-pion decay mode of D(1285) meson in π^+-p reactions at 16 GeV/c, 25:27964
BOETTGER, P., Radiological population exposure in the environment of nuclear power plants, 25:26746
BOGARD, D. D., Noble gas abundances in lunar material, 25:27308
BOGDANOV, D. D., Proton emitter studies in region of Z > 50, 25:28300 (CERN-70-30(Vol.1), pp 457-86)
BOGDANOV, N. V., Atomic power plant with water-cooled, graphite-moderated reactor for combined power and heat generation, 25:28538
BOGITCH, Seymour, Neuro-muscular tests of aging in Hiroshima subjects, 25:27053
BOGNER, G., Superconducting dc quadrupole lens, 25:28111 (KFK-1218)
BOHMANN, W., Concept for a small nuclear steam-generating system with an integrated construction, 25:28641
BOLES, Larry A., Prog. rpt. on simulation and measurement of solar-flare proton exposures, final, 11/68--8/69, 25:26920 (AD-711041)
BOLESLAVSKAYA, G. I., Stabilization of drift waves by a nonuniform high-frequency field, 25:27741
BOLOTIN, H. H., Coulomb excitation of levels in ^{105}Pd, 25:28423
BOMMER, J., Proposal of $d^3/_2$-$^1p^3/_2$ analogue states in ^{49}Ca, 25:28230
BONCH-OSMOLOVSKAYA, N. A., Ytterbium-169 levels in ^{169}Lu decay, 25:28433
BONCH-OSMOLOVSKII, A. G., Non-linear regime of radiation instability development of relativistic electron rings, 25:28116 (JINR-P9-5622)
BONDARENKO, A. V., Atomic power plant with water-cooled, graphite-moderated reactor for combined power and heat generation, 25:28538
BONDORF, J. P., Resonant fission with damping, 25:28445 (CERN-70-30(Vol.1), pp 553-66)
BONETTI, A., Solar-wind discontinuities from Feb. 24 to Feb. 28, 1969, 25:27557
BONN, J., Measurement of the spin and nuclear magnetic moment of ^{20}Na, 25:28209 (CERN-70-30(Vol.1), pp 383-5)
BOOKHART, T. W., Correction of inspection data for part misalignment utilizing a small computer, 25:28908 (Y-1755)
BOONE, M. L. M., Gas target source for neutron radiation therapy, 25:26883
BOOS, A. H., Search for spontaneously fissioning isomers produced with 600 MeV protons, 25:28306 (CERN-70-30(Vol.1), pp 575-87)
BOOTH, D. J., General-relativistic and Newtonian gravitational energy transfer, 25:28089
BOOTH, N., Interaction between electron and ion modes and feedback stabilization, 25:27765
BOOTHROYD, Milton Woodall, Improvements in or relating to nuclear reactors, 25:28649
BORG, H., Precipitation pattern for auroral keV electrons and protons, 25:27576
BORG, Hans, Anisotropy for 1- and 6-keV positive ions in upper ionosphere, 25:27604
BORG, I. Y., Results of postshot exploration of the Greeley Event, 25:26412 (UCRL-50979)
BORG, S., Evidence for high-spin three quasiparticle state in ^{133}I produced in fission, 25:28331 (CERN-70-30(Vol.2), pp 1012-14)
Experimental techniques for nuclear structure studies in the Tin-region at OSIRIS, 25:28107 (CERN-70-30(Vol.2), pp 1003-5)
Levels in doubly-even tellurium isotopes, 25:28330 (CERN-70-30(Vol.2), pp 1010-11)
Neutron hole states in the tin-region, 25:28329 (CERN-70-30(Vol.2), pp 1008-10)
Proton states in the tin-region, 25:28328 (CERN-70-30(Vol.2), pp 1006-7)
BORGE, H., Variations in low-energy electron spectrum and relation to magnetic activity, 25:27582
BORGGREEN, J., Production and decay properties of thorium and protactinium isotopes of mass 221-225 formed in heavy ion reactions, 25:28304 (CERN-70-30(Vol.1), pp 545-6)
BORGGREEN, Joern, Search for new islands of fission isomerism, 25:28305 (CERN-70-30(Vol.1), pp 567-74)
BORGMAN, C. R., System that enables PDP-9 computer to utilize CDC-160A computer as a peripheral controller, 25:28885 (SC-DR-70-856)
BORGSTEDT, Hans Ulrich, Reactions of V--Zr--Cr and V--Ti--Cr alloys in liquid sodium having low oxygen activities, 25:27174
BORISOV, E. A., Vapour-phase radiation-initiated thermal oxidation of benzene by molecular oxygen with fast electron irradiation, 25:26284
BORODAI, B. I., Effect of low frequency fluctuations on superconducting tunnelling, 25:27649
BOROVEC, R. T., Illiac III Reference Manual. Vol. I, 25:28851 (COO-2118-5)
BORSOS, Tibor, Abrogation of passively transferred tumor immunity in vivo by antigenically related tumor cells, 25:26663
BORST-PAUWELS, G. W. F. H., Uptake of ^{32}P phosphate by red blood cells, 25:26589
BOSE, S., Effect of x-rays on plant growth, flowering, and fruiting in Impatiens balsamina L, 25:27086
M_3 generation of some M_2 mutants in rice, 25:26701
Segregation pattern in the M_3 generation of rice, 25:26688
Transition quadrupole moments and the variable-moment-of-inertia model for even--even nuclei, 25:28517
BOSTROEM, L., Calculation of differential angular correlation factors for non-coaxial electric and magnetic fields, 25:27919
Effects of coaxial magnetic and electric fields on time-integral PAC with special reference to rare-earth isotopes, 25:27918
BOSTROM, Carl O., Entry of low-energy solar protons into the magnetosphere, 25:27542
BOTBOL, Moises, Determination of thallium in microsamples of natural vanadates of uranium by anodic redissolution, 25:26151 (CNEA-288)
BOTEZ, G., Spectrophotometric characterization of DNA after irradiation in vivo. VI, 25:27020
BOTTERO, G., Importance of bone marrow scintiscans in the detection of skeletal metastases, 25:26847
Unusual radiological features in 4 cases of bone metastasis, 25:26846
BOUBELIK, M., Comparison of colony-forming performance of bone marrow cells in syngeneic and allogeneic cellular environment within a single host, 25:26670
BOUDART, M., Surface and bulk carburization of tungsten single crystals, 25:27225
BOUET, J., Portable electronic unit associated with an ionization chamber, 25:26459
BOULGER, F. W., [Recent research on] metalworking, 25:27194
BOUTRON, P., Uniaxial stress experiments and magnetoelastic interactions in rare earths, 25:27889
BOUZOU, Georges, Precipitation of Pu C_2O_4, 25:26345
BOVA, L., Experimental study of a gas jet penetrating a liquid coolant and impinging on a heated surface, 25:26418 (ANL-7734)
BOWLING, T. S., Rocket-borne D-region probe measurements, 25:27565
BOWMAN, C. D., Threshold photoneutron cross sections for ^{206} ^{207} ^{208}Pb, ^{56} ^{57}Fe, ^{52} ^{53}Cr, ^{24} ^{25} ^{26}Mg, and ^{19}F, 25:28413
BOXER, L. W., Power reactor strategies and their effect on fuel cycle requirements, 25:28714
BOXERMAN, Stuart B., Statistical analysis of radioisotope scan data, 25:26856
BOYD, Charles M., Treatment doses of ^{131}I-labeled chloroquine analog in normal and malignant melanoma dogs, 25:26882
BRAEUER, N., In-beam nuclear magnetic resonance of 159 μs level in ^{119}Sn, 25:28380
BRAJOVIC, V., Neutron inelastic scattering and neutron diffraction at the Vinca heavy water reactor, 25:28779
BRAMLEY, E. N., Effects of electric fields and ion drag in middle-latitude F region, 25:27529
BRANDICOURT, G., Status report on the study of the upper neutron shields of PHENIX on 4/15/69, 25:28677 (ORNL-tr-2451)
BRANDT, N. B., Superconductivity at high pressure, 25:27655
BRANDT, P. W. T., Cardiac catheterization. III, 25:26854
BRANDT, R., Search for spontaneously fissioning isomers produced with 600 MeV protons, 25:28306 (CERN-70-30(Vol.1), pp 575-87)
BRANDT, R. A., Regge asymptotic behavior in quantum field theory, 25:28072
BRANNON, Richard Bland, Response of equine lymphocytes to x-irradiation, 25:26903
BRANSON, N. J. B. A., High-resolution radio observations of Venus at 6 cm, 25:27434
BRAR, H. S., Fertile dwarf and three other mutants in Cicer, 25:26718
BRAUN, Arnim, Oxygen effect in γ-irradiated DNA, 25:26637
BRAVERMAN, Lewis E., Duration of radioactivity in the milk of a nursing mother following /sup 99m/ Tc administration, 25:26839
BRENDL, J., Effect of gamma irradiation on the rehydration capacity of freeze-dried meat, 25:27144
BRENNAN, J. T., Response of stem cells to 14 MeV neutrons, 25:26958
BRESSAN, O. J., Electron--electron scattering in electrical resistivity of In, 25:27660
BREUSOV, O. N., Reaction of oxides of rare earth elements with boron during shock compression, 25:27291
BREWER, Peter G., Distribution of some chemical elements

between dissolved and particulate phases in the ocean, 25:26190 (NYO-4150-9)
BRIGGS, G. G., Thorium metal production, 25:27180 (NLCO-1080)
BRIGGS, R. J., Effects of cold plasma on relativistic electron layer, 25:27746
BRINI, D., OSO-G satellite instrumentation for measurements of cosmic x-rays in energy range from 25 to 190 keV, 25:26478
BRINKMAN, A. C., X-ray observations between 1 and 55 A of the Feb. 25th flare, 25:27357
BRISSOT, R., On-line isotope separator device connected to Melusine reactor, 25:26551
BRITT, H. C., Resonance structure in the $^{88}Sr(p,p')$ octupole transition, 25:28240
BROCK, J. R., Attachment of trace substances on atmospheric aerosols, 25:26383 (CONF-700601-, pp 373-80)
BROCK, R. D., Differential mutation of β-galactosidase gene of E. coli, 25:26722
BRODY, A. D., Reaction $\pi^- p \rightarrow \pi^+ A^-$ at cms energies 1640 to 1760 MeV, 25:27962
BRODY, T. A., Sum rules for Moshinsky brackets, 25:28506
BRODY, Thomas Bergman, Identification of two-cell populations required for immunocompetence, 25:26669
BRODZINSKI, R. L., Measurement of radiation exposure of astronauts by radiochemical techniques, 25:26178 (BNWL-SA-3608)
Prog. rpt. on measurement of radiation exposure of astronauts, 10/5/70--1/3/71, 25:26187 (BNWL-1183-7)
BROENSTAD, K., Morphology and dynamics of auroral-zone electron precipitation, 25:27583
BROMMUNDT, G., Ionospheric plasma drifts derived from wake measurements, 25:27585
BRONCA, G., Protection of large superconducting coils, 25:27663 (ORNL-tr-2436)
BROOKS, I. B., Development of ion exchange processes for the removal of radionuclides from milk, 25:26335 (RO/EERL-71-1)
BROOMFIELD, A. M., ZPR-3 assemblies 48: 48A, and 48B: the study of a dilute plutonium-fueled assembly and its variants, 25:28752 (ANL-7759)
BROWDER, F. N., Nuclear safety in American radiochemical processing plants, 25:26780
BROWER, John H., Effects of gamma radiation on the larval midgut of the Indian-meal moth, Plodia interpunctella (Lepidoptera: Phycitidae), 25:26916
BROWN, Lowell S., Current algebra and analyticity, 25:28027 (RLO-1388-602)
BROWN, M. R., Ion-implantation doping of zinc sulphide thin films, 25:27844
BROWN, R. A., Anomalies in distorted-wave Born-approximation analysis of $^{140}Ce(d,p)^{141}Ce$, 25:28429
BROWN, R. C., Isotope effects in close-packed metals and in alkali halides, 25:26241
BROWN, R. T., Measurements in a nonequilibrium plasma boundary layer, 25:27685
BROWNE, J. C., Fine structure of the isobaric analogs of the ground and second excited states of ^{63}Ni, 25:28237
BROWNELL, Charles, Two new gregarine parasites from the spatangoid-urchin Brisaster latifrons, 25:28880 (RLO-1750-59)
BROZMANOVA, J., Effect of 5-FU posttreatment of sensitivity to ultraviolet radiation and course of messenger RNA synthesis in E. coli, 25:27123
BRU, A., Problems in use of short-lived radioelements, 25:26763
BRUAUX, P., Electrophoresis and immunoelectrophoresis patterns from proteins of irradiated meat, fish, and fowl egg, 25:26631
BRUCE, G. S., Estimation of the dose to skin from radioactive particulate contamination of clothing, 25:26748
BRUGOVITZKY, Edith, Effect of pre-irradiation on growth substances in Brassica oleracea, 25:26651
BRUICE, T. C., Acyl transfer reactions from and to the ureido functional group. IV. Neighboring carboxyl group general acid catalysis in the hydrolysis of an O-acylisourea (2-amino-8-carboxy-4-oxo-3,1,4-benzoxazine), 25:26253
BRUINS, Paul F., Polyblends and composites. Conference held at Brooklyn, New York, June 6--7, 1969, 25:27271
BRUSCAGLI, C., Effect of ionizing radiation on the heart, 25:26961
BRUZZI, L., Containment design criteria for sodium cooled fast reactors, 25:28739 (RT/ING-(70)25)
BUCHACEK, Robert, Mechanistic implications of the role of phenol in the uranium(IV)--chlorine(III)--phenol reaction, 25:26266
BUCHANAN, R., Shielded x-ray microprobe for the analysis of radioactive samples, 25:26156
BUCHAU, Jurgen, Airborne ionospheric and optical measurements of noontime aurora, 25:27597
BUCHER, E., Hyperfine enhanced nuclear magnetic cooling in Van Vleck paramagnetic intermetallic compounds, 25:27666
Neutron crystal-field spectroscopy in rare-earth metallic compounds, 25:27893
BUCKLEY, J. L., Rocket twilight observations of H I 1216-A horizon brightening near 150 km, 25:27615
BUCKLEY, John D., Composition and microstructure of stabilized hafnium dioxide, 25:27296
BUCURESCU, D., Reaction $^{86}Sr(tau,\alpha)^{85}Sr$ at E/sub tau/ = 17.5 MeV, 25:28277
BUDDEMEIER, R. W., Radiocarbon in the sea, 25:26398 (RLO-2225-T-20-2)
BUECHLER, Frederiksen P., Lymph node scanning with radioactive Au, 25:26851
BUGYAKI, L., Electrophoresis and immunoelectrophoresis patterns from proteins of irradiated meat, fish, and fowl egg, 25:26631
BUHL, J., Brain scanning: cerebral scintigraphy, 25:26850
BUKIN, A. D., Evidence for electron-positron pair electroproduction, 25:27994
BULATOV, B. P., Trends of development of modern semiconductor ionizing radiation detectors, 25:26461
BULKIN, Yu. M., Standardized line of pressure-vessel type boiling-water reactors, 25:28716
BULL, J. W. D., Interpretation of brain scans by computer analysis, 25:26824
BULLAMORE, J. R., Calcium-47 in feces, 25:26586
BULLOUGH, R., Isotope effects in close-packed metals and in alkali halides, 25:26241
BUNCHER, C. Ralph, Smallest forms of papillary carcinoma of thyroid. A study of 141 microcarcinomas less than 0.1 cm in greatest dimension, 25:26898
BUNGE, Mario, Virtual processes and virtual particles: real or fictitious, 25:28064
BUNN, W. B., Material forming and welding nuclear pressure vessels, 25:27196
BUNNETT, J. F., Bromine scrambling accompanying base-catalyzed isomerization of 1,2,4-tribromobenzene, 25:26221
Isomerization and disproportionation of trihalobenzenes catalyzed by potassium anilide in liquid ammonia, 25:26222
BURDIASHVILI, M. Sh., Distribution of a pulsed current in a cylindrical conductor of variable conductivity, 25:27721
BURG, Constant, Restoration of the hybrid effect suppressed by whole-body irradiation, 25:26985
BURGESS, Edward Eugene, Physical, chemical, and biological control of alfalfa weevil, 25:26913
BURGESS, James Henry, Improvements in or relating to methods and apparatus for inserting rods into a frame, 25:28652
BURGOV, N. A., Capture of neutrons by Rh, Ta, and Au, 25:28437
BURKE, William L., Gravitational radiation damping of slowly moving systems calculated using matched asymptotic expansions, 25:28086
BURLOT, A., Irradiation risks with /sup 99m/Tc, 25:26766
BURN, Thomas, Nonlinear behavior of the one-dimensional weak beam--plasma system, 25:27710
BURNASHOVA, V. V., Study of the zirconium--nickel--aluminum system, 25:27258
BURNIER, P., Protection of large superconducting coils, 25:27663 (ORNL-tr-2436)
BURRIS, J. R., 1000-MWe LMFBR accident analysis and safety system design study. Topical report. candidate secondary containment support systems, 25:28730 (BAW-1349)
BURTON, Ben S., Prog. rpt. on simulation and measurement of solar-flare proton exposures, final, 11/68--8/69, 25:26920 (AD-711041)
BURTON, Frederick Glenn, Possible role of crystals in origins of life, 25:28906 (UR-49-1444)
BURTON, K. S., Mean lives and angular correlations in ^{57}Co with $^{54}Fe(\alpha,p\gamma)^{57}Co$ reaction, 25:28281
BUSCH, C. E., States in ^{17}O via neutron-polarization measurements in $^{13}C(\alpha,n)^{16}O$ reaction, 25:28202
BUSCH, G., Change of sign of Hall coefficient in liquid alloys, 25:27212
Crystal-field splitting and spin waves in antiferromagnetic CeSb, 25:27881
BUSCH, H., Brain scanning: cerebral scintigraphy, 25:26850
BUSEV, A. I., Extraction methods in analytical chemistry of Mo, 25:26344
BUSHONG, Stewart C., Gonadal dose in male radiotherapy patients, 25:26759
BUSUOLI, G., Thermoluminescent dosimeter of LiF incorporated in silicone rubber, 25:26539
BUTLER, B. L., Advanced filament-wound carbon composite, 25:28888 (SC-DR-710192)
BUTLER, Gilbert W., Fragment production in interaction of 5.5-GeV protons with U, 25:28426
BUTT, B. A., Estimating the size of populations of codling moths, 25:27155
BUXTON, G. V., Radiation chemistry of low-temperature aqueous glasses. IV, 25:26310
BUZZI, Umberto, Fuel element replacement apparatus for use in conjunction with a vertical-channel nuclear reactor, 25:28825
BYERS, J. A., Explosive instabilities in simulated plasmas, 25:27736
BYRD, Gene G., Spectrophotometry of Nova Serpentis 1970, 25:27322
BYRD, James Donald Jr., Flux flow in superconducting thin films, 25:27645
BYRER, T. G., [Recent research on] metalworking, 25:27194
BYRNE, M., Hydrogen- and deuterium-evolution reactions on gold in acid solutions, 25:26231

C

CABROL, Ch., Radioactive aerosols characteristics in French U mines, 25:26773

CACACE, Fulvio, Reactions of helium tritide ions with gaseous hydrocarbons. V. cis- and trans-1,2-dimethylcyclopropane. Unambiguous evidence for gaseous protonated cyclopropanes, 25:26321

CAHILL, Daniel F., Tritium: some effects of continuous exposure in utero on mammalian development, 25:26925

CAILLIAU, M., Mass-differences in neutron-rich Sr Region, 25:28294 (CERN-70-30(Vol.1), pp 321-9)

CALAPAJ, G. G., Strontium-90/Ca and $^{137}Cs/K$ in diet and passage through human milk, 25:26581

CALDER, I. R., Observations recorded by the cosmic-ray detector during the solar flare of Feb. 25, 1969, 25:27471

CALFEE, John D., Importance of fabrication technology in translation of fiber and matrix properties to advanced composites, 25:27278

CALLAHAN, A., Coherent K-d interactions at 12.6 GeV/c, 25:27967

CAMERON, A. G. W., Construction of mass formulas designed to be valid for neutron-rich nuclei, 25:28293 (CERN-70-30(Vol.1), pp 275-306)

Dynamics of the rapid neutron capture process, 25:27310 (CERN-70-30(Vol.2), pp 735-57)

CAMERON, Harry M., Thermal cycling on a 3-in.-diameter Nb--1 percent Zr to 316 stainless steel transition joint, 25:27179 (N-71-10454)

CANIZ, P., Effective four-body interaction in light nuclei, 25:28482

CAMPBELL, C. E., Effects of lateral substrate fields on helium monolayers, 25:27634 (RLO-1388-604)

Ground state of ^4He monolayers adsorbed on inert substrate, 25:27633 (RLO-1388-603)

w^{-1} sum rules and long range correlation in binary solutions, 25:27632 (RLO-1388-599)

Substrate mediated interaction between adsorbed atoms, 25:27635 (RLO-1388-605)

CAMPBELL, J. E., [Recent research on] mechanical properties of metals, 25:27236

CAMPBELL, P. G. C., Allylic and homoallylic oxidation of cyclohexene and cyclohexene-3,3,6,6-d_4 by palladium(II) salts. Evidence for competing symmetrical and oxypalladation intermediates, 25:26256

CAMPBELL, W. F., Effects of γ radiation on Penicillium expansum. I, 25:27084

CANDIDI, M., Solar-wind discontinuities from Feb. 24 to Feb. 28, 1969, 25:27557

CANELLI, Edmondo, ^{32}P autoradiography used to measure phosphate uptake by individual algae, 25:26596

CANNING, R. G., Kinetics in solvent extraction of metals, 25:26342

CANNON, C. J., Calculations of two-dimensional models of the lower solar chromosphere, 25:27371

CANNON, T. M., Multiple muons deep underground, 25:27954

CANO, R., Local density measurements by nonlinear mixing of electromagnetic waves, 25:27684

CANON, R. F., Deformation of UO_2 at high temperatures, 25:27287

CANONICO, Domenic A., Titanium--zirconium--germanium brazing alloy, 25:27229

CANOSSI, G. C., Scintigraphy of carcinoma using $^{197}HgCl_2$, 25:26832

CAPITELLI, M., Contribution of electronic excitation to specific heats of high-temperature gases, 25:27692

CAPRI, A. Z., First-order wave equation for integral spin, 25:27975

CARDINALE, K. G., Evaluation of /sup 99m/Tc-DTPA prepared by three different methods, 25:26840

CARDOSO, M. H., Decay of some nuclei far from the stability line studied with standard spectroscopic techniques, 25:28322 (CERN-70-30(Vol.2), pp 939-47)

CARIOU, J. M., Significance of scattering in calibrating apparatus for the measurement of fluences and neutron dose equivalents, 25:26483

CARLE, P., Levels in doubly-even tellurium isotopes, 25:28330 (CERN-70-30(Vol.2), pp 1010-11)

CARLETON, N. P., Excitation of nitrogen by fast protons and electrons, 25:27616

CARLSON, David H., ^{60}Co teletherapy of pituitary adenomas, 25:26872

CARLSON, R. W., Extreme-ultraviolet dayglow of Jupiter, 25:27432

CARLYLE, David C., Passive feedback stabilization, 25:27771

CARMICHAEL, G. D. T., Correlation of measured and calculated strains in top-half of Oldbury prestressed concrete pressure vessel R1, 1965--1970, 25:28528 (RD/B/N-1784)

CARNEIRO, A., External heavy ion source for Berkeley 88-inch cyclotron, 25:28120 (UCRL-20406)

CARRAZ, L. C., Short-lived isomers of ^{130}I and ^{130}Cs decaying via metastable states of ^{130}Xe and ^{130}Ba, 25:28342 (CERN-70-30(Vol.2), pp 1119-21)

CARRE, Jean-Claude, Measurement of the kinetic parameters of the MINERVE reactor from analysis of the neutron fluctuations, 25:28755 (CEA-N-1406)

Measurement of the transfer function of a reactor by reactivity modulation, 25:28754 (CEA-N-1405)

CARREGAL, Enrique J. A., Acute effects of x-radiation on spinal cord motoneurons. A functional and ultrastructural study in the cat, 25:26941

CARSTEN, Arland L., Decrements in the visual acuity of rhesus monkeys (Macaca mulatta) as a delayed effect of occipital cortex irradiation, 25:26991

CARTER, J. C., SAS1A: a computer code for the analysis of fast-reactor power and flow transients, 25:28727 (ANL-7607)

CARTER, K. W., Search for high-spin states in ^{27}Al, 25:28208 (ANU-P-521)

CARY, E. E., Effect of dietary selenium on the survival of rats exposed to chronic whole body irradiation, 25:27032

CASABE, Jaime, Determination of thallium in microsamples of natural vanadates of uranium by anodic redissolution, 25:26151 (CNEA-288)

CASEY, Charles P., Hydroformylation of 3-methyl-1-hexene-3-d_1. Evidence against direct formylation of a methyl group in the oxo reaction, 25:26228

CASHMORE, R. J., Reaction $\pi^- p \rightarrow \pi^+ A^-$ at cms energies 1640 to 1760 MeV, 25:27962

CASON, John L., Neutron radiography with ^{252}Cf in forensic science, 25:26437 (BNWL-SA-2865)

CASSAGNOU, Y., Interest of analog state studies in deformed nuclei, 25:28472

CASSINELLI, Joseph P., Extended model atmospheres for the central stars of planetary nebulae, 25:27314

CASTAGNET, Antonio C., Nuclear techniques and equipment in hydrology, 25:26353 (CONF-680112-, pp 37-52)

Uses of irradiation in agricultural production in Argentina, 25:27133 (CONF-680112-, pp 241-3)

CASTEL, B., Coupling of quasiparticles and anharmonic vibrations: A = 33 and 34, 25:28249

Projected Hartree--Fock and core-particle coupling for A = 29 and 30, 25:28280

CASTEL, Norman, Protection of DNA against ionizing radiation, 25:26801

CASTLEBERRY, P. J., Charged particle emission following pion capture in nuclei, 25:28178

CASTRO, Joseph R., Results in treatment of pure seminoma of the testis, 25:26891

CATALANO, E., Investigations into the Eu--Eu_2O_3, the Eu--Pt-Eu_2O_3, the Sm--Sm_2O_3, and the Yb--Yb_2O_3 systems, 25:27302

CATALINI, Nicola, Influence of the thymus in the regenerative process of cervical lymph nodes in irradiated mice, 25:26996

CATCHINGS III, Robert M., Magnetization and electrical conductivity studies of some transition metal oxide glasses, 25:27901

CATER, E. D., Infrared spectra of UO and UO_2 vapor condensed in rare-gas matrices, 25:26260 (COO-1182-34)

CAVALLINI, A., Thermoluminescent dosimeter of LiF incorporated in silicone rubber, 25:26539

CAVALLO, G., Neutral-pion decay and the gamma radiation from our galaxy, 25:27404

CAVALLO, V., Use of /sup 99m/Tc for cerebral scintigraphy, 25:26818

CAVENDISH, J. H., Thorium metal production, 25:27180 (NLCO-1080)

CAYGILL, Wayne M., Aqueous humor dynamics following pituitary irradiation in diabetic patients with retinopathy, 25:27037

CAYLA, J., Synoviothesis (synoviotherapy by radioisotopes) studies of more than 400 cases and future prospects, 25:26873

CERNANSKY, Barbara Ann, ESR of deuterated DL-tartaric acid single crystals irradiated at low temperatures, 25:26306

CERNY, Joseph, Isospin purity and delayed-proton decay: ^{17}Ne and ^{33}Ar, 25:28195

Nuclear isospin. Proceedings of the conference, Asilomar--Pacific Grove, California, March 13--15, 1969, 25:28455

CERUTTI, P. A., X-radioinduced thymine damage in Micrococcus radiodurans, 25:26643

CERVOS-NAVARRO, J., Acute changes of CNS caused by ionizing rays, 25:26987

CETTO, Ana M., Self-interaction corrections in a nonrelativistic stochastic theory of quantum mechanics, 25:27941

CHADDERTON, L. T., Annealing of damage produced by boron ion implantation of silicon single crystals, 25:27863

CHAKRABARTY, A. M., Merodiploidy and expression of episomal genes in Pseudomonas putida, 25:28849 (COO-1683-32)

CHAKRABORTY, B., Coupling of waves in nonuniform plasma, 25:27825

CHAKRAVORTY, S., Micromagnetism in Pd--Cr and V--Mn alloys, 25:27890

CHALABREYSSE, J., Medical examinations made after inhalation of natural U soluble compounds. II, 25:26607

CHALLINOR, B. A., Longitudinal variations of midlatitude ionosphere produced by neutral-air winds. I, 25:27507

CHALMERS, Joseph S., Optical-potential scattering of nucleons by carbon at medium energies, 25:28199

CHAMBERS, S., Steam-generating heavy-water reactor as energy source for power and water production when coupled to multi-stage-flash or vapour recompression

distillation plant, 25:28642
CHAMBLISS, Carlson R., Photoelectric photometry of the dwarf Cepheid HD 199757, 25:27319
CHAMPION, Robert Morrell, Shipboard irradiation of shrimp, 25:27158
CHAN, L. H., Marine geochemistries of the uranium isotopes, ^{230}Th, and ^{231}Pa, 25:26399 (TID-25674)
CHANDRASEKHAR, Saroj, Radiation, infection, and macrophage function. IV. Effect of radiation on the proliferative abilities of mononuclear phagocytes in tuberculous lesions of rabbits, 25:27001
CHANG, Ko Chang, Clinical study on the value of a scoring system of the scanning images in liver cirrhosis, 25:26862
Medical study of Korean atomic bomb survivors, 25:27060
Uptake- and metabolic studies of the labelled compounds in malignant tumors, 25:26859
CHANG, M. D., Uptake- and metabolic studies of the labelled compounds in malignant tumors, 25:26859
CHANG, Y., Effects of radiation pasteurization on Salmonella. II, 25:27164
CHANMUGAM, G., Magnetic field decay of neutron stars, 25:27344
CHANNIN, Donald Jones, Resonant phonon scattering in KCl:Li, 25:28863 (NYO-2391-111)
CHAPMAN, A. B., Genetic effects of cumulative maternal irradiation on growth and age at sexual maturity in rats, 25:26965
CHAPPELL, C. R., Ogo 5 measurements of the plasmasphere during observations of stable auroral red arcs, 25:27622
CHAPUIS, A., Alpha spectrometer for measuring the degree of radioactive equilibrium between ^{222}Rn and its daughter products in U mines, 25:26503
Radioactive aerosols characteristics in French U mines, 25:26773
CHAPUT, Raymond L., Miniature pig performance after fractionated supralethal doses of ionizing radiation, 25:26928
CHARBONNEAU, Serge, COREGRAF 2: adjustment and comparison with experiment, 25:28654 (CEA-N-1344(2))
CHARLTON, D. E., Energy dissipation near an interface: a more realistic approach to electron range and stopping power, 25:27835
CHATTERJI, A. K., Effects of radiation on safflower, 25:27083
CHATTERS, R. M., Application of nuclear techniques to the recovery of faded photographs, 25:26287
CHAUMONT, J., Half-lives of the new isotopes ^{99}Rb, ^{98}Sr, and ^{145} ^{146}Cs, 25:28388
CHAVAUDRA, J., Irradiation risks with /sup 99m/Tc, 25:26766
CHECHETKIN, V. M., Thermodynamics under conditions of hot matter neutronization and the hydrodynamic stability of stars at late stages of evolution, 25:27335
CHEGORYAN, M. A., Polarization in two-nucleon stripping reactions at low energies, 25:28496
CHEKIN, B. V., Distribution of electric field in conducting cylinder with electrodes of finite size, 25:27492
CHELNOKOV, L. P., Investigation of α decay of isotopes of element 105, 25:28350 (KFK-tr-350)
CHEN, C. H., Induction of chromosomal aberrations in pig kidney cells by far-red light, 25:26727
CHEN, C. S., Parametric excitation in an inhomogeneous plasma, 25:27814
CHEN, Etang, Annihilator of energy--momentum spectra in quantum field theory, 25:28069
CHEN, F. C., Does W_i scale, 25:27995
CHEN, F. F., Plasma control with infrared lasers, 25:27758
CHEN, Hsi-tseng, States of intermediate charge symmetry as low-lying, 0^+ collective excitation of medium weight nuclei, 25:28490
CHENG, H., Impact picture and the eikonal approximation, 25:28011
CHENG, Hung, Impact picture and the eikonal approximation, 25:28045 (DESY-71/6)
CHERDANTSEV, P. A., Energy surfaces during fission of ^{226}Ra, ^{238}U, and ^{246}Cf, 25:28395
CHERIAN, M. G., Preparation and properties of six rat red cell hemoglobins, 25:28866 (NYO-3976-5)
CHERKASHIN, A. I., Effect of period v transition metals on the structure and properties of titanium, 25:27223
Effect of small additions of vanadium and nickel on some properties of cast titanium, 25:27220
CHERNILIN, Yu. F., Nuclear data for thermonuclear reactors, 25:27792 (IAE-1986)
CHERNOV, G. P., Observations of solar radio bursts with high spectral resolution, 25:27398
CHERNYSHEV, A. S., Effect of spin--spin and spin--orbit forces on the decoupling parameters, 25:28484
CHICHEPORTICHE, Armand, Circuit for detecting coincidences between pulses by the means of sequential graphs, 25:26546 (CEA-R-4166)
CHIKUI, Shumpei, Electrometric determination in chromatographic development. III, 25:26173
CHILDRESS, C. E., Manual for ASTM A-533 grade B, class 1 steel (HSST plate 03) provided to the International Atomic Energy Agency, 25:27181 (ORNL-TM-3193)
CHILDS, R. L., Application of DOT--MORSE coupling to the analysis of three-dimensional SNAP shielding problems, 25:28784 (ORNL-TM-3365)
CHIN, G. Y., Cast permanent magnets of Co_5RE type with mixtures of Ce and Sm, 25:27883
CHIRKO, V. I., Elastic scattering of protons on iron and cobalt, 25:28263
CHITA, D., Potato plants obtained from irradiated tubers, 25:26737
CHIVERS, H. J. A., Power spectrum of scintillations of a two-component radio source, 25:27474
CHIZHOV, V. P., Microtron type electron accelerator, 25:28136
CHKHUBIANISHVILI, E. I., Effect of x rays on the nucleus and DNA dill stem, 25:27081
X ray effects on leaf cell size in vegetables, 25:27091
CHO, Mann, Total cross sections for kilovolt neutrons of even--odd nuclei in he region of the 3s strength-function resonances, 25:28279
CHOI, J. K., Mutation breeding of tomato. I, 25:26735
CHOU, S., Analysis of ion implanted diamond, 25:27358
CHOU, T. W., Effects of γ radiation on Penicillium expansum. I, 25:27084
CHOU, Tsong-wen, Effects of gamma radiation in Penicillium, 25:27085
CHRETIEN, M., Statistical physics, phase transitions, and superfluidity. II, 25:27912
CHRISTENSEN, E. R., Surface roughened fuel rods in large, fast gas-cooled reactors, 25:28696
CHRISTIE, Raymond K., Observed seismic data, Calabash event, 25:26401 (NVO-1163-218)
CHRISTOFFERSEN, G. B., Wave--particle interaction in single-ended Q machine, 25:27693
CHRISTOPHERSEN, P., Pitch-angle dependence of auroral electron fluxes in keV range, 25:27577
CHRISTOPHERSEN, Peter, Anisotropy for 1- and 6-keV positive ions in upper ionosphere, 25:27604
CHRYSOCHOIDES, N. G., Experience and research with the Greek reactor, 25:28774
CHU, Florence C. H., Review of experience with irradiation of brain metastasis, 25:26895
CHU, T. K., Collisional drift instabilities, 25:27729
Conference on feedback and dynamic control of plasmas, Princeton, N. J., 6/70. I, 25:27752
Feedback stabilization of the transverse Kelvin--Helmholtz instability, 25:27772
Remote feedback stabilization of drift instability by microwaves, 25:27766
CHU, Y. Y., Study of some neutron-deficient nuclides with high resolution x-ray detector and mass separation, 25:28321 (CERN-70-30(Vol.2), pp 931-8)
CHUCHKOV, E. A., Solar cosmic-ray increase on 25 Feb.--5 Mar., 1969, 25:27470
CHUDAKOV, A. E., Propagation of solar and galatic cosmic rays of low energies in interplanetary medium, 25:27469
CHULTEM, D., Deposition of uranium in the bones of animals, 25:26744
CHUMAK, A. S., Effect of homotransplantation of bone marrow on the healing of liver wounds in severe combined radiation trauma, 25:27005
CHUNG, Suh Urk, Spin formalisms, 25:28007 (CERN-71-8)
CHUNG, Sung Koo, Studies on amylase and protease activities of Aspergilli by uv-irradiation method, 25:27097
CHUPP, W. W., Mechanical features of electron-ring compressors, 25:28118 (UCRL-20177)
CHURCH, Hugh W., Climatology of atmospheric diffusion prediction variables, 25:28881 (SC-DC-713920)
CHURCHWELL, Edward Bruce, Radio recombination lines of H, He, and C, 25:27349
CHUYANOV, V. A., Feedback stabilization of the rarefied plasma cyclotron instability, 25:27776
CHYBICKI, M., Ionization currents induced by corpuscular radiations in liquid dielectrics, 25:26471
CICOGNANI, G., Containment design criteria for sodium cooled fast reactors, 25:28739 (RT/ING-(70)25)
CINTRA, Sebastiao Hermano Leite, Reactivity of U_3O_8/Al dispersions, 25:27294
Thermal cycling test for plates containing dispersions, 25:27251
CIOCANEL, A., New experimental data for neutron polarization from $^{11}B(\alpha,n_0)^{14}N$ reaction, at low energies, 25:28192
CLADIS, John B., Multiply coupled oscillations of field lines in magnetosphere, 25:27623
CLAEYS, F., Electrophoresis and immunoelectrophoresis patterns from proteins of irradiated meat, fish, and fowl egg, 25:26631
CLAPS, M., Analytical method for representing cylindrical B_4C absorbers in two-dimensional diffusion calculations, 25:28820 (EUR-4556)
WIGNER: program for calculation of mean thermal cross sections in reactor core and for punching of load data for calculating the epithermal cross sections, 25:28803 (EUR-4555)
CLARK, A. G., Reaction K-P → ΛK+K- and the generalized Veneziano model, 25:28042
CLARK, D. J., External heavy ion source for Berkeley 88-inch cyclotron, 25:28120 (UCRL-20406)
CLARK, Ervil Delwyn, Reactions of the sea anemone, anthopleura xanthogrammica, to electromagnetic radiations in the visible, ultraviolet, and x-ray ranges, 25:26912
CLARK, Willie E., Engineering materials list, 25:26414 (TID-4100(Suppl.62))

CLARKE, J. F., Feedback control of Kruskal--Shafranov modes, 25:27762
Measuring poloidal magnetic field in diffuse toroidal pinches, 25:27795
CLARKE, Reginald, Effect of γ-irradiation on beef myoglobin, 25:27139
CLARKE, W. B., Mass-spectrometric search for Ne and Ar isotopes in ternary fission of ^{235}U, 25:28419
CLAUSNITZER, G., Study of isobaric analogue resonances in elastic scattering of polarized protons from ^{88}Sr, ^{90}Zr, ^{92}Zr, ^{94}Zr,^{92}Mo, ^{142}Ce, ^{144}Nd, ^{146}Nd, 25:28239
CLEAVER, J. E., DNA repair and radiation sensitivity in xeroderma pigmentosum cells, 25:26634
COATS, R. B., Theoretical analysis of extensive air showers. V, 25:27477
COBB, Donald Dean, Proposed extension of the Regge pole model to include the isotopic spin symmetry, 25:28055
COCHI, C., Equipment for remote control of gamma scanning in a hot cell, 25:26550 (RT/ING-(71)1)
COCHRAN, Gordon Vance, Light variations of close binaries conforming to the Roche model, 25:27330
COE, R. J., United States utility experience with intermediate light-water reactors, 25:28577
COFFMAN, F. E., Beta--gamma band mixing in ^{152}Sm, 25:28430
COHEN, A. S., Chicago air pollution systems analysis program, 25:28840 (ANL-ES-CC-8)
COHEN, H. A., Derivation of the Pryce--Foldy--Wouthuysen transformation, 25:27937
COHEN, Marvin B., Unique case of amebic abscess of the liver, 25:26843
COHEN, Norman, Retention and distribution of ^{210}Pb in the adult baboon, 25:26610
COHEN, Robert, Geomagnetic field inclination determined by calibrating the Faraday rotation of an incoherently scatter signal, 25:27611
COHEN, Saul G., Repair and damage by mercaptans in ^{60}Co γ-ray irradiation of organic compounds in aqueous solution, 25:26291
COINER, Diane, Comparison of Schilling test and plasma level of cyanocobalamin ^{57}Co, 25:26853
COLE, Nancy C., Titanium--zirconium--germanium brazing alloy, 25:27229
COLE, R. M., Transduction in group a streptococci by ultraviolet irradiated bacteriophages, 25:27110
COLEMAN, James R., Effects of metals on cells, subcellular elements, and macromolecules. Proceedings of the 2nd conference on toxicity, Rochester, N. Y., June 12--16, 1969, 25:26608
COLEMAN, L. F., Washout of gaseous iodine species, 25:26376 (CONF-700601-, pp 271-88)
COLEMAN, N. L., Effect of concentration gradients on the performance of a nuclear sediment concentration gage, 25:26544
COLEMAN, P. J., Magnetic and electric field changes across the shock and in the magnetosheath, 25:27539
COLEMAN, Paul J. Jr., Geomagnetic storms at ATS 1, 25:27544
COLLETT, Wells I., Nuclear reactor power monitor system, 25:28672
COLLEY, D. C., Anti-lambda production in 10 GeV/c K^+ proton interactions, 25:27966
$K^0\pi^+p$ final state produced in K^+p interactions at 10 GeV/c, 25:27968
COLLIN, G. J., Ion-molecule reactions in the condensed-phase radiolysis of hydrocarbon mixtures. III. Reactions of $i\text{-}C_4H_9^+$ and $tert\text{-}C_4H_9^+$ ions originating from neopentane, 25:26309
COLLINS, R. A., Adsorption of uranium on tungsten single crystal planes, 25:27237
Adsorption of zirconium on tungsten single crystal planes, 25:27241
COLON, A. E., Transduction in group a streptococci by ultraviolet irradiated bacteriophages, 25:27110
COMAY, E., Current semiempirical mass equations and improved shell model nuclear masses, 25:28291 (CERN-70-30(Vol.1), pp 165-216)
COMBES, J. M., Class of analytic perturbations for Schrodinger Hamiltonians. I, 25:27926 (CNRS-CPT-70-P-352)
CONARD, Robert A., Immunohematological studies of Marshall Islanders sixteen years after fallout radiation exposure, 25:27058
CONDE, J. F. G., Quality control, inspection, and testing of Series I metallurgical fuels for first charge of Dragon reactor, 25:26438 (DP-Report-432)
CONGER, B. V., Response of rice to γ-rays and fission neutrons, 25:27070
CONLON, Frank B., Summary of federal regulations for packaging and transportation of radioactive materials, 25:26445 (BRH/DMRE-71-1)
CONSOLE, M., WIGNER: program for calculation of mean thermal cross sections in reactor core and for punching of load data for calculating the epithermal cross sections, 25:28803 (EUR-4555)
CONSOLI, T., Hot dense plasmas formed by laser focusing on a target, 25:27724
CONSTANTIN, M. J., Response of rice to γ-rays and fission neutrons, 25:27070
CONSTANTINIDES, M. G., Radioisotopes production program at the Nuclear Research Center Democritos, Athens, 25:28772
CONSTANTINIDIES, E., Observed redistribution of E-region ionization by neutral winds, 25:27516
CONWAY, B. E., H_2O--D_2O solvent isotope effects in volume and expansivity behavior of some organic and inorganic ions, 25:26259
COOGAN, Philip S., Relative sensitivity of various areas of the retina to laser radiation, 25:26940
COOK, P. A., Relativistic harmonic oscillators with intrinsic spin structure, 25:27973
COOK, William Jackson Jr., Fatty acids in an irradiated chicken product, 25:26647
COOKE, D., Collection efficiency of water droplets in AgCl aerosol, 25:26370 (CONF-700601-, pp 161-7)
COOLEY, James Louis, Effects of chronic irradiation and temperature on aquatic snail, 25:26915
COOPER, P. K., Repair following uv irradiation of E. coli, 25:27112
COOPERSTOCK, F. I., General-relativistic and Newtonian gravitational energy transfer, 25:28089
COPPERSMITH, W. Carlton, Reactor protection system diversity, 25:28697 (CENPD-11)
COPPEY, J., Radiobiological study of the formation of interferon in the kidney cells of monkeys infected with NDV, 25:27113
CORBEAN, Stela, Uranium determination in crop soils by neutron activation, 25:26197
CORBIN, J. C., Modified feedback control method applied to edge oscillations in Q machine, 25:27770
CORLEO, G., Reaction $^{40}Ar(d,p)^{41}Ar$ at deuteron energy below Coulomb barrier, 25:28251
CORNIDES, Istvan, Application of stable isotopes in medical and biological experiments, 25:26572
CORNWELL, R. L., Immunity to Dictyocaulus viviparus in calves. III, 25:26918
Immunity to Dictyocaulus viviparus in calves. II, 25:26919
CORONITI, F. V., Fast time-resolved spectral analysis of vlf banded emissions, 25:27621
CORTEGIANO, H., Isoracemization of N-carbobenzoxyamino acid ester derivatives, 25:26257
COSMAN, E. R., Analysis of elastic and inelastic analogue-state resonances using coupled optical equations, 25:28236
Particle-core structure in the spectra of the strontium nuclei, 25:28234
Resonance structure in the $^{88}Sr(p,p')$ octupole transition, 25:28240
COSTA, S., High-energy photoprotons from beryllium, 25:28194
COSTANTINI, V., Nonlinear effects in quantum electrodynamics, 25:28070
COSTA OLIVEIRA, Jaime M., Measurement of the kinetic parameters of the MINERVE reactor from analysis of the neutron fluctuations, 25:28755 (CEA-N-1406)
Measurement of the transfer function of a reactor by reactivity modulation, 25:28754 (CEA-N-1405)
COTEA, V., Beta radioactivity in some wines from Transylvania and Dobruja, 25:26618
COTEA, Victoria, Beta radioactivity in some wines from Transylvania and Dobruja, 25:26618
COTSAFTIS, M., Feedback stabilization of a Vlasov plasma, 25:27753
COTTEREAU, Marie-Joseph, Effect of vibrational excitation of N_2 molecules on frequency of e--N_2 elastic collisions in nitrogen plasma, 25:27711
COTTON, Joseph Bernard, Anodising Be, 25:27172
COTTS, R. M., Self-diffusion in molten Li, 25:26239
COULSON, L., Charged particle emission following pion capture in nuclei, 25:28178
COURTADE, Elpiniki Tsinga, Effects of unilateral and bilateral renal irradiation on parameters related to renal hypertension, 25:26652
COUSINS, C. S. G., Axial ratios of hexagonal metals, 25:27240
COUSSOT, Gerard, Electronic lattice structure by positron annihilation in insulators, 25:27865 (CEA-R-4138)
COVARRUBIAS, A., Factors determining introduction of nuclear power stations in developing countries, 25:28723
COVER, R. E., Isoracemization of N-carbobenzoxyamino acid ester derivatives, 25:26257
COWLS, R. S., Manned planetary missions with reusable nuclear shuttles, 25:28789
COX, A. F. J., Ion-implantation doping of zinc sulphide thin films, 25:27844
CRACIUN, T., Study of irradiation effects on mitosis in lucerne in R_0, R_1, and R_2, 25:26732
CRAFT, Harold Dumont Jr., Pulse profiles and dispersion measures of twelve pulsars, 25:27350
CRAGG, D. A., Evolution of pumping groups used on Rutherford Laboratory ^3He Refrigerator, 25:27664 (RHEL/R-208)
CRAIG, R. S., Magnetic and electrical characteristics of $REPd_2$ intermetallic compounds, 25:27870
CRAIG, Shirley S., Electron microscopic changes following canine cardiac allografts: the effects of irradiation, 25:26677
CRAMER, R., Irradiation of oncogenic viruses, 25:27111
CRANCON, J., On-line isotope separator device connected to Melusine reactor, 25:26551
CRANDELL, M. E., Optical properties of cr--mn and cr--v alloys, 25:27442

CRAVIOTO, Humberto, Acute effects of x-radiation on spinal cord motoneurons. A functional and ultrastructural study in the cat, 25:26941
CREPIN, Y., Myelo-retentive capacities and immunocompetence of bone marrow cells of the mouse cultivated in vitro, 25:26942
CRESPI GONZALEZ, Maria Alicia, St. Laurent des Eaux Power Reactor, 25:28534
CRISCUOLO, L., TIGER: program for the calculation of thermal cross sections in light-water nuclear reactor, 25:28802 (EUR-4554)
CROIZAT, H., Proliferative activity of stem cells in bone-marrow after irradiations, 25:26956
CROKE, E. J., Chicago air pollution systems analysis program, 25:28840 (ANL-ES-CC-8)
CROWLEY, Joseph M., Geometrical limitations in plasma feedback systems, 25:27754
CSAJKA, M., Retention of radionuclides on metal sulphide precipitates, 25:26199
CSATH, G., Determination of impurities in thorium and zirconium compounds by neutron activation analysis, 25:26192
CSIK, Jose Bela, Economic--finanical experience in Argentina with power reactor construction, 25:28573
CULBERT, H. V., Ferromagnetism of $ZrZn_2$, 25:27875
CULHANE, J. L., Solar flare iron line emission at 1.9 A, 25:27386
CULLEN, Thomas J., Cast permanent magnets of Co, Cu, and Ce: process and performance characteristics, 25:27184
CUNSOLO, A., Reaction $^{40}Ar(d,p)^{41}Ar$ at deuteron energy below Coulomb barrier, 25:28251
CUNY, Yvette, Interpretation of the solar continuum from 1680 to 600 A, 25:27370
CUSHING, Colbert E., Cycling of ^{65}Zn by Columbia River periphyton in a closed lotic microcosm, 25:26593
CUSSON, R. Y., EVALIN: CDC FORTRAN IV code to perform an extended variational approximation for light and intermediate nuclei, 25:28439 (AECL-3801)
CUTTS, Burton, Improvements in or relating to nuclear reactor fuel elements, 25:28837
CVRTILA, D., Some factors influencing uptake of ^{75}Se-selenomethionine by pancreatic tissues of the rat, 25:26591
CYR, Clifford R., Hydroformylation of 3-methyl-1-hexene-3-d_1. Evidence against direct formylation of a methyl group in the oxo reaction, 25:26228
CZAIKOWSKI, Peter-Michael, Properties of thermoluminescence detectors during irradiation with fast electrons, 25:26525
CZAPSKI, Gideon, Prog. rpt. on nature of oxygen containing radicals in radiation chemistry and photochemistry of aqueous solutions, 9/70--7/71, 25:26290 (NYO-3753-19)
CZECHOWSKY, P., Substorm influences on vhf continuous wave auroral backscatter, 25:27554
CZYZ, W., Scattering of composite particles at very high energy, 25:28073

D

DABEK-SZRENIAWSKA, Malgorzata, Effect of uv irradiation, merthiolate, and thymol on interferential properties of tick-borne encephalitis virus, 25:27102
D'ABREU, F. M. Marques, Organoleptic chemical and microbiological aspects of irradiated Portuguese sausages, 25:27159
DAEHNICK, W. W., Elastic scattering of ^{16}O by ^{46}Ti, ^{40}Ca, ^{27}Al, ^{12}C, ^{7}Li, and ^{6}Li, 25:28196
DAINTON, F. S., Radiation chemistry of low-temperature aqueous glasses. IV, 25:26310
DAKIN, James T., Experimental study of omega neutral decays, 25:27961 (PURC-4159-16)
DALKAROV, O. D., Possible quasinuclear nature of heavy mesonic resonances, 25:28026 (NP-18774)
DALLIMORE, P. J., Spectroscopic factors from $^{124}Sn(d,p)^{125}Sn$ above and below the Coulomb barrier, 25:28286 (ANU-P-511)
DALY, K. R., Effect of temperature on survival of γ-irradiated seeds of Arabidopsis thaliana, 25:27071
DALZIEL, R., ESRO I satellite observations of 1 to 30 MeV protons during the 25th Feb. 1969 solar event, 25:27561
Observations of 45 to 450 keV electrons during the period Feb. 24--Mar. 3, 1969, 25:27568
DAMERAU, W., ESR studies of x-irradiated single crystals of N-benzoylalanine, 25:26292
DAMKJAER, A., Compound-nucleus aspects of beta decays with high Q values, 25:28443 (CERN-70-30(Vol.1), pp 421-33)
DANA, M. Terry, Scavenging of soluble dye particles by rain, 25:26368 (CONF-700601-, pp 137-47)
D'ANDREA, A., Effective four-body interaction in light nuclei, 25:28482
D'ANGELO, F., Immunological modifications induced by radiotherapy, 25:26668
DANILYAN, G. V., Capture of neutrons by Rh, Ta, and Au, 25:28437
DANNENBERG, Arthur M. Jr., Radiation, infection, and macrophage function. IV. Effect of radiation on the proliferative abilities of mononuclear phagocytes in tuberculous lesions of rabbits, 25:27001
DANOS, M., Isospin impurities in the nuclear ground states, 25:28516
DANYUSHCHENKOV, I. A., Influence of structure and testing conditions on the mechanical properties of low-alloyed molybdenum, 25:27221
DARLE, Nils, Xenon-133 clearance and liver blood flow, 25:26576
DAS, H. A., Determination of lead in milk powder, 25:26203
Determination of sodium in ultrabasic rocks, 25:26204
DAS GUPTA, M. K., Centimeter and decimeter solar bursts in relation to S component of solar radio emission, 25:27364
Recurrence of 10.7-cm solar flux and of sunspot activity over 11-year solar cycle, 25:27362
DASH, J. G., Effects of lateral substrate fields on helium monolayers, 25:27634 (RLO-1388-604)
DASTIN, S., Advanced filamentry composites for primary aircraft structures, 25:27307
DAUGHERTY, J. D., HIPAC as a source of highly stripped heavy ions, 25:28128 (WASH-1159, pp 88-112)
DAVEY, W. G., ZPR-3 assemblies 48: 48A, and 48B: the study of a dilute plutonium-fueled assembly and its variants, 25:28752 (ANL-7759)
DAVEY, William Robert, Beta Cephei stars: analysis of radial oscillations, 25:27327
DAVIDESCU, D., Uranium in vine and wine, 25:26615
DAVIDESCU, V., Uranium in vine and wine, 25:26615
DAVIDSON, David Edward Jr., Effects of prior whole-body gamma irradiation on protein biosynthesis in rat liver, 25:27006
DAVIDSON, L. A., Analysis of ion implanted diamond, 25:27858
DAVIDSON, R. C., Heating of counterstreaming ion beams in an external magnetic field, 25:27672
DAVIDSON, W. F., Cross section of $^{25}Mg(tau,\gamma)^{28}Si$ reaction, 25:28206 (ANU-P-508)
Spectroscopic factors from $^{124}Sn(d,p)^{125}Sn$ above and below the Coulomb barrier, 25:28286 (ANU-P-511)
DAVIES, A. G., Determination of ^{137}Cs and ^{134}Cs in samples from the Windscale effluent treatment plant, 25:26177 (PG-Report-965)
DAVIES, J. A., Use of channeling-effect techniques to locate interstitial foreign atoms in silicon, 25:27857
DAVIES, J. V., Radiation studies of aryl glycosides. II, 25:26304
Radiation studies of aryl glycosides. III, 25:26305
DAVINI, V., Use of /sup 99m/Tc for cerebral scintigraphy, 25:26818
DAVIS, J. R., Resonances in $^{29}Si(p,\gamma)^{30}P$ reaction, 25:28207 (ANU-P-517)
DAVIS, T. Neil, Aspects of auroral morphology, 25:27550
DAVISON, J., Genetic effects of cumulative maternal irradiation on growth and age at sexual maturity in rats, 25:26965
DAWSON, J. M., Anomalous heating of plasma electrons, 25:27675
Heating of counterstreaming ion beams in an external magnetic field, 25:27672
DAY, P. R., Pathogenicity resulting from mutation at the b locus of Ustilago maydis, 25:27072
DAY, W. C., Project pre-Gondola II summary report, 25:26407 (PNE-1112)
DE, P. K., Stress corrosion cracking of Zr in methanol/hydrochloric acid solutions, 25:27173
DE AISENBERG, E. Y., Nuclear spectroscopy of iodine isotopes with a greater than or equal to 134, 25:28336 (CERN-70-30(Vol.2), pp 1057-68)
DEAN, J. M., Distribution of ingested ^{65}Zn in marine crustaceans, 25:26604
DEBENEDETTI, A., Effects of x rays and visible light on the reconstitution of the early potentials of the isolated frog eye, 25:27004
DE BENI, G. F., Some experimental results on the sorption of caesium by tungsten and graphite, 25:27201 (EUR-4549)
DEBERNARDI, M., Experimental determination of the turbulent diffusivity coefficient in a bundle of rods with and without spacer grids, 25:28819 (EUR-4552)
DEBERTIN, K., Relative measurements of activity with Ge(Li) detectors, 25:26191
DE BOER, F. W. N., Decay of some nuclei far from the stability line studied with standard spectroscopic techniques, 25:28322 (CERN-70-30(Vol.2), pp 939-47)
DE BORTOLI, M. C., Sampling of radioactive deposition through ion-exchange resins, 25:26559
DECKER, J. F., Dynamic stabilization of a two-stream instability, 25:27788
DEEHR, C. S., Relation of low-energy particle precipitation to luminous aurora, 25:27578
DE FERNANDEZ, M. Luisa H., Fruit pests in Bolivia, 25:27130 (CONF-680112-, pp 129-42)
DE GEER, L.-E., Experimental techniques for nuclear structure studies in the Tin-region at OSIRIS, 25:28107 (CERN-70-30(Vol.2), pp 1003-5)
Neutron hole states in the tin-region, 25:28329 (CERN-70-30(Vol.2), pp 1008-10)
DEGLI ANTONI, G., High-energy solar electrons, 25:27574
DE GRAAFF, W., X-ray observations between 1 and 55 A of the Feb. 25th flare, 25:27357
DEGROSSI, Oswaldo J., Thyroid tumour scanning with $^{197}HgCl_2$, 25:26823
DEHNHARD, D., Evidence for splitting of a bound isobaric analog state in ^{58}Co, 25:28228

DEHNHARDT, W., Lifetime measurements on neutron deficient even--even isotopes of Xe and Ba, 25:28319 (CERN-70-30(Vol.2), pp 905-10)
DE JAGER, C., High energy flare radiation, 25:27354
DE JONGE, S., Parity assignments of some ^{98}Mo resonances, 25:28402
DE KOCK, P. R., Configuration mixing and effective charges, 25:28245
DE KONING, J., Determination of sodium in ultrabasic rocks, 25:26204
DE LA CAMARA, Santiago Norena, Prestressed concrete pressure vessels for nuclear reactors, 25:28684
DELAND, Frank H., Patterns for differentiation of posterior fossa neoplasms as detected by brain scans, 25:26820
DE LANGE, J. C., Production and decay properties of some shortlived cobalt nuclei, 25:28214 (CERN-70-30(Vol.2), pp 1105-13)
DELANO, M. D., Dynamics of the rapid neutron capture process, 25:27310 (CERN-70-30(Vol.2), pp 735-57)
DE LA PENA-AUERBACH, L., Self-interaction corrections in a nonrelativistic stochastic theory of quantum mechanics, 25:27941
DELBARRE, F., Synoviothesis (synoviotherapy by radioisotopes) studies of more than 400 cases and future prospects, 25:26873
DE LEEUW, S., Improvements in use of ^{6}Li(n,α)t reaction for in-core neutron spectrum measurements, 25:28753 (BLG-450)
DE LEEUW-GIERTS, G., Improvements in use of ^{6}Li(n,α)t reaction for in-core neutron spectrum measurements, 25:28753 (BLG-450)
DELL'ANTONIO, G. F., Structure of the algebra associated to free fields, 25:28080
DEL MARMOL, P., Reassessment of some neutron yields from the longer-lived delayed neutron emitters, 25:28211 (CERN-70-30(Vol.1), pp 517-18)
DE LOTTO, I., Problems connected with the graphical interaction operator-computer, 25:28860 (LA-tr-71-28)
DEL VAL COB, J. L., Electronic instrumentation and control of the Jose Cabrera power reactor, 25:28535
DE MAEYER, E., Production of circulating rat interferon in mice--rat radiochimeras, 25:26995
DE MAEYER-GUIGNARD, J., Production of circulating rat interferon in mice--rat radiochimeras, 25:26995
DE MARIA, D., Scintigraphy of carcinoma using $^{197}HgCl_2$, 25:26832
DEMIN, A. G., Investigation of α decay of isotopes of element 105, 25:28350 (KFK-tr-350)
DEMIN, V. E., Determining portion of fission attributable to epithermal neutrons, 25:28817
DEMIRKHANOV, R. A., Distribution of a pulsed current in a cylindrical conductor of variable conductivity, 25:27721
DEMOISE, Charles F., Immunohematological studies of Marshall Islanders sixteen years after fallout radiation exposure, 25:27058
DENAVIT, J., Longitudinal oscillations of Lorentzian electron gas, 25:27822
DENEGRI, D., Coherent K-d interactions at 12.6 GeV/c, 25:27967
DENENBERG, Victor H., Conference on post-natal development of phenotype, Liblice, Czech., 9/67, 25:26696
DENIG, R., Some studies on neutron-rich nuclei, 25:28326 (CERN-70-30(Vol.2), pp 985-1000)
DERIAN, L., Radiation experiment on a model of a finned tubular fuel element. I, 25:27267 (UJV-2371.R,T.)
DESAI, Puloma A., Induced mutations in Triticum durum, 25:26710
DE SALAS, G. N. B., Thin layer chromatography of various radiopharmaceuticals, 25:26179 (CNEA-285)
DESANDRE-NAVARRE, Christian, Neutron collimator, 25:28153
DESER, S., Statistical physics, phase transitions, and superfluidity. II, 25:27912
DESHPANDE, Narayan V., Neutral stability of an incompressible magnetohydrodynamic half-jet at low Reynolds number, 25:27486
DESILVA, A. W., Plasma diagnostics by light scattering, 25:27680
DE SOUZA SANTOS, Tharcisio D., Reduction of powdered U_3O_8 by liquid Al, 25:27284
DE SOUZA SANTOS, Tharcisio Damy, Thermal cycling test for plates containing dispersions, 25:27251
DETCH, J. L. Jr., Proton--proton elastic scattering from 9.6 to 13.6 MeV, 25:27957
DETCH, J. Lewis Jr., Accurate cross-section measurements of reactions T(p,p)T, T(p,d)D, T(p,^{3}He)N, and T(p,p')T at 13.600 MeV, 25:28164 (LA-4576)
DE TOLLIS, B., Nonlinear effects in quantum electrodynamics, 25:28070
DETRAZ, C., Angular momentum transfer in $^{18}O(^{3}He,t)^{18}F$, 25:28173
Isospin purity at high excitation energies, 25:28190
DEUBLEIN, D., Experiences at KWL with steam producing up to first fuel element replacement, 25:28585
DEUTSCH, R. W., Experimental and theoretical investigation of nuclear fission induced by low-energy nuclear particles. Progress report, 25:28355 (TID-25659)
DEUTSCHMANN, M., S-wave interference in the f^0 resonance region, 25:28018
DEVDARIANI, A. Z., Cross section for excitation of the Cs II resonance lines in the Cs^+ + He process near the threshold, 25:27454
DEVILLERS, Christian, ANISN system: description and service instructions for ANISN discrete ordinate program and subroutines, 25:28149 (ORNL-tr-2419)
DE VILLIERS, P. D., Radiation dose with the orthometric view in x-ray pelvimetry, 25:26831
DEVLIN, T. J., Automatic target cycling system for total cross section measurements, 25:28115 (PURC-4159-17)
DEVRIES, R. M., Decay of ^{110}Sb, ^{111}Sb, ^{112}Sb, ^{113}Sb, and ^{114}Sb, 25:28332 (CERN-70-30(Vol.2), pp 1015-21)
DEWAN, Edmond M., Dynamic stabilization of plasma instabilities, 25:27777
DEWEY, W. C., Chromosomal aberrations and mortality of x-irradiated mammalian cells: emphasis on repair, 25:26723
D'EYE, Royston Walter Mastin, Improvements in or relating to nuclear reactor fuel elements, 25:28837
DE YOUNG, D. S., Two-dimensional simulation of flare-associated disturbances in the solar wind, 25:27629
DEZAFRA, Robert L., Measurement of lifetime and g factors in the OH and OD free radicals, 25:26243
DHAR, D. N., Effect of irradiation on larvae of nematode, 25:26909
DHARKAR, S. D., Effect of gamma irradiation on postharvest physiology of five banana varieties grown in India, 25:27165
DIAMOND, S. A., Rotation of a glow discharge in a homopolar device, 25:27701
DIBAI, E. A., Observations of comet-shaped nebulae and globules, 25:27337
DI CHIARA, F., Personnel dosimetry with ^{7}LiF Teflon discs, 25:26527
DICKEY, J. M., Leed studies of Ar crystals on Nb (100) surface, 25:27235
DIEHL, Richard Curtis, Stripping and pickup reactions between masses 90 and 120, 25:28374
DIENSTBIER, Z., Biochemical changes in serum of intact and irradiated dogs after intravenous AET administration, 25:26935
DI LELLA, V., Immunological modifications induced by radiotherapy, 25:26668
DILWORTH, C., High-energy solar electrons, 25:27574
DI MENZA, R., Small low-temperature organic-cooled and moderated reactors to be coupled to desalination plant, 25:28792
DIMIC, V., Report on research programs at the reactor TRIGA Mark II at the Inst. Jozef Stefan, Ljubljana, 25:28778
DIN, G. U., Resonances in $^{29}Si(p,\gamma)^{30}P$ reaction, 25:28207 (ANU-P-517)
DING, A., Secondary rainbows and interference in elastic scattering of H^+ by Ar, 25:27458
DINGLE, A. Nelson, Scavenging of tracer in severe storms, 25:26361 (CONF-700601-, pp 21-35)
DI TORO, M., Reaction $^{40}Ar(d,p)^{41}Ar$ at deuteron energy below Coulomb barrier, 25:28251
DITTO, S. J., Use of actuators as logic elements in relation to fail-safe design, 25:28741
DJORDJEVIC, Bozidar, Changes in biological effectiveness of a fast neutron beam with depth in tissue-equivalent material, 25:26906
DNESTROVSKII, Yu. N., Velocity distribution of rapid ions with superthermal velocity in a nonisothermal plasma, 25:27722
DOBBING, John, Vulnerability of developing brain: I. Some lasting effects of x-irradiation, 25:26946
DOBROWOLNY, M., Dynamic stabilization of drift waves in a collisionless plasma by ac electric fields, 25:27779
DOBRY, H., Problem of automatic dose planning, 25:26761
DOBSON, Ernest L., Proliferative and phagocytic capacity of the reticuloendothelial system of sublethally irradiated mice, 25:26947
DODD, N. J. F., Osmunda regalis. II, 25:27069
DOHERTY, A. E., Explosive welding of tubular components, 25:27186
DOHERTY, J. E., Internal friction studies in some titanium and zirconium based alloys, 25:27215
DOI, Akira, Fission-gas release from nuclear fuels with in-pile gas-loop, 25:28821
DOI, Yoshikuni, Liquid hydrogen target utilizing a small mechanical refrigerator, 25:28138
DOLINSKII, E. I., Peripheral model for nuclear reactions, 25:28498
DOLLFUS, M.-A., Ocular occupational accidents caused by ionizing radiation, 25:26783
DOMBERG, H., Pneumatic system for activation analysis with short-lived radionuclides, 25:26189 (KFK-1293)
DOMON, Masaharu, Effects of ultraviolet light on mouse L cells, 25:26989
DONALDSON, W., Angular structure of quasar 3C 147, 25:27351
ESRO I satellite observations of 1 to 30 MeV protons during the 25th Feb. 1969 solar event, 25:27561
DONATI, D. R., Adaptation of gamma-ray spectral analysis program for PDP-9 computer, 25:26500
DONATI, Donald R., Techniques for compiling large FORTRAN programs for a PDP-9 computer, 25:26555
DONATI, E., Appearance of skin haemangioma 15 years after radiation lesion, 25:27049
DONATI, Robert M., Combined surgical and radiation injury. IV. Effect of antimicrobials on the wound healing pattern of the x-irradiated rat, 25:26932
DONNELLY, Warren H., Bushwhacking, licensure, and Senator

XUM

Bartlett, 25:26787
DONOGHUE, T. R., States in ^{17}O via neutron-polarization measurements in $^{13}C(\alpha,n)^{16}O$ reaction, 25:28202
DONOHUE, J. T., Pure states, polarized targets, and baryon spin determination, 25:28040
DONTA, Sam, Lack of polarity of DNA injection by Escherichia coli phage lambda, 25:26692
DOO, V. Y., Corrosion and passivation of thin molybdenum films, 25:27171
DOOSE, C., Cold neutron source in Juelich, 25:28767
DORE, M. A., Gamma radiation characteristics of plutonium dioxide fuel, 25:27305 (N-70-35897)
DORENBUSCH, W. E., L = 0 transitions to 0^+ states of N = 29 nuclei, 25:28229
DORENBUSCH, William E., Intermediate-coupling and additional excitation modes, 25:28518
DOROSHKEVICH, A. G., Mixmaster universes and the cosmological problem, 25:27428
DORY, R. A., Feedback control of Kruskal--Shafranov modes, 25:27762
DOSCHERHOLMEN, Alfred, Chronic myelogenous leukemia in Hodgkin's disease: immunofluorescence of cells, 25:26964
DOSKOCILOVA, D., Structure of chlorinated poly(vinyl chloride). I. Determination of the mechanism of chlorination from infrared and NMR spectra, 25:26246
DOSSETT, J. S., 1000-MWe LMFBR accident analysis and safety system design study. Candidate primary containment safety features. Topical report, 25:28733 (BAW-1352)
DOST, M., A comparison of analogue resonance studies and coulombstripping in ^{208}Pb, 25:26366
DOSTAL, M., Acute toxic and radioprotective effects of cystamine combined with either AET or serotonine, 25:26793
DOUGHTY, William E., Acute radiation injury in neonatally thymectomized germ-free mice. Hematopoietic and morphologic consequences, 25:26937
DOUIS, M., Presentation of shielding materials, 25:26776
DOUSSET, M., Notes on safety norms, 25:26764
DOVBENKO, A. G., Optimum parameters of ^{238}U neutron optical potential, 25:28403
DRAGT, Alex J., Solar-cycle modulation of the radiation-belt proton flux, 25:27624
DRAKE, R. L., Processes influencing evolution of droplet or aerosol spectrum, 25:26385 (CONF-700601-, pp 385-402)
DRAPER, Lawrence R., Graft-versus-host reaction modified by in vitro preincubation of marrow with subcellular antigen, 25:26662
DREISSIGACKER, H-L., Expected development of methods for enriching uranium in Europe, 25:26424 (CONF-700557-3)
DREMIN, A. N., Reaction of oxides of rare earth elements with boron during shock compression, 25:27291
DREMOV, V. V., MHD-rotation of conducting fluid in cylindrical vessel, 25:27500
DRESSER, D. W., Preparation of radioactive bovine anti-mouse lymphocyte antibody, 25:26667
DRESSLER, G., Materials for the nuclear reactor technology, 25:27213
DRESSLER, John L., Videotype sampling in the feedback stabilization of electromechanical equilibria, 25:27761
DRIEDGER, A. A., Cell survival and x-ray-induced DNA degradation in Micrococcus radiodurans, 25:26627
DRIVER, C., Electroproduction of single π^+ mesons on hydrogen, 25:27950 (DESY-71/9)
DROBYSHEV, V. N., Reaction of oxides of rare earth elements with boron during shock compression, 25:27291
DROSCHA, H., Particle accelerator vacuum chambers in aluminum oxide ceramics, 25:28131
DRUIN, V. A., Investigation of α decay of isotopes of element 105, 25:28350 (KFK-tr-350)
DRUMMOND, J. L., Reaction of PTFE with liquid sodium, potassium, and NaK alloy, 25:26211 (TRG-Report-2104)
DUBININ, N. P., Mechanism of ring chromosome formation and somatic crossing-over, 25:26721
Modification of the chemical and radiative mutagenesis and metabolism, 25:26733
DUBININA, L. G., Modification of the chemical and radiative mutagenesis and metabolism, 25:26733
DUBOIS, Q. B., 1000-MWe LMFBR accident analysis and safety system design study. Topical report. candidate secondary containment support systems, 25:28730 (BAW-1349)
DUCKWORTH, J. P., Prog. rpt., 10--12/70, 25:26355 (SRO-344-11)
DUDA, F., Analyzer of $\gamma\gamma$ coincidences with semiconductor detectors, 25:26504
DUDOK, E. P., Effect of gibberelline on growth of chlorophyll in germs, 25:27064
DUDOVA, I., Sign of astatine ion charge in $HClO_4$--$H_2Cr_2O_7$ solutions, 25:26209 (JINR-P12-5644)
DUFFAR, M., Significance of scattering in calibrating apparatus for the measurement of fluences and neutron dose equivalents, 25:26483
DUFFY, Dick, Marine manganese nodules studied using nuclear reactor, 25:28764
DUFRESNE, Jacques, Fuel element replacement apparatus for use in conjunction with a vertical-channel nuclear reactor, 25:28825
DUGAN, V. L., Kinetic analysis of spore inactivation in a composite heat and gamma radiation environment, 25:27101
DUHM, H. H., Angular momentum transfer in $^{18}O(^3He,t)^{18}F$, 25:28173
DUJOVNE, Carlos A., Changes in liver and spleen scans of patients during treatment with two hypolipidemic drugs, 25:26830
DUKE, C. L., Compound-nucleus aspects of beta decays with high Q values, 25:28443 (CERN-70-30(Vol.1), pp 421-33)
DULFER, G. H., Decay studies of neutron deficient Ga and Zn isotopes, 25:28338 (CERN-70-30(Vol.2), pp 1075-9)
DUM, Christain Thomas, Nonlinear Landau damping and beat wave trapping, 25:27824
DUMAN, E. L., Exchange interaction of multi-electron atoms, 25:27444
DUNLAP, B. D., Magnetic behavior of conducting Am systems, 25:27922
DUNN, A. R., Determination of solar Doppler widths by Goldberg's method, 25:27367
DUNN, Adrian, Interference of tissue solubilizers with liquid scintillation counting fluors, 25:26463
DURAND, Alain, Coulomb scattering of high energy particles by a cylindrical block, 25:27987
DURCANSKY, Georg, Dislocation structure of a Ni single crystal with magnetic small-angle scattering of neutrons, 25:27246 (JUL-675-FF)
DUTCZAK, Krzysztof, Studies on the effect of constant magnetic field on tobacco mosaic virus synthesis in tobacco leaves, 25:27106
DUTILH, C. E., Determination of lead in milk powder, 25:26203
DUTTA, A. K., Relation between nuclear binding and excitation energies, 25:28515
DUTTA, S. M., Induction of mutation in Streptococcus diacetilactis by nitrosoguanidine and ultraviolet irradiation, 25:27121
DUTTON, D. M., Wide latitude processing of Tri-X-Ortho oscillographic film, 25:28854 (EGG-1183-1465)
DWIGHT, A. E., Alloy chemistry of thorium, uranium, and plutonium compounds, 25:27263
DWIGHT, K., Magnetic properties of europium: pressure and impurity effects, 25:27874
DWURAZNY, Antoni, Spark chambers in high-energy physics. II, 25:26514
DYER, F. F., Labeling of copper wire with /sup 110m/Ag for subsequent identification, 25:26322
DYER, P., Inelastic proton decay of the g/sub 9/2/ analogue resonance in ^{209}Bi, 25:28367
DYUMIN, N. E., Dispersion of first sound in superfluid ^3He--^4He solutions due to damping of the normal component, 25:27640
DZHELEPOV, B. S., Decay of ^{169}Lu, 25:28436
Decay of ^{66}Ge, 25:28272
Excitation of ^{169}Tm levels, 25:28432
DZHIKAEV, Yu. K., Macroscopic electrodynamics and thermal effects in the superconductor intermediate state, 25:27647
DZUBAY, T. G., Evidence for splitting of a bound isobaric analog state in ^{58}Co, 25:28228
DZYUBA, B. M., Wave function and bound energy of nuclei $^3H(^3He)$ taking into account tensor interaction of nucleons, 25:28162 (IAE-2000)

E

EARLY, Ann M., NAL 1970 archaeological survey, 25:28862 (NAL-55)
EASLEY, James D., Analysis of the treatment of Stage I and Stage II carcinomas of the uterine cervix, 25:26893
EASTERDAY, R. J., Correction of inspection data for part misalignment utilizing a small computer, 25:28908 (Y-1755)
EASTERLY D. G., Development of ion exchange processes for the removal of radionuclides from milk, 25:26335 (RO/EERL-71-1)
EASTMAN, D. E., Intrinsic metallic character of rare-earth pnictides, 25:27879
Photoemission studies of rare-earth and uranium compounds, 25:27876
EBERLE, Helen, Effect of nalidixic acid on semiconservative replication and repair synthesis after ultraviolet irradiation in Escherichia coli, 25:27125
EBERT, M., Osmunda regalis. II, 25:27069
ECCLES, D., Longitudinal variation of midlatitude ionosphere produced by neutral-air winds. II, 25:27508
Longitudinal variations of midlatitude ionosphere produced by neutral-air winds. I, 25:27507
ECK, John S., Resolution of phase-equivalent discrete ambiguities in optical-model analysis of ^{16}O + ^{16}O, 25:28197
ECKARD, Royce D., Analog-to-digital converter to digitize voltage transients, 25:28903 (UCRL-73103)
ECKELMAN, W. C., Evaluation of /sup 99m/Tc-DTPA prepared by three different methods, 25:26840
ECKER, B., Ion acceleration with high ν/γ electron beams, 25:27696 (WASH-1159, pp 204-18)
ECKER, G., Lorentz-covariant Lagrangians and causality, 25:28068
ECKERT, Hans G., Reactivity measurements using the continuous run technique, 25:28799 (CEA-N-1385)
ECKSTEIN, R. R., Method and device used for the safe

handling and storing of fragile x-ray diffraction specimens, 25:26449 (MLM-1790)
EDDY, N. W., Gamma rays in coincidence with K x rays of Cs and Ba fission products of ^{252}Cf, 25:28416
EDEN, R. J., Asymptotic properties of scattering amplitudes and their experimental consequences, 25:28100
EDGINGTON, David N., Concentration of radium, thorium, and uranium by tropical marine algae, 25:26597
EDLAND, Robert W., Glioblastoma multiforme. An analysis of the results of postoperative radiotherapy alone versus radiotherapy and concomitant 5-fluorouracil, 25:26689
EDMAN, R., Demand of uranium enrichment services for Sweden's nuclear power program, 1975--1985, 25:26395 (CONF-700903-15)
EDWARDS, M. I., Quality control, inspection, and testing of Series I metallurgical fuels for first charge of Dragon reactor, 25:26438 (DP-Report-432)
EDWARDS, R. A., Physiology of disks of irradiated tomato fruit. I, 25:27067
EFIMOV, I. A., Capture of neutrons by Rh, Ta, and Au, 25:28437
EFREMOV, A. V., Lie fields, 25:28081
EFROS, V. D., Wave function and bound energy of nuclei ^{3}H(^{3}He) taking into account tensor interaction of nucleons, 25:28162 (IAE-2000)
EGAMI, T., Domain walls in ferromagnetic Dy and Tb, 25:27873
EGGEN, O. J., Narrow- and broad-band photometry of red stars. VI, 25:27317
EHLERMANN, D., Radiation preservation of fish. I, 25:27146
Radiation preservation of fish. II, 25:27148
Radiation preservation of fish. III, 25:27147
EHRET, R., Pneumatic system for activation analysis with short-lived radionuclides, 25:26189 (KFK-1293)
EHRICKE, Krafft A., Perspective and systems engineering of manned planetary flight, 25:28787
EHRLICH, Margarete, Photographic dosimetry and x- and gamma rays, 25:26532
EIDENS, J., Identification of μ s isomers among primary fission fragments, 25:28325 (CERN-70-30(Vol.2), pp 967-84)
EILAND, H. M., Neutron cross sections and strength functions of ^{147}Sm and ^{150}Sm, 25:28349 (KAPL-P-3930)
EINSTEIN, F. W. B., Crystal and molecular structure and vibrational spectrum of the vanadium(V) oxide trinitrate--acetonitrile complex, $VO(NO_3)_3.CH_3CN$, 25:26235
EISEN, F. H., Annealing of damage in ion implanted gallium arsenide, 25:27862
Annealing of damage produced by boron ion implantation of silicon single crystals, 25:27863
Flux and fluence dependence of disorder produced during implantation of ^{11}B in Si, 25:27864
EISENHARDT, William, Photochemical transformations of small-ring carbonyl compounds. XXVIII. 1,5-hydrogen transfer in the photochemistry of aroylaziridines, 25:26250
EISENTRAUT, Kent J., Method of separating the rare earths by fractional co-distillation of their volatile chelate derivatives, 25:26336
EISMONT, O. A., Motion of alternate layers of conducting liquid and nonconducting gas in a transverse magnetic field, 25:27494
EISNER, J. H., Importance and technique of fast breeder reactors, 25:28651
EJIRI, H., Isobaric analogue resonant (p,γ) reactions on ^{92}Mo, 25:28359
EKSTROEM, C., Atomic-beam measurements in the rare-earth region, 25:28298 (CERN-70-30(Vol.1), pp 387-94)
EKSTROM, M. P., Numerical image restoration, 25:28902 (UCRL-73080)
EKWALL, Per, Fuel assemblies for nuclear reactors, 25:28695
EL-ASSALY, F. M., Levels of ^{137}Cs in man in U.A.R. during year 1970, 25:26740 (NP-18728)
ELAYATHU, N. S. D., Developments in oxidation and corrosion resistant materials, 25:27176 (INIS-mf-9)
ELBEK, Bent, Some new aspects of deformed nuclei, 25:28317 (CERN-70-30(Vol.2), pp 829-45)
EL-BISI, H. M., Effects of radiation pasteurization on Salmonella. II, 25:27164
EL-GARHY, M., Review of research activities using the UA-RR-1, 25:28777
EL GAVKHARI, A., Polarization during photoproduction of electron--positron pairs, 25:27996
ELIOFF, T., Bevatron external proton beam facilities, 25:28119 (UCRL-20194)
ELIZAROV, O. I., Analyzer of $\gamma\gamma$ coincidences with semiconductor detectors, 25:26504
EL KADY, Ahmed, Marine manganese nodules studied using nuclear reactor, 25:28764
ELKIND, M. M., Response of stem cells to 14 MeV neutrons, 25:26958
ELLETT, W. H., Absorbed fractions for small volumes containing photon-emitting radioactivity, 25:26752
ELLIS, A. E., 9/2-[514] state in ^{185}Re, 25:28287 (ANU-P-518)
ELLIS, J. L., Isobaric analog states for neutron spectroscopic factors, 25:28474
Polarization measurements for ^{88}Sr(p,p)^{88}Sr near isobaric analog resonances, 25:28238
Polarization measurements for ^{92}Zr(p,p)^{92}Zr near isobaric analog resonances, 25:28368
ELLIS, R. F., Measurement of drift-wave potential oscillations in the presence of temperature oscillations, 25:27809
ELLSAESSER, Hugh W., Air pollution: our ecological alarm and blessing in disguise, 25:28901 (UCRL-73063)
ELO, D., External heavy ion source for Berkeley 88-inch cyclotron, 25:28120 (UCRL-20406)
EL-RAEY, Mohamed, Eclipse measurements near 1.2 cm wavelength on Sept. 11, 1969, 25:27379
ELSAESSER, Klaus, Time-asymptotic perturbation theory in weak plasma turbulence. I, 25:27810
Time-asymptotic perturbation theory in weak plasma turbulence. II, 25:27811
EL-SHANSHOURY, I., Review of research activities using the UA-RR-1, 25:28777
ELTON, R. C., Atomic processes, 25:27705
ELYAPERUMAL, E., Stress corrosion cracking of Zr in methanol/hydrochloric acid solutions, 25:27173
EMEL'YANOV, I. Ya., Fast response control of reactor power on basis of γ radiation intensity, 25:28822
Monitoring of power distribution in nuclear reactor cores, 25:28699
EMERY, E. W., Interpretation of brain scans by computer analysis, 25:26824
EMMETT, M. B., Application of DOT--MORSE coupling to the analysis of three-dimensional SNAP shielding problems, 25:28784 (ORNL-TM-3365)
EMRICH, Dieter, Diagnosis of organ function in nuclear medicine, 25:26829
ENDOW, J. S., Critical evaluation of /sup 99m/Tc--Fe--ascorbic acid complex as a renal scanning agent, 25:26848
ENDRISS, M., Spectator particles and resonances, 25:28365
ENDT, P. M., Gamma-ray transitions in light nuclei, 25:28224
ENGE, H. A., Analysis of elastic and inelastic analogue-state resonances using coupled optical equations, 25:28236
ENGEL, A. R., Solar particle event of Feb. 25, 1969, 25:27560
ENGEL, Niels N., Alloy phase stability criteria, 25:27261
ENGELKE, Ray, Development of the WKB approximation by use of transformations, 25:27938
ENGELMANN, Ch., Determination of C in high-purity Si, 25:26202
ENGELMANN, J., Spectra and time history of protons in interplanetary space, Feb. 25--28, 1969, 25:27558
ENGELMANN, Peter, Investigation of neutron physics of steam-cooled fast reactors at SNEAK, 25:28659
ENGELMANN, Rudolf J., Priorities in scavenging research, 25:26359 (CONF-700601-, pp 6-10)
Scavenging prediction using ratios of concentrations in air and precipitation, 25:26391 (CONF-700601-, pp 475-85)
ENGLAND, J. B. A., Manufacturing process for silicon surface barrier radiation detectors, 25:26456 (ANU-P-516)
Particle identification using ORTEC 423 identifier, 25:26490 (ANU-P-514)
ENGLARO, G. C., Personnel dosimetry with ^{7}LiF Teflon discs, 25:26527
ENINGER, J. E., HIPAC as a source of highly stripped heavy ions, 25:28128 (WASH-1159, pp 88-112)
ENOCH, Jay M., Retinal cone receptor as an ideal light collector, 25:28850 (COO-1701-16)
ENTREKIN, J. L., Follow-on test on project firescan as an RTG heat source search and detection system, 25:26428 (SC-DR-710095)
ENWALL, E., Crystal and molecular structure and vibrational spectrum of the vanadium(V) oxide trinitrate--acetonitrile complex, $VO(NO_3)_3.CH_3CN$, 25:26235
EPLER, E. P., Use of actuators as logic elements in relation to fail-safe design, 25:28741
EPPLEY, R. E., Straightforward elucidation of complex shell-model states by β decay of nuclei far from stability, 25:28299 (CERN-70-30(Vol.1), pp 435-46)
EPSTEIN, B., Compactness by bounded L/sub p/-variation, 25:28890 (SC-RR-70-852)
ERDAL, B. R., Isomerism in odd and odd--odd nuclei with mass number 185 less than or equal to A less than or equal to 191, 25:28335 (CERN-70-30(Vol.2), pp 1045-55)
Properties of low-lying levels in even Pt and Os nuclei, 25:28334 (CERN-70-30(Vol.2), pp 1031-43)
ERKELENZ, K., One boson exchange potential and nuclear matter properties, 25:28448 (CERN-70-30(Vol.2), pp 1133-5)
ERKO, V. F., Excitation functions of He I spectral lines, 25:27463
ERMAKOV, A. I., Investigation of low-frequency plasma oscillations by means of amplitude modulation of microwave radiation, 25:27816
ERNST, H., Radiotherapy of vocal-cord leukoplakia, 25:26868
ERRAMUSPE, H. J., Fabrication of semiconductor detectors of Si(Li) for nuclear reactions, 25:26457 (CNEA-287)
ERSHOV, Yu. I., Role of energy dependence in problems of transport theory, 25:28159
ERU, I. I., Uhf methods for investigation of the dynamic

characteristics of thin superconducting films, 25:27652
ESEL'SON, B. N., Normal component density of ^3He--^4He solution at temperatures down to 0.4°K, 25:27639
ESIN, S. K., Azimuthal asymmetry of magnetic field strength of Erevan synchrotron electromagnet, 25:28139
ESSENBERG, Margaret K., Studies on the mechanism of hydrogen transfer in the coenzyme B_{12} dependent dioldohydrase reaction. II, 25:26225
ESTERL, John E., Isospin purity and delayed-proton decay: ^{17}Ne and ^{33}Ar, 25:28195
ESTON DE ESTON, Tede, Conference on biological effects of radiations, Sao Paulo, 10/69, 25:27036 (CONF-691057)
ESTRADA A., Raul, Uses of radioisotopes in agriculture in Ecuador, 25:27134 (CONF-680112-, pp 245-6)
ETOURNEAU, Jean, Crystal structure of the boron--thorium system. A new boride with type YB_{66} structure, 25:27301
ETTEMEYER, R., Special features of measurements and control for nuclear power stations compared with conventional plants, 25:28675
EVANGELISTI, F., OSO-G satellite instrumentation for measurements of cosmic x-rays in energy range from 25 to 190 keV, 25:26478
EVANS, D., Analysis of the reaction $\pi^+p \rightarrow rho^0\Delta^{++}$ at 11.7 GeV/c incident momentum, 25:27960 (DESY-71/8)
EVANS, J. H., Analysis of the New Brunswick Laboratory Sample Cask, 25:26450 (ORNL-TM-3298)
EVANS, M., 9/2-[514] state in ^{185}Re, 25:28287 (ANU-P-518)
EVANS, R. E., Absorption of hf radio waves reflected at oblique incidence from the ionosphere in winter, 25:27595
EVANS, R. M., [Recent research on] metals joining, 25:27193
EVANS, Richard G., Changes in biological effectiveness of a fast neutron beam with depth in tissue-equivalent material, 25:26906
EVERLING, F., Aluminum-25 levels from the $^{24}Mg(p,\gamma)^{25}Al$ reaction, 25:28276
EVIASHINA, L. M., Disturbances in ionosphere F region during red aurora of type A, 25:27511
EVLASHIN, L. S., Disturbances in ionosphere F region during red aurora of type A, 25:27511
EVWARAYE, Andrew Oteku, Angular distribution of photoneutrons from deuterium, 25:28165

F

FABERGE, Alexander C., Polyvinyl chloride impressions for indirect carbon replicas in electronic microscopy, 25:28858 (LA-tr-71-25)
FACCHINI, U., Mechanism of fission of heavy nuclei, 25:28504
FADIN, V. S., Pair production in collisions of high-energy charged particles, 25:27997
FAESSLER, A., Fluorescence excitation of ultra-soft x-ray emission spectra using synchrotron radiation, 25:27827 (DESY-70/59)
FAGER, J. E., Preliminary processing of multiplexed two-parameter gamma-spectrometer data, 25:26501
FAIRBANKS, Norman P., Method for producing stoichiometric uranium dioxide compositions, 25:27274
FAIRHALL, A. W., Radiocarbon in the sea, 25:26398 (RLO-2225-T-20-2)
FALCOZ, Claude, Precipitation of Pu C_2O_4, 25:26345
FAL'KO, I. I., Investigation of the superconducting state of niobium--titanium solid solutions, 25:27646
FAL'KOVSKII, L. A., Damping of magnetic surface levels in superconductors, 25:27653
FALLIEROS, S., E1 transitions from analog states in ^{90}Zr, 25:28360
FALTENS, Andris, Non-intercepting monitor of beam current and position, 25:28117 (UCRL-20166)
FANELLI, A., Radiographic and scintigraphic methods for the study of hydatids of the kidneys, 25:26816
FARAFONOV, G. W., Regeneration of cell populations of intestinal epithelium after irradiation, 25:27033
FARAG, Mohammed K., Storage temperature effects on the proteolytic activity of radiation-surviving bacteria in oysters, 25:27114
FARFALETTI-CASALI, Flavieno, Fuel element replacement apparatus for use in conjunction with a vertical-channel nuclear reactor, 25:28825
FARKAS, Jozsef, Effect of ionizing radiation on the keeping quality of sliced pork, 25:27136 (NP-tr-1932)
FARRELL, H. H., Leed studies of Ar crystals on Nb (100) surface, 25:27235
FARRER, Donald N., Decrements in the visual acuity of rhesus monkeys (Macaca mulatta) as a delayed effect of occipital cortex irradiation, 25:26991
FAUCITANO, Antonio, Intermolecular and intramolecular free valence transfer in gamma irradiated crystalline hexadecanoic and cis-9-octadecenoic acids, 25:26312
FAUCITANO MARTINOTTI, Fausta, Intermolecular and intramolecular free valence transfer in gamma irradiated crystalline hexadecanoic and cis-9-octadecenoic acids, 25:26312
FAVRET, Ewald A., Uses of ionizing radiations in the genetics of vegetable plants, 25:26686 (CONF-680112-, pp 95-111)
FAY, G., Phenomenological foundation of quantum logic, 25:27949
FAYEK, Mohamed Khorshid, Magnetic structure of a manganese-substituted zinc ferrite by neutron diffraction, 25:28857 (INR-1269)
FAZZINI, P. F., Effect of ionizing radiation on the heart, 25:26961
FEATES, F. S., Surface complexes formed by thermal and radiolytic adsorption of gases on graphite, 25:26286
FEDDER, Joel A., Comparison of kinetic and hydrodynamic models of an expanding ion exosphere, 25:27613
FEDOR, L. S., Interpretation of ionospheric radio drift measurements. III, 25:27596
FEDOROVA, T. A., Influence of irradiation on the urinary excretion of deoxycytidine and beta-aminoisobutyric acid in monkeys, 25:26999
FEDOTOV, S. I., Nonrotational states of odd-N deformed nuclei in region 153 less than or equal to A less than or equal to 171, 25:28346 (JINR-E4-5567)
FEDRO, A. J., Magnetic properties of the system Au_4R(R = Er, Tm, and Yb), 25:27872
FEIL, J., Reactor physics design technique for burnable poison and enrichment-zoned cores, 25:28663
FEINSTEIN, Richard B., X-ray beam profiles and oral radiography, 25:26817
FEIZ, Iraj, Deuterium isotope study of electrogenerative hydrogenation. Mechanism of hydrogenation of ethylene at positive potentials, 25:26230
FEJES, I., Expanding neutral hydrogen in Virgo, 25:27352
FELDBERG, Stephen, Thorium fluoride complexes. Determination of the stability constants using the fluoride ion activity electrode, 25:26268
FELDMAN, Isaac, Uranyl ion-adenine nucleotides complexes, 25:26271
FELDSHTEIN, Ya. I., Auroral oval planetary energetics, 25:27523
FENDLER, J. H., Pulse radiolytic investigations of hydroxy-radical reactivities in micellar solutions, 25:26295
FENYES, T., Nuclear spectroscopy of some light Tl isotopes, 25:28339 (CERN-70-30(Vol.2), pp 1081-91)
FEOKTISTOV, A. I., Positron decay in ^{190}Au and ^{188}Ir, 25:28392
FEOLA, J. M., RBE of negative pions in 2-day-old ascites tumors, 25:26938
FERGUSON, D. F., Tsuruga: triumph of teamwork, 25:28542
FERGUSON, S. M., Isobaric analogue resonant (p,γ) reactions on ^{92}Mo, 25:28359
FERON, J. L., Uniaxial stress experiments and magnetoelastic interactions in rare earths, 25:27889
FERON, M., Studies on the Mediterranean fruit fly in Tunisia, 25:26573
FERRANTE, E., Nuclear fuel characterization, 25:27293 (RT/ING-(70)21)
FERRARI, Harry M., Austenitic stainless steels for use in nuclear reactors, 25:27214
FERRARI, I., Stage sensitivity and dose response in human leukocytes, 25:26628
FERREIRA, C. A. Goncalves, Organoleptic chemical and microbiological aspects of irradiated Portuguese sausages, 25:27159
FERRERO, L., High-energy photoprotons from beryllium, 25:28194
FESENKO, E. E., Action of uv radiation on proteins, 25:26644
FESER, K., Fluorescence excitation of ultra-soft x-ray emission spectra using synchrotron radiation, 25:27827 (DESY-70/59)
FESSENDEN, P., Nuclear-state widths of medium-weight nuclei in the continuum, 25:28268
FESSLER, N., Superconducting dc quadrupole lens, 25:28111 (KFK-1218)
FESSLER, Theodore E., Excited states of ^{138}Ce, 25:28414
FETTICH, Janez, Effect of therapeutical roentgen irradiation on animal skin from great distance, 25:26973
FETTWEIS, P., Reassessment of some neutron yields from the longer-lived delayed neutron emitters, 25:28211 (CERN-70-30(Vol.1), pp 517-18)
FICARRA, Anthony, Autoantibodies to intrinsic factor: their determination and clinical usefulness, 25:26676
FICK, D., Levels in ^5He excited in the elastic d--^3H scattering, 25:28168
FICOCELLI, E., Contribution of electronic excitation to specific heats of high-temperature gases, 25:27692
FIDONE, I., Local density measurements by nonlinear mixing of electromagnetic waves, 25:27684
Propagation of electromagnetic waves in a plasma with a sheared magnetic field, 25:27821
FIGDOR, Sanford K., Automated calculation of ^{14}C and ^{35}S radioactivity in biological samples by external standardization and a computer program, 25:26184
FIGULI, J., Influence of gamma irradiation on some physical and chemical properties of gluten proteins, 25:26656
FILBY, W. G., Radiation studies of aryl glycosides. III, 25:26305
Radiation studies of aryl glycosides. II, 25:26304
FILIPPOV, G. F., Energy levels of three-particle system, 25:28163 (ITF-70-100-P)
FILIPPOV, S. S., Fluid flow with temperature-dependent transport coefficients in plane channels, 25:27498
FILIPPOV, V. F., Effect of small additions of V, Cr, and Mn on [structure and] properties of cast Zr, 25:27230

FILJAK, K., Some factors influencing uptake of ^{75}Se-selenomethionine by pancreatic tissues of the rat, 25:26591

FILONI, Sergio, Influence of the thymus in the regenerative process of cervical lymph nodes in irradiated mice, 25:26996

FINCKH, E., Spin assignment for two isobaric analog resonances in ^{76}Se from the neutron decay, 25:28241

FINGER, M., Isomerism in odd and odd--odd nuclei with mass number 185 less than or equal to A less than or equal to 191, 25:28335 (CERN-70-30(Vol.2), pp 1045-55)

Properties of low-lying levels in even Pt and Os nuclei, 25:28334 (CERN-70-30(Vol.2), pp 1031-43)

FINK, R. W., Neutron activation cross sections for As, Br, Rb, and Sr isotopes at 14.4 MeV, 25:28282

FINKELSTEIN, J., Necessity of exotic mesons, parity doublets, or Regge cuts, 25:28033

Self-consistent rising cross-sections, 25:28012

FINLAY, R., Angular momentum transfer in ^{18}O(^{3}He,t)^{18}F, 25:28173

FISCHER, G. J., SAS1A: a computer code for the analysis of fast-reactor power and flow transients, 25:28727 (ANL-7607)

FISCHER, R., Comparison of various steam circuits and optimization of steam temperature for sodium-cooled fast breeders, 25:28750

Concept for a small nuclear steam-generating system with an integrated construction, 25:28641

FISHER, L. M., Dopplerons in cadmium, 25:27900

FISHER, Leslie John, Peak versus average power in microwave induction of lenticular cataracts, 25:26971

FISHER, R. K., Resonance cones in field pattern of rf probe in warm anisotropic plasma, 25:27683

FISHER, S. B., Effects of high flux neutron irradiation on the microstructure of metals, 25:27266 (RD/B/N-1812)

FISHER, Shalom, Reversed field equilibria in axially symmetric electron current layers, 25:27798

FITZGIBBON, G. C., Enthalpy of formation of uranium tetrachloride, 25:26263

FLECK, C. M., Neutron temperature during power surge of TRIGA Mark II reactor, 25:28770

FLEISCHMANN, Hans H., Perpendicular injection of relativistic electron beams into magnetic mirrors, 25:27688 (WASH-1159, pp 193-5)

FLEISCHMANN, R., Study of isobaric analogue resonances in elastic scattering of polarized protons from ^{88}Sr, ^{90}Zr, ^{92}Zr, ^{96}Zr, ^{92}Mo, ^{142}Ce, ^{144}Nd, ^{146}Nd, 25:28239

FLEMONS, R. S., Attachment of thermocouples to zircaloy tubes by induction brazing, 25:27182 (R-69-CAP-8)

FLETCHER, Gilbert H., Analysis of the treatment of Stage I and Stage II carcinomas of the uterine cervix, 25:26893

Cancer of the uterine cervix; Janeway lecture, 1970, 25:26886

Ureteral strictures after radiation therapy for carcinoma of the uterine cervix, 25:27052

FLOM, Richard, Correlation between brain tumor detectability on brain scan and protein levels of the spinal fluid, 25:26828

FLORES, J., Sum rules for Moshinsky brackets, 25:28506

FLYNN, Robert W., Particle diffusion in turbulent electric fields, 25:27673

FOCKE, B., In-beam nuclear magnetic resonance of 159 μs level in ^{115}Sn, 25:28380

FODOR-CSANYI, P., Dependence of the light output of liquid scintillation systems on spectral properties of components, 25:26462

FOGELBERG, B., Energy levels in ^{114} ^{116} ^{118} ^{120} ^{122}Cd populated in decay of Ag isotopes, 25:28337 (CERN-70-30(Vol.2), pp 1069-74)

FOGL, J., Reactions of metal ions with carboxy derivatives of phenylfluorone, 25:26174

FOISSEL, P., Interest of analog state studies in deformed nuclei, 25:28472

FOMINENKO, V. P., Microtron type electron accelerator, 25:28136

FONER, S., Magnetic properties of dilute Pd(Gd) alloys, 25:27921

FONTES, P., Production cross sections of Li and Be isotopes in ^{12}C by high-energy protons and alpha particles, 25:28182

FORD, M. R., Estimation of dose to gonads from gamma emitters present in the body, 25:26760

FORKOSCH, John, Least-squares analysis of the uncertainty principle, 25:27944

FORMAN, L., Independent cesium yields in ^{236}U fission: identification of ^{144}Cs, 25:28307 (CERN-70-30(Vol.1), pp 589-99)

FORMAN, P. R., Dynamic stabilization of the z pinch, 25:27789

FORNACIARI, P., Strategy and tactics in nuclear fuel management, 25:28543

FORRESTER, David A., Neutron stability against convection in general relativity, 25:27325

Some relativistic integral theorems, 25:27324

FORSTER, William O., Chemical budget of Columbia River, 25:28879 (RLO-1750-41)

FORTUIN, J. J. H., Two genes controlling mitotic intragenic recombination and recovery from uv damage in Aspergillus nidulans. I, 25:26709

FORTUNE, H. T., An experimental test of the Barshay--Temmer theorem via the reactions ^{10}B(α,^{7}Li/sub gs/)^{7}Be/sub gs/ and ^{10}B(α,^{7}Be/sub gs/)^{7}Li/sub gs/, 25:28176

FORYS, M., Gas phase radiolysis of hydrogen sulphide, 25:26315

FOSS, M. H., Output program used with on-line data collection, 25:26510

FOSTER, D. Graham Jr., Neutron total cross sections, 2.5 to 15 MeV. II, 25:28169

Neutron total cross sections, 2.5 to 15 MeV. I, 25:28170

FOSTER, R. E. Jr., Fission yields and branching ratios of ^{85}Kr in thermal neutron fission of ^{233}U, ^{235}U, ^{239}Pu, and ^{241}Pu, 25:28383

FOSTER, Stanley C., Radiotherapy of primary lymphoma of the orbit, 25:26890

FOTI, A., Reaction ^{40}Ar(d,p)^{41}Ar at deuteron energy below Coulomb barrier, 25:28251

FOUCHER, R., Isomerism in odd and odd--odd nuclei with mass number 185 less than or equal to A less than or equal to 191, 25:28335 (CERN-70-30(Vol.2), pp 1045-55)

Mass-differences in neutron-rich Sr Region, 25:28294 (CERN-70-30(Vol.1), pp 321-9)

Properties of low-lying levels in even Pt and Os nuclei, 25:28334 (CERN-70-30(Vol.2), pp 1031-43)

FOWLER, Jack, Motion of Rifle Gap Dam Rifle, Colorado; Project Rulison underground nuclear detonation, 25:26410 (PNE-R-47)

FOWLER, S. W., Distribution of ingested ^{65}Zn in marine crustaceans, 25:26604

FOX, J. D., Spreading of the antianalogue states in ^{91}Nb, 25:28363

FRAAS, A. P., ORNL isotope kilowatt program, 25:26433

FRAAS, H., Comparison of pion electroproduction data with vector meson dominance predictions, 25:27982 (DESY-71/12)

Electroproduction of ω-meson as a test of the rhoωγ-vertex, 25:27981 (DESY-71/11)

FRADIN, F. Y., Ferromagnetism of $ZrZn_2$, 25:27875

Magnetic properties of dilute alloys of scandium, 25:27878

FRAIPONT, Donald F., Disc-based operating system for mass spectrometry experiments, 25:26556

FRAMPTON, P. D., Quality control, inspection, and testing of Series I metallurgical fuels for first charge of Dragon reactor, 25:26438 (DP-Report-432)

FRANCIA, M., Nuclear fuel characterization, 25:27293 (RT/ING-(70)21)

FRANCOIS, Bernard, Process for preparation of ceramics of fissionable materials, 25:27273

FRANK, L. A., Comments on a proposed magnetospheric model, 25:27607

Relationship of plasma sheet, ring current, trapping boundary, and plasmapause near magnetic equator and local midnight, 25:27631

FRANKLIN, R. N., Microwave reflexion from longitudinally magnetized plasma-filled coaxial waveguide, 25:27813

FRATIELLO, Anthony, Proton magnetic resonance cation solvation study of uranyl perchlorate, uranyl nitrate, and uranyl perchlorate--hydrochloric acid solutions in water--dimethyl sulfoxide--acetone mixtures, 25:26212

FRAZIER, P., External heavy ion source for Berkeley 88-inch cyclotron, 25:28120 (UCRL-20406)

FRED, Richard K., Proliferative and phagocytic capacity of the reticuloendothelial system of sublethally irradiated mice, 25:26947

FREDERICK, L. G., Reliability from the supplier's viewpoint, 25:28521 (AECL-3670, pp 39-44)

FREDRICKS, R. W., Fast time-resolved spectral analysis of vlf banded emissions, 25:27621

Magnetic and electric field changes across the shock and in the magnetosheath, 25:27539

FREEMAN, R., Electron density measurements in the thermal plasma of the magnetosphere, 25:27566

FREIDBERG, J. P., Dynamic stabilization of the screw pinch, 25:27749

FREIFELDER, David, Interruption of DNA injection by x-irradiation of phage lambda, 25:26693

Lack of polarity of DNA injection by Escherichia coli phage lambda, 25:26692

FREMLIN, J. H., Applications of nuclear physics, 25:28379

FREOUR, P., Applications of thermo and photoluminescent phenomena in health physics, 25:26528

FREUND, Juergen, Optimization of condensation process based on Carnot cycle liquid-metal MHD converters, 25:27479

FREVEL, L. K., Oxidation of 2-methoxyethanol to methoxyacetic acid by nitric acid solutions, 25:26223

FREWER, Hans, Technology and economics of the nuclear power plants constructed by Kraftwerk Union, 25:28526 (CONF-700550-, Paper 4)

FREY, Perry A., Studies on the mechanism of hydrogen transfer in the coenzyme B_{12} dependent diol dehydrase reaction. II, 25:26225

FRIDENSHTEIN, A. Ya., Fibroblast colonies in splenic cultures of irradiated mice, 25:26905

FRIED, Maurice, Program of FAO/IAEA in food and agriculture, 25:27128 (CONF-680112-, pp 1-7)

FRIEDLANDER, H. N., Importance of fabrication technology in translation of fiber and matrix properties to advanced composites, 25:27278

FRIEDMAN, A. M., Instabilities of a high-pressure plasma contained by a dense blanket of neutral gas, 25:27744

FRIEDMANN, E., Factors determining introduction of nuclear

power stations in developing countries, 25:28723
FRIEDRICH, H. B., Infrared spectra of UO and UO_2 vapor condensed in rare-gas matrices, 25:26260 (COO-1182-34)
FRIHAGEN, J., High-latitude F-region irregularities, 25:27519
FRINDEL, E., Proliferative activity of stem cells in bone-marrow after irradiations, 25:26956
FROHNER, F. H., Total cross sections for kilovolt neutrons of even--odd nuclei in he region of the 3s strength-function resonances, 25:28279
FROLOV, S. D., Study of supersonic MHD-channel flows with compression shock, 25:27489
FRYE, Roger E., Disc-based operating system for mass spectrometry experiments, 25:26556
FRYXELL, R. E., Determination of solidus-liquidus temperatures in the UO/sub 2+x/ system (-0.50 < x < 0.20), 25:27292 (GEMP-714)
FU, Jerry H. M., Surface potential of a photoemitting plate, 25:27360
FUCHS, H., Proposal of $d^3/_2{}^{-1}p^3/_2$ analogue states in ^{40}Ca, 25:28230
FUDA, Michael G., Separable-expansion method for the three-nucleon system, 25:28510
FUHS, G. Wolfgang, ^{33}P autoradiography used to measure phosphate uptake by individual algae, 25:26596
FUJIEDA, Junichiro, Superhigh voltage irradiation of bladder tumor, 25:26876
FUJII, Tadao, Liquid hydrogen target utilizing a small mechanical refrigerator, 25:28138
FUJIMURA, Kimio, Nonrelativistic composite particle model for mesons, 25:28030
FUJIMURA, O., Computer controlled dynamic cineradiography, 25:26557
FUJIMURA, Tadato, Evaluation of integrity for fast neutron irradiation embrittlement of JPDR pressure vessel, 25:28682 (JAERI-1202)
FUJINO, N., Electron probe microanalysis of Ti(C,N) and Zr(C,N) in steel, 25:26160
FUJIWARA, M., Hot electron confinement in a cusped magnetic field by ECRH wrapping, 25:27677
FUKUDA, Masasi, Radiorestorative chemicals and their clinical application, 25:26812
FUKUOKA, Noboru, Shallow traps in p-type germanium converted from n-type by electron irradiation, 25:27843
FUKUSHIMA, Hiroyuko, Spectrochemical determination of ^{235}U, 25:26170
FUKUSHIMA, Yoshihiro, Four-body correlations in light nuclei, 25:28505
FUKUSHIMA, Yutaka, Experiments and calculations for gamma rays streaming through penetration in shielding structure, 25:27829
FULIGNI, F., OSO-G satellite instrumentation for measurements of cosmic x-rays in energy range from 25 to 190 keV, 25:26478
FULRATH, Richard M., High-temperature phase equilibria in the $PbTiO_3$--$PbZrO_3$ system, 25:27295
FULTZ, S. C., LRL (Livermore) 100-MeV linear electron accelerator and facility, 25:28123 (UCRL-73075)
FUNG, P. C. W., Weak-turbulence analysis of the two-stream instability, 25:27740
FUNK, Jack, Earth departure technique for use in manned interplanetary missions using NERVA engine, 25:28788
FUNKHOUSER, J. G., Noble gas abundances in lunar material, 25:27308
FURCHTGOTT, Ernest, Prog. rpt. on long-term effects of radiation, final, 2/68--7/70, 25:26922 (ORO-3260-3-A)
FURLAN, M., Improvement in alkaline sucrose density gradient sedimentation of mammalian cell DNA, 25:26629
FURNICA, Gh., IR spectrophotometric study of changes induced by gamma irradiation in structure of proteins and nucleic acids, 25:26660
FURNICA, M., Spectrophotometric characterization of DNA after irradiation in vivo. VI, 25:27020
FURSOV, G. L., Structure of electron clusters in an injector with a step-like varying wave phase velocity, 25:28112 (KHFTI-70-17)
FURSOV, V. N., Role of variety in mutagenesis of cotton, 25:26728
FURTH, H. P., Feedback control problems in tokamaks, 25:27763
FURUICHI, S., Analysis of Kantor amplitudes and recent low-energy proton--proton scattering experiments, 25:28046
FURUSAWA, Yoichi, Present situation of development of food irradiation in USA and other foreign countries, 25:27142
FYKIN, L. E., X-ray- and neutron-diffraction study of ordering in some alloys of the titanium--zirconium--oxygen system, 25:27297

G

GABALLAH, I., Theoretical method for calculation of two-phase flow with change of phase in a flash evaporation, 25:26420 (KFK-1300)
GABESKIRIYA, V. Ya., Investigation of Pu isotopes build-up in Novo-Voronezh APS fuel, 25:28532
GABRIEL, M., Magnetic field decay of neutron stars, 25:27344
GACHOK, V. P., Integral representations of vacuum expectation values with account for local commutativity, 25:28082
GAFFEY, C. T., Response of maximal and submaximal action potentials from frog sciatic nerve to 200-kV x-rays, 25:26993
GAGLIONE, P., Sampling of radioactive deposition through ion-exchange resins, 25:26559
GAI, E. V., Spinning top problem in quantum mechanics, 25:27927 (FEI-203)
GAIVORONSKAYA, T. V., Angular correlation of nucleons generated during reactions of decaying deuterons, 25:28487
GALES, S., High resolution detection unit for charged particles, 25:28141
GALKIN, A. A., Effect of low frequency fluctuations on superconducting tunnelling, 25:27649
GALKOVSKAYA, K. F., Influence of ionizing irradiation in radiation leucosogenesis, 25:26904
GALLAGHER, P. K., Cast permanent magnets of Co_5RE type with mixtures of Ce and Sm, 25:27883
GALLAGHER, W. J., LRL (Livermore) 100-MeV linear electron accelerator and facility, 25:28123 (UCRL-73075)
GALLARDO, Juan Carlos, Dual symmetric theory and the harmonic oscillator model of hadrons, 25:28021
GALLOIS, G., Belgonucleaire and Siemens PWRs for small and medium power reactors, 25:28717
GALSTER, S., Elastic electron--deuteron scattering and electric neutron form factor at four momentum transfers: 5 $Fermi^{-2} < q^2 < 14\ Fermi^{-2}$, 25:27980 (DESY-71/7)
GALUS, Z., Redox processes of U(VI), (V), (IV), and (III) in acetate buffers, 25:26265
GAMALYA, I. A., Energy surfaces during fission of ^{226}Ra, ^{238}U, and ^{246}Cf, 25:28395
GAMBHIR, Y. K., Quasiparticle description for indium, 25:28357 (UJV-2540-F)
GAMBINO, R. J., ^{139}La NMR studies in $LaIn_3$, 25:27920
Intrinsic metallic character of rare-earth pnictides, 25:27879
GAMKRELIDZE, L. M., Effect of ionizing radiation on wheat, 25:27082
GAMMEL, John L., Pade approximant in theoretical physics, 25:28063
GANE, N. F. C., Radioinduced fibrosarcoma, 25:27044
GANGADHARAN, S., Nuclear methods in trace analysis: a review, 25:26186 (BARC-529)
GANGULY, A. K., Nuclear charge distribution in fission fragments, 25:28508
GANGULY, S., Electron density distributions in lower ionospheric regions, 25:27526
GANIVET, M., Determination of traces of iron, nickel, and chromium in plutonium nitrate solutions, 25:26154 (RFP-Trans-76)
GAPONIUK, P. Ya., Changes of plasma kinase activity in irradiated animals, 25:27030
GARBAGNA, P., Betatron therapy of pulmonary neoplasms, 25:26874
GARCIA, Enrique E., Determination of thallium in microsamples of natural vanadates of uranium by anodic redissolution, 25:26151 (CNEA-288)
GARCZYNSKI, W., Haag's theorem, 25:28083
GARDNER, M. C., Evaluation of Project Shoal site, 25:26403 (NVO-1229-105(Pt.1))
GARIBYAN, G. M., Detection of x-ray transition radiation by means of a streamer chamber, 25:26515
GARRISON II, James Carlton, Energetics of active transcellular calcium transport by chorioallantoic membrane of the embryonic chick, 25:28905 (UR-49-1440)
GARSCADDEN, A., Feedback experiments on multimode ionization waves, 25:27773
GARSIDE, L., Renormalization constants in the random-phase approach, 25:28509
GARST, D. M., Optimizing thermal and radiation effects for bacterial inactivation, 25:27099
GARY, S. P., Instabilities in perpendicular collisionless shock waves, 25:27731
GASIDLO, J. M., ZPR-3 assemblies 48: 48A, and 48B: the study of a dilute plutonium-fueled assembly and its variants, 25:28752 (ANL-7759)
GAUKLER, K. H., Conference on x-ray optics and microanalysis, Tuebingen, Ger., 9/68, 25:26155
GAUTSCH, O., Some experimental results on the sorption of caesium by tungsten and graphite, 25:27201 (EUR-4549)
GAVALAS, G. R., Effect of temperature nonuniformity on positive column, 25:27714
GAVIN, Basil F., Sputter-type Penning discharge for metallic ions, 25:28137
GAVRILOV, K. A., Investigation of α decay of isotopes of element 105, 25:28350 (KFK-tr-350)
GAVRILYUK, V. I., Stabilization of magnetic field in an iron $\pi\sqrt{2}$ β spectrometer, 25:26502
GAWLOWSKI, J., Reaction of neon ions with ethylene, 25:26314
GAZZERA, Giuseppe, Cancer of the uterine cervix, 25:26871
GEERAETS, Walter J., Radiation effects on the eye, 25:27047
GEHRZ, R. D., Mass loss from M stars, 25:27315
GEIER, P. W., Population response to sterile-release procedures for pest control, 25:27153
GEIGER, G., Cooperation of reinforced-concrete construction and steel construction, 25:27188
GELASHVILI, K. D., Changes in ovaries of mice following γ

irradiation, 25:27028
GELIN, R., Uranium demand and supply, 25:26396 (CONF-700903-16)
GELLAI, B., Vapor pressure isotope effect of H_2S/D_2S, 25:26248
GELLER, Lester M., Audiogenic seizure susceptibility of rats x-irradiated in utero during first one-third of pregnancy, 25:26968
GENDRIN, R., Wave-packet propagation and application to dispersion characteristics and to mechanisms of Pc 1 events, 25:27605
GENKIN, I. L., Correlation of fluctuations in gravitating media, 25:27430
GENSINI, P., Asymptotic lower bound of crossing-even amplitudes and dispersion relations for their inverses, 25:28098
GENTILE, Erberto Francisco, Reactivity of U_3O_8/Al dispersions, 25:27294
Thermal cycling test for plates containing dispersions, 25:27251
GENTLE, K. W., Plasma waves and echoes, 25:27800
GENTRY, W. Ronald, Differential cross sections for excitation of resolved vibrational states in $H^+ + H_2(v = 0)$ nonreactive collisions, 25:27450
GEORGE III, Frederick W., Post-irradiational recurrent epidermoid carcinoma of the uterine cervix, 25:26887
GEORGESCU, Iulia I., Radioactivity of seston and waters of Black Sea and alga (Cystoseria barbata) from Rumanian continental shelf during 1964--1967, 25:26745
GEORGESCU, L., Potato plants obtained from irradiated tubers, 25:26737
GEORGESCU, P., Spectrophotometric characterization of DNA after irradiation in vivo. VI, 25:27020
GERARD, F., Response of glass dosimeters to strong γ radiations, 25:26521
GERBER, G. B., Proteolytic activity in isolated perfused liver of normal and x-irradiated rats, 25:26984
GERLING, W., Co-existence of different structures in various domains of the periodic table, 25:28447 (CERN-70-30(Vol.2), pp 1129-32)
GERMER, John H., Hydraulic control rod drive system, 25:28676
GERMER, L. H., Adsorption of hydrogen on W (100), 25:27226
GERRARD, Martha, Developments abroad on radioisotope-powered cardiac pacemakers, 25:26434
Selected abstracts of world literature on production and industrial uses of radioisotopes, 25:26427 (ORNL-IIC-30(Pt.4))
GERUSCHKAT, K., Comparison of various steam circuits and optimization of steam temperature for sodium-cooled fast breeders, 25:28750
GERVAIS, R. L., Space shuttles and interplanetary missions. Based on shuttle, precursor missions, and planetary and lunar space station sessions of AAS 16th annual meeting, June 8--10, 1970, Anaheim, California, 25:28786
Space stations. Based on space station, safety, and international sessions of AAS 16th annual meeting, June 8--10, 1970, Anaheim, California, 25:26784
GHALIB, S. A., Nuclear power industry of the United Kingdom, 25:28524 (CONF-700550-, Paper 2)
GHOSE, M., M_3 generation of some M_2 mutants in rice, 25:26701
Segregation pattern in the M_3 generation of rice, 25:26688
GHOSH, Nandini, Effect of irradiation on yeast ribosomes, 25:26633
GIACCHETTI, G., Analysis of UO_2--Mo and UO_2--Zircaloy fuel cermets, 25:26157
GIAMATI, Charles C., Expanded FORTRAN 4 program for elastic scattering analyses, 25:28450 (N-70-42846)
GIANNINI, M., Use of a PDP-9 computer in nuclear spectroscopy measurements, 25:26496
GIARD, P., Radiotherapy heart disorders, 25:27048
GIBB, F. R., Dose-related local and systemic effects of inhaled ^{238}Pu and ^{239}Pu dioxide in dogs, 25:26929
GIBBONS, D. F., Internal friction studies in some titanium and zirconium based alloys, 25:27215
GIBBONS, J. F., Analysis of ion implanted diamond, 25:27858
GIBBS, W. R., Nuclear-state widths of medium-weight nuclei in the continuum, 25:28268
GIBERTINI, Giancarlo, Influence of the thymus in the regenerative process of cervical lymph nodes in irradiated mice, 25:26996
GIBSON, R. D., Tearing-mode instability, 25:27751
GIBSON, Thomas A. Jr., Far-out collection program. Project Schooner, 25:26404 (PNE-527)
GIERULA, J., Multiple meson production at super-high energies, 25:28050
GIESE, A. C., Nucleic acid and protein synthesis during regeneration in ultraviolet-treated Blepharisma, 25:26648
GIESE, Clayton F., Differential cross sections for excitation of resolved vibrational states in $H^+ + H_2(v = 0)$ nonreactive collisions, 25:27450
GIESSEN, B. C., Conference on developments in the structural chemistry of alloy phases, Cleveland, 10/67, 25:27260
Constitution of non-equilibrium alloys after rapid quenching from the melt, 25:27264
GILAT, Jacob, Effects of nuclear shells and angular momentum in evaporative deexcitation, 25:28266
GILES, Robert Duncan, Anodising Be, 25:27172
GILL, A. B., Nuclear desalination program annual progress report on activities sponsored by the Atomic Energy Commission for period ending October 31, 1970, 25:28790 (ORNL-4668)
GILLIS, Peter P., Elastic precursor decay in tantalum, 25:27216
GIMESI, O., Retention of radionuclides on metal sulphide precipitates, 25:26199
GINGERICH, K. A., Mass spectrometric determination of the heats of atomization of NdO_2, NdBO, and $NdBO_2$ and upper values for the dissociation energies of NdAg and Nd_2, 25:26273
GINGO, P. J., Gamma radiation characteristics of plutonium dioxide fuel, 25:27305 (N-70-35897)
GINZBURG, N. I., Superconductivity at high pressure, 25:27655
GINZBURG, V. L., Propagation of electromagnetic waves in plasmas, 25:27803
GIUDICI, T., Acyl transfer reactions from and to the ureido functional group. IV. Neighboring carboxyl group general acid catalysis in the hydrolysis of an O-acylisourea (2-amino-8-carboxy-4-oxo-3,1,4-benzoxazine), 25:26253
GIVENS, R. S., Aliphatic semidiones. XV. 2,3-semidiones derived from the bicyclo[n,1.0]alkanes, 25:26254
GLANCY, D. L., Cardiac catheterization. III, 25:26854
GLASGOW, Dale W., Neutron total cross sections, 2.5 to 15 MeV. II, 25:28169
Neutron total cross sections, 2.5 to 15 MeV. I, 25:28170
GLAUDEMANS, P. W. M., Configuration mixing and effective charges, 25:28245
GLEESON, L. J., Low-energy cosmic rays near Earth, 25:27473
Solar sources and the cosmic-ray transport equation, 25:27361
GLENCROSS, W. M., Satellite-borne x-ray spectroheliograph, 25:26484
GNITRO, M., Quasiparticle description for indium, 25:28357 (UJV-2540-F)
GNEUSS, G., Tensor polarizability in the giant dipole resonance region and collective behaviour, 25:28489
GOBLE, Robert L., Current algebra and analyticity, 25:28027 (RLO-1388-602)
GODA, Shiro, Absorption behavior of radionuclides, mainly rare earth elements, in seawater, 25:26339
GOEDBLOED, J. J., Gamma irradiation of lithium-drifted silicon, 25:27852
GOERING, Harlan L., Stereochemistry of allylic rearrangements. XVI. Stereochemistry of ion-pair return in the trans-α,γ-methylphenylallyl p-nitrobenzoate system, 25:26224
GOLAY, Marcel J., Underwater Arctic oil transport, 25:28795
GOLD, R. E., Weldability and elevated temperature stability of refractory metal alloys. II, 25:27208 (N-71-10352)
Weldability and elevated temperature stability of refractory metal alloys. V, 25:27178 (N-71-10353)
GOLDBLATT, Maxwell, Vibrational spectrum and force field of osmium tetroxide, 25:26258
GOLDE, A., Irradiation of oncogenic viruses, 25:27111
GOLDENBAUM, G. C., Plasma diagnostics by light scattering, 25:27680
GOLDIN, Gerald A., Nonrelativistic current algebras as unitary representations of groups, 25:27972
GOLDMAN, Martin V., Stability of a trapped-particle equilibrium, 25:27733
GOMEZ, Hector R., Nuclear techniques and equipment in hydrology, 25:26353 (CONF-680112-, pp 37-52)
GONZALEZ, Mario, Results in treatment of pure seminoma of the testis, 25:26891
GOOD, P. D., Quality control, inspection, and testing of Series I metallurgical fuels for first charge of Dragon reactor, 25:26438 (DP-Report-432)
GOODIN, L. J., Photoreversal of ultraviolet-induced division delay in Saccharomyces cerevisiae, 25:27080
GOODMAN, C. D., A search for isospin mixing using the (^3He,t) reaction, 25:28232
GOODRICH, R. S., Observations of grain boundaries with the field ion microscope, 25:27253
GOPASYUK, S. I., Relationship between velocity fields and magnetic fields in the solar atmosphere, 25:27394
GOPINATH, N., Supervoltage radiation response in epidermoid carcinoma of the esophagus, 25:26896
GORBACHEV, B. I., Orientation in physical pairs of galaxies, 25:27420
GORBONOSOV, A. E., Plasma oscillations and metastable states in Josephson tunnel junctions, 25:27651
GORDON, Gilbert, Mechanistic implications of the role of phenol in the uranium(IV)--chlorine(III)--phenol reaction, 25:26266
GORDON, Julius, Participation of three cell types in the anti-sheep red blood cell response in vitro. Separation of antigen-reactive cells from the precursors of antibody-forming cells, 25:26665
GORDON, Milton P., TMV--RNA photoreactivation, 25:26653
GORDON, S. A., Induction of chromosomal aberrations in pig kidney cells by far-red light, 25:26727

XUM

GORDON, Solon A., Concentration of radium, thorium, and uranium by tropical marine algae, 25:26597
GOREN, R., Effect of gamma radiation on the synthesis of scopoletin and scopolin in grapefruit peel in relation to radiation damage, 25:27079
GORLOV, G. V., Elastic neutron scattering at small angles, 25:28500
GORMAN, D. J., Energy levels in ^{239}Np, 25:28415
GOTTLIEB, Charles Frederick, Effect of radiation dose, dose rate, and quality on the immune response, 25:26679
GOTTSCHALK, Alexander, Correlation between brain tumor detectability on brain scan and protein levels of the spinal fluid, 25:26828
GOUD, J. V., Mutagenesis in sorghum, 25:26715
GOUDSMIT, P. F. A., Decay of some nuclei far from the stability line studied with standard spectroscopic techniques, 25:28322 (CERN-70-30(Vol.2), pp 939-47)
GOULD, R. J., Neutral-pion decay and the gamma radiation from our galaxy, 25:27404
GOULD, W., Resonance cones in field pattern of rf probe in warm anisotropic plasma, 25:27683
GOULDING, B. J., 1000-MWe LMFBR accident analysis and safety system design study. Topical report. Effects of irradiation-induced metal swelling on the reference design, 25:28685 (BAW-1355)
GOURDON, C., Torsatron without toroidal field coils as a solution of the divertor problem, 25:27793
GOUTIER, R., Effects of novocain on the isolated perfused heart of rats after x-irradiation, 25:26798
GOVIER, D. A., Inactivation by uv radiation of RNA from potato virus X, 25:27108
GOYAL, L. N., Illiac III Reference Manual. Vol. I, 25:28851 (COO-2118-5)
GRABISCH, K., Proposal of $d^3/_2{}^{-1}p^3/_2$ analogue states in ^{40}Ca, 25:28230
GRAEFFE, R., Preparation of Josephson junctions by plasma oxidation of Nb, 25:27659
GRAESSLER, H., S-wave interference in the f^0 resonance region, 25:28018
GRAEVSKII, E. Ya., Radiosensitizing action of N-ethylmaleimide, 25:26640
GRAHAM, C. D. Jr., Domain walls in ferromagnetic Dy and Tb, 25:27873
GRAHAM, Ernest S., Decrements in the visual acuity of rhesus monkeys (Macaca mulatta) as a delayed effect of occipital cortex irradiation, 25:26991
GRAHAM, Walter H., Electron microscopic changes following canine cardiac allografts: the effects of irradiation, 25:26677
GRANATA, G., Propagation of electromagnetic waves in a plasma with a sheared magnetic field, 25:27821
GRANT, A. Kerr, Radiation enterocolitis, 25:26811
GRANT, Paul M., Dependence of the E_1 reflectivity structure in EuO on temperature and doping, 25:27895
GRAPENGIESSER, B., Q-values of some nuclides on the neutron-rich side of stability, 25:28296 (CERN-70-30(Vol.1), pp 341-51)
GRAPPENGIGSSER, B., Neutron-rich nuclides obtained using OSIRIS facility, 25:28340 (CERN-70-30(Vol.2), pp 1093-1103)
GRARD, R. J. L., Photoelectron sheath near a planar probe in interplanetary space, 25:27359
GRASS, F., Spectrophotometric studies on plutonium(IV) complexes in aqueous and mixed organic--nitric acid systems, 25:26274
GRAUL, E. H., RBE of fast neutrons on influence of cataract development, 25:26945
GRAW, G., Study of isobaric analogue resonances in elastic scattering of polarized protons from ^{88}Sr, ^{90}Zr, ^{92}Zr, ^{94}Zr, ^{92}Mo, ^{142}Ce, ^{144}Nd, ^{148}Nd, 25:28239
GRAYBILL, S. E., Ion momentum analysis of collectively accelerated ion species, 25:27697 (WASH-1159, pp 219-26)
GRAYSTON, M. J., Cell survival and x-ray-induced DNA degradation in Micrococcus radiodurans, 25:26627
GREBINSKII, S. D., Effect of gibberelline on growth of chlorophyll in germs, 25:27064
GREEDAN, J. E., Magnetic and electrical characteristics of $REPd_3$ intermetallic compounds, 25:27870
GREEN, A. E. S., Semiempirical generalized one-boson-exchange potentials, 25:28513
Ultraviolet emissions from atomic nitrogen in the aurora, 25:27617
GREEN, J. M., Statistical model calculations of ^{56}Fe neutron cross section, 25:28218 (NP-18674)
GREEN, James D., Gonadal dose in male radiotherapy patients, 25:26759
GREEN, John H., Prog. rpt. on marine products development irradiator program: irradiated fresh shrimp shipping studies, annual, 10/67--9/68, 25:27138 (TID-25543)
GREEN, Pauline, Lunar and solar daily variation of the geomagnetic field at Watheroo, Western Australia, 25:27503
GREGOLI, Silvano, Electron transfer in γ-irradiated nucleotides and proflavine, 25:26638
GREINER, W., Nuclear molecules formed in elastic ^{16}O + ^{16}O scattering, 25:28171 (CERN-70-30(Vol.1), pp 601-2)
GREMERET, Roger, Process for preparation of ceramics of fissionable materials, 25:27273
GRENCH, R. E., Photographic method for determining velocity distributions within thermal plumes, 25:28839 (ANL/ES-4)
GREVE, A., Center to limb variation of the separation of the Mg II, H_2, and K_2 emission peaks, 25:27372
GREVESSE, N., [Fe I] lines: their transition probabilities and occurrence in sunspots, 25:27365
GREYSON, N. D., Detection of bronchopleural fistulas by radionuclide fog inhalation, 25:26833
GRIDASOV, V. I., Dynamic accelerated proton beam characteristics in IHEP 70-GeV accelerator, 25:28133
GRIDNEV, G. F., Energy resolution for dE/dx detectors, 25:26485
GRIEM, Hans R., Methods of experimental physics. IX, 25:27689
GRIFFITH, Michael G., Reactions of the hydrogen atom in solution. III. The photolysis of thiols. Studies of tritium-labeled thiols. 25:26251
GRIFFITHS, V. G., Electrolytic process for ultra-fine beryllium [powder], 25:27192
GRIGOR'EV, E. P., Palladium-99 γ radiation, 25:28431
Ytterbium-169 levels in ^{169}Lu decay, 25:28433
GRIMES, S. M., Nuclear level densities and reaction mechanisms from continuum neutron spectra, 25:28285
GRIMES, W. R., Molten Salt Reactor Experiment (MSRE): chemical aspects, 25:28636
GRIMLEY, Eugene B., Mechanistic implications of the role of phenol in the uranium(IV)--chlorine(III)--phenol reaction, 25:26266
GRIMM, G., Radiogenic bone injuries in mandibles of adult rabbits. II, 25:27003
GRIN, Yu. T., Calculation of quadrupole moments, deformations, and shape of light nuclei within K-harmonic method, 25:28180
GRINDLAY, J. E., New studies of Cherenkov radiation in extensive air showers, 25:27952
GRINGAUZ, K. I., Variations of solar-wind fluxes, 25:27535
GRISHAEV, I. A., Structure of electron clusters in an injector with a step-like varying wave phase velocity, 25:28112 (KHFTI-70-17)
GRITTON, Eugene C., Gaseous-fueled nuclear reactors for electrical power production, 25:28635
GRIZHKO, V. M., Structure of electron clusters in an injector with a step-like varying wave phase velocity, 25:28112 (KHFTI-70-17)
GROBMAN, W. D., Intrinsic metallic character of rare-earth pnictides, 25:27879
GROBMAN, Warren D., Thermopower of dilute alloys of cerium in lanthanum, 25:27877
GRODZINS, Lee, Recent work on stripping and pickup of electrons by fast heavy ions, 25:28126 (WASH-1159, pp 34-41)
GROENIER, W. S., Equipment for the dissolution of core material from sheared power reactor fuels, 25:26327 (ORNL-TM-3194)
GROMOV, K. Ya., New isotopes ^{176}Os and ^{177}Os, 25:28386
GROS, M., Spectra and time history of protons in interplanetary space, Feb. 25--28, 1969, 25:27558
GROSFELD, Jay L., Reversal of liver scan image after right-sided renal radiotherapy, 25:26884
GROSS, E. P., Statistical physics, phase transitions, and superfluidity. II, 25:27912
GROSS, R., Linearized version of the Hartree--Fock method, 25:28519
GROSS, R. A., Plasma heating by strong shock waves, 25:27670
GROSSE, E., Spectator particles and resonances, 25:28365
GROSSI, V., Effects of x rays and visible light on the reconstitution of the early potentials of the isolated frog eye, 25:27004
GROSSMAN, Herbert Harry, Effect of chronic low level gamma radiation of polytrichum commune hedw, 25:27075
GROSSMANN, V., Effects of novocain on the isolated perfused heart of rats after x-irradiation, 25:26798
GROSSOLEIL, J., X-ray induced polymerization of gaseous vinyl chloride, 25:26282
GROTHE, K.-T., Radiation induced chromosomal aberrations and growth inhibition in some agricultural plant species, 25:27093
GROVER, J. Robb, Effects of nuclear shells and angular momentum in evaporative deexcitation, 25:28266
GROZOVSKAYA, V. A., Influence of dietary calcium and fluorine on the radioresistance of bacillus-carrying animals, 25:27016
GRUBE, M., Efficiency of x-ray luminescence and thermoluminescence of lithium fluoride crystals, 25:27838 (ANL-Trans-874)
GRUBER, O., Dynamic stabilization experiment on a linear screw pinch, 25:27790
GRUENBEIN, W., Multiple pulse radiolysis: successive accumulation of two hydrated electrons in oxygen, nitrobenzene, and nitromethane, 25:26308
GRUENEWALD, Th., Use of mannitol in the dosimetry of gamma radiation, 25:26523
GRUETER, J. W., Identification of μ s isomers among primary fission fragments, 25:28325 (CERN-70-30(Vol.2), pp 967-84)
GRYPEOS, M. E., Estimate of binding energy of ^{16}O with matrix elements of effective interaction, 25:28181
GRYZINSKI, Michal, Classical theory of atomic collisions. II, 25:27449 (INR-P-1217)
GUARINO, Angelo, Reactions of helium tritide ions with gaseous hydrocarbons. V. cis- and trans-1,2-dimethylcyclopropane. Unambiguous evidence for gaseous

protonated cyclopropanes, 25:26321
GUBAREVA, A. V., Influence of ionizing irradiation in radiation leucosogenesis, 25:26904
GUBIN, V. A., Rate of initial formation of microcolonies in gamma irradiation of SOTs cells in various phases of mitotic cycle, 25:26907
GUENIN, M., Practical use of algebraic concepts in quantum field theory, 25:28084
GUENTHERODT, H.-J., Change of sign of Hall coefficient in liquid alloys, 25:27212
GUERTIN, R. P., Magnetic properties of dilute Pd(Gd) alloys, 25:27921
GUESS, T. R., Advanced filament-wound carbon composite, 25:28888 (SC-DR-710192)
GUEST, G. E., Stability of microwave-heated plasmas, 25:27743
GUILBOT, A., Development of certain physico-chemical properties of the starch granule as a function of irradiation conditions, 25:26623
GUILLEMOT, M., Deformation of electron distribution function, 25:27823
GUINTRAND, Claude, Optimized dynamic control of irradiation loop of PEGASE reactor, 25:28768
GUMINSKI, Tadeusz, Prolonged exposure to ionizing radiation in boy with aplastic anaemia, 25:27054
GUNION, J. F., Analysis of meson--baryon scattering processes related by SU(3) in a unitarized Veneziano model, 25:28041
Multi-particle eikonal model with high energy s-channel helicity conservation, 25:28034
GUNION, John F., Dual description of production processes by unitarity, 25:28044
GUNSALUS, I. C., Merodiploidy and expression of episomal genes in Pseudomonas putida, 25:28849 (COO-1683-32)
GUPTA, S. P., Investigation of daytime lower ionosphere over equator, 25:27520
GUREVICH, I. I., Two-frequency precession of muonium in magnetic field, 25:27446
GUREVICH, S. M., Weldability of certain Mo alloys, 25:27185
GURTOVENKO, E. A., Effect of macroturbulence on Fraunhofer line profiles, 25:27400
Problem of the flare-like emission in sodium lines, 25:27380
GUSEINOV, O. Kh., X-ray sources in binary systems, 25:27342
GUSTAFSON, Philip F., Nuclear power and thermal pollution: Zion, Ill, 25:28622
GUSTAFSSON, Christer, Shell model parameters of Z = 114 region, 25:28311 (CERN-70-30(Vol.2), pp 654-75)
GUSTAFSSON, G., Auroral luminosity patterns over northern Scandinavia, 25:27581
GUSTAFSSON, G. A., Relation of low-energy particle precipitation to luminous aurora, 25:27578
GUTKIN, T. I., Stabilization of drift waves by a nonuniform high-frequency field, 25:27741
GUTKOWSKI, D., Analytic properties and bound-state degeneracy in nonlocal potentials, 25:28094
GUTWEIN, E. E., Alpha-particle autoradiography of alkaline phosphatase inhibition by cadmium, 25:26574
GUYMON, R. H., MSRE procedures for period between examination and ultimate disposal, 25:28711 (ORNL-TM-3253)
GUZEI, L. S., Phase equilibria in the system vanadium--tantalum--hafnium, 25:27247
GUZMAN, J. A., Evaluation of the impedance probe method of shock speed measurement, 25:28867 (SC-DR-710086)
GYORGYI, Sandor, Simple method for determining the concentration of serum thyroxine by competitive displacement analysis, 25:26568
GYULAI, J., Lattice location and dopant behavior of Group II and VI elements, 25:27856

H

HA, Chung Woo, Application of large gamma radiation source to the treatment of parasites in human excreta, 25:27126
HAAG, R., Report on ergodic states, 25:28078
Structure analysis of quantum field theory, 25:28077
HAAKE, Fritz, Density operator and multitime correlation functions for open systems, 25:27936
HAASE, J., Brain scanning: cerebral scintigraphy, 25:26850
HAASE, Jens, Detection of space-occupying intracranial lesions, 25:26852
HABERSTICH, A., Dynamic stabilization of the z pinch, 25:27789
HACMAN, D., Absolute determination and axial radial distribution of burn-up for reactor lattice cells, 25:28766
HADLEY, J. H. Jr., Positron annihilation in irradiated teflon, 25:27306
HAEBERLI, W., Polarization measurements for $^{88}Sr(p,p)^{88}Sr$ near isobaric analog resonances, 25:28238
Polarization measurements for $^{92}Zr(p,p)^{92}Zr$ near isobaric analog resonances, 25:28368
HAEBLER, D. V., Reactor instrumentation, 25:28674
HAERENDEL, G., Evidence for magnetic field aligned currents during the substorms of Mar. 18, 1969, 25:27620
Magnetospheric electric fields, 25:27545
HAFTEL, Michael I., Off-shell effects in nuclear matter, 25:28520
HAGA, I., Aspects of boiling-water medium-power reactors, 25:28637
HAGEN, Ulrich, Oxygen effect in γ-irradiated DNA, 25:26637
HAGYARD, M. J., Analytic solutions to the Unno transfer equations, 25:27368
HAHN, R. L., α decay from high-spin isomers in ^{153}Ho and ^{155}Ho, 25:28418
Search for new α-emitters with N = 86 and N = 87, 25:28303 (CERN-70-30(Vol.1), pp 533-44)
HAI, F., Neutron production in plasma focus discharge, 25:27799
HAIDUC, C., Critical heat flux under conditions prevailing in a boiling-water reactor, 25:28660
HAIGHT, R. C., Coulomb excitation of the first 2^+ state of ^{24}Mg, 25:28283
HAIS, I. M., Decrease in pethidine demethylating activity of isolated rat liver microsomes following whole-body x-irradiation, 25:27034
HAKURA, Yukio, PFP observations. I, 25:27363
HALDAR, P. K., Supervoltage radiation response in epidermoid carcinoma of the esophagus, 25:26896
HALES, J. M., Phoretic processes in scavenging, 25:26387 (CONF-700601-, pp 411-22)
Washout of SO_2 from plume of a coal-fired power plant, 25:26378 (CONF-700601-, pp 293-303)
HALL, J. D., Instrument manual for prototype wet concrete analyzer, 25:26540 (ORO-3842-3)
HALL, R. A., Effects of fallout in agriculture, 25:26786
HALL, R. O. A., Self-irradiation damage in α-plutonium, 25:27837 (AERE-R-6506)
HALL, R. W., High-resolution radio observations of Venus at 6 cm, 25:27434
HALLE, Lars, Swedish nuclear manufacturing industries: today and tomorrow, 25:28525 (CONF-700550-, Paper 3)
HALLER, W. A., Californium-252 neutron activation for terrestrial, sea floor, and possible planetary surface analysis, 25:26188 (BNWL-SA-3803)
HALPERN, B., Myelo-restorative capacities and immunocompetence of bone marrow cells of the mouse cultivated in vitro, 25:26942
HALPERN, I., Isobaric analogue resonant (p,γ) reactions on ^{92}Mo, 25:28359
HALPERN, S. E., Critical evaluation of /sup 99m/Tc--Fe--ascorbic acid complex as a renal scanning agent, 25:26848
HALPERN, T., Hyperfine interactions: tables of isotropic and anisotropic parameters for the atoms hydrogen to bismuth, 25:27441 (ANL-7784)
HALPERN, Yuval, Electrophilic reactions at single bonds. III, 25:26226
HAMADA, K., Raman spectra of chlorofluorosilanes in gaseous, liquid, and solid state; anomalous ^{35}Cl, ^{37}Cl isotope intensity effects in splitting of totally symmetrical SiCl stretching mode in $SiCl_3F$ and $SiCl_2F_2$, 25:26218
HAMANN, D. R., Investigation of Kondo alloys and compound by the superconductive proximity effect, 25:27662
HAMILTON, J. H., Beta--gamma band mixing in ^{152}Sm, 25:28430
HAMLET, Peter, Optical bleaching of trapped electrons in γ-irradiated alkaline ice. Location of energy levels. 25:26298
HAMOUDA, I., Review of research activities using the UA-RR-1, 25:28777
HAMPL, J., Elimination of ^{131}I-labelled heterologous antigen after total body x-irradiation, 25:26944
HAMPL, V., Collection efficiency of water droplets in AgCl aerosol, 25:26370 (CONF-700601-, pp 161-7)
HANADA, Reimon, Recovery of low-temperature fast neutron irradiated tungsten, 25:27228
HANAWALT, P. C., Repair following uv irradiation of E. coli, 25:27112
HAND, T. W., Controlled avalanche caused by electron cyclotron acceleration, 25:27698
HANDLER-BERNICH, E., Interaction between thymidylic acid and sulfhydrylamine radioprotectors, 25:26279
HANGAY, Gyoergy, Radiation sterilization of an ophthalmic ointment containing hydrocortisone and chloramphenicol. IV, 25:27161
HANNA, Stanley S., Analog resonances formed in isospin forbidden reactions and splitting of the E1 giant resonance, 25:28222
HANSEN, Luisa F., Search for an imaginary isovector interaction in the optical model potential in ^3He induced reactions, 25:28461
HANSEN, P. G., Alpha decay of neutron deficient isotopes of mercury and radon and their daughters, 25:28302 (CERN-70-30(Vol.1), pp 523-31)
Compound-nucleus aspects of beta decays with high Q values, 25:28443 (CERN-70-30(Vol.1), pp 421-33)
Delayed-proton emission from neutron-deficient isotopes of xenon and mercury, 25:28301 (CERN-70-30(Vol.1), pp 487-96)
HANSEN, U., Influence of coated-particle structure in thermal-neutron-spectrum energy range, 25:28658
HANSEN, Wayne Richard, Polonium-210 in soils and plants, 25:26684
HANSON, G. T., Electrolytic process for ultra-fine beryllium [powder], 25:27192

XUM

HARA, M., Thyroid crisis following ^{131}I therapy, 25:26881
HARA, Toshihiko, Scintigraphy of lung cancer using ^{203}Hg, 25:26842
HARADA, A., Analysis of Zircaloy, 25:26171
HARASZTI, Maria, Radiation sterilization of an ophthalmic ointment containing hydrocortisone and chloramphenicol. IV, 25:27161
HARDAWAY III, John B., Ionic domain for Y_2O_3-doped ThO_2 at low oxygen activities, 25:27286
HARDY, J. C., Isospin purity and delayed-proton decay: ^{17}Ne and ^{33}Ar, 25:28195
HARDY, K. A., Moessbauer effect in 121.2-keV transition in ^{147}Sm, 25:28420
HARIHARAN, P. V., X-radioinduced thymine damage in Micrococcus radiodurans, 25:26643
HARMANEC, P., Evolution of close binaries. VI, 25:27334
HARMER, R. S., Utility of (Pr,Nd)Co_5 alloy for permanent magnets, 25:27886
HARMSEN, Aa., Brain scanning: cerebral scintigraphy, 25:26850
HARNEY, H. L., A comparison of analogue resonance studies and coulombstripping in ^{208}Pb, 25:28366
HARPER, Boyd Elbert Jr., Experimental investigation of neutron pulses through an interface and moderator lattice, 25:28818
HARRINGTON, Peter Bryan, Sound absorbing devices, 25:28832
HARRIS, Charles W., Method of seperating the rare earths by fractional co-distillation of their volatile chelate derivatives, 25:26336
HARRIS, Edward G., Hydromagnetic stability of Bennett pinch, 25:27748
HARRIS, J. S., Annealing of damage in ion implanted gallium arsenide, 25:27862
HARRIS, K. K., Ogo 5 measurements of the plasmasphere during observations of stable auroral red arcs, 25:27622
HARRIS III, William Franklin, Ecological aspects of responses of Liriodendron tulipifera L. and Acer saccharinum L. to fast neutron radiation and reduced light, 25:27076
HARRISON, H. F. A., Highly stripped ions in laser sources, 25:27723 (WASH-1159, pp 162-7)
HARRISON, R. G., Anti-inflammatory effect of benzydamine, 25:26806
HARRISS, Robert C., Mechanisms of iodine injection from the sea surface, 25:26380 (CONF-700601-, pp 319-24)
HART, Hiram E., Discrete formulation and error minimization in applying the integro-differential equation approach to mono-compartment data, 25:26580
HARTWIG, Edward C., Non-intercepting monitor of beam current and position, 25:28117 (UCRL-20166)
HARVEY, J. D., Influence of breakup channels on the analysis of deuteron stripping reactions, 25:28512
HARVEY, Karen L., Explosive phase of solar flares, 25:27382
HARVEY, M., Coupling of quasiparticles and anharmonic vibrations: A = 33 and 34, 25:28249
HAS, M., The measurement of energy levels' width in the 6-9 MeV region, 25:28219 (NRCN-254)
HASEGAWA, A. T., Dose reduction factor for radiation lethality in mice as a function of the dose of mercaptoethylamine, 25:26924
HASEGAWA, Akira, Chemical and hygienic studies on natural radioactive spa, 25:26743
HASEGAWA, Ryusuke, Two currents conduction in Kondo alloys, 25:28844 (CALT-822-28)
HASHIMOTO, T., Management of effluents from JAPC's nuclear power stations, 25:28624
HASHIMOTO, Y., Effect of radiation on the spore germination of the cellular slime mold Dictyostelium discoideum, 25:27065
HASSELGREN, A., Reaction $^{73}Ge(n,\gamma)^{74}Ge$, 25:28258
HASTE, Glenn, Feedback experiments in a hot electron plasma, 25:27775
HASUIKE, J. K., Development of ion exchange processes for the removal of radionuclides from milk, 25:26335 (RO/EERL-71-1)
HATA, Taeko, Application of pharmacology to animal group psychology, 25:28874 (ORNL-tr-2447)
HATTA, Osamu, Balneotherapy of radiation injury. XXVIII, 25:26897
HATTULA, J., Gamma transitions in ^{152}Sm, 25:28397
HAUG, P. K., Renormalization constants in the random-phase approach, 25:28509
HAUSER, J. J., Investigation of Kondo alloys and compound by the superconductive proximity effect, 25:27662
HAVENSTEIN, G. B., Genetic effects of cumulative maternal irradiation on growth and age at sexual maturity in rats, 25:26965
HAVLICEK, F., Effect of Prussian Blue combined with pilocarpine on ^{137}Cs excretion in rats, 25:26583
HAWKINS, C., Scattering of electrons by electrostatic fluctuations in a magnetized plasma, 25:27699
HAYASHI, Kozi, Two-phase region in TiC--Mo--30 percent Ni alloys, 25:27298
HAYASHI, Masatoshi, Age of fission neutrons to indium resonance in water and polyethylene, 25:28157
HAYASHI, Takeo, Deviation from the xi approximation in the beta transition of ^{122}Sb, 25:28412
Magnetic moments of three excited states in ^{149}Pm, 25:28381
HAYASHI, Tohru, Sulfur-35 uptake of gastric wall and excretion into gastric juice in rats, 25:26605
HAYE, C., Influence of irradiation dose on latency time of cataracts in rabbits, 25:27027
HAYODOM, V., Standard neutron irradiation facility experience in Thailand, 25:27062 (IAEA-R-459)
HAZELTINE, R. D., Diffraction radiation by a line charge moving past a comb, 25:28483
HEAMES, T. J., SAS1A: a computer code for the analysis of fast-reactor power and flow transients, 25:28727 (ANL-7607)
HEDGECOCK, P. C., Evidence for magnetic field aligned currents during the substorms of Mar. 18, 1969, 25:27620
Solar particle event of Feb. 25, 1969, 25:27555
HEDIN, G., Energy levels in ^{114} ^{116} ^{118} ^{120} ^{122}Cd populated in decay of Ag isotopes, 25:28337 (CERN-70-30(Vol.2), pp 1069-74)
Possible nuclear co-existence in odd-mass Ir nuclei, 25:28324 (CERN-70-30(Vol.2), pp 957-65)
HEFFNER R., Isobaric analogue resonant (p,γ) reactions on ^{92}Mo, 25:28359
HEGARTY, A. F., Acyl transfer reactions from and to the ureido functional group. IV. Neighboring carboxyl group general acid catalysis in the hydrolysis of an O-acylisourea (2-amino-8-carboxy-4-oxo-3,1,4-benzoxazine), 25:26253
HEGYELI, Ruth Johnsson, Artificial heart program conference, Washington, D. C., 6/69, 25:26899
HEIDEMANN, A., Experiments at the Munich research reactor FRM, 25:28775
HEINLOTH, K., Electroproduction of single π^+ mesons on hydrogen, 25:27950 (DESY-71/9)
HELLERSTEIN, Lewis J., Study of human radiation sensing and dark adaptometry using x-rays, 25:27039
HELLING, G., Nuclear molecules formed in elastic ^{16}O + ^{16}O scattering, 25:28171 (CERN-70-30(Vol.1), pp 601-2)
HELM, William T., Prog. rpt. on Amchitka bioenvironmental program, annual, 7/69--6/70, 25:28841 (BMI-171-133)
HELPPI, H., Gamma transitions in ^{152}Sm, 25:28397
HENDEL, H. W., Collisional drift instabilities, 25:27729
Conference on feedback and dynamic control of plasmas, Princeton, N. J., 6/70. I, 25:27752
Feedback stabilization of the transverse Kelvin--Helmholtz instability, 25:27772
Remote feedback stabilization of drift instability by microwaves, 25:27766
HENDERSON, C. E., Joshua lattice physics subsystem, 25:28801 (DP-MS-70-78)
HENDERSON, J., Blood of patients with gynecologic cancer following irradiated Streptokinase-Streptodornase, 25:26632
HENGLEIN, A., Multiple pulse radiolysis: successive accumulation of two hydrated electrons in oxygen, nitrobenzene, and nitromethane, 25:26308
Secondary rainbows and interference in elastic scattering of H^+ by Ar, 25:27458
HENRY, J. J., Capacitance gage for dimensional measurement, 25:28910 (Y-1783)
HENRY, R., Irradiation of hands during preparation of /sup 99m/Tc and /sup 113m/In labeled compounds, 25:26768
HENSLEY, D. C., Measurement of the mass of ^9Li, 25:28175
HENSLEY, W. R., Preparation of control tape for an R-THETA inspection machine, 25:28907 (Y-1725)
HERBERT, Sarah Mary, Chemical and conformational studies of gamma-irradiated lysozyme, 25:26646
HERENDEEN, Robert Albert, Paraelectric resonance in KCl:Li^+, 25:26215 (NYO-2150-59)
HERMAN, Herbert, Prog. rpt. on fatigue-enhancement of diffusion, annual, 6/70--5/71, 25:28870 (NYO-4097-2)
HERMAN, J. A., X-ray induced polymerization of gaseous vinyl chloride, 25:26282
HERNANDEZ, H. P., Mechanical features of electron-ring compressors, 25:28118 (UCRL-20177)
HEROLD, H., Dynamic stabilization experiment on a linear screw pinch, 25:27790
HERRING, J. R. H., Satellite-borne x-ray spectroheliograph, 25:26484
HERRMANN, G., Some studies on neutron-rich nuclei, 25:28326 (CERN-70-30(Vol.2), pp 985-1000)
HERTING, Sv. E., Lymph node scanning with radioactive Au, 25:26851
HERZOG, W., Some studies on neutron-rich nuclei, 25:28326 (CERN-70-30(Vol.2), pp 985-1000)
HESS, A. L., ZPR-3 assemblies 48: 48A, and 48B: the study of a dilute plutonium-fueled assembly and its variants, 25:28752 (ANL-7759)
HESS, Tom, Neutron--proton interaction in odd--odd deformed nuclei, 25:28514
HETENYI, G. Jr., H-2-glucose as tracer in turnover studies, 25:26602
HEUSENER, G., Optimization of sodium-cooled fast breeders by nonlinear programming methods, 25:28655 (EURFNR-830)
HEUSLER, A., Spectator particles and resonances, 25:28365
HEUSS, Kurt, Contribution to irradiation planning in electron therapy of bronchial carcinoma, 25:26757
Radiation treatment planning for a 42 MeV betatron, 25:26865
HEVEZI, J. M., Gas target source for neutron radiation therapy, 25:26883
HEYNEN, V., Total photoproduction cross section of hadrons

on nuclei, 25:27953
HICKS, D. L., Compactness by bounded L/sub p/-variation, 25:28890 (SC-RR-70-852)
HIDDLESTON, H. R., Isobaric analog resonances in proton scattering from ^{86}Kr, 25:28242
Isobaric analog resonances in proton elastic scattering from ^{110}Cd, ^{112}Cd, and ^{114}Cd, 25:28370
Isobaric analog resonances in proton elastic and inelastic scattering from ^{130}Te, 25:28427
Neutron particle-hole states in ^{130}Te, 25:28369
HIDY, G. M., Theory of diffusive and impactive scavenging, 25:26382 (CONF-700601-, pp 355-71)
HIGGINS, R. B., Modulated decay in a two-level quantum system, 25:27939
HIGHTOWER, B. G., Population dynamics of the screw-worm fly, 25:27152
HIGHTOWER, W. H., Joshua lattice physics subsystem, 25:28801 (DP-MS-70-78)
HILARIS, Basil S., Review of experience with irradiation of brain metastasis, 25:26895
HILDEBRAND, B. P., Pulsed-laser holography for analysis of particle size and distribution, 25:26373 (CONF-700601-, pp 213-16)
HILF, E., Construction of mass formulas designed to be valid for neutron-rich nuclei, 25:28293 (CERN-70-30(Vol.1), pp 275-306)
HILL, E. R., Gyro and synchrotron radiation in vacuum and isotropic plasma, 25:27706
HILL, K. L., Index to experimental data of neutron-induced reactions, 25:28356 (UCRL-50400(Vol.3))
HILL, Leslie R., Energy partitioning during hypervelocity impact on rocks, 25:26354 (SC-R-70-4402)
HILL, Wilma S., Prog. rpt. on marine products development irradiator program: irradiated fresh shrimp shipping studies, annual, 10/67--9/68, 25:27138 (TID-25543)
HILLIARD, R. K., Scavenging of aerosol particles by sprays, 25:26372 (CONF-700601-, pp 187-204)
HILLSINGER, William R., Dosage tolerance of pelvic structures with ^{60}Co rotation radiation therapy, 25:26894
HINGORANI, S. B., Determination of ruthenium in fallout samples, 25:26181
HINTZ, E., Collisionless shock waves in laboratory plasmas, 25:27690
HIRAI, Masamitsu, Optical study of an ionic crystal by means of pulsed electron irradiation. IV, 25:27846
HIRAMOTO, Toshiyuki, Scintillation camera based on delay-line time conversion, 25:26486
HIRAOKA, T., Paired ionization chambers for measurement of neutrons and gamma rays, 25:26538
HIRAOKA, Toru, Pulsed neutron experiment on FCA I-5, 25:28759 (JAERI-Memo-4272)
HIRATA, Masanobu, Scintigraphy of lung cancer using ^{203}Hg, 25:26842
HIRAYAMA, Toshinari, Effect of precipitates on fatigue strength, 25:27231
HIRSCH, R. H., Longitudinal oscillations of Lorentzian electron gas, 25:27822
HISANO, Kingo, Determination by x-ray fluorescence of barium and strontium in barium carbonate of industrial grade, 25:26167
HISLOP, J. S., Determination of fluorine in rock materials by γ-activation and radiochemical separation, 25:26193
HIYAMA, Tetsuo, Thermal neutron reactor study group, 25:28712
HIYAYAMA, Hiroshi, Rare-earth elements spot-lighted by development of their separation techniques, 25:26343
HJORT, S. A., Rotational states in ^{168}Yb, ^{169}Yb, and ^{170}Yb, 25:28394
HNAKE, W., Program for solution of the stationary neutron transport equation with spherical symmetry, 25:28147 (JUL-683-MA)
HOAGLAND, R. G., Fracture mechanisms and radiation effects, 25:27270
HOCEVAR, C. J., THETA1-B: a computer code for nuclear reactor core thermal analysis, 25:28737 (IN-1445)
HOCH, Michael, Thermodynamic properties of ternary refractory carbides. III, 25:27283 (N-71-10590)
HOCHBERG, S., Faddeev's equations in the SU(3) representation of a three-particle state, 25:28056
HOCHMANNOVA, J., Carotenoids synthesized by uv-induced mutants of Mycobacterium phlei, 25:26687
HOCKING, L. M., Recent calculations of collision efficiencies, 25:26384 (CONF-700601-, pp 381-3)
HOEBERICHTS, J. A., Uptake of ^{32}P phosphate by red blood cells, 25:26589
HOEGILD, P., Spatial distribution of defects in ion bombarded silicon and germanium, 25:27861
HOEGLUND, A., Lifetimes of excited nuclear levels, 25:28341 (CERN-70-30(Vol.2), pp 1115-18)
HOEHNE, K., Electroproduction of single π^+ mesons on hydrogen, 25:27950 (DESY-71/9)
HOELD, A., Analytical model for describing the frequency response and stability behavior of light-water moderator pressurized power reactors, 25:28665
HOFFER, Paul B., Correlation between brain tumor detectability on brain scan and protein levels of the spinal fluid, 25:26828
HOFFMAN, Joseph, Early and late effects of tritiated thymidine upon the replication of splenic lymphocytes, 25:26994
HOFFMANN, Alain, COREGRAF 2: adjustment and comparison with experiment, 25:28654 (CEA-N-1344(2))
HOFFMANN, G., Diagnostic value of the quotients of precordial over prepulmonary counting rate from Na^{131}I, 25:26822
HOFMANN, G., Electroproduction of single π^+ mesons on hydrogen, 25:27950 (DESY-71/9)
HOFMANN, P., Fission product yield in the fission of ^{235}U, ^{238}U, ^{239}Pu, and ^{241}Pu with neutrons of different energies, 25:28354 (NP-18723)
HOFMANN, P. L., Prog. rpt. on environmental engineering, 10--12/70, 25:28710 (HEDL-TME-71-26)
HOFNER, W., Efficacy of additional shielding in telecobalt therapy, 25:26779
HOGAN, Mary Elizabeth Mogge, SU(3) x SU(3) chiral Lagrangian model for anti KN interactions, 25:28037
HOGAN, W., Argand-diagram analysis of Pomeron coupling to KN and anti KN system, 25:28035
HOGAN, W. A., Conservative trapping of charged particles in a static magnetic field, 25:27674
HOGE, Kenneth G., Elastic precursor decay in tantalum, 25:27216
HOGLUND, B. M., Experimental study of a gas jet penetrating a liquid coolant and impinging on a heated surface, 25:26418 (ANL-7734)
HOLINDE, K., One boson exchange potential and nuclear matter properties, 25:28448 (CERN-70-30(Vol.2), pp 1133-5)
HOLLAND, I. B., Co-transduction of a pleiotropic mutation affecting colicin E2 refractivity, uv sensitivity, recombination proficiency, and surface properties of E. coli K12, 25:26707
HOLLAS, C. L., Isobaric analog resonances in proton scattering from ^{86}Kr, 25:28242
Isobaric analog resonances in proton elastic scattering from ^{110}Cd, ^{112}Cd, and ^{114}Cd, 25:28370
Isobaric analog resonances in proton elastic and inelastic scattering from ^{130}Te, 25:28427
Neutron particle-hole states in ^{130}Te, 25:28369
HOLLECK, H., Stoichiometry shift in an oxide fuel element at high burnup, 25:28690 (EURFNR-836)
HOLLEY, C. E. Jr., Enthalpy of formation of uranium tetrachloride, 25:26263
HOLLIDAY, J., Quality control, inspection, and testing of Series I metallurgical fuels for first charge of Dragon reactor, 25:26438 (DP-Report-432)
HOLLINGSWORTH, Dorothy R., Neuro-muscular tests of aging in Hiroshima subjects, 25:27053
HOLLINGSWORTH, J. William, Neuro-muscular tests of aging in Hiroshima subjects, 25:27053
HOLM, G., Levels in doubly-even tellurium isotopes, 25:28330 (CERN-70-30(Vol.2), pp 1010-11)
HOLM, G. B., Evidence for high-spin three quasiparticle state in ^{133}I produced in fission, 25:28331 (CERN-70-30(Vol.2), pp 1012-14)
Experimental techniques for nuclear structure studies in the Tin-region at OSIRIS, 25:28107 (CERN-70-30(Vol.2), pp 1003-5)
Neutron hole states in the tin-region, 25:28329 (CERN-70-30(Vol.2), pp 1008-10)
Proton states in the tin-region, 25:28328 (CERN-70-30(Vol.2), pp 1006-7)
Tin-132-region studied by means of OSIRIS facility, 25:28327 (CERN-70-30(Vol.2), pp 1001-3)
HOLMGREN, L.-A., Pitch-angle dependence of auroral electron fluxes in keV range, 25:27577
HOLSTEIN, B. R., Chiral symmetry and nonleptonic-radiative hyperon decay, 25:28004
HOLSTON, J. A., Study of irradiated-pasteurized fishery products, 25:27149
HOLZER, Thomas E., Comparison of kinetic and hydrodynamic models of an expanding ion exosphere, 25:27613
HOLZER, Thomas Edward, Stellar winds and related flows, 25:27328
HOMMERICH, K. W., Radiotherapy of vocal-cord leukoplakia, 25:26868
HONECK, H. C., Joshua lattice physics subsystem, 25:28801 (DP-MS-70-78)
HONECKER, R., Four-pion decay mode of D(1285) meson in π^+-p reactions at 16 GeV/c, 25:27964
HONES, Edward W. Jr., Experimental observations in the magnetotail during an interplanetary disturbance, 25:27546
HONIG, A. L., 1000-MWe LMFBR accident analysis and safety system design study. Candidate emergency decay heat removal systems. Topical report, 25:28732 (BAW-1351)
HONIG, H., 1000-MWe LMFBR accident analysis and safety system design study. Topical report. candidate secondary containment support systems, 25:28730 (BAW-1349)
HONIG, Milton Leslie, Synthesis and isomerization of deuterated cyclobutenes, 25:26219
HOOGEVEEN, Joh. Th., Thermoconductometric investigation of phosphatidylcholine in aqueous tertiary butanol solutions in the absence and presence of metal ions, 25:26272
HOOKE, W. H., Divergence of ion velocity in the E region due to vertical winds, 25:27610
HOOPER, M. B., Isospin coupling in deuteron stripping reactions, 25:28462
HOOTMAN, H. E., Californium-252 shielding guide, 25:27828 (DP-1246)

XUM

HOPEWELL, J. W., Vulnerability of developing brain: I. Some lasting effects of x-irradiation, 25:26946
HOPFENBERG, H. B., Transport of fixed gases in radiation-stabilized poly(vinyl chloride), 25:26280
HOPKINS, B. J., Surface potential of H on W (100), (110), and (112) single crystal surfaces, 25:27234
HORD, C. W., Mariner 6 and 7 ultraviolet spectrometer experiment: upper atmosphere data, 25:27433
HORGAN, A. M., Oxygen adsorption, reconstruction, and thin oxide film formation on Ni, Fe, W, and Mo, 25:27224
HORIKAWA, M., Comparative studies on rejoining of DNA-strand breaks, 25:26953
HORLITZ, E., Program for solution of the stationary neutron transport equation with spherical symmetry, 25:26147 (JUL-683-MA)
HORN, J., Evolution of close binaries. V, 25:27331
HORNBY, I. W., Correlation of measured and calculated strains in top-half of Oldbury prestressed concrete pressure vessel R1, 1965--1970, 25:28528 (RD/B/N-1784)
HORNSEY, Shirley, Survival of jejunal crypt cells after radiation, 25:26957
HORNSHOEJ, P., Alpha decay of neutron deficient isotopes of mercury and radon and their daughters, 25:28302 (CERN-70-30(Vol.1), pp 523-31)
Compound-nucleus aspects of beta decays with high Q values, 25:28443 (CERN-70-30(Vol.1), pp 421-33)
Delayed-proton emission from neutron-deficient isotopes of xenon and mercury, 25:28301 (CERN-70-30(Vol.1), pp 487-96)
HORSCH, F., Prompt gamma transitions in primary fragments from neutron-induced fission, 25:28320 (CERN-70-30(Vol.2), pp 917-30)
HORTON, P. H., Development of nuclear reactor bearings for 1500°F space operation, 25:27200 (CONF-691114-7)
HOSAIN, Fazle, Ionic /sup 135m/Ba: a new agent for bone scanning, 25:26835
HOSEK, B., Radioprotective effect of AET, serotonine, natrium-fluoro-acetate, and histamine in mice, 25:26800
HOSOKAWA, M., Hot electron confinement in a cusped magnetic field by ECRH wrapping, 25:27677
HOUCK, Clarence W., Titanium--zirconium--germanium brazing alloy, 25:27229
HOURS, R., Radioisotopes, general concepts, 25:26316
HOUSTON, J. E., Characterization of the ionic species incident on the cathode in a glow discharge, 25:28891 (SC-RR-710122)
HOWARD, James O., Block in-plant radiation by design, 25:28572
HOWARTH, John L., Acute radiation injury in neonatally thymectomized germ-free mice. Hematopoietic and morphologic consequences, 25:26937
HOWERTON, R. J., Index to experimental data of neutron-induced reactions, 25:28356 (UCRL-50400(Vol.3))
HOY, Gilbert R., Prog. rpt. on coincidence-Moessbauer studies of solid state phenomena, 6/70--5/71, 25:28864 (NYO-3973-8)
HRADIL, J., Problems of excretion analysis after repeated internal contamination with strontium radioisotopes, 25:26585
HRASTNIK, B., Deexcitation of the 662-keV state in ^{137}Ba by the internal Compton effect, 25:28422
HRDLICKA, Z., Neutron radiography and its application, 25:26439 (UJV-2545-R,T)
HREBIK, F., Observations of chromospheric flares at Ondrejov, 25:27391
HREN, J. J., Measurements of atomic order with the field-ion microscope, 25:27252
HSU, F. H., Positron annihilation in irradiated tefion, 25:27306
HU, Michael J. C., SLAC spiral reader system, 25:26511
HUANG, H. S., Optimum control of heat exchangers with internal heat generation, 25:26421
HUBBARD, H. W., Statistical model calculations of ^{56}Fe neutron cross section, 25:28218 (NP-18674)
HUBER, H., Electron optics of sagittaire, 25:28142
HUBER, Max G., Microscopic analysis of (γ,p) and (γ,n) reactions at medium photon energies, 25:28488
HUDGENS, C. R., Method and device used for the safe handling and storing of fragile x-ray diffraction specimens, 25:26449 (MLM-1790)
HUEBEL, H., Levels in ^{194}Pt, ^{196}Pt, and ^{198}Pt, 25:28425
HUEBSCHER, D., Some studies on neutron-rich nuclei, 25:28326 (CERN-70-30(Vol.2), pp 985-1000)
HUEFNER, Joerg, Microscopic calculation for the escape width of analog states, 25:28466
The role of the anti-analog state in the decay of the analog state, 25:28467
HUFFMAN, F., Effects of intracorporeal heat and radiation on dogs, 25:26931
HUG, Otto, Dominant lethal mutations in descendants of irradiated male mice. I, 25:26726
HUGHES, T. A., E1 transitions from analog states in ^{90}Zr, 25:28360
HUGHES, T. H., VENUS: a two-dimensional coupled neutronics-hydrodynamics computer program for fast-reactor power excursions, 25:28728 (ANL-7701)
HULL, Andrew P., Radiation in perspective: some comparisons of the environmental risks from nuclear- and fossil-fueled power plants, 25:28627
HULLY, Richard, JOANIE: a multianalyzer program for pulse height analysis, 25:26495
HULTBERG, S., Rotational bands in ^{171} ^{173} ^{175}Hf from (particle, xn) reactions, 25:28323 (CERN-70-30(Vol.2), pp 949-55)
HULTGREN, Ake, Recovery of Pu and U from reactor fuel elements, 25:26346
HULTQVIST, Bengt, Anisotropy for 1- and 6-keV positive ions in upper ionosphere, 25:27604
HUMES, R. M., Absorbed fractions for small volumes containing photon-emitting radioactivity, 25:26752
HUNDHAUSEN, A. J., Heat conduction and nonsteady phenomena in the solar wind, 25:27628
Observation of the Feb. 26, 1969 interplanetary shock wave, 25:27570
Plasma measurements across the bow shock and in the magnetosheath, 25:27537
Solar-wind disturbances associated with solar activity, 25:27534
Two-dimensional simulation of flare-associated disturbances in the solar wind, 25:27629
HUNSTEIN, W., Radiation (^{90}Sr) induced pulmonary carcinoma in rats, 25:26921 (LF-tr-49)
HUNT, D. C., Restricted release of plutonium. Part 2. Theory, 25:26782
Restricted release of plutonium: Part 1. Observational data, 25:26781
HUNT, Dale E., Biologic activity of daunomycin in microbial systems, 25:27100
HUNTER, D. O., Effects on neutron irradiation, at thermal reactor temperatures, on the propagation velocity of ultrasonic waves in A533-B steel, 25:27268 (WHAN-FR-38)
HUNTZICKER, James J., Magnetic transition, heat capacity, and thermodynamic properties of UO_2 from 5 to 350°K, 25:26264
HUPF, H. B., Generator /sup 83m/Kr, 25:26320
HURDUS, M. H., Delayed neutron emission from selenium isotopes, 25:28212 (CERN-70-30(Vol.1), pp 519-20)
HURT, H. D., Effect of dietary selenium on the survival of rats exposed to chronic whole body irradiation, 25:27032
HURT, N. E., Jordan algebras and quantizable dynamical systems, 25:27945
HURTER, A., Chicago air pollution systems analysis program, 25:28840 (ANL-ES-CC-8)
HURT III, S. S., Prog. rpt. on research reactor, 10--12/70, 25:28762 (ORNL-TM-3369)
HUTCHENS, R. D., Magnetic and electrical characteristics of $REPd_3$ intermetallic compounds, 25:27870
HUTSON, R. L., Proton--proton elastic scattering from 9.6 to 13.6 MeV, 25:27957
HYATT, William Dennis, Low-temperature annealing of electron irradiated germanium, 25:27850
HYDE, E. K., Production and decay properties of thorium and protactinium isotopes of mass 221-225 formed in heavy ion reactions, 25:28304 (CERN-70-30(Vol.1), pp 545-6)
HYDE, Earl K., Fragment production in interaction of 5.5-GeV protons with U, 25:28426
Search for new islands of fission isomerism, 25:28305 (CERN-70-30(Vol.1), pp 567-74)
HYLAND, R. E., Cavity reactor engineering mockup critical experiment, 25:28761 (NASA-CR-72409)
HYNDS, R. J., Low-energy proton measurements in interplanetary space, 25:27559

I

IBRAGIMOV, A. P., Changes in carbohydrates and organic acids in leaves and roots of cotton and maize plants in dependence on the dose of presowing gamma irradiation of seeds, 25:27074
ICHIKAWA, Michio, Analysis of instrumentation data from IFA-150 irradiated in HBWR, 25:28692 (JAERI-Memo-4248)
ICHIKAWA, Yoichi, New phenomenon of usefulness in the radioimmunoassay of plasma adrenocorticotropic hormone, 25:26675
IDEHARA, T., Oscillation due to collision-induced instability in mercury plasma, 25:27802
IDENO, Kazumi, Nonrandom distributions of neutron resonance levels, 25:28421
IGLESIAS, F. C., Nuclear spectroscopy of iodine isotopes with a greater than or equal to 134, 25:28336 (CERN-70-30(Vol.2), pp 1057-68)
IGNATENKO, M. M., Efficiency of a three-dimensional MHD-channel, 25:27490
IIJIMA, Soichi, Smallest forms of papillary carcinoma of thyroid. A study of 141 microcarcinomas less than 0.1 cm in greatest dimension, 25:26898
IIO, Masaaki, Scintigraphy of lung cancer using ^{203}Hg, 25:26842
IIZAWA, Katsuyuki, Gamma-ray spectroscopy of ^{74}As, 25:28278
IKEBUCHI, Hideharu, Chemical and hygienic studies on natural radioactive spa, 25:26743
IKEGAMI, H., Hot electron confinement in a cusped magnetic field by ECRH wrapping, 25:27677
IKUTA, Takashi, Calculation of x-ray production in alloy targets using Monte Carlo method, 25:27836
ILAKOVAC, K., Deexcitation of the 662-keV state in ^{137}Ba by the internal Compton effect, 25:28422
ILARI, O., Measurement of β-active gases in the air,

25:26488
ILLARIONOV, A. F., Thomson scattering as a cooling mechanism for the solar corona, 25:27401
IMAI, T., Thyroid crisis following ^{131}I therapy, 25:26881
IMAZU, S., Effect of helical instability on the radial density and potential distribution, 25:27738
IMSHENNIK, V. S., Thermodynamics under conditions of hot matter neutronization and the hydrodynamic stability of stars at late stages of evolution, 25:27335
INADA, T., Paired ionization chambers for measurement of neutrons and gamma rays, 25:26538
INDGIN, Sidney N., Eccrine poroma, 25:27055
INDYKUL, V. P., Transverse particle diffusion in stochastic fields, 25:27719
INGEMARSSON, A., Polarization of 3- level in ^{40}Ca, 25:28256
INGRAND, J., Synoviothesis (synoviotherapy by radioisotopes) studies of more than 400 cases and future prospects, 25:26873
INOUE, Kiyoshi, Fission-gas release from nuclear fuels with in-pile gas-loop, 25:28821
INOUE, Nobuko, Adsorption of uranium in artificial seawater with titanic acid, 25:26350
INZELT, Gy, Dependence of the light output of liquid scintillation systems on spectral properties of components, 25:26462
IONESCU, M., Effect of gamma-rays on some pea species, 25:27089
IOTTI, Robert Charles, Cluster-model evaluation of neutron cross sections for light-weight nuclei, 25:28167
IRELAND, Rosalee, Relative susceptibilities of caffeine-sensitive and caffeine-resistant strains of Candida albicans to inactivation and mutation by ultraviolet radiation, 25:27073
IRIE, Goro, Superhigh voltage irradiation of bladder tumor, 25:26876
IRVING, J., Correlation of measured and calculated strains in top-half of Oldbury prestressed concrete pressure vessel R1, 1965--1970, 25:28528 (RD/B/N-1784)
ISAACS, H. S., Ionic range of ThO_2--1b wt. percent Y_2O_3 at high oxygen activities, 25:26262
ISAACS, L. L., Magnetic properties of dilute alloys of scandium, 25:27878
ISHIDA, H., Computer controlled dynamic cineradiography, 25:26557
ISHIDA, Y., Oscillation due to collision-induced instability in mercury plasma, 25:27802
ISHII, Daido, Activation analysis for B, 25:26198
Activation analysis for Li, 25:26196
ISHII, K., Suppression of drift instability by rf electric field, 25:27787
ISHIKAWA, I., $4\pi\beta$--γ coincidence absolute measurement of nuclides emitting soft conversion electrons in appreciable proportions, 25:26464
ISHIKAWA, N., Flow of a liquid metal coolant past a heat generating cylinder, 25:26422
ISHKHANOV, B. S., Photoneutron reactions on copper, 25:28260
ISOUM, M., Photosensitizing effect of trisoralen on DNA synthesis, 25:26808
ITAGAKI, Shinjiro, Decay of 14-min ^{112}In, 25:28406
ITAKURA, T., Management of effluents from JAPC's nuclear power stations, 25:28624
ITAYA, Mitsuo, Even-parity states of ^{16}O, 25:28191
IVANCHENKO, V. G., Calculating cross-sections of $^{16}O(\gamma,n)^{15}O$ reactions, 25:28186
Change in solubility of Ce, Pr, and Nd in Cr as a function of temperature, 25:27238
IVANCHENKO, Yu. M., Effect of low frequency fluctuations on superconducting tunnelling, 25:27649
IVANOV, A. A., Influence of high-frequency field on plasma instabilities, 25:27781
IVANOV, G. R., Normal color indices of Cepheids. III, 25:27340
IVANOV, U. I., Apparatus for study of motion of conducting emulsions in electric and magnetic fields, 25:27501
IVANOV, V. I., Radiation biophysical investigations of Arabidopsis thaliana. III, 25:26736
IVANOV-KHOLODNI, G. S., Ionization of e region by precipitating electrons, 25:27527
IVANTER, I. G., Two-frequency precession of muonium in magnetic field, 25:27446
IVASCU, M., Reaction $^{88}Sr(tau,\alpha)^{88}Sr$ at E/sub tau/ = 17.5 MeV, 25:28277
IVASHCHENKO, R. K., Influence of structure and testing conditions on the mechanical properties of low-alloyed molybdenum, 25:27221
IWAMASA, R. T., Oxidation of 2-methoxyethanol to methoxyacetic acid by nitric acid solutions, 25:26223
IWASAKI, Tamiko, Effects of fast neutrons and ^{60}Co γ-rays on Artemia, 25:26917
IYER, M. R., Nuclear charge distribution in fission fragments, 25:28508
IZUMI, M., Thyroid crisis following ^{131}I therapy, 25:26881
IZVORANU, M., Changes in the concentration of free amino acids in the liver of irradiated and partially hepatectomized rats, 25:27022

J

JABLON, Seymour, Childhood cancer in relation to prenatal exposure to atomic-bomb radiation, 25:27043
JACKA, F., Stable auroral red arcs observed from Adelaide during 1967-69, 25:27525
JACKSON, A. D., Model space calculation of the quasi-particle interaction for nuclear matter, 25:28453 (NYO-4032-37)
JACKSON, M. R., Scavenging by snow and ice crystals, 25:26367 (CONF-700601-, pp 121-36)
JACOBI, K. W., Eye changes caused by fast neutrons (15 MeV) and the protective action of chemicals, 25:27014
JACOBI, S., Cladding monitoring in sodium-cooled reactors by detection of delayed neutrons, 25:28698 (NP-18778)
JACOBS, Camille, Application of nuclear techniques to the recovery of faded photographs, 25:26287
JACOBSEN, T., High-latitude F-region irregularities, 25:27519
JACQUEMART, Rene, Reactivity measurements using the continuous run technique, 25:28799 (CEA-N-1385)
JAENECKE, Joachim, Shell-model description of Coulomb displacement energies in the light nuclei, 25:28479
JAGT, T., Lymph node scanning with radioactive Au, 25:26851
JAHNKE, U., Spin assignment for two isobaric analog resonances in ^{78}Se from the neutron decay, 25:28241
JAKEWAYS, R., Observations recorded by the cosmic-ray detector during the solar flare of Feb. 25, 1969, 25:27471
JAMES, A. Everette Jr., Patterns for differentiation of posterior fossa neoplasms as detected by brain scans, 25:26820
JAMES, A. P., Cell survival and x-ray-induced DNA degradation in Micrococcus radiodurans, 25:26627
JAMNE, E., Well reactor, 25:28793
JANCSO, G., Vapor pressure isotope effect of H_2S/D_2S, 25:26248
JANES, G. S., HIPAC as a source of highly stripped heavy ions, 25:28128 (WASH-1159, pp 88-112)
JANIK, R., Monochromatic method for measurement of mean proton energy in 665 MeV beam, 25:26505 (JINR-P13-5636)
JANIN, Guy, Numerical experiments with one-dimensional gravitational system by Euler-type method, 25:27412
JANUSZAJTIS, Andrzej, Applicability of the theory of initial recombination to liquid filled ionization chambers, 25:26472
JAQUEN, J., Electron optics of sagittaire, 25:28142
JARLSKOG, Cecilia, Radiative corrections to beta decay, 25:28493
JARMIE, Nelson, Proton--proton elastic scattering from 9.6 to 13.6 MeV, 25:27957
JASSBY, D. L., Feedback stabilization of the transverse Kelvin--Helmholtz instability, 25:27772
JAVID, Manucher, Glioblastoma multiforme. An analysis of the results of postoperative radiotherapy alone versus radiotherapy and concomitant 5-fluorouracil, 25:26889
JAYARAMAN, Swaminathan, Radiation damage and repair after whole-body or partial--body irradiations of T. molitor larvae, 25:26914
JEDLICKA, Pavel, Reaction of nervous tissue to application of ionizing radiation, 25:27056
JEFFERTS, K. B., Interstellar $^{12}C^{18}O$, $^{13}C^{18}O$, and $^{12}C^{18}O$, 25:27402
JENNINGS, P. J., Electron diffraction at crystal surfaces. IV, 25:27256
JENSEN, V. O., Wave--particle interaction in single-ended Q machine, 25:27693
JEPPESEN, P., Lymph node scanning with radioactive Au, 25:26851
JESPERSEN, M., Electron density observations during the PCA event of 25 Feb. 1969, 25:27564
JETER, T. R., Independent cesium yields in ^{236}U fission: identification of ^{145}Cs, 25:28307 (CERN-70-30(Vol.1), pp 589-99)
JETT, J. H., Proton--proton elastic scattering from 9.6 to 13.6 MeV, 25:27957
JIBUTI, M. V., Tri-axial periodic modulated structure in metallic alloys, 25:27249
JINNO, Kiyokatsu, Activation analysis for B, 25:26198
Activation analysis for Li, 25:26196
JOASOO, A., Use of serum thyroxine in assessment of thyroid function, 25:26857
JOBES, M., Anti-lambda production in 10 GeV/c K^+ proton interactions, 25:27966
$K^0_s p$ final state produced in K^+p interactions at 10 GeV/c, 25:27968
JOENSSON, J. O., Magnetic moment and hyperfine structure of ^{103}Ag, 25:28396
JOHANNESSON, Nils, Kinematic singularities in multi-particle processes derived from basic properties of spinor amplitudes, 25:28099
JOHANNSEN, K., Multiregion heat transfer analysis for displaced central, corner, and side elements of unbaffled LMFBR fuel rod bundles, 25:28661
JOHANSSON, A., Excited states of ^{40}Ca, 25:28255
JOHANSSON, N. G. E., Chemical transport of silicon and germanium during anneal treatment, 25:27909
JOHANSSON, Thomas, Two-centre potential and the (del V x p vector)^2 term, 25:28312 (CERN-70-30(Vol.2), pp 676-88)
JOHNSON, H. E., Galactic winds, 25:27403
JOHNSON, H. M., Environmental cracking in high-strength materials, 25:27175

XUM

JOHNSON, R. C., Influence of breakup channels on the analysis of deuteron stripping reactions, 25:28512
JOHNSON, R. G., Photoreversal of ultraviolet-induced division delay in Saccharomyces cerevisiae, 25:27080
JOHNSON, W. H. Jr., Feasibility of direct mass determinations of short half-life isotopes, 25:26547 (CERN-70-30(Vol.1), pp 307-19)
JOHNSON, W. S., Analysis of ion implanted diamond, 25:27858
JOHNSON, Wallace E., Energy partitioning during hypervelocity impact on rocks, 25:26354 (SC-R-70-4402)
JOHNSSON, J.-E., Content of noradrenaline and 5-hydroxytryptamine in rat after ionizing radiation, 25:26959
JOHNSTON, R. C., Canadian approach to designing and building foreign nuclear power stations, 25:28718
JOHSON, B., Delayed-proton emission from neutron-deficient isotopes of xenon and mercury, 25:28301 (CERN-70-30(Vol.1), pp 487-96)
JOLLEC, Claude, Use of microelectronics in linear circuits for nuclear spectrometry, 25:26494
JONEK, J., Influence of x-rays upon the mitotic activity and DNA synthesis in endometrial glandular epithelium, 25:26659
JONES, A. D. W., Low-lying excited states of ^{29}Al. III, 25:28267
JONES, Colin Elliott, Effect of stress on luminescence spectrum of irradiated silicon, 25:27849
JONES, D. Llanwyn, Analysis of transient elf disturbances within Earth--ionosphere cavity, 25:27592
Magnitude of sources of transient excitation of Schumann resonances, 25:27591
JONES, Heber D., Neutron--proton interaction in odd--odd deformed nuclei, 25:28514
JONES, K. L., Origin of storm increases of midlatitude F-layer electron concentration, 25:27510
Storm-time variation of F2-layer electron concentration, 25:27509
JONES, R. A., Influence of field-aligned currents on auroral-electron temperatures, 25:27603
JONES, R. M., Immunity to Dictyocaulus viviparus in calves. II, 25:26919
Immunity to Dictyocaulus viviparus in calves. III, 25:26918
JONES, Ray, SCOLDS: Spark chamber on-line data system, 25:26512
JONES, T., Radiation protection around the medical cyclotron at Hammersmith Hospital, 25:26775
JONES, T. B., Absorption of hf radio waves reflected at oblique incidence from the ionosphere in winter, 25:27595
JONES, W. D., Plasma expansion into a vacuum, 25:27709
JONES, William Benjamin, Distorted wave effects in pion interactions with nuclei, 25:28048
JONES, William Elvin, Relationship between x-ray induced teratogeny and chromosome aberrations in golden hamster embryos, 25:26982
JONGSMA, H. W., Production and decay properties of some shortlived cobalt nuclei, 25:28214 (CERN-70-30(Vol.2), pp 1105-13)
JONSCHER, A. K., Space-charge waves in solids, 25:27805
JONSON, B., Compound-nucleus aspects of beta decays with high Q values, 25:28443 (CERN-70-30(Vol.1), pp 421-33)
Low-lying states in odd-mass polonium isotopes, 25:28333 (CERN-70-30(Vol.2), pp 1023-9)
JOOS, H., Relativistic scalar quark model with strong binding, 25:28022 (DESY-71/10)
JORDAN, K. C., Technique for direct measurement of thermal power in assay calorimeters, 25:26548 (MLM-1780)
JOSEFSSON, L., Nuclear district heating: a study for the town of Lund, 25:28574
JOSHI, S. K., Cross-sections and reaction rates for electron-impact ionization of lithiumlike and sodiumlike positive ions, 25:27443
JOSLIN, W. Murray, Review of engineering standards development for nuclear power systems, 25:28536
JOVIC, Dj., Neutron inelastic scattering and neutron diffraction at the Vinca heavy water reactor, 25:28779
JOYCE, Glenn, Nonlinear behavior of the one-dimensional weak beam--plasma system, 25:27710
JOYET, G., Thorium-series in cigarettes and in lungs of smokers, 25:27046
JUDGE, D. L., Extreme-ultraviolet dayglow of Jupiter, 25:27432
JULIAN, Glenn M., Excited states of ^{138}Ce, 25:28414
JULIEN, R., LET parameter and radiolysis of Fe^{2+} solutions by low-energy protons, 25:26288 (LB/G-2937)
JULLIEN, P., Production of circulating rat interferon in mice--rat radiochimeras, 25:26995
JUNG, H. H., Total neutron cross sections of gross fission products, 25:28404
JUNKER, J., Plasma displacement due to dipole current near high-beta plasma, 25:27774
JURASKOVA, Vera, Study of recovery processes in haemopoietic tissue after irradiation, 25:26678
JURCEVIC, M., Deexcitation of the 662-keV state in ^{137}Ba by the internal Compton effect, 25:28422
JURETSCHKE, H. J., Extraordinary Hall effect in paramagnetic gadolinium, 25:27908
JURNEY, E. T., Nuclear levels in ^{177}Lu and ^{175}Lu, 25:28424
JUST, G., Measuring effective renal plasma flow by means of whole-body clearance of ^{131}I-hippuric acid, 25:26825

K

KABACHNIK, N. M., Electroexcitation of ^{32}S in region of dipole resonance, 25:28220 (UJV-2553-F)
KADLEC, J., Radiation experiment on a model of a finned tubular fuel element. I, 25:27267 (UJV-2371.R,T.)
KADZIKIEWICZ, Teodora, Induction of auxotrophic mutation in Streptomyces erythreus IA 64-575, 25:26699
KAELLNE, J., Excited states of ^{40}Ca, 25:28255
Polarization of 3$^-$ level in ^{40}Ca, 25:28256
KAERCHER, K. H., Efficacy of additional shielding in telecobalt therapy, 25:26779
KAESTNER, P. C., User's manual for two-dimensional axisymmetric transient heat conduction material ablation computer program, 25:28883 (SC-DR-70-510)
KAFALAS, J. A., Magnetic properties of europium: pressure and impurity effects, 25:27874
KAFFRELL, N., Some studies on neutron-rich nuclei, 25:28326 (CERN-70-30(Vol.2), pp 985-1000)
KAFKA, P., Belgonucleaire and Siemens PWRs for small and medium power reactors, 25:28717
KAGANOV, M. I., Dependence of the electron dislocation stopping power in a superconductor on temperature and velocity, 25:27648
KAHAN, R. S., Effect of gamma radiation on the synthesis of scopoletin and scopolin in grapefruit peel in relation to radiation damage, 25:27079
KAHANA, S., Survey of (p,t) reactions in 1p shell, 25:28204
KAHN, B., Radiological surveillance studies at a boiling water nuclear power reactor, 25:28625
KAINDL, G., Moessbauer effect study of hyperfine interactions in ^{149}Nd, 25:27924
KAISER, G. D., Asymptotic properties of scattering amplitudes and their experimental consequences, 25:28100
KAJANI KANTHA, K. R., Autoantibodies to intrinsic factor: their determination and clinical usefulness, 25:26676
KAJI, Keisuke, Relation between the polymer conformation and the elastic modulus of the crystalline region of polymer, 25:26281
KAKEHI, Hirotake, Contribution of low-energy gamma emitters to the scintigram, 25:26849
KAKIHANA, Hidetake, Adsorption of uranium in artificial seawater with titanic acid, 25:26350
KALACHEVA, Z. F., Energy distribution of α-particles in p + ^{11}B → 3α reaction, 25:28184
KALDOR, Andrew, Matrix isolation study of borazine and boroxine. A vibrational analysis, 25:26233
KALIBERDA, S. G., Some pecularities of cognition of microworld, 25:27929 (ITF-70-62-E)
KALIBERDA, V. S., Velocity distribution of stars of equal mass in clusters, 25:27336
KALISH, R., Particle-core structure in the spectra of the strontium nuclei, 25:28234
KALISH R., Resonance structure in the ^{88}Sr(p,p') octupole transition, 25:28240
KALMAN, Bela, Effect of ionizing radiation on the keeping quality of sliced pork, 25:27136 (NP-tr-1932)
KALPAKCHIEVA, R., New isotopes of iridium, 25:28348 (JINR-P6-5617)
KALUZA, Jozef, Radiomimetic effect of actinomycin C on tumors of glial origin, 25:26908
KALVIUS, G. M., Magnetic behavior of conducting Am systems, 25:27922
KAMDAR, M. H., Adsorption-induced brittle fracture in liquid--metal environments, 25:27243
KAMERMANS, T., Production and decay properties of some shortlived cobalt nuclei, 25:28214 (CERN-70-30(Vol.2), pp 1105-13)
KAMETANI, Katsuaki, Chemical and hygienic studies on natural radioactive spa, 25:26743
KAMIMURA, Masayasu, Four-body correlations in light nuclei, 25:28505
KAMINKER, D. M., Neutron transport by a moving medium, 25:28815 (BNWL-tr-66)
KAMMLOTT, G. W., Investigation of Kondo alloys and compound by the superconductive proximity effect, 25:27662
KANAZAWA, Mamoru, Shallow donor state produced by proton bombardment of silicon, 25:27847
KANBAI, G. G., Retrograde injury of the retina by ionizing radiation, 25:26902
KANDA, Keiji, Age of fission neutrons to indium resonance in water and polyethylene, 25:28157
KANE, R. P., Relationship between H ranges at equatorial and middle latitudes, 25:27504
KANEKO, Shobu, Hydromagnetic stability of Bennett pinch, 25:27748
KANG, Shin Koo, Changes of salivary gland function after ^{60}Co irradiation, 25:27061
KANGILASKI, Mihkel, Effects of hydride precipitation of the tensile properties of irradiated Zircaloy-2. Final report, 25:27198 (BMI-X-10276)
KANNO, Takuji, Solubility of TTA--uranyl chelate, 25:26340
KAPITOLA, J., Difference in dried thyroid block of ^{131}I uptake in male and female rats, 25:26601
KAPITONOV, I. M., Photoneutron reactions on copper, 25:28260
KAPUS, Istvan, Simple method for determining the

concentration of serum thyroxine by competitive displacement analysis, 25:26568
KAPUSTA, A. B., MHD-rotation of conducting fluid in cylindrical vessel, 25:27500
KARAEV, R., Theory of excited states of deformed even--even nuclei, 25:28501
KARAM, J. D., Properties of bacteriophage T4 mutants defective in gene 30 (deoxyribonucleic acid ligase) and the rII gene, 25:26708
KARATAEV, V. D., Inspection of the laminates with the beam of electrons, 25:26542
KARLSSON, E., Calculation of differential angular correlation factors for non-coaxial electric and magnetic fields, 25:27919
Effects of coaxial magnetic and electric fields on time-integral PAC with special reference to rare-earth isotopes, 25:27918
KARNAUKHOV, V. A., Proton emitter studies in region of Z > 50, 25:28300 (CERN-70-30(Vol.1), pp 457-86)
KARNIK, R. R., Method of assigning the vibration bands by progressive isotope exchange, 25:26216
KARNOWSKY, Maurice M., Determination of the activation energy for precipitation of Al_6Mn in Al--3.4 w/o Mn alloy, 25:28889 (SC-RR-70-356)
KAROW, P., Electroproduction of single π^+ mesons on hydrogen, 25:27950 (DESY-71/9)
KARR H., Dynamic stabilization of the z pinch, 25:27789
KARTHA, Mukund, Reversal of liver scan image after right-sided renal radiotherapy, 25:26884
KARYAKIN, A. V., Determination of Sm microimpurity in Eu oxide, 25:26162
KASAHARA, Atsushi, Radiation injury and recovery in mice, 25:26980
KASCHL, G. Th., Further indications for t-dependence of angular distributions, 25:28174
KASE, Paul G., Radiation model of man for analysis of future space missions, 25:26778
KASHCHEI, V. A., Uhf methods for investigation of the dynamic characteristics of thin superconducting films, 25:27652
KASHCHUK, V. A., Effect of period v transition metals on the structure and properties of titanium, 25:27223
Effect of small additions of V, Cr, and Mn on [structure and] properties of cast Zr, 25:27230
Effect of small additions of vanadium and nickel on some properties of cast titanium, 25:27220
KASHEVS'KA, O. M., Change in solubility of Ce, Pr, and Nd in Cr as a function of temperature, 25:27238
KASHUBA, I. E., Parameters of optical nuclear model according to elastic scattering of polarized neutrons, 25:28248
KASPER, John S., Crystal structure of the boron--thorium system. A new boride with type YB_{66} structure, 25:27301
KASTNER, J., Relationship between encapsulation and apparent fast neutron-induced fading in TLD, 25:26536
KATO, Hiroo, Childhood cancer in relation to prenatal exposure to atomic-bomb radiation, 25:27043
KATO, Yoshio, Effects of fast neutrons and ^{60}Co γ-rays on Artemia, 25:26917
KATOH, L. M., Illiac III Reference Manual. Vol. I, 25:28851 (COO-2118-5)
KATSUMATA, Kazuo, Binding of ^{131}I-insulin to mitochondria, 25:26575
KATSUME, Michito, Superhigh voltage irradiation of bladder tumor, 25:26876
KATYKHIN, G. S., Palladium-99 γ radiation, 25:28431
KAUFMAN, Stephen J., Selective inhibition of cells in the immune response by actinomycin D, 25:26671
KAVANAGH, R. W., Mass and half-life of ^9C, 25:28187
KAW, P. K., External control of ion waves in a plasma by high-frequency fields, 25:27807
KAWABE, T., Energy analysis of cesium ions in Q machine, 25:27686
KAWADE, Kiyoshi, Gamma-ray spectroscopy of ^{76}As, 25:28278
KAWAKAMI, Hiroyasu, Application of activation analysis in hot spring chemistry and sanitary chemistry, 25:26195
KAWAKISHI, Shunro, Effects of γ-irradiation on the enzyme relating to the development of characteristic odor of onions, 25:26620
KAWAMURA, Shoichi, Comparative study on Zr oxide for preparation of /sup 113m/In generator, 25:26341
KAWASAKI, K., Low-latitude DS component of geomagnetic storm field, 25:27619
KAWASE, Yoichi, Excited states of ^{52}Cr and ground state spin of ^{52}V in the decay of ^{52}V, 25:28250
Two-phonon states in ^{104}Pd, 25:28382
KAWASHIMA, K., Paired ionization chambers for measurement of neutrons and gamma rays, 25:26538
KAYE, J. H., Preliminary processing of multiplexed two-parameter gamma-spectrometer data, 25:26501
KAYLOR, John D., Prog. rpt. on marine products development irradiator program: irradiated fresh shrimp shipping studies, annual, 10/67--9/68, 25:27138 (TID-25543)
KAZACHKOVSKII, O. D., Capture of neutrons by Rh, Ta, and Au, 25:28437
KAZAKOVA, L. Ya., Optimum parameters of ^{238}U neutron optical potential, 25:28403
KAZARINOV, Yu. M., Proton form factors, 25:27991
KAZATCHEVSKAYA, T. V., Ionization of e region by precipitating electrons, 25:27527
KAZDA, Stanislav, Conference on post-natal development of phenotype, Liblice, Czech., 9/67, 25:26696
KE, Charles H., Inactivation and reactivation of hemocyanin by radiolytic OH and e/sub aq⁻/, 25:26302
KEAM, R. F., Perturbation treatment of Bethe--Salpeter equation for tightly bound fermion--antifermion systems, 25:27971
KEAN, D. C., Search for high-spin states in ^{27}Al, 25:28208 (ANU-P-521)
KEANE, J. A., States in ^{17}O via neutron-polarization measurements in $^{13}C(\alpha,n)^{16}O$ reaction, 25:28202
KEEGAN, J., Quality control, inspection, and testing of Series I metallurgical fuels for first charge of Dragon reactor, 25:26438 (DP-Report-432)
KEEHN, Robert J., Neuro-muscular tests of aging in Hiroshima subjects, 25:27053
KEEN, B. E., Feedback stabilization of various plasma instabilities, 25:27767
Preliminary results on the dynamic stabilization of the drift-dissipative instability, 25:27786
KEENEY, W. P., ZPR-3 assemblies 48: 48A, and 48B: the study of a dilute plutonium-fueled assembly and its variants, 25:28752 (ANL-7759)
KEEP, C. W., Surface complexes formed by thermal and radiolytic adsorption of gases on graphite, 25:26286
KELLER, Donald L., Prog. rpt. on development of fuels and technology for advanced reactors, 10--12/70, 25:28686 (BMI-1898)
KELLER, L. L. Jr., Worldwide correlation of soil and population, 25:26429 (SC-R-7121)
KELLEY, D. M., Maps of vertical F layer drifts caused by horizontal winds, 25:27588
KELLY, H. J., Niobium alloy development with B, Hf, and W, 25:27227
KELLY, J. C., Bremsstrahlung spectrum of energetic β particles traversing single crystals in lattice-directed trajectories, 25:27832
KELLY, Lola S., Proliferative and phagocytic capacity of the reticuloendothelial system of sublethally irradiated mice, 25:26947
KELLY, R. J., Nuclear generating unit performance: an operator viewpoint, 25:28547 (AECL-3670, pp 13-20)
KELLY, W. H., Straightforward elucidation of complex shell-model states by β decay of nuclei far from stability, 25:28299 (CERN-70-30(Vol.1), pp 435-46)
KELSEY, C. A., Gas target source for neutron radiation therapy, 25:26883
KELSON, I., Isobaric spin in nuclear fission, 25:28477
KEMP, D. T., Analysis of transient elf disturbances within Earth--ionosphere cavity, 25:27592
Magnitude of sources of transient excitation of Schumann resonances, 25:27591
KENDALL, James Michael, Stability domains in nonlinear point reactor dynamics, 25:28800 (COO-2109-3)
KENDYSH, I. N., Role of radiosensitive tissues in the mechanism of post-radiation gluconeogenesis, 25:26963
KENNEL, C. F., Fast time-resolved spectral analysis of vlf banded emissions, 25:27621
KENNEL, C. R., Magnetic and electric field changes across the shock and in the magnetosheath, 25:27539
KENT, A., Tearing-mode instability, 25:27751
KENT, Thomas H., Effects of altered propulsion on rat small intestinal flora, 25:26975
KEREK, A., Levels in doubly-even tellurium isotopes, 25:28330 (CERN-70-30(Vol.2), pp 1010-11)
KERIMOV, B. K., Polarization during photoproduction of electron--positron pairs, 25:27996
KERKER, M., Collection efficiency of water droplets in AgCl aerosol, 25:26370 (CONF-700601-, pp 161-7)
KERMAN, A. K., Allowed neutron decay of highly excited $(T_0+1/2)$ compound nucleus states, 25:28460
Analysis of elastic and inelastic analogue-state resonances using coupled optical equations, 25:28236
Low-energy neutron--oxygen scattering derived from two-body forces, 25:28198
Microscopic calculation for the escape width of analog states, 25:28466
The role of the anti-analog state in the decay of the analog state, 25:28467
KERMODE, M. W., Numerical calculation of S-state energy eigenvalues for a local potential, 25:27933
KERN, S., Magnetic susceptibility of Eu_2O_3, 25:27896
KERNAN, A., Reaction $\pi^-p + \nu^\Delta-$ at cms energies 1640 to 1760 MeV, 25:27962
KESKE, R. G., Aliphatic semidiones. XV. 2,3-semidiones derived from the bicyclo[n,1.0]alkanes, 25:26254
KESKE, Robert G., Aliphatic semidiones. XVI. Semidiones derived from the bicyclo[n.1.1]alkanes, 25:26255
KESNER, Jay, Trapping and containment of a cesium plasma in a magnetic mirror, 25:27671
KEVAN, Larry, Optical bleaching of trapped electrons in γ-irradiated alkaline ice. Location of energy levels, 25:26298
KEY, Charles R., Smallest forms of papillary carcinoma of thyroid. A study of 141 microcarcinomas less than 0.1 cm in greatest dimension, 25:26898
KHABAKHPASHEV, A. G., Evidence for electron-positron pair electroproduction, 25:27994
KHAKIMOV, A. A., Operational experience with VK-50 reactor facility, 25:28579
KHALKIN, V., Sign of astatine ion charge in $HClO_4$--$H_2Cr_2O_7$ solutions, 25:26209 (JINR-P12-5644)

XUM

KHAMBANONDA, P., Standard neutron irradiation facility experience in Thailand, 25:27062 (IAEA-R-459)
KHAN, Faiz M., Variable block-surface-distance (BSD) for adjustment of shadow size in mantle therapy, 25:26892
KHAN, M. A., Prospects of intermediate-size power reactors, 25:28583
KHARITONOV, Yu. P., Investigation of a decay of isotopes of element 105, 25:28350 (KFK-tr-350)
KHARLAMOV, A. G., Loop for radiation study of electrical conductivity of materials in the VVR reactor, 25:26765
KHATRI, A. A., Studies in Trichoderma glaucum with special reference to the effects of thermal neutrons, gamma, and ultraviolet radiation, 25:27088
KHOLODOV, A. G., Change in solubility of Ce, Pr, and Nd in Cr as a function of temperature, 25:27238
KHORUZHII, S. S., Global and local structure of relativistic quantum systems, 25:27931 (JINR-E2-5575)
KHURSHUDYAN, L. S., Fast detector of a relativistic charged particle passage, 25:26513
KIBARSKA, T., Biochemical activity of Asp. niger under effects of x-rays, 25:27094
KIDMAN, R. B., Group constants for fast reactor calculations, 25:28657 (HEDL-TME-71-36)
KIDO, Yasumasa, Chemical and hygienic studies on natural radioactive spa, 25:26743
KIENLE, P., Single-particle analog state anomalies in the scattering of protons from ^{197}Au, ^{196}Pt, and ^{184}W, 25:28371
KILIAN, K., Levels in ^{5}He excited in the elastic d--^{3}H scattering, 25:28168
KILIAN, Peter, Economical and technical properties of the sodium-cooled high-power breeder reactor with carbide fuel, 25:28664
KILSBY, E. R., Tsuruga: triumph of teamwork, 25:28542
KILTHAU, Gustave F., PDP-8 series studies of dynamic relocations of radioactive isotopes, 25:26473
KIM, Jin Yong, Medical study of Korean atomic bomb survivors, 25:27060
KIM, K. I., Parameters of asynchronous liquid-metal MHD generator, 25:27484
KIM, M. Z., Mutation breeding of tomato. I, 25:26735
KIM, S. C., First nuclear power plant in Korea, 25:28539
KIMBALL, C. W., Magnetic properties of the system Au_xR(R = Er, Tm, and Yb), 25:27872
KIMURA, Hiroshi, Recovery of low-temperature fast neutron irradiated tungsten, 25:27228
KIMURA, Itsuro, Average cross section for the ^{232}Th(n,f), 25:28409
Measurements of average cross sections for some threshold reactions for neutrons with fission-type reactor spectrum, 25:28273
KIMURA, Motoharu, Pile physics experiment by means of TOF neutron diffraction, 25:28769
KING, D. A., Oxygen adsorption, reconstruction, and thin oxide film formation on Ni, Fe, W, and Mo, 25:27224
KING, F. J., Study of irradiated-pasteurized fishery products, 25:27149
KING, J., Electric charge of interacting cosmic-ray particles at sea level, 25:27475
KING, J. W., Longitudinal variation of midlatitude ionosphere produced by neutral-air winds. II, 25:27508
KING, L. D. Percival, Kinetic intense neutron generator reactor, 25:28650
KING, Marcia J., s-channel helicity conservation constraints on t-channel exchanges, 25:28028 (SU-1206-242)
KIRIBUCHI, Mitsunori, Conservative treatment of retinoblastoma, 25:26880
KIRILLOVA, M. M., Optical properties of tungsten single crystals, 25:27899
KIRITANI, S., Computer controlled dynamic cineradiography, 25:26557
KIROV, A. G., Distribution of a pulsed current in a cylindrical conductor of variable conductivity, 25:27721
KIRSANOVA, R. V., Genetics and selection of Beauveria bassiana (Bals.) Vuill., an entomopathogenic fungus. I, 25:26703
KIRSCH, W., Unilateral determination of effective renal plasma flow by radioisotopes, 25:26826
KIRYUKHINA, A. I., Hydrogen ionization and the excitation of quiescent prominences, 25:27395
KISELEV, V. I., Actinium aerosols determination in the air in the presence of other radioactive substances, 25:26394
KISS, Istvan, Effect of ionizing radiation on the keeping quality of sliced pork, 25:27136 (NP-tr-1932)
KISTNER, O. C., Lifetime measurements on neutron deficient even--even isotopes of Xe and Ba, 25:28319 (CERN-70-30(Vol.2), pp 905-10)
KITA, Tomitaro, Application of pharmacology to animal group psychology, 25:28874 (ORNL-tr-2447)
KITABATAKE, Takashi, Medical 6 MeV linear accelerator, 25:28132
KITAGAWA, Toshio, Medical 6 MeV linear accelerator, 25:28132
KITAMI, Toyokichi, Liquid hydrogen target utilizing a small mechanical refrigerator, 25:28138
KITAMURA, Isao, Gamma-ray spectroscopy of ^{76}As, 25:28278
KITAYAMA, Shigeru, Macromolecular synthesis in Micrococcus radiodurans during postirradiation incubation, 25:26639
KITAZUME, Mitsuyuki, Experiments and calculations for gamma rays streaming through penetration in shielding structure, 25:27829
KITCHEN, W. J. Jr., Properties of vanadium dioxide thermal filaments, 25:27906
KLAPISCH, R., Half-lives of the new isotopes ^{99}Rb, ^{98}Sr, and ^{145} ^{146}Cs, 25:28388
Special experimental techniques used in the study of nuclei far from stability, 25:28290 (CERN-70-30(Vol.1), pp 21-45)
KLAPISHEVSKAYA, Z. B., Vapour-phase radiation-initiated thermal oxidation of benzene by molecular oxygen with fast electron irradiation, 25:26284
KLECZKOWSKI, A., Inactivation by uv radiation of RNA from potato virus X, 25:27108
KLEIN, H., Elastic electron--deuteron scattering and electric neutron form factor at four momentum transfers: 5 Fermi^{-2} < q^2 < 14 Fermi^{-2}, 25:27980 (DESY-71/7)
Quasielastic electron--deuteron scattering for four pulse transfers in range 0.2 (GeV/c)^2 < q^2 < 0.85(GeV/c)^2, 25:27951 (NP-18725)
KLEIN, S., Effect of gamma irradiation on the rehydration capacity of freeze-dried meat, 25:27144
KLEMM, A., Self-diffusion of liquid ^{6}Li and ^{7}Li, 25:26238
Separative fluodiffusion, 25:26242
KLEYKAMP, H., Experimental contribution to Jost mechanisms in solid-state reactions, 25:26210 (KFK-1312)
Stoichiometry shift in an oxide fuel element at high burnup, 25:28690 (EURFNR-836)
KLIMEK, H., Histological examination of parodontium after irradiation of the rat trunk at a dose of 600 r, 25:26960
KLIMENKO, A. S., Elastic scattering of protons on iron and cobalt, 25:28263
KLIMKIEWICZ, Z., Influence of x-rays upon the mitotic activity and DNA synthesis in endometrial glandular epithelium, 25:26659
Ribonucleic acid synthesis in endometrial epithelium in mice after whole-body x-ray irradiation, 25:27031
KLING, Charles L., Reactor protection system diversity, 25:28697 (CENPD-11)
KLOPP, William D., Long-time creep behavior of tantalum--10 tungsten in high vacuum, 25:27207 (N-70-42045)
KLOTZ, Paul, Thorium fluoride complexes. Determination of the stability constants using the fluoride ion activity electrode, 25:26268
KLOZENBERG, J. P., Reply to comment on negative diffusion in coefficients in quasi-linear theory, 25:27713
KNAPIK, Jerzy, Spark chambers in high-energy physics. II, 25:26514
KNAPP, G. S., Ferromagnetism of $ZrZn_2$, 25:27875
KNAPP, J., Calculation of the factors of resonance self-shielding in fissile materials, 25:28503
KNAUF, Philip Andrew, Modification of anion and cation permeability of the human red cell membrane by amino and sulfhydryl reactive reagents, 25:28904 (UR-49-1429)
KNIZHNIKOV, V. A., Influence of dietary calcium and fluorine on the radioresistance of bacillus-carrying animals, 25:27016
KNORR, Georg, Nonlinear behavior of the one-dimensional weak beam--plasma system, 25:27710
KNOTT, K., Ionospheric plasma drifts derived from wake measurements, 25:27585
KNYAZEV, V. M., Universal magnetic spectrometer with 0.15 percent resolving power at maximum pulse of 60 GeV/c, 25:26507 (NP-18764)
KOBA, Z., Graphical illustration of isospin analysis in single-pion production, 25:28039
Veneziano n-point function, 25:28014
KOBAYASHI, Kathuhei, Average cross section for the ^{232}Th(n,f), 25:28409
KOBAYASHI, Katsuhei, Measurements of average cross sections for some threshold reactions for neutrons with fission-type reactor spectrum, 25:28273
KOBE, Donald H., Maximum-overlap orbitals, an energy variational principle, and perturbation theory, 25:28511
KOBYLINSKII, N. A., Photoproduction of eta mesons on nucleons at high energies, 25:27989
KOBZENKO, G. F., Change in solubility of Ce, Pr, and Nd in Cr as a function of temperature, 25:27238
KOCH, E. E., Optical absorption of gaseous methane, ethane, propane, and butane, and reflection of solid methane and ethane in the vacuum ultraviolet, 25:28853 (DESY-SR-71/1)
KOCH, L., Spectra and time history of protons in interplanetary space, Feb. 25--28, 1969, 25:27558
KOCHETOV, A. B., Calculation of quadrupole moments, deformations, and shape of light nuclei within K-harmonic method, 25:28180
KOCMIERSKA-GRODZKA, D., Proteolytic activity in isolated perfused liver of normal and x-irradiated rats, 25:26984
KOCZYNSKI, A., X and gamma thermoluminescent dosimeter for accidental personnel dosimetry purposes, 25:26516 (CLOR-82/D)
KODAIRA, Tsuneo, Evaluation of integrity for fast neutron irradiation embrittlement of JPDR pressure vessel,

XUM

25:28682 (JAERI-1202)
KOECK, George P., Dosage tolerance of pelvic structures with ^{60}Co rotation radiation therapy, 25:26894
KOENE, B. K. S., Decays of /sup 70a/Cu, /sup 70b/Cu, and ^{67}Ni, 25:28221
KOEPP, C., Influence of real dead-time simulation on dynamic behavior of computer model of automatically controlled Na-2 reactor, 25:28804 (EURFNR-835)
KOERNER, Gerald S., Stereochemistry of allylic rearrangements. XVI. Stereochemistry of ion-pair return in the trans-α,γ-methylphenylallyl p-nitrobenzoate system, 25:26224
KOESSLER, Franz, Biophysical studies with luminous bacteria. IV, 25:27122
Biophysical studies with luminous bacteria. V, 25:27120
KOESTER, L., Experiments at the Munich research reactor FRM, 25:28775
KOH, Chang Soon, Uptake- and metabolic studies of the labelled compounds in malignant tumors, 25:26859
KOHNO, Isao, Elastic scattering of carbon and nitrogen ions, 25:28274
KOIZUMI, Yoshinobu, Design and performance of double emitter type self-powered neutron detectors, 25:26458
KOJ, A., Acute-phase reactants and lysosomal enzymes in the blood of rats with experimental inflammation or radiation injury, 25:26979
KOJIMA, Shoji, Suppression of longitudinal electron oscillation by beam modulation, 25:27702
KOKAME, Jun, Reaction (p,t) on even--even deformed nuclei, 25:28411
KOLDEWIJN, P., Decay of some nuclei far from the stability line studied with standard spectroscopic techniques, 25:28322 (CERN-70-30(Vol.2), pp 939-47)
KOLEMENSKII, A. A., Radiation effects on dynamics of relativistic electron rings, 25:28114 (NP-18634)
KOLESAR, D. C., TOPLYR: two-dimensional thermal energy transport code, 25:28856 (HEDL-TME-71-39)
KOLINSKY, M., Structure of chlorinated poly(vinyl chloride). I. Determination of the mechanism of chlorination from infrared and NMR spectra, 25:26246
KOLK, B., Contact density of conduction electrons in iron and the isomer shift of ^{57}Fe, 25:28247
KOLLMANN, George, Mechanism of action of radiation protective agents: in vivo distribution and metabolism of cysteamine-S-phosphate (MEAP), 25:26805
Protection of DNA against ionizing radiation, 25:26801
KOLMANOVA, A., Carotenoids synthesized by uv-induced mutants of Mycobacterium phlei, 25:26687
KOLOSOV, V. I., Structure of electron clusters in an injector with a step-like varying wave phase velocity, 25:28112 (KHFTI-70-17)
KOLYADIN, V. I., Loop for radiation study of electrical conductivity of materials in the VVR reactor, 25:28765
KOMAR, A. P., Microtron type electron accelerator, 25:28136
KOMAROV, V. V., Angular correlation of nucleons generated during reactions of decaying deuterons, 25:28487
Convergence of infinite series of nonrelativistic contributions for (n--d) scattering amplitude, 25:28166
Energy distribution of α-particles in p + ^{11}B + 3α reaction, 25:28184
Resonance narrowing effect in two-particle interactions, 25:28497
KOMAROVSKII, A. N., Construction of nuclear installations, 25:28531
KOMAROVSKII, V. A., Relative values of oscillator strengths of spectral lines, 25:27445
KOMOLOV, I. S., Rate of initial formation of microcolonies in gamma irradiation of SOTs cells in various phases of mitotic cycle, 25:26907
KONDO, Yasuhiro, Optical study of an ionic crystal by means of pulsed electron irradiation. IV, 25:27846
KONECKI, J., Influence of x-rays upon the mitotic activity and DNA synthesis in endometrial glandular epithelium, 25:26659
Ribonucleic acid synthesis in endometrial epithelium in mice after whole-body x-ray irradiation, 25:27031
KONIJN, J., Decay of some nuclei far from the stability line studied with standard spectroscopic techniques, 25:28322 (CERN-70-30(Vol.2), pp 939-47)
KONISHI, Toshio, Pulsed neutron experiment on FCA I-5, 25:28759 (JAERI-Memo-4272)
KONKASHBAEV, I. K., Thermonuclear combustion wave, 25:27820
KONONENKO, A. M., Regeneration of cell populations of intestinal epithelium after irradiation, 25:27033
KONOPLEV, K. A., Neutron transport by a moving medium, 25:28815 (BNWL-tr-66)
KONOPLYA, S. P., Role of variety in mutagenesis of cotton, 25:26728
KONSTANTINOV, L. V., Fast response control of reactor power on basis of γ radiation intensity, 25:28822
Monitoring of power distribution in nuclear reactor cores, 25:28699
KONSTANTINOV, O. V., Dopplerons in cadmium, 25:27900
KONSTANTINOVIC, J., Neutron inelastic scattering and neutron diffraction at the Vinca heavy water reactor, 25:28779
KONTOR, N. N., Solar cosmic-ray increase on 25 Feb.--5 Mar., 1969, 25:27470
KOOL, W. H., Gamma irradiation of lithium-drifted silicon, 25:27852
KORBA, Alvin, Thermoluminescent dosimeter badge, 25:26524
KORDYUKEVICH, V. O., Decay of neutron defficient isotopes of Pt, Ir, and Os, 25:28389
KORKISCH, Johann, Selective ion-exchange separation of alkali metals, 25:26337
Separation of scandium from rare earth elements, 25:26338
KORNILOV, I. I., X-ray- and neutron-diffraction study of ordering in some alloys of the titanium--zirconium--oxygen system, 25:27297
KOROGODIN, V. I., Growth patterns of uv-irradiated E. coli B in saline, 25:27119
KOROLEV, A. M., Magnetic dipole and electric quadrupole moments of odd-mass nuclei, 25:28499
KOROLEVA, L. V., Qualitative leucocyte changes due to total x-ray irradiation, 25:26901
KORTZEBORN, Robert N., Scavenging of aerosols by rain, 25:26388 (CONF-700601-, pp 433-46)
KORZH, I. A., Parameters of optical nuclear model according to elastic scattering of polarized neutrons, 25:28248
KORZHOV, L. N., Actinium aerosols determination in the air in the presence of other radioactive substances, 25:26394
KOSACHEVSKII, L. Ya., Propagation of shear waves in conducting viscous-plastic medium, 25:27497
KOSSLER, J., Particle-core structure in the spectra of the strontium nuclei, 25:28234
KOSTELECKY, R., Magnetic susceptibility of Eu_2O_3, 25:27896
KOSTENKO, P. P., Study of supersonic MHD-channel flows with compression shock, 25:27489
KOSTIKAS, A., Experimental physics research at the Democritos reactor, 25:28781
KOSTOMAROV, D. P., Velocity distribution of rapid ions with superthermal velocity in a nonisothermal plasma, 25:27722
KOSTRITSA, A. A., Decrease of critical mass of a reactor, 25:28809
KOSTRITZA, A. A., Neutron transport by a moving medium, 25:28815 (BNWL-tr-66)
KOSTYAKOVA, E. B., Investigation of planetary nebulae in the near ultraviolet region of the spectrum, 25:27338
KOTANSKI, A., Quark model additivity frame, 25:28017
KOTULOVA, Daniela, Protease activity changes in rabbit lung macrophages, spleen cells, and polymorphonuclear leucocytes after whole-body x-irradiation, 25:27035
KOURILEK, K., Biochemical changes in serum of intact and irradiated dogs after intravenous AET administration, 25:26935
KOVACH, William Stephen, Effects of dust and Lyman-alpha radiation on evolution of planetary nebulae, 25:27323
KOVACIC, Roger T., Miniature pig performance after fractionated supralethal doses of ionizing radiation, 25:26928
KOVACS, C. J., Mitotic delay in two biochemically different G1 cell populations in cultured roots of pea (Pisum sativum), 25:27063
KOVACS, J., Isoracemization of N-carbobenzoxyamino acid ester derivatives, 25:26257
KOWALSKI, Mieczyslaw, Genetic analysis by transduction of Rhizobium meliloti mutants, 25:27103
Transducing phages of Rhizobium meliloti, 25:27104
KOWARSKI, A., Determination of integrated plasma concentrations and true secretion rates of human growth hormone, 25:26579
KOWNACKA, Ludwika, Origin and evolution of the radioactive clouds, 25:26357 (CLOR-81/D)
KOYAMA, Shin-Ichiro, Gross theory of beta-decay and the nuclei far from the region of beta-stability, 25:28442 (CERN-70-30(Vol.1), pp 397-419)
KOYAMA, Takeko, Protein synthesis in lens and its disturbance. II, 25:26649
KOZAK, Danuta, Molybdenum recovery from alkaline slag, 25:26348
KOZINSKI, Andrzej W., Early intracellular events in the replication of bacteriophage T4 deoxyribonucleic acid. V. Further studies on T4 protein-deoxyribonucleic acid complex, 25:26570
KOZODAEV, A. M., Regulator for high voltage capacitor bank, 25:28108 (ITEF-761)
KOZYRENKO, V. E., Longitudinal end effects in MHD channels at arbitrary R/sub m/ numbers, 25:27483
KRACIK, B., Decay of ^{90}Nb, /sup 89m,89/Nb, /sup 85m,85/Y and /sup 85m/Sr, 25:28215 (CERN-70-30(Vol.2), pp 1137)
KRACIKOVA, T. I., Decay of /sup 110m/Ag to ^{110}Cd, 25:28435
KRAEMER, W., Aspects of boiling-water medium-power reactors, 25:28637
KRAEMMER, A. B., Parton theory based on the dual resonance model, 25:28002
KRAJEWSKI, B., Tropospheric scavenging of ^{90}Sr and ^{3}H, 25:26389 (CONF-700601-, pp 447-63)
KRAMER, Simon, Oxygen effect on the production of radiation-induced myelitis in rats, 25:26966
KRAMMER, M., Relativistic scalar quark model with strong binding, 25:28022 (DESY-71/10)
KRANE, Kenneth Saul, Gamma transitions between collective states of even--even nuclei, 25:28434
KRASNIKOV, V. D., Structure of electron clusters in an injector with a step-like varying wave phase velocity, 25:28112 (KHFTI-70-17)

KRASNOBAEV, K. V., Static solar HII zone, 25:27399
KRASNOPEVCEVA, N. G., Recovery of yeast after irradiation and protein synthesis, 25:27096
Role of high energy compounds in the processes of postirradiation recovery of yeast, 25:27095
KRASNOV, Yu. K., Motion of vortexes in superconductors of the second kind, 25:27650
KRASSA, R. F., OGO 5 measurements of Lyman alpha sky background, 25:27414
KRATZ, K. L., Some studies on neutron-rich nuclei, 25:28326 (CERN-70-30(Vol.2), pp 985-1000)
KREJCI, J., Elimination of ^{131}I-labelled heterologous antigen after total body x-irradiation, 25:26944
KREY, P. W., Tropospheric scavenging of ^{90}Sr and ^{3}H, 25:26389 (CONF-700601-, pp 447-63)
KRIEGER, H. L., Radiological surveillance studies at a boiling water nuclear power reactor, 25:28625
KRIKORIAN, J., Protection of large superconducting coils, 25:27663 (ORNL-tr-2436)
KRIKS, H.-J., Proportional counter for detection of exoelectrons, 25:26487
KRIMIGIS, S. M., Low-energy cosmic rays near Earth, 25:27473
KRISHNAMOORTHY, P. N., Methods of effluent control in nuclear plants, 25:28623
KRISHNAMURTHY, G. T., Demonstration of collateral pathways after superior vena caval obstruction with the scintillation camera, 25:26844
KRISHNAN, R., Transmission electron microscopic studies of cold-rolled zirconium, 25:27245 (INIS-mf-15)
KRISHNASWAMI, R., Relationship between response to radiations and nature of polyploidy in some crop plants, 25:27087
KRISYUK, E. M., Determination of specific release of radon by protective enclosures in premises, 25:26356
KRIVSKY, L., Observations of chromospheric flares at Ondrejov, 25:27391
KRIZ, S., Evolution of close binaries. V, 25:27331
KROH, J., Influence of LET on radical yields in frozen aliphatic alcohols, 25:26311
KROKOWSKI, E., Effects of ionizing radiation on the eye, 25:27013
KRUEGER, G. J., Self-diffusion of liquid ^{6}Li and ^{7}Li, 25:26238
KRUER, W. L., Anomalous heating of plasma electrons, 25:27675
KRUGER, M., Air handling plant of Obrigheim nuclear power station, 25:28545
KRYLOVA, L. M., Motion of a plasma cluster in a channel with variable inductance, 25:27485
KRYSL, V., Difference method of solution of two-dimensional multigroup time-independent diffusion equations, 25:28607 (ZJE-101)
KRYUKOVA, L. N., Decay of neutron defficient isotopes of Pt, Ir, and Os, 25:28389
KRZYWICKI, J., Histological examination of parodontium after irradiation of the rat trunk at a dose of 600 r, 25:26960
KUBO, Vicki, Proton magnetic resonance cation solvation study of uranyl perchlorate, uranyl nitrate, and uranyl perchlorate--hydrochloric acid solutions in water--dimethyl sulfoxide--acetone mixtures, 25:26212
KUCEROVA, M., Sequellae of intrauterine radiation exposure in girl 4 years and 6 months after exposure, 25:27057
KUCKUCK, H., Superconducting dc quadrupole lens, 25:28111 (KFK-1218)
KUDRYASHOV, V. I., Elastic and inelastic scattering in A = 23 to 35 region, 25:28261
KUDRYASHOV, Yu. B., Express methods of initial selection and study of chemical means of protection from radiation injury, 25:27024
KUEBRICH, John P., Mechanism of the benzoin condensation, 25:26220
KUENZI, H. U., Change of sign of Hall coefficient in liquid alloys, 25:27212
KUGLER, E., Delayed-proton emission from neutron-deficient isotopes of xenon and mercury, 25:28301 (CERN-70-30(Vol.1), pp 487-96)
KUGLER, G., Mass-spectrometric search for Ne and Ar isotopes in ternary fission of ^{235}U, 25:28419
KUGLER, M., Scaling and dilation invariance, 25:28057
KUHN, A. T., Hydrogen- and deuterium-evolution reactions on gold in acid solutions, 25:26231
KUILA, R. K., Induction of mutation in Streptococcus diacetilactis by nitrosoguanidine and ultraviolet irradiation, 25:27121
KULIK, I. O., Plasma oscillations and metastable states in Josephson tunnel junctions, 25:27651
KULINSKII, V. I., Antiradioprotective effect of catecholamines, 25:26804
Influence of radioprotectors on the content of catecholamines in mouse tissues, 25:27017
KULKARNI, A. K., Development of high temperature ceramic materials, 25:27280 (INIS-mf-12)
KULLMANN, D., Superconducting dc quadrupole lens, 25:28111 (KFK-1218)
KUMAMOTO, Yoshikazu, Effects of fast neutrons and ^{60}Co γ-rays on Artemia, 25:26917
KUMAR, Krishna, New aspects of intermediate nuclei, 25:28316 (CERN-70-30(Vol.2), pp 779-812)
KUMAR, Naresh, Effective nuclear interactions and level properties for the lighter nuclei in the 1p-shell, 25:28452 (NP-18717)
KUMAR, S., Researches on ceramic materials in india, 25:27281 (INIS-mf-13)
KUMP, P., Lifetime measurements on neutron deficient even--even isotopes of Xe and Ba, 25:28319 (CERN-70-30(Vol.2), pp 905-10)
KUMPF, H., Steam generating assembly for use in the interior of a pressure vessel of a pressurized water nuclear reactor, 25:28751
KUNA, P., Changes of heart frequency and blood pressure in rabbits after application of cystamine, aminoethylisothiouronium bromide hydrobromide, and of their mixture in radioprotective doses, 25:26794
KUNIKE, M., Charge exchange between a negative ion and high-energy proton, 25:27456
KUNITSKII, Yu. A., Emissivity of diborides of transition metals from Groups IV--VI, 25:27290
KUNKEL, Wulf B., Energy flux in incompressible magnetohydrodynamic plane waves, 25:27487
KUNSELMAN, R., Kaon mass measurement from kaonic atom x-ray energies, 25:28031
KUNZ, E., Ionizing radiation exposure from diagnostic procedures, 25:26788
KUNZE, J. F., Cavity reactor engineering mockup critical experiment, 25:28761 (NASA-CR-72409)
KUO, L. Y., Large isospin mixing in ^{16}O states near 18 MeV, 25:28188
KUPRYASHKIN, V. T., Stabilization of magnetic field in an iron $\pi\sqrt{2}$ β spectrometer, 25:26502
KURABE, M., Feasibility of the sea-bottom atomic power stations, 25:28630
KURATH, D., Survey of (p,t) reactions in 1p shell, 25:28204
KURODA, P. K., Distribution of low-mass fission yields in 14.8-MeV neutron induced fission of ^{238}U and ^{232}Th, 25:28385
Yields of Ru isotopes from spontaneous fission of ^{238}U, 25:28384
KUROHARA, Samuel S., Post-irradiational recurrent epidermoid carcinoma of the uterine cervix, 25:26887
KURUSU, Akira, Radiation exposure, aging, and immunity. II, 25:26664
KURYUSHKINA, A. A., Mutagenesis induced by uv-irradiation in B. subtilis, 25:26729
KURZEKA, W. J., Development of nuclear reactor bearings for 1500°F space operation, 25:27200 (CONF-691114-7)
KUTSAROVA, T., New isotopes of iridium, 25:28348 (JINR-P6-5617)
KUTSCHERA, W., Lifetime measurements on neutron deficient even--even isotopes of Xe and Ba, 25:28319 (CERN-70-30(Vol.2), pp 905-10)
On- and off-beam gamma spectroscopy on neutron deficient isotopes of Ge, Se, Br, and Kr, 25:28213 (CERN-70-30(Vol.2), pp 911-15)
KUZ'MA, Yu. B., Phase equilibria in the titanium--vanadium--boron and titanium--manganese--boron systems, 25:27300
X-ray study of the chromium--manganese--boron system, 25:27299
KUZMENKO, G. N., Fibroblast colonies in splenic cultures of irradiated mice, 25:26905
KUZNETSOV, E. A., Variational principle and canonical variables in magnetohydrodynamics, 25:27488
KUZNETSOVA, S. M., Phase equilibria in the system vanadium--tantalum--hafnium, 25:27247
KUZNIETZ, Moshe, Effect of substitutional anions on magnetic properties of UN and GdN, 25:27880
Photoemission studies of rare-earth and uranium compounds, 25:27876
KVASNICKOVA, E., Decrease in pethidine demethylating activity of isolated rat liver microsomes following whole-body x-irradiation, 25:27034
KVICALA, J., Observations of chromospheric flares at Ondrejov, 25:27391
KYRAL, V., Biochemical changes in serum of intact and irradiated dogs after intravenous AET administration, 25:26935
KYRIAKOPOULOS, E., Infinite multiplets with SU(3), 25:28058
KYSER, D. F., Annealing study of EuO films doped with Fe Eu, 25:27898

L

LAASANEN, A. T., Polarization parameter K*p elastic scattering GeV/c, 25:27963
LACIS, Andrew Andreja, White-dwarf envelope structure and its effect on the thermal cooling rate, 25:27332
LACOURLY, G., Estimate of the risk of internal contamination in man by radioactive water pollution, 25:26747
LACOURLY, S., Wave-packet propagation and application to dispersion characteristics and to mechanisms of Pc 1 events, 25:27605
LACRUCHE, Gilbert, Neutron collimator, 25:28153
LADENBAUER-BELLIS, I. M., Decay of ^{76}Br, 25:28246
Level structure of ^{109}Cd from decay of ^{109}In, 25:28428
LAFFERTY, R. H. Jr., ^{90}Sr heat sources, 25:26432
LAFFERTY, Robert H. Jr., Flow measurements with radioisotopes, 25:26435

LAFONTAINE, A., Electrophoresis and immunoelectrophoresis patterns from proteins of irradiated meat, fish, and fowl egg, 25:26631
LAGERCRANTZ, Carl, Spin trapping of radicals formed by γ-irradiation of sodium phosphite in solid state, 25:26313
LALIBERTE, L. H., H_2O--D_2O solvent isotope effects in volume and expansivity behavior of some organic and inorganic ions, 25:26259
LALOVIC, D., Pomeranchuk singularity in the Veneziano model and unitarity, 25:28020
LAM, D. J., Magnetic behavior of conducting Am systems, 25:27922
Magnetic properties of dilute alloys of scandium, 25:27878
LAM, F. L., Repair and damage by mercaptans in ^{60}Co γ-ray irradiation of organic compounds in aqueous solution, 25:26291
LAM, S. H., Similarities between ion waves in plasmas and gravity waves in incompressible fluids, 25:27806
LAMBERT, D. L., Emission (lambda 4097.3 NIII) in the chromospheric spectrum, 25:27373
LAMBERT, F., Myelo-restorative capacities and immunocompetence of bone marrow cells of the mouse cultivated in vitro, 25:26942
LAMBERTSON, Glen R., Printed-circuit steering coils, 25:28116 (UCRL-20165)
LAMBORN, B. N. A., Conservative trapping of charged particles in a static magnetic field, 25:27674
LAMBREV, V. G., Instrumental activation analysis of Au, Br, Mn, Na, Ta, and W, 25:26200
LANCMAN, H., Internal bremsstrahlung accompanying orbital-electron capture in ^{7}Be, 25:28200
LANDAHL, H. D., Dose reduction factor for radiation lethality in mice as a function of the dose of mercaptoethylamine, 25:26924
LANDMARK, B., Electron density observations during the PCA event of 25 Feb. 1969, 25:27564
LANDOLT, R., Alpha-particle autoradiography of alkaline phosphatase inhibition by cadmium, 25:26574
LANDSHOFF, P. V., Non perturbative parton model of current interactions, 25:28015
Partons and duality in deep inelastic lepton scattering, 25:28001
LANDSTREET, J. D., Search for optical circular polarization in the Crab Nebula, 25:27348
LANEGRASSE, L., Alpha spectrometer for measuring the degree of radioactive equilibrium between ^{222}Rn and its daughter products in U mines, 25:26503
LANG, Joseph Edward, Macdowell symmetry, conspiracy, and fermion Regge trajectories, 25:28092
LANGE, D., Use of an analogue circuit for on-line correction in simultaneous double-tracer studies, 25:26569
LANGE-HESSE, G., Substorm influences on vhf continuous wave auroral backscatter, 25:27554
LANGER, Stanley H., Deuterium isotope study of electrogenerative hydrogenation. Mechanism of hydrogenation of ethylene at positive potentials, 25:26230
LANIER, Sidney F., Subject headings used by the USAEC Division of Technical Information, 25:28892 (TID-5001(10th Rev.))
LANSFORD, R. M., Illiac III Reference Manual. Vol. I, 25:28851 (COO-2118-5)
LANTZ, T. E., Radiation chemistry of low-temperature aqueous glasses. IV, 25:26310
LANZEROTTI, L. J., Access of solar particles to synchronous altitude, 25:27541
LAPIDUS, L. I., Proton form factors, 25:27991
LAPIERRE, Ch. M., Influence of substances which change the rate of depolymerization of a collagen gel on its radiosensitivity, 25:26802
LAPONCHE, Bernard, COREGRAF 2: adjustment and comparison with experiment, 25:28654 (CEA-N-1344(2))
LAPPIN, P. W., Relative sensitivity of various areas of the retina to laser radiation, 25:26940
LARMORE, L., Space shuttles and interplanetary missions. Based on shuttle, precursor missions, and planetary and lunar space station sessions of AAS 16th annual meeting, June 8--10, 1970, Anaheim, California, 25:28786
Space stations. Based on space station, safety, and international sessions of AAS 16th annual meeting, June 8--10, 1970, Anaheim, California, 25:26784
LARSSON, Alf, Recovery of Pu and U from reactor fuel elements, 25:26346
LARTIGUE, J., Fuel-cycle evaluation criteria for an intermediate-power reactor, 25:28722
LASHINSKY, Herbert, Dynamic stabilization of plasma instabilities, 25:27777
LASHMORE-DAVIES, C. N., Plasma stabilization by feedback, 25:27756
Stabilization of a low-density plasma in a simple magnetic mirror by feedback control, 25:27757
LASSMAN, G., ESR studies of x-irradiated single crystals of N-benzoylalanine, 25:26292
LASZTITY, R., Influence of gamma irradiation on some physical and chemical properties of gluten proteins, 25:26656
LATARJET, R., Irradiation of oncogenic viruses, 25:27111
LATTA, R. E., Determination of solidus-liquidus temperatures in the UO/sub 2+x/ system (-0.50 < x < 0.20), 25:27292 (GEMP-714)
LATTERY, J. E., Project pre-Gondola III, phase II summary report, 25:26408 (PNE-1117)
LAU, Y. Y., Effects of cold plasma on relativistic electron layer, 25:27746
LAUBERT, Roman, Pauli excitation of atoms in collision, 25:27453
LAUER, R. S., Photometric determination of rare earths of Y subgroup, 25:26161
LAUGHLIN, John S., Changes in biological effectiveness of a fast neutron beam with depth in tissue-equivalent material, 25:26906
LAUSCHER, P., Four-pion decay mode of D(1285) meson in π⁺⁻p reactions at 16 GeV/c, 25:27964
LAVEISSIERE, Francoise, Isotopic electricity generators, 25:26423 (CEA-Bib-190)
LAVROVA, V. V., Dopplerons in cadmium, 25:27900
LAWERGREN, B., Some M1 transitions with Δ = 1 in ^{24}Mg, ^{27}Al and ^{28}Si, 25:28225
LAWES, R. A., Laser illumination system for Hough--Powell device, 25:26509 (RHEL/R-212)
LAWIN, H., Identification of μ s isomers among primary fission fragments, 25:28325 (CERN-70-30(Vol.2), pp 967-84)
LAWRENCE, J. H., RBE of negative pions in 2-day-old ascites tumors, 25:26938
LAX, Melvin, Fluctuation and coherence phenomena in classical and quantum physics, 25:27947
LAXMINARAYANA, H., Induction of mutation in Streptococcus diacetilactis by nitrosoguanidine and ultraviolet irradiation, 25:27121
LAYMAN, R. W., Nonlinear perturbations and electron scattering in a beam plasma, 25:27703
Scattering of electrons by electrostatic fluctuations in a magnetized plasma, 25:27699
LAZAREV, B. G., Dimensional effect in magnetization of strong superconductors, 25:27644 (KHFTI-70-8)
LAZAREV, N. V., Regulator for high voltage capacitor bank, 25:28108 (ITEF-761)
LAZUTIN, E. V., Photoneutron reactions on copper, 25:28260
LEACHMAN, R. B., Nuclear-state widths of medium-weight nuclei in the continuum, 25:28268
LEARY, H. J. Jr., Infrared spectra of UO and UO_2 vapor condensed in rare-gas matrices, 25:26260 (COO-1182-34)
LEBEDEVA, N. S., Elastic neutron scattering at small angles, 25:28500
LEBOWITZ, Jacob, Internal bremsstrahlung accompanying orbital-electron capture in ^{7}Be, 25:28200
LECCISOTTI, A., Use of /sup 99m/Tc for cerebral scintigraphy, 25:26818
LECLOUX, M., How to use the code, COMET, 25:27202 (EUR-4562)
LEE, Arthur Clair, Delayed effects of canine ovarian irradiation, 25:27009
LEE, Bae Ham, Studies on amylase and protease activities of Aspergilli by uv-irradiation method, 25:27097
LEE, H. C., EVALIN: CDC FORTRAN IV code to perform an extended variational approximation for light and intermediate nuclei, 25:28439 (AECL-3801)
LEE, Hyun Duk, Application of large gamma radiation source to the treatment of parasites in human excreta, 25:27126
LEE, Jang Kyu, Clinical study on the value of a scoring system of the scanning images in liver cirrhosis, 25:26862
Medical study of Korean atomic bomb survivors, 25:27060
Uptake- and metabolic studies of the labelled compounds in malignant tumors, 25:26859
LEE, Kenneth, Annealing study of EuO films doped with Fe Eu, 25:27898
LEE, L. H., Corrosion and passivation of thin molybdenum films, 25:27171
LEE, R., Effects of intracorporeal heat and radiation on dogs, 25:26931
LEE, S. P. Y., Faddeev's equations in the SU(3) representation of a three-particle state, 25:28056
LEE, T. H., Physiology of disks of irradiated tomato fruit. I, 25:27067
LEE, Un Chul, General energy-dependent transport equation with fission, 25:28155
LEE, W. W., Longitudinal oscillations of Lorentzian electron gas, 25:27822
LEE, William David, Effect of pressure on luminescence of helium II, 25:27636
LEEPER, D. B., Chromosomal aberrations and mortality of x-irradiated mammalian cells: emphasis on repair, 25:26723
LEETZ, H.-K., First experiences in the use of a computer system in clinical radiation physics, 25:26755
LEFEVRE, B. G., Field-ion studies of microstructures and transformations in long-range-ordered alloys, 25:27255
LEFFEK, K. T., Secondary kinetic isotope effects in bimolecular nucleophilic substitutions. IV, 25:26217
LEFORT, Marc, Search for superheavy elements on accelerator ALICE, 25:28315 (CERN-70-30(Vol.2), pp 723-33)
LEGEAY, G., Influence of irradiation dose on latency time of cataracts in rabbits, 25:27027
LE GOFF, P., Velocities of particles of a refractory material injected into an arc plasma jet, 25:28859 (LA-tr-71-27)

LEGVOLD, S., Electrical resistivity and magnetization of Gd--Th and Gd--Mg alloys, 25:27871
LEHMAN, Roger H., Thorium induced carcinoma of the maxillary sinus, 25:27050
LEHMANN, B., In-beam nuclear magnetic resonance of 159 μs level in ^{115}Sn, 25:28380
LEHMANN, Jeanne, Uranium alloys, 25:27195
LEHNERT, Shirley, X-ray-induced single-strand breaks in DNA of E. coli B/r: effect of irradiation and postirradiation conditions, 25:26655
LEHRHEUER, W., High-temperature brazing of thermoelements and pipe ducts on reactor plugs for reactor experiments, 25:27177 (JUL-681-RX)
LEIGH, J. R., 9/2-[514] state in ^{185}Re, 25:28287 (ANU-P-518)
LEIPZIGER, S., Flow of a liquid metal coolant past a heat generating cylinder, 25:26422
LEITER, D., Classical charged tachyons and their electromagnetic interaction, 25:27984
LEJSEK, K., Decrease in pethidine demethylating activity of isolated rat liver microsomes following whole-body x-irradiation, 25:27034
LEMAITRE, J., Cyclic variation of volume of the heart, 25:26566 (CEA-CONF-1711)
LEMOINE, A., Velocities of particles of a refractory material injected into an arc plasma jet, 25:28859 (LA-tr-71-27)
LENER, J., Distribution of radioactive ^{99}Mo in tissue of test animals, 25:26598
LENGEMANN, F. W., Atomic energy techniques to increase productivity of domestic livestock, 25:26578 (CONF-680112-, pp 153-66)
LENGEROVA, Alena, Comparison of colony-forming performance of bone marrow cells in syngeneic and allogeneic cellular environment within a single host, 25:26670
LENHART, K. G., Ground observations of the solar event of Feb. 25, 1969, 25:27553
LENZ, F., Diagnostic value of the quotients of precordial over prepulmonary counting rate from ^{24}Na^{131}I, 25:26822
LENZ, P., Ureteral injuries after obstetric--gynecologic intervention and radiation, 25:26814
Urologic management of injuries to the bladder after gynecologic radiotherapy, 25:26813
LEO, R. A., Vacuum polarization tensor and equal-time commutators in quantum electrodynamics, 25:28074
LEONARD, C. G., Transduction in group a streptococci by ultraviolet irradiated bacteriophages, 25:27110
LEPECHINSKY, D., Dynamic stabilization of the drift dissipative instability by an inhomogeneous rf field, 25:27780
LESKI, R., Population studies of the cherry fruit fly, Rhagoletis cerasi L, 25:27150
LESSMANN, G. G., Weldability and elevated temperature stability of refractory metal alloys. V, 25:27178 (N-71-10353)
Weldability and elevated temperature stability of refractory metal alloys. II, 25:27208 (N-71-10352)
LESTRINGUEZ, J., Production cross sections of Li and Be isotopes in ^{12}C by high-energy protons and alpha particles, 25:28182
LETT, J. T., Production of strand breaks in mammalian DNA by x-rays: at different stages in the cell cycle, 25:26625
LEV, A., Role of configuration states in isospin forbidden proton decays of T = 3/2 states, 25:28179
LEVENE, Martin B., Pituitary radiotherapy, 25:27041
LEVENTHAL, J. J., Energetics of HeH$^+$ formed in H_2^+--He collisions, 25:27452
LEVER, A. B. P., Far-infrared and electronic spectra of some bis-ethylenediamine and related complexes of copper(II) and the relevance of these data to tetragonal distortion and bond strengths, 25:26232
LEVI, C., Interest of analog state studies in deformed nuclei, 25:28472
LE VIET BIN, Determination of Sm microimpurity in Eu oxide, 25:26162
LEVIN, Gilbert V., Automated primary productivity measurements in water bodies, 25:28867 (NYO-3993-1)
LEVINE, A. M., Dynamic stabilization of a two-stream instability, 25:27788
LEVITIN, M. M., Genetics and selection of Beauveria bassiana (Bals.) Vuill., an entomopathogenic fungus. I, 25:26703
Mutability of fungi, 25:26698
LEVITSKII, S. M., Electron-beam relaxation in a plasma, 25:27700
LEVY, Peter M., Dependence of the s--f exchange coupling parameter on rare-earth atomic number, 25:27892
LEVY, R. H., HIPAC as a source of highly stripped heavy ions, 25:28128 (WASH-1159, pp 88-112)
LEVY-LEBLOND, J.-M., Stability of zero-mass particles, 25:27979
LEWAK, G. J., Interaction of electrostatic waves in collisionless plasmas, 25:27812
Penetration to second order of an electrostatic field into a warm plasma, 25:27707
LEWIS, E. E., Transient heat conduction model for reactor fuel elements, 25:28662
LEWIS, M. B., Nuclear data sheets for A = 208, 25:28375
LEWIS, P., Reliability factors affecting power plant mechanical equipment, 25:28549 (AECL-3670, pp 45-55)
LEWIS, P. B., Nonlinear perturbations and electron scattering in a beam plasma, 25:27703
LHERMITTE, Roger M., Radar observations of convective storm circulation and its relation to precipitation scavenging, 25:26360 (CONF-700601-, pp 13-20)
LIACOPOULOS-BRIOT, M., Myelo-restorative capacities and immunocompetence of bone marrow cells of the mouse cultivated in vitro, 25:26942
LIE, T. N., Detection of highly stripped heavy ions in a low-pressure linear pinch device, 25:27678 (WASH-1159, pp 172-83)
LIEBERMAN, Lionel M., Radiolabeled cholesterol as an adrenal scanning agent, 25:26845
Treatment doses of ^{131}I-labeled chloroquine analog in normal and malignant melanoma dogs, 25:26882
LIEBOWITZ, H., Fracture. An advanced treatise. III, 25:27170
LIGGETT, G., Isomer ratio for (b,xn,yp,γ) reactions, 25:28502
LIGOU, J., Integral equation of transport in one-dimensional cyclindrical geometry. I, 25:28145 (EIR-188)
LIKHODED, L. Ya., Mutagenesis induced by uv-irradiation in B. subtilis, 25:26729
LIKTENSHTEIN, V. Kh., Feedback stabilization of the rarefied plasma cyclotron instability, 25:27776
LILLEY, E. M., Electrical resistance of ytterbium as a function of temperature and pressure, 25:27867 (UCRL-51006)
LIMA, F. W., Application of the retaining ion technique to separation of ions by electrophoretic focusing ions, 25:26351
LIN, David H. Y., Most primitive precursor cells of hemopoietic system, 25:28898 (UCRL-20613)
LIN, K. Y., Low-energy theorems for Compton scattering on targets of arbitrary spin, 25:27993
LINDAHL, A., Alpha decay of neutron deficient isotopes of mercury and radon and their daughters, 25:28302 (CERN-70-30(Vol.1), pp 523-31)
Experimental Q-values far from stability, 25:28295 (CERN-70-30(Vol.1), pp 331-40)
LINDAHL-KIESSLING, K., Chromosome and chromatid-type aberrations induced by ^{60}Co irradiation and tritiated uridine in human leukocyte cultures, 25:26636
LINDALEN, H. R., Low-energy solar protons during the Feb. 25, 1969 event, 25:27573
Proton precipitation in noon--midnight meridian, 25:27579
LINDAUER, Erwin, Review of methods for handling of stationary neutron transport problem, 25:28151 (TUBIK-21)
LINDBERG, K., Development of transient fatty liver after release from ten-day stay in hypoxia, 25:26967
LINDER, W., Measurement of the spin and nuclear magnetic moment of ^{20}Na, 25:28209 (CERN-70-30(Vol.1), pp 383-5)
LINDGREN, Alice Marilyn Lindell, Effect of x-irradiation on the wound response of the rat lens epithelium, 25:27000
LINDGREN, I., Atomic-beam measurements in the rare-earth region, 25:28298 (CERN-70-30(Vol.1), pp 387-94)
LINDGREN, N. E., Feedback suppression of drift-centrifugal waves in mirror-confined plasma, 25:27768
LINDGREN, R. G., Effect of temperature nonuniformity on positive column, 25:27714
LINDGREN, S., Particle fluxes and field configuration after major particle injection of January 28, 1967, 25:27584
LINDMAN, E. L., Generalized boundary conditions of plasma feedback systems, 25:27755
LINDSTROM, D. P., Fine structure of the isobaric analogs of the ground and second excited states of ^{63}Ni, 25:28237
LINDUP, Rhona, Radioinduced fibrosarcoma, 25:27044
LINSAY, Ernest C., Stereochemistry of allylic rearrangements. XVI. Stereochemistry of ion-pair return in the trans-α,γ-methylphenylallyl p-nitrobenzoate system, 25:26224
LINSON, Lewis M., Electrostatic electron oscillations in cylindrical, non-neutral plasmas, 25:27808
LIPTAK, Ya., Ytterbium-169 levels in ^{169}Lu decay, 25:28433
LIRAN, S., Current semiempirical mass equations and improved shell model nuclear masses, 25:28291 (CERN-70-30(Vol.1), pp 165-216)
LISMAN, F. L., Fission yields and branching ratios of ^{85}Kr in thermal neutron fission of ^{233}U, ^{235}U, ^{239}Pu, and ^{241}Pu, 25:28383
LISON, R., High-temperature brazing of thermoelements and pipe ducts on reactor plugs for reactor experiments, 25:27177 (JUL-681-RX)
LIST, R. J., Use of natural radioactivities to estimate large-scale precipitation scavenging, 25:26390 (CONF-700601-, pp 465-74)
LISTON, J., Radiation destruction of Vibrio parahaemolyticus, 25:27115
LISZKA, L., Variations in low-energy electron spectrum and relation to magnetic activity, 25:27582
LITTLE, John B., Irradiation of primary human amnion cell cultures: effects on DNA synthesis and progression through the cell cycle, 25:26630
LIUKKONEN, E., Energy levels of ^{176}Yb, 25:28398
LIUZZO, Joseph A., Storage temperature effects on the proteolytic activity of radiation-surviving bacteria in oysters, 25:27114
LJUBICIC, A., Deexcitation of the 662-keV state in ^{137}Ba by

the internal Compton effect, 25:28422
LOCATELLI, Paolo, Intermolecular and intramolecular free valence transfer in gamma irradiated crystalline hexadecanoic and cis-9-octadecenoic acids, 25:26312
LOCKETT, G. E., Using high-temperature reactor for power generation below 500 MW(e), 25:28719
LOCKWOOD, J. A., Comments on solar activity, 27-day variation, and long-term modulation of cosmic-ray intensity, 25:27389
LODDING, A., Differential diffusion of impurities in isotopic lithium matrices, 25:26240
LODHI, M. A. K., Dynamical correlation in ^{6}Li and inelastic electron scattering, 25:28201
LOHNER, H., Pneumatic system for activation analysis with short-lived radionuclides, 25:26189 (KFK-1293)
LOMINSKI, I., Long-chain mutants of Streptococcus faecalis induced by ultraviolet irradiation, 25:26731
LOMSADZE, Yu. M., Some pecularities of cognition of microworld, 25:27929 (ITF-70-62-E)
LONG, Everett, Gas cooled nuclear reactors, 25:28831
LONG, J. K., ZPR-3 assemblies 48: 48A, and 48B: the study of a dilute plutonium-fueled assembly and its variants, 25:28752 (ANL-7759)
LOPEZ, A., Alpha spectrometer for measuring the degree of radioactive equilibrium between ^{222}Rn and its daughter products in U mines, 25:26503
Radioactive aerosols characteristics in French U mines, 25:26773
LOREN, Robert B., Spectrophotometry of Nova Serpentis 1970, 25:27322
LORENZ, Erhard, Effect of radionuclide contamination on the calibration of ^{99}Mo, 25:26317
LORIKYAN, M. P., Detection of x-ray transition radiation by means of a streamer chamber, 25:26515
LOU, K. H., Bevatron external proton beam facilities, 25:28119 (UCRL-20194)
LOVBERG, Ralph H., Methods of experimental physics. IX, 25:27689
LOVELACE, C., K^{+}p Reggeized phase shift analysis, 25:28043
LOVELOCK, David, Einstein tensor and its generalizations, 25:28085
LOVERA, G., 27-day oscillation in cosmic-ray intensity and shorter periodicities, 25:27472
LOWER, Richard R., Electron microscopic changes following canine cardiac allografts: the effects of irradiation, 25:26677
LOZHKIN, O. V., Energy resolution for dE/dx detectors, 25:26485
LUCA, I., Beta radioactivity in some wines from Transylvania and Dobruja, 25:26618
LUCARONI, A., Effects of x rays and visible light on the reconstitution of the early potentials of the isolated frog eye, 25:27004
LUECKE-HUHLE, Christine, Oxygen effect in γ-irradiated DNA, 25:26637
LUENGO, C. A., Electron--electron scattering in electrical resistivity of In, 25:27660
LUFFIN, Jean, COREGRAF 2: adjustment and comparison with experiment, 25:28654 (CEA-N-1344(2))
LUKIERSKI, J., Description of N-theta sector in Lee model, 25:28067
LUM, G. S., In-vitro studies of rat viruses. II, 25:27117
LUNA, Robert E., Climatology of atmospheric diffusion prediction variables, 25:28881 (SC-DC-713920)
LUND, E., Neutron-rich nuclides obtained using OSIRIS facility, 25:28340 (CERN-70-30(Vol.2), pp 1093-1103)
Q-values of some nuclides on the neutron-rich side of stability, 25:28296 (CERN-70-30(Vol.1), pp 341-51)
LUNDE, P. K. M., Determination of blood flow in rabbit femur by radioactive microspheres, 25:26577
LUPES, Mircea E., Mechanism of the benzoin condensation, 25:26220
LUUKKO, A., Energy levels of ^{24}Mg, 25:28259
LUZANOV, V. M., Change in the functional state of erythropoiesis during prolonged fractionated irradiation, 25:27015
LWOWSKI, Walter, Infrared spectroscopic study of the photolytic decomposition of methyl azidoformate, 25:26236
LYNCH, Anthony, Vulnerability of developing brain: I. Some lasting effects of x-irradiation, 25:26946
LYONS, L., Reaction K^{-}P → AK^{+}K^{-} and the generalized Veneziano model, 25:28042
LYUBIMOV, G. P., Solar cosmic-ray increase on 25 Feb.--5 Mar., 1969, 25:27470
LYUBIMOV, V. A., Universal magnetic spectrometer with 0.15 percent resolving power at maximum pulse of 60 GeV/c, 25:26507 (NP-18764)
LYUTI, I. N., Stabilization of magnetic field in an iron πγ2 β spectrometer, 25:26502

M

MACDONALD, Douglas E., Damping of dislocations in niobium by phonon viscosity, 25:27905
MACDONALD, R. A., Molecular dynamical studies of the phase transformation of iron under pressure, 25:28895 (TID-25683)
MACFARLANE, D. R., SAS1A: a computer code for the analysis of fast-reactor power and flow transients, 25:28727 (ANL-7607)
MACFARLANE, Ronald D., Beta-neutrino correlations and recoil nuclear alignment effects in light delayed particle emitters, 25:28210 (CERN-70-30(Vol.1), pp 447-55)
MACGREGOR, M. H., Evidence for linear meson systematics with baryon number N = 2, 25:28010
Hadron rotational levels, 25:28009
MAC GREGOR, Malcolm H., Hadron spectroscopy, 25:28008 (UCRL-73073)
MACHIYAMA, Yoshihiko, Medical 6 MeV linear accelerator, 25:28132
MACHTA, L., Use of natural radioactivities to estimate large-scale precipitation scavenging, 25:26390 (CONF-700601-, pp 465-74)
MACIAS-MARQUES, M. I., Mass-differences in neutron-rich Sr Region, 25:28294 (CERN-70-30(Vol.1), pp 321-9)
MACKELLAR, Alan D., Low-energy neutron--oxygen scattering derived from two-body forces, 25:28198
MACKINTOSH, R. S., Inelastic scattering of very low energy pions from nuclei, 25:28244
MACMAHON, T. D., Energy released by beta radiation following fission. I, 25:28407
MACRAE, A. U., Isothermal annealing of boron implanted silicon, 25:27854
MACRES, V. G., Shielded x-ray microprobe for the analysis of radioactive samples, 25:26156
MACVITTIE, Thomas Joseph, Radiation-induced residual injury in the hematopoietic system of the mouse, 25:26981
MADDOCK, R. D., Analysis of the reaction π^{+}p → rho^{0}Δ^{++} at 11.7 GeV/c incident momentum, 25:27960 (DESY-71/8)
MADSEN, V. A., Charged-exchange reactions, 25:28457
MAECK, W. J., Fission yields and branching ratios of ^{85}Kr in thermal neutron fission of ^{233}U, ^{235}U, ^{239}Pu, and ^{241}Pu, 25:28383
MAEHARA, Nobutoshi, Role of leukocytes in production of interferon, 25:26986
MAEKAWA, Hiroshi, Pulsed neutron research. III, 25:28161
MAEZAWA, Kiyoshi, Two basic modes of interaction between the solar wind and the magnetosphere, 25:27630
MAGDON, Erwin, Effect of ionizing radiation on DNA x RNA hybridization, 25:26641
MAGEE, Tommy Joe, Defect studies in neutron and gamma-irradiated silicon, 25:27848
MAGRI, V., STAZ-2: program for thermohydraulic analysis of channel of water-moderated and cooled nuclear reactor core operating in stationary state, 25:28679 (EUR-4553)
MAGYARI, E., Exactly solvable quantum-mechanical N-body problem, 25:27934
MAHAUX, C., Fine structure of analog resonances, 25:28463
MAHESHWARI, P. N., Nuclear structure studies of ^{51}V by ^{50}Ti(^{3}He,d) reaction, 25:28231
MAHUNKA, I., Nuclear spectroscopy of some light Tl isotopes, 25:28339 (CERN-70-30(Vol.2), pp 1081-91)
MAHUNKA, M., Nuclear spectroscopy of some light Tl isotopes, 25:28339 (CERN-70-30(Vol.2), pp 1081-91)
MAILLET, Ennemond, Method of and apparatus for the production of power, 25:28747
MAIN, Robert, Status and outlook for arc-discharge sources, 25:28124 (WASH-1159, pp 1-10)
MAIRLE, G., Further indications for t-dependence of angular distributions, 25:28174
MAISURADZE, N. A., Defect annealing in neutron irradiated niobium, 25:27269
MAIYA, P. S., Surface relaxation kinetics of uranium dioxide, 25:27288
MAJ, Zbigniew, Studies on the effect of constant magnetic field on tobacco mosaic virus synthesis in tobacco leaves, 25:27106
MAJLING, L., Electroexcitation of ^{32}S in region of dipole resonance, 25:28220 (UJV-2553-F)
MAK, D., H-2-glucose as tracer in turnover studies, 25:26602
MAKAR, Michael, Immunohematological studies of Marshall Islanders sixteen years after fallout radiation exposure, 25:27058
MAKAROV, A. M., Unsteady magnetohydrodynamic flow of a viscoplastic medium over an infinite plate, 25:27496
MAKHANKOV, V. G., Non-linear regime of radiation instability development of relativistic electron rings, 25:28110 (JINR-P9-5622)
MAKIEJ, Boleslaw, Mechanism of superconductivity, 25:27661
MALEK, I., Carotenoids synthesized by uv-induced mutants of Mycobacterium phlei, 25:26687
MALIK, S. K., Stability of the screw pinch with Hall current, 25:27732
MALIN, S. R. C., Lunar and solar daily variation of the geomagnetic field at Watheroo, Western Australia, 25:27503
MALKE, H., Characteristics of transducing group A streptococcal bacteriophages A5 and A25, 25:27098
MALKOV, E. I., Constraints on the partial amplitudes of an annihilation channel, 25:28097
MALMSKOG, S. G., Lifetimes of excited nuclear levels, 25:28341 (CERN-70-30(Vol.2), pp 1115-18)
Possible nuclear co-existence in odd-mass Ir nuclei, 25:28324 (CERN-70-30(Vol.2), pp 957-65)
MALOV, L. A., Nonrotational states of odd-N deformed nuclei in region 153 less than or equal to A less than or equal to 171, 25:28346 (JINR-E4-5567)
MALOVICHKO, I. I., Respiration and oxidative

phosphorylation of bone marrow tissue of irradiated rabbits after homotransplantation of bone marrow elements, 25:27019
MAMACOS, James, Changes in biological effectiveness of a fast neutron beam with depth in tissue-equivalent material, 25:26906
MANCIULEA, S., Effect of γ-ray microdoses on some metabolic indexes during white rat adaptation to hypothermia, 25:27023
MANDELZWEIG, V. B., Possible quasinuclear nature of heavy mesonic resonances, 25:28026 (NP-18774)
MANDY, Stephen H., Eccrine poroma, 25:27055
MANIKAS, G., Radiation-induced sterility in the control of the olive fruit fly, 25:27151
MANILOFF, Jack, Effects of metals on cells, subcellular elements, and macromolecules. Proceedings of the 2nd conference on toxicity, Rochester, N. Y., June 12--16, 1969, 25:26608
MANKU, G. C. S., Formation constants of some metal complexes of 5,7-diiodo-8-hydroxyquinoline, 25:26214
MANN, A., Linearized version of the Hartree--Fock method, 25:28519
MANN, A. K., Comments on the letter limits on the electromagnetic production of heavy leptons, 25:27998
MANN, S., Nuclear safety in American radiochemical processing plants, 25:26780
MANNO, V., Conference on intercorrelated satellite observations related to solar events, Noordwijk, Netherlands, 9/69, 25:27531
MANSON, A. H., Particle influx and midlatitude nighttime E region at solar minimum, 25:27601
Seasonal variation of electron densities below 100 km at midlatitudes. IV, 25:27512
MANTOVANI, E., Far-infrared and electronic spectra of some bis-ethylenediamine and related complexes of copper(II) and the relevance of these data to tetragonal distortion and bond strengths, 25:26232
MANUZIO, Caterina, Diagrams for the determination of the risk of failure of structures, 25:28872 (ORNL-tr-2133)
MARCH, N. H., Isotope effects in close-packed metals and in alkali halides, 25:26241
MARCHI, F., Effect of ionizing radiation on the heart, 25:26961
MARCORELLI, E., Cylindrical adenoma of the parotid gland, 25:26866
MARENKOV, O. S., Generalization of γ-albedo calculations on basis of similarity theory, 25:27831
MARFINA, K. G., Changes in carbohydrates and organic acids in leaves and roots of cotton and maize plants in dependence on the dose of presowing gamma irradiation of seeds, 25:27074
MARGEN, P. H., Conceptual design of medium-output integrated PWR produced from components series intended for larger units, 25:28639
MARGOLIS, B., Coherent and incoherent reactions and diffraction, 25:27978
MARGVELASHVILI, P. I., Regeneration of K^0 mesons on deuteron at high energies, 25:28049
MARIANI, F., Interplanetary magnetic field measured by Pioneer 8 during the Feb. 25, 1969 event, 25:27556
MARINICH, A. M., Optimization of parameters for small nuclear power sources containing water-cooled, water-moderated reactors, 25:28640
MARIPUU, S., Titanium-51 ground-state analogue, 25:28226
MARK, Herman F., New composites: morphology and properties, 25:27277
MARK, J. E., Volume dependence of C_2 correction in the Mooney--Rivlin elastic equation of state, 25:26285
MARKEEV, A. K., Observations of solar radio bursts with high spectral resolution, 25:27398
MARKI, A., Incidence-rate and types of chlorophyll mutants in flax induced by gamma rays and some alkylating agents, 25:27090
MARKIV, V. Ya., Study of the zirconium--nickel--aluminum system, 25:27258
MARKOVITS, P., Radiobiological study of the formation of interferon in the kidney cells of monkeys infected with NDV, 25:27113
MARQUES DE SOUZA, J. A., United Kingdom reactors available for commercial operations, 25:28720
MARSCHAL, A., Determination of C in high-purity Si, 25:26202
MARSDEN, P. L., Observations recorded by the cosmic-ray detector during the solar flare of Feb. 25, 1969, 25:27471
MARSH, Spinks H., ^{60}Co teletherapy of pituitary adenomas, 25:26872
MARSHALL, Alan, Measurement of lifetime and g factors in the OH and OD free radicals, 25:26243
MARSHALL, Dannis Albert George, Improvements in or relating to filters, 25:28829
MARSHALL, T. C., Microwave scattering from plasmas, 25:27679
MARTENS, Christopher S., Mechanisms of iodine injection from the sea surface, 25:26380 (CONF-700601-, pp 319-24)
MARTIAL-LASFARGUES, C., Myelo-restorative capacities and immunocompetence of bone marrow cells of the mouse cultivated in vitro, 25:26942
MARTIN, D. L., Cast permanent magnets of Co, Cu, and Ce: process and performance characteristics, 25:27884
MARTIN, David, Mechanism of action of radiation protective agents: in vivo distribution and metabolism of cysteamine-S-phosphate (MEAP), 25:26805
MARTIN, M. J., Nuclear data sheets for A = 209, 25:28376
Nuclear data sheets for A = 211, 25:28377
MARTIN, S., Coulomb displacement energies for excited states in nuclei around ^{28}Si, 25:28243
MARTIN, William J., Irradiation apparatus in combination web handling means, 25:26417
MARTINCHUK, E. L., Change in solubility of Ce, Pr, and Nd in Cr as a function of temperature, 25:27238
MARTINELLI, P., Radioactive analysis techniques, 25:26164
MARTINKOVA, J., Effects of novocain on the isolated perfused heart of rats after x-irradiation, 25:26798
MARTINS, A. A. R. Lopes, Organoleptic chemical and microbiological aspects of irradiated Portuguese sausages, 25:27159
MARTKOPLISHVILI, G. S., Defect annealing in neutron irradiated niobium, 25:27269
MARTY, D., Torsatron without toroidal field coils as a solution of the divertor problem, 25:27793
MARUYAMA, T., Effect of helical instability on the radial density and potential distribution, 25:27738
MARUYAMA, Takashi, Effects of fast neutrons and ^{60}Co γ-rays on Artemia, 25:26917
MARUYAMA, Yosh, Variable block-surface-distance (BSD) for adjustment of shadow size in mantle therapy, 25:26892
MARX, E., Pair annihilation at a potential barrier in time, 25:27985
MASCHKE, E. K., Torsatron without toroidal field coils as a solution of the divertor problem, 25:27793
MASEK, V., Radiation experiment on a model of a finned tubular fuel element. I, 25:27267 (UJV-2371.R,T.)
MASKER, Warren, Effect of nalidixic acid on semiconservative replication and repair synthesis after ultraviolet irradiation in Escherichia coli, 25:27125
MASON, Warren P., Damping of dislocations in niobium by phonon viscosity, 25:27905
MASS, W. J., Magnetic properties of the system Au_4R(R = Er, Tm, and Yb), 25:27872
MASSE, P., Spectra and time history of protons in interplanetary space, Feb. 25--28, 1969, 25:27558
MASSETH, F. X., 1000-MWe LMFBR accident analysis and safety system design study. Candidate primary containment safety features. Topical report, 25:28733 (BAW-1352)
MATCHES, Jack R., Radiation destruction of Vibrio parahaemolyticus, 25:27115
MATE, Z., Nuclear spectroscopy of some light Tl isotopes, 25:28339 (CERN-70-30(Vol.2), pp 1081-91)
MATHESON, A. F., Secondary kinetic isotope effects in bimolecular nucleophilic substitutions. IV, 25:26217
MATHIEU, Jacques, Mean gamma ray energy necessary to create ion pairs in dielectric liquids, 25:26293
MATHUR, K. C., Cross-sections and reaction rates for electron-impact ionization of lithiumlike and sodiumlike positive ions, 25:27443
MATHUR, S. C., Adaptation of gamma-ray spectral analysis program for PDP-9 computer, 25:26500
MATHUR, Suresh C., Techniques for compiling large FORTRAN programs for a PDP-9 computer, 25:26555
MATIJEVIC, E., Collection efficiency of water droplets in AgCl aerosol, 25:26370 (CONF-700601-, pp 161-7)
MATIN, A., Problems of introducing small and medium power reactors to developing countries with particular reference to the creation of a special nuclear fund, 25:28540
MATLACK, George M., Methods of chemical analysis for FBR uranium--plutonium oxide fuel and source materials, 25:26153 (LA-4622)
MATOUSEK, V., Comparison of colony-forming performance of bone marrow cells in syngeneic and allogeneic cellular environment within a single host, 25:26670
MATSUBARA, Tadao, Studies on analysis of rare earths. II, 25:26168
MATSUI, Hiroshi, Studies on analysis of rare earths. II, 25:26168
MATSUKURA, Shigeru, New phenomenon of usefulness in the radioimmunoassay of plasma adrenocorticotropic hormone, 25:26675
MATSUMURA, Tetsuo, Analysis of Zircaloy, 25:26171
MATSUNAGA, Sakuro, Temperature dependence of critical current in Nb_3Sn ribbon, 25:27658
MATSUURA, O. T., Impulsiveness of microwave bursts and its association with sunspot types, 25:27381
MATSUYAMA, Akira, Macromolecular synthesis in Micrococcus radiodurans during postirradiation incubation, 25:26639
Radiosensitivity of Streptomyces cacaoi spores, 25:27068
MATSUZAWA, H., Paired ionization chambers for measurement of neutrons and gamma rays, 25:26538
MATTERN, J., Some technical aspects and economy of AEG--BWR fuel cycle, 25:28721
MATTHEWS, D. L., Relation between integral electron flux and current in retarding-potential plasma probes, 25:27682
MATTHEWS, J. R., Calculation of stress in fast reactor fuel elements, 25:27285
MATTHEWS, R. W., Evaluation of the ceric--cerous system as an impurity-insensitive megarad dosimeter, 25:26526
MATTHIAS, Bernd T., High-temperature superconductivity, 25:27656
MATTHIAS, E., In-beam nuclear magnetic resonance of 159 μs

XUM

level in ^{119}Sn, 25:28380
MATTINGLY, Alice, Repair of irradiated transforming deoxyribonucleic acid in wild type and a radiation-sensitive mutant of Micrococcus radiodurans, 25:27124
MATUDA, Kozi, Quadrupole effects in NMR spectra on ^{12}B and ^{13}N, 25:27923
MAUDERLI, Walter, Effect of radionuclide contamination on the calibration of ^{99}Mo, 25:26317
MAURER, Hans A., Reliability analysis for the evaluation of reactor systems, 25:28740
MAVROYANNAKIS, E., Measurement of the coefficient of gamma absorption of materials used for nuclear constructions, 25:27826 (DEMO-70/11)
MAXFIELD, William S., Synergism between radiation and estrogen in the production of mammary cancer in the rat, 25:27011
MAY, P., Unilateral determination of effective renal plasma flow by radioisotopes, 25:26826
MAYER, J. W., Lattice location and dopant behavior of Group II and VI elements, 25:27856
MAYER, L., Calculation of flux distributions in reactor sub-regions with generalized multiple collision probabilities, 25:28805 (EURFNR-898)
MAYERS, G. L., Isoracemization of N-carbobenzoxyamino acid ester derivatives, 25:26257
MAZUR, A., Preparation and properties of six rat red cell hemoglobins, 25:28866 (NYO-3976-5)
Prog. rpt., 6/70--5/71, 25:28865 (NYO-3976-4)
MAZURIK, V. K., Influence of irradiation on the urinary excretion of deoxycytidine and beta-aminoisobutyric acid in monkeys, 25:26999
MCADOO, Stewart F. Jr., Earth departure technique for use in manned interplanetary missions using NERVA engine, 25:28788
MCCARTHY, Shaun Leaf, Superconductivity of zirconium--transition metal coumpounds, 25:27654
MCCAULEY, James E., Two new gregarine parasites from the spatangoid-urchin Brissaster latifrons, 25:28880 (RLO-1750-59)
MCCLAIN, W. C., Salt mine repository for radioactive wastes, 25:26453
MCCLAIN, William James, Investigation of the use of a digital computer for processing radioisotope scan data, 25:26834
MCCLURE, D. A., Coulomb excitation of levels in ^{105}Pd, 25:28423
MCCLURE, J. W., Nuclear level densities and reaction mechanisms from continuum neutron spectra, 25:28285
MCCORMACK, J. D., Scavenging of aerosol particles by sprays, 25:26372 (CONF-700601-, pp 187-204)
MCCREA, W. H., Doubts about Mach's principle, 25:28065
MCCULLOUGH, Edwin Charles, Qualitative and quantitative features of the terrestrial solar ultraviolet radiation environment, 25:26517 (COO-1105-164)
MCDIARMID, I. B., Evidence for a solar-wind origin of auroral ions from low-energy ion measurements, 25:27618
MCDONALD, Frank B., Satellite observations of solar cosmic rays, 25:27533
MCDONALD, P. T., Correlation of linkage groups with chromosomes in the mosquito, Aedes aegypti, 25:26694
Cytogenetics of two radiation-induced, sex-linked translocations in the yellow-fever mosquito, Aedes aegypti, 25:26719
MCDONALD, R. E., Low-lying excited states of ^{29}Al. III, 25:28267
MCDONNELL, John J., Aliphatic semidiones. XV. 2,3-semidiones derived from the bicyclo[n,1.0]alkanes, 25:26254
MCDOWELL, Robin S., Vibrational spectrum and force field of osmium tetroxide, 25:26258
MCFADDEN, J. T., Automatic target cycling system for total cross section measurements, 25:28115 (PURC-4159-17)
MCGLASSON, W. B., Physiology of disks of irradiated tomato fruit. I, 25:27067
MCGONNAGLE, Warren J., Nondestructive testing, 25:26440
MCGRATH, R. G., Westinghouse experience with medium-size reactors and some factors to be considered in selecting a nuclear plant, 25:28638
MCGRATH, Robert L., Properties of analog resonances formed in direct reactions decaying via isospin-forbidden modes, 25:28223
MCGUIRE, T. R., Intrinsic metallic character of rare-earth pnictides, 25:27879
Magnetic and magneto-optical properties of Fe-doped EuO films, 25:27897
MCGURTY, James A., Method for producing stoichiometric uranium dioxide compositions, 25:27274
MCHARRIS, Wm. C., Straightforward elucidation of complex shell-model states by β decay of nuclei far from stability, 25:28299 (CERN-70-30(Vol.1), pp 435-46)
MCHENRY, J. R., Effect of concentration gradients on the performance of a nuclear sediment concentration gage, 25:26544
MCINTYRE, L. C. Jr., Mean lives and angular correlations in ^{57}Co with ^{56}Fe(α,pγ)^{57}Co reaction, 25:28281
MCKENZIE, J. M., Tentative method for expressing radiation hardness, 25:26560 (SC-DR-710045)
MCKISIC, James Michael, Application of the dispersive sum rule method to meson systems, 25:28029
MCLEMORE, R. H., Hurricane protection design, 25:28629
MCLENNAN, D. J., Bromine scrambling accompanying base-catalyzed isomerization of 1,2,4-tribromobenzene, 25:26221
MCMILLAN, J. A., Hyperfine interactions: tables of isotropic and anisotropic parameters for the atoms hydrogen to bismuth, 25:27441 (ANL-7784)
MCMILLAN, Juan A., Electron paramagnetic resonance spectroscopy, 25:28838 (ANL-7764)
MCNALLY, J. Rand Jr., Fusion chain reactions. I, 25:27796
Fusion chain reactions. II, 25:27797
Fusion chain reactions. III, 25:27725
MCNEAL, R. A., SAS1A: a computer code for the analysis of fast-reactor power and flow transients, 25:28727 (ANL-7607)
MCNIFF, E. J. Jr., Magnetic properties of dilute Pd(Gd) alloys, 25:27921
MCPHERSON, R., Tabulation of gamma--gamma directional-correlation coefficients, 25:28401
MCRAE, E. G., Electron diffraction at crystal surfaces. IV, 25:27256
MCRAE, J., Iron-59 distribution in normal and x-irradiated mice, 25:27012
MCVEAN, R. L., ZPR-3 assemblies 48: 48A, and 48B: the study of a dilute plutonium-fueled assembly and its variants, 25:28752 (ANL-7759)
MECKONI, V. N., Role of heavy-water reactors in Indian nuclear power program, 25:28580
MEDER, L. F., Exactly solvable quantum-mechanical N-body problem, 25:27934
MEDVEDEV, A. I., Decay of ^{169}Lu, 25:28436
MEDYANIK, I. A., Function of the brain cortex symmetric areas in irradiated animals, 25:28075
MEHLTRETTER, J. P., Studies of granular velocities. II, 25:27366
MEIJER, B. J., Decay of some nuclei far from the stability line studied with standard spectroscopic techniques, 25:28322 (CERN-70-30(Vol.2), pp 939-47)
MEIN, P., Propagation of magneto-acoustic waves along the gravitational field in an isothermal atmosphere, 25:27393
MEKJIAN, A. Z., Isospin impurity in bound states, 25:28476
MELCHER, J. R., Feedback stabilization of hydromagnetic continua: review and prospects, 25:27759
MELEKA, A. H., Electron beam welding. principles and practice, 25:27197
MELESHKO, E. A., Two-frequency precession of muonium in magnetic field, 25:27446
MELLO, P. A., Extension of a schematic theory of nuclear reactions to include isospin and isobaric analogue resonances, 25:28492
MELLON, D. W., Electrical resistivity and magnetization of Gd--Th and Gd--Mg alloys, 25:27871
MELNICAK, P., Scintigraphic localisation of the kidneys for percutaneous renal biopsy, 25:26821
MELNICHEKO, V. V., Structure of electron clusters in an injector with a step-like varying wave phase velocity, 25:28112 (KHFTI-70-17)
MELVIN, J. G., Design and development for reliability, 25:28554 (AECL-3670, pp 89-96)
MELZER, E., Compressor for a high pressure helium circuit for cooling high temperature fuel elements during irradiation experiments, 25:28833
MENDEZ, F., Inhibition of ribosomal RNA synthesis in x-irradiated HeLa cells, 25:26983
MENEGHETTI, J. R., Mechanical features of electron-ring compressors, 25:28118 (UCRL-20177)
MENKES, C., Synoviothesis (synoviotherapy by radioisotopes) studies of more than 400 cases and future prospects, 25:26873
MENTZEN, Bernard F., Infrared absorption of crystalline thorium tetraformates. I. Characterization of thorium tetraformates in the solid state by infrared spectroscopy, 25:26270
Infrared absorption of crystalline thorium tetraformates. II. Detection of polymorphic transitions by infrared spectroscopy: interpretation of the delta(CCO) vibrational mode splitting in the carboxylic group of thorium tetraformates, 25:26269
MENYUK, N., Magnetic properties of europium: pressure and impurity effects, 25:27874
MERCADO, A. L., 1000-MWe LMFBR accident analysis and safety system design study. Candidate emergency decay heat removal systems. Topical report, 25:28732 (BAW-1351)
MERIDIES, R., Ureteral injuries after obstetric--gynecologic intervention and radiation, 25:26814
Urologic management of injuries to the bladder after gynecologic radiotherapy, 25:26813
MERRY, M. W. J., Seasonal variation of electron densities below 100 km at midlatitudes. IV, 25:27512
MERTE, H.-J., Problems of industrial medicine in ophthalmology. I and II, 25:27051
MERZ, Timothy, Chromosomal rejoining in absence of unscheduled DNA synthesis, 25:26724
METCALF, Harold, Measurement of lifetime and g factors in the OH and OD free radicals, 25:26243
METZ, Charles F., Methods of chemical analysis for FBR uranium--plutonium oxide fuel and source materials, 25:26153 (LA-4622)
MEYER, G., Inactivation by uv light of Polyoma virus: cell surface antigen, 25:27107
MEYER, H., Total photoproduction cross section of hadrons

on nuclei, 25:27953
MEYER, J., Compressor for a high pressure helium circuit for cooling high temperature fuel elements during irradiation experiments, 25:28833
MEYER, O., Lattice location and dopant behavior of Group II and VI elements, 25:27856
MEYER, Walter, Argument for a recoverable high-level waste container, 25:26454
MICHEL, W., Thermal conductivity of sintered carbides at elevated temperature, 25:27289
MICHELSEN, K., Determination of blood flow in rabbit femur by radioactive microspheres, 25:26577
MICHELSEN, P., Wave--particle interaction in single-ended Q machine, 25:27693
MIESTERL, J., Neutron temperature during power surge of TRIGA Mark II reactor, 25:28770
MIGDAL, E., Gas phase radiolysis of hydrogen sulphide, 25:26315
MIGEON, C. J., Determination of integrated plasma concentrations and true secretion rates of human growth hormone, 25:26579
MIGNECO, E., Parity assignments of some ^{98}Mo resonances, 25:28402
MIKHAILOVSKII, A. B., Instabilities of a high-pressure plasma contained by a dense blanket of neutral gas, 25:27744
MIKI, Masamichi, Aging characteristics of Cu--30 percent Ni--Be--Ti alloys, 25:27232
MILEY, George H., Direct conversion of nuclear radiation energy, 25:27480
MILIVOJEVIC, Katarina, Effect of total body gamma irradiation on the percutaneous absorption of radiocesium, 25:26595
MILKEY, R. W., Origin of flare produced hard x rays, 25:27385
MILLER, B., Plasma heating by strong shock waves, 25:27670
MILLER, C. Samuel, Thermionic properties of refractory intermetallic compounds in the binary systems chromium--rhenium, molybdenum--rhenium, and tungsten--rhenium, 25:27911
MILLER, D. W., Aluminum-25 levels from the ^{24}Mg(p,γ)^{25}Al reaction, 25:28276
MILLER, H. H., Chromosomal aberrations and mortality of x-irradiated mammalian cells: emphasis on repair, 25:26723
MILLER, J. R., Evidence for a solar-wind origin of auroral ions from low-energy ion measurements, 25:27618
MILLER, L. P., Influence of radioprotectors on the content of catecholamines in mouse tissues, 25:27017
MILLER, Morton W., Effects of metals on cells, subcellular elements, and macromolecules. Proceedings of the 2nd conference on toxicity, Rochester, N. Y., June 12--16, 1969, 25:26608
MILLER, O. A., Investigation of Pu isotopes build-up in Novo-Voronezh APS fuel, 25:28532
MILLER, R. H., Pair correlations in stellar systems, 25:27321
MILLER, Richard A., Unusual rotation of a sunspot Sept. 30 to Oct. 8, 1969, 25:27375
MILLER, Robert C. Jr., Early intracellular events in the replication of bacteriophage T4 deoxyribonucleic acid. V. Further studies on T4 protein-deoxyribonucleic acid complex, 25:26570
MILLNER, A. R., Nonlinear stabilization of a continuum, 25:27760
MIL'MAN, Yu. V., Influence of structure and testing conditions on the mechanical properties of low-alloyed molybdenum, 25:27221
MIMINOSHVILI, Z. N., Decay of ^{97}Zr, 25:28438
MINAMI, S., Imaginary parts of Regge trajectories, duality concept, and meson--nucleon scattering, 25:28036
MINAMISONO, Tadanori, Quadrupole effects in NMR spectra on ^{12}B and ^{12}N, 25:27923
MINCIONE, G., Effect of ionizing radiation on the heart, 25:26961
MINEHART, R. C., Charged particle emission following pion capture in nuclei, 25:28178
MINGUZZI, A., Vacuum polarization tensor and equal-time commutators in quantum electrodynamics, 25:28074
MINN, Hokee, Green's function of time-energy dependent neutron transport equation, 25:28154
Pulsed energy dependent neutron transport, 25:28156
MINOR, Gregory C., Nuclear reactor power monitor system, 25:28672
MINOR, Michael M., Nuclear levels in ^{177}Lu and ^{175}Lu, 25:28424
MINUSHKIN, B., Ionic range of ThO_2--15 wt. percent Y_2O_3 at high oxygen activities, 25:26262
MISCHKE, R. E., Automatic target cycling system for total cross section measurements, 25:28115 (PURC-4159-17)
MISKELL, R. V., Cubic interpolation for numerically controlled machines, 25:28909 (Y-1782)
MISRA, S., Calorimetric investigation of long-range ordering in the cadmium--mercury system, 25:27248
MISTRY, V. D., Isobaric analog resonances in proton scattering from ^{86}Kr, 25:28242
MISTRY, V. D., Isobaric analog resonances in proton elastic scattering from ^{110}Cd, ^{112}Cd, and ^{114}Cd, 25:28370
Isobaric analog resonances in proton elastic and inelastic scattering from ^{130}Te, 25:28427
Neutron particle-hole states in ^{130}Te, 25:28369
MISUSTOVA, J., Radioprotective effect of AET, serotonine, natrium-fluoro-acetate, and histamine in mice, 25:26800
MITCHELL, N. T., Radioactivity in surface and coastal waters of the British Isles, 1969, 25:26397 (FRL-7)
MITCHNER, M., Measurements in a nonequilibrium plasma boundary layer, 25:27685
MITROFANOV, I. E., Photoneutron cross sections of ^{203}Tl and ^{205}Tl, 25:28391
MITROKHOVICH, N. F., Positron decay in ^{196}Au and ^{188}Ir, 25:28392
MITSONIAS, C., Experience and research with the Greek reactor, 25:28774
MITTA, A. E. A., Thin layer chromatography of various radiopharmaceuticals, 25:26179 (CNEA-285)
MITTELSTAEDT, James Stanley, Detoxifying effect of gamma radiation on venom in rabbits, 25:26674
MITTING, W., Interest of analog state studies in deformed nuclei, 25:28472
MITTMANN, H. U., Secondary rainbows and interference in elastic scattering of H^+ by Ar, 25:27458
MIYAKE, S., Dynamic control of cusp loss, 25:27676
MIYASE, H., Isobaric analog states in (γ,p) reactions on N = 50 nuclei, 25:28227
Isobaric analog states in (γ,p) reactions on N = 82 nuclei, 25:28362
MIYASE H., Isobaric analog states in (γ,p) reactions on Sn isotopes, 25:28361
MIZOBUCHI, Akira, Quadrupole effects in NMR spectra on ^{12}B and ^{12}N, 25:27923
MIZUNO, Junya, Role of electronic resonance states in heavy particle atomic collisions, 25:27462
MIZUNO, Tomomi, Analysis of Zircaloy, 25:26171
MIZUTANI, J., Studies on γ-radiolysis of sulphur-containing amino acids. II, 25:26294
MIZZI, C., Cause of a type of magnetic variation on quiet days, 25:27602
MLEKODAJ, R. L., Anomalies in distorted-wave Born-approximation analysis of ^{140}Ce(d,p)^{141}Ce, 25:28429
MO, Y. K., Electrophilic reactions at single bonds. III, 25:26226
MOCHIZUKI, Yoshio, Thorium, its toxicity and the counter-measure for safety, 25:26603
MODUGNO, G., Nuclear fuel characterization, 25:27293 (RT/ING-(70)21)
MOELLENSTEDT, G., Conference on x-ray optics and microanalysis, Tuebingen, Ger., 9/68, 25:26155
MOELLER, Peter, Effects of P_3 and P_5 distortions on fission barriers of superheavy elements, 25:28313 (CERN-70-30(Vol.2), pp 689-99)
MOGHISSI, A. A., Generator /sup 83m/Kr, 25:26320
MOH, C. C., Frequency and behavior of mutants induced by gamma irradiation in beans, 25:26685 (CONF-680112-, pp 85-93)
MOHAN, Radhe, Isospin impurities in the nuclear ground states, 25:28516
MOHAPATRA, R. N., Ets + 3π decay puzzle, 25:27992
MOLDAUER, P. A., Analog fine structure and asymmetry, 25:28468
MOLEA, M., New experimental data for neutron polarization from ^{11}B(α,n_0)^{14}N reaction, at low energies, 25:28192
MOLZAHN, D., Search for spontaneously fissioning isomers produced with 600 MeV protons, 25:28306 (CERN-70-30(Vol.1), pp 575-87)
MONCASSOLI, A. M., WIGNER: program for calculation of mean thermal cross sections in reactor core and for punching of load data for calculating the epithermal cross sections, 25:28803 (EUR-4555)
MONNAND, E., Short-lived isomers of ^{136}I and ^{138}Cs decaying via metastable states of ^{136}Xe and ^{138}Ba, 25:28342 (CERN-70-30(Vol.2), pp 1119-21)
MONSELISE, S. P., Effect of gamma radiation on the synthesis of scopoletin and scopolin in grapefruit peel in relation to radiation damage, 25:27079
Relationship between radiation damages to citrus fruits and changes in enzymes and other constituents of the peel, 25:27135 (IAEA-R-362-F)
MONTAGNIER, L., Irradiation of oncogenic viruses, 25:27111
MONTGOMERY, D., Search for spontaneously fissioning isomers produced with 600 MeV protons, 25:28306 (CERN-70-30(Vol.1), pp 575-87)
MONTGOMERY, David, Negative diffusion coefficients in quasi-linear theory, 25:27712
MONTGOMERY, M. D., Observation of the Feb. 26, 1969 interplanetary shock wave, 25:27570
MONTGOMERY, Michael D., Heat conduction and nonsteady phenomena in the solar wind, 25:27628
MONTROLL, Elliott W., Lectures on the Ising model of phase transitions, 25:27913
MOON, Ronald L., High-temperature phase equilibria in the $PbTiO_3$--$PbZrO_3$ system, 25:27295
MOON SUC KYONG, Medical study of Korean atomic bomb survivors, 25:27060
MOORE, Fred C., Spectator particles and resonances, 25:28365
MOORE, J., Technological status of steam-generating heavy-water reactor, 25:28581
MOORE, J. S., Radiation studies of aryl glycosides. III, 25:26305
Radiation studies of aryl glycosides. II, 25:26304
Radiation studies of aryl glycosides. I, 25:26303
MOORE, James S., Review of engineering standards

development for nuclear power systems, 25:28536
MOORE, R. V., Nuclear power, 25:28544
MOORE, R. W., 1000-MWe LMFBR accident analysis and safety system design study. Accident-initiating conditions. Part 1. Flow abnormalities. Topical report, 25:28731 (BAW-1350)
1000-MWe LMFBR accident analysis and safety system design study, 25:28729 (BAW-1342)
MOORTHY, V. K., Development of high temperature ceramic materials, 25:27280 (INIS-mf-12)
Influence of microstructure on properties of ceramic products, 25:27282 (INIS-mf-14)
MOOS, H. W., Rocket twilight observations of H I 1216-A horizon brightening near 150 km, 25:27615
MORAVEK, F., Late consequences of whole-body irradiation, 25:26943
MORAWETZ, Herbert, Catalysis of ionic reactions by polyelectrolytes. III. Quenching of uranyl ion fluorescence by iron(II) ions in poly(vinylsulfonic acid) solution, 25:26267
MOREAU, J., Protection of large superconducting coils, 25:27663 (ORNL-tr-2436)
MOREEN, Harry A., Superdislocations in Ni_3V, 25:27250
MOREH, R., Forward elastic scattering of 9 MeV gamma rays, 25:28358
Level structure of ^{50}Ti and ^{51}Ti using ^{49}Ti(n,γ) and ^{50}Ti(n,γ) reactions, 25:28284
MORENO, G., Solar-wind discontinuities from Feb. 24 to Feb. 28, 1969, 25:27557
MORGAN, G. L., Aluminum-25 levels from the ^{24}Mg(p,γ)^{25}Al reaction, 25:28276
MORGAN, Karl Z., History of radiation protection, 25:26774
MORGAN, M. Granger, Laboratory model for radio-star scintillation and other diffraction phenomena, 25:27612
MORGAN, S. H. Jr., Coulomb corrections to Bethe--Heitler cross sections for electron--nucleus bremsstrahlung, 25:28451 (N-71-10999)
MORI, K. J., Radioprotective effect of reticuloendothelial system blockade in mice, 25:26926
MORI, Yoshihiro, Analysis of zirconium compound, 25:26150
MORIER, Francis, COREGRAF 2: adjustment and comparison with experiment, 25:28654 (CEA-N-1344(2))
MORIKAWA, G. K., Axially symmetric hydromagnetic equilibria with spherical plasma--vacuum interfaces, 25:27691
MORINAGA, H., On- and off-beam gamma spectroscopy on neutron deficient isotopes of Ge, Se, Br, and Kr, 25:28213 (CERN-70-30(Vol.2), pp 911-15)
MORISHIGE, Toshiko, Effect of ^{95}Zr--^{95}Nb on mice. IV, 25:26962
MORISHIMA, Atsuyoshi, Analysis of instrumentation data from IFA-150 irradiated in HBWR, 25:28692 (JAERI-Memo-4248)
MORISHIMA, Hiroshi, Primary process in the direct action of ionizing radiation on proteins: electron paramagnetic resonance of a glycylglycine single crystal γ-irradiated at 77°K, 25:26300
MORITZ, J., Elastic electron--deuteron scattering and electric neutron form factor at four momentum transfers: 5 Fermi^{-2} < q^2 < 14 Fermi^{-2}, 25:27980 (DESY-71/7)
MOROSON, H., Improvement in alkaline sucrose density gradient sedimentation of mammalian cell DNA, 25:26629
MOROSON, Harold, X-ray-induced single-strand breaks in DNA of E. coli B/r: effect of irradiation and postirradiation conditions, 25:26655
MOROZ, B. B., Role of radiosensitive tissues in the mechanism of post-radiation gluconeogenesis, 25:26963
MOROZOV, I. I., Influence of dose rate and conditions of α-irradiation on radiosensitivity of E. coli B/R, B, and B/sub s-I/, 25:27118
MOROZOV, V. M., Elastic neutron scattering at small angles, 25:28500
MORRIS, D., External heavy ion source for Berkeley 88-inch cyclotron, 25:28120 (UCRL-20406)
MORRIS, D. M., Crystal and molecular structure and vibrational spectrum of the vanadium(V) oxide trinitrate--acetonitrile complex, $VO(NO_3)_3.CH_3CN$, 25:26235
MORRIS, James F., Freeze, melt valve and dispensing system for Cs, 25:26413 (N-71-10455)
MORRISON, B. C., Rheology of fresh, aged, and gamma-irradiated egg white, 25:26923
MORRISON, G. C., Comparison of spectroscopic factors from (p,p$_0$) and (d,p) reactions on barium isotopes, 25:28372
Lifetime of 981-keV state in ^{8}Li, 25:28203
Proton-induced analog resonances, 25:28469
MORRISON, G. C.., Single-particle analog state anomalies in the scattering of protons from ^{197}Au, ^{198}Pt, and ^{184}W, 25:28371
MORRISON, H. Gail, Photoreversal of ultraviolet-induced division delay in Saccharomyces cerevisiae, 25:27080
MORRISON, Jasper J., Triaxial bidirectional integrating 4-level acceleration amplitude recorder, 25:28900 (UCRL-72748)
MORRISON, Roderick Gordon, Gamma compensated fission thermocouple, 25:26466
MORROW, P. E., Dose-related local and systemic effects of inhaled ^{238}Pu and ^{239}Pu dioxide in dogs, 25:26929
MORSE, R. L., Numerical simulation of the weibel instability in one and two dimensions, 25:27737
MORTIMER, M. J., Self-irradiation damage in α-plutonium, 25:27837 (AERE-R-6506)
MORTLAND, J. E., [Recent research on] metals joining, 25:27193
MORTON, Jane I., Radiation sensitivity of New Zealand black mice and the development of autoimmune disease and neoplasia, 25:26952
MORUCCI, M., Immunological modifications induced by radiotherapy, 25:26668
MORUZZI, V. L., Intrinsic metallic character of rare-earth pnictides, 25:27879
Magnetic and magneto-optical properties of Fe-doped EuO films, 25:27897
MOSELEY, B. E. B., Repair of irradiated transforming deoxyribonucleic acid in wild type and a radiation-sensitive mutant of Micrococcus radiodurans, 25:27124
MOSELEY, John, Oxygen ion--ion neutralization reaction as related to tropical ultraviolet nightglow, 25:27698
MOSER, P., Study of internal friction peaks in molybdenum after irradiation with neutrons at 270°K, 25:27199 (CEA-CONF-1671)
MOSES, J. D., Fine structure of the isobaric analogs of the ground and second excited states of ^{63}Ni, 25:28237
MOSHER, J. M., Mass and half-life of ^{9}C, 25:28187
MOSHINSKY, M., Extension of a schematic theory of nuclear reactions to include isospin and isobaric analogue resonances, 25:28492
MOSS, C. E., Isospin purity at high excitation energies, 25:28190
MOSS, Eugene C., Discrepancies of film badges, 25:26537
MOSZKOWSKI, S. A., Statistical model calculations of ^{56}Fe neutron cross section, 25:28218 (NP-18674)
MOSZYNSKI, M., Subnanosecond timing in nuclear spectroscopy, 25:26491 (INR-1213)
MOTLEY, R. W., Energy analysis of cesium ions in Q machine, 25:27686
Measurement of drift-wave potential oscillations in the presence of temperature oscillations, 25:27809
MOTTA, M., Tensorial formulation and geometric interpretation of a multi level multi channel formula for nuclear resonances, 25:28454 (RT/FI-(70)38)
MOUSSA, A., Short-lived isomers of ^{130}I and ^{138}Cs decaying via metastable states of ^{130}Xe and ^{138}Ba, 25:28342 (CERN-70-30(Vol.2), pp 1119-21)
MOVSISYAN, L. M., Phase equation for electron motion in a traveling-wave field with synchronous energy as an independent variable, 25:27946
MOWATT, R. S., Isomers of ^{148}Pm and neutron capture in ^{147}Pm, 25:28373
MOYER, C. B., User's manual for two-dimensional axisymmetric transient heat conduction material ablation computer program, 25:28883 (SC-DR-70-510)
MOYER, Charles E. Jr., Isomerization and disproportionation of trihalobenzenes catalyzed by potassium anilide in liquid ammonia, 25:26222
MOZZHUKHIN, A. V., Decay of ^{66}Ge, 25:28272
MRAZ, J., Calcifications after x irradiation of DHT-sensitized rats. I, 25:26933
Development of calcifications after whole-body irradiation in rats sensitized with DHT. II, 25:26977
Development of calcifications after whole-body irradiation in rats sensitized with DHT. I, 25:26978
MRINAK, J., Scintigraphic localisation of the kidneys for percutaneous renal biopsy, 25:26821
MUELLER, G. L. J., Modified feedback control method applied to edge oscillations in Q machine, 25:27770
MUELLER, H., Measurement of the spin and nuclear magnetic moment of ^{20}Na, 25:28209 (CERN-70-30(Vol.1), pp 383-5)
MUELLER, H. J. W., Derivative amplitudes in photoproduction, 25:28000
MUELLER, H.-G., Gel filtration studies of uv-irradiated ribonuclease A. II, 25:26658
Gel filtration studies on uv-irradiated ribonuclease A. III, 25:26661
MUELLER, J., Fluorescence excitation of ultra-soft x-ray emission spectra using synchrotron radiation, 25:27827 (DESY-70/59)
MUELLER, M., Measurement of neutron spectra within the 1 eV to 10 keV energy range by means of the sandwich technique, 25:28656 (EURFNR-842)
MUELLER, R. A., Conceptual studies of a 1000-MWe nuclear power station with a steam-cooled, fast breeder reactor, 25:28634 (NP-18782)
Danger contained in a steam-cooled fast breeder reactor and the dose value released to the environment in a severe accident, 25:28738 (NP-18781)
MUELLER-WARMUTH, W., Self-diffusion of liquid ^{6}Li and ^{7}Li, 25:26238
MUENCH, G., Distribution of gas and dust in the Orion Nebula, 25:27312
MUENZNER, R., Radiation preservation of fish. I, 25:27146
Radiation preservation of fish. III, 25:27147
Radiation preservation of fish. II, 25:27148
MUKHERJEE, D., Effect of x-rays on plant growth, flowering, and fruiting in Impatiens balsamina L, 25:27086
MUKHERJI, Anil, Thorium fluoride complexes. Determination of the stability constants using the fluoride ion activity electrode, 25:26268
MUKHOPADHYAY, P., Transmission electron microscopic studies of cold-rolled zirconium, 25:27245 (INIS-mf-15)
MUKSINOVA, K. N., Change in the functional state of

erythropoiesis during prolonged fractionated irradiation, 25:27015
MULAC, A. J., Evaluation of the impedance probe method of shock speed measurement, 25:28887 (SC-DR-710086)
MULLANEY, Henry, Geographic distribution of ionospheric evening anomaly and relation to neutral winds, 25:27515
MULLER, K.-N., Total cross sections for kilovolt neutrons of even--odd nuclei in he region of the 3s strength-function resonances, 25:28279
MUMFORD, George S., Binary stars among cataclysmic variables. XII, 25:27320
MUNDT, F. D., Eddy current measurements with a coil encircling a two-conductor rod, 25:28911 (Y-1787)
MUNRO, T. R., Site of the target region for radiation-induced mitotic delay in cultured mammalian cells, 25:26927
MURAKAMI, M., Measuring poloidal magnetic field in diffuse toroidal pinches, 25:27795
MURAKAMI, Tetsuo, Application of pharmacology to animal group psychology, 25:28874 (ORNL-tr-2447)
MURAMATSU, Susumu, Late injuries induced by radiation. II, 25:26976
MURATA, Kenji, Calculation of x-ray production in alloy targets using Monte Carlo method, 25:27836
MURATA, Motoi, Changes of genetic loads in experimental populations of Drosophila melanogaster with radiation histories, 25:26705
MURAV'EV, V. F., Influence of high-frequency field on plasma instabilities, 25:27781
MURAV'EVA, V. V., Decay of ^{92}Zr, 25:28438
Decay of neutron defficient isotopes of Pt, Ir, and Os, 25:28389
MURAYAMA-OKABAYASHI, Fumiko, A series of hybrid cells containing different ratios of parental chromosomes formed by two steps of artificial fusion, 25:26700
MURDAY, J. S., Self-diffusion in molten Li, 25:26239
MURDIN, J., Rocket-borne D-region probe measurements, 25:27565
MURPHY, Edward J., Prog. rpt. on marine products development irradiator program: irradiated fresh shrimp shipping studies, annual, 10/67--9/68, 25:27138 (TID-25543)
MURPHY, Terence M., TMV--RNA photoreactivation, 25:26653
MURRAY, I. P. C., Use of serum thyroxine in assessment of thyroid function, 25:26857
MURRAY, J., Liquid scintillation counting of $^{14}CO_2$ in toluene/Triton X-100 system, 25:26180
MURZINA, L. D., Change in the functional state of erythropoiesis during prolonged fractionated irradiation, 25:27015
MUSIALOWICZ, T., X and gamma thermoluminescent dosimeter for accidental personnel dosimetry purposes, 25:26516 (CLOR-82/D)
MUSIN, M. A., Monochromatic method for measurement of mean proton energy in 665 MeV beam, 25:26505 (JINR-P13-5636)
MUSIOL, G., Decay of ^{90}Nb, /sup 89m,89/Nb, /sup 85m,85/Y and /sup 85m/Sr, 25:28215 (CERN-70-30(Vol.2), pp 1137)
MUSTARD, G. L., Precise computerized in-line compressible flow metering, 25:28855 (GAT-T-1649)
MYACHKOVA, S. A., Scattering of neutrons on Mg, 25:28265
MYASNIK, M. N., Growth patterns of uv-irradiated E. coli B in saline, 25:27119
Influence of dose rate and conditions of α-irradiation on radiosensitivity of E. coli B/R, B, and B/sub s-I/, 25:27118
MYDLIK, M., Scintigraphic localisation of the kidneys for percutaneous renal biopsy, 25:26821
MYZNIKOV, K. P., Dynamic accelerated proton beam characteristics in IHEP 70-GeV accelerator, 25:28133

N

NACHTMANN, O., Phenomenological investigation of inelastic electron--proton scattering, 25:27999
NADZHAKOV, E., New isotopes of iridium, 25:28348 (JINR-P6-5617)
NAGAI, Hiroyuki, Even-parity states of ^{18}O, 25:28191
NAGANO, Yasuiti, Role of leukocytes in production of interferon, 25:26986
NAGASAKI, Ryukichi, Recrystallization of V--20 percent Ti alloy, 25:27259
NAGASE, Katsuya, Influence on liver of radiation, 25:26955
NAGATA, H., Comparative studies on rejoining of DNA-strand breaks, 25:26953
NAGATSU, Chizuko, Radiosensitivity of Streptomyces cacaoi spores, 25:27068
NAGORCKA, B. N., Experimental investigation of ^{16}O + ^{12}C nuclear burning at stellar energies, 25:27309 (ANU-P-471)
NAJAM, M. R., Cross section of ^{25}Mg(tau,γ)^{29}Si reaction, 25:28206 (ANU-P-508)
NAJZER, M., Report on research programs at the reactor TRIGA Mark II at the Inst. Jozef Stefan, Ljubljana, 25:28778
NAKAGAWA, Haruo, Age of fission neutrons to indium resonance in water and polyethylene, 25:28157
NAKAGAWA, Tsutomu, Transport of fixed gases in radiation-stabilized poly(vinyl chloride), 25:26280
NAKAHARA, Hiromichi, Calculation of kinetic energy and most-probable charge in fission, 25:28408
NAKAJIMA, Shyunji, Elastic scattering of carbon and nitrogen ions, 25:28274
NAKAJIMA, Tokunosuke, Spectrochemical determination of ^{235}U, 25:26170
NAKAMOTO, Kazuo, Metal isotope effect on metal--ligand vibrations. VI. Metal complexes of 8-hydroxyquinoline, 25:26234
NAKAMURA, S., Radioprotective effect of reticuloendothelial system blockade in mice, 25:26926
NAKAMURA, Wataru, Role of leukocytes in production of interferon, 25:26986
NAKAMURA, Yoshihara, Suppression of longitudinal electron oscillation by beam modulation, 25:27702
NAKANISHI, T., Studies on the distribution of chemical elements in geochemical samples by an activation autoradiographic method, 25:26194
NAKANO, Masafumi, Pulsed neutron experiment on FCA I-5, 25:28759 (JAERI-Memo-4272)
NAKANO, Y., Effect of helical instability on the radial density and potential distribution, 25:27738
NAKATA, Hiroshi, Analysis of energy-loss data for 0.2 to 0.5-MeV/amu p, α, and N in Se, 25:27833
NAMATAME, Hiroshi, Evaluation of integrity for fast neutron irradiation embrittlement of JPDR pressure vessel, 25:28682 (JAERI-1202)
NAMBOODIRI, M. N., Limiting cross sections for fission isomers with nanosecond lifetimes produced in heavy-ion reactions, 25:28399
NAMIKI, Kazuko, Effects of γ-irradiation on the enzyme relating to the development of characteristic odor of onions, 25:26620
NAMIKI, M., Studies on γ-radiolysis of sulphur-containing amino acids. II, 25:26294
NAMIKI, Mikio, Nonrelativistic composite particle model for mesons, 25:28030
NAMIKI, Mitsuo, Effects of γ-irradiation on the enzyme relating to the development of characteristic odor of onions, 25:26620
NANDA, S., Topology for Minkowski space, 25:28061
NARAIN, Prem, Treatment of carcinoma penis by radium mould, 25:26863
NARITA, Kiichi, Analysis of Zircaloy, 25:26171
NAROSKA, B., Total photoproduction cross section of hadrons on nuclei, 25:27953
NARYSHKIN, M. A., Characteristics and quantitative prediction of cumulative storage of ^{90}Sr in arboreal plants, 25:26616
NASIM, M., Environmental aspects of Karachi Nuclear Power Plant, 25:28626
NASKIDASHVILI, I. A., Defect annealing in neutron irradiated niobium, 25:27269
NASLAIN, Roger, Crystal structure of the boron--thorium system. A new boride with type YB_{66} structure, 25:27301
NASTA, A., Study of irradiation effects on mitosis in lucerne in R_0, R_1, and R_2, 25:26732
NATHSCHLAEGER, P., Problem of numerical calculations for reactors, 25:28808
NATSIK, V. D., Dependence of the electron dislocation stopping power in a superconductor on temperature and velocity, 25:27648
NAUMANN, R. A., Levels in ^{194}Pt, ^{196}Pt, and ^{198}Pt, 25:28425
NAVE, M. F. F., Impulsiveness of microwave bursts and its association with sunspot types, 25:27381
NAYAR, K. M. D., Mutagenesis in sorghum, 25:26715
NAZAROV, N. I., Investigation of low-frequency plasma oscillations by means of amplitude modulation of microwave radiation, 25:27816
NDOCKO, V. B., Low energy boron implantation profiles in silicon from junction depth measurements, 25:27855
NEDVIDEK, J., Incorporation of radiophosphorus into nucleic acids of frog embryo, 25:26617
NEEL, J., Protection of large superconducting coils, 25:27663 (ORNL-tr-2436)
NE'EMAN, Yuval, Time-reversal symmetry violation and the oscillating universe, 25:27424
NEFEDOV, V. V., Scattering of neutrons on Mg, 25:28265
NEGELE, J. W., ^{41}Sc--^{41}Ca Coulomb energy difference, 25:28253
NEILSON, George Walter, ESR in gamma-irradiated single crystals of unsaturated aliphatic hydrocarbons, 25:26301
NEKRASOV, V. V., Instrumental activation analysis of Au, Br, Mn, Na, Ta, and W, 25:26200
NEKRASOVA, I. V., Radiosensitizing action of N-ethylmaleimide, 25:26640
NELSON, D. M., Photographic method for determining velocity distributions within thermal plumes, 25:28839 (ANL/ES-4)
NELSON, D. S., Iron-59 distribution in normal and x-irradiated mice, 25:27012
NELSON, John B., Prog. rpt. on simulation and measurement of solar-flare proton exposures, final, 11/68--8/69, 25:26920 (AD-711041)
NELSON, R. D., X-ray comparison of beta plutonium grain size, 25:27244 (BNWL-1545)
NELSON, William H., Structural condition status report, 25:26400 (NVO-99-12)
NEMTSEVA, L. S., Mechanism of ring chromosome formation and

somatic crossing-over, 25:26721
NERESON, N., Magnetic properties of CeBi, NdBi, TbBi, and DyBi, 25:27887
NERODENKO, M. M., Weldability of certain Mo alloys, 25:27185
NERUDA, O., Problems of excretion analysis after repeated internal contamination with strontium radioisotopes, 25:26585
NESBITT, E. A., Cast permanent magnets of Co_5RE type with mixtures of Ce and Sm, 25:27883
NESS, N. F., Interplanetary magnetic field measured by Pioneer 8 during the Feb. 25, 1969 event, 25:27556
NESSIN, N., Some M1 transitions with $\Delta = 1$ in ^{26}Mg, ^{27}Al and ^{28}Si, 25:28225
NETTLES, P. H., Measurement of the mass of ^{9}Li, 25:28175
NEUDATCHIN, V. G., Electroexcitation of ^{32}S in region of dipole resonance, 25:28220 (UJV-2553-F)
NEUHOLD, John M., Prog. rpt. on Amchitka bioenvironmental program, annual, 7/69--6/70, 25:28841 (BMI-171-133)
NEW, I. B. Jr., Maintenance of on-line computers used with nuclear production reactors, 25:28797
NEWKIRK, L. R., Hyperfine magnetic interactions in Fe--Ga solid solutions, 25:28843 (CALT-822-27)
Moessbauer study of BiF_3 type ordering in metastable FeGa alloys, 25:28842 (CALT-822-26)
NEWLAND, J. E., Heat source capsule fabrication technology program: September 1970--January 1971, 25:26425 (MLM-1796)
NEWMAN, Leonard, Thorium fluoride complexes. Determination of the stability constants using the fluoride ion activity electrode, 25:26268
NEWMAN, R. C., Defects produced in n-type silicon by electron irradiation, 25:27845
NEWTON, A. A., Plasma displacement due to dipole current near high-beta plasma, 25:27774
NEWTON, J. O., 9/2-[514] state in ^{185}Re, 25:28287 (ANU-P-518)
NICA, Alexandru, Theory and practice of lubrication systems, 25:26416
NICKELS, Robert J., Beta-neutrino correlations and recoil nuclear alignment effects in light delayed particle emitters, 25:28210 (CERN-70-30(Vol.1), pp 447-55)
NICKLOW, R. M., Spin-wave dispersion relation in rare-earth metals, 25:27888
NICOLAE, M., Recording and uses of α-particle tracks in cellulose nitrate, 25:26474
NICOLATO, A., Betatron therapy of pulmonary neoplasms, 25:26874
NICOLIN, A., Daunomycin influence on Ehrlich ascites cancer, 25:26990
NICOLINO, R., Inhibition of ribosomal RNA synthesis in x-irradiated HeLa cells, 25:26983
NIEDZIELSKI, J., Reaction of neon ions with ethylene, 25:26314
NIELSEN, H. B., Parton theory based on the dual resonance model, 25:28002
NIELSEN, O. B., Alpha decay of neutron deficient isotopes of mercury and radon and their daughters, 25:28302 (CERN-70-30(Vol.1), pp 523-31)
Compound-nucleus aspects of beta decays with high Q values, 25:28443 (CERN-70-30(Vol.1), pp 421-33)
Experimental Q-values far from stability, 25:28295 (CERN-70-30(Vol.1), pp 331-40)
NIELSEN, P., Wave--particle interaction in single-ended Q machine, 25:27693
NIELSON, C. W., Numerical simulation of the weibel instability in one and two dimensions, 25:27737
NIEWENHUIS, Robert J., Morphologic and functional changes in testicular interstitial tissue of the rat after cryptorchidism or x irradiation, 25:27008
NIFENECKER, Herve, Effect of charge on ^{252}Cf fission fragments on neutron emission process, 25:28288 (CEA-R-4121)
NIGH, W. G., Kinetics of the pyrolysis of beryllium hydride, 25:26278
NIKAIDO, O., Comparative studies on rejoining of DNA-strand breaks, 25:26953
NIKIFOROVA, G. P., Relative values of oscillator strengths of spectral lines, 25:27445
NIKITIN, M. K., Palladium-99 γ radiation, 25:28431
NIKOLAEV, A. I., Radiosensitivity of the inductive and productive phases of antibody, 25:26680
NIKOLOV, Iv., Radioprotective effect of AET and serotonin in growing rats, irradiated fractionally with small doses of roentgen rays, 25:26807
NIKOLOV, N. S., Normal color indices of Cepheids. III, 25:27340
NIKOL'SKII, G. M., Inner corona polarization during solar eclipse of 9/22/68, 25:27397
NILOLOV, N. A., Resonances of a plane plasma condenser in crossed electric and magnetic fields, 25:27718
NIP, Hans C. H., Bremsstrahlung spectrum of energetic β particles traversing single crystals in lattice-directed trajectories, 25:27832
NISCE, Lourdes Z., Review of experience with irradiation of brain metastasis, 25:26895
NISHI, Tomota, Calculation of kinetic energy and most-probable charge in fission, 25:28408
NISHIDA, Atsuhiro, DP 2 and polar substorm, 25:27606
Two basic modes of interaction between the solar wind and the magnetosphere, 25:27630
NISHIDA, Y., Suppression of drift instability by rf electric field, 25:27787
NISHIGAKI, Minoru, Effect of Zr on stability of a Ti--15 Mo base beta alloy, 25:27233
Isothermal transformation of Ti--Mo binary alloy, 25:27257
NISHIGORI, Nobuko, Calculation of x-ray production in alloy targets using Monte Carlo method, 25:27836
NISHIKAWA, Yasuharu, Absorption behavior of radionuclides, mainly rare earth elements, in seawater, 25:26339
NISHIMURA, H., Studies on γ-radiolysis of sulphur-containing amino acids. II, 25:26294
NISHIMURA, Hiroyuki, Effects of γ-irradiation on the enzyme relating to the development of characteristic odor of onions, 25:26620
NITSCHKE, J. M., Recoil atom mass analyser (RAMA), 25:28106 (CERN-70-30(Vol.1), pp 153-62)
NIX, J. R., Theoretical predictions for superheavy nuclei, 25:28309 (CERN-70-30(Vol.2), pp 605-44)
NIZHNIK, G. V., Comparison of the effectiveness of a single and fractionated irradiation of spermatozoids on prenatal death in rabbits, 25:26954
NOBLE, J. V., Energy dependence of direct isospin-violating (d,α) reactions, 25:28459
NOERDLINGER, Peter D., Relativistic acceleration of charged particles by an electromagnetic pulse, 25:27715
NOHARA, Norimasa, Scintillation camera based on delay-line time conversion, 25:26486
NOLEN, J. A. Jr., Comparison of spectroscopic factors from (p,p_0) and (d,p) reactions on barium isotopes, 25:28372
NOLTE, E., On- and off-beam gamma spectroscopy on neutron deficient isotopes of Ge, Se, Br, and Kr, 25:28213 (CERN-70-30(Vol.2), pp 911-15)
NOMEROVANNAYA, L. V., Optical properties of tungsten single crystals, 25:27899
NORCO, J. E., Chicago air pollution systems analysis program, 25:28840 (ANL-ES-CC-8)
NORK, W. E., Evaluation of Project Shoal site, 25:26403 (NVO-1229-105(Pt.1))
NORMAN, J., Effects of intracorporeal heat and radiation on dogs, 25:26931
NORMAN, K., Electron density measurements in the thermal plasma of the magnetosphere, 25:27566
NOSEK, J., Haemolysis of red blood cells in propylene glycol solutions in miners from uranium mines, 25:26588
Inorganic phosphorus in red blood cells of miners in uranium mines, 25:26582
NOSKOV, M. M., Optical properties of tungsten single crystals, 25:27899
NOTZ, D., Total photoproduction cross section of hadrons on nuclei, 25:27953
NOVAK, Arthur F., Storage temperature effects on the proteolytic activity of radiation-surviving bacteria in oysters, 25:27114
NOVAK, L., Radioprotective effect of AET, serotonine, natrium-fluoro-acetate, and histamine in mice, 25:26800
NOVIKOV, I. D., Mixmaster universes and the cosmological problem, 25:27428
NOVOTEL'NOVA, N. S., Mutability of Verticillium, 25:26689
NUSSBAUMER, H., [Fe I] lines: their transition probabilities and occurrence in sunspots, 25:27365
NUSSINOV, S., Scaling and dilation invariance, 25:28057
NUZHDIN, N. I., Comparison of the effectiveness of a single and fractionated irradiation of spermatozoids on prenatal death in rabbits, 25:26954
NYQVIST, H., Atomic-beam measurements in the rare-earth region, 25:28298 (CERN-70-30(Vol.1), pp 387-94)

O

OAKEY, Neil S., Beta-neutrino correlations and recoil nuclear alignment effects in light delayed particle emitters, 25:28210 (CERN-70-30(Vol.1), pp 447-55)
OBATA, Y., Studies on γ-radiolysis of sulphur-containing amino acids. II, 25:26294
OBERBECK, Peter Ernst Rudolf, ORBIT: Online Reduced Bandwidth Information Transmission, 25:28846 (COO-1469-178)
OBERHAUSEN, E., Unilateral determination of effective renal plasma flow by radioisotopes, 25:26826
O'BRIEN, Brian J., Auroral electron characteristics deduced from ground-based observations, 25:27590
O'BRIEN, K. P., Cardiac catheterization. III, 25:26854
OCHKUR, A. P., Generalization of γ-albedo calculations on basis of similarity theory, 25:27831
Method and technique of gamma--gamma logging of underground boreholes in mercury and iron ore deposits, 25:26352 (CONF-630513-1)
OCHSENFELD, W., Aqueous reprocessing of fuel elements of fast breeder, 25:26326 (KFK-911)
ODA, Toshiyuki, Application of activation analysis in hot spring chemistry and sanitary chemistry, 25:26195
ODEN, L. L., Niobium alloy development with B, Hf, and W, 25:27227
ODERA, Masatoshi, Elastic scattering of carbon and nitrogen ions, 25:28274
O'DONNELL, P. J., Anti-inflammatory effect of benzydamine, 25:26806

OEKROES, Istvan, Combined histochemical procedure to distinguish between mesenchymal and epithelial reticular cells in the rat thymus under the light microscope, 25:26654
OERDOEGH, M., Determination of impurities in thorium and zirconium compounds by neutron activation analysis, 25:26192
OESCHGER, H., Use of natural radioactivities to estimate large-scale precipitation scavenging, 25:26390 (CONF-700601-, pp 465-74)
OESTLUND, H. Goete, Prog. rpt. on tritiated hydrogen and its compounds in the environment, 3/71, 25:26393 (ORO-3944)
OFFERMANN, D., Atomic oxygen and carbon dioxide in the lower thermosphere, 25:27609
OGATA, Noboru, Adsorption of uranium in artificial seawater with titanic acid, 25:26350
OGAWA, Naotake, Comparative study on Zr oxide for preparation of /sup 113m/In generator, 25:26341
OGAWA, Yutaka, Recrystallization of V--20 percent Ti alloy, 25:27259
OGII, P. E., Effect of homotransplantation of bone marrow on the healing of liver wounds in severe combined radiation trauma, 25:27005
OGINO, Noriyuki, Regional lung function tests using ^{131}I and ^{133}Xe double isotope method, 25:26841
OGIRIMA, Masahiko, Effect of precipitates on fatigue strength, 25:27231
OHBA, Ichiro, Nonrelativistic composite particle model for mesons, 25:28030
OHKAKU, Noboru, Metal isotope effect on metal--ligand vibrations. VI. Metal complexes of 8-hydroxyquinoline, 25:26234
OHKAWA, Tihiro, Convection cell produced by low-frequency flute instabilities, 25:27734
Plasma convection produced by ion-driven drift instability, 25:27735
OHKI, K., Location and size of a solar hard x-ray burst on Sept. 27, 1969, 25:27384
OHKUBO, Makio, Nonrandom distributions of neutron resonance levels, 25:28421
OHLEN, Gunnar, Odd-particle effect on the fission barrier, 25:28314 (CERN-70-30(Vol.2), pp 700-8)
OHMORI, Kazuo, Vertebral column of inbred mice treated with x-rays or FCdR, 25:26997
OHMURA, Yamichi, Shallow donor state produced by proton bombardment of silicon, 25:27847
OHMURO, Hiroshi, Superhigh voltage irradiation of bladder tumor, 25:26876
OHYAMA, Harumi, Restoration of radiation damage in rat thymocytes, 25:26936
OKADA, Yoshio, A series of hybrid cells containing different ratios of parental chromosomes formed by two steps of artificial fusion, 25:26700
OKAGAWA, Seigo, Primary cooling water decomposition in reactors, 25:28758 (JAERI-1204)
OKAMOTO, Hironobu, Calculation of kinetic energy and most-probable charge in fission, 25:28408
OKANO, Kotoyuki, Excited states of ^{52}Cr and ground state spin of ^{52}V in the decay of ^{52}V, 25:28250
Two-phonon states in ^{104}Pd, 25:28382
OKAZAKI, M., Potential contribution of nuclear power to on-site generation of electric and steam power in Japanese industries, 25:28582
OKUDA, Shigeo, Recovery of low-temperature fast neutron irradiated tungsten, 25:27228
OKUNO, Hideki, Liquid hydrogen target utilizing a small mechanical refrigerator, 25:28138
OLAH, George A., Electrophilic reactions at single bonds. III, 25:26226
OLDANO, C., 27-day oscillation in cosmic-ray intensity and shorter periodicities, 25:27472
OLDENBERG, O., Excitation of nitrogen by fast protons and electrons, 25:27616
OLDFIELD, M. L. G., Microwave reflexion from longitudinally magnetized plasma-filled coaxial waveguide, 25:27813
OLIVAIN, J., Deformation of electron distribution function, 25:27823
OLIVIERI, E., Effective four-body interaction in light nuclei, 25:28482
OLIVO, Oliviero Mario, Migration and survival of fibroblast culture in chicken following exposure to x irradiation, 25:26642
OLLIS, D. F., Surface and bulk carburization of tungsten single crystals, 25:27225
OLMR, J., Observations of chromospheric flares at Ondrejov, 25:27391
OLOFSON, C. T., [Recent research on] metalworking, 25:27194
OLSEN, Birthe, Simple program for pulse-height analysis with time-sharing for routines using the peripheral units, 25:26497
OLSMATS, M., Atomic-beam measurements in the rare-earth region, 25:28298 (CERN-70-30(Vol.1), pp 387-94)
OLSON, B. L., Magnetic and magneto-optical properties of Fe-doped EuO films, 25:27897
OLSON, E. C., Determination of solar Doppler widths by Goldberg's method, 25:27367
OLSON, Ronald E., Oxygen ion--ion neutralization reaction as related to tropical ultraviolet nightglow, 25:27608
OLTMAN, B. G., Relationship between encapsulation and apparent fast neutron-induced fading in TLD, 25:26536
OMHOLT, A., Relation of low-energy particle precipitation to luminous aurora, 25:27578
OMNES, R., Antimatter in the universe, 25:27426
ONGARO, D., Strontium-90/Ca and $^{137}Cs/K$ in diet and passage through human milk, 25:26581
ONISHI, Hiroshi, Spectrophotometric determination of traces of uranium in sodium, 25:26152 (JAERI-Memo-4267)
ONISHI, Naoki, Neutron--proton interaction in odd--odd deformed nuclei, 25:28514
OORT, J. H., Absence of radio emission from Maffei I, 25:27405
OOSTEROM, M. G., Determination of sodium in ultrabasic rocks, 25:26204
OPHEL, T. R., Computer reduction of complex spectra, 25:26489 (ANU-P-487(2))
Nuclear spectroscopy instrumentation, 25:28102 (ANU-P-502)
OPUCHLIK, M., Effects of nuclear radiation on semiconductor elements, 25:26561
ORLANDINI, Kent A., Selective ion-exchange separation of alkali metals, 25:26337
Separation of scandium from rare earth elements, 25:26338
ORLOFF, J., Elastic scattering of ^{16}O by ^{48}Ti, ^{40}Ca, ^{27}Al, ^{12}C, ^{7}Li, and ^{6}Li, 25:28196
ORLOV, B. N., Proton scattering on ^{24}Mg, ^{25}Mg, and ^{26}Mg, 25:28264
ORLOV, Yu. V., Calculation of three-body model vertex part $^{3}H + n + d$, 25:28047
ORTEGA, R. F., Fuel-cycle evaluation criteria for an intermediate-power reactor, 25:28722
ORVEDAHL, Walter, Prog. rpt. on computer project, final, 6/59--3/70, 25:28877 (ORO-2572-27)
ORZALESI, C. A., Regge asymptotic behavior in quantum field theory, 25:28072
OSADCHUK, R., Zirconium-base alloys, 25:27190
OSAWA, Yasuo, Fission-gas release from nuclear fuels with in-pile gas-loop, 25:28821
OSBORNE, T. S., Response of rice to γ-rays and fission neutrons, 25:27070
OSHIMA, Keiichi, Trends in utilization of radiation and radioisotopes, 25:26276
OSMAN, A., Three-body model for ^{6}Li induced reactions, 25:28486
OSOKINA, R. M., Isotopic effects in photonuclear reactions, 25:28393
OSTAPENKO, V. P., Cylindrical linear MHD machine in open-cycle regime, 25:27481
OSTERBERG, Charles L., Chemical budget of Columbia River, 25:28879 (RLO-1750-41)
OSTERTAG, B., Radiation-induced modifications in nervous system, 25:26972
OSTROWSKA-KRYSIAK, Barbara, Induction of auxotrophic mutation in Streptomyces erythreus IA 64-575, 25:26699
OSWALD, Patrick, Restoration of the hybrid effect suppressed by whole-body irradiation, 25:26985
OSZUSZKY, F., Future management of radioactive wastes in Austria, 25:26451 (SGAE-RT-33/1970)
OTANI, Shitoshi, Effect of Zr on stability of a Ti--15 Mo base beta alloy, 25:27233
Isothermal transformation of Ti--Mo binary alloy, 25:27257
OTGONSUREN, O., Deposition of uranium in the bones of animals, 25:26744
OTH, Daniel, Restoration of the hybrid effect suppressed by whole-body irradiation, 25:26985
OTHMER, Siegfried, Electron spin resonance spectrum of FCN- and HCN- in KCl, 25:26289 (NYO-2150-60)
OTT, A., Differential diffusion of impurities in isotopic lithium matrices, 25:26240
OTT, Edward, Nonlinear Landau damping and beat wave trapping, 25:27824
OTTEN, E. W., Measurement of the spin and nuclear magnetic moment of ^{20}Na, 25:28209 (CERN-70-30(Vol.1), pp 383-5)
On-line measurements of spin and moments of nuclear ground states, 25:27914 (CERN-70-30(Vol.1), pp 361-81)
OTTO, G., Investigations on superconducting diffusion layers with an electron beam microprobe, 25:26159
OTTO, G. W., Technique for direct measurement of thermal power in assay calorimeters, 25:26548 (MLM-1780)
OVCHARENKO, O. N., Dimensional effect in magnetization of strong superconductors, 25:27644 (KHFTI-70-8)
OVCHARENKO, V. I., Energy levels of three-particle system, 25:28163 (ITF-70-100-P)
OWMAN, Ch., Content of noradrenaline and 5-hydroxytryptamine in rat after ionizing radiation, 25:26959
OYAMA, Kiyoshi, Determination by x-ray fluorescence of barium and strontium in barium carbonate of industrial grade, 25:26167
OYAMADA, Masayuki, Pile physics experiment by means of TOF neutron diffraction, 25:28769
OYVIN, I. A., Qualitative leucocyte changes due to total x-ray irradiation, 25:26901
OZANNE, P. G., Calcium uptake by subterranean clover bur shown by using ^{45}Ca, 25:26614
OZEMRE, A. Y., Utilization of TR-1 research reactor of Cekmece Nuclear Research Center, 25:28776
OZEROV, R. P., X-ray- and neutron-diffraction study of ordering in some alloys of the titanium--zirconium--oxygen system, 25:27297

OZIEWICZ, M., Description of N-theta sector in Lee model, 25:28067
OZIN, G. A., Raman spectra of chlorofluorosilanes in gaseous, liquid, and solid state; anomalous ^{35}Cl, ^{37}Cl isotope intensity effects in splitting of totally symmetrical SiCl stretching mode in $SiCl_3F$ and $SiCl_2F_2$, 25:26218

P

PAC, Pong Youl, General energy-dependent transport equation with fission, 25:28155
Green's function of time-energy dependent neutron transport equation, 25:28154
PACKER, J. E., Radiolysis of oxygenated cysteine solutions at neutral pH, 25:26307
PADHYE, M. R., Method of assigning the vibration bands by progressive isotope exchange, 25:26216
PADWA, Albert, Photochemical transformations of small-ring carbonyl compounds. XXVIII. 1,5-hydrogen transfer in the photochemistry of aroylaziridines, 25:26250
PAGE, D. E., Conference on intercorrelated satellite observations related to solar events, Noordwijk, Netherlands, 9/69, 25:27531
Introduction to the ESRO spacecraft, 25:27552
PAITASH, T. P., Phase equilibria in the titanium--vanadium--boron and titanium--manganese--boron systems, 25:27300
PAKHTUSOVA, E. V., Evidence for electron-positron pair electroproduction, 25:27994
PALEVSKY, H., Scattering of high energy protons from nuclei, 25:27958
PALMER, David Ray, Inelastic neutrino--nucleon scattering at high energy and Sugawara model, stress tensor, and spectral sum rules, 25:28006
PALMER, R. S., Modified feedback control method applied to edge oscillations in Q machine, 25:27770
PALMIERI, J. N., Neutron--proton scattering at 152 MeV, 25:27956
PALMS, J. M., Neutron activation cross sections for As, Br, Rb, and Sr isotopes at 14.4 MeV, 25:28282
PANCHOLI, S. C., Nuclear data sheets for A = 211, 25:28377
PANDEY, Girish Chandra, Rayleigh's problem in magnetohydrodynamics with suction, 25:27491
PANIGRAHY, P., Micromagnetism in Pd--Cr and V--Mn alloys, 25:27890
PANOV, D. A., Feedback stabilization of the rarefied plasma cyclotron instability, 25:27776
PAPADOPOULOS, K., Heating of counterstreaming ion beams in an external magnetic field, 25:27672
PAPAGIANNIS, Michael D., Geographic distribution of ionospheric evening anomaly and relation to neutral winds, 25:27515
PAPINEAU, L., Interest of analog state studies in deformed nuclei, 25:28472
PAPPALARDO, G., Reaction $^{40}Ar(d,p)^{41}Ar$ at deuteron energy below Coulomb barrier, 25:28251
PARCHEV, N., Biochemical activity of Asp. niger under effects of x-rays, 25:27094
PARK, P. Kilho, Chemical budget of Columbia River, 25:28879 (RLO-1750-41)
PARKER, C. Warren Jr., Prog. rpt. on simulation and measurement of solar-flare proton exposures, final, 11/68--8/69, 25:26920 (AD-711041)
PARKER, F. T., Moessbauer effect in 121.2-keV transition in ^{147}Sm, 25:28420
PARKER, Harriet Inez, Intermediates in the biosynthetic conversion of thebaine to codeine in Papaver somniferum, 25:28899 (UCRL-20624)
PARKER, R. R., Nonlinear stabilization of a continuum, 25:27760
PARKIN, J., Use of serum thyroxine in assessment of thyroid function, 25:26857
PARKINSON, J. H., Satellite-borne x-ray spectroheliograph, 25:26484
PARKINSON, T. D., Auroral intensity ratio of O I (6300 A) and O I (5577 A), 25:27600
Phase and amplitude study of auroral pulsations, 25:27599
PARKOS, Gerald R., Nuclear reactor power monitor system, 25:28672
PARKS, George K., Acceleration and precipitation of Van Allen electrons during magnetospheric substorms, 25:27551
PARLANGE, J.-Y., Derivation of connection formula using partial Wronskian, 25:27817
PARMENTIER, C., Irradiation risks with /sup 99m/Tc, 25:26766
PARRY, A., United Kingdom reactors available for commercial operations, 25:28720
PARSIGNAULT, D. R., Radial diffusion observations in the Earth's outer radiation belt, 25:27626
PASHEV, Il., Biochemical activity of Asp. niger under effects of x-rays, 25:27094
PASHLEY, R. D., Lattice location and dopant behavior of Group II and VI elements, 25:27856
PASNICU, C., Beta radioactivity in some wines from Transylvania and Dobruja, 25:26618
PASQUALINI, Christiane Dosne, Leukemogenic effect of x rays in BALB mice, 25:27021
PASQUALINI, L., High-energy photoprotons from beryllium, 25:28194
PASSATORE, G., Mathematical approach to the derivation of the theoretical optical potential, 25:28096
PASSELL, L., Neutron crystal-field spectroscopy in rare-earth metallic compounds, 25:27893
PASSOW, Hermann, Red blood cell: penetration, distribution, and toxic actions of heavy metals, 25:26609
PATAU, Jean-Paul, Mean gamma ray energy necessary to create ion pairs in dielectric liquids, 25:26293
PATERLINI, V., TIGER: program for the calculation of thermal cross sections in light-water nuclear reactor, 25:28802 (EUR-4554)
WIGNER: program for calculation of mean thermal cross sections in reactor core and for punching of load data for calculating the epithermal cross sections, 25:28803 (EUR-4555)
PATERSON, Christopher A., Efflux of ^{22}Na and ^{86}Rb from crystalline lens, 25:26606
PATTERSON, J. R., Experimental investigation of $^{16}O + ^{12}C$ nuclear burning at stellar energies, 25:27309 (ANU-P-471)
PATTERSON, John W., Ionic domain for Y_2O_3-doped ThO_2 at low oxygen activities, 25:27286
PATTERSON, L. K., Pulse radiolytic investigations of hydroxy-radical reactivities in micellar solutions, 25:26295
PAULIKAS, G. A., Solar particle observations over the polar caps, 25:27540
PAUNEL, F., Potato plants obtained from irradiated tubers, 25:26737
PAVLOV, V. S., Capture of neutrons by Rh, Ta, and Au, 25:28437
PAVLOVIC, P., Apochromatic method for measurement of mean proton energy in 657 MeV beam, 25:26506 (JINR-P13-5637)
Monochromatic method for measurement of mean proton energy in 665 MeV beam, 25:26505 (JINR-P13-5636)
PAVLOVSCHI, Gh., Uranium in vine and wine, 25:26615
PAVLOVSKAYA, E. D., Structure of Galaxy and visible picture of the Milky Way, 25:27411
PAVONE, D., Enthalpy of formation of uranium tetrachloride, 25:26263
PAYNE, G. L., Analog spin mixing in ^{49}Sc, 25:28235
PEACOCK, D. W., Nuclear energy and electrical generation, 25:28527 (DUN-SA-166)
PEARCE, J. B., Mariner 6 and 7 ultraviolet spectrometer experiment: upper atmosphere data, 25:27433
PECORINI, Victorio, Thyroid tumour scanning with $^{197}HgCl_2$, 25:26823
PEDERSEN, Mogens, Detection of space-occupying intracranial lesions, 25:26852
PEGG, C., Effects of intracorporeal heat and radiation on dogs, 25:26931
PEHRSON, David L., Engineering view of the LRL OCTOPUS computer network, 25:28896 (UCID-15754)
PEISKER, M., Influence of storage period between drying and irradiation on action of x-rays in resting barley seeds. II, 25:27092
PENCEA, C., New experimental data for neutron polarization from $^{11}B(\alpha,n_0)^{14}N$ reaction, at low energies, 25:28192
PENDLETON, Hugh, Deterministic quantum interference experiments, 25:27942
PENKIN, N. P., Relative values of oscillator strengths of spectral lines, 25:27445
PENNER, H., Histological identification of irradiated potatoes, 25:27145
PENNEYS, Neal S., Eccrine poroma, 25:27055
PENNY, S. K., EDITOR: processing code for ENDF/B format data, 25:28148 (ORNL-TM-3266)
PENZIAS, A. A., Interstellar $^{12}C^{16}O$, $^{13}C^{16}O$, and $^{12}C^{18}O$, 25:27402
PERCEVAL, F., Deformation of electron distribution function, 25:27823
PERELYGIN, V. P., Deposition of uranium in the bones of animals, 25:26744
PERESLEGINA, N. V., Solar cosmic-ray increase on 25 Feb.--5 Mar., 1969, 25:27470
PEREZ, J. D., Analog spin mixing in ^{49}Sc, 25:28235
PERFILOV, N. A., Energy resolution for dE/dx detectors, 25:26485
PERINI, A., Estimate of the dose of ionogenic radiations absorbed by airport personnel carrying out the ground operations connected with the transport of packages containing radioactive materials, 25:26770
PERKINS, F. W., Remote feedback stabilization of drift instability by microwaves, 25:27766
PERKINS, R. W., Californium-252 neutron activation for terrestrial, sea floor, and possible planetary surface analysis, 25:26188 (BNWL-SA-3803)
In-cloud scavenging analysis from cosmogenic radionuclide measurements, 25:26364 (CONF-700601-, pp 69-97)
Stable elements of the atmosphere as tracers of precipitation scavenging, 25:26365 (CONF-700601-, pp 99-108)
PERKINS, S. T., Index to experimental data of neutron-induced reactions, 25:28356 (UCRL-50400(Vol.3))
PERKINS, W. A., High-frequency instabilities, 25:27727
PEROTTI, Angelo, Intermolecular and intramolecular free valence transfer in gamma irradiated crystalline hexadecanoic and cis-9-octadecenoic acids, 25:26312

PERRET, William R., Gasbuggy seismic source and surface motion, 25:26405 (PNE-1002)
PERRIA, C., Use of /sup 99m/Tc for cerebral scintigraphy, 25:26818
PERRICOS, D. C., Experience and research with the Greek reactor, 25:28774
Reassessment of some neutron yields from the longer-lived delayed neutron emitters, 25:28211 (CERN-70-30(Vol.1), pp 517-18)
PERRIN, Alfred James, Improvements in heat exchangers, 25:28749
PERRIN, James S., Effects of hydride precipitation of the tensile properties of irradiated Zircaloy-2. Final report, 25:27198 (BMI-X-10276)
PERRIN, R. C., Isotope effects in close-packed metals and in alkali halides, 25:26241
PERRON, C., Production cross sections of Li and Be isotopes in ^{12}C by high-energy protons and alpha particles, 25:28182
PERSHIN, I. I., Universal magnetic spectrometer with 0.15 percent resolving power at maximum pulse of 60 GeV/c, 25:26507 (NP-18764)
PERSSON, S. E., Distribution of gas and dust in the Orion Nebula, 25:27312
PESKOVATSKII, S. A., Uhf methods for investigation of the dynamic characteristics of thin superconducting films, 25:27652
PETERLIN, Tatjana M., Bunching of neutrons in the MeV region in high resolution neutron spectroscopy, 25:26493
PETERS, Hannah, Late effects of irradiation in infancy on the mouse ovary, 25:26930
PETERS, Martin Charles, Improvements in heat exchangers, 25:28749
PETERS, Richard, Thorium induced carcinoma of the maxillary sinus, 25:27050
PETERSEN, Aage, Deterministic quantum interference experiments, 25:27942
PETERSON, James R., Oxygen ion--ion neutralization reaction as related to tropical ultraviolet nightglow, 25:27608
PETIN, V. G., Influence of dose rate and conditions of α-irradiation on radiosensitivity of E. coli B/R, B, and B/sub s-I/, 25:27118
PETRICH, G. F., Magnetic and magneto-optical properties of Fe-doped EuO films, 25:27897
PETRIE, L. M., EDITOR: processing code for ENDF/B format data, 25:28148 (ORNL-TM-3266)
PETRINA, D. Ya., Model Hamiltonian of theory of superconductivity, 25:27643 (ITF-70-90-E)
PETROV, L. A., Proton emitter studies in region of $Z > 50$, 25:28300 (CERN-70-30(Vol.1), pp 457-86)
PETTIGREW, George L., Summary of federal regulations for packaging and transportation of radioactive materials, 25:26445 (BRH/DMRE-71-1)
PETYREK, P., Calcifications after x irradiation of DHT-sensitized rats. I, 25:26933
Comparison of the action of certain radioprotective compounds on the weight loss of submaxillary glands with their effect on rat lethality, 25:26795
Development of calcifications after whole-body irradiation in rats sensitized with DHT. I, 25:26978
Development of calcifications after whole-body irradiation in rats sensitized with DHT. II, 25:26977
Effect of time between radioprotective compound administration and irradiation on weight loss of submaxillary gland, 25:26792
PFIRSCH, D., Existence of shock-like solutions of Korteweg--De Vries equation, 25:27818
Existence of stationary shock waves in collisionless plasmas, 25:27708
PFLASTERER, G. R., Prog. rpt. on SEFOR, 11/70--1/71, 25:28757 (GEAP-10010-27)
PHELPS, Robert T., Methods of chemical analysis for FBR uranium--plutonium oxide fuel and source materials, 25:26153 (LA-4622)
PHILIP, W. S., Quality assurance in relation to nuclear power plants, 25:28550 (AECL-3670, pp 59-63)
PHILIPP, Hermann, Bibliographies in nuclear science and technology, Sect. 13, No. 7, 1970, 25:26443 (AED-C-13-7)
PHILLIPS, G. O., Radiation studies of aryl glycosides. III, 25:26305
Radiation studies of aryl glycosides. II, 25:26304
Radiation studies of aryl glycosides. I, 25:26303
PHILLIPS, J. A., Dynamic stabilization of the z pinch, 25:27789
PHILLIPS, K. J. H., Solar flare iron line emission at 1.9 A, 25:27386
PHIPPS, P. B. P., Annealing study of EuO films doped with Fe Eu, 25:27898
PICHON, R., Study of internal friction peaks in molybdenum after irradiation with neutrons at 27°K, 25:27199 (CEA-CONF-1671)
PICRAUX, S. T., Low temperature channeling measurements of ion implantation lattice disorder in single crystal silicon, 25:27859
PIEKARSKA, A., Influence of LET on radical yields in frozen aliphatic alcohols, 25:26311
PIEPER, Steven Charles, Calculations of three-body scattering amplitudes, 25:28101
PIESCH, E., New developments and aspects in phosphate glass dosimetry, 25:26519 (NP-18747)
Personnel monitoring with radiophotoluminescent dosimeters, 25:26518 (NP-18746)
PIIPARINEN, M., Energy levels of ^{28}Mg, 25:28259
PIKE, Chester D., Printed-circuit steering coils, 25:28116 (UCRL-20165)
PIKETTY, C. A., Relativistic corrections to the asymmetry of high-energy neutrons emitted in polarized muon capture by nuclei, 25:28183
PILUSO, C. J., Search for high-spin states in ^{27}Al, 25:28208 (ANU-P-521)
PINCOCK, G. D., Cavity reactor engineering mockup critical experiment, 25:28761 (NASA-CR-72409)
PINKEL, Benjamin, Gaseous-fueled nuclear reactors for electrical power production, 25:28635
PINKERTON, Arthur, Changes in biological effectiveness of a fast neutron beam with depth in tissue-equivalent material, 25:26906
PINSKY, Steven M., Correlation between brain tumor detectability on brain scan and protein levels of the spinal fluid, 25:26828
PINTER, G. F., Analysis of the reaction $\pi^+p \to rho^0\Delta^{++}$ at 11.7 GeV/c incident momentum, 25:27960 (DESY-71/8)
PIOTROWSKI, A., Nuclear spectroscopy of some light Tl isotopes, 25:28339 (CERN-70-30(Vol.2), pp 1081-91)
PISKAREV, I. M., Photoneutron reactions on copper, 25:28260
PISTONI, G., Nonlinear effects in quantum electrodynamics, 25:28070
PITTEWAY, M. L. V., Interpretation of ionospheric radio drift measurements. III, 25:27596
PITTILLO, Robert F., Biologic activity of daunomycin in microbial systems, 25:27100
PIXBERG, H. U., Measuring effective renal plasma flow by means of whole-body clearance of ^{131}I-hippuric acid, 25:26825
PIZZELLA, G., Differential energy spectrum of geomagnetically trapped protons with Injun 5 satellite, 25:27625
PLACANICA, A., Immunological modifications induced by radiotherapy, 25:26668
PLAKAS, Chris, Automated primary productivity measurements in water bodies, 25:28867 (NYO-3993-1)
PLAVEC, M., Evolution of close binaries. V, 25:27331
PLAVKO, A. V., Proton scattering on ^{24}Mg, ^{25}Mg, and ^{26}Mg, 25:28264
PLEITER, F., Contact density of conduction electrons in iron and the isomer shift of ^{57}Fe, 25:28247
PLESHANOV, A. S., Optimum magnetohydrodynamic flows, 25:27493
PNIEWSKI, J., Hypernuclei and hypernuclear spectroscopy, 25:28051
POBO, L. G., Ion cyclotron resonance studies of ionic reactions in ethane and of hydrogen exchange in D_2--C_2H_6 and H_2--C_2D_6 mixtures, 25:26249
POCHIN, E. E., Development of quantitative bases for radiation protection, 25:27042
PODLUBNYI, L. I., Spectrum of the inelastic collision integral in molecular mixtures, 25:27459
POGGENBURG, J. K., Ionic /sup 135m/Ba: a new agent for bone scanning, 25:26835
POGGIOLI, R. S., Model space calculation of the quasi-particle interaction for nuclear matter, 25:28453 (NYO-4032-37)
POGUTSE, O. P., Stabilizing effect of a high-frequency magnetic field on the trapped-particle instability, 25:27745
POHL, B. A., Nuclear level densities and reaction mechanisms from continuum neutron spectra, 25:28285
POICHAR, R. M., Carbon-12 states using $^{11}B(^3He,d)^{12}C$ reaction, 25:28205
POITER, R., Reactor physics design technique for burnable poison and enrichment-zoned cores, 25:28663
POKORNA, I., Scintigraphic localisation of the kidneys for percutaneous renal biopsy, 25:26821
POLIKANOV, S. M., Emissions of ^6He through nuclear fission by heavy ions, 25:28351 (KFK-tr-352)
POLKINGHORNE, J. C., Non perturbative parton model of current interactions, 25:28015
Partons and duality in deep inelastic lepton scattering, 25:28001
POLONIS, D. H., Superdislocations in Ni_3V, 25:27250
POLUEKTOV, N. S., Extraction-photometric determination of uranyl ions, 25:26163
Photometric determination of rare earths of Y subgroup, 25:26161
POLYAKOVA, G. N., Excitation functions of He I spectral lines, 25:27463
POLYANSKII, V. N., Reactions (d,p) of Ti and Cr isotopes, 25:28269
POOLE, D. M., Microanalysis with a proton-probe, 25:26158
POPA, P., Absolute determination and axial radial distribution of burn-up for reactor lattice cells, 25:28766
POPHAM, Mary G., Interpretation of brain scans by computer analysis, 25:26824
POPOV, Yu. P., Alpha decay of resonance states of ^{148}Sm, 25:28347 (JINR-P3-5553)
Reaction (n,α): new channel for studying nature of neutron resonances, 25:28345 (JINR-E3-5483)
POPOVA, A. M., Convergence of infinite series of nonrelativistic contributions for (n--d) scattering

XUM

amplitude, 25:28166
Energy distribution of α-particles in p + ^{11}B → 3α reaction, 25:28184
POPOVA, T. I., Decay of ^{66}Ge, 25:28272
POPP, Diana M., Genetic effect on radiation sensitivity consistent with a single gene locus hypothesis, 25:26690
POPP, R. A., Genetic effect on radiation sensitivity consistent with a single gene locus hypothesis, 25:26690
POPPOFF, I. G., Ionosphere of Mars below 80 km altitude. I, 25:27431
PORA, E. A., Effect of γ-ray microdoses on some metabolic indexes during white rat adaptation to hypothermia, 25:27023
PORGES, Karl G., Neutron flux plotting device, 25:26460
PORTER, Richard F., Matrix isolation study of borazine and boroxine. A vibrational analysis, 25:26233
POSKANZER, A. M., Fragment production in interaction of 5.5-GeV protons with U, 25:28426
POSPISIL, J., Biochemical changes in serum of intact and irradiated dogs after intravenous AET administration, 25:26935
POSPISIL, M., Individual differences in the radiation tolerance of rats and their relationship to the differences in the pre-irradiation stress response, 25:27029
POST, Joseph, Early and late effects of tritiated thymidine upon the replication of splenic lymphocytes, 25:26994
POSTAN, A., Coupling processes in D and E regions at low and medium frequencies. III, 25:27565
POSTMA, A. K., Effect of solubilities of gases on their scavenging by raindrops, 25:26374 (CONF-700601-, pp 247-59)
Washout of gaseous iodine species, 25:26376 (CONF-700601-, pp 271-88)
POSTNIKOV, V. V., Fast response control of reactor power on basis of γ radiation intensity, 25:28822
Monitoring of power distribution in nuclear reactor cores, 25:28699
POTAPKIN, V. I., Fast response control of reactor power on basis of γ radiation intensity, 25:28822
POUND, A. W., Induced cell proliferation and the initiation of skin tumour formation in mice by ultraviolet light, 25:26809
POUNDS, K. A., Satellite-borne x-ray spectroheliograph, 25:26484
POVH, B., Lifetime measurements on neutron deficient even--even isotopes of Xe and Ba, 25:28319 (CERN-70-30(Vol.2), pp 905-10)
POWELL, D. L., Spectroscopic factors from ^{124}Sn(d,p)^{125}Sn above and below the Coulomb barrier, 25:28286 (ANU-P-511)
PRABHU, Rashmiraj Balkrishna, Theory of superfluid Fermi systems, 25:27637
PRADDAUDE, H. C., Magnetic properties of dilute Pd(Gd) alloys, 25:27921
PRADEL, J., Radioactive aerosols characteristics in French U mines, 25:26773
PRAKASH, Satya, Subbaraya, B. H., Investigation of daytime lower ionosphere over equator, 25:27520
PRASAD, N., Effects of radiation on safflower, 25:27083
PRASAD, S. S., Ultraviolet emissions from atomic nitrogen in the aurora, 25:27617
PRATCHETT, A. G., Determination of fluorine in rock materials by γ-activation and radiochemical separation, 25:26193
PRATO, F. S., Tabulation of gamma--gamma directional-correlation coefficients, 25:28401
PRATT, Michael W., Prediction of the dosage to man from the fallout of nuclear devices. VII. Estimation of the maximum dose rate from the continuous release of radionuclides to the biosphere, 25:26751 (UCRL-50163(Pt.7))
PRATT, R. F., Acyl transfer reactions from and to the ureido functional group. IV. Neighboring carboxyl group general acid catalysis in the hydrolysis of an O-acylisourea (2-amino-8-carboxy-4-oxo-3,1,4-benzoxazine), 25:26253
PREECE, C. M., Adsorption-induced brittle fracture in liquid--metal environments, 25:27243
PRENTICE, A. J. R., Angular momentum problem in star formation, 25:27326
PREPEJCHAL, W., Photographic method for determining velocity distributions within thermal plumes, 25:28839 (ANL/ES-4)
PRESTON, Alan, Control of radioactive pollution in North Sea oyster fishery, 25:26742
PRESTON, D., Shielded x-ray microprobe for the analysis of radioactive samples, 25:26156
PREUSSNER, A., Cold neutron source in Juelich, 25:28767
PREVITE, J. J., Effects of radiation pasteurization on Salmonella. II, 25:27164
PREVITI, G., STAZ-2: program for thermohydraulic analysis of channel of water-moderated and cooled nuclear reactor core operating in stationary state, 25:28679 (EUR-4553)
PRIESMEYER, H. G., Total neutron cross sections of gross fission products, 25:28404
PRIEUR-DREVON, M., High-dynamic range rise time to amplitude converter, 25:26545 (CEA-N-1430)
PRIGENT, R., Portable electronic unit associated with an ionization chamber, 25:26459
PRIKHODTSEVA, V. P., Decay of ^{66}Ge, 25:28272
PRILUTSKII, O. F., Ionization and heating of intergalactic gas, 25:27429
PRINCE, Norman, Nuclear reactor standpipes, 25:28830
PRINDLE, Austin L., Far-out collection program. Project Schooner, 25:26404 (PNE-527)
PROCHAZKA, Z., Elimination of ^{131}I-labelled heterologous antigen after total body x-irradiation, 25:26944
PROCUREUR, J., Relativistic corrections to the asymmetry of high-energy neutrons emitted in polarized muon capture by nuclei, 25:28183
PRODI, Vittorio, Particle-free space in Stefan flow, 25:26386 (CONF-700601-, pp 403-10)
PROKOF'EV, A. I., Photoneutron cross sections of ^{203}Tl and ^{205}Tl, 25:28391
PROKOPENKO, V. S., Elastic proton scattering on medium-A nuclei, 25:28262
Elastic scattering of protons on iron and cobalt, 25:28263
PROPERZIO, William S., X-ray fluoroscopic screens: history, crystal kinetics, preliminary report on aging, 25:26815 (BRH/DMRE-71-2)
PROTASOVA, L. F., Palladium-99 γ radiation, 25:28431
PROTO, G. R., Properties of vanadium dioxide thermal filaments, 25:27906
PRUDNIKOV, E. D., Flame-spectrophotometric determination of microquantities of Li, Rb, Cs, and Sr in water, 25:26176
PRUESS, K., Nuclear molecules formed in elastic ^{16}O + ^{16}O scattering, 25:28171 (CERN-70-30(Vol.1), pp 601-2)
PRYOR, R. J., Joshua lattice physics subsystem, 25:28801 (DP-MS-70-78)
PRYOR, William A., Reactions of the hydrogen atom in solution. IV. Photolysis of deuterated thiols, 25:26252
Reactions of the hydrogen atom in solution. III. The photolysis of thiols. Studies of tritium-labeled thiols, 25:26251
PRZYTULA, M., Alpha decay of resonance states of ^{148}Sm, 25:28347 (JINR-P3-5553)
PSHENICHNYI, G. A., Generalization of γ-albedo calculations on basis of similarity theory, 25:27831
PSKOVSKII, Yu. P., Photometric aspects of Type I supernovae, 25:27339
PUCCI, R., Possibility of a single positron bound state in an electron liquid, 25:27447
PUCHEAULT, J., LET parameter and radiolysis of Fe^{2+} solutions by low-energy protons, 25:26288 (LB/G-2937)
PUCHEROV, N. N., Elastic scattering of protons on iron and cobalt, 25:28263
PUESCHEL, C. R., Application of the retaining ion technique to separation of ions by electrophoretic focusing ions, 25:26351
PUHALLA, J. E., Pathogenicity resulting from mutation at the b locus of Ustilago maydis, 25:27072
PULATIV, D. D., Emissions of ^{4}He through nuclear fission by heavy ions, 25:28351 (KFK-tr-352)
PULLMAN, I., Interaction between thymidylic acid and sulfhydrylamine radioprotectors, 25:26279
PUPP, C., Mass spectrometric determination of the heats of atomization of NdO_2, NdBO, and $NdBO_2$ and upper values for the dissociation energies of NdAg and Nd_2, 25:26273
PURCELL, T., Paramagnetic defects in TiO_2 produced by radiation, 25:27853
PURO, Jaakko, Changes in frequency of crossing-over in x-irradiated Drosophila melanogaster females, 25:26713
PURSIHEIMO, V., Energy levels of ^{176}Yb, 25:28398
PUSTOVALOV, V. V., Wave function and bound energy of nuclei ^{3}H(^{3}He) taking into account tensor interaction of nucleons, 25:28162 (IAE-2000)
PUTTARUDRAIAH, Sathyavathiamma Magadi, Operating characteristics of disc-focus dense plasma, 25:27794
PUTZ, F., Problem of numerical calculations for reactors, 25:28808
PYNE, H., Reactor physics design technique for burnable poison and enrichment-zoned cores, 25:28663
PYSTINA, K. A., Mutability of Verticillium, 25:26689
PYTTE, T., Morphology and dynamics of auroral-zone electron precipitation, 25:27583

Q

QUAGLIANO, James V., Prog. rpt. on structual studies of metal coordination compounds, 1959--69, 25:28894 (TID-25682)
QUALE, Andreas, Dynamical approach to the clock paradox, 25:28062
QUECHON, H., Influence of irradiation dose on latency time of cataracts in rabbits, 25:27027
QUEENER, S. F., Merodiploidy and expression of episomal genes in Pseudomonas putida, 25:28849 (COO-1683-32)
QUICK, Martin Vinicombe, Improvements in and relating to graphite moderated nuclear reactors, 25:28828
QUINN, Colin P., Deuterium isotope study of electrogenerative hydrogenation. Mechanism of hydrogenation of ethylene at positive potentials, 25:26230
QUINN III, James L., Correlation between brain tum

detectability on brain scan and protein levels of the spinal fluid, 25:26828
QUIRK, William Joseph, Computer simulations of processes in galactic dynamics, 25:27406
QURESHI, Z. A., Ability of sterilized irradiated males of D. cucurbitae COQ. and D. zonatus (Saunders) to compete with normal males, 25:27154

R

RABADJIJA, L., Some factors influencing uptake of ^{75}Se-selenomethionine by pancreatic tissues of the rat, 25:26591
RABASA, S. L., Leukemogenic effect of x rays in BALB mice, 25:27021
RABENSTEIN, D., Experiments at the Munich research reactor FRM, 25:28775
RACH, Klaus, Basic concepts for the use of radioactivity in medicine, 25:26790
RACZKIEWICZ, J., Results of x-ray irradiation of thymus gland in Myasthenia gravis, 25:26677
RADEBOLD, Reinhart, Condensation process based on Carnot cycle for liquid-metal MHD converters, 25:27478
RADKE, L. F., Interactions of cloud condensation nuclei and ice nuclei with cloud and precipitation elements, 25:26362 (CONF-700601-, pp 37-48)
RADTSIG, A. A., Charge exchange between negative and positive ions, 25:27455
RADUCANU, E., Uranium in vine and wine, 25:26615
RAENSCH, J., Analysis of UO_2--Mo and UO_2--Zircaloy fuel cermets, 25:26157
RAGHAVAN, P., New method for differential perturbed angular correlation measurements, 25:27917
RAGHAVAN, R. S., New method for differential perturbed angular correlation measurements, 25:27917
RAGNARSSON, Ingemar, Extrapolations to Z = 40 - 60 region of elements, 25:28318 (CERN-70-30(Vol.2), pp 847-82)
RAGUSA, S., Electric polarizability of the nucleon and the harmonic-oscillator symmetric quark model, 25:27983
RAI, K. S., Correlation of linkage groups with chromosomes in the mosquito, Aedes aegypti, 25:26694
Cytogenetics of two radiation-induced, sex-linked translocations in the yellow-fever mosquito, Aedes aegypti, 25:26719
RAIKO, V. I., Extraction and shaping of ion beams in plasma sources, 25:26549 (ORNL-tr-2462)
RAITT, W. J., Ionospheric measurements during the Feb. 25, 1969 solar proton event, 25:27567
RAJU, M. R., RBE of negative pions in 2-day-old ascites tumors, 25:26938
RALPH, B., Metallurgical applications of the field-ion microscope, 25:27254
RAMA, P. G., Analytical method for representing cylindrical B_4C absorbers in two-dimensional diffusion calculations, 25:28820 (EUR-4556)
RAMAYYA, A. V., Beta--gamma band mixing in ^{152}Sm, 25:28430
RAMQVIST, Lars, Electronic structure of cubic refractory carbides, 25:27907
RANCITELLI, L. A., Stable elements of the atmosphere as tracers of precipitation scavenging, 25:26365 (CONF-700601-, pp 99-108)
RANDALL, B. A., Differential energy spectrum of geomagnetically trapped protons with Injun 5 satellite, 25:27625
RANDER, J., Ion acceleration with high ν/γ electron beams, 25:27696 (WASH-1159, pp 204-18)
RANDERIA, B. V., Advances in preservation of food by irradiation, 25:27166
RANDOLPH, D. D., Material forming and welding nuclear pressure vessels, 25:27196
RANGANATHAN, B., Induction of mutation in Streptococcus diacetilactis by nitrosoguanidine and ultraviolet irradiation, 25:27121
RAO, B. Ramachandra, Characteristics of travelling ionospheric perturbations over Waltair, 25:27530
Dependence of horizontal drift and anisotropy of irregularities on the relative spacing of the aerials, 25:27517
RAO, G. S., Calorimetric investigation of long-range ordering in the cadmium--mercury system, 25:27248
RAO, M. G., Mutagenesis in sorghum, 25:26715
RAO, N. K., Materials for reactor technology, 25:27204 (INIS-mf-3)
RAO, P. Venugopala, Neutron activation cross sections for As, Br, Rb, and Sr isotopes at 14.4 MeV, 25:28282
RAO, S. V. K., Influence of microstructure on properties of ceramic products, 25:27282 (INIS-mf-14)
RAO, T. H., Kinetics of the high-temperature oxidation of dispersion-strengthened nickel--niobia alloys, 25:27279 (INIS-mf-11)
RAO, V. U. S., Magnetic and electrical characteristics of $REPd_3$ intermetallic compounds, 25:27870
RAOULT, Norbert, Use of microelectronics in linear circuits for nuclear spectrometry, 25:26494
RAPAPORT, J., L = 0 transitions to 0$^+$ states of N = 29 nuclei, 25:28229
RAPP, Herbert J., Abrogation of passively transferred tumor immunity in vivo by antigenically related tumor cells, 25:26663
RAPPAY, Gyoergy, Combined histochemical procedure to distinguish between mesenchymal and epithelial reticular cells in the rat thymus under the light microscope, 25:26654
RAPP DE ESTON, Veronica, Conference on biological effects of radiations, Sao Paulo, 10/69, 25:27036 (CONF-691057)
RASHCHENKIN, A. P., Excitation in the gap of a linear induction machine operating with variable-velocity wave field, 25:27482
RASMUSSEN, I. L., Experimental Q-values far from stability, 25:28295 (CERN-70-30(Vol.1), pp 331-40)
RASMUSSEN, J. O., Rotational bands in ^{171} ^{173} ^{175}Hf from (particle, xn) reactions, 25:28323 (CERN-70-30(Vol.2), pp 949-55)
RASMUSSEN, P., Brain scanning: cerebral scintigraphy, 25:26850
RASSOW, Juergen, Electron deep therapy by pendulum irradiation. V, 25:26867
Film dosimetry of high-energy rays. III, 25:26756
New telecentric small angle pendulum technique, specific for primarily unscattered electrons, 25:26878
RATER, D. L., Numerical image restoration, 25:28902 (UCRL-73080)
RATHJE, J., Electroproduction of single π^+ mesons on hydrogen, 25:27950 (DESY-71/9)
RATNER, B. S., Calculating cross-sections of ^{16}O(γ,n)^{15}O reactions, 25:28186
RATNIKOVA, V. A., Effect of macroturbulence on Fraunhofer line profiles, 25:27400
RATZEL, W., Comparison of various steam circuits and optimization of steam temperature for sodium-cooled fast breeders, 25:28750
RAWSON, D. E., Results of postshot exploration of the Greeley Event, 25:26412 (UCRL-50579)
READING, J. F., Low-energy neutron--oxygen scattering derived from two-body forces, 25:28198
REDDI, C. Raghava, Characteristics of travelling ionospheric perturbations over Waltair, 25:27530
REES, M. H., Influence of field-aligned currents on auroral-electron temperatures, 25:27603
REGAN, J. D., Two mechanisms of repair of uv-damaged DNA in vertebrate cells, 25:26635
REICH, F. R., Pulsed-laser holography for analysis of particle size and distribution, 25:26373 (CONF-700601-, pp 213-16)
REID, George C., Current problems in polar-cap absorption, 25:27548
REIN, James E., Methods of chemical analysis for FBR uranium--plutonium oxide fuel and source materials, 25:26153 (LA-4622)
REINKE, Peter, Economical and technical properties of the sodium-cooled high-power breeder reactor with carbide fuel, 25:28664
REIQUAM, H., European interest in acidic precipitation, 25:26377 (CONF-700601-, pp 289-92)
REISER, M., Intensity and phase-space limitations of various heavy-ion acceleration methods, 25:28130 (WASH-1159, pp 227-51)
REKALO, M. P., Meson photoproduction on neutrons at high energies, 25:27990
REMO, J. L., Empirical solar continuum models, 25:27369
RENKAS, M., External heavy ion source for Berkeley 88-inch cyclotron, 25:28120 (UCRL-20406)
RENSINK, M. E., Explosive instabilities in simulated plasmas, 25:27736
RESHAMWALA, A. S., Contribution of powder metallurgy techniques to materials science, 25:27205 (INIS-mf-19)
RESTIGNOLI, M., Argand-diagram analysis of Pomeron coupling to KN and anti KN system, 25:28035
REUTER, W., Preparation and structure of Fe-doped EuO films, 25:27894
REYNOLDS, G. M., Carbon-12 states using ^{11}B(^{3}He,d)^{12}C reaction, 25:28205
REYNOLDS, M. C., Optimizing thermal and radiation effects for bacterial inactivation, 25:27099
REYNOLDS, Miles Jr., Project Rulison post-shot investigations, 25:26409 (PNE-R-45)
REZANKA, I., Level structure of ^{109}Cd from decay of ^{109}In, 25:28428
Rotational bands in ^{171} ^{173} ^{175}Hf from (particle, xn) reactions, 25:28323 (CERN-70-30(Vol.2), pp 949-55)
REZWANI, V., Tensor polarizability in the giant dipole resonance region and collective behaviour, 25:28489
RIBE, F. L., Feedback stabilization of high-β, sharp-boundaried plasma column, 25:27764
RICH, Kenneth E., Uranyl ion-adenine nucleotides complexes, 25:26271
RICHARD, Patrick, Proton emission from isobaric analog resonances and isobaric analog resonances effects in (d,p) and (p,d) cross sections, 25:28471
RICHARDS, J. F., Rheology of fresh, aged, and gamma-irradiated egg white, 25:26923
RICHARDS, James F., Effect of γ-irradiation on beef myoglobin, 25:27139
RICHARDSON, M. J., Solution of Mathieu equation in WKB approximation, 25:27935
RICHARDSON, R. W., States of intermediate charge symmetry as low-lying, 0$^+$ collective excitation of medium weight nuclei, 25:28490
RICHES, A. C., Effects of x irradiation and antilymphocyte serum on responses to tumor allografts, 25:26666
RICHMAN, C., RBE of negative pions in 2-day-old ascites

XUM

tumors, 25:26938
RICHTER, A., An experimental test of the Barshay--Temmer theorem via the reactions $^{10}B(\alpha,^{7}Li/sub\ gs/)^{7}Be/sub\ gs/$ and $^{10}B(\alpha,^{7}Be/sub\ gs/)^{7}Li/sub\ gs/$, 25:28176
RICHTER, W., UV spectrum of $^{120}Sn^{35}Cl$ molecule in region between 2800 and 3450 A, 25:26244
RICKARD, J. J., High-velocity and intermediate-velocity H I clouds, 25:27416
RIDNER, A. E., Electron--electron scattering in electrical resistivity of In, 25:27660
RIECK, H. G., Californium-252 neutron activation for terrestrial, sea floor, and possible planetary surface analysis, 25:26188 (BNWL-SA-3803)
RIEDESEL, R. G., Manned planetary missions with reusable nuclear shuttles, 25:28789
RIEDL, P., Efficacy of additional shielding in telecobalt therapy, 25:26779
RIEDLER, W., Measurements of low-energy auroral particles from Feb. 23 to Mar. 2, 1969, 25:27569
Pitch-angle dependence of auroral electron fluxes in keV range, 25:27577
Precipitation pattern for auroral keV electrons and protons, 25:27576
Variations in low-energy electron spectrum and relation to magnetic activity, 25:27582
RIEDLER, Willi, Anisotropy for 1- and 6-keV positive ions in upper ionosphere, 25:27604
RIEGEL, D., In-beam nuclear magnetic resonance of 159 μs level in ^{119}Sn, 25:28380
RIEWE, F., Semiempirical generalized one-boson-exchange potentials, 25:28513
RILEY, P. J., Isobaric analog resonances in proton scattering from ^{86}Kr, 25:28242
Isobaric analog resonances in proton elastic scattering from ^{110}Cd, ^{112}Cd, and ^{114}Cd, 25:28370
Isobaric analog resonances in proton elastic and inelastic scattering from ^{130}Te, 25:28427
Neutron particle-hole states in ^{130}Te, 25:28369
RIMONDI, O., Thermoluminescent dosimeter of LiF incorporated in silicone rubber, 25:26539
RINGEARD, Claude, Use of microelectronics in linear circuits for nuclear spectrometry, 25:26494
RINGKOB, Thomas Paul, Estimation of meat composition by gamma rays and effects of parental size on lambs, 25:26571
RINGLEE, R. J., Survey of experience with equipment availability, 25:28548 (AECL-3670, pp 23-37)
RIOU, Michel, Search for superheavy elements on accelerator ALICE, 25:28315 (CERN-70-30(Vol.2), pp 723-33)
RIOV, J., Effect of gamma radiation on the synthesis of scopoletin and scopolin in grapefruit peel in relation to radiation damage, 25:27079
Relationship between radiation damages to citrus fruits and changes in enzymes and other constituents of the peel, 25:27135 (IAEA-R-362-F)
RIPPMANN, Ernst T., Influence of different traumas on pregnancy in laboratory mouse, 25:28873 (ORNL-tr-2445)
RISHBETH, H., F-layer dynamo, 25:27598
Maps of vertical F layer drifts caused by horizontal winds, 25:27588
Origin of storm increases of midlatitude F-layer electron concentration, 25:27510
Polarization fields produced by winds in equatorial F region, 25:27586
RISTORI, C., On-line isotope separator device connected to Melusine reactor, 25:26551
RITTENBERG, V., Scaling and duality in strong interactions, 25:28016
RIVERS, R. J., Analyticity structure of simple single-particle exchange models for high-energy interactions, 25:28013
RIZEK, J., Electroexcitation of ^{32}S in region of dipole resonance, 25:28220 (UJV-2553-F)
ROBBINS, John A., Model for variations with particle size of halogen-ion ratios in marine aerosols, 25:26381 (CONF-700601-, pp 325-51)
ROBERT, Kearny Quinn Jr., In-beam internal conversion spectroscopy, 25:28271
ROBERTS, Geoffrey Alfred, Improvements in and relating to graphite moderated nuclear reactors, 25:28828
ROBERTS, J. J., Chicago air pollution systems analysis program, 25:28840 (ANL-ES-CC-8)
ROBERTS, J. T., Potential demand for nuclear power in developing countries, 25:28541
ROBERTS, J. T. A., Deformation of UO_2 at high temperatures, 25:27287
ROBERTS, R. G., Analysis of meson--baryon scattering processes related by SU(3) in a unitarized Veneziano model, 25:28041
Dual description of production processes by unitarity, 25:28044
Multi-particle eikonal model with high energy s-channel helicity conservation, 25:28034
ROBERTSON, C. E., Interactions of cloud condensation nuclei and ice nuclei with cloud and precipitation elements, 25:26362 (CONF-700601-, pp 37-48)
ROBERTSON, J. S., Extracorporeal irradiation of blood by beta-emitting isotopes: principles of dose calculations, 25:26754
ROBILLARD, J., Use of /sup 99m/Tc and its compounds, 25:26765
ROBINSON, E. A., Raman spectra of chlorofluorosilanes in gaseous, liquid, and solid state; anomalous ^{35}Cl, ^{37}Cl isotope intensity effects in splitting of totally symmetrical SiCl stretching mode in $SiCl_3F$ and $SiCl_2F_2$, 25:26218
ROBSON, D., General remarks, 25:28465
RODGER, K. S., Space-charge waves in solids, 25:27805
RODIONOVA, T. V., Extraction methods in analytical chemistry of Mo, 25:26344
RODRIGUEZ, P., Irradiation effects on reactor structural materials, 25:27265 (INIS-mf-5)
ROEDERER, Juan G., Trapped particle population changes associated with solar events, 25:27543
ROESCHERT, G., Proposal of $d^{3}/_{2}$-$1p^{3}/_{2}$ analogue states in ^{49}Ca, 25:28230
ROGERS, R. F., Safety summary report: LLD-1 package, 25:26446 (DPSPU-71-124-1)
ROGOZKIN, V. D., Reaction of hypophyseal-adrenal system to ionizing radiation, 25:26998
ROHAN, Paul Edward, Comparisons of transport and diffusion theory calculations of performance characteristics for large fast reactors, 25:28812
ROHDE, Robert Sterbenz, Temporal Landau damping and wave echoes in collisionless plasma, 25:27819
ROHRMANN, C. A., Fission-product xenon and krypton: an opportunity for large-scale utilization, 25:26347
ROIZIN, Leon, Decrements in the visual acuity of rhesus monkeys (Macaca mulatta) as a delayed effect of occipital cortex irradiation, 25:26991
ROLLAND, P., Dynamic stabilization of the drift dissipative instability by an inhomogeneous rf field, 25:27780
ROMAGNOLI, R., Scintigraphy of carcinoma using $^{197}HgCl_2$, 25:26832
ROMANOVSKII, E. A., Energy distribution of α-particles in p + ^{11}B + 3α reaction, 25:28184
ROMASHKO, O. O., Reaction of hypophyseal-adrenal system to ionizing radiation, 25:26998
ROMBERG, G. P., Photographic method for determining velocity distributions within thermal plumes, 25:28839 (ANL/ES-4)
RONAMI, G. N., Phase equilibria in the system vanadium--tantalum--hafnium, 25:27247
RONAY, Maria, Fatigue of high-strength materials, 25:27242
RONEN, A., Repair of alkylation-induced damage in E. coli and its bacteriophage lambda, 25:27109
RONSIVALLI, L. J., Study of irradiated-pasteurized fishery products, 25:27149
ROONEY, T. A., Infrared spectra of UO and UO_2 vapor condensed in rare-gas matrices, 25:26260 (COO-1182-34)
ROOS, P. G., A search for isospin mixing using the (^{3}He,t) reaction, 25:28232
ROS, J., High-dynamic range rise time to amplitude converter, 25:26545 (CEA-N-1430)
ROSE, Fred L., Cycling of ^{65}Zn by Columbia River periphyton in a closed lotic microcosm, 25:26593
ROSEN, A., Atomic-beam measurements in the rare-earth region, 25:28298 (CERN-70-30(Vol.1), pp 387-94)
Hyperfine structure of ^{51}Cr, 25:28252
ROSENBLUTH, M. N., Diffraction radiation by a line charge moving past a comb, 25:28483
Feedback stabilization of high-β, sharp-boundaried plasma column, 25:27764
ROSENOW, Ulf, Simulation of moving beam therapy and grid size in electronic calculation of single fields and standard plans of telecobalt therapy, 25:26758
ROSENSTEIN, Laurence, Absorbed dose rates in growing feline bone from continuous exposure to low levels of ^{90}Sr, 25:26612
ROSENTHALL, L., Detection of bronchopleural fistulas by radionuclide fog inhalation, 25:26833
ROSENTHALL, Leonard, Combined inferior vena cavography, iliac venography, and lung imaging with /sup 99m/Tc albumin macroaggregates, 25:26837
ROSHCHUPKIN, D. I., Action of uv radiation on proteins, 25:26644
ROSIEK, O., Regeneration of proliferative activity in progeny of murine lymphoma cells L5178Y irradiated with x-rays, 25:26974
ROSS, D. K., Gravitational red-shift, 25:27347
ROSS, D. W., Stabilizing effect of a high-frequency magnetic field on the trapped-particle instability, 25:27745
ROSS, R. T., Reaction K-P + AK+K- and the generalized Veneziano model, 25:28042
ROSSIGNOL, Jean-Luc, Intragenic recombination of ascospore color mutants in Ascobolus and its relationship to the segregation of outside markers, 25:26695
ROSTOKER, Norman, Acceleration and stripping of ions by intense relativistic electron beams, 25:27694 (WASH-1159, pp 184-9)
ROTHENBERG, Sheldon P., Autoantibodies to intrinsic factor: their determination and clinical usefulness, 25:26676
ROTHWELL, P., Longitudinal variation of midlatitude ionosphere produced by neutral-air winds. II, 25:27508
ROUCAYROL, J.-C., Synoviothesis (synoviotherapy by radioisotopes) studies of more than 400 cases and future prospects, 25:26873
ROULLIER, Francoise, Measurement of the kinetic parameters of the MINERVE reactor from analysis of the neutron fluctuations, 25:28755 (CEA-N-1406)
ROUX, A., Wave-packet propagation and application to

XUM

dispersion characteristics and to mechanisms of Pc 1 events, 25:27605
ROUX, Andre, Wigner energy in irradiated oxides BeO, MgO, Al_2O_3, and SiO_2, 25:27839 (CEA-N-1171)
ROWLAND, T. J., Quadrupolar effects in ^{51}V NMR of V-based transition-metal alloys, 25:27916
ROY, R. R., Gamma rays in coincidence with K x rays of Cs and Ba fission products of ^{252}Cf, 25:28416
ROZENBLATT, Shmuel, Induction of cellular DNA synthesis by supercoiled SV40 DNA in x-irradiated mouse 3T3 cells, 25:26691
ROZENTAL, I. L., Ionization and heating of intergalactic gas, 25:27429
ROZGON, M. I., Radiosensitivity of the inductive and productive phases of antibody, 25:26680
RUBACHEV, P. G., Influence of irradiation on the urinary excretion of deoxycytidine and beta-aminoisobutyric acid in monkeys, 25:26999
RUBINSTEIN, H. R., Scaling and duality in strong interactions, 25:28016
RUD, V. I., Investigation of α decay of isotopes of element 105, 25:28350 (KFK-tr-350)
RUDAVSKII, E. Ya., Dispersion of first sound in superfluid ^3He--^4He solutions due to damping of the normal component, 25:27640
RUDDY, Frank H., Limiting cross sections for fission isomers with nanosecond lifetimes produced in heavy-ion reactions, 25:28399
RUDENKO, V. N., Inspection of the laminates with the beam of electrons, 25:26542
RUDNICKI, Tadeusz, Serum amino acids in rats in the course of acute radiation injury, 25:26624
RUDSTAM, G., Compound-nucleus aspects of beta decays with high Q values, 25:28443 (CERN-70-30(Vol.1), pp 421-33)
Neutron-rich nuclides obtained using OSIRIS facility, 25:28340 (CERN-70-30(Vol.2), pp 1093-1103)
Q-values of some nuclides on the neutron-rich side of stability, 25:28296 (CERN-70-30(Vol.1), pp 341-51)
RUESTER, R., Effects of electric fields and ion drag in middle-latitude F region, 25:27529
Electron concentration in the midlatitude F layer, 25:27528
Solution of ionospheric continuity equations and equations of motion for particles, 25:27521
RUETHER, W., Eye changes caused by fast neutrons (15 MeV) and the protective action of chemicals, 25:27014
RBE of fast neutrons on influence of cataract development, 25:26945
RUF, R., Heavy-water-cooled and-moderated boiling-water reactor, 25:28645
RUH, F., Cooperation of reinforced-concrete construction and steel construction, 25:27188
RUHENSTROTH-BAUER, Gerhard, Spleen, liver, plasma, and erythrocytes of whole-body irradiated rats, 25:26600
RUMI, R. F., Alpha decay of resonance states of ^{146}Sm, 25:28347 (JINR-P3-5553)
RUMYANTSEV, G. Ya., Principle of boundary sources in neutron transport theory, 25:28160
RUNDQUIST, D. E., Carbon-12 states using $^{11}B(^3He,d)^{12}C$ reaction, 25:28205
RUNGE, E.-G., Electrical facilities of Braunschweig research and measuring reactor, 25:28771
New repositioning drives for source-range detectors for startup channels of reactor FMRB, 25:28773
RUPPE, Charles R., Irradiation apparatus in combination web handling means, 25:26417
RUSS, John C., Review of engineering standards development for nuclear power systems, 25:28536
RUSSELL, C. T., Magnetic and electric field changes across the shock and in the magnetosheath, 25:27539
RUSSELL, Glen A., Aliphatic semidiones. XV. 2,3-semidiones derived from the bicyclo[n,1.0]alkanes, 25:26254
Aliphatic semidiones. XVI. Semidiones derived from the bicyclo[n.1.1]alkanes, 25:26255
RUSSKIKH, V. S., Photoneutron cross sections of ^{203}Tl and ^{205}Tl, 25:28391
RUTHERFORD, P. H., Feedback control problems in tokamaks, 25:27763
RYAN, Lois M., Radiation model of man for analysis of future space missions, 25:26778
RYBACHENKO, V. F., Wave function and bound energy of nuclei $^3H(^3He)$ taking into account tensor interaction of nucleons, 25:28162 (IAE-2000)
RYDBERG, B., Evidence for high-spin three quasiparticle state in ^{133}I produced in fission, 25:28331 (CERN-70-30(Vol.2), pp 1012-14)
Experimental techniques for nuclear structure studies in the Tin-region at OSIRIS, 25:28107 (CERN-70-30(Vol.2), pp 1003-5)
Levels in doubly-even tellurium isotopes, 25:28330 (CERN-70-30(Vol.2), pp 1010-11)
Proton states in the tin-region, 25:28328 (CERN-70-30(Vol.2), pp 1006-7)
RYDE, H., Rotational bands in ^{171} ^{173} ^{175}Hf from (particle, xn) reactions, 25:28323 (CERN-70-30(Vol.2), pp 949-55)
Rotational states in ^{168}Yb, ^{169}Yb, and ^{170}Yb, 25:28394
RYDER, J., Maintenance from the station operator's point of view, 25:28551 (AECL-3670, pp 65-70)
RYDING, G., Equilibrium charge-state distribution of heavy ions (1 to 14 MeV), 25:28127 (WASH-1159, pp 45-57)
RZAZEWSKI, K., Interaction of harmonic oscillators with radiation field, 25:27928 (INR-P-1203)
RZEWUSKI, J., Hilbert spaces of functional power series, 25:28066

S

SAAL, Fortuna, Leukemogenic effect of x rays in BALB mice, 25:27021
SAARI, Donald G., Implications of the inverse-square-law model, 25:27422
SACCO, M., Radiographic and scintigraphic methods for the study of hydatids of the kidneys, 25:26816
SACCOMANNO, Geno, Histologic types of lung cancer among uranium miners, 25:27045
SACHS, Francis L., Engineering materials list, 25:26414 (TID-4100(Suppl.62))
SACHS, Peter L., Distribution of some chemical elements between dissolved and particulate phases in the ocean, 25:26190 (NYO-4150-9)
SACK, Horst, Electron deep therapy by pendulum irradiation. V, 25:26867
SADOVOI, A. A., Wave function and bound energy of nuclei $^3H(^3He)$ taking into account tensor interaction of nucleons, 25:28162 (IAE-2000)
SADOYAN, K. A., Azimuthal asymmetry of magnetic field strength of Erevan synchrotron electromagnet, 25:28139
SAEGUSA, Kenji, Contribution of low-energy gamma emitters to the scintigram, 25:26849
SAETTA-MENICHELLA, E., Mechanism of fission of heavy nuclei, 25:28504
SAFAEVA, I. B., Radiosensitivity of the inductive and productive phases of antibody, 25:26680
SAFIYASOV, Zh. S., Growth patterns of uv-irradiated E. coli B in saline, 25:27119
SAFRONOVA, U. I., Use of Coulomb Green functions in atomic calculations. I, 25:27465
SAGAN, Leonard A., Human radiation exposures from nuclear power reactors, 25:26741
SAH, R. C., Bevatron external proton beam facilities, 25:28119 (UCRL-20194)
SAIFUDDIN, Recent high-energy p-p scattering experiments and the optical-model predictions, 25:28052
SAIKI, Masamichi, Marine ecology and atomic energy, 25:26683
SAIMONGKOL, U., Standard neutron irradiation facility experience in Thailand, 25:27062 (IAEA-R-459)
SAITO, Haruo, Shallow traps in p-type germanium converted from n-type by electron irradiation, 25:27843
SAITO, T., Isobaric analog states in (γ,p) reactions on Sn isotopes, 25:28361
Isobaric analog states in (γ,p) reactions on N = 50 nuclei, 25:28227
Isobaric analog states in (γ,p) reactions on N = 82 nuclei, 25:28362
SAITO, Toshimi, Influence on liver of radiation, 25:26955
SAKANOUE, M., Studies on the distribution of chemical elements in geochemical samples by an activation autoradiographic method, 25:26194
SAKON, Tomosaburo, Development of atomic energy, 25:28584
SAKURADA, Ichiro, Relation between the polymer conformation and the elastic modulus of the crystalline region of polymer, 25:26281
SAKUTA, Masaaki, Ocean nuclear-power plant, 25:28643
SALADIN, J. X., Coulomb excitation of the first 2^+ state of ^{24}Mg, 25:28283
SALAGEAN, O., New experimental data for neutron polarization from $^{11}B(\alpha,n_0)^{14}N$ reaction, at low energies, 25:28192
SALLACH, R. A., Reaction of Mulberry with various gases, 25:27210 (SC-DR-710124)
SAL'MAN, Kh., Energy distribution of α-particles in p + ^{11}B + 3α reaction, 25:28184
SALSIG, W. W., Mechanical features of electron-ring compressors, 25:28118 (UCRL-20177)
SALUNKHE, D. K., Effects of γ radiation on Penicillium expansum. I, 25:27084
SALZANO, F. J., Ionic range of ThO_2--15 wt. percent Y_2O_3 at high oxygen activities, 25:26262
SALZMANN, D., Forward elastic scattering of 9 MeV gamma rays, 25:28358
SAMAIN, A., Dynamic stabilization of a confined plasma, 25:27778
SAMPERIO, Jorge Gutierrez, Cooperative program on the investigation of the Med Fly in Central America, 25:27131 (CONF-680112-, pp 143-50)
SAMPSON, Richard J., Smallest forms of papillary carcinoma of thyroid. A study of 141 microcarcinomas less than 0.1 cm in greatest dimension, 25:26898
SAMSONOV, G. V., Emissivity of diborides of transition metals from Groups IV--VI, 25:27290
SAMUELS, Larry D., Reversal of liver scan image after right-sided renal radiotherapy, 25:26884
SAMUELSSON, Erik Lennart Mauritz, Decay of excited nuclear states studied by electron directional correlation methods, 25:28410
SANATHANAN, C. K., SAS1A: a computer code for the analysis of fast-reactor power and flow transients, 25:28727 (ANL-7607)
SANCISI, R., Correlation between gas and dust, 25:27415
SANDBERG, G., Effects of intracorporeal heat and radiation

on dogs, 25:26931
SANDHU, S. S., Fertile dwarf and three other mutants in Cicer, 25:26718
SANDS, Jean, Vulnerability of developing brain: I. Some lasting effects of x-irradiation, 25:26946
SANDU, M. A., Photometric determination of rare earths of Y subgroup, 25:26161
SANG, Y. N., Lactic dehydrogenase level of rats exposed to γ irradiation, 25:26803
SANGAL, S. P., Spectrophotometric determination of Pr, Nd, Sm, and Eu using chromotrope 2 R as a chromogenic reagent, 25:26165
SANGUINETI, M., Scintiscanning with /sup 99m/Tc pertechnate perfusion, 25:26838
SANINA, A. V., Radiation biophysical investigations of Arabidopsis thaliana. III, 25:26736
SANMARTIN, Juan R., Similarities between ion waves in plasmas and gravity waves in incompressible fluids, 25:27806
SANN, H. J., Lifetime measurements on neutron deficient even--even isotopes of Xe and Ba, 25:28319 (CERN-70-30(Vol.2), pp 905-10)
SANNAZZARI, G. L., Importance of bone marrow scintiscans in the detection of skeletal metastases, 25:26847
SANNER, L., Magnetic moment and hyperfine structure of ^{103}Ag, 25:28396
SANNER, Tore, Transfer of radiation energy from macromolecules to sulfur compounds. A comparison between the trapping efficiency of a thiol and its corresponding disulfide, 25:26299
SANO, Hogara, Medical 6 MeV linear accelerator, 25:28132
SANTESSON, B., Chromosome and chromatid-type aberrations induced by ^{60}Co irradiation and tritiated uridine in human leukocyte cultures, 25:26636
SANTO, R., Coulomb displacement energies for excited states in nuclei around ^{28}Si, 25:28243
SANZONE, M., High-energy photoprotons from beryllium, 25:28194
SAPRE, A. B., Partial pistilloidy in rice following irradiation, 25:26702
SARACHEK, A., Relative susceptibilities of caffeine-sensitive and caffeine-resistant strains of Candida albicans to inactivation and mutation by ultraviolet radiation, 25:27073
SARGENT, F. P., Radiation chemistry of low-temperature aqueous glasses. IV, 25:26310
SARKAR, S. K., Centimeter and decimeter solar bursts in relation to S component of solar radio emission, 25:27364
Recurrence of 10.7-cm solar flux and of sunspot activity over 11-year solar cycle, 25:27362
SASAKI, Fukashi, X-ray and fast-electron scattering factors for light atomic systems, 25:27460
SASAKI, Go, Mechanical properties of laves phases, 25:27211 (UCRL-20301)
SASTRI, J. Hanumath, Dependence of horizontal drift and anisotropy of irregularities on the relative spacing of the aerials, 25:27517
SASTRY, K. S. R., Higher order interference effects in hindered allowed β-decay and the matrix element ratio C/sub v/[1]/C/sub A1/[I], 25:28480
SATCHER, David, Effects of ^{131}I and x radiation on chromosomes of peripheral blood leukocytes, 25:26730
SATO, Fumiaki, Late injuries induced by radiation. II, 25:26976
SATO, Fumiko, Gradual development of radioprotection in HeLa S_3 cells during treatment with β-mercaptoethylguanidine, 25:26797
SATO, H., Effect of helical instability on the radial density and potential distribution, 25:27738
SATO, Matsuki, Studies on analysis of rare earths. II, 25:26168
SATO, Shosaku, Superhigh voltage irradiation of bladder tumor, 25:26876
SATO, T., Dynamic control of cusp loss, 25:27676
Thyroid crisis following ^{131}I therapy, 25:26881
SATO, Tomotaro, Sprout inhibition of potatoes, 25:27167
SATO, Yasuo, Combination therapy of malignant tumors, 25:26885
SATPATHY, L., Shape-fluctuation model of ground-state bands in even--even nuclei, 25:28481
SATPATHY, M., Shape-fluctuation model of ground-state bands in even--even nuclei, 25:28481
SAVINOVA, I. R., Investigation of reactions in solid phases in the systems Y_2O_3--Al_2O_3 and Y_2O_3--Ga_2O_3 with luminescence spectra of Eu, 25:27303
SAWA, Zdzislaw P., Energy levels in ^{70}Ga, 25:28254
SAWSON, J. M., External control of ion waves in a plasma by high-frequency fields, 25:27807
SAYED, A. M., Annual occupational radiation exposure dose levels, 25:26749 (NP-18732)
SAZANOV, A. A., Inner corona polarization during solar eclipse of 9/22/68, 25:27397
SCALIA, A., Analytic properties and bound-state degeneracy in nonlocal potentials, 25:28094
SCALIA, M., Effective four-body interaction in light nuclei, 25:28482
SCARF, F. L., Fast time-resolved spectral analysis of vlf banded emissions, 25:27621
Magnetic and electric field changes across the shock and in the magnetosheath, 25:27539
SCARLAT, F., Incoherent space charge accelerated in betatron, 25:28143
SCHAAP, Ward B., Prog. rpt. on electrochemical research in amine solvents, final, 3/71, 25:28845 (COO-256-102)
SCHAARE, W., Proportional counter for detection of exoelectrons, 25:26487
SCHAECHTER, L., Absolute determination and axial radial distribution of burn-up for reactor lattice cells, 25:28766
SCHAEFFER, O. A., Noble gas abundances in lunar material, 25:27308
SCHAEFFER, R. C., Role of recombination in pre-dawn enhancement of lambda 6300 A [O I] airglow, 25:27514
Stable auroral red arcs observed from Adelaide during 1967-69, 25:27525
SCHAFER, Kenneth Lisle Jr., Visual effects of ionizing radiation in moth, 25:26910
SCHAPIRA, J. P., High resolution detection unit for charged particles, 25:28141
SCHARER, J., Deformation of electron distribution function, 25:27823
SCHARFF-GOLDHABER, Gertrude, Some interesting aspects of the VMI model, 25:28446 (CERN-70-30(Vol.2), pp 813-27)
SCHATZ, A., Radiological population exposure in the environment of nuclear power plants, 25:26746
SCHEID, W., Achromatic lesions induced by x-rays in chromosomes of Vicia faba, 25:26725
Distribution of x-ray-induced achromatic lesions within and between arms of M-chromosome of Vicia faba, 25:26734
Nuclear molecules formed in elastic ^{16}O + ^{16}O scattering, 25:28171 (CERN-70-30(Vol.1), pp 601-2)
SCHEIDER, B., Structure of chlorinated poly(vinyl chloride). I. Determination of the mechanism of chlorination from infrared and NMR spectra, 25:26246
SCHENTER, R. E., Group constants for fast reactor calculations, 25:28657 (HEDL-TME-71-36)
SCHERZ, H., Use of mannitol in the dosimetry of gamma radiation, 25:26523
SCHICK, M., Effects of lateral substrate fields on helium monolayers, 25:27634 (RLO-1388-604)
Ground state of ^3He monolayers adsorbed on inert substrate, 25:27633 (RLO-1388-603)
Substrate mediated interaction between adsorbed atoms, 25:27635 (RLO-1388-605)
SCHIELTZ, Jon D., Ionic domain for Y_2O_3-doped ThO_2 at low oxygen activities, 25:27286
SCHIFFER, J. P., Coulomb energies, 25:28475
Shell-model structure of ^{209}Bi, 25:28417
Single-particle analog state anomalies in the scattering of protons from ^{197}Au, ^{196}Pt, and ^{184}W, 25:28371
SCHILDKNECHT, D., Comparison of pion electroproduction data with vector meson dominance predictions, 25:27982 (DESY-71/12)
SCHINDLER, K., Existence of stationary shock waves in collisionless plasmas, 25:27708
Tearing instabilities in the magnetosphere, 25:27547
SCHLAPP, D. M., Cause of a type of magnetic variation on quiet days, 25:27602
SCHLOSSER, K., Future management of radioactive wastes in Austria, 25:26451 (SGAE-RT-33/1970)
SCHMAHL, Edward Joseph, Io, an Alfven-wave generator, 25:27435
SCHMETS, J. J., Experience acquired in fluid bed preparation of UF_6 in view of reactor fuel processing, 25:26207 (BLG-448)
SCHMID, E. D., Substituent effect on ir intensities of CH stretching vibrations of benzene derivatives, 25:26247
SCHMIDT, D., Electroproduction of single π^+ mesons on hydrogen, 25:27950 (DESY-71/9)
SCHMIDT, E. G., Photometric study of four classical Cepheids, 25:27318
SCHMIDT, Frederic C., Prog. rpt. on electrochemical research in amine solvents, final, 3/71, 25:28845 (COO-256-102)
SCHMIDT, K. H., Elastic electron--deuteron scattering and electric neutron form factor at four momentum transfers: 5 $Fermi^{-2} < q^2 < 14$ $Fermi^{-2}$, 25:27980 (DESY-71/7)
SCHMIDT, Willfred, Oxidations of aqueous Chromium(II). II. Chromium-carbon bond, 25:26229
SCHMIEDER, H., Aqueous reprocessing of fuel elements of fast breeder, 25:26326 (KFK-911)
SCHMITZ, G., Cladding monitoring in sodium-cooled reactors by detection of delayed neutrons, 25:28698 (NP-18778)
SCHMITZ, Gerald L., Thorium induced carcinoma of the maxillary sinus, 25:27050
SCHMITZ, W., Ureteral injuries after obstetric--gynecologic intervention and radiation, 25:26814
Urologic management of injuries to the bladder after gynecologic radiotherapy, 25:26813
SCHMITZ-FEUERHAKE, Inge, Use of gamma cascade isotopes in three dimensional function measurements in vivo and layer scintigraphy, 25:26465
SCHMORAK, M. R., Nuclear data sheets for A = 207, 25:28378
SCHNEIDER, E. E., Controlled avalanche caused by electron cyclotron acceleration, 25:27698
SCHNEIDER, G. R., Kinetics of the pyrolysis of beryllium hydride, 25:26278
SCHOLER, M., Effect of Alfven waves on MHD fast shocks, 25:27387
SCHOTT, O., Effects of technical improvements on patient

doses in x-ray diagnosis, 25:26858
SCHOTTENFELD, David, Incidence of multiple primary cancers. IV. Cancers of the female breast and genital organs, 25:27038
SCHOWEN, Richard L., Mechanism of the benzoin condensation, 25:26220
SCHRADER, Richard, Production of tungsten powder from mechanically activated tungstic acid, 25:27183
SCHREIBER, B., Spin assignment for two isobaric analog resonances in ^{74}Se from the neutron decay, 25:28241
SCHREIBER, D. S., Paramagnetism of high-concentration manganese in bcc vanadium, 25:27891
SCHREIBEROVA, O., Difference in dried thyroid block of ^{131}I uptake in male and female rats, 25:26601
SCHREINER, P. A., Reaction K-P + AK*K- and the generalized Veneziano model, 25:28042
SCHRIEWER, J., Equivalence relation for resonance absorption based on numerically calculated collision probabilities. I, 25:28666
SCHROEDER, Ellinor, Effect of ionizing radiation on DNA x RNA hybridization, 25:26641
SCHROEDER, Guenter, Influence of different crystal models on thermal neutron scattering in beryllium oxide and graphite, 25:28158
SCHROEDER, Johannes Horst, Dominant lethal mutations in descendants of irradiated male mice. I, 25:26726
SCHROEDER, K., Optical properties of cr--mn and cr--v alloys, 25:27442
SCHUBERT, B., Radiotherapy of vocal-cord leukoplakia, 25:26868
SCHUBERT, Jack, Inactivation and reactivation of hemocyanin by radiolytic OH and e/sub aq-/, 25:26302
SCHUETTE, D., Co-existence of different structures in various domains of the periodic table, 25:28447 (CERN-70-30(Vol.2), pp 1129-32)
SCHULMAN, L. S., Gravitational shock waves from tachyons, 25:28088
SCHULZE, H., Influence of lattice defects on backscattering of protons and helium ions from niobium single crystals, 25:27840 (IPP-7/3)
SCHULZ-EKLOFF, G., Pressure dependence and mechanisms of nitrogen activation on iron, 25:26245
SCHUMACHER, M., Compton scattering of gamma rays by electrons bound in heavy atoms, 25:27461
SCHUMANN, G., Ionospheric plasma drifts derived from wake measurements, 25:27585
SCHUSTER, Nick A., Multiple detector neutron logging apparatus, 25:26541
SCHUSTER, Ronald E., Proton magnetic resonance cation solvation study of uranyl perchlorate, uranyl nitrate, and uranyl perchlorate--hydrochloric acid solutions in water--dimethyl sulfoxide--acetone mixtures, 25:26212
SCHUTZENDUBEL, W. G., Design details of boiler for 330 MW HTGR power station, 25:28631
SCHWARTZ, J. J., Shell-model structure of ^{209}Bi, 25:28417
SCHWARZ, H., Reliability factors affecting power plant mechanical equipment, 25:28549 (AECL-3670, pp 45-55)
SCHWARZ, K., Efficiency of x-ray luminescence and thermoluminescence of lithium fluoride crystals, 25:27838 (ANL-Trans-874)
SCHWEBEL, J. C., Illiac III Reference Manual. Vol. I, 25:28851 (COO-2118-5)
SCHWEICKERT, H., Measurement of the spin and nuclear magnetic moment of ^{20}Na, 25:28209 (CERN-70-30(Vol.1), pp 383-5)
SCIOCCHETTI, G., Measurement of β-active gases in the air, 25:26488
SCOPINARO, G., Scintiscanning with /sup 99m/Tc pertechnate perfusion, 25:26838
SCOTT, B. C., In-cloud scavenging analysis from cosmogenic radionuclide measurements, 25:26364 (CONF-700601-, pp 69-97)
SCOTT, J. H., 1000-MWe LMFBR accident analysis and safety system design study. Accident-initiating conditions. Part 1. Flow abnormalities. Topical report, 25:28731 (BAW-1350)
1000-MWe LMFBR accident analysis and safety system design study. Accident initiating conditions. Part 2. reactivity insertions, 25:28735 (BAW-1360)
1000-MWe LMFBR accident analysis and safety system design study, 25:28729 (BAW-1342)
SCOTT, W. D., Interactions of cloud condensation nuclei and ice nuclei with cloud and precipitation elements, 25:26362 (CONF-700601-, pp 37-48)
SCOTT, William A., Immunohematological studies of Marshall Islanders sixteen years after fallout radiation exposure, 25:27058
SCRUTCHFIELD, W., Effects of radiation pasteurization on Salmonella. II, 25:27164
SCUMPU, N., Effect of gamma-rays on some pea species, 25:27089
SEAGONDOLLAR, L. W., Aluminum-25 levels from the ^{24}Mg(p,γ)^{25}Al reaction, 25:28276
SEAGREN, R. D., Shipping-cask evaluation, 25:26452
SEBAOUN, E., Cyclic variation of volume of the heart, 25:26566 (CEA-CONF-1711)
SEBILLOTTE, P., Low energy boron implantation profiles in silicon from junction depth measurements, 25:27855
SEDLIAKOVA, M., Effect of 5-FU posttreatment of sensitivity to ultraviolet radiation and course of messenger RNA synthesis in E. coli, 25:27123
SEEGER, A., Intermediate state in type-II superconductors, 25:27657
SEEGER, P. A., Mass law with model-based shape-dependent shell terms, 25:28441 (CERN-70-30(Vol.1), pp 217-62)
SEEMANN, K. W., Neutron cross sections and strength functions of ^{147}Sm and ^{150}Sm, 25:28349 (KAPL-P-3930)
SEGALOFF, Albert, Synergism between radiation and estrogen in the production of mammary cancer in the rat, 25:27011
SEGGEWIES, H., Air handling plant of Obrigheim nuclear power station, 25:28545
SEGLER, Samuel Louis, Scattering of pions and protons from complex nuclei, 25:27959
SEIBEL, Hugo R., Electron microscopic changes following canine cardiac allografts: the effects of irradiation, 25:26677
SEIDEL, T. E., Isothermal annealing of boron implanted silicon, 25:27854
SEIDMAN, D. N., Prog. rpt. on defects in metal crystals, annual, 2/71, 25:27866 (NYO-3504-56)
SEITZ, H., A modified schiffer procedure for spectroscopic factors from analogue resonances, 25:28473
SEKIGUCHI, Akira, Design and performance of double emitter type self-powered neutron detectors, 25:26458
SEKSO, M., Some factors influencing uptake of ^{75}Se-selenomethionine by pancreatic tissues of the rat, 25:26591
SELIN, E., Nuclear structure of ^{23}Ne and ^{21}Ne, 25:28257
Rotational states in ^{168}Yb, ^{169}Yb, and ^{170}Yb, 25:28394
SELPH, Frank B., Planning for superhilac timeshare operation with both heavy and light ion beams, 25:28122 (UCRL-20633)
SEMAGIN, V. N., Importance of the conditioned reflex method in neuroradiology, 25:26949
SEMONIN, R. G., Collection efficiencies of raindrops for submicron particulates, 25:26369 (CONF-700601-, pp 151-60)
SEMOV, M. P., Flame-spectrophotometric determination of microquantities of Li, Rb, Cs, and Sr in water, 25:26176
SEN, S., Researches on ceramic materials in india, 25:27281 (INIS-mf-13)
SEO, Takeshi, Magnetic moments of three excited states in ^{149}Pm, 25:28381
SEREBRENNIKOV, Yu. M., Fast response control of reactor power on basis of γ radiation intensity, 25:28822
SEREBRYAKOV, S. G., Convergence of infinite series of nonrelativistic contributions for (n--d) scattering amplitude, 25:28166
SEREBRYAKOV, V. V., Sum rules for πn-scattering, 25:28024 (NP-18766)
SERGEEV, Yu. A., Optimization of parameters for small nuclear power sources containing water-cooled, water-moderated reactors, 25:28640
SESSLER, A. M., Diffraction radiation by a line charge moving past a comb, 25:28483
SEUNG, H. C., Lactic dehydrogenase level of rats exposed to γ irradiation, 25:26803
SEXL, R. U., Lorentz-covariant Lagrangians and causality, 25:28068
SEXTRO, R. G., Isospin purity and delayed-proton decay: ^{17}Ne and ^{33}Ar, 25:28195
SEYDEWITZ, H. H., Substituent effect on ir intensities of CH stretching vibrations of benzene derivatives, 25:26247
SEYFFERTH, L., Medium-power boiling-water reactors for developing countries, 25:28715
SEYMOUR, A. E., Radiation enterocolitis, 25:26811
SHA, W. T., SAS1A: a computer code for the analysis of fast-reactor power and flow transients, 25:28727 (ANL-7607)
VENUS: a two-dimensional coupled neutronics-hydrodynamics computer program for fast-reactor power excursions, 25:28728 (ANL-7701)
SHABALIN, E., IBR: fast pulsed reactor, 25:28760 (JPRS-52907)
SHAEFFER, James, Chromosomal rejoining in absence of unscheduled DNA synthesis, 25:26724
SHAEFFER, James Dennis, X-ray-induced unscheduled DNA synthesis in mammalian cells, 25:27002
SHAFFER, J. C., Magnetic properties of the system Au_4R(R = Er, Tm, and Yb), 25:27872
SHAFFER, R. M., Wide latitude processing of Tri-X-Ortho oscillographic film, 25:28854 (EGG-1183-1465)
SHAH, Dinesh O., Lipid-metal ion interaction in monomolecular films, 25:26213
SHAH, Vasant L., Spectrophotometric determination of Pr, Nd, Sm, and Eu using chromotrope 2 R as a chromogenic reagent, 25:26165
SHAIKH, M. Rafi, Long-chain mutants of Streptococcus faecalis induced by ultraviolet irradiation, 25:26731
SHAKED, H., Utilization of research reactors in Israel, 25:28780
SHAKIN, C. M., Microscopic calculation for the escape width of analog states, 25:28466
The role of the anti-analog state in the decay of the analog state, 25:28467
SHALAK, N. I., Determination of specific release of radon by protective enclosures in premises, 25:26356
SHAMALY, A., First-order wave equation for integral spin, 25:27975
SHAMRAY, A. E., Respiration and oxidative phosphorylation

of bone marrow tissue of irradiated rabbits after homotransplantation of bone marrow elements, 25:27019
SHANU, R. E., Large isospin mixing in ^{16}O states near 18 MeV, 25:28188
SHAND, W. A., Ion-implantation doping of zinc sulphide thin films, 25:27844
SHAPIRO, Bernard, Mechanism of action of radiation protective agents: in vivo distribution and metabolism of cysteamine-S-phosphate (MEAP), 25:26805
Protection of DNA against ionizing radiation, 25:26801
SHAPIRO, I. S., Possible quasinuclear nature of heavy mesonic resonances, 25:28026 (NP-18774)
SHAPKINA, Yu. S., Flame-spectrophotometric determination of microquantities of Li, Rb, Cs, and Sr in water, 25:26176
SHARIPOV, Sh., Theory of excited states of deformed even--even nuclei, 25:28501
SHARMA, B. D., Irradiation effects on reactor structural materials, 25:27265 (INIS-mf-5)
SHARMA, R. P., Combined effect of physical and chemical mutagens on mutation frequency in Aspergillus nidulans, 25:26717
Increased mutation frequency and wider mutation spectrum in barley induced by combining gamma-rays with ethyl methane sulphonate, 25:26716
SHARMA, U., Supervoltage radiation response in epidermoid carcinoma of the esophagus, 25:26896
SHAROV, A. S., Structure of Galaxy and visible picture of the Milky Way, 25:27411
SHARP, G. W., Ogo 5 measurements of the plasmasphere during observations of stable auroral red arcs, 25:27622
SHARP, John D., Interruption of DNA injection by x-irradiation of phage lambda, 25:26693
Lack of polarity of DNA injection by Escherichia coli phage lambda, 25:26692
SHASHURIN, I. P., Electron-beam relaxation in a plasma, 25:27700
SHAW, J. L., Microanalysis with a proton-probe, 25:26158
SHAW, M. L., X-ray observations between 1 and 55 A of the Feb. 25th flare, 25:27357
SHAW, Michael Kevin, Gas cooled nuclear reactors, 25:28831
SHCHEGLOVSKI, Z., New isotopes of iridium, 25:28348 (JINR-P6-5617)
SHCHELUKHIN, E. M., Distribution of electric field in conducting cylinder with electrodes of finite size, 25:27492
SHCHEPETNOV, R. V., Variations of solar-wind fluxes, 25:27535
SHCHERBIN, V. N., Elastic proton scattering on medium-A nuclei, 25:28262
Reactions (d,p) of Ti and Cr isotopes, 25:28269
SHCHETKIN, I. S., Investigation of the superconducting state of niobium--titanium solid solutions, 25:27646
SHCHINOV, B. G., Non-linear regime of radiation instability development of relativistic electron rings, 25:28110 (JINR-P9-5622)
SHCHUKIN, A. A., Weldability of certain Mo alloys, 25:27185
SHEA, M. A., Proposed solar proton event classification system, 25:27356
Solar proton event classification system, 25:27388
SHELINE, Raymond K., Neutron--proton interaction in odd--odd deformed nuclei, 25:28514
Nuclear levels in ^{177}Lu and ^{175}Lu, 25:28424
SHEN, Jacob, Electrophilic reactions at single bonds. III, 25:26226
SHENNAN, John Vincent, Improvements in or relating to nuclear reactor fuel elements, 25:28837
SHENOY, G. K., Magnetic behavior of conducting Am systems, 25:27922
SHEPARD, J. S., Stage sensitivity and dose response in human leukocytes, 25:26628
SHERIDAN, W. F., Excitation of nitrogen by fast protons and electrons, 25:27616
SHERIEF, M. K., Spectrophotometric studies on plutonium(IV) complexes in aqueous and mixed organic--nitric acid systems, 25:26274
SHERWOOD, R. C., Cast permanent magnets of Co_5RE type with mixtures of Ce and Sm, 25:27883
SHESLER, Albert T., Reactor protection system diversity, 25:28697 (CENPD-11)
SHEVCHENKO, V. G., Photoneutron reactions on copper, 25:28260
Universal magnetic spectrometer with 0.15 percent resolving power at maximum pulse of 60 GeV/c, 25:26507 (NP-18764)
SHIBATA, Toshikazu, Age of fission neutrons to indium resonance in water and polyethylene, 25:28157
Measurements of average cross sections for some threshold reactions for neutrons with fission-type reactor spectrum, 25:28273
SHIBUYA, N., Location and size of a solar hard x-ray burst on Sept. 27, 1969, 25:27384
SHIBUYA, Seiji, Determination of microamounts of Ag in Cu, Al, and their alloys by solvent extraction--atomic absorption spectrophotometry, 25:26169
SHIDA, Y., On- and off-beam gamma spectroscopy on neutron deficient isotopes of Ge, Se, Br, and Kr, 25:28213 (CERN-70-30(Vol.2), pp 911-15)
SHIGEMATSU, Tsunenobu, Absorption behavior of radionuclides, mainly rare earth elements, in seawater, 25:26339
SHIHABI, Zakariya Kamel, Effects of ionizing radiations on albumin biosynthesis and cell permeability, 25:27007
SHIJO, Yoshio, Spectrophotometric determination of Be and Ga with chromazurol S and certyltrimethylammonium chloride, 25:26172
SHIKHLYAROV, K. K., Detection of x-ray transition radiation by means of a streamer chamber, 25:26515
SHIKHOV, S. B., Role of energy dependence in problems of transport theory, 25:28159
SHIKITA, Mikio, Gradual development of radioprotection in HeLa S_3 cells during treatment with β-mercaptoethylguanidine, 25:26797
SHIMA, Kiyoshi, Radiation, infection, and macrophage function. IV. Effect of radiation on the proliferative abilities of mononuclear phagocytes in tuberculous lesions of rabbits, 25:27001
SHIMIZU, Ryuichi, Calculation of x-ray production in alloy targets using Monte Carlo method, 25:27836
SHIRAIWA, T., Electron probe microanalysis of Ti(C,N) and Zr(C,N) in steel, 25:26160
SHIRVAITIS, A. I., Radiation dosimeter with semiconductor detectors, 25:26529
SHODA, K., Isobaric analog states in (γ,p) reactions on N = 50 nuclei, 25:28227
Isobaric analog states in (γ,p) reactions on Sn isotopes, 25:28361
Isobaric analog states in (γ,p) reactions on N = 82 nuclei, 25:28362
SHOEMAKER, Clara B., Structural properties of some sigma-phase related phases, 25:27262
SHOEMAKER, David P., Structural properties of some sigma-phase related phases, 25:27262
SHOR, Roberta, ^{90}Sr heat sources, 25:26432
SHORE, Moris L., Proliferative and phagocytic capacity of the reticuloendothelial system of sublethally irradiated mice, 25:26947
SHORT, R. D., Non perturbative parton model of current interactions, 25:28015
SHOUP, R., Spreading of the antianalogue states in ^{91}Nb, 25:28363
SHRAGER, P., On-line high energy physics analysis with a PDP-9, 25:28135
SHRESTHA, K. L., Sporadic-e and atmospheric pressure waves, 25:27524
SHUKHMAN, V. A., Motion of vortexes in superconductors of the second kind, 25:27650
SHUKLA, P. K., Propagation of an electromagnetic pulse through inhomogeneous plasma, 25:27801
SHULTS, Gary W., Process for inactivating enzymes in meat to be stabilized by radiation, 25:27163
SHURTLEFF, W. W., Computerized ultrasonic data acquisition system, 25:28884 (SC-DR-70-680)
SIBBEL, R., Faddeev's equations in the SU(3) representation of a three-particle state, 25:28056
SIDOROV, V. A., Evidence for electron-positron pair electroproduction, 25:27994
SIDWELL, Ronald Arden, Pi^+-p backward elastic scattering from 2.18 to 5.25 GeV/c, 25:27965
SIEBOLD, P., Photographic method for determining velocity distributions within thermal plumes, 25:28839 (ANL/ES-4)
SIEGEL, Benjamin V., Radiation sensitivity of New Zealand black mice and the development of autoimmune disease and neoplasia, 25:26952
SIEGEL, Stan, Is the effective charge correction larger for a neutron than for a proton, 25:28456
SIEGEL, Stanley Gordon, Effective operators in nuclei, 25:28189
SIEVERS, Robert E., Method of separating the rare earths by fractional co-distillation of their volatile chelate derivatives, 25:26336
SIFFERT, P., Low energy boron implantation profiles in silicon from junction depth measurements, 25:27855
SIGMAR, D. J., Stability of microwave-heated plasmas, 25:27743
SIGURBJOERNSSON, Bjoern, Induced mutations in plants, 25:26697
SIGURD, D., Chemical transport of silicon and germanium during anneal treatment, 25:27909
SIJS, Arnold, Dynamic tests on tangential pipe fittings. I, 25:28871 (ORNL-tr-1991)
SILENOK-BEL'SKII, G. A., Plasma motion across inhomogeneous magnetic field, 25:27720
SILL, L. R., Magnetic properties of the system Au_4R(R = Er, Tm, and Yb), 25:27872
SIMENOG, I. V., Energy levels of three-particle system, 25:28163 (ITF-70-100-P)
SIMMS, P. C., Beta--gamma circular polarization correlation and nuclear matrix elements of ^{76}As, 25:28216 (COO-1746-54)
SIMOES, J. Henriques, Organoleptic chemical and microbiological aspects of irradiated Portuguese sausages, 25:27159
SIMON, Barry Martin, Quantum mechanics for Hamiltonians defined as quadratic forms, 25:27940
SIMON, M., Radiation doses at the altitude of supersonic transport flights, 25:26750 (ORNL-tr-2455)
SIMONEN, T. C., Feedback stabilization of the transverse Kelvin--Helmholtz instability, 25:27772
Remote feedback stabilization of drift instability by microwaves, 25:27766

XUM

SIMONEN, Thomas C., Feedback applications to basic plasma instability experiments, 25:27769
SIMONS, Daniel J., Automated primary productivity measurements in water bodies, 25:28867 (NYO-3993-1)
SIMONYAN, N. V., Growth patterns of uv-irradiated E. coli B in saline, 25:27119
SIMPSON, Erik E., Evolutionary models of stars of 15 and 30 M solar mass, 25:27316
SIMS, J. S., Ionosphere of Mars below 80 km altitude. I, 25:27431
SINCHESKUL, B. F., Influence of, and allowance for, background in photographic photometry, 25:27341
SINCHESKUL, V. N., Influence of, and allowance for, background in photographic photometry, 25:27341
SINCLAIR, Warren K., Relation of protein synthesis to radiation-induced division delay in Chinese hamster cells, 25:26626
SINGER, Sidney, Association of energetic storm particles with interplanetary shock waves, 25:27571
Interaction of solar energertic particles with the Earth's bow shock and magnetopause, 25:27538
SINGH, B., Effects of γ radiation on Penicillium expansum. I, 25:27084
Tabulation of gamma--gamma directional-correlation coefficients, 25:28401
SINGH, H. P., Calorimetric investigation of long-range ordering in the cadmium--mercury system, 25:27248
SINGH, K. P., Propagation of an electromagnetic pulse through inhomogeneous plasma, 25:27801
SINGH, Kunwar Suresh, Effect of irradiation on larvae of nematode, 25:26909
SINGH, M., Decay of ^{110}Sb, ^{111}Sb, ^{112}Sb, ^{113}Sb, and ^{114}Sb, 25:28332 (CERN-70-30(Vol.2), pp 1015-21)
SINGH, Mohanjit, L-shell photoelectric cross-sections for low energy gamma-rays in lead, 25:27830
SINGH, R. N., Propagation of an electromagnetic pulse through inhomogeneous plasma, 25:27801
SINKEVICH, O. A., Motion of a plasma cluster in a channel with variable inductance, 25:27485
SIPOS, L., Redox processes of U(VI), (V), (IV), and (III) in acetate buffers, 25:26265
SIROTA, N. N., Process of reaction diffusion of silicon into niobium, 25:27239
SIRUGUE, M., Constraints imposed upon a state of a system that satisfies the K.M.S. boundary condition, 25:27925 (CNRS-CPT-70-P-325)
SISTEMICH, K., Identification of μ s isomers among primary fission fragments, 25:28325 (CERN-70-30(Vol.2), pp 967-84)
SIVARAMAKRISHAN, K. S., Irradiation effects on reactor structural materials, 25:27265 (INIS-mf-5)
SIVUKHIN, D. V., Duration of charged particles containment in a trap with magnetic mirror, 25:27669 (IAE-1972)
SJOEBERG, N.-O., Content of noradrenaline and 5-hydroxytryptamine in rat after ionizing radiation, 25:26959
SKIBOWSKI, M., Optical absorption of gaseous methane, ethane, propane, and butane, and reflection of solid methane and ethane in the vacuum ultraviolet, 25:28853 (DESY-SR-71/1)
SKILES, Durward D., Energy flux in incompressible magnetohydrodynamic plane waves, 25:27487
SKOBOV, V. G., Dopplerons in cadmium, 25:27900
SKOGMO, David G., Generalized integrated circuit, 25:28886 (SC-DR-710033)
SKOLKA, H., Radioactivity of seston and waters of Black Sea and alga (Cystoseria barbata) from Rumanian continental shelf during 1964--1967, 25:26745
SKOVLI, G., Observations of electrons in Aurorae satellite, 25:27580
SKOVLI, Gunnar, Auroral particles and ground observations during the Feb. 25th solar event, 25:27572
SLATER, James M., Ureteral strictures after radiation therapy for carcinoma of the uterine cervix, 25:27052
SLATKIN, D. N., Extracorporeal irradiation of blood by beta-emitting isotopes: principles of dose calculations, 25:26754
SLAUGHTER, Barbara G., Disc-based operating system for mass spectrometry experiments, 25:26556
SLEBOCKA, H., Influence of LET on radical yields in frozen aliphatic alcohols, 25:26311
SLETTEN, A., Auroral-zone x-ray events and their relation to polar magnetic substorms, 25:27593
SLEZARIKOVA, V., Effect of 5-FU posttreatment of sensitivity to ultraviolet radiation and course of messenger RNA synthesis in E. coli, 25:27123
SLINN, W. G. N., Phoretic processes in scavenging, 25:26387 (CONF-700601-, pp 411-22)
SLOUKA, V., Linkage of radiocerium to blood serum proteins studied by dialysis techniques, 25:26584
SMALL, Gary D., Partial purification of photoreactivating enzyme from Euglena gracilis, 25:26619 (COO-1793-6)
SMALL, L. F., Distribution of ingested ^{65}Zn in marine crustaceans, 25:26604
SMART, D. F., Proposed solar proton event classification system, 25:27356
Solar proton event classification system, 25:27388
SMIDT, F. A. Jr., Fracture mechanisms and radiation effects, 25:27270
SMIRNOV, B. M., Charge exchange between negative and positive ions, 25:27455
Exchange interaction of multi-electron atoms, 25:27444
Ionization constant of the Penning process, 25:27457
SMIRNOV, M. N., Recovery of yeast after irradiation and protein synthesis, 25:27096
Role of high energy compounds in the processes of postirradiation recovery of yeast, 25:27095
SMIRNOV, O. N., Determining portion of fission attributable to epithermal neutrons, 25:28817
SMITANANDA, Nitaya, Iron-59 distribution in normal and x-irradiated mice, 25:27012
SMITH, C. L., Distribution of some chemical elements between dissolved and particulate phases in the ocean, 25:26190 (NYO-4150-9)
SMITH, D. F., Weak-turbulence analysis of the two-stream instability, 25:27740
SMITH, H., Angular structure of quasar 3C 147, 25:27351
SMITH, H. A., Beta--gamma circular polarization correlation and nuclear matrix elements of ^{76}As, 25:28216 (COO-1746-54)
SMITH, J. L., Explosive instabilities in simulated plasmas, 25:27736
SMITH, M. E. Jr., Use of natural radioactivities to estimate large-scale precipitation scavenging, 25:26390 (CONF-700601-, pp 465-74)
SMITH, Margaret M., Expanded FORTRAN 4 program for elastic scattering analyses, 25:28450 (N-70-42846)
SMITH, P. A., Observations of 45 to 450 keV electrons during the period Feb. 24--Mar. 3, 1969, 25:27568
SMITH, Richard J., Engineering materials list, 25:26414 (TID-4100(Suppl.62))
SMITH, Sheila Maynard, Kornberg polymerase and the repair of irradiated T4 bacteriophage, 25:27105
SNAPE, G., On-line high energy physics analysis with a PDP-9, 25:28135
SNELL, A. H., Deep inelastic collisions and Auger processes, 25:27437 (WASH-1159, pp 113-19)
SNELLING, J. B., Circuit for measuring frequency dependent complex admittance and impedance, 25:28882 (SC-DR-68-796)
SNIPES, Wallace, Free radicals in pyrimidines: ESR of a γ-irradiated single crystal of 5-nitrouracil, 25:26296
SNYDER, W. S., Estimation of dose to gonads from gamma emitters present in the body, 25:26760
SOBOLEV, V. I., Normal component density of ^{3}He--^{4}He solution at temperatures down to 0.4°K, 25:27639
SODICOFF, Marvin, Colony-forming units in rat parabionts, 25:26939
SOERAAS, F., Low-energy solar protons during the Feb. 25, 1969 event, 25:27573
Proton precipitation in noon--midnight meridian, 25:27579
SOFER, D. H., Radium and radon dosimetry, 25:26769
SOKOL, Daniel, Ground water safety evaluation. Project Gasbuggy, 25:26406 (PNE-1009)
SOKOLOV, I. N., Standardized line of pressure-vessel type boiling-water reactors, 25:28716
SOKOLOV, S. N., Process of reaction diffusion of silicon into niobium, 25:27239
SOKOLOVA, I. G., Phase equilibria in the system vanadium--tantalum--hafnium, 25:27247
SOKOLOVSKAYA, E. M., Phase equilibria in the system vanadium--tantalum--hafnium, 25:27247
SOLIANI, G., Vacuum polarization tensor and equal-time commutators in quantum electrodynamics, 25:28074
SOLODOVCHENKO, S. I., Plasma motion across inhomogeneous magnetic field, 25:27720
SOLOMATINA, E. K, Variations of solar-wind fluxes, 25:27535
SOLOMON, A. I., Group theory of superfluidity, 25:27641
SOLOV'EV, S. P., X-ray- and neutron-diffraction study of ordering in some alloys of the titanium--zirconium--oxygen system, 25:27297
SOLOV'EV, V. G., Nonrotational states of odd-N deformed nuclei in region 153 less than or equal to A less than or equal to 171, 25:28346 (JINR-E4-5567)
SOLOV'EV, Yu. A., Operational experience with VK-50 reactor facility, 25:28579
SON, U. T., Measurements of atomic order with the field-ion microscope, 25:27252
SONDHEIMER, James H., Discrete formulation and error minimization in applying the integro-differential equation approach to mono-compartment data, 25:26580
SONNABEND, E., Testing of dental Roentgen apparatuses to their radiation safety, 25:26772
SONNICHSEN, J. C. Jr., TOPLYR: two-dimensional thermal energy transport code, 25:28856 (HEDL-TME-71-39)
SOOD, B. S., L-shell photoelectric cross-sections for low energy gamma-rays in lead, 25:27830
SOOD, S. K., Scavenging by snow and ice crystals, 25:26367 (CONF-700601-, pp 121-36)
SORENSEN, R. A., Theoretical considerations on nuclei far from stability, 25:28289 (CERN-70-30(Vol.1), pp 1-19)
SOROKIN, A. A., Decay of ^{97}Zr, 25:28438
Decay of neutron defficient isotopes of Pt, Ir, and Os, 25:28389
SOROKIN, A. I., Proton scattering on ^{24}Mg, ^{25}Mg, and ^{26}Mg, 25:28264
SOUFFRIN, Suzy, Abundances and reddening of nuclei of Seyfert galaxies, 25:27418
SPALDING, J. F., Genetic effect on radiation sensitivity consistent with a single gene locus hypothesis, 25:26690

SPALEX, G. C., Gas target source for neutron radiation therapy, 25:26883
SPALTHOFF, W., Nuclear magnetic resonance studies of metal hydrides, 25:26261 (ORNL-tr-2439)
SPANGLER, Glenn Edward, Interaction of electrons with vorticity in heat-flushed He II, 25:27638
SPAVENTI, S., Some factors influencing uptake of ^{75}Se-selenomethionine by pancreatic tissues of the rat, 25:26591
SPEAR, R. H., Search for high-spin states in ^{27}Al, 25:28208 (ANU-P-521)
SPECHT, G., Electroproduction of single π^+ mesons on hydrogen, 25:27950 (DESY-71/9)
SPECKER, Steven Robert, Applications of optimal control theory to space--time reactor kinetics, 25:28813
SPEJEWSKI, E. H., Levels in ^{194}Pt, ^{196}Pt, and ^{198}Pt, 25:28425
SPENCER, Derek W., Distribution of some chemical elements between dissolved and particulate phases in the ocean, 25:26190 (NYO-4150-9)
SPENCER, J. E., Analysis of elastic and inelastic analogue-state resonances using coupled optical equations, 25:28236
SPERANZA, Maurizio, Reactions of helium tritide ions with gaseous hydrocarbons. V. cis- and trans-1,2-dimethylcyclopropane. Unambiguous evidence for gaseous protonated cyclopropanes, 25:26321
SPERBER, D., Isomer ratio for (b,xn,yp,γ) reactions, 25:28502
SPERBER, Gunnar, Analysis of reduced density matrices in coordinate representation. I, 25:27466
Analysis of reduced density matrices in coordinate representation. II, 25:27467
SPICER, B. M., Cross section of ^{28}Mg(tau,γ)^{28}Si reaction, 25:28206 (ANU-P-508)
SPILLING, P., Reaction ^{86}Sr(tau,α)^{88}Sr at E/sub tau/ = 17.5 MeV, 25:28277
SPINRAD, Hyron, Stellar content of the nuclei of nearby galaxies. I, 25:27409
SREENIVASAN, A., Effect of gamma irradiation on post-harvest physiology of fruits, 25:27140
Effect of gamma irradiation on postharvest physiology of five banana varieties grown in India, 25:27165
Effect of gamma radiation on wheat starch and its components, 25:26621
Susceptibility to amylolysis of gamma-irradiated wheat, 25:26622
SREE RAMULU, K., Comparison of mutation induction in diploid and tetraploid rice, 25:26714
SREE RANGASAMY, S. R., Comparison of mutation induction in diploid and tetraploid rice, 25:26714
SRINIVASAN, T. K. K., Infrared spectroscopic study of the photolytic decomposition of methyl azidoformate, 25:26236
SRIVASTAVA, B. S., Ultra-violet induced mutations to growth factor requirement and penicillin resistance in a blue-green alga, 25:26712
SRIVASTAVA, Y., Argand-diagram analysis of Pomeron coupling to KN and anti KN system, 25:28035
STADELMAIER, H. H., Metal-rich metal-metalloid phases, 25:27304
STADLER, David R., Intragenic recombination of ascospore color mutants in Ascobolus and its relationship to the segregation of outside markers, 25:26695
STADSNES, J., Auroral-zone x-ray events and their relation to polar magnetic substorms, 25:27593
STAGAT, R. W., Semiempirical generalized one-boson-exchange potentials, 25:28513
STAHL, D., Analytical model for describing the frequency response and stability behavior of light-water moderator pressurized power reactors, 25:28665
STAMM, H., Blood of patients with gynecologic cancer following irradiated Streptokinase-Streptodornase, 25:26632
Effect of ionizing irradiation on blood coagulation factor activity, 25:26900
STAMPA, L., Nuclear fuel characterization, 25:27293 (RT/ING-(70)21)
STANLEY, James P., Reactions of the hydrogen atom in solution. IV. Photolysis of deuterated thiols, 25:26252
STANNETT, V., Transport of fixed gases in radiation-stabilized poly(vinyl chloride), 25:26280
STARKOV, G. V., Auroral oval planetary energetics, 25:27523
STAUNING, Peter, Auroral particles and ground observations during the Feb. 25th solar event, 25:27572
STEFAN, Horia, Calculation of temperature effects on reactor neutron spectra, 25:28814
STEFANICKA-WIECHOWA, Alina, Radiomimetic effect of actinomycin C on tumors of glial origin, 25:26908
STEFANOVIC, J., Protease activity changes in rabbit lung macrophages, spleen cells, and polymorphonuclear leucocytes after whole-body x-irradiation, 25:27035
STEFFE, Dirl H., Concentration variation of some trace metals in precipitation from great plains thunderstorms, 25:26366 (CONF-700601-, pp 109-20)
STEFUNKOVA, E., Effect of 5-FU posttreatment of sensitivity to ultraviolet radiation and course of messenger RNA synthesis in E. coli, 25:27123
STEIGMAN, G., Neutrino limits on antimatter sources of energy in Seyfert galaxies, 25:27417
STEIN, Nelson, Results and interpretation of analog resonance experiments, 25:28470
STEIN, Robert F., Reflection, refraction, and coupling of MHD waves, 25:27392
STEIN, S., Preparation and properties of six rat red cell hemoglobins, 25:28866 (NYO-3976-5)
STEINBERG, M. S., Charge invariance and electron mass from the ultimate speed experiment, 25:27988
STEINBERG, P. H., Polarization parameter K$^+$p elastic scattering GeV/c, 25:27963
STEINER, L. F., Estimating the size of populations of sterile pest tephritidae in release programs, 25:27156
Estimating the size of populations of codling moths, 25:27155
Mediterranean fruit fly research in Hawaii, 25:27157
STELTS, Marion L., Search for an imaginary isovector interaction in the optical model potential in ^{3}He induced reactions, 25:28461
STELZER, F., Cold neutron source in Juelich, 25:28767
STEMPIN'SKI, M., Alpha decay of resonance states of ^{146}Sm, 25:28347 (JINR-P3-5553)
STENERSON, R. O., Multiple muons deep underground, 25:27954
STENFLO, Lennart, Effect of dissipation on nonlinear coupling phenomena, 25:27815
STENSGAARD, I., Spatial distribution of defects in ion bombarded silicon and germanium, 25:27861
STEPANOV, A. M., Design and calculation of ITEP 2-meter liquid-hydrogen bubble chamber, 25:26508 (NP-18787)
STEPHENS, D. R., Electrical resistance of ytterbium as a function of temperature and pressure, 25:27867 (UCRL-51006)
STEPHENS, Joseph R., Alloy softening in group VIA metals alloyed with Re, 25:27209 (N-71-11662)
STEPHENS, Ralph Edmund, X-ray-induced prophase reversion in neuroblasts of Chorotophaga viridifasciata, 25:26911
STEPHENS, S. A., Analysis of the low frequency radio continuum in the galaxy, 25:27419
STEPHENSON, J., Estimation of the dose to skin from radioactive particulate contamination of clothing, 25:26748
STERN, R. A., Electron--ion collision effects on parametric instability, 25:27782
STERNBERG, Joseph, Irradiation and radiocontamination during pregnancy, 25:27040
STEVENS, D. C., Estimation of the dose to skin from radioactive particulate contamination of clothing, 25:26748
STEVENS, G., Multiple pulse radiolysis: successive accumulation of two hydrated electrons in oxygen, nitrobenzene, and nitromethane, 25:26308
STEVENS, G. A., Rocket observations of protons and α-particles, 25:27563
STEVENSON, M. G., 1000-MWe LMFBR accident analysis and safety system design study, 25:28729 (BAW-1342)
STEWART, James A., Influence of translational entropy of activation on reaction rates in isotopic solvents, 25:26227
STEWART, K. B., Rail accident statistics pertinent to the shipment of radioactive materials, 25:26447 (HW-76299)
STEWART, K. W. C., Coupling of quasiparticles and anharmonic vibrations: A = 33 and 34, 25:28249
Projected Hartree--Fock and core-particle coupling for A = 29 and 30, 25:28280
STEYAERT, J., External heavy ion source for Berkeley 88-inch cyclotron, 25:28120 (UCRL-20406)
STILES, Lynn F. Jr., Effect of electric field and temperature on radiative lifetime of F center, 25:27841 (NYO-3463-23)
STILLER, H., Cold neutron source in Juelich, 25:28767
STOCK, E., Koebner phenomenon-like manifestation of a retothel sarcoma of the skin following x-ray treatment, 25:26875
STOCKMAN, Godfried, Dynamic tests on tangential pipe fittings. I, 25:28871 (ORNL-tr-1991)
STOCKTON, J. R., EDITOR: processing code for ENDF/B format data, 25:28148 (ORNL-TM-3266)
STODDARD, D. H., Californium-252 shielding guide, 25:27828 (DP-1246)
STOJANOVIC, Dragoslav, Effect of total body gamma irradiation on the percutaneous absorption of radiocesium, 25:26595
STORK, D. H., Reaction K-P $\rightarrow$ AK$^+$K$^-$ and the generalized Veneziano model, 25:28042
STORRER, J., Belgonucleaire and Siemens PWRs for small and medium power reactors, 25:28717
STRAKER, E. A., Application of DOT--MORSE coupling to the analysis of three-dimensional SNAP shielding problems, 25:28784 (ORNL-TM-3365)
STRANGE, John Ruble, Dose-rate effects in the prenatally irradiated rat, 25:26951
STRAUSS, Harry W., Changes in liver and spleen scans of patients during treatment with two hypolipidemic drugs, 25:25830
STRAUSZ, R., Levels in ^{5}He excited in the elastic d--^{3}H scattering, 25:28168
STRICKLAND, P., Radioinduced fibrosarcoma, 25:27044
STRITTMATTER, P. A., Neutrino limits on antimatter sources of energy in Seyfert galaxies, 25:27417
STRNAT, K. J., Utility of (Pr,Nd)Co$_5$ alloy for permanent magnets, 25:27886

XUM

STROBEL, Darrell F., Diurnal variation of nitric oxide in the upper atmosphere, 25:27614
STROJNY, E. J., Oxidation of 2-methoxyethanol to methoxyacetic acid by nitric acid solutions, 25:26223
STRONGIN, M., Leed studies of Ar crystals on Nb (100) surface, 25:27235
STROUD, A. N., Induction of chromosomal aberrations in pig kidney cells by far-red light, 25:26727
STRUB, Rene, Gas turbine and nuclear reactor plants, 25:28647
STRUMINSKA, Jadwiga, Prolonged exposure to ionizing radiation in boy with aplastic anaemia, 25:27054
STRUVEN, Warren C., Control and monitoring of the SLAC Accelerator utilizing a PDP-9 system, 25:28134
STUEGER, R., Heavy-water-cooled and-moderated boiling-water reactor, 25:28645
STUTIUS, W., Crystal-field splitting and spin waves in antiferromagnetic CeSb, 25:27881
STUTZ, E., Radiation (^{90}Sr) induced pulmonary carcinoma in rats, 25:26921 (LF-tr-49)
SUBBA RAO, M., Determination of ruthenium in fallout samples, 25:26181
SUD, S. P., Decay of ^{134}Cs, 25:28405
SUDA, S. C., Difficulties and approaches in the development of inventory control for nuclear material safeguards, 25:26444 (BNL-15601)
SUDAN, R. N., Existence of shock-like solutions of Korteweg--De Vries equation, 25:27818
SUEHIRO, Teruo, Reaction (p,t) on even--even deformed nuclei, 25:28411
SUEMITSU, H., Analysis of Kantor amplitudes and recent low-energy proton--proton scattering experiments, 25:28046
SUGAHARA, T., Comparative studies on rejoining of DNA-strand breaks, 25:26953
Survival of lethally-irradiated mice, 25:26934
SUGAWARA, M., Isobaric analog states in (γ,p) reactions on N = 50 nuclei, 25:28227
Isobaric analog states in (γ,p) reactions on Sn isotopes, 25:28361
Isobaric analog states in (γ,p) reactions on N = 82 nuclei, 25:28362
SUGII, Atsushi, Comparative study on Zr oxide for preparation of /sup 113m/In generator, 25:26341
SUGIMOTO, Kenzo, Quadrupole effects in NMR spectra on ^{12}B and ^{12}N, 25:27923
SUGIYAMA, Kazusuke, Decay of 14-min ^{112}In, 25:28406
SUGIYAMA, Yasuharu, Reaction (p,t) on even--even deformed nuclei, 25:28411
SUITS, J. C., Annealing study of EuO films doped with Fe Eu, 25:27898
SUKHAREVSKII, B. Ya., Investigation of the superconducting state of niobium--titanium solid solutions, 25:27646
SULEK, P., Apochromatic method for measurement of mean proton energy in 657 MeV beam, 25:26506 (JINR-P13-5637)
Monochromatic method for measurement of mean proton energy in 665 MeV beam, 25:26505 (JINR-P13-5636)
SUMMERS, Peter W., Scavenging of SO_2 by convective storms, 25:26379 (CONF-700601-, pp 305-18)
SUMMERS, Robert W., Effects of altered propulsion on rat small intestinal flora, 25:26975
SUN, C., Production of strand breaks in mammalian DNA by x-rays: at different stages in the cell cycle, 25:26625
SUNIER, J. W., Decay of ^{110}Sb, ^{111}Sb, ^{112}Sb, ^{113}Sb, and ^{114}Sb, 25:28332 (CERN-70-30(Vol.2), pp 1015-21)
SUN-TSZIN-YAN, G. Ya., Investigation of α decay of isotopes of element 105, 25:28350 (KFK-tr-350)
SUSANNA, A., Estimate of the dose of ionogenic radiations absorbed by airport personnel carrying out the ground operations connected with the transport of packages containing radioactive materials, 25:26770
SUSHKO, V. N., Global and local structure of relativistic quantum systems, 25:27931 (JINR-E2-5575)
SUSLOV, Yu. P., New values for Kβ branching coefficients, 25:28494
Relativistic evaluation of electron capture exchange effect, 25:28495
SUSSKIND, L., Parton theory based on the dual resonance model, 25:28002
SUTTON, D., Crystal and molecular structure and vibrational spectrum of the vanadium(V) oxide trinitrate--acetonitrile complex, $VO(NO_3)_3.CH_3CN$, 25:26235
SUZUKI, David T., Detection of putative deletions in proximal heterochromatin of Drosophila, 25:26720
SUZUKI, Hisashi, Two-phase region in TiC--Mo--30 percent Ni alloys, 25:27298
SUZUKI, Komei, Evaluation of integrity for fast neutron irradiation embrittlement of JPDR pressure vessel, 25:28682 (JAERI-1202)
SUZUKI, Kunio, Determination of pore distributions in tungsten and tungsten carbide powders by mercury-porosimeter, 25:27218
SUZUKI, Masashi, Thorium, its toxicity and the counter-measure for safety, 25:26603
SUZUKI, Nobuo, Solubility of TTA--uranyl chelate, 25:26340
SVATOS, J., Polarization of μ Cephei and graphite core--ice mantle grains, 25:27408
SVEDMYR, Erik, Evidence for thymic dependence of PHA-reactive cells in spleen and lymph nodes and independence in bone marrow, 25:26673
SVESTKA, Zdenek, Particle event forecasting, 25:27355
SVISTUNOV, V. M., Effect of low frequency fluctuations on superconducting tunnelling, 25:27649
SWAIM, William R., Chronic myelogenous leukemia in Hodgkin's disease: immunofluorescence of cells, 25:26964
SWANENBURG, B. N., OGO-5 measurements of electrons above 500 MeV, 25:27575
SWANSON, Carl D., European liquid metal cooled breeder reactor instrumentation: a trip summary, 25:28667 (HEDL-SA-170)
SWIFT, Daniel W., Possible mechanisms for formation of the ring-current belt, 25:27627
SWIFT-HOOK, D. T., Cylindrical probe in a flowing plasma, 25:27681
SWINDLE, D. L., Distribution of low-mass fission yields in 14.8-MeV neutron induced fission of ^{238}U and ^{232}Th, 25:28385
Yields of Ru isotopes from spontaneous fission of ^{238}U, 25:28384
SWINEHART, James H., Oxidations of aqueous Chromium(II). II. Chromium-carbon bond, 25:26229
SWINGS, J. P., [Fe I] lines: their transition probabilities and occurrence in sunspots, 25:27365
SYED, Ibrahim B., Ionic /sup 135m/Ba: a new agent for bone scanning, 25:26835
SYMONDS, N., Kornberg polymerase and the repair of irradiated T4 bacteriophage, 25:27105
SYMONS, G. D., Experimental investigation of ^{16}O + ^{12}C nuclear burning at stellar energies, 25:27309 (ANU-P-471)
SYUNYAEV, R. A., Thomson scattering as a cooling mechanism for the solar corona, 25:27401
SZABADHAZY, A., Retention of radionuclides on metal sulphide precipitates, 25:26199
SZABO, E., Determination of impurities in thorium and zirconium compounds by neutron activation analysis, 25:26192
SZIRMAI, E., Blood of patients with gynecologic cancer following irradiated Streptokinase-Streptodornase, 25:26632
Effect of ionizing irradiation on blood coagulation factor activity, 25:26900
SZTRAKA, Helen, Simple method for determining the concentration of serum thyroxine by competitive displacement analysis, 25:26568

T

TABAKIN, Frank, Off-shell effects in nuclear matter, 25:28520
TABOR, W. H., Prog. rpt. on research reactor, 10--12/70, 25:28762 (ORNL-TM-3369)
TACHIBANA, Takehiko, A series of hybrid cells containing different ratios of parental chromosomes formed by two steps of artificial fusion, 25:26700
TAFF, L. M., Decays of /sup 70a/Cu, /sup 70b/Cu, and ^{67}Ni, 25:28221
TAGGART, R., Superdislocations in Ni_3V, 25:27250
TAGGI, R., Effect of gamma irradiation on the pectic substances of strawberries at different maturity stages, 25:27160
TAHA, Issam A., Catalysis of ionic reactions by polyelectrolytes. III. Quenching of uranyl ion fluorescence by iron(II) ions in poly(vinylsulfonic acid) solution, 25:26267
TAKADA, Kenjiro, Four-body correlations in light nuclei, 25:28505
TAKAGI, T., Studies on the distribution of chemical elements in geochemical samples by an activation autoradiographic method, 25:26194
TAKAHASHI, Fuminobu, Pile physics experiment by means of TOF neutron diffraction, 25:28769
TAKAHASHI, Kohji, Gross theory of beta-decay and the nuclei far from the region of beta-stability, 25:28442 (CERN-70-30(Vol.1), pp 397-419)
TAKAHISA, Michio, Determination of microamounts of Ag in Cu, Al, and their alloys by solvent extraction--atomic absorption spectrophotometry, 25:26169
TAKAKURA, T., Location and size of a solar hard x-ray burst on Sept. 27, 1969, 25:27384
TAKAMATSU, Kunio, Liquid hydrogen target utilizing a small mechanical refrigerator, 25:28138
TAKAMURA, Saburo, Recovery of low-temperature fast neutron irradiated tungsten, 25:27228
TAKASHIMA, Yoshimasa, Proportion of ^{32}P produced by ^{31}P(n,γ) and ^{32}S(n,p) reactions in phosphorus--sulfur compounds, 25:26318
TAKEDA, Yasushi, Decay of 14-min ^{112}In, 25:28406
TAKETANI, Kiyoaki, Analysis of instrumentation data from IFA-150 irradiated in HBWR, 25:28692 (JAERI-Memo-4248)
TAKEUCHI, Tsugio, Spectrophotometric determination of Be and Ga with chromazurol S and cetyltrimethylammonium chloride, 25:26172
TAKO, Jozsef, Simple method for determining the concentration of serum thyroxine by competitive displacement analysis, 25:26568
TALAGUS, V. S., X-ray study of the chromium--manganese--boron system, 25:27299
TALBERT, W. L. Jr., Experimental techniques using ISOL systems (review of operating systems), 25:28105 (CERN-70-30(Vol.1), pp 109-41)

XUM

Recent studies of short-lived gaseous fission products and their daughters, 25:28343 (CERN-70-30(Vol.2), pp 1125-7)
TANI, Thomas M., Far-out collection program. Project Schooner, 25:26404 (PNE-527)
TAN, Teresita, Participation of three cell types in the anti-sheep red blood cell response in vitro. Separation of antigen-reactive cells from the precursors of antibody-forming cells, 25:26665
TANAHASHI, Goro, Air shower observation, 25:27468
TANAKA, Eiichi, Scintillation camera based on delay-line time conversion, 25:26486
TANAKA, Kiyoshi, X-ray and fast-electron scattering factors for light atomic systems, 25:27460
TANAKA, T., Comparative studies on rejoining of DNA-strand breaks, 25:26953
Survival of lethally-irradiated mice, 25:26934
TANANAEV, A. V., Measurements of the velocity profile in crossed electric and magnetic fields, 25:27502
TANIBAYASHI, M., Suppression of drift instability by rf electric field, 25:27787
TANIGUCHI, Kaoru, Fission-gas release from nuclear fuels with in-pile gas-loop, 25:28821
TANIGUCHI, Masayuki, Analysis of Zircaloy, 25:26171
TANNER, T. M., Stable elements of the atmosphere as tracers of precipitation scavenging, 25:26365 (CONF-700601-, pp 99-108)
TARAKANOVA, M. P., Influence of irradiation on the urinary excretion of deoxycytidine and beta-aminoisobutyric acid in monkeys, 25:26999
TARASENKO, A. G., Radiosensitizing action of N-ethylmaleimide, 25:26640
TARASOV, S. I., Determination of specific release of radon by protective enclosures in premises, 25:26356
TARESKI, V. G., Illiac III Reference Manual. Vol. I, 25:28851 (COO-2118-5)
TASHCHYAN, A. A., Pulse-time fluctuation in large scintillation counters, 25:26482
TASHJIAN, Benjamin M., Reactor protection system diversity, 25:28697 (CENPD-11)
TASSO, H., Dynamic stabilization of MHD instabilities, 25:27784
TATSUMI, Yukichi, Shallow traps in p-type germanium converted from n-type by electron irradiation, 25:27843
TAUBE, Henry, Oxidations of aqueous Chromium(II). II. Chromium-carbon bond, 25:26229
TAVERNA, Carla, Electron transfer in γ-irradiated nucleotides and proflavine, 25:26638
TAVONI, R., Containment design criteria for sodium cooled fast reactors, 25:28739 (RT/ING-(70)25)
TAYLOR, Benjamin J., Stellar content of the nuclei of nearby galaxies. I, 25:27409
TAYLOR, E. A., Sterile insect release to control and eradicate insect populations, 25:27129 (CONF-680112-, pp 123-8)
TAYLOR, H. W., Tabulation of gamma--gamma directional-correlation coefficients, 25:28401
TAYLOR, I. J., Some M1 transitions with Δ = 1 in ^{26}Mg, ^{27}Al and ^{28}Si, 25:28225
TAYLOR, J. B., Plasma stabilization by feedback, 25:27756
TAYLOR, J. F., Survival time and dose-response following supralethal irradiation of dogs, 25:26992
TAYLOR, W. R., Design and development of packagings for low enriched fuel bundles, 25:26442 (AECL-3803)
Thermal test calculations for packages of steel construction, 25:26441 (AECL-3802)
TEICHMANN, J., Dynamic stabilization of the drift dissipative instability by an inhomogeneous rf field, 25:27780
TEITELBAUM, L., On-line high energy physics analysis with a PDP-9, 25:28135
TEMPEL, K., Rat kidney under whole-body irradiation and 2,4,6-triethyleniemino-s-triazine, 25:26645
TENDOLKAR, G. S., Contribution of powder metallurgy techniques to materials science, 25:27205 (INIS-mf-19)
TENENBAUM, J., Level structure of ^{50}Ti and ^{51}Ti using ^{49}Ti(n,γ) and ^{50}Ti(n,γ) reactions, 25:28284
TERADA, Osamu, Two-phase region in TiC--Mo--30 percent Ni alloys, 25:27298
TERASIMA, Toyozo, Gradual development of radioprotection in HeLa S_3 cells during treatment with β-mercaptoethylguanidine, 25:26797
TERENETSKII, K. O., Reactions (d,p) of Ti and Cr isotopes, 25:28269
TER HAAR, D., Angular momentum problem in star formation, 25:27326
TERLECKI, J., Ionization chamber with mixture of N-hexane and carbon tetrachloride for phantom measurements of photon, 25:26531
TER-NERSESYANTS, V. E., Excitation of ^{169}Tm levels, 25:28432
TESKE, Richard G., Solar soft x rays and solar activity. ii. soft x ray emission during solar flares, 25:27383
TEUCHERT, E., Influence of coated-particle structure in thermal-neutron-spectrum energy range, 25:28668
THEIS, J. D., Advanced filament-wound carbon composite, 25:28888 (SC-DR-710192)
THEISS, S., Aqueous reprocessing of fuel elements of fast breeder, 25:26326 (KFK-911)
THEOBALD, J. P., Parity assignments of some ^{98}Mo resonances, 25:28402
THOLEN, A., Cold neutron source in Juelich, 25:28767
THOMAS, C. W., In-cloud scavenging analysis from cosmogenic radionuclide measurements, 25:26364 (CONF-700601-, pp 69-97)
Stable elements of the atmosphere as tracers of precipitation scavenging, 25:26365 (CONF-700601-, pp 99-108)
THOMAS, D. Brynmor, Effects of x irradiation and antilymphocyte serum on responses to tumor allografts, 25:26666
THOMAS, G. E., OGO 5 measurements of Lyman alpha sky background, 25:27414
THOMAS, G. R., ESRO I satellite observations of 1 to 30 MeV protons during the 25th Feb. 1969 solar event, 25:27561
Observations of 45 to 450 keV electrons during the period Feb. 24--Mar. 3, 1969, 25:27568
THOMAS, Kenneth C., Austenitic stainless steels for use in nuclear reactors, 25:27214
THOMAS, Paul, Effect of gamma irradiation on post-harvest physiology of fruits, 25:27140
Effect of gamma irradiation on postharvest physiology of five banana varieties grown in India, 25:27165
THOMAS, Roger J., Solar soft x rays and solar activity. ii. soft x ray emission during solar flares, 25:27383
THOMAS L., Lower ionosphere, 25:27522
THOMASSEN, K. I., Feedback stabilization in plasmas, 25:27742
Feedback systems on linear THETA pinches with helical fields, 25:27726 (LA-4598)
THOMMES, Michael M., Concentration of radium, thorium, and uranium by tropical marine algae, 25:26597
THOMPSON, C. L., EDITOR: processing code for ENDF/B format data, 25:28148 (ORNL-TM-3266)
THOMPSON, G. E., Decay of ^{110}Sb, ^{111}Sb, ^{112}Sb, ^{113}Sb, and ^{114}Sb, 25:28332 (CERN-70-30(Vol.2), pp 1015-21)
THOMPSON, R. G., Determination of integrated plasma concentrations and true secretion rates of human growth hormone, 25:26579
THOMPSON, Stanley G., Method of obtaining americium, 25:26319
THOMPSON, W. J., Isobaric analog states for neutron spectroscopic factors, 25:28474
R-matrix analysis of proton inelastic scattering through isobaric analog resonances, 25:28364
THORP, J. M., Washout of SO_2 from plume of a coal-fired power plant, 25:26378 (CONF-700601-, pp 293-303)
THORSON, Theodore Melvin, Response of streptozotocin diabetic rats to ionizing radiation, 25:27010
THRELFALL, E. J., Co-transduction of a pleiotropic mutation affecting colicin E2 refractivity, uv sensitivity, recombination proficiency, and surface properties of E. coli K12, 25:26707
THROOP, M. J., Lifetime of 981-keV state in ^{9}Li, 25:28203
THUNELL, J., Nuclear district heating: a study for the town of Lund, 25:28574
TIBELL, G., Excited states of ^{40}Ca, 25:28255
TILGER, Clarence A., SCOLDS: Spark chamber on-line data system, 25:26512
TILLMAN, P. W. Jr., Aluminum-25 levels from the ^{24}Mg(p,γ)^{25}Al reaction, 25:28276
TILTON, Elvin W., Effects of gamma radiation on the larval midgut of the Indian-meal moth, Plodia interpunctella (Lepidoptera: Phycitidae), 25:26916
TIMOFEEFF-RESSOVSKY, H. A., Radiation biophysical investigations of Arabidopsis thaliana. III, 25:26736
TIMOFEEV, V. D., Vapour-phase radiation-initiated thermal oxidation of benzene by molecular oxygen with fast electron irradiation, 25:26284
TINDALE, John Basil, Improvements in or relating to methods and apparatus for inserting rods into a frame, 25:28652
TITIRICI, M., Reaction ^{88}Sr(tau,α)^{85}Sr at E/sub tau/ = 17.5 MeV, 25:28277
TITRAN, Robert H., Long-time creep behavior of tantalum--10 tungsten in high vacuum, 25:27207 (N-70-42045)
TKACZYK, W., Possibility of detectable fluxes of cosmic γ rays with energy above 10^{19} eV, 25:27423
TOBARI, Izuo, Changes of genetic loads in experimental populations of Drosophila melanogaster with radiation histories, 25:26705
TODD, R. R., Straightforward elucidation of complex shell-model states by β decay of nuclei far from stability, 25:28299 (CERN-70-30(Vol.1), pp 435-46)
TOERNQUIST, N., Graphical illustration of isospin analysis in single-pion production, 25:28039
TOITA, Yukio, Spectrophotometric determination of traces of uranium in sodium, 25:26152 (JAERI-Memo-4267)
TOKAREV, Yu. I., Standardized line of pressure-vessel type boiling-water reactors, 25:28716
TOKAREVSKII, V. V., Elastic proton scattering on medium-A nuclei, 25:28262
Reactions (d,p) of Ti and Cr isotopes, 25:28269
TOKUDA, Sei, Acute radiation injury in neonatally thymectomized germ-free mice. Hematopoietic and morphologic consequences, 25:26937
TOLLEFSRUD, P. B., Isospin impurities of some ^{19}F states observed via ^{15}N(α,α$_i$)^{15}N* (2.311 MeV), 25:28177
TOLLIER, M. Th., Development of certain physico-chemical properties of the starch granule as a function of

XUM

irradiation conditions, 25:26623
TOMBRELLO, T. A., Mass and half-life of ^{9}C, 25:28187
Measurement of the mass of ^{9}Li, 25:28175
TOMLINSON, L., Delayed neutron emission from selenium isotopes, 25:28212 (CERN-70-30(Vol.1), pp 519-20)
TON, Hendrik, Lifetimes of excited states in heavy nuclei, 25:28353 (NP-18695)
TONE, Hirohito, Primary cooling water decomposition in reactors, 25:28758 (JAERI-1204)
TONUMA, Tadao, Elastic scattering of carbon and nitrogen ions, 25:28274
TOOHIG, T. E., BNL summer study on AGS utilization, 1970, 25:28104 (BNL-16000)
TORR, D. G., Ionosphere during a solar eclipse, 25:27587
TORR, Marsha R., Ionosphere during a solar eclipse, 25:27587
TORRANCE, D. J., Traumatic intrapericardial herniation of the transverse colon masquerading as a pericardial effusion on the scan, 25:26836
TOTH, K. S., α decay from high-spin isomers in ^{153}Ho and ^{154}Ho, 25:28418
Search for new α-emitters with N = 86 and N = 87, 25:28303 (CERN-70-30(Vol.1), pp 533-44)
TOTH, Z., Radioisotopic scintigraphy in diagnosis of liver abscess, 25:26860
Value of radioisotope scintigraphy in the diagnosis of liver cirrhosis, 25:26861
TOUCHE, J., Torsatron without toroidal field coils as a solution of the divertor problem, 25:27793
TOWE, Agnes M., Intragenic recombination of ascospore color mutants in Ascobolus and its relationship to the segregation of outside markers, 25:26695
TOXEN, A. M., ^{139}La NMR studies in $LaIn_3$, 25:27920
TRACANELLA, Roberto Barata, Reactivity of U_3O_8/Al dispersions, 25:27294
TRACY, B. L., Half-lives of the new isotopes ^{99}Rb, ^{98}Sr, and ^{145} ^{146}Cs, 25:28388
TRAN THANH MINH, Decay of ^{90}Nb, /sup 89m,89/Nb, /sup 85m,85/Y and /sup 85m/Sr, 25:28215 (CERN-70-30(Vol.2), pp 1137)
TRAUT, H., Achromatic lesions induced by x-rays in chromosomes of Vicia faba, 25:26725
Distribution of x-ray-induced achromatic lesions within and between arms of M-chromosome of Vicia faba, 25:26734
TRAUTMANN, N., Some studies on neutron-rich nuclei, 25:28326 (CERN-70-30(Vol.2), pp 985-1000)
TRAVAGLINI, M., Containment design criteria for sodium cooled fast reactors, 25:28739 (RT/ING-(70)25)
TRAVIS, James Carlus, Serum protein and hemoglobin alterations in gamma-irradiated Spanish goat, 25:26970
TREACY, P. B., Beam optics calculations for cyclotron-tandem injection system, 25:28103 (ANU-P-519)
TREBICHAVSKY, I., Incorporation of radiophosphorus into nucleic acids of frog embryo, 25:26617
TREFALL, H., Auroral-zone x-ray events and their relation to polar magnetic substorms, 25:27593
Morphology and dynamics of auroral-zone electron precipitation, 25:27583
Morphology of auroral-zone x-ray events. I, 25:27594
TREFILOV, V. I., Influence of structure and testing conditions on the mechanical properties of low-alloyed molybdenum, 25:27221
TREHAN, P. N., Decay of ^{134}Cs, 25:28405
TREIBER, H., Levels in ^{5}He excited in the elastic d--^{3}H scattering, 25:28168
TREIMAN, S. B., Phenomenology of weak interactions, 25:28003 (PURC-4159-22)
TRETTER, Patricia K., Radiotherapy of primary lymphoma of the orbit, 25:26890
TRIBUKAIT, B., Development of transient fatty liver after release from ten-day stay in hypoxia, 25:26967
TRIPATHI, A. N., Cross-sections and reaction rates for electron-impact ionization of lithiumlike and sodiumlike positive ions, 25:27443
TRIVELPIECE, A. W., Production of multiply stripped ions in magnetically confined high-energy electron clouds, 25:27439 (WASH-1159, pp 147-55)
TROEIM, J., Electron density observations during the PCA event of 25 Feb. 1969, 25:27564
TROFIMOV, A. K., Investigation of reactions in solid phases in the systems Y_2O_3--Al_2O_3 and Y_2O_3--Ga_2O_3 with luminescence spectra of Eu, 25:27303
TROITSKAYA, V. A., Variations of solar-wind fluxes, 25:27535
TRON, L., Nuclear spectroscopy of some light Tl isotopes, 25:28339 (CERN-70-30(Vol.2), pp 1081-91)
TROSKO, J. E., Photosensitizing effect of trisoralen on DNA synthesis, 25:26808
TROUT, E. Dale, X-ray fluoroscopic screens: history, crystal kinetics, preliminary report on aging, 25:26815 (BRH/DMRE-71-2)
TROYON, F., Dynamic stabilization of high-beta plasmas, 25:27783
TRUE, William W., Nuclear isospin. Proceedings of the conference, Asilomar--Pacific Grove, California, March 13--15, 1969, 25:28455
TRURAN, J. W., Construction of mass formulas designed to be valid for neutron-rich nuclei, 25:28293 (CERN-70-30(Vol.1), pp 275-306)
Dynamics of the rapid neutron capture process, 25:27310 (CERN-70-30(Vol.2), pp 735-57)
TSAI, D. H., Molecular dynamical studies of the phase transformation of iron under pressure, 25:28895 (TID-25683)
TSAP, T. T., Relationship between velocity fields and magnetic fields in the solar atmosphere, 25:27394
TSENG, Linda, Influence of translational entropy of activation on reaction rates in isotopic solvents, 25:26227
TSUCHIHASHI, Keiichiro, Comparison of thermal neutron cross sections, 25:28344 (JAERI-1200)
TSUEI, C. C., Hyperfine magnetic interactions in Fe--Ga solid solutions, 25:28843 (CALT-822-27)
Moessbauer study of BiF_3 type ordering in metastable FeGa alloys, 25:28842 (CALT-822-26)
TSUI, J. B. Y., Utility of (Pr,Nd)Co_5 alloy for permanent magnets, 25:27886
TSUJI, Hideo, Balneotherapy of radiation injury. XXVII, 25:26950
TSUKAHARA, Iwao, Determination of microamounts of Ag in Cu, Al, and their alloys by solvent extraction--atomic absorption spectrophotometry, 25:26169
TSUNODA, Y., Magnetic structure of α-Ho_2C_3, 25:27904
TSYPIN, V. S., Instabilities of a high-pressure plasma contained by a dense blanket of neutral gas, 25:27744
TSYTOVICH, V. N., Bremsstrahlung of relativistic plasma, 25:27687 (NP-18758)
Non-linear regime of radiation instability development of relativistic electron rings, 25:28110 (JINR-P9-5622)
Plasma bremsstrahlung from relativistic particles in a turbulent plasma, 25:27704 (NP-18759)
TU, K. N., Preparation and structure of Fe-doped EuO films, 25:27894
TUBIANA, M., Proliferative activity of stem cells in bone-marrow after irradiations, 25:26956
TUCK, A. G., Derivation and use of experimental efficiency graphs for γ spectrometry in the Physics Department at the Radiochemical Centre, 25:26492 (RCC-M-211)
TUCKER, P. A., Heat source capsule fabrication technology program: September 1970--January 1971, 25:26425 (MLM-1796)
TULL, Robert G., Spectrophotometry of Nova Serpentis 1970, 25:27322
TUMANYAN, A. R., Azimuthal asymmetry of magnetic field strength of Erevan synchrotron electromagnet, 25:28139
TUNALEY, J. K. E., Photoelectron sheath near a planar probe in interplanetary space, 25:27359
TUNG, Do Kim, Sign of astatine ion charge in $HClO_4$--$H_2Cr_2O_7$ solutions, 25:26209 (JINR-P12-5644)
TUNG, M. A., Rheology of fresh, aged, and gamma-irradiated egg white, 25:26923
TUPPER, B. O. J., Cosmological models in an extension of Yilmaz' theory of gravitation, 25:28087
TURBERFIELD, K. C., Neutron crystal-field spectroscopy in rare-earth metallic compounds, 25:27893
TURCOTTE, D. L., Rotation of a glow discharge in a homopolar device, 25:27701
TUREKIAN, K. K., Marine geochemistries of the uranium isotopes, ^{230}Th, and ^{231}Pa, 25:26399 (TID-25674)
TURNIPSEED, Marvin Roy, Fetal and ovarian effects of gamma irradiation in female cotton rats, 25:26988
TUSCANY, R., Current possibilities of biologic dosimetry, 25:26771
TUURNALA, T., Energy levels of ^{176}Yb, 25:28398
TYAPKIN, Yu. D., Tri-axial periodic modulated structure in metallic alloys, 25:27249
TYRROFF, H., Nuclear spectroscopy of some light Tl isotopes, 25:28339 (CERN-70-30(Vol.2), pp 1081-91)

U

UCHIDA, Shunsuke, Experiments and calculations for gamma rays streaming through penetration in shielding structure, 25:27829
UCHIYAMA, Yuichi, Pulsed neutron research. III, 25:28161
UDSETH, H., Differential cross sections for excitation of resolved vibrational states in $H^+ + H_2(v = 0)$ nonreactive collisions, 25:27450
UEDA, Hiroshi, Protective effect of inosine against radiation injury, 25:26799
UEDA, Kazuo, Temperature dependence of critical current in Nb_3Sn ribbon, 25:27658
UEDA, Masayasu, Optical study of an ionic crystal by means of pulsed electron irradiation. IV, 25:27846
UEDA, Toshio, Medical 6 MeV linear accelerator, 25:28132
UEHARA, Shinichi, Excited states of ^{52}Cr and ground state spin of ^{52}V in the decay of ^{52}V, 25:28250
Two-phonon states in ^{104}Pd, 25:28382
UGGERHOEJ, E., Use of channeling-effect techniques to locate interstitial foreign atoms in silicon, 25:27857
UGLUM, J. R., Ion momentum analysis of collectively accelerated ion species, 25:27697 (WASH-1159, pp 219-26)
UHL, J. E., Characterization of the ionic species incident on the cathode in a glow discharge, 25:28891 (SC-RR-710122)
UJIMOTO, Kikujiro, Proportion of ^{32}P produced by $^{31}P(n,\gamma)$ and $^{32}S(n,p)$ reactions in phosphorus--sulfur compounds, 25:26318
ULLALAND, S., Morphology of auroral-zone x-ray events. I, 25:27594

XUM

ULLRICH, R., Multiregion heat transfer analysis for displaced central, corner, and side elements of unbaffled LMFBR fuel rod bundles, 25:28661
ULMER, David D., Effects of metals on protein structure, 25:26237
ULMER, Melville Paul, Gamma rays and distribution of cosmic rays in the Galaxy, 25:27407
UMARCHODGAEV, E. M., Changes of plasma kinase activity in irradiated animals, 25:27030
UMEZAWA, H., 4πβ--γ coincidence absolute measurement of nuclides emitting soft conversion electrons in appreciable proportions, 25:26464
UNDEUTSCH, Walter, Development of fibrosarcoma following x-irradiation in early infancy, 25:27059
UNGER, W. E., Nuclear safety in American radiochemical processing plants, 25:26780
UPHOFF, Delta E., Graft-versus-host reaction modified by in vitro preincubation of marrow with subcellular antigen, 25:26662
UPMALIS, A., Calculation and design of boilers in nuclear power stations, 25:28748
URAKUBO, Goro, Chemical and hygienic studies on natural radioactive spa, 25:26743
URBANETS, Ya., Ytterbium-169 levels in ^{169}Lu decay, 25:28433
URSU, V., IR spectrophotometric study of changes induced by gamma irradiation in structure of proteins and nucleic acids, 25:26660
USAMI, Akira, Radiation and mechanical damage of diffused layer of silicon solar cells, 25:26564
USAMI, S., Surface potential of H on W (100), (110), and (112) single crystal surfaces, 25:27234

V

VAESSEN, Franz, Concrete pressure vessel reactors, 25:28823
VAGENAKIS, Apostolos G., Duration of radioactivity in the milk of a nursing mother following /sup 99m/ Tc administration, 25:26839
VAIDYANATH, L. R., High conductivity coppers, 25:27187
VAINSHTEIN, L. A., Thermal model of solar corona active regions, 25:27396
VAKIL, U. K., Effect of gamma radiation on wheat starch and its components, 25:26621
Susceptibility to amylolysis of gamma-irradiated wheat, 25:26622
VAKULOV, P. V., Propagation of solar and galatic cosmic rays of low energies in interplanetary medium, 25:27469
VALENTIN, Pierre, Effect of vibrational excitation of N_2 molecules on frequency of e--N_2 elastic collisions in nitrogen plasma, 25:27711
VALENTINI, Anna Fiorella, Migration and survival of fibroblast culture in chicken following exposure to x irradiation, 25:26642
VALET, Guenter, Spleen, liver, plasma, and erythrocytes of whole-body irradiated rats, 25:26600
VALEYRE, J., Dosimetry during handling of /sup 113m/In generators, 25:26767
VALI, Gabor, Entry of freezing nuclei into precipitation, 25:26363 (CONF-700601-, pp 49-68)
VALLI, K., Production and decay properties of thorium and protactinium isotopes of mass 221-225 formed in heavy ion reactions, 25:28304 (CERN-70-30(Vol.1), pp 545-6)
VALTANCOLI, A., Experimental determination of the turbulent diffusivity coefficient in a bundle of rods with and without spacer grids, 25:28619 (EUR-4552)
VAMPOLA, A. L., Solar particle observations over the polar caps, 25:27540
VAN ALBADA, G. B., Corrections to previously published photographic observations of Sirius B, 25:27346
VAN AS, D., Measurement and analysis of radioactive fallout over South Africa, 25:26613
VAN BEEK, H. F., Rocket observations of protons and α-particles, 25:27563
VAN CANEGHEM, P., Influence of substances which change the rate of depolymerization of a collagen gel on its radiosensitivity, 25:26802
VAN DEN BERGH, Sidney, Optical studies of Cassiopeia A. II, 25:27313
VANDENBURGH, D. E., United States utility experience with intermediate light-water reactors, 25:28577
VAN DER BORGHT, O., Ruthenium-106 in marine and freshwater organisms in laboratory conditions, 25:26587
VAN DER STICHELEN ROGIER, M., Electrophoresis and immunoelectrophoresis patterns from proteins of irradiated meat, fish, and fowl egg, 25:26631
VAN DER WESTHUIZEN, M., Measurement and analysis of radioactive fallout over South Africa, 25:26613
VANDLIK, J., Nuclear spectroscopy of some light Tl isotopes, 25:28339 (CERN-70-30(Vol.2), pp 1081-91)
VAN KLINKEN, J., Decays of /sup 70a/Cu, /sup 70b/Cu, and ^{67}Ni, 25:28221
VAN PARADIJS, J. A., Curve of growth analysis of delta Cep, 25:27345
VAN PUYMBROECK, S., Ruthenium-106 in marine and freshwater organisms in laboratory conditions, 25:26587
VAN'T HOF, Jack, Mitotic delay in two biochemically different G1 cell populations in cultured roots of pea (Pisum sativum), 25:27063
VAN'T VEER, F., Spectral type of brightest component of triple system 44 i Bootis, 25:27343
VAN VELZE, P., Structure and working of the on-line system for SNEAK data processing and control of experiments, 25:28756 (EURFNR-803)
VAN WALLENDAEL, S., Thermoluminescent dosimetry, 25:26522
VANZANI, V., Nuclear rearrangement processes in an exact N-body theory, 25:28485
VARGA, Stefan, Radionuclide x-ray fluorescence analysis. II, 25:26175
VARMA, Vijay M., Treatment doses of ^{131}I-labeled chloroquine analog in normal and malignant melanoma dogs, 25:26882
VARSHNI, Y. P., Transition quadrupole moments and the variable-moment-of-inertia model for even--even nuclei, 25:28517
VASILIEV, G. Y., Neutron transport by a moving medium, 25:28815 (BNWL-tr-66)
VASSAL, G., Protection of large superconducting coils, 25:27663 (ORNL-tr-2436)
VASU, K. I., Kinetics of the high-temperature oxidation of dispersion-strengthened nickel--niobia alloys, 25:27279 (INIS-mf-11)
VAVILOVA, V. V., X-ray- and neutron-diffraction study of ordering in some alloys of the titanium--zirconium--oxygen system, 25:27297
VEADO, Juarez Tavora, Two applications of the microhardness test, 25:27222
VELINOV, P., Variations of the cosmic-ray layer in the lower ionosphere, 25:27513
VENKOVA, Ts., New isotopes of iridium, 25:28348 (JINR-P6-5617)
VERHEUL, H., Decay studies of neutron deficient Ga and Zn isotopes, 25:28338 (CERN-70-30(Vol.2), pp 1075-9)
Production and decay properties of some shortlived cobalt nuclei, 25:28214 (CERN-70-30(Vol.2), pp 1105-13)
VERNOV, S. N., Propagation of solar and galatic cosmic rays of low energies in interplanetary medium, 25:27469
Solar cosmic-ray increase on 25 Feb.--5 Mar., 1969, 25:27470
VERON, M. P., Statistically complete sample of radio-sources at 1400 MHz, 25:27353
VERON, P., Statistically complete sample of radio-sources at 1400 MHz, 25:27353
VESPIGNANI, G., OSO-G satellite instrumentation for measurements of cosmic x-rays in energy range from 25 to 190 keV, 25:26478
VIALETTES, H., Significance of scattering in calibrating apparatus for the measurement of fluences and neutron dose equivalents, 25:26483
VIANO, G. A., Harmonic analysis of scattering amplitude and Poincare model of Lobacevskij geometry, 25:28091
VIERS, M., Cyclic variation of volume of the heart, 25:26566 (CEA-CONF-1711)
VIKLICKY, V., Comparison of colony-forming performance of bone marrow cells in syngeneic and allogeneic cellular environment within a single host, 25:26670
VINCENT, Russell A. Jr., Chromosomal rejoining in absence of unscheduled DNA synthesis, 25:26724
VINEN, W. F., Topics in superfluids, 25:27642
VINITCHI, V., Critical heat flux under conditions prevailing in a boiling-water reactor, 25:28660
VIOLA, V., Intensity and phase-space limitations of various heavy-ion acceleration methods, 25:28130 (WASH-1159, pp 227-51)
VIOLINI, G., Argand-diagram analysis of Pomeron coupling to KN and anti KN system, 25:28035
VIROT, Andre, Uranium alloys, 25:27195
VISEK, W. J., Effect of dietary selenium on the survival of rats exposed to chronic whole body irradiation, 25:27032
VISHNYAKOV, V. A., Structure of electron clusters in an injector with a step-like varying wave phase velocity, 25:28112 (KHFTI-70-17)
VISHNYAKOV, V. I., Unsteady magnetohydrodynamic flow of a viscoplastic medium over an infinite plate, 25:27496
VITOUX, D., Coulomb excitation of the first 2$^+$ state of ^{24}Mg, 25:28283
VITTORI, Ottavio A., Particle-free space in Stefan flow, 25:26386 (CONF-700601-, pp 403-10)
VLADIMIROV, Yu. A., Action of uv radiation on proteins, 25:26644
VLEGGAAR, Constance M., Measurement and analysis of radioactive fallout over South Africa, 25:26613
VODICKA, I., Comparison of the action of certain radioprotective compounds on the weight loss of submaxillary glands with their effect on rat lethality, 25:26795
Development of calcifications after whole-body irradiation in rats sensitized with DHT. II, 25:26977
Effect of time between radioprotective compound administration and irradiation on weight loss of submaxillary gland, 25:26792
VOELK, H., Magnetospheric electric fields, 25:27545
VOGT, O., Crystal-field splitting and spin waves in antiferromagnetic CeSb, 25:27881
VOITOVITSKII, V. K., Comparative study of ability of chromosomes in cells of two sublines of Ehrlich ascites tumor to recovery after x irradiation, 25:26704
VOKROUHLICKY, L., Changes of heart frequency and blood pressure in rabbits after application of cystamine,

XUM

aminoethylisothiouronium bromide hydrobromide, and of their mixture in radioprotective doses, 25:26794
VOLKE, J., Regeneration of cell populations of intestinal epithelium after irradiation, 25:27033
VOLOSHKO, A. Yu., Plasma motion across inhomogeneous magnetic field, 25:27720
VONBERG, D. D., Radiation protection around the medical cyclotron at Hammersmith Hospital, 25:26775
VON BRENTANO, P., Spectator particles and resonances, 25:28365
VON EGIDY, T., Experiments at the Munich research reactor FRM, 25:28775
VON EHRENSTEIN, D., Comparison of spectroscopic factors from (p,p0) and (d,p) reactions on barium isotopes, 25:28372
VONGTAMA, Vitune Y., Post-irradiational recurrent epidermoid carcinoma of the uterine cervix, 25:26887
VON MEERWALL, E., Paramagnetism of high-concentration manganese in bcc vanadium, 25:27891
Quadrupolar effects in ^{51}V NMR of V-based transition-metal alloys, 25:27916
VON PLATEN, Ch., Measurement of the spin and nuclear magnetic moment of ^{20}Na, 25:28209 (CERN-70-30(Vol.1), pp 383-5)
VON ZAHN, U., Atomic oxygen and carbon dioxide in the lower thermosphere, 25:27609
VOOK, F. L., Low temperature channeling measurements of ion implantation lattice disorder in single crystal silicon, 25:27859
VORONIN, V. S., Change in the functional state of erythropoiesis during prolonged fractionated irradiation, 25:27015
VORONINA, S. M., Concentration distribution of binary mixtures in films moving along the walls of round pipes in the presence of an external nonuniform magnetic field, 25:27499
VOURVOPOULOS, G., Spreading of the antianalogue states in ^{91}Nb, 25:28363
VRBSKY, J., Reactions of metal ions with carboxy derivatives of phenylfluorone, 25:26174
VUORINEN, A., Absolute activity measurements of radioactive nuclides, 25:26185
VYSOTSKII, G. L., Polarization in two-nucleon stripping reactions at low energies, 25:28496

W

WADMARK, Lars Olof Tor, Improvements in and relating to water-cooled nuclear reactors, 25:28836
WAGMAN, J., Current semiempirical mass equations and improved shell model nuclear masses, 25:28291 (CERN-70-30(Vol.1), pp 165-216)
WAGNER, F., K+p Reggeized phase shift analysis, 25:28043
WAGNER, Henry N. Jr., Ionic /sup 135m/Ba: a new agent for bone scanning, 25:26835
Patterns for differentiation of posterior fossa neoplasms as detected by brain scans, 25:26820
WAGNER, J., Problem of numerical calculations for reactors, 25:28808
WAGNER, Raymond L., Spectrophotometry of Nova Serpentis 1970, 25:27322
WAGNER, Rosemarie A., Airborne ionospheric and optical measurements of noontime aurora, 25:27597
WAHL, H., Some experimental results on the sorption of caesium by tungsten and graphite, 25:27201 (EUR-4549)
WAKABAYASHI, Masaru, Intracavitary radiation therapy under hyperbaric oxygenation, 25:26869
WAKAT, M. A., Catalogue of γ-rays emitted by radionuclides, 25:28400
WALD, Francine J., Extraordinary Hall effect in paramagnetic gadolinium, 25:27908
WALDRON, W., Reliability factors affecting power plant mechanical equipment, 25:28549 (AECL-3670, pp 45-55)
WALI, Kameshwar C., s-channel helicity conservation constraints on t-channel exchanges, 25:28028 (SU-1206-242)
WALKER, J. C., Moessbauer effect in 121.2-keV transition in ^{147}Sm, 25:28420
WALKER, J. C. G., Influence of field-aligned currents on auroral-electron temperatures, 25:27603
WALKER, W. H., Isomers of ^{146}Pm and neutron capture in ^{147}Pm, 25:28373
WALL, A. N., Sum rules for πN-scattering, 25:28024 (NP-18766)
WALLACE, Robert H., Relationship between encapsulation and apparent fast neutron-induced fading in TLD, 25:26536
WALLACE, W. E., Magnetic and electrical characteristics of $REPd_3$ intermetallic compounds, 25:27870
WALMOD-LARSEN, O., Experimental investigations of the release of radioactivity under accidental conditions in a reactor containment building, 25:28763 (RISO-205)
WALSH, J. E., Nonlinear perturbations and electron scattering in a beam plasma, 25:27703
Scattering of electrons by electrostatic fluctuations in a magnetized plasma, 25:27699
WALSH, John R., Comparison of Schilling test and plasma level of cyanocobalamin ^{57}Co, 25:26853
WALTER, J. F., Pair annihilation at a potential barrier in time, 25:27985
WALTER, W. Q., Correction of inspection data for part misalignment utilizing a small computer, 25:28908 (Y-1755)
WALTERS, G. M., Explosive instabilities in simulated plasmas, 25:27736
WALZE, H., Structure and working of the on-line system for SNEAK data processing and control of experiments, 25:28756 (EURFNR-803)
WAND, Y., Level structure of ^{50}Ti and ^{51}Ti using $^{49}Ti(n,\gamma)$ and $^{50}Ti(n,\gamma)$ reactions, 25:28284
WANG, Maw-song, Mechanism of the benzoin condensation, 25:26220
WANNBERG, B., Atomic-beam measurements in the rare-earth region, 25:28298 (CERN-70-30(Vol.1), pp 387-94)
Magnetic moment and hyperfine structure of ^{103}Ag, 25:28396
WAPSTRA, A. H., Determination of atomic masses for far unstable nuclei by extrapolation, 25:28292 (CERN-70-30(Vol.1), pp 263-73)
WARD, T. E., Distribution of low-mass fission yields in 14.8-MeV neutron induced fission of ^{238}U and ^{232}Th, 25:28385
WARDASZKO, T., Measurement of β-active gases in the air, 25:26488
WARDMAN, P., Ion recombination and delayed emission in the pulse radiolysis of liquid isopentane solutions at low temperature, 25:26297
WARNER, G. G., Estimation of dose to gonads from gamma emitters present in the body, 25:26760
WARNER, R. A., Straightforward elucidation of complex shell-model states by β decay of nuclei far from stability, 25:28299 (CERN-70-30(Vol.1), pp 435-46)
WARULIK, Wojciech, Molybdenum recovery from alkaline slag, 25:26348
WASCHER, Robert E., Block in-plant radiation by design, 25:28572
WASLEY, Richard J., Elastic precursor decay in tantalum, 25:27216
WATAGHIN, G. V., Model of expanding universe, 25:27421 (ITF-70-105-E)
WATANABE, Noboru, Pile physics experiment by means of TOF neutron diffraction, 25:28769
WATARI, T., Dynamic control of cusp loss, 25:27676
WATARI, W., Analysis of Kantor amplitudes and recent low-energy proton--proton scattering experiments, 25:28046
WATERBURY, Glenn R., Methods of chemical analysis for FBR uranium--plutonium oxide fuel and source materials, 25:26153 (LA-4622)
WATERSON, R. H., Axial buckling measurements in BNL Mark II stacks, 25:28806 (RD/B/N-1837)
Manganese reaction rate measurements in [Berkeley Nuclear Lab.] reactors, 25:28816 (RD/B/N-1518)
WATSON, E. L., Rheology of fresh, aged, and gamma-irradiated egg white, 25:26923
WATT, F., Controlled avalanche caused by electron cyclotron acceleration, 25:27698
WDOWCZYK, J., Muon bundles in extensive air showers, 25:27476
Possibility of detectable fluxes of cosmic γ rays with energy above 10^{19} eV, 25:27423
Theoretical analysis of extensive air showers. V, 25:27477
WEAVER, Charles L., Development of ion exchange processes for the removal of radionuclides from milk, 25:26335 (RO/EERL-71-1)
WEBBER, John C., Molecular spectrum of sunspots, 25:27374
WEBER, G., Koebner phenomenon-like manifestation of a retothel sarcoma of the skin following x-ray treatment, 25:26875
WEBSTER, John H., Post-irradiational recurrent epidermoid carcinoma of the uterine cervix, 25:26887
WEDDE, T., Effects of auroral electrojet on fast electrons in upper atmosphere, 25:27589
WEEKS, R. A., Paramagnetic defects in TiO_2 produced by radiation, 25:27853
WEGENER, D, Elastic electron--deuteron scattering and electric neutron form factor at four momentum transfers: 5 Fermi^{-2} < q^2 < 14 Fermi^{-2}, 25:27980 (DESY-71/7)
WEIDENMUELLER, Hans A., Determination of spectroscopic factors, 25:28464
WEIDINGER, A., Spin assignment for two isobaric analog resonances in ^{76}Se from the neutron decay, 25:28241
WEIDMANN, J., Special features of measurements and control for nuclear power stations compared with conventional plants, 25:28675
WEIGEL, M., Renormalization constants in the random-phase approach, 25:28509
WEINER, J. H., Particle method for the numerical solution of the time-dependent Schroedinger equation, 25:27932
WEINHOUSE, Sidney, Proceedings of the sixty-second annual meeting of the American Association for Cancer Research, April 8--10, 1971, Chicago, Illinois, 25:26789
WEINSTEIN, S., Neutron cross sections and strength functions of ^{147}Sm and ^{150}Sm, 25:28349 (KAPL-P-3930)
WEISE, H. P., Secondary rainbows and interference in elastic scattering of H^+ by Ar, 25:27458
WEISE, Wolfram, Microscopic analysis of (γ,p) and (γ,n) reactions at medium photon energies, 25:28488
WEISENBERGER, W. H., Low temperature channeling measurements of ion implantation lattice disorder in single crystal silicon, 25:27859

XUM

WEISS, E. R., Critical evaluation of /sup 99m/Tc--Fe--ascorbic acid complex as a renal scanning agent, 25:26848
Demonstration of collateral pathways after superior vena caval obstruction with the scintillation camera, 25:26844
WEISSMAN, Donald D., X-ray beam profiles and oral radiography, 25:26817
WELCH, B., Flux and fluence dependence of disorder produced during implantation of ^{11}B in Si, 25:27864
WELFORD, W. T., Laser illumination system for Hough--Powell device, 25:26509 (RHEL/R-212)
WELLUM, R., Energy released by beta radiation following fission. I, 25:28407
WELSH, L. B., ^{139}La NMR studies in $LaIn_3$, 25:27920
WENDELN, D. E., Heat source capsule fabrication technology program: September 1970--January 1971, 25:26425 (MLM-1796)
WENE, Clas-Otto, Proton hole states excited by monoenergetic gamma-quanta, 25:28217 (LUNP-7013)
WENZEL, Werner, Possibility of nuclear energy for metallurgical and chemical processes, 25:28791
WEPSIC, Harold T., Abrogation of passively transferred tumor immunity in vivo by antigenically related tumor cells, 25:26663
WERKHOVEN, C. H. E., Calcium uptake by subterranean clover bur shown by using ^{45}Ca, 25:26614
WERNER, H., Incorporation of radiostrontium by pigs. II, 25:26594
WERNICK, J. H., Cast permanent magnets of Co_5RE type with mixtures of Ce and Sm, 25:27883
WESSELIUS, P. R., Correlation between gas and dust, 25:27415
WEST, Charles D., New phenomenon of usefulness in the radioimmunoassay of plasma adrenocorticotropic hormone, 25:26675
WEST, Lewis R., Observed seismic data, Calabash event, 25:26401 (NVO-1163-218)
WESTGAARD, L., Q-values of some nuclides on the neutron-rich side of stability, 25:28296 (CERN-70-30(Vol.1), pp 341-51)
WESTPHAL, H., Materials for the nuclear reactor technology, 25:27213
WESTPHAL, Hartmut, Production of tungsten powder from mechanically activated tungstic acid, 25:27183
WESTRUM, Edgar F. Jr., Magnetic transition, heat capacity, and thermodynamic properties of UO_2 from 5 to 350°K, 25:26264
WESTWOOD, A. R. C., Adsorption-induced brittle fracture in liquid--metal environments, 25:27243
WETZEL, R., Effect of uv-irradiation on DNA in dependence of DNA structure, 25:26657
WETZEL, Robert G., Role of carbon in hard-water lakes, 25:28847 (COO-1599-32)
WEXLER, S., Ion cyclotron resonance studies of ionic reactions in ethane and of hydrogen exchange in D_2--C_2H_6 and H_2--C_2D_6 mixtures, 25:26249
WEYMOUTH, Richard J., Electron microscopic changes following canine cardiac allografts: the effects of irradiation, 25:26677
WHALEN, B. A., Evidence for a solar-wind origin of auroral ions from low-energy ion measurements, 25:27618
WHALEN, James A., Airborne ionospheric and optical measurements of noontime aurora, 25:27597
WHAN, R. E., Preferential etching of ion-bombarded GaAs, 25:27860
WHEELWRIGHT, E. J., Cation-exchange conversion of hydroxylamine sulfate to hydroxylamine nitrate, 25:26208 (BNWL-CC-2180)
WHITE, Patricia, Kornberg polymerase and the repair of irradiated T4 bacteriophage, 25:27105
WHITEHAIR, L. A., Radiation preservation of foods, 25:27132 (CONF-680112-, pp 221-39)
WHITEHEAD, J. D., Divergence of ion velocity in the E region due to vertical winds, 25:27610
WHITEHILL, Don Earl, Electron excitation--gamma decay reaction in heavy nuclei, 25:28491
WHITTEN, C. L., LRL (Livermore) 100-MeV linear electron accelerator and facility, 25:28123 (UCRL-73075)
WHITTEN, R. C., Ionosphere of Mars below 80 km altitude. I, 25:27431
WHITTLE, Philip R., Aliphatic semidiones. XV. 2,3-semidiones derived from the bicyclo[n,1.0]alkanes, 25:26254
Aliphatic semidiones. XVI. Semidiones derived from the bicyclo[n.1.1]alkanes, 25:26255
WIBBERENZ, G., Protons and α-particles during the Feb. 25, 1969 solar event, 25:27562
WICHMANN, Erich, Bibliographies in nuclear science and technology, Sect. 13, No. 7, 1970, 25:26443 (AED-C-13-7)
WIDELL, Bjoern, Fuel manufacturing in Sweden, 25:27272 (CONF-700903-18)
WIDEROEE, R., Advanced treatment schemes with high-energy radiation considering the oxygen effects on anoxic tumor cells, 25:26864
WIDNER, M., Plasma expansion into a vacuum, 25:27709
WIECH, G., Fluorescence excitation of ultra-soft x-ray emission spectra using synchrotron radiation, 25:27827 (DESY-70/59)
WIENHARD, K., Study of isobaric analogue resonances in elastic scattering of polarized protons from ^{88}Sr, ^{90}Zr, ^{92}Zr, ^{94}Zr,^{92}Mo, ^{142}Ce, ^{144}Nd, ^{146}Nd, 25:28239
WIERBICKI, Eugene, Process for inactivating enzymes in meat to be stabilized by radiation, 25:27163
WIGGINS, Peter F., Marine manganese nodules studied using nuclear reactor, 25:28764
WIGMANS, M. E. J., Decay studies of neutron deficient Ga and Zn isotopes, 25:28338 (CERN-70-30(Vol.2), pp 1075-9)
WIIK, T., Preparation of Josephson junctions by plasma oxidation of Nb, 25:27659
WILCOX, John M., Magnetic-field variation in interplanetary space, 25:27536
WILD, J. P., Gyro and synchrotron radiation in vacuum and isotropic plasma, 25:27706
WILDE, R. E., Infrared spectroscopic study of the photolytic decomposition of methyl azidoformate, 25:26236
WILDER, D. R., Ionic domain for Y_2O_3-doped ThO_2 at low oxygen activities, 25:27286
WILDER, David R., Composition and microstructure of stabilized hafnium dioxide, 25:27296
WILEY, A. L. Jr., Gas target source for neutron radiation therapy, 25:26883
WILHELM, I., Alpha decay of resonance states of ^{148}Sm, 25:28347 (JINR-P3-5553)
WILL, Clifford M., Relativistic gravity in the solar system. I, 25:27358
WILLIAMS, Clyde M., Effect of radionuclide contamination on the calibration of ^{99}Mo, 25:26317
WILLIAMS, D. R., Determination of fluorine in rock materials by γ-activation and radiochemical separation, 25:26193
WILLIAMS, J. M., Ion-implantation doping of zinc sulphide thin films, 25:27844
WILLIAMS, K. R., Effects of high flux neutron irradiation on the microstructure of metals, 25:27266 (RD/B/N-1812)
WILLIAMS, N., Comparison of spectroscopic factors from (p,p_0) and (d,p) reactions on barium isotopes, 25:28372
WILLIS, J. C., Effect of concentration gradients on the performance of a nuclear sediment concentration gage, 25:26544
WILLIS, R. A., Carcinogenic effects of radiations on the uterus, 25:26827
WILLMORE, A. P., Electron density measurements in the thermal plasma of the magnetosphere, 25:27566
WILSKY, K., Alpha decay of neutron deficient isotopes of mercury and radon and their daughters, 25:28302 (CERN-70-30(Vol.1), pp 523-31)
Compound-nucleus aspects of beta decays with high Q values, 25:28443 (CERN-70-30(Vol.1), pp 421-33)
Delayed-proton emission from neutron-deficient isotopes of xenon and mercury, 25:28301 (CERN-70-30(Vol.1), pp 487-96)
WILSON, C. W., Preparation of control tape for an R-THETA inspection machine, 25:28907 (Y-1725)
WILSON, Charles S., Radiotherapy of primary lymphoma of the orbit, 25:26890
WILSON, H. W., Energy released by beta radiation following fission. I, 25:28407
WILSON, J. J., Determination of ^{137}Cs and ^{134}Cs in samples from the Windscale effluent treatment plant, 25:26177 (PG-Report-965)
WILSON, R. C., 1000-MWe LMFBR accident analysis and safety system design study. Candidate protective features. Topical report, 25:28734 (BAW-1354)
WILSON, R. W., Interstellar $^{12}C^{16}O$, $^{13}C^{16}O$, and $^{12}C^{18}O$, 25:27402
WINDSCHITL, Harold E., Chronic myelogenous leukemia in Hodgkin's disease: immunofluorescence of cells, 25:26964
WINEINGER, T. W., THETA1-B: a computer code for nuclear reactor core thermal analysis, 25:28737 (IN-1445)
WINNINK, M., Constraints imposed upon a state of a system that satisfies the K.M.S. boundary condition, 25:27925 (CNRS-CPT-70-P-325)
WINOCOUR, Ernest, Induction of cellular DNA synthesis by supercoiled SV40 DNA in x-irradiated mouse 3T3 cells, 25:26691
WINSTON, M. A., Critical evaluation of /sup 99m/Tc--Fe--ascorbic acid complex as a renal scanning agent, 25:26848
Demonstration of collateral pathways after superior vena caval obstruction with the scintillation camera, 25:26844
WINSTON, Roland, Retinal cone receptor as an ideal light collector, 25:28850 (COO-1701-16)
WINTERS, H. F., Annealing study of EuO films doped with Fe Eu, 25:27898
WITHERS, H. R., Response of stem cells to 14 MeV neutrons, 25:26958
WITTE, M., Protons and α-particles during the Feb. 25, 1969 solar event, 25:27562
WITTKOWER, A., Equilibrium charge-state distribution of heavy ions (1 to 14 MeV), 25:28127 (WASH-1159, pp 45-57)
WITZEL, A., Statistically complete sample of radio-sources at 1400 MHz, 25:27353
WITZKE, Walter R., Alloy softening in group VIA metals alloyed with Re, 25:27209 (N-71-11662)

XUM

WIXON, Norman J., Scattering of high energy muons on electrons, 25:27955
WIZGALL, H., Investigations on superconducting diffusion layers with an electron beam microprobe, 25:26159
WOBIG, H., Dynamic stabilization of MHD instabilities, 25:27784
WOEHL, M., Molecules in sunspots, 25:27390
WOHLFARTH, E. P., Correlation effects in transition metals and alloys, 25:27868
WOLDRINGH, H. H., Extension of the derivation of the diffusion length for neutrons in a medium with small absorption, 25:28150 (RCN-134)
WOLF, G. H., Dynamic stabilization of hydrodynamic interchange instabilities: a model for plasma physics, 25:27791
WOLF, L., Multiregion heat transfer analysis for displaced central, corner, and side elements of unbaffled LMFBR fuel rod bundles, 25:28661
WOLF, M. A., Washout of SO_2 from plume of a coal-fired power plant, 25:26378 (CONF-700601-, pp 293-305)
WOLFE, Janet P., Neutron--proton scattering at 152 MeV, 25:27956
WOLFE, Saul, Allylic and homoallylic oxidation of cyclohexene and cyclohexene-3,3,6,6-d_4 by palladium(II) salts. Evidence for competing symmetrical and oxypalladation intermediates, 25:26256
WOLFE, W. A., Computer simulation of nuclear reactor system's capability, 25:28713
Special aspects of reliability and maintainability in nuclear stations, 25:28552 (AECL-3670, pp 73-81)
WOLFENDALE, A. W., Muon bundles in extensive air showers, 25:27476
Possibility of detectable fluxes of cosmic γ rays with energy above 10^{19} eV, 25:27423
Theoretical analysis of extensive air showers. V, 25:27477
WOLFF, Andre Charles, High-resolution investigation of the $^{30}Si(p,\gamma)^{31}P$ and $^{30}Si(tau,d)^{31}P$ reactions, 25:28270
WOLFSBERG, K., Independent cesium yields in ^{238}U fission: identification of ^{145}Cs, 25:28307 (CERN-70-30(Vol.1), pp 589-99)
WOLGAST, Richard C., Vacuum cryopumping a heavy ion source in a high voltage terminal, 25:28121 (UCRL-20620)
WOLSKA-WITER, M., X and gamma thermoluminescent dosimeter for accidental personnel dosimetry purposes, 25:26516 (CLOR-82/D)
WOLTER, W., Multiple meson production at super-high energies, 25:28050
WON, J. L., Mutation breeding of tomato. I, 25:26735
WONG, A. Y., Interaction between electron and ion modes and feedback stabilization, 25:27765
WONG, C., Nuclear level densities and reaction mechanisms from continuum neutron spectra, 25:28285
WONG, Cho Fai, Electrodisintegration of carbon, 25:28193
WOOD, A. C., Major shutdown of HIFAR in 1970, 25:28782
WOOD, F. C., Steam-generating heavy-water reactor as energy source for power and water production when coupled to multi-stage-flash or vapour recompression distillation plant, 25:28642
WOOD, R. E., Cavity reactor engineering mockup critical experiment, 25:28761 (NASA-CR-72409)
Neutron activation cross sections for As, Br, Rb, and Sr isotopes at 14.4 MeV, 25:28282
WOODHAM, C. H., Growth of Vicia faba roots during irradiation, 25:27066
WOOLF, N. J., Mass loss from M stars, 25:27315
WOOLLEY, R. G., Molecular quantum electrodynamics, 25:27943
WOOLSON, William Andrew, New semi-random sampling techniques for Monte Carlo calculations, 25:27834
WORSTER, J., Isotope effects in close-packed metals and in alkali halides, 25:26241
WRIGHT, Ann Elizabeth Foley, Kinetics of catalase activity in solution and in a lipoprotein complex and the relative response to ionizing radiation, 25:26650
WRIGHT, J. W., Interpretation of ionospheric radio drift measurements. III, 25:27596
WRIGHT, R. J., Distribution of low-mass fission yields in 14.8-MeV neutron induced fission of ^{238}U and ^{232}Th, 25:28385
Yields of Ru isotopes from spontaneous fission of ^{238}U, 25:28384
WRIGHT, R. Q., EDITOR: processing code for ENDF/B format data, 25:28148 (ORNL-TM-3266)
WRONSKI, Anastazy, Serum amino acids in rats in the course of acute radiation injury, 25:26624
WU, Alfred C. T., Structure of combinatorial generalization of hypergeometric functions for SU(n) states, 25:28053
WU, T. T., Impact picture and the eikonal approximation, 25:28011
WU, Tai Tsun, Impact picture and the eikonal approximation, 25:28045 (DESY-71/6)
WULLAERT, Richard A., Effects of hydride precipitation of the tensile properties of irradiated Zircaloy-2. Final report, 25:27198 (BMI-X-10276)
WYCKOFF, H. O., Design of free-air ionization chambers, 25:26469
WYDER, W. C., Heat source capsule fabrication technology program: September 1970--January 1971, 25:26425 (MLM-1796)
WYPYCH, M., Influence of LET on radical yields in frozen aliphatic alcohols, 25:26311
WYSOPOLSKI, J., X and gamma thermoluminescent dosimeter for accidental personnel dosimetry purposes, 25:26516 (CLOR-82/D)

Y

YABE, G., Potential contribution of nuclear power to on-site generation of electric and steam power in Japanese industries, 25:28582
YACOB, A., Extraterrestrial ring current under very quiet magnetic conditions, 25:27518
YADROVSKII, E. L., Isotopic effects in photonuclear reactions, 25:28393
YAKUSHINA, A. I., Influence of structure and testing conditions on the mechanical properties of low-alloyed molybdenum, 25:27221
YAMADA, Eiichi, Dose measurement of ^{90}Sr-applicator, 25:26870
YAMADA, Masami, Gross theory of beta-decay and the nuclei far from the region of beta-stability, 25:28442 (CERN-70-30(Vol.1), pp 397-419)
YAMADA, Shigeru, Deviation from the xi approximation in the beta transition of ^{122}Sb, 25:28412
YAMADA, Takeshi, Restoration of radiation damage in rat thymocytes, 25:26936
YAMADA, Yukio, Pile physics experiment by means of TOF neutron diffraction, 25:28769
YAMAGATA, Masao, Items of tests and experiments for nuclear ship Mutsu, 25:28796
YAMAGISHI, Tomejiro, Normal mode expansion in neutron thermalization theory with a simple scattering kernel, 25:28152
YAMAKI, Hideo, Experiments and calculations for gamma rays streaming through penetration in shielding structure, 25:27829
YAMAMOTO, Katsumune, Primary cooling water decomposition in reactors, 25:28758 (JAERI-1204)
YAMAMURO, Nobuhiro, Pulsed neutron research. III, 25:28161
YAMAUCHI, S., Thermodynamic properties of ternary refractory carbides. III, 25:27283 (N-71-10590)
YANAGISAWA, K., Effect of radiation on the spore germination of the cellular slime mold Dictyostelium discoideum, 25:27065
YANG, I. C., Radiocarbon in the sea, 25:26398 (RLO-2225-T-20-2)
YANG, W. J., Optimum control of heat exchangers with internal heat generation, 25:26421
YAN'KOV, G. B., Nuclear data for thermonuclear reactors, 25:27792 (IAE-1986)
YAO, Tsu, Unitary irreducible representations of SU(2,2). III, 25:28054
YAP, S. P., Nonrelativistic composite particle model for mesons, 25:28030
YASHIKI, Mikio, Absorption behavior of radionuclides, mainly rare earth elements, in seawater, 25:26339
YATSISHIN, V. P., Model Hamiltonian of theory of superconductivity, 25:27643 (ITF-70-90-E)
YATSUN, V. A., Consequence of Gribov--Froissart formula, 25:27930 (ITF-70-101-E)
YEARGERS, Edward, Prog. rpt. on spin interactions between slow electrons and amino acid films, 6/68--2/71, 25:26277 (ORO-3799-7)
YEH, Tyan, Axially symmetric hydromagnetic equilibria with spherical plasma--vacuum interfaces, 25:27691
YELLOWLEES, John Mackinlay, Improvements in and relating to graphite moderated nuclear reactors, 25:28828
YEW, N. C., Shielded x-ray microprobe for the analysis of radioactive samples, 25:26156
YIOU, F., Production cross sections of Li and Be isotopes in ^{12}C by high-energy protons and alpha particles, 25:28182
YOKOUCHI, Ichiro, Primary cooling water decomposition in reactors, 25:28758 (JAERI-1204)
YONAS, G., Ion acceleration with high v/γ electron beams, 25:27696 (WASH-1159, pp 204-18)
Ion production with intense electron beams, 25:27695 (WASH-1159, pp 196-203)
YONEZAWA, M., Analysis of Kantor amplitudes and recent low-energy proton--proton scattering experiments, 25:28046
YOSHIDA, S., Calculation of nucleon widths of the lowest T = 3/2 states of ^{13}N and ^{13}C, 25:28172
YOSHIKAWA, S., Low-frequency instabilities, 25:27728
YOSHINARI, Takehisa, Optical study of an ionic crystal by means of pulsed electron irradiation. IV, 25:27846
YOSHIOKA, M., Studies on the distribution of chemical elements in geochemical samples by an activation autoradiographic method, 25:26194
YOSHIOKA, T., Management of effluents from JAPC's nuclear power stations, 25:28624
YOUNG, A. W., Radiocarbon in the sea, 25:26398 (RLO-2225-T-20-2)
YOUNG, J. A., In-cloud scavenging analysis from cosmogenic radionuclide measurements, 25:26364 (CONF-700601-, pp 69-97)
YOUNGBLOOD, D. H., Lifetime of 981-keV state in ^{6}Li, 25:28203
YOUNGDAHL, C. K., SASIA: a computer code for the analysis of fast-reactor power and flow transients, 25:28727 (ANL-7607)

YUDIN, N. P., Electroexcitation of ^{32}S in region of dipole resonance, 25:28220 (UJV-2553-F)
YUDIN, V. A., Dopplerons in cadmium, 25:27900
YUHARA, Hiroshi, Thermal neutron reactor study group, 25:28712
YUHAS, John M., Biological factors affecting the radioprotective efficiency of S-2-[3-aminopropylamino] ethylphosphorothioic acid (WR-2721).LD/sub 50(30)/ doses, 25:26796
YUILE, C. L., Dose-related local and systemic effects of inhaled ^{238}Pu and ^{239}Pu dioxide in dogs, 25:26929
YUILE, Charles L., Tritium: some effects of continuous exposure in utero on mammalian development, 25:26925
YUN, Sik Hong, Magnetostatic sunspot model with twisted field, 25:27378
New empirical model of a sunspot umbra, 25:27376
YUN, Taik Koo, Medical study of Korean atomic bomb survivors, 25:27060
YURCHENKO, L. V., Genetics and selection of Beauveria bassiana (Bals.) Vuill., an entomopathogenic fungus. I, 25:26703
YUR'EV, Z. N., Vapour-phase radiation-initiated thermal oxidation of benzene by molecular oxygen with fast electron irradiation, 25:26284

Z

ZABELIN, A. I., Operational experience with VK-50 reactor facility, 25:28579
ZACHARIASEN, F., Self-consistent rising cross-sections, 25:28012
ZAEHRINGER, J., Noble gas abundances in lunar material, 25:27308
ZAFIRATOS, C. D., $^{24}Mg(\alpha,d)^{26}Al$: a test of the $\Delta T = 0$ selection rule, 25:28233
Isospin purity at high excitation energies, 25:28190
ZAIDI, S. A. A., Inelastic proton decay of the g/sub 9/2/ analogue resonance in ^{209}Bi, 25:28367
ZAIDINS, C. S., Isospin purity at high excitation energies, 25:28190
ZAIKIN, Yu. I., Loop for radiation study of electrical conductivity of materials in the VVR reactor, 25:28765
ZAITSEVA, N. G., New isotopes ^{176}Os and ^{177}Os, 25:28386
Nuclear spectroscopy of some light Tl isotopes, 25:28339 (CERN-70-30(Vol.2), pp 1081-91)
ZAK, W. M., Experimental investigations of the release of radioactivity under accidental conditions in a reactor containment building, 25:28763 (RISO-205)
ZAKHAROV, I. A., Genetic control of radioresistance of the cell and some general problems of genetics, 25:27116
ZAKHAROV, V. E., Variational principle and canonical variables in magnetohydrodynamics, 25:27488
ZAKHAROVA, N. P., Loop for radiation study of electrical conductivity of materials in the VVR reactor, 25:28765
ZAKOPALOVA, I., Individual differences in the radiation tolerance of rats and their relationship to the differences in the pre-irradiation stress response, 25:27029
ZAKOWICZ, W., Interaction of harmonic oscillators with radiation field, 25:27928 (INR-P-1203)
ZALETAEV, S. P., Apparatus for study of motion of conducting emulsions in electric and magnetic fields, 25:27501
ZALEWSKI, K., Quark model additivity frame, 25:28017
ZAMICK, Larry, Is the effective charge correction larger for a neutron than for a proton, 25:28456
ZANFAGNA, B., Local density measurements by nonlinear mixing of electromagnetic waves, 25:27684
ZARUBIN, P. P., Elastic and inelastic scattering in A = 23 to 35 region, 25:28261
Proton scattering on ^{24}Mg, ^{25}Mg, and ^{26}Mg, 25:28264
ZATS, A. V., Excitation functions of He I spectral lines, 25:27463
ZAVGORODNII, V. A., Spectra of protons in $^{238}U(t,pf)$ reaction, 25:28390
ZAWADZKI, E. M., Penetration to second order of an electrostatic field into a warm plasma, 25:27707
ZBAR, Berton, Abrogation of passively transferred tumor immunity in vivo by antigenically related tumor cells, 25:26663
ZECCHIN, R., Personnel dosimetry with ^{7}LiF Teflon discs, 25:26527
ZEIDMAN, B., An experimental test of the Barshay--Temmer theorem via the reactions $^{10}B(\alpha,^{7}Li/sub\ gs/)^{7}Be/sub\ gs/$ and $^{10}B(\alpha,^{7}Be/sub\ gs/)^{7}Li/sub\ gs/$, 25:28176
ZELDES, N., Current semiempirical mass equations and improved shell model nuclear masses, 25:28291 (CERN-70-30(Vol.1), pp 165-216)
ZEL'DOVICH, Ya. B., Growth of perturbations in an expanding universe of free particles, 25:27427
ZELENOV, B. A., Dynamic accelerated proton beam characteristics in IHEP 70-GeV accelerator, 25:28133
ZELENY, V., Comparison of colony-forming performance of bone marrow cells in syngeneic and allogeneic cellular environment within a single host, 25:26670
ZELIN, V. A., Dynamic accelerated proton beam characteristics in IHEP 70-GeV accelerator, 25:28133
ZELIOLI-LANZINI, Francesco, Difference of action between hepatic extracts and small doses of roentgen rays on the mitotic activity of the partially hepatectomized liver, 25:26948
ZEPP, Gerard, Propagation of an electromagnetic wave in a superconducting coaxial cylindrical guide, 25:27665
ZEPPENFELD, K., Nonvertical interband transitions in graphite, 25:27902
ZETTERLUND, S., Calculation of differential angular correlation factors for non-coaxial electric and magnetic fields, 25:27919
ZHILEIKO, G. I., Phase equation for electron motion in a traveling-wave field with synchronous energy as an independent variable, 25:27946
ZHIL'TSOV, V. A., Feedback stabilization of the rarefied plasma cyclotron instability, 25:27776
ZHULIN, I. A., Interdisciplinary investigations of the auroral phenomena, 25:27549
ZIEGLER, James F., Determination of surface impurity concentration profiles by nuclear backscattering, 25:26183
ZIEMBA-ZAK, B., Regeneration of proliferative activity in progeny of murine lymphoma cells L5178Y irradiated with x-rays, 25:26974
ZIEMER, Paul L., Relationship between encapsulation and apparent fast neutron-induced fading in TLD, 25:26536
ZIFF, E. C., Auroral intensity ratio of O I (6300 A) and O I (5577 A), 25:27600
ZIJLSTRA, H., Critical fields determining magnetic coercivity in microparticles of $SmCo_5$ and $LaCo_5$, 25:27882
ZIL'BERMAN, L. A., Effect of low frequency fluctuations on superconducting tunnelling, 25:27649
ZIMA, T. E., Decrease of critical mass of a reactor, 25:28809
ZIMACEK, J., Scintigraphic localisation of the kidneys for percutaneous renal biopsy, 25:26821
ZIMIN, E. P., Motion of alternate layers of conducting liquid and nonconducting gas in a transverse magnetic field, 25:27494
ZINOV'EV, L. P., Deuteron acceleration in LA9-injector of JINR synchrocyclotron, 25:28109 (JINR-P9-5610)
ZIOCK, K. O. H., Charged particle emission following pion capture in nuclei, 25:28178
ZIRWER, D., Effect of uv-irradiation on DNA in dependence of DNA structure, 25:26657
ZIVANOVIC, M., Neutron inelastic scattering and neutron diffraction at the Vinca heavy water reactor, 25:28779
ZOERNER, William, Hydrostatic extrusion of hard core clad rod, 25:28869 (NYO-4078-3)
ZOHTA, Yasuhito, Shallow donor state produced by proton bombardment of silicon, 25:27847
ZRELOV, V. P., Apochromatic method for measurement of mean proton energy in 657 MeV beam, 25:26506 (JINR-P13-5637)
Monochromatic method for measurement of mean proton energy in 665 MeV beam, 25:26505 (JINR-P13-5636)
ZUCKER, A., Possible single impact source for multiply charged ions, 25:27438 (WASH-1159, pp 141-6)
ZUK, W. M., Experimental investigation of $^{16}O + ^{12}C$ nuclear burning at stellar energies, 25:27309 (ANU-P-471)
ZURSTADT, D. H., SPECTR: a program for handling and analyzing multichannel pulse height spectra, 25:26499
ZVERKO, J., Spectrum and quantitative analysis of Ap star alpha Draconis, 25:27333
ZWALLY, H. Jay, Spark source, 25:28129 (WASH-1159, pp 168-71)
ZWIRN, P., Cyclic variation of volume of the heart, 25:26566 (CEA-CONF-1711)
ZYRYANOVA, L. N., New values for Kβ branching coefficients, 25:28494

XUM

SUBJECT INDEX

Cross references are included in cumulative subject indexes and in *Subject Headings Used by the USAEC Division of Technical Information* (USAEC report TID-5001).

The reader is also referred to *Guide to Abstracting and Indexing for Nuclear Science Abstracts* (USAEC report TID-4576).

Most headings in the subject index are specific materials, things, and processes. The headings are followed by modifiers that describe the properties of, or processes applied to, the headings.

All index entries cite *NSA* volume and abstract numbers; volume number precedes the colon and the abstract number follows it. The designation (R) following the abstract number indicates a progress report; (P) indicates a patent; and (T) indicates a translation. Abstracts for reports other than progress reports carry no letter designation. Report numbers, where applicable, are included in parentheses after the abstract number of the citation. Published literature (journal article or book) can be identified by the absence of a report number.

Ideas presented in the original literature, rather than key words, have been indexed. The indexers have selected what seemed the most probable and logical place to look for typical information. Since it is not always possible to anticipate where a user would look for information, the cumulative indexes include numerous cross references. Consideration of synonymous or closely related terms will prove valuable.

Information is indexed for the greatest use to the greatest number of users. This requires that a topic be indexed to headings that most specifically describe it and not ordinarily to the headings that describe its ultimate use or to the general class headings that include the specific headings. For example, information on boiler design for the Fermi Fast Breeder Reactor would be indexed under the headings BOILERS and FERMI FAST BREEDER REACTOR but not necessarily under the headings REACTORS, FAST or REACTORS, BREEDER.

General or broad headings are reserved for general summaries, reviews, comprehensive reports, and similar literature.

Subject Heading Styles

Generally, the direct form of subject entry is used rather than inverted headings; e.g., AMINO ACIDS rather than ACIDS, AMINO; HELIUM ISOTOPES He-4 rather than HELIUM—ISOTOPES He-4 or HELIUM—He-4 ISOTOPES. Note, however, that in some cases parenthetic modifying terms or inverted headings such as NEUTRONS, FAST, are used where the alphabetical arrangement of a direct entry would cause information to be scattered. In addition, organic compounds are usually entered in the index in the inverted form to facilitate grouping like or related compounds with the parent compounds; e.g., BENZENE, BROMO- rather than BROMOBENZENE. In general, the nomenclature used is that of the subject indexes to *Chemical Abstracts*.

Alphabetization

Subject headings are alphabetized word by word. Parenthetic qualifiers, numbers, and Greek letters within subject headings are disregarded in alphabetizing unless there are two or more headings that are otherwise identical, in which case the qualifier, numerical progression, or spelled names for the Greek letters determine the order.

Examples:

M-Capture
  see ELECTRON CAPTURE
MAGNESIUM
MAGNESIUM ALLOYS AND SYSTEMS
MANGANESE FLUORIDES
MANGANESE FLUORIDES MnF_2
MESONS
MESONS (π)
MESONS (ρ)
1-PENTANOL
2-PENTANOL

Modifying Phrases

The modifiers appearing under a subject heading are written specifically to show the relation between the item being indexed and the heading. The modifier therefore contains a maximum of useful information. Although the modifier begins with the word judged to be of greatest use to the greatest number of users, there is still need for the searcher to consider all modifiers under the heading(s) of interest.

Modifiers usually form meaningful phrases when combined with the subject heading. Some are intended to be read following the subject heading, e.g., the entry HYDROGEN—sorption by charcoal should be read "hydrogen sorption by charcoal." As a result of placing the important word first, however, many modifiers must be rearranged for smooth reading, e.g., FORMALDEHYDE—yields in radiolysis of ethyl ether, effects of deuterium on, should be read "effects of deuterium on formaldehyde yields in radiolysis of ethyl ether" and URANIUM—crystal structure of, effect of cooling rate on allotropic transformations in, should be read "effect of cooling rate on allotropic transformations in crystal structure of uranium."

Special characters are added to modifiers in the fields of physics and reactor technology; if the modifier does not establish the experimental or theoretical character of a reference, a symbol (E), (T), or (E/T) is placed immediately after the modifying phrase and before the abstract number.

XUM

Physical States and Configurations of Materials

The specific physical state, if other than normal, or the geometric configuration of the material is included in the modifying phrase; e.g., information on liquid metals is indexed under the specific metal with "liquid" in the modifier and carbon crucibles is indexed under CARBON with "crucibles" appropriately placed in the modifier. The information on carbon crucibles is also indexed under CRUCIBLES.

Nomenclature of Inorganic Compounds

Inorganic compounds are indexed to subject headings in the direct form. Cations are listed in the order of increasing valence for polycationic salts of varying valence and in alphabetic order for polycationic salts in which all cations have the same valence; e.g., SODIUM ALUMINUM SILICATES and POTASSIUM SODIUM SULFATES. If more than one anionic species is presented in a compound, the anions are arranged alphabetically, e.g., BERYLLIUM FLUORIDE HYDROXIDES.

Nomenclature of Organic Compounds

Organic compounds are indexed by subject headings based on the indexes to *Chemical Abstracts* except in the area of enzymes, in which specific enzymes, named according to the 1964 recommendations of the International Union of Biochemistry, are used. In many cases nonproprietary names for drugs are used as subject headings, and cross references are made from the systematic chemical names. Subject headings for hormones appear in the inverted style at HORMONES.

Nomenclature of Life Sciences

Subject headings for plants are names of phyla with one exception: members of the Phylum Tracheophyta are indexed under class or subclass names. Scientific names (genus and species) are used as the initial, or file, word in the modifying phrase. Scientific names are omitted only when the name is not available in the literature or cannot be found in available references.

Subject headings for animals are the names of phyla with the following exceptions: (1) members of Phylum Arthropoda and Phylum Chordata are indexed under appropriate class name, and (2) common names are used for members of Class Mammalia.

Subject headings are entered for various classes of commodities, and specific products are identified in the file-word position of the modifier. In the following examples, approved subject headings are capitalized and typical modifier file words are listed in lower case.

Example 1	Example 2
CEREALS	MEATS
bread	beef
flour	fish
oats	mutton
rice	pork
rye	poultry
wheat	seafood

Diseases, pathological conditions, and in vitro studies of atypical cells and tissues are indexed under subject headings for the organism affected, under the appropriate anatomical structure of physiological phenomenon affected, and under the appropriate disease heading. Subject headings for diseases (defined as any deviation from the norm) are DISEASES; DISEASES, INFECTIOUS; DISEASES, NEOPLASTIC; DISEASES, PHYSIOLOGICAL; DISEASES, PLANT; and DISEASES, TRAUMATIC.

Diseases of mixed etiology are treated in the following manner: neoplastic diseases that are also classified as infectious or physiological are indexed under DISEASES, NEOPLASTIC; diseases in which a microorganism is the etiologic agent are classified under DISEASES, INFECTIOUS; physiological anomalies that are neither neoplastic nor infectious are indexed under DISEASES, PHYSIOLOGICAL; the acute radiation syndrome, nonspecific radiation injuries, trauma, and wounds or incisions inflicted mechanically are indexed under DISEASES, TRAUMATIC.

Specific diseases or pathological conditions are named in the file-word position of the modifier, in the author's terminology, and are set off from the remainder of the modifier by commas. Neoplasms are designated as benign or malignant in the file-word position when more specific information is not available.

Multicomponent Alloys and Other Systems

Multicomponent alloys and systems, except well-known trade names, are indexed under a subject heading for each component in the form "element systems" for nonmetals or "element alloys and systems" for metals. The modifier begins with element symbols for each component arranged alphabetically. In addition, if significance is placed on the base metal of the alloy, this is indicated by adding "-base" to the element symbol.

Example: A 1.5C, 12Cr, 0.25V, 0.8Mo, bal Fe alloy is indexed as

```
CARBON SYSTEMS
  C--Cr--Fe-base--Mo--V, ...
CHROMIUM ALLOYS AND SYSTEMS
  C--Cr--Fe-base--Mo--V,...
IRON ALLOYS AND SYSTEMS
  C--Cr--Fe-base--Mo--V, ...
MOLYBDENUM ALLOYS AND SYSTEMS
  C--Cr--Fe-base--Mo--V, ...
VANADIUM ALLOYS AND SYSTEMS
  C--Cr--Fe-base--Mo--V, ...
```

Well-known alloys, such as ZIRCALOY-2, are indexed under the trade name; cross references from each component of the alloy to the trade name appear in cumulative indexes.

Multicomponent systems in which nonmetallic elements are present in large percentage and which are commonly referred to as systems or mixtures are indexed in a manner similar to alloys.

Example: A tungsten–silicon preparation is indexed as

```
TUNGSTEN ALLOYS AND SYSTEMS
  Si--W, ...
SILICON SYSTEMS
  Si--W, ...
```

Multicompound systems and mixtures of inorganic compounds are indexed under the subject heading for each component compound; the modifiers begin with an alphabetical listing of compound formulas.

Example: A lead titanate–lead zirconate mixture is indexed as

```
LEAD TITANATES
  PbTiO3--PbZrO3
LEAD ZIRCONATES
  PbTiO3--PbZrO3
```

XUM

A mixed system of compounds and elements is indexed by a combined form of the preceding conventions; e.g., a dispersion of copper and alumina would be indexed as

ALUMINUM OXIDES
  Al_2O_3--Cu, ...
COPPER ALLOYS AND SYSTEMS
  Al_2O_3--Cu, ...

Mixtures of organic compounds are indexed under subject headings for each component of the mixture; the modifiers begin with an alphabetical listing of compound names.

Example:

ACETIC ACID
  acetic acid--BF_3, ...
BORON FLUORIDES
  acetic acid--BF_3, ...

Example:

BENZENE, CHLORO-
  bromophenol--chlorobenzene, ...
PHENOL, BROMO-
  bromophenol--chlorobenzene, ...

If modifiers for alloys and systems are included with other modifiers under the same subject heading, they are filed last.

Example:

CARBON SYSTEMS
  deposition on nuclear fuel particles
  molecular structure of
  neutron total cross section for
  sorptive properties for xenon
  Young's modulus for
  Al--C--Cr, superconductivity in
  B--C, phase studies for
  C--U--Zr, fabrication and physical properties of

Nomenclature of High Energy Physics

Information on particle-particle events is indexed under subject headings for the specific particles involved. The modifier file word *interactions* is followed by the specific interaction written in symbolic form. Particle nomenclature and symbols follow that of Rosenfeld, et al. *Data on Particles and Resonant States*, UCRL-8030 (latest revision). For consistency the incident particle is always written first. The mass (in MeV) of a resonance state is included in parentheses after the symbol to avoid ambiguity. Hyperfragments are indicated in modifiers as in the following examples: Λ-He^5, Σ-H^3, $\Lambda\Lambda$-Be^{10}. The superscript on the right indicates the total number of baryons in the composite system.

Examples:

MESONS (π^-)
  interactions $\pi^- + p \rightarrow \Lambda + K^+ + \pi^-$ at 6 GeV/c in hydrogen bubble chamber, $\Lambda K(1700)$ enhancement in, (E)
BARYONS, RESONANCE (N^*)
  production of $\Delta^{++}(1236)$ and $\Delta^0(1236)$ from $K^- + p \rightarrow K^- + p + \pi^+ + \pi^-$ interactions at 2.63 and 2.70 GeV/c, (E)
HYPERFRAGMENTS
  binding energy of $\Lambda\Lambda$-He^6, three-body α--Λ--Λ model for

Subject headings are also provided for specific models and theories.

Examples:

ELEMENTARY PARTICLE MODELS (TRIPLET)
  hadron total cross sections in quark, numerical analysis of
CURRENT ALGEBRA
  PCAC hypothesis for A_1 and rho dominance in $\pi \rightarrow e + \nu + \gamma$ decay
REGGE POLE THEORY
  predictions for polarization in $K^- + p \rightarrow$ anti $K^0 + n$, $\pi^- + p \rightarrow \pi^0 + n$, and $\pi^- + p \rightarrow$ eta + n interactions at high energies
SYMMETRY GROUPS
  SU(2) × SU(4) intermediate-coupling model for nucleon and hyperon isobars

Nomenclature of Reactor Technology

Subject headings for reactors are of three types:

(1) Specific reactors, e.g., ARGONNE RESEARCH REACTOR, SAXTON POWER REACTOR

(2) Reactors having a common physics or engineering characteristic, e.g., REACTORS, FAST; REACTORS, ORGANIC-COOLED; REACTORS, PRESSURIZED-WATER

(3) Reactors having a common purpose, e.g., REACTORS, POWER; REACTORS, RESEARCH

Information on specific reactors, type (1), is indexed under the one specific subject heading. Information on classes or types of reactors, types (2) (characteristics) and (3) (purpose), is indexed under all applicable headings. For example, information on a heavy-water-moderated organic-cooled power reactor is indexed under REACTORS, HEAVY WATER-MODERATED; REACTORS, ORGANIC-COOLED; and REACTORS, POWER.

Subject headings exist for selected reactor components, e.g., REACTOR FUEL ELEMENTS. When applicable, headings for components are indexed even though they may have been included in a modifier under a type (1) or (2) heading. The materials in reactor components are indexed when the information is peculiar to the material.

Modifier file words under reactor headings are of two primary types: one type expresses reactor characteristics, e.g., reactivity; the other, components, e.g., control rod. If no subject heading appears for a reactor component, the heading REACTORS is used, and the component is used as the modifier file word.

A

ABDOMEN
radiation dose to, of medical personnel from technetium-99m, methods for shielding against, 25:26765
ACCELERATORS
beam current in circular, maximum electron, (T), 25:28140
beam intensity limitations of various heavy-ion, 25:28130 (WASH-1159, pp 227-51)
charge stripping and pickup data for heavy-ion, 25:28126 (WASH-1159, pp 34-41)
vacuum chambers for circular, design of aluminum oxide ceramic, 25:28131
ACCELEROMETERS
design of triaxial bidirectional integrating 4-level, 25:28900 (UCRL-72748)
ACCIDENTS
statistics on US railroad, 1958 to 1961, 25:26447 (HW-76299)
ACETIC ACID
effectiveness of bladder perfusion with, for treatment of injuries following radiotherapy for gynecological tumors, 25:26813
radiosensitizing effects on tumorigenesis in skin of mice, uv, 25:26809
ACETIC ACID, [(CARBOXYMETHYLIMINO)BIS(ETHYLENENITRILO)]TETRA-
use of technetium-99m-labeled, for scanning, evaluation of effects of preparation method on usefulness of, 25:26840
ACETIC ACID, FLUORO-
sodium salt, radioprotective effects on mice in relation to body temperature and respiration, 25:26800
ACETIC ACID, IODO-
effects on survival of γ-irradiated Penicillium expansum, 25:27084
ACETONE
radiolysis of aqueous solutions of, effects of cysteine, mercaptans, or 2-mercaptoethanol on yields from γ, 25:26291
acetone--HCl--methyl sulfoxide--$UO_2(ClO_4)_2$, complex formation in aqueous solutions of, PMR studies on solvation and, 25:26212
acetone--methyl sulfoxide--$UO_2(ClO_4)_2$, complex formation in aqueous solutions of, PMR studies on solvation and, 25:26212
acetone--methyl sulfoxide--$UO_2(NO_3)_2$, complex formation in aqueous solutions of, PMR studies on solvation and, 25:26212
ACETYLENE
effects on x-radioinduced polymerization of gaseous chloroethylene, 25:26282
yields from γ radiolysis of ethylene--neon, effects of pressure on, 25:26314
ACETYLENEDICARBOXYLIC ACID
hydrogen atom reactions with powders of dihydrates of, ESR studies on yields of radicals from, 25:26301
potassium salts, hydrogen atom reactions with powders of, ESR studies on yields of radicals from, 25:26301
potassium salts, radiation effects on single crystals of dihydrate of, ESR studies on yields of radicals from γ, 25:26301
radiation effects on single crystals of dihydrate of, ESR studies on yields of radicals from γ, 25:26301
ACID PHOSPHATASE
radiation effects on activity of, in blood plasma and liver of rats, single and combined effects of turpentine and x, 25:26979
radiation effects on metabolism of, in rat kidneys in comparison to injection of TEM, whole-body x, 25:26645
ACRIDINE, 3,6-DIAMINO-
complexes with DNA, radiation effects on electron transfer in, ESR spectral studies on γ, 25:26638
ACTINIDES
nuclear energy levels in, calculations using two-center potential of equilibrium, (T), 25:28312 (CERN-70-30(Vol.2), pp 676-88)
ACTINIUM ISOTOPES Ac-209
energy levels and properties of, nuclear data sheets for, 25:28376
ACTINIUM ISOTOPES Ac-211
energy levels and properties of, nuclear data sheets for, 25:28377
ACTINIUM ISOTOPES Ac-227
determination of aerosols of, in air containing other radioactive substances, method for, 25:26394
ACTIVATION ANALYSIS
developments in neutron, using californium-252 for terrestrial, sea floor, and planetary surface studies, 25:26188 (BNWL-SA-3803)
methods for, review on, 25:26164
pneumatic system for, with short-lived radioisotopes, 25:26189 (KFK-1293)
radioisotope retention on sulfide precipitates in, 25:26199
sensitivity, principles, and uses of, review on, 25:26186 (BARC-529)
vessels for, volatility of mercury from plastic, 25:26201
ADENINE
effects on content of ATP in x-irradiated thymocytes in rats, 25:26936
ADENOSINE
radioprotective effects in bacteria, uv, 25:27122
radioprotective effects in bacteria, x, 25:27120
ADENOSINE 5'-DIPHOSPHATE
complexes with uranyl ions, NMR and titrimetric studies on, 25:26271
ADENOSINE MONOPHOSPHATES
complexes with uranyl ions, NMR and titrimetric studies on, 25:26271
radioprotective effects on rabbit eyes, cobalt-60γ and fast neutron, 25:27014
ADENOSINE 5'-TRIPHOSPHATE
complexes with uranyl ions, NMR and titrimetric studies on, 25:26271
effects of depressed synthesis of, on survival of irradiated L cells, 25:26969
effects of synthesis of, on recovery in x-irradiated yeast, 25:27095
radiation effects on content of, in thymocytes in rats, effects of adenine on x, 25:26936
ADRENAL GLANDS
radiation effects on rat, recovery from, 25:26998
scanning in dogs using cholesterol labeled with carbon-14 and iodocholesterol labeled with iodine-125, 25:26845
AEROSOLS
characterization of radioactive, in uranium mines for development of protective devices for personnel, 25:26773
particle size of marine, mathematical model for relating halogen-ion ratios in aerosols with, 25:26381 (CONF-700601-, pp 325-51)
scavenging of submicron biological, from atmosphere, equipment and method for measuring efficiency of raindrops for, 25:26369 (CONF-700601-, pp 151-60)
AET
effects on biochemistry of blood serum and tissues in x-irradiated dogs, 25:26935
radioprotective effects of, on blood pressure and heart frequency in rabbits, γ, 25:26794
radioprotective effects of, on mice, combined effects of cystamine and, 25:26793
radioprotective effects of, on rats, sublethal fractionated dose, 25:26807
radioprotective effects of, on submaxillary gland in female rats, effects of time of administrtion on γ, 25:26792
radioprotective effects of, on submaxillary glands in mice, comparison of cystamine, cysteine, noradrenaline serotonin, and tetramethylcystamine with γ, 25:26795
sodium salt, radioprotective effects on mice in relation to body temperature and respiration, 25:26800
toxic effects of, on γ-irradiated mice, combined effects of cystamine and, 25:26793
AGE
effects on survival of γ-irradiated fungi, 25:27085
effects on survival of γ-irradiated Penicillium expansum, 25:27084
effects on x-radioinduced breaks in DNA of Chinese hamster cells, 25:26625
AGING
radiation effects on mouse, x, 25:26922(R) (CRC-3260-3-A)
radioinduced, in human populations on Marshall Islands, 25:27058
AGRICULTURE
conference on nuclear energy in, Santiago, Chile, Jan. 9 to 12, 1968, 25:27127 (CONF-680112)
economic impact of marketing gamma-processes potatoes on, 25:27141
radioisotopes in, in Ecuador, 25:27134 (CONF-680112-, pp 245-6)
role in food conservation following nuclear attack, 25:26786
AIR
actinium-227 aerosol content of, containing other radioactive substances, method for determining, 25:26394
corrosive effects of dry and moist, on thin molybdenum films at 70 to 100°C, relations of silicon dioxide layer or double layer of silicon dioxide and silicon nitride with, 25:27171
AIRCRAFT
structural materials for, development of composite, 25:27307
AIRGLOW
emission of ionospheric F region equatorial uv nightglow, relation to oxygen ion--ion neutralization reaction, (E/T), 25:27608
hydrogen spectra of, horizon Lyman-α brightness at 150 km for dawn and evening twilights, (E), 25:27615
pre-dawn enhancement of 6300-A oxygen, at Adelaide, recombination-associated, (E/T), 25:27514
ALANINE, N-BENZOYL-
radiolysis of single crystals of, ESR spectral studies on radicals produced by γ, 25:26292
β-ALANINE, 2-METHYL-
radiation effects on urinary excretion of, by monkeys, γ,

XUM

25:26999
ALARM SYSTEMS
design and maintenance of ANSI standard criticality accident, 25:26553
ALASKA
ecology of Amchitka Island, freshwater invertebrate and vertebrate, 25:28841(R) (BMI-171-133)
ALBUMINS
radiation effects on metabolism of, in liver of rats, combined effects of starvation and x, 25:26984
radiation effects on rheology of egg, effects of temperature on γ, 25:26923
radiation effects on synthesis of, in rats, mechanism of, 25:27007
ALEUTIAN ISLANDS
seismotectonics of, research progress on, 25:28852(R) (CU-4203-1)
ALGORITHMS
development for correction of data for part misalignment from numerically controlled inspection machines, 25:28908 (Y-1755)
development of numerical image restoration, for use on digital computer, 25:28902 (UCRL-73080)
ALKALI METALS
separation from other elements by ion exchange of 4,4,4-trifluoro-1-(2-thienyl)-1,3-butanedione complexes in pyridine, 25:26337(P)
ALKALINE PHOSPHATASE
activity in kidney tissues, autoradiographic method of measurement of effects of cadmium on, 25:26574
radiation effects on metabolism of, in rat kidneys in comparison to injection of TEM, whole-body x, 25:26645
ALKANES
radioinduced ion pairs in, mean energy for γ, 25:26293
spectra of gaseous, absorption, 25:28853 (DESY-SR-71/1)
ALKYLATING AGENTS (BIOLOGICAL)
effects on bacteria and bacteriophages, mechanisms of repair from damaging, 25:27109
ALLOXANTIN
distribution of chromium-51-labeled, in rat bones following intravenous injection, 25:26590
ALLOYS
conference on structural chemistry of phases in, Cleveland, Ohio, Oct. 1967, 25:27260
corrosion by melting glasses in radioactive waste vitrification process, 25:26334(T) (ORNL-tr-2410, pp 143-89)
crystal structure of two-phase, field ion microscopy studies of, 25:27254
fabrication of, research on methods for, 25:27194
fatigue in high-strength, mechanisms of, 25:27242
microstructure of non-equilibrium binary and ternary, review on effects of rapid quenching from melt on, 25:27264
microstructures and transformations in long-range-ordered, field ion microscopy studies of, 25:27255
radiation effects on two-phase, field ion microscopy studies of, 25:27254
welding of hard facing and hard metal, in sodium at 580 to 700°C, self-, 25:27206 (KFK-Ext.Ber.-8/70-1)
ALPHA PARTICLES
angular and spatial distribution over polar caps, satellite observations of solar, (E), 25:27540
detection at 3 to 10 MeV, in nitrocellulose track detector, 25:26474
detection of 5- to 9-MeV, resolution of thin silicon telescope detectors for, 25:26485
detection of, development of organic-liquid ionization chambers for, 25:26471
effects on alkylbenzene--tridodecylamine solvents, 25:26330(T) (ORNL-tr-2410, pp 14-78)
effects on Arabidopsis seeds, 1 to 20-krad mutagenic, 25:26736
effects on bacteria, effects of dose rate on lethal, 25:27118
effects on frozen aliphatic alcohols, role of LET in, 25:26311
effects on gaseous hydrogen sulfide, effects of electron and proton scavengers on hydrogen yields from, 25:26315
effects on helium II, effect of pressure on luminescence from, 25:27636
effects on mitosis in Chinese hamster cells, delaying, 25:26927
energy losses in selenium, (E), 25:27833
energy spectra of 2.3 to 70 MeV, during PCA following Feb. 24-25 solar event, (E), 25:27563
energy spectra of 24- to 75-MeV/nucleon, following Feb. 25, 1969 solar event, (E), 25:27562
energy spectra of cosmic solar, satellite observation of, (E), 25:27533
intensity at synchronous altitude, temporal and spectral variations of solar, (E/T), 25:27541
monitoring in organisms, seston, and water of Black Sea off Rumanian coast during 1964 to 1967, 25:26745
production in ELMO mirror machine, 25:27438 (WASH-1159, pp 141-6)
reactions (α,Be-7) and (α,Li-7) with boron-10 at 45 MeV, test of Barshay-Temmer theorem by, 25:28176
reactions (α,d) with magnesium-24 at 28 MeV, analysis of angular distributions for ΔT = 0 selection rule, (E), 25:28233
reactions (α,n) and (α,p) with carbon-12 at 13 to 16 MeV, differential cross sections for, (E), 25:28188
reactions (α,n) with boron-11 at 3.4 to 3.7 MeV, polarization angular distributions from, (E), 25:28192
reactions (α,n) with carbon-13 at 3.4 to 4.8 MeV, angular distributions of neutron polarization in, (E), 25:28202
reactions (α,n) with iron-56 and titanium-48 at 11.5 to 22.7 MeV, neutron spectra from, (E), 25:28285
reactions (α,p) with magnesium-24 at 11.3 to 15.8 MeV, spectra and angular distributions for, (E), 25:28208 (ANU-P-521)
reactions (α,pγ) with iron-54 at 9 and 10 MeV, p-γ angular correlations from, (E), 25:28281
reactions (α,t) with lead-207 at 30 MeV, triton spectra from, (E), 25:28417
reactions (α,x) with carbon-12 at 100 to 140 MeV, production cross sections of lithium and beryllium isotopes in, (E), 25:28182
scattering by nitrogen-14 at 10.2 to 18.2 MeV, excitation functions for inelastic, (E), 25:28177
scattering by palladium-105 at 4.4 to 8 MeV with Coulomb excitation, γ spectra from inelastic, (E), 25:28423
use of high-doses of, for ablation of pituitary gland in patients with diabetes, 25:27037
ALPHA SPECTROMETERS
development of silicon surface-barrier, for measuring equilibrium of radon-222 and decay products, 25:26503
ALUMINUM
analysis for trace amounts of silver by solvent extraction and atomic absorption spectrophotometry, 25:26169
analysis of lunar surface-exposed foils of, for solar wind particles, 25:26187(R) (BNWL-1183-7)
crack propagation in, effects of mercury on, 25:27243
determination in granite by autoradiography and neutron activation, 25:26194
determination in sea floor samples by neutron activation, 25:26188 (BNWL-SA-3803)
determination in yttrium oxides by solvent extraction and spectrography, 25:26168
determination in Zircaloy, chemical method for, 25:26171
effects on spectrophotometric determination of beryllium and gallium, 25:26172
embrittlement by mercury-base zinc amalgams, 25:27243
gamma absorption coefficient of, (E), 25:27826 (DEMO-70/11)
ion reactions at 100 to 350 keV with, cross sections and Pauli-excitation mechanism of K-shell ionization in, 25:27453
meson (π) reactions at 1 GeV/c, differential and total cross sections for, (E), 25:27959
neon-ion reactions at 100 keV to 3.2 MeV with, cross sections and Pauli-excitation mechanism of K-shell ionization in, 25:27453
photon reactions at 5.4 GeV, total cross section for hadron production in, 25:27953
proton reactions at 1 GeV/c, differential and total cross sections for, (E), 25:27959
reactions of liquid, with uranium oxide to prepare uranium, reduction, 25:27284
reactions with intermetallic UAl_3, Jost mechanisms in solid-state, 25:26210 (KFK-1312)
tensile properties of, 25:27236
welding of 6061 and 5083, to Type 304 stainless steel for use as tubular transition joint, high-rate angular method for, 25:27186
ALUMINUM ALLOYS AND SYSTEMS
fatigue and fracture toughness of, 25:27236
Al--Ce, Kondo effect in intermetallic $CeAl_2$, study by superconducting proximity effect, (E), 25:27662
Al--Cr--Cu--Mg--Zn, analysis for trace amounts of silver by solvent extraction and atomic absorption spectrophotometry, 25:26169
Al--Cu--Zr, magnetic properties of $ZrCu/sub\ 2-x/Al/sub\ x/$, 25:27875
Al--Cu-base, depth distributions of 30-keV electrons and K x rays in, Monte Carlo calculation of, (T), 25:27836
Al--Mn, precipitation of, activation energy for, 25:28889 (SC-RR-70-356)
Al--Mo--Sn--Ti-base--Zr, fatigue properties of, 25:27236
Al--Mo--Ti-base--V, cracking under stress, effects of aqueous sodium chloride on, 25:27175
Al--Ni--Zr, phase studies of, 25:27258
Al--rare earths, s--f exchange coupling parameter of RAl_2, 25:27892
Al--Th, crystal structure parameters of intermetallic Th_2Al, (E), 25:27654
Al--transition metals, phase stability in, 25:27261
Al--U, analysis for trace amounts of silver by solvent extraction and atomic absorption spectrophotometry, 25:26169
Al--U, reactions of intermetallic UAl_3 in, with aluminum, Jost mechanisms in solid-state, 25:26210 (KFK-1312)
Al--U, reactions of liquid, with uranium oxide to prepare uranium, 25:27284
Al--U, separation of fission products from irradiated fuels of, by chlorination and pyrohydrolysis, 25:26332(T) (ORNL-tr-2410, pp 98-120)
Al--U_3O_8, phase studies of aluminum alloy-clad rolled fuel plates of, effects of deformation and shear

XUM

process on, 25:27294
AL--U_3O_8-base, structure of dispersions of, equipment and method for studies of, 25:27251
ALUMINUM IONS
charge state distribution in oxygen targets at 1 to 14 MeV, equilibrium, (E/T), 25:28127 (WASH-1159, pp 45-57)
ALUMINUM ISOTOPES Al-25
energy levels from magnesium-24 (p,γ) reactions, (E), 25:28276
ALUMINUM ISOTOPES Al-27
cross section data on, tables of multigroup, 25:28657 (HEDL-TME-71-36)
deuteron reactions (d,nγ) at 4 MeV, γ spectra from, (E), 25:28225
energy levels from carbon-12 (O-16,p) and magnesium-24 (α,p) reactions, search for high-spin, (E), 25:28208 (ANU-P-521)
energy-level transitions from proton reactions, branching ratios, gamma-ray angular distributions, and internal conversion coefficients for, (E/T), 25:28271
energy-level transitions in, M1, ΔT = 1, (E), 25:28225
nitrogen-14 elastic scattering at 65 to 88 MeV, optical-model analysis of differential cross sections for, (E), 25:28274
oxygen-16 elastic scattering at 36 to 48 MeV, angular distributions for, (E), 25:28196
ALUMINUM ISOTOPES Al-28
Coulomb energy differences in aluminum-28--silicon-28 isobaric analog states, 25:28243
ALUMINUM ISOTOPES Al-29
energy levels from aluminum-27 (t,p) reactions, lietimes of low-lying, (E), 25:28267
ALUMINUM OXIDES
deformation substructure in polycrystalline, 25:28878 (ORO-3328-13)
radioinduced Wigner energy storage in, neutron, 25:27839 (CEA-N-1171)
Al_2O_3--CoO--SiO_2, magnetic ordering and electric conduction in glasses of, 25:27901
Al_2O_3--Y_2O_3, phase studies of, using europium luminescence spectra as reference, 25:27303
AMERICIUM
determination in plutonium and uranium oxides by gamma counting, 25:26153 (LA-4622)
production by neutron irradiation of uranium, 25:26319(P)
separation from fission products, plutonium, and uranium by precipitation using a rare earth carrier, 25:26319(P)
AMERICIUM ALLOYS AND SYSTEMS
Am--Sb, magnetic properties of AmSb, Moessbauer-effect study of, 25:27922
AMERICIUM CARBIDES
magnetic properties of, Moessbauer-effect study of, 25:27922
AMERICIUM ISOTOPES Am-239
alpha decay of, α spectra from, (E), 25:28415
AMERICIUM ISOTOPES Am-241
cross section data on, tables of multigroup, 25:28657 (HEDL-TME-71-36)
AMERICIUM ISOTOPES Am-243
cross section data on, tables of multigroup, 25:28657 (HEDL-TME-71-36)
neon-22 reactions at 120 MeV, effective cross sections for element 105 production in, (E), 25:28350(T) (KFK-tr-350)
AMERICIUM SELENIDES
magnetic properties of, Moessbauer-effect study of, 25:27922
AMERICIUM TELLURIDES
magnetic properties of, Moessbauer-effect study of, 25:27922
AMINES
effects on systemic reactions following irradiation, 25:27036 (CONF-691057)
AMINO ACIDS
photolysis of, mechanisms of uv, 25:26644
radiation effects on content of, in rat liver, effects of dose and hepatectomy on x, 25:27022
radiation effects on films of, spin interactions in slow electron, 25:26277(R) (ORO-3799-7)
radioinduced mutations in fungus for dependency on, uv and x, 25:26703
radiolysis of aqueous solutions of sulfur-containing, effects of nitrous oxide and potassium bromide on yields from γ, 25:26294
AMMETERS
design of portable, for measuringg currents from ionization chambers, 25:26459
AMMONIA
effects on hydrogen yields from α radiolysis of gaseous hydrogen sulfide, 25:26315
effects on x-radioinduced polymerization of gaseous chloroethylene, 25:26282
AMPHIBIA
carbohydrate metabolism in developing, 25:28848(R) (COO-1631-27)
nucleic acid metabolism in developing, 25:28848(R) (COO-1631-27)
Rana sp., radiation effects on recovery of early potentials of eyes in, comparison of visible light and x, 25:27004
Rana sp., radiation effects on sciatic nerve of, dose dependence of 200-kV x, 25:26993
AMPLIFIERS
design of fast, for γ--γ coincidence spectrometers, 25:26504
AMYLOPECTINS
radiation effects on activity of, in wheat, γ, 25:26621
AMYLOSES
radiation effects on activity of, in wheat, γ, 25:26621
ANALYTICAL CHEMISTRY
conference on x-ray optics and microanalysis, Tuebingen, Germany, Sept. 9 to 14, 1968, 25:26155
ANGIOSPERMIDAE
Acer saccharinum, radiation effects on growth and photosynthesis in seedlings of, effects of reduced light on fast neutron, 25:27076
Allium sp., radiation effects on disulfide and lyase activity in, γ, 25:26620
Anethum graveolens, radiation effects on leaf cell size of, 5000 to 8000-R x, 25:27091
Anethum graveolens, radiation effects on nucleus size and DNA content of, 5000 to 10000 R, x, 25:27081
Arabidopsis thaliana, radiation effects on seeds of, effects of temperature on γ, 25:27071
Arabidopsis thaliana, radioinduced mutations for chlorophyll production and lethality, alpha, proton, and x, 25:26736
Betula sp., strontium-90 content in, formula for prediction of, 25:26616
Brassica oleracea, radiation effects on auxin content of, in X_2 generation following seed exposure, x, 25:26651
Camellia sinensis, radioisotope content of Japanese, April 1969 to April 1970, cesium-137 and strontium-90, 25:26392 (NIRS-RSD-27)
Cannabis sativa, radiation effects on growth and mitosis in, x, 25:27093
Carthamus tinctorius, radiation effects on cytological and morphologica properties of, effects of dose and dose rate on x, 25:27083
chromosome aberration and mutation induction in seeds of, economics of EMS, 25:26657
Cicer arietinum, radioinduced mutations in, genetic mapping of x, 25:26718
Citurs paradisi, radiation effects on scopoletin and scopolin synthesis in, gamma, 25:27079
Crepis capillaris, radioinduced chromosome aberrations in, gamma, fast neutron, and x, 25:26721
Crepis capillaris, radioinduced mutations in chromosomes of, comparison of ethylenimine induced mutations with, 25:26733
Glycine sp., radioinduced mutations in, for early maturation, increased yield, and resistance to nematodes, scab, and viruses, γ, 25:26706
Gossypium hirsutum, radiation effects on ploidy in, thermal neutron, gamma, x, 25:27087
Gossypium sp., radiation effects on carbohydrates and organic acids in leaves and roots of, following seed exposure, effects of dose on γ, 25:27074
Gossypium sp., radiation effects on mutagenesis of seeds of, effects of variety on γ and thermal neutron, 25:26728
Hordeum sp., radioinduced mutations for disease resistance, 25:26686 (CONF-680112-, pp 95-111)
Hordeum vulgare, radiation effects on growth of, following seed exposure, experience of Standard Neutron Irradiation Facility in Thailand in determining neutron, 25:27062 (IAEA-R-459)
Hordeum vulgare, radiation effects on ploidy in, thermal neutron, gamma, x, 25:27087
Hordeum vulgare, radioinduced mutations in, effects of EMS on gamma, 25:26716
Hordeum vulgare, radiosensitivity of seeds of, effects of storage temperature on x, 25:27092
Impatiens balsamina, radiation effects on germination and growth of seeds of, 30-kR x, 25:27086
Lactuca sativa, radiation effects on leaf cell size of, 5000 to 8000-R x, 25:27091
Linum sp., radiation effects on growth and mitosis in, x, 25:27093
Linum usitatissimum, mutation induction in, for chlorophyll production using endoxan, ethylmethanesulfonate, nitrosomethylurea, and triethylenemelamine, 25:27090
Linum usitatissimum, radioinduced mutations for chlorophyll production in, gamma, 25:27090
Liriodendron tulipifera, radiation effects on growth and photosynthesis in seedlings of, effects of reduced light on fast neutron, 25:27076
Lucerne sp., radiation effects on mitosis in, effects of doses of 500 to 15,000 R on gamma, 25:26732
Lycopersicum sp., radiation effects on physiology of, effects of cutting and vacuum infiltration on γ, 25:27067
Lycopersicum sp., radioinduced mutations for breeding in, gamma, 25:26735
Nicotiana glutinose, synthesis of TMV in leaves of, effects of magnetic fields on, 25:27106
Nicotiana rustica, radiation effects on ploidy in, thermal neutron, gamma, x, 25:27087
Oryza latifolia, radioinduced mutations for viable

reproduction in sterile hybrids of, γ, 25:26702
Oryza minuta, radioinduced mutations for viable reproduction in sterile hybrids of, γ, 25:26702
Oryza sativa, radiation effects on seed germination and survival of plants of, β and x, 25:27078
Oryza sativa, radioinduced morphological abnormalities in, exposed as seeds, β, γ, and x, 25:27077
Oryza sativa, radioinduced mutations for color and morphological changes in, x, 25:26688
Oryza sativa, radioinduced mutations in, for economic value, comparison of ethyl sulfate and x, 25:26701
Oryza sativa, radiosensitivity of, effects of dose rate, oxygen, storage, and water content on fission neutron and γ, 25:27070
Oryza sp., radioinduced mutations for chlorophyll production in diploid and tetraploid, x, 25:26714
Phaseolus vulgaris, radioinduced mutation frequencies for chlorophyll and morphology in, comparison of acute and chronic γ, 25:26685 (CONF-680112-, pp 85-93)
Pisum sativum, radioinduced mitotic delay in, effects of protein synthesis on γ, 25:27063
Pisum sp., radiation effects on chlorophyll content, growth, and respiration in, effects of gibberellin on x, 25:27064
Pisum sp., radiation effects on germination and pollen viability in, gamma, 25:27089
Pisum sp., radioinduced chromosome aberration in, gamma, 25:27089
radioinduced chromosome aberrations and mutations in seeds of, economics of γ and x, 25:26697
Raphanus sativus, radiation effects on growth and mitosis in, x, 25:27093
Secale cereale, radiation effects on growth and mitosis in, x, 25:27093
Solanum tuberosum, radioinduced mutations for morphological changes in leaves, stalks, and tubers of, 1000 to 120,000-R x, 25:26737
Sorghum sp., radioinduced mutations in, economics of gamma, 25:26715
Spinacia oleracea, radiation effects on leaf cell size of, 5000 to 8000-R x, 25:27091
Trifolium sp., calcium-45 uptake by seeds of, 25:26614
Triticium sp., radiation effects on chlorophyll content, growth, and repiration in, effects of gibberellin on x, 25:27064
Triticum aestivium, radiation effects on ploidy in, thermal neutron, gamma, x, 25:27087
Triticum durum, radioinduced mutations in, frequency of fast neutron and γ, 25:26710
Triticum sp., radiation effects on activity of amylose, amylopectin, and starch in, γ, 25:26621
Triticum sp., radiation effects on amylolysis in, effects of doses of 20 to 200 Krad on γ, 25:26622
Triticum sp., radiation effects on growth of 1000 to 8000 R, x, 25:27082
Triticum sp., radiation effects on physicochemical properties of, 25:27133 (CONF-680112-, pp 241-3)
Vicia faba, radioinduced lesions in chromosomes of, use of electron microscope scanning to visualize x, 25:26725
Vicia faba, radioinduced lesions in chromosomes of, distribution of x, 25:26734
Vicia faba, radioinduced stimulation of growth in roots of, effects of auxin and dose rate on γ, 25:27066
Vitis sp., uranium content of, 25:26615
Zea mays, radiation effects on carbohydrates and organic acids in leaves and roots of, following seed exposure, effects of dose on γ, 25:27074
Zea mays, radiation effects on chlorophyll content, growth, and respiration in, effects of gibberellin on x, 25:27064

ANIMALS
radiation effects on eyes of laboratory, effects of age and dose on, 25:27013
radiation effects on, protective effects of mercamine against ionizing, 25:27024
radiosensitivity of jejunal crypt cells of intestines in, effects of dose rate on whole-body, 25:26957

ANTENNAS
performance of rf probes, for diagnostics of warm anisotropic plasmas, 25:27683
spacing of five, dependence of horizontal drift and anisotropy of ionospheric irregularities on relative, (E), 25:27517

ANTIBODIES
effectiveness of iodine-125-labeled bovine antilymphocytic serum, for prolonging skin grafts, 25:26667
radiation effects on differentiation of, from bone marrow progenitors in mice, 25:26669
radiation effects on production of, in mice spleen cells, x, 25:26680
radioimmunoassay for binding and blocking anti-intrinsic, in human blood serum and gastric juice, diagnosis of pernicious anemia by, 25:26676

ANTIGENS
elimination from blood of chickens, preparation of iodine-131-labeled human blood serum for studies of, 25:26944
radiation effects on inactivation of surface of polyoma, effects of dose on uv, 25:27107
radiation effects on, in Naja naja snake venom, γ, 25:26674

ANTI-INFLAMMATORY DRUGS
effectiveness of solutions of, for treatment of radioinduced bladder inflammations, 25:26810

ANTIMONY
determination by photometry using carboxy derivatives of 2,6,7-trihydroxy-9-phenyl-3H-xanthen-3-one, 25:26174
determination in marine silts by neutron activation and γ spectroscopy, 25:26190(R) (NYO-4150-9)
determination in sea floor samples by neutron activation, 25:26188 (BNWL-SA-3803)
gamma absorption coefficient of, (E), 25:27826 (DEMO-70/11)

ANTIMONY ALLOYS AND SYSTEMS
Am--Sb, magnetic properties of AmSb, Moessbauer-effect study of, 25:27922
Be--Nb--Sb--Zr-base, properties for use as structural material for reactors, 25:27190(P)
Ce--Sb, crystal-field splitting and spin waves in CeSb, 25:27881
Ce--Sb--Y, thermal capacity of Ce/sub x/Y/sub 1-x/Sb at 1.5 to 70°K, 25:27881
Gd--Sb, electron band structure of GdSb, intrinsic metallic character in, 25:27879
La--Sb, thermal capacity of LaSb at 1.5 to 70°K, 25:27881
Pr--Sb, crystal field levels in PrSb, neutron inelastic scattering study of, 25:27893
Sb--Y, electron band structure of YSb, intrinsic metallic character in, 25:27879

ANTIMONY IONS
effects on silicon and germanium at 10 to 400 keV, distribution of defects induced in, 25:27861
implantation in silicon single crystals at 200 keV, lattice disorder induced in, 25:27859

ANTIMONY ISOTOPES Sb-110
beta decay of, half-life for, (E), 25:28332 (CERN-70-30(Vol.2), pp 1015-21)

ANTIMONY ISOTOPES Sb-111
beta decay of, half-life for, (E), 25:28332 (CERN-70-30(Vol.2), pp 1015-21)

ANTIMONY ISOTOPES Sb-112
beta decay of, half-life for, (E), 25:28332 (CERN-70-30(Vol.2), pp 1015-21)

ANTIMONY ISOTOPES Sb-113
beta decay of, half-life for, (E), 25:28332 (CERN-70-30(Vol.2), pp 1015-21)

ANTIMONY ISOTOPES Sb-114
beta decay of, half-life for, (E), 25:28332 (CERN-70-30(Vol.2), pp 1015-21)

ANTIMONY ISOTOPES Sb-121
energy levels of, analysis of nonrandom distributions of neutron resonance, (T), 25:28421

ANTIMONY ISOTOPES Sb-122
beta decay of, beta--gamma angular correlations in, (E/T), 25:28412

ANTIMONY ISOTOPES Sb-123
energy levels of, analysis of nonrandom distributions of neutron resonance, (T), 25:28421

ANTIMONY ISOTOPES Sb-133
beta decay of, Q value for, (E), 25:28296 (CERN-70-30(Vol.1), pp 341-51)

ARGENTINA
radiation processing of agricultural products in, review of, 25:27133 (CONF-680112-, pp 241-3)

ARGON
effects on yields from electron pulse and γ radiolysis of aqueous solutions of phenyl glucopyranoside, 25:26304
electron correlation and density in, calculations using restricted Hartree--Fock approximation, 25:27467
plasma of, electron density and temperature measurements in boundary layer of nonequilibrium, 25:27685
proton elastic scattering by, at 10 and 25 eV, secondary rainbows and interference in, (E), 25:27458
scattering by helium atoms, total cross sections for elastic, (T), 25:27444
scattering by nitrogen molecules, differential cross sections for, (E), 25:27451
sorption of crystalline, on niobium (100) crystal surface, LEED studies of, 25:27235

ARGON IONS
reactions with aluminum at 100 to 350 keV, cross sections and Pauli-excitation mechanisms of K-shell ionization in, 25:27453

ARGON ISOTOPES
abundance in lunar surface materials, (E), 25:27308
production in uranium-235 ternary neutron fission, mass-spectrometric search for, 25:28419

ARGON ISOTOPES Ar-33
beta and delayed-proton decay of, half-life and γ and proton spectra from, (E), 25:28195

ARGON ISOTOPES Ar-37
distribution in atmosphere, estimation of large-scale precipitation scavenging using vertical, 25:26390 (CONF-700601-, pp 465-74)

ARGON ISOTOPES Ar-40
deuteron reactions (d,p) at 1.96 MeV, angular distributions for, (E), 25:28251

ARGON ISOTOPES Ar-41
energy levels from argon-40 (d,p) reactions, spectroscopic factors for, (E), 25:28251

ARKANSAS NUCLEAR ONE POWER REACTOR, UNIT 2
design parameters of, revised and additional data on, 25:28620 (DOCKET-50368-8)
operations aspects of, revised and additional data on, 25:28620 (DOCKET-50368-8)
ARSENIC
determination by photometry using carboxy derivatives of 2,6,7-trihydroxy-9-phenyl-3H-xanthen-3-one, 25:26174
determination in sea floor samples by neutron activation, 25:26188 (BNWL-SA-3803)
determination in silicon by alpha scattering at 4 MeV, 25:26163
ARSENIC ISOTOPES As-75
energy levels of, analysis of nonrandom distributions of neutron resonance, (T), 25:28421
neutron reactions (n,2n) at 14.4 MeV, activation cross section for, (E), 25:28282
neutron reactions (n,α) at 14.4 MeV, activation cross section for, (E), 25:28282
neutron reactions (n,p) at 14.4 MeV, activation cross section for, (E), 25:28282
proton reactions (p,α) at 5 to 13 MeV, excitation functions for, (E), 25:28268
proton reactions (p,n) at 3 and 3.2 MeV, neutron spectra from, (E), 25:28241
ARSENIC ISOTOPES As-76
beta decay of, branching ratios, gamma spectra, and log-ft values for, (E), 25:28278
beta decay of, β-γ circular polarization correlation and nuclear matrix elements for, (E), 25:28216 (COO-1746-54)
ARYLSULPHATASE
radiation effects on activity of, in blood plasma and liver of rats, single and combined effects of turpentine and x, 25:26979
ASCORBIC ACID
complexes with iron, evaluation of metastable technetium-99-labeled, for kidney scanning, 25:26848
ASTATIDES
oxidation by dichromates in dilute perchloric acid solutions, production of positively charged ion by, 25:26209 (JINR-P12-5644)
ASTATINE
oxidation by dichromates in dilute perchloric acid solutions, production of positively charged ion by, 25:26209 (JINR-P12-5644)
ASTATINE ISOTOPES At-207
energy levels and properties of, nuclear data sheets for, 25:28378
ASTATINE ISOTOPES At-208
energy levels and properties of, nuclear data tables for, 25:28375
ASTATINE ISOTOPES At-209
energy levels and properties of, nuclear data sheets for, 25:28376
ASTATINE ISOTOPES At-211
energy levels and properties of, nuclear data sheets for, 25:28377
ASTRON DEVICE
E-layer equilibria in, reversed field, (T), 25:27798
E-layer in, cold plasma effects on negative mass instability in, (T), 25:27746
ASTRONAUTS
radiation exposure of, radiochemical methods for measurement of, 25:26178 (BNWL-SA-3608)
radiation exposure of, radiochemical methods for measurement of, 25:26187(R) (BNWL-1183-7)
radiation protection programs for, 25:26784
radiation protection programs for, use of radiation shielded human phantom and computer calculations for, 25:26778
ASTROPHYSICS
inverse-square law in, implications of, (T), 25:27422
ATMOSPHERE
cloud growth in, mathematical models for, 25:26385 (CONF-700601-, pp 385-402)
cloud rise in, mechanisms for nuclear explosion-produced, 25:26357 (CLOR-81/D)
contamination of, 25:28901 (UCRL-73063)
contamination of Chicago area, systems analysis program for control and measurement of, 25:28840 (ANL-ES-CC-8)
diffusion in, climatology of prediction variables in, 25:28881 (SC-DC-713920)
diffusion of iodine into marine, from sea surface, mechanisms of, (E), 25:26380 (CONF-700601-, pp 319-24)
effects of neutral composition of, on electron density and behavior of midlatitude ionospheric F region, (T), 25:27528
gas and particle scavenging from, by precipitation, method for predicting efficiency of, 25:26391 (CONF-700601-, pp 475-85)
nitrogen-oxide density in upper, theoretical model of diurnal variation of, (T), 25:27614
plasma transport in upper, (T), 25:27328
radioactivity measurements in, scintillation detector for beta, 25:26488
radioisotope distribution in, estimation of large-scale precipitation scavenging using natural, 25:26390 (CONF-700601-, pp 465-74)
trace substance distribution in, factors affecting, (T), 25:26383 (CONF-700601-, pp 373-80)
tritium content of Miami, Florida and Fairbanks, Alaska, June 1970 to March 1971, 25:26393(R) (ORO-3944)
ATMOSPHERIC PRECIPITATION
acidity of Scandanavian, effects of European stack-released sulfur dioxide on, (E), 25:26377 (CONF-700601-, pp 289-92)
aerosol scavenging by, effects of phoretic processes on submicron, 25:26387 (CONF-700601-, pp 411-22)
conference on scavenging by, Richland, Wash., June 2 to 4, 1970, 25:26358 (CONF-700601)
effects of convective storm-contained, on sulfur dioxide scavenging, (E), 25:26379 (CONF-700601-, pp 305-18)
effects on scavenging of particles from atmosphere, stable elements tracer studies of, (E), 25:26365 (CONF-700601-, pp 99-108)
ice particle content in hailstones and raindrops, effects of rainfall rate on, 25:26363 (CONF-700601-, pp 49-68)
particle scavenging by, design of indium tracer experiments for studying, 25:26361 (CONF-700601-, pp 21-35)
particle scavenging by, research priorities in, 25:26359 (CONF-700601-, pp 6-10)
particle scavenging by, use of pulse Doppler radar method for studying, 25:26360 (CONF-700601-, pp 13-20)
particle size spectra and velocity distribution in, pulse Doppler radar method for measurement of, 25:26360 (CONF-700601-, pp 13-20)
radioisotope scavenging by, effects of precipitation rate and ocean proximity on cosmogenic, (E), 25:26364 (CONF-700601-, pp 69-97)
silver content of hail, from Nebraska and South Dakota, absorption spectrophotometric measurements of, 25:26366 (CONF-700601-, pp 109-20)
strontium-90 scavenging from troposphere by, 25:26389 (CONF-700601-, pp 447-63)
tritium scavenging from troposphere by, 25:26389 (CONF-700601-, pp 447-63)
ATOMIC ABSORPTION SPECTROMETRY
methods for, review on, 25:26164
ATOMIC ENERGY
effects on marine ecology, review of, 25:26683
ATOMIC ENERGY, LEGAL ASPECTS
regulations for industrial, medical, and research handling of radioactive materials in Australia, 25:26738
regulations for packaging and shipping of radioactive materials, summary of U.S, 25:26445 (BRH/DMRE-71-1)
ATOMIC MODELS
density matrices for electronic systems, definitions and basic formulas for reduced, 25:27466
ATOMIC PHYSICS
bibliography on surface and vacuum physics, 25:27440
ATOMIC STRUCTURE
calculations of, use of one- and two-particle Coulomb Green functions in, 25:27465
ATOMS
electron localization in, use of information theory in, 25:27464
electron scattering factors for light, calculation using configuration-interaction and Hartree--Fock wave functions, 25:27460
hyperfine-interaction parameters for Z = 1 to 83, tables of isotropic and anisotropic, 25:27441 (ANL-7784)
interactions between multielectron, potential for exchange, (T), 25:27444
ion reactions with, electronic resonance states in negative, (T), 25:27462
reactions between ground-state and metastable, temperature effects on Penning ionization in, (E/T), 25:27457
reactions with ions, merging-beams method for study of, 25:27448 (IAE-2001)
x radiation from, tables of abundance, energy, and half-life of, (E), 25:28400
ATUCHA POWER REACTOR
construction of, planning and cost studies on, 25:28573
AURORAE
characteristics of, ESRO-I/AURORAE data on, (E), 25:27552
electric-field measurement in ionospheric, balloon electrostatic-probe, (E), 25:27545
electron acceleration and precipitation during magnetospheric substorms, (E/T), 25:27551
electron spectra and pitch-angle distribution in, ground-based observations of, (E), 25:27590
electron temperature in, effects of field-aligned currents on, (E/T), 25:27603
ion intensity in early-evening, solar-wind origin of primary proton and helium, (E/T), 25:27618
morphology of, (E/T), 25:27550
nitrogen excitation cross sections in, 5- to 25-keV-proton and .045- to 25-keV-electron, (E), 25:27616
nitrogen intensity in, excitation of 1134-, 1200-, 1493-, 1743-A far-uv from, atomic, (E/T), 25:27617
observations of noontime, airborne ionospheric and optical measurements of, (E), 25:27597
oxygen emission of 6300 to 6364 A in Type A, at 300 to 400 km associated with sporadic-F layer, (E/T), 25:27511
oxygen emissions of 5577 and 6300 A, intensity ratio in quiet arc at 120 to 330 km, (E), 25:27600
oxygen green-line emission in, relation to phase and

XUM

amplitude of pulsations, (E/T), 25:27599
particle spectra in midnight luminous, comparison of electron and proton, (E), 25:27578
properties of, x-ray and electron interdisciplinary analysis of, (E), 25:27549
stable red arcs associated with intense magnetic storms, plasmasphere proton density during, (E), 25:27622
stable red arcs in, observations from Adelaide, Sept. 1967 to Oct. 1969, (E), 25:27525
AURORAL ZONE
charged particles at 300 to 500 km in ionospheric, Geiger--Mueller observations during Feb. 25, 1969 solar event, (E), 25:27572
electron fluxes in, 10 and 80 degree pitch-angle distribution of magnetic activity-dependent low energy, (E), 25:27577
electron precipitation morphology and dynamics, from bremsstrahlung measurements, (E), 25:27583
electron-energy spectra variations of 1 to 6 keV in, relation to magnetic activity of, (E), 25:27582
energy release during polar substorms in, determination from photographs, (E), 25:27523
luminosity patterns over northern Scandinavia, relation to 1 to 13 keV electron and proton fluxes, (E), 25:27581
particle measurements during Feb.-Mar. 1969 in, low-energy electron and proton, (E), 25:27569
precipitation patterns over northern polar cap, keV electron and proton, 1968, (E), 25:27576
proton precipitation at high-latitude noon--midnight meridian, relation to geomagnetic activity, (E), 25:27579
radio-wave backscatter in, correlation with polar electrojet, vhf continuous, (E/T), 25:27554
x-radiation events in midnight, dynamics of polar magnetic substorm-related, (E), 25:27594
x-radiation events in midnight, relation to polar magnetic substorms, (E), 25:27593
AUSTRIA
radioactive waste management in, plans for future, 25:26451 (SGAE-RT-33/1970)
AUTORADIOGRAPHY
method for measurement of alkaline phosphatase activity in kidney tissues following addition of lead-210 to metal salt stain, 25:26574
AVES
chickens, radiation effects on antigen elimination from blood of, x, 25:26944
AVIATION PERSONNEL
radiation dose to supersonic transport, effects of cosmic radiation, heavy primary particles, and solar radiation and flares on, 25:26750(T) (ORNL-tr-2455)
radiation dose to, from ground operations handling of radioactive materials in transit, 25:26770
AVR REACTOR
boilers for, design parameters of helically wound tube, 25:28748

B

B-66 (NIOBIUM ALLOY)
stability at high temperatures, long-term thermal, 25:27208 (N-71-10352)
BABOONS
lead-210 distribution and retention in organs and tissues of, following intravenous injection, 25:26610
BACTERIOPHAGES
A25, radioinduced damage to head of, mechanisms of repair by host cell following uv, 25:27098
A5, radioinduced damage to head of, mechanisms of repair by host cell following uv, 25:27098
lambda, radiation effects on DNA polarity in, x, 25:26692
lambda, radiation effects on DNA release by, x, 25:26693
lambda, radiation effects on repair of, comparison of alkylating agents with uv, 25:27109
radiation effects on virulent, transduction of group A streptococcus to streptomycin resistance following uv, 25:27110
radiosensitivity of transducing Rhizobium meliloti, uv, 25:27104
T4, radiosensitivity of mutants of, defective in deoxyribonucleic acid ligase and rII gene, uv, 25:26708
T4, radiosensitivity of, effects of Kornberg polymerase on uv, 25:27105
BAILLY POWER REACTOR, UNIT 1
design parameters of, requested additional information on, 25:28619 (DOCKET-50367-12)
operations aspects of, requested additional information on, 25:28619 (DOCKET-50367-12)
BARIUM
abundance in lunar surface materials, (E), 25:27308
determination by electroconductivity method following chromatographic separation from alkali metals, 25:26173
determination by potentiometric titration using ion-selective electrodes, 25:26166
determination in barium carbonate by x ray fluorescence, 25:26167
BARIUM CARBONATES
analysis for barium and strontium by x ray fluorescence, 25:26167
BARIUM ISOTOPES
gamma--x-ray spectra of, from californium-252 spontaneous fission, 25:28416
BARIUM ISOTOPES Ba-126
energy levels from cadmium-114 (O-16,4n) reactions, deformation parameters and lifetimes for 2+, (E), 25:28319 (CERN-70-30(Vol.2), pp 905-10)
energy-level transitions from cadmium-114 (O-16,4n) reactions, probabilities for E2, (E), 25:28319 (CERN-70-30(Vol.2), pp 905-10)
BARIUM ISOTOPES Ba-128
energy levels from cadmium-116 (O-16,4n) reactions, deformation parameters and lifetimes for 2+, (E), 25:28319 (CERN-70-30(Vol.2), pp 905-10)
energy-level transitions from cadmium-116 (O-16,4n) reactions, probabilities for E2, (E), 25:28319 (CERN-70-30(Vol.2), pp 905-10)
BARIUM ISOTOPES Ba-130
proton elastic scattering at 7 to 12 MeV with isobaric analog excitation, comparison of spectroscopic factors to (d,p) reactions, 25:28372
BARIUM ISOTOPES Ba-132
energy level at 662 keV, internal Compton effect in decay of, (E), 25:28422
proton elastic scattering at 7 to 12 MeV with isobaric analog excitation, comparison of spectroscopic factors to (d,p) reactions, 25:28372
BARIUM ISOTOPES Ba-134
energy levels from cesium-134 beta decay, spin--parity assignments for, (E), 25:28405
proton elastic scattering at 7 to 12 MeV with isobaric analog excitation, comparison of spectroscopic factors to (d,p) reactions, 25:28372
BARIUM ISOTOPES Ba-135
use of metastable, for diagnosis of bone lesions in man, methods for, 25:26835
BARIUM ISOTOPES Ba-136
proton elastic scattering at 7 to 12 MeV with isobaric analog excitation, comparison of spectroscopic factors to (d,p) reactions, 25:28372
BARIUM ISOTOPES Ba-138
energy levels from cesium-138 beta decay, lifetimes and spin--parity assignments for, (E), 25:28342 (CERN-70-30(Vol.2), pp 1119-21)
proton elastic scattering at 7 to 12 MeV with isobaric analog excitation, comparison of spectroscopic factors to (d,p) reactions, 25:28372
BARIUM ISOTOPES Ba-140
determination of, 4π β--γ coincidence method for, 25:26464
BARIUM ISOTOPES Ba-141
beta decay of, Q value for, (E), 25:28296 (CERN-70-30(Vol.1), pp 341-51)
BARIUM OXIDES
reactions with lead chlorides, Jost mechanisms in solid-state, 25:26210 (KFK-1312)
BARYONS
interactions with mesons, baryon spin determination from polarized, 25:28040
interactions with mesons, eikonal model from unitarized Veneziano model for, 25:28041
BARYONS, RESONANCE
decay of, spin formalisms for, 25:28007 (CERN-71-8)
energy level diagrams for, rotational, 25:28009
production by polarized particles, additivity frame in quark model for, 25:28017
properties of, systematics of, 25:28010
properties of, systematics of, 25:28008 (UCRL-73073)
BARYONS, RESONANCE (N*)
decay rates from partial-wave analysis of $\pi^- + p \rightarrow \Lambda^- + \pi^-$ interactions at 1640 to 1760 MeV, 25:27962
production in $\pi + N \rightarrow \pi + N^*$, s-channel helicity conservation constraints on t-channel exchanges in, (T), 25:28028 (SU-1206-242)
production in $\pi^+ + p \rightarrow rho^0 + \Delta^{++}$ at 11.7 GeV/c/differential and total cross sections for, (E/T), 25:27960 (DESY-71/8)
production of Δ(1236) in $K^+ + p \rightarrow K^0 + \pi^+ + p$ interactions at 10 GeV/c, (E), 25:27968
BARYONS, RESONANCE (Y*)
production of Σ(1385) in $\pi^- + p \rightarrow K^+ + \Sigma(1385)$ interactions at 2.75 to 14.0 GeV/c, cross sections for, (E), 25:28038
BEARINGS
book: Theory and Practice of Lubrication Systems, 25:26416
materials for nuclear reactor, for operation in space at 1500°F, evaluation of, 25:27200 (CONF-691114-7)
BEHAVIOR
radiation effects on audiogenic seizure susceptibility in offspring of rats, in utero x, 25:26968
BENZENE
radioinduced thermal oxidation of, with oxygen, electron, 25:26284
reactions with radiolytic hydroxyl radicals, effects of micellar solutions on, 25:26295
BENZENE, ALKYL-
effects as diluent on stability of tridodecylamine, 25:26330(T) (ORNL-tr-2410, pp 14-78)

alkylbenzene--tridodecylamine, radiolysis of, plutonium-239 α, 25:26330(T) (ORNL-tr-2410, pp 14-78)
BENZENE, NITRO-
radiolysis of aqueous solutions of,yields of hydrated electrons from electron pulse, 25:26308
BENZYDAMINE
radioprotective effects of, on skin inflammation in rabbits, 25:26806
BERYLLIUM
book: Electrolytic Process for Ultra-Fine Beryllium, 25:27192
determination by spectrophotometry, effects of thorium, uranium, and other metals on, 25:26172
electron correlation and density in, calculations using restricted Hartree--Fock approximation, 25:27467
passivation for corrosion protection by anodization, 25:27172(P)
photon reactions at 1.5 to 5.7 GeV, total cross section for hadron production in, 25:27953
properties of fibers of, for use in composites, 25:27278
radiation effects on electric conductivity of, fast and thermal neutron, 25:28765
shear constant for, calculation from axial ratios, 25:27240
x-ray K-emission spectrum excited by synchrotron radiation, (E), 25:27827 (DESY-70/59)
BERYLLIUM ALLOYS AND SYSTEMS
Be--Cu, fabrication and uses of high conductivity, 25:27187
Be--Cu, fatigue strength of, effects of fine precipitates on, 25:27231
Be--Cu--Nb--Zr-base, properties for use as structural material for reactors, 25:27190(P)
Be--Cu-base--Ni--Ti, properties of, aging and mechanical, 25:27232
Be--Fe-base, structure in aging, model for tri-axial periodic modulated, 25:27249
Be--Nb--Sb--Zr-base, properties for use as structural material for reactors, 25:27190(P)
Be--Nb--Sn--Zr-base, properties for use as structural material for reactors, 25:27190(P)
Be--Nb--Te--Zr-base, properties for use as structural material for reactors, 25:27190(P)
Be--transition metals-base, properties for use as structural material for reactors, 25:27190(P)
Be--Zr-base, properties of brazing alloy of, for attaching low profile thermocouples to Zircaloy fuel sheaths, 25:27182 (R-69-CAP-8)
Be-base--Cu, embrittlement by mercury-base--sodium alloys at 25°C, 25:27243
Be-base--Ni, properties for use in welding heat resisting metals, 25:27177 (JUL-681-RX)
BERYLLIUM HYDRIDES
pyrolysis of BeH_2, kinetics of, 25:26278
radiation effects on pyrolysis of BeH_2, x, 25:26278
BERYLLIUM ISOTOPES Be-7
determination in feces and urine of astronauts by γ spectroscopy, 25:26178 (BNWL-SA-3608)
distribution in atmosphere, estimation of large-scale precipitation scavenging using vertical, 25:26390 (CONF-700601-, pp 465-74)
electron-capture decay of, internal bremsstrahlung spectra from, (E), 25:28200
production by carbon-12 (p,x) and (α,x) reactions, cross sections for, (E), 25:28182
BERYLLIUM ISOTOPES Be-8
nuclear binding energy, deformation, quadrupole moments, radii, and shape of, (T), 25:28180
BERYLLIUM ISOTOPES Be-9
cross section data on, tables of multigroup, 25:28657 (HEDL-TME-71-36)
helium-3 reactions (He-3,d) at 22 MeV, isospin dependence of angular distributions for, (E), 25:28174
meson (π^-) capture with charged particle emission, particle spectra and branching ratios for, (E), 25:28178
photon reactions (γ,p) at 56 MeV, proton spectra and cross sections for, (E), 25:28194
production by carbon-12 (p,x) and (α,x) reactions, cross sections for, (E), 25:28182
BERYLLIUM ISOTOPES Be-10
production by carbon-12 (p,x) and (α,x) reactions, cross sections for, (E), 25:28182
BERYLLIUM OXIDES
neutron scattering by, cross sections, phonon spectra, and scattering law from different crystal models for thermal, (T), 25:28158
properties of, 25:27281 (INIS-mf-13)
properties of composites of, 25:27277
radioinduced Wigner energy storage in, neutron, 25:27839 (CEA-N-1171)
BETA DECAY
interference effects in hindered allowed, behavior of matrix elements for higher-order, (T), 25:28480
neutrinos in, relativistic extension of droplet theory of elementary particle structure for, (T), 25:27970
probability relative to electron capture, calculations of, (T), 25:28494
Q values for, development of β--γ spectrometer for measuring, 25:28296 (CERN-70-30(Vol.1), pp 341-51)
radiative corrections in, (T), 25:28493
strength functions for high Q-value, review of, (T), 25:28443 (CERN-70-30(Vol.1), pp 421-33)
theory in region far from stability, gross, (T), 25:28442 (CERN-70-30(Vol.1), pp 397-419)
BETA PARTICLES
detection of, development of organic-liquid ionization chambers for, 25:26471
dose calculations for strontium-90, in extracorporeal irradiation of blood, 25:26754
dose to abdomen, face, and hands of medical personnel using technetium-99m, methods for shielding against, 25:26765
dose to chest and gonads of medical personnel during technetium-99m scintigraphy, 25:26766
dose to feline bones following chronic ingestion of strontium-90, 25:26612
dose to medical personnel from handling technetium-99m, devices for protection against, 25:26776
dose to medical personnel from preparation of technetium-99m-labeled compounds, 25:26768
dose to normal and melanoma tissues in dogs following injection of iodine-131-labeled chloroquine analog, absorbed, 25:26882
dose to skin following particulate contamination of clothing, estimation of, 25:26748
dosimetry of strontium-90 applicator, for use in therapy, 25:26870
effects on chromosomes in human leukocytes, aberrant, 25:26730
effects on frozen aliphatic alcohols, role of LET in, 25:26311
effects on human eyes, effects of dose on, 25:26870
effects on lungs of rats, carcinogenic, 25:26921(T) (LF-tr-49)
effects on morphological abnormalities in rice exposed as seeds, 25:27077
effects on seed germination and survival of rice plants, 25:27078
effects on visual system of noctuid moths, combined effects of light and, 25:26910
monitoring in organisms, seston, and water of Black Sea off Rumanian coast during 1964 to 1967, 25:26745
reactions with single crystals, effects of channeling on bremsstrahlung spectra from, (T), 25:27832
BETA SOURCES
activity measurements in atmosphere, scintillation detector for, 25:26488
dose distribution in water around 75 point, computer calculations for, 25:26753
BETA SPECTROMETERS
design of, for directional correlation measurements, 25:28410
development of β--γ coincidence, for measuring total nuclear decay energies, 25:28296 (CERN-70-30(Vol.1), pp 341-51)
magnetic field in √2 π, stabilization of, 25:26502
BETATRONS
space-charge acceleration in 8- and 25-MeV, effects of resonant phenomena on incoherent, 25:28143
BEVATRON
beam splitting system for, septum magnet, 25:28119 (UCRL-20194)
BEVERAGES
wines, radioisotope content of Transylvania, 25:26618
wines, uranium content of, 25:26615
BEZNAU POWER REACTOR, UNIT 1
operations history for, 25:28638
BIBLIOGRAPHIES
on decontamination methods, 25:26443 (AED-C-13-7)
on hafnium and zirconium, 25:27191
on plasma physics, 25:27667
on plasma physics, 25:27668
on plutonium with appendix on transplutonium elements, Feb. 1971, 25:27168
on plutonium with appendix on transplutonium elements, Jan. 1971, 25:27169
on production and industrial uses of radioisotopes, Oct. through Dec. 1970, 25:26427 (ORNL-IIC-30(Pt.4))
on surface and vacuum physics, 25:27440
BIG ROCK POINT POWER REACTOR
operations history for 1963 to 1970, review of, 25:28577
operations history for May to October 1967, 25:28561 (DOCKET-50155-78)
BIOLOGICAL MATERIALS
analysis for carbon-14 and sulfur-35, external standardization method for automatic liquid scintillation spectroscopic, 25:26184
book: Effects of Metals on Cells, Subcellular Elements, and Macromolecules, 25:26608
BIOLOGICAL MODELS
development of anthropomorphic Monte Carlo computer, for estimation of absorbed dose in gonads from γ source implanted elsewhere in body, 25:26760
development of demographic, for determining population response to radiosterilized male technique for pest control, 25:27153
BIOLOGY
research progress in, AEC, 25:26205
BIPHENYL
biphenyl--2-methylbutane, radiolysis at -120°C, delayed emission and ion recombination in pulse, 25:26297

BISMUTH
determination by photometry using carboxy derivatives of 2,6,7-trihydroxy-9-phenyl-3H-xanthen-3-one, 25:26174
BISMUTH ALLOYS AND SYSTEMS
Bi--Ce, magnetic structure of CeBi, neutron-diffraction study of, 25:27887
Bi--Dy, magnetic structure of DyBi, neutron-diffraction study of, 25:27887
Bi--Nd, magnetic structure of NdBi, neutron-diffraction study of, 25:27887
Bi--Pr, crystal field levels in PrBi, neutron inelastic scattering study of, 25:27893
Bi--Tb, magnetic structure of TbBi, neutron-diffraction study of, 25:27887
BISMUTH ISOTOPES Bi-207
energy levels and properties of, nuclear data sheets for, 25:28378
energy-level transitions in, electron conversion ratios for, (E), 25:28352 (N-71-10060)
BISMUTH ISOTOPES Bi-208
energy levels and properties of, nuclear data tables for, 25:28375
energy levels and transitions from stripping and pickup reactions, spectroscopic factors for, (E), 25:28417
BISMUTH ISOTOPES Bi-209
deuteron reactions (d,t) at 20 MeV, triton spectra from, (E), 25:28417
energy levels and properties of, nuclear data sheets for, 25:28376
energy levels from lead-208 proton resonances, inelastic proton decay of isobaric analog, (T), 25:28367
helium-3 reactions (He-3,α) at 28 MeV, alpha spectra from, (E), 25:28417
BISMUTH ISOTOPES Bi-211
energy levels and properties of, nuclear data sheets for, 25:28377
BITUMINOUS MATERIALS
gamma absorption coefficient of, (E), 25:27826 (DEMO-70/11)
BLACK BODY RADIATION
relation to gamma radiation with energy above 10^{19} eV, (T), 25:27423
BLACK SEA
radioactivity monitoring in organisms, seston, and water of, off Rumanian coast during 1964 to 1967, 25:26745
BLADDER
radiation dose tolerance of human, during rotation therapy, γ, 25:26894
radioinduced injuries of human, following therapy for gynecological tumors, methods for treatment of, 25:26813
radioinduced injuries of human, methods for treatment of, 25:26810
radiotherapy of tumors of human, effectiveness of high-energy x, 25:26876
BLAST EFFECTS
measurement of long-range air, from Pre-Gondola III Phase II explosion, 25:26408 (PNE-1117)
measurement of Pre-Gondola II Event, 25:26407 (PNE-1112)
BLOOD
circulation in bones of rabbits, use of strontium-85-labeled plastic microspheres for measurement of, 25:26577
circulation in human lungs, tracer technique for scanning, 25:26819
circulation in liver of cats, xenon-133 clearance studies on, 25:26576
clotting time of human, following addition of γ-irradiated clotting factors, 25:26900
effects of loss of, on survival of x-irradiated mice, 25:26934
radiation dose to human, calculations of strontium-90 β, 25:26754
radiation effects on coagulation of, in man following cancer therapy, effects of dose on, 25:26668
radiation effects on thromboelastogram of human, following addition of γ-irradiated varidase, 25:26632
sampling, design of small portable constant withdrawal pump for, 25:26579
BLOOD CELLS
formation in mice, role of bone marrow stem cells in, 25:28898 (UCRL-20613)
phosphorus accumulation in, of uranium miners, 25:26582
radiation effects on immune reactions in peripheral, in human populations on Marshall Islands, correlation of aging and fallout, 25:27058
BLOOD PLASMA
circulation time through kidneys, effectiveness of iodine-131-labeled hippuran in combination with external gamma radiation for measuring, 25:26826
flow through kidneys, development of catheterless method using iodine-131 for measurement of, 25:26825
radiation effects on activity of lysosomal enzymes and content of glycoproteins in, of rats, single and combined effects of turpentine and, 25:26979
radiation effects on corticosterone content of rat, recovery from, 25:26998
radiation effects on esterase activity of rat, effects of pH on, 25:26600
radioimmunoassay for ACTH in human, antibody binding method for, 25:26675
BLOOD PLATELETS
radiation effects on, in man following cancer therapy, effects of dose on, 25:26668
BLOOD PRESSURE
radiation effects on, of rabbits, protective effects of AET and cystamine against γ, 25:26794
BLOOD SERUM
cerium-141 binding to proteins in, review on dialysis methods for studying, 25:26584
labeling with iodine-131 for use in antigen elimination studies, 25:26944
radiation effects on proteins in, of goats, acute and chronic γ, 25:26970
radioimmunoassay for binding and blocking anti-intrinsic factor antibodies in human, diagnosis of pernicious anemia by, 25:26676
thyroxine content of human, development of iodine-125 labeling method for determining, 25:26568
BLOOD VESSELS
scanning of human, for diagnosis of vascular diseases, methods for technetium-99 in, 25:26838
BLOWERS
design of high pressure low flow helium, for fuel element irradiation test loop, 25:28833
BOILERS
design for molten salt and liquid metal cooled reactor, 25:28746(P)
design parameters for 330 MW(e) high temperature gas cooled reactor, 25:28631
design parameters of power reactor, 25:28748
design parameters of pressure vessel enclosed, for pressurized water reactors, 25:28751(P)
BOLIVIA
insect radiosterilization in, methods for, 25:27130 (CONF-680112-, pp 129-42)
BONE MARROW
effects of transplants of, on leukosis in irradiated mice, 25:26904
effects of transplants of, on recovery of rabbits from combined liver and radiation injuries, 25:27005
function of stem cells of, in development of blood cells, 25:28898 (UCRL-20613)
radiation effects on colony formation in allogeneic and syngeneic transplants of spleen cells and, in mice, γ, 25:26670
radiation effects on differentiation of immunoresponsive cells from progenitors in, of mice, 25:26669
radiation effects on growth of stem cells of, in spleen of rats following injection, x, 25:26939
radiation effects on hematopoiesis in mouse, effects of intraperitoneal injection of milk on x, 25:26678
radiation effects on immune reactions and myeloid functions in, of mice, effects of phytohemagglutinin on x, 25:26942
radiation effects on iron-59 distribution and uptake in, of mice, effects of immune reactions on x, 25:27012
radiation effects on mouse, effects of balneotherapy on mixed gamma and neutron, 25:26950
radiation effects on oxidative phosphorylation and respiration in rabbit, after homotransplantation of bone marrow elements, 25:27019
radiation effects on stem cells in, of mice, partial- and whole-body x, 25:26956
radiation effects on, in mammals, review on latent whole-body, 25:26943
scanning for localization of neoplastic metastases in, use of gold-198 colloids for, 25:26847
thorium-228 accumulation in human, 25:26603
use of transplants of, in experimental radiation pathology, 25:27036 (CONF-691057)
BONES
blood flow in, of rabbits, use of strontium-85-labeled plastic microspheres for measurement of, 25:26577
chromium-51 uptake by rat, following intravenous injection of labeled alloxantin, methods for determining, 25:26590
lead-210 distribution in, of baboons and rats, 25:26610
molybdenum-99 distribution and retention in rat, following subcutaneous injection, 25:26598
plutonium-239 uptake by, of dogs following inhalation of labeled plutonium oxide, 25:26599
radiation dose rate to feline, following chronic ingestion of strontium-90, 25:26612
radiation dose to pregnant patients during pelvimetry, orthometric view for reduction of x, 25:26831
radiation effects on differentiation of rib, in progeny of mice, effects of in utero 2'-deoxy-5-fluorocytidine and x, 25:26997
radiation effects on growth of rat mandible, 1200-R x, 25:27025
radiation effects on rat mandibular, 1200-R x, 25:27026
radioinduced damage to mandibular, in chick embryos, x, 25:27018
radioinduced injuries in lower jaw, of rabbits, effects of dose and time on, 25:27003
radioisotope content of, in humans in South Africa during 1963 to 1967, methods for calculating fallout, 25:26613
radiotherapy of joint diseases in human, effectiveness of synovial injection of gold-198, phosphorus-32, or yttrium-90 for, 25:26873
scanning of human, for diagnosis of lesions,

XUM

effectiveness of barium-135m for, 25:26835
uranium content of, of fossil animals and mice, 25:26744
zinc-65 uptake and distribution in endochondral growth sites of, in rats, 25:26611
BOROHYDRIDES
radiosensitizing effects on collagen gel, x, 25:26802
BORON
determination by prompt neutron activation using an americium--beryllium source, 25:26198
determination in Zircaloy, chemical and instrumental methods for, 25:26171
effects on fabrication and oxidation of niobium alloys, 25:27227
implants in diamond single crystals, analysis, 25:27858
reactions with rare earth oxides, effects of shock waves and temperature on, 25:27291
x-ray K-emission spectrum excited by synchrotron radiation, (E), 25:27827 (DESY-70/59)
BORON CARBIDES
reactivity worth of cylinder shaped, (E/T), 25:28820 (EUR-4556)
BORON IONS
implantation in silicon at 15 keV, proton energy-loss measurements of distribution of, 25:27855
implantation in silicon at 150 keV, high-temperature isothermal annealing studies of, 25:27854
implantation in silicon at 200 keV, flux and fluence dependence of lattice disorder induced in, 25:27864
implantation in silicon single crystals at 100 to 400 keV, annealing of damage induced in, 25:27863
BORON ISOTOPES B-10
alpha reactions (α,Be-7) and (α,Li-7) at 45 MeV, test of Barshay-Temmer theorem by, 25:28176
cross section data on, tables of multigroup, 25:28657 (HEDL-TME-71-36)
effects on ir spectra of borazine and boroxine, 25:26233
meson (π^-) capture with charged particle emission, particle spectra and branching ratios for, (E), 25:28178
BORON ISOTOPES B-11
alpha reactions (α,n) at 3.4 to 3.7 MeV, polarization angular distributions from, (E), 25:28192
helium-3 reactions (He-3,d) at 22 MeV, isospin dependence of angular distributions for, (E), 25:28174
helium-3 reactions (He-3,d) with carbon-12 at 44 MeV, deuteron spectra and angular distributions for, (E), 25:28205
proton reactions (p,3α) at 2 MeV, multiparticle-reaction analysis of energy distributions from, (T), 25:28184
reactions with gold-197 and praseodymium-141, cross-section limits for fission isomer excitation in, (E), 25:28399
reactions with zinc-64 at 43 MeV with alpha and proton evaporation, statistical analysis for shell and angular momentum effects in, (T), 25:28266
BORON ISOTOPES B-12
nuclear magnetic resonance in molybdenum, niobium, tantalum, titanium borides, tungsten, and zirconium borides, coupling constants and spectra from, (E), 25:27923
nuclear quadrupole moment from NMR studies, (E), 25:27923
BORON OXIDES
B_2O_3--Fe_2O_3--Li_2O--Na_2O, magnetic ordering and electric conduction in glasses of, 25:27901
B_2O_3--Fe_2O_3--Na_2O, magnetic ordering and electric conduction in glasses of, 25:27901
BORON SYSTEMS
B--Cr--Mn, phase diagram at 800°C, isothermal, 25:27299
B--epoxy, properties for use in aircraft structures, 25:27307
B--Hf--Nb-base--W, strength at 1200°C, 25:27227
B--Mn--Ti, phase diagrams at 800 and 1400°C, isothermal, 25:27300
B--Ti--V, phase diagrams at 800 and 1400°C, isothermal, 25:27300
BOSONS
group theory of superfluid system of, 25:27641
wave equations for finite-mass, first order, 25:27975
BRAIN
metastases radiotherapy of metastases in human, combined effects of corticosteroids and γ and x, 25:26895
radiation effects on developing rat, x, 25:26946
radiation effects on edema development in monkey, x, 25:26987
radiation effects on noradrenaline and serotonin levels in, of rats, whole-body x, 25:26959
radiation effects on reflexes of rat, 1-R dose, 25:26949
radioinduced aberrations in, of human progeny following maternal uterine therapy, x, 25:27057
radioinduced necrosis in, of man following therapy, x, 25:27041
radiotherapy of tumors of, development of nervous tissue reactions following, 25:27056
scanning for diagnosis of infected lesions of, in man using technetium-99m, 25:26818
scanning of human, computer evaluation of mercury-197, 25:26824
scanning of human, for diagnosis of lesions and malignancies, effectiveness of, 25:26850
scanning of human, for diagnosis of tumors, comparison of gamma camera and rectilinear scanner for technetium-99m, 25:26852
scanning of human, for diagnosis of tumors, methods for technetium-99, 25:26828
scanning using mercury-197, technetium-99, xenon-133, and ytterbium-169, international methods for, 25:26855
BRASS
analysis for trace amounts of silver by solvent extraction and atomic absorption spectrophotometry, 25:26169
crack propagation in, effects of mercury on, 25:27243
tensile properties of α-, 25:27236
BREEDING (BIOLOGICAL)
radiation effects on plant, description of joint FAO/IAEA program on, 25:27128 (CONF-680112-, pp 1-7)
BREMSSTRAHLUNG
dose calculation for bronchial carcinoma therapy, techniques for 43-MeV betatron, 25:26757
emission from relativistic plasma, theory for, 25:27687 (NP-18758)
emission from turbulent plasma, theory for, 25:27704 (NP-18759)
intensity in auroral zone associated with electron precipitation morphology and dynamics, (E), 25:27583
production by beta particles traversing single crystals, effects of channeling on spectra of, (T), 25:27832
reactions (γ,n) with A = 19 to 208 nuclei near threshold energies, cross sections and resonance parameters for, (E), 25:28413
reactions (γ,n) with deuterium up to 125 MeV, angular distributions for, (E), 25:28165
reactions (γ,n) with thallium-203 and -205 at 30 MeV endpoint energy, cross sections for, (E), 25:28391
reactions (γ,p) with cerium-140, lanthanum-139, praseodymium-141, and samarium-144 with isobaric analog excitation, proton spectra from, (E), 25:28362
reactions (γ,p) with molybdenum-92, strontium-88, yttrium-89, and zirconium-90 with isobaric analog excitation, proton spectra from, (E), 25:28227
reactions (γ,p) with tin-116, -118, -120, and -124 with isobaric analog excitation, proton spectra from, (E), 25:28361
reactions with even tin isotopes, isotope effects on giant dipole resonance in, (T), 25:28393
BROMINE
content ratio to chlorine and iodine in marine aerosols, mathematical model for demonstrating aerosol particle size dependence of, 25:26381 (CONF-700601-, pp 325-51)
determination in woven fabric by neutron activation, 25:26200
BROMINE IONS
charge state distribution in oxygen targets at 1 to 14 MeV, equilibrium, (E/T), 25:28127 (WASH-1159, pp 45-57)
BROMINE ISOTOPES Br-72
half-life for, (E), 25:28213 (CERN-70-30(Vol.2), pp 911-15)
BROMINE ISOTOPES Br-76
beta and electron-capture decay of, γ singles and coincidence spectra from, (E), 25:28246
BROMINE ISOTOPES Br-79
neutron reactions (n,2n) at 14.4 MeV, activation cross section for, (E), 25:28282
neutron reactions (n,α) at 14.4 MeV, activation cross section for, (E), 25:28282
BROMINE ISOTOPES Br-81
neutron reactions (n,2n) at 14.4 MeV, activation cross section for, (E), 25:28282
neutron reactions (n,α) at 14.4 MeV, activation cross section for, (E), 25:28282
neutron reactions (n,p) at 14.4 MeV, activation cross section for, (E), 25:28282
BROMINE ISOTOPES Br-82
exchange in base-catalyzed isomerization of tribromobenzene, 25:26221
BROMINE ISOTOPES Br-87
neutron decay of, half-lives and yields from delayed-, (E), 25:28211 (CERN-70-30(Vol.1), pp 517-18)
BROMINE ISOTOPES Br-88
neutron decay of, yields from delayed-, (E), 25:28211 (CERN-70-30(Vol.1), pp 517-18)
BROMINE ISOTOPES Br-90
beta decay of, half-life for, (E), 25:28326 (CERN-70-30(Vol.2), pp 985-1000)
BROMINE ISOTOPES Br-91
beta decay of, half-life for, (E), 25:28326 (CERN-70-30(Vol.2), pp 985-1000)
BROMINE ISOTOPES Br-92
beta decay of, half-life for, (E), 25:28326 (CERN-70-30(Vol.2), pp 985-1000)
BROOKHAVEN ALTERNATING-GRADIENT SYNCHROTRON (AGS)
experimental facilities for, 1970 summer study on post-conversion, 25:28104 (BNL-16000)
operating parameters of post-conversion, 25:28104 (BNL-16000)
research program at, 1970 summer study on post-conversion, 25:28104 (BNL-16000)
BRYOPHYTA
Polytrichum commune, radiation effects on gametophores, spores, and sporocytes, chronic low-dose γ, 25:27075
BUBBLES
diffusion in helium- and krypton-ion-irradiated copper

XUM

foils, 25:27842 (RD/B/N-1850)
BUILDING MATERIALS
gamma absorption coefficients, (E), 25:27826 (DEMO-70/11)
radioinduced hardening in reactor, review of, 25:27265 (INIS-mf-5)
BUTADIENE POLYMERS
radioinduced crosslinking of, volume dependence of C_2 correction in equation of state for products from γ, 25:26285
BUTANE, 2-METHYL-
biphenyl--2-methylbutane, radiolysis at -120°C, delayed emission and ion recombination in pulse, 25:26297
1,3-BUTANEDIONE, 4,4,4-TRIFLUORO-1-(2-THIENYL)-
complexes with alkali metals, ion-exchange separation of, from other elements, 25:26337(P)
solvent properties for uranium, 25:26340
tert-BUTYL RADICALS
yields of ions of, from γ radiolysis of liquid 2,2-dimethylpropane, kinetics of reactions of electron scavengers and hydrocarbons with, 25:26309
sec-BUTYLAMINE
effects on survival of γ-irradiated Penicillium expansum, 25:27084
BUTYRIC ACID, 2-AMINO-4-(METHYLSELENYL)-
distribution of selenium-75-labeled, in rat pancreas, effects of intravenously injected pancreozymin and secretin on, 25:26591

C

C-129Y (NIOBIUM ALLOY)
stability at high temperatures, long-term thermal, 25:27208 (N-71-10352)
CACTINOMYCIN
effects on glial tumor cells, damaging, 25:26908
CADARACHE REACTORS
irradiation loop of PEGASE, optimization of control of, (T), 25:28768
CADARACHE REACTORS (RAPSODIE)
fuel elements for, decladding of irradiated, by chopping and crushing at high temperatures, 25:26332(T) (ORNL-tr-2410, pp 98-120)
CADMIUM
complexes with 5,7-diiodo-8-quinolinol, formation constants of, 25:26214
determination in sea floor samples by neutron activation, 25:26188 (BNWL-SA-3803)
determination in Zircaloy, chemical and instrumental methods for, 25:26171
effects on activity of alkaline phosphatase in kidney tissues, 25:26574
failure under stress, effects of mercury on, 25:27243
gamma absorption coefficient of, (E), 25:27826 (DEMO-70/11)
perturbed angular correlation in ferromagnetic gadolinium for noncoaxial magnetic and electric fields, 25:27919
shear constant for, calculation from axial ratios, 25:27240
surface resistance oscillations in magnetic field of single-crystal plates of, Doppler-shifted, (E/T), 25:27900
CADMIUM ALLOYS AND SYSTEMS
Cd--Cu, fabrication and uses of high conductivity, 25:27187
Cd--Hg, ordering of ω-phase, at 81°K, calorimetric study of long-range, 25:27248
CADMIUM IONS
implantation in silicon at 50 keV, outdiffusion, lattice location, and electrical behavior of, 25:27856
CADMIUM ISOTOPES
energy levels from (d,p) and (d,t) reactions, spectroscopic factors for, (E), 25:28374
CADMIUM ISOTOPES Cd-108
energy levels from resonances in silver-107 ($p,,\alpha$) reactions, widths for compound-nucleus, (E), 25:28268
CADMIUM ISOTOPES Cd-109
energy levels from indium-109 decay, spin parity assignments for, (E), 25:28428
CADMIUM ISOTOPES Cd-110
energy levels from isomeric silver-110 beta decay, spin-parity assignments for, (E), 25:28435
energy levels from resonances in silver-109 (p,α) reactions, widths for compound-nucleus, (E), 25:28268
energy-level transitions from isomeric silver-110 beta decay, K-conversion coefficients and multipolarities for, (E), 25:28435
energy-level transitions in, multipole mixing ratios for, (E), 25:28434
proton elastic scattering at 6 to 11 MeV with isobaric analog excitation, excitation functions for, 25:28370
CADMIUM ISOTOPES Cd-111
magnetic hyperfine fields in iron and nickel, differential perturbed angular correlation measurements of, 25:27917
CADMIUM ISOTOPES Cd-112
energy levels from indium-112 beta and electron-capture decay, spin--parity assignments for, (E), 25:28406
proton elastic scattering at 6 to 11 MeV with isobaric analog excitation, excitation functions for, 25:28370
CADMIUM ISOTOPES Cd-114
energy levels from silver-114 beta decay, spin--parity assignments for, (E), 25:28337 (CERN-70-30(Vol.2), pp 1069-74)
energy-level transitions from silver-114 beta decay, probabilities for E2, (E), 25:28337 (CERN-70-30(Vol.2), pp 1069-74)
proton elastic scattering at 6 to 11 MeV with isobaric analog excitation, excitation functions for, 25:28370
CADMIUM ISOTOPES Cd-116
energy levels from silver-116 beta decay, spin--parity assignments for, (E), 25:28337 (CERN-70-30(Vol.2), pp 1069-74)
energy-level transitions from silver-116 beta decay, probabilities for E2, (E), 25:28337 (CERN-70-30(Vol.2), pp 1069-74)
CADMIUM ISOTOPES Cd-118
energy levels from silver-118 beta decay, spin--parity assignments for, (E), 25:28337 (CERN-70-30(Vol.2), pp 1069-74)
energy-level transitions from silver-118 beta decay, probabilities for E2, (E), 25:28337 (CERN-70-30(Vol.2), pp 1069-74)
CADMIUM ISOTOPES Cd-120
energy levels from silver-120 beta decay, spin--parity assignments for, (E), 25:28337 (CERN-70-30(Vol.2), pp 1069-74)
energy-level transitions from silver-120 beta decay, probabilities for E2, (E), 25:28337 (CERN-70-30(Vol.2), pp 1069-74)
CADMIUM OXIDES
reactions with zinc sulfide, Jost mechanisms in solid-state, 25:26210 (KFK-1312)
CAFFEINE
effects on colony formation by uv-irradiated L cells of mice, 25:26989
effects on mutability and survival of uv-irradiated Candida albicans, 25:27073
CALCIFICATION
radioinduced, in rats, effects of dihydrotachysterol on x, 25:26978
radioinduced, in rats, effects of dihydrotachysterol on x, 25:26933
radioinduced, in rats, effects of dose and dihydrotachysterol on γ, 25:26977
CALCIUM
abundance in lunar surface materials, (E), 25:27308
complexes with lecithins in aqueous butanol solutions, properties of, 25:26272
content relative to strontium-90 in human diet and transport through maternal milk, 25:26581
determination by electroconductivity method following chromatographic separation from alkali metals, 25:26173
determination by potentiometric titration using ion-selective electrodes, 25:26166
determination in thorium nitrates and zirconium nitrates by neutron activation, 25:26192
determination in yttrium oxides by solvent extraction and spectrography, 25:26168
effects on gamma-radiosensitivity in rats, 25:27016
effects on luminescence and thermoluminescence efficiency of lithium fluoride crystals, (E), 25:27838(T) (ANL-Trans-874)
electron correlation and density in, calculations using restricted Hartree--Fock approximation, 25:27467
meson (π^-) capture with charged particle emission, particle spectra and branching ratios for, (E), 25:28178
reactions of zinc fluoride and, with thorium fluoride to prepare thorium, reduction, 25:27180 (NLCO-1080)
transport by chorioallantoic membrane of embryonic chick, energetics of active transcellular, 25:28905 (UR-49-1440)
CALCIUM FLUORIDES
lattice structure of, positron-annihilation study of, (E/T), 25:27865 (CEA-R-4138)
properties for thermoluminescent dosimetry, review of, 25:26522
CALCIUM HYDRIDES
spectral absorption lines of, in sunspot spectra, (E), 25:27390
spectral absorption lines of, in sunspot spectra, (E/T), 25:27374
CALCIUM ISOTOPES Ca-40
energy levels from potassium-39 (d,n) reactions, isobaric analog, (E), 25:28230
energy levels of, calculation using renormalized RPA, (T), 25:28509
meson (μ) capture by, relativistic corrections to asymmetry of high-energy neutrons from polarized, (T), 25:28183
oxygen-16 elastic scattering at 36 to 48 MeV, angular distributions for, (E), 25:28196
proton differential inelastic scattering cross sections at 185 MeV, angular distributions from, (E), 25:28255
proton inelastic scattering at 185 MeV, polarization angular distributions from, (E), 25:28256
CALCIUM ISOTOPES Ca-41
Coulomb energy difference between scandium-41 and, (T), 25:28253

CALCIUM ISOTOPES Ca-45
uptake by seeds of subterranean clover, 25:26614
CALCIUM ISOTOPES Ca-47
accumulation in feces of man, γ counting method for estimating, 25:26586
CALCIUM ISOTOPES Ca-48
energy levels of, calculation using renormalized RPA, (T), 25:28509
CALCIUM OXIDES
CaO--HfO_2-base, composition and microstructure of, 25:27296
CALIFORNIUM ISOTOPES Cf-246
fission of, energy surfaces for, (T), 25:28395
CALIFORNIUM ISOTOPES Cf-252
fission of, charge distribution in spontaneous, (T), 25:28508
fission of, effects of fission fragment charge on x-ray and neutron emission following spontaneous, (E), 25:28288 (CEA-R-4121)
fission of, fragment kinetic-energy distributions in spontaneous, (T), 25:28408
fission of, γ--x-ray coincidence spectra of fragments from spontaneous, (E), 25:28416
radiation properties of, 25:27828 (DP-1246)
shielding guide for, 25:27828 (DP-1246)
use as neutron source in portable radiographic camera for detecting contraband material, 25:26437 (BNWL-SA-2865)
CALORIMETERS
calibration heater for assay, 25:26548 (MLM-1780)
CALUTRONS
experimental facilities at Orsay, description of, 25:28106 (CERN-70-30(Vol.1), pp 153-62)
use on-line, review of experimental techniques for, (E), 25:28105 (CERN-70-30(Vol.1), pp 109-41)
CANDU REACTOR
maintenance of, requirements for access for, 25:28551 (AECL-3670, pp 65-70)
operation of, computer system for evaluation of component reliability during, 25:28575
operation of, maintenance procedures for reliability in, 25:28551 (AECL-3670, pp 65-70)
CARBAMIC ACID, METHYLDITHIO-
sodium salt, effects on radiation stability of poly(vinyl chloride) films, 25:26280
CARBOHYDRATES
radiation effects on content of, in leaves and roots of corn and cotton plants following seed exposure, effects of dose on γ, 25:27074
CARBON
abundance in H II regions, (E), 25:27349
determination in plutonium oxide--uranium oxide fuels, evaluation of methods for, 25:26153 (LA-4622)
determination in silicon by α particles, deuteron, γ proton, and helium-3 activation, 25:26202
mechanical properties of filament-wound composite of, 25:28888 (SC-DR-710192)
meson (π) reactions at 1 GeV/c, differential and total cross sections for, (E), 25:27959
meson (π^-) capture with charged particle emission, particle spectra and branching ratios for, (E), 25:28178
neon-ion reactions at 100 to 350 keV with, cross sections and Pauli-excitation mechanism of K-shell ionization in, 25:27453
nucleon elastic scattering at 142, 210, and 330 MeV, optical potential analysis of, (T), 25:28199
photon reactions at 1.5 to 5.7 GeV, total cross section for hadron production in, 25:27953
proton reactions at 1 GeV/c, differential and total cross sections for, (E), 25:27959
radio recombination lines of, in H II regions, (E), 25:27349
role in hardwater lakes, 25:28847 (COO-1599-32)
spectra of C I 1561- and 1657-A lines of, in upper Martian atmosphere, uv, (E), 25:27433
x-ray K-emission spectrum excited by synchrotron radiation, (E), 25:27827 (DESY-70/59)
CARBON DIOXIDES
analysis for carbon-14 by liquid scintillation counting using toluene--Triton X-100, 25:26180
content in lower thermosphere, performance of helium-cooled ion source for determination of, (E), 25:27609
reactions of radiolytic, with graphite, formation of surface complexes in, 25:26286
reactions with niobium--uranium--zirconium alloy at 27 to 1000°C, kinetics of, 25:27210 (SC-DR-710124)
scavenging from atmosphere by raindrops, laboratory studies of, 25:26375 (CONF-700601-, pp 261-9)
spectra of ionized A-X and B-X bands of, in upper Martian atmosphere, uv, (E), 25:27433
CARBON ISOTOPES C-9
half-life of, 25:28187
mass of, 25:28187
CARBON ISOTOPES C-12
abundance in interstellar carbon monoxide, (E), 25:27402
alpha reactions (α,n) and (α,p) at 13 to 16 MeV, differential cross sections for, (E), 25:28188
alpha reactions (α,x) at 100 to 140 MeV, production cross sections for lithium and beryllium isotopes in, (E), 25:28182
carbon-12 elastic scattering at 70 MeV, optical-model analysis of differential cross sections for, (E), 25:28274
cross section data on, tables of multigroup, 25:28657 (HEDL-TME-71-36)
electron reactions (e,e'p) at 45.9 MeV, proton angular distributions and energy spectra from, (E), 25:28193
energy levels from boron-11 (He-3,d) reactions, spin--parity assignments for, (E), 25:28205
helium-3 reactions (He-3,p) at 2.48 to 3.25 MeV at 34°, cross sections and polarization for, (T), 25:28496
meson (μ) capture by, relativistic corrections to asymmetry of high-energy neutrons from polarized, (T), 25:28183
meson reactions (π^+,p) with, distorted-wave effects for differential cross sections for, (T), 25:28048
nitrogen-14 elastic scattering at 65 to 88 MeV, optical-model analysis of differential cross sections for, (E), 25:28274
nuclear binding energy, deformation, quadrupole moments, radii, and shape of, (T), 25:28180
oxygen-16 elastic scattering at 36 to 48 MeV, angular distributions for, (E), 25:28196
oxygen-16 reactions (^{16}O,p) (^{16}O,α) at 4.54 to 8.53 MeV, total and partial cross sections for, (E), 25:27309 (ANU-P-471)
oxygen-16 reactions (O-16,p) at 25.4 to 26.3 MeV, spectra and angular correlations for, (E), 25:28208 (ANU-P-521)
photon reactions (γ,p) with, cross sections for, (E/T), 25:28193
proton reactions (p,x) at 150 and 600 MeV, production cross sections for lithium and beryllium isotopes in, (E), 25:28182
proton reactions at 1 GeV, multiple diffractive model for, 25:28073
reactions (C-12,f) with gold-197 and uranium-238 at 82 MeV, analysis of helium-6 emission in, (E), 25:28351(T) (KFK-tr-352)
reactions with cerium-142, lead, neodymium-144, and praseodymium-141, cross-section limits for fission isomer excitation in, (E), 25:28399
reactions with copper-63 at 55 MeV with alpha and proton evaporation, statistical analysis for shell and angular momentum effects in, (T), 25:28266
scattering by carbon-12 at 70 MeV, optical-model analysis of differential cross sections for elastic, (E), 25:28274
scattering by silicon-28 at 49.3 to 83.5 MeV, optical-model analysis of differential cross sections for elastic, (E), 25:28274
CARBON ISOTOPES C-13
abundance in interstellar carbon monoxide, (E), 25:27402
alpha reactions (α,n) at 3.4 to 4.8 MeV, angular distributions of neutron polarization in, (E), 25:28202
electron reactions (e,e'p) at 43 MeV, proton angular distributions and energy spectra from, (E), 25:28193
energy levels of, calculation of nucleon widths for lowest T = 3/2, (T), 25:28172
helium-3 reactions (He-3,d) at 22 MeV, isospin dependence of angular distributions for, (E), 25:28174
photon reactions (γ,p) with, cross sections for, (E/T), 25:28193
CARBON ISOTOPES C-14
content in seawater at various worldwide locations, 25:26398 (RLO-2225-T-20-2)
determination in biological materials by automatic liquid scintillation spectroscopy using external standardization, 25:26184
determination in carbon dioxide by liquid scintillation counting using toluene--Triton X-100, 25:26180
incorporation in polyethylene glycol for determining secretion of mineral elements of milk, 25:26578 (CONF-680112-, pp 153-66)
use as tracer in plasma glucose turnover studies in eviscerated and nephrectomized rats, comparison of tritium with, 25:26602
use of cholesterol-incorporated, for scanning adrenal glands in dogs, 25:26845
use of MEG-labeled, for determination of time of development of radioprotection in x-irradiated HeLa cells, 25:26797
CARBON MONOXIDES
spectra of a-X and A-X and ionized B-X bands of, in upper Martian atmosphere, uv, (E), 25:27433
spectral line radiation from interstellar, of different isotopic composition, (E), 25:27402
CARBON SYSTEMS
C--Co--Mo-base, weldability of, 25:27185
C--Fe--Mo-base, weldability of, 25:27185
C--Hf--Zr, thermodynamic properties of compound of, at 2440°K, 25:27283 (N-71-10590)
C--Ir--Mo-base, weldability of, 25:27185
C--Mo-base, weldability of, 25:27185
C--Mo-base--Ni, weldability of, 25:27185
CARBON TETRACHLORIDE
effects on hydrogen yields from α radiolysis of gaseous hydrogen sulfide, 25:26315
CARBOXYPEPTIDASE
radiation effects on activity of rat blood plasma, x, 25:27030

XUM

CARDIAC PACEMAKERS
design and development of radioisotope-powered, research program for, 25:26426(R) (NUMEC-4189-4)
development of radioisotope-fueled, in Australia, France, Switzerland, and United Kingdom, 25:26434
CAROTENOIDS
radioinduced mutations for production in Mycobacterium phlei, uv, 25:26687
CARTILAGE
zinc-65 distribution in, of bones in rats, 25:26611
CATALASE
radioinduced inactivation of, in solution, protective effects of glycerol against γ, 25:26650
radiosensitivity of lipoprotein-complexed, in vitro, role of molecular orientation of complex in reduced γ, 25:26650
CATS
blood flow in liver of, xenon-133 clearance studies on, 25:26576
radiation effects on spinal cord motoneurons of, x, 25:26941
CATTLE
immunity to Dictyocaulus viviparus in, effects of vaccination with x-irradiated larvae on, 25:26918
immunity to Dictyocaulus viviparus in, effects of vaccination with x-irradiated larvae on, 25:26919
CAVITIES
formation by Greeley Event, postshot drill hole data on, 25:26412 (UCRL-50979)
ground water flow into Greeley Event, postshot measurements of, 25:26412 (UCRL-50979)
reentry into Rulison Event chimney, summary of operations for, 25:26409 (PNE-R-45)
size of Gasbuggy Event, calculations from seismic data, 25:26405 (PNE-1002)
Cb-752 (NIOBIUM ALLOY)
stability at high temperatures, long-term thermal, 25:27208 (N-71-10352)
CELLS
book: Effects of Metals on Cells, Subcellular Elements, and Macromolecules, 25:26608
effects of hematopoietic stem, on radioactivity in mice, 25:26952
radiation effects on components of, 25:27036 (CONF-691057)
radiation effects on DNA synthesis in human amnion, sensitizing effects of trisoralen on uv, 25:26808
radiation effects on glial tumor, comparison of effects of actinomycin C with x, 25:26908
radiation effects on immunocompetent, in lymph nodes, spleen, and thymus of mice following bone marrow reconstitution, x, 25:26672
radiation effects on interstitial, in testes of rats, functional and morphological studies on cryptorchidism and x, 25:27008
radiation effects on phytohemagglutinin response of mouse bone marrow, lymph node, and spleen, effects of thymus on x, 25:26673
radiation injuries to erythroid and myeloid, in hematopoietic system of mice, x, 25:26981
radioinduced differentiation of epithelial and mesenchymal, in rat thymus gland, light microscopy whole-body x, 25:26654
radiosensitivity of populations of mouse spleen, effects on selective inhibition of, 25:26671
sensitivity of immune mouse spleen, to dactinomycin, effects on selective inhibition of, 25:26671
CELLS, CULTURED
radiation effects on antigenicity of guinea pig tumor, x, 25:26663
radiation effects on DNA synthesis in human amnion,effects of dose and growth rate on x, 25:26630
radiation effects on formation of fibroblast in mouse spleen, effects of dose on, 25:26905
radiation effects on growth of, in mouse leukemic lymphoblasts, x, 25:26974
radiation effects on migration and survival of chicken fibroblast, 1000 to 120,000-R, x, 25:26642
radiation effects on molecular weight of DNA in Ehrlich ascites, use of guanidinium chloride in alkaline sucrose gradient for determination of x, 25:26629
radiation effects on proliferation of SOTs, effects of mitotic stage on gamma, 25:26907
radiation effects on survival of ascited tumor, RBE for meson (π⁻), 25:26938
radioinduced breaks in DNA of Chinese hamster, effects of age on x, 25:26625
radioinduced chromosome aberrations in Chinese hamster, repair mechanisms of x, 25:26723
radioinduced chromosome aberrations in Ehrlich ascites, x, 25:26704
radioinduced chromosome aberrations in rat kangaroo kidney, repair mechanisms of x, 25:26724
radioinduced damage in DNA of vertebrate, effects of cell type and postirradiation conditions on repair mechanisms of uv, 25:26635
radioinduced delay of mitosis in Chinese hamster, effects of dose and protein synthesis on x, 25:26626
radioinduced inhibition of DNA synthesis in, analysis of viral induced DNA synthesis in cells following x, 25:26691
radioinduced mitotic delay in Chinese hamster, determination of site of delay in α and x, 25:26927
radioinduced mutants of Ehrlich ascites, methods for hybridization of uv, 25:26700
radioinduced single strand breaks in DNA of Ehrlich ascites, hamster lung, and porcine kidney, mechanisms of repair in x, 25:26953
radioinduced unscheduled DNA synthesis in, effects of dinitrophenol and puromycin on uv and x, 25:27002
radiosensitivity of antibody forming, 25:26665
radiosensitivity of DNA of human xeroderma pigmentosum, repair replication for uv, 25:26634
radiosensitivity of Ehrlich ascites carcinoma, effects of N-ethylmaleimide and cysteamine on x, 25:26640
CELLS, HeLa
radiation effects on reproduction of, RBE for fast neutron, 25:26906
radiation effects on RNA synthesis in, inhibitory x, 25:26983
radiation effects on survival of, effects of temperature on protective effects of MEG against x, 25:26797
CELLS, L
radiation effects on mouse, effects of mitotic phase on uv, 25:26989
radiation effects on synchronized, effects of depressed macromolecular synthesis on recovery from, 25:26969
radioinduced mutants of, methods for hybridization of uv, 25:26700
radioinduced single strand breaks in DNA of, mechanisms of repair in x, 25:26953
CEMENTS
determination in wet concrete, radiometric instrument for, 25:26540 (ORO-3842-3)
CENTRAL AMERICA
med fly radiosterilization in, cooperative program for, 25:27131 (CONF-680112-, pp 143-50)
CENTRIFUGES
testing of large-capacity, in natural uranium production plant, 25:26330(T) (ORNL-tr-2410, pp 14-78)
testing of, for use in fuel reprocessing, 25:26331(T) (ORNL-tr-2410, pp 79-97)
CERAMIC MATERIALS
properties of, effects of microstructure on electric, magnetic, mechanical, and thermal, 25:27282 (INIS-mf-14)
research in India during present decade, review of, 25:27281 (INIS-mf-13)
research on ferro-electric, ferro-magnetic, and oxide, in India, 25:27281 (INIS-mf-13)
CEREALS
wheat, radiation processing effects on insect infestation in, 25:27143
CERIUM
determination by photometry using carboxy derivatives of 2,6,7-trihydroxy-9-phenyl-3H-xanthen-3-one, 25:26174
determination in yttrium oxides by solvent extraction and spectrography, 25:26168
effects on magnetic susceptibility of scandium, 25:27878
nitrogen-14 reactions with, cross-section limit for fission isomer excitation in, (E), 25:28399
solubility in chromium, effects of temperature on, 25:27238
CERIUM ALLOYS AND SYSTEMS
Al--Ce, Kondo effect in intermetallic $CeAl_2$, study by superconducting proximity effect, (E), 25:27662
Bi--Ce, magnetic structure of CeBi, neutron-diffraction study of, 25:27887
Ce--Co--Cu--Fe--Sm, magnetic properties of, 25:27883
Ce--Cu, Hall coefficient and electric conductivity of liquid, 25:27212
Ce--La-base, thermoelectric power at 4.2 to 350°K of Kondo system, 25:27877
Ce--Pd, magnetic and electric properties of $CePd_3$ at 4 to 300°K, 25:27870
Ce--Sb, crystal-field splitting and spin waves in CeSb, 25:27881
Ce--Sb--Y, thermal capacity of Ce/sub x/Y/sub 1-x/Sb at 1.5 to 70°K, 25:27881
CERIUM ISOTOPES Ce-138
beta decay of isomeric, half-life for, 25:28342 (CERN-70-30(Vol.2), pp 1119-21)
energy level scheme from praseodymium-138 decay, (E), 25:28414
CERIUM ISOTOPES Ce-140
deuteron reactions (d,p) at 12 MeV, anomalies in DWBA analysis of, (E), 25:28429
energy levels from photoexcitation, radiative widths for isobaric analog, (E), 25:28362
oxygen-16 reactions with, cross-section limit for fission isomer excitation in, (E), 25:28399
photon reactions (γ,p) with isobaric analog excitation, proton spectra from, (E), 25:28362
CERIUM ISOTOPES Ce-141
binding to blood serum proteins, review on dialysis methods for studying, 25:26584
energy levels from cerium-140 (d,p) reactions, anomalous spin assignments for, (E), 25:28429
CERIUM ISOTOPES Ce-142
carbon-12 reactions with, cross-section limit for fission isomer excitation in, 25:28399
proton elastic scattering using polarized beams, isobaric analog resonances in, (E), 25:28239

CERIUM ISOTOPES Ce-144
content in Japanese airborne dusts and soils, April 1969 to April 1970, 25:26392 (NIRS-RSD-27)
separation from irradiated aluminum--uranium and uranium--zirconium fuels by chlorination and pyrohydrolysis, 25:26332(T) (ORNL-tr-2410, pp 98-120)
separation of plutonium from, by solvent extraction using tridodecylamine, 25:26330(T) (ORNL-tr-2410, pp 14-78)
CESIUM
determination of trace amounts of, in hydrofluoric acid and spectrophotometry, 25:26176
encapsulation of, design of dispensing system with freeze--melt valve for vacuum, 25:26413 (N-71-10455)
plasma of, injection and confinement in magnetic mirrors, (E), 25:27671
plasma of, ion energy analysis in Q devices, 25:27686
scavenging of aerosol particles of water-soluble, by aqueous sprays, (E), 25:26372 (CONF-700601-, pp 187-204)
separation from milk by moving-bed ion exchange, 25:26335 (RO/EERL-71-1)
separation from other fission products by ion exchange, 25:26337(P)
separation of plutonium from, by solvent extraction using tridodecylamine, 25:26330(T) (ORNL-tr-2410, pp 14-78)
sorption by nuclear and pyrolytic graphite and tungsten powders at 600 to 800°C, cesium vapor pressure from, 25:27201 (EUR-4549)
vaporization from graphite, (E), 25:28633(R) (GA-10399)
CESIUM IONS
reactions with helium, cross sections for excitation of Cs II resonance lines near threshold in, (T), 25:27454
CESIUM ISOTOPES
effects on kinetics of isotope diffusion in cesium chloride, 25:26241
gamma--x-ray spectra of, from californium-252 spontaneous fission, 25:28416
CESIUM ISOTOPES Cs-134
beta decay of, angular correlations, branching ratios, decay energies, gamma spectra, and log-ft values for, (E), 25:28405
determination in Windscale effluent by isotope dilution and γ spectrometry, 25:26177 (PG-Report-965)
CESIUM ISOTOPES Cs-135
energy-level transitions from xenon-135 beta decay, conversion coefficients, K-L+... values, and multipolarities for, (E), 25:28336 (CERN-70-30(Vol.2), pp 1057-68)
CESIUM ISOTOPES Cs-137
content and transport in San Juan Basin ground water following Gasbuggy Event, safety evaluation of, 25:26406 (PNE-1009)
content in Japanese airborne dusts and soils, April 1969 to April 1970, 25:26392 (NIRS-RSD-27)
content in Japanese powdered milk, tea, vegetables, and water, April 1969 to April 1970, 25:26392 (NIRS-RSD-27)
content of human bones and milk in South Africa during 1963 to 1967, methods for calculating, 25:26613
content of man in Egypt during 1970, whole-body counting of, 25:26740 (NP-18728)
content of wine in Transylvania, 25:26618
content relative to potassium in human diet and transport through maternal milk, 25:26581
determination in Windscale effluent by isotope dilution and γ spectrometry, 25:26177 (PG-Report-965)
energy-level transitions from xenon-137 beta decay, conversion coefficients, K/L+... values, and multipolarities for, (E), 25:28336 (CERN-70-30(Vol.2), pp 1057-68)
excretion in rats, combined effects of prussian blue and pilocarpine on, 25:26583
radiation dose from particles of, following clothing contamination, 25:26748
radiation effects on sorption through rat skin, effects of contamination timing on 600 rad cobalt-60 γ, 25:26595
separation from irradiated aluminum--uranium and uranium--zirconium fuels by chlorination and pyrohydrolysis, 25:26332(T) (ORNL-tr-2410, pp 98-120)
transport through human food chains following nuclear attack, 25:26786
CESIUM ISOTOPES Cs-138
yield in neutron fission of uranium-235, (E), 25:28307 (CERN-70-30(Vol.1), pp 589-99)
CESIUM ISOTOPES Cs-139
beta decay of, Q value for, (E), 25:28296 (CERN-70-30(Vol.1), pp 341-51)
energy-level transitions from xenon-139 beta decay, conversion coefficients K/L+... values, and multipolarities for, (E), 25:28336 (CERN-70-30(Vol.2), pp 1057-68)
yield in neutron fission of uranium-235, (E), 25:28307 (CERN-70-30(Vol.1), pp 589-99)
CESIUM ISOTOPES Cs-141
yield in neutron fission of uranium-235, (E), 25:28307 (CERN-70-30(Vol.1), pp 589-99)
CESIUM ISOTOPES Cs-142
yield in neutron fission of uranium-235, (E), 25:28307 (CERN-70-30(Vol.1), pp 589-99)
CESIUM ISOTOPES Cs-143
yield in neutron fission of uranium-235, (E), 25:28307 (CERN-70-30(Vol.1), pp 589-99)
CESIUM ISOTOPES Cs-145
beta decay of, half-life for, (E), 25:28388
yield in neutron fission of uranium-235, (E), 25:28307 (CERN-70-30(Vol.1), pp 589-99)
CESIUM ISOTOPES Cs-146
beta decay of, half-life for, (E), 25:28388
CHARGED-PARTICLE BEAMS
interactions with plasma, if oscillations from, 25:27816
monitoring of current and position of, design and performance of device for, 25:28117 (UCRL-20166)
steering coils for, printed-board, 25:28116 (UCRL-20165)
CHARGED PARTICLES
coupling to tensor and electromagnetic fields, causality in Lorentz-covariant Lagrangian for, (T), 25:28068
detection of relativistic, position-sensitive silicon detector with secondary emission foil for, 25:26513
identification using ORTEC 423 identifier with telescope detector, 25:26490 (ANU-P-514)
pair annihilation at potential barrier in time in external electromagnetic field, probability for, (T), 25:27985
scattering by cylindrical block at high energies, Coulomb, (T), 25:27987
stopping powers for use with cavity ionization chambers, 25:26533
CHEMICAL REACTIONS
Jost mechanisms in solid-state, 25:26210 (KFK-1312)
CHEMISTRY
research progress in, AEC, 25:26205
CHERENKOV RADIATION
emission from cosmic EAS, angular, spectral, and temporal properties of, (E), 25:27952
CHILE
insect radiosterilization in, methods for, 25:27130 (CONF-680112-, pp 129-42)
power reactors for, economic aspects of, 25:28723
CHIMERAS
radiation effects on production of interferon in mouse, following injection of Newcastle disease virus, 25:26995
CHIPMUNKS
radiation effects on population mechanics of, in natural environments, γ, 25:26682(R) (NYO-2579-20)
CHLORAMPHENICOL
effects on wound healing patterns following combined x radiation and surgical injury to rats, 25:26932
radioprotective effects on germinating spores of Streptomyces, γ and uv, 25:27068
CHLORINE
content ratio to bromine and iodine in marine aerosols, mathematical model for demonstrating aerosol particle size dependence of, 25:26381 (CONF-700601-, pp 325-51)
determination by potentiometric titration using ion-selective electrodes, 25:26166
determination in plutonium oxide--uranium oxide pellets, 25:26153 (LA-4622)
determination in Zircaloy, chemical method for, 25:26171
reactions of trivalent, with tetravalent uranium, mechanism of effects of phenol on, 25:26266
CHLORINE IONS
charge state distribution in oxygen targets at 1 to 14 MeV, equilibrium, (E/T), 25:28127 (WASH-1159, pp 45-57)
CHLORINE ISOTOPES Cl-33
energy levels from argon-33 decay, isospin purity of, (E), 25:28195
energy levels of, calculation using intermediate coupling vibrational model with anharmonic core and quasiparticle effects, (T), 25:28249
energy levels of, role of configuration states in isospin-forbidden proton decay of T = 3/2, 25:28179
CHLORINE ISOTOPES Cl-37
effects on Raman spectra of gaseous, liquid, and solid chlorofluorosilanes, 25:26218
CHLORINE ISOTOPES Cl-38
content of cosmogenic, in rainwater, effects of precipitation rate and ocean proximity on, (E), 25:26364 (CONF-700601-, pp 69-97)
CHLORINE ISOTOPES Cl-39
content of cosmogenic, in rainwater, effects of precipitation rate and ocean proximity on, (E), 25:26364 (CONF-700601-, pp 69-97)
CHLORMERODRIN
effectiveness of mercury-197-labeled, for kidney localization in man in comparison with other diagnostic methods, 25:26821
use of mercury-197-labeled, for brain scanning, computer evaluation of, 25:26824
CHLOROPHYLL
radiation effects on corn, pea, and wheat seedling, effects of gibberellin on x, 25:27064
CHLOROPHYTA
radioisotope concentration by tropical marine, 25:26597
zinc-65 uptake by Columbia River, effects of ion concentration on, 25:26593
CHLOROQUINE
effectiveness of injections of iodine-131-labeled analog of, for therapy of malignant melanomas, 25:26882
5α-CHOLESTAN-3β-OL
reactions of monolayers of saturated and unsaturated,

XUM

with osmium tetroxide, potassium permanganate, and uranyl acetate, effects of variables on, 25:26213
CHOLESTEROL
reactions of monolayers of saturated and unsaturated, with osmium tetroxide, potassium permanganate, and uranyl acetate, effects of variables on, 25:26213
CHROMIUM
abundance in α Dra, (E), 25:27333
cross section data on, tables of multigroup, 25:28657 (HEDL-TME-71-36)
determination in plutonium nitrate solutions by atomic absorption spectrophotometry, 25:26154(T) (RFP-Trans-76)
determination in thorium nitrates and zirconium nitrates by neutron activation, 25:26192
determination in yttrium oxides by solvent extraction and spectrography, 25:26168
determination in Zircaloy, chemical method for, 25:26171
neutron elastic scattering at 3.2 MeV using polarized beam, optical-model analysis of, (T), 25:28248
reactions of divalent, with hydrogen peroxide in presence of 2-propanol, yields of hydroxyl radicals from, 25:26290(R) (NYO-3753-19)
solvent properties for cerium, neodymium, and praseodymium, effects of temperature on, 25:27238
CHROMIUM ALLOYS AND SYSTEMS
properties for use as fuel cans for fast breeder reactors, 25:27213
Al--Cr--Cu--Mg--Zn, analysis for trace amounts of silver by solvent extraction and atomic absorption spectrophotometry, 25:26169
B--Cr--Mn, phase diagram at 800°C, isothermal, 25:27299
Cr--Cu, fabrication and uses of high conductivity, 25:27187
Cr--Fe--Mo, fatigue strength of, effects of fine precipitates on, 25:27231
Cr--Pd, mictomagnetism in fcc, 25:27890
Cr--Re, hardness of, effects of composition and temperature on decreasing, 25:27209 (N-71-11662)
Cr--Re, thermionic work functions of, 25:27911
Cr--Ti--V, compatibility with flowing sodium at 500 to 600°C, 25:27174
Cr--Ti-base, internal friction at 4 to 300°K, 25:27215
Cr--V, reflectance spectra of, measurement and band model of, 25:27442
Cr--V--Zr, compatibility with flowing liquid sodium at 500 to 600°C, 25:27174
Cr--Zr-base, microstructure of, 25:27230
Cr--Zr-base, properties of, electric and mechanical, 25:27230
Cr-base--Mn, reflectance spectra of, measurement and band model of, 25:27442
CHROMIUM ISOTOPES Cr-50
deuteron reactions (d,p) at 13.6 MeV, distorted-wave analysis of differential cross sections from, (E/T), 25:28269
proton elastic scattering at 6.9 MeV, optical-model analysis of angular distributions from, (E), 25:28262
CHROMIUM ISOTOPES Cr-51
distribution in rat bones following intravenous injection of labeled alloxantin, methods for determining, 25:26590
energy levels from chromium-50 (d,p) reactions, angular-momentum transfer, spectroscopic factors, and spin--parity assignments for, (E/T), 25:28269
energy-level density from titanium-48 (α,n) and vanadium-51 (p,n) reactions, (E), 25:28285
nuclear magnetic moment of, determination from hyperfine structure, (E), 25:28252
CHROMIUM ISOTOPES Cr-52
deuteron reactions (d,p) at 13.6 MeV, distorted-wave analysis of differential cross sections from, (E/T), 25:28269
energy levels from vanadium-52 decay, (E), 25:28250
helium-3 reactions (He-3,p) at 11 MeV, angular distributions for L = 0 transitions in, (E), 25:28229
photon reactions (γ,n) near threshold energy, cross section and resonance parameters for, (E), 25:28413
proton elastic scattering at 6.9 MeV, optical-model analysis of angular distributions from, (E), 25:28262
CHROMIUM ISOTOPES Cr-53
energy levels from chromium-52 (d,p) reactions, angular-momentum transfer, spectroscopic factors, and spin--parity assignments for, (E/T), 25:28269
neutron total cross sections and resonance parameters at 10 to 250 keV, (E/T), 25:28279
photon reactions (γ,n) near threshold energy, cross section and resonance parameters for, (E), 25:28413
CHROMIUM ISOTOPES Cr-54
energy-level transitions from proton reactions, branching ratios, gamma-ray angular distributions, and internal conversion coefficients for, (E/T), 25:28271
CHROMOSOMES
aberration induction in seed, economics of EMS, 25:26697
radiation effects on cross-over frequency in, of Drosophila melanogaster, x, 25:26713
radioinduced aberration of Ehrlich ascites tumor cell, x, 25:26704
radioinduced aberration of pea, gamma, 25:27089
radioinduced aberrations in, biological dosimetry using, 25:26771
radioinduced aberrations in, of human progeny following maternal uterine therapy, x, 25:27057
radioinduced aberrations of Chinese hamster cell, repair mechanisms of x, 25:26723
radioinduced aberrations of Crepis, gamma, fast neutron, and x, 25:26721
radioinduced aberrations of hamster embryo, relation to teratogeny of x, 25:26982
radioinduced aberrations of human leukocyte, comparison of tritium and γ, 25:26636
radioinduced aberrations of human leukocyte, effects of dose on x, 25:26628
radioinduced aberrations of human leukocyte, effects of dose and dose rate on iodine-131 β, γ, x, 25:26730
radioinduced aberrations of lymphocyte, in dogs following implantation of plutonium-238-powered circulatory assist device, γ and neutron, 25:26931
radioinduced aberrations of rat kangaroo kidney cell, repair mechanisms of x, 25:26724
radioinduced aberrations of seed, economics of γ and x, 25:26697
radioinduced aberrations of, in kidney cells of swine far-red, 25:26727
radioinduced aberrations of, in mammals, review on latent whole-body, 25:26943
radioinduced lesions in Vicia, distribution of x, 25:26734
radioinduced lesions of Vicia, use of electron scanning to visualize x, 25:26725
radioinduced mutations in Crepis seed, effects of stage of cell cycle on, 25:26733
radioinduced translocation aberrations of mosquito, 25:26694
radioinduced translocations in, of male mice, cytogenetical studies on x, 25:26711
CHROMOSPHERE
magnetic fields in, relation to velocity fields, (E), 25:27394
models of lower, two-dimensional, (E), 25:27371
spectra of transition region with photosphere, (E/T), 25:27370
spectra of, 4097.3 N III emission in, (E), 25:27373
spectra of, from 1680 to 600 A, (E/T), 25:27370
CHRYSOPHYTA
phosphate uptake in, phosphorus-33 autoradiographic study of, 25:26596
zinc-65 uptake by Columbia River, effects of ion concentration on, 25:26593
CIRCUITS
analog-to-digital converter to digitize voltage transients, 25:28903 (UCRL-73103)
development for measuring frequency dependent complex admittance and impedance, 25:28882 (SC-DR-68-796)
feasibility of generalized integrated, 25:28886 (SC-DR-710033)
CITRIC ACID
radiation effects on content of, in leaves and roots of corn and cotton plants following seed exposure, effects of dose on γ, 25:27074
CIVILIAN DEFENSE
program in USSR, translation of handbook on, 25:26785(T) (ORNL-tr-2306)
CLOTHING
radioactive particulate contamination of, estimation of dose to skin following beta, 25:26748
CLOUDS
condensation and ice nuclei in atmospheric, effects of atmospheric precipitation on, 25:26362 (CONF-700601-, pp 37-48)
effects on atmospheric scavenging, mathematical model for prediction of, 25:26391 (CONF-700601-, pp 475-85)
formation of dust, by Pre-Gondola II Event, (E), 25:26407 (PNE-1112)
formation of dust, by Pre-Gondola III Phase II explosion, measurement of, 25:26408 (PNE-1117)
gas and particulate scavenging by rain, kinetic theory of, 25:26382 (CONF-700601-, pp 355-71)
particles and water droplets in, evolving size spectra of, (T), 25:26385 (CONF-700601-, pp 385-402)
CNIDARIA
Anthopleura xanthogrammica, radiation effects on behavior of, effects of dose on uv, x, and visible, 25:26912
COATINGS
properties of protective, effects of composition, heat tretment, surface finish, and working on, 25:27176 (INIS-mf-9)
thickness measurements of light-element, on heavy-element backing, electron backscatter method for, 25:26542
COBALT
complexes with 5,7-diiodo-8-quinolinol, formation constants of, 25:26214
determination in marine silts by neutron activation and γ spectroscopy, 25:26190(R) (NYO-4150-9)
determination in sea floor samples by neutron activation, 25:26188 (BNWL-SA-3803)
determination in thorium nitrates and zirconium nitrates by neutron activation, 25:26192
determination in Zircaloy, chemical method for, 25:26171
hardness of irradiated and unirradiated, hot, 25:27236
COBALT ALLOYS AND SYSTEMS
hardness of irradiated and unirradiated, hot, 25:27236
mechanical properties at 400 to 800°C, 25:27203 (INIS-

mf-2)
C--Co--Mo-base, weldability of, 25:27185
Ce--Co--Cu--Fe--Sm, magnetic properties of, 25:27883
Co--Cu--rare earths, casting and properties of permanent magnets of, 25:27184
Co--Cu-base, Kondo effect in, study by superconducting proximity effect, (E), 25:27662
Co--La, magnetic coercivity of $LaCo_5$ particles, domain-wall pinning in, 25:27882
Co--misch metal--Sm, preparation and magnetic properties of permanent magnets of, 25:27884
Co--Nd--Pr, magnetic properties of $Pr_{0.87}Nd_{0.13}Co_5$, 25:27886
Co--Pt, ordering in intermetallic PtCo, field ion microscopy studies of, 25:27252
Co--Sm, magnetic coercivity of $SmCo_5$ particles, domain-wall pinning and nucleation in, 25:27882
Co--Sm, magnetization discontinuities in Co_5Sm particles, 25:27885
Co--Sn, crystal structure parameter of intermetallic Sn_2Co, (E), 25:27654
Co--TaC--TiC--WC, thermal conductivity of sintered, at 200 to 700°C, 25:27289
Co--WC, thermal conductivity of sintered, at 200 to 700°C, 25:27289
Co--Y, magnetization discontinuities in Co_5Y particles, 25:27885
Co--Zr, superconductivity of intermetallic, (E), 25:27654

COBALT HYDRIDES
spectral absorption lines of, in sunspot spectra, (E), 25:27390

COBALT ISOTOPES Co-57
effectiveness of cyanocobalamin-incorporated, for diagnosis of vitamin B_{12} deficiency diseases in man, comparison of Schilling test with, 25:26853
energy levels from iron-54 (α,p) reactions, lifetimes and spin assignments for, (E), 25:28281
energy-level transitions from iron-54 (α,p) reactions, multipolarities for, (E), 25:28281
use of cyanocobalamin-incorporated, for radioimmunoassay of binding and blocking anti-intrinsic factor antibodies in human blood serum and gastric juice, 25:26676

COBALT ISOTOPES Co-58
energy level near 5.75 MeV, splitting of isobaric analog, (E), 25:28228

COBALT ISOTOPES Co-59
meson (π^-) capture with charged particle emission, particle spectra and branching ratios for, (E), 25:28178
proton elastic scattering at 6.9 MeV, optical-model analysis of angular distributions from, (E), 25:28262
proton elastic scattering at 6.9 MeV, optical-model analysis of cross-section and polarization angular distributions from, (E), 25:28263
proton reactions (p,n) at 7.8 to 14.7 MeV, neutron spectra from, (E), 25:28285

COBALT ISOTOPES Co-60
content of oysters in estuary of North Sea in relation to distance from nuclear power plant, 25:26742
radiation dose from particles of, following clothing contamination, 25:26748
use for therapy of pituitary adenomas in man, methods for, 25:26872

COBALT ISOTOPES Co-62
beta decay of, gamma energies and intensities, branching ratios, and log-ft values for, (E), 25:28214 (CERN-70-30(Vol.2), pp 1105-13)

COBALT ISOTOPES Co-63
beta decay of, gamma energies and intensities, branching ratios, and log-ft values for, (E), 25:28214 (CERN-70-30(Vol.2), pp 1105-13)

COBALT OXIDES
Al_2O_3--CoO--SiO_2, magnetic ordering and electric conduction in glasses of, 25:27901

COINCIDENCE CIRCUITS
analysis of, sequential graphs for binary, 25:26546 (CEA-R-4166)

COINCIDENCE MEASUREMENTS
method for determination of radioisotopes that emit conversion electrons, 4π β--γ, 25:26464

COLLAGEN
radioinduced polymerization of gel, protective and sensitizing effects of chemical substances in relation to x, 25:26802

COLLIMATORS
design for neutrons, 25:28153(P)

COLLISION PROCESSES
theory of atomic elastic, classical, 25:27449 (INR-P-1217)

COLUMBIA RIVER
chemical inputs in, 25:28879 (RLO-1750-41)
thermal discharge from Hanford reactors into, effects on feeding activities and growth of fish, 25:26681 (BNWL-1528)
zinc-65 cycling by periphyton in, 25:26593

COMPOSITE MATERIALS
conference on, New York, June 6 to 7, 1969, 25:27271
development for use in aircraft structures, 25:27307
fabrication technology of, review on, 25:27278
morphology and properties of, 25:27277

COMPTON EFFECT
cooling mechanism for solar corona, (T), 25:27401

COMPUTER PROGRAMS
ANISN, for solving Boltzmann equation in one dimension in plane, cylindrical, or spherical geometry, in FORTRAN IV, 25:28149(T) (ORNL-tr-2419)
ASTHMA, for two-dimensional axisymmetric transient heat conduction material ablation, 25:28883 (SC-DR-70-510)
COL HEAT, for simulating thermal effects on rivers from thermal effluents from proposed nuclear power plants, development of, 25:28710(R) (HEDL-TME-71-26)
COLD, for experimentation on graphical system of communication between operator and computer, problems in, 25:28860(T) (LA-tr-71-28)
COMET, for calculation of mechanical and thermal stresses in fuel element cladding, FORTRAN IV for IBM 360/65, 25:27202 (EUR-4562)
COREGRAF 2, for neutron flux distribution in gas cooled graphite moderated reactors, 25:28654 (CEA-N-1344(2))
EDITOR, for processing ENDF/B format data, 25:28148 (ORNL-TM-3266)
EVALIN, for calculating intrinsic states of A < 165 nuclei by extended Hartree--Fock variational methods, in FORTRAN IV for CDC 6600, 25:26439 (AECL-3801)
FITTER, for lithium-drifted germanium gamma ray line shape fitting, for S360/50, 25:26489 (ANU-P-487(2))
for determining optical potentials for neutron elastic scattering and total cross sections, (T), 25:28403
for investigating the effects of auroral electrojet on absorption and scattering of ionospheric fast electrons, (T), 25:27589
for measurement of radioisotope distribution in animals as function of time following intravenous injection for IBM 360, 25:26580
for on-line and off-line analysis of complex spectra, for IBM 1800, 25:26489 (ANU-P-487(2))
for pulse height analysis with time sharing, for PDP-8/I, 25:26497
for solution of stationary neutron transport equation with spherical symmetry, 25:28147 (JUL-683-MA)
GASPAN, for lithium-drifted germanium gamma spectral analysis, for PDP-9, 25:26500
INCRED, for linear and nonlinear least squares fitting of spectra, for S360/50, 25:26489 (ANU-P-487(2))
INVARA, POPDEN, and SHAZ, for evaluating hazards to man from earth impaction of space power system radioactive capsules, 25:26429 (SC-R-7121)
JN-METD1, for solving neutron transport problems by j/sub n/ method, 25:28146 (EUR-4601)
JOANIE, for pulse height analysis, for PDP-9, 25:26495
MLINA, for gamma ray line shape fitting, for IBM 1800, 25:26489 (ANU-P-487(2))
PEEL, for gamma ray line shape fitting, for S360/50, 25:26489 (ANU-P-487(2))
SAS1A, for analysis of fast reactor power and coolant flow transients, FORTRAN for CDC 3600 and IBM 360, 25:28727 (ANL-7607)
SCATLE, for optical-model analysis of elastic scattering data with automatic search, in FORTRAN IV, 25:28450 (N-70-42846)
SCOLDS, for data acquisition from magnetostrictive spark chambers, in FORTRAN, 25:26512
SPECTR, for handling and analyzing multichannel pulse height spectra, in FORTRAN, 25:26499
STAZ-2, for thermohydraulics of water cooled and moderated reactor cooling channel, FORTRAN 2 for IBM 704, 25:28679 (EUR-4553)
THETA1-B, for effects of coolant loss accident conditions on pressurized water reactor fuel elements, for IBM 360/75, 25:28737 (IN-1445)
TIGER, for thermal neutron spectrum in water moderated fuel elements, FORTRAN 4 for IBM 7040, 25:28802 (EUR-4554)
TOPLYR, for thermal and hydraulic behavior of subsurface thermal plumes in large bodies of water, development of, 25:28710(R) (HEDL-TME-71-26)
VENUS, for calculation of energy release in fast reactor power excursions, FORTRAN for IBM 360, 25:28728 (ANL-7701)
WIGNER, for calculation of mean thermal neutron cross sections for reactor cores, FORTRAN 4 for IBM 7040, 25:28803 (EUR-4555)

COMPUTERS
conference on, fall 1970 DECUS, 25:26498
conference on, spring 1969, DECUS, 25:26554
conference on, spring 1970 DECUS, 25:26558
description of Lawrence Radiation Laboratory's OCTOPUS computer network, 25:28896 (UCID-15754)
design and components of, research progress on studies of, 25:28877(R) (ORO-2572-27)
Illiac III Reference Manual, 25:28851 (COO-2118-5)
maintenance of on-line, for production reactor control, 25:28797
use for simulation of spaced-antenna ionospheric radio-drift measurements, (E/T), 25:27596
use of CDC-160A, as peripheral controller for PDP-9 computer at Sandia Laboratory, 25:28885 (SC-DR-70-856)

CONCRETES
analysis of wet, for cement, radiometric instrument for, 25:26540 (ORO-3842-3)

XUM

uses of reinforced, in conjunction with steel for construction, 25:27188
CONDENSERS
thermal insulation for ice cooled, for pressurized water reactor containment system, 25:28700(P)
CONNECTICUT YANKEE POWER REACTOR
cooling system piping for, revised in-service inspection requirements for, 25:28592 (DOCKET-50213-102)
core for safety limits for, 25:28594 (DOCKET-50213-104)
core for, design parameters and operations aspects of zircaloy clad assemblies and neptunium target rods in, 25:28593 (DOCKET-50213-103)
design characteristics of, 25:28544
instrumentation for, calibration requirements for pressurizer level, 25:28592 (DOCKET-50213-102)
operation of, low pressure trip setpoint for, 25:28594 (DOCKET-50213-104)
operations history for 1967 to 1970, review of, 25:28577
pressure vessel for, revised in-service inspection requirements for, 25:28592 (DOCKET-50213-102)
radioactive effluents from, revised technical specifications for gaseous and liquid, 25:28592 (DOCKET-50213-102)
CONNECTORS (ELECTRIC)
standardization of signal, for nuclear instruments, 25:26552
CONVERSION ELECTRONS
detection and measurement for determination of radioisotopes, coincidence method for, 25:26464
COPPER
analysis for trace amounts of silver by solvent extraction and atomic absorption spectrophotometry, 25:26169
complexes with 5,7-diiodo-8-quinolinol, formation constants of, 25:26214
cross section data on, tables of multigroup, 25:28657 (HEDL-TME-71-36)
determination by photometry using carboxy derivatives of 2,6,7-trihydroxy-9-phenyl-3H-xanthen-3-one, 25:26174
determination in sea floor samples by neutron activation, 25:26188 (BNWL-SA-3803)
determination in thorium nitrates and zirconium nitrates by neutron activation, 25:26192
determination in yttrium oxides by solvent extraction and spectrography, 25:26168
determination in Zircaloy, chemical method for, 25:26171
effects on spectrophotometric determination of beryllium and gallium, 25:26172
fabrication and uses of high conductivity, 25:27187
identification of electric cables of, by labeling with silver-110m, 25:26322
inert-gas bubble precipitation and diffusion on dislocations in foils of, 25:27842 (RD/B/N-1850)
meson (π) reactions at 1 GeV/c, differential and total cross sections for, (E), 25:27959
neutron elastic scattering at 3.2 MeV using polarized beam, optical-model analysis of, (T), 25:28248
photon reactions (γ,p) at 17.6 MeV with natural, energy spectra from, (E), 25:28217 (LUNP-7013)
photon reactions at 5.4 GeV, total cross section for hadron production in, 25:27953
proton reactions at 1 GeV/c, differential and total cross sections for, (E), 25:27959
thermal capacity at 1.5 to 20°K, 25:27910
COPPER ALLOYS AND SYSTEMS
Ag--Cu, fabrication and uses of high conductivity, 25:27187
Al--Cr--Cu--Mg--Zn, analysis for trace amounts of silver by solvent extraction and atomic absorption spectrophotometry, 25:26169
Al--Cu--Zr, magnetic properties of ZrCu/sub 2-x/Al/sub x/, 25:27875
Al--Cu-base, depth distributions of 30-keV electrons and K x rays in, Monte Carlo calculation of, (T), 25:27836
Be--Cu, fabrication and uses of high conductivity, 25:27187
Be--Cu, fatigue strength of, effects of fine precipitates on, 25:27231
Be--Cu--Nb--Zr-base, properties for use as structural material for reactors, 25:27190(P)
Be--Cu-base--Ni--Ti, properties of, aging and mechanical, 25:27232
Be-base--Cu, embrittlement by mercury-base--sodium alloys at 25°C, 25:27243
Cd--Cu, fabrication and uses of high conductivity, 25:27187
Ce--Co--Cu--Fe--Sm, magnetic properties of, 25:27883
Ce--Cu, Hall coefficient and electric conductivity of liquid, 25:27212
Co--Cu--rare earths, casting and properties of permanent magnets of, 25:27184
Co--Cu-base, Kondo effect in, study by superconducting proximity effect, (E), 25:27662
Cr--Cu, fabrication and uses of high conductivity, 25:27187
Cu--Te, fabrication and uses of high conductivity, 25:27187
Cu--transition metals, phase stability in, 25:27261
Cu-base--Fe, Kondo effect in, study by superconducting proximity effect, (E), 25:27662
Cu-base--Mn, Kondo effect in, study by superconducting proximity effect, (E), 25:27662
COPPER ISOTOPES
effects on kinetics of isotope diffusion in copper, 25:26241
COPPER ISOTOPES Cu-62
beta and electron-capture decay of, gamma energies and intensities, branching ratios, and log-ft values for, (E), 25:28214 (CERN-70-30(Vol.2), pp 1105-13)
COPPER ISOTOPES Cu-63
carbon-12 reactions at 55 MeV with alpha and proton evaporation, statistical analysis for shell and angular momentum effects in, (T), 25:28266
cross section data on, tables of multigroup, 25:28657 (HEDL-TME-71-36)
effects on ir spectra of copper oxinates, 25:26234
photon reactions (γ,2n) at 1974 MeV, structure and energy dependence of differential cross sections for, (E), 25:28260
photon reactions (γ,n) at 10.84 MeV, structure and energy dependence of differential cross sections for, (E), 25:28260
photon reactions (γ,np) at 16.72 MeV, structure and energy dependence of differential cross sections for, (E), 25:28260
proton elastic scattering at 6.9 MeV, optical-model analysis of angular distributions from, (E), 25:28262
COPPER ISOTOPES Cu-65
cross section data on, tables of multigroup, 25:28657 (HEDL-TME-71-36)
effects on ir spectra of copper oxinates, 25:26234
photon reactions (γ,2n) at 17.82 MeV, structure and energy dependence of differential cross sections for, (E), 25:28260
photon reactions (γ,3n) at 28.66 MeV, structure and energy dependence of differential cross sections for, (E), 25:28260
photon reactions (γ,n) at 9.91 MeV, structure and energy dependence of differential cross sections for, (E), 25:28260
photon reactions (γ,np) at 17.11 MeV, structure and energy dependence of differential cross sections for, (E), 25:28260
proton elastic scattering at 6.9 MeV, optical-model analysis of angular distributions from, (E), 25:28262
COPPER ISOTOPES Cu-67
energy levels and transitions from nickel-67 decay, (E), 25:28221
COPPER ISOTOPES Cu-70
beta decay of isomeric, gamma spectra, β--γ coincidences, and log ft for, (E), 25:28221
CORRONEL 230
corrosion by melting glasses in radioactive waste vitrification process, 25:26334(T) (ORNL-tr-2410, pp 143-89)
CORROSION-RESISTANT ALLOYS
properties of, effects of coating, composition, heat treatment, surface finish, and working on, 25:27176 (INIS-mf-9)
COSMIC PARTICLES
decay of π^0, comparison with galactic γ flux for γ spectra from, (T), 25:27404
detection of 0.31-MeV protons in near-Earth interplanetary space and anisotropy, 25:27473
detection of multiple meson (μ), deep underground, (E), 25:27954
electric charge of interacting, at sea level, producing energy transfers greater than or equal to 25 GeV in steel targets, (E), 25:27475
energy spectra of electrons above 500 MeV, OGO-5 satellite data on, (E), 25:27575
COSMIC RADIATION
detection of gamma rays with energy above 10^{19} eV, (T), 25:27423
distribution in the Galaxy, (E), 25:27407
effects of proton event of Feb. 25, 1969, (E), 25:27553
intensity of, 6-, 12-, and 27-day oscillation in, (E), 25:27472
modulation of galactic and solar, in interplanetary space, (T), 25:27361
modulation of primary, relation to 27-day and 11-year variations, (T), 25:27389
propagation of low-energy galactic, in interplanetary space, (E), 25:27469
solar-flare effects on galactic, (E/T), 25:27532
variations in layer of galactic, in lower ionospheric D region, (T), 25:27513
COSMIC RADIO SOURCES
distribution of extragalactic, between -5 and +70°, (E), 25:27353
model for scintillation and diffraction phenomena of, ionosphere, magnetosphere, and solar wind, (T), 25:27612
spectral index of extragalactic, between -5 and 70°, (E), 25:27353
spectral scintillations to 1.0 Hz of two-component Cyg-A, cosine modulations of power, (E/T), 25:27474
COSMIC RAY TELESCOPES
operation of satellite-borne solar x-ray, 25:26484
COSMIC SHOWERS
Cherenkov radiation from EAS, angular, spectral, and temporal properties of, (E), 25:27952
detection of 1 to 10 TeV meson (μ), deep underground,

XUM

(E), 25:27954
detection of extensive, atmospheric scintillation, (E), 25:27468
meson production in, angular distribution for multiple, 25:28050
mesons (μ) bundles in extensive, (T), 25:27476
mesons (μ) distribution in extensive, TeV-range, (E), 25:27477
mesons (ν) distribution in extensive, TeV-range, (E), 25:27477
COSMOLOGY
arrow of time in, (T), 25:27424
fluctuations in gravitating media, correlation of, (T), 25:27430
gravitational interactions in expanding universe, (T), 25:27427
inverse-square law in, implications of, (T), 25:27422
model featuring oscillating Universe, (T), 25:27428
models in extension of Yilmaz gravitational theory, (T), 25:28087
observations in, discrete algebraic theories of limits on, (T), 25:27425
COUMARIN
radiation effects on synthesis of, in grapefruit skin, gamma, 25:27079
CRAB NEBULA
polarization in, search for optical circular, (E), 25:27348
CRACKS
propagation in fatigued high-strength meterials, mechanisms of, 25:27242
CRATERS
formation by Pre-Gondola II Event, measurements of, 25:26407 (PNE-1112)
formation by Pre-Gondola III Phase II explosion, measurements of, 25:26408 (PNE-1117)
CRITICAL ASSEMBLIES
control rods in ZPR-3 assemblies 48 and 48A, reactivity worth of boron carbide, (E), 25:28752 (ANL-7759)
critical mass of ZPR-3 assemblies 48, 48A, and 48B, (E), 25:28752 (ANL-7759)
Doppler effect measurements in ZPR-3 assemblies 48 and 48B, 25:28752 (ANL-7759)
experiments in SNEAK, on-line system for data processing and control of, 25:28756(T) (EURFNR-803)
neutron buckling in AGR-type lattices, measurement of axial, (E/T), 25:28806 (RD/B/N-1837)
neutron fission ratios in ZPR-3 assemblies 48 and 48B, (E), 25:28752 (ANL-7759)
neutron reaction rate measurements in ZPR-3 assembly 48, foil irradiations for, 25:28752 (ANL-7759)
neutron reaction rate traverses in ZPR-3 assemblies 48, 48A, and 48B, (E), 25:28752 (ANL-7759)
neutron reaction rates in AGR-type lattices, measurement of manganese, 25:28816 (RD/B/N-1518)
neutron spectra in ZPR-3 assembly 48, (E), 25:28752 (ANL-7759)
physics measurements in SNEAK, for steam cooled fast reactors, 25:28659
physics measurements in ZPR-3 assemblies 48, 48A, and 48B, summary of, 25:28752 (ANL-7759)
physics parameter measurements in Cavity Reactor Critical Experiment, 25:28761 (NASA-CR-72409)
reactivity for bare sphere and cylinder shaped cores of FCA, pulsed neutron analysis of negative, (E/T), 25:28759 (JAERI-Memo-4272)
reactivity of ZPR-3 assemblies 48 and 48B, effects of heterogeneity and sodium voids on, (E), 25:28752 (ANL-7759)
reactivity worth measurements in ZPR-3 assemblies 48, 48A, and 48B, 25:28752 (ANL-7759)
CROPS
radiation effects on production of, description of joint FAO/IAEA program for studies on, 25:27128 (CONF-680112-, pp 1-7)
yield of cereal and vegetable, use of plant mutation by ethyl sulfonates and ionizing radiation for improved, 25:26686 (CONF-680112-, pp 95-111)
CROTON OIL
radiosensitizing effects on tumorigenesis in skin of mice, uv, 25:26809
CRUSTACEA
Artemia salina, radiation effects on, comparison of fast neutron and gamma, 25:26917
Crago sp., zinc-65 distribution in tissues of, following ingestion, 25:26604
Euphausia sp., zinc-65 distribution in tissues of, following ingestion, 25:26604
radioactivity monitoring in, of Black Sea off coast of Romania during 1964 to 1967, 25:26745
CRYOGENICS
cooling to low temperatures, using hyperfine fields and nuclear adiabatic demagnetization in Van Vleck paramagnetic intermetallic compounds, (E/T), 25:27666
CRYSTAL RIVER POWER REACTOR, UNIT 3
design of, hurricane protection requirements in, 25:28629
CRYSTAL STRUCTURE
Ising model of, lectures on, 25:27913
CRYSTAL VIOLET
effects on determination of uranium by extraction--photometry, 25:26163
CRYSTALS
proton channeling in fluorite, 25:27851
role in origins of life, study of adsorption, catalysis, and pyrophosphate formation by hydroxyapatite to investigate possible, 25:28906 (UR-49-1444)
CULTURE MEDIA
effects of saline, on uv-irradiated bacteria, 25:27119
effects on alpha-radiosensitivity of bacteria, 25:27118
effects on survival of γ-irradiated fungi, 25:27085
CURIUM ISOTOPES Cm-244
cross section data on, tables of multigroup, 25:28657 (HEDL-TME-71-36)
CURRENT ALGEBRA
mesons (rho) and (sigma) bootstrap in π + π interactions in, 25:28027 (RLO-1388-602)
theory for nonrelativistic, as unitary representations of groups, 25:27972
CYANIDES
determination by potentiometric titration using ion-selective electrodes, 25:26166
CYANOGEN FLUORIDES
spectra of radiolytic ionic, ESR, 25:26289 (NYO-2150-60)
CYANOPHYTA
Phormidium mucicola, radioinduced mutations in, uv, 25:26712
CYCLOHEXANE
solvent properties for uranyl complex with 4,4,4-trifluoro-1-(2-thienyl)-1,3-butanedione, radiometric determination of, 25:26340
CYCLOPHOSPHAMIDE
effects on flax plants, mutagenic, 25:27090
CYCLOPROPANE, 1,2-DIMETHYL-
reactions with helium tritide ions from tritium beta decay, 25:26321
CYCLOTRON RADIATION
emission from isotropic plasma, general formula for, (T), 25:27706
CYCLOTRONS
design of microtron, 25:28136(P)
experimental facilities and research program at ALICE, for transactinide element production and identification, 25:28315 (CERN-70-30(Vol.2), pp 723-33)
ion source for Berkeley 88-inch, external PIG-type heavy, 25:28120 (UCRL-20406)
radiation protection methods for personnel of, used for therapy and radioisotope production, 25:26775
CYLINDERS
temperature distribution in solid heat-generating, cooled by flowing liquid metal, method for calculating, 25:26422
CYSTAMINE
radioprotective effects of, on blood pressure and heart frequency in rabbits, γ, 25:26794
radioprotective effects of, on mice, combined effects of AET or serotonin and, 25:26793
radioprotective effects of, on submaxillary glands in mice, comparison of AET, cysteine, noradrenaline, serotonin, and tetramethylcystamine with γ, 25:26795
radioprotective effects on catecholamine content in mouse tissues, 25:27017
radioprotective effects on DNA, 25:26801
toxic effects of, on γ-irradiated mice, combined effects of AET or serotonin and, 25:26793
CYSTEAMINE
effects on radiosensitivity of Ehrlich ascites cells, 25:26640
hydrochloride, radiation effects on binding to diammonium deoxythymidylate, 25:26279
radioprotective effects on animals, 25:27024
radioprotective effects on rabbit eyes, cobalt-60 γ and fast neutron, 25:27014
toxicity to mice in radioprotective doses, effects of temperature on, 25:26924
CYSTEINE
effects on radiolysis of aqueous solutions of acetone or 2-propanol, 25:26291
hydrochloride, radiation effects on binding to diammonium deoxythymidylate, 25:26279
radiolysis of oxygenated aqueous solutions at pH = 7, reactions of transient species in pulse, 25:26307
radioprotective effects of, on submaxillary glands in mice, in comparison of AET, cystamine, noradrenaline, serotonin, and tetramethylcystamine with γ, 25:26795
CYTIDINE, 2'-DEOXY-
radiation effects on urinary excretion of, by monkeys, γ, 25:26999
CYTIDINE, 2'-DEOXY-5-FLUORO-
effects on differentiation in vertebral column of, progeny of mice, in utero, 25:26997

D

D-43 (NIOBIUM ALLOY)
stability at high temperatures, long-term thermal, 25:27208 (N-71-10352)
DACTINOMYCIN
effects on immune spleen cells in mice, effects on selective inhibition of sensitizing, 25:26671

effects on recovery from x-radioinduced prophase reversion in grasshopper embryos, 25:26911
DAMS
damage from Rulison Event-produced ground motion, measurement and prediction of, 25:26402 (JAB-99-78)
motion of base of Rifle Gap, Colo., from Rulison Event, equipment for measurement of, 25:26410 (PNE-R-47)
response of Fort Peck, Montana, to Pre-Gondola III Phase II explosion, measurements of structural, 25:26408 (PNE-1117)
DATA ACQUISITION SYSTEMS
description of on-line PDP-9, for missing mass spectrometer, 25:28135
description of PDP-7, for spark chambers, 25:26510
development of computerized ultrasonic, 25:28884 (SC-DR-70-680)
development of PDP-9 computer on-line, for nuclear structure studies, 25:26555
requirements for nuclear power plant reliability, 25:28553 (AECL-3670, pp 83-8)
DATA PROCESSING SYSTEMS
description of PDP-8 computer-based, for mass spectrometer, 25:26556
development for dose calculations and measurements in clinical radiation physics, 25:26755
development for use with radioisotope scans, 25:26834
operation of on-line, for control of reactor experiments, 25:28756(T) (EURFNR-803)
DATA TABULATIONS
gamma--gamma directional-correlation coefficients, (T), 25:28401
hyperfine-interaction parameters for atoms having Z = 1 to 83, 25:27441 (ANL-7784)
nuclear binding energies, shape coefficients, and spin--parity assignments from liquid-drop-model calculations of γ process, (T), 25:28441 (CERN-70-30(Vol.1), pp 217-62)
nuclear data sheets for A = 207, 25:28378
nuclear data sheets for A = 208, 25:28375
nuclear data sheets for A = 209, 25:28376
nuclear data sheets for A = 211, 25:28377
of multigroup cross sections, 25:28657 (HEDL-TME-71-36)
radiation emitted by atoms and radionuclides, x and gamma, (E), 25:28400
DAUNOMYCIN
effects on development of Erlich ascites tumors in x-irradiated mice, 25:26990
effects on radiosensitivity of Streptococcus faecalis, 25:27100
DECANOIC ACID
effects on solvent properties of tridodecylamine for neptunium and plutonium, 25:26333(T) (ORNL-tr-2410, pp 121-42)
DECONTAMINATION
bibliography on methods for, 25:26443 (AED-C-13-7)
DENMARK
radiation processing of food in, development of programs for, 25:27142
DEOXYRIBONUCLEASE
radiation effects on metabolism of, in rat kidneys in comparison to injection of TEM, whole-body x, 25:26645
DEOXYRIBONUCLEASE II
radiation effects on metabolism of, in rat kidneys in comparison to injection of TEM, whole-body x, 25:26645
DEUTERIUM
effects on allylic and homoallylic oxidation of cyclohexene by palladium(II), 25:26256
effects on benzoin condensation in methanol, 25:26220
effects on changes of structure of water caused by organic and inorganic ions, 25:26259
effects on conversion of propanediol to propionaldehyde by dioldehydrase and coenzyme B_{12}, 25:26225
effects on hydroformylation of 3-methyl-1-hexene, 25:26228
effects on hydrogen evolution on gold electrodes in acid solutions, 25:26231
effects on hydrolysis of 2-amino-8-carboxy-4-oxo-3,1,4-benzoxazine, 25:26253
effects on ir and NMR spectra of chlorinated poly(vinyl chloride), 25:26246
effects on ir spectra of benzene derivatives, 25:26247
effects on ir spectra of borazine and boroxine, 25:26233
effects on ir spectra of ethylenediamine complexes of copper, 25:26232
effects on ir spectra of tribromobenzene, 25:26222
effects on isomerization of cyclobutene, 25:26219
effects on lifetime and g factors of substates in excited hydroxyl radicals, 25:26243
effects on oxidation of 2-methoxyethanol to methoxyacetic acid by nitric acid solutions, 25:26223
effects on quantum yields from photolysis of trans-N-tert-butyl-2-phenyl-3-benzoylaziridine, 25:26250
effects on reactions of dimethylaniline with methyl p-toluenesulfonate in nitrobenzene, effects of temperature on, 25:26217
effects on reactions of hydrogen atoms produced by photolysis of thiols, 25:26252
effects on spectra of photolyzed methyl azidoformate, 25:26236
effects on spectra of vanadium oxide trinitrate complex with acetonitrile, 25:26235
effects on vapor pressure of hydrogen sulfide, 25:26248
exchange between benzoin and methanol, 25:26220
exchange between heavy water and alcohols in oxidation of aqueous chromium(II), 25:26229
exchange in hydrogenation of ethylene, 25:26230
exchange with hydrogen in benzohydroxamic acid, method for assignment of vibration bands by progressive, 25:26216
exchange with hydrogen in deuterium--ethane and hydrogen--deuterium-labeled ethane mixtures, ion cyclotron resonance studies on ionic reactions in, 25:26249
exchange with hydrogen in dimethyl sulfoxide solutions of bicyclo[3.1.0]hexanesemidione, kinetics of, 25:26254
exchange with hydrogen in dimethyl sulfoxide solutions of potassium tert-butoxide and semidiones, 25:26255
exchange with hydrogen in reactions of alkanes with superacids, 25:26226
exchange with hydrogen in the pentachlorophenyl ester of N-carbobenzoxy-S-benzyl-L-cysteine, 25:26257
photon reactions (γ,n) up to 125 MeV, angular distributions for, (E), 25:28165
plasma of, neutron production in focus discharge, (E), 25:27799
DEUTERONS
interactions e + d → e + p + n at high energies, cross sections, angular distributions, and neutron electric form factors from, (E), 25:27951 (NP-18725)
interactions e + d, electric neutron form factor from cross sections for, (T), 25:27980 (DESY-71/7)
interactions K_2^0 + d → K_1^0 + d at high energies, differential cross section and phase of amplitude for, (T), 25:28049
interactions K^- + d → K^- + π^+ + π^- + d at 12.6 GeV/c, production of L and Q in, (E), 25:27967
interactions n + d → t, three-body model vertex part of virtual, (T), 25:28047
interactions n + d at 20 to 60 MeV, convergence of nonrelativistic graphs for elastic scattering, 25:28166
interactions π + d at 3.65 and 3.75 GeV, cross sections for elastic, 25:28073
reactions (d,2n) with neptunium-237 at 9 to 14 MeV with excitation of fission isomers, energy spectra and isomer ratio for, (E), 25:28355(R) (TID-25659)
reactions (d,3n) with tungsten-186 at 12 to 19.6 MeV, gamma spectra from, (E), 25:28287 (ANU-P-518)
reactions (d,α) with light nuclei, mechanism in isospin-violating direct, (T), 25:28459
reactions (d,n) with potassium-39 at 4.7 MeV, neutron time-of-flight spectra from, (E), 25:28230
reactions (d,nγ) with aluminum-27 and sodium-23 at 4 MeV, γ spectra from, (E), 25:28225
reactions (d,p) and (d,t) with lutetium-176 at 12 MeV, γ spectra from, (E), 25:28424
reactions (d,p) with argon-40 at 1.96 MeV, angular distributions for, (E), 25:28251
reactions (d,p) with chromium-50 and -52 and titanium-48 and -49 at 13.6 MeV, distorted-wave analysis of differential cross sections from, (E/T), 25:28269
reactions (d,p) with curium-140 at 12 MeV, anomalies in DWBA analysis of, (E), 25:28429
reactions (d,p) with nuclei near 20 MeV, adiabatic treatment of, (T), 25:28512
reactions (d,p) with nuclei, isobaric analog resonance effects in, 25:28471
reactions (d,p) with tin-124 at 5.1 to 12.0 MeV, angular distributions for, (E), 25:28286 (ANU-P-511)
reactions (d,pf) with plutonium-239 at 13 MeV, optical-model analysis of probability for, (T), 25:28445 (CERN-70-30(Vol.1), pp 553-66)
reactions (d,t) with A = 94 to 110 nuclei at 17 MeV, angular distributions for, (E), 25:28374
reactions (d,t) with bismuth-209 at 20 MeV, triton spectra from, (E), 25:28417
scattering by phosphorus-31 at 8 and 12 MeV, optical-model analysis of angular distributions from elastic, (E), 25:28270
scattering by tritium at 3.2 to 12.3 MeV using polarized beam, excitation functions and analyzing power for elastic, (E), 25:28168
DIAMONDS
ion implantations in single crystal, analysis of, 25:27858
DIDO REACTORS
maintenance of HIFAR, during 1970, 25:28782
neutron source in FRJ-2, construction and operation of cold, 25:28767
DIELECTRICS
conductivity in liquid, conference on, 25:26470
DIET
polonium-210 contamination of vegetable component of human, potential long-term hazards to man from, 25:26684
radioisotope content of human, derived from freshwater food chain, establishment of MPC in ecosystem for control of specific, 25:26747
DIFFUSION
research progress on fatigue-enhancement of, 25:28870(R) (NYO-4097-2)
DIFOLATAN
effects on survival of γ-irradiated Penicillium expansum, 25:27084

DIGESTIVE SYSTEM
radiation effects on, ionizing, 25:27036 (CONF-691057)
DIODES
radiation effects on IMPATT, gamma and neutron, 25:26562
DIRECT ENERGY CONVERSION DEVICES
book: Direct Conversion of Nuclear Radiation Energy, 25:27480
DISEASES, INFECTIOUS
abscesses, radiodiagnosis of human liver, effectiveness of gold-198 colloids or iodine-131-labeled rose bengal scanning for, 25:26860
amebic abscess, radiodiagnosis and evaluation of drug therapy of, in human liver, use of colloidal gold-198 scanning for, 25:26843
hydatidosis, radiodiagnosis of kidney, in man using combined radiography and scintigraphy, 25:26816
radiodiagnosis of infected brain lesions in man using technetium-99m, 25:26818
tuberculosis, radiation effects on proliferation of phagocytes in lesions in rabbits, tritium tracer study, 25:27001
DISEASES, NEOPLASTIC
adenocarcinomas, radiation effects on growth of transplanted mammary, in mice in comparison to effects of antilymphocyte serum, x, 25:26666
adenomas, radiotherapy of pituitary gland, cobalt-60 gamma, 25:26872
adenomas, radiotherapy of salivary gland, effectiveness of pre- and post-operative, 25:26866
cancer, radioinduced in human lungs following occupational exposure, gamma, 25:27045
cancer, therapy of uterine, comparison of medical, radiation, and surgical methods for, 25:26871
carcinoma, radiotherapy planning for bronchial, phantom method for 43-MeV betatron electron and bremsstrahlung, 25:26757
carcinomas, conference on etiology of, 25:26791
carcinomas, histology of papillary, in human thyroid of atomic bomb survivors, 25:26898
carcinomas, radiodiagnosis of human lung, effectiveness of scanning with glutathione-treated mercury-203-labeled mercury chlorides for, 25:26842
carcinomas, radiodiagnosis of human, effectiveness of mercury-197-labeled bichloride scintigraphy for, 25:26832
carcinomas, radioinduced mammary, in rats, synergism between diethylstilbestrol and, 25:27011
carcinomas, radioinduced, in animals and man, 25:27036 (CONF-691057)
carcinomas, radioinduced, in human breast and genital organs following therapy, 25:27038
carcinomas, radioinduced, in human maxillary sinus following diagnostic thorium administration, 25:27050
carcinomas, radioinduced, in human uterus following x-ray diagnostic procedures, 25:26827
carcinomas, radioinduced, in lungs of rats following implantation of strontium-90, 25:26921(T) (LF-tr-49)
carcinomas, radioinduced, in mice, effects of dose on late γ, neutron, and x, 25:26976
carcinomas, radioinduced, in rats, radium and x, 25:26827
carcinomas, radiotherapy of cervical, in man, evaluation of combined surgery and, 25:26886
carcinomas, radiotherapy of human cervical, recurrence following, 25:26887
carcinomas, radiotherapy of human esophagus, methods for cobalt-60 gamma, 25:26896
carcinomas, radiotherapy of human pelvic, complications following rotation γ, 25:26894
carcinomas, radiotherapy of human penis, use of radium-226 molds for contact γ, 25:26863
carcinomas, radiotherapy of human uterus, use of combined hyperbaric oxygen intracavitary and external beam γ, 25:26869
carcinomas, radiotherapy of Stages I and II of human cervical, complications following, 25:26893
conference on research on, Chicago, 1971, 25:26789
Erlich ascites tumors, radiation effects on development of, in mice, combined effects of daunomycin and x, 25:26990
fibrosarcomas, radioinduced, in man following childhood therapy of hemangioma, x, 25:27059
fibrosarcomas, radioinduced, in man following therapy, 25:27044
glioblastoma multiforme, radiotherapy of human, following surgery, combined effects of 5-fluorouracil and γ, 25:26889
gliomas, radiodiagnosis of human brain, by scanning, effectiveness of, 25:26850
hemangiomas, radioinduced, following therapy, latent, 25:27049
hemangiomas, radiotherapy of, in children, development of fibrosarcomas following x, 25:27059
leukemia, occurrence in man exposed in utero to atomic bombing at Hiroshima and Nagasaki, 25:27043
leukemia, radioinduced, in animals and man, 25:27036 (CONF-691057)
leukemia, radioinduced, in man, 25:26964
leukemia, radioinduced, in mice, effects of splenectomy on x, 25:27021
leukosis, radioinduced mouse, effects of bone marrow autotransplants on, 25:26904
luteomas, radioinduced, in ovaries of mature mice following exposure in infancy, x, 25:26930
lymphoma, radiation effects on growth of cells of, in mice, x, 25:26974
lymphomas, radiotherapy of human orbital, effectiveness of x, 25:26890
malignant, occurrence in man exposed in utero to atomic bombing at Hiroshima and Nagasaki, 25:27043
malignant, radiodiagnosis of human lymph node, effectiveness of colloidal radioactive gold scanning for, 25:26851
malignant, radioinduced, in human bones and lungs, thorium-228, 25:26603
malignant, radiotherapy of deep-seated, using fractionated-dose high-energy electrons while breathing hyperbaric oxygen, 25:26864
malignant, radiotherapy of human nose and paranasal sinus, use of radiosensitizing drugs and surgery with gamma, 25:26885
melanomas, radiotherapy of human, by endolymphatic administration of iodine-131-labeled ethiodol, 25:26888
melanomas, radiotherapy using injected iodine-131-labeled chloroquine analog in dogs, 25:26882
meningiomas, radiodiagnosis of human brain, by scanning, effectiveness of, 25:26850
metastases, localization in human bone marrow, use of colloidal gold-198 scanning for, 25:26847
metastases, radiodiagnosis in human bones, effectiveness of radiography for, 25:26846
metastases, radiodiagnosis of human brain, by scanning, effectiveness of, 25:26850
metastases, radiotherapy of human brain, combined effects of corticosteroids and γ and x, 25:26895
nodules, radiodiagnosis of human thyroid, effectiveness of mercury-197-labeled mercury dichloride for, 25:26823
retinoblastoma, radiotherapy of human, effectiveness of electron beam, radon-222 contact, and x, 25:26880
sarcomas, radiotherapy of human skin, Koebner phenomenon-like occurrence following x, 25:26875
seminomas, radiotherapy of testicular, in man, effectiveness of γ, 25:26891
tumors, diagnosis in brain of man using radioisotope scanning and spinal fluid protein analysis, 25:26828
tumors, radiodiagnosis of human brain, scintigraphic patterns for, 25:26820
tumors, radiodiagnosis of human brain, using technetium-99m, comparison of gamma camera and rectilinear scanner for, 25:26852
tumors, radioinduced, in skin of mice, sensitizing effects of acetic acid, croton oil, and xylene on uv, 25:26809
tumors, radiotherapy of brain and spinal cord, development of nervous tissue reactions following, 25:27056
tumors, radiotherapy of gynecological, effects on bladder, 25:26813
tumors, radiotherapy of human bladder, effectiveness of high-energy x, 25:26876
tumors, radiotherapy of human bladder, telecentric small-angle pendulum method for fast electron, 25:26867
tumors, radiotherapy of human renal, telecentric small-angle pendulum method for fast electron, 25:26867
tumors, radiotherapy of pulmonary, in man, evaluation of 42-MeV betatron, 25:26874
tumors, radiotherapy of recurrent human gynecological, telecentric small-angle pendulum method for fast electron, 25:26867
tumors, radiotherapy of, variable block-surface-distance for adjustment of shadow size in mantle field, 25:26892
tumors, scanning of human, preparation of selenium-75-labeled selenite, niobium-95-labeled oxalate, iodine-131-labeled iodouracil, and iodine-131-labeled fibrinogen for, 25:26859
Wilms' tumors, radiotherapy of, in right kidney of human children, injuries to liver following, 25:26884
DISEASES, PHYSIOLOGICAL
anemia, diagnosis of pernicious, in humans, radioimmunoassay method for, 25:26676
anemia, radiation effects on patients with Fanconi type aplastic, chronic radium, 25:27054
anemia, radiodiagnosis of pernicious, in man, comparison of effectiveness of cobalt-57-labeled cyanocobalamin plasma level test Schilling test for, 25:26853
arthritis, radiotherapy of human, effectiveness of synovial injections of gold-198, phosphorus-32, or yttrium-90 for, 25:26873
cataracts, radioinduced in eyes of rabbits, effects of average power in relation to dose on, 25:26971
cataracts, radioinduced in personnel by cyclotrons, radioisotopes, x-ray generators, and γ-ray generators, 25:26783
cataracts, radioinduced, in eyes of rabbits, protective effects of chemicals against cobalt-60γ and fast neutron, 25:27014
cataracts, radioinduced, in eyes of rabbits, RBE for fast neutron, 25:26945
cataracts, radioinduced, in human eyes following postoperative treatment for prevention of pterygium

XUM

recurrence, β, 25:26870
cataracts, radioinduced, in rabbits, RBE for 14-MeV neutron, 25:27027
cirrhosis, radiodiagnosis of human liver, effectiveness of gold-198 colloids or iodine-131-labeled rose bengal scanning for, 25:26861
dermatitis, radioinduced, in human skin following therapy, development of eccrine poroma in area of, 25:27055
diabetes, radiosensitivity of rats with, induced by streptozotocin, x, 25:27010
diabetic retinopathy, radioinduced pituitary ablation for treatment of, effects on aqueous humor dynamics, 25:27037
diaphragmatic hernia, radiodiagnosis in man using technetium-99 scanning, 25:26836
eccrine poroma, development in human skin in area of chronic radiodermatitis, 25:27055
edema, radioinduced, in brain of monkeys, x, 25:26987
enterocolitis, radioinduced, in man, pathology and treatment of, 25:26811
fistulae, radiodiagnosis of post-surgical bronchopleural, in man, use of inhaled technetium-99-labeled albumin for, 25:26833
hyperlipemia, radiodiagnosis in liver and spleen of man using technetium-99m, 25:26830
hypertension, radioinduced renal, in rats following bilateral or unilateral exposure of kidneys, evaluation of physiological parameters related to x, 25:26652
hyperthyroidism, radiotherapy using iodine-131, occurrence of thyroid crisis in patients following, 25:26881
inflammations, radioinduced, on rabbit skin, protective effects of benzydamine against x, 25:26806
lesions, radiodiagnosis of human bone, using barium-135m, 25:26835
leukopenia, radioinduced, in man, therapeutic effects of taurine, uridine monophosphates, and vitamin B_4 on, 25:26812
leukoplakia, radiotherapy of human vocal cord, effects of dose and histological origin on effectiveness of, 25:26868
Myasthenia gravis, radiotherapy of human, by thymus gland exposure, effects of x, 25:26877
myelitis, radioinduced, in rats, effects of oxygen on x, 25:26966
myocardial infarctions, radiodiagnosis of human, effectiveness of iodine-131-labeled sodium iodide for, 25:26822
pterygium, radiotherapy of human, for prevention of postoperative recurrence, β, 25:26870
pulmonary embolism, radiodiagnosis in man using technetium-99 scanning, 25:26837
radiodiagnosis in pelvic area in pregnant patients, orthometric view for dose reduction during x, 25:26831
radioinduced, in human progeny following maternal uterine therapy, x, 25:27057
thyroid crisis, occurrence in man following iodine-131 therapy of hyperthyroidism, 25:26881

DISEASES, TRAUMATIC
burns, effects on life span of erythrocytes, nitrogen-15 method for studying, 25:26572
lesions, radiodiagnosis of human brain, by scanning, effectiveness of, 25:26850
lesions, radiodiagnosis of, data analysis method for use in, 25:26856
radiation injuries, development in lower jaws of rabbits, effects of dose and time on, 25:27003
radiation injuries, development in man following diagnosis, x, 25:26788
radiation injuries, effects of antibiotics on healing patterns of combined surgical and x, 25:26932
radiation injuries, induced in human bladder following therapy for gynecological tumors, methods for treatment of, 25:26813
radiation injuries, induced in human ureter following therapy, surgical methods for treatment of, 25:26814
radiation injuries, methods for treatment of human bladder, following therapy, 25:26810
radiation injuries, treatment of human cardiac and myocardial, developed after radiotherapy, 25:27048
radiation injury, effectiveness of balneotherapy of, 25:26897
wounds, radiation effects on response of lens epithelium of rats to, x, 25:27000

DISPERSION RELATIONS
sum rules for π + K + π + K, anti K + K + anti K + K, and K + K + K + K interactions, 25:28029

DOGS
heart volume variations in, use of iodine-131 in measurement of, 25:26566 (CEA-CONF-1711)
plutonium-239 distribution in tissues of, following inhalation of plutonium oxide, 25:26599
radiation dose absorbed by normal and melanoma tissues of, following injection of iodine-131-labeled chloroquine analog, 25:26882
radiation dose to mongrel, from implanted plutonium-238-powered circulatory assist device, γ and neutron, 25:26931
radiation effects on biochemistry of blood serum and tissues in, effects of AET on x, 25:26935
radiation effects on estrus and fertility of beagle, following ovarian exposure, delayed x, 25:27009
radiation effects on immune reactions in, following heart transplants, ultrastructural electron microscopy studies on x, 25:26677
radiation effects on leukocytes and lymph nodes of, plutonium-238 and plutonium-239 dioxide α and γ, 25:26929
radiation effects on liver in, effects of dose on γ, 25:26955
radiation effects on mortality of beagle, effects of dose on neutron and gamma, 25:26992
radioinduced chromosome aberrations in lymphocytes of mongrel, following implantation of plutonium-238-powered circulatory assist device, γ and neutron, 25:26931

DOUNREAY FAST REACTOR
design characteristics of, 25:28544

DRESDEN POWER REACTOR, UNIT 1
operations history for 1960 to 1969, review of, 25:28577
operations incident of March 11, 1971, failure of primary drum low level scram relay, 25:28557 (DOCKET-50010-84)
site for, environmental radiation monitoring program for, 25:28525

DRESDEN POWER REACTOR, UNIT 2
cooling system piping for, revised in-service inspection requirements for, 25:28600 (DOCKET-50237-154)
electrical systems for, seismic test program for, 25:28598 (DOCKET-50237-152)
fuel elements for, evaluation of failed, 25:28598 (DOCKET-50237-152)
instrumentation for, seismic test program for, 25:28598 (DOCKET-50237-152)
neutron flux distribution for, asymmetrical, 25:28598 (DOCKET-50237-152)
operations incident of April 4, 1971, wiring error on backup power supply to injection valves of low pressure coolant injection system, 25:28566 (DOCKET-50237-155)
operations incident of February 26, 1971, loss of electric power to low pressure coolant injection system, 25:28565 (DOCKET-50237-151)
operations incident of February 3, 1971, malfunction of 2/3 A standby gas treatment system, 25:28564 (DOCKET-50237-145)
pressure vessel for, revised in-service inspection requirements for, 25:28600 (DOCKET-50237-154)
protection systems for, corrective maintenance for, 25:28598 (DOCKET-50237-152)
pumps for, vibration criteria for supports of jet, 25:28598 (DOCKET-50237-152)
radioactive waste disposal system, requested additional information on, 25:28598 (DOCKET-50237-152)
technical specifications for, revised, 25:28597 (DOCKET-50237-148)
technical specifications for, revised, 25:28596 (DOCKET-50237-146)
turbine electrohydraulic control system for, additional pressure sensors for oil piping of, 25:28599 (DOCKET-50237-153)

DRESDEN POWER REACTOR, UNIT 3
cooling system piping for, revised in-service inspection requirements for, 25:28605 (DOCKET-50249-64)
pressure vessel for, revised in-service inspection requirements for, 25:28605 (DOCKET-50249-64)
turbine electrohydraulic control system for, additional pressure sensors for oil piping of, 25:28599 (DOCKET-50237-153)

DROPS
collision efficiencies of liquid, calculations of, 25:26384 (CONF-700601-, pp 381-3)
size spectra of water, in atmospheric aerosols, mathematical models for evolving, 25:26385 (CONF-700601-, pp 385-402)

DUNGENESS B REACTORS
design characteristics of, 25:28544

DUSTS
angular-momentum losses of clouds of, during star formation, (T), 25:27326
distribution in Milky Way, relation to gases, (E), 25:27415
distribution in Orion Nebula, (E), 25:27312
dynamic processes in galaxies, computer simulation of, (T), 25:27406
radioisotope content of Japanese, April 1969 to April 1970, cerium-144, cesium-137, and strontium-90, 25:26392 (NIRS-RSD-27)
scavenging of atmospheric, efficiency of raindrops for, (E/T), 25:26371 (CONF-700601-, pp 169-86)

DYES
use of fluorescent, as tracers for measuring scavenging efficiency of rainwater, 25:26368 (CONF-700601-, pp 137-47)

DYSPROSIUM
determination in plutonium oxide--uranium oxide pellets by emission spectroscopy, 25:26153 (LA-4622)
determination in yttrium oxides by solvent extraction and spectrography, 25:26168
effects on magnetic susceptibility of scandium, 25:27878
magnetic domain walls in, calculations of spin structure and energy of, 25:27873
magnetic properties of, effects of uniaxial stress on, 25:27889

spin-wave dispersion relations of, neutron inelastic scattering study of, 25:27888
DYSPROSIUM ALLOYS AND SYSTEMS
Bi--Dy, magnetic structure of DyBi, neutron-diffraction study of, 25:27887
Dy--Pd, magnetic properties of $DyPd_3$ at 4 to 300°K, 25:27870
DYSPROSIUM ISOTOPES Dy-156
helium-3 reactions (He-3,6n), (He-3,7n), (He-3,α4n)), (He-3,α5n), (He-3,p6n), and (He-3,p7n) at 68 to 98 MeV, yield curves for, (E), 25:28303 (CERN-70-30(Vol.1), pp 533-44)
DYSPROSIUM ISOTOPES Dy-160
energy-level transitions in, multipole mixing ratios for, (E), 25:28434
DYSPROSIUM ISOTOPES Dy-164
energy levels from terbium-164 beta decay, (E), 25:28326 (CERN-70-30(Vol.2), pp 985-1000)
energy levels of, deformation parameters for 4+, (E/T), 25:28411
proton reactions (p,t) at 51.7 MeV, spectra and DWBA analysis of differential cross sections from, (E/T), 25:28411

E

EARTH
distance to Moon, effects of an anisotropic gravitational mass on, (T), 25:27358
EARTHQUAKES
effects on Midwest Fuel Recovery Plant, 25:26325 (DOCKET-50268-7)
effects on safety of West Valley Processing Plant, 25:26324 (DOCKET-50201-68)
ECOSYSTEMS
radiation effects on marine, in relation to waste disposal, review of, 25:26683
radioisotope transport time in, calculations of, 25:26751 (UCRL-50163(Pt.7))
ECUADOR
radioisotopes in agriculture in, 25:27134 (CONF-680112-, pp 245-6)
EDDY CURRENT TESTING
instrumentation for, coil encircling two-conductor rod, 25:28911 (Y-1787)
method for materials, review of, 25:26440
EGGS
radiation effects on proteins of, role of immunoelectrophoresis and starch gel electrophoresis to determine, 25:26631
radiation effects on rheology of albumin of, effects of temperature on γ, 25:26923
EGYPT
cesium-137 content of man during 1970 in, whole-body counting of, 25:26740 (NP-18728)
radiation dose received by atomic energy personnel in, during 1962 through 1969, 25:26749 (NP-18732)
ELAIDIC ACID
elaidic acid--palmitic acid, radiolysis at -196°C, ESR studies on kinetics of radical transformation in γ, 25:26312
ELECTRIC CAPACITORS
properties of plane plasma-filled, in crossed electric and magnetic fields, (T), 25:27718
ELECTRIC CHARGES
Lorentz invariance of, 25:27988
ELECTRIC DISCHARGE
current--voltage characteristics of positive column, effect of temperature nonuniformities on, (T), 25:27714
ionization waves in positive column, feedback control of, (T), 25:27773
plasma drift instabilities in, stabilization using rf electric fields, (E), 25:27787
plasma drift-dissipative instabilities in afterglow, dynamic stabilization of, (E), 25:27786
plasma helical instabilities in positive column, effect on density and potential distribution, (T), 25:27738
ELECTRIC FIELDS
currents observations during Mar. 18, 1969 substorms from barium cloud releases at 12.4 R/sub E/, (E), 25:27620
effects of east-west, on midlatitude ionospheric F2 layer, (T), 25:27529
effects on electron density and behavior of midlatitude ionospheric F region, (T), 25:27528
electric-conducting emulsions in, motion of, (E), 25:27501
measurement in auroral ionosphere, balloon electrostatic-probe, (E), 25:27545
measurements of magnetospheric, ion-cloud and sounding-rocket, (E), 25:27545
properties around planar probes in interplanetary space, photoemission and probe surface parameters affecting, (T), 25:27359
variations across bow shock and magnetosheath, (E), 25:27539
ELECTRIC GENERATORS
design standards for power reactor auxiliary diesel, 25:28705
ELECTRIC PROBES
current in retarding-potential plasma, relation to integral electron flux in ionosphere, (E/T), 25:27682
theory of cylindrical, in flowing plasma, 25:27681
use of Langmuir, for measurement of drift-wave potential oscillations in plasma, (T), 25:27809
uses in nondestructive testing, 25:26440
ELECTROJETS
effects of auroral, on fast electron absorption and scattering in upper atmosphere, (T), 25:27589
relation of intensity of auroral, with low-latitude DS-current component during intense geomagnetic storms, (E/T), 25:27619
ELECTROMAGNETIC FIELDS
charged-particle coupling to, causality in Lorentz-covariant Lagrangian for, (T), 25:28068
charged-particle pair annihilation at potential barrier in time in external, probability for, (T), 25:27985
effect of solar-wind flux variation on, Jan. 21 to March 21, 1969, (E), 25:27535
ELECTROMAGNETIC LENSES
design of 12-cm bore superconducting dc quadrupole, 25:28111 (KFK-1218)
ELECTROMAGNETIC WAVES
interactions in plasma, electron density measurement by nonlinear, (T), 25:27684
propagation in bounded cold plasma, (T), 25:27804
propagation in Earth--ionospheric cavity, technique for analysis of transient elf, (E/T), 25:27592
propagation in Earth-ionospheric cavity, amplitude-frequency spectra of elf transient, (E/T), 25:27591
propagation in inhomogeneous plasma, (T), 25:27801
propagation in plasma with sheared magnetic fields, (T), 25:27821
propagation in plasma, theory for, 25:27803
ELECTRON BEAMS
book: Electron Beam Welding, 25:27197
injection into magnetic mirrors, relativistic, (E), 25:27688 (WASH-1159, pp 193-5)
interactions with gases, ion acceleration in, (E), 25:27696 (WASH-1159, pp 204-18)
interactions with magnetized plasma, electron scattering by electrostatic fluctuations in, (E), 25:27699
interactions with plasma, highly ionized ion production by relativistic, (E), 25:27694 (WASH-1159, pp 184-9)
interactions with plasma, ion momentum analysis from, (E), 25:27697 (WASH-1159, pp 219-26)
interactions with plasma, ion production in, (E), 25:27695 (WASH-1159, pp 196-203)
interactions with plasma, nonlinear perturbations and electron scattering in, (E), 25:27703
interactions with plasma, nonlinear properties of one-dimensional, (T), 25:27710
interactions with plasma, relaxation processes in, (E), 25:27700
interactions with plasma, suppression of longitudinal electron oscillations by beam modulation, (E), 25:27702
radiation emission effects in dynamics of relativistic, 25:28114 (NP-18634)
stability of E-layer, cold plasma effects on negative mass, (T), 25:27746
ELECTRON CAPTURE
effects of exchange and overlapping in, relativistic corrections to, (T), 25:28495
probability relative to beta decay, calculations of, (T), 25:28494
ELECTRON GAS
oscillations in Lorentzian, Landau damping of longitudinal, (T), 25:27822
positron interactions with, bound states in, (T), 25:27447
ELECTRON MICROSCOPY
bibliography on surface and vacuum physics, 25:27440
book: Electron Microscopy 1968, Vol II, 25:26565
conference on, abstracts of papers presented at fourth European Regional, 25:26565
specimen preparation for, polyvinyl chloride impressions for indirect carbon replicas for, 25:28858(T) (LA-tr-71-25)
ELECTRON PAIRS
production by gamma quanta in nuclear fields, polarization effects on cross sections for, (T), 25:27996
ELECTRON PARAMAGNETIC RESONANCE
principles of, 25:28838 (ANL-7764)
ELECTRON PROBE MICROANALYSIS
equipment for irradiated reactor fuel elements, 25:26157
equipment for radioactive samples, 25:26156
ELECTRON-RING ACCELERATORS
beam dynamics in, radiation emission effects in electron, 25:28114 (NP-18634)
beam injection in printed circuit steering coils for, 25:28116 (UCRL-20165)
electron ring instability in, non-linear regime of, (T), 25:28110 (JINR-P9-5622)
performance as source of highly-ionized heavy ions, 25:27439 (WASH-1159, pp 147-55)
radiation losses in, diffraction radiation by line charge moving past comb in model of, (T), 25:28483
ring compressor for, mechanical features of, 25:28118 (UCRL-20177)

XUM

ELECTRON TUBES
voltage stabilization circuit for thyratron, 25:28108 (ITEF-761)
ELECTRONS
absorption and scattering in ionosphere, effects of auroral electrojet on fast, (T), 25:27589
angular and spatial distribution over polar caps, satellite observations of solar, (E), 25:27540
anticorrelation with auroral structures during high magnetic activity, (E), 25:27581
anticorrelation with geomagnetic index, auroral zone, (E), 25:27582
bleaching of trapped radiolytic, in alkaline ice, 25:26298
density and temperature in magnetosphere during Feb. 25, 1969 proton event, Langmuir probe, (E), 25:27566
detection of, based on x-ray transition radiation detection using streamer chamber, 25:26515
dose calculation for bronchial carcinoma therapy, techniques for 43-MeV betatron, 25:26757
dose fractionation scheme for high-energy, in therapy of deep-seated neoplasms, 25:26864
dosimetry for therapy, use of computer calculations in, 25:26761
dosimetry of 42-MeV betatron, for therapy using tissue-equivalent phantoms, 25:26865
dosimetry of, properties of calcium fluoride and lithium fluoride thermoluminescent dosimeters for, 25:26525
effectiveness for preservation of trout, effects of dose on, 25:27148
effectiveness for therapy of human retinoblastomas, 25:26880
effectiveness of 10-MeV, for preservation of carp, effects of dose on, 25:27147
effects of pulsed, on aqueous solutions of nitrobenzene, nitromethane, and oxygen, yields of hydrated electrons from, 25:26308
effects of pulsed, on aqueous solutions of phenyl glucopyranoside, effects of scavengers on production of transient species in, 25:26304
effects of pulsed, on single crystals of potassium chloride, spectral studies on, (E/T), 25:27846
effects of pulsed, on substituted aryl glycosides, rate constants for reactions of hydrated electrons and hydroxyl radicals produced by, 25:26305
effects of radiolytic hydrated, on activity of hemocyanins, 25:26302
effects on amino acid films at 40 to 1000 eV, spin interactions in, 25:26277(R) (ORO-3799-7)
effects on color stability and storage life of beef, effects of sodium tripolyphosphate on, 25:27162
effects on n-type germanium at 1.1 MeV and 5°K, low-temperature annealing of defects induced in, 25:27850
effects on n-type silicon at 2 MeV and low temperatures, infrared study of defects induced in, 25:27845
effects on p-type germanium at 1.5 MeV, shallow traps induced in, 25:27843
effects on properties and shelf life of gwyniads, effects of dose on, 25:27146
effects on silicon, luminescence spectrum induced in, 25:27849
effects on thermal oxidation of benzene with oxygen, 25:26284
effects on tissue physiology of citrus fruits, 25:27135 (IAEA-R-362-F)
energy dissipation in matter near plane and spherical interfaces, model for, 25:27835
energy of classical, Maxwell equations and special relativity for, (T), 25:27986
energy spectra above 500 MeV, OGO-5 satellite data on cosmic, (E), 25:27575
energy spectra of 45 to 450 keV, Feb. 23 to Mar. 2, 1969 ESRO data at northern high latitudes of trapped and precipitated, (E), 25:27568
energy spectra of cosmic solar, satellite observation of, (E), 25:27533
energy spectra of precipitated-auroral, in presence of x-ray components, (E), 25:27549
flux enhancements from solar activity Dec. 1969 to June 1969, high-energy, (E), 25:27574
flux in mid-latitude nighttime, precipitation, (E), 25:27601
fluxes in polar ionosphere, scatter and magnetic disturbance-dependence of, (E), 25:27580
intensity at 300 to 500 km in auroral zone, Geiger--Mueller observations during Feb. 25, 1969 solar event, (E), 25:27572
intensity during Feb. 25, 1969 solar flare, ESRO-II observations of, (E), 25:27471
intensity increase in Feb. 25-Mar. 5, 1969 of solar cosmic-ray, (E), 25:27470
interaction of solar energetic, with bow shock and magnetopause, (E), 25:27538
interactions e + d + e + p + n at high energies, cross sections, angular distributions, and neutron electric form factors from, (E), 25:27951 (NP-18725)
interactions e + d, electric neutron form factor from cross sections for, (T), 25:27980 (DESY-71/7)
interactions e + N, comparison of vector-meson dominance predictions with ν production in, 25:27982 (DESY-71/12)
interactions e + p + e' + π+ + n at 4 to 5.4 GeV, differential cross sections for, (E), 25:27950 (DESY-71/9)
interactions e + p, distributions of transverse momenta in inelastic, (T), 25:27974
interactions e + p, proton form factors and radius from, (T), 25:27991
interactions e + p, scale invariance of proton inelastic structure function from, 25:27995
interactions e + p, structure function and scaling behavior of inelastic, 25:27999
interactions e+ + e- + e+ + e- + e+ + e- at 2 x 510 MeV, cross section and angular distribution for, (E), 25:27994
interactions e- + e- + e- + e- + K+ + K-, double-logarithmic approximation for cross sections for, 25:27997
interactions e+ + e- + e+ + e- + K+ + K-, double-logarithmic approximation for cross sections for, 25:27997
interactions e- + e- + e- + e- + μ+ + μ-, double-logarithmic approximation for cross sections of, 25:27997
interactions e+ + e- + e+ + e- + μ+ + μ-, double-logarithmic approximation for cross sections of, 25:27997
interactions e+ + e- + e+ + e- + π+ + π-, double-logarithmic approximation for cross sections of, 25:27997
interactions e- + e- + e- + e- + π- + π-, double-logarithmic approximation for cross sections for, 25:27997
interactions e+ + e- at high energies, spectral sum rules in Sugawara model with modified stress tensor for cross sections for hadron production in, (T), 25:28006
interactions e+ + e-, limits on production and decay modes of heavy leptons from, 25:27998
interactions μ+ + e + μ+ + e at 10.1 GeV/c in emulsions, cross sections for, (E), 25:27955
interactions μ- + e + μ- + e at 5.0 and 14.5 GeV/c in emulsions, cross sections for, (E), 25:27955
interactions with cosmic microwave background, ultraviolet radiation from, (T), 25:27429
ionization of lithiumlike and sodiumlike ions, (T), 25:27443
mass of, rest, 25:27988
modulation of magnetospheric trapped, relation of coupled magnetic-field-line oscillations to, (T), 25:27623
momentum of classical, Maxwell equations and special relativity for, (T), 25:27986
motion in traveling-wave field, phase equation for, considering space charge, 25:27946
motion of coupled ionospheric, equation of, 25:27521
photobleaching of trapped radiolytic, in alkaline glasses, 25:26310
precipitation patterns for keV, auroral, over northern polar cap, 1968, (E), 25:27576
radial diffusion in outer radiation belts, observations of May-June 1967 bimodal, (E/T), 25:27626
reactions (e,e'2p) with nuclei, study of proton-proton correlations by, (T), 25:28491
reactions (e,e'p) with carbon-12 at 45.9 MeV, proton angular distributions and energy spectra from, (E), 25:28193
reactions (e,e'p) with carbon-13 at 43 MeV, proton angular distributions and energy spectra from, (E), 25:28193
reactions of hydrated, in electron pulse and γ radiolysis of aqueous solutions of substituted aryl glycosides, rate constants for, 25:26305
reactions with diatomic molecules, inelastic collision integral for, (T), 25:27459
reactions with nitrogen in aurorae at .045 to 25 keV, excitation cross sections for, (E), 25:27616
scattering by heavy nuclei with γ emission, study of low-lying excited states by inelastic, (T), 25:28491
scattering by light atoms and ions, configuration-interaction and Hartree--Fock calculations of factors for, 25:27460
scattering by nuclei at 0.2 to 2.0 MeV, Coulomb corrections to Bethe--Heitler cross sections for bremsstrahlung production by, (T), 25:28451 (N-71-10999)
scattering by sulfur-32 in giant resonance region, microscopic calculation of form factors for inelastic, (T), 25:28220 (UJV-2553-F)
scattering in graphite, inelastic, 25:27902
scattering inelastically by lithium-6, analysis using nucleon--nucleon correlation, (T), 25:28201
spectra in midnight luminous aurorae, comparison with proton, (E), 25:27578
trapping of radiolytic, in water-walled cavity in alkaline glasses, 25:26310
use for food processing, review of principles involved and wholesomeness considerations in, 25:27132 (CONF-680112-, pp 221-39)
use for radiotherapy, telecentric small angle pendulum technique for, 25:26878
use for therapy of abdominal tumors, telecentric small-angle pendulum method for, 25:26867
yields of hydrated, from pulse radiolysis of aqueous solutions of nitrobenzene, nitromethane, and oxygen,

XUM

25:26308
ELECTROSTATIC FIELDS
interactions of three, in collisionless plasma, (T), 25:27812
penetration of semi-infinite Vlasov plasma, (T), 25:27707
ELEMENT 105
alpha decay of, half-life and α energy for, (E), 25:28350(T) (KFK-tr-350)
production in neon-22 reactions with americium-243 at 120 MeV, effective cross sections for, (E), 25:28350(T) (KFK-tr-350)
ELEMENT 110
potential-energy surfaces for, effects of asymmetric distortions in single-particle potential on, (T), 25:28313 (CERN-70-30(Vol.2), pp 689-99)
ELEMENTARY PARTICLE MODELS
composite, meson internal dynamics in nonrelativistic, Schroedinger equation for, 25:28030
composite, π electromagnetic form factor and p-wave ground-state spin-orbit force in nonrelativistic, Schroedinger equation for, 25:28030
droplet, elementary particle structure in relativistic extension of, 25:27970
dual harmonic oscillator, general vertex for hadrons in, 25:28021
dual resonance, for strong interactions, scaling of, 25:28016
dual resonance, parton theory based on, 25:28002
eikonal, formulation with high-energy s-channel helicity conservation, 25:28034
multiperipheral, self-consistent rising cross sections from absorptive corrections in, 25:28012
one-particle-exchange, for high-energy interactions, analyticity structure of, 25:28013
parton, current interactions in nonperturbative, 25:28015
parton, for deep inelastic lepton--nucleon interactions, 25:28001
parton, formulation based on dual resonance model, 25:28002
Veneziano, eikonal model from unitarity corrections to generalized, 25:28034
Veneziano, eikonal-like pole-cut model from unitarity corrections to, 25:28044
Veneziano, Pomeranchuk singularity in unitarized, 25:28020
Veneziano, symmetric representations of n-point functions in, 25:28014
Veneziano, test from $K^- + p \to \Lambda + K^+ + K^-$ interactions at 3.3 GeV/c, 25:28042
ELEMENTARY PARTICLE MODELS (BOOTSTRAP)
mesons (rho) and (sigma) production in π + π interactions in, current algebra and analyticity for, 25:28027 (RLO-1388-602)
ELEMENTARY PARTICLE MODELS (TRIPLET)
additivity frame identification with Jackson frame in quark, experimental consequences of, 25:28017
dynamics of relativistic scalar quark, for mesons, 25:28022 (DESY-71/10)
ELEMENTARY PARTICLES
interactions at high energies, analyticity structure of one-particle-exchange model for, 25:28013
interactions at high energies, limiting partial cross sections for, 25:27974
interactions in multiperipheral model with absorptive corrections, self-consistent rising cross sections for, 25:28012
interactions in nonperturbative parton model, 25:28015
interactions of two Dirac spinor, model with harmonic oscillator structure for linear, 25:27973
interactions of, variational principle based on Faddeev equations and analytic structure in total energy of T-matrix for calculations of amplitudes of three-body, (T), 25:28101
production of, diffraction and Regge pole behavior of multiple, 25:27969 (PURC-4159-19)
reactions with nuclei, production of high-energy particles from, 25:27978
spin formalisms for, 25:28007 (CERN-71-8)
stability of zero-mass, 25:27979
strong interactions at high energies, model of complex separable potential for, 25:28019
strong interactions of, Cabibbo angle in theory for symmetry-breaking semi-, (T), 25:28059
strong interactions of, interference between Coulomb and, 25:28100
structure of, relativistic extension of droplet theory for, (T), 25:27970
symmetry for, reduction with respect to iso-Poincare subgroup for unitary irreducible representations of SU(2,2), (T), 25:28054
theory for tightly bound spin-$^1/_2$ fermion--antifermion systems of small total mass, perturbation treatment of Bethe--Salpeter equation for, (T), 25:27971
wave equations for integral-spin and finite-mass, first-order, 25:27975
weak interactions of, Cabibbo angle in theory for strangeness-changing, 25:28059
weak interactions of, review on, 25:28003 (PURC-4159-22)
ELEMENTARY PARTICLES (TRIPLET)
flux in sea-level cosmic radiation, (E), 25:27475
ELEMENTS
abundances relative to solar system, r-process calculations of, (T), 25:28441 (CERN-70-30(Vol.1), pp 217-62)
content in rainwater, precipitation scavenging studies of origin and quantity of, (E), 25:26365 (CONF-700601-, pp 99-108)
hyperfine-interaction parameters for Z = 1 to 83, tables of isotropic and anisotropic, 25:27441 (ANL-7784)
EMBRYOS
radioinduced abnormalities in hamster, in relation to radioinduced chromosome aberrations, x, 25:26982
radioinduced damage to mandibular in chick, x, 25:27018
ENGINEERING
engineering materials list, 25:26414 (TID-4100(Suppl.62))
ENVIRONMENT
radioactivity of, review of potential effects on man, 25:27042
research programs on, review on AEC, 25:26205
ENZYMES
inactivation of proteolytic, in beef prior to γ-radiation processing, method for, 25:27163(P)
purification of photoreactivating Euglena, 25:26619 (COO-1793-6)
radiation effects on biochemistry of, in dogs, effects of AET on x, 25:26935
radiation effects on pethidine demethylating, in rat liver microsomes, x, 25:27034
radiation effects on, in citrus fruits following processing, 0.5 and 1.5 MeV-electrons and γ, 25:27135 (IAEA-R-362-F)
radioinduced inactivation of autolytic, in processed food, 25:27132 (CONF-680112-, pp 221-39)
radioinduced inactivation of, review of mechanisms of, 25:26644
EPITHELIUM
radiation effects on insects larvae, effects of dose on gamma, 25:26916
radiation effects on regeneration of mouse intestinal, effects of dose on x, 25:27033
radiation effects on testicular, in guinea pigs following long distance skin therapy, x, 25:26973
EPOXY RESINS
B--epoxy, properties for use in aircraft structures, 25:27307
EQUIPMENT AND PROCEDURES
control tape for continuous-path numerically controlled inspection machine, preparation of, 25:28907 (Y-1725)
ERBIUM
determination by photometry using 1,10-phenanthroline and salicylfluorone, 25:26161
determination in yttrium oxides by solvent extraction and spectrography, 25:26168
ERBIUM ALLOYS AND SYSTEMS
Au--Er, magnetic properties of Au_4Er at 6 to 300°K, (E/T), 25:27872
Er--Pd, magnetic properties of $ErPd_3$ at 4 to 300°K, 25:27870
ERBIUM IONS
implantation in zinc sulfide films at 200 keV, detection using luminescence, 25:27844
ERBIUM ISOTOPES Er-151
beta decay of, half-life for, (E), 25:28303 (CERN-70-30(Vol.1), pp 533-44)
ERBIUM ISOTOPES Er-164
energy levels from isomeric thulium-164 beta decay, spin-parity assignments for, (E), 25:28322 (CERN-70-30(Vol.2), pp 939-47)
ERBIUM ISOTOPES Er-166
energy levels of, analysis of nonrandom distributions of neutron resonance, (T), 25:28421
ERYTHROCYTES
heavy metal uptake by, membrane penetration mechanisms during, 25:26609
ion permeability of membranes of, effects of amino and sulfhydryl reactive reagents on, 25:28904 (UR-49-1429)
life span of, in burn patients, nitrogen-15 method for studying, 25:26572
phosphorus-32 uptake by, methods for determining, 25:26589
radiation effects on esterase activity in extract of rat, effects of pH on whole-body x, 25:26600
radiation effects on rat, effects of dietary selenium on whole-body gamma, 25:27032
ERYTHROPOIESIS
radiation effects on rat, effects of dose fractionation on gamma, 25:27015
ESTERASES
radiation effects on activity of, in extracts of erythrocytes, liver, spleen, and blood plasma of rats, effects of pH on whole-body x, 25:26600
ETHANE
yields from γ radiolysis of liquid 2,2-dimethylpropane, effects of additives on, 25:26309
ETHANESULFONIC ACID
effects on cereal and vegetable plants, mutagenic, 25:26686 (CONF-680112-, pp 95-111)
ETHANOL
radiolysis of frozen aqueous solutions of, role of LET in

XUM

yields from α, β, and γ, 25:26311
radioprotective effects on germinating spores of Streptomyces, γ and uv, 25:27068
ETHANOL, 2-MERCAPTO-
effects on radiolysis of aqueous solutions of acetone or 2-propanol, 25:26291
ETHENESULFONIC ACID
sodium salt, polymers, effects on fluorescence of uranyl compounds, 25:26267
ETHIODIZED OIL
use of iodine-131-labeled, for therapy of malignant melanomas in man, 25:26888
ETHYL SULFATES
effects on β-galactosidase gene of Escherichia, mutagenic, 25:26722
effects on rice, mutagenic, 25:26701
effects on segregation pattern in rice, mutagenic, 25:26688
ETHYLAMINE, 2,2'-DITHIOBIS[N,N-DIMETHYL-
radioprotective effects of, on submaxillary gland in female rats, effects of time of administrtion on γ, 25:26792
radioprotective effects of, on submaxillary glands in mice, comparison of AET, cystamine, cysteine, noradrenaline, and serotonin with γ, 25:26795
ETHYLENE
radiation effects on production of, in fruits, γ, 25:27140
radiation effects on production of, in tomatoes, effects of cutting and vacuum infiltration on γ, 25:27067
ethylene--Ne, radiolysis of, effects of pressure on yields from γ, 25:26314
ETHYLENE, CHLORO-
radioinduced polymerization of gaseous, effects of additives on kinetics of x, 25:26282
ETHYLENE, CHLORO-, POLYMERS
radiation stability of films of, effects of sodium methyldithiocarbamate on γ, 25:26280
ETHYLENE POLYMERS
neutron slowing-down in, analysis of ages to indium resonance from, (E), 25:28157
radiation effects on elastic moduli of, γ, 25:26281
ETHYLENE, TETRAFLUORO-, POLYMERS
gamma absorption coefficients of Teflon, (E), 25:27826 (DEMO-70/11)
radiation effects on positron annihilation in Teflon, gamma, 25:27306
reactions with liquid potassium, potassium--sodium alloy, and sodium, 25:26211 (TRG-Report-2104)
ETHYLENIMINE
effects on chromosomes of Crepis seeds, mutagenic, 25:26733
EUMYCOTA
Ascobolus immersus, radioinduced mutations in ascospores of, genetic mapping of uv and x, 25:26695
Aspergillus nidulans, radioinduced mutations in, effects of EMS on gamma, 25:26717
Aspergillus nidulans, radiosensitivity of, genetic mapping of uv, 25:26709
Aspergillus niger, radiation effects on biochemical activity of, 7000-R x, 25:27094
Aspergillus niger, radioinduced mutations for increased amylase and proteinase activity in, uv, 25:27097
Aspergillus oryzae, radioinduced mutations for increased amylase and proteinase activity in, uv, 25:27097
Aspergillus usamii, radioinduced mutations for increased amylase and proteinase activity in, uv, 25:27097
Beauveria bassiana, radioinduced mutations for amino acid dependency in, uv and x, 25:26703
Candida albicans, radiation effects on inactivation and mutation in caffeine-resistant and caffeine-sensitive strains of, uv, 25:27073
fungi, radioinduced mutations in phytopathogenic, analysis of genes of uv, 25:26698
Osmunda regalis, radiation effects on spores of, effects of nitric oxide, oxygen, and water on, 25:27069
Penicillium expansum, radiation effects on survival of, effects of age, culture media, and temperature on γ, 25:27085
Penicillium expansum, radiosensitivity of, effects of age, culture media, radiosensitizers, and temperature on γ, 25:27084
Saccharomyces cerevisiae, radiation effects on mitosis in, effects of photoreactivation on uv, 25:27080
Saccharomyces ellipsoides, radiation effects on, role of ATP synthesis in recovery from x, 25:27095
Saccharomyces ellipsoideus, radiation effects on, role of protein synthesis in recovery from x, 25:27096
Streptomyces cacaoi, radiation effects on germinating spores of, protective effects of chloramphenicol, ethanol, freezing, and mitomycin against γ and uv, 25:27068
Streptomyces erythreus, radioinduced mutations in, for auxotrophy, uv, 25:26699
Trichoderma glaucum, radioinduced mutations for gliotoxin production and physical change in, thermal neutron, gamma, and uv, 25:27088
Ustilago maydis, radioinduced mutations in, for pathogenicity, uv, 25:27072
Verticillium dahliae, radioinduced mutations for morphological and sporulation changes in, effects of doses of 200,000 to 300,000 R on γ, 25:26689
yeasts, radioinduced dissociation of ribosomes of, effects of magnesium ions on x, 25:26633
EUROPE
uranium enrichment in, economics and development prospects of methods for, 25:26424(T) (CONF-700557-3)
EUROPIUM
determination by spectrophotometry, 25:26165
determination in plutonium oxide--uranium oxide pellets by emission spectroscopy, 25:26153 (LA-4622)
determination in yttrium oxides by solvent extraction and spectrography, 25:26168
magnetic properties of, effects of pressure on transition temperatures, 25:27874
EUROPIUM ALLOYS AND SYSTEMS
Eu--Eu_2O_3, phase studies of, 25:27302
Eu--Eu_2O_3--Pt, phase studies at 1500°C, 25:27302
Eu--Pd, magnetic properties of $EuPd_3$ at 4 to 300°K, 25:27870
EUROPIUM ISOTOPES Eu-145
energy levels from gadolinium-145 beta and electron-capture decay, complex shell-model, (E/T), 25:28299 (CERN-70-30(Vol.1), pp 435-46)
EUROPIUM OXIDES
analysis for trace amounts of samarium by crystal phosphor luminescence method, 25:26162
magnetic susceptibility down to 4°K, 25:27896
reflectivity peak of intrinsic and gadolinium-doped single crystals of, temperature dependence of E_1, 25:27895
Eu_2O_3--Y_2O_3, magnetic susceptibility down to 4°K, 25:27896
Eu--Eu_2O_3, phase studies of, 25:27302
Eu--Eu_2O_3--Pt, phase studies at 1500°C, 25:27302
EuO-base--Fe, magnetic and optical properties of doped films of, 25:27897
EuO-base--Fe, magnetic properties of doped films of, effects of annealing on, 25:27898
EuO-base--Fe, preparation and structure of doped films of, 25:27894
EUROPIUM SULFIDES
photoemission spectral study of f states and valence bands in, 25:27876
EXOSKELETONS
zinc-65 distribution in, of euphausiids and shrimp following ingestion, 25:26604
EXOSPHERE
electron-energy spectra at northern high-latitude, precipitated and trapped 45 to 450 keV, (E), 25:27568
ion density and velocity flowing in, comparison of hydrodynamic and kinetic models of expanding, (T), 25:27613
EXPERIMENTAL BREEDER REACTOR-II
fuel pins for, fabrication and irradiation testing of plutonium nitride--uranium nitride, 25:28687 (BMI-1898, Sect.A)
EXPLOSION CLOUDS
origin and thermodynamics of radioactive, 25:26357 (CLOR-81/D)
EXPONENTIAL PILES
neutron spectra for beryllium oxide (BeO) moderated, time-of-flight method for measurement of, (E/T), 25:28769
EYES
effects of radioinduced pituitary ablation on aqueous humor dynamics in, of humans with diabetic retinopathy, 25:27037
electrolyte efflux from lens of rabbit, design of constant perfusion device for tracer studies on, 25:26606
protein synthesis in lens of rabbit, effects of naphthalene and x radiation on, 25:26649
radiation damage of rat, effects of dose rate and prenatal exposure on gamma, 25:26951
radiation effects on animal and human, effects of age and dose on, 25:27013
radiation effects on human, protection against γ, ir, microwave, uv, and x, 25:27047
radiation effects on rabbit, protective effects of chemicals against cataract-inducing cobalt-60γ and fast neutron, 25:27014
radiation effects on recovery of early potentials of, in frogs, comparison of visible light and x, 25:27004
radiation effects on recurrence of postoperative pterygium of human, effects of dose on β, 25:26870
radiation effects on retina of Rhesus monkey, laser, 25:26940
radiation effects on wound response in lens epithelium of, rat, x, 25:27000
radiation effects on, in personnel of nuclear industries, measures for protection against, 25:26783
radiation protection measures for, 25:27013
radiation protection methods for human, during cobalt-60 γ therapy, 25:26779
radioinduced cataracts in human, effects on dose on β, 25:26870
radioinduced cataracts in rabbits, RBE for fast neutron, 25:26945
radioinduced injuries in retina of, lethal and sublethal, 25:26902
radiotherapy of lymphoma of orbit of, in man, effectiveness of x, 25:26890

XUM

zinc-65 distribution in, of euphausiids and shrimp following ingestion, 25:26604

F

FACE
radiation dose to, of medical personnel from technetium-99m, methods for shielding against, 25:26765
FALLOUT
analysis and collection of long-range, from Schooner Event, program for, 25:26404 (PNE-527)
analysis for ruthenium-103 and ruthenium-106 by β counting method, 25:26181
content in human environment, method for estimation of maximum permissible, 25:26751 (UCRL-50163(Pt.7))
effects on aging, immune reactions, and peripheral blood of human populations on Marshall Islands, correlation of, 25:27058
radioisotope content of long-range, from Schooner Event, data tabulation on, 25:26404 (PNE-527)
sampling of radioactive, development of column collector for, 25:26559
FAST CERAMIC REACTOR
core for, design and kinetic analyses of, 25:28691(R) (GEAP-10028-37)
fuel elements for, development during November 1970 to January 1971, 25:28691(R) (GEAP-10028-37)
safety of, transient overpower and coolant loss effects on, 25:28691(R) (GEAP-10028-37)
FATS
content in meats, γ attenuation method for measuring, 25:26571
FATTY ACIDS
radiation effects on, in canned chicken pet food products, 25:26647
FECES
analysis of astronaut, by neutron activation and γ spectroscopy, 25:26187(R) (BNWL-1183-7)
analysis of astronaut, for beryllium-7, sodium-22, and sodium-24 by γ spectroscopy, 25:26178 (BNWL-SA-3608)
calcium-47 accumulation in human, γ counting method for estimating, 25:26586
lead-210 excretion in, of baboons, 25:26610
FEDERAL REPUBLIC OF GERMANY
dental x-ray equipment survey in, evaluation of, 25:26772
nuclear power plant development in, 25:28526 (CONF-700550-, Paper 4)
nuclear power plant development in, review of, 25:28644
FERMI FAST BREEDER REACTOR
emergency systems for, secondary containment requirements for liquid sodium, 25:28587 (DOCKET-50016-107)
operations history for December 1970, 25:28559 (DOCKET-50016-109)
operations history for November 1970, 25:28558 (DOCKET-50016-108)
FERMIONS
gauge-invariant quasi-free states of system of, application of Kubo--Martin--Schwinger automorphisms to, 25:27925 (CNRS-CPT-70-P-325)
theory for tightly bound spin-$^1/_2$ fermion--antifermion systems of small total mass, perturbation treatment of Bethe--Salpeter equation for, (T), 25:27971
FETUSES
radiation effects on, in cotton rats, γ, 25:26988
radioinduced disorders in, following accidental contamination or therapy of mother, 25:27040
strontium-89 uptake by, of sows following ingestion, 25:26594
FIBRINOGEN
labeling with iodine-131 for use in tumor scanning, 25:26859
radiation effects on content of, in blood plasma of rats, single and combined effects of turpentine and x, 25:26979
FIELD EMISSION MICROSCOPES
heating of specimens in, calculation, 25:27866(R) (NYO-3504-56)
uses in metallurgy, review on, 25:27254
FIELD THEORY
charged-particle coupling to tensor field in, causality in Lorentz-covariant Lagrangian for, (T), 25:28068
constraints imposed on system satisfying Kubo--Martin--Schwinger boundary condition, 25:27925 (CNRS-CPT-70-P-325)
particle coupling to massless rank-two tensor field in, causality in Lorentz-covariant Lagrangian for point, (T), 25:28068
theory for relativistic, ergodic states in, 25:28078
FILMS
processing of Tri-X-Ortho oscillographic, wide latitude, 25:28854 (EGG-1183-1465)
FILTERS
design with honeycomb activated carbon layers, for removal of radioactive particles from air streams, 25:28829(P)
FINS
deformation of Magnox fuel element, from spontaneous expansion and thermal cycling, development of strut theory for defining, 25:26415 (TRG-Report-2121)
FISSION
isomerism in, search for islands of, 25:28305 (CERN-70-30(Vol.1), pp 567-74)
mechanism of heavy-nucleus, description of, (T), 25:28504
theory of resonant, optical-model, (T), 25:28445 (CERN-70-30(Vol.1), pp 553-66)
theory of, isobaric spin in, 25:28477
FISSION FRAGMENTS
analysis of uranium-235, on-line isotope separator for, 25:26551
charge distributions of, model for, (T), 25:28508
charge effects on x-ray and neutron emission following californium-252 fission, (E), 25:28288 (CEA-R-4121)
charges of, calculation of most-probable, (T), 25:28408
gamma spectra of, from thermal neutron capture by uranium-235, (E), 25:28325 (CERN-70-30(Vol.2), pp 967-84)
gamma spectra of, from uranium-235 thermal fission, (E), 25:28320 (CERN-70-30(Vol.2), pp 917-30)
gamma--x-ray coincidence spectra of, from californium-252 spontaneous fission, (E), 25:28416
kinetic energies of, calculations of, (T), 25:28408
production in thorium-232 neutron fission, relative yields of, (E), 25:28409
x-ray spectra and lifetimes of, from thermal neutron capture by uranium-235, (E), 25:28325 (CERN-70-30(Vol.2), pp 967-84)
FISSION PRODUCTS
beta decay of uranium-235, energy released by, (E), 25:28407
neutron cross sections of gross, from neutron irradiation of enriched uranium, total, (E), 25:28404
release from uranium oxide (UO_2) fuel, effects of high temperature on, (E), 25:28821
separation from americium by precipitation using a rare earth carrier, 25:26319(P)
separation of cesium from other, by ion exchange, 25:26337(P)
yields from plutonium-239, plutonium-241, uranium-235, and uranium-238 neutron fission, (E), 25:28354 (NP-18723)
FISSIONABLE MATERIAL
preparation of porous, from powders, compression and sintering method for, 25:27273(P)
resonance self-shielding in, method of calculating, (T), 25:28503
FLOWMETERS
development of computerized in-line compressible-fluid, 25:28855 (GAT-T-1649)
FLUID FLOW
electrohydrodynamic, velocity profile measurements in crossed electric and magnetic fields, 25:27502
magnetohydrodynamic supersonic channel, with compression shock, (T), 25:27489
magnetohydrodynamic unsteady, of viscoplastic medium over infinite plate, (T), 25:27496
magnetohydrodynamic, concentration distribution of binary mixtures in films moving along walls of round pipes in, (T), 25:27499
magnetohydrodynamic, efficiency of three-dimensional channel for, (T), 25:27490
magnetohydrodynamic, electric field distribution in conducting cylinder with finite electrodes, 25:27492
magnetohydrodynamic, energy flux in incompressible plane waves, (E), 25:27487
magnetohydrodynamic, neutral stability of incompressible half-jet at low Reynolds number, (T), 25:27486
magnetohydrodynamic, optimization of, 25:27493
magnetohydrodynamic, Rayleigh's problem with suction in, (T), 25:27491
magnetohydrodynamic, shear wave propagation in visco-plastic medium, (T), 25:27497
magnetohydrodynamic, variational principle and canonical variables in, (t), 25:27488
magnetohydrodynamic, velocity profile measurements in crossed electric and magnetic fields, 25:27502
magnetohydrodynamic, with temperature-dependent transport coefficients in plane channels, (T), 25:27498
turbulent diffusivity coefficient for rod type bundle arranged fuel assemblies, effects of spacer grid configurations on, (E/T), 25:28819 (EUR-4552)
FLUORINE
determination by potentiometric titration using ion-selective electrodes, 25:26166
determination in lunar fines and standard rocks by γ activation and radiochemical separation, 25:26193
determination in plutonium oxide--uranium oxide pellets, 25:26153 (LA-4622)
effects on gamma-radiosensitivity in rats, 25:27016
FLUORINE IONS
implantation into gallium arsenide at 300 keV, annealing of damage induced in, 25:27862
FLUORINE ISOTOPES F-17
energy levels from neon-17 decay, isospin purity of, (E), 25:28195
energy levels of, role of configuration states in isospin-forbidden proton decay of T = 3/2, 25:28179
FLUORINE ISOTOPES F-18
energy levels from nitrogen-14 alpha resonances, isospin impurities of, (E), 25:28177

FLUORINE ISOTOPES F-19
energy-level transitions from proton reactions, branching ratios, gamma-ray angular distributions, and internal conversion coefficients for, (E/T), 25:28271
helium-3 reactions (He-3,Li-7) and (He-3,Be-7) at 39 to 42 MeV at 165°, correlations in excitation functions for, (E), 25:28190
photon reactions (γ,n) near threshold energies, cross section and resonance parameters for, (E), 25:28413
reactions with gold-197, cross-section limits for fission isomer excitation in, (E), 25:28399
FLUORITES
proton channeling in crystals of, 25:27851
FOOD
disposal and use following nuclear attack, criteria for, 25:26786
radiation processing for extension of storage life of, development of programs in Denmark, Holland, and USA for, 25:27142
radiation processing of, description of joint FAO/IAEA program on, 25:27128 (CONF-680112-, pp 1-7)
radiation processing of, on flavor and shelf life following, 25:27143
radiation processing of, review of ionizing, 25:27166
radiation processing of, review of principles involved and wholesomeness considerations in electron, γ, and x, 25:27132 (CONF-680112-, pp 221-39)
FOOD CHAINS
fission product transport through human, following nuclear attack, 25:26786
radioactive contamination of freshwater, in relation to human diet and hazards to man, establishment of MPC for, 25:26747
radioisotope transport through, to man, 25:26751 (UCRL-50163(Pt.7))
FOOD IRRADIATION FACILITIES
design and construction of, in Argentina, 25:27133 (CONF-680112-, pp 241-3)
development of portable shipboard γ, for processing shrimp, 25:27158
FORBUSH DECREASES
effects of proton solar event, Feb. 25, 1969, (E), 25:27553
relation to 11-year intensity variations, (T), 25:27389
FORENSIC SCIENCE
copper wire identification by labeling with silver-110m, 25:26322
FORT ST. VRAIN POWER REACTOR, UNIT 1
boilers for, design parameters of, 25:28631
design parameters of, revised and additional data on, 25:28608 (DOCKET-50267-28)
operations aspects of, revised and additional data on, 25:28608 (DOCKET-50267-28)
site for, environmental radiation survey during January to December 1970, 25:28608 (DOCKET-50267-28)
FOSSILS
uranium content of bones of animal, 25:26744
FRANCIUM ISOTOPES Fr-207
energy levels and properties of, nuclear data sheets for, 25:28378
FRANCIUM ISOTOPES Fr-208
energy levels and properties of, nuclear data tables for, 25:28375
FRANCIUM ISOTOPES Fr-209
energy levels and properties of, nuclear data sheets for, 25:28376
FRANCIUM ISOTOPES Fr-211
energy levels and properties of, nuclear data sheets for, 25:28377
FREE RADICALS
radiation effects on distribution of, in phosphate soluble fraction of lysozymes, tracer studies on γ, 25:26646
radioinduced production in deuterated dl-tartaric acid monocrystals, ESR spectral studies on γ and x, 25:26306
spectra of radiolytic, in proteins, EPR, 25:26300
yields from γ radiolysis of 5-nitrouracil, ESR studies on, 25:26296
yields from γ radiolysis of N-benzoylalanine, ESR spectral studies on structure of, 25:26292
FRICTION
book: Theory and Practice of Lubrication Systems, 25:26416
FRUITS
bananas, radiation processing effects on acceptability and ripening of, 20 to 40-krad gamma, 25:27165
oranges, radiation processing effects on maturation of, 25:27134 (CONF-680112-, pp 245-6)
radiation processing effects on ethylene production, respiration, and shelf life of, γ, 25:27140
radiation processing of citrus, tissue physiology following electron and γ, 25:27135 (IAEA-R-362-F)
strawberries, radiation effects on oxygen uptake and pectin metabolism in, effects of maturity on γ, 25:27160
FS-85 (NIOBIUM ALLOY)
stability at high temperatures, long-term thermal, 25:27208 (N-71-10352)
FUEL CAPSULES
fabrication and testing of strontium-90 heat source, for thermoelectric generators, 25:26432
fabrication of Pioneer and Transit heat source, equipment and methods for, 25:26425 (MLM-1796)

G

GADOLINIUM
cadmium perturbed angular correlation in ferromagnetic, for noncoaxial magnetic and electric fields, 25:27919
determination in plutonium oxide--uranium oxide pellets by emission spectroscopy, 25:26153 (LA-4622)
determination in yttrium oxides by solvent extraction and spectrography, 25:26168
effects on magnetic susceptibility of scandium, 25:27878
effects on temperature coefficient of saturation magnetization of Co_5RE permanent magnet alloys, 25:27883
Hall coefficient of thin oriented films of paramagnetic, extraordinary, (E), 25:27908
magnetic properties of, effects of uniaxial stress on, 25:27889
spin-wave dispersion relations of, neutron inelastic scattering study of, 25:27888
GADOLINIUM ALLOYS AND SYSTEMS
Gd--Pd, magnetic and electric properties of $GdPd_3$ at 4 to 300°K, 25:27870
Gd--Pd-base, magnetic moments at 1.5 to 4.2°K, effects of gadolinium content on, 25:27921
Gd--Sb, electron band structure of GdSb, intrinsic metallic character in, 25:27879
Gd-base--Mg, magnetic periodic ordering of, from electric conductivity and magnetization measurements, 25:27871
Gd-base--Th, magnetic periodic ordering of, from electric conductivity and magnetization measurements, 25:27871
GADOLINIUM ISOTOPES Gd-145
beta and electron-capture decay of, complex shell-model states in, (E/T), 25:28299 (CERN-70-30(Vol.1), pp 435-46)
GADOLINIUM ISOTOPES Gd-158
energy levels of, deformation parameters for 4+, (E/T), 25:28411
proton reactions (p,t) at 51.7 MeV, spectra and DWBA analysis of differential cross sections from, (E/T), 25:28411
GADOLINIUM NITRIDES
magnetic properties of GdN, effects of anion substitution on, 25:27880
GADOLINIUM OXIDES
reactions with boron, effects of shock waves and temperature on, 25:27291
GADOLINIUM SULFIDES
photoemission spectral study of f states and valence bands in, 25:27876
GAGES AND METERS
development of capacitance gage for dimensional measurement, 25:28910 (Y-1783)
GALAXIES
density fluctuations in, (T), 25:27430
dynamic processes in, computer simulation of, (T), 25:27406
evolution of one-dimensional gravitational water-bag models, (T), 25:27412
gas flow in spherically symmetric, steady radial, (T), 25:27403
model for nuclei of M31, M32, and M81, (E), 25:27409
orientation in physical pairs of, (T), 25:27420
oscillations along axis of symmetry in, stability of, (T), 25:27410
radio emission from Maffei I, search for, (E), 25:27405
stellar content of nuclei of M31, M32, and M81, (E), 25:27409
GALLIUM
determination by spectrophotometry, effects of thorium, uranium, and other metals on, 25:26172
GALLIUM ALLOYS AND SYSTEMS
Fe--Ga, Moessbauer spectra of solid solutions of, 25:28843 (CALT-822-27)
Fe--Ga, Moessbauer study of BiF_3 type ordering in metastable, 25:28842 (CALT-822-26)
Ga--Ni-base, electron correlation effects in Ni_3Ga, 25:27868
Ga--V, superconducting diffusion layers in, electron microprobe studies on, 25:26159
Ga--Zr, superconductivity of intermetallic, (E), 25:27654
GALLIUM ARSENIDES
radiation damage in, annealing of 200-keV proton and 300-keV fluorine-ion, 25:27862
radiation damage in, etching of 400-keV xenon-ion, 25:27860
radiation effects on current flow of epitaxial laser diodes of, 76 and 300°K neutron, 25:26563
GALLIUM ISOTOPES Ga-63
beta decay of, branching ratios and log-ft values for, (E), 25:28338 (CERN-70-30(Vol.2), pp 1075-9)
GALLIUM ISOTOPES Ga-66
energy levels from germanium-66 decay, spin-parity assignments for, (E), 25:28272
GALLIUM ISOTOPES Ga-70
energy levels from gallium-69 (d,p) and zinc-70 (p,nγ)

XUM

reactions, (E), 25:28254
GALLIUM ISOTOPES Ga-72
energy levels of, (E), 25:28254
GALLIUM OXIDES
Ga_2O_3--Y_2O_3, phase studies of, using europium luminescence spectra as reference, 25:27303
GAMMA CAMERAS
data processing system for dynamic function studies, PDP-8 computer-based, 25:26473
development of, international, 25:26855
performance for brain scanning with technetium-99m, 25:26852
performance for lung scanning using technetium-99-labeled microaggregated albumin, 25:26837
performance for technetium-99m scintigraphy of collateral blood veins in man, 25:26844
GAMMA RADIATION
albedo calculations of, generalization on basis of similarity theory, 25:27831
detection of cosmic, with energy above 10^{19} eV, (T), 25:27423
distribution in the Galaxy, (E), 25:27407
dose distribution in moving beam telecobalt therapy, electronic calculation of, 25:26758
dose of hands of medical personnel from handling indium-113m, methods for shielding against, 25:26767
dose to abdomen, face, and hands of medical personnel using technetium-99m, methods for shielding against, 25:26765
dose to chest and gonads of medical personnel during technetium-99m scintigraphy, 25:26766
dose to dogs from implanted plutonium-238-powered circulatory assist device, 25:26931
dose to feline bones following chronic ingestion of strontium-90, 25:26612
dose to gonads from source implanted elsewhere in body, development of Monte Carlo computer model for estimating absorbed, 25:26760
dose to medical personnel from preparation of indium-113m and technetium-99m-labeled compounds, 25:26768
dose to personnel from handling indium-113m and technetium-99m, devices for protection against, 25:26776
dose to tissues in dogs following injection of iodine-131-labeled chloroquine analog, absorbed, 25:26882
dosimetry for therapy, use of computer calculations in, 25:26761
dosimetry in mixed neutron field, paired ionization chambers for, 25:26538
dosimetry of, development of glasses for colorimetric, 25:26521
dosimetry of, development of liquid-filled ionization chambers for, 25:26531
dosimetry of, thermoluminescent dosimeter for personnel accident, 25:26516 (CLOR-82/D)
dosimetry using photographic film, procedures for, 25:26532
effectiveness for measuring renal plasma flow in combination with iodine-131-labeled hippuran in comparison to PAH clearance method, 25:26826
effectiveness of radium-226 applicator, for therapy of carcinomas of human penis, 25:26863
effects of prompt and delayed, on fast response of reactor control system, 25:28822
effects on 5-nitrouracil, ESR studies on free radicals produced by, 25:26296
effects on ability of male fruit flies to compete with normal males, 25:27154
effects on acceptability and ripening of bananas, effects of fruit maturity and temperature on, 25:27165
effects on activity of catalase complexed with lipoprotein, role of molecular orientation of complex in protective effects of complex formation against inhibitory, 25:26650
effects on activity of catalase in solution, protective effects of glycerol against inhibitory, 25:26650
effects on activity of lactate dehydrogenase in rat tissues, protective effects of injection of methylene blue against, 25:26803
effects on amylolysis in wheat, effects of doses of 20 to 200 Krad on enhancing, 25:26622
effects on amylose, amylopectin, and starch in wheat, enhancing, 25:26621
effects on antigenicity of snake venum in mice and rabbits, detoxifying, 25:26674
effects on aqueous solutions of acetone or 2-propanol, 25:26291
effects on aqueous solutions of hydrogen peroxide and 2-propanol, reactions of radicals from, 25:26290(R) (NYO-3753-19)
effects on aqueous solutions of phenyl glucopyranoside, effects of radical scavengers on yields from, 25:26304
effects on Aspergillus, mutagenic, 25:26717
effects on bacillus carrying rats, effects of dose fractionation on damaging, 25:27016
effects on bacteria in relation to spacecraft sterilization, 25:27101
effects on bacteria, effects of humidity, temperature, and dose rate on lethal, 25:27099
effects on bacteria, lethal, 25:27115
effects on barley, mutagenic, 25:26716
effects on beagle dogs, effects of dose on lethal, 25:26992
effects on biochemical structure of proteins and nucleic acids, 25:26660
effects on blood pressure and heart frequency in rabbits, protective effects of AET and cystamine against, 25:26794
effects on bone marrow in mice, effects of balneotherapy on pathological, 25:26950
effects on brain metastases in man, combined effects of corticosteroids and, 25:26895
effects on β-galactosidase gene of Escherichia, mutagenic, 25:26722
effects on calcification in rats, effects of dose and dihydrotachysterol on, 25:26977
effects on carbohydrates and organic acids in leaves and roots of corn and cotton plants following seed exposure, effects on dose on, 25:27074
effects on cesium-137 sorption through skin of rats, effects of contamination timing on 600 rad cobalt-60, 25:26595
effects on chemical and physical properties of gluten proteins, 1-Mrad damaging, 25:26656
effects on chemical and physical properties of starch, degratory, 25:26623
effects on chemical blood clotting factors, 25:26900
effects on chlorophyll production and morphology of beans, comparison of frequencies of acute and chronic mutagenic, 25:26685 (CONF-680112-, pp 85-93)
effects on chromosomes and chromatids in human leukocytes, aberrant, 25:26636
effects on chromosomes in human leukocytes, aberrant, 25:26730
effects on chromosomes in seeds, aberrant and mutagenic, 25:26697
effects on chromosomes of Crepis, aberrant, 25:26721
effects on chromosomes, pollen, and germination of peas, aberrant and stimulatory, 25:27089
effects on cis- and trans-9-octadecenoic acids and hexadecanoic acid, ESR studies on kinetics of radical transformation in, 25:26312
effects on colony formation in allogeneic and syngeneic bone marrow and spleen cell transplants in mice, 25:26670
effects on color stability and storage life of beef, effects of sodium tripolyphosphate on, 25:27162
effects on cotton, effects of variety on mutagenic, 25:26728
effects on crosslinking of polybutadiene, 25:26285
effects on deuterated di-tartaric acid monocrystals, ESR of free radicals produced by, 25:26306
effects on dissociation of infective and oncogenic functions of polyoma and simian viruses, 25:27111
effects on dissociation of infective and oncogenic functions of Rous sarcoma, 25:27111
effects on disulfide and lyase activity in onions, inhibitory, 25:26620
effects on DNA and nucleoproteins, effects of oxygen on degratory, 25:26637
effects on Drosophila chromosomes, mutagenic and lethal, 25:26720
effects on elastic moduli of polyethylenes, 25:26281
effects on electron between DNA and proflavine complexes, ESR spectral studies on, 25:26638
effects on erythrocytes and leukocytes of rats, lethal, 25:27032
effects on Escherichia coli, recombination, refractivity, and uv sensitivity of mutagenic, 25:26707
effects on ethylene-neon, effects of pressure on yields from, 25:26314
effects on eyes in rabbits in comperions to fast neutrons, protective effects of chemicals against cataract-inducing, 25:27014
effects on fecundity of laboratory and natural populations of snails, effects of dose rate on, 25:26915
effects on fetuses, ovaries, and reproductive capacity of cotton rats, effects of dose on, 25:26988
effects on flax plants, mutagenic, 25:27090
effects on frozen aliphatic alcohols, role of LET in, 25:26311
effects on function and morphology of mouse ovaries, damaging, 25:27028
effects on functional state and morphology of erythropoiesis in rats, 25:27015
effects on fungi, lethal, 25:27085
effects on fungi, mutagenic, 25:27088
effects on gametophores, spores, and sporocytes of Polytrichum (moss), chronic low-dose, 25:27075
effects on germinating spores of Streptomyces, protective effects of chloramphenicol, ethanol, freezing, and mitomycin against, 25:27068
effects on germination of spores of slime molds, effects of auto-inhibitor on enhancing, 25:27065
effects on germination, growth, and fruit size of tomatoes, mutagenic, 25:26735
effects on glassy alkaline ice, bleaching of trapped electrons from, 25:26298
effects on glioblastoma multiforme in man, combined effects of postoperative 5-fluorouracil and, 25:26889
effects on glucose and glycogen production in rat liver, 25:26963

effects on glycylglycine, ESR studies on free radicals produced by, 25:26300
effects on hemocyanins, role of hydrated electrons and hydroxyl radicals in, 25:26302
effects on hemoglobin and serum proteins in goats, acute and chronic, 25:26970
effects on human bone marrow during therapy, protective effects of inosine against, 25:26799
effects on human eye, review on, 25:27047
effects on human lungs, carcinogenic, 25:27045
effects on human pelvic structures during rotation therapy, effects of dose on, 25:26894
effects on immune reactions in mice, effects of dose and dose rate on, 25:26679
effects on immune spleen cells in mice, effects on selective inhibition of sensitizing, 25:26671
effects on IMPATT diodes, 25:26562
effects on larvae epithelium of insects, effects of dose on damaging, 25:26916
effects on leaves, stalks, and tubers of potatoes, effects of dose on mutagenic, 25:26737
effects on liquid 2,2-dimethylpropane, kinetics of reactions of electron scavengers and hydrocarbons with ions produced by γ, 25:26309
effects on lithium-drifted boron-doped silicon, 25:27852
effects on liver in dogs, effects of dose on pathological, 25:26955
effects on lymphocyte chromosomes in dogs following implantation of plutonium-238-powered circulatory assist device, 25:26931
effects on mice, effects of dose on late neoplastic, 25:26976
effects on mice, protective and toxic effects of cystamine with or without AET of serotonin, 25:26793
effects on miniature swine, effects of dose and dose fractionation on lethal, 25:26928
effects on mitosis in lucerne cells, effects of doses of 500 to 15,000 R on damaging, 25:26732
effects on mitosis in pea roots, effects of protein synthesis on delaying, 25:27063
effects on morphological abnormalities in rice plants, 25:27077
effects on morphology and sporulation in fungi, 200,000 to 300,000-R mutagenic, 25:26689
effects on mortality rates of rats, effects of hypothermic condition on, 25:27023
effects on myoglobin of beef, damaging, 25:27139
effects on n-type silicon, structure of defects induced in, 25:27848
effects on organoleptic properties and shelf life of fruits, 25:27140
effects on organoleptic properties and storage life of shrimp, 25:27136(R) (TID-25543)
effects on oxygen uptake and pectin metabolism in strawberries, effects of maturity on, 25:27160
effects on oxygenated aqueous solutions of cysteine at pH = 7, 25:26307
effects on phosphate soluble fraction of lysozymes, chemical and conformational studies on, 25:26646
effects on physiology of tomatoes, effects of cutting and vacuum in filtration on, 25:27067
effects on ploidy in crop plants, 25:27087
effects on population mechanics of chipmunks and pocket gophers in natural environments, 25:26682(R) (NYO-2579-20)
effects on positron annihilation in Teflon, 25:27306
effects on proliferation of SOTs cells, 25:26907
effects on protein synthesis by liver microsomal fractions in rats, subsequent whole-body, 25:27006
effects on proteolytic activity of bacteria growing on oysters, 25:27114
effects on quality of shrimp following shipboard exposure, 25:27158
effects on rat, effects of dose rate and prenatal exposure on, 25:26951
effects on rehydration capacity of freeze-dried meat, effects of dose on, 25:27144
effects on reproductive capacity of olive fruit flies, 25:27151
effects on reticuloendothelial system of mice, effects of glucan on inhibitory, 25:26947
effects on RFM mice, lethal, 25:26690
effects on rheology of albumin of eggs, effects of temperature on, 25:26923
effects on rice seeds, effects of dose rate, oxygen, storage, and water content on, 25:27070
effects on roots of Vicia faba, effects of auxin and dose rate on stimulating, 25:27066
effects on S-allyl-L-cysteine sulfoxide and S-propyl-L-cysteine sulfoxide, effects of nitrous oxide and potassium bromide on yields from, 25:26294
effects on salivary gland functions in man, use of sialography to evaluate, 25:27061
effects on Salmonella typhimurium in relation to antibiotic resistance, sensitivity, and virulence, mutagenic, 25:27164
effects on scopoletin and scopolin synthesis in grapefruit skin, 25:27079
effects on seeds of Arabidopsis, effects of temperature on, 25:27071
effects on seminoma of testis in man, therapeutic, 25:26891
effects on shrimp, lethal, 25:26917
effects on silicon, luminescence spectrum induced in, 25:27849
effects on single crystals of acetylenedicarboxylic acid and its potassium salt, ESR studies on yields of radicals from, 25:26301
effects on single crystals of, ESR spectral studies on radicals produced by, 25:26292
effects on skin of man, latent pathological, 25:27049
effects on solid aryl glucosides, ESR spectral studies on, 25:26303
effects on solid sodium phosphite, 25:26313
effects on Sorghum, mutagenic, 25:26715
effects on soybean maturation, yield, and resistance to nematodes, scab, and viruses, mutagenic, 25:26706
effects on spermatozoids of rabbits, effects of dose and dose rate on lethal, 25:26954
effects on spores of Penicillium expansum, effects of age, culture media, radiosensitizers, and temperature on lethal, 25:27084
effects on stability of modified poly(vinyl chloride) films, 25:26280
effects on sterile hybrids of rice, mutagenic, 25:26702
effects on storage life and wholesomeness of cod and haddock fillets and shrimp, 25:27149
effects on storage life and wholesomeness of pork, 25:27136(T) (NP-tr-1932)
effects on storage life and wholesomeness of potatoes, 25:27141
effects on submaxillary gland in female rats, effects of time of administration on protective effects of AET cystamine, or tetramethylcystamine against, 25:26792
effects on submaxillary glands and survival of rats, comparative effects of radioprotective compounds against, 25:26795
effects on substituted aryl glycosides, rate constants for reactions of hydrated electrons and hydroxyl radicals produced by, 25:26305
effects on survival of mice, role of thymectomy in recovery from, 25:26937
effects on synthesis of nucleic acids and proteins in Micrococcus radiodurans, dose dependence of, 25:26639
effects on thymine in DNA of Micrococcus radiodurans, repair of, 25:26643
effects on tissue physiology of citrus fruits, 25:27135 (IAEA-R-362-F)
effects on titanium oxide, production and annealing of paramagnetic defects in, 25:27853
effects on urinary excretion of beta-amino-isobutyric acid and deoxycitidine in monkeys, 25:26999
effects on varidase behavior in man following addition to blood, 25:26632
effects on visual system of noctuid moths, combined effects of light and, 25:26910
effects on wheat, mutagenic, 25:26710
emission by radioisotopes, tables of abundance, energy, half-life, and production mode of, (E), 25:28400
emission from Milky Way, comparison of γ spectra from cosmic π^0 decay with, (T), 25:27404
monitoring in organisms, seston, and water of Black Sea off Rumanian coast during 1964 to 1967, 25:26745
radiation effects on survival of larvae and pupae of alfalfa weevil, comparison of biological and chemical control with, 25:26913
reactions (γ,p) with natural copper at 17.6 MeV, energy spectra from, (E), 25:28217 (LUNP-7013)
reactions with dielectric liquids, measurement of mean energy for production of ion pairs in, 25:26293
reactions with lead at 84, 145, and 279 keV, L-shell photoelectric cross sections for, (E), 25:27830
scattering by lead and uranium at 9 MeV, cross section for elastic, (E), 25:28358
scattering by lead at 661.6 keV, differential cross sections for Compton, (E/T), 25:27461
spectra from plutonium dioxide fuels, 25:27305 (N-70-35897)
streaming through shielding apertures, (E/T), 25:27829
transport in spheres, cylinders, and planes, computer program for solving one-dimensional Boltzmann equation for, (T), 25:28149(T) (ORNL-tr-2419)
use for food processing, review of principles involved and wholesomeness considerations in, 25:27132 (CONF-680112-, pp 221-39)
use for parasitic decontamination of human excreta, 25:27126
use for radiotherapy, comparison with 30-MeV fast neutron beam, 25:26879
use for sterilization of codling moths, estimation of size of populations for sterile release programs, 25:27155
use for therapy of carcinomas of human uterus by combining intracavitary cobalt-60 applicators and external beams, 25:26869
use of cobalt-60, for therapy of carcinomas of human esophagus, methods for, 25:26896
use of therapy of neoplasms of human nose and paranasal sinuses, effectiveness of radiosensitizing drugs and surgery with, 25:26885
uses in nondestructive testing, review of, 25:26440

GAMMA SPECTROMETERS
coincidence circuits for, using on-line computers,

25:26504
data analysis for lithium-drifted germanium, computer program for, 25:26500
data analysis for lithium-drifted germanium, PDP-8 computer for, 25:26496
data processing of multiplexed two-parameter, PDP-9 computer for preliminary, 25:26501
development of β--γ coincidence, for measuring total nuclear decay energies, 25:28296 (CERN-70-30(Vol.1), pp 341-51)
efficiency graph for sodium iodide scintillation, construction and use of, 25:26492 (RCC-M-211)
performance of sodium iodide crystal, for burnup measurements of pin type fuel elements, 25:28766
standardization of liquid, for carbon-14 and sulfur-35 determination in biological samples, method for external, 25:26184

GAMMA SPECTROSCOPY
spectra fitting for, computer programs for, 25:26489 (ANU-P-487(2))

GAS CENTRIFUGES
uranium enrichment in European, economics of and prospects for, 25:26424(T) (CONF-700557-3)

GAS FLOW
magnetohydrodynamic laminar boundary layer at nonconducting surface in, (T), 25:27495
magnetohydrodynamic, motion of alternate layers of conducting liquid and nonconducting gas in transverse magnetic field in, (T), 25:27494
measurements using radioisotopes, review of methods for, 25:26435

GASEOUS DIFFUSION PLANTS
uranium enrichment in European, economics of and prospects for, 25:26424(T) (CONF-700557-3)

GASES
determination of total, in mixed oxide fuel pellets, 25:26153 (LA-4622)
distribution in Milky Way, relation to dust, (E), 25:27415
distribution in Orion Nebula, (E), 25:27312
distribution of toxic, in atmospheric aerosols, (T), 25:26383 (CONF-700601-, pp 373-80)
dynamic processes in galaxies, computer simulation of, (T), 25:27406
effects of liquid coolant-penetrating jets of, on temperature transients in heated walls, (E), 25:26418 (ANL-7734)
electron beam interactions with, ion acceleration in, (E), 25:27696 (WASH-1159, pp 204-18)
electron beam interactions with, ion production in, (E), 25:27695 (WASH-1159, pp 196-203)
heating and ionization of intergalactic, by ultraviolet radiation, (T), 25:27429
motion in spherically symmetric galaxies, (T), 25:27403
scavenging from atmosphere by raindrops, effects of gas solubility on, (T), 25:26374 (CONF-700601-, pp 247-59)
scavenging of atmospheric aerosol, method for predicting efficiency of precipitation, 25:26391 (CONF-700601-, pp 475-85)
scavenging of atmospheric, by rain clouds and raindrops, kinetic theory of, 25:26382 (CONF-700601-, pp 355-71)

GASTRIC JUICE
radioimmunoassay for binding and blocking anti-intrinsic factor antibodies in human, diagnosis of pernicious anemia by, 25:26676
sulfur-35 secretion in rat, effects of ulcers, steroid hormones, and inflammation suppressive drugs on, 25:26605

GENES
locus for γ-radiosensitivity of RFM mouse, 25:26690
mapping for gamma-radioinduced heterochromatin deletion mutations in Drosophila, 25:26720
mapping in uv and x-radioinduced mutations in Ascobolus, 25:26695
mapping in uv-radioinduced mutants of phytopathogenic fungi, 25:26698
mapping in x-radioinduced mutants of Cicer, 25:26718
mapping of uv-radioinduced, of radiosensitive mutations in Aspergillus, 25:26709
radioinduced translocations in, of mosquitoes for genetic control, x, 25:26719

GENETICS
book: Post-Natal Development of Phenotype, 25:26696
conference on post-natal development of phenotype, 25:26696

GEOMAGNETIC FIELDS
correlation between quiet-day H ranges at equatorial and midlatitude, 1964, (E), 25:27504
effects of configuration of, on injected solar-particle propagation following Jan. 28, 1967 solar flare, (E), 25:27584
inclination of, determination by calibration of Faraday rotation of incoherently scattered signals, 25:27611
morphology of auroral polar substorms, comparison with DP 2 fluctuations, (E/T), 25:27606
pulsations in, ATS 1 observations of storm-time, (E), 25:27544
pulsations in, origin and mechanisms of Pc1, associated with magnetospheric particle behavior, (T), 25:27605
relation of activity in, to auroral proton precipitation at high-latitude noon--midnight meridian, (E), 25:27579
solar-activity effect on disturbances in, (E), 25:27534
variations at Watheroo, Western Australia 1919-1958, lunar and solar daily, (E), 25:27503
variations due to solar wind-induced plasma motion across bow shock and in magnetosheath, (E), 25:27537
variations on quiet days, abnormal and regular, (E/T), 25:27602

GERMANIUM
determination by photometry using carboxy derivatives of 2,6,7-trihydroxy-9-phenyl-3H-xanthen-3-one, 25:26174
radioinduced defects in n-type, low-temperature annealing of 5°K 1.1-MeV electron, 25:27850
radioinduced defects in, channeling study of distribution of 10- and 400-keV heavy-ion, 25:27861
radioinduced shallow traps in antimony-doped p-type, annealing study of 1.5-MeV electron, 25:27843
transport to silicon during anneal, 25:27909

GERMANIUM ALLOYS AND SYSTEMS
Fe--Ge, Hall coefficient and electric conductivity of liquid, 25:27212
Ge--Ti-base--Zr, properties for use in brazing graphite or refractory metals, 25:27229(P)

GERMANIUM ISOTOPES Ge-66
beta and electron-capture decay of, branching ratios, gamma spectra, and log-ft values for, (E), 25:28272

GERMANIUM ISOTOPES Ge-68
energy levels from oxygen reactions with nickel, spin-parity assignments for, (E), 25:28213 (CERN-70-30(Vol.2), pp 911-15)

GERMANIUM ISOTOPES Ge-71
energy-level transitions from proton reactions, branching ratios, gamma-ray angular distributions, and internal conversion coefficients for, (E/T), 25:28271

GERMANIUM ISOTOPES Ge-73
neutron capture by, Q-value, excitation energies, and energies and intensities of γ rays from thermal, (E), 25:28258

GERMANIUM ISOTOPES Ge-74
energy-level transitions of, vibrational model for scheme of, (T), 25:28258

GLANDS
submaxillary, radiation effects on, in female rats, effects of time of administration on protective effects of AET, cystamine, or tetramethylcystamine against γ, 25:26792

GLASS
corrosive effects of melting, on alloys in radioactive waste vitrification process, 25:26334(T) (ORNL-tr-2410, pp 143-89)
magnetic ordering and electric conduction in transition-metal-oxide, 25:27901

GLOBULINS
radiation effects on content of, in blood plasma of rats, single and combined effects of turpentine and x, 25:26979

GLOW DISCHARGES
cathode environment in, characterization of, 25:28891 (SC-RR-710122)

GLUCANS
effects on γ-irradiated mice, 25:26947

GLUCOPYRANOSIDE, PHENYL
radiolysis of aqueous solutions of, effects of radical scavengers on yields of glucose and phenol from γ, 25:26304
radiolysis of aqueous solutions of, effects of scavengers on kinetics of production and decay of transient species in electron pulse, 25:26304

GLUCOSE
metabolism in rats, comparison of carbon-14 and tritium in tracer studies on, 25:26602
radiation effects on production of, in rat liver, x, 25:26963
radiation effects on tolerance to, in diabetic rats, x, 25:27010
yields from γ radiolysis of aqueous solutions of phenyl glucopyranoside, effects of radical scavengers on, 25:26304

GLUCOSIDES
radiolysis of solid aryl, ESR spectral studies on yields from, 25:26303

β-GLUCURONIDASE
radiation effects on activity of, in blood plasma and liver of rats, single and combined effects of turpentine and x, 25:26979

GLUTARALDEHYDE
radioprotective effects on collagen gel, x, 25:26802

GLUTEN
radiation effects on chemical and physical properties of, 1-Mrad γ, 25:26656

GLYCERIDES
radiation effects on, in canned chicken pet food products, 25:26647

GLYCEROL
radioprotective effects on catalase activity in vitro, γ, 25:26650

GLYCINE, N-GLYCYL-
radiolysis of monocrystals of, ESR studies on free radicals from γ, 25:26300

GLYCOGEN
radiation effects on production of, in rat liver, x, 25:26963

XUM

GLYCOSIDES
radiolysis of aqueous solutions of substituted aryl, rate constants for reactions of hydrated electrons and hydroxyl radicals in electron pulse and γ, 25:26305
GOATS
radiation effects on hemoglobin and serum proteins in, acute and chronic γ, 25:26970
GOLD
determination in sea floor samples by neutron activation, 25:26188 (BNWL-SA-3803)
determination in woven fabric by neutron activation, 25:26200
effects on spectrophotometric determination of beryllium and gallium, 25:26172
field-ion microscopy of vacancies in, 25:27866(R) (NYO-3504-56)
photon reactions at 5.4 GeV, total cross section for hadron production in, 25:27953
GOLD ALLOYS AND SYSTEMS
Au--Er, magnetic properties of Au_4Er at 6 to 300°K, (E/T), 25:27872
Au--Tm, magnetic properties of Au_4Tm at 6 to 300°K, (E/T), 25:27872
Au--Yb, magnetic properties of Au_4Yb at 6 to 300°K, (E/T), 25:27872
GOLD ISOTOPES
effectiveness of colloidal, for diagnosis of human lymph node malignancies, 25:26851
energy-level transitions in, probabilities of E2, (E), 25:28341 (CERN-70-30(Vol.2), pp 1115-18)
use for function studies of human liver, 25:26862
GOLD ISOTOPES Au-184
beta and electron-capture decay of, γ spectra from, (E), 25:28425
beta decay of, positron spectrum and Q value for, (E), 25:28295 (CERN-70-30(Vol.1), pp 331-40)
GOLD ISOTOPES Au-185
alpha-decay of, half-lives for, (E), 25:28335 (CERN-70-30(Vol.2), pp 1045-55)
GOLD ISOTOPES Au-186
beta and electron-capture decay of, γ spectra from, (E), 25:28425
half-lives of isomeric, (E), 25:28335 (CERN-70-30(Vol.2), pp 1045-55)
GOLD ISOTOPES Au-187
electron-capture decay of, half-lives for, (E), 25:28335 (CERN-70-30(Vol.2), pp 1045-55)
GOLD ISOTOPES Au-188
electron-capture decay of, γ spectra from, (E), 25:28425
GOLD ISOTOPES Au-189
half-lives of isomeric, (E), 25:28335 (CERN-70-30(Vol.2), pp 1045-55)
GOLD ISOTOPES Au-194
beta decay of, Fermi plots, gamma spectra, and log-ft values from, (E), 25:28392
GOLD ISOTOPES Au-197
boron-11 reactions with, cross-section limit for fission isomer excitation in, (E), 25:28399
carbon-12 fission at 82 MeV, analysis of helium-6 emission in, (E), 25:28351(T) (KFK-tr-352)
fluorine-19 reactions with, cross-section limit for fission isomer excitation in, (E), 25:28399
neutron capture by, gamma spectra from resonance, (E), 25:28437
nitrogen-14 reactions with, cross-section limit for fission isomer excitation in, (E), 25:28399
oxygen-16 fission at 137 MeV, analysis of helium-6 emission in, (E), 25:28351(T) (KFK-tr-352)
oxygen-16 reactions with, cross-section limit for fission isomer excitation in, (E), 25:28399
proton elastic and inelastic scattering at 13 to 17 MeV, analog resonance anomalies in, (E), 25:28371
GOLD ISOTOPES Au-198
effectiveness for diagnosis of liver abscesses in man, 25:26860
effectiveness for diagnosis of liver cirrhosis in man, 25:26861
effectiveness for therapy of joint diseases in human bones by synovial injection, 25:26873
energy levels from gold-197 neutron capture, skin--parity assignments for, (E), 25:28437
use for scanning bone marrow for localization of metastases, 25:26847
use of colloids of, for scanning human liver for diagnosis and evaluation of drug therapy of amebic abscess, 25:26843
GOLD ISOTOPES Au-200
beta decay of isomeric, lifetimes of high-spin energy levels of mercury-200 from, (E), 25:28353 (NP-18695)
GONADS
radiation dose to, from source implanted elsewhere in body, development of Monte Carlo computer model for estimating absorbed γ, 25:26760
radiation dose to, of man during therapy, 25:26759
radiation dose to, of medical personnel during technetium-99m scintigraphy, γ, 25:26766
radiation effects on, 25:27036 (CONF-691057)
GOPHERS
radiation effects on population mechanics of, in natural environments, γ, 25:26682(R) (NYO-2579-20)
GRANITES
analysis for aluminum, iron, manganese, and sodium by autoradiography and neutron activation, 25:26194
GRAPHITE
configuration of blocks to facilitate easy removal from reactors, 25:28828(P)
electron inelastic scattering study of nonvertical interband transitions in single crystals of natural, 25:27902
neutron flux through interface of styrofoam with, time and space dependence of thermal, (E), 25:28818
neutron flux through lattice of, time and space dependence of, (E), 25:28818
neutron scattering by, cross sections, phonon spectra, and scattering law from different crystal models for thermal, (T), 25:28158
radiation effects on dimensional stability of boronated and hafnated, neutron, (E), 25:28633(R) (GA-10399)
radiation effects on electric conductivity of, fast and thermal neutron, 25:28765
radiolytic oxidation by carbon dioxide or oxygen, surface complexes in, 25:26286
sorptive properties of nuclear and pyrolytic, for cesium at 600 to 800°C, 25:27201 (EUR-4549)
GRAVITATION
energy transfer in general relativity theory, Newtonian, 25:28089
evolution of galactic water-bag models, (T), 25:27412
inverse-square law in Newtonian, (T), 25:27422
potential energy in relativistic stars, (T), 25:27324
spectral redshift in, Schwarzschild-metric calculation of, 25:27347
theory of, cosmological models in extension of Yilmaz, 25:28087
GRAVITATIONAL FIELDS
coupling to energy--momentum tensor, causality in Lorentz-covariant Lagrangian for, (T), 25:28068
GRAVITATIONAL RADIATION
damping of slowly moving systems, matched asymptotic expansion method for calculating, (T), 25:28086
emission as shock waves from tachyons, general relativity predictions for, (T), 25:28088
GROUND
motion from Calabash Event, calculated psuedo-relative velocity spectra from measurements of, 25:26401 (NVO-1163-218)
motion from Gasbuggy Event, measurement of surface, 25:26405 (PNE-1002)
motion from Rulison Event at Rifle Gap Dam, Colo., equipment for measurement of, 25:26410 (PNE-R-47)
motion from Rulison Event, measurement and prediction of damage to structures from, 25:26402 (JAB-99-78)
motion from underground nuclear explosions, summary of 1957 to 1970 data on, 25:26411 (SC-DC-713865)
motion of Pre-Gondola II area, measurements of, 25:26407 (PNE-1112)
motion of Pre-Gondola III Phase II area, measurements of, 25:26408 (PNE-1117)
GROUND WATERS
contamination of San Juan Basin, by Gasbuggy Event, safety evaluation of, 25:26406 (PNE-1009)
effectiveness of hot spring, for therapy of radiation injuries of Japanese bomb survivors, 25:26897
flow into Greeley Event chimney, postshot measurements of, 25:26412 (UCRL-50979)
flow of Argentine, review of radioisotope tracer studies of, 25:26353 (CONF-680112-, pp 37-52)
GROUP THEORY
method of dynamical, for treating superfluid Bose system, 25:27641
GUANIDINE
effects on bacteria, mutagenic, 25:27121
GUANIDINE, 1,1'-(DITHIODIETHYLENE)DI-
radioprotective effects on DNA, 25:26801
GUANIDINE, 2-MERCAPTOETHYL-
radioprotective effects on HeLa cells, x, 25:26797
GUANIDINE, 1-METHYL-3-NITRO-1-NITROSO-
effects on β-galactosidase gene of Escherichia, mutagenic, 25:26722
GUANIDINE, 1,1'-PENTAMETHYLENEDI-
radioprotective effects on DNA, 25:26801
GUANOSINE
radioprotective effects in bacteria, uv, 25:27122
GUINEA PIGS
radiation effects on antigenicity of tumor cells in, x, 25:26663
radiation effects on hematopoiesis and testicle epithelium in, following long distance skin therapy, x, 25:26973
GYMNOSPERMIDAE
Pinus sp., strontium-90 content in, formula for prediction of, 25:26616

H

H.B. ROBINSON POWER REACTOR, UNIT 2
control elements for, physics tests for revised core positions of part-length, 25:28567 (DOCKET-50261-55)
operations incident of March 14, 1971, failure of turbine bearings due to loss of lubrication, 25:28569 (DOCKET-50261-57)
operations incident of March 8, 1971, difficulties with

XUM

lube oil system of emergency diesel generators, 25:28568 (DOCKET-50261-56)
safety injection system for, tests on modified, 25:28570 (DOCKET-50261-58)
HI REGIONS
characteristics of, surrounding planetary nebulae, (E/T), 25:27323
expansion of, in Virgo, (E), 25:27352
survey of high- and intermediate-velocity, (E), 25:27416
HII REGIONS
characteristics of, surrounding planetary nebulae, (E/T), 25:27323
origin of, surrounding Cas A, (E), 25:27313
properties of static solar, (E), 25:27399
radio recombination lines of carbon, helium, and hydrogen in, (E), 25:27349
HADRONS
decay of, spin formalisms for, 25:28007 (CERN-71-8)
electroproduction in parton model, 25:28002
energy level diagrams for, rotational, 25:28009
form factors in parton model, 25:28002
interactions at high energies, group theoretical model with isotopic-spin-symmetry extension of Regge pole model for, (T), 25:28055
interactions at high energies, phi^3 field theory for, 25:28045 (DESY-71/6)
interactions of, impact picture and eikonal approximation in phi^3 theory for, 25:28011
interactions with leptons at high energies, review on, 25:28005
production in $e^+ + e^-$ interactions at high energies, spectral sum rules in Sugawara model with modified stress tensor for cross sections for, (T), 25:28006
production in photon reactions with nuclei at 1.5 to 5.7 GeV, total cross sections for, 25:27953
spectroscopy of, 25:28008 (UCRL-73073)
theory for, general dual vertex in harmonic oscillator model and dual local electromagnetic current in, 25:28021
HAFNIUM
analysis for zirconium, review on methods for, 25:26150
determination in Zircaloy, instrumental method for, 25:26171
determination in zirconium, review on methods for, 25:26150
production and uses of, review on, 25:27191
separation from zirconium, review on methods for, 25:26150
HAFNIUM ALLOYS AND SYSTEMS
B--Hf--Nb-base--W, strength at 1200°C, 25:27227
C--Hf--Zr, thermodynamic properties of compound of, at 2440°K, 25:27283 (N-71-10590)
Fe--Hf, mechanical properties of Laves phase $HfFe_2$, 25:27211 (UCRL-20301)
Hf--Ir, superconductivity of intermetallic Hf_2Ir, (E), 25:27654
Hf--Nb-base, strength at 1200°C, 25:27227
Hf--Nb-base--W, oxidation resistance at 1200°C, 25:27227
Hf--Ta--V, phase diagram of, 25:27247
HAFNIUM CARBIDES
electron band structure of, (E/T), 25:27907
HAFNIUM ISOTOPES Hf-169
beta and electron-capture decay of, half-lives for, (E), 25:28321 (CERN-70-30(Vol.2), pp 931-8)
HAFNIUM ISOTOPES Hf-171
energy levels from (particle,xn) reactions, spin--parity assignments for rotational, (E/T), 25:28323 (CERN-70-30(Vol.2), pp 949-55)
HAFNIUM ISOTOPES Hf-173
energy levels from (particle,xn) reactions, spin--parity assignments for rotational, (E/T), 25:28323 (CERN-70-30(Vol.2), pp 949-55)
HAFNIUM ISOTOPES Hf-175
energy levels from (particle,xn) reactions, spin--parity assignments for rotational, (E/T), 25:28323 (CERN-70-30(Vol.2), pp 949-55)
HAFNIUM ISOTOPES Hf-176
energy levels of, deformation parameters for 4^+, (E/T), 25:28411
proton reactions (p,t) at 51.7 MeV, spectra and DWBA analysis of differential cross sections from, (E/T), 25:28411
HAFNIUM ISOTOPES Hf-177
energy levels of, analysis of nonrandom distributions of neutron resonance, (T), 25:28421
HAFNIUM OXIDES
CaO--HfO_2-base, composition and microstructure of, 25:27296
HfO_2-base--MgO, composition and microstructure of, 25:27296
HfO_2-base--Y_2O_3, composition and microstructure of, 25:27296
HAIR
analysis by neutron activation, 25:26195
HALDEN BOILING REACTOR
fuel rod assembly irradiation in, data analysis from IFA-150, 25:28692 (JAERI-Memo-4248)
HALIDES
content in rainwater, precipitation scavenging studies of origin and quantity of, (E), 25:26365 (CONF-700601-, pp 99-108)
HAMSTERS
radioinduced abnormalities in embryos of, in relation to radioinduced chromosome aberrations, x, 25:26982
HANDS
radiation dose to, from preparation of indium-113m- and technetium-99m-labeled compounds, 25:26768
radiation dose to, of medical personnel from handling indium-113m, methods for shielding against γ, 25:26767
radiation dose to, of medical personnel from technetium-99m, methods for shielding against, 25:26765
HANFORD PRODUCTION REACTORS
thermal discharge from, effects on feeding activities and growth of fish in Columbia river, 25:26681 (BNWL-1528)
HAPTOGLOBINS
radiation effects on content of, in blood plasma of rats, single and combined effects of turpentine and x, 25:26979
HARDENING
research progress on particle size distribution effects in precipitation, 25:28897(R) (UCLA-34-P-172-1)
HAWAII
research on longevity, reproduction, and culture media of Mediterranean fruit fly in, for radiation control programs, 25:27157
HEART
function studies, use of tracer techniques in, 25:26567 (STI/PUB-263)
radiation effects on biochemistry of, in dogs, effects of AET on x, 25:26935
radiation effects on immune reactions in dogs following transplants of, ultrastructural electron microscopy studies on x, 25:26677
radiation effects on noradrenaline and serotonin levels in, of rats, whole-body x, 25:26959
radiation effects on novocaine action in isolated rat, following whole-body exposure to 600 R or 1000 R, x, 25:26798
radiation effects on, in rabbits, localization of, 25:26961
radiation effects on, of rabbits, protective effects of AET and cystamine against γ, 25:26794
radiation effects on, of rats following exposure in utero, tritium β, 25:26925
radiodiagnosis of diseases in human, by angiocardiography, 25:26854
radioinduced lesions in human, following therapy, treatment of, 25:27048
scanning of human, for diagnosis of vascular diseases, methods for technetium-99 in, 25:26838
scanning of pericardium of, using phosphorus-32, international methods for, 25:26855
volume of dog, use of iodine-131 in measurement of variations of, 25:26566 (CEA-CONF-1711)
HEART, MECHANICAL
book: Artificial Heart Program Conference, 25:26899
conference on current program for development of, 25:26899
implantation of plutonium-238-powered, in dogs, γ and neutron dose and temperature rise in body following, 25:26931
HEAT EXCHANGERS
temperature control in internal heat-generating, method for optimum, (E/T), 25:26421
HEAT EXCHANGERS (LIQUID-LIQUID)
design of liquid metal heated tubular, with means for prevention of localized overheating, 25:28749(P)
HEAT SOURCES
detection and location of earth-impacted simulated radioisotope, performance of Firescan equipment for airborne, 25:26428 (SC-DR-710095)
power measurements of, calorimetric method for, 25:26548 (MLM-1780)
HEAT TRANSFER
calculation and measurement of critical, for water-cooled rod bundles under transient operating conditions, 25:26419(R) (GEAP-10221-5)
calculation of fuel element to pressurized water, two-region lumped parameter model for transient, (T), 25:28662
measurements of enhanced surface tubes and operations at four-effect Vertical Tube Evaporator Pilot Plant, 25:28893(R) (TID-25679)
HEAT TRANSFER SYSTEMS
blowers for fuel element irradiation, design of high pressure low flow helium, 25:28833
sampling system for nine-rod, design and installation of three-subchannel, 25:26419(R) (GEAP-10221-5)
HEATED EFFLUENTS
control methods for nuclear power plants, 25:28623
control of nuclear power plant, 25:28621 (STI/PUB-261)
control of nuclear power plant, 25:28624
economics for urban heating systems using, in Sweden, 25:28574
effects of power plant, on Lake Michigan, 25:28622
effects on feeding activities and growth of fish in Columbia River, 25:26681 (BNWL-1528)
effects on flow and temperature of surface waters, COL HEAT and TOPLYR programs for simulation of, 25:28710(R) (HEDL-TME-71-26)
environmental effects of nuclear power plant, 25:28527 (DUN-SA-166)
monitoring of nuclear power plant, 25:28624

XUM

velocity distributions within plumes of, photographic method for determining, 25:28839 (ANL/ES-4)
HELIUM
abundance in H II regions, (E), 25:27349
cesium-ion reactions with, cross sections for excitation of Cs II resonance lines near thresholds in, (T), 25:27454
electron correlation and density in, calculations using restricted Hartree--Fock approximation, 25:27467
energy spectra of cosmic solar nuclei of, satellite observations of, (E), 25:27533
hydrogen-ion (H_2^+) reactions at 1.7 to 12.5 eV with, energy distributions of helium hydride ions (HeH^+) formed in, (E), 25:27452
interaction between adsorbed atoms of, substrate mediated, (T), 25:27635 (RLO-1388-605)
plasma of, dynamic stabilization of drift-dissipative instabilities in afterglow, (T), 25:27786
radio recombination lines of, in H II regions, (E), 25:27349
scattering by helium atoms, total cross sections for elastic, (T), 25:27444
specific heat of high-temperature, effect of electron excitation on, 25:27692
HELIUM IONS
bubble formation and diffusion in copper foils bombarded by 8-keV, 25:27842 (RD/B/N-1850)
intensity of He^+ and He^{++} in early-evening proton aurora, solar-wind origin of primary, (E/T), 25:27618
reactions with hydrogen molecules at 100 eV to 30 keV, excitation functions of He I spectral lines emitted in, (E), 25:27463
scattering from niobium single crystals at 100 keV, effects of lattice defects on back-, 25:27840 (IPP-7/3)
scattering from ytterbium implants in silicon at 1 MeV, flux-peaking effect in back-, 25:27857
HELIUM ISOTOPES
abundance in lunar surface materials, (E), 25:27308
HELIUM ISOTOPES He-3
binding energy of, calculation using K-harmonics method, 25:28162 (IAE-2000)
neutron elastic scattering at 1, 3.6, and 6 MeV, cluster-model analysis of, (T), 25:28167
neutron reactions (n,p) at 1, 3.6, and 6 MeV, cluster-model analysis of, (T), 25:28167
reactions (He-3,6n), (He-3,7n), (He-3,α4n), (He-3,α5n), (He-3,p6n), and (He-3,p7n) with dysprosium-156 at 68 to 98 MeV, yield curves for, (E), 25:28303 (CERN-70-30(Vol.1), pp 533-44)
reactions (He-3,α) with bismuth-209 at 28 MeV, alpha spectra from, (E), 25:28417
reactions (He-3,α) with strontium-86 at 17.5 MeV, DWBA analysis of angular distributions from, (E), 25:28277
reactions (He-3,d) with beryllium-9, boron-10, and carbon-13 at 22 MeV, isospin dependence of angular distributions for, (E), 25:28174
reactions (He-3,d) with boron-11 at 44 MeV, deuteron spectra and angular distributions for, (E), 25:28205
reactions (He-3,d) with lead-207 at 30 MeV, deuteron spectra from, (E), 25:28417
reactions (He-3,d) with silicon-30 at 12 MeV, spectra and DWBA analysis of differential cross sections for, (E), 25:28270
reactions (He-3,d) with titanium-50 at 10 MeV, deuteron spectra and angular distributions for, (E), 25:28231
reactions (He-3,d) with zirconium-90 at 24.8 MeV, deuteron spectra and angular distributions for, (E), 25:28363
reactions (He-3,γ) with magnesium-26 at 4.44 to 8.26 MeV, differential cross sections for, (E), 25:28206 (ANU-P-508)
reactions (He-3,Li-7) and (He-3,Be-7) with fluorine-19 at 39 to 42 MeV at 165°, correlations in excitation functions for, (E), 25:28190
reactions (He-3,p) with carbon-12 at 2.48 to 3.25 MeV at 34°, cross sections and polarization for, (T), 25:28496
reactions (He-3,p) with chromium-52 at 11 MeV, angular distributions for L = 0 transitions in, (E), 25:28229
reactions (He-3,p) with titanium-50 at 10 MeV, angular distributions for L = 0 transitions in, (E), 25:28229
reactions (He-3,t) with iron-56 at 25 MeV, analysis for isospin mixing in cross sections for, (E), 25:28232
reactions (He-3,t) with oxygen-18 at 16 MeV, triton spectra from, (E), 25:28173
reactions with nuclei, analysis for imaginary isovector term in optical potential for, (T), 25:28461
scattering by silicon-30 at 12 MeV, optical-model analysis of angular distributions from elastic, (E), 25:28270
thermal capacity of monolayers of, on graphite, effects of lateral substrate fields on, 25:27634 (RLO-1388-604)
He-3--He-4, normal-component density of solutions of, from lambda point down to 0.4°K, 25:27639
He-3--He-4, sound dispersion in superfluid solutions of, due to damping of normal component, 25:27640
He-3--He-4, sum rules and long-range correlations in binary solutions of liquid, 25:27632 (RLO-1388-599)
HELIUM ISOTOPES He-4
electron interactions with vorticity with heat-flushed superfluid, 25:27638
energy levels of monolayers of, on inert substrate, ground-state, 25:27633 (RLO-1388-603)
luminescence of liquid II, effect of pressure on alpha-particle induced, (E), 25:27636
scattering by helium-4, multiple diffractive model for elastic, 25:28073
thermal capacity of monolayers of, on graphite, effects of lateral substrate fields on, 25:27634 (RLO-1388-604)
He-3--He-4, normal-component density of solutions of, from lambda point down to 0.4°K, 25:27639
He-3--He-4, sound dispersion in superfluid solutions of, due to damping of normal component, 25:27640
He-3--He-4, sum rules and long-range correlations in binary solutions of liquid, 25:27632 (RLO-1388-599)
HELIUM ISOTOPES He-5
energy levels from resonances in tritium--deuteron elastic scattering, (E), 25:28168
HELIUM ISOTOPES He-6
beta decay of, half-life for, (E), 25:28351(T) (KFK-tr-352)
HELIUM TRITIDES
reactions of ionic, from tritium beta decay with dimethylcyclopropane, 25:26321
HEMAGGLUTININS
effects on x-irradiated bone marrow cells of mice, 25:26942
HEMATOPOIESIS
radiation effects on, in guinea pigs following long distance skin therapy, x, 25:26973
radiation effects on, in mice, recovery from x, 25:26980
HEMATOPOIETIC SYSTEM
development of mammalian, function of bone marrow stem cells in, 25:28898 (UCRL-20613)
radiation injuries to mouse, as evidenced in residual injury in erythroid and myeloid systems, x, 25:26981
HEME
analysis for nitrogen-15 for life span studies on erythrocytes in burn patients, mass spectrometric, 25:26572
HEMOCYANINS
radiation effects on activity of, role of hydrated electrons and hydroxyl radicals in γ, 25:26302
HEMOGLOBIN
nature of rat red cell, research studies on, 25:28865(R) (NYO-3976-4)
preparation and properties of six rat red cell, 25:28866 (NYO-3976-5)
radiation effects on, in goats, acute and chronic γ, 25:26970
HEMOLYSIN
radiation effects on formation of, in mice following bone marrow reconstitution, 25:26672
HEPTANE
radioinduced ionization currents in, measurement of alpha and beta, 25:26471
solvent properties for uranyl complex with 4,4,4-trifluoro-1-(2-thienyl)-1,3-butanedione, radiometric determination of, 25:26340
3,5-HEPTANEDIONE, 2,2,6,6-TETRAMETHYL-
complexes with rare earths, separation by fractional distillation, 25:26336(P)
HEXANE
radioinduced ionization currents in, measurement of alpha and beta, 25:26471
solvent properties for uranyl complex with 4,4,4-trifluoro-1-(2-thienyl)-1,3-butanedione, radiometric determination of, 25:26340
HIGH-ENERGY PHYSICS
High Energy Physics Index. Vol. 9, No. 5, 25:27976
High Energy Physics Index. Vol. 9, No. 7, 25:27977
HIGH-TEMPERATURE GAS-COOLED REACTOR EXPERIMENT
design characteristics of, 25:28544
fuels for, quality control and testing of, 25:26438 (DP-Report-432)
HIGH-TEMPERATURE LATTICE TEST REACTOR
physics parameters of HTGR lattices in, (E/T), 25:28633(R) (GA-10399)
HIROSHIMA
atomic bombing of, effects of age on neuro-muscular function of survivors of, 25:27053
atomic bombing of, leukemia incidence in man exposed in utero to, 25:27043
HISTAMINE
sodium salt, radioprotective effects on mice in relation to body temperature and respiration, 25:26800
HOLMIUM
determination in yttrium oxides by solvent extraction and spectrography, 25:26168
spin-wave dispersion relations of, neutron inelastic scattering study of, 25:27888
HOLMIUM ALLOYS AND SYSTEMS
Ho-Pd, magnetic and electric properties of $HoPd_3$ at 4 to 300°K, 25:27870
HOLMIUM CARBIDES
magnetic structure of alpha-Ho_2C_3, neutron-diffraction study of, 25:27904
HOLMIUM ISOTOPES Ho-150
beta decay of, half-life for, (E), 25:28303 (CERN-70-30(Vol.1), pp 533-44)

HOLMIUM ISOTOPES Ho-153
alpha decay of isomeric, α energy and half-life for, (E), 25:28418
alpha decay of, energy and half-life for, (E), 25:28303 (CERN-70-30(Vol.1), pp 533-44)
HOLMIUM ISOTOPES Ho-154
alpha decay of isomeric, α energy and half-life for, (E), 25:28418
alpha decay of, energy and half-life for, (E), 25:28303 (CERN-70-30(Vol.1), pp 533-44)
HORMONES
effects of duodenal, on selenium-75 distribution in rat pancreas, 25:26591
effects on systemic reactions following irradiation, 25:27036 (CONF-691057)
HORMONES, ADRENAL
corticoids, effects on radioinduced nervous tissue reactions following therapy of human brain and spinal cord tumors, 25:27056
corticosteroids, effects combined with γ or x radiotherapy on brain metastases in man, 25:26895
corticosterone, radiation effects on content of, in adrenal glands and plasma of rats, 25:26998
epinephrine, determination by radioisotope derivative method using iodine-125, 25:26182
epinephrine, radioprotective effects on mice, effects of catecholamines on, 25:26804
isopropylnoradrenaline, effects on radioprotective effects of noradrenaline in irradiated mice, 25:26804
noradrenaline, radioprotective effects on mice, efects of catecholamines on, 25:26804
norepinephrine, determination by radioisotope derivative method using iodine-125, 25:26182
norepinephrine, radiation effects on level of, in tissues of rats, whole-body x, 25:26959
norepinephrine, radioprotective effects of, on submaxillary glands in mice, comparison of AET, cystamine, cysteine, serotonin, and tetramethylcystamine with γ, 25:26795
HORMONES, PANCREATIC
insulin, binding of iodine-131-labeled, to isolated mitochondria, effects of acetaldehyde, 2,4-dinitrophenol, glutathione, and palmitic acid on, 25:26575
insulin, radiation effects on activity of, in muscles, x, 25:27010
HORMONES, PITUITARY
adrenocorticotropic, radioimmunoassay of human blood plasma, antibody binding method for, 25:26675
growth hormone, measurement of secretion rate in man, using iodine-131 as tracer and portable blood sampler, 25:26579
HORMONES, PLANT
auxins, effects on root growth in γ-irradiated Vicia faba, 25:27066
gibberellin, effects on x-irradiated corn, pea, and wheat seedlings, 25:27064
indole-3-acetic acid, radiation effects on content of, in cabbage plants in X_2 generation following seed exposure, x, 25:26651
HORMONES, SEX
androgens, radiation effects on production of, by interstitial cells in testes of rats, x, 25:27008
diethylstilbestrol, effects on development of mammary carcinomas in rats, synergism between radiation and, 25:27011
testosterone, radiation effects on production of, by interstitial cells in testes of rats, x, 25:27008
HORMONES, THYROID
thyroxine, content of human blood serum, development of iodine-125 labeling method for determining, 25:26568
thyroxine, evaluation of serum, for diagnosis of thyroid function in man, 25:26857
triiodothyroxine, evaluation of iodine-125-labeled, for diagnosis of thyroid function in man, 25:26857
HUMBOLDT BAY POWER REACTOR
fuel burnup for, technical specification definitions for average and maximum, 25:28589 (DOCKET-50133-55)
operations history for 1963 to 1968, review of, 25:28577
operations incident of March 13, 1971, blown fuse in automatic circuit for off-gas isolation valve, 25:28560 (DOCKET-50133-53)
personnel for, authorization for revised high radiation access control methods for, 25:28588 (DOCKET-50133-54)
HYBRIDS
radioinduced in Ehrlich ascites cells and L cells, methods for uv, 25:26700
HYDRAZINE
radiosensitizing effects on collagen gel, x, 25:26802
HYDROCHLORIC ACID
effects on x-radioinduced polymerization of gaseous chloroethylene, 25:26282
acetone--HCl--methyl sulfoxide--$UO_2(ClO_4)_2$, complex formation in aqueous solutions of, PMR studies on solvation and, 25:26212
HCl--methanol, corrosive effects on annealed and cold-worked zirconium, 25:27173
HYDROCYANIC ACID
spectra of radiolytic ionic, ESR, 25:26289 (NYO-2150-60)
HYDROFLUORIC ACID
analysis for cesium, lithium, rubidium, and strontium by spectrophotometry, 25:26176
reactions with plutonium in tridodecylamine solutions, precipitation, 25:26330(T) (ORNL-tr-2410, pp 14-78)
HYDROGEN
determination in Zircaloy, 25:26171
electric discharges in, effect of temperature nonuniformity on positive column, (T), 25:27714
helium-ion reactions at 100 eV to 30 keV with molecular, excitation functions of He I spectral lines emitted in, (E), 25:27463
hydrogen-ion(H^-) reactions with atomic, electronic resonance states in, (T), 25:27462
ionization in prominences, (E), 25:27395
Lyman-α emission from interstellar neutral, (E), 25:27413
Lyman-α sky background, OGO-5 measurements of, (E), 25:27414
plasma of, dynamic stabilization of drift-dissipative instabilities in afterglow, (T), 25:27786
proton reactions at 10 eV with molecular, differential cross sections for excitation of resolved vibrational states in, (E), 25:27450
radio recombination lines of, in H II regions, (E), 25:27349
reactions of atomic, with acetylenedicarboxylic acid and its potassium salt powders, ESR studies on yields of radicals from, 25:26301
reactions with mechanically activated tungsten oxide at 700°C to prepare tungsten powder, reduction, 25:27183
solar-wind interactions with interstellar, (T), 25:27328
sorption by tungsten (100), (110), and (112) monocrystal surfaces, effects on surface potentials, 25:27234
sorption on tungsten (100) crystal surfaces, model for calculation of, 25:27226
spectra of H I 1216-A line of, in upper Martian atmosphere, uv, (E), 25:27433
spectra of, in airglow, horizon Lyman-α brightness at 150 km for dawn and evening twilights in, (E), 25:27615
target of, design and operation of liquid, 25:28138
yields of atoms of, from γ radiolysis of ethylene--neon, effects of pressure on, 25:26314
yields of molecules of, from α radiolysis of gaseous hydrogen sulfide, effects of electron and proton scavengers on, 25:26315
HYDROGEN IONS (H^-)
proton reactions above 10 keV with, charge exchange in, (T), 25:27456
reactions with hydrogen atoms, electronic resonance states in, (T), 25:27462
HYDROGEN IONS (H_2^+)
production in ELMO mirror machine, 25:27438 (WASH-1159, pp 141-6)
reactions with helium at 1.7 to 12.5 eV, energy distributions of helium hydride ions (HeH^+) formed in, (E), 25:27452
HYDROGEN PEROXIDES
reactions with chromium, iron, titanium, and vanadium in presence of 2-propanol, yields of hydroxyl radicals from, 25:26290(R) (NYO-3753-19)
H_2O_2--2-propanol, radiolysis of aqueous solutions of, reactions of radicals from γ, 25:26290(R) (NYO-3753-19)
HYDROGEN SULFIDES
radiolysis of gaseous, effects of electron and proton scavengers on molecular hydrogen yields from α, 25:26315
HYDROMAGNETIC WAVES
Alfven-wave effects on fast, in interplanetary space, (T), 25:27387
generation by Io, (T), 25:27435
propagation along the gravitational field in solar atmosphere, (T), 25:27393
propagation at a density step in solar atmosphere, (T), 25:27392
HYDROXYL (HO)
effects of radiolytic, on activity of hemocyanins, 25:26302
reactions in electron pulse and γ radiolysis of aqueous solutions of substituted aryl glycosides, rate constants for, 25:26305
reactions of radiolytic, with benzene, effects of micellar solutions on, 25:26295
HYDROXYLAMINE
nitrate, preparation from hydroxylamine sulfate by cation-exchange process, 25:26208 (BNWL-CC-2180)
nitrate, reactions with tetravalent plutonium, effects of iron on, 25:26206 (ARH-1920)
HYPERFINE STRUCTURE
lectures on uses of, in nuclear and solid-state physics research, 25:27915 (NP-18702)
HYPERFRAGMENTS
gamma spectroscopy of, 25:28051
properties of, review of experimental studies on, 25:28051
HYPERONS
decay of, chiral symmetry for nonleptonic radiative, 25:28004
HYPERONS (A)
interactions π + Λ + π + Σ(Λ), SU(3) x SU(3) chiral Lagrangian model for total cross sections of, (T), 25:28037
interactions π + Λ, SU(3) x SU(3) chiral Lagrangian model

XUM

for scattering lengths for, (T), 25:28037
HYPERONS (anti Λ)
production in K+ + p interactions at 10 GeV/c, generalized Veneziano model and Reggeized multiperipheral model for, (E/T), 25:27966
HYPERONS (Σ)
interactions π + Σ → π + Σ, SU(3) x SU(3) chiral Lagrangian model for total cross sections of (T), 25:28037
HYPERONS (Σ-)
production in π- + p → K + Σ- interactions at 2.75 to 14.0 GeV/c, cross sections for, (E), 25:28038
HYPOXIA
effects on radiosensitivity of mice, 25:26967

I

ICE
content of particles of, in clouds, effects of atmospheric precipitation on, 25:26362 (CONF-700601-, pp 37-48)
content of particles of, in raindrops and hailstones, effects of rainfall rate on, 25:26363 (CONF-700601-, pp 49-68)
radiolysis of glassy alkaline, bleaching of trapped electrons from γ, 25:26298
scavenging efficiency of crystals of, for polystyrene latex and sodium chloride particles, (E), 25:26367 (CONF-700601-, pp 121-36)
ILLINOIS
archaeological survey of National Accelerator Laboratory site, 25:28862 (NAL-55)
IMMUNE REACTIONS
radiation effects on, in blood of human populations on Marshall Islands, correlation of aging and fallout, 25:27058
radiation effects on, in bone marrow cells of mice, effects of phytohemagglutinin on x, 25:26942
radiation effects on, in dogs following heart transplants, x, 25:26677
radiation effects on, in mice to transplanted mammary carcinomas in comparison to effects of antilymphocyte serum, x, 25:26666
radiation effects on, in mice, effects of dose and dose rate on fission neutron, γ, x, 25:26679
radiation effects on, in mice, effects of preincubation with bone marrow on, 25:26662
radiation effects on, in Oesophagostomum, effects of dose on x, 25:26909
radiation effects on, relation of age to, 25:26664
radiation effects on, to injected bacterial endotoxin and viruses in mice, whole-body x, 25:26986
radiation effects on, to parental and hybrid tumor transplants in mice, whole-body ionizing, 25:26985
IMMUNITY
genetic control of, in mice, 25:26985
INCOLOY 800
hardness of irradiated and unirradiated, hot, 25:27236
INCONEL 600
corrosion by melting glasses in radioactive waste vitrification process, 25:26334(T) (ORNL-tr-2410, pp 143-89)
INDEXES
to data on neutron-induced reactions in Experimental Cross Section Information Library, 25:28356 (UCRL-50400(Vol.3))
INDIAN POINT POWER REACTOR, UNIT 1
operations history for 1962 to 1969, review of, 25:28577
operations incident of April 4, 1971, malfunction of time-delay switch for high pressure boron addition system pump, 25:28556 (DOCKET-50003-67)
INDIUM
determination by photometry using carboxy derivatives of 2,6,7-trihydroxy-9-phenyl-3H-xanthen-3-one, 25:26174
determination in sea floor samples by neutron activation, 25:26188 (BNWL-SA-3803)
electric conductivity of normal and superconducting, evidence for electron--electron scattering in, 25:27660
use as tracer for studying precipitation scavenging and severe storms, 25:26361 (CONF-700601-, pp 21-35)
INDIUM ALLOYS AND SYSTEMS
Hg--In, effects on fracture strength of aluminum, 25:27243
In-base--La, lanthanum-139 NMR study of LaIn3 exchange-enhanced susceptibility, 25:27920
INDIUM ISOTOPES
energy levels from (d,p) and (d,t) reactions, spectroscopic factors for, (E), 25:28374
INDIUM ISOTOPES In-109
beta and electron-capture decay of, γ spectra from, (E), 25:28428
INDIUM ISOTOPES In-111
energy levels from cadmium-110 proton resonances, spectroscopic factors for isobaric analog, (E), 25:28370
INDIUM ISOTOPES In-112
beta and electron-capture decay of, branching ratios, decay curves, gamma spectra, and log-ft values for, (E), 25:28406
INDIUM ISOTOPES In-113
energy levels from cadmium-112 proton resonances, spectroscopic factors for isobaric analog, (E), 25:28370
sorptive properties of isomeric, for hydrous zirconium oxide and zirconium oxide for use in generators, 25:26341
use of metastable, for scanning lungs for blood circulation, 25:26819
INDIUM ISOTOPES In-114
decay of isomeric, double internal conversion in, (E), 25:28410
INDIUM ISOTOPES In-115
energy levels from cadmium-114 proton resonances, spectroscopic factors for isobaric analog, (E), 25:28370
energy levels of, quasiparticle description of, (T), 25:28357 (UJV-2540-F)
proton reactions (p,α) at 5 to 13 MeV, excitation functions for, (E), 25:28268
INDIUM ISOTOPES In-131
beta decay of, half-life and gamma energies for, (E), 25:28329 (CERN-70-30(Vol.2), pp 1008-10)
INDOLE, 3-(2-AMINOETHYL)-5-METHOXY-
radioprotective effects on catecholamine content in mouse tissues, 25:27017
INFORMATION CENTERS
activities of Nuclear Desalination, during November 1969 through October 1970, 25:28790(R) (ORNL-4668)
subject heading for NSA, 25:28892 (TID-5001(10th Rev.))
INFRARED OPTICAL SYSTEMS
performance of airborne Firescan, for detecting and locating earth-impacted simulated radioisotope heat sources, 25:26428 (SC-DR-710095)
INFRARED RADIATION
effects on human eye, review on, 25:27047
emission from Seyfert galaxies, (T), 25:27417
INOSINE
radioprotective effects in bacteria, uv, 25:27122
radioprotective effects on human bone marrow, reaction mechanisms for γ, 25:26799
INSECTA
Aedes aegypti, radioinduced translocation aberrations of chromosomes in, 25:26694
Aedes aegypti, radioinduced translocations in genes of, genetic control following x, 25:26719
Anastrepha sp., radiosterilization of, methods used in Bolivia, Chile, and Peru, 25:27130 (CONF-680112-, pp 129-42)
Carpocapsa pomonella, control using radiosterilized male technique, 25:27129 (CONF-680112-, pp 123-8)
Carpocapsa pomonella, estimation of population size for radiation control programs, 25:27155
Ceratitis capitata, estimation of population size during radiation control programs using radiosterilized male release technique, 25:27156
Ceratitis capitata, estimation of size of populations of, in Tunisia using phosphorus-32 as tracer, 25:26573
Ceratitis capitata, research on longevity, reproduction, and culture media of, for control programs using radiosterilized male technique in Hawaii, 25:27157
Ceratitis sp., radiosterilization of, methods used in Bolivia, Chile, and Peru, 25:27130 (CONF-680112-, pp 129-42)
Chortophaga viridifasciata, radioinduced prophase reversion in embryos of, effects of dactinomycin on recovery from x, 25:26911
Cochliomyia hominivorax, population dynamics in Texas and Mexico, effects of radiosterilized male technique on, 25:27152
control of, review of efficiency of radiosterilized male technique for, 25:27129 (CONF-680112-, pp 123-8)
control using radiosterilized male technique, conference on, 25:27137 (STI/PUB-223)
Dacus cucurbitae, estimation of population size during radiation control programs using radiosterilized male release technique, 25:27156
Dacus cucurbitae, radiosterilization effects on ability of male to compete with normal males, γ, 25:27154
Dacus dorsalis, estimation of population size during radiation control programs using radiosterilized male release technique, 25:27156
Dacus oleae, control using radiosterilized male technique, 25:27151
Dacus oleae, ratio of radiosterilized, to normal flies, effects on damage to fruit of, 25:27151
Dacus zonatus, radiosterilization effects on ability of male to compete with normal males, γ, 25:27154
Drosophila melanogaster, radiation effects on cross-over frequency in chromosomes of, x, 25:26713
Drosophila melanogaster, radioinduced mutations in genetic load of, x, 25:26705
Drosophila sp., radioinduced mutations for heterochromatin deletion in, genetic mapping of gamma, 25:26720
Heliothis zea, radiation effects on visual system of, combined effects of light and beta, gamma, and x, 25:26910
Hypera postica, radiation effects on survival of larvae and pupae of, effects of dose on γ, 25:26913
Plodia interpunctella, radiation effects on epithelium of larvae of, effects of dose on gamma, 25:26916

radiation control of pest, using sterile release technique, 25:27153
radiosterilization of med flies in Central America, cooperative program for, 25:27131 (CONF-680112-, pp 143-50)
radiosterilization of parasitic, in human excreta, gamma, 25:27126
radiosterilization of, description of joint FAO/IAEA program on, 25:27128 (CONF-680112-, pp 1-7)
Rhagoletis cerasi, control in Poland using radiosterilized male technique, 25:27150
Rhagoletis cerasi, population dynamics of, in Poland, phosphorus-32 tracer study of, 25:27150
Tenebrio molitor, radiation damage to larvae of, effects of age, dose, dose fractionation, partial-body and whole-body exposure on repair of x, 25:26914
Tenebrio molitor, radiation effects on life span of adults, following exposure of larvae, x, 25:26914
use as food by fish in Columbia River, effects of heated effluents on, 25:26681 (BNWL-1528)

INSTRUMENTS
radiation hardness of, method for measuring 14-MeV neutron, 25:26560 (SC-DR-710045)

INTERFERON
radiation effects on content of blood of mice following injection of Newcastle disease virus, whole-body x, 25:26986
radiation effects on formation of, in monkey kidney cells infected with Newcastle disease virus, 25:27113
radiation effects on production of, in mice transplanted with rat bone marrow, 25:26995

INTERMETALLIC COMPOUNDS
crystal structure of sigma-phase related phases in, 25:27262

INTERSTELLAR MATERIAL
distribution in Milky Way, (E/T), 25:27411
distribution of gas and dust in Orion Nebula, (E), 25:27312
electron densities in, (E/T), 25:27419
evidence for source of extraterrestrial hydrogen emission, (E), 25:27413
properties of graphite core--ice mantle grains in, (E/T), 25:27408

INTESTINES
effects of hormones of duodenal, on selenium-75 distribution in rat pancreas, 25:26591
radiation dose tolerance of human, during rotation therapy, γ, 25:26894
radiation effects on growth of bacteria in small, in rats, effects of peristalsis on x, 25:26975
radiosensitivity of jejunal crypt cells of, in animals, effects of dose rate on whole-body, 25:26957
radiosensitivity of stem cells of, in mice, comparison of 14-MeV-neutron and x, 25:26958

INVARIANCE PRINCIPLES
dilation invariant field theory, scaling of, 25:28057
isospin purity at high excitation energies as evidenced by cross correlations of mirror-channel fluctuations in fluorine-19 (He-3,Li-7) and (He-3,Be-7) reactions, (E), 25:28190
Lorentz invariance of electric charge, 25:27988
scale invariance in dual resonance model for strong interactions, 25:28016

IODINE
content ratio to bromine and chlorine in marine aerosols, mathematical model for demonstrating aerosol particle size dependence of, 25:26381 (CONF-700601-, pp 325-51)
determination by potentiometric titration using ion-selective electrodes, 25:26166
diffusion into marine atmosphere from sea surface, mechanisms of, (E), 25:26380 (CONF-700601-, pp 319-24)
scavenging of aerosol particles of water-soluble, by aqueous sprays, (E), 25:26372 (CONF-700601-, pp 187-204)
scavenging of particulate fission product, from air by aqueous sprays, (E), 25:26376 (CONF-700601-, pp 271-88)
separation from milk by moving-bed ion exchange, 25:26335 (RO/EERL-71-1)

IODINE IONS
charge state distribution in oxygen targets at 1 to 14 MeV, equilibrium, (E/T), 25:28127 (WASH-1159, pp 45-57)

IODINE ISOTOPES I-125
effects on ability of bovine antilymphocytic serum antibody to prolong skin grafts, 25:26667
use as tracer for determining iodine metabolism in cattle, 25:26578 (CONF-680112-, pp 153-66)
use for determination of serum thyroxine, simplification of method for, 25:26568
use for radioimmunoassay of ACTH in human blood plasma, antibody binding method for, 25:26675
use of iodocholesterol-incorporated, for scanning adrenal glands in dogs, 25:26845
use of triiodothyroxine incorporated, for diagnosis of thyroid function in man, 25:26857

IODINE ISOTOPES I-131
binding to isolated mitochondria, effects of acetaldehyde and ethyl alcolol on, 25:26575
content in West Valley Processing Plant environs milk, Oct. 1970 to Jan. 1971, 25:26355(R) (SRO-344-11)
content in West Valley Processing Plant stack effluents, Oct. 1969 to Jan. 1970, 25:26355(R) (SRO-344-11)
effectiveness for diagnosis of liver abscesses in man, 25:26860
effectiveness for diagnosis of liver cirrhosis in man, 25:26861
effectiveness of hippuran-incorporated, for measuring renal plasma flow in combination with external gamma radiation in comparison to PAH clearance method, 25:26826
effectiveness of injections of chloroquine analog-incorporated, for therapy of malignant melanomas, 25:26882
effectiveness of sodium iodide incorporated, for diagnosis of myocardial infarction in man, 25:26822
effects of endolymphatic administration of ethiodol-incorporated, on malignant melanomas in man, therapeutic, 25:26888
energy levels from tellurium-130 proton resonances, widths and spectroscopic factors for, (E), 25:28427
incorporation in fibrinogen for use in tumor scanning, 25:26859
incorporation in human serum albumin for use in antigen elimination studies, 25:26944
incorporation in iodouracil for use in tumor scanning, 25:26859
transport through human food chains following nuclear attack, 25:26786
uptake by thyroid gland in rats, effects of dried thyroid ingestion and sex on, 25:26601
use as tracer for determining iodine metabolism in cattle, 25:26578 (CONF-680112-, pp 153-66)
use as tracer for measurement of growth hormone secretion rate in man, 25:26579
use for kidney scanning, review on international methods for, 25:26855
use for measuring renal plasma flow, development of catheterless method for, 25:26825
use for scanning lungs for blood circulation, 25:26819
use for scanning thyroid gland, review on international methods for, 25:26855
use for therapy of hyperthyroidism in man, occurrence of thyroid crisis following, 25:26881
use of serum albumin-incorporated, for measuring dog heart volume variations, 25:26566 (CEA-CONF-1711)
use with xenon-133 for scanning blood circulation in human lungs,, 25:26841

IODINE ISOTOPES I-132
beta decay of, Q value for, (E), 25:28296 (CERN-70-30(Vol.1), pp 341-51)
use for scanning thyroid gland, review on international methods for, 25:26855

IODINE ISOTOPES I-133
isomeric energy level in, spin--parity assignment for, (E), 25:28331 (CERN-70-30(Vol.2), pp 1012-14)

IODINE ISOTOPES I-134
beta decay of, beta and gamma spectra from, (E), 25:28336 (CERN-70-30(Vol.2), pp 1057-68)
energy level at 79.5 keV, lifetime of, (E), 25:28341 (CERN-70-30(Vol.2), pp 1115-18)

IODINE ISOTOPES I-135
beta decay of, gamma spectra, Kurie plots, and Q values for, (E), 25:28296 (CERN-70-30(Vol.1), pp 341-51)
energy-level transitions from tellurium-135 beta decay, multipolarities for, (E), 25:28328 (CERN-70-30(Vol.2), pp 1006-7)

IODINE ISOTOPES I-136
beta decay of isomeric, half-life for, 25:28342 (CERN-70-30(Vol.2), pp 1119-21)

IODINE ISOTOPES I-137
neutron decay of, half-lives and yields from delayed-, (E), 25:28211 (CERN-70-30(Vol.1), pp 517-18)

IODINE ISOTOPES I-139
beta decay of, half-life for, (E), 25:28326 (CERN-70-30(Vol.2), pp 985-1000)

IODINE ISOTOPES I-140
beta decay of, half-life for, (E), 25:28326 (CERN-70-30(Vol.2), pp 985-1000)

IODINE ISOTOPES I-141
beta decay of, half-life for, (E), 25:28326 (CERN-70-30(Vol.2), pp 985-1000)

ION-ACOUSTIC WAVES
propagation in plasma, detection of, (E/T), 25:27800
propagation in plasma, existence of shock-like solutions of Korteweg--de Vries equation for, 25:27818

ION PAIRS
radioinduced production in dielectric liquids, mean energy for γ, 25:26293

ION SOURCES
beam extraction and shaping systems for plasma, design of, 25:26549(T) (ORNL-tr-2462)
conference on heavy, Washington, D. C., 3/70, 25:27436 (WASH-1159)
description of spark, for heavy ions, 25:28129 (WASH-1159, pp 168-71)
design and performance of PIG-type heavy, for Berkeley 88-inch cyclotron, 25:28120 (UCRL-20406)
design of sputter-type Penning discharge, for metallic ions, 25:28137(P)
development of arc discharge heavy, 25:28124 (WASH-1159, pp 1-10)
development of HIPAC highly-stripped heavy, 25:28128

XUM

(WASH-1159, pp 88-112)
operation and performance of multiply charged heavy, review on, 25:28125 (WASH-1159, pp 13-33)
performance of ELMO mirror machine, for multiply-charged ions, 25:27438 (WASH-1159, pp 141-6)
performance of Univ. of Maryland electron ring injection and containment device, 25:27439 (WASH-1159, pp 147-55)
test bench for multicharged, 25:28113 (LYCEN-7054)
vacuum system for Super Hilac, differentially cryopumped, 25:28121 (UCRL-20620)
IONOSPHERE
auroral-electrojet effects on fast electron absorption and scattering in upper atmosphere, (T), 25:27589
characteristics of northern polar, ESRO-I/AURORAE data on, (E), 25:27552
charged-particle injection into, magnetospheric trapped, (T), 25:27623
conference on intercorrelated satellite observations and solar activity, Noordwijk, Netherlands, 9/69, 25:27531
D region, behavior of quiet-day midlatitude, (E), 25:27522
D region, cosmic-ray layer variations in lower, galactic, (T), 25:27513
D region, coupling processes at low and medium frequencies, (E/T), 25:27505
D region, electron density and irregularities in equatorial daytime, using Langmuir and plasma-noise probes, (E), 25:27520
D region, electron density during Feb. 25, 1969 PCA event, solar flare-associated, (E), 25:27564
D region, electron-density distributions in, from multifrequency A_1-absorption, (E/T), 25:27526
D region, electron-density variations below 100 km at midlatitude, seasonal, (E/T), 25:27512
D region, ion-density profiles from 60 to 70 km in, following onset of Feb. 25, 1969 solar-proton event, (E), 25:27565
E region, absorption of oblique incidence-reflected hf radio waves, in winter, (E), 25:27595
E region, coupling processes at low and medium frequencies, (E/T), 25:27505
E region, electron-density distributions in lower, from multifrequency A_1-absorption, (E/T), 25:27526
E region, electron-density variations below 100 km at midlatitude, seasonal, (E/T), 25:27512
E region, ionization by precipitating electrons at middle latitudes at high solar-zenith angle, (E), 25:27527
E region, ionization redistribution and electron-density variations by neutral winds in, observations of, (E), 25:27516
E region, particle influx in mid-latitude nighttime, at solar minimum, (E), 25:27601
electric field mapping into magnetosphere, (E/T), 25:27545
electrojet in, effect on vhf continuous-wave auroral backscatter, polar, (E/T), 25:27554
electromagnetic-wave propagation in Earth--ionospheric cavity, amplitude-frequency spectra of elf transient, (E/T), 25:27591
electromagnetic-wave propagation in Earth--ionospheric cavity, technique for analysis of transient elf, (E/T), 25:27592
electron density before and after Feb. 25, 1969 solar-proton event, (E), 25:27567
electron density variations above F-layer peak at midlatitudes in northern and southern hemispheres, (E/T), 25:27508
electron flux in, relation to current in satellite-borne retarding-potential probes, integral, (E/T), 25:27682
electron scatter in day-to-day maximum fluxes in polar, (E), 25:27580
electron temperature in auroral, effect of field-aligned currents on auroral, (E/T), 25:27603
electron-density measurements using Faraday rotation and ionosonde data, (E/T), 25:27611
F region, dynamo-current phenomena in, (E/T), 25:27596
F region, effects of partial solar eclipses on ionization of, (T), 25:27587
F region, electron concentration in, origin of storm increases of midlatitude, (T), 25:27510
F region, electron density and behavior of midlatitude, effects of electric fields, neutral air winds, and atmospheric composition changes on, (T), 25:27528
F region, electron density in, effects of low-energy particle flux and spectra steepness on, (E), 25:27582
F region, electron-density irregularities in high-latitude, in situ observations of, (E), 25:27519
F region, maps of horizontal wind-produced vertical drifts in midlatitude, (T), 25:27588
F region, polarization fields in equatorial sunrise and sunset, neutral-air wind-produced, (E/T), 25:27586
F region, SAR arcs in, observations from Adelaide, Sept. 1967 to Oct. 1969, (E), 25:27525
F region, uv equatorial nightglow in, relation to oxygen ion--ion neutralization reaction, (E/T), 25:27608
F2 layer, electron concentration at midlatitude, storm-time variation phenomena of, (E/T), 25:27509
F2 layer, electron density in midlatitude, effects of electric fields and ion drag in, (T), 25:27529
F2 layer, evening anomaly of midlatitude, global neutral-wind-associated, (E/T), 25:27515
F2 layer, perturbation characteristics over Waltair, phase-path technique for analysis of traveling, (E/T), 25:27530
irregularities in, use of spaced aerials for comparison of horizontal drift and anisotropy parameters of, (E/T), 25:27517
model for, to study scintillation and diffraction phenomena of cosmic radio sources, (T), 25:27612
nitrogen-oxide density in lower, theoretical model of diurnal variation of, (T), 25:27614
observations of noontime aurorae, airborne ionospheric and optical measurements of, (E), 25:27597
oxygen emissions of 5577 and 6300 A in auroral, intensity ratio in quiet arc at 120 to 330 km, (E), 25:27600
particle measurements during Feb. 23 to Mar. 2, 1969 in auroral, low-energy electron and proton, (E), 25:27569
particle motions in, solution of coupled time-dependent continuity equations for, 25:27521
particle observation over polar caps, solar, (E), 25:27540
plasma drift variations in midlatitude northern and southern hemispheric, neutral-air wind-produced longitudinal, (E/T), 25:27507
plasma-drift measurements in, using satellite-produced wakes, (E), 25:27585
polar-cap absorption during Feb. 25, 1969 solar proton event, (E), 25:27553
polar-cap absorption following Feb. 24-25 solar event, energy spectra of 2.3- to 70-MeV protons and α particles during, (E), 25:27563
polar-cap absorption in, characteristics of, (E/T), 25:27548
proton anisotropy in upper, magnetic-field aligned 1- to 6-keV, (E), 25:27604
radio-drift measurements in, simulation of spaced-antenna, (E/T), 25:27596
radio-wave propagation beneath inhomogeneous anisotropic, elf and vlf, (E/T), 25:27506
solar-flare effects on, (E/T), 25:27532
sporadic E, ion velocity due to vertical winds in, divergence of, (E/T), 25:27610
sporadic E, relation of ionization, cold fronts, and microbarometric acitivity in, (E/T), 25:27524
sporadic F, relation to auroral-oxygen emission of 6300 to 6364 A at 300 to 400 km, (E/T), 25:27511
IONS
charge stripping and pickup data for fast heavy, 25:28126 (WASH-1159, pp 34-41)
cross sections and reaction rates for electron-impact ionization of lithiumlike and sodiumlike, (T), 25:27443
density and velocity flow in expanding exosphere, comparison of hydrodynamic and kinetic models of, (T), 25:27613
electron scattering factors for light, calculation using configuration-interaction and Hartree--Fock wave functions, 25:27460
motion of coupled ionospheric, equation of, 25:27521
production by relativistic electron beams, (E), 25:27694 (WASH-1159, pp 184-9)
production of highly charged, review of methods and mechanisms of, 25:27437 (WASH-1159, pp 113-19)
proton reactions above 10 keV with negative, charge exchange in, (T), 25:27456
reactions between negative and positive, charge exchange and excitation in, (T), 25:27455
reactions with atoms of negative, electronic resonance states in, (T), 25:27462
reactions with atoms, merging-beams method for study of, 25:27448 (IAE-2001)
reactions with intermediate nuclei at 210 MeV, cross sections for delayed protons from heavy, (E/T), 25:28300 (CERN-70-30(Vol.1), pp 457-86)
velocity in ionospheric sporadic-E region due to vertical winds, divergence of, (E/T), 25:27610
IRIDIUM
nitrogen-14 reactions with, cross-section limit for fission isomer excitation in, (E), 25:28399
IRIDIUM ALLOYS AND SYSTEMS
C--Ir--Mo-base, weldability of, 25:27185
Hf--Ir, superconductivity of intermetallic Hf_2Ir, (E), 25:27654
Ir--Mo, superconductivity of intermetallic Mo_3Ir, (E), 25:27654
Ir--Ti, superconductivity of intermetallic Ti_3Ir, (E), 25:27654
Ir--Zr, superconductivity of intermetallic, (E), 25:27654
IRIDIUM ISOTOPES Ir-179
beta decay of, half-life for, (E), 25:28348 (JINR-P6-5617)
IRIDIUM ISOTOPES Ir-180
beta decay of, half-life for, (E), 25:28348 (JINR-P6-5617)
IRIDIUM ISOTOPES Ir-181
beta decay of, half-life for, (E), 25:28348 (JINR-P6-5617)
IRIDIUM ISOTOPES Ir-182
beta and electron-capture decay of, half-life and gamma energies and intensities from, (E), 25:28348 (JINR-P6-5617)

IRIDIUM ISOTOPES Ir-183
electron-capture decay of, half-life and gamma energies and intensities from, (E), 25:28348 (JINR-P6-5617)
IRIDIUM ISOTOPES Ir-185
half-lives of isomeric, (E), 25:28335 (CERN-70-30(Vol.2), pp 1045-55)
IRIDIUM ISOTOPES Ir-186
half-lives of isomeric, (E), 25:28335 (CERN-70-30(Vol.2), pp 1045-55)
IRIDIUM ISOTOPES Ir-187
half-lives of isomeric, (E), 25:28335 (CERN-70-30(Vol.2), pp 1045-55)
IRIDIUM ISOTOPES Ir-188
beta decay of, Fermi plots and log-ft values from, (E), 25:28392
IRIDIUM ISOTOPES Ir-189
electron-capture decay of, gamma energies and intensities from, (E), 25:28389
energy levels from platinum-189 electron-capture decay, lifetimes and spin--parity assignments for, (E), 25:28324 (CERN-70-30(Vol.2), pp 957-65)
half-lives of isomeric, (E), 25:28335 (CERN-70-30(Vol.2), pp 1045-55)
nuclear deformation of, (E), 25:28324 (CERN-70-30(Vol.2), pp 957-65)
IRIDIUM ISOTOPES Ir-191
energy levels from platinum-191 electron-capture decay and osmium-191 beta decay, lifetimes and spin--parity assignments for, (E), 25:28324 (CERN-70-30(Vol.2), pp 957-65)
half-lives of isomeric, (E), 25:28335 (CERN-70-30(Vol.2), pp 1045-55)
nuclear deformation of, (E), 25:28324 (CERN-70-30(Vol.2), pp 957-65)
IRIDIUM ISOTOPES Ir-193
energy levels from osmium 193 beta decay, lifetimes and spin--parity assignments for, (E), 25:28324 (CERN-70-30(Vol.2), pp 957-65)
nuclear deformation of, (E), 25:28324 (CERN-70-30(Vol.2), pp 957-65)
IRIDIUM ISOTOPES Ir-194
beta decay of isomeric, lifetimes of high-spin energy levels of platinum-194 from, (E), 25:28353 (NP-18695)
IRIDIUM ISOTOPES Ir-196
beta decay of isomeric, lifetimes of high-spin energy levels of platinum-196 from, (E), 25:28353 (NP-18695)
IRON
cadmium-111 hyperfine field in, differential perturbed angular correlation measurements of, 25:27917
complexes with 5,7-diiodo-8-quinolinol, formation constants of, 25:26214
complexes with ascorbic acid, evaluation of metastable technetium-99-labeled, for kidney scanning, 25:26848
complexes with lecithins in aqueous butanol solutions, properties of, 25:26272
cross section data on, tables of multigroup, 25:28657 (HEDL-TME-71-36)
determination by photometry using carboxy derivatives of 2,6,7-trihydroxy-9-phenyl-3H-xanthen-3-one, 25:26174
determination in granite by autoradiography and neutron activation, 25:26194
determination in marine silts by neutron activation and γ spectroscopy, 25:26190(R) (NYO-4150-9)
determination in plutonium nitrate solutions by atomic absorption spectrophotometry, 25:26154(T) (RFP-Trans-76)
determination in plutonium oxide--uranium oxide pellets by spectrophotometry, 25:26153 (LA-4622)
determination in yttrium oxides by solvent extraction and spectrography, 25:26168
determination in Zircaloy, chemical method for, 25:26171
effects of divalent, on fluorescence of uranyl compounds in presence of poly(vinylsulfonate), 25:26267
effects of trivalent, on reduction of tetravalent plutonium by hydroxylamine nitrate, 25:26206 (ARH-1920)
effects on spectrophotometric determination of beryllium and gallium, 25:26172
gamma absorption coefficient of, (E), 25:27826 (DEMO-70/11)
neutron elastic scattering at 3.2 MeV using polarized beam, optical-model analysis of, (T), 25:28248
phase transformation under pressure, molecular dynamical studies of, 25:28895 (TID-25683)
plasma of, production by laser-beam irradiation of, (E), 25:27723 (WASH-1159, pp 162-7)
production of, use of process heat reactors in, 25:28791
radiation effects on frature of, neutron, 25:27270
reactions of divalent, with hydrogen peroxide in presence of 2-propanol, yields of hydroxyl radicals from, 25:26290(R) (NYO-3753-19)
sorptive properties and surface film reactions with oxygen, 25:27224
spectral lines of, in sunspots, (E), 25:27365
IRON ALLOYS AND SYSTEMS
mechanical properties at 400 to 800°C, 25:27203 (INIS-mf-2)
Be--Fe-base, structure in aging, model for tri-axial periodic modulated, 25:27249
C--Fe--Mo-base, weldability of, 25:27185
Ce--Co--Cu--Fe--Sm, magnetic properties of, 25:27883
Cr--Fe--Mo, fatigue strength of, effects of fine precipitates on, 25:27231
Cu-base--Fe, Kondo effect in, study by superconducting proximity effect, (E), 25:27662
EuO-base--Fe, magnetic and optical properties of doped films of, 25:27897
EuO-base--Fe, magnetic properties of doped films of, effects of annealing on, 25:27898
EuO-base--Fe, preparation and structure of doped films of, 25:27894
Fe--Ga, Moessbauer spectra of solid solutions of, 25:28843 (CALT-822-27)
Fe--Ga, Moessbauer study of BiF_3 type ordering in metastable, 25:28842 (CALT-822-26)
Fe--Ge, Hall coefficient and electric conductivity of liquid, 25:27212
Fe--Hf, mechanical properties of Laves phase $HfFe_2$, 25:27211 (UCRL-20301)
Fe--Nb, mechanical properties of Laves phase $NbFe_2$, 25:27211 (UCRL-20301)
Fe--Ni, electron correlation effects in Invar, 25:27868
Fe--Ni--Ti, fatigue strength of, effects of fine precipitates on, 25:27231
Fe--Pt, ordering in intermetallic FePt and $FePt_3$, field ion microscopy studies of, 25:27252
Fe--Ta, mechanical properties of Laves phase $TaFe_2$, 25:27211 (UCRL-20301)
Fe--Ti, mechanical properties of Laves phase $TiFe_2$, 25:27211 (UCRL-20301)
Fe--Zr, mechanical properties of Laves phase $ZrFe_2$, 25:27211 (UCRL-20301)
Fe--Zr, superconductivity of intermetallic Zr_3Fe, (E), 25:27654
IRON IONS
spectral lines due to Fe XXV in solar flares, (E), 25:27386
IRON ISOTOPES Fe-54
alpha reactions (α,pγ) at 9 and 10 MeV, p-γ angular correlations from, (E), 25:28281
effects on ir spectra of iron oxinates, 25:26234
IRON ISOTOPES Fe-55
content of oysters in estuary of North Sea in relation to distance from nuclear power plant, 25:26742
energy-level transitions from proton reactions, branching ratios, gamma-ray angular distributions, and internal conversion coefficients for, (E/T), 25:28271
IRON ISOTOPES Fe-56
alpha reactions (α,n) at 11.5 to 22.7 MeV, neutron spectra from, (E), 25:28285
detection in solar wind, (T), 25:27328
energy levels from neutron reactions (n,n) with iron-56, 25:28218 (NP-18674)
helium-3 reactions (He-3,t) at 25 MeV, analysis for isospin mixing in cross sections for, (E), 25:28232
neutron reactions (n,γ), (n,2n), and (n,np), cross sections for, (T), 25:28218 (NP-18674)
neutron reactions (n,n) and (n,p), cross sections and energy levels of iron-56 and manganese-56 from, (T), 25:28218 (NP-18674)
photon reactions (γ,n) near threshold energy, cross section and resonance parameters for, (E), 25:28413
proton elastic scattering at 6.9 MeV, optical-model analysis of cross-section and polarization angular distributions from, (E), 25:28263
proton elastic scattering at 6.9 MeV, optical-model analysis of angular distributions from, (E), 25:28262
IRON ISOTOPES Fe-57
effects on ir spectra of iron oxinates, 25:26234
nuclear isomer shift in, (E), 25:28247
photon reactions (γ,n) near threshold energy, cross section and resonance parameters for, (E), 25:28413
IRON ISOTOPES Fe-58
proton elastic scattering at 6.9 MeV, optical-model analysis of angular distributions from, (E), 25:28262
IRON ISOTOPES Fe-59
radiation effects on uptake and distribution of, in bone marrow and spleen of mice, effects of immune reactions on x, 25:27012
use as tracer for hemoglobin studies in sheep, 25:26578 (CONF-680112-, pp 153-66)
IRON ORES
well logging in deposits of, equipment and method for gamma--gamma, 25:26352(T) (CONF-630513-1)
IRON OXIDES Fe_2O_3
B_2O_3--Fe_2O_3--Li_2O--Na_2O, magnetic ordering and electric conduction in glasses of, 25:27901
B_2O_3--Fe_2O_3--Na_2O, magnetic ordering and electric conduction in glasses of, 25:27901
IRON SULFATES
radiolysis of aqueous solutions of, by protons at 30 to 400 keV, LET parameters in, 25:26288(T) (LB/G-2937)
IRRADIATION FACILITIES
design for continuous irradiation of chemically treated materials, 25:26417(P)
design of 15,000-Curie cobalt-60, for studies on diluents and solvents used in fuel reprocessing, 25:26330(T) (ORNL-tr-2410, pp 14-78)
ISOTOPE EFFECTS
kinetics of solvent, effects of translational entropy of activation on, 25:26227

XUM

J

JAPAN
nuclear power plant development in, technical and economic aspects of, 25:28584
nuclear power plants in, technical and economic aspects of ocean siting of, 25:28643
power requirements for 1965 to 1985, 25:28582
radiation dose from hot spring waters at Misasa Spa area, 25:26743
radiation monitoring in, April 1969 to April 1970, 25:26392 (NIRS-RSD-27)
JAPANESE MATERIALS TESTING REACTOR
coolant for, decomposition rate of water, 25:28758 (JAERI-1204)
JAPANESE POWER DEMONSTRATION REACTOR
pressure vessel for, evaluation of fast neutron embrittlement of steel, 25:28682 (JAERI-1202)
JAPANESE POWER DEMONSTRATION REACTOR II
fuel rod assembly for, irradiation testing of, 25:28692 (JAERI-Memo-4248)
JOSE CABRERA POWER REACTOR
control system for, diagrams of electronic circuits in, 25:28535
cost analysis for, 25:28578
design parameters of, 25:28578
operations history for April 1969 to April 1970, 25:28578
JOSEPH M. FARLEY POWER REACTOR, UNIT 1
design parameters of, revised and additional data on, 25:28618 (DOCKET-50348-19)
operations aspects of, revised and additional data on, 25:28618 (DOCKET-50348-19)
JOSEPH M. FARLEY POWER REACTOR, UNIT 2
design parameters of, revised and additional data on, 25:28618 (DOCKET-50348-19)
operations aspects of, revised and additional data on, 25:28618 (DOCKET-50348-19)
JUPITER (PLANET)
airglow spectra in upper atmosphere of, 300- to 1300-A extreme-uv, (E/T), 25:27432
ionospheric interaction with Io, (T), 25:27435

K

KARACHI POWER REACTOR
radioactive waste disposal system for, 25:28626
site for, environmental radiation monitoring program for, 25:28626
KIDNEYS
blood plasma flow in, effectiveness of iodine-131-labeled hippuran in combination with gamma radiation for measuring, 25:26826
function studies, use of tracer techniques in, 25:26567 (STI/PUB-263)
lead-210 distribution in, of baboons and rats, 25:26610
molybdenum-99 distribution and retention in rat, following subcutaneous injection, 25:26598
plasma flow through, development of catheterless method using iodine-131 whole-body clearance for measurement of, 25:26825
radiation effects on biochemistry of, in dogs, effects of AET on x, 25:26935
radiation effects on metabolism of DNAses and phosphatases in rat, in comparison to TEM, whole-body x, 25:26645
radiation effects on rat, in relation to physiological mechanisms for development of renal hypertension, x, 25:26652
radiation protection methods for human, during cobalt-60 γ therapy, 25:26779
radiodiagnosis of hydatidosis of, in man using combined radiography and scintigraphy, 25:26816
radiotherapy of Wilms' tumor in, of children, development of liver injuries following, 25:26884
scanning of human, effectiveness of mercury-197-labeled neohydrin for, in comparison to other diagnostic methods, 25:26821
scanning using iodine-131, international methods for, 25:26855
scanning using metastable technetium-99-labeled ascorbic acid--iron complexes, 25:26848
KRYPTON
determination in gaseous effluents from dissolution of aluminum--plutonium fuels, method for, 25:26331(T) (ORNL-tr-2410, pp 79-97)
electron correlation and density in, calculations using restricted Hartree--Fock approximation, 25:27467
properties and uses of fission-product, 25:26347
scattering by helium atoms, total cross sections for elastic, (T), 25:27444
separation from xenon, 25:26347
KRYPTON IONS
bubble formation and diffusion in copper foils bombarded by 50-keV, 25:27842 (RD/B/N-1850)
KRYPTON ISOTOPES
abundance in lunar surface materials, (E), 25:27308
KRYPTON ISOTOPES Kr-74
energy levels from oxygen reactions with nickel, spin-parity assignments for, (E), 25:28213 (CERN-70-30(Vol.2), pp 911-15)
KRYPTON ISOTOPES Kr-76
energy levels from oxygen reactions with nickel, spin-parity assignments for, (E), 25:28213 (CERN-70-30(Vol.2), pp 911-15)
KRYPTON ISOTOPES Kr-78
energy levels from oxygen reactions with nickel, spin-parity assignments for, (E), 25:28213 (CERN-70-30(Vol.2), pp 911-15)
KRYPTON ISOTOPES Kr-83
production of metastable, rubidium-83 generator for, 25:26320
KRYPTON ISOTOPES Kr-85
activity measurements in atmosphere, scintillation detector for, 25:26488
content in West Valley Processing Plant stack effluents, Oct. 1969 to Jan. 1970, 25:26355(R) (SRO-344-11)
yields from thermal fission of uranium-233 and -235 and plutonium-239 and -241, (E), 25:28383
KRYPTON ISOTOPES Kr-86
proton elastic and inelastic scattering at 4.8 to 10.1 MeV with isobaric analog excitation, excitation functions for, (E), 25:28242

L

LA CROSSE BOILING-WATER REACTOR
operations incident of April 14, 1971, unscheduled shutdown from procedural error during power and flow safety system test, 25:28555 (DOCKET-1155-112)
LACTATE DEHYDROGENASE
radiation effects on activity of, and isoenzymes of, in rat tissues, protective effects of injected methylene blue against γ, 25:26803
LANTHANUM
determination by photometry using 1,10-phenanthroline and salicylfluorone, 25:26161
determination by photometry using carboxy derivatives of 2,6,7-trihydroxy-9-phenyl-3H-xanthen-3-one, 25:26174
determination in marine silts by neutron activation and γ spectroscopy, 25:26190(R) (NYO-4150-9)
determination in yttrium oxides by solvent extraction and spectrography, 25:26168
LANTHANUM ALLOYS AND SYSTEMS
Ce--La-base, thermoelectric power at 4.2 to 350°K of Kondo system, 25:27877
Co--La, magnetic coercivity of $LaCo_5$ particles, domain-wall pinning in, 25:27882
In-base--La, lanthanum-139 NMR study of $LaIn_3$ exchange-enhanced susceptibility, 25:27920
La--Sb, thermal capacity of LaSb at 1.5 to 70°K, 25:27881
LANTHANUM ISOTOPES La-138
energy levels of, analysis of nonrandom distributions of neutron resonance, (T), 25:28421
LANTHANUM ISOTOPES La-139
nuclear magnetic resonance in $LaIn_3$ at 1.6 to 300°K, 25:27920
photon reactions (γ,p) with isobaric analog excitation, proton spectra from, (E), 25:28362
LANTHANUM ISOTOPES La-140
determination of, 4π β--γ coincidence method for, 25:26464
LANTHANUM ISOTOPES La-141
energy level at 190.3 keV, lifetime of, (E), 25:28341 (CERN-70-30(Vol.2), pp 1115-18)
LANTHANUM OXIDES
reactions with boron, effects of shock waves and temperature on, 25:27291
LARVAE
radiation damage of Tenebrio, repair of x, 25:26914
radiation effects on epithelium of, effects of dose on gamma, 25:26916
radiation effects on survival of larval and pupae of alfalfa Hypera weevil, effects of dose on γ, 25:26913
LARYNX
radiation protection methods for human, during cobalt-60 γ therapy, 25:26779
LASER RADIATION
effects on retina of eyes of Rhesus monkeys, damaging, 25:26940
interactions with plasma, use for stabilizing lf waves in, (T), 25:27758
reactions with metal targets, plasma production in, (E), 25:27723 (WASH-1159, pp 162-7)
reactions with solid targets, plasma production in, (E), 25:27724
scattering on plasma in Tokamak devices, poloidal magnetic field measurement from, (T), 25:27795
LASERS
book: Statistical Physics, Phase Transitions, and Superfluidity, 25:27912
coherence phenomena in classical and quantum physics, 25:27947
design for illumination of HPD for measurement of bubble chamber particle tracks, 25:26509 (RHEL/R-212)
radiation effects on current flow of epitaxial gallium arsenide diodes, 76 and 300°K neutron, 25:26563
use of pulsed, in holographic method for measuring

distribution and size of aerosol particles, 25:26373 (CONF-700601-, pp 213-16)
LEAD
carbon-12 reactions with, cross-section limit for fission isomer excitation in, 25:28399
complexes with lecithins in aqueous butanol solutions, properties of, 25:26272
determination in powdered milk by photon activation, 25:26203
determination in yttrium oxides by solvent extraction and spectrography, 25:26168
gamma absorption coefficient of, (E), 25:27826 (DEMO-70/11)
gamma elastic scattering at 9 MeV, cross section for, (E), 25:28358
meson (π) reactions at 1 GeV/c, differential and total cross sections for, (E), 25:27959
meson (π⁻) capture with charged particle emission, particle spectra and branching ratios for, (E), 25:28178
neutron reactions with, pulsed, (E), 25:28161
photon reactions at 84, 145, and 279 keV with, L-shell photoelectric cross sections for, (E), 25:27830
photon scattering at 661.6 keV by bound electrons in, differential cross sections for, (E/T), 25:27461
proton reactions at 1 GeV/c, differential and total cross sections for, (E), 25:27959
superconducting proximity effect of, study of Kondo effect using, (E), 25:27662
superconductivity recovery in thin films, 25:27652
uptake by erythrocytes, mechanisms for membrane penetration during, 25:26609
LEAD CHLORIDES
reactions with barium oxide, Jost mechanisms in solid-state, 25:26210 (KFK-1312)
LEAD ISOTOPES Pb-204
neutron inelastic scattering by, cross sections for fast, (E), 25:28273
neutron reactions (n,2n) with, cross sections for fast, (E), 25:28273
LEAD ISOTOPES Pb-206
photon reactions (γ,n) near threshold energy, cross section and resonance parameters for, (E), 25:28413
LEAD ISOTOPES Pb-207
alpha reactions (α,t) at 30 MeV, triton spectra from, (E), 25:28417
energy levels and properties of, nuclear data sheets for, 25:28378
energy-level transitions in, conversion coefficients for, (E), 25:28410
helium-3 reactions (He-3,d) at 30 MeV, deuteron spectra from, (E), 25:28417
photon reactions (γ,n) near threshold energy, cross section and resonance parameters for, (E), 25:28413
proton inelastic scattering at 14 to 18 MeV with isobaric analog excitation, excitation functions for, (E), 25:28365
LEAD ISOTOPES Pb-208
energy levels and properties of, nuclear data tables for, 25:28375
energy levels from analog resonances and coulomb stripping, comparison of spectroscopic factors for, 25:28366
energy levels of, calculation using renormalized RPA, (T), 25:28509
photon reactions (γ,n) near threshold energy, cross section and resonance parameters for, (E), 25:28413
proton scattering at 19.3 GeV/c, multiple diffractive model for, 25:28073
LEAD ISOTOPES Pb-209
energy levels and properties of, nuclear data sheets for, 25:28376
LEAD ISOTOPES Pb-210
distribution and retention in baboons and rats following intravenous injection, half-life values for, 25:26610
distribution in atmosphere, estimation of large-scale precipitation scavenging using vertical, 25:26390 (CONF-700601-, pp 465-74)
LEAD ISOTOPES Pb-211
energy levels and properties of, nuclear data sheets for, 25:28377
LEAD OXIDES
PbO--TiO_2--ZrO_2, phase studies above 900°C, use of heating curves in, 25:27295
LEAVES
radiation effects on cell size of dill, lettuce, and spinach, x, 25:27091
radioinduced mutations for morphological changes in potato, 1000 to 120,000-R x, 25:26737
LECITHINS
complexes with calcium, iron, mercury, lead, or uranyl ions in aqueous butanol solutions, properties of, 25:26272
reactions of monolayers of saturated and unsaturated, with osmium tetroxide, potassium permanganate, and uranyl acetate, effects of variables on, 25:26213
LEPTONS
interactions with hadrons at high energies, review on, 25:28005
interactions with nucleons, parton and dual model for deep inelastic, 25:28001
production and decay modes of heavy, from $e^+ + e^-$ interactions, limits on, 25:27998
LEUCINE
uptake of carbon-14-labeled, by lens protein, effects of naphthalene and x radiation on, 25:26649
LEUKOCYTES
count in peripheral blood of x-irradiated rats and parabiotic partners, 25:26939
radiation effects on count of, in blood of mice following injection of Escherichia coli endotoxin, whole-body x, 25:26986
radiation effects on proliferation of mononuclear, in tuberculous lesions of rabbits, tritium tracer study, 25:27001
radiation effects on protease activity in rabbit, whole-body x, 25:27035
radiation effects on rat, effects of dietary selenium on whole-body gamma, 25:27032
radiation effects on, of dogs, plutonium-238 and plutonium-239 dioxide α and γ, 25:26929
radioinduced changes in preparations of, from whole-body x-irradiated rabbits and rats, 25:26901
radioinduced chromosome aberrations in human, effects of dose and dose rate on iodine-131 β, γ, x, 25:26730
radioinduced chromosome and chromatid aberrations in human, comparison of tritium and γ, 25:26636
radiosensitivity of human, effects of age on x, 25:26628
LIGHT
effects on behavior of sea anemones, 25:26912
effects on chromosomes of kidney cells of swine, aberrant far-red, 25:26727
effects on recovery of early potentials of eyes in frogs, comparison of x radiation and, 25:27004
effects on uv-inactivated ribonucleic acid isolated from tobacco mosaic virus, photoreactivating, 25:26653
propagation in mixmaster universes, (T), 25:27428
scattering on plasma, diagnostic use of, (E/T), 25:27680
LIMESTONE
gamma absorption coefficient of marble, (E), 25:27826 (DEMO-70/11)
LINEAR ACCELERATORS
beam injection in 2-GeV electron, using step-like varying wave phase velocity, 25:28112 (KHFTI-70-17)
beam optics for electron, for x-ray therapy, 25:28142
description of LRL 100-MeV electron, 25:28123 (UCRL-73075)
ion source for Super Hilac, vacuum cryopumping for, 25:28121 (UCRL-20620)
operation and performance of 6-MeV electron, for radiotherapy, 25:28132
operation of Super Hilac, for simultaneous acceleration of heavy and light ions, 25:28122 (UCRL-20633)
power supply for preinjector for 25-MeV proton, stabilization circuit for, 25:28108 (ITEF-761)
LINGEN POWER REACTOR
maintenance of, review of first loading, 25:28585
operations of, review of first loading, 25:28585
LIPOPROTEINS
complexes with catalase, γ-radiosensitivity of, 25:26650
LIQUID FLOW
magnetohydrodynamic rotation of conducting, in cylindrical vessel, (T), 25:27500
magnetohydrodynamic, motion of alternate layers of conducting liquid and nonconducting gas in transverse magnetic field in, (T), 25:27494
measurements using radioisotopes, review of methods for, 25:26435
transient analysis in fast reactor cores, SAS1A code for, 25:28727 (ANL-7607)
LIQUID METAL FAST BREEDER REACTOR
accidents in 1000 MW(e), analysis of reactivity insertion, 25:28735 (BAW-1360)
accidents in 1000 MW(e), methods and models for analysis of, 25:28729 (BAW-1342)
containment for 1000 MW(e), candidate safety features for primary, 25:28733 (BAW-1352)
containment for 1000 MW(e), candidate support systems for secondary, 25:28730 (BAW-1349)
coolant combustion accidents in, release and transport of aerosols and energy from sodium, (E/T), 25:28726(R) (AI-AEC-12986)
coolant flow in 1000 MW(e), accident initiating malfunctions affecting, 25:28731 (BAW-1350)
core components for 1000 MW(e), radiation effects on deformation and expansion of, 25:28685 (BAW-1355)
core meltdown in 1000 MW(e), candidate emergency decay heat removal systems for, 25:28732 (BAW-1351)
engineered safeguards for 1000 MW(e), methods and models for design of, 25:28729 (BAW-1342)
fuel elements for, development of stainless steel clad plutonium oxide (PuO_2)--uranium oxide (UO_2), 25:28691(R) (GEAP-10028-37)
fuel elements for, slug-flow heat transfer to displaced, (T), 25:28661
fuel reprocessing for, evaluation of methods for core dissolution after shearing in, 25:26327 (ORNL-TM-3194)
fuels for, creep testing of ceramic, 25:28689 (BMI-1898, Sect.C)
fuels for, development during October through December 1970, 25:28686(R) (BMI-1898)
fuels for, development of plutonium nitride--uranium nitride, (E), 25:28687 (BMI-1898, Sect.A)

XUM

fuels for, high temperature irradiation performance of, (E/T), 25:28688 (BMI-1898, Sect.B)
kinetics of, effects of sodium coolant boiling on, (E/T), 25:28726(R) (AI-AEC-12986)
protective system for 1000 MW(e), candidate design and performance requirements for, 25:28734 (BAW-1354)
protective systems for 1000 MW(e), methods and models for design of, 25:28729 (BAW-1342)
safety programs during October to December 1970, 25:28726(R) (AI-AEC-12986)
transients in, SAS1A code for analysis of power and coolant flow, 25:28727 (ANL-7607)
LIQUIDS
conductivity in dielectric, conference on, 25:26470
radioinduced ion pairs in dielectric, measurement of mean energy for γ, 25:26293
radioinduced ionization currents in dielectric, analysis of, 25:26472
LITHIUM
determination by prompt neutron activation using an americium--beryllium source, 25:26196
determination of trace amounts of, in hydrofluoric acid and spectrophotometry, 25:26176
meson (π^-) capture with charged particle emission, particle spectra and branching ratios for, (E), 25:28178
LITHIUM FLUORIDES
luminescence and thermoluminescence efficiency of crystals of, effects of magnesium and calcium on, (E), 25:27838(T) (ANL-Trans-874)
LITHIUM ISOTOPES Li-6
alpha decay of, vertex function for virtual, (T), 25:28185
cross section data on, tables of multigroup, 25:28657 (HEDL-TME-71-36)
effects on diffusion in liquid lithium-7, NMR studies on, 25:26238
effects on diffusion in molten lithium, NMR studies on, 25:26239
effects on diffusion of impurities of gold-195 and sodium-22 in solid matrix,, 25:26240
effects on diffusion of liquid lithium under argon pressure in presence of iron, 25:26242
effects on paraelectric resonance spectra of lithium-doped potassium chlorides, 25:26215 (NYO-2150-59)
electron inelastic scattering by, analysis using nucleon--nucleon correlations, (T), 25:28201
energy levels of calculation of transition probabilities using nucleon--nucleon correlations, (T), 25:28201
oxygen-16 elastic scattering at 36 to 48 MeV, angular distributions for, (E), 25:28196
production by carbon-12 (p,x) and (α,x) reactions, cross sections for, (E), 25:28182
reactions with nuclei, three-body model for, (T), 25:28486
scattering by nuclei, three-body model for elastic, (T), 25:28486
LITHIUM ISOTOPES Li-7
effects on diffusion in liquid lithium-6, NMR studies on, 25:26238
effects on diffusion in molten lithium, NMR studies on, 25:26239
effects on diffusion of impurities of gold-195 and sodium-22 in solid matrix,, 25:26240
effects on diffusion of liquid lithium under argon pressure in presence of iron, 25:26242
oxygen-16 elastic scattering at 36 to 48 MeV, angular distributions for, (E), 25:28196
production by carbon-12 (p,x) and (α,x) reactions, cross sections for, (E), 25:28182
proton reactions (p,α) with, multi-level R-matrix analysis of, (T), 25:28452 (NP-18717)
LITHIUM ISOTOPES Li-8
energy level at 981 keV from deuterium (Li-7,p) reactions, lifetime of, (E), 25:28203
LITHIUM ISOTOPES Li-9
mass of, (E), 25:28175
LITHIUM NITRATES
complexes with tetravalent plutonium in aqueous methanol solutions, spectrophotometric studies on, 25:26274
LITHIUM OXIDES
B_2O_3--Fe_2O_3--Li_2O--Na_2O, magnetic ordering and electric conduction in glasses of, 25:27901
LIVER
blood flow in, of cats, xenon-133 clearance studies on, 25:26576
function studies, use of tracer techniques in, 25:26567 (STI/PUB-263)
lead-210 distribution in, of baboons and rats, 25:26610
molybdenum-99 distribution and retention in rat, following subcutaneous injection, 25:26598
radiation effects on activity of lysosomal enzymes and content of glycoproteins in, of rats, single and combined effects of turpentine and x, 25:26979
radiation effects on albumin metabolism and proteolytic activity in, of rats, combined effects of starvation and x, 25:26984
radiation effects on biochemistry of, in dogs, effects of AET on x, 25:26935
radiation effects on esterase activity in extract of rat, effects of pH on whole-body x, 25:26600
radiation effects on protein synthesis by microsomal fractions in, of rats, subsequent whole-body γ, 25:27006
radiation effects on regeneration of, in partially hepatectomized rats in comparison to effects of liver extracts, x, 25:26948
radiation effects on RNA synthesis in rat, hybridization method for determining dose effect on, 25:26641
radiation effects on, of rabbits, effects of bone marrow transplants on recovery following combined injury and, 25:27005
radiation effects on, of rats following exposure in utero, tritium β, 25:26925
radioinduced injuries of dog, pathogenesis and recovery from γ, 25:26955
radioinduced injuries of dog, use of radiography for evaluation of γ, 25:26955
radioinduced injury to, following therapy of Wilms' tumor in right kidney of human children, 25:26884
scanning for determination of extent of gamma radioinduced injuries of dog, use of iodine-131-labeled Rose Bengal and gold-198 colloids for, 25:26955
scanning for diagnosis and evaluation of drug therapy of amebic abscess in human, use of gold-198 colloids for, 25:26843
scanning for diagnosis of hyperlipemia using technetium-99m, 25:26830
scanning of human, effectiveness of gold-198 colloids or iodine-131-labeled rose bengal for diagnosis of abscesses by, 25:26860
scanning of human, effectiveness of gold-198 colloids or iodine-131-labeled rose bengal for diagnosis of cirrhosis by, 25:26861
scanning using gold isotopes for function studies of human, scoring system for, 25:26862
thorium-228 accumulation in human, 25:26603
LUBRICATION
book: Theory and Practice of Lubrication Systems, 25:26416
LUNAR MATERIALS
ages for Apollo 11 and 12, cosmic-ray exposure, (E), 25:27308
analysis of fines from Apollo 11 for fluorine by γ activation and radiochemical separation, 25:26193
rare-gas abundances in Apollo 11 and 12, (E), 25:27308
uranium content of, analysis of solar wind foils for estimation of, 25:26187(R) (BNWL-1183-7)
LUNGS
function studies, use of tracer techniques in, 25:26567 (STI/PUB-263)
plutonium-239 uptake by, of dogs following inhalation of labeled plutonium oxide, 25:26599
radiation effects on human, following cigarette smoking, thorium-232 alpha and gamma, 25:27046
radioinduced cancer in human, following occupational exposure, gamma, 25:27045
radioinduced carcinomas in, of rats following implantation of strontium-90, 25:26921(T) (LF-tr-49)
scanning blood perfusion and ventilation in, using iodine-131 and xenon-133 with dual scintillation counters, 25:26841
scanning for measurement of blood circulation and ventilation time in, of man, use of iodine-131 or indium-113m with xenon-133 for simultaneous, 25:26819
scanning for tumor localization in, use of glutathione-treated mercury chloride labeled with mercury-203 for, 25:26842
uranium retention in human, following inhalation of soluble compounds, ICRP threshold levels for determining degree of contamination based on natural, 25:26607
LUTETIUM
determination in yttrium oxides by solvent extraction and spectrography, 25:26168
separation from ytterbium, effects of copper ions on electrophoretic focusing ion, 25:26351
LUTETIUM ISOTOPES Lu-168
beta and electron-capture decay of, half-lives for, (E), 25:28321 (CERN-70-30(Vol.2), pp 931-8)
LUTETIUM ISOTOPES Lu-169
beta and electron-capture decay of, branching ratios, log-ft values, and Q values for, (E), 25:28436
beta and electron-capture decay of, branching ratios, gamma spectra, log-ft values, and Q values for, (E), 25:28433
energy levels from hafnium-169 beta and electron-capture decay, spin--parity assignments for, (E), 25:28321 (CERN-70-30(Vol.2), pp 931-8)
LUTETIUM ISOTOPES Lu-172
energy-level transitions in, multipolarities for, 25:28410
LUTETIUM ISOTOPES Lu-175
energy levels from lutetium-176 (d,t) reactions, (E), 25:28424
LUTETIUM ISOTOPES Lu-176
deuteron reactions (d,p) and (d,t) at 12 MeV, particle spectra from, 25:28424
neutron capture by, γ spectra from thermal, (E), 25:28424
LUTETIUM ISOTOPES Lu-177
energy levels from lutetium-176 (d,p) and (n,γ) reactions, (E), 25:28424

LYASES
radiation effects on activity of onion, γ, 25:26620
LYMPH NODES
plutonium-239 uptake by, of dogs following inhalation of labeled plutonium oxide, 25:26599
radiation effects on melanoma cells in human, following endolymphatic administration of iodine-131-labeled ethiodol, β, 25:26888
radiation effects on regeneration in mouse cervical, effects of thymus shielding on x, 25:26996
radiation effects on, in man following uterine cervix cancer therapy, 25:26886
radiation effects on, of dogs, plutonium-238 and plutonium-239 dioxide α and γ, 25:26929
scanning of human, effectiveness of colloidal radioactive gold for, 25:26851
LYMPHOCYTES
radiation effects on replication of rat spleen, tritium beta, 25:26994
radiation effects on survival of cultured, effects of phytohemagglutinin on x, 25:26903
LYSOZYME
radiation effects on phosphate soluble fraction of, chemical and conformational studies on γ, 25:26646

M

MACHINE TOOLS
control of development of third-order interpolation method for continuous-path numerical, 25:28909 (Y-1782)
MAGNESIUM
abundance in lunar surface materials, (E), 25:27308
complexes with 5,7-diiodo-8-quinolinol, formation constants of, 25:26214
determination by electroconductivity method following chromatographic separation from alkali metals, 25:26173
determination in sea floor samples by neutron activation, 25:26188 (BNWL-SA-3803)
determination in yttrium oxides by solvent extraction and spectrography, 25:26168
effects on luminescence and thermoluminescence efficiency of lithium fluoride crystals, (E), 25:27838(T) (ANL-Trans-874)
effects on x-radioinduced dissociation of yeast ribosomes, 25:26633
electron correlation and density in, calculations using restricted Hartree--Fock approximation, 25:27467
meson (π^-) capture with charged particle emission, particle spectra and branching ratios for, (E), 25:28178
shear constant for, calculation from axial ratios, 25:27240
MAGNESIUM ALLOYS AND SYSTEMS
Al--Cr--Cu--Mg--Zn, analysis for trace amounts of silver by solvent extraction and atomic absorption spectrophotometry, 25:26169
Gd-base--Mg, magnetic periodic ordering of, from electric conductivity and magnetization measurements, 25:27871
MAGNESIUM FLUORIDES
lattice structure of, positron-annihilation study of, (E/T), 25:27865 (CEA-R-4138)
MAGNESIUM HYDRIDES
spectral absorption lines of, in sunspot spectra, (E), 25:27390
spectral absorption lines of, in sunspot spectra, (E/T), 25:27374
MAGNESIUM ISOTOPES Mg-24
alpha reactions (α,d) at 28 MeV, analysis of angular distributions for $\Delta T = 0$ selection rule, (E), 25:28233
alpha reactions (α,p) at 11.3 to 15.8 MeV, spectra and angular distributions for, (E), 25:28208 (ANU-P-521)
energy level from oxygen-16 Coulomb excitation, transition probability and quadrupole moment of first 2^+, (E), 25:28283
energy levels from sodium-23 (p,α) reactions at 590 to 1810 keV, spin-parity assignments and formation parameters for, (E), 25:28259
energy-level transitions from sodium-23(d,n) reactions, M1, $\Delta T = 1$, (E), 25:28225
meson (π^-) inelastic scattering at low energies, (T), 25:28244
neutron inelastic scattering at 14.2 MeV, cross sections and neutron spectra from, (E), 25:28265
photon reactions (γ,n) near threshold energy, cross section and resonance parameters for, (E), 25:28413
proton elastic and inelastic scattering at 5.94 MeV, angular distributions and spectra from, (E), 25:28264
proton reactions (p,γ) at 1201 and 1485 keV, Q value for, (E), 25:28276
MAGNESIUM ISOTOPES Mg-25
photon reactions (γ,n) near threshold energy, cross section and resonance parameters for, (E), 25:28413
proton elastic and inelastic scattering at 5.84 to 6.03 MeV, angular distributions and spectra from, (E), 25:28264
MAGNESIUM ISOTOPES Mg-26
helium-3 reactions ($He-3,\gamma$) at 4.44 to 8.26 MeV, differential cross sections for, (E), 25:28206 (ANU-P-508)
photon reactions (γ,n) near threshold energies, cross section and resonance parameters for, (E), 25:28413
proton elastic scattering at 5.84 to 6.03 MeV, angular distributions from, (E), 25:28264
MAGNESIUM OXIDES
lattice structure of, positron-annihilation study of, (E/T), 25:27865 (CEA-R-4138)
radioinduced Wigner energy storage in, neutron, 25:27839 (CEA-N-1171)
HfO_2-base--MgO, composition and microstructure of, 25:27296
MAGNET COILS
protection of large superconducting, 25:27663(T) (ORNL-tr-2436)
MAGNETIC FIELDS
direction of interplanetary, correlation with propagation path of Feb. 25, 1969 solar-flare particles, (E), 25:27559
effect of activity of, on low energy auroral electron flux at 10 and 80 degree pitch-angle distribution, (E), 25:27577
effects of extremely quiet, on ring-current enhancements, 1932--1969, (E), 25:27518
effects on synthesis of TMV in tobacco leaves, 25:27106
electric-conducting emulsions in, motion of, (E), 25:27501
intensity during solar-particle event of Feb. 25, 1969, Pioneer 8 measurement of interplanetary, 25:27556
intensity during solar-particle event of Feb. 25, 1969, HEOS-I measurement of interplanetary, 25:27555
oscillation modulation of trapped particles in magnetosphere, coupled, (T), 25:27623
variation and structure in interplanetary space, solar-flare-related, (E/T), 25:27536
variations across bow shock and magnetosheath, (E), 25:27539
MAGNETIC MATERIALS
conference on, sixteenth annual, Miami Beach, Nov. 17-20, 1970, 25:27869
MAGNETIC MIRROR MACHINES
plasma cyclotron instabilities in OGRA II, feedback stabilization of, (E), 25:27776
plasma instabilities in, boundary, conditions for convective wave, (E/T), 25:27750
MAGNETIC MIRRORS
charged-particle confinement in, duration equations for, 25:27669 (IAE-1972)
charged-particle injection and trapping in static, (T), 25:27674
electron beam injection into, relativistic, (E), 25:27688 (WASH-1159, pp 193-5)
plasma drift centrifugal waves in, feedback suppression of, (E), 25:27768
plasma injection and confinement in, cesium, (E), 25:27671
plasma production by injection of molecular ions in, 25:27725
plasma stabilization using feedback systems, low-density, (T), 25:27757
MAGNETIC STORMS
current observations during Mar. 18, 1969 substorms from barium cloud releases at 12.4 R/sub E/, electric- and magnetic-field, (E), 25:27620
effects of increases of midlatitude F-layer electron concentration, (T), 25:27510
effects of proton solar event, Feb. 25, 1969, (E), 25:27553
effects of substorms on vhf continuous-wave auroral backscatter, (E/T), 25:27554
effects on plasma sheet and solar wind, May 1, 1967 weak sc, (E), 25:27546
effects on plasmasphere proton density associated with stable auroral red arcs, (E), 25:27622
energy release of polar substorms, determination from photographs of aurorae, (E), 25:27523
morphology of DP 2 fluctuations and polar substorms, (E/T), 25:27606
particle events of Feb. 26, 1969, May 1967, and Jan. 10, 1968, relation to interplanetary shock waves, solar proton, (E/T), 25:27571
particle-density variations in radiation belts during, solar event-associated energetic, (E/T), 25:27543
properties of, at ATS 1, (E), 25:27544
relation of low-latitude DS-current component and auroral-electrojet intensity during intense, (E/T), 25:27619
relation of polar substorms to midnight auroral-zone x-ray events, (E), 25:27593
relation of polar substorms to midnight auroral-zone x-ray events, (E), 25:27594
solar-flare effects on geomagnetic, crochet, (E/T), 25:27532
variation phenomena of electron concentration in F2 layer, (E/T), 25:27509
MAGNETIC TESTING
method for materials, review of, 25:26440
MAGNETISM
conference on, sixteenth annual, Miami Beach, Nov. 17-20, 1970, 25:27869
MAGNETOHYDRODYNAMIC GENERATORS
condensation process for liquid-metal, fundamentals of

XUM

single-stage two-phase, (T), 25:27478
condensation process for, optimization of single-stage two-phase, based on Carnot cycle for liquid-metal, 25:27479
end effects in channels at arbitrary R/sub m/ numbers, boundary-value problems for longitudinal, 25:27483
excitation in gap of linear induction, operating with variable-velocity wave field, 25:27482
magnetic field distributions in cylindrical linear, in open-cycle regime, (E/T), 25:27481
parameters of asynchronous liquid-metal, (T), 25:27484
plasma cluster motion in channel with variable inductance, (T), 25:27485
MAGNETOPAUSE
model of polar cusp relationship with plasma sheet, (T), 25:27607
position variations in, geomagnetic-field variations due to solar wind-induced, (E), 25:27537
proton interaction with, intercomparison of interplanetary space, magnetosheath, and magnetotail energetic solar, (E), 25:27538
MAGNETOSHEATH
interaction of protons in, with bow shock and magnetopause, (E), 25:27538
model of polar cusp relationship with plasma sheet, (T), 25:27607
plasma measurements across bow shock in, (E), 25:27537
variations in electric and magnetic fields in, (E), 25:27539
MAGNETOSPHERE
characteristics of distant, HEOS-I data on, (E), 25:27552
charged-particle modulation in, coupled magnetic-field-line oscillations, relation to trapped, (T), 25:27623
conference on intercorrelated satellite observations and solar activity, Noordwijk, Netherlands, 9/69, 25:27531
currents in, observations during Mar. 16, 1969 substorms from barium cloud releases at 12.4 R/sub E/ of field-aligned, (E), 25:27620
electric fields in, ion-cloud and sounding-rocket measurement of, (E), 25:27545
electron plasma density and temperature in, Langmuir probe data during Feb. 25, 1969 event of, (E), 25:27566
electron-energy spectra above 500 MeV in, OGO-5 measurements of cosmic, (E), 25:27575
electron-trough position near local midnight and magnetic equatorial plane, interrelation with near-Earth plasma sheet of >40-keV, (E), 25:27631
magnetic substorms in, correlation with radiation-belt electron acceleration and precipitation, (E/T), 25:27551
magnetic-field variations on quiet days, abnormal and regular, (E/T), 25:27602
model for, to study scintillation and diffraction phenomena of cosmic radio sources, (T), 25:27612
model of, (T), 25:27607
plasma instabilities in, associated with topological variations of magnetic-field configuration, (T), 25:27547
plasma instabilities of neutral sheet in tail, (T), 25:27547
plasma sheet termination in pre- and post-midnight, near magnetic equator, structure of near-Earth, (E), 25:27631
position variations of bow shock in, geomagnetic-field variations due to solar wind-induced, (E), 25:27537
proton density in plasmasphere during magnetic storm-associated stable auroral red arcs, (E), 25:27622
proton intensity at synchronous altitude in, temporal and spectral variations of solar, (E/T), 25:27541
proton interaction with bow shock, intercomparison of interplanetary space, magnetosheath, and magnetotail energetic solar, (E), 25:27538
proton penetration into, interplanetary and magnetospheric measurements of low-energy solar, (E/T), 25:27542
pulsation propagation through cold plasma and high-energy proton density, spectral shape of Pc1, (T), 25:27605
radio-wave spectral analysis of vlf-banded chorus and narrowband emissions, OGO 5 fast time-resolved, (E), 25:27621
relation of low-latitude DS-current component and auroral-electrojet intensity during intense geomagnetic storms, (E/T), 25:27619
solar-wind discontinuity interaction with magnetosheath, Feb. 24-28, 1969, (E/T), 25:27557
solar-wind interaction with, basic modes of, (E/T), 25:27630
trapping-boundary position near local midnight and magnetic equatorial plane, interrelation with near-Earth plasma sheet, (E), 25:27631
variations in electric and magnetic fields across bow shock, (E), 25:27539
MAGNETOTAIL
disturbances in plasma sheet, effects of weak sc, (E), 25:27546
interaction of protons in, with bow shock and magnetopause, (E), 25:27538
model of polar cusp relationship with plasma sheet, (T), 25:27607
MAGNETS
casting and properties of cobalt--copper--rare earth alloy, 25:27184
fabrication and properties of cobalt--misch metal--samarium, 25:27884
properties of cast permanent, of Co_5RE type, 25:27883
properties of permanent, of $(Pr,Nd)Co_5$ alloy, 25:27886
MAINE YANKEE POWER REACTOR
design parameters of, requested additional data on, 25:28615 (DOCKET-50309-33)
operations aspects of, requested additional data on, 25:28615 (DOCKET-50309-33)
MALEIMIDE, N-ETHYL-
effects on radiosensitivity of Ehrlich ascites cells, 25:26640
MAMMALIA
radiation effects on bone marrow and chromosomes in, review on latent whole-body, 25:26943
radioisotope distribution in tissues of, as function of time following intravenous injection, computer calculations for, 25:26580
MAMMARY GLANDS
radiation effects on development of carcinomas in, of rats, synergism between diethylstilbestrol and, 25:27011
MAN
calcium-47 accumulation in feces of, γ counting method for estimating, 25:26586
cesium-137 content of, in Egypt during 1970, 25:26740 (NP-18728)
collateral blood vein development in, following obstruction of superior vena cava, use of gamma camera with technetium-99m-labeled sodium pertechnetate for demonstration of, 25:26844
conference on vision problems in, in relation to working efficiency, 25:27051
effectiveness of balneotherapy for treatment of blood dyscrasias and high blood pressure in, over 20 years following exposure to atomic bomb, 25:26897
leukemia incidence in, exposed in utero to atomic bombing at Hiroshima and Nagasaki, 25:27043
polonium-210 ingestion in contaminated diet, potential long-term hazards from, 25:26684
radiation dose during diagnostic fluoroscopic radiography of, effects of screen components on x, 25:26815 (BRH/DMRE-71-2)
radiation dose to blood of, calculations of strontium-90 β, 25:26754
radiation dose to gonads of, during therapy, 25:26759
radiation dose to skin of, following particulate contamination of clothing, β, 25:26748
radiation dose to, during x-radiography in relation to diagnostic accuracy, 25:26858
radiation dose to, following ingestion of contaminated food from freshwater food chain in relation to establishment of MPC for freshwater ecosystem, 25:26747
radiation dose to, following release of radioisotopes to biosphere, method for calculation of, 25:26751 (UCRL-50163(Pt.7))
radiation dose to, regulations for maximum permissible, 25:26764
radiation dose tolerance of pelvic structures of, during rotation therapy, γ, 25:26894
radiation effects on blood coagulation in, following cancer therapy, effects of dose on, 25:26668
radiation effects on bone marrow in, during therapy, protective effects of inosine against γ, 25:26799
radiation effects on children with Fanconi type aplastic anemia, chronic radium, 25:27054
radiation effects on eyes of, effects of age and dose on, 25:27013
radiation effects on eyes of, protection against γ, ir, microwave, uv, and x, 25:27047
radiation effects on lungs of, following cigarette smoking, thorium-232 alpha and gamma, 25:27046
radiation effects on neuro-muscular function of, following exposure to atomic bomb blast, effects of age on, 25:27053
radiation effects on progeny of, following maternal uterine therapy, aberrant and clinical x, 25:27057
radiation effects on salivary gland function in, cobalt-60 gamma, 25:27061
radiation effects on sarcomas on skin of, Koebner phenomenon-like occurrence following therapeutic x, 25:26875
radiation effects on, following exposure to nuclear explosions at Hiroshima and Nagasaki, medical study of, 25:27060
radiation effects on, review of effects of dose and dose rate on genetic and somatic ionizing, 25:27042
radiation hazards to, from diagnosis, x, 25:26788
radiation hazards to, from earth impaction of space power system radioactive capsules, computer programs for evaluating, 25:26429 (SC-R-7121)
radiation protection of eyes, kidneys, and larynx in, during cobalt-60 γ therapy, shielding methods for, 25:26779
radiation sensing ability following dark adaptation, tests of x, 25:27039
radiodiagnosis of hydatidosis of kidney of, using combined radiography and scintigraphy, 25:26816

radioinduced carcinomas in breast and genital organs following therapy, 25:27038
radioinduced carcinomas of maxillary sinus of, following diagnostic thorium administration, 25:27050
radioinduced chromosome aberrations in leukocytes of, effects of dose and dose rate on iodine-131, β, γ, x, 25:26730
radioinduced dermatitis in, following therapy, development of eccrine poroma in area of, 25:27055
radioinduced enterocolitis in, pathology and treatment of, 25:26811
radioinduced fibrosarcomas in, following childhood therapy of hemangiomas, x, 25:27059
radioinduced fibrosarcomas in, following therapy, 25:27044
radioinduced hemangioma following therapy of, latent, 25:27049
radioinduced injuries in bladder of, following therapy for gynecological tumors, methods for treatment of, 25:26813
radioinduced injuries in bladder of, methods for treatment of, 25:26810
radioinduced injuries in liver of children following therapy for Wilms' tumor in right kidney, 25:26884
radioinduced injuries of ureter in, surgical methods for treatment of, 25:26814
radioinduced leukopenia in, effectiveness of taurine, uridine monophosphates, and vitamin B_6 for treatment of, 25:26812
radioinduced myelogenous leukemia in, 25:26964
radioinduced necrosis in brain of, following therapy, x, 25:27041
radioinduced papillary microcarcinomas in thyroid of, following atomic bombing of Hiroshima and Nagasaki, 25:26898
radioinduced pituitary ablation in, with diabetic retinopathy, effects on aqueous humor dynamics in eyes, 25:27037
radioinduced strictures in ureter of, following therapy for cervical carcinoma, 25:27052
radioisotope excretion in urine of, following internal contamination from nuclear explosions, problems in measuring, 25:26585
radioisotope transport from diet to maternal milk of, contamination of infant following cesium-137 and strontium-90, 25:26581
radiotherapy for prevention of postoperative recurrence of pterygium in, β, 25:26870
radiotherapy of abdominal tumors in, telecentric small-angle pendulum method for fast electron, 25:26867
radiotherapy of adenomas of parotid glands of, effectiveness of pre- and post-operative, 25:26866
radiotherapy of bladder tumors of, effectiveness of high-energy x, 25:26876
radiotherapy of brain and spinal cord tumors in, development of nervous tissue reactions following, 25:27056
radiotherapy of carcinomas of esophagus of, methods for cobalt-60 gamma, 25:26896
radiotherapy of carcinomas of penis of, effectiveness of radium-226 contact γ, 25:26863
radiotherapy of carcinomas of uterus in, effectiveness of combined use of cobalt-60 intracavitary applicators and external beam gamma for, 25:26869
radiotherapy of cervical cancer in, review of dosimetry and response following, 25:26886
radiotherapy of cervical carcinomas in, complications following, 25:26893
radiotherapy of cervical carcinomas in, recurrence following, 25:26887
radiotherapy of deep-seated neoplasms of, dose-fractionation scheme for high-energy electrons for, 25:26864
radiotherapy of glioblastoma multiforme in, combined effects of postoperative 5-fluorouracil and γ, 25:26889
radiotherapy of hyperthyroidism using iodine-131 in, occurrence of thyroid crisis following, 25:26881
radiotherapy of joint diseases in, effectiveness of synovial injections of gold-198, phosphorus-32, or yttrium-90 for, 25:26873
radiotherapy of lung tumors in, evaluation of 42-MeV betatron, 25:26874
radiotherapy of lymphoma of orbit in, effectiveness of x, 25:26890
radiotherapy of malignant neoplasms of nose and paranasal sinuses of, use of radiosensitizing drugs and surgery with gamma, 25:26885
radiotherapy of melanomas in, by endolymphatic administration of iodine-131-labeled ethiodol, 25:26888
radiotherapy of pituitary adenomas in, methods for cobalt-60 gamma, 25:26872
radiotherapy of retinoblastoma of, comparison of effectiveness of radon-222 implant, electron, and x, 25:26880
radiotherapy of seminoma of testis in, effectiveness of γ, 25:26891
radiotherapy of vocal cord leukoplakia in, effects of dose and histological condition on effectiveness of, 25:26868
scanning of brain of, for infected lesions using technetium-99m, 25:26818
technetium-99m content of milk of, as function of time following injection of tracer dose, 25:26839
thorium-228 accumulation in bone marrow, liver and spleen of, 25:26603
uranium retention in lungs of, following inhalation in soluble compounds, ICRP threshold levels for determining degree of contamination based on natural, 25:26607

MANGANESE
determination in granite by autoradiography and neutron activation, 25:26194
determination in marine silts by neutron activation and γ spectroscopy, 25:26190(R) (NYO-4150-9)
determination in ocean floor samples by γ spectroscopy, 25:28764
determination in sea floor samples by neutron activation, 25:26188 (BNWL-SA-3803)
determination in thorium nitrates and zirconium nitrates by neutron activation, 25:26192
determination in woven fabric by neutron activation, 25:26200
determination in yttrium oxides by solvent extraction and spectrography, 25:26168
determination in Zircaloy, chemical method for, 25:26171

MANGANESE ALLOYS AND SYSTEMS
Al--Mn, precipitation of, activation energy for, 25:28889 (SC-RR-70-356)
B--Cr--Mn, phase diagram at 800°C, isothermal, 25:27299
B--Mn--Ti, phase diagrams at 800 and 1400°C, isothermal, 25:27300
Cr-base--Mn, reflectance spectra of, measurement and band model of, 25:27442
Cu-base--Mn, Kondo effect in, study by superconducting proximity effect, (E), 25:27662
Mn--V, mictomagnetism in bcc, 25:27890
Mn--V, paramagnetism of bcc, NMR and susceptibility study of, 25:27891
Mn--Zr-base, microstructure of, 25:27230
Mn--Zr-base, properties of, electric and mechanical, 25:27230

MANGANESE FLUORIDES
lattice structure of, positron-annihilation study of, (E/T), 25:27865 (CEA-R-4138)

MANGANESE IONS
implantation in zinc sulfide films at 200 keV, detection using luminescence, 25:27844

MANGANESE ISOTOPES Mn-54
energy-level transitions from proton reactions, branching ratios, gamma-ray angular distributions, and internal conversion coefficients for, (E/T), 25:28271

MANGANESE ISOTOPES Mn-55
cross section data on, tables of multigroup, 25:28657 (HEDL-TME-71-36)
energy-level transitions from proton reactions, branching ratios, gamma-ray angular distributions, and internal conversion coefficients for, (E/T), 25:28271
nuclear magnetic resonance in vanadium--manganese alloys, 25:27891

MANGANESE ISOTOPES Mn-56
energy levels from neutron reactions (n,p) with iron-56, (T), 25:28218 (NP-18674)

MANGANESE ZINC FERRATES
magnetic structure of, neutron diffraction study of, 25:28857 (INR-1269)

MANNITOL
properties for use in gamma radiation dosimeters, 25:26523

MARS (PLANET)
atmosphere of, altitudinal analysis of ultraviolet spectrum of upper, (E), 25:27433
ionosphere of, model of ion chemistry below 80 km of, (T), 25:27431

MARSHALL ISLANDS
radiation effects on aging, immune reactions, and peripheral blood of populations on, correlation of fallout, 25:27058

MASERS
book: Statistical Physics, Phase Transitions, and Superfluidity, 25:27912
coherence phenomena in classical and quantum physics, 25:27947

MASS SPECTROMETERS
data collection and processing system for, PDP-8 computer-based, 25:26556
description of on-line isotope separator for analysis of uranium-235 fission fragments, 25:26551
design of peak-matching, for direct mass determination of short half-life radioisotopes, 25:26547 (CERN-70-30(Vol.1), pp 307-19)

MATHEMATICAL PHYSICS
transport equations in, exact analytic solutions of, (T), 25:27948

MATHEMATICS
bound variation compactness theorem, 25:28890 (SC-RR-70-852)

MATTER
nuclei in neutron, calculations of amounts of, (T), 25:27311 (CERN-70-30(Vol.2), pp 759-68)

MATTER, ANTI-
aggregations of, in the Universe, (T), 25:27426

XUM

MEATS
beef, radiation processing effects on color of, γ, 25:27139
beef, radiation processing of, effects of sodium tripolyphosphate and dose rate on color stability following electron and γ, 25:27162
beef, radiation processing of, methods for inactivation of proteolytic enzymes prior to γ, 25:27163(P)
fat content in, γ attenuation method for measuring, 25:26571
fish, radiation effects on proteins of, role of immunoelectrophoresis and starch gel electrophoresis to determine, 25:26631
fish, radiation processing effects on shelf life and taste of gwyniad, 10-MeV electron, 25:27146
fish, radiation processing effects on taste and shelf life of trout, 10-MeV electron, 25:27148
fish, radiation processing of, review of ionizing, 25:27166
pork, radiation processing effects on organoleptic properties and storage life of, γ, 25:27136(T) (NP-tr-1932)
pork, radiation processing of Portuguese sausage, bacterial count, chemical and organoleptic changes, and storage life following x, 25:27159
poultry, radiation processing of chicken for use as pet food, fatty acid composition following, 25:26647
radiation effects on proteins of, role of immunoelectrophoresis and starch gel electrophoresis to determine, 25:26631
radiation effects on rehydration capacity of, effects of dose and timing on γ, 25:27144
seafood, radiation processing effects on 27 strains of Vibrio found in, γ, 25:27115
seafood, radiation processing effects on organoleptic properties and storage life of shrimp, 25:27138(R) (TID-25543)
seafood, radiation processing effects on proteolytic activity of stored oysters, 25:27114
seafood, radiation processing effects on shelf life and taste of carp, 10-MeV electron, 25:27147
seafood, radiation processing of cod and haddock fillets and shrimp, effects on organoleptic properties and storage life of γ, 25:27149
seafood, radiation processing of shrimp, facility for shipboard γ, 25:27158
MECHANICS
equilibrium states of statistical, ergodic states for, 25:28078
MEDICAL PERSONNEL
licensing x-ray, status of legislation in USA in 1971 concerning standards for, 25:26787
radiation dose to abdomen, face, and hands of, from technetium-99m, methods for shielding against, 25:26765
radiation dose to chest and gonads of, during technetium-99m scintigraphy, γ, 25:26766
radiation dose to hands of, from handling indium-113m, methods for shielding against γ, 25:26767
radiation dose to, from handling short-lived radioisotopes, 25:26763
radiation dose to, from preparation of indium-113m- and technetium-99m labeled compounds, 25:26768
radiation dose to, from short-lived radioisotopes, conference on protection, 25:26762
radiation dosimetry for, development of standardization procedure for film badges used in, 25:26756
radiation hazards to, during angiocardiography, x, 25:26854
radiation production of dental, recommendations for, 25:26772
radiation protection of podiatric, recommendations for, 25:26777
radiation protection of, Australian codes of practice for, 25:26738
radiation protection of, during handling of indium-113m and technetium-99m, design of devices for, 25:26776
MEDICINE
book: Diagnosis of Organ Function in Nuclear Medicine (German), 25:26829
book: Radioactivity in Medicine, 25:26790
conference on cancer research, Chicago, 1971, 25:26789
conference on ophthalmology, 25:27051
conference on tracer techniques for dynamic studies in, 25:26567 (STI/PUB-263)
radiation dose calculations and measurements in, development of computer system for handling, 25:26755
research progress in, AEC, 25:26205
x-ray equipment in dental, survey of, in West Germany, 25:26772
MELAMINE, TRIETHYLENE-
effects of injected, on metabolism of DNAses and phosphatases in rat kidneys in comparison to whole-body x radiation, 25:26645
effects on Dictyocaulus viviparus larvae, immunity in vaccinated calves following attenuating, 25:26918
effects on Dictyocaulus viviparus larvae, immunity in vaccinated calves following attenuating, 25:26919
MERCHANT VESSELS
design parameters of nuclear submarine, for petroleum transport tankers, 25:28795
economics of nuclear submarine, for petroleum transport tankers, 25:28795
MERCURY
alpha decay of, half-lives, Q values, reduced widths, and spectra from, (E), 25:28302 (CERN-70-30(Vol.1), pp 523-31)
complexes with lecithins in aqueous butanol solutions, properties of, 25:26272
determination by neutron activation, effects of volatility from plastic containers on, 25:26201
determination in hot spring waters in Japan by neutron activation, 25:26195
determination in marine silts by neutron activation and γ spectroscopy, 25:26190(R) (NYO-4150-9)
effects on crack propagation in aluminum and brass, 25:27243
effects on embrittlement of dilute zinc alloys, 25:27243
effects on failure of cadmium under stress, 25:27243
plasma of, oscillations from collision-induced instabilities in, (E), 25:27802
uptake by erythrocytes, mechanisms for membrane penetration during, 25:26609
effects on brittle fracture of zinc, 25:27243
MERCURY ALLOYS AND SYSTEMS
Hg-base--Zn, effects of amalgams of, on embrittlement of aluminum, 25:27243
Cd--Hg, ordering of w-phase, at 81°K, calorimetric study of long-range, 25:27248
Hg--In, effects on fracture strength of aluminum, 25:27243
Hg-base--Na, effects on embrittlement of beryllium--copper alloys, 25:27243
MERCURY CHLORIDES
use of mercury-197-labeled, for scintigraphy of carcinomas in man, 25:26832
MERCURY IONS
implantation in silicon at 50 keV, outdiffusion, lattice location, and electrical behavior of, 25:27856
MERCURY ISOTOPES Hg-179
proton decay of, half-life of delayed-, (E), 25:28301 (CERN-70-30(Vol.1), pp 487-96)
MERCURY ISOTOPES Hg-181
nuclear spin-parity assignments from delayed-proton decay of, (E), 25:28301 (CERN-70-30(Vol.1), pp 487-96)
proton decay of, half-life and energy spectra from delayed-, (E), 25:28301 (CERN-70-30(Vol.1), pp 487-96)
MERCURY ISOTOPES Hg-183
nuclear parity assignment from delayed-proton decay of, (E), 25:28301 (CERN-70-30(Vol.1), pp 487-96)
proton decay of, half-life of delayed-, (E), 25:28301 (CERN-70-30(Vol.1), pp 487-96)
MERCURY ISOTOPES Hg-184
beta and electron-capture decay of, γ spectra from, (E), 25:28425
MERCURY ISOTOPES Hg-185
beta and electron-capture decay of, half-lives for, (E), 25:28335 (CERN-70-30(Vol.2), pp 1045-55)
MERCURY ISOTOPES Hg-186
beta and electron-capture decay of, γ spectra from, (E), 25:28425
MERCURY ISOTOPES Hg-187
beta and electron-capture decay of, half-lives for, (E), 25:28335 (CERN-70-30(Vol.2), pp 1045-55)
MERCURY ISOTOPES Hg-188
beta and electron-capture decay of, γ spectra from, (E), 25:28425
MERCURY ISOTOPES Hg-189
electron-capture decay of, half-lives for, (E), 25:28335 (CERN-70-30(Vol.2), pp 1045-55)
MERCURY ISOTOPES Hg-193
energy-level transitions in, conversion coefficients and multipolarities for, (E), 25:28339 (CERN-70-30(Vol.2), pp 1081-91)
MERCURY ISOTOPES Hg-197
effectiveness of mercury dichloride-incorporated, for scanning of thyroid nodules for differential diagnosis, 25:26823
effectiveness of neohydrin-incorporated, for kidney localization in comparison with other diagnostic methods, 25:26821
use for brain scanning, review on international methods for, 25:26855
use of chlormerodrin-incorporated, for brain scanning, computer evaluation of, 25:26824
use of mercury bichloride-incorporated, for scintigraphy of carcinomas in man, 25:26832
MERCURY ISOTOPES Hg-198
energy levels from isomeric thallium-198 beta decay, lifetimes of high-spin, (E), 25:28353 (NP-18695)
MERCURY ISOTOPES Hg-200
energy levels from isomeric gold-200 beta decay, lifetimes of high-spin, (E), 25:28353 (NP-18695)
MERCURY ISOTOPES Hg-203
separation from solutions by retention on mercury sulfide precipitates, 25:26199
use of mercury chloride-incorporated, for scanning lungs for tumor localization, effects of addition of glutathione to tracer on results of, 25:26842
MESIC ATOMS
x-ray spectra from chlorine K-, (E), 25:28031
MESONS
dynamics of, Schroedinger equation in nonrelativistic

composite model for internal, 25:28030
interactions with baryons, eikonal model from unitarized Veneziano model for, 25:28041
interactions with mesons, exotic mesons, Regge cuts, and parity doublets for, 25:28033
interactions with polarized baryons, baryon spin determination from, 25:28040
mass spectra and form factors in SU(3) infinite multiplet model, 25:28058
model of, strong binding in quark, 25:28022 (DESY-71/10)
production in nucleon interactions in nuclear emulsions and cosmic jets, multiple, 25:28050
Regge trajectories for, properties of imaginary part of, 25:28036

MESONS (eta)
decay eta → 3π, models for Dalitz-plot distribution and rate of, 25:27992

MESONS (f)
decay angular distribution of, s-wave interference for, 25:28018

MESONS (K)
interactions anti K + K → anti K + K, dispersive sum rule method for scattering lengths for, (T), 25:28029
interactions anti K + N → anti K + N, SU(3) chiral Lagrangian model for total cross sections of, (T), 25:28037
interactions anti K + N → π + Σ(Λ), SU(3) x SU(3) chiral Lagrangian model for total cross sections of, (T), 25:28037
interactions anti K + N, SU(3) x SU(3) chiral Lagrangian model for scattering lengths for, (T), 25:28037
interactions K + K → K + K, dispersive sum rule method for scattering lengths and resonance spectrum for, (T), 25:28029
interactions K + N, imaginary part of Regge trajectories for, 25:28036
interactions π + K → π + K, dispersive sum rule method for SU(3) x SU(3) symmetry breaking, off-shell corrections, scattering lengths, and mass and width of kappa in, (T), 25:28029

MESONS (K-)
interactions K- + d → K- + π+ + π- + d at 12.6 GeV/c, production of L and Q in, (E), 25:27967
interactions K- + N → K + π + N, graphical illustration of isospin analysis of, 25:28039
interactions K- + N, Argand diagram analysis of s-channel helicity amplitudes of, 25:28035
interactions K- + p → Λ + K+ + K- at 3.3 GeV/c, test of generalized Veneziano model from, 25:28042
interactions K- + p → π- + Y*+, eikonal-like pole-cut model for, 25:28044
mass of, x-ray energy shift from 4f--3d transition in chlorine for determining, (E), 25:28031

MESONS (K°)
content of, in neutral kaon beam, (T), 25:27424
interactions K_2^0 + d → K_1^0 + d at high energies, differential cross section and phase of amplitude for, (T), 25:28049
regeneration K_2^0 → K_1^0 on deuterons at high energies, differential cross section and phase of amplitude for, (T), 25:28049

MESONS (anti K°)
content of, in neutral kaon beam, (T), 25:27424

MESONS (K+)
interactions K+ + N → K + π + N, graphical illustration of isospin analysis of, 25:28039
interactions K+ + N, Argand diagram analysis of s-channel helicity amplitudes of, 25:28035
interactions K+ + p → K° + π+ + p at 10 GeV/c, cross sections and decay distributions for Δ(1236), K*(890), and K*(1420) production in, (E), 25:27968
interactions K+ + p at 1.60 to 3.31 GeV/c, polarization parameter or elastic, (E), 25:27963
interactions K+ + p at 10 GeV, generalized Veneziano model and Reggeized multiperipheral model for anti Λ production in, (E/T), 25:27966
interactions K+ + p below 2 GeV/c, Reggeized phase shift analysis of, 25:28043

MESONS (kappa)
coupling with pseudoscalar mesons and baryons in nonconserved vector current theory, 25:28023 (NP-18763)
decay kappa → K + p in nonconserved vector current theory, 25:28023 (NP-18763)

MESONS (μ)
capture by calcium-40, carbon-12, silicon-28, and sulfur-32, relativistic corrections to asymmetry of high-energy neutrons from polarized, (T), 25:28183
detection of multiple cosmic, deep underground, (E), 25:27954
distribution in extensive air showers, (T), 25:27476
distribution in extensive air showers, TeV-range, (E), 25:27477

MESONS (μ-)
interactions μ- + e → μ- + e at 5.0 and 14.5 GeV/c in emulsions, cross sections for, (E), 25:27955
production of μ+--μ- pairs by gamma quanta in nuclear fields, polarization effects on cross sections for, (T), 25:27996

MESONS (μ+)
interactions μ+ + e → μ+ + e at 10.1 GeV/c in emulsions, cross sections for, (E), 25:27955
production of μ+--μ- pairs by gamma quanta in nuclear fields, polarization effects on cross sections for, (T), 25:27996
spin precession in muonium in magnetic fields, two-frequency, (E), 25:27446

MESONS (ω)
coupling constant for rhoωγ, electroproduction of ω as test of, 25:27981 (DESY-71/11)
decay ω → 2π° + γ, branching ratio for, (E), 25:27961 (PURC-4159-16)
decay ω → eta + γ, upper limit for branching ratio for, (E), 25:27961 (PURC-4159-16)
decay ω → π° + γ, branching ratio for, (E), 25:27961 (PURC-4159-16)
electroproduction of, test of mass dependence of rhoωγ coupling constant from, 25:27981 (DESY-71/11)

MESONS (ρ)
coupling constant for rhoωγ, electroproduction of ω as test of, 25:27981 (DESY-71/11)
distribution in extensive air showers, TeV-range, (E), 25:27477
form factor of, Schroedinger equation in nonrelativistic composite model for electromagnetic, (T), 25:28030
interactions π + d at 3.65 and 3.75 GeV, cross sections for elastic, 25:28073
interactions π + K → π + K, dispersive sum rule method for SU(3) x SU(3) symmetry breaking, off-shell corrections, scattering lengths, and mass and width of kappa in, (T), 25:28029
interactions π + Λ → π + Σ(Λ), SU(3) x SU(3) chiral Lagrangian model for total cross sections of, (T), 25:28037
interactions π + Λ, SU(3) x SU(3) chiral Lagrangian model for scattering lengths for, (T), 25:28037
interactions π + N → π + N*, s-channel helicity conservation constraints on t-channel exchanges in, (T), 25:28028 (SU-1206-242)
interactions π + N → π + π + N, graphical illustration of isospin analysis of, 25:28039
interactions π + N, effects of imaginary part of Regge trajectories on differential cross sections for backward, 25:28036
interactions π + π, current algebra and analyticity for bootstrap of rho and sigma in, (T), 25:28027 (RLO-1388-602)
interactions π + π, s-channel helicity conservation constraints on t-channel exchanges in, (T), 25:28028 (SU-1206-242)
interactions π + π, sum rules for partial-wave amplitudes of, 25:28024 (NP-18766)
interactions π + π, unitarized model with CDD poles for P-wave amplitudes of, 25:28032
interactions π + Σ → π + Σ, SU(3) x SU(3) chiral Lagrangian model for total cross sections of (T), 25:28037
interactions with atmospheric nuclei in extensive air showers, (T), 25:27476
production in e + N interactions, comparison of vector-meson dominance model with, 25:27982 (DESY-71/12)
production in γ + N interactions, derivative amplitudes for, 25:28000
reactions with aluminum, carbon, copper, and lead at 1 GeV/c, differential and total cross sections for, (E), 25:27959
scattering lengths for, SU(3) x SU(3) chiral Lagrangian model for, 25:28037
spin-orbit force for p-wave ground state of, Schroedinger equation in nonrelativistic composite model for, (T), 25:28030

MESONS (π-)
capture by Z = 3 to 82 nuclei with charged particle emission, particle spectra and branching ratios for, (E), 25:26178
effects on survival of ascites tumor cells in mice, RBE for, 25:26938
interactions π- + p → Δ- + π+ at 1640 to 1760 MeV, partial-wave analysis of, (E/T), 25:27962
interactions π- + p → eta + n, duality concept for imaginary part of Regge trajectories for, 25:28036
interactions π- + p → K+ + Σ(1385) at 2.75 to 14.0 GeV/c, cross sections for, (E), 25:28038
interactions π- + p → K+ + Σ- at 2.75 to 14.0 GeV/c, cross sections for, (E), 25:28038
interactions π- + p → π- + p + D°, D° → π+ + π+ + π- + π- at 16 GeV/c, cross section for, (E), 25:27964
interactions π- + p → π- + p at 2.38 to 3.00 GeV/c, differential cross sections and angular distributions for backward, (E), 25:27965
scattering by magnesium-24 at low energies, inelastic, (T), 25:28244

MESONS (π°)
decay of cosmic, comparison with galactic γ flux for γ spectra from, (T), 25:27404
interactions π+ + π° → π+ + π°, scattering amplitude and length of forward, 25:28025 (NP-18768)

MESONS (π+)
interactions π+ + p → K+ + Y*+, eikonal-like pole-cut model for, 25:28044
interactions π+ + p → π+ + p + D°, D° → π+ + π+ + π- + π- at 16 GeV/c, cross section for, (E), 25:27964
interactions π+ + p → π+ + p at 2.18 to 5.25 GeV/c,

differential cross sections and angular distributions for backward, (E), 25:27965
interactions $\pi^+ + p \rightarrow rho^0 + \Delta^{++}$ at 11.7 GeV/c, total and differential cross sections for, (E/T), 25:27960 (DESY-71/8)
interactions $\pi^+ + \pi^0 \rightarrow \pi^+ + \pi^0$, scattering amplitude and length of forward, 25:28025 (NP-18768)
production in $e + p \rightarrow e' + \pi^+ + n$ interactions at 4 to 5.4 GeV, differential cross sections for, (E), 25:27950 (DESY-71/9)
reactions (π^+,p) with carbon-12, distorted-wave effects for differential cross sections for, (T), 25:28048
MESONS (rho)
coupling constant for rhoww, electroproduction of w as test of, 25:27981 (DESY-71/11)
production in w + w interactions, current algebra and analyticity for bootstrap for, (T), 25:28027 (RLO-1388-602)
production in $\pi^+ + p \rightarrow rho^0 + \Delta^{++}$ at 11.7 GeV/c/differential and total cross sections for, (E/T), 25:27960 (DESY-71/8)
MESONS, RESONANCE
decay $D^0 \rightarrow \pi^+ + \pi^+ + \pi^- + \pi^-$ and $D^0 \rightarrow eta + \pi^+ + \pi^-$, upper limit for ratio of, (E), 25:27964
decay of, spin formalisms for, 25:28007 (CERN-71-8)
energy level diagrams for, rotational, 25:28009
existence of heavy, as nonrelativistic bound state of N - anti N system, 25:28026 (NP-18774)
mass and width of kappa in $\pi + K \rightarrow \pi + K$ interactions, dispersive sum rule method for calculating, (T), 25:28029
production by polarized particles, additivity frame in quark model for, 25:28017
production in K + K + K + K interactions, dispersive sum rule method for, (T), 25:28029
production in $\pi + \pi$ interactions, s-channel helicity conservation constraints on t-channel exchanges in, (T), 25:28028 (SU-1206-242)
production of A_1, additivity frame in quark model for, 25:28017
production of $D^0(1285)$ in $\pi^+ + p$ and $\pi^- + p$ interactions at 16 GeV/c, (E), 25:27964
production of $K^*(890)$ and $K^*(1420)$ in $K^+ + p \rightarrow K^0 + \pi^+ + p$ interactions at 10 GeV/c, (E), 25:27968
production of L and Q in $K^- + d \rightarrow K^- + \pi^+ + \pi^- + d$ interactions at 12.6 GeV/c, (E), 25:27967
production of sigma in $\pi + \pi$ interactions, current algebra and analyticity for bootstrap for, (T), 25:28027 (RLO-1388-602)
properties of, systematics of, 25:28008 (UCRL-73073)
systematics of, 25:28010
METALS
book: Effects of Metals on Cells, Subcellular Elements, and Macromolecules, 25:26608
complexes of, research progress on structural studies of, 25:28894(R) (TID-25682)
defects in crystals of, research program on, 25:27866(R) (NYO-3504-56)
deposition of, field ion microscopy studies of vapor, 25:27189
determination in plutonium oxide--uranium oxide pellets by emission spectroscopy, 25:26153 (LA-4622)
effects of liquid, on brittle fracture of solid alloys and metals, 25:27243
fabrication of, research on methods for, 25:27194
fatigue in high-strength, mechanisms of, 25:27242
properties for use in reactors, selection and improvement of, 25:27219
radiation effects on fracture of, neutron, 25:27270
radiation effects on fuel cladding, high-flux fast neutron, 25:27266 (RD/B/N-1812)
temperature distribution in coolants of liquid, flowing past solid heat-generating cylinder, method for calculating, 25:26422
METEORITES
ages of stone, cosmic-ray exposure, (E), 25:27308
METHACRYLIC ACID, METHYL ESTER, POLYMERS
gamma absorption coefficients of Plexiglas, (E), 25:27825 (DEMO-70/11)
METHANE
yields from γ radiolysis of ethylene--neon, effects of pressure on, 25:26314
yields from γ radiolysis of liquid 2,2-dimethylpropane, effects of additives on, 25:26309
METHANE, IODO-
scavenging of gaseous fission product, from air by aqueous sprays, (E), 25:26376 (CONF-700601-, pp 271-88)
METHANE, NITRO-
radiolysis of aqueous solutions of, yields of hydrated electrons from electron pulse, 25:26308
METHANESULFONIC ACID, ETHYL ESTER
effects on Aspergillus, mutagenic, 25:26717
effects on β-galactosidase gene of Escherichia, mutagenic, 25:26722
effects on flax plants, mutagenic, 25:27090
METHANESULFONIC ACID, METHYL ESTER
effects on barley, mutagenic, 25:26716
METHANOL
HCl--methanol, corrosive effects on annealed and cold-worked zirconium, 25:27173
METHYL RADICALS, CHLORO-
yields from γ radiolysis of ethylene--neon, effects of pressure on, 25:26314
METHYL SULFOXIDE
acetone--HCl--methyl sulfoxide--$UO_2(ClO_4)_2$, complex formation in aqueous solutions of, PMR studies on solvation and, 25:26212
acetone--methyl sulfoxide--$UO_2(ClO_4)_2$, complex formation in aqueous solutions of, PMR studies on solvation and, 25:26212
acetone--methyl sulfoxide--$UO_2(NO_3)_2$, complex formation in aqueous solutions of, PMR studies on solvation and, 25:26212
METHYLAMINE
effects on x-radioinduced polymerization of gaseous chloroethylene, 25:26282
METHYLENE BLUE
radioprotective effects in rats, γ, 25:26803
MEXICO
radiation effects on population dynamics of screw-worm flies in, 25:27152
MIAMISBURG AREA (OHIO)
radiation monitoring of environment of during 1970, 25:26739(R) (MLM-1795)
MICA
research in India during present decade, 25:27281 (INIS-mf-13)
MICE
cysteamine-S-phosphate distribution and metabolism in tissues of, phosphorus-32 and sulfur-35 double tracer study of, 25:26805
fighting episodes of, effects of third party on, 25:28874(T) (ORNL-tr-2447)
hematopoietic cell formation in, role of bone marrow stem cells in, 25:28898 (UCRL-20613)
pregnancy in laboratory, effects of traumas on, 25:28873(T) (ORNL-tr-2445)
radiation effects on aging in, x, 25:26922(R) (ORO-3260-3-A)
radiation effects on ascites tumor cells in, RBE for meson (π^-), 25:26938
radiation effects on blood, bone marrow, liver, lymph nodes, and spleen of, recovery from x, 25:26980
radiation effects on catecholamine content in tissues of, protective effects of cystamine and mexamine against, 25:27017
radiation effects on colony formation in allogeneic and syngeneic bone marrow and spleen cell transplants in, γ, 25:26670
radiation effects on development of Erlich ascites tumors in, combined effects of daunomycin and x, 25:26990
radiation effects on development of nervous system in, in utero x, 25:26972
radiation effects on differentiation in vertebral column of progeny of, effects of in utero 2'-deoxy-5-fluorocytidine and x, 25:26997
radiation effects on differentiation of immunoresponsive cells from bone marrow progenitors in, 25:26669
radiation effects on erythropoiesis in, effects of immune reactions on x, 25:27012
radiation effects on fertility span and reproductive capacity of mature, following exposure in infancy, x, 25:26930
radiation effects on fibroblast formation in spleen cultures of, 25:26905
radiation effects on function and morphology of ovaries of, low-dose gamma, 25:27028
radiation effects on hematopoiesis in bone marrow and spleen of, effects of intraperitoneal injection of milk on x, 25:26678
radiation effects on hematopoietic system of, as evidenced by residual injury in erythroid and myeloid systems, x, 25:26981
radiation effects on immune reactions and myeloid functions in, effects of phytohemagglutinin on x, 25:26942
radiation effects on immune reactions in, effects of dose and dose rate on fission neutron, γ, x, 25:26679
radiation effects on immune reactions in, effects of preincubation with bone marrow on, 25:26662
radiation effects on immune reactions to injected Escherichia coli endotoxin and Newcastle disease virus in, whole-body x, 25:26986
radiation effects on immune reactions to parental and hybrid tumor transplants in, whole-body ionizing, 25:26985
radiation effects on immunocompetent cells in lymph nodes, spleen, and thymus of, x, 25:26672
radiation effects on interferential activity of encephalitis virus in, comparison of thymol with uv, 25:27102
radiation effects on iron-59 uptake and distribution in bone marrow and spleen of, effects of immune reactions on x, 25:27012
radiation effects on L cells of, effects of DNA synthesis phase on uv, 25:26989
radiation effects on mitosis and DNA in endometrial glandular epithelium of, 600-R x, 25:26659
radiation effects on phytohemagglutinin response of bone marrow, lymph node, and spleen cells of, effects of thymus on x, 25:26673
radiation effects on production of interferon in,

transplanted with rat bone marrow, 25:26995
radiation effects on regeneration in cervical lymph nodes of, effects of thymus shielding on x, 25:26996
radiation effects on regeneration of intestinal epithelium cells of, effects of dose on x, 25:27033
radiation effects on regeneration of proliferative activity in cultured lymphoma cells of, x, 25:26974
radiation effects on reproductive behavior and spermatogenesis in male, following subcutaneous injection of zirconium-95--niobium-95, 25:26962
radiation effects on reticuloendothelial system of, effects of glucan on γ, 25:26947
radiation effects on RNA synthesis in endometrial epithelium of, whole-body x, 25:27031
radiation effects on stem cells in bone marrow of, partial- and whole-body x, 25:26956
radiation effects on survival of, effects of subsequent bleeding on x, 25:26934
radiation effects on survival of, role of thymectomy in recovery from γ, 25:26937
radiation effects on survival of, therapeutic effects of taurine, uridine monophosphates, and vitamin B_6 on, 25:26812
radiation effects on, protective and toxic effects of cystamine with or without AET on serotonin on γ, 25:26793
radiation injuries to bone marrow in, effects of balneotherapy on mixed gamma and neutron induced, 25:26950
radiation protection effectiveness of AET, histamine, serotonin, and sodium fluoroacetate for, 25:26800
radiation protection using cysteamine, dose reduction factor for x, 25:26924
radiation protection using cysteamine-S-phosphate, relation of metabolism and tissue distribution to mechanism of, 25:26805
radiation protection, using adrenaline, noradrenaline, or phenylephrine, effects of catecholamines on, 25:26804
radioinduced carcinomas in, effects of dose on late γ, neutron, and x, 25:26976
radioinduced chromosome translocations in male, cytogenetical studies on x, 25:26711
radioinduced dominant lethal mutations in, effects of dose and dose fractionation on whole-body x, 25:26726
radioinduced leukemia in, comparison of phosphorus-32 and x, 25:27021
radioinduced leukosis in, effects of bone marrow autotransplants on, 25:26904
radioprotective efficiency of cystaphos in, biological factors in x, 25:26796
radiosensitivity of antibody forming cells of, effects of inductive and productive phases on x, 25:26680
radiosensitivity of RFM, use of H-2 genotype to determine γ, 25:26690
radiosensitivity of spleen cells of, effects on selective inhibition of γ, 25:26671
radiosensitivity of stem cells of intestinal mucosa in, comparison of 14-MeV neutron and x, 25:26958
radiosensitivity of, effects of hematopoietic stem cells on, 25:26952
radiosensitivity of, effects of hypoxia on, 25:26967
survival of x irradiated, effects of reticuloendothelial system blockage on, 25:26926
uranium content of bones of, 25:26744

MICHIGAN, LAKE
thermal effects of power plant effluents in, 25:28622

MICROORGANISMS
radiation effects on growth of, in processed food, 25:27132 (CONF-680112-, pp 221-39)
radiosensitivity of, review of, 25:27116

MICROSOMES
radiation effects on pethidine demethylating system in rat liver, x, 25:27034
radiation effects on protein synthesis by fractions of liver, in rats, subsequent whole-body γ, 25:27006

MICROWAVE EQUIPMENT
electromagnetic wave propagation in superconducting coaxial cylindrical guide, (T), 25:27665

MICROWAVES
cosmic background, ultraviolet radiation from interactions with cosmic-ray electrons, (T), 25:27429
effects on cataract induction in eyes of rabbits, effects of average power in relation to dose on, 25:26971
effects on human eye, review on, 25:27047
reflection from longitudinally magnetized plasma in coaxial waveguide, (E), 25:27813
scattering on plasma, diagnostic use of, (E/T), 25:27679
use for remote feedback stabilization of plasma drift waves in Q devices, 25:27766

MIDWEST FUEL RECOVERY PLANT
safety of, seismic analysis of, 25:26325 (DOCKET-50268-7)

MILK
analysis of powdered, for lead by photon activation, 25:26203
iodine-131 content of West Valley Processing Plant environs, Oct. 1970 to Jan. 1971, 25:26355(R) (SRO-344-11)
radioisotope content of Japanese powdered, April 1969 to April 1970, cesium-137 and strontium-90, 25:26392 (NIRS-RSD-27)
radioisotope content of, in South Africa during 1963 to 1967, methods for calculating fallout, 25:26613
radioisotope transport from diet to human, cesium-137 and strontium-90, 25:26581
separation of cesium, iodine, and strontium from, by moving-bed ion exchange, 25:26335 (RO/EERL-71-1)
technetium-99m content of human, as function of time following injection of tracer dose, 25:26839

MILKY WAY
brightness distribution in, (E/T), 25:27411
cosmic-ray distribution in, (E), 25:27407
electron densities in interstellar clouds, (E/T), 25:27419
expanding neutral hydrogen in Virgo, (E), 25:27352
gamma radiation from, comparison of γ spectra from cosmic π^0 decay with, (T), 25:27404
gamma-ray flux in, (E), 25:27407
gases in, relation to dust distribution, (E), 25:27415
Lyman-α background, OGO-5 measurements of, (E), 25:27414
matter distribution in, (E/T), 25:27411
radio continuum in, analysis of low-frequency, (E/T), 25:27419
radio survey of high- and intermediate-velocity H I clouds, (E), 25:27416
structure of, (E/T), 25:27411

MILLSTONE POINT POWER REACTOR, UNIT 1
construction of, extension of completion date on provisional permit for, 25:28602 (DOCKET-50245-21)
construction of, request for completion date change in provisional permit for, 25:28603 (DOCKET-50245-65)
trip circuits for shutdown of, additional information on, 25:28604 (DOCKET-50245-66)

MINERALS
analysis by neutron activation, 25:26188 (BNWL-SA-3803)

MINES
radioactive aerosol characterization in uranium, in relation to development of protective devices for personnel, 25:26773

MISCH METAL
Co--misch metal--Sm, preparation and magnetic properties of permanent magnets of, 25:27884

MISSOURI RIVER
temperture of, model for simulating effects of thermal effluents from power plants on, 25:28710(R) (HEDL-TME-71-26)

MITOCHONDRIA
iodine-131 and iodine-131-labeled insulin binding to isolated, effects of acetaldehyde, 2,4-dinitrophenol, glutathione, and palmitic acid on, 25:26575

MITOMYCIN C
radioprotective effects on germinating spores of Streptomyces, γ and uv, 25:27068

MITOSIS
effects of stage of, on proliferation in gamma-irradiated cells, 25:26907
radiation effects on flax, hemp, radish, and rye, x, 25:27093
radiation effects on lucerne cell, effects of doses of 500 to 15,000 R on gamma, 25:26732
radiation effects on mouse endometrial glandular epithelium, 600-R x, 25:26659
radiation effects on yeast, effects of photoreactivation on uv, 25:27080
radiation effects on, in lens epithelium of rats, x, 25:27000
radiation effects on, in mouse L cells, uv, 25:26989
radioinduced delay of Chinese hamster cell, determination of site of delay in α and x, 25:26927
radioinduced delay of Chinese hamster cell, effects of dose and protein synthesis on x, 25:26626
radioinduced delay of pea root, effects of protein synthesis on γ, 25:27063
radioinduced prophase reversion during, in grasshopper embryos, effects of RNA synthesis on recovery from x, 25:26911

MIXERS
design for use in reprocessing irradiated fuel elements, 25:26330(T) (ORNL-tr-2410, pp 14-78)

MOLECULES
book: Effects of Metals on Cells, Subcellular Elements, and Macromolecules, 25:26608
electron localization in, use of information theory in, 25:27464
electron reactions with diatomic, inelastic collision integral for, (T), 25:27459
nuclear magnetic relaxation of adsorbed, theory of intermolecular, 25:28875(T) (ORNL-tr-2457)
nuclear magnetic relaxation of adsorbed, theory of intermolecular, 25:28876(T) (ORNL-tr-2458)
reactions with molecules in multitemperature mixtures, inelastic collision integral for, (T), 25:27459

MOLLUSCA
Anodonta anatina, rubidium-106 uptake and distribution in, effects of temperature on, 25:26587
Littorina littorea, rubidium-106 uptake and distribution in, effects of temperature on, 25:26587
Lymnaea stagnalis, rubidium-106 uptake and distribution in, effects of temperature on, 25:26587
Mytilus edulis, rubidium-106 uptake and distribution in, effects of temperature on, 25:26587
Ostrea sp., radioactive contamination in estuary of North Sea, cobalt-60, iron-55, and zinc-65, 25:26742

XUM

Physa heterostropha, radiation effects on fecundity of laboratory and natural populations of, effects of dose rate on γ, 25:26915
Purpura lapillus, rubidium-106 uptake and distribution in, effects of temperature on, 25:26587
Viviparis contectus, rubidium-106 uptake and distribution in, effects of temperature on, 25:26587
MOLTEN SALT REACTOR EXPERIMENT
coolant salt for, chemical aspects of, 25:28636
decommissioning program for, procedures for abnormal conditions and surveillance requirements for Phase 3 of, 25:28711 (ORNL-TM-3253)
fuel salt for, chemical aspects of, 25:28636
MOLYBDENUM
boron-12 NMR in, quadrupole effects on spectra and coupling constants from, (E), 25:27923
corrosion of thin films of, by dry and moist air and fluorochemical liquid coolant and deionized water at 70 to 100°C, effects of silicon dioxide layer or double layer of silicon dioxide and silicon nitride on, 25:27171
cross section data on, tables of multigroup, 25:28657 (HEDL-TME-71-36)
determination by photometry using carboxy derivatives of 2,6,7-trihydroxy-9-phenyl-3H-xanthen-3-one, 25:26174
determination in sea floor samples by neutron activation, 25:26188 (BNWL-SA-3803)
determination in Zircaloy, chemical method for, 25:26171
effects on electric conductivity, microhardness, and microstructure of titanium, 25:27223
hardness of irradiated and unirradiated, hot, 25:27236
internal friction peaks in irradiated, relations with relaxation phenomena, 25:27199 (CEA-CONF-1671)
separation from slag by leaching and fractional precipitation, 25:26348
separation methods for, review on, 25:26344
sorptive properties and surface film reactions with oxygen, 25:27224
MOLYBDENUM ALLOYS AND SYSTEMS
hardness of irradiated and unirradiated, hot, 25:27236
mechanical properties of low-alloy Type TSM-2A sheet, effects of structure and testing methods on, 25:27221
properties for use as fuel cans for fast breeder reactors, 25:27213
Al--Mo--Sn--Ti-base--Zr, fatigue properties of, 25:27236
Al--Mo--Ti-base--V, cracking under stress, effects of aqueous sodium chloride on, 25:27175
C--Co--Mo-base, weldability of, 25:27185
C--Fe--Mo-base, weldability of, 25:27185
C--Ir--Mo-base, weldability of, 25:27185
C--Mo-base, weldability of, 25:27185
C--Mo-base--Ni, weldability of, 25:27185
Cr--Fe--Mo, fatigue strength of, effects of fine precipitates on, 25:27231
Ir--Mo, superconductivity of intermetallic Mo_3Ir, (E), 25:27654
Mo--Ni, ordering in intermetallic Ni_4Mo, field ion microscopy studies of, 25:27252
Mo--Ni--TiC-base, phase studies of two-phase region in, 25:27298
Mo--Os, superconductivity of intermetallic Mo_3Os, (E), 25:27654
Mo--Re, hardness of, effects of composition and temperature on decreasing, 25:27209 (N-71-11662)
Mo--Re, thermionic work functions of, 25:27911
Mo--Re--W-base, tensile properties of welds in, at high temperatures, 25:27178 (N-71-10353)
Mo--Re--W-base, weldability of arc cast and powder metallurgy, 25:27178 (N-71-10353)
Mo--Ti-base, mechanical properties of, effects of aging on, 25:27233
Mo--Ti-base, phase transformation of metastable β-, isothermal, 25:27257
Mo--Ti-base, stability of metastable β-, effects of zirconium additions on, 25:27233
Mo--Ti-base--Zr, mechanical properties of, effects of aging on, 25:27233
Mo--Zr-base, internal friction at 4 to 300°K, 25:27215
MOLYBDENUM ISOTOPES Mo-92
neutron reactions (n,p) with, cross sections for fast, (E), 25:28273
photon reactions (γ,p) with isobaric analog excitation, proton spectra from, (E), 25:28227
proton elastic scattering using polarized beams, isobaric analog resonances in, (E), 25:28239
proton reactions (p,γ) at 5.9 MeV with isobaric analog excitation, γ spectra from, (E), 25:28359
MOLYBDENUM ISOTOPES Mo-94
deuteron reactions (d,t) at 17 MeV, angular distributions for, (E), 25:28374
MOLYBDENUM ISOTOPES Mo-96
deuteron reactions (d,t) at 17 MeV, angular distributions for, (E), 25:28374
MOLYBDENUM ISOTOPES Mo-99
determination of breakthrough, in technetium-99m generators, effects of contamination on calibration for counting for, 25:26317
distribution and retention in rat organs following subcutaneous injection, 25:26598
energy levels from neutron resonances in molybdenum-98, spin--parity assignments for, (E), 25:28402
MOLYBDENUM ISOTOPES Mo-100
deuteron reactions (d,t) at 17 MeV, angular distributions for, (E), 25:28374
MONKEYS
radiation effects on edema development in brain of, x, 25:26987
radiation effects on interferon formation and virus replication in kidney cells of, 25:27113
radiation effects on retina of, laser, 25:26940
radiation effects on urinary excretion of beta-aminoisobutyric acid and deoxycitidine by, γ, 25:26999
radiation effects on visual acuity in, effects of dose on x, 25:26991
radiation effects on, measurement of simulated solar flare proton, 25:26920(R) (AD-711041)
MONTE CARLO METHOD
sampling techniques for calculations with, new semi-random, 25:27834
MOON
effects on diurnal variations of geomagnetic field at Watheroo, Western Australia, (E), 25:27503
photoelectron sheath around, photoemission and surface parameters affecting, (T), 25:27359
MOUTH
radiation dose to tissues of human, during dental radiography, methods for reduction of x, 25:26817
MUCOSA
radiosensitivity of stem cells of intestinal, in mice, comparison of 14-MeV neutron and x, 25:26958
MUONIUM
hyperfine splitting in, determination from two-frequency meson (μ^+) spin precession, 25:27446
MUSCLES
radiation effects on function of, in atomic bomb survivors on Hiroshima, effects of age on, 25:27053
radiation effects on insulin activity in, x, 25:27010
zinc-65 distribution in, of euphausiids and shrimp following ingestion, 25:26604
MUTATIONS
induction in cereals for improved yield using ethyl sulfonates and ionizing radiation, 25:26686 (CONF-680112-, pp 95-111)
induction in Escherichia by BUdR, 2-aminopurine, DES, EMS, and guanidine, 1-methyl-3-nitro-1-nitroso, 25:26722
induction in flax plants for chlorophyll production using endoxan, ethylmethanesulfonate, nitrosomethylurea, and triethylenemelamine, 25:27090
induction in seeds by EMS, economics of, 25:26697
radioinduced dominant lethal, in mice, effects of dose and dose fractionation on x, 25:26726
radioinduced in Aspergillus for increased amylase and proteinase activity, economics of uv, 25:27097
radioinduced, in Arabidopsis for chlorophyll production and lethality, alpha, proton, and x, 25:26736
radioinduced, in ascospores of Ascobolus for color variations, uv and x, 25:26695
radioinduced, in Aspergillus for radiosensitivity, effects of incubation and temperature on uv, 25:26709
radioinduced, in Aspergillus, effects of EMS on gamma, 25:26717
radioinduced, in Bacillus, effects of transformation ability on uv, 25:26729
radioinduced, in bacteria for acid production, enzyme activity, and milk coagulation, comparison of nitrosoguanidine induced mutations with uv, 25:27121
radioinduced, in barley, effects of EMS on gamma, 25:26716
radioinduced, in beans for chlorophyll and morphology, comparison of frequencies of acute and chronic γ, 25:26685 (CONF-680112-, pp 85-93)
radioinduced, in blue-green alga, uv, 25:26712
radioinduced, in Cicer, genetic mapping of x, 25:26718
radioinduced, in cotton seeds, γ and thermal neutron, 25:26728
radioinduced, in Crepis seed, review of cellular mechanisms of, 25:26733
radioinduced, in diploid and tetraploid rice for chlorophyll production, x, 25:26714
radioinduced, in Drosophila for heterochromatin deletions, genetic mapping of gamma, 25:26720
radioinduced, in Drosophila melanogaster for changes in genetic load, x, 25:26705
radioinduced, in Escherichia coli, refractivity, recombination, and uv sensitivity of γ, 25:26707
radioinduced, in Escherichia, gamma, 25:26722
radioinduced, in flax plants for chlorophyll production, gamma, 25:27090
radioinduced, in fungi for amino acid dependency, uv and x, 25:26703
radioinduced, in fungi for gliotoxin production and physical change, thermal neutron, gamma, and uv, 25:27088
radioinduced, in fungi for pathogenicity, uv, 25:27072
radioinduced, in fungi, for morphological and sporulation changes, effects of doses of 200,000 to 300,000 R on γ, 25:26689
radioinduced, in leaves, stalks, and tubers of potatoes for morphological changes, 1000 to 120,000-R x, 25:26737
radioinduced, in Mycobacterium phlei for carotenoid production, uv, 25:26687

radioinduced, in phytopathogenic fungi, gene mapping of uv, 25:26698
radioinduced, in Rhizobium, for symbiotic activity, uv, 25:27103
radioinduced, in rice for color and morphological changes, x, 25:26688
radioinduced, in rice for economic value, comparison of ethyl sulfate and x, 25:26701
radioinduced, in rice for reproduction, γ, 25:26702
radioinduced, in Salmonella typhimurium, effects of dose on antibiotic resistance, sensitivity, and virulence of γ, 25:27164
radioinduced, in seeds, economics of γ and x, 25:26697
radioinduced, in Sorghum, economics of gamma, 25:26715
radioinduced, in soybeans for early maturation, increased yield, and resistance to nematodes, scab, and viruses, γ, 25:26706
radioinduced, in Streptococcus for chain formation, uv, 25:26731
radioinduced, in Streptomyces erythreus for auxotrophy uv, 25:26699
radioinduced, in tomatoes for breeding, gamma, 25:26735
radioinduced, in wheat, frequency of fast neutron and γ, 25:26710
radiosensitivity of phage T4, defective in deoxyribonucleic acid ligase and rII gene, uv, 25:26708
MUTSU REACTOR
operation of, summary of tests and experiments for initial, 25:28796
MYOGLOBIN
radiation effects on beef, γ, 25:27139
MYXOMYCOTA
Dictyostelium discoideum, radiation effects on germination of spores of, effects of auto-inhibitor on γ, 25:27065
MZFR (SIEMENS REACTOR)
maintenance during 1967 to 1971, 25:28586
operations during 1967 to 1971, 25:28586

N

NAGASAKI
atomic bombing of, leukemia incidence in man exposed in utero to, 25:27043
NALIDIXIC ACID
effects on DNA of uv-irradiated bacteria, 25:27125
NAPHTHALENE
effects on protein synthesis in cultured rabbit lens, carbon-14 tracer study, 25:26649
NATURAL WATERS
radioisotope content and radiation dose from, at Misasa Spa area, Japan, 25:26743
NEBULAE
dust and gas distribution in Orion, (E), 25:27312
observations of comet-shaped, and globules, (E), 25:27337
NEMATODA
Dictyocaulus viviparus, radiation effects on larvae of, immunity in vaccinated calves following attenuating x, 25:26919
Dictyocaulus viviparus, radiation effects on larvae of, immunity in vaccinated calves following attenuating x, 25:26918
Oesophagostomum columbianum, radiation effects on immune reactions and survival of, effects of dose on x, 25:26909
radiosterilization of parasitic, in human excreta, gamma, 25:27126
NEODYMIUM
determination by spectrophotometry, 25:26165
determination in yttrium oxides by solvent extraction and spectrography, 25:26168
dissociation energy of gaseous Nd_2, upper limit for, 25:26273
neodymium-145 magnetic hyperfine fields in compounds of, Moessbauer-effect study of, 25:27924
neodymium-145 magnetic hyperfine fields in, Moessbauer-effect study of, 25:27924
solubility in chromium, effects of temperature on, 25:27238
NEODYMIUM ALLOYS AND SYSTEMS
neodymium-145 magnetic hyperfine fields in, Moessbauer-effect study of, 25:27924
Ag--Nd, dissociation energy of gaseous NdAg, upper limit for, 25:26273
Bi--Nd, magnetic structure of NdBi, neutron-diffraction study of, 25:27887
Co--Nd--Pr, magnetic properties of $Pr_{0.83}Nd_{0.13}Co_5$, 25:27886
Nd--Pd, magnetic properties of $NdPd_3$ at 4 to 300°K, 25:27870
NEODYMIUM BORATES
vaporization heats of gaseous NdBO and $NdBO_2$, 25:26273
NEODYMIUM CHLORIDES
$NdCl_3$--YCl_3-bae, neodymium-145 magnetic hyperfine fields in hexahydrate of, Moessbauer-effect study of, 25:27924
NEODYMIUM ISOTOPES Nd-134
decay of, half-life and γ spectra for, (E), 25:28387
NEODYMIUM ISOTOPES Nd-135
decay of, half-life and γ spectra for, (E), 25:28387
NEODYMIUM ISOTOPES Nd-139
beta and electron-capture decay of isomeric, complex shell-model states in, (E/T), 25:28299 (CERN-70-30(Vol.1), pp 435-46)
NEODYMIUM ISOTOPES Nd-144
carbon-12 reactions with, cross-section limit for fission isomer excitation in, 25:28399
energy levels from samarium-147 (n,α) reactions, (E), 25:28345 (JINR-E3-5483)
proton elastic scattering using polarized beams, isobaric analog resonances in, (E), 25:28239
NEODYMIUM ISOTOPES Nd-145
magnetic hyperfine fields of 72.5-keV gamma rays in paramagnetic salts and intermetallic compounds of neodymium, Moessbauer-efect study of, 25:27924
NEODYMIUM ISOTOPES Nd-146
energy levels of, analysis of nonrandom distributions of neutron resonance, (T), 25:28421
proton elastic scattering using polarized beams, isobaric analog resonances in, (E), 25:28239
NEODYMIUM ISOTOPES Nd-149
beta decay of, γ singles and coincidence spectra and perturbed angular correlations from, (E), 25:28381
NEODYMIUM ISOTOPES Nd-150
energy levels of, analysis of nonrandom distributions of neutron resonance, (T), 25:28421
NEODYMIUM OXIDES
reactions with boron, effects of shock waves and temperature on, 25:27291
vaporization heat of gaseus NdO_2, 25:26273
NEON
electron correlation and density in, calculations using restricted Hartree--Fock approximation, 25:27467
neon-ion reactions at 100 to 350 keV with, cross sections and Pauli-excitation mechanism of K-shell ionization in, 25:27453
NEON IONS
reactions with aluminum at 100 keV to 3.2 MeV, cross sections and Pauli-excitation mechanism of K-shell ionization in, 25:27453
NEON ISOTOPES
abundance in lunar surface materials, (E), 25:27308
production in uranium-235 ternary neutron fission, mass-spectrometric search for, 25:28419
NEON ISOTOPES Ne-17
beta and delayed-proton decay of, half-life and γ and proton spectra from, (E), 25:28195
NEON ISOTOPES Ne-20
energy levels of, effects of ground-state correlations on, (T), 25:28505
neutron capture by cross sections, gamma spectra, and Q values for thermal, (E/T), 25:28257
neutron capture by, cross sections and Q values for thermal, (E), 25:28275
NEON ISOTOPES Ne-21
energy levels from neon-20 thermal-neutron capture, Nilsson-model analysis of, (E/T), 25:28257
energy-level transitions from neon-20 (n,γ) reactions, energies and intensities of, (E), 25:28275
neutron capture by, cross sections and Q values for thermal, (E), 25:28275
NEON ISOTOPES Ne-22
energy-level transitions from neon-21 (n,γ) reactions, energies and intensities of, (E), 25:28275
neutron capture by, cross sections and Q values for thermal, (E), 25:28275
neutron capture by, cross sections, gamma spectra, and Q values for thermal, (E/T), 25:28257
reactions with americium-243 at 120 MeV, effective cross sections for element 105 production in, (E), 25:28350(T) (KFK-tr-350)
NEON ISOTOPES Ne-23
energy levels from neon-22 thermal-neutron capture, Nilsson-model analysis of, (E/T), 25:28257
energy-level transitions from neon-22 (n,γ) reactions, energies and intensities of, (E), 25:28275
NEON SYSTEMS
ethylene--Ne, radiolysis of, effects of pressure on yields from γ, 25:26314
NEPTUNIUM
separation from aqueous fuel processing solutions by solvent extraction using tridodecylamine, 25:26333(T) (ORNL-tr-2410, pp 121-42)
separation from plutonium by solvent extraction using tridodecylamine in decanoic acid, 25:26333(T) (ORNL-tr-2410, pp 121-42)
separation from soils by ion exchange, 25:26197
NEPTUNIUM ISOTOPES Np-235
energy levels from americium-239 and plutonium-235 decays, lifetimes and Nilsson assignments for, (E), 25:28415
NEPTUNIUM ISOTOPES Np-237
cross section data on, tables of multigroup, 25:28657 (HEDL-TME-71-36)
deuteron reactions (d,2n) at 9 to 14 MeV with excitation of fission isomers, energy spectra and isomer ratio for, (E), 25:28355(R) (TID-25659)
Moessbauer spectra in americium compounds, 25:27922
NERVES
radiation effects on frog sciatic, dose dependence of

XUM

200-kV x, 25:26993
NERVOUS SYSTEM
radiation effects on development of, in embryos of mice, in utero x, 25:26972
radiation effects on function of, in atomic bomb survivors on Hiroshima, effects of age on, 25:27053
radioinduced reactions in human, following therapy of brain and spinal cord tumors, effects of dose and corticoids on, 25:27056
NETHERLANDS
radiation processing of food in, development of programs for, 25:27142
NEUTRINOS
emission from Seyfert galaxies, (T), 25:27417
emission from stars undergoing neutronization, (T), 25:27335
interactions ν + N at high energies, damped residue function and asymptotic limit of scaling function in duality model for inelastic, (T), 25:28006
mass of, radiative corrections to, (T), 25:28493
stability of, 25:27979
theory in beta decay, relativistic extension of droplet theory of elementary particle structure in, (T), 25:27970
NEUTRON BEAMS
collimator for, 25:28153(P)
NEUTRON CROSS SECTIONS
calculation of mean thermal, computer program for, 25:28803 (EUR-4555)
comparison of group cross sections and Westcott parameters for thermal, JNDC, UK, and ENDF/B files, (T), 25:28344 (JAERI-1200)
data file on, computer program for processing ENDF/B, 25:28148 (ORNL-TM-3266)
data library of group constants for fast reactor calculations, 25:28657 (HEDL-TME-71-36)
NEUTRON SOURCES
design of gas-target, for 10^{13}n/sec flux, 25:26883
design of helium cooled liquid hydrogen moderated thermal, 25:28767
development for radiography, review on, 25:26439 (UJV-2545-R,T)
gamma/neutron ratio from, effects of indium, rhodium, and sulfur foils on, 25:27062 (IAEA-R-459)
oscillator for, design of very-high-frequency, (E), 25:28161
NEUTRON SPECTROMETERS
development of high-resolution, for inelastic scattering studies using vibrating crystal for beam bunching, 25:26493
NEUTRON STARS
magnetic-field decay in, (T), 25:27344
nuclei in, calculations of amounts of, (T), 25:27311 (CERN-70-30(Vol.2), pp 759-68)
x-ray emission from, in binary systems, (T), 25:27342
NEUTRONS
buckling in AGR-type assemblies, axial, (E/T), 25:28806 (RD/B/N-1837)
detection of gamma-compensated self-powered detector for in-core, 25:26458
dose to dogs from implanted plutonium-238-powered circulatory assist device, 25:26931
dose to polymeric materials, ASTM standard method for calculation of, 25:26535
dosimetry of, lithium fluoride thermoluminescent badge for personnel, 25:26524(P)
dosimetry of, review of instruments and methods for, 25:26534
dosimetry of, scattering corrections for, 25:26483
effects of 14 MeV, on eyes of rabbits, RBE for cataractogenic, 25:27027
effects on beagle dogs, effects of dose on lethal, 25:26992
effects on bone marrow in mice, effects of balneotherapy on pathological, 25:26950
effects on devices, method for measuring, 25:26560 (SC-DR-710045)
effects on dimensional stability of boronated and hafnated graphite, (E), 25:28633(R) (GA-10399)
effects on epitaxial gallium arsenide laser diodes at 76 and 300°K, 25:26563
effects on faded photographs, tintypes, and glass-plate negatives, 25:26287
effects on fracture of iron and steel, review on, 25:27270
effects on IMPATT diodes, 25:26562
effects on lymphocyte chromosomes in dogs following implantation of plutonium-238-powered circulatory assist device, 25:26931
effects on mice, effects of dose on late neoplastic, 25:26976
effects on microhardness of potassium chloride, 25:27222
effects on miniature swine, effects of dose and dose fractionation on lethal, 25:26928
effects on oxidation of graphite by carbon dioxide or oxygen, 25:26286
effects on oxides, Wigner energy storage in, 25:27839 (CEA-N-1171)
effects on seedling growth following exposure of barley seeds, experience of Standard Neutron Irradiation Facility in Thailand in determining, 25:27062 (IAEA-R-459)
effects on silicon, luminescence spectrum induced in, 25:27849
effects on stem cells of intestinal mucosa in mice, comparison of x radiation and 14-MeV, 25:26958
effects on titanium oxide, production and annealing of paramagnetic defects in, 25:27853
electric polarizability of, symmetric quark model for, 25:27983
flux calculations for reactors, development of synthesis methods for, (T), 25:28808
flux distribution in gas cooled graphite moderated reactors, adjusted computer program for, (E/T), 25:28654 (CEA-N-1344(2))
flux distribution in reactor sub-regions, analysis of multiple collision probabilities for, (T), 25:28805 (EURFNR-898)
flux distribution in reactors, development of device for plotting, 25:26460(P)
flux measurements of, scattering corrections for, 25:26483
flux measurements using activation detectors, ASTM standard method for, 25:26476
flux measurements, gamma-compensated fission thermocouple for, 25:26466(P)
flux transients, analysis of reactor kinetics from, (E/T), 25:28755 (CEA-N-1406)
form factor from e + d → e + p + n interactions at high energies, (E), 25:27951 (NP-18725)
form factor from e + d elastic scattering, electric, (T), 25:27980 (DESY-71/7)
interactions γ + n → Δ^0 + π^0 at high energies, models for, (T), 25:27990
interactions γ + n → n + eta at high energies, pole--cut model for, (T), 25:27989
interactions γ + n → p + π^- at high energies, isotopic structure of N* decay amplitudes from, (T), 25:27990
interactions γ + n → p + rho−, OPE amplitude and rho$\pi\gamma$ coupling constants from, 25:27990
interactions n + d → t, three-body model vertex part of virtual, (T), 25:28047
interactions n + p → n + p at 152 MeV, differential cross sections and angular distributions for, (E), 25:27956
reaction rates in AGR-type lattices, measurement of manganese, 25:28816 (RD/B/N-1518)
reactions (n,α) with nuclei as tool for studying neutron resonances, 25:28345 (JINR-E3-5483)
reactions (n,α) with samarium-147, α spectra from, (E), 25:28347 (JINR-P3-5553)
reactions (n,f) with uranium-235, yields of cesium-138, -139, -141, -142, -143, and -145 in, (E), 25:28307 (CERN-70-30(Vol.1), pp 589-99)
reactions (n,γ) and (n,p) with phosphorus-sulfur compounds, production of recoil phosphorus-32 by, 25:26318
reactions (n,γ), (n,2n), and (n,np) with nuclei, computer program for calculating cross sections for, (T), 25:28218 (NP-18674)
reactions (n,n) and (n,p) with iron-56, cross sections and energy levels of iron-56 and manganese-56 from, (T), 25:28218 (NP-18674)
reactions with A = 45 to 61 nuclei at 10 to 250 keV, total cross sections and resonance parameters for, (E/T), 25:28279
reactions with lead, natural uranium, and poisoned and pure water, pulsed, (E), 25:28161
reactions with nuclei, index to data in Experimental Cross Section Information Library, 25:28356 (UCRL-50400(Vol.3))
reactions with uranium-238 at 0.075 to 15 MeV, optical-model analysis of, (T), 25:28403
scattering by oxygen-16, elastic phase-shift calculations using two-body forces, (T), 25:28198
scattering by praseodymium chalcogenides and pnictides, inelastic, 25:27893
scattering of, collimation corrections in small-angle, (T), 25:28144 (RT/FIMA-69-5)
slowing down of, normal mode expansion with a simple scattering kernel for, (T), 25:28152
spectra in beryllium oxide (BeO) moderated system, time-of-flight method for measurement of, (E/T), 25:28769
spectra in fast reactors, resonance absorbers for measurement of 0.001 to 10 keV, (E/T), 25:28656(T) (EURFNR-842)
spectra in reactors, temperature effects on, (T), 25:28814
spectra measurements in reactors, use of lithium-6(n,α)t reaction for in-core, (E), 25:28753 (BLG-450)
transport equation for, transfer matrix method for solution of, 25:28798 (NYU-4090-1)
transport equation in one-dimensional cylindrical geometry, polynomial approximation and linear anisotropic diffusion for integral, 25:28145 (EIR-188)
transport equation with spherical symmetry, computer program for solution of stationary, 25:28147 (JUL-683-MA)
transport in bounded media, boundary-sources method for solving Boltzmann's equation for, (T), 25:28160
transport in finite media, exact analytic solutions for, (T), 25:27948
transport in homogeneous nonconcave media, solution of integral equation for, (T), 25:28159

XUM

transport in spheres and slabs, computer program for solution by j/sub n/ method, 25:28146 (EUR-4601)
transport in spheres, cylinders, and planes, computer program for solving one-dimensional Boltzmann equation for, (T), 25:28149(T) (ORNL-tr-2419)
transport of, Green's function for solution of time--energy-dependent, (T), 25:28154
transport of, solution of equations for time--energy-dependent, (T), 25:28156
transport problems for, review on methods for treatment of stationary, 25:28151 (TUBIK-21)
transport with fission, solution of general anisotropic energy-dependent equation for, (T), 25:28155
use for activation analysis of elements in tissues of farm animals, 25:26578 (CONF-680112-, pp 153-66)

NEUTRONS, EPITHERMAL
reactions (n,f) with uranium-235, reactivity measurement method for determination of, 25:28817
reactions with gross fission products from neutron irradiation of enriched uranium, total cross sections for, (E), 25:28404

NEUTRONS, FAST
dosimetry in mixed gamma field, paired ionization chambers for, 25:26538
effects on chromosomes of Crepis, aberrant, 25:26721
effects on defect production in niobium, annealing recovery from, (E), 25:27269
effects on deformation and expansion of liquid metal cooled fast breeder reactor core components, 25:28685 (BAW-1355)
effects on electric conductivity of beryllium and graphite, 25:28765
effects on embrittlement of A302B steel, 25:28682 (JAERI-1202)
effects on eyes in rabbits in comparison to gamma radiation, protective effects of adenosine monophosphate, cysteamine, and serotonin against cataract-inducing, 25:27014
effects on eyes of rabbits, RBE for pathological, 25:26945
effects on fuel cladding metals at high fluxes, 25:27266 (RD/B/N-1812)
effects on growth and photosynthesis in seedlings of silver maple and yellow poplar, effects of reduced light on, 25:27076
effects on mechanical properties and swelling of stainless steel fuel element cladding, (E), 25:28691(R) (GEAP-10028-37)
effects on n-type silicon, structure of defects induced in, 25:27848
effects on reproduction of HeLa cells, RBE for, 25:26906
effects on shrimp, lethal, 25:26917
effects on sound velocity in Type A533B steel at 503 to 550°F, 25:27268 (WHAN-FR-38)
effects on wheat, mutagenic, 25:26710
flux measurements using aluminum activation detectors, ASTM standard method for, 25:26481
flux measurements using iron activation detectors, ASTM standard method for, 25:26477
flux measurements using nickel activation detectors, ASTM standard method for, 25:26479
flux measurements using sulfur activation detectors, ASTM standard method for, 25:26480
interactions n + d at 20 to 60 MeV, convergence of nonrelativistic graphs for elastic scattering, 25:28166
production for use in therapy, design criteria of facility for, 25:26883
reaction with Z = 1 to 94 nuclei at 2.5 to 15 MeV, total cross sections for, (E), 25:28170
reactions (n,α), (n,p), and (n,2n) with A = 75 to 88 nuclei, activation cross sections for, (E), 25:28282
reactions (n,f) with plutonium-239, uranium-235, and uranium-238, fission yields from, (E), 25:28354 (NP-18723)
reactions (n,f) with thorium-232 and uranium-238 at 14.8 MeV, low-mass fission yields in, (E), 25:28385
reactions (n,f) with uranium-235 at 15.5 MeV, barrier parameters for, (T), 25:28504
reactions (n,f) with uranium-238 at 14 MeV, gamma spectra from technetium products of, (E), 25:28326 (CERN-70-30(Vol.2), pp 985-1000)
reactions (n,p) with helium-3 at 1, 3.6, and 6 MeV, cluster-model analysis of, (T), 25:28167
reactions (n,p), (n,α), and (n,2n) with nuclei, cross sections for, (E), 25:28273
reactions with osmium-192 at 14 MeV, gamma spectra from, (E), 25:28326 (CERN-70-30(Vol.2), pp 985-1000)
reactions with Z = 1 to 94 nuclei, effects of nuclear deformation on total cross sections for, (T), 25:28169
scattering by heavy nuclei at small angles, analysis of reported anomalies in elastic, (T), 25:28500
scattering by helium-3 at 1, 3.6, and 6 MeV, cluster-model analysis of elastic, (T), 25:28167
scattering by magnesium-24 at 14.2 MeV, cross sections and neutron spectra from, (E), 25:28265
scattering by Z = 22 to 40 nuclei at 3.2 MeV using polarized beam, optical-model analysis of elastic, (T), 25:28248
use for radiotherapy, comparison with cobalt-60 gamma beam, 25:26879

NEUTRONS, FISSION
effects on immune reactions in mice, effects of dose and dose rate on, 25:26679
effects on rice seeds, effects of dose rate, oxygen, storage, and water content on, 25:27070
slowing down in polyethylene and water, analysis of ages to indium resonance from, (E), 25:28157

NEUTRONS, FUSION
production in focus discharges in deuterium, (E), 25:27799

NEUTRONS, INTERMEDIATE
capture by gold-197, rhodium-103, and tantalum-181, gamma spectra from, (E), 25:28437

NEUTRONS, PILE
reactions (n,f) with thorium-232, average cross sections and yields from, (E), 25:28409
reactions (n,f) with uranium-235, mass-spectrometric search for argon and neon isotopes in ternary, 25:28419

NEUTRONS, THERMAL
capture by germanium-73, Q-value, excitation energies, and energies and intensities of γ rays from, (E), 25:28258
capture by lutetium-176, γ spectra from, (E), 25:28424
capture by neon-20 and -22, cross sections, gamma spectra, and Q values for, (E/T), 25:28257
capture by neon-20, -21, and -22 and nitrogen-14, cross sections and Q values for, (E), 25:28275
capture by promethium-147, ground-state and isomeric cross sections for, (E), 25:28373
capture by titanium-49 and -50, γ spectra and angular correlations from, (E), 25:28284
diffusion in water, effects of turbulence on, (E/T), 25:28815(T) (BNWL-tr-66)
diffusion length in media with small absorption, first-order corrections to, (T), 25:28150 (RCN-134)
effects on cotton, effects of variety on mutagenic, 25:26728
effects on electric conductivity of beryllium and graphite, 25:28765
effects on fungi, mutagenic, 25:27088
effects on ploidy in crop plants, 25:27087
flux measurements using activation detectors, ASTM standard method for, 25:26475
flux through graphite moderator lattice and graphite-styrofoam interface, time and space dependence of, (E), 25:28818
reactions (n,f) with nuclei, method for predicting prompt neutron yields from, (T), 25:28355(R) (TID-25659)
reactions (n,f) with plutonium-239, plutonium-241, and uranium-235, fission yields from, (E), 25:28354 (NP-18723)
reactions (n,f) with plutonium-239, uranium-233, and uranium-235, charge distributions in, (T), 25:28508
reactions (n,f) with plutonium-239, uranium-233, and uranium-235, prompt neutron yields from, (T), 25:28355(R) (TID-25659)
reactions (n,f) with uranium-233 and -235 and plutonium-239 and -241, krypton-85 branching ratios and yields in, (E), 25:28383
reactions (n,f) with uranium-235, gamma and x-ray spectra from products of, (E), 25:28325 (CERN-70-30(Vol.2), pp 967-84)
reactions (n,f) with uranium-235, gamma spectra from fragments from, (E), 25:28320 (CERN-70-30(Vol.2), pp 917-30)
reactions (n,f) with uranium-235, potential-energy contours and fragment kinetic-energy and most-probable-charge distributions from, (T), 25:28408
reactions with samarium-147 and -150, total cross sections, strength functions and resonance parameters for, (E), 25:28349 (KAPL-P-3930)
scattering by beryllium oxide and graphite, cross sections, phonon spectra, and scattering law for different crystal models for, (T), 25:28158
spectra in reactor lattices, effects of heterogeneous structure of coated particle fuels on, (T), 25:28658
spectrum in water moderated reactor fuel elements, computer program for, 25:28802 (EUR-4554)

NEVADA
site of Shoal Event in, recommendations for disposal of, 25:26403 (NVO-1229-105(Pt.1))

NEVADA TEST SITE
ground motion from underground nuclear explosions at, damage to buildings in Las Vegas and southern Nevada from, (E), 25:26400 (NVO-99-12)

NICKEL
cadmium-111 hyperfine field in, differential perturbed angular correlation measurements of, 25:27917
complexes with 5,7-diiodo-8-quinolinol, formation constants of, 25:26214
cross section data on, tables of multigroup, 25:28657 (HEDL-TME-71-36)
determination in plutonium nitrate solutions by atomic absorption spectrophotometry, 25:26154(T) (RFP-Trans-76)
determination in sea floor samples by neutron activation, 25:26188 (BNWL-SA-3803)
determination in yttrium oxides by solvent extraction and spectrography, 25:26168
determination in Zircaloy, chemical method for, 25:26171
effects on electric and mechanical properties and

XUM

microstructure of cast titanium, 25:27220
gamma absorption coefficient of, (E), 25:27826 (DEMO-70/11)
sorptive properties and surface film reactions with oxygen, 25:27224
structure of deformed single crystal, magnetic small-angle neutron scattering method for studies of dislocation, 25:27246 (JUL-675-FF)
NICKEL ALLOYS AND SYSTEMS
mechanical properties at 400 to 800°C, 25:27203 (INIS-mf-2)
properties for use as fuel cans for fast breeder reactors, 25:27213
welding in sodium at 580 to 700°C, self-, 25:27206 (KFK-Ext.Ber.-8/70-1)
Al--Ni--Zr, phase studies of, 25:27258
Be--Cu-base--Ni--Ti, properties of, aging and mechanical, 25:27232
Be-base--Ni, properties for use in welding heat resisting metals, 25:27177 (JUL-681-RX)
C--Mo-base--Ni, weldability of, 25:27185
Fe--Ni, electron correlation effects in Invar, 25:27868
Fe--Ni--Ti, fatigue strength of, effects of fine precipitates on, 25:27231
Ga--Ni-base, electron correlation effects in Ni_3Ga, 25:27868
Mo--Ni, ordering in intermetallic Ni_4Mo, field ion microscopy studies of, 25:27252
Mo--Ni--TiC-base, phase studies of two-phase region in, 25:27298
Nb_2O_5--Ni-base, oxidation of dispersion-strengthened, at 700 to 950°C, kinetics of, 25:27279 (INIS-mf-11)
Ni--Rh, electron correlation effects in, 25:27868
Ni--Ti-base, internal friction at 4 to 300°K, 25:27215
Ni--TiC-base, phase studies of two-phase region in, 25:27298
Ni--Zr, superconductivity of intermetallic Zr_2Ni, (E), 25:27654
Ni-base--V, dislocations in Ni_3V precipitates in, super, 25:27250
NICKEL HYDRIDES
spectral absorption lines of, in sunspot spectra, (E), 25:27390
NICKEL ISOTOPES Ni-58
effects on ir spectra of nickel oxinates, 25:26234
nitrogen-14 elastic scattering at 84 MeV, optical-model analysis of differential cross sections for, (E), 25:28274
proton elastic scattering at 6.9 MeV, optical-model analysis of angular distributions from, (E), 25:28262
NICKEL ISOTOPES Ni-59
energy-level density from cobalt-59 (p,n) and iron-56 (α,n) reactions, (E), 25:28285
energy-level transitions from proton reactions, branching ratios, gamma-ray angular distributions, and internal conversion coefficients for, (E/T), 25:28271
NICKEL ISOTOPES Ni-60
oxygen-16 reactions (O-16,2n), (O-16,2p), and (O-16,pn) at 42 to 52 MeV, excitation functions for gamma rays from, (E), 25:28213 (CERN-70-30(Vol.2), pp 911-15)
proton elastic scattering at 6.9 MeV, optical-model analysis of angular distributions from, (E), 25:28262
NICKEL ISOTOPES Ni-61
neutron total cross sections and resonance parameters at 10 to 250 keV, (E/T), 25:28279
proton elastic scattering at 6.9 MeV, optical-model analysis of angular distributions from, (E), 25:28262
NICKEL ISOTOPES Ni-62
effects on ir spectra of nickel oxinates, 25:26234
energy levels from cobalt-62 beta decay and copper-62 beta and electron-capture decay, skin--parity assignments for, (E), 25:28214 (CERN-70-30(Vol.2), pp 1105-13)
energy levels from copper-63(γ,p) reactions, spin--parity assignments for, (E), 25:28217 (LUNP-7013)
proton elastic scattering at 2.4 to 2.7 MeV with isobaric analog excitation, excitation function for, (E), 25:28237
proton elastic scattering at 6.9 MeV, optical-model analysis of angular distributions from, (E), 25:28262
NICKEL ISOTOPES Ni-63
energy levels from cobalt-63 beta decay, spin--parity assignments for, (E), 25:28214 (CERN-70-30(Vol.2), pp 1105-13)
energy levels from nickel-62 proton scattering, isobaric analog, (E), 25:28237
NICKEL ISOTOPES Ni-64
energy levels from copper-65(γ,p) reactions, spin--parity assignments for, (E), 25:28217 (LUNP-7013)
proton elastic scattering at 6.9 MeV, optical-model analysis of angular distributions from, (E), 25:28262
NICKEL ISOTOPES Ni-67
beta decay of, gamma spectra, β--γ coincidences, and log ft for, (E), 25:28221
NICOTINIC ACID
effects on determination of uranium by extraction--photometry, 25:26163
NIMONIC 75
corrosion by melting glasses in radioactive waste vitrification process, 25:26334(T) (ORNL-tr-2410, pp 143-89)
NINE MILE POINT POWER REACTOR
operation of, safety limits and environmental monitoring requirements for 1850 MW(t), 25:28595 (DOCKET-50220-62)
NIOBIUM
boron-12 NMR in, quadrupole effects on spectra and coupling constants from, (E), 25:27923
determination by photometry using carboxy derivatives of 2,6,7-trihydroxy-9-phenyl-3H-xanthen-3-one, 25:26174
diffusion of silicon in, by reactive processes, 25:27239
dislocation damping by phonon viscosity in, <111> wave attenuation study of, 25:27905
effects on electric conductivity, microhardness, and microstructure of titanium, 25:27223
hardness of irradiated and unirradiated, hot, 25:27236
nitrogen-12 NMR in, quadrupole effects on spectra and coupling constants from, (E), 25:27923
oxidation during glow discharge, for Josephson junction fabrication with lead, 25:27659
proton and helium-ion backscattering from single crystals of, effects of lattice defects on, 25:27840 (IPP-7/3)
radiation effects on defect production in, at 120 to 500°K, annealing recovery from fast neutron, 25:27269
sorptive properties of (100) crystal surface of, for argon crystals, LEED studies of, 25:27235
welding to niobium, testing of filler alloys for, 25:27177 (JUL-681-RX)
welding to tantalum, testing of filler alloys for, 25:27177 (JUL-681-RX)
NIOBIUM ALLOYS AND SYSTEMS
fabrication of, effects of boron additions on, 25:27227
mechanical properties at 400 to 800°C, 25:27203 (INIS-mf-2)
oxidation of, effects of boron additions on, 25:27227
B--Hf--Nb-base--W, strength at 1200°C, 25:27227
Be--Cu--Nb--Zr-base, properties for use as structural material for reactors, 25:27190(P)
Be--Nb--Sb--Zr-base, properties for use as structural material for reactors, 25:27190(P)
Be--Nb--Sn--Zr-base, properties for use as structural material for reactors, 25:27190(P)
Be--Nb--Te--Zr-base, properties for use as structural material for reactors, 25:27190(P)
Fe--Nb, mechanical properties of Laves phase $NbFe_2$, 25:27211 (UCRL-20301)
Hf--Nb-base, strength at 1200°C, 25:27227
Hf--Nb-base--W, oxidation resistance at 1200°C, 25:27227
Nb--Sn, critical current in ribbon of, temperature dependence of, 25:27658
Nb--Sn, superconducting diffusion layers in, electron microprobe studies on, 25:26159
Nb--Ti, magnetization of superconducting, dimensional effect in, (E), 25:27644 (KHFTI-70-8)
Nb--Ti, superconducting transition in solid solutions of, 25:27646
Nb--Ti--Zr, magnetization of superconducting, dimensional effect in, (E), 25:27644 (KHFTI-70-8)
Nb--Ti-base, internal friction at 4 to 300°K, 25:27215
Nb--U-base--Zr, reactions with carbon dioxide, nitrogen, oxygen, and water vapor at 27 to 1000°C, kinetics of, 25:27210 (SC-DR-710124)
Nb--Zr, magnetization of superconducting, dimensional effect in, (E), 25:27644 (KHFTI-70-8)
Nb--Zr-base, internal friction at 4 to 300°K, 25:27215
Nb-base--Zr, hardness of irradiated and unirradiated, hot, 25:27236
Nb-base--Zr, properties of tubular coextruded joints of stainless steel to, effects of thermal cycling at 300 to 1600°F on, 25:27179 (N-71-10454)
NIOBIUM CARBIDES
electron band structure of, (E/T), 25:27907
NIOBIUM ISOTOPES Nb-91
energy levels from zirconium-90(He-3,d) reactions, antianalog, (E), 25:28363
NIOBIUM ISOTOPES Nb-93
neutron reactions (n,2n) with, cross sections for fast, (E), 25:28273
NIOBIUM ISOTOPES Nb-95
effects on reproductive behavior and spermatogenesis in male mice following subcutaneous injection, 25:26962
incorporation in oxalate for use in tumor scanning, 25:26859
separation from irradiated aluminum--uranium and uranium--zirconium fuels by chlorination and pyrohydrolysis, 25:26332(T) (ORNL-tr-2410, pp 98-120)
separation of plutonium from, by solvent extraction using tridodecylamine, 25:26330(T) (ORNL-tr-2410, pp 14-78)
NIOBIUM ISOTOPES Nb-97
energy levels from zirconium-97 beta decay, spin--parity assignments for, (E), 25:28438
NIOBIUM OXALATES
labeling with niobium-95 for use in tumor scanning, 25:26859
NIOBIUM OXIDES
properties of, 25:27281 (INIS-mf-13)
Nb_2O_5--Ni-base, oxidation of dispersion-strengthened, at 700 to 950°C, kinetics of, 25:27279 (INIS-mf-11)
NITRIC ACID
complexes with tetravalent plutonium in aqueous methanol solutions, spectrophotometric studies on, 25:26274
solvent properties for stainless steel-clad uranium dioxide pellets, 25:26330(T) (ORNL-tr-2410, pp 14-78)

XUM

NITROGEN
argon-atom scattering by molecular, differential cross sections for, (E), 25:27451
density at 85 to 150 km in ionosphere, theoretical model of diurnal variation of atomic and molecular ionized, (T), 25:27614
determination in plutonium oxide--uranium oxide pellets by spectrophotometry, 25:26153 (LA-4622)
determination in Zircaloy, 25:26171
diffusion in plutonium nitride--uranium nitride fuels, self, (E), 25:28687 (BMI-1898, Sect.A)
excitation in aurorae, 5- to 25-keV-proton and .045- to 25-keV-electron, (E), 25:27616
implants in diamond single crystals, analysis, 25:27858
intensity in aurorae, excitation of 1134-, 1200-, 1493-, and 1743-A far-uv from, atomic, (E/T), 25:27617
plasma of, effects of vibrational excitation on frequency of electron--molecule collisions in, (T), 25:27711
reactions with niobium--uranium--zirconium alloy at 27 to 1000°C, kinetics of, 25:27210 (SC-DR-710124)
specific heat of high-temperature, effect of electron excitation on, 25:27692
NITROGEN IONS
energy losses in selenium, effective atomic number for, (E), 25:27833
reactions with aluminum at 100 to 350 keV, cross sections and Pauli-excitation mechanisms of K-shell ionization in, 25:27453
NITROGEN ISOTOPES
exchange during adsorption on iron films at 350°C and 2 to 20 torr, 25:26245
NITROGEN ISOTOPES N-12
nuclear magnetic resonance in niobium, tantalum, titanium borides, and zirconium borides, coupling constants and spectra from, (E), 25:27923
NITROGEN ISOTOPES N-13
energy levels of, calculation of nucleon widths for lowest T = 3/2, (T), 25:28172
energy levels of, role of configuration states in isospin-forbidden proton decay of T = 3/2, 25:28179
NITROGEN ISOTOPES N-14
alpha inelastic scattering at 10.2 to 18.2 MeV, excitation functions for, (E), 25:28177
neutron capture by, Q values for thermal, (E), 25:28275
reactions with cerium, gold-197, and iridium, cross-section limits for fission isomer excitation in, (E), 25:28399
scattering by carbon-12 and aluminum-27 at 65 to 88 MeV, optical-model analysis of differential cross sections for elastic, (E), 25:28274
scattering by nickel-58 and silicon-28 at 84 MeV, optical-model analysis of differential cross sections for elastic, (E), 25:28274
NITROGEN ISOTOPES N-15
determination in heme for life span studies on erythrocytes in burn patients, mass spectrometric, 25:26572
effects on spectra of vanadium oxide trinitrate complex with acetonitrile, 25:26235
energy-level transitions from nitrogen-14 (n,γ) reactions, energies and intensities of, (E), 25:28275
use as tracer for nonprotein nitrogen studies in ruminants, 25:26578 (CONF-680112-, pp 153-66)
NITROGEN OXIDES NO
density at 85 to 150 km in ionosphere, theoretical model of diurnal variation of ionized and NO, (T), 25:27614
effects on survival of irradiated spores of Osmunda regalis, 25:27069
effects on x-radioinduced polymerization of gaseous chloroethylene, 25:26282
NITROGEN OXIDES NO_2 OR N_2O_4
scavenging from atmosphere by raindrops, laboratory studies of, 25:26375 (CONF-700601-, pp 261-9)
NITROGEN OXIDES N_2O
effects on yields from electron pulse and γ radiolysis of aqueous solutions of phenyl glucopyranoside, 25:26304
effects on yields from γ radiolysis of S-allyl-L-cysteine sulfoxide and S-propyl-L-cysteine sulfoxide, 25:26294
NORTH ANNA POWER REACTOR, UNIT 1
containment spray system for, modifications for periodic flow testing of, 25:28617 (DOCKET-50338-29)
site for, construction permit provisions for protection of, 25:28616 (DOCKET-50338-28)
NORTH ANNA POWER REACTOR, UNIT 2
containment spray system for, modifications for periodic flow testing of, 25:28617 (DOCKET-50338-29)
NORWAY
nuclear power plant development in, 25:28523 (CONF-700550-, Paper 1)
NOVAE
spectrophotometry of Serpentis 1970 near maximum light, (E), 25:27322
NOVO VORONEZH POWER REACTOR, UNIT 1
fuels for, effects of burnup on plutonium build-up in, (E/T), 25:28532
NOZZLES
uranium enrichment using separation, in Europe, economic evaluation of, 25:26424(T) (CONF-700557-3)
NUCLEAR AUXILIARY POWER SYSTEMS
design of conceptual 25 kW(e) zirconium hydride thermoelectric reactor, for space missions, 25:28783 (AI-AEC-Memo-12717)
heat sources for, computer programs for evaluating hazards to man following earth impaction of, 25:26429 (SC-R-7121)
power cycles for, development of radioisotope-fueled organic and steam, 25:26433
NUCLEAR ELECTRIC MOMENTS
calculations for 5d-shell nuclei, using pure shell model configurations, 25:28245
NUCLEAR EXPLOSIONS, UNDERGROUND
cavity formation by Greeley Event, postshot drill hole data on, 25:26412 (UCRL-50979)
ground motion from Nevada Test Site, damage to structures in Las Vegas and southern Nevada from, (E), 25:26400 (NVO-99-12)
ground motion from, summary of 1957 to 1970 data on, 25:26411 (SC-DC-713865)
ground motions from Calabash Event, calculated pseudo-relative velocity spectra from measurements of, 25:26401 (NVO-1163-218)
NUCLEAR ISOMERS
production of spontaneously fissioning, cross sections for, (E), 25:28306 (CERN-70-30(Vol.1), pp 575-87)
NUCLEAR MAGNETIC RESONANCE
perturbed angular correlation for rare-earth ions, effects of coaxial magnetic and electric fields on time-integral, (T), 25:27918
perturbed angular correlation in ferromagnetic materials, effects of noncoaxial magnetic and electric fields on, 25:27919
NUCLEAR MATERIALS MANAGEMENT
safeguards for, inventory control problems in, 25:26444 (BNL-15601)
NUCLEAR MATTER
binding energy of, calculation using one-boson exchange potential of, (T), 25:28448 (CERN-70-30(Vol.2), pp 1133-5)
binding energy of, off-shell effects on, (T), 25:28520
quasi-particle interaction in, model space calculation of, (T), 25:28453 (NYO-4032-37)
NUCLEAR MODELS
Fermi gas, effects of spin--spin and spin--orbit forces on decoupling parameter in, (T), 25:28484
intermediate coupling, extension to 2p-1h excitation modes, (T), 25:28518
optical, computer program for analysis of elastic scattering, (T), 25:28450 (N-70-42846)
unified, energy-level transitions in heavy deformed nuclei in, probabilities for, 25:28353 (NP-18695)
variable-moment-of-inertia, review of, (T), 25:28446 (CERN-70-30(Vol.2), pp 813-27)
NUCLEAR PHYSICS
book: Applications of Nuclear Physics, 25:28379
hyperfine interactions in, lectures on, 25:27915 (NP-18702)
NUCLEAR POWER PLANTS
book: Construction of Nuclear Installations, 25:28531
buildings and structures for, fabrication methods for concrete, 25:28531
construction of, quality assurance planning for, 25:28550 (AECL-3670, pp 59-63)
control system for, design requirements of, 25:28675
design of, reliability techniques used in, 25:28521 (AECL-3670, pp 39-44)
development in Germany, review of, 25:28644
development in Japan, technical and economic aspects of, 25:28584
development in Norway, 25:28523 (CONF-700550-, Paper 1)
development in Sweden, 25:28525 (CONF-700550-, Paper 3)
development in United Kingdom, 25:28524 (CONF-700550-, Paper 2)
development in West Germany, 25:28526 (CONF-700550-, Paper 4)
development of, conference on, 25:28522 (CONF-700550)
development of, economics for worldwide, 25:28533
development of, review of, 25:28544
effluents from, control methods for radioactive and thermal, 25:28623
effluents from, control of chemical, radioactive, and thermal, 25:28621 (STI/PUB-261)
environmental effects of, 25:28527 (DUN-SA-166)
environmental effects of U. S, 25:28530
environmental effects of, comparison of fossil fueled plants to, 25:28627
operation of, conference on equipment and systems reliability in, 25:28546 (AECL-3670)
operation of, effects of component reliability and maintainability on, 25:28554 (AECL-3670, pp 89-96)
operation of, effects of component reliability and maintainability on, 25:28552 (AECL-3670, pp 73-81)
operation of, effects of radiation environments on, 25:28572
operation of, performance criteria for, 25:28547 (AECL-3670, pp 13-20)
operation of, reliability analysis methods for evaluation of, 25:28553 (AECL-3670, pp 83-8)
personnel for, licensing requirements for, 25:28725
power conversion system for, description of stored liquid heat source for auxiliary, 25:28745(P)
radiation dose to human populations from, 25:26741
radioactive contamination of oysters in vicinity of, 25:26742

XUM

safety aspects of, 25:28544
safety criteria for, 25:28675
site for, environmental radiation monitoring program for, 25:28625
sites for, technical and economic aspects of ocean, 25:28643
sites for, technical and economic aspects of sea-bottom, 25:28630
siting of, U.S. AEC seismic and geologic standards for criteria for, 25:28628
standards for, review of programs for development of, 25:28536
thermal effluents from Sweden, economics of urban heating system using, 25:28574
thermal effluents from, development of COL HEAT and TOPLYR programs for simulating ecological effects of, 25:28710(R) (HEDL-TME-71-26)
thermal effluents from, model for evaluating ecological effects of methods for, 25:28710(R) (HEDL-TME-71-26)
NUCLEAR REACTION ANALYSIS
sensitivity, principles, and uses of, review on, 25:26186 (BARC-529)
NUCLEAR REACTIONS
analog resonances in charge-exchange, 25:28457
analog resonances in deformed region, 25:28472
analog resonances in isospin forbidden, 25:28222
analog resonances in, asymmetry in fine structure of, (T), 25:28468
analog resonances in, fine structure of, (T), 25:28463
analog resonances in, microscopic calculation of escape widths of, (T), 25:28466
analog resonances in, modified Schiffer procedure for determination of spectroscopic factors for, (T), 25:28473
analog resonances in, R-matrix analysis for neutron spectroscopic factors for, (T), 25:28474
analog resonances in, role of anti-analog state in decay of, (T), 25:28467
analog resonances in, survey on experiments interpretations of, 25:28470
analog resonances in, survey on theories for, 25:28465
coherent and incoherent, for high-energy physics, 25:27978
compound nucleus excitation with particle and gamma emission in, isomer ratio for, (T), 25:28502
compound nucleus states in, allowed neutron decay of, (T), 25:28460
deuteron decay in compound, nucleon angular correlations in, (T), 25:28487
giant resonance excitation, splitting of E1, 25:28222
rearrangement mechanism of, exact N-body theory for, 25:28485
resonances in, tensoral formulation of multi-level, multi-channel formula for, (T), 25:28454 (RT/FI-(70)38)
schematic theory of, extension to isospin formalism and isobaric analog resonances, 25:28492
three-body model for lithium-6-induced, (T), 25:28486
NUCLEAR REACTIONS (DIRECT)
analog resonances in stripping and pick-up, on light nuclei, 25:28458
analog resonances in, properties of, 25:28223
analog resonances in, proton decay of, 25:28471
cross sections for single-nucleon transfer, peripheral-model calculations of, (T), 25:28498
resonance narrowing effects in three-particle final-state, (T), 25:28497
theory of deuteron stripping, isospin coupling in, 25:28462
two-nucleon stripping at low energies, polarization effects in, (T), 25:28496
NUCLEAR STRUCTURE
calculations for A = 6 to 9 nuclei using shell model with effective interactions, (T), 25:28452 (NP-18717)
calculations of, in transition regions, (T), 25:28447 (CERN-70-30(Vol.2), pp 1129-32)
calculations using charge-independent pairing Hamiltonian, states of intermediate charge symmetry in, (T), 25:28490
calculations using RPA, renormalization constants in, (T), 25:28509
description for deformed even-even nuclei using collective quadrupole excitations, (T), 25:28501
description using data on Coulomb energies, 25:28475
isobaric analog states in, review of formalism for description of, (T), 25:28507
nucleon--antinucleon bound state, existence of heavy meson resonance as, 25:28026 (NP-18774)
research at OSIRIS facility, experimental techniques for, (E), 25:28107 (CERN-70-30(Vol.2), pp 1003-5)
review of experimental data and theoretical predictions concerning, (T), 25:28449 (ISS-70/17)
shape-fluctuation model of ground-state bands in even-even nuclei, 25:28481
NUCLEAR THEORY
calculation of maximum-overlap orbital using energy variational principle and perturbation theory, 25:28511
conference on nuclear isospin, 25:28455
energy splittings of parallel and antiparallel n-p coupling states in deformed odd-odd nuclei, 25:28514
Hartree-Fock method in, linearized version of, 25:28519
model space calculation of the quasi-particle interaction for nuclear matter, 25:28453 (NYO-4032-37)
Moshinsky brackets in, derivation of sum rules and symmetry relations for generalized and ordinary, 25:28506
neutron and proton effective charge corrections in, 25:28456
nucleon--nucleon interaction in, description using one-boson exchange potential, (T), 25:28448 (CERN-70-30(Vol.2), pp 1133-5)
one-boson-exchange potentials in, analysis of semiempirical generalized, 25:28513
relation between nuclear binding and excitation energies, 25:28515
shape-fluctuation model of ground-state bands in even-even nuclei, 25:28481
three-nucleon system in, separable-expansion method for, 25:28510
NUCLEI
beta decay of A approximately 132, half-lives and Q values for, (T), 25:28327 (CERN-70-30(Vol.2), pp 1001-3)
beta decay of neutron-deficient Z = 47 to 78, Q values for, (E), 25:28297 (CERN-70-30(Vol.1), pp 353-60)
binding energy of light, effective four-body nucleon interaction for, 25:28482
content in neutron stars, calculations of, (T), 25:27311 (CERN-70-30(Vol.2), pp 759-68)
Coulomb displacement energies of light, shell-model calculations for, (T), 25:28479
Coulomb displacement energies of, systematics of, (T), 25:28478
decay probability for electron capture relative to beta decay, calculations of, (T), 25:28494
decoupling parameters for A = 159 to 183, effects of spin--spin and spin--orbit forces on, (T), 25:28484
deuteron reactions (d,α) with light, mechanism in isospin-violating direct, (T), 25:28459
deuteron reactions (d,p) near 20 MeV, adiabatic treatment of, (T), 25:28512
deuteron reactions (d,p) with, isobaric analog resonance effects in, 25:28471
electric quadrupole moments of odd-mass spherical, generalized Bohr-model description with core excitation for, 25:28499
electron inelastic scattering with γ emission in heavy, study of low-lying excited states by, (T), 25:28491
electron reactions (e,e'2p) with, study of proton-proton correlations by, (T), 25:28491
electron scattering at 0.2 to 2.0 MeV, Coulomb corrections to Bethe--Heitler cross sections for bremsstrahlung production by, (T), 25:28451 (N-71-10999)
electron-capture decay of Z = 14 to 98, relativistic corrections to exchange and overlap effects in, (T), 25:28495
elementary particle reactions with, production of high-energy particles from, 25:27978
energy levels for odd-N A = 153 through 171, calculation using superfluid model and Woods-Saxon potential, (T), 25:28346 (JINR-E4-5567)
energy levels in heavy even--even, lifetimes of 2+ and 4+ rotational, (E), 25:28353 (NP-18695)
energy levels of A < 165, computer program for calculating intrinsic, (T), 25:28439 (AECL-3801)
energy levels of A = 3, study by method of reciprocal interaction parameter expansion of, (T), 25:28163 (ITF-70-100-P)
energy levels of beta-unstable, conference on properties and structure of, (E/T), 25:28308 (CERN-70-30(Vol.2))
energy levels of deformed, effects of Coriolis coupling on Nilsson, (T), 25:28317 (CERN-70-30(Vol.2), pp 829-45)
energy levels of even--even, isospin impurities in ground-state, (T), 25:28516
energy levels of even--even, transition quadrupole moments in variable-moment-of-inertia model for, (T), 25:28517
energy levels of even-even, shape-fluctuation model of ground-state bands of, (T), 25:28481
energy levels of light, effects of ground-state correlations on, (T), 25:28505
energy levels of, effect of Coulomb distortions on isospins of ground-state, (T), 25:28476
energy-level transitions in A = 186 to 196, multipole mixing ratios for, (T), 25:28316 (CERN-70-30(Vol.2), pp 779-812)
energy-level transitions in A = 90 to 92 and 140 to 142, review of, (E), 25:28343 (CERN-70-30(Vol.2), pp 1125-7)
energy-level transitions in heavy deformed, unified model for probabilities of, (T), 25:28353 (NP-18695)
energy-level transitions in light, analog to anti-analog, 25:28224
energy-level transitions in Z = 7 to 21, calculations of E2, (T), 25:28189
energy-level transitions in, tables of abundances, energies, half-lives, and production modes of, (E), 25:28400
energy-level transitions in, tables of gamma--gamma directional-correlation coefficients for, (T),

XUM

25:28401
half-lives of A = 440 to 480, Strutinsky-shell-correction calculation of, (T), 25:28310 (CERN-70-30(Vol.2), pp 646-53)
half-lives of A = 75 to 147, (E), 25:28340 (CERN-70-30(Vol.2), pp 1093-1103)
heavy-ion reactions at 210 MeV with intermediate, cross sections for delayed protons from, (E/T), 25:28300 (CERN-70-30(Vol.1), pp 457-86)
helium-3 reactions with, analysis for imaginary isovector term in optical potential for, (T), 25:28461
internal conversion coefficients at 50 keV to 10 MeV for Z = 3 to 30, (E/T), 25:28271
isomers of Z = 83 to 92, cross sections for production of spontaneously fissioning, (E), 25:28306 (CERN-70-30(Vol.1), pp 575-87)
lifetimes of heavy deformed, delayed coincidence method for measuring, (E), 25:28353 (NP-18695)
magnetic dipole moments of odd-mass spherical, generalized Bohr-model description with core excitation for, 25:28499
magnetic moments and spins of short-lived, methods for determining, (E), 25:27914 (CERN-70-30(Vol.1), pp 361-81)
mass formulas for neutron-rich, pairing and shell corrections for, (T), 25:28293 (CERN-70-30(Vol.1), pp 275-306)
masses of Garvey--Kelson, liquid-drop, and shell-model equations for, (T), 25:28291 (CERN-70-30(Vol.1), pp 165-216)
masses of highly unstable, extrapolation procedures for determining, (T), 25:28292 (CERN-70-30(Vol.1), pp 263-73)
masses of, calculations using liquid-drop model with shell terms based on Nilsson model with Strutinsky normalization and BCS pair correlations, (T), 25:28441 (CERN-70-30(Vol.1), pp 217-62)
masses of, method for direct determination of, 25:26547 (CERN-70-30(Vol.1), pp 307-19)
neutron elastic scattering by heavy, analysis of reported small-angle anomalies in, (T), 25:28500
neutron fission of, method for predicting prompt neutron yields from thermal, (T), 25:28355(R) (TID-25659)
neutron reactions (n,α) with, as tool for studying neutron resonances, 25:28345 (JINR-E3-5483)
neutron reactions with, index to data in Experimental Cross Section Information Library, 25:28356 (UCRL-50400(Vol.3))
neutron total cross sections for Z = 1 to 94, effects of nuclear deformation in fast, (T), 25:28169
neutron total cross sections of Z = 1 to 94, at 2.5 to 15 MeV, (E), 25:28170
nuclear electric quadrupole moments of Z = 7 to 21, (T), 25:28189
nuclear quadrupole moments of A = 182 to 196, (T), 25:28316 (CERN-70-30(Vol.2), pp 779-812)
photon elastic and inelastic scattering by even-even, collective model analysis of tensor polarizability in giant resonance region, (T), 25:28489
photon reactions (γ,n) and (γ,p) at 40 to 140 MeV, shell model analysis with short-range nucleon-nucleon correlations, (T), 25:28488
photon scattering by, amplitude and differential cross section for, 25:28070
production of, review of methods for, (T), 25:28309 (CERN-70-30(Vol.2), pp 605-44)
properties far from the beta-stability valley, review of, (T), 25:28444 (CERN-70-30(Vol.1), pp 497-516)
properties far from the region of beta stability, conference on, (E/T), 25:28440 (CERN-70-30(Vol.1))
properties of highly unstable, review of experimental techniques for studying, (E), 25:28290 (CERN-70-30(Vol.1), pp 21-45)
properties of Z = 20 to 120, liquid-drop-model calculations of binding energies, shape coefficients, and spin--parity assignments, (T), 25:28441 (CERN-70-30(Vol.1), pp 217-62)
properties of, review of theoretical predictions of chemical, (T), 25:28309 (CERN-70-30(Vol.2), pp 605-44)
proton elastic and inelastic scattering at 6 to 17.5 MeV by A = 23 to 35, core-excitation analysis of differential and integrated cross sections from, (T), 25:28261
proton elastic and inelastic scattering with isobaric analog excitation, review on, 25:28469
proton elastic and inelastic scattering with isobaric analog excitation, determination of spectroscopic factors in, 25:28464
proton reactions (p,d) with, adiabatic treatment of, (T), 25:28512
proton reactions (p,d) with, isobaric analog resonance effects in, 25:28471
proton reactions (p,t) with 1p-shell, analysis using zero-range DWBA, 25:28204
proton reactions at 1 GeV, experimental studies of nucleon correlations from, 25:27958
radii of A = 3, dependence on interaction parameter of, (T), 25:28163 (ITF-70-100-P)
stability of, far from stability line, (T), 25:28289 (CERN-70-30(Vol.1), pp 1-19)
stability of, review of theoretical predictions of, (T), 25:28309 (CERN-70-30(Vol.2), pp 605-44)

NUCLEI (CELLS)
radiation effects on size of dill plants, x, 25:27081
NUCLEIC ACID
labeling with phosphorus for use in metabolism studies, 25:26617
radiation effects on biochemical structure of, effects of dose on gamma, 25:26660
radiation effects on synthesis of, in Blepharisma during regeneration, carbon-14 tracer study of uv, 25:26648
radiation effects on synthesis of, in Micrococcus radiodurans, dose dependence of gamma, 25:26639
NUCLEIC ACID, DEOXYRIBO-
complexes with proflavine, radiation effects on electron transfer in, ESR spectral studies on γ, 25:26638
effects of depressed synthesis of, on survival of irradiated L cells, 25:26969
metabolism in frog eggs, preparation of phosphorus-labeled-nucleic acids for studies of, 25:26617
molecular weight of mammalian, tritium effects on, 25:26592
radiation damage to thymine in, of Micrococcus radiodurans, repair of γ, 25:26643
radiation effects on content of dill plants, x, 25:27081
radiation effects on molecular weight of, in Ehrlich ascites cells, use of guanidinium chloride in alkaline sucrose gradient for determination of x, 25:26629
radiation effects on mouse endometrial glandular epithelium, 600-R x, 25:26659
radiation effects on polarity of phage lambda, x, 25:26692
radiation effects on release of, by phage lambda, x, 25:26693
radiation effects on semiconservative replication of bacteria, effects of nalidixic acid on uv, 25:27125
radiation effects on synthesis of, in human amnion cells, effects of dose and growth rate on x, 25:26630
radiation effects on synthesis of, in human cells, photosensitizing effects of trisoralen on uv, 25:26808
radiation effects on synthesis of, in lens epithelium of rats, x, 25:27000
radiation effects on transforming bacteria, repair of uv, 25:27124
radiation effects on, in hepatectomized rats, effects of dose and time on, 25:27020
radioinduced breaks in Chinese hamster cell, effects of age on x, 25:26625
radioinduced crosslinks and double single strand breaks in, effects of oxygen on γ, 25:26637
radioinduced damage in vertebrate cell, effects of cell type and postirradiation conditions on repair of uv, 25:26635
radioinduced damage of, protective effects of cysteine, GED, and pentamethylene diguanidine against ionizing, 25:26801
radioinduced degradation of Micrococcus radioduran, x, 25:26627
radioinduced degradation of, uv, 25:26657
radioinduced inactivation of virus, uv, 25:26691
radioinduced inhibition of synthesis of, analysis of viral induced DNA synthesis in cells following x, 25:26691
radioinduced single strand breaks in bacteria, effects of dose rate, oxygen, and temperature on x, 25:26655
radioinduced single strand breaks in Ehrlich ascites cell, hamster lung cell, L cell, and porcine kidney cell, mechanisms of repair in x, 25:26953
radioinduced unscheduled synthesis of, in mammalian cells, effects of dinitrophenol and puromycin on uv and x, 25:27002
radioprotective effects in bacteria, uv, 25:27122
repair replication in uv-irradiated human xeroderma pigmentosum cells, 25:26634
replication in bacteriophage T4, preparation of tritium labeled thymidine for studies of, 25:26570
NUCLEIC ACID, RIBO-
effects of depressed synthesis of, on survival of irradiated L cells, 25:26969
metabolism in frog eggs, preparation of phosphorus-labeled-nucleic acids for studies of, 25:26617
radiation effects on synthesis of messenger, effects of 5-fluorouracil and uracil on uv, 25:27123
radiation effects on synthesis of, in endometrial epithelium of mice, whole-body x, 25:27031
radiation effects on synthesis of, in HeLa cells, inhibitory x, 25:26983
radiation effects on synthesis of, in rat livers, methods for determining, 25:26641
radioinduced inactivation of infectivity of, isolated from tobacco mosaic virus, photoreactivation of uv, 25:26653
radioinduced inactivation of, from potato virus X, effects of wavelength on uv, 25:27108
radioprotective effects in bacteria, uv, 25:27122
radioprotective effects in bacteria, x, 25:27120
synthesis in cultured lymphocytes, effects of, on response of lymphocytes to x radiation, 25:26903
synthesis in grasshopper embryos, effects on recovery from x-radioinduced prophase reversion of, 25:26911
NUCLEOGENESIS
cross sections for $^{16}O + ^{12}C$ burning, (E), 25:27309

XUM

(ANU-P-471)
γ-process abundances in, relative to solar system, (T), 25:28441 (CERN-70-30(Vol.1), pp 217-62)
models of, for antimatter concentrations in Universe, (T), 25:27426
r process in, dynamics of, (T), 25:27310 (CERN-70-30(Vol.2), pp 735-57)
NUCLEONS
electric polarizability of, symmetric quark model for, 25:27983
interactions anti K + N → anti K + N, SU(3) chiral Lagrangian model for total cross sections of, (T), 25:28037
interactions anti K + N → π + Σ(Λ), SU(3) x SU(3) chiral Lagrangian model for total cross sections of, (T), 25:28037
interactions anti K + N, SU(3) x SU(3) chiral Lagrangian model for scattering lengths for, (T), 25:28037
interactions e + N, comparison of vector-meson dominance predictions with ω production in, 25:27982 (DESY-71/12)
interactions γ + N → Δ⁰ + ω, OPE amplitude and ωπγ coupling constants from, 25:27990
interactions γ + N, derivative amplitudes for ω production, 25:28000
interactions in light nuclei, effective four-body, 25:28482
interactions in nuclear emulsions at TeV range, multiple meson production in, 25:28050
interactions K + N, imaginary part of Regge trajectories for, 25:28036
interactions K⁺ + N → K + π + N, graphical illustration of isospin analysis of, 25:28039
interactions K⁻ + N → K + π + N, graphical illustration of isospin analysis of, 25:28039
interactions K⁺ + N, Argand diagram analysis of s-channel helicity amplitudes of, 25:28035
interactions K⁻ + N, Argand diagram analysis of s-channel helicity amplitudes of, 25:28035
interactions N + N → N + π + N, graphical illustration of isospin analysis of, 25:28039
interactions ν + N at high energies, damped residue function and asymptotic limit of scaling function in duality model for inelastic, (T), 25:28006
interactions π + N → π + N*, s-channel helicity conservation constraints on t-channel exchanges in, (T), 25:28028 (SU-1206-242)
interactions π + N → π + π + N, graphical illustration of isospin analysis of, 25:28039
interactions π + N, effects of imaginary part of Regge trajectories on differential cross sections for backward, 25:28036
interactions with leptons, parton and dual model for deep inelastic, 25:28001
scattering by carbon at 142, 210, and 330 MeV, optical potential analysis of elastic, (T), 25:28199
NUCLEOPROTEINS
radioinduced crosslinks and double single strand breaks in, effects of oxygen on γ, 25:26637

O

OBRIGHEIM POWER REACTOR (GERMANY)
ventilation system for, design parameters of, 25:28545
OIL SHALES
energy partitioning in, during hypervelocity impact by projectiles, two-material Eulerian code for studying, (T), 25:26354 (SC-R-70-4402)
OLDBURY REACTORS
design characteristics of, 25:28544
pressure vessel for Unit 1, strains in top of prestressed concrete, (E/T), 25:28528 (RD/B/N-1784)
OLEIC ACID
oleic acid--urea, radiolysis of clathrate compounds of, at -196°C, ESR studies on kinetics of radical transformation in γ, 25:26312
OOCYTES
radiation effects on, in ovaries of beagle dogs, delayed x, 25:27009
ORGANIC ACIDS
radiation effects on content of, in leaves and roots of corn and cotton plants following seed exposure, effects of dose on γ, 25:27074
ORGANS
function studies using nuclear medicine, 25:26829
scanning for diagnosis of lesions, data analysis method for use in, 25:26856
zinc-65 uptake and distribution in, of rats, 25:26611
ORNL RESEARCH REACTOR
maintenance during October to December 1970, 25:28762(R) (ORNL-TM-3369)
operations during October to December 1970, 25:28762(R) (ORNL-TM-3369)
OSKARSHAMN POWER REACTOR
design parameters of, 25:28637
OSMIUM ALLOYS AND SYSTEMS
Mo--Os, superconductivity of intermetallic Mo_3Os, (E), 25:27654
OSMIUM ISOTOPES Os-176
beta decay of, gamma spectra and half-lives for, (E), 25:28322 (CERN-70-30(Vol.2), pp 939-47)
half-life of, (E), 25:28386
OSMIUM ISOTOPES Os-177
half-life of, (E), 25:28386
OSMIUM ISOTOPES Os-178
half-life of, (E), 25:28386
OSMIUM ISOTOPES Os-179
electron-capture decay of, half-life and gamma energies and intensities from, (E), 25:28348 (JINR-P6-5617)
half-life of, (E), 25:28386
OSMIUM ISOTOPES Os-180
electron-capture decay of, half-life and gamma energies and intensities from, (E), 25:28348 (JINR-P6-5617)
half-life of, (E), 25:28386
OSMIUM ISOTOPES Os-181
electron-capture decay of, half-life and gamma energies and intensities from, (E), 25:28348 (JINR-P6-5617)
half-life of, (E), 25:28386
OSMIUM ISOTOPES Os-182
electron-capture decay of, half-life and gamma energies and intensities from, (E), 25:28348 (JINR-P6-5617)
energy level at 119.8 keV, lifetimes of, (E), 25:28334 (CERN-70-30(Vol.2), pp 1031-43)
energy-level transitions in, probabilities for E2, (E), 25:28334 (CERN-70-30(Vol.2), pp 1031-43)
OSMIUM ISOTOPES Os-183
electron-capture decay of, half-life and gamma energies and intensities from, (E), 25:28348 (JINR-P6-5617)
OSMIUM ISOTOPES Os-184
energy level at 127 keV, lifetime of, (E), 25:28334 (CERN-70-30(Vol.2), pp 1031-43)
energy-level transitions in, probabilities for E2, (E), 25:28334 (CERN-70-30(Vol.2), pp 1031-43)
OSMIUM ISOTOPES Os-185
electron-capture decay of, gamma energies and intensities from, (E), 25:28389
half-lives of isomeric, (E), 25:28335 (CERN-70-30(Vol.2), pp 1045-55)
OSMIUM ISOTOPES Os-186
energy-level transitions in, multipole mixing ratios for, (E), 25:28434
OSMIUM ISOTOPES Os-188
energy-level transitions in, multipole mixing ratios for, (E), 25:28434
OSMIUM ISOTOPES Os-190
energy-level transitions in, multipolarities for, 25:28410
energy-level transitions in, multipole mixing ratios for, (E), 25:28434
OSMIUM ISOTOPES Os-192
energy levels from neutron reactions with osmium-192, spin--parity assignments for, (E), 25:28326 (CERN-70-30(Vol.2), pp 985-1000)
neutron reactions at 14 MeV, gamma spectra from, (E), 25:28326 (CERN-70-30(Vol.2), pp 985-1000)
OSMIUM OXIDES
reactions with monolayers of saturated and unsaturated cholestanol, cholesterol, and lacithins, effects of variables on, 25:26213
OSTEICHTHYES
Alburnis lucidus, rubidium-106 uptake and distribution in, effects of temperature on, 25:26587
Oncorhynchus tshawytscha, feeding activities and growth of Columbia River, effects of heated effluents on, 25:26681 (BNWL-1528)
OTTO HAHN REACTOR
boilers for, design parameters cross counterflow once through, 25:28748
OUABAIN
effects on rubidium-86 and sodium-22 efflux from lens of rabbits, 25:26606
OVARIES
radiation effects on mouse, low-dose gamma, 25:27028
radiation effects on, in beagle dogs, delayed x, 25:27009
radiation effects on, in cotton rats, γ, 25:26988
radioinduced luteomas and premature aging in, of mature mice following exposure in infancy, x, 25:26930
OXALIC ACID
reactions with plutonium in tridodecylamine solutions, precipitation, 25:26330(T) (ORNL-tr-2410, pp 14-78)
OXYGEN
activity for anionic conduction in thorium dioxide--yttrium oxide at 775 to 1000°C, 25:27286
content in lower thermosphere, performance of helium-cooled ion source for determination of atomic, (E), 25:27609
density at 85 to 150 km in ionosphere, theoretical model of diurnal variation of molecular ionized, (T), 25:27614
determination by neutron activation, pneumatic system for, 25:26189 (KFK-1293)
determination in mixed oxide fuel pellets, 25:26153 (LA-4622)
determination in Zircaloy, 25:26171
effects of moist, on cracking of Type H-11 steel under stress, 25:27175
effects on electron-sensitivity of neoplasms, hyperbaric, 25:26864
effects on gamma sensitivity of carcinomas of human uterus, 25:26869

XUM

effects on γ radiosensitivity of rice seeds, 25:27070
effects on γ-irradiated DNA and nucleoproteins, 25:26637
effects on reactions of flowing liquid sodium with refractory alloys at 500 to 600°C, 25:27174
effects on survival of irradiated spores of Osmunda regalis, 25:27069
effects on x-radioinduced myelitis in rats, 25:26966
effects on x-radioinduced polymerization of gaseous chloroethylene, 25:26282
effects on x-radioinduced single strand breaks in DNA of bacteria, 25:26655
emission of auroral green-line, relation to phase and amplitude of pulsations, (E/T), 25:27599
emissions of 5577 and 6300 A, intensity ratio in quiet auroral arc at 120 to 330 km, (E), 25:27600
meson (π^-) capture with charged particle emission, particle spectra and branching ratios for, (E), 25:28178
radiation effects on uptake of, by strawberries, effects of maturity on γ, 25:27160
radioinduced reactions with benzene, electron, 25:26284
radiolysis of aqueous solutions of, yields of hydrated electrons from electron pulse, 25:26308
reactions of radiolytic, with graphite, formation of surface complexes in, 25:26286
reactions with niobium--uranium--zirconium alloy at 27 to 1000°C, kinetics of, 25:27210 (SC-DR-710124)
sorption by and surface film reactions with iron, molybdenum, nickel, and tungsten, 25:27224
spectra of O I 1304-, 1356-, and 2972-A lines of, in upper Martian atmosphere, uv, (E), 25:27433
spectra pre-dawn enhancement of airglow at 6300 A at Adelaide, recombination-associated, (E/T), 25:27514
spectral emission of 6300 to 6364 A, at 300 to 400 km associated with sporadic-F layer, (E/T), 25:27511
spectral emission of 6300-A and green-line 5577-A, observations in SAR arcs, (E), 25:27525

OXYGEN IONS
reactions with aluminum at 100 to 350 keV, cross sections and Pauli-excitation mechanisms of K-shell ionization in, 25:27453

OXYGEN IONS (O^+)
density at 85 to 150 km in ionosphere, theoretical model of diurnal variation of, (T), 25:27614
neutralization reaction $O^+ + O^-$, relation to ionospheric F region uv equatorial nightglow, (E/T), 25:27608

OXYGEN IONS (O^-)
neutralization reaction $O^+ + O^-$, relation to ionospheric F region uv equatorial nightglow, (E/T), 25:27608

OXYGEN ISOTOPES O-16
abundance in interstellar carbon monoxide, (E), 25:27402
binding energy of, calculation using matrix elements of the effective interaction, (T), 25:28181
cross section data on, tables of multigroup, 25:28657 (HEDL-TME-71-36)
energy levels from resonances in carbon-12 (α,p) and (α,n) reactions, isospin mixing in, (E), 25:28188
energy levels of, calculation using renormalized RPA, (T), 25:28509
energy levels of, shell-model calculations of even-parity, (T), 25:28191
neutron elastic scattering by, phase-shift calculations using two-body forces, (T), 25:28198
nuclear binding energy, deformation, quadrupole moments, radii, and shape of, (T), 25:28180
oxygen-16 elastic scattering by, formation of nuclear molecules in, (T), 25:28171 (CERN-70-30(Vol.1), pp 601-2)
oxygen-16 elastic scattering by, resolution of phase-equivalent discrete ambiguities in optical-model analysis of, 25:28197
photon reactions (γ,n) at 15.8 to 22.15 MeV, mathematical-statistics analysis of cross sections and yield curves for, (T), 25:28186
proton elastic scattering at 17 GeV/c, multiple diffractive model for, 25:28073
reactions (^{16}O,p) and (^{16}O,α) at 4.54 to 8.53 MeV with carbon-12, total and partial cross sections for, (E), 25:27309 (ANU-P-471)
reactions (O-16,2n), (O-16,2p), and (O-16,pn) with nickel-60 at 42 to 52 MeV, excitation functions for gamma rays from, (E), 25:28213 (CERN-70-30(Vol.2), pp 911-15)
reactions (O-16,4n) with palladium-110 at 75 MeV, gamma spectra from, (E), 25:28319 (CERN-70-30(Vol.2), pp 905-10)
reactions (O-16,f) with gold-197 and uranium-238 at 137 MeV, analysis of helium-6 emission in, (E), 25:28351(T) (KFK-tr-352)
reactions (O-16,p) at 25.4 to 26.3 MeV, spectra and angular correlations for, (E), 25:28208 (ANU-P-521)
reactions with cerium-140 and gold-197, cross-section limits for fission isomer excitation in, (E), 25:28399
scattering by aluminum-27, calcium-40, carbon-12, lithium-6, lithium-7, and titanium-48 at 13 to 16 MeV, angular distributions for elastic, (E), 25:28196
scattering by oxygen-16, formation of nuclear molecules in elastic, (T), 25:28171 (CERN-70-30(Vol.1), pp 601-2)

OXYGEN ISOTOPES O-17
energy levels from resonances in carbon-13 (α,n) reactions, spin--parity assignments for, (E), 25:28202

OXYGEN ISOTOPES O-18
abundance in interstellar carbon monoxide, (E), 25:27402
effects on ir and Raman spectra of osmium oxides, 25:26258
effects on ir spectra of uranium oxide vapors trapped in rare gas matrices, 25:26260 (COO-1182-34)
exchange in ion-pair return in trans-α,γ-methylphenylallyl p-nitrobenzoate system, 25:26224
helium-3 reactions (He-3,t) at 16 MeV, triton spectra from, (E), 25:28173

OXYGEN SYSTEMS
O--Ti--Zr, structure and ordering in, x-ray and neutron diffraction studies of, 25:27297

OYSTER CREEK POWER REACTOR, UNIT 1
design characteristics of, 25:28544

P

PACKAGING
regulations for radioactive material, summary of U.S, 25:26445 (BRH/DMRE-71-1)
regulations for safe, of radioactive materials, review of, 25:26452

PALISADES POWER REACTOR
radioisotopes for, correction in possession limit for cesium-137, 25:28607 (DOCKET-50255-37)

PALLADIUM ALLOYS AND SYSTEMS
Ce--Pd, magnetic and electric properties of $CePd_3$ at 4 to 300°K, 25:27870
Cr--Pd, mictomagnetism in fcc, 25:27890
Dy--Pd, magnetic properties of $DyPd_3$ at 4 to 300°K, 25:27870
Er--Pd, magnetic properties of $ErPd_3$ at 4 to 300°K, 25:27870
Eu--Pd, magnetic properties of $EuPd_3$ at 4 to 300°K, 25:27870
Gd--Pd, magnetic and electric properties of $GdPd_3$ at 4 to 300°K, 25:27870
Gd--Pd-base, magnetic moments at 1.5 to 4.2°K, effects of gadolinium content on, 25:27921
Ho-Pd, magnetic and electric properties of $HoPd_3$ at 4 to 300°K, 25:27870
Nd--Pd, magnetic properties of $NdPd_3$ at 4 to 300°K, 25:27870
Pd--Pr, magnetic properties of $PrPd_3$ at 4 to 300°K, 25:27870
Pd--Si--transition metals, two currents conduction in, 25:28844 (CALT-822-28)
Pd--Sm, magnetic properties of $SmPd_3$ at 4 to 300°K, 25:27870
Pd--Tb, magnetic properties of $TbPd_3$ at 4 to 300°K, 25:27870
Pd--Tm, magnetic properties of $TmPd_3$ at 4 to 300°K, 25:27870
Pd--Yb, magnetic properties of $YbPd_3$ at 4 to 300°K, 25:27870

PALLADIUM HYDRIDES
nuclear magnetic resonance at -190 to 300°C, 25:26261(T) (ORNL-tr-2439)

PALLADIUM ISOTOPES
energy levels from (d,p) and (d,t) reactions, spectroscopic factors for, (E), 25:28374

PALLADIUM ISOTOPES Pd-99
beta and electron-capture decay of, branching ratios, gamma spectra, log-ft values, and Q values for, (E), 25:28431

PALLADIUM ISOTOPES Pd-104
energy levels from resonances in rhodium-103 (p,α) reactions, widths for compound-nucleus, (E), 25:28268
energy levels from rhodium-104 and -104m decay, two-phonon, (E), 25:28382

PALLADIUM ISOTOPES Pd-105
alpha inelastic scattering at 4.4 to 8 MeV with Coulomb excitation, γ spectra from, (E), 25:28423
energy levels from, alpha Coulomb excitation, transition probabilities for, (E), 25:28423

PALLADIUM ISOTOPES Pd-108
deuteron reactions (d,t) at 17 MeV, angular distributions for, (E), 25:28374

PALLADIUM ISOTOPES Pd-110
deuteron reactions (d,t) at 17 MeV, angular distributions for, (E), 25:28374
oxygen-16 reactions (O-16,4n) at 75 MeV, gamma spectra from, (E), 25:28319 (CERN-70-30(Vol.2), pp 905-10)

PALMITIC ACID
radiolysis at -196°C, ESR studies on kinetics of radical transformation in γ, 25:26312
elaidic acid--palmitic acid, radiolysis at -196°C, ESR studies on kinetics of radical transformation in γ, 25:26312
palmitic acid--urea, radiolysis of clathrate compounds of, at -196°C, ESR studies on kinetics of radical transformation in γ, 25:26312

PANCREAS
selenium-75 distribution in rat, effects of intravenously injected pancreozymin and secretin on, 25:26591

PAPER
properties of, radiometric gage for measuring, 25:26543(P)

XUM

PARAFFIN
gamma absorption coefficient of, (E), 25:27826 (DEMO-70/11)
PARANASAL SINUSES
radioinduced carcinomas of human maxillary, following diagnostic thorium administration, 25:27050
PARTICLE COLLECTORS
development of column, for radioactive fallout, 25:26559
PARTICLE TRACKS
analysis of hydrogen bubble chamber, SLAC spiral reader system for, 25:26511
measurement of bubble chamber, laser illumination system for HPD for, 25:26509 (RHEL/R-212)
PARTICLES
collision efficiencies of solid, calculations of, 25:26384 (CONF-700601-, pp 381-3)
diffusion and motion of aerosol, effects of temperature on, 25:26386 (CONF-700601-, pp 403-10)
distribution and size of aerosol, pulsed-laser holographic method for measurement of, 25:26373 (CONF-700601-, pp 213-16)
motion of coupled ionospheric neutral, equation of, 25:27521
scavenging of atmospheric aerosol, by rainwater, numerical model for studying, 25:26388 (CONF-700601-, pp 433-46)
scavenging of atmospheric aerosol, method for predicting efficiency of precipitation, 25:26391 (CONF-700601-, pp 475-85)
scavenging of atmospheric, by rain clouds and raindrops, kinetic theory of, 25:26382 (CONF-700601-, pp 355-71)
scavenging of atmospheric, research priorities in research on, 25:26359 (CONF-700601-, pp 6-10)
scavenging of submicron aerosol, effects of phoretic processes on precipitation, (T), 25:26387 (CONF-700601-, pp 411-22)
size spectra of solid, in atmospheric aerosols, mathematical models for evolving, 25:26385 (CONF-700601-, pp 385-402)
PEACH BOTTOM POWER REACTOR, UNIT 1
administrative controls for, revised technical specifications for, 25:28591 (DOCKET-50171-82)
operations history for February 1971, 25:28562 (DOCKET-50171-83)
personnel for, revised technical specifications for, 25:28591 (DOCKET-50171-82)
PECTINESTERASE
radiation effects on activity of, in strawberries, effects of maturity on γ, 25:27160
PECTINS
radiation effects on metabolism of, in strawberries, effects of maturity on, 25:27160
PENETRANT TESTING
method for nondestructive inspection of materials, review of, 25:26440
PENICILLAMINE
effects on x-radiosensitivity of collagen gel, 25:26802
radiolysis of oxidized or reduced, on Sephadex at 77°K, ESR studies on x, 25:26299
PERSONNEL
hemogram studies of uranium mining, 25:26588
licensing requirements for nuclear power plant, 25:28725
phosphorus accumulation in red blood cells of uranium mining, 25:26582
radiation dose received by atomic energy, in Egypt during 1962 through 1969, 25:26749 (NP-18732)
radiation hazards to industrial, Australian regulations for protection against, 25:26738
radiation hazards to, in nuclear industries and uranium mines, protective measures against, 25:26783
radiation protection methods for cyclotron, 25:26775
radioinduced cancer in lungs of uranium mining, following occupational exposure, gamma, 25:27045
PERU
insect radiosterilization in, methods for, 25:27130 (CONF-680112-, pp 129-42)
PHAEOPHYTA
Cystoseria barbata, radioactivity monitoring in, of Black Sea off coast of Romania during 1964 to 1967, 25:26745
Fucus vesiculosus, rubidium-106 uptake and distribution in, effects of temperature on, 25:26587
radioisotope concentration by tropical marine, 25:26597
PHANTOMS
development of radiation shielded astronaut, for planning radiation protection programs for space flight, 25:26778
electron dosimetry in Alderson-Rando, 42-MeV betatron, 25:26865
functional studies in tissue-equivalent, using double tracer method, 25:26569
radiation scattering measurements on liver and thyroid, γ, 25:26849
PHARMACEUTICALS
analysis of radio-, for radioactive impurities, use of thin-layer chromatography in, 25:26179 (CNEA-285)
preparation of radioisotope-labeled, for nuclear medicine, 25:26829
PHASE STUDIES
book: Statistical Physics, Phase Transitions, and Superfluidity, 25:27912
Ising model of transitions, lectures on, 25:27913
PHENIX FAST REACTOR
shielding for, evaluation of design options for top, (T), 25:28677(T) (ORNL-tr-2451)
PHENOL
effects on reactions of tetravalent uranium with trivalent chlorine, mechanism of, 25:26266
yields from γ radiolysis of aqueous solutions of phenyl glucopyranoside, effects of radical scavengers on, 25:26304
PHENOL, 2,4-DINITRO-
effects on unscheduled DNA synthesis in x-irradiated mammalian cultured cells, 25:27002
PHENYLEPHRINE
radioprotective effects on mice, effects of catecholamines on, 25:26804
PHOSPHATES
uptake in diatom cultures, use of phosphorus-33 autoradiography for studies of, 25:26596
PHOSPHINE, TRIOCTYL-
solvent properties for rare earths, 25:26338(P)
PHOSPHOLIPIDS
radiation effects on, in canned chicken pet food products, 25:26647
PHOSPHORIC ACID, BIS(2-ETHYLHEXYL) ESTER
solvent properties for rare earths, 25:26338(P)
solvent properties for rare earths, 25:26342
PHOSPHORIC ACID, TRIBUTYL ESTER
separation of ruthenium from, by extraction chromatography using dibutyl phosphate--potassium hydroxide, 25:26330(T) (ORNL-t--2410, pp 14-78)
solvent properties for rare earths, 25:26338(P)
PHOSPHOROTHIOIC ACID, S-(2-AMINOETHYL) ESTER
distribution and metabolism in tissues of mice, phosphorus-32 and sulfur-35 double tracer study of, 25:26805
radioprotective effects on mice in relation to metabolism and tissue distribution, mechanism of, 25:26805
PHOSPHOROTHIOIC ACID, S-2-(3-AMINOPROPYLAMINO)ETHYL ESTER
radioprotective efficiency in mice, biological factors in, 25:26796
PHOSPHORUS
accumulation in red blood cells of uranium miners, 25:26582
determination in plutonium oxide--uranium oxide pellets by spectrophotometry, 25:26153 (LA-4622)
implants in diamond single crystals, analysis, 25:27858
PHOSPHORUS IONS
effects on silicon and germanium at 10 to 400 keV, distribution of defects induced in, 25:27861
PHOSPHORUS ISOTOPES
incorporation into nucleic acids of frog eggs for studies on nucleic acid metabolism, 25:26617
PHOSPHORUS ISOTOPES P-29
Coulomb energy differences between phosphorus-29--silicon-29 isobaric analog states, 25:28243
energy levels of, calculation using projected Hartree--Fock basis and core-particle coupling, (T), 25:28280
PHOSPHORUS ISOTOPES P-30
energy levels from silicon-29(p,γ) reactions, resonance and bound, (E), 25:28207 (ANU-P-517)
PHOSPHORUS ISOTOPES P-31
deuteron elastic scattering at 8 and 12 MeV, optical-model analysis of angular distributions from, (E), 25:28270
energy levels from proton resonances in silicon-30, spin assignments and strengths for, (E), 25:28270
energy levels from silicon-30 (He-3,d) reactions, l values, spectroscopic factors, and spin--parity assignments for, (E), 25:28270
energy levels from silicon-30 (p,γ) reactions, lifetimes and spin--parity assignments for, (E), 25:28270
energy-level transitions from proton resonances in silicon-30, branching ratios for, (E), 25:28270
energy-level transitions from silicon-30 (p,γ) reactions, branching and mixing ratios for, (E), 25:28270
PHOSPHORUS ISOTOPES P-32
effectiveness for therapy of joint diseases in human bones by synovial injection, 25:26873
effects on mice, effects of dose fractionation on leukemogenic, 25:27021
production of recoil, by neutron reactions (n,γ) and (n,p) in phosphorus-sulfur compounds, 25:26318
uptake by erythrocytes, methods for determining, 25:26589
use as tracer for determining rate of dispersal of cherry fruit flies in Poland, 25:27150
use as tracer for estimating population size of Mediterranean fruit fly in Tunisia, 25:26573
use for heart scanning, review on international methods for, 25:26855
PHOSPHORUS ISOTOPES P-33
incorporation in diatom cultures for use in measuring phosphate uptake, 25:26596
PHOTOGRAPHY
radioinduced recovery of faded paper photographs, tintypes, and glass-plate negatives in, neutron, 25:26287
PHOTOMETRY
background effects in stellar, (E/T), 25:27341
PHOTONS
absorption in small volumes of target tissues from interstitial radioisotope sources, computer

XUM

calculations of, 25:26752
interactions γ + γ, amplitudes from vacuum polarization tensor in quantum electrodynamics, 25:28070
interactions γ + N → Δ⁰ + ω, OPE amplitude and ωπγ coupling constants from, 25:27990
interactions γ + n → Δ⁰ + π⁰ at high energies, models for, (T), 25:27990
interactions γ + n → n + eta at high energies, pole--cut model for, (T), 25:27989
interactions γ + n → p + π⁻ at high energies, isotopic structure of N* decay amplitudes from, (T), 25:27990
interactions γ + n → p + rho⁻, OPE amplitude and rhoπγ coupling constants from, 25:27990
interactions γ + N, derivative amplitudes for π production, 25:28000
interactions γ + p → p + eta at high energies, pole--cut model for, (T), 25:27989
reactions (γ,2n) with copper-63 at 19.74 MeV, structure and energy dependence of differential cross sections for, (E), 25:28260
reactions (γ,2n) with copper-65 at 17.82 MeV, structure and energy dependence of differential cross sections for, (E), 25:28260
reactions (γ,3n) with copper-65 at 28.66 MeV, structure and energy dependence of differential cross sections for, (E), 25:28260
reactions (γ,n) and (γ,p) with nuclei at 40 to 140 MeV, shell model analysis with short-range nucleon-nucleon correlations, (T), 25:28488
reactions (γ,n) with copper-63 at 10.84 MeV, structure and energy dependence of differential cross sections for, (E), 25:28260
reactions (γ,n) with copper-65 at 9.91 MeV, structure and energy dependence of differential cross sections for, (E), 25:28260
reactions (γ,n) with oxygen-16 at 15.8 to 22.15 MeV, mathematical-statistics analysis of cross sections and yield curves for, (T), 25:28186
reactions (γ,np) with copper-63 at 16.72 MeV, structure and energy dependence of differential cross sections for, (E), 25:28260
reactions (γ,np) with copper-65 at 17.11 MeV, structure and energy dependence of differential cross sections for, (E), 25:28260
reactions (γ,p) with beryllium-9 at 56 MeV, proton spectra and cross sections for, (E), 25:28194
reactions (γ,p) with carbon-12 and -13, cross sections for, (E/T), 25:28193
reactions with aluminum at 5.4 GeV, total cross section for hadron production in, 25:27953
reactions with beryllium at 1.5 to 5.7 GeV, total cross section for hadron production in, 25:27953
reactions with carbon at 1.5 to 5.7 GeV, total cross section for hadron production in, 25:27953
reactions with copper at 5.4 GeV, total cross section for hadron production in, 25:27953
reactions with gold at 5.4 GeV, total cross section for hadron production in, 25:27953
reactions with silver at 5.4 GeV, total cross section for hadron production in, 25:27953
reactions with titanium at 1.5 to 5.7 GeV, total cross section for hadron production in, 25:27953
scattering by even-even nuclei, collective model analysis of tensor polarizability in giant resonance region, (T), 25:28489
scattering by nuclei, amplitude and differential cross section for Delbrueck, 25:28070
scattering on arbitrary-spin targets, low-energy theorems for Compton, 25:27993
spectra from cosmic π⁰ decay, comparison with galactic γ flux for, (T), 25:27404
stability of, 25:27979

PHOTOSPHERE
emission of sodium lines, intense flare-like, (E/T), 25:27380
granular velocities in, (E), 25:27366
model for, empirical continuum, (T), 25:27369
spectra of transition region with chromosphere, (E/T), 25:27370
spectra of, effect of macroturbulence on Fraunhofer lines in, (T), 25:27400

PHOTOSYNTHESIS
radiation effects on, in seedlings of silver maple and yellow poplar, effects of reduced light on fast neutron, 25:27076

PHYSICS
Pade Approximant in Theoretical Physics, 25:28063
research progress in, AEC, 25:26205

PHYTOHEMAGGLUTININ
effects on synthesis of proteins and RNA in cultured lymphocytes, effects of, on response of lymphocytes to x radiation, 25:26903

PILGRIM POWER REACTOR
operation of, notice of AEC consideration of license for, 25:28613 (DOCKET-50293-47)
piping systems for, withdrawal of requests for information on weld reinforcement for, 25:28614 (DOCKET-50293-48)
safety report on, Advisory Committee of Reactor Safeguards, 25:28612 (DOCKET-50293-46)

PILOCARPINE
effects on cesium-137 excretion in rats, combined effects of prussian blue and, 25:26583

PINCH DEVICES
ion detection in low-pressure linear, highly ionized, (E), 25:27678 (WASH-1159, pp 172-83)
plasma instabilities in bumpy theta, dynamic stabilization of, (T), 25:27785
plasma stabilization in linear theta, using feedback systems, (T), 25:27726 (LA-4598)

PINCH EFFECT
plasma stability in screw, with Hall current, (T), 25:27732
stability of Bennett, hydromagnetic, (T), 25:27748
stabilization of linear screw, dynamic, (E), 25:27790
stabilization of m = 1 mode screw, dynamic, (T), 25:27749
stabilization of z-, dynamic, (E/T), 25:27789

PIPE FITTINGS
testing of tangential, 25:28871(T) (ORNL-tr-1991)

PIPES
crack initiation and growth in reactor cooling system, effects of low-cycle fatigue on, (E), 25:28680(R) (GEAP-10207-23)
failure in reactor cooling systems, probability analysis of, 25:28680(R) (GEAP-10207-23)

PITUITARY GLAND
radioinduced ablation in patients with diabetic retinopathy, effects on aqueous humor flow rates of high-dose α, 25:27037

PLACENTA
strontium-89 uptake by, of sows following ingestion, 25:26594

PLANETARY NEBULAE
atmospheres of central stars of, model, (T), 25:27314
electron densities and temperatures in, (E), 25:27338
evolution of, effects of dust and Lyman-α radiation on, (E/T), 25:27323

PLANETS
surface analysis of, by neutron activation, 25:26188 (BNWL-SA-3803)

PLANTS
polonium-210 uptake from soil by crop, transfer coefficients for, 25:26684

PLASMA
bibliography on, 25:27667
bibliography on, 25:27668
book: Methods of Experimental Physics. Vol. 9. Plasma Physics. Part A, 25:27689
boundary layer of nonequilibrium, electron density and temperature in, (E), 25:27685
boundary of, hydromagnetic equilibria of vacuum, (T), 25:27691
charged-particle acceleration by electromagnetic pulse, relativistic, (T), 25:27715
charged-particle beam interactions with, lf oscillations from, 25:27816
charged-particle trapping in static mirror fields, (T), 25:27674
collisions in nitrogen, effects of vibrational excitation on frequency of electron--molecule collisions in, (T), 25:27711
collisions in, effects on parametric instabilities in, (T), 25:27782
conference on feedback and control of, Princeton, N. J., 6/70, 25:27752
confinement in cusp magnetic fields, dynamic control of losses in, (E/T), 25:27676
confinement in magnetic-mirror traps, duration equations for, (T), 25:27669 (IAE-1972)
confinement in static mirror fields, charged particle injection and trapping in, (T), 25:27674
confinement of hot electron, in cusped magnetic fields, (E), 25:27677
confinement of injected cesium, in magnetic mirrors, (E), 25:27671
convection cells produced by low-frequency flute instabilities, (T), 25:27734
convection produced by ion-driven drift instabilities, (T), 25:27735
current distribution in cylindrical, with variable conductivity, pulsed, (T), 25:27721
diagnostics in Q devices, energy analysis of cesium ions, 25:27686
diagnostics of nonequilibrium boundary layer of, electron density and temperature, (E), 25:27685
diagnostics of warm anisotropic, using resonance cones in field pattern of rf probes, 25:27683
diagnostics of, Langmuir probe measurement of drift-wave potential oscillations in, (T), 25:27809
diagnostics using feedback stabilization, (E/T), 25:27769
diagnostics using light scattering, (E/T), 25:27680
diagnostics using microwave scattering, (E/T), 25:27679
diagnostics using nonlinear mixing of electromagnetic waves, electron density, (T), 25:27684
diffusion in stochastic fields, transverse, (T), 25:27719
diffusion of turbulent, in electric fields, (T), 25:27673
electric discharges in, effect of temperature nonuniformity on positive column, (T), 25:27714
electric potential of photo-emitting plate in

XUM

interplanetary, surface, (T), 25:27360
electron acceleration by microwaves in crossed fields at electron cyclotron resonant frequency, (E), 25:27698
electron beam equilibria in, E-layer, (T), 25:27798
electron beam in cold, negative mass instability of E-layer, (T), 25:27746
electron beam interactions with magnetized, electron scattering by electrostatic fluctuations in, (E), 25:27699
electron beam interactions with suppression of longitudinal electron oscillations by beam modulation, (E), 25:27702
electron beam interactions with, highly ionized ion production by relativistic, (E), 25:27694 (WASH-1159, pp 184-9)
electron beam interactions with, ion acceleration in, (E), 25:27696 (WASH-1159, pp 204-18)
electron beam interactions with, ion momentum analysis from, (E), 25:27697 (WASH-1159, pp 219-26)
electron beam interactions with, ion production in, (E), 25:27695 (WASH-1159, pp 196-203)
electron beam interactions with, nonlinear perturbations and electron scattering in, (E), 25:27703
electron beam interactions with, nonlinear properties of one-dimensional, (T), 25:27710
electron beam interactions with, relaxation processes in, (E), 25:27700
electron distribution function for, effect of electrostatic wave damping on, (E), 25:27823
expansion into vacuum, computer simulation of, (T), 25:27709
heating by strong shock waves, (E/T), 25:27670
heating of electrons by large hf electric fields, anomalous, (E/T), 25:27675
heating of ions by two-stream instabilities in external magnetic fields, (T), 25:27672
injection and confinement of cesium, in magnetic mirrors, (E), 25:27671
interactions with electrostatic fields, penetration in, (T), 25:27707
ion detection in low-pressure linear pinch, highly ionized, (E), 25:27678 (WASH-1159, pp 172-83)
ion velocity distribution in non-isothermal, relation to Maxwellian distribution, (T), 25:27722
ionization waves in positive column, feedback control of, (T), 25:27773
kinetic theory for non-resonant region, quasi-linear, 25:27717
kinetic theory of, modification of quasi-linear equations for, (T), 25:27739
kinetic theory of, negative diffusion coefficients in quasi-linear, 25:27713
kinetic theory of, negative diffusion coefficients in quasi-linear, 25:27712
kinetic theory of, quasi-linear equations for wave number spectra in, 25:27716
kinetics of, atomic processes in, (T), 25:27705
motion across inhomogeneous magnetic fields, effects of particle velocity distribution on, (T), 25:27720
oscillations in beam--plasma system, microwave radiations from, 25:27816
oscillations in cylindrical non-neutral, electrostatic electron, (T), 25:27808
oscillations in Lorentzian electron gas, Landau damping of longitudinal, (T), 25:27822
oscillations in, Langmuir probe measurement of drift-wave potential, (T), 25:27809
production by laser irradiation of targets, (E), 25:27724
production by molecular ion injection and trapping in magnetic mirrors, 25:27725
production of highly ionized, by laser-beam irradiation, (E), 25:27723 (WASH-1159, pp 162-7)
properties of plane condensers, in crossed electric and magnetic fields, (T), 25:27718
radiations from isotropic, cyclotron and synchrotron, (T), 25:27706
radiations from relativistic, theory for bremsstrahlung, 25:27687 (NP-18758)
radiations from turbulent, theory for bremsstrahlung, 25:27704 (NP-18759)
relaxation processes in electron beam--plasma system, (E), 25:27700
shock wave propagation in collisionless, instabilities from, (T), 25:27731
shock waves in collisionless, existence of, (T), 25:27708
simulation of expanding, into vacuum, (T), 25:27709
simulation of Weibel instability in one and two dimensions, numerical, (T), 25:27737
specific heat of helium and nitrogen, effect of electron excitation on, 25:27692
stability in magnetic mirrors, boundary conditions for convective wave, (E/T), 25:27750
stability in perpendicular collisionless shock waves, (T), 25:27731
stability in positive columns, effect of helical, on radial density and potential distribution, (T), 25:27738
stability of Bennett pinch, hydromagnetic, (T), 25:27748
stability of collisional, drift wave, (E/T), 25:27729
stability of collisional, universal drift, (T), 25:27747
stability of counterstreaming ion beams, heating by two-stream instabilities in external magnetic fields, (T), 25:27672
stability of high-beta, magnetohydrodynamic, (E/T), 25:27730
stability of high-pressure, in dense blanket of neutral gas, (T), 25:27744
stability of linear pinch, tearing-mode, (T), 25:27751
stability of microwave-heated, (T), 25:27743
stability of screw-pinch, with Hall current, (T), 25:27732
stability of simulated, explosive, (T), 25:27736
stability of trapped-particle equilibrium, (T), 25:27733
stability of, classification of lf, (E/T), 25:27728
stability of, convection from ion-driven drift, (T), 25:27735
stability of, convective cells from flute, (T), 25:27734
stability of, effect of electron--ion collisions on parametric, (T), 25:27782
stability of, numerical simulation of Weibel, (T), 25:27737
stability of, theory of hf, 25:27727
stability of, weak-turbulence analysis of two-stream, (T), 25:27740
stabilization in Q devices using remote feedback by microwaves, (E/T), 25:27766
stabilization in Q devices, passive feedback, (E), 25:27771
stabilization in tokamak devices, feedback control problems in, (T), 25:27763
stabilization of collisionless multi-mode drift centrifugal waves in mirror-confined, feedback, (E), 25:27768
stabilization of cyclotron instabilities in OGRA II device, feedback, (E), 25:27776
stabilization of drift and ion acoustic instabilities, feedback, (E/T), 25:27767
stabilization of drift instabilities in discharges, by rf electric fields, (E), 25:27787
stabilization of drift waves by nonuniform hf electromagnetic fields, (T), 25:27741
stabilization of drift waves in collisionless, by ac electric fields, (T), 25:27779
stabilization of drift-dissipative instabilities by inhomogeneous rf fields, (T), 25:27780
stabilization of drift-dissipative instabilities in afterglow, dynamic, (E), 25:27786
stabilization of edge oscillations in Q devices, using feedback, (E), 25:27770
stabilization of electromechanical equilibria, videotype sampling in feedback, (T), 25:27761
stabilization of electrostatic instabilities in, dynamic, (T), 25:27777
stabilization of electrostatic instabilities in, feedback, (T), 25:27756
stabilization of high-β columns, feedback, (E), 25:27774
stabilization of high-β sharp boundaried column in helical fields, feedback, (T), 25:27764
stabilization of high-β, dynamic, (T), 25:27783
stabilization of hot electron, feedback, (E), 25:27775
stabilization of interchange instabilities in, dynamic, (E/T), 25:27791
stabilization of ion and electron modes in, feedback, (E), 25:27765
stabilization of ionization waves in positive columns, using feedback, (T), 25:27773
stabilization of Kelvin--Helmholtz instabilities in Q devices, feedback, (E/T), 25:27772
stabilization of Kruskal--Shafranov modes in, feedback, (T), 25:27762
stabilization of linear screw pinch, dynamic, (E), 25:27790
stabilization of linear theta pinches, by feedback systems, (T), 25:27726 (LA-4598)
stabilization of $m = 1$ instabilities in bumpy theta pinch, dynamic, (T), 25:27785
stabilization of magnetically confined, using hf potential, (T), 25:27778
stabilization of magnetohydrodynamic instabilities, dynamic, (T), 25:27784
stabilization of magnetohydrodynamic instabilities using nonlinear feedback, (T), 25:27760
stabilization of MHD instabilities using feedback, review of, 25:27759
stabilization of mirror-confined, using feedback, (T), 25:27757
stabilization of screw pinch $m = 1$ mode, dynamic, (T), 25:27749
stabilization of trapped-particle instability in, effect of hf magnetic fields on, (T), 25:27745
stabilization of two-stream instabilities in, dynamic, (E), 25:27788
stabilization of Vlasov, feedback, (T), 25:27753
stabilization of z-pinch, dynamic, (E/T), 25:27789
stabilization of, conference on, 25:27752
stabilization of, generalized boundary conditions for feedback systems for, (T), 25:27755
stabilization of, geometric limitations of feedback systems for, 25:27754
stabilization of, quasi-linear equations for, (T), 25:27739

XUM

stabilization using feedback, diagnostic use of, (E/T), 25:27769
stabilization using feedback, review of, 25:27742
stabilization using hf fields, ordinary- and helicon-wave, (T), 25:27781
stabilization using two carbon dioxide laser beams, (T), 25:27758
thermonuclear combustion waves in dense, existence of, (T), 25:27820
turbulence in, time-asymptotic perturbation theory for weak, (T), 25:27810
turbulence in, time-asymptotic perturbation theory for weak, (T), 25:27811
wave coupling in nonuniform, transverse and longitudinal, (T), 25:27825
wave coupling in, correction formula for electromagnetic and Bohm--Gross, (T), 25:27817
wave damping by external hf fields, ion, (T), 25:27807
wave damping in collisionless, standing wave measurement of Landau, (E), 25:27819
wave damping in, effect on electron distribution function, (E), 25:27823
wave echoes in collisionless, standing wave measurement of, (E), 25:27819
wave echoes in, detection of, (E/T), 25:27800
wave excitation by collisional instabilities in partially ionized mercury, (E), 25:27802
wave excitation in inhomogeneous, parametric, (T), 25:27814
wave instabilities in, theory for hf, 25:27727
wave interactions in collisionless, three electrostatic, (T), 25:27812
wave interactions in simulated, explosive instabilities from, (T), 25:27736
wave interactions in, dissipation effects on coupling coefficients for nonlinear, (T), 25:27815
wave interactions in, nonlinear Landau damping and beat wave trapping in, (T), 25:27824
wave interactions with charged particles in open-ended Q devices, (E/T), 25:27693
wave propagation in bounded cold, electromagnetic, (T), 25:27804
wave propagation in dense, existence of thermonuclear combustion, (T), 25:27820
wave propagation in inhomogeneous, electromagnetic, (T), 25:27801
wave propagation in sheared magnetic fields, electromagnetic, (T), 25:27821
wave propagation in, electron and ion acoustic, (E/T), 25:27800
wave propagation in, existence of shock-like solutions of Korteweg--de Vries equation for ion acoustic, 25:27818
wave propagation in, relation of gravity waves in incompressible fluids to ion, (T), 25:27806
wave propagation in, theory for electromagnetic, 25:27803
wave propagation in, time-asymptotic perturbation theory for weakly turbulent, (T), 25:27810
wave propagation in, Vlasov theory for weakly turbulent, (T), 25:27811
wave reflection from longitudinally magnetized coaxial waveguide, microwave, (E), 25:27813

PLASMA ACCELERATORS
design and performance of disc focus, 25:27794
jet rotation in glow discharge mode of homopolar, (E), 25:27701
neutron production in focus discharge, with and without axial magnetic fields, (E), 25:27799

PLASMA JETS
diagnostics of, theory of cylindrical probe for, 25:27681
particle velocity of refractory material injected into arc, 25:28859(T) (LA-tr-71-27)

PLASMA, SOLID-STATE
wave propagation in, space-charge, (T), 25:27805

PLASMAPAUSE
position near local midnight and magnetic equatorial plane, interrelation with near-Earth plasma sheet, (E), 25:27631

PLATES
deformation from spontaneous expansion and thermal cycling, development of strut theory for defining, 25:26415 (TRG-Report-2121)
neutron transport in flat, boundary-sources method for solving Boltzmann's equation for, (T), 25:28160

PLATINUM
alpha decay of, half-lives, Q values, reduced widths, and spectra from, (E), 25:28302 (CERN-70-30(Vol.1), pp 523-31)
radioinduced defects in, field-ion microscopic study of 20- and 30-keV platinum-ion, 25:27866(R) (NYO-3504-56)

PLATINUM ALLOYS AND SYSTEMS
Co--Pt, ordering in intermetallic PtCo, field ion microscopy studies of, 25:27252
Eu--Eu_2O_3--Pt, phase studies at 1500°C, 25:27302
Fe--Pt, ordering in intermetallic FePt and $FePt_3$, field ion microscopy studies of, 25:27252
Pr--Pt, nuclear magnetic cooling of $PrPt_5$, using hyperfine field, 25:27666
Pt-base--Rh, fabrication of Pioneer and Transit heat source capsule components of, equipment and methods for, 25:26425 (MLM-1796)

PLATINUM IONS
effects on platinum at 20 to 30 keV, field-ion microscopic study of, 25:27866(R) (NYO-3504-56)

PLATINUM ISOTOPES
energy-level transitions in, branching ratios for E2, (T), 25:28316 (CERN-70-30(Vol.2), pp 779-812)

PLATINUM ISOTOPES Pt-182
energy levels of, spin--parity assignments for, (E), 25:28334 (CERN-70-30(Vol.2), pp 1031-43)

PLATINUM ISOTOPES Pt-184
energy levels from gold-184 decay, transition probabilities for, (E), 25:28425
energy levels of, spin--parity assignments and lietimes for, (E), 25:28334 (CERN-70-30(Vol.2), pp 1031-43)
energy-level transitions in, probabilities for E2, (E), 25:28334 (CERN-70-30(Vol.2), pp 1031-43)

PLATINUM ISOTOPES Pt-185
electron-capture decay of, half-lives for, (E), 25:28335 (CERN-70-30(Vol.2), pp 1045-55)

PLATINUM ISOTOPES Pt-186
energy levels from gold-186 decay, transition probabilities for, (E), 25:28425
energy levels of, spin--parity assignments and lietimes for, (E), 25:28334 (CERN-70-30(Vol.2), pp 1031-43)
energy-level transitions in, probabilities for E2, (E), 25:28334 (CERN-70-30(Vol.2), pp 1031-43)

PLATINUM ISOTOPES Pt-188
electron-capture decay of, gamma energies and intensities from, (E), 25:28389
energy levels from gold-188 decay, transition probabilities for, (E), 25:28425
energy levels of, spin--parity assignments and lietimes for, (E), 25:28334 (CERN-70-30(Vol.2), pp 1031-43)
energy-level transitions in, probabilities for E2, (E), 25:28334 (CERN-70-30(Vol.2), pp 1031-43)

PLATINUM ISOTOPES Pt-189
electron-capture decay of, gamma energies and intensities from, (E), 25:28389
half-lives of isomeric, (E), 25:28335 (CERN-70-30(Vol.2), pp 1045-55)

PLATINUM ISOTOPES Pt-190
energy levels of, spin--parity assignments and lietimes for, (E), 25:28334 (CERN-70-30(Vol.2), pp 1031-43)
energy-level transitions in, probabilities for E2, (E), 25:28334 (CERN-70-30(Vol.2), pp 1031-43)

PLATINUM ISOTOPES Pt-192
energy levels of, spin--parity assignments for, (E), 25:28334 (CERN-70-30(Vol.2), pp 1031-43)

PLATINUM ISOTOPES Pt-194
energy levels from isomeric iridium-194 beta decay, lifetimes of high-spin, (E), 25:28353 (NP-18695)
energy-level transitions in, multipole mixing ratios for, (E), 25:28434

PLATINUM ISOTOPES Pt-196
energy levels from iridium-196m beta decay, lifetimes of high-spin, (E), 25:28353 (NP-18695)
energy-level transitions in, multipole mixing ratios for, (E), 25:28434
proton elastic and inelastic scattering at 13 to 17 MeV, analog resonance anomalies in, (E), 25:28371

PLOWSHARE PROJECT
effects of Pre-Gondola II Event in, summary of measured air blast, cloud development, cratering, and seismic, 25:26407 (PNE-1112)
effects of Pre-Gondola III Phase II Event in, summary of measured air blast, cloud development, cratering, geologic, and seismic, 25:26408 (PNE-1117)
fallout from Schooner Event in, program for collection and analysis of long-range, 25:26404 (PNE-527)
ground motion from Rulison Event in, at Rifle Gap Dam, Colo., (E), 25:26410 (PNE-R-47)
ground motion from Rulison Event in, measurement and prediction of structural damage from, 25:26402 (JAB-99-76)
ground water contamination from Gasbuggy Event in, evaluation of San Juan Basin, 25:26406 (PNE-1009)
reentry operations for Rulison Event chimney in, summary of, 25:26409 (PNE-R-45)
seismic source function and surface motion from Gasbuggy Event in, measurement of, 25:26405 (PNE-1002)

PLUTONIUM
bibliography on, Feb. 1971, 25:27168
bibliography on, Jan. 1971, 25:27169
complexes of tetravalent, with lithium nitrate or nitric acid in aqueous methanol solutions, spectrophotometric studies on, 25:26274
determination in oxides by controlled potential coulometry, 25:26153 (LA-4622)
grain size of α-, β-, and γ-, effects of heat treatments and phase transformations on, 25:27244 (BNWL-1545)
packaging and shipping of metallic, design and safety evaluation of LLD-1 container for, 25:26446 (DPSPU-71-124-1)
radiation effects on electric conductivity of α-, expression for relation of holding time in liquid helium with self-, 25:27837 (AERE-R-6506)
reduction of tetravalent, by hydroxylamine nitrate, effects of iron on, 25:26206 (ARH-1920)
release to environment following unrestricted release within enclosures, model for calculations of hazards

XUM

from, 25:26782
release to environment following unrestricted release within enclosures, hazards from, 25:26781
separation from americium by precipitation using a rare earth carrier, 25:26319(P)
separation from aqueous fuel processing solutions by solvent extraction using tridodecylamine, 25:26333(T) (ORNL-tr-2410, pp 121-42)
separation from aqueous solutions by continuous precipitation as oxalate, 25:26345(P)
separation from fission products by solvent extraction using tridodecylamine, 25:26330(T) (ORNL-tr-2410, pp 14-78)
separation from irradiated fuels by Purex Process, 25:26326 (KFK-911)
separation from neptunium by solvent extraction using tridodecylamine in decanoic acid, 25:26333(T) (ORNL-tr-2410, pp 121-42)
separation from plutonium dioxide--uranium dioxide fuels by solvent extraction using TBP in presence of sulfuric acid, 25:26330(T) (ORNL-tr-2410, pp 14-78)
separation from tridodecylamine by precipitation using hydrofluoric acid or oxalic acid, 25:26330(T) (ORNL-tr-2410, pp 14-78)
separation from uranium in acidic solutions from reactor fuel reprocessing, selective solvent extraction process for, 25:26346(P)
PLUTONIUM ALLOYS AND SYSTEMS
properties of intermetallic compounds of, chemical and structural, 25:27263
PLUTONIUM FLUORIDES PuF_4
reduction by sulfur dioxide, effects of uranium hexafluoride on kinetics of, 25:26332(T) (ORNL-tr-2410, pp 98-120)
PLUTONIUM ISOTOPES
determination in plutonium dioxide by mass spectrometry, 25:26153 (LA-4622)
determination in plutonium dioxide--uranium dioxide pellets by mass spectrometry, 25:26153 (LA-4622)
PLUTONIUM ISOTOPES Pu-235
electron-capture decay of, γ spectra and half-life for, (E), 25:28415
PLUTONIUM ISOTOPES Pu-238
content of atmosphere and river water at Miamisburg, Ohio during 1970, 25:26739(R) (MLM-1795)
cross section data on, tables of multigroup, 25:28657 (HEDL-TME-71-36)
determination by α spectrometry, 25:26153 (LA-4622)
effects on leukocytes and lymph nodes of dogs following inhalation, 25:26929
use as heat source in implantable cardiac pacemakers, 25:26434
PLUTONIUM ISOTOPES Pu-239
cross section data on, tables of multigroup, 25:28657 (HEDL-TME-71-36)
deuteron fission at 13 MeV, optical-model analysis of probability for, (T), 25:28445 (CERN-70-30(Vol.1), pp 553-66)
distribution in tissues of dogs following inhalation of plutonium oxide-incorporated, 25:26599
effects on leukocytes and lymph nodes of dogs following inhalation, 25:26929
neutron fission of, charge distribution in thermal, (T), 25:28508
neutron fission of, fission yield from fast, (E), 25:28354 (NP-18723)
neutron fission of, fission yield from thermal, (E), 25:28354 (NP-18723)
neutron fission of, krypton-85 branching ratios and yields in thermal, (E), 25:28383
neutron fission of, prompt neutron yield from thermal, (T), 25:28355(R) (TID-25659)
PLUTONIUM ISOTOPES Pu-240
cross section data on, tables of multigroup, 25:28657 (HEDL-TME-71-36)
energy levels of, analysis of nonrandom distributions of neutron resonance, (T), 25:28421
PLUTONIUM ISOTOPES Pu-241
cross section data on, tables of multigroup, 25:28657 (HEDL-TME-71-36)
fission barrier of, odd-particle effects on, (T), 25:28314 (CERN-70-30(Vol.2), pp 700-8)
neutron fission of, fission yield from thermal, (E), 25:28354 (NP-18723)
neutron fission of, krypton-85 branching ratios and yields in thermal, (E), 25:28383
PLUTONIUM ISOTOPES Pu-242
cross section data on, tables of multigroup, 25:28657 (HEDL-TME-71-36)
PLUTONIUM NITRATES
analysis of solutions of, for chromium, iron, and nickel by atomic absorption spectrophotometry, 25:26154(T) (RFP-Trans-76)
PLUTONIUM NITRIDES
PuN--UN, irradiation testing of fuels of, 25:28687 (BMI-1898, Sect.A)
PuN--UN, radiation effects on high temperature swelling, fission gas release, and microstructure of, (E/T), 25:28688 (BMI-1898, Sect.B)
PuN--UN, self-diffusion of nitrogen in, (E), 25:28687 (BMI-1898, Sect.A)
PLUTONIUM OXALATES
precipitation of, apparatus for continuous process for, 25:26345(P)
precipitation of, simulation tests on continuous, 25:26330(T) (ORNL-tr-2410, pp 14-78)
PLUTONIUM OXIDES PuO_2
analysis of fuel and source materials of, evaluation of chemical methods for, 25:26153 (LA-4622)
gamma spectra of fuels of, 25:27305 (N-70-35897)
metabolism of plutonium-239-labeled, in dogs, 25:26929
preparation of pyrolytic carbon-coated fuel particles of, method for, 25:27275(P)
PuO_2--UO_2, preparation of enriched fuels of, method for, 25:27276(P)
toxic effects of inhaled plutonium-239-labeled, in dogs, 25:26599
PuO_2--UO_2, analysis of fuel and source materials of, evaluation of chemical methods for, 25:26153 (LA-4622)
PuO_2--UO_2, creep of, effects of microstructure, stress, temperature, and fission process on, (E), 25:28689 (BMI-1898, Sect.C)
PuO_2--UO_2, dissolution by sealed-tube method, 25:26153 (LA-4622)
PuO_2--UO_2, properties of fuels of, mechanical, physical, and thermal, (E), 25:28691(R) (GEAP-10028-37)
PuO_2--UO_2, radiation effects on high temperature swelling, fission gas release, and microstructure of, (E/T), 25:28688 (BMI-1898, Sect.B)
PuO_2--UO_2, radiation effects testing of fuels of, 25:28691(R) (GEAP-10028-37)
PuO_2--UO_2, reprocessing of fuels of, by halide volatilization process, 25:26332(T) (ORNL-tr-2410, pp 98-120)
PuO_2--UO_2, stoichiometry shift in mixed, effects of burnup on, (E/T), 25:28690(T) (EURFNR-836)
POINT BEACH POWER REACTOR, UNIT 1
operations incident of March 28, 1971, unscheduled venting of containment system, 25:28571 (DOCKET-50266-46)
POLONIUM
alpha decay of, half-lives, Q values, reduced widths, and spectra from, (E), 25:28302 (CERN-70-30(Vol.1), pp 523-31)
POLONIUM ISOTOPES Po-201
energy levels from radon-205 alpha decay and decay of isomeric polonium-201, spin--parity assignments for, (E), 25:28333 (CERN-70-30(Vol.2), pp 1023-9)
POLONIUM ISOTOPES Po-203
energy levels from radon-207 alpha decay and astatine-203 electron-capture decay, spin--parity assignments for, (E), 25:28333 (CERN-70-30(Vol.2), pp 1023-9)
POLONIUM ISOTOPES Po-205
energy levels from radon-209 alpha decay and astatine-205 electron-capture decay, spin--parity assignments for, (E), 25:28333 (CERN-70-30(Vol.2), pp 1023-9)
POLONIUM ISOTOPES Po-207
energy levels and properties of, nuclear data sheets for, 25:28378
energy levels from astatine-207 electron-capture decay, spin--parity assignments for, (E), 25:28333 (CERN-70-30(Vol.2), pp 1023-9)
energy-level transitions from astatine-207 electron-capture decay, multipolarities for, (E), 25:28333 (CERN-70-30(Vol.2), pp 1023-9)
POLONIUM ISOTOPES Po-208
energy levels and properties of, nuclear data tables for, 25:28375
POLONIUM ISOTOPES Po-209
energy levels and properties of, nuclear data sheets for, 25:28376
energy levels from astatine-209 electron-capture decay, spin--parity assignments for, (E), 25:28333 (CERN-70-30(Vol.2), pp 1023-9)
energy-level transitions from astatine-209 electron-capture decay, multipolarities for, (E), 25:28333 (CERN-70-30(Vol.2), pp 1023-9)
POLONIUM ISOTOPES Po-210
content of atmosphere and river water at Miamisburg, Ohio during 1970, 25:26739(R) (MLM-1795)
determination in lunar surface-exposed solar wind foils, 25:26187(R) (BNWL-1183-7)
ingestion by man in contaminated diet, potential long-term hazards from, 25:26684
sorption in agricultural soils following contamination, distribution coefficients for fallout, 25:26684
uptake from soil by crop plants, transfer coefficients for, 25:26684
POLONIUM ISOTOPES Po-211
energy levels and properties of, nuclear data sheets for, 25:28377
POLYMERS
conference on polyblend, New York, June 6 to 7, 1969, 25:27271
elastic moduli of crystalline regions of, effects of molecular conformation on, 25:26281
neutron dose to, ASTM standard method for calculation of, 25:26535
radioinduced curing of, survey on, 25:26283
POLYPHOSPHATES
effects on color stability of electron- and γ-radiation processed beef, 25:27162

XUM

POPULATIONS
radiation dose to human, from nuclear power plants, 25:26741
radiation effects on aging, immune reactions, and peripheral blood of human, on Marshall Islands, correlation of fallout, 25:27058
radiation hazards to human, from medical uses, comparison of hypothetical exposure from nuclear industries with, 25:26774
radiation hazards to, in environment of nuclear power plants, 25:26746
PORCELAIN
gamma absorption coefficient of, (E), 25:27826 (DEMO-70/11)
POROSIMETERS
design of neutron radiometric, with borehole-effects compensation, 25:26541(P)
POSITRONS
annihilation in gamma-irradiated Teflon, 25:27306
annihilation in single insulator crystals, angular correlation of gamma rays from, (E/T), 25:27865 (CEA-R-4138)
interactions $e^+ + e^- \rightarrow e^+ + e^- + e^+ + e^-$ at 2 x 510 MeV, cross section and angular distribution for, (E), 25:27994
interactions $e^+ + e^- \rightarrow e^+ + e^- + K^+ + K^-$, double-logarithmic approximation for cross sections for, 25:27997
interactions $e^+ + e^- \rightarrow e^+ + e^- + \mu^+ + \mu^-$, double-logarithmic approximation for cross sections of, 25:27997
interactions $e^+ + e^- \rightarrow e^+ + e^- + \pi^+ + \pi^-$, double-logarithmic approximation for cross sections of, 25:27997
interactions $e^+ + e^-$ at high energies, spectral sum rules in Sugawara model with modified stress tensor for cross sections for hadron production in, (T), 25:28006
interactions $e^+ + e^-$, limits on production and decay modes of heavy leptons from, 25:27998
interactions with electron liquid, bound states in, (T), 25:27447
POTASSIUM
content ratio to sodium in urine of rats as indicator of biological stress, tracer study of, 25:27029
content relative to cesium-137 in human diet and transport through maternal milk, 25:26581
efflux from rabbit lens, design of constant perfusion device for tracer studies on, 25:26606
reactions of liquid, with poly(tetrafluoroethylene), 25:26211 (TRG-Report-2104)
POTASSIUM ACID PHOSPHATES
radiation effects on, yields of recoil phosphorus-32 from neutron, 25:26318
POTASSIUM ALLOYS AND SYSTEMS
K--Na, reactions of liquid, with poly(tetrafluoroethylene), 25:26211 (TRG-Report-2104)
POTASSIUM BROMIDES
effects on yields from γ radiolysis of S-allyl-L-cysteine sulfoxide and S-propyl-L-cysteine sulfoxide, 25:26294
POTASSIUM CHLORIDES
effects of pulsed electrons on single crystals of, spectral studies on, (E/T), 25:27846
phonon scattering in lithium-doped, using heat pulses and microwave phonon generation, resonant, 25:28863 (NYO-2391-111)
radiation effects on microhardness of, relations of microhardness with neutron, 25:27222
radioinduced F centers in, effects of electric field and temperature on radiative lifetime of excited, 25:27841 (NYO-3463-23)
radiolysis of potassium cyanide-doped, ESR spectra of FCN^- and HCN^- from x, 25:26289 (NYO-2150-60)
POTASSIUM FLUORIDES
radioinduced F centers in, effects of electric field and temperature on radiative lifetime of excited, 25:27841 (NYO-3463-23)
POTASSIUM ISOTOPES K-39
deuteron reactions (d,n) at 4.7 MeV, neutron time-of-flight spectra from, (E), 25:28230
POTASSIUM ISOTOPES K-40
content of wine in Transylvania, 25:26618
POTASSIUM PERMANGANATES
reactions with monolayers of saturated and unsaturated cholestanol, cholesterol, and lacithins, effects of variables on, 25:26213
POTASSIUM SULFATES
radiation effects on, yields of recoil phosphorus-32 from neutron, 25:26318
POTASSIUM THIOCYANATES
effects on yields from electron pulse and γ radiolysis of aqueous solutions of phenyl glucopyranoside, 25:26304
POWDER METALLURGY
methods for consolidation and fabrication of metals and metal--nonmetal aggregates and particles, 25:27205 (INIS-mf-19)
POWER CYCLES
development of radioisotope-fueled organic Rankine, for 1 to 10 kW(e) power systems, 25:26433
development of radioisotope-fueled steam, for 1 to 10 kW(e) power systems, 25:26433
POWER PLANTS
availability of, equipment reliability factors affecting, 25:28549 (AECL-3670, pp 45-55)
availability of, survey of information collection procedures on, 25:28548 (AECL-3670, pp 23-37)
coolant water from, computer program for computing temperature distribution in large water bodies from discharge of, 25:28856 (HEDL-TME-71-39)
environmental effects of U. S, 25:26530
sulfur dioxide emissions from coal-fired, scavenging by rainwater and snow of, (E), 25:26378 (CONF-700601-, pp 293-303)
PRASEODYMIUM
determination by spectrophotometry, 25:26165
determination in yttrium oxides by solvent extraction and spectrography, 25:26168
solubility in chromium, effects of temperature on, 25:27238
PRASEODYMIUM ALLOYS AND SYSTEMS
Bi--Pr, crystal field levels in PrBi, neutron inelastic scattering study of, 25:27893
Co--Nd--Pr, magnetic properties of $Pr_{0.87}Nd_{0.13}Co_5$, 25:27886
Pd--Pr, magnetic properties of $PrPd_3$ at 4 to 300°K, 25:27870
Pr--Pt, nuclear magnetic cooling of $PrPt_5$, using hyperfine field, 25:27666
Pr--Sb, crystal field levels in PrSb, neutron inelastic scattering study of, 25:27893
Pr--Tl, nuclear magnetic cooling of $PrTl_3$, using hyperfine field, 25:27666
PRASEODYMIUM ARSENIDES
crystal field levels in, neutron inelastic scattering study of, 25:27893
PRASEODYMIUM ISOTOPES Pr-133
decay of, half-life and γ spectra for, (E), 25:28387
PRASEODYMIUM ISOTOPES Pr-134
beta and electron-capture decay scheme, (E), 25:28387
PRASEODYMIUM ISOTOPES Pr-135
beta and electron-capture decay scheme, (E), 25:28387
PRASEODYMIUM ISOTOPES Pr-138
beta and electron-capture decay of ground-state and isomeric, γ spectra from, (E), 25:28414
PRASEODYMIUM ISOTOPES Pr-139
energy levels from neodymium-139 beta and electron-capture decay, complex shell-model, (E/T), 25:28299 (CERN-70-30(Vol.1), pp 435-46)
PRASEODYMIUM ISOTOPES Pr-141
carbon-12 reactions with, cross-section limit for fission isomer excitation in, 25:28399
energy levels from photoexcitation, radiative widths for isobaric analog, (E), 25:28362
energy levels of, analysis of nonrandom distributions of neutron resonance, (T), 25:28421
photon reactions (γ,p) with isobaric analog excitation, proton spectra from, (E), 25:28362
PRASEODYMIUM ISOTOPES Pr-144
energy levels from photoexcitation, radiative widths for isobaric analog, (E), 25:28362
PRASEODYMIUM PHOSPHIDES
crystal field levels in, neutron inelastic scattering study of, 25:27893
PRASEODYMIUM SELENIDES
crystal field levels in, neutron inelastic scattering study of, 25:27893
PRASEODYMIUM SULFIDES
crystal field levels in, neutron inelastic scattering study of, 25:27893
PRASEODYMIUM TELLURIDES
crystal field levels in, neutron inelastic scattering study of, 25:27893
PRECIPITATORS
capacity of continuous, tests on, 25:26330(T) (ORNL-tr-2410, pp 14-78)
PRESSURE VESSELS
construction of reactor, regulatory criteria standards for, 25:28537
design of cylinder shaped prestressed reinforced concrete, 25:28823(P)
development of reactor prestressed concrete, review of, 25:28684
fabrication of steel reactor, review of US methods for, 25:27196
materials for, problems in selection of, 25:27204 (INIS-mf-3)
radiation effects on embrittlement of A302B steel, evaluation of fast neutron, 25:28682 (JAERI-1202)
strain in top of prestressed concrete, comparison of measured and calculated long-term variations of, (E/T), 25:28528 (RD/B/N-1784)
thermal shock limits for coolant loss accidents in water cooled power reactor, standards for, 25:28683
PRINCETON SYNCHROTRON
experimental facility for, on-line PDP-9 computer for missing mass spectrometer, 25:28135
PROCAINE
effects on isolated rat hearts following whole-body x-irradiation, 25:26798
PROMETHIUM ISOTOPES Pm-141
energy levels from samarium-141 beta and electron-capture decay, complex shell-model, (E/T), 25:28299 (CERN-70-30(Vol.1), pp 435-46)

XUM

PROMETHIUM ISOTOPES Pm-147
neutron capture by, ground-state and isomeric cross sections for thermal, (E), 25:28373
use as heat source in cardiac pacemakers, 25:26434
PROMETHIUM ISOTOPES Pm-148
beta decay of ground-state and isomeric, γ spectra from, (E), 25:28373
PROMETHIUM ISOTOPES Pm-149
energy levels from neodymium-149 decay, magnetic moments of, (E), 25:28381
PROPANE, 2-CHLORO-2-METHYL-
yields from γ radiolysis of liquid 2,2-dimethylpropane, effects of additives on, 25:26309
PROPANE, 2,2-DIMETHYL-
radiolysis of liquid, kinetics of reactions of electron scavengers and hydrocarbons with ions produced by γ, 25:26309
PROPANE, 2-METHYL-
yields from γ radiolysis of liquid 2,2-dimethylpropane, effects of additives on, 25:26309
1-PROPANOL
radiolysis of frozen aqueous solutions of, role of LET in yields from α, β, and γ, 25:26311
2-PROPANOL
radiolysis of aqueous solutions of, effects of cysteine, mercaptans, or 2-mercaptoethanol on yields from γ, 25:26291
radiolysis of frozen aqueous solutions of, role of LET in yields from α, β, and γ, 25:26311
H_2O_2--2-propanol, radiolysis of aqueous solutions of, reactions of radicals from γ, 25:26290(R) (NYO-3753-19)
PROPENE
yields from γ radiolysis of liquid 2,2-dimethylpropane, effects of additives on, 25:26309
PROPENE, 2-METHYL-
effects on hydrogen yields from α radiolysis of gaseous hydrogen sulfide, 25:26315
yields from γ radiolysis of liquid 2,2-dimethylpropane, effects of additives on, 25:26309
yields of ions of, from γ radiolysis of liquid 2,2-dimethylpropane, kinetics of reactions of electron scavengers and hydrocarbons with, 25:26309
PROPRANOLOL
effects on radioprotective effects of adrenaline and noradrenaline in mice, 25:26804
PROTACTINIUM ISOTOPES Pa-222
decay products of, energies, intensities, and half-lives of alpha, (E), 25:28304 (CERN-70-30(Vol.1), pp 545-6)
PROTACTINIUM ISOTOPES Pa-223
decay products of, energies, intensities, and half-lives of alpha, (E), 25:28304 (CERN-70-30(Vol.1), pp 545-6)
PROTACTINIUM ISOTOPES Pa-224
decay products of, energies, intensities, and half-lives of alpha, (E), 25:28304 (CERN-70-30(Vol.1), pp 545-6)
PROTACTINIUM ISOTOPES Pa-225
decay products of, energies, intensities, and half-lives of alpha, (E), 25:28304 (CERN-70-30(Vol.1), pp 545-6)
PROTACTINIUM ISOTOPES Pa-231
geochemistry of, studies of marine, 25:26399 (TID-25674)
PROTACTINIUM ISOTOPES Pa-238
beta decay of, gamma spectra from, (E), 25:28326 (CERN-70-30(Vol.2), pp 985-1000)
PROTECTIVE OINTMENTS
radiosterilization of ophthalmic, containing chloramphenicol and hydrocortisone, effective dose for, 25:27161
PROTEINASES
radiation effects on activity of rabbit leukocyte, macrophage, and spleen cell, whole-body x, 25:27035
PROTEINS
cerium-141 binding to blood serum, review on dialysis methods for studying, 25:26584
effects of depressed synthesis of, on survival of irradiated L cells, 25:26969
effects of synthesis of, on recovery in x-irradiated yeast, 25:27096
effects on mitosis in γ-irradiated pea roots, delaying, 25:27063
effects on x-radioinduced delay of mitosis in Chinese hamster cells, 25:26626
radiation effects on biochemical structure of, effects of dose on gamma, 25:26660
radiation effects on biochemistry of, in dogs, effects of AET on x, 25:26935
radiation effects on egg, fish, and meat, role of immunoelectrophoresis and starch gel electrophoresis to determine, 25:26631
radiation effects on metabolism of, in rats, x, 25:26624
radiation effects on synthesis of, by liver microsomal fractions in rats, subsequent whole-body γ, 25:27006
radiation effects on synthesis of, in Blepharisma during regeneration, carbon-14 tracer study of uv, 25:26648
radiation effects on synthesis of, in Micrococcus radiodurans, dose dependence of gamma, 25:26639
radioinduced inactivation of, review of mechanisms of uv, 25:26644
synthesis in cultured lymphocytes, effects of, on response of lymphocytes to x radiation, 25:26903
synthesis in cultured rabbit lenses, effects of naphthalene and x radiation on, carbon-14 tracer study, 25:26649
PROTONS
angular and spatial distribution over polar caps, satellite observations of solar, (E), 25:27540
anisotropy in upper ionosphere, energetic electron flux-associated magnetic-field aligned 1- to 6-keV, (E), 25:27604
channeling in fluorite crystals, 25:27851
classification and forecasting of solar events, (T), 25:27355
density of solar 500-keV, effect on magnetic-field configuration following Jan. 28, 1967 solar flare, (E), 25:27584
detection at 657 MeV, design and performance of Cherenkov detector for, 25:26506 (JINR-P13-5637)
detection at 665 MeV, design and performance of Cherenkov detector for, 25:26505 (JINR-P13-5636)
detection of 0.31-MeV cosmic, in near-Earth interplanetary space and anisotropy, 25:27473
directional measurements of interplanetary low-energy, during Feb. 25, 1969 solar flare, (E), 25:27559
distribution in cold-plasma magnetosphere, effect on Pc1 propagation, (T), 25:27605
effects on aqueous solutions of iron sulfates at 30 to 400 keV, LET parameters in, 25:26288(T) (LB/G-2937)
effects on Arabidopsis seeds, 1 to 20-krad mutagenic, 25:26736
effects on gallium arsenide at 200 keV, annealing of damage induced in, 25:27862
effects on monkeys, measurement of simulated solar flare, 25:26920(R) (AD-711041)
effects on silicon at 200 to 400 kV, shallow donor state induced in, 25:27847
effects on silicon solar cells at 40 keV, 25:26564
electric polarizability of, symmetric quark model for, 25:27983
emission during solar flares, classification system for, (T), 25:27388
emission from meson reactions (π^+,p) with carbon-12, distorted-wave effects for differential cross sections for, (T), 25:28048
energy losses in selenium, (E), 25:27833
energy spectra of 1- to 30-MeV, over northern polar cap during Feb. 25, 1969 solar event, (E), 25:27561
energy spectra of 2.3 to 70 MeV, during PCA following Feb. 24-25 solar event, (E), 25:27563
energy spectra of 30- to 120-MeV, following Feb. 25, 1969 solar event, (E), 25:27562
energy spectra of cosmic solar, satellite observations of, (E), 25:27533
energy spectra of trapped 0.3- to 74-MeV, Aug. 29 to Nov. 15, 1968, (E), 25:27625
flare-position effect of, on Earth's particle flux, solar, (T), 25:27355
flux in radiation belts, neutron source decay solar-cycle modulation in, (T), 25:27624
fluxes of 1 to 13 keV, relation to auroral luminosity patterns over northern Scandinavia, (E), 25:27581
form factors from e + p interactions, (T), 25:27991
injection into magnetosphere, mechanism responsible for formation of ring current, (T), 25:27627
intensity at 300 to 500 km in auroral zone, Geiger--Mueller observations during Feb. 25, 1969 solar event, (E), 25:27572
intensity at synchronous altitude, temporal and spectral variations of solar, (E/T), 25:27541
intensity during Feb. 25, 1969 solar flare, ESRO-II observations of low-energy, (E), 25:27471
intensity in deep magnetosphere, effect of low-energy solar, (E/T), 25:27541
intensity in early-evening proton aurora, solar-wind origin of primary, (E/T), 25:27618
intensity increase in Feb. 25-Mar. 5, 1969 of solar cosmic-ray, (E), 25:27470
intensity of >360-MeV and >30-MeV solar, directional measurements aboard HEOS-I during Feb. 25, 1969 solar event, (E), 25:27560
intensity over northern polar cap of 100 keV to 6 MeV, following Feb. 25, 1969 solar event, (E), 25:27573
interaction of solar energetic, with bow shock and magnetopause, (E), 25:27538
interactions e + p → e' + π^+ + n at 4 to 5.4 GeV, differential cross sections for, (E), 25:27950 (DESY-71/9)
interactions e + p, distributions of transverse momenta in inelastic, (T), 25:27974
interactions e + p, proton form factors and radius from, (T), 25:27991
interactions e + p, scale invariance of proton inelastic structure function from, 25:27995
interactions e + p, structure function and scaling behavior of inelastic, 25:27999
interactions γ + p → p + eta at high energies, pole--cut model for, (T), 25:27989
interactions K^- + p → Λ + K^+ + K^- at 3.3 GeV/c, test of generalized Veneziano model from, 25:28042
interactions K^- + p → π^- + Y^{*+}, eikonal-like pole-cut model for, 25:28044
interactions K^+ + p at 1.60 to 3.31 GeV/c, polarization parameter or elastic, (E), 25:27963
interactions K^+ + p at 10 GeV, generalized Veneziano model and Reggeized multiperipheral model for anti Λ

production in, (E/T), 25:27966
interactions K^+ + p below 2 GeV/c, Reggeized phase shift analysis of, 25:28043
interactions n + p → n + p at 152 MeV, differential cross sections and angular distributions for, (E), 25:27956
interactions n + p at 25 to 50 MeV, Kantor amplitudes for $^3P_0$ phase shift for, (E/T), 25:28046
interactions p + p → p + p at 9.690 to 13.600 MeV, differential cross sections for, (E), 25:27957
interactions p + p above 10 GeV, optical-model calculations of, (E/T), 25:28052
interactions p ≠ p as proposed test of impact picture of hadron dynamics, 25:28045 (DESY-71/6)
interactions p + p at 25 to 50 MeV, Kantor amplitudes for $^3P_0$ phase shift for, (E/T), 25:28046
interactions p + p, cross sections for elastic, 25:28073
interactions p + p, distributions of transverse momenta in inelastic, (T), 25:27974
interactions π^- + p → Δ^- + π^+ at 1640 to 1760 MeV, partial-wave analysis of, (E/T), 25:27962
interactions π^- + p → eta + n, duality concept for imaginary part of Regge trajectories for, 25:28036
interactions π^- + p → K^+ + Σ(1385) at 2.75 to 14.0 GeV/c, cross sections for, (E), 25:28038
interactions π^- + p → K^+ + Σ^- at 2.75 to 14.0 GeV/c, cross sections for, (E), 25:28038
interactions π^+ + p → K^+ + Y^{++}, eikonal-like pole-cut model for, 25:28044
interactions π^+ + p → π^+ + p + D^0, D^0 → π^+ + π^+ + π^- + π^- at 16 GeV/c, cross section for, (E), 25:27964
interactions π^- + p → π^- + p + D^0, D^0 → π^+ + π^+ + π^- + π^- at 16 GeV/c, cross section for, (E), 25:27964
interactions π^+ + p → π^+ + p at 2.18 to 5.25 GeV/c, differential cross sections and angular distributions for backward, (E), 25:27965
interactions π^- + p → π^- + p at 2.38 to 3.00 GeV/c, differential cross sections and angular distributions for backward, (E), 25:27965
interactions π^+ + p → rho^0 + Δ^{++} at 11.7 GeV/c, total and differential cross sections for, (E/T), 25:27960 (DESY-71/8)
modulation of magnetospheric trapped, relation of coupled magnetic-field-line oscillations to, (T), 25:27623
nitrogen excitation in aurorae by, 5 to 25 keV, (E), 25:27616
penetration into magnetosphere, interplanetary and magnetospheric measurements of low-energy solar, (E/T), 25:27542
precipitation at high-latitude noon--midnight meridian, relation to geomagnetic activity, (E), 25:27579
precipitation patterns for keV, auroral, over northern polar cap, 1968, (E), 25:27576
radius from e + p interactions, (T), 25:27991
reactions (p,3α) with boron-11 at 2 MeV, multiparticle-reaction analysis of energy distributions from, (T), 25:28184
reactions (p,α) with arsenic-75, indium-115, rhodium-103, silver-107, silver-109 and yttrium-89 at 5 to 13 MeV, excitation functions for, (E), 25:28268
reactions (p,α) with lithium-7, multi-level R-matrix analysis of, (T), 25:28452 (NP-18717)
reactions (p,α) with sodium-23 at 590 to 1810 keV, angular distributions from, (E), 25:28259
reactions (p,d) and (p,He-3) with tritium at 13.6 MeV, angular distributions for, (E), 25:28164 (LA-4576)
reactions (p,d) with nuclei adiabatic treatment of, (T), 25:28512
reactions (p,d) with nuclei, isobaric analog resonance effects in, 25:28471
reactions (p,f) with radium-226 at 13 MeV, fragment kinetic-energy distributions from, (T), 25:28408
reactions (p,γ) with magnesium-24 at 1201 and 1485 keV, Q value for, (E), 25:28276
reactions (p,γ) with molybdenum-92 at 5.9 MeV with isobaric analog excitation, γ spectra from, (E), 25:28359
reactions (p,γ) with silicon-29 at 0.9 to 2.2 MeV, γ spectra from, (E), 25:28207 (ANU-P-517)
reactions (p,γ) with silicon-30 up to 2 MeV, Q value and gamma angular distributions and spectra from, (E), 25:28270
reactions (p,γ) with titanium-50 at 1.3 to 1.4 MeV, excitation function for, (E), 25:28226
reactions (p,n) with arsenic-75 at 3 and 3.2 MeV, neutron spectra from, (E), 25:28241
reactions (p,n) with cobalt-59 and vanadium-51 at 7.8 to 14.7 MeV, neutron spectra from, (E), 25:28285
reactions (p,t) with 1p-shell nuclei, analysis using zero-range DWBA, 25:28204
reactions (p,t) with dysprosium-164, gadolinium-158, hafnium-176, tungsten-184, and ytterbium-172 at 51.7 MeV, spectra and DWBA analysis of differential cross sections from, (E/T), 25:28411
reactions (p,x) with carbon-12 at 150 and 600 MeV, production cross sections for lithium and beryllium isotopes in, (E), 25:28182
reactions with aluminum, carbon, copper, and lead at 1 GeV/c, differential and total cross sections for, (E), 25:27959
reactions with carbon-12 at 1 GeV, multiple diffractive model for, 25:28073
reactions with hydrogen molecules at 10 eV, differential cross sections for excitation of resolved vibrational states in, (E), 25:27450
reactions with lead-208 at 19.3 GeV/c, multiple diffractive model for, 25:28073
reactions with negative ions above 10 keV, charge exchange in, (T), 25:27456
reactions with nuclei at 1 GeV, experimental studies of nucleon correlations from, 25:27958
reactions with uranium at 5.5 GeV, energy spectra of fragments from, (E), 25:28426
scattering by A = 23 to 35 nuclei at 6 to 17.5 MeV, core-excitation analysis of differential and integrated cross sections from elastic and inelastic, (T), 25:28261
scattering by A = 88 to 146 nuclei using polarized beams, isobaric analog resonances in elastic, (E), 25:28239
scattering by argon at 10 and 25 eV, secondary rainbows and interference in elastic, (E), 25:27458
scattering by barium-130, -132, -134, -136, and -138 at 7 to 12 MeV with isobaric analog excitation, comparison of spectroscopic factors with (d,p) reactions, 25:28372
scattering by cadmium-110, -112, and -114 at 6 to 11 MeV with isobaric analog excitation, excitation functions for elastic, (E), 25:28370
scattering by calcium-40 at 185 MeV, differential cross sections for inelastic, (E), 25:28255
scattering by calcium-40 at 185 MeV, polarization angular distributions from inelastic, (E), 25:28256
scattering by cobalt-59 and iron-56 at 6.9 MeV, optical-model analysis of cross-section and polarization angular distributions from elastic, (E), 25:28263
scattering by gold-197, platinum-196, and tungsten-184 at 13 to 17 MeV, analog resonance anomalies in elastic and inelastic, (E), 25:28371
scattering by krypton-86 at 4.8 to 10.1 MeV with isobaric analog excitation, excitation functions for elastic and inelastic, (E), 25:28242
scattering by lead-207 at 14 to 18 MeV with isobaric analog excitation, excitation functions for, (E), 25:28365
scattering by magnesium-24, -25, and -26 at 5.84 to 6.03 MeV, angular distributions and spectra from elastic and inelastic, (E), 25:28264
scattering by medium-A nuclei at 6.9 MeV, optical-model analysis of angular distributions from elastic, (E), 25:28262
scattering by nickel-62 at 2.4 to 2.7 MeV with isobaric analog excitation, excitation function for elastic, (E), 25:28237
scattering by nuclei with isobaric analog excitation, determination of spectroscopic factors in elastic and inelastic, 25:28464
scattering by nuclei with isobaric analog excitation, review on elastic and inelastic, 25:28469
scattering by oxygen-16 at 17 GeV/c, multiple diffractive model for elastic, 25:28073
scattering by strontium-86 at 4.5 to 7.5 MeV, excitation functions for elastic and inelastic, (E), 25:28234
scattering by strontium-88 at 4.5 to 8.6 MeV with isobaric analog excitation, proton polarization from elastic, (E), 25:28238
scattering by strontium-88 at 8 to 12 MeV with isobaric analog excitation, excitation functions for elastic and inelastic, (E), 25:28240
scattering by strontium-88 with isobaric analog excitation, analysis using coupled optical equations, (T), 25:28236
scattering by tellurium-130 at 7.8 to 12 MeV with isobaric analog excitation, excitation functions for elastic and inelastic, (E), 25:28427
scattering by tellurium-130 to 10.2 to 10.8 MeV, proton spectra and angular distributions for inelastic, (E), 25:28369
scattering by titanium-50 at 1.3 to 1.4 MeV, excitation function for elastic, (E), 25:28226
scattering by tritium at 13.6 MeV using polarized beam, asymmetry and angular distribution for elastic, (E), 25:28164 (LA-4576)
scattering by tritium at 13.6 MeV, angular distribution for elastic, (E), 25:28164 (LA-4576)
scattering by zirconium-90 with isobaric analog excitation, R-matrix analysis of inelastic, (T), 25:28364
scattering by zirconium-92 at 4.7 to 8.6 MeV with isobaric analog excitation, proton polarization in elastic, (E), 25:28368
scattering from niobium single crystals at 100 keV, effects of lattice defects on back-, 25:27840 (IPP-7/3)
scattering from phosphorus-ion implanted diamonds, back-25:27858
solar events involving, proposed classification of, 25:27356
spectra in midnight luminous aurorae, comparison with proton, (E), 25:27578
spectral emission in solar radiation, flare-associated high-energy, (E/T), 25:27354
spectral intensity in interplanetary space, Feb. 25-28, 1969, (E), 25:27558
structure function for, scale invariance of inelastic,

25:27995
PROTOZOA
Blepharisma intermedium, radiation effects on synthesis of nucleic acids and proteins in, during regeneration, carbon-14 tracer study of uv, 25:26648
Euglena gracilis, purification of photoreactivating enzyme from, 25:26619 (COO-1793-6)
gregarine species parasitic on spatangoid urchins, description of new, 25:26880 (RLO-1750-59)
PRUSSIAN BLUE
effects on cesium-137 excretion in rats, combined effects of pilocarpine and, 25:26583
PULSARS
dispersion measures for twelve, (E), 25:27350
pulse profiles for twelve, (E), 25:27350
PULSE CONVERTERS
design of wide-range rise time-to-amplitude, 25:26545 (CEA-N-1430)
PUPAE
radiation effects on survival of larvae and pupae of alfalfa weevil, effects of dose on γ, 25:26913
PURINE, 2-AMINO-
effects on β-galactosidase gene of Escherichia, mutagenic, 25:26722
PUROMYCIN
effects on unscheduled DNA synthesis in x-irradiated mammalian cultured cells, 25:27002
PYRETHRINS
synthesis of radioactive, in Ecuador, 25:27134 (CONF-680112-, pp 245-6)
PYRIDOXAL
radioprotective effects on collagen gel, x, 25:26802
PYROCATECHOL
radiation effects on content of, in mice tissues, protective effects of cystamine and mexamine against, 25:27017

Q

Q DEVICES
ion energy analysis in double ended, cesium, 25:27686
plasma injection and confinement in, cesium, (E), 25:27671
plasma instabilities in, feedback stabilization of Kelvin--Helmholtz, (E/T), 25:27772
plasma stabilization by remote feedback using microwaves, (E/T), 25:27766
plasma stabilization in, passive feedback, (E), 25:27771
plasma stabilization of edge oscillations in, using feedback, (E), 25:27770
plasma wave--charged particle interactions in single-ended, (E/T), 25:27693
QUANTUM ELECTRODYNAMICS
model for interactions in, multiple diffractive scattering, 25:28073
vacuum polarization tensor and equal-time commutators in, 25:28074
vacuum polarization tensor in, amplitudes for photon interactions from fourth-rank, 25:28070
QUANTUM FIELD THEORY
algebra associated with free relativistic fields in, structure of, 25:28080
eikonal approximation and impact picture in phi^3 theory, 25:28045 (DESY-71/6)
energy--momentum spectra in, annihilator of, 25:28069
functional power series in, Hilbert spaces of, 25:28066
Haag theorem in, 25:28083
impact picture and eikonal approximation in phi^3 theory for hadron interactions, 25:28011
Lagrangians in axiomatic, algebraic concepts for, 25:28084
lectures on axiomatic, 25:28076
Lee model in, field operator with continuous spectrum of asymptotic energies for N--theta sector in, 25:28067
model for axiomatic, vector Lie fields, 25:28081
Pade approximants for, book on, 25:28063
quantization of nonlinear field, 25:28071
Regge asymptotic behavior in, mechanism for origin of, 25:28072
renormalization in, conference on, 25:28060 (IC-69/121)
structural analysis of, review of, 25:28077
theory for relativistic, ergodic states in, 25:28078
vacuum expectation values with account of local commutativity in, integral representations of, 25:28082
virtual particles and processes in, 25:28064
Wightman functionals in, moments problem and continual integral representations of, 25:28079
QUANTUM MECHANICS
book: Statistical Physics, Phase Transitions, and Superfluidity, 25:27912
decay in two-level system, modulated, 25:27939
density operator and multitime correlation functions for open systems, 25:27936
derivation of Pryce--Foldy--Wouthuysen transformation, 25:27937
development of WKB approximation using transformations, 25:27938
energy eigenvalues for local potential, numerical calculation of S-state, (T), 25:27933
fluctuation and coherence phenomena in classical and, 25:27947
Hamiltonian for interaction of molecular system with electromagnetic field, 25:27943
Hamiltonians as quadratic forms in, 25:27940
harmonic oscillator interactions with radiation field, 25:27928 (INR-P-1203)
interference experiments in, deterministic, 25:27942
Jordan algebras for dynamic systems in, 25:27945
Mathieu equation in WKB approximation, solution of, (T), 25:27935
oscillator problem in, exactly solvable N-body, 25:27934
phenomenological foundation of quantum logic, 25:27949
restrictions on partial-wave amplitudes from Grobov--Froissart formula, 25:27930 (ITF-70-101-E)
Schroedinger equation in, particle method for numerical solution of time-dependent, 25:27932
Schroedinger Hamiltonian for one-body problem in, class of analytic perturbations for, 25:27926 (CNRS-CPT-70-P-352)
spinning-top problem in, 25:27927 (FEI-203)
stochastic theory of, self-interaction corrections in nonrelativistic, 25:27941
structure of relativistic quantum systems, global and local, 25:27931 (JINR-E2-5575)
uncertainty principle in, least-squares analysis of, 25:27944
use in cognition of microcosmos, 25:27929 (ITF-70-62-E)
QUASARS
angular structure of 3C 147, (E), 25:27351
spectral redshift of, Schwarzschild-metric calculation of gravitational, 25:27347
8-QUINOLINOL, 5,7-DIIODO-
complexes with metals, formation constants of, 25:26214

R

RABBITS
blood flow in bones of, use of strontium-85-labeled plastic microspheres for measurement of, 25:26577
radiation effects on blood pressure and heart frequency of, protective effects of AET and cystamine against γ, 25:26794
radiation effects on eyes in, protective effects of chemicals against cataract-inducing cobalt-60γ and fast neutron, 25:27014
radiation effects on heart of, localization of, 25:26961
radiation effects on oxidative phosphorylation and respiration in bone marrow of, after homotransplantation of bone marrow elements, effects of doses of 1200 to 1250 R on, 25:27019
radiation effects on proliferation of phagocytes in tuberculous lesions of, tritium tracer study, 25:27001
radiation effects on protease activity in leukocytes, macrophages, and spleen cells of, whole-body x, 25:27035
radiation effects on spermatozoids of, effects of dose and dose rate on γ, 25:26954
radiation effects on, effects of bone marrow transplants on recovery following combined liver injury and, 25:27005
radioinduced cataracts in eyes of, effects of average power in relation to dose on microwave, 25:26971
radioinduced cataracts in eyes of, RBE for 14-MeV neutron, 25:27027
radioinduced cataracts in eyes of, RBE for fast neutron, 25:26945
radioinduced changes in leukocyte preparations from, following whole-body exposure, x, 25:26901
radioinduced inflammation on skin of, protective effects of benzydamine against x, 25:26806
radioinduced injuries in lower jaws of, effects of dose and time on, 25:27003
RADAR
performance of pulse Doppler, for studying storm circulation and precipitation scavenging, 25:26360 (CONF-700601-, pp 13-20)
RADIATION
conference on biological effects of, 25:27036 (CONF-691057)
dose to bones and body of man following release of radioisotopes to biosphere, method for calculation of ionizing, 25:26751 (UCRL-50163(Pt.7))
dose to gonads of man during therapy, 25:26759
dose to hospital personnel from handling short-lived radioisotopes, 25:26763
dose to man following ingestion of food from contaminated freshwater food chain, correlation between MPC for radioisotopes in freshwater ecosystem and, 25:26747
dose to man from nuclear power plants, calculations of, 25:26741
dose to man, regulations for maximum permissible, 25:26764
effectiveness for therapy of cancer of cervix, 25:26871
effectiveness for therapy of vocal cord leukoplakia in man, effects of dose and histological condition on, 25:26868
effects of nuclear explosions, on human thyroid, carcinogenic, 25:26898
effects on adrenal glands in rats, recovery from, 25:26998

effects on albumin synthesis and cell permeability in rats, mechanism of, 25:27007
effects on animals, injurious, 25:27024
effects on antibody forming cells, 25:26665
effects on biphenyl--2-methylbutane solutions at -120°C, delayed emission and ion recombination in pulse, 25:26297
effects on blood coagulation in man following cancer therapy, effects of dose on, 25:26668
effects on bone marrow and chromosomes in mammals, review on latent, aberrant, leukemic, and tumorogenic, 25:26943
effects on brain reflexes in rats, effects of 1-R dose on damaging, 25:26949
effects on carcinomas of human uterine cervix, complications following therapeutic, 25:26893
effects on catecholamine content in mouse tissue, 25:27017
effects on cereal and vegetable plants, mutagenic, 25:26686 (CONF-680112-, pp 95-111)
effects on cervical cancer in man, intercavitary radium and external, 25:26886
effects on chromosomes of Crepis seeds, mutagenic, 25:26733
effects on chromosomes of mosquitoes, aberrant, 25:26694
effects on conjunctival, pulmonary, and renal tissues, 25:27036 (CONF-691057)
effects on curing of polymers, survey on, 25:26283
effects on development of mammary carcinomas in rats, synergism between diethylstilbestrol and, 25:27011
effects on differentiation of immunoresponsive cells from bone marrow progenitors in mice, 25:26669
effects on DNA in hepatectomized rats, effects of dose and time on, 25:27020
effects on DNA, protective effects of cystamine, GED, and pentamethylene diguanidine against degratory, 25:26801
effects on embryonic development of animals and man, 25:27036 (CONF-691057)
effects on eyes in animals and man, effects of age and dose on, 25:27013
effects on fibroblast formation in cultures of mouse spleen following exposure of mice, 25:26905
effects on fibrosarcoma incidence in man following radiotherapy, 25:27044
effects on fish and food, 25:27166
effects on food, carcinogenic and mutagenic, 25:27143
effects on formation of hyperproducing virions, 25:27111
effects on free fatty acids, phospholipids, sterols, sterol esters, and triglycerides in canned chicken pet food products, 25:26647
effects on heart in rabbits, localization of, 25:26961
effects on hematopoiesis in mice, effects of bone marrow transplants and dose on, 25:26904
effects on human breast and genital organs following therapy of neoplasms, carcinogenic, 25:27038
effects on human cervical carcinomas incidence of ureteral strictures following therapeutic, 25:27052
effects on human cervical carcinomas, recurrence following therapeutic, 25:26887
effects on human fetus following accidental contamination or therapy of mother, review of, 25:27040
effects on human ureter following therapy, surgical methods for treatment of, 25:26814
effects on immune reactions in mice following transplantation of parental and hybrid tumors, 25:26985
effects on immune reactions in mice, effects of preincubation with bone marrow on lethal, 25:26662
effects on insect fruit pests in Bolivia, Chile, and Peru, sterilizing, 25:27130 (CONF-680112-, pp 129-42)
effects on interferon formation and virus replication in monkey kidney cells infected with Newcastle disease, 25:27113
effects on intestinal tract of man, pathology and treatment of, 25:26811
effects on jejunal crypt cells of intestines in animals, effects of dose rate on whole-body, 25:26957
effects on life span of animals and man, 25:27036 (CONF-691057)
effects on liver in human children following therapy for Wilms' tumor in right kidney, 25:26884
effects on lower jaws in rabbits, effects of dose and time on, 25:27003
effects on man exposed in nuclear explosions at Hiroshima and Nagasaki, medical study of, 25:27060
effects on man, leukemogenic, 25:26964
effects on man, review of effects of dose and dose rate on genetic and somatic, 25:27042
effects on mice, effects of hematopoietic stem cells on lethal, 25:26952
effects on mice, effects of hypoxia on, 25:26967
effects on microorganisms, genetic control of, 25:27116
effects on nerve tissues, 25:27036 (CONF-691057)
effects on nervous tissue following therapy of human brain and spinal cord tumors, effects of corticoids on, 25:27056
effects on neuro-muscular function of atomic bomb survivors on Hiroshima, effects of age on, 25:27053
effects on oxidative phosphorylation and respiration in rabbit bone marrow after homotransplantation of bone marrow elements, effects of doses of 1200 to 1250 R on, 25:27019
effects on parodontium of rats following trunk exposure, 25:26960
effects on proliferation of phagocytes in tuberculous lesions of rabbits, tritium tracer study, 25:27001
effects on proteins of eggs, fish, and meat, role of immunoelectrophoresis and starch gel electrophoresis to determine, 25:26631
effects on rabbits, effects of bone marrow transplants on recovery following combined liver injury and, 25:27005
effects on rats, protective effects of AET or serotonin against sublethal fractionated dose, 25:26807
effects on reproductive capacity of insects, review of, 25:27129 (CONF-680112-, pp 123-8)
effects on reproductive capacity of insects, use of sterile male technique for, 25:27128 (CONF-680112-, pp 1-7)
effects on reproductive capacity of screw-worm flies in relation to population dynamics in Mexico and Texas, 25:27152
effects on retina, lethal and sublethal, 25:26902
effects on RNA synthesis in rat livers, use of DNA x RNA hybridization technique for determining, 25:26641
effects on sprouting of potatoes, inhibitory, 25:27167
effects on Streptococcus faecalis, effects of daunomycin on, 25:27100
effects on survival of bacteria in ophthalmic ointment containing chloramphenicol and hydrocortisone, effective dose for, 25:27161
effects on survival of spores of Osmunda regalis, effects of nitric oxide, oxygen, and water on, 25:27069
effects on synchronized L cells, effects of depressed macromolecular synthesis on recovery from, 25:26969
hazards to human population from medical uses, comparison of hypothetical exposure from nuclear industries with, 25:26774
hazards to human populations in environs of nuclear power plants, 25:26746
hazards to personnel in nuclear industries and uranium mines, 25:26783
use for control of insect pests, conference on, 25:27137 (STI/PUB-223)
use for inhibition of sprouting in potatoes, methods for detecting, 25:27145
use for insect control using radiosterilized male technique, description of model for population response to, 25:27153
use for sterilization of fruit flies, estimation of population size for sterile release programs, 25:27156
use for sterilization of med flies in Central America, cooperative program on, 25:27131 (CONF-680112-, pp 143-50)
use for sterilization of Mediterranean fruit flies in Hawaii, 25:27157

RADIATION CHEMISTRY
uses in industry in Japan, review on, 25:26276

RADIATION DETECTORS
book: Applications of Nuclear Physics, 25:28379
corrections for scattering in neutron dosimetry and flux measurements, 25:26483
design and performance of telescope, for particle identification using ORTEC 423 identifier, 25:26490 (ANU-P-514)
design of gamma-compensated self-powered, for in-core neutrons, 25:26458

RADIATION DETECTORS, ACTIVATION
neutron flux measurements using aluminum, ASTM standard method for fast, 25:26480
neutron flux measurements using aluminum, ASTM standard method for fast, 25:26481
neutron flux measurements using iron, ASTM standard method for fast, 25:26477
neutron flux measurements using nickel, ASTM standard method for fast, 25:26479
neutron flux measurements using, ASTM standard method for thermal, 25:26475
neutron flux measurements using, ASTM standard method for, 25:26476
neutron flux measurements using, for calculation of dose, ASTM standard method for, 25:26535
performance of sandwich, for measurement of 0.001 to 10 keV neutron spectra, (E/T), 25:26656(T) (EURFNR-842)

RADIATION DETECTORS, BUBBLE CHAMBER
design of ITEP 2-meter liquid hydrogen, 25:26508 (NP-18787)
particle tracks in hydrogen, SLAC spiral reader system for, 25:26511
particle tracks in, laser illumination system for HPD for measurement of, 25:26509 (RHEL/R-212)

RADIATION DETECTORS, CHERENKOV
design and performance using monochromatic method, for protons at 665 MeV, 25:26505 (JINR-P13-5636)
design and performance with apochromatic prism doublet for protons at 657 MeV, 25:26506 (JINR-P13-5637)

RADIATION DETECTORS, DIELECTRIC TRACK
particle tracks in nitrocellulose, recording of 3- to 10-MeV alpha, 25:26474

RADIATION DETECTORS, GEIGER-MUELLER
bases for, ANSI standard, 25:26468
development for carbon-14 tracer studies of photosynthesis in phytoplankton, 25:28867 (NYO-3993-1)

XUM

RADIATION DETECTORS, IONIZATION CHAMBER
ammeter for, design of portable, 25:26459
design and performance of paired, for simultaneous neutron and gamma dosimetry, 25:26538
design of standard free-air, for x-rays at 50 to 500 keV, 25:26469
development of heptane- and hexane-filled, for detection of alpha and beta particles, 25:26471
development of liquid-filled, for gamma and x-ray dosimetry, 25:26531
development of liquid-filled, for medical dosimetry, 25:26530
ionization currents in liquid, 25:26472
materials for cavity, review of stopping powers of, (E/T), 25:26533
standardization of voltage charger and quartz-fiber, ANSI, 25:26467
RADIATION DETECTORS, PROPORTIONAL
development and testing of multiwire, 25:27959
development for detection of exoelectrons, 25:26487
RADIATION DETECTORS, SCINTILLATION
design of OSO-G satellite-borne, for measurement of cosmic x ray at 25 to 190 keV, 25:26478
development for measurement of beta sources in atmosphere, 25:26488
efficiency graph for sodium iodide, for gamma spectroscopy, construction and use of, 25:26492 (RCC-M-211)
light output of liquid, effects of spectral characteristics of components on, 25:26462
solvent interactions with scintillators in liquid, interference effects from, 25:26463
time fluctuations in large, 25:26482
timing properties for subnanosecond half-life measurements, 25:26491 (INR-1213)
RADIATION DETECTORS, SEMICONDUCTOR
design of antimony trisulfide, for dosimetry, 25:26529
development of, review on, 25:26461
timing properties for subnanosecond half-life measurements, 25:26491 (INR-1213)
RADIATION DETECTORS, SEMICONDUCTOR (GERMANIUM)
performance of lithium-drifted, for relative measurements of gamma activity of radioisotopes, 25:26191
RADIATION DETECTORS, SEMICONDUCTOR (SILICON)
design of position-sensitive with secondary emission foil, for relativistic charged particles, 25:26513
fabrication of lithium-drifted, 25:26457 (CNEA-287)
manufacturing process for surface-barrier, 25:26456 (ANU-P-516)
resolution of telescope for alpha particles of 5 to 9 MeV, 25:26485
RADIATION DETECTORS, SPARK CHAMBER
data acquisition and control for magnetostrictive, computer program for, 25:26512
data acquisition system for, PDP-7, 25:26510
design and operation of wide-gap, review on, 25:26514
development for plotting neutron flux distributions in reactors using fission foils, 25:26460(P)
performance of streamer, for detecting x-ray transition radiation from electrons, 25:26515
RADIATION DOSE
calculation and measurement in clinical radiation physics, development of computer system for, 25:26755
maximum permissible, for supersonic aviation personnel, factors affecting, 25:26750(T) (ORNL-tr-2455)
RADIATION DOSIMETERS
development of, based on thermally stimulated currents and depolarization in nonluminescent near-insulating solids, 25:26520(R) (NYO-3409-9)
operation and performance for neutrons and neutrons in gamma fields, review on, 25:26534
RADIATION DOSIMETERS, BIOLOGICAL
chromosome aberrations as, 25:26771
RADIATION DOSIMETERS, CHEMICAL
development of mannitol, for gamma dosimetry, 25:26523
performance of ceric--cerous, for megarad dosimetry, effects of impurities on, 25:26526
RADIATION DOSIMETERS, COLORIMETRIC
calibration of glass, for gamma dosimetry, 25:26521
development of glass, for gamma dosimetry, 25:26521
RADIATION DOSIMETERS, EXOELECTRON
readout of, development of proportional detector for, 25:26487
RADIATION DOSIMETERS, PHOTOGRAPHIC FILM
characteristics and use for gamma and x rays, 25:26532
errors in commercial badge, 25:26537
performance for radiotherapy personnel, development of standardization procedure for improving, 25:26756
RADIATION DOSIMETERS, PHOTOLUMINESCENT
characteristics of, 25:26528
development of phosphate glass, new aspects in, 25:26519 (NP-18747)
performance of silver-activated phosphate glass, for personnel monitoring, 25:26518 (NP-18746)
readout system for phosphate glass, differential, 25:26519 (NP-18747)
RADIATION DOSIMETERS, THERMOLUMINESCENT
characteristics of, 25:26528
design and performance of manganese-activated calcium fluoride, for personnel x and gamma accident dosimetry, 25:26516 (CLOR-82/D)
design of discs of lithium fluoride, incorporated in silicone rubber, 25:26539
design of personnel badge of lithium fluoride, for neutrons, 25:26524(P)
development of lithium-7-fluoride Teflon personnel, 25:26527
performance of calcium fluoride and lithium fluoride, for fast electrons, 25:26525
properties of calcium fluoride, review of, 25:26522
response of, role of encapsulation in apparent fast neutron-induced fading of, 25:26536
sensitivity to ultraviolet radiation, 25:26517 (COO-1105-164)
RADIATION DOSIMETRY
methods for radium and radon, physical data for, 25:26769
RADIATION MONITORING
program for nuclear power plant site, 25:28626
program for nuclear power plant site, 25:28625
RADIATION PROTECTION
bases for quantitative, development of, 25:27042
developments in, history of, 25:26774
equipment and methods for, of podiatrists during diagnosis, recommendations for, 25:26777
equipment for medical personnel handling indium-113m and technetium-99m, design of, 25:26776
methods for cyclotron personnel, 25:26775
methods for medical personnel handling short-lived radioisotopes, conference on, 25:26762
methods for patients during cobalt-60 γ therapy, 25:26779
programs for astronauts, use of radiation shielded human phantom and computer calculations for, 25:26778
recommendations for, of patients and personnel in dentistry, 25:26772
recommendations of ICRP, 25:27036 (CONF-691057)
standards for patients and medical personnel in Australia, 25:26738
RADIATION-SCATTERING ANALYSIS
sensitivity for constructing surface impurity profiles, 25:26183
sensitivity, principles, and uses of, review on, 25:26186 (BARC-529)
RADIATION TARGET CANS
fabrication of fuel irradiation capsule for EBR-2, 25:28687 (BMI-1898, Sect.A)
RADIATION TARGET CHAMBERS
design for spectroscopy measurements, 25:28102 (ANU-P-502)
design using surface-barrier detectors, 25:28141
RADIATION TARGETS
cycling system for total cross section measurements, automatic, 25:28115 (PURC-4159-17)
design and operation of liquid hydrogen, using mechanical refrigerator, 25:28138
design of tritium gas, for production of 10^{13} n/sec, 25:26883
x-ray production in, Monte Carlo calculation of, (T), 25:27836
RADIO WAVES
absorption of oblique incidence-reflected hf, in winter ionosphere, (E), 25:27595
correlation of 10.7-cm flux with sunspot activity over 11-year solar cycle, 27-day periodicity of, (E/T), 25:27362
emission of solar, relation of 606- to 8800-MHz solar radio bursts to S-component phase of, Nov. 1966 to April 1969, (E), 25:27364
propagation beneath inhomogeneous anisotropic ionosphere, elf and vlf, (E/T), 25:27506
scattering of vhf continuous auroral, correlation with polar electrojet of back-, (E/T), 25:27554
spectral analysis of vlf-banded chorus and narrowband emissions, OGO 5 fast time-resolved, (E), 25:27621
spectral emission during proton solar event, Feb. 25, 1969, (E), 25:27553
RADIOACTIVE MATERIALS
analysis by electron microprobe methods, equipment for, 25:26156
deposition on soil surfaces following earth impaction of space power system radioactive capsules, computer programs for evaluating hazards to man from, 25:26429 (SC-R-7121)
handling and storage of, contained in x-ray diffraction specimens, design and use of equipment for safe, 25:26449 (MLM-1790)
handling by airport personnel, estimation of dose from, 25:26770
handling of, Australian codes of practice for, 25:26738
packaging and shipping of, review of regulations for safe, 25:26452
packaging and shipping of, summary of U.S. regulations for, 25:26445 (BRH/DMRE-71-1)
radon emission from, in confined spaces, methods for measurement of, 25:26356
shipping of, US railroad accident data for use in developing safe equipment and methods for, 25:26447 (HW-76299)
RADIOACTIVE WASTE
analysis of Windscale neutralized liquid, for cesium-134 and cesium-137 by isotope dilution and γ spectrometry, 25:26177 (PG-Report-965)

control of nuclear power plant, 25:28624
decontamination of liquid, from laundries by bacteria and ozonation, 25:26329(T) (ORNL-tr-2410, pp 1-13)
disposal in seas, methods for safe management of, 25:26683
disposal into aquatic environment of UK, 1969, 25:26397 (FRL-7)
disposal methods for nuclear power plants, 25:28623
disposal of high-level solidified, in salt mines, requirements for recoverable containers for, 25:26454
disposal of solidified high-level, in salt mines, USAEC program for, 25:26453
disposal of, summary of USAEC regulations on, 25:26455
disposal requirements for nuclear power plants, 25:28621 (STI/PUB-261)
disposal system for nuclear power plant, 25:28626
monitoring of nuclear power plant, 25:28624
packaging and transport of high-level vitrified, for disposal in Asse Salt Mine, safety evaluation of, 25:26448 (KFK-1263)
processing and disposal of liquid, into Danube River from future Austrian power reactor, economics and safety of, 25:26451 (SGAE-RT-33/1970)
processing of, research progress in, 25:26328(T) (ORNL-tr-2410)
release from power reactors, environment effects of, 25:28527 (DUN-SA-166)
removal from gas streams, honeycomb activated carbon filter for, 25:28829(P)
treatment of, bacterial, evaporation, ion exchange, and precipitation methods for, 25:26329(T) (ORNL-tr-2410, pp 1-13)
treatment of, design of β--γ installation for semi-industrial, 25:26329(T) (ORNL-tr-2410, pp 1-13)
vitrification of solutions of, operation and performance of equipment for, 25:26334(T) (ORNL-tr-2410, pp 143-89)

RADIOACTIVITY
measurements in Cattaraugus Creek, New York waters during Oct. 1969 to Jan. 1970, 25:26355(R) (SRO-344-11)
monitoring in coastal and surface waters of UK, 1969, 25:26397 (FRL-7)
monitoring in environs of West Valley Processing Plant, Oct. 1969 to Jan. 1970, 25:26355(R) (SRO-344-11)
standardization methods for, manual on, 25:26455

RADIOAPPLICATORS
use of radium-226, for contact therapy of carcinomas of human penis, γ, 25:26863

RADIOBIOLOGY
book: Applications of Nuclear Physics, 25:28379

RADIOCHEMICAL ANALYSIS
sensitivity, principles, and uses of, review on, 25:26186 (BARC-529)

RADIOCHEMICAL PROCESSING PLANTS
safety procedures in USA, 25:26780

RADIOCHEMISTRY
book: Applications of Nuclear Physics, 25:28379

RADIOGRAPHY, BIOMEDICAL
effectiveness for diagnosis of bone metastases from unidentified neoplasms, 25:26846
equipment for, development of PDP-9 computer-controlled, 25:26557
licensing technicians using diagnostic, status in USA in 1971 of standards for, 25:26787
radiation dose to man in, in relation to diagnostic accuracy, x, 25:26858
radiation dose to oral tissues during diagnostic dental, beam profiles for reduction of x, 25:26817
radiation dose to patients during diagnostic fluoroscopic, effects of screen components on x, 25:26815 (BRH/DMRE-71-2)

RADIOGRAPHY, INDUSTRIAL
camera for neutron, using californium-252 source for detecting contraband material, development of portable, 25:26437 (BNWL-SA-2865)
development and uses of neutron, literature survey on, 25:26439 (UJV-2545-R,T)

RADIOISOTOPE SCANNERS
development with coincidence detectors for function measurements using gamma cascade isotopes, 25:26465
performance for brain scanning with technetium-99m, 25:26852

RADIOISOTOPE SCANNING
data analysis for, development of statistical method for, 25:26856
data processing system for using digital computer, 25:26834
effectiveness for diagnosis of brain lesions and malignancies, 25:26850
effectiveness of low energy γ emitters in, 25:26849
methods for, review of international, 25:26855
methods in nuclear medicine, 25:26829

RADIOISOTOPES
activity measurements on, 25:26185
activity measurements using lithium-drifted germanium detectors, relative gamma, 25:26191
bibliography on production and industrial uses of, Oct. through Dec. 1970, 25:26427 (ORNL-IIC-30(Pt.4))
book: Radioactivity in Medicine, 25:26790
conference on industrial and research uses of, Rio de Janeiro, Brazil, June 23 to 27, 1970, 25:26436
content in long-range fallout from Schooner Event, data tabulation on, 25:26404 (PNE-527)
content of hot spring waters at Misasa Spa, Japan, 25:26743
content of human aquatic food chain in relation to radiation dose and hazards to man, establishment of MPC for, 25:26747
detection and measurement of, review on, 25:26316
distribution in animal tissues as function of time following intravenous injection, computer calculations of, 25:26580
effectiveness for differentiation of tumors of posterior cranial fossa in man, effects of age and anatomical location on, 25:26820
effects on human fetus following accidental contamination or therapy of mother, review of, 25:27040
gamma radiation from, tables of abundance, energy, half-life, and production mode of, (E), 25:28400
half-life measurements of, timing properties of radiation detectors or subnanosecond, 25:26491 (INR-1213)
hazards to personnel handling, protective measures against, 25:26783
masses of short-lived, method for direct determination of, 25:26547 (CERN-70-30(Vol.1), pp 307-19)
production of, review on, 25:26316
radiation dose absorbed in small-volume target tissues from interstitial photon-emitting, computer calculations of, 25:26752
release to biosphere, method for calculation of radiation dose to man following, 25:26751 (UCRL-50163(Pt.7))
separation from solutions by retention on sulfide precipitates, quantitative, 25:26199
standardization for clinical and biological uses, methods for, 25:26455
use as tracers in research on productivity of farm animals, review of, 25:26578 (CONF-680112-, pp 153-66)
use for diagnosis, 25:27036 (CONF-691057)
use in agriculture in Ecuador, 25:27134 (CONF-680112-, pp 245-6)
use in research on marine ecology, review of, 25:26683
use of two simultaneously administered, with different γ energies for functional studies, development of method for, 25:26569
uses as excitation sources in x-ray fluorescence analysis, 25:26175
uses in hydrology in Argentina, review of, 25:26353 (CONF-680112-, pp 37-52)

RADIOMETRIC ANALYSIS
methods for, review on, 25:26164

RADIOMETRIC TESTING
instrument for, design of, 25:26543(P)
method for materials, review of, 25:26440

RADIOPROTECTIVE COMPOUNDS
radiation effects on binding between thymidylic acid and sulfhydrylamine, 25:26279

RADIOTHERAPY
book: Radioactivity in Medicine, 25:26790
comparison of Co-60 gamma and fast neutron, 25:26879
dose distribution calculations for moving beam telecobalt, development of method for, 25:26758
dose distribution in tissues during electrons, gamma, and x, computer calculations of, 25:26761
field shaping for, variable block-surface-distance for adjustment of shadow size in, 25:26892
planning 42-MeV betatron electron, using tissue-equivalent phantoms, 25:26865

RADIUM
dosimetry of, evaluation of physical data for, 25:26769
effects on patients with aplastic anemia of Fanconi type, chronic, 25:27054
effects on uterus of rats, carcinogenic, 25:26827

RADIUM ISOTOPES Ra-207
energy levels and properties of, nuclear data sheets for, 25:28378

RADIUM ISOTOPES Ra-208
energy levels and properties of, nuclear data tables for, 25:28375

RADIUM ISOTOPES Ra-209
energy levels and properties of, nuclear data sheets for, 25:28376

RADIUM ISOTOPES Ra-211
energy levels and properties of, nuclear data sheets for, 25:28377

RADIUM ISOTOPES Ra-226
concentration by tropical marine algae, 25:26597
fission of, energy surfaces for, (T), 25:28395
proton fission at 13 MeV, fragment kinetic-energy distributions in, (T), 25:28408

RADON
alpha decay of, half-lives, Q values, reduced widths, and spectra from, (E), 25:28302 (CERN-70-30(Vol.1), pp 523-31)
dosimetry of, evaluation of physical data for, 25:26769
emission from materials in enclosed spaces, methods for measurement of, 25:26356

RADON ISOTOPES Rn-207
energy levels and properties of, nuclear data sheets for, 25:28378

RADON ISOTOPES Rn-208
energy levels and properties of, nuclear data tables for, 25:28375

RADON ISOTOPES Rn-209
energy levels and properties of, nuclear data sheets for, 25:28376
RADON ISOTOPES Rn-211
energy levels and properties of, nuclear data sheets for, 25:28377
RADON ISOTOPES Rn-222
effectiveness for contact therapy of human retinoblastomas, 25:26880
monitoring in uranium mines, alpha spectrometer for, 25:26503
RAINWATER
aerosol scavenging by drops of, numerical model for studying, 25:26388 (CONF-700601-, pp 433-46)
effects on cloud condensation nuclei and ice nuclei content in clouds, (E), 25:26362 (CONF-700601-, pp 37-48)
efficiency for scavenging stack-released sulfur dioxide from coal-fired power plant plumes, (E), 25:26378 (CONF-700601-, pp 293-303)
efficiency of drops of, for scavenging atmospheric gases, effects of gas solubility on, 25:26374 (CONF-700601-, pp 247-59)
efficiency of drops of, for scavenging carbon dioxide, nitrogen dioxide, and sulfur dioxide trace gases from atmosphere, (E), 25:26375 (CONF-700601-, pp 261-9)
efficiency of drops of, for scavenging of atmospheric dusts, (E/T), 25:26371 (CONF-700601-, pp 169-86)
efficiency of drops of, for scavenging submicron biological aerosols, equipment and method for measuring, 25:26369 (CONF-700601-, pp 151-60)
gas and particulate scavenging by drops of, kinetic theory of, 25:26382 (CONF-700601-, pp 355-71)
ice particle content in drops of, effects of rainfall rate on, 25:26363 (CONF-700601-, pp 49-68)
particle scavenging from atmosphere by, uranin and rhodamine dye tracer studies of, 25:26368 (CONF-700601-, pp 137-47)
radioisotope content of Japanese, April 1969 to April 1970, cesium-137 and strontium-90, 25:26392 (NIRS-RSD-27)
radioisotope scavenging by, effects of precipitation rate and ocean proximity on cosmogenic, (E), 25:26364 (CONF-700601-, pp 69-97)
silver content of Nebraska and South Dakota, absorption spectrophotometric measurements of, 25:26366 (CONF-700601-, pp 109-20)
stable element content of, origin and quantity of, (E), 25:26365 (CONF-700601-, pp 99-108)
RARE EARTH ALLOYS AND SYSTEMS
Al--rare earths, s--f exchange coupling parameter of RAl_2, 25:27892
Co--Cu--rare earths, casting and properties of permanent magnets of, 25:27184
RARE EARTH IONS
perturbed angular correlation in NMR of, effects of coaxial magnetic and electric fields on time-integral, (T), 25:27918
RARE EARTHS
complexes with 5,7-diiodo-8-quinolinol, formation constants of, 25:26214
determination in hot spring waters in Japan by neutron activation, 25:26195
nuclear masses and quadrupole moments for Z = 40 to 60, Strutinsky shell-correction calculations of, (T), 25:28318 (CERN-70-30(Vol.2), pp 847-82)
nuclear spin and Nilsson-model level assignments for, atomic-beam measurements of, (E/T), 25:28298 (CERN-70-30(Vol.1), pp 387-94)
production, sources, and uses of, review on, 25:26343
separation by fractional distillation of volatile complexes with 2,2,6,6-tetramethyl-3,5-heptanedione, 25:26336(P)
separation from scandium by ion exchange as complex with organic phosphorus compounds, 25:26338(P)
separation from seawater by sorption on vessel walls and other materials, 25:26339
separation from uranium-barren sulfate leach liquors by solvent extraction using DEHPA, 25:26342
RARE GASES
physical properties of crystals of, calculation from interatomic exchange potential, 25:27444
RATS
cesium-137 excretion in, combined effects of prussian blue and pilocarpine on, 25:26583
chromium-51 distribution in bones of, following intravenous injection of labeled alloxantin, 25:26590
glucose metabolism in eviscerated and nephrectomized, comparison of carbon-14 and tritium tracer studies on, 25:26602
iodine-131 uptake by thyroid gland in, effects of dried thyroid ingestion and sex on, 25:26601
lead-210 distribution and retention in organs and tissues of, following intravenous injection, 25:26610
molybdenum-99 distribution and retention in bones, teeth, and organs following subcutaneous injection, 25:26598
radiation damage to eyes and testes of, effects of dose rate and prenatal exposure on, 25:26951
radiation effects on activity of lactate dehydrogenase in blood serum, heart, liver, and testis of, protective effects of injection of methylene blue against γ, 25:26803
radiation effects on adrenal glands in, recovery from, 25:26998
radiation effects on age and growth of, x, 25:26965
radiation effects on albumin metabolism and proteolytic activity in liver, combined effects of starvation and x, 25:26984
radiation effects on albumin synthesis and cell permeability in, mechanism of, 25:27007
radiation effects on amino acid content of livers of, effects of dose and hepatectomy on x, 25:27022
radiation effects on audiogenic seizure susceptibility in offspring of, effects of age on in utero, x, 25:26968
radiation effects on brain reflexes in, 1-R dose, 25:26949
radiation effects on cesium-137 sorption through skin of, effects of contamination timing on 600 cobalt-60 γ, 25:26595
radiation effects on content of ATP in thymocytes of, effects of adenine on x, 25:26936
radiation effects on development of mammary carcinomas in, synergism between diethylstilbestrol and, 25:27011
radiation effects on DNA from hepatectomized, effects of dose and time on, 25:27020
radiation effects on erythrocytes and leukocytes in, effects of dietary selenium on whole-body gamma, 25:27032
radiation effects on esterase activity in extracts of erythrocytes, liver, spleen, and blood plasma of rats, effects of pH on whole-body x, 25:26600
radiation effects on fetuses, ovaries, and reproductive capacity of cotton, γ, 25:26988
radiation effects on formation of spleen colonies following injection of isologous bone marrow in, transfer to parabiotic partner of x, 25:26939
radiation effects on functional state and morphology of erythropoiesis in, effects of dose fractionation on gamma, 25:27015
radiation effects on glucose and glycogen production in liver of, gamma, 25:26963
radiation effects on glycoprotein contents and lysosomal enzyme activity in blood plasma and liver of, single and combined effects of turpentine and x, 25:26979
radiation effects on growth of bacteria in small intestine of, effects of peristalsis on x, 25:26975
radiation effects on interstitial cells in testes of, functional and morphological studies on cryptorchidism and x, 25:27008
radiation effects on kininase activity in blood plasma of, x, 25:27030
radiation effects on leukocyte count in peripheral blood of, x, 25:26939
radiation effects on liver regeneration in partially hepatectomized, in comparison to effects of liver extracts, x, 25:26948
radiation effects on mandible bone and dentin growth in, 1200-R x, 25:27025
radiation effects on mandibular condyle of, 1200-R x, 25:27026
radiation effects on metabolism of DNAses and phosphatases in kidneys of, in comparison to injection of TEM, whole-body x, 25:26645
radiation effects on mortality of, effects of hypothermic condition on gamma, 25:27023
radiation effects on noradrenaline and serotonin levels in tissues of, whole-body x, 25:26959
radiation effects on novocaine action in isolated heart of, following whole-body exposure to 600 or 1000 R, x, 25:26798
radiation effects on parodontium in, 25:26960
radiation effects on pethidine demethylating system in liver microsomes of, x, 25:27034
radiation effects on protein metabolism in, x, 25:26624
radiation effects on protein synthesis by liver microsomal fractions in, subsequent whole-body γ, 25:27006
radiation effects on replication of spleen lymphocytes in, tritium beta, 25:26994
radiation effects on RNA synthesis in livers of, hybridization method for determining dose effect on, 25:26641
radiation effects on submaxillary gland of, effects of time of administration on protective effects of AET, cystamine, or tetramethylcystamine against γ, 25:26792
radiation effects on submaxillary glands and survival of, comparative radioprotective effects of AET, cystamine, cysteine, noradrenaline, serotonin, and tetramethylcystamine against γ, 25:26795
radiation effects on weight of brains of, x, 25:26946
radiation effects on weight of heart and liver of neonatal, following exposure in utero, tritium β, 25:26925
radiation effects on wound response in lens epithelium of, x, 25:27000
radiation effects on, protective effects of AET or serotonin against sublethal fractionated dose, 25:26807
radiation effects on, use of sodium/potassium ratios in urine to determine x, 25:27029
radiation injuries to, effects of antibiotics on wound healing patterns following combined surgical and x, 25:26932

radioactivity of bacillus carrying, effects of dietary calcium and fluorine on gamma, 25:27016
radioinduced calcification in, effects of dihydrotachysterol on x, 25:26933
radioinduced calcifications in, effects of dihydrotachysterol on, 25:26978
radioinduced calcifications in, effects of dose and dihydrotachysterol on γ, 25:26977
radioinduced carcinomas in lungs of, following implantation of strontium-90, 25:26921(T) (LF-tr-49)
radioinduced carcinomas in uterus of, radium and x, 25:26827
radioinduced changes in leukocyte preparations from, following whole-body exposure, x, 25:26901
radioinduced differentiation of epithelial and mesenchymal cells in thymus gland of, light microscopy whole-body x, 25:26654
radioinduced myelitis in, effects of oxygen on x, 25:26966
radioinduced renal hypertension in, following bilateral or unilateral exposure of kidneys, evaluation of physiological parameters related to x, 25:26652
radiosensitivity of streptozotocin-induced diabetic, x, 25:27010
selenium-75 distribution in pancreas of, effects of pancreozymin and secretin on, 25:26591
sulfur-35 uptake by gastric mucosa and secretion in gastric juice of, with stomach ulcers, effects of steroid hormones and inflammation suppressive drugs on, 25:26605
zinc-65 uptake and distribution in endochondral growth sites in bones of, 25:26611
zinc-65 uptake and distribution in organs and tissues of, 25:26611

REACTIVITY
distribution of, effects of reactor control rod vibrations on, (T), 25:28835
measurement by multiplication method of negative, comparison with calculations of, (E/T), 25:28759 (JAERI-Memo-4272)
measurement of reactor, continuous run method for, (E/T), 25:28799 (CEA-N-1385)
stability domains for nonlinear point reactor, (T), 25:28800 (COO-2109-3)
transfer functions for research reactors, modulation method for measurement of, (E/T), 25:28754 (CEA-N-1405)

REACTOR CONTAINMENT STRUCTURES
aircraft crashes into, analysis of impact loadings from, 25:28611 (DOCKET-50289-34)
design of concrete secondary, 25:28831(P)
design of sodium cooled fast, (T), 25:28739 (RT/ING-(70)25)
loading conditions from explosive accidents, calculation from underwater TNT explosion of, 25:28733 (BAW-1352)
penetrations in primary, design standards for instrument line, 25:28678

REACTOR CONTAINMENT SYSTEMS
design for 1000 MW(e) steam cooled fast breeder, effects of maximum credible accident on, (T), 25:28738 (NP-18781)
design of ice condenser for pressurized water reactor, 25:28700(P)
gas control methods for water cooled power, design standards for coolant loss accident, 25:28702
radioactivity distribution in research reactor, during accident release, 25:28763 (RISO-205)

REACTOR CONTROL ELEMENTS
design of helium vented rod type, for liquid sodium cooled reactors, 25:28673(P)
drive system for rod type, description of hydraulic, 25:28676(P)
drives coupling system for liquid metal cooled reactors, 25:28670(P)
drives for liquid sodium cooled, description of coupling system for, 25:28671(P)
drives for pressurized water, description of part length, 25:28668 (WCAP-7406)
position monitoring of pressurized water, analog system for, 25:28669 (WCAP-7571)
reactivity worth of boron carbide rod, 25:28752 (ANL-7759)
reactivity worth of cylinder shaped boron carbide (B_4C), (E/T), 25:28820 (EUR-4556)
vibrations of rod type, effects on reactivity of, (T), 25:28835

REACTOR CONTROL SYSTEMS
computers for, maintenance of on-line, 25:28797
design of power monitoring, 25:28672(P)
design of pressurized water, 25:28697 (CENPD-11)
design of, use of actuators as logic elements in fail-safe, 25:28741
design requirements of power reactor, 25:28675
development of protective, review of, 25:28674
instrumentation for sodium cooled, development of, 25:28667 (HEDL-SA-170)
operation of pressurized water, 25:28697 (CENPD-11)
performance of fast liquid metal cooled, analysis of real dead-time effects on computer simulation of automatic, 25:28604(T) (EURFNR-835)
performance of γ radiation actuated, effects of prompt and delayed γ radiation on fast response, 25:28822

REACTOR EXPERIMENTAL FACILITIES
control of, model for optimization of, (T), 25:28768

REACTOR FUEL ELEMENTS
analysis of molybdenum- and Zircaloy-clad oxide, development of electron microprobe for, 25:26157
assembly of pins into grid-containing wrappers, method for, 25:28652(P)
burnout of water-cooled bundles of, under transient operating conditions, (E/T), 25:26419(R) (GEAP-10221-5)
burnup of pin type, γ-scanning device for measurement of axial and radial, 25:28766
cladding and pressure tubes for, problems in selection of materials for, 25:27204 (INIS-mf-3)
cladding for mixed uranium oxide (UO_2)--plutonium oxide (PuO_2) fast, development and testing of stainless steel, 25:28691(R) (GEAP-10028-37)
cladding for, COMET code for calculation of mechanical and thermal stresses in, 25:27202 (EUR-4562)
cladding for, properties of austenitic stainless steel, 25:27214(P)
cladding materials for fast breeder, development of, (E/T), 25:28632(T) (EURFNR-824)
coolant flow in rod type bundle, effects of spacer grid configurations on turbulent, (E/T), 25:28819 (EUR-4552)
coolant flow in water cooled nine rod assemblies of, effects of grid and spacer configurations on, (E), 25:28681(R) (GEAP-10221-6)
coolant flow through clusters of, method for control of, 25:28649(P)
creep testing of fast ceramic, 25:28689 (BMI-1898, Sect.C)
design of assemblies of bundles of spaced rod, for steam cooled fast reactors, 25:28695(P)
design of finned Magnox-clad uranium-235-enriched, 25:27267 (UJV-2371.R,T.)
design of gas cooled vented pin type bundle, 25:28694(P)
design of packed bed pyrolytic carbon coated particles in resin filler, 25:28826(P)
design of spaced 19 rod assemblies of, 25:28827(P)
design of spaced 19 rod bundle arranged assemblies of, 25:28824(P)
design parameters of silicon carbide sheathed, with means for absorbing fission products between preventing reactions between sheath and fuel, 25:28837(P)
development of fast breeder, fabrication and irradiation testing programs for, 25:28632(T) (EURFNR-824)
development of sodium-bonded stainless steel clad plutonium nitride--uranium nitride, (E), 25:28687 (BMI-1898, Sect.A)
end retaining member for, with means for control of longitudinal thermal expansion, 25:28834(P)
explosion in liquid sodium of uranium oxide (UO_2), mechanical energy conversion efficiency and particle size distribution from, (E), 25:28726(R) (AI-AEC-12986)
fabrication of coated particle type gas cooled, for recycle testing, 25:28633(R) (GA-10399)
fabrication of packed bed pyrolytic carbon coated particles in resin filler, 25:28826(P)
fabrication of plutonium oxide (PuO_2)--uranium oxide (UO_2) pellet type, 25:28757(R) (GEAP-10010-27)
fabrication of Zircaloy-2-clad uranium dioxide, review of Swedish methods for, 25:27272 (CONF-700903-18)
failure in sodium cooled reactors, delayed neutron monitoring for detection of, (E/T), 25:28698 (NP-18778)
failure of, system for monitoring, 25:28703
fission gas release from ruptured pin-type, effects on temperatures in adjacent fuel pins, (E), 25:26418 (ANL-7734)
gamma scanning of, remote control equipment for, 25:26550 (RT/ING-(71)1)
grid locking device for liquid metal cooled rod type, 25:28693(P)
heat transfer characteristics of gas cooled rod, effects of surface roughening on, (T), 25:28696
heat transfer in nine rod assemblies of, effects of grid and spacer configuration on, 25:28681(R) (GEAP-10221-6)
heat transfer to displaced liquid metal cooled, single-rod multiregion analysis of slug-flow, (T), 25:28661
heat transfer to water cooled, two-region lumped parameter model for transient, (T), 25:28662
inspection of plutonium oxide (PuO_2)--uranium oxide (UO_2) pellet type, 25:28757(R) (GEAP-10010-27)
neutron spectrum in water moderated, computer program for thermal, 25:28802 (EUR-4554)
performance of defected mixed uranium oxide (UO_2)--plutonium oxide (PuO_2) in flowing sodium, (E), 25:28691(R) (GEAP-10028-37)
performance of stainless steel clad plutonium nitride--uranium nitride, during transient irradiation, (T), 25:28687 (BMI-1898, Sect.A)
preparation of uranium-base alloy, method for, 25:27195(P)
radiation effects on dimensional stability of Magnox-clad uranium-235-enriched, 25:27267 (UJV-2371.R,T.)
radiation effects on performance of fast, at high

temperature, (E/T), 25:28688 (BMI-1898, Sect.B)
radiation effects testing of mixed uranium oxide (UO_2)--plutonium oxide (PuO_2) fast, 25:28691(R) (GEAP-10028-37)
reprocessing by selective solvent extraction, separation of uranium and plutonium in, 25:26346(P)
reprocessing cycle development for gas cooled, (E), 25:28633(R) (GA-10399)
shipping container for irradiated, method for calculation of temperature of steel, 25:26441 (AECL-3802)
shipping of dissolver samples of, safety evaluation of New Brunswick Laboratory Sample Cask for, (T), 25:26450 (ORNL-TM-3298)
shipping of unirradiated bundles of Candu-type, design and testing of packaging for, 25:26442 (AECL-3803)
stoichiometry shift in mixed uranium oxide (UO_2)--plutonium oxide (PuO_2), effects of burnup on, (E/T), 25:28690(T) (EURFNR-836)
stress in Type 316 stainless steel-clad oxide fast, computer calculation of, 25:27285
structure of dispersion plate-type, thermal cycling tests for studies of, 25:27251
temperature distribution in liquid metal-cooled, method for calculating, 25:26422

REACTOR FUELS
chemical aspects of fused salt, 25:28636
cycle management for, procedures and strategy for optimum economic, 25:28543
cycle requirements in western Europe, effects of power reactor strategies on, (T), 25:28714
cycles in Mexico for 540 to 660 MW(e) power reactor, comparison of reactor types for optimum economic, 25:28722
development of fast breeder, fabrication and irradiation testing programs for, 25:28632(T) (EURFNR-824)
development of fast, during October through December 1970, 25:28686(R) (BMI-1898)
dissolution of core material from sheared, evaluation of methods for, 25:26327 (ORNL-TM-3194)
fission gas diffusion and bubble growth in, (E/T), 25:28688 (BMI-1898, Sect.B)
fission gas release from uranium oxide (UO_2), effects of high temperature on, (E), 25:28821
microstructure and properties of, development of methods for characterization of, 25:27293 (RT/ING-(70)21)
quality control and testing of Dragon, 25:26438 (DP-Report-432)
radiation effects testing of coated particle, 25:28633(R) (GA-10399)
reprocessing of coated particle, fluid bed oxidation procedures in, (E), 25:28633(R) (GA-10399)
reprocessing of fast breeder, extraction and separation of plutonium and uranium in Purex Process for, 25:26326 (KFK-911)
reprocessing of spent, using tridodecylamine, effects of alkylbenzene diluents on, 25:26330(T) (ORNL-tr-2410, pp 14-78)
reprocessing of, large-scale recovery and use of xenon from, 25:26347
reprocessing of, research progress in, 25:26328(T) (ORNL-tr-2410)
reprocessing of, role of radiolysis of process solutions in, 25:26349
reprocessing of, starting materials for fluidized-bed preparation of uranium hexafluoride from, 25:26207 (BLG-448)
reprocessing of, tests on centrifugal extractor for use in, 25:26331(T) (ORNL-tr-2410, pp 79-97)
resonance absorption of, equivalence relation for, (T), 25:28666
structure of coated particle, effects on thermal neutron spectra of heterogeneous, (T), 25:28656

REACTOR LOADING MACHINES
design of low profile horizontal, for vertical core reactors, 25:28825(P)
guide tubes for, description of reactor bottom penetrating, 25:28836(P)

REACTOR SAFETY
accidental release of airborne radioactivity, distribution in containment and ventilation systems of, 25:28763 (RISO-205)
accidents in boiling power reactor, assumptions for evaluation of radiation hazards from steam line break, 25:28744
accidents in boiling power reactor, assumptions for evaluation of radiation hazards from coolant loss, 25:28743
accidents in liquid metal cooled fast breeder reactor, analysis of reactivity insertion, 25:28735 (BAW-1360)
accidents in pressurized water power reactors, assumption for evaluation of radiation hazards from coolant loss, 25:28742
analysis of coolant loss accidents in pressurized water reactor, THETA1-B computer program for, 25:28737 (IN-1445)
analysis of, methods and models for Accident Analysis and Safety System Design Study, 25:28729 (BAW-1342)
coolant combustion accidents in liquid metal cooled reactors, release and transport of aerosols and energy from sodium, 25:28726(R) (AI-AEC-12986)
power excursions in fast reactors, VENUS code for calculation of energy release by, 25:28728 (ANL-7701)
reliability of circuits in systems for, methods for analysis of, 25:28740
transient analysis in fast reactor cores, SAS1A code for power and coolant flow, 25:28727 (ANL-7607)

REACTOR SAFETY EXPERIMENTS
fuel element irradiation in TREAT, analysis of stainless steel clad plutonium nitride--uranium nitride, (T), 25:28687 (BMI-1898, Sect.A)

REACTOR SIMULATORS
performance of digital computer, for fast liquid metal cooled reactor automatic control system, 25:28804(T) (EURFNR-835)

REACTORS
critical mass of, use of constant thermal neutron density zones for minimization of, (T), 25:28809
effluents from, filters for removal of radioactive particles from gaseous, 25:28829(P)
fuel loading standpipe for, coolant flow regulating valve for, 25:28830(P)
kinetics for, stability domains in nonlinear point, (T), 25:28800 (COO-2109-3)
kinetics of space-dependent, application of optimal control theory to space-time, 25:28813
lattice parameters in, JOSHUA code subsystem for, 25:28801 (DP-MS-70-78)
materials for, selection and improvement of, 25:27219
neutron cross sections for core of, computer program for calculation of mean thermal, 25:28803 (EUR-4555)
neutron flux distribution in sub-regions of, analysis of multiple collision probabilities for, (T), 25:28805 (EURFNR-898)
neutron flux distribution in, development of device for plotting, 25:26460(P)
neutron spectra in, temperature effects on, (T), 25:28814
neutron transport in, transfer matrix method for calculation of, 25:28798 (NYU-4090-1)
physics calculations for, development of synthesis methods for, (T), 25:28808
physics calculations for, difference method for solution of two-dimensional multigroup time-independent diffusion equations in, 25:28807 (ZJE-101)
pressure vessels for, description of prestressed reinforced concrete cylinder shaped, 25:28823(P)
reactivity measurements for, continuous run method for, (E/T), 25:28799 (CEA-N-1385)
reactivity of, effects of control rod vibrations on, (T), 25:28835
research progress on, AEC, 25:26205

REACTORS, AGR-TYPE
neutron buckling in lattices of, axial, (E/T), 25:28806 (RD/B/N-1837)
neutron reaction rates in lattice of, measurement of manganese, 25:28816 (RD/B/N-1518)

REACTORS, BOILING
accidents in power, assumptions for evaluation of radiation hazards from steam line break, 25:28744
accidents in power, assumptions for evaluation of radiation hazards from coolant loss, 25:28743
control of 300 to 500 MW(e), technical aspects of, 25:28721
control system for, design requirements of, 25:28675
coolant boiling in, critical heat flux for, (E/T), 25:28660
cooling systems for, testing of low-cycle fatigue life of carbon and stainless steel piping in, (E), 25:28680(R) (GEAP-10207-23)
cost analysis for 70 MW(t) open vessel well-type, for desalination, 25:28793
cost analysis for medium power, 25:28715
cost analysis for medium power, for developing countries, 25:28637
design of heavy water cooled and moderated, 25:28645(P)
design parameters for 70 MW(t) open vessel well-type, for desalination, 25:28793
design parameters for superheating heavy water moderated desalination and power, analysis of optimum economic, 25:28642
design parameters of medium power, 25:28715
development in U.S.S.R. of small and medium power, 25:28716
fuel cycle for 300 to 500 MW(e), 25:28721
startup of 300 to 500 MW(e), technical aspects of, 25:28721

REACTORS, BREEDER
containment system design for 1000 MW(e) steam cooled, effects of maximum credible accident on, (T), 25:28738 (NP-18781)
control of sodium cooled, instrumentation development for, 25:28667 (HEDL-SA-170)
coolant flow through breeder fuel clusters in, method for control of, 25:28649(P)
core optimization for sodium cooled, nonlinear programming method for, 25:28655(T) (EURFNR-830)
design parameters for mixed uranium carbide (UC)--plutonium carbide (PuC) fueled liquid sodium cooled, analysis of optimum economic, 25:28664
design parameters of 1000 MW(e) steam cooled, 25:28634 (NP-18782)
design parameters of fast, 25:28651
development during January to March 1970, 25:28632(T)

(EURFNR-824)
fuel cans for fast, properties of alloys of chromium, molybdenum, nickel, and vanadium for, 25:27213
operations aspects for mixed uranium carbide (UC)--plutonium carbide (PuC) fueled liquid sodium cooled, analysis of optimum economic, 25:28664
safety features of 1000 MW(e) steam cooled, description of, 25:28634 (NP-18782)
steam cycles for 300 MW(e) and 1000 MW(e) liquid sodium cooled fast, analysis of optimum economic, 25:28750
REACTORS, CANADA
construction for foreign country markets, 25:28718
design for foreign country markets, 25:28718
REACTORS, CANDU-TYPE
design characteristics of, 25:28544
REACTORS, FAST
containment for sodium cooled, design criteria for, (T), 25:28739 (RT/ING-(70)25)
containment system design for 1000 MW(e) steam cooled, effects of maximum credible accident on, (T), 25:28738 (NP-18781)
control of sodium cooled, instrumentation development for, 25:28667 (HEDL-SA-170)
control systems for Na-2, analysis of real dead-time effects on computer simulation of automatic, 25:28804(T) (EURFNR-835)
coolant flow through breeder fuel clusters in, method for control of, 25:28649(P)
cooling systems for, corrosion product and fission product activity levels in, (E), 25:28632(T) (EURFNR-824)
core for, thermodynamic and hydrodynamic design of, (E/T), 25:28632(T) (EURFNR-824)
core monitoring in, instrumentation and signal processing for, (E/T), 25:28632(T) (EURFNR-824)
core optimization for sodium cooled, nonlinear programming method for, 25:28655(T) (EURFNR-830)
design parameters of 1000 MW(e) steam cooled, 25:28634 (NP-18782)
design parameters of breeder, 25:28651
development during January to March 1970, 25:28632(T) (EURFNR-824)
fuel element assemblies for steam cooled, description of spaced rod bundle, 25:28695(P)
fuel elements for, method for forming assemblies of, 25:28652(P)
fuel rods for gas cooled, effects of surface roughening on heat transfer characteristics of, (T), 25:28696
fuels for, effects of high burnup on stoichiometry shift in mixed uranium oxide (UO_2)--plutonium oxide (PuO_2), (E/T), 25:28690(T) (EURFNR-836)
neutron spectra in, resonance absorbers for measurement of, (E/T), 25:28656(T) (EURFNR-842)
physics calculations for, multigroup cross section library for, 25:28657 (HEDL-TME-71-36)
physics characteristics of carbide fueled sodium cooled, transport and diffusion theory calculations of, 25:28812
physics characteristics of pulsed, 25:28760(T) (JPRS-52907)
physics measurements for steam cooled, (E), 25:28659
physics parameters of dilute plutonium fueled, (E), 25:28752 (ANL-7759)
physics parameters of, (E/T), 25:28632(T) (EURFNR-824)
power excursions in, VENUS code for calculation of energy release by, 25:28728 (ANL-7701)
safety features of 1000 MW(e) steam cooled, description of, 25:28634 (NP-18782)
safety studies on, (E/T), 25:28632(T) (EURFNR-824)
steam cycles for 300 MW(e) and 1000 MW(e) liquid sodium cooled breeder, analysis of optimum economic, 25:28750
transients in, SAS1A code for analysis of power and coolant flow, 25:28727 (ANL-7607)
REACTORS, FLUID-FUELED
design parameters of water cooled and beryllium reflected supercritical, with annular core, 25:28650(P)
stability of shutdown equilibrium state of, space independent differential-difference linear model of asymptotic, 25:28810
REACTORS, GAS-COOLED
blowers for, design of high pressure low flow, 25:28833
control system for, design requirements of, 25:28675
coolant circulation unit for, secondary pressure containment means for removable, 25:28831(P)
coolant circulator intake duct for, sound absorbing device for, 25:28832(P)
cost analysis for 250 MW(e) high temperature, 25:28719
design parameters of 250 MW(e) high temperature, 25:28719
design with closed cycle carbon dioxide gas turbine and means for turbine speed control, 25:28648(P)
design with closed cycle carbon dioxide gas turbines and two compression and expansion stages, 25:28646(P)
design with closed cycle carbon dioxide gas turbines and automatic control of throttle and gas flow, 25:28653(P)
design with closed cycle carbon dioxide gas turbine and means for maintaining constant pressure at reactor inlet, 25:28647(P)
development of 1000 MW(e) HTGR concept during September through November 1970, 25:28633(R) (GA-10399)
development of high temperature power and process heat, 25:28794
fission product release and transport in high temperature, (E/T), 25:28633(R) (GA-10399)
fuel element assemblies for, description of vented pin type bundle, 25:28694(P)
fuel elements for high temperature, fabrication and irradiation testing of recycle, (E/T), 25:28633(R) (GA-10399)
fuel elements for high temperature, plant designs and costs for reprocessing, 25:28633(R) (GA-10399)
fuel rods for fast, effects of surface roughening on heat transfer characteristics of, (T), 25:28696
neutron flux distribution in graphite moderated, adjusted computer program for, (E/T), 25:28654 (CEA-N-1344(2))
power production system for, with means for heat storage during off-peak operation, 25:28747(P)
REACTORS, GAS-FUELED
design of cavity core, with thermionic converters and turbogenerators, 25:28635(P)
REACTORS, GRAPHITE-MODERATED
design parameters for water cooled power and process heat, 25:28538
moderator assembly for, means for replacement of blocks in, 25:28828(P)
neutron flux distribution in gas cooled, adjusted computer program for, (E/T), 25:28654 (CEA-N-1344(2))
REACTORS, GREAT BRITAIN
cost analysis for low and medium output pressurized water and superheating heavy water moderated, small, 25:28720
REACTORS, HEAVY WATER-MODERATED
cost analysis for small and medium power superheating, 25:28720
design parameter of heavy water cooled boiling, 25:28645(P)
design parameters for superheating boiling desalination and power, analysis of optimum economic, 25:28642
economics in India for medium power, 25:28580
REACTORS, INDIA
development of medium power heavy water moderated, 25:28580
REACTORS, JAPAN
development of power, predicted, 25:28582
REACTORS, LIQUID METAL-COOLED
boilers for, description of, 25:28746(P)
containment for sodium cooled, design criteria for, (T), 25:28739 (RT/ING-(70)25)
control elements for, description of helium vented rod type, 25:28673(P)
control of sodium cooled, instrumentation development for, 25:28667 (HEDL-SA-170)
control rod drive coupling system for, 25:28670(P)
control rod drive system for, description of hydraulic, 25:28676(P)
control rod drives for, description of coupling system for, 25:28671(P)
core optimization for sodium cooled, nonlinear programming method for, 25:28655(T) (EURFNR-830)
design parameters for mixed uranium carbide (UC)--plutonium carbide (PuC) fueled breeder, analysis of optimum economic, 25:28664
fuel element failures in, delayed neutron monitoring for detection of, (E/T), 25:28698 (NP-18778)
fuel elements for, grid locking device for rod type, 25:28693(P)
heat exchangers for, prevention of localized overheating in, 25:28749(P)
operations aspects for mixed uranium carbide (UC)--plutonium carbide (PuC) fueled breeder, analysis of optimum economic, 25:28664
physics characteristics of carbide fueled sodium cooled, transport and diffusion theory calculations of, 25:28812
steam cycles for 300 MW(e) and 1000 MW(e) fast breeder, analysis of optimum economic, 25:28750
REACTORS, MARITIME
design parameters of submarine, for petroleum transport tankers, 25:28795
economics of submarine, for petroleum transport tankers, 25:28795
REACTORS, MOLTEN-SALT
boilers for, description of, 25:28746(P)
REACTORS, ORGANIC-COOLED
design parameters of organic moderated low temperature desalination, 25:28792
REACTORS, ORGANIC-MODERATED
design parameters of organic cooled low temperature desalination, 25:28792
REACTORS, PEBBLE-BED
neutron spectra in, effects of heterogeneous structure of coated particle fuels on thermal, (T), 25:28658
REACTORS, POWER
accidents in boiling, assumptions for evaluation of radiation hazards from steam line break, 25:28744
accidents in boiling, assumptions for evaluation of radiation hazards from coolant loss, 25:28743
accidents in pressurized water, assumptions for evaluation of radiation hazards from coolant loss, 25:28742
auxiliary power supplies for, design standards for diesel generator set, 25:28705

auxiliary power supply systems for, design standards for redundant, 25:28704
boilers for, design parameters of, 25:28748
construction of, 25:28531
construction of, program in Canada for foreign country markets, 25:28718
containment heat removal system pumps for, design standards for net positive suction head for, 25:28701
containment structures for, design standards for instrument line penetrations in primary, 25:28678
containment systems for water cooled, design standards for gas control methods during coolant loss accidents in, 25:28702
control of 300 to 500 MW(e) boiling, technical aspects of, 25:28721
control system for, description of power monitoring, 25:28672(P)
core physics for pressurized water, effects of fuel enrichment and burnable poison loadings on optimum, 25:28663
cost analysis for 250 MW(e) high temperature helium cooled, 25:28719
cost analysis for boiling medium output, 25:28715
cost analysis for medium output boiling, for developing countries, 25:28637
cost analysis for medium output pressurized water, 25:28638
cost analysis in Korea of 600 MW(e), 25:28539
cost analysis in U.K. for low and medium output pressurized water and superheating heavy water moderated, small, 25:28720
cost analysis of 100 to 500 MW(e), 25:28583
cost analysis of pressurized water small and medium output, 25:28717
design of gas fueled cavity core, with thermionic converters and turbogenerators, 25:28635(P)
design of medium output pressurized water, modification of high output components for conceptual, 25:28639
design of, program in Canada for foreign country markets, 25:28718
design parameters for superheating heavy water moderated boiling desalination, analysis of optimum economic, 25:28642
design parameters for water cooled graphite moderated process heat, 25:28538
design parameters in Korea of 600 MW(e), 25:28539
design parameters of 250 MW(e) high temperature helium cooled, 25:28719
design parameters of integrated 275 MW(t) pressurized water, 25:28641
design parameters of low output water cooled and moderated, analysis of optimum economic, 25:28640
design parameters of medium output boiling, 25:28715
design parameters of small and medium output pressurized water, 25:28717
design with closed cycle carbon dioxide gas turbine and means for maintaining constant pressure at reactor inlet, 25:28647(P)
design with closed cycle carbon dioxide gas turbine and means for turbine speed control, 25:28648(P)
design with closed cycle carbon dioxide gas turbines and two compression and expansion stages, 25:28646(P)
design with closed cycle carbon dioxide gas turbines and automatic control of throttle and gas flow, 25:28653(P)
development for desalination and agro-industrial complexes during November 1969 through October 1970, 25:28790(R) (ORNL-4668)
development in Chile, economic aspects of, 25:28723
development in India of medium output heavy water moderated, 25:28580
development in Japan, predicted, 25:28582
development in Turkey, economic aspects and management requirements of, 25:28724
development in U.S.S.R. of small and medium output boiling, 25:28716
development of 100 to 500 MW(e), 25:28583
development of 1000 MW(e) HTGR concept during September through November 1970, 25:28633(R) (GA-10399)
development of high temperature helium cooled process heat, 25:28794
development of small and medium output, conference on, 25:28529 (STI/PUB-267)
economic aspects in developing countries of small and medium output, 25:28540
economics in India for heavy water moderated medium output, 25:28580
economics of thermal, review of, 25:28712
emergency core cooling system pumps for, design standards for net positive suction head for, 25:28701
fuel cycle for 300 to 500 MW(e) boiling, 25:28721
fuel cycle management for, procedures and strategy for optimum economic, 25:28543
fuel cycle requirements in western Europe, effects of development strategies on, (T), 25:28714
fuel cycles in Mexico for 540 to 660 MW(e), comparison of reactor types for optimum economic, 25:28722
management requirements in developing countries for small and medium output, 25:28540
operation of, computer simulation of effects of component reliability on, 25:28713
operations aspects for developing countries during 1970 to 1985, 25:28541
power distribution in, in-core monitoring systems for, 25:28699
power production in developing countries during 1970 to 1985, 25:28541
power production system for gas cooled, with means for heat storage during off-peak operation, 25:28747(P)
pressure vessels for water cooled, standards for thermal shock analysis of coolant loss accidents in, 25:28683
pressure vessels for, development of prestressed concrete, 25:28684
pressure vessels for, regulatory criteria standards for construction of, 25:28537
protection system for, description of power monitoring integrated, 25:28672(P)
protection system for, design and operation of, 25:28697 (CENPD-11)
protection systems for, use of actuators as logic elements in fail-safe design of, 25:28741
protective systems for, development trends in, 25:28674
safety systems in, reliability analysis of, 25:28740
startup of 300 to 500 MW(e) boiling, technical aspects of, 25:28721
steam cycles for 300 MW(e) and 1000 MW(e) liquid sodium cooled fast breeder, analysis of optimum economic, 25:28750

REACTORS, PRESSURIZED-WATER
accidents in power, assumptions for evaluation of radiation hazards from coolant loss, 25:28742
containment system for, refrigeration system and thermal insulation for ice condenser, 25:28700(P)
control rod drives for, description of part length, 25:28668 (WCAP-7406)
control rod position in, analog monitoring system for, 25:28669 (WCAP-7571)
control system for, design requirements of, 25:28675
coolant loss accident conditions in, effects on fuel element characteristics of, 25:28737 (IN-1445)
core physics for power, effects of fuel enrichment and burnable poison loadings on optimum, 25:28663
cost analysis for medium power, 25:28638
cost analysis for small and medium power, 25:28720
cost analysis for small and medium power, 25:28717
design of medium power, modification of high output components for conceptual, 25:28639
design parameters of integrated 275 MW(t), 25:28641
design parameters of small and medium power, 25:28717
frequency response of, linear one-dimensional model analysis for, (T), 25:28665
fuel element failures in, system for monitoring of, 25:28703
fuel elements for, effects of coolant loss accident conditions on, 25:28737 (IN-1445)
protection system for, design and operation of, 25:28697 (CENPD-11)
stability of, linear one-dimensional model analysis for, (T), 25:28665
steam generator for, description of pressure vessel enclosed, 25:28751(P)

REACTORS, PROCESS HEAT
cost analysis for 70 MW(t) open vessel well-type boiling, for desalination, 25:28793
design parameters for 70 MW(t) open vessel well-type boiling, for desalination, 25:28793
design parameters for superheating heavy water moderated boiling power, analysis of optimum economic, 25:28642
design parameters for water cooled graphite moderated power, 25:28538
design parameters of organic cooled and moderated low temperature desalination, 25:28792
development for desalination and agro-industrial complexes during November 1969 through October 1970, 25:28790(R) (ORNL-4668)
development for iron and steel production, 25:28791
development of high temperature helium cooled power, 25:28794

REACTORS, RESEARCH
containment system for DR-3, accident release radioactivity distribution for, 25:28763 (RISO-205)
coolant for JRR-2, decomposition rate of heavy water, 25:28758 (JAERI-1204)
design parameters of FR-3, 25:28632(T) (EURFNR-824)
development of IBR (U.S.S.R.), 25:28760(T) (JPRS-52907)
electric circuits in FMRB, schematic diagrams of, 25:28771
experimental facilities for WWR, description of materials irradiation testing, 25:28765
experimental facilities in GRR-1, design modifications and testing programs for, 25:28774
fuel elements for WWR-S Bucharest, γ-scanning device for burnup measurements of, 25:28766
kinetics of MINERVE, analysis of neutron fluctuations for, (E/T), 25:28755 (CEA-N-1406)
neutron diffraction studies in RA (Vinca), 25:28779
neutron inelastic scattering studies in RA (Vinca), 25:28779
neutron spectra measurements in, use of lithium-6(n,α)t reaction for in-core, (E), 25:28753 (BLG-450)
neutron temperature distribution in TRIGA Mark 2, measurement during power surge of power transient, (E/T), 25:28770

operation of FRM, review of, 25:28775
operation of GRR-1, 25:28774
operation of GRR-1, review of, 25:28781
operation of RA (Vinca), review of, 25:28779
operation of TR-1, review of, 25:28776
operation of UA-RR-1, review of, 25:28777
operation of Yugoslavia TRIGA Mark 2, review of, 25:28778
operations of IBR (U.S.S.R.), 25:28760(T) (JPRS-52907)
physics research in FRM, 25:28775
physics research in TR-1, 25:28776
physics research in UA-RR-1, 25:28777
physics research in Yugoslavia TRIGA Mark 2, for, 25:28778
physics research programs in GRR-1 review of, 25:28781
radioisotope production in GRR-1, review of 1962 to 1970, 25:28772
radioisotope production in TR-1, 25:28776
radioisotope production in UA-RR-1, 25:28777
remote handling equipment for FMRB, design parameters for startup radiation detector of, 25:28773
transfer functions for ERMINE, MINERVE, and ULYSSE, reactivity modulation method for measurement of, (E/T), 25:28754 (CEA-N-1405)
use in Israel for physics research, 25:28780
use of University of Maryland 10 kW pool type, for spectrographic analysis of manganese nodules, 25:28764
ventilation system for DR-3, accident release radioactivity distribution for, 25:28763 (RISO-205)

REACTORS, ROCKET
bearings for, evaluation of materials for, 25:27200 (CONF-691114-7)
uses in manned planetary missions, 25:28786
uses in manned planetary missions, comparison of expendable and reusable shuttles for, 25:28789

REACTORS, SUPERHEATING
containment system design for 1000 MW(e) steam cooled, effects of maximum credible accident on, (T), 25:28738 (NP-18781)
cost analysis for small and medium power graphite moderated, 25:28720
design parameters for heavy water moderated boiling desalination and power, analysis of optimum economic, 25:28642
design parameters of 1000 MW(e) steam cooled, 25:28634 (NP-18782)
fuel elements assemblies for steam cooled fast, description of spaced rod bundle, 25:28695(P)
physics measurements for steam cooled fast, (E), 25:28659
safety features of 1000 MW(e) steam cooled, description of, 25:28634 (NP-18782)

REACTORS, SWEDEN
uranium requirements for, to 1985, 25:26395 (CONF-700903-15)

REACTORS, SWIMMING-POOL
remote handling equipment for, design parameters for startup radiation detector of, 25:28773

REACTORS, THERMAL
economics of power, review of, 25:28712
fuel cans for, properties of zirconium alloys for, 25:27213
stability of, direct numerical solution technique for analysis of xenon-135 feedback effects on, 25:28811

REACTORS, U.S.S.R.
development of boiling small and medium power, 25:28716

REACTORS, WATER-COOLED
containment systems for power, design standards for gas control methods during coolant loss accidents in, 25:28702
cooling channels for, effects of fuel assemblies grid and spacer configurations on coolant flow and heat transfer of, (E), 25:28681(R) (GEAP-10221-6)
cooling channels of water moderated, computer program for thermal and hydraulic analysis of, 25:28679 (EUR-4553)
cooling systems for, failure mechanisms in piping of, (E/T), 25:28680(R) (GEAP-10207-23)
design parameters for graphite moderated power and process heat, 25:28538
design parameters of beryllium reflected supercritical, with annular core, 25:28650(P)
design parameters of low power water moderated, analysis of optimum economic, 25:28640
fuel elements for, effects of coolant loss accidents on transient heat transfer to, (T), 25:28662
material for, properties of austenitic stainless steel, 25:27214(P)
pressure vessels for power, standards for thermal shock analysis of coolant loss accidents in, 25:28683
refueling tube for, description of bottom penetrating, 25:28836(P)

REACTORS, WATER-MODERATED
cooling channels of water cooled, computer program for thermal and hydraulic analysis of, 25:28679 (EUR-4553)
design parameters of low power water cooled, analysis of optimum economic, 25:28640
fuel elements for, computer program for thermal neutron spectrum in, 25:28802 (EUR-4554)

REFRACTORY MATERIALS
development of super, considerations for, 25:27280 (INIS-mf-12)
properties of, effects of composition and manufacturing conditions on, 25:27280 (INIS-mf-12)

REFRIGERATION
development of pumping groups for helium-3, 25:27664 (RHEL/R-208)

REGGE POLE THEORY
dual local electromagnetic current for hadrons in, 25:28021
dual vertex for hadrons in harmonic oscillator model in, 25:28021
duality model for inelastic $\nu + N$ interactions at high energies in, damped residue function and asymptotic limit of scaling function in, 25:28096
model with isotopic spin symmetry for hadron interactions at high energies in, group theoretical, 25:28055
residue functions for $\pi + \pi$ and $\pi + N \rightarrow \pi + N^*$ interactions in, s-channel helicity conservation constraints on t-channel exchanges for, 25:28028 (SU-1206-242)
scattering amplitude in, MacDowell symmetry and conspiracy constraints for fermion trajectory and residue functions for, 25:28092
trajectories and residue functions for scattering amplitude in, MacDowell symmetry and conspiracy constraints for, 25:28092
trajectories for meson interactions with baryons, duality concept and imaginary parts of, 25:28036

RELATIVE BIOLOGICAL EFFECTIVENESS
calculation for cataractogenic effects of 14-MeV neutrons on eyes of rabbits, 25:27027

RELATIVITY THEORY
clock paradox in, dynamical theory for, 25:28062
convection in general, neutral stability against, (T), 25:27325
effect of an anisotropic gravitational mass on Earth--Moon distance, (T), 25:27358
Einstein tensor in general, generalization of, 25:28085
gravitational energy transfer in general, Newtonian, 25:28089
gravitational radiation damping of slowly moving systems in general, matched asymptotic expansion method for calculating, 25:28086
gravitational theory extension in general, cosmological models in Yilmaz, 25:28087
isomorphism between base homologies in Lorentz--Einstein, (T), 25:27425
Lagrangian function in special, causality in Lorentz-covariant, 25:28068
Mach principle in special and general, 25:28065
Minkowski space in special, topology for, 25:28061
transformations to rotating frame in, paradox in, 25:28075

REMOTE-CONTROL EQUIPMENT
design for gamma scanning of fuel rods, 25:26550 (RT/ING-(71)1)

REMOTE-HANDLING EQUIPMENT
combination of grabs, wedges, and rollers, for removal and replacement of graphite moderator blocks, 25:28828(P)
design parameters for startup radiation detector, for swimming pool research reactors, 25:28773

REPUBLIC OF KOREA
power requirements and sources, 25:28539

RETICULO-ENDOTHELIAL SYSTEM
radiation effects on mouse, effects of glucan on γ, 25:26947
radioprotective effects of, blockage in mice, x, 25:26926

RHENIUM
hardness of irradiated and unirradiated, hot, 25:27236

RHENIUM ALLOYS AND SYSTEMS
Cr--Re, hardness of, effects of composition and temperature on decreasing, 25:27209 (N-71-11662)
Cr--Re, thermionic work functions of, 25:27911
Mo--Re, hardness of, effects of composition and temperature on decreasing, 25:27209 (N-71-11662)
Mo--Re, thermionic work functions of, 25:27911
Mo--Re--W-base, tensile properties of welds in, at high temperatures, 25:27178 (N-71-10353)
Mo--Re--W-base, weldability of arc cast and powder metallurgy, 25:27178 (N-71-10353)
Re--W, hardness of, effects of composition and temperature on decreasing, 25:27209 (N-71-11662)
Re--W, thermionic work functions of, 25:27911
Re--W-base, weldability of arc cast, effects of high preheat temperatures on, 25:27178 (N-71-10353)

RHENIUM ISOTOPES Re-179
electron-capture decay of, half-life and gamma energies and intensities from, (E), 25:28348 (JINR-P6-5617)
electron-capture decay scheme for, (E), 25:28386

RHENIUM ISOTOPES Re-180
beta and electron-capture decay of, half-life and gamma energies and intensities from, (E), 25:28348 (JINR-P6-5617)

RHENIUM ISOTOPES Re-181
electron-capture decay of, half-life and gamma energies and intensities from, (E), 25:28348 (JINR-P6-5617)

RHENIUM ISOTOPES Re-185
energy level at 368.1 keV from tungsten-186 (d,3n) reaction, energy assignment and half-life for, (E), 25:28287 (ANU-P-518)

RHODAMINE B
effects on determination of uranium by extraction--photometry, 25:26163
RHODIUM ALLOYS AND SYSTEMS
Ni--Rh, electron correlation effects in, 25:27868
Pt-base--Rh, fabrication of Pioneer and Transit heat source capsule components of, equipment and methods for, 25:26425 (MLM-1796)
Rh--Zr, superconductivity of intermetallic Zr_2Rh, (E), 25:27654
RHODIUM ISOTOPES Rh-99
energy levels from palladium-99 decay, spin--parity assignments for, (E), 25:28431
RHODIUM ISOTOPES Rh-103
neutron capture by, gamma spectra from resonance, (E), 25:28437
proton reactions (p,α) at 5 to 13 MeV, excitation functions for, (E), 25:28268
RHODIUM ISOTOPES Rh-104
beta decay of ground-state and isomeric, γ singles and coincidence spectra from, (E), 25:28382
energy levels from rhodium-103 neutron capture, spin--parity assignments for, (E), 25:28437
RHODOPHYTA
radioisotope concentration by tropical marine, 25:26597
RHODOPSIN
radioinduced bleaching of, from cattle retinas, γ, 25:26910
RIBONUCLEASE
radiation effects on molecular weight of, use of gel filtration to study uv, 25:26658
radiation effects on structure of, gel filtration studies on uv, 25:26661
RIBOSOMES
radiation effects on protein synthesis by fractions of liver, in rats, subsequent whole-body γ, 25:27006
radioinduced dissociation of yeast, effects of magnesium ions on x, 25:26633
RING CURRENT
enhancement characteristics during extremely quiet magnetic conditions, 1932--1969, (E), 25:27518
formation of, mechanism responsible for magnetospheric inflation, (T), 25:27627
position near local midnight and magnetic equatorial plane, interrelation with near-Earth plasma sheet, (E), 25:27631
RIVERS
radioactive waste disposal into Danube, from future Austrian power reactor, economics and safety of, 25:26451 (SGAE-RT-33/1970)
ROBERT E. GINNA POWER REACTOR, UNIT 1
operations aspects of, revised end-of-life reactivity shutdown margin of 1.9 percent, 25:28601 (DOCKET-50244-69)
operations history for, 25:28638
ROCK DRILLING
equipment and methods for reentry into Rulison Event chimney, 25:26409 (PNE-R-45)
ROCKET REACTORS (NERVA)
development of, JCAE hearings on suspension of, 25:28785
uses in manned planetary missions, 25:28787
uses in manned planetary missions, Earth departure technique for, 25:28788
ROCKS
analysis of standard ultrabasic, for sodium by neutron activation, 25:26204
analysis of standard, for fluorine by γ activation and radiochemical separation, 25:26193
RODS
fracture of hydrostatically extruded hard core clad, effects of core to sleeve bonding on, 25:28869 (NYO-4078-3)
ROMANIA
radioactivity monitoring in Black Sea off coast of, during 1964 to 1967, 25:26745
ROOTS
radioinduced delay of mitosis in pea, effects of protein synthesis on γ, 25:27063
radioinduced growth stimulation in Vicia faba, effects of auxin and dose rate on γ, 25:27066
radioinduced mutations for morphological changes in potato, 1000 to 120,000-R x, 25:26737
ROTENONE
synthesis of radioactive, in Ecuador, 25:27134 (CONF-680112-, pp 245-6)
RUBIDIUM
determination of trace amounts of, in hydrofluoric acid and spectrophotometry, 25:26176
RUBIDIUM ISOTOPES Rb-83
preparation for use in laboratory generator for krypton-83m, 25:26320
RUBIDIUM ISOTOPES Rb-85
neutron reactions (n,2n) at 14.4 MeV, activation cross section for, (E), 25:28282
neutron reactions (n,α) at 14.4 MeV, activation cross section for, (E), 25:28282
neutron reactions (n,p) at 14.4 MeV, activation cross section for, (E), 25:28282
RUBIDIUM ISOTOPES Rb-87
neutron reactions (n,2n) at 14.4 MeV, activation cross section for, (E), 25:28282
neutron reactions (n,α) at 14.4 MeV, activation cross section for, (E), 25:28282
neutron reactions (n,p) at 14.4 MeV, activation cross section for, (E), 25:28282
RUBIDIUM ISOTOPES Rb-89
beta decay of, Q value for, (E), 25:28294 (CERN-70-30(Vol.1), pp 321-9)
RUBIDIUM ISOTOPES Rb-90
beta decay of, Q value for, (E), 25:28294 (CERN-70-30(Vol.1), pp 321-9)
beta decay of, Q value for, (E), 25:28296 (CERN-70-30(Vol.1), pp 341-51)
RUBIDIUM ISOTOPES Rb-91
beta decay of, Q value for, (E), 25:28294 (CERN-70-30(Vol.1), pp 321-9)
RUBIDIUM ISOTOPES Rb-92
beta decay of, Q value for, (E), 25:28294 (CERN-70-30(Vol.1), pp 321-9)
RUBIDIUM ISOTOPES Rb-93
beta decay of, Q value for, (E), 25:28294 (CERN-70-30(Vol.1), pp 321-9)
RUBIDIUM ISOTOPES Rb-94
beta decay of, Q value for, (E), 25:28294 (CERN-70-30(Vol.1), pp 321-9)
RUBIDIUM ISOTOPES Rb-95
beta decay of, Q value for, (E), 25:28294 (CERN-70-30(Vol.1), pp 321-9)
RUBIDIUM ISOTOPES Rb-96
beta decay of, half-life for, (E), 25:28388
beta decay of, Q value for, (E), 25:28294 (CERN-70-30(Vol.1), pp 321-9)
RUBIDIUM ISOTOPES Rb-97
beta decay of, half-life for, (E), 25:28388
RUBIDIUM ISOTOPES Rb-98
beta decay of, half-life for, (E), 25:28388
RUBIDIUM ISOTOPES Rb-99
beta decay of, half-life for, (E), 25:28388
RUPTURE
book: Fracture. An Advanced Treatise, Volume III. Engineering Fundamentals and Environmental Effects, 25:27170
RUTHENIUM
separation from TBP by extraction chromatography using dibutyl phosphate--potassium hydroxide mixture, 25:26330(T) (ORNL-tr-2410, pp 14-78)
RUTHENIUM ALLOYS AND SYSTEMS
Ru--Zr, properties of, mechanical and oxidation resistance, 25:27203 (INIS-mf-2)
RUTHENIUM ISOTOPES
energy levels from (d,p) and (d,t) reactions, spectroscopic factors for, (E), 25:28374
RUTHENIUM ISOTOPES Ru-103
determination in fallout, β counting method for, 25:26181
separation from irradiated aluminum--uranium and uranium--zirconium fuels by chlorination and pyrohydrolysis, 25:26332(T) (ORNL-tr-2410, pp 98-120)
yields from spontaneous fission of uranium-238, (E), 25:28384
RUTHENIUM ISOTOPES Ru-104
deuteron reactions (d,t) at 17 MeV, angular distributions for, (E), 25:28374
RUTHENIUM ISOTOPES Ru-106
determination in fallout, β counting method for, 25:26181
energy levels from technetium-106 beta decay, spin--parity assignments for, (E), 25:28326 (CERN-70-30(Vol.2), pp 985-1000)
separation from irradiated aluminum--uranium and uranium--zirconium fuels by chlorination and pyrohydrolysis, 25:26332(T) (ORNL-tr-2410, pp 98-120)
separation of plutonium from, by solvent extraction using tridodecylamine, 25:26330(T) (ORNL-tr-2410, pp 14-78)
uptake and distribution in freshwater and marine organisms, effects of temperature on, 25:26587
yields from spontaneous fission of uranium-238, (E), 25:28384
RUTILES
radioinduced paramagnetic defects in single-crystal, ESR study of annealing of gamma and neutron, 25:27853

S

SAFETY HAZARDS
evaluation of radiological, from earth impaction of space power system radioactive capsules, development of computer programs for, 25:26429 (SC-R-7121)
SAINT LAURENT-DES-EAUX REACTOR (EDF-4)
design parameters of, summary of, 25:28534
SALIVARY GLANDS
radiation effects on function of, in patients with head and neck tumors, cobalt-60 gamma, 25:27061
radiotherapy of adenomas of, effectiveness of pre- and post-operative, 25:26866
submaxillary, radiation effects on, in rats, comparative radioprotective effects of AET, cystamine, cysteine, noradrenaline, serotonin, and tetramethylcystamine against γ, 25:26795
SALT DEPOSITS
radioactive waste disposal in, requirements for recoverable containers for high-level solidified,

25:26454
radioactive waste disposal in, USAEC program for high-level solidified, 25:26453
SAMARIUM
determination by spectrophotometry, 25:26165
determination in plutonium oxide--uranium oxide pellets by emission spectroscopy, 25:26153 (LA-4622)
determination of trace amounts of, in europium oxide by crystal phosphor luminescence method, 25:26162
spectra of, oscillator strengths of 275 lines of absorption, 25:27445
SAMARIUM ALLOYS AND SYSTEMS
Ce--Co--Cu--Fe--Sm, magnetic properties of, 25:27883
Co--misch metal--Sm, preparation and magnetic properties of permanent magnets of, 25:27884
Co--Sm, magnetic coercivity of $SmCo_5$ particles, domain-wall pinning and nucleation in, 25:27882
Co--Sm, magnetization discontinuities in Co_5Sm particles, 25:27885
Pd--Sm, magnetic properties of $SmPd_3$ at 4 to 300°K, 25:27870
Sm--Sm_2O_3, phase studies of, 25:27302
SAMARIUM ISOTOPES Sm-141
beta and electron-capture decay of isomeric, complex shell-model states in, (E/T), 25:28299 (CERN-70-30(Vol.1), pp 435-46)
SAMARIUM ISOTOPES Sm-144
photon reactions (γ,p) with isobaric analog excitation, proton spectra from, (E), 25:28362
SAMARIUM ISOTOPES Sm-147
energy level at 121.2 keV, quadrupole and magnetic dipole moments for, (E), 25:28420
neutron cross sections, strength functions, and resonance parameters for, thermal, (E), 25:28349 (KAPL-P-3930)
neutron reactions (n,α) with, α spectra from, (E), 25:28347 (JINR-P3-5553)
neutron reactions (n,α) with, energy levels of neodymium-144 from, (E), 25:28345 (JINR-E3-5483)
SAMARIUM ISOTOPES Sm-148
energy levels from resonances in samarium-147 (n,α) reactions, α decay widths for, (E), 25:28347 (JINR-P3-5553)
SAMARIUM ISOTOPES Sm-150
energy levels from gamma resonance scattering, widths for, (E), 25:28219 (NRCN-254)
neutron cross sections, strength functions, and resonance parameters for, thermal, (E), 25:28349 (KAPL-P-3930)
SAMARIUM ISOTOPES Sm-152
energy levels of, calculation using collective quadrupole excitations, (T), 25:28501
energy-level transitions from europium-152 decay, band mixing parameters for, (E), 25:28430
energy-level transitions of, directional correlations for E2 and M2, (E), 25:28397
nuclear magnetic and quadrupole moments of, (T), 25:28316 (CERN-70-30(Vol.2), pp 779-812)
SAMARIUM OXIDES
Sm--Sm_2O_3, phase studies of, 25:27302
SAMPLING
equipment and method for atmospheric, for tritium content measurements, 25:26393(R) (ORO-3944)
SAN ONOFRE POWER REACTOR, UNIT 1
operations history for 1967 to 1970, review of, 25:28577
operations history for March 1971, 25:28563 (DOCKET-50206-111)
SAP (SINTERED ALUMINUM POWDERS)
diffusion of zinc in, relations of microhardness with solid state, 25:27222
SATELLITES
Alfven-wave generation by Io, (T), 25:27435
conference on intercorrelated satellite observations and solar activity, Noordwijk, Netherlands, 9/69, 25:27531
current in retarding-potential probes aboard, relation to ionospheric integral electron flux, (E/T), 25:27682
SAVANNAH RIVER PRODUCTION REACTORS
control systems for, maintenance of on-line computers in, 25:28797
SAXTON POWER REACTOR
containment structure for, leak rate testing schedule for, 25:28590 (DOCKET-50146-71)
radioactive effluents from, revised release limits for, 25:28590 (DOCKET-50146-71)
SCANDIUM
determination by photometry using carboxy derivatives of 2,6,7-trihydroxy-9-phenyl-3H-xanthen-3-one, 25:26174
determination in marine silts by neutron activation and γ spectroscopy, 25:26190(R) (NYO-4150-9)
magnetic susceptibility of, effects of nonmagnetic and magnetic alloying additives on, 25:27878
separation from rare earths by ion exchange as complex with organic phosphorus compounds, 25:26338(P)
separation from uranium-barren sulfate leach liquors by solvent extraction using DEHPA, 25:26342
SCANDIUM ISOTOPES Sc-41
Coulomb energy difference between calcium-41 and, (T), 25:28253
energy levels of, role of configuration states in isospin-forbidden proton decay of T = 3/2, 25:28179
SCANDIUM ISOTOPES Sc-45
neutron total cross sections and resonance parameters at 10 to 250 keV, (E/T), 25:28279
proton elastic scattering at 6.9 MeV, optical-model analysis of angular distributions from, (E), 25:28262
SCANDIUM ISOTOPES Sc-49
energy levels of, analog spin mixing in, (T), 25:28235
SCATTERING
amplitudes for multiparticle processes, kinematic singularities from spinor, 25:28099
amplitudes for three-particle-exchange interactions, asymptotic behavior of, 25:28093
amplitudes in annihilation channel, constraints on partial-wave, 25:28097
amplitudes of, bounds on asymptotic behavior of, 25:28100
amplitudes of, derivation of optical theorem for relation of total cross section to forward, 25:28090
amplitudes of, lower bounds of crossing-even, 25:28098
amplitudes of, MacDowell symmetry and conspiracy constraints for fermion Regge trajectory and residue functions for, 25:28092
amplitudes of, Poincare model of Lobacevskij geometry for t-channel expansion of, 25:28091
amplitudes of, variational principle based on Faddeev equations and analytic structure in total energy of T-matrix for calculations of three-body, 25:28101
Haag theorem in, generalized, 25:28083
potential, Faddeev equation in SU(3) representation for three-particle bound-state, 25:28056
potential, in many dimensions, partial-wave expansion method for spherical, 25:28090
potentials in, analytic properties and bound-state degeneracy in nonlocal, 25:28094
potentials in, spectrum of operator in formulation of optical, 25:28095
potentials in, time-dependent and time-independent formulations of optical, 25:28096
restrictions on partial-wave amplitudes from Grobov--Froissart formula, 25:27930 (ITF-70-101-E)
SCb-291 (NIOBIUM ALLOY)
stability at high temperatures, long-term thermal, 25:27208 (N-71-10352)
SCHIZOMYCOTA
Achromobacter sp., radiation effects on proteolytic activity of, effects of dose and temperature on gamma, 25:27114
Bacillus pumilus, radiation effects on survival of, in ophthalmic ointment containing chloramphenicol and hydrocortisone, effective dose for, 25:27161
Bacillus sp., radiation effects on proteolytic activity of, effects of dose and temperature on gamma, 25:27114
Bacillus subtilis, radioinduced mutations in, effects of transformation ability on uv, 25:26729
Escherichia coli, mutation induction by BUdR, 2-aminopurine, DES, EMS, and guanidine, 1-methyl-3-nitro-1-nitroso in, 25:26722
Escherichia coli, radiation effects on growth of, effects of saline culture medium on uv, 25:27119
Escherichia coli, radiation effects on repair of, comparison of alkylating agents with uv, 25:27109
Escherichia coli, radiation effects on semiconservative DNA replication and repair synthesis in, effects of nalidixic acid on uv, 25:27125
Escherichia coli, radiation effects on transforming DNA of, repair of uv, 25:27124
Escherichia coli, radioinduced injuries in, repair mechanisms for uv, 25:27112
Escherichia coli, radioinduced mutations in, gamma, 25:26722
Escherichia coli, radioinduced mutations in, refractivity, recombination, and uv sensitivity of γ, 25:26707
Escherichia coli, radioinduced single strand breaks in DNA of, effects of dose rate, oxygen, and temperature on x, 25:26655
Escherichia coli, radiosensitivity of B/r, B, and B(s-1) strains of, effects of culture media on alpha, 25:27118
Escherichia coli, radiosensitivity of, effects of 5-fluorouracil and uracil on uv, 25:27123
Micrococcus radiodurans, radiation damage to thymine in DNA of, repair of γ, 25:26643
Micrococcus radiodurans, radiation effects on synthesis of nucleic acids and proteins in, dose dependence of gamma, 25:26639
Micrococcus radiodurans, radioinduced degradation of DNA of, x, 25:26627
Mycobacterium phlei, radioinduced mutations for carotenoid production in, uv, 25:26687
Neisseria sp., radiation effects on proteolytic activity of, effects of dose and temperature on gamma, 25:27114
Pseudomonas putida, merodiploidy and expression of episomal genes in, 25:28849 (COO-1683-32)
Pseudomonas sp., radiation effects on proteolytic activity of, effects of dose and temperature on gamma, 25:27114
radiation effects on bioluminescence and respiration in, protective effects of adenosine and RNA against x, 25:27120
radiation effects on content of, in food products, 25:27143
radiation effects on survival of, effects of humidity, temperture, and dose rate on γ, 25:27099
radiation effects on survival of, in Portuguese smoked

sausage, x, 25:27159
radiation effects on, in relation to spacecraft sterilization, 25:27101
radioinduced growth of, in small intestine of rats, effects of peristalsis on x, 25:26975
radiosterilization of parasitic, in human excreta, gamma, 25:27126
radiosterilization of, on shrimp, effects of dose on γ, 25:27138(R) (TID-25543)
Rhizobium meliloti, radioinduced mutations in symbiotic activity in, uv, 25:27103
Rhizobium meliloti, radiosensitivity transducing phages of, uv, 25:27104
Salmonella typhimurium, radioinduced mutations in, effects of dose on antibiotic resistance, sensitivity, and virulence of γ, 25:27164
Streptococcus diacetilactis, radioinduced mutations for acid production, enzyme activity, and milk coagulation in, comparison of nitrosoguanidine induced mutations with uv, 25:27121
Streptococcus faecalis, radiation effects on survival of, in ophthalmic ointment containing chloramphenicol and hydrocortisone, effective dose for, 25:27161
Streptococcus faecalis, radioinduced mutations for chain formation in, uv, 25:26731
Streptococcus faecalis, radiosensitivity of, effects of daunomycin on, 25:27100
Streptococcus sp., effects of uv-irradiated bacteriophage on transduction of group A, to streptomycin resistance, 25:27110
Vibrio luminosus, radiation effects on bioluminescence, growth, and respiration in, protective effects of adenosine, DNA, guanosine, inosine, and RNA against uv, 25:27122
Vibrio parahaemolyticus, radiation effects on, effects of dose rate and temperature on gamma, 25:27115

SCINTILLATION CAMERAS
design and performance of, based on delay-line time conversion, 25:26486

SEAS
construction of nuclear power plants in bottom of, technical and economic aspects of, 25:28630
construction of nuclear power plants in, technical and economic aspects of, 25:28643

SEAWATER
analysis for trace metals by anodic stripping voltammetry, 25:28861(R) (MIT-905-162)
carbon-14 content of, at various worldwide locations, 25:26398 (RLO-2225-T-20-2)
diffusion of iodine into atmosphere from, mechanisms of, (E), 25:26380 (CONF-700601-, pp 319-24)
radiation monitoring of UK coastal, 1969, 25:26397 (FRL-7)
radioactivity monitoring in, of Black Sea off coast of Romania during 1964 to 1967, 25:26745
separation of rare earths and yttrium from, by sorption on vessel walls and other materials, 25:26339
sorption of uranium from, by titanic acid, 25:26350

SEDIMENTARY DEPOSITS
analysis of marine, by neutron activation, 25:26188 (BNWL-SA-3803)

SEED
chromosome aberration and mutation induction in, economics of EMS, 25:26697
radioinduced chromosome aberrations and mutations in, economics of γ and x, 25:26697
radiosensitivity of rice, effects of dose rate, oxygen, storage, and water content on fission neutron and γ, 25:27070

SEISMIC WAVES
propagation from Pre-Gondola II Event, (E), 25:26407 (PNE-1112)
propagation from Pre-Gondola III Phase II explosion, (E), 25:26408 (PNE-1117)

SELENITES
labeling with selenium-75 for use in tumor scanning, 25:26859

SELENIUM
determination by photometry using carboxy derivatives of 2,6,7-trihydroxy-9-phenyl-3H-xanthen-3-one, 25:26174
determination in sea floor samples by neutron activation, 25:26188 (BNWL-SA-3803)
effects of ingestion of, on gamma-irradiated rats, 25:27032
ion energy losses at 0.2 to 0.5 MeV/amu in, (E), 25:27833

SELENIUM IONS
implantation in silicon at 50 keV, outdiffusion, lattice location, and electrical behavior of, 25:27856

SELENIUM ISOTOPES Se-72
energy levels from oxygen reactions with nickel, spin-parity assignments for, (E), 25:28213 (CERN-70-30(Vol.2), pp 911-15)

SELENIUM ISOTOPES Se-74
energy levels from oxygen reactions with nickel, spin-parity assignments for, (E), 25:28213 (CERN-70-30(Vol.2), pp 911-15)

SELENIUM ISOTOPES Se-75
distribution of selenomethionine-incorporated, in rat pancreas, effects of intravenously injected pancreozymin and secretin on, 25:26591
energy-level transitions from proton reactions, branching ratios, gamma-ray angular distributions, and internal conversion coefficients for, (E/T), 25:28271
incorporation in selenite for use in tumor scanning, 25:26859

SELENIUM ISOTOPES Se-76
energy levels from arsenic-75(p,n) reactions, spin assignments for isobaric analog, (E), 25:28241
energy levels from arsenic-76 beta decay, spin--parity assignments for, (E), 25:28278
energy levels from bromine-76 decay, (E), 25:28246
energy levels from resonances in arsenic-75 (p,α) reactions, widths for compound-nucleus, (E), 25:28268

SELENIUM ISOTOPES Se-80
energy levels from gamma resonance scattering, widths for, (E), 25:28219 (NRCN-254)

SELENIUM ISOTOPES Se-87
neutron decay of, half-lives and neutron branching ratios for delayed, (E), 25:28212 (CERN-70-30(Vol.1), pp 519-20)

SELENIUM ISOTOPES Se-88
neutron decay of, half-lives and neutron branching ratios for delayed, (E), 25:28212 (CERN-70-30(Vol.1), pp 519-20)

SELENIUM ISOTOPES Se-89
neutron decay of, half-lives and neutron branching ratios for delayed, (E), 25:28212 (CERN-70-30(Vol.1), pp 519-20)

SEMICONDUCTOR JUNCTIONS
radiation effects on p--n, 25:26561

SEMICONDUCTORS
radiation effects on, 25:26561

SEROMUCOID
radiation effects on content of, in blood plasma of rats, single and combined effects of turpentine and x, 25:26979

SEROTONIN
radiation effects on level of, in tissues of rats, whole-body x, 25:26959
radioprotective effects of, on mice, combined effects of cystamine and, 25:26793
radioprotective effects of, on rats, sublethal fractionated dose, 25:26807
radioprotective effects of, on submaxillary glands in mice, comparison of AET, cystamine, cysteine, noradrenaline, and tetramethylcystamine with γ, 25:26795
radioprotective effects on rabbit eyes, cobalt-60γ and fast neutron, 25:27014
sodium salt, radioprotective effects on mice in relation to body temperature and respiration, 25:26800
toxic effects of, on γ-irradiated mice, combined effects of cystamine and, 25:26793

SERPUKHOV SYNCHROTRON
beam characteristics of, measurement of, 25:28133
experimental facility for, magnetic spectrometer for, 25:26507 (NP-18764)

SEWAGE
radiation processing using cobalt-60 gamma facility, 25:27126

SEYFERT GALAXIES
element abundances in nuclei of, (E), 25:27418
infrared emission from, energy sources for, (T), 25:27417
matter--antimatter annihilation in, (T), 25:27417
spectral shifts in nuclei of, (E), 25:27418

SHIELDED CONTAINERS
design and fabrication for safe shipping of radioactive materials, review of regulations for, 25:26452
design and safety of LLD-1, for packaging and shipping plutonium metal, 25:26446 (DPSPU-71-124-1)
design and testing of, for shipping unirradiated Candu-type fuel bundles, 25:26442 (AECL-3803)
design of safe, for railway shipping of radioactive materials, US railroad accident data for use in, 25:26447 (HW-76299)
requirements for recoverable, for long-term storage of high-level solidified radioactive wastes in salt repositories, 25:26454
safety evaluation of New Brunswick Laboratory Sample Cask, for shipping fuel element dissolver samples, (T), 25:26450 (ORNL-TM-3298)
safety evaluation of welded steel, for shipping high-level vitrified wastes to Asse Salt Mine, 25:26448 (KFK-1263)
temperature of steel, for shipping irradiated fuel, method for calculation of thermal test, 25:26441 (AECL-3802)

SHIELDING
calculations for SNAP space reactors, use of coupled discrete ordinates and Monte Carlo techniques for, 25:28784 (ORNL-TM-3365)
fabrication of concrete, 25:28531
gamma streaming through apertures in, (E/T), 25:27829

SHIELDING MATERIALS
radiation dose rate reduction for varying thicknesses of, 25:27828 (DP-1246)

SHIPPING
regulations for radioactive material, summary of U.S, 25:26445 (BRH/DMRE-71-1)
regulations for safe, of radioactive materials, review of, 25:26452

XUM

safety evaluation of high-level vitrified waste, to Asse Salt Mine, 25:26448 (KFK-1263)
SHOCK TUBES
design for plasma heating experiments, 25:27670
SHOCK WAVES
detection of, evaluation of impedance probe method for, 25:28887 (SC-DR-710086)
interactions with plasma, heating processes in, (E/T), 25:27670
phenomena of interplanetary, model of nonspherical, (T), 25:27629
production of collisionless, for β much less than 1, (E/T), 25:27690
propagation in collisionless plasma in magnetic fields, (T), 25:27708
propagation in interplanetary space on Feb. 26, 1969, possible correlation with Feb. 25 solar event, (E/T), 25:27570
propagation in interplanetary space, relation to Feb. 25, 1969, May 1967, and Jan. 9, 1968 solar proton events, (E/T), 25:27571
propagation in plasma, instabilities from collisionless, (T), 25:27731
SILICON
abundance in α Dra, (E), 25:27333
abundance in lunar surface materials, (E), 25:27308
analysis for arsenic by alpha scattering at 4 MeV, 25:26183
analysis for carbon by α particle, deuteron, γ photon, and helium-3 activation, 25:26202
boron-ion implantation at low energies in N-type, proton energy-loss measurements of distribution of, 25:27855
boron-ion implantation in, high-temperature isothermal annealing studies of 150-keV, 25:27854
determination in yttrium oxides by solvent extraction and spectrography, 25:26168
determination in Zircaloy, chemical method for, 25:26171
diffusion in niobium, by reactive processes, 25:27239
gamma absorption coefficient of, (E), 25:27826 (DEMO-70/11)
ion implantation in, flux and fluence dependence of lattice disorder induced in 200-keV boron, 25:27864
ion implantation of heavy Group IIB and VIA elements at 50 keV in, outdiffusion, lattice location, and electrical behavior of, 25:27856
ion-implantation-induced lattice disorder in single crystals of, proton-channeling study of 200-keV antimony, 25:27859
meson (π^-) capture with charged particle emission, particle spectra and branching ratios for, (E), 25:28178
radiation damage from boron ion implantation at 100 to 400 keV in single crystals of, annealing of, 25:27863
radioinduced defect centers in n-type, infrared study of low-temperature 2-MeV electron, 25:27845
radioinduced defects in lithium-drifted boron-doped, gamma, 25:27852
radioinduced defects in n-type, structure studies of neutron and gamma, 25:27848
radioinduced defects in, channeling study of distribution of 10- and 400-keV heavy-ion, 25:27861
radioinduced luminescence spectrum of, effects of stress and temperature on, 25:27849
radioinduced shallow donor state in n- and p-type, proton, 25:27847
transport to graphite during anneal, 25:27909
ytterbium implants in, flux-peaking effect in 1-MeV helium-ion backscattering from 60-keV, 25:27857
SILICON ISOTOPES Si-28
carbon-12 elastic scattering at 49.3 to 83.5 MeV, optical-model analysis of differential cross sections for, (E), 25:28274
Coulomb energy differences in aluminum-28--silicon-28 isobaric analog states, 25:28243
energy-level transitions from aluminum-27(d,n) reactions, M1, ΔT = 1, (E), 25:28225
meson (μ) capture by, relativistic corrections to asymmetry of high-energy neutrons from polarized, (T), 25:28183
neutron reactions (n,p) with, cross sections for fast, (E), 25:28273
nitrogen-14 elastic scattering at 84 MeV, optical-model analysis of differential cross sections for, (E), 25:28274
SILICON ISOTOPES Si-29
Coulomb energy differences between phosphorus-29--silicon-29 isobaric analog states, 25:28243
energy levels of, calculation using projected Hartree--Fock basis and core-particle coupling, (T), 25:28280
neutron reactions (n,p) with, cross sections for fast, (E), 25:28273
proton reactions (p,γ) at 0.9 to 2.2 MeV, γ spectra from, (E), 25:28207 (ANU-P-517)
SILICON ISOTOPES Si-30
energy levels of, calculation using projected Hartree--Fock basis and core-particle coupling, (T), 25:28280
helium-3 elastic scattering at 12 MeV, optical-model analysis of angular distributions from, (E), 25:28270
helium-3 reactions (He-3,d) at 12 MeV, spectra and DWBA analysis of differential cross sections from, (E), 25:28270
neutron reactions(n,α) with, cross sections for fast, (E), 25:28273
proton reactions (p,γ) up to 2 MeV, Q value and gamma angular distributions and spectra from, (E), 25:28270
SILICON NITRIDES
effects of double layer of silicon dioxide and, on passivation of thin molybdenum films, 25:27171
SILICON OXIDES
effects of double layer of silicon nitride and, on passivation of thin molybdenum films, 25:27171
effects of layer of, on passivation of thin molybdenum films, 25:27171
lattice structure of, positron-annihilation study of, (E/T), 25:27865 (CEA-R-4138)
radioinduced Wigner energy storage in, neutron, 25:27839 (CEA-N-1171)
Al_2O_3--CoO--SiO_2, magnetic ordering and electric conduction in glasses of, 25:27901
SILICON SYSTEMS
Pd--Si--transition metals, two currents conduction in, 25:28844 (CALT-822-28)
Si--V, superconducting diffusion layers in, electron microprobe studies on, 25:26159
SILTS
analysis of marine, for metals by neutron activation and γ spectroscopy, 25:26190(R) (NYO-4150-9)
diffusion of uranium-234 from deep-sea, studies of, 25:26399 (TID-25674)
transport of Argentine, review of radioisotope tracer studies of, 25:26353 (CONF-680112-, pp 37-52)
SILVER
content in hail and rain samples from Nebraska and South Dakota, absorption spectrophotometer measurements of, 25:26366 (CONF-700601-, pp 109-20)
determination in sea floor samples by neutron activation, 25:26188 (BNWL-SA-3803)
determination of trace amounts of, in aluminum, copper, and their alloys by solvent extraction and atomic absorption spectrophotometry, 25:26169
fracture strength of, effects of indium-mercury solutions on, 25:27243
photon reactions at 5.4 GeV, total cross section for hadron production in, 25:27953
SILVER ALLOYS AND SYSTEMS
Ag--Cu, fabrication and uses of high conductivity, 25:27187
Ag--Nd, dissociation energy of gaseous NdAg, upper limit for, 25:26273
SILVER CHLORIDES
scavenging of aerosol particles of, efficiency of water droplets for, (E), 25:26370 (CONF-700601-, pp 161-7)
SILVER ISOTOPES Ag-101
nuclear spin of, (E), 25:28396
SILVER ISOTOPES Ag-102
nuclear spin of, (E), 25:28396
SILVER ISOTOPES Ag-103
nuclear magnetic moment and hyperfine structure anomaly of, (E), 25:28396
SILVER ISOTOPES Ag-107
proton reactions (p,α) at 5 to 13 MeV, excitation functions for, (E), 25:28268
SILVER ISOTOPES Ag-109
proton reactions (p,α) at 5 to 13 MeV, excitation functions for, (E), 25:28268
SILVER ISOTOPES Ag-110
beta decay of isomeric, branching ratios, gamma spectra, and log-ft values from, (E), 25:28435
properties of isomeric, for labeling copper electric cable for subsequent identification, 25:26322
SILVER ISOTOPES Ag-114
beta decay of, gamma energies and intensities from, (E), 25:28337 (CERN-70-30(Vol.2), pp 1069-74)
SILVER ISOTOPES Ag-116
beta decay of, gamma energies and intensities from, (E), 25:28337 (CERN-70-30(Vol.2), pp 1069-74)
SILVER ISOTOPES Ag-118
beta decay of, gamma energies and intensities from, (E), 25:28337 (CERN-70-30(Vol.2), pp 1069-74)
SILVER ISOTOPES Ag-120
beta decay of, gamma energies and intensities from, (E), 25:28337 (CERN-70-30(Vol.2), pp 1069-74)
SINGLE CRYSTALS
beta-particle reactions with, effects of channeling on bremsstrahlung spectra from, (T), 25:27832
SKIN
radiation effects on cesium-137 sorption through rat, effects of contamination timing on 600 rad cobalt-60 γ, 25:26595
radioinduced inflammation of rabbit, protective effects of benzydamine against x, 25:26806
radioinduced tumorigenesis in mouse, sensitizing effects of acetic acid, croton oil, and xylene on uv, 25:26809
radiotherapy of sarcomas of human, Koebner phenomenon-like occurrence following x, 25:26875
SNOW
effects on cloud condensation nuclei and ice nuclei content in clouds, (E), 25:26362 (CONF-700601-, pp 37-48)
efficiency for scavenging polystyrene latex and sodium chloride particles, (E), 25:26367 (CONF-700601-, pp 121-36)
efficiency for scavenging stack-released sulfur dioxide

from coal-fired power plant plumes, (E), 25:26378 (CONF-700601-, pp 293-303)
SODIUM
analysis for uranium by solvent extraction and spectrophotometry, 25:26152 (JAERI-Memo-4267)
boiling in liquid metal cooled reactors, initiation and thermal hydraulics aspects of, (E/T), 25:28726(R) (AI-AEC-12986)
combustion in liquid metal cooled reactor accidents, release and transport of aerosols and energy from, (E/T), 25:28726(R) (AI-AEC-12986)
content ratio to potassium in urine of rats as indicator of biological stress, tracer study of, 25:27029
corrosive effects of liquid, on fast breeder reactor materials, (E/T), 25:28632(T) (EURFNR-824)
determination in granite by autoradiography and neutron activation, 25:26194
determination in standard rocks by neutron activation, 25:26204
determination in woven fabric by neutron activation, 25:26200
effects on self-welding of hard facing and hard metal alloys, nickel alloys, and stabilized ferritic steel at 580 to 700°C, 25:27206 (KFK-Ext.Ber.-8/70-1)
efflux from rabbit lens, design of constant perfusion device for tracer studies on, 25:26606
reactions of liquid, with poly(tetrafluoroethylene), 25:26211 (TRG-Report-2104)
reactions with refractory alloys at 500 to 600°C, effects of oxygen on, 25:27174
SODIUM ALLOYS AND SYSTEMS
Hg-base--Na, effects on embrittlement of beryllium--copper alloys, 25:27243
K--Na, reactions of liquid, with poly(tetrafluoroethylene), 25:26211 (TRG-Report-2104)
SODIUM CHLORIDES
effects of aqueous, on cracking of alloys and metals under stress, 25:27175
scavenging of particles of, efficiency of ice and snow crystals for, (E), 25:26367 (CONF-700601-, pp 121-36)
SODIUM FLUORIDES
radioinduced F centers in, effects of electric field and temperature on radiative lifetime of excited, 25:27841 (NYO-3463-23)
SODIUM HYDROXIDES
radiolysis of glassy ices of, bleaching of trapped electrons from γ, 25:26298
SODIUM ISOTOPES
effects on kinetics of isotope diffusion in sodium chloride, 25:26241
SODIUM ISOTOPES Na-20
alpha decay of, beta--neutrino correlations and nuclear alignment effects of β-recoil in beta-delayed, (E/T), 25:28210 (CERN-70-30(Vol.1), pp 447-55)
nuclear magnetic moment of, (E), 25:28209 (CERN-70-30(Vol.1), pp 383-5)
SODIUM ISOTOPES Na-22
abundance in lunar surface materials, (E), 25:27308
determination in feces and urine of astronauts by γ spectroscopy, 25:26178 (BNWL-SA-3608)
SODIUM ISOTOPES Na-23
cross section data on, tables of multigroup, 25:28657 (HEDL-TME-71-36)
deuteron reactions (d,nγ) at 4 MeV, γ spectra from, (E), 25:28225
proton reactions (p,α) at 590 to 1810 keV, angular distributions from, 25:28259
SODIUM ISOTOPES Na-24
content of cosmogenic, in rainwater, effects of precipitation rate and ocean proximity on, (E), 25:26364 (CONF-700601-, pp 69-97)
determination in feces and urine of astronauts by γ spectroscopy, 25:26178 (BNWL-SA-3608)
SODIUM OXIDES
B_2O_3--Fe_2O_3--Li_2O--Na_2O, magnetic ordering and electric conduction in glasses of, 25:27901
B_2O_3--Fe_2O_3--Na_2O, magnetic ordering and electric conduction in glasses of, 25:27901
SODIUM PHOSPHITES
radiolysis of solid, spin trapping of radicals formed by γ, 25:26313
SOILS
analysis for uranium by ion exchange separation of neptunium-239 after neutron activation, 25:26197
polonium-210 sorption in agricultural, distribution coefficients for fallout, 25:26684
radioactivity following earth impaction of space power system radioactive capsules, computer programs for evaluating, 25:26429 (SC-R-7121)
radioisotope content of Japanese, April 1969 to April 1970, cerium-144, cesium-137, and strontium-90, 25:26392 (NIRS-RSD-27)
separation of neptunium from, by ion exchange, 25:26197
SOLAR ACTIVE REGIONS
effect of Feb. 24-Mar. 5, 1969, on solar electron and proton cosmic-ray increase, (E), 25:27470
flare production in, relation to solar-wind disturbances, (E), 25:27534
model of coronal, thermal, (E/T), 25:27396
sunspot rotation in 10344, (E), 25:27375
SOLAR CELLS
radiation damage to silicon, 40-keV proton, 25:26564
SOLAR CORONA
cooling mechanism for, Thomson scattering as, (T), 25:27401
matter distribution in inner, (E), 25:27397
polarization during eclipse of Sept. 22, 1968 in inner, (E), 25:27397
SOLAR DISTURBANCES
cosmic-ray modulation by, primary, (T), 25:27389
SOLAR FLARES
alpha-particle energy spectra during Feb. 24-25, at 2.3 to 70 MeV, (E), 25:27563
alpha-particle energy spectra from Feb. 25, 1969, 24- to 75-MeV/nucleon, (E), 25:27562
classification system for proton events, (T), 25:27388
conference on intercorrelated satellite observations and solar activity, Noordwijk, Netherlands, 9/69, 25:27531
disturbances in solar wind associated with, propagation through interplanetary space of, (T), 25:27629
effect on solar-wind disturbances, (E), 25:27534
effects of Feb. 25, 1969 proton event on Earth and near-Earth, (E), 25:27553
effects of Feb. 25, 1969, correlation with shock wave in interplanetary space, Feb. 26, (E/T), 25:27570
effects of Feb. 25, 1969, on auroral particles at 300 to 500 km, Geiger--Mueller observations of, 25:27572
effects of Feb. 25, 1969, on interplanetary magnetic field, HEOS-I measurement of, 25:27555
effects of Feb. 25, 1969, on interplanetary magnetic field, Pioneer 8 measurement of, 25:27556
effects of Feb. 25, 1969, on ion-density profiles in ionospheric D region, (E), 25:27565
effects of Feb. 25, 1969, on ionospheric D-region electron density, (E), 25:27564
effects of Feb. 25, 1969, on ionospheric electron density, (E), 25:27567
effects of Feb. 25, 1969, on magnetospheric electron density and temperature, (E), 25:27566
effects on interplanetary and terrestrial phenomena, (E/T), 25:27532
electron flux enhancements from Feb. 25, Feb. 27, Mar. 30, and Apr. 12, 1969, high-energy, (E), 25:27574
explosive phase of, development of, (E), 25:27382
intensity of Feb. 25, 1969, x-ray observations at 1 to 55A of, (E), 25:27357
observations at Ondrejov during 1964--1968 on chromospheric, (E), 25:27391
particle flux following Jan. 28, 1967 solar flare, effect of magnetic-field configuration on propagation of, (E), 25:27584
particle intensity during Feb. 25, 1969, ESRO-II observations of low-energy protons and electrons, (E), 25:27471
position effects of proton, on Earth's particle flux, (T), 25:27355
proton anisotropy and intensity during Feb. 25, 1969, (E), 25:27559
proton directional measurements during Feb. 25, 1969, >360-MeV and >30-MeV, 25:27560
proton distributions from Feb. 25, 1969, over northern polar cap during, 1- to 30-MeV, (E), 25:27561
proton emission from, simulated effects of, on monkeys, 25:26920(R) (AD-711041)
proton energy spectra during Feb. 24-25, at 2.3 to 70 MeV, (E), 25:27563
proton energy spectra from Feb. 25, 1969, 30- to 120-MeV, (E), 25:27562
proton event from, proposed classification of, 25:27356
proton event of Feb. 25, 1969, correlation of satellite and ground-based data, (E), 25:27553
proton events from, classification and forecasting of, (T), 25:27355
proton spectra from Feb. 25, 1969, at 100 keV to 6 MeV over northern polar cap, (E), 25:27573
relation of Feb. 25, 1969, May 1967, and Jan. 9, 1968, to interplanetary shock waves, (E/T), 25:27571
relation to magnetic-field variation in interplanetary space, (E/T), 25:27536
research programs on proton-emitting, (E), 25:27363
spectra of, iron line emission at 1.9A in, (E), 25:27386
structure and environment of, model of, (E/T), 25:27354
time sequence of solar proton event, Feb. 25-28, 1969, (E), 25:27558
x-ray bursts associated with, hard, (E/T), 25:27385
x-ray emission during, (E), 25:27383
x-ray emission during, satellite-borne spectroheliograph for measuring, 25:26484
SOLAR GRANULES
spectra of, statistical analysis of high-resolution, (E), 25:27366
SOLAR PARTICLES
energy spectra of, satellite observations of, (E), 25:27533
flux increases on Feb. 25 to March 5, 1969, Venus measurements of solar electron and proton, (E), 25:27470
propagation of injected, following Jan. 28, 1967 solar flare, effect of magnetic-field configuration on, (E), 25:27584
SOLAR PROMINENCES
hydrogen ionization and excitation in, (E), 25:27395

XUM

SOLAR RADIATION
effects of proton event of Feb. 25, 1969, (E), 25:27553
propagation of low-energy, in interplanetary space, (E), 25:27469
solar-flare effects on x-ray, (E/T), 25:27532
SOLAR RADIO BURSTS
emission during explosive phase of solar flares, (E), 25:27382
observations at Ondrejov during 1964--1968, (E), 25:27391
occurrence in conjunction with sunspots of Type D, E, and F, (E/T), 25:27381
relation of 606- to 8800-MHz, to S-component phase of solar radio emission, Nov. 1966 to April 1969, (E), 25:27364
spectral observations of, high-resolution, (E), 25:27398
SOLAR SYSTEM
effect of an anisotropic gravitational mass on Earth--Moon distance, (T), 25:27358
SOLAR WIND
Alfven-wave effects on MHD fast shocks in, (T), 25:27387
conference on intercorrelated satellite observations and solar activity, Noordwijk, Netherlands, 9/69, 25:27531
disturbances in flare-associated, sources of, (E/T), 25:27532
disturbances in, effects of weak sc, (E), 25:27546
disturbances in, propagation through interplanetary space of flare-associated, (T), 25:27629
disturbances in, solar-flare-associated, (E), 25:27534
effect of discontinuities on magnetosphere, (E/T), 25:27543
effect on plasma measurements across bow shock and in magnetosheath, (E), 25:27537
flux variations of, effect on electromagnetic field from Jan. 21 to March 21, 1969, (E), 25:27535
interaction with magnetosheath, Feb. 24-28, 1969, (E/T), 25:27557
interaction with magnetosphere, basic modes of, (E/T), 25:27630
interactions with interstellar hydrogen, (T), 25:27328
model for, to study scintillation and diffraction phenomena of cosmic radio sources, (T), 25:27612
properties as energy source for primary auroral ion intensity, (E/T), 25:27618
thermal conduction in nonsteady, nonspherically symmetric, by analysis of electron energy equation, (E/T), 25:27628
SOLAR X-RAY BURSTS
emission of soft, during solar flares, (E), 25:27383
location of Sept. 27, 1969, (E), 25:27384
origin of flare-produced hard, (E/T), 25:27385
size of Sept. 27, 1969, (E), 25:27384
SOLID STATE PHYSICS
hyperfine interactions in, lectures on, 25:27915 (NP-18702)
research progress on coincidence-Moessbauer studies of, 25:28864(R) (NYO-3973-8)
SOLUTIONS
radiolysis of alkaline glassy, electron trapping in, 25:26310
SOLVENTS
electrochemical research in amine, 25:28845(R) (COO-256-102)
SOUND
absorption devices for gas ducts, 25:28832(P)
SOUTHWEST EXPERIMENTAL FAST OXIDE REACTOR
cooling system for, natural circulation testing of, 25:28707 (DOCKET-50231-75)
experimental facilities for, testing of FRED, 25:28708 (DOCKET-50231-77)
fuel elements for, fabrication and inspection of plutonium oxide (PuO_2)--uranium oxide (UO_2) pellet type, 25:28757(R) (GEAP-10010-27)
maintenance during November 1970 to January 1971, 25:28757(R) (GEAP-10010-27)
operations during November 1970 to January 1971, 25:28757(R) (GEAP-10010-27)
operations history for November 1970 to January 1971, 25:28706 (DOCKET-50231-74)
operations incident of April 10, 1971, failure of cover gas pressure control relays, 25:28709 (DOCKET-50231-78)
operations incident of April 9, 1971, failure of reactor vessel overflow valve, 25:28709 (DOCKET-50231-78)
personnel for, qualifications of operation, 25:28736 (DOCKET-50231-76)
physics measurements for pluutonium oxide (PuO_2)--uranium oxide (UO_2) fueled, (E/T), 25:28757(R) (GEAP-10010-27)
radioactive effluents for, technical specifications for release limits of, 25:28736 (DOCKET-50231-76)
startup testing of plutonium oxide (PuO_2)--uranium oxide (UO_2) fueled, 25:28757(R) (GEAP-10010-27)
SOVIET UNION
civil defense program in, translation of handbook on, 25:26785(T) (ORNL-tr-2306)
SPACE
characteristics of interplanetary, HEOS-I data on, (E), 25:27552
cosmic-ray modulation in interplanetary, galactic and solar, (T), 25:27361
cosmic-ray propagation in interplanetary, low-energy galactic and solar, (E), 25:27469
electric properties around planar probe in interplanetary, photoemission and probe surface parameters affecting, (T), 25:27359
magnetic-field direction in interplanetary, correlation with propagation path of Feb. 25, 1969 solar-flare particles, (E), 25:27559
magnetic-field variation in interplanetary, solar-flare-related, (E/T), 25:27536
plasma sheath around photo-emitting plate in interplanetary, surface electric potential from, (T), 25:27360
proton detection and anisotropy in near-Earth interplanetary, cosmic approximately0.31-MeV, (E), 25:27473
proton spectral intensity in interplanetary, Feb. 25-28, 1969, (E), 25:27558
protons in interplanetary, interaction with bow shock and magnetopause, (E), 25:27538
shock-wave propagation Feb. 26, 1969, in interplanetary, possible correlation with Feb. 25 solar event, (E/T), 25:27570
solar-wind disturbances propagation through interplanetary, flare-associated, (T), 25:27629
SPACE FLIGHT
conference on manned planetary missions, 25:28786
conference on space station safety, 25:26784
Earth departure technique for NERVA powered manned planetary missions, 25:28788
nuclear shuttle use in manned planetary, comparison of expendable and reusable, 25:28789
radiation protection programs for astronauts during, use of human radiation shielded phantom and computer calculations for, 25:26778
SPACE VEHICLES
conference on intercorrelated satellite observations and solar activity, Noordwijk, Netherlands, 9/69, 25:27531
electric potential distribution on surfaces of, in interplanetary space, (T), 25:27360
electric properties around interplanetary, photoemission and probe surface parameters affecting, (T), 25:27359
performance of ESRO-I/AURORAE, in northern polar ionosphere and aurorae, (E), 25:27552
performance of ESRO-II/IRIS, in near-polar orbit at apogee 1100 km and 350 km perigee, (E), 25:27552
performance of HEOS-I, in interplanetary space and distant magnetosphere, (E), 25:27552
power systems for, design of conceptual 25 kW(e) zirconium hydride thermoelectric reactor, 25:28783 (AI-AEC-Memo-12717)
radiosterilization of, effectiveness of γ, in combination with dry heat, 25:27101
systems engineering requirements for manned planetary missions, 25:28787
SPECTROMETERS
circuits or nuclear, microelectronic, 25:26494
design of magnetic, for elementary particle interaction studies, 25:26507 (NP-16764)
SPECTROSCOPY
data handling and analysis for multichannel pulse analyzer, computer program for, 25:26499
spectra fitting for, computer programs for, 25:26489 (ANU-P-487(2))
SPERM
radiation effects on viability of rabbit, effects of dose and dose rate on γ, 25:26954
SPERMATOGENESIS
radiation effects on, of male mice following subcutaneous injection of zirconium-95--niobium-95, 25:26962
SPINAL CORD
radiation effects on cat, x, 25:26941
radioinduced lesions in, of embryos of mice, in utero x, 25:26972
radiotherapy of tumors of, development of nervous tissue reactions following, 25:27056
SPLEEN
effects of removal of mouse, on incidence of radioinduced leukemia, 25:27021
function studies, use of tracer techniques in, 25:26567 (STI/PUB-263)
lead-210 distribution in, of baboons and rats, 25:26610
molybdenum-99 distribution and retention in rat, following subcutaneous injection, 25:26598
radiation effects on colony formation in allogeneic and syngeneic transplanted, in mice, γ, 25:26670
radiation effects on esterase activity in extract of rat, effects of pH on whole-body x, 25:26600
radiation effects on formation of fibroblast colonies in cultures of mouse, following exposure of mice, 25:26905
radiation effects on hematopoiesis in mouse, effects of intraperitoneal injection of milk on x, 25:26678
radiation effects on hematopoietic colony formation in rat, following injection of isologous bone marrow, x, 25:26939
radiation effects on iron-59 distribution and uptake in, of mice, effects of immune reactions on x, 25:27012
radiation effects on protease activity in rabbit, whole-body x, 25:27035
scanning for diagnosis of hyperlipemia using technetium-99m, 25:26830
thorium-228 accumulation in human, 25:26603

SPORES
radiation effects on germinating Streptomyces, protective effects of chloramphanicol, ethanol, freezing, and mitomycin against γ and uv, 25:27068
radiation effects on germination of slime mold, effects of auto-inhibitor on γ, 25:27065
radiation effects on Polytrichum (moss), chronic low-dose γ, 25:27075
radiation effects on, of Osmunda regalis, effects of nitric oxide, oxygen, and water on, 25:27069
radiation effects on, of Penicillium expansum, effects of age, culture media, radiosensitizers, and temperature on γ, 25:27084
radioinduced mutations in fungi, gene mapping of uv, 25:26698
SPRAYS
efficiency of aqueous, for scavenging aerosol particles, (E), 25:26372 (CONF-700601-, pp 187-204)
efficiency of aqueous, for scavenging fission product iodine particles and methyl iodide from air, 25:26376 (CONF-700601-, pp 271-88)
STACK DISPOSAL
iodine-131 release from West Valley Processing Plant, Oct. 1969 to Jan. 1970, 25:26355(R) (SRO-344-11)
krypton-85 release from West Valley Processing Plant, Oct. 1969 to Jan. 1970, 25:26355(R) (SRO-344-11)
sulfur dioxide emissions from coal-fired power plant, scavenging by rainwater and snow of, (E), 25:26378 (CONF-700601-, pp 293-303)
STAINLESS STEEL
fatigue properties of Type 316, 25:27236
gamma absorption coefficient of 18/8, (E), 25:27626 (DEMO-70/11)
hardness of irradiated and unirradiated, hot, 25:27236
mechanical properties of carburized and nitrided, 25:27236
properties for use as cladding, fuel, and reactor core components, 25:27204 (INIS-mf-3)
properties of austenitic, for use in water-cooled reactors and as fuel element cladding, 25:27214(P)
properties of tubular coextruded joints of niobium--zirconium alloy to, effects of thermal cycling at 300 to 1600°F on, 25:27179 (N-71-10454)
radiation effects on swelling and mechanical properties of Type 304, Type 316, and Type 347, fast neutron, (E), 25:28691(R) (GEAP-10028-37)
welding of outer jacket of Type 316, and inner liner of tantalum for use as reactor boiler tubing, explosive method for, 25:27186
welding of Type 304, to 6061 and 5083 aluminum for use as tubular transition joint, high-rate angular method for, 25:27186
welding to titanium for use as transition joints for spacecraft fuel systems, explosive method for, 25:27186
STANDARDS
alarm systems, criticality accident ANSI, 25:26553
connectors for nuclear instruments, ANSI coaxial electric, 25:26552
control of combustible gas concentrations in containment following coolant loss accidents, AEC Safety Guide 7 1971 on, 25:28702
description of NBS radioactivity, 25:26455
diesel generator set capacity for standby power supplies, AEC Safety Guide 9 1971 on, 25:28705
dosimeter and voltage charger, quartz-fiber electrometer-type, 25:26467
Geiger--Mueller detector bases, 25:26468
instrument line penetrations in primary reactor containment, AEC Safety Guide 11 1971 on, 25:28678
ionization chambers, design of free-air, 25:26469
neutron dose to polymeric materials and application of threshold-foil measurements, ASTM D 2365-68, method of calculation of, 25:26535
neutron flux measurements by radioactivation of aluminum, ASTM E 266-70, method for fast, 25:26481
neutron flux measurements by radioactivation of iron, ASTM E 263-70, method for fast, 25:26477
neutron flux measurements by radioactivation of sulfur, ASTM E 265-70, method for fast, 25:26480
neutron flux measurements by radioactivation of sulfur, ASTM E 264-70, method for fast, 25:26479
neutron flux measurements by radioactivation techniques, ASTM E 261-70, method for, 25:26476
neutron flux measurements by radioactivation techniques, ASTM E 262-70, method for thermal, 25:26475
nuclear pressure vessels, supplementary criteria for ASME code-constructed, 25:28537
personnel selection and training, AEC Safety Guide 8 1971 on, 25:28725
power sources and distribution systems, AEC Safety Guide 6 1971 for independence between redundant standby, 25:28704
pumps for reactor emergency core cooling and containment heat removal systems, AEC Safety Guide 1 1970 on net positive suction head for, 25:28701
radiological consequences of coolant loss accidents in boiling reactor, AEC Safety Guide 3 1970 on assumptions for evaluation off potential, 25:28743
radiological consequences of coolant loss accidents in pressurized water reactor, AEC Safety Guide 4 1970 on assumptions for evaluation of potential, 25:28742
radiological consequences of steam line break accidents in boiling water reactors, AEC Safety Guide 5 1971, on assumptions for evaluation of potential, 25:28744
siting criteria for nuclear power plants, seismic and geologic, 25:28628
thermal shocks to reactor pressure vessels, AEC Safety Guide 2 1970 in limits for, 25:28683
STANFORD LINEAR ACCELERATOR
control and monitoring system for, PDP-9 computer-based, 25:28134
STAR CLUSTERS
star velocity distribution in, equal-mass, (T), 25:27336
STARCHES
radiation effects on activity of, in wheat, γ, 25:26621
radiation effects on hydrolysis of, in wheat, effects of doses of 20 to 200 Krad on γ, 25:26622
radioinduced degradation of macromolecules of, effects of temperature and water content on γ, 25:26623
STARS
atmosphere of delta Cep, curve of growth analysis for, (E), 25:27345
atmospheres of central, of planetary nebulae, (T), 25:27314
brightness variations in binary, among cataclysmic variables, (E), 25:27320
color indices of Cepheids, (E/T), 25:27340
convection in relativistic, neutral modes of, (T), 25:27325
diameters of, from lunar occultations, (E), 25:27329
distribution and spectral classification of, in nuclei of M31, M32, and M81, (E), 25:27409
distribution in Milky Way, (E/T), 25:27411
dust shells associated with M giant and supergiant, (E/T), 25:27315
dynamic processes in galaxies, computer simulation of, (T), 25:27406
envelope structure of white-dwarf, effects on thermal cooling rate, (E/T), 25:27332
evolution of 15- and 30-solar-mass, models for, (T), 25:27316
evolution of β Cephei, (T), 25:27327
evolution of close binary, mass exchange in, (T), 25:27334
evolution of close binary, rapid mass losses in, (T), 25:27331
formation of, angular momentum problem in, (T), 25:27326
light polarization of μ Cephei, (E/T), 25:27408
light variations of close-binary, conforming to Roche model, (E), 25:27330
luminosities for old disk-population red, (E/T), 25:27317
mass loss from M giant and supergiant, (E/T), 25:27315
neutronization in central regions of, thermodynamics of hot matter, (T), 25:27335
pair correlations in systems of, (T), 25:27321
photographic observations of Sirius B, corrections to previous, (E), 25:27346
photometry of dwarf Cepheid HD 199757, photoelectric, (E), 25:27319
photometry of field, near Cas A, (E), 25:27313
photometry of four classical Cepheids, (E), 25:27318
photometry of, background effects in, (E/T), 25:27341
pressure of relativistic, integral theorems for, (T), 25:27324
radial oscillations of β Cephei, linear nonadiabatic analysis of, (T), 25:27327
spectra of Arcturus, iron lines in, (E), 25:27365
spectra of α Dra, (E), 25:27333
spectral type of brightest component of triple system 44 i Boo, (E), 25:27343
stability at late evolutionary stages, hydrodynamic, (T), 25:27335
temperatures for old disk-population red, (E/T), 25:27317
velocity distribution of equal-mass, in clusters, (T), 25:27336
x-ray emission from neutron stars in binary systems, (T), 25:27342
STATISTICS
equilibrium states in statistical mechanics, ergodic states for, 25:28078
Pade approximants for, book on, 25:28063
STEAM
H_2O--steam, flow in evaporator channels with change of phase, equations for calculation of, 25:26420 (KFK-1300)
STEAM-GENERATING HEAVY-WATER-MODERATED REACTOR
design characteristics of, 25:28581
operations history for February 1968 to August 1970, 25:28581
STEAM POWER PLANTS
environmental effects of fossil fueled, comparison of nuclear power plants to, 25:28627
STEEL
analysis for titanium and zirconium carbide or nitride inclusions by electron probe methods, 25:26160
crack initiation and growth in carbon and Type 304 stainless, effects of low-cycle fatigue on, (E), 25:28680(R) (GEAP-10207-23)
cracking of Type 300 M, under stress, effects of environment on, 25:27175

XUM

cracking of Type 4340, under stress, effects of aqueous sodium chloride on, 25:27175
cracking of Type H-11, under stress, effects of humidified oxygen on, 25:27175
cracking of Type H-11, under stress, effects of water on, 25:27175
fabrication and mechanical properties of heavy-section ASTM A533B, manual on, 25:27181 (ORNL-TM-3193)
fabrication of reactor pressure vessels of, review of US methods on, 25:27196
fatigue and fracture toughness of armor, 25:27236
hardness of irradiated and unirradiated Type A302B, hot, 25:27236
joining of, research on, 25:27193
microstructure of heavy-section ASTM A533B, after heat treatment, 25:27181 (ORNL-TM-3193)
production of, use of process heat reactors in, 25:28791
properties of austenitic and ferritic, for use in pressure vessels, 25:27204 (INIS-mf-3)
radiation effects on embrittlement of A302B, evaluation of fast neutron, 25:28682 (JAERI-1202)
radiation effects on frature of, neutron, 25:27270
radiation effects on mechanical properties of austenitic and ferritic, recovery from, 25:27265 (INIS-mf-5)
radiation effects on sound velocity in Type A533B, at 503 to 550°F, fast neutron, 25:27268 (WHAN-FR-38)
uses in construction in conjunction with reinforced concrete, 25:27188
welding of German Type 1.4541, filler alloy development for, 25:27177 (JUL-681-RX)
welding of stabilized ferritic, in sodium at 580 to 700°C, self-, 25:27206 (KFK-Ext.Ber.-8/70-1)

STELLAR WIND
flow problems in, (T), 25:27328

STELLARATORS
plasma stabilization in high-β, feedback, (T), 25:27764

STEMS
radioinduced mutations for morphological changes in potato, 1000 to 120,000-R x, 25:26737

STEROLS
radiation effects on, in canned chicken pet food products, 25:26647

STOMACH
sulfur-35 uptake by mucosa of rat, effects of ulcers and treatment with steroid hormones and inflammation suppressive drugs on, 25:26605

STORAGE RINGS
beam current in electron, maximum, (T), 25:28140
beam dynamics in, radiation emission effects in electron, 25:28114 (NP-18634)

STREPTODORNASE--STREPTOKINASE
radiation effects on activity in human blood, use of thromboelastogram for determining γ, 25:26632

STREPTOMYCIN
effects on wound healing patterns following combined x radiation and surgical injury to rats, 25:26932

STRONTIUM
abundance in α Dra, (E), 25:27333
determination by electroconductivity method following chromatographic separation from alkali metals, 25:26173
determination in barium carbonate by x ray fluorescence, 25:26167
determination of trace amounts of, in hydrofluoric acid and spectrophotometry, 25:26176
separation from milk by moving-bed ion exchange, 25:26335 (RO/EERL-71-1)

STRONTIUM ISOTOPES Sr-84
neutron reactions (n,2n) at 14.4 MeV, activation cross section for, (E), 25:28282

STRONTIUM ISOTOPES Sr-85
energy levels from strontium-86 (He-3,α) reactions, spin--parity assignments for, (E), 25:28277
energy levels from yttrium-85 beta and electron-capture decay and strontium-85 isomeric transitions, spin--parity assignments for, (E), 25:28215 (CERN-70-30(Vol.2), pp 1137)
use of plastic microsphere-incorporated, for measurement of blood flow in rabbit bones, 25:26577

STRONTIUM ISOTOPES Sr-86
energy levels from gamma resonance scattering, widths for, (E), 25:28219 (NRCN-254)
helium-3 reactions (He-3,α) at 17.5 MeV, DWBA analysis of angular distributions from, (E), 25:28277
neutron reactions (n,2n) at 14.4 MeV, activation cross section for, (E), 25:28282
proton elastic and inelastic scattering at 4.5 to 7.5 MeV, excitation functions for, (E), 25:28234

STRONTIUM ISOTOPES Sr-87
energy levels from resonances in strontium-86 proton scattering, particle-core structure of isobaric analog, (E), 25:28234

STRONTIUM ISOTOPES Sr-88
neutron reactions (n,2n) at 14.4 MeV, activation cross section for, (E), 25:28282
neutron reactions (n,p) at 14.4 MeV, activation cross section for, (E), 25:28282
photon reactions (γ,p) with isobaric analog excitation, proton spectra from, (E), 25:28227
proton elastic and inelastic scattering at 8 to 12 MeV with isobaric analog excitation, excitation functions for, (E), 25:28240
proton elastic and inelastic scattering with isobaric analog excitation, analysis using coupled optical equations, (T), 25:28236
proton elastic scattering at 4.5 to 8.6 MeV with isobaric analog excitation, proton polarization from, (E), 25:28238
proton elastic scattering using polarized beams, isobaric analog resonances in, (E), 25:28239

STRONTIUM ISOTOPES Sr-89
excretion in urine of man following internal contamination from nuclear explosions, problems in measuring, 25:26585
transport through human food chains following nuclear attack, 25:26786
uptake by fetuses, placenta, and tissues of sows following ingestion, 25:26594
use for bone scanning, review on international methods for, 25:26855

STRONTIUM ISOTOPES Sr-90
content and transport in San Juan Basin ground waters following Gasbuggy Event, safety evaluation of, 25:26406 (PNE-1009)
content in Japanese airborne dusts and soils, April 1969 to April 1970, 25:26392 (NIRS-RSD-27)
content in Japanese powdered milk, tea, vegetables, and water, April 1969 to April 1970, 25:26392 (NIRS-RSD-27)
content of birch and pine trees, 25:26616
content of human bones and milk in South Africa during 1963 to 1967, methods for calculating, 25:26613
content of wine in Transylvania, 25:26618
content relative to calcium in human diet and transport through maternal milk, 25:26581
excretion in urine of man following internal contamination from nuclear explosions, problems in measuring, 25:26585
half residence time of, in troposphere, calculation of, 25:26389 (CONF-700601-, pp 447-63)
metabolism in bones of cats following chronic ingestion, isodensitometric evaluation of absorbed dose rates from, 25:26612
production and uses as heat source in thermoelectric generators, review of, 25:26432
radiation dose from particles of, following clothing contamination, 25:26748
scavenging from troposphere by atmospheric precipitation, 25:26389 (CONF-700601-, pp 447-63)
transport through human food chains following nuclear attack, 25:26786

STRONTIUM ISOTOPES Sr-93
beta decay of, Q value for, (E), 25:28294 (CERN-70-30(Vol.1), pp 321-9)

STRONTIUM ISOTOPES Sr-94
beta decay of, Q value for, (E), 25:28294 (CERN-70-30(Vol.1), pp 321-9)

STRONTIUM ISOTOPES Sr-95
beta decay of, Q value for, (E), 25:28294 (CERN-70-30(Vol.1), pp 321-9)

STRONTIUM ISOTOPES Sr-97
beta decay of, half-life for, (E), 25:28388

STRONTIUM ISOTOPES Sr-98
beta decay of, half-life for, (E), 25:28388

STRUCTURES
damage from Rulison Event-produced ground motion, measurement and prediction of, 25:26402 (JAB-99-78)
damage to Las Vegas and southern Nevada, from ground motions produced by underground nuclear explosions at Nevada Test Site, (E), 25:26400 (NVO-99-12)
failure of, diagrams for determining risk of, 25:28872(T) (ORNL-tr-2133)

STYRENE POLYMERS
neutron flux through graphite-styrofoam interface, time and space dependence of thermal, (E), 25:28818
scavenging of particles of latex-type, efficiency of ice and snow crystals for, (E), 25:26367 (CONF-700601-, pp 121-36)

SUBMARINES
design parameters of merchant nuclear, for petroleum transport tankers, 25:28795
economics of merchant nuclear, for petroleum transport tankers, 25:28795

SULFATES
determination by potentiometric titration using ion-selective electrodes, 25:26166

SULFIDES
radiation effects on activity of onion, γ, 25:26620

SULFUR
determination in plutonium oxide--uranium oxide pellets by spectrophotometry, 25:26153 (LA-4622)

SULFUR DIOXIDES
effects of European stack-released, on acidity of atmospheric precipitation in Scandanavia, (E), 25:26377 (CONF-700601-, pp 289-92)
reactions with plutonium hexafluoride, effects of uranium hexafluoride on kinetics of reduction, 25:26332(T) (ORNL-tr-2410, pp 98-120)
scavenging from atmosphere by precipitation in convective storms, airborne and ground measurements of, 25:26379 (CONF-700601-, pp 305-18)
scavenging from atmosphere by raindrops, laboratory studies of, 25:26375 (CONF-700601-, pp 261-9)

XUM

scavenging of coal-fired power plant stack-released, by rainwater and snow, (E), 25:26378 (CONF-700601-, pp 293-303)
SULFUR FLUORIDES
effects on hydrogen yields from a radiolysis of gaseous hydrogen sulfide, 25:26315
effects on x-radioinduced polymerization of gaseous chloroethylene, 25:26282
SULFUR ISOTOPES S-32
electron inelastic scattering in giant resonance region, microscopic calculation of form factors for, (T), 25:26220 (UJV-2553-F)
meson (μ) capture by, relativistic corrections to asymmetry of high-energy neutrons from polarized, (T), 25:28183
SULFUR ISOTOPES S-33
energy levels of, calculation of E2 transition rates using shell model with configuraton mixing, (T), 25:28245
energy levels of, calculation using intermediate coupling vibrational model with anharmonic core and quasiparticle effects, (T), 25:28249
SULFUR ISOTOPES S-34
energy levels of, calculation using intermediate coupling vibrational model with anharmonic core and quasiparticle effects, (T), 25:28249
SULFUR ISOTOPES S-35
determination in biological materials by automatic liquid scintillation spectroscopy using external standardization, 25:26184
uptake by gastric mucosa and secretion in gastric juice of rats with stomach ulcers, effects of steroid hormones and inflammation suppressive drugs on, 25:26605
SUN
activity of Feb. 25, 1969, experiments and performance of ESRO-I, ESRO-II, and HEOS-I during, (E), 25:27552
activity over 11-year cycle of, association of 27-day periodicity of 10.7-cm flux and sunspot activity during, (E/T), 25:27362
atmosphere of, MHD wave reflection, refraction, and coupling at density steps in, (T), 25:27392
conference on intercorrelated satellite observations and solar activity, Noordwijk, Netherlands, 9/69, 25:27531
cycles in, associated with modulated radiation-belt proton flux, (T), 25:27624
eclipses ofDec. 25, 1954 and Aug. 11, 1961, relation to F-region ionospheric ionization, (T), 25:27587
effects of activity of, Dec. 1968 to June 1969, on high-energy electron enhancements, (E), 25:27574
effects on diurnal variations of geomagnetic field at Watheroo, Western Australia, (E), 25:27503
H II region associated with properties of static, (E), 25:27399
iron abundance in, (E), 25:27365
microwave emission during eclipse of Sept. 11, 1969, (E), 25:27379
observation of, during Feb. 25, 1969 proton event, (E), 25:27553
particle emission from, flare-associated high-energy, (E/T), 25:27354
relation of sunrise at magnetic conjugate point with airglow pre-dawn enhancement of OI 6300 A, (E/T), 25:27514
spectra of, center-limb variations of separation of MgII, H, and K_2 emission peaks, (E/T), 25:27372
spectra of, Doppler widths from Goldberg's method, (E), 25:27367
wave propagation in atmosphere of, magneto-acoustic, (T), 25:27393
SUNSPOTS
activity of, correlation with 10.7-cm solar flux over 11-year solar cycle, 27-day periodicity of, (E/T), 25:27362
magnetic fields in, (E/T), 25:27377
microwave emission during eclipse of Sept. 11, 1969, (E), 25:27379
model for, magnetostatic, (T), 25:27378
observation of, during Feb. 25, 1969 proton event, (E), 25:27553
relation of D, E, and F, to impulsive microwave bursts, (E/T), 25:27381
rotation of, in plage region 10344, (E), 25:27375
spectra of umbrae of, molecular, (E), 25:27390
spectra of, iron lines in, (E), 25:27365
spectra of, molecular, (E/T), 25:27374
structure of, internal, (T), 25:27378
umbrae of, model for, (E/T), 25:27376
Unno transfer equation for Stokes parameters in Milne--Eddington atmosphere, solutions to, 25:27368
velocities in, radial, (E/T), 25:27377
SUPERCONDUCTIVITY
book: Statistical Physics, Phase Transitions, and Superfluidity, 25:27912
research on, review of, 25:27642
theory of Type-I and Type-II, 25:27661
theory of, model Hamiltonian of, 25:27643 (ITF-70-90-E)
SUPERCONDUCTORS
dynamic characteristics of thin films, uhf methods for study of, 25:27652
electromagnetic and thermal effects in intermediate-state of Type-I, equations for related, (T), 25:27647
electron dislocation stopping power in, dependence on temperature and velocity of, 25:27648
electron--electron interaction in, 25:27936
intermediate state in Type-II, possibility of, 25:27657
Josephson junction fabrication using plasma oxidation of niobium, 25:27659
Josephson tunnel junctions in, plasma oscillations and metastable states in, 25:27651
magnetic flux flow in thin films, 25:27645
magnetic surface level damping in, 25:27653
properties of, at high pressure, 25:27655
transition temperature in, review of high, 25:27656
tunneling in, effect of low-frequency fluctuations on, 25:27649
vortex motion in Type-II, 25:27650
SUPERFLUIDITY
book: Statistical Physics, Phase Transitions, and Superfluidity, 25:27912
group theory of, 25:27641
research on, review of, 25:27642
theory of Fermi systems in, 25:27637
SUPERNOVA REMNANTS
stars near Cas A, UBV photometry of field, (E), 25:27313
SUPERNOVAE
light curve for Kepler's, (E), 25:27339
photometry of Type I, (E), 25:27339
SURFACE-ACTIVE AGENTS
radiolysis of aqueous solutions of, reactions of hydroxyl radicals in pulse, 25:26295
SURFACE WATERS
ecological effects of thermal effluents on, CCL HEAT and TOPLYR programs for simulation of, 25:28710(R) (HEDL-TME-71-26)
flow of Argentine, review of radioisotope tracer studies of, 25:26353 (CONF-680112-, pp 37-52)
radiation monitoring of UK, 1969, 25:26397 (FRL-7)
radiation monitoring of West Valley Processing Plant environs, Oct. 1969 to Jan. 1970, 25:26355(R) (SRO-344-11)
temperature effects on Mississippi and Missouri Rivers of thermal effluents from power plants, model for simulating, 25:28710(R) (HEDL-TME-71-26)
SURFACES
analysis for impurities by nuclear backscattering methods, 25:26183
bibliography on surface and vacuum physics, 25:27440
SURGERY
methods for treatment of radioinduced ureter lesions, 25:26814
SURRY POWER REACTOR, UNIT 1
site for, wind direction and velocity measurements during November 1967 to July 1969, 25:28610 (DOCKET-50280-38)
SURRY POWER REACTOR, UNIT 2
site for, wind direction and velocity measurements during November 1967 to July 1969, 25:28610 (DOCKET-50280-38)
SUSPENSIONS
concentrations of sedimentary, performance of x radiometric gage for measurement of, 25:26544
SWEDEN
nuclear power plant development in, 25:28525 (CONF-700550-, Paper 3)
uranium demand and supply in, for nuclear power plant development to 1985, 25:26396 (CONF-700903-16)
uranium enrichment requirements in, for nuclear power plant development to 1985, 25:26395 (CONF-700903-15)
SWINE
radiation effects on survival of miniature, effects of dose and dose fractionation of pulsed mixed γ and neutron, 25:26928
radioinduced chromosome aberrations in kidney cells of, far-red, 25:26727
strontium-89 distribution in fetuses, placentas, and tissues of, following ingestion, 25:26594
SYMMETRY GROUPS
SU(1,1) x SU(2), model with isotopic spin extension of Regge pole model for hadron interactions at high energies in, 25:28055
SU(2,2), model with isotopic spin extension of Regge pole model for hadron interactions at high energies in, 25:28055
SU(2,2), representations for particles in, reduction with respect to iso-Poincare subgroup for unitary irreducible, 25:28054
SU(3) x SU(3), breaking in $\pi + K + \pi + K$ interactions, dispersive sum rule method for, 25:28029
SU(3) x SU(3), breaking in semi-strong interactions, Cabibbo angle in theory for, 25:28059
SU(3) x SU(3), chiral Lagrangian model for total cross sections and scattering lengths for meson interactions with baryons in, 25:28037
SU(n), hypergeometric functions for states of, structure of combinatorial generalization of, 25:28053
SYMMETRY GROUPS SU(3)
breaking in semi-strong interactions, Cabibbo angle in theory for, 25:28059
meson mass spectra and form factors for infinite multiplets model in, 25:28058
representation of three-particle state, Faddeev equations in, 25:28056
SYNCHROCYCLOTRONS
beam dynamics in, radiation emission effects in electron,

XUM

25:28114 (NP-18634)
beam injector for JINR, acceleration of deuterons in LA9 linac, 25:28109 (JINR-P9-5610)
SYNCHROTRON RADIATION
emission from isotropic plasma, general formula for, (T), 25:27706
use of DESY, to excite ultra-soft x-ray emission spectra, (E), 25:27827 (DESY-70/59)
SYNCHROTRONS
magnetic field in Erevan, azimuthal asymmetry of, 25:28139
SYSTEMS FOR NUCLEAR AUXILIARY POWER (SNAP)
book: Direct Conversion of Nuclear Radiation Energy, 25:27480
development in U.S. of radioisotope-fueled, data summary on, 25:26423 (CEA-Bib-190)
shielding of space reactors, coupling of discrete ordinates and Monte Carlo techniques for analysis of, 25:28784 (ORNL-TM-3365)
SYSTEMS FOR NUCLEAR AUXILIARY POWER (SNAP-7)
heat sources for, production and testing of strontium-90, 25:26432
SYSTEMS FOR NUCLEAR AUXILIARY POWER (SNAP-23)
design of Experimental Mockup System for 23A, engineering drawings for, 25:26430
design of Fueled Prototype Mockup System for 23A, engineering drawings for, 25:26431

T

T-111 (TANTALUM ALLOY)
fabrication of Pioneer and Transit heat source capsule components of, equipment and methods for, 25:26425 (MLM-1796)
stability at high temperatures, long-term thermal, 25:27208 (N-71-10352)
T-222 (TANTALUM ALLOY)
stability at high temperatures, long-term thermal, 25:27208 (N-71-10352)
TACHYONS
gravitational shock waves from, general relativity predictions for, (T), 25:28088
interactions with tardyons, Lagrangian theory for electromagnetic, 25:27984
TACHYSTEROL, DIHYDRO-
effects on calcification in whole-body x-irradiated rats, effects of time of administration on, 25:26933
effects on calcification in x-irradiated rats, 25:26978
effects on γ-radioinduced calcifications in rats, 25:26977
TANTALUM
boron-12 NMR in, quadrupole effects on spectra and coupling constants from, (E), 25:27923
determination by photometry using carboxy derivatives of 2,6,7-trihydroxy-9-phenyl-3H-xanthen-3-one, 25:26174
determination in woven fabric by neutron activation, 25:26200
elastic precursor decay in high-impact tests of, effects on dislocation density, 25:27216
hardness of irradiated and unirradiated, hot, 25:27236
nitrogen-12 NMR in, quadrupole effects on spectra and coupling constants from, (E), 25:27923
welding of inner liner of, and outer jacket of Type 316 stainless steel for use as reactor boiler tubing, explosive method for, 25:27186
welding to niobium, testing of filler alloys for, 25:27177 (JUL-681-RX)
welding to tantalum, testing of filler alloys for, 25:27177 (JUL-681-RX)
TANTALUM ALLOYS AND SYSTEMS
Fe--Ta, mechanical properties of Laves phase $TaFe_2$, 25:27211 (UCRL-20301)
Hf--Ta--V, phase diagram of, 25:27247
Ta-base--W, creep behavior at 2000 to 2600°F to 10,000 hr, effects of grain size on high-vacuum, 25:27207 (N-70-42045)
Ta-base--W, fabrication of Pioneer and Transit heat source capsule components of, equipment and methods for, 25:26425 (MLM-1796)
Ta-base--W, hardness of irradiated and unirradiated, hot, 25:27236
Ta-base--W, stability at high temperatures, long-term thermal, 25:27208 (N-71-10352)
TANTALUM CARBIDES
electron band structure of, (E/T), 25:27907
Co--TaC--TiC--WC, thermal conductivity of sintered, at 200 to 700°C, 25:27289
TANTALUM HYDRIDES
nuclear magnetic resonance at -190 to 300°C, 25:26261(T) (ORNL-tr-2439)
TANTALUM ISOTOPES Ta-170
beta decay of, gamma spectra and half-lives for, (E), 25:28322 (CERN-70-30(Vol.2), pp 939-47)
TANTALUM ISOTOPES Ta-171
beta decay of isomeric, gamma spectra and half-lives for, (E), 25:28322 (CERN-70-30(Vol.2), pp 939-47)
beta decay of, gamma spectra and half-lives for, (E), 25:28322 (CERN-70-30(Vol.2), pp 939-47)
TANTALUM ISOTOPES Ta-181
cross section data on, tables of multigroup, 25:28657 (HEDL-TME-71-36)
neutron capture by, gamma spectra from resonance, (E), 25:28437
TANTALUM ISOTOPES Ta-182
energy levels from tantalum-181 neutron capture, skin--parity assignments for, (E), 25:28437
TANTALUM OXIDES
properties of, 25:27281 (INIS-mf-13)
TARTARIC ACID
radiolysis of monocrystals of deuterated di-, ESR spectral studies on free radicals produced by low temperature γ and x, 25:26306
TAURINE
effectiveness for treatment of radioinduced leukopenia in man, 25:26812
effects on survival of irradiated mice, 25:26812
TECHNETIUM ISOTOPES
production by uranium-238 neutron fission at 14 MeV, gamma spectra from, (E), 25:28326 (CERN-70-30(Vol.2), pp 985-1000)
TECHNETIUM ISOTOPES Tc-93
energy levels from molybdenum-92 (p,γ) reactions, isobaric analog, (E), 25:28359
TECHNETIUM ISOTOPES Tc-99
content of metastable, in human milk as function of time following injection of tracer dose, 25:26839
effectiveness of ascorbic acid--iron complexes labeled with metastable, for kidney scanning, 25:26848
effectiveness of metastable, for diagnosis of infected brain lesions and cerebral neoplasms, 25:26818
production of isomeric, methods of testing for molybdenum-99 breakthrough in, 25:26317
production of, use of research reactors for, 25:28772
use of DTPA-incorporated metastable, for scanning, evaluation of effects of preparation method on usefulness of, 25:26840
use of inhaled albumin-incorporated metastable, for diagnosis of post-surgical bronchopleural fistulae in man, 25:26833
use of metastable, for bone, brain, and thyroid gland scanning, review on international methods for, 25:26855
use of metastable, for diagnosis of brain tumors in man in combination with spinal fluid protein analysis, 25:26828
use of metastable, for diagnosis of diaphragmatic hernia in man, methods for, 25:26836
use of metastable, for diagnosis of human brain tumors, comparison of gamma camera and rectilinear scanner for, 25:26852
use of metastable, for diagnosis of pulmonary embolism in man, methods for, 25:26837
use of metastable, for diagnosis of vascular diseases in man, methods for, 25:26838
use of sodium pertechnetate-incorporated metastable, for scintigraphy of collateral blood veins in man, 25:26844
use of sulfur colloid-incorporated metastable, for liver and spleen scanning, 25:26830
TEETH
molybdenum-99 distribution and retention in rat, following subcutaneous injection, 25:26598
radiation effects on parodontium of, 25:26960
TELEVISION EQUIPMENT
bandwidth compression scheme for, 25:28846 (COO-1469-178)
TELLURIUM
determination by photometry using carboxy derivatives of 2,6,7-trihydroxy-9-phenyl-3H-xanthen-3-one, 25:26174
TELLURIUM IONS
implantation in silicon at 50 keV, outdiffusion, lattice location, and electrical behavior of, 25:27856
TELLURIUM ISOTOPES Te-114
energy levels from tin-112 (α,2nγ) reactions, spin--parity assignments for, (E), 25:28330 (CERN-70-30(Vol.2), pp 1010-11)
TELLURIUM ISOTOPES Te-116
energy levels from tin-114 (α,2nγ) reactions, spin--parity assignments for, (E), 25:28330 (CERN-70-30(Vol.2), pp 1010-11)
TELLURIUM ISOTOPES Te-118
energy levels from tin-116 (α,2nγ) reactions, spin--parity assignments for, (E), 25:28330 (CERN-70-30(Vol.2), pp 1010-11)
TELLURIUM ISOTOPES Te-120
energy levels from tin-118 (α,2nγ) reactions, spin--parity assignments for, (E), 25:28330 (CERN-70-30(Vol.2), pp 1010-11)
TELLURIUM ISOTOPES Te-122
energy levels from tin-120 (α,2nγ) reactions, spin--parity assignments for, (E), 25:28330 (CERN-70-30(Vol.2), pp 1010-11)
TELLURIUM ISOTOPES Te-124
energy levels from tin-122 (α,2nγ) reactions, spin--parity assignments for, (E), 25:28330 (CERN-70-30(Vol.2), pp 1010-11)
energy-level transitions in, multipole mixing ratios for, (E), 25:28434
TELLURIUM ISOTOPES Te-126
energy levels from tin-124 (α,2nγ) reactions, spin--parity assignments for, (E), 25:28330 (CERN-70-30(Vol.2), pp 1010-11)

XUM

TELLURIUM ISOTOPES Te-128
energy levels from antimony-128 beta decay, spin--parity assignments for, (E), 25:28330 (CERN-70-30(Vol.2), pp 1010-11)
TELLURIUM ISOTOPES Te-130
energy levels from antimony-130 beta decay, spin--parity assignments for, (E), 25:28330 (CERN-70-30(Vol.2), pp 1010-11)
energy levels from gamma resonance scattering, widths for, (E), 25:28219 (NRCN-254)
energy levels from proton inelastic scattering, (E), 25:28427
energy levels from proton inelastic scattering, spectroscopic factors and spin-parity assignments for, (E), 25:28369
proton elastic and inelastic scattering at 7.8 to 12 MeV with isobaric analog excitation, excitation functions for, (E), 25:28427
proton inelastic scattering at 10.2 to 10.8 MeV, proton spectra and angular distributions for, (E), 25:28369
TELLURIUM ISOTOPES Te-132
energy levels from antimony-132 beta decay, spin--parity assignments for, (E), 25:28330 (CERN-70-30(Vol.2), pp 1010-11)
TELLURIUM ISOTOPES Te-133
beta decay of, Q value for, (E), 25:28296 (CERN-70-30(Vol.1), pp 341-51)
TELLURIUM SYSTEMS
Be--Nb--Te--Zr-base, properties for use as structural material for reactors, 25:27190(P)
Cu--Te, fabrication and uses of high conductivity, 25:27187
TEMPERATURE
control in coolant and walls of heat exchanger with internal heat generation, method for optimum, (E/T), 25:26421
distribution in heated wall impinged by liquid coolant-penetrating gas jet, equipment and method for measuring, 25:26418 (ANL-7734)
distribution in solid heat-generating cylinders cooled by flowing liquid metals, method for calculating, 25:26422
TERBIUM
determination in yttrium oxides by solvent extraction and spectrography, 25:26168
magnetic domain walls in, calculations of spin structure and energy of, 25:27873
magnetic properties of, effects of uniaxial stress on, 25:27889
TERBIUM ALLOYS AND SYSTEMS
Bi--Tb, magnetic structure of TbBi, neutron-diffraction study of, 25:27887
Pd--Tb, magnetic properties of $TbPd_3$ at 4 to 300°K, 25:27870
TERBIUM CARBIDES
magnetic structure of alpha-Tb_2C_3, neutron-diffraction study of, 25:27903
TERBIUM IONS
implantation in zinc sulfide films at 200 keV, detection using luminescence, 25:27844
TERBIUM ISOTOPES Tb-161
determination of, 4π β--γ coincidence method for, 25:26464
TERBIUM ISOTOPES Tb-164
beta decay of, gamma spectra from, (E), 25:28326 (CERN-70-30(Vol.2), pp 985-1000)
TESTES
radiation damage of rat, effects of dose rate and prenatal exposure on gamma, 25:26951
radiation effects on epithelium of guinea pig, following long distance skin therapy, x, 25:26973
radiation effects on interstitial cells in, of rats, functional and morphological studies on cryptorchidism and x, 25:27008
radiation effects on noradrenaline and serotonin levels in vas deferens in, of rats, whole-body x, 25:26959
radiotherapy of seminomas of human, effectiveness of γ, 25:26891
TETRACYCLINE
accumulation and fluorescence in tissues of whole-body x-irradiated rats, effects of dihydrotachysterol on, 25:26933
effects on wound healing patterns following combined x radiation and surgical injury to rats, 25:26932
TEXAS
radiation effects on population dynamics of screw-worm flies in, 25:27152
TEXTILES
analysis by neutron activation, 25:26200
THALLIUM
determination in tyuyamunites by anodic stripping after controlled-potential electrolysis, 25:26151 (CNEA-288)
THALLIUM ALLOYS AND SYSTEMS
Pr--Tl, nuclear magnetic cooling of $PrTl_3$, using hyperfine field, 25:27666
THALLIUM ISOTOPES Tl-190
electron-capture decay of, gamma spectra and half-lives for, (E), 25:28339 (CERN-70-30(Vol.2), pp 1081-91)
THALLIUM ISOTOPES Tl-191
electron-capture decay of, gamma spectra and half-lives for, (E), 25:28339 (CERN-70-30(Vol.2), pp 1081-91)
THALLIUM ISOTOPES Tl-193
electron-capture decay of, electron and gamma spectra and half-lives for, (E), 25:28339 (CERN-70-30(Vol.2), pp 1081-91)
THALLIUM ISOTOPES Tl-198
beta decay of isomeric, lifetimes of high-spin energy levels of mercury-198 from, (E), 25:28353 (NP-18695)
THALLIUM ISOTOPES Tl-203
nuclear quadrupole moment and deformation parameters for, (E), 25:28391
photon reactions (γ,n) at 30 MeV endpoint energy, cross sections for, (E), 25:28391
THALLIUM ISOTOPES Tl-205
nuclear quadrupole moment and deformation parameters for, (E), 25:28391
photon reactions (γ,n) at 30 MeV endpoint energy, cross sections for, (E), 25:28391
THALLIUM ISOTOPES Tl-207
energy levels and properties of, nuclear data sheets for, 25:28378
THALLIUM ISOTOPES Tl-208
energy levels and properties of, nuclear data tables for, 25:28375
THALLIUM ISOTOPES Tl-209
energy levels and properties of, nuclear data sheets for, 25:28376
THEBAINE
conversion to codeine in Papaver somniferum, intermediates in biosynthetic, 25:28899 (UCRL-20624)
THERMAL INSULATION
design of ice condenser, for pressurized water reactor containment system, 25:28700(P)
THERMAL TRANSFER TESTING
method for materials, review of, 25:26440
THERMIONIC CONVERTERS
development of radioisotope-fueled, data summary on international, 25:26423 (CEA-Bib-190)
THERMOCOUPLES
brazing of low profile, to Zircaloy fuel sheaths using beryllium--zirconium alloy, method for induction, 25:27182 (R-69-CAP-8)
design of gamma-compensated fission, for neutron flux measurements, 25:26466(P)
THERMOELECTRIC CONVERTERS
components for Experimental Mockup System SNAP-23A, design of, 25:26430
components for Fueled Prototype Mockup System SNAP-23A, design of, 25:26431
development and uses of strontium-90-fueled, review of, 25:26432
development of radioisotope-fueled, data summary on international, 25:26423 (CEA-Bib-190)
THERMONUCLEAR REACTIONS
energy losses in chain, 25:27797
energy losses in chain, 25:27796
THERMONUCLEAR REACTORS
data analysis for, review of, (E/T), 25:27792 (IAE-1986)
design and operation of, review of, (E/T), 25:27792 (IAE-1986)
magnetic field measurement in diffuse toroidal pinches, Thomson scattering for poloidal, (T), 25:27795
magnetic surfaces in l=3 torsatron, (T), 25:27793
THERMOSPHERE
carbon dioxide and oxygen in lower, performance of helium-cooled ion source for measurement of, (E), 25:27609
THICKNESS GAGES
performance of electron backscatter, for light-element coatings on heavy-element backing, 25:26542
THIOCYANATES
determination by potentiometric titration using ion-selective electrodes, 25:26166
THIOLS
effects on radiolysis of aqueous solutions of acetone or 2-propanol, 25:26291
THORAX
radiation dose to, of medical personnel during technetium-99m scintigraphy, γ, 25:26766
THORIUM
determination by photometry using carboxy derivatives of 2,6,7-trihydroxy-9-phenyl-3H-xanthen-3-one, 25:26174
determination of trace amounts of, in uranium-233 solutions, spectrophotometric, 25:26331(T) (ORNL-tr-2410, pp 79-97)
effects on magnetic susceptibility of scandium, 25:27878
effects on spectrophotometric determination of beryllium and gallium, 25:26172
preparation by reduction of thorium fluoride by calcium and zinc fluoride, 25:27180 (NLCO-1080)
separation of uranium-233 from irradiated, in nitric acid solutions using hydrochloric acid and TBP, 25:26331(T) (ORNL-tr-2410, pp 79-97)
uptake by erythrocytes, mechanisms for membrane penetration during, 25:26609
THORIUM ALLOYS AND SYSTEMS
properties of intermetallic compounds of, chemical and structural, 25:27263
Al--Th, crystal structure parameters of intermetallic Th_2Al, (E), 25:27654
Gd-base--Th, magnetic periodic ordering of, from electric conductivity and magnetization measurements, 25:27871

THORIUM BORIDES
crystal structure of delta-phase ThB_{66}, 25:27301
THORIUM FLUORIDES
reduction by calcium and zinc fluoride to prepare thorium, 25:27180 (NLCO-1080)
stability constants for, 25:26268
THORIUM FORMATES
phase transitions in, ir studies on, 25:26269
spectra of crystals of, ir, 25:26270
THORIUM HYDRIDES
nuclear magnetic resonance at -190 to 300°C, 25:26261(T) (ORNL-tr-2439)
THORIUM ISOTOPES Th-221
decay products of, energies, intensities, and half-lives of alpha, (E), 25:28304 (CERN-70-30(Vol.1), pp 545-6)
THORIUM ISOTOPES Th-222
decay products of, energies, intensities, and half-lives of alpha, (E), 25:28304 (CERN-70-30(Vol.1), pp 545-6)
THORIUM ISOTOPES Th-223
decay products of, energies, intensities, and half-lives of alpha, (E), 25:28304 (CERN-70-30(Vol.1), pp 545-6)
THORIUM ISOTOPES Th-228
accumulation in bone marrow, liver and spleen of man, 25:26603
effects on development of osteosarcomas in comparison with plutonium-239 and radium-226, 25:26603
THORIUM ISOTOPES Th-229
energy level transitions in, lifetimes of rotational states from, (E), 25:28353 (NP-18695)
energy levels in, lifetimes of rotational, (E), 25:28353 (NP-18695)
THORIUM ISOTOPES Th-230
geochemistry of, studies of marine, 25:26399 (TID-25674)
THORIUM ISOTOPES Th-232
concentration by tropical marine algae, 25:26597
effects on human lungs of cigarette smokers, damaging, 25:27046
neutron fission at 14.8 MeV, low-mass yields in, (E), 25:28385
neutron fission of, average cross sections and yields from, (E), 25:28409
THORIUM NITRATES
analysis for trace amounts of impurities by neutron activation, 25:26192
THORIUM OXIDES
properties of, 25:27281 (INIS-mf-13)
THORIUM OXIDES ThO_2
effects on incidence of carcinoma of human maxillary sinuses following diagnostic administration, 25:27050
preparation of microspheres of, kinetics of, 25:26333(T) (ORNL-tr-2410, pp 121-42)
preparation of pyrolytic carbon-coated fuel particles of, method for, 25:27275(P)
ThO_2--Y_2O_3, ionic transference numbers of electrolytes of, at high oxygen activities, 25:26262
ThO_2--Y_2O_3, oxygen activity for anionic conduction in $Th_{0.85}Y_{0.15}O_{1.925}$, at 775 to 1000°C, 25:27286
THREE MILE ISLAND POWER REACTOR, UNIT 1
buildings and structures for, safety analysis of aircraft impact loadings on, 25:28611 (DOCKET-50289-34)
THROMBIN
radiation effects on activity in human blood clotting time cobalt-60 γ, 25:26900
THULIUM
determination in yttrium oxides by solvent extraction and spectrography, 25:26168
THULIUM ALLOYS AND SYSTEMS
Au--Tm, magnetic properties of Au_4Tm at 6 to 300°K, (E/T), 25:27872
Pd--Tm, magnetic properties of $TmPd_3$ at 4 to 300°K, 25:27870
THULIUM ISOTOPES Tm-156
alpha decay of, energy and half-life for, (E), 25:28303 (CERN-70-30(Vol.1), pp 533-44)
THULIUM ISOTOPES Tm-158
beta decay of, gamma spectra and half-lives for, (E), 25:28322 (CERN-70-30(Vol.2), pp 939-47)
THULIUM ISOTOPES Tm-159
beta decay of, gamma spectra and half-lives for, (E), 25:28322 (CERN-70-30(Vol.2), pp 939-47)
THULIUM ISOTOPES Tm-160
beta decay of, gamma spectra and half-lives for, (E), 25:28322 (CERN-70-30(Vol.2), pp 939-47)
THULIUM ISOTOPES Tm-162
beta and electron-capture decay of, half-lives for, (E), 25:28321 (CERN-70-30(Vol.2), pp 931-8)
THULIUM ISOTOPES Tm-164
beta decay of isomeric, gamma spectra and half-lives for, (E), 25:28322 (CERN-70-30(Vol.2), pp 939-47)
THULIUM ISOTOPES Tm-169
energy levels from ytterbium-169 decay, spin--parity assignments for, (E), 25:28432
energy-level transitions from ytterbium-169 decay, multipolarities for, (E), 25:28432
THULIUM ISOTOPES Tm-176
beta decay of, thulium-176 half-life and energy levels of ytterbium-176 from, (E), 25:28398
energy levels of, spin and parity for ground-state, (E), 25:28398
half-life of isomeric, (E), 25:28398
half-life, (E), 25:28398
THYMIDINE
labeling with tritium for use in studies on DNA replication, 25:26570
THYMIDINE MONOPHOSPHATES
radiation effects on binding to sulfhydrylamines, 25:26279
THYMINE
radiation damage to, in DNA of Micrococcus radiodurans, repair of γ, 25:26643
THYMOL
effects on interferential activity of encephalitis virus in mice, stimulating, 25:27102
THYMUS GLAND
effects on regeneration in cervical lymph nodes of x-irradiated mice, 25:26996
radioinduced differentiation of epithelial and mesenchymal cells in rat, light microscopy whole-body x, 25:26654
removal from γ-irradiated mice, effects of, on survival, 25:26937
THYROID GLAND
function studies, use of tracer techniques in, 25:26567 (STI/PUB-263)
iodine-131 uptake by, in rats, effects of dried thyroid ingestion and sex on, 25:26601
radioinduced papillary microcarcinomas in, of atomic bomb survivors, 25:26898
scanning using iodine-131, iodine-132, and technetium-99, international methods for, 25:26855
TIN
determination by photometry using carboxy derivatives of 2,6,7-trihydroxy-9-phenyl-3H-xanthen-3-one, 25:26174
determination in yttrium oxides by solvent extraction and spectrography, 25:26168
determination in Zircaloy, chemical method for, 25:26171
effects on spectrophotometric determination of beryllium and gallium, 25:26172
TIN ALLOYS AND SYSTEMS
Al--Mo--Sn--Ti-base--Zr, fatigue properties of, 25:27236
Be--Nb--Sn--Zr-base, properties for use as structural material for reactors, 25:27190(P)
Co--Sn, crystal structure parameter of intermetallic Sn_2Co, (E), 25:27654
Nb--Sn, critical current in ribbon of, temperature dependence of, 25:27658
Nb--Sn, superconducting diffusion layers in, electron microprobe studies on, 25:26159
TIN ISOTOPES
energy levels from (d,p) and (d,t) reactions, spectroscopic factors for, (E), 25:28374
TIN ISOTOPES Sn-110
energy levels from antimony-110 beta decay, spin--parity assignments for, (E), 25:28332 (CERN-70-30(Vol.2), pp 1015-21)
TIN ISOTOPES Sn-111
energy levels from antimony-111 beta decay, spin--parity assignments for, (E), 25:28332 (CERN-70-30(Vol.2), pp 1015-21)
TIN ISOTOPES Sn-112
energy levels from antimony-112 beta decay, spin--parity assignments for, (E), 25:28332 (CERN-70-30(Vol.2), pp 1015-21)
TIN ISOTOPES Sn-113
energy levels from antimony-113 beta decay, spin--parity assignments for, (E), 25:28332 (CERN-70-30(Vol.2), pp 1015-21)
sorptive properties for hydrous zirconium oxide and zirconium oxide for use in generators, 25:26341
TIN ISOTOPES Sn-114
energy levels from antimony-114 beta decay, spin--parity assignments for, (E), 25:28332 (CERN-70-30(Vol.2), pp 1015-21)
photon reactions with, isotope effects on giant dipole resonance in, (T), 25:28393
TIN ISOTOPES Sn-115
energy level at 726 keV, measurement of magnetic moment using in-beam NMR, 25:28380
TIN ISOTOPES Sn-116
energy levels from photoexcitation, radiative widths for isobaric analog, (E), 25:28361
energy levels from resonances in indium-115 (p,α) reactions, widths for compound-nucleus, (E), 25:28268
photon reactions (γ,p) with isobaric analog excitation, proton spectra from, (E), 25:28361
TIN ISOTOPES Sn-118
energy levels from photoexcitation, radiative widths for isobaric analog, (E), 25:28361
photon reactions (γ,p) with isobaric analog excitation, proton spectra from, (E), 25:28361
photon reactions with, isotope effects on giant dipole resonance in, (T), 25:28393
TIN ISOTOPES Sn-120
effects on uv spectra of tin chlorides, 25:26244
energy levels from gamma resonance scattering, widths for, (E), 25:28219 (NRCN-254)
energy levels from photoexcitation, radiative widths for isobaric analog, (E), 25:28361
photon reactions (γ,p) with isobaric analog excitation, proton spectra from, (E), 25:28361
photon reactions with, isotope effects on giant dipole resonance in, (T), 25:28393

XUM

TIN ISOTOPES Sn-122
photon reactions with, isotope effects on giant dipole resonance in, (T), 25:28393
TIN ISOTOPES Sn-124
deuteron reactions (d,p) at 5.1 to 12.0 MeV, angular distributions for, (E), 25:28286 (ANU-P-511)
energy levels from photoexcitation, radiative widths for isobaric analog, (E), 25:28361
photon reactions (γ,p) with isobaric analog excitation, proton spectra from, (E), 25:28361
photon reactions with, isotope effects on giant dipole resonance in, (T), 25:28393
TIN ISOTOPES Sn-125
energy levels from tin-124 (d,p) reactions, spectroscopic factors and l values for, (E), 25:28286 (ANU-P-511)
TIN ISOTOPES Sn-129
energy levels from indium-129 beta decay, (E), 25:28329 (CERN-70-30(Vol.2), pp 1008-10)
TIN ISOTOPES Sn-133
beta decay of, half-life for, (E), 25:28328 (CERN-70-30(Vol.2), pp 1006-7)
TISSUES
dose distribution from beta and electron radioisotope point sources in, measurement using adaptation of computer calculations in water for, 25:26753
radiation dose absorbed in small volumes of target, from interstitial radioisotope photon sources, computer calculations of, 25:26752
strontium-89 uptake by, of sows following ingestion, 25:26594
transplants of parental and hybrid tumor, in mice, effects of whole-body irradiation on immune reactions to, 25:26985
zinc-65 uptake and distribution in, of rats, 25:26611
TITANIUM
determination by photometry using carboxy derivatives of 2,6,7-trihydroxy-9-phenyl-3H-xanthen-3-one, 25:26174
determination in sea floor samples by neutron activation, 25:26188 (BNWL-SA-3803)
determination in Zircaloy, chemical method for, 25:26171
effects on magnetic susceptibility of scandium, 25:27878
effects on spectrophotometric determination of beryllium and gallium, 25:26172
electric conductivity of, effects of molybdenum, niobium, and yttrium on, 25:27223
hardness of, effects of molybdenum, niobium, and yttrium on micro-, 25:27223
mechanical properties and uses of, 25:27203 (INIS-mf-2)
microstructure of, effects of molybdenum, niobium, and yttrium on, 25:27223
microstruture of cast, effects of nickel or vanadium additions on, 25:27220
neutron elastic scattering at 3.2 MeV using polarized beam, optical-model analysis of, (T), 25:28248
photon reactions at 1.5 to 5.7 GeV, total cross section for hadron production in, 25:27953
properties of cast, effects of nickel or vanadium additions on electric and mechanical, 25:27220
reactions of trivalent, with hydrogen peroxide in presence of 2-propanol, yields of hydroxyl radicals from, 25:26290(R) (NYO-3753-19)
welding to stainless steel for use as transition joints for spacecraft fuel systems, explosive method for, 25:27186
TITANIUM ALLOYS AND SYSTEMS
joining of, research on, 25:27193
mechanical properties at 400 to 800°C, 25:27203 (INIS-mf-2)
Al--Mo--Sn--Ti-base--Zr, fatigue properties of, 25:27236
Al--Mo--Ti-base--V, cracking under stress, effects of aqueous sodium chloride on, 25:27175
B--Mn--Ti, phase diagrams at 800 and 1400°C, isothermal, 25:27300
B--Ti--V, phase diagrams at 800 and 1400°C, isothermal, 25:27300
Be--Cu-base--Ni--Ti, properties of, aging and mechanical, 25:27232
Cr--Ti--V, compatibility with flowing sodium at 500 to 600°C, 25:27174
Cr--Ti-base, internal friction at 4 to 300°K, 25:27215
Fe--Ni--Ti, fatigue strength of, effects of fine precipitates on, 25:27231
Fe--Ti, mechanical properties of Laves phase $TiFe_2$, 25:27211 (UCRL-20301)
Ge--Ti-base--Zr, properties for use in brazing graphite or refractory metals, 25:27229(P)
Ir--Ti, superconductivity of intermetallic Ti_3Ir, (E), 25:27654
Mo--Ti-base, mechanical properties of, effects of aging on, 25:27233
Mo--Ti-base, phase transformation of metastable β-, isothermal, 25:27257
Mo--Ti-base, stability of metastable β-, effects of zirconium additions on, 25:27233
Mo--Ti-base--Zr, mechanical properties of, effects of aging on, 25:27233
Nb--Ti, magnetization of superconducting, dimensional effect in, (E), 25:27644 (KHFTI-70-8)
Nb--Ti, superconducting transition in solid solutions of, 25:27646
Nb--Ti--Zr, magnetization of superconducting, dimensional effect in, (E), 25:27644 (KHFTI-70-8)
Nb--Ti-base, internal friction at 4 to 300°K, 25:27215
Ni--Ti-base, internal friction at 4 to 300°K, 25:27215
O--Ti--Zr, structure and ordering in, x-ray and neutron diffraction studies of, 25:27297
Ti--transition metals, phase stability in, 25:27261
Ti--V-base, crystallization at 500 to 1100°C, 25:27259
Ti-base--V, internal friction at 4 to 300°K, 25:27215
TITANIUM BORIDES
boron-12 NMR in, quadrupole effects on spectra and coupling constants from, (E), 25:27923
nitrogen-12 NMR in, quadrupole effects on spectra and coupling constants from, (E), 25:27923
TITANIUM CARBIDES
determination as inclusions in steels by electron probe methods, 25:26160
electron band structure of, (E/T), 25:27907
Co--TaC--TiC--WC, thermal conductivity of sintered, at 200 to 700°C, 25:27289
Mo--Ni--TiC-base, phase studies of two-phase region in, 25:27298
Ni--TiC-base, phase studies of two-phase region in, 25:27298
TITANIUM HYDROXIDES
sorptive properties for uranium in seawater, 25:26350
TITANIUM ISOTOPES Ti-46
neutron reactions (n,p) with, cross sections for fast, (E), 25:28273
proton elastic scattering at 6.9 MeV, optical-model analysis of angular distributions from, (E), 25:28262
TITANIUM ISOTOPES Ti-47
neutron reactions (n,p) with, cross sections for fast, (E), 25:28273
neutron total cross sections and resonance parameters at 10 to 250 keV, (E/T), 25:28279
proton elastic scattering at 6.9 MeV, optical-model analysis of angular distributions from, (E), 25:28262
TITANIUM ISOTOPES Ti-48
alpha reactions (α,n) at 11.5 to 22.7 MeV, neutron spectra from, (E), 25:28285
deuteron reactions (d,p) at 13.6 MeV, distorted-wave analysis of differential cross sections from, (E/T), 25:28269
neutron reactions (n,p) with, cross sections for fast, (E), 25:28273
neutron resonance parameters at 10 to 250 keV, (E/T), 25:28279
oxygen-16 elastic scattering at 36 to 48 MeV, angular distributions for, (E), 25:28196
proton elastic scattering at 6.9 MeV, optical-model analysis of angular distributions from, (E), 25:28262
TITANIUM ISOTOPES Ti-49
deuteron reactions (d,p) at 13.6 MeV, distorted-wave analysis of differential cross sections from, (E/T), 25:28269
energy levels from titanium-48 (d,p) reactions, angular-momentum transfer, spectroscopic factors, and spin--parity assignments for, (E/T), 25:28269
neutron capture by, γ spectra and angular correlations from thermal, (E), 25:28284
neutron total cross sections and resonance parameters at 10 to 250 keV, (E/T), 25:28279
proton elastic scattering at 6.9 MeV, optical-model analysis of angular distributions from, (E), 25:28262
TITANIUM ISOTOPES Ti-50
energy levels from titanium-49 (d,p) reactions, angular-momentum transfer, spectroscopic factors, and spin--parity assignments for, (E/T), 25:28269
energy levels from titanium-49 thermal neutron capture, spin--parity assignments for, (E), 25:28284
helium-3 reactions (He-3,d) at 10 MeV, deuteron spectra and angular distributions for, (E), 25:28231
helium-3 reactions (He-3,p) at 10 MeV, angular distributions for L = 0 transitions in, (E), 25:28229
neutron capture by, γ spectra and angular correlations from thermal, (E), 25:28284
proton elastic scattering at 1.3 to 1.4 MeV, excitation function for, (E), 25:28226
proton elastic scattering at 6.9 MeV, optical-model analysis of angular distributions from, (E), 25:28262
proton reactions (p,γ) at 1.3 to 1.4 MeV, excitation function for, (E), 25:28226
TITANIUM ISOTOPES Ti-51
energy levels from titanium-50 thermal neutron capture, spin--parity assignments for, (E), 25:28284
TITANIUM NITRIDES
determination as inclusions in steels by electron probe methods, 25:26160
TITANIUM OXIDES
radioinduced paramagnetic defects in single-crystal, ESR study of annealing of gamma and neutron, 25:27853
spectral absorption lines of, in sunspot spectra, (E/T), 25:27374
$PbO--TiO_2--ZrO_2$, phase studies above 900°C, use of heating curves in, 25:27295
TOKAI-MURA POWER REACTOR
effluents from, control and monitoring of radioactive and thermal, 25:28624
TOKAMAK DEVICES
electromagnetic wave propagation in T-3, with sheared magnetic fields, (T), 25:27821
magnetic field measurement in, Thomson scattering for

XUM

poloidal, (T), 25:27795
plasma stabilization in, feedback control problems in, (T), 25:27763
TRACER TECHNIQUES
conference on, for dynamic studies in medicine, 25:26567 (STI/PUB-263)
development for measuring gas and liquid flows using radioisotopes, review of, 25:26435
TRANSACTINIDE ELEMENTS
fission barrier of, odd-particle effects on, (T), 25:28314 (CERN-70-30(Vol.2), pp 700-8)
half-lives for, odd-particle effects on alpha and spontaneous-fission, (T), 25:28314 (CERN-70-30(Vol.2), pp 700-8)
half-lives of A = 440 to 480, Strutinsky-shell-correction calculation of, (T), 25:28310 (CERN-70-30(Vol.2), pp 646-53)
production and identification of, methods for, (E), 25:28315 (CERN-70-30(Vol.2), pp 723-33)
properties of Z less than 121, liquid-drop-model calculations of binding energies, shape coefficients, and spin--parity assignments, 25:28441 (CERN-70-30(Vol.1), pp 217-62)
properties of, conference on, (E/T), 25:28308 (CERN-70-30(Vol.2))
properties of, shell-model calculations of, (T), 25:28311 (CERN-70-30(Vol.2), pp 654-75)
TRANSFERASES
effects on repair of uv-irradiated phage T4, 25:27105
TRANSITION METAL ALLOYS AND SYSTEMS
Al--transition metals, phase stability in, 25:27261
Be--transition metals-base, properties for use as structural material for reactors, 25:27190(P)
Cu--transition metals, phase stability in, 25:27261
Pd--Si--transition metals, two currents conduction in, 25:28844 (CALT-822-28)
Ti--transition metals, phase stability in, 25:27261
transition metals--V-base, vanadium-51 NMR in, quadrupole effects in, 25:27916
TRANSITION METAL BORIDES
microstructure of metal-rich phases in, 25:27304
thermal emissivity of Groups IV and VI, 25:27290
TRANSITION METAL CARBIDES
microstructure of metal-rich phases in, 25:27304
TRANSITION METAL NITRIDES
microstructure of metal-rich phases in, 25:27304
TRANSITION METAL OXIDES
microstructure of metal-rich phases in, 25:27304
TRANSITION RADIATION
detection of x-ray, from electrons using streamer chamber, 25:26515
TRANSPORT THEORY
exact analytical solution of equations in, (T), 25:27948
TRANSURANIUM ELEMENTS
bibliography on, Feb. 1971, 25:27168
bibliography on, Jan. 1971, 25:27169
electron-capture decay of Z < 99, relativistic corrections to exchange and overlap effects in, 25:28495
properties of, liquid-drop-model calculations of binding energies, shape coefficients, and spin--parity assignments, 25:28441 (CERN-70-30(Vol.1), pp 217-62)
TRIDODECYLAMINE
separation of plutonium from, by precipitation using hydrofluoric acid or oxalic acid, 25:26330(T) (ORNL-tr-2410, pp 14-78)
solvent properties for neptunium and plutonium, effects of decanoic acid on, 25:26333(T) (ORNL-tr-2410, pp 121-42)
solvent properties for plutonium, 25:26330(T) (ORNL-tr-2410, pp 14-78)
stability of, effects of alkylbenzene diluents on, 25:26330(T) (ORNL-tr-2410, pp 14-78)
alkylbenzene--tridodecylamine, radiolysis of, plutonium-239 α, 25:26330(T) (ORNL-tr-2410, pp 14-78)
TRIOXSALEN
effects on uv-radioinduced synthesis of DNA in human amnion cells, photosensitizing, 25:26808
TRITIUM
abundance in lunar surface materials, (E), 25:27308
beta decay of, reactions of dimethylcyclopropane with helium tritide ions from, 25:26321
binding energy of, calculation using K-harmonics method, 25:28162 (IAE-2000)
binding energy of, calculation using separable-expansion method, (T), 25:28510
content and transport in San Juan Basin ground waters following Gasbuggy Event, safety evaluation of, 25:26406 (PNE-1009)
content in atmosphere and atmospheric moisture at Miami, Florida and Fairbanks, Alaska, June 1970 to March 1971, 25:26393(R) (ORO-3944)
content of atmosphere and river water at Miamisburg, Ohio during 1970, 25:26739(R) (MLM-1795)
deuteron elastic scattering at 3.2 to 12.3 MeV using polarized beam, excitation functions and analyzing power for, (E), 25:28168
distribution in troposphere, calculations for 1963 to 1966, 25:26389 (CONF-700601-, pp 447-63)
effects on chromosomes and chromatids in human leukocytes, aberrant, 25:26636
effects on conversion of propanediol to propionaldehyde by dioldehydrase and coenzyme B_{12}, 25:26225
effects on development of rats following in utero exposure, β, 25:26925
effects on molecular weight of mammalian DNA, 25:26592
effects on reactions of radicals produced by photolysis of propanethiol, 25:26251
effects on replication of spleen lymphocytes in rats, 25:26994
exchange between benzoin and methanol, 25:26220
exchange with hydrogen in carboxypeptidase A, conalbumin, metallothionein, and transferrin, effects of metals on, 25:26237
half residence time of, in stratosphere and troposphere, calculation of, 25:26389 (CONF-700601-, pp 447-63)
incorporation in thymidine for use in studies on DNA replication, 25:26570
monitoring in environment near nuclear plants, development of sampling equipment for, 25:26393(R) (ORO-3944)
proton elastic scattering at 13.6 MeV using polarized beam, asymmetry and angular distributions for, (E), 25:28164 (LA-4576)
proton elastic scattering at 13.6 MeV, angular distributions for, (E), 25:28164 (LA-4576)
proton reactions (p,d) and (p,He-3) at 13.6 MeV, angular distributions for, (E), 25:28164 (LA-4576)
scavenging from troposphere by atmospheric precipitation and vapor exchange with oceans, 25:26389 (CONF-700601-, pp 447-63)
use as tracer in plasma glucose turnover studies in eviscerated and nephrectomized rats, comparison of carbon-14 with, 25:26602
TRITONS
decay t + n + d, three-body model vertex part of virtual, (T), 25:28047
reactions (t,pf) with uranium-238 at 12.54 MeV, proton coincidence spectra from, (E), 25:28390
TROPOSPHERE
strontium-90 content and distribution in, calculations for 1963 to 1966, 25:26389 (CONF-700601-, pp 447-63)
tritium content distribution in, calculations for 1963 to 1966, 25:26389 (CONF-700601-, pp 447-63)
TSURUGA POWER REACTOR
construction of, 25:28576
construction of, summary of problems in, 25:28542
effluents from, control and monitoring of radioactive and thermal, 25:28624
operation of, review of initial, 25:28576
startup testing for, 25:28576
TUNGSTEN
boron-12 NMR in, quadrupole effects on spectra and coupling constants from, (E), 25:27923
carburization of monocrystalline, by hydrocarbons at 2000°K, mechanisms of bulk and surface, 25:27225
determination by photometry using carboxy derivatives of 2,6,7-trihydroxy-9-phenyl-3H-xanthen-3-one, 25:26174
determination in plutonium oxide--uranium oxide pellets by spectrophotometry, 25:26153 (LA-4622)
determination in woven fabric by neutron activation, 25:26200
determination in Zircaloy, chemical method for, 25:26171
electron band structure of single crystals of, from optical and dielectric properties, 25:27899
electron diffraction at crystal surfaces of, LEED method for calculating intensity of, 25:27256
grain boundaries in, field ion microscopy studies of, 25:27253
hardness of irradiated and unirradiated, hot, 25:27236
particle size measurement of powdered, effects of packing methods, porosities, and sample weights on, 25:27217
pore size distribution in powdered, mercury porosimeter determination of, 25:27218
preparation by hydrogen reduction of mechanically activated tungsten oxide at 700°C, 25:27183
radiation damage in, field-ion microscopic study of 20-keV tungsten-ion, 25:27866(R) (NYO-3504-56)
recovery of fast neutron irradiated, at 15 to 420°K, electric conductivity study of, 25:27228
sorptive properties and surface film reactions with oxygen, 25:27224
sorptive properties of monocrystalline, for hydrogen, 25:27226
sorptive properties of powdered, for cesium at 600 to 800°C, 25:27201 (EUR-4549)
sorptive properties of single crystal planes of, for uranium, 25:27237
sorptive properties of single crystal planes of, for uranium, 25:27241
surface potential on (100), (110), and (112) crystal surfaces of, effects of hydrogen sorption on, 25:27234
tensile properties at high temperatures, 25:27178 (N-71-10353)
weldability of, effects of high preheat temperatures on, 25:27178 (N-71-10353)
TUNGSTEN ALLOYS AND SYSTEMS
hardness of irradiated and unirradiated, hot, 25:27236
B--Hf--Nb-base--W, strength at 1200°C, 25:27227
Hf--Nb-base--W, oxidation resistance at 1200°C, 25:27227
Mo--Re--W-base, tensile properties of welds in, at high temperatures, 25:27178 (N-71-10353)
Mo--Re--W-base, weldability of arc cast and powder

XUM

metallurgy, 25:27178 (N-71-10353)
Re--W, hardness of, effects of composition and temperature on decreasing, 25:27209 (N-71-11662)
Re--W, thermionic work functions of, 25:27911
Re--W-base, weldability of arc cast, effects of high preheat temperatures on, 25:27178 (N-71-10353)
Ta-base--W, creep behavior at 2000 to 2600°F to 10,000 hr, effects of grain size on high-vacuum, 25:27207 (N-70-42045)
Ta-base--W, fabrication of Pioneer and Transit heat source capsule components of, equipment and methods for, 25:26425 (MLM-1796)
Ta-base--W, hardness of irradiated and unirradiated, hot, 25:27236
Ta-base--W, stability at high temperatures, long-term thermal, 25:27208 (N-71-10352)
TUNGSTEN CARBIDES
particle size measurement of powdered, effects of packing methods, porosities, and sample weights on, 25:27217
pore size distribution in powdered, mercury porosimeter determination of, 25:27218
Co--TaC--TiC--WC, thermal conductivity of sintered, at 200 to 700°C, 25:27289
Co--WC, thermal conductivity of sintered, at 200 to 700°C, 25:27289
TUNGSTEN IONS
effects on tungsten at 20 keV, field-ion microscopic study of, 25:27866(R) (NYO-3504-56)
TUNGSTEN ISOTOPES W-172
beta decay of, gamma spectra and half-lives for, (E), 25:28322 (CERN-70-30(Vol.2), pp 939-47)
TUNGSTEN ISOTOPES W-182
cross section data on, tables of multigroup, 25:28657 (HEDL-TME-71-36)
TUNGSTEN ISOTOPES W-183
cross section data on, tables of multigroup, 25:28657 (HEDL-TME-71-36)
TUNGSTEN ISOTOPES W-184
cross section data on, tables of multigroup, 25:28657 (HEDL-TME-71-36)
energy levels of, deformation parameters for 4+, (E/T), 25:28411
energy-level transitions in, multipolarities for, 25:28410
proton elastic and inelastic scattering at 13 to 17 MeV, analog resonance anomalies in, (E), 25:28371
proton reactions (p,t) at 51.7 MeV, spectra and DWBA analysis of differential cross sections from, (E/T), 25:28411
TUNGSTEN ISOTOPES W-186
cross section data on, tables of multigroup, 25:28657 (HEDL-TME-71-36)
deuteron reactions (d,3n) at 12 to 19.6 MeV, gamma spectra from, (E), 25:28287 (ANU-P-518)
TUNGSTEN OXIDES
reduction of mechanically activated WO_3, by hydrogen at 700°C to prepare tungsten powder, 25:27183
TUNISIA
Mediterranean fruit fly population in, use of phosphorus-32 as tracer in estimation of, 25:26573
TURKEY
power reactors for, economic aspects and management requirements of, 25:28724
TURKEY POINT POWER REACTOR, UNIT 3
operation of, analysis of Florida power capacities and requirements from delay of, 25:28606 (DOCKET-50250-43)
TURKEY POINT POWER REACTOR, UNIT 4
operation of, analysis of Florida power capacities and requirements from delay of, 25:28606 (DOCKET-50250-43)
TURPENTINE
effects on glycoprotein contents and lysosomal enzyme activity in blood plasma and liver of rats, combined effects of x radiation and, 25:26979
TYUYAMUNITES
analysis for thallium by anodic stripping after controlled-potential electrolysis, 25:26151 (CNEA-288)

U

ULTRASONIC TESTING
method for materials, review of, 25:26440
ULTRAVIOLET RADIATION
characteristics of polar, 25:26517 (COO-1105-164)
dosimetry of solar, sensitivity of thermoluminescent dosimeters for, 25:26517 (COO-1105-164)
effects on amylase and proteinase activity in Aspergillus, mutagenic, 25:27097
effects on ascosperes of Ascobolus, mutagenic, 25:26695
effects on Bacillus, effects of transformation ability on mutagenic, 25:26729
effects on bacteria and bacteriophages, mechanisms of repair from damaging, 25:27109
effects on bacteria, mutagenic, 25:27121
effects on behavior of sea anemones, dose dependence of, 25:26912
effects on bioluminescence, growth, and respiration in bacteria, 25:27122
effects on blue-green algs in relation to growth factor requirements and penicillin resistance, mutagenic, 25:26712
effects on carotenoids of Mycobacterium phlei, mutagenic, 25:26687
effects on chain formation in Streptococcus, mutagenic, 25:26731
effects on dissociation of infective and oncogenic functions of polyoma and simian viruses, 25:27111
effects on DNA of human xeroderma pigmentosum cells, repair replication in, 25:26634
effects on DNA of vertebrate cells, effects of cell type and postirradiation conditions on repair mechanisms of, 25:26635
effects on DNA structure, degratory, 25:26657
effects on DNA synthesis in human amnion cells, photosensitizing effects of trisoralen on, 25:26808
effects on DNA synthesis in viruses, inactivating, 25:26691
effects on Escherichia coli (bacteria), tracer studies on repair mechanisms for, 25:27112
effects on fungi, lethal and mutagenic, 25:26703
effects on fungi, mutagenic, 25:27072
effects on fungi, mutagenic, 25:27088
effects on genes of Aspergillus, mutagenic, 25:26709
effects on germinating spores of Streptomyces, protective effects of chloramphenicol, ethanol, freezing, and mitomycin against, 25:27068
effects on growth of bacteria, 25:27119
effects on γ-induced mutants of Escherichia coli, 25:26707
effects on heating and ionization of intergalactic gas, (T), 25:27429
effects on human eye, review on, 25:27047
effects on hybridization in Ehrlich ascites cells and L cells, mutagenic, 25:26700
effects on inactivation and mutation in caffeine-resistant and caffeine-sensitive strains of Candida albicans, 25:27073
effects on inactivation of RNA from potato virus X, effects of wavelength on, 25:27108
effects on inactivation of surface antigens of polyoma virus, effects of dose on, 25:27107
effects on interferential activity of encephalitis virus in mice, stimulating, 25:27102
effects on mitosis in yeasts, effects of photoreactivation on lethal, 25:27080
effects on molecular weight of ribonuclease, 25:26658
effects on morphology of bacteriophages, damaging, 25:27098
effects on mouse L cells, 25:26989
effects on mRNA synthesis in bacteria, 25:27123
effects on phage T4, effects of Kornberg polymerase on damaging, 25:27105
effects on proteins, review of mechanisms of inactivating, 25:26644
effects on ribonucleic acid isolated from tobacco mosaic virus, inactivating, 25:26653
effects on Rous sarcoma virions, nonirradiated virus inhibition following, 25:27111
effects on semiconservative DNA replication and repair synthesis in bacteria, 25:27125
effects on skin of mice, sensitizing effects of acetic acid, croton oil, and xylene on tumorigenic, 25:26809
effects on spores of phytopathogenic fungi, lethal and mutagenic, 25:26698
effects on Streptomyces erythreus, mutagenic, 25:26699
effects on structure of ribonuclease A, 25:26661
effects on symbiotic activity in Rhizobium, mutagenic, 25:27103
effects on synthesis of nucleic acids and proteins in Blepharisma during regeneration, carbon-14 tracer study, 25:26648
effects on T4 phage mutants defective in deoxyribonucleic acid ligase and rII gene, 25:26708
effects on transducing phages of Rhizobium meliloti, 25:27104
effects on transduction of group A streptococcus to streptomycin resistance by exposure of virulent bacteriophages, 25:27110
effects on transforming DNA in bacteria, damaging, 25:27124
effects on transforming DNA in Euglena, effects of time on repair of, 25:26619 (COO-1793-6)
effects on unscheduled DNA synthesis in kangaroo rat cultured cells, 25:27002
excitation of 1134-, 1200-, 1493-, and 1743-A far-, from auroral atomic nitrogen, (E/T), 25:27617
relation of ionospheric F region equatorial, to oxygen ion--ion neutralization reaction, (E/T), 25:27608
spectra of Martian upper atmosphere, altitudinal analysis of, (E), 25:27433
UNITED KINGDOM
nuclear power plant development in, 25:28524 (CONF-700550-, Paper 2)
radiation monitoring of aquatic environment, 1969, 25:26397 (FRL-7)
UNITED STATES
radiation processing of food in, development of programs for, 25:27142
UNIVERSE
antimatter in, (T), 25:27426
expansion of, isomorphism between base homologies in, (T), 25:27425
model of expanding, including Hubble effect, (T),

XUM

25:27421 (ITF-70-105-E)
model of mixmaster, (T), 25:27428
oscillations of, time-reversal symmetry violation in, (T), 25:27424
perturbations in expanding, of free particles, (T), 25:27427
URACIL
effects on mRNA synthesis and uv-radiosensitivity in bacteria, 25:27123
URACIL, 5-FLUORO-
effects combined with γ radiotherapy on glioblastoma multiforme in man, postoperative, 25:26889
effects on gamma-radiosensitivity of human neoplasms, 25:26885
effects on mRNA synthesis and uv-radiosensitivity in bacteria, 25:27123
URACIL, IODO-
labeling with iodine-131 for use in tumor scanning, 25:26859
URACIL, 5-NITRO-
radiolysis of, ESR studies on free radicals produced by γ, 25:26296
URANIUM
complexes with 5,7-diiodo-8-quinolinol, formation constants of, 25:26214
content of bones of fossil animals and mice, 25:26744
content of vines and wines, 25:26615
demand and supply in Sweden to 1985, 25:26396 (CONF-700903-16)
determination by complexation of uranyl ions with nicotinic acid and crystal violet or rhodamine B, extraction--photometric, 25:26163
determination by photometry using carboxy derivatives of 2,6,7-trihydroxy-9-phenyl-3H-xanthen-3-one, 25:26174
determination in bone samples by neutron activation, 25:26744
determination in oxides by controlled potential coulometry, 25:26153 (LA-4622)
determination in plutonium oxide--uranium oxide pellets by spectrophotometry, 25:26153 (LA-4622)
determination in sodium by solvent extraction and spectrophotometry, 25:26152 (JAERI-Memo-4267)
determination in soils by ion-exchange separation of neptunium-239 after neutron activation, 25:26197
determination in Zircaloy, chemical method for, 25:26171
effects on hemolysis of red blood cells in miners, measurement of, 25:26588
effects on spectrophotometric determination of beryllium and gallium, 25:26172
enrichment in Europe, economics and development prospects of methods for, 25:26424(T) (CONF-700557-3)
enrichment requirements to fuel proposed Swedish power reactors, 25:26395 (CONF-700903-15)
gamma elastic scattering at 9 MeV, cross section for, (E), 25:28358
neutron reactions with natural, spectra from pulsed, (E), 25:28161
oxidation and reduction in acidic acetate buffers, polarographic studies on, 25:26265
preparation by reduction of uranium oxide with liquid aluminum or aluminum--uranium alloy, 25:27284
proton reactions at 5.5 GeV, energy spectra of fragments from, (E), 25:28426
radiation effects on dimensional stability of Magnox-clad fuel elements of uranium-235-enriched, 25:27267 (UJV-2371.R,T.)
reactions of tetravalent, with trivalent chlorine, mechanism of effects of phenol on, 25:26266
reprocessing of natural, hydrodynamic testing of large capacity centrifugal extractors for, 25:26330(T) (ORNL-tr-2410, pp 14-78)
retention in human lungs following inhalation in soluble compounds, ICRP threshold levels for determining degree of contamination based on natural, 25:26607
separation from americium by precipitation using a rare earth carrier, 25:26319(P)
separation from aqueous solutions by solvent extraction using 4,4,4-trifluoro-1(2-thienyl)-1,3-butanedione, 25:26340
separation from irradiated fuels by Purex Process, 25:26326 (KFK-911)
separation from plutonium dioxide--uranium dioxide fuels by solvent extraction using TBP, 25:26330(T) (ORNL-tr-2410, pp 14-78)
separation from plutonium in acidic solutions from reactor fuel reprocessing, selective solvent extraction process for, 25:26346(P)
sorption by tungsten single crystal planes, mechanisms of, 25:27237
sorption from seawater by titanic acid, 25:26350
URANIUM ALLOYS AND SYSTEMS
preparation for use as fuel in carbon dioxide-cooled reactors, 25:27195(P)
properties of intermetallic compounds of, chemical and structural, 25:27263
Al--U, analysis for trace amounts of silver by solvent extraction and atomic absorption spectrophotometry, 25:26169
Al--U, reactions of intermetallic UAl_3 in, with aluminum, Jost mechanisms in solid-state, 25:26210 (KFK-1312)
Al--U, reactions of liquid, with uranium oxide to prepare uranium, 25:27284
Al--U, separation of fission products from irradiated fuels of, by chlorination and pyrohydrolysis, 25:26332(T) (ORNL-tr-2410, pp 98-120)
Nb--U-base--Zr, reactions with carbon dioxide, nitrogen, oxygen, and water vapor at 27 to 1000°C, kinetics of, 25:27210 (SC-DR-710124)
U--Zr, separation of fission products from irradiated fuels of, by chlorination and pyrohydrolysis, 25:26332(T) (ORNL-tr-2410, pp 98-120)
URANIUM CARBIDES
preparation of pyrolytic carbon-coated fuel particles of, method for, 25:27275(P)
radiation effects on high temperature swelling, fission gas release, and microstructure of, (E/T), 25:28688 (BMI-1898, Sect.B)
URANIUM CHLORIDES UCl_4
enthalpy of formation of, 25:26263
URANIUM FLUORIDES UF_6
effects on plutonium hexafluoride reduction by sulfur dioxide, kinetics of, 25:26332(T) (ORNL-tr-2410, pp 98-120)
preparation from spent fuels, fluidized-bed, 25:26207 (BLG-448)
URANIUM HYDRIDES
nuclear magnetic resonance at -190 to 300°C, 25:26261(T) (ORNL-tr-2439)
URANIUM ISOTOPES
determination in plutonium dioxide--uranium dioxide pellets by mass spectrometry, 25:26153 (LA-4622)
determination in uranium dioxide by mass spectroscopy, 25:26153 (LA-4622)
URANIUM ISOTOPES U-232
analysis of solutions of, for trace amounts of thorium, spectrophotometric, 25:26331(T) (ORNL-tr-2410, pp 79-97)
separation from irradiated thorium in nitric acid solutions using hydrochloric acid and TBP, 25:26331(T) (ORNL-tr-2410, pp 79-97)
URANIUM ISOTOPES U-233
cross section data on, tables of multigroup, 25:28657 (HEDL-TME-71-36)
neutron fission of, charge distribution in thermal, (T), 25:28508
neutron fission of, krypton-85 branching ratios and yields in thermal, (E), 25:28383
neutron fission of, prompt neutron yield from thermal, (T), 25:28355(R) (TID-25659)
URANIUM ISOTOPES U-234
cross section data on, tables of multigroup, 25:28657 (HEDL-TME-71-36)
diffusion from deep-sea sediments, studies of, 25:26399 (TID-25674)
energy levels of, analysis of nonrandom distributions of neutron resonance, (T), 25:28421
geochemistry of, studies of marine, 25:26399 (TID-25674)
neutron fission threshold from uranium-233 (t,pf) reactions, (E), 25:28390
URANIUM ISOTOPES U-235
cross section data on, tables of multigroup, 25:28657 (HEDL-TME-71-36)
determination of, spectrochemical method for, 25:26170
energy level transitions in, lifetimes of rotational states from, (E), 25:28353 (NP-18695)
energy levels in, lifetimes of rotational, (E), 25:28353 (NP-18695)
fission of, energy released by beta radiation of products following, (E), 25:28407
neutron fission at 15.5 MeV, barrier parameters for, (T), 25:28504
neutron fission in reactor spectrum, mass-spectrometric search for argon and neon isotopes in ternary, 25:28419
neutron fission of, charge distribution in thermal, (T), 25:28508
neutron fission of, fission yield from fast, (E), 25:28354 (NP-18723)
neutron fission of, fission yield from thermal, (E), 25:28354 (NP-18723)
neutron fission of, gamma and x-ray spectra from products of thermal, (E), 25:28325 (CERN-70-30(Vol.2), pp 967-84)
neutron fission of, gamma spectra from fragments from thermal, (E), 25:28320 (CERN-70-30(Vol.2), pp 917-30)
neutron fission of, krypton-85 branching ratios and yields in thermal, (E), 25:28383
neutron fission of, on-line isotope separator for analysis of fission fragments from thermal, 25:26551
neutron fission of, potential-energy contours and fragment kinetic-energy and most-probable-charge distributions from thermal, (T), 25:28408
neutron fission of, prompt neutron yield from thermal, (T), 25:28355(R) (TID-25659)
neutron fission of, reactivity measurement method for determination of, 25:28817
neutron fission of, yields of cesium-138, -139, -141, -142, -143, and -145 in, (E), 25:28307 (CERN-70-30(Vol.1), pp 589-99)
resonance self-shielding factors for, calculations of, (T), 25:28503
URANIUM ISOTOPES U-236
cross section data on, tables of multigroup, 25:28657

(HEDL-TME-71-36)
potential-energy surfaces for, effects of asymmetric distortions in single-particle potential on, (T), 25:28313 (CERN-70-30(Vol.2), pp 689-99)
URANIUM ISOTOPES U-238
carbon-12 fission at 82 MeV, analysis of helium-6 emission in, (E), 25:28351(T) (KFK-tr-352)
concentration by tropical marine algae, 25:26597
cross section data on, tables of multigroup, 25:28657 (HEDL-TME-71-36)
energy levels from protactinium-238 beta decay, spin--parity assignments for, (E), 25:28326 (CERN-70-30(Vol.2), pp 985-1000)
fission of, energy surfaces for, (T), 25:28395
fission of, ruthenium-130 and -106 yields from spontaneous, (E), 25:28384
geochemistry of, studies of marine, 25:26399 (TID-25674)
neutron elastic scattering and total cross sections at 0.075 to 15 MeV, optical-model analysis of, (T), 25:28403
neutron fission at 14 MeV, gamma spectra from technetium products of, (E), 25:28326 (CERN-70-30(Vol.2), pp 985-1000)
neutron fission at 14.8 MeV, low-mass yields in, (E), 25:28385
neutron fission of, fission yield from fast, (E), 25:28354 (NP-18723)
oxygen-16 fission at 137 MeV, analysis of helium-6 emission in, (E), 25:28351(T) (KFK-tr-352)
triton fission at 12.54 MeV, coincidence-proton spectra from, (E), 25:28390
URANIUM ISOTOPES U-239
neutron fission threshold from uranium-238 (t,pf) reactions, (E), 25:28390
URANIUM LEACH SOLUTIONS
separation of lanthanides, scandium, and yttrium from uranium-barren, by solvent extraction using DEHPA, 25:26342
URANIUM NITRIDES
magnetic properties of UN, effects of anion substitution on, 25:27880
radiation effects on high temperature swelling, fission gas release, and microstructure of, (E/T), 25:28688 (BMI-1898, Sect.B)
reactions with zirconium oxide, Jost mechanisms in solid-state, 25:26210 (KFK-1312)
PuN--UN, irradiation testing of fuels of, 25:28687 (BMI-1898, Sect.A)
PuN--UN, radiation effects on high temperature swelling, fission gas release, and microstructure of, (E/T), 25:28688 (BMI-1898, Sect.B)
PuN--UN, self-diffusion of nitrogen in, (E), 25:28687 (BMI-1898, Sect.A)
URANIUM OXALATES
precipitation of, continuous, 25:26330(T) (ORNL-tr-2410, pp 14-78)
URANIUM OXIDES
properties of, 25:27281 (INIS-mf-13)
scavenging of aerosol particles of insoluble, by aqueous sprays, (E), 25:26372 (CONF-700601-, pp 187-204)
URANIUM OXIDES UO
spectra of rare gas matrix-trapped vapors of, ir, 25:26260 (COO-1182-34)
URANIUM OXIDES UO_2
analysis of fuel and source materials of, evaluation of chemical methods for, 25:26153 (LA-4622)
analysis of molybdenum- or Zircaloy-clad irradiated, electron beam microprobe equipment for, 25:26157
creep of, effects of microstructure, stress, temperature, and fission process on, (E), 25:28689 (BMI-1898, Sect.C)
diffusion in stoichiometric, at 1660 to 2035°C, sinusoidal profile relaxation method for studying surface and vapor-phase, 25:27288
fabrication of Zircaloy-2-clad fuel elements of, review of Swedish methods for, 25:27272 (CONF-700903-18)
fission gas diffusion and bubble growth in, (E/T), 25:28688 (BMI-1898, Sect.B)
gamma absorption coefficient of, (E), 25:27826 (DEMO-70/11)
lattice structure of, positron-annihilation study of, (E/T), 25:27865 (CEA-R-4138)
magnetic transition of, at 5 to 350°K, 25:26264
mechanical properties to 1800°C, four-point bending method for studying effects of grain size and strain rate on, 25:27287
phase studies of solidus--liquidus temperatures for nonstoichiometric, 25:27292 (GEMP-714)
preparation of porous, from powders, compression and sintering method for, 25:27273(P)
preparation of pyrolytic carbon-coated fuel particles of, method for, 25:27275(P)
preparation of stoichiometric dispersion of, in refractory metal or refractory metal alloy matrix, sintering method for, 25:27274(P)
properties for use as fuel, effects of microstructure on, 25:27282 (INIS-mf-14)
PuO_2--UO_2, preparation of enriched fuels of, method for, 25:27276(P)
radiation effects on high temperature swelling, fission gas release, and microstructure of, (E/T), 25:28688 (BMI-1898, Sect.B)
solubility of stainless steel-clad, in nitric acid solutions, 25:26330(T) (ORNL-tr-2410, pp 14-78)
spectra of rare gas matrix-trapped vapors of, ir, 25:26260 (COO-1182-34)
stoichiometry control of, (E), 25:28688 (BMI-1898, Sect.B)
thermodynamic properties of, at 5 to 350°K, 25:26264
uptake by erythrocytes, mechanisms for membrane penetration during, 25:26609
PuO_2--UO_2, analysis of fuel and source materials of, evaluation of chemical methods for, 25:26153 (LA-4622)
PuO_2--UO_2, creep of, effects of microstructure, stress, temperature, and fission process on, (E), 25:28689 (BMI-1898, Sect.C)
PuO_2--UO_2, dissolution by sealed-tube method, 25:26153 (LA-4622)
PuO_2--UO_2, properties of fuels of, mechanical, physical, and thermal, (E), 25:28691(R) (GEAP-10028-37)
PuO_2--UO_2, radiation effects on high temperature swelling, fission gas release, and microstructure of, (E/T), 25:28688 (BMI-1898, Sect.B)
PuO_2--UO_2, radiation effects testing of fuels of, 25:28691(R) (GEAP-10028-37)
PuO_2--UO_2, reprocessing of fuels of, by halide volatilization process, 25:26332(T) (ORNL-tr-2410, pp 98-120)
PuO_2--UO_2, stoichiometry shift in mixed, effects of burnup on, (E/T), 25:28690(T) (EURFNR-836)
URANIUM OXIDES U_3O_8
reduction by liquid aluminum or aluminum--uranium alloy to prepare uranium, 25:27284
Al--U_3O_8, phase studies of aluminum alloy-clad rolled fuel plates of, effects of deformation and shear process on, 25:27294
Al--U_3O_8-base, structure of dispersions of, equipment and method for studies of, 25:27251
URANIUM SULFIDES
photoemission spectral study of f states and valence bands in, 25:27876
URANYL ACETATES
reactions with monolayers of saturated and unsaturated cholestanol, cholesterol, and lecithins, effects of variables on, 25:26213
URANYL COMPOUNDS
complexes with 4,4,4-trifluoro-1-(2-thienyl)-1,3-butanedione, solubility in various solvents, radiometric determination of, 25:26340
complexes with adenosine 5'-diphosphate, adenosine monophosphate, and adenosine 5'-triphosphate, NMR and titrimetric studies on, 25:26271
complexes with lecithins in aqueous butanol solutions, properties of, 25:26272
fluorescence of, effects of poly(vinylsulfonate) and ferrous ions on, 25:26267
URANYL NITRATES
acetone--methyl sulfoxide--$UO_2(NO_3)_2$, complex formation in aqueous solutions of, PMR studies on solvation and, 25:26212
URANYL PERCHLORATES
acetone--HCl--methyl sulfoxide--$UO_2(ClO_4)_2$, complex formation in aqueous solutions of, PMR studies on solvation and, 25:26212
acetone--methyl sulfoxide--$UO_2(ClO_4)_2$, complex formation in aqueous solutions of, PMR studies on solvation and, 25:26212
UREA
oleic acid--urea, radiolysis of clathrate compounds of, at -196°C, ESR studies on kinetics of radical transformation in γ, 25:26312
palmitic acid--urea, radiolysis of clathrate compounds of, at -196°C, ESR studies on kinetics of radical transformation in γ, 25:26312
UREA, 1-METHYL-1-NITROSO-
effects on flax plants, mutagenic, 25:27090
URETER
radioinduced strictures in human, following therapy for cervical carcinomas, 25:27052
URIDINE, 5-BROMO-2'-DEOXY-
effects on β-galactosidase gene of Escherichia, mutagenic, 25:26722
effects on gamma-radiosensitivity of human neoplasms, 25:26885
URIDINE MONOPHOSPHATES
effectiveness for treatment of radioinduced leukopenia in man, 25:26812
effects on survival of irradiated mice, 25:26812
URINE
analysis of astronaut, by neutron activation and γ spectroscopy, 25:26187(R) (BNWL-1183-7)
analysis of astronaut, for beryllium-7, sodium-22, and sodium-24 by γ spectroscopy, 25:26178 (BNWL-SA-3608)
radiation effects on excretion of beta-aminoisobutyric acid and deoxycitidine in monkey, γ, 25:26999
radioisotope excretion in, of man following internal contamination from nuclear explosions, problems in measuring, 25:26585
UTERUS
radiation dose tolerance of human, during rotation therapy, γ, 25:26894
radioinduced carcinomas of rat, radium and x, 25:26827
radiotherapy of cancer of cervix of human, evaluation of

XUM

combined surgery and, 25:26886
radiotherapy of cancer of cervix of, effectiveness of, 25:26871
radiotherapy of carcinoma of cervix of human, recurrence following, 25:26887
radiotherapy of carcinomas of cervix of human, incidence of ureteral strictures following, 25:27052
radiotherapy of Stages I and II carcinomas of cervix of human, complications following, 25:26893

V

VACUUM
bibliography on surface and vacuum physics, 25:27440
VACUUM SYSTEMS
design for Super Hilac ion source, 25:28121 (UCRL-20620)
VACUUM VESSELS
design of aluminum oxide ceramic, for circular accelerators, 25:28131
VALVES
design of coolant flow regulating, for fuel loading standpipes, 25:28830(P)
design of freeze--melt, for use in vacuum encapsulation of cesium, 25:26413 (N-71-10455)
VAN ALLEN RADIATION BELTS
electron acceleration and precipitation during magnetospheric substorms, (E/T), 25:27551
electron intensity profile in outer, outward motion of, (E/T), 25:27626
electron radial diffusion in outer, observations of May-June 1967 bimodal, (E/T), 25:27626
particle-density variations in, solar event-associated energetic, (E/T), 25:27543
proton energy spectra in, trapped 0.3- to 74-MeV, Aug. 29 to Nov. 15, 1968, (E), 25:27625
proton flux in, neutron source decay solar-cycle modulation in, (T), 25:27624
ring-current enhancement characteristics during extremely quiet magnetic conditions, 1932--1969, (E), 25:27518
VAN DE GRAAFF ACCELERATORS
beam injection in EN tandem, from cyclotron, optics calculations for, 25:28103 (ANU-P-519)
charge state distributions of heavy ions in stripping target in tandem, equilibrium, 25:28127 (WASH-1159, pp 45-57)
VANADIUM
crystallization at 500 to 1100°C, 25:27259
determination by photometry using carboxy derivatives of 2,6,7-trihydroxy-9-phenyl-3H-xanthen-3-one, 25:26174
determination in sea floor samples by neutron activation, 25:26188 (BNWL-SA-3803)
determination in yttrium oxides by solvent extraction and spectrography, 25:26168
effects on electric and mechanical properties and microstructure of cast titanium, 25:27220
effects on spectrophotometric determination of beryllium and gallium, 25:26172
hardness of irradiated and unirradiated, hot, 25:27236
reactions of tetravalent, with hydrogen peroxide in presence of 2-propanol, yields of hydroxyl radicals from, 25:26290(R) (NYO-3753-19)
VANADIUM ALLOYS AND SYSTEMS
hardness of irradiated and unirradiated, hot, 25:27236
properties for use as fuel cans for fast breeder reactors, 25:27213
Al--Mo--Ti-base--V, cracking under stress, effects of aqueous sodium chloride on, 25:27175
B--Ti--V, phase diagrams at 800 and 1400°C, isothermal, 25:27300
Cr--Ti--V, compatibility with flowing sodium at 500 to 600°C, 25:27174
Cr--V, reflectance spectra of, measurement and band model of, 25:27442
Cr--V--Zr, compatibility with flowing liquid sodium at 500 to 600°C, 25:27174
Ga--V, superconducting diffusion layers in, electron microprobe studies on, 25:26159
Hf--Ta--V, phase diagram of, 25:27247
Mn--V, mictomagnetism in bcc, 25:27890
Mn--V, paramagnetism of bcc, NMR and susceptibility study of, 25:27891
Ni-base--V, dislocations in Ni_3V precipitates in, super, 25:27250
Si--V, superconducting diffusion layers in, electron microprobe studies on, 25:26159
Ti--V-base, crystallization at 500 to 1100°C, 25:27259
Ti-base--V, internal friction at 4 to 300°K, 25:27215
transition metals--V-base, vanadium-51 NMR in, quadrupole effects in, 25:27916
V--Zr-base, internal friction at 4 to 300°K, 25:27215
V--Zr-base, microstructure of, 25:27230
V--Zr-base, properties of, electric and mechanical, 25:27230
VANADIUM CARBIDES
electron band structure of, (E/T), 25:27907
magnetic susceptibility at 77 to 300°K, 25:27910
superconductivity of, search for, 25:27910
thermal capacity at 1.5 to 20°K, 25:27910
VANADIUM ISOTOPES V-51
energy levels from titanium-50 proton resonances, isobaric analog, (E), 25:28226
energy levels from titanium-50(He-3,d) reactions, spectroscopic factors for, (E), 25:28231
neutron reactions(n,α) with, cross sections for fast, (E), 25:28273
nuclear magnetic resonance in vanadium--manganese alloys, 25:27891
nuclear magnetic resonance in vanadium--transition metal alloys, quadrupole effects in, 25:27916
proton elastic scattering at 6.9 MeV, optical-model analysis of angular distributions from, (E), 25:28262
proton reactions (p,n) at 7.8 to 14.7 MeV, neutron spectra from, (E), 25:28285
VANADIUM ISOTOPES V-52
beta decay of, γ singles and coincidence spectra from, (E), 25:28250
nuclear spin and parity of, (E), 25:28250
VANADIUM OXIDES
electrical switching in VO_2 thin films, thermal filaments in, (E/T), 25:27906
VEGETABLES
onions, radiation processing effects on sprouting of, 25:27143
potatoes, identification of radiation processed, methods for, 25:27145
potatoes, radiation processing effects on inhibition of sprouting during storage, gamma, 25:27141
potatoes, radiation processing effects on sprouting of, 7 to 15-Krad, 25:27167
potatoes, radiation processing effects on sprouting and storage life of, 25:27133 (CONF-680112-, pp 241-3)
potatoes, radiation processing effects on sprouting of, 25:27143
radioisotope content of Japanese, April 1969 to April 1970, cesium-137 and strontium-90, 25:26392 (NIRS-RSD-27)
VEINS (BLOOD)
scintigraphy of collateral human, following obstruction of superior vena cava, use of gamma camera with technetium-99m-labeled sodium pertechnetate for, 25:26844
VELA PROJECT
site of Shoal Event in, recommendations for disposal of, 25:26403 (NVO-1229-105(Pt.1))
VENOMS
radiation effects on antigenicity of Naja naja snake, in mice and rabbits, γ, 25:26674
VENTILATION
radioactivity distribution in research reactor, during accident release, 25:28763 (RISO-205)
systems for nuclear power plants, design parameters of, 25:28545
VENUS (PLANET)
atmosphere of, model, (E), 25:27434
radio observations at 6 cm of, high-resolution, (E), 25:27434
surface pressures for, (E), 25:27434
surface temperatures of, (E), 25:27434
water vapor in lower atmosphere of, (E), 25:27434
VERMONT YANKEE POWER REACTOR
owners of, financial statements of, 25:28609 (DOCKET-50271-49)
VERTEBRAL COLUMN
radiation effects on differentiation in progeny of mice, effects of in utero 2'-deoxy-5-fluorocytidine and x, 25:26997
VIBRATIONS
effects on reactivity of control rod, 25:28835
VIRUSES
encephalitis, radiation effects on interferential activity of, in mice, comparison of thymol with uv, 25:27102
L-S, radiation effects on infectivity of, effects of temperature on x, 25:27117
Newcastle disease, radiation effects on replication of, in monkey kidney cells, 25:27113
polyoma, radiation effects on inactivation of surface antigens of, effects of dose on uv, 25:27107
polyoma, radioinduced dissociation of infective and oncogenic functions of, γ, uv, and x, 25:27111
potato X, radioinduced inactivation of RNA from, effects of wavelength on uv, 25:27108
radioinduced inactivation of DNA in, uv, 25:26691
Rous sarcoma, radioinduced dissociation of infective and oncogenic functions of, γ, 25:27111
RV, radiation effects on infectivity of, effects of temperature on x, 25:27117
simian 40, radioinduced dissociation of infective and oncogenic functions of, γ, uv, and x, 25:27111
TMV, effects of magnetic fields on synthesis in tobacco leaves, 25:27106
TMV, uv-inactivation of ribonucleic acid isolated from, photoreactivation following, 25:26653
VISION
conference on work-connected hazards to, in man, 25:27051
radiation effects on monkey, effects of dose on x, 25:26991
radiation effects on physiology of noctuid moth, combined effects of light and beta, gamma, and x, 25:26910
sensitivity of mechanisms contributing to directional, 25:28850 (COO-1701-16)

VITAMIN B GROUP
B_{12}, sorption by human intestine, comparison of effectiveness of cobalt-57-labeled cyanocobalamin plasma level test and Schilling test for diagnosis of, 25:26853
B_6, effectiveness for treatment of radioinduced leukopenia in man, 25:26812
B_6, effects on survival of irradiated mice, 25:26812
cyanocobalimin, use of cobalt-57-labeled, for immunoassay of binding and blocking anti-intrinsic antibodies in human blood serum and gastric juice, 25:26676
VK-50 REACTOR
design characteristics of, 25:28579
operations history for, 25:28579

W

WATER
analysis for cesium, lithium, rubidium, and strontium by spectrophotometry, 25:26176
analysis for mercury and rare earths by neutron activation, 25:26195
content of particles of, in clouds, effects of atmospheric precipitation on, 25:26362 (CONF-700601-, pp 37-48)
corrosive effect of deionized, on thin molybdenum films at 70 to 100°C, relations of silicon dioxide layer or double silicon dioxide and silicon nitride layer with, 25:27171
decomposition rate in reactor environment, 25:28758 (JAERI-1204)
determination in mixed oxide fuel pellets, 25:26153 (LA-4622)
diffusion of evaporating drops of, in Stefan flow, effects of temperature on, 25:26386 (CONF-700601-, pp 403-10)
dose distribution from radioisotope beta and electron point sources in, computer calculation of, 25:26753
effects on cracking of Type H-11 steel under stress, 25:27175
effects on γ radiosensitivity of rice seeds, 25:27070
effects on γ, radioinduced degradation of starch molecular, 25:26623
effects on survival of irradiated spores of Osmunda regalis, 25:27069
effects on x-radioinduced polymerization of gaseous chloroethylene, 25:26282
efficiency of droplets of, for scavenging silver chloride aerosol particles, (E), 25:26370 (CONF-700601-, pp 161-7)
neutron diffusion in, effects of turbulence on, (E/T), 25:28815(T) (BNWL-tr-66)
neutron reactions with poisoned, spectra from pulsed, (E), 25:28161
neutron reactions with, pulsed, (E), 25:28161
neutron slowing-down in, analysis of ages to indium resonance from, (E), 25:28157
sediment concentration in, performance of x radiometric gage for measuring suspended, 25:26544
H_2O--steam, flow in evaporator channels with change of phase, equations for calculation of, 25:26420 (KFK-1300)
WATER-d_2
decomposition rate in reactor environment, 25:28758 (JAERI-1204)
effects on volume and expansivity of some organic and inorganic ions, 25:26259
WATER SUPPLIES
radioisotope content of Japanese, April 1969 to April 1970, cesium-137 and strontium-90, 25:26392 (NIRS-RSD-27)
WATER VAPOR
abundance in lower cytherean atmosphere, (E), 25:27434
reactions with niobium--uranium--zirconium alloy at 27 to 1000°C, kinetics of, 25:27210 (SC-DR-710124)
spectral absorption lines of, in sunspot spectra, (E), 25:27390
WELDING
book: Electron Beam Welding, 25:27197
WELL LOGGING
equipment and method for gamma--gamma, of boreholes in iron ore and mercury deposits, 25:26352(T) (CONF-630513-1)
equipment and method for neutron, development of borehole-effects compensation, 25:26541(P)
WEST VALLEY PROCESSING PLANT
design modification schedule for, 25:26323 (DOCKET-50201-67)
environs monitoring during Oct. 1970 to Jan. 1971, 25:26355(R) (SRO-344-11)
safety analysis revisions for, 25:26324 (DOCKET-50201-68)
WHOLE-BODY COUNTERS
effectiveness of liquid scintillation, for studies on animal productivity, 25:26578 (CONF-680112-, pp 153-66)
WIND
effect of horizontal, on ionospheric midlatitude F-region vertical drifts, maps of, (T), 25:27588
effect of neutral-air, on electron density in midlatitude northern and southern hemispheric ionosphere, (E/T), 25:27508
effect of neutral-air, on longitudinal drift variations in midlatitude northern and southern hemispheric ionosphere, (E/T), 25:27507
effect on distribution of ionization in ionospheric E region, (E), 25:27516
effects of neutral air, on electron density and behavior of midlatitude ionospheric F region, (T), 25:27528
effects of neutral-air, on equatorial F-region polarization, (E/T), 25:27586
effects on Midwest Fuel Recovery Plant, 25:26325 (DOCKET-50268-7)
effects on safety of West Valley Processing Plant, 25:26324 (DOCKET-50201-68)

X

X RADIATION
characteristics of auroral, during study of precipitated-electron spectra, (E), 25:27549
detection and measurement of cosmic, at 25 to 190 keV, OSO-G satellite instrumentation for, 25:26478
detection at 50 to 500 keV, design of standard free-air ionization chamber for, 25:26469
detection by man following dark adaptation, tests of, 25:27039
dose to man during diagnostic fluoroscopic radiography, effects of screen components on, 25:26815 (BRH/DMRE-71-2)
dose to oral tissues during dental radiography, methods for reduction of, 25:26817
dose to patients in relation to diagnostic accuracy, methods for reducing, 25:26858
dose to pregnant patients during pelvimetry, orthometric view for reduction of, 25:26831
dosimetry for therapy, use of computer calculations in, 25:26761
dosimetry of, development of liquid-filled ionization chambers for, 25:26531
dosimetry of, thermoluminescent dosimeter for personnel accident, 25:26516 (CLOR-82/D)
dosimetry using photographic film, procedures for, 25:26532
effectiveness for therapy of human retinoblastomas, 25:26880
effectiveness of superhigh voltage, for therapy of bladder tumors, 25:26876
effects on age and growth of rats, 25:26965
effects on aging in mice, 25:26922(R) (ORO-3260-3-A)
effects on albumin metabolism and proteolytic activity in liver of rats, combined effects of starvation and, 25:26984
effects on alkali metal halides, radiative lifetime of excited F centers induced in, 25:27841 (NYO-3463-23)
effects on amino acid content in livers of rats, effects of dose and hepatectomy on, 25:27022
effects on antibody formation in mouse spleen cells, 25:26680
effects on antigenicity of tumor cells in guinea pigs, 25:26663
effects on Arabidopsis seeds, 1 to 20-krad mutagenic, 25:26736
effects on ascosperes of Ascobolus, mutagenic, 25:26695
effects on audiogenic seizure susceptibility in offspring of rats, in utero, 25:26968
effects on auxin content of cabbage plants in X_2 generation following seed exposure, 25:26651
effects on bacterial count, chemical and organoleptic changes, and storage life of Portuguese smoked sausage, 25:27159
effects on barley seeds, effects of water content on, 25:27092
effects on behavior of leukocyte preparations from whole-body exposed rabbits and rats, 25:26901
effects on behavior of sea anemones, dose dependence of, 25:26912
effects on binding between thymidylic acid and sulfhydrylamines, 25:26279
effects on biochemical activity of anastomose cultures of fungi, 25:27094
effects on biochemistry of blood serum and tissues in dogs, effects of AET on, 25:26935
effects on bioluminescence and respiration in bacteria, 25:27120
effects on blood, bone marrow, lymph nodes, liver, and spleen of mice, recovery from, 25:26980
effects on brain metastases in man, combined effects of corticosteroids and, 25:26895
effects on brain of man, necrotic, 25:27041
effects on brain of monkeys, edematous, 25:26987
effects on calcification in rats, effects of dihydrotachysterol on, 25:26978
effects on cell DNA synthesis, analysis of viral induced DNA synthesis in cells following inhibiting, 25:26691
effects on cell size of dill, lettuce, and spinach leaves, 25:27091
effects on chlorophyll content, growth, and respiration in corn, pea, and whet seedlings, effects of gibberellin on, 25:27064
effects on chlorophyll production in diploid and

tetraploid rice, mutagenic, 25:26714
effects on chromosome translocations in male mice, cytogenetical studies on, 25:26711
effects on chromosomes in human leukocytes, aberrant, 25:26730
effects on chromosomes in seeds, aberrant and mutagenic, 25:26697
effects on chromosomes of Chinese hamster cells, aberrant and lethal, 25:26723
effects on chromosomes of Crepis, aberrant, 25:26721
effects on chromosomes of Ehrlich ascites tumor cells, aberrant, 25:26704
effects on chromosomes of hamster embryos, abnormalities resulting from, 25:26982
effects on chromosomes of human leukocytes, effects of age and dose on aberrant, 25:26628
effects on chromosomes of rat kangaroo kidney cells, effects of dose and dose rate on aberrant, 25:26724
effects on chromosomes of Vicia, aberrant, 25:26725
effects on chromosomes of Vicia, aberrant, 25:26734
effects on Cicer, mutagenic, 25:26718
effects on content of ATP in rat thymocytes, effects of adenine on lethal, 25:26936
effects on content of glycoproteins in blood plasma and liver of rats, single and combined effects of turpentine and, 25:26979
effects on cross-over frequency in chromosomes of Drosophila melanogaster, 25:26713
effects on cytological and morphological properties of safflower, 25:27083
effects on deuterated dl-tartaric acid monocrystals, ESR of free radicals produced by, 25:26306
effects on developing brains in rats, latent damping, 25:26946
effects on development of Erlich ascites tumors in mice, combined effects of daunomycin and, 25:26990
effects on development of fibrosarcomas following therapy for hemangiomas in human children, 25:27059
effects on development of nervous system in embryos of mice, effects of age on in utero, 25:26972
effects on Dictyocaulus viviparus larvae, immunity in vaccinated calves following attenuating, 25:26918
effects on Dictyocaulus viviparus larvae, immunity in vaccinated calves following attenuating, 25:26919
effects on differentiation in vertebral column of, progeny of mice, in utero, 25:26997
effects on dissociation of infective and oncogenic functions of polyoma and simian viruses, 25:27111
effects on DNA in Chinese hamster cells, effects of age on degratory, 25:26625
effects on DNA in mammalian cells, mechanisms of repair in degratory, 25:26953
effects on DNA of bacteria, degratory, 25:26655
effects on DNA of Micrococcus radiodurans, degratory and lethal, 25:26627
effects on DNA polarity in phage lambda, degratory, 25:26692
effects on DNA release by phage lambda, inhibiting, 25:26693
effects on DNA synthesis in human amnion cells, effects of growth rate and dose on, 25:26630
effects on Ehrlich ascites cells, effects of N-ethylmaleimide and cysteamine on, 25:26640
effects on elimination of iodine-131-labeled antigen from blood of chickens, 25:26944
effects on enzymatic pethidine demethylating system in rat liver microsomes, inhibitory, 25:27034
effects on epithelial and mesenchymal cells in thymus gland of rats, light microscopy discriminatory, 25:26654
effects on erythropoiesis in mice, effects of immune reactions on, 25:27012
effects on esterase activity in extracts of erythrocytes, liver, spleen, and blood plasma, methods for determining effects of pH on whole-body, 25:26600
effects on estrus and fertility of dogs following ovarian exposure, delayed, 25:27009
effects on fungi, lethal and mutagenic, 25:26703
effects on genes of mosquitoes, mutagenic, 25:26719
effects on genetic load in Drosophila melanogaster, mutagenic, 25:26705
effects on germination and growth of seeds, 30-kR inhibitory, 25:27086
effects on glial tumor cells, damaging, 25:26908
effects on growth and mitosis in flax, hemp, radish, and rye, 25:27093
effects on growth of bacteria in small intestine of rats, effects of peristalsis on, 25:26975
effects on growth of cultured mouse lymphoma cells, 25:26974
effects on growth of transplanted mammary adenocarcinomas in mice in comparison to effects of antilymphocyte serum, 25:26666
effects on growth of wheat, 25:27082
effects on Hela cells, protective effects of MEG against lethal, 25:26797
effects on hematopoiesis and testicular epithelium in guinea pigs following long distance skin therapy, 25:26973
effects on hematopoiesis in mice bone marrow and spleen, effects of 400 to 600 R doses on, 25:26678
effects on hematopoietic system of mice as evidenced by residual injury in erythroid and myeloid systems, 25:26981
effects on human eye, review on, 25:27047
effects on human progeny following maternal uterine therapy, aberrant and clinical, 25:27057
effects on human uterus following radiodiagnosis, carcinogenic, 25:26827
effects on immune reactions and myeloid functions in bone marrow cells of mice, effects of phytohemagglutinin on lethal, 25:26942
effects on immune reactions and survival of 3rd stage larvae of Oesophagostomum, 25:26909
effects on immune reactions in dogs following heart transplants, ultrastructural electron microscopy studies on, 25:26677
effects on immune reactions in mice, effects of dose and dose rate on, 25:26679
effects on immune reactions to injected bacterial endotoxins and viruses in mice, 25:26986
effects on immune reactions, relation of age to, 25:26664
effects on immunocompetent cells in lymph nodes, spleen, and thymus of mice following bone marrow reconstitution, 25:26672
effects on infectivity of rat viruses, effects of temperature on, 25:27117
effects on interferon production in mice transplanted with rat bone marrow, 25:26995
effects on interstitial cells in rat testes, functional and morphological studies on, 25:27008
effects on iron-59 uptake and distribution in bone marrow and spleen of mice, effects of immune reactions on, 25:27012
effects on kininase activity in blood plasma of rats, 25:27030
effects on larvae of cattle lungworms for use as vaccine, 25:26578 (CONF-680112-, pp 153-66)
effects on larvae of Tenebrio, effects of age, dose, dose fractionation, partial-body and whole-body exposure on repair of, 25:26914
effects on leukocyte count in peripheral blood of rats, 25:26939
effects on liver regeneration in partially hepatectomized rats in comparison to effects of liver extracts, 25:26948
effects on lymphoma of orbit in man, therapeutic, 25:26890
effects on lysosomal enzyme activity in blood plasma and liver of rats, single and combined effects of turpentine and, 25:26979
effects on man following diagnosis, genetic and somatic, 25:26788
effects on mandible bone and dentin growth in rats, inhibitory, 25:27025
effects on mandibular condyle in rats, damaging, 25:27026
effects on mandibular development in chick embryos, damaging, 25:27018
effects on metabolism of DNAses and phosphatases in rat kidneys in comparison to TEM, 25:26645
effects on mice, dose reduction factors for cysteamine lethal, protection against, 25:26924
effects on mice, effects of dose fractionation on leukemogenic, 25:27021
effects on mice, effects of dose on late neoplastic, 25:26976
effects on mice, mutagenic and lethal, 25:26726
effects on mice, protective effects of reticuloendothelial system against lethal, 25:26926
effects on mice, radioprotective efficiency of cystaphos against, 25:26796
effects on migration and survival of fibroblast cells of chickens, effects of doses of 1000 R to 120,000 R on, 25:26642
effects on mitosis and DNA in mouse endometrial glandular epithelium, inhibitory, 25:26659
effects on mitosis in Chinese hamster cells, delaying, 25:26927
effects on mitosis in Chinese hamster cells, effects of dose and protein synthesis on delaying, 25:26626
effects on molecular structure of collagen gel, protective and sensitizing effects of chemical substances in relation to polymerizing, 25:26802
effects on molecular weight of DNA in Ehrlich ascites cells, use of guanidinium chloride in alkaline sucrose gradient for determination of, 25:26629
effects on morphological abnormalities in rice exposed as seeds, 25:27077
effects on motoneurons of spinal cord of cats, damaging, 25:26941
effects on Myasthenia gravis progression in humans by exposure of thymus gland, 25:26877
effects on noradrenaline and serotonin levels in tissues of rats, whole-body, 25:26959
effects on novocaine action in hearts of rats, dose effect on whole-body, 25:26798
effects on nucleus size and DNA content of dill plants, damaging, 25:27081
effects on ovaries of mature mice following exposure in infancy, latent pathological, 25:26930
effects on penicillamine on Sephadex at 77°K, 25:26299

effects on phytohemagglutinin response of bone marrow, lymph node, and spleen cells of mice, effects of thymus on, 25:26673
effects on ploidy in crop plants, 25:27087
effects on polymerization of gaseous chloroethylene, effects of additives on, 25:26282
effects on potassium cyanide-doped potassium chloride crystals, ESR spectra of FCN⁻ and HCN⁻ from, 25:26289 (NYO-2150-60)
effects on protease activity in leukocytes, macrophages, and spleen cells of rabbits, 25:27035
effects on protein metabolism in rats, 25:26624
effects on protein synthesis in cultured rabbit lens, carbon-14 tracer study, 25:26649
effects on pyrolysis of beryllium hydride, 25:26278
effects on rat kidneys in relation to physiological mechanisms for development of renal hypertension, 25:26652
effects on rats of, effects of antibiotics on wound healing patterns following combined surgical and, 25:26932
effects on rats, damaging, 25:27029
effects on rats, effects of dihydrotachysterol on whole-body calcifying, 25:26933
effects on recovery of early potentials of eyes in frogs, comparison of visible light and, 25:27004
effects on regeneration in cervical lymph nodes of mice, effects of thymus shielding on, 25:26996
effects on regeneration of intestinal epithelium cells of mice, 25:27033
effects on ribosomes of yeast, effects of magnesium ions on dissociating, 25:26633
effects on rice, mutagenic, 25:26701
effects on RNA synthesis in endometrial epithelium of mice, autoradiographic technique for determining, 25:27031
effects on sarcomas on human skin, Koebner phenomenon-like occurrence following therapeutic, 25:26875
effects on sciatic nerve of frogs, 25:26993
effects on seed germination and survival in rice plants, 25:27078
effects on segregation pattern in rice, mutagenic, 25:26688
effects on skin of man, latent pathological, 25:27049
effects on skin of rabbits, protective effects of benzydamine against inflammatory, 25:26806
effects on spinal cord of rats, effects of oxygen on pathological, 25:26966
effects on spleen colony formation following injection of isologous bone marrow in rats, transfer to parabiotic partners of, 25:26939
effects on stem cells in bone marrow of mice, partial- and whole-body, 25:26956
effects on stem cells of intestinal mucosa in mice, comparison of 14-MeV neutron and, 25:26958
effects on streptozotocin-induced diabetic rats, 25:27010
effects on survival of cultured lymphocytes, effects of phytohemagglutinin on, 25:26903
effects on survival of mice, effects of subsequent bleeding on, 25:26934
effects on synthesis of messenger and ribosomal RNA in HeLa cells, inhibitory, 25:26983
effects on unscheduled DNA synthesis in mammalian cells, effects of dinitrophenol and puromycin on, 25:27002
effects on uterus of rats, carcinogenic, 25:26827
effects on visual acuity in monkeys, latent, 25:26991
effects on visual system of noctuid moths, combined effects of light and, 25:26910
effects on wound response in lens epithelium of rats, 25:27000
effects on yeast, damaging, 25:27095
effects on yeast, damaging, 25:27096
emission by atoms, tables of abundance, energy, and half-life for, (E), 25:28400
emission from binary systems containing a black hole, neutron star, or white dwarf, (T), 25:27342
emission from coronal active regions, (E/T), 25:27396
emission from Sun, satellite-borne spectroheliograph for measuring, 25:26484
excitation of ultra-soft emission spectra by DESY synchrotron radiation, (E), 25:27827 (DESY-70/59)
hazards to medical personnel during angiocardiography, 25:26854
observations of Feb. 25, 1969 solar flare at 1 to 55A, soft, (E), 25:27357
production in alloy targets, Monte Carlo calculation of, (T), 25:27836
prophase reversion induction in grasshopper embryos by, effects of dactinomycin on recovery from, 25:26911
scattering by light atoms and ions, configuration-interaction and Hartree--Fock calculations of factors for, 25:27460
solar-flare effects on bursts of solar, (E/T), 25:27532
spectral emission in solar, high-energy, (E/T), 25:27354
use for food processing, review of principles involved and wholesomeness considerations in, 25:27132 (CONF-680112-, pp 221-39)
uses in nondestructive testing, review of, 25:26440

X-RAY EMISSION ANALYSIS
conference on x-ray optics and microanalysis, Tuebingen, Germany, Sept. 9 to 14, 1968, 25:26155
equipment and method for, using proton probe as excitation source, 25:26158
X-RAY EQUIPMENT
design for use by podiatrists, 25:26777
design for use in dental radiography, 25:26817
development of PDP-9 computer-controlled, for dynamic cineradiography, 25:26557
fluoroscopic screen stability evaluation, 25:26815 (BRH/DMRE-71-2)
survey of dental, in West Germany, evaluation of, 25:26772
X-RAY FLUORESCENCE ANALYSIS
methods for, review on, 25:26164
radioisotope uses as excitation sources in, 25:26175
3H-XANTHEN-3-ONE, 2,6,7-TRIHYDROXY-9-PHENYL-
uses of carboxy derivatives of, in photometric determination of metals, 25:26174
XENON
properties and uses of fission-product, 25:26347
scattering by helium atoms, total cross sections for elastic, (T), 25:27444
separation from krypton, 25:26347
separation from spent fuels, economics of, 25:26347
XENON IONS
effects on gallium arsenide at 400 keV, etching of damage in, 25:27860
XENON ISOTOPES
abundance in lunar surface materials, (E), 25:27308
XENON ISOTOPES Xe-115
nuclear spin-parity assignments from delayed-proton decay of, (E), 25:28301 (CERN-70-30(Vol.1), pp 487-96)
proton decay of, half-life and statistical-model analysis of energy spectra from delayed-, (E), 25:28301 (CERN-70-30(Vol.1), pp 487-96)
XENON ISOTOPES Xe-117
nuclear spin-parity assignments from delayed-proton decay of, (E), 25:28301 (CERN-70-30(Vol.1), pp 487-96)
proton decay of, half-life of delayed-, (E), 25:28301 (CERN-70-30(Vol.1), pp 487-96)
XENON ISOTOPES Xe-120
energy levels from palladium-108 (O-16,4n) reactions, deformation parameters and lifetimes for 2⁺, (E), 25:28319 (CERN-70-30(Vol.2), pp 905-10)
energy-level transitions from palladium-108 (O-16,4n) reactions, probabilities for E2, (E), 25:28319 (CERN-70-30(Vol.2), pp 905-10)
XENON ISOTOPES Xe-122
energy levels from palladium-110 (O-16,4n) reactions, deformation parameters and lifetimes for 2⁺, (E), 25:28319 (CERN-70-30(Vol.2), pp 905-10)
energy-level transitions from palladium-110 (O-16,4n) reactions, probabilities for E2, (E), 25:28319 (CERN-70-30(Vol.2), pp 905-10)
XENON ISOTOPES Xe-133
energy-level transitions from iodine-133 beta decay, conversion coefficients and multipolarities for, (E), 25:28336 (CERN-70-30(Vol.2), pp 1057-68)
use as tracer for measuring total liver blood flow in cats, 25:26576
use for brain scanning, review on international methods for, 25:26855
use for scanning lungs for ventilation, 25:26819
use with iodine-131 for scanning ventilation in human lungs, 25:26841
XENON ISOTOPES Xe-134
energy-level transitions from iodine-134 beta decay, conversion coefficients and multipolarities for, (E), 25:28336 (CERN-70-30(Vol.2), pp 1057-68)
XENON ISOTOPES Xe-135
effects on power oscillations in thermal reactors, direct numerical solution technique for analysis of, 25:28811
XENON ISOTOPES Xe-136
energy levels from iodine-136 beta decay, lifetimes and spin--parity assignments for, (E), 25:28342 (CERN-70-30(Vol.2), pp 1119-21)
energy-level transitions from iodine-136 beta decay, conversion coefficients, K/L+... values, and multipolarities for, (E), 25:28336 (CERN-70-30(Vol.2), pp 1057-68)
XENON ISOTOPES Xe-139
beta decay of, beta and gamma spectra from, (E), 25:28336 (CERN-70-30(Vol.2), pp 1057-68)
XYLENE
radiosensitizing effects on tumorigenesis in skin of mice, uv, 25:26809

Y

YANKEE POWER REACTOR
operations history for 1960 to 1970, review of, 25:28577
YTTERBIUM
determination by photometry using 1,10-phenanthroline and salicylfluorone, 25:26161
determination in yttrium oxides by solvent extraction and spectrography, 25:26168
electric conductivity of, effects of pressure on, (E/T), 25:27867 (UCRL-51006)
separation from lutetium, effects of copper ions on electrophoretic focusing ion, 25:26351

YTTERBIUM ALLOYS AND SYSTEMS
Au--Yb, magnetic properties of Au_4Yb at 6 to 300°K, (E/T), 25:27872
Pd--Yb, magnetic properties of $YbPd_3$ at 4 to 300°K, 25:27870
Yb--Yb_2O_3, phase studies of, 25:27302
YTTERBIUM IONS
implantation in silicon at 60 keV, 1-MeV helium-ion backscattering study of, 25:27857
YTTERBIUM ISOTOPES Yb-156
alpha decay of, energy and half-life for, (E), 25:28303 (CERN-70-30(Vol.1), pp 533-44)
YTTERBIUM ISOTOPES Yb-157
alpha decay of, energy and half-life for, (E), 25:28303 (CERN-70-30(Vol.1), pp 533-44)
YTTERBIUM ISOTOPES Yb-158
beta decay of, gamma spectra and half-lives for, (E), 25:28322 (CERN-70-30(Vol.2), pp 939-47)
YTTERBIUM ISOTOPES Yb-160
beta decay of, gamma spectra and half-lives for, (E), 25:28322 (CERN-70-30(Vol.2), pp 939-47)
YTTERBIUM ISOTOPES Yb-162
electron-capture decay of, half-lives for, (E), 25:28321 (CERN-70-30(Vol.2), pp 931-8)
YTTERBIUM ISOTOPES Yb-163
beta decay of, gamma spectra and half-lives for, (E), 25:28322 (CERN-70-30(Vol.2), pp 939-47)
YTTERBIUM ISOTOPES Yb-168
energy levels from lutetium-168 beta and electron-capture decay, spin-parity assignments for, (E), 25:28321 (CERN-70-30(Vol.2), pp 931-8)
energy levels of, spin-parity assignments for, (E), 25:28394
energy-level transitions from lutetium-168 beta and electron-capture decay, lifetimes and relative intensities as function of mode of production of lutetium-168, (E), 25:28321 (CERN-70-30(Vol.2), pp 931-8)
YTTERBIUM ISOTOPES Yb-169
electron-capture decay of, conversion-electron and gamma spectra, branching ratios, and log-ft values for, (E), 25:28432
energy levels from erbium-167 (α,2n) reactions, Coriolis-coupling analysis of, (E/T), 25:28394
energy levels from lutetium-169 decay, spin-parity assignments for, (E), 25:28436
energy levels from lutetium-169 decay, spin-parity assignments for, (E), 25:28433
energy-level transitions from erbium-167 (α,2n) reactions, Coriolis-coupling analysis of mixing ratios and probabilities for, (E/T), 25:28394
energy-level transitions from lutetium-169 decay, multipolarities for, (E), 25:28433
energy-level transitions from lutetium-169 decay, conversion coefficients and multipolarities for, (E), 25:28436
nuclear magnetic moment of, (T), 25:28394
use for brain scanning, review on international methods for, 25:26855
YTTERBIUM ISOTOPES Yb-170
energy levels of, spin-parity assignments for, (E), 25:28394
YTTERBIUM ISOTOPES Yb-172
energy levels of, deformation parameters for 4+, (E/T), 25:28411
proton reactions (p,t) at 51.7 MeV, spectra and DWBA analysis of differential cross sections from, (E/T), 25:28411
YTTERBIUM ISOTOPES Yb-174
energy levels of, analysis of nonrandom distributions of neutron resonance, (T), 25:28421
YTTERBIUM ISOTOPES Yb-176
decay of isomeric, (E), 25:28398
energy levels from thulium-176 beta decay, spin and parity for, (E), 25:28398
YTTERBIUM OXIDES
reactions with boron, effects of shock waves and temperature on, 25:27291
Yb--Yb_2O_3, phase studies of, 25:27302
YTTRIUM
abundance in lunar surface materials, (E), 25:27308
effects on electric conductivity, microhardness, and microstructure of titanium, 25:27223
separation from seawater by sorption on vessel walls and other materials, 25:26339
separation from uranium-barren sulfate leach liquors by solvent extraction using DEHPA, 25:26342
YTTRIUM ALLOYS AND SYSTEMS
Ce--Sb--Y, thermal capacity of Ce/sub x/Y/sub 1-x/Sb at 1.5 to 70°K, 25:27881
Co--Y, magnetization discontinuities in Co_9Y particles, 25:27885
Sb--Y, electron band structure of Ysb, intrinsic metallic character in, 25:27879
YTTRIUM CHLORIDES
$NdCl_3$--YCl_3-base, neodymium-145 magnetic hyperfine fields in hexahydrate of, Moessbauer-effect study of, 25:27924
YTTRIUM ISOTOPES Y-89
photon reactions (γ,p) with isobaric analog excitation, proton spectra from, (E), 25:28227
proton reactions (p,α) at 5 to 13 MeV, excitation functions for, (E), 25:28268
YTTRIUM ISOTOPES Y-90
effectiveness for therapy of joint diseases in human bones by synovial injection, 25:26873
radiation dose from particles of, following clothing contamination, 25:26748
YTTRIUM ISOTOPES Y-91
use as tracer for determining calcium metabolism in chickens, 25:26578 (CONF-680112-, pp 153-66)
YTTRIUM ISOTOPES Y-97
beta decay of, half-life for, (E), 25:28388
YTTRIUM ISOTOPES Y-98
beta decay of, half-life for, (E), 25:28388
YTTRIUM OXIDES
analysis for rare earths and other metals by solvent extraction and spectrography, 25:26168
reactions with boron, effects of shock waves and temperature on, 25:27291
Al_2O_3--Y_2O_3, phase studies of, using europium luminescence spectra as reference, 25:27303
Eu_2O_3--Y_2O_3, magnetic susceptibility down to 4°K, 25:27896
Ga_2O_3--Y_2O_3, phase studies of, using europium luminescence spectra as reference, 25:27303
HfO_2-base--Y_2O_3, composition and microstructure of, 25:27296
ThO_2--Y_2O_3, ionic transference numbers of electrolytes of, at high oxygen activities, 25:26262
ThO_2--Y_2O_3, oxygen activity for anionic conduction in $Th_{0.85}Y_{0.15}O_{1.925}$, at 775 to 1000°C, 25:27286

Z

ZINC
complexes with 5,7-diiodo-8-quinolinol, formation constants of, 25:26214
content in hail and rain samples from Nebraska and South Dakota, absorption spectrophotometer measurements of, 25:26366 (CONF-700601-, pp 109-20)
determination in marine silts by neutron activation and γ spectroscopy, 25:26190(R) (NYO-4150-9)
determination in thorium nitrates and zirconium nitrates by neutron activation, 25:26192
diffusion in sintered aluminum powder, relations of microhardness with solid state, 25:27222
electron correlation and density in, calculations using restricted Hartree--Fock approximation, 25:27467
fracture in liquid metal environments, adsorption-induced brittle, 25:27243
neutron elastic scattering at 3.2 MeV using polarized beam, optical-model analysis of, (T), 25:28248
shear constant for, calculation from axial ratios, 25:27240
ZINC ALLOYS AND SYSTEMS
embrittlement of dilute, by mercury, 25:27243
Al--Cr--Cu--Mg--Zn, analysis for trace amounts of silver by solvent extraction and atomic absorption spectrophotometry, 25:26169
Hg-base--Zn, effects of amalgams of, on embrittlement of aluminum, 25:27243
Zn--Zr, electron correlation effects in $ZrZn_2$, 25:27868
Zn--Zr, magnetic properties of $ZrZn_2$, 25:27875
ZINC FLUORIDES
reactions of calcium and, with thorium fluoride to prepare thorium, reduction, 25:27180 (NLCO-1080)
ZINC IONS
implantation in silicon at 50 keV, outdiffusion, lattice location, and electrical behavior of, 25:27856
ZINC ISOTOPES Zn-63
energy levels from gallium-63 beta decay, spin--parity assignments for, (E), 25:28338 (CERN-70-30(Vol.2), pp 1075-9)
ZINC ISOTOPES Zn-64
boron-11 reactions at 43 MeV with alpha and proton evaporation, statistical analysis for shell and angular momentum effects in, (T), 25:28266
effects on ir spectra of zinc oxinates, 25:26234
neutron reactions (n,p) with, cross sections for fast, (E), 25:28273
proton elastic scattering at 6.9 MeV, optical-model analysis of angular distributions from, (E), 25:28262
ZINC ISOTOPES Zn-65
content of oysters in estuary of North Sea in relation to distance from nuclear power plant, 25:26742
distribution in tissues of euphausiids and shrimp following ingestion, 25:26604
energy levels from gallium-65 beta decay, spin--parity assignments for, (E), 25:28338 (CERN-70-30(Vol.2), pp 1075-9)
separation from solutions by retention on zinc sulfide precipitates, 25:26199
uptake and distribution in endochondral growth sites of bones in rats, 25:26611
uptake and distribution in organs and tissues of rats, 25:26611
uptake by algae in Columbia River, effects of ion concentration on, 25:26593
ZINC ISOTOPES Zn-66
energy levels from gamma resonance scattering, widths for, (E), 25:28219 (NRCN-254)

energy-level transitions from proton reactions, branching ratios, gamma-ray angular distributions, and internal conversion coefficients for, (E/T), 25:28271
proton elastic scattering at 6.9 MeV, optical-model analysis of angular distributions from, (E), 25:28262
ZINC ISOTOPES Zn-67
proton elastic scattering at 6.9 MeV, optical-model analysis of angular distributions from, (E), 25:28262
ZINC ISOTOPES Zn-68
effects on ir spectra of zinc oxinates, 25:26234
ZINC ISOTOPES Zn-70
energy levels from isomeric copper-70 decay, spins and parities of, (E), 25:28221
proton elastic scattering at 6.9 MeV, optical-model analysis of angular distributions from, (E), 25:28262
ZINC SULFIDES
ion implantation and luminescence of manganese, terbium, and erbium in thin films of, 25:27844
reactions with cadmium oxide, Jost mechanisms in solid-state, 25:26210 (KFK-1312)
ZION POWER REACTOR, UNIT 1
thermal effluents from, effects on Lake Michigan, 25:28622
ZION POWER REACTOR, UNIT 2
thermal effluents from, effects on Lake Michigan, 25:28622
ZIRCALOY
analysis of, survey of methods for, 25:26171
brazing of fuel sheaths of, to low profile thermocouples using beryllium--zirconium alloy, method for induction, 25:27182 (R-69-CAP-8)
ZIRCALOY-2
tensile properties of fast neutron-irradiated, effects of zirconium hydride orientation on, 25:27198 (BMI-X-10276)
ZIRCONATES
production and uses of, review on, 25:27191
ZIRCONIUM
abundance in lunar surface materials, (E), 25:27308
analysis for hafnium, review on methods for, 25:26150
corrosion cracking of annealed and cold-worked, in hydrochloric acid--methanol mixtures, resistance to stress, 25:27173
determination by photometry using carboxy derivatives of 2,6,7-trihydroxy-9-phenyl-3H-xanthen-3-one, 25:26174
determination in hafnium, review on methods for, 25:26150
effects on spectrophotometric determination of beryllium and gallium, 25:26172
effects on stability of metastable β-molybdenum--titanium alloy, 25:27233
microstructure of crystal bar, transmission electron microscopy study of effects of cold rolling on, 25:27245 (INIS-mf-15)
neutron elastic scattering at 3.2 MeV using polarized beam, optical-model analysis of, (T), 25:28248
production and uses of, review on, 25:27191
separation from hafnium, review on methods for, 25:26150
sorption by tungsten single crystal planes, mechanisms of, 25:27241
ZIRCONIUM ALLOYS AND SYSTEMS
mechanical properties at 400 to 800°C, 25:27203 (INIS-mf-2)
production and uses of, review on, 25:27191
properties for cladding and structural uses in nuclear reactors, 25:27176 (INIS-mf-9)
properties for use as cladding, fuel, and reactor core components, 25:27204 (INIS-mf-3)
properties for use as fuel cans for thermal reactors, 25:27213
radiation effects on mechanical properties of, recovery from, 25:27265 (INIS-mf-5)
Al--Cu--Zr, magnetic properties of ZrCu/sub 2-x/Al/sub x/, 25:27875
Al--Mo--Sn--Ti-base--Zr, fatigue properties of, 25:27236
Al--Ni--Zr, phase studies of, 25:27258
Be--Cu--Nb--Zr-base, properties for use as structural material for reactors, 25:27190(P)
Be--Nb--Sb--Zr-base, properties for use as structural material for reactors, 25:27190(P)
Be--Nb--Sn--Zr-base, properties for use as structural material for reactors, 25:27190(P)
Be--Nb--Te--Zr-base, properties for use as structural material for reactors, 25:27190(P)
Be--Zr-base, properties of brazing alloy of, for attaching low profile thermocouples to Zircaloy fuel sheaths, 25:27182 (R-69-CAP-8)
C--Hf--Zr, thermodynamic properties of compound of, at 2440°K, 25:27283 (N-71-10590)
Co--Zr, superconductivity of intermetallic, (E), 25:27654
Cr--V--Zr, compatibility with flowing liquid sodium at 500 to 600°C, 25:27174
Cr--Zr-base, microstructure of, 25:27230
Cr--Zr-base, properties of, electric and mechanical, 25:27230
Fe--Zr, mechanical properties of Laves phase $ZrFe_2$, 25:27211 (UCRL-20301)
Fe--Zr, superconductivity of intermetallic Zr_2Fe, (E), 25:27654
Ga--Zr, superconductivity of intermetallic, (E), 25:27654
Ge--Ti-base--Zr, properties for use in brazing graphite or refractory metals, 25:27229(P)
Ir--Zr, superconductivity of intermetallic, (E), 25:27654
Mn--Zr-base, microstructure of, 25:27230
Mn--Zr-base, properties of, electric and mechanical, 25:27230
Mo--Ti-base--Zr, mechanical properties of, effects of aging on, 25:27233
Mo--Zr-base, internal friction at 4 to 300°K, 25:27215
Nb--Ti--Zr, magnetization of superconducting, dimensional effect in, (E), 25:27644 (KHFTI-70-8)
Nb--U-base--Zr, reactions with carbon dioxide, nitrogen, oxygen, and water vapor at 27 to 1000°C, kinetics of, 25:27210 (SC-DR-710124)
Nb--Zr, magnetization of superconducting, dimensional effect in, (E), 25:27644 (KHFTI-70-8)
Nb--Zr-base, internal friction at 4 to 300°K, 25:27215
Nb-base--Zr, hardness of irradiated and unirradiated, hot, 25:27236
Nb-base--Zr, properties of tubular coextruded joints of stainless steel to, effects of thermal cycling at 300 to 1600°F on, 25:27179 (N-71-10454)
Ni--Zr, superconductivity of intermetallic Zr_2Ni, (E), 25:27654
O--Ti--Zr, structure and ordering in, x-ray and neutron diffraction studies of, 25:27297
Rh--Zr, superconductivity of intermetallic Zr_2Rh, (E), 25:27654
Ru--Zr, properties of, mechanical and oxidation resistance, 25:27203 (INIS-mf-2)
U--Zr, separation of fission products from irradiated fuels of, by chlorination and pyrohydrolysis, 25:26332(T) (ORNL-tr-2410, pp 98-120)
V--Zr-base, internal friction at 4 to 300°K, 25:27215
V--Zr-base, microstructure of, 25:27230
V--Zr-base, properties of, electric and mechanical, 25:27230
Zn--Zr, electron correlation effects in $ZrZn_2$, 25:27868
Zn--Zr, magnetic properties of $ZrZn_2$, 25:27875
ZIRCONIUM BORIDES
boron-12 NMR in, quadrupole effects on spectra and coupling constants from, (E), 25:27923
nitrogen-12 NMR in, quadrupole effects on spectra and coupling constants from, (E), 25:27923
production and uses of, review on, 25:27191
ZIRCONIUM CARBIDES
determination as inclusions in steels by electron probe methods, 25:26160
electron band structure of, (E/T), 25:27907
production and uses of, review on, 25:27191
ZIRCONIUM HYDRIDES
effects of orientation of platelets of, on tensile properties of Zircaloy-2, 25:27198 (BMI-X-10276)
nuclear magnetic resonance at -190 to 300°C, 25:26261(T) (ORNL-tr-2439)
ZIRCONIUM ISOTOPES Zr-89
energy levels from niobium-89 beta decay, spin--parity assignments for, (E), 25:28215 (CERN-70-30(Vol.2), pp 1137)
ZIRCONIUM ISOTOPES Zr-90
energy levels from niobium-90 beta and electron-capture decay, spin--parity assignments for, (E), 25:28215 (CERN-70-30(Vol.2), pp 1137)
energy levels from resonances in yttrium-89 (p,α) reactions, widths for compound-nucleus, (E), 25:28268
energy levels of, E1 transitions of analog, (T), 25:28360
helium-3 reactions (He-3,d) at 24.8 MeV, deuteron spectra and angular distributions for, (E), 25:28363
photon reactions (γ,p) with isobaric analog excitation, proton spectra from, (E), 25:28227
proton elastic scattering using polarized beams, isobaric analog resonances in, (E), 25:28239
proton inelastic scattering with isobaric analog excitation, R-matrix analysis of, (T), 25:28364
ZIRCONIUM ISOTOPES Zr-91
energy levels from zirconium-90 proton scattering, spectroscopic factors for isobaric analog, (T), 25:28364
ZIRCONIUM ISOTOPES Zr-92
proton elastic scattering at 4.7 to 8.6 MeV with isobaric analog excitation, proton polarization in, (E), 25:28368
proton elastic scattering using polarized beams, isobaric analog resonances in, (E), 25:28239
ZIRCONIUM ISOTOPES Zr-94
proton elastic scattering using polarized beams, isobaric analog resonances in, (E), 25:28239
ZIRCONIUM ISOTOPES Zr-95
effects on reproductive behavior and spermatogenesis in male mice following subcutaneous injection, 25:26962
separation from irradiated aluminum--uranium and uranium--zirconium fuels by chlorination and pyrohydrolysis, 25:26332(T) (ORNL-tr-2410, pp 98-120)
separation of plutonium from, by solvent extraction using tridodecylamine, 25:26330(T) (ORNL-tr-2410, pp 14-78)
ZIRCONIUM ISOTOPES Zr-97
beta decay of, singles and γ--γ and γ--e coincidence spectra, branching ratios, and log-ft values for, (E), 25:28438

ZIRCONIUM NITRATES
analysis for trace amounts of impurities by neutron activation, 25:26192
ZIRCONIUM NITRIDES
determination as inclusions in steels by electron probe methods, 25:26160
production and uses of, review on, 25:27191
ZIRCONIUM OXIDES
production and uses of, review on, 25:27191
reactions with uranium nitride, Jost mechanisms in solid-state, 25:26210 (KFK-1312)
sorption by isomeric indium-113 and tin-113 for use in generators, 25:26341
PbO--TiO_2--ZrO_2, phase studies above 900°C, use of heating curves in, 25:27295
ZIRCONIUM SILICIDES
production and uses of, review on, 25:27191

REPORT NUMBER INDEX

Reports, conference papers and proceedings, numbered translations, and patents are included in this index. Each item is listed by report number; this is followed by the abstract number and a brief notation regarding public availability. The index entries show which reports are on file in the institutions listed on the back of the front cover (Dep.), which reports have been published in open-literature journals (journal citation), and which reports can be purchased (source and price). Whenever a report is identified by more than one number, the availability is given under the primary number, and a cross reference is given under the secondary report number.

The report number codes apply to USAEC reports unless designated otherwise. Non-USAEC reports are identified by parenthetical notes after the report codes; e.g., (non-AEC), (British), (Canadian), (French). The note (Misc.) identifies the codes used for both USAEC and non-USAEC reports. Patents are listed under the heading "PATENTS"; the country of origin is included in parentheses.

A comprehensive list of both USAEC and non-USAEC report codes is contained in the latest revision of TID-85, *Report Number Series Used by the Division of Technical Information in Cataloging Reports.* This information is also included in the Cumulative Report Number Index (issued annually).

Availability of USAEC Reports

All USAEC Reports abstracted in *Nuclear Science Abstracts* are available through one or more of the following sources:

(1) University and public libraries in the United States. A list of these organizations appears on the inside front cover of each issue of *NSA*.

(2) NCR Microcard Editions in Microcard and micronegative form. Orders and inquiries should be sent to: Order Processing Department, 365 South Oak Street, West Salem, Wisconsin 54669.

(3) National Technical Information Service, U. S. Department of Commerce, Springfield, Virginia 22151.

(4) Superintendent of Documents, U. S. Government Printing Office, Washington, D. C. 20402.

(5) National Cash Register Co., P. O. Box 3111, Oak Ridge, Tenn. 37830, in micronegative form. Purchase details available on request.

Availability of Non-USAEC Reports

U. S. Reports. Reports of U. S. Government agencies are available to the public from the National Technical Information Service (NTIS). If specific availability is not shown, inquiries may be directed to NTIS.

Non-U. S. Reports. Reports of atomic energy organizations of other countries are available from NTIS for U. S. sale only. Specific availability in the country of origin is shown, when known, at the report number entry. Otherwise, inquiries should be made to the organizations listed below:

AUSTRALIA

Australian Atomic Energy Commission Research Establishment. Available upon request from the Library, Australian Atomic Research Establishment, Private Mail Bag, Sutherland, New South Wales, Australia.

BELGIUM

Centre d'Étude de l'Energie Nucléaire. Available upon request to individuals and organizations from the Centre d'Etude de l'Energie Nucléaire (C.E.N.), Studiecentrum voor Kernenergie (S.C.K.), Technical Information Dept., MOL-DONK (Belgium).

CERN

CERN European Organization for Nuclear Research. Available without charge from CERN European Organization for Nuclear Research, Geneva 23, Switzerland. Copies are deposited in libraries throughout the world.

FRANCE

Commissariat à l'Energie Atomique. Inquiries for reports numbered 1-2199 should be addressed to Service Central de Documentation du C.E.A., Centre d'Etudes Nucléaires de Saclay, Boîte postale n° 2, 91. GIF-sur-YVETTE, FRANCE. Reports numbered 2200 and above are available from La Documentation Française, 31 quai Voltaire, 75, PARIS (7e), FRANCE.

Service Central de Protection contre les Rayonnements Ionisants. Copies are available from Ministere de la Santé Publique, Service Central de Protection contre les Rayonnements Ionisants, B.P. n° 78 Le Vesinet (France) Telex 25667.

GERMANY

Deutsches Elektronen-Synchrotron DESY. Copies are available from Deutsches Elektronen-Synchrotron DESY, Dokumentation, 2000 Hamburg 52, Notkestieg 1, Germany.

Gesellschaft für Kernforschung mbH (KFK). Copies are available from Gesellschaft für Kernforschung mbH, 75 Karlsruhe, Postfach 947, Germany. Copies are also deposited in many national nuclear centers in the world.

Kernforschungsanlage. Copies may be ordered from Zentralbibliothek der Kernforschungsanlage Jülich, Jülich, Bundesrepublik Deutschland.

Hahn-Meitner-Institute für Kernforschung. Available without charge from Hahn-Meitner-Institute für Kernforschung Ber-

lin, Bibliothek, Glienicker Strasse 100, 1 Berlin 39, Germany. Copies are deposited in many national nuclear centers in the world.

Johann-Wolfgang-Goethe Universität, Frankfurt Am Main, Institut für Kernphysik, (IKF). Copies are available from Gmelin Institut, 40–42 Varrentrappstrasse, Frankfurt (Main), West Germany.

ISRAEL

Israel Atomic Energy Commission. Available without charge from Israel Atomic Energy Commission, Soreq Nuclear Research Centre, Yavne, Israel.

ITALY

Centro Informazioni Studi Esperienze (CISE). For sale at CISE Press Office, Casella Postale 3986, Milano, Italy. Copies are deposited in the libraries of various nuclear centers in Italy and abroad.

Comitato Nazionale per l'Energia Nucleare. Copies are available from Comitato Nazionale per l'Energia Nucleare, Divisione Affari Internazionali e Studi Economici, Ufficio Pubblicazioni, Via Belisario, 15, Roma, Italy.

JAPAN

Japan Atomic Energy Research Institute (JAERI). Available from the Staff Supply Cooperative of Japan Atomic Energy Research Institute (JAERI), Tokai-mura, Naka-gun, Ibaraki-ken, Japan. Copies are deposited in depositories in Tokyo, Nagoya, and Osaka.

Nagoya University. Copies are available from Research Information Center, Institute of Plasma Physics, Nagoya University, Nagoya, Japan.

University of Tokyo. Available free of charge from Institute for Nuclear Study, University of Tokyo, Tanashi-Machi, Kitatama-gun, Tokyo, Japan.

NETHERLANDS

Reactor Centrum Nederland. For sale by Reactor Centrum Nederland, 112 Scheveningseweg, 's-Gravenhage, The Netherlands. Copies are deposited in university libraries in Holland and in many national nuclear centers in the world.

NEW ZEALAND

Institute of Nuclear Sciences. Copies are available from Librarian, N. Z. Institute of Nuclear Sciences, D.S.I.R., Private Bag, Lower Hutt, New Zealand. Copies are deposited in other countries.

PAKISTAN

Atomic Energy Center. Copies are available from Atomic Energy Center, P. O. Box 658, Lahore, (West Pakistan).

POLAND

Reports of the Polish nuclear institutes are published by the Nuclear Energy Information Center of the Government Commissioner for Use of Nuclear Energy. Copies are available free of charge from Nuclear Energy Information Center, Palace of Culture and Science, Warsaw, Poland.

SPAIN

Junta de Energia Nuclear. "JEN" reports are available without charge from Servicio de Documentation, Junta de Energia Nuclear, Ciudad Universitaria, Madrid (3), España.

SWITZERLAND

Eidgenössisches Institut für Reaktorforschung. "EIR" reports are available from Eidgenössisches Institut für Reaktorforschung, c/o Bibliothek, 5303 Würenlingen/Switzerland.

TURKEY

Turkish Atomic Energy Commission. Copies are available free of charge from T.A.E.C., Çekmece Nuclear Research Center, P. O. Box 1, Airport, Istanbul, Turkey.

Conferences

Published conference proceedings as well as individual unpublished papers from conferences are included in this index. A CONF number is assigned to the conference if published proceedings are received and also if only a single paper is received. The base number used is year-month-sequence. Thus, the number CONF-650101 indicates that the conference was held in 1965, in January, and that this was the first January 1965 conference so received. This number would be assigned to complete published proceedings. If individual papers are received, the base number is extended to include a paper number, e.g., CONF-650101-1. As additional papers are received, they will be assigned consecutive numbers in the series, CONF-650101-1, CONF-650101-2, etc. This numbering system ensures that all papers received from a conference will be associated with that conference in this index.

If published proceedings are received after the receipt of individual papers, the complete proceedings will be abstracted and the abstract number will appear in this index with the base CONF number.

Abbreviations Used in Availability Column

AECL	Reports of the Atomic Energy of Canada Limited are for sale by the Scientific Document Distribution Office, Atomic Energy of Canada Limited, Chalk River, Ontario, Canada.
CFSTI	See NTIS
DENM	Reports of the Atomic Energy Commission Research Establishment, Risö, are available on exchange from the Library, Danish Atomic Energy Commission, Risö, Roskilde, Denmark. Also for sale at the price shown from Jul. Gjellerup, Booksellers, 87 Sölvgade, Kobenhavn K., Denmark. Reports of Danatom are available on loan from Research Establishment, Risö, Roskilde, Denmark. Copies are available from Danatom, Aurehojvej 2, Hellerup, Denmark.
Dep.	AEC reports so designated are maintained in the organizations listed on the inside front cover of *NSA*. Prior to July 1, 1965, reports were deposited either in printed copy form or in microform. After that time, all reports have been in the form of micronegatives. Reports from other countries so designated are available in the United States at the organizations listed on the inside front cover of *NSA*.

DTIE Available from the U. S. Atomic Energy Commission, Division of Technical Information Extension, P. O. Box 62, Oak Ridge, Tennessee 37830. (Conference papers are available on loan only.)

EM Blueprints of AEC engineering drawings are available from NTIS, U. S. Department of Commerce, Springfield, Virginia 22151. Current prices of the CAPE-packages may be obtained from this address. TID-4100, available from the Division of Technical Information Extension, P. O. Box 62, Oak Ridge, Tennessee 37830, contains information on all the CAPE-packages for sale.

EUR For sale by Centrale de vente des publications des Communautés européennes 37, rue Glesener-Luxembourg.

GPO For sale by the Superintendent of Documents, Government Printing Office, Washington, D. C. 20402.

IAEA Available from the International Atomic Energy Agency, Vienna, Austria, and from its sales agencies in various countries throughout the world. A list of these agencies is found in each STI/DOC and STI/PUB publication.

NORW Reports from Forsvarets Forskningsinstitutt are available from Norwegian Defense Research Establishment, Library, P. O. Box 25, Kjeller, Norway.

"KR" reports are available on an exchange basis from the Library, Institutt for Atomenergi, Box 40, Kjeller, Norway.

Reports of the Norwegian Reactor School are available from the Library, Institutt for Atomenergi, P. O. Box 40, Kjeller, Norway.

NRC For sale by the National Research Council of Canada, Ottawa, Ontario, Canada.

NTIS For sale by the National Technical Information Service (NTIS), U. S. Department of Commerce, Springfield, Virginia 22151 at the following prices for eye legible copy:

1–300 pages	$3.00
301–600 pages	$6.00
601–900 pages	$9.00

Documents over 900 pages have special prices which may be obtained from NTIS. Microfiche copy of each separately bound document can be purchased for $0.95.

Reports issued by organizations outside the United States will be sold by NTIS *only to purchasers within the United States.*

Purchasers outside the United States may acquire such reports from the sources described elsewhere in these columns.

OECD Available from O. E. C. D., Publications 2, rue, André-Pascal, 75 Paris 16^{e}, France, and from its sales agencies in various countries throughout the world. A list of these agencies is found in each OECD publication.

SWED "AE" reports are for sale from Aktiebolaget Atomenergi, Library Section, Box 43041, Stockholm 43, Sweden. Microcopy of these reports is available from the International Documentation Center, Tumba, Sweden.

Reports of the VDDIT-series may be obtained from Aktiebolaget Atomenergi, Information Office, Scientific and Technical Information, Box 43041, Stockholm 43, Sweden.

Other series are not generally available to the public. Organizations in the Atomic Energy field may obtain copies from Aktiebolaget Atomenergi.

UK United Kingdom Atomic Energy Authority reports generally may be purchased from Her Majesty's Stationery Office, P. O. Box 569, London S.E.1. Copies of many UKAEA reports (particularly earlier ones) may be purchased in microcopy form from Micro Methods Ltd., East Ardsley, Wakefield, Yorkshire, England. Copies of UKAEA reports are deposited with the National Lending Library for Science and Technology and 10 public libraries in England; with the USAEC and (through USAEC) with NTIS; and in most national nuclear centers throughout the world. In the USA, UKAEA reports are available on a subscription basis, by subject category, from UNIPUB, Inc., P. O. Box 433, New York, N. Y. 10016, USA.

UN Mail orders should be directed to the Sales Section, Room 1059, United Nations Headquarters, New York, New York 10017.

ZAED Available from Zentralstelle für Atomkernenergie Dokumentation, 6000 Frankfurt/Main 90, P. O. Box 901069, Westendstr. 21, West Germany

Report No.	Abstract No.	Availability
AD-	(Misc.)	
711041	25-26920	NTIS, 20p.
AEC-tr-		
7102/1	25-26275	Dep. NTIS
AECL-	(Canadian)	
3670	25-28546	AECL $2.50
3749	25-28373	Can. J. Phys.; 49: 108-17(1 Jan 1971)
3801	25-28439	Dep. NTIS (U. S. Sales Only). AECL $2.50, 116p.
3802	25-26441	Dep. NTIS (U. S. Sales Only). AECL $0.50, 10p.
3803	25-26442	Dep. NTIS (U. S. Sales Only). AECL $0.50, 9p.
AED-C-	(Non-AEC)	
13-7	25-26443	Dep. NTIS (U. S. Sales Only), 46p.
AERE-R-	(British)	
6506	25-27837	Dep. NTIS, 13p.
AFML-TR-	(Non-AEC)	
69-209(Pt. 3)	25-27283	See N-71-10590
AI-AEC-		
12986	25-28726	Dep. NTIS, 41p.
AI-AEC-Memo-		
12717	25-28783	Dep. NTIS, 176p.
ANL-		
7607	25-28727	Dep. NTIS, 294p.
7701	25-28728	Dep. NTIS, 114p.
7734	25-26418	Dep. NTIS, 42p.
7759	25-28752	Dep. NTIS, 158p.
7764	25-28838	Dep. NTIS, 112p.
7784	25-27441	Dep. NTIS, 14p.
ANL-Trans-		
874	25-27838	Dep. NTIS
ANU-P-	(Australian)	
471	25-27309	Dep. NTIS (U. S. Sales Only), 19p.
487(2)	25-26489	Dep. NTIS (U. S. Sales Only), 81p.
502	25-28102	Dep. NTIS (U. S. Sales Only), 39p.
508	25-28206	Dep. NTIS (U. S. Sales Only), 8p.
511	25-28286	Dep. NTIS (U. S. Sales Only), 20p.
514	25-26490	Dep. NTIS (U. S. Sales Only), 25p.
516	25-26456	Dep. NTIS (U. S. Sales Only), 43p.
517	25-28207	Dep. NTIS (U. S. Sales Only), 18p.
518	25-28287	Dep. NTIS (U. S. Sales Only), 6p.
519	25-28103	Dep. NTIS (U. S. Sales Only), 14p.
521	25-28208	Dep. NTIS (U. S. Sales Only), 24p.
ARH-		
1920	25-26206	Dep. NTIS, 15p.
BARC-	(Non-AEC)	
529	25-26186	Dep. NTIS (U. S. Sales Only), 57p.
BAW-	(Misc.)	
1342	25-28729	Dep. NTIS, 117p.
1349	25-28730	Dep. NTIS, 127p.
1350	25-28731	Dep. NTIS, 103p.
1351	25-28732	Dep. NTIS, 85p.
1352	25-28733	Dep. NTIS, 90p.
1354	25-28734	Dep. NTIS, 68p.
1355	25-28685	Dep. NTIS, 233p.
1360	25-28735	Dep. NTIS, 37p.
BLG-	(Belgian)	
448	25-26207	Dep. NTIS (U. S. Sales Only), 13p.
450	25-28753	Dep. NTIS (U. S. Sales Only), 15p.
BMI-	(Misc.)	
171-133	25-28841	Dep. NTIS, 15p.
1898	25-28686	Dep. NTIS, 110p.
BMI-X-		
10276	25-27198	Dep. NTIS, 25p.
BNL-		
15601	25-26444	Dep. NTIS, 14p.
16000	25-28104	Dep. NTIS, 385p.
BNWL-		
1183-7	25-26187	Dep. NTIS, 39p.
1528	25-26681	Dep. NTIS, 68p.
1545	25-27244	Dep. NTIS, 14p.
BNWL-CC-		
2180	25-26208	Dep. NTIS, 13p.
BNWL-SA-		
2865	25-26437	Dep. NTIS, 17p.
3608	25-26178	Dep. NTIS, 12p.
3803	25-26188	Dep. NTIS, 15p.
BNWL-tr-		
66	25-28815	Dep. NTIS
BRH/DMRE-	(Non-AEC)	
71-1	25-26445	GPO $0.50
71-2	25-26815	GPO $0.60
CALT-		
822-26	25-28842	Dep. NTIS, 13p.
822-27	25-28843	Dep. NTIS, 22p.
822-28	25-28844	Dep. NTIS, 7p.
CAPE-		
2063	25-26430	EM
2064	25-26431	EM
CEA-Bib-	(French)	
190	25-26423	Dep. NTIS (U. S. Sales Only), 44p.
CEA-CONF-	(French)	
1671	25-27199	Dep. NTIS (U. S. Sales Only), 16p.
1711	25-26566	Dep. NTIS (U. S. Sales Only), 14p.
CEA-N-	(French)	
1171	25-27839	Dep. NTIS (U. S. Sales Only), 95p.
1341	25-26328	For translation see ORNL-tr-2410
1344(2)	25-28654	Dep. NTIS (U. S. Sales Only), 155p.
1349	25-28677	For translation see ORNL-tr-2451
1358	25-28149	For translation see ORNL-tr-2419
1385	25-28799	Dep. NTIS (U. S. Sales Only), 39p.
1405	25-28754	Dep. NTIS (U. S. Sales Only), 82p.
1406	25-28755	Dep. NTIS (U. S. Sales Only), 56p.
1430	25-26545	Dep. NTIS (U. S. Sales Only), 12p.
CEA-R-	(French)	
4121	25-28288	Dep. NTIS (U. S. Sales Only), 166p.
4138	25-27865	Dep. NTIS (U. S. Sales Only), 142p.
4166	25-26546	Dep. NTIS (U. S. Sales Only), 55p.
CENPD-	(Non-AEC)	
11	25-28697	
CERN-	(European Organization for Nuclear Research)	
70-30(Vol. 1)	25-28440	
70-30(Vol. 2)	25-28308	
71-8	25-28007	Dep. NTIS (U. S. Sales Only), 81p.
CLOR-	(Polish)	
81/D	25-26357	Dep. NTIS (U. S. Sales Only), 47p.
82/D	25-26516	Dep. NTIS (U. S. Sales Only), 22p.
CNEA-	(Argentinean)	
285	25-26179	Dep. NTIS (U. S. Sales Only), 7p.
287	25-26457	Dep. NTIS (U. S. Sales Only), 31p.
288	25-26151	Dep. NTIS (U. S. Sales Only), 11p.
CNRS-CPT-	(French)	
70-P-325	25-27925	Dep. CFSTI (U. S. Sales Only), 14p.
70-P-352	25-27926	Dep. NTIS (U. S. Sales Only), 18p.
CONF-630513-	(5th All-Union Scientific-Technical Geophysical Conference, Novosibirsk, U.S.S.R., May 31-June 5, 1963)	
1	25-26352	Dep. NTIS (U. S. Sales Only)
CONF-660314-	(20th Annual Symposium on Fundamental Cancer Research, Houston, Tex., Mar. 7--9, 1966)	
	25-26791	Baltimore; Williams and Wilkins Company (1967). 786p. $16.00
CONF-660843-	(1st Symposium of the International Study Group for Ergophthalmology, Munich, Germany, Aug, 14-19, 1966)	
(Vol.1)	25-27051	Basel; S. Karger AG (1969). 395p. $17.75
CONF-670853-	(Panel on Insect Ecology as Related to Control of Noxious Insects by The Sterile-Male Technique, Vienna, Austria, Aug. 7-11, 1967)	
	25-27137	See STI/PUB-223
CONF-670997-	(Conference on The Post-Natal Development of Phenotype, Prague, Czechoslovakia, Sept. 18-22, 1967)	
	25-26696	London; Butterworth and Company Limited (1970). 420p. 160s
CONF-671092-	(Conference on Developments in the Structural Chemistry of Alloy Phases, Cleveland, Ohio, Oct. 16, 1967)	
	25-27260	New York; Plenum Publishing Corporation (1969). 298p. $12.50
CONF-671093-	(S.I.F. Congress Conference, Bologna, Italy, Oct. 1967)	
1	25-28860	See LA-tr-71-28

Report No. Abstract No. Availability

CONF-680112- (Conference on the Application of Nuclear Energy to Agricultural Productivity, Santiago, Chile, Jan. 9-12, 1968)
25-27127

CONF-680535- (14th National Conference of the Italian Association for Health Physics and Protection from Radiation, Formia, Italy, May 29-31, 1968)
24 25-26559 Minerva Fisiconucl.; 13: 219-24 (Jul-Sep 1969)

CONF-680601- (14th Annual Meeting of the American Nuclear Society, Toronto, Ontario, Canada, June 9-13, 1968)
59 25-28761 See NASA-CR-72409

CONF-680675- (2nd Symposium of the International Study Group for Ergophthalmology, Amsterdam, Netherlands, June 18, 1968)
(Vol.2) 25-27051 Basel; S. Karger AG (1969). 395p. $17.75

CONF-680942- (4th European Regional Conference on Electron Microscopy, Rome, Italy, Sept. 1-7, 1968)
(Vol.2) 25-26565 Rome; Tipografia Poliglotta Vaticana (1968). 609p

CONF-680983- (International Conference on Conduction Processes in Dielectric Liquids, Grenoble, France, Sept. 17-19, 1968)
25-26470 Paris; Centre National de la Recherche Scientifique (1970). 541p

CONF-680984- (5th International Congress on X-Ray Optics and Microanalysis, Tubingen, Germany, Sept. 9-14, 1968)
25-26155 Berlin; Springer-Verlag (1969). 622p. $54.50

CONF-690310- (2nd Conference on Nuclear Isospin, Pacific Grove, Calif., Mar. 13-15, 1969)
25-28455 New York; Academic Press, Inc. (1969). 866p. $22.00

CONF-690455- (Conference on Transport Processes in Inorganic Nonmetallic Raw Material and Structure of these Materials, Mainz, Germany, Apr. 10-11, 1969)
1 25-26210 See KFK-1312

CONF-690510- (DECUS Symposium, Wakefield, Mass., May 12-13, 1969)
25-26554 Maynard, Mass.; Digital Equipment Computer Users Society (1969). 390p

CONF-690621- (2nd Conference on Toxicity, Rochester, N.Y., June 12-16, 1969)
25-26608 Springfield, Ill.; Charles C Thomas, Publisher (1970). 410p

CONF-690651- (Polyblends and Composites Conference, Brooklyn, N. Y., June 6-7, 1969)
25-27271 Appl. Polym. Symp.; No. 15, 1-292(1970)

CONF-690655- (Artificial Heart Program Conference, Washington, D.C., June 9-13, 1969)
25-26899 Bethesda, Md.; Department of Health, Education, and Welfare (1969). 1139p. GPO $10.00

CONF-690820- (Informal Meeting on Renormalization Theory, Trieste, Italy, Aug. 25029, 1969)
(Summ.) 25-28060 See IC-69/121

CONF-690971- (3rd Intercorrelated Satellite Observations Related To Solar Events, Noordwijk, The Netherlands, Sept. 16-19, 1969)
25-27531 New York; Springer-Verlag New York Inc. (1970). 644p. $38.20

CONF-691056- (Symposium on The Irradiation of Potatoes, Brussels, Belgium, Oct. 1-2, 1969)
25-27141 Brussels, Bureau EURISOTOP (1970). 173p

CONF-691057- (Biological Effects of Radiation Conference, Sao Paulo, Brazil, Oct. 6-17, 1969)
25-27036

CONF-691114- (90th Annual Meeting on American Society of Mechanical Engineers, Los Angeles, Calif., Nov. 16-20, 1969)
7 25-27200 ASME, New York $1.50

CONF-700117- (20th Annual Conference on Nuclear Spectroscopy and Nuclear Structure, Leningrad, U.S.S.R., Jan. 28-Feb. 5, 1970)
1 25-28163 See ITF-70-100-P

CONF-700204- (IAEA Meeting on Research Reaction Utilization, Rome, Italy, Feb. 2-6, 1970)
3 25-28781 pp 57-72 of Research Reactor Utilization. Vol. 1. Vienna; International Atomic Energy Agency (1970)
4 25-28776 pp 117-22 of Research Reactor Utilization. Vol. 1. Vienna; International Atomic Energy Agency (1970)
5 25-28779 pp 185-206 of Research Reactor Utilization. Vol. 1. Vienna; International Atomic Energy Agency (1970)
6 25-28774 pp 27-45 of Research Reactor Utilization. Vol. 1. Vienna; International Atomic Energy Agency (1970)
7 25-28780 pp 89-116 of Research Reactor Utilization. Vol. 1. Vienna; International Atomic Energy Agency (1970)
10 25-28778 pp 167-76 of Research Reactor Utilization. Vol. 1. Vienna; International Atomic Energy Agency (1970)
11 25-28772 pp 47-56 of Research Reactor Utilization. Vol. 1. Vienna; International Atomic Energy Agency (1970)
12 25-28775 pp 225-49 of Research Reactor Utilization. Vol. 1. Vienna; International Atomic Energy Agency (1970)
13 25-28777 pp 149-66 of Research Reactor Utilization. Vol. 1. Vienna; International Atomic Energy Agency (1970)

CONF-700218- (Symposium on Materials Science Research, Bangalore, India, Feb. 24, 1970)
1 25-27203 See INIS-mf-2
4 25-27176 See INIS-mf-9
5 25-27280 See INIS-mf-12
7 25-27245 See INIS-mf-15
11 25-27204 See INIS-mf-3
12 25-27282 See INIS-mf-14
13 25-27279 See INIS-mf-11
14 25-27205 See INIS-mf-19
15 25-27281 See INIS-mf-13
16 25-27265 See INIS-mf-5

CONF-700337- (Conference on Heavy Ion Sources, Washington, D.C., Mar. 13, 1970)
25-27436 See WASH-1159

CONF-700503- (3rd International Conference on Magnet Technology, Hamburg, Germany, May 19-22, 1970)
9 25-28111 See KFK-1218

CONF-700505- (2nd Congress of the International Radiation Protection Association, Brighton, England, May 3-8, 1970)
19 25-26773 Radioprotection; 5: 263-70(1970)
20 25-26760 Radioprotection; 5: 271-80(1970)
21 25-26747 Radioprotection; 5: 281-91(1970)
22 25-26503 Radioprotection; 5: 293-304(1970)
23 25-26607 Radioprotection; 5: 305-10(1970)
24 25-26483 Radioprotection; 5: 311-22(1970)

CONF-700524- (Digital Equipment Corporation Users Society Spring Symposium, Atlantic City, N.J., May 4, 1970)
25-26558 Maynard, Mass.; Digital Equipment Computer Users' Society (1970). 361p

CONF-700550- (International Power System Fair and Symposium, Oslo, Norway, May 19-24, 1970)
25-28522

CONF-700552- (Meeting on the Problems Concerning the Protection of Personnel Handling Short-Lived Radioelements in Hospitals, Saclay, France, May 12, 1970)
25-26762 J. Biol. Med. Nucl.; Special No., 1-22(1970)

CONF-700556- (Italian-Polish Meeting, Warsaw, Poland, May 26-June 6, 1970)
1 25-27293 See RT/ING-(70)21

CONF-700557- (Meeting on Mechanical Flow Processes in Gas Centrifuges, Porz-Wahn, Germany, May 14, 1970)
3 25-26424 Dep. NTIS (U. S. Sales Only)

Report No. Abstract No. Availability

CONF-700601- (Precipitation Scavenging Meeting, Richland, Wash., June 2-4, 1970)
25-26358 Dep. NTIS, 508p.

CONF-700616- (Symposium on Feedback and Dynamic Control of Plasmas, Princeton, N.J., June 18-19, 1970)
(Vol.1) 25-27752 New York; American Institute of Physics (1970). 374p

CONF-700624- (Conference on Anelastic Effects Due to Defects and Phase Transformations in Solids, Lausanne, Switzerland, June 24, 1970)
3 25-27199 See CEA-CONF-1671

CONF-700641- (1st Brazilian Symposium on Radioisotopes, Rio de Janeiro, Brazil, June 23-27, 1970)
(Abstr.) 25-26436 Rio de Janeiro; Comissao Nacional de Energia Nuclear (1970). 64p

CONF-700643- (16th Annual Meeting on Space Station and Manned Planetary Exploration, Anaheim, Calif., June 8-10, 1970)
25-26786 Tarzana, Calif.; American Astronautical Society (1970). 484p
25-26784 Tarzana, Calif.; American Astronautical Society (1970). 602p

CONF-700646- (Radioisotope Production Technology Development Meeting, Oak Ridge, Tenn., June 2-3, 1970)
1 25-26452 Isotop. Radiat. Technol.; 8: 350-9 (1971)

CONF-700648- (3rd Conference on Statistical Physics and Physical Kinetics, L'vov, U.S.S.R., June 1970)
3 25-27643 See ITP-70-90-E

CONF-700810- (Symposium on Environmental Aspects of Nuclear Power Stations, New York, N.Y., Aug. 10-14, 1970)
25-28621 See STI/PUB-261

CONF-700815- (Conference on the Properties of Nuclei Far from the Region of Beta-Stability, Leysin, Switzerland, Aug. 31-Sept. 4, 1970)
(Vol.1) 25-28440 See CERN-70-30(Vol.1)
(Vol.2) 25-28308 See CERN-70-30(Vol.2)

CONF-700833- (Symposium on Dynamics Studies with Radioisotopes in Clinical Medicine and Research, Rotterdam, Netherlands, Aug. 31-Sept. 4, 1970)
25-26567 See STI/PUB-263
1 25-26566 See CEA-CONF-1711

CONF-700903- (4th Foratom Congress on Industrial Aspects of the Nuclear Fuel Cycle in Europe, Stockholm, Sweden, Sept. 21-23, 1970)
15 25-26395 Dep. NTIS (U. S. Sales Only), 3p.
16 25-26396 Dep. NTIS (U. S. Sales Only), 14p.
18 25-27272 Dep. NTIS (U. S. Sales Only), 6p.

CONF-700905- (Symposium on Developments in the Management of Low and Intermediate Level Radioactive Wastes, Aix-en-Provence, France, Sept. 7-11, 1970)
13 25-26451 See SGAE-RT-33/1970

CONF-701041- (Symposium on Reliability, Chalk River, Ontario, Canada, Oct. 14-15, 1970)
25-28546 See AECL-3670

CONF-701042- (38th National Meeting of the Operations Research Society of America, Detroit, Mich., Oct. 27-30, 1970)
1 25-26444 See BNL-15601

CONF-701046- (Small and Medium Power Reactors Symposium, Oslo, Norway, Oct. 12-16, 1970)
25-28529 See STI/PUB-267

CONF-701101- (Fall Joint Computer Conference, Houston, Tex., Nov. 19-21, 1970)
25-26498 Maynard, Mass.; Digital Equipment Computer Users Society (1970). 335p

CONF-701104- (16th Annual Conference on Magnetism and Magnetic Materials, Miami Beach, Fla., Nov. 17-20, 1970)
25-27869 J. Appl. Phys.; 42: 1243-1816(15 Mar 1971)

CONF-701119- (12th Symposium on Rock Mechanics, Rolla, Mo., Nov. 16-18, 1970)
1 25-26354 See SC-R-70-4402

Report No. Abstract No. Availability

CONF-710106- (Conference on Fundamental Interactions at High Energy, Coral Gables, Fla., Jan. 20-22, 1971)
6 25-28008 See UCRL-73073

CONF-710210- (Seminar on Test Requirements for Packaging for the Transport of Radioactive Materials, Vienna, Austria, Feb. 8-12, 1971)
1 25-26441 See AECL-3802
2 25-26442 See AECL-3803

CONF-710212- (Analog-to-Digital Symposium, Albuquerque, N.Mex., Feb. 2, 1971)
1 25-28903 See UCRL-73103

CONF-710301- (3rd Conference on Neutron Cross Sections and Technology, Knoxville, Tenn., Mar. 15-17, 1971)
2 25-28349 See KAPL-P-3930

CONF-710302- (Meeting on New Development in Reactor Mathematics and Applications, Idaho Falls, Idaho, Mar. 29-31, 1971)
1 25-28801 See DP-MS-70-78

CONF-710304- (Symposium on Natural and Manmade Radiation in Space, Las Vegas, Nev., Mar. 1-5, 1971)
5 25-26178 See BNWL-SA-3608
6 25-28784 See ORNL-TM-3365

CONF-710305- (100th Annual AIME Centennial Meeting, New York, N.Y., Mar. 1-4, 1971)
1 25-27180 See NLCO-1080

CONF-710307- (Meeting of the Seismological Society of America, Riverside, Calif., Mar. 25, 1971)
1 25-26411 See SC-DC-713865

CONF-710308- (National Particle Accelerator Conference, Chicago, Ill., Mar. 1-3, 1971)
1 25-28123 See UCRL-73075
2 25-28116 See UCRL-20165
3 25-28117 See UCRL-20166
4 25-28118 See UCRL-20177
5 25-28120 See UCRL-20406
6 25-28119 See UCRL-20194
10 25-28122 See UCRL-20633
12 25-28121 See UCRL-20620

CONF-710309- (Conference on the Phenomenology of Particle Physics, Pasadena, Calif., Mar. 25-26, 1971)
1 25-28003 See PURC-4159-22

CONF-710402- (Meeting on Neutron Sources and Applications, Augusta, Ga., Apr. 18-21, 1971)
2 25-26188 See BNWL-SA-3803

CONF-710405- (62nd Meeting of the American Association for Cancer Research, Chicago, Ill., Apr. 8-10, 1971)
(Abstr.) 25-26789 Proc. Amer. Ass. Cancer Res.; 12: 1-123(Mar 1970)

CONF-710409- (17th Annual Meeting and Equipment Exposition, Los Angeles, Calif., Apr. 26-30, 1971)
1 25-28900 See UCRL-72748

CONF-710410- (8th Space Congress Conference, Cocoa Beach, Fla., Apr. 20-23, 1971)
1 25-28901 See UCRL-73063

CONF-710412- (Instrument Society of America Meeting, Richland, Wash., Apr. 13, 1971)
1 25-28667 See HEDL-SA-170

CONF-710413- (American Physical Society Meeting, Washington, D.C., Apr. 26-29, 1971)
1 25-27969 See PURC-4159-19

CONF-710506- (IEEE Region 6th Conference, Sacramento, Calif., May 11-13, 1971)
1 25-28902 See UCRL-73080

CONF-710507- (Symposium on Flow--Its Measurement and Control in Science and Industry, Pittsburgh, Pa., May 9-14, 1971)
1 25-28855 See GAT-T-1649

COO-
38-740 25-26694 Genetics; 66: 475-85(Nov 1970)
38-746 25-26719 Genetics; 66: 635-51(Dec 1970)
256-102 25-28845 Dep. NTIS, 12p.
1105-164 25-26517 Dep. NTIS, 129p.
1182-34 25-26260 Dep. NTIS, 26p.
1469-178 25-28846 Dep. NTIS, 87p.
1599-32 25-28847 Dep. NTIS, 35p.

Report No.	Abstract No.	Availability
1631-27	25-28848	Dep. NTIS, 12p.
1683-32	25-28849	Dep. NTIS, 10p.
1701-16	25-28850	Dep. NTIS, 8p.
1746-54	25-28216	Dep. NTIS, 27p.
1764-64	25-28507	Rend. Scu. Int. Fis. Enrico Fermi; 40: 380-427([1970])
1793-6	25-26619	Dep. NTIS, 11p.
2109-3	25-28800	Dep. NTIS, 47p.
2118-5	25-28851	Dep. NTIS, 106p.
CU-	(Misc.)	
4203-1	25-28852	Dep. NTIS, 10p.
DEMO-	(Greek)	
70/11	25-27826	Dep. NTIS (U. S. Sales Only), 15p.
DESY-	(German)	
70/59	25-27827	Dep. NTIS (U. S. Sales Only), 11p.
71/6	25-28045	Dep. NTIS, 11p.
71/7	25-27980	Dep. NTIS (U. S. Sales Only), 38p.
71/8	25-27960	Dep. NTIS (U. S. Sales Only), 35p.
71/9	25-27950	Dep. NTIS (U. S. Sales Only), 49p.
71/10	25-28022	Dep. NTIS (U. S. Sales Only), 37p.
71/11	25-27981	Dep. NTIS (U. S. Sales Only), 24p.
71/12	25-27982	Dep. NTIS (U. S. Sales Only), 18p.
DESY-SR-	(German)	
71/1	25-28853	Dep. NTIS (U. S. Sales Only), 11p.
DOCKET-1155-	(LaCrosse Boiling Water Reactor) (AEC)	
112	25-28555	Dep. NTIS, 2p.
DOCKET-50003-	(Indian Point Station; See Also DOCKET-50247, DOCKET-50286) (Non-AEC)	
67	25-28556	Dep. NTIS, 2p.
DOCKET-50010-	(Dresden Nuclear Power Station; See also DOCKET-50237 and DOCKET-50249) (Non-AEC)	
84	25-28557	Dep. NTIS, 2p.
DOCKET-50016-	(Enrico Fermi Atomic Power Plant) (Non-AEC)	
107	25-28587	Dep. NTIS, 3p.
108	25-28558	Dep. NTIS, 14p.
109	25-28559	Dep. NTIS, 12p.
DOCKET-50133-	(Humboldt Bay Power Plant) (Non-AEC)	
53	25-28560	Dep. NTIS, 2p.
54	25-28588	Dep. NTIS, 4p.
55	25-28589	Dep. NTIS, 4p.
DOCKET-50146-	(Saxton Nuclear Experimental Corporation) (Non-AEC)	
71	25-28590	Dep. NTIS, 4p.
DOCKET-50155-	(Big Rock Point Reactor) (Misc.)	
78	25-28561	Dep. NTIS, 11p.
DOCKET-50171-	(Peach Bottom Atomic Power Station; See also DOCKET-50277 and DOCKET-50278) (Non-AEC)	
82	25-28591	Dep. NTIS, 28p.
83	25-28562	Dep. NTIS, 9p.
DOCKET-50201-	(West Valley Reprocessing Plant--Formerly Spent Fuel Processing Plant) (Misc.)	
67	25-26323	Dep. NTIS, 2p.
68	25-26324	Dep. NTIS, 15p.
DOCKET-50206-	(San Onofre Nuclear Generating Station) (Misc.)	
111	25-28563	Dep. NTIS, 6p.
DOCKET-50213-	(Connecticut Yankee Atomic Power Plant) (Misc.)	
102	25-28592	Dep. NTIS, 10p.
103	25-28593	Dep. NTIS, 10p.
104	25-28594	Dep. NTIS, 7p.
DOCKET-50220-	(Nine Mile Point Nuclear Station) (Non-AEC)	
62	25-28595	Dep. NTIS, 58p.
DOCKET-50231-	(Southwest Experimental Fast Oxide Reactor) (Non-AEC)	
74	25-28706	Dep. NTIS, 29p.
75	25-28707	Dep. NTIS, 32p.
76	25-28736	Dep. NTIS, 7p.
77	25-28708	Dep. NTIS, 28p.
78	25-28709	Dep. NTIS, 5p.
DOCKET-50237-	(Dresden Nuclear Power Station, See also DOCKET-50249) (Non-AEC)	
145	25-28564	Dep. NTIS, 2p.
146	25-28596	Dep. NTIS, 177p.
148	25-28597	Dep. NTIS, 180p.
151	25-28565	Dep. NTIS, 2p.
152	25-28598	Dep. NTIS, 36p.
153	25-28599	Dep. NTIS, 4p.
154	25-28600	Dep. NTIS, 3p.
155	25-28566	Dep. NTIS, 4p.

Report No.	Abstract No.	Availability
DOCKET-50244-	(Robert Emmett Ginna Nuclear Power Plant, Formerly Brookwood Nuclear Station) (Non-AEC)	
69	25-28601	Dep. NTIS, 5p.
DOCKET-50245-	(Millstone Point Nuclear Power Station) (Non-AEC)	
21	25-28602	Dep. NTIS, 3p.
65	25-28603	Dep. NTIS, 5p.
66	25-28604	Dep. NTIS, 2p.
DOCKET-50249-	(Dresden Nuclear Power Station; See also DOCKET-50237) (Non-AEC)	
63	25-28599	See DOCKET-50237-153
64	25-28605	Dep. NTIS, 3p.
DOCKET-50250-	(Turkey Point, See also DOCKET-50251) (Non-AEC)	
43	25-28606	Dep. NTIS, 7p.
DOCKET-50251-	(Turkey Point, See also DOCKET-50250) (Non-AEC)	
39	25-28606	See DOCKET-50250-43
DOCKET-50255-	(Palisades Plant) (Non-AEC)	
37	25-28607	Dep. NTIS, 3p.
DOCKET-50261-	(H. B. Robinson) (Non-AEC)	
55	25-28567	Dep. NTIS, 8p.
56	25-28568	Dep. NTIS, 2p.
57	25-28569	Dep. NTIS, 5p.
58	25-28570	Dep. NTIS, 2p.
DOCKET-50266-	(Point Beach Nuclear Plant) (Non-AEC)	
46	25-28571	Dep. NTIS, 3p.
DOCKET-50267-	(Fort St. Vrain Nuclear Generating Station) (Non-AEC)	
28	25-28608	Dep. NTIS, 286p.
DOCKET-50268-	(Midwest Fuel Recovery Plant) (Non-AEC)	
7	25-26325	Dep. NTIS, 26p.
DOCKET-50271-	(Vermont Yankee Nuclear Power Station) (Non-AEC)	
49	25-28609	Dep. NTIS, 158p.
DOCKET-50280-	(Surry Power Station, See also DOCKET-50281) (Non-AEC)	
38	25-28610	Dep. NTIS, 54p.
DOCKET-50281-	(Surry Power Station, See also DOCKET-50280) (Non-AEC)	
38	25-28610	See DOCKET-50280-38
DOCKET-50289-	(Three Mile Island Nuclear Station) (Non-AEC)	
34	25-28611	Dep. NTIS, 83p.
DOCKET-50293-	(Pilgrim Nuclear Power Station) (Non-AEC)	
46	25-28612	Dep. NTIS, 4p.
47	25-28613	Dep. NTIS, 4p.
48	25-28614	Dep. NTIS, 2p.
DOCKET-50309-	(Maine Yankee Atomic Power Company) (Non-AEC)	
33	25-28615	Dep. NTIS, 163p.
DOCKET-50338-	(North Anna Power Station; See also DOCKET-50339) (Non-AEC)	
28	25-28616	Dep. NTIS, 5p.
29	25-28617	Dep. NTIS, 6p.
DOCKET-50339-	(North Anna Power Station; See also DOCKET-50338) (Non-AEC)	
27	25-28616	See DOCKET-50338-28
28	25-28617	See DOCKET-50338-29
DOCKET-50348-	(Joseph M. Farley Nuclear Plant, Units 1 and 2, Formerly Seala Nuclear Plant, See also DOCKET-50364) (Non-AEC)	
19	25-28618	Dep. NTIS, 293p.
DOCKET-50364-	(Joseph M. Farley Nuclear Plant, Units 1 and 2, See also DOCKET-50348) (Non-AEC)	
13	25-28618	See DOCKET-50348-19
DOCKET-50367-	(Bailly Generating Station Nuclear 1), (Non-AEC)	
12	25-28619	Dep. NTIS, 300p.
DOCKET-50368-	(Arkansas Nuclear One) (Non-AEC) (Unit 2)	
8	25-28620	Dep. NTIS, 258p.
DP-		
1246	25-27828	Dep. NTIS, 82p.
DP-MS-		
70-78	25-28801	Dep. NTIS, 8p.
DP-Report-	(British)	
432	25-26438	Dep. NTIS (U. S. Sales Only), 81p.
DPC-		

Report No.	Abstract No.	Availability
71-8	25-28555	See DOCKET-1155-112
DPSPU-		
71-124-1	25-26446	Dep. NTIS, 66p.
DUN-SA-		
166	25-28527	Dep. NTIS, 12p.
E-	(Misc.)	
5607	25-28450	See N-70-42846
5680	25-27209	See N-71-11662
5798	25-27179	See N-71-10454
5884	25-26413	See N-71-10455
EGG-		
1183-1465	25-28854	Dep. NTIS, 47p.
EIR-	(Swiss)	
188	25-28145	Dep. NTIS (U. S. Sales Only), 54p.
ENDF-		
142	25-28148	See ORNL-TM-3266
143	25-28657	See HEDL-TME-71-36
EUR-	(European Atomic Energy Community)	
4167	25-26326	See KFK-911
4549	25-27201	Dep. NTIS (U. S. Sales Only). EUR FF 4.45, 22p.
4552	25-28819	Dep. NTIS (U. S. Sales Only). EUR Lit. 500,-, 26p.
4553	25-28679	Dep. NTIS (U. S. Sales Only). EUR Lit. 1.250, 72p.
4554	25-28802	Dep. NTIS (U. S. Sales Only). EUR Lit. 1.560, 88p.
4555	25-28803	Dep. NTIS (U. S. Sales Only). EUR Lit. 2.180, 128p.
4556	25-28820	Dep. NTIS (U. S. Sales Only). EUR Lit. 750,-, 38p.
4562	25-27202	Dep. NTIS (U. S. Sales Only). EUR FF 11,-, 74p.
4601	25-28146	Dep. NTIS (U. S. Sales Only). EUR F.Fr. 13.80, 90p.
EURFNR-	(European Atomic Energy Community)	
803	25-28756	Dep. NTIS
824	25-28632	Dep. NTIS
830	25-28655	Dep. NTIS
835	25-28804	Dep. NTIS
836	25-28690	Dep. NTIS
842	25-28656	Dep. NTIS
898	25-28805	Dep. NTIS (U. S. Sales Only), 22p.
FEI-	(Russian)	
203	25-27927	Dep. NTIS (U. S. Sales Only), 7p.
FRDC/FEWP/P-	(British)	
(70)559	25-27266	See RD/B/N-1812
FRL-	(British)	
7	25-26397	Dep. NTIS (U. S. Sales Only), 33p.
GA-	(Misc.)	
10399	25-28633	Dep. NTIS, 99p.
GAT-T-		
1649	25-28855	Dep. NTIS, 18p.
GEAP-	(Misc.)	
10010-27	25-28757	Dep. NTIS, 62p.
10028--37	25-28691	Dep. NTIS, 109p.
10207-23	25-28680	Dep. NTIS, 58p.
10221-5	25-26419	Dep. NTIS, 26p.
10221-6	25-28681	Dep. NTIS, 18p.
GEMP-	(Misc.)	
714	25-27292	Dep. NTIS, 38p.
GESP-	(Non-AEC)	
31	25-28761	See NASA-CR-72409
HEDL-SA-		
170	25-28667	Dep. NTIS, 22p.
HEDL-TME-		
71-26	25-28710	Dep. NTIS, 23p.
71-36	25-28657	Dep. NTIS, 299p.
71-39	25-28856	Dep. NTIS, 41p.
HW-		
76299	25-26447	Dep. NTIS, 72p.
IAE-	(Russian)	
1972	25-27669	Dep. NTIS (U. S. Sales Only), 47p.
1986	25-27792	Dep. NTIS (U. S. Sales Only), 36p.
2000	25-28162	Dep. NTIS (U. S. Sales Only), 20p.
2001	25-27448	Dep. NTIS (U. S. Sales Only), 23p.
IAEA-R-	(International Atomic Energy Agency)	
362-F	25-27135	NTIS (U. S. Sales Only), 5p.
459	25-27062	NTIS (U. S. Sales Only), 6p.
IC-	(Italian)	
69/121	25-28060	
IN-		
1445	25-28737	Dep. NTIS, 112p.
INIS-mf-	(International Atomic Energy Agency)	
2	25-27203	NTIS (U. S. Sales Only), 18p.
3	25-27204	NTIS (U. S. Sales Only), 15p.
5	25-27265	NTIS (U. S. Sales Only), 16p.
9	25-27176	NTIS (U. S. Sales Only), 23p.
11	25-27279	NTIS (U. S. Sales Only), 46p.
12	25-27280	NTIS (U. S. Sales Only), 11p.
13	25-27281	NTIS (U. S. Sales Only), 23p.
14	25-27282	NTIS (U. S. Sales Only), 10p.
15	25-27245	NTIS (U. S. Sales Only), 14p.
19	25-27205	NTIS (U. S. Sales Only), 25p.
INR-	(Non-AEC)	
1213	25-26491	Dep. NTIS (U. S. Sales Only), 211p.
1269	25-28857	Dep. NTIS (U. S. Sales Only), 74p.
INR-P-	(Polish)	
1203	25-27928	Dep. NTIS (U. S. Sales Only), 18p.
1217	25-27449	Dep. NTIS (U. S. Sales Only), 132p.
IPP-	(Non-AEC)	
7/3	25-27840	Dep. NTIS (U. S. Sales Only), 38p.
ISS-	(Italian)	
70/17	25-28449	Dep. NTIS (U. S. Sales Only), 29p.
ITEF-	(Russian)	
761	25-28108	Dep. NTIS (U. S. Sales Only), 11p.
ITF-	(Russian)	
70-62-E	25-27929	Dep. NTIS (U. S. Sales Only), 22p.
70-90-E	25-27643	Dep. NTIS (U. S. Sales Only), 21p.
70-100-P	25-28163	Dep. NTIS (U. S. Sales Only), 72p.
70-101-E	25-27930	Dep. NTIS (U. S. Sales Only), 20p.
70-105-E	25-27421	Dep. NTIS (U. S. Sales Only), 11p.
JAB-	(Non-AEC)	
99-78	25-26402	Dep. NTIS, 183p.
JAERI-	(Japanese)	
1200	25-28344	Dep. NTIS (U. S. Sales Only), 13p.
1202	25-28682	Dep. NTIS (U. S. Sales Only), 17p.
1204	25-28758	Dep. NTIS (U. S. Sales Only), 11p.
JAERI-Memo-	(Japanese)	
4248	25-28692	Dep. NTIS (U. S. Sales Only), 26p.
4267	25-26152	Dep. NTIS (U. S. Sales Only), 10p.
4272	25-28759	Dep. NTIS (U. S. Sales Only), 22p.
JINR-	(Russian)	
E2-5575	25-27931	Dep. NTIS (U. S. Sales Only), 78p.
E3-5483	25-28345	Dep. NTIS (U. S. Sales Only), 22p.
E4-5567	25-28346	Dep. NTIS (U. S. Sales Only), 17p.
P3-5553	25-28347	Dep. NTIS (U. S. Sales Only), 16p.
P6-5617	25-28348	Dep. NTIS (U. S. Sales Only), 23p.
P7-5161	25-28350	For translation see KFK-tr-350
P7-5192	25-28351	For translation see KFK-tr-352
P9-5610	25-28109	Dep. NTIS (U. S. Sales Only), 18p.
P9-5622	25-28110	Dep. NTIS (U. S. Sales Only), 33p.
P12-5644	25-26209	Dep. NTIS (U. S. Sales Only), 8p.
P13-5636	25-26505	Dep. NTIS (U. S. Sales Only), 25p.
P13-5637	25-26506	Dep. NTIS (U. S. Sales Only), 28p.
JPL-TR-	(Non-AEC)	
32-1481	25-27305	See N-70-35897
JPRS-	(Non-AEC)	
52907	25-28760	NTIS
JUL-	(German)	
675-FF	25-27246	Dep. NTIS (U. S. Sales Only), 76p.
681-RX	25-27177	Dep. NTIS (U. S. Sales Only), 49p.
683-HA	25-28147	Dep. NTIS (U. S. Sales Only), 24p.
KAPL-P-		
3930	25-28349	Dep. NTIS, 7p.
KFK-	(German)	
911	25-26326	Dep. NTIS (U. S. Sales Only), 121p.
1179	25-28804	For translation see EURFNR-835
1181	25-28690	For translation see EURFNR-836
1188	25-28756	For translation see EURFNR-803
1218	25-28111	Dep. NTIS (U. S. Sales Only), 11p.
1233	25-28656	For translation see EURFNR-842
1238	25-28655	For translation see EURFNR-830
1263	25-26448	Dep. NTIS (U. S. Sales Only), 69p.
1270/1	25-28632	For translation see EURFNR-824
1293	25-26189	Dep. NTIS (U. S. Sales Only), 13p.
1300	25-26420	Dep. NTIS (U. S. Sales Only), 30p.
1312	25-26210	Dep. NTIS (U. S. Sales Only), 17p.
1334	25-28805	See EURFNR-898
KFK-Ext.Ber.-	(West German)	
8/70-1	25-27206	NTIS (U. S. Sales Only), 21p.

XUM

Report No.	Abstract No.	Availability
KFK-tr-	(German)	
350	25-28350	Dep. NTIS (U. S. Sales Only)
352	25-28351	Dep. NTIS (U. S. Sales Only)
KHFTI-	(Russian)	
70-8	25-27644	Dep. NTIS (U. S. Sales Only), 11p.
70-17	25-28112	Dep. NTIS (U. S. Sales Only), 11p.
L-	(Misc.)	
6015	25-28352	See N-71-10060
LA-		
4576	25-28164	Dep. NTIS, 123p.
4598	25-27726	Dep. NTIS, 14p.
4622	25-26153	Dep. NTIS, 155p.
LA-tr-		
71-25	25-28858	Dep. NTIS
71-27	25-28859	Dep. NTIS
71-28	25-28860	Dep. NTIS
LB/G-	(British)	
2937	25-26288	Dep. NTIS (U. S. Sales Only)
LF-tr-		
49	25-26921	Dep. NTIS
LUNP-	(Swedish)	
7013	25-28217	Dep. NTIS (U. S. Sales Only), 24p.
LYCEN-	(French)	
7054	25-28113	Dep. NTIS (U. S. Sales Only), 46p.
M-	(Misc.)	
436	25-28451	See N-71-10999
MIT-	(Misc.)	
905-162	25-28861	Dep. NTIS, 31p.
MLM-		
1780	25-26548	Dep. NTIS, 12p.
1790	25-26449	Dep. NTIS, 9p.
1795	25-26739	Dep. NTIS, 51p.
1796	25-26425	Dep. NTIS, 104p.
N-	(Misc.)	
70-35897	25-27305	NTIS, 37p.
70-42045	25-27207	NTIS, 22p.
70-42846	25-28450	NTIS, 110p.
71-10060	25-28352	NTIS, 40p.
71-10352	25-27208	NTIS, 171p.
71-10353	25-27178	NTIS, 110p.
71-10454	25-27179	NTIS, 11p.
71-10455	25-26413	NTIS, 6p.
71-10590	25-27283	NTIS, 30p.
71-10999	25-28451	NTIS, 104p.
71-11662	25-27209	NTIS, 27p.
NAL-		
55	25-28862	Dep. NTIS, 9p.
NASA-CR-	(Misc.)	
1608	25-27208	See N-71-10352
1611	25-27178	See N-71-10353
72409	25-28761	Dep. NTIS, 23p.
110136	25-27305	See N-70-35897
111120	25-27283	See N-71-10590
NASA-TM-X-	(Misc.)	
2118	25-27179	See N-71-10454
2126	25-26413	See N-71-10455
NASA-TN-D-	(Misc.)	
6000	25-28450	See N-70-42846
6038	25-28451	See N-71-10999
6044	25-27207	See N-70-42045
6057	25-28352	See N-71-10060
7000	25-27209	See N-71-11662
NCRP-	(Non-AEC)	
25	25-26534	Superintendent of Documents, GPO, Washington, D. C
27	25-26533	Superintendent of Documents, GPO, Washington, D. C
28	25-26455	Superintendent of Documents, GPO, Washington, D. C
NIRS-RSD-	(Japanese)	
27	25-26392	Dep. NTIS (U. S. Sales Only), 17p.
NLCO-		
1080	25-27180	Dep. NTIS, 57p.
NP-	(AEC File No. for Non-AEC Reports)	
18634	25-28114	Dep. NTIS (U. S. Sales Only), 28p.
18674	25-28218	
18695	25-28353	Dep. NTIS (U. S. Sales Only), 99p.
18702	25-27915	Dep. NTIS (U. S. Sales Only), 363p.
18717	25-28452	Dep. NTIS (U. S. Sales Only), 221p.
18723	25-28354	Dep. NTIS (U. S. Sales Only), 155p.
18725	25-27951	Dep. NTIS (U. S. Sales Only), 77p.
18728	25-26740	Dep. NTIS (U. S. Sales Only), 4p.
18732	25-26749	Dep. NTIS (U. S. Sales Only), 4p.
18746	25-26518	Dep. NTIS (U. S. Sales Only), 32p.
18747	25-26519	Dep. NTIS (U. S. Sales Only), 29p.
18758	25-27687	Dep. NTIS (U. S. Sales Only), 36p.
18759	25-27704	Dep. NTIS (U. S. Sales Only), 33p.
18763	25-28023	Dep. NTIS (U. S. Sales Only), 8p.
18764	25-26507	Dep. NTIS (U. S. Sales Only), 16p.
18766	25-28024	Dep. NTIS (U. S. Sales Only), 11p.
18768	25-28025	Dep. NTIS (U. S. Sales Only), 10p.
18774	25-28026	Dep. NTIS (U. S. Sales Only), 12p.
18778	25-28698	Dep. NTIS (U. S. Sales Only), 21p.
18781	25-28738	Dep. NTIS (U. S. Sales Only), 57p.
18782	25-28634	Dep. NTIS (U. S. Sales Only), 70p.
18787	25-26508	Dep. NTIS (U. S. Sales Only), 22p.
NP-tr-	(AEC File No. for Non-AEC Translations)	
1932	25-27136	Husipar; 19: No. 3, 101-4(May--Jun 1970)
NRCN-	(Israel)	
254	25-28219	NTIS (U. S. Only), 46p.
NUMEC-		
4189-4	25-26426	Dep. NTIS, 36p.
NVO-		
99-12	25-26400	Dep. NTIS, 134p.
1163-218	25-26401	Dep. NTIS, 66p.
1229-105 (Pt.1)	25-26403	Dep. NTIS, 42p.
NYO-		
2150-59	25-26215	Dep. NTIS, 122p.
2150-60	25-26289	Dep. NTIS, 84p.
2391-111	25-28863	Dep. NTIS, 106p.
2579-20	25-26682	Dep. NTIS, 47p.
3270-47	25-28563	See DOCKET-50206-111
3399-242	25-28028	See SU-1206-242
3409-9	25-26520	Dep. NTIS, 36p.
3463-23	25-27841	Dep. NTIS, 135p.
3504-56	25-27866	Dep. NTIS, 21p.
3753-19	25-26290	Dep. NTIS, 34p.
3973-8	25-28864	Dep. NTIS, 16p.
3976-4	25-28865	Dep. NTIS, 4p.
3976-5	25-28866	Dep. NTIS, 22p.
3993-1	25-28867	Dep. NTIS, 144p.
4032-37	25-28453	Dep. NTIS, 23p.
4075-10	25-28868	Dep. NTIS, 6p.
4078-3	25-28869	Dep. NTIS, 37p.
4097-2	25-28870	Dep. NTIS, 12p.
4150-9	25-26190	Dep. NTIS, 13p.
NYU-		
4090-1	25-28798	Dep. NTIS, 16p.
ORNL-		
4668	25-28790	Dep. NTIS, 32p.
ORNL-IIC-		
30(Pt.4)	25-26427	Dep. NTIS, 37p.
ORNL-TM-		
3193	25-27181	Dep. NTIS, 58p.
3194	25-26327	Dep. NTIS, 64p.
3253	25-28711	Dep. NTIS, 41p.
3266	25-28148	Dep. NTIS, 33p.
3298	25-26450	Dep. NTIS, 58p.
3365	25-28784	Dep. NTIS, 25p.
3369	25-28762	Dep. NTIS, 36p.
ORNL-tr-		
1991	25-28871	Dep. NTIS
2133	25-28872	Dep. NTIS
2306	25-26785	Dep. NTIS
2410	25-26328	Dep. NTIS
2419	25-28149	Dep. NTIS
2436	25-27663	Dep. NTIS
2439	25-26261	Dep. NTIS
2445	25-28873	Dep. NTIS
2447	25-28874	Dep. NTIS
2451	25-28677	Dep. NTIS
2455	25-26750	Dep. NTIS
2457	25-28875	Dep. NTIS
2458	25-28876	Dep. NTIS
2462	25-26549	Dep. NTIS
ORO-		
2572-27	25-28877	Dep. NTIS, 43p.
3260-3-A	25-26922	Dep. NTIS, 16p.
3328-13	25-28878	Dep. NTIS, 13p.
3799-7	25-26277	Dep. NTIS, 67p.
3842-3	25-26540	Dep. NTIS, 101p.
3944	25-26393	Dep. NTIS, 9p.
PATENTS	(British)	
1,165,689	25-28836	
1,219,146	25-26346	
1,222,653	25-27172	
1,224,248	25-26345	

XUM

Report No.	Abstract No.	Availability
1,224,278	25-28823	
1,224,856	25-28746	
1,225,360	25-28830	
1,225,460	25-28670	
1,225,470	25-28824	
1,225,487	25-28831	
1,225,751	25-28829	
1,225,771	25-28832	
1,225,782	25-28652	
1,225,947	25-28673	
1,225,967	25-28749	
1,225,970	25-28837	
1,226,021	25-28694	
1,226,106	25-28649	
1,226,207	25-28826	
1,226,264	25-28828	
1,226,308	25-28825	
1,226,514	25-28671	
1,226,826	25-28695	
1,226,919	25-28693	
1,226,929	25-28827	
1,226,930	25-28700	
1,227,386	25-28747	
1,227,505	25-27275	
1,227,580	25-28647	
1,227,606	25-28646	
1,227,929	25-28153	
1,228,317	25-27276	
1,228,390	25-27195	
1,228,610	25-28834	
1,228,616	25-28653	
1,228,617	25-28648	
1,228,694	25-26543	
PATENTS	(Canadian)	
859,053	25-27190	
866,999	25-28751	
867,000	25-28645	
PATENTS	(French)	
1,593,817	25-28745	
PATENTS	(Russian)	
244,519	25-28136	
PATENTS	(U. S.)	
3,546,454	25-26541	
3,546,455	25-26460	
3,554,693	25-26338	
3,554,709	25-26337	
3,554,773	25-27163	
3,554,867	25-26319	
3,558,440	25-26336	
3,558,935	25-28635	
3,562,480	25-26524	
3,563,728	25-27214	
3,564,081	25-27273	
3,564,238	25-26417	
3,564,246	25-26466	
3,565,591	25-27229	
3,565,760	25-28672	
3,566,185	25-28137	
3,573,036	25-27274	
3,573,166	25-28676	
3,573,167	25-28650	
PG-Report-	(British)	
965	25-26177	Dep. NTIS (U. S. Sales Only). UK 25p, 13p.
PNE-		
527	25-26404	Dep. NTIS, 17p.
1002	25-26405	Dep. NTIS, 74p.
1009	25-26406	Dep. NTIS, 38p.
1112	25-26407	Dep. NTIS, 116p.
1117	25-26408	Dep. NTIS, 68p.
PNE-G-		
73	25-26405	See PNE-1002
74	25-26406	See PNE-1009
PNE-R-		
45	25-26409	Dep. NTIS, 28p.
46	25-26402	See JAB-99-78
47	25-26410	Dep. NTIS, 32p.
PRDC-EF-		
87	25-28558	See DOCKET-50016-108
88	25-28559	See DOCKET-50016-109
PURC-		
4159-16	25-27961	Dep. NTIS, 129p.
4159-17	25-28115	Dep. NTIS, 14p.
4159-19	25-27969	Dep. NTIS, 19p.
4159-22	25-28003	Dep. NTIS, 23p.
R-	(Misc.)	
69-CAP-8	25-27182	
591	25-28218	See NP-18674
RCC-M-	(British)	
211	25-26492	Dep. NTIS (U. S. Sales Only), 15p.
RCN-	(Dutch)	
134	25-28150	Dep. NTIS (U. S. Sales Only), 6p.
RD/B/N-	(British)	
1518	25-28816	Dep. NTIS (U. S. Sales Only), 43p.
1784	25-28528	Dep. NTIS (U. S. Sales Only), 55p.
1812	25-27266	Dep. NTIS (U. S. Sales Only), 24p.
1837	25-28806	Dep. NTIS (U. S. Sales Only), 49p.
1850	25-27842	Dep. NTIS (U. S. Sales Only), 20p.
RFP-Trans-		
76	25-26154	Dep. NTIS
RHEL/R-	(British)	
208	25-27664	Dep. NTIS (U. S. Sales Only). UK 17p, 11p.
212	25-26509	Dep. NTIS (U. S. Sales Only). UK 50p, 36p.
RISO-	(Danish)	
205	25-28763	Dep. NTIS (U. S. Sales Only), 117p.
RLO-		
1388-599	25-27632	Dep. NTIS, 18p.
1388-602	25-28027	Dep. NTIS, 11p.
1388-603	25-27633	Dep. NTIS, 25p.
1388-604	25-27634	Dep. NTIS, 10p.
1388-605	25-27635	Dep. NTIS, 27p.
1750-41	25-28879	Dep. NTIS, 27p.
1750-59	25-28880	Dep. NTIS, 14p.
2225-T-20-2	25-26398	Dep. NTIS, 43p.
RO/EERL-	(Non-AEC)	
71-1	25-26335	GPO $0.50
RPC/RPNK/P-	(British)	
(70)80	25-28806	See RD/B/N-1837
(71)7	25-28816	See RD/B/N-1518
RT/BIO-	(Italian)	
(70)33	25-27160	Ind. Conserve; 45: No. 1, 23-8(Jan-Mar 1970)
RT/FI-	(Italian)	
(70)38	25-28454	Dep. NTIS (U. S. Sales Only), 33p.
RT/FIMA-	(Italian)	
69-5	25-28144	NTIS (U. S. Sales Only), 28p.
RT/ING-	(Italian)	
(70)21	25-27293	Dep. NTIS (U. S. Sales Only), 15p.
(70)25	25-28739	Dep. NTIS (U. S. Sales Only), 28p.
(71)1	25-26550	Dep. NTIS (U. S. Sales Only), 22p.
RT/PROT-	(Italian)	
(70)6	25-26770	Securitas; 54: 821-40(1969)
SAM-TR-	(Non-AEC)	
70-38	25-26920	See AD-711041
SC-DC-		
713865	25-26411	Dep. NTIS, 8p.
713920	25-28881	Dep. NTIS, 18p.
SC-DR-		
68-796	25-28882	Dep. NTIS, 12p.
70-510	25-28883	Dep. NTIS, 215p.
70-680	25-28884	Dep. NTIS, 29p.
70-856	25-28885	Dep. NTIS, 95p.
710033	25-28886	Dep. NTIS, 26p.
710045	25-26560	Dep. NTIS, 42p.
710086	25-28887	Dep. NTIS, 15p.
710095	25-26428	Dep. NTIS, 24p.
710124	25-27210	Dep. NTIS, 20p.
710192	25-28888	Dep. NTIS, 41p.
SC-R-		
70-4402	25-26354	Dep. NTIS, 23p.
7121	25-26429	Dep. NTIS, 65p.
SC-RR-		
70-356	25-28889	Dep. NTIS, 44p.
70-852	25-28890	Dep. NTIS, 16p.
710122	25-28891	Dep. NTIS, 36p.
SGAE-RT-	(Non-AEC)	
33/1970	25-26451	Dep. NTIS (U. S. Sales Only), 16p.
SM-	(Misc.)	
147/4	25-26442	See AECL-3803
147/5	25-26441	See AECL-3802
SRO-	(Misc.)	
344-11	25-26355	Dep. NTIS, 7p.
STI/PUB-	(International Atomic Energy Agency)	
223	25-27137	IAEA $4.00
261	25-28621	IAEA $25.00
263	25-26567	IAEA $24.00

XUM

Report No.	Abstract No.	Availability
267	25-28529	IAEA $14.00
SU-	(Misc.)	
1206-242	25-28028	Dep. NTIS, 34p.
TID-		
4100(Suppl. 62)	25-26414	
5001(10th Rev.)	25-28892	Dep. NTIS, 272p.
25543	25-27138	Dep. NTIS, 103p.
25659	25-28355	Dep. NTIS, 35p.
25672	25-27480	Hinsdale, Ill.; American Nuclear Society (1970). 528p. $34.90
25674	25-26399	Dep. NTIS, 35p.
25679	25-28893	GPO $1.00
25682	25-28894	Dep. NTIS, 20p.
25683	25-28895	Dep. NTIS, 36p.
TRG-Report-	(British)	
2104	25-26211	Dep. NTIS (U. S. Sales Only). UK 6p, 5p.
2121	25-26415	Dep. NTIS (U. S. Sales Only). UK 35p, 49p.
TT-	(Misc.)	
70-55010/1	25-26275	See AEC-tr-7102/1
TUBIK-	(German)	
21	25-28151	Dep. NTIS (U. S. Sales Only), 268p.
UCID-		
15754	25-28896	Dep. NTIS, 32p.
UCLA-		
34-P-172-1	25-28897	Dep. NTIS, 31p.
UCRL-		
20165	25-28116	Dep. NTIS, 2p.
20166	25-28117	Dep. NTIS, 3p.
20177	25-28118	Dep. NTIS, 3p.
20194	25-28119	Dep. NTIS, 4p.
20301	25-27211	Dep. NTIS, 69p.
20406	25-28120	Dep. NTIS, 10p.
20613	25-28898	Dep. NTIS, 49p.
20620	25-28121	Dep. NTIS, 5p.
20624	25-28899	Dep. NTIS, 105p.
20633	25-28122	Dep. NTIS, 9p.
50163(Pt.7)	25-26751	Dep. NTIS, 77p.
50400(Vol. 3)	25-28356	Dep. NTIS, 812p.
50979	25-26412	Dep. NTIS, 31p.
51006	25-27867	Dep. NTIS, 13p.
72748	25-28900	Dep. NTIS, 8p.
73063	25-28901	Dep. NTIS, 6p.
73073	25-28008	Dep. NTIS, 85p.
73075	25-28123	Dep. NTIS, 8p.
73080	25-28902	Dep. NTIS, 5p.
73103	25-28903	Dep. NTIS, 53p.
UJV-	(Czechoslovakian)	
2540-F	25-28357	Dep. NTIS (U. S. Sales Only), 31p.
2553-F	25-28220	Dep. NTIS (U. S. Sales Only), 22p.
UR-		
49-1128	25-26271	pp 117-29 of Effects of Metals on Cells, Subcellular Elements, and Macromolecules. /Maniloff, Jack (ed.). Springfield, Ill.; Charles C Thomas, Publisher (1970)
49-1429	25-28904	Dep. NTIS, 132p.
49-1440	25-28905	Dep. NTIS, 104p.
49-1444	25-28906	Dep. NTIS, 106p.
WANL-PR(P)-	(Misc.)	
14	25-27208	See N-71-10352
17	25-27178	See N-71-10353
WASH-		
1159	25-27436	Dep. NTIS, 260p.
WCAP-	(Misc.)	
7406	25-28668	Dep. NTIS, 23p.
7571	25-28669	Dep. NTIS, 17p.
WHAN-FR-		
38	25-27268	Dep. NTIS, 23p.
Y-		
1725	25-28907	Dep. NTIS, 56p.
1755	25-28908	Dep. NTIS, 40p.
1762	25-28909	Dep. NTIS, 54p.
1783	25-28910	Dep. NTIS, 26p.
1787	25-28911	Dep. NTIS, 87p.
ZJE-	(Czechoslovakian)	
101	25-28807	Dep. NTIS (U. S. Sales Only), 20p.

☆U. S. GOVERNMENT PRINTING OFFICE: 1971—436-215/28

XUM

UNITED STATES ATOMIC ENERGY COMMISSION

NUCLEAR SCIENCE ABSTRACTS

Volume 25
Numbers 7-12

Abstracts 12921-28911

April—June
1971

Division of Technical Information

XUM

STAFF OF NUCLEAR SCIENCE ABSTRACTS

John W. Norris
Managing Editor

Donald D. Davis
Assistant Managing Editor

David E. Bost
Production Manager

Sidney F. Lanier
Subject Heading Specialist

J. Paul Meredith
Descriptive Cataloging Specialist

Frederick E. Marsh, Jr.
Computer Index Coordinator

Clara L. Fox
Corporate Author Specialist

Helen W. White
Report Number Specialist

Section Editors

Everett J. Hoffman
Chemistry

Robert C. Kelly
Engineering; Earth Sciences; Metals, Ceramics, and Other Materials

Lee M. Thompson
General Physics

Charles E. Stuber
High Energy Physics; Instrumentation

Donald D. Davis
Life Sciences

Lawrence T. Whitehead
Nuclear Physics

James M. Jacobs
Reactor Technology

Evaluators

Thomas S. Chapman
Rose V. Jermain
John H. Mitchell
Mary H. Newman
Polly C. Summers

Abstractors

F. S. Armstrong*
Ellis R. Bedford
Mary M. Brown
Jane G. Buchanan
D. Lamar Cason
Gloria M. Caton
David C. Cunningham
James R. Dulaney
Helga B. Gerstner
Mary C. Grissom
Phyllis C. Hansen
Carolyn D. Houston
Elaine E. Huber
Rose V. Jermain
W. Hugh Kinser, Jr.
Lisbeth C. Lieberman
Betty L. McDowell
Patricia B. McEwen
Fay M. Martin
William D. Matheny
Dora H. Moneyhun
Jean F. Peckham
Henry D. Raleigh
Mona H. Raridon
Julia S. Redford
Jessie W. Rushing
Robert W. Rutkowski
Francis L. Sachs
Lila B. Smith
Anne G. Ward
Helen L. Ward
Milton O. Whitson
Juanita Wilson

*Atomic Energy of Canada, Ltd.

Charles R. Bruce
Publishing Coordinator

Communication concerning the editorial policy and content of *Nuclear Science Abstracts* should be addressed to the Managing Editor, *Nuclear Science Abstracts*, USAEC Division of Technical Information Extension, P. O. Box 62, Oak Ridge, Tennessee 37830.

Use of funds for printing this publication approved by the Director of the Bureau of the Budget, June 26, 1969.

XUM

UNITED S[illegible]
GOVERNMENT PRI[illegible] OFFICE
DIVISION
PUBLIC DOC[illegible]NTS
WASHINGTON, D[illegible]
OFFICIAL BUS[illegible]

POSTAGE AND FEES PAID
U. S. GOVERNMENT PRINTING OFFICE

AEC Critical Review Series

Aerodynamic Characteristics of Atmospheric Boundary Layers

ERICH J. PLATE, Argonne National Laboratory and Karlsruhe University

May 1971

In the last few decades many meteorologists, physicists, and engineers have contributed to such an extent to our understanding of atmospheric boundary layers that a reasonably complete physical picture of the flow proce[illegible] is available. In this book Professor Plate has summarized what [illegible]nown about mean flow conditions and has developed his subject in f[illegible] chapters covering four aspects of boundary layers. For each of th[illegible]reas, recent research is surveyed and integrated into a coherent acc[illegible] of mean properties of wind and temperature fields. A series of su[illegible]ions is given for future research to extend the limits of our knowl[illegible] with particular emphasis on laboratory experiments.

1. Neutrally Stratified Boundary Layer over Uniform Terrain
2. Stratified Atmospheric Boundary Layer near the Ground
3. Free-Convection Layer
4. Two-Dimensional Disturbed Boundary Layers

Subject and Author Indexes

198 pages, 7 [illegible] inches
Library of Co[illegible]s Catalog Card Number: 70-611329

Available for [illegible] as TID-25465 from
National T[illegible]al Information Service
U. S. Depar[illegible]t of Commerce
Springfield, [illegible]nia 22151

XUM